Tenth International Technical Conference on Experimental Safety Vehicles

U.S. Department of Transportation

National Highway Traffic Safety Administration

England

Tenth International Technical Conference on Experimental Safety Vehicles

Sponsored by:

U.S. Department of Transportation
National Highway Traffic Safety Administration

Hosted by:

The Department of Transportation of Her Majesty's Government

Held at:

Oxford, England, July 1-4, 1985

U.S. Department of Transportation

National Highway Traffic Safety Administration

Foreword

This report of the proceedings of the Tenth International Technical Conference on Experimental Safety Vehicles was prepared by the National Highway Traffic Safety Administration, U.S. Department of Transportation.

We wish to thank the authors and all those responsible for the excellence of the material submitted, which aided materially in the preparation of this report.

For clarity and because of some translation difficulties, a certain amount of editing was necessary. Apologies are, therefore, offered where the transcription is not exact.

Participants List

AUSTRALIA

McCaul, K.A.
NH & MRC Road Accident Research

Pound, F.R.
General Motors Holdens Ltd.

BELGIUM

Akiba, T.
JSAE Brussels

Foggini, B.F.
CCHC

Gerryn, C.
Ford of Europe Inc.

Hachiya, M.
Nissan Motor Co. Ltd.

Henssler, H.
Commission of the European Communities

Masani, M.
Toyota Motor Corporation

Meganck, A.M.
Honda Motor Co. Ltd.

Mizuno, Y.
Nissan Motor Co. Ltd.

Moritake, T.
Toyota Motor Corporation

Murao, Y.
Daihatsu Motor Co. Ltd.

Nishikawa, T.
Nissan Motor Co. Ltd.

Ono, K.
Mazda Motor Corporation

Shibagaki, Mr.
Mazda Motor Corporation

Silvestri, G.
Commission of the European Communities

Van Driessche, H.
Honda Motor Co. Ltd.

CANADA

Boulding, R.W.
Hastings & Boulding Engineering

Welbourne, E.R.
Transport Canada

DENMARK

Rasmussen, I.
Ministry of Justice

FEDERAL REPUBLIC OF GERMANY

Backhaus, Mr.
Audi

Bendig, U.
Engineer

Brasche, W.
Ford Werke

Brenner, R.
TRW Repa GmbH

Breuer, B.J.
Automotive Engineering Institute
Technische Hochschule Darmst

Chikamori, S.
Mitsubishi Motor Corporation

Daniel-Holther, G.
Leiter Verkehrsredaktion NDR

Danner, M.
HUK-Verband

Elmar, E.V.
Audi

Embleu, Mr.
Volkswagen Werke AG

Fellerer, J.
Bayerische Motoren Werke AG

Fohl, A.H.
TRW Repa GmbH

Friedel, B.
Federal Highway Research Institute

Grosch, I.
Daimler-Benz AG

Gunter, Z.
Adam Opel AG

Haberl, J.
Bayerische Motoren Werke AG

Heger, A.
Technical University of Berlin

Heinz, K.
Sekurit Glas Union GmbH

Helbach, W.E.
TRW Repa GmbH

Herkommer, B.
TRW Repa GmbH

Heydenreich, R.
BMW-AG Sparte Motorrad

Hoefs, H.O.
HCF Porsche AG

Honl, W.D.
TRW Repa GmbH

Hummel, T.
HUK-Verband

Kallieris, D.
Institute for Legal Medicine

Klaus, G.
Volkswagenwerk AG

Koch, Dr.
Institut fuer Zweiradsicherheit

Kraft, H.J.
Bayerische Motoren Werke AG

Kruger, H.J.
TUV Rheinland e.V.

Kuiperback, J.
Department of Road Research

Kunert, H.
Sekurit Glas Union GmbH

Langwieder, K.
HUK-Verband

Leyer, H.
Volkswagen Werke AG

Loebich, R.
Audi AG

Merlino, C.J.
Merco Inc.

Mitzkus, J.E.
TRW Repa GmbH

Nilsson, K.E.
Bayern Chemie GmbH

Peters, B.
TRW Repa GmbH

Pfanzeder, D.
Bayerische Motoren Werke AG

Praxenthaler, H.
Federal Highway Research Institute

Reidelbach, W.
Daimler-Benz AG

Reinschild, K.W.R.
Motor Presse Club

Roehl, E.
TUEV Rheinland

Roesler, H.
Bayerische Motoren Werke AG

Rompe, K.
Institute for Traffic Safety

Schmid, W.
Daimler-Benz AG

Schwellenbach, M.
Fordwerke

Seiffert, U.W.
Wolkswagenwerk AG

Sorsche, J.H.S.
Daimler-Benz AG

Sporner, A.
HUK-Verband

Stamm, R.
Federal Ministry of Transportation

Strakerjan, Mr.
Daimler-Benz AG

Sturtz, G.
Daimler-Benz AG

Timmermann, A.
Forschungsgemeinschaft

Vogel, C.V.
Elbatainer

von Manteuffel, P.
Verband der Automobilindustrie e.V.

Weisbarth, H.P.
BMW AG

Wezel, U.E.
Porsche

Wierschem, F.
Porsche

Yanagimoto, M.
NSK Technical Centre Europe

FRANCE

Bellisai, G.B.
Klippan France

Bluet, J.C.B.
Directeur du Centre Evaluation ONSER

Bohers, Mr.
Pas Etudes Recherches Reglementations

Bourdillon, T.B.
UTAC

Cesari, D.
ONSER

Chenevez, A.
Regie Renault

Chillon, C.
Peugeot SA

Cord, P.P.
Society National des Poudres & Exp.

Dargaud, R.D.
UTAC

Dejeammes, M.
ONSER

Edouard, A.
Peugeot

Genestier, J.
UTAC

Gratadour, M.
PSA Etudes et Recherches

Guasco, R.G.
CLEPA

Hartemann, F.H.
PSA/Renault

Helary, Mr.
Renault

Leroy, J.
ONSER-Laboratoire de Chocs

Mauron, M.G.
Peugeot SA

Moreau de St. Martin, J.M.
ONSER

Phelps, J.L.
BPICA

Provensal, J.L.
Renault

Sasaki, S.
JAMA

Soret, P.
Renault

Tarriere, C.T.
PSA/Renault

Verriest, J.P.
ONSER

Wilson, E.C.
BPICM

Yermont, Y.V.
Renault

GREAT BRITAIN

Adams, J.B..lf BL Technology Ltd.

Allum, D.R.T.
3 M

Ashley, C.
Motor Industry Research Association

Ashton, S.J.
University of Birmingham

Austin, D.A.
Norton Motors, Ltd.

Bacon, D.G.C.
Motor Industry Research Association

Baker, D.H.
Ford Motor Company, Ltd.

Barnes, K.B.
SMMT

Bates, H.J.
Transport & Road Research Laboratory

Baxter, W.L.
Automotive Engineering Consultant

Bentley, J.T.
Freight Rover Ltd.

Berry, J.M.
Department of Transport

Betterton, C.
Austin Rover Group, Ltd.

Beulich, H.
BMW Motor Cycles

Bischoff, W.W.
Consultant

Black, C.D.
Jaguar Cars Ltd.

Bothwell, P.W.
Caliber Design Ltd.

Bothwell, R.
Caziber Design, Ltd.

Brabin, E.J.
Brabin Consultants, Ltd.

Breen, J.M.
Imperial College

Brindle, L.R.
Cranfield Institute of Technology

Bulmer, C.H.
BL Technology Limited

Burford, G.W.
Automobile Association

Burgess, R.
Aston Martin Lagonda

Burgess, T.M.
Transport & Road Research Laboratory

Cart, J.
Lucas Girling Ltd.

Charles, J.M.
Ford Motor Company Ltd.

Charlick, B.E.
Ford Motor Company Ltd.

Chinn, B.P.
Transport & Road Research Laboratory

Clarke, C.S.
Transport & Road Research Laboratory

Clarke, S.L.
Institute of Consumer Ergonomics

Clifton, J.T.
Department of Transport

Colbourne, N.J.
Rolls Royce Motors Ltd.

Coles, R.E.
Society of Motor Manufacture & Trades, Ltd.

Connell, P.C.
Kawasaki Motors (UK) Ltd.

Cooke, A.C.
Rolls Royce Motors Ltd.

Copeland, R.
Jaguar Cars Limited

Cornelius, D.F.
Transport & Road Research Laboratory

Cutting, E.J.
Ford Motor Company Ltd.

Dale, K.J.
Motor Industry Research Association

Dancocks, H.P.
Austin Rover Group Ltd.

Davies, G.O.
Austin Rover Group Ltd.

Davies, J.G.
BL Technology Limited

Davis, R.J.
Bedford Commercial Vehicles

Dixon, W.H.
SMMT Ltd.

Doe, G.T.
Lotus Cars Ltd.

Donne, G.L.
Transport & Road Research Laboratory

Dovey, J.
Jaguar Cars Limited

Dowling, M.J.
Austin Rover Group Ltd.

Dunn, E.
Department of Transport

Eaton, M.A.
Vehicle Inspectorate DTp

Edwards, H.G.
Vehicle Inspectorate DTp

Edwards, K.C.
Austin Rover Group Ltd.

Elliot-Smith, A.G.
Austin Rover Group Ltd.

Ellis, S.L.
Aston Martin Lagonda

Else, R.
Britax Wingard Ltd.

Fenn, M.A.
Transport & Road Research Laboratory

Foot, D.J.
Department of Transport

Fowler, J.E.
Austin Rover Group Ltd.

Fulford, I.W.G.
Spafax Supplies Ltd.

Furness, J.W.
Chairman, Tenth International Technical Conference on Experimental Safety Vehicles

Galer, M.D.
Institute for Consumer Economics

Gazeley, I.
Motor Industry Research Association

Gebbels, D.R.
Austin Rover Group Ltd.

Gibson, D.A.K.
Talbot Motor Co. Ltd.

Gidlow, W.
Jaguar Cars Limited

Giles, A.R.
Austin Rover Group Ltd.

Gloyns, P.F.
Vehicle Safety Consultants

Goater, J.H.
Transport & Road Research Laboratory

Goldsmith, R.
Aston Martin Lagonda Ltd.

Gould, D.G.
Ford Motor Company Ltd.

Green, D.H.
Ford Motor Company Ltd.

Green, F.
Thames Valley Police

Grew, N.D.
Austin Rover Group Ltd.

Grime, G.
University College of London

Grimes, A.J.
Department of Transport

Hall, L.C.
Royal Military College of Science

Happian-Smith, J.
Brunel University

Hardy, R.N.
Cranfield Impact Centre

Harms, P.L.
Transport & Road Research Laboratory

Harris, J.A.
Transport & Road Research Laboratory

Harvey, D.W.
Vehicle Inspectorate DTp

Haslegrave, C.M.
University of Nottingham

Hassan, A.A.
Cranfield Institute of Technology

Hayes, H.R.M.
Child Accident Prevention Trust

Hercher, H.
Girling Bremsen

Hill, D.
Kawasaki Motors (UK) Ltd.

Hill, K.J.
The Middlesex Polytechnic

Hobbs, C.A.
Transport & Road Research Laboratory

Hope, A.
Journalist

Hopes, P.D.
Transport & Road Research Laboratory

Horsfall, J.A.C.
R.B. Hawkins & Assoc. Ltd.

Hosier, B.F.
British Standards Institution

Houston, D.J.
Automobile Association

Jacobson, M.A.I.
Automobile Association

James, S.K.
Bedford Trucks

Jefferies, A.
Monsanto

Jelly, R.D.
Lotus Cars Ltd.

Jeyes, J.A.
Department of Transport

Jones, A.N..
Jaguar Cars Ltd.

Jones, D.V.
Department of Transport

Jones, G.
Austin Rover Group Ltd.

Jones, T.C.
Jaguar Cars Ltd.

Kecman, D.
Cranfield Impact Centre

Kemp, R.N.
Kemp & Wilkins

Kershaw, K.
Renault Truck Industries

Knight, M.
University of Birmingham

Langdon, M.G.
Transport & Road Research Laboratory

Last, D.
Renault Truck Industries

Lawrence, G.J.L.
Transport & Road Research Laboratory

Lee, J.
Ford Motor Company Ltd.

Leigh, D.G.
Austin Rover Group Ltd.

Lewis, R.W.
Ford Motor Company, Ltd.

Logan, E.
Secretary to F.C. Munns

Lontay, R.G.R.
Bedford Commercial Vehicles

Lovell, P.J.
Royal Automobile Club

Lowne, R.W.
Transport & Road Research Laboratory

Lyness, D.J.
Department of Transport

Macaulay, M.D.
Brunel University

Mackay, M.
University of Birmingham

Manton, S.M.
Austin Rover Group Ltd.

Martin, J.K.
Open University

Mason, D.E.
Austin Rover Group Ltd.

McCallum, J.
Leyland Trucks

McConachie, E.I.
Austin Rover Group Ltd.

Meades, J.K.
Transport & Road Research Laboratory

Mills, P.J.
Transport & Road Research Laboratory

Mills, R.
Ogle Design Ltd.

Mitchell, C.G.B..
Transport & Road Research Laboratory.

Moore, G.G.
Austin Rover Group Ltd.

Munns, F.C.M.
Consultant Engineer

Murphy, P.B.
Department of Transport

Nakajima, N.
Kawasaki Motors (UK) Ltd.

Neilson, I.D.
Transport & Road Research Laboratory

Ng, P.
Ford Motor Company Ltd.

Nigogosian, L.V.
Thorn EMI Datatech

O'Leary, M.
Transport & Road Research Laboratory.

Oliver, C.M.
Bedford Commercial Vehicles

Oliver, R.J.
Department of Transport

O'Reilly, P.N.J.
Department of Transport

Osbourne, D.J.
Austin Rover Group Ltd.

Osman, D.F.H.
Austin Rover Group Ltd.

Otubushin, A.
ICE

Owen, M.G.
Morgan Motor Company Ltd.

Oxley, R.N.
Austin Rover Group Ltd.

Parkes, A.M.
University of Birmingham

Patience, C.J.
Automobile Association

Pendry, M.J.
Austin Rover Group Ltd.

Pennells, P.J.
Pilkington Glass Ltd.

Penoyre, S.
Transport & Road Research Laboratory

Peppercorn, J.
Thorn EMI Ltd.

Persicke, B.
Project Engineer

Petty, S.P.F.
Transport & Road Research Laboratory

Phipps, W.
University of Birmingham

Platten, G.
Ogle Design Ltd.

Prince, A.W.J.
Bedford Commercial Vehicles

Randle, J.N.
Jaguar Cars Limited.

Rattenbury, S.J.
Vehicle Safety Consultants

Rees, D.B.
Bedford Commercial Vehicles

Rees, M.
Brunel University

Renolds, A.K.
Department of Transport

Renouf, M.A.
Transport & Road Research Laboratory

Riley, B.S.
Transport & Road Research Laboratory

Roberts, A.K.
Transport & Road Research Laboratory

Robertson, A.J.
Cranfield Institute of Technology

Robertson, N.K.B.
ICE

Robins, T.L.
I Mech E

Rogers, N.M.
Motorcycle Association

Rothman, G.S.
Consultant

Roy. A.P.
The Middlesex Polytechnic

Sabey B.E.
Transport & Road Research Laboratory

Sadeghi, M.M.
Cranfield Impact Centre

Sadler, S.
Jaguar Cars Limited

Salter, R.N.P.
Austin Rover Group Ltd.

Santilli, R.
Transport & Road Research Laboratory

Savage, G.T.
The Middlesex Polytechnic

Scholes, D.B.
Jaguar Cars Limited

Searle, J.A.
Motor Industry Research Association

Seymour, D.
Austin Rover Group Ltd.

Shirley, W.E.
Austin Rover Group Ltd.

Simmonds, G.R.W.
Ford Motor Company Ltd.

Skuse, P.V.
Austin Rover Group Ltd.

Slater, D.F.
Rolls Royce Motors Ltd.

Smales, H.
Mintex Ltd.

Smith, C.A.
University of Birmingham

Smith, R.
Jaguar Cars Limited

Spragg, D.J.
Department of Transport

Stone, J.W.
Austin Rover Group Ltd.

Stone, K.
Ford Motor Company Ltd.

Stubbs, J.A.
Automobile Association

Suthurst, G.D.
Ford Motor Company Ltd.

Symes, M.
Institute for Consumer Ergonomics

Tavazza, G.
Pirelli Ltd. (Italy)

Taylor, C.T.
Bendix Ltd.

Teece, B.G.
Jaguar Cars Limited

Thomas, P.
Institute for Consumer Ergonomics

Thomas, P.M.
I Mech E

Thornadtsson, T.B.
Saab

Tidbury, G.H.
Cranfield Impact Centre

Tomlin, C.T.V.
Consultant

Tribbick, D.
Austin Rover Group Ltd.

Turner, S.P.
Royal Automobile Club

Twiss, M.K.
University of Birmingham.

Wall, J.G..gl Transport & Road Research Laboratory

Waller, J.A.
Bedford Commercial Vehicles

Ward, E.G.
Hope Technical Dev. Ltd.

Waters, M.H.L.
Transport & Road Research Laboratory

Watson, P.M.F.
Transport & Road Research Laboratory

White, D.M.
Cranfield Impact Centre

White, R.J.
Department of Transport

Yates, R.
Department of Trade & Industry

INDIA

Mohan, D.
Indian Institute of Technology

ITALY

Ardoino, P.L.
Fiat Auto SpA

Chirico, D.
Alfa Romeo Auto SpA

Ferrero, G.C.
Fiat Auto SpA

Gilardi, M.
Fiat Research Corporation

Landsberg, E.
Alfa Romeo Auto SpA

Maestripieri, L.
Alfa Romeo Auto SpA

Pastorino, A.
Fiat Auto SpA

Rossi, F.R.
Centrale Motorizzazione

Schinaia, Mr.
Centrale Motorizzazione

JAPAN

MINISTRY OF INTERNATIONAL TRADE & INDUSTRY

Takeda, S.T.

MINISTRY OF TRANSPORT

Kanbe, T.
Shimodaira, T.
Takegawa, K.

DAIHATSU

Ogawara, H.

FUJI

Obayashi, S.O.
Oshita, S.P.
Otake, M.O.

HONDA

Higuchi, K.
Makino, N.
Nakajima, Z.
Nakamura, Y.
Noaki, H.
Sano, S.
Shiraishi, S.
Yamamoto, T.

JARI

Fukuda, S.F.
Goto, K.G.
Miyazaki, K.M.
Nishimi, T.N.

KANTO SEIKI

Endo, H.

KAWASAKI

Kusaka, K.

MAZDA

Kurimoto, K.

MITSUBISHI

Yoshida, S.

NISSAN

Kawata, H.
Maeda, K.
Marumo, N.
Morita, S.M.
Tokuda, T.
Yabuta, K.

ROMEO KOJYO

Romeo, D.J.

SUZUKI

Igarashi, M.
Oshima, T.
Takokoro, H.

TAKATA

Nakayama, Y.
Takada, J.
Takada, K.

TOKAI RIKA

Teraoka, F.

TOYOTA

Kondo, Y
Nomura, K.N.
Osaka, K.O.
Yamaguchi, S.Y.

YAMAHA

Yamamoto, N.Y.

THE NETHERLANDS

Blaauw, G.J.
Volvo Car Corporation
fl Edelman, A.
Institute for Road Safety Research

Hoekstra, P.W.
Department of Road Transport

Huyskens, C.G.
TNO

Jacobs, P.W.A.
Volvo Car Corporation

Janssen, E.G.
TNO

Maltha, J.
TNO

Roelfsema, A.
Volvo Car Corporation

Slagter, E.E.S.
Directie Verueers Veiugheid

Takashima, Y.
Tokai Rika Co. Ltd.

Van Kempen, L.T.B.
Institute for Road Safety Research

Wismans, J.S.H.
TNO

SWEDEN

Aldman, B.
Chalmers University of Technology

Almquist, R.K.A.
Volvo Car Corporation

Anderlind, K.T.
SAAB, Scania AB

Bengtson, S.W.
Volvo Car Corporation

Berntsson, B.
Volvo Car Corporation

Bohlin, N.B.
Volvo Car Corporation

Eklund, E.S.O.
Swedish Road Safety Office

Eriksson, A.
Volvo Car Corporation

Everson, J.
Volvo Car Corporation

Gustausson, B.H.
SAAB, Scania AB

Gustavsson, H.H.
Folksam Insurance Company

Hansson, P.T.
Volvo Car Corporation

Ivarsson, J.E.
Volvo Car Corporation

Jonsson, B.M.
SAAB, Scania AB

Kajzer, J.
Chalmers University of Technology

Karlbrink, L.K.
Volvo Car Corporation

Lousund, P.
Chalmers University of Technology

Mellander, H.M.
Volvo Car Corporation

Nilsson, M.
Volvo Car Corporation

Nilsson, B.
Volvo Car Corporation

Nilsson Ehle, A.E.
Volvo Car Corporation

Nordgren, C.
Association of Automobile Manufactuers & Wholesalers

Norin, H.
Volvo Car Corporation

Nygren, A.
Folksam Insurance Company

Skotte, L.G.
Volvo Car Corporation

Strandberg, L.
National Road & Traffic Research Institute

Tingvall, C.T.
Folksam Insurance Company

Turbell, T.
Swedish Road & Traffic Research

UNITED STATES

Alderson, S.W.
Humanoid Systems

Anderson, T.E.
General Motors Research Laboratories

Appleby, M.R.
Automobile Club of Southern California

Arning, K.H.
Ford Motor Company

Betka, M.C.
Talley Defense Systems, Inc.

Borlaug-Phillips, K.
Congressional Staff (U.S. Senate)

Brantman, R.
Breed Corporation

Breed, A.K.
Breed Corporation

Breed, D.
Breed Corporation

Breed, R.
Breed Corporation

Camp, L.W.
Ford Motor Company

Carr, T.J
Motor Vehicle Manufacturers Association

Detloff, C.A.
General Motors Corporation

Digges, K.
U.S. Department of Transportation

Donohue, R.J.
General Motors Corporation

Dunn, L.
Congressional Staff (U.S. Senate)

Egbers, R.G.
ARCO Chemical Company

Eppinger, R.H.
U.S. Department of Transportation

Evans, L.
General Motors Research Laboratories

Fancher, P.S
University of Michigan

Finkelstein, M.M., Conference Chairman
U.S. Department of Transportation

Finnegan, D.B.
Congressional Staff (U.S. House of Representatives)

Fish, J.
Congressional Staff (U.S. House of Representatives)

Fitzpatrick, M.U.
Fitzpatrick Engineering

Gambardella, C.B.
Consultant Automotive Engineer

Gorte, C.B.
Ford Motor Company

Griswold, C.J.
General Motors Company Ltd.

Haase, O.H.
EI DuPont de Nemours & Co.

Hackney, J.R.
U.S. Department of Transportation

Haenchen, D.K.
Volkswagen of America, Inc.

Hale, C.
American Honda Motor Co. Inc.

Harrington, T.
American Honda Motor Co. Inc.

Hayashi, T.
Nissan Research & Development

Hedlund, J.H.
U.S. Department of Transportation

Henderson, D.B.
Automobile Importers of America

Henson, S.E.
Ford Motor Company

Hespeler, G.M.
Mercedes Benz of North America

Hight, P.V.
Accident & Safety Consultant

Hitchcock, R.J
U.S. Department of Transportation

Howell, L.J.
General Motors Research Laboratories

Howland, A.
Ford Motor Company

Johannessen, H.G.
OmniSafe Inc.

Jones, I.S.
Insurance Institute for Highway Safety

Kahn, H.
Automotive News

Kelleher, B.J.
Calspan Advanced Technology

Kennebeck, J.W.
Volkswagen of America Inc.

King, W.K.
Ford Motor Company

Kirchoff, G.F.
Morton Thiokol Inc.

Koike, J.
Yamaha Motor Corporation

Komatsu, S.
American Honda Motor Co. Inc.

Lake, L.C.
ANSI/ISO/Yamaha Motor Corp./S

Lau, I.V.
General Motors Research Laboratories

Lehman, Hon. William
Chairman, Subcommittee on Transportation
U.S. House of Representatives

Lisowski, J.I.
Morgan, Melhuish & Lisowski

Maugh, R.E.
Ford Motor Company

McGrath, T.C.
Breed Corporation

McGuigan, D.G.
Ford Motor Company

Melvin, J.W.
University of Michigan

Miller, P.M.
MGA Research Corporation

Negro, A.
Fiat

Nicholson, R.M.
U.S. Department of Transportation

Nield, G.C.
Automobile Importers of America

Ohari, S.O.
Japanese Translator

O'Toole, S.O.
General Motors Inc.

Perry, D.J.
Subaru of America Inc.

Petrucelli, E.
American Association for Automotive Medicine

Prasad, P.
AVET, Ford Motor Company Ltd.

Riley, W.R.
Warner Riley Enterprises Inc.

Rinehart, C.F.
Congressional Staff (U.S. House of Representatives)

Robbins, R.W.
Consultant

Rockow, R.
Dynamic Sciences Corporation

Romeo, D.J.
Romeo Kojyo Co. Inc.

Satsuma, K.
American Honda Motor Co. Inc.

Shapiro, W.
Volvo of America Corporation

Sheets, P.A.
Kawasaki Motors Corporation

Shimizu, T.S.
MMC Services Inc.

Shively, J.C., Jr.
U.S. Department of Transportation

Smith, R.L.
Vector Enterprises Inc.

Smreker, J.P.
Volkswagen of America, Inc.

Sparrrow, F.T.
Purdue University

Stalnaker, R.L.
Ohio State University

Steed, D.
U.S. Department of Transportation

Thibault, L.E.
University of Pennsylvania

Tobin, T.W.

Utans, P.
Subaru of America Inc.

Verrastro, G.J.V.
Somers, Hall & Verrastro

Versace, J.
Ford Motor Company

Viano, D.C.
General Motors Research Laboratories

Walsh, M.J.
Calspan Advanced Technology

Warner, J.C.
Warner & McCauley

Wasko, R.J.
Motor Vehicle Manufacturers Association

Waterman, D.
National Transportation Safety Board

Willen, W.R.W.
American Honda Motor Co. Inc.

Wilson, R.A.
General Motors Corporation

Wiseman, H.A.B.
University of Miami

Yamada, T.A.
Mike Masaoka Associates

Zellner, J.W.
Dynamic Research Inc.

Ziwica, K.
BMW of North America Inc.

Contents

FOREWORD iii
PARTICIPANTS v

SECTION 1: OPENING CEREMONIES
Welcoming Address
Sir Peter Lazarus
Permanent Secretary
U.K. Department of Transport 1

Keynote Address:
Diane K. Steed
Administrator
National Highway Traffic Safety Administration
U.S. Department of Transportation 2

SPECIAL SESSION: AWARDS PRESENTATIONS
Diane K. Steed, Chairman, United States 5

SECTION 2: GOVERNMENT STATUS REPORTS
John W. Furness, Chairman, United Kingdom

United States:
Michael M. Finkelstein
Associate Administrator for Research and Development
National Highway Traffic Safety Administration
U.S. Department of Transportion 11

Canada:
E. R. Welbourne
Chief, Vehicle Systems
Road Safety Directorate
Transport Canada 15

European Experimental Vehicle Committee:
Prof. Dr. Bernd Friedel
Chairman of EEVC 17

Federal Republic of Germany:
Prof. Dr. Heinrich Praxenthaler
President
Federal Highway Research Institute 19

Italy:
Dr. Franco Rossi
Direttore Centrale Motorizzazione
Direzione Generale M.C.T.C.
Ministero Dei Trasporti 22

France:
Jean Moreau de Saint-Martin
Director
Organisme National de Sécurite Routiére 23

The Netherlands:
Pieter W. Hoekstra
Deputy Head
Staff Division for Technical Affairs
Department of Road Transport 25

Sweden:
Prof. Dr. Bertil Aldman
Swedish Transport Research Delegation
Chalmers University of Technology 26

Japan:
Takashi Shimodaira
Deputy Director of the Engineering and Planning Division, Regional Transport Bureau
Ministry of Transport 27

United Kingdom:
David Lyness
Head of Vehicle Standards and Engineering Division
Department of Transport 29

SECTION 3: PROGRESS WITH AND DISCUSSION ON SAFETY DEVELOPMENTS FOR ROAD VEHICLES
Michael M. Finkelstein, Chairman, United States

A Demonstration Car with Improvements for Pedestrian Protection
C.A. Hobbs, G.J.L. Lawrence, and C.S. Clarke 31

A Motorcycle Demonstrating Improved Safety Features
P.M. Watson 39

Driver Airbag Police Fleet Demonstration Program—A 24-Month Progress Report
D. Romeo and J. Morris 45

Panel Discussion on Airbag Technology
"Optimizing Airbag Performance, Tuning to the Characteristics of Specific Vehicles, Application in Small Cars at Driver and Passenger Positions, Prospects in Vehicles with Two Seating Positions and Bench Seats, Reducing System Costs and FMVSS 208 Injury Criteria"
A.K. Breed
President, Breed Corporation, United States
(Statement) 55

Roger Maugh, Director Automotive Safety, Ford Motor Company, United States
(Statement) 59

Prof. W. Reidelbach, Director, Daimler-Benz Passenger Car Body Basic Research, Federal Republic of Germany
(Statement) 64

David Romeo, President, Romeo-Kojyo Company, United States
(Statement) 65

Panel Discussion on Safety Belt Developments
"Issues that Manufacturers Will Be Facing as They Comply with the Requirements of FMVSS 208"

C. Detloff, Engineer in Charge, General Motors Safety Belt Design Program, United States
(Statement) 66

H.G. Johannessen, Consultant, Omni Safe, Inc., United Sates
(Statement) 68

S. Sano, Research Engineer, Honda R&D, Japan
(Statement) 72

Dietmar K. Haenchen, Executive Engineer, Volkswagen of America
(Statement) 74

SECTION 4: TECHNICAL SESSIONS

SESSION ONE: BIOMECHANICS AND DUMMY DEVELOPMENT
Chairman: Jean Leroy, France

Biomechanics:
Biomechanics of Diffuse Brain Injuries
L.E. Thibault and
T.A. Gennarelli
University of Michigan, United States 79

Effects of Different Types of Headrests in Rear-End Collisions
A. Nygren,
H. Gustafson, and
C. Tingvall
Folksam R&D Division
Karolinska Hospital, Dept. of ENT
Stockholm, Sweden 85

Production of Injury in Blunt Frontal Impact
R. Eppinger and
J. Marcus
National Highway Traffic Safety Administration, United States 90

Thoracic Impact: A Viscous Tolerance Criterion
D. Viano and
I. Lau
Biomedical Science Department
General Motors Research Laboratories 104

Modelling the Lateral Impact of the Thorax in Car Side Impact Accidents
M. Langdon
Transport and Road Research Laboratory, United Kingdom 114

Validity of Thoracic Injury Criteria
Based on the Number of Rib Fractures
J.P. Verriest and
A. Chapon
O.N.S.E.R., France 124

Synthesis of Pelvic Fracture Criteria
for Lateral Impact Loading
M. Haffner
National Highway Traffic Safety Administration, United States 132

Dummy Development:
The Eurosid Side Impact Dummy
The EEVC Ad Hoc Group on Dummies 153

Advanced Anthropomorphic Test Device Concept Definition
J. Melvin
Dept. of Mechanical Engineering and Applied Mechanics
University of Michigan, United States 165

A New Dummy for Pedestrian Test
B. Aldman and
J. Kajzer
Department of Traffic Safety, Chalmers University of Technology, Sweden 176

Head and Neck Injuries in Human Cadavers
from Lateral Impacts
M. Walsh and
B. Kelleher
Calspan Corporation, United States 186

SESSION TWO: CRASH AVOIDANCE
Chairman: Robert M. Nicholson, United States

Discerning the State of Crash Avoidance
in the Accident Experience
A.C. Malliaris
National Highway Traffic Safety Administration, United States 199

Optimum Luminances and Areas of Rear-Position-Lamps
and Stop Lamps
H.J. Schmidt-Clausen
Technical University, Darmstadt,
Federal Republic of Germany 220

Evaluation of Headlamp Beam Patterns
Using the Ford CHESS Program
M. Perel
National Highway Traffic Safety Administration, United States 225

A Study of Laser Radar
H. Kawata,
H. Endo, and
Y. Eto
Nissan Motor Co., Ltd., Japan 230

Car Controls for Physically Handicapped Drivers
C. Haslegrave
Motor Industry Research Association, United Kingdom 235

The Prevention of Bead Dislodgement of Tyres and the
Importance of Limited Run Flat Capability on Safety
G. Tavazza
Pirelli Coordinamento Pneumatici, Italy 243

Modification of Vehicle Handling Performance by
Four-Wheel Steering System
S. Sano,
Y. Furukawa, and
S. Shiraishi
Honda Motor Co., Ltd., Japan 248

Maneuverability and New Suspension for
Four-Wheel Drive Vehicles
M. Otake,
S. Obayashi,
M. Kubota, and
Y. Nozawa
Subaru Engineering Division,
Fuji Heavy Industries, Ltd., Japan 262

Behaviour of a Vehicle During Turning
Y. Vermont
Renault, France 269

An Instrument to Measure Scattered Light
Due to Windshield Wear
A. Timmermann
Forschungsgemeinschaft Auto-Sicht-Sicherheit,
Federal Republic of Germany 276

The Development of Drowsiness Warning Devices
K. Yabuta,
H. Iizuka,
T. Yanagishima,
Y. Kataoka, and
T. Seno
Nissan Motor Co., Ltd., Japan 282

Tire Pressure Warning System
Y. Uemura,
S. Oshita,
T. Konno,
T. Kobuna, and
Y. Yoshida
Subaru Engineering Division,
Fuji Heavy Industries, Ltd. 288

Aspects of Subjective/Objective Correlation
Regarding Vehicle Tyres
L. Breindle
Technology Assessment Applied Psychology
Cranfield Intitute of Technology, United Kingdom 294

Tire Performance Measurements—Wet and Dry
L. Emery
National Highway Traffic Safety Admimistration, United States 300

Accident Avoidance—Crosswind Sensitivity of
Some Streamlined Cars
M. Jacobson, Consultant
The Automobile Association, United Kingdom 310

SESSION THREE: OCCUPANT PROTECTION FOR FRONTAL IMPACT
Chairman: Dr. Kennerly H. Digges, United States

Efficient Energy Absorption of Automobile Side Rails
S. Yamaguchi,
H. Kato, and
T. Okazaki
Toyota Motor Corporation, Japan 321

Collapse Behavior Development of Body Components
R. Brasche,
G. Giazitzis, and
H. Schmitt
Ford-Werke AG, Federal Republic of Germany 326

Advanced Concepts for Driver Air Cushion Systems
G. Kirchoff,
R. Carr,
R. Wheelwright, and
G. Adams
Morton Thiokol, Inc., United States 332

Injury Criteria for Combined Restraint Systems
L. Grösch
Daimler-Benz AG, Federal Republic of Germany 338

A Modified Steering Wheel to Reduce Facial Injuries and Associated Test Procedures
S. Petty
Transport and Road Research Laboratory
United Kingdom 342

Improved Crashworthiness Independent of Belts or Airbags
R. Wilson
Environmental Activities Staff, General Motors,
United States 347

An Impact Test Programme Using Six Models of Lower-Medium-Sized Cars
S. Penoyre
Transport and Road Research Laboratory,
United Kingdom 357

A Free-Flight Headform Impact Device for Evaluating the Energy Absorption Characteristics of Vehicle Interiors
K. Dale and
K. Clemo
Motor Industry Research Association, United Kingdom 362

New Car Assessment Program Results and the Risk of Injury in Actual Accidents
I. Jones,
R. Whitfield, and
D. Carroll
Insurance Institute for Highway Safety, United States 371

A Review of the Effects of Belt Systems, Steering Assemblies, and Structural Design on the Safety Performance of Vehicles in the New Car Assessment Program
J. Hackney
National Highway Traffic Safety Administration, United States 380

Accident Research and Frontal Testing
M. Danner
HUK-Verband, Federal Republic of Germany 413

Results of Crash Tests According to the ECE/GRCS Regulation Proposal Concerning 50km/h Frontal Impact Against the Rigid 30° Barrier
E. Faerber and
K. Glaeser
Federal Highway Research Institute,
Federal Republic of Germany 415

The Characteristics of Frontal Impacts in Real-World Accidents
F. Hartemann,
J. Foret-Bruno,
C. Henry, and
G. Faverjon
Laboratoire de Physiologie et de Biomechanique,
Peugeot SA/Renault, France
C Got,
A. Patel, and
J. Coltat
Institute de Recherche Othopedique
Hospital Raymond Poincare, France 424

Testhouse Experiences with the Draft ECE Regulation for Head-On Collisions
C. Huijskens,
J. Maltha, and
A. Dyche
Research Institute for Road Vehicles TNO,
The Netherlands 432

Comparison of 0° and Oblique Tests
J. Hackney
National Highway Traffic Safety Administration, United States 436

Applying Computer Techniques in the Design and Development of an Occupant Restraint System
N. Grew
Austin Rover Group, Ltd., United Kingdom 436

The Use of the DRACR Airbag Simulation Model as a Design Tool
L. Skötte,
H. Mellander, and
D. Biss
Volvo Car Corporation, Sweden 448

An Analytical Management of Frontal Crash Impact Response
K. Kurimoto,
S. Takeda, and
H. Uehara
Mazda Motor Corporation, Japan 454

Evaluation of Frontal Occupant Protection Using the Passenger/Driver Simulation Model
L. Stucki,
D. Cohen, and
C. Ragland
National Highway Traffic Safety Administration, United States 459

Comparative Evaluation of the MVMA2D and MADYMO2D
Occupant Simulation Models with
MADYMO-Test Comparisons
P. Prasad
Ford Motor Company, United States 480

The Safe Transportation of Wheelchair Occupants
in the United Kingdom
S. Petty
Transport and Road Research Laboratory,
United Kingdom 488

Discerning the State of Crashworthiness in
the Accident Experience
A.C. Malliaris
National Highway Traffic Safety Administration, United States 491

SESSION FOUR: ACCIDENT INVESTIGATION AND ITS RELEVANCE TO LEGISLATION
Chairman: R. Stamm, Federal Republic of Germany

The Causes of Injury in Car Accidents—
An Overview of a Major Study Currently
Underway in Britain
M. Galer and
S. Clarke
Accident Research Unit
Institute for Consumer Ergonomics, United Kingdom
G. Mackay and
S. Ashton
Accident Research Unit
Birmingham University, United Kingdom 513

Large Scale Data Collection Systems—
The NASS Experience
R. Richardson and
F. Costello
National Highway Traffic Safety Administration, United States 525

Five Years of New Car Assessment Program:
Balance and Current Conclusions
J. Provensal,
F. Hartemann, and
C. Tarriere
Regie Nationale Des Usines Renault, France 530

An Aid for the Assessment of Biomechanical Values
with High Scatter and Uncertain Limit Values
Dr. W. Schmid
Daimler-Benz AG, Federal Republic of Germany 543

Car Size and Safety: Results from Analyzing
U.S. Accident Data
L. Evans
Transportation Research Department
General Motors Research Laboratories,
United States 548

Rating System for Serious Consequences (RSC)
Due to Traffic Accidents. Risk of Death
or Permanent Disability

H. Gustafsson,
A. Nygren, and
C. Tingvall
Folksam Research and Development Division, Sweden
A. Nygren and
C. Tingvall
Karolinska Hospital, Department of ENT., Sweden 556

Seatbelt Research and Legislation
in The Netherlands
L. van Kampen
Institute for Road Safety Research SWOV
The Netherlands 560

The Effects of Mandatory Seatbelt Use
in Great Britain
S. Ashton and
G. Mackay
Accident Research Unit
Department of Transportation and Highway Engineering
University of Birmingham, United Kingdom
P. Thomas and
M. Galer
Accident Research Unit
Institute for Consumer Ergonomics, United Kingdom
P. Harms
Transport and Road Research Laboratory,
United Kingdom 567

Collison Types and Characteristics of Bus
Accidents—Their Consequences for the Bus
Passengers and the Accident Opponent
K. Langwieder,
M. Danner, and
T. Hummel
Automobile Engineering Department
HUK-Verband, Federal Republic of Germany 585

Fatality Rates in Toyota Cressidas with Automatic Belts
C. Nash and
B. Eisemann
National Highway Traffic Safety Administration, United States 594

Trends and Forecasts of the Japanese
Traffic Accident Situation
K. Takegawa
Traffic Safety Policy Office,
Director-General's Secretariat
Management and Coordination Agency, Japan 597

SESSION FIVE: OCCUPANT PROTECTION IN SIDE IMPACT
Chairman: I.D. Neilson, United Kingdom

The Safety Performance of Production Vehicles
in Side Impacts
H. Gabler III
Transportation Systems Center, United States
J. Hackney
National Highway Traffic Safety Administration, United States 607

Load Transfer from the Striking Vehicle in Side and Pedestrian Impacts
B. Aldman and
J. Kajzer
Chalmers University of Technology
T. Anderlind
Saab Car Division
M. Maimqvist
National Testing Institute of Sweden
H. Mellander
Volvo Car Corporation
T. Turbell
Swedish Road and Traffic Research Institute 620

Side Impact Aggressiveness Attributes
M. Monk and
D. Willke
National Highway Traffic Safety Administration, United States 637

Volvo Side Impact Testing
M. Nilsson,
K. Andersson,
J. Korner, and
A. Nilsson-Ehle
Automotive Safety Center
Volvo Car Corporation, Sweden 649

Side Impact Testing
J. Gratadour
Peugeot, France 658

Testing the Side Impact Tests: Method and Some Initial Results
S. Henson,
M. Huang,
R. Hultman,
I. Parekh,
E. Grush, and
J. Pike
Environmental and Safety Engineering Staff
Ford Motor Company, United States 667

Results of the Motor Vehicle Manufacturers Association Component and Full-Vehicle Side Impact Test Procedure Evaluation Program
R. Wasko
Motor Vehicle Manufacturers Association, United States
R. Wilson
General Motors Corporation, United States 716

A Comparison of European and American Test Devices and Test Parameters for Lateral Impacts
F. Klaus,
R. Sinnhuber, and
G. Hoffmann
Volkswagenwerk AG, Federal Republic of Germany 727

Occupant Response Sensitivity Analyses Using a Lumped Mass Model in Simulation of Car-to-Car Side Impacts
T. Trella,

Transportation Systems Center, United States
J. Kanianthra
National Highway Traffic Safety Administration, United States 755

Inclusion of Crashworthiness in Concept Design
G. Suthurst and
P. Ng
Ford Motor Company, United Kingdom
M. Sadeghi
Cranfield Impact Centre, United Kingdom 772

Development and Testing of Optimized
Deformation Structures
F. Kramer and
A. Heger
Technische Universitat,
Federal Republic of Germany 779

Status of the MADYMO Crash Victim Simulation
Package 1985
J. Wismans,
T. Hoen, and
L. Wittebrood
Research Institute for Road Vehicle TNO
The Netherlands 784

Validation of the EEVC Mobile Deformable
Barrier for Side Impact Testing
D. Cesari and
J. Bloch
O.N.S.E.R. France
W. Sievert and
E. Pulwitt
Federal Highway Research Institute (BASt)
Federal Republic of Germany
I. Neilson and
A. Hobbs
Transport and Road Research Laboratory,
United Kingdom 794

The CCMC Mobile Deformable Barrier for
Lateral Collison Testing
D. Gebbels 811

Fabrication and Validation of a Mobile
Deformable Barrier for Side Impact
H. Le Guen,
R. Dargaud, and
T. Bourdillon
Union Technique de l'sAutomobile, du Motocycle,
et du Cycle (UTAC), France 822

SESSION SIX: SAFETY DEVELOPMENTS OF GOODS VEHICLES AND BUSES
Chairman: L. Strandberg, Sweden

Improved Commercial Vehicle Conspicuity
and Signalling Systems
R. Smith,
W. Burger,
K. Ziedman, and
M. Mulholland
Vector Enterprises, Inc., United States 841

The MVMA Investigation into the Complexities of Heavy Truck Splash and Spray Problem
C. Gorte
Ford Motor Company, United States
R. Joyner
General Motors Corporation, United States
K. Pedersen
International Harvester Company, United States
C. McConnell
Motor Vehicle Manufacturers Association, United States 848

An Evaluation of the Obstacle-Avoidance Capabilities of Articulated Commercial Vehicles
P. Fancher
Transportation Research Institute
University of Michigan, United States 863

Test Procedures and Evaluation Criteria for the Handling Characteristics of Heavy Commercial Vehicles
K. Rompe and
B. Heibing
Institute for Traffic Safety,
TÜV Rheinland e.V., Colgne,
Federal Republic of Germany 873

Tractor Semitrailer Unit for the Future
P. Soret
Renault Véhicules Industriels, France 880

Protecting Car Occupants, Pedestrians, and Cyclists in Accidents Involving Heavy Goods Vehicles by Using Front Underrun Bumpers and Sideguards
B. Riley,
S. Penoyre, and
H. Bates
Transport and Road Research Laboratory,
United Kingdom 883

Load Restraint for the Protection of Occupants in Light Vans Including Car Derivatives
D. Bacon and
I. Gazeley
Motor Industry Research Association,
United Kingdom 896

Severe Coach Accident Survey
C. Thomas,
F. Hartemann, and
C. Tarriere
Laboratory of Physiology and Biomechanics of
Peugeot SA/Renault, France
P. Botto,
C. Got, and
A. Patel
Orthopaedic Research Institute,
Hospital Raymond Poincare, France 904

Optimisation of a Bus Superstructure from the Rollover Safety Point of View
D. Kecman
Faculty of Mechanical Engineering, University of Belgrade, Yugoslavia
G. Tidbury
Cranfield Impact Centre, United Kingdom 914

Improvements for Bus Safety
K. Rompe and
H. Krüger
Institute for Traffic Safety, TÜV, Federal Republic of Germany 919

Heavy Truck Safety—What We Know
H. Seiff
Motor Vehicle Manufacturers Association, United States 925

Heavy Trucks Aggressivity for Road Users—In Search of Improved Safety
M. Dejeammmes
O.N.S.E.R., France 930

P.S.V. Rollover Stability
D. White
Cranfield Impact Centre, United Kingdom 936

SESSION SEVEN: PEDESTRIAN PROTECTION
Chairman: Dr. Franco R. Rossi, Italy

General Problems Concerning Car-Pedestrian Collision
A. Costanzo
School of Medicine and Surgery, Rome University, Italy 943

Vehicle Pedestrian Head Impacts: A Computer Method for Rating a Profile Without Previous Mathematical Modelization
D. Lestrelin,
F. Brun-Cassan,
A. Fayon, and
C. Tarriere
Laboratory of Physiology and Biomechanics, Peugeot SA/Renault, France 949

Computer Simulations of a Range of Car-Pedestrian Collisions
G. Suthurst
Ford Motor Company, United Kingdom
R. Hardy
Cranfield Impact Centre, United Kingdom 955

Pedestrian Injury Protection by Car Design
EEVC Ad Hoc Group on Pedestrian Protection 965

Experiemental and Mathematical Simulation of
Pedestrian-Vehicle and Cyclist-Vehicle Accidents
E. Janssen and
J. Wismans
Research Institute for Road Vehicles TNO,
The Netherlands 977

Experimental Research on Pedestrian Protection
Using a Mobile Deformable Barrier
L. Maestripieri
Alfa Romeo Auto S.p.A., Italy 988

Research Concentrated on an Experimental
Method for Protecting Pedestrians
K. Maeda,
H. Isobe,
Y. Sakuma, and
Y. Kurihara
Nissan Motor Company, Ltd., Japan 999

The Influence of Car Design on Pedestrian Protection
H. Harris
Transport and Road Research Laboratory,
United Kingdom
N. Grew
Austin Rover Group Ltd., United Kingdom 1009

Evaluation of a Pedestrian Compatible Bumper
B. Kelleher and
M. Walsh
Calspan Corporation, United States
R. Vergara and
J. Herridge
Battelle Corporation, United States
R. Eppinger
National Highway Traffic Safety Administration, United States 1023

An Experimental Study of a Modified Compliant Bumper
B. Aldman and
J. Kajzer
Department of Traffic Safety
Chalmers University of Technology, Sweden
O. Bunketorp
Chalmers University of Technology, and
Department of Orthopaedic Surgery,
University of Göteborg, Sweden
R. Eppinger
National Highway Traffic Safety Administration, United States 1035

Simplified Test Recommendations for
Pedestrian Protection
J. Harris
Transport and Road Research Laboratory
United Kingdom 1041

Experimental Simulation of the Pedestrian Impact
G. Stürtz
Daimler-Benz AG, Federal Republic of Germany 1045

SESSION EIGHT: SAFETY DESIGN OF 2-WHEELED VEHICLES
Chairman: Y. Nakamura, Japan

Leg Protection for Riders of Motorcycles
B. Chinn and
P. Hopes
Transport and Road Research Laboratory,
United Kingdom
M. Macaulay
Brunel University, United Kingdom 1055

Application of Fluidics Technology to the
Development of Antilock Brakes for Motorcycles
R. Purves
Jet Propulsion Laboratory
California Institute of Technology, United States 1058

Accidents of Motorcyclists—Increase of Safety
By Technical Measures on the Basis of Knowledge
Derived from Real-Life Accidents
M. Danner,
K. Langwieder, and
A. Sporner
HUK-Verband, Automobile Engineering Department,
Federal Republic of Germany 1072

Analysis of Straight Running Stability of Motorcycles
T. Nishimi,
A. Aoki, and
T. Katayama
Japan Automobile Research Institute, Inc., Japan 1080

The Protective Effect of a Specially Designed
Suit for Motorcyclists
B. Aldman and
J. Kajzer
Chalmers University of Technologoy, Sweden
H. Gustafsson
Folksam Traffic Safety Group, Sweden
A. Nygren and
C. Tingvall
Folksam Traffic Safety Group, and
Karolinska Hospital, Sweden 1095

A Study of Motorcycle Leg Protection
H. Tadokoro
Motor Rider Protection Subcommittee
Japan Automobile Manufacturers Association, Japan
S. Fukuda and
K. Miyazaki
Japan Automobile Research Institute, Japan 1100

Aspects of Motorcycle Braking
G. Donne and
P. Watson
Transport and Road Research Laboratory,
United Kingdom 1109

Motorcycle Rider Protection in Frontal Impacts
B. Chinn,
G. Donne, and
P. Hopes
Transport and Road Research Laboratory,
United Kingdom 1116

Motorcycle Conspicuity in Daylight
G. Donne
Transport and Road Research Laboratory,
United Kingdom
E. Fulton
Institute for Consumer Ergonomics, United Kingdom
P. Stroud
Loughborough University of Technology,
United Kingdom 1119

A Feedback Control Method for Antilock Brake Design
J. Zellner and
D. Chiang
Dynamic Research, Inc., United States 1122

Measurement of Motorcycle Riders's Eye Locations
M. Motoki and
T. Asah
Japan Automobile Research Institute, Inc.,
Japan 1129

Cycle and Light-Powered Two-Wheeler Accidents
European Experimental Vehicles Committee 1152

SECTION 5: TRENDS AND PRIORITIES IN VEHICLE DEVELOPMENT IN RELATION TO ROAD SAFETY
Chairman: M.R. Dunn, United Kingdom

Panel Member Statements

A. Chenevez, Renault, France
(Statement) 1207

H. Kraft, BMW, Federal Republic of Germany
(Statement) 1207

Dr. E. Landsberg, Alfa Romeo, Italy
(Statement) 1208

S. Takeda, Ministry of International Trade,
Japan
(Statement) 1208

I.D. Neilson, Transport and Road Research Laboratory,
United Kingdom
(Statement) 1210

R. Hitchcock, National Highway Traffic
Safety Administration, United States
(Statement) 1210

SECTION 6: CONFERENCE SUMMARY

Dr. C. Ashley,
Motor Industry Research Association,
United Kingdom
Summary 1213

SECTION 7: CLOSING REMARKS

Michael M. Finkelstein, United States 1217

John Furness, United Kingdom 1217

Section 1
Opening Ceremonies

Welcoming Address:

Sir Peter Lazarus
Permanent Secretary, United Kingdom
Department of Transport

It is my very great pleasure to open this conference today and to welcome you all on behalf of the Government of the United Kingdom to this Tenth Experimental Safety Vehicle Conference and to the University and City of Oxford.

Experimental Safety Vehicle Conferences have played an important role in stimulating the development of safer vehicles, and I congratulate the Government of the United States and in particular NHTSA for being so farsighted in sponsoring these conferences since 1971.

We have here today a considerable number of the world's experts directly involved in improving the safety features of vehicles, as well as those who are influential for ensuring that the momentum of progress made in this field in recent years will continue into the future.

Your past efforts have resulted in considerable progress being made in this important area of vehicle design. However, in spite of these improvements there is much still to be done. The public expects a constant flow of improvements to make life safer for all classes of road users—motorist, cyclist, and pedestrian. For this reason I welcome particularly your discussions on reducing the adverse effect of the motor vehicle on other road users.

It is 11 years since an Experimental Safety Vehicle Conference was held in this country. In the intervening period there have been many changes in design. Cars, even though they are lighter in weight to aid better fuel economy, incorporate many more safety features for the protection of their occupants than at the time of the 1974 Conference. I congratulate industry on the inventiveness it has shown in reconciling these often conflicting demands arising from considerations of safety, economy, and the environment.

However, we cannot be complacent, and this conference will highlight several areas in which we can—indeed, must—make progress toward designs that provide even greater safety for both vehicle occupants and other road users.

I note with interest how the subject matter of these conferences has developed over the years. The early conferences dealt solely with safety features on cars. This conference extends the discussion to include safety problems associated with trucks, buses, motorcycles, and pedal cycles, which are widely used as personal transport in many parts of the world.

In this country, injuries to motorcyclists and their passengers are a matter of grave concern, and we must find ways to improve the safety of this group of road users. I am very heartened, therefore, to see the conference will be considering safety features for motorcycles and, in particular, I note that antilock braking systems for motorcycles are now being actively developed.

Even though improvement in the design of cars for safety is very important and will remain so, progress must be made with safer designs for all types of road vehicles.

I would like to remind you of one event that has taken place in this country that we consider one of the most effective measures taken in our battle to reduce injuries and fatalities arising from road accidents. I am referring, of course, to the compulsory wearing of seatbelts. In the 2 years since this requirement has become compulsory, we have seen a large reduction in deaths and serious injuries (17 percent fewer deaths, 22 percent fewer injuries), and you will be hearing more of our experience during the conference.

One of the most important benefits of this conference is that it will further encourage the free exchange of information and stimulate the cooperation necessary for the rapid development of safer vehicles. I would, therefore, like to thank the Institution of Mechanical Engineers for organising this conference on behalf of the Department

of Transport and for their efforts in preparing the Conference facilities. I am sure you will find much to interest you during the next 4 days, and I hope you will enjoy and benefit from your brief stay in this ancient university city.

Keynote Address:

Diane K. Steed
U.S. Department of Transportation, National Highway Traffic Safety Administration

It is indeed a special privilege to be here in the United Kingdom, home of the English Parliament, Buckingham Palace, and, this week especially, Wimbledon. As said earlier, I have been looking forward for quite some time to joining you at this conference.

I bring you personal greetings from U.S. Secretary of Transportation Elizabeth Dole, who very much wanted to attend this important safety conference to express personally our country's strong commitment to vehicle safety. I know it is a commitment that all of us share. As Secretary Dole has often said, safety is her highest priority. My own commitment to highway safety is no less absolute.

Over the past decade of cooperative safety research effort, we have seen many technological advances in automotive safety. Most of the safety improvements on today's vehicles were made possible through research of the governments, private industry, and individuals represented at this conference. We appreciate these contributions, and we have all benefited from them. These combined efforts have contributed substantially to the reduction of deaths and injuries resulting from motor vehicle crashes.

The critical goal of improved safety can best be realized when government and the private sector cooperate. We do not look on industry as an adversary—we consider industry a key partner in the common goal of improved motor safety.

It is government's job to regulate—and appropriately so—but it is the manufacturers who bring the experience, the resources, and the expertise necessary to design and build the safer automobiles of the future. And industry is doing just that.

Manufacturers throughout the world are working toward the development of new technologies. Germany is giving us the opportunity to look at technology in the real world by offering airbags as optional equipment in some of its automobiles. Japanese automakers have devised improvements in the comfort and performance of safety belts. Italy is studying ways to reduce vehicle weight without sacrificing vehicle safety. Major safety improvements in production design are being tested in Sweden, including advanced energy-absorbing front structures and improved safety designs for other vehicle subsystems. France has underway exciting work on designs for the 3-point safety belt. In the United Kingdom, research is producing new information on skidding and loss of control, as well as new concepts on barrier design.

These efforts—and the list could go on and on—are reducing traffic fatalities and serious injuries, and I applaud these achievements. The engineers in this room seldom make the headlines, but you are quietly and effectively laying the foundation for a better, safer tomorrow for all of us.

In the United States, we are also striving to be innovative in motor vehicle safety. One of our concerns is making certain that our limited research dollars are properly directed to a balanced safety program and the most important safety issues.

To respond to this concern—and because we know government does not have all the answers—I am working now to establish a Motor Vehicle Safety Research Advisory Committee. This will be a joint effort between government and the private sector to advise me on important safety issues of mutual concern. The committee will consist of motor vehicle safety research experts selected from the ranks of automotive manufacturers, academic institutions, trade associations, and government. It will coordinate safety research to avoid duplication and encourage innovation. Initially the committee will concentrate on occupant crash protection and heavy truck safety. These two areas, we believe, are most appropriate at present for coordinated research.

There are three other important subjects I would like to discuss with you:

1. Our increased emphasis on international harmonization
2. Secretary Dole's decision on our Standard No. 208 on occupant protection
3. Our dedication to continued international cooperation

In 1982 we announced our commitment to harmonizing our safety regulations with other countries. We recognized then that differences in test procedures, performance standards, and compliance criteria were unnecessarily complicating and increasing the costs of producing automobiles in a world market.

International harmonization is an important goal of this administration. In that regard, I am pleased to announce that I have established a new Office of International Harmonization at NHTSA. To give it appropriate visibility and increased emphasis, I have placed this new office under my direct supervision. I recognize the importance of international harmonization—and am making this a priority in our 1986 budget.

In the past 3 or 4 years, we have seen many benefits from our participation in the work of the Group of Experts on the Construction of Vehicles. Two cases in point are the common symbols on vehicle control displays and recent changes we have made in lighting standards. These are small breakthroughs, but accomplishments in minor areas such as these are the forerunners of compatibility in more complex areas—such as brake designs and side impact harmonization.

We will continue to work toward eliminating conflicting regulations that make it burdensome for manufacturers to construct cars for both domestic and foreign markets. Those differences serve as nontariff trade barriers that restrict international commerce and increase costs to consumers and industry alike.

In some cases, harmonization will promote increased production, marketing flexibility, and cost savings for vehicle manufacturers, and ultimately for consumers, without compromising safety. In fact, international harmonization can actually promote safety by upgrading standards and encouraging the sharing of safety technology by removing the differences between domestic and imported vehicles.

My pledge to you today is increased emphasis on international harmonization, and I know that through our joint efforts great accomplishments can be achieved in the future.

Now I want to discuss briefly the background and rationale behind Secretary Dole's decision on the 208 standard on occupant protection. This was one of the toughest, most complex policy decisions in which I have ever had a part. The Secretary's goal from the outset was to do what was best for the motoring public and to save as many lives as possible as quickly as possible.

Last July when Secretary Dole announced her ruling, it was one of the most significant decisions of her administration. It calls for automatic crash protection—either automatic belts, airbags, or other new technology—to be phased in beginning with 1987 model cars. The decision also encourages States to pass mandatory safety belt use laws, with a provision that if by April 1, 1989, two-thirds of the population is covered by mandatory use laws, the automatic protection requirements will be rescinded. Her decision was a major achievement in the history of occupant protection because, for the first time, the regulation is actually saving lives.

Of particular interest to those of you at this conference is the emphasis this decision gives to the development of new safety technology. For each car built with nonbelt technology, manufacturers will receive extra credit toward their percentage requirement if they use something other than automatic safety belts to protect the driver. In other words, manufacturers get extra credit for the installation of airbags, protective interiors, or other nonbelt technology that meets the test requirements of the rule.

We believe there is a definite advantage in the initial stages of compliance to encourage a variety of automatic protection technologies. This will promote the development of what may be better alternatives in the future than what might otherwise be developed.

The Secretary's decision is not an either/or decision—either automatic devices or belt use laws. It means both. We know the decision resulting in the enactment of State belt use laws already has saved many lives and prevented countless injuries. In New York, the first State to have a mandatory belt use law, fatalities are already down an impressive 27 percent. I hope to be able to report to you at our next conference that most U.S. citizens are protected by belt use laws.

Finally I want to discuss another priority of ours—to encourage continued international cooperation and technology sharing. I believe all of us agree that we can all benefit from collaboration on safety research projects. What each of us may find difficult to do alone we can and have accomplished together.

In the area of transportation, no country has a monopoly on the best ideas or most advanced technology. Therefore, we support an active international research and development program to foster data and technology sharing.

Independent, uncoordinated research and development can be wasteful and redundant. It can lead to development of safety technologies that may not always be suitable for worldwide application. International cooperation, on the other hand, can lead to the development and expanded use of improved safety equipment on a global scale.

And international cooperation does not lie exclusively with federally sponsored projects. American scientists and engineers from the private sector engage in a great many cooperative international ventures. Often they work through the universities or the industrial firms that employ them, with the Federal Government acting—at most—as a catalyst. An important goal of this administration is to encourage such private sector cooperation.

The benefits we will derive from international cooperation and from conferences such as this are crucial because they eventually filter down to improve the quality of life for all people. This research—this sharing of knowledge—is an essential investment in our future—one we must wisely and responsibly nurture.

I want to close my remarks today by extending to you a very personal invitation to my Nation's capital. In May 1987 the United States will host the Eleventh Experimental Safety Vehicle Conference in Washington, D.C. We have

already started our preliminary planning, and I know the conference will be challenging and professionally stimulating. I hope we can provide you with an equal measure of hospitality that our British colleagues have shown us this week.

Through continuing communications we will move closer to the spirit of international cooperation that is this conference's stated purpose and our sincere goal. There is mutual interest in these important areas we have discussed this week. There will be mutual benefit, and we in the United States pledge to all delegates present at this conference our mutual cooperation.

Awards Presentations

Safety Awards for Engineering Excellence

In recognition of and appreciation for extraordinary contributions in the field of motor vehicle safety engineering and for distinguished service to the motoring public.

Italy

Dott. Ing. Lamberto Maestripieri
Manager of the Alfa Romeo Safety Laboratory

Dr. Maestripieri has been working actively for improved passive and active safety since joining Alfa Romeo in 1967. He was directly involved in the development of the Safety Laboratory established by Alfa Romeo at its Experimental Center and in 1970 was appointed head of the laboratory. Dr. Maestripieri has conducted both theoretical and experimental research on improved vehicle structural performance in frontal and side impacts, weight reduction without sacrificing safety, and reductions in noise and air pollution. He was responsible for the design, development, and testing of the Alfa Romeo Synthesis Vehicle (S.V.A.R.), which was presented at the Ninth ESV Conference in Kyoto. By these many efforts, Dr. Maestripieri has made a major contribution to vehicle safety.

Federal Republic of Germany

Professor Dr.-Ing. Klaus Rompe
Director of the Institute for Traffic Safety, TUV Rheinland

Professor Rompe has made significant research contributions in the areas of active safety. First he analyzed passenger car handling characteristics by comprehensive computer programs. Then he initiated the development and application of objective test procedures for these characteristics. In comprehensive comparative test programs for passenger cars, cars and trailers, trucks, and truck combinations, he developed the necessary evaluation criteria and test procedures needed for a better understanding of the driver-vehicle-environment system, for investigations of the causes of accidents. Professor Rompe also investigated the view conditions of the drivers, especially for night driving, the interaction phenomena in a car crash with two and more passengers, and improved passenger protection in bus crashes. For these many safety accomplishments, Professor Rompe is deserving of special recognition.

France

Francois Hartemann
Head of Section on Accident Research Investigation, Laboratory of Physiology and Biomechanics, Peugeot-Renault

In 1970 Mr. Hartemann was appointed head of the Research Unit created by Peugeot and Renault to conduct detailed analyses of accident data. In this position Mr. Hartemann has made major contributions to vehicle safety by his work on the relationship between driver fatigue and accidents, the effects of collision force in frontal and side impacts, the definition and validation of test procedures, and improvements in the efficiency of the 3-point seat belt. Many of the results of these research efforts have been incorporated in production vehicles, resulting in a reduction in deaths and injuries. Through his research work, Mr. Hartemann has made a significant contribution to improved vehicle safety.

Jean Leroy
Manager, Laboratoire des Chocs et de Biomecaniquee, Organisme National de Securite Routiere

Mr. Leroy has had a long and distinguished career in furthering vehicle safety. His work with Renault involved accident analysis, improved restraint systems, deformable vehicle structures, and improved interior padding. His work with ONSER addressed improved protection for motor car users as well as research to improve the road environment. Mr. Leroy is well recognized both nationally and internationally for his expert participation in international working groups and scientific and technical societies. His contributions have resulted in major improvements in the safety performance of vehicles. Therefore, he is especially deserving of this award.

Sweden

Hans A. Norin
Senior Safety Engineer
Volvo Car Corporation

Through lectures, technical papers, and presentations, Mr. Norin has taken part in and deepened the international traffic safety debate with special emphasis on child safety and side collisions. The work of the Volvo Car Accident Research Group for which Mr. Norin is responsible has led to major safety improvements in production car design. Some examples are improved steering column systems, advanced energy-absorbing front structures, improved gas tank design and location, improved safety belt systems, and improved safety designs for doors, seats, suspension systems, and other vehicle subsystems. For these many impressive safety accomplishments, Mr. Norin is deserving of the special recognition.

Dr. Bertil Aldman
Professor, Department of Traffic Safety, Chalmers University of Technology

Dr. Aldman has been instrumental in the design of protective devices of various types. His research has influenced the development of 3-point seat belt systems, automatically locking retractors, and crash helmets and protective clothing for motorcyclists. He designed the first rear-facing child seat and presented it at the Stapp Conference in 1964 and participated in the development of booster cushions for children. Together with a team in France, he is currently involved in the design of a new type of pedestrian dummy, which will be presented during the Tenth ESV Conference. Dr. Aldman has published over 200 technical papers covering subjects

from first-aid and hospital care, the biomechanics of trauma, the design of protection devices, to definitions and theories as a basis for road safety research. For these many safety contributions, Dr. Aldman is especially deserving of receiving the award for engineering excellence.

United Kingdom

Gwilym Jones

Manager, Vehicle Legislation and Safety Research, Austin Rover Group
Product Engineering

Mr. Jones began his career working in car development and then specialized in vehicle testing, particularly braking and handling. As a result of this work, he was appointed Chief Experimental Engineer and then assumed responsibility, for the Vehicle Safety Engineering Department. In conjunction with this responsibility he is also managing the vehicle legislation aspects of car design and development. His major contributions to vehicle safety include research work on the skidding behavior of vehicles, vehicle handling, loss of control, and future trends in improved protection in frontal impact. Mr. Jones has been chairman of the SMM&T Car Safety Technical Committee for the past 4 years. Because of Mr. Jones's significant contributions to vehicle safety, he is recognized for his accomplishments by this award for engineering excellence.

Gunter Persicke

Ing., F.I. Plant E., Quinton Hazell Ltd.

For the past 20 years, Mr. Persicke has been particularly interested in the development of hydraulic shock absorbers and their application to a wide range of safety problems. Mr. Persicke has developed a versatile and inexpensive design for use in the design of barriers and bridge parapets, truck bumpers, and truck front and rear underride protection. Many of these applications are now in production and in use. Mr. Persicke currently leads a development team at Quinton Hazell developing suspension energy absorbers to provide controlled but variable rates of damping to improve handling and ride for road vehicles. For his significant contribution to vehicle safety, Mr. Persicke is deserving of special recognition.

G.D. Suthurst

Ford Motor Company Limited, Research and Engineering Centre

Mr. Suthurst joined Ford in 1963 in its Passenger Vehicle Research Department. He has been involved with vehicle safety since 1968 and has managed Body and Safety Research for the past 8 years. During this time he has been associated with initial development of a collapsible steering column used in the Cortina; design, development, and fabrication of the Ford demonstration car of 1974 to show the protection possible without restraints and the resulting loss of interior space; initial development of adjustable B-pillar seatbelt mountings; and development of computer optimization programs for simulating side impacts and pedestrian impacts. His research group is the focus for developments within Ford for improving the safety of cars and bridges the gap between outside research and production design. For his major contributions to vehicle safety, Mr. Suthurst is deserving of special recognition.

Japan

Kenichiro Nomura
Project Manager, Toyota Motor Corporation

Mr. Nomura has been manager of Toyota vehicle safety research and development since 1979. The results of much of this research can be found in Toyota production vehicles. Mr. Nomura was the project manager of Toyota ESV-III, which was introduced and exhibited during the Ninth ESV Conference in Kyoto. The ESV-III incorporated advanced accident prevention electronic developments such as the supermonitoring display, the radar-autodrive system, and the back sonar and antiglare mirrors. These latter two systems now appear in production vehicles. Because of his dedication to automotive safety, Mr. Nomura is selected to receive this award for engineering excellence.

Tomokazu Tokuda
General Manager, Research Department No. 1, Vehicle Research Laboratory Central Engineering Laboratories Nissan Motor Company, Ltd.

Mr. Tokuda has had a distinguished career with the Nissan Motor Company since 1958. As general manager of the Research Department, Vehicle Research Laboratory, Mr. Tokuda has conducted research in all areas of vehicle technology including safety, fuel economy, and weight reductions. As a part of his work, he developed the NRV II (Nissan Research Vehicle II), which was introduced and exhibited during the Ninth ESV Conference in Kyoto. The NRV II featured advanced technologies to lighten the driver's tasks as well as improved accident avoidance and occupant protection, energy and resource savings, and significant vehicle weight reductions. Mr. Tokuda is certainly deserving of the award for engineering excellence.

Shoichi Sano
Staff Engineer and Manager for Research Section Tochigi R&D Center, Wako R&D Institute Honda R&D Co., Ltd.

Mr. Sano, as the chief engineer for development of the Honda ESV project, contributed immeasurably to the completion of the compact 1,500-pound advanced technology ESV. Since completion of the ESV project in 1974, Mr. Sano has actively participated in the development of an airbag system for Honda small cars. His current effort to advance the accident avoidance capabilities of production cars has centered on the development of a four-wheel steering system. Mr. Sano is now leading a major effort to develop this new four-wheel steering system for commercial production cars. Because of these major safety research efforts, Mr. Sano is most deserving of special recognition.

The Netherlands

Dr. Johan G. Kuiperbak (Retired)

Director, Department of Road Transport
Ministry of Transport and Public Works
The Netherlands

Upon Dr. Kuiperbak's retirement from the Netherlands Ministry of Transport and Public Works, it is appropriate that we recognize his many years of effort to improve vehicle safety on the world's highways. Dr. Kuiperbak has been an active supporter of the ESV Program through his participation in the European Experimental Vehicles Committee and through his support and participation in the International Technical Conferences on Experimental Safety Vehicles. Dr. Kuiperbak's major contributions to road and vehicle safety are recognized by this special award.

Sweden

Nils Bohlin (Retired)

Senior Engineer for Automobile Safety
AB Volvo

Mr. Bohlin received the NHTSA Award for Engineering Excellence in 1979 for his many contributions to automotive safety. Now on his retirement, we are especially pleased to again recognize his outstanding research work over the years. Mr. Bohlin has been instrumental in advancing the state of the art in safety engineering and development. His contributions have indeed been impressive and have directly affected the safety performance of production vehicles.

United Kingdom

J.W. Furness (Retired)

Chief Mechanical Engineer
Department of Transport

Mr. Furness has had a long and distinguished career in furthering the cause of vehicle and road safety. His efforts in the harmonization of vehicle safety regulations are worthy of special recognition. As Chief Mechanical Engineer for the United Kingdom Department of Transport during the past 10 years, Mr. Furness has brought a keen insight to all the environmental aspects of motor vehicle safety, emissions, noise, weight, and fuel consumption. Because of Mr. Furness's major contribution to improved vehicle and road safety, he is most deserving of this special recognition.

Federal Republic of Germany

Professor Dr.-Ing. Willi Reidelbach (Retired)
Director, Passenger Car Body Basic Research,
Daimler-Benz A.G.

Professor Reidelbach initiated the Daimler-Benz accident analysis effort resulting in mathematical models that permitted evaluation of occupant behavior in all accident modes. The results were incorporated in vehicle design to improve structural integrity and controlled stiffness of the passenger compartment while reducing the weight of the car bodies. Professor Reidelbach's work in the area of car-to-car compatibility and driver/vehicle interaction in both real life as well as mathematical models is a yardstick for the designers today. As the Daimler-Benz safety officer for the Body Division, he was most influential in the design, testing, and final installations of the Daimler-Benz SRS System. For his many years of productive safety engineering, Professor Reidelbach is especially deserving of special recognition.

Italy

Dott. Ing. Giacomo Pocci (Retired)
Head of Studies and Research
General Administrative Department
Department of Civil Motorization
and Licensed Transports Ministry of Transport

Dr. Pocci has been an active and productive participant in vehicle safety improvement since 1955. His contributions include not only his impressive work for the Italian Ministry of Transport but also his performance as chairman of Working Party 29 of the ECE, his chairmanship of Working Group 6 of the EEVC, and other impressive research contributions to international groups and committees. Dr. Pocci has published many significant technical papers covering all aspects of vehicle safety. It is appropriate that he receive this special recognition.

Section 2
Government Status Reports

John W. Furness, Chairman, United Kingdom

Status Report of the United States

Michael M. Finkelstein
Associate Administrator for Research and Development, U.S. Department of Transportation, National Highway Traffic Safety Administration

Introduction

It is my pleasure to present the U.S. Government Status Report on our progress in automotive safety.

Since the Kyoto conference in November 1982, the National Highway Traffic Safety Administration's (NHTSA) automotive safety program has undergone several significant changes with encouraging results.

Of most importance has been Secretary Dole's decision of July 1984 on FMVSS 208, with the resulting efforts in many States to require the mandatory use of safety belts. In the near term, these laws will have a greater impact on highway safety than anything else we can do. However, we are also excited by the prospects offered by passive protection—both airbags and automatic safety belts.

Major efforts are also progressing throughout the United States to get drinking drivers off our highways. The decade of the 1980's has witnessed impressive reductions in the proportion of intoxicated drivers involved in fatal crashes.

Taken together, these steps have resulted in changes in vehicles and driving habits. The combination has been paying off. Last year witnessed the lowest fatal accident rate ever measured in the United States, and highway fatalities have declined by more than 11 percent from the levels we reported in Kyoto only 3 years ago.

The Accident Environment

Since 1980 the fatality rate per 100 million vehicle kilometers of travel in the United States has declined from 2.1 to 1.6 in 1984, the lowest rate ever recorded in the United States. The total number of traffic fatalities decreased from 51,091 in 1980 to an estimated 44,250 in 1984, while travel increased by approximately 3 percent per year.

A major goal in NHTSA's continuous effort to reduce the number of traffic fatalities and injuries has been to increase the use of occupant restraints in passenger vehicles. Within the past few years, almost all States have adopted mandatory child restraint laws with very encouraging results. In 1979 only 11 percent of young children in car accidents were restrained; by 1983 the proportion had increased to 48 percent.

Following on this achievement, mandatory safety belt use laws are being enacted throughout the United States. As of June 15, 1985, mandatory safety belt use laws for front seat passenger car occupants have been enacted in 13 States and legislation is pending in many others. The first law took effect in January 1985 in New York.

Another NHTSA priority is the reduction of drunk driving on the Nation's highways. Since 1980 the number of drivers who were involved in fatal accidents and had a BAC of .10 or above has been decreasing steadily. In addition, although traffic fatalities decreased during all periods of the day between 1980 and 1984, the reduction during nighttime hours, 6 p.m. to 6 a.m., was 19.2 percent, as compared to 3.4 percent during daytime hours.

Accident Data Collection and Analysis

The accident data cited throughout this report are derived from the Fatal Accident Reporting System (FARS) and the National Accident Sampling System (NASS). Both of these accident data collection systems are operated by NHTSA's National Center for Statistics and Analysis.

FARS is a computerized data base containing information on all fatal motor vehicle accidents occurring in the United States. The system became operational in 1975 and currently has records on almost 500,000 fatalities. FARS data are acquired directly from each State's operational records. The FARS file provides the most comprehensive, detailed, and accurate data available on the U.S. national motor vehicle fatality toll.

NASS is a network of 50 experienced, highly trained accident investigation teams that collect data on a nationally representative sample of police-reported accidents. Data are compiled and evaluated from detailed accident site inspections, measurements and assessments of damaged vehicles, driver interviews, medical records, autopsy data, and other pertinent State records. The NASS system collects information in significantly greater detail, both in number of variables and precision of observations, than existing records or systems. NASS presently has more than 40,000 accidents in the file from 1979 through 1984.

Crashworthiness Research

Since Kyoto, crashworthiness research at NHTSA has concentrated principally on the reduction of harm resulting from lateral crashes. We have completed most of our research on chest injuries resulting from contact with the vehicle interior. We are now attempting to increase our understanding of side crash protection, addressing other types of injuries, particularly head contacts with interior objects and ejections. Our other major project initiated since Kyoto has been a frontal protection project. Initially it was addressing unrestrained occupants, but the changing environment with respect to mandatory belt use laws has us expanding this project to cover restrained occupants as well. The foundation for much of our crashworthiness research is our biomechanics program, which is now completing work on the Side Impact Dummy (SID) and exploring the possibility of expanding the capabilities of the Hybrid III. Finally we have been exploring the feasibility of aftermarket airbag systems as well as encouraging the introduction of airbags from vehicle manufacturers.

Side Protection

Since Kyoto, the research reported on the Moving Deformable Barrier (MDB) was completed. A detailed test procedure for conducting perpendicular side impact tests using the MDB has been made available.

In addition to full system tests, a component test procedure was developed to simulate the interaction of the human thorax with the side door interior.

In a joint effort by NHTSA and Motor Vehicle Manufacturers Association (MVMA), a coordinated study of side impact accident data was completed and the predominant side impact injury categories were defined. Analyses of the accident data provided insight into the sources of injury and the injury-causing mechanisms in side impacts.

Frontal Protection

The major activity in our frontal crashworthiness research program is the accurate assessment of the safety problems associated with both restrained and unrestrained occupants of passenger cars involved in frontal impacts. The current effort focuses on the analytical characterization of the in-use vehicle fleet to identify present injury mechanisms, alternative countermeasures, and to predict the effectiveness of these countermeasures.

In addition to these efforts, a study of the safety performance parameters of production vehicles for restrained occupants is continuing. Belt systems, steering assemblies, and frontal structural energy management designs are being carefully examined from the New Car Assessment Program test results.

With an increasing number of mandatory safety belt use laws in the States and the effect of FMVSS 208, it is expected that a much larger percentage of U.S. vehicle occupants will be restrained. The different problems faced by unrestrained and restrained occupants will be closely examined in the course of our research.

Biomechanics

In biomechanics we have initiated several efforts to investigate injury production in frontal impacts for both the driver and passenger.

Trauma assessment technology efforts have also been very active. The design, development, testing, evaluation, and documentation efforts on the SID have been completed. This has been complemented by the recent publication of the Thoracic Trauma Index (TTI), which links the SID's impact response measures to the probability of producing various levels of thoracic injury.

Airbag Fleet Demonstration Programs

NHTSA, in cooperation with State police agencies, is conducting two demonstration projects to support research, manufacturing, and testing of retrofit airbags. The first project uses conventional airbag technology in retrofit kits developed by the Romeo-Kojyo Company of Tempe, Arizona.

Our second retrofit project began in March 1984 with the Breed Corporation. This project requires the production of retrofit driver airbag systems using a mechanical rather than an electrical signal to initiate inflation.

The Department of Transportation is also interested in gaining more experience with original equipment airbag systems. To this end, in March 1983 DOT signed an interagency agreement with the General Services Administration (GSA) to purchase 5,000 model-year 1985 Ford Tempos equipped with driver-side airbags, virtually all of which have been delivered and are currently on the road.

Crash Avoidance Research

Crash avoidance research continues to receive considerable attention at NHTSA. Several of our research programs have reached the point where we have been able to quantify safety benefits in terms of predicting actual accident reductions. In other areas we are focusing our efforts on the development of the technical framework and data bases necessary to insure that our activities are addressing well-defined safety problems and that they will yield useful results.

Work continues on the development and refinement of the data bases that will be used for problem identification and establishing research priorities. We are concentrating on developing large-scale crash data files that focus on the precrash events leading up to the accidents. We are particularly interested in identifying vehicle maneuvers and driver actions in the 3- to 5-s time period immediately prior to the crash.

Lighting and Visibility

In the report at the Kyoto conference, earlier research on rear-lighting systems was described where we established the effectiveness of a high-mounted brake lamp in reducing rear-end collisions. Since then a regulation has been promulgated that will require all passenger cars manufactured on or after September 1, 1985, to be equipped with a single center high-mounted brake lamp.

In current research, we are assessing the photometric requirements contained in Federal Motor Vehicle Safety Standard 108 that deals with the intensity of presence and brake lamps. During the past 2 years NHTSA's headlight research has been directed toward improving the light distribution pattern of low beam headlights. In a recently completed experimental study, a new low beam was found to offer potentially better lighting in comparison with typical U.S. and European beam patterns. Comparison of the results of the experiment and an analytical evaluation of the same beam patterns using the Comprehensive Headlamp Environment Systems Simulation model indicated the need for a more comprehensive approach to headlamp evaluation. At the present time, a program is underway to examine improved measures and procedures for evaluating headlamp performance in the context of the driver-vehicle-roadway system.

Research to examine approaches for reducing crashes by increasing vehicle conspicuity is continuing. Preliminary results from a fleet study involving nearly 4,000 tractor-trailer units indicate that reflectorization of trailers may be an effective means of reducing the number of crashes of other vehicles into trailers. In another fleet study, the use of daytime running lights will be evaluated to determine if the benefits of this countermeasure in reducing multiple-car crashes apply to U.S. roadway and environmental conditions.

Handling and Stability

In handling and stability, we have just concluded extensive research on the influence of brake balance on vehicle yaw instability. Several new computer simulations have been developed to predict lateral position and yaw deviation as a result of rear axle lock. Open loop experiments with an instrumented variable brake balance vehicle have been conducted to confirm the simulations. In addition, human factors testing has been performed to investigate the effects of brake balance on the driver's ability to maintain vehicle brake control during braking with rear axle lock.

Finally, under our crash avoidance research program, a joint project has been initiated between NHTSA and the National Aeronautics and Space Administration for the development of an advanced radar crash warning system. The program is being conducted at the Johnson Space Flight Center in Houston, Texas, and is expected to be completed 18 months from now. A prototype system suitable for vehicle test and evaluation will be available at the completion of the project.

Heavy Duty Vehicle Safety Research

The goal of the heavy duty vehicle safety program is to improve the accident avoidance capabilities and crashworthiness of vehicles with gross vehicle weight ratings in excess of 10,000 lb through improvements in vehicle performance and driver/vehicle interaction. Even though they comprise only 3 to 4 percent of the motor vehicle fleet, heavy trucks continue to be involved in more than 10 percent of the fatal accidents.

Current heavy truck research focuses primarily on high priority crash avoidance programs aimed at improving

the dynamic performance of heavy vehicles in braking and steering maneuvers. A core level brake research program continues to seek ways to improve the safety performance of both air and hydraulically braked trucks in accident avoidance maneuvers involving braking, i.e., improved stopping capability without compromising directional stability.

Driver and Pedestrian Safety Research

While most of the activity we are focusing attention on at this conference deals with motor vehicle safety research, NHTSA has an active program addressing the behavioral components of traffic safety. Our major efforts these past few years have continued to concentrate on impaired driving problems and on safety belt and child restraint use.

Alcohol Safety Research

The goal of the alcohol safety program is to develop procedures that effectively reduce alcohol-impaired driving and related accidents.

Alcohol safety is focused on the following four areas:

- General Deterrence—Development of combined enforcement, public information, adjudication, and licensing programs designed to increase public perception of DWI detection risk among the general population
- Specific Deterrence—Development of programs directed at identified drunk drivers and designed to prevent future DWI offenses
- Prevention—Development of education, public information, and local community training programs designed to instill responsible attitudes toward drinking and driving and promote cooperative action for avoiding DWI
- Intervention—Development of programs designed to identify techniques that will enable and motivate third parties (e.g., bartenders, hosts/hostesses, drinking companions) to take action in a drinking situation that will deter potential DWI incidents

We are also beginning to initiate more work on drug-impaired driving, a potentially significant problem in the United States and many European countries.

Safety Belt Use Research

The enactment of mandatory belt use laws by State governments has brought about a revamping of the agency's program to foster increased safety belt use. Rather than relying almost exclusively on educational and persuasive efforts to motivate drivers and passengers to buckle up voluntarily, attention is now focused on providing educational information for States considering belt use laws and assisting those States that have such laws to develop programs to implement them in the most effective manner. Research concentrates mainly on: (1) assessing the impact of these laws through the analyses of crash data and tracking use rates; (2) exploring the situational and demographic variables associated with nonuse of belts; and (3) field testing and evaluating both traditional and innovative techniques to achieve higher belt use rates.

Vehicle Safety Standards

Since the Ninth ESV Conference in Japan, some significant changes have occurred in our Federal Motor Vehicle Safety Standards (FMVSS).

In the crashworthiness area, in July 1984 we reinstated the FMVSS 208 requirements for automatic occupant crash protection. Automatic crash protection will be required in 10 percent of new 1987 models, 25 percent of new 1988 models, 40 percent of new 1989 models, and in all new cars starting with 1990 models.

However, if mandatory safety belt usage laws meeting specified conditions are passed by a sufficient number of States, effective not later than September 1, 1989, the automatic crash protection requirements will be rescinded.

FMVSS 205 was amended to permit antilacerative glass/plastic windshields and other windows in U.S. cars. Some U.S. car models are already being sold with glass/plastic windshields as an option or as standard equipment.

In the near future, NHTSA is considering crashworthiness improvements in the side impact area. Every attempt will be made to include full consideration of the worldwide efforts underway in side impact protection research.

Finally, we have recently issued a proposal to permit the use of the Hybrid III anthropomorphic test dummy, and to ultimately have it replace the dummy currently used in U.S. crash tests.

In the crash avoidance area, we have issued a proposal for a new hydraulic brake systems standard for passenger cars. This new FMVSS is the culmination of several years of our work with the GRRF, and represents a significant attempt by the United States to harmonize European and U.S. brake system regulations.

We have issued several amendments to the FMVSS 108 to harmonize rear lamp photometrics and headlamp height with the European requirements. Additionally, we now permit replaceable bulb headlamps in the United States, a major step toward international harmonization; and we have proposed adoption of a U.S. version of the H-4 headlamp bulb.

The United States has just proposed that devices be installed on heavy trucks and trailers to reduce the splash and spray from the tires when driving on wet roads. Included in the proposal are spray suppressant flaps behind the wheels, and side skirts on both sides of the vehicle wheels.

International Harmonization

NHTSA is committed to fostering international harmonization of motor vehicle safety standards. This policy is, of course, tempered by legal and procedural requirements that the agency must follow and by concern that motor vehicle safety in the United States not be compromised.

Our efforts are directed toward controls and displays, lighting, and brakes. The agency has issued amendments to the controls and displays standard and the lighting standard and recently proposed a new harmonized standard for passenger car brakes.

FMVSS 101, Controls and Displays, was amended on July 27, 1984, by changing several identification requirements to agree with the symbols recommended by the International Standards Organization (ISO).

On November 26, 1984, FMVSS 108, Lamps, Reflective Devices, and Associated Equipment, was amended to bring the requirements into closer harmony with those of ECE.

The agency recently published, on May 10, 1985, a notice of proposed rulemaking that proposes a new standard, FMVSS 135, Passenger Car Brake Standards, which would replace FMVSS 105, Hydraulic Brake Systems for passenger cars. The new standard would differ from the existing one primarily in that it contains a revised and shortened test procedure based on a draft harmonized international procedure developed by ECE.

With regard to future endeavors, the agency has under serious consideration the question of establishing a new standard for side impact protection of occupants of passenger cars.

ECE/WP29, through its Group of Rapporteurs on Crashworthiness (GRCS), is also studying the problem. The United States, as a participating member, has offered to test both the anthropomorphic device and movable deformable barrier that are decided on by the GRCS in the interest of furthering harmonized requirements for both devices.

Status Report of Canada

Eric R. Welbourne
Chief, Vehicle Systems, Road Safety and Motor Vehicle Regulation Directorate,
Transport Canada

Introduction

As many of you are aware, Canada has been an interested observer of the ESV and RSV programs almost from their beginnings. We have participated in most of the conferences, which continue to provide unequalled opportunities for the exchange of research information relating directly to the development of safer motor vehicles. I am pleased to have this opportunity to contribute to that exchange by telling you something of recent work in Canada.

The design, construction, and performance of motor vehicles manufactured in or imported to Canada are regulated by the Federal Government under the authority of the Motor Vehicle Safety Act of 1970. The associated Canada Motor Vehicle Safety Standards (CMVSS) are, for the most part, either identical or compatible with the corresponding U.S. Federal Motor Vehicle Safety Standards. In a few instances, compliance with the relevant ECE regulation is an acceptable alternative to compliance with the North American standard.

The high level of harmonization of standards between the United States and Canada is a logical consequence of the integration of vehicle manufacturing in the two countries, which followed the conclusion in 1965 of the Canada-U.S. Automotive Products Agreement. This high level of harmonization offers certain evident advantages to Canada but does not relieve the Federal Government of two important obligations arising from its regulatory role. The first is to determine whether the net social and economic benefits of adopting a specific U.S. standard are likely to be positive in Canada. A second obligation is to determine whether current and proposed U.S. standards are sufficient for Canadian needs. Such considerations have, in the past, led to significant differences in the specific requirements of Canadian and U.S. standards in such areas as occupant protection, lighting, heavy truck braking, and exhaust emissions. They have also resulted in the development of several standards having no equivalents in the United States.

Perhaps more importantly in the present context, these obligations have continued to provide the principal motivation for a modest research and development

program in support of the Canada Motor Vehicle Safety Standards. The resources now available are such that we can usually consider only one major topic in crash avoidance and one in crashworthiness at any given time. I would therefore like to describe briefly the work we have been doing; first, on daytime running lights and, second, on the improvement of occupant protection.

Daytime Running Lights (DRL)

The Directorate first became interested in the potential of daytime running lights as a crash avoidance countermeasure in 1973. Following a review of the existing literature, our first thoughts concerned the feasibility of conducting a properly controlled field experiment to measure effectiveness and obtain associated cost data. In fact, we began a series of studies, addressing many of the specific questions relating to the costs and effectiveness of DRL, that was completed in 1984.

From these studies and the results that had been obtained from DRL use in Finland and Sweden, we concluded the general use of daytime running lights in Canada would lead to important reductions in the number of accidents involving two or more vehicles or a single vehicle and another road user. In our view, the favorable results obtained in Scandinavia had little to do with the lower levels of ambient illumination in the more northerly latitudes of those countries; it had much to do with the high proportion of collisions that are associated with perceptual errors on the part of drivers and other road users under all lighting conditions. It was further apparent that these accident reductions (equivalent to a 3 to 6 percent reduction in all accidents) could be obtained at a very modest cost, provided that the measure was not implemented simply by the use of existing lighting systems with low beam headlights on.

A comprehensive discussion paper that deals with several options for the implementation of general DRL use in Canada is substantially complete and will be published shortly. Following a review of its contents with various interest groups, it is hoped that a decision will be made quickly on implementation.

Improvement of Occupant Protection

Following the introduction of the first provincial laws requiring the use of seatbelts, a study was undertaken of the injury experience of passenger vehicle occupants restrained by 3-point belt systems. The results of this study, and a review of the literature on the performance of 3-point belt systems, suggested that the effectiveness of current systems could be improved significantly with little increase in either their cost or their complexity. The principal areas for improvement were the incidence of head and facial impacts with the vehicle interior, the thoracic loading induced by the upper torso belt, and the internal abdominal injuries induced by the lapbelt.

It did not appear there was any particular difficulty in designing a belt system to give the desired performance (some existing systems were evidently very good). The problem was simply that the current design-based standards for seatbelts permitted the use of a wide range of designs, many having obviously unsatisfactory features from a biomechanical viewpoint. It was also evident the use of the existing set of three performance criteria (HIC, maximum chest acceleration, and maximum femur load), specified in CMVSS and FMVSS 208 for passive restraint systems, offered no panacea. From some tests of our own and from an analysis of data from other sources, we determined that those criteria can be met readily by the use of belt systems that provide very poor control of occupant motion during a collision yet impose very high restraining forces on the occupant. Indeed, it became clear that under some circumstances the criteria could be met with a completely unrestrained test dummy.

The general problem then was to develop a set of performance criteria that addressed the actual injury experience of restrained occupants. That is what we set out to do, accepting as a practical constraint that those criteria would be applied in the context of the standard 48km/h frontal barrier crash. We then turned to the specific problems of defining performance criteria and developing the means of determining compliance with them. Within the scope of the present short report, it is not feasible to describe the development work in any detail. Much of it has been described elsewhere. For present purposes I shall, therefore, simply summarize the current status of the work.

Using a modified General Motors Hybrid III dummy, we are presently proposing performance criteria to address closed head injuries, facial bone fractures, and thoracic injuries in the standard barrier test collision. The basic Hybrid III head has been substantially modified to incorporate a frangible facial insert of methyl methacrylate and a compliant chin of silicon rubber. The original covering of the head has been replaced by a featureless skin of nominally uniform thickness. The Hybrid III chest has been replaced with a new structure that more closely approaches the shape of the human thorax. Its compliance distribution is based on the results of human volunteer tests and cadaver data. The deflection response to blunt mid-sternal impacts is essentially the same as that of the original Hybrid III chest.

An interim criterion for the prevention of closed head injuries has been proposed. It is based on a linear combination of the instantaneous value of the resultant translational acceleration of the head and the rotational acceleration of the head in the sagittal plane. Facial bone fractures are controlled by the frangible insert, which

fails at an impact energy level based on available cadaver data. Thoracic injury is presently controlled by specifying a maximum chest compression at mid-sternum.

No dynamic criterion has been proposed to control loading of the soft tissue of the abdomen. Instead, a separate static test procedure has been developed that provides a quantitative measure of the fit of the lapbelt in relation to the anterior/superior iliac spines. The procedure uses the standard H-point machine, modified to accept pelvic and thoracic forms. A small number of these accessory sets has been produced and the participation of interested agencies in evaluating the proposed procedures and hardware will be sought shortly.

We believe the U.S. administration's recent acceptance of the Hybrid III dummy as a compliance test device is a significant step toward the specification of more relevant and comprehensive criteria for the performance of occupant protection systems. As we approach a first series of crash tests to evaluate the developments I have described, we are optimistic the results will contribute to some long overdue progress in that direction.

Other Activities

Although I do not wish to take any more time than is necessary, it would be remiss of me not to mention at least a major cooperative research project presently in progress in Canada. The project, which is funded jointly by the Federal and provincial governments and industry, seeks to provide objective data on the implications of more uniform weight and dimensional regulations for commercial vehicles in Canada. The research addresses the effects of vehicle weight and dimensional variations on the stability and control characteristics of the vehicles themselves and their effects on the strain and deflection response of pavements. The availability of a common base of objective information should facilitate the more uniform acceptance of vehicle configurations offering improved safety and operational efficiency. I would be glad to provide additional information to anyone who would like to know more about the work.

Status Report of the European Experimental Vehicles Committee (EEVC)

Prof. Dr. Bernd Friedel
Chairman, European Experimental Vehicles Committee (EEVC)

When we met in Kyoto in November 1982, we stated in the Status Report of the European Experimental Vehicles Committee (EEVC) that the considerations in Europe with respect to occupant protection are based on the compulsory use of the seatbelt. In this respect, a number of changes have been successfully introduced since 1982. In some European countries, it has been possible to achieve drastic increases in seatbelt usage rates on the front seats: up to 90 percent and even more. These high rates, apart from various other factors, certainly contributed to injury mitigations and further reductions in the number of traffic deaths in particular.

Apart from these positive developments with regard to the number of accident-involved injured and killed persons, a series of problems had to be dealt with since the Ninth ESV Conference. We will have to take care that, under the pressure of other urgent problems, the safety of our cars does not lose in importance. Environmental problems and their discussion doubtless are growing in importance. We all know that extensive and serious attempts at improving the quality of the air have to be made—still, we should not give up and cease developing, making demands for, and introducing automotive engineering solutions to improve road safety.

As you know, the European Communities (EEC) have declared 1986 as the year of road safety in Europe. For several international bodies, the subject of occupant protection has remained under discussion, i.e., the work for a global test in a frontal collision has continued along with priority discussion on side impact and pedestrian protection at the Economic Commission for Europe (ECE).

For passenger protection in frontal collisions, it has been proved that a big step forward had been taken. It now seems necessary to implement the available scientific knowledge into political decisions to improve also the protection of passengers in side collisions and the safety of pedestrians and two-wheelers. It is our conviction that differences of existing opinions cannot be harmonized by further research alone. It needs a stern resolve and firm will, with its reflection in policies, to achieve solutions for all parties concerned.

Upon an extensive inquiry of NHTSA, EEVC proposed after the last ESV conference cooperation in the field of research between Europe and the United States. It was

our opinion the following tasks were to be dealt with by cooperative efforts:

- NHTSA participation in the EEVC ad hoc group on side impact dummies
- Participation in the EEVC ad hoc group on pedestrian safety
- Clarification of national viewpoints and interests with regard to the compatibility of cars
- NHTSA establishment of bilateral contacts with partners in different European countries to deal with special studies by joint efforts, e.g., Advanced Motorcycle Brake System, Driver Performance Measurement Systems, and Heavy Truck Control and Dynamic Stability

Efforts initiated to improve cooperation have just started. Despite our good intentions, however, it must be admitted that cooperation was more difficult than we expected, partly due to the traveling costs involved.

As mentioned before, special efforts were invested in the development of a side impact dummy for a study and evaluation of occupant protection in side impacts. A set of specifications and requirements for the EUROSID, as the dummy is called, was drawn up by an EEVC ad hoc group under the chairmanship of Mr. Neilson (TRRL) and published in 1984. The Commission of the European Communities (EEC) has sponsored in their large biomechanics programme intensive research concerning the comparison of different side impact dummies. Those studies formed the basis of the common attempt to develop a special European side impact dummy. Various institutions were engaged to produce specific parts of this dummy (e.g., pelvis, neck, and shoulder). We are pleased to demonstrate a prototype of the EUROSID at this conference. A validation program concerning the EUROSID is set up, in particular to investigate whether this dummy would meet the abovementioned EEVC specifications. The involvement of EEC will still be continued and the validation work will probably be undertaken with the contribution by EEC. After finishing this task, the dummy will be available for a wider use in side impact testing. NHTSA, the car industry, and other interested bodies are then invited to collaborate and participate. It is hoped that arrangements can be made for production of the EUROSID.

Efforts were made by several European research institutions to advance the work on the mobile barrier with a deformable front face, which had been proposed by a working group of EEVC. The barrier is built with a polyurethane hard foam block and will be exhibited during this conference. It seems the test device performs according to EEVC specifications for the perpendicular crash mode mentioned by our Working Group 6. For 2 years the ECE group of rapporteurs of vehicle structures (ECE/GRCS) have based the draft regulations for side impact tests on this EEVC barrier.

As stated at the Kyoto conference, EEVC dealt with the subject of "Cycle and Light-powered Two-wheeler Accidents" within new Working Group 8. An extensive report was published in 1984 that outlined the following:

- Detailed presentation of numbers of accidents involving cyclists and riders of light-powered two-wheelers
- Description of injury-influencing parameters
- Current knowledge on human tolerances (with special relevance for two-wheelers)
- Injury prevention measures and related consequences for other road users

Among the results one will find proposed improvements of two-wheelers and other vehicles (e.g., lighting equipment, braking performance of bicycles, energy-absorbing materials in front structures of cars, and underrun-guards on heavy goods vehicles). In general there seem to be no big discrepancies in measures to protect pedestrians and two-wheelers. General recommendations and recommendations for future research are outlined. We hope the EEVC report will be included in the proceedings of this conference.

Suggestions and proposals with respect to pedestrian protection are reviewed and discussed within an EEVC ad hoc group under the chairmanship of Mr. Moreau de Saint-Martin (ONSER). Thus the state of the art of pedestrian safety continues to be kept up to date despite the completion of the work of EEVC Working Group 7 (the report was published and disseminated at the ESV conference in Kyoto, 1982). The ad hoc group concentrated on the following factors in particular: accident analysis, injury mechanism, human tolerances, and possible methods to test and evaluate the effectiveness of pedestrian protection measures.

It was further attempted to draft guidelines for the design of cars related to stiffness and shape and to list priorities for further research. With respect to the guidelines, the idea was that although they should be introduced soon, the points to be considered in the long run should also be taken into account. There will be a report about this presented at the conference.

We have come to this year's ESV conference to present and discuss the results and suggestions arrived at by EEVC since the last conference. We have also come to exchange new research findings and information obtained at other places, e.g., in the United States and Japan. We trust this exchange will deepen our understanding and insight and also our acceptance of the need for further car safety improvements. The possibilities of cooperative efforts should be studied thoroughly and coordinated so as to fully concentrate our resources on priority problems—the protection of passengers in lateral collisions and the protection of pedestrians and two-wheelers.

Status Report of the Federal Republic of Germany

Prof. Dr. Heinrich Praxenthaler
President, Federal Highway Research Institute

When the Ninth ESV Conference was held in 1982 in Japan, we stressed the necessity of continuing our efforts to improve motor vehicle safety, to save energy and raw materials, and to reduce further the impacts on our environment in close collaboration with the car industry. Since that conference, efforts to improve environmental conditions by vehicle measures have gained prominence.

Since 1982 the trend of road traffic accidents in the Federal Republic of Germany is marked by an increase in accidents of about 9.3 percent, with injury accidents remaining more or less unchanged. A noticeable decline in fatal accidents took place in 1984, amounting to about 12 percent compared with 1982. Based on the mileage figures, which have risen by about 5 percent since 1982, these figures gain special importance. Concerning car occupants from 1982 to 1983, there was an alarming increase in fatalities, but an encouraging decrease took place from 1983 to 1984 resulting in an overall drop in the number of car occupant fatalities by about 8.6 percent since 1982.

Of special importance in this connection is that from the summer of 1984, noncompliance with the seatbelt usage law by front seat occupants incurs a fine of DM40. Because of this measure, belt usage rates changed between March and September 1984: on motorways from 81 percent to 97 percent and on rural roads from 62 percent to 94 percent. In urban areas the rates rose spectacularly, from 47 percent to 88 percent. There has been no decline in these figures so far; they even continued to increase slightly up to March 1985.

In 1984 the Federal Government presented a comprehensive program for improving road safety. It strongly appeals for road users to be more circumspect in traffic, drive more relaxed, and be regardful of others. Federal states and communities, associations and industry, and companies and societies are asked to support road safety to an even greater extent than before. Higher financial commitments are also needed because road safety efforts cannot be the sole responsibility of the state. One does not rely so much on more rules and regulations but on strengthening road users' individual and joint responsibilities for human life and health. That is why traffic education measures and safety campaigns are priority concerns of the Federal Government. Still, additional regulations are considered to be indispensable. Young car drivers and young two-wheel riders are marked by above-average learner risks. The introduction of a probationary driving license and a graduated driving permit for motorcycles is to effect more caution by learners during their first years of driving practice. The pleasure enjoyed in taking risks must be controlled and more relaxed attitudes displayed with respect to traffic.

Among other things, motorcyclists will have to comply with the mandated use of low lights during daylight hours, and mofa riders will be required to wear safety helmets. The seatbelt usage law has now been made compulsory for occupants in rear seating positions, but they are not fined for the time being. A model test will demonstrate whether it is possible to reduce the number of traffic signs on roads. The introduction of antilock braking systems for heavy-duty trucks and coaches has been set as an aim; the same applies to in-car displays that visually or acoustically remind drivers of buckling up and to the further standardization of seatbelt locking systems.

On the road sector, accident black spots, the construction of bypasses and cycle lanes, and influencing drivers by means of variable message signs are in the foreground. Further improvements to the emergency medical services system are also being undertaken.

In the field of accident research, activities of the Federal Government, car industry, and motor vehicle insurers can again be mentioned at this ESV conference. Further improvements to occupant protection continue to be an issue of general concern, especially in side collisions, from the viewpoint of the compatibility of cars and the protection of other road users, i.e., pedestrians and two-wheel riders. We are confronted here with the problem of designing front and side structures, based on detailed accident analyses, to optimize deformation values, bearing in mind the other road users.

The accident research efforts of the German motor vehicle insurers (HUK Association) are continued in the field of interior safety. In addition, studies on active safety, driver training, and the rating of the safety of driver groups and car categories are becoming increasingly important.

The HUK Association's accident research data base, revised in 1980, has been extended and presently comprises about 11,000 accidents occurring since 1980. Roughly 2,000 car accidents in which belts had been used, 3,000 single car crashes, 4,000 two-wheeler accidents, and 2,000 truck and bus accidents are available for accident research. These retrospective studies are increasingly undertaken in direct collaboration with the police and accident clinics. A study of 200 car frontal collisions in which occupants had been belted again confirmed the high protective effect of this restraint system; this effect may, however, be bettered by additional measures, such as preloaders and the use of airbags or steering column and wheel design alterations. Another study revealed that belt usage in rear seating positions could protect about 350 car occupants in Germany per year against fatal injuries and about 4,000 against major injuries.

Work on the sector of active safety concentrates on describing the accident characteristics in relation to the interactive driver-car behavior and particularly on the possible benefits of an antilock system. Based on the outcome of these initial studies, the motor vehicle insurers have been granting a premium rebate of 10 percent in the case of complete vehicle insurance policies for antilock braking system-equipped cars, trucks, and buses. Concrete studies into the effectiveness of such vehicles are envisaged for 1985-86.

It is also an objective of the HUK Association's accident research to use accident research findings for the benefit of driver training. In collaboration with other institutions, it has been possible to derive knowledge from studies on actual accidents, such as, for instance, the distribution of accidents with respect to categories of motorcycles, and consider them in the proposed revision of the regulations applying to the operating permit for motorized two-wheelers and the probationary driving license.

An analysis of 1,100 truck accidents with respect to exterior safety and partner protection has been completed by collaboration with the Research Association Motor Vehicle Techniques (FAT); work on the truck front structures is being continued by means of a second series of 14 crash tests and shows that practicable solutions are possible. An analogous study on truck occupant safety was started early in 1985.

Further research efforts of the HUK Association will aim at reducing injuries despite buckling up and at obtaining improved biomechanical safety criteria. Improved starting points for an approach to the safety rating of different car models in a crash can be expected to emerge from new methods of evaluation. A project extending over several years is expected to lead to information about accident frequency characteristics for particular car models and the accident consequences therefrom; it is also expected to provide tips, particularly for automotive engineers, as to necessary remedial measures.

The accident research efforts of the state have primarily been concentrated on continuing the numerous projects started since the last ESV conference. At-the-scene accident investigations undertaken since 1973 have been continued. These include special evaluations with respect to truck accidents, pedestrian accidents, and accidents involving motorized two-wheelers.

Roughly 30,000 rear-end collisions, each involving two cars, respectively, were analyzed to study the effects of two additional high-mounted stoplights. This analysis revealed no noticeable effects on accidents, either in terms of frequency or severity. A fact that attracted attention is the disproportionately high percentage of rear-end accidents in which both cars involved were equipped with additional high-mounted stoplights. An analysis of about 8,000 rear-end accidents involving between three and five cars also did not provide a confirmation of the effect of these lights.

A pilot study on the definition of critical situations with respect to driver-car behavior has been completed. Furthermore, reconstructions of accidents have been started to determine characteristic driving maneuvers in the phase preceding a crash and in the direct precrash phase.

The effects of safety helmets for motorized two-wheel riders were analyzed in laboratory tests and at-the-scene accident investigations. The main questions concerned the impact points and the resulting head injuries. On the whole, the studies clearly confirmed the helmet's positive effects on safety, which mitigates considerably the severity of injuries. The benefits of a safety helmet for riders of light-powered two-wheelers were also confirmed. A study of protective clothing demonstrated its positive effects; these mainly consist of mitigating open wounds and the danger of infection whereby otherwise protracted healing processes are shortened.

An extensive research project, "Design of Cars Affording Optimum Occupant Protection from the Viewpoint of the Economy," sponsored by the Federal Ministry for Research and Technology, was undertaken to study the optimization of the safety-related design aspects of cars, taking economic viewpoints into account. A mathematical simulation program was developed for this purpose. Occupant injuries were studied and evaluated in addition to the cost of design and production and changes in operating costs. Among other things, the results demonstrate that by optimizing requirements, considerable safety gains are still attainable without an increase in costs.

All efforts toward optimization presuppose belt usage by occupants. It is clearly important that car structures be adjusted to the restraint system employed. If that is not the case, a part of the restraint system's benefit is wasted.

It was further recognized that occupant protection in side collisions can be even partially achieved by designing car front structures accordingly, i.e., attenuating the aggressiveness of the impacting car. Based on experience acquired by car manufacturers, such improvements appear to be possible.

It must be the objective of future efforts to develop test methods taking the protection of both the occupants of the impacting car and those of the impacted car into consideration, thus simulating car behavior in an actual accident more realistically than is possible by means of head-on collisions against a rigid barrier.

In another side collision project, a deformable element of a movable barrier was developed in accordance with EEVC specifications. The barrier is currently being tested in collaboration with institutes in France and Great Britain.

In a new series of tests, the studies on the interaction of car occupants were continued. With respect to the frontal

collision, it has been possible to demonstrate that an interaction load can be totally avoided if occupants in rear seating positions are belted. To avoid such loads in the rear-end collision, the stiffening and additional upholstering of the backs of front seats should be required.

Furthermore, the variations of data measured on the car and dummy in collisions against a rigid barrier at a speed of 50km/h were determined. The scatter for the vehicle loading remained clearly below 10 percent and that for the protection criteria HIC and SI between 22 and 33 percent. It still must be clarified how the scatter should be taken into account in the legal regulations applying to full-scale tests.

Accident analyses revealed that it appears appropriate to incorporate clear evidence of the elimination of submarining into the corresponding regulation on frontal collisions.

Since no method is known at present by which the aggressiveness of vehicles with respect to pedestrians can be adequately described, a proposal for a standardized pedestrian test was worked out in collaboration with other European research institutions. Based on accident statistics, dummy positions and collision speeds were determined in particular and their applicability studied in a global test. In cooperation with experts from Switzerland, recommendations with respect to vehicle design considerations for the protection of the pedestrian were developed for the responsible ECE group.

A number of the projects mentioned were undertaken in close cooperation between state authorities and the car industry. The wide range of the car industry's own activities is the topic of numerous contributions to this conference.

The objective of safety was enlarged years ago by including in a farsighted manner the three well-known E-factors—energy, environment, and economy.

The last conferences paid special tribute to the achievements of the car industry in the field of more economical vehicles. We are accustomed to their existence and often forget how difficult the path toward fuel economy has been and that the favorable energy situation today is also due to fuel savings in motor vehicle traffic.

Environmental problems regarding the car are characterized above all by noise pollution and exhaust emissions. In EEC countries, the noise emission limits for motor vehicles were reduced in the past years, based on ISO measurements. The noise emission limits for motor vehicles should be lowered still further. In the past years, the car industry, with the decisive support of the Federal Government, developed commercial vehicles to the production stage with a noise emission level comparable to that of cars. An important condition of mass production and the corresponding demand for these vehicles was the establishment of binding criteria in respect to a noise-controlled commercial vehicle. It is important for the Federal Government to increase the proportion of such noise-controlled trucks in the total number of registered vehicles.

The extent to which measures of traffic restraint can contribute to mitigating the noise exposure of the residential population is currently being studied.

In the Federal Republic of Germany, particularly because of exhaust emissions, environmental impacts caused by cars have become an issue of symbolic character. "Waldsterben" is spreading and has become an alarming concern. This is not the place to talk about the stony path to an emission-controlled car. Facts have compelled us to act and emotions have aggravated the situation, but nobody should believe it is primarily the domestic policy conflict that has determined our outlook. All responsible forces of the Federal Republic want resolute efforts to be undertaken to reduce the levels of air pollution and want automotive engineering to contribute its share. We are also convinced that this recognition will soon spread to countries that are not yet alarmed by damage to their forests. What matters is not only the protection of our forests but the protection of human beings.

Although activities aim mainly at the new environmentally acceptable car, the roughly 25 million cars with internal combustion engines on our roads are also the objective of our efforts. No efforts should be spared to obtain noticeable emission reductions by means of subsequent alterations to the combustion system of cars.

Furthermore, the annual emission control introduced in January 1985, in association with optimal engine adjustment, will reduce emission levels. The customary interval between two emission controls has thus been reduced by half. This control concept also applies to cars with catalytic converters until a suitable test method becomes available.

The emission behavior of diesel engines with respect to gaseous emissions is essentially superior to internal combustion engines without an exhaust gas cleaning system. However, the Federal Government is presently working on a concept of reducing the gaseous pollutants, and especially the noxious particles, emitted by diesel vehicles.

Economy also stands for the moderate price of a car. We still regard a car as a means affording freedom that should be owned by many citizens. The production of emission-controlled cars has its price just as safety does. So that those who contribute to environmental protection are not put at a disadvantage, the state provides support and assistance. This is the approach we chose; it is in no way unusual since state incentives and state subsidies are given in many areas, not only in our country.

Concepts and activities today largely concentrate on environmental and competitive objectives. These matters should not, however, push the issue of safety out of the limelight, which was the problem of original concern at

ESV conferences. Each time we face conflicting aims, there is the danger that the permanent objectives, pursued for so long, are inadmissibly pushed aside by current issues. For that reason, the ESV conferences continue to be meaningful and significant.

Status Report of Italy

Dr. Franco Rossi
Direttore Centrale Motorizzazione, Direzione Generale M.C.T.C., Ministero dei Trasporti

Analysis of Accidents

In the past few years, the Italian domestic statistics have shown a slight decrease in casualties due to road accidents and a practically stable situation with regard to injuries. This notwithstanding, it appears further improvement is still possible.

In this connection, it should be pointed out that accident distribution according to type varies from one country to another. It is, therefore, necessary that an international accident data bank be established so the international regulatory bodies can determine priorities of intervention and evaluate the effectiveness of provisions adopted. Lack of such a data bank is a gap in the legislative procedure that both the EEC (European Economic Community) and ECE (Economic Commission for Europe) must fill. EEC has already stated that a road accident and safety data bank should be established at the community level.

General Provisions

Road Infrastructures

Our country has been developing a General Transport Plan that also takes road safety into account.

The Italian political authority will, therefore, have some guidelines available for the priority actions aimed at improving the infrastructures and reducing road fatalities.

Statistics show that whereas the Italian motorway network is more than adequate, the secondary road network perhaps does not compare with that of some other nations when related to traffic density. This is an area in which considerable effort will have to be made in the future.

Motor Vehicle Regulations

With regard to technical provisions concerning motor vehicles, Italy has adopted as many as 55 ECE regulations and 46 corresponding Community Directives. These are practically all the legislative documents issued by the international intergovernmental bodies. As a result of the experience gained from such instruments, we think careful consideration should be given to future amendments.

The criteria that have formed the present regulatory policy, based on geometric protection concepts, are no longer adequate in view of the evolution of accident investigation and vehicle test techniques.

We think it is necessary to evaluate the means—for example, biomechanics, dummies, and mathematical models—now available. Development of integrated test methods to evaluate overall vehicle behavior is, in our opinion, a more adequate response to the need to improve the motor vehicle fleet.

The Italian Government thinks, however, that efforts made so far to improve vehicles have already yielded considerable results and that further progress will require extensive investigation.

It is necessary to point out here the need to improve use of the vehicle through more shrewd traffic management to reach the main goal of reducing accidents and their effects.

The Human Factor

Finally, as far as the last and most important safety factor—MAN—is concerned, it should be noted that in our country a great many initiatives are underway to raise the public consciousness about traffic safety and to educate road users.

The Ministero dei Lavori Pubblici has declared 1985 the "Year of Road Safety," thus anticipating of one year the initiative of the European community. This means that throughout 1985 and 1986 the efforts of many of our national bodies will be focused on traffic problems.

In particular, the Ministero dei Trasporti has set up a permanent Commission on Road Safety, chaired by the Minister of Transport, whose tasks are—

- To examine the Italian road safety situation
- To propose a Road Safety Plan that will take into account the most recent technical progress in the areas of standardization and information

- To express opinions on provisions and initiatives concerning road safety and environment protection

Investigation committees will be established within this Commission to examine and discuss specific problems.

Active Safety

With regard to active safety, consideration has been given at the international level to braking regulations.

To extend antilock systems even to medium/small class vehicles, the possibility of approving simplified antilock systems was advocated during appropriate meetings.

In addition to the braking performance of a vehicle obtained with traditional means, these devices permit excellent stability on low-adhesion courses even though their cost is within acceptable limits.

In the past few years, Italy has conducted extensive investigations of braking, which have resulted in concrete proposals about replacement linings. Since vehicle safety shall be insured over many years of use, a test method has been devised for spare linings to assess braking performance and to insure they are fully interchangeable with original linings.

This is particularly important because the average life of in-use vehicles is increasing. The Italian Government also favors the addition, where possible or necessary, of conformity standards and in-use vehicle inspection standards to the existing approval regulations.

It is also necessary to investigate whether spare parts must be original equipment and, if so, which ones, or if they must at least have the same characteristics as the original parts.

Passive Safety

In the period from the Ninth ESV Conference to this conference, research activity was directed mainly to exposed road users and to assessing and setting up test instruments for occupant protection in side collisions.

In the session devoted to pedestrians, Alfa Romeo will, in fact, present a paper on the results of overall tests conducted with suitably instrumented dummies. Italy also participated in the three EEVC Working Groups (Pedestrian Protection, Bicyclists and Moped-Riders Protection, and European Side Impact Dummy). The evaluation of the results obtained by these groups is included in the schedule of the Congress.

Mention should also be made of the significant contribution to the solution of safety problems given by the GRCS, GRDP, and WP29, chaired by representatives of the Italian administration.

Exhaust Emissions and Noise

Italy is providing an active contribution to international work on new emission limits and test methods.

For applicability at the national level, community decisions are awaited to harmonize the Italian regulations with European legislation.

Regarding the technology to be adopted to reduce emission limits, legislation should be enacted to permit the use of techniques already tried in the United States, and other solutions should be adopted during research that will yield excellent results in terms of exhaust emissions and represent valid alternatives.

When investigating new motor vehicle regulations, an analysis should always be made of the cost/benefit of possible solutions to take account of the user's requirements and industrial impact.

As far as noise pollution is concerned, Italy has adopted promptly the latest EEC tightened requirements, thus showing its consciousness and availability.

Generally speaking, the Italian Government is of the opinion that to further protect the environment from motor vehicle pollution and noise, action should be taken in regard to traffic density and organization.

Status Report of France

Jean Moreau de Saint-Martin
Director, Organisme National de Sécurite Routiére

Road safety remains an overriding preoccupation of the French government, which is sustaining and developing its effort in this direction and achieving positive results in consequence. In 1983 some 11,946 people were killed in road accidents, the first time the figure had dropped below the 12,000 mark since 1964. This trend continued in 1984, when 11,685 people were killed and 284,907 injured (73,314 of them seriously) in 202,637 accidents. The level of risk has decreased correspondingly, since the number of vehicles on the road continues to increase slightly. It is difficult to give an exact measure for the level of risk, however, since recent research shows the volume of traffic using secondary roads has been considerably underestimated in past

assessments. Once this has been rectified, the level of risk will certainly work out to less than four deaths per 100 million vehicle-kilometers.

French road safety policy is largely devoted to measures aimed at influencing the behavior of road users and at encouraging local authority officials and opinion leaders to take action in support of road safety. This policy does not rule out other possibilities for taking steps of a more general nature, such as measures for improving vehicle safety. The main elements in the government's policy are—

(1) The "Réagir" (React) campaign provides for all serious accidents to be investigated administratively and technically to identify all the factors that might have played a role in the accident, as well as to propose preventive measures and to counteract the tendency of public opinion to treat road accidents as events of no importance. This program aims to have 10,000 accidents analyzed per year.

(2) The "Objectif Moins 10 percent" (Objective 10 percent Less) program is an incentive scheme aimed at local authorities (at both departmental and big city levels) that links the level of subsidies allocated to each local community taking part to their success in reducing the number of road accidents causing personal injury by 10 percent. Since the scheme was launched in 1983, some 80 departments and as many urban authorities of over 50,000 inhabitants have committed themselves to this objective, and several have already succeeded in reducing the number of accidents by 10 percent.

(3) A new drinking and driving law passed in 1983 will make it easier to carry out breathalyzer tests and render penalties more effective.

(4) Following extensive consultations with motorcyclists, changes were introduced on January 1, 1985, in the administrative classification of motorcycles and the corresponding driving licenses. Motorized two-wheelers are now divided into three categories:
- Mopeds: under 50cc, designed to give a maximum speed of 45km/h, minimum age 14
- Small motor bikes: less than 125cc and 13hp, minimum age 17 for an AL license (16 for bikes of under 80cc with a maximum speed of 75km/h)
- Motor bikes: over 125cc, maximum power 100hp, open to 18-year-olds with an A license

In addition, new regulations were laid down concerning two-wheelers' lights and indicators (officially approved headlights, lateral reflectors at rear).

(5) Additional regulations were introduced for heavy goods vehicles:
- Rules concerning rear bumpers were harmonized with the EEC directive.
- Lorries of 10 t and over must be equipped with speed limitation devices corresponding to the permitted maximum.
- Lateral bars are mandatory to prevent pedestrians and cyclists from being run down.
- For the same reason, additional rear-view mirrors are now mandatory to comply with the new EEC directive.

Furthermore, the "lorries for the future" project (which forms part of the "Virages" program) is going ahead and its effect on road safety will be evaluated shortly.

(6) The following measures have been taken in respect to motor cars:
- Safety laminated windscreens have been made compulsory.
- Mandatory roadworthiness tests are to be introduced shortly for all cars that have been involved in accidents, as well as for all secondhand cars over 5 years old each time they change hands.
- An agreement has been reached with motor manufacturers and importers to refrain from advertisements stressing maximum speeds that exceed legal limits.
- All motorists are now subject to stiffer speed restrictions when it is raining.

In addition, with a view to taking advantage of the latest technical developments for making driving easier, a tender has been launched inviting manufacturers to bid for the supply of six types of driving aid. They are concerned with information about road conditions, drivers' lack of attentiveness, avoiding obstacles, additional devices for near rear-view vision, limits on visibility and speed in fog, danger of skidding, and loss of tire pressure.

To improve the protection of car occupants in head-on collisions, France and West Germany have proposed a joint program of experiments aimed at a more accurate and realistic assessment of protection when new official standards are laid down in the future. As far as side-on collisions are concerned, France is participating in the studies and consultations that are taking place at a European level, such as those being conducted by the European Experimental Vehicles Committee. The results of some of this research will be presented at this conference, along with those of other research work dealing with all aspects of the fight against road accidents.

To complete this summary of current developments and initiatives, I should point out that ONSER (the National Road Safety Agency) and IRT (the Transport

Research Institute) have been merged into a new public research establishment, with a view to giving greater scope for developing transport research in general and road safety research in particular.

Status Report of the Netherlands

Pieter W. Hoekstra
Ministry of Transport and Public Works,
The Netherlands

For the first time representing our Government at an ESV conference in many years, it is my pleasure to present here a short statement on Dutch policy and activities regarding safety of road vehicles. After many years of following at some distance the experimental work on safer vehicles, the Netherlands has become more involved in the past few years; both as far as research work by private institutions is concerned, such as governmental activities in planning and sponsoring such work and other measures, and through contribution to and preparation of international requirements.

One of the reasons for this involvement is the remaining number of traffic casualties. As in most countries, the total number of both killed and injured in traffic has gone down from an absolute maximum of 3,264 killed in 1972 and 72,167 injured in 1971 to 1,710 killed and 52,212 injured in 1982, both lowest figures since 1966. (For 1984, 1,610 casualties are indicated, but a recent study says that the development is less positive; the registration rate seems to have diminished.)

Nevertheless these figures represent an enormous amount of harm and misery, and, of course, material or financial damage (recently a figure of 7 milliard guilders, or some 1.5 milliard pound sterling has been calculated for 1984).

Among these remaining casualties in our country in 1982, 260 pedestrians were killed and 5,117 were injured by road vehicles (15.2 and 9.8 percent). Figures for bicyclists are especially high in our country: 372 (21.7 percent) resp. 12,897 (24.7 percent); for mopeds: 143 (8.4 percent) killed and 12,380 (23.7 percent) injured. These categories amount to 45.3 percent killed and 58.2 percent injured; a large part of them crashed with cars (50 percent if private cars are considered, 80 percent if HGV's and vans are included). EEVC produced reports on these problem areas during the Ninth ESV Conference in Kyoto 1982 (pedestrians) and at IRCOBI, Delft 1984, and this ESV Conference 1985, regarding bicyclists and moped riders.

Consequently, the Dutch Government gives high value to the vulnerable road users: children, elderly, handicapped, pedestrians, cyclists, moped riders, and drivers of motorcycles. For pedestrians and cyclists, we work on the outside/front construction of cars; for handicapped, on easier and safer transportation in road vehicles through fixation of better constructed wheelchairs. At the same time, we think that by changing car designs, much can be gained for people in cars. These road users also deserve our special attention because roughly one out of every two road traffic casualties was seated in a car.

Some of the measures under consideration, after the introduction in recent years of a front seatbelt use obligation, helmet use for mopeds and motorcycles, and safety seats and systems for children, are the following:

1. Extra mirror for the off-side of HGV-cabs
2. Slow-moving vehicle warning plate
3. Side reflection for bicycles (January 1, 1987)
4. Improved side protection on HGV's for pedestrians and two-wheelers
5. Making cars less aggressive toward pedestrians and two-wheelers
6. Draft ECE regulation on side protection in passenger cars
7. Installation of seatbelts in the rear of cars (1987 or 1988)

Of course such proposals form only part of our traffic safety policy. Many other activities aim at preventing accidents:

- Physical planning (towns, roads)
- New types of restricted areas (like "woonerf"), the so-called 30km/h zones
- Antialcohol campaigns and measures
- Education
- Emergency services
- Improved organization of and communication within the Administration at all levels

For 1984 and 1985 a National Traffic Safety Scheme was published, listing among others some 125 measures, problems, and research areas. This scheme will be updated yearly to provide a continuous guideline and program of work. (A summary was published in 1984 by UNO/ECE in Doc. TRANS/SCI/GE.20/R.223.)

We look forward to a fruitful conference, where once more information may be brought forward that will help us, motor vehicle manufacturers as well as governments, to make decisions that will benefit the road users in traveling more safely than today. We count on international cooperation in research as well as in drawing up new legal requirements, preferably on the basis of internationally harmonized and recognized requirements as set up in ECE WP29 and/or EEC.

Status Report of Sweden

Professor Dr. Bertil Aldman
Swedish Transport Research Delegation,
Chalmers University of Technology

The positive trend in Sweden, indicated by decreasing numbers of police-reported road accidents since 1970, was unfortunately broken 2 years ago. In 1983 the number of injury-producing accidents increased by 3.7 percent from the previous year. An additional increase of 4 percent was reported in 1984. The accidents of last year resulted in 717 fatalities, 4,882 severely and 10,792 slightly injured people. The number of accidents was highest in built-up areas where an increase by 6 percent was reported. One explanation for this unfortunate development may be that the number of vehicles on the roads is increasing again after some years with almost constant numbers.

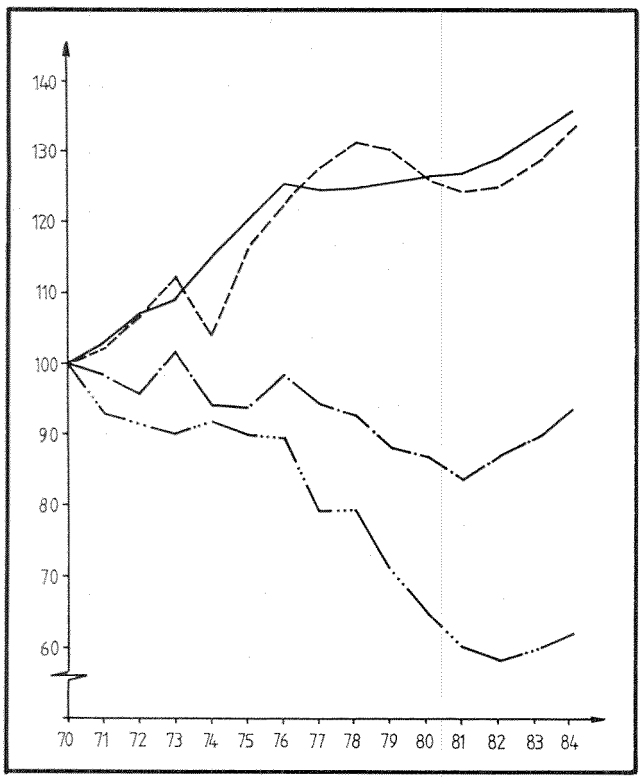

Figure 1. The development of vehicle registration, fuel consumption and casualties 1970-1984.

The negative trend for two-wheelers was particularly disturbing, and in December 1983 the Swedish Government appointed a special group of experts to deal with this problem. Its task was to initiate coordinated efforts toward better safety for pedal- and motorcyclists. The actual work was carried out by three subgroups, and some of their proposals have already been implemented.

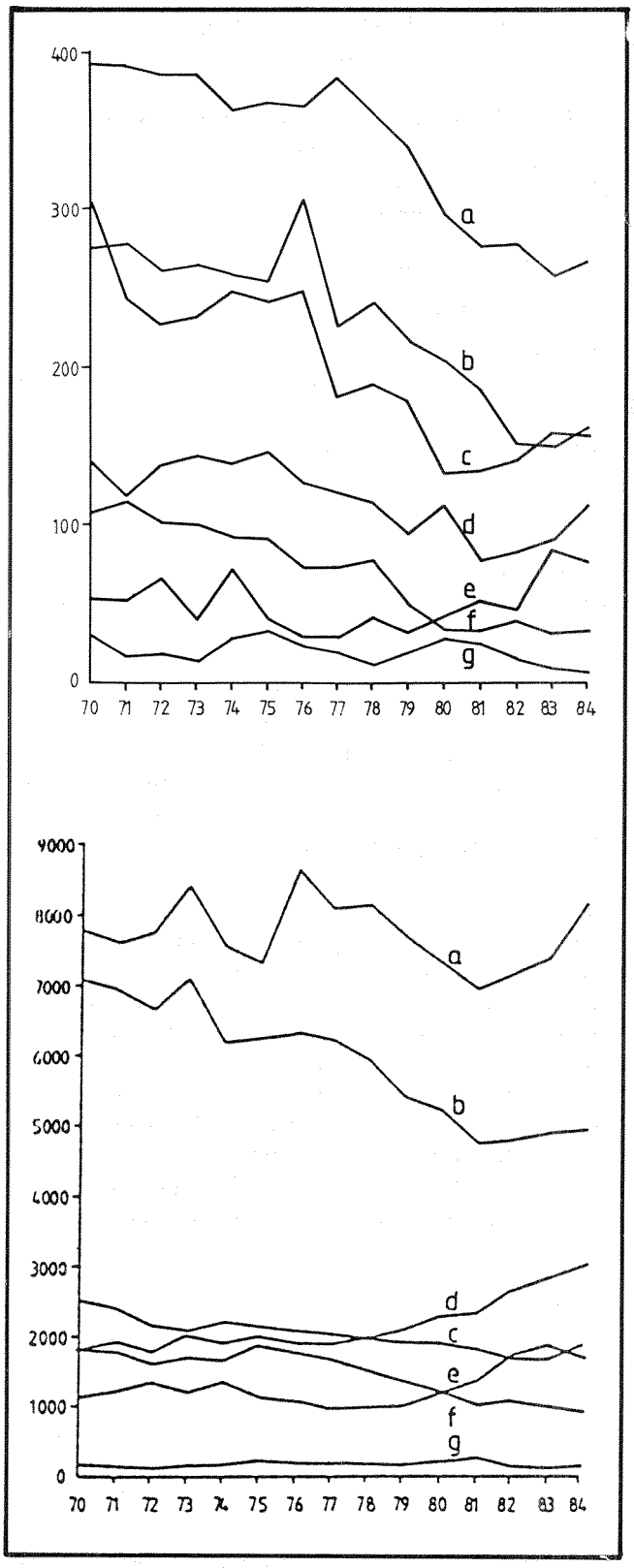

Figure 2. Number of people killed (top) and injured (bottom) in road accidents 1970-1984.

The recommendations regarding motorcyclists include the following items:

- Improved training for driving instructors and additional training for the staff carrying out driving tests will be instituted.
- Motoryclists will be taught how to drive with a pillion passenger and will have more driving hours on rural roads before they get their license.
- They will be trained in estimating their vehicle's turning capacity and be taught the technique and hazards involved in turning, particularly with a pillion passenger.
- They will also be trained in using the vehicle's full braking capacity both when going straight and during evasive maneuvers. Driving tests will include braking from 50, 70, and 90km/h.
- Condensed, 1-day courses will be available for continued training of those holding a driver's license for motorcyclists.
- A standard will be prepared for type approval of protective clothing for motorcyclists.
- Measures will be taken to improve the visibility of motorcycles.

Status Report of Japan

Takashi Shimodaira
Deputy Director of the Engineering and Planning Division, Land Transport Engineering Department, Regional Transport Bureau, Ministry of Transport

It is a pleasure to know that a series of ESV international conferences have produced many fruitful results since the first ESV international conference was held in Paris in 1971. Also, it is a pleasure to see that the ESV conferences have been playing a significant role in enhancing the safety of motor vehicles.

Nevertheless, in view of the current situation in which a great number of persons are killed or injured due to road traffic accidents, we believe the furtherance and strengthening of traffic safety measures are indispensable to insure the healthy and cultural living of people.

As for the trend of road traffic accidents in Japan, the number of annual casualties was on the decrease after 1970 when a peak number was reported. This trend was reversed in 1980. Since then the number of annual casualties has been on the increase. The government-conducted forecast survey of traffic accidents in the future reveals this increase trend will continue. It estimates the number of casualties will reach about 10,600 in 1990, while the number of accidents will reach about 576,000 in the same year. According to statistics of road traffic accidents in 1984, the death toll was 9,262, representing 7.7 persons per a population of 100,000. Furthermore the number of persons injured reached 644,000, representing 536 per a population of 100,000. When the accident cases were broken down according to the category of accidents, motor-vehicle to motor-vehicle accidents accounted for about 80 percent. Also, the majority of these accidents were head-on accidents and rear-end accidents. In regard to other kinds of accidents, motor-vehicle accidents involving pedestrians accounted for about 15 percent, whereas those accidents involving motor vehicles accounted only for about 5 percent.

The foregoing statistics of road traffic accidents classified by the category of accidents show that motor-vehicle to motor-vehicle accidents far outnumber other kinds of accidents. However, as far as motor vehicle fatalities are concerned, the combined number of the killed pedestrians and bicycle riders accounts for 40 percent. This fact behooves Japan to exert more efforts on safety measures for pedestrians and so forth than other countries.

With a view to preventing road traffic accidents and tackling its countermeasures with efforts of the whole Nation, the Fundamental Law Related to Traffic Safety Measures was enacted in 1970. Based on this law, the traffic safety basic planning has been made at intervals of 5 years. Moreover, wide-ranging safety measures, including keeping the traffic safety facilities in good condition, have been promoted totally and powerfully. At present, the Third Planning, which covers a period of fiscal years 1981 through 1985, is underway. A wide variety of measures have been promoted with emphasis placed on realizing a safe, comfortable traffic society—one that makes it possible for people and motor vehicles to co-exist and that is benefiting the motor vehicle society.

As a concrete road traffic safety measure achieved recently, the use of seatbelts by drivers and passengers of motor vehicles becomes a statutory obligation effective September 1985. It is expected that the rate of wearing seatbelts will increase sharply and fatalities owing to road traffic accidents will decrease significantly with this statutory provision.

On the other hand, as for the safety measures from the viewpoint of motor vehicle construction, they have been progressing steadily toward a stage of practical use, based

on the technical development accomplished through ESV and RSV vehicles. Concretely, we can cite the following accident preventive measures:

(1) Measures where the drivers' ability to prevent accidents is assisted from the side of motor vehicles, the reduction in drivers' burdens, the use of abnormality warning devices for systems, and so forth

(2) Measures to enhance accident preventive performance inherent in motor vehicles themselves, improvements of controllability, stability and braking performance, the use of fail-safe mechanisms, the installation of impact-absorbing-type bumpers, and so forth

Furthermore, for safety measures in the event of accidents we can cite the following:

(1) Occupant protective measures, the use of devices that take into consideration insuring a safe space for occupants, the restraint of occupants and impact reduction, and so forth

(2) Preventive measures for motor vehicle fires, the prevention of fuel leakage in the event of collisions, etc., the adoption of flame-resisting materials of interior appointments, and so forth

From now on, it is expected the number of various systems incorporating electronic control equipment will increase rapidly. Hence we believe it is urgently needed to make these systems safer and more reliable.

Regarding the motor vehicle safety standards in Japan, they are to be stipulated progressively in accordance with the Second Enlargement and Strengthening Targets of motor vehicle safety standards set forth in October 1980. We have been exerting efforts to further the research activities necessary for achieving these targets.

As an example of revisions of the safety standards, the maximum permissible luminous intensity of headlamps was raised in October 1983. Also, the performance requirements of other lamps were harmonized with international standards.

In addition, draft standards were completed as to the following subjects in June 1985, while taking into consideration the harmonization with those standards of other nations:

(1) Enlargement of categories of motor vehicles where the installation of seatbelts is compulsory and enlargement of applicable seats

(2) Installation of front windshields made of penetration-resistant, laminated glass, as has been the case with European countries and the United States

(3) Strengthening of fuel leakage preventive requirements in the event of rear-end collisions

With respect to these draft standards, in accordance with the GATT Agreement, we have already notified those persons concerned in the relevant nations so we may hear their comments.

With a view to promoting the importation of foreign-made motor vehicles, the government of Japan has been endeavoring to further the rationalization and internationalization of our standards and certification systems.

Concretely, as for the certification procedures, we have stipulated the following measures for the sake of convenience for overseas motor vehicle manufacturers:

(1) Dispatch of examining officials abroad

(2) Acceptance of results of tests conducted by foreign official testing institutes

(3) Handling system of small quantity motor vehicles

Since August 1983 the type designation system has been drastically simplified.

With regard to implementation of motor vehicle standards, the government of Japan has been paying thorough consideration to various aspects, such as insuring of safety, harmonization with the standards of foreign countries, and hearing opinions from those in foreign countries concerned with the process of preparing the standards.

In October 1983 as many as 12 items of the Safety Regulations for Road Vehicles were revised to attain harmonization with the counterpart standards in European nations and the United States.

Besides the aforesaid measures, we have been taking all possible measures, including positive participation in the WP29 as the international uniform standards planning activities.

With respect to the drafting activities for international uniform standards for motor vehicles, we intend to participate positively in their activities in the future through meetings of the ECE WP29. Thus, we are determined to make our utmost efforts to fulfill an international role as the second largest motor-vehicle-producing nation.

Status Report of the United Kingdom

David Lyness
Head of Vehicle Standards and
Engineering Division, United Kingdom
Department of Transport

I have pleasure in reporting that since the 1982 Experimental Safety Vehicle Conference in Kyoto, there has been progress both through the introduction of new regulations and the fruition of research work toward improving the safety of vehicle occupants, pedestrians, motorcyclists, and other road users in the United Kingdom.

Compulsory Seatbelt Wearing

At the Kyoto conference, it was announced the United Kingdom intended to introduce compulsory wearing of seatbelts for front seat occupants in cars and similar vehicles with effect from 31 January 1983. In our view, this has been a very successful measure. Since the implementation of this law, we have observed a consistently high wearing rate (well in excess of 90 percent) among those required to do so. This in itself is a very impressive result when compared with the wearing rate of around 35 percent in 1982, the year before the new regulation went into effect, and compares very favourably with the wearing rates reported by most other countries.

Our regulations have been introduced for 3 years, ending January 1986, after which they will lapse unless renewed by Parliament. Parliamentary debate on whether compulsion should continue will take place toward the end of the year. Already the pros and cons of the existing requirements are a matter of public controversy, and much has been written about certain side effects. The facts remain, however, that in the first 23 months of compulsion, February 1983 to December 1984, there were 690 (17 percent) fewer deaths and 12,153 (22 percent) fewer injuries to front seat occupants of cars and light vans compared with the corresponding period before the regulations.

These results were achieved with the seatbelts on the current car fleet and show that the current designs of seatbelts perform well. However, there is room for improvement in seatbelt design. For example, TRRL is investigating methods of reducing the forward movement of a seatbelt wearer without causing injury. There is reason to believe that quite small changes in the detailed design of seatbelts could bring substantial additional benefits in future years.

Rear Seatbelts

The restraining of rear seat passengers provides further scope for reducing casualties. At present we are considering making mandatory the fitting of rear seatbelts, with child restraints or disabled persons' belts as permissible alternatives.

Improved Design of Steering Wheels

Information from accident studies and other research work has shown that drivers wearing seatbelts can be subject to injuries of up to AIS 2 due to the face hitting the steering wheel. Later in the week, TRRL will report on the work they have carried out aimed at reducing this type of injury. A modified test procedure has been developed using the standard pendulum procedure but with an aluminum honeycomb-faced head form. We believe tests have shown that the modifications suggested by TRRL can be readily incorporated into vehicle design and that such changes will produce worthwhile benefits.

Accident Studies

For well over 10 years, the United Kingdom has had programmes running, almost continuously, to collect and analyse data relating to car accidents. Although such exercises are costly and difficult to finance, we are at present in the process of planning to extend this work until about 1989. The current studies are carried out for the Department of Transport and other sponsors by the Universities of Birmingham and Loughborough, using data collected by the universities and by the Department's Vehicle Inspection Division. This work will be described to you in more detail during the course of the conference.

Current Levels of Car Occupant Protection

TRRL has carried out a series of tests on six models of recent design by leading manufacturers around the world. The tests included front and side impacts and checked much of the interior for resistance to head form impact. When compared with earlier and similar tests on designs of 10 years ago, I am pleased to report there has been a distinct improvement in occupant safety, particularly from frontal impacts, even if not from side impacts. It is encouraging to report that a number of manufacturers

are designing well in advance of the current mandatory requirements. The test programme and the results will be presented in a TRRL paper later.

Side Impact Protection

At the Kyoto conference, we expressed concern that it had not been practicable to establish minimum mandatory standards for side impact performance. Sadly that is still the case. The work on a manikin and deformable barrier essential for a mandatory requirement continues, but there is still some way to go before we have a practical test. As an alternative to the full-scale test, we in Britain consider that more attention should be given to subsystem requirements—at least as an interim measure. For example, it would be feasible to legislate against unnecessarily stiff armrests, which can be tne cause of internal injuries. We have put this idea to ECE with the proposal it should become a common European requirement. We believe such a measure will constitute a worthwhile, albeit a small, step in reducing injuries from side impact. We intend to continue searching for similar areas where worthwhile improvements can be made.

Pedestrian Protection

It is now possible to put forward a set of design guidelines for the frontal area and bonnet (hood) tops of cars. Designs following these guidelines should much reduce the severity of leg injuries and soften the impact at many places likely to be struck by the heads of both children and adults. In the outdoor exhibition, you can see how these guidelines can be applied, for example, to an Austin metro. TRRL will present a detailed description of this work. There are several papers later in the conference dealing with pedestrian protection, and I draw attention in particular to that from EEVC. I urge all manufacturers to take note of this important exhibit and of the guidelines, which indicate a potential saving of some 33-1/3 percent of serious injuries and 10 percent of fatalities.

Motorcycles

Motorcyclists and pillion passengers in the United Kingdom comprise about 30 percent of the total number of motor vehicle users killed, this despite the fact that motorcycles amount to less than 3 percent of motor vehicle traffic. In the United Kingdom, we have been working on several ideas to improve the safety of motorcycles. In particular I would draw your attention to the antilock braking system that is now undergoing service trials with several police forces in this country. The leg guard shown is an advanced design that has performed well under test and is a design we believe with a little more work could be incorporated in production machines. These developments give the prospect of major improvements in motorcycle safety in the long term. More immediately we intend to introduce the newly agreed ECE standard for wet braking into our national regulations.

Buses and Coaches

In general, buses and coaches have a very good accident record, but there are some areas that need attention. One such area is a standard for the structural strength of coaches to mitigate the results of rollover accidents. There has been a very recent agreement in ECE to a suitable specification for structural strength, and we intend to introduce this specification into our national rules for the construction of coaches.

Goods Vehicles

A great deal of progress has been made to improve the safety of heavy lorries. At Kyoto it was reported we were investigating a basis for U.K. requirements for underrun guards and sideguards for lorries and trailers. We now have mandatory requirements for sideguards to be fitted to all new lorries and trailers and to existing heavy trailers. Rear underrun protection is also required on all new lorries and trailers. We are also investigating the practical application of front underrun devices to commercial vehicles. On display is an example of a device developed by TRRL and industry that has proved satisfactory under test. We continue to encourage the fitting of antilock braking systems to heavy goods vehicles, and over 80 percent of trailers are now being fitted with antilocks as standard equipment.

Finally, we have made mandatory antispray devices on all new trailers, and these requirements will be progressively extended to new motor vehicles (October 1985) and existing trailers in 1986/87.

Section 3
Progress With and Discussion on Safety Developments for Road Vehicles

Michael M. Finkelstein, Chairman, United States

PSC1—A Demonstration Car with Improvements for Pedestrian Protection

C.A. Hobbs,
G.J.L. Lawrence, and
C.S. Clarke
Transport and Road Research Laboratory, Department of Transport, Crowthorne, Berkshire, United Kingdom

Abstract

A demonstration pedestrian safety car has been produced based on the Austin Metro car. The modifications did not require the use of materials not already familiar to the motor industry, and changes to the car's styling were limited. The modifications have been shown to give substantial improvements in the level of protection offered to adult and child pedestrians up to impact speeds of 40km/h. In particular, the most frequently injured body region, the lower limbs, was afforded much increased protection. Tests on the head impact area indicated that worthwhile reductions in child head injuries could be expected. It should be possible for modifications of the type made to this car to be incorporated in other production cars, in which case significant reductions in pedestrian injuries could be expected.

Introduction

Following a cooperative project carried out by TRRL and Austin Rover(1), it was decided to produce a demonstration pedestrian safety car (PSC1) designed to give improved protection to adult and child pedestrians in impacts up to 40km/h (25mph) (Figure 1). The car was based on the Austin Metro, this being the car chosen for much of the earlier work. The modifications were carried out without using new materials or manufacturing techniques—the aim being to demonstrate that worthwhile improvements in pedestrian protection could be achieved without radically altering a current car. No attempt has been made to incorporate any safety features for car occupants. It is recognised that pedestrian safety requirements would need to be integrated with those of other road users. The effectiveness of the modifications was tested by impacting the car into adult and child pedestrian dummies. Additional headform impact tests were carried out to check those parts of the head impact area not hit by the dummy heads.

This project was carried out by TRRL in cooperation with Austin Rover Group Ltd. and DA & PR Simpson Ltd.

Pedestrian Accidents

Of the 60,000 U.K. pedestrian casualties each year, about three-quarters are hit by cars, most of them hit by the front. About 35 percent of the casualties are children under the age of 15, and 20 percent are under 10(2).

Figure 1. PSC1—pedestrian safety car

Accidents with impact speeds below 30km/h (19mph) have been shown to result in predominantly minor (AIS 1)(3) injuries, with those above 30km/h being predominantly more severe than minor(4). The transition from predominantly survivable to predominantly fatal injury is between 50 and 60km/h. Further analysis predicted that a car front that eliminated serious injuries induced by vehicle contact, at speeds up to 40km/h, would result in a 30 to 40 percent reduction in the number of seriously injured pedestrians(5).

The most frequently injured parts of the body are the lower limbs and head, with fatal injuries being predominantly to the head. In general, injuries to the lower legs and knees result from impact with the bumper. The upper legs and pelvis are injured by the leading edge of the bonnet, and the head from contact with the windscreen, its surround, the scuttle, bonnet, or wing tops. The stiff areas, which are of particular concern, are the windscreen surround, joints between bonnet and scuttle or bonnet and wing, and the bonnet where it is supported by a stiff frame or where there are stiff structures close to its underside. On the scuttle, the wiper spindles present the additional risk of penetrating injury.

Because of the Metro's short bonnet length, most adult heads would impact the windscreen. Head contact with the bonnet top and scuttle should be restricted to children and short adults. The stiffest part of the bonnet is at the hinge mounts. Immediately below the bonnet are the carburettor, the rocker cover with its oil filter, the brake master cylinder, and the battery. These could each be contacted if the head hit the bonnet above them.

Modifications To Improve Pedestrian Safety

Bumper Area

Because of the high initial force necessary to displace a complete bumper assembly, a locally compliant bumper was required. Adoption of a tall bumper-air dam assembly should give a large leg contact area, and if the lower edge were contacted first, then this should overcome foot to ground friction early in the impact. Early tests showed that the most uniform bending moment in the adult's lower leg was obtained if the bumper to air dam force was split in the ratio 60:40.

The high cost of manufacturing a mould prevented the production of a new bumper skin; therefore, standard mouldings were used. Tests on a range of plastic bumpers in current use showed that without their inner steel reinforcements, most could be adapted to give good leg impact characteristics. The Metro bumper was found to be slightly stronger than desirable, but by removing internal flanges and returns it could be weakened sufficiently. To make the bumper assembly taller, it was combined with an air dam taken from the Metro Turbo, which was positioned immediately below the leading edge of the bumper. As an energy-absorbing medium to go behind the bumper-air dam skin, it was found the best characteristics were obtained using a low-density, rigid polyurethane foam, cored to reduce its stiffness. A maximum crush depth of 150mm was provided. As the polyurethane foam was produced using the bumper-air dam as a mould, it was possible to use it to support the assembly along its length. Additional sliding clips were fitted between the bumper ends and the front wings. Although this construction performed satisfactorily, the use of a weaker outer skin and stiffer foam would be preferable.

Even though a bumper of this type has local compliance when hit by the almost line contact of a leg, much larger forces would be generated when hit by a wide object. Such a bumper could be satisfactory for other types of impact. However, additional strengthening may be needed behind the crushable bumper.

Bonnet Leading Edge

Although the leading edge of the Metro's bonnet is not itself sufficiently strong to pose a problem for pedestrians, it is supported by the bonnet lock platform, which is supported by the radiator that sits on the lower front cross member. To reduce the effect of this support, the bonnet was extended 75mm forward. The bonnet lock platform and radiator were left where they were though it was necessary to extend the platform forward to support the grille. An advantage of extending the bonnet was the ability to accommodate the extra bumper crush depth without the need for it to protrude unduly.

Headlight and Grille Area

The headlights, grille, and front wings were extended forward to correspond with the bonnet leading edge but were softened to reduce their potential to cause injury. Metro headlights are mounted in enclosed units with internal beam adjustment. The mounting arrangement was changed to allow the headlight units to collapse rearward if impacted. The mountings for the grille were arranged so it would not form a strut supporting the bonnet leading edge. To remove the hazard of their stiff leading edges, the front wings were made with separate leading edge sections that could break away on impact. Though these leading edges are steel on the demonstration car, in production they could be made in plastic.

Bonnet

With the bonnet area, the most difficult problem is posed by the closeness of under-bonnet structures. As a crush depth of up to 100mm is required to achieve satisfactory decelerations for an adult head, adequate clearance over stiff structures is essential. Clearance can be achieved in three ways: the components could be lowered, the bonnet could be raised, or a mechanism could be incorporated that would detect the initial impact and elevate the bonnet in anticipation of head contact.

With the Metro, lowering the under-bonnet structures is not feasible. Although the carburettor and oil filter could be moved, moving the rocker cover would involve lowering or tilting the engine. Lowering would result in insufficient ground clearance, and both would be technically difficult. The brake master cylinder is mounted vertically above the servo on the bulkhead. Space limitations make moving them difficult. On the other hand, lowering the battery would not be difficult.

The third option, that of elevating the bonnet at the time of an accident, has been considered and work is in hand to develop such a system. If a satisfactory method could be developed, other measures such as improving the scuttle and windscreen lower edge may prove unnecessary.

In the demonstration car, the second option has been adopted. The rear of the bonnet has been raised by 50mm. This has provided adequate clearance at the bonnet's rear for an adult head impact. Toward the centre of the bonnet, where a child's head would impact, clearance is also increased. As there was little increase in clearance toward the front of the bonnet, the battery was lowered, even though the likelihood of head contact in this area is small.

To eliminate the stiff joint between the bonnet and wing, the joint was taken over the side of the car. The line of the new bonnet joint was dictated by the inner wing panel and styling considerations. With a new design, it would be desirable to have the joint a little lower.

The bonnet strengthening frame on the Metro is essentially V-shaped with two top hat sections going between the centrally mounted bonnet lock at the front and the two hinges at the rear corners. An additional strengthening plate spans the V about halfway up the bonnet (Figure 2). For head impact considerations, an ideal bonnet would have almost uniform stiffness. To achieve this, a considerable amount of work would be needed on the development of a strengthening frame. In the time available, it was necessary to modify the existing frame in an attempt to achieve satisfactory performance. This was done by drilling holes along the edge of the top hat sections adjacent to the bonnet skin. The cross plate was weakened by slitting it lengthwise and shortened so that it did not reinforce the top hat sections. At the front, the bonnet lock and antirattle pads were mounted on collapsible pillars (Figure 3).

Windscreen Surround and Scuttle Area

The windscreen surround is stiff and presents a narrow contact area. Any major improvement in the crush characteristic of the windscreen pillar would almost certainly result in a reduction in driver visibility and possibly in roof strength. Although improvements to the leading edge of the roof should be possible, there has been insufficient time for this area to be considered.

The lower windscreen edge forms part of the scuttle where there is more potential for improvement. On the Metro, the scuttle is cantilevered out from the lower windscreen edge and is relatively soft, other than at the windscreen edge. However, mounted on the scuttle are exposed windscreen wiper spindles. As the bonnet could not be extended rearward over the scuttle area without a redesign of the hinging arrangement, a new scuttle panel

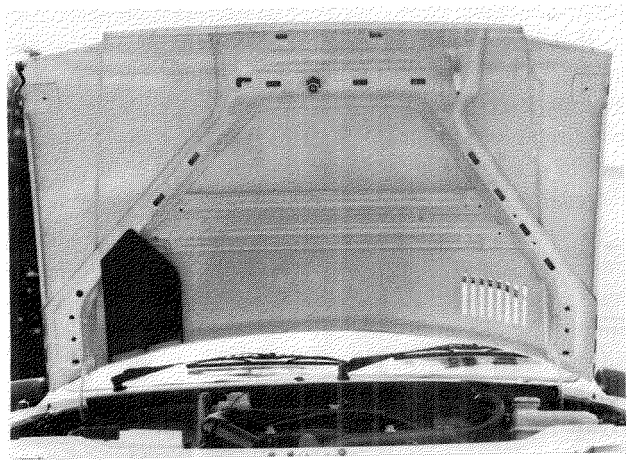

Figure 2. Metro bonnet frame

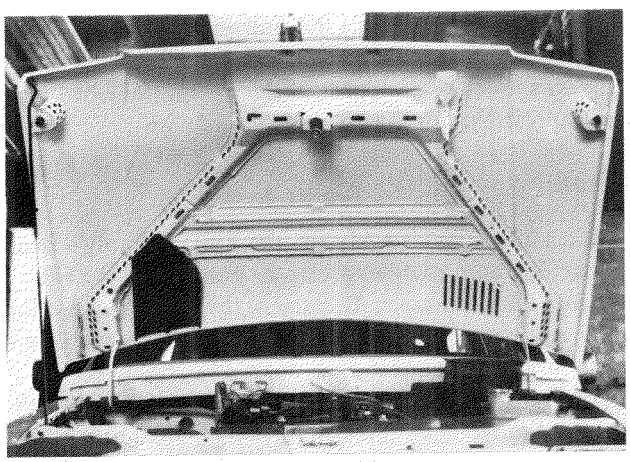

Figure 3. PSC1 bonnet frame

was fitted above the original. The original scuttle panel was angled downward and the wiper spindles repositioned to increase their clearance beneath the new scuttle. The panel was then used to support the new scuttle panel above it. This arrangement provided for collapse of both panels, as a sandwich, as well as collapse of the top panel. In this way, the scuttle was prevented from bottoming out on the spindles. The windscreen edge itself was weakened by slotting the return in which the windscreen rubber locates.

Safety Performance Evaluation—Dummy Tests

A prototype of PSC1 was tested by being impacted at 40km/h (25mph) into a 50th percentile adult pedestrian dummy(6) and a 50th percentile 6-year-old child dummy. These tests were each carried out on the centreline of the car and offset toward the side, virtually in line with the centre of the car's headlight. For comparison, the same tests were carried out on a standard Metro.

The child and adult dummies were instrumented to measure accelerations of the head, thorax, and pelvis and to measure the bending moment in the middle of the upper and lower leg first hit by the car. On the adult dummy, additional measurements were made of the bending moments at the hip and the top of the lower leg, and of acceleration at the knee.

Because of the way the car was modified, the original tests were carried out with the bonnet leading edge mounted about 40mm too low. Subsequent centreline tests were performed with the bonnet leading edge at the correct height and with the bumper weakened by additional coring of the foam.

The target limits for the head have been taken as a Head Injury Criterion (HIC)(7) of 1,000 or agreement with the Wayne State criteria(8). Preferably the head should not sustain an acceleration of over 80g for a period exceeding 3ms. For the thorax and pelvis, a Severity Index (SI)(9) of 1,000 and an acceleration of 60g for 3ms have been taken. For the knee, a limit of 60g for 3ms was used with the rest of the lower limbs having a limit of 200Nm for 3ms(6).

Head

With the standard Metro, the child dummy's head impacted about halfway along the bonnet and the adult's head on the windscreen. Because of the forward extension of the bonnet on the modified car, the impacts were a little further forward.

With the child dummy and the modified car, while the forward movement of the body had resulted in the head moving vertically downward, the head had not started moving in the direction of travel of the car by the time it hit the bonnet. By this time, the pelvis was travelling at about the speed of the car. As the body became horizontal, forces transmitted up the spine caused the head to accelerate suddenly toward the pelvis. Because of the inelastic nature of the dummy's spine, this resulted in high vertical accelerations on the head at precisely the same time the head hit the bonnet. This is a phenomenon not seen before and is probably not a realistic representation of a human, where the spine is slightly elastic. Because of the short duration of this vertical acceleration, about 2ms, only a small time difference is required to reduce substantially the effect on the head's resultant acceleration.

With the child impacted on the standard Metro's centreline, the head hit the bonnet above the central plate of the bonnet frame. This gave an HIC value of nearly 1,300 and a 3ms exceedence level of about 140 (Table 1). When the child was impacted toward the side of the car, the head hit the bonnet near to, but not over, part of the V frame. In this case, the HIC was about 1,000 and the 3ms level about 100. In neither case was any contact made with any structure below the bonnet. With the modified car, the head accelerations were a little lower but were affected, as previously stated, by the timing of the force transmitted up the spine.

With the adult, the centreline test on the standard car gave an HIC of about 600 and the side test gave one of nearly 700. The 3ms exceedences were about 80 and 100, respectively (Table 2). With the modified car, the head accelerations were slightly higher, though still acceptable.

When tested, the bonnet frame on the modified car was unaltered in the child's head impact area. Modifications carried out later should reduce the child dummy's head acceleration, but their effectiveness has not yet been checked with the dummy.

Thorax

In general, the thorax was not found to be a problem area and indeed accident data support this assertion. However, with the standard Metro, the 3ms exceedence level on the child was slightly high at around 70g. The initial modifications brought these levels down. However, they appeared to be closely related to what happened to the legs, and subsequent alterations to the bumper increased the accelerations to this level again.

Pelvis and Hip

On the adult dummy, pelvic accelerations and hip bending moments with both the standard and modified cars were low and did not give cause for concern. With the child, however, the standard car gave very high pelvic accelerations with 3ms exceedence levels of around 130 and 150 for the centreline and offset impacts, respectively. In both cases, the SI was above 2,000.

Table 1. Results of car to child dummy tests at 40km/h (25mph)

Car		Metro		PSC1		PSC1*	
Impact Location		Centre	Side	Centre	Side	Centre	Target Level
HEAD							
HIC		1,277	1,019	852	973	853	1,000
Peak acc.	(g)	159	136	139	143	132	300
3ms exceed.	(g)	141	105	119	116	119	80-140
10ms exceed.	(g)	56	72	60	59	57	65
THORAX							
SI		705	410	372	403	469	1,000
3ms exceed.	(g)	72	70	64	62	70	60
PELVIS							
SI		2,059	2,067	975	841	973	1,000
3ms exceed.	(g)	131	149	81	81	87	60
UPPER LEG							
3ms exceed.	(Nm)	558	612	182	177	136	200
LOWER LEG							
3ms exceed.	(Nm)	265	340	212	214	162	200

* Following correction to ride height and weakening of bumper

The modified car gave much lower values, with a 3ms exceedence level of about 80g and SI's of under 1,000. Later modifications to reduce leg accelerations increased the 3ms exceedence level to nearly 90g. Post-impact examination of the bonnet revealed that the frontal extention of the bonnet frame had resulted in a locally stiff area, at the point where the extension was joined to the original frame. In the impact, a plastic hinge was formed at this point, and it is thought this allowed the pelvis to partly interlock with the bonnet. This could have given rise to higher than necessary accelerations. On the demonstration car, the bonnet frame has been modified in an attempt to avoid this hinge, and tests will be carried out to see whether these modifications have improved the situation.

Legs

With the standard car, the leg accelerations and bending moments were all very high. In impacts at this speed, it is clear that very serious damage would be done to a pedestrian's legs. For the child, upper leg bending moments of around 600Nm were measured. The lower leg bending moments were also high at between 260 and 340Nm. With the adult, the highest bending moments occurred at the top of the lower leg. Here the 3ms exceedence levels were about 500Nm.

The modified car gave a greatly improved performance. With the child, initial tests gave 3ms exceedences for the upper leg of under 200Nm and for the lower leg of just over 200Nm. Subsequent centreline tests with the bumper weakened slightly more gave even better results, with a 3ms exceedence level of around 135Nm for the upper leg and 160Nm for the lower leg. Although improvements were made for the adult, particularly to the top of the lower leg, it was not possible to get the levels as low as would have been desirable. Nevertheless, the leg injuries that would be sustained in a severe impact such as this would have been substantially reduced in severity.

Safety Performance Evaluation—Headform Tests

To check those parts of the head impact area not hit by the dummy, headform impact tests at 11m/s were carried out. This impact velocity is toward the top of the range of expected head impact velocities. The only headform presently available for use with the air gun was adult size.

The headform impacts were carried out on both the standard Metro and the modified car at the following locations:

- Scuttle midway between the nearside wiper spindle and the windscreen lower corner
- Scuttle over the offside wiper spindle
- Scuttle at the base of the windscreen pillar
- Scuttle at the windscreen lower edge

Table 2. Results of car to child dummy tests at 40km/h (25mph)

Car		Metro		PSC1		PSC1*	
Impact Location		Centre	Side	Centr	Side	Centre	Target Level
HEAD							
HIC		597	676	770	617	750	1,000
Peak acc.	(g)	114	125	133	134	122	300
3ms exceed.	(g)	78	98	111	79	105	80-140
10ms exceed.	(g)	44	43	41	51	47	65
THORAX							
SI		60	67	93	67	64	1,000
3ms exceed.	(g)	17	23	25	21	19	69
PELVIS							
SI		187	115	93	107	123	1,000
3ms exceed.	(g)	43	30	28	35	33	60
HIP							
3ms exceed.	(Nm)	141	105	119	104	114	200
UPPER LEG							
3ms exceed.	(Nm)	370	226	244	246	195	200
KNEE							
3ms exceed.	(g)	146	134	116	107	89	60
LOWER LEG-TOP							
3ms exceed.	(Nm)	507	477	387	303	280	200
LOWER LEG-MIDDLE							
3ms exceed.	(Nm)	336	282	345	296	261	200

* Following correction to ride height and weakening of bumper

- Bonnet over the V frame midway between the hinge and the bonnet lock
- Bonnet over the midpoint of the frame centre plate
- Bonnet over the hinge mount
- Bonnet over the original bonnet to wing joint, halfway along the bonnet

Scuttle Midway Between the Nearside Wiper Spindle and the Windscreen Lower Corner

On the standard Metro, an HIC of just under 800 was recorded with a 3ms exceedence level of almost 100g (Table 3). With the modified car, although the impact velocity of the headform was a little higher, the HIC was reduced to nearly 700 and the 3ms exceedence level to below 80g.

Scuttle Over the Offside Wiper Spindle

The main purpose in testing at the wiper spindle was to check whether the scuttle panel bottomed out on the spindle top. Although the standard Metro gave an HIC of about 900 and a 3ms exceedence level of 100g, this is not representative of what would happen to a human head. With a real head, the wiper spindle would penetrate causing very serious injury. With the modified car, the acceleration levels were higher, partly because of the greater inertia of moving two panels and partly because the lower panel had been unintentionally stiffened when the test car was modified. A correctly made scuttle should be somewhat softer, though this has not yet been tested. More importantly, the upper panel did not contact the spindle and, as expected, both panels collapsed together with some extra collapse of the top panel. In an impact

Table 3. Results of comparative headform impact tests

Location		Scuttle Panel		Over Wiper Spindle		Scuttle Corner		Windscreen Edge	
Car		Metro	PSC1	Metro	PSC1	Metro	PSC1	Metro	PSC1
Impact Vel.	(m/s)	10.7	11.6	10.4	11.3	10.4	10.6	10.3	
HIC		83	715	911	1,224	4,677	4,987	827	
Peak acc.	(g)	111	79	121	118	316	335	97	N/A
3ms exceed.	(g)	99	79	191	109	233	216	93	
10ms exceed.	(g)	65	67	69	85	47	48	75	

Location		Bonnet V frame		Bonnet Centre Plate		Bonnet Over Hinge		Bonnet Over Wing Joint	
Car		Metro	PSC1	Metro	PSC1	Metro	PSC1	Metro	PSC1
Impact Vel.	(m/s)	10.0	11.1	10.4	10.1	10.3	10.7	10.5	10.8
HIC		1,834	937	1,243	874	2,035	1,120	1,071	1,078
Peak acc.	(g)	158	115	147	109	198	112	127	131
3ms exceed.	(g)	146	102	135	105	152	105	114	102
10ms exceed.	(g)	51	69	64	68	52	79	74	79

with a human head, there would not be a penetrating injury, though accelerations would be higher than desirable.

Scuttle at the Base of the Windscreen Pillar

No attempt has been made to improve this area. On the Metro, the main box section from the front of the car joins the A-pillar just below this point. A major redesign of the car would be required to make improvements, in the absence of a bonnet elevating mechanism. On both the standard and modified cars, HIC values of between 4,500 and 5,000 were recorded with 3ms exceedence levels over 200g. In the few head contacts that might occur in this area, serious injury should be expected.

Scuttle at the Windscreen Lower Edge

Tests on the standard Metro gave an HIC value of around 800 and a 3ms exceedence of about 90g. However, this area gives a concentrated line loading so that localised forces could cause serious damage to the human head. The weakening of the windscreen edge should reduce this effect. Unfortunately, as stated previously, this area on the test prototype was unintentionally stiffened during modification and so was not suitable for testing.

Bonnet Over the V Frame Midway Between the Hinge and the Bonnet Lock

On the standard car, an HIC of about 1,800 and a 3ms exceedence of about 150g was measured. With the modified car, the HIC was reduced to about 950 and the 3ms exceedence to about 100g. A more radical redesign of the bonnet frame would probably be needed to improve on these figures.

Bonnet Over the Midpoint of the Centre Plate

By slitting the centre plate along its length combined with the weaker V frame, the HIC was reduced from about 1,250 to 900 with the 3ms exceedence level from

135g to 105g. Further reductions may be possible by increasing the separation between the half plates.

Bonnet Over the Hinge Mount

Where the hinge mounts onto the bonnet, the frame is necessarily stiff to resist hinge forces. On the standard Metro, an HIC of over 2,000 and a 3ms exceedence of 150g were recorded. The modified car gave an HIC of about 1,100 and a 3ms exceedence of about 100g. This was thought to be due to the reduced support given by the bonnet to wing joint, because of its greater distance from the hinge. Following the weakening of the V frame, which was extended around the hinge area, head accelerations at the hinge should be reduced even further. To date, it has not been possible to retest this area.

Bonnet Over the Original Bonnet to Wing Joint, Halfway Along the Bonnet

When impacted by the adult headform, the standard and modified cars gave similar HIC values of just under 1,100. Although the 3ms exceedence level was lower on the modified car, it was still over 100g. However, examination of the acceleration traces showed that for the modified car, the acceleration remained at about 35g for the first 6ms, which corresponded to a deflection of 60mm. The amount of kinetic energy absorbed in this period was more than that required to decelerate a child's head from 11m/s to rest. So it would appear that moving the bonnet joint over the side of the wing has been of benefit to the child. If protection were to be adequately provided for the adult, the joint would have to be lower on the wing, and structures under the bonnet at this point would also have to be lower.

Conclusion

The production of this demonstration pedestrian safety car has shown that substantial reductions can be readily made to the pedestrian injury-producing potential of a small car, at impact speeds up to 40km/h (25mph).

Modifications to the front of the car resulted in substantially reduced loads on the lower limbs and pelvis, particularly for the child. Although protection of the head impact areas is not complete, again worthwhile improvements were made. The problem of the head contacting stiff structures below the bonnet skin was eliminated, except in the unlikely event of an adult head hitting the bonnet at its edge. With a little further work, it should be possible to arrange for the bonnet stiffness to be even more uniform. The modifications to the scuttle were seen to prevent penetrating injuries to the head, but improvements in the areas of the roof leading edge, the windscreen pillars, and the scuttle at the base of the pillars were not attempted at this stage.

The modifications incorporated in this car have not required the use of new materials or technologies and have not radically altered the car's styling. Any additional cost in manufacturing the car would probably be small. If cars in production were built with the characteristics of this car, significant reductions in pedestrian injuries could be expected.

References

1. Harris, J., and N.D. Grew, "The influence of car design on pedestrian protection," Proceedings Tenth International Technical Conference on Experimental Safety Vehicles, Oxford, 1985.
2. Department of Transport, *Road Accidents in Great Britain 1983,* London, H M Stationery Office, 1984.
3. American Association for Automotive Medicine, *The Abbreviated Injury Scale* (1980 revision), Morton Grove, IL: AAAM, 1980.
4. Ashton, S.J., and G.M. Mackay, "Some characteristics of the population who suffer trauma as pedestrians when hit by cars and some resulting implications," Proceedings Fourth International IRCOBI Conference, Goteborg, Sweden, 1979.
5. Ashton, S.J., "A preliminary assessment of the potential for pedestrian injury reduction through vehicle design," Proceedings 24th Stapp Car Crash Conference, Troy, 1980.
6. Fowler, J.E., and J. Harris, "Practical vehicle design for pedestrian protection," Proceedings Ninth International Technical Conference on Experimental Safety Vehicles, Kyoto, 1982.
7. Newman, J.A., "On the use of the Head Injury Criterion (HIC) in protective headgear evaluation," Proceedings 19th Stapp Car Crash Conference, Warrendale, Pennsylvania, 1975.
8. Patrick, L.M., H.R. Lissmer, and E.S. Gurdjian, "Survival by design—head protection," Proceedings 7th Stapp Car Crash Conference, Springfield, Illinois, 1963.
9. Gadd, C.W., "Use of a weighted-impulse criterion for estimating injury hazard," Procedures of the Tenth Stapp Car Crash Conference, New York, 1966.

Acknowledgement

The authors would like to thank Austin Rover Group Ltd. for their contribution to the work and to DA & PR Simpson Ltd., Camberley, for their help in developing the car and for carrying out the modifications.

ESM2—A Motorcycle Demonstrating Improved Safety Features

P.M. Watson
Transport and Road Research Laboratory, Department of Transport, Crowthorne, Berkshire, United Kingdom

Abstract

This paper gives details of safety features that have been incorporated in the second United Kingdom Safety Motorcycle (ESM2). Progress on research and adoption of those features fitted to ESM1 exhibited at the Seventh International Technical Conference on Experimental Safety Vehicles in 1979 is outlined.

An assessment is made of the benefits of four of these features in relation to the saving of casualties.

Introduction

At the Seventh International Technical Conference on Experimental Safety Vehicles in Paris, June 1979, the United Kingdom exhibited their first Experimental Safety Motorcycle (ESM1)(1). This vehicle incorporated six features that were in the prototype development stage to provide solutions to the problems of motorcycle safety derived from a number of studies since 1974.

On the occasion of the Tenth International Technical Conference on Experimental Safety Vehicles, the United Kingdom now exhibits their second Experimental Safety Motorcycle (ESM2). This vehicle is based on a BMW 800cc twin-cylinder motorcycle, which is in service with a number of police forces. ESM2 has seven safety features and shows the progress made on those originally fitted to ESM1. The features are—

- Improvements in braking
- Daytime conspicuity aids
- Forward impact restraint system
- Safety fairing with leg protection
- Nonspill fuel system
- Interlocked parking stands
- Digital speedo and instruments

Brakes

ESM1 was fitted with an antilock brake system to both wheels using a system (developed by TRRL) that had originally been designed for cars. The control system was electronic. The motorcycles fitted with this system gave excellent results when tested but the device was very much in the experimental stage at that time. ESM2 is fitted with an antilock brake system to both wheels that has been developed by Lucas/Girling. This is a fully productionised, developed system. The control is mechanical and contained within each separate unit. Motorcycles are now being fitted with these units for use by police forces, and a number are already in service. This exercise is part of a field trial to assess the performance of motorcycle antilock from the point of view of effectiveness, reliability, and rider reaction.

A paper, Aspects of Motorcycle Braking(2), by Donne and Watson is being presented at this conference and gives details of some experiments with antilock brakes. The Transport and Road Research Laboratory has been promoting their use on motorcycles for 20 years.

ESM1 was also fitted with sintered metal brake pads to the calipers of the disc brakes. The problem of having inconsistent braking(3) when the discs were wet could be prevented by replacing the standard pads of that time with the sintered metal alternative. Today the problem has largely been overcome by developments in industry in response to regulations that will require new motorcycles to be tested with the brake system both dry and wet. Unfortunately there is no such requirement for replacement pad linings, whose users may have problems with inconsistent brake performance if they fit replacements of a lower standard.

In the exhibition associated with this conference, the United Kingdom is showing an experimental version of a mechanical brake incorporating a simple antilock system still under development. Promising results from experiments have been obtained on good dry surfaces and wet slippery surfaces without wheel-locking. We consider this system is best exploited on light machines with low performance. Simple antilock systems have not yet been developed for these vehicles.

Conspicuity

Studies by the Transport and Road Research Laboratory conclude that in many accidents between motorcycles and other vehicles, the other-vehicle driver did not see the motorcycle in time to avoid a collision. The subject of motorcycle conspicuity has been widely studied in many countries by researchers during the past decade, and it is generally agreed that other road users not seeing motorcycles is a major problem.

It is not possible to identify another single motorcycle safety problem that is a contributory cause in over 30 percent of casualty accidents. Particular attention has been paid to this topic to find solutions to improve the situation. Details of the joint study by The Institute of

Consumer Ergonomics and TRRL are given in the paper, "Motorcycle Conspicuity in Daylight,"(4) by Donne, Fulton, and Stroud, which is in the proceedings of this conference.

The two main options for conspicuity aids are rider-based and machine-based features. Of the rider-based options, a fluorescent jacket or waistcoat has been found to be the most effective. However, fluorescence decays with exposure to light, and garments must be stored away from light to prolong their effectiveness. Because of this decay, they need to be replaced fairly frequently. A further disadvantage with all rider-based options is that for each journey, the rider has a choice whether or not to wear the conspicuity aid. For this reason, machine-based options are to be preferred because they provide the conspicuity aid as a permanent feature. The use of headlamps has considerable appeal because they are machine-based and are generally fitted as standard. Research has shown that the use of large, powerful headlamps is beneficial but small headlamps provide no benefit. In Great Britain, over half the motorcycle population has a capacity of 150cm^3 or less and is neither likely nor required to have headlamps of adequate dimensions to provide effective conspicuity. Consequently, a requirement to use headlamps in daytime is unlikely to be of overall benefit because small machines may be put to increased risks. One solution would be to require better headlamps for small machines. One problem with headlamps is that they can be switched to full beam and cause glare in daylight. Results show the most effective machine-based option assessed was a pair of daytime running lamps, and the combined wattage required can be as low as 16 watts. ESM2 is equipped with a pair of these lamps, which has been shown to be effective for all machines. Some 80 percent of new police service machines are now supplied with this equipment. The situation for nighttime conspicuity continues to be a problem where, despite considerable effort, no adequate solution is apparent. Between one-third and one-half of motorcycle casualties occur at night because the risk per mile at night is twice as high as during the day, although the accident sites are similar. The possible introduction of two level lighting systems (Dim/Dip) for new vehicles in Great Britain may now provide an opportunity for motorcycles to be identified more easily in traffic because of the variations in light output between them and other vehicles. Future research on nighttime conspicuity will study this new system, which at present appears to be the only available option that may provide a solution.

Frontal Impacts

A frontal impact on a standard unmodified motorcycle at 30mph causes a rider to be ejected horizontally headfirst at 28mph. Fatal accidents often occur when a hard obstacle is in the path of the rider's head.

A solution to this problem is to provide a restraint system that operates for this type of impact, to reduce the rider's kinetic energy and control his trajectory. A total restraint system would not be acceptable because, in some accident situations, it is preferable for the rider to part from his machine.

ESM1 was fitted with an experimental chest pad restraint system that produced excellent results in tests for frontal impacts. It required fairly major design changes to the frame and fuel tank to assemble the unit, and it also detracted from the general appearance of the motorcycle. The paper supporting ESM1 particularly examined the problems associated with the initiation device for airbags for motorcycle applications and concluded these problems should be solved before further work could be justified on a system that otherwise had much to offer.

Further research into bag initiation by sensing vehicle deceleration concluded this could not be engineered to provide a reliable restraint system that would fire when required without inadvertent activation. Of other methods studied, it was decided to proceed using the forward movement of the seated rider as the sensor. From studies of rider trajectories in frontal impact, it became clear that a significant force was generated on the saddle by the rider moving forward at impact. This force is used to move the saddle forward a short distance against an energy absorber; this movement operates a mechanical switch that provides current to fire the cartridge, which inflates the bag in the centre of the handlebar mounting.

This system has been tested successfully on a full-scale impact rig and on a complete motorcycle with dummy rider at 50km/h into the side of a car at 90°.

With this airbag frontal impact protection system, the rider's forward velocity was significantly reduced when compared with that in a similar test on an unmodified machine.

The airbag provides the restraint system for the rider relative to his motorcycle, but other work shows that some features need attention if the best use is to be made of the airbag as a restraint. First, the stiffness of the front end components has a marked effect on the pitch of the motorcycle during impact. Cast wheels are stiffer than spoked wheels, and it has been found that because of this the pitch of the motorcycle on impact is greater when it has a cast wheel. This could detract from the effectiveness of the restraint system. Second, it is preferable for the motorcyclist to ride down in the restraint system during the soft crush of the vehicle. Third, the interaction between the knees of the rider and the padding of the safety fairing also helps to reduce the kinetic energy of the rider and is part of his trajectory control. Fourth, as pitch of the motorcycle is undesirable, a second load path has been introduced high on the motorcycle that takes the form of a tubular structure in the fairing headlamp surround, and this transmits some of the load to the main frame.

These features, together with the airbag and rider-movement initiation system, form the basis of a viable frontal impact protection system that would not require drastic redesign of the motorcycle, particularly if a fairing is fitted. It is not claimed that this system has yet been optimised. Although there is no problem with fully inflating the bag prior to the rider reaching it, consideration must be given to using a bag larger than the 70 l-devices used in these tests. Inflation of the bag was by firing a cartridge, but a system using high-pressure stored gas should be evaluated in terms of bag inflation rate, cost, and serviceability. The fairing screen forms part of the bag reaction system and could be designed as a yielding structure to assist rider deceleration. This may permit the inflation time to be increased, which could reduce the effect of a secondary impact.

ESM2 is fitted with the forward impact restraint system described. A machine that is fitted with the system and has been impacted into the side of a car is also on display.

A paper by Chinn, Donne, and Hopes, "Motorcycle Rider Protection in Frontal Impact,"(5) is in the proceedings of this conference.

Leg Protection

The high incidence of serious injuries to the legs directed attention to possible methods for reducing the severity of these injuries. ESM1 was fitted with a safety fairing to provide a survival space for the legs on impact and a progressive crush to prevent the rider being ejected unnecessarily violently into the obstacle struck. Work on leg protection devices has since been carried out on light, medium, and heavy motorcycles. This work is summarised in the paper, "Leg Protection for Riders of Motorcycles,"(6) by Chinn, Macaulay, and Hopes, which is presented at this conference. Results are given for damage to the dummy leg and of changes in head velocity after the motorcycle impact. These are for different designs of a leg protection device and are compared with results for unmodified motorcycles. The results show clearly that for the tests conducted, a worthwhile reduction in injury severity and head velocity is to be expected when motorcycles are fitted with such leg protectors. While at this point it is not claimed that the required characteristics for leg protection have been optimised, the importance must be stressed of the design of the device in absorbing some of the kinetic energy of the rider and motorcycle during the impact.

ESM2 is fitted with a BMW RT fairing that has been modified to contain the leg protection device on both sides within the outer skin panels of the fairing. It is felt that this demonstrates leg protection can be adopted within a fairing without detracting from the appearance of the vehicle.

Safety Fairing

ESM2 is fitted with a safety fairing. The top part is a standard BMW RT fairing modified to receive the new instrument pack. The lower part has been restyled so the leg protection devices can be contained within the inner and outer skin panels. The forward impact test motorcycle incorporates the leg protection cones, which can be seen inside the fairing together with the tubular framework that provides the second load path for frontal impact. The inner skin panels of ESM2 cover these features and also supply the crush zone for the riders' knees in forward impacts. On the outside, the fairing is painted white as an aid to conspicuity, and the twin daytime running lamps are positioned on either side of the headlamp. The smooth line of the fairing with no external projections provides the best available solution for primary impact with a pedestrian.

Further work on the fairing is needed to provide controlled yield of the windscreen for part of the occupant ride-down with the airbag restraint system. Further research will show if the airbag stowage position is more effective if it is contained within the fairing rather than in its present position.

It is considered that this safety fairing offers significant protection in impacts without detracting from the visual image of what is acceptable for a motorcycle.

Other Features

Digital Speedo and Instruments

ESM1 was fitted with a speedometer with a 1-in-high digital display. Experiments had shown that a significant difference exists in the time riders take to read their speedometers and this depends on the type of instrument fitted. The time taken to read a large-dial instrument was reduced by 0.58s when a digital display was used. During this time saved, a distance of 8m is covered at 48km/h, which allows the rider to concentrate more fully on the road scene.

ESM2 is also fitted with a digital display speedometer, adapted from a unit produced for a car, supplied by Lucas. This also provides a tachometer and fuel gauge display together with warning lights. A warning light is lit on the panel if a system failure develops in either of the antilock brake units to alert the rider the machine is back to standard brakes. At this stage, the speedometer is also switched off as a further warning of a failure. This failure warning system is now being developed so the speedometer is a constant on-vehicle monitor that the antilock brakes are functioning. A separate failure warning lamp will also be provided. This section of the instrument display is considered to be a part of the antilock brake system.

Fuel System

Reports on accidents show that in the case of motorcycles, 30 percent involve spillage of fuel from the machine; in one-third of these, spillage is reported to be excessive. The incidence of fire in motorcycle accidents is higher than for cars, and spillage of fuel is an unnecessary hazard if it can be avoided easily. The Transport and Road Research Laboratory has developed a simple system using two fixed tubes inside the petrol tank that shut off the fuel supply to the fuel lines if the machine falls over on either side (Figure 1). Designs are available using this principle for both gravity feed systems and pumped feed systems. ESM2 is fitted with a gravity-fed system. The petrol tap positions have also been resited to forward takeoff points to overcome the external protrusions provided by the original taps. A single tap is now provided in the centre position of the fuel tank. This fuel tap is operated by a solenoid valve that turns the fuel on when the ignition is switched on. Similarly, the fuel is turned off when the ignition is switched off.

A habit with some riders is not to refuel their motorcycle until they have gone on to the reserve fuel position. This can be a hazard in some instances as the engine loses power until the fuel supply is resumed, which can lead to accidents. No manually operated reserve fuel supply is available on ESM2 because a fuel gauge is fitted.

Interlocked Stands

Accidents have been caused by drivers riding off from rest with the side stand down, so requirements are in hand for the vehicle to be constructed to prevent this. The side stand on ESM2 is automatically returned when the clutch is operated and is additionally provided with an interlock with the ignition circuit. The centre stand is also fitted with an ignition interlock, but a manual override is provided that locks the stand down so the engine can be run for servicing while the machine is raised on its centre stand. A better solution would be to have the centre stand also hand-operated so the rider could use it while still astride the motorcycle. More effective use of the main stand could result on heavy motorcycles where frequently only the side stands are used for convenience. This was not found to be possible on ESM2 because of the cylinder layout.

Assessment

Accident and casualty data in Great Britain have shown that motorcycles are 10 times more likely to be involved in a casualty accident per mile travelled than are cars (not allowing for rider and driver age differences). In 1983, there was a total of 64,494 casualties among their

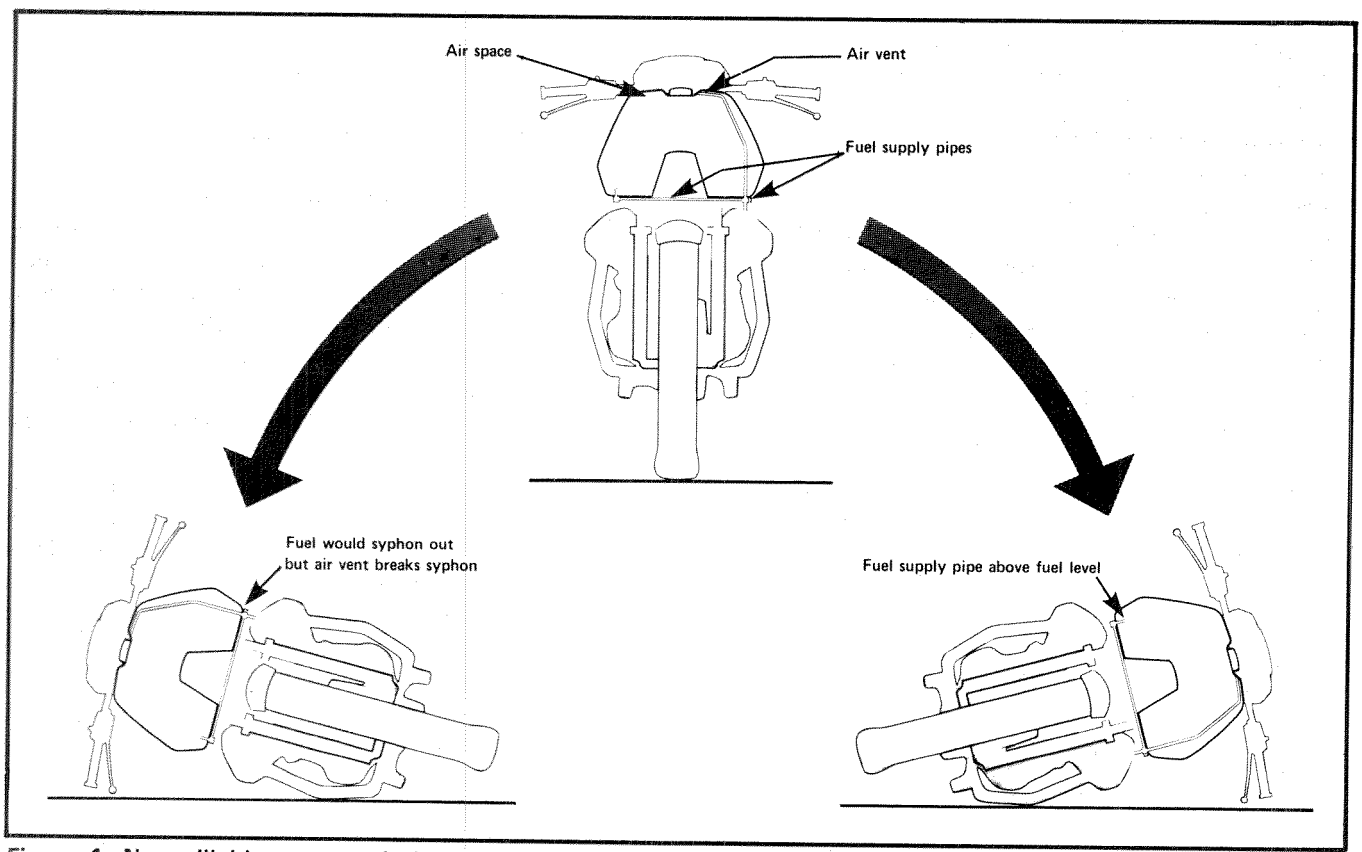

Figure 1. Nonspillable motorcycle fuel tank

riders and passengers, of which 963 were fatal. In this year, the casualty rate was slightly up on previous years but the total number of casualties was lower. The trend of reducing motorcycle mileage continued in 1983, and the casualty savings for the year appear to be due mainly to this reduction. The reasons for the decline in motorcycling in recent years are not clear, but the recession could be one of the variables producing this trend. If in subsequent years the motorcycle mileage increases, as has occurred previously, the increase would contain a larger portion of inexperienced riders, which would tend to increase the accident rate, thus producing a disproportionate rise in casualties.

There are certain safety features that can be incorporated in a motorcycle to provide part solutions to problems that exist, and estimates of effectiveness can be made from the data available. Of the accident avoidance and rider protection systems on ESM2, it is worth speculating on four features and the value of each of them independently. This is done in terms of casualty savings using 1983 data and assumes that all motorcycles would be fitted with these systems (Table 1).

Although the features are considered independently in the analysis, the effect of applying one treatment to the vehicle would reduce the number of available accidents that the other features could benefit from. Improved daytime conspicuity, which has the best cost-benefit, would reduce the present quantifiable accidents that would benefit from the other three features. Conversely, other benefits exist that cannot be quantified by the data. The introduction of antilock brakes would contribute to reducing the 6,000 accidents involving skidding in adverse conditions. It is not possible to quantify the potential savings on dry roads arising from skidding or from underbraking due to the fear of a skid. Work at the Laboratory toward reducing leg injuries has shown in the tests carried out to simulate leg injury accidents that with correctly designed leg protectors, the rider's head velocity is reduced compared with results from a similar test on an unmodified motorcycle. In some of these accidents, a reduction in head injury severity would also be expected.

Frontal impact research has considered the motorcycle hitting an object normal to its direction of travel. The research work on leg protection has shown that on an unmodified motorcycle if the object struck is inclined at 30° either side of normal, the trajectory of the rider is virtually the same as a frontal impact. The frontal impact accounts for 60 percent of motorcycle collisions, and for these the restraint system could assist in reducing the rider's kinetic energy.

The work on motorcycle safety at the Transport and Road Research Laboratory is aimed at providing viable solutions to problems identified by research without departing from the image of a motorcycle. Although this task is far from complete, there has been some notable progress made since the first safety motorcycle exhibit ESM1 in 1979. A preliminary consideration of possible costs and savings for antilocking brakes, by protection, forward trajectory control, and daytime conspicuity suggests that all are likely to be worthwhile and deserve further development for general use.

Acknowledgments

The work described in this paper forms part of the programme of the Transport and Road Research Laboratory and is published by permission of the Director.

References

1. Watson, P.M.F., "Features of the experimental safety motorcycle ESM1," Proceedings Seventh International Technical Conference on Experimental Safety Vehicles, Paris, June 1979.
2. Donne, G.L., and P.M.F. Watson, "Aspects of motorcycle braking," Proceedings Tenth International Technical Conference on Experimental Safety Vehicles, Oxford, July 1985.
3. Donne, G.L., "The performance of motorcycle disc brakes when wet," Department of Transport, TRRL Report LR 1121, Crowthorne, 1984.
4. Donne, G.L., E.J. Fulton, and P.G. Stroud, "Motorcycle conspicuity in daylight," Proceedings Tenth International Technical Conference on Experimental Safety Vehicles, Oxford, July 1985.
5. Chinn, B.P., G.L. Donne, and P.D. Hopes, "Motorcycle rider protection in frontal impacts," Proceedings Tenth International Technical Conference on Experimental Safety Vehicles, Oxford, July 1985.
6. Chinn, B.P., M.A. Macaulay, and P.D. Hopes, "Leg protection for riders of motorcycles," Proceedings Tenth International Technical Conference on Experimental Safety Vehicles, Oxford, July 1985.
7. "Road accidents Great Britain 1983," HMSO.

Table 1. Preliminary estimates of costs and savings for safety features

	Number of accidents	Estimated cost of accidents £m/yr	Estimated number of casualties saved or with reduced injury severity	Estimated cost of injuries saved £m/yr	Estimated equipment cost £/motorcycle	Estimated cost to fit 250,000 new machines/yr £m/yr	Remarks
Daytime conspicuity	18,000	72[2]	6,000	26	10	2.5	Original equipment or retro-fit
Anti-lock brakes	12,000	52[2]	6,000	26	Large M/C 200 Small M/C 25	32.5	Treatment 150,000 Large 100,000 Small
Leg protection	38,000[1]	90[1]	(5,282 serious converted to slight) (7,778 slight)	37	75-300	19-75	Safety fairing cost Large machine £300 Medium machine £75(3)
Forward impact	42,000	183[2]	8,500	37	15	3.75 have to be fitted	Safety fairing would also

(1) 65% serious casualities. 60% slight casualties
(2) Using average casualty cost

(3) Quotation from commercial supplier producing from limited tooling

Using 1983 Casualty Data[1] Riders and Passengers of Two-Wheeled Motor Vehicles				
	Fatal	963	Cost £'s of Casualities	Fatal 150,045
	Serious	20,317		Serious 6,950
	Slight	43,214		Slight 170
	All severities	64,494	Average all severities	4,370

Driver Airbag Police Fleet Demonstration Program— A 24-Month Progress Report

David J. Romeo
Romeo Kojyo Company Inc.

John B. Morris
U.S. Department of Transportation, National Highway Traffic Safety Administration

Abstract

The objective of this program is to design, test, evaluate, manufacture, and install in 500 state highway patrol vehicles a driver airbag retrofit system.

Airbag system benefits are universally accepted. However, the costs, complexities, and availabilities of these systems are widely misunderstood. This program takes much of the mystery out of the airbag and demonstrates to fleet operators and the public at large that airbag technology, components, and systems do presently exist and can be acquired at a reasonable cost.

Detailed information on system design, selection of vehicles and states to participate, as well as sled testing and full-scale crash testing are presented as SAE Paper 841216, "Driver Airbag Police Fleet Demonstration Program—A 15-Month Progress Report" by the same authors. The present paper reviews very briefly those aspects of the program and places emphasis on the field experience of the 500-car fleet, which to this point has experienced 18 actual airbag deployment crashes (16 of which have occurred in the past 9 months).

Program Discussion

The primary goals of this program were to design, test, and evaluate a driver airbag retrofit system, and using production hardware to manufacture sufficient kits for demonstration purposes, and to install these kits into police vehicles in a number of State Highway Patrols.

Retrofitting the driver's side with an airbag system was not overly difficult; the essential production components already existed. It was accomplished by replacing the existing steering wheel with an airbag wheel, installing crash sensors, providing a proper electrical circuit, and adding a knee restraint to the instrument panel. The retrofitted vehicle appears little different from the original vehicle.

To make retrofit kits available for this program, engineering effort was required to finalize design of airbag components (airbag, module, steering wheel, crash sensors, and knee restraint). These components, with the addition of minor brackets and cosmetic components peculiar to each type vehicle, complete the retrofit kit. Once design was finalized, these components needed some additional minor tooling for limited production, and parts needed to be produced in sufficient quantities to enable evaluation testing and retrofit of selected demonstration vehicles.

The system consists of sensor(s), wiring, diagnostics, connectors, steering wheel, gas generator, airbag and all module components including the cosmetic cover, and a knee restraint. The system design consists (to the extent possible) of commercially available production components. The gas generator, airbag, and sensor are production designs and heretofore have been subjected to acceptable automobile manufacturer's qualification tests and specifications.

The project was initiated April 15, 1983. A review of the program through April 1985 is presented here. Topics to be discussed include—

- Selection of States
- Selection of Vehicles
- System Design
- Sled Testing
- Crash Testing
- Installation of the Retrofit System
- Field Experience to Date

Selection of States

When funding for the program was committed, NHTSA sent letters to each of the States regarding their interest in participation. Approximately 20 States responded positively and the selection of six States was made, based on earlier commitments, earnestness expressed, and geographical location (there was an effort to represent as wide a range of locations, e.g., west, southwest, midwest, etc., as possible).

Vehicle availability, type, and scheduling were considered. The States originally participating in the program were Arizona, California, Ohio, Maryland, Mississippi, and Wisconsin. Later in the program, the system was modified to include improved installation procedures and a new diagnostic. At that time, the New York State, New York City, and River Vale, N.J., police fleets were added.

Selection of Vehicles

Two basic car types were included—the Ford Panther and the Chrysler M-body. Both represented Ford's and Chrysler's V-8 engine, rear-wheel drive, full-size cars. Ford versions of this vehicle include the Ford LTD up to

1982, Ford LTD Crown Victoria, Mercury Gran Marquis, and, with some front end change, the Lincoln Town Car. This vehicle has been manufactured without change from 1979 to the present. The Chrysler M-body has been sold since 1982 as the Plymouth Gran Fury and at least since 1981 as the Dodge Diplomat. It was formerly sold as the Chrysler Le Baron and presently is the Chrysler 5th Avenue.

System Design

The latest system (see Figure 1) consists of the following items: two front sensors, a safing sensor, and wiring with protective shielding in the engine compartment that passes through the firewall and plugs into a diagnostic unit mounted in the occupant compartment. From the diagnostic unit, wiring leads go to (1) power and ground, (2) a readiness indicator light, and (3) up the steering column through a special coiled connector to a four-spoke airbag steering wheel. The wheel, which mounts using a hub fabricated to fit the column shaft, has two horn buttons mounted on the upper spokes. The airbag module is attached to the special wheel using four allen-head cap screws and consists of the gas generator, the nylon airbag, metal mounting components, and a highly developed reinforced cover assembly.

The knee restraint is mounted over the lower part of the instrument panel on the driver's side and consists of a sheet metal frame, energy-absorbing foam, and a vinyl cover colored to match the vehicle interior.

A photograph of the system mounted in a police cruiser is shown as Figure 2.

The sensors and diagnostic system were supplied by the Technar Corporation of Arcadia, California. The steering wheel and airbag module were supplied by Takata Corporation of Tokyo, Japan, and the gas generator was supplied by Bayern Chemie GmbH of Ottobrunn, West Germany.

Sled Testing

A total of 31 sled tests were run using the HYGE facility at the Transportation Research Center, TRC, in Marysville, Ohio. Twenty-two tests were run with the

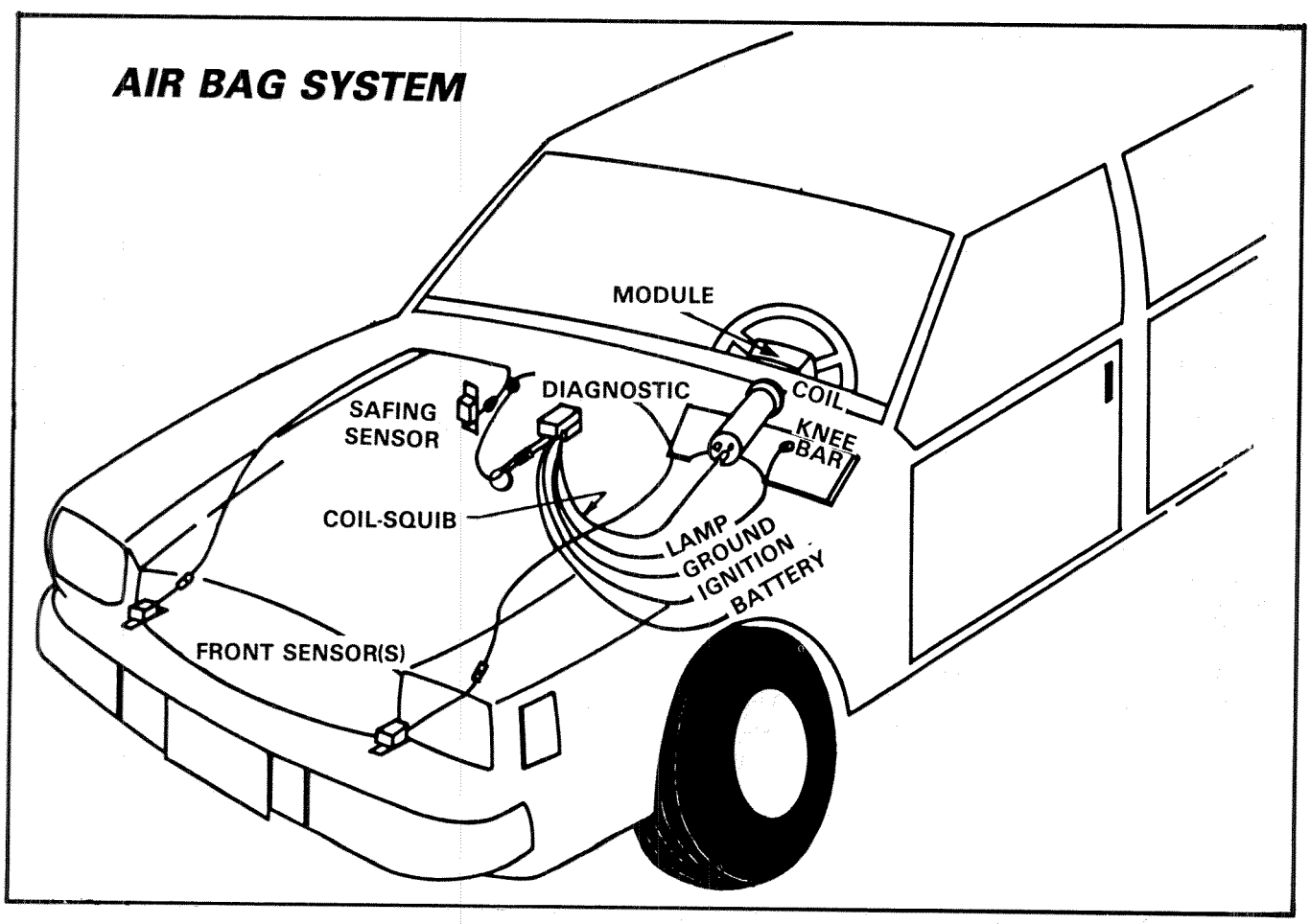

Figure 1. Airbag system

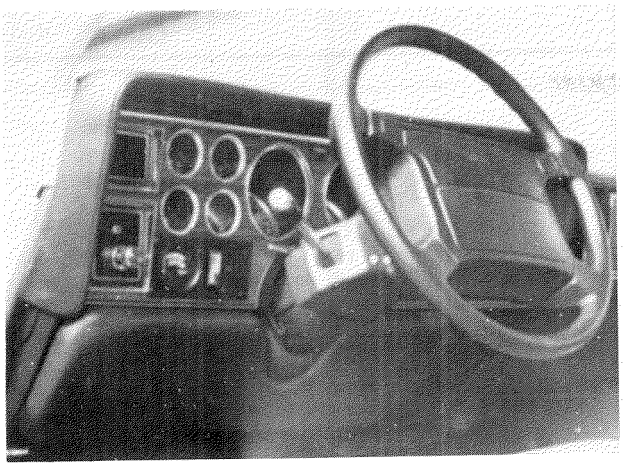

Figure 2. Typical Romeo Kojyo airbag system installation

Ford body buck and crash pulse and nine with the Dodge. A detailed discussion of these tests is beyond the scope of this paper, but is available through NHTSA. Only a brief summary of results is presented here.

The tests on the Ford body were run first to finalize system design. Once this was accomplished, the remaining tests were run to study effects of test dummy size and to simulate crash speed, crash angle, and a range of restraint configurations.

The airbag system, that is, the steering wheel, airbag module, and knee restraint, were tested alone and in combination with lapbelt only, and with lapbelt plus shoulder belt. The belt restraint configurations were also tested without the airbag. Two other comparisons were made. The 50th percentile dummy was tested with no restraint system, and finally the airbag was tested without the knee restraint.

These results are summarized below for the 50th percentile head, chest, and femur load results.

Sled test results, Ford LTD, 32.5mph

	HIC	C_R	Femur*
Unrestrained	2,401	59g's	2,754lb
Lapbelt	2,584	44	410
Lapbelt/Airbag	468	43	702
Lap/Shoulder Belt	865	36	433
Lap/Shoulder/Airbag	510	35	427
Airbag	209	38	1,690
Airbag, w/o Knee Bar	263	40	3,002

*max value, left or right leg

It is clear that results for the unrestrained case are very poor (the reader's knowledge of injury criteria, i.e., HIC, C_R, and femur loads is assumed). As can be seen further, the lapbelt controls leg loads and improves chest results but plays no role in controlling injury to the head. The airbag and lapbelt work well in combination and provide superior protection to the head than does the lap and shoulder belt.

Crash Testing

Seven full-scale tests were conducted between September 1983 and January 1984 to evaluate the performance of the driver airbag system. The results of these tests are summarized in Table 1. A description of each of these tests is presented in the previously mentioned SAE paper.

Results of crash tests with the 1982 Ford LTD were better than anticipated, while results with the Dodge Diplomat were satisfactory but not as good. To a lesser degree, these results were seen in the sled tests, which used nearly the same crash pulse.

Regarding overall system performance and design in the two vehicles, the following remarks can be made:

- Sensor closure time was sufficiently early in both vehicles.
- The bag position was excellent. Therefore, although some improvement in chest ride down, that is $-C_R$, would result from removal of the bag straps, there is strong reluctance to do so since it is believed that the bag straps are important in locating the bag.

Installation of the Retrofit System

When police cruisers are purchased and received from the automobile dealers, they are cars that have been assembled with special police package options such as heavy-duty springs, shocks, radiator, and a large engine. However, before the vehicles are put into service, they are prepared by police technicians at special facilities and receive radio equipment, sirens, light bars, bumper bars, decals, and various other equipment. The point is, each highway patrol agency has its own skilled mechanics, technicians, radio men, and garage facilities. These men and facilities were used for installation of the airbag retrofit systems.

For each vehicle type, a detailed set of installation instructions was written and supplied to the police agencies. In addition to these instructions, a few days were spent at each State facility demonstrating installation of the first half-dozen systems. After installation in the first one or two cars was completed, the technicians took over installation responsibility with Romeo Kojyo and NHTSA representatives in attendance to answer specific questions. This methodology worked very well in every State, and comments or feedback from the installers were used to improve on the installation method.

Table 1. Crash test results

Test	1	2	3	4	5	6	7
Date	9/1/83	9/9/83	10/3/83	12/1/83	12/8/83	12/13/83	1/6/84
Vehicle	Ford	Ford	Dodge	Ford	Ford	Dodge	Dodge
Speed, mph	29.7	30.3	29.4	30.1	35.4	29.4	29.9
Mode	Barrier	Barrier	Barrier	Pole	Barrier	Barrier	Pole
Restraint	NAB/KB	AB/KB	AB/KB	AB/KB	AB/KB/3PT	AB/KB	AB/KB
Sensor Closure,MS		20	24	20	16	16	16
HIC	821	470	991	306	866	919	950
$C_{R,}$ g's	55	48	54	38	43	61	59
Femur, lb							
left	1,448	1,775	1,420	1,700	672	1,820	1,610
right	1,485	1,356	1,420	2,000	820	1,585	2,290

NAB - nondeployed airbag module/steering wheel
AB - airbag
KB - knee bar

Field Experience

Maintenance

No major problems associated with any of the system components have occurred. A few minor problems arose that required changes to the system itself or to its installation procedure. These were discussed in the earlier paper.

Accidents Involving Airbag-Equipped Vehicles

Appendix A presents a synopsis of the airbag deployment crashes as of April 15, 1985. Photographs of some of these crashes are shown in Figures 3-5. Attempts have been made to analyze and categorize the 18 deployments using several different approaches (see Table 2). Two methods were selected. The first was by crash type, frontal or frontal offset, versus undercarriage or suspension impacts. The second method was whether a higher sensor threshold could have been used.

The second method of comparison is clearly subjective and necessarily includes such important factors as whether or not the belt was worn, and whether or not police cruisers should be considered as a separate group because of the hard use to which they are subjected.

With regard to belt use, it was a condition of each State participating in the program to have a strict belt use policy. However, 100 percent belt use was not an allowable assumption, and a goal of the design was to provide adequate protection for both belted and unbelted officers.

From Table 2, it is seen that by counting all undercarriage accidents and the two impacts with deer, it might be argued that in nine of the deployments supplemental airbag protection may not have been needed. It is interesting to note, however, that with the exception of the initiation threshold level of the first deployment, there were positive reactions from the officers who were driving the vehicles.

The deployment threshold of the crash sensors used in this program was established to accommodate the general driving public. Following the first airbag deployment, the question arose as to whether the threshold level should be raised for police vehicles, which, as previously mentioned, are subjected to harder than normal use. To further complicate matters, two police fleets, California and Arizona, use pusher bars attached to the front of the vehicle. Test data indicate that pusher bars lower the deployment threshold 2 to 3mph compared to cars without pusher bars.

From an engineering standpoint, it was concluded that an increase in the threshold level of the crash sensors could be accepted. Accordingly, the higher level threshold sensors were incorporated into the California Highway Patrol vehicles and into the newer systems provided to the State Police of New York and to the New York City Police.

Currently, two airbag deployment strategies are being used in the study: a deployment threshold intended for the general driving public and a higher deployment threshold possibly more suitable for police use. During the remainder of the program, the two deployment strategies will be evaluated.

The program will continue for at least 1 more year. During this time, we expect to gather valuable information on the types of accidents in which the airbag deploys, the injury prevention capability of the system, and the appropriate sensor threshold for vehicles depending on the use to which they are put.

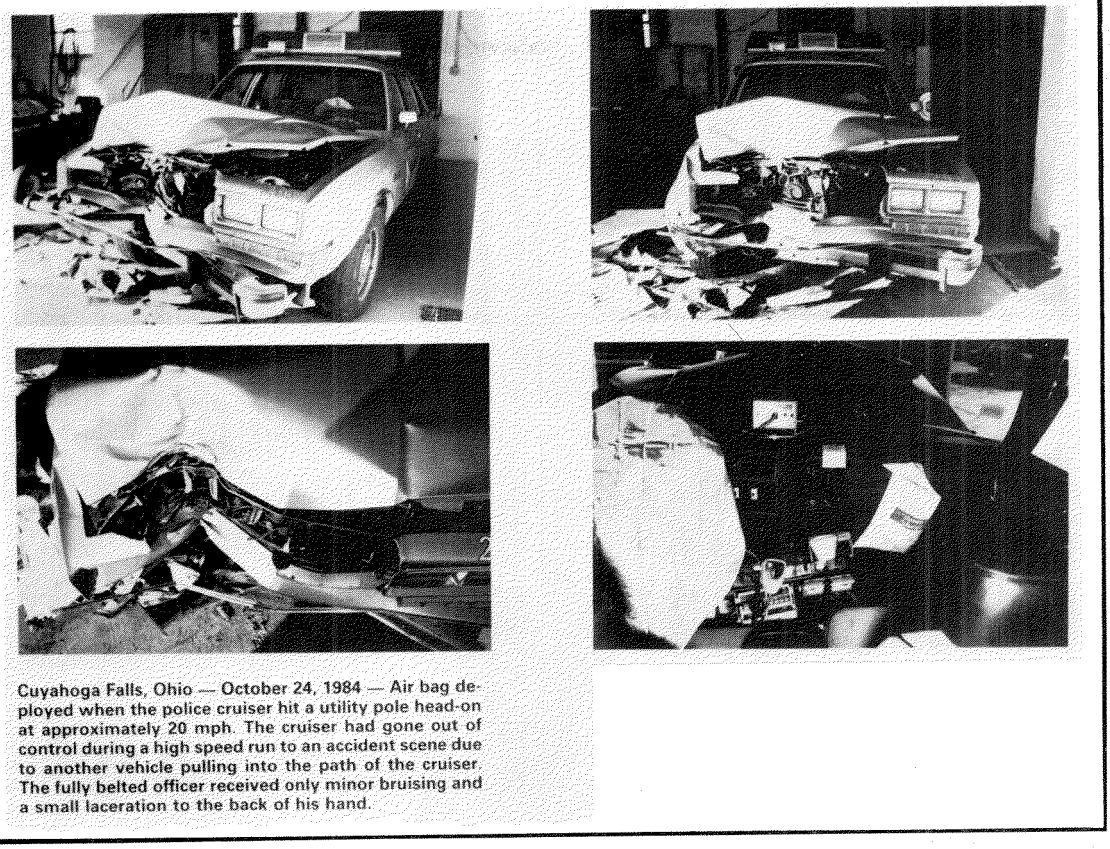

Cuyahoga Falls, Ohio — October 24, 1984 — Air bag deployed when the police cruiser hit a utility pole head-on at approximately 20 mph. The cruiser had gone out of control during a high speed run to an accident scene due to another vehicle pulling into the path of the cruiser. The fully belted officer received only minor bruising and a small laceration to the back of his hand.

Figure 3. Police fleet airbag deployments

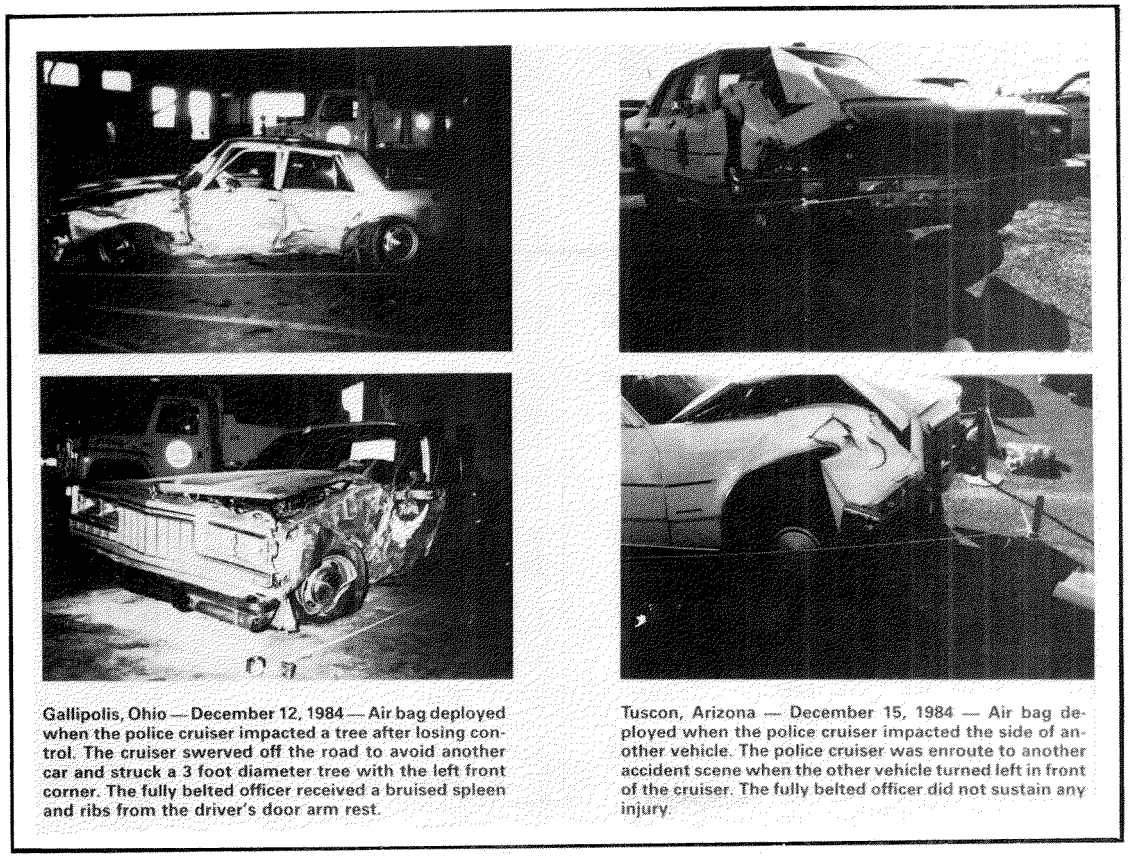

Gallipolis, Ohio — December 12, 1984 — Air bag deployed when the police cruiser impacted a tree after losing control. The cruiser swerved off the road to avoid another car and struck a 3 foot diameter tree with the left front corner. The fully belted officer received a bruised spleen and ribs from the driver's door arm rest.

Tuscon, Arizona — December 15, 1984 — Air bag deployed when the police cruiser impacted the side of another vehicle. The police cruiser was enroute to another accident scene when the other vehicle turned left in front of the cruiser. The fully belted officer did not sustain any injury.

Figure 4. Police fleet airbag deployments

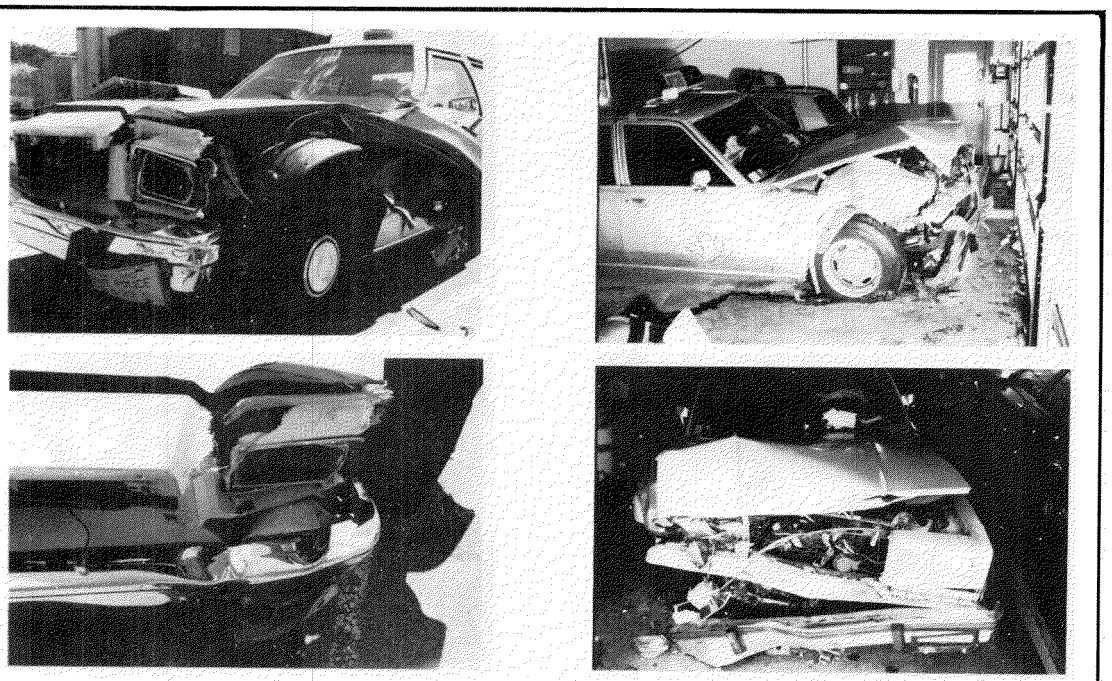

Elkridge, Maryland — September 4, 1984 — Air bag deployed when the police cruiser impacted a car stopped in a travel lane on the expressway as a result of a previous accident. Another car had swerved in front of the police cruiser leaving the cruiser without an avoidance path. Impact speed was estimated at 45 mph. The two officers in the front seat of the cruiser were both fully belted and neither received appreciable injury.

Marion, Ohio — January 22, 1984 — The police cruiser was parked heading south. Its occupants were attending another accident. A northbound vehicle, whose driver was distracted by the first accident and lost control of the car, struck the police cruiser head-on. The air bag deployed. The two police officers were belted and uninjured.

Figure 5. Police fleet airbag deployments

Table 2.

Crash	Date	State	Vehicle Type	Object Struct	Velocity Change mph
1	4/11/84	CA	Dodge	Rough Road	6
2	6/29/84	AZ	Ford	Car	10
3	7/25/84	WI	Ply	Embankment	6
4	8/25/84	OH	Ply	Ramp	6
5	9/04/84	MD	Ford	Car	12
6	9/12/84	MS	Ford	Car	10
7	10/10/84	OH	Ply	Deer	6
8	10/24/84	OH	Ply	Pole	16
9	11/10/84	MS	Ford	Ditch	10
10	12/12/84	OH	Ply	Tree	18
11	12/15/84	AZ	Ford	Car	13
12	1/22/85	OH	Ply	Car	13
13	1/24/85	MD	Ford	Car	10
14	1/31/85	AZ	Ford	Rock Wall	7
15	2/09/85	CA	Dodge	Car	8
16	3/10/85	MS	Ford	Ditch	10
17	3/29/85	MD	Ford	Culvert	9
18	4/9/85	MD	Ford	Deer	8

Conclusion

1. In 450 police vehicles, approximately 20 million vehicle-miles, there has been no occurrence of airbag deployment without a reportable accident.
2. There have been approximately 25 to 30 accidents, of varying intensity, involving the airbag-equipped police vehicles, resulting in 18 deployments.
3. There have been no significant injuries of consequence in any of the accidents.
4. In no case has an accident occurred in which the airbag should have deployed and did not.
5. Evaluation of the system will continue at least through July 1986.

Appendix A

Police Airbag Retrofit Experience

4-11-84 Sacramento, California—Airbag deployed while in hot pursuit on a dirt roadway. The driver was wearing a lapbelt and received bruises on inner wrist and upper right inner arm. The car was driven from the scene by the police officer. The vehicle was a 1983 Dodge Diplomat. The airbag was deployed after running through a ditch and striking large stones in the roadway. The pusher bar on the police car bumper was found to reduce the deployment threshold speed for this type of accident. These pusher bars are unique to the California police cars, and the airbag sensors of all California cars have been adjusted for this difference. The investigation is by Dynamic Science.

6-29-84 Cordes Jct., Arizona—Airbag deployed when an unoccupied 1983 Ford Crown Victoria police cruiser was pushed into the rear of a 1980 Cadillac Eldorado as a result of the airbag car being rear-ended by a 1979 Dodge van. The airbag police vehicle had stopped the Cadillac for a traffic violation. The ignition was on and the engine was running in the unoccupied police car at the time of impact; therefore, the airbag system was ready for activation. Only minor injuries occurred to the driver of the van and both occupants of the Cadillac. The police officer was not injured. The investigation is by Dynamic Science.

7-25-84 Reedsburg, Wisconsin—Airbag deployed when the undercarriage of the 1984 Plymouth Gran Fury impacted an embankment while chasing a motorcyclist across a golf course. The fully belted officer received abrasions and contusions to the inner wrists/forearms and biceps that did not require treatment. The car bottomed out with such force that the officer driving was thankful for the airbag deployment. The officer drove the car away after apprehending the cyclist. The investigation is by Calspan, Buffalo, NY.

8-25-84 Ironton, Ohio—Airbag deployed when the torsion bar bracket (undercarriage) of the 1984 Plymouth Gran Fury dug into the entrance ramp of an asphalt church driveway. The police cruiser had slowed from an 80+mph pursuit down to an estimated 35mph when the impact occurred. The impact produced an estimated 15mph delta-V and left a gouge in the pavement approximately 30in in length and 2-½in deep. The cruiser did not sustain any deformation in the impact; the crash energy was dissipated by the stiff torsion bar bracket trenching the pavement. The fully belted officer sustained an abrasion to his inner left forearm but was otherwise uninjured. He braked the cruiser to a controlled stop after the impact and apprehended the suspect, who tried to hide behind the church. The cruiser was driven from the scene. The officer, when asked if he would spend $500 for an airbag in his personal car, replied, "Yes." The investigation is by University of Tennessee.

9-4-84 Elkridge, Maryland—Airbag deployed when the 1982 Ford police cruiser impacted a car stopped in a travel lane on the expressway as a result of a previous accident. Another car had swerved in front of the police cruiser, leaving the cruiser without an avoidance path. The left front corner of the cruiser impacted the right front corner of the stopped car (perpendicular impact) at an estimated 45mph. The left front fender of the cruiser was peeled away from the car structure, the driver door was distorted and sprung, and roof buckling occurred over the B-pillar. The two officers in the front seat of the cruiser were both fully belted and neither received appreciable injury. The driver incurred a minor lower back strain and a contusion to the left arm and left knee. The Maryland State Police associated with this incident were favorably impressed with the airbag performance. The investigation is by Calspan, Washington, DC.

9-12-84 Magee, Mississippi—Airbag deployed when the 1984 LTD Crown Victoria Ford police

cruiser impacted the left front corner of a 1980 Chevrolet Caprice as it pulled from a parking lot into the path of the cruiser. The impact speed was about 15mph and inflicted about 8in of crush to the right front of the cruiser. The police officer was unbelted at the time of the impact and received an abrasion to the inner left arm and chest. The police officer was leaning to his right over the console with his left arm on the steering wheel when the deployment occurred. The driver of the Chevrolet left the scene of the accident prior to questioning and apparently was not appreciably injured. The investigation is by Dynamic Science.

10-10-84 Ashland, Ohio—Airbag deployed when the 1983 Plymouth Gran Fury impacted a 120 lb deer (four-point buck) with the right front corner of the cruiser at an estimated 50mph. The maintenance man driving the cruiser was not injured. The cruiser sustained 3in of buckling to the hood and fender, and the grille and right front headlight assembly were shattered. The damage to the cruiser is estimated at over $1,000. The investigation is by University of Michigan.

10-24-84 Cuyahoga Falls, Ohio—Airbag deployed when the 1983 Plymouth Gran Fury hit a utility pole head-on at approximately 20mph. The cruiser had gone out of control during a high-speed run to an accident scene due to another vehicle pulling into the path of the cruiser. The police cruiser sustained 23in of crush in the right front. The fully belted officer received only minor bruising and a small laceration to the back of his hands as a result of their contact with internally mounted radar equipment. The damage to the police cruiser is estimated at $3,700. The investigation is by University of Michigan.

11-10-84 Lucedale, Mississippi—Airbag deployed when the 1984 Ford LTD police cruiser left the roadway, grazed a pole, right front wheel dug into the dirt (which appears to have initiated the deployment), and then hit a tree. The cruiser had lost control enroute to an accident scene when another vehicle pulled into the path of the cruiser. The fully belted driver received a swollen lip and scratch to the eye during the accident event. The investigation is by University of Tennessee.

12-12-84 Gallipolis, Ohio—Airbag deployed when the 1983 Plymouth Gran Fury police cruiser impacted a tree after losing control. Another car turned in front of the cruiser as the cruiser passed through an intersection while enroute to an accident scene. The cruiser swerved off the road to avoid the other car and struck a 3ft-diameter tree with the left front corner. The motion of the cruiser continued, with the tree producing about 6in of damage (crush) down the left side of the cruiser. The cruiser separated from the tree before coming to its final rest position. The fully belted police officer received a bruised spleen and ribs from the driver's door armrest. The police officer was very pleased with the airbag performance in this crash. The investigation is by Calspan, Buffalo, NY.

12-15-84 Tucson, Arizona—Airbag deployed when the 1983 Ford Crown Victoria police cruiser impacted the side of a 1974 Oldsmobile Cutlass. The police cruiser was enroute to another accident scene when the Oldsmobile turned left in front of the cruiser. The impact produced about 5in of crush to the front of the police cruiser and about 8in of crush to the right side of the Oldsmobile. The fully belted police officer did not sustain any injury whatsoever. He was particularly pleased that he "didn't even have any bruises." The investigation is by Dynamic Science.

1-22-85 Marion, Ohio—A 1983 Plymouth Gran Fury police cruiser was parked heading southbound off the road on U.S. 23 just north of State Road #231. Its occupants, two police officers, were attending another accident. A northbound Ford Granada, whose driver was distracted by the first accident and lost control of the car, struck the police cruiser head-on in a full frontal collison. The airbag deployed. The two police officers in the Gran Fury were belted and uninjured. The driver of the Granada was also belted and uninjured. The investigation is by University of Michigan.

1-24-85 Clement, Maryland—A 1984 Ford LTD Crown Victoria police cruiser struck the right side of a 1979 Oldsmobile Cutlass Station Wagon. The airbag in the Ford deployed. The driver of the police cruiser had a contusion on the inside left upper arm and small laceration on the outside surface of the right hand. The right front passenger had a small contusion of the right knee. Both officers stated they were belted. The impact speed was about 10mph. There was 18in of crush to the side of the Oldsmobile. The investigation is by Calspan, Washington, DC.

1-31-85 Globe, Arizona—A 1983 Ford LTD Crown Victoria police cruiser struck an embankment and rotated. The airbag deployed as the left

front corner of the vehicle was displaced rearward about 7in. There was about $1,500 damage. The unbelted driver suffered a minor abrasion to the left arm and an abrasion and contusion on the left side of the forehead from the roof rail. The investigation is by Dynamic Science.

2-9-85 Los Angeles, California—A 1983 Dodge Diplomat police cruiser was stopped on Interstate 5 as its driver (a police officer) was out of the vehicle assisting a motorist with a disabled car. The unoccupied police cruiser was struck in the rear by a third vehicle travelling in the same direction, and moved forward into the rear of the disabled vehicle. The bag deployed during the frontal strike by the police cruiser. All parties involved received minor injuries except for a lower leg fracture to one pedestrian. The police cruiser was totaled. The investigation is by Dynamic Science.

3-10-85 Starkville, Mississippi—Airbag deployed when the Ford Crown Victoria police cruiser went off the road and impacted a shallow ditch in the pursuit of a high-speed subject. The driver was lapbelted but had about 2 to 3ft of slack in the shoulder belt to facilitate the radar equipment that had been in use. The driver incurred a black left eye, contusion to the left eyelid, and redness to the left side of his face. The right front passenger was not belted and received a sprained ankle and sore wrist (apparently from windshield contact). Both occupants were very positive about the airbag performance in this crash. The investigation is by University of Tennessee.

Summary of the Accident Experience of 1970 Vehicles Equipped with Airbags as of July 1, 1985

Fleet Vehicles*	
1972 Mercury's	831
1973 Chevrolet's	1,000
1975 Volvo's	75
Privately-owned Vehicles	
1974-76 GM Cars (Buick, Cadillac, and Oldsmobile)	10,281

Airbag Crash Experience**

As of July 1, 1985, NHTSA knows of 279 airbag deployment crashes. The vehicles involved had 397 front seat occupants, sitting behind airbags, who had the following injury levels:

None-Minor (AIS 0-1)	321
Moderate-Serious (AIS 2-3)	53
Severe-Critical (AIS 4-5)	4
Fatal (including 2 drownings)	12

In these accidents, the airbag vehicles had primary damage as follows:

Front	208
Side	49
Undercarriage	22

NHTSA also has information on 161 accidents involving airbag vehicles where the vehicle frontal deceleration was not great enough to deploy the airbag. The vehicles involved had 220 front seat occupants who had the following injury levels:

None-Minor	196
Moderate-Severe	10
Serious-Critical	0
Fatal	2

In these accidents, the airbag vehicles experienced primary damage as follows:

Front	106
Side	33
Undercarriage	2
Rear	8
Rollover	3

Exposure: The following is an estimate of the number of vehicle-years of operation of automobiles equipped with airbags. It was made using data on new car sales, registration data from R.L. Polk, and general vehicle scrappage data.

Models	**Car Years of Operation (1-1-84)**
1972 Mercury Fleet	8,088
1973 Chevrolet Fleet	9,205
1974-76 GM Cars	84,008

* The data include a very small number of vehicles with prototype airbag systems, including a 1980 Oldsmobile and a small number of 1982 Lincolns.

** Some data may be missing due to individuals who did not wish to provide us with information and vehicles that had been repaired prior to an investigation.

Summary of the Accident Experience of 1983 and Later Airbag-Equipped Vehicles as of October 1, 1985

Fleet Vehicles	
1985 Ford Tempo's-U.S. Gov't.	5,300
1983-1985 Police Car Retrofits	530
1985 Other Fleets (1)	2,100
Privately-Owned	
1983-85 Mercedes	11,500 (latest estimate)

Airbag-Equipped Vehicle Exposure

Vehicle	**Total Estimated Mileage**
Tempo's-U.S. Gov't.	25 million
Tempo's-Other Fleets	10 million
Police Fleets	21 million
Mercedes-Benz	Unknown

Results of Fleet Experience to Date

Experience with the current generation airbag fleet has been very positive. The airbags deployed in cases where crash protection was desirable, and there have been no failures to deploy when needed. Airbags have deployed only in accidents where they were designed to deploy. When airbags deployed, injuries were relatively minor.

(1) Airbag-equipped Ford Tempo's in private fleets.
(2) There were two deployments in police cars struck while parked with engines running.
(3) Some data may be missing because individuals were unwilling to provide information or vehicles had been repaired prior to the investigation.
(4) The accident notification criteria and level of injury information available on nondeployment accidents vary with each fleet of cars.

Deployment Accidents (**)

D/P — Driver/Front Passenger

	Accidents	AIS-0	AIS-1	AIS-2	AIS-3	AIS-4	AIS-5	AIS-6
Tempo-Gov't	16	4/1	9/2	3/0	0/0	0/0	0/0	0/0
Police Cars (2)	20	4/1	14/3	0/0	0/0	0/0	0/0	0/0
Mercedes (3)	5	2/0	3/0	0/1	0/0	0/0	0/0	0/0
Others (3)	2	0/0	1/0	0/0	0/0	0/0	0/0	0/0
Total	43	10/2	27/5	3/1	0/0	0/0	0/0	0/0

Primary Damage Area in Deployment Accidents: Front - 34; Side - 3; Undercarriage - 6

Nondeployment Accidents

	AIS-0	AIS-1	AIS-2	AIS-3	AIS-4	AIS-5	AIS-6
Tempo's U. S. Gov't	178	7	0	0	0	0	0
Police Cars	2	0	0	0	0	0	0
Mercedes	0	2	0	0	0	0	0
Others	0	0	0	0	0	0	0
Total	180	9	0	0	0	0	0

The Breed All-Mechanical Airbag Module

Allen Breed
Breed Corporation

For almost a quarter of a century, Breed Corporation has engaged in the quest of finding simple mechanical solutions to complicated engineering problems in both the military ordnance and civilian arenas. In the field of automotive safety, Breed Corporation pioneered retrofit installation of conventional electrical driver side airbags. We are presently producing the electrical crash sensors used in the airbag-equipped Ford Tempo/Topaz vehicles. However, my presentation today will focus on our all-mechanical airbag module.

We approach our problems analytically. Our standard procedure is to develop a computer simulation, via math modelling, as our major problem-solving and design tool. Once we arrive at a mathematical solution, we design as simple a mechanical device as possible for use in the field. That is the road—long, tortuous, and hard as it is—that we followed in the airbag case.

We developed three basic proprietary computer math model simulations for our airbag work. First was our sensor simulation model to predict the sensor trigger time for various types of crash sensors. We further developed our VODS 1 and VODS 3 (Vehicle Occupant Dynamics Simulator) models to predict the occupant injury measures for various vehicle crashes and occupant sizes as a function of airbag system design. In conjunction with these computer models, we worked with our own extensive automobile proving ground crash library of more than 1,000 instrumented crashes. With these tools, we constructed an acceptable sensor response curve for a sensor mounted outside the crush zone—in the steering wheel for the driver side and in the instrument panel for the passenger side. We designed a sensor with a response curve that would not allow the airbag to deploy in minor accidents or bumps, but would act in sufficient time in a crash to keep injury levels well below those specified in FMVSS 208. We then built such a sensor and married it to a simple mechanical military type initiator. Finally, we placed our Breed Sensor/Initiator inside the gas generator itself to create, with the addition of a fabric bag, the Breed All-Mechanical Airbag Module.

Figure 1 depicts the Breed All-Mechanical Sensor/Initiator. In a crash with a deceleration of more than four G's, the ball-sensing mass will move forward. If airbag deployment is needed, the ball will push the bias lever far enough to release a cocked firing pin, which initiates a prime, thereby initiating the gas-generating material and inflating the airbag. We build two separate and independent sensor/initiators into each of our units to provide high statistical reliability.

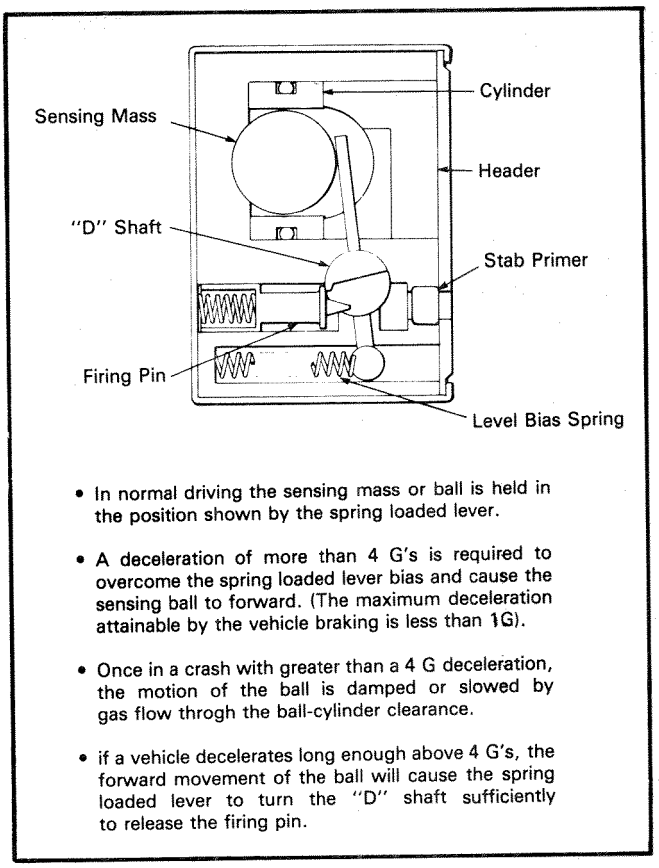

Figure 1. Breed airbag crash sensor initiator

Most airbag systems place crash sensors in the vehicle's frontal crush zone (Figure 2). In a crash, these sensors act as an electric switch connecting the battery to an electric squib in the gas generator, which then initiates airbag deployment. These conventional systems also require electrical wiring connecting the sensors to the battery and up the steering column; a slip ring; an electric squib; an auxiliary power supply; and an electronic diagnostic system that monitors all airbag wiring and components for opens or shorts. All of these elements are eliminated in our All-Mechanical Airbag Module (Figure 3). As such, it is substantially simpler to both build and install, providing higher reliability at significantly less cost.

When working with individual automobile manufacturers, we design an appropriate airbag system, using our computer math modelling to define the desired knee bolster, steering column, gas generator, sensor, and airbag characteristics for the specific vehicle under consideration.

Because of confidentiality arrangements, it is not possible to discuss our present activities with specific automobile manufacturers. We can, however, talk in detail about our crash test results in a demonstration contract we have with Mike Finkelstein's Office of

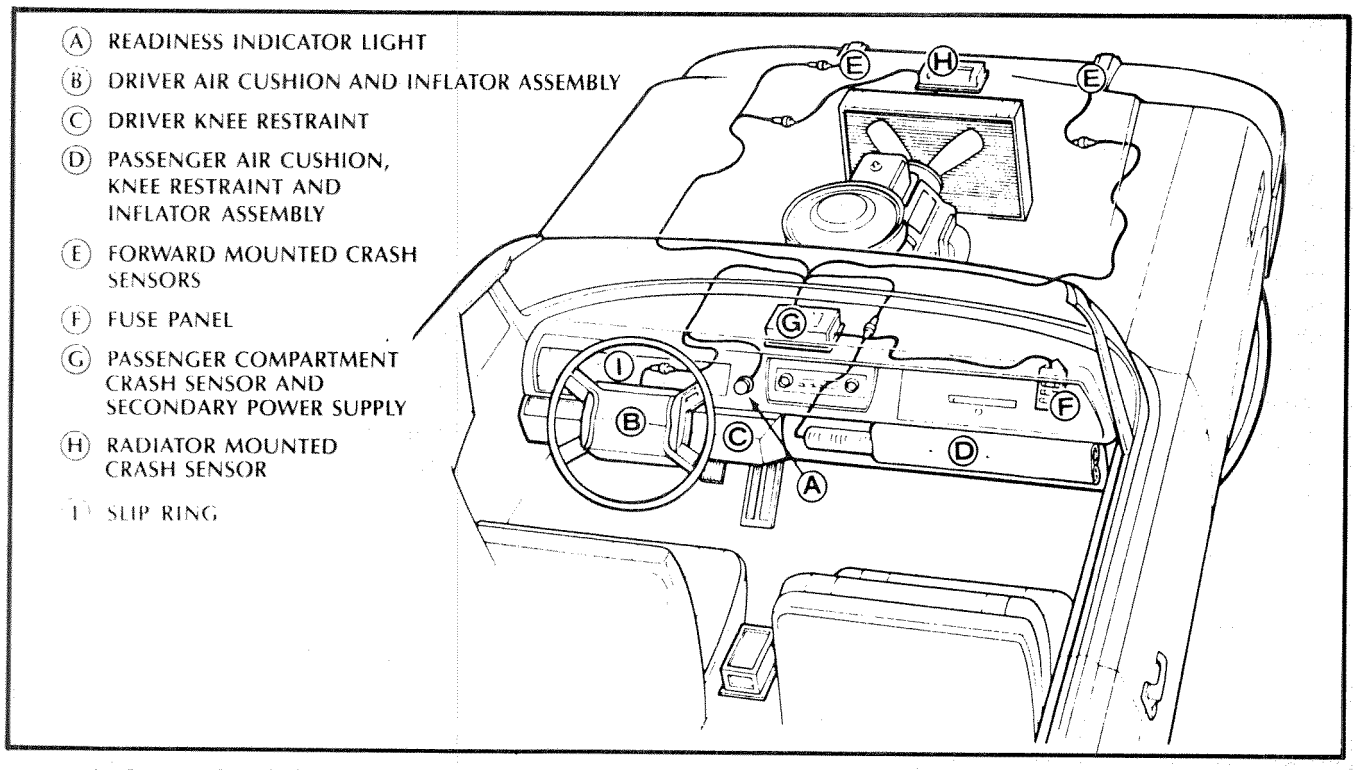

Figure 2. Conventional air cushion safety system

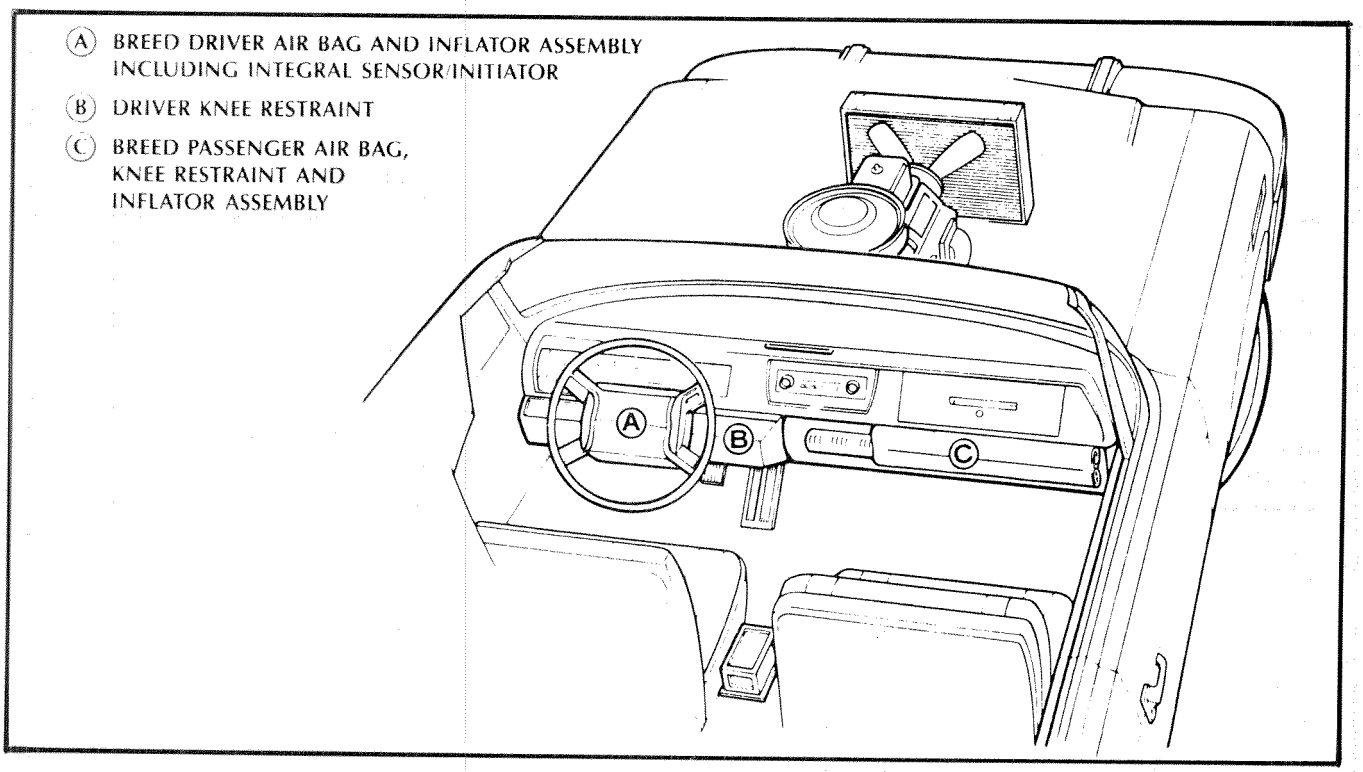

Figure 3. Breed airbag module

Research & Development at the National Highway Traffic Safety Administration. We now have had and analyzed five successful crash tests of our driver side All-Mechanical Compact Airbag System retrofitted into three Ford LTD's, a Dodge Diplomat, and a Chevrolet Impala. The test results are summarized in Table 1. Suffice it to say, the dummy injury levels achieved in these tests have been highly satisfactory.

We have also run a series of Chevrolet Impala sled tests, again with excellent results. Table 2 highlights these results. Probably the two most significant sled test conclusions are that: (1) the Breed All-Mechanical Compact Airbag System provides highly effective crash protection on its own, and (2) when used in conjunction with a 2- or 3-point belt system, it dramatically improves the performance of the seatbelt system.

Finally, I would like to address the five specific points presented to all panelists.

1. In considering optimum airbag performance, how critical is it to tune an airbag system to the characteristics of a specific vehicle?

An airbag system must at least be tuned to each generic vehicle type, based on the stiffness of the crash pulse and the occupant seating position. The use of sophisticated computer math modelling is critical to tuning an airbag system for specific vehicle types. To optimize airbag performance, we must concern ourselves with the candidate vehicle's crash pulse, its interior ergonomics, the steering column and knee bolster characteristics, the sensor and gas generator response curves, and the airbag size and venting parameters.

Table 1. Breed all-mechanical airbag crash tests

NATURE OF CRASH TEST	DATE	HIC	CHEST G'S	LEFT FEMUR	RIGHT FEMUR
1979 Ford LTD 30 mph Frontal Barrier	6/26/84	247	44	1,450	1,820
1979 Ford LTD 12 mph Frontal Barrier	7/26/84	25	20	1,100	1,015
1980 Ford LTD 30 mph Centerline	8/08/84	187	43	1,350	1,310
1983 Dodge Diplomat 30 mph Frontal Barrier	12/20/84	461	49	2,100	1,500
1983 Chevrolet Impala 30 mph Frontal Barrier	1/10/85	289	44	1,850	1,000

Table 2. Chevrolet Impala sled test results

		50% Male and 5% Female 30mph Barrier Equivalent Velocity					
Test Condition	Injury Measures	Breed A/B System Only	Breed A/B Sys. & 2-pt	Breed A/B Sys. & 3-pt	3-Point Belt Only	2-Point Belt Only	No Restraint
50% Male 30mph	HIC	215	160	291	855	734	651
	Chest G	32	30	39	39	72	90
	Femur L	1,080	750	670	170	290	2,540
	Femur R	1,250	460	460	390	500	1,220
5% Female 30mph	HIC	551	228	585	1,635		
	Chest G	46	45	51	58		
	Femur L	550	340	300	300		
	Femur R	700	280	500	200		

After analyzing many crash pulses, it appears the response curve of the Breed All-Mechanical Sensor/Initiator probably will remain the same from vehicle to vehicle. After all, the crash pulse that activates the interior crash sensor is the same pulse that propels the occupants forward.

2. Airbag applications in small cars, both at the driver and passenger position.

We believe we will be able to supply suitable All-Mechanical Compact Airbag Modules for the driver and passenger side of small cars as well as large ones, if steering column and dash intrusions are not severe.

Using our sensor and VODS models, we have analyzed more than 600 crashes of various types of vehicles, including many small cars. The spectrum of crashes included head-on barrier and pole crashes, angled crashes, and car-to-car collisions. Results indicated that in all but two cases, the Breed All-Mechanical Airbag System would have kept injury measures below 80 percent of the requirements of FMVSS 208. Even for the two cases, the FMVSS limits were not exceeded(1).

3. Prospects for passenger airbag systems in vehicles with two designated seating positions and in vehicles with bench seats.

To date, we have dealt only with vehicles having two designated front seating positions. We believe the automobile manufacturers will follow the Federal administrative rule providing for active seatbelt protection for a center front seat passenger.

4. Prospects for reducing system costs.

There have been at least three independent cost estimates to date of the driver side Breed All-Mechanical Airbag Module. A summary breakdown of these estimates is shown in Table 3. The first column is our own estimate, based on an automated production volume of 1 million units per year. The second is by Mr. Ed Clary, a retired senior automotive engineer, at the same 1 million per year production rate; the third is an in-depth cost analysis under an independent NHTSA contract by Corporate Tech Planning along with Pioneer Engineering. This last set of figures is based on 300,000 units per year only and does not assume automated production.

Each of these estimates confirms that the Breed All-Mechanical Airbag Module would be substantially less expensive than conventional electrical airbag systems.

For the passenger side, a Breed All-Mechanical Airbag Module should cost, at maximum, no more than double that of the driver side. Accordingly, if current overall production were to exceed 300,000 units per year, the cost to any individual car manufacturer for a complete driver and passenger side Breed All-Mechanical Airbag Module System would be under $165. And, if current overall production were to exceed 1 million units per year, a complete driver and passenger module system would drop to under a $95 dealer cost.

5. FMVSS 208 injury criteria and its impact on airbags.

We were pleased to see a General Motors proposal in the recent DOT/NHTSA proposed rulemaking that suggested different injury level limits for airbag/belt restraints. For a new injury level measurement of chest deflection, General Motors suggested a 3in chest deflection limit for distributed loading restraint systems such as airbags and a 2in chest deflection limit for the lap/shoulder belt. We agree. We also feel the occupant safety industry, automobile manufacturers, insurance companies, con-

Table 3. Independent cost estimates of drivers side Breed all-mechanical compact airbag module

	BREED	CLARY	CTP/ PIONEER
(Units Per Year)	(1 Million)	(1 Million)	(300,000)
Sensor	$ 5.00	$ 7.56	$11.49
Gas Generator	15.00	25.21	16.45
Airbag/Cover/Mounting Plate	8.00	8.00	20.35
Total Manufacturing Cost	28.00	40.77	48.29
Manufacturer Profit (15%)	4.00	6.12	7.24
Cost to Distributor/Dealer	32.00	46.89	55.53
Dealer Profit (30%)	10.00	14.07	16.66
Installation	5.00	5.00	8.05
Total Cost to Consumer	$47.00	$65.96	$80.24

sumer groups, and the government should now focus on establishing different injury criteria for airbag restraints, active and passive seatbelt restraints, and friendly interior protection systems because of the different character of loadings produced by these systems. Current evidence indicates that present safety criteria of 1,000 HIC and 60 chest G's are conservative estimates for injury criteria using an airbag system.

I would like to thank our Chairman, Mike Finkelstein, for inviting me to participate in this panel discussion about state-of-the-art airbag technology. I would be happy to answer any questions you might have.

Acknowledgments

I wish to acknowledge the invaluable contribution provided by Thomas C. McGrath, Jr., Dr. Russel Brantman, Dr. Ria Breed, and Ms. Cynthia Werthamer in the preparation of this paper.

References

1. Brantman, Russel, and David Breed, "Use of computer simulation in evaluating airbag system performance," SAE Paper 851188, Washington, D.C., May 1985.

Supplemental Driver Airbag System—Ford Motor Company Tempo and Topaz Vehicles

Roger E. Maugh
Director, Automotive Safety Office,
Ford Motor Company

Abstract

This paper describes Ford's supplemental airbag system that is available to commercial fleet users in the United States on Tempo and Topaz car lines. Several key components of the system were based on designs used in a 1981 experimental program. Design considerations in adapting that experimental system to a smaller production vehicle are presented.

In my discussion, I would like to describe the supplemental driver-side airbag system currently being sold as a commercial fleet option in the United States on Ford's Tempo and Topaz compact front-wheel-drive car lines. This system went into production early this year. It was developed in part on the basis of experience we gained with an experimental design originally developed for the full-size 1981 Lincoln Town Car. The Town Car is a large luxury car, approximately 43in (1,088mm) longer and 1,540 lb (700kg) heavier than the Tempo/Topaz. Since the focus of our panel discussion is on airbag technology and optimizing airbag system performance, I would like to describe a few of the changes Ford made during a nearly 2-year program to adapt the experimental Lincoln-based airbag system to the much smaller Tempo/Topaz vehicles.

First, the Ford supplemental driver-side airbag system consists of—

- An airbag module mounted in the steering wheel
- A unique steering wheel and column
- An airbag readiness indicator light
- Five crash sensors mounted in four locations
- A unique wiring harness
- An electronic diagnostic module

Each of these airbag system components had to be redesigned and/or recalibrated in order to work in the smaller Tempo/Topaz models.

The process of redesigning the airbag system for the Tempo/Topaz involved two basic aspects of system performance:

- Meeting crash sensing requirements
- Meeting occupant restraint requirements, including
  - — Inflation geometry/dynamics
  - — Dummy test "injury criteria" (with and without belts)

Let's discuss these in more detail. First, the Tempo Topaz crash sensing system has been designed to do the following:

- To detect and deploy in frontal impacts above a 14mph (22.4kph) perpendicular barrier crash equivalent
- To not deploy in frontal impacts below an 8mph (12.8kph) perpendicular barrier crash equivalent
- To detect impacts that are concentrated inboard (pole), outboard (offset and angular), high (truck), and low (fixed object)
- To differentiate between impact and nonimpact signals
- To supply the firing signal to the bag assembly on a timely basis

To meet these objectives, the sensing system uses three primary sensors and two secondary sensors. All of the primary sensors are located across the front of the vehicle; two are mounted low outboard and one is mounted high at the vehicle centerline. One of the two

secondary sensors, which confirm the crash, is mounted at this same high centerline position and the other is mounted back on the dash panel.

Electrically, the three primary sensors are wired in parallel and the two secondary sensors are wired in parallel. The firing circuit consists of a series loop formed by the parallel group of primary sensors, the ignitor, the parallel group of two secondary sensors, and the battery. Firing occurs when any primary sensor and any secondary sensor are simultaneously closed for at least 3ms.

The sensors, which are manufactured by the Breed Corporation, use a bias magnet to hold a ball that, at a specified deacceleration, will pull away from the magnet and move through a tube to touch two electrical contacts that close the circuit. These sensors are sealed in a shock-mounted assembly so the motion of the ball is not impeded by off-axis vibrations.

Selection of the sensor design for each location is an iterative process. The first step is to run a series of crash tests to obtain the vehicle's crash signature at the desired sensor locations. This is followed by computer modeling of the crash sensor by the sensor manufacturer to select the sensor component specifications that will provide the sensor design objectives specified by Ford. Design variables within the sensor, such as magnet bias, ball-to-tube clearance, and ball travel, can be adjusted to meet the design objectives. The final system design can then be confirmed by an additional series of fully instrumented crash tests.

On the Tempo/Topaz program, we ran 17 crash tests at different speeds and angles to get crash signatures at a number of prospective sensor locations. Some locations were eliminated, based on the lack of a good acceleration signal at that point. Based on these data and modeling work by the sensor manufacturer, sensor locations and tentative "calibrations" were selected as follows:

	Location	Calibration (at Location)
Primary Sensors		
Left	Left front fender apron	10mph (16kph)
Center	Center of radiator support	10mph (16kph)
Right	Right front fender apron	10mph (16kph)
Secondary "Safing" Sensor		
Forward	Center of radiator support	3.5mph (5.6kph)
Rear	Centerline of dash panel	1.1mph (1.8kph)

I should point out that when we identify a primary sensor calibration as 10mph (16kph), the speed refers to the speed of the test device used by the sensor manufacturer to insure compliance with Ford's 14mph (22.4kph) closure design objective. In other words, the 10mph (16kph) haversine test device pulse is equivalent to an actual 14mph (22.4kph) crash pulse in terms of causing sensor closure.

Each sensor must pass six individual production acceptance checks—three for insuring that it will close or fire at a 10mph (16kph) velocity change with soft/medium/hard g (haversine) pulse widths—and three for insuring that it will not close or fire when subjected to 6.5mph (10.4kph) velocity change with soft/medium/hard g (haversine) pulse widths. And might I add that all of these checks are performed twice on every sensor shipped to Ford, once during the manufacturing process and again after final sensor assembly.

After the sensors were designed by the sensor manufacturer, the system was subjected to a series of nine validation crash tests. The test program included crashes at various speeds and types. For example, we ran angular, perpendicular, truck underride, car-to-car, and pole-type tests. The end result of this process is shown on the attachment. For all crash pulses above the shaded area, sensors will close and a firing signal will occur (such as the 31mph and the 14.8mph pulses shown on the chart). For crash pulses in the shaded area, sensor closure and a firing signal may occur. For all crash pulses below the shaded area (about 8mph), no closure or firing will occur.

The system was also tested in the laboratory and on the track for durability, corrosion resistance, and other normal vehicle operating conditions. However, even with all of this test and development work, we still need extensive on-the-road experience to confirm our sensing system design. This is one of the primary benefits we hope to get from the NHTSA-GSA fleet program and the other fleet units now going into service.

The second major area of airbag system performance involved in redesigning the system for the Tempo/Topaz was to meet the occupant restraint requirements. As I mentioned earlier, this involved—

- Inflation geometry and dynamics
- Dummy test injury criteria (with and without belts)

Since the basic relationship between the driver and the steering wheel is essentially common in most cars, it was initially assumed that the driver airbag module developed experimentally for the Lincoln could be used with little change for the Tempo/Topaz installation. A study of the crush characteristics of the Tempo/Topaz showed that even though it is substantially smaller than the 1981 Lincoln, there is still sufficient crush space—approximately 24in (610mm)—with its resultant delay of the crash pulse reaching the occupant compartment—to permit the use of the nonaggressive bag fill incorporated in the original Lincoln airbag design. However, a crash test identified another reason for making significant changes to the Lincoln airbag module. The experimental Lincoln design used a firm unvented airbag that transmitted virtually all of the dummy energy into the steering column. It was concluded that the smaller Tempo/Topaz

models needed a softer bag that would absorb some energy through a vent system.

Our engineers also decided to add a strap system to the bag to control bag shape during inflation. These two bag changes (vents and straps) required a comprehensive sled test program to evaluate alternative bag sizes, inflator calibration levels, and vent sizes. Following the sled test program, our engineers selected a 26-½in (64.8cm) diameter bag with two 1.1in (28mm) vents and the original experimental Lincoln inflator or gas generator calibration.

This package was then put through a series of development crash tests primarily aimed at confirming that the 30mph (48kph) belted and unbelted GSA contract requirements would be met. Typical test levels for the system at this point in the program were as follows:

30mph (48kph) Perpendicular Barrier Test Results

Driver	Belted	Unbelted
HIC	823	524
Chest G	46	47
Left Femur (#)	414	1,663
Right Femur (#)	1,346	1,750

Throughout the development program, the primary focus had been on meeting the 30mph (48kph) contract criteria, although several tests had been run at 35mph (56kph) with HIC results (belted) within the 1,000 range.

Just before production startup, production level vehicles were tested at 30mph (48kph) to demonstrate the contract requirements had been met. In addition, we tested one at 35mph (56kph) to confirm the results were not out of line at this higher speed.

The results were good at 30mph (48kph) but not what we expected or wanted for 35mph (56kph) tests.

	30mph (48kph)		35mph (56kph)
	Belted	Unbelted	Belted
HIC	653	721	1,202
Chest G	49	58	55
Left Femur	675	1,258	967
Right Femur	898	1,198	1,922

At this point, it was clear that if we wanted lower test results at 35mph (56kph), we were going to have to soften the bag some more. Another sled test series was run to evaluate the effects of larger vents at different speeds, belted and unbelted. From this work, it was determined that 1.6in (40mm) vents could be used to provide lower test results at 35mph (56kph) for the belted configuration and still not "strike thru" at 30mph (48kph) for the unbelted configuration.

New production level vehicles were then prepared and tested with the revised 1.6in (40mm) vent system.

	30mph (48kph)		35mph (56kph)
	Belted	Unbelted	Belted
HIC	540	377	550
Chest G	52	52	52
Left Femur	505	1,340	452
Right Femur	622	1,804	1,175

Test results were acceptable, and production started in January 1985. We are satisfied that the Tempo/Topaz airbag provides good supplemental protection at test speeds up to at least 35mph (56kph). Although we have not tested the system at test speeds above 35mph (56kph), we believe it also will provide added protection at higher speeds.

Designing the supplemental airbag system to meet NHTSA's injury criteria at both 30 and 35mph (48/56kph) probably affected its performance characteristics at other speeds. As test speeds increase, the possibility of upper torso or head "strike thru" also increases. As we move ahead to future airbag installations, we think it will be important for NHTSA and manufacturers to learn more about injury thresholds when impacting airbags and the relationship between test speed and "strike thru" to be sure we aren't sacrificing real-world protection just to satisfy an artificial test objective.

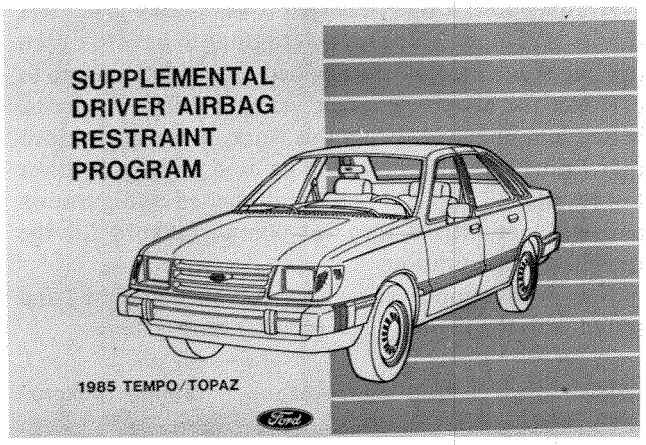
SUPPLEMENTAL
DRIVER AIRBAG
RESTRAINT
PROGRAM
1985 TEMPO/TOPAZ
Ford

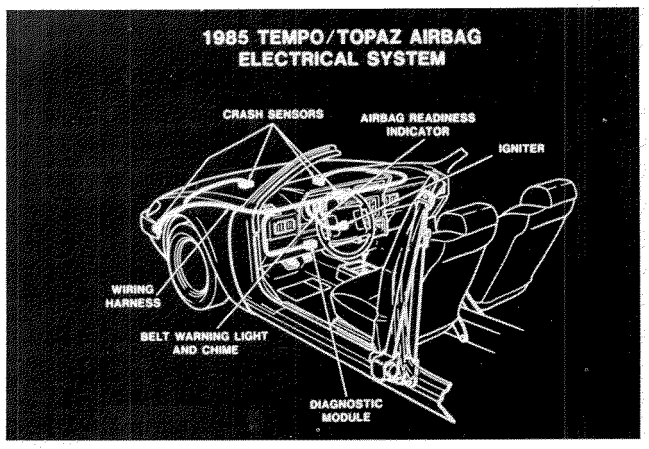
1985 TEMPO/TOPAZ AIRBAG
ELECTRICAL SYSTEM
CRASH SENSORS
AIRBAG READINESS
INDICATOR
IGNITER
WIRING
HARNESS
BELT WARNING LIGHT
AND CHIME
DIAGNOSTIC
MODULE

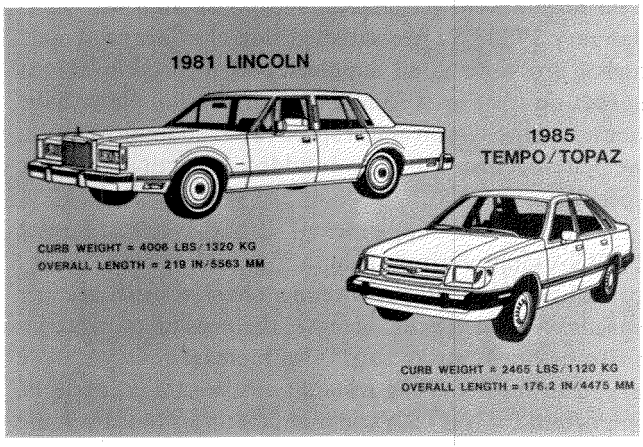
1981 LINCOLN
1985
TEMPO/TOPAZ
CURB WEIGHT = 4008 LBS/1320 KG
OVERALL LENGTH = 219 IN/5563 MM
CURB WEIGHT = 2465 LBS/1120 KG
OVERALL LENGTH = 176.2 IN/4475 MM

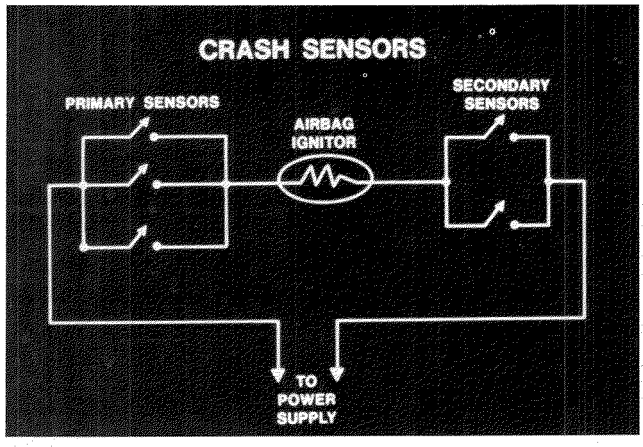
CRASH SENSORS
PRIMARY SENSORS
AIRBAG
IGNITOR
SECONDARY
SENSORS
TO
POWER
SUPPLY

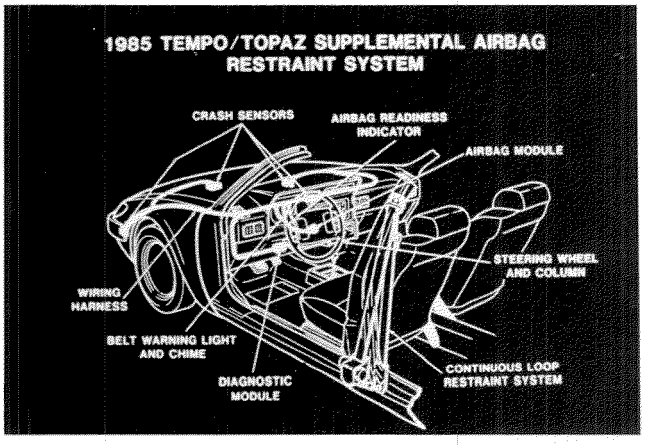
1985 TEMPO/TOPAZ SUPPLEMENTAL AIRBAG
RESTRAINT SYSTEM
CRASH SENSORS
AIRBAG READINESS
INDICATOR
AIRBAG MODULE
STEERING WHEEL
AND COLUMN
WIRING
HARNESS
BELT WARNING LIGHT
AND CHIME
DIAGNOSTIC
MODULE
CONTINUOUS LOOP
RESTRAINT SYSTEM

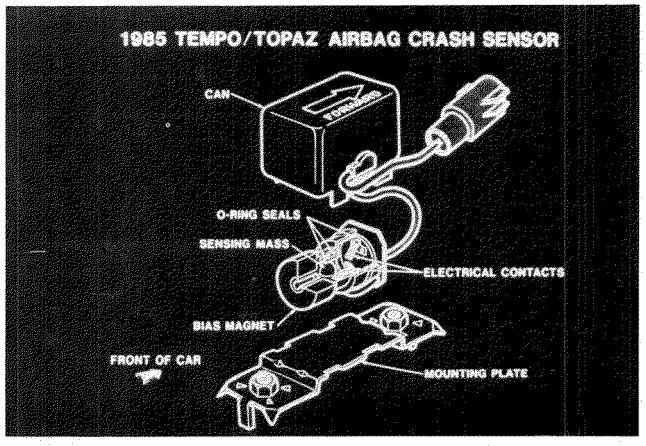
1985 TEMPO/TOPAZ AIRBAG CRASH SENSOR
CAM
O-RING SEALS
SENSING MASS
ELECTRICAL CONTACTS
BIAS MAGNET
FRONT OF CAR
MOUNTING PLATE

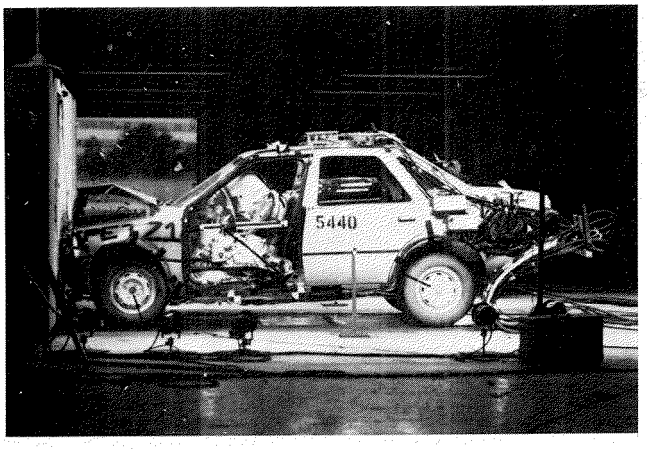

FMVSS 208 INJURY CRITERIA

HIC ≤ 1000
CHEST g ≤ 60*
FEMUR LOAD ≤ 2250#

* ALLOWS PEAKS ABOVE 60 FOR A CUMULATIVE PERIOD NOT TO EXCEED 3 MILLISECONDS

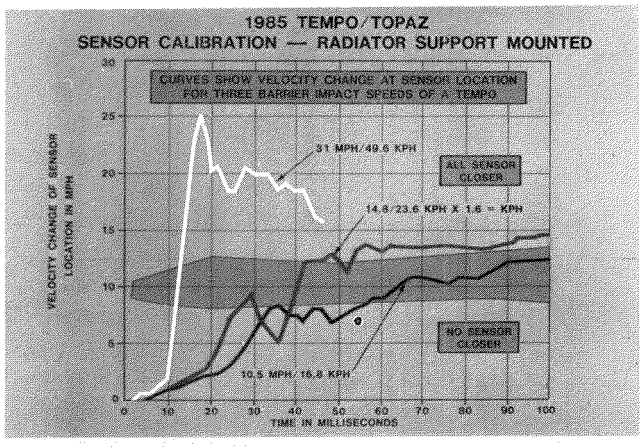

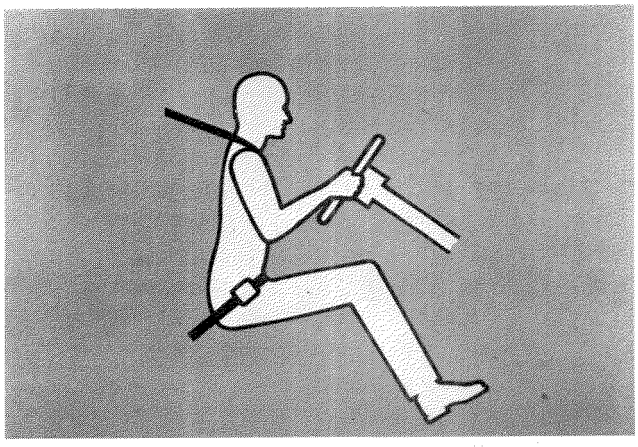

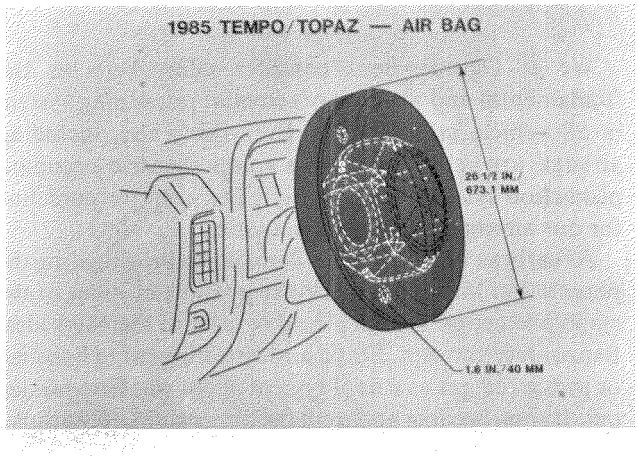

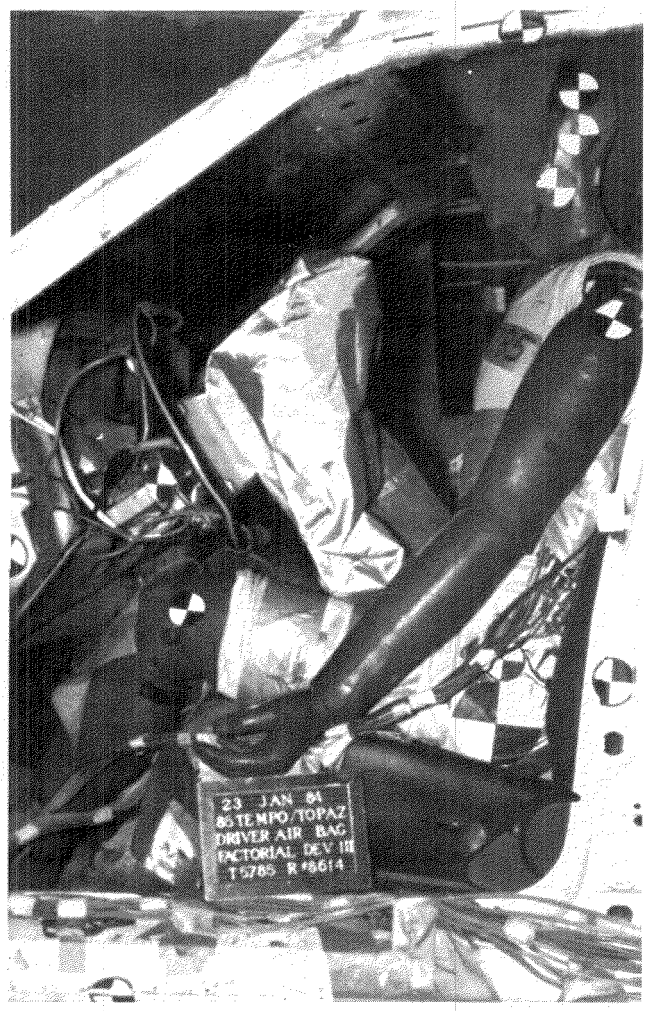

The Daimler-Benz Supplemental Restraint System

Prof. Dr. Ing. W. Reidelbach
Daimler-Benz AG

We at Daimler-Benz consider safety belts as the fundamental and absolutely essential restraining system in all vehicle crash modes. Everything else, including airbags, are supplements to a comprehensive occupant protection system. This principle has been the guideline for our airbag development activities.

As early as 1966, Daimler-Benz began investigating the potential of airbags as a further possible element of the crash protection system already a part of the Mercedes-Benz safety concept. Static airbag testing using liquified or pressured gas as a deployment agent was first carried out. It soon became apparent the dimensions of the bulky devices available at this time were impractical for installation in Mercedes-Benz passenger cars.

In 1969 we turned to an entirely new technology of bag deployment and materials because of our earlier experience and knowledge; in 1970 we initiated the development of a solid propellant gas generator that could be packaged into the hub of the Mercedes-Benz steering wheel without sacrificing the protective function of the kinetic energy-absorbing elements of the wheel. This was done in cooperation with Bayern-Chemie, and later with Morton-Thiokol. Today a German or an American gas generator is used to inflate the 60-liter driver airbag.

To trigger the system, we have selected an electronic solid state deceleration sensor. The prime function of the sensor is to measure deceleration forces and determine whether the impact speed is above the predetermined triggering threshold. If the threshold has been exceeded, the triggering signal will initiate the firing sequence. The

sensor is also responsible for monitoring and registering system readiness.

Considerable testing of the performance of the components and the total system has been conducted since 1970, including thousands of gas generator performance tests, static bag inflation tests, impact simulations on sleds, and full-scale crash tests. Several hundred company cars were equipped with the driver airbag system and field tested.

In 1980 the mileage accumulated during field operation of the test fleet exceeded 80 million road kilometers, and the system was released for production.

We started offering as an option the Supplemental Restraint System (a driver airbag system, together with an emergency tensioning belt retractor for the passenger) in December 1980 on the S-class models only, then, in spring 1982, on all models in certain European countries. For model year 1984, the system was offered also in the United States and Canada. As of June 1985, about 60,000 Mercedes-Benz cars with driver airbags had been delivered worldwide, about 14,000 of these in North America.

The functional reliability of the system has proved very satisfactory. We were informed on accidents with or without airbag deployment. All nondeployment cases occurred at a very low impact severity level, i.e., below the triggering threshold.

In all cases with an impact severity level at or above the threshold, the bag was inflated. There was no inadvertent deployment. The system has functioned as designed.

The Police Fleet Airbag Retrofit Program

David Romeo
Romeo Kojyo Co., Inc.

The Police Fleet Airbag Retrofit Program has been progressing successfully. With initial placement of systems into police vehicles in December 1983 and approximately 450 airbag-equipped vehicles on the road, there have been—

1. No occurrences of airbag deployment without a reportable accident
2. Approximately 25 to 30 accidents of varying intensity resulting in 18 deployments
3. No significant injuries in any of the accidents
4. No cases where an accident occurred in which the airbag should have deployed and did not

Evaluation of the system is continuing.

Since a progress report on the program was submitted to the conference in written form (paper by Romeo and Morris), no further discussion of the program will be presented. Instead, this presentation will respond to the chairman's specific areas of interest, which were—

1. Considerations for optimizing airbag performance. How critical is it to tune an airbag system to the characteristics of a specific vehicle?
2. Airbag application in small cars both at the driver and passenger position.
3. Prospects for passenger airbag systems in vehicles with two designated seating positions and in vehicles with bench seats.
4. Prospects for reducing system costs.
5. FMVSS 208 injury criteria and its impact on airbags.

Succinctly these concerns are addressed as follows:

1. Optimizing airbag performance.

From the standpoint of designing an airbag system less sensitive to vehicle design considerations than manual belts, there is less need to tune. The need to tune an airbag is driven more by subjecting its performance to FMVSS 208 dummy criteria evaluation (as opposed to the manual belt, which has no such requirement) than it is to any inherent sensitivity of airbag systems to vehicle differences. (One acknowledged exception to this are systems that use sensors located remote from the crush zone.)

Quite a bit has been said by automobile manufacturers regarding the difficulty of fitting an airbag to different cars. It is interesting to note, however, that there is in fact little or no difference across car line in the systems offered by each of the three companies that produce driver airbags. These car lines range in size from compact to luxury.

2. Airbag use in small cars was addressed very recently by John B. Morris in a paper entitled "Airbags For Small Cars," SAE Paper 851200, May 1985.

He compared predicted driver airbag performance in a large car, full size, or Ford LTD versus a subcompact Chevrolet Chevette. The fatality risk for drivers of cars of these classes based on an analysis for two vehicle crashes by Cerrelli (see above paper) is five times greater for the small car. Yet, airbag restraint capability degrades only from 17.9 to 35.6 percent of allowable HIC and 47 to 65 percent of allowable C_R between these cars.

Therefore, the obvious conclusion is that although on an absolute basis airbag system performance is degraded in a small car, on a relative basis the potential benefits of the airbag in the small car are far greater than they are in a large car. Putting it another way, both my Toyota Corolla and my Datsun Pickup have airbags.

3. With regard to passenger airbag systems, with recent FMVSS 208 exemption for automatic protection for the center front passenger, one can forget about a full bench seat (three front passengers) airbag system. Besides, airbag technology is now being led by the Europeans (spelled Mercedes and BMW) and they do not have a bench seat. For the right front passenger, introduction of airbag systems are imminent.
4. Cost reduction can be effected in two ways:
   - Make the system simpler
   - Make a large number of systems

Holding quantity of production constant, i.e., 1,000/yr, 10,000/yr, 100,000/yr, etc., the recently reintroduced "all-mechanical system" promises a cost reduction of approximately 15 percent through elimination of diagnostic, wiring harness, and connector coil. Holding system design constant and increasing production from 1,000/yr to 10,000/yr or 100,000/yr shows cost reductions of 50 and 75 percent, respectively. It is obvious, therefore, that in the near future quantity considerations will overwhelm all others with regard to potential cost reduction.

5. Regarding FMVSS 208, it has been concluded that the evaluation criteria of this rule are clearly inadequate for making comparable evaluations of the performance of belt and airbag systems. This is due primarily to the concentrated versus the distributed loading capabilities of belts versus airbags. An excellent discussion of this point appears in the proceedings of the 20th Stapp Car Crash Conference in a paper by Walsh and Romeo, "Results of Cadaver and Anthropomorphic Dummy Tests in Identical Crash Situations."

Passive Safety Belt Developments

Clement A. Detloff
General Motors, Fisher Guide Division

Abstract

The U.S. Department of Transportation National Highway Traffic Safety Administration MVSS 208 requirement for passive restraints and dynamic performance on 1987 vehicles confronted virtually every auto manufacturer selling in the U.S. market with the problem of equipping vehicles with passive restraint systems. This presentation touches on some of the problems and concerns associated with providing a passive belt system.

Introduction

From a manufacturing standpoint, the U.S. requirement for passive restraints in 1987 U.S. vehicles has created more changes to safety belt restraints and more challenge for the related businesses than any action since safety belts were legislated into U.S. vehicles in 1968. For the vehicle manufacturer, the performance of the restraint system in the vehicle becomes an added concern since the injury performance criteria required in the standard must be met by all vehicles. Dynamic performance repeatability and the ability to meet requirements at different test facilities with different test personnel present some concern. For the hardware manufacturer, the compliance to world seatbelt laws covering the components must still be met along with the added requirements of the vehicle manufacturer to assure vehicle system dynamic performance compliance.

System Selection

The selection of any restraint system must take into consideration complying with the MVSS 208 requirements, providing overall safety to the system users, and also providing a usable and marketable product to the customer. The user comfort and convenience of the system is a major concern as well as compatibility with the vehicle, such as rear seat passenger entry, driver visibility, and overall appearance. GM's previous experience with the passive safety belt systems and other passive restraint systems has not been good from a customer acceptance standpoint. Air restraint and passive safety belt vehicles produced by General Motors in the past were difficult to market due to lack of customer acceptance, and the sales projections were not achieved. Although some limited clinical data indicate that acceptance of passive restraint systems has improved and our state-of-the-art safety belt systems are more acceptable to the potential buyer, we do not have clinical data to definitely establish the system that customers prefer today. The time limitations to meet the 1987 production also provide limitations in tooling and manufacturing of some possible restraint systems. In addition, the interior styling and general configuration of a vehicle can provide some limiting factors. Examples are door frames or frameless glass. The differences in legal requirements between countries also provide some concern and limitations with regard to system selection. They have an effect on anchorage locations and actual performance of system hardware.

Body-Mounted 2-Point Passive Belt Systems

Body-mounted retractor 2-point passive restraint systems (Figure 1) use a single retractor that is body-mounted in the center of the vehicle with the upper or shoulder belt anchor located on the upper frame or B-pillar. Instrument panel knee bolsters or knee restraints are required with the system. The B-pillar-mounted anchor requires a power means to move the anchor forward on a guide track to allow vehicle entry and exit. From an engineering standpoint, the system presents limitations on center seating positions, use of center-mounted consoles, and proper placement of anchorages for optimum dynamic performance. Also, webbing tends to drag across the occupants when the system is operated during entry and exit. This type of system does not generally provide an emergency release latch, but an emergency or override of the retractor lock could be provided.

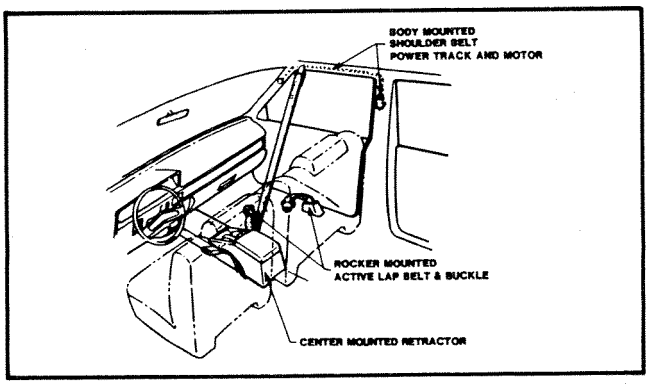

Figure 1. Body-mounted 2-point passive belt system

Door-Mounted 2-Point Passive Belt System

Door-mounted retractor 2-point restraint systems (Figure 2) use a single retractor mounted on the tunnel with an emergency release latch assembly mounted in the door area of the vehicle with instrument panel knee bolsters. The upper or shoulder anchorage of this system is door-mounted and moves with the door to allow for entry and exit. Two-point systems present some unique challenges both from a performance standpoint and from an engineering standpoint. From a performance standpoint, this type of system presents engineers additional challenges to provide adequate protection for various size occupants through the full range of seat adjustment travel. Like all restraint systems, these systems require tuning each vehicle system to assure performance over the full range considering all variables.

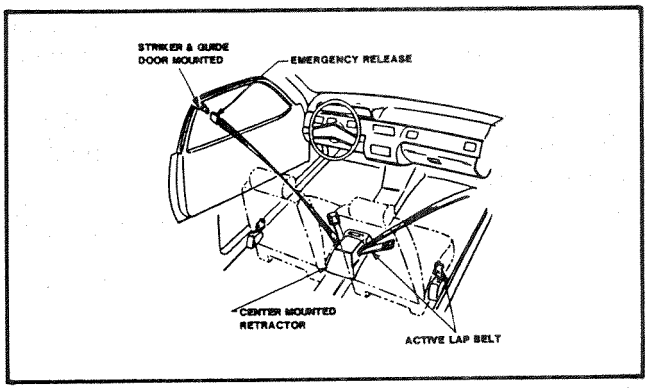

Figure 2. Door-mounted 2-point passive belt system

Door-Mounted 3-Point Passive Belt Systems

The door-mounted 3-point system (Figure 3) would use two door-mounted retractors with the shoulder belt and lapbelt anchorages located on the door, allowing the belts to move with the door for entry and exit and providing conventional safety belt restraint for the two outboard front seat occupants. By using door-mounted retractors, a center seating position still can be incorporated and the intrusion on center console space is eliminated. The instrument panel knee restraints are not required in most cases; however, in some specific vehicles, such a restraint may be required to insure proper dynamic performance. Dynamic performance with 3-point systems is similar to the conventional manual system; however, placement of anchorages and the use of any belt snubber has to be tuned to the vehicle to assure proper kinematics. This system allows flexibility of anchorage locations.

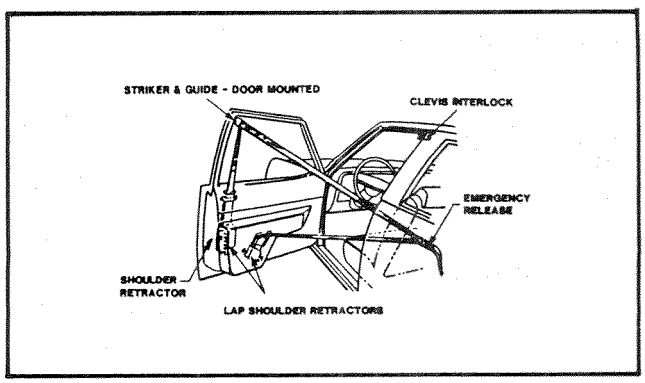

Figure 3. Door-mounted 3-point passive belt system

Complementary Interiors

The passive interior concept (Figure 4) would not require the use of conventional restraint systems to meet

the performance criteria but would use occupant kinematics and the interior services of the vehicle to control energy absorption. Any such system would be considered supplemental to the 3-point lap/shoulder belt system that would be provided in the vehicle, and its use would be recommended.

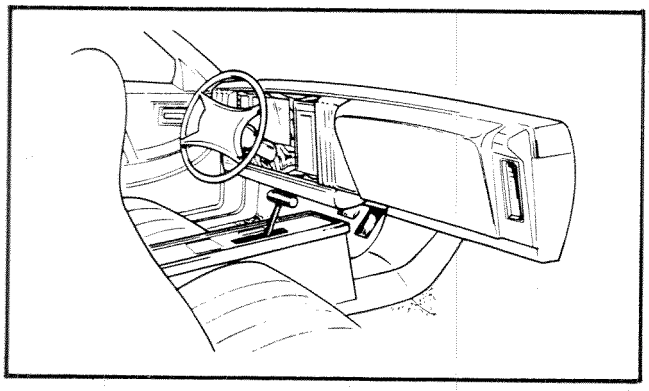

Figure 4. Complementary interior

Summary

In conclusion, various systems can be used to comply with the passive requirements. Any system requires evaluation of the vehicle configuration, vehicle crash performance, compatibility with vehicle environment, and overall acceptability aimed at the vehicle purchased to assure acceptance in the marketplace.

Automatic Belt Restraint Systems for Motor Vehicle Occupants

H. George Johannessen, P.E.
OmniSafe, Inc.

Abstract

Following early U.S. Government regulatory action requiring passive occupant crash protection for vehicle occupants covered by Motor Vehicle Safety Standard 208, intensive development began on passive seatbelts as promising alternatives to the inflatable systems being considered. The general types of passive seatbelt systems are identified. Passive systems that have been offered to date as optional installations in production car lines are described. Design considerations are discussed. Recent usage rates of installed passive systems are compared with manual belts.

Introduction

The U.S. Congress enacted the Highway Traffic Safety Act of 1966 to address the problem of traffic fatalities and injuries on American roadways. The National Highway Safety Bureau was quickly established to carry out the provisions of the new law. (The National Highway Safety Bureau later became the National Highway Traffic Safety Administration.) The late Dr. William Haddon, Jr., was appointed to head the new agency. He was a medical doctor with a long and distinguished role in public health and traffic safety in the State of New York. He viewed traffic fatalities and injuries as a public health problem of epidemic proportions that could best be overcome by passive means—that is, by means requiring no overt action on the part of the parties affected. He cited past examples of successful passive solutions to major public hazards, such as inoculation of entire populations to overcome dread diseases, pasteurization of milk, and use of automatic sprinkler systems to control fires.

Passive Systems for Passenger Cars

In November 1970, the U.S. Federal Motor Vehicle Safety Standard 208, which addresses vehicle occupant crash protection, was amended to incorporate the original requirements for passive restraints in the front seating positions of all passenger cars manufactured on or after the first day of July 1973 for sale in the U.S. car market. Challenges to these original requirements and original effective date resulted in a series of subsequent actions from 1970 to the present by legislative and judicial branches of the U.S. Government, in addition to the responsible regulatory agency, NHTSA, which reconsidered and revised requirements and effective installation schedules for passive occupant protection. The most recent action calls for passive occupant protection in front outboard seating positions on a phased-in schedule with installations in a minimum of 10 percent of the manufacturers' car build after September 1, 1986, 25

percent after September 1, 1987, 40 percent after September 1, 1988, and 100 percent after September 1, 1989. The passive requirement will be rescinded if States representing two-thirds of the Nation's population enact mandatory seatbelt usage laws before April 1, 1989, that will be in effect and enforced by September 1989.

The passive system for vehicle occupant protection that received immediate attention following the issuance of the original rulemaking in 1970 was the inflatable restraint, or airbag. Alternative noninflatable means, however, were considered as well. Many categories of such noninflatable passive candidate systems were identified, as shown in Table 1. These included transparent shields, deployable nets and blankets, cushions, restraining arms and barriers, integrated seat systems, and seatbelt systems.

Table 1. Noninflatable automatic occupant restraints

- Transparent Shields
- Deployable Nets
- Deployable Blankets
- Integrated Seat Systems
- Restraining Arms
- Cushions
- Seatbelt Systems

Developmental Passive Seatbelts

Of these various categories, passive seatbelts showed the greatest promise by far. Passive seatbelts were developed in many variations. Several distinctive classes may be identified. These are listed in Table 2. They may be 2-point, 3-point, or 4-point systems based on the number of load-bearing connections to vehicle structure. They may be all mechanical or may be all or partially motorized. They may have retractors located in either inboard or outboard locations and fixed anchors located either inboard or outboard. Some may require knee bolsters to control lower body movement. All must have some provision to permit disengaging the seatbelt after an accident. Prototypes of all these classes of systems have been developed and installed in production cars.

Table 2. Typical automatic seatbelt systems

2-POINT — Passive Shoulder Belt Only

3-POINT — Passive Lap and Shoulder Belts

4-POINT – Separate Passive Lap and Shoulder Belts

- Mechanical and Motorized Models in All Types

Installations in Production Car Lines

Some of the more promising developmental designs have been offered to the public in production cars. These are described in Table 3. The first production model to appear was a 2-point system, installed as an extra-cost option in a Volkswagen Rabbit in model year 1975 and subsequent years. Figure 1 shows the conceptual design of the Rabbit installation. This system includes a 2-point

Table 3. Production automatic seatbelt systems

CAR LINE	MODEL YEAR INTRODUCED	TYPE
VW RABBIT	1975	2-POINT
GM CHEVETTE	1978 ½	2-POINT
GM CHEVETTE	1980	3-POINT
TOYOTA	1981	2-POINT — MOTORIZED

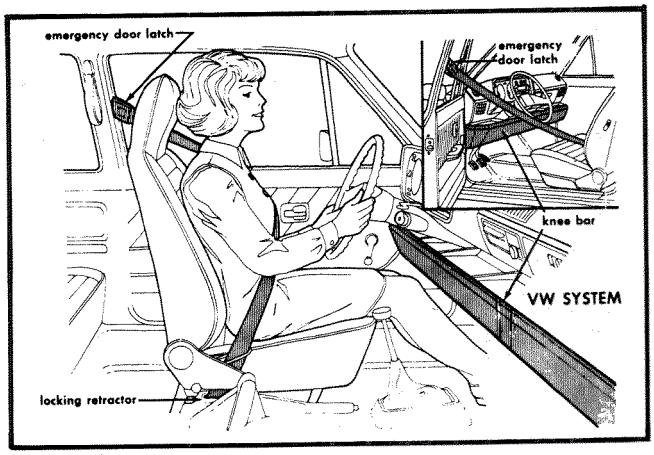

Figure 1. First automatic seatbelt system in production car line

upper torso belt with the retractor inboard and the fixed anchor attached outboard on the door. The door connection incorporates a buckle for emergency disconnection. The buckle has an electrical interlock with the starter system to insure that the buckle is connected in normal driving use. The lower body movement is controlled by a knee bolster and a specially designed seat pan. Figure 2 shows the appearance of the VW system as installed in the Rabbit.

The first production installation in a car produced in the United States appeared in the Chevette manufactured by the Chevrolet Division of General Motors in model year 1978. It was quite similar to the VW installation in the Rabbit, except that it used a seat of conventional design and included a manual lapbelt. Figure 3 shows the conceptual design, with a passive 2-point shoulder belt, a knee bolster, and a lapbelt.

Figure 2. VW automatic seatbelt installation

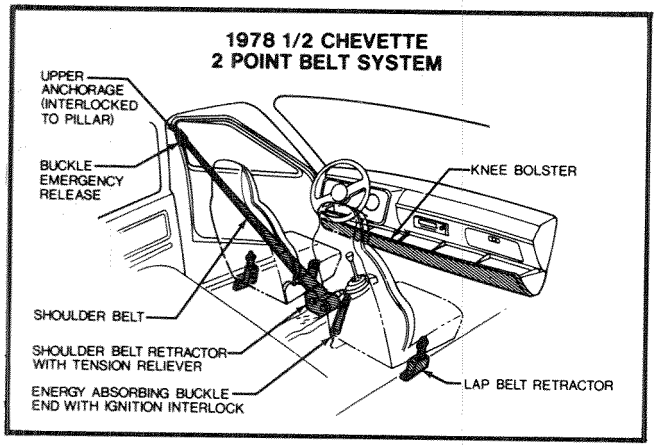

Figure 3. First automatic seatbelt system in U.S. domestic production car line

The next production installation appeared in the Chevette in model year 1980. This was a 3-point system with an inboard retractor and two fixed anchor points on the door. Figure 4 shows the conceptual design of this system. A buckle on the lower anchor on the door was provided for emergency release. This buckle also incorporated a switch to provide an electrical connection with a buzzer to insure that the buckle was engaged during normal use.

The most recent automatic system has been installed in the Toyota Cressida since model year 1981. It is a 2-point system with an inboard emergency-locking retractor and an outboard anchor location on the B-pillar. Figure 5 shows the conceptual design of the Toyota system. A manual belt is included to control lower body movement. The lower portion of the instrument panel provides a knee bolster as well. The motorized outboard anchor point is routed along the roof rail and the upper portion of the A-pillar. This action moves the shoulder belt forward out of the way for easy occupant ingress into the vehicle, and then returns it to don the shoulder belt on the occupant after he is seated and the door is closed. The

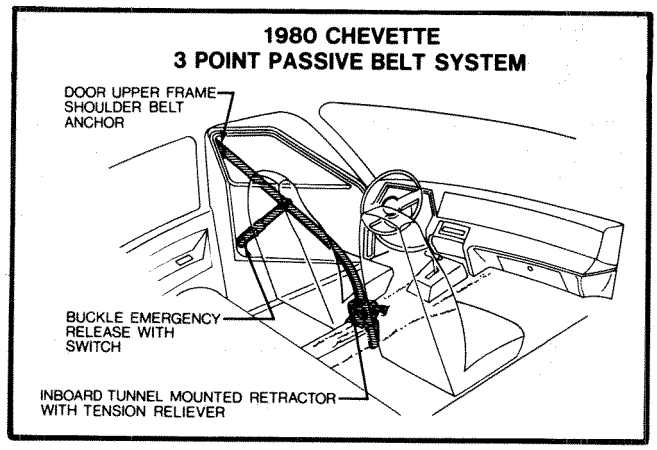

Figure 4. Second generation automatic seatbelt system in U.S. domestic production car line

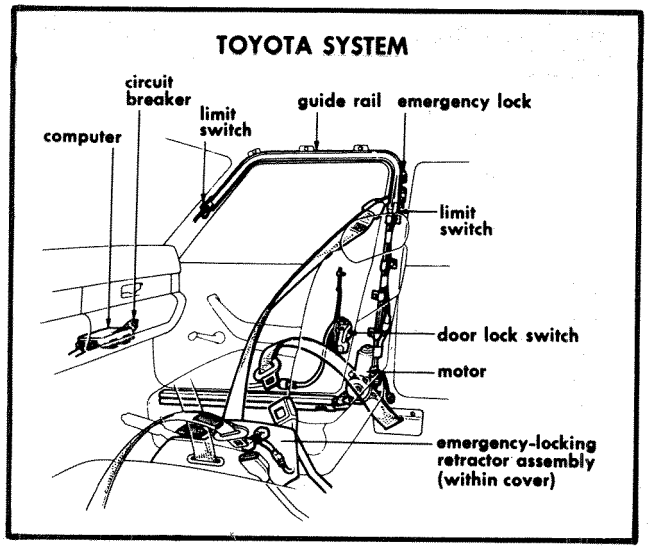

Figure 5. Motorized automatic system

traverse of the belt has been carefully timed to move the belt quickly, yet not so quickly as to startle the occupant. Figure 6 shows the relative movement and location of the motorized shoulder belt.

Design Considerations for Automatic Seatbelt Systems

The general design considerations for all seatbelts are shown in Table 4. The list includes performance in accidents and evasive maneuvers, simplicity in design and operation, reliability, durability, vulnerability to damage during normal use or in accidents that could render them inoperable, comfort during use, convenience in use, packaging size and shape for accommodation in the vehicle, esthetics, and cost. Automatic seatbelts have the added requirement for automatic donning and doffing.

In any given system design, tradeoffs inevitably are encountered such that optimization of one variable is

Figure 6. Toyota automatic shoulder belt system

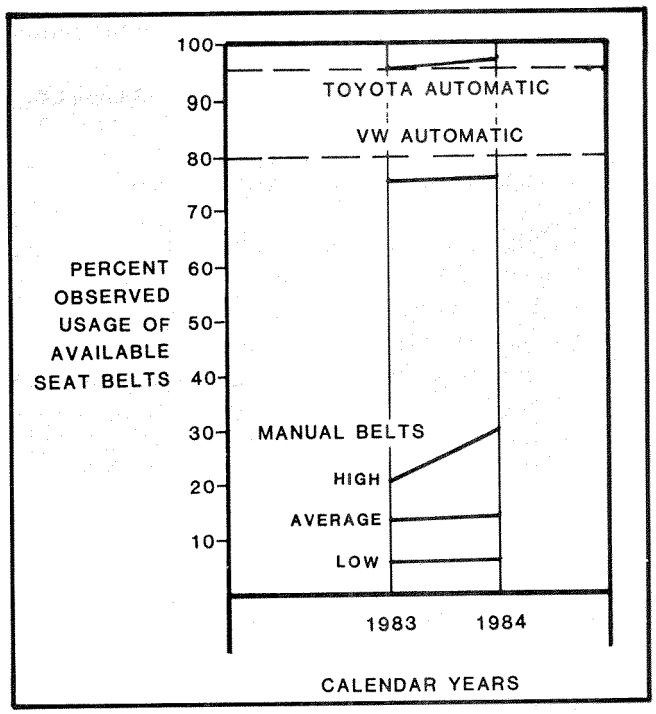

Figure 7. Recent seatbelt usage rates in US.A.

accompanied by some sacrifice in optimization of another. Some obvious examples are (1) the possible degradation of performance in emergencies for the sake of increased comfort in normal usage by means of a tension-relieving device on the shoulder belt, and (2) the possible decrease in simplicity and reliability for the sake of increased convenience and improved stowage through the use of retractors.

Table 4. Design considerations

● Performance in Emergency Events
● Reliability
● Durability
● Vulnerability to Damage
● Simplicity in Operation
● Comfort
● Convenience
● Packaging
● Esthetics
● Cost

Usage and Performance

The usage rates and performance of these automatic seatbelts in the field have been very satisfactory. Figure 7 shows the usage rates for automatic systems as compared with the usage rates for manual belts, representing data obtained in the ongoing program sponsored by the National Highway Traffic Safety Administration in which usage rates are monitored in 19 cities across the United States. Average driver usage of manual belts in these 19 cities increased from 13.3 percent in 1983 to 14.4 percent in 1984 and 15.3 percent in the last quarter of 1984. The upward trend was due mainly to the intensive efforts of NHTSA and others in the safety community to increase seatbelt usage in the United States. Usage rates varied appreciably from one city to another in the 19-city study, with a low rate in 1984 of 7.1 percent and the highest rate of 30.1 percent. The principal predictors of usage, in the absence of mandatory use laws, are age and sex of the driver (with the greatest usage in the age range of 25 to 49, and women consistently being more frequent users than men); size of car (with greater usage in smaller cars); foreign versus domestic U.S. cars (with drivers of foreign cars more than two times as likely to be wearing seatbelts); and the age of the car (with seatbelts more likely to be in use in later model cars).

The usage rate for the VW system has persisted in the range of 80 percent through the years since 1975, when it was introduced, with observed usage rates of 75 percent in 1983 and 76 percent in 1984. The Toyota Cressida system has done even better, with usage rates of more than 95 percent observed in the NHTSA 19-city program. The Chevette system's usage rates are in the same general range as the VW, but somewhat lower.

Performance data for these systems in accidents are limited because of the relatively short time they have been exposed on the roadways and the relatively small number involved in accidents. The data acquired to the present through the National Accident Sampling System operated in the United States by NHTSA, referred to as the NASS data, indicate the performance of these automatic systems

in the real world is generally comparable to the performance of manual systems.

The Future of Automatic Seatbelts

The key to the need for automatic belts is the usage rate of seatbelts. In the many countries and jurisdictions around the world having mandatory seatbelt use laws, starting with Australia in 1970 and including England more recently, usage rates of 75 to 95 percent are achieved with manual seatbelt systems when minimal—but continuing—enforcement is observed and nominal fines are imposed. In the State of New York, where a mandatory usage law became fully effective on the first day of January of this year, the usage rate is becoming acceptably high. Seatbelt performance in New York, in terms of reduction in fatalities and serious injuries, has followed the patterns observed in other countries having successful mandatory use laws.

Automatic seatbelts are not inherently better performers than manual belts, but they do appear to induce higher usage rates when installed as extra-cost options. The public acceptance of automatic seatbelts when installed as standard equipment remains to be seen. The degree of success in enacting and enforcing mandatory seatbelt usage laws in the United States will determine whether automatic seatbelt systems will be required in the long term.

Safety Belt Development

S. Sano
Honda Research & Development

Last summer, NHTSA issued a rule under MVSS 208 that created the regulation to equip automobiles with passive restraints under a phase-in schedule.

Beginning with model year 1987, 10 percent of all automobiles sold will be equipped with passive restraints. That percentage will increase unless enough States representing more than two-thirds of the entire U.S. population pass legislation mandating seatbelt use by drivers and passengers.

I believe the ideal situation would be the use of manual 3-point seatbelts in conjunction with the adoption of seatbelt use laws by all the States. It is my hope that effective regulation will be in place, as I feel this is the most effective way of providing adequate protection to automobile occupants, rather than by mandatory regulation requiring automatic restraints beginning with the 1987 model year.

We are, of course, preparing to comply with the passive restraint requirement and are considering an automatic seatbelt. Before considering what type of system should be used, at this point I would like to discuss the requirements of a system and the utilization of it.

First, I want to discuss the occupant protection performance, especially the performance of the system in restraining a driver or occupant at the moment of impact. Discussions for the passive belt system have involved both the 2- or 3-point types. However, the important issue is not whether the system is 2-point or 3-point, but how efficiently the automatic system works for a particular car; that is, how efficiently any system can be integrated with other crashworthy characteristics of an automobile, such as crush characteristics, impact duration, and the survivability space available for the occupants.

Another consideration surrounds the system performance during a postcrash emergency escape, either by the occupants or by outside rescue personnel. This relates to the selection of a detachable or nondetachable system and to the related issues of decreased seatbelt usage by user tampering or disconnection of the system. I do not think that whether the system is detachable or nondetachable will have a lasting influence on the restraint usage rate, especially in the long term. For example, during model year 1974, there was a starter-interlock device that was adopted for improving seatbelt usage rates. This rate was raised for a short period, but the interlock system was subsequently defeated, and there does not appear to be any significant difference in the usage rate of seatbelts between the 1974 models and any other year model.

It is my opinion that adopting a nondetachable system for the purpose of improving the restraint usage rates might have the same results as the earlier use of the interlock. Furthermore, it is quite possible that users would subvert the restraint system by removing the belts, which would require a subsequent replacement by any future vehicle owners that would want the protection of the system. The most effective way to improve the rate of restraint system usage is to adopt legislation making seatbelt or restraint use mandatory, which would certainly make the question of whether to use the detachable or nondetachable system no longer a point of discussion.

When considering most emergency escapes in accident situations or rescue of an occupant by outside personnel, it is obvious the detachable system is far superior to the nondetachable system. Because of these considerations, I

am proceeding toward the adoption of a detachable system as my passive restraint system of choice.

There are two considerations affecting acceptance by consumers. One is that the car equipped with a passive restraint system will be acceptable from a cost/benefit standpoint on the open marketplace, and the second is that the system will be used in an unaltered configuration. In the initial stages of the phase-in program, there will be a mixture of cars with passive restraints and cars with the current active seatbelts on the market. This will allow consumers to choose from among them. During the phase-in period, especially before most of the cars being sold are equipped with the passive system, we can assume that those who decide to purchase the cars with the passive belts will have the intention and desire to use that system.

If a consumer, given the choice, decides to purchase a car with the passive restraint, he has considered the benefits and determined they outweigh any detriments such as increased cost, perceived difficulty in entering and exiting the vehicle, or what we may call the spiderweb appearance of the vehicle's interior.

The degree of perceived benefit of the automatic system will depend on the mind-set of the purchaser. People who presently use seatbelts regularly and like the manual system will probably not care for an automatic system; while people who don't like the inconvenience of manual belts but use them because of the perceived safety benefits will most likely prefer an automatic system. Finally, people who are uninformed or simply don't care about the added safety of seatbelts probably won't like the automatic restraint system and are most likely the ones who will take the opportunity to disengage or defeat the system.

As a consequence, we feel the focus during the phase-in period will be on those consumers who do utilize seatbelts, although they feel seatbelts are difficult or inconvenient to use.

Next, I would like to discuss the motorized system. Certainly a motorized system will improve the application and removal situation when a vehicle occupant enters or exits the automobile; however, it does not eliminate all the problems of putting on and removing a belt. Moreover, certain discomforts will be generated for some occupants, such as the belt rubbing against a user's face or neck since the belt moves automatically regardless of user's intention.

A motorized unit will increase the cost substantially when compared to the cost of the belt itself, either under the present system or a nonmotorized passive restraint system. Additionally, there is no doubt a system that has simple component parts will have superior reliability when compared to the complexity of the motorized system.

Again it is very difficult to evaluate the cost/benefit of the passive restraint systems. Because no system is a perfect system in every aspect, one approach could be to evaluate various manufacturers' systems over a period of time.

We began to develop the automatic seatbelt system in the early 1970's and exhibited a motorized version 11 years ago at the ESV meeting held here in England. We abandoned that system after an evaluation program because of concern about injury-causing potential from the positioning of the mechanical arm.

Since that time, we have tried many different combinations, such as a motorized arm operating on the door side, a motorized arm operating from the mid-portion of the car interior, a system without a motorized arm, one with a convenience hook, another system with an ELR set in the middle of the automobile interior as well as an ELR on the door, 2-point systems, 3-point systems, and every combination of all the elements mentioned.

From our extensive experience, we concluded no perfect system exists that is acceptable and satisfies every single consideration. The 2-point restraint system and the motorized arm system are not favored by people accustomed to the traditional manual belts, since space is further restricted by a knee bolster and is not considered by those persons as a benefit. System users are influenced apparently more by the discomforts caused by the passive restraint system than by any improvement of the putting on or removal of the system.

Therefore, we consider the simple, nonmotorized 3-point passive restraint system that is similar to the current manual belt system to be the most adequate during the phase-in period.

However, we are well aware that the situation concerning development of automatic restraints keeps changing. We are keeping an open mind as to appropriate forms of automatic restraints that are most desirable from the standpoint of safety, efficiency, and comfort, and will change the system any time substantial and significant advancements are made in accordance with our ongoing research programs.

Dietmar K. Haenchen
Volkswagen-Research

I would like to talk about four related topics:

1. VW seatbelt features
2. Belt use in VW Rabbits
3. Performance of automatic and manual belts in the field
4. Whether measures to improve the vehicle structure for 35mph barrier crashes would result in improved accident statistics

Let me now describe the main features of the Volkswagen belt systems:

Slide 1. You are all familiar with the manual belt. Note that in VW's 3-point belt system, the buckle is mounted to the seat. This assures good fit of the belt in all seating positions.

Slide 2. The VW automatic belt has the same geometry of the upper torso belt. In this case, the retractor is mounted under the seat. This also assures good fit because the belt moves with the seat when it is adjusted. The lower torso restraint is provided by the knee bolster.

Slide 3. The advantage of this simple automatic belt is that it is easy to use—just open the door, get into the car, and close the door.

When we introduced this automatic belt system in 1975, we were curious how this system would perform in the field. Although crash test data indicated good performance, real-world performance could have differed due to the many accident types we have in the real world.

When using the collective Fatal Accident Reporting System (FARS) data from 1975 through 1983, it turned out the overall effectiveness of automatic belts in VW Rabbits is about 19 percent better than the effectiveness of manual belts.

Slide 4. Observed belt usage in Volkswagen Rabbits has been relatively high for both the manual and automatic belts, as shown in this slide. It is around 30 percent for manual belts and around 80 percent for automatic belts.

However, belt use in severe accidents is much lower, due to the fact that those occupants who don't wear seatbelts also tend to be more involved in severe accidents.

Slide 5. John van Dyke of NHTSA's Center for Statistics and Analysis investigated whether the difference in fatality rates is compatible with the observed usage rate for both restraint systems. Using belt use data from accident statistics in three different States, he assumed that both the manual and automatic belts in Rabbits are 45 percent effective in preventing fatalities and serious injuries. Van Dyke concluded that the 19 percent fatality rate difference is reasonably consistent with the difference in observed usage rates.

Slide 6. Volkswagen researchers recalculated the data the other way round. Taking the FARS data and using the 45 percent effectiveness of both belt systems, they calculated the usage rate.

As you can see in the slide, there is good agreement of the calculated usage rate with the observed usage rate. Van Dyke concluded that, "This evidence supports the conclusion that the lower fatality rate for occupants of automatic restraint Rabbits is attributable to the higher restraint use by these occupants."

With this in mind, it is obvious that further significant decreases in traffic fatalities and serious injuries can be achieved if we continue to increase belt use.

Slide 7. This slide illustrates the remaining lifesaving potential of seatbelts. For reasons of simplicity, we have assumed an effectiveness of 50 percent for all belts.

The first column shows zero lifesavings if no belts are worn; the second shows 25 percent usage (this is about the usage we see in accidents with Rabbits with manual belts); and the third shows the 50 percent usage that we see in accidents with Rabbits with automatic belts. The last column shows the improvement we would get with 100 percent belt use.

Mandatory belt use laws have reduced fatalities and injuries in many countries, and I am convinced they will also work in the United States.

Let me touch the topic of improving seatbelt performance by modification of the vehicle structure.

Using computer simulation, Volkswagen researchers developed force-deflection curves that would give optimum injury criteria for 3-point belts in 30mph barrier tests. Two optimized structures were developed, one for a seatbelt system without preloader and one for a seatbelt system with preloader. Both of these systems had about the same overall benefit.

Slide 8. The diagrams show the force-deflection curves of the vehicle front structure. In the left diagram, we see the optimum curve of the vehicle without preloader; in the central diagram is the system with preloader. The dashed lines represent a present vehicle structure.

Our researchers also calculated a force-

deflection curve for an optimum performance of the belt system at the 35mph barrier impact velocity. As you can see in the right diagram, this optimized curve is very different from the present curve. The optimized structure for the 35mph system requires a very high initial force to achieve the optimum performance.

It is obvious that such a structure would be very aggressive to other vehicles, especially in side impacts. Consequently, the overall safety benefit in the field would be produced by such a structure.

Let me conclude with a summary:

1. Manual and automatic belts show similar effectiveness when worn.
2. The difference in overall effectiveness between manual and automatic belts is basically related to the difference in belt use only. Mandatory belt use laws will help to further increase the effectiveness of both types of belt systems.
3. Optimizing the vehicle structure to improve injury criteria for 35mph crashes does not necessarily lead to better overall accident performance in the field.

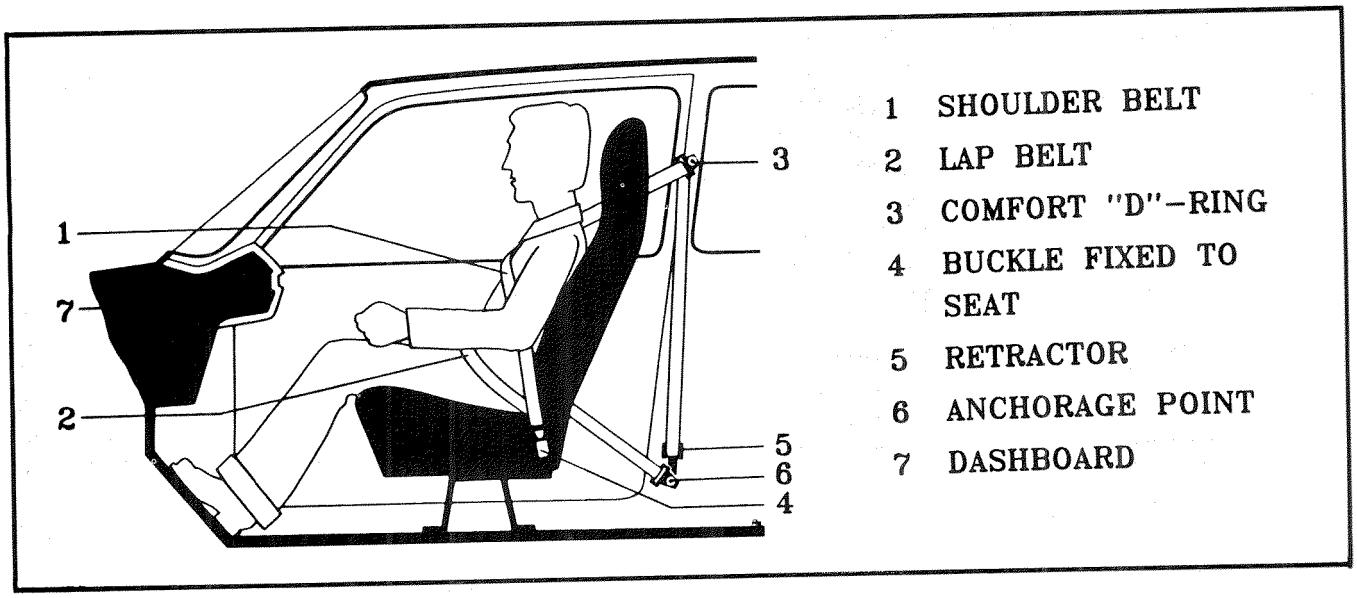

Slide 1. Three point belt

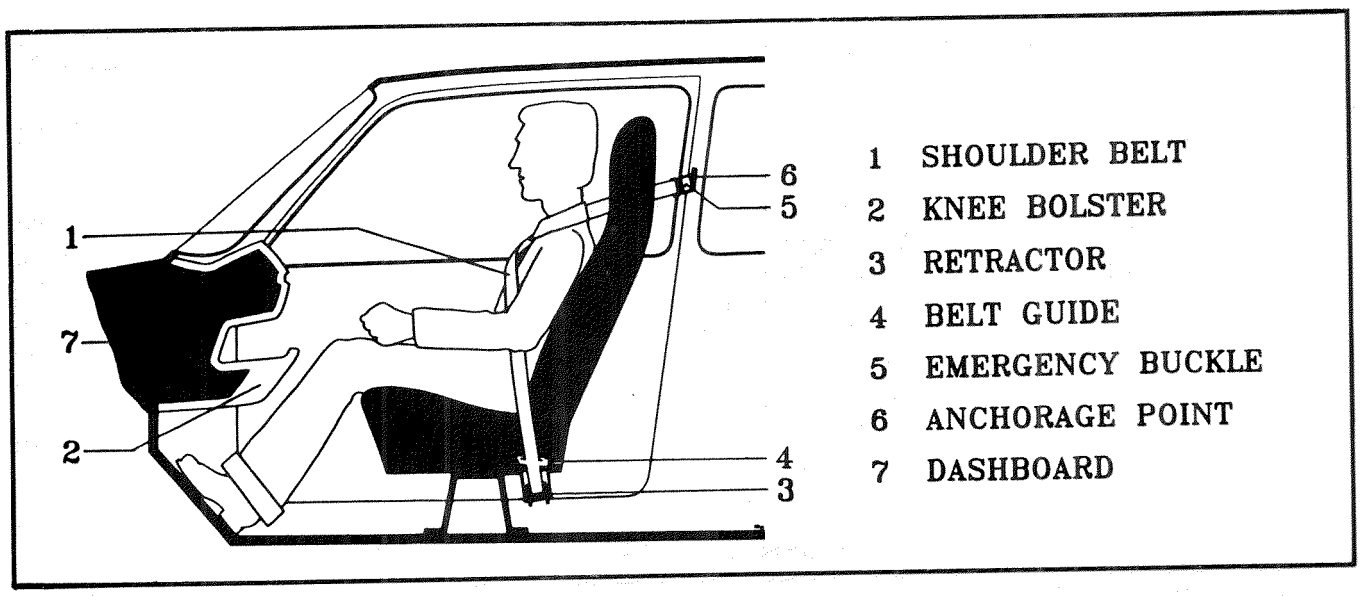

Slide 2. Restraint Automatic

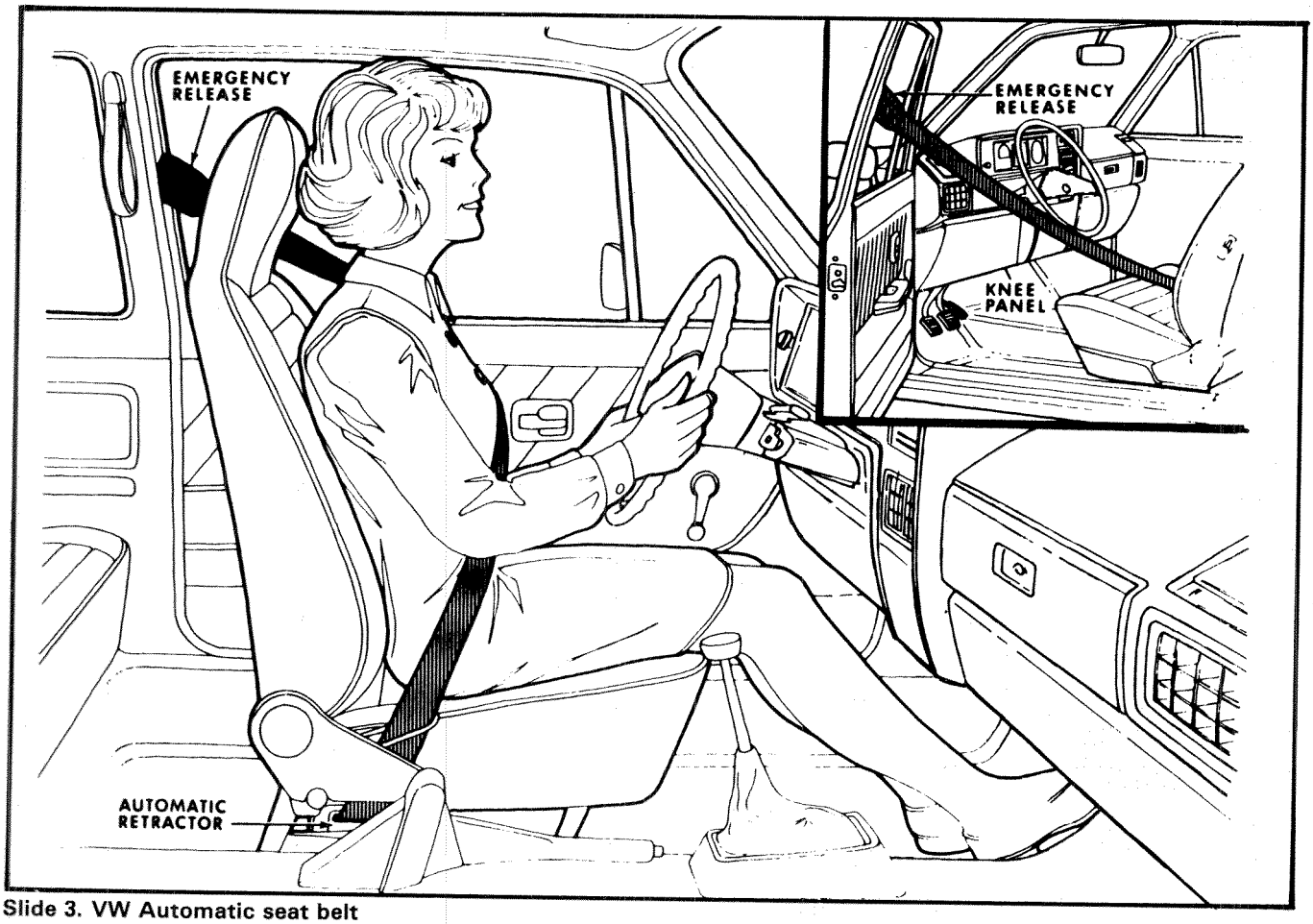

Slide 3. VW Automatic seat belt

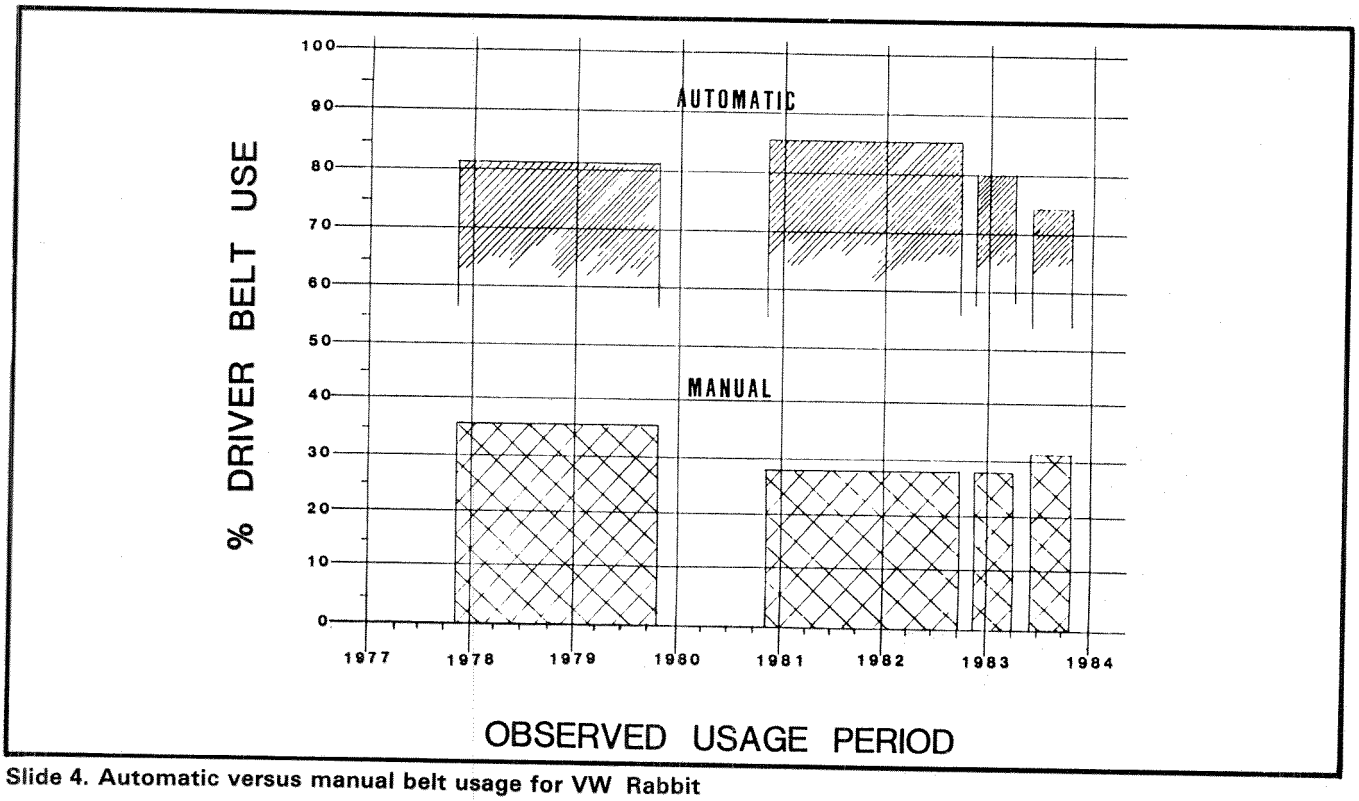

Slide 4. Automatic versus manual belt usage for VW Rabbit

NHTSA-STUDY ON VW-AUTOMATIC SYSTEM **RA**

(VAN DYKE: VOLKSWAGEN RESTRAINT SYSTEMS AND FATALITY-RATES)

ASSUMPTION: TWO-POINT-BELT WITH KNEE-BAR AS EFFICIENT AS THREE-POINT-BELT

CONCLUSION: DIFFERENT FATALITY-RATES OF THE SYSTEMS DEPEND ON DIFFERENT USAGE RATE

THE ASSUMPTION HOLDS, IF THE COMPUTED AND THE OBSERVED USAGE RATES CORRESPOND

Slide 5. NHTSA study on VW automatic system RA

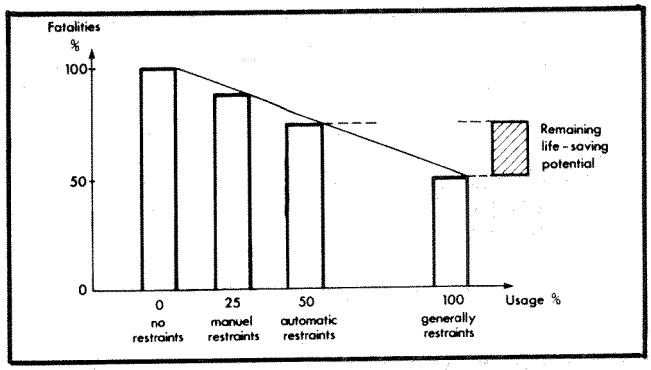

Slide 7. Decrease of fatalities

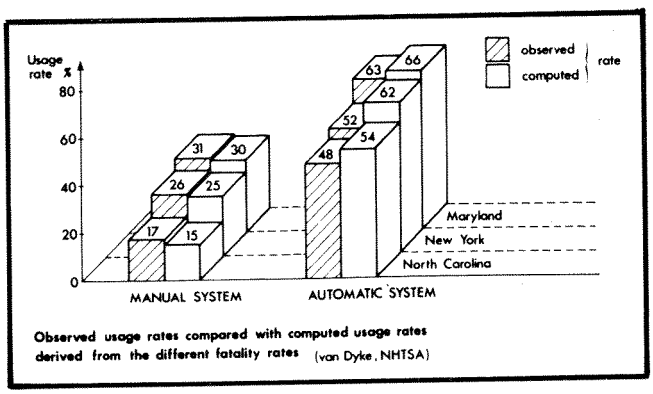

Slide 6. Automatic versus manual belt system

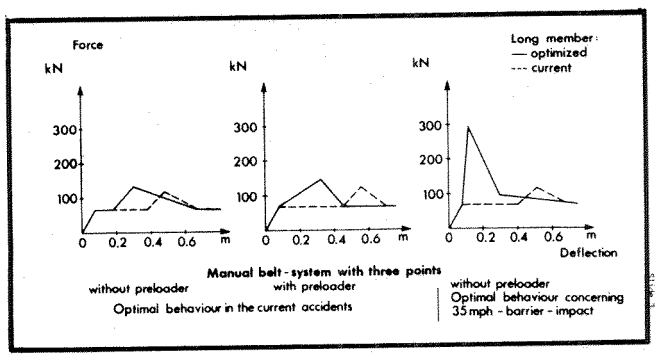

Slide 8. Force-deflection of the long member

Section 4 Technical Sessions

Frontal Crash Protection and Pedestrian Protection

Technical Session No. 1

Biomechanics and Dummy Development

Jean Leroy, Chairman, France

Biomechanics of Diffuse Brain Injuries

Lawrence E. Thibault
Thomas A. Gennarelli
University of Pennsylvania

Abstract

This report discusses the development of brain injury tolerance criteria based on the study of three model systems: the primate, inanimate physical surrogates, and isolated tissue elements. Although we are equally concerned with the neural and neurovascular tissue components of the brain, the report will focus on the former and, in particular, the axonal elements. Under conditions of distributed, impulsive, angular acceleration loading, the primate model exhibits a pathophysiological response ranging from mild cerebral concussion to massive, diffuse white matter damage with prolonged coma. When physical models are subjected to identical loading conditions it becomes possible to map the displacements and calculate the associated strains and stresses within the field simulating the brain. Correlating these experimental models leads to predictive levels of tissue element deformation that may be considered as a threshold for specific mechanisms of injury. Isolated tissue studies in the axon then serve to confirm the relationship between ultimate strain, for example, and the pathophysiological consequences. At this time, we have found that elongating strains of between 5 and 10 percent at strain rates of greater than 50sec^{-1} produce membrance depolarization and a concomitant decrease in excitability that recovers in minutes. The degree of depolarization is directly proportional to the magnitude of the stretch. Further, total structural failure of the axonal membrane (diameters 400-750.jmm) occurs between 25 and 50 percent elongation at comparable strain rates. These observations are in reasonable agreement with the estimations of critical strains obtained from the primate and physical model studies.

Introduction

The development of head injury tolerance criteria for specific forms of brain injury remains one of the many challenging problems in the biomechanics of central nervous system trauma. Part of this problem is to describe the variety of head injuries that occur and to associate with each injury a severity index. Additionally, it becomes necessary to elucidate the mechanisms that produce each injury and to develop tolerance (or failure) criteria for the components that constitute the brain. Finally, a method to relate the kinematics of dynamic mechanical loading of the head to the deformations of the brain tissue is required.

This report will discuss the use of three model systems selected to address these issues and, further, it will focus on diffuse brain injury. Although the neural and neurovascular tissue injuries may be of equal importance in terms of injury severity, the scope of this study is restricted to the axonal structures of the brain. The three models therefore include the primate, simplified, inanimate, structural models of the skull brain system, and isolated axonal tissue preparations. Previous studies have found(1,2,3) that inertial loading, and in particular rotational acceleration, is capable of producing diffuse injury to the brain of the primate. We have more recently shown that the severity of this injury can be varied to include mild cerebral concussion as well as prolonged coma with axonal damage bilaterally in the hemispheres and in the corpus colossum and brain stem. Results to date suggest that as the brain experiences inertial loading

with significant rotational components it undergoes a deformation that depends not only on the details of the loading but obviously on the local geometry and the tissue material and structural properties.

Simple physical models of the skull-brain structure under carefully controlled inertial loading experiments allow one to study the temporal and spatial variation of these deformations as a function of the magnitude, direction, and time history of the rotational accelerations. These deformations result in strains and stresses that, when excessive, are manifested in functional and structural changes in the tissue elements. To demonstrate the latter, it is most practical to use isolated tissue elements. We will discuss the giant axon of the squid as a model of axonal structures of the brain. Electron miscroscopic examination of the brain's deep white matter reveals intracellular injury to the axons in the regions of the nodes of Ranvier, and this particular injury has been associated with prolonged coma(4). Although the squid axon is non-myelinated, we feel it is a reasonable model for this nodal region that is probably the most vulnerable from a structural point of view. Changes in the electrophysiology of the axon under conditions of variable strain-rate uniaxial extension are then related to the animal and physical model results.

Methods

Primate Model

A standard 6in diameter HYGE® (Bendix) shock tester has been modified in the following manner:

- The stroke length was reduced to 3.125in.
- The internal acceleration and deceleration metering pins were redesigned to produce the desired acceleration-time characteristics.
- A kinematic linkage was designed that converts the translational motion of the HYGE thrust column into an angular motion.
- A helmet system was designed to rigidly couple the primate head to the kinematic linkage.

This system is used to provide controlled inertial loading to the primate as well as the physical models. Figure 1 depicts the kinematic linkage whose angular displacement is set at approximately 65°. Also shown in the figure is a typical acceleration-time history expressed as tangential acceleration.

The primates used in these studies were baboons ranging in weight from approximately 5 to 10kg. Standard physiological monitoring was performed including intracranial pressure, arterial pressure, respiration, respiratory carbon dioxide, respiratory oxygen, EKG, EEG, and multimodality evoked potentials. Upon sacrifice, both light and electron microscopic studies were performed on the brain tissue. With particular emphasis on the axonal structures, the lesions are mapped according to anatomic location and degree of severity.

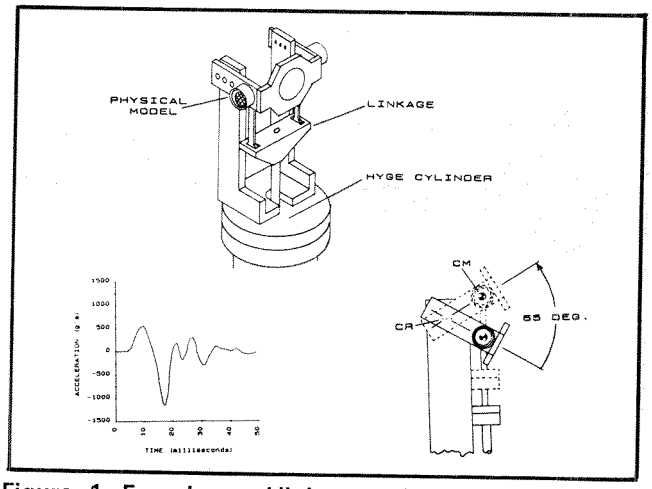

Figure 1. Experimental linkage and typical acceleration profile

Fresh brain weights are recorded in all cases immediately post-mortem and in this study range from approximately 110 to 170g.

The rotational axis was varied to include the three mutually perpendicular planes of sagittal, coronal, and horizontal.

Physical Models

A surrogate brain material in the form of a silicone-based gel, known as Silicone Gel System (Dow Corning), was used for these studies. The material is supplied as a two-part mix of polymer and catalyst. By varying the relative concentrations of these two components, it is possible to alter the modulus of elasticity of the gel by several orders of magnitude. For these experiments, the material properties were closely matched to brain tissue. The gel is an optically transparent substance cast at room temperature and can be layered with no mechanical discontinuity (i.e., the gel in a liquid state will adhere to a polymerized surface upon curing). It is therefore possible to cast the surrogate brain in layers and print or paint an orthogonal grid on selected surfaces that can be entrained in depth within the model. As depicted in Figure 2, both idealized right circular cylindrical geometries, as well as realistic skull boundaries, can be studied.

The physical models are mechanically fastened to the kinematic linkage of the HYGE system in such an orientation that deformations of the grid within the gel can be filmed in the plane of interest. Photography is performed at 4,000 frames per second on 16mm film. Individual frames of interest are printed and then digitized using a Hewlett Packard 9836 computer and bit pad. From the digitized data, one can then compute the field parameters of displacement, strain, and stress at node points within the grid. Therefore, both the strains and strain-rates at a particular location can be determined for any given loading condition.

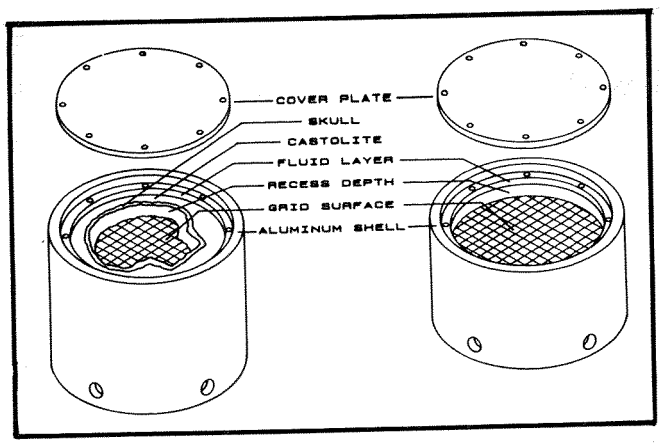

Figure 2. Construction of the physical models

Isolated Tissue

A system has been developed that permits one to study the electrophysiology, morphology, biochemistry, and transport properties of the giant axon of the squid as a function of variable strain-rate and variable magnitude of stretch in uniaxial extension.

Approximately 5cm of dissected axon is mounted in a chamber where glass cannulae are inserted through small cuts in the membrane. As portions of the membrane are allowed to dry to the glass cannula, a tight grip is formed between the glass and the internal circumference of the axon. This procedure produces a viable length of axon of approximately 1.5cm, which is immersed in the physiologically suitable fluid. The glass cannulae are part of platens that on one end attach to an isometric force transducer and on the other to a movable linkage. The linkage is driven by an audio speaker that can be programmed to move a predetermined displacement at a given velocity. This constitutes a small materials testing machine with a specimen environmental chamber. For purposes of this study, a wire electrode is inserted axially into the preparation to obtain membrane potential measurements. The system is depicted schematically in Figure 3. The entire device is integrated onto the movable

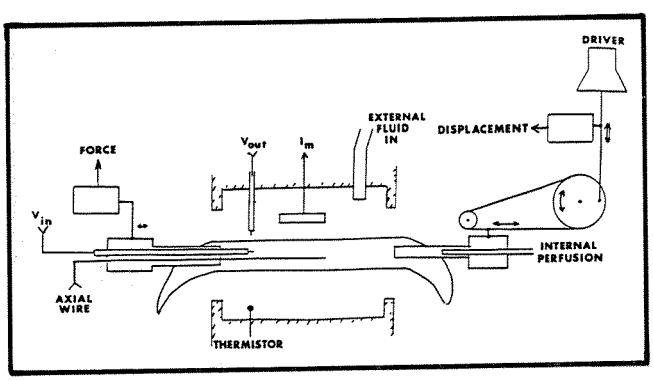

Figure 3. Experimental apparatus for isolated tissue studies

stage of an inverted phase contrast microscope. With this arrangement, it is then possible to obtain axonal mechanical properties as well as the neural tissue element electrophysiological response to mechanical stimulation.

Results

Primate Model

Thus far we have been able to programmably reproduce the following brain injuries in the primate model:

1. The acute subdural hematoma with varying degrees of severity.
2. Cerebral concussion from mild to periods of unconsciousness of up to 2 hours.
3. Diffuse axonal injury with prolonged coma.

The subdural hematoma as part of a class of neurovascular injuries will not be presented here.

The cerebral concussion and diffuse axonal injuries are shown in Figure 4. These same data are presented in Figure 5 where the peak rotational acceleration is shown plotted against the change in angular velocity. The data are scaled based on Holbourn's(5) suggested relationship as a function of brain mass to an average human brain of approximately 1,400g.

In the case of cerebral concussion, the period of unconsciousness varied from less than 1 minute to approximately 2 hours. For those animals listed as having diffuse axonal injury with prolonged coma, the longest survivor was sacrificed at 6 weeks. At this point in our experiments, the threshold levels for cerebral concussion and diffuse axonal injury when scaling the primate data to man appears to be 5,000 rad/s^2 (75 rad/s) and approximately 15,000 rad/s^2 (150 rad/s), respectively. The symbols □ and x in both figures refer to diffuse axonal injury and cerebral concussion.

Physical Model

Depicted in Figure 6 are the digitized and computer-reconstructed still frames of the grid deformations within an idealized riqht circular cylindrical geometry. Time is shown beneath each frame and is expressed in milliseconds. As the frames are presented, the cylinder is rotating in a counterclockwise direction. Recalling the asymmetric acceleration-time history character of the loading, the peak deformation is seen to occur at a point that temporally corresponds to the peak of the tangential deceleration waveform. Once the deformation field is digitized, the computation of the field parameters can be performed. Shown in Figure 7 is a plot of one component of the nonlinear strain tensor, E_{12}, as a function of the nondimensional cylinder radius. This type of analysis is

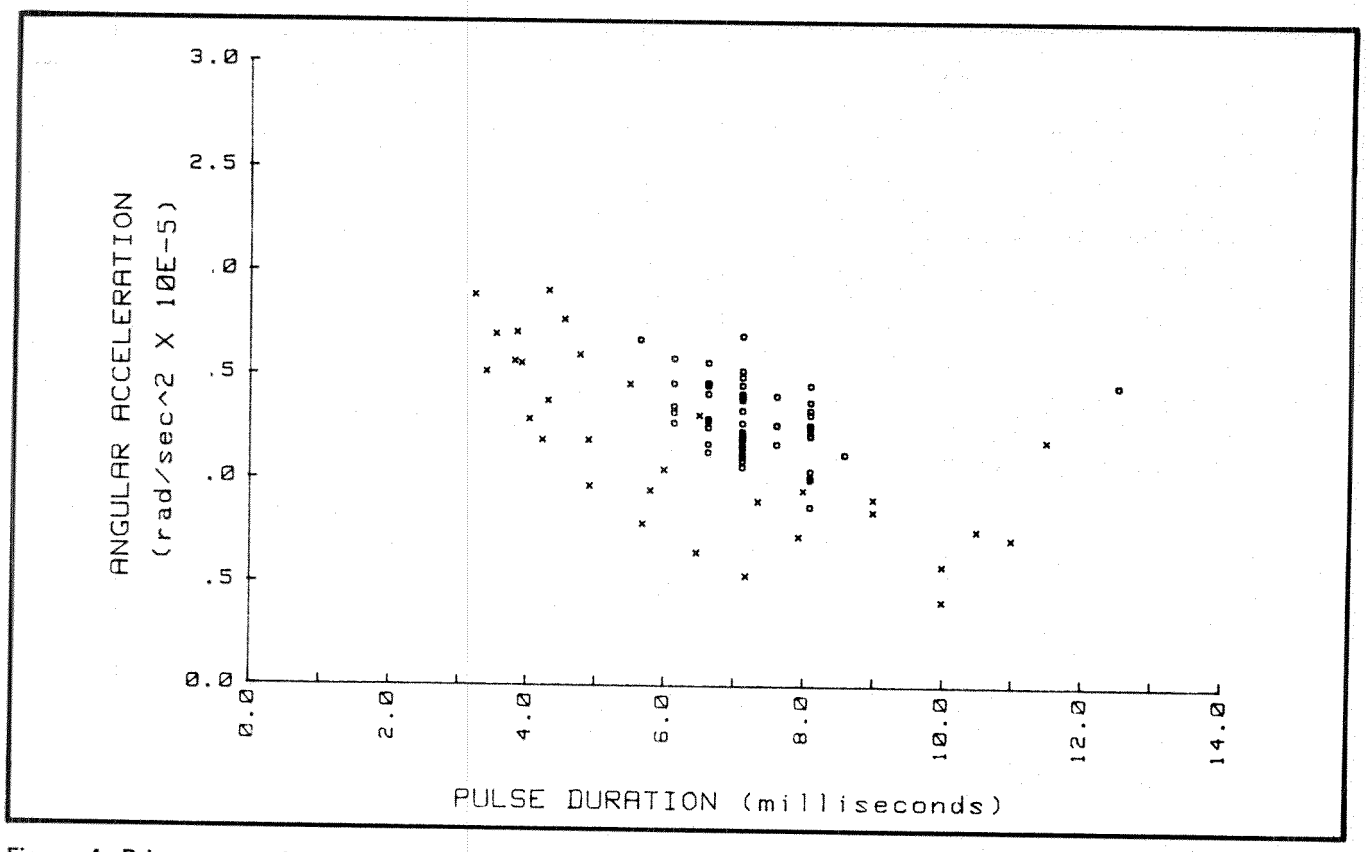

Figure 4. Primate experiments—angular acceleration versus pulse duration

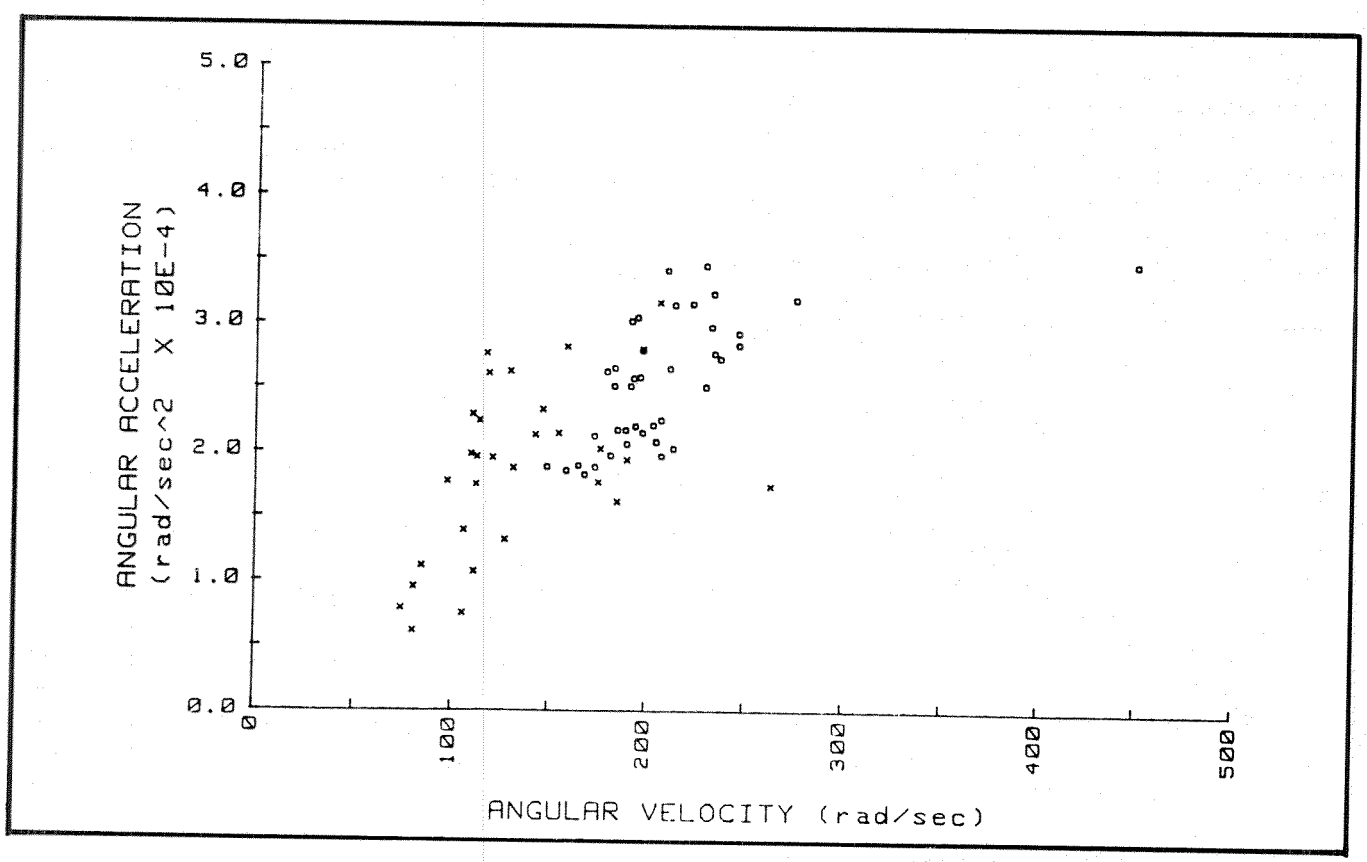

Figure 5. Primate experiments—angular acceleration versus angular velocity

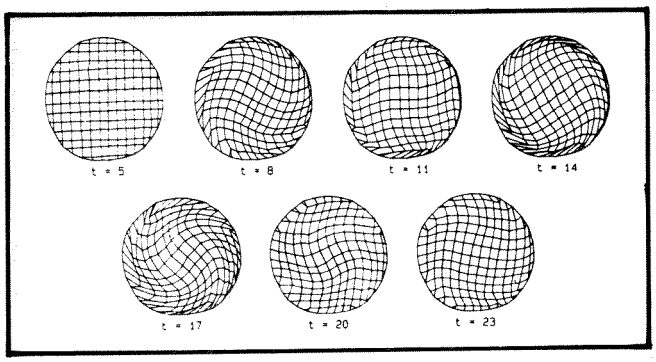

Figure 6. Digitized reconstruction of still frames for the right circular cylinder model

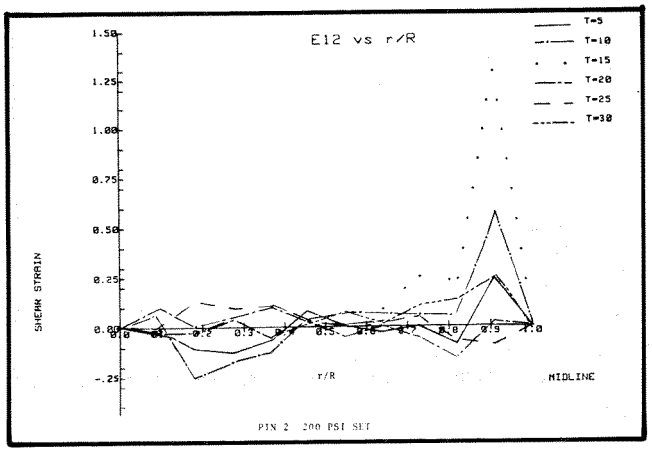

Figure 7. Strain versus nondimensional radius

presented to demonstrate the somewhat asymmetric strain field expected in the case of a noncentroidal rotation and to show an example of the many kinds of analysis that can be performed with the physical model data.

Figure 8 represents a comparison of the maximum elongating strains in three cylindrical models of different radii as a function of the peak rotational acceleration. The curves are labeled A, B, and C, representing cylinder diameters of 11.12cm, 7.94cm, and 6.35cm. Experiments such as these enable one to test scaling relationships such as the one proposed by Holbourn given as

$$\frac{\ddot{\Theta}_m}{\ddot{\Theta}_p} = \left(\frac{M_p}{M_m}\right)^{2/3}$$

Figure 9 shows the relationship between the maximum strain and the peak rotational acceleration when this scaling relationship is applied. The data in this case are scaled to the average brain mass of the baboon from the mass of each of the three cylinder models.

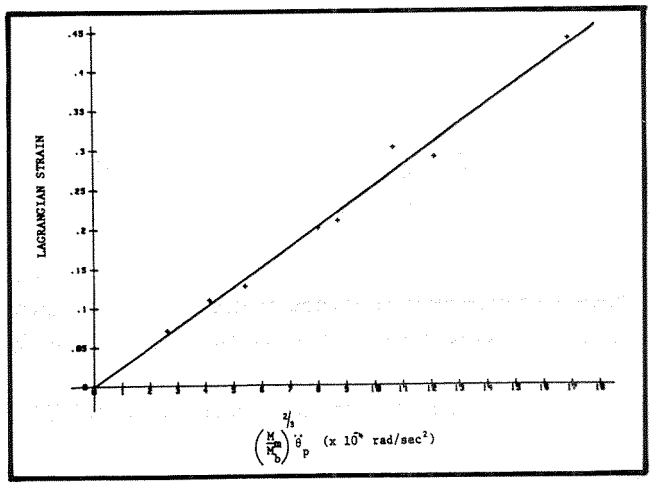

Figure 8. Strain versus angular acceleration for three cylindrical models A, B, and C of mass m_1, m_2, and m_3

Figure 9. Strain versus angular acceleration from the three cylinder experiments scaled to the primate brain mass

Isolated Tissue

Figure 10 shows examples of the mechanical testing performed on the giant axon of the squid. The load-elongation curve exhibits the nonlinear behavior characteristic of soft tissue. Hysteresis and stress-relaxation studies also depicted are representative of the viscoelastic behavior of this class of biological materials. Under conditions of high strain-rate uniaxial extension, there is an associated depolarization of the axon. Figure 11 shows two such experiments where the magnitude of the axial elongation is increased from approximately 15 percent in the first case to 30 percent in the second study. A proportionate increase in the depolarization is observed. We believe that this phenomena and the accompanying decrease in membrane excitability are analogous to the cerebral concussion observed in the primate model. Figure 12 shows the time course of recovery of the resting membrane potential following a high strain-rate ($50s^{-1}$) uniaxial extension (20 percent). The exponential

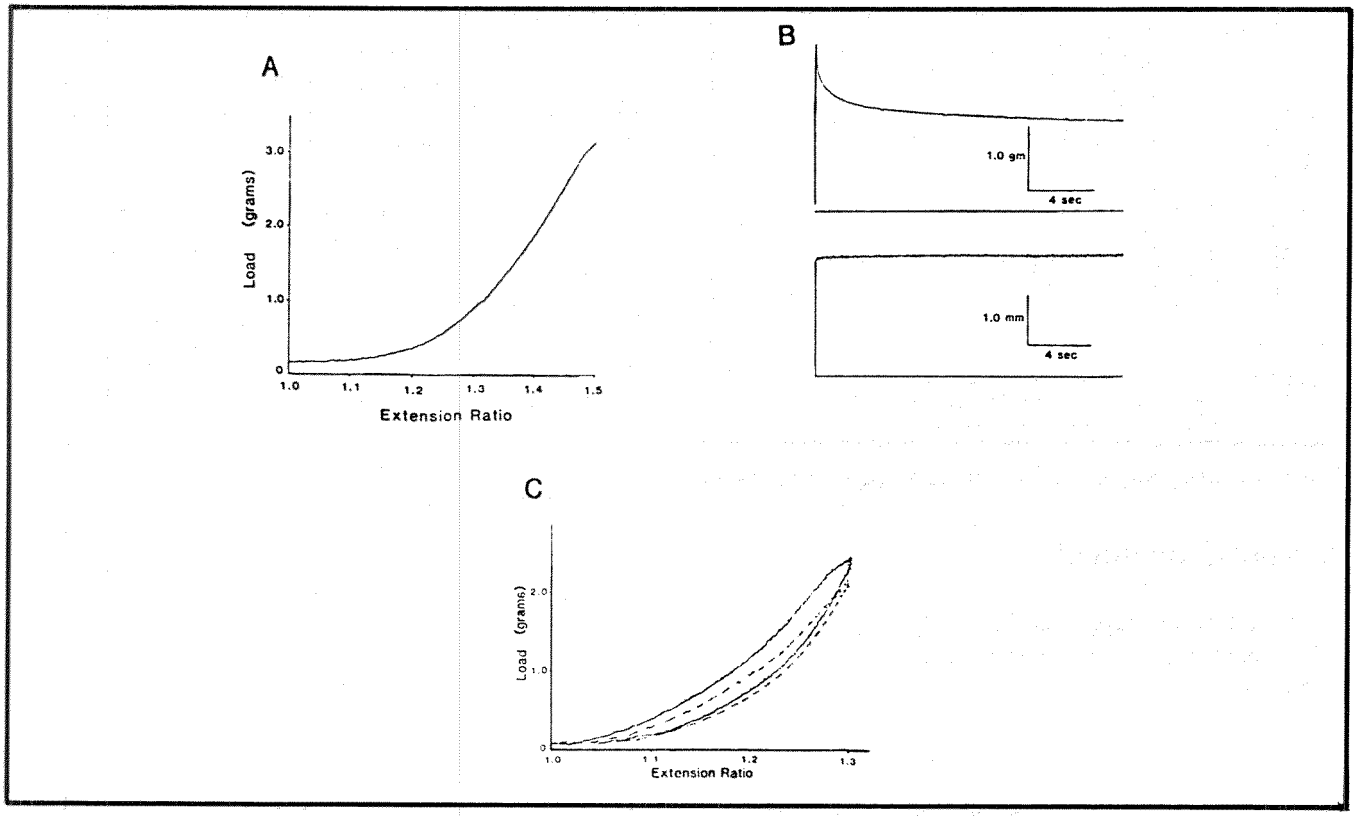

Figure 10. Mechanical properties of the isolated squid giant axon

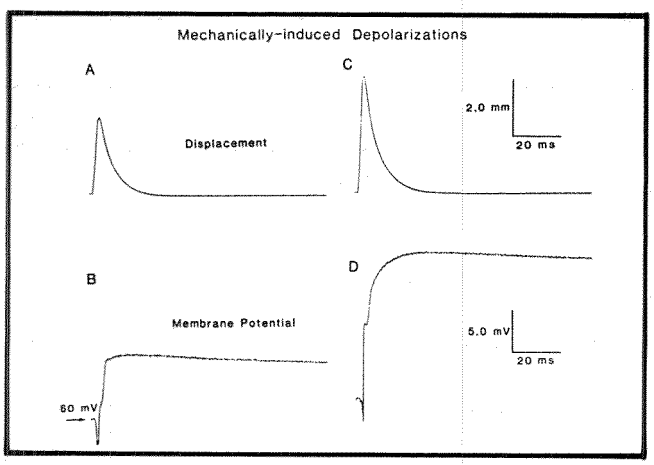

Figure 11. Changes in membrane potential associated with high strain-rate uniaxial elongation

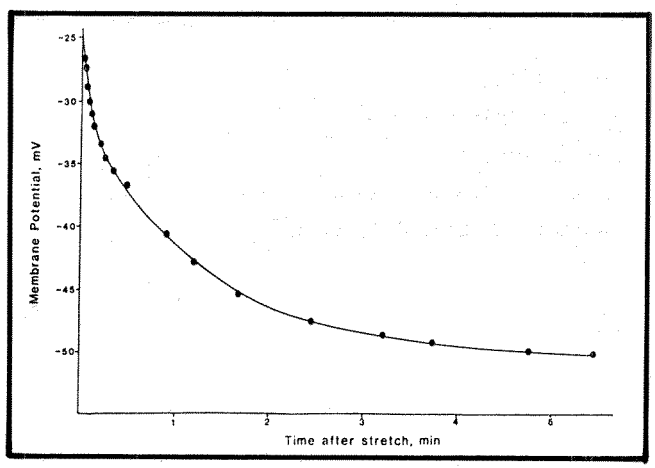

Figure 12. Membrane potential time course of recovery following mechanical stimulation

recovery has a characteristic time constant of the order of several minutes.

Discussion

The experiments described herein are designed to provide methods of improving on existing head injury tolerance criteria and to develop model systems whereby it is possible to study the mechanisms of injury with the ultimate goal of therapeutic intervention. These two distinctly different objectives share a common approach that we describe as the cellular basis for injury from both the biomechanics and pathophysiological points of view.

Figure 13 represents our first approach to developing injury criteria based on tissue response to mechanical strain. The physical models, which are highly idealized at this point, enable one to transform the inertial loading data into tissue deformation. The predicted thresholds for cerebral concussion and diffuse axonal injury ap roximate the isolated tissue response.

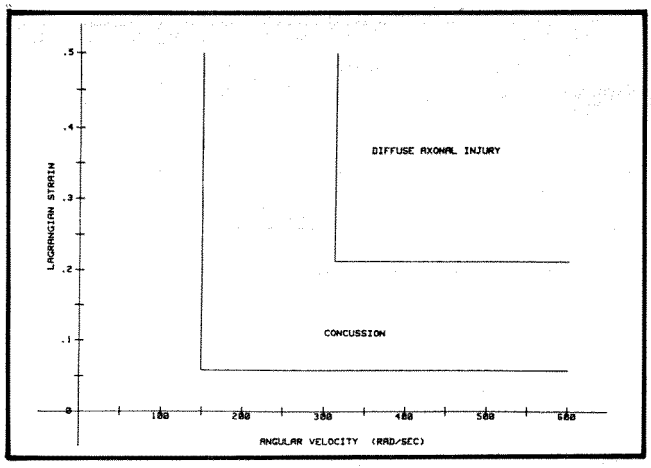

Figure 13. Langrangian strain versus angular velocity

Acknowledgement

This work was supported in part by NHTSA of the U.S. Department of Transportation, Contract DTNH 22-82-C07187.

References

1. Higgins, L.S., and R.A. Schmall,"A device for the investigation of head injury effected by non-deforming head accelerations," Proceedings 11th Stapp Car Crash Conference, Soc. Auto. Eng., New York, pp. 57-72, October 1967.
2. Ommaya, A.K., F. Taas, and P. Yarnell, "Head injury in the chimpanzee. 1. Biodynamics of traumatic unconsciousness," *J. Neurosurg*, 39:2:152-166, August 1973.
3. Gennarelli, T.A., L.E. Thibault, and A.K. Ommaya, "Pathophysiological response to rotational and translational accelerations of the head," Proceedings 16th Stapp Car Crash Conference, Soc. Auto. Eng., New York, pp. 296-308, 1972.
4. Gennarelli, T.A., L.E. Thibault, J.H. Adams, D.I. Graham, C.J. Thompson, and R.P. Marcincin, "Diffuse axonal injury and traumatic coma in the primate," *Annals of Neurology*, Vol. 12, pp. 564-574, 1982.
5. Holbourn, A.H.S., "Mechanics of head injuries," Lancet (2), pp. 438-441, 1943.

Effects of Different Types of Headrests in Rear-End Collisions

Ake Nygren,
Hans Gustafsson, and
Claes Tingvall
Folksam Traffic Safety Group, Karolinska Hospital, Stockholm, Sweden

Abstract

Nygren(1) showed that whiplash injuries in rear-end collisions often lead to permanent disability. Ten percent of those initially complaining about neck pain after a rear-end collision had remaining problems 5 years after the accident and were judged as permanently, medically disabled.

It was also shown that fitted headrests had little effect in preventing whiplash injuries. Fixed headrests reduced the incidence of whiplash injuries by 24 percent, while adjustable headrests reduced the risk by only 14 percent. The results of whiplash injuries in terms of permanent disability were not affected by headrest fitting and type.

The present study is based on 339,675 accidents and determines if the variations of the effects of headrests in different car models could be explained by their type and position.

Background

Neck pain seems to be an increasing problem in Sweden(2). No other diagnosis has so increased its proportion among those leading to sickness or disablement pensions during the past 5 years. The origin of such neck problems is mostly occupational strain injuries, but trauma will accelerate this problem. Nygren(1) showed that neck injuries due to car accidents led to disablement pensions to a higher degree than was recognized earlier. This paper discusses neck injuries in car accidents, especially those coded as AIS 1 in rear-end accidents.

Severe neck injuries in car accidents occur mostly among unbelted car occupants, while slight neck injuries occur among belted ones in frontal collisions(3,4). One specially defined slight neck injury occurs among car occupants in rear-end collisions(3). This problem was discussed in the fifties and sixties, and at that time vehicle manufacturers started designing headrests to extend the seat back.

Neck injuries in rear-end collisions are supposed to be a noncontact injury(5). The crash causes the trunk to accelerate in a forward direction. The unsupported head cannot follow this motion, which results in a hyperextension of the head. The head moves backward and sharply around its initial position and then rapidly

forward. Normally this type of injury leaves no visibly palpable or radiologically distinguishable indication of injury. That could explain why the medical society has not taken this type of injury into special consideration. There are no investigations or treatment recommended for this type of injury. Nevertheless, it is the second most common diagnosis among car occupants with permanent disability(1).

Neck injuries in rear-end collisions often occur in accidents with low speed(6,7). The initial pulse of acceleration when the rear bumper of the car is struck is apparently sufficient to bring about forces producing injury.

The injuries are supposed to be ligament or muscle damage with bleeding. This bleeding may cause an inflammation that can influence the cervical nerves(3). These patients have pain, weakness or abnormal response in the shoulder areas or upper back areas enervated by the cervical nerves. Some authors have reported headache, blurred eyesight, hearing disturbance, or other symptoms involving the central nervous system(5,8).

This type of injury often occurs in accidents of low severity, which might explain why car manufacturers until quite recently have not done much to improve headrests. The injury-reducing effect is 24 percent for fixed headrests and 14 percent for adjustable ones. These figures are fairly low(1).

Objectives

The aim of this study was to investigate the effectiveness of different types of headrests. Special attention was paid to—

- Investigation of the outcome of rear-end collisions in cars with the same construction except type of headrests
- Adjustment of headrests in real traffic
- Evaluation of the influence of the starting year of production on the incidence of neck injuries in rear-end collisions
- Evaluation of the influence of the weight of the car on the incidence of neck injuries in rear-end collisions
- Evaluation of the influence of the horizontal and vertical position of the headrest on the incidence of neck injuries in rear-end collisions

Material and Methods

The material consists of data from car accidents reported during a 5-year period to Folksam, the largest motor insurance company in Sweden with a market share of 27 percent. The study comprises 339,675 private cars involved in accidents. In these cars, 8,592 drivers and 5,878 passengers were injured or killed.

The accident reports contain data about impact direction, and 90 percent of the reports with bodily injuries also contain hospital records or doctors' certificates. The material has been used in a thesis(1) in which a more detailed description of the material can be found.

For this presentation, special measurements made by Autograph in Sweden(9) have been added to the computerized data, such as the vertical and horizontal position of the headrests to the head of a normal-size dummy. Horizontal and vertical positions were collected for 39 car models.

The horizontal position was defined as the distance between the head (base of the skull) and the lowest position of the headrest. The vertical distance is the distance between the highest position of the headrest and the head (Figure 1). A roadside observation study, where cars were stopped by the police, was conducted to evaluate the normal position of adjustable headrests.

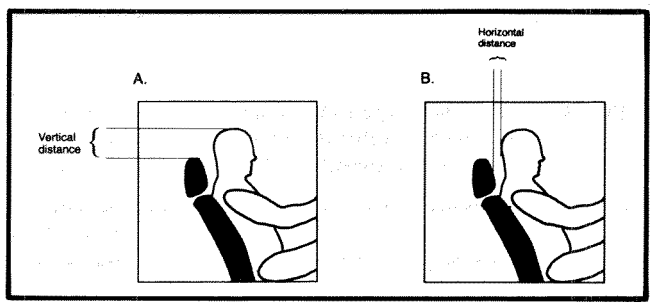

Figure 1. Headrest, vertical (A) distance and horizontal (B) distance
SOURCE: Autograph HB, Sweden

Results

Table 1 shows the severity of injuries in rear-end collisions correlated to different car weights. It can be seen that the injury severity is fairly low expressed in ISS, especially in large cars. The majority of ISS 1-3 is neck injuries.

Table 2 shows the risk of medical disability is much higher for neck injuries in rear-end collisions than for other injuries coded as AIS 1.

Table 3 shows the coefficient of variation for neck injuries in rear-end collisions compared to other directions of impact for 39 car models with headrests. The results show that the incidence of neck injuries in rear-end collisions is more dependent on car model than neck injuries in other directions of impact.

The variation of incidence of neck injuries in rear-end collisions is due to a number of factors, e.g., car weight, horizontal position between head and headrest, as well as

Table 1. Injury severity in rear-end collisions correlated to car weight

Type of car	N	ISS 1-4	ISS 5-10	ISS 11-	Fatally injured
Small car	344	91.0	8.4	0.3	0.3
Medium-size car	763	92.3	6.2	1.2	0.4
Large car	405	94.3	5.2	0.5	0.0

Table 2. Risk of medical disability >10% among car occupants who sustained neck injury in rear-end collisions (AIS 1) compared to all injuries coded as AIS 1 except whiplash

Type of injury	Risk of permanent medical disability
All injuries except neck injuries	0.1%
Neck pain due to rear-end collision	9.6%

Table 3. Coefficient of variation for 39 car models with headrests, a comparison between rear-end and other directions of impact

	Rear-end impact	Other direction
Total CV in %	58	47

vertical position. To study the influence of these three variables, a regression model was fitted to the data.

$$Y = \alpha + \beta_1 x_1 + \beta_2 x_2 + \beta_3 x_3 + \varepsilon$$

Y = Frequency of neck injuries in rear-end collisions

X_1 = Vertical distance between the head of a normal-size dummy and the headrest (see Figure 1)

X_2 = Horizontal distance between dummy head and headrest (see Figure 1)

X_3 = Car weight

ε = Error term

$$Y = 0.101 + 0.0295\, X_1 - 0.00012\, X_2 - 0.0695\, X_3$$
$$(2.05) \qquad (-0.042) \qquad (-2.68)$$

$R^2 = 0.27$

The coefficient of variation of injuries in rear-end collisions was 58 percent. The model explains 27 percent of the variance, which is fairly low. The rest of the variation was due to reasons other than difference in position of headrest and car weight. The car weight and vertical distance were significant, but the horizontal distance between head and headrest was nonsignificant. The range of the horizontal distance was 7-15 and of the vertical distance 4-15 (1 = 2cm).

In Figure 2 it can be seen that the injury frequency of neck injuries in rear-end collisions increased with increased vertical position.

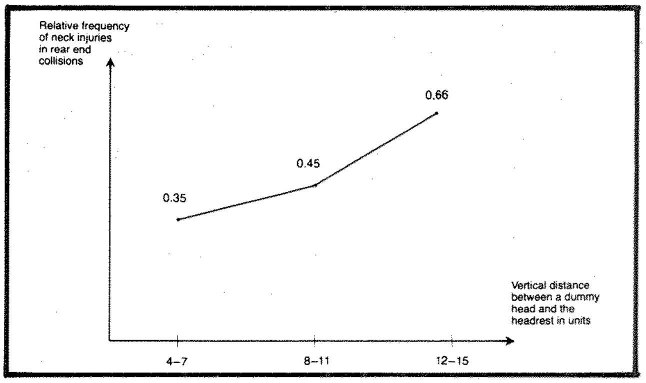

Figure 2. Relative frequency of neck injuries in rear-end collisions correlated to the vertical distance between headrest and dummy head (1 unit vertical distance = 2 cm.)

In connection with the analysis of the relationship of how the position of the headrest affects the incidence of neck injuries a pilot study was made in real traffic. One hundred eighty-seven cars with adjustable headrests were stopped by the police, and it was found that 83 percent of the drivers had their headrests in the lowest or second lowest position. This indicates that the analysis of the position of the headrest in vertical and horizontal distance to the head is adequate.

The variation of incidence of neck injuries correlated to the starting year of production of the studied cars can be seen in Figure 3. The incidence of neck injuries varies for cars with different starting years of production, but there is no reduction of injuries in newer cars.

To determine what happens in newer car models concerning neck injuries, two car makes were studied. The relative incidence of neck injuries in three model year

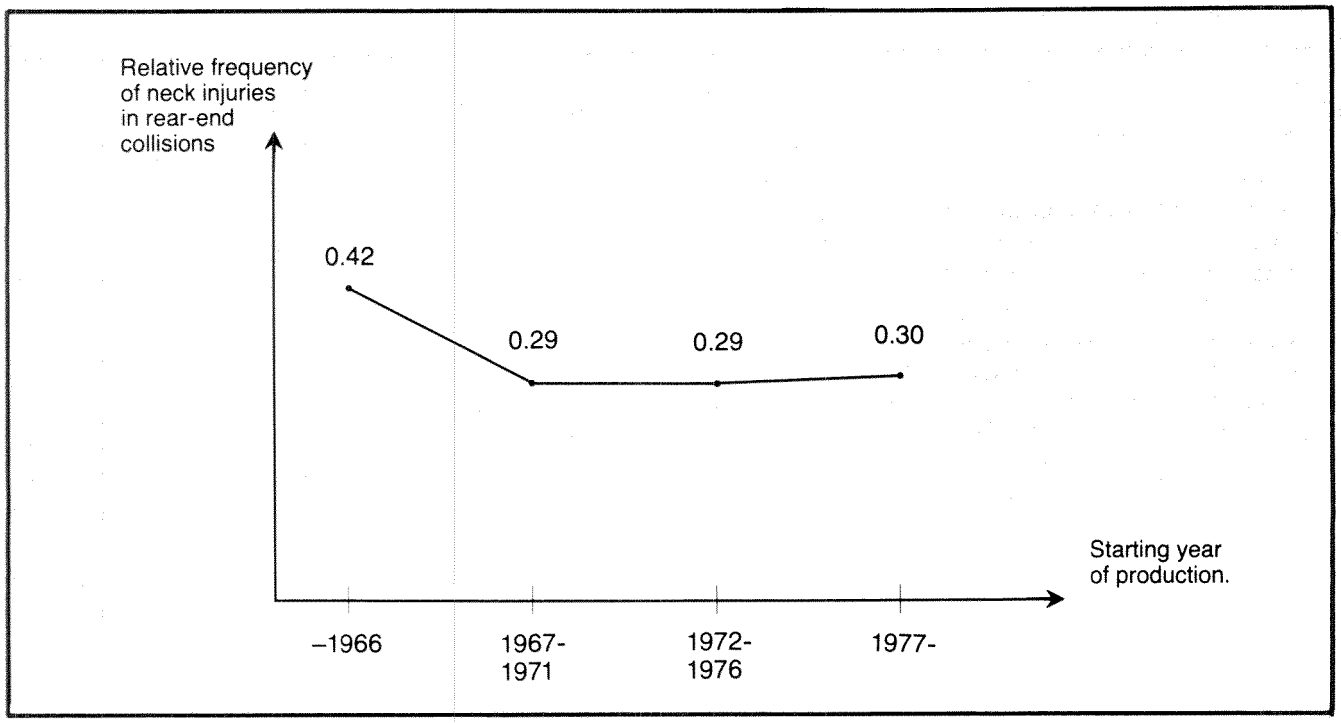

Figure 3. Relative frequency of neck injuries (AIS = 1) in rear-end collisions for different starting years of production

periods for each make was studied where the car models were similar during the period but with different types of headrests. It can be seen that Car A has a reduction of injuries for newer models while there is no such reduction for Car B. This explains why the total incidence of neck injuries does not decrease for newer models. It also indicates that the knowledge of how the headrest really functions is low. Further studies, therefore, are necessary.

Discussion

Neck injuries classified as AIS 1 have not been recognized earlier as a special medical problem. Nygren(1) showed that neck injury is a common reason among car occupants for medical as well as financial disability. It could be estimated that so-called minor neck injuries (AIS 1) cost Swedish insurance companies 100 million

Table 4. Relative frequency of neck injuries in rear-end collisions for two car makes with different headrest designs

Type of car	Production start	N	Relative frequency of neck injuries in rear-end collisions
Car A			
No Headrest	-1969	11,439	0.52
Adjustable	1970-1974	49,003	0.44
Fixed	1975-1983	30,499	0.28
Car B			
No headrest	-1973	11,760	0.37
Fixed	1974-1979	16,714	0.33
Adjustable	1980-	3,863	0.50

kronor a year and society at least the same sum. Measures taken by the car industry and the medical society have not had the desired effect on incidence of neck injuries in rear-end crashes.

In a rear-end collision, the occupant of the struck car will accelerate forward. The unsupported head cannot follow that movement immediately. The head will bend backward in relation to the torso and then flex forward. During that time, the ligaments, muscles, nerves, and vessels of the neck can be damaged. For a person with degenerative changes in the neck, the damage may be even worse. The patient will have problems relating from the neck, but only about half of those injured will go to the doctor immediately. In many cases, medical care is delayed by 3 days or more. This phenomenon with late-appearing symptoms leads to the fact that the patients with such neck injuries go to different doctors, e.g., to the doctor at the emergency care, at their work, to the family doctor, or to a specialist in either neurology, orthopedic surgery, or neurosurgery. The different specialists give different treatments, and no specialty recognizes neck injury as a big problem. The normal course of neck problems in rear-end collisions can be seen in Figure 4.

Rear-end collisions normally cause little damage, and the repair costs are also low(6,7). That is probably why the car industry, until recently, has looked upon neck injuries in rear-end collisions as a very small problem, since many manufacturers make studies only on accidents above a certain repair cost.

This study shows that the vertical distance between head and headrest is important. Owners having cars with adjustable headrests must be instructed how to fix the headrest in a correct position. Since the effectiveness varies, it is important to study rear-end collisions, both under experimental conditions and in real life.

The actual analysis shows there are characteristics other than just the position of the headrest that are important in reducing such injuries. These characteristics must be found to increase the effectiveness of the headrest and avoid neck injuries in rear-end collisions. It has been shown earlier that fixed headrests are more effective than adjustable ones(1). This could be explained by the fact that fixed headrests are in a better position than adjustable ones.

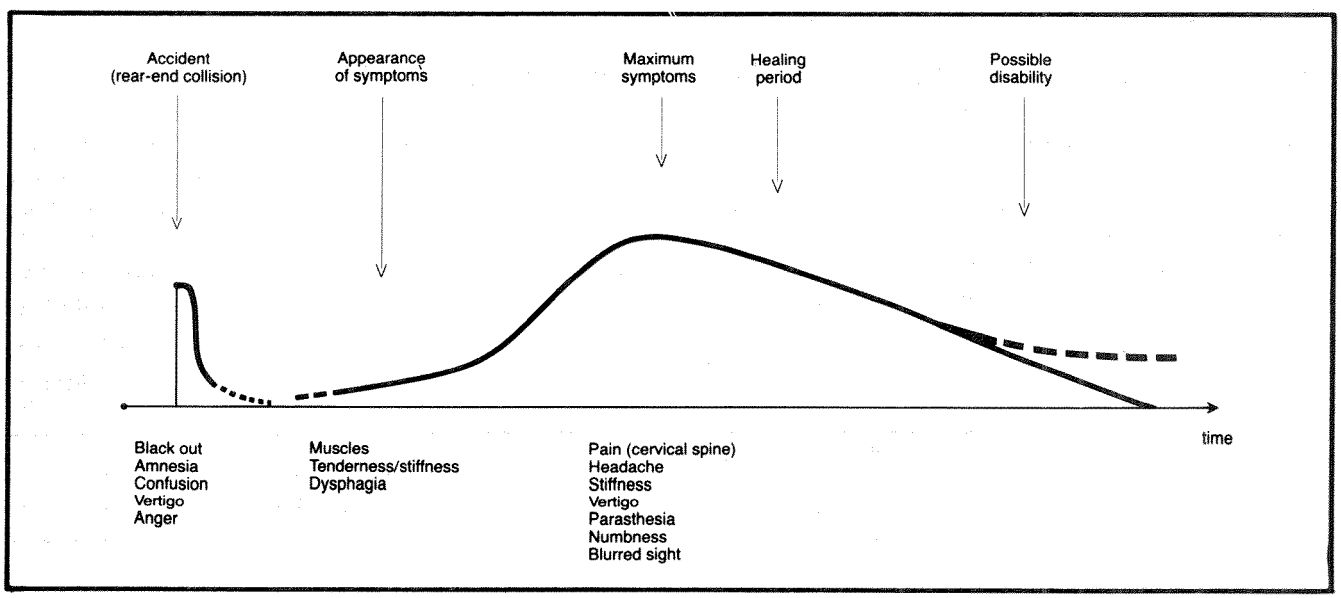

Figure 4. Normal course of neck pain (AIS 1) after rear-end collisions (according to Spangfort)

Conclusions

1. Neck injuries classified as AIS 1 are a great medical problem, especially those that occur in rear-end collisions.
2. Headrests have a certain influence on the incidence of neck injuries in rear-end collisions.
3. There are big differences in effectiveness between different types of headrests shown in a large-scale study.
4. There is no reduction of neck injuries in rear-end collisions for newer car constructions.
5. The vertical position has some influence on the incidence of neck injuries in rear-end collisions.
6. Adjustable headrests are normally adjusted in the lowest position.
7. The weight of the car influences the risk of neck injuries in rear-end collisions.
8. Further studies on headrests, both experimentally and in real life accidents, are necessary.

References

1. Nygren, A., "Injuries to car occupants—some aspects of the interior safety of cars," *Acta Oto-Laryngologica*, Suppl. 395, 164 p., 1984.
2. Belastningsskador i arbetet, 1984:3 Arbetarskyddsstyrelsen ISA Informationsystem om arbetsskador.
3. States, J.D., "Soft tissue injuries of the neck. Human neck: anatomy, injury mechanisms and biomechanics," SAE SP-438, Warrendale, Pennsylvania, pp. 37-43, 1979.
4. Huelke, D.F., E.A. Moffat, R.A. Mendelsohn, and J.W. Melvin, "Cervical fractures and fracture dislocations: an overview. Human Neck: anatomy, injury mechanisms and biomechanics," SAE SP-438, Warrendale, Pennsylvania, pp. 9-15, 1979.
5. Kahane, C.J., "Evaluation of head restraint. Federal motor vehicle safety standard 202," U.S. Department of Transportation, National Highway Traffic Safety Administration, Washington, D.C., 1982.
6. Langwieder, K., S.H. Backaitis, W. Fan, S. Partyka, and A. Ommaya, "Comparative studies of neck injuries of car occupants in frontal collisions in the United States and in the Federal Republic of Germany," Proceedings 25th Car Crash Conference, San Francisco, pp. 71-127, 1981.
7. Portnoy, H.D., J.H. McElhaney, J.W. Melvin, and P.D. Croissant, "Mechanism of cervical spine injury in auto accidents," American Association for Automotive Medicine, 15th Conference, Colorado Springs, October 1971.
8. Roca, P.D., "Ocular manifestations of whiplash injuries," American Association for Automotive Medicine, 15th Conference, Colorado Springs, October 1971.
9. Autograph HB, Personal information and drawings, Helsingborg, Sweden.
10. Spangfort, E., Department of Orthopedic Surgery, Huddinge Sjukhus, Sweden.

Production of Injury in Blunt Frontal Impact

Rolf H. Eppinger and Jeffrey Marcus

U.S. Department of Transportation, National Highway Traffic Safety Administration

Introduction

Blunt thoracic impact as experienced by automobile occupants in frontal impact has received considerable research attention over the past 20 years. These efforts have provided the basis for the development of test dummy impact response specifications as well as evaluation criteria to be used in conjunction with the dummy to evaluate the hazard of various crash situations. This paper will attempt to extend the current understanding of thoracic injury production by examining the results of 82 impact tests to determine the effects that several fundamental parameters have on the production of injuries in the thorax.

Pendulum Tests

While several pioneering efforts investigated the interaction of the driver with the steering system during a frontal crash, most notably those of Gadd(1) and Patrick(2) that led to the development of the characteristics of the energy-absorbing steering column, the efforts of Kroel(3,4), Nahum(5), Neathery(6), and Lobdell(7), using well-controlled pendulum impacts, have led to the current understanding of the dynamics of the thorax under impact conditions and have provided the basis for the generally accepted relationship between thoracic chest compression and the severity of the expected thoracic injuries.

Characterizations of the thoracic response were made by cross-plotting the observed impact force imparted by the pendulum to the thorax against the observed normalized thoracic chest compression (chest compression divided by the original chest depth) for repeated tests in two distinct impact situations: a 51.5-lb linear pendulum striking the thorax at an initial velocity of either 14 or 21ft/s.

Additional testing with various pendulum speeds and masses provided sufficient data for the authors to observe and propose the relationship between chest compression and the degree of thoracic injury severity(6), the severity measure being the Abbreviated Injury Scale. This relationship is linear in nature and combines deflection together with age as the independent variables predicting injury severity. Viano(8), after reexamination of the experimental pendulum impact data as well as extensive manipulations of Lobdell's thoracic model, concluded

that chest deflection was still the most viable injury measure.

Examination of one of Viano's figures (reproduced here as Figure 1), however, reveals that for all averaged injuries in the AIS severity classifications of 3 or greater, the averaged normalized chest deflection is almost uniformly 40 percent. The proposed linear regression model linking AIS with chest deflection merely passes through the midpoint of this vertical portion of the data and the lower injury data points. A truer characterization of the injury versus deflection relationship would show injuries increasing in severity up to the 40 percent deflection level; then any additional increase in injury severity would not be accompanied by an increase in chest deflection.

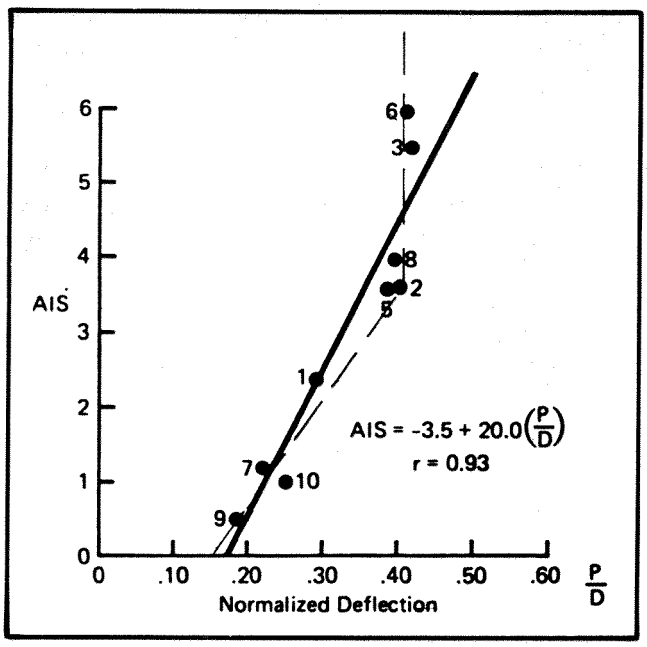

Figure 1. Averaged normalized deflection versus averaged AIS (8)

Since the Viano plot used averages of grouped data that might have masked the real characteristic, a graph (Figure 2) of deflection versus AIS using the individual test points was examined. This also shows the reduced dependence of high AIS injuries on chest deflection. It appears that the thorax reaches its maximum deflection limit at about the AIS 3 level and that other factors influence whether the injury outcome is more serious. This bottoming phenomenon was also recognized by Viano in a subsequent analysis(9)

Energy Considerations

Since the Kroell series of pendulum tests were well controlled and many of the geometrical conditions invariant, i.e., the impact pendulum remained a flat, 6in diameter rigid surface and the point of impact remained

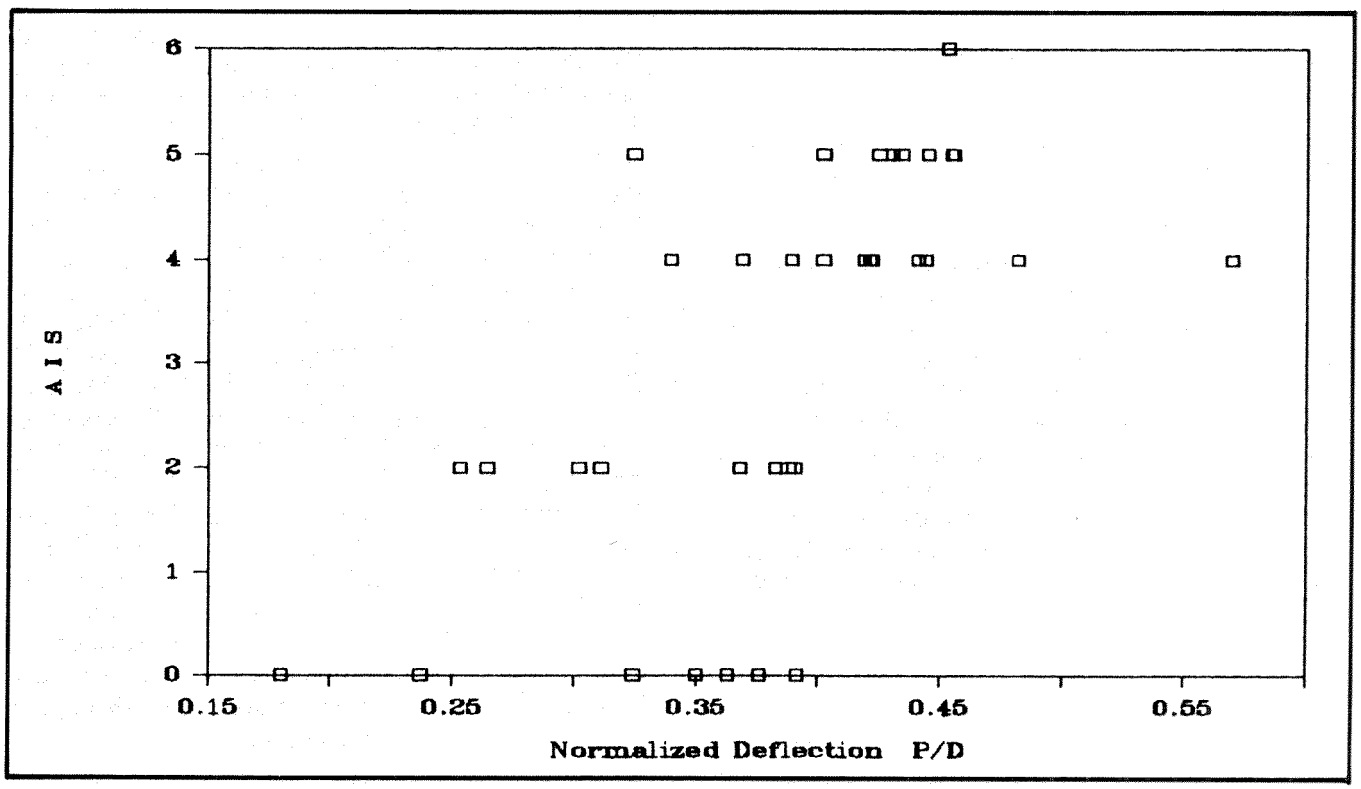

Figure 2. Normalized deflection versus AIS: 6in diameter pendulum

at the fourth costal interspace, it was decided to investigate if thoracic injury (AIS) is a function of the amount of energy that the thorax absorbed in each test. Since rigid pendulums of known masses traveling at known initial velocities struck cadavers of known weight and stature, it was assumed that both momentum and energy balances could be made using reasonable assumptions. These assumptions were: (1) the pendulum was effectively a rigid body and therefore could not absorb energy internally, (2) the pendulum interacted only with the thoracic mass, which is some constant proportion of the total body mass, (3) there is a point during the impact event at which all of the thoracic mass is traveling at a common velocity with the pendulum, (4) as a result of 1 and 3 and enforcing the conservation of energy, the difference between the initial kinetic energy of the pendulum and the kinetic energy of the pendulum and the thorax at the time of common velocity must be absorbed by the thorax, and (5) it is this absorbed energy that produces injury. Analytically, the absorbed energy was calculated using the following relationship . (A detailed derivation of this relationship is given in Appendix A.)

$$E_{abs} = ((k * M_s) / (M_p + k * M_s)) * E_{pend}$$

where:

E_{abs} is the thoractic absorbed energy

k is ratio of active thoracic mass to total body mass (determined to be 0.35)

M_p is mass of the striking pendulum

M_s is mass of the subject

E_{pend} is the initial kinetic energy in the penduluim

Assuming that larger and more massive subjects would be able to sustain greater doses of energy than smaller and less massive subjects, it was decided to develop a parameter, called specific absorbed energy (SAE), calculated by dividing the thoracic absorbed energy by the total body mass of the test specimen. This can be viewed as a primitive or overall energy density function. The relationship of this parameter versus AIS is shown in Figure 3.

Several interesting things can be noted when comparing this figure with Figure 2. First, it can be seen in Figure 2 that the greater portion of the AIS>=4 injuries occur at a normalized chest deflection between 40 and 45 percent while in Figure 3 for these same tests the specific absorbed energy continues to increase. This suggests that while the thoracic deflection capacity is limited to approximately a 45 percent level, the thorax continues to have the capacity to absorb ever greater quantities of energy. Second, it can be seen that as the quantity of specific absorbed energy increases, the likelihood of higher and higher levels of thoracic injury increases, suggesting that this parameter better explains the production of injury in the thorax and may indeed be the causal factor

Additional Data

Over the past several years, NHTSA and other organizations have sponsored several programs that have impacted cadaveric specimens in a variety of simulated frontal collisions. The impact conditions range from pendulum tests very similar to the Kroell tests but which have used impact surfaces of different areas(10) or a diagonal torso belt strap(11) to sled impact tests using either a 2-point shoulder harness(12) or an airbag restraint(13) with knee bar. Five human volunteer pendulum impacts by Patrick(14) are also included. (Table 1 summarizes the type, number, source, and essential parameters of all of the tests used in this analysis.) Since the specific absorbed energy explained the production of injury so well in the Kroell pendulum tests, it was decided to analyze the additional available tests to see if this parameter could explain injury production in these conditions as well.

Several additional processing techniques, which are described in Appendixes B and C, were developed to calculate the specific absorbed energy for these other test conditions. The results are shown in Figure 4 where the SAE from all tests is cross-plotted against AIS. It is interesting to note there appears to be a progression of increased energy-absorbing capacity as one considers first the 6in diameter pendulum tests, then the increased area pendulum tests, the belt tests, and the airbag tests. This increased energy-absorbing capability is greatest when comparing the airbag to the 6in pendulum where it can be seen that it requires approximately six times more absorbed energy to produce the same level injury in an airbag test than it does in a pendulum test. Figure 5 graphically illustrates this point. Here, all calculated pendulum SAE's were multiplied by 6, the belt-related SAE's were multiplied by 1.25, and the airbag SAE values were left unchanged. The data were replotted against each observed AIS. This process significantly compresses the spread in the data and shows that the relationship between specific absorbed energy and injury is similar for a variety of restraint types except for the various constant factors.

Additional Factors Influencing Injury

The available data for all of the tests analyzed for SAE were further scrutinized for factors that might explain the large differences in absorbed energy needed to produce a certain level of injury. The first and most obvious

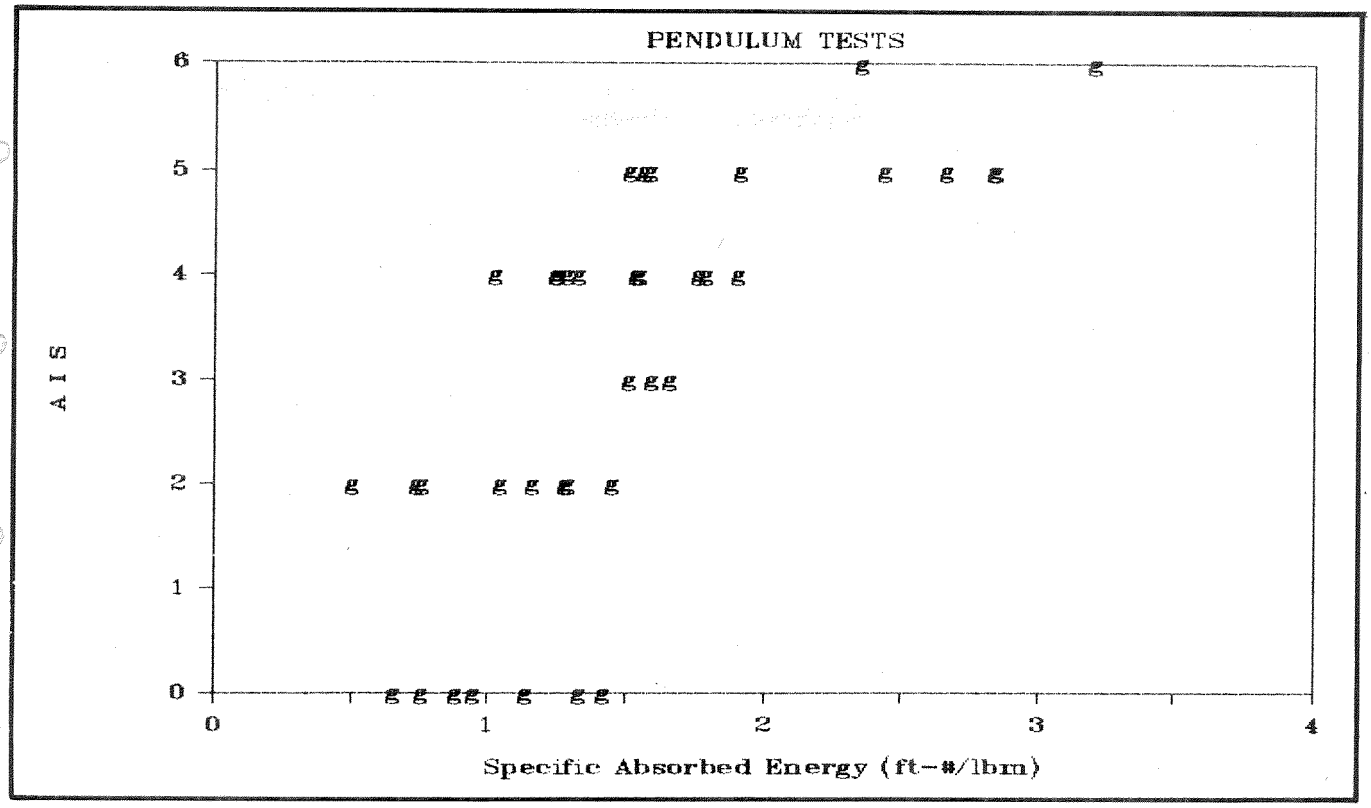

Figure 3. Specific absorbed energy versus AIS

difference between the various tests was that the impact contact area varied greatly. Reasoning that, if a certain dose of energy were to be delivered to the thorax, it would produce more injury if it were delivered through a small contact area than if it were delivered through a large area because the local energy density would be higher, all SAE's were divided by the area of the contact surface delivering the impact force. The exact area of each type of pendulum face was calculated and approximations were made for both the shoulder belts and the airbag systems. Figure 6 shows the result of this effort. Clearly, consideration of area effects alone does little to explain the large differences in absorbed energy tolerances between the various restraint configurations.

Further analysis of the data revealed that the time required for the body to acquire the absorbed energy varied considerably over the variety of test conditions. Therefore, using the reasoning that, if a certain dose of energy were delivered in a short time period, it would be more harmful than if it were delivered over a longer period of time, the SAE's were divided by the observed time thus generating a larger value of shorter time durations. Figure 7 shows the result of this effort. Again, this factor by itself does not provide any better explanation of the events.

Since the arguments supporting the influence of area and time duration were both considered reasonable, it was decided to evaluate their combined influence. This was done by dividing the specific absorbed energy by the product of the effective contact area and the time duration. It can be seen in Figure 8 that this function, SAE/(A*T), does make the different restraint-loading conditions cluster around the same level for each of the various injury severity levels.

Discussion

The above analysis strongly suggests that the production of trauma in the thorax is dependent on three factors:(1) the amount of energy (nonkinetic) that the thorax absorbs during an impact, (2) the area over which the impact forces are applied to the thorax, and (3) the length of time needed for the thorax to acquire the nonkinetic energy delivered to it. Since the analysis identifying these factors was totally an empirical one, additional theoretical and experimental evidence characterizing the effects of these factors in producing structural failures would provide additional support for the validity of this proposed injury production hypothesis.

The first factor, the amount of absorbed nonkinetic energy per pound of body weight, is clearly analogous to a variety of strain energy or energy density functions that are the basis of several currently employed failure criteria. It can be reasoned that the process of an automotive crash event start- with the subject possessing

Table 1. Thoracic injury analysis data — specific absorbed energy

TEST #	TEST TYPE	IMPACTOR AREA (IN 2)	IMPACTOR VEL (m/s)	IMPACTOR MASS (Kg)	AGE (yrs)	SUBJECT MASS (Kg)	AIS (Tx)	Epend (#-ft)	Eabs Tx (#-ft)	EabTx/Wt (#-ft/lbm)	dT to Max d or F (msec)	E/WAdT #-ft (lbm-ft 2-msec)	Reference
42fm	RIGID PEND(CAD)	28.27	4.87	23.00	61	54.4	0	200.48	90.80	0.76	23.80	0.1624	(2),(3)
45fm	RIGID PEND(CAD)	28.27	5.05	23.00	64	64.0	2	215.57	106.36	0.76	27.00	0.1425	(2),(3)
60fm	RIGID PEND(CAD)	28.27	4.34	23.00	60	79.4	2	159.22	87.12	0.50	25.80	0.0985	(2),(3)
53fm	RIGID PEND(CAD)	28.27	5.23	23.00	75	77.1	2	231.21	124.82	0.74	27.70	0.1353	(2),(3)
19fm	RIGID PEND(CAD)	28.27	6.71	23.40	19	71.4	2	387.21	199.97	1.27	20.00	0.3242	(2),(3)
20fm	RIGID PEND(CAD)	28.27	6.70	23.40	29	56.5	0	386.06	176.82	1.42	28.00	0.2588	(2),(3)
63fm	RIGID PEND(CAD)	28.27	7.00	23.40	53	88.2	4	421.40	239.70	1.24	20.00	0.3146	(2),(3)
64fm	RIGID PEND(CAD)	28.27	6.93	23.40	72	63.0	2	413.02	200.37	1.45	15.00	0.4909	(2),(3)
22fm	RIGID PEND(CAD)	28.27	6.71	23.40	72	74.8	4	387.21	204.46	1.24	25.20	0.2511	(2),(3)
18fm	RIGID PEND(CAD)	28.27	6.71	23.40	78	65.8	4	387.21	192.06	1.33	21.00	0.3218	(2),(3)
15fm	RIGID PEND(CAD)	28.27	6.88	23.40	80	53.1	4	407.08	180.20	1.54	20.00	0.3929	(2),(3)
13fm	RIGID PEND(CAD)	28.27	7.42	23.40	81	76.2	5	473.49	252.20	1.50	25.10	0.3053	(2),(3)
21ff	RIGID PEND(CAD)	28.27	7.30	23.10	45	68.6	4	452.42	230.58	1.53	28.40	0.2740	(2),(3)
12ff	RIGID PEND(CAD)	28.27	7.72	23.10	67	62.6	4	505.98	246.30	1.79	20.00	0.4555	(2),(3)
14ff	RIGID PEND(CAD)	28.27	7.82	23.10	76	57.6	5	519.17	241.94	1.91	27.70	0.3511	(2),(3)
37fm	RIGID PEND(CAD)	28.27	9.83	23.00	48	73.9	5	816.81	432.35	2.66	14.00	0.9676	(2),(3)
31fm	RIGID PEND(CAD)	28.27	10.20	23.00	51	74.8	5	879.45	468.16	2.84	20.00	0.7246	(2),(3)
24fm	RIGID PEND(CAD)	28.27	9.66	23.00	65	81.6	5	788.80	436.93	2.43	20.00	0.6199	(2),(3)
32fm	RIGID PEND(CAD)	28.27	10.00	23.00	75	54.5	6	845.30	383.22	3.20	21.90	0.7434	(2),(3)
46fm	RIGID PEND(CAD)	28.27	7.30	19.10	46	94.8	0	374.08	237.41	1.14	27.00	0.2148	(2),(3)
36fm	RIGID PEND(CAD)	28.27	7.20	19.10	52	74.8	4	363.90	210.40	1.28	19.60	0.3323	(2),(3)
34fm	RIGID PEND(CAD)	28.27	8.23	19.10	64	59.0	4	475.46	247.00	1.90	20.00	0.4847	(2),(3)
11ff	RIGID PEND(CAD)	28.27	6.72	19.60	60	59.1	2	325.30	167.03	1.28	20.00	0.3272	(2),(3)
54ff	RIGID PEND(CAD)	28.27	6.70	19.60	49	37.2	5	323.36	129.07	1.58	24.90	0.3226	(2),(3)
23ff	RIGID PEND(CAD)	28.27	8.25	19.60	58	61.2	4	490.28	256.02	1.90	20.00	0.4843	(2),(3)
25fm	RIGID PEND(CAD)	28.27	14.70	5.50	65	54.4	5	436.80	338.90	2.83	10.00	1.4424	(2),(3)
26fm	RIGID PEND(CAD)	28.27	11.90	1.90	75	63.5	0	98.89	91.10	0.65	12.50	0.2657	(2),(3)
28fm	RIGID PEND(CAD)	28.27	15.45	1.60	54	68.0	0	140.37	131.52	0.88	13.80	0.3245	(2),(3)
30ff	RIGID PEND(CAD)	28.27	13.30	1.60	52	40.8	2	104.02	93.54	1.04	10.80	0.4915	(2),(3)
51FM(RB)	RIGID PEND(CAD)	28.27	6.66	10.50	60	82.3	0	171.17	171.17	0.95	28.00	0.1720	(2),(3)
56FM(RB)	RIGID PEND(CAD)	28.27	7.00	10.50	65	74.1	2	189.09	189.09	1.16	22.00	0.2686	(2),(3)
52FM(RB)	RIGID PEND(CAD)	28.27	7.20	10.50	65	51.8	4	200.05	200.05	1.76	25.00	0.3577	(2),(3)
50FM(RB)	RIGID PEND(CAD)	28.27	7.30	10.50	66	60.1	5	205.65	205.65	1.56	23.90	0.3315	(2),(3)
58fm(RB)	RIGID PEND(CAD)	28.27	7.00	10.50	68	69.1	4	189.09	189.09	1.24	23.00	0.2755	(2),(3)
48fm(RB)	RIGID PEND(CAD)	28.27	7.00	10.50	69	64.5	0	189.09	189.09	1.33	21.00	0.3232	(2),(3)
55ff	RIGID PEND(CAD)	28.27	9.92	19.55	46	81.0	6	707.06	418.48	2.35	16.00	0.7476	(2),(3)
62fm	RIGID PEND(CAD)	28.27	6.93	9.98	76	50.0	4	176.15	112.18	1.02	28.30	0.1836	(2),(3)
119FM	RIGID PEND(CAD)	28.27	13.40	4.25	69	65.0	3	280.47	236.32	1.65	NA		(2),(3)
121FM	RIGID PEND(CAD)	28.27	13.40	4.25	66	68.2	3	280.47	238.08	1.59	NA		(2),(3)
123FM	RIGID PEND(CAD)	28.27	13.40	4.25	58	72.3	3	280.47	240.14	1.51	NA		(2),(3)
LMP1	RIGID PEND(VOL)	28.27	2.40	10.00		73.0	0	21.17	15.21	0.09	37.00	0.0130	(14)
LMP2	RIGID PEND(VOL)	28.27	3.40	10.00		73.0	0	42.49	30.53	0.19	31.00	0.0312	(14)
LMP3	RIGID PEND(VOL)	28.27	4.20	10.00		73.0	0	64.83	46.59	0.29	28.00	0.0528	(14)

Table 1. continued

TEST #	TEST TYPE	IMPACTOR AREA (IN 2)	IMPACTOR VEL (m/s)	IMPACTOR MASS (Kg)	AGE (yrs)	SUBJECT MASS (Kg)	AIS (Tx)	Epend (#-ft)	Eabs Tx (#-ft)	EabTx/Wt (#-ft/lbm)	dT to Max d or F (msec)	E/WAdT #-ft (lbm-ft 2-msec)	Reference
LMP4	RIGID PEND(VOL)	28.27	2.40	10.00		73.0	0	21.17	15.21	0.89	37.00	0.0130	(14)
LMP5	RIGID PEND(VOL)	28.27	2.40	10.00		73.0	0	21.17	15.21	0.09	37.00	0.0130	(14)
LMP6	RIGID PEND(VOL)	28.27	3.40	10.00		73.0	0	42.49	30.53	0.19	31.00	0.0312	(14)
LMP7	RIGID PEND(VOL)	28.27	3.40	10.00		73.0	0	42.49	30.53	0.19	31.00	0.0312	(14)
LMP8	RIGID PEND(VOL)	28.27	4.60	10.00		73.0	0	77.77	55.89	0.35	27.00	0.0657	(14)
CM25	RIGID PEND(CAD)	80.00	7.60	23.40	55	85.5	4	496.74	278.69	1.48	18.00	0.1482	(10)
CM29	RIGID PEND(CAD)	80.00	7.55	23.60	71	68.6	2	494.41	249.34	1.65	NA		(10)
CM30	RIGID PEND(CAD)	80.00	7.51	23.60	66	84.1	2	489.19	271.51	1.47	16.00	0.1651	(10)
CM31	RIGID PEND(CAD)	80.00	7.19	23.60	57	73.2	1	448.39	233.40	1.45	19.00	0.1373	(10)
CM32	RIGID PEND(CAD)	54.00	7.33	23.60	60	57.3	3	466.02	214.03	1.70	12.00	0.3775	(10)
CM33	RIGID PEND(CAD)	54.00	7.42	23.60	70	59.5	1	477.53	223.85	1.71	14.00	0.3257	(10)
CM34	RIGID PEND(CAD)	28.27	6.39	23.60	55	64.1	2	354.16	172.60	1.22	22.00	0.2834	(10)
CM35	RIGID PEND(CAD)	28.27	7.73	23.60	69	68.2	2	518.27	260.61	1.74	18.00	0.4915	(10)
CM36	RIGID PEND(CAD)	54.00	10.14	23.60	61	72.7	2	891.81	462.68	2.89	17.00	0.4538	(10)
CM37	RIGID PEND(CAD)	54.00	10.10	23.60	57	46.8	4	884.79	362.50	3.52	16.00	0.5868	(10)
CM38	RIGID PEND(CAD)	80.00	10.10	23.60	49	44.1	4	884.79	349.86	3.61	10.00	0.6491	(10)
CM39	RIGID PEND(CAD)	54.00	8.98	23.60	65	70.4	2	699.44	357.26	2.31	18.00	0.3417	(10)
CM40	RIGID PEND(CAD)	54.00	10.95	23.60	61	83.6	2	1039.98	575.67	3.13	20.00	0.4173	(10)
UCSD226	BELT PEND(CAD)	37.00	6.57	23.60	31	49.1	4	374.39	157.75	1.41	18.00	0.3051	(11)
UCSD227	BELT PEND(CAD)	37.00	6.77	23.60	54	60.5	2	397.53	188.00	1.38	20.00	0.2689	(11)
UCSD236	BELT PEND(CAD)	37.00	7.24	24.70	50	54.1	3	475.84	206.49	1.65	16.00	0.4005	(11)
UCSD244	BELT PEND(CAD)	37.00	7.53	27.10	60	72.1	5	564.73	272.30	1.62	20.00	0.3162	(11)
UCSD245	BELT PEND(CAD)	37.00	6.37	27.10	50	90.9	5	404.14	218.24	1.02	20.00	0.1977	(11)
WS3022	AIR BAG(CAD)	100.00			66	72.2	5		1110.00	6.99	41.00	0.2454	(13)
WS3026	AIR BAG(CAD)	100.00			54	50.0	0		728.60	6.62	47.00	0.2029	(13)
WS3032	AIR BAG(CAD)	100.00			56	96.4	2		2075.50	9.79	45.00	0.3132	(13)
WS3035	AIR BAG(CAD)	100.00			63	74.0	1		1468.80	9.02	44.00	0.2953	(13)
WS3038	AIR BAG(CAD)	100.00			68	83.2	4		2094.20	11.44	39.00	0.4224	(13)
WS3039	AIR BAG(CAD)	100.00			67	60.0	0		1095.90	8.30	44.00	0.2717	(13)
WS3040	AIR BAG(CAD)	100.00			61	87.7	1		1471.70	7.63	55.00	0.1997	(13)
WS3041	AIR BAG(CAD)	100.00			66	60.9	0		582.90	4.35	45.00	0.1392	(13)
WSU F16	BELT(CAD)	37.00			60	80.9	2		947.58	5.32	70.00	0.2960	(12)
WSU F18	BELT(CAD)	37.00			21	60.0	0		532.22	4.03	61.00	0.2572	(12)
WSU F19	BELT(CAD)	37.00			65	56.4	1		512.11	4.13	70.00	0.2296	(12)
WSU F20	BELT(CAD)	37.00			29	95.9	2		1398.75	6.63	68.00	0.3794	(12)
WSU F21	BELT(CAD)	37.00			56	51.4	2		546.21	4.83	62.00	0.3034	(12)
WSU F23	BELT(CAD)	37.00			63	70.5	2		1170.12	7.55	50.00	0.5876	(12)
WSU F25	BELT(CAD)	37.00			58	74.5	2		1277.36	7.79	55.00	0.5511	(12)
WSU F26	BELT(CAD)	37.00			63	52.3	2		922.72	8.02	58.00	0.5384	(12)

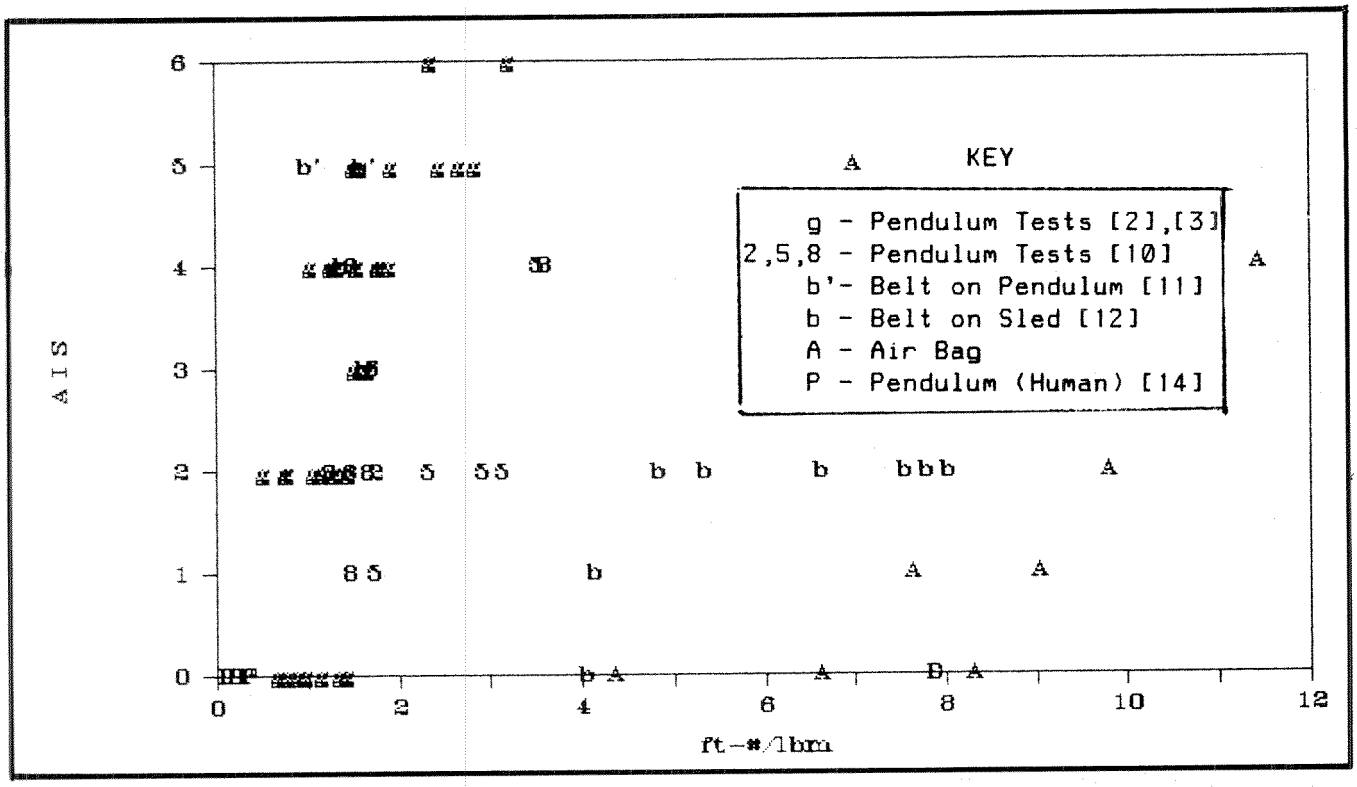

Figure 4. Specific absorbed energy versus AIS (all available tests)

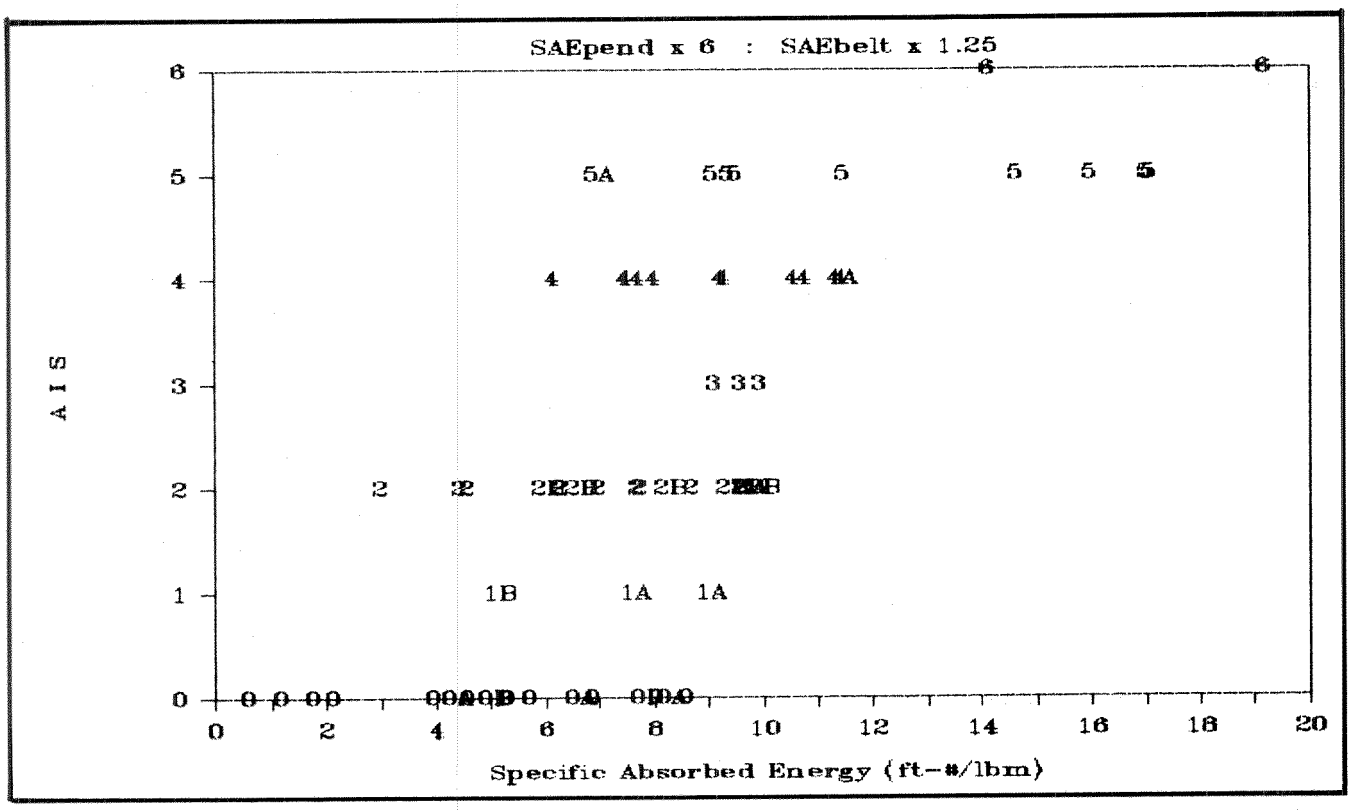

Figure 5. Artificially adjusted specific absorbed energy versus AIS

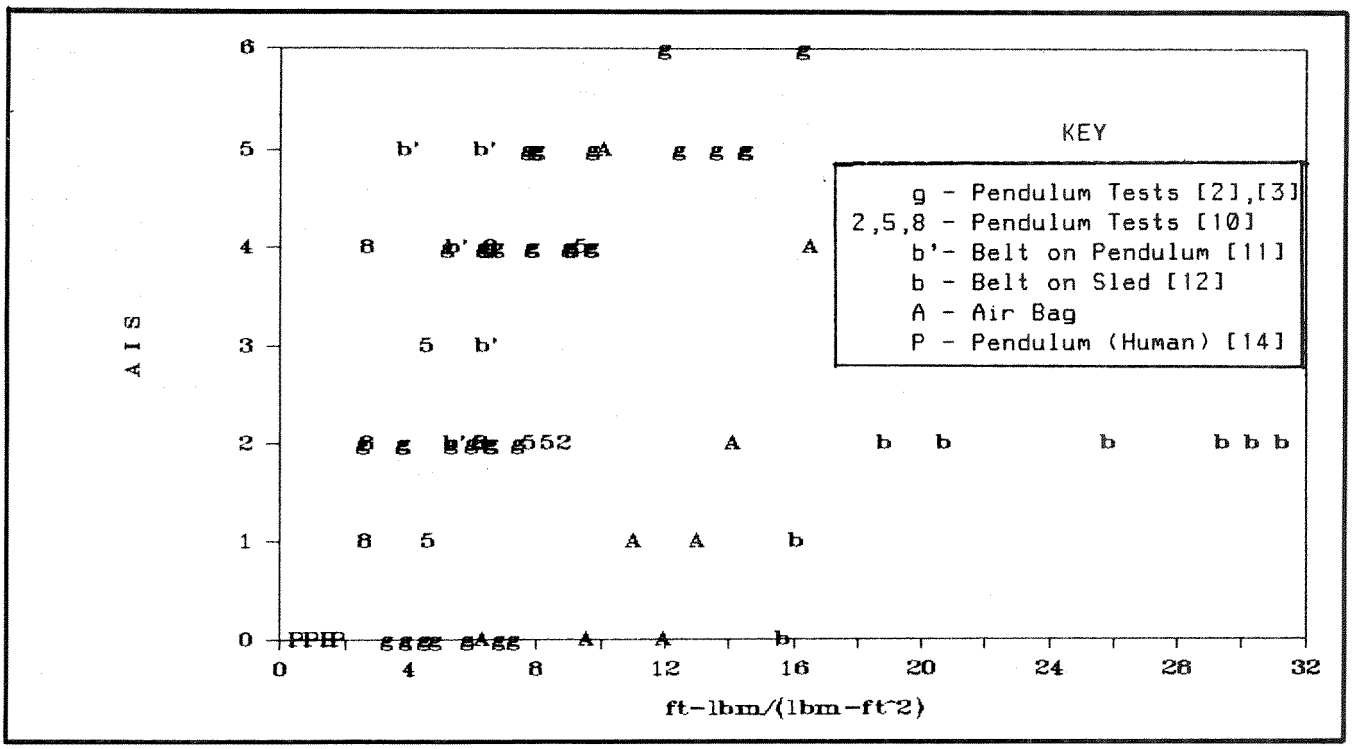

Figure 6. Specific absorbed energy/area versus AIS

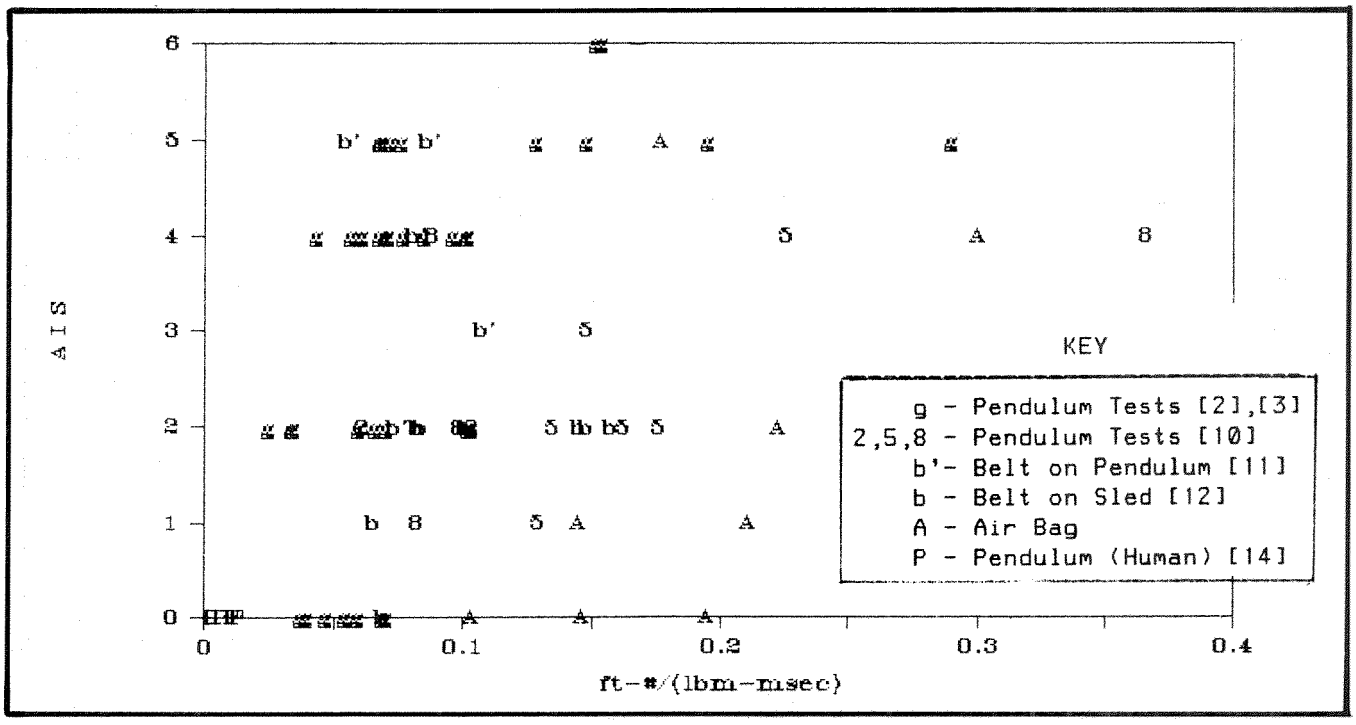

Figure 7. Specific absorbed energy/time versus AIS

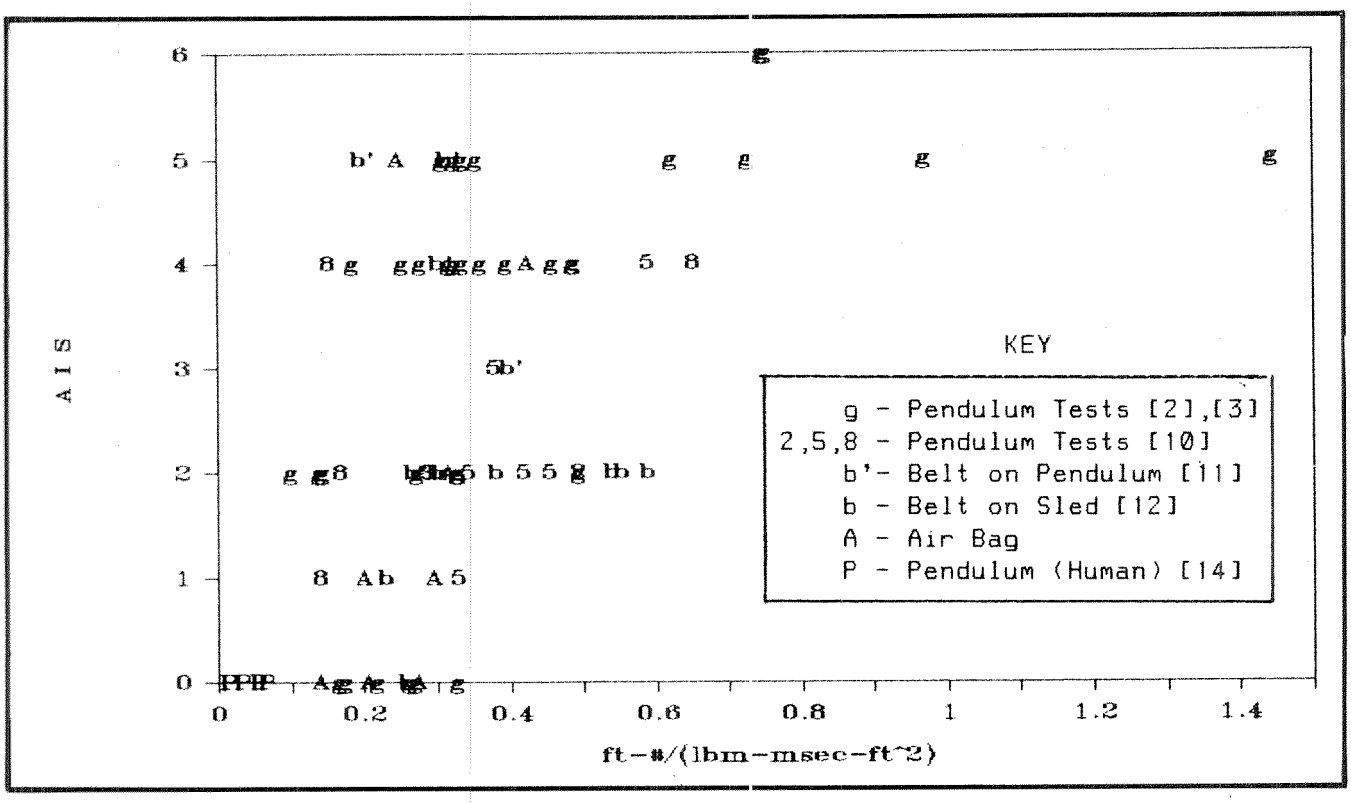

Figure 8. Specific absorbed energy/(area * time) versus AIS

a specific amount of kinetic energy and that after the event is over, this kinetic energy is no longer present. The principle of the conservation of energy requires that this kinetic energy either be removed from the body or converted into other forms of energy within the body. Therefore, as the internalized absorbed energy exceeds the energy capacity of the structure, it could be expected that it will fail and the extent of failure would be proportional to the degree to which the absorbed energy exceeds the threshold capacity.

Arguments in support of the observed effects of area can be easily derived from simple beam theory by considering two extreme loading conditions of a simply supported beam: a point force loading the beam exactly midspan and a load equal to the point load but uniformly loading the beam over its entire length. Beam theory shows that the outer fiber stresses and strains are twice as high for the point load than for the uniformly distributed load condition. Therefore, the point-loaded beam would fail at a load of one-half the load of the uniformly loaded beam if a maximum stress or strain failure mechanism were in effect.

A possible explanation of why area increases by themselves do not explain the injury variation seen in the experimental data can also be derived from the beam theory. That is, beam theory also shows that the deflection of the uniformly loaded beam is only 62 percent that of the point-loaded beam and therefore the effective stiffness and the natural frequency of the uniformly loaded beam is higher. This would imply that under similar time histories of total load, the uniformly loaded beam would respond quicker and, if the time allowed to absorb the energy is also critical, this quicker response would offset some of the gains obtained by increasing the area. The pendulum tests that varied the impactor surface area bear out this phenomenon of faster response with greater area. The data indicate that the average time to acquire the absorbed energy when using the 26in^2 impactor was 20ms. This decreased to 16.2 and 15.7ms as the area was increased to 56 and 80in^2, respectively. The pendulum belt tests also confirm this effect with an 18.8ms absorption period as compared to 21.5 for all the Kroell tests.

Other arguments in support of time dependence can be found or developed. Alternative experimental evidence can be offered by examining the work of McElhaney(15) in which he tested human and bovine femurs to failure at strain rates between 0.001 and 1,000 percent/s. He observed that both the energy to failure and the strain at failure decrease at strain rates above 1 percent/s. This critical strain rate is well below those experienced in thoracic impacts. Reduced energy-absorbing capacity as a function of strain rate may also be a factor in soft tissue failures. Alternative qualitative arguments in support of time dependence can be made by considering the Kroell tests. Since most of the AIS>=4 injuries were produced at close to the maximum chest deflection, which can be surmised to be close to the point at which the posterior surface of the sternum contacts the anterior surface of the

spinal column, the higher rates of loading would either require the internal organs to displace more rapidly from their normal positions and produce organ failure due to higher stresses, strains, and inertial forces or cause physical crushing of the organs due to the increased inability of the organs to move rapidly out of the way because of their visco-elastic stiffening behavior at high loading rates.

The airbag and torso belt tests examined in this analysis have, by virtue of the "ride down effect," greatly extended energy absorption time periods (averages of 45 and 62ms for the bag and belt, respectively) while maintaining contact areas similar to impact events of much shorter duration. Since the total specific absorbed energies for the sled belt and bag tests were much greater than with the short duration events, but the injuries were equivalent, it can be deduced that modulation of the energy absorption time periods has a profound effect on injury production.

The instrumentation and experimental techniques employed by the studies used in this analysis were not designed to measure energy transfers directly and, therefore, all results presented herein were calculated from the data by using a variety of assumptions and judgments. These assumptions and judgments may have contributed to both systematic and random errors in the calculated values of the independent variables finally considered significant, i.e., absorbed energy, area of contact, and time duration, and ultimately degrade somewhat the quality of the injury severity-dose relationship as presented in Figure 8. However, even in light of these computational uncertainties, it is felt that the strength of the proposed injury hypothesis is undeniable because of the diverse data it is capable of explaining.

Conclusions and Recommendations

This study strongly suggests that the severity of injury produced in the thorax is proportional to the amount of specific energy that the thorax must absorb during an impact and inversely proportional to the area over which the impact energy is either delivered or extracted and the length of time over which this is all accomplished. The magnitude and diversity of the impact data used in this analysis lend greatly to the support of the proposed injury production hypothesis and suggest that further investigations should be pursued that will directly address the viability of the hypothesis. The rationale for the selection of specific measurements in these studies should be guided in part by their demonstrated capability in measuring the parameters identified in this study.

Since the specific absorbed energy, the area over which it is delivered, and the time required to transfer the impact energies are not measures currently available from test dummies, direct evaluation of thoracic impact hazards using the proposed injury hypothesis is not possible at this time. Initiation of efforts to make specific absorbed energy a realizable dummy-based measurement is recommended as are continued efforts to develop injury relationships based on current body-based measures.

The lack of capability in current test dummies to measure these factors directly should, however, not preclude their use because they can be deduced by analytical methods or by additional dedicated experimental instrumentation. It is therefore recommended and encouraged that the proposed injury production hypotheses be considered in the development of automotive safety systems.

References

1. Gadd, C.W., and L.M. Patrick, "System versus laboratory impact tests for estimating injury hazard," SAE Automotive Engineering Congress, 680053, Detroit, January 1968.
2. Patrick, L.M., H.J. Mertz, and C.K. Kroell, "Cadaver, knee, chest and head impact loads," Proceedings 11th Stapp Car Crash Conference, SAE Paper 670913, October 1967.
3. Kroell, C.K., D.C. Schneider, and A.M. Nahum, "Impact tolerance and response of the human thorax," Proceedings 15th Stapp Car Crash Conference, SAE Paper 710851, November 1971.
4. Kroell, C.K., D.C. Schneider, and A.M. Nahum, "Impact tolerance and response of the human thorax II," Proceedings 18th Stapp Car Crash Conference, SAE Paper 741187, Warrendale, Pennsylvania, 1974.
5. Nahum, A.M., D.C. Schneider, and C.K. Kroell, "Cadaver skeletal response to blunt impact," Proceedings 19th Stapp Car Crash Conference, SAE Paper 75150, Warrendale, Pennsylvania, 1975.
6. Neathery, R.F., C.K. Kroell, and H.J. Mertz, "Prediction of thoracic injury from dummy responses," Proceedings 19th Stapp Car Crash Conference, SAE, Warrendale, Pennsylvania, 1975.
7. Lobdell, T.E., C.K. Kroell, D.C. Schneider, W.E. Hering, and A.M. Nahum, *Impact Response of the Human Thorax; Human Impact Response,* edited by King and Mertz, Plenum Press, New York, 1973.
8. Viano, D.C. "Evaluation of biomechanical response and potential injury from thoracic impact; aviation space and environmental medicine," Vol. 49, No. 1, ASEMCG 49(1) 1-348, 1978.
9. Viana, D.C. "Thoracic injury potential," Proceedings 3rd IRCOBI Conference, Lyon, France, September 1978.
10. Walsh, M.J., and B.J. Kellerher, Progress reports to NHTSA under Contract No. DTNH 22-83-C-47019, "Thoracic/abdominal trauma from impact with steering assembly/instrument panel," October 1983-May 1985.

11. Schneider, D.C., "Analysis of human cadaver and ATD blunt thoracic impacts," Final report, as contained with Occupant Injury Criteria Assessment Report to August 10, 1982, Biokinetics and Assoc. Ltd., Ottawa, Canada, Document R82-9.
12. Cheng, R., K. Yang, R.S. Levine, and A.I. King, "Dynamic impact loading of the femur under passive restrained condition," Proceedings 28th Stapp Car Crash Conference, SAE Paper 841661, p.152, Warrendale, Pennsylvania, November 1984.
13. Cheng, R., K. Yang, R.S. Levine, A.I. King, and R.M. Morgan, "Injuries to the cervical spine caused by a distributed frontal load to the chest," Proceedings 26th Stapp Car Crash Conference, SAE, Warrendale, Pennsylvania, October 1982.
14. Patrick, L.M., "Impact force-deflection of the human thorax," Proceedings 25th Stapp Car Crash Conference, SAE Paper 811014, Warrendale, Pennsylvania, 1981.
15. McElhaney, J.H., and E.F. Byars, "Dynamic response of biological materials," Amer. Soc. Mech. Eng., 655-WA/HUF-9.

Appendix A

Computation of SAE for Pendulum Tests

In a pendulum test, a rigid impactor of known mass and known initial velocity struck a stationary test subject. In this study, it was assumed that the effective mass of the thorax was 35 percent of total body mass. This figure has been reported and used by others(1,2,3,4,5,6,7). The impactor struck the test subject and some time later the test subject and the impactor moved with a common velocity. From momentum considerations

$$M_p\ v_i = (M_e + M_p)\ v_f$$

where:

M_p = mass of pendulum

M_e = effective mass of the thorax

v_i = initial pendulum velocity

v_f = final speed of pendulum and thorax

rearranging

$$v_f = \frac{M_p\ V_i}{(M_e + M_p)}$$

Now perform an energy balance on the system.

$$E_i = E_f = E_{ke} + E_{abs}$$

where:

E_i = initial energy

E_f = final energy

E_{abs} = absorbed energy

E_{ke} = kinetic energy

then

$$\tfrac{1}{2} M_p v_i^2 + \tfrac{1}{2} (M_p + M_e)\ v_f^2 + E_{abs}$$

after substitution

$$E_{abs} = \frac{M_p}{(M_p + M_e)}\ E_i$$

$$\text{Specific Absorbed Energy} = \text{SAE} = E_{abs} / M_{total}$$

M_{toal} = Total Body Mass

Appendix B

Computation of SAE for Airbag Tests

Calculation of absorbed energy for airbag tests was based on energy and impulse-momentum considerations. Seven frontal tests were performed on the sled at Wayne State University at a nominal 30mph impact speed. The airbag was a standard production General Motors airbag mounted on a standard production airbag steering wheel. The wheel in turn was mounted on a horizontal, rigid, nonstroking column. The airbag was fully inflated prior to the test, and there was no venting of the gas in the bag.

In addition to the standard signals recorded from the test subject (9 head accelerations, 12 thoracic accelerations, 3 pelvic accelerations, and pulmonary pressure), a number of data signals were recorded external to the test subject. Data of interest from this group included the initial sled velocity, the deceleration of the sled, the pressure within the airbag, the compressive load on the steering column, and the impact force on each knee.

Human cadaveric test subjects were used. The test subjects were unrestrained except for the airbag and knee bolsters. In the following analysis, it was assumed that frictional forces were negligible, and that all forces that stopped the test subject were measured by the three load cells present (steering column, left knee, right knee). It was also assumed that energy absorption by the knee bolsters was negligible.

The first step in computing thoracic absorbed energy was to determine the effective thoracic mass. This determination used impulse-momentum. Recall that

$$\int F(t)\ dt = \int M_e\ dv = I$$

where

$F(t)$ = force at time t

M_e = effective mass

dv = differential velocity

dt = differential time

I = impulse

It was determined that when the steering column force was at maximum, the test subject had stopped (dv = test velocity) and begun to rebound. The three forces (left knee, right knee, steering column) were integrated from time = 0 (t_1) to the time of maximum steering column force (t_2).

$$M_e \Delta v = \int_{t_1}^{t_2} F_{SC}\, dt$$

where

M_e = effective thoracic mass

Δv = change in velocity of thorax (= test speed in the test analyzed)

F_{SC} = steering column force

t_2 = time of max F_{SC}

t_1 = time 0 (= 0)

$$M_e = \frac{\int_{t_1}^{t_2} F_{SC}\, dt}{\Delta v}$$

When this analysis was performed, the resulting thoracic masses as a percentage of total body weight ranged from 39 to 57 percent, with most values closely clustered around 50 percent. It was decided to set the effective thoracic mass in airbag tests to 50 percent of the total body mass.

Having determined an effective thoracic mass, and knowing the initial speed of the sled (and the test subject), the initial thoracic kinetic energy was computed as:

$$KE_o = \frac{M_e v_o^2}{2}$$

where

KE_o = kinetic energy

M_e = effective thoracic mass

v_o = initial velocity

At some point during the test, the thorax stopped (velocity = 0) and began to rebound away from the airbag. When the velocity was 0, the thoracic kinetic energy was also 0. It was assumed that when airbag pressure reached its maximum value the thorax had stopped and begun to rebound.

Now consider the work done by the airbag on the sled. Given the pressure and initial volume of the airbag it was possible to calculate the change in potential energy of the gas in the bag. Then, given the force of the airbag on the steering column as a function of time, and the velocity of the steering column (rigidly mounted to the sled), the work of the airbag on the column was calculated.

The energy balance for the system is

$$KE_o = PE_{AB} + W_{SC} + KE_{t_2} + E_{abs}$$

where

KE_o = initial kinetic energy in thorax

PE_{AB} = change in potential energy of the gas in the airbag

W_{SC} = work done on the steering column by the airbag

KE_{t_2} = kinetic energy at time t_2

E_{abs} = absorbed energy in the thorax

It was assumed that when airbag pressure was at its maximum, the thorax had stopped and thus thoracic kinetic energy was 0.

$$E_{abs} = KE_o - PE_{AB} - W_{SC}$$

By knowing the test subject's initial velocity and effective thoracic mass, KE_o was computed.

Changes in potential energy of the gas in the airbag were computed knowing the pressure time history and initial volume of the system. It was assumed that the impact occurred so quickly that there was no heat transfer and no mass lost, i.e., an adiabatic event. The change in energy of the gas therefore was

$$PE = \int_{V_2}^{V_1} P\, dV$$

where

PE = change in potential energy

P = pressure (absolute)

V_1 = initial volume

V_2 = volume at peak pressure

The following is true for a perfect gas undergoing adiabatic compression.

$$pv^n = \text{constant}$$

For air (used to inflate the airbag in these tests) n = 1.4.

$$P_1V_1^{1.4} = P_2V_2^{1.4} = C$$

P_1, P_2, and V_1 are known.

$$V_2 = \left(\frac{C}{P_2}\right)^{(1/1.4)}$$

$$P(V) = \frac{C}{V^{1.4}}$$

$$PE = \int_{V_1}^{V_2} P\,dv = C\int_{V_1}^{V_2} V^{1.4}\,dV$$

$$= \frac{-C\,V^{-0.4}}{0.4}\Bigg|_{V_1}^{V_2}$$

$$= \frac{-c^{1.4}(V_2^{-0.4} - V_1^{-0.4})}{0.4}$$

This represented the total change in potential energy of the gas within the airbag. However, some of this change arose from work done by the atmosphere on the airbag.

$$PE_{total} = PE_{AB} + \int P_{atm}\,dV$$

PE_{total} = total change in the potential energy of the gas in the airbag

PE_{AB} = change in potential energy of gas due to work done by thorax on the airbag

P_{atm} = absolute atmospheric pressure (constant)

$$PE_{AB} = PE_{total} - P_{atm}(V_2 - V_1)$$

To compute the work done on the steering column, the signal from the steering column load cell was used as well as the sled acceleration signal.

$$\text{Work} = \int F\,dx$$

$$= \int F\frac{dx}{dt}\,dt$$

$$= \int F\,v\,dt$$

where

F = force

dx = displacement of sled with respect to laboratory reference frame.

$\frac{dx}{dt}$ = v = velocity with respect to laboratory reference frame.

dt = incremental time

In the case at hand, F was the steering column load cell measurement, and v(t) was the integrated sled acceleration subtracted from the initial sled velocity. The time limits ranged from $t_1 = 0$ to t_2 = time of maximum pressure in the airbag.

$$W_{SC} = \int_{t_1}^{t_2} F_{SC}\,v(t)\,dt$$

Thus, knowing an effective thoracic mass, an initial velocity, and an initial airbag volume, the thoracic absorbed energy was computed using the steering column load signal, sled acceleration signal, and airbag pressure signal.

$$E_{abs} = KE_o - PE_{AB} - W_{SC}$$

The specific absorbed energy was obtained by dividing the absorbed energy by the total body mass.

SAE = Specific Absorbed Energy = E_{abs}/M_{total}

M_{total} = Total Body Mass

Appendix C

Computation of SAE for Belt Tests

The belted tests used in this study were nominal 30mph frontal sled tests conducted by Wayne State University. The restraint system was a 2-point belt (i.e., there was no lap belt) with knee bolsters. The knee bar was segmented and mounted on load cells so the load imposed on each knee could be measured. In addition, the tension in the belt was measured as well as the sled acceleration.

The first step was to compute an effective thoracic mass. This was accomplished in a manner similar to that used with the airbag system using impulse momentum.

$$M_{total}\,v_i = I_{LK} + I_{RK} + I_{thorax}$$

where

M_{total} = total subject mass

v_i = initial velocity

I_{LK} = impulse of left knee

I_{RK} = impulse of right knee

I_{thorax} = impulse of thorax

where impulse - $\int F\ dt$

The above relationship assumed that the test subject stopped when time equaled the upper time limit of the integration. Examination of the data revealed that this assumption was invalid because, when belt force peaked, some sled velocity remained. The assumption was then changed to be that the test subject had the same velocity as the sled at peak belt force. This changed the impulse-momentum relationship to be

$$M_{total}\,\Delta v + \int_{t_1}^{t_2} F_{LK}\,dt + \int_{t_1}^{t_2} F_{RK}\,dt + \int_{t_1}^{t_2} F_{thorax}\,dt$$

where

Δv = change in velocity of thorax
initial sled velocity - sled velocity at time = t_2

F_{LK} = force on left knee

F_{RK} = force on right knee

F_{thorax} = force on thorax

t_1 = 0

t_2 = time of peak thoracic force

While the horizontal forces acting on each knee were directly measured in these tests, the force acting on the thorax was available only indirectly through the belt tension force. It was assumed that the thoracic force-time signal had an identical signature, and differed in magnitude only by a constant when compared to the belt tension force.

$$F_{thorax} = c\,F_{belt\ tension}$$

where c is a proportionality constant. To determine c

$$M\Delta v = \int F_{LK}\,dt = \int F_{RK}\,dt = c\int F_{belt\ tension}\,dt$$

$$c = \frac{M\Delta v - I_{RK} - I_{LK}}{\int F_{belt\ tension}\,dt}$$

The value of c ranged from 1.5 to 1.98, clustering around 1.95. These values give confidence that the assumptions are valid.

The effective thoracic mass is then

$$M_e = \frac{c\,F_{belt\ tension}\,dt}{\Delta v}$$

Now consider the energy balance of the thorax.

$$KE_o = KE_{t_2} + E_{belt} + W_{sled} + E_{abs}$$

where

KE_o = initial kinetic energy of thorax

KE_{t_2} = kinetic energy of thorax at time t_2

E_{belt} = strain energy absorbed by belt

W_{sled} = work done on the sled by belt

E_{abs} = energy absorbed by the thorax

If m_e is the effective thoracic mass, then the kinetic energy at any time is

$$\frac{M_e\,v^2}{2}$$

The velocity of the sled just prior to impact was used to compute the initial kinetic energy KE_o. The velocity used to compute ke_{t2} was the sled's velocity at time t_2 (time of maximum belt force)

The strain energy absorbed by the belt was

$$E_{belt} = \frac{K\,x^2}{2}$$

where

K = stiffness of belt (=10,416lbs/ft
This is equivalent to 6% strain at 2,500lb for a 4ft belt

x = total elongation of belt

$$= \frac{F_{tension}}{K}$$

$F_{tension}$ = peak belt tension

$$E_{belt} = \frac{(F_{tension})^2}{2\,K}$$

The work done on the sled by the belt was computed in a manner similar to the computation of the work done by an airbag on the sled. Here

$$W_{sled} = c \int_{t_1}^{t_2} F_{belt\ tension}\ v(t)\ dt$$

$v(t)$ = sled velocity

Next the SAE was computed

$$E_{abs} = KE_o - KE_{t_2} - E_{belt} - W_{sled}$$

$$= \tfrac{1}{2} M_e (v_o^2 - v_{t_2}^2) - \frac{F_{tension}^2}{2k} - c \int_{t_1}^{t_2} F_{belt\ tension}\ v(t)\ dt$$

$$SAE = E_{abs} / M_{total}$$

where

M_{total} = total Body Mass

Thoracic Impact: A Viscous Tolerance Criterion

David C. Viano and
Ian V. Lau
General Motors Research Laboratories

Abstract

There are currently two accepted criteria for assessment act exposures. Our studies have shown an interaction between the deformation velocity and level of compression during impact, resulting in a greater compression tolerance for low-speed impact than for high-speed loadings. High-speed thoracic impact can cause critical or fatal injury in physiologic experiments before exceeding the acceleration or compression tolerance. The velocity-sensitive tolerance is represented by the maximum product of velocity of deformation and compression, which is derivable from the chest compression response. As the magnitude of this "viscous" response increases, the risk of serious or fatal injury increases. This paper discusses the analysis of available literature and results from our laboratory and demonstrates the need for a viscous tolerance criterion to assess chest impact protection in high-velocity impact.

Introduction

Whole-Body Deceleration Tolerance

To provide improved protection of military personnel exposed to rapid decelerations, Stapp(1) conducted a series of rocket-sled experiments demonstrating the whole-body tolerance with belt restraints. Information from these experiments on the long-duration, whole-body deceleration tolerance and information from other tests enabled Eiband(2) to demonstrate that the whole-body deceleration tolerance increased as the duration of the exposure decreased. This led to a well-accepted deceleration tolerance (Figure 1), which for the first time information over orders of magnitude in duration of deceleration. However, the tolerance was based primarily on accelerations measured on the sled fixture, not on the test subject. The data did provide useful guidelines for the development of restraint systems for occupant protection in crash situations involving military and civilian personnel.

The basis for the whole-body deceleration tolerance criterion is Newton's second law where the deceleration of a rigid mass is in proportion to the force on the moving mass. Thus, the greater the deceleration, the greater the force and risk of injury. The increase in tolerable deceleration for shorter durations of exposure implies a based on an equivalent energy transfer, since an equivalent change in velocity (V) can be achieved by reciprocal changes in the level and duration of acceleration (for a velocity change (V=AT) the deceleration (A) can increase the duration (T) decreases).

Force Tolerance

In the early 1960's, automotive safety engineers were seeking information on the force tolerance of the thorax.

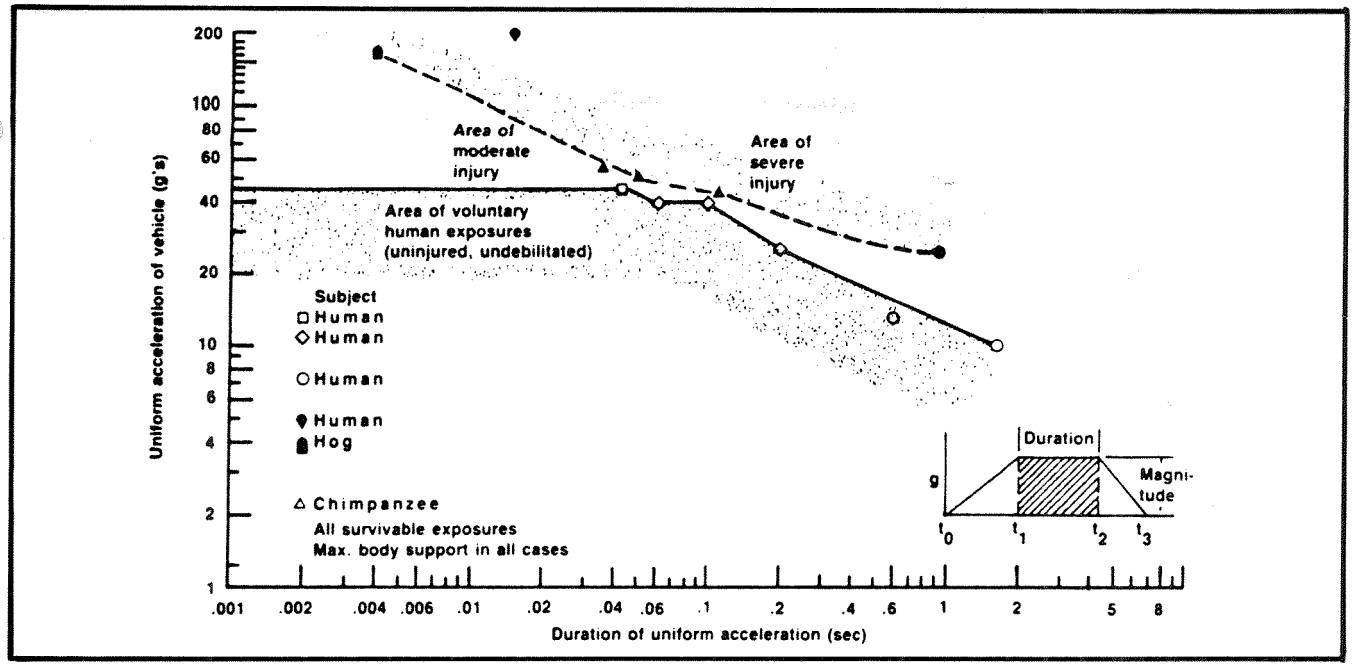

Figure 1. Duration and magnitude of vehicle decelerations endured by various subjects(2)

This information was needed to develop the energy-absorbing steering column. The energy-absorbing column included a device that limited force to a maximum level beyond which the structure would deform and absorb energy as it compressed. However, the available human tolerance data (see the review by Snyder(3)) did not provide specific information on the appropriate yield force for the system. The basic safety objective was to design the yield force as high as practical, consistent with tolerance, to maximize the energy-absorbing capacity and extend the range of safety function of the system.

Faced with uncertain information on the force tolerance of the chest, a collaborative program was undertaken between General Motors Research Laboratories and Wayne State University to develop a crash simulation facility and conduct experiments on human tolerance in automotive crash situations. The first series of experiments by Patrick et al.(4) involved sled tests with embalmed cadavers simulating the response of an unrestrained occupant interacting with load-measuring surfaces. Head, chest, and knee contacts against padded load-cells provided the first information on human tolerance to impact force. The resulting force tolerance of the thoracic rib cage provided the necessary information to biomechanically design the energy-absorbing element in the steering system.

Subsequent experiments by Gadd and Patrick(5) with prototype energy-absorbing steering system confirmed that a 3.29kN (740-lb) maximum hub force on the sternum and an 8.00kN (1,800-lb) maximum load on the shoulders and chest allowed column compression with only minor risk of skeletal damage in the rib cage for a impact. These experiments provided new human tolerance data and enabled the introduction of the energy-absorbing steering column which has proven to be a highly effective built-in safety feature for driver protection(6).

Chest Compression Tolerance

In the course of the cadaver impact experiments, it became clear that the concept of whole-body deceleration and force did not adequately describe the response of the thorax during blunt impact. In fact, force applied to the sternum was shown to compress the chest, thus bending the ribs and leading to fractures when the level of compression exceeded the tolerance of the rib cage. Analysis by Kroell(7) of a large series of blunt thoracic impact experiments confirmed that the maximum acceleration of the thoracic spine was a poor indicator of injury potential for blunt frontal thoracic loading and that the maximum level of chest compression was a superior predictor of chest injury (Figure 2).

Kroell's tests(7) with human volunteers showed that chest compression up to 20 percent during moderately long duration loading produced no detectable injury and was fully reversible. Impact tests with human cadavers at of compression greater than 20 percent showed that as the compression increased, the risk of skeletal fractures in the rib cage increased. At 40 percent compression, there was multiple skeletal injury indicative of flail chest. As protective function of the rib cage was destroyed by multiple fractures causing an unstable structure, direct loading of intrathoracic vital organs was possible (Figure 3) and there was risk of injury to the heart, lung, and great vessels (see the discussion by Viano(8)). Analysis of these

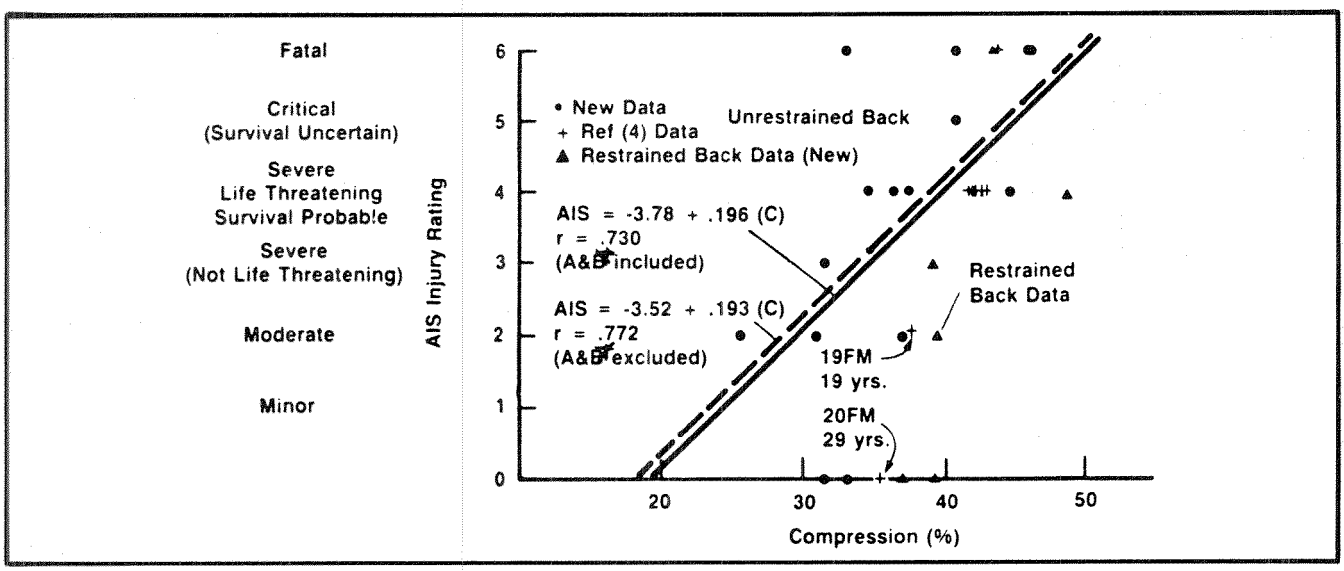

Figure 2. Injury rating and chest compression for University of California, San Diego, unembalmed cadavers subjected to blunt frontal impact(7). A and B are the responses of the 19- and 20-year old subjects

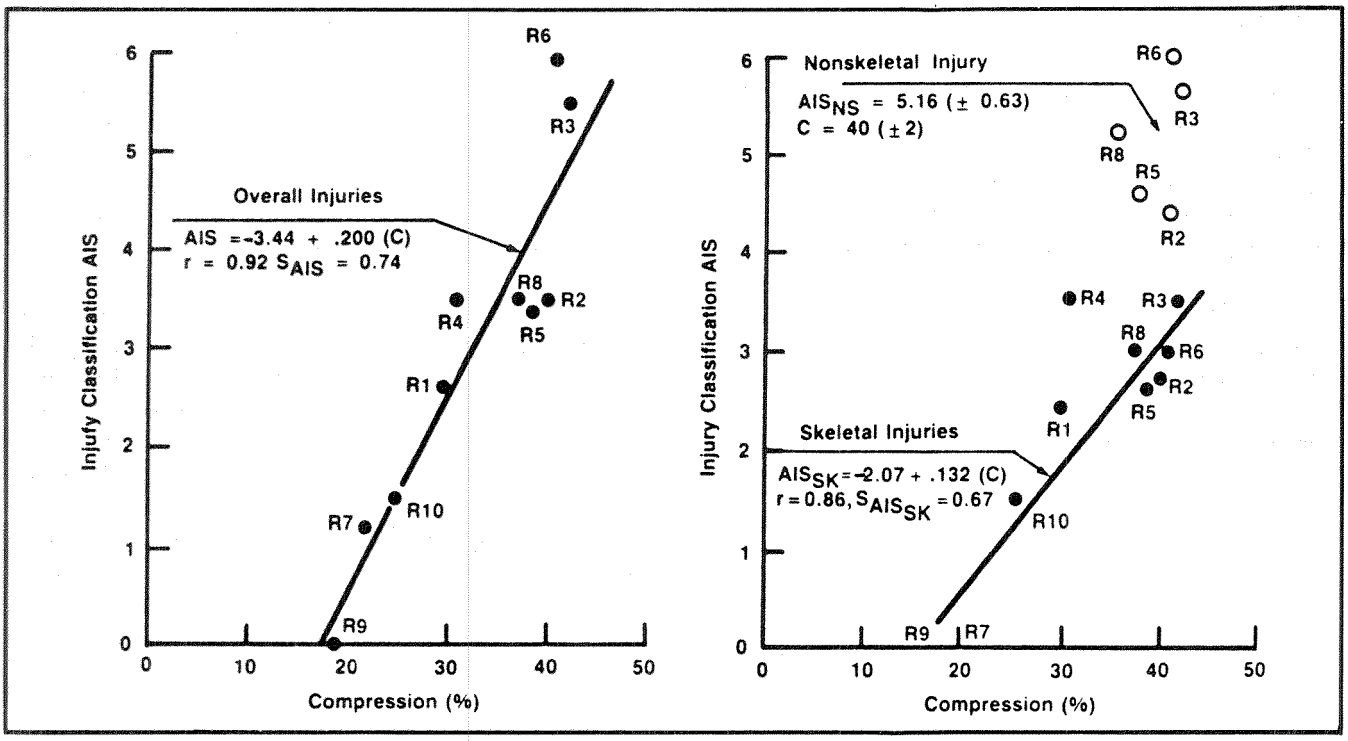

Figure 3. Injury rating and chest compression for University of California, San Diego, unembalmed cadavers subjected to blunt frontal impact showing increased severity of rib fractures with compression and cluster of soft tissue injuries at high compressions where the stability of the ribcage is compromised(8). Each point represents the average response of a group of similar tests identified by R1-R10(8)

data led Neathery et al.(9) to develop a criterion of maximum chest compression for the evaluation of injury risk for blunt frontal impact.

Evaluation of the time-varying force and compression response of the chest in human cadaver experiments also provided information on the dynamic stiffness of the thorax. The experimental data on biomechanical responses allowed Neathery(10) to define corridors predicting the impact response of the 50th percentile male cadaver. These data were pivotal to the development by Foster et al.(11) of an improved anthropomorphic test device with chest biofidelity, and ultimately led to the

Hybrid III dummy chest. Improved thoracic stiffness and structure have allowed the Hybrid III to be identified as most appropriate test tool to be used for the evaluation of the steering system in a wide range of sled test environments (see Horsch and Viano(12)).

In an effort to further understand the mechanisms of soft tissue injury, the literature was reviewed for various impact exposures, including experimental simulations of blast-wave injury. A comprehensive series of physiologic experiments on lateral thoracic impact confirmed a new observation: the chest compression tolerance is not a fixed maximum value for a wide range of impact velocities. In fact, the experiments by Jonsson and Clemedson(13) suggested that as the velocity of impact increased, the tolerance to chest compression decreased, at least on the basis of lung injury.

Since impacts in the range of 5m/s to 20m/s are possible in high-speed automotive collisions, the sufficiency of a single maximum value for chest compression was studied by Lau and Viano(14) in a series of experiments. In these tests, the liver was the target organ, and the experiment was set up to attain a maximum level of 16 percent abdominal compression, which was well within the range of tolerable compression for a volunteer in a moderate duration loading. The rate of abdominal compression was varied from 5m/s to 20m/s to study the influence of the velocity of compression. The experiments confirmed an increasing risk of liver injury severity as the of abdominal compression increased (Figure 4). The experiments confirmed that the velocity of compression was an important factor in injury assessment.

Subsequent physiologic experiments by Kroell et al.(15) and Lau and Viano(16) involving blunt thoracic impact

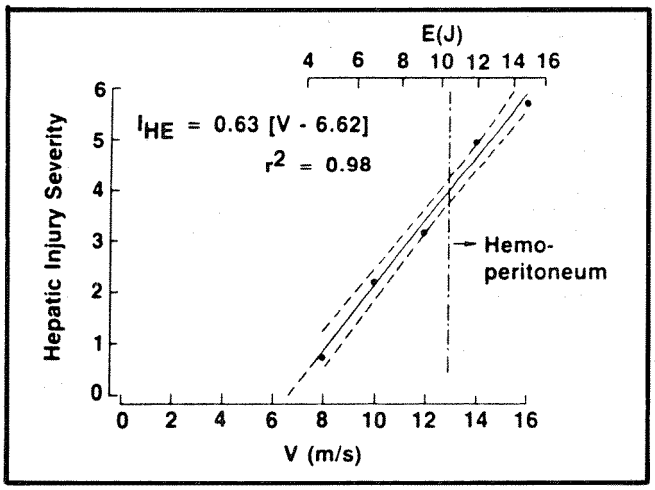

Figure 4. Hepatic injury severity and impact velocity for a fixed maximum compression. The maximum viscous response is the product of forced velocity of compression and 16% maximum compression (14). Impacts above 12m/s resulted in severe hemoperitoneum, bleeding in the abdomen

substantiated an interrelationship between chest compression and velocity of compression. These two responses were critical to the severity of skeletal or internal thoracic injury. Analysis of other physiologic experiments by Lau et al.(17) found that velocity of impact in the range of 13m/s to 24m/s was an important factor for nonpenetrating thoracic injury leading to ventricular fibrillation. Similar findings of the importance of the velocity of compression were identified in a series of open thoracic impacts of the heart by Stein et al.(18). The risk of fatal cardiac arrhythmias was found to increase with the velocity of cardiac compression.

Viscous Tolerance

The concept of a viscous tolerance (deformation velocity and compression sensitive tolerance) for soft tissues in the body was first proposed by Viano and Lau(19) who analyzed a large series of frontal thoracic impact experiments. The physiologic experiments included velocities of compression in the range of 5m/s to 22m/s and maximum thoracic compressions of 4 to 55 percent. On the basis of occurrence of critical-fatal injury, the experiments confirmed a velocity and compression sensitive tolerance to chest impact. Although the chest could withstand 50 percent compression for loadings of 5m/s velocity of deformation, the tolerance decreased significantly to 20 percent at velocities of 20m/s. Further analysis of the data showed that the maximum of the product of velocity of deformation and compression was an effective predictor of injury risk (Figure 5). The maximum viscous response was defined as VC max = [V(t) * C(t)] max and was shown to be a measure of the energy dissipated by viscous elements in the thorax. Probit analysis defined an effective maximum viscous

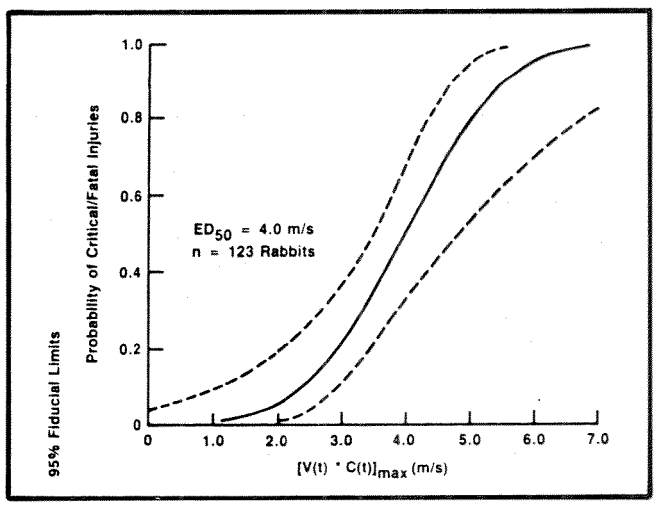

Figure 5. Probit analysis of critical-fatal injury risk and maximum viscous response for blunt frontal impact (19)

response for 50 percent occurrence of critical-fatal thoracic injury in the physiologic model at VC max = [V(t) * C(t)] = 4.0m/s.

Over the years of research on mechanisms of thoracic and soft-tissue injury, it has been increasingly evident that the body cannot be considered a rigid structure and that injury criteria based on whole-body acceleration are inadequate predictors of injury risk. It is now clear that the body is a deformable structure and at low speeds of impact (< 5m/s) the tolerance to rib cage damage and risk of crush injury can be evaluated by the maximum compression of the chest. This is primarily the case for belt-restrained occupants where tight coupling to the vehicle deceleration involves low speeds of chest compression. However, for high speeds of thoracic deformation (> 5m/s) typical of the unrestrained or those in high-speed side impacts, the quasi-static maximum compression tolerance does not adequately reflect the viscous properties of the chest and thus soft-tissue injury risks. For these types of impact, both the compression and velocity of deformation are important responses that relate to injury.

In more recent physiologic experiments by Horsch et al.(20) and Lau et al.(21) on upper-abdominal injury with steering wheel contact, the viscous response was found to be the superior predictor of severity and time of occurrence of liver injury. It also demonstrated more clearly the important biomechanical responses of the abdomen during steering wheel contact. These studies showed that liver injury by steering wheel contact occurred prior to maximum compression of the abdomen or maximum acceleration of the spine, but at the same time as the peak of the abdominal viscous response (see Lau et al.(21)). The viscous criterion has also been found by Rouhana et al.(22) to be the biomechanical response predictive of abdominal injury due to lateral impact.

In the following sections, the viscous response will be defined as the time-varying product of the velocity of deformation and compression and will further demonstrate that the maximum of this biomechanical response is an important predictor of injury. However, the viscous response and tolerance should be considered a supplement to the currently accepted maximum chest compression criterion that reflects the quasi-static or crush limit of the thorax.

Definitions

A lateral view of the thorax is shown in Figure 6, where coordinates y_1, y_2, and, y_3 represent the displacement of the skin covering the anterior chest wall, the sternum, and vertebral spine, respectively (Table 1). Chest compression (C) is defined as the difference in the displacement of the anterior skin and spine ($y = y_1 - y_3$) normalized by the initial exterior thickness of the thorax (D). The velocity

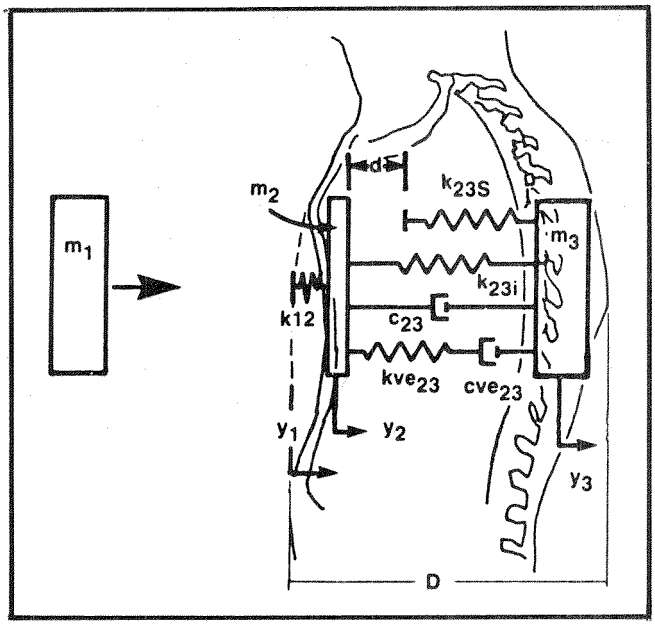

Figure 6. Lateral view of thorax with Lobdell's thoracic model(25) superimposed showing the sternal and spinal masses, and the spring and dashpot elements representing the thoracic compliance

of chest compression (V) is defined as the time rate of change of the relative displacement between the anterior skin and spine. The viscous response (VC) is defined as the time-varying product of the velocity of chest deformation and compression.

Energy Concepts for Injury Risk

Stored Energy

Simple mechanical analogs of the biomechanical response of the thorax can be used to discuss injury risks during frontal thoracic impact. A portion of the thorax can be represented by an elastic spring (see Figure 6). The spring response demonstrates how an increase in compression is associated with an increase in force, energy stored, and risk of reaching the elastic limit of the element.

When the elastic response of the thorax is represented by a spring, the energy stored (E_e) during compression is defined as the integral of the compressive force (F) during the deflection (y) it causes:

$$E_e(t) = \int_0^y F(t)\, dy \qquad \text{(Equation 1)}$$

Since force in a linear spring is proportional to the deflection of the endpoints (F(t)y(t)) and the incremental

Table 1. Definition of biomechanical responses

Variable	Response
$y_1(t)$	Skin Displacement
$y_2(t)$	Sternal Displacement
$y_3(t)$	Spinal Displacement
$\dot{y}_1(t)$	Skin Velocity
$\dot{y}_2(t)$	Sternal Velocity
$\dot{y}_3(t)$	Spinal Velocity
$\ddot{y}_1(t)$	Sternal Acceleration
$\ddot{y}_2(t)$	Spinal Acceleration
D	Chest Depth
$y(t) + y_1(t) - y_3(t)$	Chest Deflection
$C(t) + y(t)/D$	Chest Compression
$V(t) + \dot{y}(t)$	Velocity of Deformation
$\dot{C}(t) + V(t)/D$	Compression Rate
$V(t)C(t) + \dot{y}(t)y(t)/D$	Viscous Response

deflection is given by $dy = (dy/dt)dt = ydt$, Equation (1) reduces to:

$$E_e(t) = \int_o^t y(t)\ \dot{y}(t)\ dt \qquad \text{(Equation 2)}$$

Recognizing that the differential of y^2 is equal to the integrand of Equation (2) $(d/dt\ (y^2 = 2yy)$, Equation (2) reduces to:

$$E_e(t) = \tfrac{1}{2}\int_o^t d/dt\ (y^2(t))\ dt = \tfrac{1}{2}\int_o^t d\ (y^2 t)) \qquad \text{(Equation 3)}$$

However, Equation (3) is uniquely solved assuming a zero initial deflection or compression of the thorax, such that Equation (3) equals:

$$E_e(t) = \tfrac{1}{2}\ y^2(t)) \qquad \text{(Equation 4)}$$

Thus, the energy stored in compressing the elastic components of the thorax is directly proportional to the square of the time-varying deflection. Normalizing the deflection by the initial thickness of the chest implies that the stored elastic energy is proportional to the square of thoracic compression ($E_e \sim C^2$). Since compression derives this function, stored energy is determined by compression ($E_e \sim C$).

The maximum compression criterion essentially establishes a biomechanical response represented by compression of a spring. Load on the spring and stored energy in spring determine the risk of reaching the deformation limit or the energy capacity of the thorax, which is proportional to the compression of the spring. During impact, force applied to the chest accelerates body masses and compresses the spring elements. Since it is not possible to a priori separate the inertial and elastic components of force from the total load, compression is the measurable response and meaningful biomechanical parameter of injury risk.

Absorbed Energy

The viscous elements of the thorax can be represented by a mechanical dashpot (see Figure 6), and the absorbed energy (E_v) associated with deformation of the element is proportional to the force (F) acting across it:

$$E_v(t) = \int_o^y F(t)\ dy \qquad \text{(Equation 5)}$$

In this case, the force developed by a viscous dashpot due to deformation of the endpoints is proportional to the velocity of deformation $(F(t)\ \dot{y}(t))$. Recognizing again that the differential deflection is given by $dy = (dy/dt)\ dt = \dot{y}dt$, Equation (5) reduces to:

$$E_v(t) = \int_o^t \dot{y}^2(t)\ dt \qquad \text{(Equation 6)}$$

In the case of Equation (6), it is not possible to find a unique solution. However, if we recognize that the differential of $y\dot{y}$ is $d/dt\ (y\dot{y}) = \dot{y}\dot{y} + y\ddot{y}$, it is possible to reduce Equation (6) to the form:

$$E_v(t) = \int_o^t d\ (y(t)\ \dot{y}(t)) - \int_o^t y(t)\ \ddot{y}(t)\ dt \qquad \text{(Equation 7)}$$

The first integral of Equation (7) can be solved by direct integration so that the energy absorbed by the viscous elements representing the thoracic response during dynamic compression takes on the form:

$$E_v(t) = y(t)\ \dot{y}(t) - R(y, \ddot{y}) \qquad \text{(Equation 8)}$$

where the residual function in Equation (8) is given by: $R(y, y) = \int^t y(t)\ddot{y}(t)\ dt$. The first term in Equation (8) for the absorbed energy is related to the product of velocity of deformation and compression when the deflection is normalized ($E_v \sim \dot{y}y \sim VC$). Thus, absorbed energy is related to the viscous response. Maximum elastic (stored energy) limit is proportional to the square of maximum compression, and the maximum viscous (dissipated energy) limit is proportional to the maximum product of the deformation velocity and compression.

Strain Energy Analogy for the Viscous Response

Impact of an elastic material can cause the propagation of a wave. The principles of impulse and momentum can be used to define the stress, strain, and energy in the material. The velocity of propagation of the elastic wave

is $c = (E/\rho)^{1/2}$ where E is Young's modulus and ρ is density. There is a relationship (see Hudson and Housner(23)) between the velocity of deformation (V) of the impacted surface and the stress (σ) developed, such that $\sigma = (E\rho)^{1/2}V$. Since the strain (ε) is proportional to the foreshortening of the external dimensions, it is equal to the compression of the material, and $\varepsilon = C$. The strain energy is given by: $E\varepsilon = \frac{1}{2}\sigma\varepsilon = \frac{1}{2}(\rho\tau 5\varepsilon = C$. In this case, the propagation of an elastic wave due to an instantaneous surface velocity of deformation causes strain energy in the material in proportion to the product of the velocity of deformation times compression ($E_e \sim VC$). Thus, there is another mechanical basis of VC as a measure of the intensity of the energy density in a material during dynamic loading.

Although neither of the previous analogies represent a rigorous theoretical demonstration of the fundamental basis for the viscous response, a mechanical basis has been shown for the product of the two biomechanical responses (VC) as a proportional measure of intensity of a material response to dynamic loads.

Response of a Viscoelastic Thoracic Model

Lobdell's viscoelastic model(24,25) of the human cadaver chest provides another means of demonstrating the biomechanical importance of the viscous response. Using the parameters and responses defined in (24), the following two cases were simulated: Case 1, Impact Mass 20kg and Impact Velocity 7m/s, and Case 2, 4kg Mass and Impact Velocity of 15m/s. These two cases have identical kinetic energy of the impacting mass. The results of the simulation are shown in Figures 7 and 8, and maximum response values are tabulated in Table 2. There is a dramatic difference in response maxima for the two cases, which provide insight into the dynamic response of the thorax. Both cases resulted in a maximum compression of 30 percent. However, the maximum in velocity of chest compression and viscous response were nearly double in the low-mass, high-velocity impact simulation. Interestingly, there was nearly a doubling in dissipated energy in

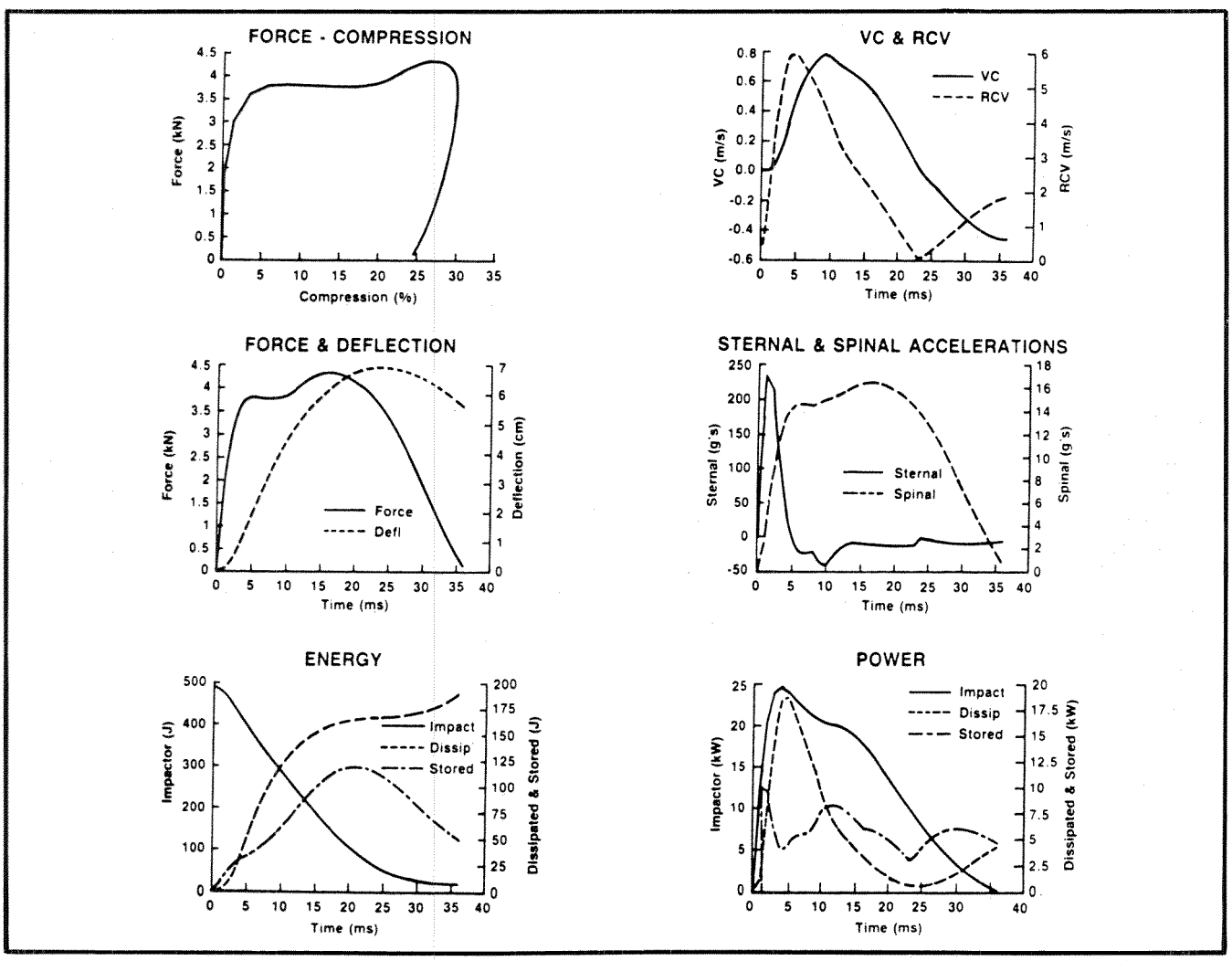

Figure 7. Thoracic impact responses for a 20kg impactor striking the chest at 7m/s

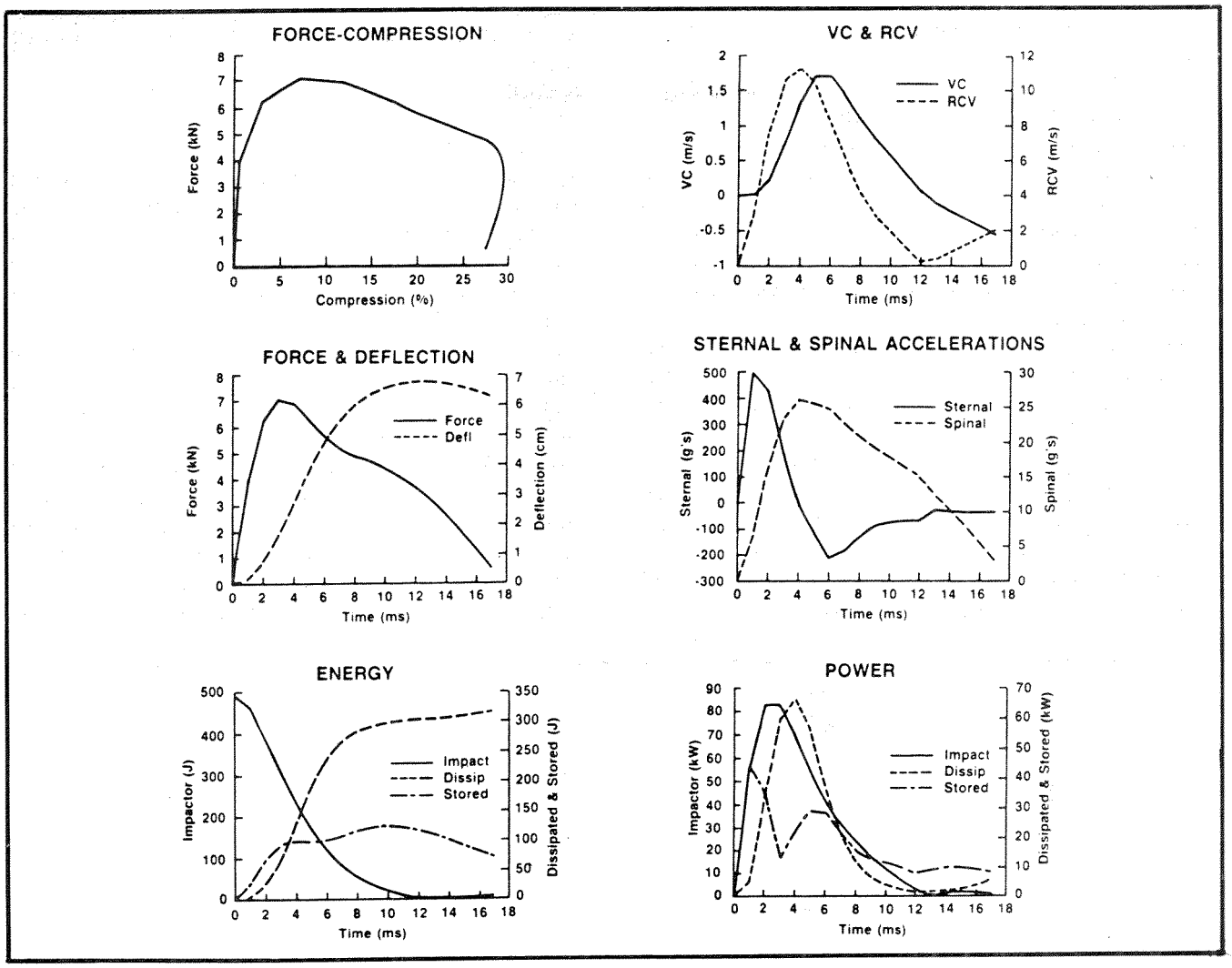

Figure 8. Thoracic impact responses for a 4kg impactor striking the chest at 15m/s

Table 2. Simulated response of a visco-elastic model of the thorax

Impact Parameters	Case 1	Case 2
Mass (kg)	20.	4.
Velocity (m/s)	7.	15.
Responses		
Force (kN)	4.2	7.0
Compression %	30.0	30.0
Rel. Chest Velocity (m/s)	5.8	11.0
Viscous (m/s)	0.8	1.7
Sternal Acc. (g)	230.0	500.0
Spinal Acc. (g)	16.0	28.0
Diss. Energy (J)	180.0	310.0
Stored Energy (J)	120.0	105.0
Diss. Power (kW)	18.0	65.0
Stored Power (kW)	7.5	58.0

the high-velocity impact with a reduction in energy stored in the elastic components. Sternal and spinal accelerations were greater in the high-velocity impact, as was the peak in load on the sternum.

In these two cases, the peaks in chest compression were arrived at by two substantially different deformation responses, one with nearly a doubling in the viscous response. The maximum viscous response occurred much earlier than the maximum in chest compression. On the basis of our previous experimental research(19,21), there would be a greater risk of soft-tissue injury in the low-mass, high-velocity impact even though the maximum compression is similar and within the tolerable level. Soft-tissue injury associated with a high viscous response would occur earlier than maximum chest compression. The two simulations demonstrate the variability in response associated with thoracic impact and show how the viscous response is a useful supplemental biomechanical response.

Analysis of Cadaver Data

The series of blunt frontal impact tests conducted at the University of California at San Diego (UCSD) under contract to the General Motors Research Laboratories represents one of the most comprehensive sets of data available. The response of the chest during blunt frontal impact was measured by transducers attached to the subject and by analysis of high-speed photographs of the impact event. Compression of the chest was determined by film analysis, and the time histories of the responses have been published and discussed in many papers (see, for example, Kroell(7) and (8-10)).

The viscous response of the cadavers was determined from the published chest deflection data, and examples of the viscous response are shown in Figure 9 for the tests used to develop response corridors for the human cadaver and to develop the Hybrid III dummy chests(7,10,11). Eight tests were conducted with a 23.4kg mass and impact velocity of 6.7m/s, and four tests were conducted with a 23.4kg mass and impact velocity of 4.27m/s. These data demonstrate that the peak viscous response occurs earlier (at 10ms) than the maximum compression (at 30ms) in the cadaver subject. Kroell(7) has shown that rib fractures occur progressively with compression, the first fracture occurring as early as 9.2ms and the second at 13.6ms in an event like this that takes 30ms to reach maximum compression. It is interesting that the maximum viscous response occurs at about the same time as the initiation of skeletal damage.

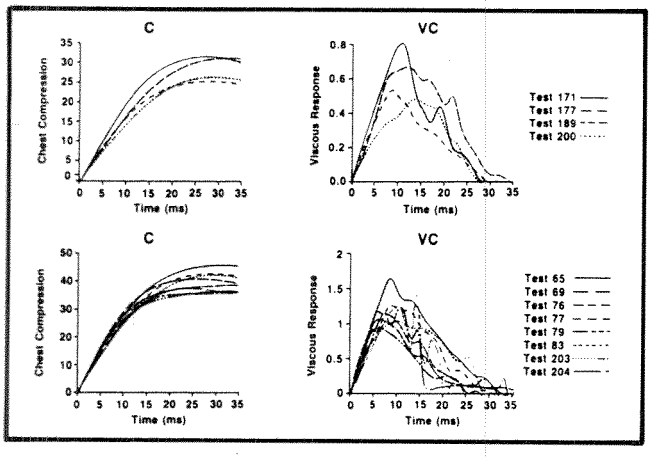

Figure 9. Compression and vicous response of University of California, San Diego, cadavers subjected to blunt frontal impact by a 23.1kg mass striking at 4.9m/s (top curves) of 7.2m/s (bottom curves)(7)

Determining the average maximum viscous response subjects exposed to a range of similar tests (see Viano(8) for groupings of tests) allowed the maximum viscous response to be correlated with the risk of critical injury (Figure 10). There is reasonable correlation between the

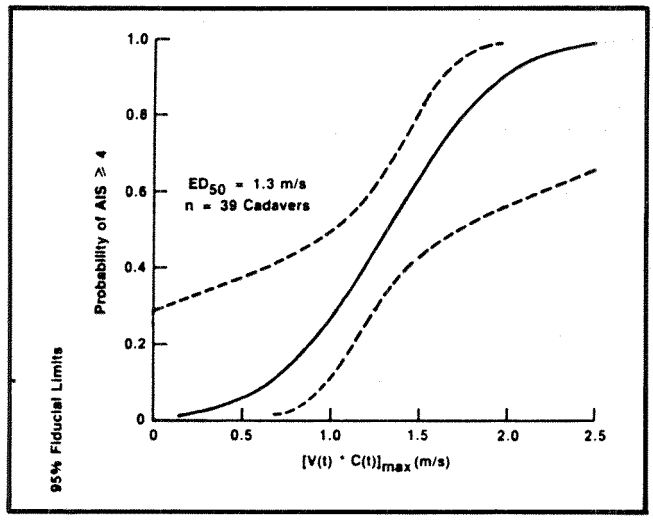

Figure 10. Analysis of critical injury risk (AIS 3) and maximum viscous response for blunt frontal impact of University of California, San Diego, unembalmed cadavers(7)

maximum viscous response and the risk of critical-fatal injury. The effective viscous dose for 50 percent critical injury is VC = 1.3m/s. The viscous response in the high-low-mass simulation of the previous section was VC max = 1.7. Based on the analysis of the UCSD data, there be a high probability (75 percent) of critical-fatal injury. In contrast, the low-velocity, high-mass impact would have a low probability (15 percent) of injury even though injury risk would be similar on the basis of compression.

Evaluation of the Viscous Response in the Hybrid III Dummy

One of the important instrumentation and response features of the Hyrid III dummy(11) is the biofidelity of the chest compression response and a transducer that measures the chest deflection. During a frontal impact, the Hybrid III chest deflects in a manner similar to the response of the human cadaver(10,11), and an analog signal of the deflection is produced. The computation of chest compression is done by normalizing the deflection data by chest depth. This is accomplished by analog to digital conversion of a deflection response and computer processing. Differentiation of the deflection response results in the velocity of deformation, and multiplication of the compression and the velocity of deformation results in the viscous response. A computer program was developed(27) to process Hybrid III and other test subject chest deflection data into the responses. Evaluation of the viscous response from the Hybrid III dummy is underway; however, a tolerance level for dummy testing has not been established.

References

1. Stapp, J.P., "Voluntary human tolerance levels," *Impact Injury and Crash Protection*, E.S. Gurdjian, W.A. Lange, L.M. Patrick, and L.M. Thomas (eds.) Charles C. Thomas, Springfield, Illinois, pp. 308-349, 1970.
2. Eiband, A.M., "Human tolerance to rapidly applied acceleration: a survey of the literature," National Aeronautics and Space Administration, Washington, D.C., NASA Memo No. 5-19-59E, 1959.
3. Snyder, R.G., "State-of-the-art—human impact tolerance," SAE Paper 700398, New York, 1970 (revised 1970, reprinted 1972).
4. Patrick, L.M., H.J. Mertz, Jr., and C.K. Kroell, "Cadaver knee, chest and head impact loads," Proceedings 11th Stapp Car Crash Conference, SAE New York,pp. 168-182, 1969.
5. Gadd, C.W., and L.M. Patrick, "Systems versus laboratory impact tests for estimating injury hazard," SAE Paper 680053, New York, 1968.
6. *Occupant Crash Interaction with the Steering System,* SAE Special Publication SP-507, 1982 International Congress and Exposition, D.C., Viano (ed)., SAE, Warrendale, Pennsylvania, 1982.
   - Kahane, C.J., "Evaluation of current energy-absorbing steering assemblies," SAE Paper 820473.
   - Horsch, J.D., K. Petersen, and D.C. Viano, "Laboratory study of factors influencing the performance of energy-absorbing steering systems," SAE Paper 820475.
   - Hess, R.L., K. Weber, and J. Melvin, "Review of research on thoracic impact tolerance and injury criteria related to occupant protection," SAE Paper 820480.
7. *The Human Thorax - Anatomy, Injury, and Biomechanics*, SAE Special Publication P-67, 1976.
   - Patrick, L.M., "Frontal force impact tolerance of the human thorax."
   - Kroell, C.K., "Thoracic response to blunt frontal loading," SAE, Warrendale, Pennsylvania.
8. Viano, D.C., "Thoracic injury potential," in 3rd International Meeting on the Simulation and Reconstruction of Impacts in Collisions Proceedings, Bron, France, pp. 142-156, International Research Committee on the Biokinetics of Impacts, 1978.
9. Neathery, R.F., C.K. Kroell, and H.J. Mertz, "Prediction of thoracic injury from dummy responses," Proceedings 19th Stapp Car Crash Conference, SAE Paper 751151, Warrendale, Pennsylvania, pp. 195-316, 1975.
10. Neathery, R.F., "An analysis of chest impact response data and scaled performance recommendations," Proceedings 18th Stapp Car Crash Conference, SAE Paper 741188, Warrendale, Pennsylvania, pp. 459-493, 1974.
11. Foster, J.K., J.O. Kortge, and M.J. Wolanin, "Hybrid III - a biomechanically-based crash test dummy," Proceedings 21st Stapp Car Crash Conference, SAE Paper 770938, Warrendale, Pennsylvania, pp. 975-1014, 1977.
12. Horsch, J.D., and D.C. Viano, "Influence of the surrogate in laboratory evaluation of energy-absorbing steering system," Proceedings 28th Stapp Car Crash Conference, P-152, Paper 841660, Warrendale, Pennsylvania, pp. 261-274, 1984.
13. Jonsson, A., C.J. Clemedson, A.B. Sundquist, and E. Arvebo, "Dynamic factors influencing the production of lung injury in rabbits subjected to blunt chest wall impact," *Avia Space Environ. Med.*, 50:325-337, 1979.
14. Lau, V.K., and D.C. Viano, "Influence of impact velocity on the severity of nonpenetrating hepatic injury," *J. Trauma* 21:115-123, 1981.
15. Kroell, C.K., M.E. Pope, D.C. Viano, et al., "Interrelationship of velocity and chest compression in blunt thoracic impact," Proceedings 25th Stapp Car Crash Conference, SAE Paper 811016, Warrendale, Pennsylvania, 1981.
16. Lau, V.K., and D.C. Viano, "Influence of impact velocity and chest compression on experimental pulmonary injury severity in an animal model," *J. Trauma* 21: 1022-1028, 1981.
17. Lau, V.K., D.C. Viano, and D.B. Doty, "Experimental cardiac trauma - ballistics of a captive bolt pistol," *J. Trauma* 21(1):39-41, 1981.
18. Stein, P.D., H.N. Sabbah, D.C. Viano, and J.J. Vostal, "Response of the heart to nonpenetrating cardiac trauma," *J. Trauma* 22:364-373, 1982.
19. Viano, D.C., and V.K. Lau, "Role of impact velocity and chest compression in thoracic injury," *Avia Space Environ. Med.*, 16-21, 1983.
20. Horsch, J.D., I.V. Lau, D.C. Viano, and D.V. Andrzejak, "Mechanism of abdominal injury by steering wheel loadings," in review for the Proceedings 29th Stapp Car Crash Conference, SAE, Warrendale, Pennsylvania, 1985.
21. Lau, I.V., J.D. Horsch, D.C. Viano, and D.V. Andrzejak, "Mechanism of liver injury by steering wheel loading," for submission to the *J. Trauma*, 1985.
22. Rouhana, S.W., I.V. Lau, and S.A. Ridella, "Influence of velocity and forced compression on the severity of abdominal injury in blunt, nonpenetrating lateral impact," General Motors Research Report No. GMR-4763, 1985.
23. Housner, G.N., and D.E. Hudson, *Applied Mechanics and Dynamics*, D. Van Nostrand Company, New Jersey, 2nd Edition, 1959.

24. Viano, D.C., "Evaluation of biomechanical response and potential injury from thoracic impact," *Avia Space Environ Med.*, 49:125-135, 1978.
25. Lobdell, T.F., "Impact response of the human thorax," Proceedings of the Symposium "Human Impact Response Measurement and Simulation," General Motors Research Laboratories, New York-London: Plenum Press, pp. 201-245, 1972.
26. Kroell, C.K., D.C. Schneider, and A.M. Nahum, "Impact tolerance and response of the human thorax II," Proceedings 18th Stapp Car Crash Conference, SAE Paper 741187, Warrendale, Pennsylvania, 1974.
27. Viano, D.C., and I.V. Lau, "Thoracic impact: a viscous tolerance criterion," General Motors Research Publication, June 1985.

Modelling the Lateral Impact of the Thorax in Car Side Impact Accidents

M.G. Langdon
Transport and Road Research Laboratory
Crowthorne, United Kingdom

Abstract

As part of the development of a simulation model for side impact accidents, it has been necessary to develop a model of the human thorax. This is required to provide both the correct dynamic interface with the simulation of the car structure and a reasonable criterion of injury probability. In terms of designing structures (such as additional padding) that will maximise occupant protection, it is important to have a good understanding of the dependence of injury on the time history of the impact forces.

It is only possible to develop a complete model of a system as complex as the thorax in terms of a step-by-step simulation. However, an analytical model has also been developed to describe the third order mass/spring/damper system that forms a major subsystem in the step-by-step simulation. This differs from the ordinary second order mass/spring/damper system by having an additional spring in series with the damper, which gives a softer response to a sudden impact. Detailed characteristics of the system have been derived, including an analysis of the dependence of peak deflection (probably a good measure of injury probability) on the duration of an applied impulse force.

Background

There is currently much interest in the problem of occupant protection in side impact accidents. Experimental data on the effects of such accidents are required, both to obtain a better understanding of the problem and be able to set safety standards to which production cars must conform. There are two practical methods by which such data can be obtained.

One is to examine the results of real accidents, in which occupant injuries and damage to the vehicles are easily measured. A major disadvantage of this approach is that the kinematic inputs are not controllable and are not always easy to deduce accurately from the evidence available.

The alternative is to crash vehicles deliberately under controlled conditions with instrumented dummies providing substitutes for human vehicle occupants. Because of constraints of cost and staff time, it is possible only to carry out a limited number of such experiments, and in the interpretation of the results there is some uncertainty about how well results obtained from dummies represent the likelihood that particular injuries, or fatalities, would have been sustained by human occupants.

To increase the number of "experiments" that can be carried out with limited resources, recourse is now made to mathematical modelling of various aspects of vehicle crashes. This is usually in the form of a numerical step-by-step simulation, though analytical models are sometimes useful for improving understanding of specific problems. The great advantage of mathematical models is that once a model has been developed, a large number of "experiments" can be carried out relatively quickly and cheaply. The development of the model can by itself frequently provide a useful insight into the fundamental processes occurring during an impact. However, the development of useful models is a skilled and time-consuming process, and great care has to be taken to insure that the final model provides an adequate representation of reality.

This paper describes the development of models to represent injury to the thorax suffered by the occupants of a car during side impact accidents.

Purpose of the Models

The long-term objective of the simulation programme is to produce a model of side impact that can investigate the relative usefulness of modifying various features of

vehicle design, such as the relative stiffness of various structural components and the provision of energy-absorbing padding to protect the occupants at points of impact. The starting point was a simulation model developed by British Leyland (now Austin-Rover) for the Morris Marina(1). The vehicle part of the model performed well and produced some useful and interesting results, but it rapidly became apparent that further progress would require a more sophisticated model of the dynamic behaviour and injury tolerance of the human thorax.

The accuracy with which the dynamic behaviour of the occupant is represented becomes important when the impacting part of the car structure is relatively light and soft, as for example with thin sheet metal or foam padding. In such cases, it is important to have a good model of the effect of the occupant on the car structure, as well as of the car structure on the occupant. In fact, the occupant and the car should be considered merely as distinguishable parts of an overall dynamic system. Current work is therefore concentrated on the development of models to represent the dynamics of the human thorax in lateral impact.

The initial design of a thorax simulation model was based on the mechanical design for the thorax of the EUROSID dummy(2). This consists of three relatively massive steel ribs, with an additional connection to the spine box provided by a spring/damper system. The model has proved very useful, and the current objectives of the research based on it are—

- To provide a suitable thorax submodel for eventual incorporation in an overall side impact model to investigate ways of improving vehicle design for safety
- To obtain a better understanding of the dynamic characteristics of the thorax substructure in the EUROSID dummy, leading eventually to design improvements in the dummy that can provide a closer match to the characteristics of a human thorax
- To develop a criterion for chest injury that takes full account of the time history of the imposed forces

Two basic models are being developed. One is a step-by-step simulation that attempts to model the human thorax in as much detail as is practicable and necessary. The other is an analytical model of the basic three degree of freedom mass/spring/damper system that represents the movement of the ribs relative to the spine (or alternatively the dynamics of the layer of skin covering the ribs). This has proved useful for providing a full understanding of the dynamic characteristics of parts of the more complex step-by-step model, and for deriving appropriate numerical values for some of the parameters in that model.

An Analytical Model of the Thorax

Description of the Model

The mechanical layout of the system represented by the analytical model is shown in Figure 1a. It consists of two masses, m and M, representing the ribs and torso, connected by a spring with spring constant k_1. This

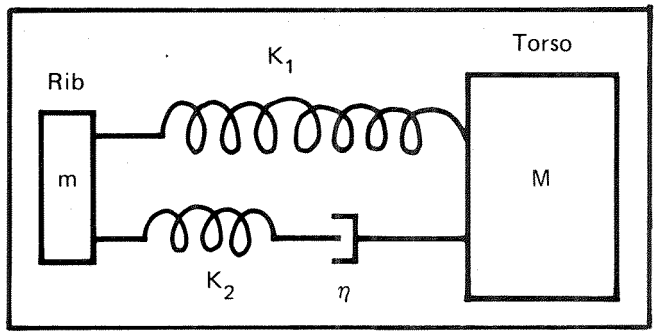

Figure 1a. Layout of system represented by the analytical model

system on its own would have no damping, which would be unrealistic, so damping is provided by a viscous damper, with damping coefficient η. If this damper were connected rigidly to the rib mass (m), it would give an instantaneous large force ($=\eta V$) if the rib were struck by an impactor to give an initial velocity V. This type of behaviour is not observed in actual impactor experiments on cadavers, where the rise in the restoring force exerted by the ribs is relatively slow, suggesting a "rubbery" type of structure. This type of characteristic can be obtained by putting an additional spring (spring constant k_2) in series with the viscous damper. This is the precise type of model used to develop a physical description of rubber elasticity.

In practice there will inevitably be a small mass at the connection between the spring k_2 and the damper. Simulation of the system with such a mass shows that provided the mass is small (e.g., less than 0.2 of the rib mass), it has little effect on the overall behaviour of the system. As its inclusion would seriously complicate the analytical model, such a mass has been omitted for the present.

The characteristics of the system are best evaluated in terms of the impulse response, which describes the behaviour of the system after the rib mass m has been given an initial velocity (e.g., by being struck by an impactor) and no further external forces are applied to the system. If y represents the distance between the rib mass m and the torso mass M, the characteristic equation for the system is:

$$\dddot{y} + k_2\ddot{y}/\eta + (k_1 + k_2)\,\dot{y}/M_0 + k_1k_2y/M_0\eta = 0 \qquad (1)$$

The Newtonian dot notation is used to indicate differentiation with respect to time.

M_o is the reduced mass: $M_o = Mm/M+m)$. If the torso is rigidly clamped so that effectively $M \to \infty$, then the reduced mass M_o becomes equal to the rib mass m.

This is a third order dynamic equation; the inclusion of the damper mass in the model would have led to a considerably more complex fourth order equation.

Following the method used in the well-known second order equation, it is convenient to express this equation in terms of an undamped natural frequency (which provides the dimensional scaling for systems with different frequencies) and two nondimensional parameters. The parameters chosen are:

Undamped (angular) natural frequency

$$\omega_o = \sqrt{k_1/M_o} \qquad (2a)$$

(The undamped natural fraguency $f_o = \omega_o / 2\pi$)

Nondimensional damping constant

$$\eta_s = \eta / M_o\omega_o \qquad (2b)$$

(Note: η_s differs by a factor of two from the corresponding nondimensional parameter normally used in the second order equation.)

Spring ratio $\quad r = k_2/k_1 \qquad (2c)$

This leads to the parametric equation:

$$\dddot{y} + R\omega_o\ddot{y}/\eta_s + (1+R)\omega_o^2\dot{y} + R\omega_o^3 y/\eta_s + 0 \qquad (3)$$

An alternative type of third order dynamic model that has been used to represent the thorax is shown in Figure 1b. This consists of a conventional second order spring/damper system, involving the spring K_1 and damper η, with an additional spring K_2 placed in series with this system. The characteristic equation for the overall system, with no external forces acting, is:

$$\dddot{y} + (k_1+K_2)\ddot{y}/\eta + K_2\dot{y}/M_o + K_1K_2y/M_o\eta + 0 \qquad (4)$$

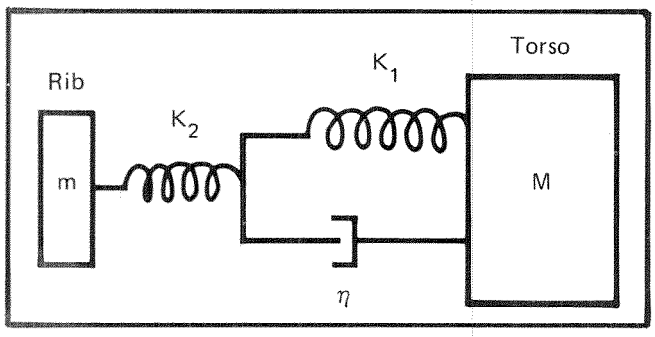

Figure 1b. Layout of alternative model

This can be expressed in terms of the undamped natural frequency ω_o and two nondimensional parameters by making the substitutions:

$$\omega_o^2 = [R/(1+R)]\ K_1/M_o \qquad (5a)$$

$$\eta_s = [R/(1+R)]^2\ \eta/M_o\omega_o \qquad (5b)$$

$$R = K_2/K_1 \qquad (5c)$$

The resultant parameterised equation is identical to the parameterised equation (3) for the system shown in Figure 1a, showing that with an appropriate choice of component values the two systems are dynamically identical.

Solution of the Model Equation—Impulse Response

The third order dynamic equation is solved by making the assumption that the solution is of the form:

$$y = Ae^{-\alpha t} \qquad (6)$$

(Since the equation is third order, there will be three pairs of values of α and A, and the general solution will be the sum of these three solutions.) Substituting this value of y, and its first, second, and third differential w.r.t. time in Equation 3, leads to the cubic equation:

$$\alpha^3 - R\omega_o\alpha^2/\eta_s + (1+R)\omega_o^2\alpha - R\omega_o^3/\eta_s = 0 \qquad (7)$$

This can be solved by the classical method, which involves a substitution of variable to eliminate the term in $a\alpha^2$. The solution is easy to program on a computer, but is not simply expressible in elementary terms. It can be shown that the solution has only three real roots when λ_s lies in the range:

$$(a - b) < \eta_s(a + b) \qquad (8)$$

where

$$a = R^2(R^2 + 20R-8)/8(1+R)^3$$

$$b = R^2\sqrt{R(R-8)^3}/8(1+R)^3$$

The expression for b in the above inequality is only real when $R>8$, so all solutions (for any value of λ_s) must include complex roots when $R<8$.

The complete solution for the case with complex roots is:

$$y = Ae^{-\alpha t} + e^{-\varepsilon t}(B\cos\omega t + C\sin\omega t) \qquad (9)$$

where A, B, and C are arbitrary constants that can be derived from the initial conditions. The parameters ε and ω are the real and imaginary parts of the complex roots of α.

$$\alpha_1 = \varepsilon - i\omega \qquad (10a)$$

$$\alpha_2 = \varepsilon + i\omega \qquad (10b)$$

When the system is excited by an (infinitesimally short) impulse of value I, the initial velocity of the rib mass is V = I/m, and the arbitrary constants have values:

$$A = 2\varepsilon I/m\,[(\varepsilon - \alpha)^2 + \omega^2] \qquad (11a)$$

$$B = -A$$

$$C = I(\alpha^2 - \varepsilon^2 + \omega^2)/m\omega\,[(\varepsilon - \alpha)^2 + \omega^2] \qquad (11b)$$

When all roots are real, the motion is nonoscillatory (over-damped), and the complete solution is:

$$y = Ae^{-\alpha_1 t} + Be^{-\alpha_2 t} + Ce^{-\alpha_3 t} \qquad (12)$$

The arbitrary constant A is given by:

$$A = I(\alpha_2 + \alpha_3)/m(\alpha_1 - \alpha_2)(\alpha_1 - \alpha_3) \qquad (13)$$

The values of B and C are found similarly by equations that are symmetrical with Equation 13.

Using the above equations, it is possible to calculate the impulse response characteristics of the system for any values of η_s and R. It is convenient to work with a "normalised" system for which the undamped (angular) natural frequency ω_o is unity, and to examine the response to an impulse giving unit velocity to the rib mass. The response for other conditions can then easily be calculated by simple scaling. If the real system has an undamped (angular) natural frequency of ω_o (calculated from Equation 2a or 5a), and suffers an impulse giving an initial velocity V, then actual values of time, displacement, or acceleration are found from the normalised values as follows:

Time: $$\text{actual} = T_{\text{normalised}}/\omega_o \qquad (14a)$$

Displacement: $$y_{\text{actual}} = y_{\text{normalised}} \times V/\omega_o \qquad (14b)$$

Acceleration: $$\ddot{y}_{\text{actual}} = \ddot{y}_{\text{normalised}} \times V \times \omega_o \qquad (14c)$$

The quantity y refers to the second differential of the distance between the rib mass and the torso mass, and only represents an absolute acceleration if the torso is clamped. If the torso is free to move, the absolute accelerations of the ribs and torso are found from:

Rib acceleration

$$a_{\text{rib}} = \frac{M_o\ddot{y}}{m} = \frac{M}{M+m}\ddot{y} \qquad (15a)$$

Torso acceleration

$$a_{\text{torso}} = \frac{-M_o\ddot{y}}{M} = \frac{m}{M+m}\ddot{y} \qquad (15b)$$

Figure 2 shows contours of specific values of maximum displacement, plotted as a function of the dimensionless parameters η_s and R. The region in which the solution of Equation 7 has all real roots (over-damping) is shown for interest. It will be noted that although the form of the solution changes at the boundaries of this region, there are no discontinuities in the contours. It will also be seen that when R is greater than 8, there are always two values of η_s that give critical damping (the boundary between over-damping and oscillatory solutions of Equation 3).

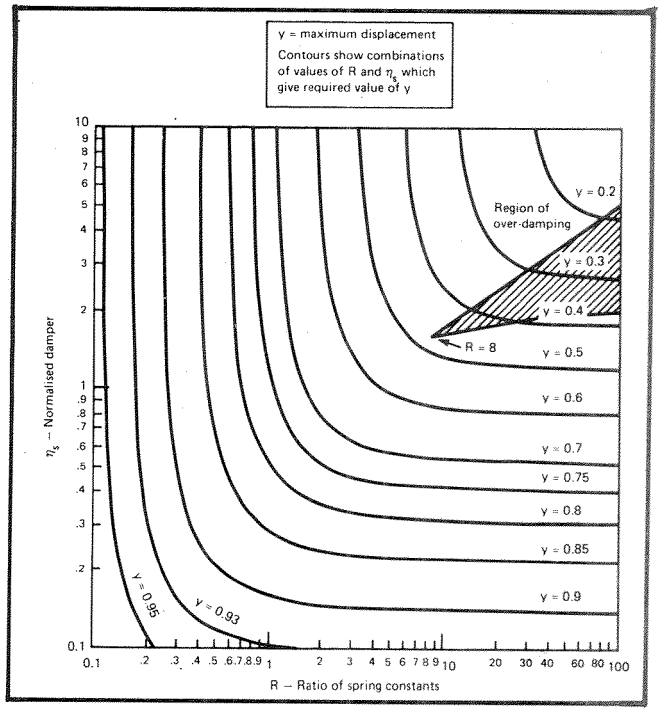

Figure 2. Analytical model—contours of maximum displacement after excitation by a unit impulse

Frequency Response

An alternative (but equivalent) method of representing the behaviour of the system is in terms of its long-term response to a constant amplitude sinusoidal input force. If the rib mass is subjected to a sustained sinusoidal force

F·sin ωt, then the relative rib displacement will also vary sinusoidally with angular frequency ω, after the initial transients have damped out. The displacement can be represented by the equation:

$$y = A \sin \omega t + B \cos \omega t \qquad (16)$$

This has an overall amplitude $\sqrt{A^2 + B^2}$, and a phase angle relative to the input force of ϕ, where tab = (B/A) (17)

The values of A and B are found by equating coefficients in the dynamic equation (3), modified to include the effect of the driving force. The values derived are:

$$A = \frac{F}{M} \cdot \frac{[\omega^2\eta_s^2[(1+R)\omega_o^2 - \omega^2] + R^2\omega_o^2(\omega_o^2 - \omega^2)]}{\{\omega^2\eta_s^2[(1+R)\omega_o^2 - \omega^2]^2 + R^2\omega_o^2(\omega_o^2 - \omega^2)^2\}} \qquad (18)$$

$$B = -\frac{F}{m} \cdot \frac{R^2\omega\omega_o^3\eta_2}{\{\omega^2\eta_2^2[(1+R)\omega_o^2 - \omega^2]^2 + R^2\omega_o^2(\omega_o^2 - \omega^2)^2\}}$$

Figure 3 shows the impulse response for a typical third order system (normalised with $\omega_o = 1$), and the corresponding frequency response plotted separately for the amplitude and phase characteristics. The impulse and frequency responses are mathematically related by the Fourier Integral transform. If the function y(t) represents the response at time (t) following an impulse at time t=0, and Y(f) represents the frequency response, then:

$$Y(f) = \int_o^\infty y(t) \cdot e^{-i2\pi ft}\, dt \qquad (19)$$

(the lower limit of integration should be $-\infty$, but as it is assumed that y = 0 for all time before the impulse, the lower limit can be set to zero.) i represents the imaginary number $\sqrt{-1}$

The function Y(f) derived from this equation is a complex number that contains both the amplitude and phase response. The relationship of Equation 19 is not in fact required to derive the frequency response listed in Equations 16 to 18 (though it is of course satisfied by these equations), but it is useful in further development of the theory of the system dynamics.

Response to Finite Length Pulses

Having evaluated the impulse response of the system, it is possible to calculate the response for any known input. Since the system is linear (i.e., the parameters m, M, k_1, k_2,η are assumed to remain constant for any finite displacements), the effects of a large number of infinitesimal impulses are strictly additive, provided that the effect of the different times of the impulses (i.e., phases)

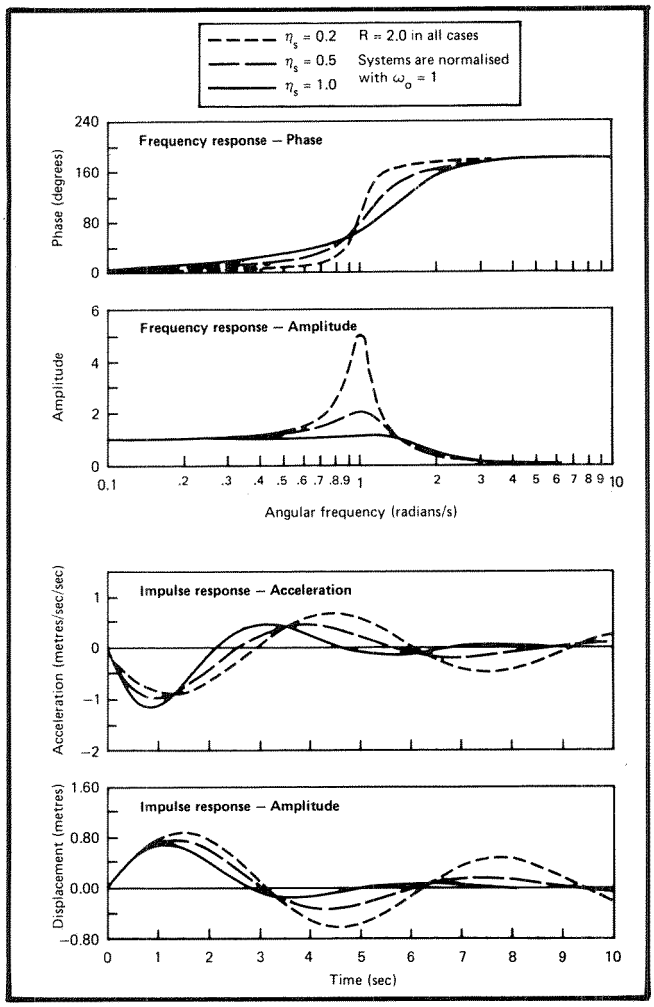

Figure 3. Impulse and frequency response of a third order dynamic system

are taken into consideration. If h(t) is the impulse response (i.e., y = h(t) at a time t after a unit impulse) and x(t) is the actual input at time t, then the response of the system at time t is given by the convolution integral:

$$y(t) = \int_o^t x(\tau)\, h(t - \tau) d\tau \qquad (20)$$

Response to Rectangular Impulses

If the input is a rectangular impulse of amplitude $x(\tau) = I/T_o$ for $0 < \tau < T_o$ and zero for all other time (i.e., it has a total impulse of I spread over a time T_o), then the response can be calculated directly from the impulse response (Equation 9 or 12, depending on whether the solution is oscillatory or not) and the convolution equation (20).

For the exponential terms in the impulse response having the form h(t) = A exp ($-\alpha t$), the overall response becomes:

$$y(t) + \frac{I}{m} \cdot \frac{A}{\alpha T_o} [1 - \exp(\alpha t)]$$

For $0<t<T_o$ (21a)

and

$$y(t) = \frac{I}{m} \frac{A}{\alpha T_o} \exp(-\alpha t) [\exp(\alpha T_o) - 1]$$ (21b)

for $t>T_o$

For the trigonometric terms in the impulse response (when an oscillatory solution is obtained) having the form $h(t) \exp(-\varepsilon t) [B \cos \omega t + C \sin \omega t]$, the overall response can be calculated either by direct integration of the convolution equation (20), or by rewriting the impulse response in terms of complex exponential functions (see Equation 10): the constants B and C also become complex in this case to give an overall real result and substituting the values in Equation 21a or 21b. The results for these trigonometric terms are:

$$y(t) = \frac{I}{m} \frac{1}{(\varepsilon^2 + \omega^2)T_o}$$

$$\{ [\varepsilon B + \omega C] [1 - \exp(-\varepsilon t) \cos \omega t] -$$

$$[\varepsilon C - \omega B] \exp(-\omega t) \sin \omega t\}$$

for $0<t<T_o$ (22a)

$$y(t) = \frac{I}{m} \frac{\exp(-\varepsilon t)}{(\varepsilon^2 + \omega^2)T_o}$$

$$\{[\varepsilon B + \omega C] [\exp(\varepsilon T_o) \cos \omega(t-T_o) - \cos \omega t]$$

$$+ [\varepsilon C - \omega B] [\exp(\varepsilon T_o) \sin \omega(t - T_o) - \sin \omega t]\}$$

for $t>T_o$ (22b)

These equations can be differentiated with respect to time t to find the velocity and acceleration responses to a rectangular impulse input.

Response to Half Sine Wave Impulses

A more realistic input is a half sine wave having the form:

$$x(\tau) = I \sin(\pi \tau / T_o) \text{ for } 0<\tau<T_o$$ (23)

and zero for all other time.

As for the rectangular pulse, this has a total impulse of I. It is again possible to calculate the response by direct integration of the convolution equation, but the result is rather more complicated.

For each exponential term, $h(t) = A \exp(-\alpha t)$, in the impulse response, the overall response is:

$$y(t) = \frac{I}{m} \frac{\pi T_o A}{2(\alpha^2 T_o + \pi^2)}$$

$$\{\alpha \sin \frac{\pi t}{T_o} - \frac{\pi}{T_o} \cos \frac{\pi t}{T_o} + \frac{\pi}{T_o} \exp(-\alpha t)\}$$

for $0<t<T_o$ (24a)

and

$$y(t) = \frac{I}{m} \frac{\pi^2 A \exp(-\alpha t)}{2(\alpha^2 T_o + \pi^2)}$$

$$[\exp(\alpha T_o) + 1]$$

for $t>T_o$ (24b)

These equations can be differentiated with respect to time (t) to find the velocity and acceleration responses to a half sine wave impulse input.

The expressions for the overall response from the trigonometric terms become very complicated, and numerical evaluation is best performed by complex arithmetic on a computer, using Equations 2a and 2b with the appropriate complex values substituted for A and α.

Figure 4 shows how the peak deflection of the rib mass varies as the duration of a half sine wave impulse is increased, keeping the overall impulse constant. Curves are shown for a range of values of η_s between 0.2 and 5.0, for a fixed value of spring ratio R = 2. (As before the system is normalised, with $\omega_o = 1$). The present EUROSID design is intended to have a value of η_s a little less than 2. Figure 4 also includes a dotted curve showing the displacement that would occur if a static force was applied equal to the peak force arising in the impulsive input. It will be seen that all the curves are asymptotic to this static deflection value for large values of the impulse duration.

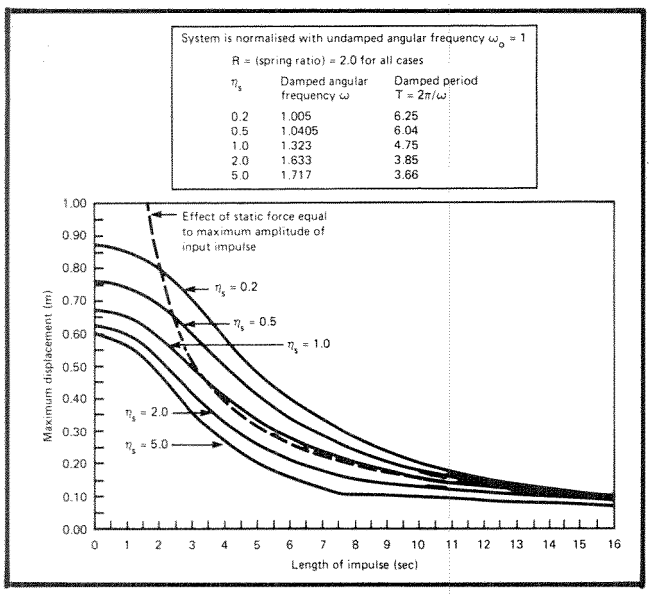

Figure 4. Responses of third order dynamic system to half-sine wave input impulses of different durations

The maximum displacements initially decrease rather slowly as the impulse length is increased, and it requires a pulse length approximately equal to the period of the system to reduce them to half value. (The period ω varies with η_s. See box in the figure.) The curves are at their steepest in this region. If padding is used to increase the length of the impulse, the increase in effectiveness for increasing thickness is obviously at its maximum here.

Similar curves are obtained with rectangular impulses, although the curves fall off rather more steeply. A pulse length of about 0.7 of the system period is required to reduce the peak displacement to half the value for a very short impulse. With a rectangular impulse, the discontinuity in slope of the curve for $\eta s = 5.0$ is much stronger; it occurs when the maximum value of displacement is at the second maximum of the displacement/time curve instead of the first.

Response to an Arbitrarily Complex Input

For input pulses with shapes more complex than the half sine wave, it does not appear worthwhile to attempt to calculate the output response by a purely analytic method. In principle it would be possible to use a direct numerical integration of the convolution equation (20), but the Fast Fourier Transform provides a much quicker method. Convolution in the time domain transforms into multiplication in the frequency domain. The impulse response h(t) and the input waveform x(t) are therefore transformed by means of Equation 19, and the product at each frequency of these transforms H(f).X(f) is then the transform of the output response Y(f). The output time response can then be recovered by the inverse transform.

$$y(t) = \int_{-\infty}^{\infty} Y(f)e^{i2\pi ft}df \qquad (25)$$

Computer programs to implement the Fast Fourier Transform are now widely available, and the methodology is well described in the literature(3).

However, if the impulse response is formed by the sum of a number of exponential terms (real or complex), as in the model under discussion, a much simpler numerical method can be used to find the output response. Consider the contribution to the total response contributed by the term $A \exp(-\alpha t)$, and suppose that the input waveform is sampled at a large number of times separated by intervals of Δt. Further, suppose that the total contribution from this term to the system output (e.g., rib displacement) after n intervals is S_n.

After a further period Δt, in the absence of any input, this displacement would have decayed to $S_n.\exp(-\alpha\Delta t)$. However, if the system is subjected to an average force F_n in the interval, it will have received an additional impulse $F_n\Delta t$, which will give a response $AF_n\Delta t/m$. The total response after n+1 intervals is therefore:

$$S_{n+1} = S_n \cdot \exp(-\alpha\Delta t) + AF_n\Delta t/m \qquad (26)$$

If t is very small, the exponential term can be approximated:

$$\exp(-\alpha\Delta t) \rightarrow 1 - \alpha\Delta t \quad \text{as } \alpha\Delta t \rightarrow 0 \qquad (27)$$

and Equation 26 can be simplified to:

$$S_{n+1} = S_n + (AF_n/m - \alpha S_n)\Delta t \qquad (28)$$

If the input is zero for all times before the time corresponding to n=0, and S_o is set to zero, this equation provides a simple iterative method of calculating the contribution by each term, and hence the overall system response, for all subsequent times.

When the overall solution is oscillatory and contains trigonometric terms, it is simplest to replace the trigonometric terms by the corresponding complex exponentials, and use these directly in complex versions of Equations 26 or 28. For example, the trigonometric form of the impulse function:

$$h(t) = A\exp(-\alpha t) + \exp(-\varepsilon t)[B\cos\omega t + C\sin\omega t] \qquad (9)$$

becomes

$$h(t) = A\exp(-\alpha_1 t) + B'\exp(-\alpha_2 t) + C'\exp(-\alpha_3 t) \qquad (29)$$

where

$$\alpha_1 = \alpha \text{ (the real term is unchanged)} \qquad (30a)$$

$$\alpha_2 = \varepsilon - i\omega \quad (30b)$$

$$\alpha_3 = \varepsilon + i\omega \quad (30c)$$

$$B' = 1/2(B-iC) \quad (30d)$$

$$C' = 1/2(B+iC) \quad (30e)$$

The complex exponentials $\exp(-\alpha_2 t)$ and $\exp(-\alpha_3 t)$ represent vectors rotating in the complex plane. The amplitude of the vector decreases at a rate controlled by the parameter ε, while the rate of rotation is controlled by the parameter ω.

When Equations 26 or 28 are evaluated and the results for all the terms are summed, it is found that the imaginary terms cancel out and vanish, leaving a result that is wholly real. The use of complex variables may therefore, if desired, be regarded solely as a mathematical device to simplify the calculations required, and need not concern the user of the results.

If the maximum rib displacement could be regarded as providing a measure of injury severity, the above method for calculating the response to any arbitrary input could be used as the basis for a new injury criterion. It would be much faster to calculate than exceedences or HICs, as well as appearing to be based on sounder physical principles.

Step-by-Step Simulation Model

The analytical model described above has proved useful for obtaining a better understanding of the operation of subsystems with up to three dynamic components (springs or dampers). However, a model of this type would become very complicated and difficult to use if extended to more complicated systems, and parts of the solution would require numerical methods of solution. (For example, solution of the equation to give the impulse function is only possible by numerical methods when the highest power of α exceeds four.) Furthermore it would be virtually impossible to include nonlinear components in the model, at least without losing most of the features that have made it so tractable.

The alternative type of model for solving more complicated problems is the step-by-step simulation. It takes more time to run than an analytic model and does not provide the same degree of insight in simple situations, but there are no fundamental limits to the complexity of the problem to which it can be applied, other than those set by the storage capacity and available running time of the computer. Programs have been written using the Advanced Computer Simulation Language (ACSL). With this the operator effectively has to write out a set of simultaneous equations that define the problem, provide initial values for all variables that are to be integrated, and set a step length. The ACSL system then automatically carries out a step-by-step integration of the set of equations and provides facilities for accessing any required variables at suitable time intervals. Outside the dynamic section of the program that performs the integrations, the operator may include ordinary Fortran coding, including access to Fortran subroutines, so the system is extremely flexible in use.

Systems Investigated

The basic model used in the step-by-step simulation is shown in Figure 5. The rib structure is identical to that investigated in the analytical model. Between the rib mass and the impacting mass, there is an additional spring/damper system to represent the skin. This could also be

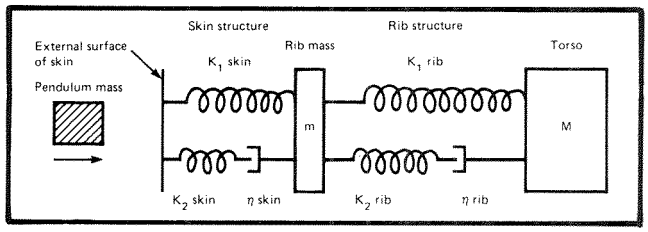

Figure 5.

used to represent the effect of padding, if required. This system is similar to the spring/damper used for the ribs, except that it is stiffer and the main spring (k_1-skin) is nonlinear. The force/compression characteristic is represented by the equation:

$$\text{Spring force} = k_{1\text{-skin}}.x.x_o/(x_o-x) \quad \text{for } x>0 \quad (31)$$

$$= 0 \quad \text{for } x<0$$

where x represents the compression of the skin, and x_o is a maximum compression, nearly equal to the initial skin thickness.

For small deflections, the skin behaves as a linear spring, with spring constant k_1-skin, but when the compression approaches a value x_o the spring becomes progressively stiffer so that the compression can never exceed x_o.

Typical values of the skin parameters used to simulate a foam covering used in tests on a dummy rib are:

$k_{1\text{-skin}}$ 200 kN/metre

$k_{2\text{-skin}}$ 4000 kN/metre

η-skin 250 Newtons/metre per second

x_o 10 mm

The spring parameters of the main rib system have been selected to conform approximately to some cadaver results, though more work is required to optimise the match of the simulation system to the experimental results. The rib mass is equated to the rib mass of the EUROSID dummy, and is rather large compared with the skeletal mass of human ribs. The parameters relating to one rib of the first prototype EUROSID dummy (one-third of a complete thorax) are:

$k_{1\text{-rib}}$ 15 kN/metre

$k_{2\text{-rib}}$ 33 kN/metre

η-rib 250 kN/metre per second

m-rib 1 Kg

i.e. ω_o = 122.5 radius/sec (19.5Hz)

R = 2.2

η_s =2.04

ω = 205 radius/sec (33Hz)

This basic thorax simulation has been built into a number of simulation programmes representing various possible test situations. These include:

i) Pendulum impact when the spine box (torso) is clamped

ii) Pendulum impact when the spine box is free to move

iii) Excitation by square wave or half sine wave impulses of varying pulse length (c.f., similar impulsive inputs to the analytical model)

iv) Impact of the whole thoracic system into a fixed wall; impact from horizontal motion corresponds to the "Heidelberg" test; impact from a vertical drop corresponds to the "Peugeot/Renault" tests

The dynamic outputs from the system can be filtered within the programme, if required, to produce results that are fully compatible with the results from experimental work. At present a second order Butterworth filter is incorporated, but more complex filters can easily be provided by the ACSL system if required.

The thoracic simulation has also been used as part of a complete vehicle side-impact simulation, but it is not intended to carry out further work on simulating vehicle impacts until a full comparison has been made between the simulation model and experiments with dummies and cadavers. At present the role of the model is seen as providing help in matching dummy and cadaver characteristics and obtaining a better understanding of the criteria for thoracic injury.

A number of problems or potential problems with the dummy thorax have been investigated by the simulation model.

Effects of Changing the Skin Characteristics

When a dummy rib is impacted by a pendulum, the measured accelerations on the rib or spine differ markedly from the smooth curve predicted by the simple analytical model (Figure 3), due to an additional higher frequency oscillation. This is caused by "bouncing" between the pendulum and rib, in the system formed by the pendulum and rib masses, and the skin elasticity. A similar acceleration waveform is shown by the simulation. The actual shape of the waveform can be altered significantly by changes in the skin characteristics. However, the displacement waveform, and particularly the peak displacement, are affected only slightly by such changes, provided that the "skin bounce" frequency is high compared with the fundamental response frequency of the rib structure. This would be expected from a consideration of the analytical model's response to impulses of different durations (Figure 4).

It is clear that if it is required to match the acceleration response of various parts of the dummy thorax with the responses recorded in cadaver experiments, then it is important to produce exactly the "right" characteristics for the skin covering the ribs. If, however, the injury effects on the dummy can reasonably be related to the peak displacement (compression) of the rib structure, then it may be much less important to "fine-tune" the skin characteristics to produce a dummy that can give a reliable measure of injury likelihood in crash experiments.

Effect of Rib Mass

An accelerometer attached to the pendulum used to provide the impact on a dummy will record an initial high-peak acceleration, followed by a series of oscillations due to "bounce" between the pendulum and rib mass. This initial peak is still apparent, though its amplitude is decreased, even if the output response is heavily filtered. The peak is reproduced on the simulation but is generally absent in cadaver experiments. The reason for this discrepancy is the high mass of the dummy rib, compared with the lower mass of the bony rib structure in a human cadaver. In the human, there is effectively a small concentrated mass in the bony rib, backed up by the distributed mass of various organs lying between the rib and the spine. This mass is set in motion gradually as the rib moves and will have quite a different effect on the acceleration of the pendulum.

The difference in mechanical layout clearly has implications on the degree to which the "lumped-mass" dummy can accurately reproduce the motion of a real human thorax. The important matter is whether this simplified model of the human chest incorporated in the dummy can still give a useful measure of the likelihood of injury under a wide range of crash conditions. This

problem will be investigated by the simulation model in the near future.

Effect of "Lateral Inertia" on Dummy Rib Mass

The values of spring constants and masses in a dummy rib system can easily be measured in quasi-static experiments. However, experiments on an instrumented dummy to determine the damper characteristics during the pendulum gave peculiar results, suggesting initially that the main spring k_1 has highly nonlinear characteristics in a dynamic (as opposed to quasi-static) situation. This seemed unlikely as the spring is a simple steel coil, but it now seems probable that the effect is due to a "lateral inertia" effect. (In this case, "lateral" is relative to the "left-right" direction of impact; in absolute terms, it is the "anterior-posterior" inertia.) When the rib is struck by a pendulum so that the springs are compressed (Figure 6), the steel strip forming the dummy rib deforms as well as being pushed away from the impulse, and part of it is accelerated in the a-r direction after a slight time delay.

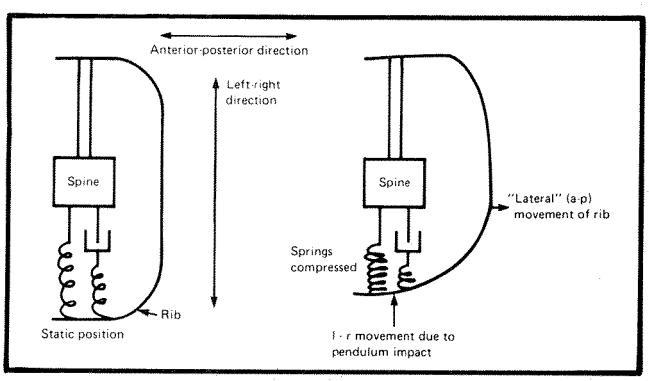

Figure 6.

Since the rib has a substantial distributed mass, a force is required to produce this acceleration, and this force is seen as an apparent increase in the mass of the rib at the attachment point of the springs. (The rib mass is represented by a single point mass at this location in the models.) In subsequent motion, the rib oscillates in the a-p direction with its own natural frequency (as well as any frequencies forced on it), and the effective mass at the spring attachment point varies widely.

The effect of this "lateral inertia" can be included in the (one dimensional) simulation by adding an additional mass attached only to the rib mass by an undamped (or very slightly damped) spring. The simulation has been used to check the correctness of the original hypothesis that a "lateral inertia" effect is the likely cause of the discrepancies in experimental results.

Preliminary results have suggested not only that the hypothesis is correct, but that the effect may improve the "fit" of the model to the results of cadaver tests. It seems likely that the additional mass can represent the effects in the human body of massive organs within the rib cage, which are only loosely coupled to the rib structure.

Discussion

A discrete element model can be built that appears to respond to a side impact in a similar way to the rib system of the human thorax. Two springs and a viscous damper are required to obtain a reasonable match of the dynamic response. There are two possible configurations for these elements (Figures 1a and 1b), but it can be shown that with an appropriate choice of parameters the two configurations can always be designed to give identical dynamic characteristics. A full analysis of this three-element model has been carried out by analytical methods, including its response to rectangular and half sine wave impulses of various durations.

The results have the following important implications for the design of padding. In most accidents in which there is no significant penetration of the vehicle structure, the total velocity change to which the occupant is subjected is largely unaffected by vehicle design. The importance of padding, or the inclusion of crushable or deformable elements in the vehicle structure, is to change the time over which the velocity change is applied. The analysis of the effect on rib crush of varying the impulse duration suggests that for thoracic injury, padding has little effect unless it can stretch the impulse out to a time that is at least half the natural frequency of the rib structure.

As well as providing a useful insight into the mechanics of the rib system and the probable effectiveness of padding in reducing injury, the analytical model also appears to provide a method for calculating an injury index based on sound physical principles, and would be much easier to calculate than the present method of exceedences.

To investigate the characteristics of more complicated systems such as a rib system covered by an elastic skin, a step-by-step simulation model has been developed. This is currently being used as an aid to the design of the thorax for the EUROSID dummy. It has thrown considerable light on the significance of the "skin" characteristics in modifying the acceleration response of the ribs in pendulum impact tests and has emphasised the importance of reducing the mass of the steel ribs near the point of impact. The simulation is currently being "tuned" to give the best possible fit to the results of cadaver tests. Because of the large number of variable parameters in the step-by-step model, a trial-and-error method of adjusting parameters would have been very time-consuming. The analytic model was therefore used to estimate probable

values of many of the parameters for the initial simulation runs.

The next stage of research will attempt to evaluate the performance of the human thorax in terms of a transfer function from input force (at the ribs) to rib deflection, rather than in terms of an equivalent mass/spring/damper system. It would then be possible to set up a simulation using this transfer function directly and compare the results (for a wide range of input impulses) with those of a dummy-equivalent simulation. This would provide information on the relative significance for injury estimation of remaining differences between the dummy and human characteristics.

References

1. Emmerson, W.C., and J.E. Fowler, "The application of computer simulation in vehicle safety," Proceedings Fifth International Technical Conference on Experimental Safety Vehicles, London, pp. 712-720, 1974.
2. Neilson, I.E., et al., "Development of the EUROSID side impact dummy," Proceedings Tenth International Technical Conference on Experimental Safety Vehicles, Oxford, 1985.
3. Jenkins, G.M., and D.G. Watts, "Spectral analysis and its applications," Holden Day, 1968.

Validity of Thoracic Injury Criteria Based on the Number of Rib Fractures

Jean-Pierre Verriest and
André Chapon
Organisme National de Sécurité Routière
Laboratoire des Chocs et de Biomécanique

Abstract

Most of the thoracic injury criteria proposed these past years are based mainly on the analysis of data obtained from experiments with human cadavers and are related principally to rib fractures. And yet, the actual threat to life incurred in real accidents results from lesions to intrathoracic viscerae that are not necessarily correlated with the number of rib fractures. Moreover, the injuries sustained by cadavers during experiments are mainly rib fractures. In these cases, visceral lesions are unusual and not necessarily identical with those sustained by real accident victims.

Preliminary results of measurements concerning rib strength and dynamic behavior of the cadaver thorax in frontal impacts show the rib cage offers a low resistance against compression and the vertebral column acts as a stop. The combination of these various data leads to questioning the validity of thoracic injury criteria based on the number of rib fractures observed on human cadavers.

Introduction

Thoracic injuries rank second, after head injuries, among the causes of fatalities or of severe impairment of vital ability in traffic accident victims. Injury criteria are needed to design protective devices and to evaluate their efficiency. In a recent review of biomechanical research, Aldman(1) defines such injury criteria as follows: they are a mechanical variable, or a group of mechanical variables, whose value enables an estimation of the injury risk for the considered body segment, for the road user submitted to an impulsive mechanical sollication similar to those found in traffic accidents. Numerous epidemiological and experimental studies have tried to better know the thoracic tolerance to impact and to define a corresponding injury criterion. The use of human cadavers as experimental subjects has spread these past years in the various laboratories involved in the research, maybe because of the problems resulting from the use of other substitutes, such as animals (involving scientific, ethical, and financial problems). This human substitute is thought to be reliable since it reproduces the anatomy of the living human accurately: therefore, there is practically no scaling problem. Besides, the human cadaver is considered to be more fragile than the living human from the point of view of resistance to injury; this means that protective devices defined from criteria based on the cadaver should

be all the more efficient for the living human. However, the reserves and recommendations made, among others, by some specialists in this field(3) and that are related to the limits of validity of cadaver data tend to be dropped. Everyone knows that a cadaver has no muscular activity, its blood does not flow, its heart does not beat, and its brain does not work. But the only corrective parameters that are presently included in data processing are age and weight.

In the discussion opposing the tenants of either deflection or force or acceleration as a physical variable to be measured to estimate the injury risk, there is a tendency to forget a main point which is the variety of injury mechanisms, to keep a sole lesion only which is the number of rib fractures. However, there are some arguments in the clinical and in the biomechanical fields as well to carry things further. The objective of this paper is to debate some of these from the analysis of accidentological data and preliminary results obtained from experiments performed in our laboratory.

Particularities of Thoracic Anatomy

The body segment concerned in this paper is thorax in the wide meaning of the word, i.e., the thoracic cage and its internal organs, including liver and spleen, which are sheltered behind the grid provided by ribs. The thoracic vertebral column is excluded from our discussion. The sketches of Figure 1 show how the various intra-thoracic organs are arranged in relation to the bony structure. It is important to notice the respective positions of the different organs and also the external and internal size of the thoracic cage. The space between the anterior face of dorsal vertebrae and the posterior face of sternum accounts for about 46 percent of the anterio-posterior diameter at the mid-sternum level. At the upper third, this space is only 39 percent; and at the lower third, it widens up to 48 percent. In other words, when the thorax sustains a frontal impact inducing a deflection of about 45 percent, the sternum comes into contact with the vertebral column. For an external diameter of 22cm, this deflection is about 10cm. It is also noted that the heart and major vessels are located in the median zone comprised between the sternum and the column, where the space is the most reduced.

Overview of General Injury-Producing Mechanism

During a traffic accident, since the trunk has a certain kinetic energy, it comes into contact with a more or less hard obstacle that applies on the thoracic wall a force that tends to crush the chest. This force opposes the inertia of masses in motion, fluid or solid, the elasticity of structures that are compressed, and their viscous resistance to rate of motion. Within the organs, this force induces various stresses (tensile, compressive, shearing, twisting) that can locally overrun the strength of tissues and hence produce injuries.

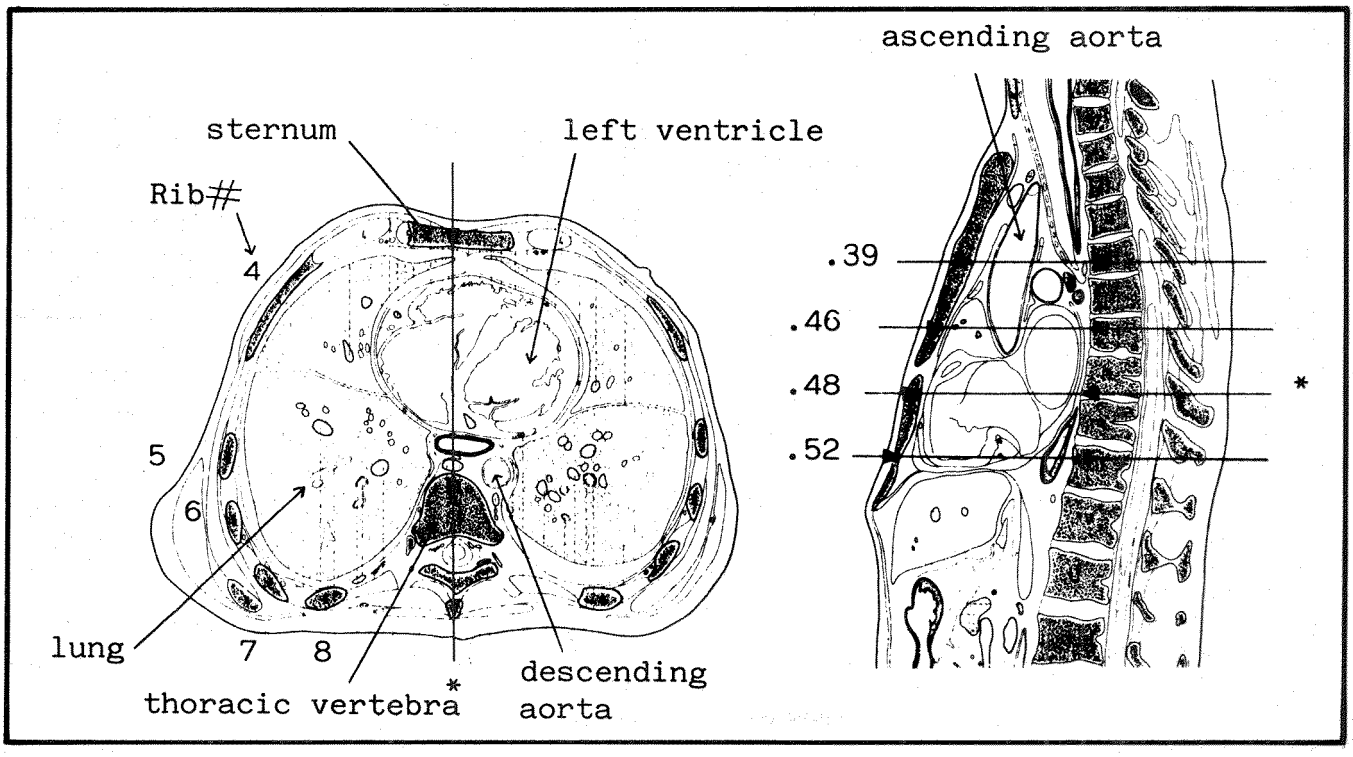

Figure 1. Transverse (left) and sagittal (right) sections of a human thorax

Schematically, during a frontal impact against the sternum, the first event is the initiation of the anterior wall motion. Then, once the speeds of both the thoracic wall and the impactor are equalized, the wall begins to deflect. This flexion mainly applies a bending stress to the ribs but also makes them rotate downwards about the axis of the costo-vertebral joint. The bending stresses can exceed the resistance of ribs, which break. According to the degree of crushing, intra-thoracic organs, especially the heart and the major vessels, are then compressed. The fluids inside them are flown out to other places, which opposes the compression through their inertia and the resistance of the vessels to the flow. Once the cavities are completely collapsed, the walls of organs are subsequently submitted to compression, which they resist by their elasticity and viscosity. But these organs may also be pushed aside in the adjacent cavities. Then they compress the adjoining organs and especially exert stretchings on their attachments up to rupture. The phenomenon is slightly different in the case of lateral impact since the viscerae are not jammed between two hard structures. The heart is perhaps better protected than in the case of frontal impact. Since not all organs have the same mechanical properties, the same mass, they behave differently. When observing inside motions through high speed x-rays(5,6), it can be seen that the heart behaves like a solid (few deformations and large motions), whereas the liver is more comparable with a fluid (large deformations, small motions). The intra-thoracic organs may also be submitted to stresses resulting from remote impacts, for example, at the abdominal level. In this case, the mechanism can be the intrusion of abdominal organs, which push thoracic organs up, and the propagation of a pressure wave.

Typology of Thoracic Injuries in Real Accidents

Injuries sustained by victims of a thoracic trauma in a traffic accident have largely been described in surgery and traumatology journals. Special synthesis reviews have been issued(7) and the case study from Huelke(8) gives a survey of possible injuries. Without entering into all the details, it seems necessary to underline some points of importance for the following discussion.

It is well established that rib fractures are found in nearly all cases. Their severity is related to their consequences on the respiratory function, which is altered if fractures are numerous and, above all, if they constitute an unstable flap preventing the normal expansion of the rib cage. When the fracture is open, it may result in organs being punctured subsequently to a very large local deformation. On the whole, however, the severity of rib fractures remains limited, thanks to techniques of respiratory aid now available.

The severity of the thoracic injury lies mainly in heart wounds and ruptures of major vessels. Among lesions resulting in an immediate death (before admission to the hospital), according to Gilroy(9), wounds to the heart and to main thoracic vessels are fatal in 57 out of 144 cases (34 aorta ruptures, 16 ruptures of the myocardium, and 7 of other vessels). Similar results are found in results of autopsies made by Sivard(10) of 100 road victims who died before admission to the hospital: 32 fatal lesions were of intra-thoracic origin. Liver and spleen lesions, such as laceration, tearing, or rupture, are severe because they produce hemorrhages— often profuse.

Other lesions, less impressive since they do not lead to large structural damages, may severely impair the functional ability. Disturbances of the heart electric conduction, such as fibrillation or block, are fatal if they are not attended very rapidly(11). Diffuse lesions of the lung parenchyma corresponding to ruptures of air-cells or pulmonary lobules are characterized by the parenchyma being flooded by a blood/air mixture. Depending on their size, these lesions prevent exchanges between blood and air and prove to be much more severe than macroscopic bronchial ruptures or lung lacerations, which are easier to detect and to treat(12). They often are only suspected when there is no indication for a surgical operation to treat a macroscopic lesion.

But the main point with respect to the present discussion is the association of visceral lesions with bone lesions, especially rib fractures. When an accident victim sustains a large number of rib fractures, there often is an underlying endo-thoracic lesion, either because broken pieces of ribs have perforated the tegument of an organ or, more simply, because the thoracic internal organs have been extensively compressed.

But this relationship is far from following an absolute rule: deep crushes of the costal grid without visible underlying lesion can be observed. On the contrary, the thoracic impact may produce very severe injuries to internal organs without any fracture or with a few. For example, among the 27 cases of immediate death reported by Sivard(10), which show 34 lesions of the heart and major vessels, 7 are mentioned without fracture. Out of 35 fatal wounds or ruptures of the liver, 19 are associated with fractures but 16 are not. Similarly, Chesneau(13) reports that out of 7 ruptures of the aorta, 3 are not associated with any fracture. Out of 10 nonfatal cases of rupture of the aorta isthmus reported by Caillard(14), 7 are without fracture.

What is true for vascular lesions applies also to lung parenchyma lesions. In a case report of 73 severe thoracic-injured admitted to the hospital with multiple rib fractures and/or a thoracic visceral lesion (AIS $\geq$ 3), Anselmet(15) notes that below 7 rib fractures, there are as many cases with visceral lesions (hemo and/or pneumothorax) as cases without lesion. As concerns the upper abdominal viscerae and depending on various authors,

only 10 to 30 percent of the lesions of the liver and spleen are associated with fractures of respectively right and left lower ribs(15,16).

Rib fractures, then, are neither a necessary nor a sufficient factor to involve severe intra-thoracic lesions. The absence of fracture is especially obvious in young subjects, whose ribs are much more flexible than older subjects.

Within the frame of using the number of rib fractures as an indicator of the severity of intra-thoracic and upper abdominal injuries, it would be necessary to establish relationships likely to exist between bone fractures and visceral lesions from the analysis of injury associations in real accident victims.

Topology of Injuries Produced Experimentally

Experimental works are necessary to evaluate human tolerance, and to establish injury criteria for accidentological surveys does not provide accurate characteristics of the input signal, and variation sources are too numerous. For obvious reasons, traumas can only be studied with substitutes of the living man. This is why many experimental studies have used human cadavers as a model. The injuries reported in most studies carried out with cadavers are rib fractures. In frontal impact and with a 3-point belt or in accident reconstruction, there is never or almost never intra-thoracic lesions(17,18, 19,20,21). On the other hand, the number of rib fractures is always higher in experimental subjects than in real accident victims as shown by accident reconstructions(22) or by the estimation of the input signal applied to real accident victims(23). This difference is due mainly to the age of the subjects available and also to their state of health before death. Impacts with a rigid striker result either in lesions to intra-thoracic viscerae(24,25) or in no lesion(26,27). In any case, a visceral lesion without a bone fracture is never reported. Moreover, when these lesions exist, they are not described accurately enough to allow a comparison with injuries sustained in real accidents. (Are lacerations of the aorta produced experimentally comparable with ruptures of the aorta sustained by real accident victims?) It is rarely a point of discussion to know whether injuries are of the same type; only injury severity levels are compared through injury codings (AIS, MAIS, etc.).

From all these attempts to evaluate thoracic tolerance, two main points can be drawn out:

- The injuries cadavers are likely to show are rib fractures. Visceral lesions are not frequent and do not necessarily correspond with those found in real accidents.
- Results are very different from one subject to another and the number of rib fractures depends mainly on the experimental subject's individual characteristics.

When these results are compared with real accident data, the validity of an injury criterion based on the number of rib fractures only, even with age compensation, may be questioned.

Static Mechanical Resistance of Thorax

A protective purpose is often implicitly devoted to the thoracic cage toward the organs it shelters. This is perhaps true when the released energy is low. In fact the statical force that can be opposed to a frontal compression is due mainly to the ability of inter-costal muscles to prevent the rotation of ribs around the costo-vertebral joint. In volunteers, this force is limited to a few hundreds of Newtons for a maximal deflection of 3 to 4cm(17,28,29). The stiffness calculated for these solicitations remains nearly constant and is of about 100 to 150N/cm.

In unembalmed cadavers, the first rib fracture occurs at about 1,500 to 1,800N for a deflection of 5 to 6cm(17). During this experiment, deflection values of 10 to 11cm (i.e., 38 to 49 percent) were reached for a force of 3,700 to 5,000N, resulting in multiple fractures (see Figure 2). Unfortunately these data are incomplete: the loading curve and also the deflection values at which fractures occurred (except the first one) are unreported as well as what happens if the force exceeds 5,000N. From the tests performed at our laboratory (full results to be issued later), the resistance of an isolated rib for a 53-year-old male varies from 35 to 95N, depending on the costal level, for a deflection of about 1.2 to 4.3cm (see Figure 3 and Table 1). These data are similar to those from Schmidt(19). Ultimate force values vary because of the different loading procedures used, but the bending moments are similar. Assuming that in a frontal compression 10 pairs of ribs are loaded at the same time, the maximum resistance provided by the rib cage alone cannot exceed 600N, with a stiffness of about 200N/cm, in a plane parallel with the ribs, i.e., in a direction of 45° relatively to the direction of compression. If inter-costal muscles oppose the rotation, as stated by Kroell(24), the total normal resistance settles at about 900N (see Figure 4), and it must decrease when fractures occur. The force of several thousands of Newtons that resists to the penetration of the impacting object, such as safety belt, steering column, or dashboard, does not come from the resistance of the rib cage but from the compression of intra-thoracic organs (elasticity, load losses in fluid motions, and inertia).

Dynamic Behavior of Thorax

When analyzing what occurs in a frontal impact with belt restraint, for example, the impact object, i.e., the

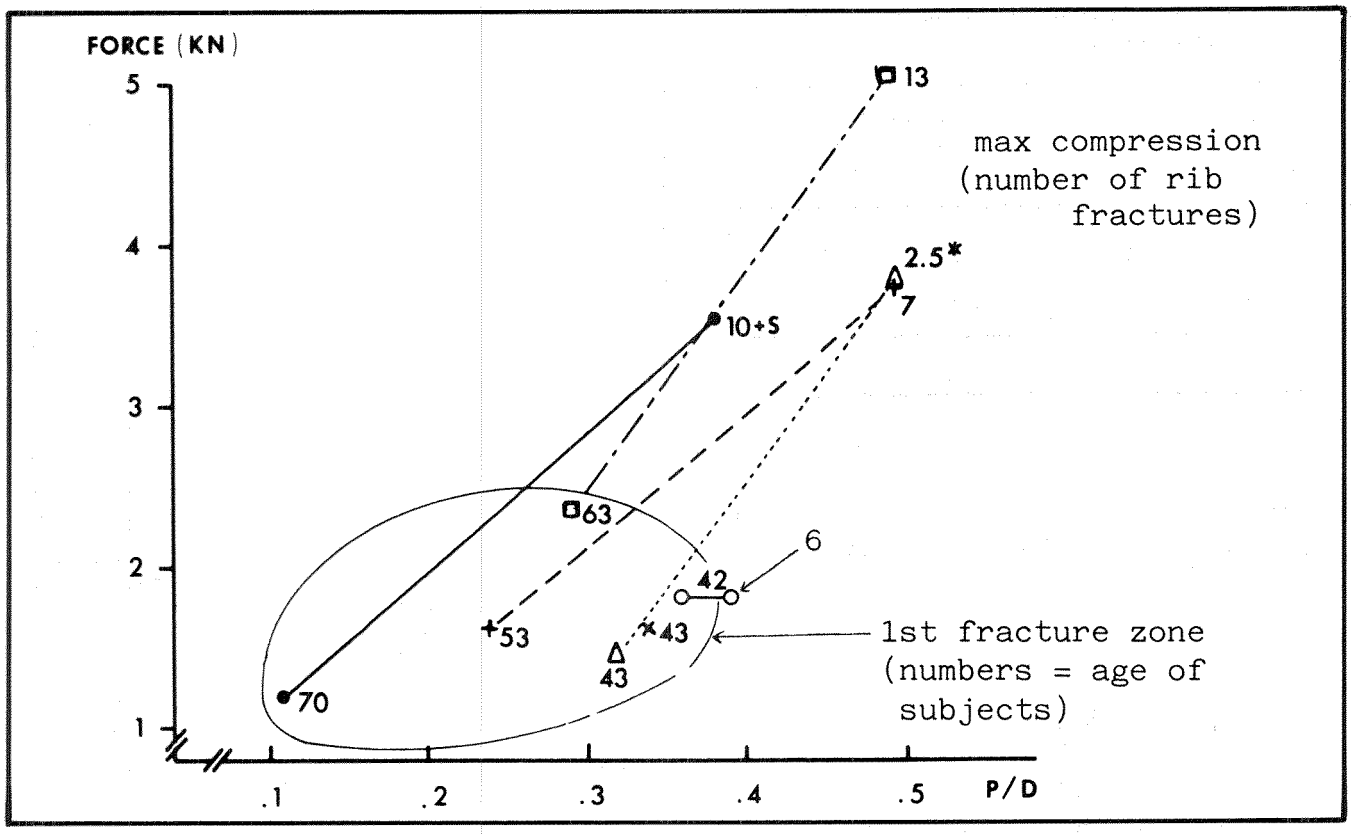

Figure 2. Static strength of human thorax

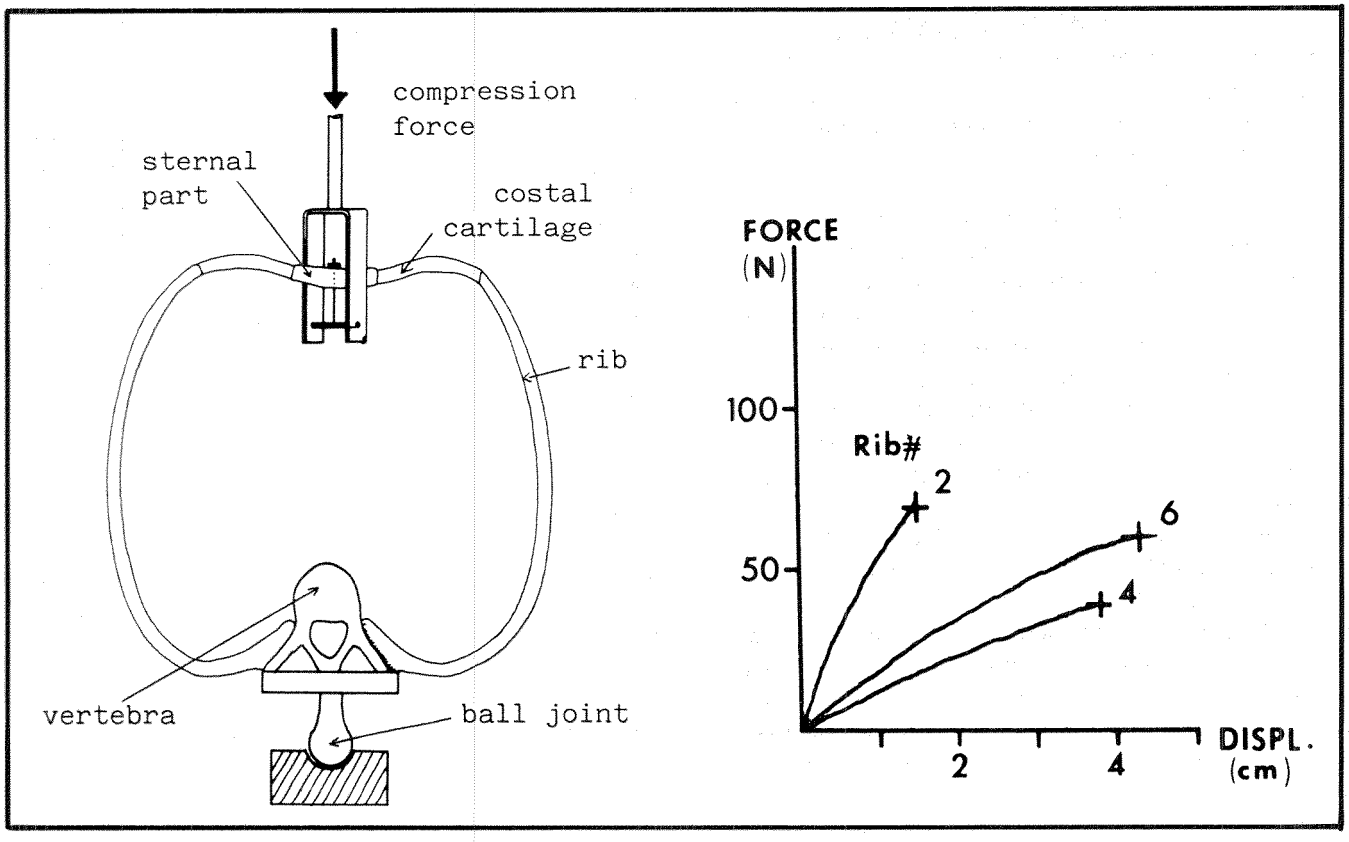

Figure 3. Compressive strength of an isolated costal ring

Table 1. Mechanical parameter values at failure for a single costal ring

Costal ring number	Ultimate force (N)	Desplacement at fracture (cm)	Average stiffness (N/cm)
2	64.9	1.6	40
4	34.6	3.7	9.3
6	56.5	4.3	13.1

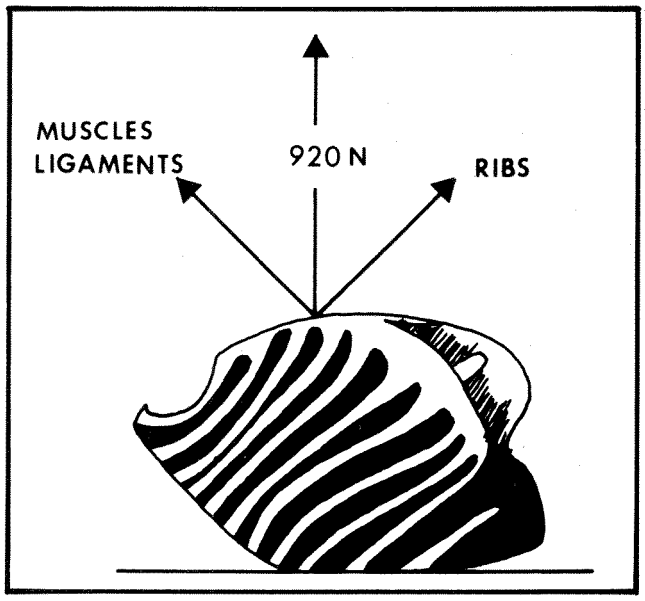

Figure 4. Maximal resistive force opposed by the ribcage (without internal organs) to a frontal static compression

belt, compresses the thoracic wall progressively. The ribs bend gradually and break depending on their specific deflection capabilities related to the costal level and the individual characteristics. Once the heart cavities and vessels are collapsed, the compression of walls and/or the forced displacement of these organs occur. It is most probably at this moment that the global thoracic stiffness increases. Force/deflection curves we established some time ago with pigs (see Figure 5) show this gradual stiffness increase(30).

For a cadaver in a similar situation (3-point belt, 45kph frontal impact, 20Gs mean deceleration), the compression force can reach 8kN whereas deflection is of 9cm (see Figure 6). Stiffness must tend toward an asymptote as the sternum comes into contact with the vertebral column, that is, for a 40 to 50 percent deflection. As soon as the sternum is stopped, there is no more deflection and hence no more rib fractures since these depend mainly on deflection. At this point, the extent of the damage to viscerae varies on the way the organs are either jammed between two hard bony structures or displaced into the

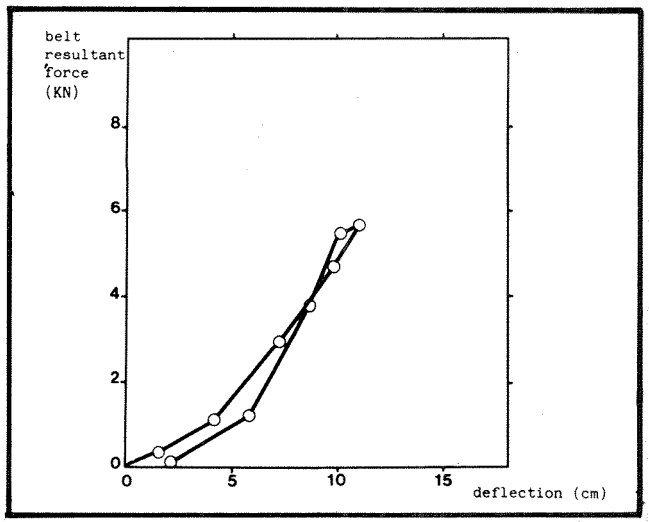

Figure 5. Load deflection curve of the thorax of a 35kg live pig submitted to a frontal impact with a 3-point belt at 45Kph. The stiffness progressively increases with deflection level(30)

side cavities. This explains why, over 40 percent penetration, a criterion based on sole deflection cannot accurately account for the severity of injuries—neither skeletal nor visceral.

In case of impact against a hard surface, the phenomena develop in a slightly different way, since, contrarily to the safety belt, there is a significant difference between the impactor speed and the thoracic wall speed. At the time of impact, an energy transfer occurs within a very short period considering the hardness of the contact. This transfer induces the wide peak of initial force(31) and injury mechanisms probably different from those induced by the safety belt. The fact is that the localization of rib fractures varies with the speed at which the thorax is compressed. But after the initial peak, if the remaining energy is still sufficient, the deflection goes on and shows a gradually increasing stiffness. The same phenomena as with the safety belt can then occur if the deflection is sufficient.

In lateral impact, mechanical phenomena are different since this stopping effect of the vertebral column does not take place. Possibilities of deflection are larger. Besides, force/deflection curves are different for frontal and lateral impacts.

Injury mechanisms are likely distinct, more related to large viscerae displacements. In this case, rib cage deflection, and hence rib fracture number, could account for tensile stress-related injuries; but the relationship between these two types of injury has to be established.

Besides, a series of studies conducted by Lau(32,33,34) on animals showed that visceral injury extent and severity are related to speed of compression, which, at first glance, does not apply to rib fractures.

So, to estimate the vital risk reliably, a thoracic injury criterion should not be limited to rib fracture number on

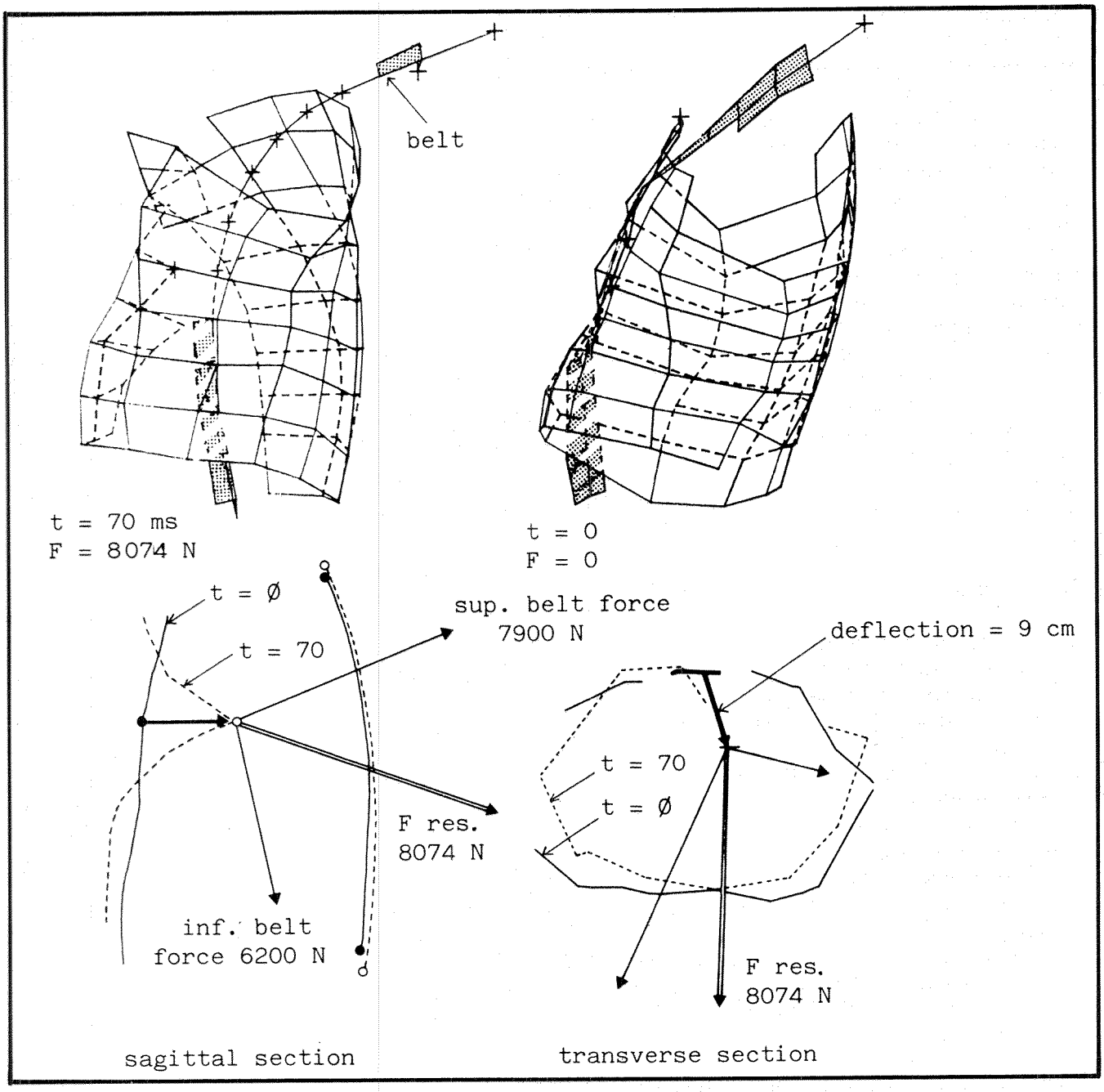

Figure 6. Frontal impact of a belted cadaver at 45kph

one hand, and should be based on more physical variables than the sole deflection level, such as speed of compression, force, and internal overpressure, for instance.

Conclusion

The injuries subsequent to an impact to the thoracic segment during a traffic accident affect the thoracic cage and the intra-thoracic and abdominal viscerae. Rib fractures are life-threatening only when they are very numerous and lead to a flailed chest or when they are open and perforate the walls of underlying organs. Lesions to the viscerae (heart, lungs, major vessels, liver, spleen), however, are nearly always severe and are responsible for a large number of fatalities. They represent the major threat to life.

A first analysis of accident logical data shows there is no relationship between the severity of visceral injuries and the number of rib fractures. This number is a factor neither necessary nor sufficient to involve a visceral lesion.

The experiments made with cadavers mainly produce bony lesions only. When visceral lesions occur, it is not clearly demonstrated that they are similar to injuries found in real accidents.

From a mechanical point of view, the resistance to compression offered by the rib cage is by far lower than the total thoracic resistance, which minimizes the protective purpose generally ascribed to the bony structure. What resists compression is elasticity, inertia, and viscosity of muscles, viscerae, and their contents. Moreover, in frontal compression, the deflection is limited to about 40 percent by the stop provided by the vertebral column. In these conditions, the number of rib fractures, which depends mainly on the bending stress these bones sustain, can only account for the injuries due to a similar mechanism, i.e., deflection.

Other lesions related to other physical variables are to be considered to estimate the vital risk.

The relevance of injury criteria based on the number of bony lesions observed on cadavers is then far from being valid.

References

1. Aldman, B., Synthesis report of the E.E.C. biomechanics programme in Benjamin, T.E.A., "Biomechanics of impacts in road accidents," Proc. Symp. Brussels, March 1983, pp. 487-540, EEC Ed. Brussels, ISBN 92-825-4328-5, 1984.
2. Patrick, L.M., and R.S. Levine, "Injury to unembalmed belted cadavers in simulated collisions," Proceedings 19th Stapp Car Crash Conference, San Diego, pp. 79-116, SAE Ed., 1975.
3. Human subjects for biomechanical research, Minutes of international workshops preceding Stapp Conferences.
4. Koritke, J.G., and H. Stick, *Atlas de coupes sériées du corps humain,* Vol. 1, Tête, cou, thorax Urban & -Schwarzenberg Ed. Munich, 1982.
5. Nusholtz, G.S., J.W. Melvin, G. Mueller, J.R. MacKenzie, and R. Burney, "Thoraco-abdominal response and injury," Proceedings 24th Stapp Car Crash Conference, pp. 187-228, SAE Ed., 1980.
6. Cooper, G.J., R. Bexon, B.P. Pearce, M.C. Stainer, R.L. Maynard, and D.E.M. Taylor, "Visualisation of heart movement following non penetrating impact using ciné and flash x-ray," Proc. VIth IRCOBI Meeting, Salon-de-Provence, pp. 313-320, 1981.
7. Mulligan, G.W.N., G.S. Pizey, D. Lane, L. Andersson, C. English, and C. Kohut, An introduction to the understanding of blunt chest trauma in "The Human Thorax—Anatomy, Injury and Biomechanics,", SAE Ed., P-67, pp. 11-36, 1976.
8. Huelke, D.F., H.W. Sherman, and M.J. Murphy, "Severe to fatal injuries to lap-shoulder belted car occupants," SAE Paper 770149.
9. Gilroy, D., "Deaths (144) from road traffic accidents occurring before arrival at hospital," *Injury*, 16, pp. 241-242, 1985.
10. Sivard, J., "Contribution à l'étude des causes de la mort dans les accidents du trafic automobile," Thèse Médecine Univ. Lyon, 1 vol., 72 p., 1976.
11. Viano, D.C., and C.G. Artinian, "Myocardial conducting system dysfunction from thoracic impact," *J. of Trauma*, 18, 6, pp. 452-459, 1978.
12. Ribet, M., "Les lésions broncho-pulmonaires dans les traumatismes graves du thorax," *Ann. Chir. Thorac. Cardio-vasc.*, 12, 1, pp. 19-34, 1973..
13. Chesneau, A.M., C. Got, C. Tarriere, F. Honnart, G. Merignargues, and A. Patel, "Les ruptures aortiques en traumatologie routière," *La Nouvelle Presse Médicale*, 4, 38, pp. 2713-2717, 1975.
14. Caillard, B., B. Letourneau, C. Freysz, C. Coulon, R. Brenot, and M. David, "Analyse d'une série de dix ruptures traumatiques aigües de l'isthme aortique," *Lyon Chirurgical*, 81, 1, pp. 20-23, 1985.
15. Anselmet, P., "Analyse des lésions du thorax et de l'abdomen chez les victimes d'accidents d'automobile. Relation entre les lésions osseuses et viscérales," (109 cas), Thèse Médecine Univ. de Marseille, 1 vol., 77 p., 1985.
16. Bot, F.J., and F. Van Faassen, Abdominal injury literature, Institut voor Wegtransport Middelen, EEC Contract NH3, 1980.
17. Fayon, A., C. Tarriere, G. Walfisch, C. Got, and A. Patel, "Thorax of 3-point belt wearers during a crash," Proceedings 19th Stapp Car Crash Conference, San Diego, pp. 195-223, SAE Ed., 1975.
18. Schmidt, G., D. Kallieris, J. Barz, and R. Mattern, "Results of 49 cadaver tests simulating frontal collision of front seat passengers," Proceedings 18th Stapp Car Crash Conference, Ann Arbor, pp. 283-293, SAE Ed., 1974.
19. Schmidt, G., D. Kallieris, J. Barz, R. Mattern, and J. Klaiber, "Neck and thorax tolerance levels of belt protected occupants in head on collisions," Proceedings 19th Stapp Car Crash Conference, San Diego, p. 225, SAE Ed., 1975.
20. Cromack, J.R., and H.H. Ziperman, "Three-point belt induced injuries: a comparison between laboratory surrogates and real world accident victims," Proceedings 19th Stapp Car Crash Conference, pp. 1-24, SAE Ed., 1975.
21. Kallieris, D., H. Mellander, G. Schmidt, J. Barz, and R. Mattern, "Comparison between frontal impact tests with cadavers and dummies in a simulated true car restrained environment," Proceedings 26th Stapp Car Crash Conference, Ann Arbor, pp. 353-367, SAE Ed., 1982.
22. Cesari, D., and M. Ramet, "Evaluation of human tolerance in frontal impact," Proceedings 23rd Stapp

Car Crash Conference, San Diego, pp. 873-914, SAE Ed., 1979.
23. Sacreste, J., G. Walfisch, A. Fayon, C. Thomas, F. Hartemann, and C. Tarriere, "Tolérance thoracique des porteurs de ceintures de sécurité," *J. Traumatologie*, 1, 2, pp. 105-113, 1980.
24. Kroell, C.K., D.C. Schneider, and A.M. Nahum, "Impact tolerance and response of the human thorax," Proceedings 18th Stapp Car Crash Conference, Ann Arbor, pp. 383-458, SAE Ed., 1974.
25. Robbins, D.H., R.J. Lehman, and K. Augustyn, "Prediction of thoracic injuries as a function of occupant kinematics," Proc. 7th E.S.V. Conf., Paris, pp. 374-383, 1979.
26. Cesari, D., M. Ramet, and J. Bloch, "Influence of arm position on thoracic injuries in side impacts," Proceedings 25th Stapp Car Crash Conference, San Diego, pp. 271-297, SAE Ed., 1981.
27. Nusholtz, G.S., J.W. Melvin, and P. Lux, "The influence of impact energy and direction on thoracic response," Proceedings 27th Stapp Car Crash Conference, San Diego, pp. 69-94, SAE Ed., 1983.
28. Stalnaker, R.L., J.H. McElhaney, V.L. Roberts, and M.L. Trollope, Human torso response to blunt trauma in *Human Impact Response,* Ed. W.F. King and H.J. Mertz, Plenum Press, New York-London, pp. 181-199 1973.
29. Lobdell, T.E., C.K. Kroell, D.C. Schneider, W.E. Hering, and A.M. Nahum, Impact response of the human thorax in *Human Impact Response,* Ed. W.F. King and H.J. Mertz, Plenum Press, New York-London, pp. 201-245 1973.
30. Verriest, J.P., A. Chapon, and R. Trauchessec, "Cinephotogrammetrical study of porcine thoracic response to belt applied load in frontal impact. Comparison between living and dead subjects," Proceedings 25th Stapp Car Crash Conference, San Francisco, pp. 499-545, SAE Ed., 1981.

Synthesis of Pelvic Fracture Criteria for Lateral Impact Loading

Mark Haffner
U.S. Department of Transportation, National Highway Traffic Safety Administration

Abstract

Two candidate functions for the prediction of pelvic fracture probability are created using lateral pelvic acceleration and age data from 84 cadaver impact experiments. These functions include measures of bone stress, bone strain, age, and load concentration factor. Data are analyzed using the maximum likelihood approach, and it is found that representation of the data by a Weibull distribution yields higher maximum likelihood than does the assumption of an underlying normal distribution.

Additional data are presented documenting pelvic force and acceleration responses for both cadavers and the Side Impact Dummy (SID). Systematic differences are noted and discussed.

Introduction

Lateral impact to the pelvis can result in injuries to the pelvic bone, to the hip joint, and to the soft tissue contents of the pelvic cavity. Bone fractures can occur at numerous sites on the pelvic ring: at the acetabulum, the sacro-iliac junction, the pubic symphysis, the pubic rami, and in the wing of the ilium. Within the pelvic cavity, fractures of the pelvis are associated with potentially severe injuries to the bladder and urinary tract.

Given this wide range of potential injury sites on the pelvic bone and within the pelvic cavity, it is most unlikely that a single parameter can be identified that is predictive of specific pelvic injury site and type. A more realistic goal, adopted here, is the identification of a parameter that is predictive of the occurrence of pelvic bone fracture, irrespective of fracture location.

In searching for a parameter predictive of pelvic fracture, we proceed on the assumption that a pelvic bone protection criterion will confer a large measure of protection on the contents of the pelvic cavity as well. Confirmation of this working hypothesis, however, remains for further study.

Data Resources

This analysis has drawn upon cadaveric lateral pelvic impact data from numerous sources. Table 1 presents a summary of these data resources and characterizes them by degree of applied load concentration, age range,

average age of cadavers tested, and other variables of interest.

It is important for our purposes to note several significant ways in which the ONSER(A) data set differs from the balance of the data base:

1. The average age of ONSER(A) cadaveric specimens is higher than the average age for most other data sets included.
2. Loading in the ONSER(A) series was directed to the limited area of the greater trochanter via a hemispherical rigid impactor, as distinguished from the other test series in which both the iliac wing and trochanter could be loaded by larger impact surfaces.
3. The experimental design of the ONSER(A) test series differs from that of the other test series included. The ONSER(A) series sought to identify fracture threshold for each specimen, by repeatedly testing each specimen at increasing impact severity until fracture occurred. By contrast, the other test series in the data base tested each specimen once at known impact severity, with either fracture or nonfracture reported as outcome.

The fact that a markedly different experimental design was employed in the ONSER(A) series as compared to the other test series strongly suggests that these blocks of data be separated for analysis and that distinct methods of analysis be applied to the two resulting subsets.

With regard to transducer data available, it can be noted from Table 1 that input force data are available only for the ONSER(A) and the Heidelberg test series. Some observations will be made shortly with regard to the relationship of input force to measured pelvic accelerations for these two data sets; however, it is clear from Table 1 that the only common thread available in all data sets is pelvic acceleration and that only the y (lateral) component of pelvic acceleration is available in all data sets.

With regard to data processing procedures, digital data tapes were obtained for all test series so that uniform data processing procedures could be applied to them. Following a quality control process using the "raw" data, all remaining force and acceleration data were filtered, subsampled, and refiltered[1] before being entered into the project data base for further analysis.

Previously Proposed Injury Predictive Parameters

Previous investigators have proposed both maximum applied force and maximum pelvic acceleration fracture criteria for lateral pelvic impact. Cesari, et al.(2) have proposed a 10kN (3ms clip) limit on impact force for a 76kg male and 4kN (3ms) for a 5th percentile female. These values are based on the data obtained from their older subject population. Also, these limits are associated with the specific concentrated trochanter loading protocol of the ONSER(A) cadaver tests. Tarriere et al.(9) conducted a series of lateral drop tests using cadaver subjects and reported pelvic fractures associated with resultant peak pelvic accelerations of 62 to 120g. Peak resultant pelvic accelerations associated with nonfracture ranged up to 135g. Harris(10) discussed the potential interaction during impact of lateral loadings acting on

1 Raw digital data were filtered with a 300Hz antialiasing Butterworth filter whose roll-off characteristics satisfied SAE J 211B. The data were then subsampled at 1,600SPS, and finally operated on with a finite impulse response filter with passband frequency = 100Hz, stopband frequency = 189Hz, passband ripple = 0225db, and stopband gain = 100db.

Table 1. Summary of data resources utilized in project data base

Organization	Description of Test Environment	Degree of Load Concentration on Pelvis	Number of Tests (Number of Fractures) male	female	Age Range male	female	Average Age male	female	Transducer Data Reported	References
Onser(A)	Rigid Impactor Strikes on Trochanter of Stationary Seated subjects	Concentrated	7 (4)	5 (3)	61-85	63-79	71	70	Force & Pelvic ay	1,2,3
Heidelberg	Rigid and Padded Impacts with Sled-Mounted Flat Wall	Distributed	23 (2)	11 (2)	17-79	17-60	39	34	Force & Pelvic ax,ay,az	4
FAT	Moving Deformable Barrier into Opel Vehicles; Nearside Impact	Distributed	29 (2)	6 (0)	21-64	26-42	38	35	Pelvic ax,ay,az	5,6
Onser(B) (BMD Series)	Moving Deformable Barrier into Rabbit Vehicles; Nearside Impact	Distributed	3 (0)	2 (1)	43-55	39-40	50	40	Pelvic ay	7
HSRI	Rigid and Padded Sled Tests	Distributed	7 (0)	3 (1)	62-84	45-75	71	59	Pelvic ax,ay,az	8

the iliac crest and on the hip joint. A tolerance value of 6kN for the sum of both the iliac crest and trochanter forces was proposed for specific use with the TRRL side impact dummy.

The EUROSID dummy now under development(3) employs three force transducers in the pelvic segment: one at the anatomical location of the pubic symphysis, and upper and lower transducers at the anatomical location of the junction between the iliac wing and the sacrum. Selection of one or a combination of outputs from these transducers for injury predictive purposes has not been finalized. The pelvis is also designed to accommodate a triaxial accelerometer for use with acceleration-based pelvic injury criteria.

Formulation of New Predictive Parameters

As has been pointed out by Nuscholtz, et al.(11), the interactions of the femur, pelvis, and associated soft tissue during lateral pelvic impact are complex. A fundamental source of variability appears to exist in the anatomy of the hip joint because rotation of the femoral head in the acetabulum during impact is a relatively unpredictable function of (a) initial femur and pelvic bone geometry, (b) degree of entrapment of the proximal femur by the impacting surface, and (c) variations in soft tissue thickness and distribution. Nuscholtz et al. properly caution that a generalized injury predictive parameter may be difficult to identify. Notwithstanding the variability inherent in pelvic response and injury patterns, however, we have attempted to isolate some of the confounding factors and quantify the extent of variability remaining in the data.

In formulating new fracture predictive parameters, we have elected to pursue two parallel analysis approaches. The first approach (denoted Approach 1) utilizes maximum bone stress as a primary explanatory variable, and also considers specimen age, specimen sex, and degree of applied load concentration for inclusion in analysis. The second approach (denoted Approach 2) substitutes maximum bone strain for maximum stress in the predictive function.

A brief discussion of the rationale for consideration of these variables follows

1. Maximum Stress

Numerous solid material failure theories (e.g., maximum stress, maximum strain, maximum strain energy, maximum distortion energy, etc.) are available for application. For brittle materials, the maximum stress failure theory is generally favored. The maximum stress theory predicts failure when the largest principal stress reaches the uniaxial tensile or compressive failure stress. The efficacy of using a stress-related variable instead of raw applied force was suggested by Cesari(2). He hypothesized that many lateral pelvic fractures were linked to excessive bending stress in the frequently fractured pubic rami. In pursuing this hypothesis, he computed area moments of inertia of ilio-pubic ramus cross-sections (I_x) from undamaged portions of tested pelvic specimens, and successfully correlated fracture force (F) and (I_x) for fractured specimens (r = .96). The governing equation for simple bending is:

$$(1) \quad \sigma + \frac{M}{(I_x/y)}$$

σ = ultimate tensile stress induced by bending of ramus

M = applied moment

I_x/y = area moment of inertia of ramus divided by offset from neutral axis

The moment applied to each specimen M = (F)(d), where d is a characteristic moment arm. Therefore, the above expression can be written:

$$(2) \quad \frac{\sigma}{d} = \frac{F}{(I_x/y)}$$

The high linear correlation and near zero intercept reported by Cesari between F and (I_x/y) implies that:

$$(3) \quad \frac{\sigma}{d} \cong \text{constant}$$

If d is a weak function of subject size and sex, the hypothesis advanced is upheld.

In the present effort, we have found it useful to invoke the equal stress-equal velocity scaling law to treat the experimental data (hereafter called subject data). The equal stress-equal velocity scaling law for geometrically similar models assumes that both density and modulus of elasticity are invariant and that the following relationships follow between subject data and data scaled for a specimen of standard size and mass. If we define:

$$(4) \quad \frac{\ell_{sub}}{\ell_{std}} = \lambda$$

ℓ_{sub} = characteristic length of subject

ℓ_{std} = characteristic length of standard specimen

(5) then:

$$F_{std} = \frac{F_{sub}}{\lambda^2} \qquad \text{for force}$$

(6) $a_{std} = \lambda a_{sub}$ for acceleration

(7) $M_{std} = \frac{M_{sub}}{\lambda^3}$ for mass

Using (4) and (5):

(8) $$\frac{F_{std}}{(\ell_{std})^2} = \frac{F_{sub}}{(\ell_{sub})^2} \equiv S$$

Note in Equation (8) that the terms have units of force per unit area or stress, and thus that stress induced in the standard specimen and subject specimen are equal for the same test velocity (stress scales 1 to 1).

If, for convenience, we write equation (8) as:

(9) $$F_{std} = (S)(\ell_{std})^2$$

we can observe that F_{std} is a measure of subject stress, adjusted only by a constant $(\ell_{std})^2$

Thus we would propose $F_{std} = F_{sub}/\lambda^2$ as a measure of pelvic bone stress magnitude, which might have potential for fracture prediction.

For an isotropic specimen as assumed here:

λ is simply $\left(\frac{M_{sub}}{M_{std}}\right)^{1/3}$ from equation 7 and:

(10)

$$F_{std} + F_{sub} / \left(\frac{M_{sub}}{76}\right)^{2/3} \quad \begin{cases} M_{sub} \text{ in Kg} \\ M_{std} = 76 \text{ Kg} \end{cases}$$

In analogous fashion, using (6) and (7):

(11) $$a_{std} = \left(\frac{M_{sub}}{M_{std}}\right)^{1/3} (a_{sub})$$

Multiplying the right hand side of (11) by the quantity we obtain:

$$\frac{M_{sub}}{M_{sub}} = \text{unity}$$

(12) $$a_{std} = \left(\frac{1}{M_{std}}\right)^{1/3} \frac{(M_{sub}\ a_{sub})}{(M_{sub})^{2/3}}$$

The quanity $M_{sub}\ a_{sub}$ has units of force, and $M_{sub}^{2/3}$ can be expressed as:

$$[\rho_{sub}\ \ell_{c_{sub}}^3]^{2/3} = (\rho_{sub})^{2/3}\ \ell_{c_{sub}}^2$$

where ρ_{sub} is subject density and $\ell_{c_{sub}}$ is a characteristic subject length.

Thus:

$$a_{std} \approx \frac{1}{M_{std}^{1/3}\ \rho_{sub}^{2/3}} \left(\frac{F_{sub}}{\ell_{c_{sub}}^2}\right) \quad (13)$$

Since M_{std} is a constant and ρ_{sub} is also invariant, equation (13) is of the form:

$$a_{std} = (\text{constant})(\text{stress}) \quad (14)$$

We thus propose $a_{std} = \lambda a_{sub}$ as an alternative measure of pelvic bone stress. For an assumed isotropic specimen, Equation (11) may be used with $M_{std} = 76$kg to yield:

$$a_{std} = a_{sub} \left(\frac{M_{sub}}{76}\right)^{1/3} \quad \{M_{sub} \text{ in Kg} \quad (15)$$

The above approach to the determination of λ does not, however, take into account variation in subject build; i.e., a short, stocky specimen and a tall, thin specimen each of equal mass would each yield the same λ. The following method is proposed to improve the estimation of λ when subject height and mass are known.

The body is considered as a cylinder of mass M, density ρ, height H, and diameter D. The diameter of a subject may be estimated as:

$$D_{sub} = 2 \left(\frac{M_{sub}}{\pi \rho_{std} H_{sub}}\right)^{1/2} \quad (16)$$

Similarly, the diameter of the standard specimen is:

$$D_{std} = 2 \left(\frac{M_{std}}{\pi \rho_{std} H_{std}}\right)^{1/2} \quad (17)$$

Then since $\rho_{sub} = \rho_{std}$

$$\lambda = \frac{D_{sub}}{D_{std}} \left[\left(\frac{M_{sub}}{M_{std}}\right)\left(\frac{H_{std}}{H_{sub}}\right)\right]^{1/2} \quad (18)$$

For $M_{std} = 76$ Kg and $H_{std} = 1.75$ m:

$$\lambda = \left[\left(\frac{M_{sub}}{76}\right)\left(\frac{1.75}{H_{sub}}\right)\right]^{1/2} \quad \begin{cases} M_{sub} \text{ in Kg} \\ H_{sub} \text{ in m} \end{cases} \quad (19)$$

and using (5):

$$F_{std} = \frac{F_{sub}}{(M_{sub} / 76)(1.75 / H_{sub})} \quad (20)$$

In analogus fashion, using (19) and (6):

$$a_{std} = \left[\left(\frac{M_{sub}}{76}\right)\left(\frac{1.75}{H_{sub}}\right)\right]^{1/2} (a_{sub}) \quad \begin{matrix} M_{sub} \text{ in Kg} \\ H_{sub} \text{ in m} \end{matrix} \quad (21)$$

Implementation of Equations (10) and (15) is denoted scaling method A. Implementation of Equations (20) and (21) is denoted scaling method B. Both methods have been used for processing subject data; results will be presented below in the Analysis section.

Since bone is a viscoelastic material, bone stress may be considered to be a function of both strain and strain rate. The strain rate dependence of bone has received considerable research attention. Evans(12) reports the experiments of McElhaney and Byars (1965) and McElhaney (1966). The experiments conducted were constant velocity compression tests on cattle and human femoral bone. At strain rates exceeding 1cm/cm/s, the investigators found that ultimate compressive stress and modulus of elasticity increased while strain at fracture decreased. (Ultimate compressive stress at 1cm/cm/s was 22 percent greater than at .01cm/cm/s; ultimate strain decreased 31 percent.

A lateral pelvic deflection of .5cm (.2in) in 20ms would correspond to a strain of approximately 2 percent and a strain rate of approximately 1.1cm/cm/s. Thus, it appears likely that the pelvic bone exhibits significant rate sensitivity in the automotive crash environment. The inclusion of strain rate sensitivity in a pelvic fracture model is, therefore, desirable.

2. Maximum Strain

A maximum strain failure criterion is also a likely candidate for consideration. In the present application, maximum strain will be calculated via a lumped parameter pelvic model as discussed under Approach 2 below.

3. Age Effects

Evans(12) reports the data of Messerer (1880), who investigated the static bending strength of fresh cortical bone specimens from the tibia, femur, and humerus of male and female subjects. Ultimate bending stress increased to a maximum in the range of 20 to 30 years of age and declined steadily thereafter. The ratio of male femur ultimate bending stress at 75 years of age to that at 24 years of age is approximately .81; the corresponding ratio for females tested was .85. Yamada(13) cites data for static bending of fresh cortical bone and reports maximum ultimate bending stress occurring for specimens in the range 20 to 40 years of age, with strength declining thereafter. The ratio of ultimate bending stress reported at 70 to 79 years of age to that at 20 to 29 years is .80.

Thus, it is concluded that age effects upon probability of pelvic bone fracture are significant and should be incorporated into our pelvic fracture model.

4. Sexual Differences

In the bending data of Messerer reported above, sexual differences in ultimate bending stress can be assessed. The ratio of female ultimate bending stress to male ultimate stress for a given age range is approximately .90 for the femur and 1.0 for the tibia. Yamada reports no significant sexual differences in compressive strength or bending strength in samples of cortical bone.

The absence of significant sexual difference in ultimate bending stress suggests strongly that the lower pelvic fracture forces reported by Cesari(2) for females as compared to males is largely due to smaller female pelvic bone cross-sectional areas. As was discussed earlier, when Cesari normalized the male and female fracture forces in terms of a measure of stress, the male and female data were observed to overplot.

Therefore, it is tentatively concluded that the use of a stress-related variable should permit male and female data to be merged for analysis.

The possibility exists, however, that the scaling laws we are proposing will not fully accommodate the differing pelvic geometries of male and female specimens. (The scaling law requires geometric similarity.) It is therefore proposed that the extent to which male and female data does overplot be observed before reaching a conclusion on the suitability of this scaling approach.

5. Degree of Load Concentration

The pelvic load concentration factor has been mentioned as an important potential influence upon fracture potential.

It may be recalled that two main load paths exist into the laterally impacted pelvis, through the acetabulum via the trochanter and through the iliac wing. The ONSER(A) data can be considered as defining the pelvic fracture tolerance for the trochanter load path. However, in the balance of the experimental data (and presumably in the vehicle environment), load is transmitted in some proportion through both paths. A pelvic accelerometer cannot distinguish which load path or paths are active but responds to net applied force. Thus, pelvic accelerations as measured from the ONSER(A) experiments should not be interpreted in the same way as pelvic accelerations measured in distributed load experiments.

A simplified schematic drawing illustrating this point is shown in Figure 1. The pelvis is shown assumed as a rigid body of mass M with crushable elements at the trochanter and iliac wing locations. Let us say that we know the "trochanter" will fail at force F_1, and that the "iliac wing" will fail at some force F_2. For argument, we will assume that these failures are independent. In case (a) similar to the ONSER(A) configuration, we would associate acceleration F_A/M with pelvic fracture. In case (b), where the iliac wing carries external load, we would associate pelvic acceleration $(F_A+F_B)/M$ with the same fracture. Clearly, the nature of load distribution is a significant input to the interpretation of an acceleration-based pelvic fracture criterion.

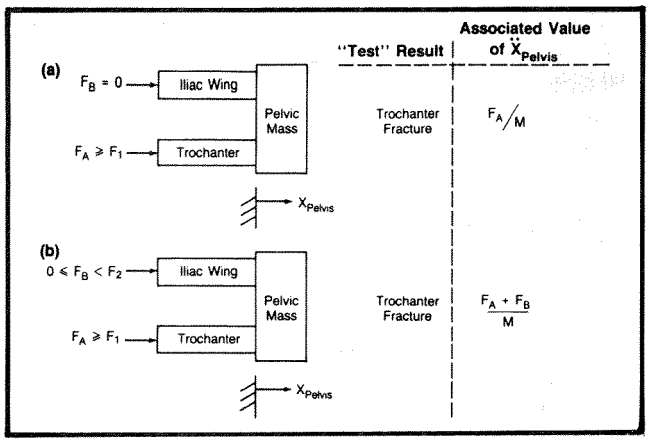

Figure 1. Schematic illustration of concentrated and distributed lateral pelvic loading

Summarizing our discussions relative to candidate parameters for inclusion in our fracture predictive function, it is postulated that probability of pelvic fracture is a function of the following variables:

1. A stress measure as quantified by a standardized (scaled) peak applied force or standardized (scaled) peak pelvic acceleration (Approach 1)
2. A strain measure as quantified by the output of a lumped parameter model (Approach 2)
3 Age of specimen
4. Degree of applied load distribution (concentrated or distributed)

Data Analysis and Results

Before proceeding with the analysis, it is of interest to look at the relationship between recorded force and acceleration for the limited number of ONSER(A) and Heidelberg tests in which both were recorded. (Only the lateral component of force F_y was measured. Also, only the y component of acceleration was utilized in analysis because (a) a_y is the only measurement available in all of the data, and (b) incorporation of resultant acceleration into the analysis was investigated and shown to yield no significant improvement in predictive capability.)

Typical overplots of force and acceleration traces from the ONSER(A) series are shown in Figures 2 and 3. (Note that the peaks of the force traces have been artificially scaled to match the peaks of the acceleration traces so that trace shapes can readily be compared.) As may be observed, there is lag in acceleration response initially, but force and acceleration peaks tend to coincide in time. Substantial differences exist, however, in the shapes of force and acceleration traces during the unloading phase.

Figure 4 shows the relationship between peak force and peak acceleration (scaled according to method A) for the 11 ONSER(A) tests in the data base for which both signals are available. The good correlation observed (r = .89) suggests that if (as has been proposed by Cesari) an injury criterion can be developed using peak applied force, then it should be possible to use pelvic acceleration to construct a similar predictive function.

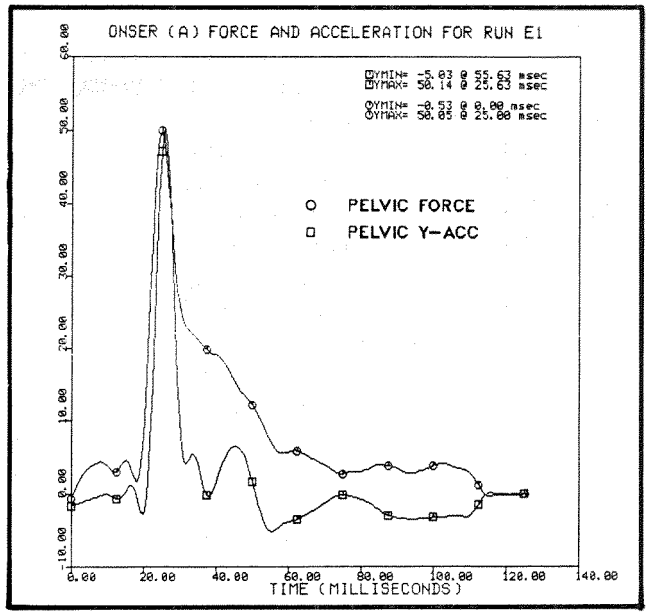

Figure 2. Pelvic force and pelvic Y-acceleration overlay for ONSER (A) test E1

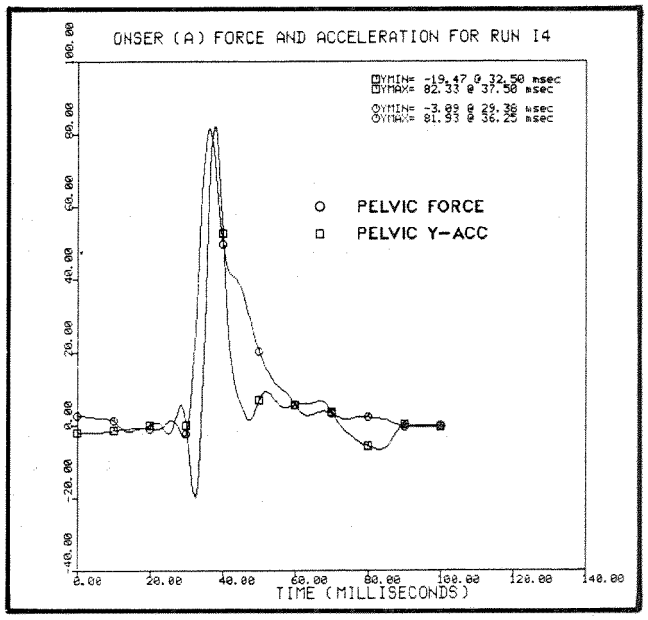

Figure 3. Pelvic force and pelvic Y-acceleration overlay for ONSER (A) test I4

Figures 5 and 6 present analogous overplots of force and acceleration for two Heidelberg tests—one rigid and one padded. The interesting and typical differences observed between these two tests will be discussed further in Appendix B, but for the moment we can observe that peak force and peak acceleration again tend to coincide in time. Figure 7 presents peak-scaled force vs. peak-

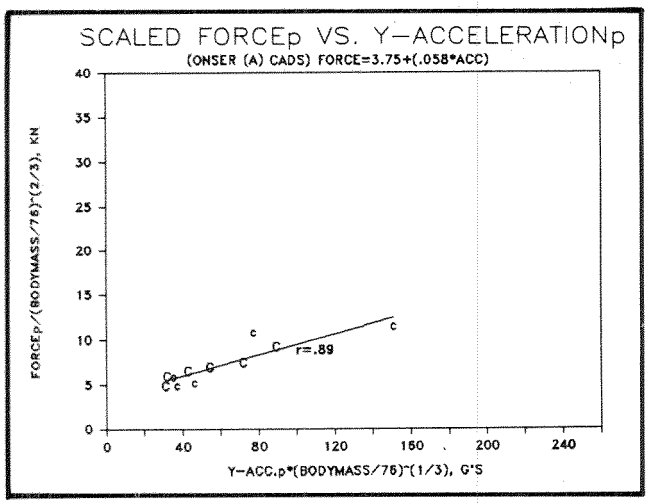

Figure 4. Scaled peak pelvic force versus scaled peak pelvic Y-acceleration for ONSER (A) tests

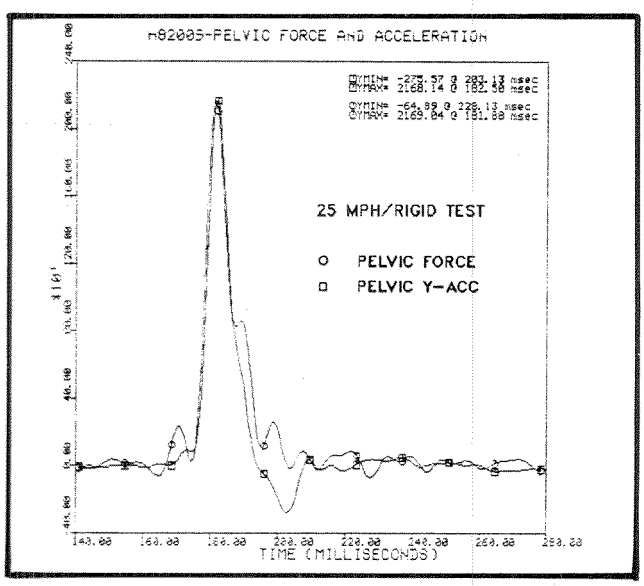

Figure 5. Pelvic force and pelvic Y-acceleration for Heidelberg test H82009

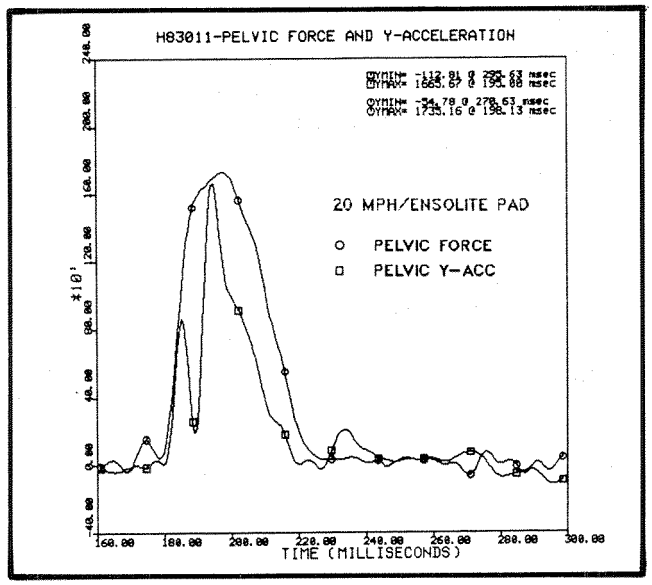

Figure 6. Pelvic force and pelvic Y-acceleration for Heidelberg test H83011

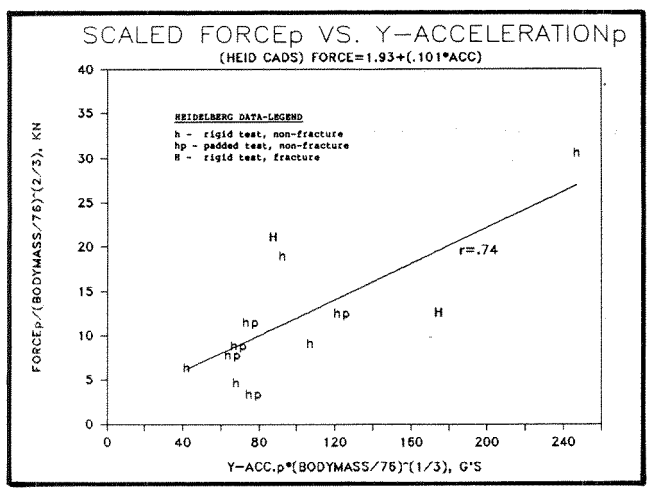

Figure 7. Scaled peak pelbic force vs. scaled peak pelvic y-acceleration for heidelberg tests.

scaled acceleration for available Heidelberg data. Correlation between them is not as high (r = .74) as the correlation found for the ONSER(A) data.

In general, it has not been possible to utilize force data to construct a predictive function from the non-ONSER(A) data. This is because excluding the ONSER(A) data, the number of cases of fracture for which force data is available is very small (0 male, 2 female). In any case, the force data as measured from the Heidelberg tests would not be comparable to the ONSER(A) force data, since the measured Heidelberg forces were applied via a large contact plate that spanned the pelvis and thigh.

As has been discussed, the ONSER(A) data have been separated from the other available data (see Table 1) for purposes of analysis. Analysis thus concentrated on the use of acceleration data as obtained from the Heidelberg, FAT, ONSER(B), and HSRI data sets.

Heidelberg, FAT, ONSER(B), and HSRI Data—Approach 1

The stress variable $a_{std} = (a_{subp})(\lambda)$ is plotted in Figure 8 against age, where we recall from Equation (19) that:

$$\lambda = \left[\left(\frac{M_{sub}}{76}\right)\left(\frac{1.75}{H_{sub}}\right)\right]^{1/2} \quad \begin{cases} M_{sub} \text{ in Kg} \\ H_{sub} \text{ in m} \end{cases}$$

and where a_{subp}, M_{sub} and H_{sub} are the peak y pelvis acceleration, body mass, and height for each test.

In Figure 8, each nonfracture test is plotted as a dot, while each fracture test carries the initial of its source according to the following code:

H—Heidelberg
B—ONSER(B)
F—FAT
S—HSRI

Based on the known decrease of ultimate bone strength with age presented earlier, a series of lines are drawn on Figure 8 with slope m = $-0.5g/_{yr}$ corresponding to a 20 percent reduction in ultimate stress between the ages of 24 and 75 years. It is then postulated that the zone between each pair of lines represents a region of nearly constant fracture probability. Since the equation of each line is of the form:

(22) $(a_{subp})(\lambda) + (.5)(age) = constant$

we further postulate that:

Probability of Pelvic Fracture
$= f[a_{subp} * \lambda + (.5)(age)]$

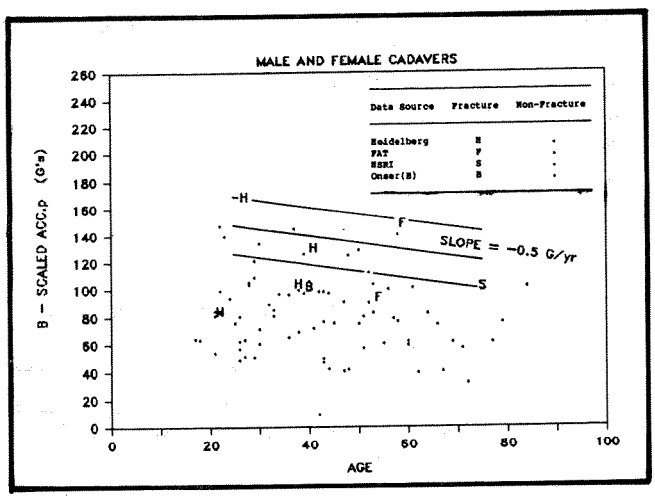

Figure 8. B-scaled acceleration versus specimen age—distributed load data

Since the data being considered are quantal or "censored," as defined by Ran et al.(14), we have applied the maximum likelihood approach discussed there, and have adopted a Weibull distribution as representative of the data. Figure 9 represents the result of analysis of the available distributed load data. For any selected fracture probability and age, a "tolerable" value of peak B-scaled acceleration = $a_{std} = \lambda a_{subp}$ can be read from the figure. For example, for a selected 20 percent probability of pelvic fracture at 40 years of age, we may find a_{std} = 143g. Similarly, for 10 percent fracture probability and 40 years of age, a_{std} = 103g. These "standard" values, we may

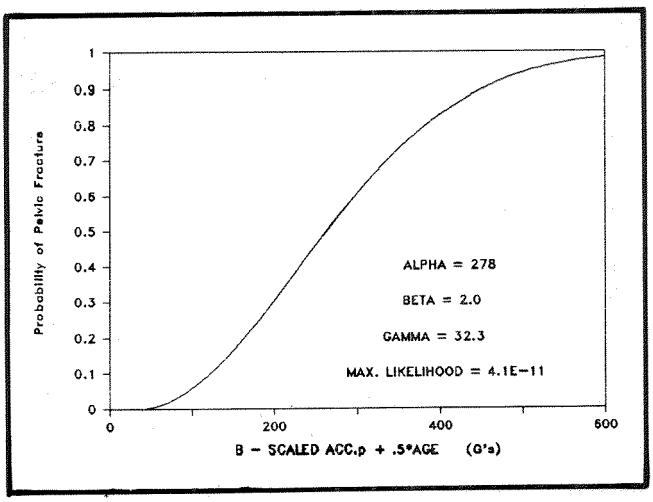

Figure 9. Probability of pelvic fracture from Weibull analysis of distributed load data—approach 1

recall, are for a specimen of mass = 76kg and height = 1.75m.

We may also note on Figure 9 the values of α, β, and γ as computed by the Weibull program for best fit to the data, and the maximum likelihood number of 4.1×10^{-11} associated with this computation. Figure 10 presents the computed probability density function. The fact that this function is not symmetrical confirms that the underlying distribution is not normal. However, we found it of interest to impose normality upon the data, observe the results, and compare them to the Weibull computations. (A probit analysis program was used for normal distribution computations.)

This comparison is presented in Figures 11 and 12, where it may be clearly seen that the Weibull distribution is right-shifted as compared to the normal distribution. Also of interest is the fact that the maximum likelihood number calculated for the imposed normal distribution

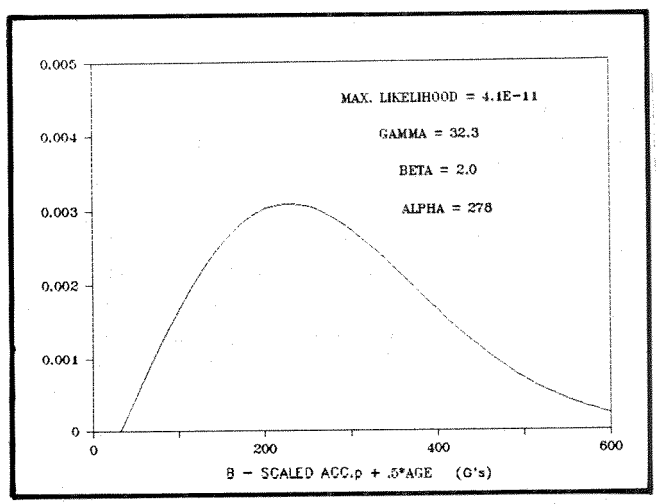

Figure 10. Weibull probability density function associated with Figure 9

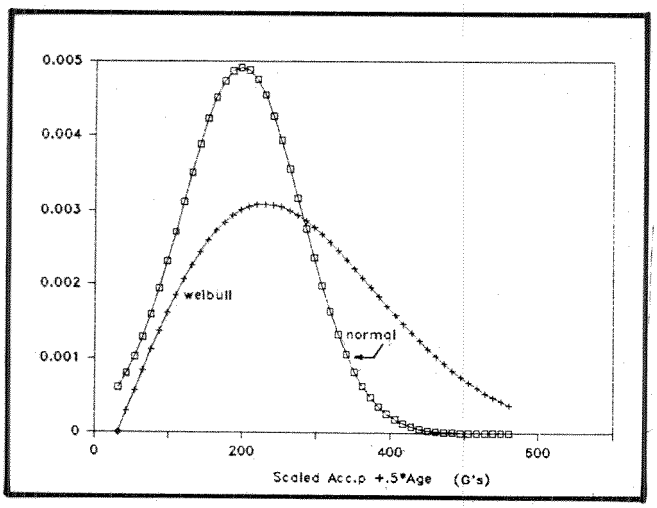

Figure 11. Comparison of Weibull and normal probability density functions calculated

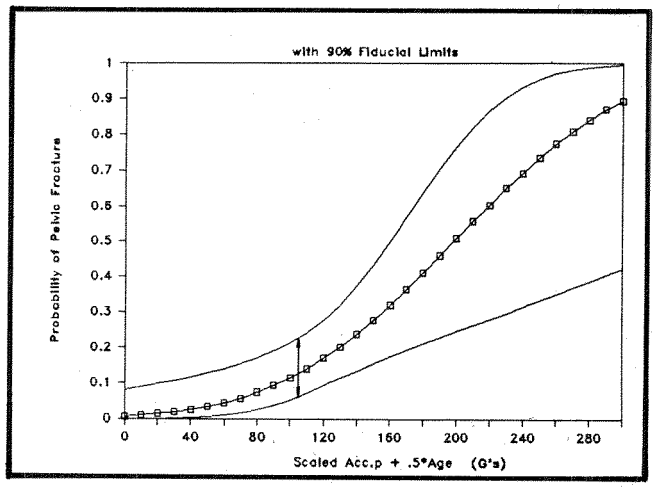

Figure 13. Fiducial limits on probability of pelvic fracture as computed from imposed normal distribution

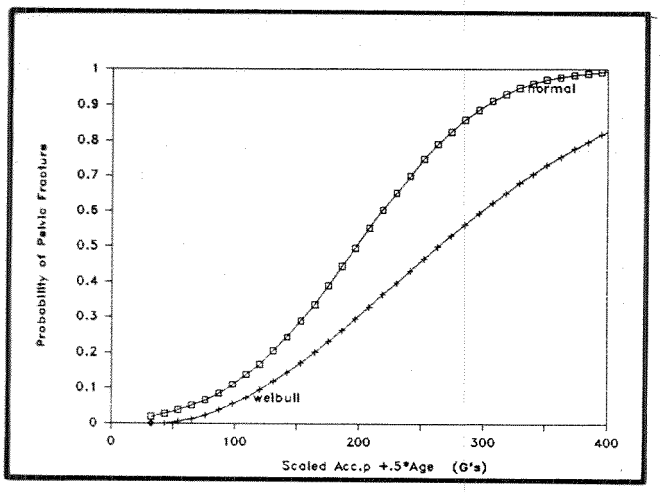

Figure 12. Comparison of pelvic fracture probabilities computed from Weibull and normal distributions—distributed load data—approach 1

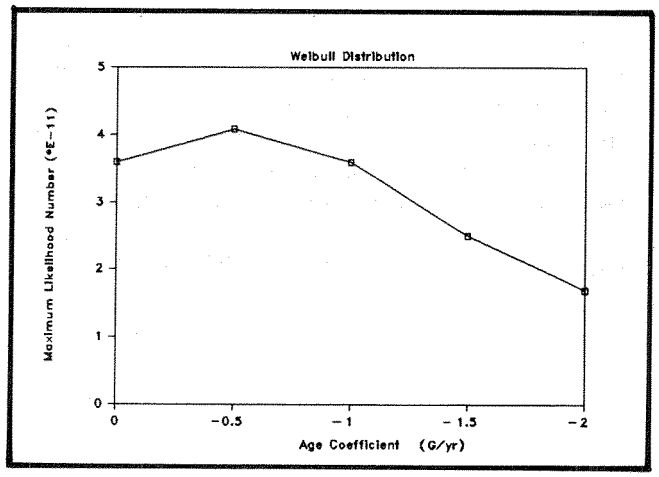

Figure 14. Maximum likelihood number versus age coefficient—Weibull analysis—approach 1

was 6.0 x 10^{-16}, lower than that for the Weibull computation, indicating that the Weibull function provides a better fit to our data.

With regard to confidence intervals, the algorithm for their computation is not presently available for the Weibull distribution. However, 90 percent fiducial limits have been computed for reference for the normal distribution assumption and are provided in Figure 13.

Further, as a check that the value of the coefficient on age m was correctly deduced as -0.5, a series of Weibull fits to the data were run for m = 0, -0.5, -1.0, -1.5, and -2.0. As indicated by Figure 14, maximum likelihood did indeed occur for m = -0.5, thus providing support for our selection process for m.

Heidelberg, FAT, ONSER(B), and HSRI Data—Approach 2

Approach 1 above operates on maximum pelvic acceleration as a measure of maximum stress. The utility of this approach tends to be limited, however, by the variability inherent in the measurement of a peak quantity. In Approach 2, a straightforward scheme was sought that would minimize dependence on this peak measurement. Toward this end, a lumped parameter one dimensional linear model was constructed as shown in Figure 15. Mass M_1 is associated with struck side upper leg mass, and M_2 is associated with the "pelvic mass" upon which the pelvic accelerometer is attached.

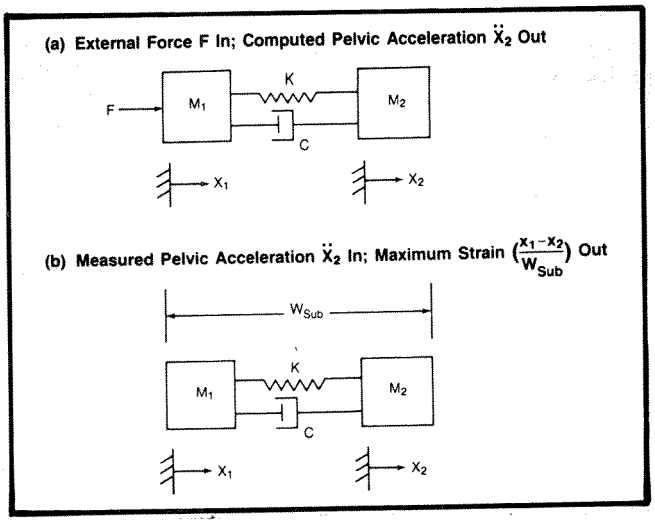

Figure 15. Model construct for pelvic injury assessment

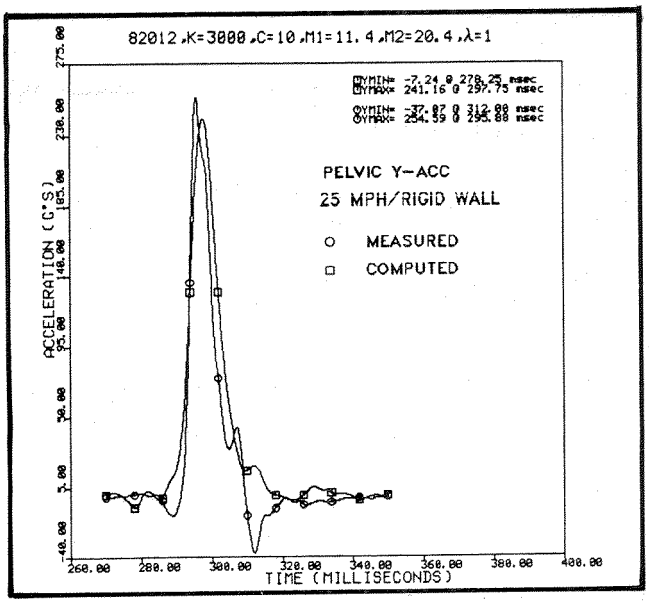

Figure 16. Comparison of measured pelvic Y-acceleration to that computed using two-mass model of Figure 15(a)—Heidelberg test H82012

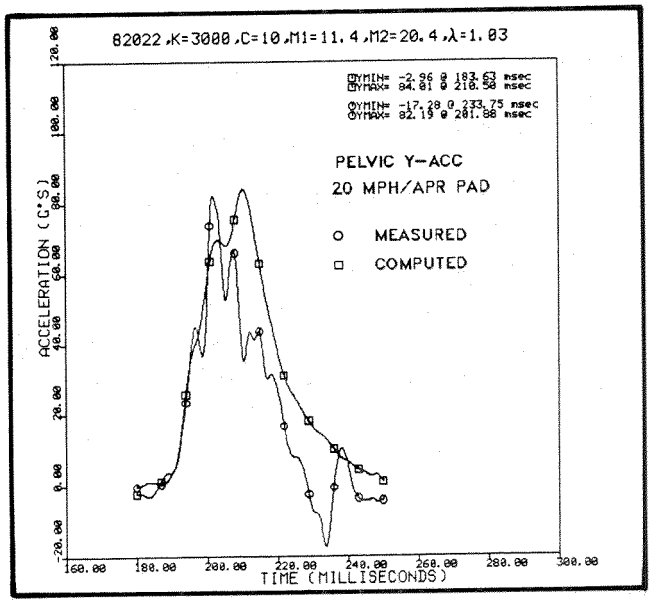

Figure 17. Comparison of measured pelvic Y-acceleration to that computed using two-mass model of Figure 15(a)

There is a basis for the formulation of a model in this configuration in the work of (11), wherein impedance plots for the laterally impacted pelves of three cadavers are reported. This simple construct should not be thought of as a literal model of the laterally impacted pelvis, but rather as a useful device for injury predictive purposes along the lines of the Brinn and Staffeld Effective Displacement Index(15) or the HSRI Maximum Strain Criterion(16).

Our operating premise is that if the model is "run backwards," i.e., if measured pelvic acceleration is provided as input to the model at M_2 (see Figure 15b), that a function of resulting maximum "pelvic" strain $(X_1\text{-}X_2)_{max}/W_{sub}$ can be utilized in a fracture predictive function (W_{sub} is subject pelvic width). Specifically, if we denote the quantity $(X_1\text{-}X_2)_{max}/W_{sub}$ as MPS or Maximum Pelvic Strain, we postulate that:

Probability of Pelvic Fracture = f[MPS+(n)(age)]

where n is an age coefficient relative to reduction of ultimate strain with age.

To select reasonable values for parameters M_1, M_2, K, and C, the model was first exercised in the "forward" direction (see Figure 15a), using the 12 Heidelberg cadaver runs for which both force and acceleration data were available. (Parameters were scaled according to the mass and height of each specimen using scaling method B.) Initial parameter estimates were deduced from the impedance plots of (11); adjustment by trial and error then resulted in the determination of a parameter set for which observed and computed pelvic accelerations were reasonably matched for both a rigid case (H82012) and an APR padded case (H82022), as shown in Figures 16 and 17, respectively. The parameter set selected was as follows:

M_1 = 11.4 lb, M_2 = 20.4 lb, K = 3,000 lb/in, and C = 10 lb-s/in.

Because this model exercise showed output pelvic acceleration to be more sensitive to change in total mass than to change in K or C, and since the influence of strain on fracture predictive capability was being investigated, three sets of standard parameters were selected for further use, with three possible values for C, as shown in Table 2.

As a final preparatory step before exercising the model, the standard parameters of Table 2 were B-scaled

Table 2. Standard parameter sets chosen for exercise of MPS model

Set No.	M_1(lb)	M_2(lb)	K(lb/in)	C(lb-sec/in)
1	11.4	20.4	3000	5
2	11.4	20.4	3000	10
3	11.4	20.4	3000	20

for each subject in the data base to create a file of subject specific parameters using the following relationships:

$$M_{1\ sub} = \lambda^3 M_{1\ std} \quad (23)$$

$$M_{2\ sub} = \lambda^3 M_{2\ std} \quad (24)$$

$$K_{sub} = \lambda K_{std} \quad (25)$$

$$C_{sub} = \lambda^2 C_{std} \quad (26)$$

where the value of λ for each subject was obtained from Equation (19).

A listing of the calculated subject specific model parameters may be found in Appendix A.

As shown in Figure 15(b), and using actual subject pelvic acceleration data as input to mass M_2, the model was exercised three times for each qualifying subject in the data base, once for each of the three parameter sets of Table 2. For each model run, the quantities $V_{max} = (\dot{X}_1 - \dot{X}_2)_{max}$ and maximum strain were calculated (see listings in Appendix A). The maximum strain (MPS) for each subject was calculated as follows:

$$MPS_{sub} = \frac{(X_1 - X_2)_{max}}{\lambda W_{std}} \quad (27)$$

where W_{std} is the pelvic bispinous breadth for a standard specimen = 22.5cm (8.84in) and λW_{std} is therefore equal to W_{sub}, or subject pelvic width.

Using a method analogous to that employed in Approach 1, the MPS values calculated for each subject using the model were then plotted versus corresponding subject age data. Three plots were thus created corresponding to the three parameter sets of Table 2. Figure 18 presents the plot for parameter set 3. Again, using methods analogous to those employed earlier, three candidate fracture probability functions were created for the three parameter sets as follows:

For Set 1: Probability of Pelvic Fracture
= f (MPS + .035 * age)

For Set 2: Probability of Pelvic Fracture
= f (MPS + .030 * age)

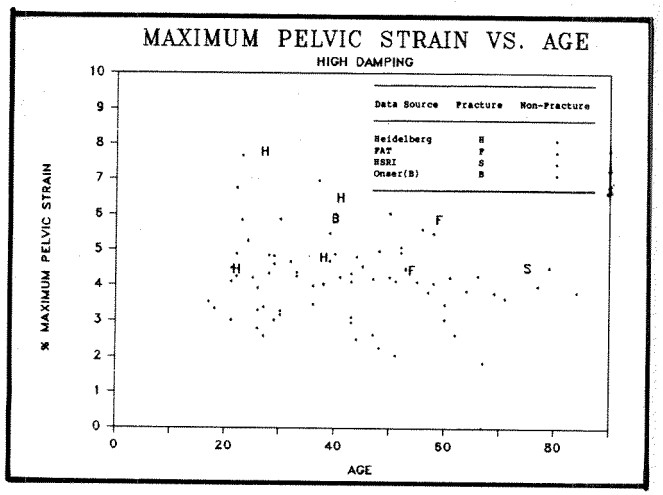

Figure 18. Computed maximum pelvic strain versus specimen age—parameter set #3—distributed load data

For Set 3: Probability of Pelvic Fracture
= f (MPS + .025 * age)

All three sets were submitted for Weibull analysis and computation of maximum likelihood numbers. The highest maximum likelihood, computed for parameter set 3, was 1.1×10^{-9}.

Figures 19 and 20 present the Weibull probability function and distribution, respectively, for parameter set 3 computations. We may note using Figure 19 that the value of MPS corresponding to 20 percent fracture probability at 40 years of age is approximately 6.1 percent, and that the corresponding value of MPS for 10 percent fracture probability and 40 years of age is approximately 4.8 percent

It is also of interest to compare the best maximum likelihood number arising from Approach 2 to that computed from Approach 1. These are shown in Table 3.

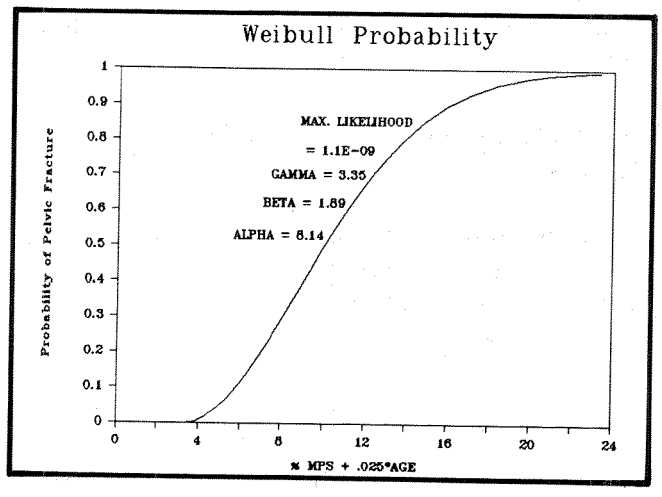

Figure 19. Probability of pelvic fracture from Weibull analysis of distributed load data, approach 2, parameter set #3 (M_1 = 11.4 lb, M_2 = 20.4 lb, k = 3,000 lb/in, C = 20 lb-sec/in).

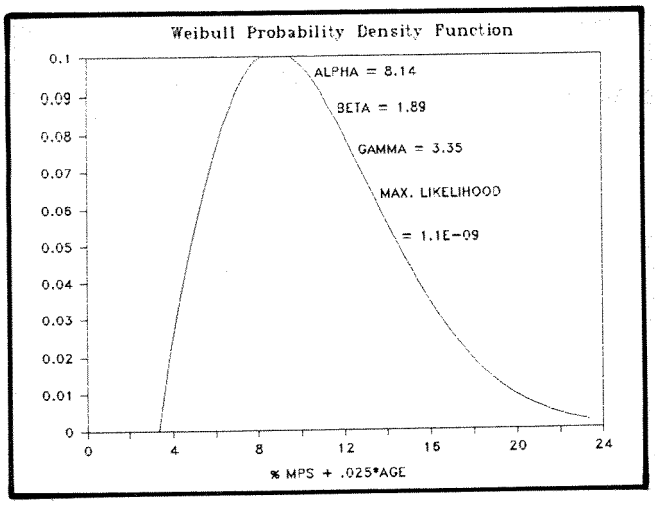

Figure 20. Weibull probability density function associated with Figure 19

Table 3. Comparison of maximum likelihood numbers

Approach No.	Maximum Likelihood Number
1	4.1×10^{-11}
2	1.1×10^{-9}

It is concluded, based on the higher maximum likelihood number achieved for the MPS approach, that the incorporation of additional information from the acceleration pulse into the predictive function increases its predictive power.

Finally, we have cross-plotted the values of the predictive functions for the two approaches (Weibull computations) for all qualifying subjects and present the results in Figure 21. We may observe that differences do exist in the relative ordering of the data by the two approaches; however, these differences are not large.

Incorporation of ONSER(A) Data Into the Analysis

As has been previously discussed, the ONSER(A) data have been separated from the balance of the data for purposes of analysis because—

- Unlike the other data sets, it is not quantal (or censored) in nature.
- Unlike the other data sets, concentrated loads were applied to the pelvis.

In subjecting each specimen to increasing impact severity until fracture occurred, Cesari sought to define the fracture tolerance of each specimen. For each specimen, we may presume that the severity of the last nonfracture test underestimates specimen tolerance, while

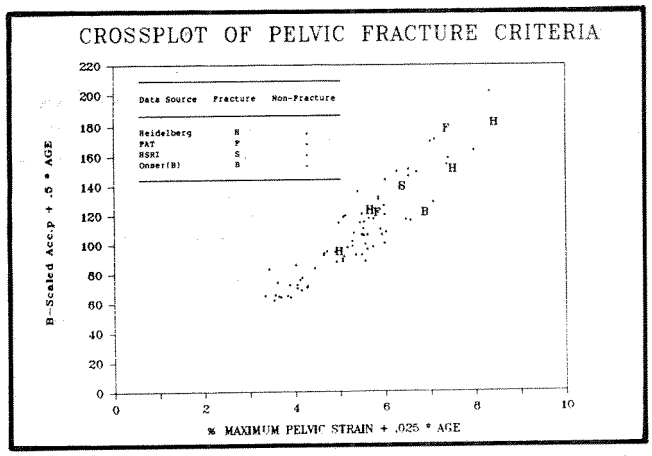

Figure 21. Crossplot of two candidate lateral pelvic fracture criteria

the severity of the fracture-inducing test overestimates specimen tolerance to some degree. Therefore, we take as the best estimate of fracture tolerance for each specimen the average response of the last nonfracture test and the fracture test. Four test pairs are available for examination. Scaled acceleration data for specimens D, E, I, and J are presented on Figure 22 (results for E are anomalous in that last nonfracture response is higher than fracture response; the higher value is thus taken as the fracture response estimate). The range of estimates for scaled acceleration associated with fractures thus ranges from 41g (D) to 79g (I). Since all of these tests are narrowly grouped in age, we plot the above scaled acceleration range on Figure 8 at age = 69 years and present the result as Figure 23. It is immediately apparent that ONSER(A) fracture estimates plot very low in the distribution of other available data.

A similar presentation using MPS as the response variable is presented in Figure 24, and the corresponding fracture estimate range is plotted on Figure 18 as Figure 25. Again, the fracture range estimate plots very low in the distribution of the other data.

It is concluded that ONSER(A) fractures occurred at significantly lower measured pelvic accelerations than in the other data sets. In fact, the highest fracture estimate in the ONSER(A) set corresponds to about a 5 percent fracture probability level in the main data set.

Discussion

It is believed that a probable explanation for the result found in the previous section may be found in Figure 1. That is, for concentrated loading to the trochanter as schematically shown in 1(a), acceleration associated with fracture is minimized.

The fact, however, that the fracture distributions for the ONSER(A) data are so different compared to the balance of the data base points to the conclusion that the

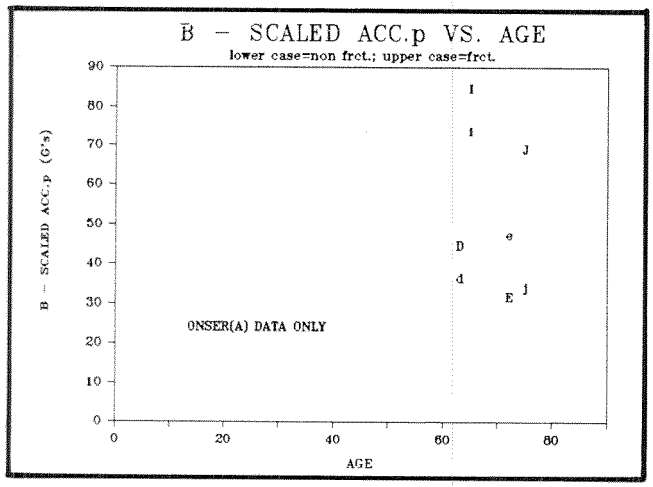

Figure 22. Nonfracture/fracture data pairs from ONSER (A) test series

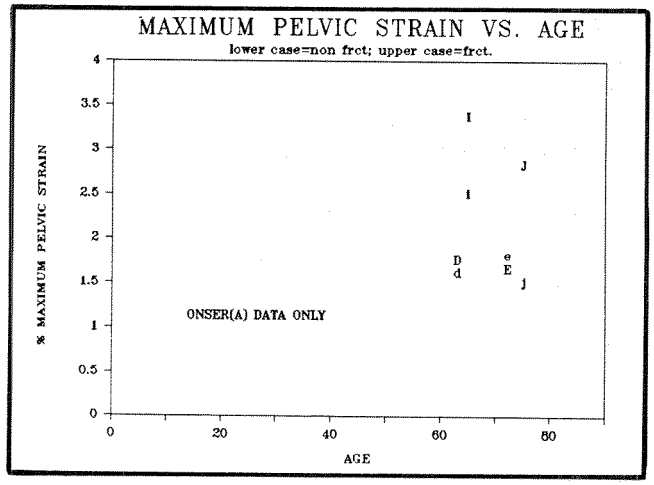

Figure 24. Nonfracture/fracture data pairs from ONSER (A) test series

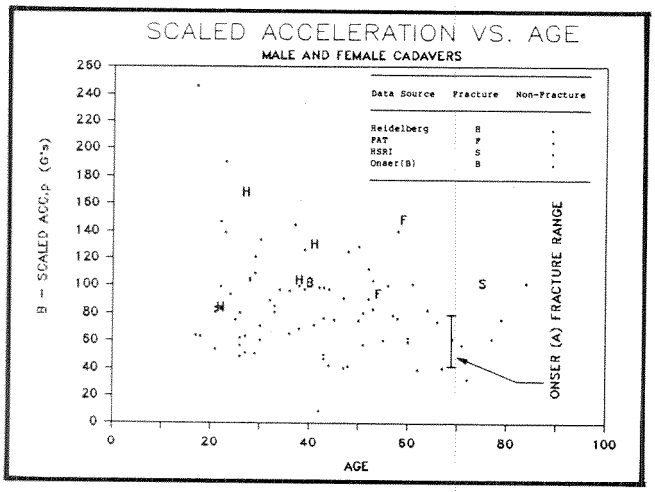

Figure 23. Superposition of ONSER (A) fracture range estimate on distributed load data—approach 1

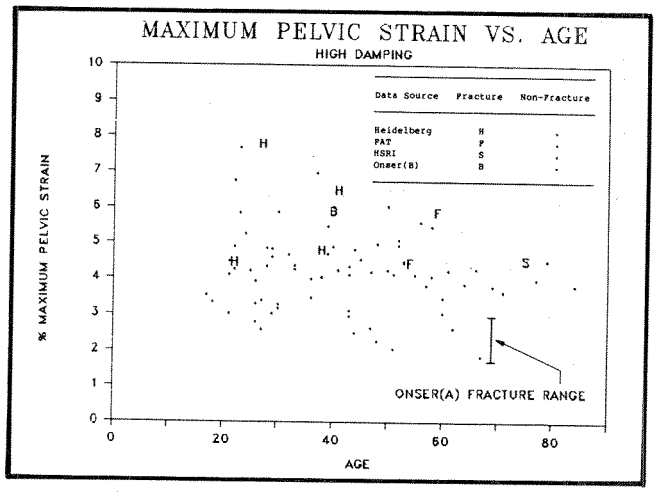

Figure 25. Superposition of ONSER (A) fracture range estimate on distributed load data—approach 2

ONSER(A) impact tests involved a degree of load concentration significantly higher than that realized in the vehicle environment. It will be recalled the tests used in our analysis involved rigid walls and three types of vehicle interiors (Opel, Rabbit, and Volvo). Yet in no case did a pelvic fracture occur at a response level as low as the estimated ONSER(A) fracture range.

The ONSER(A) data are, of course, most valuable in that the data define the load tolerance of one of the two major pelvic load paths. Investigation would also appear to be warranted into the load tolerance of the "other" load path through the iliac wing and into the effects of superposition of distributed loads as typically found in the vehicle environment.

It is recognized that any acceleration measure reflects the net force acting on the measured body. Thus, a pelvic acceleration measurement would be expected to be influenced to some degree by other forces acting on the pelvis during the impact event (e.g., horizontal seat interface force and horizontal shear force between the abdomen and pelvis). Some insight into the magnitude of this potential source of variability can be obtained by reference to Figure 4. Despite the presumed existence of seat and internal shear forces, a high correlation is obtained between peak applied force and peak pelvic acceleration. This result implies, for the ONSER(A) test condition at least, that the vector sum of the seat and shear forces is a predictable function of impact severity level. However, the extent of variability introduced into pelvic acceleration measurement in other environments more typical of the vehicle interior deserves further study before this observation can be generalized.

The data base is heavily biased toward nonfracture outcome. There is a need for additional fracture data to improve confidence in our fracture probability estimates, especially at higher fracture probabilities.

Male and female data have been merged for analysis, as have data from rigid and padded test conditions. The availability of further fracture data would permit a more detailed examination of the validity of this approach.

There is no doubt that a force-based approach to pelvic injury prediction exists as a strong alternative or adjunct to the acceleration-based proposals advanced here. The lack of a substantial body of comparable sets of force data have precluded our investigation of this alternative. When such data become available, a maximum likelihood analysis could provide a rational basis for ranking the effectiveness of the two approaches.

Summary and Conclusion

Two functions predictive of pelvic fracture due to distributed lateral impact have been synthesized from available data. The functions utilize the lateral component of pelvic acceleration as measured on 84 male and female cadaveric subjects from four major test series.

The second function, which incorporates the time history of measured acceleration, has been found to offer higher predictive power than does the first, which operates on peak acceleration magnitude alone. Age has been included as an explanatory variable in both approaches, and the value of its inclusion has been confirmed by the analysis.

All data have been analyzed using maximum likelihood methods. It has been confirmed that representation of the data by a Weibull distribution yields higher maximum likelihood than does the assumption that the data are normally distributed.

The degree of load distribution on the impacted pelvis has been identified as an important variable controlling pelvic tolerance to fracture. Acquisition of additional data defining the force tolerance of the pelvic bone under distributed loading conditions appears to be desirable.

Acknowledgments

Several individuals have made important contributions to the work reported here.

Deserving special mention, Margaret Hayden of Chi Associates painstakingly assembled the data base (see Appendix A) and artfully conducted innumerable queries of the data in the process of creating the presentations found throughout this paper.

Ranga Rangarajan of the Automated Science Group, Inc. implemented the MPS model under difficult time constraints and assisted in interpretation of early results.

Dominique Cesari of ONSER graciously provided a data tape of his [ONSER(A)] experiments for analysis, and Nabih Alem of UMTRI processed these data into the NHTSA format for our use.

Jeffrey Marcus and Richard Morgan of NHTSA developed many of the software routines that were extensively used on this project and that contributed materially to its progress.

Rolf Eppinger of NHTSA provided the benefit of many discussions during the course of the work.

Last, but certainly not least, Beulah Evans of NHTSA expertly prepared the manuscript for publication.

References

1. Cesari, D., M. Ramet, and P. Clair, "Evaluation of pelvic fracture tolerance in side impact," Proceedings 24th Stapp Car Crash Conference, SAE Paper 801306, 1980.
2. Cesari, D., and M. Ramet, "Pelvic tolerance and protection criteria in side impact," Proceedings 26th Stapp Car Crash Conference, SAE Paper 821159, 1982.
3. Cesari, D., R. Bouquet, and R. Zac, "A new pelvis design for the European side impact dummy," Proceedings 28th Stapp Car Crash Conference, SAE Paper 841650, 1984.
4. Kallieris, D., R. Mattern, G. Schmidt, and R. Eppinger, "Quantification of side impact responses and injuries," Proceedings 25th Stapp Car Crash Conference, SAE Paper 811009, 1981.
5. Klaus, G., and D. Kallieris, "Side impact—a comparison between HSRI, APROD, and HYBRID II dummies and cadavers," Proceedings 27th Stapp Car Crash Conference, SAE Paper 831630, 1983.
6. Klaus, G., R. Sinnhuber, G. Hoffmann, D. Kallieris, and R. Mattern, "Side impact—a comparison between dummies and cadavers, correlations between cadaver loads and injury severity," Proceedings 28th Stapp Car Crash Conference, SAE Paper 841655, 1984.
7. Cesari, D., and A. Johnson, "Evaluation of improved protection and dummy biofidelity in side impact," Proceedings Ninth International Technical Conference on Experimental Safety Vehicles, U.S. Department of Transportation, 1982.
8. Robbins, D., R. Lehman, and K. Augustyn, "Prediction of thoracic injuries as a function of occupant kinematics," Proceedings Seventh International Technical Conference on Experimental Safety Vehicles, U.S. Department of Transportation, 1979.
9. Tarriere, C., G. Walfisch, A. Fayon, J. Rosey, C. Got, A. Patel, and A. Delmas, "Synthesis of human tolerances obtained from lateral impact simulations," Proceedings Seventh International Technical Conference on Experimental Safety Vehicles, U.S. Department of Transportation, 1979.

10. Harris, J., "The design and use of the TRRL side impact dummy," Proceedings 20th Stapp Car Crash Conference, SAE Paper 760802, 1976.
11. Nuscholtz, G., N. Alem, and J. Melvin, "Impact response and injury of the pelvis," Proceedings 26th Stapp Car Crash Conference, SAE Paper 821160, 1982.
12. Evans, F. Gaynor, *Mechanical Properties of Bone,* Charles C. Thomas, Springfield, Illinois, 1973.
13. Yamada, H., *Strength of Biological Materials,* Williams and Wilkins, Baltimore, Maryland, 1970.
14. Ran, A., M. Koch, and H. Mellander, "Fitting injury versus exposure data into a risk function," 1984 International IRCOBI Conference on the Biomechanics of Impacts, IRCOBI Secretariat, Bron, France.
15. Brinn, J., and S. Staffeld, "The effective displacement index—an analysis technique for crash impacts of anthropometric dummies," Proceedings 15th Stapp Car Crash Conference, SAE, 1971.
16. Stalnaker, R., J. McElhaney, R. Snyder, and V. Roberts, "Door crashworthiness criteria," U.S. Department of Transportation, National Highway Traffic Safety Administration, DOT-HS-800 534, June 1971.

Key to Codes in Appendix A

General Table

NA	Data not available or rejected

Test No. Prefix Codes

H	-	HEIDELBERG
CES	-	ONSER(A)
F	-	FAT
BMD	-	ONSER(B)
7	-	HSRI

Test Type Codes

SLD	-	SLED
OPL	-	OPEL
BAS	-	ONSER (B) BASELINE RABBIT
MOD	-	ONSER (B) MODIFIED RABBIT
IMP	-	RIGID IMPACTOR

Impacted Surface Codes

RIG	-	RIGID
APR	-	APR PADDING
ENSO	-	ENSOLITE PADDING
VDR	-	VOLVO DOOR
MCI	-	MINICARS PADDING
SRL	-	FIBERGLASS HONEYCOMB PADDING
RAB	-	RABBIT DOOR
OPL	-	OPEL DOOR

Sex Codes

M	-	MALE
F	-	FEMALE
D	-	DUMMY

In AIS Column * = AIS 0

Appendix A. Lateral pelvic impact database, April 1985

Test No.	Tst Typ	Speed MPH	Imp Surf.	Sex	Age	Body Mass KG	Height Meters	ACC. yP G's	Force yP (KN)	AIS	A-Scaled ACC(G's)	A-Scaled Force(KN)	Lamda	B-Scaled ACC(G's)	B-Scaled Force KN	M1 (1lb)	M2 (1lb)	K (1lb/in)	C (1lb-sec/in)	Max Strain (in/in #10 2)	VMAX (in/sec)
H82008	SLD	20.0	APR	M	61	99	1.73	90.0	NA	*	98.3	NA	1.149	103.4	NA	17.30	30.96	3448	26	4.33	72.42
H8106D	SLD	20.0	RIG	D	NA	76	1.75	114.9	NA	*	1.8	NA	1.000	1.8	NA	NA	NA	NA	NA	NA	NA
H8105D	SLD	20.0	RIG	D	NA	76	1.75	130.6	NA	*	1.8	NA	1.000	1.8	NA	NA	NA	NA	NA	NA	NA
H8103D	SLD	15.0	APR	D	NA	76	1.75	49.0	NA	*	1.8	NA	1.000	1.8	NA	NA	NA	NA	NA	NA	NA
H8102D	SLD	15.0	RIG	D	NA	76	1.75	50.8	NA	*	1.8	NA	1.000	1.8	NA	NA	NA	NA	NA	NA	NA
H81027	SLD	25.3	RIG	M	30	77	1.80	137.0	NA	*	137.6	NA	0.992	136.0	NA	11.14	19.94	2977	20	5.95	97.58
H81021	SLD	15.0	APR	F	48	57	1.65	48.7	NA	*	44.2	NA	0.892	43.4	NA	8.09	14.48	2676	16	2.36	25.98
H8101D	SLD	14.0	RIG	D	NA	76	1.75	45.2	NA	*	1.8	NA	1.000	1.8	NA	NA	NA	NA	NA	NA	NA
H81016	SLD	25.0	RIG	M	22	77	1.75	148.3	NA	*	148.9	NA	1.007	149.3	NA	11.63	20.80	3020	20	6.85	103.37
H81015	SLD	14.6	APR	M	44	73	1.73	44.8	NA	*	44.2	NA	0.987	44.2	NA	10.96	19.61	2961	19	2.58	16.21
H81012	SLD	20.0	APR	F	33	46	1.55	105.8	NA	*	89.5	NA	0.827	87.5	NA	6.44	11.52	2480	14	4.45	51.16
H81011	SLD	20.0	APR	M	43	59	1.65	111.3	NA	*	102.3	NA	0.907	101.0	NA	8.52	15.25	2722	16	4.42	71.5
H81006	SLD	20.0	RIG	M	37	82	1.70	139.4	NA	*	143.0	NA	1.054	146.9	NA	13.34	23.88	3162	22	7.05	81.01
H81004	SLD	20.0	RIG	M	56	80	1.65	97.1	NA	*	98.8	NA	1.057	102.6	NA	13.45	24.07	3170	22	5.67	62.87
H81002	SLD	21.0	RIG	M	57	65	1.65	85.2	NA	*	80.9	NA	0.953	81.2	NA	9.85	17.63	2858	18	3.89	51.55
H80024	SLD	21.0	RIG	M	24	65	1.75	104.0	NA	*	98.7	NA	0.925	96.2	NA	9.02	16.14	2774	17	5.33	41.5
H80023	SLD	21.0	SRL	F	41	82	1.60	68.0	NA	*	69.7	NA	1.087	73.9	NA	14.63	26.18	3260	24	4.33	55.6
H80021	SLD	20.0	SRL	M	29	63	1.80	58.7	NA	*	55.1	NA	0.898	52.7	NA	8.25	14.76	2693	16	3.12	27.88
H80020	SLD	19.0	APR	F	26	67	1.68	53.0	NA	*	50.8	NA	0.960	50.9	NA	10.08	18.03	2879	18	2.89	26.8
H80018	SLD	19.3	APR	M	21	61	1.65	61.0	NA	*	56.7	NA	0.923	56.3	NA	8.96	16.03	2768	17	3.12	32.46
H80017	SLD	15.0	RIG	M	38	70	1.75	74.3	NA	*	72.3	NA	0.960	71.3	NA	10.08	18.03	2879	18	4.11	37.53
H80014	SLD	14.0	RIG	F	60	84	1.68	60.2	NA	*	62.2	NA	1.075	64.7	NA	14.15	23.31	3224	23	3.14	49.61
H80011	SLD	14.0	RIG	M	27	89	1.88	51.5	NA	*	54.3	NA	1.045	53.8	NA	13.00	23.25	3134	22	2.67	26.72
FAT5D	OPL	31.1	OPL	D	NA	76	1.75	NA	NA	*	1.8	NA	1.000	1.8	NA	NA	NA	NA	NA	NA	NA
FAT4D	OPL	31.1	OPL	D	NA	76	1.75	NA	NA	*	1.8	NA	1.000	1.8	NA	NA	NA	NA	NA	NA	NA
FAT3D	OPL	31.1	OPL	D	NA	76	1.75	NA	NA	*	1.8	NA	1.000	1.8	NA	NA	NA	NA	NA	NA	NA
FAT2D	OPL	31.1	OPL	D	NA	76	1.75	NA	NA	*	1.8	NA	1.000	1.8	NA	NA	NA	NA	NA	NA	NA
FAT1D	OPL	31.1	OPL	D	NA	76	1.75	NA	NA	*	1.8	NA	1.000	1.8	NA	NA	NA	NA	NA	NA	NA
F8412	OPL	28.0	OPL	M	54	68	1.78	100.5	NA	3	96.8	NA	0.939	94.3	NA	9.43	16.87	2816	18	4.42	56.13
F8411	OPL	28.0	OPL	M	64	76	1.73	84.2	NA	*	84.2	NA	1.007	84.8	NA	11.65	20.85	3022	20	3.94	49.47
F8410	OPL	28.0	OPL	M	53	74	1.73	86.0	NA	*	85.2	NA	0.994	85.5	NA	11.19	20.03	2982	20	4.57	62.8
F8409	OPL	28.0	OPL	M	25	95	1.88	71.9	NA	*	77.5	NA	1.079	77.6	NA	14.33	25.65	32.38	23	4.31	53.06
F8407	OPL	28.0	OPL	F	27	61	1.60	70.1	NA	*	65.1	NA	0.937	65.7	NA	9.39	16.80	2812	18	3.48	43.41
F8406	OPL	28.0	OPL	M	30	60	1.75	70.7	NA	*	65.3	NA	0.889	62.8	NA	8.00	14.31	2666	16	3.36	44.8
F8405	OPL	24.8	OPL	M	60	64	1.70	66.2	NA	*	62.5	NA	0.931	61.6	NA	9.20	16.47	2793	17	3.57	43.33
F8404	OPL	24.8	OPL	M	51	60	1.68	90.8	NA	*	83.9	NA	0.908	82.5	NA	8.54	15.28	2725	16	4.21	54.51
F8402	OPL	31.1	OPL	M	33	73	1.88	88.0	NA	*	86.8	NA	0.946	83.3	NA	9.65	17.27	2838	18	4.35	49.52
F8041	OPL	31.1	OPL	M	36	91	1.75	90.2	NA	*	95.8	NA	1.094	98.7	NA	14.94	26.73	3283	24	4.07	91.66
F8329	OPL	31.1	OPL	M	38	77	1.78	102.4	NA	*	102.4	NA	0.999	101.9	NA	11.36	20.33	2997	20	4.14	91.8
F8328	OPL	31.1	OPL	M	44	88	1.85	95.5	NA	*	100.3	NA	1.047	99.9	NA	13.07	23.38	3140	22	4.89	87.27
F8327	OPL	31.1	OPL	M	53	62	1.70	115.4	NA	*	107.8	NA	0.916	105.8	NA	8.77	15.70	2749	17	4.53	76.93
F8326	OPL	31.1	OPL	M	32	82	1.70	86.8	NA	*	89.0	NA	1.054	91.5	NA	13.34	23.88	3162	22	4.74	51.69
F8319	OPL	37.3	OPL	M	40	82	1.75	147.0	NA	*	150.8	NA	1.039	152.7	NA	12.78	22.86	3116	22	6.1	115.2
F8318	OPL	24.8	OPL	M	26	63	1.83	92.7	NA	*	87.1	NA	0.891	82.6	NA	8.07	14.43	2673	16	4.01	45.12
F8317	OPL	37.3	OPL	M	50	85	1.72	122.7	NA	*	127.4	NA	1.067	130.9	NA	13.84	24.76	3200	23	6.12	91.17
F8315	OPL	24.8	OPL	F	36	60	1.64	73.6	NA	*	68.0	NA	0.918	67.6	NA	8.81	15.77	2754	17	3.55	56.13
F8314	OPL	37.3	OPL	M	23	80	1.92	196.5	NA	*	199.9	NA	0.980	192.5	NA	10.71	19.17	2939	19	7.74	157.62
F8313	OPL	24.8	OPL	F	26	51	1.59	68.7	NA	*	60.1	NA	0.859	59.0	NA	7.24	12.95	2578	15	3.4	30.12
F8306	OPL	31.1	OPL	M	59	60	1.69	164.3	NA	2	151.9	NA	0.904	148.6	NA	8.43	15.08	2712	16	5.87	137.97
F8305	OPL	31.1	OPL	F	42	60	1.62	109.0	NA	*	100.7	NA	0.923	100.7	NA	8.98	16.07	2770	17	NA	NA

Appendix A, continued

Test No.	Tst Typ	Speed MPH	Imp Surf.	Sex	Age	Body Mass KG	Height Meters	ACC. yP G's	Force yP (KN)	AIS	A-Scaled ACC(G's)	A-Scaled Force(KN)	Lamda	B-Scaled ACC(G's)	B-Scaled Force KN	M1 (1lb)	M2 (1lb)	K (1lb/in)	C (1lb-sec/in)	Max Strain (in/in #10 2)	VMAX (in/sec)
F8304	OPL	31.1	OPL	M	28	61	1.72	117.0	NA	*	108.7	NA	0.904	105.7	NA	8.41	15.05	2711	16	4.94	73.25
F8303	OPL	31.1	OPL	M	52	68	1.72	120.3	NA	*	115.9	NA	0.954	114.8	NA	9.90	17.72	2862	18	5.03	68.45
F8302	OPL	31.1	OPL	M	22	65	1.75	109.3	NA	*	103.7	NA	0.925	101.1	NA	9.02	16.14	2774	17	4.97	60.17
F8301	OPL	31.1	OPL	F	39	57	1.73	147.4	NA	*	133.9	NA	0.871	128.4	NA	7.53	13.48	2613	15	5.55	98.73
F8213	OPL	31.1	OPL	M	47	90	1.70	84.4	NA	*	89.3	NA	1.104	93.2	NA	15.34	27.46	3312	24	4.27	66.97
F8211	OPL	31.1	OPL	M	29	59	1.77	127.1	NA	*	116.8	NA	0.876	111.4	NA	7.67	13.72	2628	15	4.91	77.06
F8210	OPL	31.1	OPL	M	29	70	1.84	131.9	NA	*	128.3	NA	0.936	123.5	NA	9.35	16.73	2808	18	4.68	118.61
F8207	OPL	31.1	OPL	M	58	68	1.65	146.3	NA	*	141.0	NA	0.974	142.5	NA	10.54	18.86	2922	19	5.55	100.93
F8206	OPL	31.1	OPL	M	23	63	1.75	155.3	NA	*	145.9	NA	0.910	141.4	NA	8.60	15.40	2731	17	5.94	112.23
F8205	OPL	31.1	OPL	M	43	77	1.78	79.2	NA	*	79.5	NA	0.998	79.0	NA	11.33	20.28	2994	20	4.2	51.73
H8405D	SLD	20.0	RIG	D	NA	76	1.75	225.7	NA	*	225.7	NA	1.000	225.7	NA	NA	NA	NA	NA	NA	NA
H8404D	SLD	20.0	RIG	D	NA	76	1.75	239.0	NA	*	239.0	NA	1.000	239.0	NA	NA	NA	NA	NA	NA	NA
H8403D	SLD	15.0	RIG	D	NA	76	1.75	47.3	NA	*	47.3	NA	1.000	47.3	NA	NA	NA	NA	NA	NA	NA
H8402D	SLD	20.0	RIG	D	NA	76	1.75	133.4	NA	*	133.4	NA	1.000	133.4	NA	NA	NA	NA	NA	NA	NA
H8401D	SLD	18.0	RIG	D	NA	76	1.75	100.7	NA	*	100.7	NA	1.000	100.7	NA	NA	NA	NA	NA	NA	NA
H84008	SLD	20.0	ENSO	M	79	64	1.68	83.4	NA	*	78.8	NA	0.938	78.2	NA	9.41	16.84	2814	18	4.59	47.52
H8306D	SLD	20.0	RIG	D	NA	76	1.75	204.2	37.16	*	204.2	37.2	1.000	204.2	37.16	NA	NA	NA	NA	NA	NA
H8305D	SLD	20.0	APR	D	NA	76	1.75	82.3	10.50	*	82.3	10.5	1.000	82.3	10.50	NA	NA	NA	NA	NA	NA
H8304D	SLD	15.0	RIG	D	NA	76	1.75	125.5	21.14	*	125.5	21.1	1.000	125.5	21.14	NA	NA	NA	NA	NA	NA
H8303D	SLD	20.0	ENSO	D	NA	76	1.75	51.4	8.38	*	51.4	8.4	1.000	51.4	8.38	NA	NA	NA	NA	NA	NA
H83031	SLD	16.8	VDR	M	43	62	1.70	56.8	NA	*	53.1	NA	0.916	52.1	NA	8.77	15.70	2749	17	3.2	31.56
H83030	SLD	11.2	VDR	M	42	86	1.88	11.0	NA	*	11.5	NA	1.026	11.3	NA	12.32	22.05	3079	21	NA	NA
H8302D	SLD	20.0	ENSO	D	NA	76	1.75	70.1	11.48	*	70.1	11.5	1.000	70.1	11.48	NA	NA	NA	NA	NA	NA
H83021	SLD	22.4	VDR	M	38	58	1.65	115.6	NA	2	105.6	NA	0.900	104.0	NA	8.31	14.87	2700	16	4.78	81.06
H83020	SLD	20.0	ENSO	F	17	52	1.52	74.7	6.06	*	65.8	7.8	0.887	66.2	7.71	7.95	14.22	2660	16	3.63	36.44
H8301D	SLD	16.8	ENSO	D	NA	76	1.75	65.7	8.98	*	65.7	9.0	1.000	65.7	8.98	NA	NA	NA	NA	NA	NA
H83016	SLD	22.0	VDR	M	52	68	1.70	96.7	NA	*	93.2	NA	0.960	92.8	NA	10.08	18.03	2879	18	5.16	56.5
H83012	SLD	20.0	ENSO	M	34	77	1.78	99.4	NA	*	99.8	NA	0.999	99.3	NA	11.36	20.33	2997	20	NA	NA
H83011	SLD	20.0	ENSO	M	26	61	1.88	74.3	7.69	*	69.0	NA	0.865	64.3	NA	7.37	13.20	2594	15	NA	NA
H83010	SLD	16.8	ENSO	F	30	56	1.75	85.3	2.80	*	77.0	NA	0.858	73.2	NA	7.21	12.90	2575	15	3.27	53.35
H82022	SLD	20.0	APR	M	50	77	1.68	75.0	11.60	*	75.3	NA	1.029	77.2	NA	12.42	22.22	3087	21	4.32	49.11
H82021	SLD	20.0	APR	M	48	99	1.80	113.2	15.00	*	123.6	NA	1.125	127.4	NA	16.25	29.07	3376	25	5.06	115.79
H82020	SLD	19.4	RIG	M	41	73	1.80	135.0	NA	2	133.2	NA	0.966	130.5	NA	10.29	18.41	2899	19	6.48	179.19
H82019	SLD	14.4	RIG	F	47	67	1.65	43.9	5.86	*	42.1	NA	0.967	42.5	NA	10.31	18.45	2901	19	2.72	22.14
H82018	SLD	14.4	RIG	F	28	85	1.80	103.1	9.91	*	107.0	NA	1.043	107.5	NA	12.93	23.13	3128	22	4.42	81
H82016	SLD	19.4	RIG	M	21	50	1.88	106.4	14.37	*	92.5	NA	0.783	83.3	NA	5.47	9.79	2349	12	4.57	69.17
H82015	SLD	14.4	RIG	M	18	69	1.83	70.1	4.39	*	67.9	NA	0.933	65.4	NA	9.25	16.54	2798	17	3.43	34.43
H82014	SLD	20.0	RIG	F	22	61	1.77	94.4	18.18	3	87.7	NA	0.892	84.2	NA	8.09	14.47	2675	16	4.44	96.24
H82012	SLD	25.0	RIG	M	17	75	1.73	248.1	30.26	*	247.0	NA	1.001	248.2	NA	11.42	20.44	3002	20	9.9	202.2
H82009	SLD	25.0	RIG	F	27	51	1.65	199.6	9.68	3	174.7	NA	0.844	168.4	NA	6.85	12.25	2531	14	7.76	108.49
F8204	OPL	31.1	OPL	F	40	60	1.58	115.5	NA	*	106.7	NA	0.935	108.0	NA	9.32	16.68	2805	17	4.98	74.64
F8203	OPL	31.1	OPL	M	21	68	1.73	91.0	NA	*	87.7	NA	0.951	86.6	NA	9.82	17.57	2854	18	4.19	62.4
F8123	OPL	31.1	OPL	M	22	71	1.78	89.1	NA	*	87.1	NA	0.958	85.4	NA	10.03	17.96	2875	18	4.35	53.73
BMD05	BAS	40.0	RAB	F	39	64	1.70	107.0	NA	*	101.0	NA	0.931	99.6	NA	9.20	16.47	2793	17	4.77	61.16
BMD04	BAS	40.0	RAB	M	51	71	1.57	58.5	NA	*	57.2	NA	1.020	59.7	NA	12.11	21.68	3061	21	2.15	46.18
BMD03	MOD	40.0	RAB	M	55	73	1.74	64.2	NA	*	63.3	NA	0.983	63.1	NA	10.82	19.37	2949	19	4.19	34.01
BMD02	MOD	40.0	RAB	M	43	71	1.75	51.1	NA	*	50.0	NA	0.967	49.4	NA	10.29	18.42	2900	19	3.06	18.47
BMD01	BAS	40.0	RAB	F	40	59	1.67	112.8	NA	3	103.7	NA	0.902	101.7	NA	8.36	14.97	2706	16	5.89	71.78
77T098	SLD	20.0	MCI	M	71	59	1.68	65.8	NA	*	60.5	NA	0.901	59.3	NA	9.33	14.90	2702	16	3.72	26.02
77T095	SLD	20.0	MCI	M	77	93	1.83	59.2	NA	*	63.3	NA	1.083	64.1	NA	14.47	25.89	3248	23	4.07	41.01

Appendix A, continued

Test No.	Tst Typ	Speed MPH	Imp Surf.	Sex	Age	Body Mass KG	Height Meters	ACC. yP G's	Force yP (KN)	AIS	A-Scaled ACC(G's)	A-Scaled Force(KN)	Lamda	B-Scaled ACC(G's)	B-Scaled Force KN	M1 (1lb)	M2 (1lb)	K (1lb/in)	C (1lb-sec/in)	Max Strain (in/in #10 2)	VMAX (in/sec)
77T092	SLD	20.0	RIG	F	45	58	1.78	89.5	NA	·	81.8	NA	0.867	77.6	NA	7.43	13.29	2601	15	4.61	53.23
77T089	SLD	20.0	RIG	M	66	55	1.73	89.6	NA	·	80.4	NA	0.857	76.8	NA	7.17	12.82	2570	15	4.37	39.97
76T042	SLD	25.0	MCI	F	58	64	1.78	86.7	NA	·	81.9	NA	0.911	79.0	NA	8.61	15.41	2732	17	4.16	50.59
76T039	SLD	20.0	MCI	M	72	74	1.88	35.9	NA	·	35.6	NA	0.953	34.2	NA	9.85	17.63	2858	18	NA	NA
76T034	SLD	19.6	MCI	M	62	59	1.83	48.2	NA	·	44.3	NA	0.862	41.6	NA	7.31	13.08	2587	15	2.71	19.57
76T029	SLD	15.0	MCI	M	67	63	1.68	45.6	NA	·	42.8	NA	0.931	42.4	NA	9.19	16.44	2792	17	1.94	53.75
76T011	SLD	20.0	RIG	M	69	75	1.70	63.4	NA	·	63.1	NA	1.008	63.9	NA	11.67	20.89	3024	20	3.88	58.71
76T010	SLD	19.6	RIG	M	84	88	1.62	93.0	NA	·	97.7	NA	1.117	103.9	NA	15.89	28.43	3351	25	3.9	83.8
76T009	SLD	25.8	RIG	F	75	44	1.55	125.6	NA	4	104.7	NA	0.809	101.6	NA	6.04	10.80	2427	13	4.51	131.21
CESZ2	IMP	32.3	RIG	M	67	58	1.67	NA	NA	3	NA	NA	0.894	NA	NA	8.15	14.59	2683	16	NA	NA
CESZ1	IMP	28.3	RIG	M	67	58	1.67	NA	NA	·	NA	NA	0.894	NA	NA	8.15	14.59	2683	16	NA	NA
CESY2	IMP	33.5	RIG	M	74	100	1.75	NA	NA	2	NA	NA	1.147	NA	NA	17.21	30.79	3441	28	NA	NA
CESX2	IMP	33.0	RIG	F	54	56	1.62	NA	NA	3	NA	NA	0.892	NA	NA	8.10	14.49	2677	16	NA	NA
CESX1	IMP	28.4	RIG	F	54	56	1.62	NA	NA	·	NA	NA	0.892	NA	NA	8.10	14.49	2677	16	NA	NA
CESW2	IMP	18.6	RIG	M	85	68	1.7	56.2	6.48	2	54.2	7.0	0.960	53.9	7.04	10.08	18.03	2879	18	2.1	32.67
CSV2	IMP	17.2	RIG	M	61	50	1.62	49.2	4.95	3	42.8	6.5	0.843	41.5	6.97	6.83	12.22	2529	14	1.52	54.14
CEST2	IMP	21.5	RIG	F	79	44	1.44	38.1	4.16	3	31.8	6.0	0.839	32.0	5.91	6.73	12.04	2516	14	1.7	13.74
CESS4	IMP	27.6	RIG	M	79	64	1.64	NA	6.44	3	NA	7.2	0.948	NA	7.17	9.71	17.38	2844	18	NA	NA
CESS3	IMP	25.3	RIG	M	79	64	1.64	NA	6.07	·	NA	6.8	0.948	NA	6.76	9.71	17.38	2844	18	NA	NA
CESR5	IMP	31.4	RIG	M	80	82	1.8	NA	10.24	2	NA	9.7	1.024	NA	9.76	12.25	21.92	3073	21	NA	NA
CESR4	IMP	29.3	RIG	M	80	82	1.8	NA	10.14	·	NA	9.6	1.024	NA	9.67	12.25	21.92	3073	21	NA	NA
CESO6	IMP	26.2	RIG	M	70	79	1.6	NA	6.2	3	NA	6.0	1.066	NA	5.45	13.82	24.73	3199	23	NA	NA
CESO5	IMP	23.5	RIG	M	70	79	1.6	NA	5.62	·	NA	5.5	1.066	NA	4.94	13.82	24.73	3199	23	NA	NA
CESN7	IMP	25.5	RIG	M	54	86	1.84	NA	9.06	3	NA	7.7	1.037	NA	7.76	12.73	22.78	3112	22	NA	NA
CESN6	IMP	23.4	RIG	M	54	86	1.84	NA	9.08	·	NA	7.7	1.037	NA	7.76	12.73	22.78	3112	22	NA	NA
CESL4	IMP	27.7	RIG	M	71	85	1.75	145.4	12.44	·	150.9	10.7	1.058	153.8	10.31	13.48	24.13	3173	22	NA	NA
CESK3	IMP	21.7	RIG	M	75	55	1.71	NA	NA	·	NA	NA	0.861	NA	NA	7.27	13.00	2582	15	NA	NA
CESJ3	IMP	22.0	RIG	M	75	63	1.77	76.4	6.6	3	71.8	8.5	0.905	69.2	9.13	8.46	15.14	2716	16	2.83	44.33
CESJ2	IMP	19.0	RIG	M	75	63	1.77	37.7	5.28	·	35.4	6.8	0.905	34.1	7.30	8.46	15.14	2716	16	1.52	23.37
CESI5	IMP	24.9	RIG	M	65	63	1.81	94.7	8.16	2	89.0	10.5	0.895	84.8	11.54	8.18	14.64	2686	16	3.38	62.34
CESI4	IMP	24.7	RIG	M	65	63	1.81	82.3	9.58	·	77.3	12.3	0.895	73.7	11.95	8.18	14.64	2686	16	2.51	79.3
CESH4	IMP	23.7	RIG	M	69	86	1.75	NA	NA	2	NA	NA	1.064	NA	NA	13.72	24.56	3191	23	NA	NA
CESH3	IMP	21.5	RIG	M	69	86	1.75	NA	NA	·	NA	NA	1.064	NA	NA	13.72	24.56	3191	23	NA	NA
CESF3	IMP	21.7	RIG	F	59	55	1.52	NA	NA	·	NA	NA	0.913	NA	NA	8.67	15.51	2738	17	NA	NA
CESE2	IMP	19.3	RIG	F	72	60	1.55	33.5	4.17	3	31.0	4.9	0.944	31.6	4.68	9.59	17.17	2832	18	1.66	24.29
CESE1	IMP	15.7	RIG	F	72	60	1.55	50.1	4.54	·	46.3	5.3	0.944	47.3	5.09	9.59	17.17	2832	18	1.81	38.14
CESD2	IMP	19.1	RIG	F	63	52	1.6	51.5	NA	3	45.4	NA	0.865	44.6	NA	7.38	13.21	2595	15	1.76	36.78
CESD1	IMP	15.5	RIG	F	63	52	1.6	42.0	3.86	·	37.0	5.0	0.865	36.3	5.16	7.38	13.21	2595	15	1.62	24.72
CESC3	IMP	24.5	RIG	M	69	78	1.73	NA	7.28	2	NA	7.2	1.019	NA	7.01	12.06	21.58	3057	21	NA	NA
CESC2	IMP	19.9	RIG	M	69	78	1.73	NA	8.39	·	NA	8.2	1.019	NA	8.08	12.06	21.58	3057	21	NA	NA
CESB2	IMP	18.6	RIG	F	84	70	1.54	NA	NA	2	NA	NA	1.023	NA	NA	12.21	21.84	3069	21	NA	NA
CESB1	IMP	13.0	RIG	F	84	70	1.54	NA	NA	·	NA	NA	1.023	NA	NA	12.21	21.84	3069	21	NA	NA
CESA4	IMP	25.5	RIG	F	70	58	1.67	NA	NA	3	NA	NA	0.894	NA	NA	8.15	14.59	2683	16	NA	NA
CESA3	IMP	18.6	RIG	F	70	58	1.67	NA	NA	·	NA	NA	0.894	NA	NA	8.15	14.59	2683	16	NA	NA

Appendix B

Comparison of Cadaver and Dummy Lateral Impact Pelvic Data

1. Comparison of Peak Responses

A limited amount of data is available from the Heidelberg data set that permits comparison of cadaver and SID dummy force and acceleration responses. Figures B-1 and B-2 present peak force versus peak acceleration data for Heidelberg cadavers and Heidelberg SID dummies, respectively. It may be noted that the slope of the line fitting the dummy data (.196KN/g) is approximately twice the slope of the least squares fit to the cadaver data (.101KN/g). This result suggests that the dummy generates higher peak pelvic interface force for a given level of peak pelvic acceleration response.

To investigate this indication further, dummy and cadaver data were segregated by test speed and by impacting surface (rigid or padded), and the ratios of average dummy peak responses to average cadaver peak responses for each test condition were calculated and plotted. Figure B-3 presents these computed acceleration ratios. It may be noted that the ratio of peak dummy acceleration to peak cadaver acceleration ranges from 1.0 to 1.7 for rigid impacts and remains stable at a lower value of approximately .85 for padded impacts.

Figure B-4 presents corresponding computed force ratios. Although data are very limited and should be interpreted with caution, the dummy appears to generate

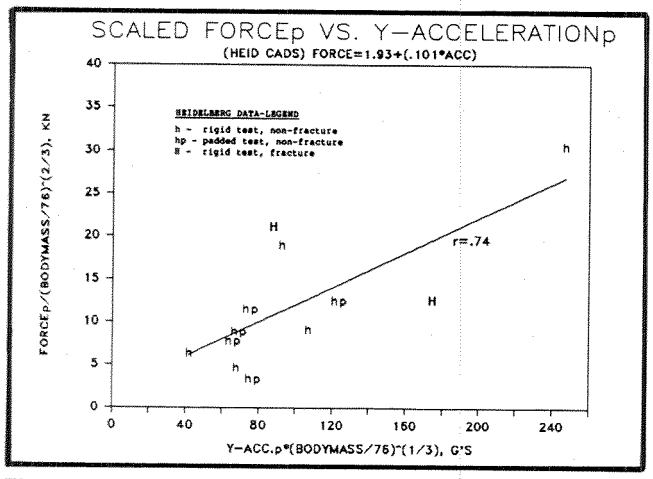

Figure B-1. Scaled peak pelvic forces versus scaled peak pelvic Y-acceleration for Heidelberg cadaver tests

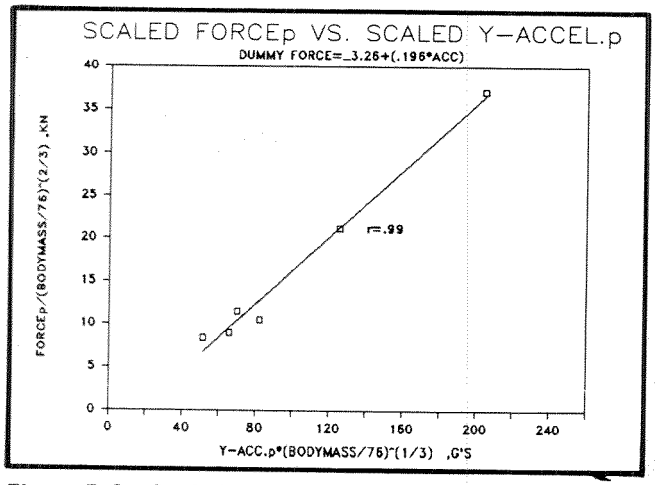

Figure B-2. Scaled peak pelvic force versus scaled peak pelvic Y-acceleration for Heidelberg SID dummy tests

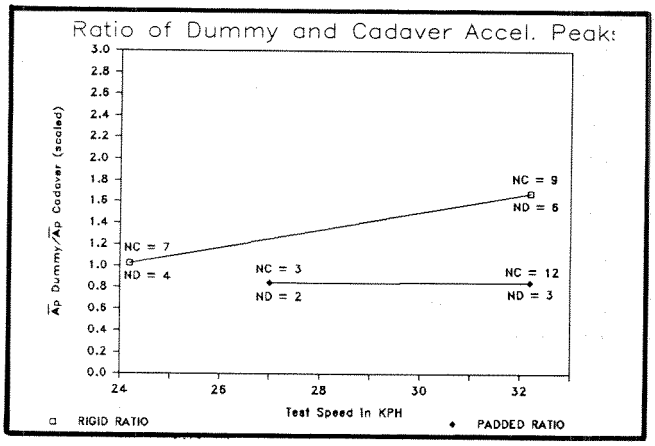

Figure B-3. Ratios of SID dummy and cadaver peak accelerations—Heidelberg data (NC and ND are number of cadaver tests and number dummy tests, respectively, included in ratio of determination at each data point)

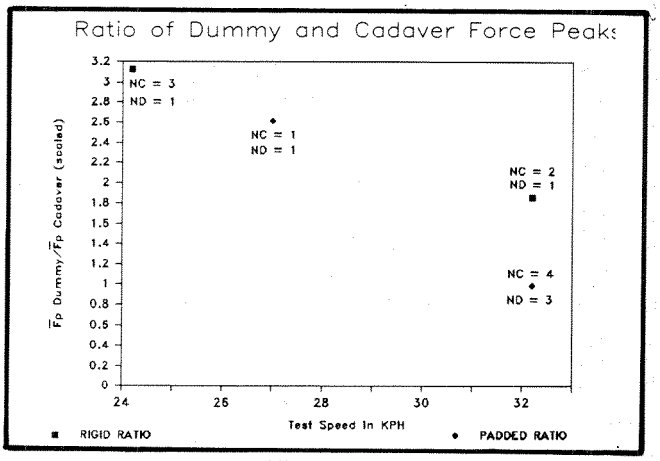

Figure B-4. Ratios of SID dummy and cadaver peak forces-Heidelberg data

higher interface force than does the cadaver at all test speeds. Also, the force ratio exhibits a trend toward reduction with increasing test speed. However, more data would be desirable to confirm these observations.

2. Comparison of Pulse Shape

Thus far, we have compared only the behavior of peak force and peak acceleration responses. It is also of interest to examine comparative pulse shapes for cadavers and dummies from the Heidelberg series, for both rigid and padded test conditions.

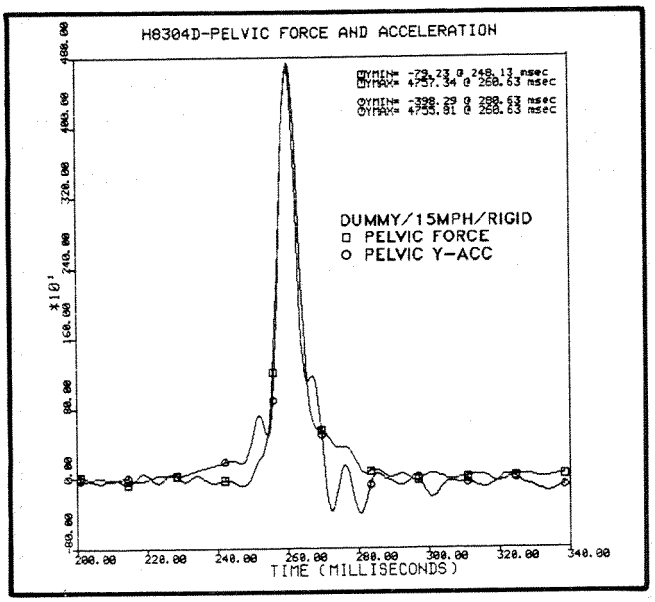

Figure B-5. Pelvic force and pelvic Y-acceleration overlay for Heidelberg SID dummy test H8304d

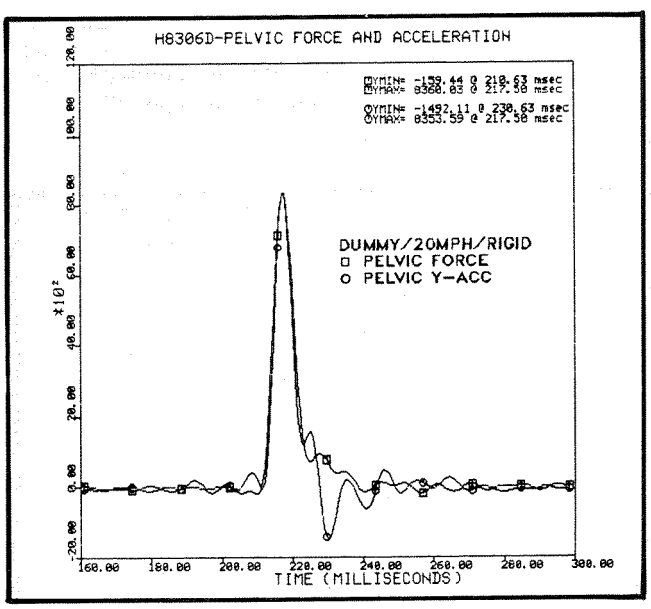

Figure B-6. Pelvic force and pelvic Y-acceleration overlay for Heidelberg SID dummy test H8306d.

A. Rigid Interface

Figures B-5 and B-6 present overplots of pelvic force and acceleration data for a 15mph dummy test and a 20mph dummy test, respectively. (Traces have been artificially scaled to equalize plotted peak amplitudes so that curve shapes can be better compared.) Figures B-7 and B-8 present comparable data for 20mph and 25mph cadaver exposures.

For all dummy and cadaver rigid tests, excellent agreement of force and acceleration curve shape is seen, and rigid body behavior is approached.

B. Padded Interface

Figures B-9 and B-10 present typical dummy tests, at 17 and 20mph, into ensolite padding. Figures B-11 and B-12 are corresponding plots for two cadavers at 20mph into ensolite.

Distinctly different characteristic acceleration pulse shapes are evidenced by the SID and by the cadavers in the padded environment. Whereas the dummy exhibits good tracking of force and acceleration up to peak force, the cadaver accelerations are seen to track force well initially, but then to dip and rise again to meet the force curve. In all cases, as was observed in the main body of the paper, peak force and peak acceleration are closely coincident in time.

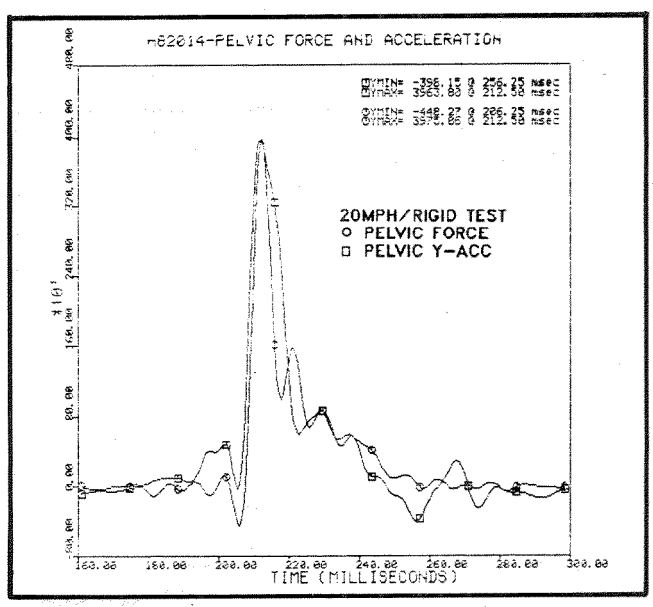

Figure B-7. Pelvic force and pelvic Y-acceleration overlay for Heidelberg cadaver test H82014

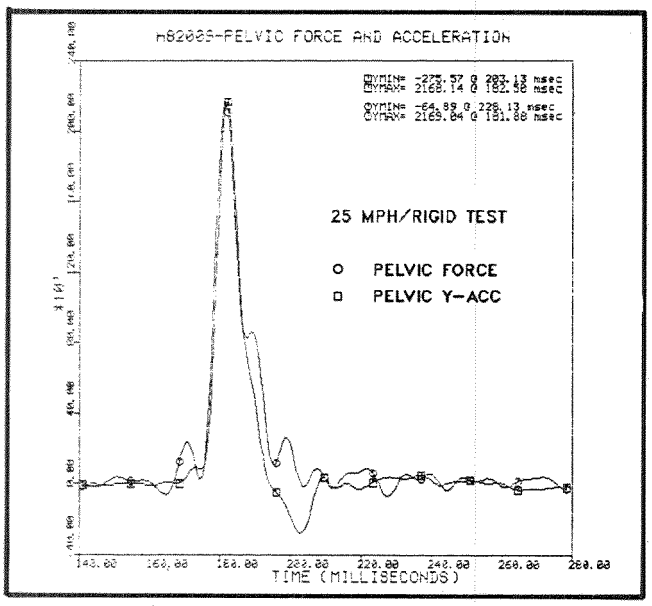

Figure B-8. Pelvic force and pelvic Y-acceleration overaly for Heidelberg cadaver test H82005

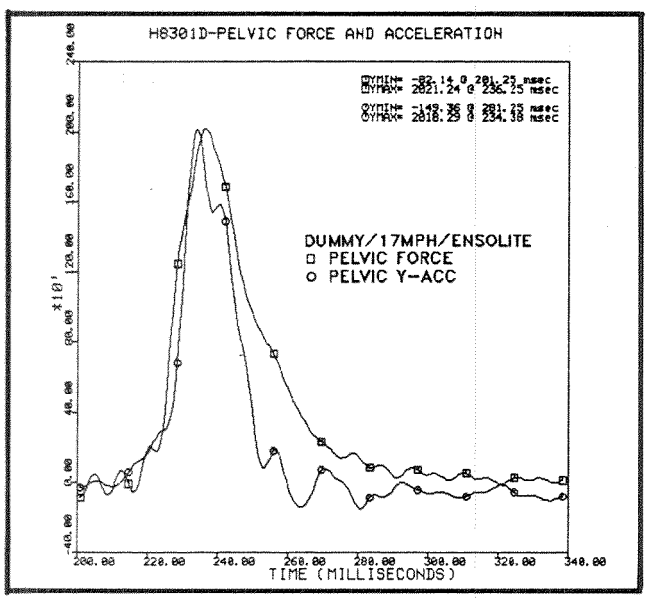

Figure B-9. Pelvic force and pelvic Y-acceleration overlay for Heidelberg SID dummy test H8301d

It is interesting to speculate as to why the differences noted above occur in the padded environment and not in the rigid environment. This difference could be related to additional compliance in the structure of the human hip joint or could be due to differences in phasing of horizontal shear forces acting between the abdomen and pelvis.

Although not pursued here, these observed differences should be better understood for input to the development of advanced side impact dummy concepts.

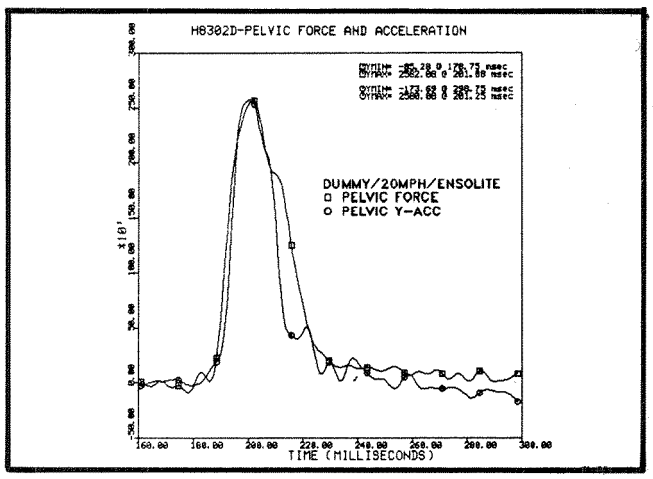

Figure B-10. Pelvic force and pelvic Y-acceleration overlay for Heidelberg SID dummy test H8302d

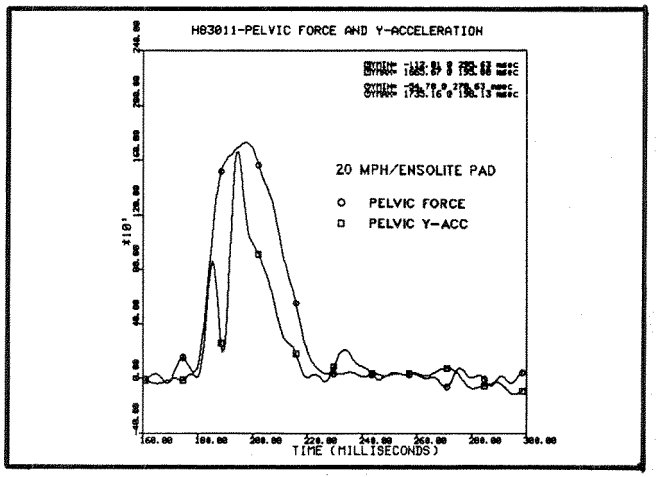

Figure B-11. Pelvic force and pelvic Y-acceleration overlay for Heidelberg cadaver test H83011

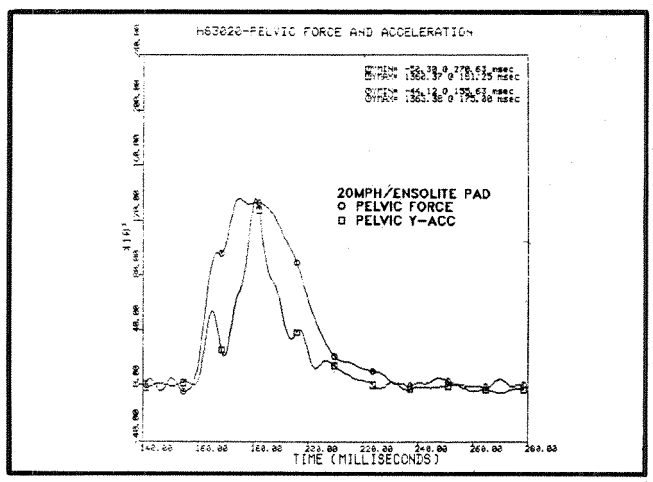

Figure B-12. Pelvic force and pelvic Y-acceleration overlay for Heidelberg cadaver test H83020.

The EUROSID Side Impact Dummy

L. Neilson and
R. Lowne
Transport and Road Research Laboratory, United Kingdom

C. Tarrière,
F. Bendjellal, and
D. Gillet
Association Peugeot S.A./Renault, France

J. Maltha
Instituut voor Wegtransportmiddelen—TNO, Netherlands

D. Cesari and
R. Bouquet
Organisme National de Sécurité Routière, France

Abstract

EUROSID is the side impact dummy that has been designed and has now been almost completely developed by a group of European research laboratories working together under the auspices of the European Experimental Vehicles Committee (EEVC). It represents a bringing together of components and ideas from the three experimental side impact dummies sponsored by the EEC[1] as part of their Biomechanics Programme. These were produced by APR (Peugeot-Renault), ONSER, and MIRA. This paper describes the evolution of the EUROSID dummy and discusses the advances in biofidelity, the responses of its various components to impact, and the types of measurements it can record.

Introduction

When the EEVC first recommended a side impact test in its report to the Fifth ESV Conference(1), which included the use of dummies, there was no suitable dummy available. At that time, the only dummy designed for use in side impacts was the TRRL side impact dummy(2). This was regarded more as a dynamic load-measuring device than a dummy. While being built to 50th percentile male dimensions and weight, it made no pretense of being biomechanically correct in its response.

A symposium was organised by the EEC in 1975 to establish priorities for improving vehicle legislation. Following this the Biomechanics Programme was set up, with some help from EEVC members. It was partially funded by the EEC to expedite ongoing research, which was thought to be necessary as a basis for the safety aspects of this legislation(3). One of the recognised priorities included in the programme was the development of a suitable side impact dummy.

Projects undertaken within this programme included an accident investigation studying specifically side impacts, studies of biomechanical performance required for the design of dummies, and the development of three independent side impact dummies. The three side impact dummies are described in detail elsewhere(4,5,6), but their essential details are given below.

APROD (APR)

The head was a standard Hybrid III head. The neck was a modified version of Hybrid III. The chest was based on the rib cage of the Part 572 dummy but with the posterior ends of the ribs attached in two groups of three to the ends of pistons, which could traverse laterally inside cylinders attached to the spine. Chest compression was determined by measuring the movement of the pistons in their cylinders. The shoulders were modified forms of the Part 572 design to allow and encourage greater upwards and forwards rotation. Modified arms were used but the remainder was of the Part 572 design.

MIRA

The head, neck, legs, and arms were of the Part 572 design. The shoulder was a complex unit incorporating a sliding and rotating clavicle. The chest comprised six spring steel ribs, of which the force on each could be measured. The pelvis could measure acceleration and the force applied at the ilium, great trochanter, and the pubic symphysis.

ONSER

This was essentially a standard ONSER 50 frontal impact dummy with a new chest and shoulder design to adapt it for side impact use. The shoulder was a sprung sliding and pivoting unit and the chest was of moulded polyurethane foam on rigid spine. A transducer was incorporated for measuring lateral compression of the chest.

TNO Abdomen

TNO designed an abdomen based on cadaver tests performed by the Peugeot-Renault Association (APR)(7)

1. Financial support was also given by the governments of the participating countries (France, the Netherlands, and the United Kingdom).

that could in principle be used in any side impact dummy incorporating the standard Part 572 lumbar spine interface. In practice, the prototypes produced had the correct dimensions to fit the Part 572 pelvis and therefore could be used only with the APROD. The abdomen was designed to have the correct force-penetration characteristics at an appropriate impact velocity and incorporated switches to indicate when critical levels of penetration and force had been exceeded.

Side Impact Dummy Specification

During the final phase of the Biomechanics Programme, the three prototype dummies were evaluated and compared with each other, with the side impact dummy developed by HSRI for NHTSA(8), and with the available cadaver test findings. The results, being part of the Biomechanics Programme, were presented at the EEC Biomechanics Seminar in 1983(3,9).

At the same time, the EEVC Ad-Hoc Group on Dummies was drawing up an agreed specification for a side impact dummy, which evolved as the programme progressed(10).

A Unified European Side Impact Dummy

At the conclusion of the EEC Biomechanics Programme, the EEVC Ad-Hoc Group on Dummies coordinated the development of a single side impact dummy, which evolved by adopting the most successful principles of the three prototype dummies. The detailed side impact accident investigation(11) provided information on the location, cause, and type of injuries to car occupants in side impacts. This provided a guide to the requirements and priorities in the design of the side impact dummy. The distribution of injuries to struck-side occupants in side impacts is given in Table 1.

These results show that ideally the dummy should be capable of registering the likelihood of injury to the head, chest, abdomen, pelvis, and legs.

Table 1. Distribution of injuries to struck-side occupants in side impacts

Body region	Number of cases	
	AIS≥3	AIS≥4
Head and face	16	11
Neck	1	0
Chest	15	5
Abdomen	12	7
Pelvis	3	0
Legs	6	1

These results, the comparison testing of the three European prototypes(9), and the side impact dummy specification enabled the EEVC Ad-Hoc Group to coordinate the development of a unified side impact dummy. Various laboratories worked on the different body parts, which were combined into a European side impact dummy. This has come to be known as EUROSID. The sources of its component parts are now discussed briefly.

Head

The Hybrid III head was found to be closest in performance to the lateral drop tests performed with cadavers and was chosen for the dummy without further development.

Neck

The APROD 82 neck came closest in kinematics to the volunteer and cadaver results. The Peugeot-Renault Association was continuing its development of this neck, and therefore the developed version of the APROD neck was chosen for EUROSID.

Chest

Injuries to the chest are caused by excessive force or compression. On balance, the Ad-Hoc Group considered compression to be the parameter most closely related to injury risk in side impact. The APROD chest was considered to be the best at measuring deflection while being closest to the biomechanical performance references. However, the APROD design had some mechanical problems, at least in its earliest version, and it subdivided the chest into only two discrete areas. Accident studies showed that serious internal injuries can sometimes be associated with relatively few fractured ribs, three or four, suggesting that concentrated forces could cause injury whereas the same force over the whole rib cage would not. However, it is also desirable to keep to a minimum the number of instrumentation channels and the complexity of the chest design. It was decided that a new chest could be developed by TRRL in consultation with Peugeot-Renault and TNO based on the design principles of the APROD chest but with the chest divided into three discrete areas, and chest deflection would be measured in each area.

Shoulder

None of the shoulders from the prototype dummies were found to be satisfactory with regard to mechanical reliability or in reproducing the observed cadaver re-

sponses. The Ad-Hoc Group felt there was a need for arms on the side impact dummy and therefore a need for a fully articulating shoulder. This would help to achieve the correct inertial effect and the appropriate mass distribution and would enable correct engagement with the diagonal strap of a seatbelt. It was decided to have arms and shoulders if these proved practical to design. ONSER tests on cadavers in the Biomechanics Programme demonstrated that the chest is less liable to injury if the arm is trapped between the chest and an impactor(12). The "worst case" condition, which is the usual situation for legislative testing, is therefore with the chest exposed. For this reason, the specification calls for a shoulder that, when struck laterally, moves forward to expose the chest to a more direct impact. TRRL agreed to include the development of a new shoulder to meet the requirement of the specification as part of the thorax development.

Abdomen

The performance of the TNO abdomen was close to that specified from the tests on cadavers. No other abdomen has been or was being developed, and the Ad-Hoc Group agreed that TNO should develop the abdomen for EUROSID by small modifications to improve its performance and to adapt it to fit the EUROSID chest and pelvis.

Pelvis

None of the three prototype dummy pelves were satisfactory. When struck by a rigid impactor, they all produced a far higher force than the cadavers when similarly tested. The Ad-Hoc Group felt that force was the parameter most closely related to injury potential for the pelvis. Acceleration would only be related to force by a constant factor if the effective mass remained constant and the pelvis was not trapped by the seat or car structure. Only the MIRA pelvis could measure force but its instrumentation was complex and no further work was proposed to improve this pelvis. ONSER had planned to develop a force-measuring pelvis and agreed to produce the pelvis for EUROSID to the Ad-Hoc Group specification.

Legs

Although leg fractures feature regularly in side impacts, no suitable instrumented femur had been developed and this area was given a lower priority than the other four body areas. It was agreed that Part 572 legs would be used for EUROSID at this stage.

Arms

Arm injury was not considered to be sufficiently serious to warrant instrumentation. Part 572 arm dimensions would be used, modified only insofar as this affected the performance of the chest and shoulder.

Design and Performance of Specialised EUROSID Components

Neck

The first version of the APROD dummy neck (1982 version) was developed from a biomechanical data base derived from volunteers and from human subjects (cadavers).

Data from experiments with volunteers came from tests performed by Ewing(13). Their aim was to study the dynamic response of the head-neck system when the entire body was subjected to an acceleration of the +Gy type. Experiments involving cadavers, performed in the same test conditions as those used by Ewing, were performed in the Association Peugeot-Renault Laboratory. The tests selected for the design of this neck are shown in Table 2. They enable a direct comparison to be made between the cadaver and volunteers' responses.

The sled deceleration for the two types of tests met the conditions of HOLD (High rate of Onset, Long Duration).

Table 2. Test conditions for cadaver and volunteer tests

CADAVER TESTS		
Test	Average peak sled acceleration	Initial velocity of the sled
MS 234 MS 235 MS 239 MS 240	7.55g (74.06 m/s_2)	6.08 m/s
VOLUNTEER TESTS		
Test	Average peak sled acceleration	Initial velocity of the sled
1594 1921 1922 1926 1924	7.07g (69.4 m/s_2)	6.408 m/s

The characteristics of these tests are described in detail in (14) as is the description of the design of this 1982 version.

Technological problems arose at the time of tests performed with the neck, especially cable breakage, the separation and even the shearing of the buffers at the interface plates, and seizing-up of the half-spheres.

To remedy these problems and improve biofidelity of the neck for high impact severities, a second version was developed in the APR Laboratory, this being the version developed for EUROSID.

Development of APROD Neck for EUROSID

During cadaver tests, under the conditions defined above, it was observed that the subject sustained no injuries either to the cervical spine or to bone joints.

This led, therefore, to more violent experimental conditions than those of earlier tests ($74 m/s^2$ and 6.08m/s). These severities could not be obtained from volunteers but were necessary to improve the neck design up to injury level.

Three tests with cadavers were performed in 1983 in the following test conditions.

Table 3. Test conditions for 1983 cadaver tests

Test	Peak sled acceleration		Initial velocity of the sled
	g	m/s_2	m/s
249	12.02	117.91	6.11
297	14.02	137.53	6.22
298	13.06	128.11	6.11

Biomechanical Data Base

The following such data were used in the development of this EUROSID neck.

A { — Ewing data from volunteer tests
— APR data from cadaver tests

B { — APR data from cadaver tests described in table 3 above

The results of APR tests are published in a separate paper(15). A description of the EUROSID neck is given in the following section.

Description of EUROSID Neck

This version is composed of three parts:

- A neck/trunk interface piece
- A head/neck interface piece
- A central section made of rubber that links the two interfaces to one another

Figure 1 illustrates various neck sections, showing the components of each part.

Each interface is made up of two plates; an exterior one ((3) or (1) in Figure 1) and an intermediary one(2) bonded to the central part. Linking of the two plates is by means of a sphere, which, in fact, constitutes a point of rotation to replicate head neck kinematics.

Two types of buffers are interposed between the plates: the section CC (Figure 1) illustrates this. Those buffers that are triangular act as buffers at the end of travel.

The central component(5) and these buffers are all part of the same system. The circular buffers modulate the shearing or rotational movement in relation to the centre of the half-sphere.

Figure 2 shows the neck/trunk interface in its final position.

The central part of the neck, simulating the cervical vertebral column, allows flexion and extensions. The neck prototype, which has been developed, has the following stiffness characteristics:

- Central part and triangular section buffers: 70 shores
- Buffers(6) with a circular section: 70 shores

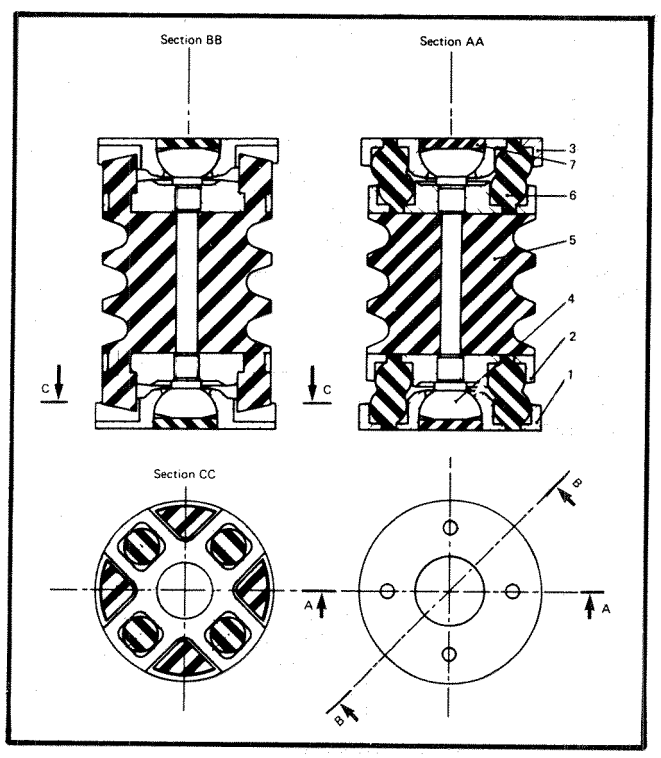

Figure 1. EUROSID neck

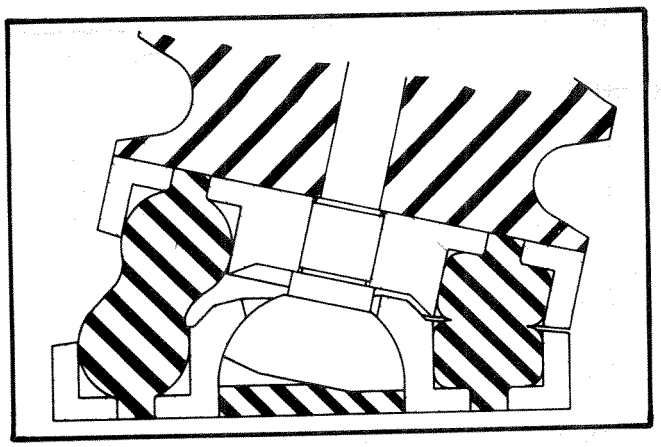

Figure 2. Neck-thorax interface

Figure 3 shows the various possibilities of simple movements of the different parts of the neck.

It can be said that this set-up represents a system having two pivots and three modes of deformation.

The two pivots are represented by the centre of the half-spheres.

The three modes of deformation possible for such a neck are:

- Simple lateral flexion (of the central part)
- Translation and rotation (relative movements of the interface plates)
- Extension of the central part

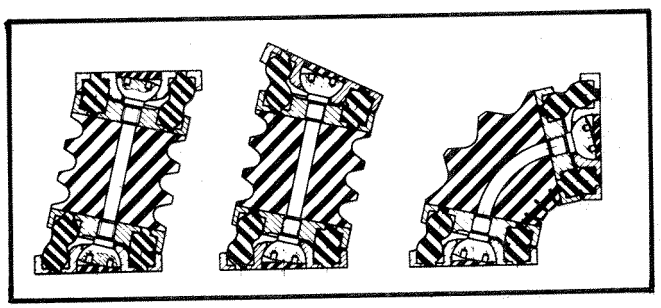

Figure 3. Possible neck deformation modes

The play that exists around the buffers and the compliance of these latter may give rise to torsion—a rotation around the neck's vertical axis. This matter will be discussed when the processing of available data is completed.

Mechanical Behaviour Tests

With a view to studying the whole system's mechanical behaviour (resistance to impact of the various neck components), particularly violent tests were performed with the neck attached to an APROD dummy.

The characteristics of these tests were as follows.

The dummy is decelerated laterally against a rigid wall (at 90° where it is subjected to an impact velocity (V_i) of approximately 20m/h. This is a high-violence impact, which is reflected in a lateral thoracic acceleration$_{\gamma T}$(3ms) of about 180g.

Table 4 summarizes the parameters of these tests.

The results of these tests show that—

(i) In the two tests, no deterioration was observed either in terms of welding of components or in terms of rubber parts of the neck.

(ii) From the point of view of kinematics, test 2346 C1, where the stiffnesses of the prototype were respectively 60 and 50 shores, shows that the displacements of the head/neck system are much greater than for test 2346 C2.

Validation Tests

Currently, side impact tests using cadavers and the APROD dummy equipped with the second version of the neck (stiffness of 70 shores) are in hand.

The principle of these tests is exactly the same as that of the preceding tests (study of the head/neck response when the body is subjected to an acceleration of the type +Gy).

Table 4. Characteristics of mechanical behaviour tests

Test	V_i to which the dummy was subjected		Stiffnesses used		Peak horizontal acceleration measured at APROD's thorax (γT)		γT (3ms)	
			Central part and triangular buffers	Buffers (6)				
	km/h	m/s			g	m/s^2	g	m/s^2
2346 C1	31,4	8,73	60 sh	50 sh	184	1805.04	132	1294.92
2346 C2	31,4	8,73	70 sh	70 sh	176	1726.56	120	1177.2

The method used, on the other hand, is slightly different:

- More appropriate instrumentation that is also more reliable (a different array of transducers in relation to the anatomical coordinate frame)
- More flexible conditions of studying head-neck kinematics (cameras fixed to the laboratory, more highly developed camera calibration methods)

The results of these tests, as well as a simple specification for the dummy neck, will be the subject of another paper presented at the 1985 ESV Conference(15).

Shoulder

The specification for the shoulder is given in detail in (10), but briefly it requires that the shoulder when struck laterally moves forward and possibly upward to expose the chest, under a relatively low force. It should include a representation of the clavicle and should return to a positive neutral position.

The dynamic behaviour of cadaver shoulders when impacted laterally is given from tests performed by Peugeot-Renault, and a force-deflection corridor has been proposed (Figure 6(9)). The quasi-static lateral compression of the shoulder with respect to the spine at a maximum force of 200N was found to be about 55mm with volunteers(16).

To encourage forward rotation of the shoulder when struck laterally, the centre of rotation must be posterior to the point of impact. However, there is no such position, using a fixed radius arm for the clavicle, that would allow the upper arm to clear the front of the chest and permit full rotation of the clavicle. It was also found that an initial transverse movement of the clavicle caused the inner flesh of the upper arm to bind on the chest flesh, inhibiting the subsequent forward rotation required. The solution found to these problems was to design the clavicle as a cam so that as the shoulder rotates forward, the instantaneous center of rotation moves forward allowing the arm to clear the chest (Figure 4). The shoulder is made from polypropylene and has survived rigid wall impacts of 9m/s (20m/h).

The maximum compression at the acromion with respect to the spine under 200N force was found to be 190mm. Lateral impact tests on the shoulder have been performed with a 23.4kg impactor, suspended on four wires, at 4.3m/s. The results are shown in Figure 5 together with the cadaver corridor. The dotted lines extend the corridor beyond the range of the cadaver tests.

New upper arms were built with the metal skeleton positioned towards the inner surface and with Sorbothane flesh, in order to reduce the inertia spike. It can be seen that for 90° impacts, the force-deceleration curves correspond to the cadaver corridor.

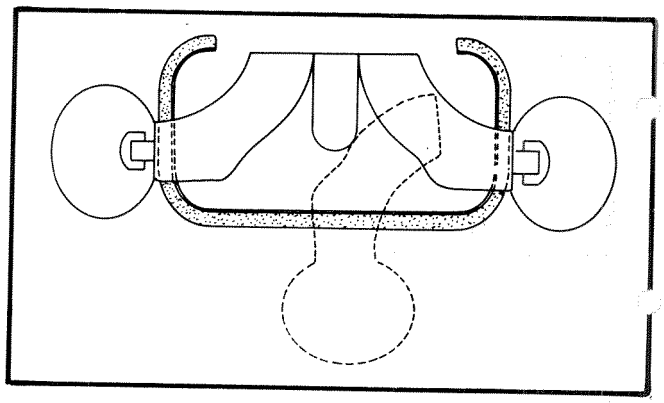

Figure 4. Diagram of shoulder cam (top view)

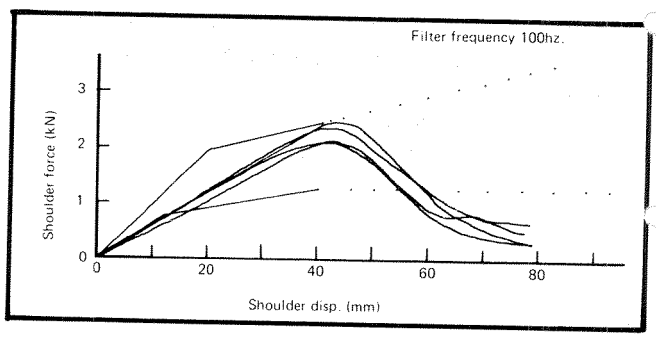

Figure 5. Force displacement results for lateral impacts to the shoulder with a 23.4kg pendulum at 4.3m/s

Table 5 shows the peak forces generated for non-impacts. It can be seen that the shoulder cam works well for perpendicular impacts and for impact directions aft of perpendicular. At impact directions of 10° or more of perpendicular, the peak force rises and the arm does not rotate forward.

Chest

The design requirements given(10) call for a chest divided into three separate regions or ribs, of which the deflection of each can be measured. There are three prime sources of cadaver reference tests that have been used as the performance basis for the chest. These are (i) the cadaver drop tests performed by the Peugeot-Renault Association(4) from which force-deflection and force-time corridors have been obtained(4,17,18), (ii) the impactor tests performed on cadaver tests by HSRI (now UMTRI)(8) from which impactor force and rib acceleration curves have been obtained, and (iii) the rigid and padded wall tests performed at Heidelberg for NHTSA(19), which give impact force, rib, and spine acceleration curves(20).

The APROD rib, piston, and cylinder concept for the chest mechanism has been adapted for the EUROSID chest. The pistons have been increased in length so the

Table 5. Peak shoulder force in pendulum impacts

Direction of impact	Perpendicular				Aft			Forward		
	90°	90°	90°	90°	100°	110°	120°	80°	70°	60°
Peak force (kN)	2.37	2.17	2.55	2.14	1.84	1.64	1.64	3.04	4.58	4.91

separation between the two bearings inside the cylinder is now much greater (Figure 6). This has eliminated the occasional occurrence of piston jamming seen with earlier designs. However, this has also meant that the chest can collapse from one side only. To make the dummy suitable for testing on both sides of a vehicle, the rib-piston assemblies are individual units that can be removed easily from the spine and inverted so the piston is now on the opposite side of the dummy. The three rib-piston assemblies are identical, which means they can be calibrated off the dummy and replaced individually if necessary.

A mathematical model of the thorax(21) was used to help with the development of the EUROSID chest. It became clear at an early stage that it was necessary to incorporate damping into the chest and also in the representation of the skin. The model used is shown in Figure 7.

The objective was to find appropriate values for the spring stiffnesses, damper coefficient, and rib mass that would match the model response to the three cadaver bases. Rib response was found to be critically dependent on the flesh characteristics and rib mass, but relatively unaffected by the rib spring and damper factors. Also thorax force-time curves were the only responses available for all three cadavar bases. Therefore, this was the response used primarily as the basis for selecting the chest spring and damper properties.

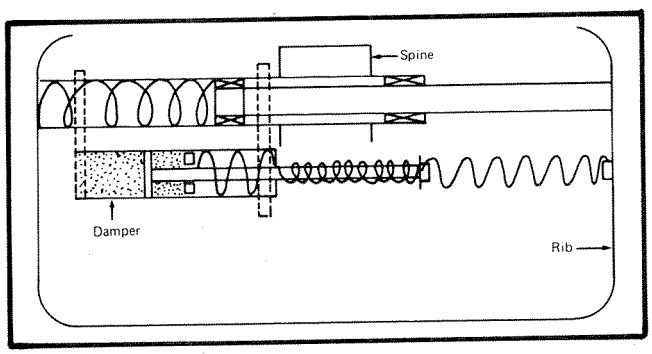

Figure 6. Diagram of rib—piston—damper module

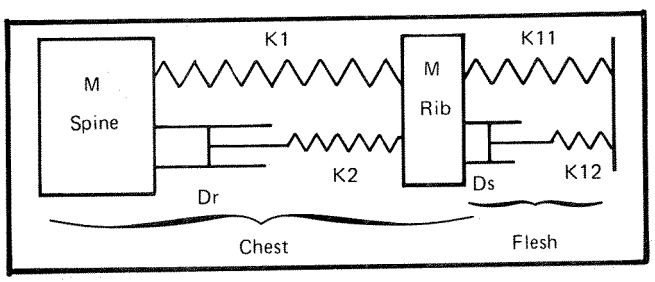

Figure 7. Mathematical model of thorax

Despite the incorporation of a damper into the model, no combination of springs and damper could be found that would give a good match to all three data bases. Either this representation of the thorax is too simple or the cadaver data bases are incompatible. Simulations using the model suggested that suitable initial values for these components would be K1 = 15kN/m, K2 = 30kN/m, and Dr = 250N/m/s.

Preliminary testing using a pendulum impactor showed that, mechanically, this design worked well. However, the provision of a pivot between the rib and piston made the thorax more sensitive to impact direction than if the link were solid. A supplementary leaf spring was provided behind the main rib to prevent plastic bending of the rib at this point.

Some difficulty was experienced in obtaining a suitable damper since most commercially available shock absorbers are carefully designed to produce a rising force coefficient with stroke. Armstrong Patents have developed a suitable adjustable damper by modifying a production model.

Simulations of the pendulum impact on the thorax suggested there would be a high inertia spike at the start of the impactor force curve, caused by the rapid acceleration required to raise the velocity of the rib over a very short period. This prediction was confirmed by the first pendulum impacts onto the thorax. The model showed this could only be reduced significantly by reducing the mass of the rib as much as practical or by the addition of an unrealistic amount of flesh to the side of the thorax. The effective mass of the ribs was reduced by replacing the solid steel pistons with hollow aluminum pistons. This inertia spike was further controlled by the use of 10mm sorbothane as flesh attached to each rib.

The deflection of each rib is measured by using a reflecting graticule attached to the piston and an optical transducer attached to the cylinder, following the method used on the APROD dummy.

The results of the HSRI cadaver tests using a 23.4kg impactor(8) have been normalised following the method

given by Mertz(17) adapted for a two-mass system. Performance corridors generated from these normalised curves, together with the impactor and spine accelerations measured in tests on the prototype thorax, are shown in Figures 8 and 9. As predicted by the simulation model for the spring and damper coefficients chosen, these values of thoracic acceleration rise above the maxima of the corridors. However, the pulse duration and general shape of the curves are in close agreement with the cadaver results.

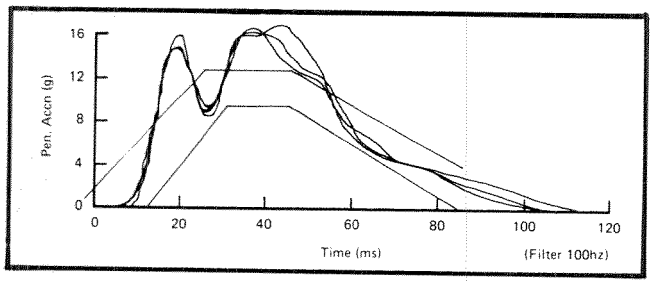

Figure 8. Acceleration of impactor striking prototype thorax at 4.3m/s compared with corridor derived from HSRI cadaver tests

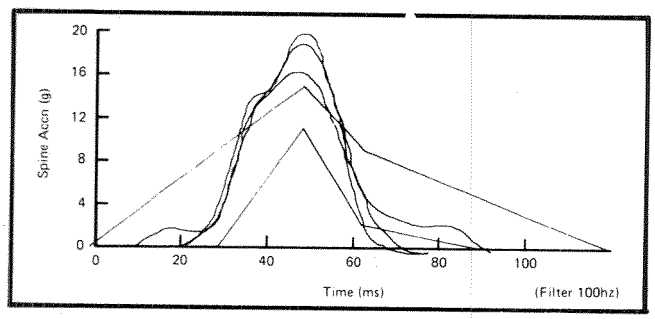

Figure 9. Spine acceleration for pendulum impacts to thorax at 4.3m/s compared with corridor derived from HSRI cadaver tests

Preliminary testing with the first prototype thorax attached to a Part 572 pelvis and legs, following the procedure used in the Heidelberg study(19,20), showed some anomalous results. The spine acceleration in the 15m/h (6.7m/s) and 20m/h (8.9m/s) rigid wall tests showed two distinct pulses. Close examination of the relative times of the spine acceleration and the rib acceleration and displacement showed that the first spine acceleration pulse occurred before the rib-piston springs had compressed (Figures 10 and 11), suggesting that the shoulder might be transmitting a significant force to the spine. A repeat of the test at 15mi/h (6.7m/s) with the shoulder held forward produced a spine acceleration duration that was much closer to cadaver results(20), although the amplitude was slightly too high compared to the cadavers (Figure 12).

It appears that, at impact speed of 15mi/h (6.7m/s) or greater, while the shoulder does rotate forward, it does

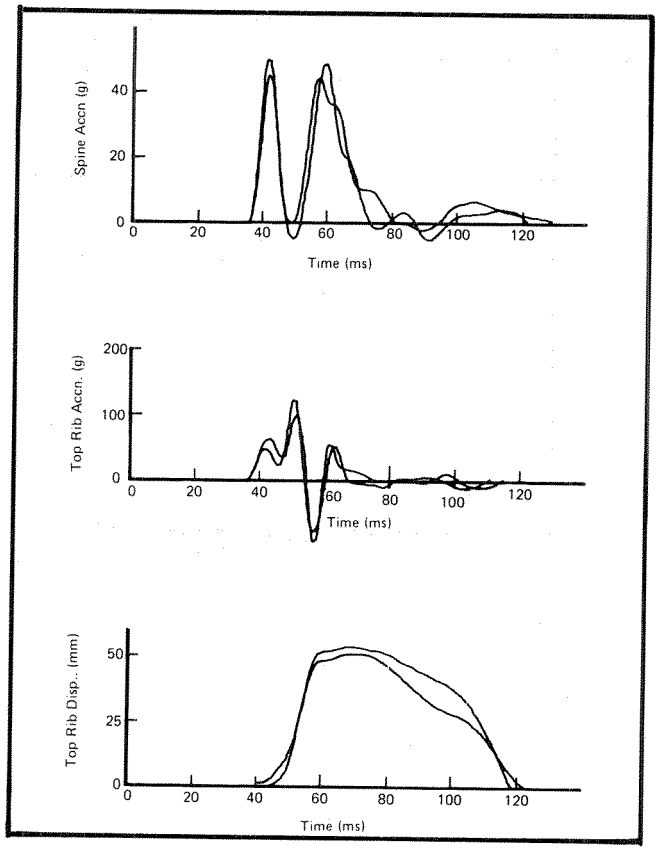

Figure 10. Rigid wall test on EUROSID thorax—15m/h

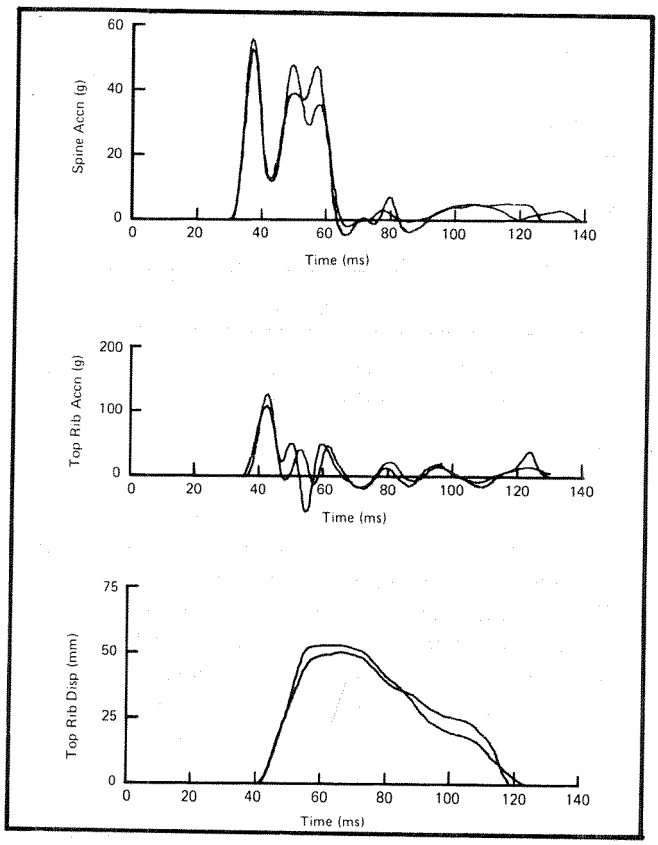

Figure 11. Rigid wall test on EUROSID thorax—20m/h

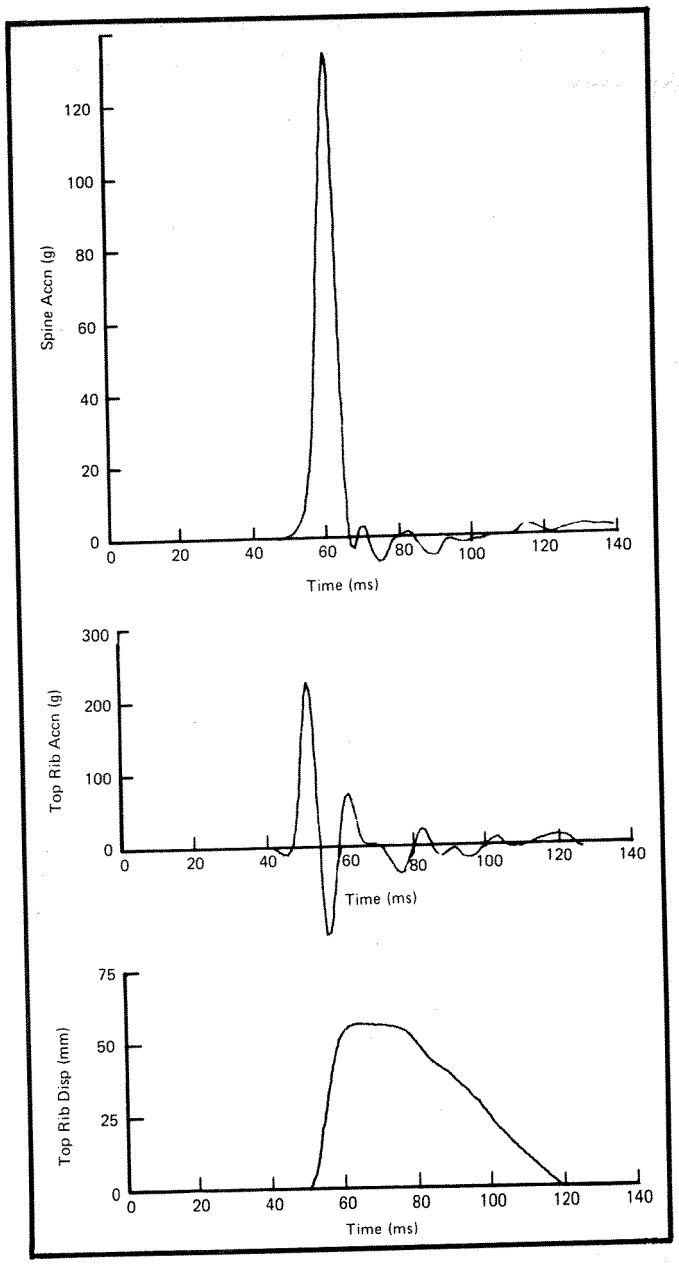

Figure 12. Rigid wall test on EUROSID thorax with shoulder rotated forward—15 mi/h

not do so sufficiently rapidly if the whole torso, including the shoulder, strikes a flat rigid plate.

This shoulder-induced spike was not observed in a 15m/h (6.7m/s) padded impact where the APR padding block top surface was below the shoulder. It should be noted, perhaps, that in most vehicles, the shoulder will be in the area of the side glazing and above the metal structure of the door.

A revised prototype thorax is under construction with more accurate dimensions and mass, and this will be tuned to the published cadaver data.

Remarks on the Thorax

A prototype thorax has been constructed whose shoulder can rotate forward, taking the arm clear of the side of the chest and with a rib cage that can measure deflection on three individual rib units. The chest is tuneable by means of replaceable springs and adjustable dampers, and can withstand repeated 20m/h (8.9m/s) rigid wall impacts without failure or jamming.

Abdomen

The abdomen section for the EUROSID side impact dummy should interact in a humanlike manner with any structural component of a tested car in a side impact to assure correct kinematics of the complete dummy (biofidelity). In addition, the abdomen section must measure the injury parameters or detect exceedance of the set human tolerance limits (measurement function)(10,22). The EUROSID abdomen has been designed by TNO on the basis of lateral drop tests of various cadavers impacting a rigid armrest, which were performed by the Association Peugeot-Renault(23,7).

Peugeot-Renault defined from the cadaver tests a force-deflection corridor that is valid for the mid-abdomen (120mm space between lower rib and iliac wing of pelvis) impacted by a 7cm-wide flat armrest at a velocity of 6.3mi/s. They also established tolerance values of a maximum force on the abdomen of 4,500N and a maximum allowed penetration of 40mm, both corresponding with an AIS 3 value(22). These formed the design requirements for the hardware (Figure 13).

The principle of the EUROSID abdomen section is a metal drum that is rigidly attached to the lumbar spine-thorax box interface of the dummy. This drum is covered by a flexible material up to the outside contour of the abdomen that allows a penetration of 40mm before "bottoming out". Between this flesh-simulating material

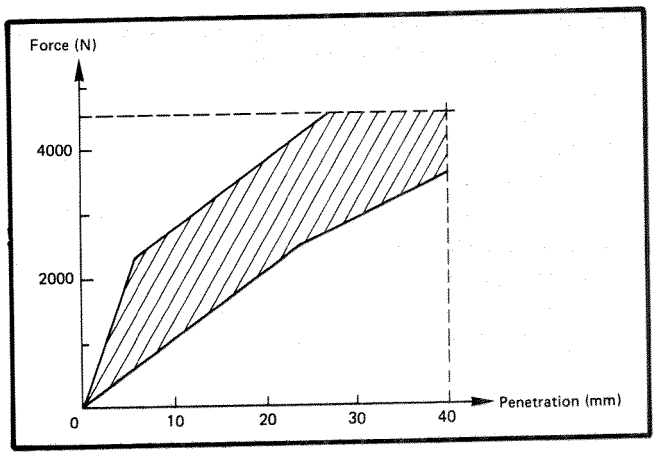

Figure 13. Force-deflection corridor for abdomen section, based on APR cadaver tests

and the rigid drum are located three vertical steel leaf-spring switch units. These switch units can be individually adjusted to trigger at an externally applied force level of 4,500N.

To obtain correct biofidelity up to the point at which the tolerance levels are exceeded, it was necessary to add to the flesh-simulating polyurethane foam a certain amount of mass. This mass is obtained by moulding a total of 1.5kg of small lead pellets in the outside contour at the impacted side (Figure 14). The resulting force-deflection response is then of a degressive form fitting into the design corridor. The first series of prototypes as described by Maltha(7) were tested by various laboratories in Europe and the United States. These tests showed some shortcomings with respect to the response and interference of the mass-carrying rubber/lead slab in side bending of the dummy.

For this reason and to obtain a better interfacing with the EUROSID pelvis and thorax sections, the abdomen has recently been completely redesigned. This redesigned abdomen has not yet been tested, but there is good confidence that the response will be in the design corridor and the switches can be easily calibrated to the correct force-trigger level.

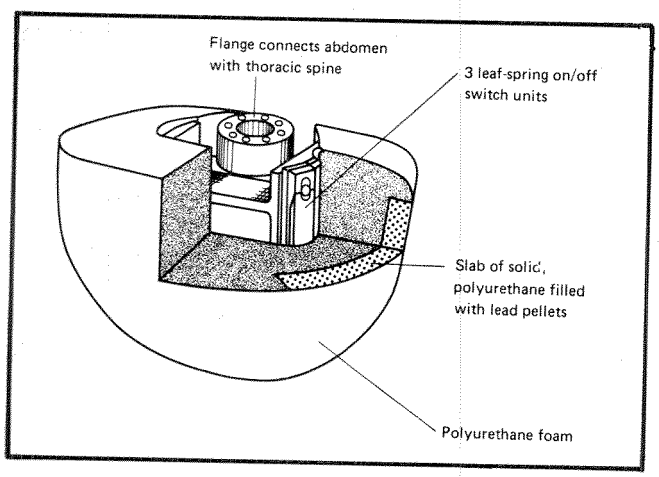

Figure 14. TNO abdomen section with lead pellets on impacted side

Pelvis

Main Specifications for the Pelvis of the EUROSID Dummy

The external shape of the pelvic bone should be realistic the legs of the Part 572 dummy at the level of the upper extremities of the femur force transducer and to the torso at the lower extremity of the Part 572 lumbar spine.

The external slope of the pelvic bone should be realistic and, especially, it must be representative of the shape of the human pelvis at the points directly involved in a side impact and at the interactions with the car seat as well as at the iliac crests where the seatbelt fits around the pelvis. Its design should consider the deformation capability of the pelvis bones as well as of the flesh.

The motion capability of the femurs relative to the pelvis is considered of great importance, and an abduction of 30° seems the value to be considered in the design of the hip joint.

The EUROSID should permit the measurement of pelvic acceleration, if possible, at the same locations as on the Part 572.

The flesh in the area at the side of the pelvis liable to be struck should be sufficient to comply with the likely requirements and sufficiently durable that it should not deteriorate significantly during many impacts.

Design of the EUROSID Pelvis

The geometry of the pelvic girdle was analyzed by Reynolds et al., and this study was followed by a plaster model of the 50th percentile male pelvis(24).

The shape of the EUROSID pelvic bones is based on this model: Figure 15 shows the EUROSID pelvic bone.

The external shape and the important points such as the pubic symphysis, the H point, and the center of L1 are in the same location on the EUROSID pelvis as on the human pelvic model. The hip articulation of the EUROSID pelvis is intentionally different from the human one: to minimize the effect of the leg position on the pelvic loading, the external forces are transmitted to the pelvis along an axle passing through the hip ball joint. To increase the energy absorption capability, the EUROSID pelvis has the part of the flesh that is directly compressed by the impact made from Sorbothane.

The EUROSID pelvis is designed to measure pelvic compressive forces as well as pelvic acceleration. The compressive force is measured in the pubic symphysis area with a force transducer and on the iliac wing with a strain gauge. The pelvic acceleration is measured at the same location as on the Part 572 dummy.

Results of Validation Tests

The new pelvis of EUROSID was tested in conditions similar to the cadavers used for pelvic tolerance study in side impacts(25).

A series of eight tests at four different speeds (25, 30, 35, and 40km/h) were conducted with the same impactor used for cadaver tests.

Test results show a great sensitivity of the pubic force to the increasing of the impactor speed. When the impactor speed increases from 25 to 40km/h, the maximum of the pubic force is increased by 260 percent. This is important because in side impacts the speed of the side

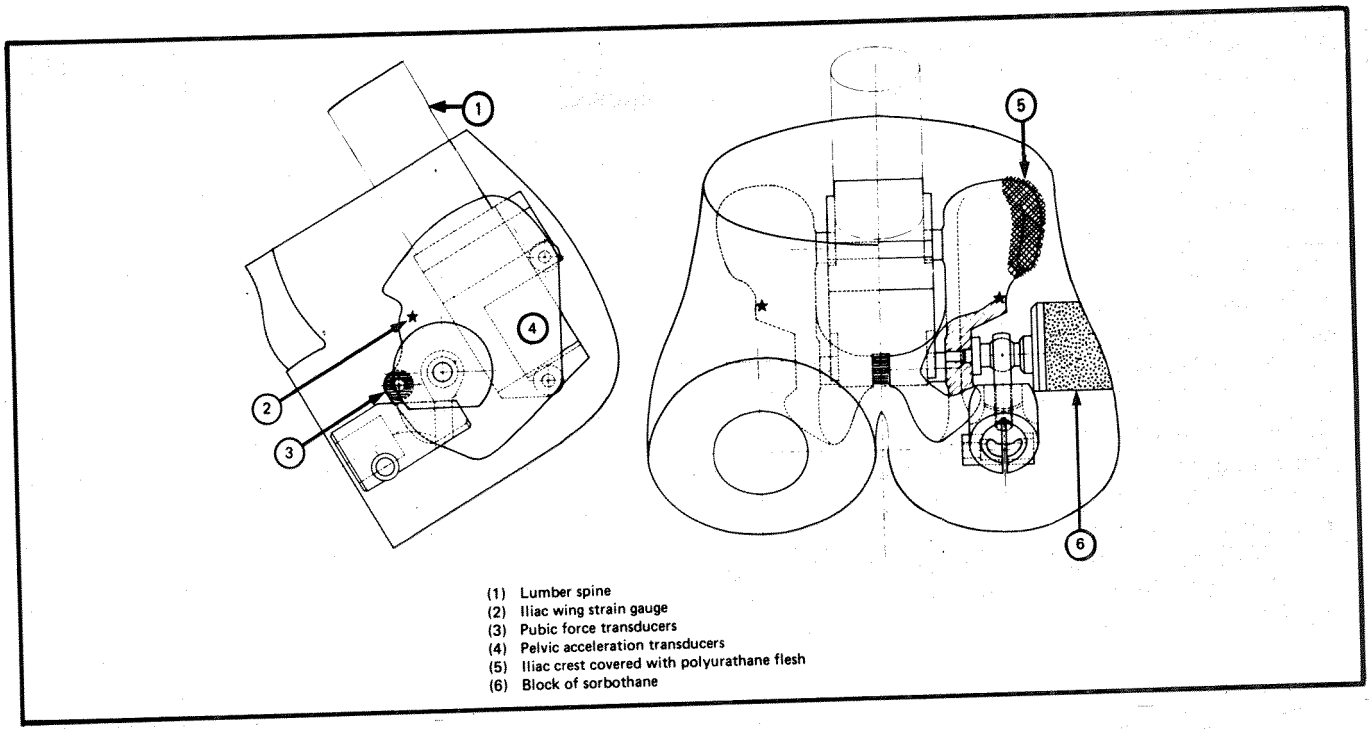

Figure 15. EUROSID pelvis diagram

panel at the time of contact with the occupant is the parameter that is considered related to the severity of the impact, and the motion of this side panel is simulated by the impactor.

The only parameter that was recorded on dummies and on cadavers in all the tests is the transverse pelvic acceleration. Figure 16 presents the maximum values of pelvic transverse acceleration of cadavers and side impact dummies relatively to impact speed. This figure shows clearly that the EUROSID pelvis sustained for the same impact speed a higher acceleration than the cadavers but lower than the other side impact dummies. Moreover, the repeatability of results seems better for the EUROSID: for the three tests conducted at 35km/h, the average of maximum pelvic acceleration is 149.37g and the corresponding standard deviation 4.96g (3.3 percent). For the other dummies, the values vary from 4.88 percent for the ONSER dummy to 9.93 percent for the DOT-SID.

The first tests performed with a dummy fitted with this pelvis show that—

1. The compressive force recorded on the pelvis is directly related to the impact speed.
2. Compared to cadavers, the EUROSID pelvis gives higher injury parameter values but clearly lower values than other side impact dummies.
3. Although the evaluation of durability and repeatability needs a larger number of tests, the pelvis sustained 25 impacts at a speed range of 25 to 40km/h without any damage either to the skeleton or to the flesh, and three tests performed at the same conditions gave very close results.

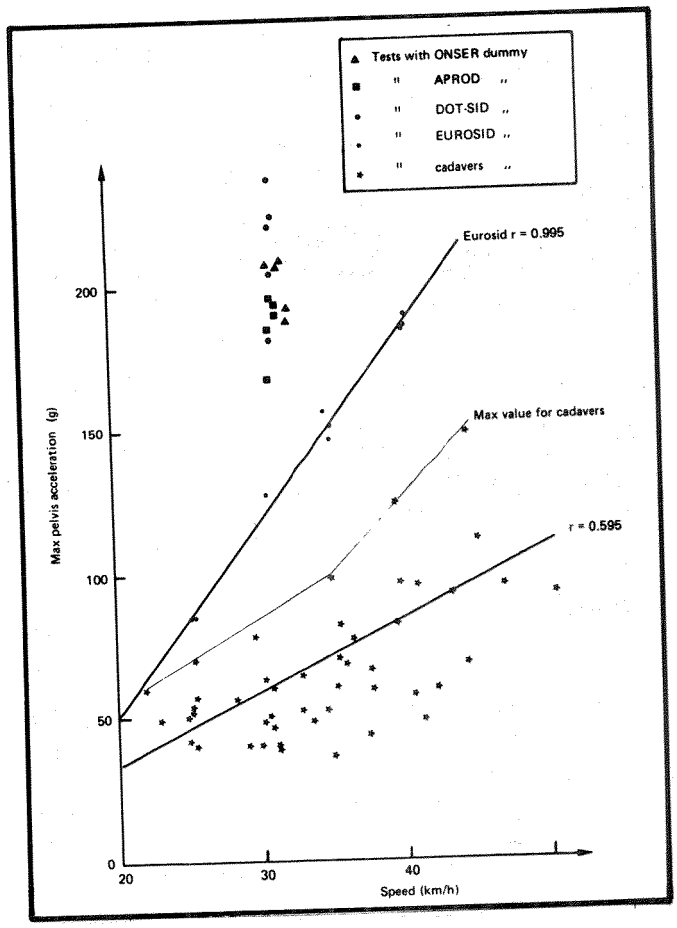

Figure 16. Pelvis acceleration versus impact speed tests with circular impactor

Conclusion

A prototype side impact dummy has been constructed from a basis of accident investigation, biomechanical studies, and the experience gained from the development and evaluation of three side impact dummies carried out in the EEC Biomechanics Programme 1978-1982. The EUROSID dummy is capable of measuring potential injury risk to the head, thorax, abdomen, and pelvis. Although test experience may suggest one or two final adjustments to the design, it may be agreed this has been a successful collaborative effort between laboratories within Europe coordinated by the EEVC Ad-Hoc Group on Dummies.

The prototype has been constructed from components produced in France, the Netherlands, and the United Kingdom, together with a head and legs purchased from the United States. This prototype will now be evaluated as a complete dummy and refined to a state where it will be usable in legislative tests, such as that proposed by ECE, and other side impact tests.

References

1. *The Future for Car Safety in Europe*, A report of the European Experimental Vehicles Committee, Proceedings Fifth International Technical Conference on Experimental Safety Vehicles, London, 1974.
2. Harris, J., "The design and use of the TRRL side impact dummy," Proceedings 20th Stapp Car Crash Conference, SAE Paper 760802, 1976.
3. EEC, "Biomechanics of impacts in road accidents," Proceedings of Seminar, Brussels, March 1983 (ed. T.E.A. Benjamin).
4. Fayon, A., C. Tarrière, G. Walfisch, M. Duprey, and H. Balthazard, "Development and performance of the APR dummy (APROD)," Proceedings Eighth International Technical Conference on Experimental Safety Vehicles, Wolfsburg, 1980.
5. Cesari, D., and R. Bouquet, "Design of ONSER side impact dummy," Proceedings EEC Seminar on Biomechanics of Impacts in Road Accidents, Brussels, 1983.
6. Haslegrave, C.M., and J.A. Searle, "Design of MIRA side impact dummy," Proceedings EEC Seminar on Biomechanics of Impacts in Road Accidents, Brussels, 1983.
7. Maltha, J., and E.G. Janssen, "Design of injury detecting abdomen section for side impact dummies," Proceedings EEC Seminar on Biomechanics of Impacts in Road Accidents, Brussels, 1983.
8. Melvin, J.W., D.H. Robbins, and J.B. Benson, "Experimental application of advanced thoracic instrumentation technique to anthropomorphic test devices," Proceedings Seventh International Technical Conference on Experimental Safety Vehicles, Paris, 1979.
9. Maltha, J., and E.G. Janssen, "EEC comparison testing of four side impact dummies," Proceedings EEC Seminar on Biomechanics of Impacts in Road Accidents, Brussels, 1983.
10. Neilson, I.D., and R.W. Lowne, "Some design requirements for side impact dummies intended for legislative testing and research," Proceedings 1984 International IRCOBI Conference, Delft.
11. Griffiths, D.K., J.M. Breen, P.D. Thomas, and S.D. Lawson, *Investigation of a Representative Sample of Real World Side-Impacts to Cars,* Final Report, EEC BiFLechanics Programme, Phase III Project UK1, University of Birmingham, 1983.
12. Cesari, D., M. Ramet, and J. Bloch, "Influence of arm position on thoracic injuries in side impact," Proceedings 25th Stapp Car Crash Conference, SAE Paper 811007, 1981.
13. Ewing, C.L., D.J. Thomas, L. Lustick, W.H. Huzzy, G.C. Willems, and P. Majewski, "Dynamic response of the human head and neck to +Gy impact acceleration," Proceedings 21st Stapp Car Crash Conference SAE Paper 770928, 1977.
14. Peugeot S.A./Renault, *Development of a More Convenient Dummy Than the Part 572 One for Side Collisions*, Final Report, EEC Biomechanics Programme Phase III, Project F10, 1981.
15. Benjellal, F., D. Gillet, C. Got, A. Patel, Y.C. Leung, S. Casson, C. Tarrière, and G. Walfisch, "Development of a dummy neck for lateral collision," Proceedings Tenth International Technical Conference on Experimental Safety Vehicles, Oxford, 1985.
16. Lowne, R.W., and A.K. Roberts. "Measurement of shoulder width reduction under side force," Appendix to "Design of MIRA Side Impact Dummy" by Haslegrave and Searle, Proceedings EEC Seminar on Biomechanics of Impacts in Road Accidents, Brussels, p.3578, 1983.
17. Mertz, H.J., *A Procedure for Normalising Impact Resource Data,* SAE Government/Industry and Exposition, Washington, D.C., SAE Paper 840884, 1984.
18. Krause, P.L., *Normalisation of Side Impact Cadaver Dynamic Response Data Utilizing Regression Techniques,* SAE Government/Industry Meeting and Exposition, Washington, D.C., SAE Paper 840883, 1984.

19. Kallieris, D., R. Mattern, G. Schmidt, and R.H. Eppinger, "Quantification of side impact responses and injuries," Proceedings 25th Stapp Car Crash Conference, SAE Paper 811009, 1981.
20. Eppinger, R.H., J.H Marcus, and R.M. Morgan, ATTAD for unrestrained left-front occupants by principal direction of force (percentages denote proportion of horizontal force IPR in each direction)
21. Langdon, M.G., "Modelling the lateral impact of the thorax in side impact accidents", Proceedings Tenth International Experimental Safety Vehicles Conference, Oxford, 1985.
22. Walfisch, G., A. Fayon, C. Tarrière, J.P. Rosey, F. Guillon, C. Got, A. Patel, and R.L. Stalnaker, "Designing of a dummy's abdomen for detecting injuries in side impact collisions," Proceedings 5th International IRCOBI Conference, Birmingham, 1980.
23. Maltha, J., and R.L. Stalnaker, "Development of a dummy abdomen capable of injury detection in side impacts," Proceedings 25th Stapp Car Crash Conference, SAE Paper 811019, 1981.
24. Reynolds, H.M., C.C. Snow, and J.W. Young, "Spatial geometry of the human pelvis," Memorandum Report AAC-119-81-5.
25. Cesari, D., M. Ramet, and P.Y. Clair, *Pelvis and Femur Human Tolerance in Side Impact,* Final Report, EEC Biomechanics Programme, Phase III, Project B2F3, 1980.

Advanced Anthropomorphic Test Device Concept Definition

John W. Melvin
The University of Michigan

Abstract

This paper summarizes the results of Phase 1, Concept Definition, of the AATD program and identifies the reasons such a new test device is needed. The following areas are addressed: (1) injury priority from accident data; (2) current dummy design, use, and potential improvements; and (3) technical characteristics and design concepts for a new AATD, its data processing, and its certification systems.

Overview

Phase 1 of the AATD program[1] has shown that there is a need to develop a new anthropomorphic test device that has humanlike response in frontal through lateral as well as rollover impact directions, interacts realistically with restraint systems and the vehicle interior, is capable of making numerous meaningful measurements of injury assessment, is durable and easily maintained, and can be certified without disassembly. Because of the necessary time lag between design and production, current dummies are not based on currently available data. A greatly improved and expanded biomechanical data base has been developed in Phase 1, and these data form the basis for defining impact response characteristics necessary to insure that the AATD will perform in a humanlike manner.

The new dummy will have significant advantages over current ATD's. First, its shape in the seated configuration will be based on actual mid-sized-male-seated anthropometry, which will contribute to more realistic interaction with the vehicle seat and other components. Second, it will have biofidelity in frontal, oblique, lateral, and vertical impacts, to be achieved through such features as a deformable face, a multidirectional neck and chest, and a flexible thoracic spine. Thus, only one dummy will be needed for crash-testing purposes, and it will give realistic trajectory, contact-point, and loading results. Its humanlike response will also allow many more meaningful engineering maesurements to be made, which will in turn greatly enhance injury assessment capability. Next, its materials will be durable, and its designs will be rugged and repeatable but cost-effective to manufacture. Materials will be selected to minimize the sensitivity of the AATD to temperature variations. Finally, the certification process will be more efficient and repeatable between laboratories, to be achieved through the use of a whole-body certification fixture with a dedicated data processing system.

[1] Primary participants in this program include N.M. Alem, O. Carsten, J. O'Day, D.H. Robbins, and K. Weber of the University of Michigan; P. Begeman, R. Cheng, A.I. King, and G.W. Nyquist of Wayne State University; R.H. Arendt, P.M. Miller, and D.J. Segal of MGA Research Corporation; J. Smrcka of Alderson Research Laboratories, Inc.; R.H. Eppinger and M. Haffner of the National Highway Traffic Safety Administration.

In the following sections, the results of various aspects of this program are summarized. First, we describe an analysis of accident data to determine the priority of injuries to be addressed, based on estimated cost to society. Then we present findings on the design and use of current ATD's along with suggestions for how dummies could be improved. Finally, we summarize the technical characteristics and design concepts proposed for the new AATD and for its data processing and certification systems.

Another major task in the AATD program, not summarized here, was a review of literature on biomechanical impact response and injury in the automotive environment. This review incorporates published research available through the end of 1984 and includes chapters on the head, spine, thorax, abdomen, pelvis, and lower extremities. Each chapter addresses the anatomy, clinical injury experience, and results of laboratory impact studies for the various regions. The experimental studies include information on biomechanical response to impact as well as injury mechanisms, tolerance, and criteria. For the full review, see Melvin and Weber(1).

Injury Priority Analysis

An analysis of the National Accident Sampling System (NASS) data for 1980 and 1981 places the cost of individual or aggregated groups of injuries in perspective relative to the cost of society for all AIS 2-6 injuries to automobile occupants. The NASS files were first augmented to incorporate an impairment factor that goes beyond the Abbreviated Injury Scale (AIS) by taking into account the consequences of an injury as determined by two panels of physicans as well as a percentage impairment based on American Medical Association guidelines(2). Then a factor was generated from an economic cost model to account for expected lifetime earnings had an individual person not been injured. The impairment factors for the actual NASS injuries were multiplied by the expected earnings factors for individual injured persons to create an Injury Priority Rating (IPR). These IPR's were then aggregated by body region, direction of force, and delta V and expressed in terms of a percentage of total IPR. Tables 1 through 3 show these distributions, which indicate the relative contribution of each grouping of injuries to the total societal cost of injuries to automobile occupants. It should be noted that the occupants sustaining these 2,262 injuries were nearly all unrestrained.

The primary conclusions from these and further bivariate analyses are as follows:

1. The combination of the head, face, and neck body regions accounts for 60 percent of the IPR to passenger car occupants.

Table 1. IPR distribution by body region

Body Region	Distribution (%)	Body Region	Distribution (%)
Head	44.6	Ankle/Foot	0.6
Face	10.5	Lower Limb	0.0
Neck	5.1	Upper Arm	1.3
Shoulder	0.3	Elbow	0.5
Chest	18.9	Forearm	1.3
Back	1.6	Wrist/Hand	0.4
Abdomen	7.5	Upper Limb	0.3
Pelvis	1.1	Whole Body	0.9
Thigh	2.1	Unknown	0.2
Knee	1.6		
Lower Leg	1.0	TOTAL	100.0

Table 2. IPR distribution by direction of force

Direction of Force	Distrubution (%)	Direction of Force	Distribution (%)
1 o'clock	4.8	9 o'clock	3.3
2 o'clock	9.8	10 o'clock	7.9
3 o'clock	3.5	11 o'clock	5.0
4 o'clock	0.0	12 o'clock	36.9
5 o'clock	0.1	Nonhorizontal	16.1
6 o'clock	0.7	Unknown	10.4
7 o'clock	0.3		
8 o'clock	1.2	TOTAL	100.0

Table 3. IPR distribution by delta V

Delta V	Distribution (%)	Delta V	Distribution (%)
1-5 mph	0.1	41-45 mph	1.5
6-10 mph	0.6	46-50 mph	0.0
11-15 mph	2.0	51-55 mph	2.7
16-20 mph	4.3	>55 mph	3.8
21-25 mph	7.0	Unknown	68.9
26-30 mph	4.9		
31-35 mph	2.6	TOTAL	100.0
36-40 mph	1.5		

2. The combination of the chest, back, and abdomen body regions accounts for 28 percent of the IPR to passenger car occupants.
3. Over one-third of driver IPR occur from collisions with a 12 o'clock direction of force. One-fifth result from collisions with nonhorizontal directions of force.
4. Oblique side collisions account for more IPR than direct side collisions. This applies both to drivers and to right-front passengers. Thus, 9 o'clock collisions account for 4.3 percent of

driver IPR but 10 and 11 o'clock collisions account for 11.9 percent. Similarly, 3 o'clock collisions account for 9.4 percent of IPR to right-front passengers; 1 and 2 o'clock collisions account for 19.2 percent.

5. Using only known values of delta V, 84 percent of the driver IPR with a 12 o'clock direction of force result from severe crashes, i.e., those with a delta V greater than 20mph. For right-front passengers, the figure is 97 percent. However, it should also be noted that, for cases with known delta V, 81 percent of driver IPR and 77 percent of right-front passenger IPR was attributable to crashes with a delta V of 45mph or less.
6. Again, using only cases with known delta V, 66 percent of driver IPR for injuries to the head, face, and neck result from severe crashes. For injuries to the chest, back, and abdomen, the comparable figure is 81 percent; for injuries to the upper extremities, 45 percent; and for injuries to the lower extremities, 93 percent. Thus, one might conclude that, for drivers, serious injuries to the upper extremities are the easiest to prevent because a higher proportion of them occur in less severe crashes. Next would come the combination of the head, face, and neck, followed by the combination of the chest, back, and abdomen, and last the lower extremities.
7. Comparison of IPR with the earlier Harm model(3) indicated that the two models were in complete agreement in assigning relative priority to the directions of force in the 1980 and 1981 NASS data. When ranking body regions, however, the IPR model gives higher priority to the head, face, and neck, and correspondingly less prominence to the chest, abdomen, and extremities. This is because of the relatively severe long-term consequences of injury to the head, face, or neck.

Because of limitations in the data, it was not always possible to depict, to the extent desired, the crash environment in which the IPR to the various body regions was incurred. In particular, the high rates of missing delta V meant that analysis of crash severity was often not possible. Another concern is with the comparatively small number of occupants in the NASS files that sustain serious injuries. The 1980 and 1981 NASS files combined have only some 2,262 injuries of severity AIS 2 or greater to passenger car occupants.[2] These injuries are sustained by 1,262 occupants. There are a total of 15,378 passenger car occupants in the combined 1980 and 1981 files. Thus, 92 percent of the occupants sustain no injuries, injuries of AIS 1, or injuries of unknown severity.

[2] This figure includes some injuries originally coded with an AIS of 7.

One solution to the shortage of cases for analysis is to incorporate additional years of NASS. It is hoped that the 1982 NASS data can be added to the existing data structure so the analyses reported here can be run with additional confidence and perhaps be extended to include such issues as contact point in more detail. Another solution would be to revise the threshold for the inclusion of cases in the NASS system or to sample at higher rates cases in which injuries greater than AIS 1 are sustained. Such a revised sampling scheme could be combined with reducing the amount of investigation carried out on cases with no injuries or minor injuries.

Finally, the reader should bear in mind that the model used here is not completely satisfactory. In particular, it does not take into account the fact that a single person may have sustained more than one injury. It is hoped to pursue the development of a multi-injury model in the future.

For further details on this analysis, see Carsten and O'Day(4).

Review of Dummy Design and Use

Dummy User Survey Results

A survey of users of the Part 572 and Hybrid III dummies was taken to determine the problems these users have encountered and their preferences for changes and improvements in dummy design. General topics included mechanical design, serviceability and maintenance, durability, certification, repeatability and reproducibility, and ease of use. The survey questionnaire was made available to a wide audience through NHTSA, SAE, ISO, and various individual contacts.

Responses were received from 38 individuals representing 29 organizations. The affiliation of the 38 respondents can be categorized as follows:

7	U.S. vehicle industry
9	Foreign vehicle industry
12	U.S. government
4	Foreign government
2	Dummy manufacturing
4	Independent research

Throughout the responses to this survey, a strong emphasis was placed on the need for a durable, stable, and repeatable test device, even at the expense of biofidelity. The lack of enthusiasm for an omnidirectional dummy, expressed by several respondents early in the survey, seemed to be based on an assumption that such a dummy could not be made to be as repeatable and reliable as a unidirectional test device, while retaining a suitable simplicity of design. Comments in later sections of the survey clearly indicated that considerable time and effort were required to prepare the Part 572 dummy for

testing, and that between-test repair, replacement, adjustment, and recalibration were frequent necessities. As the survey proceeded from theoretical design to more hands-on issues, the number of respondents decreased, but the conviction and level of detail of responses increased.

Respondents were generous with their advice as to how life with an anthropomorphic test device could be made easier. Designed-in means were needed for holding onto various parts of the dummy for transporting, positioning, and storage and for holding it fixed in space for certification tests. Also needed were visible indicators of the dummy's internal structural configuration and segment centers of mass. Joints were singled out as the assemblies in particular need of redesign. In addition, it was made clear that the performance characteristics of a dummy must be built up from the smallest components, but that performance checks of components in their assembled state were also necessary.

After reviewing the responses of this international group of dummy users, the term "advanced" in AATD begins to take on a broader meaning. Not only is there an opportunity here to advance the state of the art with regard to humanlike response and innovative instrumentation techniques, but there is a necessity to make significant design and materials improvements that will result in a more durable, repeatable, and trouble-free dummy.

Anthropometric Data and Biomechanical Response Simulation for AATD Design

This section indicates the anthropometric data available for use in developing design specifications for an AATD. The use of these data is also demonstrated in a limited simulation of dummy response using the CAL-3D crash victim simulation code(5). The parameters of particular interest are those associated with spinal flexibility and shoulder mobility, which are shown to play a major role in controlling torso and head motions and applied forces.

Anthropometric Data

Several data resources are available from the recently completed dummy anthropometry project on contract DTNH22-80-C-07502(6). These include mass and inertial properties, body surface shape, seated posture, estimations for the location of the bony structure, joint locations, and range of motion at the various joint structures. These data are all static and are for a midsized male driver in an average vehicle-seated posture. Mass and inertial properties are given for a traditional linkage and segmentation of the body in the static-seated posture. The mechanical term "linkage" implies the available data are most applicable to dummies or simulations based primarily on rigid-body mechanical models. The dummy response simulation presented later uses a lumped-mass, chain-linkage, dynamic simulation software package consisting of rigid masses connected at joint structures.

Details are given in the full report(7) of the body linkages used in the simulation, as well as data sources and methods for determining the segmentation of the shoulder, neck, thoracolumbar spine, and thorax. Of particular importance are (1) the division of the traditionally rigid thorax into one rib cage, three spinal, and two shoulder segments, and (2) the approach of coupling the rib cage to the spine to achieve mobility and rotation of the thorax with respect to the spine.

Mobility and range-of-motion data are in fair supply only for static mobility and voluntary motion. In other words, it is possible to estimate how far the segments can move with respect to each other before subjects say "ouch" or before outside forcing agents must be supplied to produce further motions. Similar quantitative data for dynamic mobility (dynamic motions voluntarily made or those that occur under the influence of an outside forcing agent, such as a deceleration device) are virtually nonexistent, except for the neck and, perhaps to a more limited extent, for the thoracic and lumbar spines. Dynamic torque data are not yet available for the thoracic and lumbar regions.

Other data necessary for simulating a dummy in a crash environment include force-deformation characteristics of various body regions and data on the crash event itself. Data sources included project literature reviews, accident data analyses, and vehicle specification packages.

Regarding the status of the anthropometry data base, it was concluded that the mass and postural data are available, but body segmentation needs to be refined to include spinal and shoulder girdle masses. The data base on joints also needs to be expanded to provide torque on joints versus relative angle of the segments. The most pressing need is for additional information on spinal flexibility and torsion properties.

Biomechanical Response Simulation

The purpose of this analysis was to study the effects of spinal and shoulder flexibility on whole-body response. Degrees of freedom not found in current dummies were added to the linkage model. Comparative results for stiff and flexible joints between the thorax components are presented for belted and unbelted occupants.

Figure 1 shows the difference in head excursion for 3-point-belted occupants with a flexible three-link thoracic spine versus a stiffer linkage similar to that used in current dummies. The positions are those at 100ms, and the more restricted forward head excursion with the stiff joints is apparent. For the unbelted case, there was a

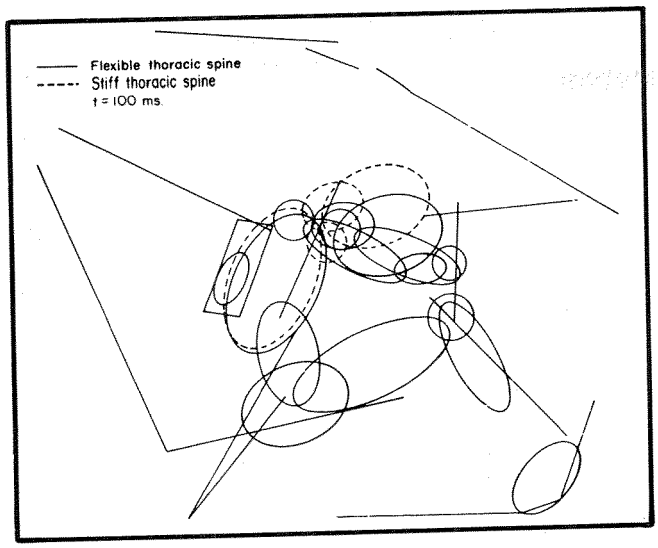

Figure 1. Effect of thoracic spine flexibility, belted case

marked reduction in the force of interaction between the thorax and the steering wheel when the shoulder masses were uncoupled from the thorax, even when the spine remained stiff.

It is clear from these exercises that crash victim simulation software can be used to study the effects of changing dummy design parameters. Specifically, it was shown that the addition of thoracic spinal flexibility has major effects on the crash victim motion. This is particularly noticeable in head excursion increases of several centimeters for belted occupants. In addition, it was shown that the uncoupling of the shoulder masses from the thorax has a major effect on the interactions of a crash victim with vehicle structures forward of the occupant, such as the steering column and the instrument panel.

ATD Critique

A review of current ATD designs was made from the standpoint of biofidelity, measurement capability, directionality, and impact testing performance. Details by body region can be found in Melvin et al.(7). Although a wide variety of currently available test devices was reviewed, primary emphasis is given here to the Hybrid III and the Side Impact Dummy (SID), since they represent test devices currently in use in research and development testing in the United States.

The Hybrid III was developed over 10 years ago, and its design is based on biomechanical knowledge available at that time. It is a frontal-loading-only ATD whose design represents an evolutionary improvement over conventional ATD design. For example, the rib cage uses the same design as the previous Hybrid II, but with altered structural stiffness to produce a humanlike impact response to midsternal moving-mass impactors. The Hybrid III also possesses humanlike hard-impact forehead response and midsagittal neck bending response. As presently configured, the Hybrid III has the greatest measurement capability of any ATD, with 44 data channels.

The SID was developed more recently than the Hybrid III and represents a modification of the chest region only in an otherwise standard (nonbiomechanical) ATD. The SID was developed to provide lateral chest response biofidelity under rigid and padded impacts. The shoulder response is included in the chest response, and, as a result, the design has no separate shoulder structure. The remainder of the SID structures are standard Part 572. Except for additional chest wall accelerations and lateral chest displacement, the SID has the same measurement capabilities as the Part 572 ATD.

Both the Hybrid III and the SID are examples of ATD's intended for use in restricted test conditions and/or directions, and as such they have only limited biofidelity in the principal directions and none in other directions. One of the most serious deficiencies of both ATD's centers around the designs of the thoraxes, both the rib cages, and the spines. The IPR analysis has indicated the great importance of the head and chest as primary sources of injury, disability, and death of unrestrained occupants. The development of effective countermeasures to minimize injury to these regions depends strongly upon having an ATD that produces realistic responses in terms of trajectories, contact points, and loadings. The combination of rigid thoracic spines with present neck designs (including that of Hybrid III) and inadequate thoracic rib-cage conformability are producing head contacts and chest/steering-system interactions that are quite unlike those in real-world crashes. All present ATD designs are quite inadequate in this respect in the crucial head/torso regions for frontal, lateral, and oblique impacts. The lack of realistic concentrated load response in the Hybrid III and SID chests is compounded for the case of shoulder-belt loading. Neither chest exhibits humanlike stiffnesses at the lower loading rates associated with belt restraint systems. This, again, will have an influence on both chest deformations and head trajectories.

To illustrate the improvement in overall effectiveness of an AATD with omnidirectional response and measurement capability in the frontal-to-lateral range, an analysis was made of the Hybrid III, SID, and AATD based solely on measurement capability and directionality. Direct-impact biofidelity was not taken into account. The IPR distribution for each body region (Table 1) was multiplied by the measurement capability of each ATD for each region, based on a rating of complete (100 percent) to partial (75 percent and 50 percent) to none (0 percent). This product was then apportioned according to the distribution of IPR to these body regions by direction of impact force. This process gave an estimate

of the proportion of the IPR addressed by each ATD in a given direction. An overall effectiveness of an ATD could then be estimated by summing these IPR proportions for the range of directions from frontal to lateral.

For the left-front unrestrained driver position, it was judged that the combination of Hybrid III and SID ATD's could address directions 11, 12, and 1 o'clock (Hybrid III) as well as 9, 10, and 3 o'clock (SID). The potential gap in the oblique direction between 10 and 11 o'clock is ignored to give the Hybrid III/SID the benefit of the doubt. The 2 o'clock PDOF, however, is not included because the SID is judged to be kinematically unreliable in far-side oblique impacts. In comparison, the AATD will be able to continuously address the full range of PDOF from 9 through 3 o'clock in a clockwise direction. In addition, the more extensive measurement capability to be available on the AATD will provide a higher level of injury assessment capability in those directions. Based on the above considerations, the AATD was found to address 90.5 percent of the total IPR (see Figure 2), while the combination of the Hybrid III and SID addressed only 43.4 percent. The AATD would thus be twice as effective as the combination of the two present ATD's.

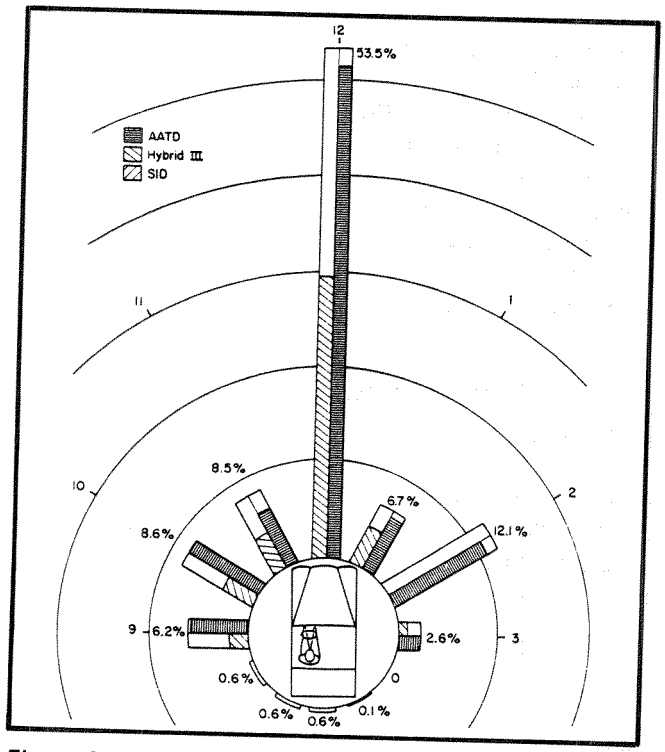

Figure 2. Estimated effectiveness of Hybrid III, SID, and ATTAD for unrestrained left-front occupants by principal direction of force (percentages denote proportion of horizontal force IPR in each direction)

Technical Characteristics and Design Concepts

This section brings together the results of our various reviews and analyses of accident data, biomechanical data, and other technical data to establish technical characteristics and to propose design concepts for the AATD and its data processing and certification systems. It is first necessary, however, to present a brief description of a major activity to develop a uniform biomechanical data base.

Biomechanical Data Base

Our ability to generate response corridors for specific body regions, but particularly for the chest, depended on the existence of a large data base whose signals could be analyzed in a uniform manner. Both previously unpublished data and those published data that warranted reanalysis were identified, consolidated, categorized, and recoded or given additional coding as appropriate. A total of 1,190 tests were initially identified by test number and source as candidates for inclusion in the data base. However, we were able to obtain and include adequate data for only 241 tests, consisting of the following:

1. A nucleus of 97 tests obtained from NHTSA that were already coded in the standard NHTSA biomechanics tape format
2. Four APR facial impacts and 41 ONSER pelvis impacts that were obtained from France on analog tapes and then digitized and coded at UMTRI
3. Fifty-eight tests conducted, digitized, and coded at UMTRI that included 26 NIOSH head axial impacts, 14 MVMA head side and frontal impacts, 11 GM whole-body sled tests, and 7 GM shoulder impacts
4. Twelve Heidelberg frontal and lateral sled tests and 5 FAT tests conducted at Heidelberg, both tapes having already been formatted

In addition, high-speed movies from 10 UMTRI thoracic tests were analyzed, and film readings were reformatted as "displacement" signals and incorporated with their corresponding sensor data. Finally, 10 Heidelberg tests containing 9 accelerometer signals were converted to the standard anatomical reference frame.

Various parameters were used as the basis for classification of the tests. These included (1) restraint type or impact surface, (2) severity of impact, in terms of impact velocity, (3) injury level, in terms of AIS rating, and (4) the subject size and condition. Test signals were further subdivided by body area, including the head, chest, spine, shoulder, and lower extremities. Once these groups were established, spectral analysis of each group was conducted to determine an appropriate filter to use for preprocessing. A procedure was developed to extract filter characteristics from the available pool of signals, and filter corners and

slopes were obtained for the near side and far side of impact for the chest and head. The area determined to have the highest priority for response characterization was the thorax, and thus emphasis was placed on generating corridors for rib and sternal accelerations. Summary data plots of chest response for a variety of test conditions (shoulder belt, airbag, rigid wall, and rigid disc) were prepared, the data having been filtered and mass-scaled. These are the basis for the performance specifications of the chest.

AATD Technical Characteristics and Design Concepts

The AATD will be designed to provide omnidirectional response in the range of ± 90° from the front in the horizontal plane. This accounts for virtually all the horizontal collision IPR and 82 percent of all IPR with known principal direction of force (PDOF). The exposure severity levels associated with cumulative values of 85 percent of the IPR are delta V's of 50mph for frontal impacts and 30mph for lateral impacts. It is expected that the AATD would be used unrestrained in such severe environments only if the vehicle structures and interiors to be tested incorporated advanced crashworthiness technology. Thus, these delta V levels are taken to be upper-limit exposure levels for the velocity of interaction with protective interior systems. The AATD will also be designed for upper-body vertical (superior-inferior) impact associated with nonhorizontal collisions. Such collisions account for 18 percent of all IPR with known PDOF.

Measurements to be made by the AATD are based on an analysis of ideal versus feasible measures. This analysis identified measures that would be desirable for injury assessment, given that an ideal test device could be developed that could reproduce all the anatomy and biomechanical responses of the human body. These were tempered by the state-of-the-art of measurement technology, and measurements were determined that would be consistent with the AATD design concepts for each body region. These measures are included in the following summaries of the desired technical characteristics and associated design concepts for the AATD, schematically presented in Figure 3.

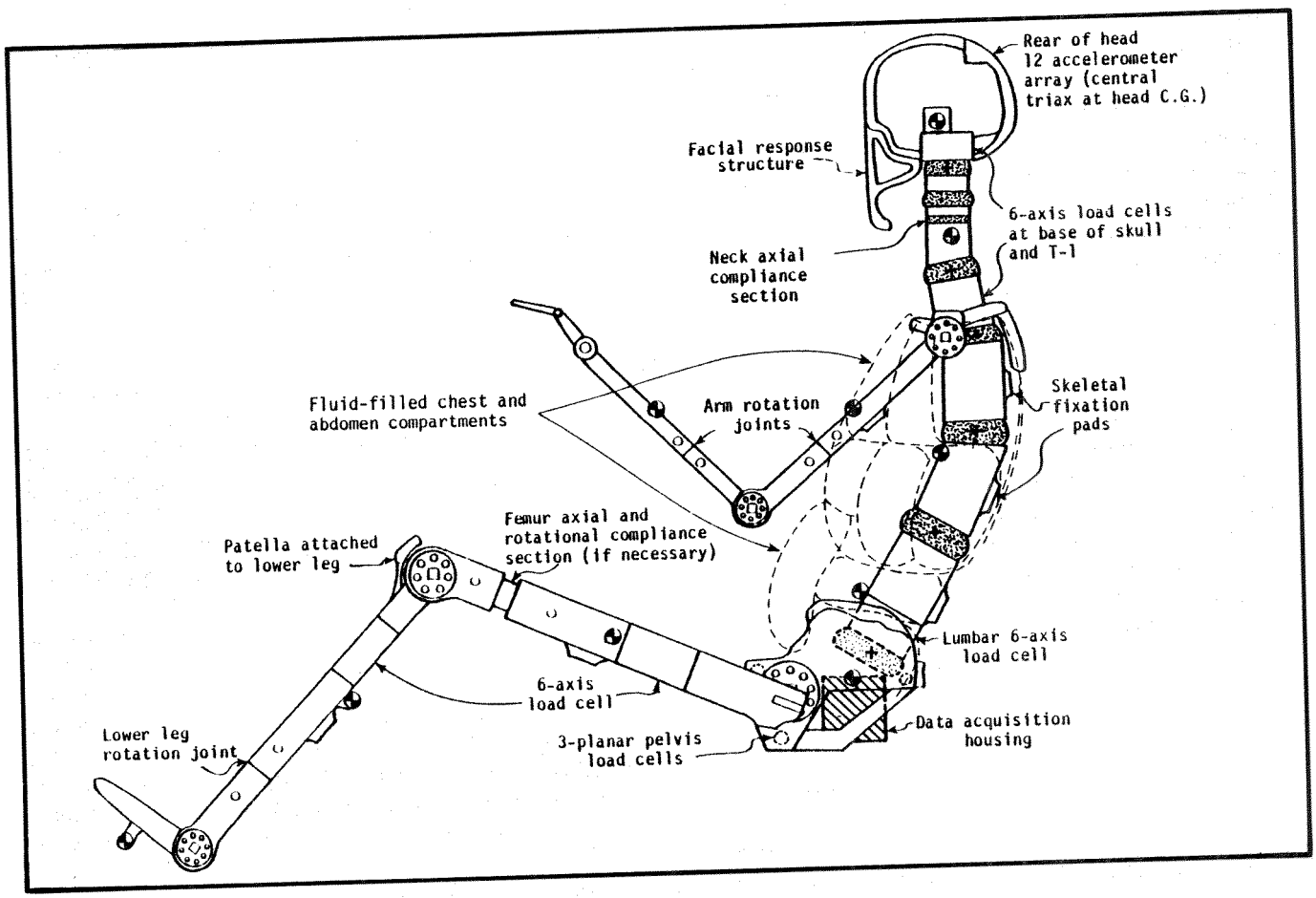

Figure 3. AATD design concepts

Head

The head will have biofidelity of response for front, side, and top rigid impacts as well as facial impact response biofidelity. Head instrumentation will consist of an array of 12 linear accelerometers to provide complete three-dimensional impact motion measurement as well as direct head center-of-gravity translational acceleration measurement. Certification testing procedures for head response will not require disassembly of the AATD.

The head will have a featureless face to aid in producing repeatable impact response. In addition, the facial structure will be designed to produce realistic head acceleration responses when the head is impacted in the face by a rigid mass. This face will be a durable structural element that can, however, be removed and replaced with an optional frangible insert for determination of facial bone fracture. The overlying soft tissue simulation of the face would similarly be replaceable with a lacerable option.

The skull of the AATD will be of cast aluminum with the front, side, and top sized to produce, in conjunction with the scalp material, biofidelity of rigid impact response. The base and rear structure of the skull will be separate from the front/side/top structure and will be designed as a mounting structure for a 12-accelerometer motion measurement array made up of four triaxial accelerometer units. As such, the base and rear structure will be very stiff to preserve the accelerometer alignment during rigid impacts to the head. The array will be configured to put one of the triaxial units at the head center of gravity for direct measurement of translational acceleration at that point and for subsequent HIC determination. The base of the skull will also serve as a mounting structure for a six-axis neck load cell.

Spine

The spine will be designed as a total system from the base of the head to the top of the pelvis. Spinal flexibility will be provided for the cervical, thoracic, and lumbar spine segments. The neck section of the spine will have biofidelity of response for frontal, lateral, and oblique indirect impacts. The specifications for these responses are based on analysis of human volunteer sled tests. These data provide static neck joint stiffness characteristics in bending (flexion, extension, and lateral), axial loading (tension and compression), and torsion, as well as dynamic head/neck junction bending moment/head-to-torso angle responses for flexion, extension, and lateral loading and accompanying head trajectory requirements. An additional requirement will be placed on matching the superior-inferior response of the head/neck system due to impacts to the top of the head. The mean force-time and acceleration-time responses of the head and spine, based on cadaver impacts, are the basis for this response requirement.

The thoracic and lumbar spine system will have biofidelity of midsagittal flexion and extension bending response based on static tests on human volunteers. The spine system will provide for adjustment of the initial spinal configuration. Six-axis load measurement (three moments and three forces) will be made at the base of the head, the base of the neck, and the base of the spine to aid in the interpretation of body loading from advanced restraint techniques.

The spinal structure will consist of a series of rigid links connected by joints at selected anatomical points. These joints will have omnidirectional motion capability and will be located at the head/neck junction, base of the neck (C7/T1), upper thorax (T4/T5), middle thorax (T8/T9), lower thorax (T12/L1), and base of the spine (L5/S1). Range-of-motion requirements in the cervical spine (75° flexion, 90° extension) require the introduction of a third neck joint near the middle of the cervical spine (C4/C5). This joint will also incorporate provisions for neck torsional stiffness and axial stiffness control.

The spine segment between T1 and T4 will provide the structural attachment for the shoulder, and the thoracic structure will be attached to the T5-T8 and T9-T12 segments. Provisions will be made at each joint to allow adjustment of the initial configuration through the use of wedge-shaped rigid blocks that can be inserted and fastened in place.

Six-axis load cells will be used at the top of the neck, base of the neck, and base of the spine to allow assessment of spinal loading due to restraint system inputs.

Shoulder

The shoulder will have a clavicle structure to carry shoulder belt and steering wheel impact loads but will also offer low lateral load resistance for side impact. The lateral stiffness and range of deflection of the shoulder will be matched to mean cadaver response. The shoulder linkage will be designed to reach its lateral deflection limit slightly after the chest reaches its lateral deflection limit.

Thorax

The thorax will be designed to provide biofidelity of response to frontal impacts for rigid disc, shoulder belt, and airbag loading conditions. Side impact response biofidelity will be required for rigid disc and rigid wall impacts. The response requirements will be met for different rates of loading as well as for different types of

loading. The response specifications are based on volunteer tests at lower impact severities and on cadaver tests at the higher levels. Mean impact force-time and acceleration-time corridors for all types of direct thoracic impacts and force-deflection corridors for rigid disc impacts are the primary specifications. They will be supplemented with static load-deflection data on volunteers. Thoracic cage deformations will be measured at multiple locations to allow the assessment of global chest deformation and deformation rates.

The thorax structure will have a thin, flexible, monolithic shell to define its shape and to provide load distribution. This shell is not intended to carry significant load and therefore will not have an influence on thoracic response. The response elements in the thorax will be an array of fluid-filled bag compartments within the shell. Each bag will be constructed of cord-reinforced rubber and will represent a flexible, constant volume reservoir. There will be five bags on each of two levels, compartmentalizing the chest into upper and lower levels with frontal, lateral, and oblique sections. Each bag will communicate with a common gas-pressure-controlled reservoir (accumulator) through a single orifice into that reservoir. One-way flow-control valves will be provided in the passages from the individual bags to the reservoir to prevent flow from one bag to another instead of into the accumulator. The bag volumes, the accumulator fluid volume and gas volume, the accumulator initial gas pressure, and the orifice size will be adjusted to produce the desired thorax response. The compartmentalization of the chest will allow positional variation of local response to better match human response to asymmetric loads such as those from shoulder belts.

Each bag will have a pressure transducer mounted in it as will the gas section of the accumulator. The bag pressure transducers will indicate the region of loading and the loading rate (related to flow rate) from the resistance to flow. The central accumulator gas pressure will indicate total global deformation of the chest independent of the region of loading. The use of well-defined materials, such as silicone fluids and nitrogen gas, to control response will minimize repeatability, reproducibility, and temperature sensitivity problems.

Abdomen

The abdomen will be a deformable system with dynamic response biofidelity based on the mean rigid armrest load-deflection response of laboratory-impacted cadavers. The deformations of the abdomen will be measured at multiple locations to indicate the degree of abdominal intrusion in frontal and lateral loading. The abdomen will be of similar general design as the thorax but with only three fluid-filled compartments, lower control pressures, and a softer outer covering.

Pelvis

The pelvis and its associated covering will be designed to exhibit rigid impact response biofidelity, based on mean force-time and acceleration-time corridors for cadavers in lateral impacts, and will have humanlike mass distribution. It will also be instrumented to sense lateral loading. The pelvic structure will be designed as a simple geometric shape for the purposes of (1) providing a lightweight, rigid structure for tying the extremities and torso together, (2) allowing lateral pelvic and hip joint load measurement, and (3) providing a protected space for housing a future data acquisition system. The anatomical details of critical points for proper restraint system engagement and interaction, such as iliac bones and ischial tuberosities, will be provided for only where needed. The mass of the pelvic structure and the accompanying soft tissue mass and stiffness will be matched to provide lateral impact biofidelity.

Lower Extremities

The legs will have knee/femur/pelvis impact biofidelity in rigid knee impacts and will have humanlike skeletal mass distribution. Soft tissue coupling to the skeletal structure will also be humanlike in response, and the knee structure will have realistic geometry. Six-axis load measurements will be made in the femoral shafts, and multiaxial loads will be measured in the lower legs. The extremity joints will be single-axis planar joints or combinations of such joints to achieve appropriate degrees of freedom. The ranges of motion of the joints will be humanlike, and the resistance characteristics will be adjustable to achieve resistance ranges from 0 to 2G. The resistive torque-angle response will be humanlike as will the joint stop characteristics.

Flesh

The flesh will be developed in conjunction with the underlying skeletal structures to insure proper overall system response, including tissue shear mobility in critical loading areas such as the buttocks and upper pelvis. The durability and stability of the flesh materials will be given special consideration.

Data Processing

The data acquisition and processing techniques that are currently used by crash and sled testing facilities to measure anthropomorphic dummy response data during impact testing were reviewed, and a number of recommendations are given regarding the development of an advanced dummy instrumentation system.

Based on the projected data channel requirements of from 72 to 100 data channels on-board the advanced dummy, and based on the present size of state-of-the-art instrumentation, the development of an on-dummy instrumentation system is recommended. This system should be designed to include integral memory but with capability to conveniently expand record times through use of external memory. The on-dummy instrumentation should be developed as a microprocessor-based system to perform on-dummy analysis and control functions as well as to allow transfer of measured data to an external computer-based test set. The on-dummy microprocessor would also function to perform self tests of individual data channels under both internal and external control.

A microprocessor-based external test set should be developed as an integral part of the advanced dummy instrumentation system. The test set should be designed to allow calibration signals to be injected into individual data channels on-board the dummy. The test set would also function to perform analysis of data channel response signals. The response signals may result from injected calibration signals or actual dummy responses generated during dummy certification tests. The test set would allow for rapid turnaround of results to provide pass/fail indications of channel performance immediately after a verification test was performed.

The advanced dummy instrumentation should be developed to meet the requirements for data systems as outlined in ISO 6487, *Road Vehicles—Techniques of Measurement in Impact Test—Instrumentation.* In specialized cases, as may apply to the nine component head accelerometer array, increased accuracy may be required. The recommended performance for the advanced dummy instrumentation is summarized in Table 4.

Procedures should be developed for use in calibrating accelerometers and other sensors. ISO 6487 should serve as a basis for the procedures. At a minimum, the following parameters should be calibrated at 6-month intervals:

- Amplitude linearity at a fixed frequency
- Amplitude response versus frequency
- Phase response

The advanced dummy instrumentation should be designed to meet specified environmental performance criteria. Recommended criteria and suggested limits are summarized in Table 5.

For further information, see Arendt et al.(8).

Table 4. Advanced dummy instrumentation requirements

Amplitude Linearity	2.5%
Amplitude Resolution	12 bits (0.02%)
Time Linearity	1%
Time Synchronization	0.1 ms
Time Zero Offset	0.1 ms
Sample Rate	8000 Hz
Record Time (per channel)	500 ms
Channel Capacity	72 expandable to 100

Table 5. Environmental specifications

Parameter	Design Limits
High Temperature	180°F.
Low Temperature	-10°F.
Temperature Shock	170°F.
Humidity	85%
Acceleration (linear)	10 G
Vibration	1 G RMS Random
Shock	500 G ½ ms (Head)
	200 G 1 ms (Chest, Pelvis)
EMI/RFI	Standard Industrial

Certification Test Procedures

The test procedures currently employed to certify the Part 572 anthropomorphic dummy for use in crash tests were reviewed, and approaches that appear promising for use with the advanced dummy are recommended below. These certification tests are intended to insure that dummy responses to impact stimuli are both repeatable and reproducible. A brief review of Hybrid III dummy certification procedures was also conducted.

Routine certification testing should be done on a completely assembled, advanced anthropomorphic dummy. Test procedures should involve dynamic exposure of the dummy to levels that are consistent with the automobile crash environment. That is, certification testing should mimic the in-use environment to the maximum extent possible. Test procedures and equipment must be developed that will allow efficient and rapid testing.

On-dummy instrumentation should be used in certification testing. It is recognized that additional electronic measurements may be necessary as a part of new test procedures; however, where possible, the sensors, instrumentation, etc., that are a part of the dummy should be utilized to provide certification test data. As this instrumentation is part of the dummy, it is reasonable that it should also be checked as a part of the certification process. However, a complete calibration of sensors is not viewed as necessary each time a dummy is certified. Rather, a calibration interval would be defined at which time all instrumentation would undergo calibration according to established procedures.

Performance criteria should include injury measures as well as engineering measures. That is, if HIC is used as an injury measure for the head, then a test procedure which results in a comparison of an HIC with established error bounds should be utilized. This approach results in a

better knowledge of error limits on the primary dummy outputs than is currently available. It should, however, be noted that measures of response in addition to injury measures may be desirable and even necessary for identification of sources of unacceptable component response.

Dummy disassembly and component level testing should be undertaken only if whole-body testing indicates a problem in meeting response limits. That is, component level testing should be undertaken as a diagnostic aid in determining a specific mechanical item in need of repair or adjustment.

For further information, see Arendt et al.(8).

Conclusion

Past dummy development has been an evolutionary process. Such a process does not allow for significant departures from traditional design solutions, because each change must take into account its effect on other dummy components that remain unchanged. Although the best aspects of past dummy designs will be drawn from for the AATD, past designs will not limit the innovative approaches to its design and development. Only by taking a fresh look at all dummy design concepts can the desired results be achieved. The technology is presently available to develop an AATD with greatly improved impact biofidelity, measurement capability, durability, maintainability, and certification ease. Design concepts, technical characteristics, and measurement requirements have been developed in Phase 1 for all body regions. These will be further developed and result in a complete prototype AATD by the end of Phase 2.

Acknowledgments

This work was conducted under contract DTNH22-83-C-07005 with the U.S. Department of Transportation, National Highway Traffic Safety Administration.

References

1. Melvin, J.W., and K. Weber, eds., *Review of Biomechanical Impact Response and Injury in the Automotive Environment,* Task B report on contract DTNH22-83-C-07005, Ann Arbor, University of Michigan Transportation Research Institute, 1985 (in press).
2. American Medical Association, Committee on Rating of Mental and Physical Impairment, *Guides to the Evaluation of Permanent Impairment*, Chicago, American Medical Association, 1971.
3. Malliaris, A.C., R. Hitchcock, and J. Hedlund, "A search for priorities in crash protection," *Crash Protection*, SP-513, pp. 1-33, SAE Warrendale, Pennsylvania, 1982.
4. Carsten, O., and J. O'Day, *Injury Priority Analysis*, Task A report on contract DTNH22-83-C-07005, Ann Arbor, University of Michigan Transportation Research Institute, 1984 (in press).
5. Fleck, J.T., and F.E. Butler, *Validation of Crash Victim Simulator*, Vol. 4, Report no. ZS-5881, Buffalo, Calspan Corporation, 1981.
6. Schneider, L.W., D.H. Robbins, M.A. Pflüg, and R.G. Snyder, *Development of Anthropometrically Based Design Specifications for an Advanced Adult Anthropomorphic Dummy Family*, 3 vols., final report on contract DTNH22-80-C-07507, Ann Arbor, University of Michigan Transportation Research Institute, 1983 (in press).
7. Melvin, J.W., D.H. Robbins, K. Weber, K.L. Campbell, and J. Smrcka, *Review of Dummy Design and Use*, Task D report on contract DTNH22-83-C-07005, Ann Arbor, University of Michigan Transportation Research Institute, 1985 (in press).
8. Arendt, R.H., D.J. Segal, and R. Cheng, *Review of Anthropomorphic Test Device Instrumentation, Data Processing, and Certification Test Procedures,* Task C report on contract DTNH22-83-C-07005, Ann Arbor, University of Michigan Transportation Research Institute, 1984 (in press).

A New Dummy for Pedestrian Test

Bertil Aldman and
Janusz Kajzer
Department of Traffic Safety, Chalmers University of Technology, Götheborg, Sweden

Dominique Cesari,
Robert Bouquet, and
R. Zac
Laboratoire des Chocs et de Biomécanique, Organisme National de Sécurité Routière, Bron, France

Introduction

Improvement of pedestrian safety is considered a priority in crash injury protection. However, analysis of evaluation methods currently available shows that present dummies are not able to give a humanlike and repeatable impact response in pedestrian tests(1).

For this reason, the Biomechanical Laboratory of ONSER in France and the Department of Traffic Safety of Chalmers University in Götheborg, Sweden, have decided to join efforts to study, design, and validate a new dummy for pedestrian testing. The lower part going from the hip joint and below was developed by Chalmers, whereas ONSER was in charge of developing the upper part.

General Characteristics of the New Pedestrian Dummy

In the agreed specifications, the new pedestrian dummy would represent the male 50th percentile for its first version. It would be symmetrical around its vertical axis especially to obtain a high repeatability. For this, it would have no arms and only one leg; however, a part of the arm weight would be included in the thorax weight.

This dummy would represent a pedestrian hit on his side. The dimensions of the dummy were selected from the main anthropometric data available(2,3,4,5) according to the parameters indicated in Figure 1. Table 1 contains the values of these parameters available in the five

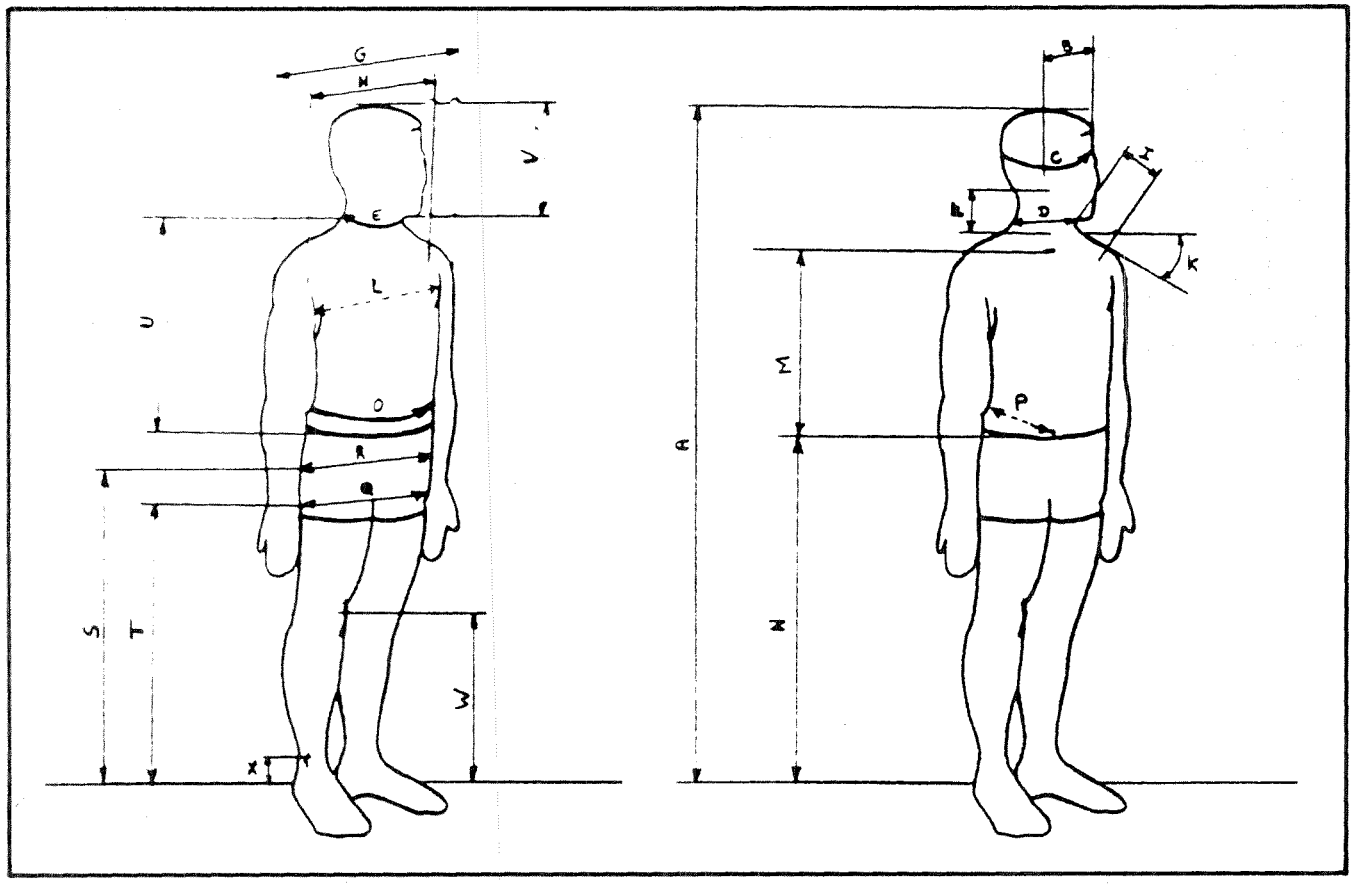

Figure 1. Dummy dimensions

selected publications and the selected values of the same parameters.

If the choice of the dimensions along the vertical axis is clear, it is much more difficult to choose the values of the diameters of the body segments: it was decided to consider the diameter of a circumference having the same length as the development of the considered body area(6), and, if there was a great difference between this value and the width of the body segment, the value of this diameter was adjusted. Table 2 gives the values of the diameters determined according to this method. On the basis of the values of these parameters, it was then possible to draw the general concept of this new pedestrian dummy as it is represented on Figure 2.

Table 1. 50th percentile male measures

	References	4	3	2	3*	5	Choice
	Weight (kg)	74 ± 1.4	81.5	73.3	74.55	-	75
A	Height	-	178.4	173.7	175.7	-	175
B	Maximum head width	15.49 ± C.51	15.6	-	-	-	15.6
C	Maximum head circumference	57.15 ± 1.27	57.6	-	57.18	-	48.7
D	Neck width	(11.6)	-	14.	-	12.1	12.1
E	Neck circumference	-	38.5	-	38.05	-	38
F	Cervical spine height	-	-	-	-	8.2	8.2
G	Shoulder width	47.47 ± 1.02	48.6	-	47.13	-	47
H	Acromial distance	-	40.9	37.1	40.02	-	40
I	Shoulder length	-	16.7	-	15.87	-	15.8
J	Shoulder angle(°)	-	-	21.1	-	-	21°
K	Acromion height (from ground)	-	146.1	-	144.04	-	144
L	Back width (between arms fork)	(33.5)	38.9	-	38.48	-	39.4
M	Belt to top of sternum	-	40.6	-	39.125	-	39.1
N	Ground to belt	-	107.2	-	105.72	-	106
O	Belt length (navel level)	83.82 (± 2.54)	88.4	-	84.43	-	88.4
P	Thickness at navel level	-	-	26.2	-	-	26.9
Q	Hip distance (great trochanter)	(37.33)	33.1	37.3	-	-	37.3
R	Iliac wings width	-	35.5	-	34.85	-	34.3
S	Ground to iliac crest	-	-	-	-	105.49	105
T	Ground to great trochanter	-	94.6	-	91.76	-	91.7
U	Belt to 7th cervical vertebra	-	47.2	-	46.15	-	45.1
V	Chin to top of head	20.5	-	-	-	-	20.5
W	Ground to knee joint	-	-	-	46.4	-	46.4
X	Ground to ankle joint	-	-	-	13.3	-	13.3

***values corrected for a 1985 body size data projection**

Table 2. Values of the diameters

	Selected from table n° 1	Humanscale Circumference	Humanscale Equivalent diameter $\frac{C}{\pi}$	Chosen value
Head	156	564	179.5	156
Shoulder	470	1163	370	400
Thorax (under the arms)	394	892	284	330
Thorax (chest level)	-	983	313	
Pelvis (great trochanter level)	373	978	311	330

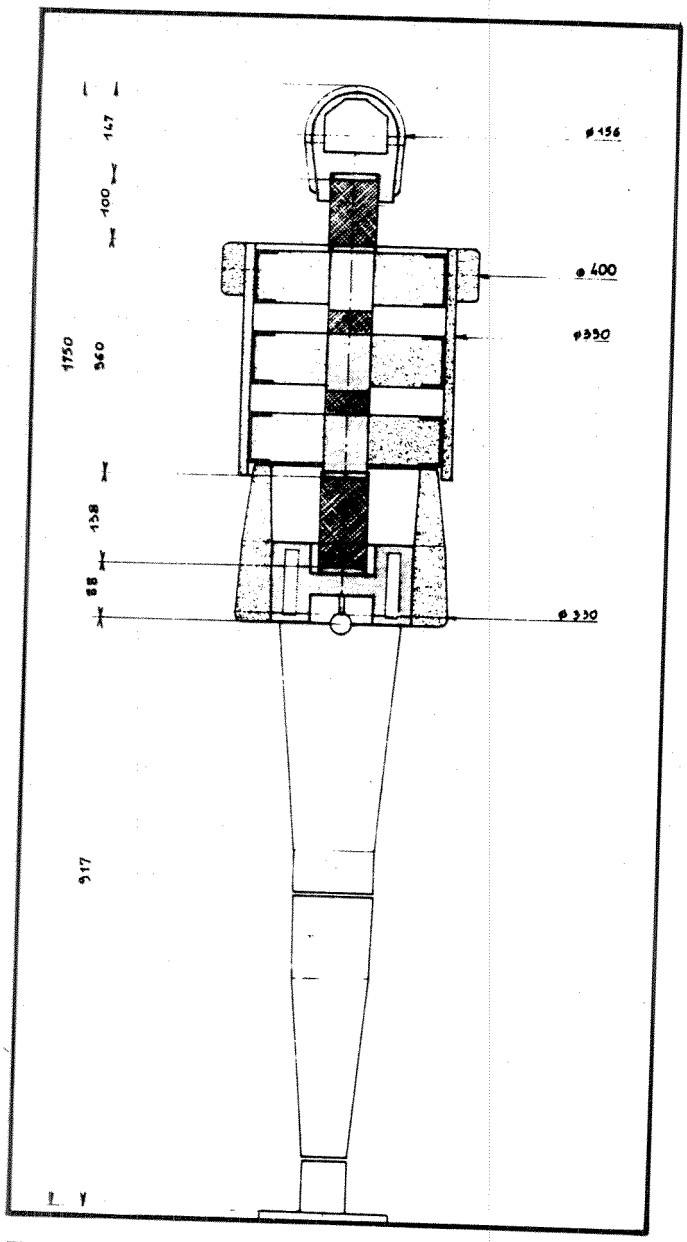

Figure 2. New dummy for pedestrian test.

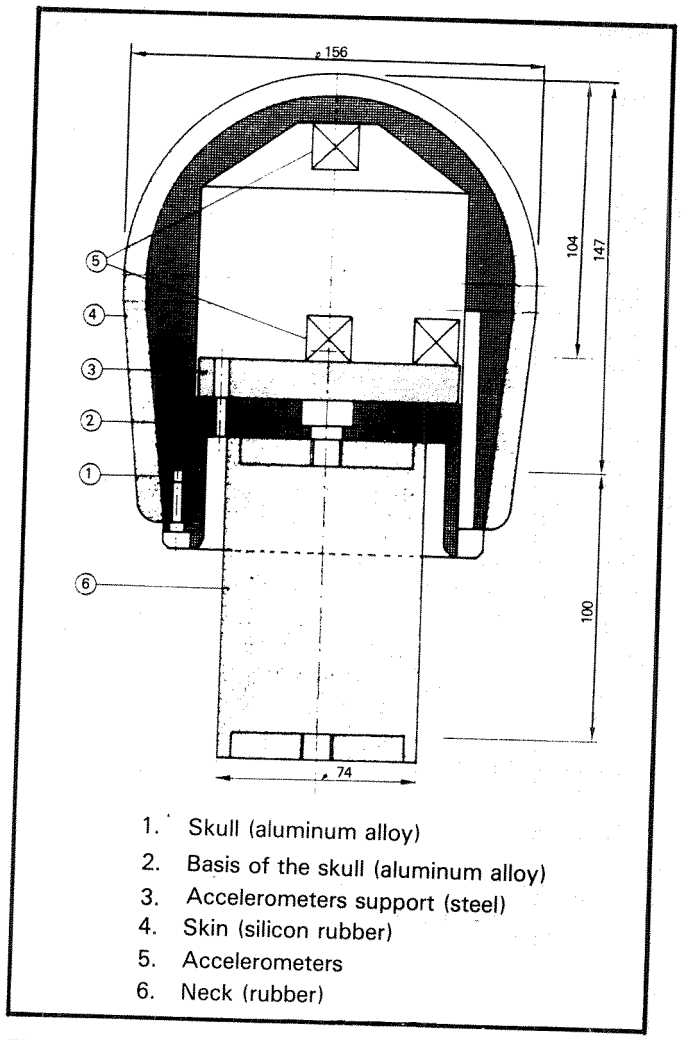

Figure 3. Head and neck assembly of the new pedestrian dummy

Part 1. The Upper Part of the Dummy (From Head to Pelvis)

The work for designing the new pedestrian dummy was divided in two parts. Part 1 includes the description of the head, the neck, the thorax, the pelvis, and the lumbar spine, which were developed by ONSER, whereas Part 2 describes the work done at Chalmers to design the hip joint and the complete leg.

Design of Head-Neck Assembly (Figure 3)

The size of the neck is the same as for the Part 572 dummy, but the stiffness characteristics are different; to give more flexibility to the neck, the rubber is softer and contains chemical adjuvant that produces a viscoelastic effect, as it was found in the same neck tested in frontal impact(7).

The skull is made of aluminum; its shape is half a hollow sphere, half continued by a trunk of cone. Accelerometers are accessible from the bottom of the head to avoid a junction plane between the sphere and the cone. The skull is covered with a 9mm-thick skin made from silicon rubber. The accelerometers plate allows five accelerometers to be screwed: one at the center of gravity and four at the periphery with an angle of 90° between each. It is also possible to screw another accelerometer at the top of the head.

The impact response of the head was evaluated in drop tests with a drop height of 25.4cm and 50cm. In these tests, one triaxial accelerometer was placed at the center of gravity and one uniaxial at the top of the skull. The results of these tests are listed in Table 3.

As indicated on Figure 4, these results were compared with the results of head cadaver tests(8) and with the

corridor of the Part 572 specification; if the response of the pedestrian dummy head is below the Part 572 corridor, it is inside the cadaver response. It is noticeable that the head sustained six impacts without damage.

Design of the Thorax

The thorax assembly is made with three identical wheels as indicated on Figure 5. Each wheel includes a central vertebra crossed by the spine cable and on which is fixed a photocell to measure the thoracic deflection. The external part is a rigid U-form rim made from fiberglass. Inside the rim, a lead plate is fixed to give a realistic mass distribution, and the rim is attached to the vertebra with a moulded soft polyurethane foam. The foam density is chosen to reproduce humanlike force-deflection characteristics. Between two following wheels, there is a polyurethane vertebra that allows a bending motion at the thoracic level. All of the thorax is covered with a 15mm-thick rubber foam, and the upper rim is covered with two other lays to reproduce the shoulders.

Design of the Pelvis

The pelvis is made in two main parts: a rigid central part attached to the lumbar spine and to the leg and a soft external part simulating the flesh (Figure 6). The rigid part is made from two rings attached to a central cylinder through three force transducers at each level. The angle between the force transducers is 120°. The upper rim represents the iliac wings and the lower one the great trochanter. With this system, it is possible to measure the forces exerted at the two levels and from any direction. It is also possible to measure pelvic acceleration at the center of gravity of the pelvis.

The flesh part is made from three lays of foam glued together and surrounding the internal metallic assembly. The thickness of the foam is chosen to give a correct external diameter to the pelvis.

The lumbar spine was generally developed for the EUROSID(9) and is made from the same rubber as the neck to give a correct erection posture to the dummy even with the soft lumbar spine. The pelvic flesh is in contact with the lower side of the lower thoracic rim.

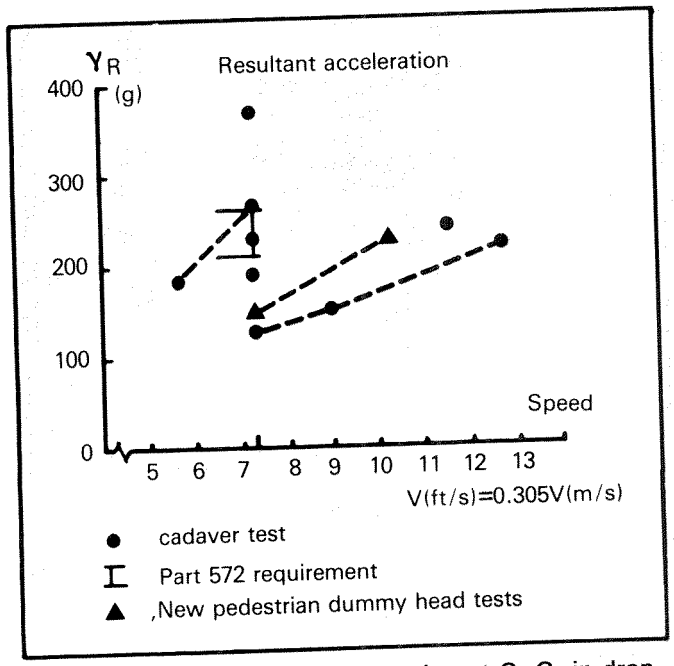

Figure 4. Head resulting acceleration at C. G. in drop tests

Table 3. Results of head drop tests

Tests	Top of Skull accelerat.	Center of Gravity Acceleration						
	γz	γx	γy	γz	γR	γR (3ms)	HIC	Speed
TMR 01	128	6.8	11.6	140	140.5	40.2	188	8km/h or 7.32ft/s
TMR 02	126	7.8	22	141	141.6	40.0	194	8
TMR 03	138	7.3	18	150	150.1	42.6	203	8
average 01-02-03	130				144		195	8
TMR 04	177	8.7	23.6	199	199.4	44.0	386	11.3km/h or 10.27ft
TMR 05	185	2.8	17.1	211.4	211.5	37.4	402	11.3
TMR 06	199	12.5	8.7	225.5	225.7	44.6	425	11.3
average 04-05-06	187				212.2		404	11.3

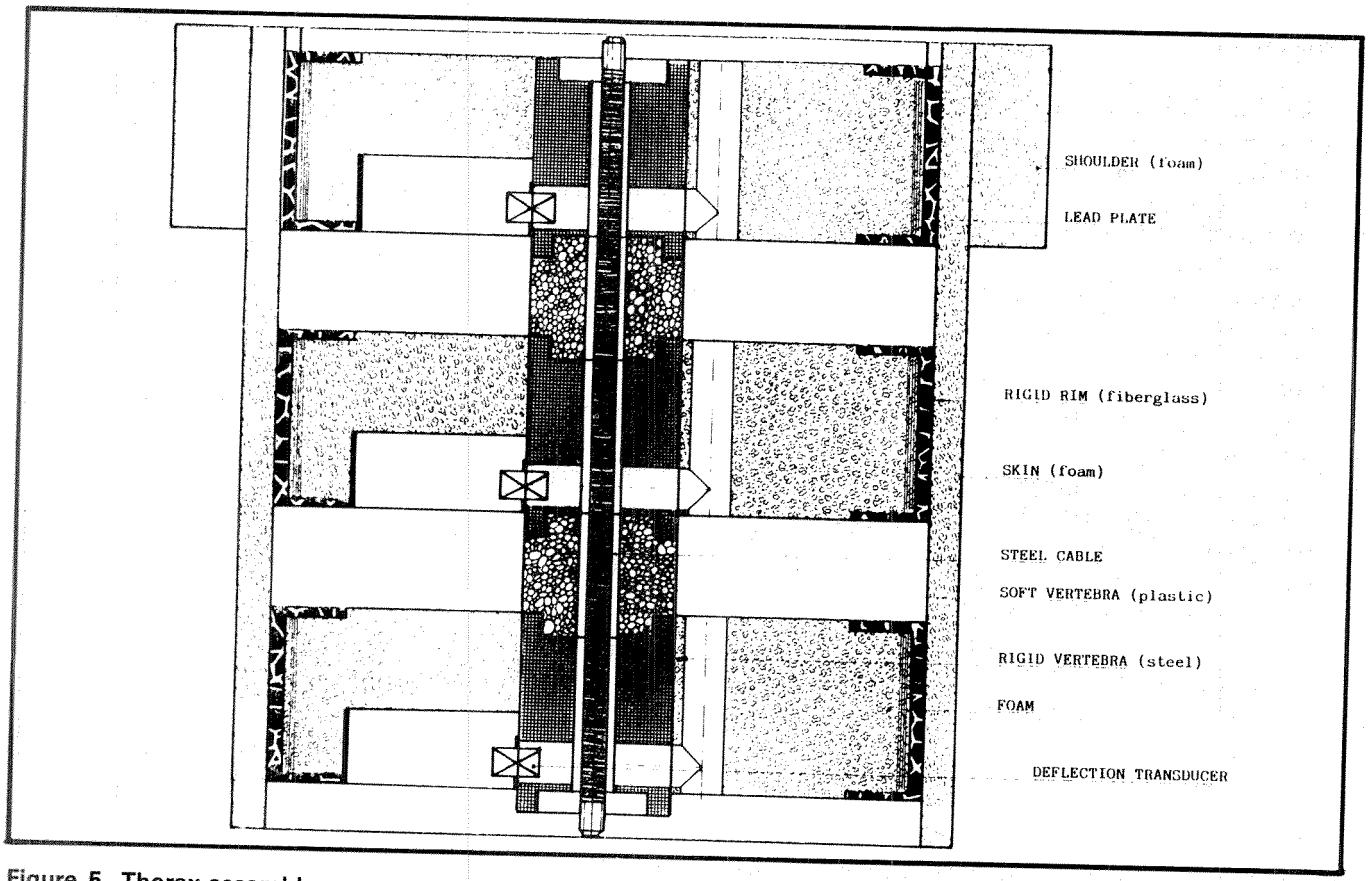

Figure 5. Thorax assembly.

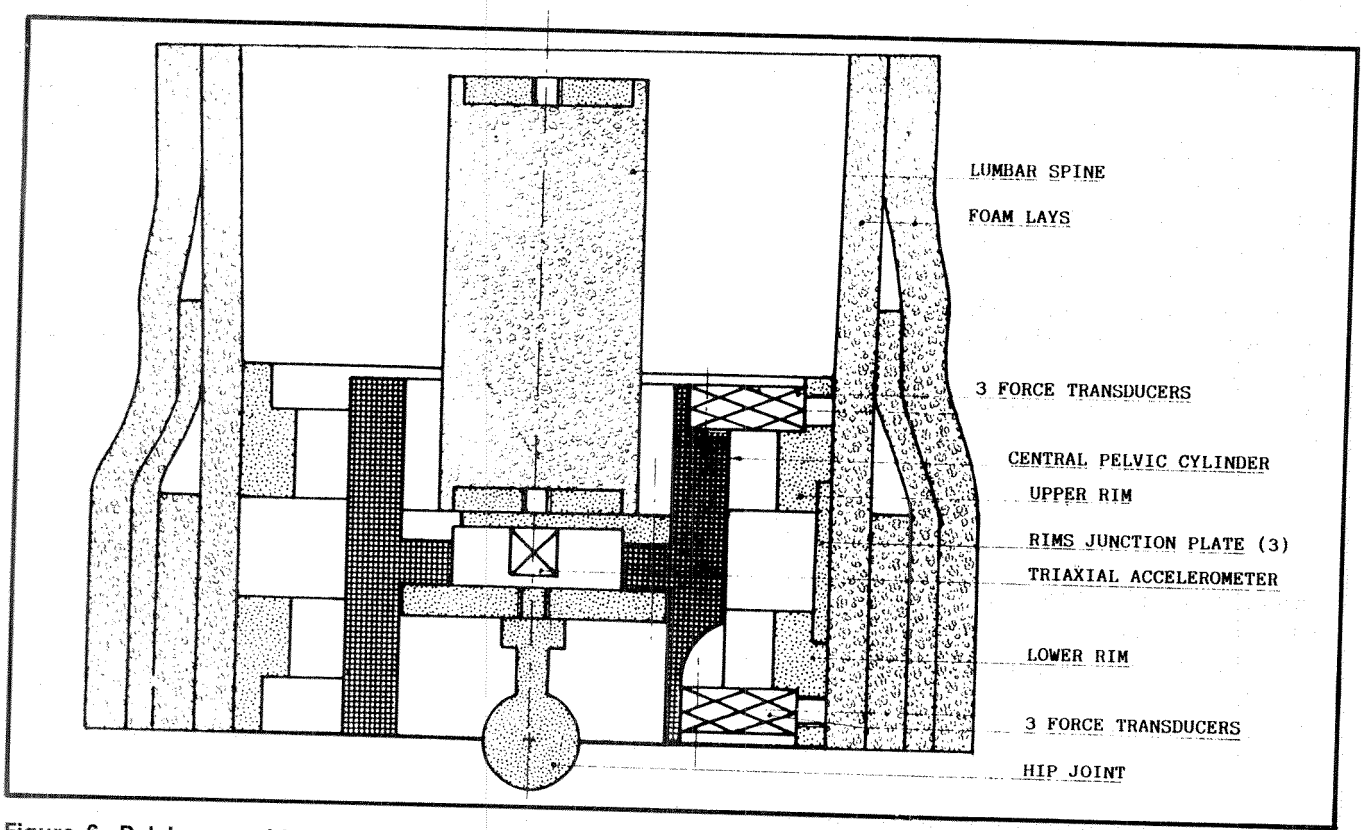

Figure 6. Pelvis assembly

References

1. CEVE, "Pedestrian injury accidents," Ninth ESV Conference, Kyoto, November 1982.
2. Haslegrave, C.M., *An Anthropometric Survey of British Drivers*, MIRA, 1978.
3. McConville, J.T., and L.L. Laubach, *Anthropometric Source Book*, Vol. 1, "Anthropometry for designers," NASA ref. Pub. 1024, 111, pp. 9-67, IV, pp. 22-66, July 1978.
4. Society of Automotive Engineers, Inc., *Technical Report J963*, SAE, 1968.
5. McConville, J.T., T.D. Churchill, Inis Kaleps, C.E. Clauser, and Jaime Cuzzi, *Anthropometric Relationships of Body and Body Segment Moments of Inertia*, December 1980.
6. Diffrient, N., A.R. Tilley, and J.C. Bardagjy, *Humanscale*, MIT Press, Massachusetts Institute of Technology, Cambridge, Massachusetts.
7. Cesari, D., and R. Bouquet, EEC Biomechanics Seminar, Session 4: "Design of ONSER side impact dummy," Bruxelles, Mars 1983.
8. Hubbard, R.P., and D.G. McLeod, "Definition and development of a crash dummy head," Proceedings 18th Stapp Car Crash Conference, Ann Arbor, Michigan, December 1974.
9. Neilson, I.D., et al., "The EUROSID side impact dummy," Tenth ESV Conference, Oxford, 1985.

Part 2. The Leg (From Hip Joint to Foot)

In normal walking, the feet are lifted one at a time with one foot not off the ground before the other touches. Studies of gait indicate that the body weight is supported only by one leg for about 80 percent of the total time(1). During this period, the vertical force against the ground varies between 80 percent and 120 percent of the static body weight(2). The reason for this varying load on the supporting foot is, of course, that the other leg has to be lifted and swung forward during this period. At the forward swing, the knee of this leg is flexed except for a very short moment when the heel hits the ground. Maximum knee flexion is 50° to 60°. From a side view, the two legs to a large extent are overlapping during this period. In a frontal view, however, the lower legs are separated by some 5 to 10cm when they pass each other.

Most of the accidents in which a person is hit by the front structure of a passenger car seem to take place in built-up areas when the pedestrian enters a traffic lane in an attempt to cross the street more or less perpendicularly. Since most adult pedestrians in this type of accident are elderly, their own velocity is quite low in relation to that of the car. The first contact between the two occurs when the most protruding part of the car front, which is usually the bumper, hits the pedestrian's lower extremities from the side.

The static level of the bumper in many cars is about 45cm above the ground. In normal driving, the bumper level is influenced by several factors. The most important is probably related to a possible application of the brakes before impact. Braking results in a more or less pronounced pitchdown of the front end of the car. This dive has its maximum about one-quarter of a second after full application of the brakes(3). This means the car will travel quite a distance from the moment the driver first observes the pedestrian and decides emergency braking is necessary until the bumper reaches its lowest position. In most pedestrian impacts, the bumper will probably not have reached its lowest position but will be at or just below the level of the knee of an adult pedestrian.

Two different positions are possible for the pedestrian's legs at the moment of impact. The swinging leg may be either the one nearest the approaching car or the one most distant. The foot of this leg will be off the ground for 80 percent of the time, and the knee of the swinging leg is more or less flexed during this period. The most probable bumper impact point will therefore be on the lower leg rather than in the knee region. Since the lower leg is not in a vertical position most of the time, the bumper contact will probably engage a larger area than if this part had been perpendicular to the bumper in its plane of motion.

Should the swinging leg be the one most distant from the car, this leg will generally first be impacted by the other leg and then by the bumper. In either case, the impact is probably distributed over a relatively large area of the swinging leg.

If, on the other hand, the bumper first hits the leg supporting the body, the contact is likely to be on its lateral or fronto-lateral aspect at or just below the knee joint. Due to the nearly vertical position of the leg, the bumper force will be concentrated over a small area. This part of the leg will in a very short time be accelerated at least to the velocity of the car at the moment of impact. Inertia of the leg and ground friction will create a bending moment about the knee, whereby the medial and cruciate ligaments are subjected to tensile and the lateral condyles to compressive forces. Shear forces will also occur, and the inertia of the foot in most cases will cause some torque about the longitudinal axis of the lower leg.

When the leg is forcibly bent in a lateral direction, the foot will come off the ground, which will substantially reduce the influence of ground friction shortly after the first contact. The lateral bending is minimal only if the point of impact is close to the center of gravity of the lower leg.

It seems the worst case would be where the bumper first impacts the leg supporting the body close to the knee. Due to the mobility in the hip joint, there is little influence on the pelvis due to the induced rotation of the legs during this first phase of the impact sequence.

The second contact between the pedestrian's body and the car front will often take place between the hip region and leading edge of the hood. If this contact is at a level close to the pedestrian's center of gravity, most of the impact energy transferred will result in a translational movement of the pedestrian body. If this second contact is with the thigh, more of the energy will result in rotation of the body in a vertical plane more or less parallel to the longitudinal axis of the vehicle. The speed at which the upper body hits the top of the hood is, therefore, mainly governed by this contact.

Rotation about the longitudinal axis of the pedestrian's body may also occur. This rotation is also of importance because the position of the nearest arm and shoulder at impact will greatly influence the kinematics of the trunk and head during this phase of the impact.

When cadavers as well as normal or slightly modified anthropometric test dummies have been used for simulated car-pedestrian impacts, it has been customary to place them with their feet separated and the dummy weight more or less loading both legs. This seems to represent a very rare accident situation. It does not represent the worst case as far as the risk for leg injuries is concerned, and this position of the legs may in some cases induce a rotation about the longitudinal axis of the body.

The presence of arms and shoulders and their construction will largely influence the later kinematics of these bodies. This may be a major source of the large scatter in recorded values of injury criteria often found in such tests. The present anthropometric dummies have, therefore, not been considered to be particularly well suited for this kind of testing.

It was mainly for the reasons mentioned above that it was decided to design and construct a new type of dummy more suitable for the assessment of car front aggressiveness in pedestrian impacts. To reduce as many as possible of the identifiable sources of scatter in recorded injury criteria, it was considered advantageous to make the dummy rotationally symmetrical about the longitudinal axis of the body. To achieve this goal completely, the dummy would have to be one-legged and the leg would have to have the characteristics of a human leg impacted on its lateral aspect. This did not seem to be a great disadvantage since the dummy would then always represent a worst case impact model.

General Requirements

The aim of this part of the work was to design and construct a rotationally symmetric mechanical representation of the lower extremity of an adult person. The appropriate dimensions were chosen to represent those of a 50th percentile U.S. male. The model should have the response characteristics of the leg of a pedestrian who is hit from the side by the front structure of a car. It should also have a similar influence on the kinematics of the upper part of this dummy as a human leg would have on a pedestrian's body in real-world accidents of this kind. Furthermore, it should be possible during tests with this dummy to record the physical parameters considered to be the most important injury criteria for this part of the body. At the present state-of-the-art, these are bending moments about the long bones and joints, tensile and shear forces at different levels, and torque about the longitudinal axis of the leg.

To be practically suitable for use under realistic test conditions, the main dummy parts would have to be strong enough not to break or distort permanently when hit by cars at speeds chosen for these tests. For this reason, the long bones are simulated by steel tubes with an outer diameter of 44.5mm and an inner diameter of 36.5mm.

The Hip Joint

This joint should attach the leg to the pelvis while allowing a 30° pendulum angle before contact is made between stiffer structures. This angle would correspond to the combined movements of the human leg with special reference to the adduction of the leg closest to the striking car. A ball and socket joint was chosen for this purpose.

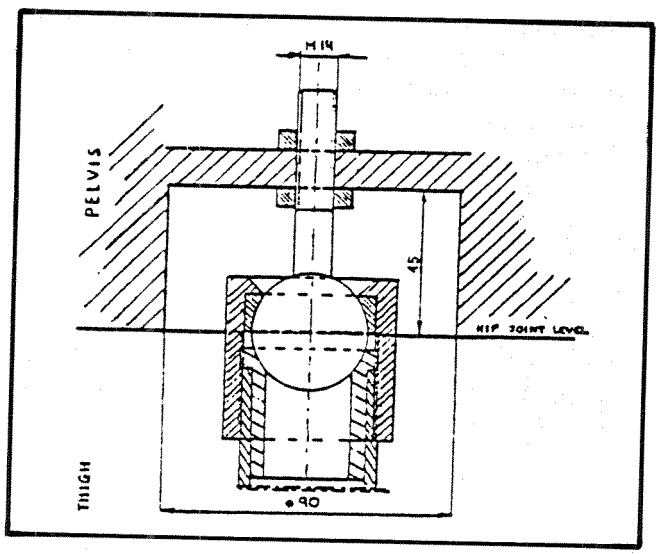

Figure 1. The hip joint.

The Knee Joint

To be able to balance the dummy on one leg and at the same time achieve, in all directions, the characteristics of a human knee struck from the side, it was decided to simulate this joint by a cylindrical steel bar inserted in the long bones. The bar is made of a standard steel (2172). Its

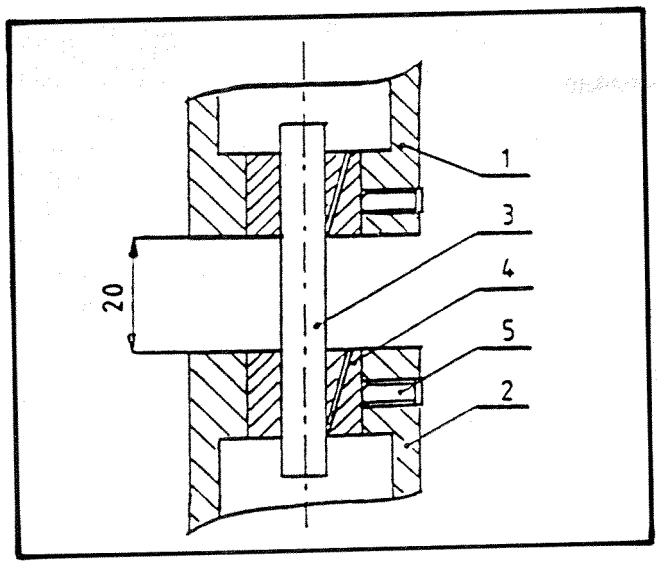

Figure 2. The knee joint

diameter is 8mm, and it is clamped in adjacent ends of the steel tubes in such a way that its free length is 20mm.

This bar will undergo plastic deformation at a bending moment of 70Nm. In a series of tests performed on cadaver legs, this bending moment was found to tear the medial collateral and the cruciate ligaments of the knee. At slightly higher bending moments, fractures of the tibial condyle were also seen(4). The angle of deformation in the knee can, for practical purposes, be used as an indication of the level of the bending moment in tests performed at the same speed. Since the inertia of the lower leg at subsequent impacts can change the angle of permanent deformation in the bar, this angle will have to be determined from film analysis of the sequence.

The Ankle Joint

This joint is similar to the knee joint, but the diameter of the steel bar is 6mm and it has a free length of 20mm. Plastical deformation of this bar will begin at 40Nm. This was found to be the average value in seven tests with cadaver legs when the foot was forced into rapid pronation. As is the case in the knee joint, a rough estimation of the bending moment about this joint can be made from the angle of deformation in tests performed at the same speed.

The Thigh

This segment is 421mm long between the centers of the joints at the hip and the knee. It has a mass of 8.2kg. The center of gravity is adjusted to its correct position at 239mm above the center of the knee joint by means of a lead weight secured by a pair of screws inside the steel tube. To adapt the thigh's contour to that of a human leg

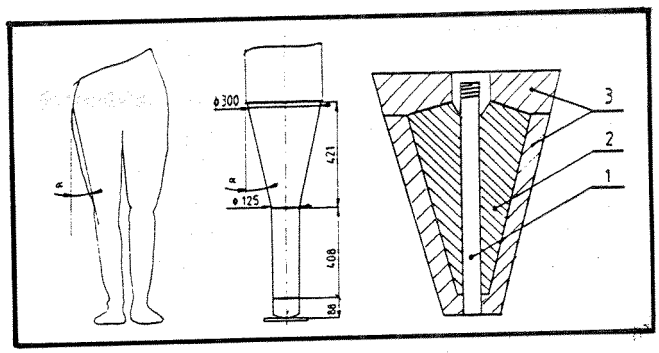

Figure 3. The thigh segment

in this aspect and to the dimensions of the pelvis, a cone of wood is placed over the steel tube. The soft parts are simulated by a 40mm-thick plastic foam with a compliance similar to that of human soft tissues, and a vinyl skin is used for additional protection. It is believed that by this design the hood edge of a car will contact this segment in a similar way as it would a pedestrian in real-world accidents.

The Lower Leg

This segment is 408mm long between the centers of the knee joint and the ankle joint. It has a mass of 3.8kg. The center of gravity is adjusted to its proper position at 231mm above the center of the ankle joint by means of a lead weight secured inside the steel tube by a pair of screws. The soft parts are simulated by a 40mm plastic foam. The damping characteristics of this foam are chosen to insure that the force pulse shape from a bumper impact is similar to that recorded in previous cadaver leg tests.

The Foot

The length of the foot segment is 88mm and has a mass of 1.1kg. The center of gravity is 30mm above ground level when placed on the simulated shoe. The soft parts are then continued from the lower leg over the ankle joint and foot. To allow the foot to tilt at low impact levels on the lower leg, the lower end of this segment has a spherical shape. In the center of this surface, there is a steel peg that fits into a hole in the center of the circular wooden plate simulating the shoe. The steel peg can transfer shear forces to the wooden plate, which has a diameter of 170mm. The simulated shoe has a lower surface of the size of a normal shoe and is covered by rubber.

The reason for not fastening the "shoe" to the foot is that, if the leg is bent, the foot will come off the ground at an early stage and leave the "shoe" on the ground to prevent it from being entangled in the front structures of the car.

Instrumentation

Ten sets of four strain gauges are glued to the metal skeleton as shown in Figure 4. Strain gauges in the B series are placed on the surface of the tube parallel with its longitudinal axis at 0°, 90°, 180°, and 270° of the circumference. They measure deformation caused by bending and shear stress. T_1 and T_2 are glued at right angles to each other and at an angle of 45° to the longitudinal axis of the tube. These measure deformation caused by torsional stress. The D gauges are glued in pairs at 0° and 180° of the circumference in such a way that one pair is parallel and the other at right angles with the longitudinal axis of the tube. They measure deformation caused by tensile stress.

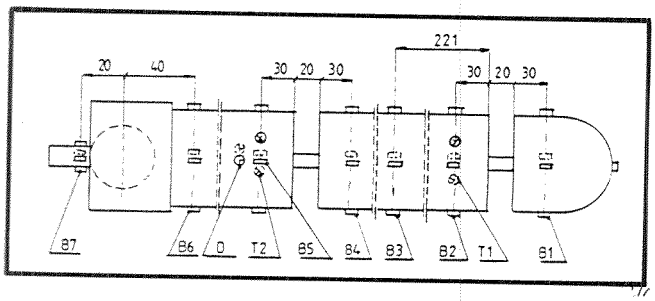

Figure 4. Distribution of strain gauges on the leg model

If the leg model is used in a general way and the impact direction is not predetermined, 17 channels will have to be recorded to enable the more complicated calculations of the various parameters. If on the other hand the impact direction can be predetermined, e.g., to be from 0°, only 10 channels will have to be recorded and still enable calculation of all the parameters.

For calculations of bending moment and shear force about the joint, the signals from corresponding strain gauges on both sides of the joints are used. Although both moments and forces are in fact nonlinear, they can be treated here as linear. Since the gauges are placed close to the joints and the masses in these regions are quite small, the error in this case can be considered as small.

A bending moment about a joint will cause deformation as illustrated in Figure 5.

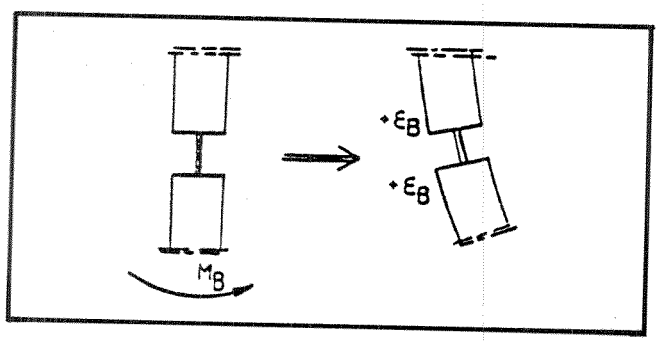

Figure 5. Deformation caused by bending stress

At impact loading of the lower leg, there is also a deformation in the shear mode, and the material will deform as shown in Figure 6.

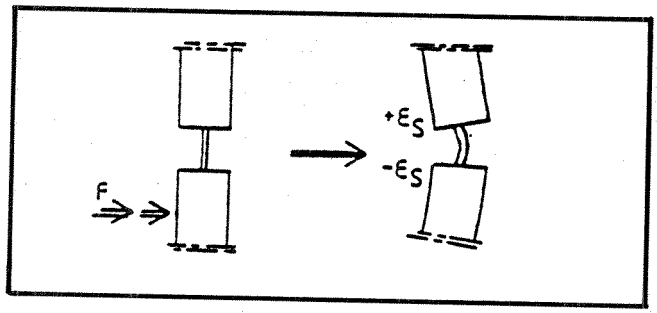

Figure 6. Deformation caused by dynamic shear stress

Each B signal has two components.
Signal B′ from above the knee contains $+\varepsilon_B$ and $+\varepsilon_S$.
Signal B″ from below the knee contains $+\varepsilon_B$ and $-\varepsilon_S$.
Deformation caused by the bending moment is then

$$\frac{B' + B''}{2}$$

Deformation caused by shear froce is then

$$\frac{B' - B''}{2}$$

In these calculations of bending moment and shear force, the measured deformation and the material constants for this model are used. Tensile force and torque can be derived directly from the deformations (D and T signals) and the corresponding material constants.

Wiring diagrams to be used if the model is impacted from a defined direction at 0°.

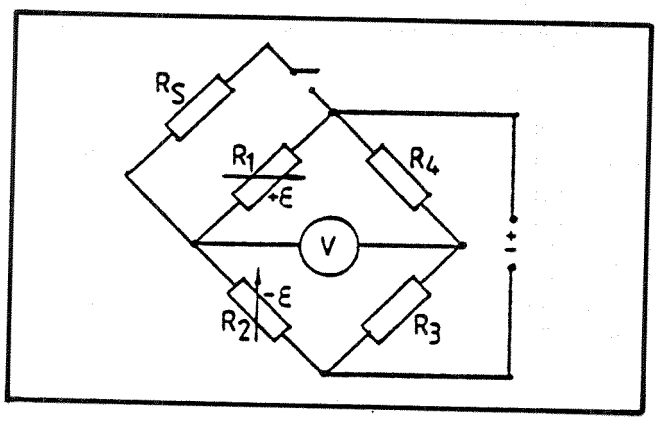

Figure 7. Wiring for strain gauges of the b series

This system is not sensitive to tensile and torsional stress.

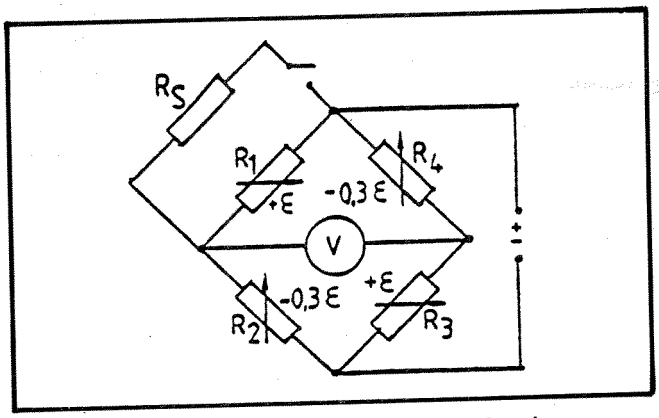

Figure 8. Wiring for strain gauges of the d series

This system is not sensitive to flexural and tensile stress.

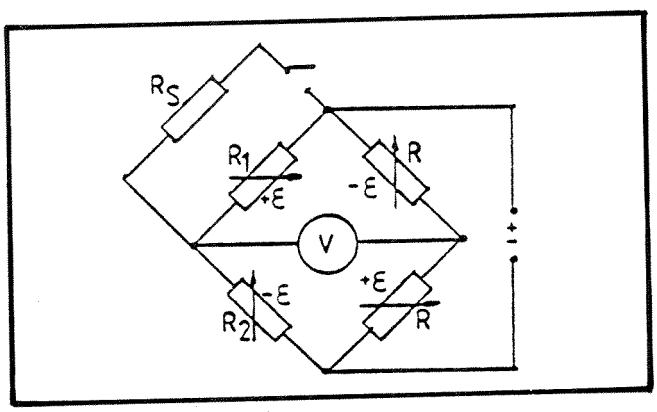

Figure 9. Wiring for the strain gauges in the t series

This system is not sensitive to flexural and tensile stress.

Wiring diagrams to be used if the model is impacted from any direction. Each set of strain gauges in the B series will have to be divided into two bridges.

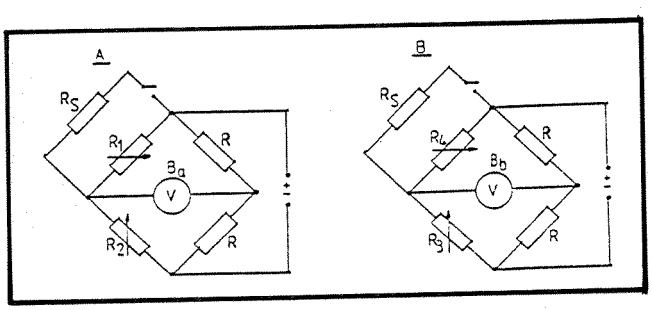

Figure 10. Wiring for the gauges in the b series

Bridge A will produce signal B_a and bridge B signal B_b. The combined deformation is: $|B| = \sqrt{B^2_a + B^2_b}$ and the sign will have to be determined from analyses of the signals and the state of deformation.

Conclusion

This paper gives the results of a first attempt to develop a round symmetrical dummy to be used in pedestrian tests.

The dummy is designed according to the latest available anthropometric and biomechanical data. Its symmetry around the vertical axis would allow it to have good repeatability for the kinematic as well as for the injury parameters. It allows a measurement of "uncommon" biomechanical parameters that are related to injury mechanisms. Its leg is instrumented to determine the distribution of forces and momenta applied to the leg.

The several body segments were tested separately, and the next phase will be the validation of this dummy in car pedestrian tests.

References

1. Zuniga, E.N., and L.A. Leavitt, "Analysis of gait: A method of measurement," In *Biomechanics IV*, Proceedings from the Fourth International Seminar on Biomechanics, University Park, Pennsylvania, Editors: Richard C. Nelson and Chauncey A. Morehouse, Macmillan, London, 1974.
2. Strandberg, Lennart, "The mechanics of slipping accidents," National Board of Occupational Safety and Health Accident Research Section, 1980.
3. Aldman, B., T. Anderlind, J. Kajzer, M. Malmqvist, H. Mellander, and T. Turbell, "Load transfer from the striking vehicle in side and pedestrian impacts," Proceedings Tenth International Technical Conference on Experimental Safety Vehicles, Oxford, 1985.
4. Aldman, B., L. Thorngren, O. Bunketorp, and B. Romanus, "An experimental model system for the study of lower leg and knee injuries in car pedestrian accidents," Proceedings Seventh International Technical Conference on Experimental Safety Vehicles, pp. 841-849, Wolfsburg, 1980.

Head and Neck Injuries in Human Cadavers From Lateral Impacts

Michael J. Walsh and
Barbara J. Kelleher
Calspan Corporation

Charles M. Severin
State University of New York at Buffalo

Abstract

Head-neck injuries occur frequently in pedestrian and occupant automotive accidents even at relatively low speeds. This paper describes the results of laboratory impact experiments using human cadavers in pedestrian/vehicle impacts and lateral-to-medial head impacts at well-known, controlled speeds. Cerebral trauma, with and without skull fracture, is discussed as a function of impact configuration and velocity. Cervical spine and cord injuries are also discussed with regard to the same parameters. Data presented include impactor mass and velocity, head acceleration measurements, complete autopsy and dissection results, and the clinical evaluation of the effect on a person of the observed trauma.

Eighteen cadavers have been exposed to lateral-to-medial head impacts by two mechanisms. Eight of the subjects were exposed to pedestrian impacts wherein their head contacted the hood of the striking vehicle, and 10 were subjected to linear impactor tests in which the head was struck by a 52lb impactor with a flat faceplate that was rigid for some experiments and padded for others. The presentation and discussions of these experiments in this paper will be directed toward the clinical results and evaluations of the trauma observed in the brains of the cadavers in addition to the measurements of accelerations and the calculations of the Head Injury Criterion (HIC) values. It must be understood at the outset that while lesions in areas of the brain can be determined in impact experiments using human cadavers, and the bodily functions that would be affected by the lesions in these various areas can be identified, the extant functions over a period of time cannot be determined. Even with sectioning of the brain and quantification of the depth (for example) of the trauma in a given area, it is not possible to ascertain the level of recovery that a living subject might be capable of achieving. It is the belief of the authors, however, that the reporting of the types of trauma to the brain and the functional impairment that may be realized (even qualitatively) from specified impacts is important as initial data base information for dissemination to the transportation safety community.

Cadaver selection criteria and the handling and testing protocols were the same for these experiments as those described in (1).

Test Procedures

The eight cadavers that were exposed to head impacts to the hoods of cars were used in pedestrian sled tests. Seven were struck on their left side and one (CM22), because of a previous left leg injury, was struck on the right side. All of these cadavers were instrumented in the head with a 9 accelerometer head mount (3-2-2-2) attached at the apex of the skull. There was also a triaxial accelerometer package installed in the mouth of the subjects. The 9 accelerometer head unit (9AU) was positioned using a Kapf stereotaxic frame that had been modified for a human skull and measurements of three points were recorded in the A-P, M-L, and S-I directions. Using this same device, measurements were taken of three points on an extension of the mouth mount. Accelerometers for the mouth were affixed to a dental impression tray, and the tray was secured in the mouth with an acrylic resin.

The 10 cadavers exposed to the lateral-to-medial head impactor tests were also instrumented with the 9AU mount on the apex of the skull, but the mouth mount was not used during these experiments. The impacting device was a flat-faced, 52lb, linearly accelerated ram with its vertical centerline aligned on the Frankfort plane. The striking surfaces ranged from 28in^2 (6in diameter), 54in^2 (6-3/4in by 8in rectangle, to 80in^2 (8in by 10in rectangle). All of the impacts were to the left side of the head of the subjects. Eight experiments were performed with the bare aluminum face of the impactor striking the lightly shrouded head, and two were performed with foam padding covering the hard aluminum face plate. With the exception of two exposures, the velocity at impact was held at approximately 13fps. The exceptions were a 7fps impact chosen to obtain a data point at the impact velocity used in test dummy certifications and an 11fps impact as an intermediate point. Table 1 presents information on the tests performed.

For the impactor experiments, the cardiovascular system of the brain was pressurized. The procedure used was one in which a catheter was inserted bilaterally into the internal carotid arteries to a level of ½in below the base of the skull. The external carotids were ligated, and the internals were tied around the catheters to form a seal. Dianeal, with a mixture of India ink and Toluidine blue, was injected and the pressure was maintained and monitored during impact. In general, good perfusion to

Table 1. Test matrix

Subject	Test Type	Velocity fps	Padding	Age	Sex	Height in	Weight lb
CM20	PED	33.0	NONE	72	M	72.0	161
CM21	PED	29.6	NONE	77	F	60.0	123
CM22	PED	28.5	NONE	71	F	62.0	156
CM23	PED	35.2	NONE	77	M	68.5	155
CM24	PED	28.0	NONE	46	M	70.0	132
CM25	IMP	13.2	NONE	55	M	72.0	188
CM26	PED	35.8	NONE	77	M	68.0	157
CM27	PED	34.5	NONE	63	M	71.0	194
CM28	PED	34.6	NONE	79	F	62.0	121
CM29	IMP	13.1	NONE	71	M	67.0	151
CM30	IMP	13.1	NONE	66	M	69.0	185
CM31	IMP	13.2	NONE	57	M	67.5	161
CM32	IMP	7.3	NONE	60	F	65.5	126
CM33	IMP	12.9	NONE	70	F	67.0	131
CM34	IMP	11.0	NONE	55	M	71.0	141
CM35	IMP	13.1	NONE	69	M	69.0	150
CM36	IMP	12.8	2.0 IN.	61	M	69.0	160
CM37	IMP	12.8	1.0 IN.	57	F	62.0	103

the brain, by the dye, was noted in all subjects allowing for an accurate evaluation of impact-induced lesions in the various regions of the brain. This technique had not been developed at the time of the pedestrian impacts and therefore was not used in those experiments. Post-mortem brain lesions were observed in some of the pedestrian subjects, but because of the lack of pressurization and staining, it is possible that some may not have been identified.

The velocities listed in Table 1 are the velocity of the head in the medial-to-lateral direction at the time of impact with the hood of the vehicle for the pedestrian tests and the velocity of the impactor just prior to contact for the impactor tests.

Clinical Results

Cerebral trauma was observed with and without skull fracture during these experiments. Skull fracture was observed in only one of the pedestrian tests (CM23) and two of the impactor tests (CM29 and CM35). A clinical description of the trauma observed is presented below along with an evaluation of the responses that could be expected based on injury to these areas of the brain. As noted earlier, the depth or extent of these responses and the temporary or residual impairment of a living person cannot be determined from these experiments with human cadavers.

Cervical spine injuries were observed in five of the eight pedestrian tests. These extension-type injuries were caused by the kinematic responses of the cadaver after the upper torso and the head had contacted the hood of the vehicle. In these cases, the cadaver, having been struck by the vehicle on the left side, would roll onto the hood and eventually be in a position where the head and the chest were flat on the hood surface. The forces that had been imparted to the lower extremities of the subject(1) caused the cadavers to rotate about the neck and put it into hyperextension.

In this section, the acceleration versus time graphs of the head impacts are presented along with a computed HIC value for each of the 18 cadavers. A narrative description of the observed trauma and a summary of the neurological deficit that would be expected from the injury follow each graph. An Abbreviated Injury Scale (AIS) code is assigned for each subject. Table 2 presents the definition of the codes as described in (2).

The peak acceleration data are resultants computed from the mouth-mounted accelerometers in the pedestrian (PED) subjects and from the 9AU mount X0, Y0, and Z0 in the impactor (IMP) subjects. They are filtered at channel class 1000 in accordance with the SAE recom-

Table 2. Abbreviated injury scale (AIS)

Code	Description
0	No Injury
1	Minor
2	Moderate
3	Serious
4	Severe
5	Critical
6	Maximum Injury - Unsurvivable in 1980
7	Injured, Unknown Severity
9	Unknown if injured

mended practice J211b. While it is understood that these instruments are not located at the head c.g., the HIC values were calculated for the purpose of having a common reference number. The mouth mount is closer to the c.g. than is the 9AU mount, but in the lateral-to-medial impacts the head translated laterally almost as a rigid body in these experiments.

The anterior and posterior longitudinal ligaments, spinal cord, left prevertebral muscles, and the sympathetic chain were severed. Cervical vertebra number 6 (CV6) was displaced anteriorly.

The subject would demonstrate quadriplegia, and probably be incontinent. He would suffer from permanent constriction of the pupils and lack of ability to perspire around the eyes. The blood vessels in the area of the eyes would be permanently dilated causing the skin in that area to feel hot (Horners syndrome). These injuries would constitute an AIS 5.

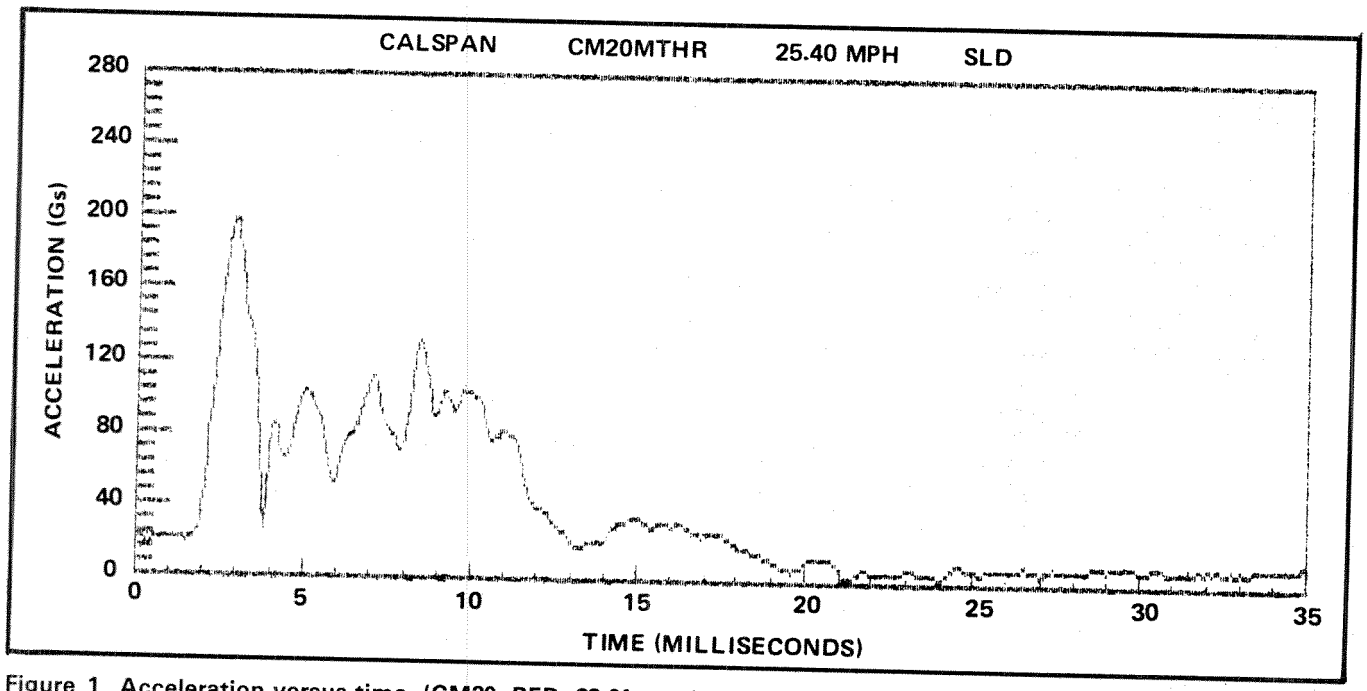

Figure 1. Acceleration versus time. (CM20, PED, 33.0fps velocity at impact. HIC = 868)

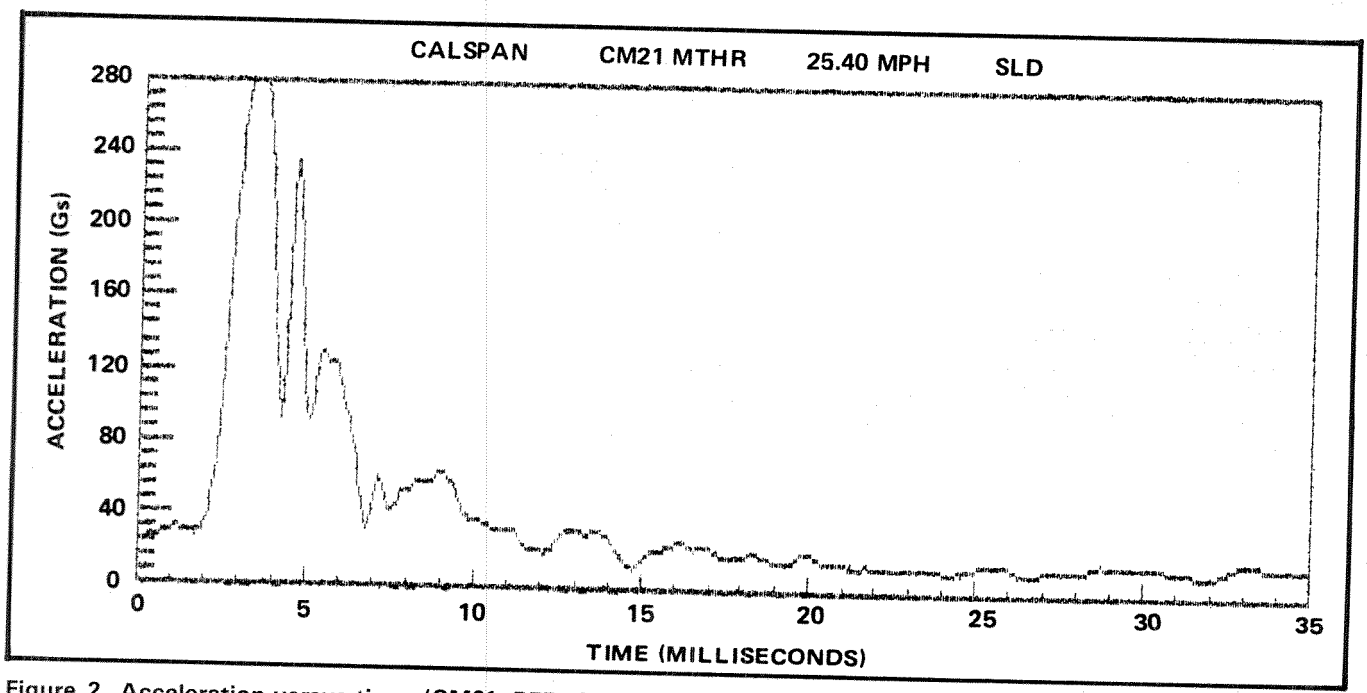

Figure 2. Acceleration versus time. (CM21, PED, 29.6fps velocity at impact. HIC = 1864)

There was a fracture of the cervical spine at CV7. TV1 was also fractured. No spinal cord involvement could be determined. There was slight traumatic subarachnoid hemorrhage on the interior surface of the right temporal lobe. Serial sections of the brain did not show any areas of hemorrhage.

The fractures of CV7 and TV1 would involve the nerves of cervical segments (CS) 7 and 8 and perhaps T1 causing damage to the ulnar nerve, thereby a loss of sensation in the ulnar region of the forearm and hand. Subarachnoid hemorrhage can cause serious damage in the living, depending on the duration and amount. It was not possible to estimate potential duration and amount in this subject. These injuries would constitute an AIS 3 in the neck and an AIS 3 in the head.

Undisplaced fractures were observed at the level of CV2-CV3 and CV7-TV1. The pedicles of CV2 were also fractured. The anterior and posterior longitudinal liga-

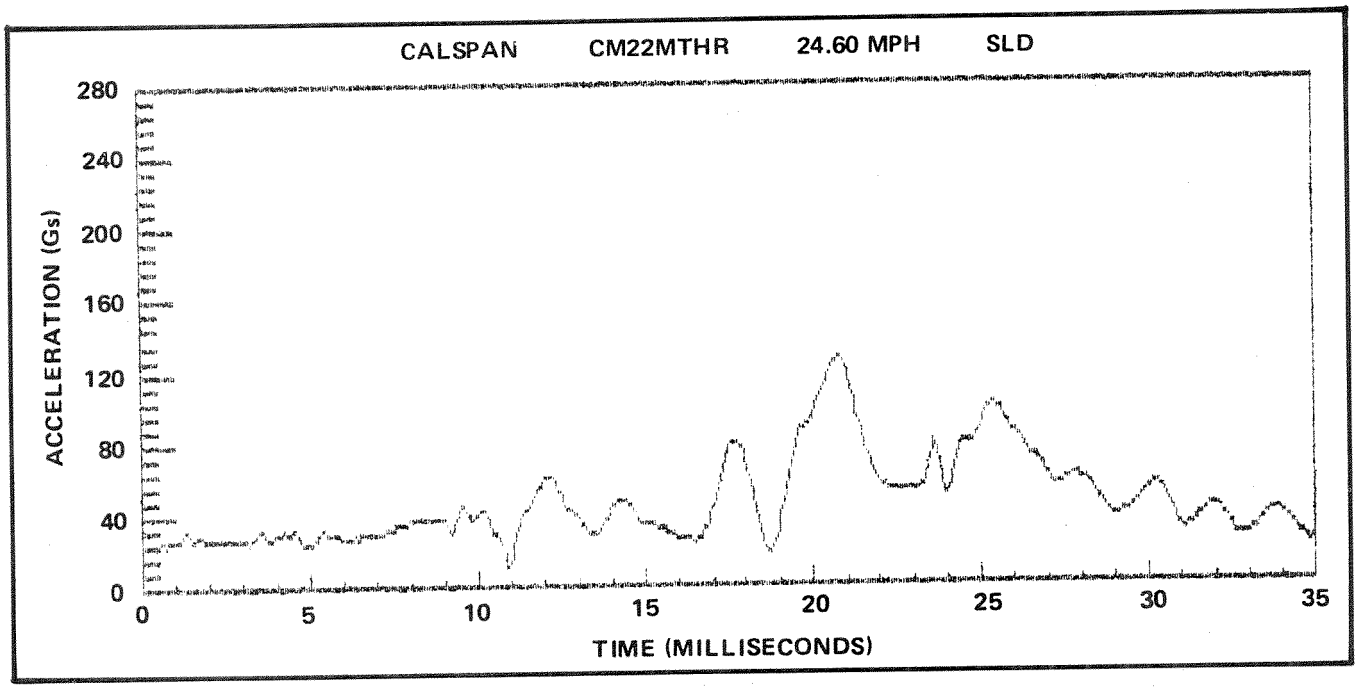

Figure 3. Acceleration versus time. (CM22, PED, 28.5fps velocity at impact. HIC = 525)

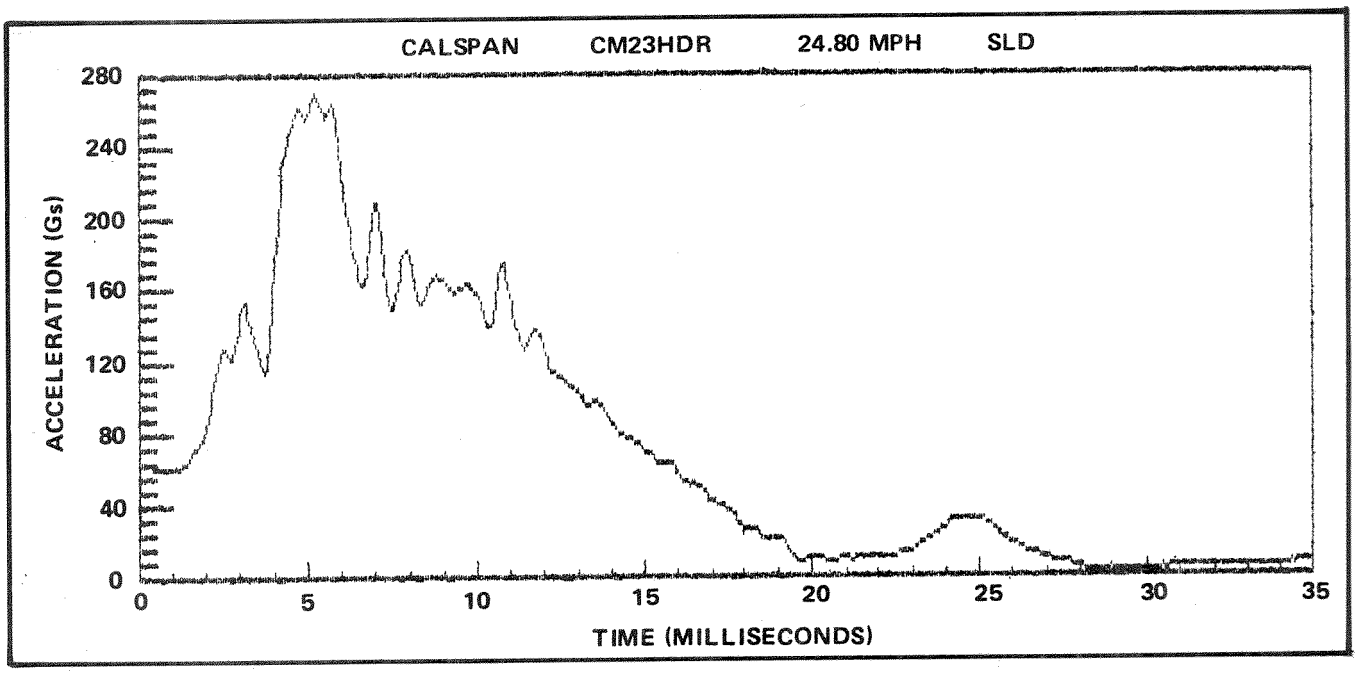

Figure 4. Acceleration versus time. (CM23, PED, 35.2fps velocity at impact. HIC = 3967)

ments were torn. Upon removal of the calvaria, there was no epidural hemorrhage present. Slight subdural bleeding was present over the brain. There was evidence of slight subarachnoid hemorrhage in the temporal lobes. Slight bleeding was seen into the ventricular cavity.

There would be a probable loss of sensation over the shoulders, on the back of the head, and on the side of the neck due to the potential nerve involvement in the kinematics during the fractures. The potential consequences of subarachnoid hemorrhage noted above hold for this subject. Also, there was no way of determining the duration or amount of bleeding that would have contributed to the bleeding that was observed into the ventricular cavity. This subject would also be assigned an AIS 3 for both the head and neck injuries.

The subject experienced fractures of the skull. There was a separation at the zygomatico-frontal suture, and the periorbita beneath the suture was lacerated. The lateral part of the frontal bone was fractured into five pieces. The opterion was displaced internally. Upon dissection, the orbital laminar (lamina papyracea) of the ethmoid bone was found to be fractured. The bony fragments were displaced interiorly with the bone piercing the periorbita. Fragments of the orbital part of the frontal bone lacerated the periorbita and extended into the periorbital fat. Branches of the opthalmic artery and veins, the optic nerve, and extraocular nerves and vessels as well as the temporal branches of the facial nerve were intact.

When the calvaria was removed, blood was found in the epidural space beneath the frontal bone fractures. This blood appeared to be caused by a laceration of the middle meningeal vessels. On the right side of the anterior cranial fossa, the orbital parts of the frontal bone were fractured at the suture between the orbital plate of the frontal bone and the lesser wing of the sphenoid bone.

Examination of the brain did not reveal any identifiable damage. The epidural hematoma would cause a displacement of the brain and thereby an increase in pressure within the cranial vault. The magnitude of these would be dependent upon the duration and amount of the hemorrhage. These could not be estimated in this subject. As noted earlier, however, there had been no attempt to pressurize nor maintain pressure on the brain during contact. These injuries would be assigned an AIS 4.

There was no injury observed to the head, brain, neck, or spinal cord of this subject. An AIS value of 0 would be assigned.

The damage involved the anterior one-third of the superior, middle, and inferior frontal gyri. The anterior one-quarter of the superior, middle, and inferior temporal gyri was also damaged.

The damage to these areas would indicate that the subject would most likely undergo personality changes. He may become indifferent. This damage would be an AIS 3.

There was a total rupture of the ligaments forming the anterior longitudinal ligament capsule of the vertebral joint between CV3 and CV4 as well as CV5 and CV6 and CV6 and CV7. The spinal cord appeared to be intact, however. The skull and brain were normal.

The potential deficit associated with this type of injury could not be assessed. However, an AIS 3 would be assigned for the neck injuries.

Examination of the neck showed a displacement between CV6 and CV7, with the intervertebral disk

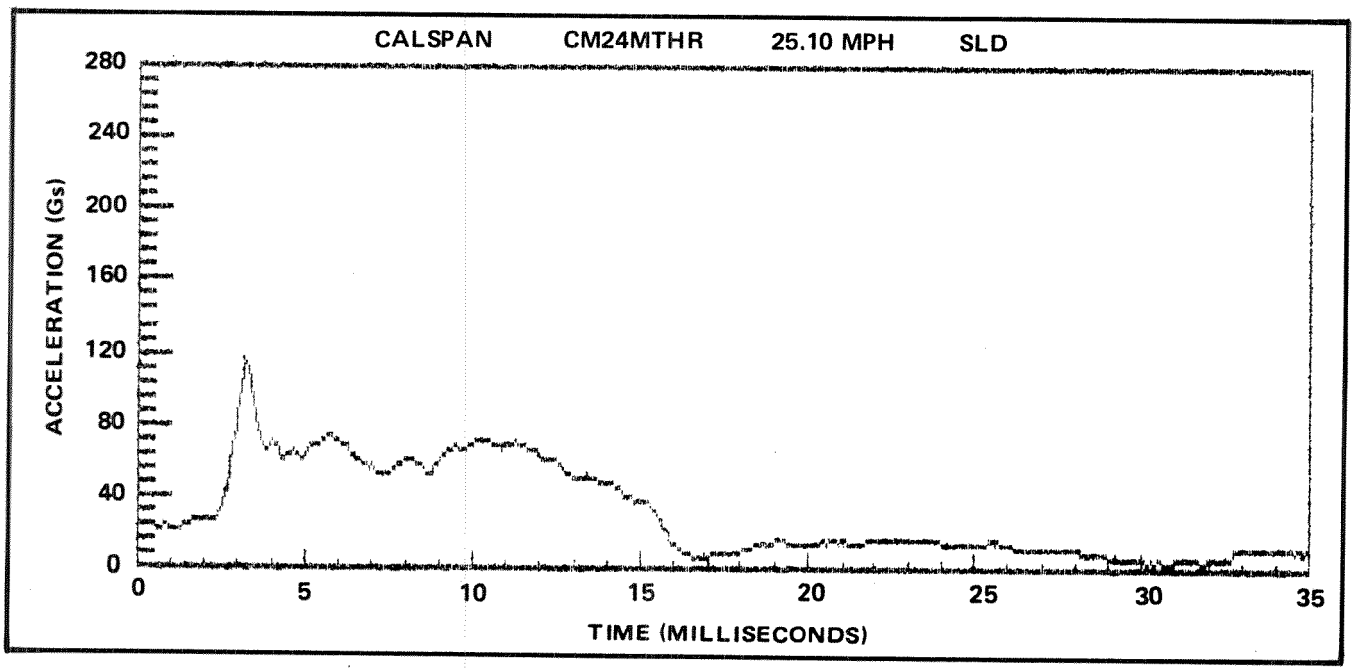

Figure 5. Acceleration versus time. (CM24, PED, 28.0fps velocity at impact. HIC = 468)

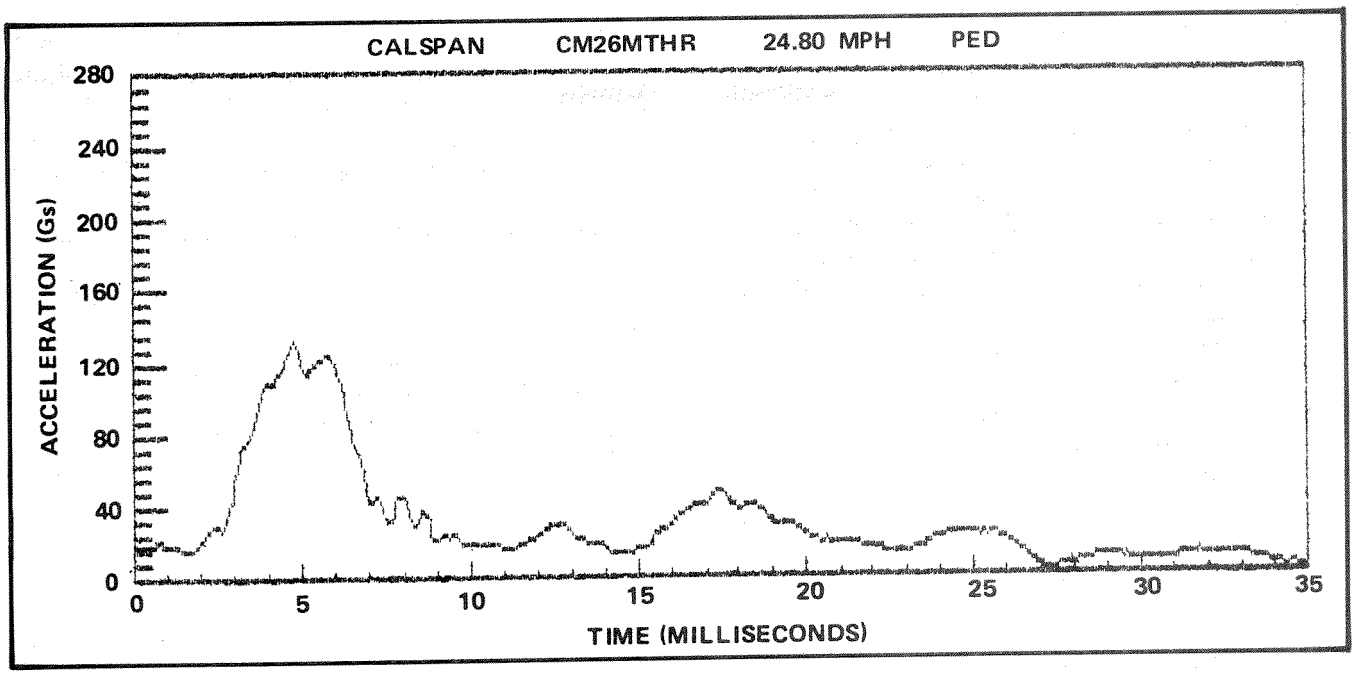

Figure 6. Acceleration versus time. (CM25, IMP, 13.1fps velocity at impact. HIC = 1021)

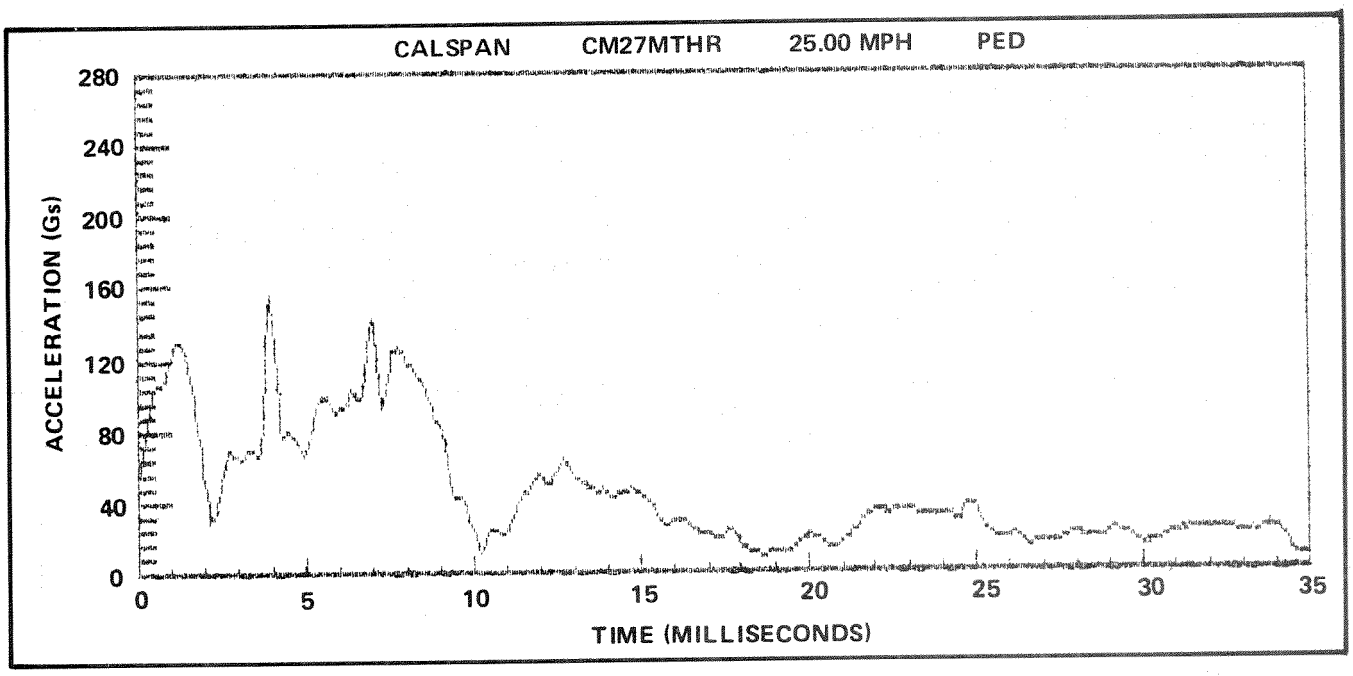

Figure 7. Acceleration versus time. (CM26, PED, 35.8fps velocity at impact. HIC = 417)

attached to CV7, which ruptured the anterior longitudinal ligament but did not sever the spinal cord. There was no damage to the skull, dura, meningeal vessels, or brain.

The potential deficit associated with this type of injury could not be assessed. These neck injuries would be an AIS 3.

There was no injury observed to the head, brain, neck, or spinal cord of this subject. An AIS value of 0 would be assigned.

This cadaver experienced a skull fracture splitting the sphenopetrosal suture in the middle cranial fossa on the left side. The greater superficial petrosal nerve on the left side was cut, and there was a contusion of the inferior part of the temporal lobe on its medial side. There was also damage to the left uncus (areas 34 and 35)(3) and to the medial part of the parahippocampal gyrus (areas 28, 35, and 36).

There would be a loss of lacrimation and a decrease in mucous production on the left side of this subject. The skull fracture would constitute an AIS 3.

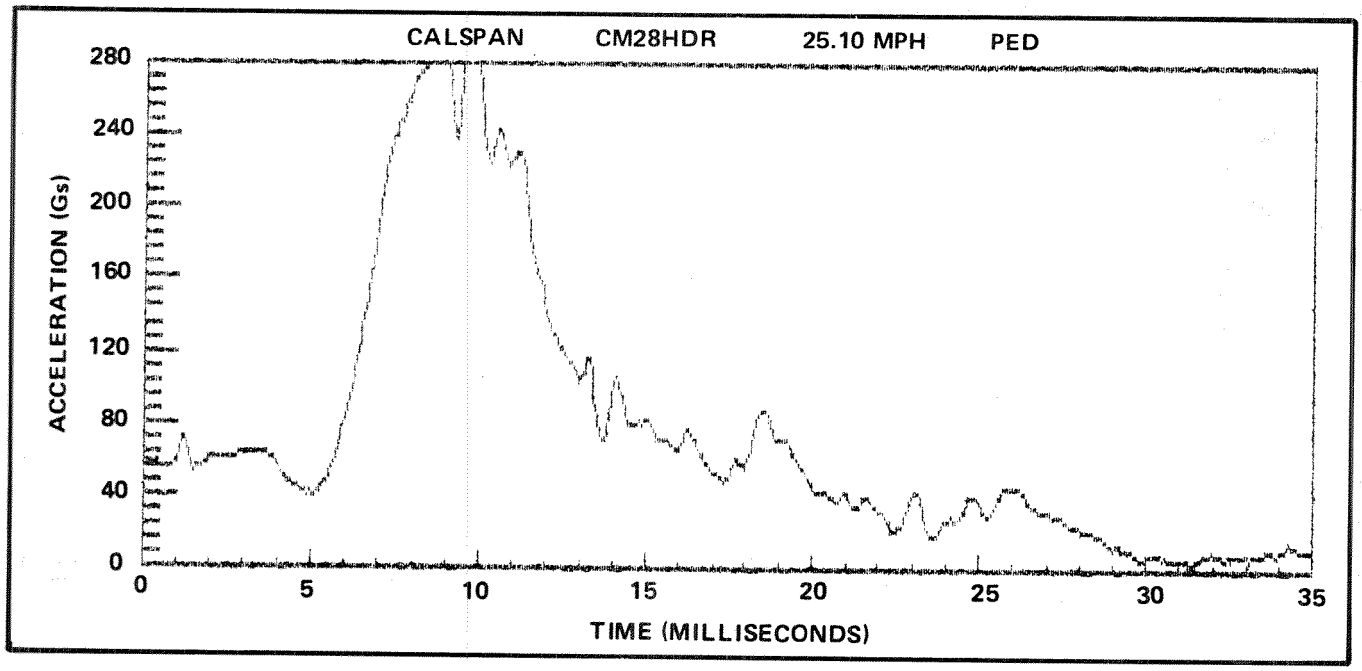

Figure 8. Acceleration versus time. (CM27, PED, 34.5fps velocity at impact. HIC = 761)

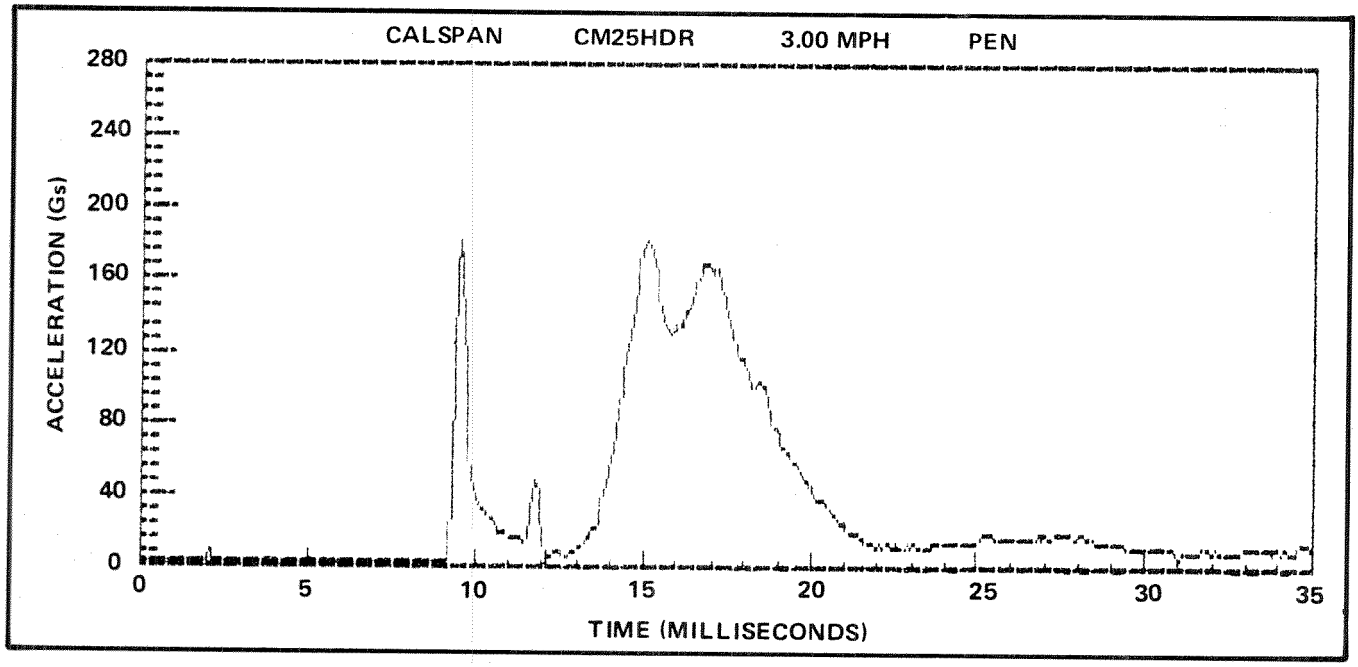

Figure 9. Acceleration versus time. (CM28, PED, 34.6fps velocity at impact. HIC + 4787)

On the right side, the subject exhibited damage to the superior lateral part of the pre- and post-central gyri and to the paracentral lobule (areas 4, 3, 1, and 2) and the pars opercularis and triangularis (areas 44 and 45). On the left side, in addition to damage to areas 4, 3, 1, 2, 44, and 45, the subject demonstrated damage to the caudal one-half of the superior frontal and middle frontal gyri (areas 6 and 8) and the superior temporal gyrus (area 22).

The damage to areas 4 and 6 would cause paresis or paralysis depending on the severity. The damage to area 8 would show no noticeable deficit, while that to areas 3, 1, and 2 would cause an inability to feel any sensations. Aphasia would be the result of the trauma to areas 44 and 45, and the aphasia notwithstanding the damage to area 22 would cause the inability to speak meaningful sentences. These brain injuries would be an AIS 3.

Multiple brain contusions were observed on this subject. In general, they were similar to those observed in CM30 with the exceptions that areas 3, 1, and 2 were not damaged but the angular gyrus on the left side (area 39)

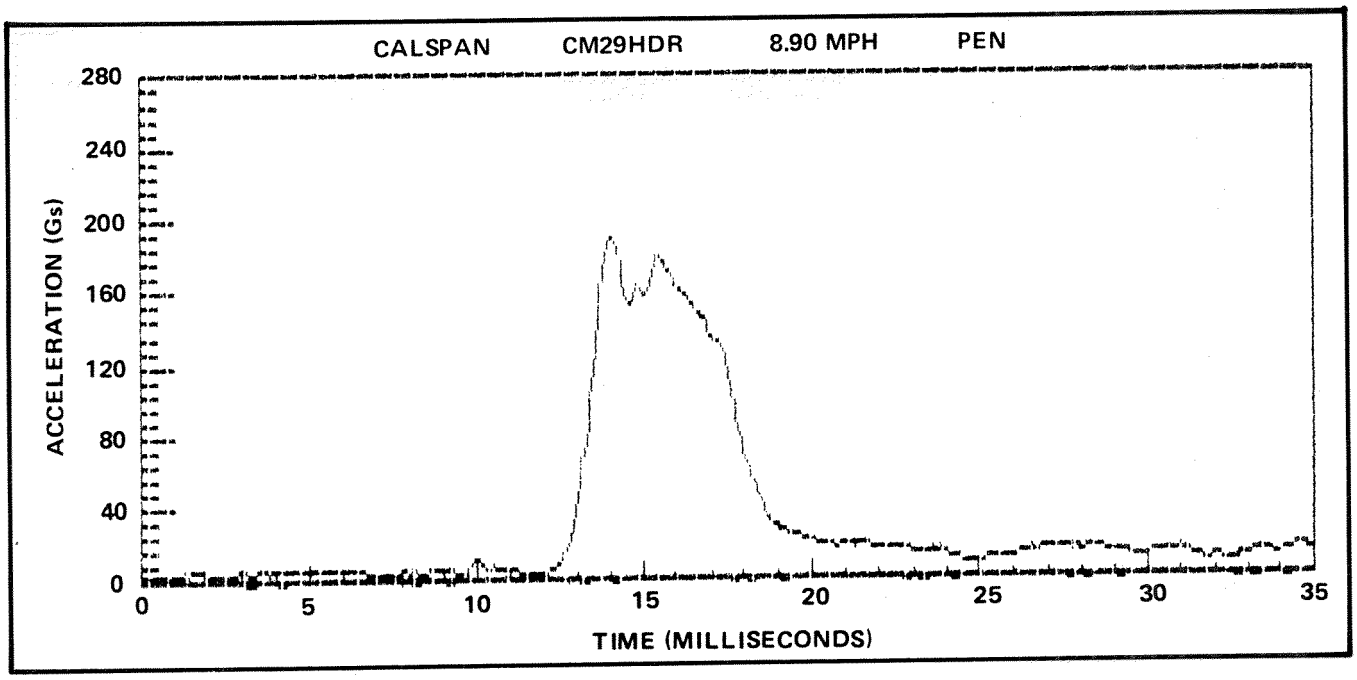

Figure 10. Acceleration versus time. (CM29, IMP, 13.2fps velocity at impact. HIC = 1290)

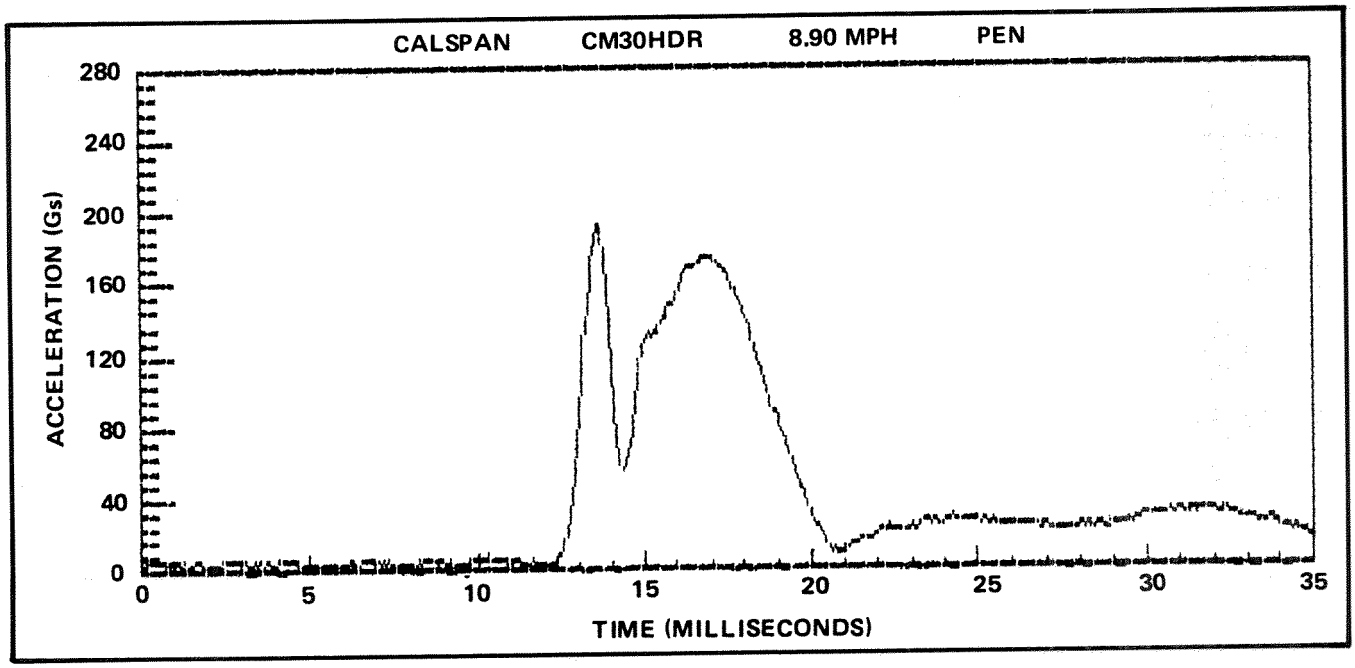

Figure 11. Acceleration versus time. (CM30, IMP, 13.1fps velocity at impact. HIC = 1306)

was damaged, in addition to the anterior temporal poles bilaterally. This subject then exhibited damage to areas 4, 6, 8, 44, 45, 39, and 22.

In addition to paresis or paralysis, aphasia, and the inability to form meaningful sentences but without the ability to feel any sensations (areas 3, 1, 2), the person would demonstrate a problem in recognizing certain written words (area 39). These injuries would constitute an AIS value of 3.

There was no damage observed during the dissection of the brain of this subject.

Since there was no identifiable damage observed, no noticeable deficit could be determined, and an AIS value of 0 would be assigned.

Brain contusions were found in the right cerebral hemisphere in the inferior part of the pre- and post-central gyri involving areas 4, 3, 1, and 2. There was some damage to the left uncus.

Paresis or paralysis (area 4) and an inability to feel sensations (areas 3, 1, and 2) in the head/neck regions would be exhibited by a subject with these types of trauma. This brain damage would be an AIS 3.

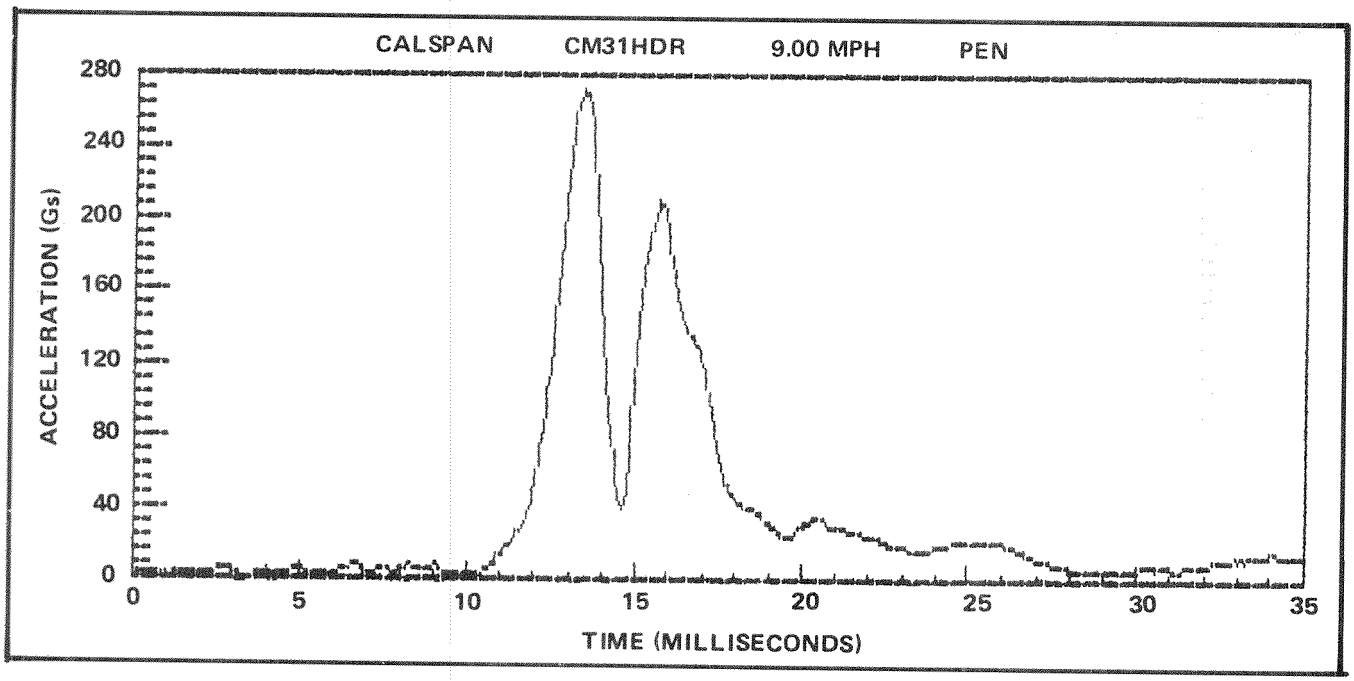

Figure 12. Acceleration versus time. (CM31, IMP, 13.2fps velocity at impact. HIC = 1545)

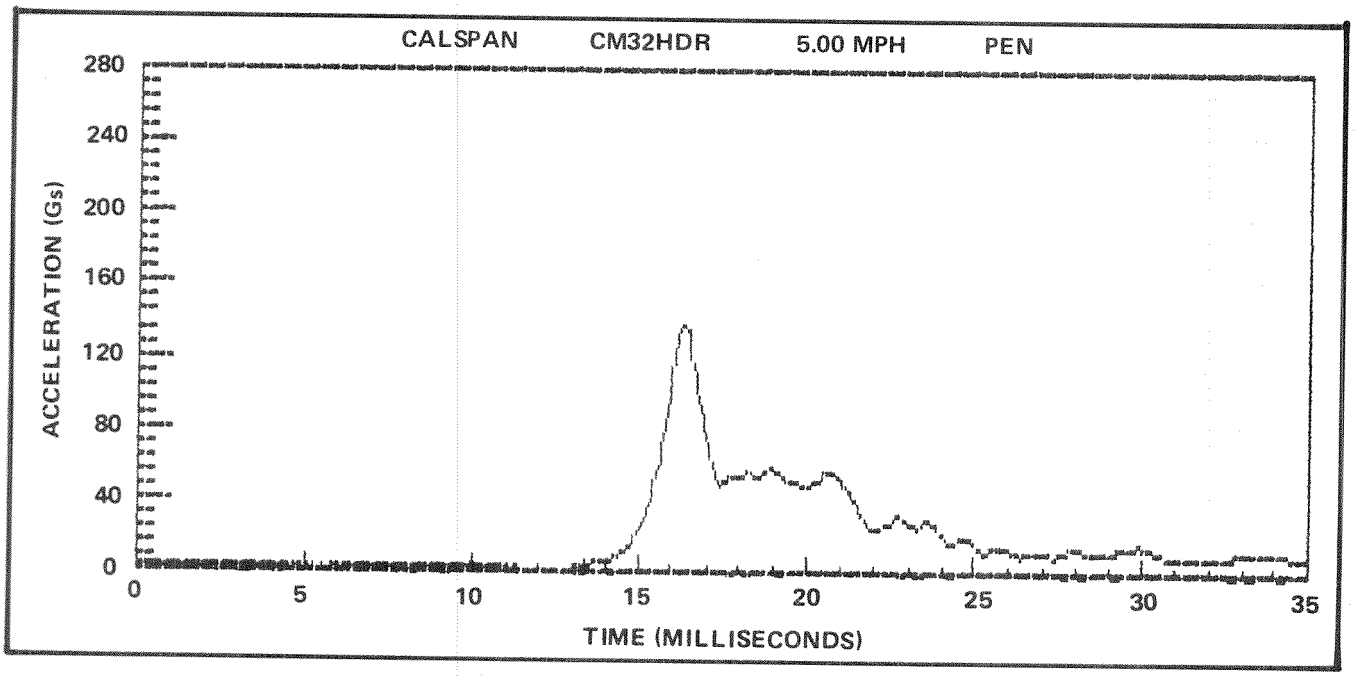

Figure 13. Acceleration versus time. (CM32, IMP, 7.3fps velocity at impact. HIC = 206)

On the right side, brain contusions of the superior and lateral parts of areas 4, 3, 1, and 2 were observed. Additionally, there was damage to the superior parietal lobule (areas 5 and 7).

The inability to feel any sensations notwithstanding areas 5 and 7 would cause a problem with the person's ability in localizing sensations. The paresis or paralysis caused by the damage to area 4 is noted. This brain damage would also be assigned an AIS value of 3.

The middle cranial fossa displayed a fracture just anterior to the petrous portion of the temporal bone. The fracture passed directly through the tegmen tympani toward the cavernous sinus. The fracture did not cross the basilar part of the occipital bone, nor the hypophyseal fossa. Upon examining the tympanic, cavity, no damage to the tympanic membrane, ossicles, chorda tympani, or facial nerve was observed. The semicircular canals were also intact. On the impacted side, contusions were

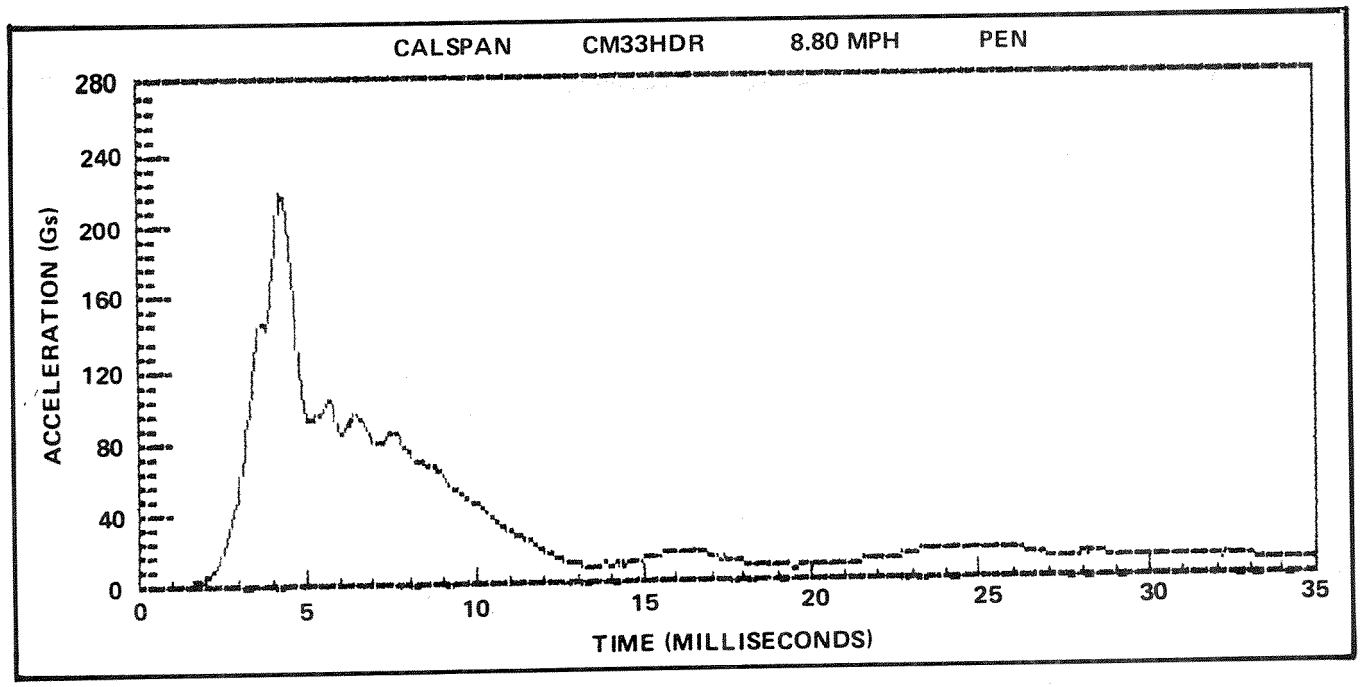

Figure 14. Acceleration versus time. (CM33, IMP, 12.9fps velocity at impact. HIC = 658)

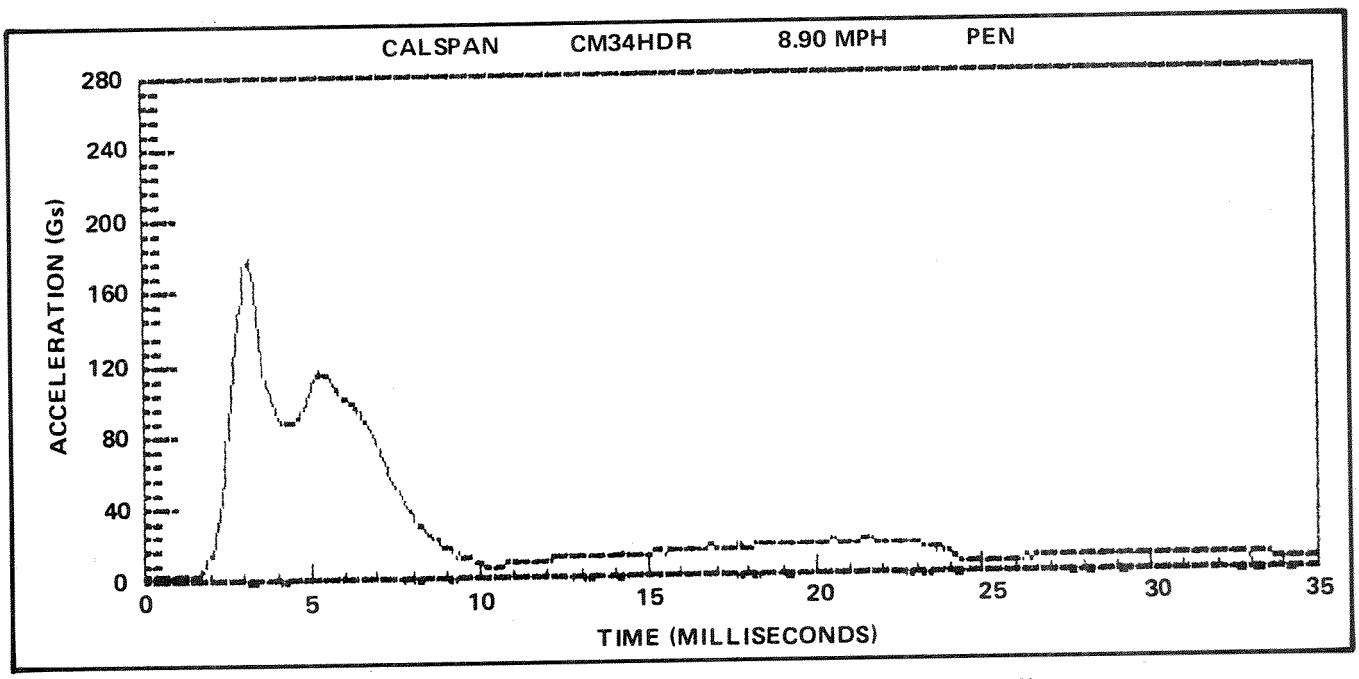

Figure 15. Acceleration versus time. (CM34, IMP, 11.0fps velocity at impact. HIC = 549)

evident on the superior portion of the central sulcus affecting areas 4 and 6 and areas 3, 1, and 2 as well as 5 and 7 in the head region. On the contrelateral side, contusions were evident on areas 3, 1, and 2 and areas 5 and 7 in the head region and in area 4 in the upper extremity region.

The effect of the contusions on this subject would be as noted in the other subjects with damage to areas 4 and 6 (paresis or paralysis), 3, 1, and 2 (inability to feel any sensation), and 5 and 7 (problem in localizing sensation). An AIS 3 would be assigned to this subject.

There was no damage observed during the dissection of the brain of this subject.

Since no trauma could be identified, no neurological deficit could be determined. An AIS of 0 would be assigned to this subject.

Brain contusions were found bilaterally on the entire frontal lobe extending posteriorly to the precentral gyrus. On the right side, damage occurred to areas 44 and 45.

Aphasia would result to some degree in this subject along with a potential for personality change. An AIS of 3 would be assigned for these brain contusions.

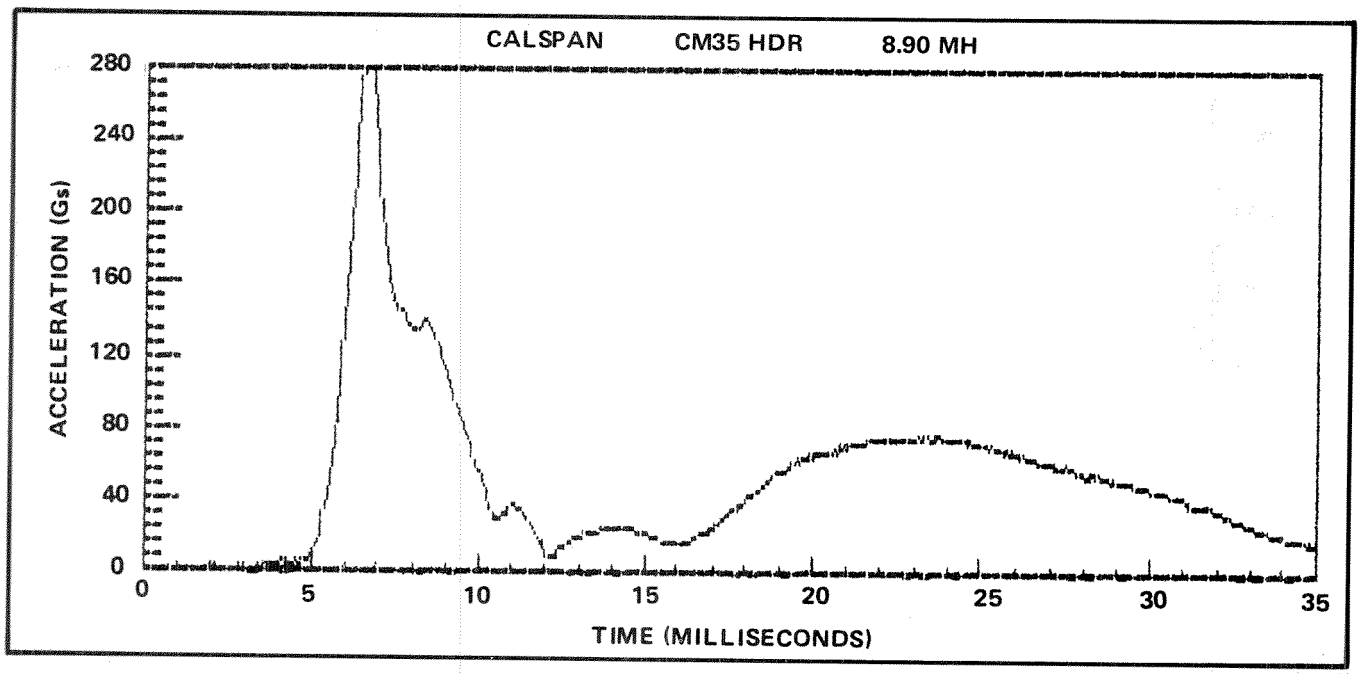

Figure 16. Acceleration versus time. (CM35, IMP, 13.1fps velocity at impact. HIC = 1284)

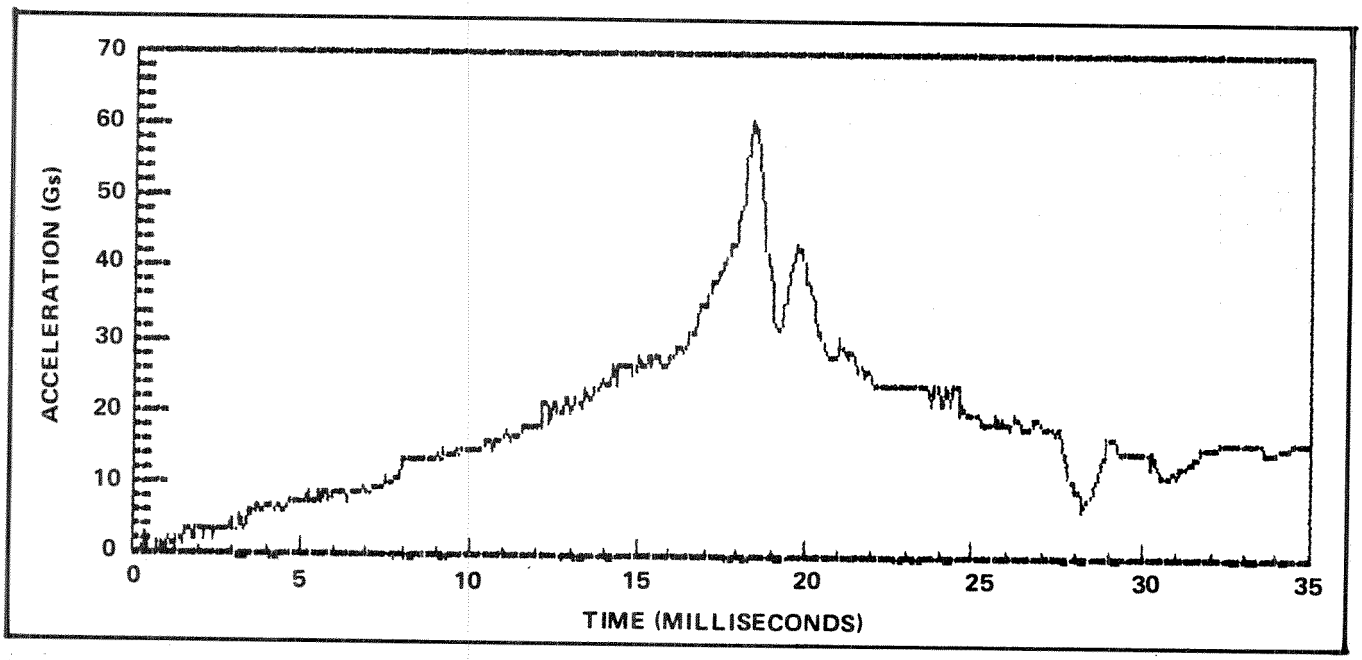

Figure 17. Acceleration versus time. (CM36, IMP, 12.7fps velocity at impact. HIC = 63)

Conclusion

With the exception of those four cadavers that experienced no discernible injury (AIS 0), and CM20 (severed spinal cord, AIS 5) and CM23 (epidural hematoma, AIS 4), all of the subjects demonstrated an AIS 3 either in the head or the neck and, in some cases, in the head and the neck. If only the head injuries are considered, a range of HIC values from 525 through 3967 produced AIS 3 level injuries. CM23 with an HIC of 3967 in addition to the epidural hematoma experienced multiple skull fractures. There is essentially no correlation demonstrated in these results between HIC value and brain injury. AIS 0 levels were observed at a range of HIC values of 63 (CM36) through 4787 (CM28). The acceleration versus time history (Figure 9) and the high-speed movies of CM28 indicate that there is no artifactual contribution that would distort the HIC calculation, but other than this value all of the AIS 0 subjects demonstrated HIC values below 500.

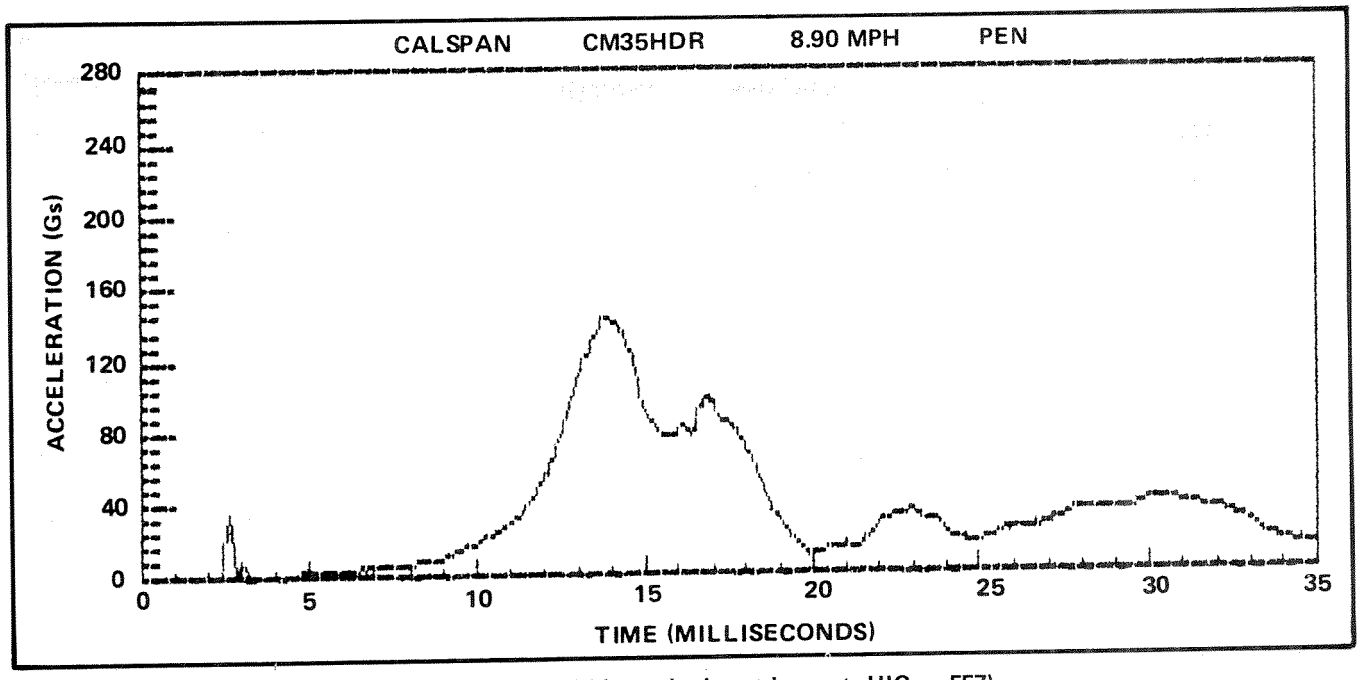

Figure 18. Acceleration versus time. (CM37, IMP, 128fps velocity at impact. HIC = 557)

These data indicate that the AIS coding for trauma to the brain is not as precise as is needed for this type of research. For example, any brain contusion is coded as an AIS 3. There are, of course, the Loss of Consciousness(L.O.C.) severity levels, but they are of no aid in assigning severity levels to injuries that are observed in cadavers that have been impacted in the laboratory. Additional effort is required to better map the thresholds of injury in head impacts and at the same time to better define injury codes for the trauma observed. A case in point might be made with a comparison of the CM34 and CM37 tests. CM34 was impacted at 11fps with a hard-faced impactor, and CM37 was struck at 12.8fps with 1in of padding on the impactor face. Essentially identical HIC values (549 and 557, respectively) were obtained, and identical AIS values of 3 were assigned. What is left undetermined in this information is whether the damage to areas 4, 3, 1, 2, 5, and 7, with the subsequent loss of the ability to localize and/or feel sensation and the paresis or paralysis, should be considered more or less severe (or equal in severity) than the damage to the entire frontal lobes and areas 44 and 45, with the potential change in personality and aphasia.

The data obtained from these 18 subjects agree in general with the data presented by Prasad and Mertz(4), especially in the area of brain damage as reported by Got et al.(5), Tarriere et al.(6), and Nahum and Smith(7,8). No attempt was made to quantify the skull thickness of the subjects reported herein, but skull fractures were experienced at HIC values of 1290 and 3967. These results agree in general with the data presented in (4) by Tarriere et al.(6), Got et al.(9), and Hodgson(10,11).

Acknowledgments

The authors acknowledge the contributions and helpful suggestions of Dr. Rolf Eppinger and Mr. Richard Morgan of the U.S. Department of Transportation, National Highway Traffic Safety Administration, and Mr. Rodolfo Vergara and Mr. John Herridge of Battelle Columbus Laboratories, as well as Mrs. Susan Enoun of the Vehicle Research and Test Center of NHTSA for supplying the head contact velocities for the pedestrian subjects.

References

1. Kelleher, B.J., M.J. Walsh, R. Vergara, J.T. Herridge, and R.H. Eppinger, "Evaluation of a pedestrian compatible bumper," Proceedings Tenth International Technical Conference on Experimental Safety Vehicles, July 1985.
2. Petrucelli, E., J.D. States, D.F. Huelke, and L.N. Hames, "Injury coding manual 1980," Final Report, Contract No. DOT-HS-8-02015, February 1980.
3. Brodmann, K., Vergleichende Lokaliastionslehre der Grosshirnrinde in Ihren Prinzipien Dargestellt auf Grund des Zellenbaues, Barth: Leipzig, 1909.
4. Prasad, P., and H.J. Mertz, "The position of the United States delegation to the ISO Working Group 6 on the use of HIC in the automotive environment," SAE Paper 851246, Washington, D.C., May 1985.
5. Got, C., A. Patel, A. Fayon, C. Tarriere, and G. Walfisch, "Results of experimental head impacts on

cadavers: the various data obtained and their relations to some measured physical parameters," Proceedings 22nd Stapp Car Crash Conference, SAE, Warrendale, Pennsylvania, 1978.

6. Tarriere, C., G. Walfisch, A. Fayon, C. Got, G. Guillon, A. Patel, and J. Hureau, "Acceleration, jerk and neck flexion angle: their respective influences on the occurrence of brain injury," ISO/TC 22/SC 12/GT-6 (USA-13) Doc. No. 118, 1982.
7. Nahum, A.M., and R.W. Smith, "An experimental model for closed head impact injury," Proceedings 20th Stapp Car Crash Conference, SAE, Warrendale, Pennsylvania, 1976.
8. Nahum, A.M., R.W. Smith, and C.C. Ward, "Intracranial pressure dynamics during head impact," Proceedings 21st Stapp Car Crash Conference, SAE, Warrendale, Pennsylvania, 1977.
9. Got, C., F. Guillon, A. Patel, F. Brun-Cassan, A. Fayon, C. Tarriere, and J. Hureau, "Morphological and biomedical study of 146 human skulls used in experimental impacts in relation with the observed injuries," Proceedings 27th Stapp Car Crash Conference, SAE, Warrendale, Pennsylvania, 1983.
10. Hodgson, V.R. and L.M. Thomas, "Breaking strength of the human skull versus impact surface curvature," Wayne State University, Detroit, DOT-HS-146-2-230, 1977.
11. Hodgson, V.R., L.M. Thomas, and J. Brinn, "Concussion levels determined by HPR windshield impacts," Proceedings 17th Stapp Car Crash Conference, SAE, Warrendale, Pennsylvania, 1973.

Technical Session No. 2

Crash Avoidance

Robert M. Nicholson, Chairman, United States

Discerning the State of Crash Avoidance in the Accident Experience

A.C. Malliaris
Office of Vehicle Research,
U.S. Department of Transportation, National Highway Traffic Safety Administration

Abstract

This paper addresses the risks of motor vehicle involvement in highway accidents. Such risks are determined from U.S. accident experience in the past 10 years. Risks are analyzed as a function of vehicle type, car market class, make, nameplate, and model year for accidents of various types and various severities. Both absolute risks, per unit exposure, and relative risks are addressed. The influence of many exposure variables is examined and necessary adjustments, to a common set of exposure conditions, are made. The control variables for this purpose are: calendar year, car age, driver's age, sex, and alcohol involvement; time and place of travel; and various roadway characteristics. Adjusted risks are reviewed versus major characteristics of cars as implied by make, nameplate, and model year. Single driver accidents and rollovers, whether pre- or post-impact, receive special attention due to their risk sensitivity to car class.

Introduction

In the past 10 years, the motor vehicle fleet in the United States has undergone significant changes in the mix of vehicle types on the road, the mix of car classes, the design and engineering of cars, and the introduction of new components and equipment. In addition, strong factors were at work in the early 1980's that individually or collectively had and have the potential to influence highway safety significantly. A depressed economy inhibited travel growth, especially for the higher risk discretionary travel. Highway safety programs, e.g., campaigns against drunken drivers and seatbelt use programs, were initiated and pursued vigorously. The questions we are addressing in this paper are whether or not and how all these changes are affecting accident risks, as determined from the accident experience of motor vehicles on U.S. roads in the past 10 years.

We treat accident risks as dependent variables where the independent variables are: calendar years, accident types, and accident severities; motor vehicle attributes such as vehicle types, market classes, makes, models, and model years; driver attributes such as age, sex, and alcohol involvement; and exposure attributes such as time, highway type and location, travel speed, roadway characteristics, etc. A companion paper (12) addresses occupant casualty risks as a function of crash attributes such as type of impact and impact severity; occupant attributes such as seating position, restraint status, and occupant age; and vehicle attributes such as those mentioned above.

Major Changes in the Motor Vehicle Fleet and Travel

In the period between the mid-1960's and the mid-1980's, the number of motor vehicles on U.S. roads grew faster than the number of drivers or the number of people in general.

Two vehicle types with particular safety problems, namely trucks and motorcycles, have grown much faster than cars. The number of trucks on U.S. roads today is about 40 million, or more than three times their number in the mid-1960's. Motorcycle registrations, approaching 6 million today, are more than four times as many by comparison to the mid-1960's. In contrast, car registrations have barely doubled in the same period.

However, significant changes took place within the car fleet. These include the introduction of radial tires, disc brakes, variable brake proportioning, and changes in the design and engineering of suspensions and steering. Furthermore, since about 1976 the entire fleet of new cars, primarily those domestically produced, was fundamentally redesigned to yield significantly lighter vehicles with predominantly front wheel drive.

Three car characteristics—weight, wheelbase, and front wheel drive—are given special consideration because they are frequently discussed and analyzed in connection with accident and casualty risks. A summary of changes in these characteristics for new cars retailed in the United States is given in Table 1, by market class. The changes refer to mean values of those characteristics between model years introduced in the early 1970's and model year 1983.

Note in Table 1 that the front wheel drive percentages are the shares in model year 1983. The same shares were virtually equal to zero for model years up to 1976. Also note that the domestically produced fleet shows substantial

Table 1. Percent change in mean weight, mean wheelbase, and percent front wheel drive of model year 1983 cars by comparison to new cars of the early 1970's

Market Class	Percent Change Mean Weight	Percent Change Mean Wheelbase	Percent* with Front Wheel Drive
U.S. Subcompact	-18.0%	-2.5%	80%
Compact	-23.5	-8.1	65
Intermediate	-22.8	-6.8	33
Standard	-11.5	-4.3	14
European Subcompact	+5.9	+1.9	99
Other	+9.9	+2.2	16
Japanese Subcompact	0.0	+1.6	72
Other	+5.8	0.0	18

*Shares in model year 1983; these were virtually zero up to model year 1976.

reductions of weight and wheelbase, all across the board, while this is not the case for the fleets of European or Japanese origin. Apparently, redesign practices and market shifts in these latter fleets, which consist of predominantly subcompact cars, led to modest increases in weight and wheelbase.

As a result of these developments, subcompact cars of U.S., European, or Japanese origin have become virtually indistinguishable, when viewed in terms of the three major characteristics discussed above. Moreover, the standard, intermediate, and compact U.S.-produced cars of model year 1983 have essentially assumed the weight and wheelbase characteristics of the intermediate, compact, and subcompact cars of the early 1970's, respectively.

Because of the prominence of car weight, wheelbase, and front wheel drive in safety reviews, we treat the changes summarized above with more detail and more quantitatively in Appendix A. In the same appendix, we also address changes that took place in the travel of motor vehicles and in the various aspects of exposure to accident risks.

Accident Involvement Risks and Risk Descriptors

Several descriptors are convenient for the characterization of the accident experience of motor vehicles, depending on the particular aspects of the problem at hand and on the availability of relevant data. Risk descriptors for accident-involved vehicles are usually expressed as:

$$R_{ijk} = V_{ijk}/E_{jk} \quad (1)$$

where

V is the number of accident-involved motor vehicles, categorized by i, j, k

E is the amount of exposure (e.g., travel) categorized by j, k

i designates accident categories including accident type (e.g., collision with other motor vehicle, collision with fixed object, overturn, etc.) and also including accident severity (e.g., fatal accident, or accident with injury only or property damage only, etc.)

j designates vehicle categories including vehicle type (e.g., car, pickup, van, heavy truck, etc.) and also including further subclassifications (e.g., car market classes, make, model, model year, etc.)

k designates travel-related exposure categories including driver attributes (e.g., age, sex, alcohol involvement) and also other travel attributes (e.g., time, day, urban or rural environment, roadway and traffic characteristics, etc.)

Risks as defined by Equation (1) are absolute. The most customary type of exposure used for risk estimation is vehicle travel, expressed in vehicle miles. However, several other alternatives may be and are being used in this paper. The number of registrations is an acceptable alternative, if differentials in travel per vehicle are not important or if means are available for taking into account such differentials whenever they appear to be important.

Another alternative applied in this paper is the concept of the conditional risk. This, as an example, addresses the question: "Given an accident in general what is the risk of this accident being fatal?"; or the question: "Given an accident in general what is the risk of this accident being a rollover?" In other words, we count the vehicles involved in fatal accidents and divide by the count of the same vehicles involved in accidents of any severity, or we count vehicles involved in rollovers and divide by the count of vehicles involved in any type of accident. In this process,

we may retain in both the numerator and denominator any desired characterization of vehicle, driver, or environmental categories.

A summation of Equation (1) over subscript i, i.e., over all accident categories, yields:

$$R_{jk} = V_{jk}/E_{jk} \quad (2)$$

Furthermore, dividing (1) by (2) yields Q_{ijk}, the conditional risk, i.e.:

$$Q_{ijk} = R_{ijk}/R_{jk} = V_{ijk}/V_{jk} \quad (3)$$

It is noted that the amount of exposure E_{jk} drops out when Equation (1) is divided by Equation (2). This is certainly a loss of rigor. However, it is compensated by a strong advantage, namely, better compatibility between numerator and denominator in the vehicle categories and exposure categories represented respectively by subscripts j and k.

Note that in the estimation of conditional risk by Equation (3), both the numerator and denominator are vehicle counts, most likely to be obtained from one and the same file or at least from very similarly structured casualty files. This minimizes the errors arising from differences in the classification of vehicular and circumstantial characteristics used in the estimation process. However, this is not the case in the estimation of absolute risks by Equation (1), where the numerator and denominator are obtained from data files of very different origins.

For example, the numerator in Equation (1) is obtained from a casualty file such as NHTSA's Fatal Accident Reporting System (FARS)(1) or NHTSA's National Accident Sampling System (NASS)(2) or from a State accident file. None of these casualty files contains information about the denominator. Values for this denominator must be assembled from other files: motor vehicle registration files such as those provided in (4) and motor vehicle travel files such as any one or several of those in (6) to (10). Because of the very dissimilar origins of the data necessary for the estimation of absolute risks, it is a challenge to achieve numerator/denominator compatibility in Equation (1).

In addition to minimizing the chances of error in risk assignments, the use of conditional risks also offers the advantage of a wider range of attributes for examination. This is particularly true for environmental and circumstantial attributes such as curving or sloping roadway, wet or dry pavement, road intersection or not, etc., which are unlikely to be available for the estimation of the denominator in Equation (1) but are available in the case of Equation (3). For the reasons discussed above, we use extensively conditional risks in conjunction with absolute risks in the exploration of the state-of-the-art in accident avoidance, discussed in this paper.

Risks of Fatal Accident Involvement

A motor vehicle's risk of involvement in a fatal accident stood at about 5.67 ± .13 per 1,000 vehicles involved in all police-reported accidents on U.S. highways. This is the mean and standard error derived from six individual values, each obtained from the data for each of the six years 1979 to 1984. It refers to all types of accidents, all categories of vehicles, and all model years. It varies very little within the specified time period (see Figure 1) in spite of the significant changes in the fleet and travel patterns discussed earlier.

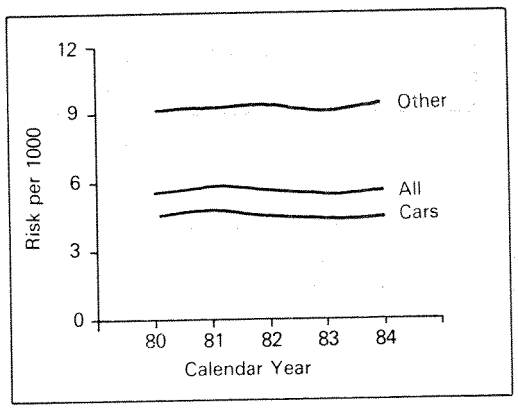

Figure 1. Risk of motor vehicle involvement in fatal accidents per 1,000 vehicles in all police-reported accidents

The data for the determination of this conditional risk are provided by two accident files of national scope, i.e., by FARS and NASS(1,2). Specifically, a total count of all vehicles involved in fatal accidents (national census) is obtained from FARS, and this is divided by a national estimate of all motor vehicles involved in all police-reported accidents, as recorded in NASS. This process is repeated for each of the calendar years 1979 to 1984.

When disaggregated by accident, vehicle, driver, or circumstantial attributes, the risk under consideration varies within a wide range. This, of course, has been known for a long time. However, the relatively recent availability of several years of FARS and NASS data of national scope provides an opportunity for quantitative results. Furthermore, the relative similarities in the structure of these files minimizes the chances of error due to incompatibilities in the classification of attributes. Risks for the two most important accident and vehicle attributes, namely accident type and vehicle type, are shown in Tables 2 and 3, respectively. These results are based on FARS and NASS data.

The risk values reported in Tables 2 and 3 are means and standard errors over the 1979 to 1984 calendar year span. Most of the characterizations are self-explanatory.

Table 2. Risk of motor vehicle involvement in fatal accidents per 1,000 vehicles in police-reported accidents as a function of accident type (first harmful event)

Accident Type	Percent of Vehicles*	Risk per Thousand in Row
Collision with Other MV	83.7 ± .27	3.83 ± .05
Collision with Object	11.7 .48	10.6 .52
Collision with Nonmotorist	2.06 .08	38.2 1.7
Overturn	1.68 .09	22.6 1.3
Other Noncollision	.87 .26	9.23 2.6
Total	100.0	5.67 .13

*In all police-reported accidents

Table 3. Risk of motor vehicle involvement in fatal accidents per 1,000 vehicles in police-reported accidents as a function of vehicle type

Vehicle Type	Percent of Vehicles*	Risk per Thousand in Row
Cars	77.8 ± .12	4.51 ± .03
Pickups	12.7 .12	7.44 .03
Vans	3.30 .13	5.47 .11
Straight Trucks	1.80 .11	7.99 .33
Combination Trucks	1.96 .06	20.0 .73
Buses	.59 .05	5.43 .33
Motorcycles	1.80 .02	25.8 .17
Total	100.0	5.67 .13

*In all police-reported accidents

Nonoccupants in Table 2 include pedestrians and bicyclists. Overturn is a rollover usually not preceded by an impact with another motor vehicle or with an object. A variety of less frequent events such as fire, explosion, immersion, etc., are included under "other noncollision." In Table 3, pickups and vans are vehicles with a gross vehicle weight rating under 10,000 lb. Straight trucks are nonarticulated trucks and vans over 10,000 lb.

It is evident in the summary of Table 2 that collision with another motor vehicle is the most frequent event but also the least risky. By reference to this, a motor vehicle's risk of fatal accident increases by a factor of 3 when a collision with an object occurs and it is 5 to 6 times higher for an overturn. Overturn as a first harmful event as well as rollover, an event subsequent to an impact, will be addressed in more detail later. The riskiest events are collisions with nonoccupants, for obvious reasons. However, the reader should note that the risk magnitude is not the only determinant of the importance of a problem. The frequency of occurrence of the circumstances that give rise to the risk is as important, if not more important. Consider, for example, the results in Table 2 to see why car collisions with other motor vehicles receive a lot of attention, in spite of the risk of fatal accident in such events being the lowest.

The summary of Table 3 shows cars running the lowest risk, in spite of their overwhelming share as vehicles in all police-reported accidents. Vans and buses show higher risks but not much higher than the risk for cars. The risks for pickups as well as for other nonarticulated trucks is about double that of cars. Much higher risks are evident for the heavy articulated trucks and also for motorcycles. Risks assigned to joint accident-vehicle type attributes show generally trends expected on the basis of the results given in Tables 2 and 3. Figure 2 displays risks for cars, pickups, and all motor vehicles as a function of accident type.

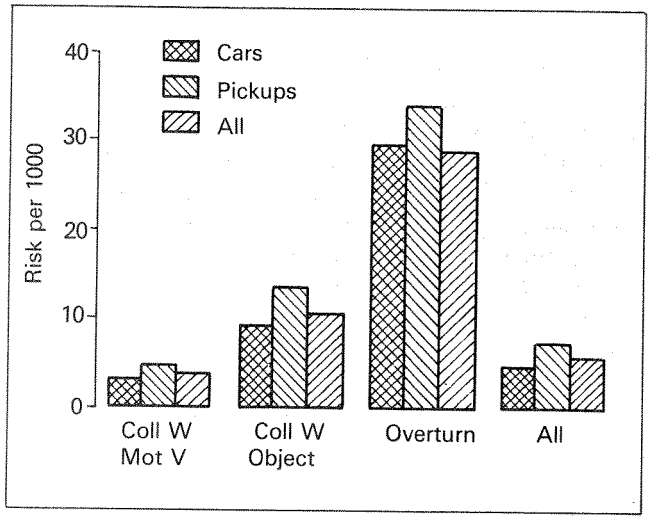

Figure 2. Risk of motor vehicle involvement in fatal accidents per 1,000 vehicles in all police-reported accidents (shown for cars, pickups, and all vehicle types, as a function of accident type)

Fatal Accident Involvement of Cars

Because of their overwhelming share of the vehicles in all police-reported accidents, cars are receiving further attention in this paper in connection with their risk of fatal accident involvement.

According to Table 3, a car's risk of involvement in a fatal accident is 4.5 ± .03 per 1,000 cars involved in all police-reported accidents. This is the mean and standard error for the 6-year period of 1979 to 1984. The smallness of the error indicates relatively little variation of the risk, whether random or systematic, in this period. This is also shown in Figure 1.

However, when this risk is resolved according to car travel attributes and type of accident, the resulting values vary within a range of two to three orders of magnitude.

This is evident in the results shown in Table 4. These are means and standard errors of car risks in the early 1980's. A difference by a factor of 2 to 3 is seen between day and night and by about 5 to 7 between urban and rural travel when all types of accidents are considered. Risks for certain types of accidents, such as overturn and collision with an object, are remarkably insensitive to car travel attributes. Risks for other types, such as collision with pedestrian and collision with motor vehicle, show a large sensitivity.

Like other vehicles, cars show fatal accidents risks that are strongly dependent on the type of accident. The last row in Table 4 quantifies this point. The highest risk is observed for overturns, followed closely by the risk in case of collision with nonmotorists. The risk in collisions with an object is three times lower than that of collisions with nonmotorists, but still three times higher than the risk of fatal accidents in car collisions with other motor vehicles.

It is common knowledge that car involvement in fatal accidents is influenced much by driver attributes. We have used the same data files as discussed above, namely the FARS and NASS, to quantify these influences, by calculating risks of car involvements in fatal accidents per 1,000 police-reported accidents, nationwide. In this case, uniform quality data are available for the 3 years 1982 to 1984. For this period, we report the mean values of risks in Table 5. The risk value 4.5 in the last row and last column of the last cluster in the table is recognized as the overall risk cited earlier. The 36 entries of this table resolve the overall risk by driver age, sex, and alcohol involvement.

The results of Table 5 quantify certain influences that have been qualitatively evident for a long time. Of the three driver attributes under consideration, alcohol has an overriding influence that makes a difference of a factor of 7 to 8, with remarkable consistency and uniformity all across the age and sex brackets. The standard errors for the mean values in Table 5 are about 3 percent in general except for the entries "With Alcohol Involvement" where the errors are about 10 percent. Furthermore, the reader should keep in mind that alcohol involvement as reported in accident files is a subject to be treated very cautiously because of potential error due to the nonuniformities in the investigation and reporting procedures.

The other two driver attributes in Table 5, namely driver's age and sex, have weaker but easily noticeable influences. Risk variation with age is minimal for all age brackets until the last, where a 40 to 50 percent jump is observed. This holds true generally, regardless of other driver attributes. Similarly, male drivers show risks about 30 to 40 percent higher than female drivers all across the driver age and alcohol involvement brackets.

Generally speaking, these influences are intuitively expected with one major exception. The young drivers, whether with or without alcohol involvement, show risks that are not higher than those of all other drivers, contrary to a commonly held notion. This is not necessarily a contradiction. Table 5 shows young drivers incurring about the same risk of fatal accident as all other drivers, given an accident. However, young drivers may have more accidents in general and thus more fatal accidents per driver, due for instance to more travel or to any other reason. Nevertheless, on a per accident basis, younger

Table 4. Resolution of risk of car involvement in fatal accidents by type of accident and travel attributes (cars in fatal accidents per 1,000 cars in all police-reported accidents)

Travel Attributes	Type of Accident (First Harmful Event)									
	Collision with Other MV		Collision with Object		Overturn		Collision with Nonmotorist		All Types	
Urban										
Day	1.1	± .1	5.4	± .4	23.7	± 4.9	10.4	± .4	1.6	± .1
Night	2.9	.1	8.0	.5	29.5	3.9	47.4	3.6	4.9	.2
All	1.6	.1	7.0	.4	26.1	2.8	22.2	.7	2.6	.1
Rural										
Day	9.3	.9	11.1	.8	32.1	3.1	44.8	9.	10.4	.8
Night	17.4	1.6	12.4	.5	36.7	5.8	409.	46.	17.6	.9
All	11.5	.5	11.9	.6	33.8	3.7	119.	22.	13.3	.3
All										
Day	2.2	.1	7.8	.4	29.9	3.5	13.4	.3	3.0	.1
Night	4.9	.3	10.0	.5	33.1	2.5	65.8	4.4	7.6	.3
All	3.0	.1	9.2	.4	31.2	1.9	20.7	.6	4.5	.1

Table 5. Resolution of risk of car involvement in fatal accidents by driver's age, sex, and alcohol involvement (cars in fatal accidents per 1,000 cars in all police-reported accidents

Driver's Age	Drivers Sex Male	Female	All
	A. No Alcohol Involvement		
16-24 Years	3.3	2.4	2.9
25-34 Years	3.1	2.2	2.7
35-64 Years	3.6	2.8	3.2
65 and Older	5.6	4.6	5.2
All	3.5	2.6	3.1
	B. With Alcohol Involvement		
16-24 Years	25.4	18.5	23.8
25-34 Years	22.9	22.4	22.3
35-64 Years	23.3	20.8	23.3
65 and Older	39.2	26.6	32.9
All	24.4	19.7	23.3
	C. Total Involvement		
16-24 Years	5.7	3.2	4.8
25-34 Years	5.5	2.8	4.4
35-64 Years	5.0	3.2	4.2
65 and Older	6.2	4.9	5.7
All	5.5	3.2	4.8

drivers are not much different than other drivers in their risk of fatal accident involvement. Another reason why young drivers do not appear overinvolved in fatal accidents is that they are more able to survive trauma(12).

So far in the discussion, we have reported risks averaged over several years in the early 1980's. We know that the overall risk of fatal accident involvement has varied little in this period as shown in the plots of Figure 1. The question remains whether specific aspects of this risk show time variations in the period under consideration. An examination of the raw data, before averaging over the calendar years, shows variations that are predominantly random and are reflected in the standard errors reported in Tables 2 to 5. In relatively few instances, there are indications of systematic increase or decrease of the risk versus calendar year. One such instance, with a rather well-pronounced time variation, is illustrated in Figure 3.

Plotted in this figure is the risk of fatal accident involvement for cars in rural daytime travel versus calendar year. The average risk over all these years is about 10 as shown in Table 4. However, according to Figure 3, this risk has been increasing substantially as the years progress from 1980 to 1984. Incidentally, a similar but weaker trend is observed for the risks either in rural

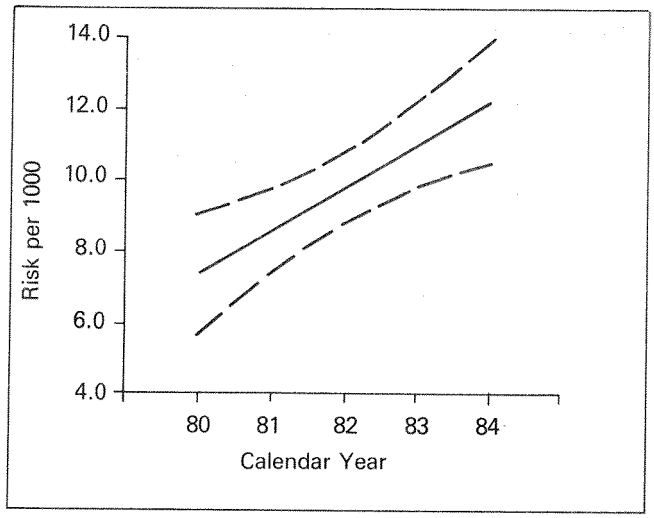

Figure 3. Risk of car involvement in fatal accidents per 1,000 cars in all police-reported accidents for rural daytime travel

travel regardless of day or night or in daytime travel regardless of urban or rural. The combination of rural and day travel amplifies the trend.

The general implication of the data shown in Figure 3 is that the exposure severity is increasing in rural travel during daytime. It is very tempting to correlate this finding and even tentatively assign it to the increasing noncompliance with the 55mph speed limit, taking place in the same period. (See, for example, Table A-6 and the related discussion in Appendix A.) However, a further review of the FARS and especially of the NASS data is required before definitive conclusions can be drawn about the rather unusual risk increase shown in Figure 3.

Car attributes may also influence the risk of fatal accident involvement. The influence of attributes such as origin of make, market class, nameplate, weight, wheelbase, etc., is reviewed and discussed in the next section. However, before closing this section, we address the conditional risk of fatal accident involvement for cars as a function of car age, and thus as a function of model year. For this purpose, we use again the fatal accident experience in FARS and the police-reported accident experience in NASS for car accident involvements in the early 1980's, combined.

We segregate the cars in four slots according to car age, i.e., according to calendar year minus model year, and we determine the risk of fatal accident involvement for each slot. The results are shown in Figure 4 for all drivers and separately for the young drivers (16 to 24 years old). These results lead to the conclusion that on a per-accident-involved driver, neither the age of the driver nor the age of the car makes much difference to the risk of the involvement being fatal.

The only obvious exception to our conclusion is the risk for the oldest cars, which is higher by 25 percent

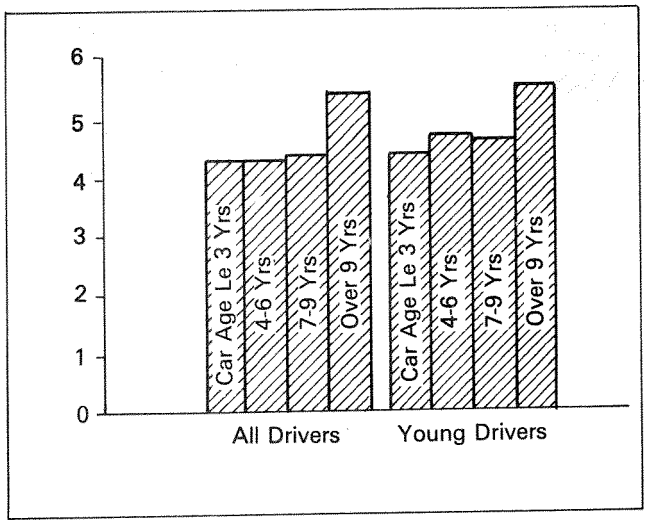

Figure 4. Risk of car involvement in fatal accidents per 1,000 cars in all police-reported accidents (shown as a function of driver age and car age)

compared to younger cars. Furthermore, it should be kept in mind that in these data, car age is covariant with car model year. Thus, due to this unavoidable ambiguity, we may state an alternative conclusion: The risk of fatal involvement per accident-involved-car does not appear to be very sensitive to the car's model year. However, even for the oldest cars, the risk may be confounded and possibly artificially increased by the fact that these cars are regularly reported by the police in fatal accidents but might be underreported in nonfatal accidents. This is especially true when the value of an old car happens to be under the threshold for reporting.

Determination of Absolute Risks

To address the influence of car attributes on car accident experience, we focus our analysis on the new cars that traveled on U.S. roads in the 1975 to 1984 period. This is also the period during which major changes took place in car attributes, as discussed earlier and as detailed further in Appendix A. For the purpose of our analysis, we define new cars as those with an age (i.e., with a calendar/model year difference) not exceeding 3 years. This is a compromise between retaining as much uniformity as possible in travel and exposure attributes while dealing with sufficiently large samples in the accident experience.

Under these constraints, we found it difficult to make the conditional risk determinations, by a combined examination of FARS and NASS data, as discussed in the last section. This is so for several reasons: NASS data for car characterization (e.g., by make and model) are not available in a form compatible with FARS data until about 1981; NASS cell populations become rather small when the accident experience is subdivided by the many combinations of car market classes, makes, nameplates, and other specific attributes, especially when these subdivisions are made on new cars only. Furthermore, there are good reasons to suspect that NASS as a sample of the national accident experience may be biased in connection with car make/model content. For example, California and the West Coast in the United States are underrepresented in NASS, while the same regions are overrepresented in imported makes.

The conclusion from the above discussion is that we may not apply Equation (3) for the task under consideration here because we have no means of obtaining reliable values for the denominator. This is an extra reason for using Equation (1), which is appropriate for the determination of absolute risks. In this section, we shall deal with Equation (1) integrated over all travel-related exposure categories, i.e., we shall drop subscript k and write for the risk:

$$R_{ij} = V_{ij}/E_j \qquad (4)$$

where i and j represent accident and vehicle-related attributes. Later we will examine the influence of circumstantial and environmental attributes represented by subscript k.

The raw data necessary for the application of Equation (4) are provided by FARS(1) for the numerator and by (4) for the denominator. FARS contains records of about 100,000 new cars involved in fatal accidents in the 10 years between 1975 and 1984. Accident type and car nameplate are known for the great majority of these cars. Furthermore, their total count is generally adequate for analyses that demand disaggregation by several attributes of interest here.

Car registrations from (4) are used to quantify the denominator in Equation (4) by car descriptor j (nameplate and model year) for each of the calendar years included in the analysis. Although car exposure in general may not be characterized accurately by car registrations alone, our constraining the analysis to new cars only introduces a uniformity in the travel per car and other attributes sensitive to car age. Furthermore, a set of adjustments are made to the risks (determined for each model year and calendar year) to bring them all under a common reference exposure.

The selected reference exposure is that experienced by 1-year-old cars in the calendar year 1980. The adjustments, detailed in the first part of Appendix B, account for travel and exposure severity variations taking place in the 10 calendar years under consideration for new cars (i.e., 1-, 2-, and 3-year-old cars). Risk adjustment factors are shown in Table B-2 of Appendix B, as a function of calendar year and car age or model year. As may be seen, the adjustments are generally small and although they may have uncertainties, these are small by comparison to the risk differentials we shall consider worth pointing out.

To achieve numerator/denominator compatibility in the application of Equation (4), we disaggregate both the

accident-involved car data (numerator) and the car registration data (denominator) by car nameplate, model year, and calendar year. We found nameplate, i.e., make and model, disaggregation more suitable than disaggregation by weight or by wheelbase. Disaggregation by weight often introduces ambiguities due to weight variations on account of optional engine sizes and other optional equipment. Furthermore, when disaggregating by weight, borderline cases may fall in one weight slot for the numerator data but in a different weight slot for the denominator data. However, the main advantages of disaggregation by nameplate are that much more information is potentially available about the car under consideration, even if this information is not always publicly available, and the number of unknowns is very small.

Risk determinations may be made at the nameplate, model year, calendar year level by straightforward applications of Equation (4), with subsequent adjustments as discussed earlier. At this level, sample sizes are generally adequate for most purposes. Given our analysis is focused on new cars, we calculate risks separately for the 1-, 2-, and 3-year-old cars, all adjusted to the common reference exposure conditions, and form the mean of the three. In the process, we obtain the standard error of this mean.

In many instances, risks for new cars, whether by nameplate or by higher levels of aggregation, are available for several calendar years within the 1975 to 1984 span. In such cases, we also calculate means and standard errors, in addition to reviewing the data for systematic variation versus calendar year. Thus, the standard errors we report are more conservative given they embrace not only purely statistical fluctuations but all other variations whether random or systematic.

Results for levels of aggregation above nameplate are obtained as follows. The raw data, whether cars in accidents or car registrations, are pooled together and the procedures described above are repeated. This leads to risk determinations for new cars aggregated by make, car body family designation, market class, origin of make, and the entire fleet of new cars. The market class designations used in this paper are those commonly used in the automotive trade literature. Furthermore, all traditional sports car nameplates and other low-volume specialty cars have been excluded from consideration because of possibly singular characteristics and circumstances.

Absolute Risks for New Cars

Results obtained according to the procedures described above are presented and discussed here for new cars. The absolute risk of fatal accident involvement per 10,000 registrations of new cars is 3.41 ± .09 when averaged over all car market classes and all types of fatal accidents that occurred in the period 1975 to 1983. First we shall resolve this risk by fatal accident type and by car market class within each accident type. The results of this resolution are shown in Figures 5 to 10. Each figure refers to a type of fatal accident. Within each figure, the risk is resolved by market class of new cars.

Keeping in mind the differences in the scales of these illustrations, we see that the principal contributions to the overall risk come from collisions with other motor vehicles and collisions with objects. Smaller contributions are made by collisions with nonmotorists and by overturns, i.e., rollovers not provoked by a preceding impact. However, these findings are evident in the accident experience alone and could be obtained from the FARS

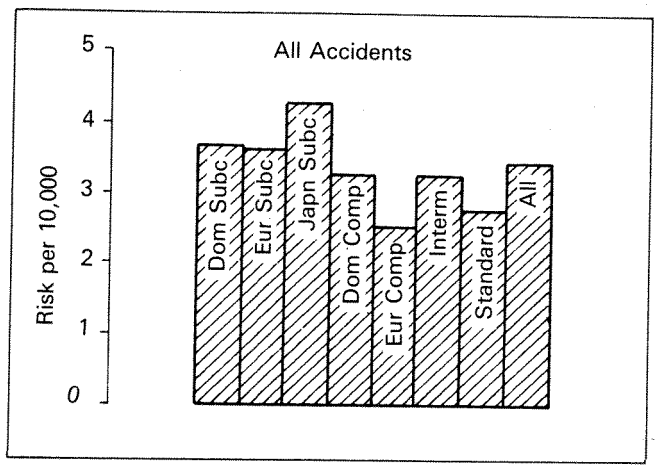

Figure 5. Risk of new car involvement in all types of fatal accidents per 10,000 new car registrations as a function of market class

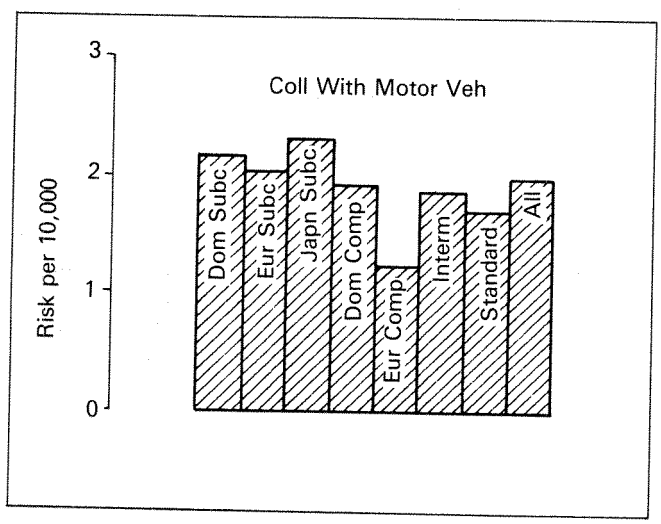

Figure 6. Risk of new car involvement in fatal collisions with other motor vehicles per 10,000 new car registrations as a function of market class

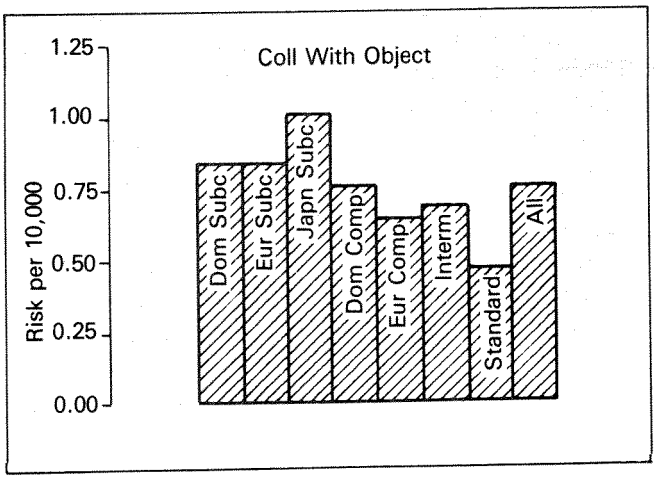

Figure 7. Risk of new car involvement in fatal collisions with objects per 10,000 new car registrations as a function of market class

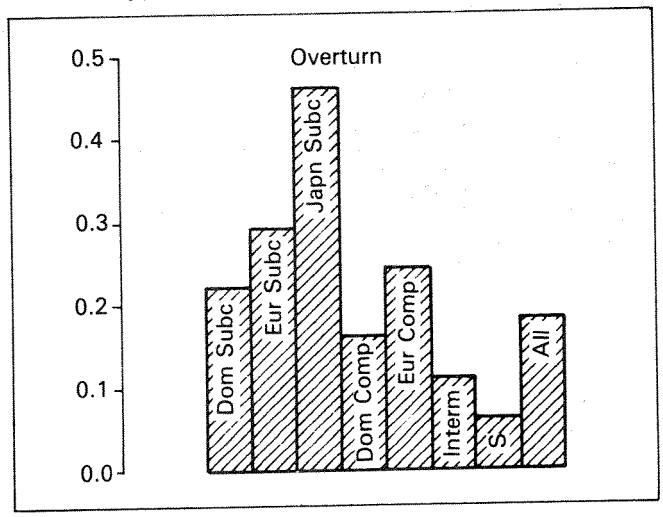

Figure 8. Risk of new car involvement in fatal overturns per 10,000 new car registrations as a function of market class

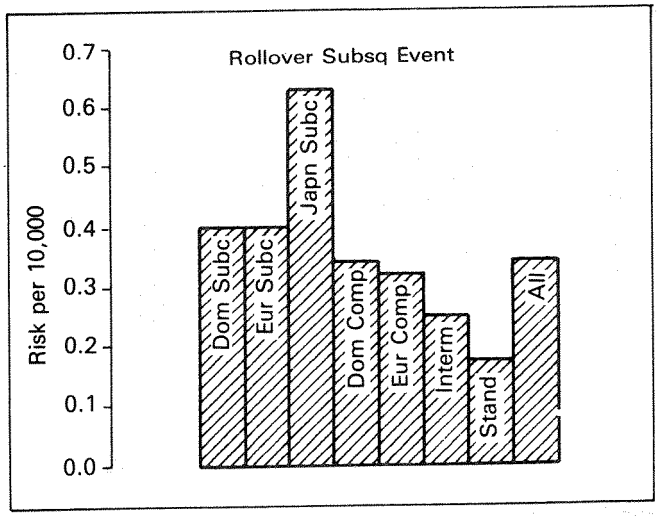

Figure 9. Fatal involvement risk of new cars in post-impact rollover per 10,000 registrations by market class

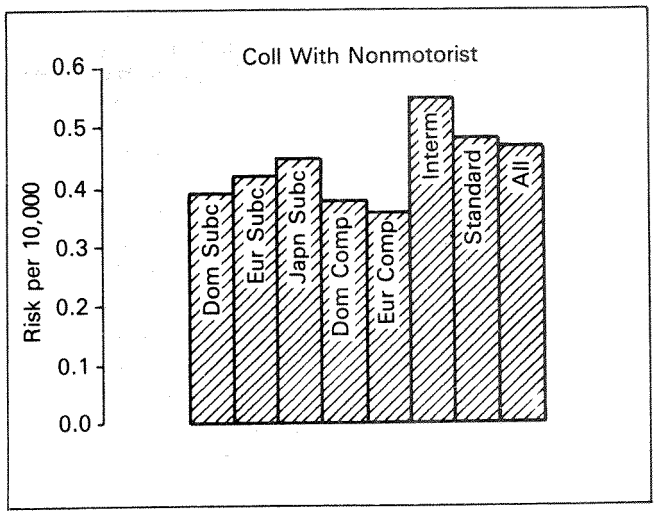

Figure 10. Risk of new car involvement in fatal collisions with nonmotorists as a function of market class

file without any additional information about exposure. The new information shown in Figures 5 to 10 is the sensitivity of these risk components and of the total risk to car attributes, as implied by the market class and origin of make designations.

It is evident that the risk of some accident types, such as collision with other motor vehicle (Figure 6) or with nonmotorist (Figure 10), shows relatively little sensitivity, while the risk of other accident types, such as collision with an object (Figure 7) and especially car overturn or rollover as a subsequent event (Figures 8 and 9), shows a high sensitivity. Car rollover, as an event subsequent to an impact with another motor vehicle or with an object, is an entirely different type of accident than overturn, which is usually not preceded by noticeable impact. These two events are mutually exclusive for all practical purposes and, when combined, they result in a risk that is a substantial component of the overall fatal accident risk with high sensitivity to car class.

Most of the sensitivities shown in Figures 5 to 10 may be established well beyond the statistical or other fluctuations that may be contained in the results. This is evident in the data shown in Table 6, which displays the risk values appearing in these figures together with their standard errors.

The data included in the overviews of Figures 5 to 10 and in Table 6 represent the national census of accident experience of over 250 million new car years. This total is subdivided into the market classes discussed above as shown in Table 7, which is formatted as Table 6 for convenience. Table 7 also presents information about the major characteristics—weight, wheelbase, and percent front wheel—drive of new cars in each of the market classes under consideration. Keep in mind that these are weighted means over the 1975 to 1983 period.

Table 6. Risks of involvement in fatal accidents per 10,000 new car registrations by market class and type of accident. Shown values are means and std. errors over calendar years 1975 to 1983

New Car Market Class	Type of Accident: Collision with Motor Vehicle	Collision with Object	Overturn	Collision with Nonmotorist	All Types*
Subcompact					
Domestic	2.17 ±.06	.84 ±.03	.22 ±.02	.39 ±.01	3.64 ±.10
European	2.03 .06	.84 .03	.29 .02	.42 .02	3.60 .08
Japanese	2.30 .09	1.01 .05	.46 .02	.45 .03	4.24 .16
Compact					
Domestic	1.92 .12	.76 .06	.16 .01	.38 .02	3.23 .20
European	1.22 .04	.64 .06	.24 .02	.36 .03	2.47 1.5
Intermediate	1.87 .03	.68 .02	.11 .01	.55 .02	3.22 .06
Standard	1.70 .07	.46 .03	.06 .01	.48 .02	2.70 .11
Entire Fleet	1.99 .05	.75 .03	.18 .01	.47 .01	3.41 .09

*Includes a rather small fraction of other types, primarily fire, explosion, and immersion

Table 7. Exposure (car years) and major characteristics of new cars by market class for the combined calendar years 1975 to 1983

New Car Market Class	Car-Years (Millions)	Mean Weight (Pounds)	Mean Wheelbase (Inches)	Percent with Front Wheel Drive
Subcompact				
Domestic	28.5	2,422	96.3	23.0
European	10.5	2,014	94.3	83.7
Japanese	29.9	2,193	93.9	37.5
Compact				
Domestic	49.5	3,087	107.4	17.3
European	5.0	2,982	104.5	22.1
Intermediate	54.5	3,640	111.5	1.0
Standard	50.6	4,119	118.6	4.6
Entire Fleet*	250.5	3,208	106.9	16.2

* Includes about 8 percent of the total not classified in the above categories for various reasons

Superimposed on the sensitivity of certain accident risks to car market class is an equally strong sensitivity to nameplates within each market class. This is especially true for new cars in the market classes of smaller cars and most strongly pronounced for accident types such as overturns, post-impact rollovers, and collisions with objects. Relevant results are given in Table 8, which displays the risks of new car involvement in these and all fatal accident types. In addition, the table displays the exposure and also the major characteristics of new cars for each entry.

Table 8. Risks of involvement per 10,000 car-years, exposure, and major characteristics of new cars by nameplate in the 1975 to 1983 period

New Car Market Class and Nameplate		Fatal Involvement Risks: Overturn	Rollover Post-Impact	Collision with Object	All Accidents	Exposure Thousands Car-Years	Mean Weight Lb	Mean Wheelbase In	Percent Front Wheel Drive
Domestic Subc. Nameplate	1	.30±.04	.46±.04	.89±.05	4.06±.14	4,683	2,072	95.4	0
	2	.14 .02	.29 .08	.82 .09	3.42 .11	3,607	2,598	97.0	0
	3	.20 .06	.37 .06	.72 .10	3.49 .20	1,594	2,782	96.0	0
	4	.31 .05	.41 .07	1.10 .11	4.40 .14	1,422	2,172	98.3	100
	5	.48 .01	.57 .08	1.05 .03	4.24 .16	901	2,059	94.0	100
European Subc. Nameplate	1	.22±.05	.35±.05	.74±.05	3.21±.18	3,075	1,973	94.6	100
	2	.39 .03	.49 .11	1.12 .11	3.98 .18	1,471	2,238	93.2	25
	3	.36 .13	.59 .08	1.03 .14	4.67 .30	814	1,768	90.0	100
	4	.29 .06	.30 .10	.66 .14	2.39 .26	684	1,837	94.1	0
	5	.52 .12	.57 .07	1.06 .18	4.86 .24	359	1,925	95.5	100
Japanese Subc. Nameplate	1	.70±.05	.63±.09	1.05±.09	4.87±.16	3,456	2,021	92.0	0
	2	.63 .06	.85 .08	1.24 .15	4.77 .24	2,800	2,591	98.0	0
	3	.46 .05	.70 .08	1.08 .14	4.35 .48	2,426	2,199	93.4	41
	4	.44 .07	.64 .10	1.29 .13	4.55 .17	2,281	2.239	94.3	11
	5	.22 .05	.36 .06	.81 .06	3.31 .19	2,009	2,152	94.3	100
Domestic Compact Nameplate	1	.21±.02	.82±.06	1.86±.14	5.96±.26	4,058	3,451	107.6	0
	2	.16 .01	.27 .02	.74 .05	3.33 .19	3,452	2,806	106.0	0
	3	.08 .01	.17 .04	.51 .07	2.87 .31	3,022	3,396	111.8	0
	4	.12 .03	.30 .05	.65 .03	3.53 .05	2,500	2,522	105.0	100
	5	.07 .01	.23 .07	.52 .03	2.88 .06	509	2,388	100.0	100
European Compact Nameplate	1	.24±.05	.18±.02	.38±.04	2.13±.12	1,351	2,980	104.1	0
	2	.19 .04	.23 .03	.51 .11	2.50 .45	1,177	3,606	109.4	0
	3	.18 .03	.32 .06	.70 .09	2.67 .17	950	2,474	102.2	100
	4	.36 .07	.48 .10	1.15 .09	3.93 .10	858	2,590	101.0	0
	5	.57 .06	.89 .09	1.58 .24	3.88 .47	696	2,797	101.9	0
Interm. and Std. Nameplate	1	.08±.01	.23±.02	.62±.03	3.15±.06	6,925	3,441	110.1	0
	2	.18 .04	.35 .05	.90 .11	4.35 .29	3,021	3,999	112.9	0
	3	.14 .03	.26 .05	.91 .09	3.81 .21	2,006	3,990	114.8	0
	4	.09 .02	.16 .03	.49 .08	3.27 .51	7,478	4,224	117.7	0
	5	.06 .02	.12 .02	.33 .06	2.06 .25	3,646	3,852	117.3	0

Risk Changes Versus Model Year

The results shown in Figures 5 to 10 and Tables 6 to 8 are averaged over all calendar years 1975 to 1983. In spite of the fact that they address new cars only, they are essentially averaged over as many as 10 model years. Given that much change has taken place in new car design during this period, the question arises whether or not the risks of fatal accident involvement are changing. To address this question, we examine the data as a function of calendar year and thus as a function of model year for new cars.

Figure 11 displays the variation of the total risk of fatal involvement in all types of accidents and for all new cars, regardless of market class. The actual data, available for each calendar year, have been treated here by a linear regression that yields the fit, shown by the solid line, and the 95 percent confidence bounds, shown by the dashed corridor. The slope is statistically significant and equal to

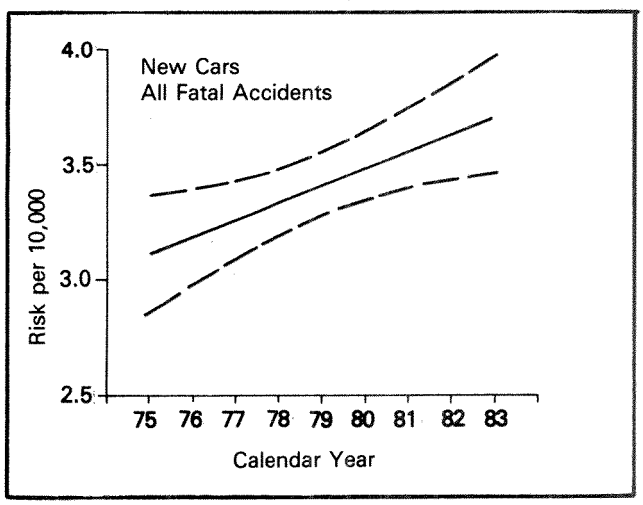

Figure 11. Risk variation versus calendar year for new cars in fatal accidents per 10,000 registrations

.076 ± .023 per year. In a 10-year period, this amounts to .76 ± .23 fatal accident involvements per 10,000 new car registrations. This is not insignificant when compared to the mean of the risk for approximately the same period: 3.41 ± .09 shown in the last entry of Table 6.

In spite of the statistical significance of the above estimates, the reader should keep in mind that the risks under consideration, obtained from the raw data for each of the past 10 calendar years, have been adjusted for variations in travel and exposure severity. These adjustments were discussed earlier and are detailed in the first part of Appendix B. Such adjustments, although well intended, could have introduced a bias that accounts for the observed increase, in part or entirely.

With full awareness of these uncertainties, and for information purposes only, we have proceeded to examine the possible origins of the estimated risk increase by fatal accident type and market class of new cars. For this purpose, we repeated the procedure discussed above in connection with Figure 11. The results are shown in Table 9 as estimates of the risk increase for a 10-year period. Only cases with statistically significant (95 percent confidence) results are shown. All other cases show the entry "none." Note that Table 9 has an entry-by-entry correspondence with Table 6. The latter displays means, while the former displays change within the 10-year period under consideration.

Influences of Car Weight, Wheelbase, and Front Wheel Drive

An examination of Table 8 leads us to believe that market class and especially nameplate designations appear to influence the risk of fatal accident involvement as much, if not more, than weight, wheelbase, or front wheel drive. To quantify these notions, we have examined the data—risk versus car weight, car wheelbase, or front wheel drive—for over 500 nameplate model year combinations, each weighted with exposure (registered car-years). We have applied log-linear regressions and have segregated the data by accident type in addition to examining them for all accident types combined.

The results of these regressions are shown in Table 10 as regression coefficients and their standard errors. The upper part of the table shows the coefficients of separate regressions, i.e., the effect of weight with no control over wheelbase variation and vice versa. The same data result in a very small, statistically nondistinguished from zero, sensitivity to front wheel drive. The striking similarity between the weight and wheelbase effects is no mystery, given these two variables are covariant in the fleet of cars. Accordingly, the question arises whether one and which one of the two effects is dominant. Thus, the risk data were also regressed versus weight and wheelbase concurrently.

The coefficients of these regressions are given in the lower part of Table 10. They show the effect of car weight when the wheelbase variation is controlled and vice versa. It is evident in these results that the car weight influence is not only small in general and smaller than the wheelbase influence, but also, contrary to a popular notion, that risk increases with weight reduction. Note in Table 10, negative coefficients indicate a risk reduction per unit weight reduction. This is what is observed for the car weight influence on accident risks for all types of accidents, except collisions with other motor vehicles where the influence is zero for all practical purposes.

Table 9. Estimates of risk increase in the last 10 years for new cars involved in fatal accidents of shown type

	Collision with Motor Vehicle	Collision with Object	Over-turn	Collision with Nonmotor Vehicle	All Types
Subcompact					
Domestic	.50 ± .17	None	None	None	.72 ± .27
European	None	None	None	None	None
Japanese	None	.41 ± .15	None	.29 ± .03	1.25 ± .47
Compact					
Domestic	1.21 ± .19	.54 ± .15	None	.17 ± .05	1.97 ± .38
European	.75 ± .02	None	None	None	None
Intermediate	None	None	None	None	None
Standard	.70 ± .09	.22 ± .06	None	.17 ± .04	1.10 ± .16
Entire Fleet	.46 ± .10	.23 ± .09	None	None	.76 ± .23

Table 10. Fatal accident risk variation for new cars by accident type as a function of car weight and wheelbase

Accident Type	Percent Risk Increase: Per 500 lb of Car Weight Reduction	Per 5 in of Wheelbase Reduction
Collision with Motor Vehicle	5.6 ± 1.3	5.2 ± 1.1
Collision with Object	11.3 2.7	12.5 1.4
Overturn	33.8 2.4	30.8 2.3
All Types	8.9 1.0	8.3 .8
	Per 500 lb of Car Weight Reduction at Fixed Wheelbase	**Per 5in of Wheelbase Reduction at Fixed Car Weight**
Collision with Motor Vehicle	1.1 ± 2.9	4.7 ± 2.4
Collision with Object	-19.1 3.9	28.7 3.2
Overturn	-20.0 5.7	48.5 4.8
All Types	-6.6 3.0	12.9 2.5

The influence of car wheelbase, at fixed car weight, appears to be substantial and quite sensitive to the type of accident. Although there may be certain physical reasons for expecting this influence, a much stronger influence may be attributed to nameplate or market class designations, as is evident in the results shown in Table 8.

Car Involvement as a Function of Accident Severity

This paper so far has addressed almost exclusively the car involvement in fatal accidents. There are obvious reasons for this emphasis. However, there are also two questions that need to be addressed: (1) Are the sensitivities observed in the fatal accident experience also evident in accidents of lesser severity? and (2) Are the results presented so far, based on the fatal accident experience recorded in FARS, seriously biased due to the FARS threshold of fatal accidents only?

To address these questions, we have analyzed the accident experience of cars in accidents of all severities as recorded in NASS and also in the accident records of several States. The NASS data have the advantage of national scope and national representativeness in general, but also have certain limitations when it comes to disaggregation of cars by nameplate—limited sample sizes and possible biases due to geographic nonuniformities of nameplate distributions.

Many States have provided NHTSA with a census of their accident records for the past 5 to 10 calendar years.[1] Collectively, these represent the experience of many millions of cars involved in accidents of known severity and known type. Several States also record the car nameplate with sufficient resolution to allow the analyses performed so far in the paper to be repeated. Other States record very general vehicle characteristics but also car make, which allows a general classification into market classes.

The complete examination of this accident experience, as a supplement to that of NHTSA's national scope files such as FARS and NASS, is a long-range project because of the enormity of the data base and the many variations of recording protocols. However, several analyses have been performed for addressing the questions raised earlier. Table 11 shows summary results concerning car propensity to overturn, a type of accident found in the FARS file to be most sensitive to car market class and nameplate.

In this table, we compare the accident experience of cars included in the records of FARS, NASS, the State of Texas, and the State of Washington. These two States have been selected for comparison with FARS because car nameplates are recorded, categorically and with a small fraction of unknowns, in a fashion most compatible with that used earlier in FARS categorization. Also the sample sizes in the State accident files are sufficiently large to allow the shown disaggregation by accident severity. This is not the case for NASS, where we show all accident severities only.

To bring the data from these many different files on a compatible basis, we employ the conditional risk descriptor of cars involved in overturns per 100 cars involved in all types of accidents. Conversion to absolute risks is obtained by multiplying the shown conditional risk with the absolute risk for all types of accidents. A review of the results in Table 11 leads us to believe that car propensity to overturn is sensitive to car attributes

1. These data bases have been provided on a professional courtesy basis. Data retrievals and analyses and any conclusions following from these analyses are the sole responsibility of the author and in no way represent the views of the States or of NHTSA.

Table11. Risk of car overturn per 100 accidents as a function of market class and accident severity. Comparison of results from the national files of FARS (1975-1983) and NASS (1981-1983) and the State accident files of Texas and Washington (1978-1983)

	Risk of Overturn per 100 Accidents							
	FARS	NASS	State of Texas			State of Washington		
Market Class	Fatal	All Severities	Property Damage	Personal Injury	Serious or Fatal	Property Damage	Personal Injury	Fatal
Subcompact								
Domestic	6.06	1.44	0.88	2.20	5.49	1.36	2.77	4.18
European	8.06	4.09	1.11	3.08	7.15	2.73	5.06	9.03
Japanese	10.85	3.46	1.54	3.84	9.24	2.32	4.34	15.20
Compact								
Domestic	4.95	1.23	0.51	1.52	4.02	1.17	2.20	8.53
European	9.72	2.45	0.92	2.38	6.03	1.22	2.72	11.52
Intermediate	3.42	.49	0.33	0.90	2.73	0.74	1.51	5.14
Standard	2.22	.34	0.17	0.64	1.63	0.47	0.98	2.35

not only in the fatal accident experience recorded in FARS but also in that of other accident files and not only for fatal accidents but for accidents of any severity. Similar results have been obtained by an examination of the accident experience in other States. Moreover, similar observations hold not only for overturn but also for other accident types that show risk sensitivity to car classes.

The Possibility of Confounding Factors

The observed sensitivity of certain accident risks to car class or nameplate is not immune from the confounding effects due to variations in the distribution of circumstantial but influential attributes among the car classes or nameplates under consideration. Included in these possible confounding factors are not only obvious attributes such as driver age and alcohol involvement or attributes such as rural or urban travel and night or day travel, but any factor that (1) has a substantial influence on the risk, and (2) has a significantly varying distribution among the car classes under examination.

A more detailed discussion of this subject is given in Appendix B in connection with Equations (B-1) to (B-8). In the same part of this appendix, we address what determinations are necessary to estimate the likelihood of confounding effects and what adjustments are appropriate to control their influence. We have applied these procedures in the examination of the data concerning sensitivity of overturn risk to car class. We selected this type of accident for a more detailed examination because of the magnitude of its sensitivity.

The number of circumstantial attributes that may influence the outcome of a car accident as an overturn is large, and their complexity is also large. We have considered the following among the most likely to be influential: the age and alcohol involvement of the driver, time of travel, urban or rural character of roadway, roadway speed limit, roadway curve occurrence, wet pavement occurrence, and topographical characteristics of travel. This last attribute was addressed by aggregating the FARS accident data into two categories by State. One category includes the States (mountainous, low population density) in which topography may promote the occurrence of overturns, while the opposite is true in the other category. The purpose of this is to control for possible effects due to nonuniformities in the geographical distribution of car classes.

We address first the distributions of these attributes and their possible variation by car market class. We did this for all accident types, whether overturns or not, and also for all single-car accidents. We selected single-car accidents for closer scrutiny because this is the pool from which the overturns are drawn. Summary results for single-car accidents are shown in Table 12. Note that for brevity in this table the shown circumstantial attributes have a binary categorization and the shown frequency values, in percent, concern the shown category. The percent value for the not shown category is obviously 100 percent minus the shown percent.

It is evident in the data of Table 12 that the distribution of circumstantial attributes among car market classes shows no significant variation or any pattern conspiring to enhance the overturn propensity of any given market class. Similar results are obtained when all accident types are considered instead of single-car accidents. The frequencies by circumstantial attribute are different, but they remain relatively insensitive to car class. On this basis alone, we may expect no substantial confounding effects on the risk determinations, unless the risk sensitivity to these attributes is overwhelming. Accordingly, we have resolved the risk of car overturn by the circumstantial attributes of interest here for each of the car market classes under consideration. These results are shown in

Table 12. Frequency of circumstantial attributes in single-car fatal accidents (FARS 1975-1983)

Market Class	Percent by Circumstantial Attribute						
	Young Driver	Alcohol Involv.	Night Travel	Rural Travel	High Speed Limit Rd.	Road Curve	Wet Pavement
Subcompact							
Domestic	26	50	69	68	66	42	18
European	29	55	70	61	60	47	14
Japanese	27	50	67	67	67	43	14
Compact							
Domestic	22	52	72	66	64	44	17
European	29	50	67	58	62	47	17
Intermediate	22	53	71	65	64	43	16
Standard	23	52	69	64	65	40	17
Entire Fleet	24	52	70	65	64	43	13

Table 13. The table also shows the overall risk for overturn, with and without adjustments.

The unadjusted overall risk is obtained from the data of Table 6 by forming the ratio of overturns/all types of accidents, for the entries appearing in Table 6. All other entries to the left of the unadjusted overall risk display values of the risk controlled for each slot of each circumstantial attribute shown in the table.

The not unexpected variation of risk according to circumstantial attributes (variation within each row) is evident. However, it is also evident that the pattern within each column is retained, for all practical purposes, regardless of the particular circumstantial attribute under consideration. This is a second indication (the first indication comes from the data of the type shown in Table 12) that no major confounding effects are to be expected. Indeed, when the overall unadjusted risk is adjusted, no major differences are observed. This is shown in the last two columns of Table 13.

The adjustment under consideration is carried out following the procedure discussed in Appendix B in connection with Equation (B-7). Very similar results are obtained when the procedure discussed above in connection with fatal car accidents is applied to car accidents of all severities. The results for all car accidents in the State of Texas, as an example, are shown in Table 14.

The above analysis leads us to the conclusion that no major confounding influences are in effect in the determination of accident involvement risks when cars are aggregated by market class. This is especially true for car involvement in overturns, where the risks appear to be quite sensitive to car market class. However, the reader should not generalize this conclusion. First, it should be kept in mind that there is no automatic assurance that all potentially influential confounding factors have been examined. In addition to possible unsuspected factors recorded in the accident files, there may be influential factors that are not recorded.

Another equally important consideration deals with the degree of desired disaggregation of the data in relation to the magnitude of the risk differentials we are attempting to examine. When relatively small differentials must be examined for a large number of classes and subclasses, the procedure of controlling for confounding factors can be very frustrating.

References

1. "Fatal accident reporting system," Automated Files, National Highway Traffic Safety Administration, Annual Issues, 1975-1984.
2. "National accident sampling system," Automated Files, National Highway Traffic Safety Administration, Annual Issues, 1979-1984.
3. "National crash severity study," Automated Files, National Highway Traffic Safety Administration, 1977-1979.
4. "National vehicle population profiles," R.L. Polk, Annual Issues, 1975-1983.
5. "Highway statistics," Federal Highway Administration, Annual Issues, 1975-1983.
6. "Nationwide personal transportation study," conducted in 1976-1977 by the U.S. Bureau of the Census for the Federal Highway Administration.
7. "Consumption patterns of household vehicles," survey conducted by the U.S. Department of Energy in 1979-1982.
8. "Truck inventory and use survey," conducted in 1977 by the U.S. Bureau of the Census.
9. "On-road fuel economy and annual travel of cars and light trucks," survey conducted in the early 1980's by the National Highway Traffic Safety Administration.

Table 13. Risk of overturn per 100 cars involved in fatal accidents (FARS 1975-1983) by market class as a function of circumstantial (driver and exposure) attributes

Car Market	Circumstantial Attributes										Overall	
Class	Youth	No Youth	Night	Day	Rural	Urban	Curve	Straight	Wet	Dry	Unadj.	Adjusted
Dom. Subcompact	6.0	4.9	6.0	4.7	8.0	2.2	9.8	4.0	4.0	5.8	6.1	5.8
Eur. Subcompact	10.6	6.5	8.4	8.0	12.1	4.1	15.7	5.5	4.3	9.4	8.1	7.7
Japanese	14.6	8.4	11.0	11.0	16.4	4.7	18.5	8.3	5.4	12.3	10.8	10.0
Dom. Compact	6.2	3.8	5.6	4.0	7.3	2.1	10.0	3.2	3.3	5.3	4.9	4.5
Eur. Compact	10.4	8.5	10.2	7.5	13.6	5.2	15.8	6.3	3.5	10.5	9.7	9.4
Dom. Interm.	4.8	3.1	4.1	3.2	5.9	1.3	8.9	2.3	1.9	4.2	3.4	3.5
Dom. Standard	3.5	2.3	3.1	2.3	4.2	1.0	6.5	1.9	2.1	2.9	2.2	2.6

Table 14. Risk of overturn per 100 cars involved in all police reported accidents (Texas 1978-1983) by market class as a function of circumatantial (driver and exposure) attributes

Car Market	Circumstantial Attributes										Overall	
Class	Youth	No Youth	Night	Day	Rural	Urban	Curve	Straight	Wet	Dry	Unadj.	Adjusted
Dom. Subcompact	1.8	1.1	3.2	0.9	8.7	0.6	11.0	1.1	1.4	1.4	1.4	1.3
Eur. Subcompact	2.7	1.3	4.0	1.3	11.6	0.9	14.2	1.3	1.8	1.9	1.9	1.8
Japanese	3.3	1.9	5.3	1.7	14.2	1.1	16.8	1.8	2.5	2.4	2.5	2.3
Dom. Compact	1.2	0.7	2.0	0.6	5.7	0.4	6.9	0.7	0.8	0.9	0.9	0.8
Eur. Compact	2.0	1.0	2.5	0.8	7.5	0.6	9.4	0.8	1.1	1.2	1.1	1.4
Dom. Interm.	0.8	0.4	1.3	0.3	3.8	0.2	4.9	0.4	0.5	0.6	0.6	0.6
Dom. Standard	0.6	0.3	0.9	0.2	2.2	0.1	3.0	0.2	0.3	0.3	0.3	0.4

10. • Stewart, J.R., et al., "Annual mileage comparisons and accident rates in North Carolina," final report to National Highway Traffic Safety Administration, 1980.
• Dutt, A.K., et al., "Annual mileage comparisons and accident rates in North Carolina," final report to National Highway Traffic Safety Administration under Contract DOT HS-803041, January 1978; also under Contract DOT HS-802428, June 1977.
11. "Fatal and injury accident rates on public roads in the United States," Federal Highway Administration, Annual Issues, 1975-1983.
12. Malliaris, A.C., "Discerning the state of crashworthiness in the accident experience," Tenth International Technical Conference on Experimental Safety Vehicles, Oxford, England, July 1985.

Appendix A

Major Changes in the Motor Vehicle Fleet and Travel

While the resident population in the United States grew at an average rate of 1.1 percent per year in the past 15 to 20 years, the number of licensed drivers grew faster, at an average rate of about 3 percent per year. An even faster growth took place in the number of registered motor vehicles and in the miles of travel of these vehicles each year. Both of these grew at a rate of about 4.5 percent per year. In addition to growth, significant changes took place during this period in the composition and major characteristics of the motor vehicle fleet.

Shifts in Fleet Shares by Vehicle Type

Between the early 1960's and 1980's, the mix of vehicle types in the fleet on the road changed significantly. In the early 1960's, vehicles other than cars were a relatively small fraction of the fleet. Since then two fleet components, trucks and motorcycles, have grown and are growing faster, as shown below:

	Registration (Millions)		
	Cars	Trucks (All Types)	Motorcycles
Early 1960's	55-65	10-13	1.3
Early 1980's	105-110	35-39	5.8

It is evident that while car registrations have barely doubled in 20 years, truck registrations have easily tripled and motorcycle registrations have more than quadrupled. Furthermore, new truck sales as a percent of all motor vehicle sales have risen from about 12 percent in the early 1960's to about 22 percent in the early 1980's.

These two vehicle types have been and still are of concern in the safety community because they are in general substantially more involved in accidents than the average vehicle type (see Table 3 in the main text). They also present special problems that are size-related. Trucks are more aggressive and motorcycles more vulnerable than the average vehicle type.

Changes in Major Car Characteristics

Three car characteristics—weight, wheelbase, and front or rear wheel drive—are singled out for general consideration because they are often discussed and analyzed in connection with accident and casualty risks. Significant changes have taken place in these characteristics in the past 10 years for most makes and market class categories, especially of the domestically produced new cars. Table A-1 shows car weight changes, and Table A-2 displays the wheelbase changes in an identical format. The growth of front wheel drive car shares is shown in Table A-3 in a similar format.

For the market class characterization in these tables, we have followed the practice of the domestic car trade literature, i.e., a classification by nameplate or car line into market class categories. European makes are classified as subcompact except for makes with a wheelbase above 100in (e.g., Mercedes Benz, Audi, BMW, Volvo, and a few others). Also, the great majority of the Japanese makes are subcompacts with few low-volume exceptions. Furthermore, we have used the R.L. Polk registration counts by nameplate and model year for obtaining the weighted means of car weight and wheelbase and for the percentages of front wheel drive cars.

Travel and Exposure Pattern Changes

Gasoline supply disruptions, the 55mph speed limit, the rising cost of highway travel, and various cycles in the economy have influenced travel and exposure patterns in the past 15 years. The resulting variations are noticeable but lesser than the changes in the motor vehicle fleet discussed above.

The average annual travel per vehicle has fluctuated by less than 5 percent in the period under consideration. However, larger fluctuations have been observed for specific vehicle categories as shown in Table A-4. The source of the data in this table is(5). The annual travel of cars, for example, shows a significant reduction between 1973 and 1974 and again between 1978 and 1981. Car travel is generally more responsive to and follows the pattern of major influencing factors.

Table A-1. Mean car weight (lbs) for cars retailed in the United States by origin of make and market class

I. New Cars by Model Year

Market Class	1977	1978	1979	1980	1981	1982	1983
Domestic Subcompact	2,597	2,453	2,425	2,393	2,118	2,211	2,125
Compact	3,415	3,231	3,047	2,756	2,651	2,708	2,612
Interm.	4,062	3,589	3,417	3,311	3,295	3,147	3,135
Standard	4,109	4,081	3,929	3,844	3,886	3,838	3,874
European Subcompact	1,994	1,897	1,989	2,098	2,032	2,085	2,071
Other	2,990	2,955	3,056	2,997	2,988	3,023	3,057
Japanese Subcompact	2,191	2,243	2,114	2,188	2,203	2,196	2,159
Other	2,673	2,740	2,834	2,849	2,887	2,886	2,851

II. All Model Years by Calendar Year

Market Class	1977	1978	1979	1980	1981	1982	1983
Domestic Subcompact		2,592	2,573	2,545	2,512	2,468	2,432
Compact		3,184	3,176	3,139	3,103	3,071	3,042
Interm.		3,946	3,861	3,802	3,753	3,703	3,637
Standard		4,379	4,347	4,325	4,311	4,285	4,259
European Subcompact		1,948	1,957	1,968	1,993	2,008	2,026
Other		2,755	2,801	2,827	2,860	2,891	2,924
Japanese Subcompact		2,187	2,188	2,184	2,183	2,187	2,187
Other		2,699	2,735	2,773	2,798	2,831	2,842

Table A-2. Registrations weighted mean car wheelbase (in) for cars retailed in the United States by origin of make and market class

I. New Cars by Model Year

Market Class	1977	1978	1979	1980	1981	1982	1983
Domestic Subcompact	95.7	96.9	96.5	96.6	95.7	96.4	95.3
Compact	110.0	108.9	106.5	105.4	103.9	102.8	101.1
Interm.	115.1	111.0	110.1	108.6	108.3	107.1	107.3
Standard	118.1	118.2	116.9	117.4	116.5	116.5	116.9
European Subcompact	94.8	93.4	93.8	94.2	95.0	96.5	96.6
Other	104.0	104.3	105.4	104.8	105.2	105.3	105.7
Japanese Subcompact	93.4	93.6	93.4	94.3	94.3	95.2	95.3
Other	104.0	104.0	104.0	100.4	103.6	103.3	103.1

II. All Model Years by Calendar Year

Market Class	1977	1978	1979	1980	1981	1982	1983
Domestic Subcompact		97.7	97.4	97.3	96.9	96.6	96.4
Compact		109.0	108.8	108.5	108.1	107.7	107.3
Interm.		115.1	114.2	113.6	113.0	112.4	111.8
Standard		122.1	121.7	121.5	121.2	120.9	120.5
European Subcompact		94.8	94.7	94.7	94.7	94.7	94.8
Other		103.4	103.7	103.9	104.0	104.2	104.4
Japanese Subcompact		93.8	93.8	93.8	93.9	94.0	94.2
Other		104.0	104.0	103.5	103.3	103.3	103.3

Table A-3. Percent of front wheel drive equipped cars retailed in the United States by origin of make and market class

I. New Cars by Model Year

Market Class	1976	1977	1978	1979	1980	1981	1982	1983
Domestic Subcompact		0.0	15.9	22.8	20.3	56..6	80.6	80.0
Compact				0.0	48.6	63.0	49.7	64.6
Interm.						0.0	27.4	33.3
Standard	0.0	3.0	0.0	2.6	14.9	13.0	13.6	14.2
European Subcompact	0.0	82.4	82.8	84.6	94.9	94.7	97.4	99.0
Other	0.0	17.6	26.8	21.1	27.7	22.3	18.2	16.0
Japanese Subcompact	0.0	27.4	27.4	37.3	42.9	51.0	59.3	72.2
Other							0.0	17.8
All Market Classes								

II. All Model Years by Calendar Year

Market Class	1976	1977	1978	1979	1980	1981	1982	1983
Domestic Subcompact		0.0	1.4	3.1	6.5	11.7	19.4	25.7
Compact			0.0	0.5	4.5	9.2	13.4	16.9
Interm.						.0.0	1.1	4.4
Standard		0.0	2.5	2.4	2.8	3.4	4.0	5.5
European Subcompact		0.0	21.9	27.8	33.1	38.8	43.2	48.1
Other		0.0	16.9	16.1	16.6	16.9	17.0	16.8
Japanese Subcompact		0.0	16.8	20.1	24.8	28.8	32.7	38.1
Other							0.0	4.4

Table A-4. Average annual travel per vehicle in thousand miles as a function of calendar year

Year	Cars	Trucks Single	Trucks Combin.	Motorcycles	All Motor Vehicles
1973	10.0	9.87	46.7	4.50	10.1
1974	9.45	8.98	49.1	4.50	9.53
1975	9.63	8.88	51.7	4.50	9.64
1976	9.76	9.37	48.3	4.50	9.84
1977	9.84	9.40	50.2	4.50	9.93
1978	10.0	9.25	49.3	4.50	10.1
1979	9.49	9.18	49.7	4.00	9.58
1980	9.14	10.1	42.7	3.14	9.41
1981	9.00	11.0	47.0	2.57	9.48
1982	9.53	9.81	50.1	2.09	9.64
1983	9.64	9.71	52.4	2.15	9.73

In the late 1960's and early 1970's, car travel showed minor fluctuations around 10,000mi per year. A significant decline occurred between 1973 and 1974 due to the oil embargo at that time. From 1974 to 1978, car travel per year increased slowly but steadily until 1979, when another oil crisis forced an abrupt reduction. This reduction was prolonged and deepened well into 1981 due to a depressed economy.

The increase of annual travel per car, starting in 1982, has coincided with the economic recovery that also started at that time. Note the annual travel for other vehicles, especially trucks, is much less discretionary and does not necessarily follow the pattern of car travel. The pattern for all motor vehicles agrees with that of cars because car travel dominates.

Annual travel per car is known to vary substantially as a function of car age (or of model year in a fixed calendar year). Variations may also exist as a function of market class. The data for a detailed and systematic examination of these patterns and their variation in the past 10 to 15 years are not at hand. However, the available information is generally consistent with the summary shown in Table A-5, which addresses relatively new cars, i.e., of age 3 years or less.

Table A-5. Annual travel per car as a function of car age and car market class

Car Market Class	1st Yr. Travel Thousand Miles/Car	Travel Ratio 2nd Yr./1st Yr.	Travel Ratio 3rd Yr./1st Yr.
Subcompact	13.2 ± .47	1.00 ± .02	.95 ± .03
Compact	12.1 .51	.91 .05	.89 .07
Intermediate	13.3 .60	.89 .02	.82 .03
Standard	13.6 .36	.91 .03	.84 .02
All	13.0 .2	.94 .02	.87 .03

The data in each entry of this table are averages of corresponding values provided by a large number of sources(2,3,6,7,9,10) spread over several years between the mid-1970's and early 1980's. The raw data in these sources have very dissimilar origins. In spite of this, fair agreement is observed for car ages up to 3 years or with respect to car market classes. This is reflected in the relatively small errors that arise when data from all these sources are averaged, as shown in Table A-5. Furthermore, no significant or systematic trend has been found in the data with respect to calendar year variations, again for car travel categorized as in Table 5.

Travel speed patterns have also changed substantially in the past 10 to 15 years. The 55mph speed limit went into effect nationwide early in 1974. Before that time, the prevailing average speed on interstate highways was about 65mph. This average speed dropped to about 57.5mph in 1974. In the following years, this speed increased steadily, slowly in the second half of the 1970's but faster in the early 1980's. Table A-6 shows the percentage of motor vehicles noncomplying with the 55mph speed limit while driving on U.S. highways(5).

Table A-6. Percent of motor vehicles on U.S. highways exceeding shown speed in the early 1980's

Year	55 Mph	65 Mph	75 Mph
1980	49.3	16.8	4.1
1981	48.5	18.4	5.2
1982	52.6	24.2	7.9
1983	54.1	25.4	8.5

Travel speed is one of the factors that influence the severity of the exposure to accident and casualty risks. Many other factors, driver, environment and vehicle-related, may also be influential with varying strengths. As an overall descriptor of exposure severity, we have considered the rate of accidents per unit travel for all vehicles on U.S. roads. Table A-7 shows how this rate has varied in the past 10 years. The source of these data is(11).

Table A-7. Fatal accidents and nonfatal injury accident rates per 100 million vehicle-miles traveled on U.S. roads by calendar year

	Accidents per 100 Million Miles	
Year	Fatal	Nonfatal Injury
1975	2.85	133.0
1976	2.87	133.3
1977	2.91	129.8
1978	2.92	135.9
1979	2.97	137.5
1980	2.96	132.8
1981	2.84	130.1
1982	2.45	123.6
1983	2.30	121.6

Appendix B

Errors and Adjustments in Risk Determinations

The most common and serious source of error in the estimation of absolute risks, by application of Equation (1), is the absence of coincidence in the categorization of attributes represented by subscripts j and k, between the numerator and denominator. The discussion following Equation (3) in the main text explains why the estimation of absolute risks is more vulnerable to such errors than the estimation of conditional risks, by application of Equation (3). The steps we have taken to minimize this type of error have been outlined in the main text in connection with absolute risk determinations.

A second, but separate, concern is the number of vehicle and exposure categories, subscripts j and k, that must be introduced to obtain the desirable resolution in the computation of risks. It is desirable, although not always feasible, to resolve the matrix jk into as many cells as necessary to obtain fairly uniform risks within each population. This, however, must be traded off against the statistically insignificant results obtained when a large number of cells yields populations that are too small.

Even after the concerns discussed above are satisfied, further adjustments may be appropriate to deal with nonuniformities in the exposure conditions relevant to risk determinations. This appendix discusses such adjustments.

We consider first a normalization procedure that is used for relatively new cars (1 to 3 years old) traveling on U.S. roads in any of the calendar years 1975 to 1983. The exposure variations experienced by these subfleets were discussed in the last section of Appendix A. Tables A-4, A-5, and A-7 display relevant data. When comparing or aggregating these subfleets, it is convenient and appropriate to normalize their accident experience to an arbitrary but common basis. For this purpose, we have selected the 1-year-old cars, under the travel and exposure severity conditions of the calendar year 1980.

In practice, normalization is performed through factors that multiply the risks of accident involvement per vehicle registration to normalize them to the reference exposure conditions. Table B-1 shows normalizing factors A and B for annual travel per car by calendar year and for exposure severity, respectively. Factor A is obtained from the car travel data shown in the first column of Table A-4, by making 1980 the reference year. Similarly, Factor B is obtained from the data of Table A-7.

Table B-1. Normalization factors by calendar year for annual travel per car (column A) and for exposure severity (columnB)

Calendar Year	A	B
1975	.95	1.04
1976	.94	1.03
1977	.93	1.02
1978	.91	1.01
1979	.96	1.00
1980	1.00	1.00
1981	1.02	1.04
1982	.96	1.21
1983	.95	1.29

The product of Factors A and B is the composite normalization factor for 1-year-old cars. This product appears in the first column of Table B-2. The other two columns of this table show the composite normalization factors for 2- and 3-year-old cars, respectively. These factors have higher values, which reflect the travel reduction taking place as the car age increases. The relevant data for these transformations are shown in the last row of Table A-5.

In addition to travel per vehicle and exposure severity in general that show variations from year to year, there are many exposure attributes that influence accident risks, even in the absence of calendar year or model year considerations. In fact, attributes such as driver age,

Table B-2. Normalization factors for travel and exposure severity by car age and calendar year

Calendar Year	Car Age 1 Year	2 Years	3 Years
1975	.99	1.05	1.14
1976	.97	1.03	1.11
1977	.95	1.01	1.09
1978	.92	.98	1.06
1979	.96	1.02	1.10
1980	1.00	1.06	1.15
1981	1.06	1.13	1.22
1982	1.16	1.23	1.33
1983	1.23	1.31	1.41

alcohol involvement, vehicle type, time of day, travel speed, etc., may have influences stronger than those addressed in the discussion so far. Accordingly, adjustments would be necessary to bring the determination of risks under exposure conditions as comparable as possible, when such comparability is desired. When necessary, these adjustments are made according to the procedure discussed below. Consider first the risks R_1 and R_2 concerning two different vehicle classes 1 and 2, as determined from aggregated data of vehicle involvements and exposure:

$$R_1 = \text{Sum } V_{1k} / \text{Sum } E_{1k} \quad \text{(B-1)}$$

$$R_2 = \text{Sum } V_{2k} / \text{Sum } E_{2k} \quad \text{(B-2)}$$

The summations in these relations are over all exposure conditions designated by k, which may represent, for example, driver age brackets, alcohol involvement, time of day, highway type, travel speed, etc. It is now helpful to introduce the exposure distribution frequencies:

$$F_{1k} = E_{1k} \text{Sum } E_{1k} \quad \text{(B-3)}$$

$$F_{2k} = E_{2k} \text{Sum } E_{2k} \quad \text{(B-4)}$$

Note that the sum of all F_{1k} or all F_{2k} values equals unity.

The use of these equations in (B-1) and (B-2) yields:

$$R_1 = \text{Sum } (F_{1k} R_{1k}) \quad \text{(B-5)}$$

$$R_2 = \text{Sum } (F_{2k} R_{2k}) \quad \text{(B-6)}$$

where the risks R_{1k} and R_{2k} are defined by Equation (1) in the main text for j = 1 and 2, respectively, and for each value of k that is of interest. Subscript i, i.e., the accident category, is dropped here for simplicity; however, the analysis is equally valid for any given or for all accident categories. Equations (B-5) and (B-6), which are fully equivalent to (B-1) and (B-2), are more informative. They show that, in each case 1 or 2, the aggregated risk is the sum of risks corresponding to individual exposure conditions, with each such risk weighted by the frequency of occurrence of the corresponding exposure condition.

When risks R_1 and R_2 are determined under aggregated exposure conditions, i.e., by Equations (B-1) and (B-2), any difference between them may be not entirely due to risk differentials under specific exposure conditions. As shown in equations (B-5) and (B-6), differences between R_1 and R_2 may arise from differences between R_{1k} and

R_{2k}, or from differences between F_{1k} and F_{2k}, or from both sources.

A numerical example will clarify these points. Let subscripts 1 and 2 represent two different vehicle types and subscripts a and b represent two different exposure conditions, say urban and rural travel. Furthermore, suppose the data we are dealing with are:

$F_{1a} = 90\%$, $F_{1b} = 10\%$; $F_{2a} = 10\%$, $F_{2b} = 90\%$

for the frequencies of occurrence of the exposure and:

$R_{1a} = 3$, $R_{1b} = 1$; $R_{2a} = 5$, $R_{2b} = 2$

for the individual risks, in accidents per unit exposure. The risks R_1 and R_2, integrated over both exposure conditions for each vehicle type, are: $R_1 = 2.8$ and $R_2 = 2.3$.

This answer may be fine if we wish to compare the risks of vehicle categories 1 and 2 under their recorded exposure conditions. However, this answer is absurd if it is meant to be a risk comparison under exposure conditions assumed to be fairly similar. It is absurd because R_{1a} is lower than R_{2a} and R_{1b} is lower than R_{2b} so R_1 is also expected to be lower than R_2, but it is not. This very substantial distortion is introduced because the frequencies of occurrence of exposure categories differ significantly between vehicle types 1 and 2.

Whenever risk calculations and comparisons, vehicle category 1 versus 2, are made over aggregated exposure conditions, it is essential as a minimum to determine and review the frequency distributions of exposure conditions for each of the vehicle categories 1 and 2. If these distributions are fairly similar, the possibility of distorted results is minimized. However, if the distributions differ substantially, then Equations (B-1) and (B-2) or their equivalent (B-5) and (B-6) as written are inappropriate for risk determinations.

Equations (B-5) and (B-6) may be used but only after an adjustment. The necessary adjustment requires that F_{1k} and F_{2k} must be made identical. This can be done either by retaining F_{1k} in (B-5) but also using the same in (B-6) instead of F_{2k}, or by retaining F_{2k} in (B-6) and also using the same in (B-5) instead of F_{1k}. These two alternatives correspond to risk comparisons either under the exposure conditions of vehicle category 1 all across the board or under those of vehicle category 2 also all across the board. A third alternative may be considered by pooling the exposure conditions of both vehicle categories together and determining a frequency distribution F_k for the pooled populations. For this alternative, the appropriate version of Equations (B-5) and (B-6) is:

$$R_1 = \text{Sum}\,(F_k R_{1k}) \quad \text{(B-7)}$$

$$R_2 = \text{Sum}\,(F_k R_{2k}) \quad \text{(B-8)}$$

Note the risks R_{1k} and R_{2k} must be determined for each exposure category k, and then used in conjunction with the common frequency distribution f_k for the determination of R_1 and R_2. Other alternatives are possible for introducing a common frequency distribution. Which alternative is selected depends on the terms under which we wish to compare risks.

Optimum Luminances and Areas of Rear-Postition Lamps and Stop Lamps

Hans-Joachim Schmidt-Clausen
Technical University Darmstadt, Federal Republic of Germany

Abstract

In static and semidynamic tests, the luminances of stop lamps and rear-position lamps were rated by test persons. Out of these results, the influence of light-intensity, area of the light-emitting surface, and observation distance on the assessment of the luminance is shown.

Introduction

Starting from the measured light-intensities as measured during ECE-type approval in Germany(1), the aging effects of lamps were looked at. These results were the basis for the static and semidynamic tests carried out in the normal traffic situation. The influence of the following parameters was investigated: light-intensity of the lamp, area of the light-emitting surface of the lamp, daytime/nighttime observation, and observation distance. As a criterion, the 9-rating scale was chosen.

Light-Intensities of Lamps

The light distribution of signal lamps is prescribed, for example, in ECE regulations. In Figure 1, a frequency distribution for the axial light-intensity is plotted for stop lamps and rear-turn-signal lamps. The plotted values are results from the test-institute in Germany. These values are gained with a so-called test voltage at the filament lamp, which is also prescribed in the regulation. The values have a normal distribution. The typical values are summarized in Table 1.

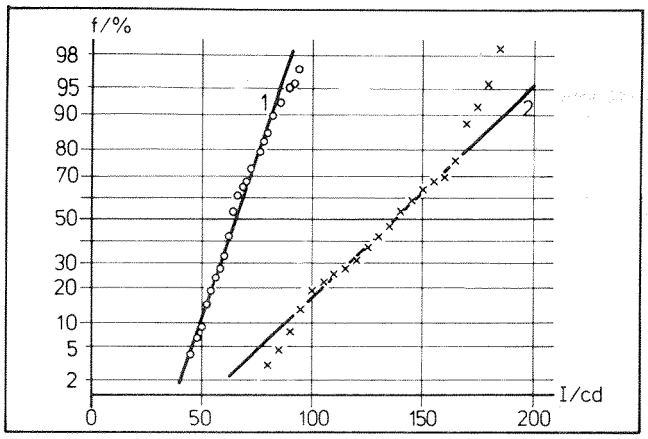

Figure 1. Frequency distribution f of light-intensity I

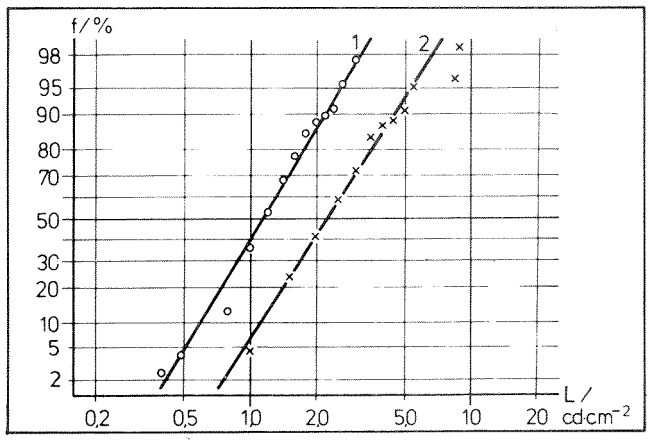

Figure 2. Frequency distribution f of luminous intensities L

Table 1.

Frequency in %	Light-intensities in cp: Stop Lamp	Light-intensities in cp: Rear-Turn-Signal Lamp
.50	65	138
16	53	99
10	49	88

These values of light-intensities were converted to luminance values. The results are plotted in Figure 2 and have a log-normal distribution.

In Table 2, the main values are summarized.

Table 2.

Frequency in %	Luminances in cp/cm²: Stop Lamp	Luminances in cp/cm²: Rear-Turn-Signal Lamp
98	3.2	6.6
50	1.2	2.3
16	0.69	1.3
10	0.59	1.1

These values as shown in Figures 1 and 2 are values measured in the laboratories. Nevertheless, these values may give an impression about the luminances of those two types of lamps.

Light-Intensities of Lamps Mounted on the Car

During a test initiated by the BAST in Germany, the light-intensities of lamps mounted on the car in use were measured(2). Some of the results are shown in the following two figures.

In Figure 3, the results of the stop lamps and rear-turn-signal lamps are plotted; in Figure 4, those for the rear-position lamps always measured with stopped engine. Each curve is represented by roughly 1,200 single measurements. The dots are the mean values as shown in Figure 1 (f = 50 percent). With increasing age, the axial light-intensities of all the described lamps are lowering. For some selected years of construction, the values for light-intensities are summarized in Table 3.

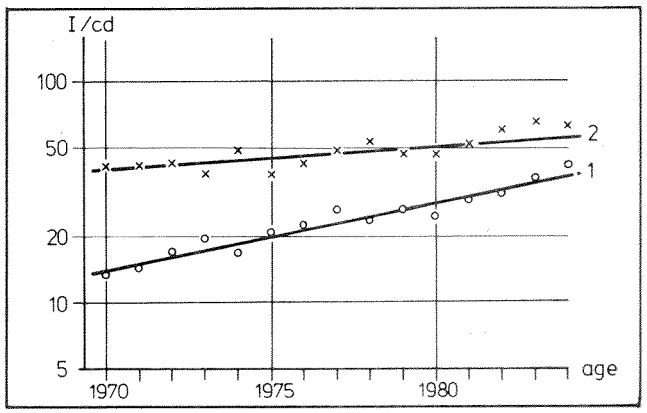

Figure 3. Light-intensity I and age of different lamps

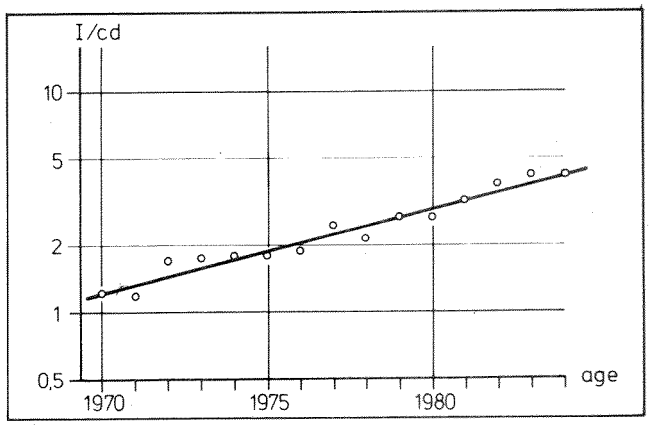

Figure 4. Light-intensity I and age of rear-position lamps

Table 3

Year of Production	Axial Light-Intensity in cp		
	Stop Lamp	Rear-Turn-Signal Lamp	Rear-Position Lamp
84	37	56	4.2
80	28	50	2.9
75	20	45	1.9

Comparing these summarized values with those in Table 1, it can be shown the mean value of the light-intensities of lamps on cars in use is roughly half the value as gained by the type approval. The same reduction will occur when comparing the luminances of the lamps in use and during type approval.

The Tests

The tests were performed statically and semidynamically. In the static test, the test person had to rate the luminance of two lamps while looking on an axial fixation spot. In the semidynamic test, the test person was moving with a car in the direction of the test fixture. At a certain distance, the test person had to rate the luminance. A dynamic test is in preparation at this moment. The areas of the test lamps could be changed between $A = 20cm^2$ and $A = 200cm^2$ in steps. The axial light-intensities of the lamps could be changed between 1cp and 1,000cp while the luminous distribution itself showed a normal curve.

The rating scale is summarized in Table 4.

Table 4

Assessment of the Luminance of Lamps	
Grade	Description
1	Too dark
2	
3	Dark
4	
5	Optimal
6	
7	Bright
8	
9	Too bright

The tests were carried out during daytime and nighttime with 10 emmetropic test persons. About 6,000 tests were conducted. The tests were made on a straight road with a neutral background during daytime and no glaring lights during nighttime. During the nighttime tests, the test persons were adapted to the luminance of a low beam. Because of this restricted kind of test, the results may be somewhat lower than those that will be gained with glare sources, street lighting, and other optical noise, etc.

Evaluation of the Tests

The results of the tests were evaluated using the common statistic method. For the evaluation of the luminances and light-intensities, a log-normal distribution was taken as a basis; for the assessments, a linear-normal distribution was used.

As an example in Figure 5, the assessments of the light-intensities I of stop lamps are plotted. The mean values x and the distribution σ of the results are shown. The regression line of the results as drawn was calculated using common statistic methods.

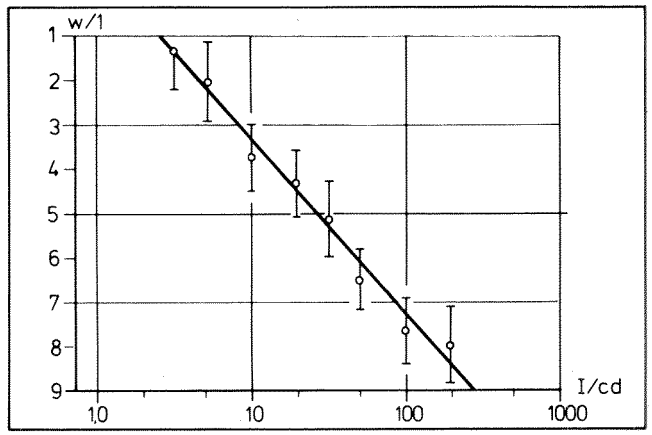

Figure 5. Assessment w of the light-intensity of a stop lamp (size of light-emitting surface of stop lamp: $A = 20cm^2$; time of test: nighttime)

Results of the Tests

Assessment of Light-Intensities

The results of the assessment of the light-intensities of stop lights are plotted in Figure 6 for daytime observation and in Figure 7 for nighttime observation. In both figures, only the results for the areas $A = 20cm^2$ and $A = 200cm^2$ are plotted. For reasons of clarity, the results for the other areas are not shown. The dotted area in both figures represents the area of light-intensities that are permitted after the ECE regulation.

For the assessment "optimal" (w = 5), the results are summarized in Table 5.

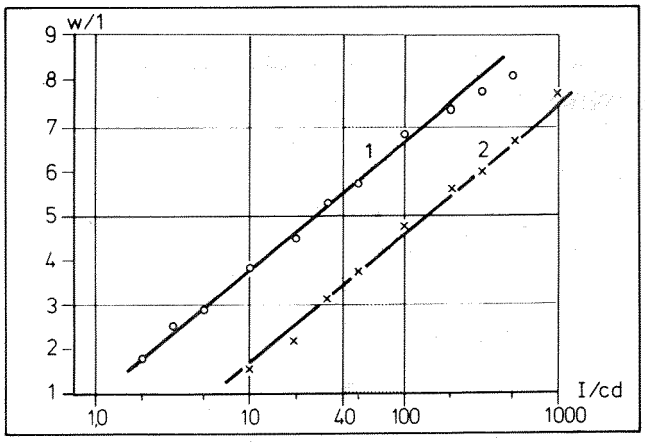

Figure 6. Assessment w of light-intensity I of stop lamps during daytime observation

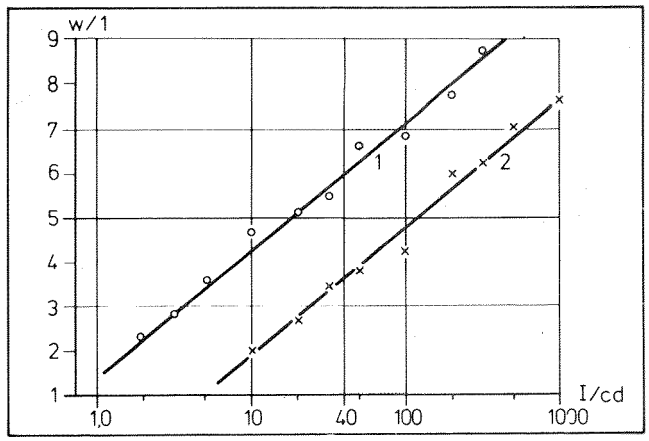

Figure 7. Assessment w of light-intensity I of stop lamps during nighttime observation

Table 5

Observation	Optimal Light-Intensities of Stop Lights in cp Area of the Light-emitting Surface in cm^2	
	20	200
nighttime	18	117
daytime	27	140

Both regression lines in the figures lie somewhat symmetric to the dotted area. In both cases, no optimal luminance can be reached with either the $20cm^2$ area nor the $200cm^2$ area.

For rear-position lamps, the results are plotted for nighttime observation only in Figure 8. The dotted area again describes the limits for the light-intensities after the ECE regulation. The light-intensities for the assessment "optimal" (w = 5) are summarized in Table 6.

Table 6.

Area of the Light-emitting Surface in cm^2	Optimal Light-Intensities of Rear-Position Lights in cp
20	5.2
200	24.3

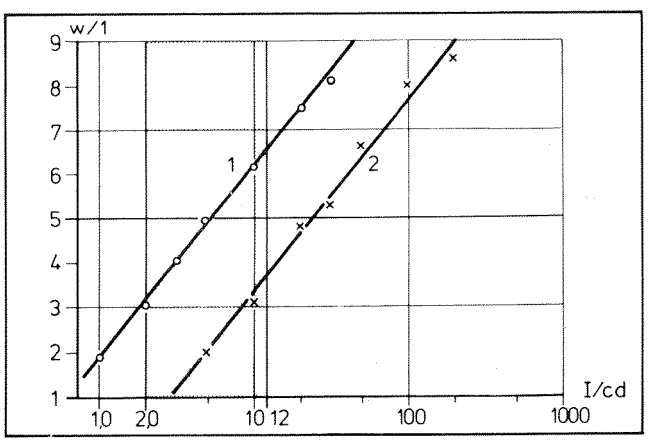

Figure 8. Assessment w of light-intensity I of rear position lamps during nighttime observation

The optimal light-intensity for rear-position lights can be reached with small areas A; for areas A = $200cm^2$, the optimum cannot be reached.

Assessment of the Luminances

For different light-emitting surfaces A, the optimum luminance L of stop lights are plotted in Figure 9. The results are plotted for daytime and nighttime observation. With increasing area A, the luminance is decreasing. The plotted results are somewhat lower than the 50 percent value in Figure 2. These results are valid for neutral backgrounds, no glare source, etc. With these influences, the optimal luminances may be higher than the results in Figure 9.

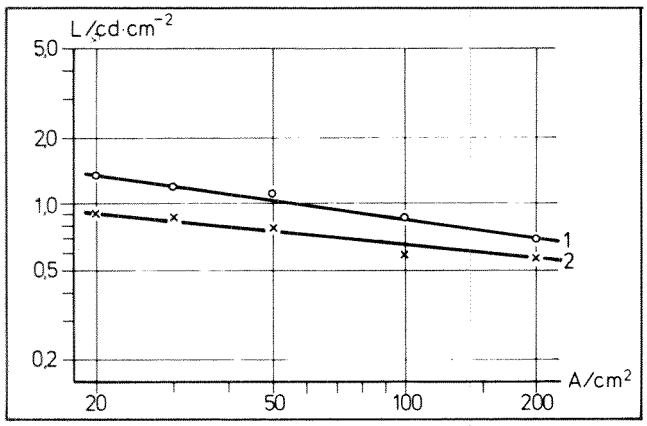

Figure 9. Luminance L and size A of a stop lamp

The results for the rear-position lamp are plotted in Figure 10 with the observation distance as a parameter. An increasing area of the lamp reduces the luminance required for the assessment "optimal." The same effect occurs with decreasing observation distance. Out of the reasons mentioned above, the necessary luminances in the real traffic situation may be higher.

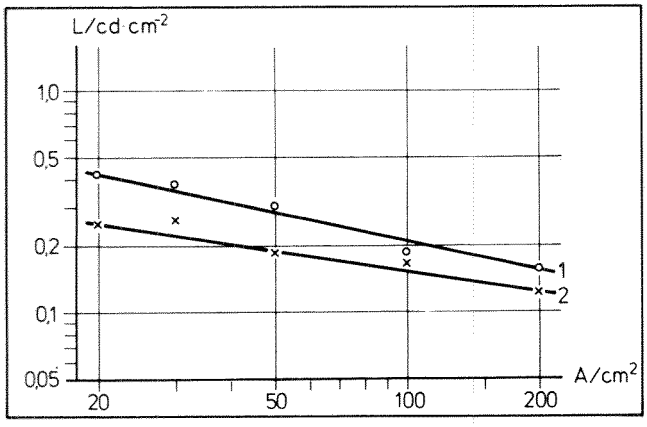

Figure 10. Luminance L and size A of a rear position lamp during nighttime observation

Influence of the Observation Distance on the Assessment

The influence of the observation distance on the assessment of the light-intensity of rear-position lamps can be shown in Figure 11, in which is plotted, with the area of the light-emitting surface A as a parameter, the dependence of the optimum light-intensity I from the observation distance d. With increasing distance d, the light-intensity must also be increased to get optimal high intensity for the lamp. Changing the distance from 25m up to 125m, the light-intensity has to be increased by 60 percent for the small area A and by 30 percent for the large area A.

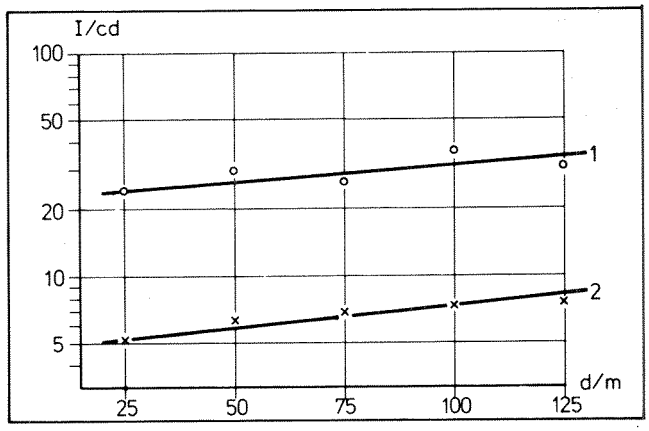

Figure 11. Light-intensity I for rear position lamps and observation distance d

Conclusion

The assessment of the luminances of stop lamps and rear-position lamps indicates that the present ECE regulations more or less fulfill, within certain areas of light-emitting surfaces, the conditions "optimal." It is nevertheless necessary to prove these results by those gained by dynamic tests.

References

1. Pollack, H., Private communication, 1985.
2. *Leuchtenüberprüfung im Verkehr,* report 1.7566, BAST, Germany, 1975.
   Leuchten- und Scheinwerferüberprüfung im Verkehr, report 1.8209, BAST, Germany, 1983.
3. Report on the "Demonstration of devices having different light-intensities and brightnesses with regard to their dazzling effects," Economic Commission of Europe, TRANS/SC 1/WP 29/GRE/R 57, 1983.

Evaluation of Headlamp Beam Patterns Using the Ford CHESS Program

Michael Perel
U.S. Department of Transportation, National Highway Traffic Safety Administration

Abstract

The Ford CHESS computer program was used to evaluate headlamp performance as a function of various influencing factors such as beam pattern, aim, and overall intensity. The degree to which the model was sensitive to headlamp, driver, and environmental variables was assessed. The results showed that only small increases in performance could be achieved by beam pattern modifications, improved aim, and increased overall intensity. Part of the difficulty in identifying performance improvements was found to be the low sensitivity of the CHESS figure of merit to changes in beam photometrics. Suggestions are made for upgrading the CHESS evaluation methodology to make the performance metrics more sensitive to differences in beam design.

Background

Recent developments in headlamp technology are making new low beam photometrics possible. The National Highway Traffic Safety Administration is interested in developing an evaluation methodology that would provide a means to compare the new beam patterns with each other and with current ones in terms of safety performance. The agency may consider the use of such a methodology to help set minimum performance requirements for headlamp systems.

Currently in the United States, we determine whether a beam is acceptable or not by whether it meets the test point specifications in the Society of Automotive Engineers standards. This approach has a number of limitations, including the difficulty of knowing what the test point values mean in terms of their influence on driver performance. In other words, test point specifications do not quantify the visibility distance or glare hazard potential of the beam. Furthermore, many beam patterns can meet the same test points but may not produce equal performance. If a new pattern is proposed that does not meet the current test point specifications, it is difficult to obtain general agreement on whether it meets minimum safety needs. Another type of problem is that current test point specifications do not permit evaluation of performance of lamps at different mounting heights or of asymmetric lamp systems.

Because of these limitations, NHTSA is exploring the possibility of developing a headlamp evaluation methodology that more directly quantifies safety performance. The performance metric most commonly used to evaluate beam patterns in the past has been target detection distance measured using static or dynamic road tests. One of the problems in conducting these tests is determining what conditions should be used. Parameters that can be varied in such studies include target type, target location, driver characteristics, headlamp aim, and roadway geometry. Because of the many variations possible, a beam that ranks high under certain test conditions might rank low if others were used. The evaluation process becomes even more complicated because there are multiple criteria for evaluating beams. In particular, a beam should provide illumination for target detection and keep glare low for oncoming motorists.

These considerations lead to the question of whether a systems evaluation should be employed that would provide a variety of conditions under which beams should be evaluated and allow tradeoffs to be made among multiple performance criteria. This approach might be thought of as analogous to the current evaluation of vehicle fuel economy where a standardized route is used to evaluate overall fuel economy over a variety of conditions. In the headlight area, this approach is somewhat similar to the Ford CHESS program (Comprehensive Headlamp Environment Systems Simulation)(1). This paper will describe some analyses conducted with CHESS in attempting to better understand whether and how it might serve as a starting point for developing an evaluation methodology. The analyses explored three general areas:

- The effects of various influencing factors on beam performance
- The role of discomfort glare in evaluating performance
- The comparison and evaluation of beam patterns

This paper discusses some of the questions suggested by these analyses that need to be addressed to develop an evaluation methodology and concludes with suggestions for future research.

Description of CHESS

The CHESS program developed by the Ford Motor Company provides a comprehensive method for quantifying headlamp photometric performance. Beam performance is evaluated in terms of a Figure Of Merit (FOM). This FOM is basically the percent of miles driven under

which three criteria for measuring performance are simultaneously met. The three performance measures are right-lane delineation visibility, pedestrian visibility, and discomfort glare. These measures are calculated for a simulated vehicle as it is "driven" over a test route representative of U.S. roadway geometries and environments. In the case of delineation visibility, the performance criterion that must be satisfied is to have visibility for a distance greater than the distance the simulated vehicle travels in 2s—time to steer the car to keep it on the road. Performance is measured based on computation of delineation contrast and comparison to the contrast needed for detection by simulated drivers. For pedestrian detection, performance is measured basically the same way—the criterion is that detection distance must be greater than the car's stopping distance. A driver is considered discomforted if the glare at the eyes is over 10 percent greater than the glare of a baseline U.S. low beam built into the model or when the subjective rating of discomfort based on the DeBoer scale reaches a value of 4 or less. In computing whether or not these criteria are met, the effects of various influencing factors such as aim, target reflectance, and driver visual characteristics are taken into account. In addition, various weightings are used to reflect the relative importance and exposure of the different components in the computation of the FOM.

As an illustration of the representative conditions under which performance is measured, Figure 1 shows how road geometry variables affect angular locations of right-delineation lines, pedestrians, and oncoming drivers. The points on the graphs illustrate where in the beam pattern the critical targets and oncoming vehicles are located. One observation from these figures is that the locations of critical targets sometimes coincide with locations of oncoming drivers—thus, this illustrates the difficulty of making the beam intense enough to detect targets without creating discomfort glare for oncoming drivers.

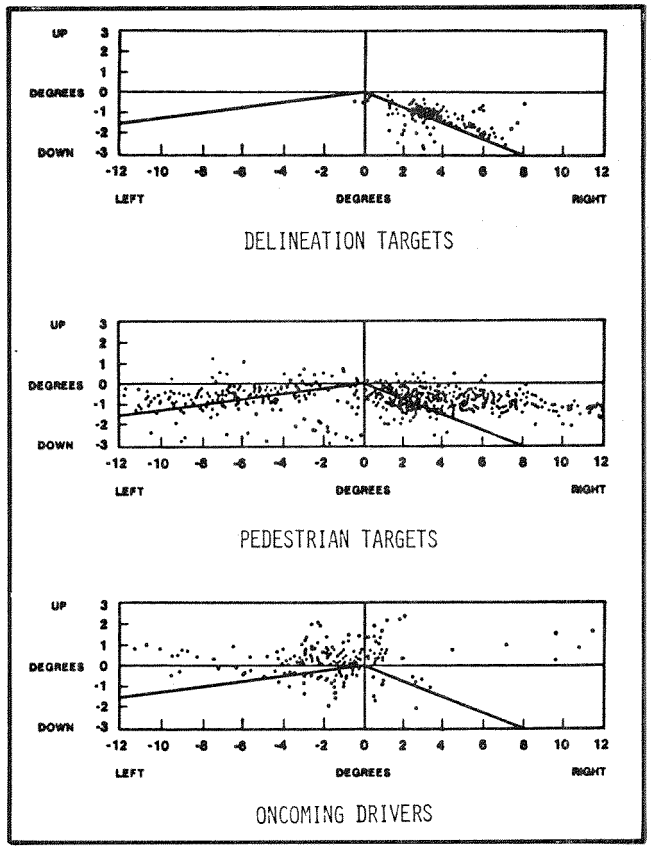

Figure 1. Distribution of angular locations of pedestrian, right-delineation lines, and oncoming drivers

Analysis of Beam Performance

One type of analysis conducted to provide information about the sensitivity of CHESS performance measures was to determine how the metrics varied when values for influencing factors or other components of CHESS were changed. This type of analysis was conducted for a number of CHESS parameters and is summarized in Table 1. It lists the qualitative degree of sensitivity that the performance metrics for a U.S. tungsten low beam have to the various factors listed. For example, the first line is the percent design intensity parameter. This parameter multiplies the overall beam intensity by a given percent. Pedestrian detection had a relatively high sensitivity to this factor, delineation had low sensitivity, drivers discomforted had high sensitivity, and the overall figure of merit shows moderate sensitivity. The delineation detection criterion was not a discriminating measure of performance for any of the factors because the required 2s criterion distance could be met under most encounters.

Another point to note in summarizing these results is that performance varies as a function of the influencing factors. The implications for improving night driving safety with beam pattern modifications is that beam performance cannot be determined in isolation from the various environmental, vehicular, and driver factors that can interact with performance. Because some beam patterns are likely to show greater sensitivity to the effects of some influencing factors than others, the relative ranking of beam performance could be affected by the choice of parameters to include in the evaluation methodology. For this reason, it is also important to reexamine the parameters of CHESS and update those that do not reflect the current driving environment.

The discomfort glare performance measure is important in the CHESS evaluation methodology. The limit of allowable discomfort is a major constraint on lamp intensity. Discomfort glare is determined from geometric consideration by calculating the beam intensity that intersects the oncoming driver's eyes in each meeting

scenario. This intensity level is compared to a criterion value to determine whether or not the driver would be discomforted.

The criterion value is based on the DeBoer rating scale, which was calibrated with a typical U.S. low beam. To calibrate the scale, a typical U.S. tungsten sealed beam was assumed to have acceptable glare. Because this low beam produced discomfort levels of 4 and above (i.e., acceptable glare) on the DeBoer scale, this value was used as the criterion.

Figure 2 shows the results of comparing several real and hypothetical low beams in terms of discomfort glare performance. The headlamps compared include, from left to right: no headlamp; a U.S. tungsten sealed beam; a European sharp cut-off beam; a modified U.S. low beam with overall higher intensity, especially in the lower right-hand quadrant; a hypothetical beam with reduced intensity in the upper left quadrant but higher lower right quadrant intensity; and a hypothetical beam with 40,000cd below horizontal and no intensity above horizontal. The lamps were evaluated under perfect aim and misaim conditions that are representative of the aim of the vehicle fleet in the early 1970's. The mean vertical aim was .75° up with a standard deviation of 1.5°. Mean horizontal aim was .08° right with a standard deviation of .86°.

The results show that, as expected, discomfort glare is an important performance measure in helping to discriminate between beams. The discomfort performance of the ECE beam is noticeably better than the other beams. The 40K beam, because of its high intensity levels, has the worst discomfort. The figure also shows the strong influence of misaim on discomfort. The difference in performance between misaim and perfect aim conditions for the same beam can be as great as the magnitude of the differences between beams. Since misaim is a fact of life for all headlamps, these results emphasize the importance of evaluating beam design under realistic misaim conditions.

An updated survey of headlamp aim of the U.S. fleet has just been completed by Olson(2). The results found that for passenger car model years 1978-1984, the mean vertical aim was .25° down with a standard deviation of 1°. Mean horizontal aim was .04° right with a standard deviation of .78°. An update of the CHESS program

Table 1. Sensitivity of performance measures to input parameters (L = low sensitivity M = moderate H = high

	Pedestrian Detection	Delineation Dection	Drivers Discomfort	FOM
Overall Intensity	H	L	H	M
Mean Vertical Aim	H	L	H	M
Mean Horizontal Aim	L	L	M	L
Vertical Aim Standard Deviation	M	L	M	M
Mounting Height	M	L	L	L
Beam Pattern	M	L	M	M
Glare Criterion	-	-	H	L
Road Illumination	H	L	L	M
Driver Alertness	M	-	-	L
Pedestrian Size	L	-	-	L

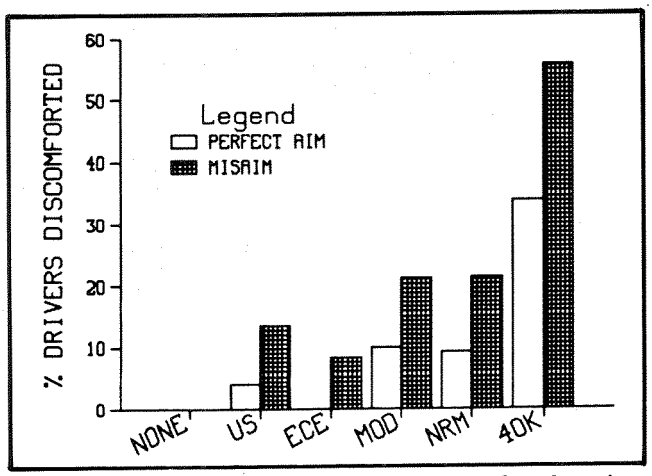

Figure 2. Discomfort glare performance of various low beams

should include these more recent data. Because of the smaller standard deviations of misaim, the more recent data would result in smaller differences between perfect aim and misaim conditions.

Another factor that affects beam performance is the level of glare beyond which drivers would subjectively rate glare as discomforting. This criterion has been studied recently by Olson and Sivak(3). Their results suggest that drivers can accept a higher intensity before they will complain of discomfort than the criterion on which the CHESS program is currently based. This finding is based on measuring glare tolerance under field conditions as opposed to laboratory testing.

The effect on performance when this discomfort glare criterion is changed according to the Michigan results is that the percent drivers discomforted for a U.S. beam pattern decreased to 5 percent from almost 17 percent with the current criterion. However, the overall FOM does not change much. This does not imply that glare is not important but that the current FOM formulation is not a very sensitive metric. It has a narrow range. Also, discomfort glare is weighted considerably less than the pedestrian detection metric in the calculation of the FOM.

The beam patterns discussed above were also compared in terms of percent pedestrians detected and overall FOM. Figure 3 shows pedestrian detection performance under unopposed traffic, unlit roadway conditions. It illustrates that misaim reduces performance slightly. Under these unopposed conditions, misaim down would reduce detection distance; misaim up would increase detection distance. The net effect, as shown in the figure, is a slight decrease in performance. The performance of the ECE beam with its sharper cutoff above horizontal is more sensitive to misaim. The 40K beam appears to be a good performer in this comparison. However, the discomfort glare of this lamp is high. When the various performance measures are combined over the entire

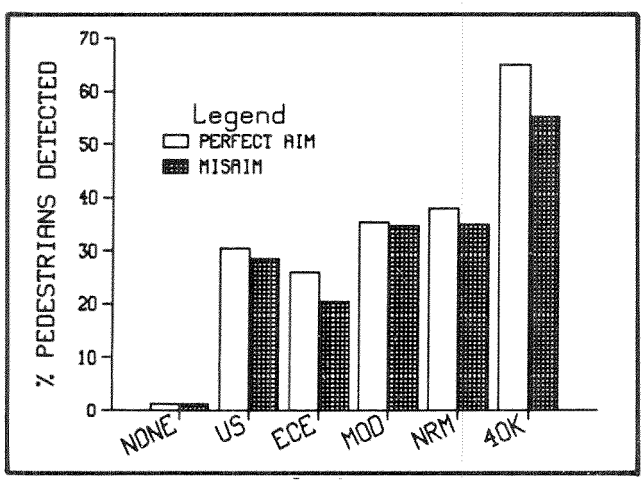

Figure 3. Pedestrian detection performance of various low beams

simulated test route to compute the FOM (Figure 4), the performance of the 40K lamp is not greatly different from the other beams. Misaim results in further reduction in the 40K lamp performance.

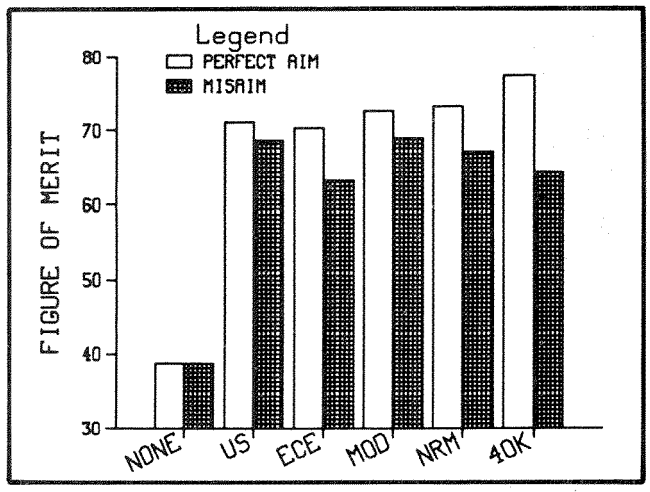

Figure 4. Merit for various low beams

None of the lamps showed any major differences when evaluated by the FOM. Larger differences among beam patterns were found with the individual performance measures than the overall FOM. Part of the reason for the lack of sensitivity of the FOM to different beam patterns is that some criteria are met by all beams and thus do not discriminate. For example, the percent delineation detected was always very high and not much different for different beam patterns. Also, the effects of the various weighting and influencing factors may wash out beam pattern differences. A beam may provide good performance under some conditions but poor performance under others. The net effect is that it is difficult to improve the overall FOM score, which takes all conditions into account. Even if we had a more sensitive FOM, there is the question of whether a major low beam improvement is possible. The inverse square law and log response of the eye mean that a large intensity is needed to gain even a small increase in detection distance. As described on a previous chart, some critical target locations coincide with oncoming drivers' eyes, further increasing the difficulty of satisfying all criteria. Finally, misaim reduces the effectiveness of beam performance.

Another observation to make from Figure 4 is that when there are no headlamps, the FOM is almost 40. In large part, this is due to delineation, and pedestrian targets can be seen from the ambient illumination and fixed roadway lighting. Thus, the CHESS program can evaluate the broader aspects of nighttime driving visibility, not just beam patterns.

Conclusion

It is difficult to identify means to make major improvements in low beam headlamp performance using CHESS. Only relatively small increases in performance could be measured due to changes in beam patterns. Small improvements in performance were also shown by modifying the various factors that interact with photometrics to upgrade performance. Although it is conceivable that other beam patterns could be envisioned that have increased performance potential, major improvements are still considered unlikely because of the underlying constraints on beam performance incorporated in CHESS. As mentioned above, these include the large increase in intensity needed for a relatively small increase in detection distance and the limits on intensity due to discomfort glare concerns. It is also possible that performance improvements are difficult to identify because of limitations in the program structure and formulation. For example, because the FOM score has a very narrow range as a function of beam pattern, performance changes due to beam modifications are difficult to detect. It may also be difficult to identify improvements because of inappropriate assumptions related to the performance criteria, test scenarios, and weighting factors used in the program calculations.

In developing a headlamp evaluation methodology using a CHESS-type approach, problems can arise in deciding which performance criteria are relevant, how to measure performance, what type of driving environment to simulate, and how to compute a performance metric. To resolve these dilemmas, a number of actions are recommended to make the tool more sensitive to safety performance differences in beam photometrics.

The performance criteria form the central basis for the evaluation methodology. It is important they reflect the safety performance required of headlamps. The criteria used in CHESS should be reviewed to make certain they reflect safety needs. Changes that might add to the safety relevance of the criteria include (1) modifying the delineation detection criterion to be a more sensitive metric, (2) adding discomfort glare from following vehicles, and (3) adding a sign detection/reading performance. The criterion level for discomfort glare needs to be reexamined and a consensus developed to determine the maximum values that could be permitted.

Once performance criteria have been identified, the methodologies and equations for computing performance need to be determined. Although some work had been performed to calibrate the formulation used to compute target detection distance and discomfort glare, additional calibration is desirable to consider a broader range of driving conditions and drivers. This type of calibration would serve as a check on the validity of the methods for evaluating performance.

Because the original CHESS development is over 10 years old, the data used to describe the influencing factors related to the driver, vehicle, and environment need to be reassessed and updated. The driving scenarios that best represent safety critical conditions should be identified, the factors that interact with beam photometrics to influence performance reviewed, and the weightings to determine the relative significance of these factors and scenarios reassessed.

Finally, a reevaluation is needed of the method for utilizing the performance metrics to arrive at a value for overall lamp performance. Consideration should be given to alternative means to compute performance that might provide greater sensitivity to beam differences. For example, the use of individual performance metrics such as pedestrians detected, or drivers discomforted, might show the relative safety benefits of the beams more directly than the FOM. Another measure that would help focus on the safety performance of beams and increase the sensitivity of the FOM to beam differences is one that gives increased weights to nonilluminated roads, curves, and other worst case conditions. With such changes, it may be possible to provide a more sensitive and safety-related evaluation of beam performance.

References

1. Bhise, V.D. et al., "Modeling vision with headlights in a systems context," SAE Paper 770238, 1977.
2. Olson, P., "Measurement of crash avoidance characteristics of vehicles in use," 1985 (in press).
3. Olson, P., and M. Sivak, "Improved low beam photometrics," NHTSA Contract DOT-HS-9-02304, Report No. DOT-HS-806 488, 1983.

A Study of Laser Radar

Hiroshi Kawata,
Hiroshi Endo, and
Yoshiyuki Eto
Nissan Motor Co., Ltd.

Abstract

Various radar systems have been proposed as collision avoidance sensors for automatic braking and warning applications. Practical use of laser radar systems is near with the introduction of high power, high reliability laser diodes.

Utilizing these new devices, a laser radar system has been adapted for measuring the distance to objects in its path. It was first shown that reflectors on the rear of the automobile possess high reflectivity and sharp directivity. Given these characteristics, a compact laser radar system was tested that employed 12W laser diodes and PIN photodiodes.

The maximum range of approximately 100m was obtained. Furthermore, the ability to discriminate other vehicles from roadside objects was achieved by detecting discontinuity in measured distance data through a microprocessor. These results show that the performance of laser radar is comparable to that of microwave radar. Considering the cost and size of the radar systems, laser radar would appear to be the more practical of the two.

Introduction

Microwave, laser, and acoustic-based radar systems that can be applied to vehicles have been proposed. Radar systems that can detect the distance of the preceding vehicles or obstacles on a highway are limited to microwave and laser-based radar systems, as they require long detection ranges. Development of microwave radar has been carried out for some time, but it is not yet practical due to its large size, high cost, etc.

On the other hand, the development of opto-electronics such as laser diodes has increased the probability of utilization, since laser radar systems can be constructed at a lower cost, while assuring higher performance than microwave radar systems.

As a fundamental experiment, reflective characteristics of the rear of a vehicle were measured. A prospect detection range of about 100m was obtained with laser power, which is nonhazardous to the naked eye. The authors have tried to construct a cheap, small-size, and practical laser radar system with a detection range exceeding 100m.

Effects of adverse weather conditions were expected, so a waterdrop and mud detector and wiper were installed on the window of a laser radar head.

A microprocessor discriminates vehicles from roadside objects by detecting their range and the relative velocity of the detected objects. Thus, the laser radar system was tested to insure its application as a sensor in collision avoidance systems or in automatic headway control systems.

This paper describes the structure and performance of the laser radar system and gives test results gained on actual roads with curves and hills and ranges in adverse weather conditions.

Laser Radar Equation

The geometry of laser radar is shown in Figure 1. A short pulse laser beam is transmitted with the divergence angle γ_0. The transmitted beam is reflected by the target, then the reflected beam diverges with the angle Φ_0 and is focused onto a detector such as photodiode. The received signal power is given by expression (1). Detector is followed by an amplifier. The range to target is given by the time difference between transmitted and received laser beams.

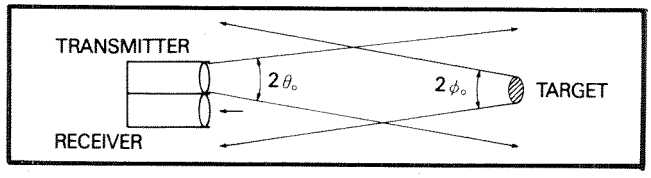

Figure 1. Geometry of laser radar

$$(1) \qquad P_r = \frac{P_t \cdot K \cdot A_t \cdot A_r \cdot T_r}{\pi^2 \, R^4 \, \theta_0^2 \, \Phi_0^2} \, e^{2\sigma R}$$

where

P_t	:	transmitted laser power
K	:	target reflectivity
A_t	:	area of target
A_r	:	receiver area
T_r	:	receiving optics transmission
R	:	range to target
Φ_0	:	transmitter half-angle divergence
Φ_0	:	reflected beam half-angle divergence
σ	:	atmospheric attenuation coefficient

Reflective Characteristics of a Vehicle

Reflective characteristics of the rear of the vehicle have been measured using a simple laser radar. As shown in Figure 2, two reflex reflectors have high reflectivity; other parts do not. Furthermore, reflex reflectors have sharp directivity; beam divergence is about 30mrad. This is very desirable in laser radar systems.

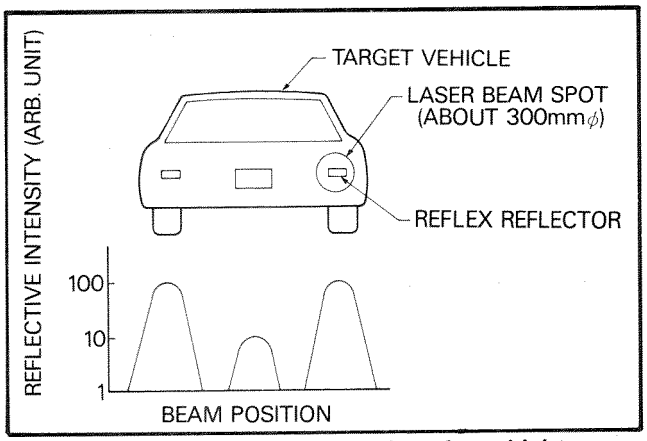

Figure 2. Reflective characteristics of a vehicle

Laser Power and Safety Aspects(1,2)

According to the IEC standard, the maximum permissible exposure value for a repetitive laser beam with a pulse width of 50ns, wavelength 900nm, is about 0.6W. Given the wheel-motion interlock system, a safety range of 1m should not pose a problem. Supposing transmitter beam divergence to be 60mrad (full angle), the diameter is 60mm at 1m range. The pupil diameter is about 7mm, so, assuming a uniform beam, the total laser power is given by:

$$P_0 \left(\frac{7}{60}\right) \leqq 0.6 \text{ (W)}$$

$$P_0 \leqq 44 \text{ (W)}$$

Actually, a uniform beam cannot be obtained, so P_0 must be less than 44W.

Laser Radar System Design

System Composition

A laser radar system is composed of a laser radar head, a display unit, and a microprocessor unit among other parts. The laser radar head is composed of a transmitter, a receiver, and a range-detecting circuit; a waterdrop and mud detector and wiper can be installed. The laser radar head provides range signals. The display unit receives the range signals and displays the range.

Range signals and vehicle velocity signals are provided for the microprocessor.

The system composition is shown in Figure 3.

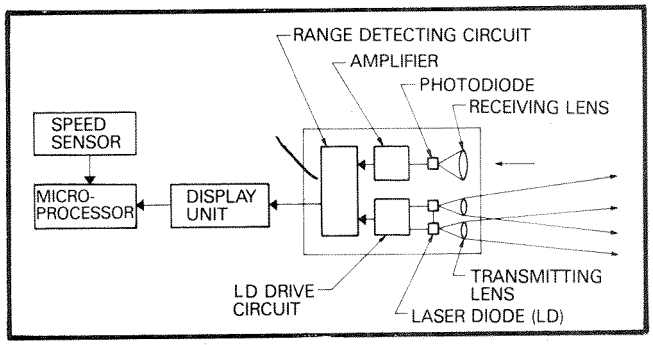

Figure 3. System composition

Transmitter

To get a wide, long detection area, two laser diodes (LD) are provided in the transmitter. Each laser diode can provide 12W peak output power.

The LD drive circuit requires high response to achieve high-range accuracy. Waveforms of drive current and laser pulse are shown in Figure 4.

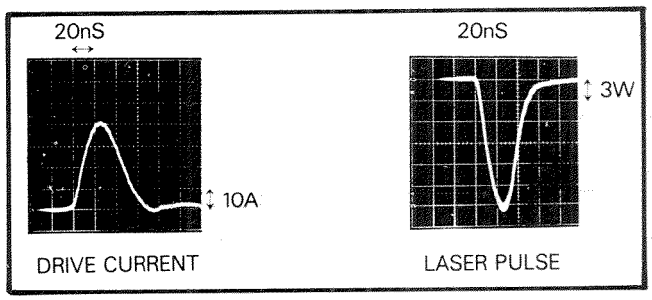

Figure 4. Waveforms of LD drive current and laser pulse

Laser beams from two laser diodes are transmitted through lenses toward the front. One laser beam has a half-intensity, full-angle divergence of 60mrad. Another laser beam has a half-intensity, full-angle divergence of 30 × 10mrad.

Irradiance distribution of the combined laser beams is shown in Figure 5. Distribution depends mainly on the characteristics of the laser diodes; it is difficult to obtain uniform distribution.

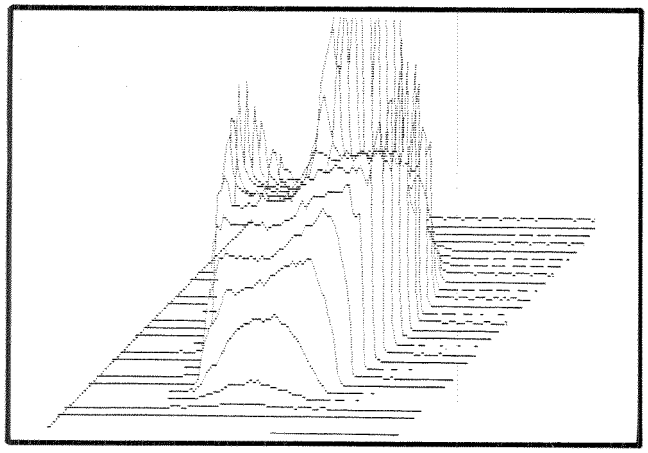

Figure 5. Irradiance distribution of laser beams

Receiver

The receiver is composed of optical parts and a signal amplifier. The structure is shown in Figure 6. Fresnel lens was chosen as a receiving lens because it covers a large area, is lightweight, and is thin. This lens is designed with a short focal length to make the laser radar head small.

The lens plate consists of two lenses, whose size is 60 × 60mm; the focal length is 40mm, respectively. Consequently, two PIN photodiodes are provided on the focal points.

Optical filters consist of infra-red filter (IR filter) and a honeycomb. An acryl-based plate is used both as an IR filter and as a fresnel lens. A honeycomb is used so as not to admit sunlight scattered by the fresnel lenses.

The signal amplifier is composed of an amplifier and an STC (sensitivity time controller). An STC is used to reject the signals reflected from fog, rain, road, etc., at close range.

Performance of the Laser Radar

Characteristics of the Laser Radar

Fundamental performance of the laser radar is shown in Table 1. A photograph of the laser radar head is shown in Figure 7.

Detection Range for a Vehicle

Detection range was measured with a passenger car as the target with two 50 × 40mm reflectors. The results are shown in Figure 8. The lane width of the highway in Japan is about 3.5m, so the vehicle in front can be detected with high reliability on a straightaway.

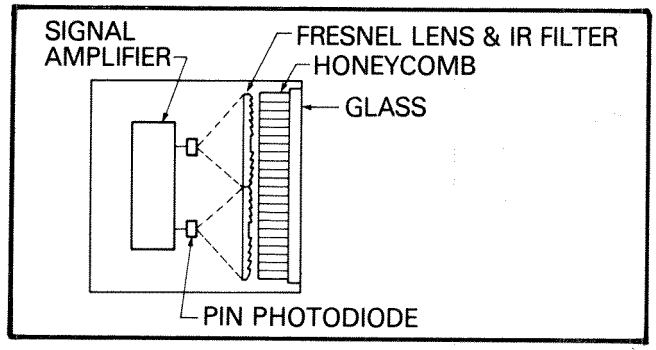

Figure 6. Receiver structure

Table 1. Characteristics of the laser radar head

Item	Description
Size	$180_W \times 80_H \times 150_L$ mm
Laser power	18 W (peak)
Beam divergence angle (full-angle)	60 mrad.
Pulse repetition cycle	6 kHz
Detecting range	about 120 m
Range resolution	1 m
Error of range	about ±2 m
Data output repetition cycle	15 ~ 30 ms
Drive voltage	10 ~ 16 V
Drive current	0.7 A

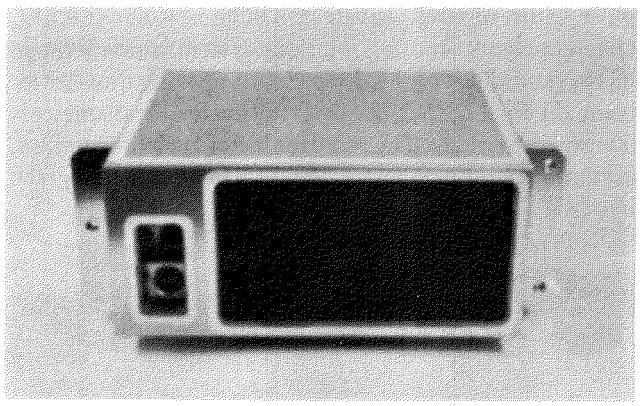

Figure 7. Laser radar head

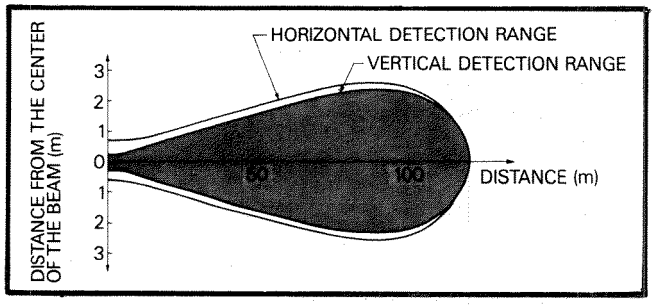

Figure 8. Detection range

Dispersion of Maximum Detection Range

Maximum detection range varies widely, as the reflected beam from the preceding vehicle is mainly from reflectors, where reflected laser power varies with their size and surface cleanliness. Results obtained on a highway are shown in Figure 9. Most of the vehicles are passenger cars or trucks. In the case of passenger cars, dispersion is relatively small. However, in the case of trucks, it is large since some trucks have muddy reflectors or large reflectors.

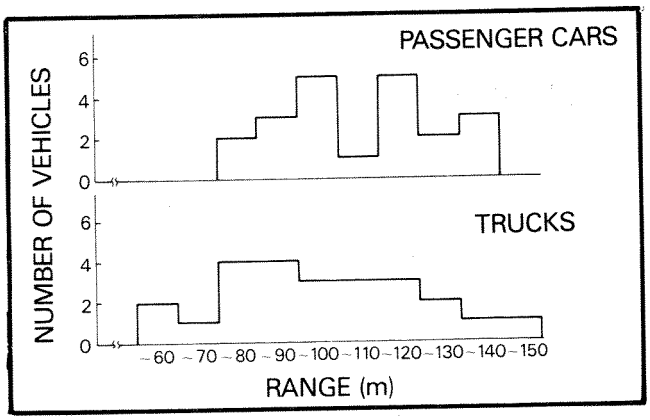

Figure 9. Dispersion of maximum detection range

Range Restriction Due to Curves and Hills

On actual roads, detection range is restricted by curves or hills. For example, in curves of a radius of 300m, maximum range is about 25m. Hills also impose range restriction; however, it is not so severe as in curves. In either case, maximum range is insufficient.

Weather Effects

It was confirmed experimentally that detection ranges in fog, rain, snow, and sunlight are restricted.

In rain, detection range is reduced by approximately a factor of two, from its clear-air value. This is caused by waterdrops on the transmitter, receiver, reflectors of the vehicles in front, and in the air, moreover, by the splashing of the vehicle in front. Based on the amount of water splashed, the detection range is sometimes reduced by approximately a factor of three. It is possible to remove waterdrops by use of a wiper, such that detection range increases about 20 percent from nonwiper values. However, in heavy rain, the wiper is not so useful. When it is raining, the transmitted laser beam is reflected by the rain. Moreover, the transmitted laser beam is scattered on the window of the transmitter and then reflected from the near-range road. An STC is necessary to sift out such useless signals.

In fog, one problem is that a transmitted laser beam is scattered and then detected by the receiver. This is also solved by an STC. Another problem is that the laser beam is attenuated by fog. The detected signal level in fog is shown in Figure 10. When the range of view is less than 100m, detection range is reduced by more than a factor of two.

There are only a few restrictions in light snow because the reflected laser beam from the snow is rejected by an STC. However, in heavy snow, it is impossible to sift out the signals from the snow; then random distance data are obtained.

Sunlight is detected by a photodiode and decreases the signal-to-noise ratio (S/N). Consequently, it causes error of range and, in the worst cases, blinding occurs. As a laser radar is designed by taking account of sunlight and noise, it operates normally under usual conditions. However, in cases when the sun is within 10° of the axis of the laser beam, the laser radar becomes blind.

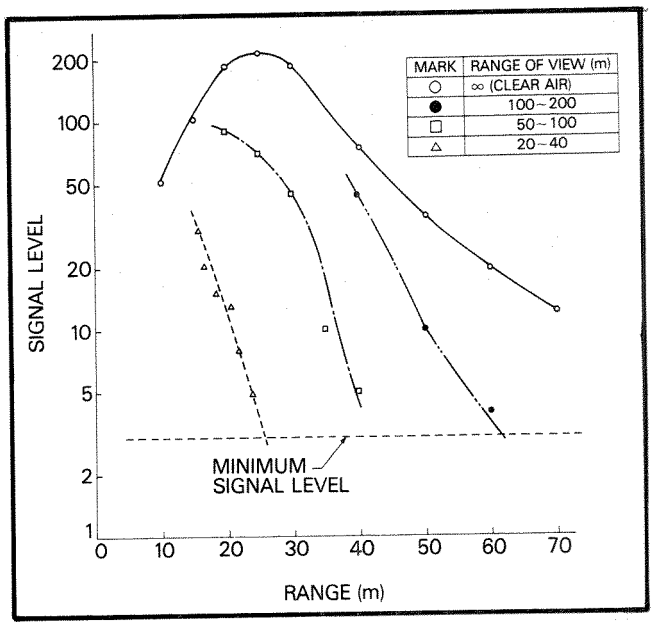

Figure 10. Signal level in fog

Window Cleaning System

As a laser radar head is provided in the front end, it is sometimes exposed to rain, snow, or muddy water. To keep the window of the laser radar head clean, a waterdrops and mud detector and a wiper are installed. The structure of the detector is shown in Figure 11.

Some of the transmitted laser beam is scattered by waterdrops or mud on the window, and the laser beam incident into the optical fiber is detected by a photodiode and then amplified. Although the detection area is limited on the path of the transmitted laser beam, the detector operates very well under ordinary adverse weather conditions. In light rain, the wiper can remove waterdrops and maintain good performance.

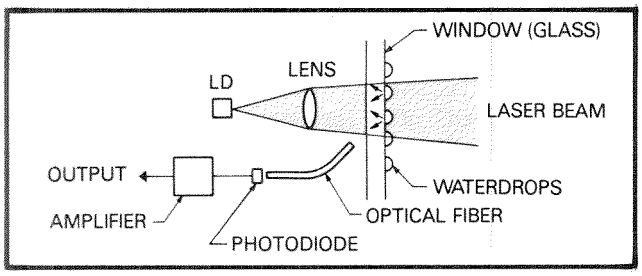

Figure 11. Structure of waterdrops and mud detector

Ranges for Other Targets

The laser radar detects many kinds of targets: roadside reflectors, guardrails, trees, roadside signs, etc. (see Figure 12). Reflectors and roadside signs have high reflectivity and ranges as long as those of vehicles are obtained. Guardrails on a highway are seldom detected. The detection range for a person is about 40m.

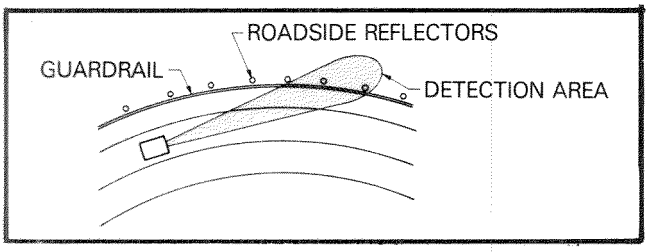

Figure 12. Roadside objects

Discrimination

Some examples of distance data on real roads are shown in Figure 13. Figure 13(a) shows data wherein a vehicle is detected on a straight road and roadside reflectors on curves. Figure 13(b) shows data when another vehicle intrudes between the preceding vehicle. Moving vehicles can be discriminated from other targets by detecting relative velocity and discontinuity in distance data. Hazard level is determined by detecting distance and relative velocity. However, lane discrimination(3,4) of the target is impossible.

Comparative Evaluation of Laser and Microwave Radar

Table 2 shows a comparative evaluation of laser and microwave radar. There is little difference in performance, but, totally evaluated, laser radar seems to be superior to microwave radar.

Conclusion

Laser radar has a detection range of approximately 100m; the capacity for discrimination between moving vehicles and roadside objects is possible. This performance is comparable with that of microwave radar. Totally evaluated, laser radar is more practical than microwave radar.

It is inevitable that the detection range of laser radar will be restricted in adverse weather conditions. Detection ranges are improved by use of a wiper; however, the original performance level cannot be obtained.

To put the laser radar system into practical use, lane discrimination of the targets and improvement in the detection ranges, especially in adverse weather conditions, must be achieved.

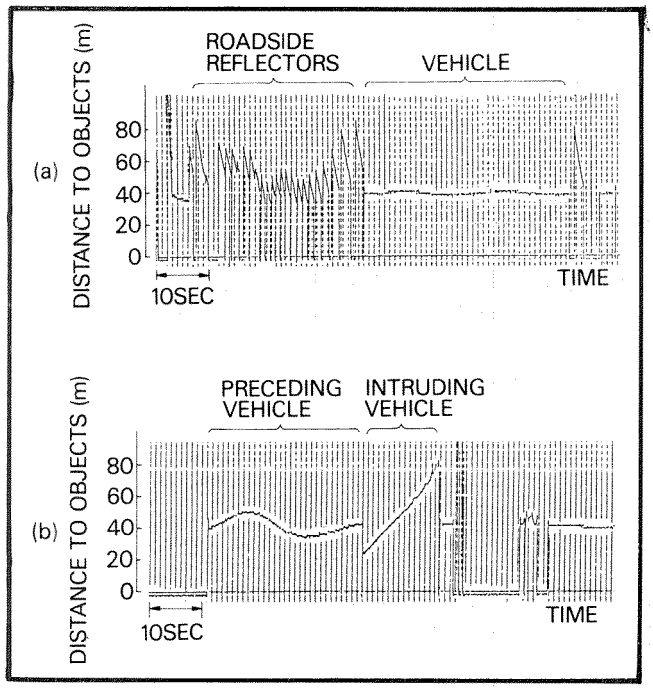

Figure 13. Distance data on real roads

Table 2. Comparative evaluation of laser and microwave radar

Item	Laser Radar	Microwave Radar (60 GHz)
Maximum range	about 100 m	←
Resolution	1 m	←
Operation in adverse weather conditions	poor	good
Cost	reasonable	expensive
Others	Poor detection range for low reflective targets Easy beam control	Poor target discrimination

Acknowledgments

The authors wish to express their gratitude to the parties concerned of Meisei Electric Co., Ltd., for frequent and stimulating assistance.

References

1. Berufsgenossenschaft Der Feinmechanik und Electrotechnik, *Unfallverhuntungs-Vorschriften VBG 93*, p.1, 1973-1.
2. American National Standard Institute, Inc., ANSI Z 136.1-1713, p. 1, 1973-4.
3. Takehana, T., et al., "Automotive radar using mm wave," C178/81, *IMech E*, 1981.
4. Kiyoto, M., et al., "A study of the automatic braking system," Seventh International Technical Conference on Experimental Safety Vehicles, June 1979.

Car Controls for Physically Handicapped Drivers

Christine M. Haslegrave*
Motor Industry Research Association

Abstract

Many physically handicapped drivers have difficulties in using ordinary car controls, and modifications need to be made to their vehicles. A review of the types of adaptations and equipment that are available for this in Europe has identified the principal aspects that need to be considered in their design. For safety and ease of use, it is important to match the characteristics of a control conversion to the driver's capabilities, taking into account the location and mode of operation of the control, together with the operating forces and the range of movement. Many of these adaptations are highly individual, and it is also important to encourage innovation and flexibility in design to increase the possibilities for severely disabled people to obtain the mobility accepted as the norm by the rest of the population.

Modern technology permits the use of sophisticated control systems, and a high degree of power assistance can be provided on steering and brakes. This raises problems such as determining the appropriate degree of feedback or "feel" on the steering wheel for drivers who have little strength in their arms. More research is needed into drivers' responses using these types of controls. In more radical conversions, such as remote steering, there may be a choice of steering characteristic, and this also needs further study.

*Now at The University of Nottingham, Department of Production Engineering and Production Management

Introduction

Physically handicapped people often need modifications to their cars to make access easier and to allow them to operate the controls safely. With recent developments in technology, many severely disabled people are now able to drive, and some conversions are highly sophisticated. In practice, the control conversions range in complexity from the simple relocation of switches to a full conversion of steering for foot operation, and possibly to the combination of all controls on a single arm-operated unit. Often the controls have to be individually tailored to the driver's needs, and conversions are typically carried out by small specialist firms. However, some of the most common adaptation equipment (such as hand-operated brake and accelerator) may be manufactured in a standard form in relatively large numbers.

A review of the control conversions used by disabled drivers in Europe was carried out in 1984, with the aim of identifying all types of control conversions that are available as well as the technical developments and research that may change their design in the future. Information was collected on the regulations and testing procedures that are applied to car adaptations in the different countries(1).

From the information obtained in various countries, it seems probable that approximately 0.5 percent of drivers are physically handicapped, and an earlier study(2) estimated that about 0.2 percent of drivers would be likely to require adaptations to their cars. In Britain, this would correspond to 70,000 drivers under 65 years of age. The numbers are relatively small compared with the total market for production cars, one reason why most special equipment is added after a production car is sold. Another reason is the diversity of handicaps, which make it unlikely a single car design could be produced suitable for even a large proportion of handicapped drivers.

The physical handicaps with the most effect on the driving task are shown in Table 1. The degree of disability arising from a particular impairment is very variable even for two people with the same medical diagnosis. In addition, some people have multiple disabilities, causing multiple handicaps. It is not a simple matter to list car conversions suitable for different types of disability. A driver with a single leg disability will probably be able to drive a car with automatic transmission, perhaps in the case of a right leg disability having the brake and accelerator pedals moved to the other side of the footwell. Similarly, a driver with a single arm disability can probably drive an ordinary car with automatic transmission, although he may find the steering easier if a knob or spinner is fitted on the steering wheel. Other more complicated conversions will need to be chosen in relation to the needs and capabilities of the individual driver.

Table 1. Principle groups of impairments affecting the driving task

- Limb disabilities which may be the loss of a limb, restricted movement of joints, or muscular impairment impairment affecting one or more limbs
- Spinal disabilities and size or reach limitations (such as dwarfism) that may affect the ability to reach the controls, or to bend or twist
- General weakness that may affect the strength needed to operate ordinary controls, or may affect walking ability and ease of getting into and out of the car
- Lack of coordination

Current Range of Control Adaptations

A wide range of equipment is now available for disabled drivers, but the cost of conversion is a critical factor that may limit the possibilities for an individual driver. Many conversions are adaptations of the ordinary foot-operated brake and/or accelerator to hand operation for drivers with leg disabilities, while a few vehicles must be controlled completely by foot operation when the driver has lost the use of both arms. Tetraplegic drivers and others with severe weakness may require very complex conversions to give a high degree of power assistance.

It is worth mentioning that in any conversion, the first consideration is the driver should have a stable seating posture (using suitable supports and restraints if necessary) with a good view of the road. This may necessitate modifications to the car seating, and sometimes to the structure of the car if the driver has a rigidly extended leg or is unable to bend his spine to adopt an ordinary seated posture. Modifications may be made to help the driver get in and out of the vehicle more easily, but these are outside the scope of this paper, which is confined to a discussion of primary control equipment.

Control conversions in Europe are usually carried out by small firms, many doing individual conversions for their customers rather than using a standardised design of control. However, several of the larger firms produce kits (usually sets of hand controls) that can be supplied to other firms, agents, or local garages. A few conversion firms specialise in a particular type of control (such as foot steering or power-assisted steering systems). In general, the vehicle manufacturers are not directly involved in conversions, which are carried out after purchase of the vehicle. Some manufacturers have organised special model specifications for customers, and a very few are more closely involved in the development of new conversion equipment and may provide a service offering approved conversions.

Brake and Accelerator Controls

The most common type of adaptation is the conversion of both brake and accelerator to hand operation, often using mechanical linkages that operate on the original pedals in the car.

In many conversions, the brake and accelerator functions are combined in a single or split lever, usually installed just under the steering wheel. The levers are normally pushed downward (axial to the steering column) to brake and upward toward the wheel to accelerate. There are some exceptions where the control may be moved radially around the wheel.

A wide variety of hand-operated controls is found, but they fall broadly into the following types:

- Push/pull levers
  - — Segment grip
  - — Ring
  - — Bar
- Rotary "twist grip"
- Electric potentiometer

Two examples are illustrated in Figure 1, which shows a bar-type lever passing below the steering wheel, and in Figure 2 which shows an accelerator ring. This is connected to the accelerator pedal by a rod passing through the centre of the steering column and operated by a light pressure of thumb or palm of the hand. The brake is operated by a different type of control.

Shoulder- and knee-operated controls have also been specially developed for individual drivers. In principle, these are similar to the hand-operated controls.

In every direct brake design found in Europe, mechanical linkages were constructed of rigid rods. Cable linkages were used only in a few designs of accelerator control. The majority of hand-control conversions are purely mechanical, but power assistance can be added to brakes, often using hydraulic servo systems.

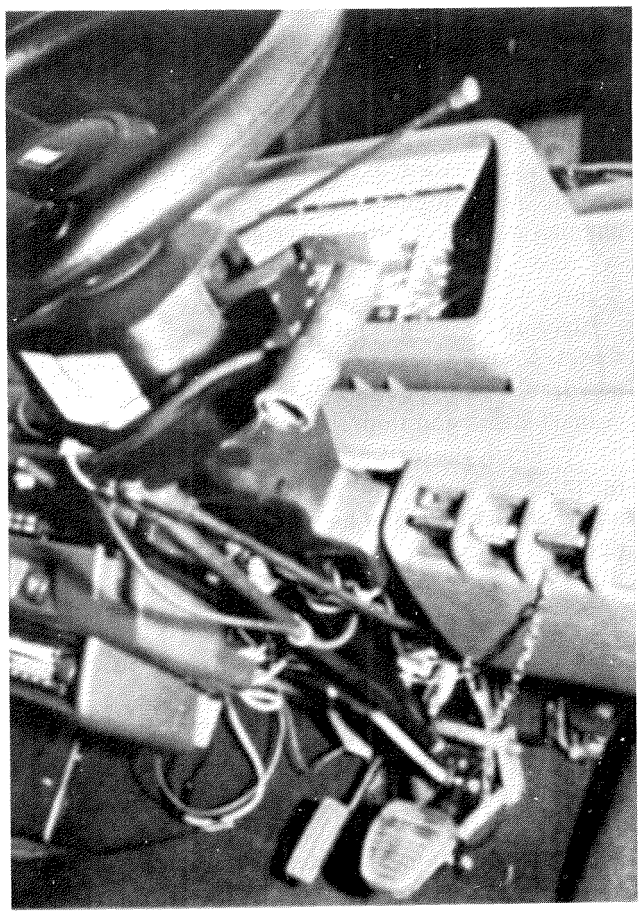

Figure 1. Bar-type hand operated brake/accelerator control

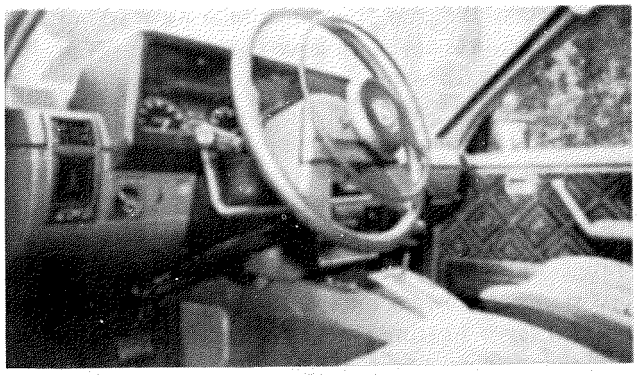

Figure 2. Accelerator ring

One conversion in Sweden is operated by compressed air, with compressors installed to act directly on the foot pedal or hand control. An electronic accelerator has been developed in France and is combined in a single control with a hydraulic brake system.

Steering

The simplest and most widespread steering aid is a knob or spinner fitted to the existing steering wheel. This is needed by anyone steering with only one hand, but may also be helpful for someone with a weak grip. Sometimes the handgrip on the spinner is moulded to fit the driver's hand or arm, and a switch panel is sometimes incorporated with the steering knob to operate minor controls.

More complex conversions to the steering system are normally made to give additional power assistance, to bring the wheel within reach, or to adapt it to foot steering.

Power-Assisted Steering

If a driver cannot choose a car with a power steering option, it is sometimes possible for a conversion firm to fit a power unit that has been designed for a different car within the car manufacturer's range, and some firms can increase the degree of power assistance of an existing system, for example by reducing effort via ratio modification. It would be of great benefit to disabled people if car manufacturers could make power steering options available on a wider range of small and less expensive cars.

A company in Britain now designs special hydraulic systems for different models of cars. During the conversion, they are able to measure the customer's steering effort in a static rig and match their steering unit to his strength.

Extended Steering Column

For small people, it is necessary to resite controls within easy reach and perhaps to fit smaller steering wheels. A conversion for someone with short arms may also include moving the steering wheel closer to the driver, and conversions are available with extended steering columns and telescopic or inclinable columns.

Foot Steering

If steering must be operated by foot, four types of systems are available commercially.

Several conversion firms fit a rotating plate system such as that shown in Figure 3. The rotating plate is positioned on the floor pan, and the foot is inserted in a slipper to turn it. It rotates in the same way as the original steering wheel, with a linkage to the car's steering column. The system is tailor-made for each individual to achieve the optimum driving position. In some conversions, the driver does not use a slipper but grips the rim of the plate with his toes or alternatively turns the plate by friction with the sole of his foot.

The second type, System Franz, was developed in Germany and uses a pedalling motion as shown in Figure 4. The pedal is connected to the normal steering system

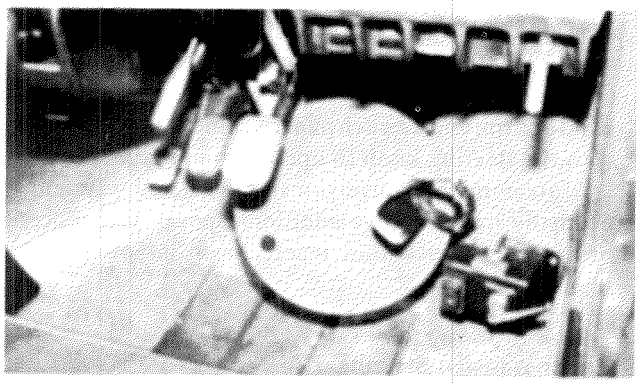

Figure 3. Rotating plate foot steering

Figure 4. System Franz foot steering

through a gear unit and is moved forward to turn right and backward to turn left.

The other two systems suitable for foot steering were designed as remote control systems and are described in the next section.

Obviously, when a driver has lost the use of his arms, many other minor controls will have to be modified when the steering is converted to foot operation. These may be operated by knee, shoulder, or head, as, for example, pushbutton switches that are fitted in the headrest to operate the turn signals.

In some conversions, the original steering wheel may be retained so the car can be driven by able-bodied people. This can be important for maintenance when the car is driven by garage staff.

Remote Steering Controls

Two systems have been developed in Britain that incorporate an operating control remote from the car steering system. These can be positioned virtually anywhere in the car and can be tailored to the individual driver with a suitable mode of operation for his disability. The Malden unit is an electronic control system using a small joystick with a gearbox mounted at the top of the steering column. Three parallel control channels are fitted for safety: two drive motors and potentiometers are fitted to turn the steering wheel, and the third is a reference channel. Three more potentiometers are turned by the gearing that turns the wheel, and their movement is compared with the movement generated by motion of the joystick potentiometer. If a discrepancy is sensed, that channel and motor is disconnected and an alarm sounds. A "reset" facility is provided to allow for temporary failures.

Steering Developments Ltd. has developed hydraulic remote control steering, which has a primary system with a hydraulic pump driven by the engine from a belt off the crankshaft. In addition, there is a backup system, which is an electrically driven hydraulic motor. The control operated by the driver is a lever, which can be placed anywhere in the car but has mostly been fitted on the car door.

Recent Developments

Joystick steering using electronic technology has also been investigated in France and Sweden but has not resulted in commercially available equipment. A team at the University of Birmingham is developing hydraulic joystick controls for small automobiles, while the I.N.S.E.R.M. Biomedical Research Unit at Montpelier has produced a single hydraulic joystick control that operates steering, brake, and accelerator. However, this uses very high technology components and is unlikely to become commercially available in the foreseeable future. In Sweden the Handikappinstitutet is working with Systemteknik to develop a servo system for quadriplegics, which operates steering, brake, and accelerator. It incorporates a hydraulic steering joystick, while the brake and accelerator are operated by a second electro-hydraulic joystick.

The past few years have seen great improvements in steering controls as many companies have introduced a range of modifications to provide additional power assistance. Some car manufacturers have also designed special servo steering units that they market for handicapped drivers. As a result of these developments, steering forces can now be reduced to as low as 4N when using a conventional steering wheel. With remote steering systems, the steering forces are reduced to virtually zero.

Electronic controls are being developed for accelerators and brakes, and more complex hydraulic systems for brakes, which means these functions will be able to be remotely controlled. They can be designed for people with little arm mobility.

Two other new developments have occurred for ancillary controls. One is infra-red sensors, which are used for switch panels and powered access functions (e.g., opening doors). The other is the introduction of voice

control by Kempf Equipements, a great advantage in combination with foot steering for drivers with both arms disabled.

The new electronic technology is on the point of being introduced and can be expected to make a big difference to the design of controls in the next few years. The groups who have the greatest difficulty in driving at present are people with problems of coordination, high tetraplegics, and those with diseases such as multiple sclerosis or muscular dystrophy, which cause severe weakness. They lack the strength to use ordinary controls but are likely to be assisted by powered steering systems or remote steering. The type of control needed but not at present commercially available is a single-handed control that operates all the car functions.

Assessment of the Driver's Requirements

When a handicapped driver chooses a car and has to consider what types of modifications will be needed, usually he will seek advice from the conversion firm or from a driver training or assessment centre. In some countries, licensing authorities and vehicle inspectors may also be involved in determining the most suitable conversion.

In many cases, these conversions are devised by medical or engineering staff who have a knowledge of the options from years of experience. There is considerable liaison between the staff of rehabilitation or assessment centres and engineers in conversion firms, which has resulted in many new developments. Often, the final design of the control system evolves through several trials, making further modifications as necessary to suit the individual driver.

Some centres are now using car simulators (or mock-ups) in which the driver's capabilities can be measured more objectively. One advantage of this is that various control layouts can be tried out quickly and easily to choose the best solution. Performance measurements can then be made using the type of control they anticipate fitting in the car. Typical measurements would be of the forces the driver is able to apply, the range and speed of movement, and the reaction time. The driver's coordination would be assessed, and it might also be necessary to assess endurance for a sustained pressure, as on the accelerator.

However, up to date, there has been little research into the levels of these measures that should be acceptable for the driving task nor into the correlation between measurements made in a simulator and performance on the road. Most research studies have concentrated on measuring the maximum forces that people can apply and on assessing these in relation to control loads in vehicles on the road. Despite this, there is still no consensus among the recommendations made by different organisations—for instance in relation to the maximum operating forces beyond which power assistance will be required.

With the wider availability of power assistance on brakes and (more recently) on steering systems, more emphasis needs to be placed on driver responses and performance using ultra-light and finger-operated controls where steering and braking forces can be virtually zero. With a light joystick control, for instance, the car's response can be very rapid, and the driver gains little feedback from the control. Similarly, servo braking can be very abrupt. Some controls are so sensitive that drivers are constantly making steering corrections, which can be tiring. Additionally, where steering is very light, it is not possible for the driver to relax with his arms resting on the wheel, and he may find this to be tiring.

Further study is needed to find how feedback or "feel" should be built into the system. In discussing this problem in relation to braking, Harden and Tenniswood(3) suggested that artificial feedback might not be the best solution, since the feedback should be a function of the specific vehicle's characteristics and nonlinearities are induced in the brake system by factors such as temperature or brake lining wear. They advocate direct feedback through the servo valve. Nishikawa et al.(4) discussed the provision of feedback in developing a power steering system for Honda.

Microprocessors and electronic control systems now make it feasible to alter the traditional steering response characteristic, and research is needed to investigate the most appropriate characteristics for drivers with various types of handicap. There is little knowledge of the degree of sensitivity or feedback acceptable for able-bodied drivers using the new types of controls, and still less for severely handicapped drivers.

Although car simulators may be useful in studying driver performance with new types of control systems, an assessment of an individual's driving ability should not be based solely on the measured criteria such as force capability and reaction time measured in a simulator. Driving is a very complex task, which cannot be completely reproduced in a simulator, and this is particularly so when reaction times are measured. Most staff involved in assessing potential drivers would agree there is no substitute for a final road test to judge the person's driving performance. However, simulators are being used more widely and have considerable advantages in assessing different options in a conversion and in providing objective measures of force capability that can be matched to control forces measured on the car itself.

Design of Controls

During the study, it was obvious a good deal of flexibility is needed in providing designs suitable for the

individual drivers, who may have very different or complicated handicaps. In many countries, converted vehicles are subjected to a technical appraisal of the control installation, and physically handicapped drivers may also be assessed while driving their converted vehicles. The inspection procedures are chiefly concerned with the suitability of the adaptation for the driver and with his ability to control the car, although they sometimes find problems with poor engineering and with installation by inexperienced fitters.

In no country visited during the study tour are there regulations or codes of practice specifying the design of the controls themselves nor of the installation, although there may be regulations prescribing the modifications or types of controls required for each type of disability. Neither is there any legislation that specifies the operating forces for controls used by handicapped drivers. It is in fact very important to encourage innovation in design in order to increase the possibilities of mobility for very severely disabled people.

However, it is possible to use the experience related by vehicle technical inspectors to promote good design of controls. During discussions with both engineers and medical staff working in this field, various problems or technical points were mentioned that have arisen with controls and/or with their installations. These have been analysed to identify the principal factors that need to be considered in the design of a control conversion, and they are listed in Table 2. They represent a summary of aspects that are important from the points of view of safety and ergonomics and that should be of concern to manufacturers and convertors. The factors fall under four main headings: ergonomics, general safety, engineering, and installation.

Table 2. Principal design factors in control conversions

ERGONOMICS
Mode of operation
Direction of operation
Location and range of movement
Operating force
Response characteristic
Relative positions of controls (separation, clearance)
GENERAL SAFETY
Stability of seating and posture
Provision of duplicate control channels or backup systems
Dangerous projections
ENGINEERING
Type of system (mechanical, hydraulic, pneumatic, electrical)
Interaction between controls in operation
Mechanical linkages (rigid or cable)
Construction techniques
Vehicle environment
Durability
INSTALLATION
Stability and rigidity of fixings and adjustments
Provision of guards or removal of original equipment
Clearance between controls, and between controls and structures
Safety of electrical connections
Facility for an able-bodied person to drive the car
Notice warning that controls have been modified

Ergonomic Factors

The ergonomic factors that need to be considered relate to the positioning and adjustments of the control, as well as to the choice of operating mode and response characteristics most suitable for different types of handicaps.

The detailed design will often need to be matched to the individual driver. Taking mode of operation as an example, a control could be operated in a linear mode, radially around the steering wheel, or in a rotary mode (such as a motorcycle throttle). The most appropriate mode would depend on the driver's disability and strength and particularly on whether certain groups of muscles had sufficient function, degree of coordination, or endurance for sustained applications.

The positioning of the control would depend on the range of movement of the driver's joints, on his mobility, and often on reaction time. Redesign of the layout or mode of operation may be sufficient to increase a driver's reaction time, just by reducing the element of movement or by overcoming difficulties of coordination. One example is a layout (described by an assessment centre as using a "paddle" action) where one foot operates the accelerator and the other the brake. This can nearly halve reaction time.

On the question of direction of operation, there are varying opinions among European organisations. It would generally be accepted, of course, that a brake control should operate forward since the driver's weight will be thrown on the control during heavy braking. However, in a few cases, the driver may need to use a different action because of his disability. Any attempt at standardisation of directions of control operations would therefore need to incorporate some flexibility.

In matching the control conversion to the driver, it is important to consider his capabilities rather than his handicaps. This can be done by determining the strength, mobility, and coordination of each limb in turn to decide which is best suited to operate each control. For example, the ordinary brake pedal in the car requires strength to operate, whereas the accelerator requires little strength but does need position control and sustained operation.

The various controls need to be considered in relation to each other to insure their relative positions are suitable and they are sensibly divided between the driver's limbs having sufficient function, so that the driving task does not overload him. The design solution needs to be tested with the driver himself either in situ or in a mock-up, if necessary making minor modifications, and seating support and posture are an important element in this.

Although emphasis has been placed here on matching the design to the driver's individual requirements, the cost of conversions is perceived by many disabled people as a major barrier to driving. There would therefore be great benefits to be gained by designing low-cost controls, perhaps by designing them to be adjustable or to fit a wider range of car models, or by using modular systems. Although this may not be feasible for the most complex conversions, it should be possible for simpler equipment—for examples, standard sets of hand-operated controls needed by larger numbers of people. If possible, adaptations should be designed to fit any model of car and not be specific to particular models.

General Safety Provisions

The general safety provisions listed are not comprehensive but highlight points where requirements may differ from those in ordinary production cars. A good seating posture is essential and needs to be established before prescribing the types of controls that will be appropriate. It has to be remembered that disabled drivers may be operating closer to the maximum limit of their capabilities than are able-bodied drivers. In the event of an engine failure, for example, the driver may lose power assistance and be unable to steer the car. Additional backup systems may be needed.

The installation of controls differs considerably between car models, requiring brackets and other fixings, often fitted on an ad hoc basis. It is not always possible to avoid encroaching on knee or other impact zones, and protection from sharp projections may then be important.

Engineering Factors

Small companies involved in manufacturing control conversions often do not have access to the sophisticated test facilities used by vehicle manufacturers. Some of the more important engineering factors that they need to take into account are given in Table 2. A few points will be mentioned in more detail.

Policies or requirements for mechanical linkages may differ between European countries. Rigid links were found to be used in virtually all direct brake systems, and in a few countries these are required for direct accelerator systems. Other countries, however, permit cable linkages on accelerator controls.

In installing special or modified control equipment, there is a danger of interaction between the new control and the original systems on the vehicle or between different parts of modified equipment. This may occur in several ways. One example that has been found in accelerator conversions for hand operation is the loss of kick-down when fitted on a vehicle with automatic transmission.

Installation

The method of installation and fixings of the control equipment in the vehicle are just as important as the design of the control unit itself. Many hand-operated controls and other ancillary controls are produced as kits, which can be fitted by people other than the manufacturers. The fixings and range of operation may differ considerably between different models of car.

Since there is an alteration of the original vehicle design, there is again the possibility of an interaction between the modified control and other controls already on the vehicle. At its simplest, the operation of a lever may restrict access to other controls at some positions in its range of travel, or there can be clearance problems between the lever and the bodywork of the car. This might result in the travel not fully covering the range of brake or accelerator operation.

Fixtures must be stable and rigid. For instance, there have been cases of adjustable steering knob fitments that do not have an adequate attachment mechanism and can be pulled away from the steering wheel. In recent car models, the increased use of plastic components and collapsible structures has tended to make installation more difficult.

Some models of car can present particular problems of installation. For example, they may have an angular offset on the steering wheel, which means the clearance between the wheel and a hand-operated control varies as the wheel is rotated. The hand reach to the control therefore varies, and it could present problems in providing sufficient travel to operate fully.

It can be useful to retain the original car equipment in addition to the converted controls. The car may need to be driven by garage mechanics during maintenance or by able-bodied members of the family. Some disabled drivers also like to have the option of using two types of controls, if for instance they are not capable of sustained pressure on an accelerator pedal for long periods of motorway driving, when they may use a hand control.

If there is any danger of a control being operated inadvertently when two types of controls are fitted, a guard should be fitted over the control, or it should be hinged out of the way or made easily removable (for example, by fitting with a wing nut). All of these solutions are frequently used when pedals are moved to the

opposite side of the footwell for left leg operation. This is particularly important for paraplegics who may not be aware of where their feet are placed and for drivers who are subject to muscle spasms.

Conclusion

1. There is now a wide range of control conversions available for production cars in Europe, permitting various modes of operation suitable for drivers with different types of handicap, although there is still need for a system in which all control functions can be operated by a single limb.
2. New techniques are being developed incorporating electronic and hydraulic systems that can provide remote-controlled and ultra-light steering, where the control can be placed in whichever position is most convenient for the driver.
3. Voice control and infra-red sensors have been developed using new technologies for the remote control of nonsafety critical functions.
4. Our knowledge of driver performance and response with the new types of controls is limited. Since it is now possible to alter the conventional control response characteristics, further research needs to be directed to determine suitable levels of feedback and of sensitivity for people with various forms of handicap.
5. The survey of control conversions currently being used in Europe has identified the various aspects of their design (relating to the ergonomics, safety, engineering, and installation) that need to be considered when a conversion is carried out.
6. It is important that designs should not be specified too rigidly. Flexibility is needed to allow for the very individual needs of drivers with different handicaps, and also to encourage innovation to permit larger numbers of severely disabled people to be able to drive.
7. One of the greatest problems perceived by disabled drivers themselves is the expense of the conversions, and there is a need for design of low-cost controls.
8. The main areas in which further study is needed are—
   - The methods of testing and assessment for handicapped drivers and the correlation between simulator measurements and road performance
   - The use of unconventional control characteristics
   - Driving performance with ultra-light steering controls
   - Ways of reducing the cost of controls and conversions

Acknowledgments

The study was carried out by the Ergonomics Department at the Motor Industry Research Association, under contract to the Vehicle Engineering Division of the Transport and Road Research Laboratory on behalf of the Vehicle Standards and Engineering Branch of the Department of Transport.

References

1. Haslegrave, C.M., *Car Control Conversions for Disabled Drivers*, TRRL Research Report No. RR29, Transport and Road Research Laboratory, Crowthorne, 1985.
2. Haslegrave, C.M., D.L. Kendall, and T.P. Hutchinson, "Personal transport for disabled people," MIRA Project Report No. 54455405, Motor Industry Research Association, Nuneaton, 1979.
3. Harden, D.H., and D.M. Tenniswood, "Advanced concepts in automobile driver controls," SAE Paper 730472, New York, 1973.
4. Nishikawa, M., Y. Toshimitsu, and T. Aoki, "A speed sensitive variable assistance power steering system," SAE Paper 790738, New York, 1979.

The Prevention of Bead Dislodgement of Tires and the Importance of Limited Run Flat Capability on Safety

G. Tavazza
Pirelli Coordinamento Pneumatici, Milano, Italy

Tire Failure and Safety

Every motorist quite rightly has the fear of a tire "blowout," especially during cornering. In this case, the cornering force exerted by one of the tires is suddenly reduced, causing a situation in which the vehicle becomes uncontrollable, especially if the tire affected is fitted to the rear axle. Furthermore, as will be seen later, due to the loss of inflation pressure, the beads of the tire will fall into the wheel well, allowing the rim flange to scrape the road and risking the possibility of becoming embedded in any surface irregularities.

Fortunately, modern car tires of tubeless design rarely blow out; instead, when damaged, they tend to lose air slowly, sometimes taking many hours to deflate to pressures significantly lower than those recommended. This phenonenon, in the absence of a good low-pressure warning device, could cause an underinflated tire to go unnoticed by the driver and precipitate a dangerous situation. In fact, should a sharp steering maneuver be executed, especially on an irregular surface, the tire beads could dislodge, giving rise to the identical conditions of a blowout but with the added risk of occurring during an emergency maneuver. It is from these types of incidents that the interest to decrease or eliminate the possibility of bead dislodgement originates.

Another potential danger for the unfortunate motorist is the necessity of immediately changing the damaged tire/wheel and fitting the spare. This, should the incident occur in a tunnel or on a busy road, can be hazardous, in which instance it is advantageous for safety reasons to be able to continue running without difficulty a short distance to arrive in a safer area to park the vehicle. This can only be achieved if no bead dislodgement has occurred and with a tire having a certain run flat performance.

The Bead Dislodgement

Examining the case of a tubeless tire, in conditions of normal use, the bead is maintained on its seating by the internal inflation pressure as shown in Figure 1.

It is accepted the bead core is considered as a ring practically radially inextensible. Thus, as the internal inflation pressure pushes the bead along the conical bead seat until it comes in contact with the flange, the rubber

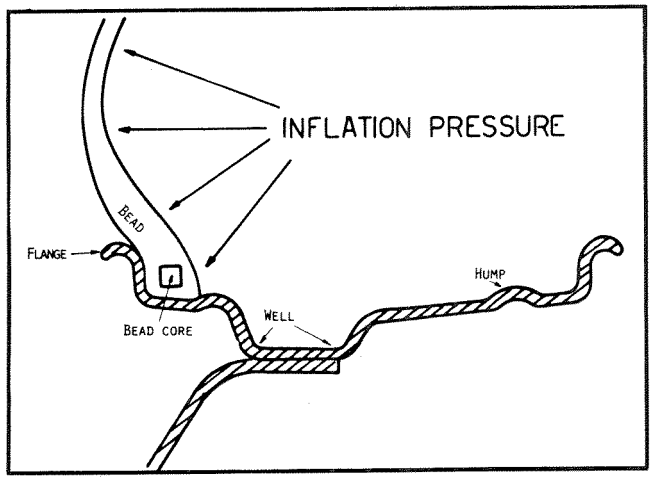

Figure 1. Internal inflation pressure on bead

between the bead core and wheel becomes compressed, giving the high contact pressure that insures the retention of air. This force effectively renders the tire locked to the wheel and capable of transmitting driving and braking torques generated by the most potent vehicles.

During cornering, the road exerts a force on the outer tire (relative to the corner) that tends to push the bead inward toward the center on the wheel as shown in Figure 2. This action can be divided into two components, an axial force that acts at the center of the bead core and an

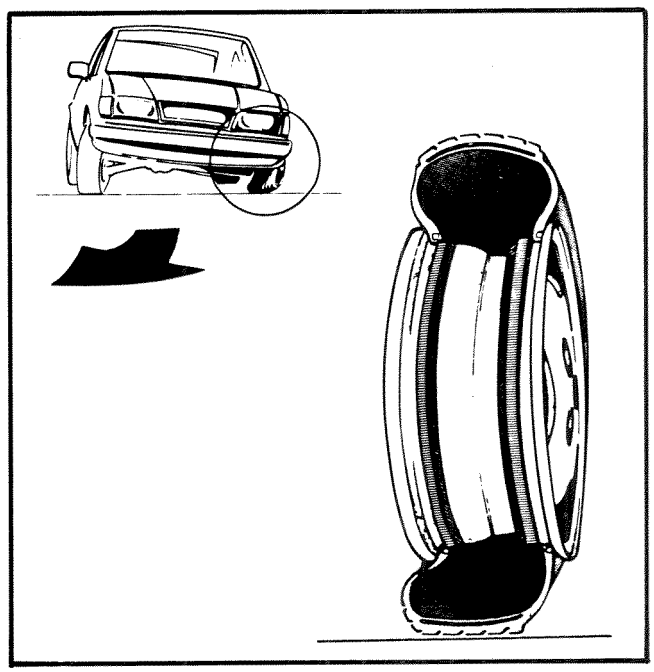

Figure 2. Effect of cornering

overturning moment (see Figure 3) that tends to turn the bead upward and inward. This rotational movement is resisted by the torsional rigidity and radial rigidity of the bead; in fact, the bead blocked from any axial movement by the hump tends to roll around the bead toe, and in doing so raises the center height of the bead core. The axial force, which tends to force the bead along its seat into the wheel well, is opposed solely by the hump. Therefore, since the bead is sufficiently rigid to resist the overturning tendencies (due to design parameters), the axial force becomes the principal cause of bead dislodgement, and the hump becomes the main obstacle to bead dislodgement.

The bead dislodgement is influenced by—

- The overload condition that affects the tire (external relative to the curve) during the cornering maneuver. This depends on suspension geometry and vehicle design.
- The grip afforded by the road surface.
- The violence at which the maneuver is performed.

These ultimate considerations explain why the laboratory tests, both static (U.S. "Push-off" test) and dynamic, are inadequate to predict the road performance of the tire/wheel unit being unable to take into account the sharp increase in load and slip angle of the affected wheel, while alternatively "on road" tests are relatively simple to perform and very realistic.

The most frequently used test is illustrated in Figure 4. The wheel being tested runs each time with the inflation pressure reduced in fixed decrements along a semicircular course at a relatively low speed (to ensure driver safety) but with high lateral acceleration due to small radius of test course (about 1.0G). The bead dislodgement usually occurs immediately after entry into the curve. With normal humps (flat or round), this dislodgement happens typically at inflation pressures of 0.7-1.1Atm.

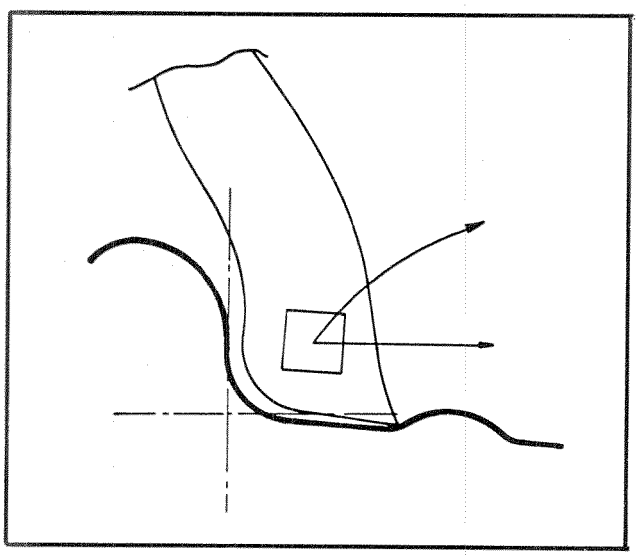

Figure 3. Overturning moment

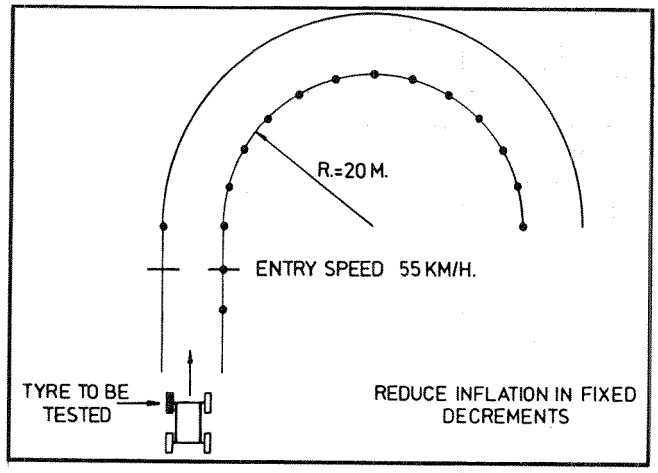

Figure 4. J-Curve roll-off test

Rims and Humps

It is obvious that increasing the diameter of the humps will certainly increase the level of bead retention but will render more difficult the seating of the beads during fitting and also (generally a less serious problem) the removal of the tire from the rim. Additionally, the fitting of tires on rims must be feasible on existing automatic fitting machines, and any variation in a fitting technique that causes an increase in operation time would be totally unacceptable in a mass production environment.

This constraint, with the exception on certain particular applications, excludes all the various solutions of split or multipiece wheels that do not require a well for fitting, systems for closing the well with inserts, or even the use of wheels with retractable pins (instead of humps), which have been used although found to suffer problems of air loss under sporty driving applications.

Other possible solutions require the use of special tires fitted to special wheels upon which, as a rule, it is not possible to mount standard tires. Solutions of this type have never really gained favor in the market since they restrict the vehicle owner to a limited range of tires or otherwise cause him to suffer the financial inconvenience of having to change wheels.

It seems the only acceptable solution is to permit the fitment of standard tires produced by a large range of manufacturers while allowing easy automatic fitting and maintaining the level of bead retention indispensable for safety reasons. This level must permit the driving in a deflated condition at reasonable speeds and lateral forces (e.g., 100Kph in a straight line and lateral acceleration of 0.2g) without bead dislodgement. The mileage attainable in this condition, as we will see later, depends only on the tire and insures the bead retention at the very low inflation pressures that even the most unexperienced motorist cannot fail to notice.

The types of humps most commonly used (Figure 5) are very similar, and unfortunately do not satisfy the criteria requested.

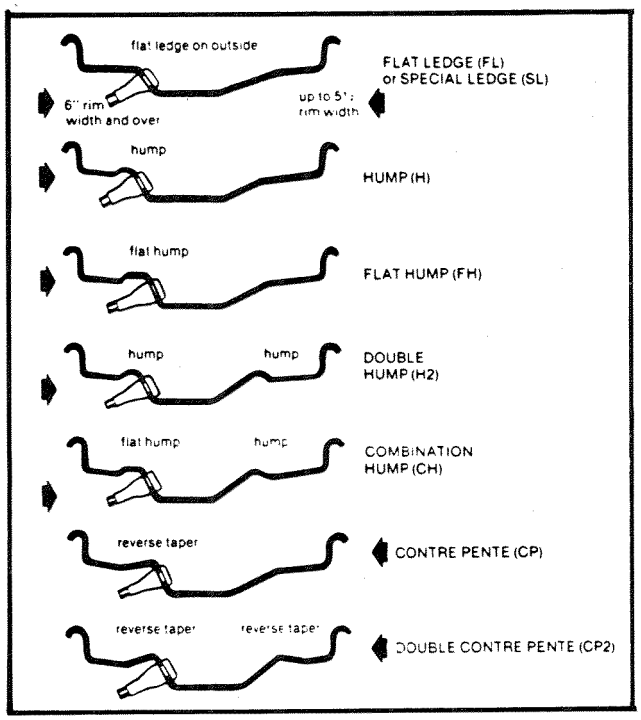

Figure 5. Types of car rims

The Asymmetric Hump Rim

Recently Pirelli and Goodyear have presented a new type of hump design, which significantly increases the level of bead retention, thereby fulfilling the safety factors listed above while satisfying the requirements of ease of fitting and compatibility with other manufacturers of tires.

The working principle is shown schematically in Figure 6. The hump can be considered as made from two rings symmetrically eccentric with respect to the hub and joined together by a straight plane. They are both of equal diameter, approximately equal to that of a standard hump, and the plane that joins the two rings has a variable inclination along the circumference (e.g., it is parallel to the axis of rotation at 90° to the section of Figure 6).

As a result of the inherent flexibility of the tire sidewalls, during the fitting operation the tire is automatically self-centering, as shown in Figure 7, ideally expanding only enough to arrive at the circumferential development of the hump, which, as stated previously, is similar to that of a normal hump. This ideal situation is realized very closely with automatic fitting where, during dome inflation, the tire is pushed simultaneously along the bead circumference.

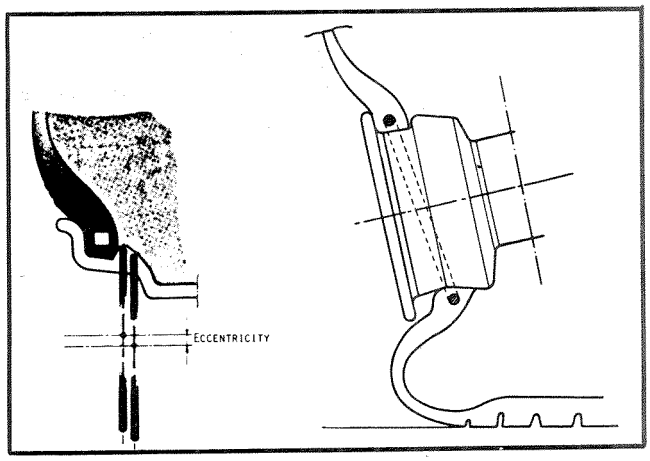

Figure 6. Working principle

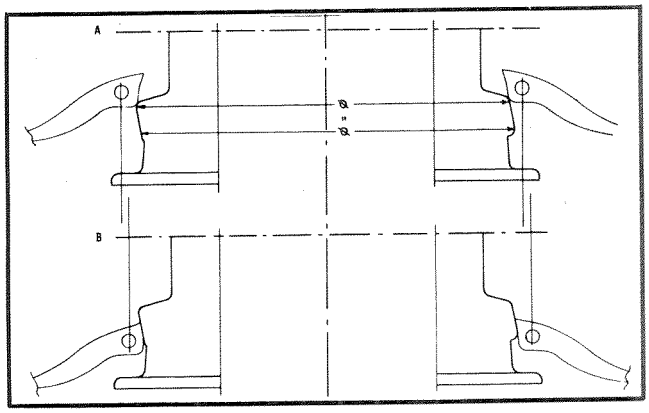

Figure 7. Mounting

During manual fitting, however, inflating through the valve, the increasing internal pressure pushes the tire in an asymmetrical manner, which causes a slight deviation from perfect self-centering. For this reason, the pop-up pressure in this condition can be slightly higher than for normal humps but always remaining within acceptable safe limits of 3-3.5bar.

During the bead dislodgement maneuver, the road applies its force to only a small section of the tire, that corresponding to the footprint area (about 30°). In such conditions, the bead is restricted from moving into the well by a barrier equal to the sum of a normal hump, plus a value of eccentricity (which usually is of the order of 2.5mm). This is far more important than the obstacle represented solely by the hump.

A selection of test results are shown in Tables 1 and 2.

The AH wheels are used as original equipment by four important European vehicle manufacturers and can be constructed in cast light alloy as well as in pressed steel.

Run Flat and Limited Run Flat

As demonstrated, wheels now exist that protect the motorist from the dangers of bead dislodgement; however,

Table 1. J-Curve roll-off test results

Car	RIM	Tire Size	Inflation at Roll-Off (Bar) Standard Rim	Special Rim	
Fiat Ritmo 65	4 ½ B 13	145SR13	0.8	0.5	*/°
Fiat Ritmo 85 S	4 ½ B 13	145SR13	0.65	0.3	*
Fiat 132	5 ½ J 14	175/70SR14	1.1	0.45	*/°
Fiat Argenta 2000 IE	5 ½ J 14	175/70SR14	1.0	0.40	*/°
Alfa Romeo Giulietta 2000	5½ J 14	185/65HR14	0.9 / 0.85	0.4 / 0.4	
Audi 200	6.0 J 15	205/60VR15	0.45 / 0.5	0.1 / 0.1	
BMW 735	6 ½ J 14	205/70VR14	0.4 / 0.45	0.0 / 0.0	°
Ford Escort XR3	5 ½ J 14	185/60HR14	0.9 / 0.9	0.35 / 0.35	*/°
Opel Kadett Caravan	5 ½ J 14	185/60HR14	0.8 / 0.7	0.1 / 0.0	
Jaguar XJ 6	7 J 15	235/60VR15	0.9 / 0.9	0.0/0.0	°
Seat Ronda	5 ½ J 14	165/65-14	0.9	0.3	*

* Rim Touches Ground
° No Roll-Off

Table 2. Rapid deflation on straight roadbed dislodgement

Car	Rim Size	Tire Size	Position	Rim Standard	A.H.
VW Jetta	5 1/2J x 14	175/65SR14	Front	No	No
			Rear	No	No
		185/60HR14	Front	No	No
			Rear	No	No
Ford Granada	6J x 14	195/70HR14	Front	Roll-Off	No
			Rear	Roll-Off	No
		195/70VR14	Front	Roll-Off	No
			Rear	No	No
DB 280S	7J x 15	205/65VR15	Front	Roll-Off	No
			Rear	Roll-Off	No
BMW 736	6 1/2J x 14	205/70VR14	Front	No	No
			Rear	No	No
Fiat Argenta	5 1/2J x 14	175/70SR14	Front	Roll-Off	No
Fiat Abarth	5 1/2J x 14	185/60HR14	Front	Roll-Off	No
			Rear	Roll-Off	No
Jaguar XJ 5.3	6 1/2J x 15	235/60VR15	Front	No	No

Test description (FMVSS110/Australia design 20)

- Dry straight road
- Vehcile with full road
- At a pre-determined point actuate rapid deflation device
- Bring the vehicle to rest under moderate braking

it remains to establish exactly how many miles a fully deflated (but still with beads in position) tire can continue running to arrive in a safe area where the wheel can be changed.

In the absence of an internal inflation pressure, the load-carrying capacity of the tire is drastically reduced by 80 to 90 percent, the sidewall and bead area come in contact with each other as shown in Figure 8, while the contact area with the road increases notably (three or four times that of the normally inflated tire), tending to lift away from the road surface in the center (C), thus increasing the contact pressure in the shoulder area (D). Occasionally, part of the sidewall comes in contact with the road surface (area B in Figure 8), which results in the relatively soft sidewall rubber compound being abraded away quite rapidly, thus cutting the tire longitudinally in this area. If, due to the geometry of the tire and width of wheel used, this does not occur, the deflated tire becomes

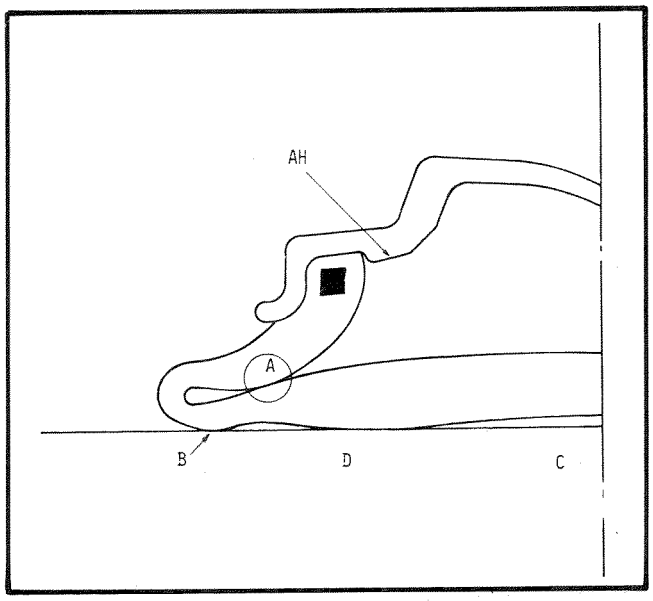

Figure 8. Sidewall and bead contact

subject to immense frictional forces in area (A), during straight running due to longitudinal chafing between the lower bead area and the part in contact with the road (particularly important on driven wheels) and during cornering due to lateral chafing between the tread and the bead.

The result of this friction generates a significant increase in temperature, which causes a rapid degradation in all the mechanical properties of the rubber compounds and temperature-sensitive reinforcing materials.

The tire failure, in the absence of sidewall damage, is seen externally as oblique cuts in the sidewall and internally as abrasion corresponding to zones of contact.

These mechanisms clearly indicate that the distance one can travel on a deflated tire diminishes rapidly with the increase in load, speed, and lateral force of the vehicle, and the situation becomes worse for a driven wheel.

Table 3 indicates a sample of test results. The speeds and lateral accelerations adopted for the tests were chosen to simulate conditions encountered by a motorist with a deflated tire searching for a safe place to change the wheel without jeopardizing the safety of other road users. The tests were all performed with the valve core removed to insure complete deflation of the tire.

It is noted that even in the most favorable conditions of a VR tire with a very low aspect ratio, the mobility afforded prior to the tire's destruction is very low.

The level of mobility of an uninflated tire can be increased in various ways. Excluding the solutions that utilize internal supporting systems necessitating multipiece wheels or the use of spray cans that require stopping the car, the simplest answer is to strengthen the tire sidewalls to obtain a self-supporting tire.

Solutions of this type have been available in the market for several years but without great success, since (prior to the introduction of AH wheels) they required special wheels, were significantly heavier (about 20 percent), and more expensive.

Table 3. Run-flat and limited run-flat (speed 100Kph in a straight line—max lateral acceleration 0.3g.)

Car	Rim	Tire Size	Tire Weight (KG)	Run-Flat Capacity (KM) Front	Rear	Tire Design
BMW 323 I	6 J 14 AH	195/60 VR 14	9.3	6.5	3.	Standard
BMW 323 I	6 J 14 AH	195/60 VR 14	9.8	32	18	Limited R.F.
BMW 323 I(*)	6 J 14 AH	195/60 VR 14	9.8	65	56	Limited R.F.
BMW 518	6 ½ J15 AH	205/60 VR 15	10.5	6	3	Standard
BMW 518	6 ½ J15 AH	205/60 VR 15	10.5	21	14	Limited R.F.
BMW 518	6 ½ J15 AH	205/60 VR 15	12.5	500	420	Self Supporting

(*) Car load of 2 passengers only

Figure 9 illustrates a section of the Pirelli self-supporting tire of which the weight and performance characteristics are listed in Table 3. In addition to the weight penalty, it also needs stating that it is not easy to tune such a robust tire to the performance comfort and rolling resistance levels currently demanded by modern motor vehicle manufacturers.

However, a run flat mobility of 20 to 30Km should be sufficient for locating a roadside area that would permit a safe wheel change. Tires providing this type of mobility, which we can refer to as limited run flat, have only a moderate increase in weight and consent to a performance almost equal to that of normal tires.

They are not self-supporting, and their run flat performance is obtained using small filters in the sidewalls and carefully choosing the structure materials. Results and characteristics are listed on Table 3.

Summarizing, it can be said that mounted on AH wheels these tires constitute a major step forward in the area of motor vehicle and road safety.

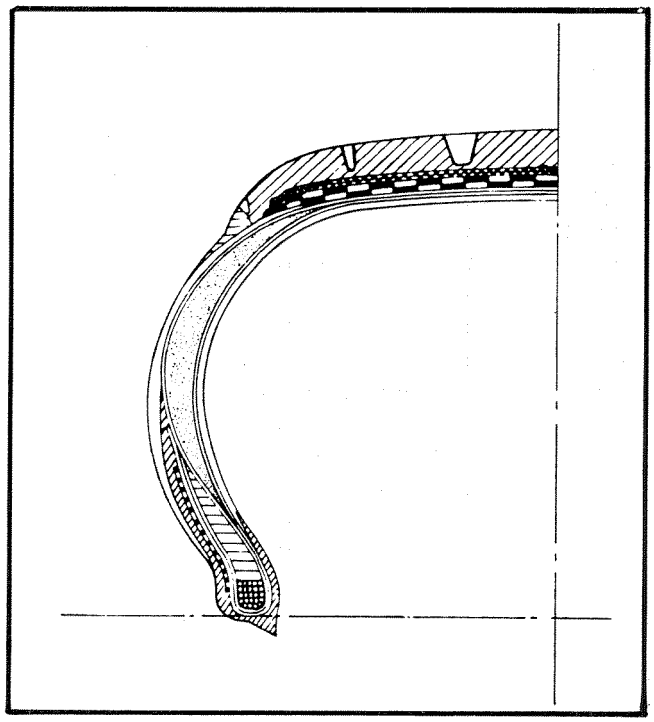

Figure 9. Pirelli self-supporting tire

Modification of Vehicle Handling Performance by Four-Wheel Steering System

Shoichi Sano,
Yoshimi Furukawa, and
Shuji Shiraishi
Honda R&D Co., Ltd.

Abstract

At past ESV conferences, we have reported on a series of studies on how the driver's control performance is affected by vehicle steering response. These studies showed that a four-wheel steering system can reduce the delay in lateral acceleration response to steering action, which may result in better control performance of the driver.

The present report examines the handling performance of an experimental vehicle fitted with a four-wheel steering system under a wider range of operating conditions. The studies were conducted using mathematical models and simulation of the driver-vehicle system, plus road tests.

The findings indicate that the four-wheel steering system may provide better vehicle handling performance than a conventional two-wheel steering system.

A vehicle incorporating this steering system may exhibit improved accident avoidance capabilities.

Introduction

This paper discusses the handling performance of a motor vehicle equipped with a four-wheel steering system. Vehicle handling performance means the overall steering performance of a driver-vehicle system, which is schematically shown in Figure 1.

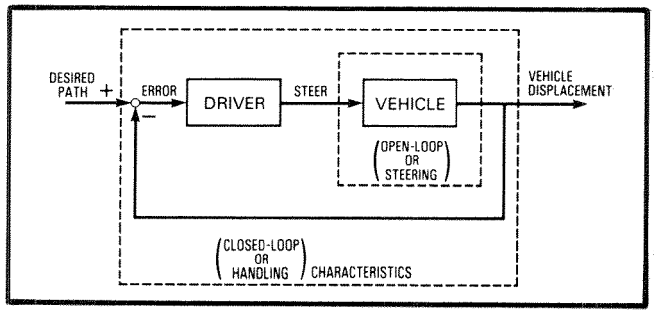

Figure 1. Driver-vehicle system

The open-loop characteristics in Figure 1 represent the steering response characteristics of a vehicle as determined with the input as a steering wheel angle and the output as vehicle motion including lateral displacement. The closed-loop characteristics are part of the "handling performance." This includes the vehicle characteristics, the driver's control performance, and the driver-vehicle closed-loop combination as shown in Figure 1. The system input is a desired course, the error is the deviation from that course, and the output is the actual vehicle path.

Sections 1 and 2 of this paper discuss research efforts to find the difference between the two-wheel and four-wheel steering systems with respect to possible vehicle steering qualities and to identify the effects of such differences on vehicle handling performance based on previous reports(1,2).

This is followed by discussions in Section 3 of computer simulation using a mathematical model of driver's steering action, conducted under a number of typical operating conditions to find vehicle handling performance; road tests to validate the simulation results; and studies based on these experiment findings to estimate the possible effects of the four-wheel steering system on driver's control performance and subjective rating.

Studies on the Handling Performance of Two-Wheel Steering Cars

Many reports are available on methods of evaluating vehicle handling performance using vehicle response parameters. Previously, the authors conducted two series of studies mostly with a lateral motion simulator. In course tracking and evasive lane change tests, it was found that a shorter delay in the phase of vehicle lateral acceleration response to steer inputs would improve the driver-vehicle system performance even if the yaw response gain and phase were kept constant(1,2).

This section first discusses how the delay in the phase of lateral acceleration response to steering action relates to the handling performance of a conventional two-wheel steering car and how this is affected by vehicle speed and design parameters. This analysis uses the two-degree of freedom car equations to calculate the frequency response (see Appendix A).

Response Delay and Vehicle Speed

The calculated effect of vehicle speed on the phase lag in the lateral acceleration response to steering action is shown in Figure 2. The vehicle specifications used in these calculations were modelled after those of a small production car, now on the market in Japan, which is of the same model as the vehicle used for road tests. The frequency bands used in Figure 2 are 0.3Hz and 0.75Hz,

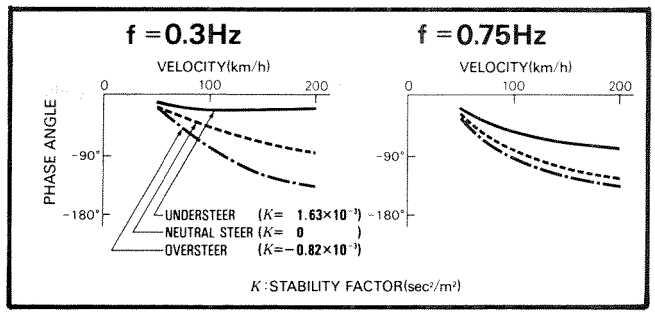

Figure 2. Effect of vehicle velocity on phase angle of lateral acceleration response

which were selected as the most typical regions in the higher and lower portions of a steering frequency range, below 1Hz. This range was selected because the steering frequency during normal driving mostly comes within 1Hz. The vehicle stability factor was alternatively set at three different levels, ranging from slight understeer to slight oversteer (see Appendix B for full details of vehicle specifications and stability factor).

The following characteristics are shown in Figure 2:

- The higher the vehicle speed, the larger the phase lag of lateral acceleration response to steering action.
- The phase delay increases as the stability factor becomes smaller and as the vehicle tends more toward oversteer characteristics.
- Vehicles with understeer characteristics have little phase delay in the lower frequency range.

Techniques To Reduce Response Delay and Their Effects

To study possible means of improving the handling performance of conventional two-wheel steering cars, the basic vehicle design parameters were varied in several ways to determine how much each contributed to the phase delay in lateral acceleration response. The vehicle specifications and typical frequency levels used for this calculation were those of the preceding section. The stability factor of the vehicle used as a reference standard was varied to three different levels, as in Figure 2. The vehicle speed was set at 110km/h (see Figure 3).

Reduction of Response Delay Relative to Vehicle Speed

To quantitatively determine the possible effects of a four-wheel steering car in terms of steering frequency range, the following paragraphs calculate the delay in the phase of lateral acceleration response to steering action from a frequency response equation for an example four-wheel steering car (see Appendix A).

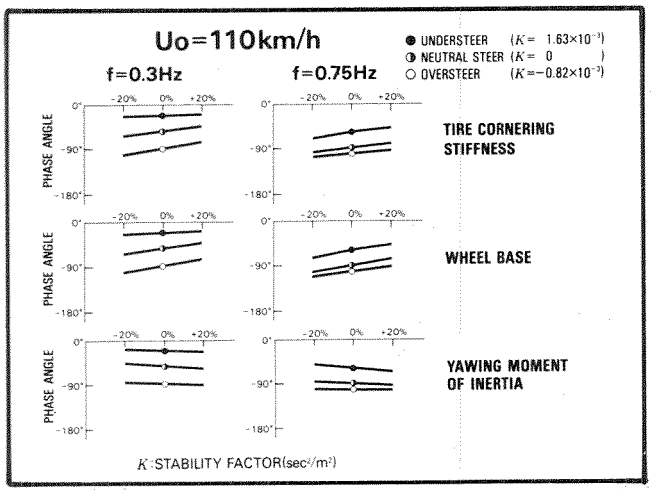

Figure 3. Effect of vehicle design parameter on phase angle of lateral acceleration response

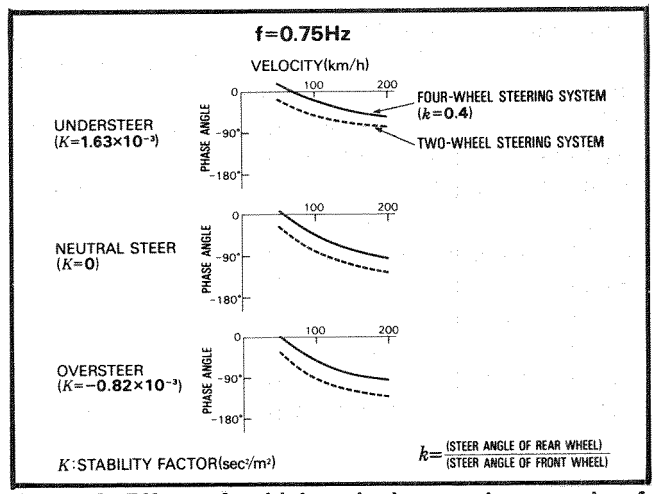

Figure 4. Effect of vehicle velocity on phase angle of lateral acceleration response by steer angle ratio of rear to front wheel

Figure 4 shows the delay in the phase of lateral acceleration at the frequency of 0.75Hz, relative to vehicle speed, for a four-wheel steering car with the same parameters and the same steady-state response gain as a two-wheel steering car.

The ratio of the rear-wheel steering angle to that of the front wheels κ was set at 0.4 level, for comparison with the two-wheel steering system. The steering angle ratio κ is considered positive when the rear wheels are steering in the same direction as the front wheels. The vehicle stability factor was set at the three different levels of Figure 2.

A. Effects of tires
   The cornering stiffness of both the front and rear tires was varied by ± 20 percent.
B. Effects of basic specifications
   The wheel base was varied ± 20 percent.
   The yawing moment of inertia was varied ± 20 percent.

The results of the calculation are as follows:

- The delay in the phase of lateral acceleration response to steering action becomes shorter as the cornering stiffness increases, as the wheel base becomes longer, and as the yawing moment of inertia decreases.
- These percentage changes in cornering stiffness and wheel base contribute almost in the same degree to the phase delay, producing an effect of around ± 10° of lag.
- The contribution of this change in yawing moment of inertia reaches its height—an effect of around ± 8°—when the vehicle has an understeer trend in the higher frequency range.

These findings indicate that the existing two-wheel steering cars can have the following trends in steering characteristics: Typical small production cars with understeer can show a longer delay in the phase of lateral acceleration response to steering action, particularly in the higher frequency range, as they run faster. The phase delay may be reduced only about 10° even if the vehicle design parameters are changed as much as some 20 percent.

This implies that in normal production cars, the improvement of vehicle handling performance may usefully involve research efforts to properly control the phase delay in lateral acceleration response in the higher frequency range. Therefore, only the typical value of 0.75Hz in the higher steering frequency range will be used in further discussion on this subject.

Reduction of Response Delay by Four-Wheel Steering System

We have reported at previous ESV conferences that the delay in the phase of lateral acceleration response to steering action may be reduced by a four-wheel steering system designed to steer the rear wheels in the same direction as the front wheels. Our reports also suggested that reduction of such a phase delay within a proper range might improve the control performance of driver-vehicle systems(1,2).

This section discusses the possible improvement of lateral acceleration response through the use of a four-wheel steering system with particular emphasis on the effects of vehicle speed variation and the steer angle ratio of rear to front wheel.

Effects of Four-Wheel Steering System

The four-wheel steering system may have the following effects: When the steering wheel is turned, a conventional two-wheel steering car places the front wheels at a slip angle in the initial stage, which gives the front wheels a

cornering force. This becomes lateral force and yawing moment for the vehicle, making it turn its heading while moving it sideways. Then a slip angle occurs between the vehicle heading and the velocity direction. This places the rear wheels at a corresponding slip angle, giving them a cornering force. Thus, the rear wheels lag a little in contributing to the lateral motion of the vehicle. The result is a delay in lateral acceleration response to steering action.

With a four-wheel steering system, on the other hand, the rear wheels take part from the first in producing a lateral force for the vehicle. Therefore, it can provide the vehicle with a quicker lateral acceleration response than the conventional two-wheel steering system.

The analytical findings are as follows:

- The four-wheel steering system can provide a shorter delay in the lateral acceleration response in any speed range whether the vehicle has understeer, neutral steer, or oversteer characteristics.
- In the higher steering frequency range, it reduces the phase delay by as much as 30° in all speed ranges. This favorable effect grows stronger as the vehicle tends more toward oversteer characteristics.

Effects of Steer Angle Ratio of Rear to Front Wheel on Phase Delay

Figure 5 shows the effects of the steer angle ratio of rear to front wheel κ noted above on the phase delay at 110km/h.

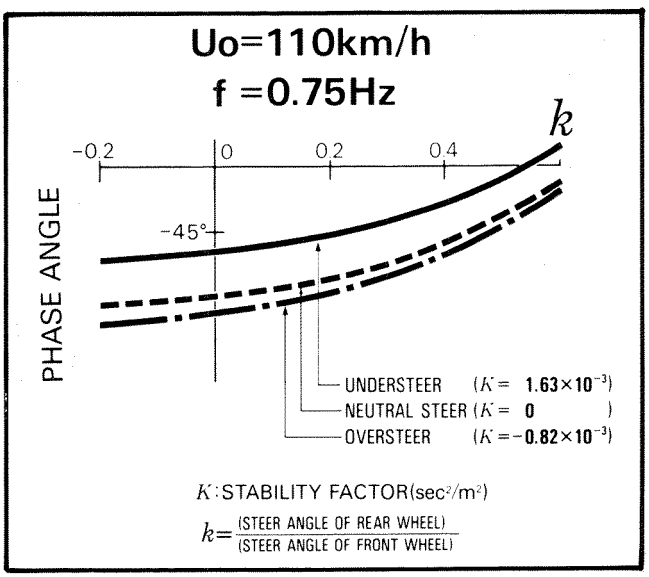

Figure 5. Effect of steer angle ratio of rear to front wheel on phase angle of lateral acceleration response

Variations in the steer angle ratio κ are significant in this higher frequency range. The phase delay decreases remarkably as the value of κ increases.

The discussions in Sections 1 and 2 may be summarized as follows:

The four-wheel steering system becomes more effective in reducing the delay in the phase of lateral acceleration as the rear-wheel steer amplitude more closely matches the front. The analyses showed that steering the rear wheels at a ratio of 0.4 to the front is about three times more effective in reducing the phase delay than a selected design parameter change. In course tracking and lane change tests, as shown previously in (1) and (2), reduction of the phase delay in lateral acceleration response may help improve vehicle handling performance. This suggests that the four-wheel steering system may provide motor vehicles with better handling performance in some driving tasks.

Effects Of Four-Wheel Steering System

This section examines the handling performance of a vehicle fitted with the four-wheel steering system using a variety of assumed operating tasks and conditions likely to occur on the road. The aim is to identify more clearly the effects of the new steering system.

Method of Study

Computer simulation with mathematical models of the driver-vehicle system was used to examine the effects of the four-wheel steering system under a wide variety of operating conditions. The simulation findings were then confirmed by road tests.

The tasks evaluating the closed-loop characteristics may be broadly divided into course tracking and course changing. The first step was to evaluate the stability of the driver-vehicle systems. Our attention was then turned to the subjects of road irregularity and lateral wind sensitivity to assess the course tracking, followed by the lane changing performance as typical of course changing tasks.

Evaluating Conditions

Table 1 shows the subjects, methods, and parameters of evaluation.

Simulation Models

For comparison with the four-wheel steering system, a two-wheel (bicycle) model as used in the preceding sections was selected for the vehicle, and a simple preview predictor model was used for driver control. Major

Table 1. Evaluating conditions

Subject	Evaluating Method and Parameters	
	Computer Simulation	Road Tests
A. Driver-vehicle system stability	Stabilty range of driver's control parameters	NIL
B. Road irregularity sensitivity	r.m.s. Value of steering Lateral deviation and heading angle Steering power spectral density	NIL
C. Lateral wind sensitivity	Maximum and cumulative values of lateral deviation and heading angle	NIL
D. Lane change performance	Range of driver's control parameters for pass through the course	NIL
	Settlement of steering patterns and vehicle motion	Settlement of steering patterns and vehicle motion

details of the driver's mathematical model used in the simulation are given below and in Appendix A.

Mathematical model

Vehicle: Bicycle model

Driver: Preview predictor model (see Reference 3)

Control parameters

1) Preview distance —L

2) Control gain —h (steering wheel angle relative to the deviation of driver's sight point from the desired course)

3) Time delay —τ (time lag between the perception of such deviation and the start of steering action)

Analytically, the driver looks at a point L meters ahead of the vehicle, finds the deviation of that point from the desired course, and turns the steering wheel for correction with the control gain h after the time delay τ seconds.

Road Tests

A test driver operated an experimental vehicle that had the steer angle ratio of rear to front wheel set at κ = 0.4. The vehicle specifications and operating conditions for the test car were identical with those for the simulation.

Driver-Vehicle System Stability

The first step in the evaluation was to analyze the stability of the driver-vehicle system.

Given a transfer function for each of the driver and vehicle, the transfer function for the driver-vehicle system can be obtained. The closed-loop system stability can be evaluated from the resulting characteristic equation (see Appendix A).

Figure 6 shows the stable range for the driver parameters preview distance L and control gain h with the time delay τ fixed at 0.2s. The results are sensitive to the time delay selected. Generally, the closed-loop response time can range from 0.15 to 0.8s, with typical values in the range of 0.25 to 0.45s(5). A nominal value of 0.2s was chosen for all the analyses based on assumed operating conditions for evasive maneuvers.

For analysis purposes, the steer angle ratio of rear to front wheel κ was set at three different levels from 0 to 0.4. As in the previous calculations, the ratio of steering wheel angle to the front-wheel steering angle η was adjusted to make the steady-state gain equal to that of the two-wheel steering car. The analysis was made at 110km/h.

Figure 6 gives the following findings:

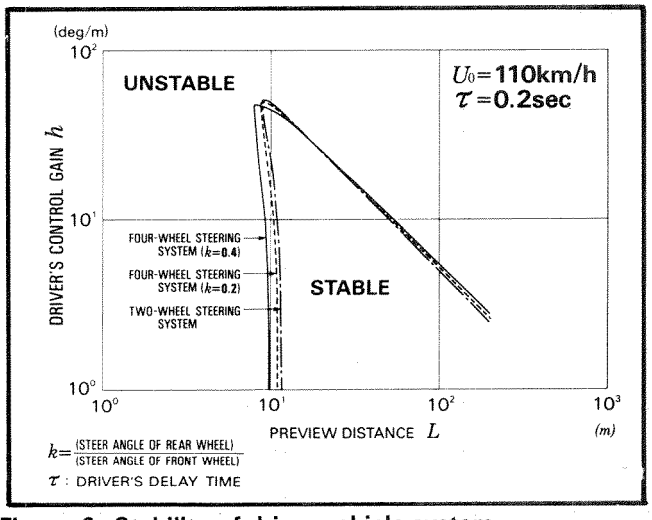

Figure 6. Stability of driver-vehicle system

- The preview distance L has a minimum value that depends on the driver time delay and vehicle speed. The four-wheel steering vehicle shows a slightly smaller minimum value of the preview distance L and, therefore, a wider range of calculated closed-loop stability than the two-wheel steering car.
- As the preview distance L becomes longer, the driver's control gain has to be made smaller to insure stability.
- The maximum value of control gain for a given length of preview distance L is little affected by the steer angle ratio of rear to front wheel κ

Sensitivity to Road Irregularity and Other External Disturbances During Straight-Ahead Driving

This section examines the driver's control action and vehicle motion when an external, lateral force is applied at random to the front and rear axles of a vehicle running straight ahead. The mathematical model of the driver described above is used.

The external disturbance used in the calculation had sufficient force to put the vehicle one full lane width (3.5m) off the desired course and give it a 1° yaw angle, after 15s, if no steering action was taken. Another feature of the external disturbance was good repeatability. The steering power spectral density was adjusted to the same level as in the road tests.

Figure 7 shows the steering and vehicle behavior when the steer angle ratio of rear to front wheel κ was varied while the driver's control gain h and preview distance L were kept constant at 5° / m and 100m, respectively. The vehicle speed was set at 110km/h. The findings are as follows.

The larger the steer angle ratio of rear to front wheel κ the less the vehicle moves sideways.

The root mean square (rms) values of steering angle, heading angle, and lateral displacement were selected as parameters for evaluating the performance of the driver-vehicle system when receiving an external disturbance. These values were divided by the rms values at κ = 0 (corresponding to the two-wheel steering car) and then made nondimensional. The results are given in Figure 8.

The four-wheel steering system does not differ appreciably from the two-wheel system in steering angle or heading angle until the steer angle ratio of rear to front wheel approaches 0.4. At κ = 0.4, the vehicle lateral deviation decreases to less than half that of the two-wheel steering system.

The most effective value of κ ıor coping with an external force is probably about 0.4. The way the vehicle lateral deviation changes relative to the level of κ is consistent with the objective and subjective ratings

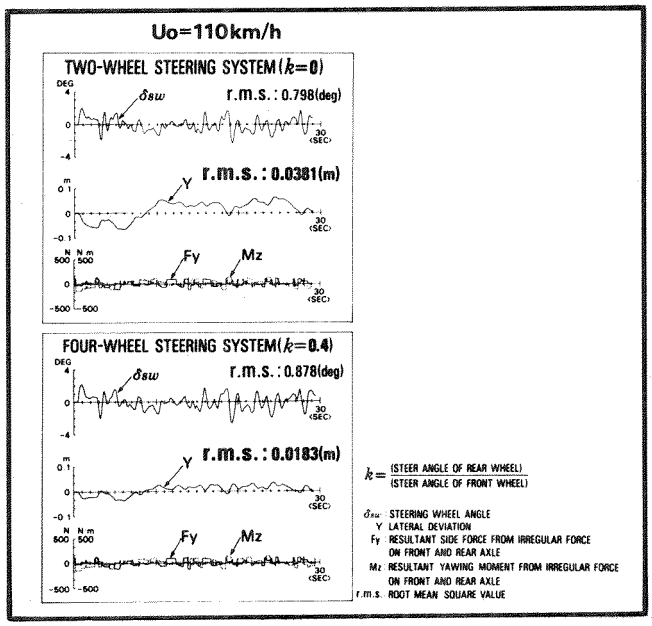

Figure 7. Maneuver on road irregularity sensitivity

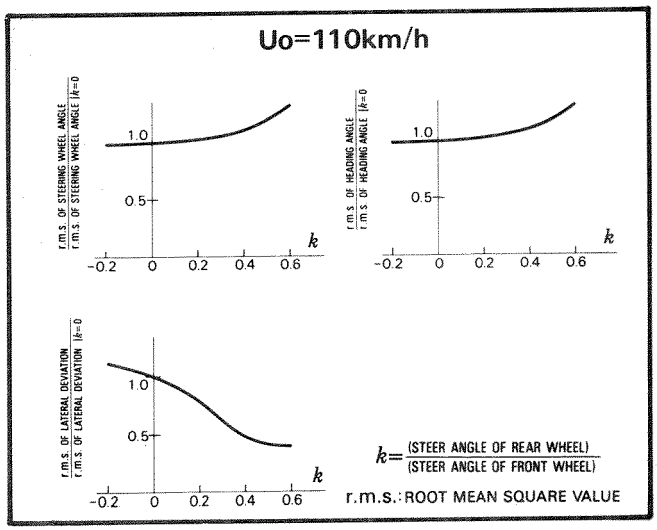

Figure 8. Effect of steer angle ratio of rear to front wheel on road irregularity sensitivity

measured in a lateral motion simulator with random course tracking tests. This was reported at previous ESV conferences (see (2) and Figure 9).

Figure 10 compares the steering power spectral densities of the four-wheel and two-wheel steering cars. In this comparison, the driver's control gain was adjusted to keep the rms value for the lateral deviation of the four-wheel steering vehicle (at κ = 0.4) virtually equal to that for the two-wheel steering car.

In the higher frequency range, the four-wheel steering car has a lower steering power spectral density amplitude than the two-wheel steering car. The power spectral density of the former reaches a peak at about 0.75Hz, and the four-wheel steering system efficiently reduces the required steering wheel amplitude at frequencies above 0.4Hz.

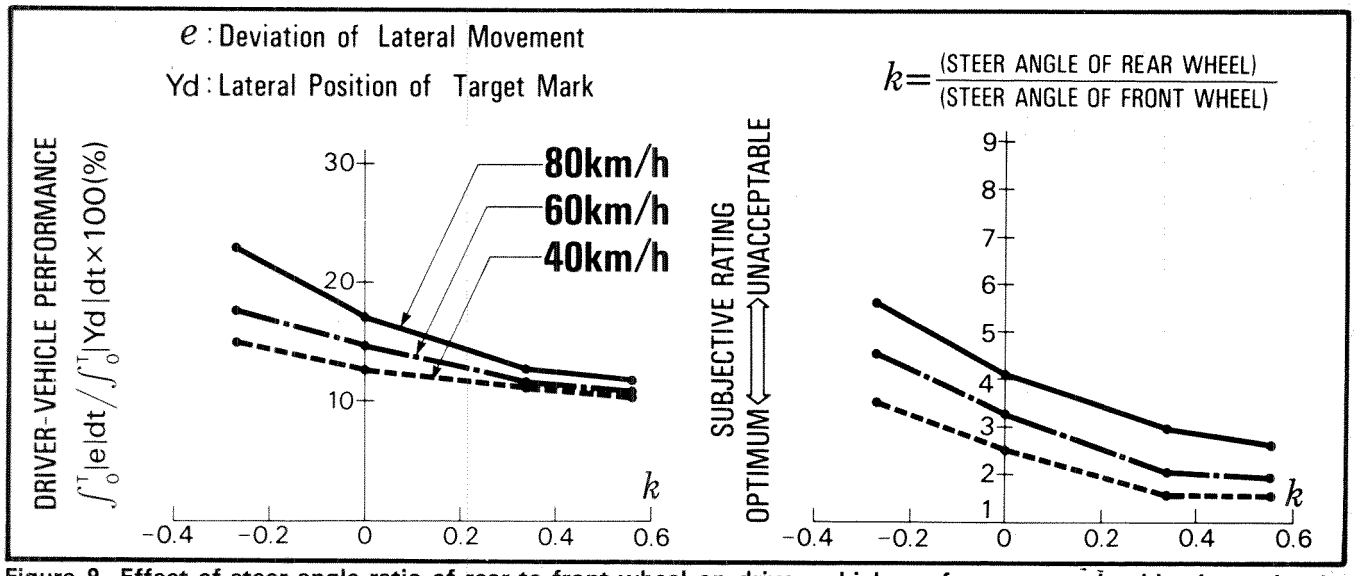

Figure 9. Effect of steer angle ratio of rear to front wheel on driver-vehicle performance and subjective rating in course tracking test

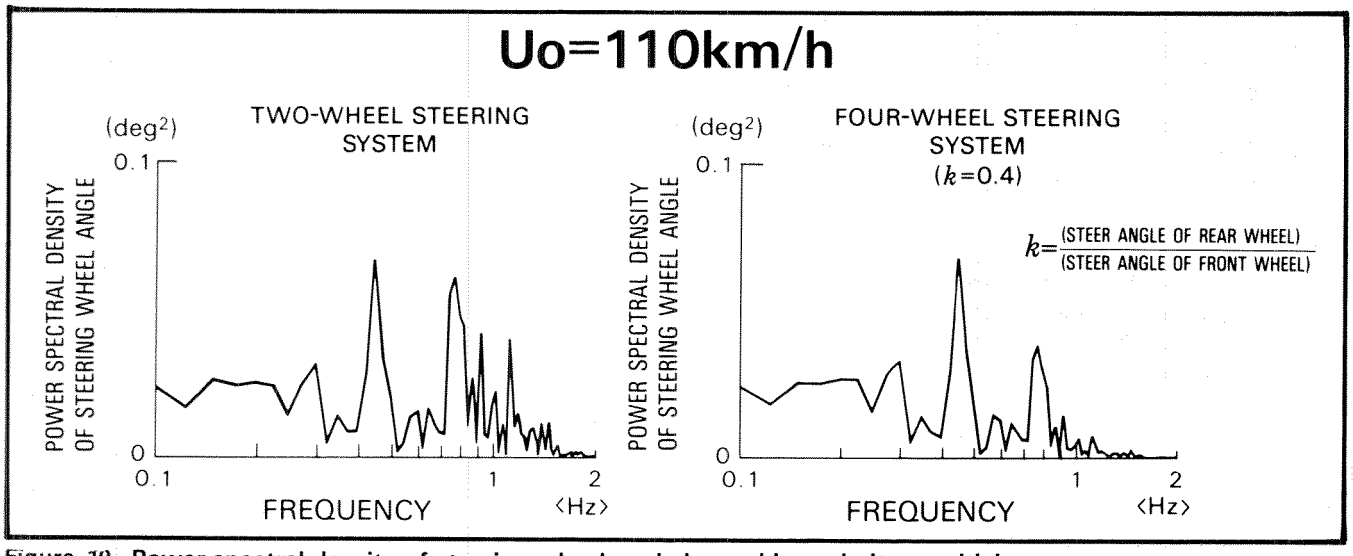

Figure 10. Power spectral density of steering wheel angle in road irregularity sensitivity

In the course tracking tests conducted on a lateral motion simulator, discussed in (2), two steering frequency ranges were considered. One was the frequency range for following the desired course, and the other related to corrective steering needed when the initial steering action failed to keep the vehicle on the desired course. The second frequency range had a peak around 0.7Hz. It was found that the amplitude of this peak was lower for the four-wheel steering car(2).

The simulation findings indicate that the four-wheel steering car requires less corrective steering to maintain the vehicle back on course.

The effects of the steer angle ratio of rear to front wheel and stability factor on the rms steering wheel angle, heading angle, and lateral deviation (see Figure 11) were investigated, i.e.,

- Vehicle lateral deviation is affected more by the steer angle ratio κ than by the stability factor K.
- But the steering wheel angle and heading angle are affected more significantly by the stability factor than by the ratio κ, if it is kept below about 0.4.

This means that use of the four-wheel steering system for vehicles with understeer characteristics should reduce the steering wheel angle, heading angle, and lateral deviation.

Lateral Wind Sensitivity

The difference between the closed-loop behavior of the four-wheel and two-wheel steering cars was calculated in

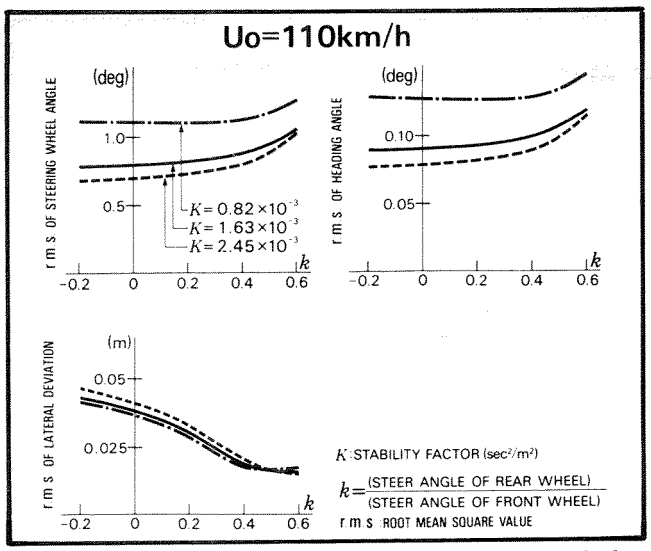

Figure 11. Effect of stability factor on road irregularity sensitivity

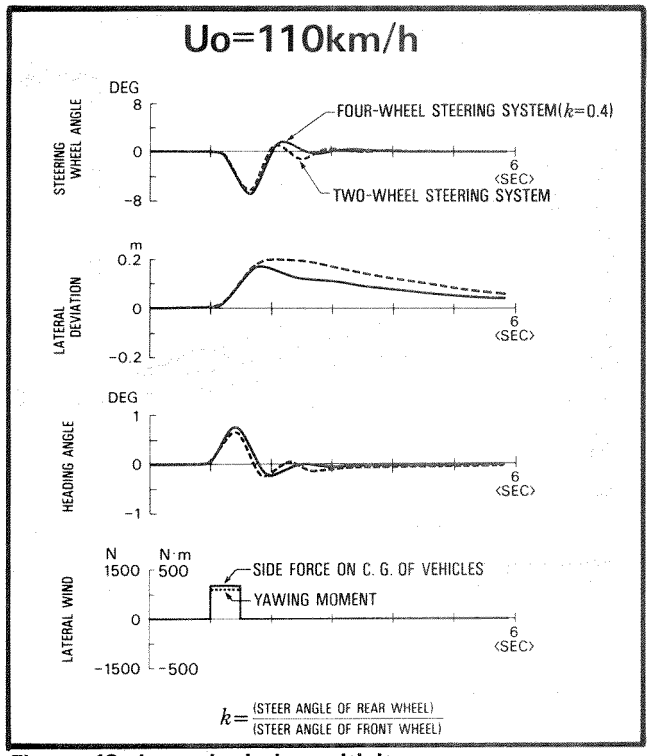

Figure 12. Lateral wind sensitivity

the presence of an external force and moment corresponding to a lateral wind. The external force and moment were made roughly equal to those a test vehicle would receive while running at 110km/h through a 15m-long lateral wind pulse with a strength of 22.5m/s.

Figure 12 compares the two-wheel steering car and the four-wheel steering car with its steer angle ratio of rear to front wheel κ set at 0.4.

The analyses show that the steering and heading angle damp faster with the four-wheel steering car.

The maximum lateral displacement of the four-wheel steering vehicle is about 20 percent less than that of the two-wheel steering vehicle. The four-wheel steering car is also some 30 percent lower than the two-wheel steering car in the cumulative value of lateral deviation—the results of integrating the lateral deviation up to the point where steering settles down.

Figure 13 shows the effects of the steer angle ratio of rear to front wheel on the maximum lateral deviation and heading angle after the closed-loop driver-vehicle is exposed to a simulated lateral wind.

The maximum heading angle becomes larger as the steer angle ratio of rear to front wheel κ increases, while the maximum closed-loop lateral deviation decreases as the value of κ increases.

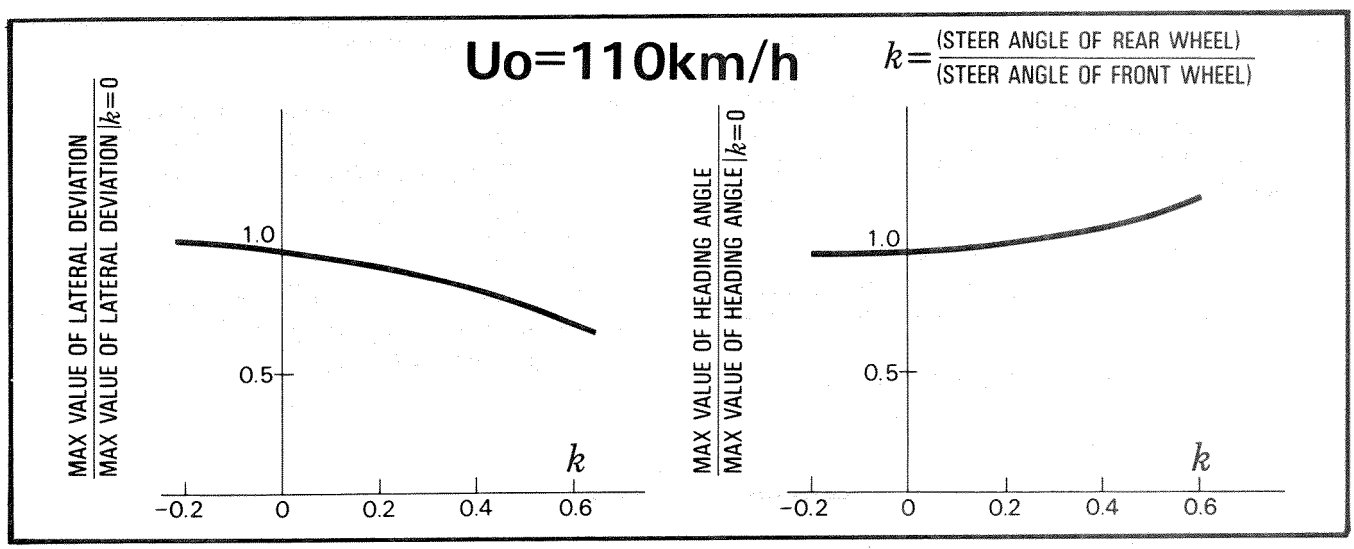

Figure 13. Effect of steer angle ratio of rear to front wheel on lateral wind sensitivity

Lane Change

Maneuverability to Pass Through Courses Marked by Traffic Cones

An attempt was made to analyze the range of driver's control parameters by which the vehicle could pass through using a simple closed-loop, driver model. In this simulation, the driver preview distance L and control gain h were varied for both the two-wheel steering car and the four-wheel steering car (at κ = 0.4). The time delay was set at 0.2.

The maneuverability was determined by whether the vehicles operated with the above driver control model could run successfully through the lane change courses, the width of which was marked by traffic cones as shown in Figure 14. A target line was used to define the course, and the vehicles were required to go through the courses without touching any of the cones. The vehicle dimensions for this calculation were fitted to the overall length and width of the test vehicles, and the vehicle speed was set at 110km/h.

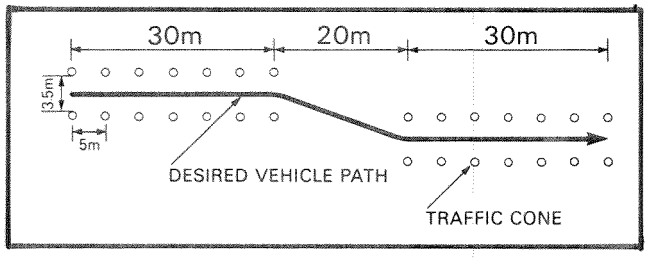

Figure 14. Course layout for lane change test

Figure 15 presents a diagram prepared by plotting the regions of successful lane change courses for the two vehicles on top of the stable ranges of driver control shown in Figure 6.

These results of computer modeling for the assumed driver time delay and vehicle speed are as follows:

- The two-wheel steering vehicle cannot change lanes successfully in a stable range of control at this speed. In other words, its motion after running through the course correctly cannot be stabilized unless the driver model control parameters change right after the lane change is over.
- The four-wheel steering vehicle, on the other hand, can change lanes using the stable range of control for the assumed conditions. These parameters enable the driver-vehicle model to go on without changing control parameters and stably run through the desired course.
- Although the steady-state response gains of the two vehicles are set equal, the four-wheel steering car requires a smaller amount of the driver control gain to run through the desired course.

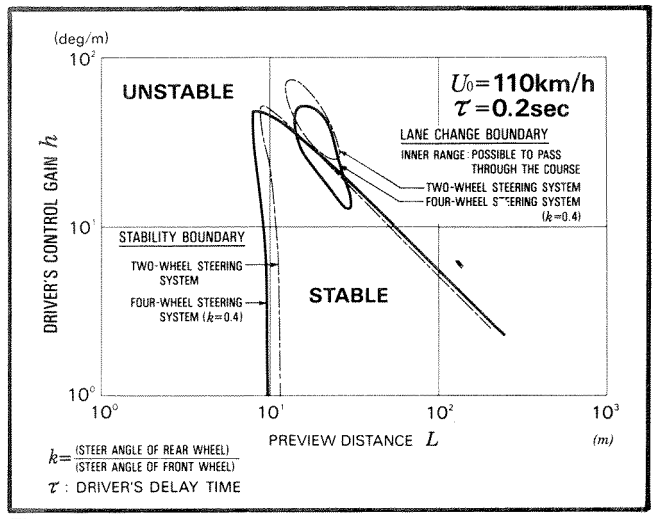

Figure 15. Task performance and stability in driver-vehicle system

Steering and Vehicle Behavior

For a lane change, from a driver control standpoint, the most desirable values of driver model parameters are probably the least control gain h and the longest preview distance L. The two vehicles can be compared in the lane change to find the difference between the systems in steering and behavior. Possibly, less control gain h and longer distance L within the stable range-parameters selected cause the driver-vehicle system to remain most stable.

The analytical findings are given in Figure 16.

The steering wheel angle, lateral acceleration, yaw velocity, and roll angle of the four-wheel steering vehicle are all less than those of the two-wheel steering car. In addition, they damp more rapidly.

Figure 16 gives the results of road tests, which show the same tendency as noted above.

Conclusion

The open-loop and closed-loop characteristics of the four-wheel steering system were analyzed by computer simulation. The results may be summarized as follows:

(1.) Open-loop characteristics of the vehicle. The four-wheel steering configuration reduces the phase lag of lateral acceleration when the rear wheels are steered in the direction of the front wheels. Steering the rear wheels at a ratio of 0.4 to the front wheels is about three times more effective in reducing this phase delay than, say, a 20 percent change in the design parameters of the conventional two-wheel steering system.

(2.) Driver-vehicle system stability. The four-wheel steering system permits the driver model preview distance to be reduced, compared with the two-

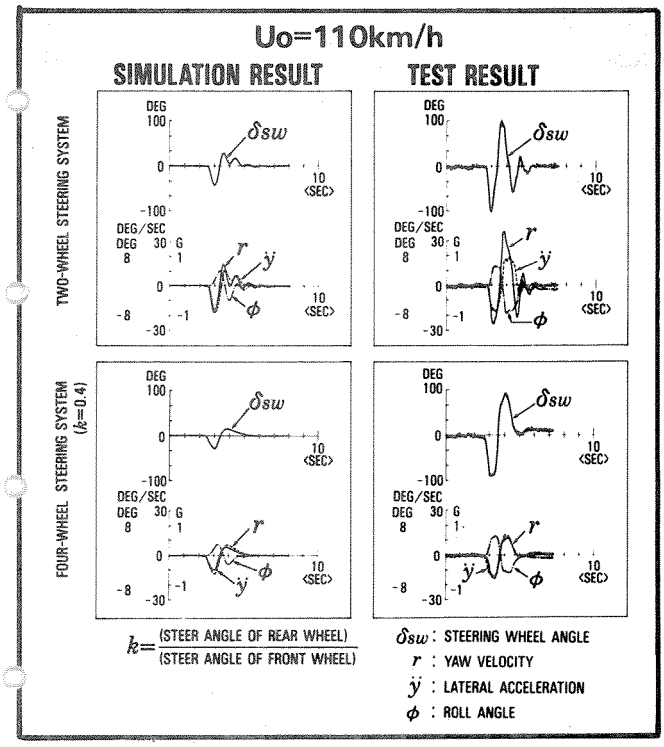

Figure 16. Lane Change Maneuver

wheel steering system. In addition, the maximum value of driver control gain for the new system does not depend on the steer angle ratio of rear to front wheel. This suggests that the new steering system might provide a slightly wider range of stability for driver-vehicle systems than the conventional two-wheel steering system.

(3.) Sensitivity to road irregularity and other external disturbances. When the steer angle ratio of rear to front wheel is set at about 0.4, the four-wheel steering system allows the corrective steering of the driver model to be reduced by about 30 percent, when countering road irregularity or other external disturbances during course tracking driving. For good lateral deviation performance, the range of steer angle ratio is up to 0.4 or so, and ratios above this level produce little effect. This trend is consistent with previous studies conducted with a lateral motion simulator.

(4.) Lateral wind sensitivity. When affected by a lateral wind, the lateral response of the four-wheel steering car damps more quickly, closed-loop. The larger the steer angle ratio, the less the lateral deviation.

(5.) Lane change. For the assumed driver model, the conventional two-wheel steering car cannot accomplish the lane change with a stable range of control parameters. However, the four-wheel steering car can follow the prescribed lane change using a stable range of model parameters.

The computed behavior of the four-wheel steering car is moderate and settles down quickly following the maneuver.

In summary, the new steering system, designed to steer the rear wheels in the same direction as the front wheels, improves the calculated control performance of the driver-vehicle system under a wide variety of operating conditions. It may provide a significant contribution to the area of active safety devices for motor vehicles in the years to come.

Appendix A
Mathematical Models

Model of a Vehicle Equipped with a Four-Wheel Steering System

Equations of Vehicle Motion

With the forward vehicle velocity given as U_o (= constant) and vehicle slip angle given as β (= small), equations of vehicle motion with 2 degrees of freedom in a coordinate system fixed to the vehicle center of gravity can be expressed as follows (see Reference (1):

$$\begin{bmatrix} I\,\dot{r} \\ m\,\dot{\beta} \end{bmatrix} = \begin{bmatrix} -\dfrac{C_f\,a^2+C_r\,b^2}{U_o} & C_r\,b-C_f\,a \\ -m+\dfrac{C_r\,b-C_f\,a}{U_o^2} & -\dfrac{C_f+C_r}{U_o} \end{bmatrix} \cdot \begin{bmatrix} r \\ \beta \end{bmatrix} + \begin{bmatrix} C_f\,a & -C_r\,b \\ \dfrac{C_f}{U_o} & \dfrac{C_r}{U_o} \end{bmatrix} \cdot \begin{bmatrix} \delta_f \\ \delta_r \end{bmatrix} \quad (1)$$

The definition of the symbols used in the equation is given in the nomenclature at the end of the appendixes.

Transfer Function for Steering Response

The right and left members of Equation (1) may be Laplace-transformed by using the relations:

$$\delta_{sw} = n\,\delta_f \quad (2)$$

$$\delta_r = k\,\delta_f \quad (3)$$

$$\ddot{y} = U_o\,(\dot{\beta}+r) \quad (4)$$

Then the transfer functions for yaw velocity response and lateral acceleration response to steering δsw can be expressed respectively as follows:

$$(5)\quad \frac{r(S)}{\delta sw(S)} = G^{r}_{\delta sw}(S) = G^{r}_{\delta sw}(O)\cdot \frac{1+Tr\,S}{1+\frac{2\zeta}{\omega n}\,S+\frac{1}{\omega n^2}\,S^2}$$

$$(6)\quad \frac{\dot{y}(S)}{\delta sw(S)} = G^{\dot{y}}_{\delta sw}(S) = G^{\dot{y}}_{\delta sw}(O)\cdot \frac{1+\frac{2\zeta'}{\omega'n}\,S+\frac{1}{\omega'^2_n}\,S^2}{1+\frac{2\zeta}{\omega n}\,S+\frac{1}{\omega n^2}\,S^2}$$

The coefficients for different terms of these transfer functions are:

$$(7)\quad G^{r}_{\delta sw}(O) = \frac{1-k}{n}\cdot\frac{Uo}{\ell\,(1+K\,Uo^2)} \qquad (7)$$

$$(8)\quad G^{\dot{y}}_{\delta sw}(O) = \frac{1-k}{n}\cdot\frac{Uo^2}{\ell\,(1+K\,Uo^2)} \qquad (8)$$

$$(9)\quad \omega n^2 = \frac{Cf\,Cr\,\ell^2\,(1+K\,Uo^2)}{m\,I\,Uo^2}$$

$$(10)\quad \zeta^2 = \frac{\{(Cf\,a^2+Cr\,b^2)\,m+(Cf+Cr)\,I\}^2}{4m\,I\,Cf\,Cr\,\ell^2\,(1+K\,Uo^2)}$$

$$(11)\quad Tr = \frac{m\,(Cf\,a-k\,Cr\,b)}{(1-k)\,Cf\,Cr\,\ell}\,Uo$$

$$(12)\quad \omega'^2_n = \frac{(1-k)\,Cf\,Cr\,\ell}{(Cf+k\,Cr)\,I}$$

$$(13)\quad \zeta'^2 = \frac{(b+k\,a)^2\,Cf\,Cr\,\ell}{4\,(1-k)\,(Cf+k\,Cr)\,I}\cdot\frac{1}{Uo^2}$$

$$(14)\quad K = \frac{Cr\,b-Cf\,a}{Cf\,Cr\,\ell^2}\,m$$

Where

$G^{r}_{\delta sw}(O)$: Steady-state gain in yaw velocity response to steering

$G^{\dot{y}}_{\delta sw}(O)$: Steady-state gain in lateral acceleration response to steering

ωn : Natural frequency of lateral motion

ζ : Damping ratio of lateral motion

Tr : Time constant (for lead) of yaw velocity

K : Vehicle stability factor.

Equations of Vehicle Motion in Ground-Fixed Coordinate System

This section derives vehicle transfer functions in a ground-fixed coordinate system o-XY, which are useful for an analysis of driver-vehicle system stability as discussed in the next section.

From Figure A-1, the following equation may be obtained:

$$\dot{Y} = Uo\,\sin(\beta+\psi) \qquad (15)$$

$$\ddot{Y} = Uo\,(\dot{\beta}+r)\,\cos(\beta+\psi) \qquad (16)$$

If vehicle motion is limited to small lateral perturbations, while running straight ahead at a constant velocity, then small angle approximations can be used, i.e.:

$$\ddot{Y} = Uo\,(\dot{\beta}+r) \qquad (17)$$

$$\dot{\psi} = r \qquad (18)$$

The right side of Equation (17) conforms with Equation (4).

Hence:

$$G^{Y}_{\delta sw}(S) = \frac{1}{S^2}\,G^{\ddot{y}}_{\delta sw}(S) = \frac{1}{S^2}\,G^{\ddot{y}}_{\delta sw}(S) \qquad (19)$$

$$G^{\psi}_{\delta sw}(S) = \frac{1}{S}\,G^{r}_{\delta sw}(S) \qquad (20)$$

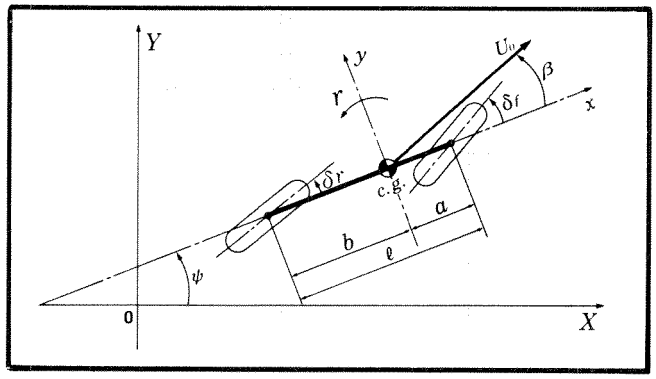

Figure A-1. Bicycle model of four-wheel steering vehicle

Analytical Model of the Driver-Vehicle System

Mathematical Model for the Driver

To analyze the handling performance of the four-wheel steering system, this paper uses a driver model, called the "preview predictor model" (see Reference (3)).

As is apparent from Equation (19), lateral vehicle position has the qualities of second-order integration. Accordingly, differential as well as proportional behavior are needed to stably control the vehicle using the driver's feedback control action. Determination of vehicle lateral deviation requires second-order integration, while the heading angle assumes characteristics similar to first-order integration as indicated in Equation (15). Typically, a motor vehicle can be easily controlled by detecting and controlling these two phenomena. This is the basic idea on which this mathematical model of drivers has been established.

As shown in Figure A-2, a driver as the mathematical model described above looks at a point L meters ahead of the vehicle, and after finding the error ε of that point from the desired course, feeds back such information to the steering wheel angle at a given gain h. It is assumed there is a delay time τ between the detection of such error and an initiating steering action.

Hence:

$$\delta sw(t)=h\ \varepsilon(t-\tau) \tag{21}$$

With the right and left members Laplace-transformed, the transfer function $G^{\delta sw}(S)$ becomes:

$$G_{\varepsilon}^{\delta sw}(S)=\frac{\delta sw(S)}{\varepsilon(S)}=h\ e^{-\tau s} \tag{22}$$

Assuming that τ is small, it follows:

$$\simeq h\ (1-\tau\ S) \tag{23}$$

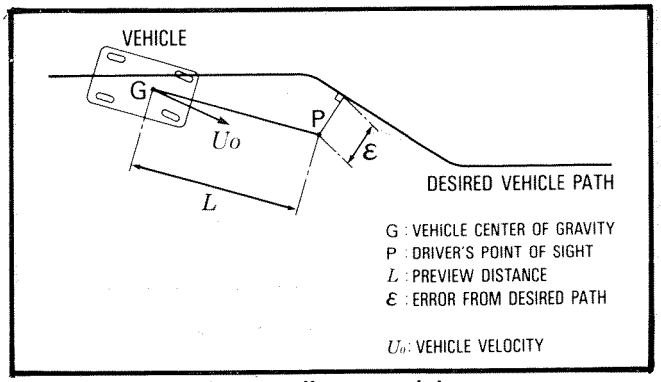

Figure A-2. Preview predictor model

With the lateral position of the desired course given as Yc, the error ε may be expressed as follows:

$$\psi \ll 1$$

$$\varepsilon \simeq Y+L\psi-Yc \tag{24}$$

The time-domain computer simulation uses Equation (21) instead of Equation (24).

Equations (23) and (24) are used in linearizing the driver-vehicle system for stability analysis, as discussed in the next subsection.

Stability Analysis of the Driver-Vehicle System

The block diagram of the driver-vehicle model discussed here is similar to Figure A-3.

From the diagram:

$$Yc(S)=\varepsilon(S)+\delta sw(S)\cdot\{G_{\delta sw}^{Y}(S)+L\ G_{\delta sw}^{\psi}(S)\} \tag{25}$$

$$Y(S)=\delta sw(S)\cdot G_{\delta sw}^{Y}(S) \tag{26}$$

$$\frac{Y(S)}{Yc(S)}=\frac{G_{\varepsilon}^{\delta sw}(S)\cdot G_{\delta sw}^{Y}(S)}{1+G_{\varepsilon}^{\delta sw}(S)\cdot\{G_{\delta sw}^{Y}(S)+L\ G_{\delta sw}^{\psi}(S)\}}$$

The characteristic equation for the driver-vehicle system as described in (27) above with the desired course as input and the lateral displacement of the vehicle as output can be expressed as follows:

$$F(S)=1+G_{\varepsilon}^{\delta sw}(S)\cdot\{G_{\delta sw}^{Y}(S)+L\ G_{\delta sw}^{\psi}(S)\}=0 \tag{27}$$

If Equations (19), (20), (23) are substituted for the appropriate terms of Equation (28), a polynomial of S raised to the fourth power can be obtained:

$$F(S)=a_0 S^4+a_1 S^3+a_2 S^2+a_3 S+a_4=0 \tag{28}$$

Where

$$a_0=n\ m\ I \tag{29}$$

$$a_1=\frac{n}{Uo}\{(C_f a^2+Cr\ b^2)\ m+(C_f+Cr)\ I\}- \tag{30}$$

$$\tau\ h\ \{(C_f+k\ Cr)\ I+L\ (C_f\ a-k\ Cr\ b)\ m\} \tag{31}$$

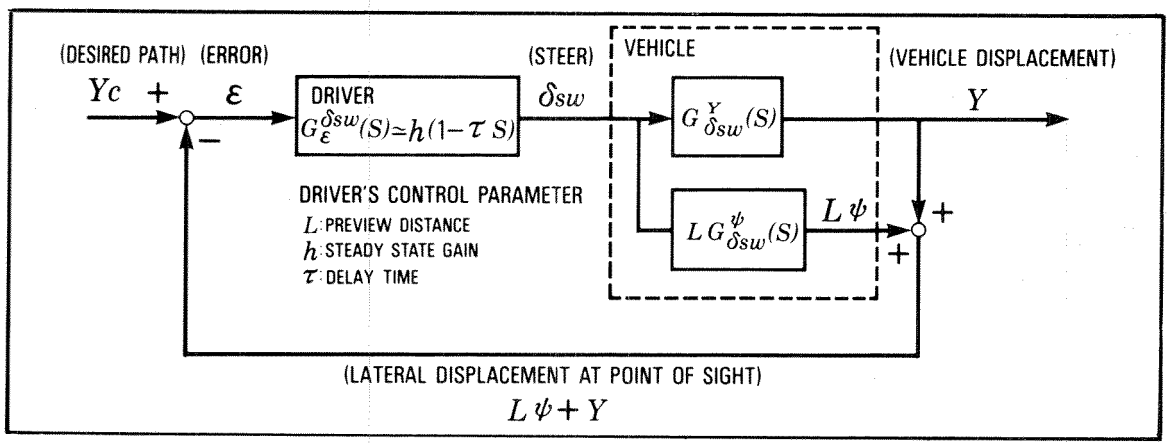

Figure A-3. Driver-vehicle system using preview predictor model

(32) $$a_2 = n\,C_f\,C_r\,\ell^2\,\frac{(1+K\,U_o^2)}{U_o^2}$$

$$h\,\{(C_f+k\,C_r)\,I+L\,(C_f\,a-k\,C_r\,b)\,m\}$$

$$-\,\tau\,h\,\frac{C_f\,C_r\,\ell}{U_o}\,\{b+k\,a+L\,(1-k)\}$$

(33) $$a_3 = h\,\frac{C_f\,C_r\,\ell}{U_o}\,\{b+k\,a+L\,(1-k)\}$$

$$-\,h\,\tau\,(1-k)\,C_f\,C_r\,\ell$$

(34) $$a_4 = h\,(1-k)\,C_f\,C_r\,\ell$$

To keep this system asymptotically stable, all roots of Equation (29) must be found in the left-half plane.

Two methods are available for identifying the stable ranges of driver's control parameters L, h, and τ; one is to directly solve Equation (29), and the other is to find such ranges from coefficients α_0, α_1, α_2, α_3 and α_4.

The second method includes a techniquts αeorem. A primary test on this particular method found that all coefficients of Equation (29) must be positive. From:

$$a_3 > 0$$

The following relation can be derived:

$$L > \tau\,U_o - \frac{b+k\,a}{1-k} \tag{35}$$

This means that the preview distance the driver has to look out ahead has a minimum value that depends on vehicle velocity and driver time delay and that a four-wheel steering system helps reduce the minimum possible preview distance, L.

Nomenclature

- a : Distance from front axle to center of gravity (C. G) of vehicle.
- b : Distance from rear axle to C. G.
- ℓ : Wheel base $(a+b)$.
- m : Vehicle mass.
- I : Yawing moment of inertia.
- n : Steer angle ratio of steering wheel to front wheel.
- k : Steer angle ratio of rear to front wheel.
- C_f : Front tires' cornering stiffness.
- C_r : Rear tires' cornering stiffness.
- U_o : Vehicle forward velocity.
- δ_{sw} : Steering wheel angle.
- δ_f : Steer angle of front wheel.
- δ_r : Steer angle of rear wheel.
- K : Stability factor.
- (X,Y) : Earth-fixed axis system.
- (x,y) : Vehicle-fixed axis system.
- ψ : Heading angle.
- β : Vehicle sideslip angle.
- r : Yaw velocity.
- $\dot{y}$: Lateral acceleration.

References

1. Sano, S., Y. Furukawa, and Y. Oguchi, "The effect of improved vehicle dynamics on driver control performance," Proceedings Seventh International Technical Conference on Experimental Safety Vehicles, 1979.
2. Sano, S., Y. Furukawa, and Y. Oguchi, "Effect of vehicle response characteristics and driver's skill level on task performance and subjective rating," Proceedings Eighth International Technical Conference on Experimental Safety Vehicles, 1980.
3. Kondo, M., and A. Agimine, "Driver's sight point and dynamics of the driver-vehicle system related in it," SAE Paper 680104.
4. McRuer, D., and D.H. Weir, "Theory of manual vehicular control," *Ergonomics*, Vol. 12, No. 4, pp. 599-633, 1969.
5. Iguchi, M., "Vehicle stability from standpoint of driver's response characteristics" (in Japanese), *Journal of the J. S. M. E.*, Vol. 62, No. 491.
6. Abe, M., "Vehicle dynamics and control" (in Japanese), Kyouritsu Pub., 1979.

Appendix B
Vehicle Specification

Table B-1. Basic specification

2WS: Two-Wheel Steering System
4WS: Four-Wheel Steering System

No.	Item		Unit	2WS	4WS
1	Vehicle Mass	: m	Kg	1280	←
2	Distance from front axle to C.G.	: a	m	0.98	←
3	Distance from rear axle to C.G.	: b	m	1.47	←
4	Yawing moment of inertia	: I	$Kg{\cdot}m^2$	1840	←
5	Wheel base	: l	m	2.45	←
6	$\frac{\text{Steering wheel angle}}{\text{Steer angle of front wheel}}$	: n		14.5	8.7
7	$\frac{\text{Steer angle of rear wheel}}{\text{Steer angle of front wheel}}$	: k		0	0.4
8	Front tires' cornering stiffness	: Cf	N/rad	66300	←
9	Rear tires' cornering stiffness	: Cr	N/rad	67400	←
10	Overall length		m	4.21	←
11	Overall width		m	1.65	←
	Stability factor	: K	sec^2/m^2	1.63×10^{-3}	←

Table B-2. Design parameters for changing stability factor

(1)

Stability Factor :K ($\times10^{-3}$)	Understeer 1.63	Neutralsteer 0	Oversteer -0.82
Front Tires' Cornering Stiffness Cf	66300	80200	86500
Rear Tires' Cornering Stiffness Cr	67400	53500	47200
			(For Fig. 3,4,5)

(2)

Stability Factor :K ($\times10^{-3}$)	More Understeer 2.45	Understeer 1.63	Less Understeer -0.82
Front Tires' Cornering Stiffness Cf	59500	66300	73300
Rear Tires' Cornering Stiffness Cr	74100	67400	60400
			(For Fig. 11)

Design Parameters for Equalizing Steady-State Response Gain

Table B-3. Design parameters for equalizing steady state response gain

$\frac{\text{Steer angle of rear wheel}}{\text{Steer angle of front wheel}}$	:k	-0.2	0	0.2	0.4	0.6
$\frac{\text{Steering wheel angle}}{\text{Steer angle of front wheel}}$	:n	17.4	14.5	11.6	8.7	5.8
						(For Fig. 5,6,8,9,11,13)

Maneuverability and New Suspension for Four-Wheel Drive Vehicles

Minoru Otake,
Shingo Obayashi,
Midori Kubota, and
Yoshiaki Nozawa
Subaru Engineering Division, Fuji Heavy Industries, Ltd.

Abstract

Four-wheel drive vehicles have recently become widely used for their enhanced safety in a variety of road conditions on the highway and snowy, wet, and gravel-covered roads.

It is well known that four-wheel drive vehicles are superior in maneuverability to two-wheel drive vehicles. We have attempted to explain this superiority by theoretical as well as experimental methods.

This paper deals with the theoretical approach in determining the difference in movements between two-wheel and four-wheel drive vehicles during cornering with varying tire-to-road-surface friction coefficients and wheel loads. Experiments were carried out on paved and snowy roads using the two types of vehicles. As a result, it has been verified quantitatively that the four-wheel drive vehicle provides higher stability with greater variations in friction coefficients and wheel loads, though the difference is only marginal under a steady state.

This paper also reports on the new suspension system developed to implement enhanced characteristic levels of a normal passenger car (vibration, ride comfort, steering stability and control, etc.) without sacrificing the unique features of the four-wheel drive system.

Introduction

The four-wheel drive vehicle, with its greater traction than two-wheel drive vehicles, was developed mainly for off-road use, but in recent years the four-wheel drive has been adopted for normal passenger cars as well. It insures safe driving not only on the snowy and unsurfaced roads but also on highways(1).

For maneuverability, however, conventional analysis based on experiments on flat roads with constant coefficient of friction is unsatisfactory for proving that the four-wheel drive vehicle is safer than two-wheel drive vehicles. We, therefore, have analyzed the movements of front-wheel, rear-wheel, and four-wheel drive vehicles with varying coefficients of road friction and wheel loads to compare and report on the safety of these types of vehicles.

This paper also reports on the practical pneumatic suspension system with height control that has been developed to insure not only a safer and more comfortable ride under high-speed cruising on the highway and on long drives, but the best performance of the four-wheel drive when used off the road.

Maneuverability Characteristics of Four-Wheel Drive Vehicles

Driving and Braking Characteristics

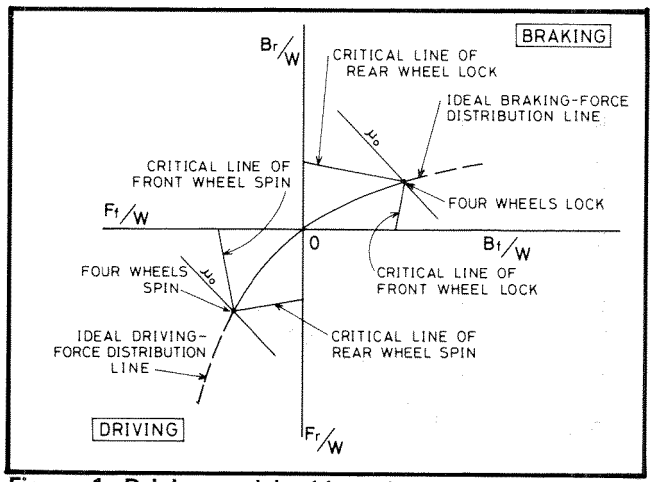

Figure 1. Driving and braking characteristics of four-wheel drive

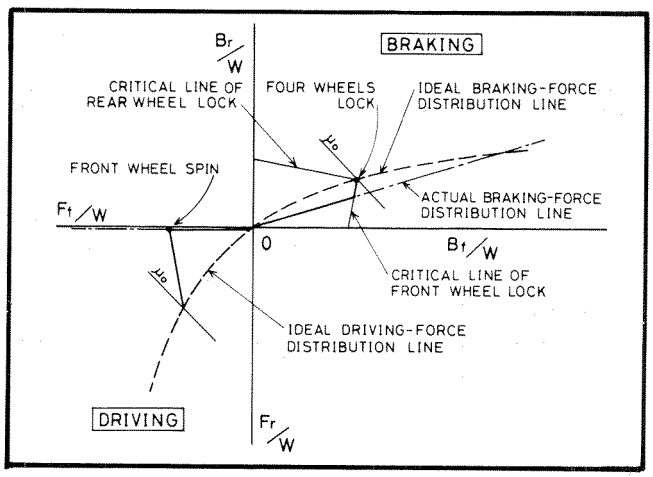

Figure 2. Driving and braking characteristics of four-wheel drive

Where:

- $B_{f\text{-}r}$: Braking-force of front and rear wheels (per wheel)
- $F_{f\text{-}r}$: Driving-force of front and rear wheels (per wheel)
- W : Vehicle weight
- μ_o : Maximum friction coefficient between tire and road surfaces

Figures 1 and 2 show driving and braking characteristics of automobiles. The four-wheel drive vehicle, in which both the front and rear wheels are connected directly to the transmission, traces theoretically an ideal braking-force distribution line during braking, insuring maximum performance regardless of road surface conditions. Though front tires cannot be steered in the two-wheel drive system while they are locked up, the four-wheel drive system allows the control of steering until all four wheels are locked, thus enhancing safety. Figure 3 shows the results of experiment.

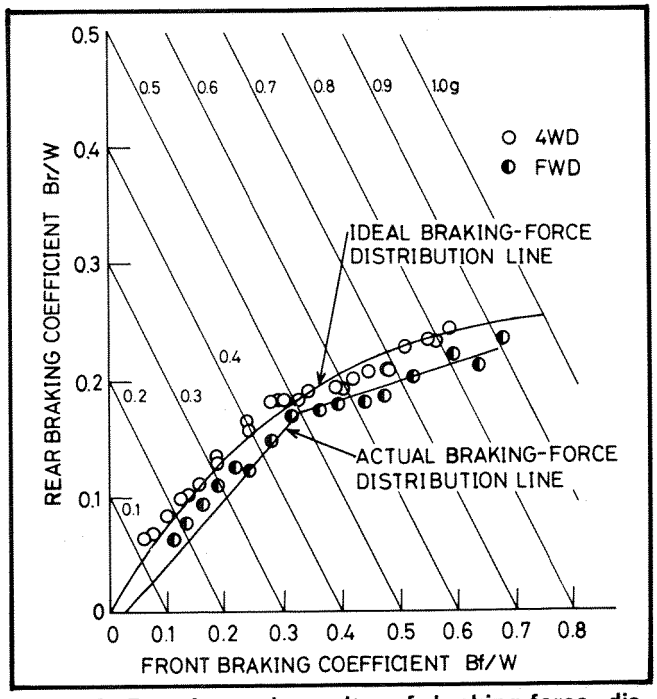

Figure 3. Experimental results of braking-force distribution

The four-wheel drive shows an ideal driving-force distribution line during driving and insures maximum traction at all times. When the equivalent traction is used in two-wheel and four-wheel drive vehicles, the four-wheel drive vehicle uses less traction per wheel, allowing greater use of cornering force.

Figure 4 shows the maximum friction coefficient (between tire and road surfaces) to maximum acceleration diagram (μ_o - α_{max} diagram) for four-wheel, front-wheel, and rear-wheel drive vehicles as obtained by calculation, from which we know the four-wheel drive vehicle is superior in its ability to transmit driving force.

Simulation Model with Three Degrees of Freedom

Figure 5 shows a two-wheel model with three degrees of freedom in a vehicle, simplified for making an analysis.

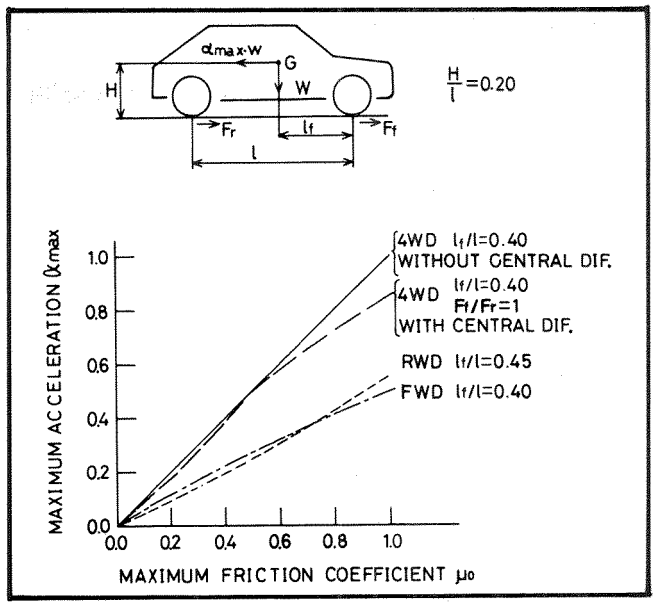

Figure 4. Maximum friction coefficient to maximum acceleration diagram

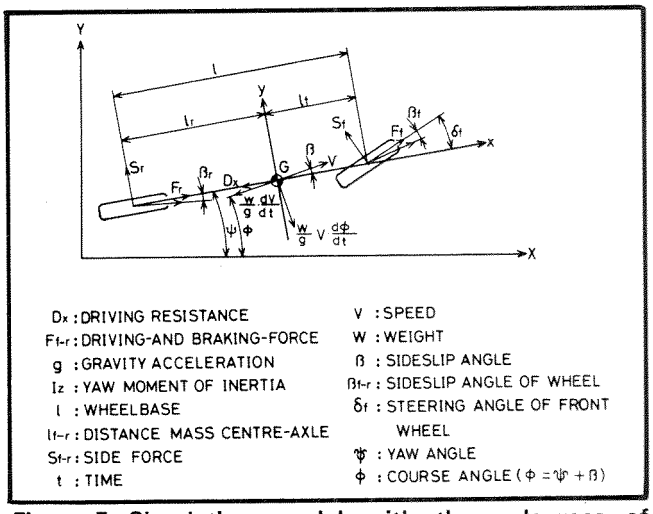

Figure 5. Simulation model with three degrees of freedom

Equations of equilibrium for vehicle longitudinal force, lateral force, and yawing moment are as follows:

Longitudinal force

$$-Dx - \left\{\left(\frac{dV}{dt}\right) - V\left(\frac{d\phi}{dt}\right)\beta\right\}\frac{W}{g} + F_f \cos\delta_f - S_f \sin\delta_f + F_r = 0 \quad (1)$$

Lateral force

$$-\left\{\left(\frac{dV}{dt}\right)\beta + V\left(\frac{d\phi}{dt}\right)\right\}\frac{W}{g} + F_f \sin\delta_f + S_f \cos\delta_f + Sr = 0 \quad (2)$$

Yawing moment

$$-I_z\left(\frac{d^2\psi}{dt^2}\right) + (F_f \sin\delta_f + S_f \cos\delta_f)\,\ell_f - S_r\,\ell_r = 0 \quad (3)$$

By applying the concept of friction circle, the relationship between tire driving and braking force $F_{f\text{-}r}$ and side force $S_{f\text{-}r}$ can be simplified as follows:

$$S_{f\text{-}r} = f_c(\mu_o \cdot L_{f\text{-}r}) \times \sqrt{1 - \left(\frac{f_{f\text{-}r}}{2} / \mu L_{f\text{-}r}\right)^2} \times 2\beta_{f\text{-}r} \quad (4)$$

Where:

- μ_o : Maximum friction coefficient between tire and road surfaces
- μ : Friction coefficient between tire and road surfaces
- $L_{f\text{-}r}$: Vertical load on front and rear wheels (per wheel)
- $f_c(\mu_o \cdot L_{f\text{-}r})$: Side force per given slip angle

From these equations, it is learned that more marked differences exist in vehicle movement between different drive systems with greater driving resistance D_x, driving force $F_{f\text{-}r}$, and wheel vertical load $L_{f\text{-}r}$, and a smaller maximum friction coefficient μ_o: the four-wheel drive system is superior in driving stability. These factors correspond, respectively, to driving on snow- and gravel-covered roads, hill climbing, and high-speed cruising on wet roads.

Figure 6 indicates simulation results of vehicle behavior when turning with a fixed steering angle and varying friction coefficients on road surfaces μ_o. It shows that the rear-wheel drive demonstrates the most drastic change in yaw velocity and a stronger tendency toward spin.

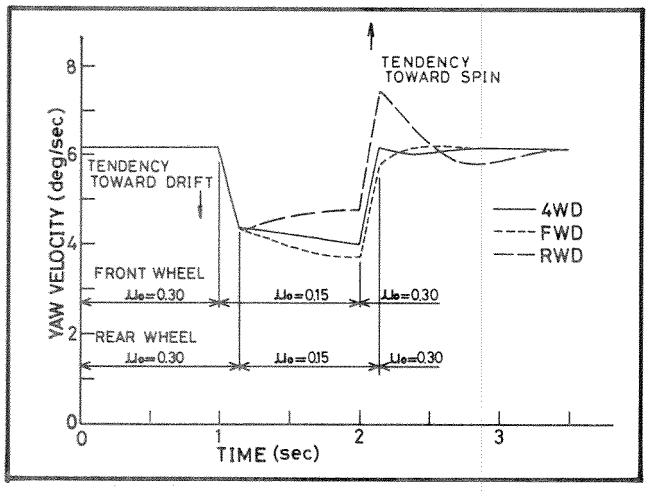

Figure 6. Theoretical simulation of vehicle behavior during turning with varying μ_o values

The front-wheel drive has greater change in yaw velocity and shows a strong drift tendency. The four-wheel drive, on the other hand, has the least change in yaw velocity, showing excellent driving stability.

The same is also true in Figure 7, which simulates vehicle behavior during turning with a fixed steering angle but varying wheel vertical loads.

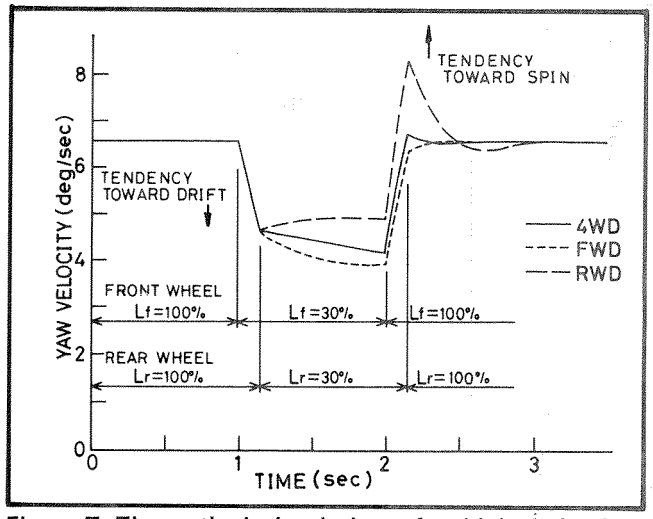

Figure 7. Theoretical simulation of vehicle behavior during turning with varying $L_{f\text{-}r}$ values

Actual Maneuverability Examples

Looking at differences in vehicle behavior between actual four-wheel and two-wheel drive vehicles when they make a steady state cornering and move up and down a snowy hill, the following are seen:

Steady State Cornering

Figure 8 shows the results of steady state cornering made by a vehicle allowing selection of either front-wheel or four-wheel drive mode, cornered in both modes. The test was conducted on both wet and dry surfaces. In both cases, the four-wheel drive has a slightly higher limit of adhesion and tends to have reduced understeer near the limit, the difference between front-wheel and four-wheel drive being marginal. This is because for a flat, smooth surface, there is no change of friction coefficient (μ_o), and there is little driving resistance.

Driving on Snowy Roads

Figure 9 shows measurements of frequency of various steering-wheel angles, steering efforts, and lateral accelerations occurring for a vehicle driven in both front-wheel and four-wheel drive modes. The vehicle was driven on a test course of approximately 5km by one driver to hold the same road impression. Maximum vehicle speed was held to the same level on a straight course.

The figure reveals that the four-wheel drive has a smaller frequency in the region of relatively small levels of steering-wheel angle, steering effort, and lateral acceleration. This indicates that the four-wheel drive tends to stay on course better, requiring little correction of steering angles along a straight line, which insures safer

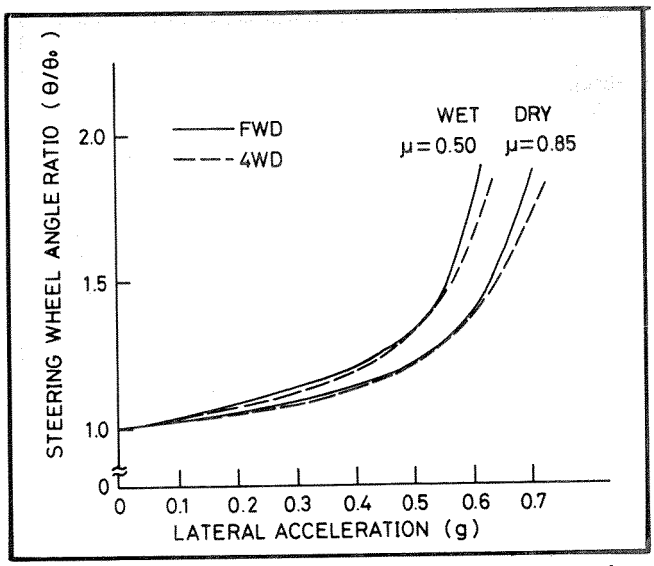

Figure 8. Experimental results of steady state cornering

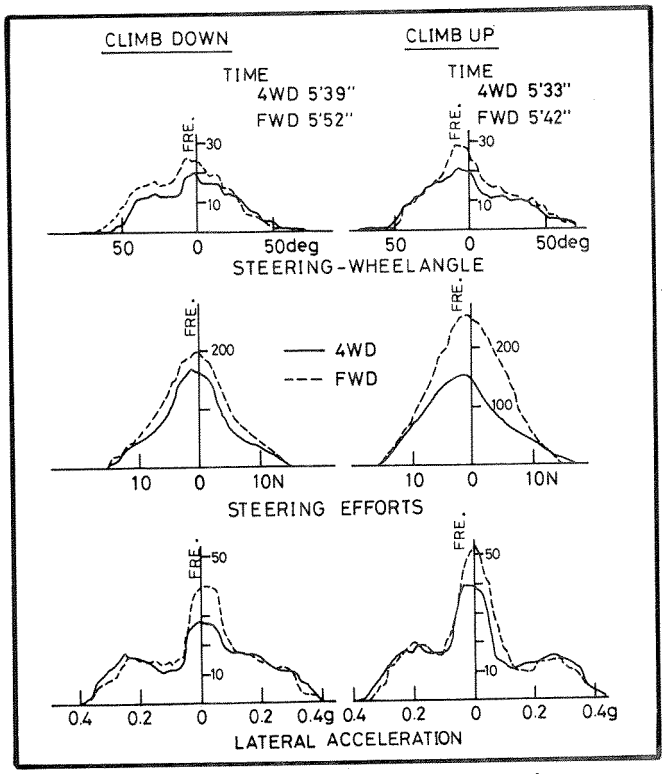

Figure 9. Experimental results of snowy roads

driving. This tendency is especially true with steering-wheel angle and steering effort when the vehicle climbs a hill, which demonstrates that the greater the driving force the more noticeable the difference between the two drive systems.

A closer examination of the results of lateral acceleration measurements shows that the four-wheel drive has a greater frequency in higher acceleration regions, as compared with the front-wheel drive, which means it is easier to handle during cornering. This agrees with the subjective evaluation results, and the four-wheel drive required shorter time than the two-wheel drive despite the fact that the vehicle was driven at the same maximum speed and driver's road impression.

Suspension System of Four-Wheel Drive Vehicles

Requirements for the Suspension System on Four-Wheel Drive Vehicles

On-Road

It is important to consider passenger comfort as well as noise characteristics, in addition to driving stability at high speeds, to insure a safe, comfortable ride on the road. These factors help to reduce fatigue of passengers. Thus, the requirements are—

- Height of vehicle center of gravity should be low.
- Sufficient suspension stroke should be provided at all times regardless of pay load.
- Spring and damper damping characteristics should be insured according to operating conditions.
- Transmission of vibration from unsprung weight should be minimized.

Off-Road

Generally speaking, off-road driving limit depends not only on traction but also on grounding and bottoming characteristics, the important factors to take into account for the suspension system on a four-wheel drive vehicle.

Excessive road shocks imparted to the vehicle body increase driver fatigue, affect driving stability, and lead to body damage. Requirements therefore include—

- Sufficient road clearance should be provided, unaffected by varying load weight.
- Sufficient suspension stroke should be provided regardless of load weight.
- Spring rate should be increased in proportion to increased load weight.
- The damper damping force should be kept at an adequately high level.

As can be observed above, design requirements for a suspension system for both on-road and off-road use tend to contradict each other in many respects.

Subaru Pneumatic Suspension System with Height Control

Outline of the System

To eliminate conflict between the requirements, we have equipped the system with several novel functions as follows:

(1) Level control that selects height at either normal or high in a range of 30mm at the front and 35mm in the rear, thereby insuring road clearance as well as low center of gravity
(2) Automatic load leveling that maintains vehicle height at a predetermined value regardless of load weight, thereby insuring sufficient suspension stroke as well as road clearance
(3) Replacement of conventional metal springs by air-spring assemblies, not only to improve the vibration damping characteristics from the unsprung weight but also to help make possible the automatic load leveling mentioned above
(4) Displacement-dependent variable damping force that improves ride comfort and stability on the road as well as driving ability off the road

Figure 10 shows the configuration of the Subaru Pneumatic Suspension System with Height Control. The system consists of the following components:

- Pneumatic springs: A rolling-diaphragm-type air spring is installed outboard the damper. This, combined with automatic load leveling, allows setting of a low spring rate for improved ride comfort. The spring rate can also be increased in proportion to load, which improves road stability with a heavy load, as well as bottoming characteristics. Should there be an air leak, the built-in bump stopper rubber comes into play to allow continued driving.

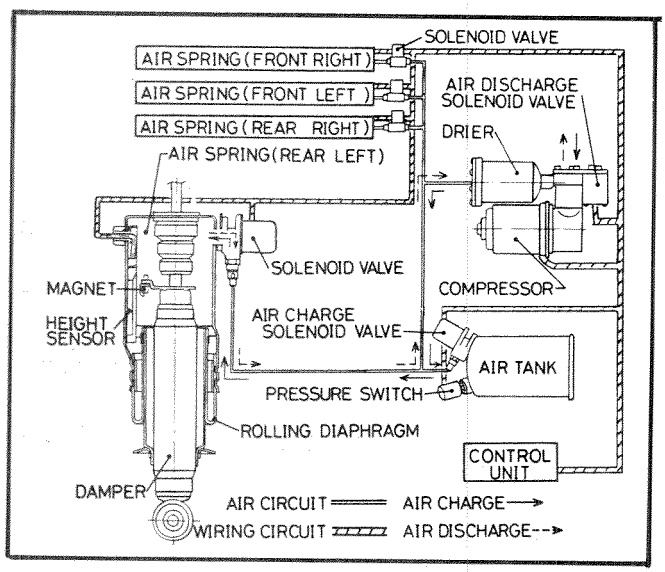

Figure 10. System diagram

- Variable damping force: Figure 11 shows the variable damping force mechanism; Figure 12 shows an example of damping force characteristics.
- Height sensor: A sensor is installed in each of the four air springs and detects suspension stroke within close tolerances, offering a means of precisely determining vehicle conditions.
- Compressor and drier: The compressor, drier, and exhaust solenoid valve are integrated into one unit. As a safety feature, the solenoid valve acts as a relief valve when delivery pressure of the

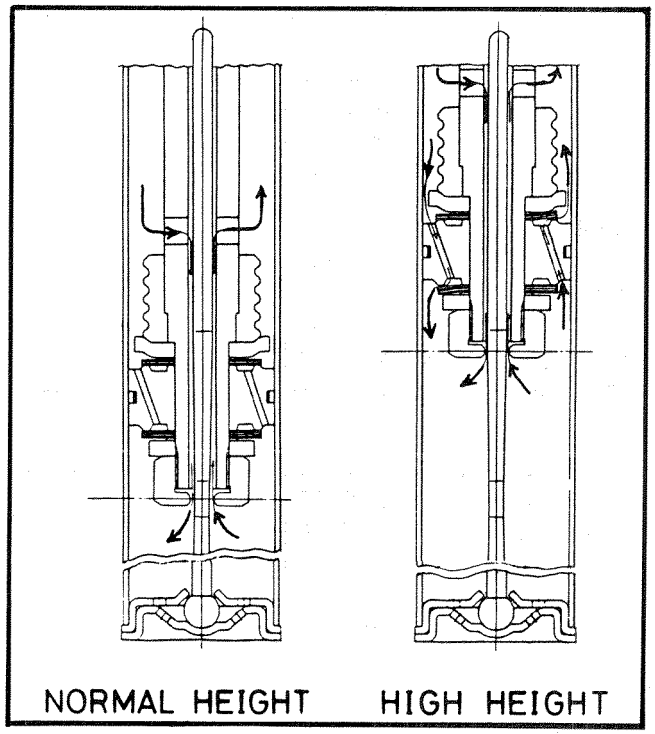

Figure 11. Variable damping force mechanism

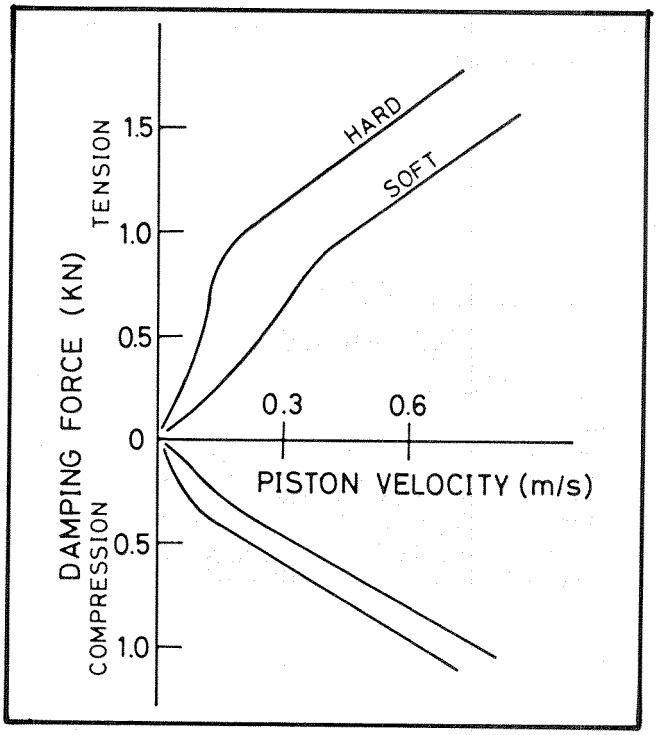

Figure 12. Damping force characteristics

compressor becomes excessive in certain unusual conditions.

- Control unit: Using a single-chip microcomputer, it enables optimum control of air springs by analyzing height-sensor and vehicle-speed signals. Figure 13 is a block diagram of the control logic.

Height Selection—The height selection switch allows the driver to select either the high or normal height, as shown in Figure 14. When vehicle speed exceeds a predetermined level while driving in high level, normal height is automatically selected to lower the center of gravity, improving driving stability at higher speeds.

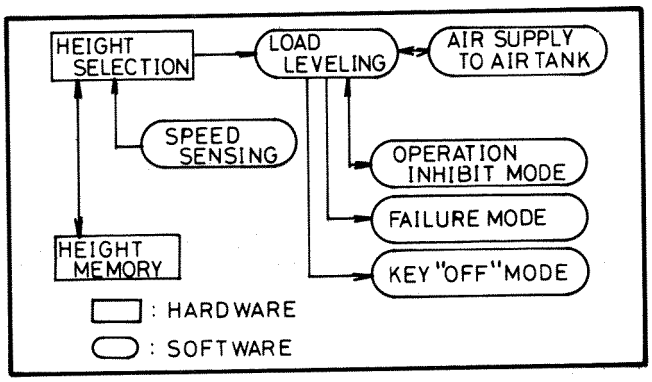

Figure 13. Block diagram of the control logic

Load Leveling—Load leveling maintains vehicle height at a predetermined level regardless of load weight. The function is activated when the height sensor transmits a signal indicating variations in car height for time duration, as shown in Table 1. It is not activated, however, when "a wheel rides on road bump," "a wheel comes off track to a lower level," or "body roll" (see Figure 15). This prevents stability and control from being deviated to right and left.

If an error occurs in the system, an indicator light flashes to warn the driver of incorrect operation, and the relevant control functions are deactivated.

Performance Evaluation

On-Road—Road stability at high speeds is improved by low vehicle height and constant vehicle position regardless of pay load and aerodynamic lift. In particular, the subjective evaluation has proved that the pneumatic suspension is extremely effective in keeping the vehicle on straight course at 100km/h or over.

The new suspension also insures good ride comfort. For example, there is little rapid pitching, such as choppy ride (see Figure 16) or vibration around 5Hz, and vibration is drastically reduced over 20Hz (see Figure 17). Noise characteristic has also been improved, as shown in Figure 18, by effectively damping or road noise.

Off-Road—When used off the road, the vehicle with the new suspension in high mode offers a wide 195mm road

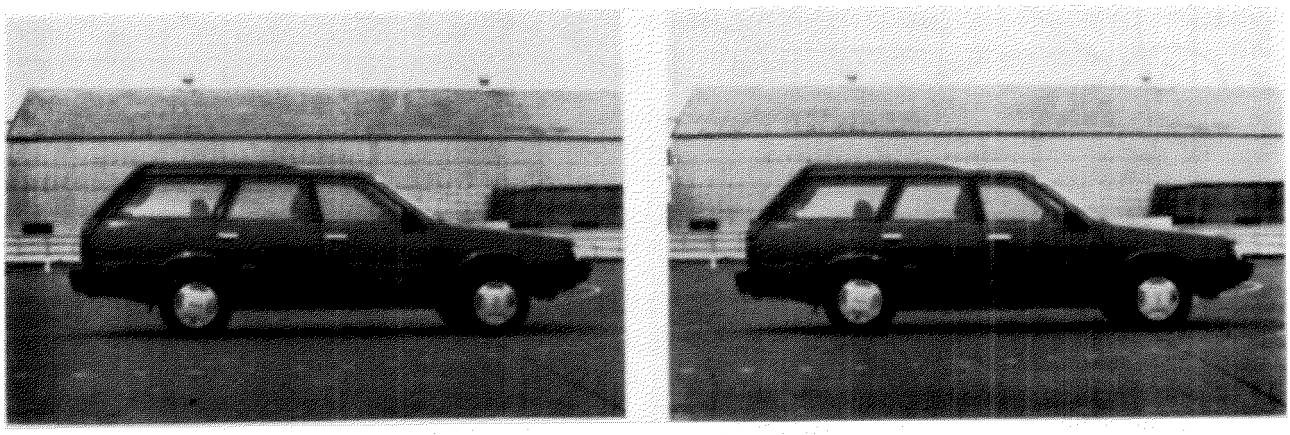

Figure 14. External view

Table 1. Time constant of height sensor signal.

Vehicle Conditions	Time Constant
Within 2 sec after ignition switch on	0.5 sec
During stationary	10 sec
Within 1 min after starting a vehicle	15 sec
1 min or more after starting a vehicle	60 sec

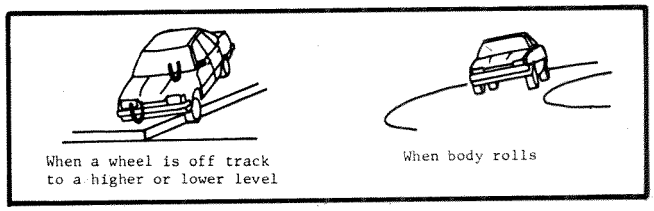

Figure 15. Examples of operation inhibit pattern

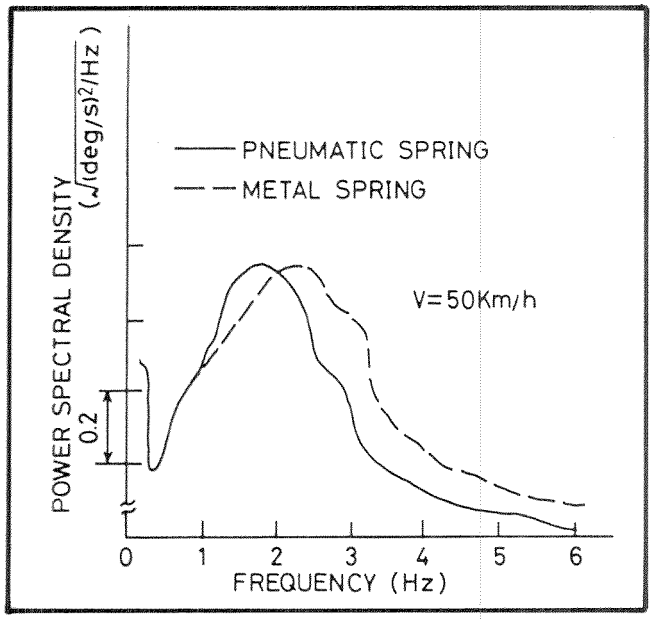

Figure 16. Body pitch rate

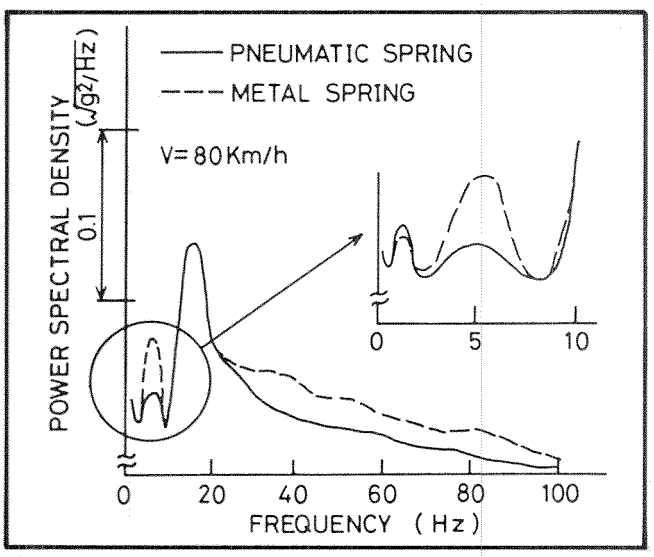

Figure 17. Vertical body vibration on Belgian road

clearance, and automatic load leveling has minimized bottoming regardless of load weight (see Figure 19). This improves driving ability as well as ride comfort on rough roads.

Conclusion

The four-wheel drive vehicle, because of its more stabilized motion on the highways and snowy and unsurfaced roads than the two-wheel drive vehicle, can insure a safer ride. By combining the four-wheel drive with the electronically controlled pneumatic suspension, sufficient stability, when used under a wider range of conditions including off-road, can be achieved together

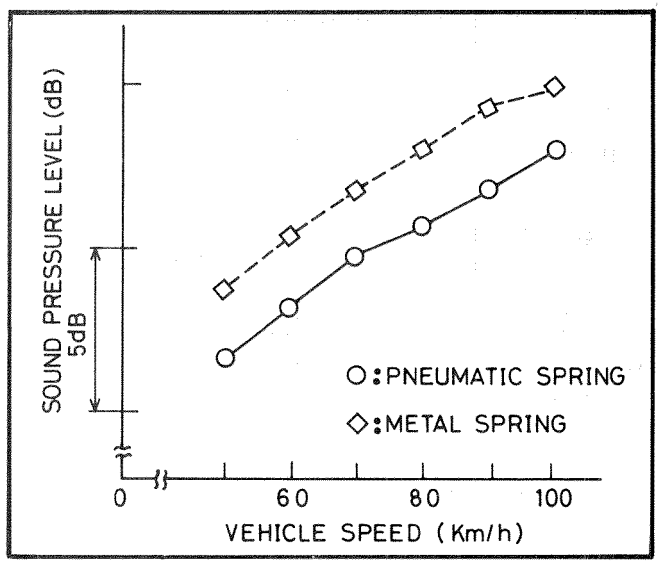

Figure 18. Interior noise

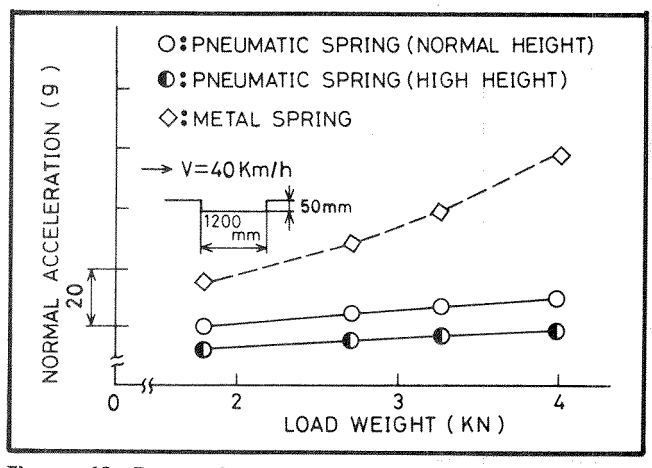

Figure 19. Bottoming characteristics

with excellent ride comfort. The combination, we believe, will provide a safer ride from both the vehicle maneuverability and human comfort viewpoints.

References

1. Matsumoto, R., et al., "Increase of driving safety through new concept 4WD vehicle," Proceedings Ninth International Technical Conference on Experimental Safety Vehicles, Kyoto, November 1982.
2. Obayashi, S., et al., "Characteristics of maneuverability of 4WD vehicles," *JSAE*, Vol. 39, No. 3, 1985.
3. Otake, M., et al., "Development of air suspension system for smaller vehicles," JSAE National Convention, Tokyo, May 1985.

Behavior of a Vehicle During Turning

Y. Vermont
Renault

Introduction

Doing things in such a way that the driver of a car is always in control of his vehicle, whatever the circumstances, is one of the goals that Regie Renault has set regarding safety:

- The behavior of the vehicle must always be consistent with the instantaneous orders given by the driver, whether he is braking, accelerating, or lifting his foot off the accelerator (a point that will be the object of this paper).
- The vehicle must inform its driver when it is nearing the point of limit.

It is easy to understand that a driver will very possibly leave the road if he takes a curve too fast. Family cars do not benefit from aerodynamic ground effects and cannot tackle a turn, without running substantial risk, at a speed greater than that producing transverse acceleration of 1g (9.81m/s2).

The natural reaction of a driver who realizes he is taking a turn too fast is to lift his foot off the accelerator and then, in some cases, to brake. Without particular technical precautions being taken, the vehicle is quite likely to skid head-to-tail.

The manufacturer, when drawing up the specifications for the axle assemblies of a car, specifies the steering geometry stresses that will improve coherence between the driver's action and the response of the vehicle. Therefore, we think we can improve car-driving safety.

The purpose of this study is to help understand—

- Why a vehicle begins a head-to-tail skid
- How the manufacturer can correct this phenomenon

Using the calculation results of a mathematical model representing the transitory behavior of a vehicle, we shall see how, by adjusting the running gear, the limit at which a car begins a head-to-tail skid can be pushed back.

The first part of this paper will be devoted to the attitude assumed by the vehicle with respect to its trajectory at stabilized speeds. In this way, we will bring in different notions needed to understand the transitory behavior of the car:

- Rigidity of the overall drift of the axle assemblies and tires
- The steering angles induced by the vehicle roll attitude
- Under- and over-steering behavior (angular dynamic)
- Behavior of the tire under load

To characterize the probable transitory stage of a car when the foot is lifted, we shall compare two static-dynamic states of the vehicle:

- Just before the foot is lifted
- The second just after, when the deceleration of the car creates longitudinal load transfers proportional to its deceleration

To maintain the trajectory, the driver must correct the angle set by the steering wheel. The greater this angle, the less stable the car will be and the higher the chances of head-to-tail skidding. If we modify the parameters defining the axle assemblies it becomes possible to have the overall rigidity of each of the axle assemblies sets evolve favorably. Although this rigidity is basically caused by the tires, it is, in fact, the evolution of the deviation between the front and rear axle rigidity that governs this behavior. The car manufacturer's margin maneuver is approximately of the same order of magnitude.

These first results were confirmed by simulations using a vehicle transitory model. This model integrates a tire model designed by Mr. Ratti, engineer at Regie Renault.

Static-Dynamic Balance of a Vehicle Turning on a Circle

Definition of Tire Drift Rigidity

If a side force is applied to a tire, the tire drifts through an angle δ. For a small angle δ, the drift and force F are in proportion to one another, so we can define a drift rigidity as $F = D \times \delta$. The drift rigidity is an increasing function of the vertical load applied to the tires.

Definition of Angular Dynamic

The angular dynamic defines the under- or over-steering behavior of the car. The test currently performed to test the under- or over-steering performance of a car is as follows. A 50m circle is traced on the ground. The test driver has to follow this line while accelerating. If he is obliged to increase the steering wheel angle, the vehicle under-steers; otherwise, it over-steers. Family car manufacturers seek to design under-steering cars. The increase of the steering angle at the steering wheel as the transverse acceleration speed increases is a natural driver reflex. In addition, it is a stability criteria for the car.

The angular dynamic of a car is the supplementary angle through which the steering wheel must be turned to keep the car on the same trajectory when transverse acceleration increases at the rate of lm/s2. A positive

angle means that the car under-steers; a negative angle means that it over-steers. The angular dynamic can be expressed either at the road wheel or at the steering wheel, through the application of the steering demultiplication ratio N.

$Ds = N \times Dr$

Let us assume a car is running at a speed V on a circle with a radius R.

- M : weight of vehicle
- M1 : weight on front axle
- M2 : weight on rear axle
- l : wheelbase
- l1 : distance from center of gravity to front axle
- l2 : distance from center of gravity to rear axle
- γt : transverse acceleration
- Ψp : vehicle yaw speed
- Y1 : transverse force on ground at front axle
- Y2 : transverse force on ground at rear axle
- D1 : front tire drift rigidity
- D2 : rear tire drift rigidity
- δ : body center of gravity drift angle
- $\delta 1$: front axle drift angle
- $\delta 2$: rear axle drift angle
- r : circle radius
- α : angle on steering wheel (expressed at road wheel)

General equations of dynamic:

$$(M1 + M2) \times \gamma t = Y1 + Y2$$

$$0 = Y1 \times l1 - Y2 \times l2$$

$$Y1 = M1 \times \gamma t$$

$$Y2 = M2 \times \gamma t$$

Tire balance equations:

$$Y1 = D1 \times \delta 11$$

$$Y2 = D2 \times \delta 12$$

Kinematic relations:

$$V \times (\alpha + \delta 1) = V \times \delta g + l1 \times \psi p$$

$$V \times \delta 2 = V \times \delta g - l2 \times \psi p$$

$$\psi p = V / R$$

$$\gamma t = V \times V / R$$

$$\alpha = l / R + \delta 2 - \delta 1$$

Finally, the angular dynamic equals the difference of the respective drift angle of the rear axle and front axle when the vehicle, traveling at a stabilized speed, is subjected to transverse acceleration of 1m/s2.

$Dr = (\delta 2 - \delta 1) / \gamma t$

If the axle drift is due only to the rigidity of the tire drift, the angular dynamic assumes a very simple expression:

$Dr = (M2/D2 - M1/D1)$

Static-Dynamic Balance of a Vehicle Traveling Around a Circle—Vehicle Attitude with Respect to Trajectory

Let us assume the vehicle is running at a stabilized speed around the circle. If the rear axle does not drift, the attitude of the vehicle on its trajectory would be in conformity with the following diagram. The center of the circle on which the vehicle is moving would be exactly in line with the rear axle. From the trace obtained, it also becomes obvious that it is essential the inner wheel turns more during turning than the outer wheel.

Because the tires drift, the attitude of the turning vehicle will conform with the following diagram. The projection from the center of the circle is now ahead of the rear axle.

Behavior of a Vehicle When the Foot Is Lifted

Static-Dynamic Approach

Let us assume the car is moving at a steady rate over a circle with radius R. Because the vehicle is understeering, the driver must turn the steering wheel (as equivalent to the road wheel), in the light of the above, through:

$\alpha v = (l/R) + (V \times V/R) \times DR$

$DR = M2/D2 - M1/D1$

Lifting the foot instantaneously results in longitudinal load transfers linked with the deceleration of the car. The drift rigidities of the axle assemblies (which as seen above depend on the vertical load supported by them) will be modified. D2 will decrease; D1 will increase. To remain on the same trajectory, the driver must decrease the angle to which the steering wheel is turned.

Stability Criterion

As a stability criterion for the car when the foot is lifted, we shall select the difference of the angle on the

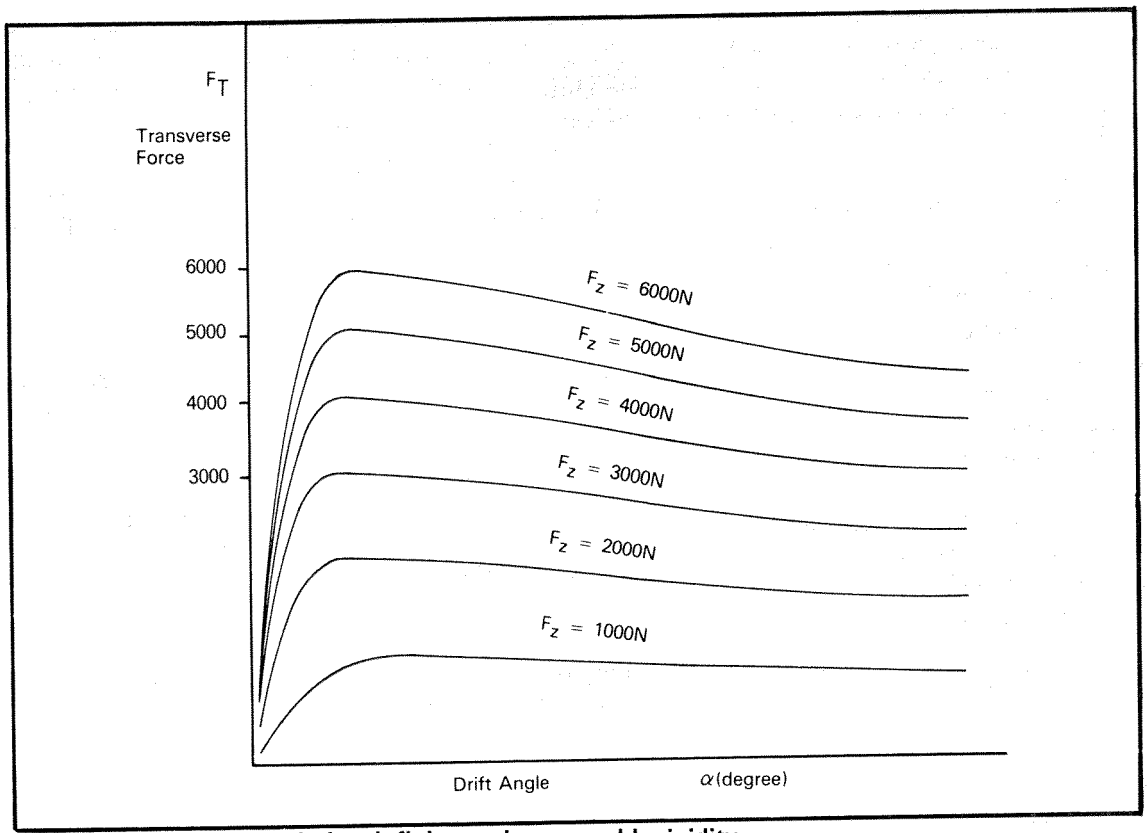

Figure 1. Vehicle on circle, infinite axle assemble rigidity

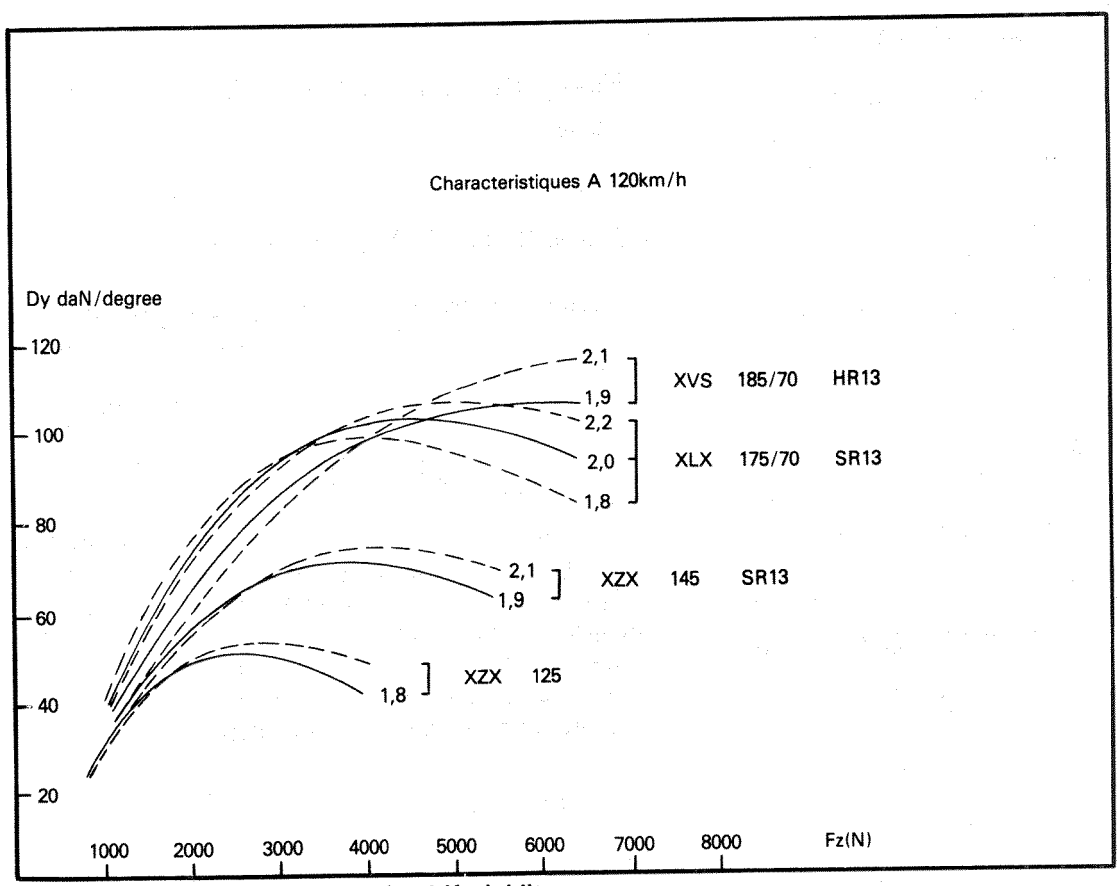

Figure 2. Vehicle on circle, low tire drift rigidity

steering wheel as required by the driver to keep to the same trajectory: the lesser the angle, the more the vehicle will be stable.

The calculation results are presented differently; in reality, we are comparing the two static-dynamic attitudes of the car before the foot is lifted and after it is lifted.

Vehicle without adjustment of running gear.

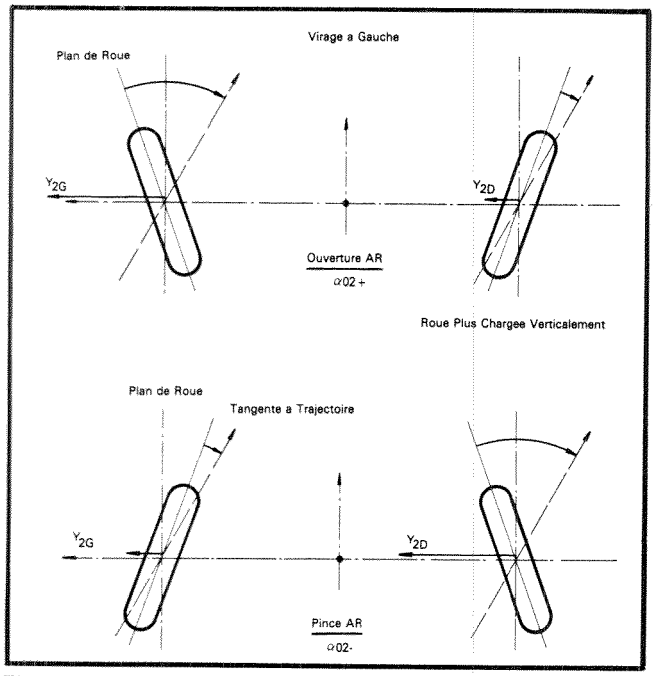

Figure 3. Two static-dynamic attitudes before and after lifting the foot (tire effect only)

Adjustment of Induced Steering Angle

If the drift rigidity of the axle assembly depends only on the tire, the automobile manufacturer would be unable to improve matters. If, effectively, the drift rigidity of the axle assembly is basically caused by the tires, the variation of the drift rigidity of a tire can be counterbalanced by a purely kinematic modification of wheel-steering angles.

We have a measuring system with which we can evaluate the steering angle of a vehicle's wheels under different stresses. On this apparatus, it is possible to impose a roll angle on the vehicle. It has been found the plane of the wheel turns in proportion to the roll angle assumed by the car.

For a given car attitude, the induced steering angles are a linear function of the roll angle. This leads to the notion of steering angles induced by roll:

eps = αir(z) / ϑ
αir : wheel steering angle
eps : induced steering coefficient
ϑ : vehicle roll (γt = λm/s^2)
z : vehicle trim

The coefficient eps depends on the car trim. The induced steering angles modify the under-steering behavior of the car. Therefore, it is normal they appear in the angular-dynamic formula:

DR = M2 / D2 - M1 / D1 + (eps2 - epsl) × ϑ

epsl: steering angle induced at front wheels
eps2: steering angle induced at rear wheels

taking into account that the sign conventions for the under-steering angles are negative at the front but positive at the rear. Controlling the wheel steering angles induced by vehicle roll forms part of the axle specifications.

Let us consider how they can be used to improve the behavior of the vehicle.

The order of magnitude if the desirable variation of the induced steering angles is not compatible with the customary kinematics of the running gear.

Therefore, we shall use another phenomenon to improve the vehicle.

Adjustment of Toe-In or Toe-Out of Axle Assembly

If we consult the technical specifications of manufacturers relative to adjusting the alignment of axle assembly, we will come to the surprising conclusion that perfect alignment is never sought after.

example of R9: 10ft toe-out at the front
30ft toe-in at the rear

As a general rule, vehicles are adjusted with toe-out at the front and toe-in at the rear.

Let us consider axle assembly adjusted with toe-in. When the car runs in a straight line, the tires drift by an angle equal to the toe-in imposed on the axle assembly and therefore develop substantial internal forces of up to 300N for a 30min wheel toe-in.

When a car rolls, the transverse forces on the ground are picked up by each wheel of the axle assembly in proportion to the rigidity of the drift of each tire. Increasing the toe-in of axle assembly is, in fact, equivalent to increasing the transverse force picked up by the outer wheel that is most heavily loaded, i.e., the wheel of the axle assembly with the greatest drift rigidity. Accordingly, the drift rigidity of the axle assembly can be increased by changing its adjustment toward a toe-in (if the axle assembly is adjusted for toe-out, then the rigidity will drop).

Adjustment of Anti-Roll Distribution

The choice of the anti-roll distribution governs the distribution of the transverse loads transfers between the front and rear running gear of the vehicle when it begins to roll. If the drift rigidity of the tire were proportional to

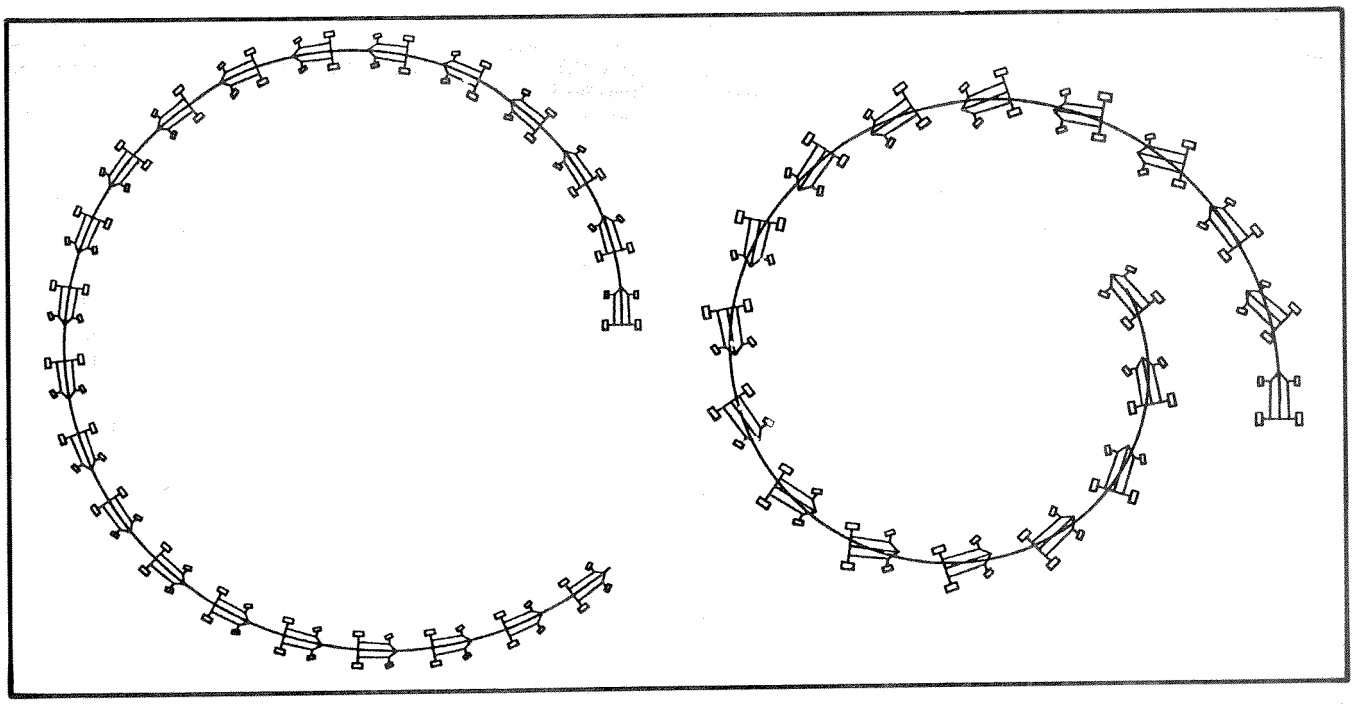

Figure 4.

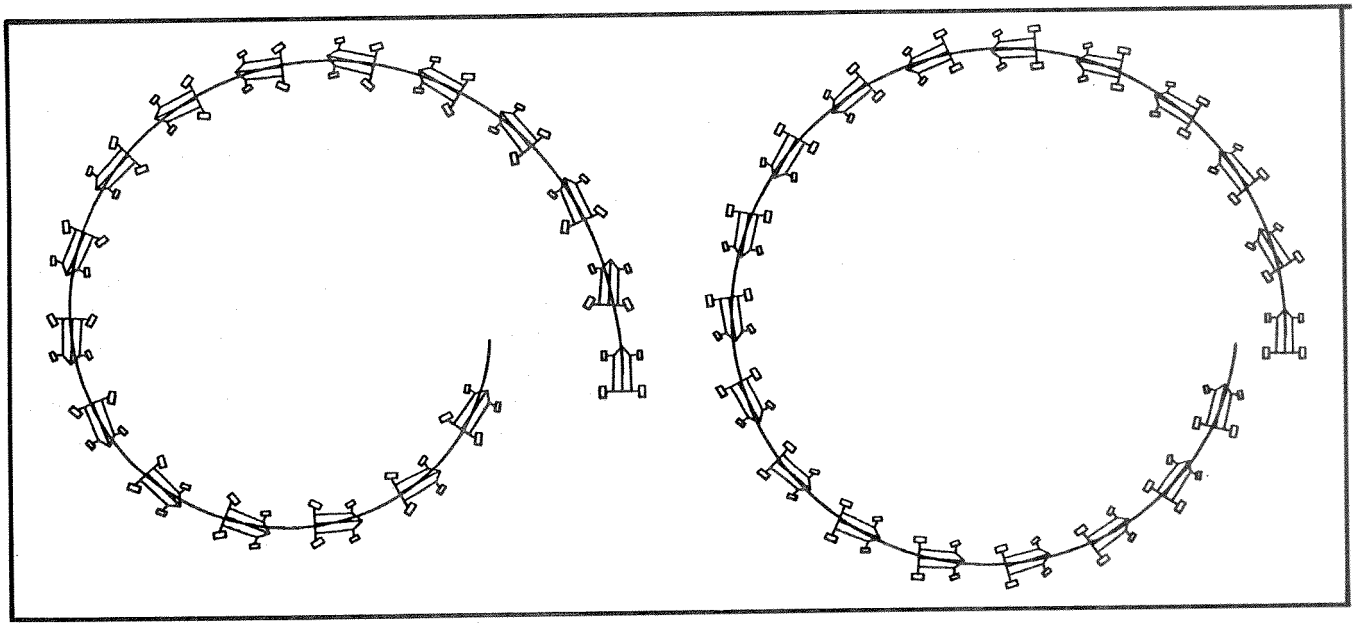

Figure 5. Internal forces for toe-in.

the vertical load it bears, the anti-roll distribution would have no effect on the behavior of the vehicle. Quite contrary to the implicit hypothesis put forward above, the tire reaches saturation point and its drift rigidity no longer increases with the load. This is understandable if we consider that the maximum transverse force with which, a tire can cope is necessarily limited by the ground adhesion coefficient.

To understand this phenomenon, one must be able to understand the operation of the tires. In the following, we give the results of tire measurement tests:

- Evolution of transverse force as a function of the drift angle
- Evolution of drift rigidity as a function of load
- Evolution of longitudinal force as a function of pseudo-slippage

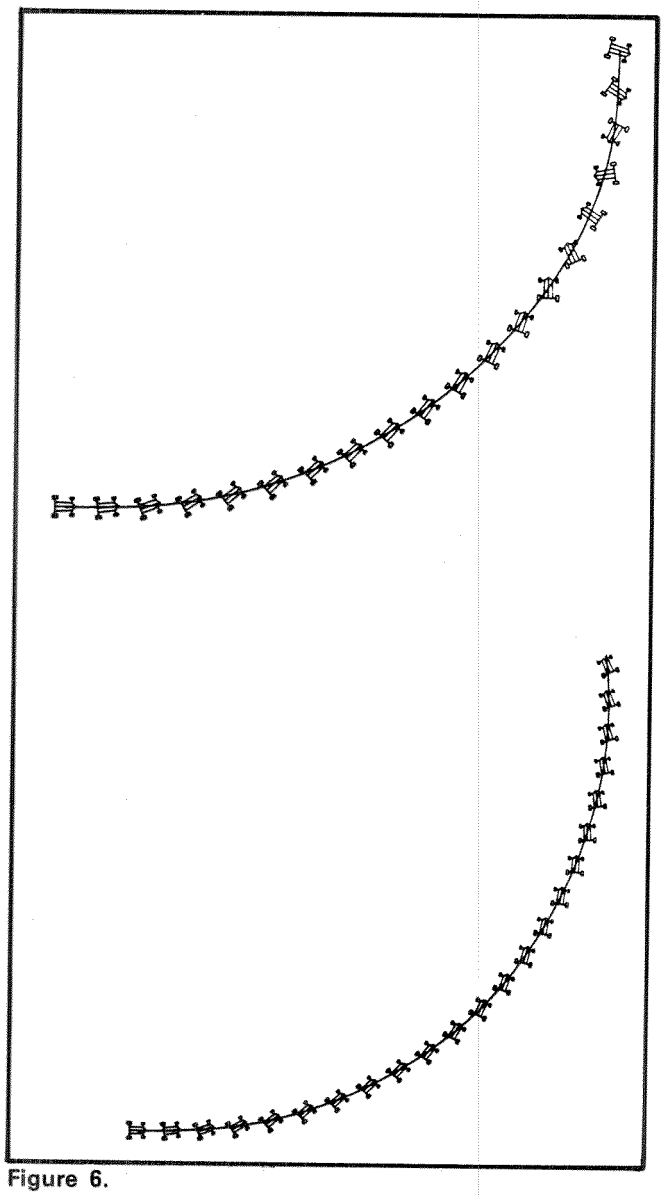

Figure 6.

- Evolution of transverse force at a given drift angle and as a function of the longitudinal force (motor power)

Taking account of the complexity of the tire's working mode, Regie Renault has developed a model of tire behavior under force (work of Mr. Ratti) which has been integrated in a simulation model of a vehicle's transitory state behavior. The results obtained with this model are presented below. The model enabled us to validate the static-dynamic approach for the improvement of behavior on lifting the foot in a car by working on—

- The analysis of the axle assembly
- The toe-in or toe-out
- The anti-roll distribution

Analysis of the Vehicle Behavior Model

Description of Model

The model takes six objects into account—the body, the four wheels, and the steering wheel.

The transverse and longitudinal Brouilhet effects are taken into account in a simplified manner: roll axis and pitch axis. The analysis of the axle assembly, including the variations of toe-in or toe-out, the steering angle variations induced as a function of the load, are incorporated in the model in the form of tables or figures. The deformation of the axle assembly under force, important phenomena we have not yet gone into, are not left out of account. We are certain they can modify the toe-in or toe-out of the axle assembly.

On the basis of the drift rigidity curves of a real tire, we adjusted the tire model. We verified that the longitudinal force variation curves as a function of pseudo-slippage were realistic, as were the transverse rigidity variation curves as a function of the longitudinal force. We were required to make this choice because we do not have a suitable measuring apparatus, which is rather to be found at a tire manufacturer. On this point, closer collaboration between car manufacturers and tire manufacturers appears essential.

Description of Simulation

The case of driving that we suggest simulating corresponds to that in which a driver is about to negotiate a motorway exit road at too high a speed, incompatible for him with the curve radius of the exit way. The speed is not excessive, but the transverse accelerations are substantial. The engine braking will generate deceleration of approximately 0.3g(3m/s2). The results of simulation confirm the improvements considered previously.

Numerical Applications

N	:	steering demultiplication ratio
αsa	:	angle on steering wheel (expressed at steering wheel)
l	:	wheel-base
γtb	:	transverse acceleration before lifting the foot
γ	:	transverse acceleration after lifting the foot

D1b : front tire drift rigidity before lifting the foot

D1a : front tire drift rigidity after lifting the foot

eps1 : steering angle induced at front wheels after (0. before)

eps2 : steering angle induced at rear wheels after (0. before)

ϑ : vehicle roll

$\alpha 01$: toe-out after at front wheels $(01 < 0)$ (rd)

$\alpha 02$: toe-in after at rear wheels $(02 > 0)$(rd)

$$\alpha sb = (1 / r + (M2 / D2b - M1 / D1b) \times \gamma tb) \times N$$
$$\alpha sa = (1 / r + (M2 / D2a - M1 / D1a) \times \gamma tb + (eps2\text{-}eps1) \times \vartheta) \times N$$

1 Vehicle Without Adjustment

D1b= 75500 N/rd
D2b= 71600 n/rd
γtb = 8.2 m/s2

D1a = 83700 N/rd
D2a = 60770 n/rd

n = 20 M1 = 549 kg M2 = 396 kg

$\alpha sb - \alpha sa$ = -16 degree

2 Vehicle With Induced Steering Angles

$\alpha sb = \alpha sa$ eps2 - eps1 = -0.12

3 Vehicle With Adjustment Of Front Toe-out, Rear Toe-in

D1b = 75500 D1a = 83700 + 1120000 × 01
D2b = 71600 D2a = 60700 + 1478000 × 02
(approximated formula)

$\alpha sb = \alpha sa$ = = > $\alpha 01 = 0.$ $\alpha 02$ = 0.023 rd
. or $\alpha 01$ = -0.018 $\alpha 02$ = 0.

Conclusion

If the simulations we have demonstrated convince you of the interest that Regie Renault has in improving the safety of the cars we put on the market, we have achieved our goal. If we believe that we can correctly control the technical factors playing a part therein, we do consider that designers are unfortunately deprived of the same latitude as computing engineers in varying the constructive parameters of the car. If we have been able to boast the advantages of a certain modification to improve the behavior when the foot is lifted, we have sometimes deliberately said nothing about the induced negative effects. Finally, everything is a question of a compromise, competition between manufacturers is severe, and the technical qualities of vehicles are improving. Let us hope safety is also improved in the process.

An Instrument To Measure Scattered Light due to Windshield Wear

Alwin Timmermann
Forschungsgemeinschaft Auto-Sicht-Sicherheit

Abstract

An instrument is described that permits the measurement of scattered light on windshields in cars in full daylight. It presents the intensities of the scattered light in the form of a diagram and calculates two indices, which can be associated with the most prominent types of wear, i.e., impact of small stones and wiper damage.

The instrument is easy to operate and permits inspection of a large number of windshields in a short time. Measurements on 300 vehicles indicate a linear increase in wear due to impact of small stones with mileage and a more-than-linear increase of wiper damage. Vehicles of identical mileage can have very different values depending on the type of use.

It is also examined how the different amounts of wear as characterized by the measured indices affect the ability of test persons to see and recognize objects on the road.

Introduction

As clear vision is of prime importance for safe driving, automobile windshields and motorcycle visors have to be of good optical quality. This is taken into account by high standards for official approval.

In actual use, both windshields and visors are exposed to the impact of small particles of sand and dust as well as the abrasive effects of cleaning efforts and scratching by fine grains that are moved over the surface by windshield wiper action.

In the case of visors, the surface will wear rather quickly. The worn surface scatters the light and may impair vision considerably (Figure 1). Motorcyclists are advised to replace their visors at reasonable intervals.

Automobile windshields, although more resistant owing to the higher hardness of glass, are nonetheless subject to wear. Figure 2 shows the typical damage in a windshield at 80,000km: The surface contains a multitude of small craters (about 180cm^2). The band of bright light is due to scattering from (locally) parallel grooves (with a statistical distribution of depths and distances) produced by the windshield wiper. These grooves extend over the entire area of the photographed glass sample. They scatter light in a direction perpendicular to them and add one or two "tails" to each light source. The tails move according to the relative position of light source, observer (or camera objective, respectively), and the direction of the grooves. Light scattered by the small craters, on the other hand,

Figure 1. Dazzling due to light scatter by a worn motorcycle visor

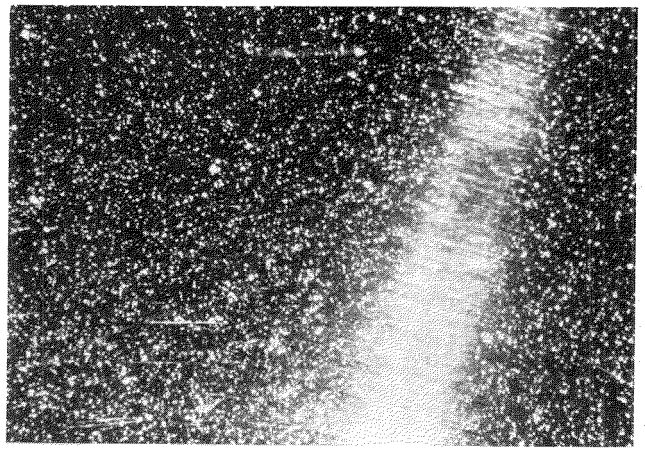

Figure 2. Surface wear on a windshield at 80,000km

appears to the observer who has his eyes accommodated to infinity, as a halo around the light source. Only few and partly contradictory data are available regarding the extent of surface damage as a function of mileage.

A recently developed instrument quantitatively measures the light scattered by surface damage while the windshield is in the car. This, for the first time, provides the capability to collect larger amounts of data. Typical values of scattering data derived from these measurements can then be correlated with the reduction in visual perception of individuals to determine the effects of worn windshields on the safety of road traffic.

Measurement of Scattered Light on Windshields in Cars

Light incident on a windshield is partially deviated from its original direction by scattering from damaged

areas of its surface (as well as films of dirt and grease). This light is called "stray light," while the portion of light transmitted without disturbance is called "useful light" (Figure 3). To characterize the scattering power, it is reasonable to take the ratio of stray light to useful light.

The human eye cannot relate the scattered light to the object from which the light originally came. The inhomogeneities of the surface appear as light sources of their own, the luminance of which is a measure for the intensity of the stray light. Divided by the intensity of the useful light, this gives us the so-called reduced luminance coefficient. Its unit is the candela per square meter and lux ($cd*m^{-2}*1x^{-1}$).

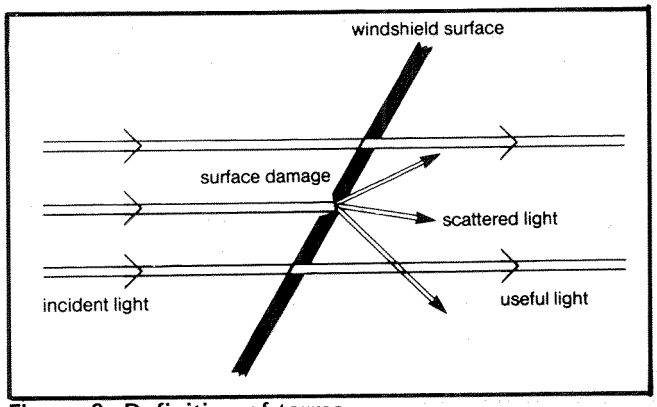

Figure 3. Definition of terms

The intensity of the stray light will depend, of course, on the scattering angle ϑ(Figure 4). Hence, values of the reduced luminance coefficient cannot be compared unless measured at the same angle. However, measurements show that the typical surface damage leads to intensities that decrease monotonously with increasing scattering angles. It seems, therefore, sufficient to restrict the measurement of stray light to a limited range of angles. The instrument is designed to utilize the angular interval from 1.5.° to 2.0° as proposed in DIN standard 4646 for the measurement of the reduced luminance coefficient.

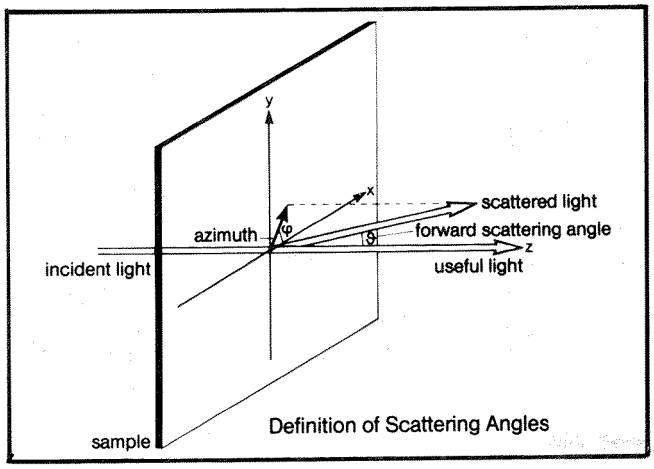

Figure 4. Definition of scattering angles

This angular interval is important for the glare while driving at night. The headlight next to the center of the road of an oncoming car 60m away and 1m lateral distance will appear at an angle of about 1.75° relative to the forward direction.

Another reason for the selection of the angular interval is that the intensity of the scattered light normally drops off rather drastically with increasing angles. The selected interval offers the advantage of higher intensities and, consequently, faster operation and higher precision. The restriction to a specified interval is necessary and sufficient to characterize the scattering power. We present our measurements taken at the interval of 1.5° to 2.0° as index values, namely as scattered light index (S.L.I.) rather than as candelas per square meter and lux.

It is desirable that the instrument discriminates between the types of windshield damage. In particular, wiper damage causes scattered light to appear as streaks that occur only in certain azimuths. Thus, a resolution of the azimuthal angle φ is required. The actual instrument based on these design considerations is shown in Figure 5 (schematic diagram) and Figure 6 (field use). A parallel light beam of 3.5cm diameter is incident on the windshield.

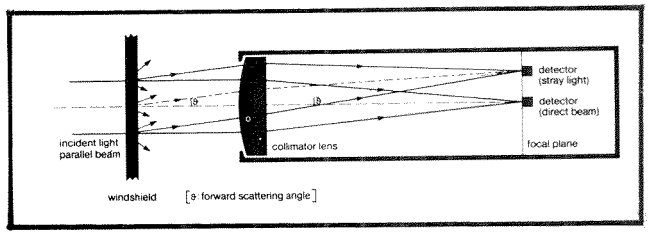

Figure 5. Schematic of the stray light measuring device

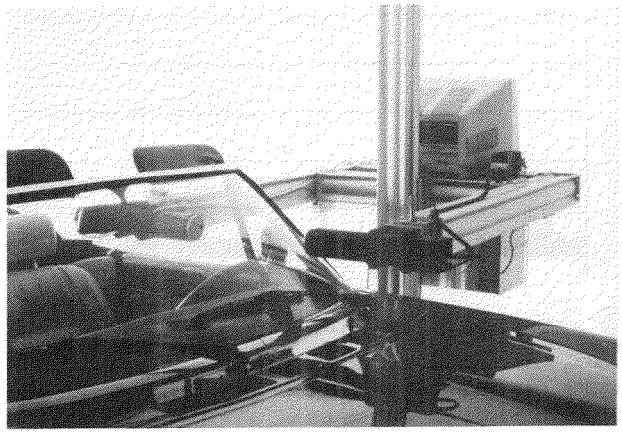

Figure 6. Instrument to measure stray-light indices on installed windshields

A collimator lens focuses the unscattered light onto a point where it is measured by a detector. The light scattered into the angle of 1.5° to 2.0° is imaged as a ring onto the focal plane. A second detector measures the scattered intensity in 250 discrete intervals, which is

equivalent to an azimuthal resolution of approximately 1.5°. The present version of the instrument takes approximately 7s for a complete measurement and automatically corrects for possible scattering within the instrument itself that may be caused by dust particles on the lenses. The S.L.I. is plotted as a function of azimuthal angle φ. Figures 7a-c show S. L. diagrams of three different samples. It can be seen that the same S.L.I., may be due to totally different azimuthal distributions.

Figure 7a shows the S.L. diagram of a glass plate damaged by dropping sand on it. The measurement was performed with the incident light perpendicular to the plate.

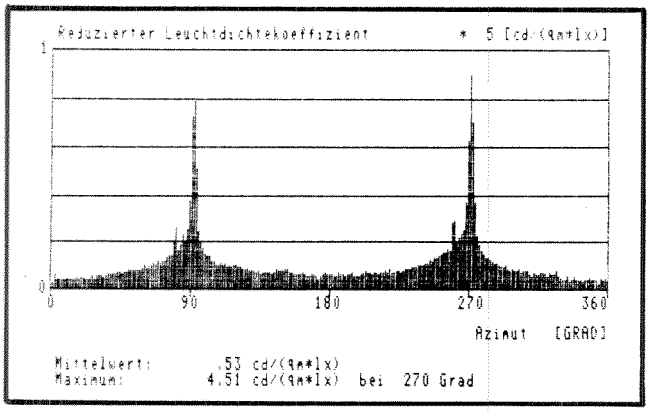

Figure 7a. Stray light diagram of a glass plate damaged by sandblast test

Figure 7b shows the S.L. diagram of a windshield after extended road use. Most of the scattered intensity is due to fine craters in the glass surface.

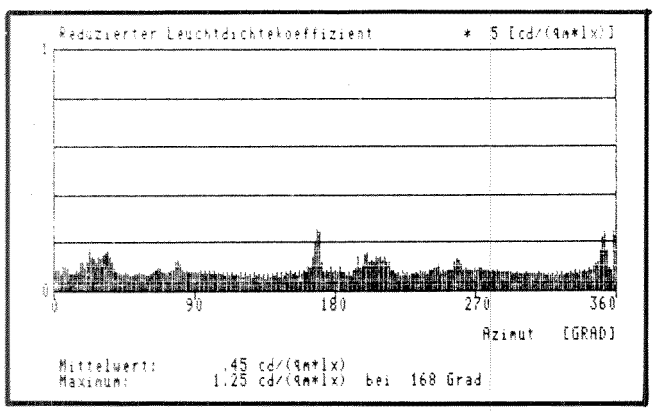

Figure 7b. Stray light diagram of a windshield after extended road use

Figure 7c shows the S.L. diagram of a windshield with damage due to wiper action. The light scattered by the resulting grooves is restricted to a narrow azimuthal range and appears as a narrow peak in the diagram.

The instrument permits the measurement of the S.L.I. while the windshield is part of the car and evaluates the scattering in the same direction in which the driver views the road.

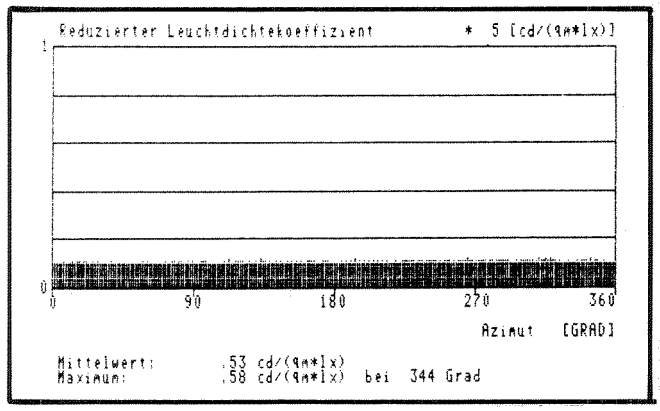

Figure 7c. Stray light diagram of a windshield with wiper damage

The geometry of the arrangement and the principle of measurement make the process of measurement insensitive to a parallel shift of the beam caused by the inclination of the windshield, which eliminates the necessity of adjusting the instrument for the measurement of windshields of varying angles of inclination. Light sources and detector systems are permanently adjusted. An electromechanical lift fits the system to the various levels of windshield position in different cars. Handling of the instrument is easy enough to be used by nontechnical personnel.

Results of Field Tests

A first set of data was obtained from 250 cars at the motor vehicle inspection station in Cologne. In the beginning, measurements were taken at various points in the main field of vision. It was found, however, that the area halfway above the steering wheel was representative of other areas, too, and measurements were subsequently restricted to this primary area. (The test was made on a voluntary basis; drivers should not be overly delayed.) The measured mean S.L.I. values as a function of mileage are presented in Figure 8, the peak values in Figure 9. For both parameters, one observes an increase with mileage as might be expected. There also is a wide variation of values, which will be discussed below.

If one tries to find a mathematical relationship between wear and mileage, one notes that the relationship is not linear in either the mean or the peak values. The peak values in particular (which are caused by scratches from the wiper blades) increase more than linearly with mileage. As peak values on averaging also enter into the mean values, this subsequently causes a nonlinear relationship of the mean values with mileage. The observed relationships can best be explained by making the following assumptions:

1. Damage to the surface of the glass by impact of stones, as an average over all vehicles, increases linearly with mileage.

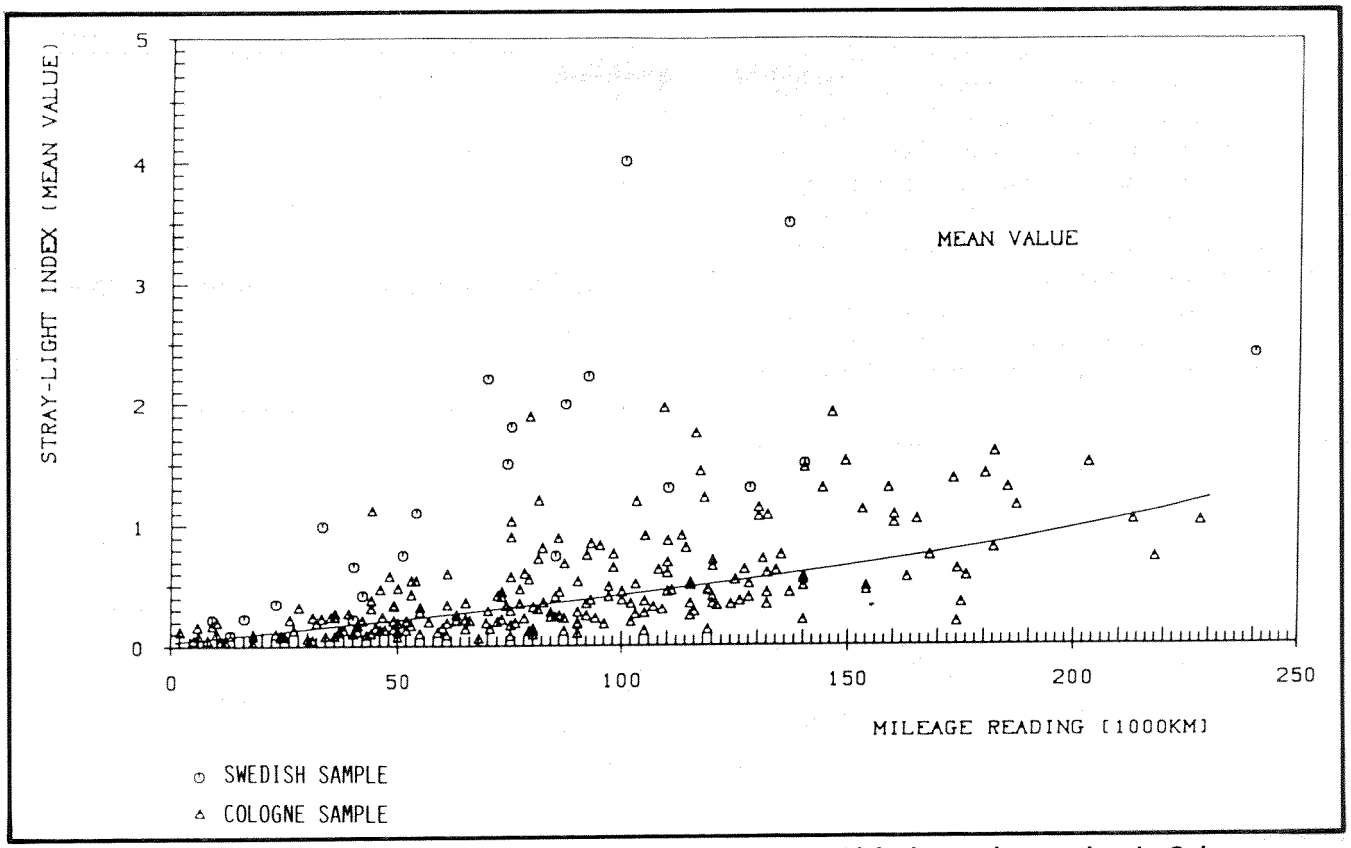

Figure 8. Distribution of mean S.L.I. values as measured at the motor vehicle inspection station in Cologne

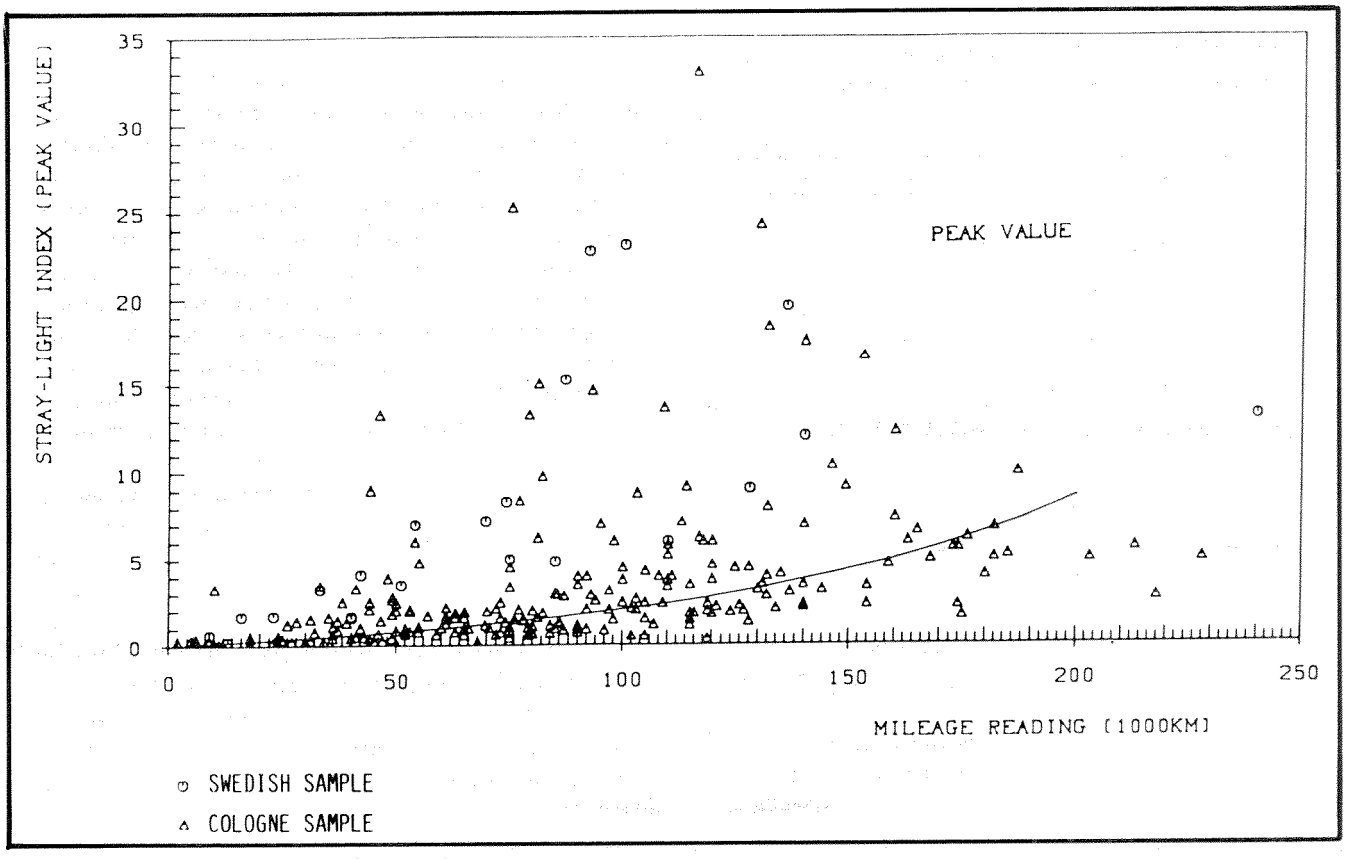

Figure 9. Distribution of peak S.L.I. values

2. An increase in wiper damage depends on the amount of previous damage already suffered at that point. The relationship between peak value and mileage would consequently be exponential.

The respective mathematical relationships in Figures 8 and 9 are represented by solid curves. Each point on the curve is chosen so that, for this particular mileage interval, half of the experimental points (Cologne sample) are above and half below.

In addition to the 250 cars from the Cologne area, a number of windshields were tested that came from other areas. Especially interesting are 25 samples from Sweden, which, at the same mileage, show three to five times higher values compared to the samples from Cologne. (The values of the Swedish samples are marked as open circles.) Such regional differences might be expected due to different road and weather conditions. To obtain a complete picture of how windshield wear affects safety, measurements will have to be made for different geographical regions.

In addition to regional influences, there is an effect on peak S.L.I. values by the amount of car care by the owner of the vehicle. It was also found that windshields of cars parked in the streets often had higher S.L.I. values than garaged cars. It is suspected that particles that collect on the windshields, and especially on the edges of the wiper blades, act as an abrasive. Dust and dirt will preferably collect in the corner between glass and wiper blade and will adhere to the glass and blade when wet. When it begins to rain and wipers are activated, abrasive material will be moved over the glass until the layers of dirt are dissolved or rinsed off. Possible remedies are covering the wiper while in the off-position and installing a ridge on the glass immediately above the off-position so that at least part of the dust and dirt particles are removed from the wiper blade.

Correlation of Measured S.L.I. Values With Loss of Perception

It is important to correlate measured values of the S.L.I. with the actual loss of perception by the individual, which will be most prominent while driving at night.

Craters caused by the impact of sand and dust particles will produce a halo around a source of light. This causes the intensity of the haze near the light source to increase, reduces contrast, and may change the state of adaptation of the eye.

Scattered light due to windshield wiper grooves appears as a "tail," which keeps changing in direction as light source, vehicle, and eye move relative to each other. This adds an additional dynamic component to the process of perception. While the psychophysiological effect of this component is not well-understood, it is nonetheless the one that causes the majority of complaints by drivers.

Light scattered by individual deep scratches and craters of 0.5 to 1.5m contribute little to the S.L.I. and reduction in contrast. However, as the relative position of the light source moves, these defects will light up suddenly and for a short time. It is this dynamic property that is most irritating to the driver and can reduce his power of concentration and his alertness.

We have made a number of tests to determine which minimum S.L.I. value will cause a noticeable reduction in the power of perception in the laboratory. Our best results were obtained by measuring the times of readaptation after dazzling and the distances at which objects are recognized using a road simulator.

Measurement of Readaptation Times Using a Mesoptometer

A standard instrument to measure the mesopic power of vision (Mesoptometer II) was used to measure the readaptation times after dazzling. It turns out these are quite sensitive to the amount of scattered light. The experimental setup is such that the test person is dazzled for 10s by a light source positioned 2° away from a given point of fixation. The object is a Landolt ring. The task is to recognize the position of the opening in the Landolt ring in the shortest possible time after the dazzling light source is switched off.

Readaptation times measured with new windshields were compared to those with used windshields of a mean average S.L.I. of 1.1. All of the 13 test persons of all age groups showed an increase in readaptation times of 6.9 to 7.9 percent. Table 1 gives the average readaptation times t_1 (new shield) and t_2 (worn shield).

It is interesting to note that among the total of 13, there are 9 cases in which the data for the worn windshield have a larger standard deviation than those with a new shield. The increase in deviation of the measured readaptation times indicates that the test person makes a stronger effort to concentrate but cannot maintain a constant level of perception. Statements of the individuals after the test confirm this impression. This means that worn windshields are a source of danger not only through an increased readaptation time, but that additional dangers may arise from an accelerated reduction in concentration.

Measurement of Detection Distances Using Simulated Road Conditions

Another series of tests to determine the influences of worn windshields in 20 subjects was made with a glare source permanently switched on. The intensity of the light was equivalent to the low beam of an approaching car. The road was simulated by a conveyer belt that

Table 1.

Testperson		Readaptation Time		Difference	Difference (%)	Signifi-cance
Sex / Age		t_1	t_2	$t_2 - t_1$	$(t_2 - t_1)/t_1$	
m	17	1.59 +/- 0.09	2.58 +/- 0.19	1.26	79%	h.s.
f	26	2.62 +/- 0.09	3.25 +/- 0.16	0.63	24%	h.s.
m	26	2.04 +/- 0.08	2.28 +/- 0.11	0.24	12%	n.s.
m	26	2.07 +/- 0.10	2.53 +/- 0.08	0.46	22%	s.
f	27	1.43 +/- 0.05	1.62 +/- 0.05	0.19	13%	s.
m	32	1.56 +/- 0.05	1.68 +/- 0.05	0.12	18%	n.s.
m	40	3.58 +/- 0.14	4.54 +/- 0.25	0.96	27%	h.s.
f	43	3.12 +/- 0.16	3.54 +/- 0.17	0.42	13%	n.s.
m	45	2.24 +/- 0.08	3.02 +/- 0.14	0.79	35%	h.s.
m	60	4.59 +/- 0.15	4.91 +/- 0.18	0.32	6.9%	n.s.
m	63	3.06 +/- 0.13	4.57 +/- 0.31	1.51	49%	h.s.
f	64	7.96 +/- 0.41	10.15 +/- 0.65	2.18	27%	s.
m	71	6.89 +/- 0.36	9.31 +/- 0.48	2.42	35%	h.s.

carried objects (cubes 20mm to the side and of low reflecting coefficient) toward the test person. At a scale 1:20, this corresponds to road conditions at night with no street lighting. The test person was told to indicate as soon as he/she believed themselves able to recognize the object. Our results show that a worn shield of S.L.I. value of 1.7 reduces the distance by 7 percent compared to a new shield.

Subjective Criteria

While measurements of S.L.I.'s of windshields were carried out, we also asked drivers as to which degree of wear they considered windshields unsafe for further use. The S.L.I.'s of such shields were between 0.5 and 1.1.

Measurement of a windshield that had been replaced by the owner because it scattered too much light (and not because of fracture) gave a mean index of 0.7 and a peak index of 6.0. These values seem to be an especially reliable indicator, as the exchange represents an expense to the owner and was certainly considered necessary. The observed correlations of measured S.L.I. values with loss of perception are summarized in Table 2.

Table 2. Threshold values for noticeable changes

Parameter	Change worn vs. new	S.L. mean	Index peak
Readaption times	6,9% - 79% prolonged	1,1	(2,8)
Detection Distances	7% shortend	1,7	(5,5)
Subjective judgement	windshield objectionable	>0,6	>4,0

Discussion

The instrument for the measurement of scattered light on windshields in cars that is presented here permits the measurement of scattered light intensities as a function of the azimuth in a fast and reliable manner. This offers the capability to inspect a large number of windshields for damage that can have a detrimental effect on road vision. Difficulties arise in the identification of large individual scratches and craters that may contribute little to the measurements but nonetheless may be irritating to the driver. On the other hand, this type of damage can be detected readily without instrument by mere visual inspection.

Loss of perception based on laboratory tests begins at an S.L.I. of 1.0. Drivers we interviewed considered windshields objectionable at a somewhat lower value of 0.5 to 1.0. It is typical for laboratory tests to result in a higher value for the threshold due to a strong interaction between concentration and physiological ability. This phenomenon is usually taken into account by so-called "field-factors" when experts give their opinions on the possible cause of accidents. Our laboratory tests measure only the correlation between loss of perception and the mean S.L.I.. The threshold peak S.L.I. value (dominated by wiper damage) at which drivers find windshields objectionable is around 5.0.

The correlation of the peak S.L.I. value and loss of perception by laboratory test is somewhat difficult. In contrast to the homogenous distribution of scattered light from craters, the light scattered from wiper damage appears only at certain azimuths, and drivers can easily see past these bright streaks of light.

The actual danger that originates in these streaks lies in the fact that they are moving as the traffic changes. This also makes it difficult to measure their effect in the laboratory. There is a lack of test parameters that can be used to estimate how such dynamic changes affect road safety. The subjective judgment by drivers indicates that the S.L.I. peak values may turn out to be the important parameter for the determination of whether or not a windshield is safe for road use.

The Development of Drowsiness Warning Devices

Keiichiro Yabuta,
Haruhiko Iizuka,
Takayuki Yanagishima,
Yukio Kataoka, and
Tetsuo Seno
Nissan Motor Co., Ltd.

Abstract

This paper describes a newly developed microcomputer-based drowsiness warning system, which detects changes in the driver's alertness through his steering behavior. In developing this system, we first quantified several levels of alertness based on such physiological factors as brain activity and blinking. Tests were then conducted in which drivers fell into different degrees of drowsiness.

Using the quantified alertness levels, we defined the "drowsy driver" and found unique steering patterns that could not be seen in normal driving. These patterns were entered into the memory unit of the microcomputer. When the sensor built into the steering wheel detects a drowsy steering pattern, the microcomputer recognizes the driver's drowsiness and activates a buzzer to warn the driver.

In this paper, the process of determining the alertness levels is explained, along with the steering characteristics of the drowsy driver.

Introduction

The continued construction of freeways in Japan in recent years and the improvement and expansion of road facilities have made it possible for drivers to enjoy pleasant, comfortable motoring. On the other hand, motorists now are more likely to drive under rather monotonous conditions, and there has been an increasing number of traffic accidents that are thought to have been caused by the driver falling asleep at the wheel.

Dozing off at the wheel is a potential danger that could befall anyone when driving under monotonous circumstances. Accidents that occur due to drowsiness, however, often tend to be of a very serious nature.

As a preventive measure against such accidents, various types of drowsiness warning devices have already been proposed by researchers at universities and other research institutions. For the most part, these devices have not been very practical because the detection system has required the attachment of an electrode to the driver's body to detect physiological reactions.

In this research, a practical drowsiness warning device has been developed by focusing on the irregularities that appear in the driver's operation of a vehicle accompanying a drop in alertness.

Prior to analyzing the driving behavior that occurs in a low alertness level, an alertness index was devised for quantifying different alertness levels. This paper will first explain the alertness index, and then the driving characteristics observed under lower alertness levels will be presented, together with a concise outline of the new drowsiness warning device.

Alertness Index

To find the characteristic driving behavior that occurs in a low alertness level, it is necessary to have some method of ascertaining when a driver's alertness level drops. However, research conducted in the field of human engineering has not yet established a method by which levels of human alertness can be grasped quantitatively.

In this study, therefore, it was first necessary to quantify levels of human alertness, and for this purpose an alertness index was formulated.

Formulation of an Alertness Index

Experimental

An experiment was conducted in which the subject's alertness level was lowered through the performance of a monotonous task. The correspondence between the results achieved by the subject during this process and different physiological reactions, including his brain waves and eyeblinking, was examined.

The experimental setup used is illustrated in Figure 1. By means of the steering wheel and the accelerator pedal, the subject controls a pursuit point with which he pursues a circular target that is moving in a circle at a uniform velocity.

Three time cycles, 50s, 20s, and 10s, were used for the circular movement of one revolution of the target circle. Measurements were taken of the subject's brain waves, blinking, facial expression, and degree of error (i.e., distance between the target circle and the pursuit point).

Formulating the Alertness Index

Special attention was focused on the subject's brain waves, blinking, and facial expression because, among the various physiological reactions of a human being, these in particular are known to vary according to the alertness level. An evaluation system was set up cor-

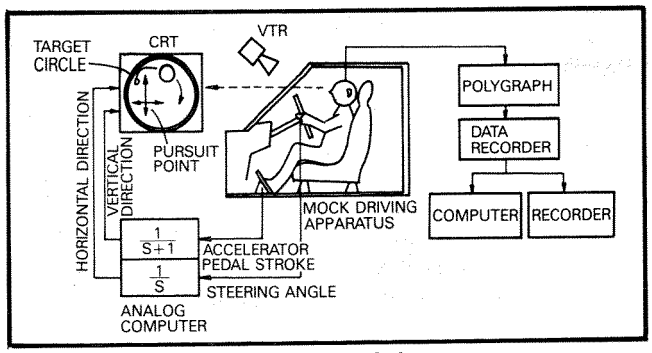

Figure 1. Schematic diagram of the test setup

responding to such variations, and a value from three points to one point was assigned accordingly, ranging from a "wide-awake state" to a "state of fuzzy consciousness just prior to falling asleep." Then, by taking the sum total of the points assigned to these three factors, seven alertness levels were ranked, ranging from "wide-awake" (nine points) to "fuzzy consciousness" (three points). Levels of human alertness were thus quantified by means of this scale (Figures 2 and 3).

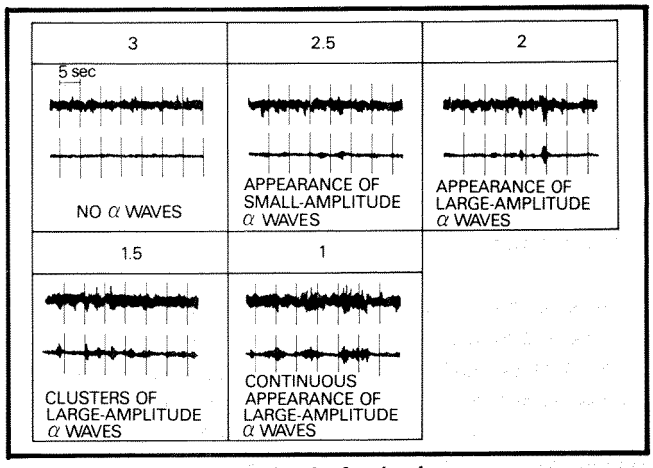

Figure 2. Evaluation criteria for brain waves

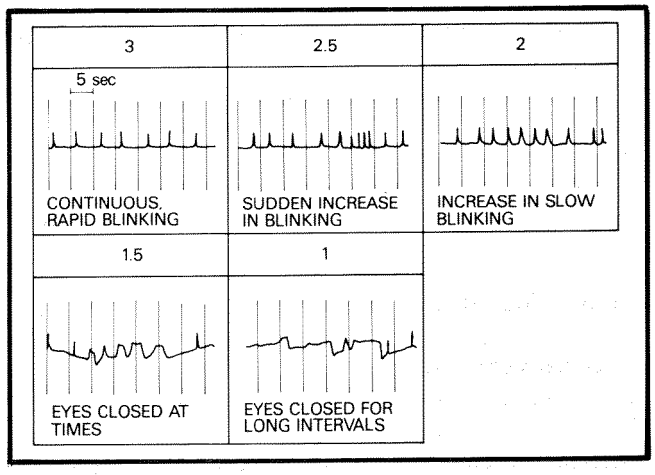

Figure 3. Evaluation criteria for blinking

Correspondence Between Alertness Levels and Control Task Results

The correspondence between the alertness level and the task results (i.e., error) is shown in Figure 4 for varying speeds of the target circle (i.e., different degrees of difficulty). The amount of error represented by the horizontal axis is an index of the off-target distance between the target circle and the pursuit point.

For an easy task (a cycle of 20s or 50s for the movement of the target circle), there is virtually no error when the alertness level is high. However, error quickly becomes conspicuous when the alertness index drops to around 6.5 ~ 6.

For a difficult task (a cycle of 10s), there is some error even if the alertness level is high. With an alertness level of 6 or lower, control becomes completely impossible.

In other words, as the alertness level drops, error increases and a person's control capability deteriorates. This confirms the appropriateness of the alertness index.

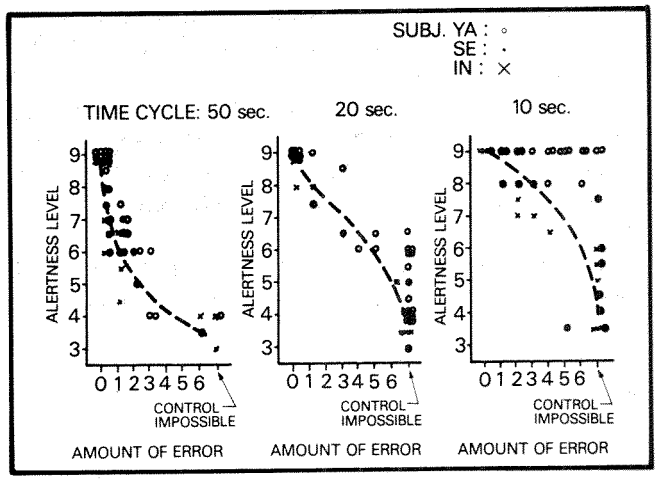

Figure 4. Correspondence between alertness level and error

Alertness Level Requiring a Warning

Using the alertness index described above, alertness levels were investigated for proving ground driving as well as for driving on ordinary roads. It was observed that the driver's alertness index fell from an initial level of 9 at the beginning of the test to between 6 ~ 7.5 after 30min of driving, regardless of whether the driver was conscious of this drop or not (Figure 5).

The relation between the alertness level and the percentage of times the driver realized he was sleepy is shown in Figure 6. The point at which a subject realized he was drowsy varied considerably depending on individual differences. However, with an alertness index of 6, the ratio was about 75 percent. With an alertness index of between 5.5 ~ 5.0, the subject was aware of being drowsy in nearly every case.

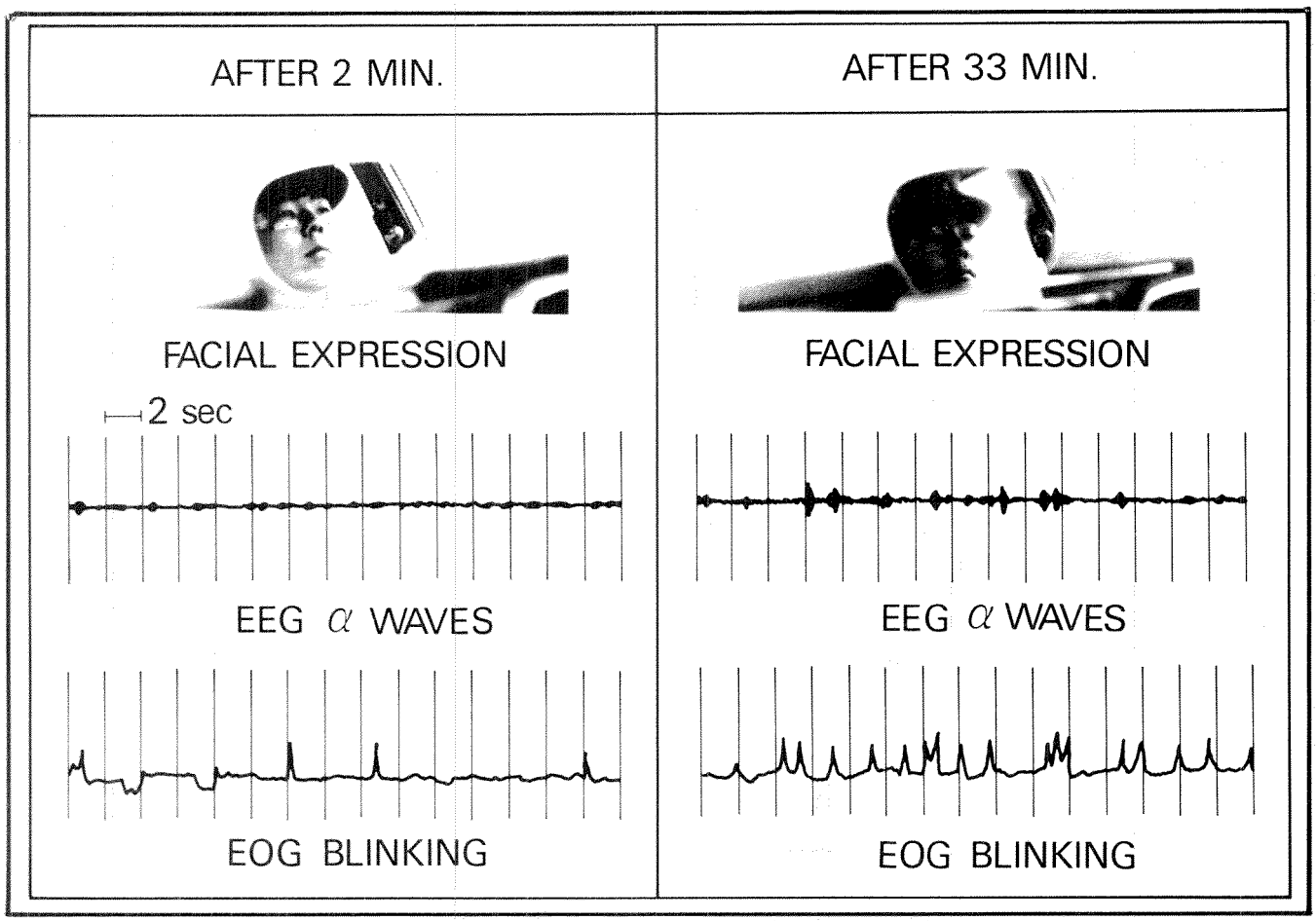

Figure 5. Example of reduced alertness level during driving

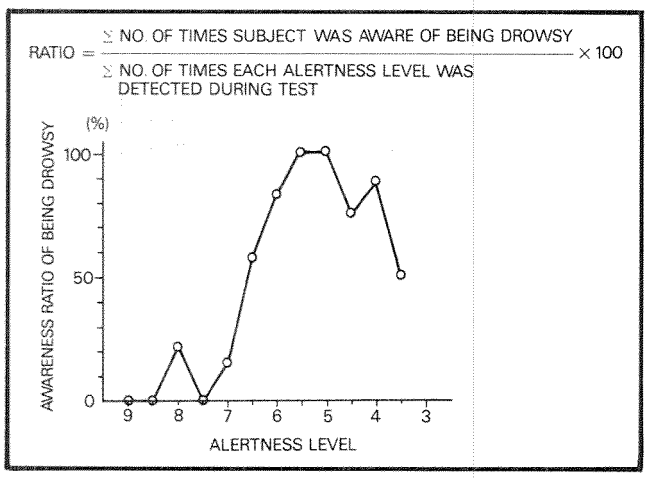

Figure 6. Relation between alertness level and awareness of drowsiness

Driving tests, which will be explained later, were also conducted under a condition of reduced alertness level using both a drive simulator and an actual vehicle. From the results of those tests and the foregoing findings, it was postulated that the alertness level that should be detected as drowsiness at the wheel, and that would not give the driver a feeling of disorientation if a warning were given, was an alertness level of 5 or lower.

The results in Figure 6 also show that for an alertness index below 4.5, the realization of drowsiness does not correlate with the alertness level and is completely unreliable.

Reduced Alertness Level Driving Test Using a Drive Simulator

This test was conducted to investigate whether or not changes would appear in the driver's operation of a vehicle accompanying a drop in alertness level (See Figures 7 and 8).

Test Procedure

The drive simulator was equipped with a color monitor that displayed the road surface, and the subject simulated a driving situation by operating the steering wheel, accelerator pedal, and brake pedal. A state of reduced alertness level was induced and recordings were made of

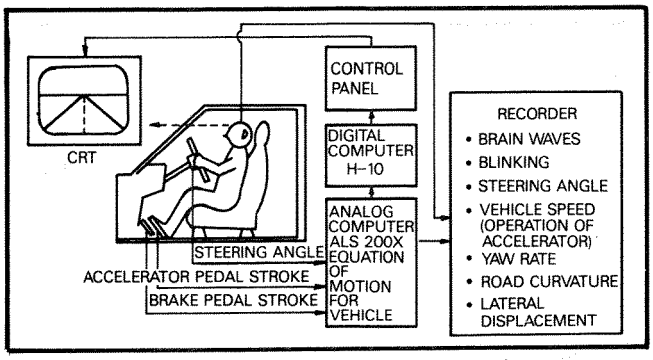

Figure 7. Schematic diagram of drive simulator

Figure 8. Photograph of drive simulator test

the subject's physiological reactions, driving actions, and vehicle behavior. The items recorded included brain waves (EEG), blinking, facial expression, steering angle, accelerator pedal stroke, vehicle speed, and side displacement.

Characteristics of Vehicle Operation Under Reduced Alertness Level

Typical examples of the test data for a wide-awake state and a reduced alertness state are shown in Figure 9.

When the subject was fully alert, he was constantly manipulating the steering wheel and the vehicle ran straight along the center line. However, when the driver's alertness level dropped, he became unable to execute minute movements of the steering wheel. The steering wheel was held stationary temporarily and then turned sharply to the right or left, producing corresponding changes in the forward direction of the vehicle. On the other hand, no substantial change was seen in the operation of the accelerator pedal.

An investigation was also made of the gripping force on the steering wheel and the driver's posture. No significant changes were observed as the driver's alertness level dropped to a state of nearly falling asleep.

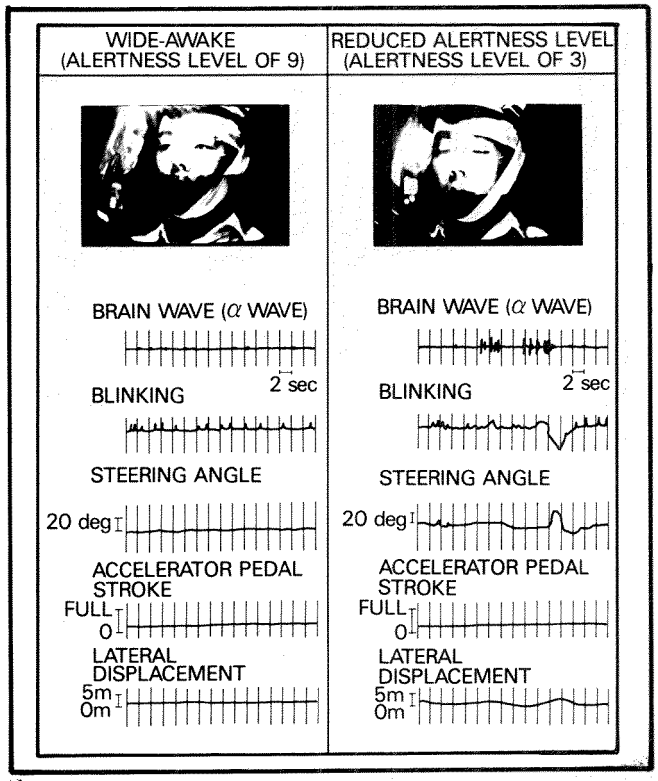

Figure 9. Examples of simulator test data

From the foregoing results, it was concluded that it would be possible to devise a method for detecting drowsiness on the basis of the driver's manipulation of the steering wheel.

Driving Test Using an Actual Vehicle

A specially outfitted test vehicle (Figure 10) was used to investigate whether the same characteristics pattern of steering wheel operation that was seen with the drive simulator would appear in a driving test using an actual vehicle. To assure safe vehicle operation during the test, a steering wheel and brake pedal were installed in the test vehicle on the passenger side. The brake pedal on the passenger side was rigged such that the fuel supply was cut off when it was depressed.

Test Procedure

The subject's alertness level was lowered through constant-speed driving on a proving ground, and a data recorder was employed to record the subject's brain waves and blinking, along with the steering angle. An examination was made of changes in the subject's manipulation of the steering wheel accompanying a drop in alertness level.

With the test vehicle as well, it was found that in a state of reduced alertness level the subject temporarily held the steering wheel stationary and then cut it sharply to the

Figure 10. Test vehicle with dual steering wheels

right or left, thus confirming the same steering pattern that was observed in the simulation test (Figure 11).

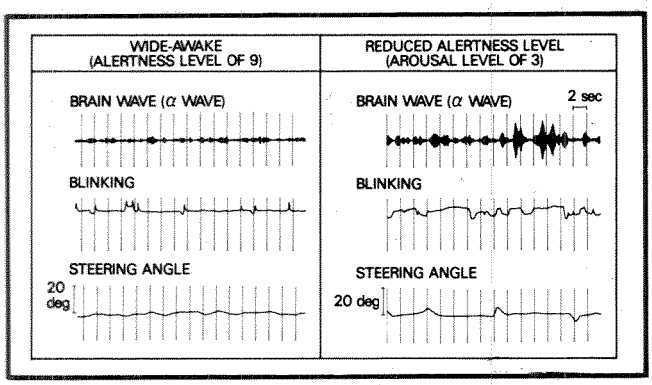

Figure 11. Examples of test driving data under reduced alertness level

Analysis of Steering Wheel Manipulation Data

Since the aforementioned tests revealed that particular characteristics occurred in the manipulating of the steering wheel in a state of reduced alertness level, an exhaustive analysis of the data was done to upgrade the performance of the drowsiness detection logic.

Analysis of Nonsteering Period

An investigation was done to determine if changes occurred in the nonsteering period when the alertness level dropped. Figure 12 shows the distribution of the nonsteering time for a wide-awake state and a reduced alertness state. As this figure indicates, no difference could be seen in the nonsteering time between these two states. It was concluded, therefore, that drowsiness at the wheel could not be detected from the nonsteering time alone.

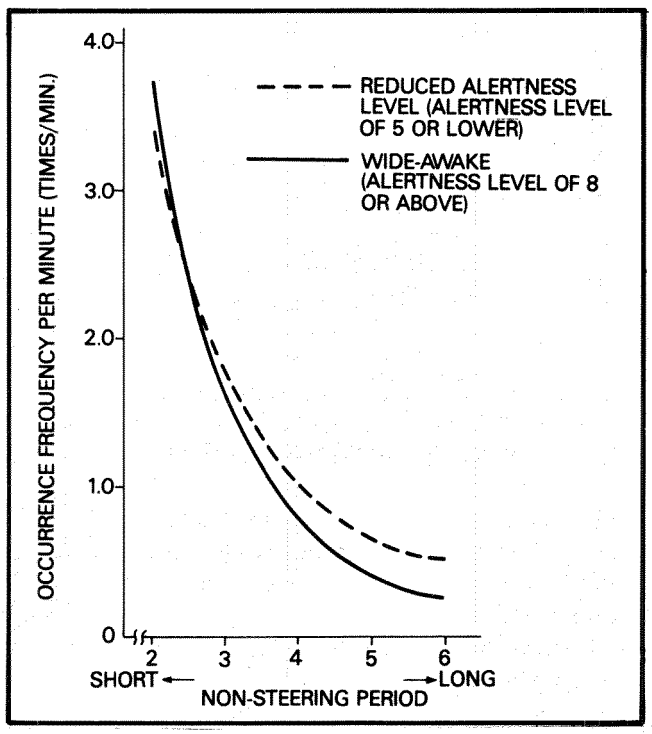

Figure 12. Difference in occurence frequencies of nonsteering period

A Steering Pattern in Which Corrective Steering Continues Following Nonsteering

The distribution of the nonsteering period in a state of reduced alertness level was found to be no different from that for a wide-awake state. However, examination of the data wave-forms revealed there tended to be a continuation of sharp, corrective steering actions following nonsteering that characterized the state of reduced alertness level, and a minute analysis of the data was done to elucidate this pattern.

A typical steering angle wave-form illustrating this characteristic is shown in Figure 13. After nonsteering, the steering wheel is turned in one direction, called the first turn hereinafter, followed by a second turn in the opposite direction.

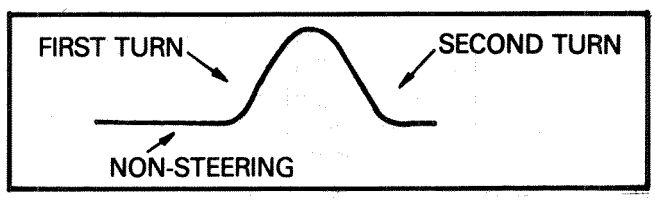

Figure 13. Steering pattern peculiar to a reduced alertness state

Figure 14 shows the occurrence frequencies of this steering pattern when the magnitude and turning speed of the first and second turns were fixed and only the nonsteering time was varied.

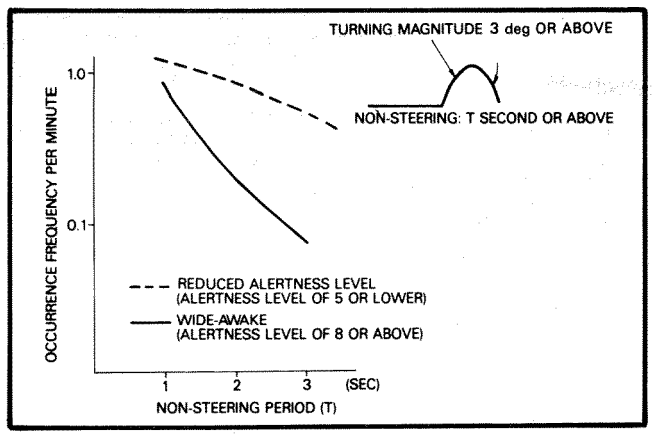

Figure 14. Occurence frequencies of steering pattern for various nonsteering periods

By making the nonsteering time longer, it became easier to distinguish between the wide-awake state and the reduced alertness state because a larger difference appeared in the occurrence frequencies. On the other hand, when the nonsteering period was set longer, the occurrence frequency dropped in the state of reduced alertness level, which indicated the possibility of a deterioration in drowsiness detection accuracy.

Figure 15 shows the occurrence frequencies of the steering pattern when the nonsteering period was fixed and the magnitude of the first and second turns was varied.

By increasing the magnitude of the turns, it became easier to distinguish between the two states, but the occurrence frequency dropped in the state of reduced alertness level. This suggested there would not be sufficient drowsiness detection accuracy.

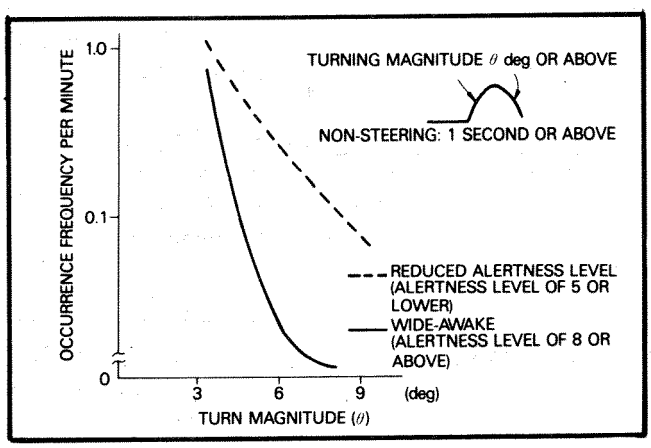

Figure 15. Occurence frequencies of steering pattern for various turn magnitudes

Figure 16 shows the occurrence frequencies when the nonsteering period and the magnitude of the first and second turns were fixed and the turning speed of the first turn was varied.

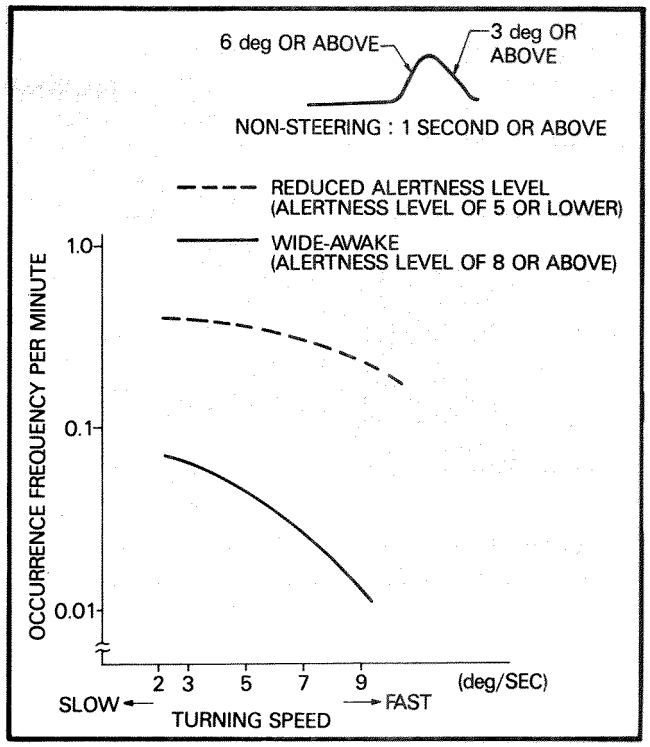

Figure 16. Occurence frequencies of steering pattern for various turning speeds

As the results explained above indicate, it was found that the steering pattern, in which corrective steering actions continue following nonsteering, would almost never appear in the wide-awake state as long as appropriate values were selected for the nonsteering time, the magnitude of the first and second turns, and the turning speed. Since the occurrence frequency in the state of reduced alertness level also became relatively small, the drowsiness detection performance was improved by incorporating multiple steering patterns into the detection logic.

Drowsiness Warning Device

A drowsiness warning device has thus been developed that detects the corrective steering pattern that appears following nonsteering and emits a warning to the driver. The practical utility of the new device has been evaluated in repeated driving tests conducted on public roads and in driving tests done under states of reduced alertness level.

In slow-speed ranges, the manipulation of the steering wheel involves many more patterns than for normal operating speeds. Therefore, to prevent mistaken operation of the warning device when the driver is wide-awake, the logic circuit has been designed so that detection is not performed at speeds below 50km/h. Furthermore, no detection is performed when the turning signals or the brakes are operated as well as during a set period of time following their operation. This precaution has been taken

to prevent the warning device from operating by mistake when a driver changes lanes or maneuvers the vehicle to avoid an obstacle on the road (Figure 17).

The drowsiness detection performance of the device was evaluated on a proving ground using a vehicle equipped with dual steering wheels.

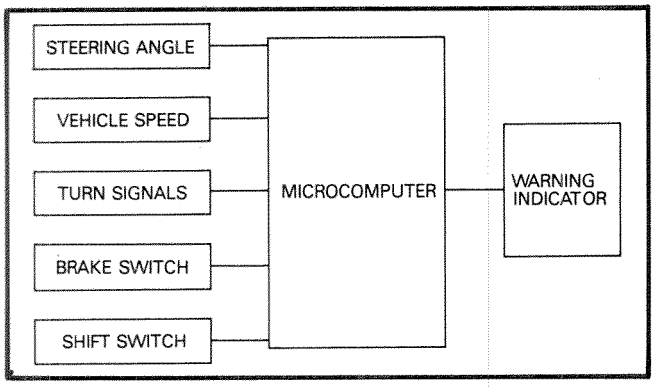

Figure 17. Block diagram of drowsiness warning device

A typical example of the test data is shown in Figure 18. At the start of the test, the driver was in a wide-awake state with an alertness index of 9. After 23min of driving, however, the alertness index had dropped to 3.5. At that point, the device detected drowsiness at the wheel and generated a warning sound that caused the driver to wake up quickly.

Conclusion

As explained in the foregoing sections, a system for quantifying human alertness levels was devised and utilized to find the vehicle operating behavior that typifies a driver in a state of reduced alertness level, particularly the characteristic steering patterns. Based on the data obtained, a practical drowsiness warning device has been developed that does not have to be attached to the driver's body.

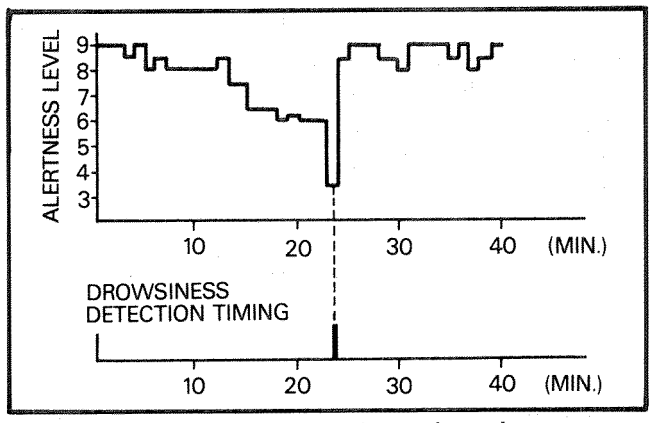

Figure 18. Examples of drowsiness detection

This indirect detection method has now made it possible to detect drowsiness at the wheel in a rather high percentage of cases, though the system is not entirely perfect. Part of the drowsiness detection logic of the new device is already being successfully incorporated into the "Safety Drive Adviser" that is available on Nissan's new Bluebird model.

To assure safety during the operation of a motor vehicle, it is essential that the driver is functioning normally and the vehicle is in proper working condition. Until recently, virtually no safety devices had been developed to check on the normal condition of the driver. It is hoped that research and development efforts in this area will see a great deal of progress in the years ahead.

Tire Pressure Warning System

Yuji Uemura,
Saiichirou Oshita,
Toshihiro Konno,
Toshiyuki Kobuna, and
Yoshihiro Yoshida
Subaru Engineering Division, Fuju Heavy Industries, Ltd.

Abstract

Low tire pressure can have adverse effects on a vehicle, such as abnormal tire wear, increased tire rolling loss, tire burst due to excessive heat generated, poor running stability due to reduced cornering power, and hydro-planing phenomenon.

The purpose of a low tire pressure warning device is to give adequate warning to a driver when tire pressure falls below the specified level, calling attention to the need for countermeasures, such as adding tire pressure or tire repairs. Thus, the equipment is to reduce the adverse effects of low tire pressure, insure safer operation, and achieve better economy.

For this, various warning devices have been developed and reported. The tire pressure warning system presented in this paper was developed to incorporate a user-friendly feature that would tell the driver which of the four wheels has low tire pressure, combined with low system price.

To achieve these targets, a combination of magnet and

Hall effect IC was selected for transmitting change in tire pressure from a rotating and vibrating tire, which also resulted in a simple control circuit.

The main components of the system are a pressure sensor using a magnet, Hall effect IC, control circuit, and alarm section, operating as follows:

- A pressure sensor is mounted on each wheel disc. When pressure falls, the magnet of the pressure sensor, as it rotates, causes a change in the magnetic field it generates.
- Each time the wheel rotates, the magnet moves across the Hall effect IC mounted on a suspension member. The IC then detects the change in the magnetic field and signals the control circuit.
- The control circuit identifies the wheel generating the signal, then operates the alarm to warn the driver.

Introduction

Maintaining proper tire pressure is essential for safe vehicle operation. Running a vehicle with low tire pressure leads to additional running cost such as abnormal tire wear, higher fuel consumption, safety hazards such as tires generating excessive heat with resultant tire burst, lower cornering power and poorer running stability, and likelihood of hydroplaning. According to a sampling survey of general road vehicles, many were found with tire pressure below that recommended of 1.8 to 2.0kgf/cm^2 (176.4 to 196kPa). As many as 12.5 percent had pressure below 1.5kgf/cm^2 (147kPa)(1).

The causes for loss of tire pressure include natural leaks over long periods, punctures, and air leaks due to rim deformation. A sudden air loss is usually sensed quickly by the driver because of a change in vehicle behavior, vibration, etc., but it may take some time to sense any difference with a gradual pressure loss. In front-wheel-drive vehicles whose rear wheel load is small, some drivers may not sense a total loss of air from a rear wheel while driving straight and are startled by the change in vehicle behavior when they attempt to steer. In such cases, warning the driver of tire pressure loss as soon as it occurs is very important for safety.

Run-flat tires that allow driving a certain distance even after pressure loss due to puncture, etc., have been developed. In Japan, their use by vehicles for the physically handicapped and police vehicles was approved in 1981(2).

Currently, such tires are still inferior to ordinary tires in terms of high-speed performance, weight, ride, cost, etc. Even the ordinary user, however, sometimes experiences difficulty or danger when attempting a wheel change to replace a punctured tire because of weather, road conditions, etc. For this reason, further improvement and commercializing run-flat tires is required. However, with this type of tire, tire pressure loss will be even more difficult for the driver to detect, and the need will be greater for an adequate tire pressure warning device.

Various tire pressure warning systems have been patented or reported(3). They can be classified roughly into the following types:

- Systems Mounted on the Wheel—Self-contained systems mounted on the wheel, with no parts installed on the vehicle body itself. There are two types, one that visually indicates tire pressure loss at the wheel center and another that warns of low tire pressure audibly with sound produced by striking the wheel rim or cap, or a spring or electrically driven bell, etc.
- Systems Indirectly Detecting Pressure Loss—Systems that detect tire pressure loss based on change in wheel rolling resistance, rate of slip, vehicle height, tire width, or tire ground contact area.
- Systems Detecting Tire Pressure Loss Mounted on the Wheel and Transmitting Signals to the Vehicle Body—Methods available to transmit signals from a rotating wheel to the vehicle body include resonance coil, electromagnetic induction, radiowave, light, and magnetism.

In developing a tire pressure warning system, we set the following targets:

- To be capable of determining, while driving, which of the four tires has abnormal tire pressure
- To have a low system price
- To make wheel changing easier
- To be maintenance-free with the alarm operating when tire pressure falls but automatically turning off once normal pressure is restored

To achieve these targets, we selected a combination of magnet and Hall effect IC from various candidate means to send signals indicating tire pressure loss from a rotating wheel to a unit mounted on the vehicle body.

General Configuration

Figure 1 shows a general configuration of the system.

A pressure sensor is mounted on the wheel disc to detect tire pressure loss. For sensing pressure, balancing between inside tire pressure acting on a silicone rubber diaphragm and reaction force of a spring in the sensor is used. When pressure falls, the spring, which is normally compressed, extends to turn and face a magnet toward the inside of the wheel. This new magnet position causes change in a magnetic field in which the Hall effect IC, mounted on the suspension member, is positioned. Once tire pressure is restored, the spring is compressed and the magnet returns to its original position. The pressure sensor has an aluminum diecast housing so its weight is

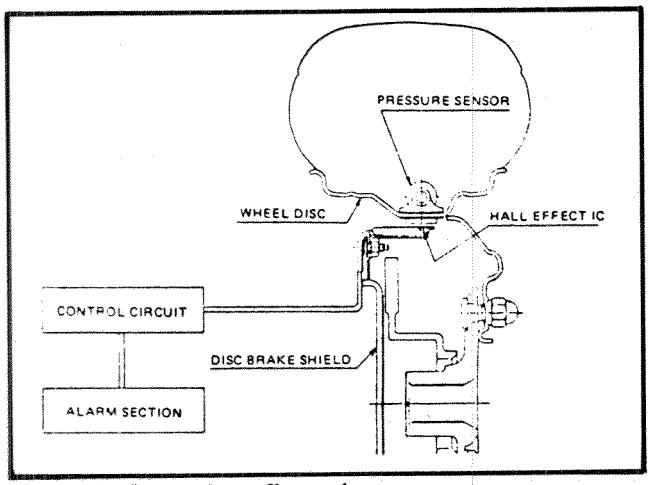

Figure 1. General configuration

within the range of ordinary adjustment for wheel balancing.

The Hall effect IC is mounted on the disc brake shield and senses a change in the magnetic field generated by the pressure sensor. This change in the magnetic field strength drives the alarm section via a control circuit and warns the driver of tire pressure loss.

The Hall effect has a temperature compensation circuit and is compact, lightweight, and resistant to vibration, making it ideal for mounting on unsprung suspension parts.

Pressure Sensor

The pressure sensor is constructed so that when a fork mounted on a slider moves according to tire pressure, it causes a magnet to turn. When the pressure is normal, the pole face of the magnet faces sideways as seen in Figure 2a.

In this position, the Hall effect IC does not sense any magnetic field, and no alarm is generated.

As tire pressure drops, the fork moves toward the right, together with the slider. As a result, the link mechanism causes a rotor carrying the magnet to turn so the magnet pole faces down (see Figure 2b).

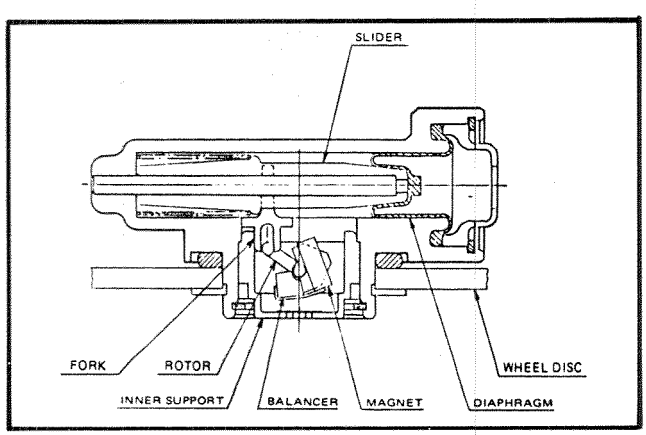

Figure 2a. During normal pressure

Then, when the IC senses the magnetic field, it sends an alarm signal. A rare earth cobalt alloy magnet is used because of less magnetic field change with temperature and because of its high magnetic force, which insures sensing even at some distance from the IC. The diaphragm used is of silicone rubber that does not harden even at temperatures as low as -40° C.

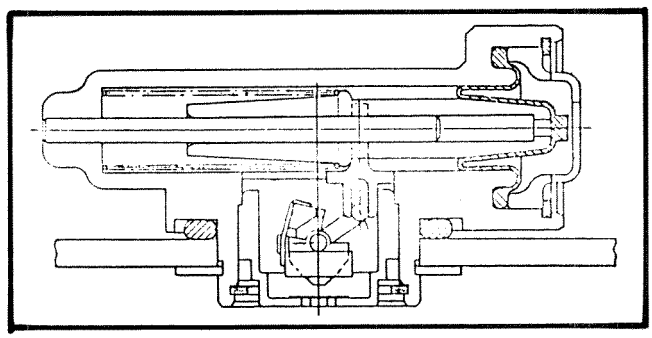

Figure 2b. During reduced pressure

With time, it is likely that a very small amount of air will pass through the diaphragm, and if the pressure sensor was made airtight, air pressure inside the sensor would equal tire inflation pressure. Then, the spring force would cause the slider to move and the magnet to turn as in Figure 2b.

Thus, it would be possible that an alarm could be generated even in the absence of tire pressure loss.

To prevent this, the pressure sensor must be open to the atmosphere but protected against entry of water and dust. These conflicting requirements have been met by a special filter mounted at the boundary between the sensor and the outside that allows air to pass but is impermeable to water.

This filter has high airflow resistance. As a result, in the event of a broken diaphragm, an alarm is generated immediately but air leakage to the outside from the sensor is obstructed by the filter, preventing any quick loss of tire pressure.

The magnet rotor is fitted with a balance weight to overcome the effects of centrifugal force during wheel rotation.

Hall Effect IC

The Hall effect device that transforms magnetic flux density to voltage making use of the Hall effect is attracting attention as a noncontract type sensor, but for improved immunity to electrical noise it is necessary to amplify the voltage signal from this device in its close proximity. It was difficult to install a Hall effect device and amplifier circuit in the form of a discrete circuit in the limited space such as a suspension part.

However, a Hall effect IC with this Hall effect device, signal amplifier circuit, etc., integrated into a single package, was recently developed to overcome this installation problem.

In this system, the Hall effect IC is used as a sensor to make noncontact detection of tire pressure change.

Figure 3 shows the transfer characteristics of the Hall effect IC used in this system. This IC, developed for automotive applications, has been designed to withstand severe operating conditions in terms of temperature range, power voltage, etc.

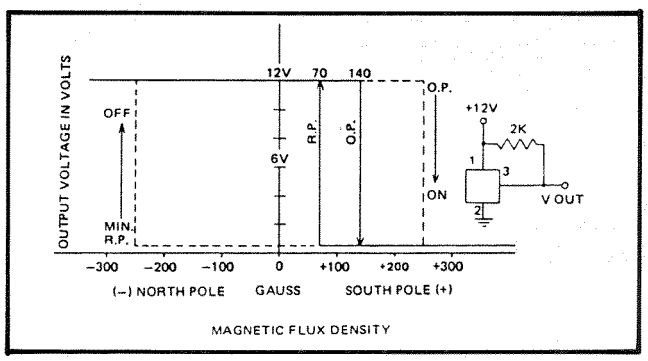

Figure 3. Transfer characteristics

Figure 4 is a functional block diagram of the Hall effect IC. This IC has a voltage regulator, temperature compensation circuit, comparator, Schmitt circuit, and output transistor. The output can be directly connected to a bipolar or CMOS logic circuit. Therefore, it was possible to simplify the control circuit that processes the output signal from this IC.

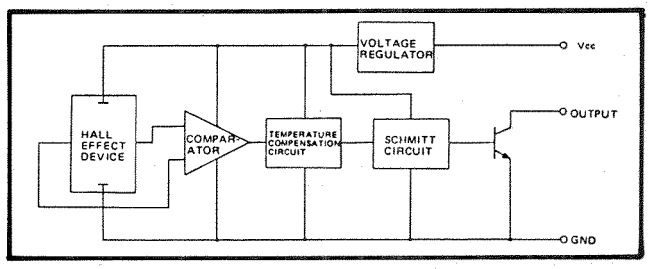

Figure 4. Functional block diagram

Figure 5 shows the Hall effect IC as mounted. The IC mounted to the disc brake shield was resin-molded for protection against vehicle body vibration, water, flying stones, etc.

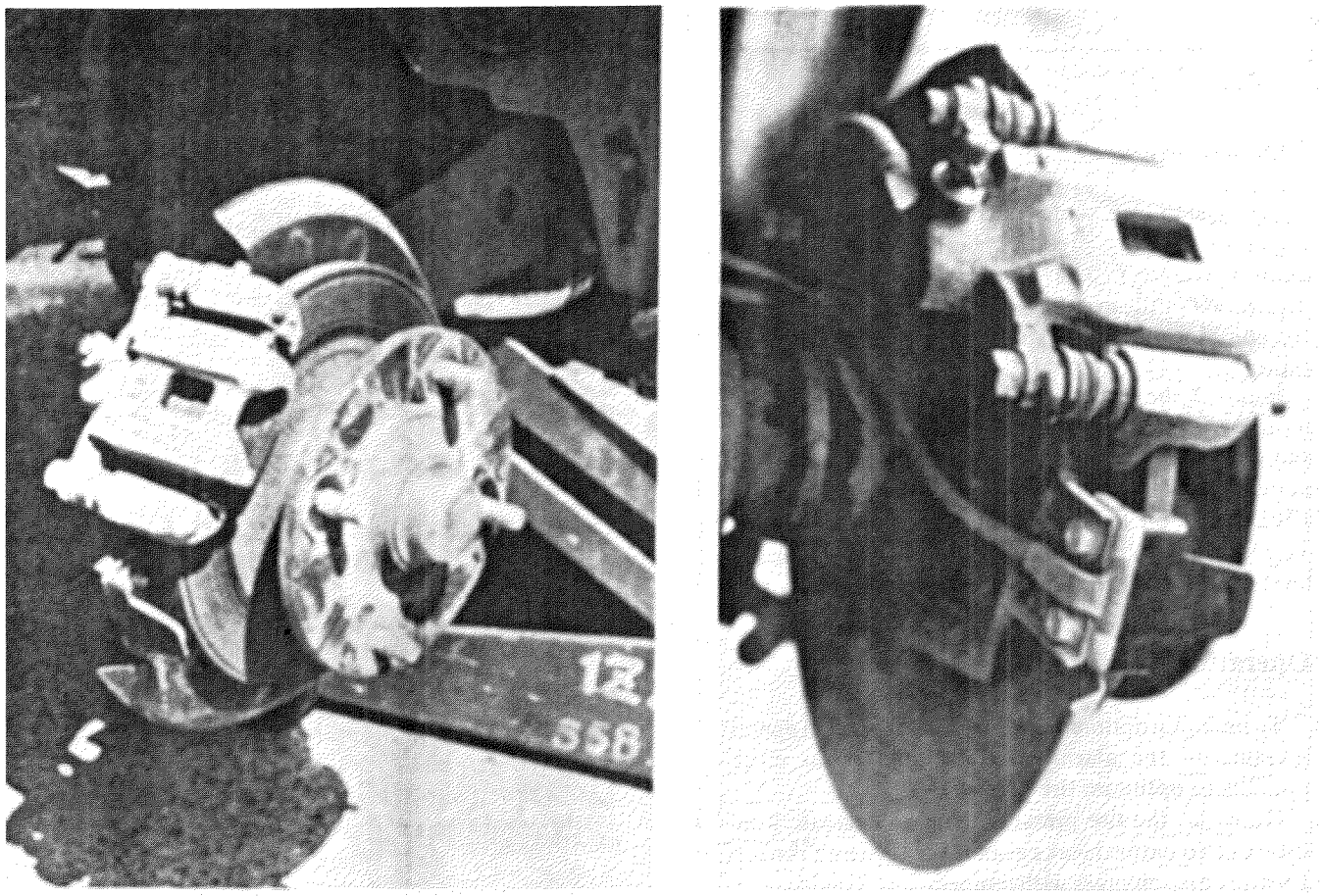

Figure 5. Hall effect IC as mounted

Control Circuit

The control circuit was formed by a hold circuit to detect change in signals coming from the Hall effect IC and a drive circuit to light an alarm lamp and sound a buzzer.

Figure 6 is a block diagram of the control circuit, which has been made as simple as possible.

The direction of the magnet in the pressure sensor fitted in the wheel disc changes as the tire pressure drops. The IC mounted to the disc brake shield detects this change of magnet direction and, as a result, the IC output voltage level also changes. The control circuit holds the IC output voltage level change and causes the alarm buzzer to flash and buzzer to sound. The alarm buzzer stops sounding after a set time, but the alarm lamp remains flashing until normal tire pressure is restored or the ignition key is turned off.

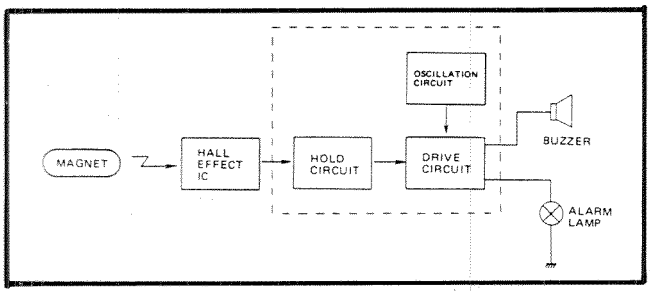

Figure 6. Control circuit block diagram

Alarm Section

This system was so designed as to positively warn the driver of low tire pressure, both visually (lamp) and audibly (buzzer). The alarm lamp, in particular, is positioned in the graphic safety monitor at the center of the combination meter so that it is readily visible at all times.

Figure 7 shows the flashing alarm lamp in the safety monitor. This alarm lamp also serves as an indicator to show 4WD mode selection. When tire pressure is at or above specified level, the lamp operates as the 4WD-FWD selection indicator (lights green when driving in 4WD mode). When tire pressure falls below specified level, the lamp of the corresponding wheel lights red.

Operating Pressure

To maintain optimum tire pressure, the actual operating pressure of the alarm system should be as close as possible to optimum tire pressure.

However, the tire pressure tends to decrease little by little due to natural leaks even if the tire itself is normal. Pressure also changes with temperature. Therefore, if the alarm operating pressure is set too closely to optimum

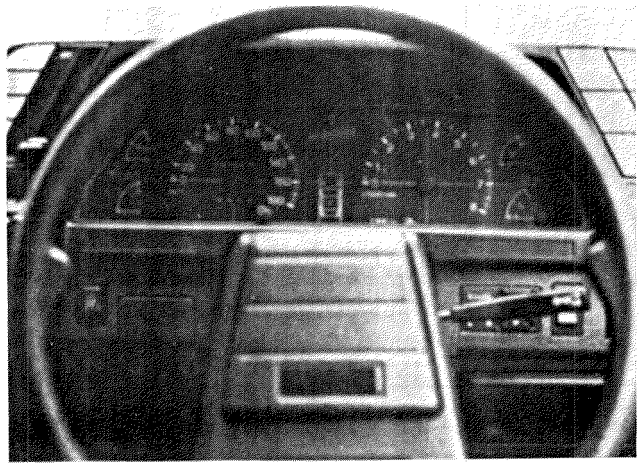

Figure 7. Safety monitor

tire pressure, alarms will be generated too frequently—to the annoyance of the driver.

The alarm operating pressure setting also depends much on vehicle and tire characteristics, and further studies and examination are required.

The operating pressure of this system can be set at any level by adjusting the reaction force of the spring in the pressure sensor.

The vehicle on which this system was installed (Figure 8) has recommended tire pressure of 2.0kgf/cm^2 (196kPa), and it can run safely under all conditions as long as the pressure is within a range from 2.3 to 1.7kgf/cm^2 (225.4 to 166.6kPa). However, when the pressure falls below 1.3kgf/cm^2 (127.4kPa), it impairs steering behavior and directional control during high-speed driving or sharp cornering.

Therefore, with these and the operating pressure setting accuracy taken into account, the operating pressure was set at 1.5kgf/cm^2 (147kPa) $\pm$ 0.1kgf/cm^2 (9.8kPa).

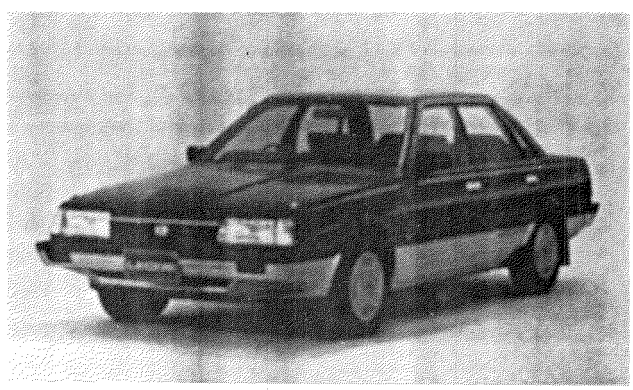

Figure 8. Test car

Results

Pressure Sensor Operating Pressure

Figure 9 shows the operating pressure of the pressure sensor. The abscissa represents the tire inflation pressure and the ordinate represents the magnetic flux density at the Hall effect IC mounted on the suspension member.

The operation point and release point of the IC used are 70 Gauss and 140 Gauss, respectively, as shown in Figure 9, and in this case the alarm turns on at 1.45kgf/cm^2 (142.1kPa) and turns off at 1.6kgf/cm^2 (156.8kPa).

This operating pressure, which is affected by the accuracy of the sensor itself, variations in Hall effect IC characteristics, and the dimensional accuracy between the pressure sensor and IC, requires full consideration in volume production of the system.

In the present system, deviation due to pressure sensor accuracy is ±0.4kgf/cm^2 (±3.9kPa), due to the Hall effect IC operating point accuracy is ±0.02kgf/cm^2 (±1.96kPa), and due to IC to pressure sensor distance accuracy (±1mm) is ±0.04kgf/cm^2 (±3.9kPa). Thus, the target value of ±0.1kgf/cm^2 (±9.8kPa) has been met.

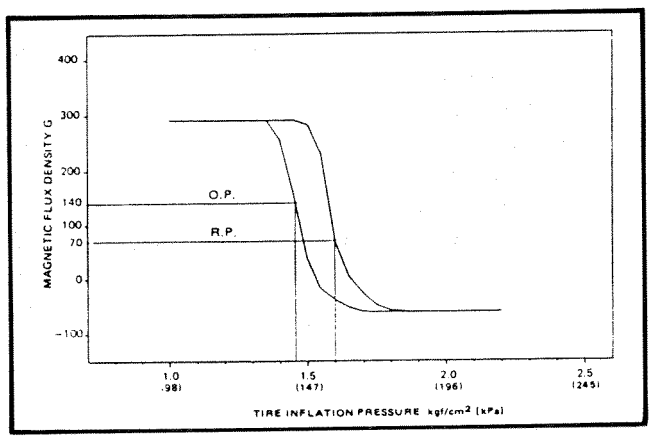

Figure 9. Pressure sensor characteristics

Change of Operating Pressure due to Speed

The pressure sensor is mounted on the wheel disc and is subjected to centrifugal force from the wheel turning. This centrifugal force not only acts directly as a force on the moving parts but also increases the frictional resistance of the sliding parts.

In this system, to minimize any operating pressure change due to centrifugal force, a balance weight is provided on the rotating parts in the pressure sensor to counter centrifugal force and resulting increase in friction force.

Figure 10 shows the change of the operating pressure due to vehicle speed.

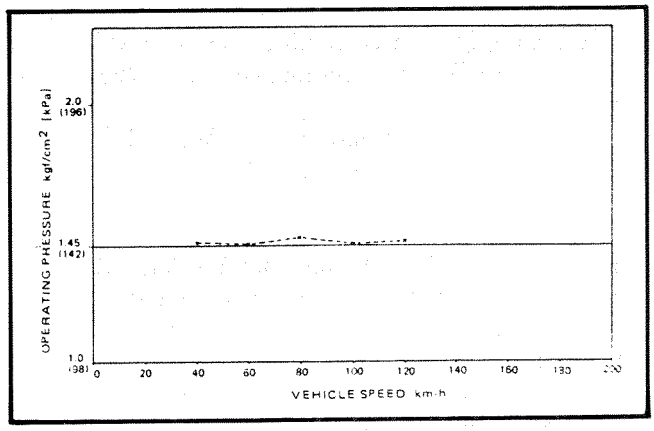

Figure 10. Operating pressure change with vehicle speed

Figure 11 shows experimental and calculated values obtained when the balance weight was changed.

By carefully selecting balance weight, it is possible to positively change alarm operating pressure with speed; that is, to raise operating pressure when speed increases so the alarm is given earlier during high-speed driving.

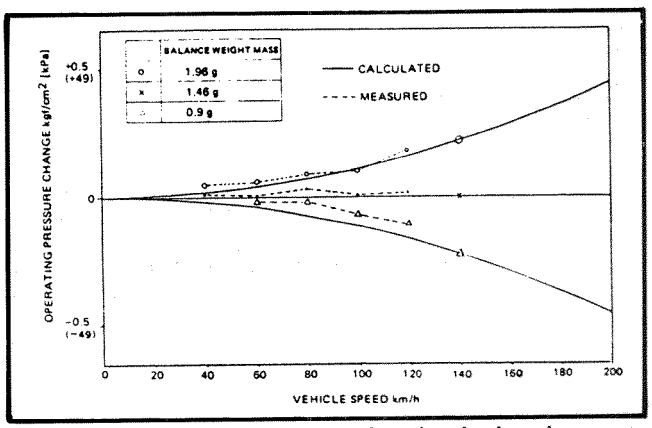

Figure 11. Change of measured and calculated operating pressure with balance weight mass change

Influence of Environment Conditions

Low Temperature

Silicone rubber of small physical change at low temperature is used for the diaphragm. No difference was observed in operating pressure between 15° C and -40° C.

High Temperature

What is most important is creep deformation of the diaphragm. A test piece of diaphragm was subjected to a

tensile load of 3kgf/cm^2 (294kPa) up to 120°C x 2,000h but permanent elongation deformation was within 20 percent.

Assuming a vehicle life of 10yr/200,000km and an ordinary and upslope running (65 percent), high-speed running (30 percent), and downslope running (5 percent), the test results and other data indicate that the temperature around the diaphragm will reach 80°C or higher for about 30h during a vehicle's lifetime. Thus, creep should not be a problem.

Water Pressure Resistance

The special filter (average pore diameter 0.6μm) separating the pressure sensor from ambient air can prevent water permeation down to a water depth of about 14m.

Test on Actual Vehicle

A vehicle (Figure 8) equipped with this system was run on in-house irregular roads for endurance testing (Belgian road, stone-paved road, and randomly waved road) over 3,000km and on snowy roads in northern Japan over 7,000km, but no change in the operating pressure was observed. No open wiring, water entry, leakage, or any other trouble were experienced.

Maintainability

The Hall effect IC's are mounted to the suspension parts as shown in Figure 5. They are protected by reinforcing members but, when removing or replacing a wheel on the vehicle, some care is necessary to avoid it striking with force at the Hall effect IC.

The pressure sensor is mounted on the rim inside, and care is necessary regarding pressure sensor location when inserting a tire lever between the wheel rim and tire bead to remove the tire.

Conclusion

The tire pressure warning system presented here adopts a simple signal processing system to make it user-friendly and at the same time achieve a low cost.

The pressure sensing accuracy of within the operating pressure ±0.1kgf/cm^2 (9.8kPa) was verified by both bench and on-vehicle tests.

References

1. Nishimura, Hiroaki, "Trend of tire pressure warning devices," *Journal of the Society of Automotive Engineer of Japan* (in Japanese), Vol.38, No.11, 1984.
2. Takahashi, Michiyoshi, and Yoshihiro Matsushita, "Current and future states of tire development," *Journal of the Society of Automotive Engineer of Japan* (in Japanese), Vol.39, No.1, 1985.
3.
   - Nishimura, Hiroaki, "The development of two simple tire warning devices," SAE Paper 840067, 1984.
   - Wazawa, Kiyoshi, and Akio Hosaka, "Development of the Nissan Alarm System of Tire Abnormal Condition (NASTAC)," *Nissan Gijutsu* (in Japanese), No.8, January 1973.
   - "Tire pressure digital display unit," *Nikkei Mechanical* (in Japanese), 1.2, p.28, 1984.
   - Kurshige, Tomoyoshi, Sumio Kobane, Hiroshi Takahashi, and Satoru Komatsu, "Low Tire Pressure Warning Device (LTPWD)," SAE Paper 820458, 1982.

Aspects of Subjective/Objective Correlation Regarding Vehicle Tyres

Dr. Lea Brindle
Cranfield Institute of Technology, Bedfordshire, England

Abstract

An introduction to vehicle steering response dynamics is followed by a discussion of the influence of pneumatic tyres on driver subjective ratings concerning vehicle steering and handling characteristics. An empirical study investigating driver sensitivity to the effects of low profile radial-ply and standard radial-ply tyres is then described.

It was found that the subjective ratings of ordinary drivers could be systematically related to objective measures of vehicle directional response. Most important in affecting favourable ratings were short lateral acceleration and yaw rate response times, and higher levels of control gain for these parameters. Low profile radial tyres were rated relatively more favourably than standard radials, mainly in respect of a combination of steering "feel," stability on dual carriageways, and roadholding

on straight roads and motorways (freeways). In contrast, standard radial-ply tyres received relatively higher ratings concerning the amount of steering return strength and the degree of comfort experienced on rural roads.

Future research directions discussed include investigating the effect of these directional response parameters on driver behaviour. Also discussed is the need for a systematic investigation of "steering aesthetics," where there would be concern for a wide range of influences on driver feedback through the vehicle's steering system. Included would be steering torque, the amount of "work done" in steering, gains and response times for lateral acceleration and yaw rate, and the linearity of response for all of these parameters.

Introduction

Overview

The introduction initially provides a presentation of aspects of the vehicle directional response dynamics necessary to facilitate an understanding of the physical consequences of change affecting vehicle steering and handling. This is followed by a discussion of the influence of pneumatic tyres on driver subjective ratings concerning vehicle steering and handling characteristics.

Vehicle Directional Response Dynamics

A description of the forces acting on the front (steered) wheels is a useful beginning for understanding the effects of pneumatic tyres on the driver/vehicle system. When the front wheels are steered, the cornering forces generated at the front of the vehicle are greater than those generated at the rear. This causes the vehicle to yaw. The cornering forces at the front (and rear) of the vehicle act via the tyres. The area where the tyre is in contact with the road is described as the "contact patch." Because of a phenomenon known as "pneumatic trail," the tyre cornering forces do not act at the centre of the contact patch. This results in the generation of "self-aligning torque," which opposes the steered force input by the driver (via the steering wheel). If the self-aligning torque is nonzero, the vehicle yaws to overcome this force and attempts to realign the steered wheels with the direction of motion of the vehicle. In general, the strength of the self-aligning torque depends on four factors. It increases as the load being applied to the tyre gets heavier. In other words, heavier cars will be more difficult to steer than lighter ones. It increases as the steered angle gets larger. It also increases for a given steer angle as the forward speed increases. Less steered angle is necessary, however, for a given cornering force as forward speed increases. Last, self-aligning torque will vary according to the geometric design of the steering system and, as we shall see, according to the type of vehicle tyre. Figure 1 shows the forces acting on the steered wheel.

The vehicle steering system can be thought of as an amplifier with similar response characteristics. Two distinct types of parameters can describe vehicle directional response. These are gains and response latencies (or response delays).

The gain of an amplifier is the ratio of output to input, or the efficiency of the system. When considering the steering system, gains operate for lateral acceleration and yaw rate response to steering wheel input. Lateral acceleration gains are defined as the lateral acceleration response per unit steering wheel angle input by the driver (ms^{-2}/Rad). Similarly, yaw rate gains are yaw rate response per unit steering wheel angle input (Rad s^{-1}/Rad). Lateral acceleration and yaw rate gains will vary according to the design of the steering geometry and type of vehicle tyre, and tend to increase as forward speed increases. The ratio of steering wheel torque to steering wheel angle input (Nm/Rad) is also influenced by the same factors (but not necessarily in the same way) as are lateral acceleration and yaw rate gains.

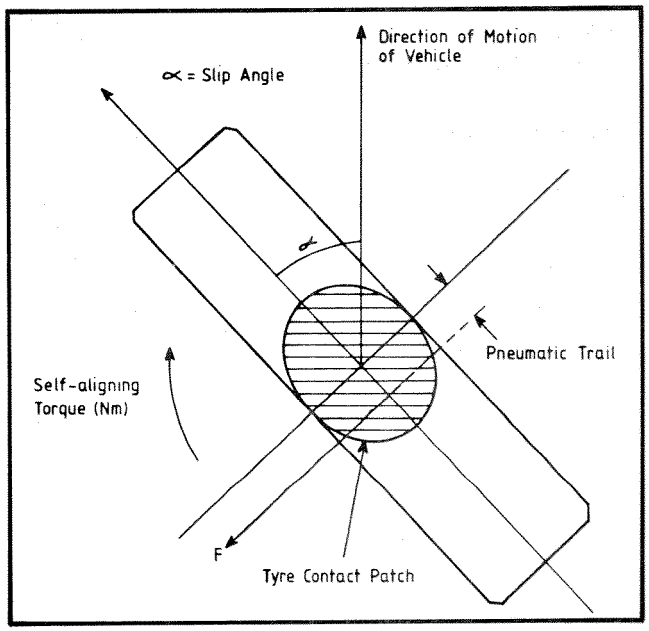

Figure 1. Forces acting on the steering wheel(10)

The other important vehicle directional response parameters are lateral acceleration and yaw rate time response to steering wheel input. These are due to the inherent time delay of mechanical systems. The measurement of these particular response parameters presents special problems since small times (which are of the order of between one-half of one second and one second for a moderately fast responding modern saloon car) are involved.

Other useful terms include transient and steady-state manoeuvres. A transient manoeuvre is one when the vehicle changes its steered direction at least once. An example of this is steering during an "S" bend. Steady-state manoeuvres are not usually encountered during normal driving but are often used by test engineers driving on vehicle proving grounds. This involves driving a vehicle during a turn with either a fixed steering wheel input or maintaining a fixed level of lateral acceleration. Open loop testing generally involves a steady-state manoeuvre, although it can involve transient manoeuvres. The term comes from control theory and refers to the fact that there is no feedback from vehicle to driver. A vehicle receiving a step input from a robot-driving machine would be a good example of an open loop system. A closed loop system is the way human factors psychologists would view the relationship between driver and vehicle—as elements in the system, each responding to feedback from the other.

Finally, some discussion of vehicle tyres is necessary. Cross-ply (or bias-ply) tyres are fitted to a minority of passenger cars nowadays. This is because the steering systems of modern cars are designed to be driven with radial-ply tyres. Radial-ply tyres last longer and generally have superior response qualities than cross-plies. However, cross-ply tyres have certain qualities that radials could do well to imitate. For example, although the roadholding limits of cross-ply tyres are lower than those of radials, cross-plies exhibit a more linear response toward the limit of their performance. Radials generally exhibit sudden break-away at their limit, a nonlinear and undesirable response. Low profile (or low aspect ratio) radial-ply tyres are a new development. These tyres are designed to put a larger area of tyre (contact patch) on the road and are generally acknowledged to have superior response qualities and higher limits of roadholding than conventional radials.

Driver Sensitivity to Vehicle Directional Response Parameters

The steering parameters most frequently reported as affecting driver opinion and driver/vehicle system are response latencies (time delays) and gain functions. A review of the literature regarding driver sensitivity to these parameters can be found in Brindle and Wilson (1983) and Brindle (1984). Brindle and Wilson showed that it was the effect on these vehicle directional response parameters that was mainly responsible for the variation in driver opinion as influenced by tyre type.

Using a methodology similar to that described in the present study, Brindle and Wilson investigated driver sensitivity to radial-ply and cross-ply (bias-ply) tyres. Following Principal Components Analysis of responses to 22 interview questions, driver opinion regarding vehicle steering and handling was reduced to nine components. Discriminant Function Analysis then performed on relatively orthogonal approximations to these nine components found three to be successful discriminators between tyre type ($p < 0.01$, canonical correlation = 0.74). It was found that drivers rated radial-ply tyres relatively more favourably than cross-ply tyres regarding a combination of perceived safety and security, control in emergencies, stability and course following on straight roads, and the amount of effort required in steering the vehicle. This was contrasted by relatively higher ratings regarding steering "feel" for drivers on cross-ply tyres.

Further analysis showed that driver opinion thus described could be systematically related to objective measures of the driver/vehicle system directional response. When lateral acceleration and yaw rate were examined, significant negative correlations were obtained between driver subjective ratings regarding both safety and effort and response time ($-0.66 < r < -0.40$, binomial probability $p < 0.001$), while significant positive correlations were obtained for gain functions on these parameters ($+0.33 < r < +0.62$, $p < 0.02$). In other words, favourable driver opinion concerning safety and effort was associated with shorter response times and higher levels of control gain. Steering "feel" was also strongly associated with both response time (positively) and control gain (negatively) and, to a lesser extent, positively with an objective measure of work expended (the product of steering wheel angle and steering wheel torque) by drivers in steering the vehicle ($+0.33 < r < +0.46$, $p < 0.07$).

Brindle (1984) explained this relationship between driver opinion and vehicle directional response parameters by examining the known engineering properties of the tyres. It was suggested that the manufacturing quality mainly responsible for the superior response characteristics (notably shorter response times) of radial-ply tyres was the higher cornering stiffness of these tyres, typically about 20 percent higher than cross-ply tyres. Thus, favourable driver opinion associated with radial tyres, which were related to short response time and higher levels of control gain, can be considered primarily attributable to this technical quality. The concept of pneumatic trail largely explains the higher levels of steering wheel torque associated with cross-plies, due to the relative movement rearward of the contact patch for these tyres. The amount of work done in steering the vehicle, also important in affecting driver opinion, was possibly affected by a combination of higher levels of steering wheel torque (as a result of increased pneumatic trail) and the high levels of steering wheel angle associated with the lower levels of control gain found for cross-ply tyres.

The Study

Research Objectives

The findings from Brindle and Wilson (op. cit.) were investigated in an expanded study examining a wider range of driver opinion. The effect of a more modern tyre contrast (low profile radials versus standard radials) on vehicle steering and handling characteristics, and the influence of these characteristics on driver opinion, was investigated under realistic driving conditions.

Research Design

A total of 46 subjects (Ss) drove a medium-size estate car (1978 Ford Cortina 1.6 L) on public roads in an independent-groups, repeated measures research design. Three treatment groups were used: 18 Ss drove using Pirelli P6 low profile "sixty series" radial-ply tyres (185/60x14) on dry roads, 18 Ss drove using Pirelli P4 "standard" radial-ply tyres (165x14) on dry roads, and 10 Ss drove using P4 radial tyres on wet roads. The route was 40.6km and included a range of rural country roads, suburban dual carriageways, and a section of motorway (freeway). Additionally, Ss drove an 8.2km practice route before commencing testing.

A total of 33 males and 13 females took part in the experiment, and Ss were aged between 18 and 60 (median 27.7 years). Driving experience ranged between 1 and 38 years (median 16.0), and driving exposure ranged between 1,000 and 25,000 miles per annum (median 11,400).

Medium-powered tests (one-way analyses of variance), carried out to check for random group assignment, failed to detect any systematic effects due to possible confounding variables (e.g., age, driving experience, miles driven per annum). The power of these tests was such that a strength of association (w^2, see Hays, ibid., p. 417) of 10 percent would have been detected at the $p < 0.05$ level ($N = 46$, $J = 3$) with a probability of 0.20 (Beta = 0.80). Groups were considered, therefore, to be adequately randomised.

Ss drove an instrumented vehicle equipped to measure steering wheel angle, lateral acceleration, yaw rate, and forward speed for a range of transient manoeuvres. These included low-, medium-, and high-speed bends and curves, and roundabouts (circles) in rural Bedfordshire and Buckinghamshire. Data were recorded on a Racal analogue tape recorder and were subsequently interpreted using a microcomputer analogue to digital routine. Ss were interviewed on a range of items both during and after each test drive.

Results

Interview data were initially analysed using Principal Components Analysis. Thus, 40 Likert scale items relating to driver subjective ratings of vehicle steering and handling, ride quality, and safety were reduced to 10 components. Before rotation, these 10 components accounted for 79.3 percent of the total variation among driver opinion. An orthogonal rotation according to the "Varimax" criterion was carried out, and relatively orthogonal simplified versions of the 10 components were subjected to Multiple Discriminant Function Analysis (DFA) for three groups. This method results in "...the reduction of multiple measurements to one or more weighted combinations having maximum potential for distinguishing among members of the different groups." (Overall and Klett, 1972, p. 280). The "Wilks" criterion for inclusion of meta-variables in a stepwise DFA was used. For further details of these multivariate statistical techniques, also see Brindle and Wilson (op. cit.).

Table 1 describes how much variance each of these 10 factors accounted for after rotation.

Table 2 shows the structure of the simplified meta-variables used in the Discriminant Function Analysis after "Varimax" rotation. A "+" in any column indicates that the respective row variable was given a weighting of +.1.0 in the composite meta-variable. Variables were thus only included in the factor structure where a "+" appears in the appropriate column. All other variables were

Table 1. Factor names, eigenvalues, and percent variance for interview data

Factor	Name	Eigenvalue	% Variance	Cum % Var
1	Rural Comfort	6.28	19.8	19.8
2	Rural Performance	5.55	17.5	37.3
3	Straight/Motorway Performance	4.55	14.3	51.6
4	Responsive/Sensitive	3.21	10.1	61.7
5	Brake in Emergency	2.96	9.3	71.0
6	Stability Dual Carriageways	2.29	7.2	78.2
7	Rural Safe	2.08	6.6	84.8
8	Effort	2.04	6.4	91.2
9	Return Strength	1.55	4.9	96.1
10	Feel	1.21	3.8	99.9

Table 2. Factor structure for the 10 meta-variables

Variable and Description		Meta-Variable									
		1	2	3	4	5	6	7	8	9	10
OPIN1	Roadholding in General										
OPIN2	Handling in General										
OPIN3	Control in Emergency Rural										
OPIN4	Quality of Ride - Rural	+									
OPIN5	Comfort - Rural Roads	+									
OPIN6	Responsivity										
OPIN7	Stability on Dual C'ways						+				
OPIN8	Return Strength									+	
OPIN9	Sensitivity on Dual C'ways				+						
OPIN10	Control in Emergency M'way										
OPIN11	Brake in Emergency M'way					+					
OPIN12	Handling Bumpy Rural Roads		+								
OPIN13	Comfort Bumpy Rural Roads	+									
OPIN14	Safety Margin Rural Roads							+			
OPIN15	Roadholding in General										
OPIN16	Handling in General										
OPIN17	Safety in General										
OPIN18	Control in Emergency - General		+								
OPIN19	Quality of Ride - General	+									
OPIN20	Comfort in General	+									
OPIN21	Responsivity in General				+						
OPIN22	Predictability in General										
OPIN23	Brake in Emergency (General)					+					
OPIN24	Handling Bumpy Rural (2)		+								
OPIN25	Roadholding Bumpy Rural (2)		+								
OPIN26	Ride Bumpy Rural Roads	+									
OPIN27	Comfort Bumpy Rural Roads	+									
OPIN28	Handling Straights and M'ways			+							
OPIN29	Roadholding Straight and M'way			+							
OPIN30	Kept on Course Straight and M'way			+							
OPIN31	Predictable Straights and M'way			+							
OPIN32	Comfort on Straights and M'way										
OPIN33	Kept on Cse Bends and Roundabouts										
OPIN34	Predictable Bends and Roundabouts										
OPIN35	Responsive Bends and Roundabouts				+						
OPIN36	Feel in General										+
OPIN37	Effort at Low Speeds								+		
OPIN38	Effort at Higher Speeds								+		
OPIN39	Likely to Buy										
OPIN40	Safety Margin in General							+			
		1	2	3	4	5	6	7	8	9	10

excluded. The criterion for assigning a weight of +1.0, or otherwise zero, was for factor loadings >0.65 in the SPSS Rotated Factor Structure matrix.

Two canonical discriminant functions were computed. The first function (which explained 67 percent of the total variance, $p < 0.05$, canonical correlation = 0.47) discriminated between P6 tyres and P4 tyres. The second function (which explained the remaining variance, $p < 0.14$, canonical correlation = 0.35) discriminated between dry and wet road conditions. Results indicated that P6 tyres were rated relatively more favourably than P4 tyres regarding a combination of steering "feel," stability on dual carriageways, and roadholding and handling on straight roads and motorways. Drivers on P4 tyres, however, expressed relatively higher ratings concerning the amount of steering return strength and the degree of comfort experienced on rural roads than drivers on P6 tyres. Drivers on dry roads expressed relatively higher ratings concerning a combination of steering return strength, responsivity and sensitivity, and roadholding and handling on straight roads and motorways than drivers on wet roads.

An analysis of the vehicle directional response parameters confirmed that response time and control gain were important parameters affecting driver subjective ratings. Since multiple correlations were made, results were examined using probabilities associated with the binomial distribution (see Hays, 1974, p. 184) for the expectation of these results due to chance. Yaw rate response time was negatively correlated with favourable

driver opinion regarding perceived safety ($-0.37 < r < -0.14$, binomial probability $p < 0.001$), and straight road and motorway performance ($-0.35 < r < 0.18$, $p < 0.02$). High levels of speed-adjusted lateral acceleration and yaw rate gain were associated with favourable ratings concerning steering "feel" ($+0.16 < r < +0.30$, $p < 0.04$), and safety ($+0.13 < r < +0.37$, $p < 0.01$). An inverse relationship was found between speed-adjusted lateral acceleration and yaw rate gain and high ratings concerning rural steering and handling ($-0.30 < r < -0.16$, $p < 0.01$), and steering responsivity and sensitivity ($-0.37 < r < -0.14$, $p < 0.04$). A marginally significant result was found suggesting a direct relationship between high ratings regarding steering responsivity and short lateral acceleration response time ($-0.22 < r < -0.11$, $p < 0.08$).

It was found additionally that, for lateral acceleration and yaw rate steering gains, standard radials had a more linear response as affected by forward speed ($r^2 = 0.91$, and 0.82, respectively) than low profile radial tyres ($r^2 = 0.84$, and 0.75). In other words, for the range tested, steering gains increased approximately linearly with increased forward speed. Results also showed that driver-adopted yaw rate had a more linear (inverse) response to forward speed ($r^2 = 0.89$) than driver-adopted lateral acceleration ($r^2 = 0.79$). These results are discussed more fully in Brindle (1984).

Conclusion

Results showed that the subjective ratings of ordinary drivers could be systematically related to objective measures of vehicle directional response. The main influences on favourable driver opinion were short response times and high levels of control gain, qualities that were, in general, associated with the superior response characteristics of low profile radial tyres. However, drivers were also sensitive to other effects of vehicle tyres, notably to rural comfort and rural steering and handling performance—qualities that were relatively more likely to be associated with standard radials than with low profile tyres. It is also possible that favourable ratings for standard radials could have been affected by the more linear lateral acceleration and yaw rate response for these tyres.

These subjective ratings by ordinary drivers match expert evaluations of the known engineering qualities of the tyres tested. Early discussions with the Technical Services Department of Pirelli U.K. Ltd. indicated that higher levels of roadholding and handling would be expected from the low profile (P6) tyres. Sandberg, Formgren, and Ohlsson (1976) reviewed several engineering reports investigating the relative merits of standard and low profile radial tyres. They concluded that standard radial tyres, apart from other benefits, would be expected to produce a higher standard of ride quality, and that low profile radials would be expected to have improved cornering stability together with some other benefits, though at the expense of ride quality. These characteristics can be seen to match the subjective ratings of ordinary drivers.

Discussion and Recommendations

The studies reported have shown that ordinary drivers are sensitive to the effect of different tyres on vehicle steering and handling. Further, it has been shown that driver subjective ratings can be systematically related to vehicle directional response parameters. This is important since, as Ray and Gibson (1983) have concluded, " . . . subjective assessments of vehicle handling performance are useful if used in conjunction with other objective test procedures," (ibid., p. 169). In conclusion, these results have a high degree of generalisability since data were collected from representative drivers under realistic closed-loop conditions. However, in addition, several research directions were indicated.

Although it has been shown that driver opinion is affected by different tyre types, the effect of this sensitivity on driver behaviour also requires investigation. For example, do drivers adjust their driving by, say, cornering faster to compensate for the superior response qualities of low profile tyres? (This question is examined in Brindle, 1985, and at length in Brindle, 1984.) Further, the effects on driver opinion and behaviour require investigation for other subsets of drivers. It is important to investigate the response for different groups, such as young versus older drivers, accident involved versus no-accident drivers, etc.

Another intriguing area involves investigating the relative effects of driver sensitivity to yaw rate and lateral acceleration response. Early indications (from both of our studies) suggest that as forward speed increases, driver-adopted yaw rate is more linear than driver-adopted lateral acceleration. Other authors have also been concerned with this distinction recently. For instance, Nakaya, Sano, Furukawa, and Oguchi (1982), using an experimental drum-type simulator with front- and rear-wheel steering, concluded from the data from three subjects "...that during evasive manoeuvres the driver attaches greater importance to the vehicle's lateral displacement as the necessary input information, while in normal driving, he puts more weight on yaw angle" (ibid., p. 109.6). It is interesting to note that lateral acceleration and yaw rate are, respectively, second- and first-order derivatives of lateral displacement and yaw heading. However, more research is required before any serious conclusions can be reached on how these parameters contribute to driver directional feedback.

Finally, it has been shown that a wide range of vehicle directional response parameters can influence driver

opinion. Previously, steering "feel" has been defined (e.g., Anderson, 1983) only in terms of "the force-feedback characteristics" (ibid., p. 16) of the steering. It is suggested that the concept of "steering feel" be broadened into that of "steering aesthetics," where there is concern for a wider range of driver feedback from the steering. Apart from steering torque, drivers have been shown to be affected by the amount of work done, lateral acceleration and yaw rate gain and response time, and the linearity of response for these parameters. This hierarchy of importance for these influences for different drivers under different driving conditions also requires clarification. It may well be that, for instance, the same characteristic may not necessarily be as important when driving on rural roads as, say, when driving on motorways.

Acknowledgments

The author would like to express his gratitude to Pirelli U.K. Ltd., which provided technical and material support for the experiments reported.

References

1. Anderson, J.M., "The evaluation of drivers' responses to a multi-characteristic power steering system," PhD Thesis, School of Automotive Studies, Cranfield Institute of Technology, England, 1982.
2. Brindle, L.R., "The influence of tyre characteristics on driver opinion and risk-taking," PhD Thesis, College of Aeronautics, Cranfield Institute of Technology, England, 1984.
3. Brindle, L.R., "Driver risk compensation and vehicle active safety," paper submitted to *Ergonomics* (in press), 1985.
4. Brindle, L.R., and W.T. Wilson, "The effects of tyre type on driver perception and risk-taking," Proceedings International Conference on Road Vehicle Handling, Institute of Mechanical Engineers, London, C134/83, 1983.
5. Hays, W.L., *Statistics for the Social Sciences*, 2nd Edition, London: Holt, Rinehart, and Winston, 1974.
6. Nakaya, H., S. Sano, Y. Furukawa, and Y. Oguchi, "Effects of vehicles' yaw and lateral acceleration responses on drivers control performance," SAE paper 82109, New York, 1982.
7. Overall, J.E., and C.J. Klett, *Applied Multivariate Statistics*, London: McGraw-Hill, 1972.
8. Ray, R.W., and P.D. Gibson, "Car handling test results: Data acquisition and analysis methods," Proceedings International Conference on Road Vehicle Handling, Institute of Mechanical Engineers, London, C126/83, 1983.
9. Sanberg, U., C. Formgren, and E. Ohlsson, "Tire dimensions: properties of wide and low versus narrow and high tires," National Swedish Road and Traffic Research Institute (VTI), Report 108A, 1976.
10. Setright, L.J.K., *Automobile Tyres*, London: Chapman and Hall, 1972.

Tire Performance Measurements—Wet and Dry

Lloyd H. Emery
U.S. Department of Transportation, National Highway Traffic Safety Administration

Abstract

Vehicle accident avoidance potential is very much dependent on the vehicle braking and cornering performance potential. In the past, much effort has been concentrated on the suspension and braking systems to raise their performance level. However, vehicle braking and cornering performance is also strongly influenced by the braking and cornering force characteristics of the vehicle tires. The study of vehicle tire dynamics has been generally limited by the absence of accurate braking and cornering tire data representative of the vehicle performance range of interest. This absence of tire performance data is particularly true in the nonlinear tire performance range of large cornering slip angles and braking slip. Accident avoidance vehicle performance research requires tire performance data representative of the tire braking and cornering forces generated by the vehicle tires when operating in the regime of large slip angles, large normal load transfers, and high braking slip, even up to locked wheel performance. The study of vehicle stability and accident avoidance through cornering and braking maneuvers requires tire performance data from 0 to 90° slip angle and from 0 to 100 percent slip for braking.

This paper reports the results of an effort by NHTSA to measure the braking and cornering forces of a P185-80R13 tire produced by Goodyear Corporation. Tire force measurements were made at the Tire Research Facility (TIRF) located at Calspan Corporation. Tire force measurements were made on both dry and wet

surfaces. Braking force was measured for each slip angle from 0 to 100 percent slip. The tire slip angle was varied over a slip angle range from 0 to 90°.

Introduction

The motivation to perform this study was the need to analyze vehicle stability and spin out performance during accident avoidance maneuvers involving steering and braking and the realization that the open literature provided insufficient tire performance data to do so effectively. Accordingly, it was decided to measure the braking and lateral forces produced by a tire when subjected to both braking and slip angle simultaneously as a function of normal load on both a wet and dry surface. The tire of interest was the Goodyear-produced P185-80R13 radial tire, which is representative both in size and construction of many tires presently being produced.

The 1984 Tire and Rim Association Manual gives this tire a rating of 1301-lb normal load at 35PSI. The measurements were performed at 30mph, at 34PSI inflation pressure, on a wet and dry surface, on the TIRF located at Calspan Corporation, Buffalo, New York. Tire force measurements reported on in this paper are the longitudinal and lateral tire forces produced by braking and cornering. These force measurements were performed at 0, 4, 12, 20, 30, 50, 60, and 90° slip angles. Tire force measurements reported on in this paper were made at the three normal loads of 250 lb, 600 lb, and 1,027 lb, at each of the above slip angles. In addition, the tire braking and lateral forces were measured as a function of braking slip from 0 to 100 percent slip. The wet friction coefficient of 0.30 was established by the usual wet ASTM tire and recommended procedure. The dry friction coefficient of 0.85 was measured by a locked ASTM tire on the dry surface.

Test Results

The braking force test results are contained in Appendix A. The lateral force test results are contained in Appendix B.

Discussion

General

The normalized braking and cornering forces of the test tire are significantly different as a function of normal load, slip angles, and slip ratio. Figures 1 through 4 have the normalized lateral force plotted as a function of normalized braking force for different slip angles and slip

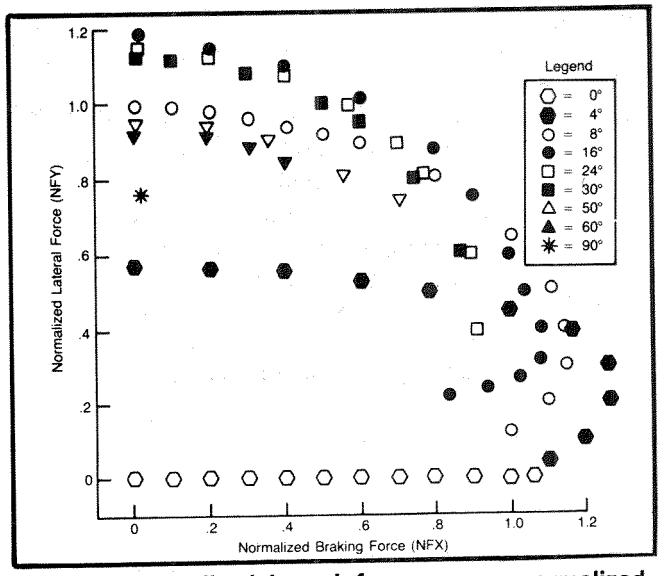

Figure 1. Normalized lateral force versus normalized braking force as a function of slip angle and percent braking slip on a dry surface with a 250 lb normal load

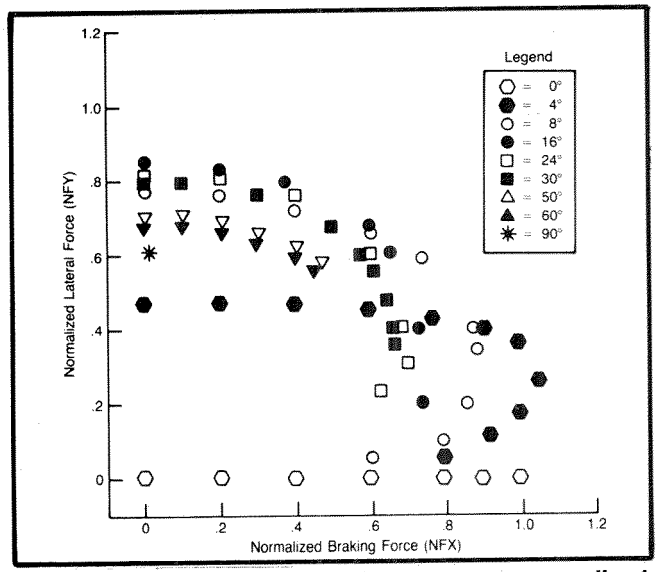

Figure 2. Normalized lateral force versus normalized braking force as a function of slip angle and percent braking slip on a dry surface with a 1,027 lb normal load

ratios for a normal load of 250 lb and 1,027 lb on both a dry and wet surface. The following observations become apparent when Figures 1 through 4 are examined.

- The normalized lateral and longitudinal forces for each slip angle are higher for the 250-lb normal load than for the 1,027-lb normal load. Thus, one can conclude this tire is more efficient at generating forces as the normal load is decreased. This observation is true for both and dry surfaces.
- The maximum normalized lateral force for both normal loads on the dry surface occurs at around the 16° slip angle at the zero slip ratio braking

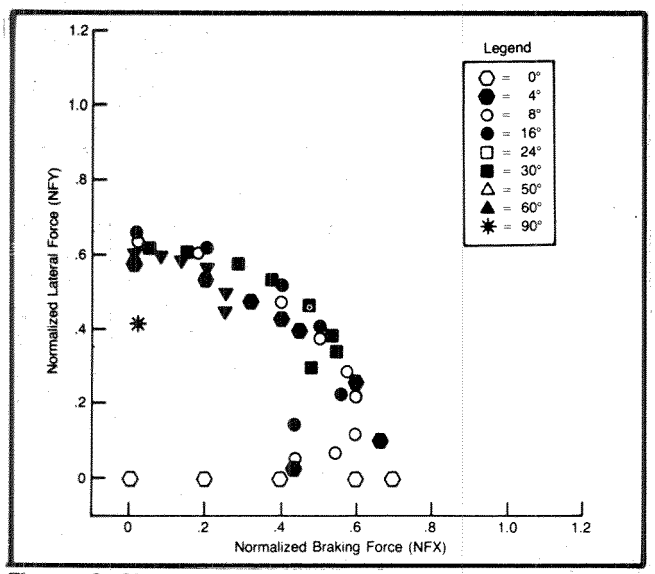

Figure 3. Normalized lateral force versus normalized braking force as a function of slip angle and percent braking slip on a wet surface with a 250 lb normal load

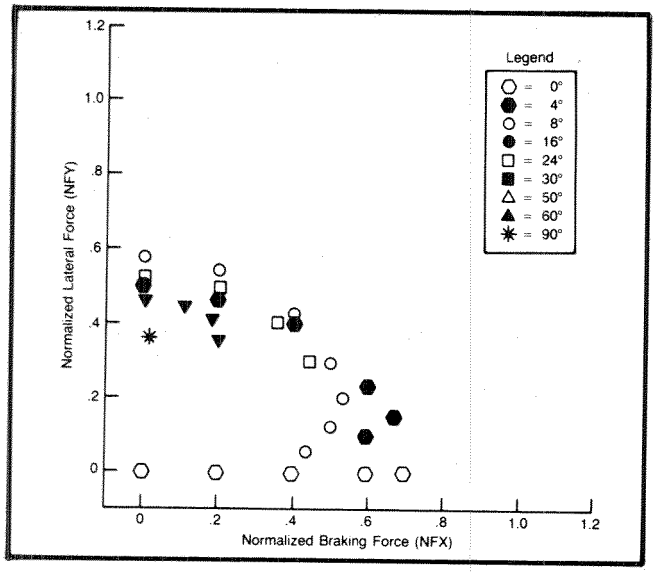

Figure 4. Normalized lateral force versus normalized braking force as a function of slip angle and percent braking slip on a wet surface with a 1,027 lb normal load

condition. Slip angles less than and greater than approximately 16° produced less normalized lateral force.

- The maximum normalized braking force on the dry surface occurred at the 4° slip angle rather than the 0° slip angle. There is presently no adequate explanation as to why the maximum normalized braking force should occur at some slip angle greater than zero. Future research will be necessary to explain this unexpected result.
- The normalized braking force on the dry surface for the 4°, 8°, and 16° slip angles shows a peak value and then a curl back to the left. The peak normalized lateral force for these three slip angle curves represents the peak normalized lateral force that occurs at some slip ratio, which is usually around 20 percent slip for straight line braking. However, the percentage slip at which the peak normalized braking force occurs increases as the slip angle increases. Examination of Appendix A clearly shows this effect.
- The peak normalized braking force on the dry surface begins to coincide with the 100 percent braking slip condition at around the 24° slip angle level.
- The normalized lateral force of about 0.76 for the 90° slip angle in Figure 1 is considerably less than the normalized braking force of about 1.05 for the 0° slip angle for the 250-lb normal load on a dry surface. A similar comparison can be made for the 1,027-lb normal load data in Figure 2. The data show that the tire is much more efficient at producing force in the longitudinal or braking mode than it is in the lateral or cornering mode. It would be interesting to rerun this experiment using wider wheels with the same tire to see if the wider wheels would increase the tire lateral force production efficiency.
- In contrast to the dry surface, the maximum normalized braking force on the wet surface for both the 250-lb and 1,027-lb normal loads occurred for the straight line braking condition rather than at some small slip angle.
- The normalized lateral forces and braking forces for all slip angles on the wet surface are much less than their counterparts on the dry surface.
- The normalized braking force on the wet surface for the 4°, 8°, and 16° slip angle with a 250-lb normal load also shows a peak value and then a curl down and to the left. The peak normalized braking force occurs at about a 20 percent braking slip for a straight line stop. The peak normalized braking force occurs at higher levels of percent braking slip as the slip angle increases. The peak normalized braking force coincides with the locked wheel condition after the 50° slip angle condition is reached.
- The normalized lateral force of about 0.4 for the 250-lb normal load and a 90° slip angle on the wet surface is again considerably less than the maximum normalized braking force of about 0.7 for the 0° slip angle condition in Figure 3. Again the tire is much more efficient at generating maximum force in the longitudinal direction compared to the lateral direction at a 90° slip angle. This tire performance characteristic is detrimental with respect to vehicle stability when the rear wheels are experiencing large slip angles.

The normalized braking force and the normalized lateral force are plotted as a function of slip angle for a locked-wheel condition in Figures 5 and 6, respectively. The maximum normalized braking force occurs not at the 0° slip angle but at about the 4° slip angle. The maximum normalized lateral force also does not occur at the 90° slip angle but at about the 60° slip angle. Again, there is no adequate explanation at the present time to explain these somewhat unexpected results.

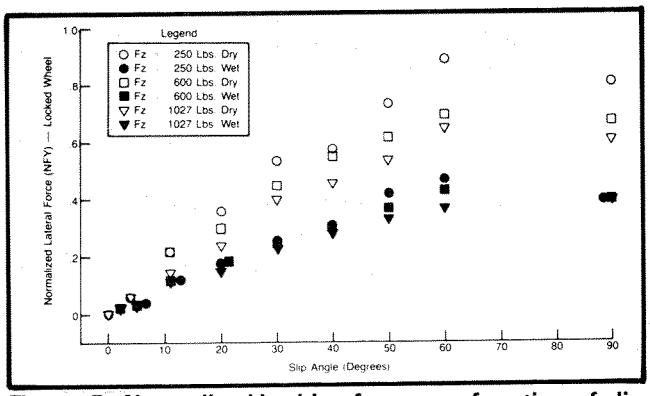

Figure 5. Normalized braking force as a function of slip angle-locked wheel

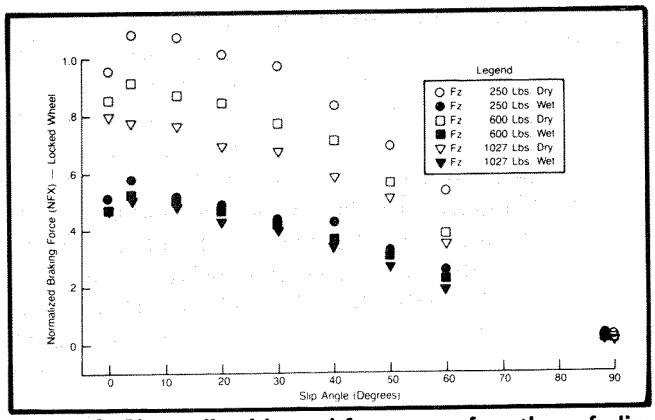

Figure 6. Normalized lateral force as a function of slip angle-locked wheel

The normalized lateral force for a normal load of 1,027 lb is plotted as a function of slip angle and braking slip in Figures 7 and 8 for a dry and wet surface, respectively. The overall normalized lateral forces are much less on the wet surface than on the dry surface; however, the normalized lateral force for very small slip angles is about the same on both the dry and wet surfaces, especially for small percentages of braking slip. The normalized lateral force has a pronounced peak at around the 8° slip angle point on the wet surface and at about the 12° slip angle point on the dry surface at the zero braking slip condition. As the percentage of braking slip increases, the peak normalized lateral force diminishes in pronouncement and occurs at larger slip angle conditions.

The locked-wheel normalized braking force is plotted as a function of the locked-wheel normalized lateral force

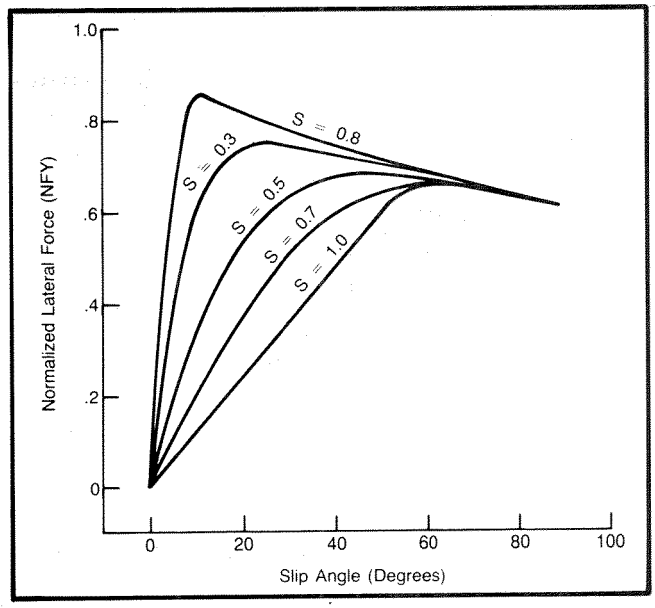

Figure 7. Normalized lateral force as a function of slip angle and percent braking slip on a dry surface with a 1,027 lb normal load

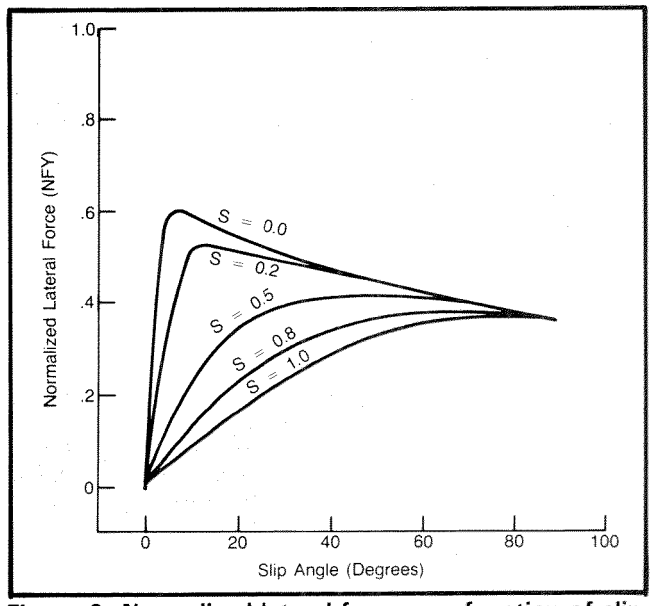

Figure 8. Normalized lateral force as a function of slip angle and percent braking slip on a wet surface with a 1,027 lb normal load

for different slip angle conditions in Figure 9. The data are plotted for three normal loads on both a wet and dry surface. Again, the normalized braking force shows a peak near the 4° slip angle and the normalized lateral force shows a peak at the 60° slip angle condition. Thus, the data show that a friction circle does not perfectly describe the braking and lateral force behavior of this tire. Both the normalized braking force and the normalized lateral force show a curl, which has never been explained.

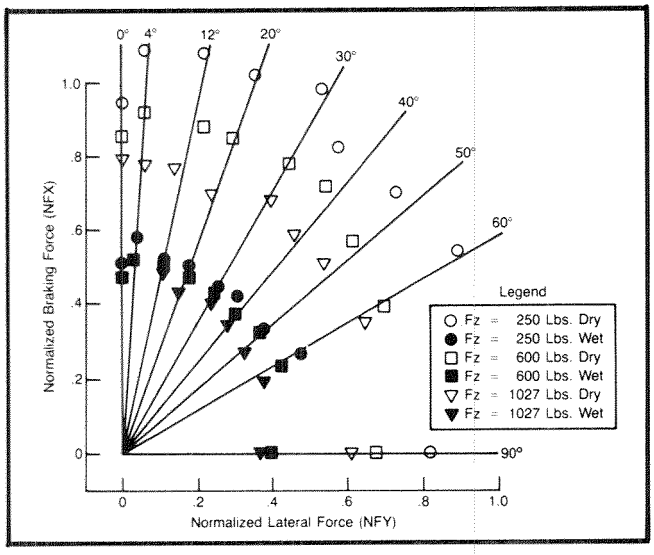

Figure 9. Normalized braking force versus normalized lateral force locked wheel

Appendix A

Examination of Appendix A reveals the following observations:

- The test data in Figure A-1 show that the test tire has a similar braking stiffness on both the wet and dry surfaces. A driver applying his brakes in a straight line braking situation would feel little difference in brake gain (vehicle deceleration versus pedal effort) between a wet and a dry surface up to about 0.2 normalized braking force. However, there is a big difference in the peak braking force between the wet and dry surfaces. The peak normalized braking force for the dry surface is about 60 percent greater (depending on normal load) than the peak normalized braking force for the wet surface. The sliding normalized brake force for the dry surface is also about 50 percent greater (depending on normal load) than the sliding normalized brake force for the wet surface. One can clearly see the increased braking potential of this tire on a dry surface versus a wet surface. It can easily be speculated that drivers can be lulled into a false sense of security when driving in the linear range on a wet surface; thus, when emergency stopping performance is needed, the expected dry deceleration potential cannot be attained. Based on these data, a locked-wheel deceleration on a wet surface may be over 40 percent less than on a dry surface. The straight line normalized braking force is largely independent of normal load on a wet surface; however, the normalized braking force is inversely proportional to normal load on the dry surface. For those vehicle designers who want to increase the straight line braking performance envelope on a dry surface, the data suggest this can be accomplished by using tires with a higher designed load range. It is also clear that the effective brake proportioning can be altered on a vehicle by the mixing of different load range, tires front to rear.
- The data in Figure A-2 represent the normalized braking force for combined cornering and braking at a 4° slip angle. The normalized braking force for the dry surface is significantly higher than the normalized braking force on the wet surface and is very much a function of normal load. The observations about A-1 are also valid here. In addition, the peak normalized braking force on the dry surface of 1.25 is very high for the lightly loaded condition of 250 lb. The peak normalized braking force for the wet surface is becoming less pronounced and is moving toward higher slip values as the slip angle increases.
- The data in Figure A-3 represent the normalized braking force for combined cornering and braking data at a 12° slip angle. The peak normalized braking force is again occurring at higher slip values as the slip angle increases. The normalized braking force for the dry surface is significantly higher than the normalized braking force on the wet surface. The normalized braking force on the dry surface is again very much a function of normal load.
- The observations made about the data in A-3 are also valid for the data in Figure A-4. The normalized braking force for the 20° slip angle data in A-4 still show a peak although the peak is occurring at about 80 percent longitudinal slip (braking). The normalized braking force on the dry surface does not show a peak for slip angles greater than 30°. The normalized braking force on the wet surface does not show a peak for slip angles greater than 50°. Also, the wet and dry normalized braking forces are starting to converge toward the same value at the 60° slip angle. Of course, the data in Figure A-8 show that the normalized braking force has converged to zero at the 90° slip angle for both wet and dry surfaces.

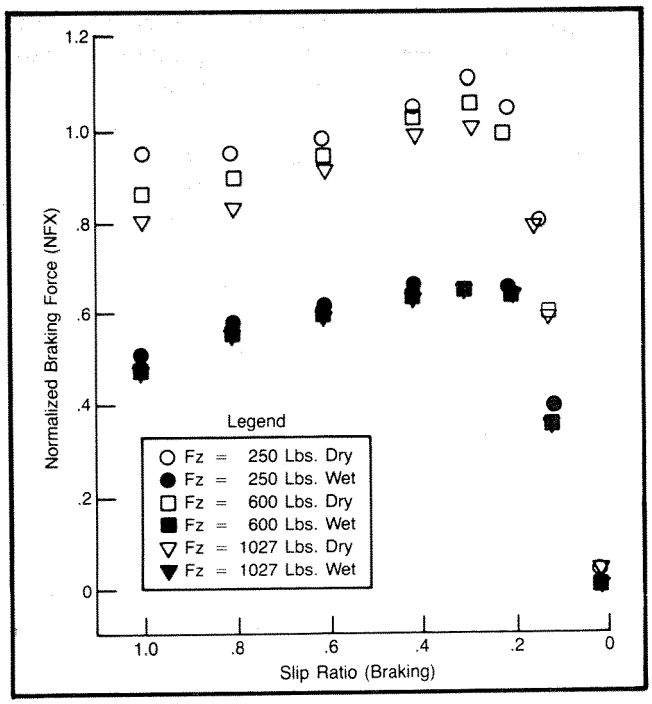

Figure A-1. Normalized braking force versus slip ratio (braking)—slip angle = 0°

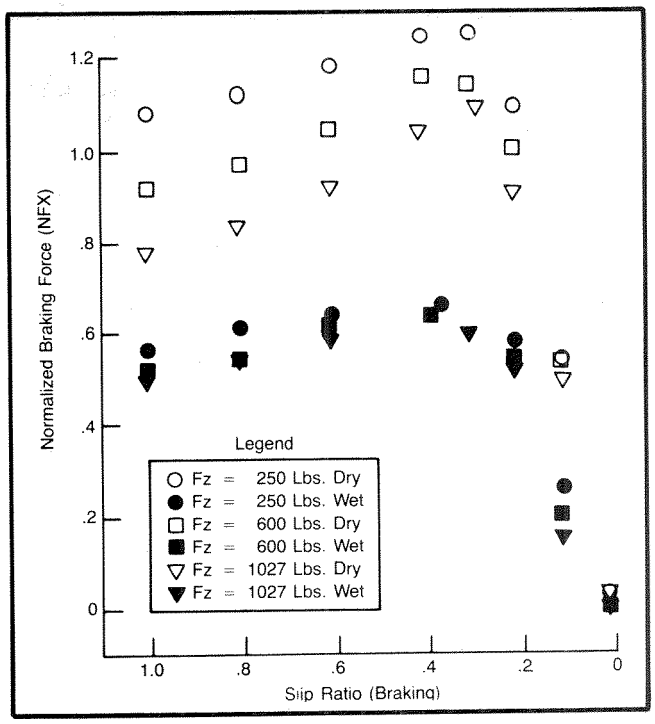

Figure A-2. Normalized braking force versus slip ratio (braking)

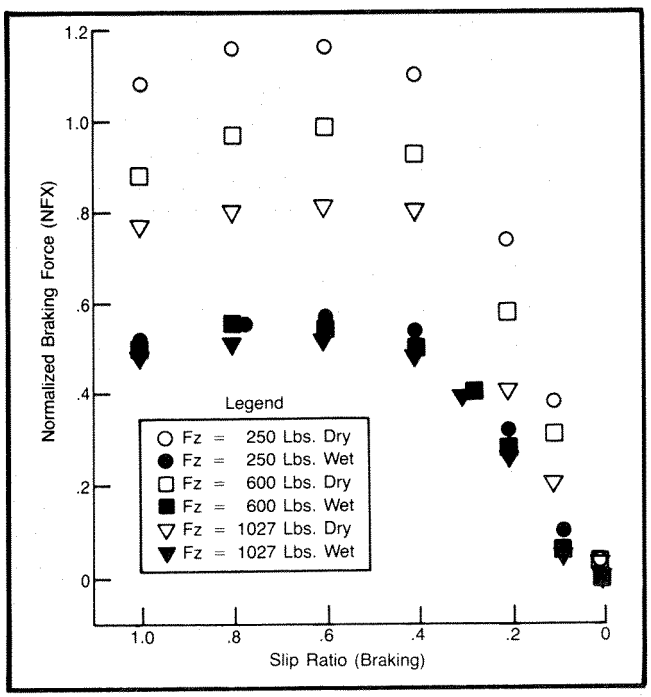

Figure A-3. Normalized braking force versus slip ratio (braking)—slip angle = 12°

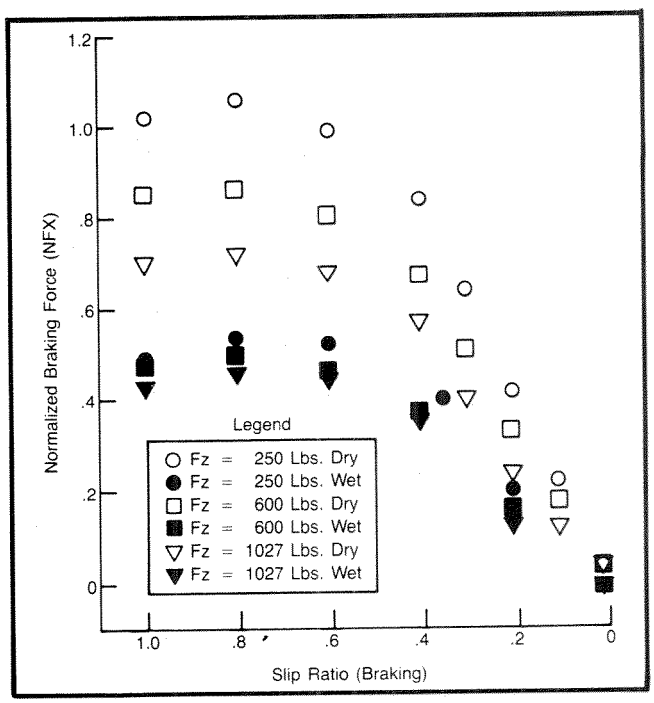

Figure A-4. Normalized braking force versus slip ratio (braking)—slip angle = 20°

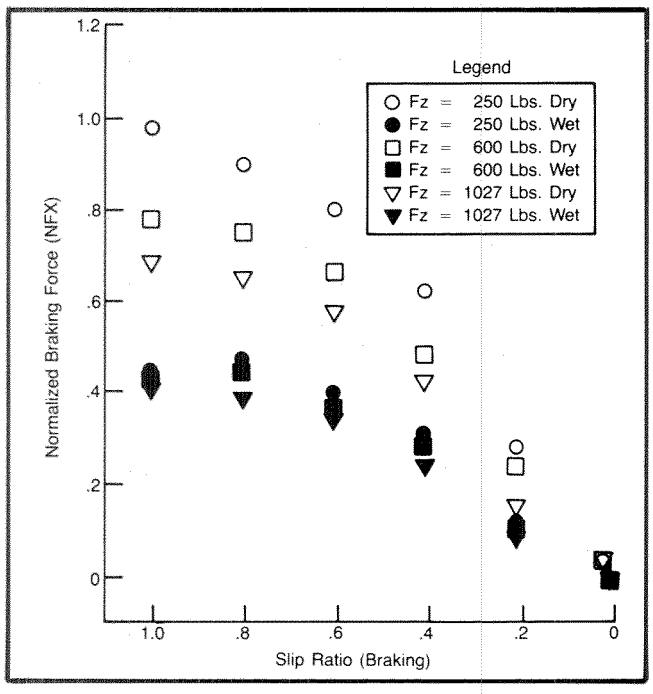

Figure A-5. Normalized braking force versus slip ratio (braking)—slip angle = 30°

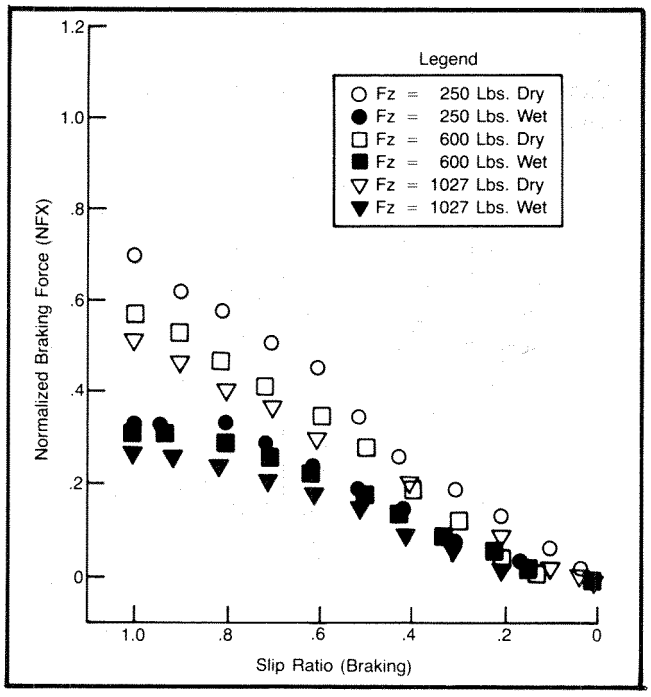

Figure A-6. Normalized braking force versus slip ratio (braking)—slip angle = 50°

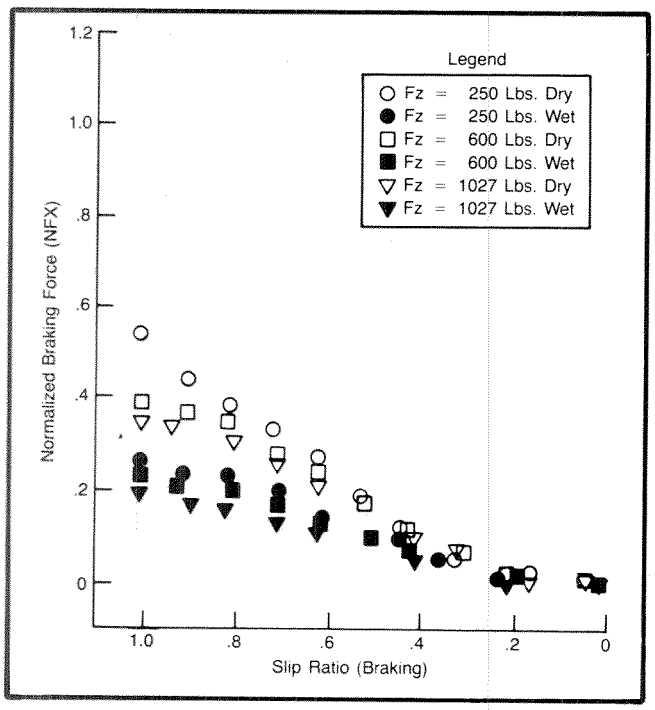

Figure A-7. Normalized braking force versus slip ratio (braking)—slip angle = 60°

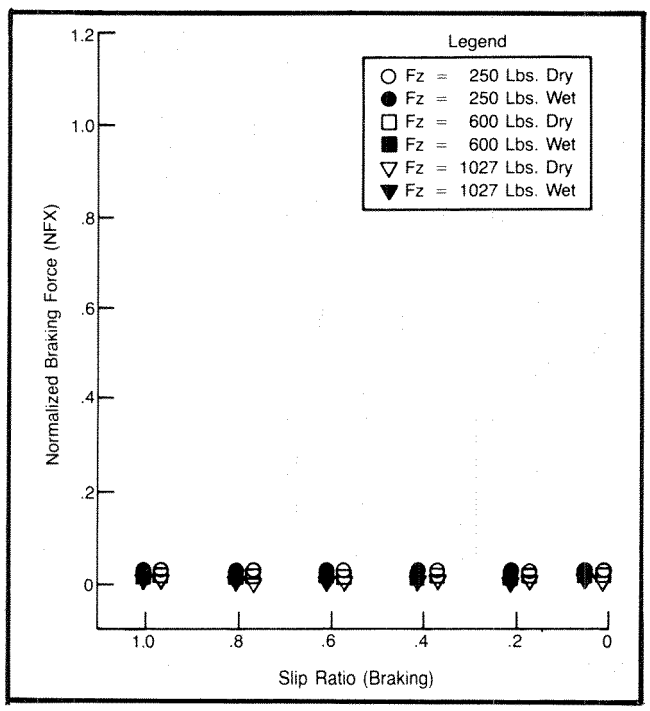

Figure A-8. Normalized braking force versus slip ratio (braking)—slip angle = 90°

Appendix B

Examination of Appendix B reveals the following observations:

- The normalized lateral force data in Figure B-1 are for combined cornering and braking at a 0° slip angle. The normalized slip force is zero on both the wet and dry surfaces regardless of the degree of braking slip. However, once the tire develops a slip angle, the normalized lateral force becomes very much a function of braking slip. The data in Figure B-2 show the normalized lateral force decreasing from around 0.5 to 0.05 as the tire goes from a free rolling condition to a locked-wheel braking condition. The data in Figure B-2 show only a limited difference between a wet and dry surface.
- The normalized lateral force in Figure B-3 is for combined cornering and braking at a 12° slip angle. The normalized lateral force is much higher on the dry surface than on the wet surface. However, the normalized lateral force on both the wet and dry surfaces again decreases rapidly as the tire approaches lockup. The data in Figures B-3 through B-8 show that as the slip angle increases, the locked-wheel normalized lateral force becomes higher and higher until it is the same value as the free rolling tire at the 90° slip angle value.
- The normalized lateral force in Figure B-8 shows higher normal load dependency on the dry surface when compared to the wet surface. It is clear from the data that the higher normalized lateral forces are achieved with lower normal loads. This effect is very prominent for the dry surface.

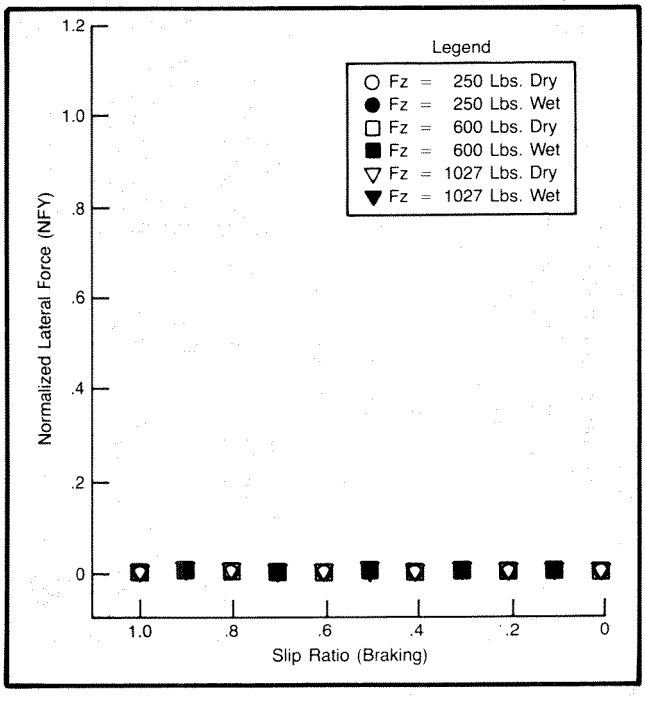

Figure B-1. Normalized lateral force versus slip ratio (braking)—slip angle = 0°

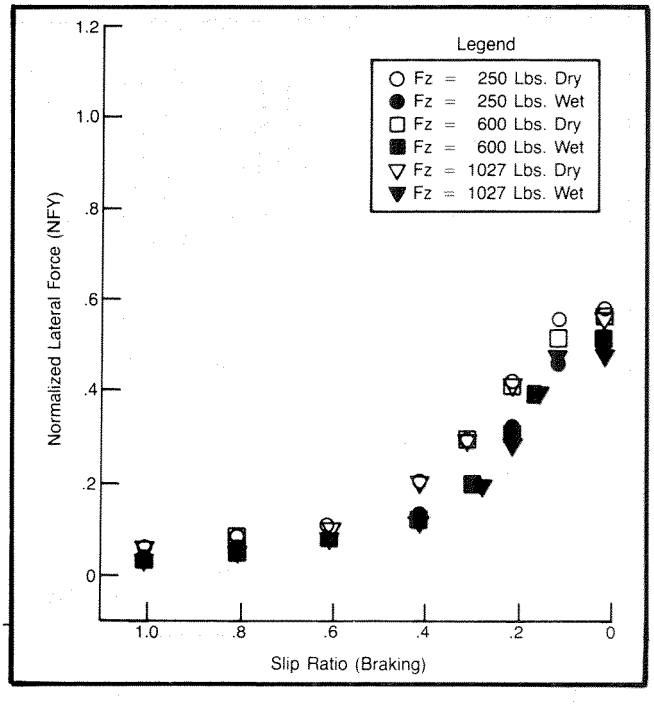

Figure B-2. Normalized lateral force versus slip ratio (braking)—slip angle = 4°

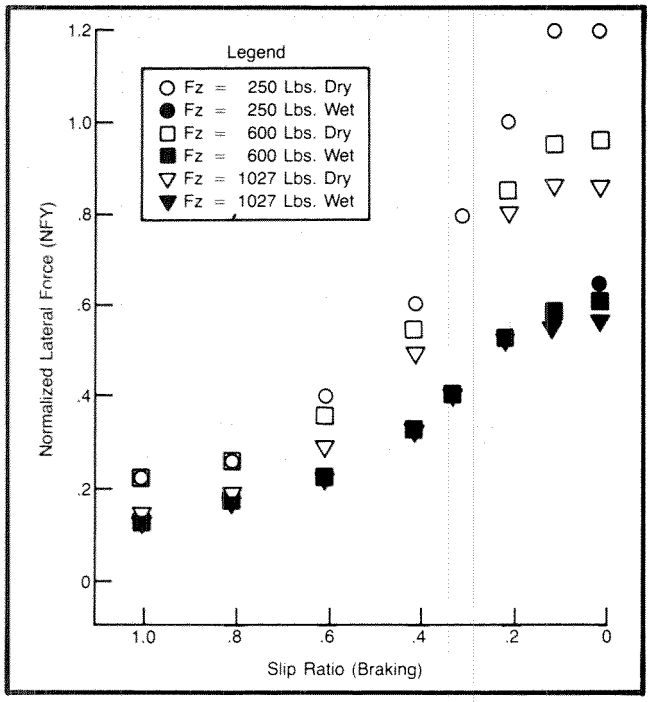

Figure B-3. Normalized lateral force versus slip ratio (braking)—slip angle = 12°

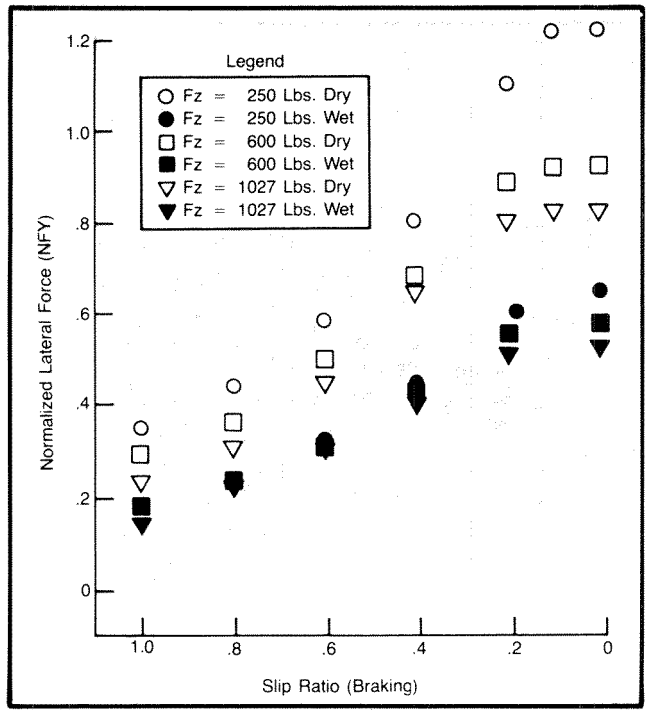

Figure B-4. Normalized lateral force versus slip ratio (braking)—slip angle = 12°

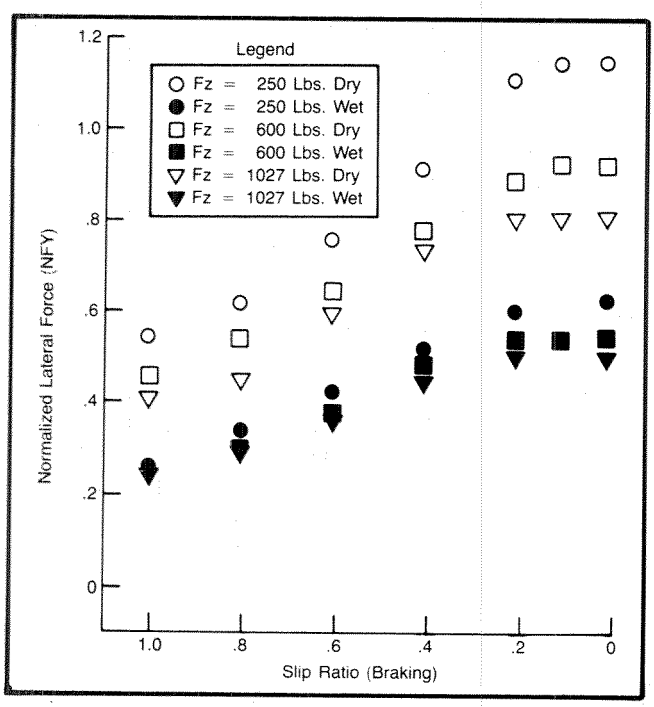

Figure B-5. Normalized lateral force versus slip ratio (braking)—slip angle = 30°

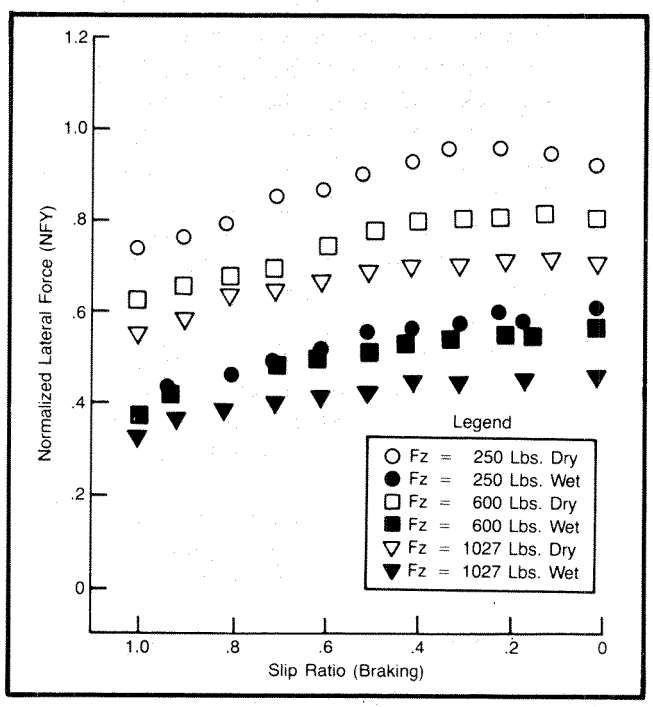

Figure B-6. Normalized lateral force versus slip ratio (braking)—slip angle = 50°

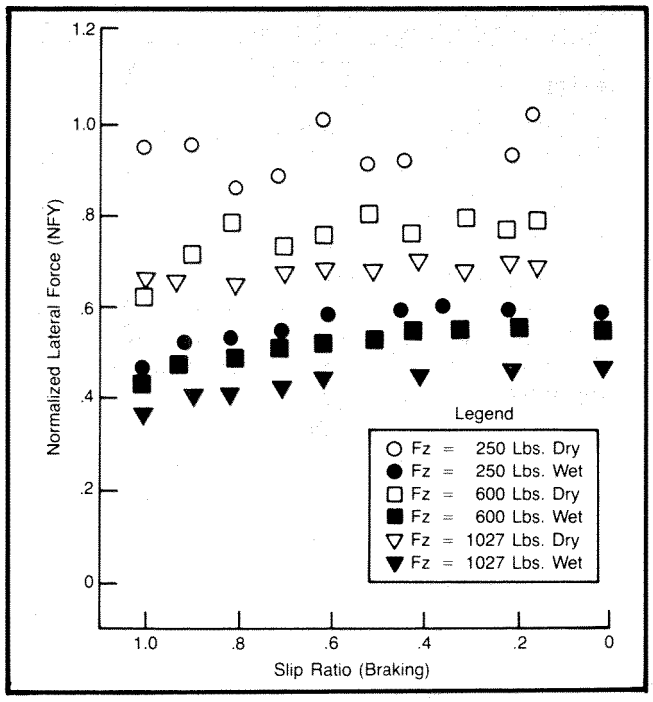

Figure B-7. Normalized lateral force versus slip ratio (braking)—slip angle = 0°

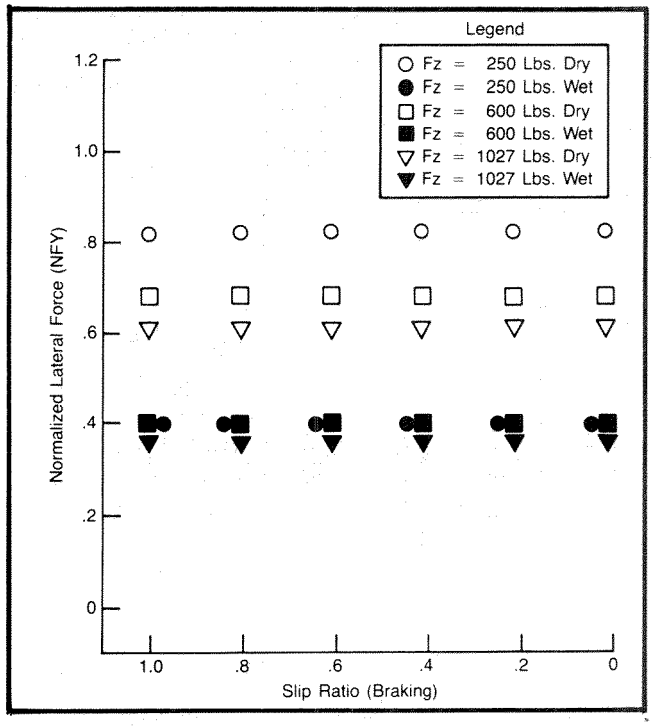

Figure B-8. Normalized lateral force versus slip ratio (braking)—slip angle + 90°

Conclusion

- Tire braking and cornering performance for the test tire, and thus the resulting vehicle performance, has been shown to be very similar on both wet and dry surfaces in the small slip angle and braking slip range. The braking and cornering performance on wet and dry surfaces has been shown to be very different in the large slip angle and braking slip range.
- The data have shown that the overall vehicle braking and cornering performance level can be increased by equipping vehicles with higher load range tires.
- The tire performance data in this study have also shown the possibility that vehicle stability during cornering and braking might be increased by equipping the rear wheels of vehicles with higher load range tires.
- Tire normalized cornering forces are largely surface-independent in the region of small slip angles (less than 4° slip angle).
- Tire normalized cornering forces are largely surface-independent in the region of small braking slip (less than 20 percent slip).
- The peak and slide normalized braking force is very much surface-dependent. The higher the friction coefficient, the higher the peak and slide values.
- The normalized lateral force is surface-dependent above 4° slip angle.
- The normalized braking force is normal load-dependent, especially on a dry surface. The lower the normal load, the higher the normalized peak and slide braking forces.
- The normalized lateral force is normal load-dependent for slip angles above 4°. The lower the normal load, the higher the normalized lateral force, especially on dry surfaces.

The above conclusions are based on the tire performance data measured in this one study.

Recommendations

- Tire design should be explored to increase wet tire braking and cornering performance.
- Tire wheel rim diameter and width, as well as tire aspect ratio, should be examined for their potential to increase tire braking and cornering performance, especially in the nonlinear, more severe, performance range.
- Tire load range should be explored as a potential tool for increasing vehicle braking and cornering performance as well as vehicle yaw stability.
- Tire normalized cornering forces are largely surface-independent in the region of small slip angles (less than 4° slip angle).

Accident Avoidance—Crosswind Sensitivity of Some Streamlined Cars

M.A. Jacobson
Consultant, The Automobile Association, United Kingdom

Abstract

This paper is based on a detailed analysis of real-life situations and is intended to highlight some of the problems that can occur with modern lightweight cars when their aerodynamic shape approaches that of an aerofoil. The problem of disappointing straight line stability when travelling at speed may be more pronounced in the United Kingdom than in Central Europe where one of the cars so flawed was conceived and developed. The topography, significantly higher crosswind speeds, the alignment of the main trunk roads relative to the prevailing winds of high speed, and the proneness for such winds to have extraordinary gust levels are cited as an explanation for the difficulties experienced by motorists when the low drag, front-engine, rear-wheel-drive car was launched in 1982/83. Progress has been made to minimise the handling problems under high speed and crosswind situations, but there is little chance of achieving better driver skill. Therefore, it must fall on the carmakers to do better and make their product fit for even morons to drive safely and be as predictable in their road manners in wet, windy weather as under less demanding conditions.

Introduction

Despite many significant advances in techniques, the information on the contributing factors to accidents or near-misses is still very scant and imprecise.

It would be wonderful if automobile engineers and those concerned with preventing road accidents could have the same feedback the aircraft industry has on the operational performance of its products and even on the causes and sequence of events leading to a near-miss or actual accident. The precision of the results obtained in forensic analysis of aircraft mishaps is beyond what can reasonably be expected in a reconstruction of road accidents. In car accidents, there are generally no precise and reliable data up to the moment of collision or impact. Motor cars do not have black boxes or flight recorders to assist an investigator in reconstructing the sequence of events, including operator errors of judgement and their consequences.

By comparison, the reconstruction of road accidents is fairly crude and remains more of an art than a science since it is often based on intuitive reasoning.

Major Contributing Factors to Road Accidents

In accident reconstructions, it is rarely possible, nor indeed necessary, to give precise answers as to what did take place, e.g., speed and driver avoidance action. The best one can hope for is to note the limiting values of the principal parameters that determine if a situation arose where an accident became inevitable or could have been avoided by a driver exercising reasonable care and competence.

The principal and interacting factors are—

- The driver, his care and attention, skill and experience, concentration and alertness, and state of well being, which includes not only drink and drug side effects, but also emotional stress
- The speed of the vehicles involved
- The road layout and special topographic features
- The dynamic characteristics of the vehicles involved
- The weather conditions, including ambient temperature, intensity, and direction of strong winds
- The condition of the tyres

Generally it is difficult to give precise values to the first two factors listed above. However, it may be possible to state a range of probable values and, by a process of iteration, give a close approximation of the most likely sequence of events that led up to the incident. In particular, the driver's reactions to a given traffic situation can span a wide range of possible options, from timid and slow to brash and erratic.

It is, regrettably, still left to professional test drivers and motoring journalists to pass judgement on the general handling characteristics of vehicles. Their approach to a car is not typical of more normal motoring. It takes most drivers quite a while to become attuned to an unfamiliar model. The insurance companies can verify that a disproportionate number of minor scrapes occur during the first few weeks following a change of car. This may be a sad reflection on how well we prepare motorists for modern fast-flowing traffic and dealing with confined parking spaces.

The only deduction one can safely come to is that wherever possible, the cars and subsystems should compensate for the inadequacy of those who drive them to get them safely out of tricky situations. In other words, make the car inherently safe even when the driver is not as competent as he or she should be.

I have chosen a particular accident, not because it was a fatal one, but because it illustrates a number of interesting features and was particularly well investigated in greater detail than most such accidents. It was a single-car accident on a well-maintained trunk road.

Accident Analysis Involving an Airborne Family Car

The case involved a young driver with only limited driving experience and on his first outing with a new 1.6-l car capable of a top speed of 101mph in wind-free conditions on a level road. He survived, but his fiancee did not. His general alertness and ability to respond to changing circumstances was poor, at least when he was subjected several months later to fairly simple tests.

There are some features of this car that make this model distinctly different from others of the same general shape and weight (2,400lb). It is front-engine, rear-wheel-drive, has all independent suspension, but does not have a very stiff floorpan, particularly on that section against which the rear suspension struts react. It has a pronounced aerodynamic shape. When travelling at speed, it has been noted and adversely reported on by several independent car testers that the early models (1982/83 build year) could be affected easily by strong winds.

Driven steadily but vigorously into a fast bend, even the 1982/83 models behave well, starting off with a mild understeer and then progressing into a mild oversteer as speed is increased, provided the throttle is kept constant. But if the driver loses confidence halfway through the bend and takes his foot off the accelerator pedal, the rear can slide out so rapidly that many motorists could find it quite difficult to regain control.

When one encounters strong crosswinds or fairly low tyre-to-road grip conditions, this model is more prone to rear-end breakaway than a comparable front-wheel-drive car.

One should not forget that the instinctive reaction of most drivers is to take their foot off the accelerator pedal when they note they have entered into a bend too fast or feel that the rear end of the car is about to drift sideways. Attempts to correct this by counter-steering are usually too late, partly because of the steering system characteristics and primarily because most drivers lack experience of "driving at the limit."

The ability to drive effortlessly and surefootedly at the limit of tyre-to-road adhesion characterises a good rally driver, for he can control a drifting car by rapid steering and throttle application. An ordinary motorist cannot.

It was considered worthwhile to compare the 1982/83 model with a 1984/85 model (in which several modifications were introduced to improve the car's behaviour) and with its direct competition (which is front-wheel-drive), and to do so not only under proving ground test conditions but also on motorways under strong crosswind conditions. Under wind-still conditions, all three behaved predictably and were at all times under perfect driver control. However, at the time of the accident, conditions were far from ideal. Under strong crosswinds, the latest version of the front-engine, rear-wheel-drive car was much improved, but even then it was still not as well balanced as its front-wheel-drive competitor. The manufacturer achieved this improvement in his later model by subtle changes in some body panels, notably stiffening the floorpan torsionally, stiffening the suspension, and lowering the ride height. Also, attempts were made to introduce a controlled amount of eddying of the airflow over the rear quarters and thereby reducing aerodynamic lift at the rear end.

The Accident Site Conditions

Although the inspection of the site and the relevant measurements were undertaken some time after the accident, clear marks were left on the road, the kerb stone, grass verges, hawthorn hedges, telegraph posts, farm gate, and the grassy bank beyond the sunken farm track. They allowed one to plot the progress of the car throughout the incident, including its trajectory while airborne. It also helped to pinpoint where the car made contact with fixed objects and to note concentrations of scattered glass from light units, dirt from under-wing areas, window glass, wheel trim, etc.

The car had come up fast along a stretch of dual carriageway, and had overtaken a slower moving vehicle while still climbing the long 1 in 12 rise. The road then levels out before dipping into the West Broughton Hollow, again at 1 in 12; it follows a wide curve.

I have safely negotiated this stretch of road in almost wind-free conditions with a wide-open throttle, reaching 86mph as I breasted the rise and 91mph as I thundered down into the hollow; the road was dry. But the test car was a 1.6-l front-wheel-drive car of a competitor's make.

Wind and Weather Conditions at the Time of the Accident

There had been some sporadic, moderate rain showers and considerable gusting of winds, with wind speeds over nearby Met Office Stations exceeding 20mph.

When the car breasted the rise, the gusty crosswinds were coming at it at an oblique angle of about 40° to 60° relative to its line of progress, but the presence of hedges on both sides of the dual carriageway and a dense windbreak of trees on the opposite side would cause the full force of the crosswind to be deflected upwards and most of it would pass over the roofline of the car.

Shortly before coming into the hollow proper, the line of fir trees stops abruptly and a car travelling westward toward Uttoxeter would suddenly be experiencing the full force of the crosswind striking the car at about 50° relative to its line of progress.

The wind speeds recorded at the time of the accident are by no means exceptionally high for the United

Kingdom. Much more severe conditions must be catered for in the overall design of a modern car.

The Condition of the Tyres

Since the car in question had only covered some 280mi prior to the accident, the tyres had hardly been bedded in and had not yet developed their full grip potential, particularly on a rapidly drying, yet still damp road surface. Table 1 gives an indication of how the surface condition of well-maintained roads influences the optimum braking one can expect. The braking distance is a measure of tyre-to-road grip.

While some tyres are "grippier" than others under thin film conditions, thanks to their special tread rubber compositions, all tyres behave very indifferently when a well-trafficked road surface is covered by only a thin film of moisture, though more and more modern tyres develop a good grip on rain-drenched roads.

Determination of Car's Speed at Moment of Leaving the Road

Skid marks were left on the road and some were clearly striation marks, indicating that the car was travelling sideways for a time. It was relatively easy to obtain values of tyre-to-road grip for the three conditions—dry, wet, and damp road surfaces—by braking to a standstill with locked wheels.

At speeds above about 60mph, there is the risk of aquaplaning when the depth of water is about 2mm; this is typical for summer rainstorms. Generally, though a thoroughly wet road tends to give a better tyre-to-road grip than when it is just damp, as, for instance, in fog or morning mist conditions or where the road is drying in patches. It requires frost, salt, and grit application and ample rainfall to open up the road surface texture and remove the thin layer of oil, diesel fuel, and abraded rubber that makes heavily trafficked roads so slippery. *Damp spells Danger.*

Table 1. Emergency braking distances for different road conditions.

The distances are the best that can be expected on well-maintained roads having either a tarmac or concrete surface. The figures are the distance, in feet, from a given initial vehicle speed to standstill and include reaction distance.

Initial speed mph	Total Braking Distance (ft.) For Different Road Surface Conditions & Sound Tyres				
	Black Ice	Damp	Wet Road		Dry Road
			1mm Tread Depth	5mm Tread Depth	
5	11	7	7	6	6
10	34	17	16	15	14
15	70	30	28	26	24
20	120	47	42	39	36
25	155	60	55	50	47
30	260	90	85	73	67
35	345	117	105	93	85
40	440	148	130	116	106
45	555	185	161	141	129
50	675	222	195	170	156
55	815	265	230	205	185
60	960	315	270	240	215
65		365	350	275	250
70		420	500	315	285
75		480	600	360	320
80		545	800	400	365
85		620	930	450	405
90		700		500	450

Depth of Water 2mm

For the road in question, typical values were found to be:

μ (dry road surface) = 0.75 to 0.8
μ (wet road, rain) = 0.6 to 0.68
μ (damp, particularly after a long dry spell) = 0.55

The striation marks indicated that the car was driven in excess of the critical speed for the curve. As long as the car is maintained at this critical speed, there exists a balance of forces: $a.r_c = v^2$

In this:

v = constant forward velocity of the car
r = radius of curvature
r_c = critical radius of curvature, i.e., the minimum radius of curvature at which a neutral steering car can be driven at constant speed v without drifting out
a = limiting lateral acceleration = μg
μ = maximum tyre-to-road grip coefficient
g = acceleration due to gravity

The radius of curvature at the critical location is around 700 to 780ft, depending on the line taken by the driver:

For the dry road condition:
v_c= critical speed = 88½mph to 96½mph
For wet and rainy conditions:
v_c= 79mph to 89mph
For damp road surface:
v_c= 76mph to 80mph

This leads to the conclusion that the car must have been travelling in excess of about 75mph when the driver lost control.

The Airborne Phase

There was ample evidence, on the spot where the car had left the road, that it had struck the kerb with the front wheels still rotating, for good tread pattern imprints were left on the kerbstone and the verge.

Striking the kerb would tilt the car very slightly upward. The aerodynamics of the car would encourage rather than suppress this attitude at takeoff. Thereafter, the car continued as a free-flying object across a sunken road, hedges, a pond, and a pasture before striking a rising grass bank some 88ft from where it took off, riccocheted off, and rolled over twice forward and once backward before coming to rest as a broken and buckled piece of machinery.

In the analysis used, the slowing-down effects due to brushing against hawthorn hedges, a telegraph pole, and the pole of a traffic sign as well as air resistance have been ignored. There was no evidence that the car had been badly dented by contact with these fixed objects.

Since the top of the hedge can yield elastically when the car first strikes it and since there were two nicks on the wooden telegraph pole, caused by the edge of the front and rear bumpers of the car, two of the points of the trajectory could be fixed only approximately. Also there was a degree of uncertainty about the actual height of the point of first strike on the soft bank some 88ft away from the takeoff point, i.e., relative to the starting point of the free-flight parabola, for the car had spun in mid-air and there was evidence that the first part of the car to make ground contact was the side of the car. It could, however, only be within a fairly narrow range.

When due correction is made for the centre of gravity position of the car, it had to be at least 7ft and no more than 8½ft below the take off point.

Altogether, seven points of the trajectory could be ascertained, of which three were only approximate. Accurately plotting them and giving the uncertain ones a realistic tolerance range confirmed that the car had followed a true parabolic trajectory and partly turned while still in free flight.

It was, therefore, considered legitimate to use a simple formula, which is familiar to those interested in ballistics.

The general formula for an object propelled like a flying projectile is:

$$\mu = R \sqrt{\frac{-g}{2\,(H - R\tan\Theta)\cos^2\Theta}}$$

in which:

μ = initial velocity at start of free flight through the air
g = acceleration due to gravity
R = range
H = height of point of impact above or below starting point
θ = angle of elevation of flying object relative to the ground at the start of its trajectory

Measurements taken on site were:

R = 88ft
H = -7½ft to -8½ft

There could be a range of values of θ; however, the scrape marks left on the hedges clearly rule out a large proportion, e.g., negative values of θ, as well as those greater than about +3°.

For R = 88 ft and H = -7 ft or -8½ft respectively

$\Theta = 0°$	μ = 91mph	μ = 82½mph
$\Theta = 1°$	μ = 82½mph	μ = 76mph
$\Theta = 2°$	μ = 76mph	μ = 71mph
$\Theta = 3°$	μ = 71mph	μ = 66½mph

Given the situation of a relatively inexperienced driver, unfamiliar with the road manners of the make of car, which is so markedly different from its predecessors and many other current motor cars, and the damp road surface on this fast downhill bend in the dual carriageway road, as well as the gusty side winds, it would be almost a

foregone conclusion that the driver would lose control of his vehicle if travelling at speeds in excess of about 80mph. It would all be over in about 1.5s, during which the car would be airborne for about 2/3s.

Why Should This Model of Car Be So Sensitive to Crosswinds?

It is not unknown for aerodynamic-shape cars to be crosswind sensitive, and a number of well-known manufacturers did have to stop selling, withdraw, or drastically modify the offending models, usually only after public pressure, severe criticism by the media, dramatic "roof bending" incidents, or fall-off in sales. In the case of the early Beetle, lack of top speed meant that the most likely and fairly disturbing feature when encountering strong and gusting crosswinds was that the car might be blown across one traffic lane when crossing an exposed road viaduct. In other words, it lacked straight line stability under crosswind conditions.

I have experienced a flip-over in three quite dissimilar models, all without suffering serious injuries, for it was a relatively long period during which lift-off or being turned on the side took place, several seconds in fact, and the slowing down to a stop was on a permanent top road surface or in cultivated fields, where the retardation was due to paint and metal being abraded by physical contact over a large surface area.

To the credit of the manufacturers of these early cars, they did eventually undertake major design changes to minimise these undesirable trends. Also the knowledge of aerodynamic forces and couples generated by strong crosswinds did not exist at the time. It is, therefore, not surprising that mistakes occurred. But since then, a great deal of factual, numerical data have been accumulated in many design studios. Racing cars have developed aerofoils to keep the rear end firmly on the ground, and air dams are now commonplace. The arguments about whether ground effect skirts gave unfair advantages to a particular racing stable could not have gone unnoticed.

The new shape car had been developed in the wind tunnel and undergone extensive proving ground and road testing in Central Europe. Apparently the test drivers and development engineers did not encounter any transient instability or other handling problems.

Limitations of Wind Tunnel Test Results

Adverse comments on the straight line stability were confined to the United Kingdom. The manufacturer concerned had placed total confidence in the results obtained during his wind tunnel testing. Also, since the car was intended for all markets in Europe and had to be very competitively priced, management did not see any need for fitting a rear end spoiler, though this is a standard and very prominent feature on all the more powerful models in this range. They use the same basic body shell.

In the early days of wind tunnel testing, the emphasis in most research departments was on reducing aerodynamic drag, and any side effects this might produce, such as unwanted aerodynamic lift and sensitivity to strong crosswinds, were barely considered to be of any relevance.

In several wind tunnels, it is difficult to yaw the test car sufficiently to simulate a strong crosswind without the wind tunnel bloc effect coming into play; moreover, this bloc effect can give very misleading numerical values. A wind tunnel will, of necessity, have limitations in tunnel cross section, shape of side walls, and power output of the wind generators. It will, therefore, be almost inevitable that when a vehicle is significantly yawed relative to the wind generator fans, some of the air blown over it in a parallel stream of uniform velocity will be deflected against the sidewalls of the wind tunnel and then be bounced back to pass over the rear end of the vehicle so being tested and thereby significantly modify the air velocity gradients in the wind tunnel. In most real-life situations, this crowding effect is absent. The greater the yaw angle, the more unreliable the wind tunnel results tend to be.

One way around this would be to use wind generators on proving grounds more extensively. Judging by the rusty state of several of them (for example, those at MIRA), they are not being used all that often, and the reasons are all too plain. The airflow mass and pressure characteristics of even very powerful compressors are puny when compared with nature. The nozzle size and the airflow velocity are such major limitations that only moderate crosswinds can be simulated. To create a yaw angle situation representative of what can take place in high winds, say a 15° to 18° angle of attack of the resultant airflow as it passes over the car's body, the speed of the vehicle as it passes the compressor exit duct nozzles at a right angle will have to be quite modest, i.e., about half the maximum speed of the car. In most modern cars, crosswind sensitivity will not occur at legal speeds in the United Kingdom, i.e., 70mph or less. However, people do motor well above that speed.

Since this 1982/83 model has neither a small air dam at the front nor anything resembling an aerofoil spoiler at the rear end, the car will experience a considerable aerodynamic lift when travelling at speed.

The effect of aerodynamic lift increases as the square of the velocity of the air flowing over the body shell. The airflow velocity over the body is the resultant of two velocities, which must be compounded by vector analysis. The first force is due to the forward speed and the second is due to crosswinds.

As long as the car travelled in the wind shadow provided by the line of trees, there was hardly any

crosswind contribution. But as the car emerged from the wind shadow of the trees and dipped into West Broughton Hollow, there was not only the additional air speed component of the gusting crosswind to be considered, but also the two effects it produced:

1. It suddenly and materially increased overall lift to around 1/10 the weight of the car, which made the steering go light, for there was then less weight acting on the front wheels, and it also lowered the effective load on the rear wheels, which provided the forward momentum.
2. Whereas in a more or less straight-ahead driving mode the centre of gravity and centre of pressure coincide, the presence of a crosswind would tend to make the car yaw in much the same way that a sailing boat reacts to wind forces.

The centre of pressure is the point at which one can consider all the wind forces to act on the car, but it does not coincide with the centre of gravity. The greater the distance between the centre of gravity (the point at which one can consider all the weight acting on the suspension to be concentrated) and the centre of pressure, the greater the leverage of crosswind forces. This creates a moment of trying to turn the car off its original straight line course. Such a moment must be resisted by sidegrip forces exerted by the tyres on the road. The sideways grip will be limited by the tyre and road surface conditions.

There is a third centre—the centre of lift at which one can assume the combined vertical lift forces to act. Ideally this centre of lift should not move as the car travels faster, nor should it be influenced by crosswinds. Should the centre of lift move rearward, then an aerodynamically induced oversteer will occur, which is exactly the opposite of what is desirable.

The car in question suffered badly from this aerodynamically induced oversteer phenomenon, particularly at higher speeds. When the winds were gusty and exceeded about 30mph mean velocity, then the sensation of crosswind wander and the need for instant and rapid countersteer would occur even at 70mph. One moment the car would be going as straight as an arrow; the next it would appear to dart off at an angle or move over bodily when passing close to a high-sided truck or coach. I have repeatedly experienced this in the United Kingdom.

This tendency is less noticeable on the continent of Europe for several reasons.

It is a little known fact that the geography and topography of Great Britain has resulted in many of the major trunk roads being so aligned that when strong crosswinds do occur, they strike traffic at an oblique angle of 15° to 90° on their North-South progress and on the East-West connecting roads on the sections where the hills provide little windbreak at around 30° to 90°, all relative to the line of progress of the vehicle.

In Central Europe, and that includes the manufacturer's proving ground area, the prevailing winds tend to be of lower intensity and less gusty inland. Also the terrain tends to be more broken up by hills, forests, and copses acting as wind force moderators.

There are, of course, exposed sections of trunk roads and motorways, but these and bridges and viaducts are liberally equipped with wind socks, which give unambiguous signals of wind intensity and direction. This gives the driver the sort of early warning that allows him to moderate his speed and thereby minimise his being blown about as he emerges from the protection of the wind shadow.

Where no such advance warning is received, it is all too easy for an average motorist to brake hard when he suddenly feels the crosswind buffeting him. This can result in a fairly sudden transfer of weight from the rear to the front. This reduces the weight on the rear tyres to the point of momentary loss of grip on the road, particularly in the damp, and the back may then slide out at an alarming rate.

Comparison of the 1982/83 Model with Previous Models

Whatever one may have thought about the previous models and their lack of all-around independent suspension and other modern refinements, hundreds of thousands of motorists all over the world proved that these three aerodynamically unrefined box cars were utterly predictable and far less affected by crosswinds; also there was no aerodynamic lift at high speed making the steering go very light.

By current standards, these earlier models are aerodynamically clumsy. Their general shape—a three-box arrangement—and the detail treatment of the body panels, windows, etc., lead to considerable eddying and absence of an uninterrupted flow of air over the body shell. In a well-streamlined body shape with smooth contours, the flow of air over the body is laminar, not turbulent, and this laminar flow follows Bernoulli's law. For airflow over the body to be continuous, that part of the airstream that passes over the bulbous (more convex) upper part of the body must meet up, a short distance behind the body, with that part that passes over the almost flat underside. The part of the airstream that has further to go over the bulbous part must, therefore, be travelling faster than the average air speed.

It is a fundamental law of nature that, as air is speeded up as it flows over the more convex part of an aerofoil (the upper part), it creates a lift. The faster the airflow, the greater this negative pressure (the lifting force). The basic principle underlying powered flight of heavier-than-air machines relies on this law of nature.

Fastback cars are particularly prone to generating lift at the rear end because the airstream on this relatively smooth contoured, very aerodynamic car remains well

attached to the upper body without much eddying or turbulence. Broken flow causes a loss of lift. In an aeroplane, this is called wing stall.

As the aerofoil approaches the stall situation, the lift diminishes to the point of collapse.

It is surprising that the manufacturer, who had ample experience of building fast motor cars for sports and rally enthusiasts, did not make a discrete rear and spoiler a standard feature across the model range. More and more competitors add simple and discretely short rear-end bustles and/or rear-end spoilers to their family cars and not only to their high-performance derivatives.

The purpose of these rear-end spoilers, which take extreme proportions on racing cars, is to insure that at speed and in crosswind conditions there is a downward force acting on the rear wheels rather than an aerodynamic lift.

This is most needed in powerful rear-wheel-drive cars, for any lowering of such downward forces reduces the tyre-to-road grip. For the same tyres, the greater the downward thrust, the greater the ability of the tyres to provide the necessary control forces. These are fore and aft for acceleration, steady speed, and braking, and sideways to hold the car on a predetermined course to prevent sliding or skidding. Absence of adequate sideways grip causes the car to be jolted by crosswinds, particularly when these are gusty and coming out of the wind shadow of tree-lined banks onto open, exposed road sections or after overtaking high-speed trucks or passing bridge parapets. The lighter the car and the more aerodynamic its shape, the more pronounced its tendency to be upset by gusty crosswinds unless spoilers are fitted.

A new industry now caters to motoring enthusiasts. Since the launch of the car, some specialist accessory manufacturers have cashed in on the reluctance of the manufacturer concerned to do it in-house. Offered are well-advertised add-on fitments to improve both the front and rear end deflection of airflow and thereby reduce crosswind sensitivity at speed. The car manufacturer concerned is now making the optional extra of stylish add-ons available through some of its major dealers, at least in some of its European markets. Does that imply this large carmaker is accepting that wind forces can be troublesome, at least in the United Kingdom, and that it is up to the carmaker to so design even his base models that they can cope with the worst that nature and press-on motorists can do to upset straight line progress?

United Kingdom Wind Conditions

Table 2 gives an indication of what the motorist in the United Kingdom has to face from time to time. The resultant wind-speed yaw angle increases rapidly as crosswind velocity rises. Moreover, what should concern the stylists and body designers and those perfecting the running gear is the rate of this increase from zero to more than 7°, which occurs as the car proceeds from the wind shadow of a tree-lined bank, or that provided by long high-sided trucks, into the full force of a crosswind of around 30mph. It takes only a fraction of a second for this transient, yet powerful, disturbance to get a hold on the car. It is the dynamic response of vehicle and driver to reestablish a new state of equilibrium, rather than the actual displacement of the car from its straight line progress, which can occasionally unnerve the ordinary motorist.

The wooliness of the response to transients is often due to there being too much compliance in the various rubber-bonded attachment points of the suspension and steering elements to the body structure.

It is of little concern to the ordinary motorist that all this may be due to either an inadequate, over-simplified mathematical model used in the early stages of product evaluation and assessment of design options or that the car will have to be tethered in an unrealistic way during wind tunnel testing. Nor is it any comfort to him that such problems will be cured by a step-by-step refinement as time goes by. Nor can one hope that the explanation will be accepted as adequate, that in mass-produced cars it may be necessary to have a considerable amount of built-in compliance to smooth assembly and that at the same time it minimises noise transmission from running gear to the passenger compartment. It will not cure the problem nor restore public confidence in some models.

Crosswind effects should not be seen in isolation, of course. It is all too easy to exaggerate the frequency of the occurrence of strong crosswinds. It is possible to draw up tables that indicate the intensity and duration of strong winds likely to occur in the United Kingdom and, e.g., Germany. The one given here is based on United Kingdom and German Met. Office records covering a 10-year period. Strong winds are not an everyday risk factor, nor do the winds always blow from the same quarter.

How Strong Are the Transient Wind Gusts Experienced in the United Kingdom?

While it would be unrealistic to demand that a carmaker design his lightweight cars to be able to proceed at almost maximum speed under every wind condition, a realisation of what the peak wind speeds can be would not come amiss. In the flying car analysed here, the peak gust speed was only 42mph and the yaw angle this induced rose in a fraction of a second from zero to 12°.

Very high winds are occasionally encountered in Scotland. Mean hourly wind speeds in excess of 70mph have been recorded at Glasgow and Edinburgh Airports,

Table 2. Annual percentage frequencies of wind near main trunk roads

General Location	Wind Force Intensity (Mean Hourly Values)						
	13 to 19 mph		20 to 24 mph	25 to 31 mph		32 to 38 mph	39mph and above
Lancashire Fells close to M6, A66	21.7 ---	40.2	18.5 ---	17.9 ---	29.6	11.7 ---	11.6 11.6
Glasgow Area M8, M73, M74	---	31.4	---	---	3.5	---	0.1
Eskdalemuir, Scotland M6, A7, A74	---	29.3	---	---	5.5	---	0.1
Edinburgh Area M8, M9, M90	---	35.3	---	---	3.5	---	0.1
Carlisle Area M6	25.3 ---	30.2	4.9 ---	1.3 ---	1.4	0.1 ---	* *
Newcastle/Tyne A1, A69	24.7 ---	32.8	8.1 ---	3.5 ---	4.2	0.7 ---	0.2 0.2
Lancashire Coast M6, M53, M56	---	44.6	---	---	8.9	---	0.3
Shropshire Plain M6, A5	21.7 ---	25.9	4.2 ---	1.1 ---	1.2	0.1 ---	* *
Nottinghamshire Plain A1, M18	23.6 ---	28.9	5.3 ---	1.3 ---	1.5	0.2 ---	* *
Nottingham/Central England M1, A46	24.6 ---	28.4	3.8 ---	0.6 ---	0.65	* ---	* *
Birmingham M5, M6, M45	18.8 ---	22.4	3.6 ---	---	1.5	---	* *
East Anglia A10, A11	29.7 ---	35.7	6.0 ---	1.4 ---	1.5	0.1 ---	* *
Bedford Area M1, A1	28.7 ---	36.4	7.7 ---	2.3 ---	2.6	0.3 ---	* *
Standted near London M11, A1, M25	25.2 ---	28.6	3.4 ---	0.5 ---	0.55	* ---	* *
London, Heathrow M3, M4, M25	22.9 ---	26.1	3.2 ---	0.7 ---	0.7	* ---	* *
Built Up Areas, Surrey M3	17.9 ---	20.2	2.3 ---	0.3 ---	0.3	* ---	* *
London, Gatwick M23, M25	22.5 ---	26.9	4.4 ---	1.1 ---	1.2	0.1 ---	* *
Dungeness, English Channel M20	---	50.3	---	---	7.5	---	0.3
Exeter A30, A38	23.1 ---	27.9	4.8 ---	1.3 ---	1.55	0.2 ---	* *
Bristol Area M4, M6	29.2 ---	39.1	9.9 ---	3.4 ---	3.9	0.5 ---	0.1 0.1
Cardiff Area M4	30.1 ---	38.2	8.1 ---	2.3 ---	2.6	0.3 ---	* *
Hamburg, Germany	---	27.4	---	---	0.8	---	
Hannover, Germany	17 ---	22.5	5.5 ---	---	1.2	---	

For the purpose of direct comparison, wind conditions are also given for two North German locations.

All these values refer to steady wind speeds averaged on an hourly basis. A gust factor of 1.6 to 2.0 has been established on many sites, where duration of such gusts may only be a few seconds at a time.

* less than 0.1 percent but more than 0.05 percent

with short gusts, lasting at least 5s, exceeding 100mph. On the Firth of Forth Road Bridge, the corresponding values were over 75mph and over 105mph.

But the southeast of the country is not spared either. Winds in excess of 55mph, gusting to over 85mph, were recorded in 1978 close to the main trunk route linking London and Dover. A little more inland, but close to the M20, these winds were 53mph, gusting to 76mph on a number of occasions.

Even the Midlands do not escape high wind speeds: 50mph winds with a minimum duration of 1 hour have been noted near Birmingham and also near Bristol, Gloucester, and further north near Shrewsbury. On a number of occasions, short-duration wind gusts of around 80mph were recorded at these locations.

Well inland, average wind speeds of between 45mph and 55mph and a duration of at least 1 or 2 hours have been recorded, particularly near Nottingham, sweeping across the main North-South motorway and its connecting spurs. Wind gusts well in excess of 80mph were also recorded in the same areas.

The more exposed areas of the West Country, Wales, and Scotland experience such high winds not for a few seconds or even minutes at a time; here it can take much longer before the ferocity of such winds abates. The same applies to the East Coast and, due to its topography, this spells trouble for motorists driving on the northern ends of the M1 and A1. The M5 and M6 motorways have been buffeted by wind gusts of over 90mph.

The topography plays a major role because it is the funnel shape of such prominent features as the English Channel, the St George's Channel, between the land masses of Ireland and Wales, and, of course, the Bristol Channel that causes an acceleration of air masses sweeping in from the Atlantic. Such hills as the Mendips and others fringing broad valleys act as deflecting vanes in turbo machinery; they redirect the wind. In short, there are far more major trunk routes in the United Kingdom that are affected by wind than in most European countries.

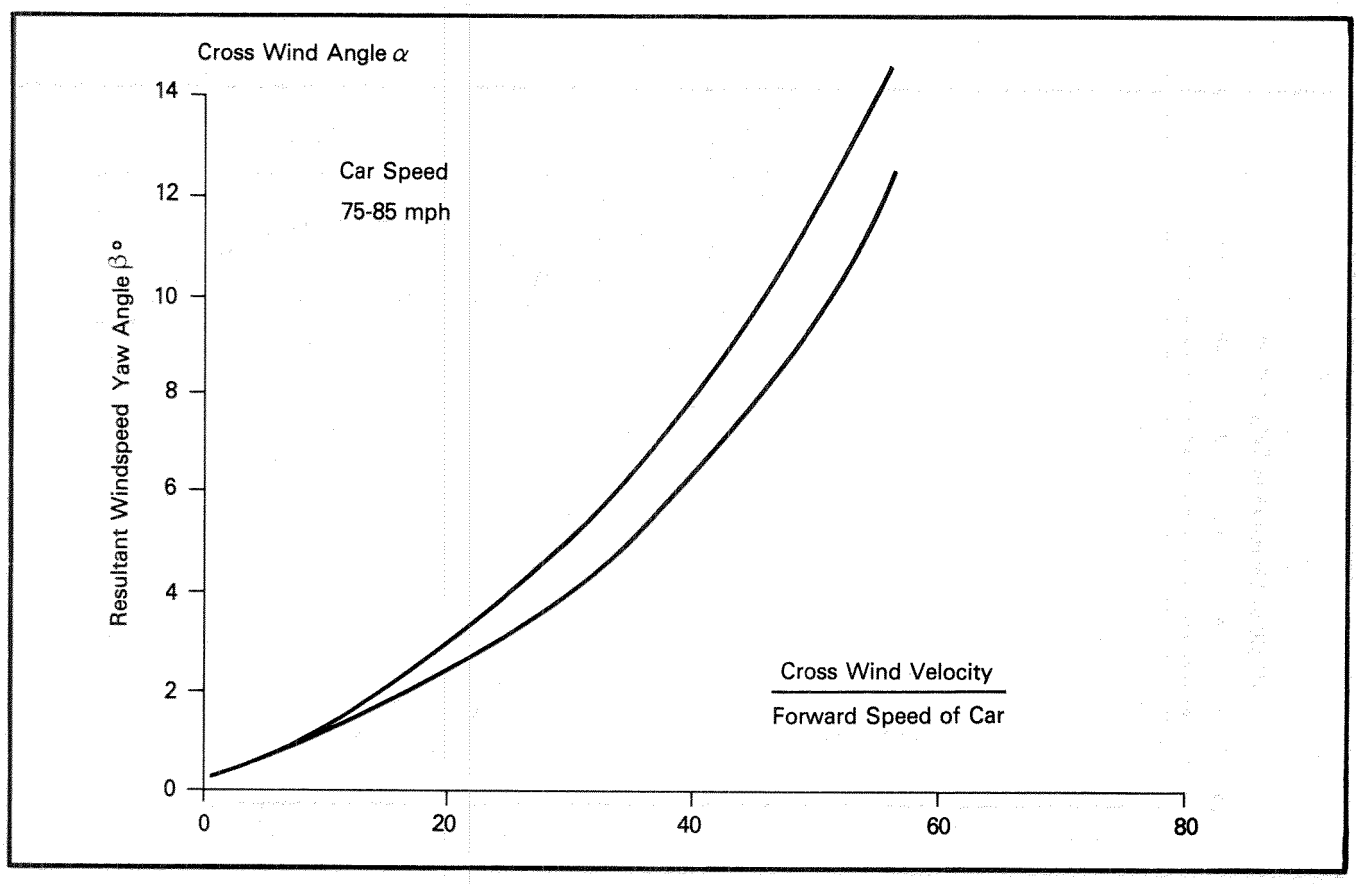

Figure 1. Angle of elevation at takeoff Θ°

Typical High Wind Speeds in Central Europe

Extreme values of wind gusts of at least 5s duration may cause concern to architects and civil engineers who have to erect tall buildings and similar structures capable of withstanding the most severe wind loading, even though they may occur only about once every 50 years. To the automotive engineer, the peak wind speeds that persist for at least 1 hour at a time, on average at least once every decade, are of more relevance. These should be included in the vehicle handling simulation, which can now be so colourfully shown in computer graphics, and therefore allow modifications to be advocated before the cars go on sale.

On the Dutch Coast, they are likely to be 50 to 55mph, yet for many places in Northern Germany, including, among others, Hamburg, Braunschweig, Hannover, Berlin, Essen, Düsseldorf, and Hildesheim, it is more likely to be around 40 to 45mph.

Geography is the prime reason why in places such as Frankfurt/Main, München, Nürnberg, Stuttgart, and Ingolstadt, it is not likely to reach 40mph. In the Danube region of Germany and Austria, wind speeds in excess of 30mph are fairly rare.

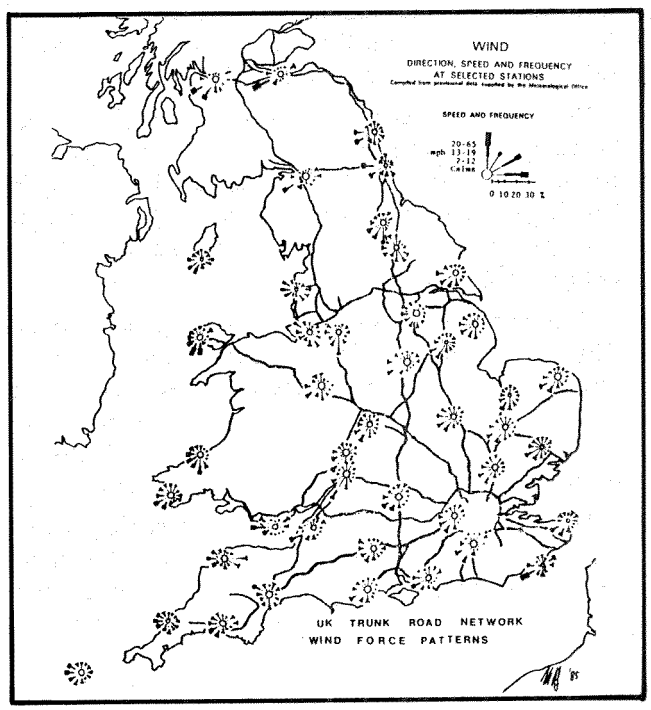

Figure 3. Wind—direction, speed, and frequency at selected stations

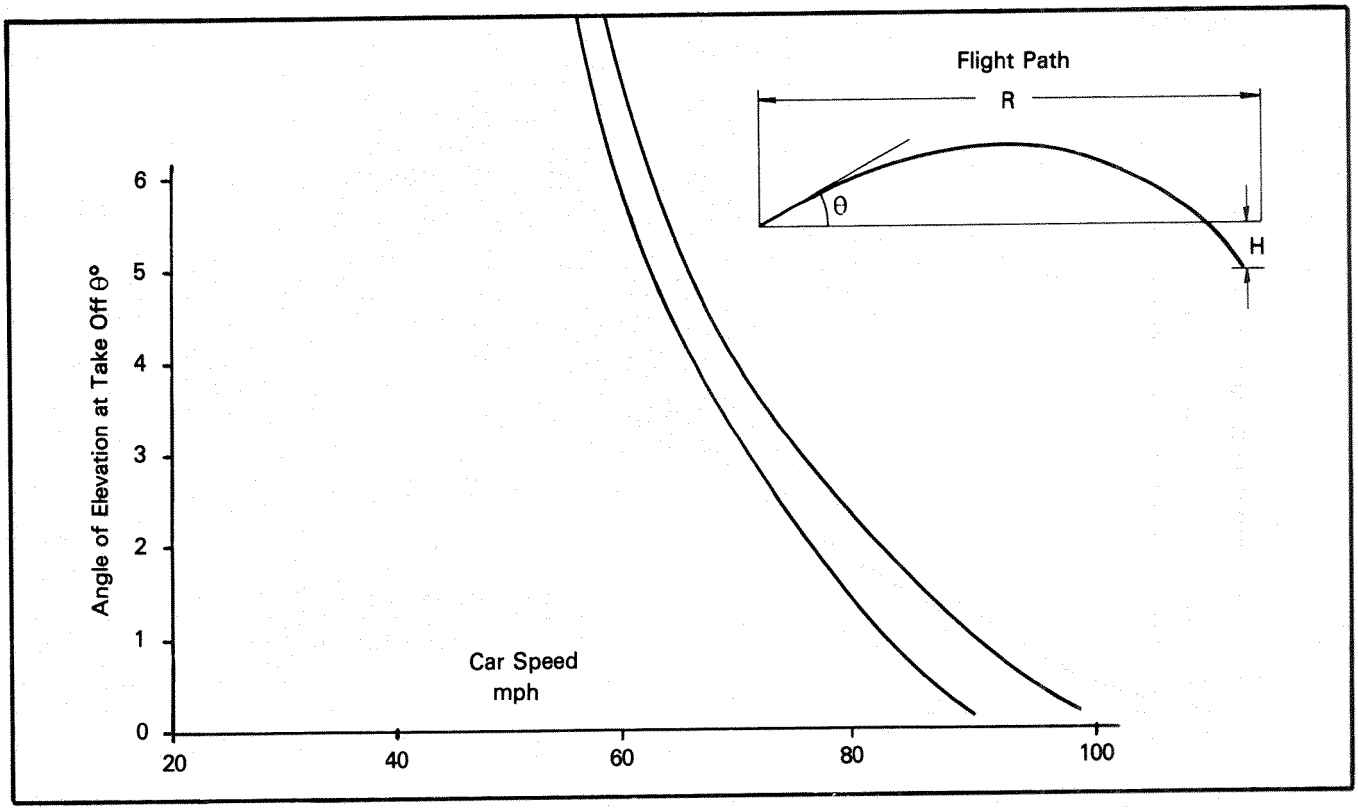

Figure 2. Crosswind angle α

Technical Session No. 3

Occupant Protection for Frontal Impact

Kennerly H. Digges, Chairman, United States

Efficient Energy Absorption of Automobile Side Rails

S. Yamaguchi,
H. Kato, and
T. Okazaki
Toyota Motor Corporation

Abstract

The method for stabilizing the axial collapse of side rails in a progressive folding mode, in which more efficient crush energy absorption was insured than in a bending mode, was examined by crush tests of closed-hat section members.

The tests have shown that the properly designed beading functions effectively and the critical collapse length of slant-mounted side rails could be estimated.

Introduction

Side rails absorb a large part of energy in head-on barrier crush tests of automobiles. The side rails deform in two different ways. One is bending deformation and the other is axial collapse in a progressive folding mode, or the axial collapse. The axial collapse absorbs crush energy more efficiently than bending and, therefore, in some cases side rails are designed to be expected to deform in the axial collapse mode for a certain length the head-on barrier crush tests. However, in many cases the side rails fail in a bending mode before the axial collapse mode reaches the expected value.

In this paper, two items are examined concerning the axial collapse stability and critical length of closed-hat section members generally used for automobile side rails.

1. Effective beading (designed dents or bulges) shapes and their arrangement to stabilize the axial collapse
2. Critical length of the axial collapse of slant-mounted side rails

Test Procedure

Figure 1 shows a schematic drawing of the test equipment. Test pieces were attached to the movable barrier and impacted to the fixed barrier. The deformation behavior of the test pieces was observed by high-speed cameras. Crush loads were measured by load cell installed on the fixed barrier face.

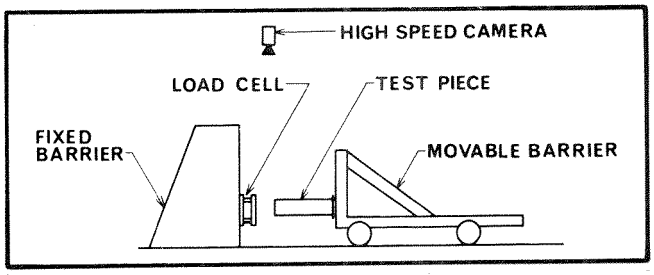

Figure 1. Test equipment

Effective Beading To Stabilize the Axial Collapse

Figure 2 schematically shows the axial collapse mode in regular folding of a closed-hat section member. In stable axial collapse, initial folding occurs near the impact end with peak and bottom lines of waves perpendicular to the axis, and subsequent foldings progress toward the other end with the same wave length (λ).

The purpose of beading is to trigger the stable axial collapse. Therefore, the foremost beading must trigger an initial folding and the other beading must trigger subsequent foldings progressively with the same wave length.

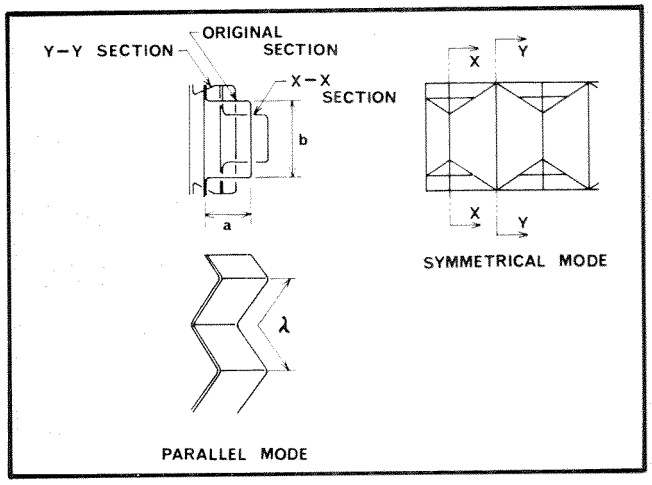

Figure 2. Axial collapse mode

Two series of tests were conducted to examine the effective beading shapes and their arrangement. One was to examine the effect of various beading shapes on a collapse mode and their proper pitches; the other was to examine the effect of combination and arrangement of the beading chosen from the previous tests. It was conducted for the members with and without the combination of beading.

Effects of Various Beading Shapes and Their Proper Pitches

Six types of test beading shapes and their expected effects are shown in Figure 3. Beading was applied to the hat-plate of the member.

Four or five beading pitches (λB) were investigated. The pitches were:

$$\lambda B = \frac{a + b}{2} \times k_i$$

where:

a : *section width*
b : *section height*
k : *coefficient*
i : *1,2,3,4,5*

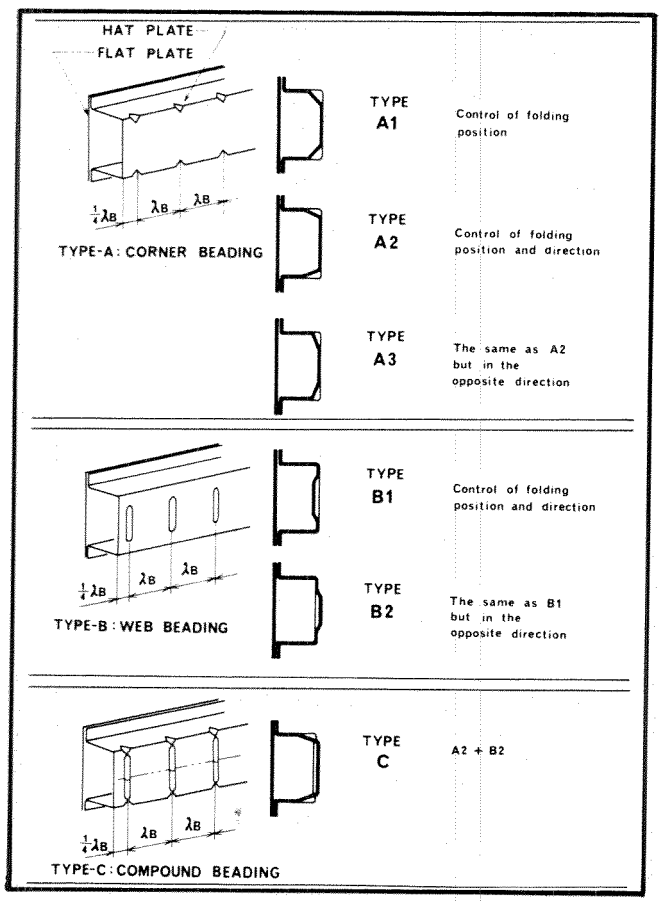

Figure 3. Beading shapes

Test results of maximum crush load (Pmax) are shown in Figure 4. The following were discovered:

1. The corner beading (A1, A2, A3) reduces the maximum crush load approximately by 20 percent.
2. The web beading (B1, B2) reduces less load than the corner beading does.
3. The compound beading (C) reduces the same load as the corner beading does, but it does not progress in subsequent foldings (see test results of folding mode).

Test results of folding mode are shown in Table 1. The table shows the following:

1. Each type of beading, except type C, had its proper pitch (λBO) to collapse the member in a regular folding mode. The proper pitch was:

$$\lambda BO(A1) = \lambda BO(A3) = \frac{a + b}{2} \times k3$$

$$\lambda BO(A2) = \lambda BO(B1) = \lambda BO(B2) = \frac{a + b}{2} \times k2$$

2. Type B1 and B2 beading folded the webs of the section in the opposite directions. Types A2 and A3 beading folded them in the same direction.
3. Type C beading did not allow the member to collapse in a progressive folding mode. All sections with the beading locally collapsed at the initial stage of the deformation, and subsequently the remaining sections between the beading were crushed. This is an extremely unstable collapse mode.
4. All the flat plates did not fold regularly.

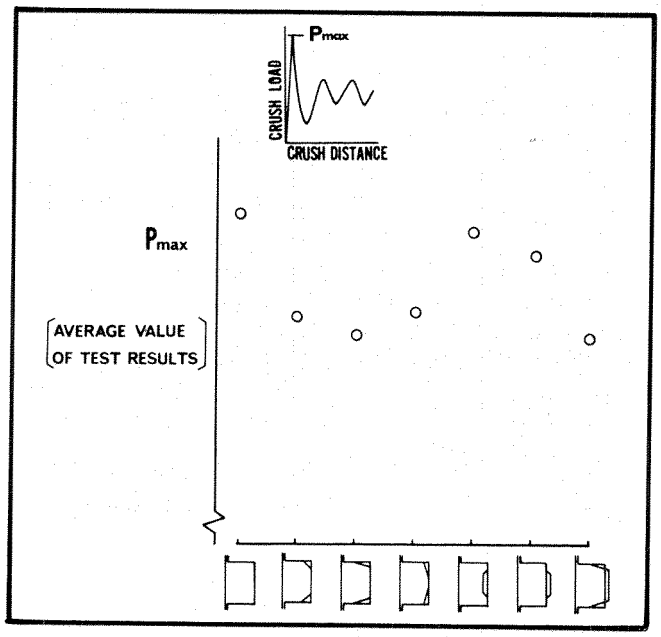

Figure 4. Maximum crush load

Table 1. Folding modes

BEADING TYPES / BEADING PITCHES	A1	A2	A3	B1	B2	C
$\frac{a+b}{2} \times k1$						
$\times k2$	HAT-PLATE / FLAT-PLATE					
$\times k3$						
$\times k4$						
$\times k5$						
NOTES						Regular folding did not occur. All the section with beading locally collapsed at first.

From the results described above, the corner beading (A1, A2, or A3) is suitable for the foremost folding point because of its low crush load. For the other folding points, the web beading (B1 or B2) is suitable because it has a relatively high crush load and regulates the folding direction.

Effect of a Beading Combination

The effect of a beading combination was examined by crush tests of the members with and without the beading. Two types of members were tested. One was straight and the other was tapered, shown in side view in Table 2. Figure 5 shows the combination and arrangement of beading. Figure 6 shows a test member schematically.

Test results are shown in Table 2 and Figures 7, 8, and 9. Both types of the members without beading failed in a bending mode, but those with the combination of beading collapsed axially in a regular progressive folding mode.

Critical Collapse Length and the Mounting Angle of Bumper-Equipped Side Rails

In many cases, side rails require positioning with some mounting angle. Therefore, designers need to estimate

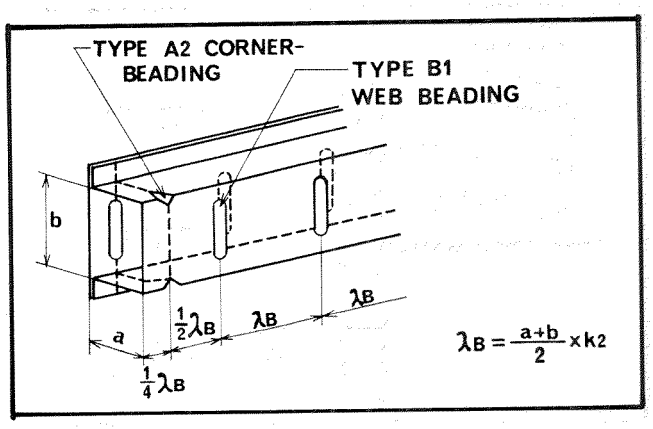

Figure 5. Combination and arrangement of beading

critical length of axial collapse to decide the angle. Slant-mounted side rails fail in two different modes shown in Figure 10. Bending mode A can be prevented by installing an appropriate reinforcement to the rear portion of side rails. Here, the collapse length, before resulting in a bending mode B, is called the critical collapse length of the side rail assembly including the bumper. The critical length was examined by crush tests for various mounting angles of the side rails.

The test side rail is shown in Figure 11. The side rail had a sufficient reinforcement to prevent the mode A bending. The tests were conducted for five levels of the mounting angles (θA and θB shown in Figure 12).

Table 2. Folding modes

SIDE VIEW OF MEMBERS \ BEADING	NO – BEADING	COMBINATION – BEADING
STRAIGHT 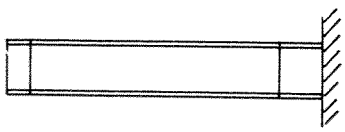	PLANE VIEW HAT – PLATE 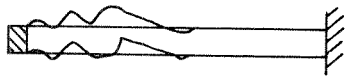 FLAT – PLATE	PLANE VIEW HAT – PLATE 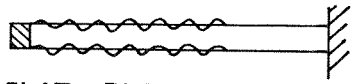 FLAT – PLATE
TAPERED 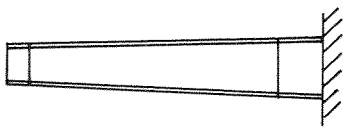	HAT – PLATE 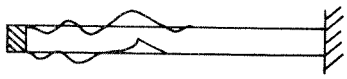 FLAT – PLATE	HAT – PLATE 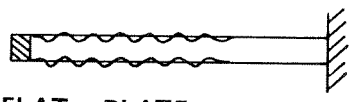 FLAT – PLATE

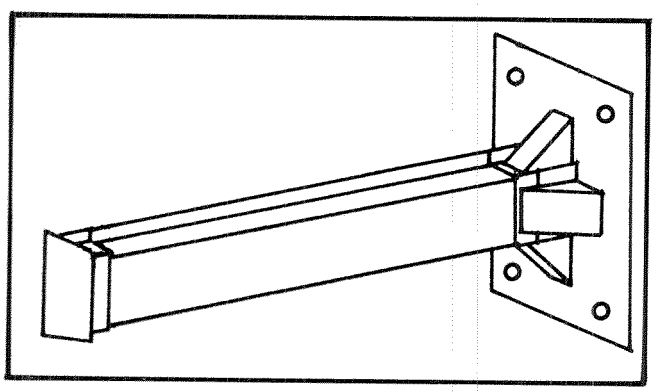

Figure 6. Test member

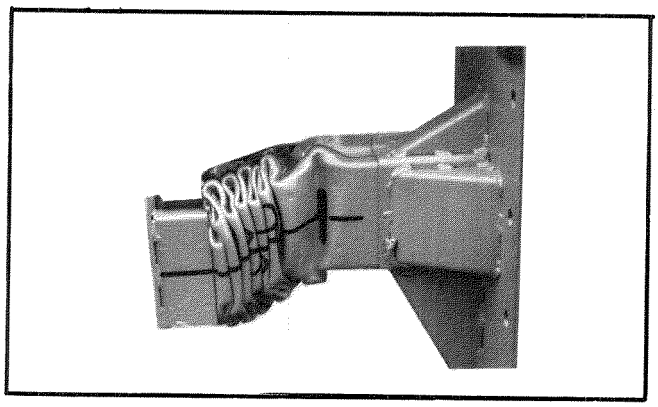

Figure 8. Hat plate of straight member with beading

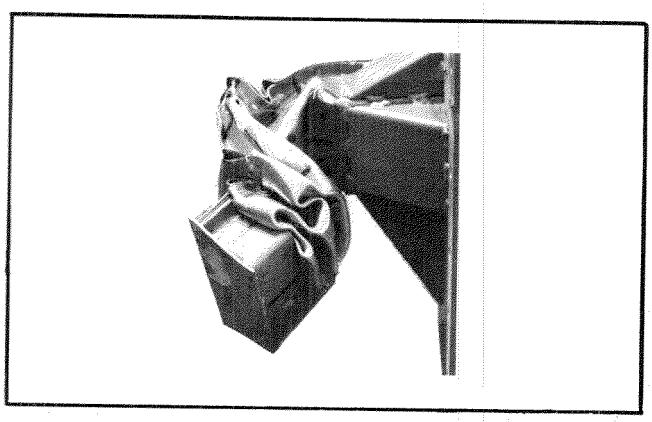

Figure 7. Straight member without beading

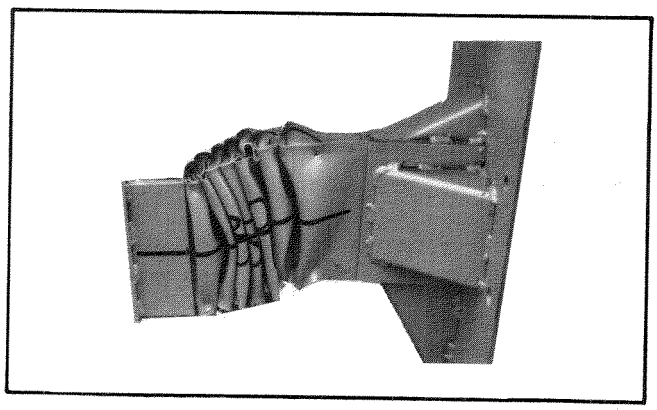

Figure 9. Flat plate of straight member with beading

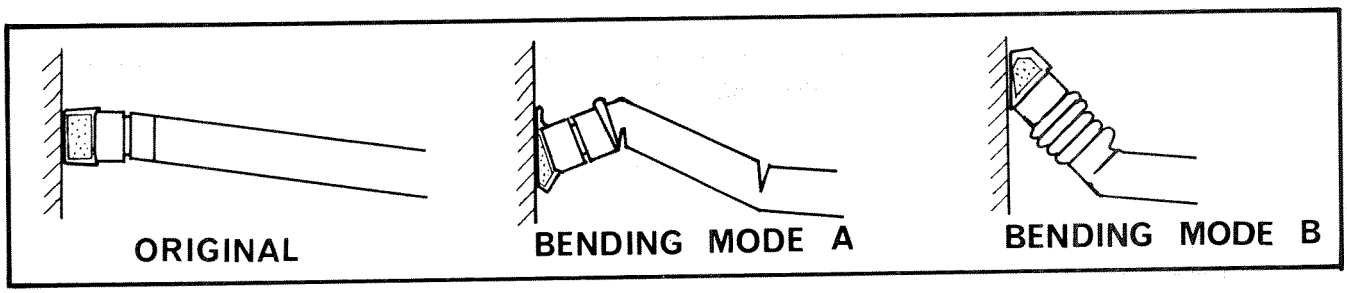

Figure 10. Bending mode of slant-mounted side rail

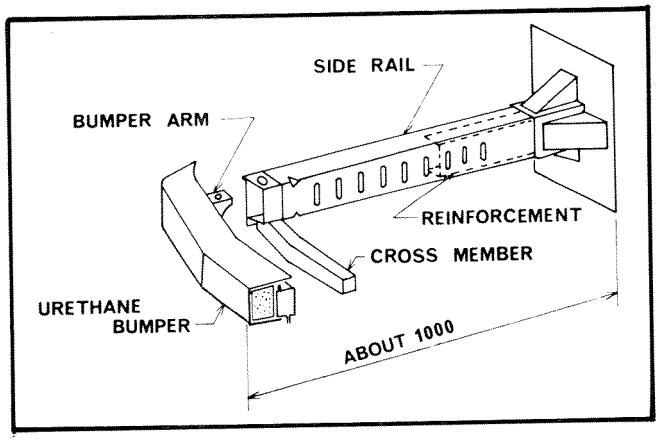

Figure 11. Test side rail assembly

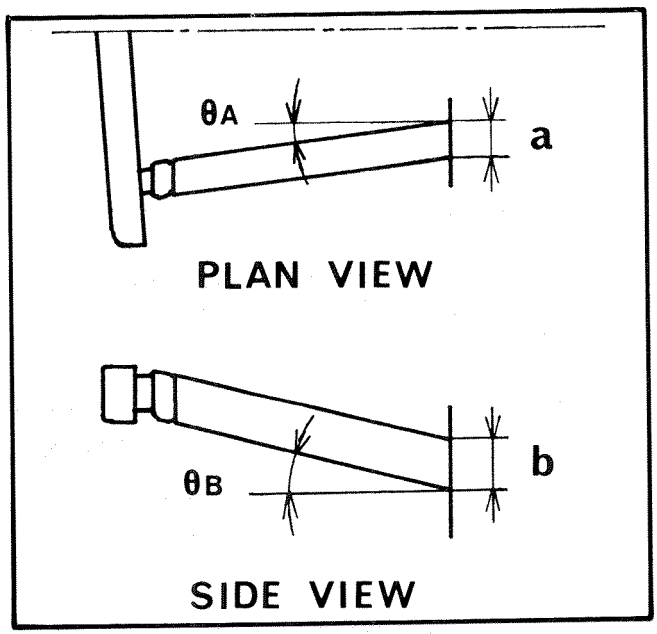

Figure 12. Mounting angle

Test results are shown in Figure 13. Dots in the figure show the mounting angles of the test side rails. The number under each dot shows the critical collapse length of the test side rail. However, the length of 600mm is the maximum value limited by dimension of test side rail. That means the critical length is 600mm or more.

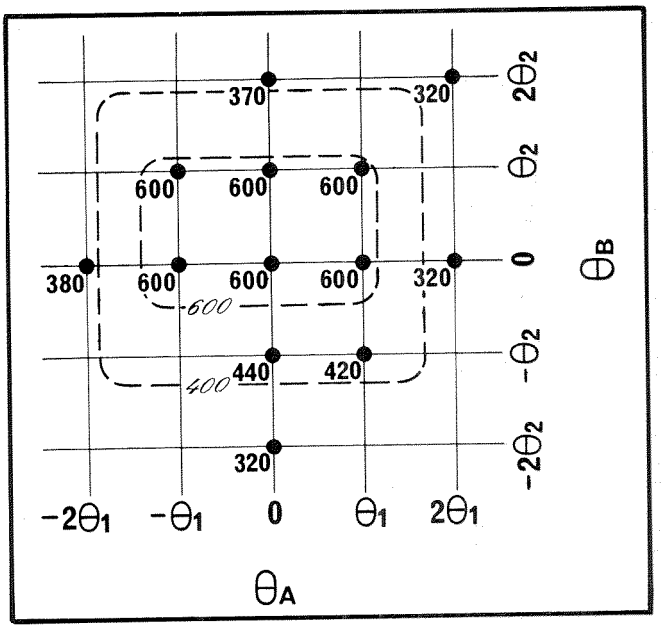

Figure 13. Critical collapse length

The figure shows that the critical length of slant-mounted side rails depends on the mounting angle and that the increase in the absolute value of the angle reduces the critical collapse length. The combination of θA and θB does not significantly affect the critical collapse length. Thus, the regions where the critical length is estimated to be 600mm and 400mm are indicated by broken lines.

Additional tests were conducted to examine the relationship of the critical collapse length and section height (b). In the case of slant-mounted side rails, the axial collapse progressing reduces the overlap (c shown in Figure 14) between the front end section and the section just collapsed.

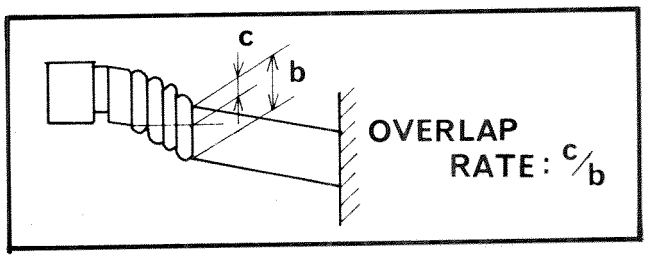

Figure 14. Overlap rate

Figure 15 shows the overlap rate, which is c divided by b, at the instant of failing in the mode B bending. This shows that the critical overlap rates are roughly the same.

Thus, the critical collapse length could be estimated for mounting angle and section height.

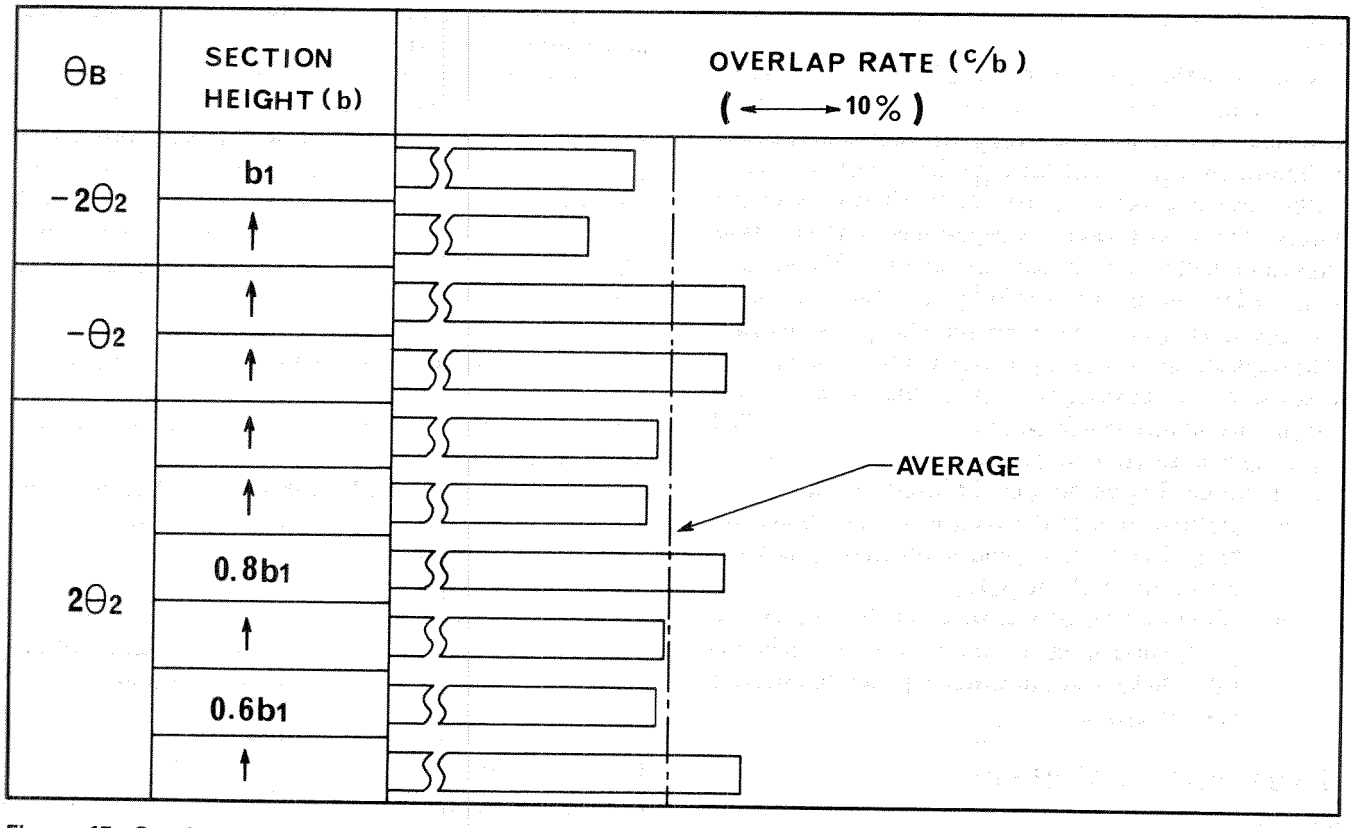

Figure 15. Overlap rates at the instant of failing in bending mode-B

Conclusion

1. Effective combination and arrangement of beading have been obtained to collapse axially closed-hat section members in a regular folding mode.
2. The critical collapse length of slant-mounted side rails could be estimated within limited conditions.

References

1. Mahmood, H.F., and A. Paluszny, "Design of thin walled columns for crash energy management—their strength and mode of collapse," SAE Paper 811302.

Collapse Behavior Development of Body Components

Reiner Brasche,
Georgios Giazitzis, and
Helmut Schmitt
Ford-Werke AG

Abstract

The development of car bodies is much affected by safety requirements, such as the FMVSS 208. Package is of major importance. In other words, space must be made available, affecting the dimensions of car front and rear end as well as the passenger compartment.

It is our objective to provide basic information about the optimal structure conditions, to study and implement better development tools, and to make use of any new methods for the benefit of the product and the safety of its users.

As a result of our development, we came across the application of analytical methods predicting rather than retesting the component form, gauge, material, and their influence on car crash behavior.

Introduction

The protection of vehicle passengers under impact conditions is mainly a function of controlled energy absorption, at least from a body engineering point of view.

Control in this sense means a minimization of passenger loading under the given change of velocity and a given deformation of space, where the permissible deformation is limited by the request for a sufficient survival space within the passenger compartment. On the other side, the injury criteria are related to the passenger's deceleration pulse and shall not exceed defined values(1). Within these boundaries, the inertia effects govern the loading of passengers as a function of chosen change of velocity. Although static tests have proven their worth in various cases of structural strength, they are unsuitable to treat the important inertia effects. These effects can be studied by using a calculation or dynamic test to do parametric investigations. Important areas of investigation are—

- Optimization of the vehicle collapse mode and body energy management for appropriate deceleration level and pulse
- Minimization of passenger loading by appropriate design of restraint systems, including safety belts, seats, instrument panel, and steering column system

Experimental Methods

The test device, Dynamic Crusher, is used to provide information about the behavior of vehicle structures, structure components, and dummy trajectories under different kinematic conditions. Measured signals are analyzed by using the data processing equipment. The following results are obtained (Table 1):

A typical example is the dummy resultant head acceleration as shown in Figure 1.

This test was conducted with a dummy fastened by a production seatbelt on production vehicle seats mounted on the sled of the Dynamic Crusher; the deceleration was about 17g mean value at an initial velocity of 41km/h. The test analysis shows the deceleration time of the sled and the resultant head deceleration curve of the dummy. The calculated Head Injury Criterion (HIC) is 283 for a time interval of 108ms.

Series of tests in this manner are evaluated and given the HIC dependence on the initial velocity and the mean deceleration. The variation can be derived with 25 percent, due to small changes of the head deceleration pulse (Figure 2).

To meet the HIC limited to 1,000, the mean deceleration shall not exceed about 24g for a 56km/h initial velocity

Table 1. Test results

• acceleration of e.g. body, engine, dummy
• velocity
• deformation of component
• displacement, dummy trajectory
• force displacement characteristic
• energy absorption
• injury criteria

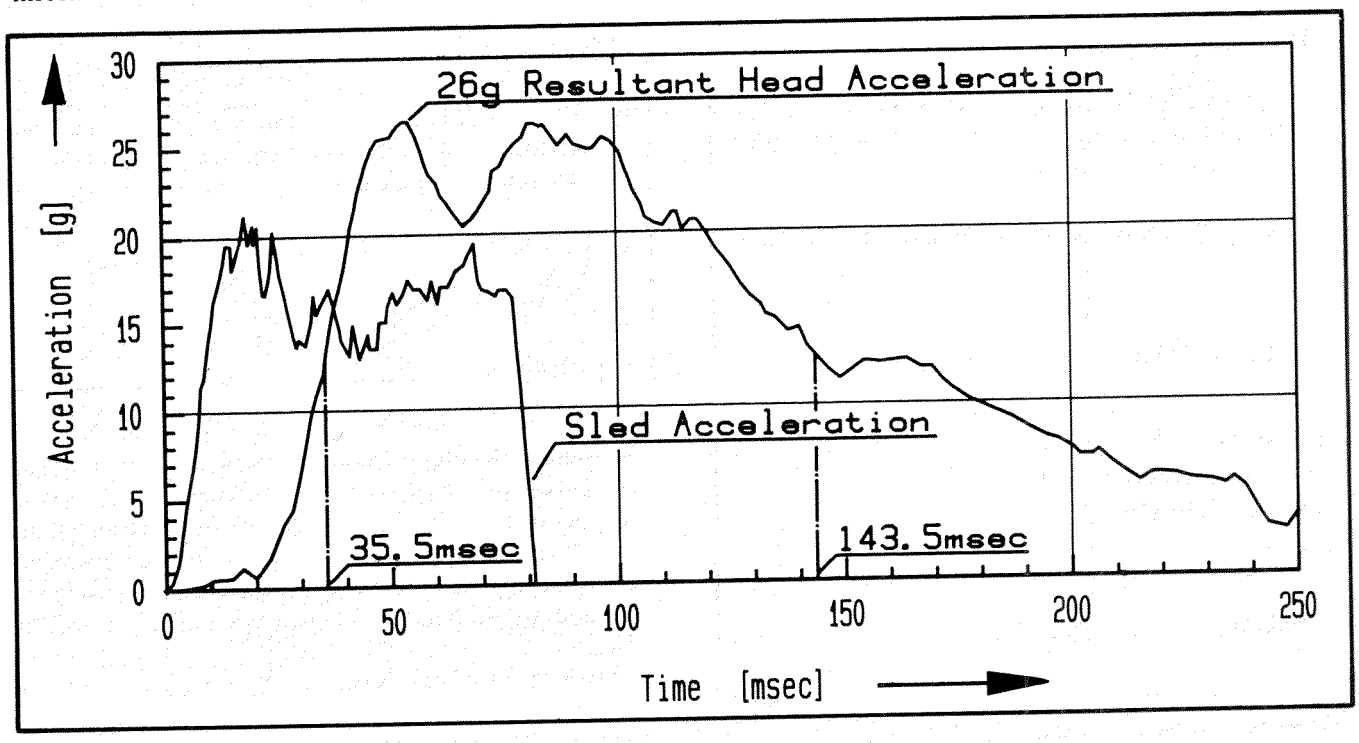

Figure 1. Dummy test result

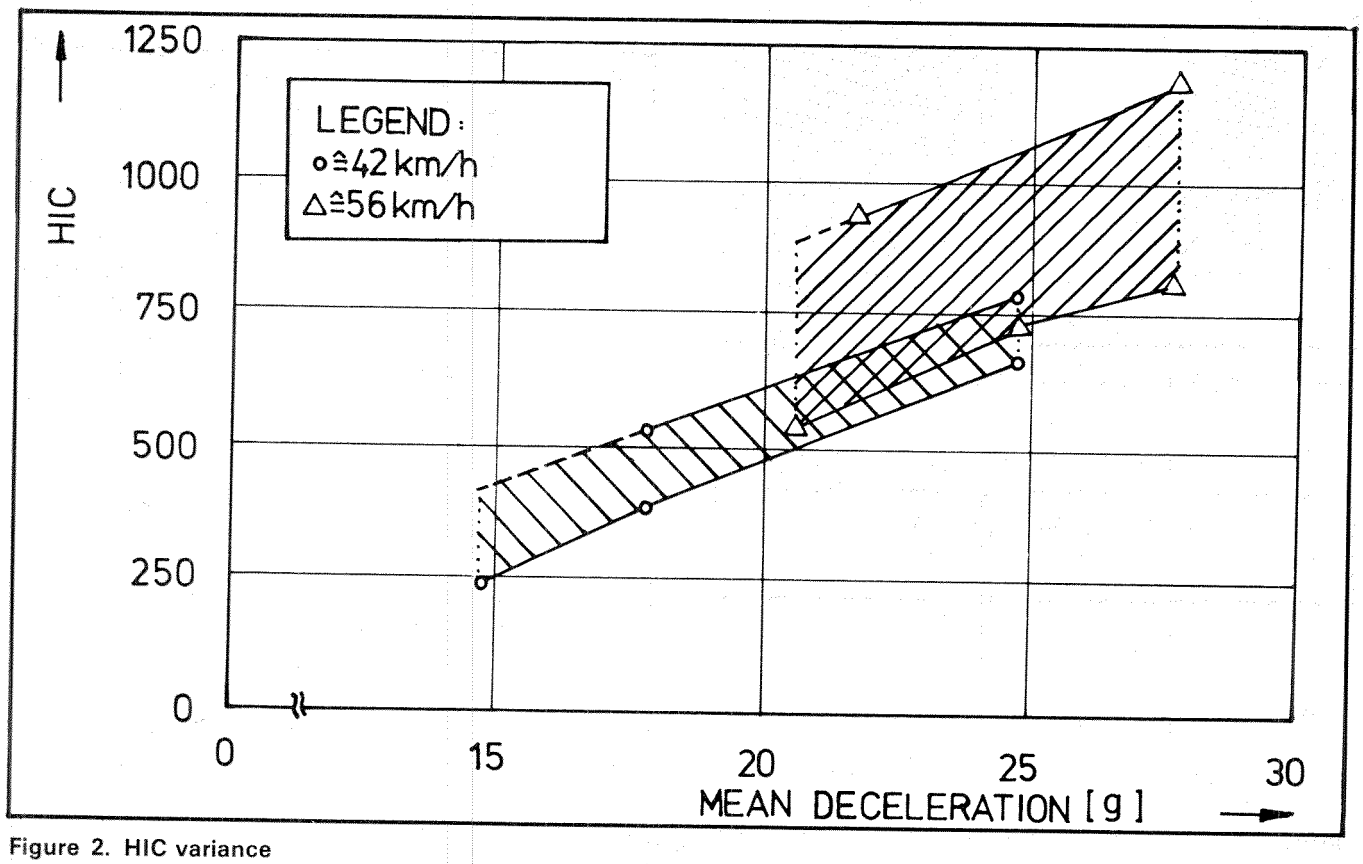

Figure 2. HIC variance

test, although single peaks can be higher. With the known mass of the vehicle, including driver, co-driver, and luggage, the mean deceleration value leads to the design requirement of sufficient structural crush space.

The structural crush of the first phase is governed mainly by the behavior of the front side rails. This behavior can be studied statically and dynamically. Figure 3 shows the sled with a mounted body side rail prepared for a dynamic test.

The figure shows a body side rail of our Scorpio vehicle prepared in a way that preformed darts reduce the peak load and insure the regular folding pattern. It should be understood that the pattern shows the final step of parametric studies as released. The energy curve and the force displacement characteristic are shown on Figure 4.

Analytical Methods

Analytical tools have the advantage of supplying information early in the development stage when physical parts are not available. There are simulation methods as shown in Table 2.

These are based on models with an appropriate mathematical description. Depending on the objectives and the availability of the above tools, the suitable one is selected.

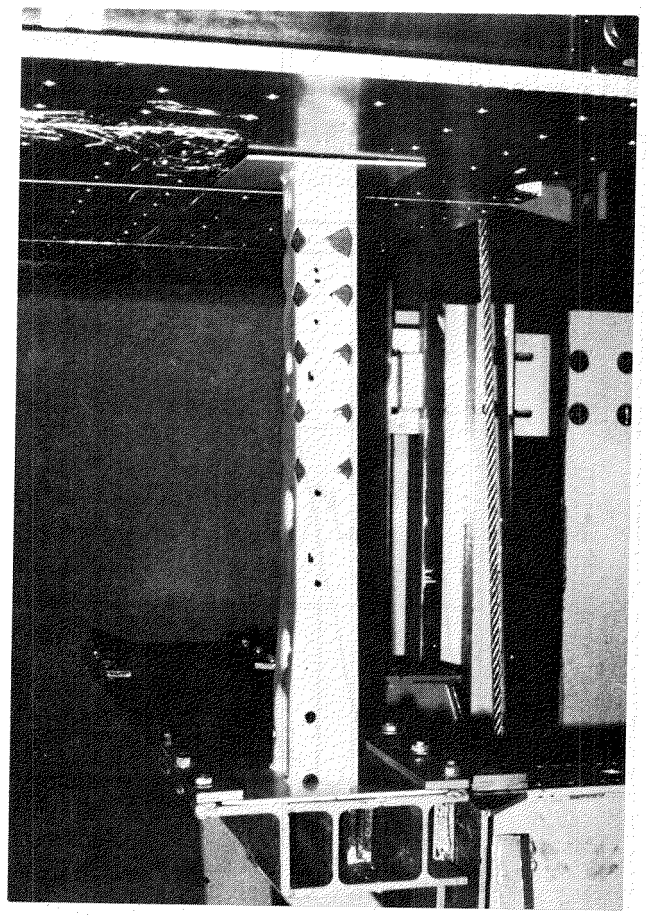

Figure 3. Scorpio body side rail—component

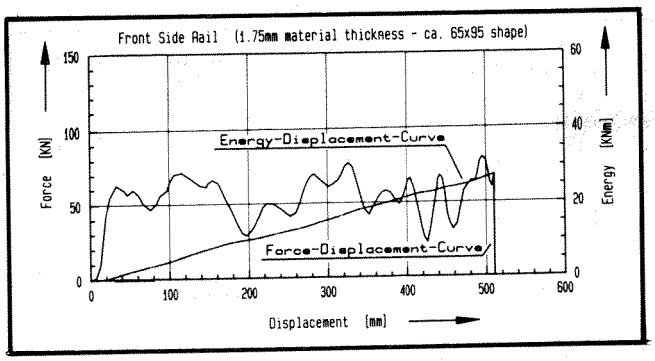

Figure 4. Scorpio front side rail-characteristic

Table 2. Analytical methods

• Spring Mass-Systems
• Finite Element Analysis
• Finite Difference Analysis

Spring Mass Models

For energy management investigations and dummy kinematic studies, the simulation tool, Ficem (in-house program), is applied. The advantages are fast preprocessing and quick turnaround of results at low cost. This tool gives the engineer information, for example, on simulation results (Table 3).

Table 3. Simulation results

• dummy displacements
• dummy velocity
• dummy deceleration
• rotation of head and chest

These results are obtained in relation to the simulation time. A typical dummy head swingline is shown on Figure 5.

Finite Element Analysis

Finite element models are used for static and dynamic analyses. As an advantage, this type of model is usually available from investigations in the field of Elastic Theory. The geometric information can be carried over. Elements, however, need to be redefined for two reasons:

- Element definition and connectivity (QUAD4-NASTRAN—TRIANGLE-WRECKER-F)
- Coarseness of model to comply with computer capacity

It is evident this tool allows the investigation of different shapes of members, material gauges, and swag patterns. Of specific interest also is the influence of small deviations of nominal surface as a result of the stamping process.

Figure 6 shows the peak load difference depending on these deviations.

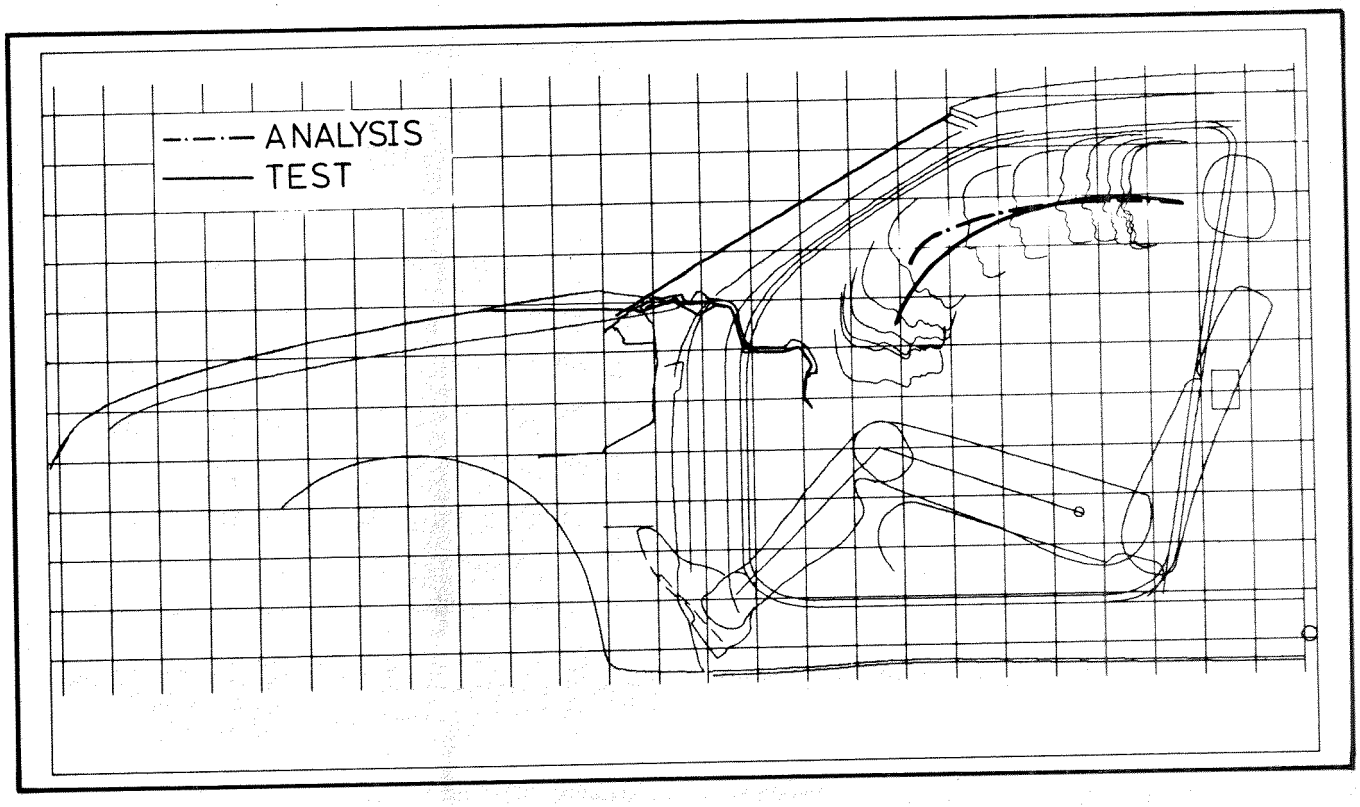

Figure 5. Dummy trajectory

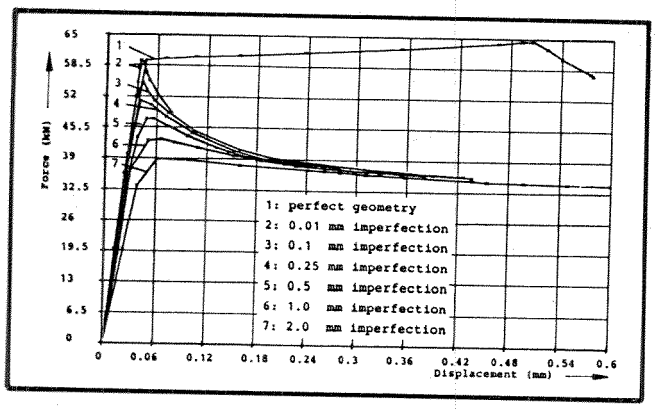

Figure 6. Influence of geometrical imperfections

It can be seen that small imperfections in the order of material gauge cause a great reduction of the peak load. The following folding process, once initiated by always-existing imperfections, is nearly independent from the above mentioned peak load reduction.

Figure 7 shows the post-peak-load behavior of a longitudinal member, as computed(2,3).

The further folding will progress until internal contact of surfaces occurs. The contact of any two points needs to be defined, for instance, with gap elements.

In this case, one has to know a priori where contact occurs or a precomputation has to be performed to define the contacting node pairs. A more effective approach exists in some codes with defining a contact surface and corresponding contact nodes. The automated way obviously will be the desire of the analyst.

Finite Difference Analysis

Finite difference methods were used successfully for continuous structures, e.g., pipes, vessels, etc. Many efforts were made to use FD also in more complex—i.e., automobile—structures.

Taking advantage of the Kirchhoff Shell Theory, which is valid for thin-shell structures, one can treat the equations of motion of a shell for an automobile body.

In the FD code that has been used(4,5), a regular mesh is formed on the shell, which helps to form these equations in a finite difference form at each mesh station. The spatial differencing requires a regular mesh, and discontinuities such as holes are hard to handle. This is an obvious disadvantage. Complex structures can be computed, however, by means of connecting shells by appropriate shell boundary conditions at corresponding edges.

Figure 8 shows such a body side rail configuration under impact load at 9ms time with computed deformation of three connected shells.

Discussion of Results

As mentioned earlier, analytical methods can be used early in the development process.

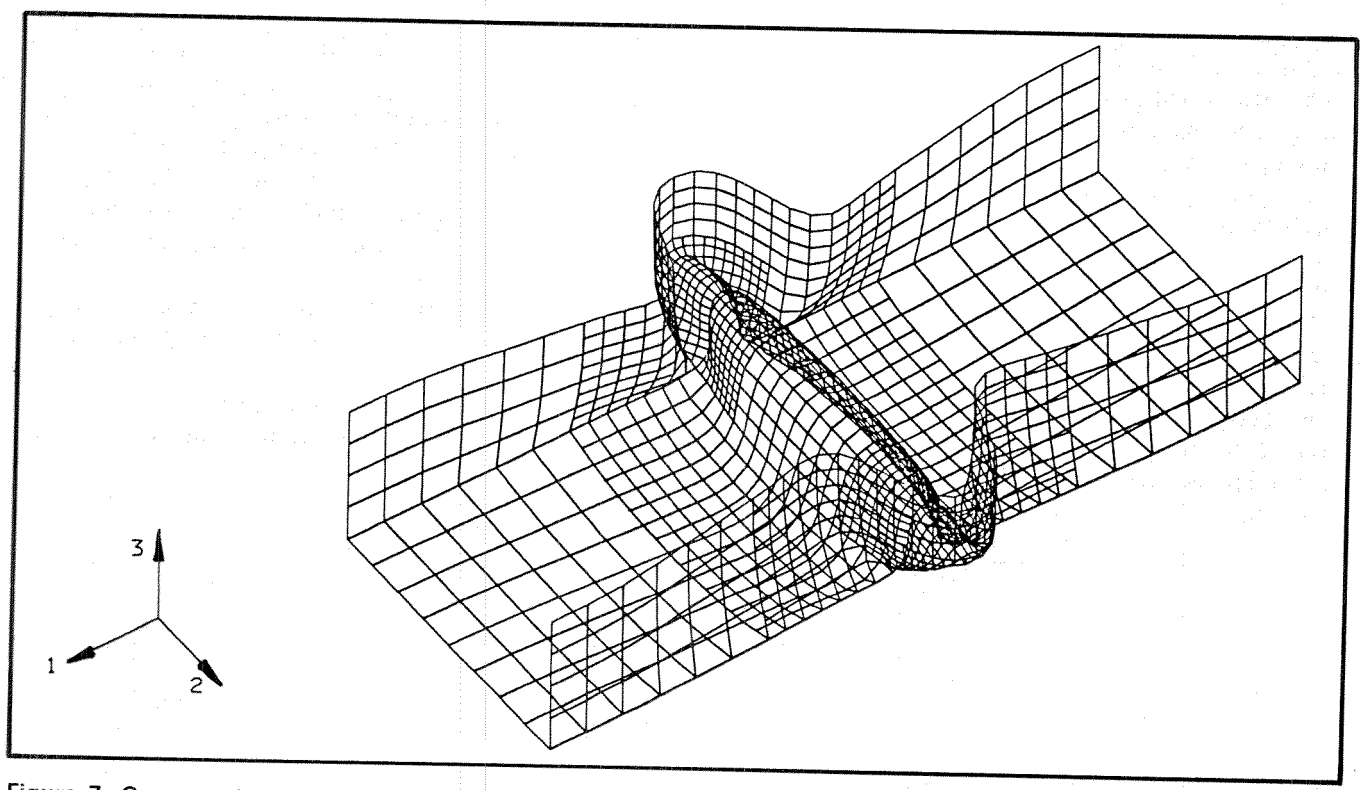

Figure 7. Computation of local fold

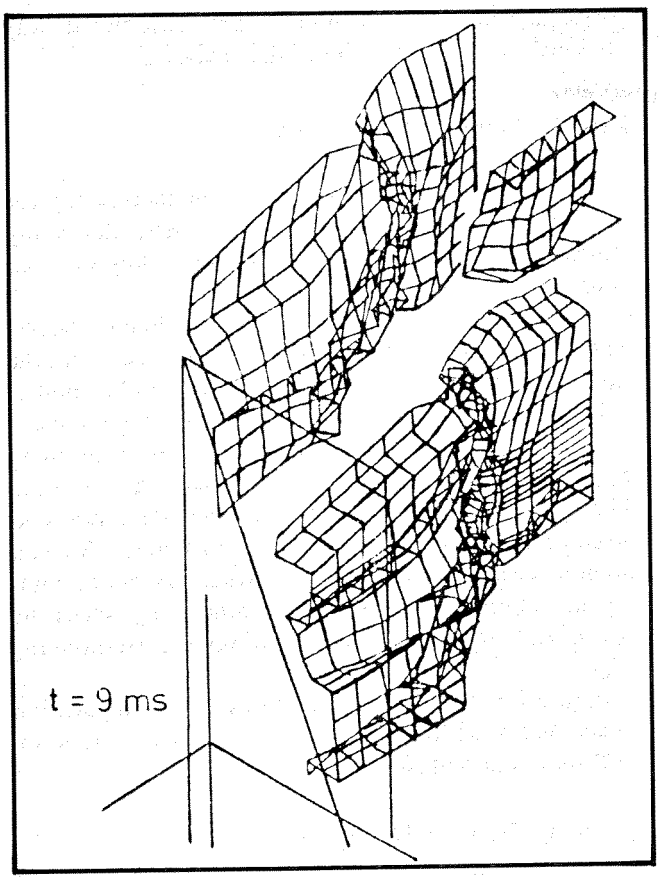

Figure 8. Finite difference shell structure

The determination of energy absorption is ruled by physical events happening in a timespan of a few milliseconds. In other words, the balance of loads needs to be established by comparing the peak load of main energy-absorbing members versus the resistance of the back-up structure. It has been shown that the FE method is providing a tool very helpful in the determination of this balance. Figure 9 shows a comparison of load versus displacement in test and calculation of a Scorpio front side member.

Depending on the use of a filter, one will see that peaks are in a close range (Figure 9). The computation code was the in-house FEM Code WRECKER-F(6).

Beyond 30mm displacement, the computation values need to be established. It must be stated that other computations have been carried out resulting in higher

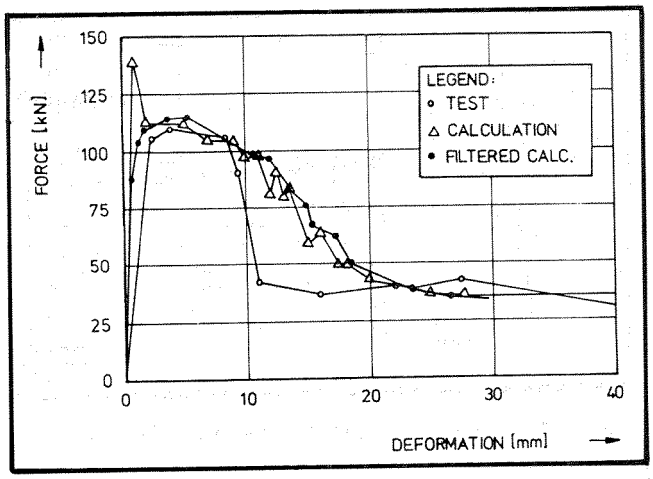

Figure 9. Scorpio front side rail—correlation

deformation. However, one has to study the effect of internal contact carefully in order not to misinterpret the results. Calculations are under way to compute the behavior of full body front and rear ends. The highly iterative computations at the order of 10,000CPU's by using a fast computer require suitable hardware. Our new Cray is yet to be used for this kind of development work.

In summary, it is concluded that analytical tools can partly replace test work.

References

1. Brasche, R., H.J. Ottersbach, and H. Schmitt, "Determination of energy absorbing members in car structures for passive safety," ISATA, Milan, 1984.
2. Hass, S., J. Helling, and H. Junker, "Finite element berechnungen, FORD- Längsträger," Internal Project Documentation, FKA, Aachen, 1984.
3. Abaqus, "User's manual; Version 4," Hibitt, Karlsson and Sorenson, Inc., Rhode Island, USA, 1982.
4. Mentor III, "User's manual," Meredith Engineering, Michigan, USA, 1979.
5. Wang, H.C., and D. Meredith, "The crush analysis of vehicle structures," *Int. J. Impact Engng.*, Vol. 1 No. 3, 1983.
6. Yeung, K.S., "Wrecker-F user's manual," Technical Report SR 84-76, Ford Motor Company, Michigan, USA.

Advanced Concepts for Driver Air Cushion Systems

G.F. Kirchoff,
R.W. Carr,
R.J. Wheelwright, and
G.V. Adams
Morton Thiokol, Inc.

Abstract

It has long been recognized that cost has been one of the major deterrents to the acceptance of airbag systems in automobiles. This paper addresses some advanced design and development approaches being evaluated by Morton Thiokol's Utah Division toward reducing design, development, and production costs of driver airbag systems. While cost reduction values are not yet available, nor are some of the design concepts proven, the approaches look quite promising.

Introduction

Morton Thiokol, Inc., is evaluating several advanced concepts for driver air cushion systems to develop a lower cost system concept than those offered today. System reduction is a result of (1) fewer components, (2) lower cost of those components, (3) component weight reduction, which reduces cost of support structure, (4) reduction in system installation cost either at the OEM or in the after-market, and (5) reduction in development, qualification, and tooling costs.

The primary ground rule during this cost reduction effort is that there is no degradation in system reliability. This includes failure of the system to function, an inadvertent function, or a failure of the system to perform the specified requirements when it functions (i.e., low inflator, slow sensing bag rip, etc.).

The approach that Thiokol has taken attempts to reduce costs in each of the five areas cited. Component cost reduction has been effected through a simpler inflator design. The reduction in components has been effected by actualization of integrating sensor concepts. Reduction in weight has been accomplished through the use of aluminum and simpler structures. Placing a sensor in the steering wheel and using a pyrotechnic actuation system are being evaluated to reduce installation costs of the airbag system. Reduction in the development cost of the airbag system is accomplished by using baseline-developed and qualified components, and modifying them for each automobile. Testing cost reduction is evaluated by using a pendulum test technique for sensor testing and developing sensor actuation times for various crash pulses. This is supported by computer performance projections to provide a total system design analysis. More details in each of these areas and the status of the Thiokol program are provided with features, approaches, and concepts rather than programmatics or actual costs.

Component Description

Inflator

The new lightweight aluminum inflator, now qualified, certified, and in production by Thiokol, is a key component to this advanced system. It consists of two forged aluminum components, a diffuser and base, joined by inertia welding on three concentric diameters. It uses a high-volume production squib, an ignition/auto ignition cartridge subassembly, sodium azide gas generant pellets, and combustion and diffuser filter and cooling screens. The design is amenable to high-volume production. Quantities anticipated in the near future are less than 300,000 annually. The gas-generating pyrotechnic used in this inflator is produced by a slurry/spray dry/pelletizing technique, which could be developed to a continuous process but is now using batches of 3,000 lb each. Any process for high-volume processing of gas generant must minimize operating personnel contact, due to the toxic and hazardous nature of the intermediate constituents, while still being able to process large uniform batches of the final pelletized product for use in the inflator.

A second inflator requirement is that it be easily tailored to meet future driver system performance specifications and the envelope and interface imposed by the steering wheel and module. Figure 1 shows those parameters established for this inflator. Also this capability must be feasible with a standard inflator and without requalification, tooling, or certification.

Module

The key features of a driver module design must minimize weight and number of components, and simplicity of design.

The module design Thiokol is evaluating features a one-piece, reinforced urethane cover and an aluminum housing, which results in a lightweight, compact unit easily attached to a steering wheel. The total weight for the module (inflator, reaction plate, bag, cover) assembly is 3.3 lb. Figure 2 shows a cutaway of this design. The module housing is stamped from an aluminum sheet and

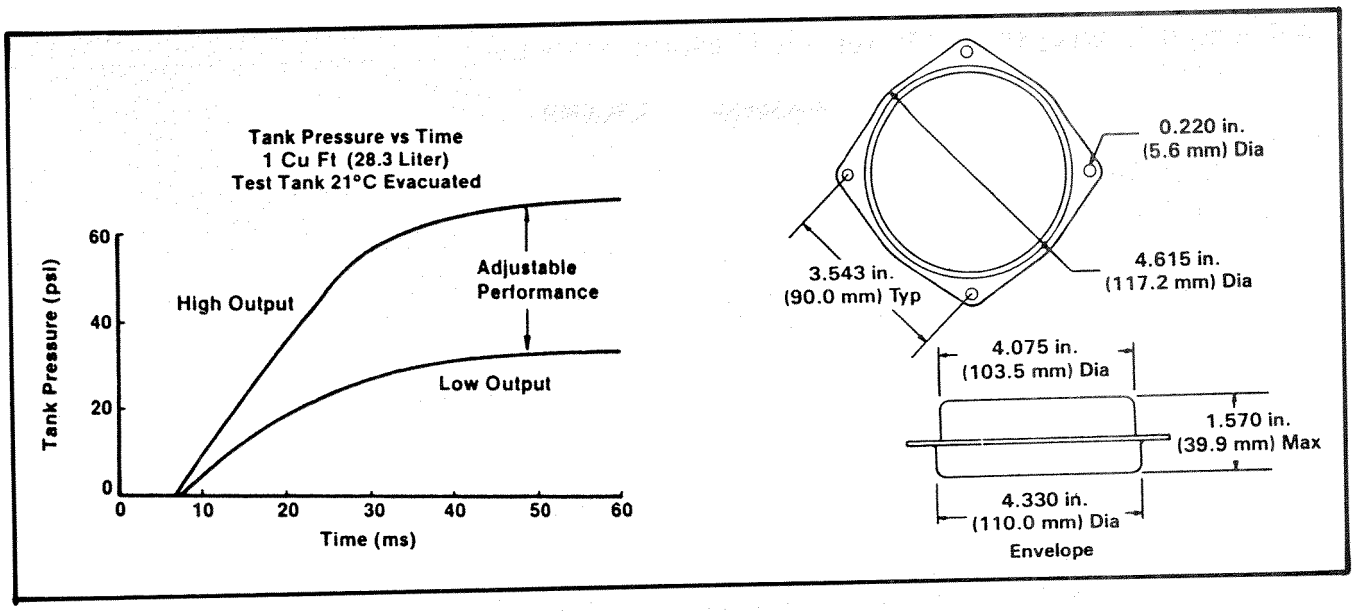

Figure 1. Advanced lightweight inflator

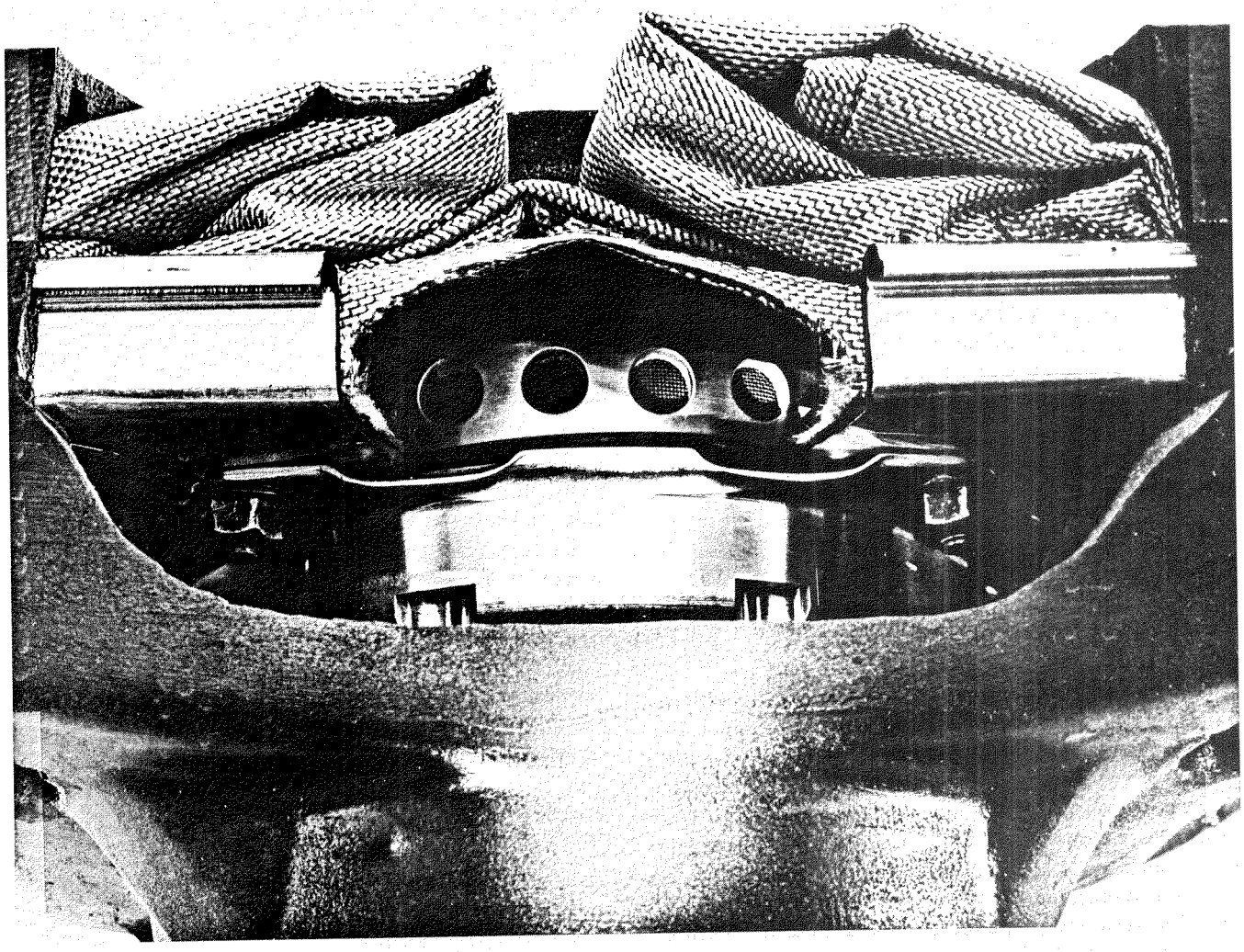

Figure 2. Thiokol module design

provides the attachment features for the remaining module components. Of these, the cover is the most difficult to manufacture. It is a single-piece, construction-reinforced, molded urethane that snaps into place over the cushion and housing and is retained by a continuous lip around the edge of the housing with a steel retainer to hold the two longest sides together. The single cover functions as both a protective cover to the airbag and a decorative cover. An internal, molded-in-place, nylon mesh provides needed reinforcement for the cover panels during deployment. Tear seams exposed just to the interior surface are being examined, however, until test results verify this concept. The more conventional approach of having tear seams on both external and internal surfaces has been selected.

Sensor/Transfer Line

The sensing element we have been evaluating with the module assembly is one of the new pseudo-integrating mechanical sensing elements with either an electrical closure switch or a mechanical firing pin with a percussion primer. The percussion primer initiates a thin-layer explosive (TLX) transfer line, which transmits a pyrotechnic shock wave to the inflator for initiation. The sensing element we have been evaluating is a gas-damped sensor being developed by Technar. A schematic of this sensing element is shown in Figure 3. The integration that takes place is a function of the travel of the "cup and mass" in the forward direction against the spring force and airflow around the cup. These impulse characteristics are shown in Figure 4, plotted to show the functioning and nonfunction regions in relation to the velocity change and time duration of the crash impulse. Other integration sensing elements available in the market are also candidates for this system.

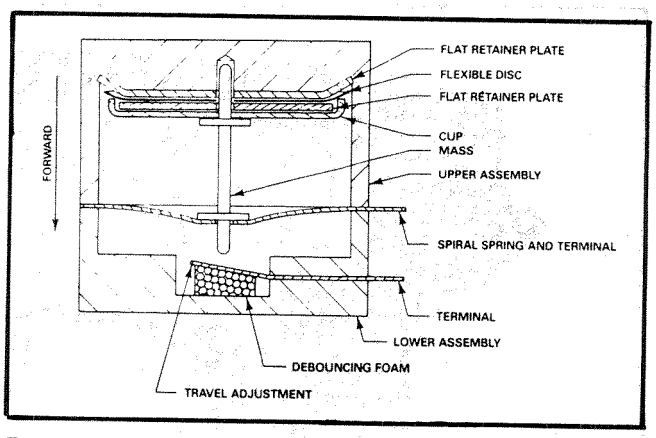

Figure 3. Technar's low-cost gas-damped sensor

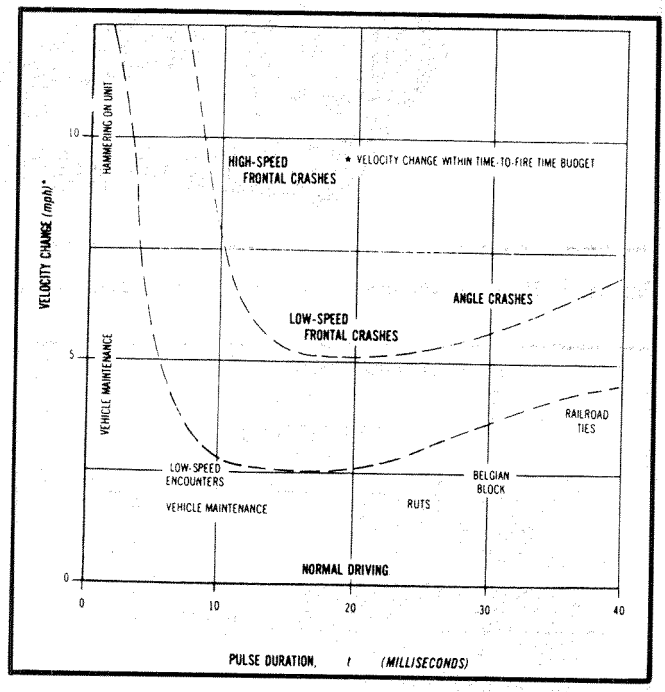

Figure 4. Crash/noncrash impulse map

Module Assembly

We are evaluating both the Pyrotechnic Sensor/Module System and the Electrical Sensor/Module System.

Pyrotechnic Sensor/Module System

The system that employs the pyrotechnic transfer is called a pyrotechnic sensor/module assembly. The sensor detects the crash environment and, through a percussion mechanism, initiates a thin-layer explosive (TLX) transfer line that transmits a pyrotechnic shock wave to the inflator for initiation. The sensor is mechanically attached to the back of the module housing, and the transfer line would be connected directly to the inflator. No changes to the steering column design are needed to accommodate this concept. A very preliminary design layout for this configuration is presented in Figure 5. The TLX transfer line, as shown in Figure 6, consists of a thin coating of reactive material on the inside of a plastic tube encased in a protective coating. When initiated by a brisant primer, a pyrotechnic impulse is transmitted along the transfer line at a velocity of 4,593ft/s. Since the length of the transfer line in this system is about 4in, the time delay between the sensor and inflator is less than 0.1ms. Inside the inflator, the transfer line is terminated adjacent to the ignition charge, so when the pyrotechnic impulse reaches that junction, the inflator fires exactly as it would if initiated electrically.

Electrical Sensor/Module System

The electrical sensor/module assembly incorporates current airbag system technology except that everything

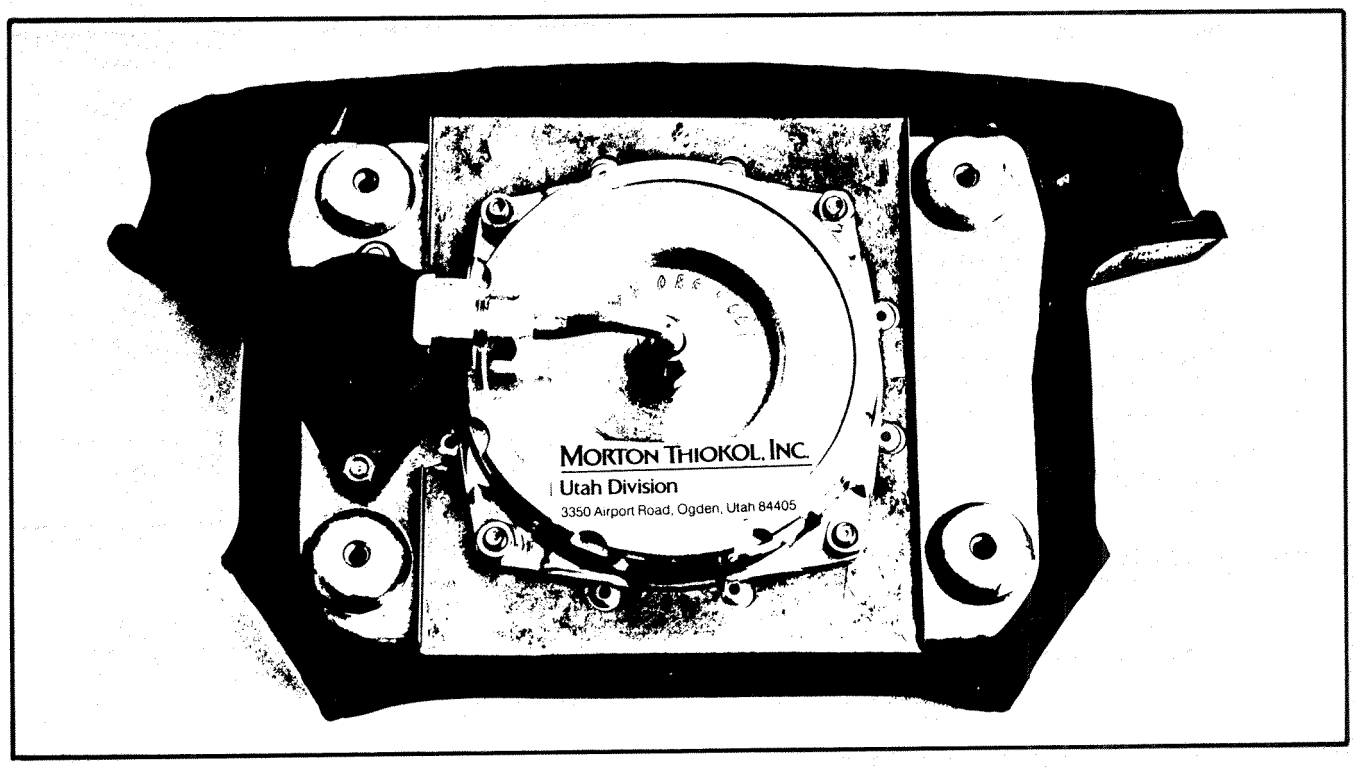

Figure 5. Preliminary design of pyrotechnic sensor/module assembly

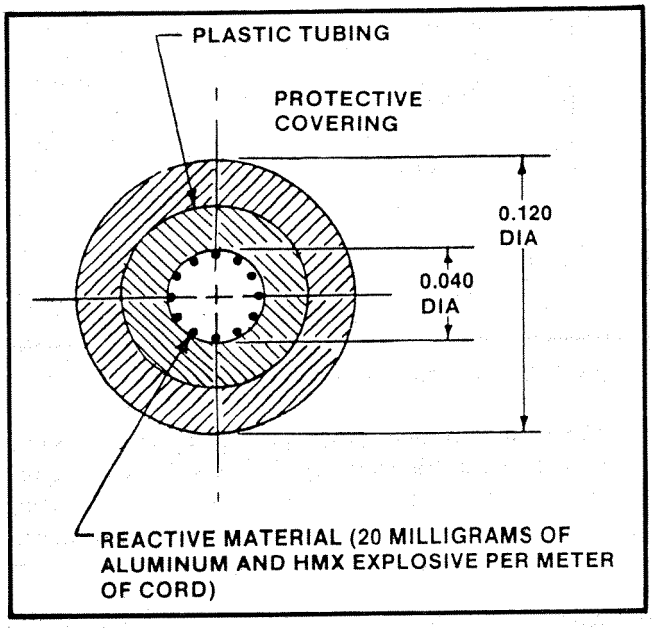

Figure 6. Cross-section view of TLX transfer tube

is contained within the module assembly. This eliminates the need for complicated interconnecting wiring harnesses and a slip ring or rotating electrical connection in the steering column. The sensor is mounted to the module housing next to the inflator (Figure 7), while on the opposite side is a cavity containing the energy storage capacitors. All components are encapsulated in a plastic cover with a foam potting material to maintain position and structural integrity during vibration and shock environments. Power from the horn ring is used to charge the capacitors where the vehicle's electrical system is energized. When the sensor functions in response to a crash impact, it closes a set of electrical contacts, allowing electrical energy from the capacitors to be applied to the electrical squib, which, in turn, fires the inflator. The added weight to the steering wheel for either the electrical or pyrotechnic concept is approximately the same and is shown in Table 1. The total assembly weight is 3.7 lb, which is a substantial reduction over that previously available.

Ease of Installation

There are two key decisions yet to be made for future driver airbag systems that affect the ease of installation. These are (1) location of the sensor—that is, can it be located in the steering wheel—and, (2) whether the inflator initiation element should be electronic or pyrotechnic. Although there are a number of ongoing programs to provide the data needed to make these decisions, the answers are not yet clear. It may be that one design approach can be selected for one automobile, while an alternate approach is suitable for others. Several elements are obvious at this point, if we wish to have a system that can be used for either. These are—

1. The inflator used must be suitable for either pyrotechnic or electrical initiation, without major development, qualification, or tooling costs.

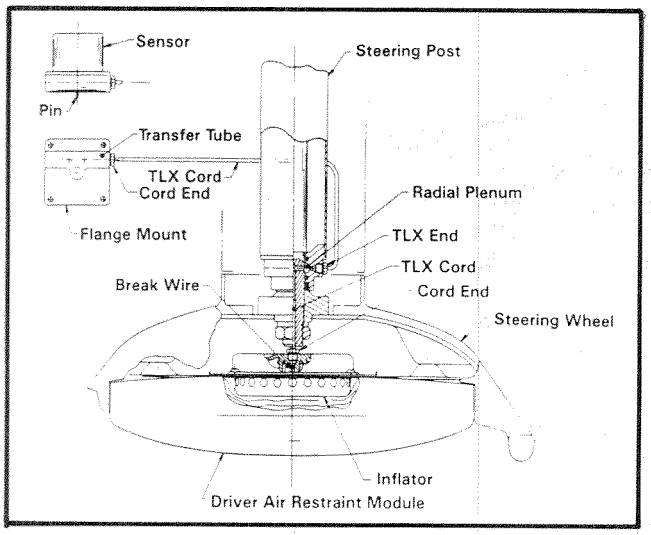

Figure 8. Layout design of driver inflator module with TLX Transfer line

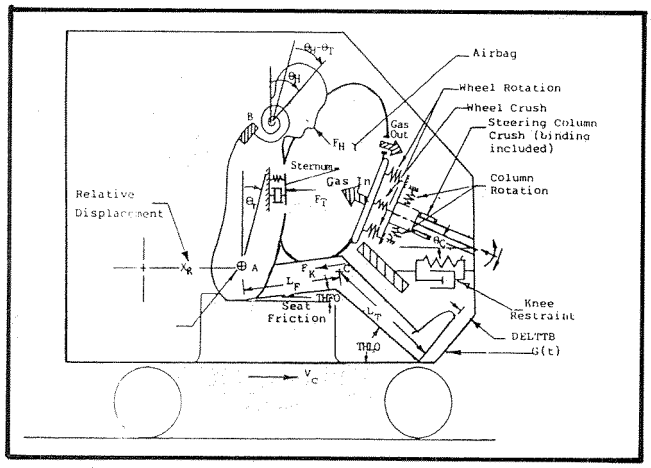

Figure 9. BDRACR computer model

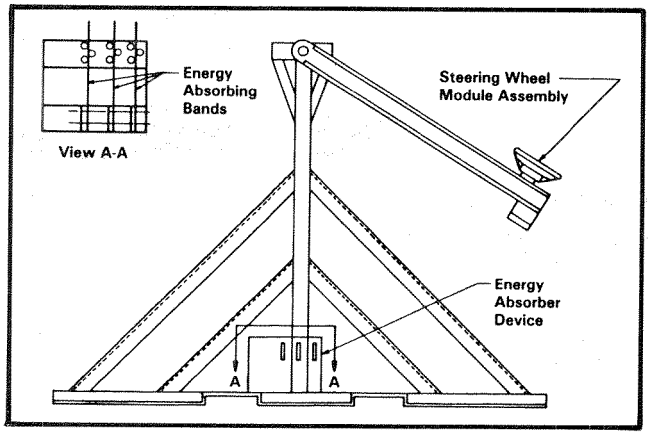

Figure 10. Pendulum test device air cushion system impact test

Development, Qualification, and Tooling

Reduction in development, qualification, and tooling costs is a major factor in selecting a driver airbag system. Further, the costs reflect the lead time required to bring the system to production readiness. There appears to be two keys to accomplishing these efforts with minimum cost. The first of these is to use developed and qualified components where possible. This is particularly true of the items that are very expensive to develop, tool, and qualify, such as the inflator and sensor. Second is the minimization of testing cost through the use of computer modeling and simplified dynamic testing, which can be used to replace more expensive sled and car crash tests.

This paper will not deal with computer modeling, which will be dealt with extensively in other papers, except to say that through the use of the BDRACR Computer Model (Figure 9) by Fitzpatrick Engineering, excellent prediction and design capabilities have been obtained with close agreement between simulated and actual results. Another feature we believe will reduce development costs is a newly devised pendulum test device now being fabricated. This device has been designed to simulate the initial portion of any given crash pulse up to 15mph through the use of a pulse generator with energy-absorbing bands. With the sensor and module assembly mounted on the pendulum (Figure 10) and impacted into the pulse generator, the sensing sequence can be simulated with an inexpensive test versus an expensive sled or car crash dynamic test. Just as in a car crash test, various sensors can be tested to provide comparative data.

In conclusion, we believe that the recent and ongoing efforts to use lighter weight, simpler inflators, simple integrating sensors, potentially simpler installations in the steering wheel, pyrotechnic initiation, and more sophisticated testing, coupled with more accurate computer perform ance modeling, offer lower cost systems than those previously available.

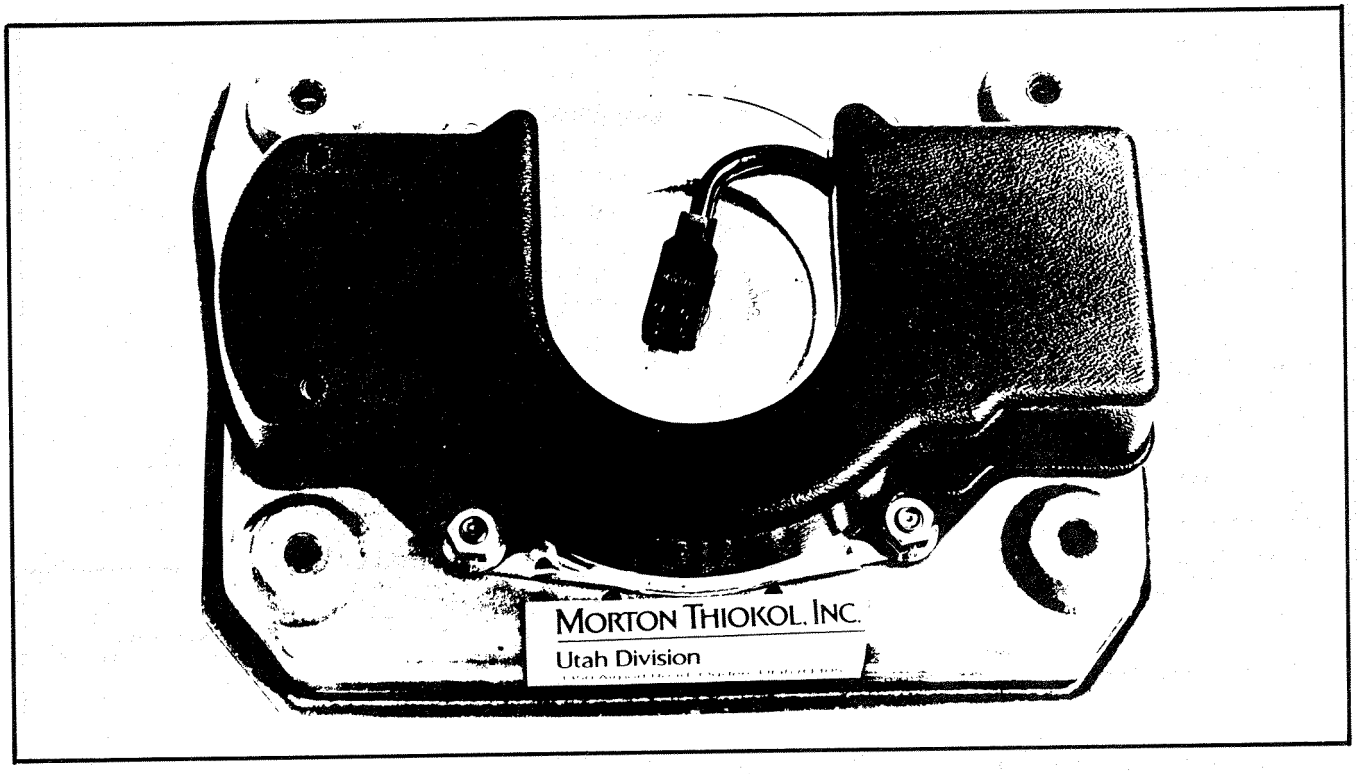

Figure 7. Electrical sensor/module assembly

Table A. Weight summary driver air cushion module

Module Assemblies	Design Description	Weight
Inflator Assembly 95501-01	Lightweight Aluminum Construction	585gms 1.3 lb
Module Assembly Without Inflator	Lightweight Reaction Plate, Bag, Attachment Hardware and Cover	906gms 2.0 lb
Sensor Assembly (No Diagnostics)	Pyrotechnic Mechanical Sensor with Transfer Line or Electrical Sensor	180gms 0.4 lb
Module Assembly With Sensor Assembly		1671gms 3.7 lb
Module Assembly Without Sensor Assembly		1491gms 3.3 lb

Thiokol has done this with the aluminum inflator.

2. There must be flexibility in sensor component placement to locate the sensor other than in the steering wheel, should this be desirable. This is obvious for the electrical system based on existing designs. It is not obvious for the pyrotechnic system. Thiokol has designed and is evaluating a rotating joint transfer line system for pyrotechnic ignition, shown in Figure 8. This concept appears adaptable to a standard steering column with minimum modification. It is not developed or qualified, though it has been conceptually proven.

These decisions will obviously have a major impact on future cost of installation of airbag systems.

Injury Criteria for Combined Restraint Systems

Dr. Lothar Grösch
Daimler-Benz, Sindelfingen

Abstract

The expected improved performance of a combined restraint system where an airbag supplements the conventional safety belt was not reflected in reduced g-values on the dummy's chest. However, by the distribution of forces over the wider area of the airbag and the corresponding reduction of the pressure exerted by the 3-point belt, improved occupant protection is actually produced. Therefore, a new method to measure the deflection of dummy ribs with strain gauges has been developed. The resulting data indicate a significantly reduced chest deflection when a combined system is used.

Similarly, a concentrated load from a steering wheel in the mouth area at a low HIC value means a higher injury risk compared to a widely distributed load from an airbag at an even higher HIC value. Consequently, an additional facial bone injury criterion based on measurements of the specific loading on the dummy's face would be useful, and an alternative calculation of HIC focusing only on that portion of the head acceleration curve assumed to have a brain-injury potential is necessary.

Chest Injury Criterion

Due to the combined effect of two restraints—a 3-point belt and an airbag—the acceleration measured in the chest of an anthropomorphic dummy is greater than with a 3-point belt alone.

Since most of the chest injuries (especially rib fractures) in real-world accidents are due to contact with the belt or with the steering wheel, it is not chest acceleration that is important for identifying the potential injury level but the deflection of the dummy's chest.

A new method, evaluated through extensive tests with different restraint systems, has been developed to measure the deflection of the dummy ribs by means of strain gauges.

Experimental Method

The sled tests were conducted at 30mph. The vehicle was equipped with an airbag, a knee bolster, and a 3-point safety belt (webbing elongation 14 percent) on the driver side.

The test device was a Hybrid II dummy, equipped with strain gauges symmetrically attached on the six ribs near the spine (Figure 1).

The dummy rib can be deflected in the sagittal or lateral direction (Figure 2). In the case of a symmetrical sagittal deflection (a), positive strains of equal magnitude S_{SAG} are measured on both measuring points. In contrast to this, the nonsymmetrical lateral deflection (b) induces a positive strain at measuring point 1 and a negative strain at measuring point 2; both of magnitude S_{LAT}.

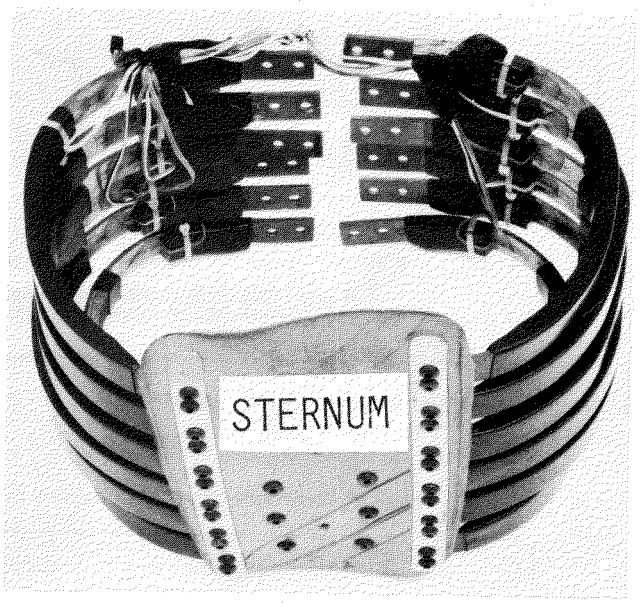

Figure 1. Location of strain gauges on dummy ribs

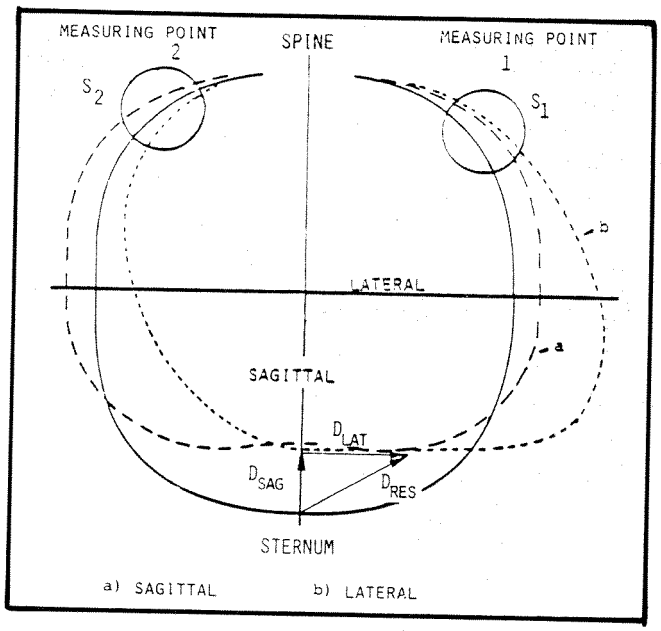

Figure 2. Measured strains if both modes of deflection occur

If both modes of deflection occur simultaneously, the measured strains are:

$$S_1 = S_{SAG} + S_{LAT} \quad \text{and} \quad S_2 = S_{SAG} - S_{LAT} \qquad (1)$$

From this, the sagittal and lateral components, respectively, can be calculated:

$$S_{SAG} = 1/2 \bullet (S_1 + S_2) \quad \text{and} \quad S_{LAT} = 1/2 \bullet (S_1 - S_2) \qquad (2)$$

They are (in linear model) proportional to the corresponding sagittal and lateral rib deflections:

$$D_{SAG} \sim S_{SAG} \quad \text{and} \quad D_{LAT} \sim S_{LAT} \qquad (3)$$

that can be determined by calibration.

The resultant deflection of each dummy rib is given by:

$$D_{RES} \sim \sqrt{S_{SAG}^2 + k^2 \bullet S_{LAT}^2} \qquad k = 0.6$$

determined by calibration (4)

The total of all rib deflections or, alternatively, the average deflection of anterior chest wall, can be regarded as a measure of chest deflection:

$$D_{TOTAL} = D_{RES}^{(1)} + \ldots + D_{RES}^{(6)} \quad D_{AV} = 1/6 \sim \qquad (5)$$

Results and Data Analysis

Three types of restraint systems were evaluated using sled tests:

a) Three-point safety belt alone without emergency tensioning retractor* (3 PT)
b) Airbag combined with 3-point belt alone (AB + 3 PT)
c) Airbag combined with 3-point belt with ETR (AB + 3 PT + ETR)

The resulting chest accelerations (Figure 3) and rib strains (Figure 4) indicate—

- Increased g-values when using the combined system without ETR (b), due to simultaneous restraint forces of belt and airbag in phase with each other
- A reduction of chest acceleration with ETR (c), due to the early restraint effect of the belt and, therefore, delayed contact with the airbag, i.e., belt and airbag out-of-phase
- In contrast to the tendency of increased chest acceleration, significantly reduced rib strains for the combined system

*To eliminate belt slack upon impact

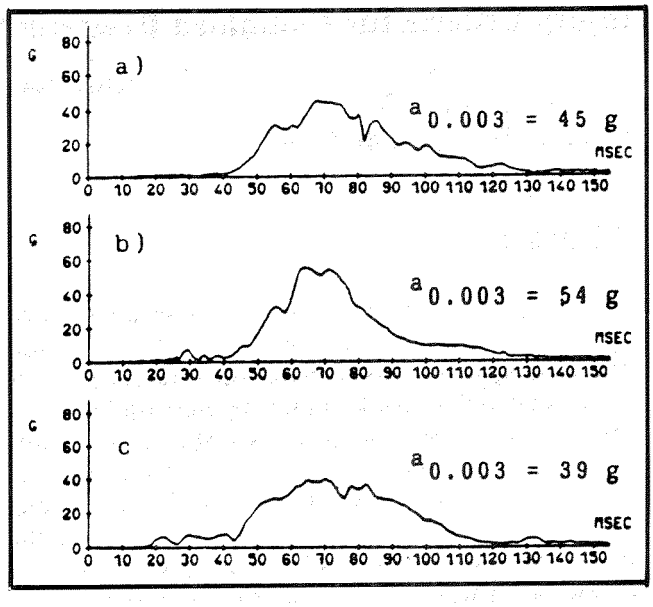

Figure 3. Resulting chest accelerations

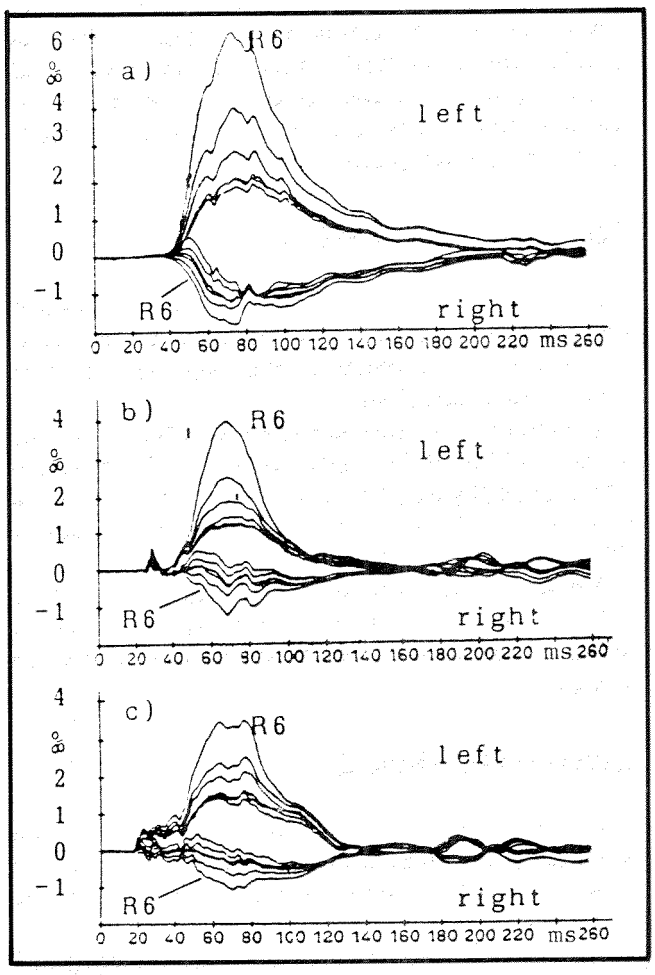

Figure 4. Resulting strain data of different restraint systems

Consistent with this, the upper torso belt load at the shoulder is significantly reduced for the combined system without ETR and slightly increased with ETR because of the delay in belt unloading from the airbag.

The separation into sagittal and lateral components of rib strains indicates—

- Nearly the same total sagittal deflection for all three restraint systems (Figure 5)
- Lateral deflections in each case higher than the sagittal, but a reduction of almost one-half when the combined system is used (Figure 6)

Furthermore, some other important facts:

- Consistent with rib fracture occurrence in real-world accidents, the lower ribs are much more stressed than the upper ones.
- By the combined system, both sagittal and lateral deflection of the lowermost rib are significantly reduced; even more with ETR.

The comparison of rib-deflection data to the chest g-values (Figure 7) indicates contradictory tendencies:

- With the combined system (b), increased chest acceleration but reduced deflection
- With an ETR in the combined system (c), lower g-values but nearly the same deflection

Because most chest injuries in real-world accidents are caused by rib deflection and not internal acceleration, the rib-deflection data are obviously more suitable for

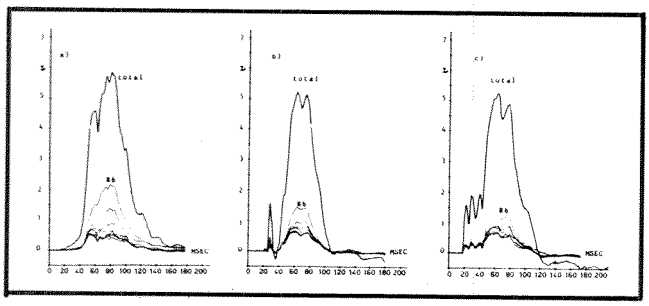

Figure 5. Saggital deflections of dummy ribs

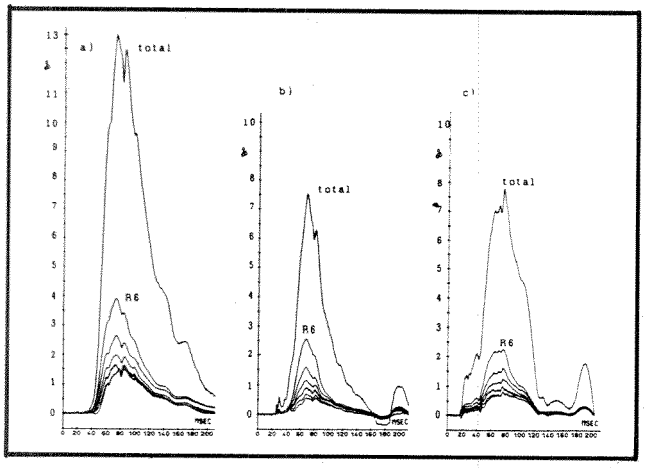

Figure 6. Lateral deflections of dummy ribs

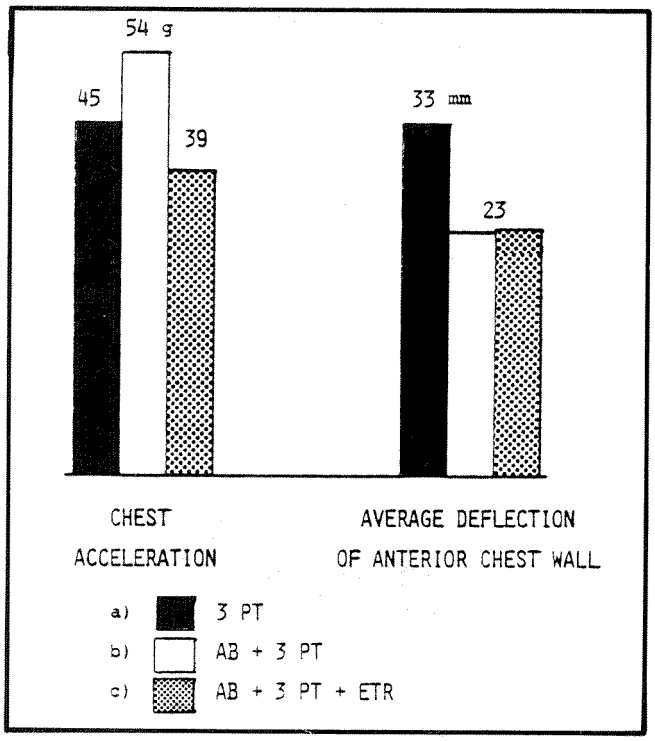

Figure 7. Comparison of restraint systems using either chest acceleration or chest wall deflection

estimating the risk of chest injury than are g-values. Therefore, the need exists for revised chest-injury criteria based on chest-deflection measurements instead of chest acceleration.

Head Injury Criterion

It is not the purpose of this paper to provide an extensive review of the pros and cons concerning the subject of HIC. Suffice it to say that—

- HIC is not adequate to evaluate the potential for facial damages, depending on both the local impact forces and differing strengths of the individual facial bones.
- The current HIC calculation can suggest that an artificially high brain-injury risk exists for a crash that has a relatively low g-level but a long-time duration (e.g., contact to airbag or non-contact events).

Head acceleration data are insufficient to predict localized fracture of the facial structure for two reasons: (1) there are a wide range of load limits for different zones in the face and (2) its incapability to detect localized hard points in the contact surface. Therefore, attempts have been made to apply various devices for pressure indication on the dummy's face (Figure 8).

Due to some difficulties in practical application—in particular where the contacting surfaces move relative to each other during an impact—it is necessary to enclose

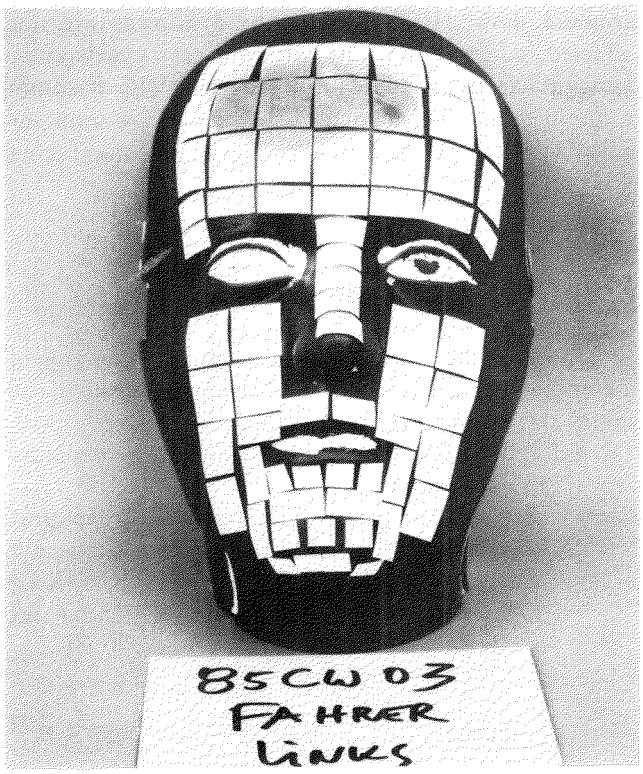

Figure 8. Dummy face with pressure-indication devices

the devices in silicon masks or nylon stockings; further improvements are in progress. The difference between static and dynamic loading makes it necessary to calibrate the device under approximately the same conditions as those under which it is used.

With the help of this pressure-indicating device, facial injury potential could be monitored. When the dummy's head contacts an airbag instead of a steering wheel, in spite of similar head accelerations and HIC values, respectively, a more than fiftyfold reduction of facial pressure was measured.

Modified Calculation of HIC

It is generally accepted that the currently used HIC formula is not able to handle the high tolerance levels in cases of long duration but low-level head acceleration pulses and, therefore, can produce an artificially high HIC. Consequently, HIC appears not to discriminate between hard steering wheel impacts, soft airbag contacts, or noncontacts, as shown in Figure 9.

In spite of similar HIC values, the actual brain-injury risk of the three head acceleration curves would be different, because the existing real-world accident data show no brain injuries with the absence of a head strike or in the case of airbag contacts. Serious brain injuries occur only with evidence of hard surface impacts. The reason for this is that most of the data points defining the Wayne-State-Tolerance-Curve (WSTC) were based on

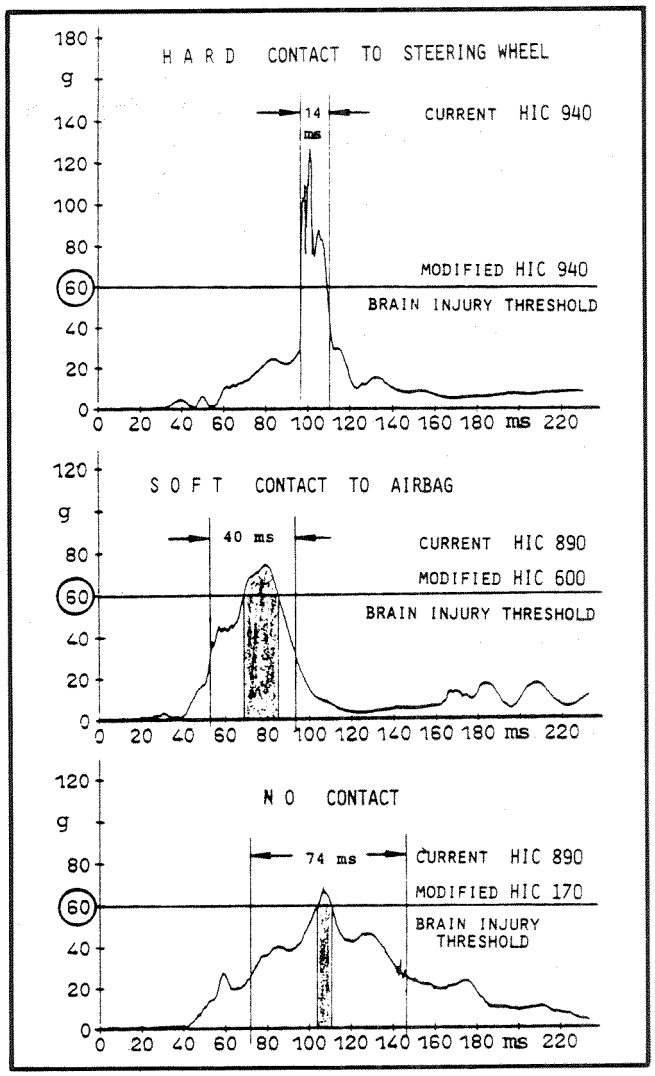

Figure 9. Head acceleration curve of different head loadings

short-duration head impacts up to 15ms, and the level of confidence is lower for those portions of the WSTC, which are analogous to noncontact events of longer duration.

Consequently, the calculation of HIC should be modified, recognizing that there exists a brain-injury threshold set to 60g by the originators of the WSTC; that, of course, simply reflects the fact that if maximum acceleration does not exceed this critical value, insufficient inertial forces are developed to produce injury. It does not matter how long the acceleration persists. Those portions of the head acceleration curve below the 60g level are assumed to be below the threshold at which brain injury occurs and should be neglected. A modified HIC calculation must focus only on that portion of the head acceleration curve assumed to have a brain-injury potential and should be limited to the specific time interval where the 60g injury threshold is exceeded as shown in the shaded portion in Figure 9.

A comparison of current and modified HIC calculations for different head loadings during rigid barrier tests is given in Table 1. It is interesting to note that only the modified HIC values are in line with the real-world accident data: HIC's of truly hard impacts are not affected, whereas those of soft contacts to airbags or noncontacts are significantly reduced. HIC becomes what it should be, namely an effective discriminator between those systems that allow hard injury-producing head impacts and those that do not.

Table 1. HIC of different loadings current and modified calculation

Head	Current		Modified	
Loading	ΔT	HIC	ΔT	HIC
Hard Impact	10ms	2220	13ms	2250
to Steering Wheel	33ms	1240	27ms	1220
or Dashboard	14ms*	940	13ms	940
Soft Contact	40ms*	890	16ms	600
to Airbag	43ms	600	7ms	150
	44ms	470	0ms	0
	51ms	1100	8ms	190
No Contact	74ms*	890	6ms	170
	38ms	630	0ms	0

*Refers to Figure 9

Summary and Conclusion

To ascertain that the improved occupant protection of a combined restraint system will also be reflected in the injury criteria, it is necessary that—

- Evaluation of the chest-injury risk be based on rib deflections
- Pressure-indicating devices be used for monitoring potential facial damages
- Calculation of HIC be limited to the specific time interval where the head acceleration exceeds the 60g level

A Modified Steering Wheel To Reduce Facial Injuries and an Associated Test Procedure

S.P.F. Petty and
M.A. Fenn
Transport and Road Research Laboratory
Department of Transport Crowthorne, United Kingdom

Abstract

Frontal and oblique-frontal impacts are responsible for about two-thirds of car occupant injuries. In those impacts, the steering assembly has been identified as one of the components most frequently hit by the driver. An in-depth study of accident injury data for the Marina car was used to identify the mode of injury. Angled barrier impact tests using an OPAT dummy as driver successfully reproduced the mode of injury.

With a 90 percent plus seatbelt wearing rate in the United Kingdom, it is desirable to develop a simple test procedure to reduce the aggressiveness of the steering wheel to the face and possibly to alleviate the deceleration pulse of the brain. A steering wheel test, based on the standard interior impact test, has been developed and evaluated on seven production car wheels and on a newly designed safer steering wheel. All the production wheels failed the test, but the safety steering wheel passed the suggested test level.

Introduction

Frontal and oblique-frontal impacts are responsible for about two-thirds of car occupant injuries. In those impacts, the steering assembly has been identified as one of the parts most frequently hit by the driver. Internationally, ECE Regulation No. 12 and FMVSS Nos. 203 and 204 were introduced to limit the *rearward* intrusion of the hub of the steering wheel into the occupant compartment in a head-on 30mph frontal barrier test and also to safely absorb the energy of the upper torso of an unbelted occupant, as defined by the SAE J944 body form, from a speed of 15mph. In recognition of the compulsory seatbelt-wearing legislation introduced in Europe with a resulting change in the mechanism and type of driver injury, Regulation No. 12 has been altered to allow the energy-absorbing column test to be optionally replaced by an energy-absorbing steering wheel. The energy absorption required has been changed from that of an upper torso to that of a hemispherical headform travelling at a maximum speed of 24.1km/h (15 mph) as defined in ECE Regulation No. 21.

At the Ninth ESV Conference, a paper by John B. Morris et al.(1) stated that although the post-standard steering system reduced the intrusion of the steering assembly into the passenger compartment by 68 percent,

it was still responsible for 27 percent of all driver serious (AIS 3-6) injuries. The key issues for the continuing injuries were given as—

- The test device does not physically simulate the driver impacting the steering assembly in actual crash situations.
- The test device is not a good human surrogate and the performance criteria are not adequate indicators of injury severity.
- The test and/or performance criteria are not able to distinguish "good" from "bad" design steering assemblies because of these inadequacies.

This paper gives the background to a project that—

- Selected a popular family-sized European car
- Assessed the United Kingdom's accident data to determine the injury mechanism for belted and unbelted drivers
- Compared the accident data with barrier tests using dummies
- Developed a test to evaluate the aggressiveness of steering wheels to the face and produced a safer steering wheel for immediate use

The car chosen for the evaluation was a British Leyland (BL) Marina. This car was nearing the end of its production so there were a sufficient number being driven in the United Kingdom to generate enough accidents to give a sample that could be studied.

Accident Data

To increase the sample size, the studies from the three United Kingdom in-depth accident teams were added together. It must be recognised that doing this gives a sample skewed to the higher energy impacts, but it is these impacts that are more likely to generate occupant injuries. One team based its sample on hospital admittances and the other two teams used accidents to which the police were called with an additional sample of accidents from which a vehicle had to be towed away.

The available sample for the Marina car was then selected for frontal and angled frontal impacts with subsets for drivers using seatbelts and those not recorded as using belts.

Belted Drivers

In the Marina, a lap and diagonal belt is a standard fitting. As there has been no comment on the reports, it is assumed that all the belted drivers were wearing a lap and diagonal belt.

Out of a total sample number of 33, 17 had *recorded* injurious head contact with the steering wheel. Because of the small numbers, the method of sampling, and varying levels of speed and injury, only trends can be considered. The most important is: "In a frontal impact, the seatbelted driver is likely to hit his head on the steering wheel."

Unbelted Drivers

The data given for unbelted drivers relate to all those drivers who could not be identified as wearing belts in the impact and will possibly include a few belted drivers. Table 1 details a relationship of impact speed change, as calculated using the Crash 2 computer program, to the number of *recorded* chest contacts with the steering wheel, to the number of car impacts in which the driver received head injury (face or cranium) from part of the car above the steering wheel, and to the total number of frontal impacts in that speed change group.

Table 1. Unbelted driver's impact data

Δv	Chest Contact with	Head Injury		Number of
mile/h	Steering Wheel	AIS 1	>AIS 1	Impacts
0-5	0	1	0	1
6-10	5	4	2	14
11-15	12	10	1	19
16-20	11	6	9	17
21-25	5	3	1	6
26-30	5	1	5	6
31-35	1	1	2	4
>35	5	0	5	5
Total	45	26	25	72

It should be noted that in seven cases, the driver's head was also identified as hitting the steering wheel. The mean impact speed for the Marina frontal impacts is within 1mi/h of the mean frontal impact speed of 14mi/h for all makes of car as given by Hobbs(2). Thus the Marina can be considered to be representative of a typical car at least in some aspects.

Analysis of the mode of injury shows differences between belted and unbelted drivers. For the belted driver, it is the head that hits the steering wheel giving cranium and/or facial injuries. For the unbelted driver, there is chest contact with the steering wheel but the head hits the A post, header rail, or top of the windscreen generating a more serious injury. With the introduction in the United Kingdom of compulsory wearing of seatbelts by front-seat occupants, the wearing rate rose from under 40 percent to over 90 percent. If the different injury mechanisms are true, there should be a significant increase in injury to the face from the steering wheel. The Rutherford Report(3) on the introduction of compulsory seatbelt wearing confirms this.

Baseline Tests

Two standard Marinas were barrier-impacted to see if the belted and unbelted modes of accident injury could be reproduced. The impacts were head-on into a wood-faced barrier angled at 30° to give maximum intrusion on the driver's side. The drivers were represented by an OPAT dummy.

Seat-Belted Driver

The dummy was restrained using a lap and diagonal inertia reel belt. The impact speed was 57km/h (36mi/h). The lapbelt held the dummy's pelvis in position, allowing its torso to jackknife forward and its head to hit the steering wheel rim, as shown on film and by paint witness marks. Early in the impact, the steering wheel rotated axially through approximately 90°. The left side of the dummy's chest hit the steering wheel rim at its strongest point where it joins the spoke, giving a high chest deceleration. The angled barrier gave some lateral and rotational motion to the car so that during the main impact, the dummy's torso moved toward the door. As a result, its head missed the steering wheel's boss and hit the weakest part of the rim.

Unbelted Driver

The impact speed for the unbelted driver was set at 38km/h (24mi/h). The accident data suggested this was above the critical speed for head injury. At impact, the dummy driver slid forward on its seat until its knee hit the fascia. The chest hit the rising bottom edge of the steering wheel rim, and its torso started to rotate upward. The top of its head hit the header rail and A post before breaking the windscreen, and its chin touched the top of the steering wheel.

The baseline data for both tests are given in Table 2.

The two tests demonstrate it is possible to reproduce the accident injury modes using a barrier test and a dummy to represent the driver. It should be noted that at almost 40km/h, the 3ms exceedance for the unbelted driver is 80g although the HIC value is low.

Table 2. Table of impact results

Driver		Unbelted	Belted
Impact Speed	km/h39.1	57.4	
	mi/h	24.3	35.7
Head			
HIC		437	1308
Peak g		148	218
3ms exceedance g		80	96
Chest			
SI		148	287
Peak g		36	52
3ms exceedance g		33	44
Femurs			
Left 8kN exceedance ms		0	0
Right 8kN exceedance ms		0	0
Car Deceleration			
1ms exceedance g		20	36

Facial Impact Into Steering Wheel

Mechanism of Impact

It was necessary to insure that the behaviour of the seat-belted dummy in the Marina baseline barrier test was typical. The angle barrier tests of six small cars at 60km/h (37mi/h) as reported by Penoyre(4) were examined. In these impacts, the dummy's head twice passed to the side of the wheel, twice contacted the rim, and twice went between the rim and the centre. In all cases, the relative motion of the head was perpendicular to the plane of the steering wheel. This is due to a combination of the upper torso of the dummy rotating downward about its hips and the intruding steering wheel rotating upward about a line along the bottom of the windscreen. Making the wheel rotate upward is a simple design solution to overcome the regulation's requirement of limited rearward intrusion in the barrier test. Thus, there is an immediate need to protect seat-belted drivers in high-energy impacts, when their heads are likely to hit the steering wheel.

Head Injuries

The injuries to the head can be divided into two broad but separable types: those to the cranium and brain, and those to the face. The brain injuries normally relate to head acceleration/time history; the facial injuries to the concentrated loading on specific bones. As the facial injuries are not normally life-threatening, they are given a lower AIS rating and have been less researched. It is likely that the low AIS rating does not adequately reflect the severe social and psychological impact of facial injuries. Nahum(5) has listed the impulse loads acting over $1in^2$ ($645mm^2$) required to break different facial bones. The lowest value given is 225 lb (1KN) for the zygomatic bones. Swearingern(6) has demonstrated that with the load evenly distributed over the head, it is possible to produce a deceleration of 300g with no bone fracture.

Thus, apart from lacerations, the head must be protected from concentrated loads and high decelerations (there is insufficient data to include the rotational injury mechanisms).

Steering Wheel Test

It is desirable that to protect unbelted drivers, the present regulations for energy-absorbing steering assemblies should continue despite their problems. In addition, the steering wheel should offer protection when it is hit by the head of a belted driver. Also, after, market wheels should be tested to the original fitment standard. Legislation "Concerning the Approval of Vehicles with Regard to their Interior Fittings" uses a head mass of 6.8kg (15 lb) and its energy is that of a mass travelling at 24.1km/h (15mi/h). For the proposed steering wheel test, the same mass and energy are retained. The hemispherical headform is replaced by a cylinder. The impacting and face of the cylinder is a disc of aluminum honeycomb with a crushing force of 200 lb/in^2. The cylinder is impacted axially square onto the plane of the wheel. The wheel is rigidly mounted or fixed on the rigidly mounted end of the steering column complete with its trim and ancillary controls. The diameter of the cylinder is 150mm (6in) and to avoid edge effects the depth of crush of the honeycomb is measured over a central area of 100mm (4in) diameter. It is proposed that the test is passed by meeting two criteria. One is that the indentations of the honeycomb do not exceed 2mm. The other is that the maximum deceleration does not exceed 80g during the impact for a cumulative period of 3ms. It should be noted this exceedance requirement may produce higher figures than that of the Interior Fittings Regulation, which specifies a continuous period of exceedance.

Wheel Test Results

Eight wheel designs were chosen to use in the test to evaluate their aggressiveness and ability to protect the head; the six from the impact tests as reported by Penoyre,(4) an Austin Metro wheel, and a safety steering wheel being developed by Sheller-Clifford in a joint development contract with TRRL to fit the Austin Metro. Each wheel design was impacted on its hub, at the join of the spoke and rim, on the mid-point of the longest unsupported part of the rim, and on the mid-point of the shortest unsupported part of the rim that did not include a join of a spoke to the rim. The results are given in Table 3. The facial injury potential of the wheels is estimated by measuring the maximum depth of the indentation into the aluminum honeycomb in 2mm steps, using a cylindrical probe 6mm in diameter. For the impacts at the join of the spokes to the rim, the level of crush is tabulated for both the spoke and rim. Where possible, the results of "in car" tests using the Motor Industry Research Association (MIRA) Mk II Free-Flight Headform Impactor has been given for comparison.

It is only on the hub impacts that the peak acceleration is greater than 80g. The channel amplitude class was set at 145g to reduce noise. For some rigid hubs, the peak level saturated giving an unrealistically low HIC value. For simplicity in Test House recording, it is recommended that the cumulative 80g for 3ms should be used. Only the Volvo padded centre spreads the load over the hexacell to give a zero crush reading. An additional 15° angled impact on this hub also gave similar results. This was due to the self-alignment of the wheel and impactor about the Z axis. However, the wheel failed in the exceedance mode.

None of the production wheels passed the proposed facial injury test at the suggested levels. Although the ideal standard should be that of zero crush of the impactor face, it is considered that a maximum crush of 2mm may have to be accepted.

The MIRA Free-Flight Headform Impactor test tends to give lower g results. Allowance must be made for one test being with a rigidly mounted wheel and a flat-faced impactor and the other with a rigid hemispherical aluminum headform hitting the steering wheel as it is fitted in the car for normal use.

The safety wheel passed all the axial impact tests with no deformation of the aluminum honeycomb and with a peak deceleration of 69g on the hub impact. Even when the wheel was angled at 30°, so that the main impulse was through the rim and down one of the most supported spokes, the crush of the honeycomb was only 1mm. Thus it seems to be possible to produce a steering wheel to production standards that protects the head from both brain and facial injuries. Eventual evidence might show that brain deceleration might still be high because for a belted occupant it is the resultant of the facial impact deceleration and head nodding deceleration, which corresponds to the restraint of the head by the neck. Although brain injuries do not seem to occur in cars from this latter deceleration, it is possible that when combined with some facial impact it can be injurious.

Alternative Test

As an alternative to the new test, a load-measuring mat that fits over a dummy's face is being evaluated. This would have the benefit of giving a load-time history at 256 points over the face. Each point is sampled once a millisecond. Such a device need not be restricted to use on a pendulum but could be developed as a standard tool for use on dummies in car crash testing.

Conclusion

1. Frontal and oblique-frontal impacts are responsible for about two-thirds of car occupant injuries. In these impacts, the steering assemblies have been identified as one of the car components most frequently struck by drivers.

Table 3. Wheel test results

Wheel Type	Impact Point	New Wheel Test Peak G	Exceedance 3ms g	Exceedance 80g ms	HIC	Faceform Penetration mm	MIRA Headform Peak g	MIRA Headform 3ms Exceedance g	MIRA Headform HIC
Austin	Hub	145*	116	4.0	713*	>6 226	62	612	
Maestro	Spoke/Rim	62	50	0	167	2-4/2-4	110	51	198
	Unsupported Rim	39	23	0	67	2-4	—	—	—
	Supported Rim	47	38	0	126	4-6	—	—	—
Renault 9	Hub	98	85	3.9	391	>6	239	19	443
	Spoke/Rim	59	49	0	148	>6/0-2	111	41	167
	Unsupported Rim	30	18	0	35	0-2	—	—	—
	Supported Rim	55	41	0	146	0-2	—	—	—
Toyota	Hub	#	#	#	#	#	134	102	602
Tercel	Spoke/Rim	67	40	0	111	0/4-6	62	37	180
	Unsupported Rim	47	23	0	63	0-2	—	—	—
	Supported Rim	35	32	0	117	4-6	—	—	—
Ford	Hub	146*	114	4.0	751*	2-4	223	53	606
Escort	Spoke/Rim	74	62	0	274	2-4/2-4	80	40	198
	Unsupported Rim	50	23	0	64	2-4	—	—	—
	Supported Rim	57	50	0	162	4-6	—	—	—
Opel	Hub	145*	112	5.0	789*	2-4	112	80	338
Cadet	Spoke/Rim	61	51	0	207	0-2/>6	43	37	151
Vauxhall	Unsupported Rim	44	26	0	79	4-6	—	—	—
Astra	Supported								
(MIRA)	Rim	42	37	0	139	4-6	—	—	—
Volvo	Hub	116	106	5.9	706	0	75	71	443
340	Spoke/Rim	54	47	0	130	0/>6	58	34	143
	Unsupported Rim	41	28	0	70	2-4	—	—	—
	Supported Rim	42	37	0	139	4-6	—	—	—
	Amgled Hub	106	97	5.9	596	0	—	—	—
Austin	Hub	144*	144	3.4	760*	>6	126	92	541
Metro	Spoke/Rim	59	53	0	219	>6/0-2	42	35	98
	Unsupported Rim	49	31	0	102	2-4	—	—	—
	Supported Rim	44	36	0	122	2-4	—	—	—
Safety	Hub	69	64	0	357	0	—	—	—
Wheel	Spoke/Rim	40	33	0	45	0/0	—	—	—
	Unsupported Rim	26	23	0	65	0	—	—	—
	Supported Rim	44	34	0	89	0	—	—	—
	30° Spoke/Rim	59	41	0	119	0-2	—	—	—

#Trim not available in UK for testing

*Low values (see text)

2. An in-depth study identified that the heads of drivers wearing seatbelts hit their steering wheels with injuries to the face and possibly to the brain in moderate-to-severe impacts. The chests of unbelted drivers hit the steering wheels, but their heads were injured by hitting either header rails, A posts, or the tops of windscreens.
3. It is possible to reproduce these two different modes of injury using an OPAT dummy driver and an angled barrier test.
4. With a 90 percent plus front seatbelt-wearing rate in the United Kingdom, it is therefore desirable to discover whether the aggressiveness of steering wheels for facial injuries can be reduced.
5. A simple impact test procedure for steering wheels has been developed, and test levels for it have been suggested. It is based on the standard interior impact test but replaces the solid hemispherical head by a flat circular face of aluminum honeycomb whose crush resistance is matched to that for the weak facial bones. The test has been evaluated on seven production car wheels and on an especially designed safer steering wheel. All the production wheels failed to pass at the suggested level, but the safer wheel did so and showed distinct improvements in several respects.

Acknowledgments

The work described in this paper forms part of the programme of the Transport and Road Research Laboratory and the paper is published by permission of the Director.

The authors wish to thank Mr. Stan Edge of Sheller-Clifford Ltd. for his help in designing and manufacturing a practical safety steering wheel.

References

1. Morris, John B. et al., "Occupant protection from impact with the steering assembly," Proceedings Ninth International Technical Conference on Experimental Safety Vehicles, Kyoto, National Highway Transportation Safety Administration, U.S. Department of Transportation, 1982.
2. Hobbs, C.A., and Paula J. Mills, "Injury probability for car occupants in frontal and side impacts," TRRL Laboratory Report 1124, Transport and Road Research Laboratory, Crowthorne, Berkshire, United Kingdom, 1984.
3. Rutherford, W.H., Personal communication on hospital-based accident study.
4. Penoyre, S., "An impact test programme using six models of lower-medium sized cars," Proceedings Tenth International Technical Conference on Experimental Safety Vehicles, Oxford, 1985.
5. Nahum, A.M. et al., "Impact tolerance of skull and face," Proceedings 12th Stapp Car Crash Conference, Detroit, Michigan, 1968.
6. Swearingen, John J., "Tolerances of the human face to crash impact," Federal Aviation Agency, Civil Aeromedical Research Institute, Oklahoma City, Oklahoma, 1965.

Improved Crashworthiness Independent of Belts or Airbags

Richard A. Wilson
General Motors Environmental Activities Staff

Abstract

Impacts to the vehicle interior are the most frequent source of occupant injury in highway accidents and generate the largest segment of the resulting total harm as calculated by the National Highway Traffic Safety Administration. Accordingly, improving the injury-mitigating properties of interior components along with the structural integrity of vehicles has significant potential for providing important safety benefits to occupants of crash-involved vehicles. This paper reviews the relative contribution of various occupant-vehicle contacts to total harm and offers some insight into the benefits that might be realized through component improvements. While such improvements are related primarily to unbelted occupants, their benefits should be considered complementary to those of safety belts and airbags since (1) some degree of nonuse of belts likely will remain even with the growing adoption of belt-use laws in the United States, and (2) belted occupants still can contact the vehicle interior in more severe crashes, as can occupants of airbag-equipped cars involved in crashes below the deployment threshold or in side impacts and rollovers.

Introduction

September 9 of next year will mark the 20th anniversary of the U.S. adoption of the National Traffic and Motor Vehicle Safety Act and establishment of the regulatory

agency now known as the National Highway Traffic Safety Administration (NHTSA). Although a number of crashworthiness improvements were well underway prior to 1966, the enactment of the safety act prompted a considerable increase in the attention given to vehicle safety by government, vehicle manufacturers, and the public. Important gains have come from this increased focus on reducing the number of deaths and injuries caused by highway crashes. However, the direction in which to advance vehicle crashworthiness further has been a subject of on-going debate for nearly two decades.

Much of this debate has been centered on automatic restraints as covered by Federal Motor Vehicle Safety Standard (FMVSS) 208, first issued as a Notice of Proposed Rulemaking in 1970. Although FMVSS 208 is often thought of as "the airbag standard," it actually carries the broader title of "Occupant Crash Protection" and its requirements for future vehicles likely will be met by three candidate approaches. Two of these, airbags and automatic belts, are well known and already have been offered as options on certain models of car. The third alternative, however, has not received as much recognition within the safety community. This approach relies on improved energy absorption and structural integrity, which are built into the vehicle. It would not use add-on systems, such as airbags or automatic belts, to meet the test performance required by the standard.

The purpose of this paper is to examine the potential for increased, built-in safety to reduce the harm to vehicle occupants caused by highway crashes. Specific safety improvements to the steering system and side impact will be discussed as well.

Assessment of Potential

An essential ingredient for any assessment of the potential for built-in safety to improve vehicle crashworthiness is some understanding of which parts of the vehicle are involved with the various body regions of the occupant and what degree of injury was produced by those occupant-to-vehicle interactions. This understanding must come from analyses of accident data, the quality and quantity of which have been improving steadily over the past decade. In February 1982, a detailed analysis of national accident data was published by NHTSA as part of the International Congress of the Society of Automotive Engineers. This significant study(1), "A Search for Priorities in Crash Protection" by A.C. Malliaris, Ralph Hitchcock, and James Hedlund, has provided a wealth of information to help guide the development and implementation of improved crash protection.

The NHTSA paper advanced the concept of total harm as a way to quantify the consequences of various occupant-to-vehicle contacts by including both the frequency and severity of the injuries. Injury severity within the National Crash Severity Study (NCSS) data was rated using the Abbreviated Injury Scale (AIS). The various injury levels ranging from minor through non-survivable (AIS 1-6) were assigned appropriate weighting factors that applied to each injury, and the weighted sum was identified as total harm. The paper provided tables that break down total harm according to a number of key variables, including crash configuration and severity, location of interior contacts, body regions injured, and injury severity.

More recently, in February of 1985, Malliaris, Hitchcock, and Hansen of NHTSA published an update and extension of the earlier work as "Harm Causation and Ranking in Car Crashes." This latter paper(2) used National Accident Sampling System (NASS) data to study what changes in casualty and risk patterns may have occurred from the late 1970's to the early 1980's. The newer study also employed a revised weighting schedule for calculating total harm from the AIS values in the data. However, in light of the conclusions of the authors that (1) no significant changes are noted between the NCSS and NASS results, and (2) no significant change in harm distribution is produced by the revised injury weighting schedule, the assessment of potential that follows will use information from the earlier work because of the more detailed breakdowns of harm distribution it provides.

Distribution of Total Harm

A review of information from the former NHTSA study provides a background for considering the potential for safety improvements. In particular, one of the tables from their paper presented a distribution of human harm according to broad categories of persons involved in highway accidents. Of course, each category of human harm is important in itself and safety improvements are desirable for all. However, as indicated by the general distribution shown in Table 1, about three-quarters of total harm relates to occupants of passenger cars, light trucks, and vans, and most of that is associated with cars.

Table 1. Distribution of harm from highway accidents (excluding property damage)

Category	Percent Total Harm
Passenger Car Occupants	60.9
Light Truck & Van Occupants	15.3
Heavy Vehicle Occupants	2.2
Motorcyclists	9.9
Pedestrians & Other Nonoccupants	11.8
Total	100.1

(From Malliaris, et al., Table 3, SAE Paper 80242)

It is particularly instructive to study in more detail those occupant-to-vehicle interactions involved in more than 60 percent of total harm to all road users. The fourth table in the NHTSA paper took the 60.9 percent total harm associated with passenger-car occupants and gave a further breakdown with respect to (1) which components of the vehicle were contacted by the various occupant body regions, (2) how much harm is related to noncontact injuries, and (3) how much harm is related to exterior contacts. That information has been condensed (see Table 2) to generate four basic categories in which to consider built-in safety improvements.

Potential for Frontal Improvements

The first observation to be made from the distribution shown in Table 2 is that over half (54 percent) of total harm to car occupants is associated with contact to frontal interior components of the vehicle. This priority on frontals is not a new finding, as evidenced by the early attention given to passenger car frontal collisions by FMVSS 208. However, the ability to break down interior contact data by body region and crash severity is more recent, providing a means to make general estimates of the potential for reducing harm through improvements to vehicle interior components. In particular, Table 11 of the Malliaris report gives a cumulative distribution of harm as a function of crash severity. That information can be viewed as upper limits on the total harm available for mitigation within various body-region/vehicle-interior contact areas and below various impact speeds.

To estimate upper bounds on the potential for built-in safety to mitigate total harm within the basic category of "front," the analysis used for Table 3 includes only those rows from Table 11 of Malliaris judged to be related primarily to vehicle interior components contacted by unbelted occupants in a frontal crash configuration. It is recognized that some portion of the values in the column labeled "Harm Pct of Total" might be associated with damage other than front (see Table 5 of Malliaris). However, since the focus of this analysis is on front interior components and component improvements likely would affect other damage directions as well, no adjustment has been made to the line items selected except for head/face contacts with A-pillars and roof edges, which exhibit a more even distribution between front and side involvements.

For convenience, Table 3 reproduces from Table 11 of Malliaris only the 20- and 30-mph columns of cumulative percent of harm. The percent of total harm for each line item is multiplied by the appropriate crash severity cumulative percentage, and the products are shown in the two columns to the right labeled "Added Calculation." The sum of these products represents the percent of the total harm associated with front interior component contacts below the indicated crash severity.

In other words, if vehicle improvements could be devised that assured all harm would be eliminated from contact with front interior components in accidents up to 20 or 30mph, Table 3 indicates a total potential of about 14 or 27 percent, respectively, exists for making reductions in overall total harm. These percentages, when compared to the 47.80 base percentage[1] for front component involvements only, represent front contact harm reduction potentials of about 29 or 57 percent, respectively.

1. The 47.8 percent total harm for front interior component contacts shown at the bottom of Tables 3, 4, and 5 is somewhat lower than the 54.0 percent given in Table 2 for the major category of front because a number of miscellaneous, small-harm value items were not encompassed by the analyses.

Table 2. Percent distribution of car occupant total harm

From Malliaris, Table 4		Basic Category	
All Frontal Interior Contacts	49.37		
A-Pillars (assume 1/2 "front")	2.23		
Roof Edges (assume 2/3 "front")	2.40	54.0	Front
All Side Interior Contacts	15.85		
A-Pillars (assume 1/2 "side")	2.24	19.3	Side
Roof Edges (assume 1/3 "side")	1.20		
Roof	2.35		
All Other Interior Contacts	4.64	14.9	Other
Noncontact	7.91		
All Exterior Contacts	11.83	11.8	Exterior*
Total	100.2%	100.0%	Total

* "Exterior" should not be equal to "ejection." As seen in Table 8 of Malliaris, only 7.4 of the 11.4 percentage points are related to occupants who were ejected.

Table 3. Potential for harm reduction in percent as a function of crash severity in miles per hour (front component contacts only)

	From Malliaris, Table 11			Added Calculation			
Item	Vehicle Contact	Body Region	Harm Pct of Total	Crash Severity 20	30	Harm % up to Crash Severity 20	30
1	Steering Assy.	Chest	11.90	x .21	.40	= 2.50	4.76
2	Steering Assy.	Abdomen	9.41	x .20	.50	= 1.88	4.71
4	Windshield	Head/Face	4.68	x .46	.66	= 2.15	3.09
5	A-Pillars	Head/Face	2.00*	x .17	.54	= 0.34	1.08
6	Inst. Panel	Lower Extr.	3.43	x .44	.73	= 1.51	2.50
7	Steering Assy.	Head/Face	3.13	x .50	.76	= .1.57	2.38
8	Roof Edges	Head/Face	1.98*	x .19	.56	= 0.38	1.11
10	Inst. Panel	Chest	2.06	x .23	.54	= 0.47	1.11
11	Inst. Panel	Abdomen	1.85	x .17	.61	= 0.31	1.13
13	Inst. Panel	Head/Face	1.65	x .61	.84	= 1.01	1.39
14	Inst. Panel	Upper Extr.	1.40	x .32	.69	= 0.45	0.97
16	Glove Comp.	Abdomen	1.23	x .02	.48	= 0.02	0.59
17	Steering Assy.	Upper Extr.	1.16	x .46	.84	= 0.54	0.97
18	Mirrors	Head/Face	1.08	x .76	.88	= 0.82	0.95
19	Glove Comp.	Chest	0.84	x .08	.55	= 0.07	0.46
	Totals		47.80%			14.02%	27.20%

*(Related to frontals only — see Malliaris, Table 5)

Since it is unlikely that all harm could be prevented by practicable improvements in occupant protection, some additional considerations for estimating a more realistic harm reduction are indicated. One assumption could be that no injuries at the minor, or AIS 1, injury level would be eliminated. For example, abrasions, contusions, and superficial lacerations are assumed still to occur. The fractions of total harm related only to AIS levels 2 through 6 can be found on Table 12 of Malliaris. Table 4 adds this assumption to the information on Table 3 and shows the harm reduction potential that remains after AIS 1 injuries are dropped from consideration.

If front interior component improvements could be devised that assured all harm having injury levels of AIS 2 or greater were eliminated in accidents up to 20 or 30mph, total harm reductions of about 11 or 23 percent, respectively, might be realized. Using only front component involvements as the base, these estimated percentages represent front contact harm reduction potentials of about 24 or 48 percent, respectively.

Additional information from Table 13 of Malliaris was used in Table 5 to evaluate a further assumption related to estimating the harm reduction potential of changes to front interior components. For each injury beyond the AIS 1's already dropped from consideration, a mitigation of only one level in the AIS rating was assumed to be achievable by improvements. Accordingly, the totals shown at the bottom right represent the percent of total harm that might be eliminated through crashworthiness improvements for unbelted occupant contact to front interior components, assuming those improvements would be successful in reducing each AIS 2 to 6 injury (occurring up to the indicated speed) by one AIS level.

The estimated potentials for reduction in overall total harm from improvements to frontal components are seen to be about 9, 13, or 17 percent for speeds up to 20, 25, or 30mph, respectively. Again, using only frontal component contacts for a baseline, these percentages represent front contact harm reduction potentials of about 19, 27, or 37 percent, respectively.

Potential for Side Improvements

Side interior contacts represent the second largest basic category of car occupant harm, accounting for about 19 percent of overall total harm. Corresponding potentials for harm reduction from side interior component improvements are estimated by Tables 6, 7, and 8, which were constructed in a manner similar to that described above for frontal components.

The nine specific side component contacts selected for Tables 6, 7, and 8 encompass nearly 14 percent of total harm. This is somewhat less than the 19 percent figure noted earlier, because the more general distribution of Table 2 includes a number of miscellaneous body region contacts not separately identified in the NHTSA tables used for the analyses in this paper.

Summary of Potential for Harm Reduction

Tables 3 through 8 have developed general estimates of the potential available for reducing car occupant total

Table 4. Potential for harm reduction in percent as a function of crash severity in miles per hour (front component contacts, AIS 2-6 only)

	From Malliaris, Table 11						Added Calculation	
				Crash Severity			Harm Pct up to Crash Severity	
Item	Vehicle Contact	Body Region	Harm Pct of Total	20	30	to drop AIS 1's**	20	30
1	Steering Assy.	Chest	11.90	x .21	.40	x .96	= 2.40	4.57
2	Steering Assy.	Abdomen	9.41	x .20	.50	x .99	= 1.86	4.66
4	Windshield	Head/Face	4.68	x .46	.66	x .67	= 1.44	2.07
5	A-Pillars	Head/Face	2.00*	x .17	.54	x .97	= 0.33	1.05
6	Inst. Panel	Lower Extr.	3.43	x .44	.73	x .66	= 1.00	1.65
7	Steering Assy.	Head/Face	3.13	x .50	.76	x .69	= 1.08	1.64
8	Roof Edges	Head/Face	1.98*	x .19	.56	x .92	= 0.35	1.02
10	Inst. Panel	Chest	2.06	x .23	.54	x .95	= 0.45	1.06
11	Inst. Panel	Abdomen	1.85	x .17	.61	x .99	= 0.31	1.12
13	Inst. Panel	Head/Face	1.65	x .61	.84	x .76	= 0.76	1.05
14	Inst. Panel	Upper Extr.	1.40	x .32	.69	x .76	= 0.34	0.73
16	Glove Comp.	Abdomen	1.23	x .02	.48	x .99	= 0.02	0.58
17	Steering Assy.	Upper Extr.	1.16	x .46	.84	x .68	= 0.36	0.66
18	Mirrors	Head/Face	1.08	x .76	.88	x .72	= 0.59	0.68
19	Glove Comp.	Chest	0.84	x .08	.55	x .96	= 0.06	0.44
	Totals		47.80%				11.35%	22.98%

*(Related to frontals only — see Malliaris, table 5)
**(Fraction for AIS 2-6 — see Malliaris, Table 12)

Table 5. Potential for harm reduction in percent as a function of crash severity in miles per hour (front component contacts, AIS 2 to 6 only, each AIS 2 to 6 lowered one level).

	From Malliaris, Table 13							Added Calculation		
				Crash Severity				Harm Reduc. up to Crash Severity		
Item	Contact	Body Region	Harm Pct of Total	20	25	30	to drop AIS 1's**	20	25	30
1	Steering Assy.	Chest	11.90	x .15	.20	.29	x .96	= 1.71	2.28	3.31
2	Steering Assy.	Abdomen	9.41	x .15	.23	.36	x .99	= 1.40	2.14	3.35
4	Windshield	Head/Face	4.68	x .42	.54	.58	x .67	= 1.32	1.69	1.82
5	A-Pillars	Head/Face	2.00*	x .09	.15	.31	x .97	= 0.17	0.29	0.60
6	Inst. Panel	Lower Ext.	3.43	x .41	.57	.66	x .66	= 0.93	1.29	1.49
7	Steering Assy.	Head/Face	3.13	x .43	.48	.61	x .69	= 0.93	1.04	1.32
8	Roof Edges	Head/Face	1.98*	x .17	.36	.39	x .92	= 0.31	0.66	0.71
10	Inst. Panel	Chest	2.06	x .18	.24	.39	x .95	= 0.35	0.47	0.76
11	Inst. Panel	Abdomen	1.85	x .13	.20	.41	x .99	= 0.24	0.37	0.75
13	Inst. Panel	Head/Face	1.65	x .51	.61	.69	x .76	= 0.64	0.76	0.87
14	Inst. Panel	Upper Ext.	1.40	x .29	.39	.62	x .76	= 0.31	0.41	0.66
16	Glove Comp.	Abdomen	1.23	x .01	.09	.32	x .99	= 0.01	0.11	0.39
17	Steering Assy.	Upper Ext.	1.16	x .40	.58	.75	x .68	= 0.32	0.46	0.59
18	Mirrors	Head/Face	1.08	x .71	.76	.81	x .72	= 0.55	0.59	0.63
19	Glove Comp.	Chest	0.84	x .05	.21	.29	x .96	= 0.04	0.17	0.23
	Totals		47.80%			(%'s)		9.23	12.73	17.48

*(Related to frontals only — see Malliaris, Table 5)
**(Fraction for AIS 2-6 — see Malliaris, Table 12)

Table 6. Potential for harm reduction in percent as a function of crash severity in miles per hour (side component contacts only).

	From Malliaris, Table 11					Added Calculation	
Item	Vehicle Contact	Body Region	Harm Pct of Total	Crash Severity 20	30	Harm % up to Crash Severity 20	30
3	Side Interior	Chest	4.94	x.52	.93	= 2.57	4.59
5	A-Pillars	Head/Face	1.66*	x.17	.54	= 0.28	0.90
8	Roof Edges	Head/Face	0.78*	x.19	.56	= 0.15	0.44
9	Side Interior	Abdomen	2.36	x.37	.79	= 0.87	1.86
15	Armrests	Abdomen	1.25	x.36	.83	= 0.45	1.04
20	Window Glass	Head/Face	.079	x.46	.96	= 0.36	0.76
21	Window Frames	Head/Face	0.77	x.90	1.00	= 0.69	0.77
23	Side Interior	Lower Ext.	0.71	x.58	.94	= 0.41	0.67
25	Roof Edges	Neck	0.57	x.01	.04	= 0.01	0.02
	Totals		13.83%			5.79%	11.05%

*(Related to left and right only see Malliaris, Table 5)

Table 7. Potential for harm reduction in percent as a function of crash severity in miles per hour (side component contacts, AIS 2 - 6 only).

	From Malliaris, Table 11						Added Calculation	
Item	Vehicle Contact	Body Region	Harm Pct of Total	Crash Severity 20	30	to drop AIS 1's**	Harm Pct up to Crash Severity 20	30
3	Side Interior	Chest	4.94	x.52	.93	x .99	= 2.54	4.55
5	A-Pillars	Head/Face	1.66*	x.17	.54	x .97	= 0.27	0.87
8	Roof Edges	Head/Face	0.78*	x.19	.56	x .92	= 0.14	0.40
9	Side Interior	Abdomen	2.36	x.37	.79	x .99	= 0.86	1.85
15	Armrests	Abdomen	1.25	x.36	.83	x .99	= 0.45	1.03
20	Window Glass	Head/Face	0.79	x.46	.96	x .52	= 0.19	0.39
21	Window Frames	Head/Face	0.77	x.90	1.00	x .96	= 0.67	0.74
23	Side Interior	Lower Ext.	0.71	x.58	.94	x .77	= 0.32	0.51
25	Roof Edges	Neck	0.57	x.01	.04	x1.00	= 0.01	0.02
	Totals		13.83%				5.45%	10.36%

*(Related to left and right only - see Malliaris, Table 5)
**(Fraction for AIS 2 thru 6 - see Malliaris, Table 12)

harm associated with contact to front and side interior components of vehicles, and the listing in Table 9 is a summary of those general estimates. The vehicle components included in the analyses are the ones most likely to be involved in nearly two-thirds of the total harm experienced by car occupants in all modes of crashes.

As mentioned previously, these potentials for harm reduction are expressed as a percentage of all the total harm to car occupants experienced for all crash modes. The values in the table would be correspondingly higher if the base for improvement is viewed as being that related only to front, side, or front-plus-side total harm, as appropriate. For example, the 24.3 percent value at the lower right of the table represents about a 40 percent reduction potential for front-plus-side interior component improvements if they could lower all AIS 2 to 6 injuries each by one AIS level.

The values shown for the potential to reduce harm by lowering AIS 2 to 6 injuries up to certain speeds may be conservative estimates. This is because the benefits of improved designs are not likely to be present at 29.9mph and absent at 30.1mph. There can be some additional potential for harm reduction manifested as some injury reduction in higher speed crashes even for the higher level injuries. As Table A-1 of reference (2) reveals, the opportunity for this effect is appreciable, since nearly half of AIS 5's and about nine-tenths of AIS 4's are survivable. Of course, the actual degree to which given improvements

Table 8. Potential for harm reduction in percent as a function of crash severity in miles per hour (side component contacts, AIS 2 to 6 only, each AIS 2 to 6 lowered one level)

	From Malliaris, Table 13			Added Calculation							
				Crash Severity				Harm Reduc. up to Crash Severity		
Item	Contact	Body Region	Harm Pct of Total	20	25	30	to drop AIS 1's**	20	25	30
3	Side Inter.	Chest	4.94	x .33	.44	.57	x .99 =	1.61	2.15	2.79
5	A-Pillars	Head/Face	1.66*	x .09	.15	.31	x .97 =	0.14	0.24	0.50
8	Roof Edges	Head/Face	0.78*	x .17	.36	.39	x .92 =	0.12	0.26	0.28
9	Side Inter.	Abdomen	2.36	x .28	.38	.56	x .99 =	0.65	0.89	1.31
15	Armrests	Abdomen	1.25	x .25	.47	.57	x .99 =	0.31	0.58	0.71
20	Wind. Glass	Head/Face	0.79	x .43	.65	.74	x .52 =	0.18	0.27	0.30
21	Wind. Frames	Head/Face	0.77	x .53	.53	.62	x .96 =	0.39	0.39	0.46
23	Side Inter.	Lower Ext.	0.71	x .43	.72	.83	x .77 =	0.24	0.39	0.45
25	Roof Edges	Neck	0.57	x .02	.04	.04	x1.00 =	0.01	0.02	0.02
	Totals	13.83%	(%'s) 3.65	5.19	6.82					

*(Related to left and right only - see Malliaris, Table 5)
**(Fraction for AIS 2-6 - see Malliaris, Table 12)

Table 9. Potential available for harm reduction (in percent of total harm)

Contact Area	Harm Pct	Total Potential Available up to 20mph	30mph	AIS2+ Potential Available up to 20mph	30mph	Assume AIS 2-6 injuries lowered one level up to 20mph	25mph	30mph
Front Int.	47.8	14.0	27.2	11.4	23.0	9.2	12.7	17.5
Side Int.	13.8	5.8	11.1	5.5	10.4	3.7	5.2	6.8
Totals	61.6%	19.8%	38.3%	16.9%	33.4%	12.9%	17.9%	24.3%

achieve these potentials will have to be observed from accident data acquired in the future.

Specific Safety Improvements

The general estimates developed above have assumed that certain reductions in injury levels actually would be accomplished within the various interior contact situations.[2] Such a hypothetical approach is useful for an overall consideration of the potential for built-in safety to provide safety benefits. However, assessing the harm reduction that might result from implementation of specific and practicable improvements to individual components of the vehicle entails estimating how much the individual crash injuries might be reduced overall through modification of particular design characteristics of the components involved.

2 The assumption that given safety improvements might yield reductions of one AIS level seems particularly reasonable for the case of head impacts which generate about 30 percent (the largest fraction) of total harm from interior contact (see Table 4 of reference 1). This judgment is supported by the basic nature of the Head Injury Criterion (HIC) used to scale the severity of head-to-vehicle contacts. Since calculation of the HIC begins with raising the measured head accelerations to the 2.5 power, even modest reductions in those impact accelerations should produce significant reductions in HIC values, along with the expectation of reduced AIS levels.

Improvements to the Steering System

As seen earlier in Table 2, the basic category of front accounts for over half (54 percent) of car occupant total harm, and a summation of items 1, 2, 7, and 17 of Table 3 indicates that occupant contact with the steering system is associated with nearly half of that (25.6 percent). In other words, about one-quarter of all harm to all car occupants in all crash modes is related to a single group of vehicle components—the steering system. This should not be surprising since most crashes are frontal and each has a driver seated directly behind a steering system. The relative importance of the steering system within the distribution of total harm prompted a more detailed study of the potential for making crashworthiness improvements in this area.

Extensive experience has been gained by General Motors during the past 20 years regarding the design, development, testing, and field evaluation of steering wheels and energy-absorbing steering columns. This experience has generated an increased understanding of the occupant's interaction with the steering system and is providing important guidance for the implementation of improved crash performance as new vehicles are de-

veloped. In particular, a number of design and performance considerations for the steering system are being identified.

The first relates to the force-versus-deflection properties of the steering column. Traditional designs have specified a more or less constant force level to compress the energy-absorption mechanism within the column. Our more recent studies suggest that a compression force that increases with increasing column stroke better recognizes the dynamic nature of the interaction of the occupant with the steering system. During the early portion of column compression, inertial forces are imposed on the torso of the occupant as the mass of the upper column and the steering wheel is accelerated toward the instrument panel. Therefore, a compounding of forces can be mitigated if the column compression force is designed to be lower at the start of the column stroke. Further, a design that provides a higher column force level toward the end of the stroke can help extend the energy-absorbing capability of the system to higher speed crashes.

Another important element in the energy-absorbing steering column system is the manner in which the stroking portion of the column is attached to the instrument panel. While this attachment must be secure enough to meet the demands of normal vehicle usage, it must also disengage readily (from a range of torso impact directions) so the column can compress in a crash. Such a quick-release attachment to the instrument panel should improve the performance of the column system over a wider range of accident configurations.

The overall interaction of the driver with the steering system can be enhanced through several other considerations. The first is maintaining control of vertical and horizontal displacement of the steering system during vehicle crush. Another is designing the knee impact area of the lower instrument panel to provide improved control of driver kinematics, which should promote both loading the column more in line with the stroking direction and reduced abdominal loads. Additionally, proper selection of steering wheel parameters such as wheel dish, hub contact areas, and force/deflection properties of the rim and spokes should, in some crashes, improve the distribution of load between the chest and shoulders of the driver and should mitigate head impacts to the rim. More crush space in the steering wheel hub should reduce the severity of potential head impacts of the belted driver.

Potential Benefits From Steering System Improvements

The Malliaris papers on total harm distribution do not include information on the specific type (i.e., fracture, concussion, laceration, etc.) of the individual injuries that were entered into their analyses using the AIS coding system. An assessment of the potential benefit from specific design changes and performance improvements such as those described above requires this more detailed knowledge, and such injury details are included in the accident data acquired through GM's Motors Insurance Corporation (MIC).

The Safety and Crashworthiness Systems group within GM's Current Product Engineering analyzed steering system improvement potential by separating the steering system total harm seen in the MIC data into cells according to specific injury type, AIS level, and body region. Injury weights used to generate the MIC total harm were identical to those used by NHTSA in its earlier study of the NCSS data. Estimates were made for how much of the harm in each cell might be mitigated by the steering system improvements under consideration. The data for drivers were analyzed separately for both the belted and unbelted conditions, and Table 10 gives the results.

The potential reductions shown in Table 10 used only steering system contact harm as the 100 percent baseline. If these steering-system-only improvements of 28.6 percent and 34.9 percent for the belted and unbelted cases are

Table 10. Potential driver harm reduction from steering system improvements (using MIC data).

Body Region	Current Percent of Steering System Harm		Portion Estimated to be Reduced	
	belted	unbelted	belted	unbelted
Head	13.4	14.9	4.2	5.4
Neck	0.4	1.5	0.0	0.0
Torso	52.4	56.4	19.8	23.6
Abdomen	16.9	15.8	4.6	4.5
Upper Ext.	7.3	4.2	0.0	0.0
Lower Ext.	2.4	2.6	0.0	0.0
Whole Body	7.2	4.6	0.0	1.4
Totals	100.0%	100.0%	28.6%	34.9%

multiplied by the 25.6 percent of total harm noted earlier for only steering system contact, a reduction in overall total harm of from 7 to 9 percent is indicated to be potentially available from steering system improvements such as were described above.

Improvements for Side Impact

Referring again to the broad distribution shown in Table 2, the basic category of side represents the second highest portion of total harm to car occupants, accounting for about 20 percent. If more specific occupant-to-vehicle contacts are examined (as in Table 6), nearly 14 percent of all harm to all car occupants in all crash modes is indicated.

In October 1980, a paper was published by Mehta, Pearson, and Wilson entitled "Side Impact Insights From General Motors Field Accident Data Base." This study(3) provided overview statistics and in-depth, case-by-case analyses of side impacts involving fatal and life-threatening injuries. The in-depth studies focused on how injuries were produced in side impacts and in what areas countermeasures might help mitigate those injuries. In general, two primary categories for countermeasures were suggested: improved energy absorption for side interiors and improved side structural integrity. Side interior improvement might allocate more space for energy-absorbing materials and/or structures in the areas of torso-to-door and head-to-roof-rail impact. Improved integrity of the side structure might include further strengthening of door hinges and latch/strikers, improved attachment of body pillars, body joint redesign, and improved welding.

Potential Benefits From Side Interior Improvements

General estimates of the potential for mitigating life-threatening and fatal (AIS 4 to 6) injuries were made during the Mehta analysis of 216 occupants in non-rollover, nonejection side impacts. Injuries to the head, torso, and lower extremities were included in the study. For 23 percent of the fatalities and 41 percent of the AIS 4 to 5 occupants, potential for injury reduction from practicable changes to the vehicle was judged present. In particular, improved interior energy absorption was estimated to have mitigation potential for 11 percent of the fatally injured and 20 percent of the AIS 4 to 5 occupants. Side structural integrity improvements were judged to have the potential to help 2 percent of the fatally injured occupants and 1 percent of those with AIS 4 to 5 injuries. Again, these judgments were very general (no specific countermeasures were identified) and injuries to all body regions were included to formulate the estimates.

Concerning a more specific benefit projection, the Field Accident Review group within GM's Current Product Engineering analyzed side impact data from the 1980-84 MIC accident files to determine what the potential reduction in total harm might be from increasing the energy absorption of the side interior. This study of MIC data, however, was limited to chest and abdomen contacts only. Specifically, the included injuries were to the chest region, the liver, the spleen, and the kidneys. The assumed modification to the side interior consisted of providing improved energy-absorbing construction in the area of occupant impact, including contoured armrests of limited protrusion. Based on earlier testing using dummies in car-to-car side impacts, an initial assumption was made that such interior changes might reduce AIS 2, 3, and 4 chest and abdomen injuries, each by one AIS level.

When the above assumptions and limitations were applied, a preliminary, computer-only data analysis indicated a potential for reduced, overall total harm of about 4.7 percentage points (a change from 9.5 to 4.8 percent). To verify the validity of the initial injury-reduction assumption, an in-depth study of those cases likely to have the greatest influence on harm reduction estimates was performed. As a result of the case-by-case review, the injury-reduction assumption was changed. The "one AIS level" reduction would still apply to all AIS 2 and 3 injuries; however, the probability of reducing AIS 4 injuries was limited to about 4 chances in 10. Also, since there is some harm reduction potential for injuries above the severity range of the first assumption, the 0.4 probability was assumed to apply also to AIS 5 injuries.

When the data were analyzed again but with the revised injury-reduction assumptions, the estimated potential for reduction in total harm from the improved energy absorption as outlined above was seen to be 2.9 percent overall. Using the original 9.5 percent value as a base, this potential reduction would represent a 30 percent improvement. As mentioned previously, only chest and abdomen contacts were included in this particular study. Any improvement for head impact from other modifications would represent additional potential for reduced harm.

Summary of Steering System and Side Interior Potential Benefits

Table 11 is a summary of the estimates of potential reductions in total harm that might be realized from improvements to two areas of the vehicle interior associated with injury to car occupants. Referring back to Tables 3 and 6, the percentages of all occupant harm produced by contact with front and side interior components in crashes below 30mph are about 27 percent and 11 percent, respectively, for a total of 38 percent. If

Table 11. Estimated harm reduction potential from interior component improvements.

Vehicle Component	Body Regions Considered	Harm Reduction for Contacts Considered	Overall Reduction in Total Harm
Steering System	All	35 percent	9 percent
Side Interior	Chest and Abdomen	30 percent	3 percent

specific improvements to just two component systems were successful in accomplishing the various AIS reductions that were judged potentially achievable, Table 11 would project nearly a one-third reduction from that total (12 parts out of 38).

Summary

This paper has reviewed car occupant harm distributions as originally developed by Malliaris, et al., of NHTSA and, by selection of appropriate line items from those distributions, has generated overall estimates of potential reductions in total harm that might be realized through vehicle crashworthiness improvements. The overall potential for harm reduction from front- and side-interior improvements alone was seen to be as much as 24 percent if those improvements were able to reduce AIS 2 to 6 injuries each by one AIS level up to crash speeds of 30mph. A general view of which occupant-interior interactions present the primary opportunities for improvement is implicit in the harm distributions themselves. In addition, specific safety improvements to the steering system and the side interior were outlined and their potential benefits discussed. About a 12 percent reduction in total harm was estimated to be potentially available from the particular countermeasures considered.

Changes to the components involved in the various safety improvement areas likely can be developed as part of the built-in crashworthiness of the vehicle's design. As such, they offer potential benefits complementary to those of add-on safety equipment such as manual belts, automatic belts, or airbags. This is important because (1) some degree of nonuse of belts likely will remain even with the growing adoption of belt-use laws in the United States, and (2) belted occupants still can contact the vehicle interior in more severe crashes, as can airbag-restrained occupants in crashes below the deployment threshold or in side impacts and rollovers.

References

1. Malliaris, A.C., R. Hitchcock, and J.H. Hedlund, "A search for priorities in crash protection," SAE Paper 820242, February 1982.
2. Malliaris, A.C., R. Hitchcock, and M. Hansen, "Harm causation and ranking in car crashes," SAE Paper 850090, February 1985.
3. Mehta, R., J.L. Pearson, and R.A. Wilson, "Side impact insights from General Motors Field Accident Data Base," Proceedings Eighth International Technical Conference on Experimental Safety Vehicles, October 1980.

An Impact Test Programme Using Six Models of Lower-Medium-Sized Care

S. Penoyre
Transport and Road Research Laboratory, Department of Transport, Crowthorne, Berkshire, United Kingdom

Abstract

This paper describes a test programme in which examples of six models of popular 1983 lower-medium-size four-door cars were subjected to front, side, and interior headform impacts to assess occupant protection.

The frontal test was a 30° angled impact into a wood-faced barrier at 60km/h using restrained OPAT dummies. The side test was a 90° impact from a CCMC deformable mobile barrier at 50km/h, using a prototype Eurosid dummy to represent the driver. The interior headform tests used a 6.8kg free-flight headform launched from an air gun at 24km/h to impact 21 points that occupants are likely to strike in an accident.

The results of these tests are summarised and used to compare the occupant protection offered by the different car models and also to see whether the average level has changed since a previous set of similar TRRL tests on 1976 cars. The more recent cars appear to provide considerably better protection in frontal impacts, mainly because of reduced intrusion and lower occupant head accelerations, but little progress has been made on improving side impact protection.

It is suggested the current levels of occupant protection could be further improved by simple, cheap design changes, e.g., fitting energy-absorbing door trims in place of standard armrests and using less aggressive steering wheels with better padding over the end of the steering column. Improvements to standard lap diagonal seatbelts, for example by fitting pretensioners, would also be worthwhile for cars sold in countries like the United Kingdom that have a high belt-wearing rate.

Introduction

This paper describes an impact test programme recently carried out on six models of European and Japanese lower-medium-size four-door cars bought new in 1983: the Renault 9, Vauxhall (GM) Astra, Volvo 340, Toyota Tercel, Austin Rover Maestro, and Ford Escort. The tests were carried out by MIRA under contract to TRRL. The purpose of the programme was to assess and compare how well these cars protect their occupants in crashes and to some degree compare the results with those from tests on 1976 cars. The tests were also intended to identify any particular strengths or weaknesses in the individual models and to suggest practicable and cheap ways in which they could be made safer. Since the tests were more demanding than those used in current safety legislation, it was hoped their results would also show whether recently designed cars are providing better occupant protection than the basic minimum required by law.

Test Procedures

The impact test procedures used in this programme were based on those TRRL has been advocating for many years(1,3); a 30° angled 60km/h frontal barrier impact, a 90° side impact mobile barrier test representing a 50km/h collision, and a set of interior tests with a free-flight headform of 6.8kg at 24km/h.

The frontal angled barrier test used OPAT dummies wearing seatbelts in both front seats of each car, the same dummies being used for each of the six tests. These tests were assessed on the same criteria as before(1,3), i.e., dummy head and chest accelerations and femur forces, and passenger compartment survival space measurements from ECE Regulation 33 (instrument panel to R point, front of passenger compartment to R point, and width of footwell through the brake pedal). OPAT dummies were used because it is felt their chest and shoulder design gives a more human-like response than the Part 572 dummy. In future frontal tests, it is likely that Hybrid III dummies will be used. However, for the reasons given in (1), it is unlikely a change from the angled barrier test to a perpendicular one will be made.

The side impact test was an updated version of the procedure previously used at TRRL(2) with a CCMC deformable barrier(4) of mass 950kg moving at 50km/h instead of the TRRL rigid barrier of mass 1,100kg moving at 35km/h. The test was a 90° impact into the driver's side of the stationary car, with the barrier face centered on the R point. The TRRL side impact dummy previously used to represent the driver was replaced with an Interim Eurosid, a prototype version of the European side impact dummy now being developed by EEVC(5). The test was mainly assessed on the dummy measurements of rib deflection and pelvis load, although the barrier's peak deceleration was also measured to give an indication of the stiffness of the struck side of the car. The Eurosid dummy is designed to give a better representation of the stiffness of the human chest than the TRRL side impact dummy, while keeping the earlier dummy's ability to measure pelvis force. The new dummy predicts chest injury from rib deflection measurements. In future tests,

it is planned to use the final Eurosid dummy rather than this interim version and to change to the EEVC deformable mobile barrier(6) rather than the CCMC design.

The interior headform impact test was also slightly updated from that previously used(1,3) since the MIRA Mark 2 Free-Flight Headform Launcher was available in place of the more awkward and bulky Mark I air gun. The new launcher is described in (7). The number of interior impact points in each car was also reduced from 25 to 21. The impacts are of the same severity as now used in ECE Regulation 21, i.e., a 6.8kg headform impacting at 24km/h and having a rigid face that is a segment of a sphere of diameter 165mm.

Frontal Impact Test Results

Table 1 summarises the results of the 60km/h frontal impact barrier tests and also gives proposed critical or tolerance values for the various parameters; figures from current or proposed legislation have been used where applicable. For head injury, the simple criterion of peak deceleration (3ms cumulative) has been used rather than HIC because it is easier to understand while (in the view of some authorities(8) being quite as good a predictor of brain injuries. A femur load tolerance value of 4kN has been used as previously; since then higher levels have been suggested but for the sake of continuity these have not been used here.

It is clear from Table 1 that Car C performed best of the six cars in this frontal impact test, with none of its measured parameters exceeding the critical values. Car F also did well, but had a passenger head acceleration of 102g, apparently due to a combination of excessive seatbelt stretch, spoolout, and too stiff a facia. Car B also had a similar though less severe (90g) passenger head to facia impact, and Cars B, D, and E all had driver's head to steering wheel rim impacts giving 87 to 95g head accelerations. Cars A, B, and D also had driver left femur loads above the 4kN level, probably from contact with the steering column or its supporting structure.

The performance of all these cars would have been improved by reducing spoolout and possibly by reducing seatbelt stretch. This might be done by using stiffer webbing, and either a web locker at the upper belt anchorage or a seatbelt pretensioner. Further improvements could be made by providing better energy-absorption capability in the areas that the occupants hit when the belt does allow such contact.

Side Impact Test Results

Table 2 summarises the results of the 50km/h side impact mobile barrier tests, with proposed critical values for the Interim Eurosid dummy used to represent the driver. These critical values are even more uncertain than usual, because the dummy was an interim version and had not been thoroughly tested to correlate its measured outputs with other side impact dummies or cadavers. A direct translation from TRRL SID to this dummy is not possible because the former has four load-measuring ribs while the latter has only two transducers measuring rib deflection. However, an approximate translation can be made, which suggests a tolerance value of 20mm for allowable rib deflection. For the pelvis, the position is even less satisfactory. Limited drop testing onto surfaces representing car doors has suggested that although the pelvis stiffness of the TRRL SID and this Eurosid are similar, the Eurosid appears to give higher measured pelvis forces than the TRRL SID. Also, work done since the pelvis tolerance load of 6kN for TRRL SID was derived(9) has suggested that this 6kN is perhaps too low; for example, cadaver tests on Onser(10) indicate a figure of 10kN for 50 percentile male subjects, and perhaps 30 percent less for females. For these six tests, a provisional critical value for pelvic load of 9kN in this Interim Eurosid dummy has been chosen.

Another difficulty arising from the use of this prototype dummy was that in one of the tests (Car A), the rib deflection measuring instrumentation failed, while in another (Car D) the ribs jammed mechanically. Chest acceleration resultant measurements can be used as a backup in such cases, although this is felt to be a worse predictor of chest injury than rib deflection. Then there is a question as to whether 3ms exceedence or Gadd Severity Index should be used. Table 2 gives values of all these quantities for all the cars.

The mobile barrier peak decelerations measured in these tests were very similar (15 to 16.7g, after filtering to 180Hz and then digitally to 60Hz). These values correspond to forces of 140 to 155kN on the 950kg barrier. They are significantly less than the force of 220kN required to deform the CCMC barrier (intended to represent the front of a typical European car) by 200mm(6). The sides of these cars, therefore, appear to be too weak to make the front of a car hitting them deform enough to absorb much of the energy in a front to side crash. Car F was the only car of the six fitted with door beams, and these do not seem to have been very effective in stiffening its side; its peak barrier deceleration of 16.7g was the same as that of Car C without beams, and measurements of intrusion in these two cars were similar.

The Car F figures for pelvis force and acceleration were satisfactorily low, better than all the other cars except Car D (where the jamming ribs probably increased the load carried by the chest while reducing the pelvis load). Car F is the only one of these cars fitted with energy-absorbing door trim at pelvis level, as an armrest, and this suggests that such trim can be effective in reducing pelvis forces. However, the Car F rib deflections and chest acceleration are not particularly low, which confirms that door beams do not necessarily reduce chest injury. This

Table 1.

Front Barrier Impact Test Results: 30° Wood-faced Barrier, 60km/h, Restrained OPAT Dummies. Results above Proposed Critical Values are Underlined.

Car (1983 models)	Instrument panel to R point	Front of passenger compartment to R point	Width of drivers footwell	Head Peak Resultant acc. (>3ms),g		Chest Peak Resultant acc. (>3ms),g		Left Femur Load kN		Right Femur Load kN	
	mm	mm	mm	Driver	Passenger	Driver	Passenger	Driver	Passenger	Driver	Passenger
Proposed Critical Value (max/min)	450 min	650 min	250 min	80 max	80 max	60 max	60 max	4 max	4 max	4 max	4 max
Car A	570	985	625	74	78	44	49	5.4	1.1	2.6	2.7
Car B	451	843	615	87	90	36	41	7.4	1.5	0.9	2.7
Car C	491	866	645	73	51	41	44	1.1	1.3	1.0	1.3
Car D	585	950	620	87	71	42	43	4.5	1.5	1.2	1.0
Car E	580	810	580	95	66	48	45	2.3	1.0	0.8	0.6
Car F	562	987	620	69	102	46	44	0.4	1.4	0.9	0.9
Average of 1983 cars	540	907	618	81	76	43	44	3.5	1.3	1.2	1.5
Average of 1976 cars (3)	435	746	367	105	84	47	45	5.9	1.5	4.3	2.3

Table 2.

Side Mobile Barrier Impact Test Results: 950kg CCMC Deformable Barrier. 50km/h :Interim Eurosid Dummy. Exceedences Underlined.

Car (1983 models)	Barrier peak acc. g (180/60Hz filter)	Upper rib deflection mm	Lower rib deflection mm	Pelvis force kN	Chest resultant acc.>3ms g	Chest Gadd severity index	Pelvis acc >3ms g	
Proposed Critical Values	20 min	20 max	20 max	9 max	60 max	500(?) max	100 max	
Car A	16.1	*	*	9.1	62	491	96	* = instrumentation failure
Car B	15.0	30.5	21.3	6.9	77	822	91	
Car C	16.7	30.0	25.6	8.3	71	529	104	
Car D	15.7	(6.9)	(3.9)	6.0	59	744	73	( ) = ribs jammed
Car E	16.2	28.4	33.2	11.5	100	781	122	
Car F	16.7	28.2	26.0	5.9	84	537	81	
Average	16.1	29.3	26.5	8.0	76	651	95	

agrees with previous TRRL work(2), which indicated that door beams produce hard areas in the door that can cause injuries, and also with more recent American work(11), which suggested that the space door beams occupy would be better used as energy-absorbing crush depth. An interesting possibility would be to use a door beam low down in the door just below the level of the driver's pelvis, where it would provide an increased side stiffness without taking up useful crush distance. Such a low beam (running back from the lower door hinge rather than the upper one) could also perhaps be supported in a side impact by a stronger seat frame and mounting to provide a worthwhile increase in occupant protection at acceptable weight and cost.

Table 2 shows that none of the cars did well in this side impact test; each car exceeded several of the proposed injury criteria, and Car E exceeded all these criteria. The consensus is that radical design changes are needed to solve this problem. These would include strengthening the side structure to resist impact, but this alone is unlikely to be effective, and it is desirable that car front structures should be softer than at present for car front to car side impacts. Finally, however, extensive energy-absorbing padding is needed to attenuate side impact loadings.

Interior Impact Results

Table 3 summarises the results of the interior free-flight headform tests. The figures given are the peak headform resultant accelerations after filtering to Channel Class 60 (i.e., 60Hz). This was chosen after a trial in which headform test results were filtered to different channel classes and their peak accelerations compared with the 3ms exceedence level. Class 60 was the frequency whose maxima corresponded most closely to the 3ms figures. Use of this 60Hz peak level is intended to overcome the well-known problem of applying the 3ms exceedence criterion (whether continuous or cumulative) to an oscillatory or spikey signal, where tiny differences in the shape of the signal can make large differences in the figure produced. It should also insure that a headform impact with a very rigid surface (e.g., the unpadded top of a steering column) cannot give an apparently safe result because the very high acceleration peak does not last for 3ms.

All the cars produced good results in the impacts with the facia top and the lower facia. The steering wheel rim impacts also gave fairly low decelerations (37 to 55g). As explained in(12), this present test with a rigid headform is not a good measure of the potential of a steering wheel for causing fracture of the facial bones. For example, a deceleration of only 40g on the 6.8kg (15 lb) headform is a force of 2.7kN (600 lb), which, if applied to a face by a narrow wheel rim over a contact area of perhaps 75x12mm (3x½in), produces a local pressure that is about twice what the facial bones can withstand(13). A test using a deformable or frangible face form (e.g., a piece of aluminum honeycomb of the correct crush strength) would therefore be preferable for measuring the safety of a steering wheel rim. The test could insure that the wheel centre, steering column end, and rim are padded to reduce face bone fractures.

The other five areas tested (header rail, cantrail, A post, B post, and steering wheel hub) all gave poor results with high headform decelerations, although there are wide variations between car models. For example, the header rail on Car A gave a mean value over five impact points of 63g, while Car E gave nearly double this at 121g. Similarly, the A post results vary from 66g (Car F) to 99g (Car E), and the steering wheel hub from 75g (Car F) to 111g (Car E). These high values for steering wheel hubs are important because these may be struck by the faces of drivers wearing seatbelts.

On all six cars, the B posts and cantrails (over the doors) gave very high levels of headform acceleration, and design changes to improve energy absorption in these areas would be very desirable. The seatbelt anchorage point on the B post might possibly be protected by using foam-filled plastic or deformable metal trims clipped to the anchorage. It may be more difficult to protect the cantrail area without unacceptable reduction of the space

Table 3.

Interior Headform Impact Test Results: Peak Resultant Acceleration, 60Hz Filter, g
: Proposed Critical Value 80g: Exceedences Underlined.

Car	Header rail mean of 5 points	Facia top: mean of 4 points	A post: mean of 2 points	Steering wheel hub	Steering wheel rim, on spoke	Lower facia: mean of 4 points	B post: mean of 2 points	Cant rail: mean of 2 points
Car A	63	45	91	94	55	61	124	141
Car B	78	47	88	94	48	31	98	114
Car C	85	35	88	91	40	31	108	117
Car D	79	45	76	107	50	51	124	98
Car E	121	48	99	111	45	29	130	119
Car F	99	58	66	75	37	55	117	120
Average	87	46	85	95	46	43	117	118
Average of 1976 cars (3)	76	61	80	84	62	71	114	97

beside the heads of occupants. Sideways head space does not usually seem to be a critical design area. Grab handles are often fitted there in the up-market versions of small cars, and several luxury saloons offer very limited head space in this direction.

Comparison With Results on Previous Cars

Although exact comparisons cannot be made with the similar tests(1,2,3) on cars produced in 1976, some trends are apparent.

In the frontal impact test, Table 1 shows the 1983 cars gave no infringements of the ECE Regulation 33 survival space requirements and lower values for dummy head accelerations (an average of 81g rather than 105g). Dummy passenger head impact levels were similar. Deceleration levels for headforms on facias have improved and so has the softness of the rims of steering wheels. However, the rigidity of the other likely head impact areas is little different.

Overall, the results of Table 1 show a fairly good level of occupant protection at 60km/h angled impact. This suggests that the 30° angled barrier test proposal at 50km/h has been largely overtaken by events.

An alternative is the U.S. New Car Assessment Program test head-on into a barrier at 35mi/h (56km/h)(14), but this does less to improve resistance to corner impact and subsequent intrusion.

For side impact protection, the introduction of European legislation is long overdue, and this may partly account for the lack of energy-absorbing door trims and other measures for protection.

Although car manufacturers can be justifiably proud of the improvements achieved in frontal barrier test results between 1976 and 1983, the fact that large numbers of car occupants are still being killed or seriously injured even when wearing seatbelts in modern designs of cars should remove any grounds for complacency. There is a wide range between the best and worst results in many of the tests, so a very significant improvement in occupant protection would result if all cars approached the levels that the best are already achieving in the various tests. It should also be possible to achieve a further improvement by using safety ideas that have not yet been introduced widely into production cars but whose value and feasibility have previously been demonstrated on experimental safety vehicles, e.g., safer steering wheels, energy-absorbing armrests and door trim, and head impact area padding. Seatbelt pretensioners are a more recent innovation of great promise.

Conclusion

1. Six models of European and Japanese 1983 lower-medium-size four-door cars have been tested in front, side, and interior impacts: the Renault 9, Vauxhall (GM) Astra, Volvo 340, Toyota Tercel, Austin Rover Maestro, and Ford Escort.
2. The results of the frontal impact tests were on average considerably better than those of similar tests carried out on 1976 cars. The most important improvements in the 1983 cars were reduced intrusion into the passenger compartment and lower occupant head decelerations. However, little progress appears to have been made in improving side impact protection.
3. A comparison of the results for the six models of car suggests that five are very similar in overall performance while the other appears to be designed to slightly less demanding standards. It is noteworthy that no one design has the best performance in many of the different aspects of safety for its occupants. In fact, a new car built with the best features from these six models would be a distinct advance on the six. Further improvements in safety can therefore be gained by attention to detail design.
4. The good average performance of these 1983 cars in this 60km/h frontal barrier impact suggests that current legislation based on 50km/h impacts is no longer having a major influence on the designs produced by competent teams, who are providing more occupant protection than the minimum standard required. Since the number of car occupants being killed is still unacceptably high, there is a clear need for a more demanding and realistic frontal impact legislative test. The long overdue introduction of European side impact legislation, and the more realistic testing of likely interior head impact areas, are also needed if legislation is to make a further contribution to car occupant safety.
5. The main safety problems for belted occupants in nearly all the six cars are—
   - In the frontal impact test, driver head injury from the steering wheel and passenger head injury from the facia
   - In the side impact test, high chest and pelvis loads
   - In the interior impact tests, excessive stiffness and lack of padding on the steering wheel hub, the header rail, and cantrails (i.e., above the windscreen and doors), and on the windscreen A post and central side pillars
6. Simple ways of reducing these safety problems would be to—
   - Improve the steering wheel design
   - Use energy-absorbing armrests and trim on the doors
   - Improve padding in the head impact areas

A more expensive safety improvement would be to use seatbelt pretensioners. However, side impact appears to be the least tractable occupant protection problem, and a

concerted effort backed by regulations is needed to improve the situation.

References

1. Neilson, I.D., S. Penoyre, and S.P.F. Petty, "Improved test procedures for front impact," Proceedings Seventh International Technical Conference on Experimental Safety Vehicles, Paris, NHTSA, U.S. Department of Transportation, 1979.
2. Neilson, I.D., S. Penoyre, S.P.F. Petty, and A.K. Dyche, "Improved test procedures for side impact," Proceedings Seventh International Technical Conference on Experimental Safety Vehicles, Paris, NHTSA, U.S. Department of Transportation, 1979.
3. Penoyre, S., "A crashworthiness rating system for cars," Proceedings Ninth International Technical Conference on Experimental Safety Vehicles, Kyoto, NHTSA, U.S. Department of Transportation, 1982.
4. CCMC, *Development of the CCMC Mobile Deformable Barrier for Lateral Collision Testing*, 1981.
5. Neilson, I.D. et al., "The Eurosid side impact dummy," Proceedings Tenth International Technical Conference on Experimental Safety Vehicles, Oxford, NHTSA, U.S. Department of Transportation, 1985.
6. Cesari, D., "European proposal for a side impact crash test procedure," SAE Paper 830464, 1983.
7. Dale, K.J., and K. Clemo, "The sub-system testing of vehicle interiors for aggressivity to occupant heads using a free flight headform impact device," Proceedings Tenth International Conference on Experimental Safety Vehicles, Oxford, NHTSA, U.S. Department of Transportation, 1985.
8. Newman, J.A., "Head injury criteria in automotive crash testing," Proceedings 24th Stapp Car Crash Conference, SAE Paper 801317, October 1980.
9. Harris, J., "The design and use of the TRRL side impact dummy," Proceedings 20th Stapp Car Crash Conference, SAE Paper 760802, 1976.
10. Cesari, D., M. Ramet, and R. Bouquet, "Tolerance of human pelvis to fracture and proposed pelvic protection criterion to be measured on side impact dummies," Proceedings Ninth International Conference on Experimental Safety Vehicles, Kyoto, NHTSA, U.S. Department of Transportation, 1982.
11. Griswold, C.J., "The development and application of side impact component test methods," SAE Paper 840887, 1984.
12. Petty, S.P.F., and M.A. Fenn, "A modified steering wheel to reduce facial injuries and an associated test procedure," Proceedings Tenth International Technical Conference on Experimental Safety Vehicles, Oxford, NHTSA, U.S. Department of Transportation, 1985.
13. Nahum, A.M. et al., "Impact tolerance of skull and face," Proceedings 12th Stapp Car Crash Conference, Detroit, SAE Paper 680785, 1968.
14. Hackney, J., and V. Quarles, "The new car assessment program—status and effect," Proceedings Ninth International Technical Conference on Experimental Safety Vehicles, Kyoto, NHTSA, U.S. Department of Transportation, 1982.

A Free-Flight Headform Impact Device for Evaluating the Energy-Absorption Characteristics of Vehicle Interiors

K.J. Dale and
K.C. Clemo
Motor Industry Research Association

Abstract

This paper reports on the design, development, and use of a test rig that enables the analysis of the aggressivity of vehicle interiors to the heads of occupants. The equipment comprises a pneumatically controlled free-flight headform device. It can be positioned inside the passenger compartment of any passenger car via any normal window or door aperture. The device fires a simulated headform prescribed in SAE J984 at speeds from 10 to 30mph. The enormous degree of flexibility in positioning enables impacts to be conducted on almost any part of the vehicle interior.

Currently, energy-absorbing characteristics of the interior of passenger cars are assessed using drop rigs or pendulums, which necessitate the dismantling of the vehicle body. This has implications for representativeness in terms of the validity of the stiffness characteristics of the section of the vehicle being tested.

The results of testing standard specimens, using all three test devices, are presented and discussed.

Introduction

In vehicle crashes, injuries to occupants are frequently sustained by the head striking the interior surfaces of the

passenger compartment. The design of the passenger compartment has a significant effect on the injuries that result from a given impact. In particular, the injury level is reduced where the impact acceleration of the head is limited by provision of resilience or energy absorption in the impact area.

A number of test methods exist to compare the ability of different vehicles to limit head injury. One method of simulating a real impact is given by a full-scale crash test using anthropomorphic dummies, such as the U.S. FMVSS 208 regulation. This comprises a variety of impact conditions, including frontal barrier, angle barrier, side impact, etc., with restrained 50th percentile male dummies in the vehicle, the dummies being fitted with accelerometers in various locations, including the head, to measure the impact accelerations.

However, this test can only mimic the behaviour of a human subject for—

- The trajectory of the dummy head
- The point of impact on the car interior for this accident configuration only

Studies of real accidents, however, show a wide variation in impact location(1). Clearly, it is impractical to carry out a full crash test at each possible head impact point and, therefore, it is necessary to supplement these with a simpler test, which can be repeated at a large number of positions on the vehicle interior.

One such test is laid down in the FMVSS 201(2) and ECE 21 regulation(3). These define the parts of a vehicle interior that must limit head acceleration during impact. They specify a test using a smooth rigid hemisphere conforming to SAE J984(4) of 6.8kg mass and 165mm diameter, striking the vehicle surface at velocities up to 24.1km/h. The impact velocity is related to the angle at which a head, connected to an imaginary torso pivoted at the H-point, strikes the surface. One established means of propelling the hemispherical headform is by mounting it on a pendulum rig or alternatively by guided drop weight rig.

The principal disadvantage using these approaches is that the vehicle to be tested must be dismantled to enable access to the selected impact positions. When dismantled, the vehicle components are mounted separately on the rig simulating as near as possible the mounting in the vehicle.

Once the component is prepared in this way, the structural integrity of the test sample is compromised, to the extent it may have a different stiffness characteristic than when it was incorporated into the vehicle body.

The MIRA Free-Flight Headform Impact Device has been designed in an attempt to provide a solution to these problems, which have also been addressed by rigs of the compressed air nodding hammer type. The device is basically a pneumatically controlled launcher of a headform conforming to SAE J984. It can be positioned inside the occupant compartment of any passenger car via any normal window or door aperture. The enormous degree of flexibility provided in positioning enables impacts to be conducted on almost any part of the vehicle interior.

One important factor in the establishment of a new piece of equipment is its correlation in performance with equipment already accepted as suitable for compliance testing to legislation requirements by the regulatory authorities.

MIRA has conducted tests using two more common rigs and the Free-Flight Headform Impact Device to access the correlation of headform deceleration characteristics between the different devices.

The MIRA Free-Flight Headform Impact Rig

Description of Equipment

The MIRA Free-Flight Headform Impact Rig consists of an instrumented headform with its associated launching apparatus and signal processing equipment. The headform is in the form of a piston and is fired from an open-ended pneumatic cylinder by a charge of low-pressure air. The rig is illustrated in Figure 1 and the launcher system in Figure 2.

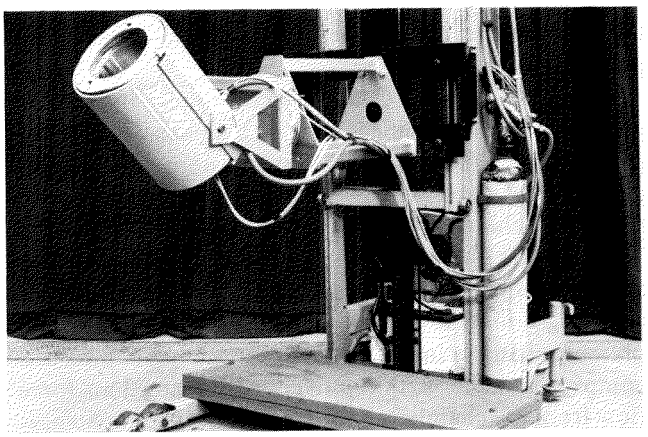

Figure 1. MIRA free-flight headform impact device

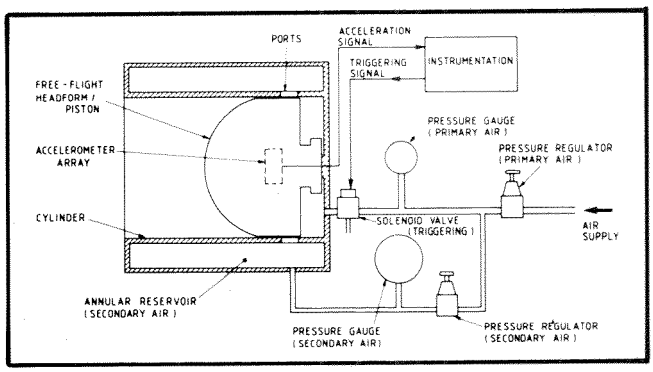

Figure 2. Schematic diagram of headform launcher system

The headform is in three parts, enclosing a central cavity that houses an accelerometer array. The central part is a steel piston of 158mm diameter, carrying two pneumatic seals. Onto the front face of this is bolted an aluminum block whose front surface forms a segment of a 165mm diameter sphere. This spherical surface subtends an arc of 140° about the piston axis.

The rear part of the headform constitutes an aluminum ballast plate designed to place the combined centre of gravity of the headform at the centre of the sphere. An array of three accelerometers is bolted to the rear face of the spherical segment with their axes aligned with the axis of the piston and two other mutually perpendicular axes, intersecting at the centre of the sphere. The combined mass of the headform and accelerometers is 6.8kg. The signal from the accelerometers is carried by an umbilical multicore cable that passes through a slot in the rear face of the headform.

The launcher consists of a cylinder of 158mm diameter and 330mm length, open at both ends. The rear end of the cylinder is fitted with a sealed plug held in position by quick-release clamps to allow the headform to be loaded from the breech. The accelerometer cable passes through a sealed gland in this plug, with approximately 2m of cable between this and the headform, the cable being wound into the space between the headform and plug. When correctly installed in the cylinder, the piston is located against a stop on the plug and held by a permanent magnet.

The outside of the cylinder incorporates an annular pressure chamber connected to the cylinder via a ring of ports in the cylinder wall. When the piston is in the firing position, the ports lie between the two piston seals, with the space behind the piston ventilated to the atmosphere. The pressure chamber may therefore be charged to the firing pressure of up to approximately 5 bar without applying a load to the piston. The arrangement of the pressure chamber in this form offers the combination of a compact launcher with relatively unrestrained air force flow from the chamber to the cylinder. The compactness of the launcher, in particular, allows impacts to be made downward onto the top of the facia panel. The piston is fired by closing the connection to the atmosphere and introducing a pulse of pressurised air onto the rear face of the piston. This moves the piston off its stop, opening the ports and allowing the air to flow from the pressure chamber into the main cylinder, firing the piston from the open end.

The pressure chamber is charged via a precision regulator from a supply of bottled nitrogen, the regulator setting being used to control the firing velocity. The air used to trigger the firing is taken from the same supply via a second regulator and an electro-pneumatic solenoid valve mounted on the plug.

The launching cylinder is mounted on an apparatus that allows it to be positioned inside a complete vehicle to simulate a wide variety of head-impact positions and directions. This is in the form of a trolley carrying an extension arm on which the cylinder is mounted, the arm being adjustable for height, using a hydraulic mechanism. The trolley is wheeled to the vehicle and the arm inserted through a suitable door, tailgate, or window aperture. A pivoting cradle on the end of the arm allows the cylinder to be aligned with the chosen impact position at a suitable firing distance. Clamps on the cradle pivots and trolley wheels and ballast on the base of the trolley minimise movement of the cylinder during firing. The trolley carries a $44ft^3$ cylinder of nitrogen that supplies the cylinder during firing, which is capable of providing a supply pressure for over 80 impacts.

The signals from the three accelerometers are passed to a MIRA instrumentation trolley where they are amplified and recorded on a Hewlett Packard HP 6942A Multi-programmer incorporating high-speed analogue to digital converter with the associated I/O circuitry and configured with HP 9816 S microcomputer.

The circuits of the three accelerometers incorporate fixed resistors inserted during calibration to represent fixed-scale values. These may be switched into the circuit and recorded before the test to enable the scale of the output signal to be determined. The switching and firing of the headform are controlled by the instrumentation trolley.

The firing velocity of the headform is generally derived from the accelerometer signal, but may also be determined by means of an extension of the rear ballast plate passing between a light source and photocell mounted on the front face of the cylinder. The extension incorporates two trailing edges a known distance apart. The output from the photocell is monitored and the time elapsed between the passage of these two edges recorded on a digital-output timer.

Test Equipment Operation and Performance

The appropriate impact point inside the vehicle is selected from the array of positions to be tested. Figure 3

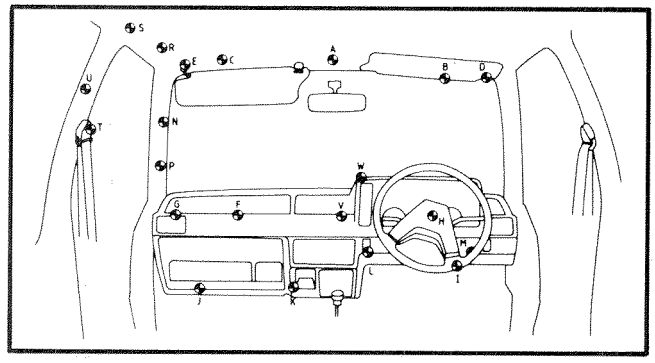

Figure 3. Typical positions selected for impact

illustrates a variety of positions where impacts can be directed.

The test rig is manoeuvred into the car to give the correct impact alignment, with the first contact of the headform on the impact point. This is checked with a small gauge that fits into the end of the cylinder and carries a two-dimensional template representing the headform. The distance of the cylinder from the impact point is selected to allow the headform to clear the cylinder before impact and prevent damage on recoil, and is normally in the range of 300 to 400mm. A small correction is made to allow for the effect of gravity on the headform in flight. With the cylinder aligned, the clamps on the support structure are tightened and the angles of the cylinder in relation to the car noted.

The cylinder is then lubricated and the headform loaded to the rear of the cylinder with the axes of the accelerometers in vertical and horizontal planes. The plug is then located on the rear of the headform and the cable wound into the annular space between them. The whole unit is then slid forward into the end of the cylinder, taking care not to trap the cable, and the plug clamps tightened. The engagement of the headform on the plug (and its correct positioning in relation to the ports) is then checked with a small gauge.

Guards are then fitted to the door apertures of the vehicle, if doors have been removed, and the cylinder charged up to the firing pressure. The firing sequence (with its safety override) is initiated, putting the calibration steps on the computer and firing the headform and recording data. The air supply is automatically disconnected and the damage noted. The headform is then fed back through the cylinder and the procedure repeated for the other impact points.

The graph of headform fore and aft acceleration shown in Figure 4 illustrates the phases that the headform

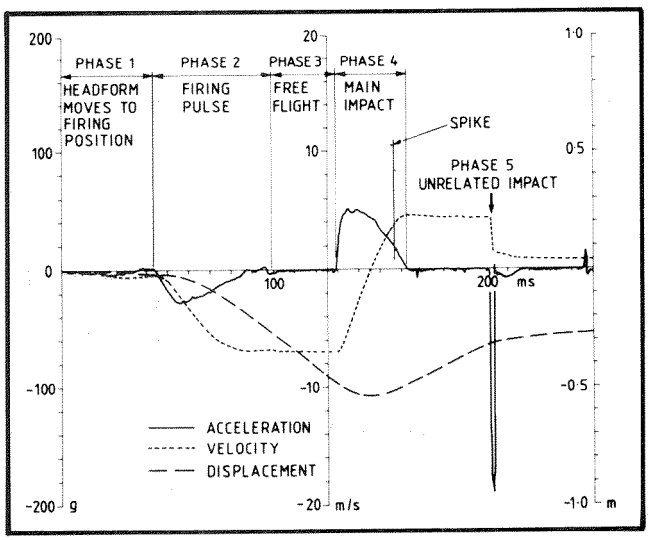

Figure 4. Various phases of headform acceleration traces

undergoes during the test. Beginning at the point where the solenoid valve operates and air is admitted behind the piston, Phase 1 represents the slow movement of the headform as the restricted airflow through the valve displaces it from its initial position toward the ports.

Phase 2 shows the increasing acceleration as the piston uncovers the ports and air transfers rapidly into the cylinder. After reaching a maximum of approximately 25g, the acceleration declines as the air charge expands.

Finally, at a displacement of 270mm, the headform emerges from the end of the cylinder and begins Phase 3, which represents the free flight of the headform to its target. The distance travelled in this phase depends on the test configuration but is generally between 200 and 500mm. The headform is subject to the effects of gravity during this phase, but this may be compensated for in setting up the test.

Phase 4 begins as the headform first decelerates as it strikes the impact point. Up to this point, the alignment of the headform has been maintained by the launcher, but during this phase the headform may rotate and cause the original alignment to be lost. Therefore, we cannot derive any useful information from the fore and aft channel beyond this point and must turn to the graph of resultant acceleration, which is not affected by the rotation of the axes. Despite this, however, analysis of high-speed cine shows most impacts appear to undergo little, if any, angular deflection during impact, so that the fore and aft trace gives an approximate indication of the penetration of the headform and the recoil velocity.

After impact, the headform falls back into the interior of the car. In doing this, further impacts occur as it strikes the launcher or the vehicle, and these often fall within the timespan of the analysis. These impacts are generally of lower severity than the main impact due to the lower velocity and can be readily distinguished. One such impact is shown on the graph as Phase 5.

The principal method of measuring headform velocity in these tests is the technique of integrating the fore and aft accelerometer signal. This is an established method used in MIRA for measuring velocity and displacement of vehicles in crash tests.

However, as a backup, a second technique is employed, using a light beam on the front face of the launcher, intersecting two surfaces on the rear of the headform. This provides a readout on a digital display from which the speed may be calculated.

However, this method proved very unpredictable in use due to the interaction of the trailing umbilical cable with the beam, and, in approximately 25 percent of the tests, this measure of velocity has been lost due to interaction of the cable before or during the timing interval.

In addition to this, the velocity calculated by this method has proved to be generally of the order of 15 percent lower than the value obtained by integration.

Examination of high-speed cine films of various impacts suggests that this may be due to the displacement of the launcher due to recoil. This displacement has a maximum amplitude of approximately 12mm and the launcher is beginning to move forward during the timing interval, so the timer speed represents only the relative velocity between the launcher and headform at this point.

The aiming of the device is good and not seriously affected by the slight distortion of the support upon firing. In a situation representing the worst possible case, with a flight distance of 430mm and the launcher axis at right angles to the arm, the headform struck a point 12mm away from its original target. Given the benefit of these tests, it is possible now to compensate for this effect in aiming the device. Clearly, it would be an advantage to have a mounting that constrains the launcher most effectively. However, this is the first of its type and the maneouverability proved extremely useful. Future models could incorporate a mounting with stiffer supports and fewer moving parts while retaining accessibility.

Signal Analysis

The results are analysed using MIRA's impact test analysis computer program. The recorded signals are variously filtered to Channel Frequency Classes (CFC) 1000 and 60 as defined in SAE Technical Report J211(5). The signals are then passed through an analogue to digital converter for analysis at a nominal sampling rate of 33 samples/ms of real time record and loaded onto disc. The accelerometer signals are recalled from disc for the period corresponding to 250ms after activation of the solenoid valve. This period includes the acceleration from the launcher, the main impact, and, in some cases, a further impact as the headform strikes other parts of the car interior.

Headform Speed

This is computed from the integration of the headform's acceleration in the firing direction, starting just before the release mechanism is operated, when the headform is known to be stationary. This may be expressed as follows:

$$v = \int_{o}^{T} a_f \cdot dt$$

Where:

a_f = acceleration in the direction of impact
t = time from a point just before release

v is drawn out as a graph against t over the time scale 0 to 250ms. The velocity of the headform just before impact may be read from the graph. Note that the graph ceases to be valid during the impact after rotation of the accelerometer axes.

The graph also computes the displacement of the headform, along the impact axis from the second integral of headform acceleration with respect to t.

The headform's velocity may also be determined by the time taken for the two trailing edges on the headform and its extension (a distance of 30mm apart) intersecting the timing light beam.

Resultant Acceleration (Magnitude of Acceleration Vector)

This may be expressed by the formula:

$$a_r = a^2_f + a^2_v l + a^2_l$$

where:

a_f = acceleration in the direction of impact
a_v = acceleration at right angles to the direction of impact and in a vertical plane
a_l = acceleration at right angles to the direction of impact and in a horizontal plane

This quantity is expressed as a graph against t, over the time scale 0 to 250ms, and, when computed, forms the basis for head injury predictions.

Head Injury Level

The computer programme conducts analysis on the normally accepted indices of head injury level required by current international legislation. These comprise the following:

80g for 3ms exceedence
Gadd Severity Index 1000
Head Injury Criterion HIC 1000

Test Equipment Used To Quantify Correlation

The most important aspect, in terms of performance, of any new device used for testing components is the correlation of the output function with other currently accepted equipment. Headform impact testing has been conducted for many years using both pendulums and drop weight rigs.

The performance comparison of the MIRA Free-Flight Headform Impact Device was conducted against that of the MIRA Head Impact Pendulum Rig and the MIRA Head Impact Drop Weight Rig. All three devices incorporate headforms to the legislative requirements, and all impacts were conducted using a standard test specimen.

Description of the Head Impact Pendulum Rig

This rig comprises a hemispherical headform mounted on a pendulum arm to simulate occupant head impacts on items such as facias, seats, etc., and is illustrated in Figure 5.

The headform is a hollow aluminum hemisphere of 165mm diameter and having an effective mass of 6.8kg. This is made in two parts and carries two accelerometers mounted symmetrically on either side of the centre-line,

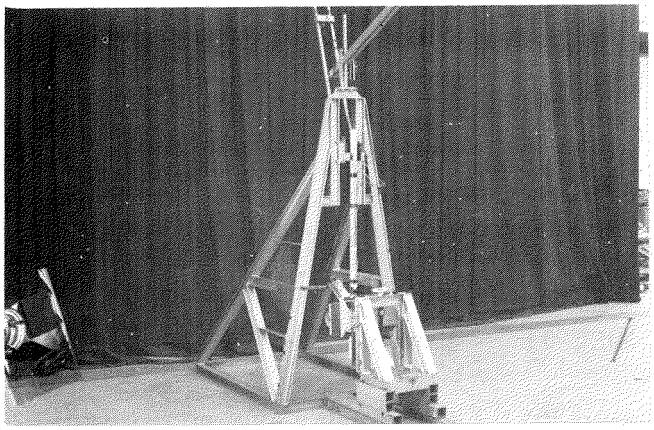

Figure 5. MIRA head impact pendulum

measuring the tangential acceleration of the headform about the arm pivot. The radius of the centre of the headform from this pivot is 1.21m.

The pendulum beam is of rectangular section and designed with counterweights below the headform and above the pivot axis to place the centre of percussion exactly at the centre of the headform.

The beam is hung from a welded steel framework via a ball bearing pivot. The frame incorporates an extension for mounting specimens and also a pivoting arm carrying an electrical release mechanism. By altering the position of the arm, the position of the pendulum and thus the drop height can be varied, allowing the impact speed to be controlled up to a maximum of approximately 24.1km/h (15mi/h).

The specimen to be tested is mounted on a support frame and positioned on the rig so as to just touch the headform when hanging free. The frame is bolted to two rails projecting from the rig to prevent movement of the specimen on impact and incorporates adjustment whereby the specimen may be raised, lowered, and tilted in the plane of the pendulum.

The speed of the pendulum immediately prior to impact is measured by a slotted blade mounted on the beam, passing between a light source and photocell fastened to the rig frame. The spacing of the leading edges is known accurately, and the signal from the photocell is amplified and fed to a timer and one channel of the instrumentation.

Description of the Head Impact Drop Weight Rig

The rig consists of a hemispherical headform that falls onto the test specimen from a given height. The headform is guided by two parallel rails and illustrated in Figure 6.

The headform is a smooth rigid aluminum hemisphere of 165mm diameter. The central cavity of the headform houses an accelerometer, measuring the acceleration in the vertical direction. The headform is bolted to a small framework supporting the guides that locate the headform in its guide rails. The headform, accelerometer, frame, and guides have a total mass of 6.8kg.

The rails are set parallel and vertical to insure precise guidance of the headform while eliminating any frictional resistance on the falling weight.

The headform is raised to the appropriate height for the chosen impact speed. An electromagnetic release mechanism is incorporated to allow the weight to be released remotely.

An accelerometer is mounted in the headform to measure the impact decelerations. Test specimens are positioned beneath the rig.

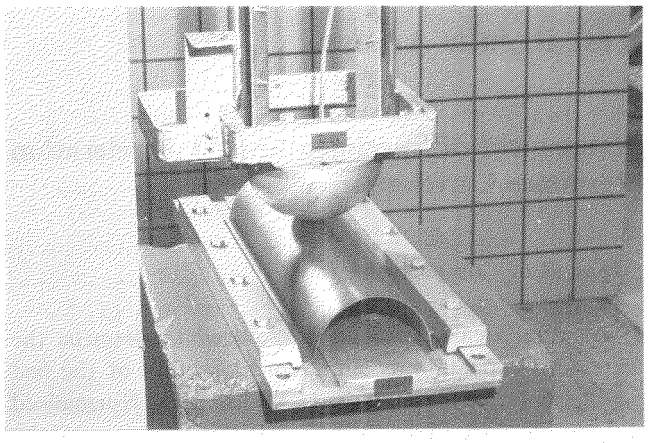

Figure 6. MIRA head impact drop rig

Description of the Calibration Specimen and Fixture

The specimens are designed to collapse as the result of impact by a standard headform to enable impact acceleration signals to be compared.

The specimens are pressed from a sheet of cold-reduced steel sheet of 0.76mm thickness and formed into a half-cylinder section. On removal from the press tool, the elasticity in the material causes the specimen to open slightly, and this elasticity is used to locate the specimen in the test fixture.

The fixture consists of a steel plate with a shallow longitudinal cavity to accept the specimen. The specimen

is constrained within the fixture by the two outer edges of the flanges pressing against the vertical walls of the cavity. Clamping plates held by four bolts secure the specimen to the fixture surface at each side. The fixture is mounted so the impact axis is perpendicular to the base at the centre of the specimen for the impact to be conducted. The arrangement is illustrated in Figure 7.

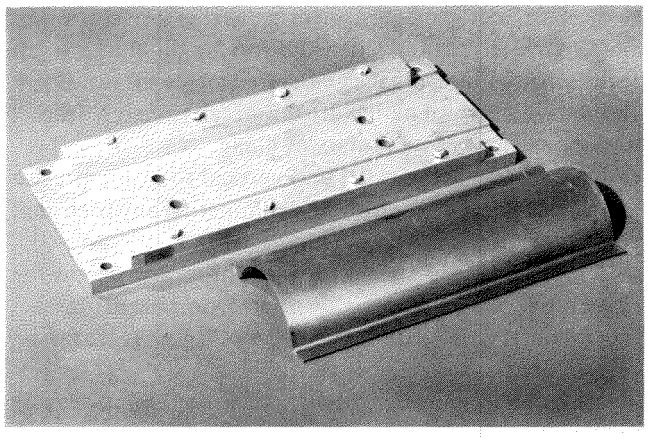

Figure 7. Calibration specimen and fixture

Test Results Analysis

Assessment of Specimen Impact Acceleration Response Correlation

Measure of Comparison

An analytical approach is required to describe the extent of repeatability and reproducibility of the test equipment. The measure used is known as the Normalised Integral Square Error (NISE). NISE is a measure of the difference between two time histories and is able to divide total NISE into phase shift, amplitude differences, and shape difference.

The equations by Donnelly et al.,(6) for NISE are:

$$NISE = 1 - \frac{2Rxy\ (o)}{Rxx\ (o) + Ryy\ (o)}$$

$$\text{where } Rxy\ (o) = \frac{1}{N} \sum_{i=1}^{N} (Xi)(Yi)$$

$$\text{where } Rxx\ (o) = \frac{1}{N} \sum_{i=1}^{N} (Xi)(Xi)$$

$$\text{where } Ryy\ (o) = \frac{1}{N} \sum_{i=1}^{N} (Yi)(Yi)$$

Xi = a digitised point of one data set
Yi = a digitised point of a second data set
N = number of digitised points in each data set

The portion of the NISE due to a phase shift between the two data sets is:

$$NISE\ (Phase) = \frac{2xy\ (t)\ max}{Rxx\ (o) + Ryy\ (o)} - \frac{2xy\ (o)}{Rxx\ (o) + Ryy\ (o)}$$

where t = a time lag

$$Rxy\ (t) = \frac{1}{N-a} \sum_{i=1}^{N-a} (Xi)(YI + a)$$

$$a = \frac{t}{\Delta t}$$

Rxy(t)max = maximum Rxy(t) for any (t)

The portion of the NISE due to a difference in amplitude only, after the phase shift has been eliminated, is:

$$NISE(0) = Pxy(t) - \frac{2\ Rxy\ (t)\ max}{Rxx\ (o) + Ryy\ (o)}$$

where Pxy (t) = correlation coefficient

$$= \frac{Rxy\ (t)\ max}{Rxx\ (o) \cdot Ryy\ (o)}$$

The portion of NISE due to a difference in shape after phase shift has been eliminated is:

NISE (Shape) = 1 - Pxy(t)

The sum of the three apportioned NISE's is then total NISE.

This approach was judged to be suitable because it is based on the principle of cumulative variance and treats each data set as a continuous whole and quantifies the difference between the two data sets over their duration.

Acceptance Criteria

Donnelly et al., reviewed the previous work on this topic and determined that a coefficient of variation of 6 percent or less was generally considered good. Using simple cases as examples, they derived allowable NISE limits of acceptability for phase, amplitude, and shape. The results of these calculations are shown in Table 1.

Table 1. Allowable NISE

	Limit of Acceptability (6%)
Phase	0.0300
Amplitude	0.0017
Shape	0.0291

For the Free-Flight Headform Impact Rig, limits of acceptability of 6 percent were adopted for both repeatability and reproducibility.

Test Result Comparison

Repeatability

The recordings of five example impacts were selected at random from a range of tests on the specimens using the Free-Flight Headform Impact Device. The acceleration data were recorded over a 100ms sample period at 33kHz sampling rate and filtered to CFC 1000. The output from three tests, for clarity, was plotted on a reduced common time base and is shown in Figure 5. The mean curve was calculated from the set of randomly selected impacts and then, to calculate the NISE, each impact was compared with the mean. The NISE was calculated for phase shift, amplitude, and shape, and the results, from these comparisons, are shown in Table 2.

Table 2. NISE comparisons for free-flight headform

	Free-Flight Headform Impact Tests			Limit of Acceptability
NISE	Sample 1	Sample 2	Sample 3	(6%)
Phase	0.00011	0.00024	0.0019	0.0300
Amplitute	0.00002	0.00021	0.00012	0.0017
Shape	0.00035	0.00011	0.00127	0.0291

The calculations for NISE (amp) and NISE (shape) were conducted without phase shift adjustment but are still well within the acceptability limits adopted. A visual comparison of the time history curves in Figure 8 shows good repeatability.

Reproducibility

The results of specimen impact tests from the MIRA Free-Flight Impact Device were compared with tests on identical specimens using the MIRA Head Impact Pendulum Rig and the MIRA Head Impact Drop Weight Rig.

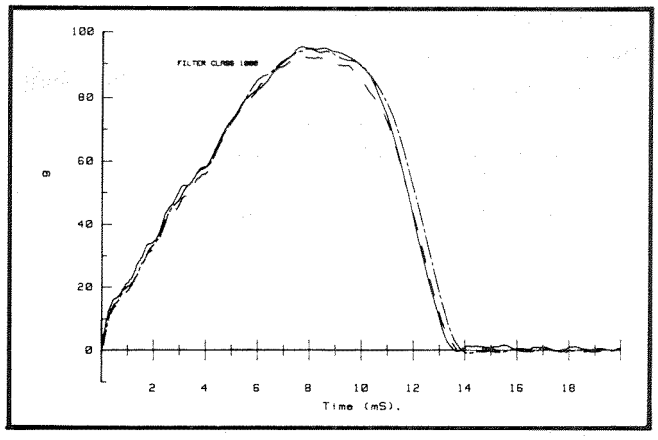

Figure 8. Curves illustrating the repeatability of the free-flight headform impact device

To enable the comparison of the different test devices, a mean curve was calculated from a set of five tests for the pendulum and drop weight rigs. The accelerations were recorded over the same sampling period and sampling rate, and filtered to the same channel class as for the Free-Flight Headform Impacts.

The NISE calculation was then conducted, comparing the mean acceleration time histories for each test device.

The calculations for NISE (amp) and NISE (shape) were conducted both with and without phase shift adjustments, and the results were well within the acceptability limit and are shown in Table 3. The curves plotted in Figure 9 are of phase shift adjusted time histories.

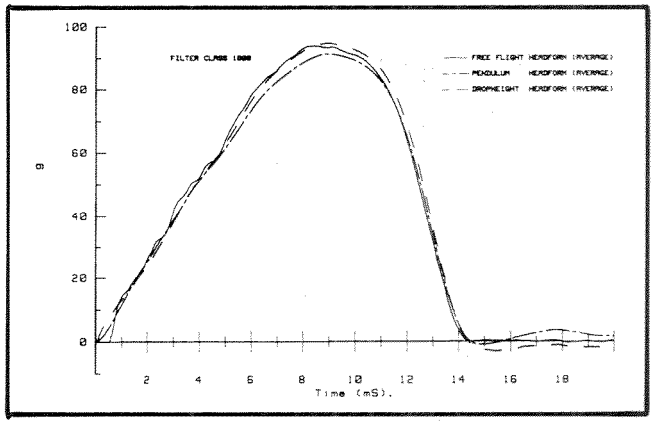

Figure 9. Curves illustrating the reproducibility of the free-flight headform against both pendulum and drop rig headforms

Table 3. NISE comparisons between different rigs

	Phase	Amplitude	Shape
Acceptability Limit (6%)	0.0300	0.0017	0.0291
Free-flight Headform vs. Pendulum	0.00015	0.00035	0.00151
Free-Flight Headform vs. Drop Weight	0.00075	0.00005	0.00288
Pendulum vs. Drop Weight	0.00087	0.00066	0.001

Therefore, the MIRA Free-Flight Headform Impact Device gives repeatable and reproducible acceleration time histories within the rigorous acceptability criteria chosen.

An additional successful aspect of the headform performance can be seen in the shape of the accelerometer traces. In designing a headform impactor of this type, it is essential that the structure be sufficiently rigid to place the natural frequency of all possible modes of vibration well above the attenuation level of the filters (i.e., 1,000Hz). Failure to achieve this causes ringing in the form of a regular ripple on the acceleration signal. Examination of the traces shows the accelerometer signals are entirely free from this effect.

Impact Velocity Variations

The Free-Flight Headform Impact Device was used when conducting a research programme in relation to head impact. The device was fired on over 100 occasions at nominally identical impact velocities, i.e., 7.2m/s. The annulus pressure required to provide this impact speed was 1.2 bar.

The pendulum and drop weight rigs have been used at MIRA for many years and, by virtue of their gravity power, have adjustable impact velocities on the basis of the release height of the headform. A series of 20 tests was conducted to verify impact speed repeatability on both the pendulum and drop weight rigs.

Table 4 shows the means and standard deviations of the tests conducted on all three rigs.

Table 4. Variations in impact velocities

	Nominal m/s	Mean	Standard Deviation
Free-Flight Headform	7.2	7.289	0.25
Pendulum Headform	6.9	6.754	0.045
Drop Weight Headform	7.2	7.317	0.017

Clearly the gravity-powered rigs show better speed control than the Free-Flight Headform Impact Device. The Free-Flight Headform produces a mean speed very close to the intended value, but there is a scatter of some 3.4 percent. Although larger than the figure for the speed variation on the gravity-powered rigs, it appears to be within acceptable limits and may well be reduced in the future by improvements in launcher design.

Discussion

The objectives in the design of the MIRA Free-Flight Headform Impact Device were to enable easy access to the interior surfaces of a passenger car and, without dismantling, conduct a series of tests to evaluate the aggressiveness of the surfaces. The characteristics of the acceleration time histories generated from these impacts were to show a close relationship to equipment currently used for the same purpose.

On completion of the commissioning trials of the device, it was used successfully in testing six saloon cars at more than 20 impact positions on their passenger compartment interiors(7). The device demonstrated its flexibility in positioning during these tests, being free to rotate up to 360° in the vertical plane and 245° in the horizontal plane.

Using the standard specimens, the tests gave extremely good correlation with the alternative test rigs used for head impacts. The repeatability and reproducibility of the deceleration pulse in terms of phase shift, amplitude, and shape were well within the coefficient of variation of the 6 percent chosen as an indication of good correlation.

The results of the work conducted to date are very encouraging, and the main objectives of the design were achieved successfully. There is, however, room for minor improvement in the repeatability of firing velocity. Design modifications have been identified, and analysis of the benefits of the proposed changes are underway.

Conclusion

The results of the tests using the MIRA Free-Flight Headform Impact Device on the interiors of a range of current vehicles(7) has illustrated the flexibility of the subsystem approach. In the area of developing improved energy-absorption characteristics of these structures, this is a tool around which test procedures could be developed, based on the analysis of accident data, and which may yield useful benefits.

Acknowledgments

The opinions, findings, and conclusions expressed in this paper are those of the authors and do not necessarily reflect the views of MIRA.

The authors wish to extend their thanks and appreciation to Mr. Phillip Degg, who conducted much of the testing.

References

1. Mallians, A.C., et al., "A search for priorities in crash protection," SAE Paper 820242, 1982.
2. Federal Regulations MVSS 201, *U.S. Federal Register*, Vol. 36, No. 232.
3. Uniform Provisions concerning the approval of vehicles with regard to their interior fittings, E/ECE/TRANS/505/Rev, 1/Add.20/Rev.1, 24, October 1980.

4. "Bodyforms for use in motor vehicle passenger compartment impact development," SAE J984, SAE Handbook, March 1967.
5. "Instrumentation for impact tests," SAE J211, SAE Handbook, June 1980.
6. Donnelly, B.R., et al., "Durability, repeatability and reproducibility of the NHTSA side impact dummy," Proceedings 27th Stapp Car Crash Conference, SAE Paper 831624, October 1983.
7. Penoyre, S., "An impact test programme for six models of lower-medium-sized cars," Proceedings 10th International Technical Conference on Experimental Safety Vehicles, Oxford, England, July 1985.

New Car Assessment Program Results and the Risk of Injury in Actual Accidents

Ian S. Jones,
R.A. Whitfield, and
Diane M. Carroll

Abstract

The risk of injury for particular car makes and models was examined in relation to their corresponding crash performance in the 35mph New Car Assessment Program's (NCAP) frontal barrier tests. Texas State accident data for the years 1980 to 1982 were used to determine the risk of driver injury in single-vehicle, fixed-object car collisions. The risk of fatal or incapacitating injury was modeled using logistic regression techniques so the effect of confounding factors such as car mass, age of driver, crash severity, and restraint use could be effectively controlled. The NCAP test results were entered in the model by using the values of Head Injury Criterion (HIC), chest deceleration (CD), and femur load as independent variables. Separate results are presented for restrained and unrestrained drivers. After controlling for the confounding effects, for restrained drivers the risk of driver injury was reduced by between 80 and 87 percent for cars with the best NCAP test results compared to cars with the worst results. The corresponding reduction for unrestrained drivers was between 21 and 36 percent. To examine the possible biomechanical causes of these statistical results, the 16mm films from the NCAP crash tests were analyzed to determine whether there were discernible differences in the trajectories of drivers for cars with good NCAP test results compared to cars with poor results. This analysis showed an obvious pattern of increasing interaction with the steering assembly with increasing HIC and CD values.

Introduction

The NCAP of the National Highway Traffic Safety Administration (NHTSA) was established in 1979 to provide consumers with comparisons of the crash protection offered by new production vehicles of the same size class. The program uses the results of full frontal barrier crash tests at 35mph with restrained anthropometric dummies in the driver and right-front passenger seat position(1). Although the program is designed to measure vehicle crashworthiness, the relevance of the single crash test and the applicability of the results to real-world crashes have been repeatedly questioned.

Previous studies have attempted to assess the relevance of the NCAP test results to real-world crashes with different degrees of success(2,3,4,5). These studies have all been criticized because they have not restricted their analyses to impacts comparable to the NCAP test configuration, and they have not been controlled sufficiently for other confounding variables.

The frequency and severity of injuries to occupants in crashes are influenced by many factors; the strongest effects include crash speed and configuration, car size or mass, and restraint use. Differences in vehicle crashworthiness are likely to have less effect on the probability of occupant injuries than some of these factors. Therefore, to assess the relevance of the NCAP crashworthiness ratings to actual crash injuries, it is necessary to separate differences in injury outcomes due to factors such as crash speed and configuration from differences due to crashworthiness. One way to do this is to identify a relatively homogeneous set of real-world crashes with characteristics similar to the 35mph frontal barrier NCAP tests and to examine—while controlling for other confounding factors—whether the various anthropometric dummy responses measured in the tests are related to the likelihood of crash injuries.

Selecting a sample of accidents that are similar to the NCAP tests makes it more likely that a relationship between crashworthiness ratings and the risk of injury will be found. At the same time, if the ratings are to be useful to consumers, it is important to establish relationships between the NCAP crashworthiness ratings and as wide a range of actual crashes as possible. Because the NCAP tests use a full frontal barrier crash configuration, it is logical to compare the test results with real-world crashes with frontal damage. An earlier analysis examined the relationship between anthropometric dummy per-

formance in the NCAP tests and risk of fatality in collisions between passenger cars(6). In the present study, these results are summarized together with other relevant literature, and the range of applicable real-world crashes is extended by examining relationships with single-vehicle, fixed-object crashes. This analysis looks at the relationship between each of the dummy response parameters measured in the NCAP tests, Head Injury Criterion (HIC), chest deceleration (CD), and femur load, and the odds of incapacitating injury or death for drivers in a sample of single-vehicle impacts of passenger cars into fixed objects.

In addition, to better understand some of the reasons for these results, a frame-by-frame analysis of driver trajectories from films of the NCAP tests was performed. The trajectory of the drivers in cars with high HIC and CD values were compared to those in cars with low values.

Literature Review

Campbell(2) examined serious and fatal injuries as a proportion of all injury for five groups of cars rated from best to worst in terms of the crashworthiness ratings published by *Consumer Reports*, which are based on the NCAP tests. Car sizes were aggregated to insure adequate sample sizes; the data base consisted of 32,602 drivers and front-seat passengers involved in crashes in North Carolina. Separate analyses were presented for drivers and front-seat passengers and for belted and unbelted occupants. No discernible relationship was detected between the crashworthiness rating based on the NCAP tests and the proportion of serious injury in highway crashes for unbelted occupants. There was a suggestion of a possible upward injury trend associated with the poorer crashworthiness ratings for belted occupants, but the results were not significant. However, as the authors point out, the data were not limited to frontal collisions, and major confounding factors such as crash severity, car mass, or driver age were not taken into account.

Jones(3) used the Fatal Accident Reporting System (FARS) data sets for 1979 through 1980 and R.L. Polk vehicle registration data to examine the fatality rates for individual car models. In that study, fatal injuries to drivers and front-seat passengers per vehicle years registered were correlated with HIC's and chest decelerations. The effects of car size were controlled by analyzing subcompact, compact, and intermediate size cars separately. Correlations bordering on statistical significance were found for subcompact cars, but the relationship disappeared with increasing car size. Similar results were found using the Highway Loss Data Institute (HLDI) relative injury claim frequencies for injury claims in excess of $500. Unfortunately, it was not possible to control for type of impact, size of car struck, age of driver, or restraint use, and the author concluded that the effects of these variables were overwhelming any possible relationships with the NCAP results.

A similar study was reported by Grush et al.(4), who used the FARS data sets for 1979-1981 and R.L. Polk vehicle registration data to compute fatalities per registered car year. HIC values, the Gillis index (a safety rating based on HIC, CD, and femur loads for both driver and passenger dummies), and the Consumers Union rating were each regressed against fatality rates for the total sample and then for restrained drivers only. The authors claimed there was no substantial relationship between fatality rate and HIC value or either of the crashworthiness ratings. However, their Table 1(4) shows that the fatality rate for cars with HIC's of less than 1,000 was 5 percent lower for unrestrained drivers and 17 percent lower for restrained drivers than for drivers of cars with HIC's greater than 1,000. The authors attempted to control for car size by analyzing small cars (<104in wheelbase) separately from large cars and to control for impact type by looking only at frontal collisions. Neither control was reported to substantially improve the strength of the relationship. However, this finding was not surprising because the effects of mass ratio and age distribution of driver, which are important and large effects, were not controlled.

In another study, Thomas et al.(5) reported no statistically significant association between various crashworthiness ratings based on results of NCAP tests for 14 French car models and the fatality rates among their occupants in frontal crashes. The fatality rates in this study were computed for crash-involved front-seat occupants aged 20 to 50 only, as the ratio of the number killed divided by the number present. The relationship between crashworthiness ratings and fatality rates was assessed using nonparametric statistical methods within groups of light, medium, and heavy model cars. The major weakness of this study was that these size groupings contained fewer than five models on average. With such small sample sizes, only a perfect correspondence of fatality rates and crashworthiness measures would have achieved statistical significance in most comparisons. It is worth noting that 12 of the 15 comparisons relating to fatality rates showed positive rank correlations between the index used and the fatality rates [(5) Table 1]. Failure to take into account explicitly the driver age and vehicle weight could have further blurred the results. Finally, no distinction was made between single- and multiple-vehicle crashes. The severity of the outcomes in collisions between two vehicles depends strongly on their relative weights, indicating a need to adjust the results for the weight of both cars in a multiple-vehicle collision.

A more comprehensive analysis of the North Carolina data, initially analyzed by Campbell(2), covering the years 1979 through 1982, was reported recently(7). Only data involving the specific make, model, and model-year

cars in the NCAP tests were included in the analyses. The effect of HIC test scores on the proportion of drivers involved in an accident who were killed or seriously injured was analyzed for belted and unbelted drivers in all types of crashes and for belted drivers in frontal crashes. The authors concluded that there was no association between the HIC parameter and injury risk. Because sample sizes for belted drivers were small, the data base was expanded to include vehicle model years other than the specific model year tested for those years where the base model had not changed. The Consumer Union Driver Protection Rating (CUDPR) was also added to the file. Statistically significant associations between CUDPR and the proportion of drivers killed or seriously injured were found for belted drivers in all types of crashes and in frontal crashes. In all other situations, the relationships were either not significant or negative. Multivariable linear and nonlinear models were used to investigate the effects of various predictor variables, including driver sex, crash type (single vehicle or multiple vehicle), car size (four categories), and crash speed (two categories). A significant effect was not found in any of the models for driver HIC; however, these models had serious limitations. Retaining nonfrontal crash configurations including side and rear impacts and rollover crashes made the models less likely to show significance for the NCAP test parameters. Modeling crash severity using two categories of crash speed (less than or greater than 50mph) may have been ineffective because the transition point was too high. Also, although four categories of car size were accommodated, no provision was made to model the mass ratio effect in multiple-vehicle crashes. Mass ratio and crash severity are two of the strongest factors in predicting injury risk; these variables were not adequately specified and their effects could mask relationships with crash test variables.

A recent study(6) used a sample of 695 crashes from FARS to determine the effect of the NCAP test results on the risk of fatality to drivers in frontal collisions between passenger cars. FARS data is outcome dependent because, for inclusion in the file, there must be a fatality in at least one vehicle. In this study, the analysis was limited to cases where there was a fatality in the other vehicle, thus the outcome of the collision in the case vehicle was not related to its inclusion in FARS. In addition, the sample was restricted to collisions involving two passenger cars of approximately equal weight, which eliminated the problem of mass differences between the vehicles.

Multiple logistic regression procedures were used to predict the odds of driver fatality. The independent or predictor variables included were the speed limit, the ratio of the two curb weights to indicate relative mass and their sum to differentiate vehicle size, driver age for the case vehicle driver and the other vehicle driver, and driver restraint use in both vehicles. The NCAP test results were modeled using the HIC and CD parameters, which were entered as rank variables to overcome problems of outlying values. The HIC and CD rankings were also summed to give a single figure of merit, SUM, to represent the overall crashworthiness of the vehicle.

The SUM parameter performed better than either HIC or CD, although all three parameters gave similar results. The combined HIC and CD parameter was significantly correlated such that vehicles with lower HIC and CD values in the NCAP crash tests had lower fatality rates than those with higher values. For all drivers, irrespective of restraint use, the risk of fatality was reduced 36 percent from 0.39 to 0.25 for cars with good crashworthiness ratings compared to those with poor ratings.

Because the number of restrained drivers in the sample was small, it was not possible to estimate a separate model for restrained drivers. Instead, the combined effects of the NCAP results and restraint use were modeled using an interaction term. In this data set, the risk of fatality for restrained drivers ranged from close to zero for cars with the lowest crashworthiness ratings to 0.58 for cars with the highest crashworthiness rating; the corresponding range for unrestrained drivers was 0.27 to 0.40.

Correlation of NCAP Test Results to Risk of Injury

For the current analysis, a sample of 6,405 single-car crashes was obtained from the Motor Vehicle Traffic Accident File of the Texas Department of Highways and Public Transportation and matched with the corresponding NCAP test results for each individual make and model of car. In addition to the HIC and CD parameters, femur load was included in this analysis. When a test result was not available for a particular model but an equivalent model had been tested, the results for the equivalent model were assigned. The data from the accident file and the dummy responses were used to estimate the odds of an incapacitating injury or death to a driver of a passenger car as a function of HIC, CD, and femur load of the tested car. The estimates were derived through multiple logistic regression(8) controlling for the simultaneous effects of driver age, vehicle mass, and crash severity. Results for restrained and unrestrained drivers were analyzed separately.

The Texas Motor Vehicle Traffic Accident File is a computerized file of all motor vehicle accidents that have been reported to the police. This analysis covers accidents occurring during the years 1980 to 1982. Only single-vehicle frontal collisions with fixed objects producing vehicle damage in the front center, front left, or front right were analyzed, so the study sample contained actual crashes with configurations comparable to the NCAP test crashes. Complete data were available for 314 restrained drivers and 6,091 unrestrained drivers. Drivers

were characterized as restrained if they were reported to be using the 3-point lapbelt and shoulder belt at the time of the accident. Drivers whose belt usage was unknown are not included in these analyses.

To fit the regression models, the logistic regression procedure from the SAS Users Group International (SUGI) Supplemental Library of the Statistical Analysis System was used(9). The dependent variable in each observation is the presence or absence of an incapacitating injury or death to the driver of a passenger car in an accident that has been reported to the police. In the Texas data, an incapacitating injury is defined as an injury that leaves the driver unable to walk or drive.

The regression equations were used to predict the log odds of an incapacitating driver injury or death. These odds are predicted as a function of driver age, vehicle mass, and crash severity as well as the HIC score, CD, and femur load derived from the NCAP tests for the particular make and model of car involved in the accident. Driver age was recoded as the years of age past age 35; for drivers 35 years of age or younger, age was recoded as zero. This function reflects the decreasing ability of older drivers to sustain a collision of a given severity without serious injury.

Vehicle mass was recoded as the difference between the mean mass of cars in the sample and the accident-involved car (2,960 lb for cars driven by restrained drivers and 3,119 lb for cars driven by unrestrained drivers). Similarly, the HIC, CD, and femur load values were transformed by subtracting the mean values found in the sample. These values for accidents involving restrained drivers were 1,000 for HIC, 50 for CD, and 912 for femur load; the corresponding figures for unrestrained drivers were 1,013 for HIC, 50 for CD, and 894 for femur load. These transformations have the effect of centering the estimates at zero for vehicles of average weight and crashworthiness. Crash severity was modeled using the TAD index, a variable in the Texas Motor Vehicle Accident File that denotes the severity of the damage sustained by each vehicle in an accident on an increasing scale of 1 to 7(10).

Regression equations were first derived with all three crash test parameters (HIC, CD, and femur load) included, while controlling for crash severity, driver age, and vehicle mass. For restrained drivers, the CD parameter proved to have a strong relationship with likelihood of injury, and neither HIC nor femur load added significantly to the model once the CD parameter was included. A similar pattern emerged for unrestrained drivers, although the femur load parameter was also significant.

Separate regression equations were derived for restrained and unrestrained drivers in which the only crash test parameter included was HIC. Using this model, the HIC parameter was statistically significant for unrestrained drivers, which suggests that it explains much the same variation as that explained by CD. However, it did not have as strong a relationship with crashworthiness in the sample as the CD parameter. The final regression coefficients were derived by dropping the nonsignificant variables: HIC and femur load in the case of restrained drivers and HIC for unrestrained drivers.

For restrained drivers, the parameter estimates given in Table 1 are based on 314 observations with 18 resulting in incapacitating injury or death. Crash severity had the strongest relationship with injury outcome followed by driver age and the CD parameter. Figure 1, which is based on these coefficients, shows the odds of an incapacitating injury or death to a hypothetical 35-year-old driver of a 3,420 lb car in crashes of differing severity at increasing levels of CD. The figure shows that for restrained drivers in very severe impacts (TADfs= 7) the risk of injury decreases substantially with decreasing CD; it drops from 0.55 for a high CD of 75g to 0.11 for the lowest CD value of 36g, which is an 80 percent reduction in risk. This reduction in injury risk is also present in the less severe impacts; for impacts of TAD severity 4, the risk drops from 0.15 to 0.02, a reduction of 87 percent.

The regression equation parameters for unrestrained drivers are shown in Table 2. In this much larger data set, there were 6,091 observations and 865 cases in which the driver was killed or sustained an incapacitating injury. Crash severity and driver age, followed by the CD

Table 1. Regression equation for injury odds for restrained drivers in a crash (chest deceleration only)

Independent Variable	Beta	Std. Error	Chi-square	p-value
Intercept	-5.7277	0.9128	39.37	.001
CD	0.0579	0.0258	5.03	.025
Crash severity	0.6360	0.1796	12.54	.001
Driver age	0.0484	0.0212	5.19	.023
Vehicle mass	3.11×10^{-5}	4.07×10^{-4}	0.01	.939

Model chi-square = 20.32 with 4 d.f.
Fraction of concordant pairs of predicted probabilities and responses; 0.74.
Rank correlation between predicted probability and response: 0.53.
N = 314 (18 severely injured or killed).

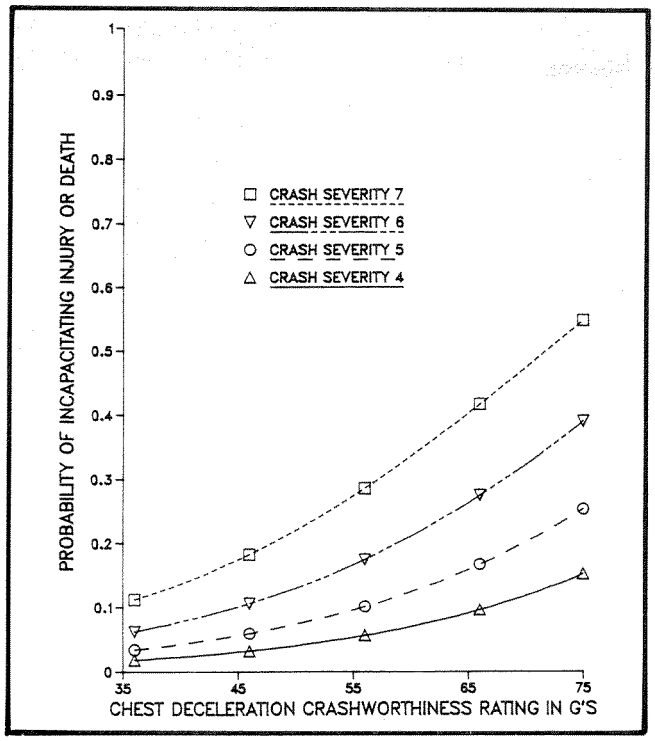

Figure 1. Probability of incapacitating injury or death for restrained drivers by NCAP chest deceleration at four levels of crash severity

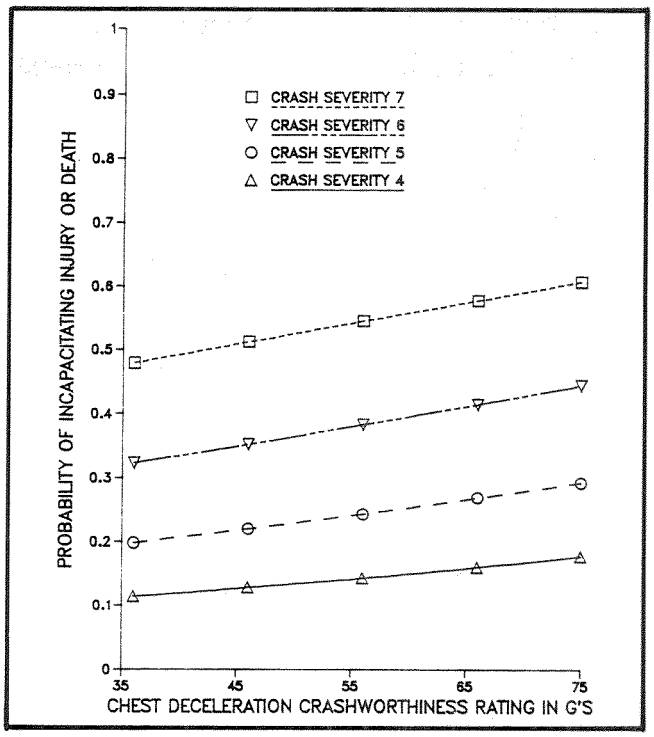

Figure 2. Probability of incapacitating injury or death for unrestrained drivers by NCAP chest deceleration at four levels of crash severity

parameter, had the strongest relationships with likelihood of injury. The parameter estimate for femur load has a negative sign, indicating that car models that had higher femur load in the NCAP tests tended to be associated with lower injury risks.

The influence of the CD measure on injury outcome is illustrated in Figure 2 using the regression coefficients from Table 2. For comparison purposes, the femur load for unrestrained drivers is set at the mean value for restrained drivers. Figure 2 shows a monotonically decreasing risk of injury with decreasing chest deceleration. For a crash of TAD severity 7, the risk of injury decreases from 0.61 for a CD of 75g to 0.48 for a CD of 36g—a reduction of 21 percent. This same trend is reflected in the lower crash severity levels; for impacts of TAD severity 4, the risk drops from 0.18 to 0.11—a reduction of 36 percent.

Table 2. Regression equation for injury odds for unrestrained drivers in a crash (chest deceleration and femur load only)

Independent Variable	Beta	Std. Error	Chi-square	p-value
Intercept	-4.5809	0.1336	1175.00	.001
CD	1.32×10^{-2}	4.11×10^{-3}	10.29	.001
Femur load	-2.48×10^{-4}	1.03×10^{-3}	5.80	.016
Crash severity	0.6566	0.0277	561.96	.001
Driver age	0.0264	0.0045	34.24	.001
Vehicle mass	-1.40×10^{-4}	6.67×10^{-5}	4.42	.036

Model chi-square = 684.05 with 5 d.f.
Fraction of concordant pairs of predicted probabilities and responses: 0.75.
Rank correlation between predicted probability and response: 0.52.
N = 6,091 (865 severely injured or killed).

Analysis of Driver Trajectories From NCAP Test Films

The analyses of the Texas data described above and the earlier FARS data(6) show that there are relationships between the NCAP test results and the risk of injury or death in frontal collisions. Both studies conclude that HIC, CD, or a combination thereof are related to the likelihood of injury in real-world crashes. To examine the possible biomechanical causes of these statistical results, the 16mm films from the NCAP tests were analyzed. The trajectories of drivers for cars with good test results (low HIC's and CD's) were compared to thise in cars with poor test results. By ranking the test results according to the driver HIC and CD values and comparing the characteristics of head and chest contact, it was possible to analyze the different trajectories that occurred from high to low HIC and CD values. Table 3 gives the NCAP crash tests for recent model years (1980-1984) ranked in descending order of a combined HIC and CD parameter (HIC' + CD'). This was computed giving equal weight to the head and chest parameters, by dividing each parameter

Table 3. Effect of driver trajectory on HIC and CD values for recent model year cars

Year/Make/Model	Driver HIC	Driver CD	Driver HIC'+CD' *	Driver Contact Points
1982 Renault Fuego	3768	50	4.77	Head hit steering wheel hub; chest hit lower rim
1984 Ford Tempo	2955	63	4.22	Head hit steering wheel hub
1980 Honda Prelude	2904	52	3.94	Face hit steering wheel hub
1980 Honda Civic	2626	54	3.71	Face hit steering wheel hub
1980 Renault LeCar	1938	85	3.63	Face hit steering wheel hub; lower rim hit chest
1980 Mazda 626	1435	101	3.45	Mouth hit upper rim; chest hit wheel
1982 Chrysler LeBaron	2644	39	3.42	Head hit steering wheel hub
1981 Toyota Starlet	1836	64	3.14	Face hit steering wheel hub; also wheel hit chest
1981Toyota Cressida	1980	55	3.08	Face hit steering wheel hub; lower rim hit chest
1984 Mitsubishi Tredia	1314	87	3.05	Chin hit upper rim; head hit dash; chest hit wheel
1984 Colt Vista	1630	71	3.05	Head hit steering wheel; wheel intruded, hit chest
1984 Renault Sportswagon	2053	43	2.91	Face hit steering wheel hub
1984 Nissan 200SX	1992	44	2.87	Face hit steering wheel hub
1980 Chrysler LeBaron	1742	54	2.82	Face hit steering wheel hub
1984 Pontiac T1000	1886	42	2.73	Face hit steering wheel hub
1980 Audi 4000	1322	70	2.72	Face hit hub, forehead hit upper rim
1984 Isuzu Impulse	1769	46	2.69	Face hit steering wheel hub
1983 Ford EXP	1744	46	2.66	Face hit steering wheel hub
1984 Nissan Stanza	1459	58	2.62	Face hit steering wheel hub
1981 VW Jetta	1210	68	2.57	Head hit upper rim
1980 Oldsmobile Cutlass	1334	62	2.57	Forehead hit upper rim; face hit hub; chest hit lower rim
1980 Subaru GLF	1087	72	2.53	Face hit upper rim; chest hit lower rim
1982 VW Quantum	1353	53	2.41	Face hit steering wheel hub
1982 Dodge Colt	932	72	2.37	Mouth hit upper rim; top of head hit dash
1980 Mercedes 240D	1262	54	2.34	Face hit hub; forehead hit upper rim; chest hit lower rim
1980 Datsun 200SX	1091	62	2.33	Mouth hit upper rim; forehead hit dash
1980 VW Rabbit	1328	48	2.29	Face hit steering wheel hub
1984 Plymouth Conquest	1118	57	2.26	Face hit upper rim; head hit dash; chest hit wheel
1984 Mercury Marquis	1094	58	2.25	Forehead hit upper rim; chest hit wheel
1983 Nissan Pulsar	1139	54	2.22	Face hit steering wheel hub
1980 Toyota Corolla	838	69	2.22	Forehead hit upper rim; chest hit steering wheel
1980 Toyota Tercel	1218	48	2.18	Forehead hit upper rim; chin hit wheel
1984 Mercedes 300 SL	890	63	2.15	Airbag - no direct contact
1983 Toyota Corolla	767	67	2.11	Face hit upper rim
1983 Mazda 626	1196	45	2.10	Face hit steering wheel hub
1981 Renault 18i	1150	45	2.09	Face hit steering wheel hub; chest hit lower rim
1982 Nissan Stanza	974	55	2.07	Forehead hit upper rim; lower rim hit chest
1981 Honda Civic	985	53	2.05	Head hit upper rim and hub; chest hit lower rim
1983 Ford T-bird	626	70	2.03	Face hit upper rim; chest hit lower rim
1982 Toyota Corona	842	59	2.02	Mouth hit upper rim; chest hit steering wheel hub
1980 Ford T-bird	988	50	2.00	Bridge of nose hit upper rim; chest hit wheel

Table 3. (continued)

Year/Make/Model	Driver HIC	CD	(HIC'+CD')*	Driver Contact Points
1984 Ford Mustang	894	55	1.99	Under nose hit upper rim; chest hit steering wheel
1984 Renault Encore	912	53	1.97	Head hit wheel; chest hit lower rim
1982 Ford Escort	950	47	1.89	Forehead hit upper rim; chin hit hub; chest hit lower rim
1983 Peugeot 505	819	52	1.86	Under nose hit upper rim; head hit dash
1983 Dodge 600	947	44	1.83	Forehead hit upper rim; face hit hub; chest hit lower rim
1980 Dodge Mirada	948	43	1.81	Forehead hit upper rim; chest hit wheel
1984 Ford LTD	646	58	1.81	Chin hit upper rim; top of head hit dash; wheel hit chest
1982 Dodge Omni	639	58	1.80	Under nose hit upper rim; chest hit wheel
1984 Mercury Cougar	652	55	1.75	Forehead hit upper rim
1981 Ford EXP	745	49	1.73	Forehead hit upper rim; chin hit hub
1983 Plymouth Reliant	656	52	1.70	Face hit upper rim; chest hit wheel
1984 Nissan 300 SX	789	45	1.69	Bridge of nose hit upper rim; forehead hit dash
1981 Plymouth Reliant	605	52	1.65	Face hit upper rim
1983 Volvo 760	719	45	1.62	Face hit upper rim; chin hit top of hub
1980 Fiat Strada	790	41	1.61	Chin hit lower rim; then forehead hit hub
1980 Chevrolet Chevette	668	45	1.57	Forehead hit upper rim
1982 Chevrolet Cavalier	708	42	1.55	Forehead hit upper rim
1982 Saab 900	734	39	1.51	Face grazed hub
1980 Cadillac Seville	623	43	1.48	Face hit upper rim
1981 Honda Civic	607	41	1.43	Top of head hit dash; no chest contact
1982 Honda Accord	500	43	1.36	Face hit upper rim; no chest contact
1982 Chevrolet Camaro	563	39	1.34	Forehead hit rim
1984 Dodge Daytona	507	37	1.25	Side of head grazed hub; no chest contact
1984 Toyota Corolla	432	41	1.25	No contact
1982 Chevrolet Celebrity	478	33	1.14	Bridge of nose grazed upper rim
1984 Pontiac Fiero	309	31	0.93	Forehead grazed upper rim

*HIC/1000 + CD/50.

by an appropriate tolerance value, i.e., HIC/1000 and CD/50. The table gives the make, model, and model year of each car and the combined driver HIC and CD values together with a brief description of the contact points.

Figure 3 gives still frames from eight of the crash tests documenting the point at which driver contact with the vehicle interior surface occurred. The pattern of contact emerges quite clearly: For tests with high HIC and CD values [(HIC' + CD') $\geq$ 3.0; Figure 3-A], excessive forward movement of the driver occurs generally involving head and chest contact with the steering assembly. The head either strikes the steering wheel hub or travels over the steering wheel such that it hits the dashboard (either produces high HIC's). High values of CD are associated with this type of trajectory because there is significant chest contact with the steering assembly.

The next group of tests[2.5 $\leq$ (HIC' + CD') $<$ 3.0; Figures 3-B and 3-C] differ in that the chest load has been reduced by using the seatbelt to limit the forward movement of the dummy and prevent chest contact with the steering assembly, although this also modifies the head trajectory so that the head moves downward and strikes the steering wheel hub, producing high HIC values. For the tests with somewhat lower HIC's [2.0 $\leq$ (HIC' + CD') $<$ 2.5; Figures 3-D and 3-E], the forward movement of the driver is further controlled by allowing higher chest loads. This, in turn, modifies the head trajectory reducing downward movement so that facial contact occurs with the steering wheel rim rather than head contact with the hub.

In the tests with even lower HIC and CD values [1.5 $\leq$ (HIC' + CD') $<$ 2.0; Figures 3-F and 3-G], the forward movement of the dummy is optimized to minimize chest deceleration while preventing significant contact of the head with the steering wheel. Finally, in those tests with the lowest HIC and CD values [(HIC' + CD') $<$ 1.5; Figure 3-H], the driver trajectory is optimized to produce extremely low chest loads and to allow only minimal or no contact between the head and steering wheel.

Discussion

The analysis of the data from the Texas study shows significant relationships between the risk of serious injury

(3-A)

1980 Honda Civic
HIC = 2626; CD = 54g; Combined = 3.71

(3-E)

1983 Toyota Corolla
HIC = 767; CD = 67g; Combined = 2.10

(3-B)

1984 Renault Sportswagon
HIC = 2053; CD = 43g; Combined = 2.91

(3-F)

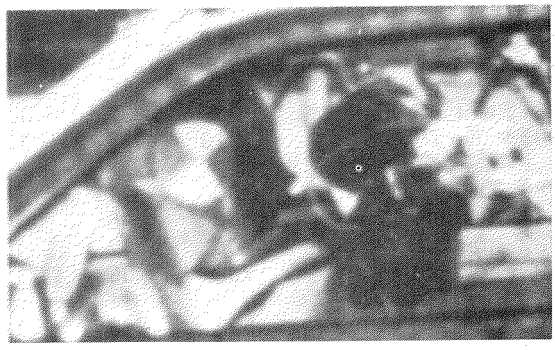

1984 Mercury Cougar
HIC = 652; CD = 55g; Combined = 1.75

(3-C)

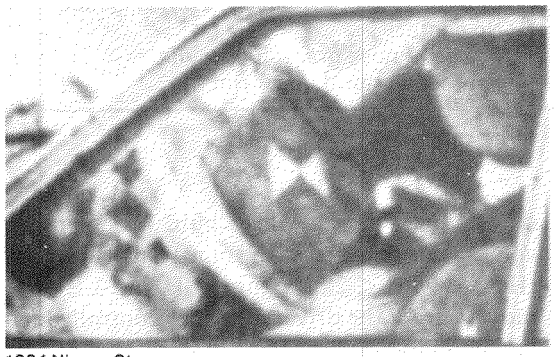

1984 Nissan Stanza
HIC = 1459; CD = 58g; Combined = 2.62

(3-G)

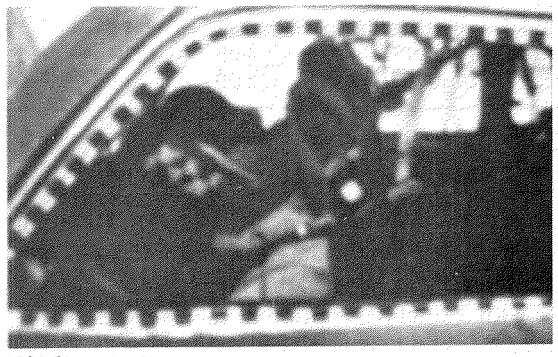

1980 Chevrolet Chevette
HIC = 668; CD = 45g; Combined = 1.57

(3-D)

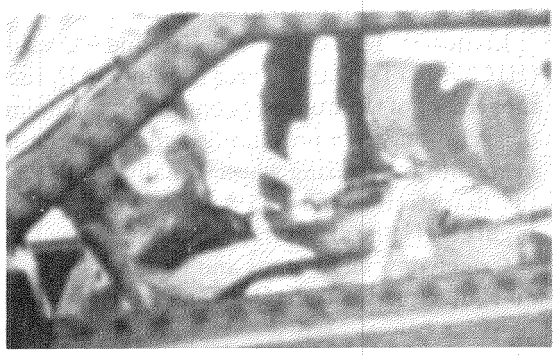

1984 Plymouth Conquest
HIC = 1118; CD = 57g; Combined = 2.26

(3-H)

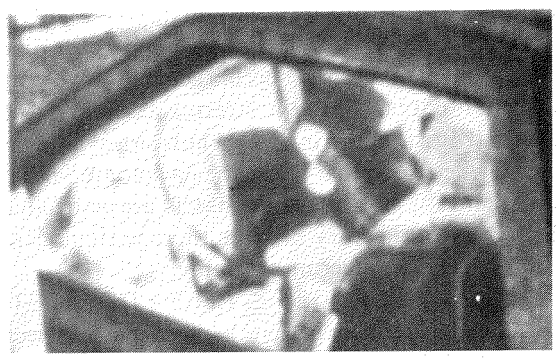

1984 Dodge Daytona
HIC = 507; CD = 37g; Combined = 1.25

Figure 3. Driver trajectory at most forward point in NCAP crash tests as a function of HIC and CD

or death for restrained drivers in frontal impacts and the results from the NCAP tests. The statistical results indicate that the CD parameter has a stronger relationship with injury risk than does HIC. The CD parameter can be expected to be the slightly better predictor of overall injury risk because it reflects both the way the front end of the car crushes and the performance characteristics of the seatbelt, whereas the HIC characterizes the head excursion. An earlier study based on FARS data showed similar trends, although the results were based on a very small sample of restrained occupants and cannot be considered as indicating a definitive result. The statistical results suggest that either the CD or HIC parameter measure driver injury risk in many frontal crash situations, but the film analysis shows that there are certain driver trajectories where a low HIC can be associated with a high CD and vice versa. Thus, for the closest relationships with overall injury risk, the anthropometric dummy parameters of HIC and CD should be used in some combination. Obviously, to relate injury to specific body regions, HIC would be the preferred parameter for head injury and CD for chest injury.

Although unrestrained drivers do not derive the same benefits from improved crashworthiness as restrained drivers, both the Texas and the earlier FARS analysis show the benefits are still considerable. It is also encouraging that both analyses show similar reductions in injury risk. The FARS analysis suggests a 32 percent reduction in risk of fatality for cars with good NCAP test results compared to those with poor results, and the Texas data suggest a corresponding reduction of 21 to 36 percent. Thus, differences in crashworthiness that produce superior performance for the restrained dummy in the 35mph NCAP tests also appear to provide improved protection (via efficient energy-absorbing steering assemblies and fascia panels) for unrestrained drivers. Although in the FARS analysis the combined HIC and CD parameter was marginally the stronger parameter for relationships with risk of fatality, the considerably larger Texas data set showed that CD was the better parameter for estimating the risk of serious injury or death and that femur load was negatively associated with risk of injury. The significance of the CD parameter suggests that the benefit for unrestrained drivers comes from the steering assembly performance. This is further indicated by the film analysis, which shows that the positioning of the dummy chest is relatively close to the steering wheel and interaction between the two often occurs in the NCAP tests.

The apparent significance of the femur load is less straightforward to explain, particularly as it suggests an increasing risk of serious injury with decreasing femur loads. However, the relative importance of the femur load parameter is considerably less than the CD parameter. One possible explanation for its apparent significance is that in a frontal impact an unrestrained occupant moves forward until the chest contacts the steering wheel and the knees strike the lower fascia panel. High femur loads could indicate early knee contact with the fascia panel, which would reduce the level of chest deceleration and hence the overall risk of serious injury or death. (This presupposes that the risk of serious injury or death due to high chest loads is greater than the risk due to high femur loads.)

The results presented here show a substantially stronger relationship between the NCAP results and occupant fatalities than has been reported previously(2,3,4,5,7). The main reasons for this are that in the present study only frontal collisions approximating the NCAP tests were used, and other confounding factors that could influence the risk of fatality or incapacitating injury in these collisions were controlled.

Conclusion

The results obtained from the New Car Assessment Program (NCAP) showed statistically significant relationships with the risk of serious injury or death in single-vehicle, fixed-object frontal impacts. Drivers of cars with better NCAP results had lower injury risk.

The NCAP tests measure crashworthiness performance with the three anthropometric dummy response parameters—HIC, CD, and femur load. Generally, CD had a stronger relationship with overall injury risk than HIC for both restrained and unrestrained drivers, although the film analysis of the driver trajectories suggests that a combination parameter of HIC and CD is desirable to avoid situations where low chest decelerations occur as a consequence of high head loads and vice versa. Femur load provided a significant negative contribution to predicting risk of injury for unrestrained drivers but not for restrained drivers.

For restrained drivers, the risk of injury decreased by between 80 and 87 percent, depending on crash severity, for cars with good NCAP test results compared to those with poor results. Unrestrained drivers did not derive as large a benefit from better crashworthiness measures as restrained drivers. For unrestrained drivers, there was a reduction in injury risk of between 21 and 36 percent, depending on crash severity, for cars with good test results compared to those with poor results.

References

1. Hackney, J., and V. Quarles, "The new car assessment program—status and effect," Proceedings Ninth International Technical Conference on Experimental Safety Vehicles, Kyoto, Japan, October 1982.
2. Campbell, B.J., "A comparison of NHTSA car safety ratings with injuries in highway crashes,"

Highway Safety Highlights, Vol. 15, No. 3, University of North Carolina Safety Research Center, 1982.
3. Jones, I.S., "Injury severity related to crash severity," Canadian Multidisciplinary Road Safety Conference II, Winnipeg, Manitoba, June 1983.
4. Grush, E.S., J.C. Marsh IV, and N.E. South, "Comparison of high speed crash test results with fatality rates," 27th Annual Proceedings of AAAM, San Antonio, Texas, October 3-6, 1983.
5. Thomas C., F. Hartemann, J.V. Foret-Bruno, C. Tarriere, C. Chillon, G. Hufschmitt, C. Got, and A. Patel, "Crashworthiness rating system and accident data: convergences and divergences," Advances in Belt Restraint Systems: Design, Performance and Usage, International Congress and Exposition, Detroit, Michigan, February 1984.
6. Zador, P.L., I.S. Jones, and M. Ginsburg, "Fatal front-to-front car collisions and the results of 35mph frontal barrier impacts," 28th Annual Proceedings of AAAM, Denver, Colorado, October 8-10, 1984.
7. Stewart, J.R., and E.A. Rodgman, "Comparisons of NCAP test results with driver injury rates in highway crashes," University of North Carolina, Highway Safety Research Center, HSRC-PR139, October 1984.
8. Walker, S.H., and D.B. Duncan, "Estimation of the probability of an event as a function of several independent variables," *Biometrika*, 54:167-179, 1967.
9. SAS Institute, Inc., *SUGI Supplemental Library, User's Guide*, 1983 Edition, Cary, North Carolina: SAS Institute Inc., 1983.
10. Traffic Accident Data Project, Technical Bulletin No.1, "Vehicle damage scale for traffic accident investigators," National Safety Council, Chicago, Illinois, 1971.

A Review of the Effects of Belt Systems, Steering Assemblies, and Structural Design on the Safety Performance of Vehicles in the New Car Assessment Program

James Hackney
U.S. Department of Transportation, National Highway Traffic Safety Administration
Carlin Ellyson
Automated Sciences Group, Inc.

Introduction

Since 1979, the National Highway Traffic Safety Administration (NHTSA) has conducted crash tests of 159 different vehicle makes and models in the New Car Assessment Program (NCAP). Each of these vehicles was crashed into a rigid barrier at a test speed of 35mph. This is 5mph faster than the prescribed speed for compliance with Federal motor vehicle safety standards. The crash tests are designed to indicate, for vehicles within the same size class, the relative levels of occupant protection and vehicle safety performance. The data from the anthropomorphic devices (Part 572 dummies) contained in the driver and passenger positions in these vehicles are regularly released as part of NHTSA's Consumer Information Program(1). Trends in these data since 1979 indicate the manufacturers have responded by incorporation of changes in their vehicle designs to lower the measures recorded on the dummies. In this paper, different vehicle parameters, along with some of these specific vehicle design changes, will be tabulated and examined in an attempt to determine their effects on the dummy responses.

Three of the major vehicle attributes that affect the safety of restrained occupants in frontal crash events are the performances of the safety belts, steering assembly, and frontal structure. The following sections will explore these three elements.

Parameters of the safety belt systems are tabulated to allow examination of the effects of belt spoolout/stretch and belt loading on occupant performance.

The performance of the steering assembly appears to be a major factor to good or poor results of the dummy in these tests. The contribution of this component relative to driver HIC is reviewed.

The energy management capability of the frontal structure of the tested vehicles is examined. It has often been debated that to perform well in the 35mph barrier crash test, the frontal structure of the vehicle must be stiffer and will therefore provide an unduly harsh environment for the occupants in other real-world crash modes(2). This aspect is examined by using parameters of the crash pulse.

The analyses are performed exclusively with electronic data collected during each vehicle test. These data include the accelerations measured on the dummy's head, the accelerations measured in the occupant compartment

(the crash pulses), and the loads measured on the torso belts. The NHTSA Crash Test Data Base is the repository of all these data and provides the analyst an opportunity for extensive comparative studies of the vehicle parameters.

Update of Dummy Responses

To allow easy comparison of all test results, the Head Injury Criterion (HIC) and the resultant acceleration on the chest (chest g's) as recorded on the restrained driver and passenger dummies are grouped into six categories as shown in Tables 1 and 2(3).

In Figure 1, the six HIC levels are compared to the recommended life-threatening injury versus HIC relationship recently developed by the U.S. Delegation to the ISO(4). In the following sections, these six levels will be applied to individual vehicles to simplify comparative analyses.

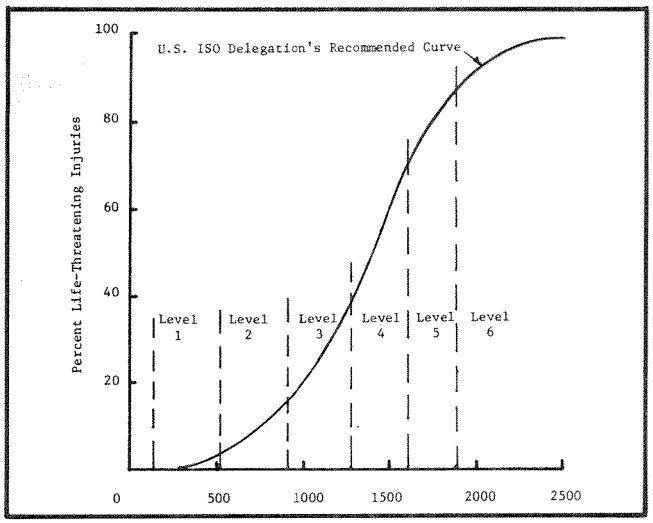

Figure 1. HIC levels shown with U.S. ISO delegation recommended curve

Table 1. HIC Levels

HIC	135 - 519	520 - 899	900 - 1254	1255 - 1574	1575 - 1859	>1860
Level	1	2	3	4	5	6

Table 2. Chest G Levels

Chest GS	17 - 37	38 - 54	55 - 68	69 - 79	80 - 90	>90
Level	1	2	3	4	5	6

In Tables 3 through 9, the NCAP results for model years (MY) 1979 through 1985 are given. (Note: Table 9 contains only those data collected and disseminated on 1985 vehicles through May 1985.) In these tables, the HIC's, chest g's, and levels are presented.

Model year trends of the NCAP data are shown in Figures 2 and 3. The distribution of the six levels are shown in Figure 2. The distribution of dummies whose responses place them in the upper three levels are shown in Figure 3. As seen in Figure 2, there have been general

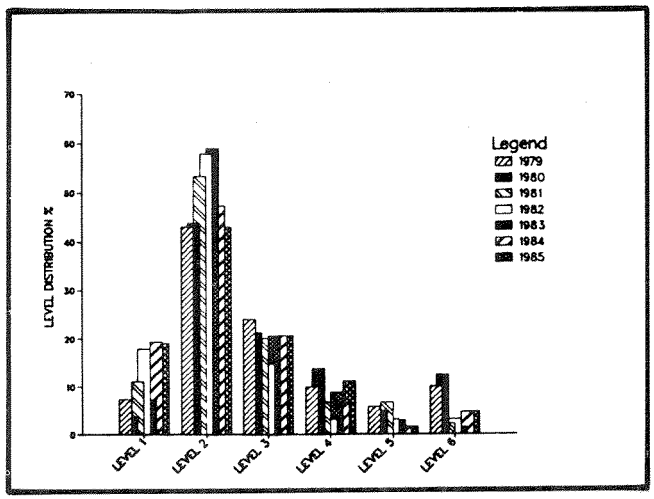

Figure 2. HIC and chest G level distribution by model year for NCAP vehicles

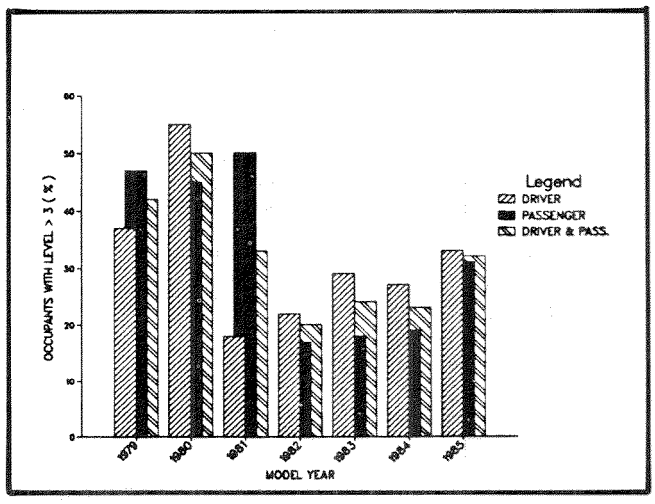

Figure 3. Percent of occupants with levels 3 by model year for NCAP vehicles

Table 3. NCAP results for 1979 MY vehicles

Vehicle Make/Body Style	Driver HIC Level	Driver Chest G Level	Passenger HIC Level	Passenger Chest G Level
Toyota Corolla				
2 dr				
Mercury Capri			770	44
2 dr hb			2	2
Oldsmobile Cutlass S	695	42	501	40
2 dr	2	2	1	2
Ford Mustang	819	41	567	33
2 dr	2	2	2	1
Buick Riviera	541	42	782	39
2 dr	2	2	2	2
Plymouth Horizon	653	52	780	38
2dr hb	2	2	2	2
Dodge Magnum	646	39	731	44
2 dr	2	2	2	2
Chevrolet Chevette	871	47	859	45
4 dr hb	2	2	2	2
Lincoln Continental	521	45	919	53
4 dr	2	2	3	2
Volkswagen Rabbit	1024	67	429	33
2 dr hb	3	3	1	1
Oldsmobile Cutlass S	997	58	799	37
2 dr	3	3	2	1
Mercury Marquis	1204	61	868	42
2 dr	3	3	2	2
Ford LTD II	1088	61	781	40
2 dr	3	3	2	2
Chevrolet Monza	1108	42	1033	41
2 dr	3	2	3	2
Ford LTD	1452	38	616	34
2 dr	4	2	2	1
Pontiac Firebird	965	42	1297	47
2 dr	3	2	4	2
Chevrolet Impala	1277	62	1254	51
4 dr	4	3	3	2
AMC Concord	1078	61	1457	69
2 dr	3	3	4	4
Ford Granada	1442	61	1279	56
4 dr	4	3	4	3
Plymouth Volare	724	40	1677	40
2 dr	2	2	5	2
Oldsmobile 98	910	59	1734	54
4 dr	3	3	5	2
Datsun 210	1358	69	1745	59
2 dr	4	4	5	3
Ford Fairmont	939	54	1583	85
4 dr	3	2	5	5
Dodge St Regis	1909	67		50
4 dr	6	3		2
Toyota Celica	849	61	1862	59
2 dr hb	2	3	6	3
Chrysler LeBaron	2402	45	1071	39
2 dr	6	2	3	2
Mercury Bobcat	723	64	1878	51
2 dr hb	2	3	6	2
Plymouth Champ	1270	72	1918	66
2 dr hb	4	4	6	3
Volvo 244 DL	1782	52	1889	61
4 dr	5	2	6	3
Ford Fiesta	1656	70	1932	48
2 dr	5	4	6	2
Honda Civic	2030	93	2093	46
2 dr	6	6	6	2
Peugeot 504	4513	63	2498	43
4 dr	6	3	6	2

Table 4. NCAP results for 1980 MY vehicles

Vehicle Make/Body Style	Driver HIC Level	Driver Chest G Level	Passenger HIC Level	Passenger Chest G Level
Chevrolet Citation	845	48	623	35
4 dr hb	2	2	2	1
Cadillac Seville	623	43	523	35
4 dr	2	2	2	1
Chevrolet Chevette	668	45	699	40
2 dr hb	2	2	2	2
Fiat Strada	790	41	962	43
4 dr hb	2	2	3	2
Dodge Mirada	948	43	959	37
2 dr	3	2	3	1
Toyota Tercel	1218	48	1179	53
2 dr	3	2	3	2
Ford T-Bird II	988	50	994	52
2 dr	3	2	3	2
Datsun 200SX	1091	62	1032	44
2 dr hb	3	3	3	2
Volkswagen Rabbit CO	1328	48	829	54
2 dr	4	2	2	2
Oldsmobile Cutlass	1334	62	1125	47
4 dr	4	3	3	2
Mercedes 240D	1262	54	1369	44
4 dr	4	2	4	2
Audi 4000	1322	70	1428	45
4 dr	4	4	4	2
Chryler LeBaron	1742	54	1252	45
2 dr	5	2	3	2
Datsun 310 GX	1059	68	2019	108
2 dr hb	3	3	6	6
Toyota Corolla	838	69	1162	92
2 dr	2	4	3	6
Honda Civic	2626	54	1506	47
2 dr hb	6	2	4	2
Subaru GLF	1087	72	2837	94
4 dr	3	4	6	6
Honda Prelude	2904	52	1759	45
2 dr hb	6	2	5	2
Renault LeCar	1938	85	1844	53
2 dr hb	6	5	5	2
Mazda 626	1435	101	2206	54
2 dr	4	6	6	2

Table 5. NCAP results for 1981 MY vehicles

Vehicle Make/Body Style	Driver HIC Level	Driver Chest G Level	Passenger HIC Level	Passenger Chest G Level
Audi 5000		43		52
4 dr		2		2
Ford EXP	745	49		53
2 dr hb	2	2		2
Honda Civic	607	41	492	35
2 dr hb	2	2	1	1
AMC Spirit	702	43	652	33
2 dr	2	2	2	1
Chrysler Imperial	976	47	590	32
2 dr	3	2	2	1
Ford Escort	618	50	1011	40
2 dr hb	2	2	3	2
Honda Civic	985	53	1391	43
4 dr hb	3	2	4	2
Volkswagen Jetta	1210	68	1272	52
4 dr	3	3	4	2
Renault 181	1150	47	1659	36
4 dr	3	2	5	1
Plymouth Reliant	605	52	1731	59
2 dr	2	2	5	3
Toyota Starlet	1836	65	1351	48
2 dr hb	5	3	4	2
Toyota Cressida	1980	55	771	50
4 dr	6	3	2	2

Table 6. NCAP results for 1982 MY vehicles

Vehicle Make/Body Style	Driver HIC Level	Driver Chest G Level	Passenger HIC Level	Passenger Chest G Level
Chevrolet Celebrity	478	33	395	21
4 dr	1	1	1	1
Honda Accord	500	43	403	29
4 dr	1	2	1	1
Volvo DL	550	45	381	35
2 dr	2	2	1	1
Chevrolet Camaro	563	39	577	32
2 dr	2	2	2	1
Toyota Celica	702	36	530	45
2 dr	2	1	2	2
Chevrolet Cavalier	708	42	821	37
2 dr hb	2	2	2	1
Lincoln Continental	757	46	728	37
4 dr	2	2	2	1
Dodge 400	520	44	756	41
2 dr	2	2	2	2
Datsun Sentra	549	43	865	46
4 dr	2	2	2	2
Saab 900	734	39	1166	35
4 dr	2	2	3	1
Chevrolet Impala	1170	40		41
4 dr	3	2		2
Ford Granada	860		1050	52
4 dr	2		3	2
Ford LTD	960	50	808	40
4 dr	3	2	2	2
Toyota Corona	842	59	828	40
4 dr	2	3	2	2
Chevrolet Chevette	1020	48	715	40
4 dr hb	3	2	2	2
Datsun Stanza	974	55	879	39
4 dr hb	3	3	2	2
Ford Escort	950	47	1070	39
4 dr hb	3	2	3	2
Volkswagen Scirocco	1482	54	683	37
2 dr	4	2	2	1
Volkswagen Quantum	1353	53	1194	41
4 dr	4	2	3	2
Dodge Omni	639	58	1703	43
4 dr hb	2	3	5	2
Mazda 626	969	47	1693	50
4 dr	3	2	5	2
Dodge Colt	932	72	1730	44
4 dr hb	3	4	5	2
Chrysler LB Conv	2644	39	697	43
2 dr	6	2	2	2
Renault Fuego	3768	50	2484	35
2 dr	6	2	6	1

Table 7. NCAP results for 1983 MY vehicles

Vehicle Make/Body Style	Driver HIC Level	Driver Chest G Level	Passenger HIC Level	Passenger Chest G Level
Pontiac Firebird	408	34	376	32
2 dr	1	1	1	1
Toyota Camry	809	48	495	40
4 dr	2	2	1	2
Volvo 760 GLE	791	45	778	41
4 dr	2	2	2	2
Toyota Tercel 4X	839	43	535	42
4 dr sw	2	2	2	2
Chevrolet Caprice	882	42	1084	47
4 dr	2	2	3	2
Ford Bronco 4X	789	49	1038	50
mpv	2	2	3	2
Peugeot 505S	819	52	1157	49
4 dr	2	2	3	2
Plymouth Reliant	656	52	1221	52
4 dr sw	2	2	3	2
Dodge 600	947	46	1010	48
4 dr	3	2	3	2
Datsun Pulsar	1139	54	1134	39
4 dr hb	3	2	3	2
Mazda 626	1196	45	1087	56
4 dr	3	2	3	3
Ford T-Bird	626	70	795	43
2 dr	2	4	2	2
Toyota Corolla	767	67	1367	43
4 dr sw	2	3	4	2
Ford LTD	609	69	957	54
4 dr	2	4	3	2
Ford EXP	1744	46	796	41
2 dr	5	2	2	2
Mitsubishi Montero 4	1641	54	1415	48
mpv	5	2	4	2
Mitsubishi Mighty MA	1475	68	1934	71
pu	4	3	6	4

trends of increases in the percentages of lower level values (levels 1 and 2) with a concurrent decrease in the percentages of levels 4, 5, and 6. Figure 3, which is considered an even better graphic presentation of the vehicle performance trend since MY1979, shows the percentage of occupants, i.e., drivers and passengers, that received HIC's greater than 1,274 and/or chest g's greater than 68. A study of the data, which are used to develop this figure, provides safety engineers and manufacturers with information on outliers (poor-performing vehicles) tested during the 7-year period.

Table 10 contains the average and median values of the HIC's and chest g's of the driver and passenger dummies for the seven MY's. As seen in the level distributions and these averages and medians, most comparisons show that later MY vehicles have improved performance. It should be noted that the median (50th percentile) values of the HIC's are often significantly lower than the average values.

Vehicle Performance by Weight Class

In the above tables and figures, the NCAP data are grouped only by MY. No distinction is made for vehicle mass. It is well known that the lighter vehicles within the traffic mix in the United States are potentially less safe(6). This is, in part, due to the higher velocity changes that the lighter vehicles experience in collisions with heavier vehicles on the roadway.

The Passenger Car Classification Subcommittee of the Transportation Research Board has completed a final report on car size definitions(7). The weight classes as recommended from the report will be used to group the NCAP vehicles. The four weight classes are—

Small	Curb Weight below 2,450 lb
Compact	Curb Weight 2,451 to 2,950 lb
Intermediate	Curb Weight 2,951 to 3,450 lb
Large	Curb Weight above 3,451 lb

Table 8. NCAP results for 1984 MY vehicles

Vehicle Make/Body Style	Driver HIC Level	Driver Chest G Level	Passenger HIC Level	Passenger Chest G Level
Pontiac Fiero	309	31	356	30
2 dr	1	1	1	1
Chevrolet Celebrity	518	31	440	28
4 dr sw	1	1	1	1
Chevrolet Cav Conv	884	43	401	29
2 dr	2	2	1	1
Toyota Corolla	432	37	602	47
2 dr	1	1	2	2
Honda Prelude	659	43	475	31
2 dr	2	2	1	1
AMC Jeep CJ-7	460	46	440	49
mpv	1	2	1	2
Chevrolet C-10	534	37	514	39
pu	2	1	1	2
Chevrolet Corvette	784	40	525	32
2 dr	2	2	2	1
Dodge Daytona	507	47	566	40
2 dr hb	1	2	2	2
Honda Civic	563	37	846	43
2 dr hb	2	1	2	2
Honda Civic	586	43	544	32
4 dr sw	2	2	2	1
Toyota Tercel	658	43	492	41
4 dr hb	2	2	1	2
Toyota Corolla	630	41	611	42
4 dr	2	2	2	2
Honda Civic CRX	571	34	959	34
2 dr	2	1	3	1
Oldsmobile Cutlass	781	40	1074	35
2 dr	2	2	3	1
Pontiac Parisienne		52	1055	48
4 dr		2	3	2
Mercury Cougar	652	55	577	37
2 dr	2	3	2	1
Nissan 300 ZX	789	45	1038	39
2 dr	2	2	3	2
Toyota Van Wagon	984	50	748	54
4 dr	3	2	2	2
Mercedes 300SD	890	63	734	44
4 dr	2	3	2	2
Renault Alliance	940	55		42
4 dr	3	3		2
Ford LTD	646	58	647	67
4 dr sw	2	3	2	3
Dodge Caravan	973	44	1200	42
3 dr	3	2	3	2
Ford Mustang	894	55	1112	38
2 dr	2	3	3	2
Plymouth Conquest	1118	57	1035	43
2 dr hb	3	3	3	2
Mercury Marquis	1094	58	1019	39
4 dr	3	3	3	2
Renault Encore	912	63	1045	67
4 dr hb	3	3	3	3
Buick Park Ave	1550	50	662	37
4 dr	4	2	2	1
AMC Jeep Cher	850	44	1548	43
mpv	2	2	4	2
Plymouth Colt Vist	1530	71	1004	45
4 dr sw	4	4	3	2

Table 8. continued

Vehicle Make/Body Style	Driver HIC Level	Driver Chest G Level	Passenger HIC Level	Passenger Chest G Level
Ford F-150	1362	48	1443	51
2 dr	4	2	4	2
Mitsubishi Tredia	1314	87	1521	57
4 dr	4	5	4	3
Nissan 200SX	1992	44	582	32
2 dr	6	2	2	1
Ford Tempo	2955	63	1104	45
4 dr	6	3	3	2
Pontiac 1000	1886	42	1306	57
4 dr hb	6	2	4	3
Datsun Stanza	1459	58	2216	53
4 dr	4	3	6	2
Isuzu Impulse	1769	46	2454	49
2 dr hb	5	2	6	2
Renault Sportwagon	2053	43	2721	52
4 dr sw	6	2	6	2

Table 9. NCAP results for 1985 MY vehicles

Vehicle Make/Body Style	Driver HIC Level	Driver Chest G Level	Passenger HIC Level	Passenger Chest G Level
Volvo DL	621	33	262	31
4 dr sw	2	1	1	1
Volvo DL	652	36	310	27
4 dr	2	1	1	1
Dodge Colt	787	42	741	32
4 dr hb	2	2	2	1
Plymouth Caravelle	685	51	760	35
4 dr	2	2	2	1
Plymouth Reliant	832	54	843	44
4 dr	2	2	2	2
Buick Somerset	1140	34	595	35
2 dr	3	1	2	1
Mitsubishi Galant		52	986	42
4 dr		2	3	2
Volkswagen Jetta	898	50	1008	51
2 dr	2	2	3	2
Mazda RX	921	40	1345	42
2 dr	3	2	4	2
Chevrolet Blazer	1036	62	1321	43
mpv	3	3	4	2
Chevrolet Spectrum	1559	51	960	56
2 dr hb	4	2	3	3
Datsun Maxima	1014	63	1500	38
4 dr sw	3	3	4	2
Subaru DL	1361	57	792	39
4 dr	4	3	2	2
Dodge Lancer	2187	38	445	30
4 dr hb	6	2	1	1
Renault Alliance	1519	62	2678	47
2 dr conv	4	3	6	2
GMC Astro	2202	70	1597	61
van	6	4	5	3

Table 10. Average and median values of HIC and chest GS for 1979 through 1985 NCAP vehicles

Model Year	Driver Average HIC	Driver Median HIC	Driver Average Chest GS	Driver Median Chest GS	Passenger Average HIC	Passenger Median HIC	Passenger Average Chest GS	Passenger Median Chest GS
1979	1248	1051	56	59	1253	1163	48	46
1980	1302	1155	58	54	1315	1171	53	46
1981	1038	976	51	50	1092	1142	44	46
1982	1026	851	47	46	957	815	39	40
1983	949	819	52	49	1011	1038	47	47
1984	1013	884	49	46	963	846	43	42
1985	1161	1014	50	51	1009	902	41	41

The vehicles in the NCAP are reported by test weight, which includes 328 lb for two dummies and a cargo weight of 100 lb for vehicles under 2,500 lb, 150 lb for vehicles between 2,500 and 3,500 lb, and 170 lb for vehicles over 3,500 lb.

The NCAP vehicles and the relevant dummy responses are grouped into these weight classifications in Tables 11 through 14. The dummy HIC's and chest g's are given for each vehicle. It should be noted that in these tables the vehicles within each weight class have been sorted. This sorting places all vehicles whose driver and passenger dummy received an HIC less than 1255 and a chest g less than 69 first in the tables. Conversely, the vehicles whose dummies recorded HIC's greater than 1254 and/or chest g's greater than 68 are last in the tables. These two groups will be referred to, relatively, as the low-risk group and the high-risk group. All subsequent tables of the four weight classes will be arranged in the same manner. Discussion will relate the safety parameters between the low- and high-risk groups.

Similar to Figures 2 and 3, the distributions for the four weight classes are shown in Figures 4 and 5. The average and median values of the HIC's and chest g's are given in Table 15.

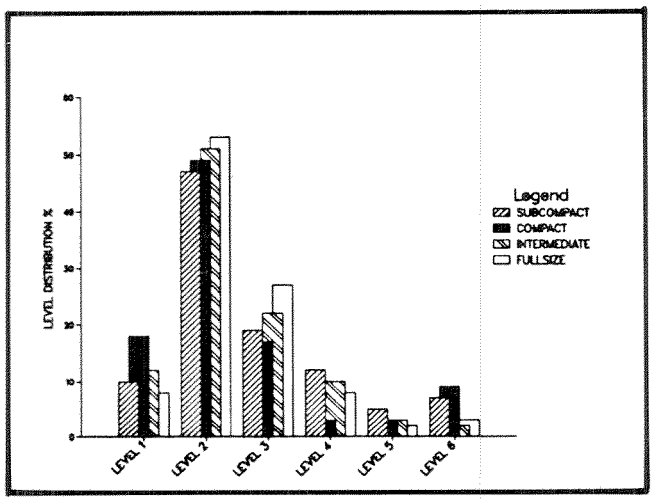

Figure 4. HIC and chest G level distribution by vehicle weight for NCAP vehicles

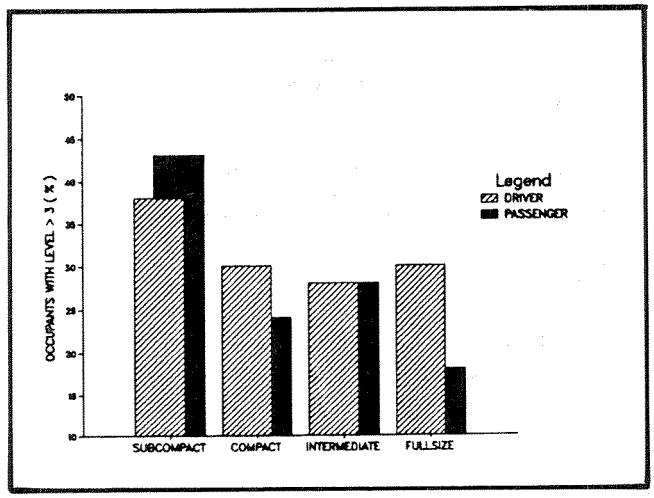

Figure 5. Percent of occupants with levels 3 by vehicle weight for NCAP vehicles

From Figures 4 and 5, the small vehicles that have been tested since 1979 show a tendency toward poorer performance than the other three weight classes. In Figure 5, the percentages of drivers and passengers for the small vehicles receiving HIC's greater than 1254 and/or chest g's greater than 68 are 38 percent and 43 percent. For the large vehicle weight class, these percentages are 30 percent and 18 percent. From Table 15, it is again noted that the median values are often significantly lower than the average values.

The remainder of this paper will present discussions of vehicle safety parameters within these selected weight groups and comparisons of the parameters between the different weight groups.

Belt Performance Parameters

The NCAP has provided the first large-scale dynamic evaluation of safety belts in today's vehicles. The experience in this program has been encouraging.

Complete failures of belt systems have occurred in only three vehicles. In each case, latching mechanisms or D-rings were the cause of the failures. Manufacturers' recalls were done on these vehicles to correct the problem.

Table 11. Dummy response data and belt performance parameters for the small vehicle weight class

NHTSA Data Base Test No.	MY	Vehicle Make/Body Style	Weight Lbs	Driver HIC Level	Driver Chest G Level	Passenger HIC Level	Passenger Chest G Level	Onset T Msec	Belt System Parameters: Driver Force Lbs	Driver Loading Lbs/Msec	Passenger Onset T Msec	Passenger Force Lbs	Passenger Loading Lbs/Msec
756	84	Renault Alliance	2460	940	55		42						
		4 dr		3	3		2						
360	81	Ford EXP	2542	745	49		53						
		2 dr hb		2	2		2						
99	79	Toyota Corolla	2651										
		2 dr											
455	82	Honda Accord	2635	500	43	403	29	38	1256	48	33	1656	51
		4 dr		1	2	1	1						
685	84	Toyota Corolla	2680	432	37	602	47	24	1990	45	26	2055	46
		2 dr		1	1	2	2						
745	84	Honda Prelude	2780	659	43	475	31	29	1223	47	25	1336	42
		2 dr		2	2	1	1						
356	81	Honda Civic	2160	607	41	492	35	25	1519	42	24	1806	48
		2 dr hb		2	2	1	1						
694	84	Honda Civic	2311	563	37	846	43	32	1059	53	29	1566	66
		2 dr hb		2	1	2	2						
523	82	Chevrolet Cavalier	2830	708	42	821	37	27	1814	56	27	1506	47
		2 dr hb		2	2	2	1						
747	84	Toyota Tercel	2440	658	43	492	41	27	1444	44	22	1602	46
		4 dr hb		2	2	1	2						
791	85	Dodge Colt	2615	787	42	741	32	31	1492	49	34	1647	60
		4 dr hb		2	2	2	1						
705	84	Honda Civic	2510	586	43	544	32	25	1239	58	20	2110	67
		4 dr sw		2	2	2	1						
590	83	Toyota Tercel 4X	2826	839	43	535	42	34	1138	26	28	1834	60
		4 dr sw		2	2	2	2						
682	84	Toyota Corolla	2610	630	41	611	42	22	1425	47	24	1445	54
		4 dr		2	2	2	2						
73	79	Chevrolet Chevette	2720	871	47	859	45	24	2244	43			
		4 dr hb		2	2	2	2						
464	82	Datsun Sentra	2455	549	43	865	46	42	1307	38	43	1489	38
		4 dr		2	2	2	2						
53	79	Plymouth Horizon	2661	653	52	780	38	44	1754	46	43	2450	50
		2 dr hb		2	2	2							
426	80	Chevrolet Chevette	2641	668	45	699	40	36	2195	59	33	2156	55
		2 dr hb		2	2	2	2						
669	84	Honda Civic CRX	2310	571	34	959	34	28	1196	59	25	1652	59
		2 dr		2	1	3	1						
797	85	Volkswagen Jetta	2844	898	50	1008	51	28	1635	43	28	1785	44
		2 dr		2	2	3	2						
206	81	Ford Escort	2590	618	50	1011	40	26	1609	38	26	1752	44
		2 dr hb		2	3	2							
194	80	Fiat Strada	2707	790	41	962	43	40	1293	37	41	1527	38
		4 dr		2	2	3	2						
525	82	Chevrolet Chevette	2827	1020	48	715	40	34	1669	53	31	1703	49
		4 dr hb		3	2	2	2						
7	79	Volkswagen Rabbit	2600	1024	67	429	33	36	1839	40	26	1847	31
		2 dr hb		3	3	1	1						
462	82	Datsun Stanza	2686	974	55	879	39	40	1496	50	38	1272	43
		4 dr hb		3	3	2	2						
452	82	Ford Escort	2584	950	47	1070	39	34	1448	39	39	1610	41
		4 dr hb		3	2	3	2						
598	83	Datsun Pulsar	2460	1139	54	1134	39	37	1559	58	33	1704	52
		4 dr hb		3	2	3	2						
122	80	Toyota Tercel	2314	1218	48	1179	53	34	1191	22	36	1598	33
		2 dr		3	2	3	2						
632	84	Renault Encore	2600	912	63	1045	67	35	1871	56	36	1801	68
		4 dr hb		3	3	3	3						

Table 11. continued

NHTSA Data Base Test No.	MY	Vehicle Make/Body Style	Weight Lbs	Driver HIC Level	Driver Chest G Level	Passenger HIC Level	Passenger Chest G Level	Belt System Parameters Driver Onset T Msec	Driver Force Lbs	Driver Loading Lbs Msec	Passenger Onset T Msec	Passenger Force Lbs	Passenger Loading Lbs Msec
445	82	Volkswagen Scirocco	2680	1482	54	683	37	38	1477	53	33	1681	39
		2 dr		4	2	2	1						
428	80	Volkswagen Rabbit CO	2767	1328	48	829	54	33	2046	53	37	2238	62
		2 dr		4	2	2	2						
790	85	Mazda RX	2873	921	40	1345	42	33	1576	53	36	1575	58
		2 dr		3	2	4	2						
563	83	Toyota Corolla	2760	767	67	1367	43	31	1522	38	28	1557	49
		4 dr sw		2	3	4	2						
273	81	Honda Civic	2456	985	53	1391	43	32	1595	52	32	1993	54
		4 dr hb		3	2	4	2						
365	81	Volkswagen Jetta	2650	1210	68	1272	52	41	2272	41	45	2286	52
		4 dr		3	3	4	2						
802	85	Chevrolet Spectrum	2346	1559	51	960	56						
		2 dr hb		4	2	3	3						
789	85	Subaru DL	2698	1361	57	792	39	25	1954	44	33	1587	62
		4 dr		4	3	2	2						
102	80	Audi 4000	2836	1322	70	1428	45	37	1891	59	36	1666	70
		4 dr		4	4	4	2						
363	81	Renault 181	2750	1150	47	1659	36	36	1364	43	29	1859	34
		4 dr		3	2	5	1						
569	83	Ford EXP	2590	1744	46	796	41	27	2624	54	29	2683	73
		2 dr		5	2	2	2						
444	82	Dodge Omni	2670	639	58	1703	43	40	825	30	34	1318	33
		4 dr hb		2	3	5	2						
526	82	Dodge Colt	2488	932	72	1730	44	42	1085	38	42	1433	41
		4 dr hb		3	4	5	2						
333	81	Toyota Starlet	2214	1836	65	1351	48	36	1521	44	31	1877	53
		2 dr hb		5	3	4	2						
35	79	Datsun 210	2425	1358	69	1745	59	39	1406	29	38	1564	28
		2 dr		4	4	5	3						
746	84	Mitsubishi Tredia	2740	1314	87	1521	57	45	1305	57	45	1642	59
		4 dr		4	5	4	3						
119	80	Datsun 310 GX	2404	1059	68	2019	108	34	1583	33	35		
		2 dr hb		3	3	6	6						
	80	Toyota Corolla	2680	838	69	1162	92						
		2 dr		2	4	3	6						
217	80	Honda Civic	2298	2626	54	1506	47	34	1333	50	33	1494	52
		2 dr hb		6	2	4	2						
133	80	Subaru GLF	2618	1087	72	2837	94						
		4 dr		3	4	6	6						
693	84	Datsun Stanza	2814	1459	58	2216	53	36	1485	45	40	1564	50
		4 dr		4	3	6	2						
799	85	Renault Alliance	2810	1519	62	2678	47						
		2 dr conv		4	3	6	2						
689	84	Pontiac 1000	2746	1886	42	1306	57	26	1850	44	32	1797	58
		4 dr hb		6	2	4	3						
33	79	Plymouth Champ	2313	1270	72	1918	6	47	803	28	46	1220	28
		2 dr hb		4	4	6	3						
216	80	Honda Prelude	2545	2904	52	1759	45	42	1541	47	38	1669	39
		2 dr hb		6	2	5	2						
218	80	Renault LeCar	2196	1938	85	1844	53	38	1581	69			
		2 dr hb		6	5	5	2						
263	79	Ford Fiesta	2185	1656	70	1932	48	24	951	47	20	1101	41
		2 dr		5	4	6	2						
94	79	Honda Civic	2166	2030	93	2093	46	32	1137	38	30	1683	40
		2 dr		6	6	6	2						

Table 12. Dummy response data and belt performance parameters for the compact vehicle weight class

NHTSA Data Base Test No.	MY	Vehicle Make/Body Style	Weight Lbs	Driver HIC Lbs	Driver Chest G Level	Passenger HIC Level	Passenger Chest G Level	Belt System Parameters: Onset T Msec	Driver Force Lbs	Driver Loading Lbs/Msec	Passenger Onset T Msec	Passenger Force Lbs	Passenger Loading Lbs/Msec
357	81	Audi 5000	3361		43		52						
		4 dr.			2		2						
157	79	Mercury Capri	3067			770	44						
		2 dr hb				2	2						
798	85	Mitsubishi Galant	3360		52	986	42						
		4 dr			2	3	2						
451	82	Chevrolet Celebrity	3273	478	33	395	21	40	1462	43	35	1495	39
		4 dr		1	1	1	1						
667	84	Pontiac Fiero	3000	309	31	356	30	21	1182	40	25	1493	60
		2 dr		1	1	1	1						
574	83	Pontiac Firebird	3330	406	34	376	32	26	1375	48	29	1458	34
		2 dr		1	1	1	1						
808	85	Volvo DL	3400	652	36	310	27	30	1629	45	24	1896	33
		4 dr		2	1	1	1						
418	82	Volvo DL	3354	550	45	381	35						
		2 dr		2	2	1	1						
661	84	Chevrolet Cav-Conv	3110	884	43	401	29	29	1530	36	28	1790	37
		2 dr		2	2	1	1						
633	84	AMC Jeep CJ-7	3180	460	46	440	49	25	1312	38	24	1741	51
		mpv		1	2	1	2						
454	82	Toyota Celica	3060	702	36	530	45	37	1670	66	38	1867	65
		2 dr		2	1	2	2						
674	84	Dodge Daytona	3000	507	47	566	40	33	1994	46	31	2396	41
		2 dr hb		1	2	2	2						
364	81	AMC Spirit	3190	702	43	652	33	23	1629	39	25	1783	50
		2 dr		2	2	2	1						
594	83	Toyota Camry	2980	809	48	495	40	30	1676	52	24	2005	46
		4 dr		2	2	1	2						
450	82	Chevrolet Camaro	3428	563	39	577	32	41	1485	42	42	1644	41
		2 dr		2	2	2	1						
255	79	Ford Mustang	2951	819	41	567	33	34	1414	25			
		2 dr		2	2	2	1						
793	85	Plymouth Caravelle	3170	685	51	760	35	42	1414	31	37	1976	30
		4 dr		2	2	2	1						
5	80	Chevrolet Citation	3260	845	48	623	35	31	1533	39	30	1521	27
		4 dr hb		2	2	2	1						
453	82	Dodge 400	3044	520	44	756	41	46	1285	41	47	1983	44
		2 dr		2	2	2	2						
794	85	Plymouth Reliant	3060	832	54	843	44	31	1216	40	38	2075	38
		4 dr		2	2	2	2						
788	85	Buick Somerset	3210	1140	34	595	35	33	1331	45	30	1645	43
		2 dr		3	1	2	1						
446	82	Saab 900	3220	734	39	1166	35	37	1216	46	39	1473	47
		4 dr		2	2	3	1						
686	84	Nissan 300 ZX	3370	789	45	1038	39	44	1431	31	43	1808	36
		2 dr		2	2	3	2						
593	83	Plymouth Reliant	2910	656	52	1221	52	43	1174	43	35	2024	27
		4 dr sw		2	2	3	2						
496	82	Toyota Corona	3040	842	59	828	40	39	1662	52	34	1832	50
		4 dr		2	3	2	2						
64	79	Chevrolet Monza	3240	1106	42	1033	41	36	1610	49	32		44
		2 dr		3	2	3	2						
514	83	Dodge 600	3110	947	46	1010	48	45	1180	39	39	2326	22
		4 dr		3	2	3	2						
599	83	Mazda 626	2900	1196	45	1087	56	34	1508	47	35	1683	41
		4 dr		3	2	3	3						
668	84	Plymouth Conquest	3170	1118	57	1035	43	47	1390	47	40	1475	40
		2 dr hb		3	3	3	2						
186	80	Datsun 200 SX	3038	1091	62	1032	44	40	1453	22	33	1412	20
		2 dr hb		3	3	3	2						

Table 12. continued

NHTSA Data Base Test No.	MY	Vehicle Make/Body Style	Weight Lbs	Driver HIC Level	Driver Chest G Level	Passenger HIC Level	Passenger Chest G Level	Belt System Parameters Onset T Msec	Driver Force Lbs	Driver Loading Lbs/Msec	Passenger Onset T Msec	Passenger Force Lbs	Passenger Loading Lbs/Msec
465	82	Volkswagen Quantum	2954	1353	53	1194	41	39	1843	62	35	1926	46
		4 dr		4	2	3	2						
665	84	Plymouth Colt Vista	2980	1530	71	1004	45	45	1488	61	41	1812	62
		4 dr sw		4	4	3	2						
470	82	Mazda 626	2900	969	47	1693	50	26	1568	30	27	1565	32
		4 dr		3	2	5	2						
207	81	Plymouth Reliant	2910	605	52	1731	59	31	1198	40	30	2292	33
		2 dr		2	2	5	3						
92	79	Ford Fairmont	3296	939	54	1583	85	36	1370	43	35	1362	39
		4 dr		3	2	5	5						
792	85	Dodge Lancer	3250	2187	38	445	30	30	1471	37	28	1626	32
		4 dr hb		6	2	1	1						
722	84	Nissan 200SX	2880	1992	44	582	32	40	1333	37	31	1538	37
		2 dr		6	2	2	1						
550	82	Chrysler LB Conv	3000	2644	39	697	43	32		65	27	2454	54
		2 dr		6	2	2	2						
334	81	Toyota Cressida	3417	1980	55	771	50	36	2235	66	38	3144	73
		4 dr		6	3	2	2						
27	79	Toyota Celica	3025	849	61	1862	59	36	1190	19	28	1532	21
		2 dr hb		2	3	6	3						
156	79	Mercury Bobcat	2998	723	64	1878	51	41	1031	24	38	1608	25
		2 dr hb		2	3	6	2						
681	84	Ford Tempo	3080	2955	63	1104	45	36	1412	51	36	1821	59
		4 dr		6	3	3	2						
579	83	Mitsubishi Mighty MA	3094	1475	68	1934	71	37	1241	23	38	1593	34
		pu		4	3	6	4						
30	79	Volvo 244 DL	3374	1782	52	1889	61	50	789	19	40	905	16
		4 dr		5	2	6	3						
743	84	Isuzu Impulse	3230	1769	46	2454	49	30	1318	38	25	1834	30
		2 dr hb		5	2	6	2						
711	84	Renault Sportwagon	3102	2053	43	2721	52	31	1526	58	30	1588	40
		4 dr sw		6	2	6	2						
118	80	Mazda 626	3066	1435	101	2206	54	38	1688	47	38	1817	40
		2 dr		4	6	6	2						
463	82	Renault Fuego	2902	3768	50	2484	35	37	1476	43	39	1230	37
		2 dr		6	2	6	1						

Table 13. Dummy response data and belt performance parameters for the intermediate vehicle weight class

NHTSA Data Base Test No.	MY	Vehicle Make/Body/Style	Weight Lbs	Driver HIC Level	Driver Chest G Level	Passenger HIC Level	Passenger Chest G Level	Belt System Parameters Onset T Msec	Driver Force Lbs	Driver Loading Lbs/Msec	Passenger Onset T Msec	Passenger Force Lbs	Passenger Loading Lbs/Msec
688	84	Chevrolet Celebrity	3590	518	31	440	28	36	1148	33	33	1337	33
		4 dr sw		1	1	1	1						
807	85	Volvo DL	3590	621	33	262	31	30	1440	37	27	1748	39
		4 dr sw		2	1	1	1						
199	79	Oldsmobile Cutlass S	3799	695	42	501	40	44	1451	39	37	2108	28
		2 dr		2	2	1	2						
613	84	Chevrolet Corvette	3680	784	40	525	32	45	1757	49	44	1802	45
		2 dr		2	2	2	1						
573	83	Volvo 760 GLE	3560	791	45	778	41	31	1668	55	25	2088	48
		4 dr		2	2	2	2						
624	84	Oldsmobile Cutlass	3700	781	40	1074	35	37	1436	33	32	2103	29
		2 dr		2	2	3	1						
471	82	Ford Granada	3430	860		1050	52	37	1370	37	34	1817	39
		4 dr		2		3	2						
612	84	Mercury Cougar	3560	652	55	577	37	34	1732	24	30	1912	35
		2 dr		2	3	2	1						
580	83	Ford Bronco 4X	3845	789	49	1038	50	29	1547	62	30	1768	65
		mpv		2	2	3	2						
588	83	Peugeot 505S	3617	819	52	1157	49	47	1110	44	37	1797	46
		4 dr		2	2	3	2						
720	84	Toyota Van Wagon	3616	984	50	748	54	22	1999	65			
		4 dr		3	2	2	2						
25	79	Oldsmobile Cutlass S	3816	997	58	799	37	37	1478	36	34	1664	32
		2 dr		3	3	2	1						
644	84	Ford LTD	3680	646	58	647	67	48	1668	44	41	1951	38
		4 dr sw		2	3	2	3						
703	84	Dodge Caravan	3791	973	44	1200	42	32	1610	54	29	1817	52
		3 dr		3	2	3	2						
271	80	Ford T-Bird II	3783	988	50	994	52	24	1776	47	23	1524	40
		2 dr		3	2	3	2						
739	84	Ford Mustang	3569	894	55	1112	38	42	3608	78	42	1662	65
		2 dr		2	3	3	2						
738	84	Buick Park Aven	3850	1550	50	662	37	50	1858	39	48	1736	37
		4 dr		4	2	2	1						
707	84	AMC Jeep Cher	3645	850	44	1548	43	29	1768	51	28	1631	47
		mpv		2	2	4	2						
606	83	Ford T-Bird	3580	626	70	795	43	43	1716	27	36	1958	22
		2 dr		2	4	2	2						
202	79	Pontiac Firebird	3909	965	42	1297	47	57	1511	40	59	1623	53
		2 dr		3	2	4	2						
600	83	Ford LTD	3563	609	69	957	54	39	1362	38	41	1674	40
		4 dr		2	4	3	2						
809	85	Datsun Maxima	3760	1014	63	1500	38	36	1561	49	33	1706	57
		4 dr sw		3	3	4	2						
801	85	Chevrolet Blazer	3900	1036	62	1321	43	27	2695	60	27	2262	53
		mpv		3	3	4	2						
136	80	Oldsmobile Cutlass	3815	1334	62	1125	47	50	2169	33	53	1259	43
		4 dr		4	3	3	2						
77	79	AMC Concord	3681	1078	61	1457	69	33	1841	49	27	2384	39
		2 dr		3	3	4	4						
137	80	Mercedes 240D	3714	1262	54	1369	44	38	1914	62	40	2107	77
		4 dr		4	2	4	2						
63	79	Plymouth Volare	3820	724	40	1677	40	31	1276	50	27	1765	35
		2 dr		2	2	5	2						
427	80	Chrysler LeBaron	3880	1742	54	1252	45	40	1735	47	39	2137	48
		2 dr		5	2	3	2						
583	83	Mitsubishi Montero 4	3873	1641	54	1415	48	36	1725	62	35	1802	67
		mpv		5	2	4	2						

Table 14. Dummy response data and belt performance parameters for the large vehicle weight class

NHTSA Data Base Test No.	MY	Vehicle Make/Body Style	Weight Lbs	Driver HIC Level	Driver Chest G Level	Passenger HIC Level	Passenger Chest G Level	Belt System Parameters Driver Onset T Msec	Driver Force Lbs	Driver Loading Lbs/Msec	Passenger Onset T Msec	Passenger Force Lbs	Passenger Loading Lbs/Msec
696	84	Chevrolet C-10	4830	534	37	514	39	30	1122	40	28	1299	31
		pu		2	1	1	2						
425	80	Cadillac Seville	4615	623	43	523	35	43	1958	48	47	2833	61
		4 dr		2	2	2	1						
528	82	Lincoln Continental	4158	757	46	728	37	40	1601	40	38	1706	40
		4 dr		2	2	2	1						
52	79	Buick Riviera	4440	541	42	782	39	49	1536	46			
		2 dr		2	2	2	2						
71	79	Dodge Magnum	4440	646	39	731	44						
		2 dr		2	2	2	2						
466	82	Chevrolet Impala	4110	1170	40		41						
		4 dr		3	2		2						
625	84	Pontiac Parisienne	4140		52	1055	48						
		4 dr			2	3	2						
335	81	Chrysler Imperial	4562	976	47	590	32	45	2751	35	40	1836	31
		2 dr		3	2	2	1						
204	79	Lincoln Continental	5362	521	45	919	53	48	1420	30	48	1492	28
		4 dr		2	2	3	2						
468	82	Ford LTD	4130	960	50	808	43	39	1182	30	35	1746	41
		4 dr		3	2	2	2						
515	83	Chevrolet Caprice	4120	882	42	1084	47	34	1421	42	34	2030	40
		4 dr		2	2	3	2						
721	84	Mercedes 300SD	4270	890	63	734	44						
		4 dr		2	3	2	2						
51	79	Mercury Marquis	4224	1204	61	868	42	44	1512	38	46	1745	38
		2 dr		3	3	2	2						
203	79	Ford LTD II	4815	1088	61	781	40	68	1917	50	44	1696	24
		2 dr		3	3	2	2						
220	80	Dodge Mirada	4136	948	43	959	37	34	1405	31	36	1392	33
		2 dr		3	2	3	1						
706	84	Mercury Marquis	4313	1094	58	1019	39	42	1193	28	43	1487	25
		4 dr		3	3	3	2						
65	79	Ford LTD	4366	1452	38	616	34	39	722	74	35	1529	37
		2 dr		4	2	2	1						
423	79	Chevrolet Impala	4179	1277	62	1254	51	68	1865	39			
		4 dr		4	3	3	2						
697	84	Ford F-150	4076	1362	48	1443	51	29	1564	32	28	1634	36
		2 dr		4	2	4	2						
66	79	Ford Granada	3950	1442	61	1279	56	37	1927	30	39	2006	27
		4 dr		4	3	4	3						
183	79	Oldsmobile 98	4709	910	59	1734	54	45	1435	38	51	1586	49
		4 dr		3	3	5	2						
182	79	Dodge St Regis	4457	1909	67		50						
		4 dr		6	3		2						
67	79	Chrysler LeBaron	4160	2402	45	1071	39	33	1469	41	29	1930	36
		2 dr		6	2	3	2						
800	85	GMC Astro	4090	2202	70	1597	61	35	2212	56	37	2736	59
		van		6	4	5	3						

Table 15. Average and median values of HIC and chest GS for four NCAP vehicle weight classes

Weight Class	Driver				Passenger			
	Average HIC	Median HIC	Average Chest GS	Median Chest GS	Average HIC	Median HIC	Average Chest GS	Median Chest GS
Small	1102	962	55	52	1185	1028	47	44
Compact	1152	867	49	47	1060	915	44	43
Intermediate	1059	860	51	51	1044	1050	44	43
Large	1121	976	51	47	959	894	44	42

Other design features contributing to high driver and passenger dummy measurements include excessive retractor spoolout, excessive belt stretch, and improper belt anchorage locations.

With continued emphasis on MUL's and with several States (and many foreign countries) having enacted such laws, it becomes increasingly important that the safety belt systems be designed to provide optimum protection for the vehicle occupants. The primary functions of the belt systems in providing this protection are to prevent or minimize occupant contact with interior surfaces and to maintain the occupant in the vehicle during a crash event. The belt system parameters in the crash involvement that are measures of these functions include the time-to-onset load on the occupant and the rate of belt loading. From the collected NCAP electronic data, these two parameters can be examined for the torso belts of the drivers and right front seat occupants. These parameters and the peak belt loads are given along with the occupant response in Tables 11 through 14 for the four selected weight classes. In these tables, the onset time is the time at which the torso belt load reaches 200 lb. The rate is the increase in load for each millisecond from 200 lb to nominally 1,000 lb. A typical illustration of these parameters is shown in Figure 6.

The average of the combined driver and passenger onset times and loading rates are given in Table 16 for the four weight classes. The ranges (minimum and maximum) of the values are also given. There appears to be a trend toward later onset times and lower load rates with increasing weight. The average values for the low- and high-risk groups are also given in this table. For all weight groups except the large, the onset times for the low-risk groups are slightly less than those of the high-risk groups.

The elements of the belt system that affect these two parameters include belt slack, belt length (the amount of belt contained on the retractor spool), how tightly the belt is wound on the spool, D-ring location (angle of belt relative to occupant torso), belt material (belt stretch), and belt web-locking mechanisms. In Table 17, the vehicles are listed that are known to have added belt web-locking mechanisms since the beginning of the NCAP (no locking mechanisms were known to have been installed in vehicles prior to the NCAP.) The web-locking

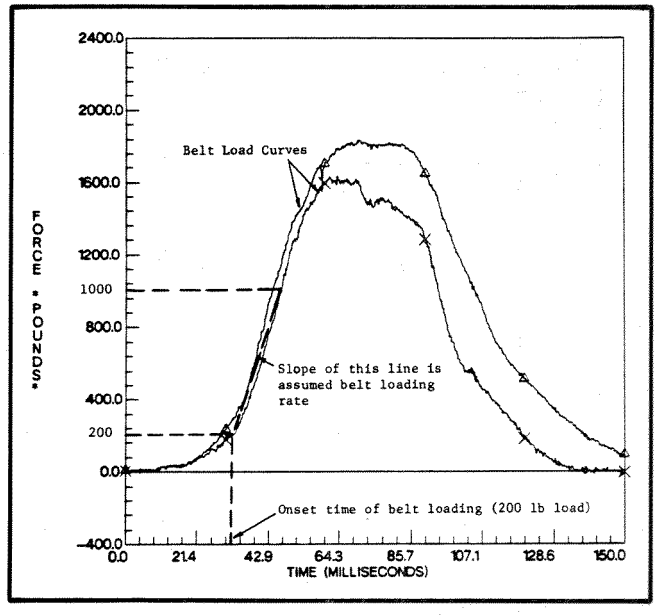

Figure 6. Illustration of belt system parameters

mechanisms should decrease the amount of spoolout and lead to an earlier belt load onset time. Comparisons of vehicle test results before and after the addition of web-locking mechanisms are given in Table 18. (Note: It is possible and probable that other design changes occurred to vehicles that may also affect the belt system and vehicle safety performance.) In this table, the belt load onset times, load rates, and peak forces for the drivers and passengers are given. Where the data are available, the addition of the web-locking mechanisms shows a decrease on the average of 20 to 30 percent in the onset time. The HIC's and chest g's are also compared in this table. Substantial decreases are noted in the driver and passenger responses. The effects of the web-locking mechanism decrease the potential for severe occupant contacts to interior vehicle compartment surfaces. All vehicles tested with web-locking mechanisms are in the low-risk group.

Steering Assembly Effects

The contact of the unrestrained driver with the steering assembly is a major contributor to injury(8). In high-

Table 16. Onset times and load rates of belt systems

		Weight Class			
		Small	Comp	Int	Large
Onset Time Msec	Average	33	35	36	40
	Minimum	20	21	17	28
	Maximum	47	50	59	68
	Avg (LR)	31	34	35	42
	Avg (HR)	35	35	38	39
Load Rate Lbs/Msec	Average	47	41	45	38
	Minimum	22	19	22	21
	Maximum	73	73	78	74
	Avg (LR)	48	41	44	37
	Avg (HR)	47	41	47	43

LR = Low risk group (HIC < 1255 and chest GS < 69)
HR = High risk group (HIC > 1254 and/or chest GS > 68)

Table 17. List of vehicles known to have belt web-locking mechanisms

Model Yrs	Vehicle
82,83,84,85	Honda Accord 4 dr
82,83,84,85	Honda Prelude
84,85	Honda Civic 2 dr
84,85	Honda Civic 4 dr
84,85	Honda Civic sw
84,85	Honda Civic CRX
84,85	Mazda 626 4 dr
85	Dodge Colt 2 dr
85	Dodge Colt 4 dr
85	Mitsubishi Sigma
85	Mitsubishi Starian
85	Mitsubishi Cordia
85	Mitsubishi Montero
85	Mitsubishi Forte

speed crash events, this will also be true of the restrained driver unless significant improvements are made to steering assembly performance. The NCAP data show significant contact will occur between the driver and the steering assembly. More than 29 percent (44 of 151) of the driver dummies in the NCAP tests had HIC measures that placed the vehicle performance in the high-risk group. In the small vehicle class, 18 of 56 (31 percent) were in the high-risk group, for the compacts 13 of 42 (32 percent), for the intermediates 6 of 30 (20 percent), and for the large vehicles 7 of 23 (30 percent).

The severity of these steering assembly impacts is dependent on several vehicle performance parameters including—

- The intrusion of the steering assembly into the occupant compartment
- The area of the head contact on the steering assembly and the force-deflection characteristics of the contact surface

Table 18. Test results of vehicles with and without web-locking mechanisms

		Driver		Passenger			Belt System Parameters				
							Driver			Passenger	
MY	Vehicle Make/Body/Year	HIC Level	Chest G Level	HIC Level	Chest G Level	Onset T Msec	Force Lbs	Loading Lbs/Msec	Onset T Msec	Force Lbs	Loading Lbs/Msec
82	Dodge Colt	932	72	1730	44	42	1085	38	42	1433	41
	4 dr hb	3	4	5	2						
*85	Dodge Colt	787	42	741	32	31	1492	49	34	1647	60
	4 dr hb	2	2	2	1						
80	Honda Prelude	2904	52	1759	45	42	1541	47	38	1669	39
	2 dr hb	6	2	5	2						
*84	Honda Prelude	659	43	475	31	29	1223	47	25	1336	42
	2 dr	2	2	1	1						
81	Honda Civic	985	53	1391	43	32	1595	52	32	1993	54
	4 dr hb	3	2	4	2						
*84	Honda Civic	586	43	544	32	25	1239	58	20	2110	67
	4 dr sw	2	2	2	1						

*With web-locking mechanisms

- The amount that the belt system reduces the velocity of the occupant before contact occurs
- Effects of the structural performance that also may lead to differences in head contact velocities

The data used in this study are restricted to the electronic information available in the NHTSA Crash Test Data Base. These data do not contain steering assembly intrusion information or force-deflection characteristics of the impacted surfaces. Film analyses and component tests are planned to collect these important data. Until these data are available, a definitive assessment of the steering assembly performance cannot be completed. Therefore, in the following paragraphs, the review does not differentiate between the attributes of the steering assemblies, belt systems, and structural performance. However, other sections of this paper do present belt system and structural attributes on the vehicles that can be examined in conjunction with these steering assembly impact data.

In addition to the HIC values, a measure of the significance of the head-to-steering-assembly impact that can be examined from the electronic data of the NCAP is the change in velocity of the head during interaction with the steering wheel rim and/or hub. This change in velocity can be determined approximately by calculating the difference between the head acceleration resultants of the driver and front seat-passenger (see Figure 7). In this approach, it is assumed that the kinematics of the front-seat passenger are the same as those of the driver until the driver head contacts the steering assembly. It is also assumed that insignificant passenger head contacts occur during the time that the driver head is in contact with the steering assembly. The change in driver head velocity for each vehicle, as calculated by this method, is given in Tables 19 through 22. If the dummy head response data do not meet the above assumptions, the velocity change parameters are omitted from the tables. For comparison, the driver HIC's and chest g's are again shown in these tables. Also in the tables, the approximate time of contact, TS, and the assumed times of disengagement of head to steering assembly, TF, are given. Estimated average g levels of the head during contact with the steering assembly are calculated from these parameters and are given as DR HD GS.

In Table 23, the average values for these steering assembly parameters are given for the total fleet and for the low- and high-risk groups. For the total fleet, these data show a decreasing trend in the change in velocity of the head and in the magnitude of the g's with increasing vehicle weight. A 15 percent lower change in velocity and a 24 percent lower DR HD GS are seen for the large vehicle weight class as compared to the small vehicle class.

In comparing the low-risk group to the high-risk group, the expected results are found. An increase of almost 50 percent in the velocity parameter and a doubling in the value of the G parameter between the low- and high-risk groups are observed.

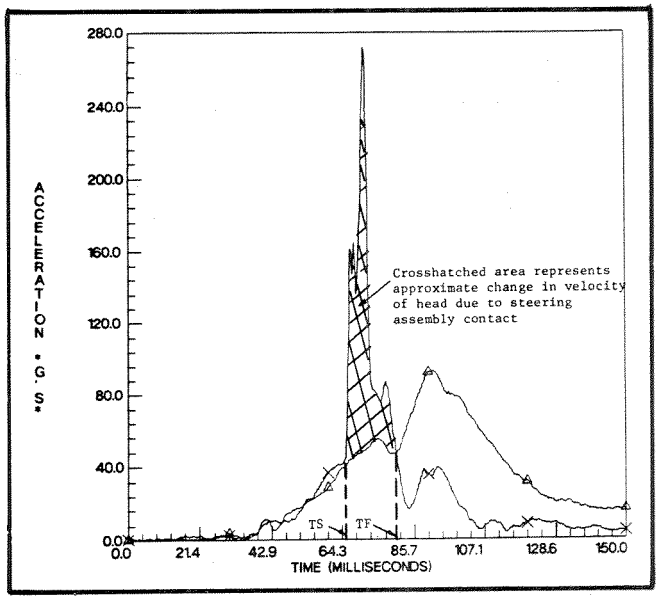

Figure 7. Overlayed resultant acceleration curves of driver passenger heads—showing parameters of steering assembly contact

Additional information of interest and possible importance is the location of the dummy driver in relation to the steering assembly. From Figure 8, the distances from the driver to the vehicle interior are defined. Values for these distances are given in Tables 19 through 22. The average values of these measurements are given in Table 24. It is interesting to note the very slight differences of the average values for the small vehicle weight class as compared to the large vehicle weight class.

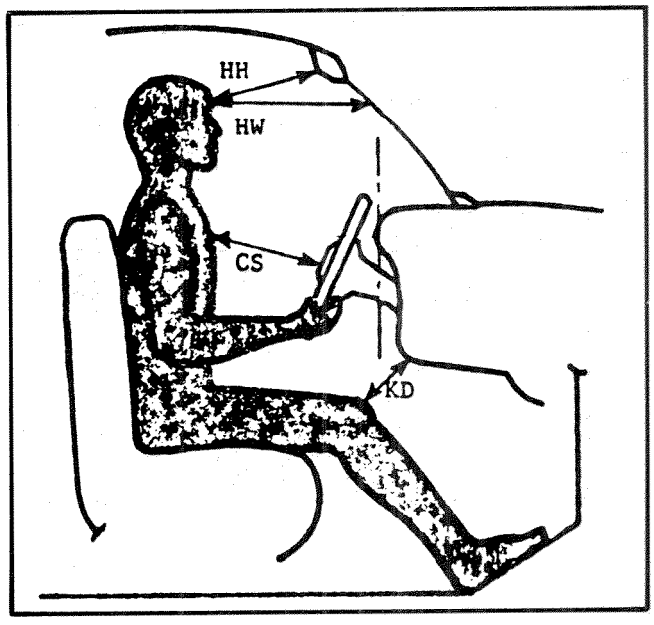

Figure 8. Driver location relative to vehicle interior

Table 19. Steering assembly parameters for the small vehicle weight class

MY	Vehicle Make/Body Style	Driver HIC Level	Driver Chest G Level	Steering ASM Parameters Delta Vel Miles/Hr	TS Msec	TF Msec	DR HD GS	Driver Location and Area of Head Contact Head Contact	Head to Header Inches	Head to Windshield Inches	Chest to Wheel Inches	Knee to Dash Inches
79	Toyota Corolla 2 dr											
81	Ford EXP 2 dr hb	745 2	49 2									
84	Renault Alliance 4 dr	940 3	55 3									
84	Toyota Corolla 2 dr	432 1	37 1					Steering wheel hub	11.20	17.50	14.60	5.00
82	Honda Accord 4 dr	500 1	43 2	3.90	75.00	92.00	10.45	Steering wheel	22.00	17.00	16.20	4.70
84	Honda Civic CRX 2 dr	571 2	34 1	7.34	64.00	94.00	11.14	Steering wheel rim	16.00	21.50	16.50	7.40
84	Honda Civic 2 dr hb	563 2	37 1	7.65	65.50	86.70	16.44	Steering wheel	17.60	24.40	18.20	6.00
79	Plymouth Horizon 2 dr hb	653 2	52 2	8.30	67.00	89.00	17.18	Steering wheel		13.90		7.00
79	Chevrolet Chevette 4 dr hb	871 2	47 2	10.26	94.00	101.00	66.75	Steering wheel	9.70	13.10	13.70	5.20
80	Fiat Strada 4 dr hb	790 2	41 2					Steering wheel	16.30	19.80	16.60	4.30
81	Ford Escort 2 dr hb	618 2	50 2	10.35	67.00	84.00	27.73	Steering wheel	11.20	16.20	13.70	3.40
81	Honda Civic 2 dr hb	607 2	41 2	7.21	70.00	97.00	12.17	Steering wheel	13.50	18.00	15.50	8.70
80	Chevrolet Chevette 2 dr hb	668 2	45 2					Steering wheel	10.60	14.90	12.90	4.70
82	Datsun Sentra 4 dr	549 2	43 2	6.91	67.00	87.00	15.74	Steering wheel	16.00	24.00	14.70	6.60
82	Chevrolet Cavalier 2 dr hb	708 2	42 2	9.24	60.00	86.40	15.94	Steering wheel rim	12.00	15.70	12.60	3.50
83	Toyota Tercel 4X 4 dr sw	839 2	43 2	19.65	64.00	98.00	26.33	Steering wheel	11.60	17.50	12.50	6.20
84	Toyota Corolla 4 dr	630 2	41 2					Steering wheel	7.50	16.40	15.20	8.00
84	Honda Civic 4 dr sw	586 2	43 2	5.24	63.50	78.00	16.46	Steering wheel	16.40	21.10	15.80	7.30
84	Honda Prelude 2 dr	659 2	43 2	14.13	68.00	88.00	32.19	Steering wheel	15.20	22.00	16.50	7.00
84	Toyota Tercel 4 dr hb	658 2	43 2	25.19	71.00	107.00	31.88	Steering wheel rim	11.50	17.20	15.50	7.20
85	Dodge Colt 4 dr hb	787 2	42 2	9.60	64.00	98.00	12.87	Steering wheel rim	14.20	20.20	15.70	7.20
85	Volkswagen Jetta 2 dr	898 2	50 2	34.06	68.00	95.00	57.47	Steering wheel	15.80	20.80	13.70	5.40
80	Toyota Tercel 2 dr	1218 3	48 2	21.49	62.00	81.00	51.54	Steering wheel				
81	Honda Civic 4 dr hb	985 3	53 2	15.71	58.00	82.00	29.83	Steering wheel	14.50	18.50	14.50	9.00
81	Renault 181 4 dr	1150 3	47 2	21.55	76.50	97.00	47.88	Steering wheel	13.50	18.00	16.20	10.50
82	Dodge Omni 4 dr hb	639 2	58 3	13.21	60.00	84.00	25.07	Steering wheel	12.50	18.50	17.20	7.50
82	Ford Escort 4 dr hb	950 3	47 2	19.92	62.00	82.50	44.27	Steering wheel	15.00	21.10	14.60	6.60
82	Chevrolet Chevette 4 dr hb	1020 3	48 2	8.15	96.00	105.00	41.26	Steering wheel	11.10	15.30	13.60	6.20
83	Toyota Corolla 4 dr sw	767 2	67 3	8.05	67.50	84.00	22.22	Steering wheel rim	13.70	17.50	14.50	3.90
83	Datsun Pulsar 4 dr hb	1139 3	54 2	16.20	67.00	86.17	38.50	Steering wheel	13.20	21.00	16.20	6.40
85	Mazda RX 2 dr	921 3	40 2	8.19	68.50	95.00	14.08	Steering wheel	12.30	16.30	15.30	7.00

Table 19, continued

MY	Vehicle Make/Body Style	Driver HIC Level	Driver Chest G Level	Steering ASM Parameters Delta Vel Miles/Hr	Steering ASM Parameters TS Msec	Steering ASM Parameters TF Msec	Steering ASM Parameters DR HD GS	Driver Location and Area of Head Contact: Head Contact	Head to Header Inches	Head to Windshield Inches	Chest to Wheel Inches	Knee to Dash Inches
79	Volkswagen Rabbit	1024	67	14.92	76.00	95.00	35.78	Steering wheel	19.00	23.50	15.00	3.80
	2 dr hb	3	3									
80	Datsun 310 GX	1059	68					Steering wheel	12.60	17.80	12.80	3.10
	2 dr hb	3	3									
81	Volkswagen Jetta	1210	68	12.91	72.00	96.13	24.37	Steering wheel	19.60	26.20	14.90	5.70
	4 dr	3	3									
82	Datsun Stanza	974	55	15.13	70.00	89.00	36.28	Steering wheel	15.10	21.50	13.00	4.60
	4 dr hb	3	3									
84	Renault Encore	912	63	9.25	69.00	82.00	32.41	Steering wheel	13.00	18.50	15.20	8.00
	4 dr hb	3	3									
80	Toyota Corolla	838	69									
	2 dr	2	4									
80	Volkswagen Rabbit CO	1328	48	12.26	76.00	88.00	46.54	Steering wheel	19.20	24.60	14.30	3.60
	2 dr	4	2									
82	Volkswagen Scirocco	1482	54	19.76	74.00	88.00	64.31	Steering wheel	14.00	19.50	15.70	7.60
	2 dr	4	2									
85	Chevrolet Spectrum	1559	51	20.69	64.00	84.00	47.12	Steering wheel	14.60	17.30	14.70	5.50
	2 dr hb	4	2									
80	Subaru GLF	1067	72					Steering wheel	16.80	22.30	13.00	4.30
	4 dr	3	4									
82	Dodge Colt	932	72	14.76	59.00	84.50	26.37	Steering wheel	11.60	15.70	12.80	7.40
	4 dr hb	3	4									
84	Datsun Stanza	1459	58	10.88	68.50	89.00	24.18	Steering wheel	17.50	23.00	16.00	5.90
	4 dr	4	3									
85	Subaru DL	1361	57	28.56	67.00	82.00	86.76	Steering wheel	13.00	17.00	14.30	4.00
	4 dr	4	3									
85	Renault Alliance	1519	62	24.89	62.00	88.00	43.61	Steering wheel hub	15.50	20.50	17.30	7.00
	2 dr conv	4	3									
79	Plymounth Champ	1270	72	16.08	64.00	85.00	34.89	Steering wheel	12.30	17.20	11.30	9.00
	2 dr hb	4	4									
79	Datsun 210	1358	69					Steering wheel		19.00		7.00
	2 dr	4	4									
80	Audi 4000	1322	70	20.77	63.00	87.00	39.43	Steering wheel		19.40	12.40	4.90
	4 dr	4	4									
83	Ford EXP	1744	46	17.44	72.00	86.00	56.76	Steering wheel	12.60	18.50	13.60	6.40
	2 dr	5	2									
81	Toyota Starlet	1836	65	19.30	70.00	83.50	65.12	Steering wheel	18.20	22.20	15.70	6.00
	2 dr hb	5	3									
79	Ford Fiesta	1656	70	19.42	19.00	43.60	35.96	Steering wheel	15.40	19.00	15.00	5.80
	2 dr	5	4									
84	Mitsubishhi Tredia	1314	87					Steering wheel rim	13.80	20.20	15.00	6.10
	4 dr	4	5									
79	Honda Civic	2030	93	17.88	60.00	80.00	40.74	Steering wheel	17.00	20.50	15.70	7.00
	2 dr	6	6									
80	Honda Prelude	2904	52	21.69	70.00	90.60	47.97	Steering wheel	19.00	25.50	18.50	5.50
	2 dr hb	6	2									
80	Honda Civic	2626	54	23.72	64.00	81.60	61.40	Steering wheel	17.10	22.60	16.00	6.00
	2 dr hb	6	2									
80	Renault Le Car	1938	85	22.87	56.00	75.80	52.62	Steering wheel	14.60	18.00	15.20	1.50
	2 dr hb	6	5									
84	Pontiac 1000	1886	42	19.86	79.50	86.00	139.17	Steering wheel	12.20	15.00	12.40	7.50
	4 dr hb	6	2									

Table 20. Steering assembly parameters for the compact vehicle weight class

MY	Vehicle Make/Body Style	Driver HIC Level	Driver Chest G Level	Steering ASM Parameters Delta Vel Miles/Hr	TS Msec	TF Msec	DR HD GS	Driver Location and Area of Head Contact: Head Contact	Head to Header Inches	Head to Windshield Inches	Chest to Wheel Inches	Knee to Dash Inches
79	Mercury Capri 2 dr hb											
81	Audi 5000 4 dr		43 2									
85	Mitsubishi Galant 4 dr		52 2									
82	Chevrolet Celebrity 4 dr	478 1	33 1					Steering wheel rim	12.80	19.00	13.50	6.70
83	Pontiac Firebird 2 dr	406 1	34 1	8.81	80.00	104.00	16.72	Steering wheel	10.00	14.70	12.70	5.60
84	Pontiac Fiero 2 dr	309 1	31 1					Steering wheel rim	11.50	18.60	13.70	6.00
82	Toyota Celica 2 dr	702 2	36 1	10.65	76.50	103.00	18.31	Steering wheel	17.59	23.60	14.10	5.60
84	AMC Jeep CJ-7 mpv	460 1	46 2	12.55	74.00	96.82	25.06	Steering wheel rim	20.50	23.20	15.00	8.00
84	Dodge Daytona 2 dr hb	507 1	47 2	8.89	84.00	97.27	30.53	Steering wheel rim	12.90	17.50	15.20	6.00
85	Volvo DL 4 dr	652 2	36 1	13.23	60.00	90.00	20.09	Steering wheel	16.70	22.20	13.50	5.90
80	Chevrolet Citation 4 dr hb	845 2	48 2	10.40	70.00	96.00	18.22	Steering wheel	14.00	18.90	15.40	7.50
81	Plymouth Reliant 2 dr	605 2	52 2	13.26	64.50	88.00	25.72	Steering wheel	13.00	17.00	15.50	4.90
79	Ford Mustang 2 dr	819 2	41 2	8.61	85.00	116.00	12.66	Steering wheel		22.00	0.00	5.00
81	AMC Spirit 2 dr	702 2	43 2	11.01	62.50	83.00	24.46	Steering wheel	13.30	18.00	15.00	11.00
82	Volvo DL 2 dr	550 2	45 2	12.12	76.00	96.00	25.09	Steering wheel				
82	Saab 900 4 dr	734 2	39 2					Steering wheel	19.50	23.50	14.50	3.60
82	Chevrolet Camaro 2 dr	563 2	39 2	10.25	83.00	97.63	31.92	Steering wheel	15.50	23.00	15.00	6.00
82	Dodge 400 2 dr	520 2	44 2					Steering wheel rim	15.50	19.20	15.00	7.00
83	Plymouth Reliant 4 dr sw	656 2	52 2	12.03	71.50	94.00	24.36	Steering wheel rim	14.50	20.40	15.50	6.70
83	Toyota Camry 4 dr	809 2	48 2	25.29	64.00	102.00	30.32	Steering wheel	12.70	18.50	13.80	5.10
84	Chevrolet Cav-Conv 2 dr	884 2	43 2	22.07	71.50	102.52	32.42	Steering wheel	9.10	15.50	15.20	5.00
84	Nissan 300 ZX 2 dr	789 2	45 2					Steering wheel rim	14.50	21.30	15.00	5.00
85	Plymouth Caravelle 4 dr	685 2	51 2	14.15	65.00	100.50	18.15	Steering wheel	14.20	19.50	14.50	6.50
85	Plymouth Reliant 4 dr	832 2	54 2	21.76	58.00	92.00	29.15	Steering wheel	12.20	16.40	13.50	5.20
85	Buick Somerset 2 dr	1140 3	34 1	15.00	79.00	101.00	31.06	Steering wheel hub	12.00	17.50	15.00	5.70
79	Toyota Celica 2 dr hb	849 2	61 3					Steering wheel	11.00	16.50	15.40	5.30
79	Chevrolet Monza 2 dr	1106 3	42 2					Dashpanel	11.00	16.50	16.10	5.50
79	Ford Fairmont 4 dr	939 3	54 2					Steering wheel	13.00	18.50	16.30	6.20

Table 20. continued

MY	Vehicle Make/Body Style	Driver HIC Level	Driver Chest G Level	Delta Vel Miles/Hr	Steering ASM Parameters TS Msec	Steering ASM Parameters TF Msec	Steering ASM Parameters DR HD GS	Driver Location and Area of Head Contact: Head Contact	Head to Header Inches	Head to Windshield Inches	Chest to Wheel Inches	Knee to Dash Inches
79	Mercury Bobcat	723	64	19.22	87.00	103.00	54.74	Steering wheel		21.50	7.10	
	2 dr hb	2	3									
82	Mazda 626	969	47	6.84	63.00	83.00	15.58	Steering wheel	13.50	18.50	14.50	6.50
	4 dr	3	2									
82	Toyota Corona	842	59	8.86	71.00	90.00	21.25	Steering wheel rim	12.50	17.00	12.00	5.70
	4 dr	2	3									
83	Dodge 600	947	46	18.58	75.00	100.57	33.10	Steering wheel	13.50	19.00	15.50	7.10
	4 dr	3	2									
83	Mazda 626	1196	45	17.77	68.00	87.52	41.48	Steering wheel	12.70	17.70	13.50	5.00
	4 dr	3	2									
80	Datsun 200 SX	1091	62					Steering wheel		22.00	16.50	6.30
	2 dr hb	3	3									
84	Plymouth Conquest	1118	57	17.97	72.00	99.00	30.32	Steering wheel rim	13.20	19.00	16.00	5.70
	2 dr hb	3	3									
82	Volkswagen Quantum	1353	53	13.96	74.00	90.00	39.81	Steering wheel	17.20	25.00	17.50	5.70
	4 dr	4	2									
83	Mitsubishi Mighty MA	1475	68	11.14	64.50	83.63	26.54	Steering wheel	16.90	21.50	15.30	5.30
	pu	4	3									
84	Plymouth Colt Vist	1530	71	23.52	65.50	82.87	61.68	Steering wheel hub	13.50	20.00	14.20	6.70
	4 dr sw	4	4									
79	Volvo 244 DL	1782	52					Steering wheel	17.90	22.80	15.10	5.30
	4 dr	5	2									
84	Isuzu Impulse	1769	46	17.87	78.00	88.00	81.42	Steering wheel	15.50	22.50	16.00	6.70
	2 dr hb	5	2									
80	Mazda 626	1435	101	14.71	55.00	81.00	25.77	Steering wheel	12.00	17.00	12.00	3.00
	2 dr	4	6									
81	Toyota Cressida	1980	55	17.18	68.00	98.00	26.09	Steering wheel	14.50	18.00	14.00	2.50
	4 dr	6	3									
82	Renault Fuego	3768	50	21.11	78.00	95.25	55.76	Steering wheel	8.70	22.00	16.50	4.70
	2 dr	6	2									
82	Chrysler LB Conv	2644	39	17.39	75.00	88.00	60.95	Steering wheel hub	13.30	18.40	15.50	8.00
	2 dr	6	2									
84	Ford Tempo	2955	63	29.82	65.50	79.95	94.01	Steering wheel	9.20	16.70	13.50	3.50
	4 dr	6	3									
84	Renault Sportwagon	2053	43	15.05	71.50	85.00	50.79	Steering wheel	18.40	22.10	17.20	4.20
	4 dr sw	6	2									
84	Nissan 200 SX	1992	44	17.55	76.50	88.50	66.63	Steering wheel	15.30	23.20	16.60	10.00
	2 dr	6	2									
85	Dodge Lancer	2187	38	21.40	66.00	88.00	44.31	Steering wheel hub	13.70	20.20	13.20	3.30
	4 dr hb	6	2									

Table 21. Steering assembly parameters for the intermediate vehicle weight class

MY	Vehicle Make/Body Style	Driver HIC Level	Driver Chest G Level	Steering ASM Parameters Delta Vel Miles/Hr	TS Msec	TF Msec	DR HD GS	Driver Location and Area of Head Contact Head Contact	Head to Header Inches	Head to Windshield Inches	Chest to Wheel Inches	Knee to Dash Inches
84	Chevrolet Celebrity 4 dr sw	518 1	31 1	9.52	81.00	114.00	13.14	Steering wheel	13.70	20.50	15.50	5.60
82	Ford Granada 4 dr	860 2						Steering wheel rim	12.40	18.70	13.70	6.50
85	Volvo DL 4 dr sw	621 2	33 1	16.72	67.00	110.00	17.72	Steering wheel	17.00	22.50	13.50	4.60
79	Plymouth Volare 2 dr	724 2	40 2	9.20	49.00	76.00	15.53	Steering wheel	11.60	15.20	13.20	7.50
79	Oldsmobile Cutlass S 2 dr	695 2	42 2	13.31	82.00	117.00	17.33	Steering wheel	13.00	19.00	13.50	8.20
83	Volvo 760 GLE 4 dr	791 2	45 2	6.41	69.00	82.00	22.46	Steering wheel	14.20	21.20	12.20	5.00
83	Ford Bronco 4X mpv	789 2	49 2	7.90	59.00	77.00	20.00	Steering wheel	12.80	17.40	10.00	5.00
83	Peugeot 505S 4 dr	819 2	52 2					Steering wheel rim	8.00	12.20	9.50	6.50
84	Chevrolet Corvette 2 dr	784 2	40 2	14.93	83.00	114.00	21.94	Steering wheel	11.00	18.00	14.00	5.50
84	Oldsmobile Cutlass 2 dr	781 2	40 2	17.59	81.00	114.37	24.02	Steering wheel	12.00	19.00	13.00	8.30
84	AMC Jeep Cher mpv	850 2	44 2	16.41	65.00	79.25	52.46	Steering wheel	18.50	23.40	13.40	5.60
79	Pontiac Firebird 2 dr	965 3	42 2					Steering wheel		22.00		8.50
80	Ford T-Bird II 2 dr	988 3	50 2	6.30	63.50	86.50	12.48	Steering wheel	14.50	19.00	13.00	6.00
84	Mercury Cougar 2 dr	652 2	55 3	10.63	91.00	111.00	24.21	Steering wheel rim	10.00	16.80	13.00	5.00
84	Ford LTD 4 dr sw	646 2	58 3	5.92	90.50	106.50	16.85	Steering wheel rim	12.50	19.30	13.40	7.10
84	Dodge Caravan 3 dr	973 3	44 2	12.46	66.00	86.88	27.18	Steering wheel	19.90	24.80	14.40	4.90
84	Toyota Van Wagon 4 dr	964 3	50 2	12.29	62.00	75.00	43.08	Steering wheel hub	13.00	17.10	13.70	7.20
84	Ford Mustang 2 dr	894 2	55 3	10.51	76.00	97.00	22.80	Steering wheel rim	11.70	18.30	14.50	5.20
79	Oldsmonile Cutlass S 2 dr	997 3	58 3	15.53	85.00	124.00	18.14	Dashpanel	13.00	19.00	13.50	8.20
79	AMC Concord 2 dr	1078 3	61 3	7.92	66.00	85.00	18.98	Steering wheel	13.70	20.00	15.70	10.60
85	Chevrolet Blazer mpv	1036 3	62 3	12.95	60.00	90.00	19.67	Steering wheel	17.20	21.60	12.50	6.20
85	Datsun Maxima 4 dr sw	1014 3	63 3	10.40	65.00	86.00	22.56	Steering wheel	13.70	20.30	15.79	7.00
80	Mercedes 240D 4 dr	1262 4	54 2	14.93	72.00	95.00	29.58	Steering wheel	17.60	22.60	14.20	4.50
83	Ford LTD 4 dr	609 2	69 4	13.18	80.00	89.00	66.72	Steering wheel rim	8.90	14.20	10.40	6.90
83	Ford T-Bird 2 dr	626 2	70 4					Steering wheel	10.50	16.20	13.10	5.40
84	Buick Park Ave 4 dr	1550 4	50 2	12.71	84.00	102.00	32.16	Steering wheel hub	15.20	22.10	15.70	8.00
80	Oldsmobile Cutlass 4 dr	1334 4	62 3	19.01	88.00	101.00	66.61	Steering wheel		22.60	12.50	7.20
80	Chrysler LeBaron 2 dr	1742 5	54 2	12.48	80.00	93.13	43.29	Steering wheel	15.60	21.50	13.20	6.30
83	Mitsubishi Montero 4 mpv	1641 5	54 2	19.62	73.00	94.00	42.57	Steering wheel	20.00	21.10	15.60	2.90
79	Peugeot 504 4 dr	4513 6	63 3	33.79	43.00	59.40	93.86	Steering wheel	16.50	20.50	14.50	10.00

Table 22. Steering assembly parameters for the large vehicle weight class

MY	Vehicle Make/Body Style	Driver HIC Level	Driver Chest G Level	Steering ASM Parameters Delta Vel Miles/Hr	Steering ASM Parameters TS Msec	Steering ASM Parameters TF Msec	Steering ASM Parameters DR HD GS	Driver Location and Area of Head Contact Head Contact	Head to Header Inches	Head to Windshield Inches	Chest to Wheel Inches	Knee to Dash Inches
84	Pontiac Parisienne		52									
	4 dr		2									
84	Chevrolet C-10	534	37	5.25	65.00	72.00	34	Steering wheel	16.50	21.90	10.80	9.20
	pu	2	1									
79	Buick Riviera	541	42					Steering wheel		21.80		7.90
	2 dr	2	2									
79	Dodge Magnum	646	39	7.61	76.00	96.00	17	Steering wheel	13.20	17.50	15.00	7.70
	2 dr	2	2									
79	Lincoln Continental	521	45	11.16	82.00	104.00	23	Steering wheel		19.20		6.00
	4 dr	2	2									
80	Cadillac Seville	623	43	12.78	83.00	118.13	17	Steering wheel	15.10	23.30	13.30	5.10
	4 dr	2	2									
83	Chevrolet Caprice	882	42	7.92	87.00	108.00	17	Steering wheel	14.70	20.20	15.00	9.20
	4 dr	2	2									
82	Lincoln Continental	757	46	8.55	80.00	104.00	16	Steering wheel	15.50	19.00	13.80	4.90
	4dr	2	2									
80	Dodge Mirada	948	43	7.01	46.00	69.00	14	Steering wheel	14.00	19.00	13.00	8.00
	2 dr	3	2									
81	Chrysler Imperial	976	47	11.63	84.00	120.00	15	Steering wheel	14.00	20.00	12.80	7.30
	2 dr	3	2									
82	Ford LTD	960	50	12.94	75.00	95.00	29	Steering wheel	14.00	20.20	13.20	6.70
	4 dr	3	2									
84	Mercedes 300SD	890	63	15.17	50.00	87.00	19	None	16.50	24.70	14.20	4.50
	4 dr	2	3									
82	Chevrolet Impala	1170	40									
	4 dr	3	2									
79	Mercury Marquis	1204	61	19.28	88.50	107.00	47	Steering wheel		22.50		7.80
	2 dr	3	3									
79	Oldsmobile 98	910	50					Steering wheel		19.60		5.60
	4 dr	3	3									
79	Ford LTD II	1088	61					Dashpanel		18.00		4.40
	2 dr	3	3									
84	Mercury Marquis	1094	58	18.89	80.00	107.00	32	Steering wheel	14.00	20.90	11.40	7.80
	4 dr	3	3									
79	Ford LTD	1452	38	23.62	74.00	103.00	37	Steering wheel	14.50	19.50	13.50	7.70
	2 dr	4	2									
84	Ford F-150	1362	48	17.78	76.00	88.00	67	Steering wheel	18.20	23.80	12.60	9.40
	2 dr	4	2									
79	Ford Granada	1442	61	6.88	77.00	91.00	22	Dashpanel	15.30	20.20	17.00	6.70
	4 dr	4	3									
79	Chevrolet Impala	1277	62					Steering wheel		19.70	16.00	8.30
	4 dr	4	3									
79	Chrysler LeBaron	2402	45	22.35	73.00	90.00	60	Steering wheel	14.00	18.20	14.00	6.20
	2 dr	6	2									
79	Dodge St Regis	1909	67									
	4 dr	6	3									
85	GMC Astro	2202	70					Steering wheel	18.00	22.50	13.40	8.00
	van	6	4									

Table 23. Average values for steering assembly parameters

Group	Weight Class	Average Values Delta Vel Miles/Hr	TS Msec	TF Msec	DR HD GS
Total Fleet	Small	15.43	67.12	87.61	38.38
	Compact	14.29	72.50	93.29	34.31
	Intermediate	13.18	72.35	94.81	30.97
	Large	13.05	74.78	97.45	29.23
Low Risk Group	Small	12.99	69.02	90.71	29.08
	Compact	13.88	72.20	96.73	26.55
	Intermediate	11.42	71.63	96.39	22.66
	Large	11.52	74.71	98.93	23.39
High Risk Group	Small	19.46	64.00	82.51	53.70
	Compact	18.39	69.79	87.35	52.81
	Intermediate	17.96	74.29	90.50	53.54
	Large	17.66	75.00	93.00	46.72

Table 24. Average dimensions for driver location

Weight Class	Driver Location Head to Header Inches	Head to Windshield Inches	Chest to Wheel Inches	Knee to Dash Inches
Small	14.44	19.26	14.84	6.06
Compact	13.86	19.68	14.49	5.87
Intermediate	13.91	19.56	13.48	6.51
Large	15.17	20.59	13.69	7.07

In addition, Tables 19 through 22 also provide data relative to the part of the steering assembly that the driver head contacted. If the contact is shown as steering wheel in the tables, the dummy head actually impacted both the rim and hub. In almost all tests, the steering wheel rim, hub, or both the rim and hub were struck. The severity of these head impacts is indicated by the resulting HIC and somewhat by the parameters as given in Tables 19 through 22.

Good performances of the restraint system and the steering assembly are both important in reducing or eliminating these impacts. The belt parameters discussed in the previous section need careful review to improve safety performance. The steering assembly must be designed to minimize intrusion and to provide a friendly environment when the head or other body part contacts occur for the restrained (and unrestrained) driver.

Structural Performance Parameters

A third vehicle attribute that can be examined from the NCAP data is the performance of the frontal structure during the crash. Safety elements that the frontal structure is expected to supply include a reasonable occupant compartment acceleration signature (crash pulse) and a collapse mode that does not cause excessive compartment intrusion. As in most safety design considerations, these elements require a compromise. The safety designer desires as much dynamic crush as possible, yet the crush must not lead to intrusion that violates the occupant space.

The crash pulse of the NCAP vehicles, as measured by accelerometers in the occupant compartment, can be analyzed to provide state-of-the-art information to the vehicle designer. Several methods can be used to examine these crash pulses. In the following paragraphs, two methods will be explored. The first method will use the simplified characteristics of the tipped equivalent square wave (TESW) as developed in (8). The second method uses the actual acceleration data highly filtered with an SAE J211B Class 30 filter.

An example of the TESW is shown in Figure 9. It is overlaid with the actual occupant compartment acceleration. The parameters from the automated process of the TESW that are preserved from the actual data are the maximum dynamic crush, the time to maximum dynamic crush (TMAX), and the time to centroid of the crash

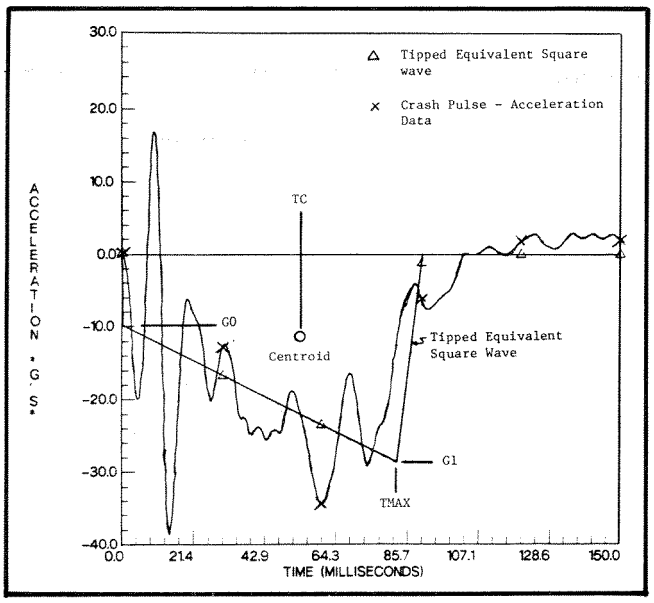

Figure 9. Tipped equivalent square wave overlayed with actual accleration data

pulse (TC). These values are given in Tables 25 through 28 for the four weight classes. In addition, g levels at the beginning of the pulse (G0) and at time of maximum crush (G1) are calculated and presented.

A further examination of the crash pulse utilizes high filtering of the actual accelerometer traces. The filtered trace is multiplied by the test weight of the vehicle and plotted against the vehicle's dynamic crush. This generates an approximate force-crush curve. From this curve, the peak force and an estimated linear stiffness of each vehicle are determined. The crush at the peak force is determined. The maximum dynamic crush is again obtained and can be compared to the equivalent value from the TESW. These parameters are also given in Tables 25 through 28 for the four weight classes.

The average values from the TESW and filtered force-crush curve for each weight class and for the low- and high-risk groups of each weight class are given in Table 29. From the average values of the crash pulse parameters for the total fleet, it is observed that, nominally, values are increasing with increasing weight (except for G0 and G1 of the TESW). In comparing the parameters of the low-risk group to the high-risk group within each weight class, it is seen that TMAX and maximum crush are the factors that show the most consistent trend. These values are larger for the low-risk groups. Except for the intermediate weight class, a similar trend of increasing peak force and increasing stiffness is also apparent from the low- to high-risk groups. From the average values of TC, G0, and G1 (which can be considered crash pulse shape functions) of the two risk groups, there appears to be a general trend toward a lower average g level and a slightly more square wave pulse shape.

Future Studies

The preceding discussions and analyses are considered preliminary and only a cursory examination of the data from NCAP. Much of these data have never been extracted from the NHTSA Crash Test Data Base and presented for review to automobile manufacturers and safety organizations in this consolidated format. It is hoped the manufacturers of the specific vehicles (along with others) will assist in a study of the tabulated information and provide comments to help validate, correct, and improve these data.

Future detailed studies of vehicle safety performance from the NCAP data planned by NHTSA Research and Development include—

1. Safety belt geometric assessments and webbing material (belt stretch) analysis. The present study was limited to data readily available in the NHTSA Crash Test Data Base. The belt anchorage locations and belt stretch information will be assembled for a large number of the NCAP vehicles. Analyses will be performed to determine the significance of these parameters.
2. Extensive film analyses of the steering assemblies. Digitized displacement-time histories of the steering assemblies are being generated from the high-speed films of the NCAP tests. These data will provide information on the relative importance of steering assembly motion and intrusion during the crash event. Tear-down studies will be performed on selected vehicles to determine the structural aspects that lead to excessive steering assembly intrusion into the occupant compartment. Component tests to measure the force-crush characteristics of rims, hubs, and columns will be conducted on a limited set of the NCAP vehicles. From these analyses and data, it is believed definitive information on the performance parameters of the steering assemblies that provide improved protection for the restrained occupant can be established.
3. Further evaluation of the crash energy management of the vehicle frontal structure. The present analysis used only the occupant compartment accelerations. Many of the NCAP tests have additional frontal structures data from multiple load cells mounted to the fixed rigid barrier. These load cell data provide a force-time distribution across the face of the vehicles. These data will be used along with some limited car-to-car and car-to-narrow-object test data to provide a better understanding of the structural performance/energy management systems of the vehicles. Again, limited tear-down studies will be conducted to identify vehicle design parameters that provide improved occupant protection.

Table 25. Structural performance parameters for the small vehicle weight class.

MY	Vehicle Make/Body Style	Driver HIC Level	Driver Chest G Level	Passenger HIC Level	Passenger Chest G Level	Crash Pulse Parameters (TESW) Tmax Msec	TC Msec	G0	G1	Crush Inches	Crash Pulse Parameters F/Displ Peak Force (Lbs)	Displ PF Inches	Max Displ Inches	Stiff Lbs/In
84	Renault Alliance	940	55		42									
	4 dr	3	3		2									
81	Ford EXP	745	49		53									
	2 dr hb	2	2		2									
79	Toyota Corolla													
	2 dr													
82	Honda Accord	500	43	403	29	92.63	53.17	-9.51	-24.70	32.55	60293.89	29.68	33.52	2031.55
	4 dr	1	2	1	1									
84	Toyota Corolla	432	37	602	47	75.75	44.24	-10.41	-31.56	27.17	90226.67	22.45	27.81	4018.59
	2 dr	1	1	2	2									
84	Honda Prelude	659	43	475	31	95.18	50.16	-13.91	-19.30	30.63	61224.27	18.77	30.80	3261.26
	2 dr	2	2	1	1									
81	Honda Civic	607	41	492	35	79.05	42.85	-15.13	-25.33	26.48	53759.92	21.30	26.30	2523.68
	2 dr hb	2	2	1	1									
84	Honda Civic	563	37	846	43									
	2 dr hb	2	1	2	2									
82	Chevrolet Cavalier	708	42	821	37	80.60	43.60	-14.92	-24.66	26.88	73877.83	22.26	27.42	3318.34
	2 dr hb	2	2	2	1									
84	Toyota Tercel	658	43	492	41	78.83	42.57	-15.38	-25.09	26.23	68306.16	24.88	26.47	2745.37
	4 dr hb	2	2	1	2									
85	Dodge Colt	787	42	741	32	81.83	45.33	-13.09	-25.63	27.75	77302.91	19.92	28.45	3879.73
	4 dr hb	2	2	2	1									
84	Honda Civic	586	43	544	32	73.00	39.35	-16.92	-27.25.	24.51	86937.40	15.95	25.04	5450.72
	4 dr sw	2	2	2	1									
83	Toyota Tercel 4X	839	43	535	42	80.88	43.11	-15.90	-23.75	26.71	74015.02	19.47	27.80	3802.12
	4 dr sw	2	2	2	2									
84	Toyota Corolla	630	41	611	42	75.75	42.65	-13.08	-28.99	26.26	78602.95	21.82	26.61	3602.88
	4 dr	2	2	2	2									
79	Chevrolet Chevette	871	47	859	45	97.95	41.63	-23.44	-8.89	25.47	107578.98	19.52	26.02	5512.49
	4 dr hb	2	2	2	2									
82	Datsun Sentra	549	43	865	46	103.88	55.16	-12.57	-18.31	34.18	54905.96	23.02	35.50	2385.54
	4 dr	2	2	2	2									
79	Plymouth Horizon	653	52	780	38	81.25	46.39	-11.19	-27.80	28.39	73969.85	29.93	32.87	2471.07
	2 dr hb	2	2	2	2									
80	Chevrolet Chevette	668	45	699	40	89.50	47.88	-14.15	-21.68	29.66	67629.29	23.04	30.55	2935.94
	2 dr hb	2	2	2	2									
84	Honda Civic CRX	571	34	959	34	78.23	41.07	-17.38	-23.51	25.38	100174.83	16.14	26.18	6207.20
	2 dr	2	1	3	1									
85	Volkswagen Jetta	898	50	1008	51	79.63	44.51	-12.94	-27.13	27.44	80656.63	17.01	26.82	4742.36
	2 dr	2	2	3	2									
81	Ford Escort	618	50	1011	40	94.28	50.72	-13.09	-20.82	31.32	57300.17	27.67	31.30	2071.05
	2 dr hb	2	2	3	2									
80	Fiat Strada	790	41	962	43	104.63	62.05	-6.69	-23.60	37.99	55669.54	33.77	37.94	1648.59
	4 dr hb	2	2	3	2									
82	Chevrolet Chevette	1020	48	715	40	88.60	45.81	-16.11	-19.78	28.14	91591.37	23.39	28.93	3916.15
	4 dr hb	3	2	2	2									
79	Volkswagen Rabbit	1024	67	429	33	82.35	47.10	-10.93	-27.57	28.85	67128.74	26.67	28.48	2516.76
	2 dr hb	3	3	1	1									
82	Datsun Stanza	974	55	879	39	91.13	51.67	-10.34	-24.24	31.46	66590.60	29.83	32.67	2232.62
	4 dr hb	3	3	2	2									
82	Ford Escort	950	47	1070	39	89.25	39.54	-23.61	-11.57	23.99	130346.38	23.86	26.08	5462.19
	4 dr hb	3	2	3	2									
83	Datsun Pulsar	1139	54	1134	39	83.63	44.24	-15.87	-22.56	27.47	77800.68	23.18	27.51	3356.37
	4 dr hb	3	2	3	2									
80	Toyota Tercel	1218	48	1179	53	93.88	48.53	-15.38	-18.87	30.15	60864.59	24.99	32.37	2435.99
	2 dr	3	2	3	2									
84	Renault Encore	912	63	1045	67	74.48	42.08	-13.03	-29.69	25.86	83520.59	22.60	25.56	3695.55
	4 dr hb	3	3	3	3									

Table 25, continued

MY	Vehicle Make/Body Style	Driver HIC Level	Driver Chest G Level	Passenger HIC Level	Passenger Chest G Level	Crash Pulse Parameters (TESW) Tmax Msec	TC Msec	G0	G1	Crush Inches	Crash Pulse Parameters F/Displ Peak Force (Lbs)	Displ PF Inches	Max Displ Inches	Stiff Lbs/In
82	Volkswagen Scirocco	1482	54	683	37	86.85	48.11	-12.44	-24.36	29.71	71205.40	22.56	29.54	3156.73
	2 dr	4	2	2	1									
80	Volkswagen Rabbit CO	1328	48	829	54	71.50	43.19	-8.36	-36.11	26.53	92062.88	26.23	28.17	3510.94
	2 dr	4	2	2	2									
85	Mazda RX	921	40	1345	42	78.38	48.36	-6.07	-34.65	29.81	114315.63	29.91	30.27	3822.33
	2 dr	3	2	4	2									
83	Toyota Corolla	767	67	1367	43	75.30	43.82	-10.81	-31.75	27.14	92909.90	21.95	27.57	4232.76
	4 dr sw	2	3	4	2									
81	Honda Civic	985	53	1391	43	85.13	43.92	-16.92	-20.52	27.05	58387.65	23.42	28.17	2493.32
	4 dr hb	3	2	4	2									
81	Volkswagen Jetta	1210	68	1272	52	80.50	46.77	-10.15	-29.35	28.73	75384.16	27.42	29.95	2749.71
	4 dr	3	3	4	2									
85	Chevrolet Spectrum	1559	51	960	56									
	2 dr hb	4	2	3	3									
85	Subaru DL	1361	57	792	39	79.13	44.94	-11.97	-28.47	27.78	77273.06	21.76	27.74	3551.41
	4 dr	4	3	2	2									
80	Audi 4000	1322	70	1428	45	76.63	44.06	-11.54	-30.42	27.37	94234.80	23.37	27.66	4033.16
	4 dr	4	4	4	2									
81	Renault 181	1150	47	1659	36	97.80	46.94	-18.34	-14.41	29.06	76638.62	17.24	28.96	4444.42
	4 dr	3	2	5	1									
83	Ford EXP	1744	46	796	41	86.85	49.07	-11.25	-25.65	30.38	70349.09	29.47	30.20	2386.79
	2 dr	5	2	2	2									
82	Dodge Omni	639	58	1703	43	92.55	53.03	-9.74	-24.92	32.87	61969.15	27.03	32.78	2292.79
	4 dr hb	2	3	5	2									
82	Dodge Colt	932	72	1730	44									
	4 dr hb	3	4	5	2									
81	Toyota Starlet	1836	65	1351	48	71.75	40.97	-12.78	-31.75	25.29	87581.18	19.50	25.55	4490.54
	2 dr hb	5	3	4	2									
79	Datsun 210	1358	69	1745	59	80.63	46.76	-10.34	-29.44	28.98	76277.56	24.55	30.35	3106.54
	2 dr	4	4	5	3									
84	Misubishi Tredia	1314	87	1521	57	86.03	49.98	-9.45	-27.32	30.54	89608.20	27.66	30.93	3239.64
	4 dr	4	5	4	3									
80	Datsun 310GX	1059	68	2019	108	78.00	44.77	-11.26	-29.24	27.32	79564.29	24.65	28.90	3228.14
	2 dr hb	3	3	6	6									
80	Toyota Corolla	838	69	1162	92									
	2 dr	2	4	3	6									
80	Honda Civic	2626	54	1506	47	72.80	40.48	-14.41	-29.00	24.71	68708.23	17.88	24.78	3843.02
	2 dr hb	6	2	4	2									
80	Subaru GLF	1087	72	2837	94	75.25	44.77	-9.11	-33.26	27.58	74578.40	26.39	27.54	2826.15
	4 dr	3	4	6	6									
84	Datsun Stanza	1459	58	2216	53	81.13	45.51	-12.53	-27.00	28.20	101029.00	24.44	28.56	4133.20
	4 dr	4	3	6	2									
85	Renault Alliance	1519	62	2678	47									
	2 dr conv	4	3	6	2									
84	Pontiac 1000	1886	42	1306	57	74.50	40.90	-15.23	-27.91	25.39	108786.09	20.78	25.45	5235.26
	4 dr hb	6	2	4	3									
79	Plymouth Champ	1270	72	1918	66	88.75	51.92	-8.87	-27.34	32.24	57870.57	31.10	32.22	1860.71
	2 dr hb	4	4	6	3									
80	Honda Prelude	2904	52	1759	45	82.60	48.07	-9.78	-28.72	29.53	71901.10	27.54	29.81	2610.49
	2 dr hb	6	2	5	2									
80	Renault LeCar	1938	85	1844	53	52.20	29.23	-19.28	-40.96	17.76	86540.27	14.26	17.97	6068.74
	2 dr hb	6	5	5	2									
79	Ford Fiesta	1656	70	1932	48	75.00	39.98	-17.05	-25.47	24.63	71541.20	15.35	24.01	4661.30
	2 dr	5	4	6	2									
79	Honda Civic	2030	93	2093	46	74.55	41.08	-14.76	-27.78	25.17	58387.43	23.45	25.18	2489.59
	2 dr	6	6	6	2									

Table 26. Structural performance parameters for the compact vehicle weight class

MY	Vehicle Make/Body Style	Driver HIC Level	Driver Chest G Level	Passenger HIC Level	Passenger Chest G Level	Crash Pulse Parameters (TESW) Tmax Msec	TC Msec	G0	G1	Crush Inches	Crash Pulse Parameters F/Displ Peak Force (Lbs)	Displ PF Inches	Max Displ Inches	Stiff Lbs/In
81	Audi 5000		43		52									
	4 dr		2	2										
79	Mercury Capri			770	44									
	2 dr hb			2	2									
85	Mitsubishi Galant		52	986	42									
	4 dr		2	3	2									
82	Chevrolet Celebrity	478	33	395	21	105.00	61.95	-6.98	-23.38	38.15	91999.55	32.57	38.07	2824.26
	4 dr	1	1	1	1									
84	Pontiac Fiero	309	31	356	30	95.40	49.32	-14.82	-18.18	30.00	78476.12	27.56	30.49	2847.86
	2 dr	1	1	1	1									
83	Pontiac Firebird	408	34	376	32	109.20	62.13	-8.61	-20.78	38.52	87122.61	35.59	38.50	2447.86
	2 dr	1	1	1	1									
85	Volvo DL	652	36	310	27	92.78	52.51	-10.28	-23.77	32.05	87198.00	30.27	32.43	2880.67
	4 dr	2	1	1	1									
82	Volvo DL	550	45	381	35	91.50	51.97	-10.28	-24.45	31.90	88691.07	29.06	32.01	3051.57
	2 dr	2	2	1	1									
84	Chevrolet Cav-Conv	884	43	401	29	84.60	47.12	-12.40	-25.29	29.03	79921.49	25.00	28.80	3196.39
	2 dr	2	2	1	1									
84	AMC Jeep CJ-7	460	46	440	49	75.38	36.86	-22.59	-19.79	22.75	97569.31	23.10	24.32	4224.38
	mpv	1	2	1	2									
82	Toyota Celica	702	36	530	45	89.00	47.70	-13.92	-21.58	29.12	110702.19	23.97	29.60	4618.04
	2 dr	2	1	2	2									
84	Dodge Daytona	507	47	566	40	90.30	56.35	-4.57	-31.13	35.10	114285.16	33.47	35.95	3414.22
	2 dr hb	1	2	2	2									
81	AMC Spirit	702	43	652	33	78.15	40.56	-18.09	-22.74	25.01	91728.32	9.57	24.84	9587.69
	2 dr	2	2	2	1									
83	Toyota Camry	809	48	495	40	80.10	45.90	-11.14	-28.51	28.17	86565.11	23.54	28.28	3677.75
	4 dr	2	2	1	2									
82	Chevrolet Camaro	563	39	577	32	100.50	58.19	-8.44	-23.66	36.27	82525.57	32.79	36.76	2516.74
	2 dr	2	2	2	1									
79	Ford Mustang	819	41	567	33	90.38	52.06	-9.51	-25.44	31.77	114024.98	29.87	31.93	3817.83
	2 dr	2	2	2	1									
85	Plymouth Caravelle	685	51	760	35	93.15	57.66	-4.90	-29.40	35.59	91426.89	34.05	35.65	2685.16
	4 dr	2	2	2	1									
80	Chevrolet Citation	845	48	623	35	91.28	51.11	-11.18	-23.75	31.48	76821.93	30.85	31.93	2490.17
	4 dr hb	2	2	2	1									
82	Dodge 400	520	44	756	41						100059.06	30.80	33.82	3248.67
	2 dr	2	2	2	2									
85	Plymouth Reliant	832	54	843	44	87.08	54.33	-4.69	-31.93	33.47	91674.73	31.49	33.06	2910.82
	4 dr	2	2	2	2									
85	Buick Somerset	1140	34	595	35						85877.80	31.14	31.81	2757.80
	2 dr	3	1	2	1									
82	Saab 900	734	39	1166	35	87.60	48.36	-12.62	-24.06	30.02	95260.48	19.76	30.35	4821.46
	4 dr	2	2	3	1									
84	Nissan 300 ZX	789	45	1038	39	90.68	55.58	-5.66	-29.50	34.24	110909.62	30.91	34.91	3587.79
	2 dr	2	2	3	2									
83	Plymouth Reliant	656	52	1221	52	99.98	56.49	-9.76	-22.25	34.92	110165.72	30.94	34.85	3560.41
	4 dr sw	2	2	3	2									
82	Toyota Corona	842	59	828	40	89.85	50.68	-10.87	-24.42	31.04	83671.59	29.95	31.80	2794.04
	4 dr	2	3	2	2									
79	Chevrolet Monza	1106	42	1033	41	100.43	48.81	-17.27	-14.60	30.18	105567.46	25.51	30.49	4137.71
	2 dr	3	2	3	2									
83	Dodge 600	947	46	1010	48									
	4 dr	3	2	3	2									
83	Mazda 626	1196	45	1087	56	88.65	53.81	-6.49	-29.76	33.41	92644.96	32.50	33.52	2851.04
	4 dr	3	2	3	3									
84	Plymouth Conquest	1118	57	1035	43	81.83	49.01	-7.98	-31.32	30.45	103237.61	28.86	30.59	3576.72
	2 dr hb	3	3	3	2									
80	Datsun 200 SX	1091	62	1032	44	82.25	48.12	-9.26	-28.53	28.90	86697.12	27.87	30.48	3111.16
	2 dr hb	3	3	3	2									

Table 26, continued

MY	Vehicle Make/Body Style	Driver HIC Level	Driver Chest G Level	Passenger HIC Level	Passenger Chest G Level	Crash Pulse Parameters (TESW) Tmax Msec	TC Msec	G0	G1	Crush Inches	Crash Pulse Parameters F/Displ Peak Force (Lbs)	Displ PF Inches	Max Displ Inches	Stiff Lbs/In
82	Volkswagen Quantum	1353	53	1194	41	80.88	44.56	-13.52	-25.45	27.13	85308.14	26.29	29.02	3244.89
	4 dr	4	2	3	2									
84	Plymouth Colt Vist	1530	71	1004	45	80.10	47.10	-9.49	-30.73	29.32	91068.20	26.10	29.58	3488.76
	4 dr sw	4	4	3	2									
82	Mazda 626	969	47	1693	50	75.68	44.42	-10.13	-32.25	27.52	91852.84	25.39	27.50	3617.42
	4 dr	3	2	5	2									
81	Plymouth Reliant	605	52	1731	59	88.20	48.00	-12.51	-23.55	29.87	114407.45	28.07	30.50	4076.34
	2 dr	2	2	5	3									
79	Ford Fairmont	939	54	1583	85	92.03	47.12	-16.26	-18.79	29.36	100524.73	22.00	29.32	4568.58
	4 dr	3	2	5	5									
85	Dodge Lancer	2187	38	445	30	89.93	54.76	-6.09	-29.09	33.47	93586.23	33.10	34.11	2827.10
	4 dr hb	6	2	1	1									
84	Nissan 200 SX	1992	44	582	32	78.53	47.66	-7.21	-33.05	29.11	107033.34	28.14	29.15	3804.25
	2 dr	6	2	2	1									
82	Chrysler LB Conv	2644	39	897	43	86.03	53.25	-5.34	-32.03	33.07	96227.71	31.47	33.23	3058.23
	2 dr	6	2	2	2									
81	Toyota Cressida	1980	55	771	50	73.75	40.93	-14.53	-28.85	25.30	159772.73	22.53	26.26	7092.00
	4 dr	6	3	2	2									
79	Toyota Celica	849	61	1862	59	90.83	48.86	-13.48	-21.44	29.93	134044.97	21.88	30.39	6126.26
	2 dr hb	2	3	6	3									
79	Mercury Bobcat	723	64	1878	51	83.13	44.64	-14.97	-23.51	27.58	82580.48	26.15	29.23	3158.42
	2 dr hb	2	3	6	2									
84	Ford Tempo	2955	63	1104	45	78.45	44.01	-12.88	-27.75	27.10	96782.16	25.38	27.91	3812.66
	4 dr	6	3	3	2									
83	Mitsubishi Mighty MA	1475	68	1934	71	74.63	36.42	-23.01	-19.92	22.54	109857.40	22.27	25.50	4933.77
	pu	4	3	6	4									
79	Volvo 244 DL	1782	52	1889	61									
	4 dr	5	2	6	3									
84	Isuzu Impulse	1769	46	2454	49	76.73	45.73	-8.72	-32.40	27.87	107411.88	26.44	27.87	4062.68
	2 dr hb	5	2	6	2									
84	Renault Sportwagon	2053	43	2721	52	83.25	46.54	-12.41	-26.02	28.77	80241.88	23.44	27.43	3422.62
	4 dr sw	6	2	6	2									
80	Mazda 626	1435	101	2206	54	73.00	44.60	-7.33	-36.57	27.62	113436.14	24.82	28.62	4570.08
	2 dr	4	6	6	2									
82	Renault Fuego	3768	50	2484	35	81.88	49.13	-7.79	-31.15	30.26	88174.20	27.61	28.80	3193.11
	2 dr	6	2	6	1									

Tables 27. Structural performance parameters for the intermediate vehicle weight class

MY	Vehicle Make/Body Style	Driver HIC Level	Driver Chest G Level	Passenger HIC Level	Passenger Chest G Level	Crash Pulse Parameters (TESW) Tmax Msec	TC Msec	G0	G1	Crush Inches	Crash Pulse Parameters F/Displ Peak Force (Lbs)	Displ PF Inches	Max Displ Inches	Stiff Lbs/In
84	Chevrolet Celebrity	518	31	440	28	101.40	59.22	-7.80	-23.66	36.50	86570.10	31.57	36.33	2742.28
	4 dr sw	1	1	1	1									
85	Volvo DL	621	33	262	31	95.33	53.29	-10.69	-22.40	32.47	92472.00	31.30	32.66	2954.38
	4 dr sw	2	1	1	1									
79	Oldsmobile Cutlass S	695	42	501	40	91.38	58.57	-2.67	-32.00	35.85	148710.23	36.68	37.54	4054.48
	2 dr	2	2	1	2									
84	Chevrolet Corvette	784	40	525	32	93.83	59.02	-3.81	-29.89	36.06	128257.33	34.62	36.09	3704.62
	2 dr	2	2	2	1									
83	Volvo 760 GLE	791	45	778	41	85.35	42.08	-19.55	-17.98	26.04	111919.20	23.86	26.54	4691.29
	4 dr	2	2	2	2									
84	Oldsmobile Cutlass	781	40	1074	35						104399.00	33.35	35.78	3130.40
	2 dr	2	2	3	1									
82	Ford Granada	860		1050	52	99.00	52.77	-12.78	-19.08	32.15	104626.53	26.42	31.86	3959.39
	4 dr	2		3	2									
84	Mercury Cougar	652	55	577	37	95.85	55.78	-8.43	-24.75	34.27	146365.94	31.87	34.79	4593.03
	2 dr	2	3	2	1									
83	Ford Bronco 4X	789	49	1038	50	81.50	40.26	-20.49	-19.07	25.08	120288.09	13.93	26.09	8637.54
	mpv	2	2	3	2									
83	Peugeot 505S	819	52	1157	49	75.25	45.45	-7.99	-34.49	26.07	123977.52	29.82	35.42	4157.93
	4 dr	2	2	3	2									
84	Toyota Van Wagon	984	50	748	54	66.50	31.32	-28.49	-20.05	19.53	111634.16	5.63	19.60	19838.31
	4 dr	3	2	2	2									
79	Oldsmobile Cutlass S	997	58	799	37									
	2 dr	3	3	2	1									
84	Ford LTD	646	58	647	67	91.80	53.34	-8.83	-25.53	32.50	132603.20	28.91	32.52	4586.20
	4 dr sw	2	3	2	3									
84	Dodge Caravan	973	44	1200	42	78.38	42.64	-15.02	-25.80	26.35	134297.00	16.98	26.77	7909.13
	3 dr	3	2	3	2									
80	Ford T-Bird II	988	50	994	52	72.80	36.33	-22.20	-21.93	22.55	172862.34	19.43	22.31	8895.94
	2 dr	3	2	3	2									
84	Ford Mustang	894	55	1112	38	93.68	55.08	-7.98	-25.84	33.71	123726.37	26.57	33.76	4656.69
	2 dr	2	3	3	2									
84	Buick Park Ave	1550	50	662	37	94.28	56.94	-6.34	-27.37	34.96	115685.74	32.77	35.04	3530.07
	4 dr	4	2	2	1									
84	AMC Jeep Cher	850	44	1548	43	82.38	46.71	-11.67	-27.37	29.02	109484.65	20.69	26.70	5292.26
	mpv	2	2	4	2									
83	Ford T-Bird	626	70	795	43	101.93	58.20	-9.04	-22.45	36.08	145814.64	33.24	36.51	4386.77
	2 dr	2	4	2	2									
79	Pontiac Firebird	965	42	1297	47	95.00	57.95	-5.75	-28.09	35.99	104640.18	33.50	34.00	2617.43
	2 dr	3	2	4	2									
83	Ford LTD	609	69	957	54	92.88	51.82	-11.26	-23.28	32.12	117709.70	28.18	34.15	4176.89
	4 dr	2	4	3	2									
85	Datsun Maxima	1014	63	1500	38	76.35	43.75	-11.70	-29.94	26.87	119063.00	24.80	26.77	4800.93
	4 dr sw	3	3	4	2									
85	Chevrolet Blazer	1036	62	1321	43	80.10	48.14	-7.84	-31.96	29.65	122072.00	20.01	23.78	6100.55
	mpv	3	3	4	2									
80	Oldsmobile Cutlass	1334	62	1125	47	96.13	58.25	-6.10	-27.43	36.28	134873.09	35.59	37.47	3789.62
	4 dr	4	3	3	2									
79	AMC Concord	1078	61	1457	69	74.25	38.61	-18.74	-23.85	23.59	114339.79	19.79	23.57	5776.78
	2 dr	3	3	4	4									
80	Mercedes 240D	1262	54	1369	44	78.25	48.28	-6.07	-34.68	29.74	159099.00	22.13	25.77	7190.23
	4 dr	4	2	4	2									
79	Plymouth Volare	724	40	1677	40	95.10	50.21	-13.95	-19.58	30.93	85033.81	29.34	31.16	3000.43
	2 dr	2	2	5	2									
80	Chrysler LeBaron	1742	54	1252	45	89.00	49.31	-12.13	-23.76	30.43	91253.77	25.98	32.34	3511.96
	2 dr	5	2	3	2									
83	Mitsubishi Montero 4	1641	54	1415	48	71.00	35.15	-23.06	-21.72	21.59	152297.72	17.70	24.10	8604.34
	mpv	5	2	4	2									

Table 28. Structural performance parameters for the large vehicle weight class

MY	Vehicle Make/Body Style	Driver HIC Level	Driver Chest G Level	Passenger HIC Level	Passenger Chest G Level	Crash Pulse Parameters (TESW) Tmax Msec	TC Msec	G0	G1	Crush Inches	Crash Pulse Parameters F/Displ Peak Force (Lbs)	Displ PF Inches	Max Displ Inches	Stiff Lbs/In
84	Chevrolet C-10	534	37	514	39	92.25	47.32	-16.01	-18.72	2956	123567.21	23.44	29.30	5270.54
	pu	2	1	1	2									
80	Cadillac Seville	623	43	523	35	93.50	49.46	-13.97	-19.85	30.22	106727.82	28.27	29.57	3775.25
	4 dr	2	2	2	1									
82	Lincoln Continental	757	46	728	37	102.60	56.64	-10.59	-20.20	34.57	124194.02	26.84	34.99	4626.35
	4 dr	2	2	2	1									
79	Buick Riviera	541	42	782	39	91.88	51.63	-11.00	-24.03	32.11	125520.65	33.39	34.38	3759.30
	2 dr	2	2	2	2									
79	Dodge Magnum	646	39	731	44	96.90	53.88	-11.01	-22.15	33.45	110056.24	32.14	33.58	3424.23
	2 dr	2	2	2	2									
82	Chevrolet Impala	1170	40		41									
	4 dr	3	2		2									
84	Pontiac Parisienne		52	1055	48									
	4 dr		2	3	2									
81	Chrysler Imperial	976	47	590	32	105.63	62.21	-7.03	-23.14	38.30	102926.55	37.72	39.96	2728.53
	2 dr	3	2	2	1									
79	Lincoln Continental	521	45	919	53	111.88	63.88	-8.20	-20.38	39.47	120445.65	36.10	39.26	3067.90
	4 dr	2	2	3	2									
82	Ford LTD	960	50	808	43	90.00	52.45	-9.54	-25.92	32.66	113246.73	27.68	32.89	4091.14
	4 dr	3	2	2	2									
83	Chevrolet Caprice	882	42	1084	47	92.70	52.65	-10.27	-24.43	32.72	104877.03	32.60	33.68	3216.66
	4 dr	2	2	3	2									
84	Mercedes 300 SD	890	63	734	44									
	4 dr	2	3	2	2									
84	Mercury Marquis	1204	61	868	42	96.25	57.85	-6.60	-26.91	36.04	113503.72	34.34	38.95	3305.74
	2 dr	3	3	2	2									
79	Ford LTD II	1088	61	781	40	102.88	60.80	-7.01	-23.87	37.32	172098.13	37.21	39.17	4625.56
	2 dr	3	3	2	2									
80	Dodge Mirada	948	43	959	37	90.00	49.50	-12.57	-23.34	30.90	124183.88	29.42	32.90	4220.52
	2 dr	3	2	3	1									
84	Mercury Marquis	1094	58	1019	39	104.13	60.18	-8.24	-22.75	37.53	119019.87	36.32	38.48	3276.92
	4 dr	3	3	3	2									
79	Ford LTD	1452	38	616	34	105.83	57.78	-11.03	-19.44	36.00	89995.27	30.74	36.11	2927.50
	2 dr	4	2	2	1									
79	Chevrolet Impala	1277	62	1254	51	80.38	43.88	-14.44	-25.46	27.19	126222.75	23.90	26.05	4845.40
	4 dr	4	3	3	2									
84	Ford F-150	1362	48	1443	51									
	2 dr	4	2	4	2									
79	Ford Granada	1442	61	1279	56	84.30	45.69	-13.98	-23.39	27.81	162329.33	26.16	28.17	6205.61
	4 dr	4	3	4	3									
79	Oldsmobile 98	910	59	1734	54	96.88	54.35	-10.41	-22.42	33.39	116811.49	30.66	36.76	3809.30
	4 dr	3	3	5	2									
79	Dodge St Regis	1909	67		50									
	4 dr	6	3		2									
79	Chrysler LeBaron	2402	45	1071	39	89.93	49.10	-12.84	-22.62	30.25	114292.36	25.16	30.91	4542.84
	2 dr	6	2	3	2									
85	GMC Astro	2202	70	1597	61	63.68	39.41	-7.12	-42.66	24.14	164073.64	23.46	24.50	6993.49
	van	6	4	5	3									

Table 29. Average values of crash pulse parameters

Group	Weight Class	TESW Parameters Tmax Msec	TC Msec	G0	G1	Crush Inches	Filtered Crash Pulse Parameters Peak Force Lbs	Crush at Peak Force (in)	Max Crush Inches	"Stiffness" Lbs/In
Total Fleet	Small	82.7	45.6	-13.2	-25.9	28.1	77906.1	23.4	28.6	3483.5
	Compact	86.9	49.4	-10.9	-26.1	30.4	97607.8	27.5	30.9	3737.1
	Intermediate	87.0	49.2	-11.9	-25.3	30.3	121931.3	26.2	30.7	5403.2
	Large	93.3	52.1	-11.2	-23.7	32.4	121830.6	30.3	33.6	4185.3
Low Risk Group	Small	85.8	46.2	-14.2	-23.3	28.4	76011.0	23.2	29.2	3449.0
	Compact	90.6	51.5	-10.5	-24.9	31.7	94031.7	28.5	32.1	3524.5
	Intermediate	87.3	48.9	-12.6	-24.5	30.1	122847.3	26.1	31.2	5900.8
	Large	96.6	54.5	-10.3	-22.9	33.8	119993.5	31.6	34.8	3860.1
High Risk Group	Small	79.3	44.9	-12.2	-28.6	27.7	79880.2	23.7	28.0	3519.5
	Compact	81.6	46.4	-11.5	-27.8	28.6	103077.1	25.9	29.1	4062.2
	Intermediate	86.7	49.5	-11.1	-26.3	30.6	120874.4	26.4	30.1	4829.1
	Large	85.7	47.3	-12.6	-25.5	29.1	134532.2	26.1	30.3	5375.6

Conclusion

NCAP has provided the most comprehensive data on vehicle crash performance ever collected. These data are resident in the NHTSA Crash Test Data Base on a VAX 11/780 computer. In the preceding sections of this paper, a preliminary review and tabulation of these data have been conducted. The following conclusions can be drawn from this review.

1. For MY vehicles 1979 through 1984, a significant improvement in restrained dummy performance is noted for recent MY vehicles (see Figure 3). (Although data are presented for some of the MY1985 vehicles, tests on all vehicles were not completed in time to be included in this paper.)
2. When the tested vehicles are separated into four weight classes, the performance of the small vehicle weight class is significantly poorer than that of the large vehicle weight class (see Figure 5). It is well known that in the accident environment the probability of serious injury or fatality is higher for the small vehicle. These data indicate that this higher probability, which definitely is associated with the higher severity exposure of the small vehicles, may also be related to the small vehicle safety design features.
3. In studying the safety belt performance parameters, the addition of a web-locking mechanism is seen to decrease significantly the time-to-belt onset loading (see Table 18). For specific vehicles, this decrease contributes to a dramatic reduction in dummy responses. With the rapidly increasing number of States and countries mandating the use of safety belts, it is important that the most efficient belt systems be made available to consumers. The web-locking mechanism or similar design to decrease the belt load onset time appears to provide the vehicle driver and occupant with improved protection.
4. Examination of driver head impacts into the steering assembly show that almost 30 percent of the restrained driver dummies in the NCAP tests had HIC values that placed the vehicle performance in the high-risk group (HIC greater than 1,254). On average, the head-to-steering-assembly impacts in the small vehicle weight class appear to be more severe than those of the other weight classes. It should be noted the severity of these impacts are dependent not only on the steering assembly parameters but also on the belt systems and structural performance of the vehicles (see Table 23). Studies are ongoing to assess the design characteristics of steering assemblies (intrusion and force-crush properties) that contribute to the excessive danger.
5. From the review of the structural performance parameters, some not unexpected conclusions are that the length of time of the crash pulse and the total crush of the vehicle during the crash are important. Trends indicate that the possibility for good safety performance is improved with long crash pulse duration and large dynamic crush. In comparing a linear stiffness parameter, a slight trend of improved performance for lower stiffness is observed (see Table 29). The data as analyzed do not indicate a significantly stiffer vehicle is required to obtain good performance in the 35mph crash tests.
6. Belts, steering assemblies, and frontal structures must perform effectively as a system. A predominant outcome of this review is that the safety performance of the vehicle is dependent on the system. With the variety of vehicle makes and models, interior occupant compartments, and exterior structural designs, the configuration of this system presently spans very wide performance corridors. Several studies have been

outlined to better locate the elements in the corridors that will improve occupant protection.

References

1. *Title II of the Motor Vehicle Information and Cost Saving Act* (15 U.S.C. 1941 et seq.).
2. Schmid, Walter, "The increase in the risk of injury in traffic accidents as a result of higher test impact speeds," Proceedings Ninth International Technical Conference on Experimental Safety Vehicles, pp. 766-771, 1982.
3. Hackney, James, and Vincent Quarles, "The new car assessment program—status and effect," Proceedings Ninth International Technical Conference on Experimental Safety Vehicles, pp. 809-824, 1982.
4. Prasad, Priya, Ford Motor Company, and Harold J. Mertz, General Motors Corp., "The position of the United States delegation to the ISO working group 6 on the use of HIC in the automotive environment," SAE Paper 851246, presented at the SAE Government/Industry Meeting and Exposition, Washington, D.C., May 20-23, 1985.
5. Eppinger, Rolf, and Susan Partyka, "Estimating fatality reductions associated with safety improvements," Proceedings Eighth International Technical Conference on Experimental Safety Vehicles, pp. 432-438, 1980.
6. Cerrelli, Ezio C., "Risk of fatal injury in vehicles of different size," NHTSA Report DOT HS 806-653, November 1984.
7. "Recommended definitions for passenger car size classification by wheelbase and weight," Final report by the Passenger Car Classification Subcommittee of the Transportation Research Board, August 1984.
8. Malliaris, A.C., Ralph Hitchcock, and Marie Hansen, "Harm causation and ranking in car crashes," SAE Paper 850090, 1985.
9. Huang, M., G.P. Lawson, B.K. Powell, and H.H. Walker, "Characteristics of vehicle deceleration time histories in the analysis of impact dynamics," SAE Paper 770013, 1977.

Accident Research and Frontal Testing

Dr.-Ing. M. Danner
HUK-Verband, Munich

Frontal collisions are still the primary reason for fatal injuries of car occupants, although the relative importance of side collisions has increased because of the protective effect of the safety belt. In classifying accidents, more attention must be given to the different sequences in car-to-car and single-car accidents and to their damage and strain criteria. However, there are problems in classifying real accidents into collision types and assessing the share that can be reproduced by standardized crash tests.

1. Each categorization of real accidents into collision types has to summarize and generalize the typical influences of each case, such as relative car masses, structure rigidity, relative speeds, direction of impact, and the movement before and after the collision. Which types of strain criteria can be combined and which have to be absolutely separated has not yet been adequately analyzed.
2. The way of dividing the collision types into a few or more (according to offset and crash angle) influences the priorities of collision types and the role of a corresponding crash test. This question has not yet been adequately resolved.
3. The comparison of accidents with crash tests is additionally impeded by the fact that crash tests are usually driven with only one moving vehicle and with an idealized distribution of forces, quite different from a real accident.
4. The international available accident materials show substantial differences. Because of the rapid car-safety development, a comparison between real accidents and corresponding crash tests is sensible only on the basis of recent accident material no older than 5 years and of accidents with belted occupants only.

There are about 3,000 single-car accidents with 1,200 belted passengers and about 1,000 car-to-car accidents with safety belts recorded in the HUK-accident material, which can be used as a basis for the questions mentioned above. In car-to-car accidents, with passenger injuries from AIS 3 in spite of fastened belts, the two collision types, "crash in longitudinal direction, centered" and "angled collision, offset less than 50 percent," dominate each with a frequency of 40 percent, which can in principle be reproduced by the 0° and 30° frontal fixed barrier test. The remaining 20 percent are accidents with high offset (offset about two-thirds) and longitudinal or angled impact direction.

Seventy percent of the frontal collisions are below a comparable barrier test speed of 50km/h; the 80 percent point is at 60km/h. In former accident material with

passengers predominantly unbelted, 90 percent of the accidents with injuries were below 60km/h. Because of the protective effect of the belt, the injury borderline has been moved to higher speeds.

In single-car accidents, however, the offset frontal impact dominates with about 60 percent, followed by the two collision types, "centered frontal fixed barrier test in longitudinal direction" and "centered, limited object impact," with 15 percent each. The rest of the accidents (about 10 percent) can be characterized as angled, distributed fixed barrier impacts. The 90 percent point of the collision speeds in single-car accidents is about 60km/h.

If an overall statement is made for the accident scene in keeping with the real-life proportions of car-to-car and single-car accidents—

- Offset accidents with clearly less than than ½ direct contact area (angled and not angled) can be estimated to account for about 40 percent of the accidents with belted injured occupants from AIS 3, followed by
- Collisions corresponding to the centered 0° frontal fixed barrier test, with almost 30 percent frequency.
- Angled frontal collisions corresponding to the 30° crash, which account for about 25 percent of all serious injuries from AIS 3.
- The rest are other collisions.

From the accident researcher's point of view, the following recommendations for safety tests are made:

1. It is not sufficient to describe the real-life frontal accident by one standardized test only. Three tests should be taken as a basis.
2. The frontal fixed barrier test should still be used as the main reference test. It covers about one-third of the real accidents with serious or fatal injuries even with fastened belts. In addition, the test can very well be reproduced and compared. A crash speed of 50km/h corresponds to the majority of accidents, but it can be seen from studies with 100 percent belted occupants that it is not altogether unjustified to increase the collision speed because of higher injury borderlines caused by the protective effect of the safety belt.
3. In addition to this test, an angled crash or an offset test is necessary, which has to be carried out in such a way that it can simulate the large problem of one-sided intrusion of the passenger compartment. This can be achieved by a 30° barrier test, but at a higher speed than 50km/h. An offset test in car-longitudinal direction with frontal contact area about one-third and a speed of 50km/h seems even more frequent in real accidents.
4. In a third test configuration, it should be considered that to reduce the injury risk in both cars involved there has to be a balance between self- and partner protection. A supplementary car-to-movable-barrier test, for example, with 50 percent offset or fully distributed, would be desirable. The test should be carried out in such a way that a movable reference-weight barrier with a specific deformation structure would show satisfying safety criteria even when it crashes against the tested car with a reference speed—according to present knowledge, about 100km/h relative speed of the two moving vehicles. This test should give indications on partner protection. We know it is difficult to realize this suggestion and to define the corresponding reference vehicle, but it should be the aim of future research to develop supplementary tests for partner protection beyond the test procedures for self-protection.

Together with the two tests mentioned before, there would thus exist basic test procedures that correspond to the real-life accident scene to a greater extent than the frontal fixed barrier test does today.

Results of Crash Tests According to the ECE/GRCS Regulation Proposal Concerning 50km/h Frontal Impact Against the Rigid 30° Barrier

E.Faerber and
K.P. Glaeser
Federal Highway Research Institute (BASt)
Federal Republic of Germany

Abstract

The Federal Highway Research Institute (BASt) has advised the Federal Minister for Transport on drawing up a draft regulation for the protection of vehicle occupants in a frontal collision. This draft regulation provides for a collision between a vehicle and the rigid 30° barrier at 50km/h.

In determining the test criteria, a number of questions had to be answered: Which calculatory and influencing possibilities are there in the application of the head protection criterion? How can the head contact be clearly determined? What spreads do the measured values for the dummy demonstrate under the same test conditions, and must these be included in the draft regulation? How frequently does submarining occur and how can submarining be measured? What other regulations can be covered by the global test proposed by this draft regulation? Do small passenger cars currently on the market already fulfill these test conditions?

Results of the following studies by the BASt concerning these aspects are introduced in this paper:

- Theoretical studies in the "Application of the Head Protection Criterion"
- Practical applications (eight crash tests) on the topic "Variance of the Measured Values"
- Accident data analysis on the topic "Frequency of Submarining"
- Trolley tests on the topic "Determination of Submarining by Measurement"
- 10 crash tests using subcompact passenger cars
- Inclusion of other ECE regulations in the global test

The draft regulation is introduced and critically assessed.

Introduction

In Europe, a large number of ECE regulations have been approved for use in testing the passive vehicle safety of vehicle components. With the ECE regulation proposed by the Group of Experts on the Construction of Vehicles(1), a regulation is planned with which the interrelationship between all the components can be tested in a full-scale test. The initial drafts for this regulation have already been critically discussed in (2).

Summary of the Regulation Content

Test Conditions

- Head-on collision, 30° barrier, initial contact on steering wheel side
- Impact speed: 48 to 50km/h
- Vehicle weight = kerb weight
- Tank 90 percent filled with nonflammable liquid (density: 0.7 to 1g/cm^3)
- One dummy (Hybrid II) on each of the front seats, seatbelts fastened
- One dummy (Hybrid II) on the rear seat behind the driver's seat unless outer rear seats fitted with 3-point belts
- All seatbelts and belt anchorages in vehicle in accordance with ECE Regulations 16 and 14.
- Height-adjustable steering wheel in normal position or, if no normal position specified by manufacturers, in middle position
- Windows closed wherever possible; open only if required for measurement purposes; window winder or other devices in position as for closed window
- Doors closed but not locked
- Longitudinal seat position: H-point 50mm ahead of R-point
- Seat height adjustment: middle position
- Seat backrests in normal position or, if no normal position specified by manufacturers, inclined at 25° to the vertical
- Dummy position: dummy symmetry plane = seat symmetry plane
  - Driver:
    - Distance to the knee: 37cm (overall)
    - Distance from the left knee to dummy symmetry plane 15cm (overall)
    - Right foot on undepressed accelerator pedal or as near as possible in front of it, heel on the floor
    - Left foot on floor alongside clutch pedal, left leg as straight as possible
    - Hands on steering wheel in "quarter to three" position
  - Passenger:
    - Legs stretched out as straight and parallel as possible

— Feet on floor or at right angles to thighs, heels on the floor
— Elbows against backrest, hands on thighs

Measured Values

- HPC (Head Performance Criterion); criterion:
  — No head-vehicle contact or
  — <1000 (calculation as for HIC, from start of head-vehicle contact to end of recording time, tolerance +250)
- Resulting acceleration of the chest; criterion: a_{3ms} 60g
- Upper thigh longitudinal forces; criterion: $F_{max} < 10kN$ and $F_{20ms} < 8kN$
- Behavior of the lapbelt (if fitted); criterion: no submarining

Further Requirements

- Door opening (as ECE-R32 and ECE-R33)
- Fuel leakage (as ECE-R34)

Special Problems in the Application of the Draft Regulation

During the discussions into the drawing up of the draft regulation, attention was paid to the following problem areas: determination of a Head Protection Criterion (HPC), the spread of the test results in full-scale tests, and detection of submarining. Results of the tests performed by the BASt will be discussed.

Head Protection Criterion

Various head protection criteria are based on the Wayne State Cerebral Concussion Tolerance Curve, which represents a borderline between translatory head loads that are dangerous to life and those not dangerous to life.

In recent studies(3), serious head and brain injuries resulting in death are divided into subdural haematoma (SDH) and diffuse axonal injuries (DAI). According to (3), both types of injury occur under the same mechanical loads, namely rotatory accelerations that differ only in their severity.

If one considers the results of this study, then the translatory acceleration of the head is, at least for severe head injuries, of minor significance. In contrast to this, however, is the fact that in vehicle safety crash tests with dummies, translatory accelerations are now almost exclusively measured and taken as the basis for protection criteria. Translatory head accelerations will also be evaluated in the ECE/GRCS draft regulation, since the uniform measurement and evaluation of rotatory accelerations does not at present appear to be sufficiently reliable.

Since the load limit for the head according to the WSU curve was evaluated using skull crash tests against steel plates, an HPC derived from the WSU curve should be applied only in the event of head contact. Head contact can, for example, be determined by measurement if electrically conducting contact zones on the head of the dummy and on the vehicle close a circuit during contact. Electrically conducting paints or foils applied to the head of the dummy have only an insignificant effect on the calibration values specified in U.S. Part 572. Despite the often noncontinuous contact circuiting, it is nevertheless normally possible to determine the start of contact with sufficient accuracy. Due to the frequent damage to the contact surfaces, however, the end of contact can usually not be determined satisfactorily. In comparative tests, it was discovered that the required contact times could not be determined with a sufficient degree of accuracy using high-speed film recordings.

The requirements for measured data recording are specified in ISO and SAE standards. The level of the requirements sets a limit to the increase in the number of channels. During the tests carried out by the BASt into this subject(4), it was discovered that large reductions in the requirements had only an insignificant influence on the HIC value. For example, the limit frequency of the low-pass filters for the head accelerations could be reduced from 1,000Hz to 300Hz, and, for certain filter types, even down to 100Hz. A reduction in the scanning rate during digitization of the measured data from the standard 8,000Hz to approximately 1,000Hz also had only a slight effect on the HIC value.

On the one hand, the HIC can be calculated from all the possible pairs of times of the measurement interval. The maximum value is then the desired HIC value. However, this method requires high computation times, even from powerful computers. For this reason, it is necessary to find suitable iterative approximation methods. When comparing the various methods, it was discovered that all the methods produced results with the required accuracy. The various methods for performing the integration required by the HIC formula affected the HIC value only insignificantly.

Because the cutoff frequency of analog and digital filters, digitization rate, and iterative calculation procedures have only minor effects on the HIC/HPC values, the cutoff frequency proposed in the ECE/GRCS draft regulation was reduced from 1,000Hz to 600Hz, and a defined calculation procedure was not demanded.

Spread of the Measured Values in Full-Scale Tests

Varied statements are made from various quarters regarding the reproducibility of the measured data from standardized crash tests.

The collision between vehicle and a rigid wall represents a more simplified type of crash than the vehicle-vehicle collision.

To be in a position to make statistically significant statements from the expected spread of the test results, it appeared necessary to perform at least eight crash tests. The vehicle used for the tests was the Opel Kadett D, built between 1979 and 1984. Used vehicles between 1 and 2 years were used. A comprehensive summary of the results has been published in (5).

In technical spheres, the normal distribution is generally used to describe the frequency distributions. A test of the measured results for normal distribution, e.g., using the chi-squared fit test, could not be carried out due to the small number of experiments. In Tables 1 and 2, spreads have been drawn up for selected parameters. The following dimensions are used in the tables for describing the distribution of the individual parameters:

- Arithmetic mean (x)
- Standard deviation (s_v)
- Coefficient of variation (cv)
- Minimum and maximum values (min., max.)

Vehicle-Related Measurements

The deformation of the front of the vehicle was measured using a measuring frame according to the displacement of 13 measuring points. The coefficients of variation of the vehicle deformation on the driver's side lay between 2 and 10 percent and, for the points with the greatest displacement, between 2 and 4 percent. The vehicle accelerations also varied by the same magnitude (see Table 1).

Table 1. Dispersion of car measurement values

	Maximum Car Deformation, Driver Side mm	Maximum Car Acceleration g	Mean Car Acceleration g	Car Velocity Change Δv km/h
min.	561	31.1	11.0	114.3
max.	533	36.7	11.7	14.9
$\bar{x}$	576	35.3	11.3	14.6
s_v	10	2.3	0.24	0.2
cv %	2	6	2	2

Table 2. Dispersion of dummy measurement values

	Head Driver		Head Passenger		Chest Driver	Chest Pass.	Femur Left	Driver Right	Femur Left	Passenger Right
	3ms Values of Resultant Acceleration g	HIC	3ms Values of Resultant Acceleration g	HIC	3ms Values of Resultant Acceleration g	3ms Values of Resultant Acceleration g	Maximum Longitudinal Forces kN	Maximum Longitudinal Forces kN	Maximum Longitudinal Forces kN	Maximum Longitudinal Forces kN
min.	45	545	38	422	34	38	0.5	1.0	0.8	4.8
max.	62	940	51	589	71	43	4.4	6.1	3.6	9.2
$\bar{x}$	51	682	43	509	41	40	1.5	3.8	1.5	6.0
s_v	7	152	4	68	12	2	1.4	2.4	1.1	1.7
cv %	13	22	10	13	29	4	94	63	74	28

Dummy-Measured Values

Selected spreads are listed in Table 2. In two tests, slight head/steering wheel contacts—in one test also a chest/steering wheel contact—were suspected but could not be proved definitely. For this reason, the HPC was not calculated according to the ECE/GRCS draft regulation (i.e., only for the duration of the contact) but was specified as an HIC as proposed in the FMVSS 208 for the entire duration of the resulting acceleration. The mean head accelerations, the HIC values, and their spreads are higher for the driver than for the front-seat passenger. This may, on the one hand, be due to the fact that in certain cases slight head/steering wheel contacts may be suspected, and, on the other hand, the movements of the two front-seat dummies differ due to the vehicle rotation.

The same effects can be observed for the chest loads.

Due to the movement of the vehicle, the two dummies moved to the left relative to the movement of the vehicle, so they moved forward in the vehicle with the right knee leading. A knee contact with higher longitudinal femur forces was therefore observed primarily for the right leg.

Regarding the forces in the left femur of the driver and front-seat passenger, the wide spread of 94 and 74 percent, respectively, can be explained by the fact that a knee contact occurred in only one and two tests, respectively. In cases where such knee contacts occurred in every test, the variances (28 percent) are considerably smaller. Due to the large forward displacement of the front-seat passenger dummy, the femur forces in this dummy were higher than in the driver dummy.

Methods for the Detection of Submarining

Submarining is defined as the sliding of the pelvis under the lapbelt loop or the riding up of the lapbelt over the crest of the ilium of vehicle occupants wearing seatbelts under frontal collision conditions. Submarining is promoted by soft seat upholstery and/or an unfavorable seatbelt geometry (small lapbelt angle) as well as misuse of the seatbelt system (belt too loose or relaxed seat position)(6).

The importance of submarining as a result of direct effects of the belt in an accident is due less to the frequency of the injury than to the seriousness of the abdominal injuries. For example, the number of cases of submarining relative to the number of injured front-seat occupants wearing seatbelts in head-on collisions in the accident material collected by the Accident Research Department in Hanover (259 cases) represented 4.6 percent; in the accident research material of Peugeot-Renault (1,073 cases), 5.8 percent. It is estimated that approximately 2 percent of all injuries with AIS $>$ 3 are abdominal injuries caused by submarining(7). For this reason, an abdominal protection criterion has been integrated into the draft ECE/GRCS guidelines for the 30° head-on collision.

Since the draft regulation proposes only a measuring method for detecting the submarining effect, although other methods are also accepted in principle, a comparative study of the measuring methods described in the draft regulation with another method used until now was carried out.

Six trolley tests were performed at 50km/h under simulated head-on collision conditions on the crash test facility of the BASt. The standard seatbelt systems of a Ford Capri II and a Citroen GS Club were fitted to the frame of a trolley so that in each case, two different measuring methods could be tested in parallel to provide a total of 12 individual results at the end of the series of tests. Steering wheel and instrument panel were not installed.

The position of the seatbelt anchorages in both vehicles lay within the limits specified in ECE Regulation 14. Film recordings were made, in which the bones of the crest of the ilium of the dummy were marked with target points, so that the sliding of the pelvis under the seatbelt during submarining could be clearly detected.

Each dummy was fitted with one of the special submarining measuring devices described below.

The one measuring method is based on a development by the Association-Peugeot-Renault (APR), in which two hook-shaped force transducers fitted with strain gauges are screwed onto the crest of the ilium of a Hybrid II dummy pelvis (Figure 1). If the lapbelt rides up over the iliac crest under submarining conditions, the transducers are subjected to a bending force, i.e., indicating abdominal loading, provided the lapbelt loads are applied vertically to the APR transducers. This measuring method conforms to that described in the ECE/GRCS draft regulation, which specifies a load limit of 800N.

The second method of detecting submarining is based on the use of a submarining indicator pelvis (SIP). Three force transducers are fitted, one above the other, into the

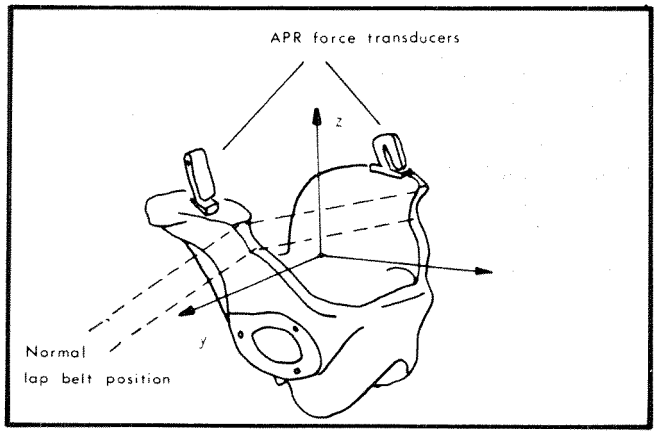

Figure 1. Dummy pelvis APR transducers

left- and right-hand ala of the ilium of the dummy pelvis, over which the lapbelt slips on collision, allowing the relative movement between pelvis and lapbelt to be deduced from the temporal relationship between the force transducer signals. This test method is only able, however, to prove whether or not submarining has taken place (Figure 2). In the event of submarining, it does not allow any statement to be made as to the size of the abdominal load.

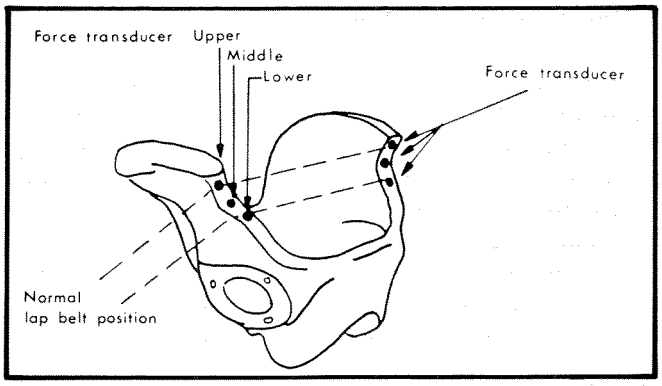

Figure 2. Submarining indicator pelvis (SIP)

As mentioned above, the decision as to wheter submarining had taken place during the test or not was based on films of the dummy movements.

This film analysis represents a suitable method of detecting submarining but is unsuitable for use in vehicle approval tests, since the test regulations make high demands on the integrity of the normal condition of the vehicle, thus forbidding the removal of the doors for filming the movement of the dummy pelvis.

Analysis of the test data has shown that the SIP method permits uncertainties in determining the sequences of movement during submarining, since the only factor for evaluation after a critical upward movement of the belt loop along the ala of the ilium is the sudden drop in the signal of the upper force transducer. From the test results, the question must certainly be posed whether, on the basis of a numerical evaluation of the signal drop, a submarining criterion such as "drop in signal in Δt" can be defined, from which submarining can be proved where the criterion is exceeded and excluded where the criterion is not exceeded. It appeared that an analysis of the temporal pattern of the lapbelt forces, which can be characterized under submarining conditions by two clear maxima with a minimum at the point when the lapbelt passes the upper force transducer of the iliac wing, in conjunction with the analysis of the temporal pattern of the upper pelvis force transducer can considerably increase the detection probability of whether or not submarining has taken place.

The APR measuring method also appears suitable for determining critical lapbelt movements. An assessment of the abdominal loads on the basis of the measured pressure forces presupposes, however, that the lapbelt forces are applied vertically to the surface of the APR transducer. Since such conditions cannot always be fulfilled, an incorrect indication of uncritical abdominal loads can be produced, although the belt forces acting on the abdomen exceed the biomechanical tolerance limits. The measuring curves of the lapbelt forces with two clear maxima under submarining conditions can also be used here, as already described above, as an additional criterion for determining submarining.

The results can be summarized as follows. The known measuring methods are not conclusive when applied alone. With the introduction of the 30° global tests by the ECE, the installation of belt force transducers should be permitted, if not even demanded, for reliable proof of the submarining-free restraint of the dummy by the safety belt. A method of interpreting a combination of measuring values from the force transducers and the belt force transducers must be worked out. The ECE Regulation 14 (Position of the Seat Belt Anchorage Points) is insufficient to prove that submarining is prevented.

Results of 10 Standardized Tests With Subcompact Cars

To investigate the applicability of the test methodology of the ECE/GRCS draft regulation and to determine to what extent subcompact cars already on the road satisfy the proposed safety requirements, a series of 10 crash tests was carried out. On the basis of the test results, an attempt should also be made to determine which existing ECE regulations are covered by the new draft regulation.

In the first three tests, no head contact measurement could be carried out, since an earlier version of the draft proposal did not permit the use of electrically conducting materials. In addition to the contact measurements, it was also possible to use the SIP from the fourth test onward. For the VW Golf, the results from one 30° and two 0° collisions were available for comparison with the results of the 0° and 30° barrier tests.

Vehicle-Measured Values

The vehicle types and certain of their technical data are shown in Table 3. The vehicles were bought second-hand and were between 1 and 1.5 years old at the time of the test. Table 4 shows the maximum vehicle deformations.

In each of the tests, the front of the vehicle on the passenger side was only slightly deformed. The deformation in the longitudinal direction of the vehicle was 10 to 30mm. Due to the one-sided loading with the 30° configuration, it is reasonable to assume that the maximum deformation would be slighter with the 0° barrier.

Table 3. Technical data of test cars

Car Type	VW Polo	Ford Fiesta	VW Golf	Peugeot 104	Citroen 2CV6	Toyota Starlet	Renault 5
Test Nr.	01,02	03,06	04	05,07	08	09	10
Unladen Kerb Weight kg	685	730	750	740	600	765	785
Length mm	3,605	3,565	3,815	3,366	3,830	3,725	3,515
Wheelbase mm	2,330	2,286	2,400	2,230	2,400	2,300	2,419

Table 4. Maximum car deformation on driver side

Car Type	VW Polo	Ford Fiesta	VW Golf	Peugeot 104	Citroen 2CV6	Toyota Starlet	Renault 5
Deformation mm	582/583	645/643	599	594/587	550	658	508

Table 5. Deceleration characteristics of the 10 ECE/GRCS regulation tests

	Car Type	VW Polo		Ford Fiesta		VW Golf	Peugeot 104		Citroen 2CV6	Toyota Starlet	Renault 5
x-Direction	Max. Accel. $a^{max.}$ g	23.7	23.9	-	31.4	26	28.5	38.3	38.2	48.6	61.7
	Duration of Accel. ms	142	120	107	148	118	118	103	117	102	82
	Average Accel. a g	9.5	11.2	13.4	9.9	12.1	12.3	14.2	12.5	14.1	17.5
	v m/s	13.3	13.2	14.1	14.4	14.0	14.2	14.3	14.3	14.1	14.1
y-Direct.	Max. Accel. $a^{max.}$ g	16.8	19.0	20.1	11.8	17.9	13.8	19.7	15.1	26.5	28.2
	v m/s	6.1	6.3	3.7	2.5	4.1	3.1	3.0	2.7	3.8	3.6

Table 5 shows selected parameters to describe the deceleration of the vehicle. As already stated, comparisons between the 0° and the 30° positions of the barrier can be made only for the VW Golf. Surprisingly, however, as shown in Table 6, there are no major differences between the two configurations. Contrary to this, however, a major research project carried out by the CCMC(9) with 71 tests and 20 different types of vehicles shows that if all models are taken into consideration, the vehicle accelerations and the velocity changes are on average noticeably higher in the 0° tests than in the 30° tests.

Table 6. Comparison 0°-30° barrier position; vehicle decelerations of VW Golf

Barrier Position	30°	0°	
Max. Accel. $a^{max.}$ g	26.0	38.9	26.9
Duration of Accel. ms	118	122	125
Δv m/s	14.8	14.6	14.6
Average Accel. a g	12.1	12.2	11.9

Dummy-Measured Values

The measured values are summarized in Table 7. In tests 2 and 9, the limit for the chest protection criterion was slightly exceeded as the driver collided with the steering wheel. In test 10, an excessive longitudinal force was measured in the right femur of the driver due to a collision with the steering column and the instrument panel (see also, section "Detection of Submarining"). As far as the other criteria were concerned, the subcompact cars available on the market in 198G4 satisfied the safety requirements.

The results for one test with the 0° barrier position and one test with the 30° barrier position were available for comparison of the dummy loads. The measured values for the dummy are shown in Table 8. In the 0° collision, the head accelerations are noticeably higher than in the 30° collision. This difference is considerably greater for all dummy-measured values in the CCMC study already mentioned(9).

The values for the HPC and abdomen protection criterion are discussed in greater detail below.

Table 7. Summary of measured protection criteria

Car type	VW Polo		VW Polo		Ford Fiesta		VW Golf		Peugeot 104		Ford Fiesta		Peugeot 104		Citroen 2CV		Toyota Starlet		Renault 5	
Test Nr.	1		2		3		4		5		6		7		8		9		10	
Dummy Position	F	BF	F	BF	F	BF	F	BF	F	BF	F	BF	F	BF	F	BF	F	BF	F	BF
Protection Criterion																				
HPC	**	***	**	0	**	0	246	0	521	0	285	0	457	0	620	0	781	0	374	0
ChPC g	48	29	78	29	52	34	36	36	42	37	52	37	41	41	36	30	71	39	56	39
FPC****left	6.0	def.	0.9	6.8	2.3	3.8	2.0	2.0	2.1	0.7	1.7	1.0	2.0	0.9	1.5	1.9	2.6	2.1	4.0	5.1
kN right	1.3	def.	4.8	0.1	2.1	7.6	4.7	1.7	6.4	1.8	3.1	1.2	3.7	1.9	9.5	1.3	8.5	1.7	15.4	7.2

* F = driver; BF = front seat passenger
** not measured; no contact measuring
*** =no head contact
**** = only maximum values

Table 8. Comparison 0° - 30° barrier position, measuring values of driver dummy (one test with VW Golf each)

Barrier Position	0°	30°
Dummy Parameter		
HIC	678*	447
t_1 ms	52	74
t_2 ms	102	149
ChPC g	38	36
FPC Right kN	0.9	2.0
Left kN	4.9	4.7

Head Protection Criterion (HPC)

As already mentioned several times, the HPC must be calculated only in the event of a head collision, and then from the beginning of the contact. For the head protection criteria HIC most widely used to date, this temporal restriction does not apply. The passenger dummies suffered no head contact during the 10 standardized tests, so the HPC was satisfied for all the tests. The HIC values calculated for the entire period of measurement are listed in Table 9. If one compares the HPC and HIC values for the driver dummies summarized in Table 10, it becomes apparent that certain HPC values are considerably lower than the HIC values. This effect occurs whenever the head contact takes place in the period t_1 to t_2 for which the HIC is calculated.

Due to its major effect on the HPC value, the measurement of head contact must be carried out with great care and accuracy. The reason for the considerable differences between HIC and HPC in test 10, for example, is that in these standardized tests, the head of the driver dummies moved between the A-pillar on the barrier side (here the left-hand A-pillar) and the rim of the steering wheel due to the angled position of the barrier. These movements generally result in simply glancing contacts and thus to contacts that are barely noticeable in the head acceleration sequence.

By analyzing acceleration traces from crash tests carried out previously in this respect, it can be stated that the difference between HIC and HPC is not as marked if a clearer and harder head collision against vehicle components occurs.

Abdomen Protection Criterion

From test 4 on, a dummy fitted with an SIP was used to record any occurrence of submarining. With the exception of one test that was performed twice, the dummy was positioned in each case on the driver's seat.

For test 3, Ford Fiesta, the occurrence of submarining was indicated by the final position of the dummy.

The recording of submarining using measurements performed in the subsequent tests, taking into consideration the seatbelt force patterns and femur forces, produced an indication of submarining in only one case (test 10, Renault R5). The reason for the slipping of the dummy under the lapbelt included the tearing of the seat out of the seat rail and thus the change, i.e., reduction, in the lapbelt angle.

The belt slipped over the right-hand ala of the ilium. This is an indication that even in the event of a 30°

Table 9. HIC-values of passenger dummy and calculated t_1 and t_2 values

Car type	VW Polo		Ford Fiesta		VW Golf	Peugeot 104		2 CV	Starlet	Renault
Test Nr.	01	02	03	06	04	05	07	08	09	10
HIC	255	255	377	570	277	606	358	470	697	657
t_1 ms	73	70	83	89	69	77	69	72	78	78
t_2 ms	162	156	154	156	164	153	156	155	163	127

Table 10. HPC and HIC values of driver dummies and calculated instants for beginning and end of integration

Car type	VW Polo		Ford Fiesta		VW Golf	Peugeot		2 CV	Starlet	Renault
Test Nr.	01	02	03	06	04	05	07	08	09	10
HIC	843	775	578	489	447	591	576	620		
t_1 ms	94	90	82	69	74	81	75	96	89	85
t_2 ms	137	130	139	125	149	125	120	133	127	122
Contact begin* ms	---	---	---	104	110	94	88	94	83	109
Contact end ms	---	---	---	128	---	146	133	158	144	118
HPC	---	---	---	285	246	521	457	620	781	374
t_1'** ms	---	---	---	104	110	94	88	96	89	109
t_2'** ms	---	---	---	120	149	124	120	133	127	120

* HPC calculation from contact start until end of recording (300ms after crash begins)
** t_1' t_2" New time instants for the begin and end of integration at HPC calculation

collision, ECE Regulation 14 (Position of the Seat Belt Anchorages) alone does not guarantee that submarining will not occur.

Inclusion of Other ECE Regulations in the Global Test

It is planned that the 30° global test will also cover a number of other ECE regulations. Annex 8 lists those regulations that will be regarded as having been satisfied if the global test is satisfactorily completed:

- ECE 11, "Door latches and hinges," complete
- ECE 12, "Steering mechanism," complete
- ECE 14, "Safety belt anchorages" for front seats
- ECE 17, "Seats and headrests" for front seats and head-on collisions
- ECE 21, "Interior fittings" for front seats and vehicle interior
- ECE 33, "Head-on collisions," complete
- ECE 34, "Fire risks" during head-on collisions

The fulfillment of these regulations is somewhat controversial. Comments on this subject have been forwarded from Great Britain and West Germany(10,11).

In tests with subcompact cars, no problems were encountered regarding the strength of the safety belts and the belt anchorage points. All the seatbelts could be opened without the use of tools, and the dummies could be removed undamaged.

During the crash tests, the doors of all the test vehicles remained closed. After the crash, at least one door, normally the passenger door, could be opened. One exception to this was the Toyota Starlet on which the locking mechanism locked the passenger door during the crash. The driver's door was also so severely damaged that it could not be opened without the use of tools.

With the exception of one vehicle, the Citroen 2 CV, the fuel tank and fuel pipes remained undamaged during and after the crash. A quasi-static rollover test on the vehicle after the crash could not be performed. On the vehicle mentioned above, a fuel pipe was damaged during the crash. The leak rate was greater than 30g/min.

In tests carried out on subcompact cars, the seat mountings frequently left something to be desired. We chose a criterion of a permanent seat forward displacement of 1cm. In 5 of the 10 vehicles tested, this forward displacement of the driver's seat was exceeded, in some cases by up to 11cm. The same applies to the passenger seat. In one case (Peugeot 104), both dummy and seat were held by the safety belt. If the seat is torn out of its mountings, the seatbelt geometry (lapbelt angle) is altered and the tendency to submarining increased. Submarining for this reason occurred in the Renault R5 test.

In standardized tests with subcompact cars, the survival area in accordance with ECE Regulation 33 was determined for the driver's side, i.e., the more severely deformed side. Since the required minimum distances were always measured relative to a fixed seat plane in the vehicle (R-point plane) and the distances quoted are really minimum distances, the permitted deformation of the foot well was exceeded on only one vehicle, a Peugeot 104. The majority of vehicles, however, exhibited severe deformations of the foot well bulkhead and instrument panel (up to 20cm). Due to the displacement of the seat caused by the collision (which was not, however, taken into consideration in the required method of measurement), the space for the vehicle occupants was in some cases considerably restricted. If, however, one considers the distances—contrary to ECE Regulation 33, but in the sense of survival area—not relative to the vehicle-related R-point plane but relative to the seat-related H-point plane, the vehicles Renault R5, Toyota Starlet, and Peugeot 104 would not have satisfied the requirements.

In the crash tests against the 30° barrier—the vehicles were fitted with dummies—the intrusion of the steering wheel into the passenger compartment could not be measured. Either the dummy collided with the steering wheel, thus preventing further intrusion of the steering

column, or, as was normally the case, the head of the dummy struck the rim of the steering wheel to the left of the steering column, thus obstructing the view to the center of the steering wheel. In some cases, however, it was nevertheless possible to deduce considerable intrusions from the film recordings. On several vehicles, the steering column was forced up sharply (e.g., on the Citroen 2 CV by 7° to the vertical). This produced a greater hazard to the occupants by the then horizontal rim of the steering wheel.

Conclusion and Discussion of the Results

The content, limitation, and application of the ECE draft regulation for the 30° head-on collision were investigated in a range of studies. The tested subcompact cars from model years 1982/83 satisfied, with few exceptions, the requirements of the proposed ECE global test for head-on collisions. It is therefore not possible to differentiate between safe and less safe vehicles using this test configuration alone. Proof of satisfaction of the requirements of the proposed global test would not automatically increase the safety of the tested vehicles. Furthermore, it is difficult to assess the safety of a vehicle with a single test.

Compared with the 0° collision, the average vehicle deceleration is less in the 30° collision(9); on the other hand, the 30° collision makes greater demands on the vehicle as far as survival area and steering column intrusion are concerned. Due to the angled collision, the dummy moves forward at an angle corresponding to the position of the barrier. As a result, no central collision with the steering wheel occurs. The dummy normally only glances the rim of the steering wheel, and the measured values for the head remain low. The more demanding test condition is presented in the 0° collision in which the possibility of a central collision with the steering wheel and steering column and correspondingly higher head and chest accelerations of the dummy exists.

In the 0° collision specified in ECE Regulations 12 and 33, no dummy is used, although the loads for the occupants will be higher than in the 30° test. In the proposed 30° collision, on the other hand, neither the intrusion of the steering wheel nor the survival area are taken into consideration, although it is to be expected that these would be higher than in the 0° test.

The following conclusions can therefore be drawn on the practical application of the draft regulation:

- The accurate determination of the start of head contact is of great importance. This is possible with a sufficient degree of accuracy. The HPC determination of the duration of head contact produces, in some cases, considera
- The accurate determination of the start of head contact is of great importance. This is possible with a sufficient degree of accuracy. The HPC determination of the duration of head contact produces, in some cases, considerably lower values than the HIC determination of the complete head acceleration pattern. The spread of the HPC values is known and has been incorporated into the draft regulation (tolerance +250).
- The measurement of chest loads and femur loads creates no problems.
- The occurrence of submarining can be detected using several methods. The two methods most frequently used to date are suitable only in combination with the interpretation of belt and, in some cases, femur forces.

The inclusion of certain other existing ECE regulations or parts thereof in the global test must be considered very carefully. Although it is correct to say that the interrelationships of the safety systems in the vehicle should be tested in full-scale tests, it should nevertheless not be forgotten that in real collisions, a wide range of collision situations occur that can and should be tested more simply and at lesser expense in component tests. The inclusion of existing regulations in the proposed global test must not cause the safety of the vehicles to deteriorate.

The requirements made on the survival area, which must be regarded as not very high in ECE Regulation 33, can be satisfied even if the seat is torn out of its mountings. The seat attachment, anchorages of the seatbelts, the strength of the safety belts and door locks, and the energy-absorption capability of the instrument panel and the steering wheel should continue to be tested in component tests, independently of the measured dummy values.

The inclusion of minimum requirements for the door-opening behaviour and leak resistance of the fuel tank in the draft regulation is planned and considered to be correct.

References

1. Economic Commission for Europe (Draft Regulation), "Uniform provisions concerning the approval of private (passenger) cars with regard to the protection of the occupants in the event of head-on collisions," GRCS TRANS, SC1, WP 29 R.23, revised version 1, August 24, 1983.
2. Neilson, I.D., Penoyre, S.P.F. Petty, "Improved test procedures for frontal impact," Proceedings Seventh International Technical Conference on Experimental Safety Vehicles, Paris, 1979.
3. Gennarelli, T.A., "Clinical and experimental head injury," *The Biomechanics of Impact Trauma*, pp. 103-116, Amalfi, 1983, ICTS 1984.

4. Faerber, E., and F. Kramer, "On the application of the HIC as a head protection criterion," Proceedings of the Tenth IRCOBI Conference, Gothenburg, 1985.
5. Faerber, E., "Streuung von Schutzkriterien in kontrollierten Aufprallversuchen gegen die starre 30°-Barriere," research reports of the Federal Highway Research Institute (BASt), Accident Research Division, FP 8267, (English version) NHTSA Highway Safety Literature, Paper 385735.
6. Adomeit, D., Neue Bewertungsgrößen für die Frontalaufprallsicherheit des gurtgesicherten Insassen," Dissertation at the Technical University of Berlin, 1980.
7. Minutes of "Submarining Frequency" Conference on 11 May 1984 at the Federal Highway Research Institute, Data from APR and Ufo MHH Hanover, unpublished.
8. Richling, P., "Vergleichende Untersuchung von-Meßmethoden zur Ermittlung von Abdominalverletzungen, Dissertation at the University of Wuppertal, 1984 (carried out at the Federal Highway Research Institute).
9. Ventre, Ph., "Results of comparative frontal crash tests," Proceedings Seventh International Technical Conference on Experimental Safety Vehicles, Paris, 1979.
10. Comments on Draft Regulation TRANS/SC 1/WP 29/GRCS R.237, Regarding the Inclusion of Other ECE Regulations, Federal Highway Research Institute, Accident Research Division, 1983, unpublished.
11. Comments on Draft Regulation TRANS/SC 1/WP 29/R.299, presented by the Government of the United Kingdom.

The Characteristics of Frontal Impacts in Real-World Accidents

F. Hartemann,
J.Y. Foret-Bruno,
C. Henry, and
G. Faverjon
Laboratoire de Physiologie et de Biomécanique, Peugeot SA/Renault Nanterre, France

C. Got,
A. Patel, and
J.C. Coltat
Orthopaedics Research Institute, Hospital Raymond Poincaré

Abstract

From a file of real-world accidents analyzed by the Peugeot SA/Renault accident investigation team, 572 frontal impacts with a ΔV of more than 35km/h were extracted. These were described and classified on the basis of a large number of criteria that make it possible to compare the degree of representativeness of an oblique test and of a perpendicular test.

This exhaustive descriptive method makes it possible to provide an objective basis for discussions concerned with the procedures of a homologation test.

The Characteristics of Frontal Impacts in Real-World Accidents

In the field of secondary safety, car manufacturers and governments aim at a common objective—that of achieving a set of solutions from among the various technical options and rulemaking procedures that can be envisaged, which will make it possible to guarantee car passengers a level of protection that covers the largest possible range of accident impact types.

Such solutions are, in principle, extremely numerous. But the energy-reducing constraints that weigh down on car manufacture have become so stringent that great attention must be given to the ultimate cost-benefit balance that can be predicted for each of the possible options.

As a means of evaluating the safety of a vehicle, the frontal impact global test is the only one that enables manufacturers to combine intelligently the whole range of factors that govern occupant protection: structure, linking features, restraint systems, seats, etc. In this respect, the global test procedure militates in favor of an optimum use of the materials consumed in the process of vehicle manufacture. With this objective in view, two types of problem remain to be solved, the biomechanical and the accidentological—

- Biomechanical Problems—That of replicating, by using a dummy on board, the kinematics of a

living occupant, and that of the interpretation of the measurements taken from this dummy, which must provide a reliable prognosis of the injury consequences the same impact would have produced upon a real accident victim.

- Accidentological Problems—That of the representativeness of the test procedure. To what type of frontal impact should the vehicle be subjected, bearing in mind that the solutions adopted by the manufacturer to guarantee protection in the test configuration used must also be effective in the maximum of other frontal configurations to which car passengers are exposed when out on the road?

Dummies are improved constantly, and the injury predictions, based on parameters that can be measured in tests, are increasingly reliable. Biomechanical problems today constitute, therefore, themes for research to comprehend more deeply, and no longer are they obstacles to the integrated test option. This is due to the fact that biomechanics is making advances through a rigorous methodology; this is an essential factor that enables exchanges between laboratories and data collected to be accumulated. The same cannot be said of accidentological work. But the representativeness of a test procedure cannot, by definition, be judged other than by reference to real-world accident data.

It is necessary that the knowledge gathered on the subject of accidents be expressed in a language common to all teams gathering and analyzing accidentological data, and that no important parameter be neglected among those that differentiate between various types of impact and that are correlated with injury severity.

In the absence of a strict standardization of the method descriptive of real impacts, accident data collected in various countries that are intensely motorized will always show up divergent patterns, which will make it easy to reach a wide range of interpretations so far as the practical meaning of a particular test procedure is concerned.

These divergent patterns appear not only because of the specificity of the methods of classification used but to a considerable extent because of the different sampling criteria of the cases studied to the peculiarities of the vehicle mix, the road network, and its environment.

The international VDI (Vehicle Deformation Index) code is a useful methodological tool for standardizing descriptions, but it is far from satisfactory for differentiating impacts in all the ways that must be considered when what is involved is the problem of matching them to a particular test mode. The accidentological justification for the latter must be based on a description of the maximum number of parameters that determine exactly the kinematics of occupants and the seriousness of their injuries. It is important to attribute to the impact categories distinguished with the help of these criteria a certain number of indications that make it possible to compare aspects of the sample described and of struck, accident location, collision type, etc.

The accidentological justifications of such a test are rooted in a detailed description such as that proposed below and cannot be based on the usual short-cut, which consists of describing accident data by indicating solely how real-world impacts are broken down into some categories of equivalent test procedures. This direct relating of one thing to another is likely to be strongly influenced by preferences for a particular procedure due to criteria that are not linked to real occupant safety considerations. It has thus been recently suggested(1) that a perpendicular test was preferable to an oblique impact as a type of test procedure since the latter represents an obstacle to the production of airbags. This kind of argument is of the same nature as those that would have us forget that a global test should be preferred to another not because it shows up better a particular means of occupant protection but because it reveals more clearly the level of safety that the model being tested will make available to those traveling in it in the real world of accidents.

Description of Frontal Impacts in the Survey Organized by Peugeot SA/Renault

Selection Criteria

Starting in 1970, 3,580 frontal impacts have been analyzed by the Peugeot SA/Renault accident investigation team. The following description concerns a subsample of cases selected on the basis of these criteria:

1. Cars equipped with 3-point seatbelts
2. Vertical location of damage of types E in the VDI (see above) system; that is, the whole of the lower part of the belt line
3. Direction of the principal force: 11, 12, 01
4. Impact violence estimated by the parameters $\frac{\Delta V}{I}$ and
5. ΔV equal to or lower than 35km/h

Criterion 2, eliminates all cases of running-under into heavy trucks—an impact type that results in most instances in deformations based upon which any estimate of the violence involved is very imprecise. It is considered that the protection of car passengers in collisions with heavy trucks raises the issue of modifications to the heavy trucks and not to the cars themselves.

Criterion 5, ΔV equal to or greater than 35km/h, enables us to use a sample of accidents in which the probability of injury is not inconsiderable. In this way,

one avoids the skew that the presence of impacts without risk for occupants can introduce into the description of impacts, which the test procedure must represent as well as possible. Such impacts without risk are the harmless ones that can, indeed, skew the description in cases where they show peculiarities of impact angle, of the degree of overlap, etc. We show in Table 1 the breakdown of cases of impact in which ΔV was equal to or lower than 35km/h, shown by direction of impact and the horizontal extent of deformation.

Category B2 includes overlap of between one-third and one-half with oblique deformation. The side member on the side opposite the impact is not solicited. This is a frequent configuration in frontal-frontal collisions. The average decelerations for values of ΔV between 45 and 55km/h are of the order of 10g.

Category C includes deformation of the entire width of the front face—an asymmetrical characteristic of head-on collisions with little degree of offset between the two vehicles. The two side members are solicited.

Table 1. Direction of principal force and horizontal location of damage for frontal impacts with $\Delta V < 35$km/h.

	11			12			01		
D	Y or Z	L or R	D	Y or Z	L or R	D	Y or Z	L or R	TOTAL
2.1	4.7	4.7	20.7	33.7	22.8	3.3	5.1	2.8	100

The classification in this table concerns 1,057 cases.

Definition of the Five Categories of Frontal Impact

The directions of impact, the geometry of deformations, and the kinematics of the vehicle and of occupants between the beginning and the end of the period of contact between the vehicle and the struck obstacle are of such wide variety in frontal impacts that any attempt at categorizing them necessarily involves an element of the arbitrary. What is important is to reduce this as much as possible by the use of technical criteria.

The five categories proposed here take account of the front-end configurations of European cars. The differences essentially have to do with the way in which the side members and the engine transmission units are solicited—a solicitation that depends on the degree of overlap at the interface with the front end of the other vehicle and on the impact violence.

Category A (Figure 1) includes impacts with overlap of between one-quarter and one-third of the front end. A single side member is solicited in one-third overlaps. This type of rectangular deformation is characteristic of collisions that are offset against another vehicle or against a fixed obstacle. The car body side is often solicited to a considerable extent.

Category B1 includes rectangular deformation that can be reproduced by impact against a barrier at 0° with overlap of between one-third and one-half. The relative rarity of this type of deformation justifies its allocation to category B2 now described.

Category D includes deformation observed in less than 20 percent of frontal impacts. Deformations of the passenger compartment are rare for ΔV values of less than 60km/h. Impacts of this category are fairly well reproduced by using the barrier at 0°.

The graphical representation of illustrating these categories is a less than ideal manner of doing so. Other variants exist for each category. In particular, the depth of penetration is arbitrarily shown since it can be less than appears or, on the contrary, greater. But constants remain and they are very precise:

1. The general appearance of deformation, which is rather rectangular or rather triangular (B2, etc.)
2. Overlap of one-quarter to one-third of the front end, overlap of one-half to two-thirds of the front end, or overlap that is total, the above applying whatever is the depth of crush
3. Angle of deformation less than 15° in categories B1 and D; between 15° and 45° in categories B2 and C

Principal Characteristics of the Categories of Frontal Impacts

Impacts by Type of Collision

Deformations that are evenly spread across the front end (category D) are relatively rare in head-on collisions (Figure 2). In 85 percent of cases, deformations are

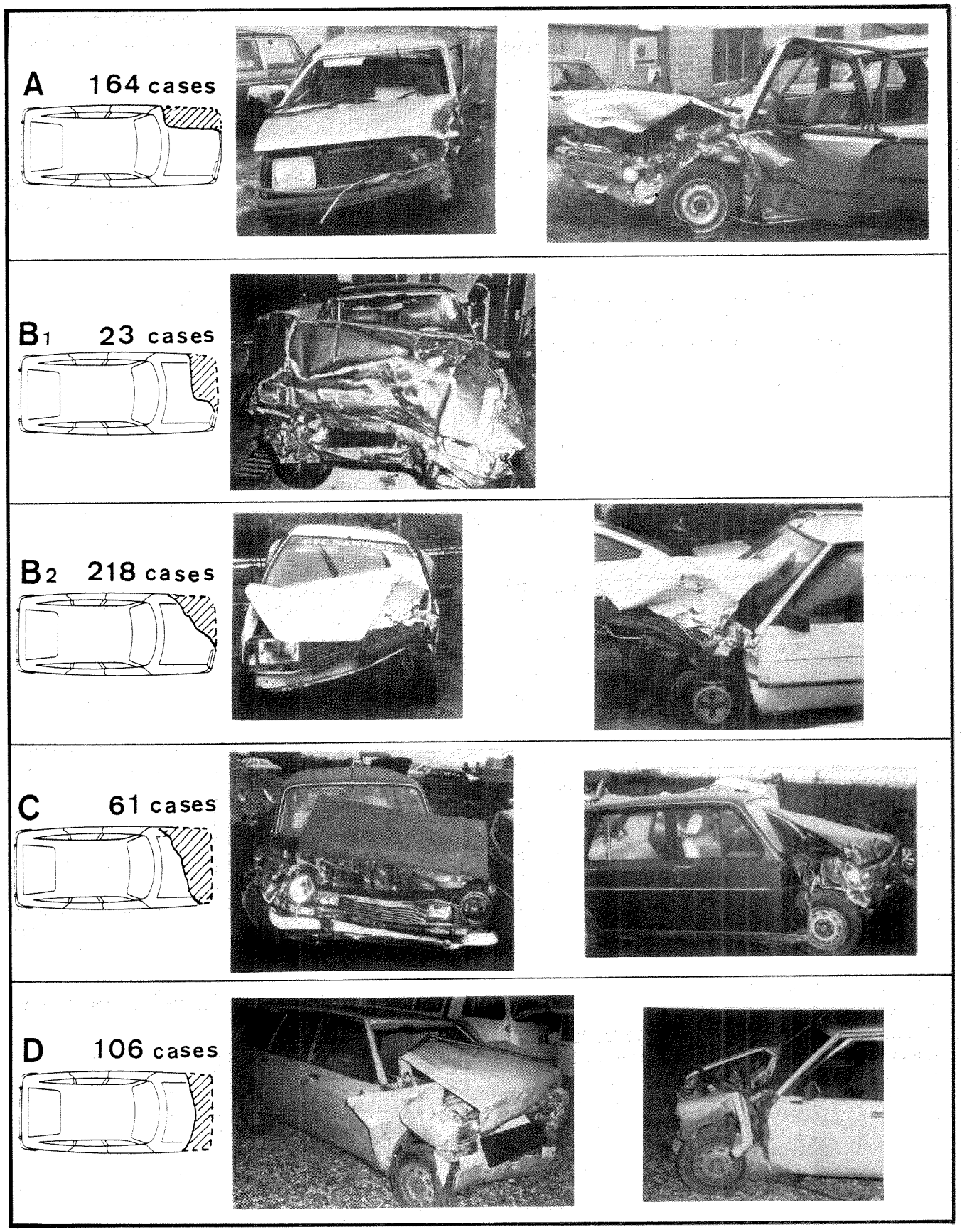

Figure 1. The five categories of frontal impact

	TYPE OF COLLISION				
	Head-on	Front to Rear	Front to Side	Front to fixed Object	TOTAL
A 164 cases	21 % 77 47 %	22 % 4 2 %	11 % 8 5 %	64 % 75 46 %	29 % 164 100 %
B_1 23 cases	52 % 188 78 %	61 % 11 4 %	32 % 24 10 %	15 % 18 7 %	42 % 241 100 %
B_2 218 cases					
C 61 cases	12 % 43 70 %	0 0 %	16 % 12 20 %	5 % 6 10 %	11 % 61 100 %
D 106 cases	15 % 53 50 %	17 % 3 3 %	41 % 32 30 %	16 % 18 17 %	18 % 106 100 %
TOTAL	100 % 361 63 %	100 % 18 4 %	100 % 76 13 %	100 % 117 20 %	100 % 572 100 %

Figure 2. Frontal impacts distribution by type of collision

	ΔV 36 to 45 km/h	ΔV 46 to 55 km/h
A 164 cases	7 g	8 g
B_1 23 cases	9 g	10 g
B_2 218 cases		
C 61 cases	10 g	12 g
D 106 cases	11 g	14 g

Figure 3. Average of mean deceleration values by type of frontal impacts

	ΔV 45 to 55 km/h	ΔV 56 to 65 km/H
A 164 cases	.71	.95
B_1 23 cases	.43	.80
B_2 218 cases		
C 61 cases	.06	.53
D 106 cases	.04	.29

Figure 4. Proportion of cases with passenger compartment intrusion exceeding 150mm in two ranges ΔV

	BELTED		UNBELTED		
	No Injury + Minor + Moderate	Severe + Fatal *	No Injury + Minor + Moderate	Severe + Fatal *	TOTAL
A 164 cases	52 30 %	12 21 %	59 33 %	41 25 %	164 29 %
B_1 23 cases	81 47 %	23 40 %	80 44 %	57 36 %	241 42 %
B_2 218 cases					
C 61 cases	11 6 %	9 15 %	17 9 %	24 15 %	61 11 %
D 106 cases	30 17 %	14 24 %	25 14 %	37 23 %	106 18 %
TOTAL	174 100 %	58 100 %	181 100 %	159 100 %	572 100 %

* Severe + fatal means M.AIS ≥ 3

Figure 5. Restrained and unrestrained drivers—severity by type of frontal impact

	ΔV (km/h)				
	36 to 45	46 to 55	56 to 65	66 to 75	TOTAL
A 164 cases	33 % 93 57 %	29 % 50 30 %	25 % 20 12 %	3 % 1 0,6 %	29 % 164 100 %
B_1 23 cases B_2 218 cases	42 % 119 49 %	45 % 79 33 %	34 % 27 11 %	47 % 16 7 %	42 % 241 100 %
C 61 cases	6 % 18 29 %	10 % 18 29 %	19 % 15 25 %	29 % 10 16 %	11 % 61 100 %
D 106 cases	19 % 55 52 %	16 % 27 25 %	22 % 17 16 %	21 % 7 7 %	18 % 106 100 %
TOTAL	100 % 285	100 % 174	100 % 79	100 % 34	100 % 572

Figure 6. Change of velocity (ΔV) by type of frontal impact

	BODY REGION				
	HEAD	THORAX	ABDOMEN	PELVIS and LEGS	TOTAL
A 164 cases	4.2	3.7	3.2	11.6	22.8
B_1 23 cases B_2 218 cases	5.3	8.5	6.9	19.6	40.2
C 61 cases	2.6	2.6	1.1	7.9	14.3
D 106 cases	4.8	4.8	4.2	9.0	22.8
TOTAL	16.9	19.6	15.3	48.1	100.0

Figure 8. Percent distribution of AIS ≥ 3 for unrestrained drivers (112 severely injured and 15 killed)

	BODY REGION				
	HEAD	THORAX	ABDOMEN	PELVIS and LEGS	TOTAL
A 164 cases	3.7	0	0	7.4	11.1
B_1 23 cases B_2 218 cases	11.1	3.7	7.4	29.7	51.9
C 61 cases	3.7	0	0	3.7	7.4
D 106 cases	7.4	3.7	7.4	11.1	29.6
TOTAL	25.9	7.4	14.8	51.9	100.0

Figure 7. Percent distribution of AIS ≥ 3 for unrestrained drivers

	HEAD CONTACT LOCATION				
	Steering Wheel	A Pillar	Other	Location Unknown	TOTAL
A 164 cases	7.5	0	3.8	9.4	20.7
B_1 23 cases B_2 218 cases	30.8	1.3	6.9	7.5	46.5
C 61 cases	6.9	0.6	0.6	1.9	10.1
D 106 cases	20.1	0	0.6	1.9	22.6
TOTAL	65.3	1.9	11.9	20.7	100.0

Figure 9. Head contact location—restrained drivers

only a fraction (about 75 percent) of all the impacts with overlap of between one-quarter and one-third of front ends. Bearing in mind that this distribution of impacts by type of collision is observed, one cannot say that the perpendicular test is representative of head-on collisions.

The high level of representation of impacts of the 0° type in collisions against the side of another vehicle (front-to-side) should also be noted. Such collisions, however, are rarely severe for the occupants of the asymmetrical; even this proportion is under estimated. In point of fact, our analysis has concerned only those cases in the sample where it has been possible to calculate the value of ΔV. In a large proportion of the collisions that resulted in category A deformation, with much offset contact, impact was followed by immediate separation of the two vehicles. In such cases, it is impossible to calculate ΔV, or it is at least rash to do so. In all of the 164 cases, the value of ΔV is known. These cases represent striking vehicle; the average level of deceleration is relatively low due to the considerable penetration into the side of the struck car.

The Average Value of Deceleration

This value increases logically with the horizontal extent of deformations. It reaches 14g between 46 and 55km/h for impacts akin to those against the barrier at 0° (Figure 3). The overestimation of average levels of deceleration by perpendicular impact has been pointed out in earlier publications(2,3,4), which have brought out the fact that the oblique impact produces decelerations of the same order of magnitude as in the majority of frontal impacts occurring in real-world accidents. But this difference in severity is not a relevant justification of the oblique impact. It could even, on the contrary, justify the choice of a 0° test for the very reason that this gives higher values to the parameters used as head and thorax injury criteria. This is, by the way, the reason given by a certain number of manufacturers for abandoning their oblique impact test.

The defect in this manner of reasoning is that of neglecting the fact that the major cause of serious injuries for restrained occupants is intrusion and that the structure's resistance to intrusion cannot be verified by means of a perpendicular impact—unless, that is, the operation is undertaken at very high speed—and obliges manufacturers to adopt solutions of which the cost-benefit analysis would be catastrophic. As witness, the first ESV models.

The intrusion measured at the level of the A-pillar exceeds 150mm in 71 percent of cases of the very offset impacts (category A, Figure 4) in which ΔV lies between 45 and 55km/h. On the other hand, in this same spread of speeds, intrusion is only observed in 4 percent of impacts with deformations spread across the whole of the front end (category D). The consequences of intrusion for restrained occupants are extremely serious (Table 2).

Intrusion provides the main explanation of the distribution of drivers who are killed or seriously injured in the various categories of frontal impact. These are as numerous in the impact categories with very little overlap (category A) as in those related to the 0° test (Figure 5)—the impacts related to the impact test contributing 55 percent of the total of the serious or fatal cases (restrained drivers).

Table 2. Severe injury and fatality rate for restrained drivers

Intrusion	ΔV (km/h)		
	46 - 55	56 - 65	66 - 75
< 150mm	.13	.31	.50
≥ 150mm	.37	.83	.94

The Breakdown of Serious Injury by Body Segment

This breakdown, being the subject of measures in tests, shows the importance of injuries of the bony pelvis, fractures of the acetabulum in general, and of the lower limbs (Figure 7).

If one takes the figure of 100 to represent the serious injuries recorded in impacts that relate to the oblique test (categories B1, B2, etc.) and if one proceeds in the same manner for the serious category D injuries (impacts related to the 0° test), one observes that an oblique test replicates more faithfully the exposure to risk of the various body segments considered (including the abdomen) than would a perpendicular test (Table 3).

The same calculation made with respect to drivers that were not restrained gives a different breakdown (Figure 8 and Table 4).

Because the seatbelt limits occupant displacement, the head/steering wheel contact is by far the most frequent among restrained drivers (Figure 9).

The above data seen as a whole do justify one of the criticisms leveled at the oblique test: this does not verify the effectiveness of head protection in an entirely satisfactory fashion.

It would only be necessary to improve it in an appropriate way for this test to become undeniably useful as a procedure.

Table 3. Breakdown of serious injuries by body segment in impacts related to the oblique test, to the 0° test, and in all impacts. Drivers restrained (retractor belts)

Impact	Body Segment				
	Head	Thorax	Abdomen	Pelvis & Lower Limbs	Total
Impacts related:					
- to 30° test	25.0	6.2	12.5	56.2	100.0
- to 0° test	25.0	12.5	25.0	37.5	100.0
All impacts	25.9	7.4	14.8	51.9	100.0

Table 4. Breakdown of serious injuries by body segment. Drivers unrestrained.

Impact	Body Segment				
	Head	Thorax	Abdomen	Pelvis & Lower Limbs	Total
Impacts related:					
- to 30° test	14.5	20.4	14.7	50.7	100.0
- to 0° test	21.0	21.0	18.4	39.5	100.0
All impacts	16.9	19.6	15.3	48.1	100.0

Conclusion

The integrated test is the optimum procedure for verifying the level of safety of a vehicle to the extent that this procedure brings in the greatest number of potential risk factors for the occupant.

For a given procedure, the fact that it produces high values for the parameters used as injury criteria is not an adequate proof of relevance. The procedure must also oblige vehicle manufacturers to adopt effective counter-measures in the greatest number of real-world accident configurations: this is the function of a "representative" test.

A description of 572 frontal impacts with a ΔV greater than 35km/h shows that the oblique test is the most representative of the sample.

It is highly desirable that accident data available to a large number of accident analysis teams should be described in the same way with a view to providing an objective basis for the decisions that must be taken by the appropriate governmental and intergovernmental bodies concerning homologation procedures.

References

1. National Highway Traffic Safety Administration, FMVSS 208, Docket 74.14 Notice 38, April 1985.
2. Ventre, Ph., "Proposal methodology for drawing-up efficient regulations," 4th International Congress on Automotive Safety, 1975.
3. Ventre, Ph., and J. Provensal, "Proposition d'une méthode d'analyse et de classification des sévérités en accidents réels," International Conference on the Biokinetics of Impacts, June 1973.
4. Tarriere, C., A. Fayon, and F. Hartemann, "The contribution of physical analysis of accidents towards interpretation of severe traffic trauma," Proceedings 19th Stapp Car Crash Conference, 1975.

Testhouse Experiences With the Draft ECE Regulation for Head-On Collisions

C.G. Huijskens,
J. Maltha, and
A. Dyche
Research Institute for Road Vehicles, TNO, Delft, The Netherlands

Abstract

TNO performed a series of well-controlled full-scale 30° angled barrier tests with Volvo 343 vehicles. In addition, a series of simplified sled tests with a Volvo 343 body mounted at angles of 15° and 19° (i.e., the angle between the longitudinal axes of the car body and sled) were conducted. The sled tests were carried out with a ΔV-time history obtained from the full-scale barrier tests. Test conditions and evaluation of the dummy results for driver and passenger were based on the new draft ECE regulation for head-on collisions and on the proposed ISO DIS 7862E for the simplified sled simulations of barrier crashes.

It was found that the ECE sled test procedure in itself is well defined and feasible with minor modifications. It should be noted that all the dummy results were low in comparison with the performance criteria in the regulation, and so, considering the dummy as a measuring instrument, the results are at the lower end of its operating range. For vehicles with different ΔV-time histories for the left and right sides during the full-scale test, it is not possible to reproduce dummy kinematics and at the same time all major injury parameters with a single mounting angle of the body on the sled and one ΔV-time history. The paper presents more details about the mounting angle and ΔV-time history problems.

Introduction

The new draft ECE regulation for occupant protection in head-on collisions specifies a 50km/h full-scale crash test against a 30° angled flat rigid barrier(1). If a vehicle type meets the requirements of this new draft regulation, it will be considered to satisfy ECE Regulations 11, 12, 14, 17, 21, 33, and 34. In case of modifications of a standard vehicle type with respect to interior fittings, a simplified equivalent impact test with a car body on a sled can be carried out (see Figure 1).

The regulation refers for the simplified sled test to an annex "test procedure with trolley," which is based on the ISO Draft International Standard 7862E(2). This standard is currently under modification by the experts of Working Group 1 of ISO/TC22/SC12 and now specifies a standard angle of 15° for mounting the vehicle body on the sled as the best representation of the 30° angled barrier test. However, this group recognizes that this standard 15° angle is not sufficiently representative for all types of vehicles and hopes to define in the future a method of calculating an equivalent angle of body mounting based on results of the 30° barrier test and more specific for the type of vehicle.

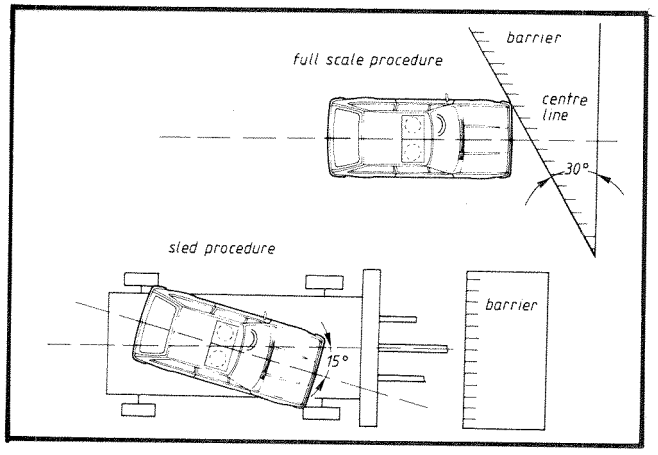

Figure 1. Test procedures of draft ECE regulation on head-on collisions

At the TNO crash facility, two full-scale 30° barrier tests, two 15° simplified sled tests, and two 19° simplified sled tests were conducted.

The vehicles and bodies in the tests were all Volvo 343, which is considered to be a good representative of a standard mid-sized European car. All tests were carried out with two Part 572 dummies and standard 3-point retractor restraint systems. The impact velocity of the full-scale tests was 50km/h, and for the sled tests the impact velocity was calculated to be 45km/h to obtain the same final ΔV-time history as measured in the full-scale tests.

The objectives of the test program were—

- To investigate the practicalities of the full-scale and sled test procedures
- To find out how closely the full-scale tests could be reproduced by the simplified sled tests at the standard angle of 15°
- To find a calculation technique for a car-specific angle in the sled test and check if this resulted in a better representation of the full-scale test
- To investigate the repeatability of the test results

Test Procedures

Barrier Tests

The full-scale 30° angled barrier tests are the baseline tests for the simplified sled test procedure. The sled tests were to be carried out with a velocity change-time history reproducing the ΔV-time curve from the barrier tests. The ΔV-time history that was to be used for the simplified sled test was established from the integration of the longitudinal accelerations of the sills. The regulation states that the impact (driver) side integrated acceleration should be reproduced within ±0.5m/s, but, due to a large difference between the left and right side ΔV-time histories (e.g., 2.2m/s at 140ms) in these full-scale tests, an average ΔV-time history of both sides was used for the velocity-time history of the sled test (see Figure 2). The accelerations were filtered at CFC 180 before integration.

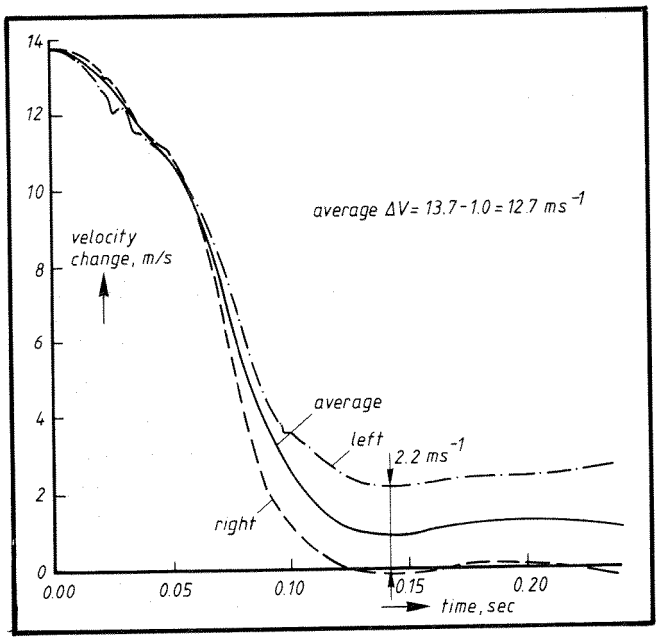

Figure 2. V-time curves of the full-scale 30°angled barrier test

Calculation of Equivalent Angle of Mounting for the Simplified Sled Test

It is recognized that the standardized 15° angle of the vehicle body mounting for the simplified sled test might not give the best possible reproduction of the full-scale barrier tests for all types of vehicles. Current discussion in the ISO Working Group led to a resolution that asked for calculation methods of a so-called Equivalent Angle, which is specific for a certain type of vehicle.

The translation angle resulting from a combined forward and sideward translation of the vehicle is defined here as a fixed angle that is the result of the ratio of the average (left and right sides) longitudinal and lateral ΔV-time histories. However, the ratio between ΔV longitudinal and ΔV lateral is a function of time. The method used to obtain the Equivalent Angle was to define the times of the most important dummy-related criteria and calculate the instantaneous translation angle at these times and then simply average it (see Table 1).

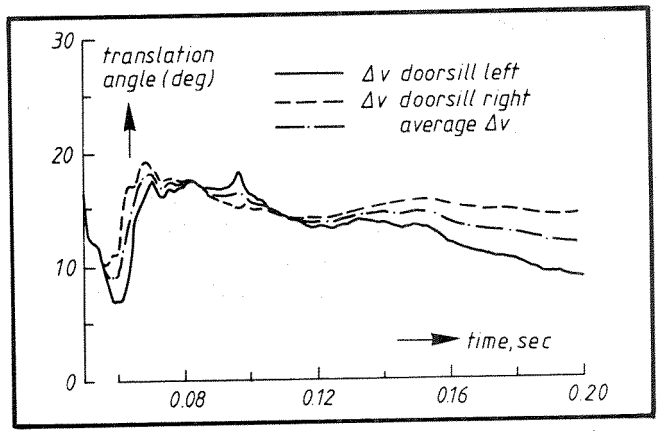

Figure 3. Calculated translation angle as function of time

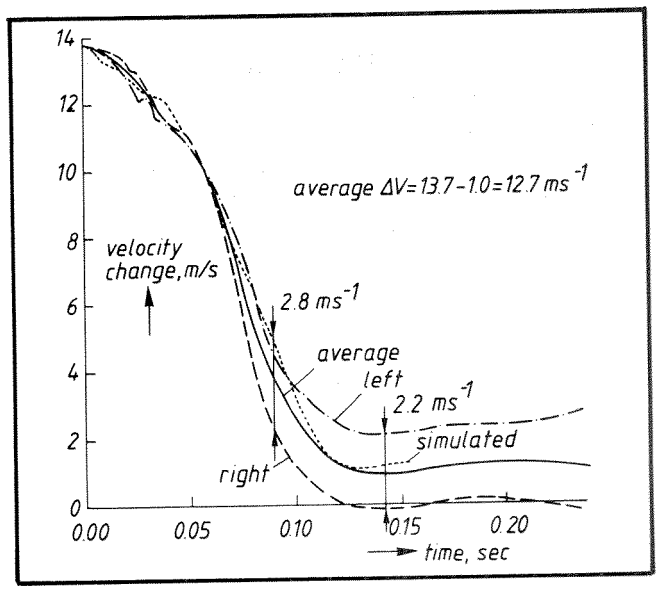

Figure 4. Simulated and full-scale V-time histories

Table 1. Optimal car body to sled mounting angles for the different criteria

Criteria	Time (ms)	Translation Angle (degrees)
max. belt loads	97	16.3
max. res. chest accn.	105	14.9
max. res. pelvis accn.	107	14.6
max. res. head accn.	135	14.3
max. head excursion	140	14.5
Average		14.9

For the Volvo 343 vehicle, this resulted in an Equivalent Angle of 14.9°.

The criteria chosen were based on the final objective of the test procedure, which is to obtain identical injury-related measurements as in the barrier test (a problem is that the injury-related measurements are dependent on the type of the vehicle and restraint used). The criteria selected were the time that maximum head, chest, and pelvis accelerations, the maximum belt loads, and the maximum head excursion occurred.

The translation angle is calculated from:

Translation Angle (t) = arctan (ΔV lateral (t)/ΔV longitudinal (t)) (1)

It was also observed that in the full-scale test, the vehicle rotated clockwise (viewed from above) during the selected time-interval (97 to 140ms) and this rotation was also a function of time (see Figure 5). The effect of the vehicle rotation on the kinematics of the dummy relative to the vehicle compartment combines with the lateral movement of the vehicle. This complicated kinematics can obviously not be exactly duplicated by one fixed angle, but a mean angle of 4° was selected to be added to the 15° Equivalent Angle. The total angle of 19° is similar to the angle of movement of the dummy relative to the vehicle, measured from high-speed film.

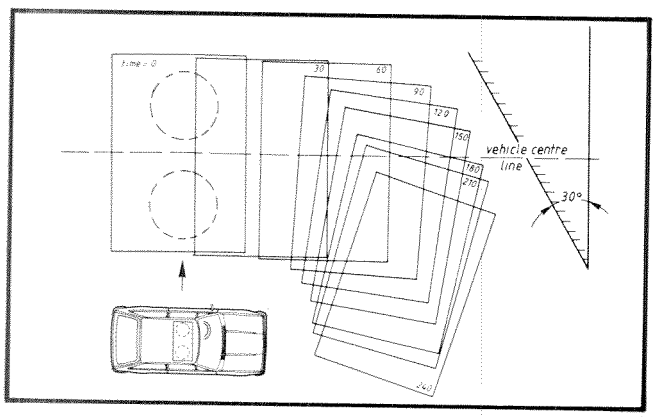

Figure 5. Top view of vehicle movement in the full-scale 30° angled barrier impact test

Simplified Sled Tests

For the simplified sled tests, a Volvo 343 body was mounted on a subframe attached to the suspension mounts and chassis. Then the body was reinforced in these critical areas by welding additional supports from these areas to the subframe. The subframe with body was bolted on the rigid sled at an angle of 15° or 19°. The center of gravity of the car body was on the longitudinal centerline of the sled. The sled was decelerated by a programmed array of steel-crumpling tubes, resulting in a ΔV-curve similar to the average ΔV-time history of the left and right sills in the full-scale tests (see Figure 4).

Results of 30° Angled Barrier Impact Test

The two tests carried out on a concrete laboratory floor covering had similar vehicle movements and dummy results. For the first part of the impact phase, the vehicle continued to move in the same direction as its initial velocity. After 60ms, the vehicle rotated clockwise (viewed from above) with a rotational velocity (yaw velocity) of 1.5rad/s at 140ms, and it also continued to move forward with a velocity of 1.0m/s at 140ms (see Figure 5).

In this 30° collision, the occupant trajectory with relation to the laboratory reference frame was in the direction of the initial movement of the car before impact for most of the time during the impact phase. The lateral displacement of the occupant relative to the vehicle was due mainly to the lateral movement of the vehicle. No contact occurred between the dummies and the vehicle, except the knees (but the femur load cells indicated no significant loads acted to the knees) and the driver's left arm.

Comparison of Sled and Full-Scale Results

General

In general, when the peak values and corresponding times of the dummy results are considered, the variation between the three different test modes (30° barrier, 15° and 19° sled tests) is within the variation between the two tests in the same test mode. This implies that both the 15° and 19° tests were reasonable representations of the 30° barrier tests as far as the overall injury parameters are concerned. It should be noted, however, that only two tests were carried out for each test mode. It should also be noted that the dummy results were low in comparison with the injury levels of the regulation, and no contact occurred between the dummies and the vehicle structure except for the knees and the driver's left arm. When the individual time histories of the dummy results and the dummy kinematics are studied in detail, differences between the test modes can be seen, which are discussed in the following sections.

Driver

The 15° sled test results were generally more like the full-scale results than the 19° sled test results. The chest acceleration and belt loads in the full-scale and 15° sled tests had slightly longer duration signals. The head accelerations in the 15° sled tests were slightly higher than in the full-scale tests, and they had more peaks and troughs in the vertical and longitudinal directions during

the arm-to-door contact period. The arm contacted the door earlier and further rearward than in the full-scale tests and 15° sled tests. Generally, the 15° sled test results, apart from the differences during the arm and knees contact times, were similar to the full-scale results except that they indicated that the sled ΔV was slightly higher by having longer signals.

Passenger

The lateral movement of the dummy during the full-scale tests and the sled tests appeared to be critical as to the way the dummy rotated out of the shoulder seatbelt. It could be analyzed from the high-speed film of the 15° sled tests that the dummy did not move as far laterally as in the full-scale tests and the rotation of the shoulders was different. The dummy tended to move in the direction of its initial velocity.

The 19° sled tests, although closer to the full-scale than the 15° tests, still did not duplicate the full-scale results exactly. The dummy accelerations and the shoulder belt loads were both lower and longer in duration in the 19° tests compared with the full-scale results. These results suggest that the overall sled velocity change was too low and also rotation of the vehicle compartment in the full-scale tests may have caused the dummy to rotate differently out of the shoulder belt.

Discussion of the Results

It can be seen from previous sections that due to the different ΔV-time histories for both vehicle sides, one ΔV reference curve (obtained by integration of the longitudinal acceleration of the vehicle) cannot be used to exactly duplicate both the driver and passenger side dummy results in the simplified sled test.

The vehicle rotation may also affect the position of the dummy relative to the seatbelt anchorages and hence the reaction of the restraint system on the dummy. The increased angle of 19° did not appear to improve the results or the seatbelt performance dummy passenger. The 19° mounting angle also produced different contact areas between the driver dummy and the vehicle, which were better at 15°. A better solution would be to carry out two separate tests for the driver and passenger with different ΔV-time histories and mounting angles.

In the sled tests, there was no attempt to simulate the movement of the vehicle other than laterally. It is known that for a perpendicular full-scale frontal impact, such effects as vehicle pitch and body distortions affect the dummy kinematics and produce different results when compared with a sled test with the same ΔV(3). These effects will combine with differences caused by the "inexact" simulation of the lateral vehicle movement in the sled test simulation. All of the dummy results were low compared with the injury criteria according to the regulation, and no head or chest contact occurred. When the dummy is considered as a measuring instrument, the variation between tests, as a percentage of the measuring range of the dummy, is low, so differences between tests are masked by random errors. The differences in dummy results in terms of mean accelerations were low but could be expected to be much higher if head and chest contact had occurred due to difference in contact areas and times, which could not be duplicated exactly.

Conclusion

1. The test procedures for testing to the draft ECE regulation are well defined and were feasible from the practical point of view.
2. The standard body mounting angle of 15° for the simplified sled tests gives overall peak and average dummy results similar to the 30° barrier tests. This may be specific for the test vehicle chosen.
3. A method used to calculate an Equivalent Angle for the Volvo 343 results in an angle of 14.9° for the relationship between the lateral and longitudinal ΔV.
4. It would appear that one fixed mounting angle and velocity time history cannot exactly reproduce both the passenger and driver results where a large difference in ΔV-time histories between the left and right sides occurs. A better method would be to define a velocity time history and calculate a mounting angle for each dummy position, then carry out a separate test for each dummy.

References

1. Draft ECE Regulation, TRANS/SC1/WP29/R.237/Rev.1, "Uniform provisions concerning the approval of private (passenger) cars with regard to the protection of the occupants in the event of a head-on collision."
2. ISO Draft International Standard 7862E, "Simplified equivalent sled test procedure for evaluating adult restraint systems in simulated head-on collisions."
3. Berge, S., B. Lundell, and M. Nilsson, "Simulation of vehicle pitch in sled testing, SAE Paper 850098.
4. Lundell, B., "Dynamic response of a belted dummy-a computer analysis of crash pulse variation," SAE Paper 840401.

Comparison of 0° and Oblique Tests

J. Hackney
U.S. Department of Transportation, National Highway Traffic Safety Administration

The accident experience in the United States as taken from the national crash severity study indicates that more than 60 percent of AIS 3 and greater injuries occur in frontal collisions that have a principal direction of force of 12 o'clock. Almost 60 percent of all frontal crash occurrences are in this clock direction. Additionally, the NCSS data show that the most prominent frontal crash mode has distributed frontal damage—more than 30 percent of AIS 3 and greater injuries occur in this crash mode. The risks associated with these 12 o'clock DOF and distributed damage crashes are higher than any other frontal collision.

Also, a predominant amount of societal harm, AIS 2 and greater (using Dr. Malliaris' definition of harm), in frontal events has a 12 o'clock PDOF. Again, the largest single contributor to harm is the distributed damage crash mode. Offset crash modes with 12 o'clock PDOF are the next largest contributors to harm. The first oblique PDOF (11 o'clock) is ranked sixth in contributing to harm. These U.S. accident data all indicate the appropriateness and support the use of the 0° barrier test.

From controlled crash tests, we can compare the relative dummy responses of 30° and 0° barrier tests. Figure 1 shows the average response for six vehicles (12 dummies) in the two test conditions. The test speed was 35mph. These responses are in terms of percent of FMVSS 208 requirements. From these data, it is quite obvious that a 30° test is essentially no requirement. For the National Highway Traffic Safety Administration or the vehicle manufacturer to use this oblique test to evaluate safety performance of present production vehicles would represent a very significant step toward reducing safety levels that exist in today's vehicle fleet.

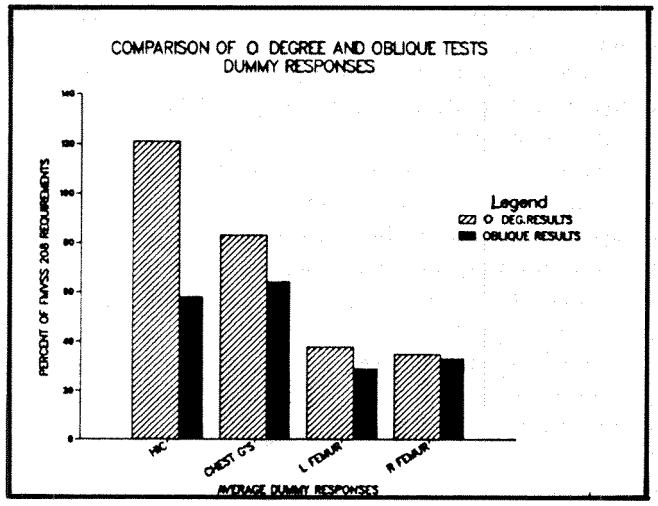

Figure 1. Comparison of 0_o and oblique test dummy responses

Applying Computer Techniques in the Design and Development of an Occupant Restraint System

N. D. Grew
Austin Rover Group Limited, BL Cars PLC, Cowley, Oxford, United Kingdom

Abstract

Computer techniques are applied in all areas of vehicle design having an influence over the speed of the design process and the efficiency and coherence of the design itself. The deployment of analytical methods removes the need for some test work and changes the role of much of the rest.

A restraint system design has implications for several vehicle areas:

- Body design
- Seat design
- Interior trim and hardware
- Steering System

and must be considered against all these as well as the structural crashworthiness of the vehicle.

At the concept stage, computer methods outline the implications of the functional specification so it can be modified if found to be unreasonable or inconsistent. As the vehicle design progresses, the requirements of the restraint system are broadly defined using programs to assess comfort and dynamic performance.

Initial sled test work is based on the realistic possibilities as determined from the dynamic simulations, and the results of these tests serve to refine the model and improve background data. These tests are deliberately

kept simple, and the computer model is used to study the effects of different impact conditions and component designs. This information is fed to design areas. This sequence of test and simulation is repeated in conjunction with prototype vehicle tests. The process means that sled tests have been effectively used and their combination with computer simulations gives a better understanding of, and confidence level in, the restraint system performance in the full vehicle test.

Introduction

The design of an occupant restraint system involves the integration of vehicle components from a variety of design areas. Each area considers the safety of the occupant as a part of its design brief, and the nature of each component affects the time required from design to tooling to manufacture.

Computer-aided design techniques can be applied in the design process, both to the specific areas of component design and to the overall restraint concept. Thus, simulation techniques can define the performance required of each component, and computer analysis can be used in the design of each component to meet the specification.

Practical testing of components and restraint system is both necessary and a legal requirement. The integration of this testing with the computer techniques is important if the strengths of the analysis methods are to be used efficiently.

The following discussion centres on the design and development of a system to protect the occupant in a frontal collision, but the principles and approach can be applied to other crash conditions.

The Concept

Once the decision has been taken to design a new model, the nature of the vehicle is defined in terms of its dimensions, levels of specification, and intended markets. The laws governing sales into those markets, competitor vehicles, and in-house policies will determine the safety performance the vehicle must meet. At this stage, therefore, it is important to insure that the nature of the vehicle concept in terms of its dimensions, etc., is compatible with the necessary safety performance and to provide some idea, to the various design areas, of the specific responsibilities that implies for them.

Once this feasibility study is completed, these responsibilities can be defined more precisely, taking into account their interaction as components of the occupant restraint system (see Figure 1).

Two types of computer simulation model will be developed: one of the structure in which the occupant is merely another constrained mass; the other of the occupant and basic interior in which the structural collapse is seen only in its effect on overall vehicle kinetics and intrusions into the passenger compartment. The first gives important data that enables the second to be

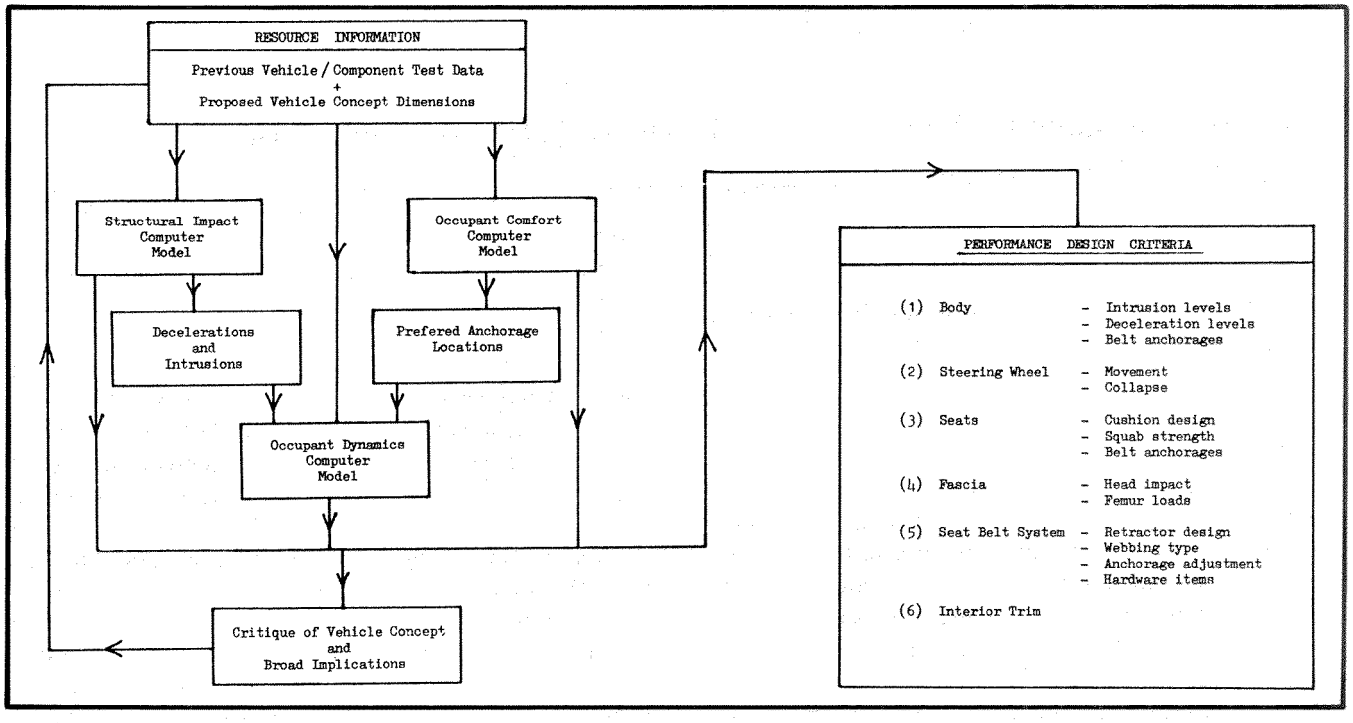

Figure 1. Application of computer simulation techniques at the vehicle concept stage

configured in a realistic manner. The results of the occupant simulations will throw light on the consequences of the structural performance and may force some changes to be made.

The structural modelling techniques involve discrete masses with appropriate constraints and stiffness elements and use CSMP (Continous System Modelling Program) and ADAMS computer programs(1).

The occupant modelling uses a version of the CALSPAN CVS program, which has been significantly modified by Austin Rover over a period of several years(2). Figure 2 shows a schematic combination of these two techniques.

Seatbelt Comfort

At this stage, the packaging hardpoints will become clear, and it is important to establish the seatbelt anchorage locations with these. For this purpose, a computer program BELTFIT is applied(3).

This program was written by MIRA (Motor Industry Research Association) to enable a user to create a seatbelt system that meets the geometric constraints of legal comfort zones and the comfort requirements of the expected range of vehicle users. The anchorages can be appraised against the selected requirements of the appropriate markets and positioned accordingly. Likewise, any necessary features such as anchorage attachment to the seat or height adjustment can be decided on by considering the variety of potential occupant sizes and postures. The program warns of certain sources of discomfort, and the pictorial representation gives the user the option to add his own experience and judgement (see Figure 3). Thus, anchorage locations, the part of the vehicle to which they are attached, and any ranges of motion can be specified and available for the design areas concerned to begin working with.

Such an anchorage arrangement gives a good basis for a seatbelt system that will perform well under accident conditions. However, other design areas need to know the parameters within which they should be operating. At the earliest stages, the simulation techniques can help to define these.

Occupant Dynamics

Figure 4 shows a simple simulation carried out at the early stages of a design concept. A restraint system from a current vehicle has been appropriately modified with a series of planes included to represent potential positions for the steering wheel during a barrier impact of the proposed vehicle. These planes are given no stiffness, but they each register the time, point, and speed of impact of the head. By carrying out a series of simulations with different webbing stiffnesses, impact trajectories are determined. These can then be used to give guidelines as to the limitations that should be set upon steering wheel movement so that the head should not strike the wheel hub.

Also, some indication of kinetic energy to be absorbed by the steering system can be gained from the impact speeds of chest and head. Typically, a trajectory using a medium webbing rate will be used as the basis of the decision so there is flexibility to alter the trajectory, if required, as the details of the restraint system become clearer and the computer model more accurate.

A similar method can be used to determine facia impact requirements for the passenger side although, generally, the headform pendulum test upon the component will be more stringent than the needs of an occupant wearing his seatbelt.

From the computer simulations carried out up to this point, the viability of the vehicle concept will have been established and critical areas identified. Some design areas will be evolving analytical component models and applying the basic guidelines from the occupant simulations in appraising their designs; for example, the facia is usually a large plastic moulding requiring a complex forming tool for which the design lead time is long. The application of finite element techniques is crucial at this stage to establish the impact, beam strength, and vibration properties (Figure 5).

From the point of view of the whole vehicle and restraint simulation models, this is the stage to carry out practical benchmark tests using modified existing components and parts that might be needed to improve the crash performance.

Sled Testing

A representation of the restraint system is set up on a sled mounted on a Hyge test rig. The deceleration pulses are taken from current structural simulation models, and appropriate controlling pin profiles are chosen or constructed to give approximations to these. In the first series of tests, the hardware will be composed of current vehicle components set in the most likely positions. This corresponds to the initial computer simulation model and will help to verify or improve it.

Using information from the computer model, some tests will differ from the standard to explore changes that the model has indicated would lead to improved performance.

The computer model can present data from areas in which it is impractical to measure, and, to help in its development, the data collected from the sled tests will be much more comprehensive than would be needed to verify standard injury criteria. Figure 6 summarises the sort of records that are made and the types of data construed from them.

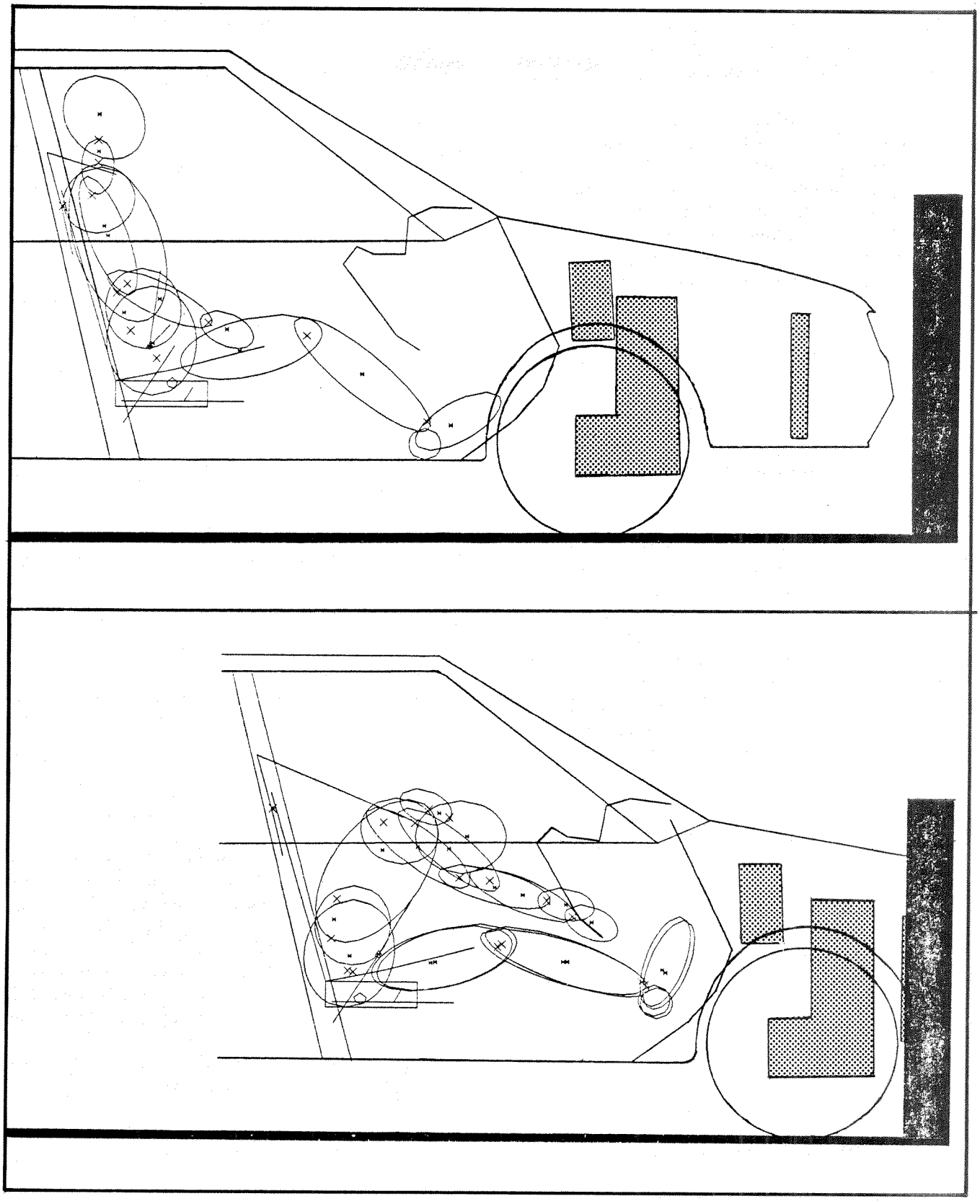

Figure 2. Schematic combination of occupant and structural simulation models

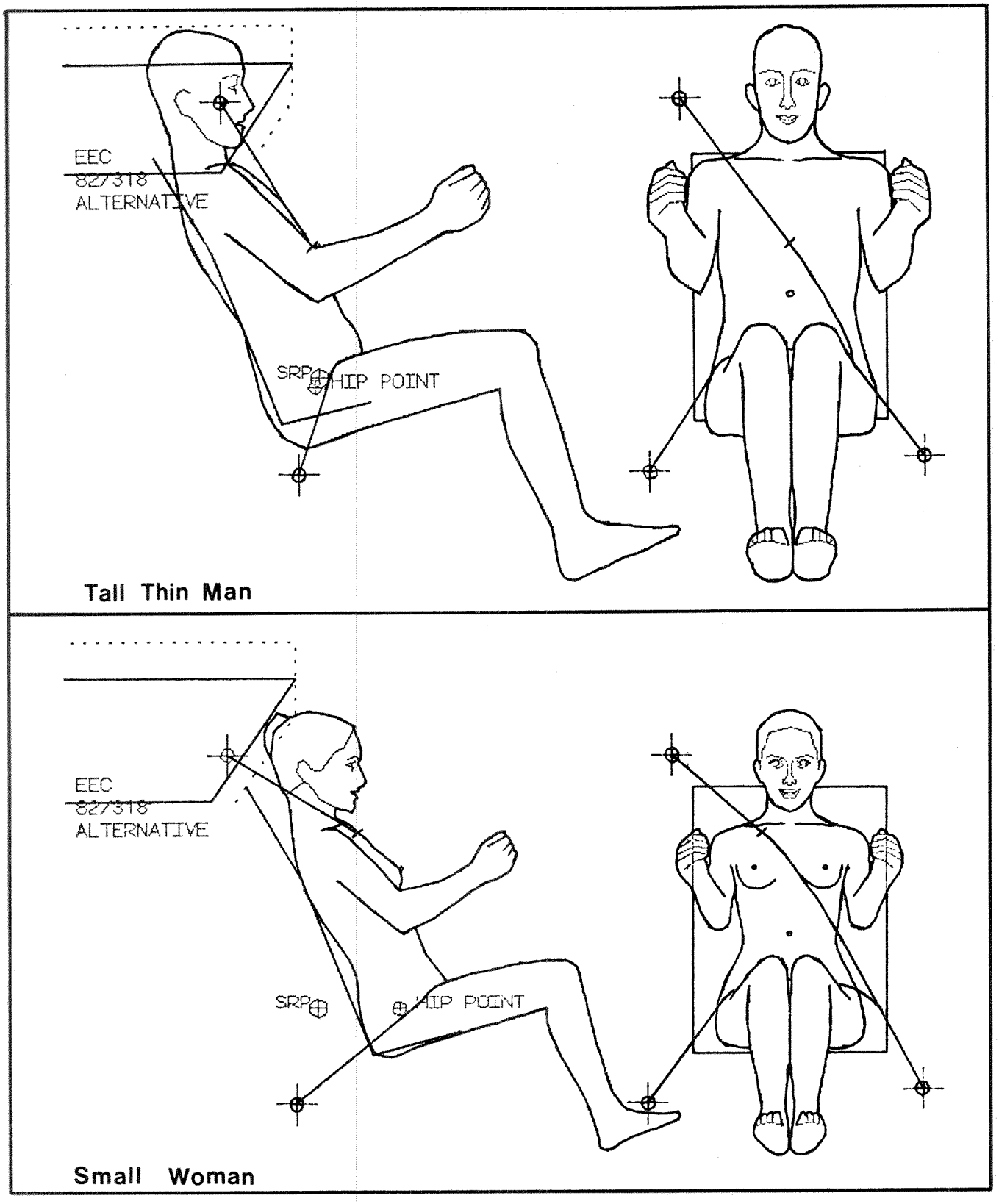

Figure 3. BELTFIT displays for assessments of seatbelt comfort

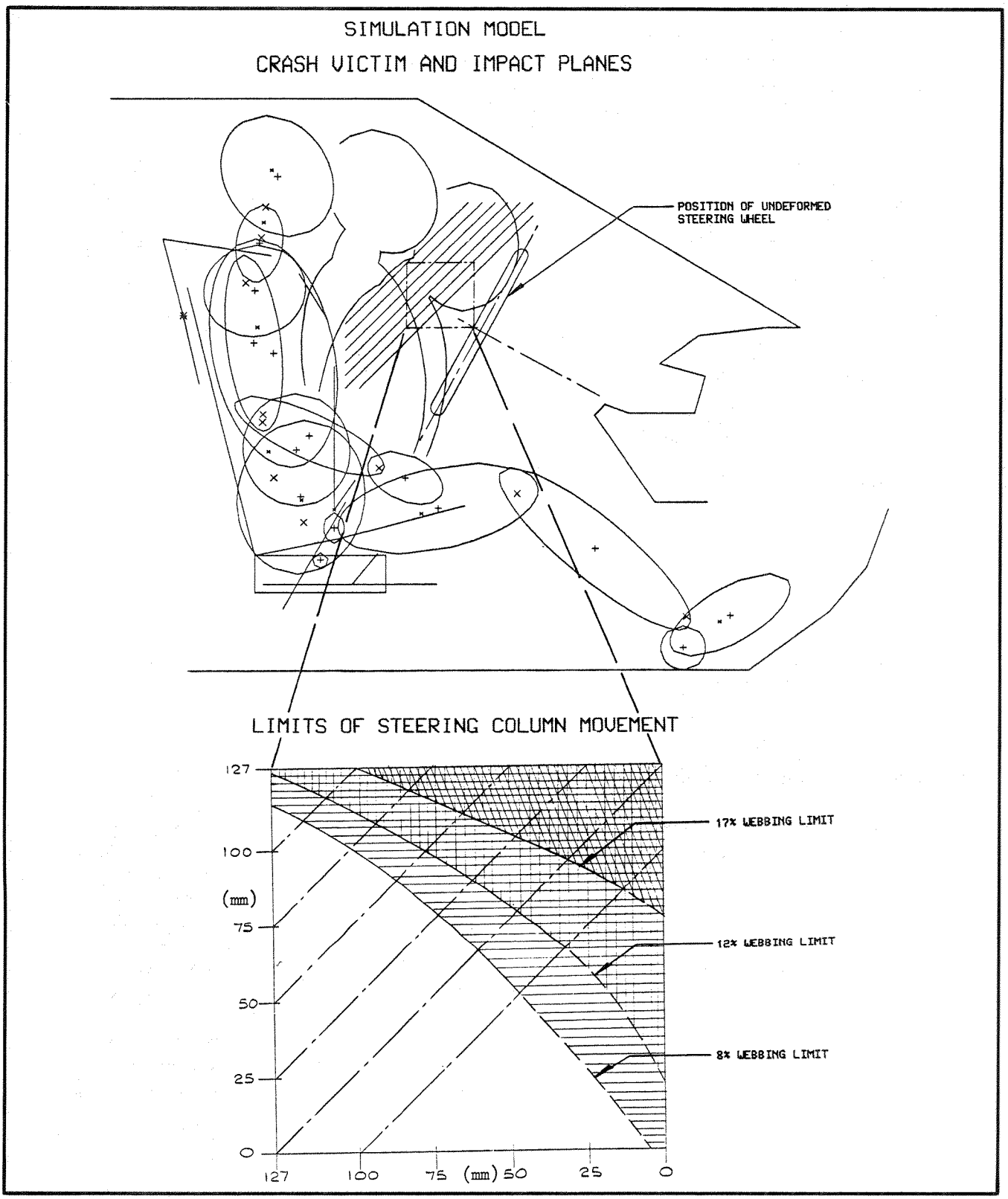

Figure 4. Simulation model of crash victim and impact planes

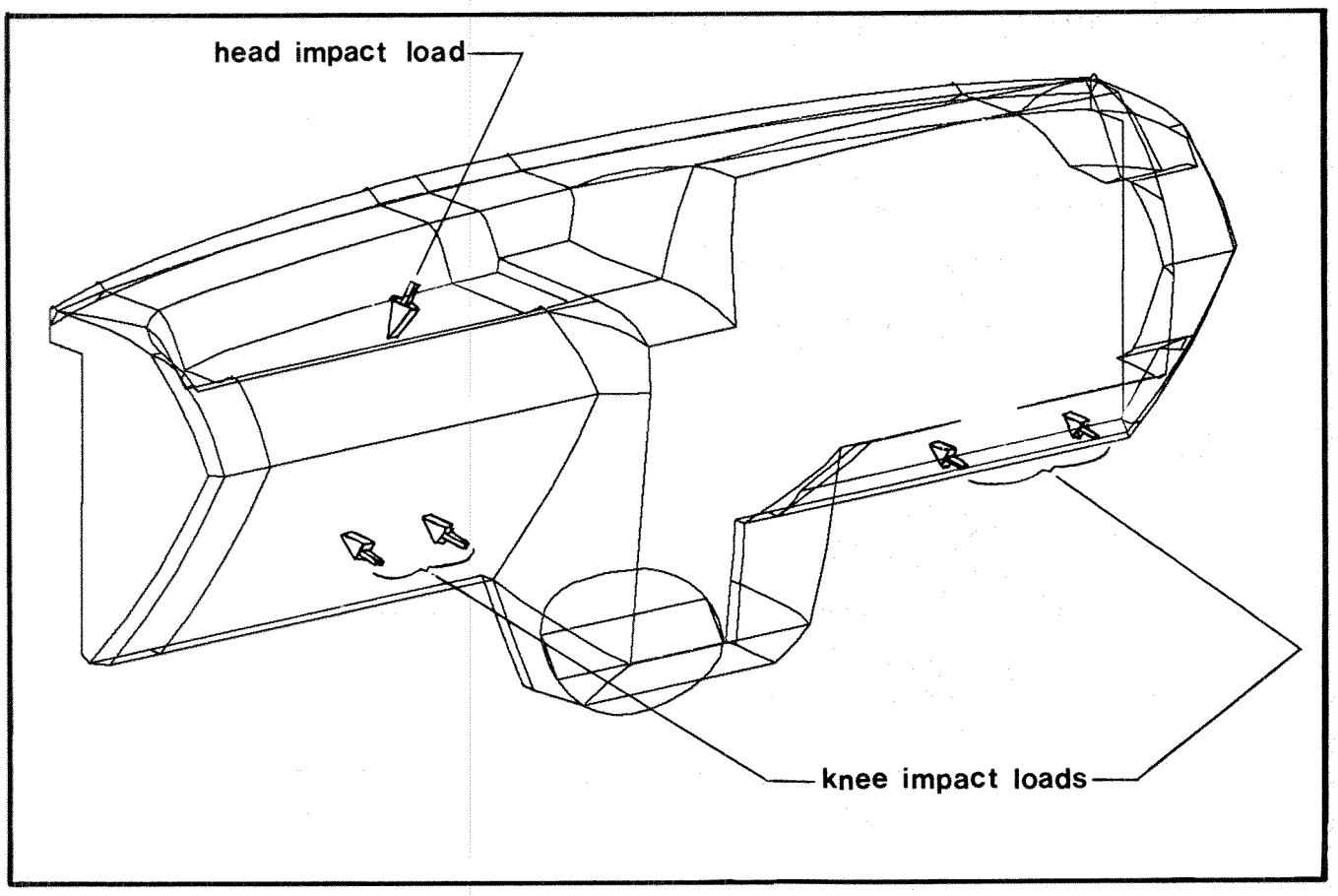

Figure 5. Fascia model for structural analysis with typical loading conditions

Developing the Computer Model

The computer model of the restraint system is modified in the light of the practical test data and by the same token helps to interpret the tests. The validated model and the enhanced understanding of the restraint system are now put to good use. Any undesirable features of the system can be ironed out in principle by changes to the model and component design areas kept informed of the results. By working in conjunction with these areas, the principles, verified on the simulation model, can be turned into features of the design. Specific loading conditions are passed from the simulation data for application on computer models of the component structure.

In parallel with this, the computer simulations of the structure will be continuing, and more definitive information will be forthcoming about the deceleration pulses and intrusion levels. These are built into the computer simulation of the occupant.

The computer model will now have changed considerably from the one that existed prior to the first sled test. To verify the model and check prototype hardware, a further series of tests is embarked upon.

A Development Example

This sequence of events is best illustrated by an example. A concept restraint system was tested as previously described, the components consisting of an inertia reel seatbelt, floor and toeboard, and current seat. In a simulated 35mph impact, a dominant and undesirable feature of the results was very high head accelerations. These were even excessive at lower speeds. The computer model had not predicted these accelerations to be as high as was found. It became evident that the lie of the lapbelt differed sufficiently from the vehicle for which the seat model had been developed to render the seat model inadequate. Alterations to the seat model brought about significant changes to the simulation results until they were similar to the test results. From this, it became evident that the dominant feature of the restraint system was a problem with the pelvis submarining. Figure 7A illustrates this and shows the test and computer simulation results. It was argued that the lack of any facia in either model was the cause of the submarining, and so a facia was built into the computer model. This caused some improvement, but submarining was still evident. Some form of pelvic restraint was then built into the simulation

	DERIVED AND MEASURED DATA	DATA SOURCES	
		TRANS-DUCERS	FILM ANALYSIS
HEAD	Tri-Axial Accelerations	X	
	Linear Velocities	X	X
	Angular Velocities		X
	Linear Displacements		X
	Angular Displacements		X
	Trajectory		X
CHEST	Tri-Axial Accelerations	X	
	Shoulder Displacement		X
	Shoulder Trajectory		X
PELVIS	Tri-Axial Accelerations	X	
	Linear Displacements		X
	Trajectory		X
FEMURS	Axial Loads	X	
KNEES	Degree of Facia Penetration		X
FEET	Contact Events	X	
BELT SYSTEM	Retractor Reelout		X
	Pillar Loop/Shoulder Belt Feed-Through		X
	Shoulder Belt/Lap Belt Feed-Through		X
	All Belt Loads	X	
	Belt Load Against Feed-Through	X	and X
INJURY CRITERIA	HIC - Head Injury Criteria	X	
	HSI - Head Severity Index	X	
	CSI - Chest Severity Index	X	
SYSTEM VERIFI-CATION	Pulse - Deceleration/Time	X	
	Velocity - Velocity Change	X	

Figure 6. List of data typically obtained from sled test for use with computer simulation

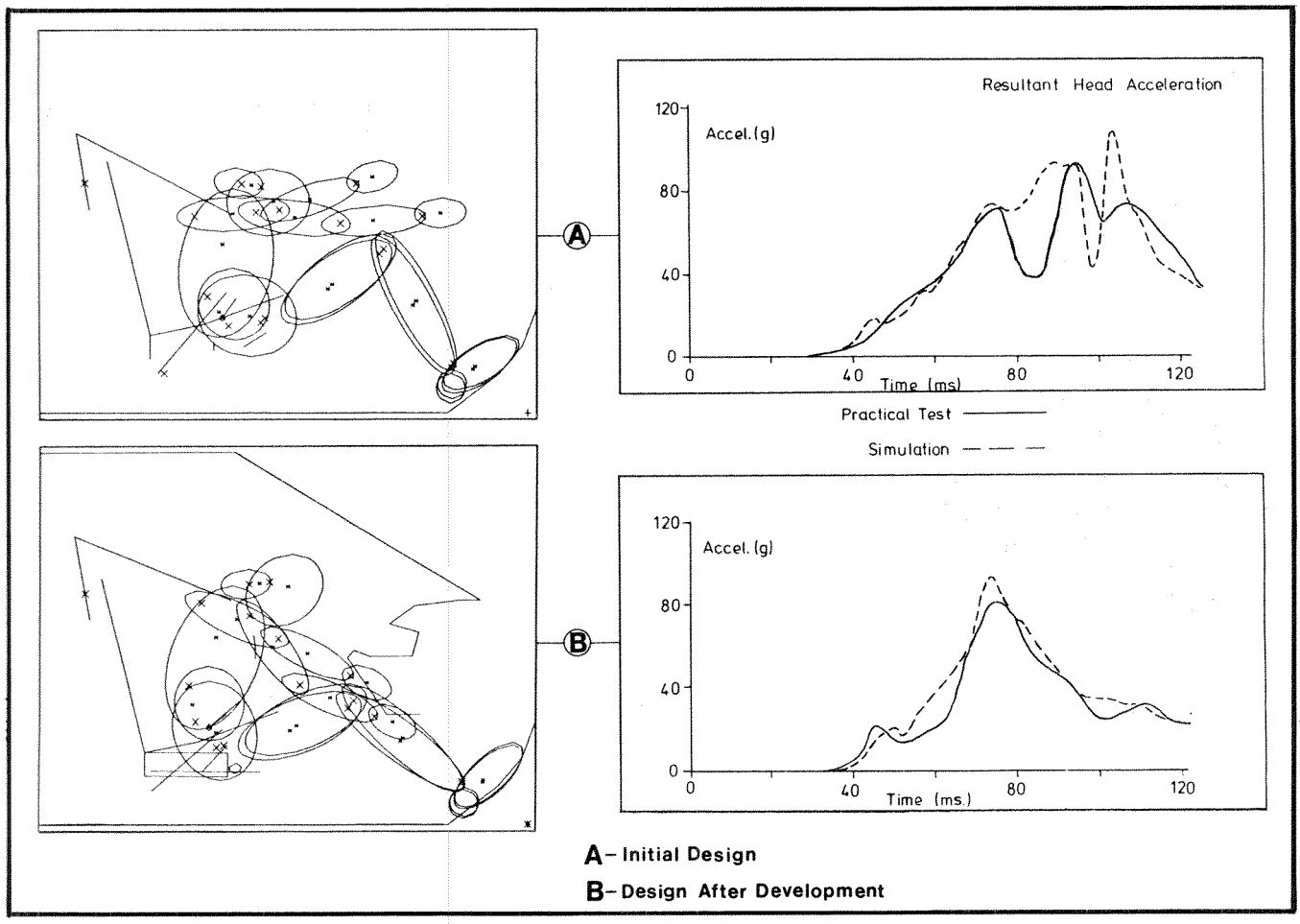

Figure 7. Example of restraint system development

seat model. The submarining was controlled (see Figure 7B). By working with the seat design area a prototype seat was evolved that would be expected to perform in practice as the computer simulation showed was needed.

A second practical sled test was carried out with this seat, other prototype hardware, and a simple foam-covered buffer representing the facia. The practical test bore out the computer simulation. The restraint system was by no means satisfactory yet, but the computer model was shown to be accurate and other changes, such as a revised deceleration pulse, could be introduced with confidence. Loading data was also passed to the seat design area so they could use it on their finite element model of the seat structure (see Figure 8).

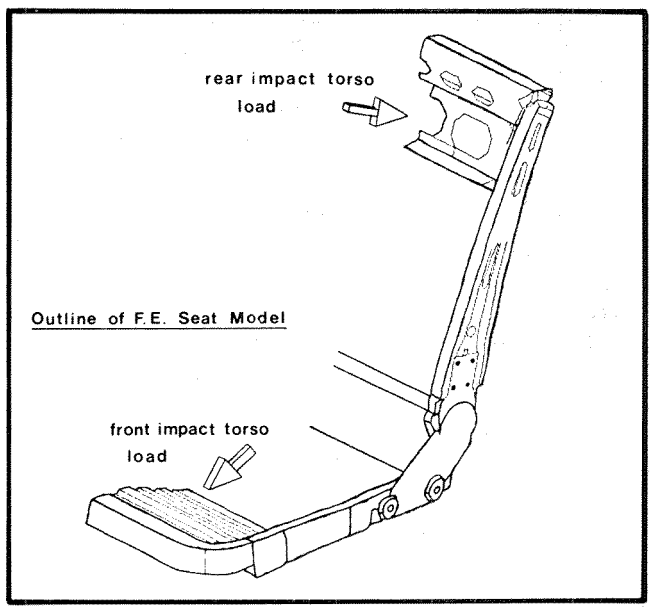

Figure 8. Seat model for structural analysis with typical loading conditions

The Interior

As has already been indicated, component areas will be using analytical methods in their designs and adopting criteria that includes data from early computer simulations and updated as the simulation model is refined.

The structural simulation of the vehicle body provides basic deceleration data to the occupant simulation, but the movements of interior features are determined by the collapse of the structure. The combination of these movements and those of the dummy and the design of these interior features are very important. Early concept simulations have given some design criteria, but the tuning of trajectories and the stiffness characteristics of the components are crucial.

Passenger Side

For simplicity, the sled tests and corresponding computer simulations represent a passenger in an undeformed interior. The consequences of intrusions can be indicated by changes to the computer model. This may mean, also, changes to the stiffness of the seatbelt webbing or even retractor to give an acceptable head trajectory for the facia movement. The computer technique is capable of including web-lock and pretensioner devices (see Figure 9).

At the same time, leg-to-facia contacts are considered, and the design requirements of peak load and absorbed energy are transmitted to facia design.

Driver Side

In a similar way, the interaction of driver and steering wheel can be modelled as an extension of the passenger model. The steering system model must include the

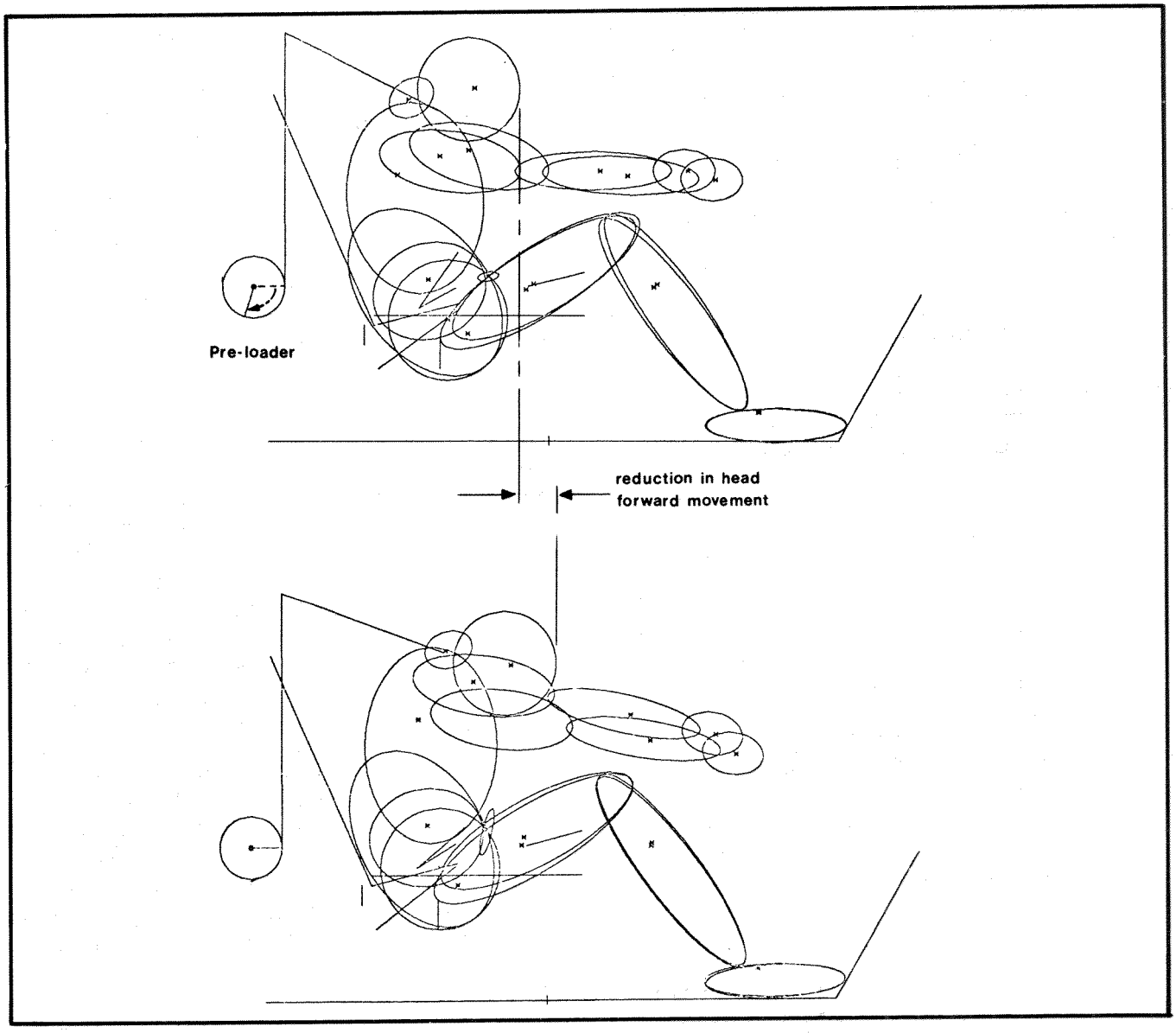

Figure 9. Simulation including Web-lock and pretensioner devices

facilities for the upper and lower rims to deform, the wheel to flex on the column, and the column to collapse (see Figure 10).

Usually the movement of the steering wheel has come to an end before the possibility of any chest or head contact and is, therefore, modelled in its final position prior to driver impact. However, the computer technique includes the facility to allow the trajectory of the wheel to be introduced if necessary.

At this stage, it is usually a case of tuning the restraint system to give a dummy movement compatible with the trajectory of the wheel. However, should the design of steering system or its movement prove difficult to match, then the need for and magnitude of any changes can be assessed using the computer model and the information fed back into the design process.

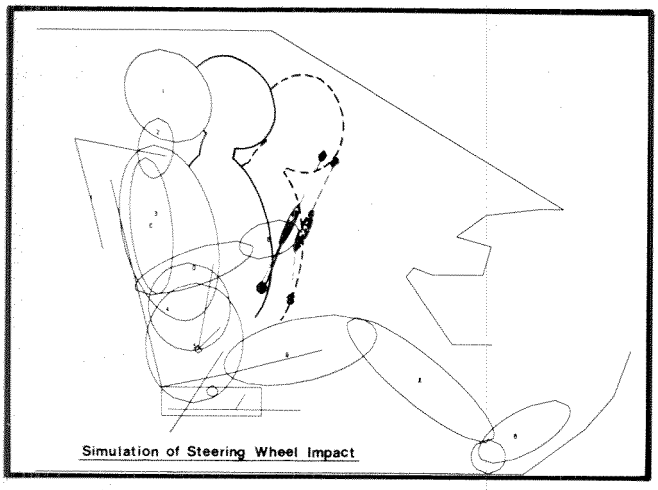

Figure 10. Simulation of steering wheel impact

Vehicle Testing

The first full prototype vehicle crash tests will take place with a reasonable confidence in the qualities of the restraint system and an awareness of the critical areas. Thus, measuring devices will be set up to give data that can be correlated with sled test and computer simulation with particular attention to the identified critical areas. In particular, the movements of parts of the interior and the interaction of the dummies with them are the subject of instrumentation as these are the least predictable features.

The results from the vehicle crash tests will be used to validate and modify the computer model with particular attention to the interior impacts and vehicle deceleration pulse. It may well be necessary to introduce vehicle pitch into the computer model input.

The computer simulation model is important, also, as an interpretive tool. The camera views of the occupants in a vehicle are limited and rarely such that data from any two can be successfully combined to give movement in orthogonal planes. The computer model can be verified against those views that are available and the direct measurements of contact, force, and acceleration. The effects and significance of events during impact can be appraised to give a more complete picture of the test.

The full vehicle crash test helps in the validation and improvement of all the analytical models applied to the vehicle and its components. Obviously the sequence of computer simulation, sled test, component analysis, and crash test will be repeated during the design process to the mutual benefit of each.

The computer simulation models can be used to assess the likely vehicle performance in impact environments either beyond the current specification or ahead of the completion of all prototype testing. For example, the angled barrier impact is less severe for the occupant in terms of vehicle deceleration levels but more severe in terms of impacted side intrusion levels and more uncertain in terms of head trajectories. The passenger (normally the nonimpacted side) will tend to move toward the centre of the vehicle with the risk of his head contacting the switchgear binnacle in front of the driver (see Figure 11). The driver will experience greater loading from the lower facia and the possibility of glancing off the wheel toward side glass or A-pillar. These features can be investigated using the occupant simulation model validated from initial vehicle 90° barrier impacts with modifications derived from similarly validated structural models.

Conclusion

Computer simulation techniques are an important part of the vehicle design process—at the outset, helping in the formulation of the concept and then assisting the actual design by analysis of systems and components. As with all analytical approaches, the need for good problem definition and specific data helps highlight design requirements and draw design areas together.

Computer simulations of the occupants in an impact situation yield data with sufficient accuracy to satisfy the analytical methods used in component design.

It is essential to integrate the test programme with the computer simulations. The practical tests establish and validate the models, and the models help interpret the tests and insure that unnecessary testing is avoided. The design process is not a simple logical progression—a motor car is more than just a machine, and marketing, styling, etc., are rarely constant points of reference. However, computer techniques are flexible, and such analytical models can adapt to changes as well as giving information on the implications of modifications. As such, these techniques help the length of the design process to be shortened or at least maintained in the face of more stringent design requirements.

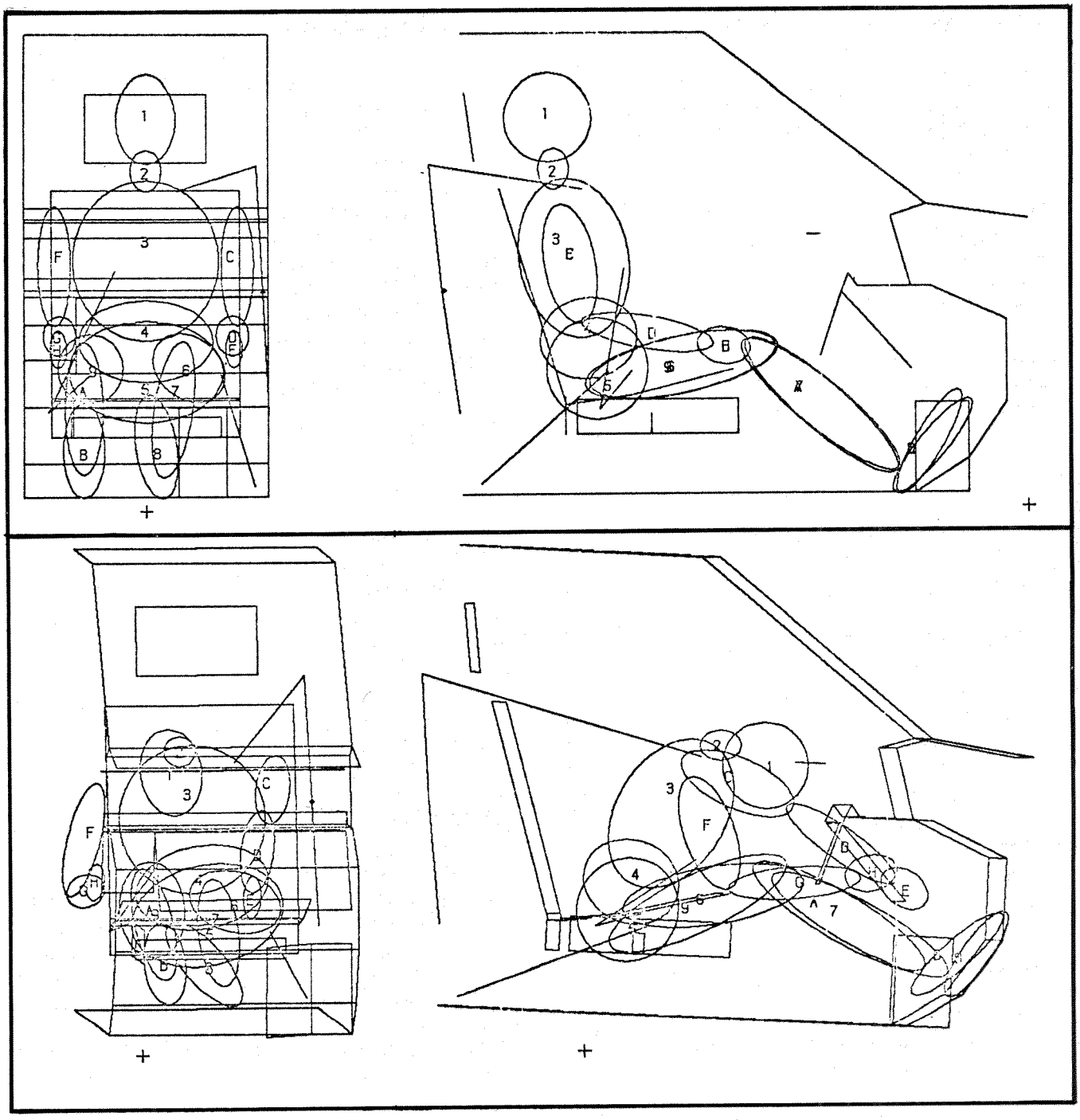

Figure 11. Angled barrier impact showing full vehicle motion

References

1. Grew, N.D., K.F. Newman, and G.G. Moore, "Using computer techniques to improve occupant protection in vehicle collisions," SEECO '84, *Dynamics in Automotive Engineering*, April 1984.
2. Newman, K.F., N.D. Grew, and G. Dowzall, "Cal 3-D: Its use in BL Cars Ltd.," Proceedings, Cal 3-D User Conference, Dearborn, Michigan, 1981.
3. "Development of a computer program to design seat belt layouts giving the greatest comfort, safety and convenience," MIRA Report No. K52012/1.

The Use of the DRACR Airbag Simulation Model as a Design Tool

Lars-Gunnar Skötte,
Hugo Mellander, and
David J. Biss
Volvo Car Corporation

Abstract

The airbag simulation program DRACR has been revised to include belt routines. The amended program is used to indicate optimal choice of parameters for a driver supplementary airbag system. As a validation, results from sled tests are given and compared with the computer runs. A good agreement is found for the values of the most essential protection criteria such as chest g's and HIC's. The model has proven to be useful in the engineering process of an airbag restraint system. The interrelationship between important input variables is easily studied. Further validation of the model by other teams is encouraged.

Introduction

The use of computers as design tools in high-tech companies is today a matter of course. Mathematical simulations of complex systems give many possibilities to study important parameters at early design stages and avoid extensive development tests, which in many cases take the form of a trial-and-error testing.

The engineering of an airbag system is a good example of where such an approach is suitable. Such a system consists of a large number of parameters, and an efficient way to handle these variables is to use a mathematical model. An early system analysis of bags, inflators, and steering system will shorten the time of development and make the process more efficient.

With this in mind, Volvo decided to start a project directed at the development and installation of a new computer model for the simulation of a driver airbag system. The model should be able to simulate the airbag inflation phase, different bag parameters, belts, different occupant sizes, etc. The DRACR model was chosen among available models to form a platform for the work. This report describes briefly the model and, more deeply, the parameter sensitivity studies and validations that have been made.

History

Volvo has been using computerized mathematical simulation models for airbag systems since 1975. The first model used a preinflated bag and in 1979 was improved to describe the inflator mass flow characteristics. In 1983, Volvo and Fitzpatrick Engineering developed a seatbelt routine and updated the DRACR model, which was then to become the Volvo DRACR model (VDRACR) described in this paper.

The VDRACR Project

The project included—

- Updating the DRACR model
- Installation, input data preparation, and debugging
- Parameter sensitivity analysis
- Design of different airbag systems for testing

Updating the DRACR Model

As the existing DRACR model did not include all capabilities required by Volvo, the model had to be improved. For example, a belt routine was added for simulation of an airbag in combination with belts. The H-point was allowed to move also in the vertical plane, and the model was changed to allow chest contact with the steering wheel through the airbag.

VDRACR Model Description

To understand the nature of the model and the results from the computer simulations, a short description of the model and its capability is presented below.

VDRACR is an acronym for Volvo DRiver Air Cushion Rotation. The model is a two-dimensional, lumped-mass computer model of a vehicle driver interacting with an airbag with or without a belt restraint system. The airbag is mounted in the steering wheel. The rotation suffix in the title means that the model simulates the rotation of the steering wheel with respect to the steering column as well as the rotation of the steering column with respect to the compartment. Different compartment geometries and occupant sizes and positions can be modeled easily. A schematic of the VDRACR model is depicted in Figure 1.

The driver is modeled by four masses: the head, the main torso, the sternal, and the lower body (pelvis and legs). The H-point is free to move in the vertical plane as well as the horizontal plane. The model simulates the pelvic girdle and torso compliance for belt interaction and sternal and chest compliance for airbag interaction. The abdomen compliance for steering wheel rim interaction is computed.

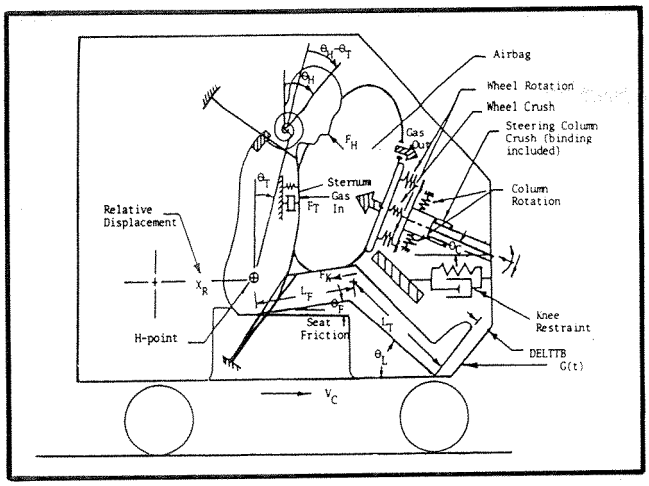

Figure 1. Schematic of VDRACR model

The airbag is modeled as an ellipsoid (actually an oblate spheroid), which is the most realistic shape of the driver airbag. The bag transmits forces from the driver head/chest to the steering wheel/column. The program uses a tabular input for the inflator gas mass flow-time properties.

The belt system in VDRACR can be used in combination with an airbag or as a stand-alone restraint system. A 2-point or 3-point belt can be simulated.

The system is described by the force-deflection properties of the webbing, the coefficient of friction between belt and latch plate, initial slack, and the amount of webbing that may stretch in each of the torso and lapbelts.

VDRACR models the steering wheel/column crush and rotation. An accurate simulation of this is important to achieve an overall simulation realism. The program calculates in each time integration interval the airbag forces and pressure before it proceeds with the steering wheel/column calculations, and in each time step the program uses a minimum energy method to determine which crush mode (steering wheel/column-rotation/crush) will occur. VDRACR models the column in a way that can be representative of most current car designs.

The model also has the capability to—

- Simulate the out-of-position driver
- Compute all the conventional protection criteria such as HIC's, chest g's, head g's, femur load, peak chest g's with 3ms clip

As a design tool, the program is oriented toward the hardware actually encountered in most design situations.

In addition, the program modules describing the performance of the various hardware components are designed to be complementary to one another. VDRACR is structured to provide balanced treatment of all the various restraint components that make up the total model.

Installation

The installation of the VDRACR model required—

- Changing the Fortran code to fit the mainframe computer at Volvo
- Creating an input file consisting of over 150 different parameters
- Building up knowledge inside Volvo of how the model was structured and how the program parameter interaction adds up to an overall system performance. It is the interaction of the major parameters affecting the driver airbag, as they vary over the range of interest, that many times has a greater effect on the results than the variation of any single parameter.

Parameter Sensitivity Analysis

The program input file consists of many different parameters. Some of these are more suitable for parameter studies and are used to optimize the airbag system, e.g., bag parameters as volume, ratio of axis, and ventilation area. Other parameters are more or less fixed because they depend on what can be delivered or developed by suppliers—for example, inflators—or are related to the vehicle. To form a basis for the sensitivity analysis, the vehicle-dependent parameters were decided and plugged into the model. The parameter sensitivity analysis was made for the overall system, and interesting parameters were varied.

For example, the interaction between chest g's, steering wheel plus steering column stroke, bag geometry and ventilation, occupant size, and inflators were varied. This is shown in Figures 2 to 4.

Figure 2 shows a plot of chest g's along with total stroke (steering wheel plus column) versus vent area for a

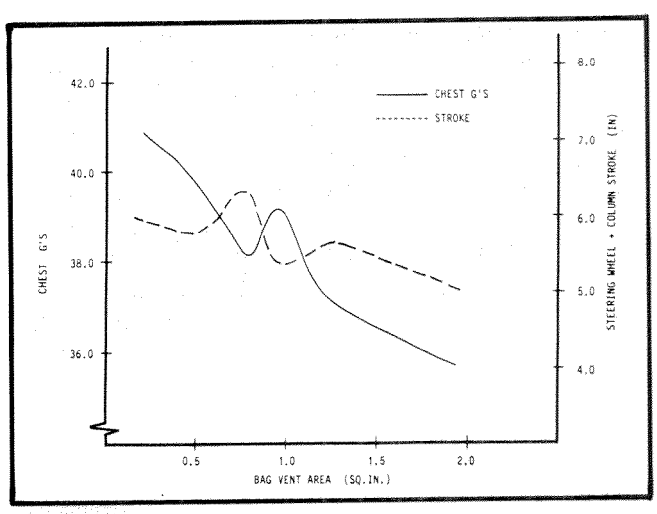

Figure 2. Chest g's and steering wheel plus column stroke versus bag vent area

67 liter bag with 280mm straps (internal straps to maintain the shape of the airbag) restraining a 50th percentile man in a 30mph barrier crash. Of interest is that chest g's and the total stroke are good mirror images of each other. Dips in the chest g's curve are matched with maxima in the total stroke and vice versa.

This appears to be the result of the program using a minimum energy approach to determine the collapse load during the program iterations. The chest g's and total stroke decrease for larger vent areas, which means that the bag dissipates energy. If the vent area is increased more than is shown in the plot, a point is reached where the chest g's raise again because there is not enough gas in the bag to prevent the occupant from bottoming out against the steering wheel.

This is actually shown in Figure 3: A 95th percentile male restrained by a 64 liter bag with 270mm straps, in a 30mph barrier test.

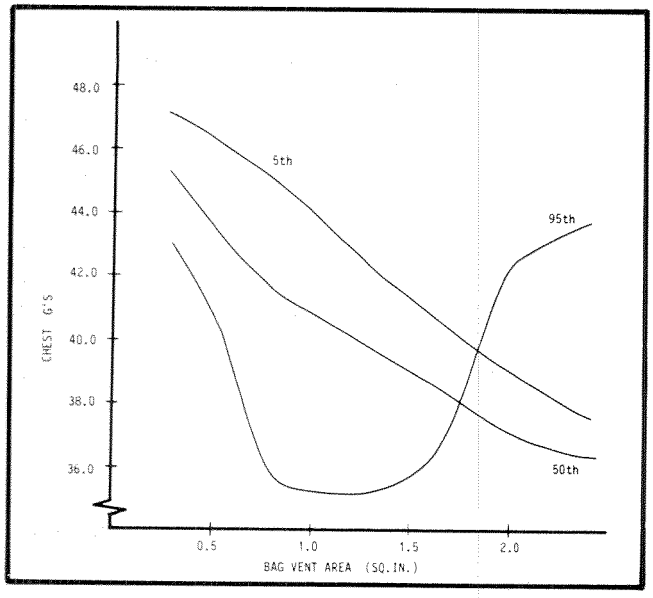

Figure 3. Chest g's versus bag vent area for a 95th, 50th, and 5th percentile driver restrained by a 64-liter airbag in a 30mph barrier crash

If the vent size is less than $0.8in^2$, the bag is too stiff for the 95th percentile which results in high chest g's. Around $1in^2$ the vent area is an optimum to get low chest g's, and above $1.5in^2$ the driver bottoms out against the steering wheel and the chest g's raise again. The 50th percentile male and the 5th percentile female are also shown in Figure 3. In these cases, the smaller driver does not bottom out as the 95th, because there is a sufficient amount of gas in the bag to protect the driver.

Figure 4 shows the chest g's versus bag vent area for a 35mph barrier crash with the driver, a 50th percentile male, restrained by a 67 liter bag with 280mm straps and a 3-point belt. Two sizes of inflator are used, 75 and 80g.

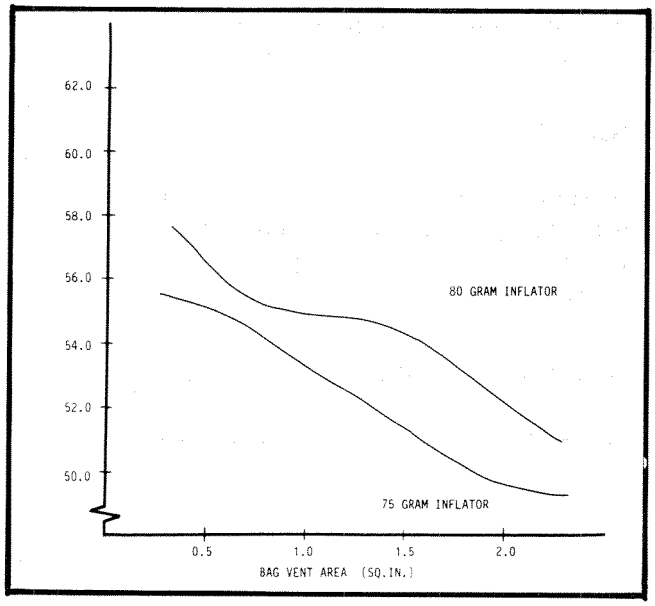

Figure 4. Chest g's versus bag vent area for a 50th percentile driver restrained by a 67-liter bag and 3-point belt in a 35mph barrier crash

In this configuration the driver receives higher chest g's with the 80g inflator as he will be more restrained. The simulations show that when a belt and an airbag are used together, the total forces on the chest are higher than if a separate system, either airbag or belt, was used. However, HIC values are decreased in tests with airbags combined with belts compared to belt-only systems due to the favorable ride down of the head.

Figures 2 to 4 demonstrate how the model gives the user the opportunity to optimize the sytem for best restraint performance.

Design of Different Airbag Systems for Testing

A number of candidate airbag systems were investigated using the optimizing procedure described above. It is important to have in mind that the objective of this work was to develop an airbag that would give protection for a 5th as well as a 95th percentile occupant and at the same time perform satisfactorily for the 50th percentile with and without a belt.

It will sometimes be easy to optimize the chest g's and HIC's for the belted 50th percentile male driver, but an unbelted 95th percentile driver may bottom out against the steering wheel with such a configuration. Also the 5th percentile female driver with belt can be overrestrained with high chest g's as a consequence. A suitable combination that meets all desirable requirements has to be found.

Over 1,000 computer analysis runs have been done, and some of the most promising combinations, depending on the availability of components and materials, were

chosen for testing and served as a basis for validation of the model.

Validation

A series of HYGE sled tests with driver airbag systems was conducted to validate the VDRACR model against experimental data. Four different test series were conducted.

General Test Conditions

50th percentile dummy, 75g inflator, bag vent area 2.65in^2.

Test Matrix

A: 35mph, 64 liter bag/280mm straps, 3-point belt
B: 35mph, 52 liter bag/220mm straps, 3-point belt
C: 30mph, 64 liter bag/280mm straps, no belt
D: 30mph, 52 liter bag/220mm straps, no belt

Results

HIC's, chest g's, head g's belt forces, chest displacements, and femur forces resulting from simulation and sled tests are compared below. Table 1 shows an overview of the results.

Figure 5 compares chest g's and HIC's from sled tests and simulations.

Examples of plots of other parameters from the tests are shown in Appendix 1.

The results show a good overall correlation. Important parameters such as chest g's, HIC's, and belt forces correlate satisfactorily.

There is a difference between simulated and experimental knee forces. This may be a result of a too stiff knee pad characteristics in the program data input.

It is important to point out that it is difficult to have an exact correlation between model input parameters and testing conditions. Some of the input parameters are results from static component tests. Dummy-related parameters such as neck and chest parameters are also

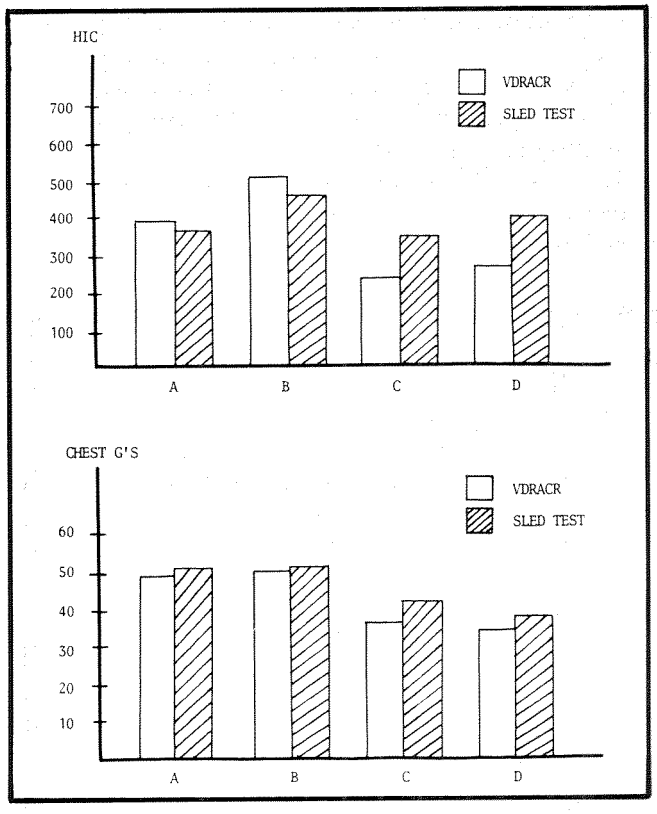

Figure 5. Chest g's and HIC from sled tests and simulations

		HIC	HEAD acc. (G)	CHEST acc. (G)	FEMUR Load (kN)	Lap Belt Load (kN)	Torso Belt Load (kN)	Chest Displ. (mm)
A	VDRACR	382	55	49	6.5	4./3	7.5	200
	Test	360	47	51	4.0/4.9	4.4	6.5	155
B	VDRACR	500	70	50	6.3	4.1	7.5	205
	Test	460	55	51	4.2/3.5	5.1	7.5	170
C	VDRACR	235	43	37	9.3	-	-	310
	Test	340	59	42	5.6/7.7	-	-	305
D	VDRACR	258	51	34	8.9	-	-	319
	Test	390	64	38	5.5/6.5	-	-	320

Table 1. Representative characteristics of structural components

hard to describe precisely. In the film, the bag shows a tendency to move up toward the windshield, which is not possible to describe in the model.

Conclusion

The VDRACR model has shown itself to be a good tool for design and development of a driver restraint airbag system. The model makes it easy to study several different airbag system parameters and their interrelationships.

Further validations should be done with different occupant sizes. Our validation is carried out against results from sled tests, and, of course, a validation against a barrier test is desirable. It is important to continue work with the model, refine the input parameters, and find methods to get improved input data for different systems guiding the event such as steering column bracket characteristics, seat cushion friction, etc.

Even if the results from sled tests and mathematical simulations are not always comparable in absolute figures, the trends suggested by the model are confirmed with the sled experiments.

The model seems capable of detecting changes in restraint system parameters and predicting trends in HIC's and chest g's, both in airbag-only exposure as well as in airbag and belt exposure.

Recommendations

A refinement of the description of the occupant is recommended. An improvement of the force balance between bag and chest is needed for simulation of a bag moving up toward the windshield, which occurred in the sled tests.

Sometimes minor algorithmical errors appear when the value of a parameter is changed. A more extensive error interrupt routine is needed. The model appears to be sensitive to changes of the integration time step, which perhaps is not relevant. The user of the model must have a good understanding of the function and capability of the model to be able to make full use of its possibilities.

Acknowledgments

The authors would like to thank the U.S. Department of Transportation, National Highway Traffic Safety Administration, for making the DRACR model available and also Fitzpatrick Engineering for their excellent work in improving the model.

References

1. Fitzpatrick Engineering, "DRACR user's manual," 1982.
2. D. Biss et al., "A systems analysis approach to airbag design and development," ESV, 1980.

Appendix 1

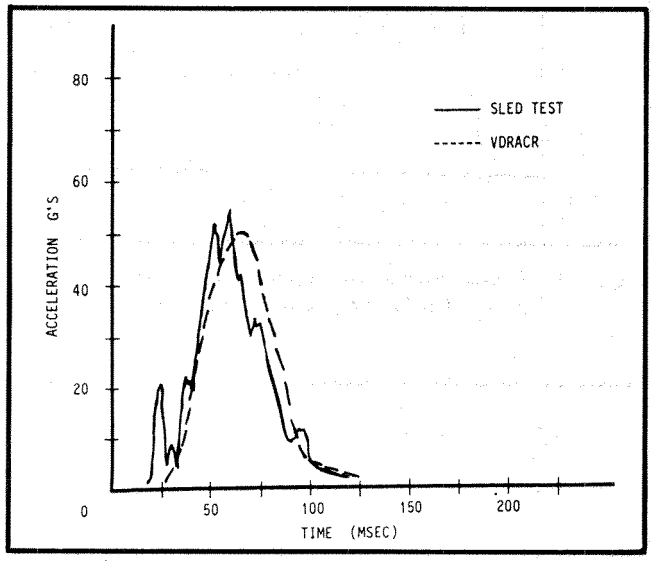

Figure 6. Chest g's versus time (35mph/50th percentile/64/64 liter bag/3-point belt)

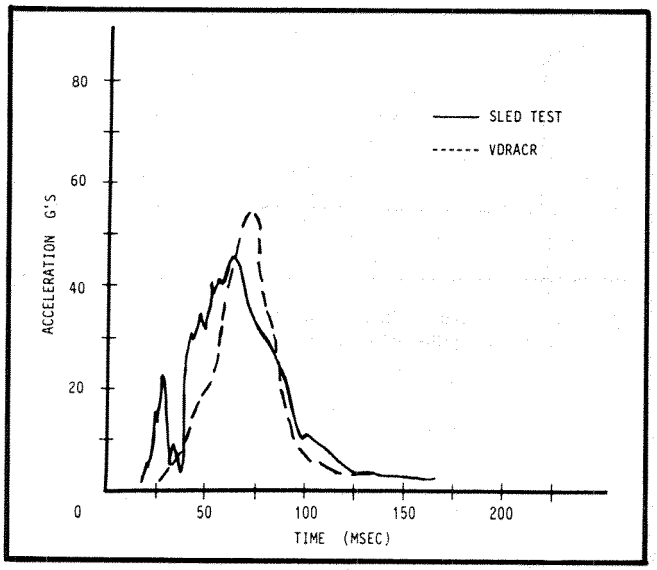

Figure 7. Head g's versus time (35mph/50th percentile/64 liter bag/3-point belt)

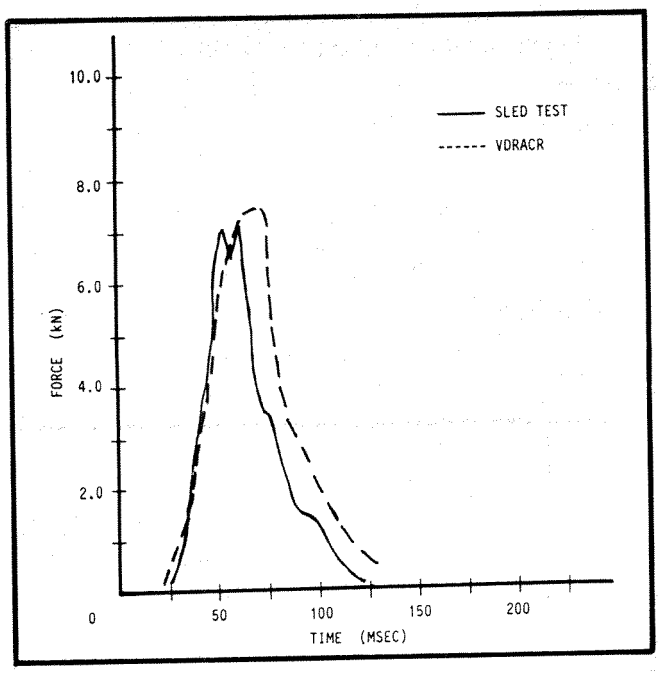

Figure 8. Torso belt load versus time (35mph/50th percentile/64 liter bag/3-point belt)

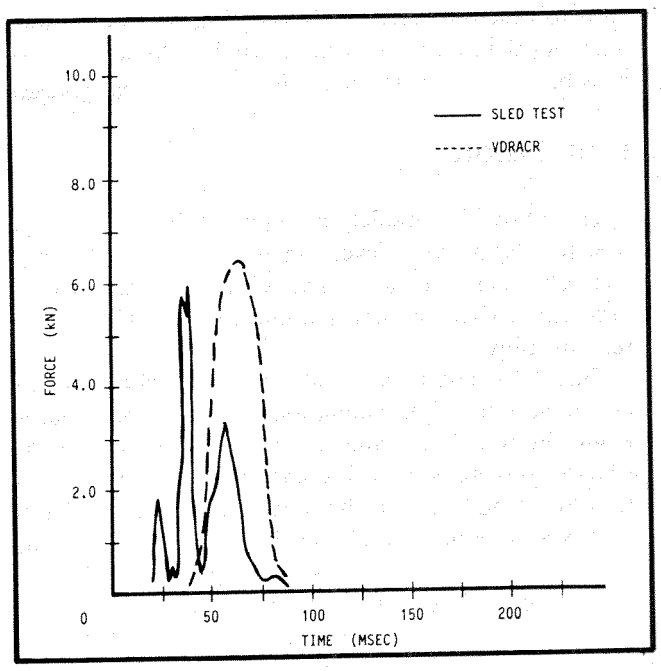

Figure 10. Femur force versus time (35mph/50th percentile/64 liter bag/3-point belt)

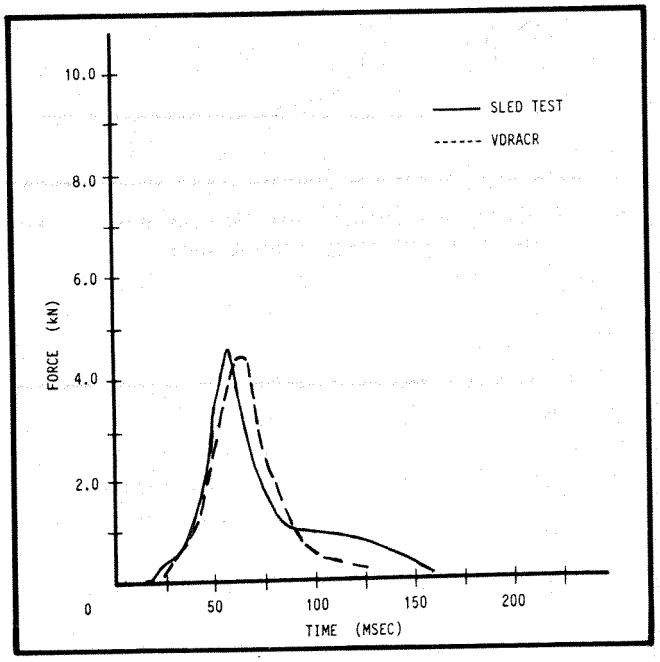

Figure 9. Lap belt load versus time (35mph/50th percentile/64 liter bag/3-point belt)

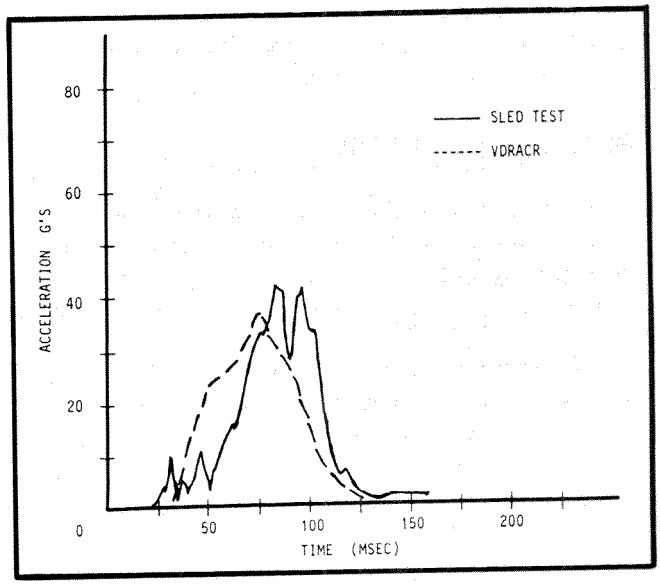

Figure 11. Chest g's versus time (35mph/50th percentile/64 liter bag/no belt)

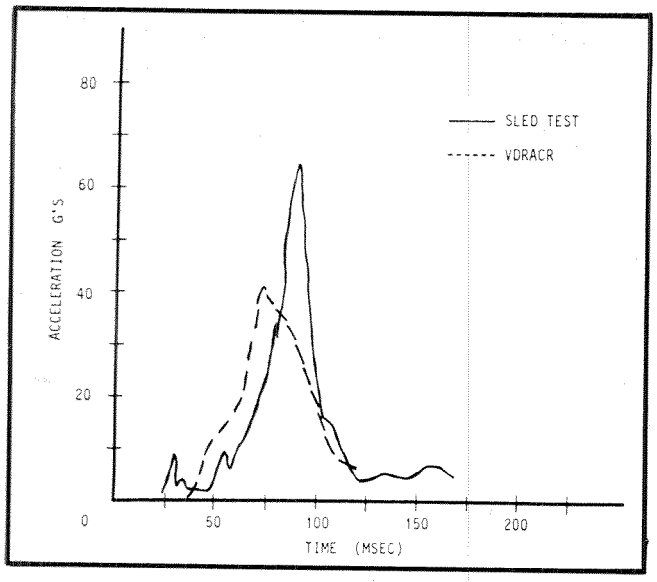

Figure 12. Head g's versus time (35mph/50th percentile/64 liter bag/no belt)

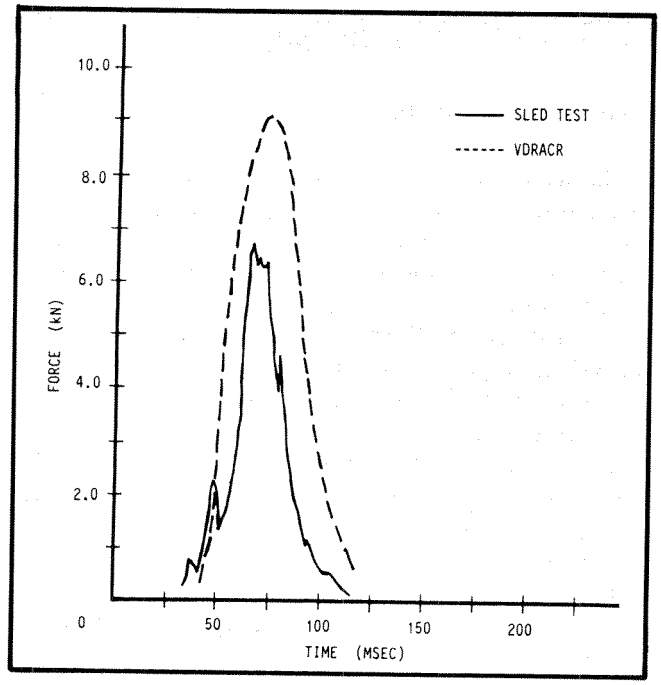

Figure 13. Femur force versus time (35mph/50th percentile/64 liter bag/no belt)

An Analytical Management of Frontal Crash Impact Response

Koji Kurimoto,
Shigemiki Takeda, and
Hisanori Uehara
Mazda Motor Corporation, Japan

Abstract

The rotational behavior of the vehicle in the vertical plane at frontal collision against a flat barrier often plays an important role with respect to an evaluation of passenger compartment integrity and occupant protection.

An analytical method to examine the degree of influence of vehicle front end parameters, both on the behavior of the vehicle and its occupant, is presented, employing a two-dimensional finite element vehicle model and a two-dimensional lumped-mass occupant model.

The feasibility of the method is discussed by comparing the calculated results with the experimented ones, in relation to the behavior of passenger compartment and its occupant injury measure.

Preface

In high-speed frontal collisions, a rotation of passenger compartment in a vertical plane, often referred to as nose dive, is often observed. The effect of this rotation, especially on an occupant behavior restrained by a seatbelt, is not very well understood. This rotation may give rise to a substantial increase of crash space, or it may degrade restraint capability of a seatbelt system, due to an additional forward movement of the seatbelt anchorage points.

This paper describes the application of a computer model to simulate both the vehicle dynamics and its interaction with the occupant in the frontal barrier crash. The vehicle is assumed to be a small passenger car, and its occupant is assumed to be restrained by a conventional 3-point seatbelt system. Each behavior at collision is treated in the vertical, two-dimensional plane.

The object of this study is to assess a method of examining the effect of changes in vehicle front end parameters on the rotation of passenger compartment and, further, on its occupant injury measure in terms of the deceleration and displacement of the occupant head.

Mathematical Modeling

General Description

Mathematical representation of an ordinary passenger car, and its occupant restrained by the conventional 3-point seatbelt, is formed on a vertical plane, assuming their kinematics in the horizontal plane have little effect on the respective performance.

In this study, the direct kinematic interaction between the vehicle and its occupant is neglected due to the relatively small influence of the occupant dynamics on that of the vehicle. Thus, the deceleration, the rotation, and the vertical displacement of the passenger compartment during collision obtained in the mathematical simulation of the vehicle model are to be fed into that of the occupant model to obtain its response.

The vehicle is represented by a combination of two-dimensional finite element beams and springs of nonlinear characteristics. A distinctive feature of this model is characterized by the consideration of bending momentum, compared to a lumped-mass and spring model.

The conventional anthropomorphic dummy is treated as an occupant, represented by a two-dimensional lumped-mass model. Here the front-seat passenger is dealt with for simplicity. The mathematical model is provided with seat and both shoulder and lapbelt anchorages. These points on the vehicle where the dummy receives respective reaction force are assumed to change their locations according to the rotation of the passenger compartment, resulting in the variation of restraining forces on the dummy during the vehicle collision.

Vehicle Model Formation

The deformation of a structural component is generally dominated either by bending deformation or by axial compression.

The bending deformation is treated by a two-dimensional finite element beam model, where each material point within a plane is identified by a curvilinear coordinate system. The cross-sectional buckling accompanying a beam bending is treated, based on the empirical relationship between a curvature change of the reference axis and the amount of buckling.

The axial deformation is treated, based on empirical equations. In cases where both the bending and axial deformation are possibly exhibited in a structural component, the condition for occurrence of axial deformation is determined by comparison of the maximum values of bending force and the maximum axial collapse force.

When any element within a structural component is connected to other components, the influence on the element is taken into consideration by including it in an internal force vector of the discrete equilibrium equation. This equation is solved by a step-by-step explicit finite difference method(1,3).

The vehicle model selected here is a certain front-engine and front-wheel-drive passenger vehicle whose mathematical model is shown in Figure 1.

The front side frame of this model consists of a curved box beam in a vertical plane, constituting local plastic hinges, and tends to undergo bending deformation during crash.

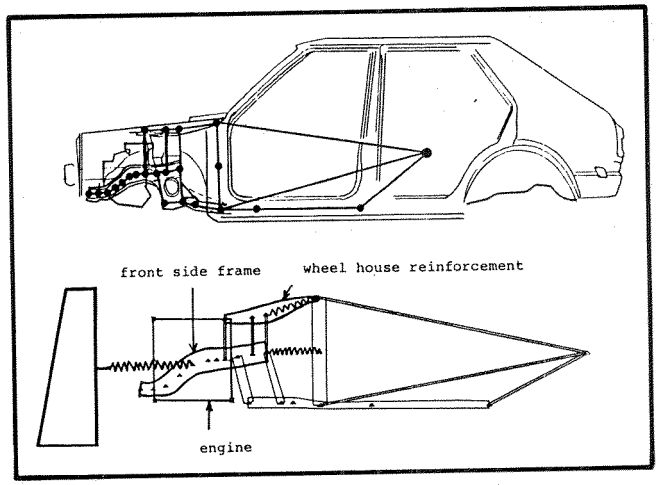

Figure 1. Schematic of vehicle model

Occupant Model Formation

A two-dimensional, five-mass, and multi-degree of freedom dynamic occupant model is employed, whose geometric, inertial, and joint characteristics are determined based on the specifications of the Part 572 hybrid dummy and on some measurements(4).

This mathematical model is provided with a seat and a conventional 3-point seatbelt system. The surface of the seat is assumed to make interaction with parts of the dummy, generating the reaction force, depending on the load versus deformation of the seat cushion in the vertical direction. Both the shoulder belt and the lapbelt are to make contact with the occupant model at two points respectively, again generating the reaction force at each point depending on the load versus relative displacement between the dummy and the respective seatbelt anchorage point on the vehicle.

This mathematical occupant model, the schematic of which is shown in Figure 2, is assumed to be stimulated by the vehicle deceleration in the longitudinal direction.

To simulate the effect of passenger compartment behavior on its occupant, the magnitudes of the deceleration, the rotation, and vertical movement of its reference point as a function of time are used as input to the occupant model. Knowing these values, the position of the bottom of the seat cushion and of the seatbelt

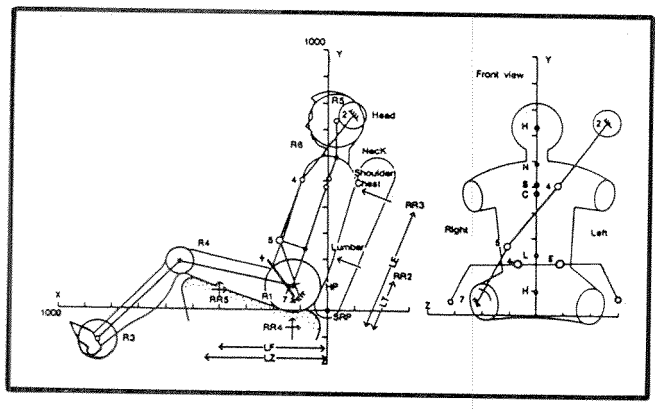

Figure 2. Schematic of occupant model

anchorage points are calculated at successive time intervals, resulting in the determination of the respective reaction force acting on the occupant based on the predetermined load versus deformation characteristics.

Simulation Fidelities

Vehicle Kinematics

Two full-scale frontal barrier crash tests at 35mph were performed with vehicles of different specifications with respect to the deformation characteristics of structural components, as shown in Table 1, obtaining different rotational behaviors of the passenger compartment.

Taking these test results into account, several computer simulations were executed on the vehicle simulation model in Figure 1. The deformation characteristics of structural components listed in Table 1 are calculated in the model based on the dimensional specification and the material property. Those of other components are estimated and adjusted by empirical methods(5).

Case	Specification	
Small Passenger Compartment Rotation	1. Wheelhouse Reinforcement	SPC 1.2t
	2. Front Side Frame (Inner)	HPC 1.0t
Large Passenger Compartment Rotation	1. Wheelhouse Reinforcement	SPC 1.0t
	2. Front Side Frame (Inner)	HPC 1.2t

Table 1. Results from sled tests and simulations

The comparison of tested and calculated results with respect to the vehicle deceleration, the rotation, and vertical movement of the passenger compartment is shown in Figures 3, 4, and 5. The results of the simulation compare reasonably to the test results.

Occupant Kinematics

The occupant behaviors at the passenger side during two full-scale barrier crash tests described above were referenced to improve the simulation fidelity of the mathematical occupant model.

To this end, several computer runs were made, where the occupant models are stimulated by the vehicle deceleration, the rotation, and the vertical movement of the passenger compartment, which were actually measured during the previously mentioned crash test.

The computed results in terms of the resultant deceleration of head and the displacement of head relative to reference point of passenger compartment on the horizontal plane are compared with those by the full-scale crash tests.

With some adjustment of restraint characteristics for the occupant, including the force versus deformation

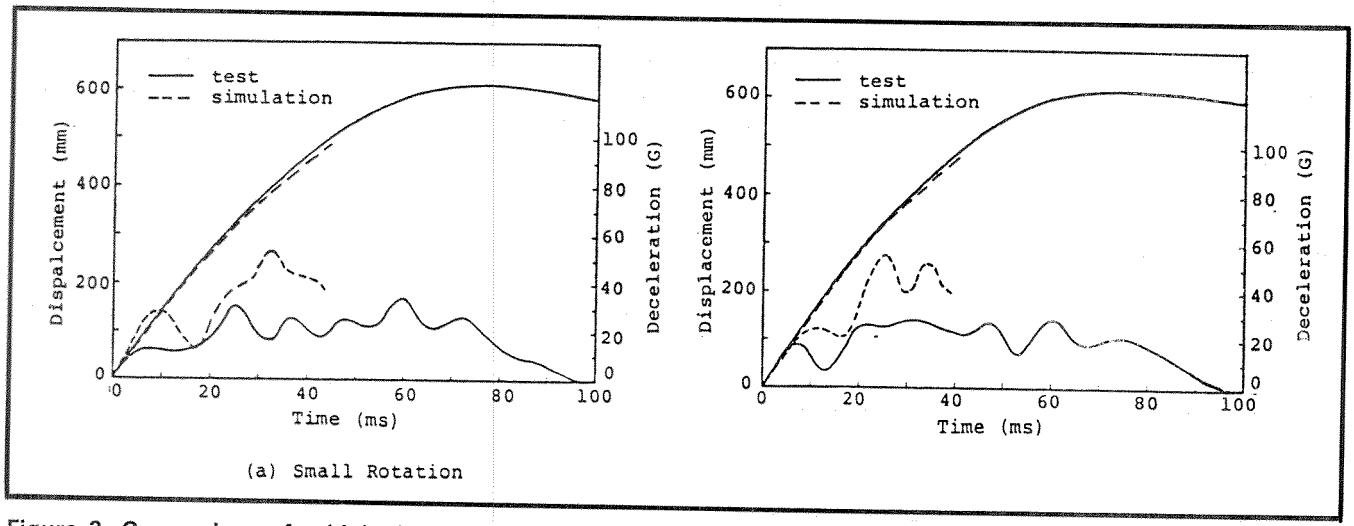

(a) Small Rotation

Figure 3. Comparison of vehicle decelerations and deformations

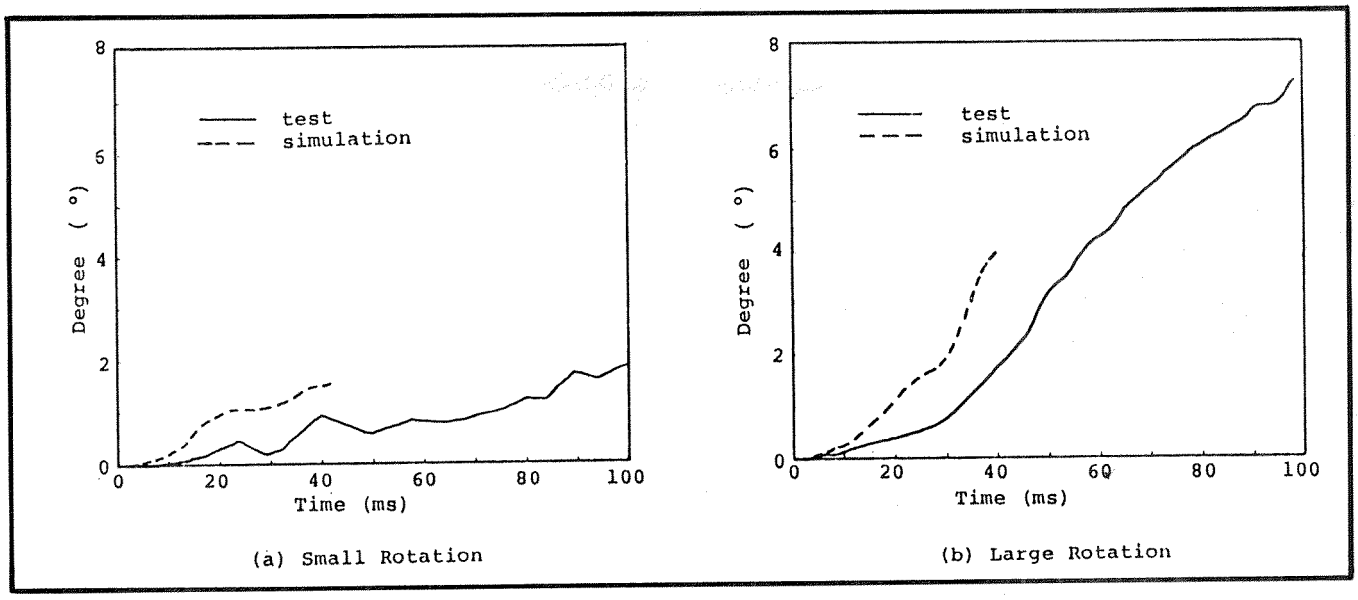

Figure 4. Comparison of passenger compartment rotations

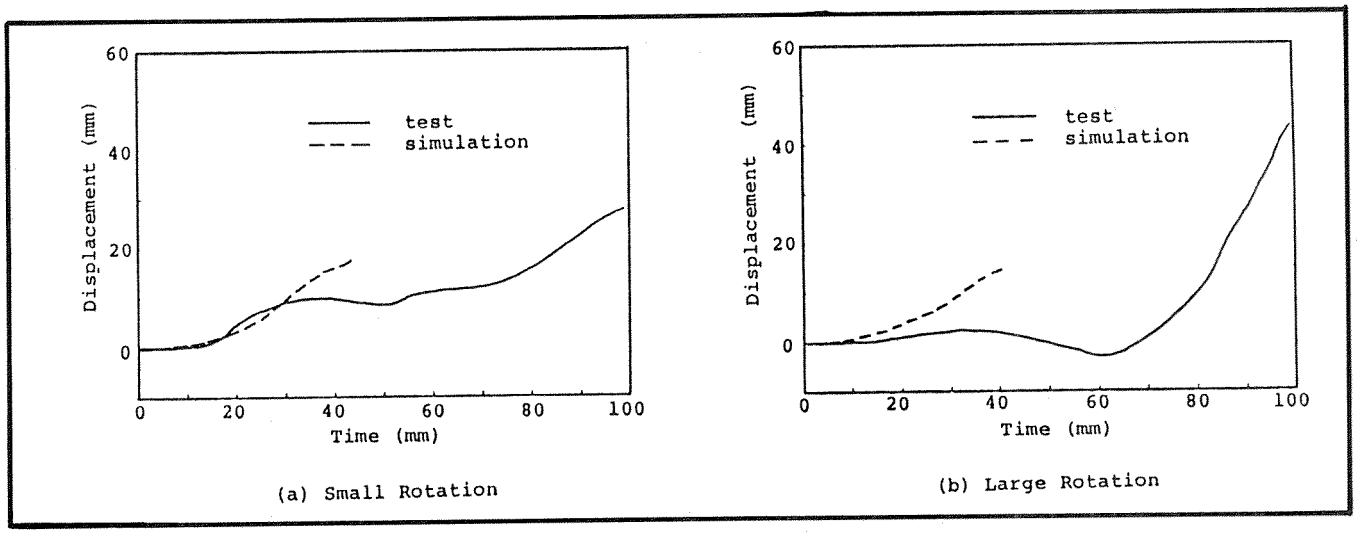

Figure 5. Comparison of passenger compartment vertical movements

characteristics for seat cushion and seatbelts as shown in Figure 6, the computation yields results in good agreement with those by the actual full-scale crash tests. The results are shown in Figures 7 and 8.

Summary and Discussion

The results in this paper indicate that cases exist where the rotation of the passenger compartment gives considerable influence on the performance of restrained occupant under specified frontal crash test, and that simulations for such cases should take the rotation into account.

It is demonstrated that the vehicle model is effectively and conveniently used by inclusion of finite element beams. Among the areas to be examined further is an improvement of vehicle response in the neighborhood of the maximum deformation or the rebound period, which is limited in the present study. An approach to this area may lie in a simplification of the model, based on closer examination of actual phenomena, by eliminating ineffective components.

It is also observed that the occupant model can be used effectively to estimate the responses to frontal crash test in the existence of rotational behavior of the vehicle by considering the displacement of connecting point of restraint devices to the vehicle.

Although there is room for improvement, the computer simulation methods presented here, both for a vehicle and its occupant, are considered acceptable for practical applications, for example, to various parametric studies.

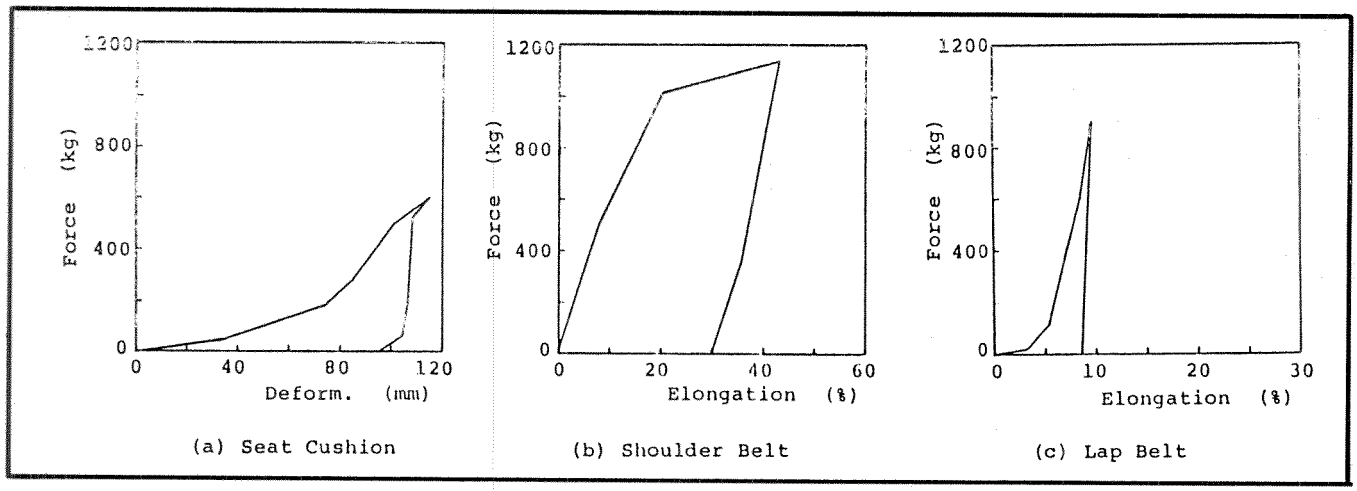

Figure 6. Restraint component characteristics

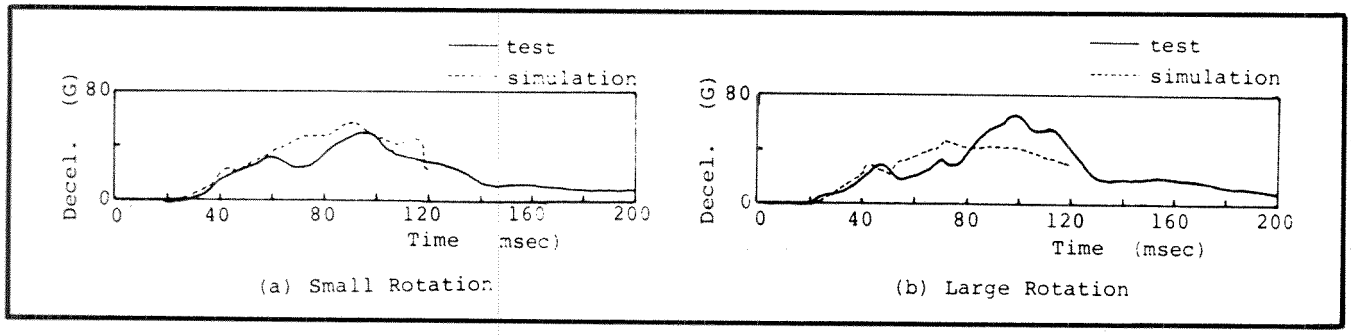

Figure 7. Comparison of head resultant decelerations

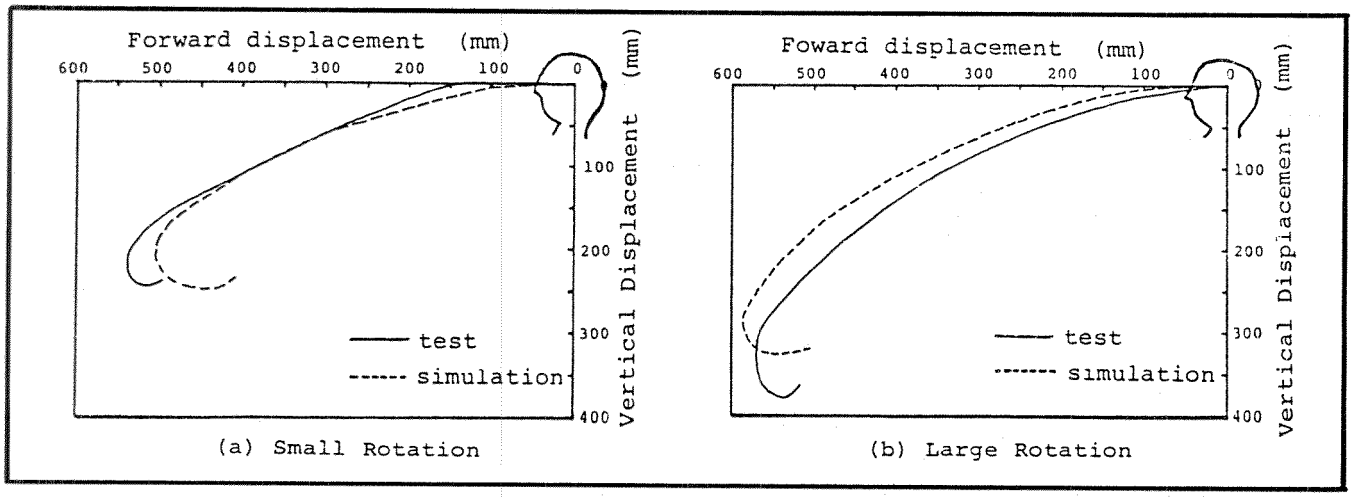

Figure 8. Comparison of relative head displacements

Acknowledgments

The authors would like to thank the related people of Mazda Motor Corporation, who gave kind suggestions in preparing this paper.

References

1. Meredith, D., et al., "Computer code for predicting the two-dimensional nonlinear dynamic response of beam structures subjected to transient loads and impacts," SAE Paper 790989, 1979.
2. Okuno, A., et al., "On an analytical crash energy management of automotive structural components," SAE Paper 830921, 1983.
3. Nakamura, K., et al., "Methodology and application of crash analysis for automotive structural components," *Proceedings of JSAE,* Vol. 832, pp. 435-442, 1983.
4. Kurimoto, K., et al., "On the optimum parameters of a seatbelt pre-loading device," Proceedings Ninth International Technical Conference on Experimental Safety Vehicles, pp. 200-205, 1982.
5. Kurimoto, K., et al., "Modeling and simulation of frontal crash impact responses," SAE Paper 810793, 1981.

Evaluation of Frontal Occupant Protection Using the Passenger/Driver Simulation Model

Lee Stucki,
Dan Cohen, and
Carl Ragland
Office of Vehicle Research,
U.S. Department of Transportation, National Highway Traffic Safety Administration

Abstract

This paper presents information on analytical procedures being developed by the National Highway Traffic Safety Administration (NHTSA) to assess the safety problem associated with occupants of passenger cars involved in frontal impacts. This analytical assessment started with the characterization of a baseline vehicle fleet consisting of specific make/model passenger car groupings representative of the in-use fleet in the United States. Newly developed analytical models have been developed and are being run in an automated mode simulating these vehicles in different frontal crash configurations. The output of these automated runs includes measures of injury severity and cause of injury, and is being used to identify the effect of different vehicle attributes on injury causation. Preliminary analytical results are presented on the relationship between steering assembly structural attributes and injury severity. Comparisons of the fleet simulation results and accident data from the National Crash Severity Study (NCSS) and the National Accident Sampling System (NASS) are also presented.

Introduction

The frontal crashworthiness research and development effort at NHTSA is aimed at assessing the safety problem associated with occupants of passenger cars involved in frontal impacts and identifying potential remedies for the problem. The approach being implemented during the present conceptual phase focuses on an analytical characterization of the in-use vehicle fleet involved in frontal crashes. This analytical characterization will be used to identify present injury mechanisms, identify alternative countermeasures, and test the effectiveness of these countermeasures.

The following major tasks were undertaken to develop analytical procedures to distinguish the baseline fleet:

- Characterization of a baseline fleet
- Identification of analytical models to simulate the baseline fleet in a crash environment
- Collection of input data related to the baseline fleet
- Automation of the analytical process to allow for efficiency in running the analytical models and analysis of the results

A detailed description of the developmental work undertaken in each of these areas was presented in a recent paper at the Society of Automotive Engineers International Congress and Exposition in Detroit(1). The following sections summarize briefly details presented in that paper.

Characterization of Baseline Fleet

The intent of this program was to select certain make/model passenger cars that represented a large proportion of vehicles in use at the time the program was initiated. The passenger cars selected were also to be highly represented in the accident files such as the National Crash Severity Study (NCSS), the National Accident Sampling System (NASS), and the Fatal Accident Reporting System (FARS). The model years selected were from 1975 to 1983. The list of specific make/model groupings (passenger cars with similar structural and interior characteristics) is presented in Table 1.

Table 1. Vehicle list—frontal protection

	Vehicle		% Fleet				
1.	76-80	Aspen/Volare	3.4	15.	75-80	Monza/Sunbird/Etc.	1.8
2.	77-81	LeBaron/Cordoba/Imperial	0.7	16.	75-79	Nova/Skylark/Etc.	3.6
3.	75-76	Dart/Valiant	0.9	17.	76-81	Chevette/T1000	3.0
4.	78-81	Omni/Horizon	1.7	18.	75-81	Camaro/Firebird	3.6
5.	75-80	Pinto/Bobcat	1.7	19.	75-81	Honda Civic	1.5
6.	78-81	Fairmont/Zephyr	1.9	20.	75-81	Toyota Corolla	2.8
7.	79-81	Mustang/Capri	1.6	21.	75-81	Subaru	1.1
8.	79-81	Ford/Mercury	1.1	22.	75-81	Datsun	2.7
9.	81	Granada/Monarch	0.2	23.	79-81	VW Rabbit	0.8
10.	80-81	T-Bird/Cougar	0.4	24.	83	Fuego	NA
11.	78-81	Malibu/Cutlass/Etc.	9.4	25.	83	Concord	NA
12.	77-81	Chevrolet	3.1	26.	83	Celebrity	NA
13.	80-81	Citation/Etc.	3.2	27.	83	Honda Accord	NA
14.	77-81	LeSabre/Electra/Etc.	4.7				

Description of Analytical Models

Occupant Simulation Model

Several analytical models are currently available capable of simulating an occupant in frontal collisions. Several models were evaluated, including the MVMA 2-D, CVS, and PADS (Passenger/Driver Simulation). It was decided to use the PADS model for simulating the driver, primarily because of the detailed steering assembly description and its relatively modest input requirements. (Comparisons of occupant kinematics and responses for PADS and MVMA 2-D are continuing for simulating the right front-seat passenger.) The PADS model has the capability to model unrestrained and restrained drivers and passengers, although at present the analytical effort focuses on the unrestrained occupant. PADS is a two-dimensional model with a four-mass (head/neck, torso, lower body, and sternum) description of the occupant. The vehicle interior compartment is described by a detailed steering assembly and seven contact planes: seat back and bottom, lower, middle, and upper instrument panel, windshield, and header (Figures 1 and 2). The model also is capable of modeling intrusion of the steering assembly, toeboard, and all contact planes except the seat back and bottom. Each contact plane is defined geometrically by its x,y coordinates, angle, and length. Mechanical properties include force-deflection, loading and unloading, surface friction, and damping. The geometric description of the steering assembly includes: x,y coordinates, column and wheel angles, column length, wheel radius, hub location relative to rim of steering wheel, and location of shear capsule and EA unit (Figure 3). Mechanical properties include force-deflection, damping and friction associated with the EA unit, column and wheel torque rotation, normal and tangential force-deflection of the wheel for head, shoulder, abdomen, and whole body loading, and hub force-deflection. A further description of PADS is contained in (2).

Crash Pulse/Intrusion Generator

Crash data matching that of the accident environment were necessary to effectively run PADS to simulate a variety of crash conditions. A crash mode generator was developed, based on a linear scaling algorithm, to

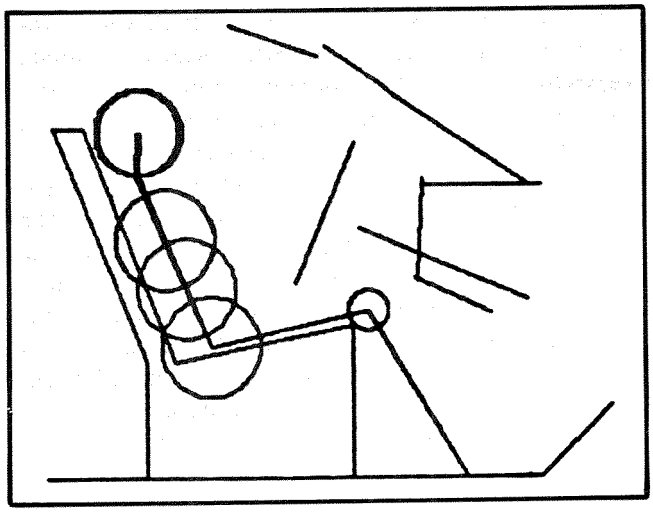

Figure 1. PADS occupant and compartment representation

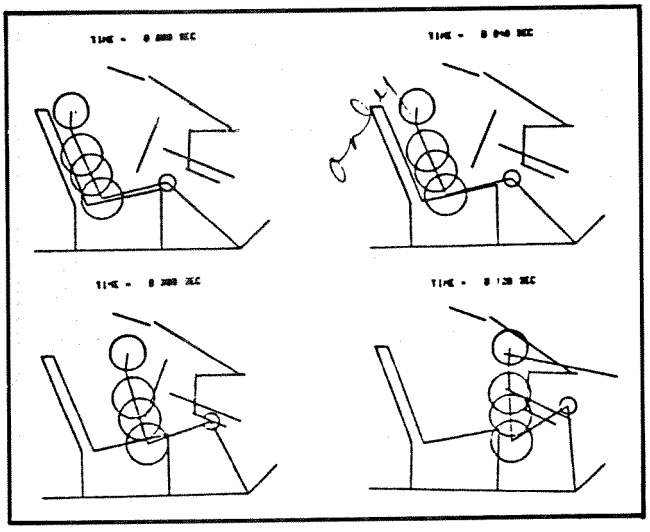

Figure 2. PADS dynamic simulation of unrestrained driver

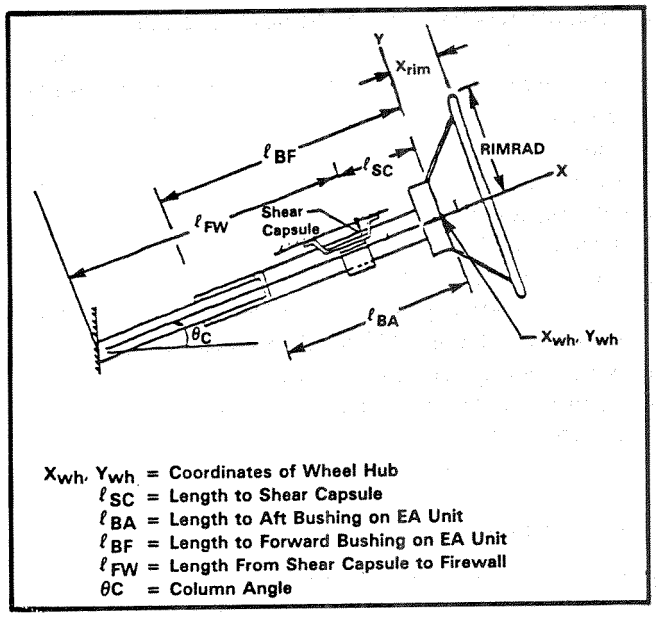

Figure 3. Steering Assembly Representation

generate a series of crash pulses representing different velocity conditions (10 to 35mph) and configuration conditions. The configuration conditions included car-to-car full frontal, car-to-car offset, and car-to-tree/pole. The crash mode scaling consists of amplitude and time scaling by an empirically derived factor dependent on the crash configuration. Algorithms to predict intrusion in different crash conditions have been developed. Further detail on these procedures are presented in this paper.

Simulation Input Data

The primary effort in developing input sets for the driver simulation involved collecting mechanical properties for the steering assembly. This consisted of three areas of testing: (1) steering column, (2) steering wheel tests conducted statically, and (3) dynamic column tests. The Transportation Systems Center (TSC) conducted these test programs as a cooperative effort with the Army Test Center for the first two programs and through a contractual effort with Batelle Columbus Laboratories for the third. Additional properties needed for driver simulation and passenger simulation include the mechanical properties of the instrument panel (lower, mid, and upper), windshield, and header. MGA Research, under contract with TSC, collected the material properties related to windshields and instrument panels. Compartment geometry data were obtained from a program being conducted at TSC(3). Occupant descriptors for the PADS model were compiled for the 5th percentile female, 50th percentile male, and 95th percentile male. All anthropometry data came from NHTSA's Advanced Dummy Program(4).

Crash testing of the 27 baseline vehicles has been conducted over the past 7 years as part of ongoing programs at NHTSA. Test data are stored in the NHTSA data base system. Twenty-five of these tests were conducted at 35mph, one at 30mph, and one at 40mph.

Automated Procedure for Simulating Fleet

Since the analytical procedure to simulate the accident environment requires the creation of numerous input files for PADS, an automated procedure was required to reduce the effort involved in their construction. Input sets required for combinations of the following parameters include: velocity (10 to 35mph), occupant sizes (5th, 50th, 95th), damage locations (distributed, offset, center),

object contact (vehicle or tree/pole), etc. The PADS Control File Generator (PCFG) was developed to automate the procedure for creating and submitting input files. The approach developed was based on storing subfiles of the car characteristics, assembling the subfiles into a complete input set, and inserting the completed input files into a run stream, which can then be submitted for computer simulation.

In addition to developing a procedure to handle effectively the creation of the input data sets, an efficient method was necessary to store and analyze the output. An output option was developed specifically for these automated runs and consists of outputting one line of data for each simulation. The line of data consists of 67 variables and includes information regarding the description of the simulation, selected simulation outputs (contact sources, contact velocities, body region involved, predicted injury levels, etc.), and run diagnostics. As a last step, this output file is converted to Statistical Analysis System (SAS) format to allow for the efficient development of tabular and graphical displays.

Structural Attributes for Crashworthiness Assessment

Identification of Attributes

The effect of the vehicle's frontal structure is being investigated by this program. Included are the effects of both the crash pulse of the compartment and the intrusion of the interior surfaces during the crash event. These are believed to be the major factors (for a given vehicle velocity change) of crash severity. Contributing to these primary factors are the collision partner stiffness, subject partner stiffness, and crash mode. This section will discuss the approach to improving structural crashworthiness, the anticipated safety improvements, and the methods used to evaluate the potential for improvement, while accounting for the complex structural parameters contributing to crashworthiness.

Data Conditioning and Crash Pulse Scaling

To evaluate potential safety improvements, crash mode and intrusion were scaled as previously mentioned. Test data for 27 vehicles tested in barrier crashes (25 at 30mph and 1 each at 30 and 40mph) were used for obtaining the starting pulse and baseline intrusion data. Crash pulse scaling was performed to obtain six velocities and three different crash modes as previously described. In addition to these 18 scaled pulses, intrusion was scaled for various objects struck (stiff, medium, or soft car or nonyielding object), which resulted in a total of 54 crash pulse/intrusion combinations for each of the 27 vehicles and 3 occupant sizes. Before performing the scaling routines, all data were carefully screened and conditioned to be consistent with observed physical phenomena. This process was accomplished by first performing film analysis to determine intrusion parameters and dynamic crush and velocity profiles for each of the vehicles. Signals from the various longitudinal accelerometers mounted in the occupant compartment, usually two to five, were processed and screened for data anomalies, such as time shift, zero bias, excessive noise, excessive data spikes (possible system or transducer overload), etc. Any observed anomalies were then, whenever possible, corrected. The pulses were next compared against film data, with one pulse chosen to represent compartment response based primarily on best agreement with film-derived dynamic displacement. This chosen pulse was further conditioned by applying a constant calibration factor that assured absolute agreement. For most of the 27 vehicles, load cell data were collected from a 36- and and a 40-segment load cell barrier. Due to early calibration problems with some of these load cells, data conditioning to obtain stiffness properties was essential for this effort. Force or load cell data were screened similarly to the crash pulse, then conditioned in the following manner based on impulse calculations. First, the time range for the impulse calculation is defined as the range of time from zero to the time when load cell response returns to zero. Impulse for the compartment pulse, using the entire mass of the vehicle, is determined over this time range. This impulse is compared against the force-time history impulse computed from the sum of the load cells, and a ratio of these impulses is determined. This ratio is used as a constant calibration factor to adjust the load cell response. This load cell response was used to obtain the maximum or peak force value (filtered at 100Hz cutoff frequency). Use of this value for obtaining intrusion will be explained in the following discussion.

After conditioning, scaling is accomplished as follows. First, the pulse is scaled to six velocities from 10 to 35mph. This is accomplished by computing a loading, unloading, and damping coefficient for a simple one-mass model. Next, crash mode scaling is performed for three modes—full frontal, half offset frontal, and pole impacts. Direct amplitude and time scaling are applied to the velocity-scaled pulse using factor, k, as follows: (Crash pulse-time) $\times$ 1/k and (Crash pulse-acceleration) $\times$ k.

Factors used are:

Crash mode	k Factor
Full frontal	1.00
Offset frontal	
-front wheel drive	0.60
-rear wheel drive	0.80
Pole	0.75

An example of velocity scaling alone compared to test data is shown in Figure 4. Velocity scaling combined with crash mode scaling is shown (compared to test data) in Figures 5 and 6.

Intrusion Analysis and Scaling

Next, an algorithm was produced for determining dynamic intrusion related to crush. As before, the baseline data for intrusion scaling were the barrier crash

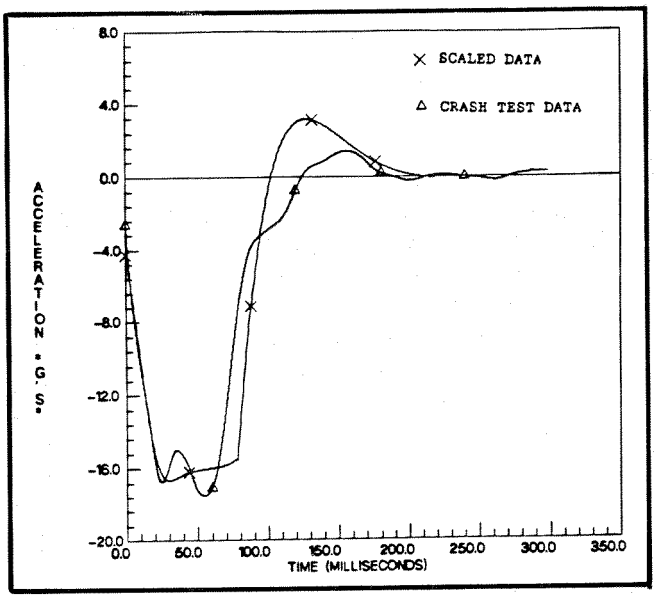

Figure 4. Velocity scaling compared to test data for 1981 AMC Concord car-to-car full frontal crash test at 25mph velocity change

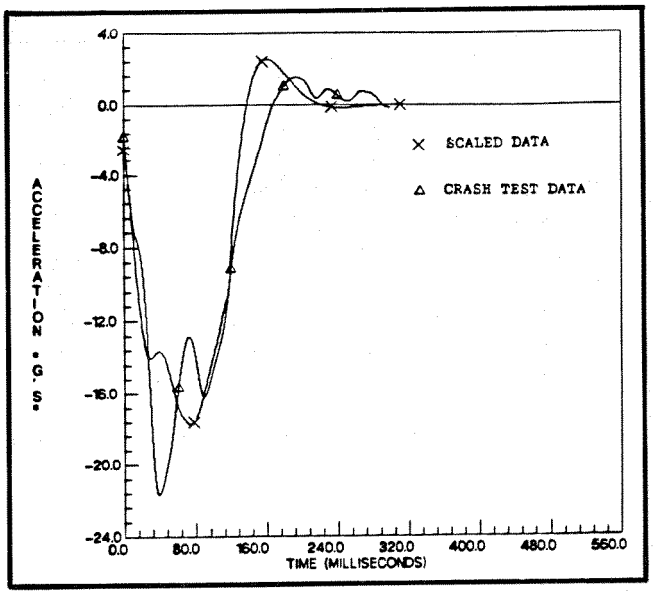

Figure 5. Velocity/crash mode scaling compared to test data for 1981 VW Rabbit car-to-car half offset crash test at 37mph

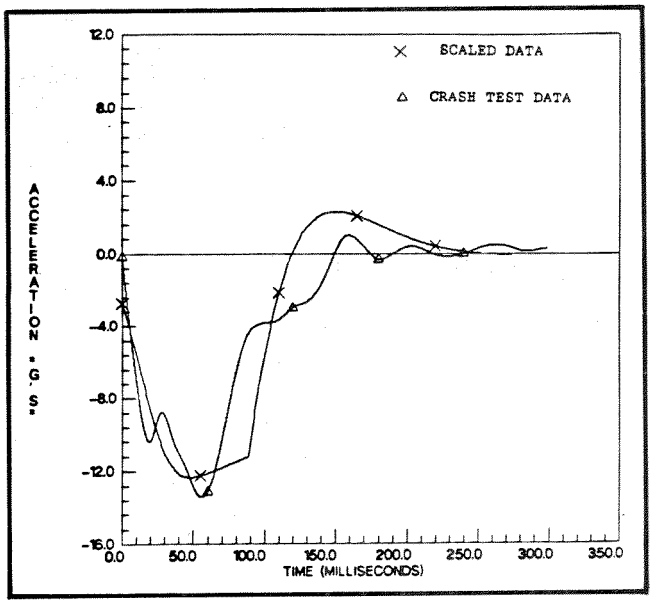

Figure 6. Velocity/crash mode scaling compared to test data for 1981 AMC Concord car-to-car half offset crash at 20mph

tests. Film analysis was performed on these data to determine the crush-related intrusion parameters. Basically, these parameters related to the onset and completion of intrusion in terms of dynamic crush of the subject vehicle. Figure 7 shows the dynamic crush, compartment velocity time, and interior intruding surface velocity time. Also shown on this plot is the film-derived onset and completion of intrusion, identified as C1 and

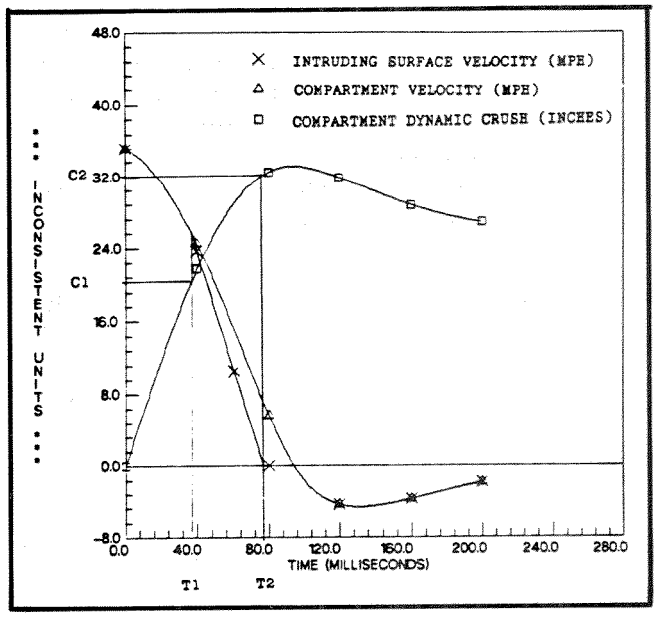

Figure 7. Intrusion relationships between compartment velocity, compartment crush, and intruding surface velocity

C2, and corresponding times T1 and T2. The extrapolation of intrusion became relatively straightforward since crush is determined directly from the velocity-scaled pulses for car-to-barrier, car-to-equivalent car, and car-to-pole type impacts. Not as straightforward, however, was intrusion scaling for car-to-car of different effective stiffness. That is where both cars do not equally share in the energy absorption and, thus, do not crush as they would in a nonyielding object-type collision. Therefore, to account for this difference, the maximum force level recorded by the summed loads from the NHTSA 36 segment load cell barrier appeared to be the best indicator of this effective stiffness. To approximate the crush sharing, the total mutual crush in a hypothetical car-to-car event is ratioed by FMAXp/(FMAXp+FMAXs), where FMAXp and FMAXs are the maximum load cell forces for a collision partner and subject car, respectively.

Evaluation Approach

Evaluation of the structure alone required an approach that would allow all other parameters to be held constant while varying the structural parameters. Since other phases of this research evaluated interior energy absorption, kinematics, etc., it seemed appropriate to ignore these factors and, as a final step, combine structure evaluation with the compartment interior evaluation. Originally, PADS was planned for this entire process, while using the above described structural input data, but the volume of runs and modeling constraints were not feasible within the time constraints. Therefore, a simpler approach was chosen, while selectively using PADS as needed. The approach chosen used PADS to relate the severity of the crash to the velocity with which a theoretical one-mass occupant would contact the interior of the occupant compartment. For purposes of visualizing this parameter, Figure 8 demonstrates the relationship between contact velocity and spacing (the distance traveled before initial contact with the interior surface). Using crash pulse scaling and PADS, a relationship of contact velocity to chest deflection and a potential injury scale were established. This was accomplished by first performing a regression analysis to derive the relationship between chest deflection and contact velocity, both determined from PADS for 18 crash mode and velocity combinations for a large and small car. This relationship, as shown in Figure 9, has an R-squared factor of .944 with a quadratic fit. Next, a regression analysis between contact velocities generated by PADS and the corresponding contact velocities calculated for a one-mass occupant was performed with the resulting linear fit shown in Figure 10. Applying this linear factor to contact velocity in Figure 9, a new quadratic relationship is derived for one-mass occupant contact velocity and chest deflection as shown in Figure 11. By using a previously

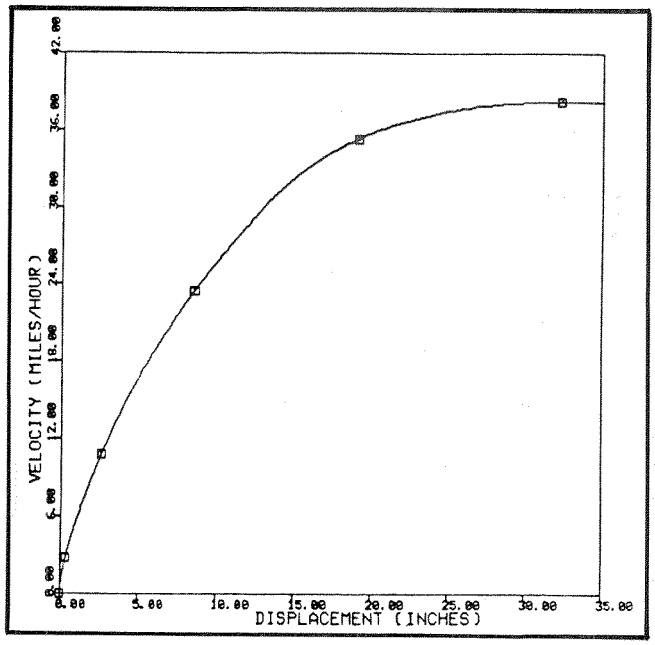

Figure 8. A plot showing contact velocity for a theoretical one-mass occupant versus spacing

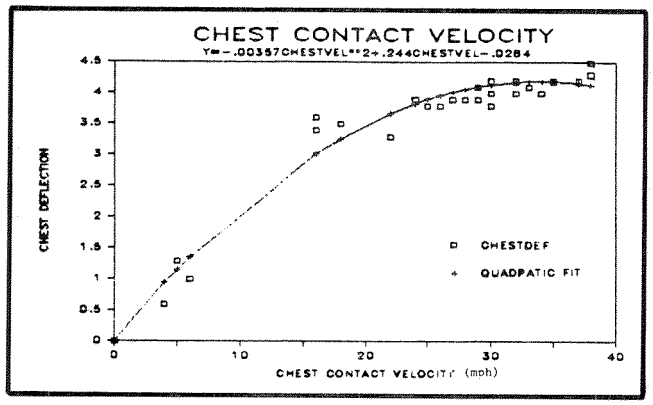

Figure 9. Chest deflection from PADS versus chest contact velocity from PADS showing a quadratic fit of data

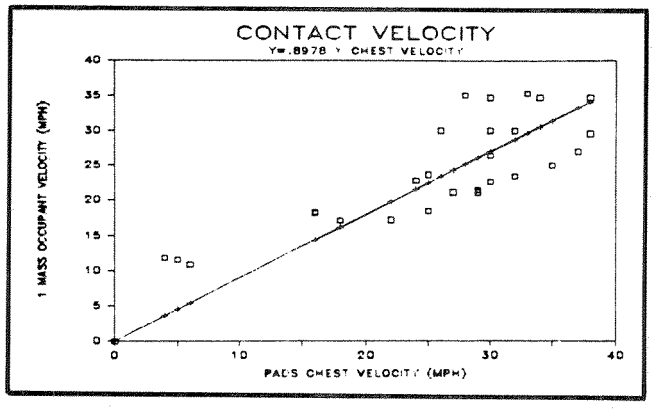

Figure 10. Contact Velocity computed from a theoretical one-mass occupant versus PADS chest contact velocity showing a straight line data fit

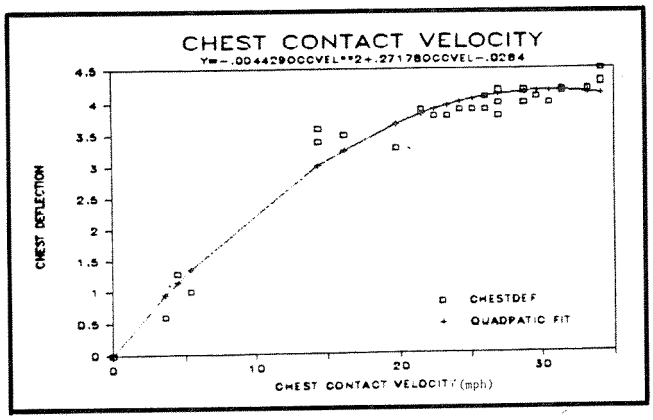

Figure 11. Chest deflection from PADS versus chest contact velocity for a theoretical one-mass occupant (derived by combining Figures 9 and 10)

derived relationship of chest deflection to injury(5), a probability of injury for contact velocity function is derived. Since this is not a true probability of injury relationship, due to other variables such as steering assembly characteristics, etc., this relationship will be referred to as a Structural Severity Index (SSI). This relationship may then be used to determine relative injury potential for a vehicle's given crash pulse and dynamic intrusion. To demonstrate the relationship of frontal structure and contact velocities, the following examples are shown. First, the effect of crash pulse without intrusion is examined using contact velocity. To make the comparisons on vehicles with similar potential for crashworthiness, the selection of 27 vehicles, shown in Table 1, was divided into six weight categories. A comparison of contact velocity versus occupant spacing is shown for the best and worst of a weight group in Figure 12A for one crash mode and velocity. This plot represents the velocity at the instant of impact with the interior surface for a theoretical one-mass occupant varying with the initial distance to the surface. To evaluate crashworthiness potential, Figure 12B shows the same two cars compared in terms of occupant contact velocity with a constant restraining force applied after a prescribed slack distance is traveled by the occupant (represening a theoretical constant force restraint). These plots are shown as extremes of crash pulse effect within a given weight class of 2,500 to 3,000 lb. Additional variations can be shown for other weight classes, and larger variations exist across weight classes (see Figure 13).

To demonstrate intrusion effects, a similar example showing contact velocities is given. To determine dynamic intrusion effects, an algorithm was developed, based on the previously discussed intrusion scaling, that combined the crash pulse with the dynamic intrusion effect to predict the theoretical contact velocity of a one-mass occupant. An example of contact velocity variations is shown in Figures 14A and 14B for two cars with different

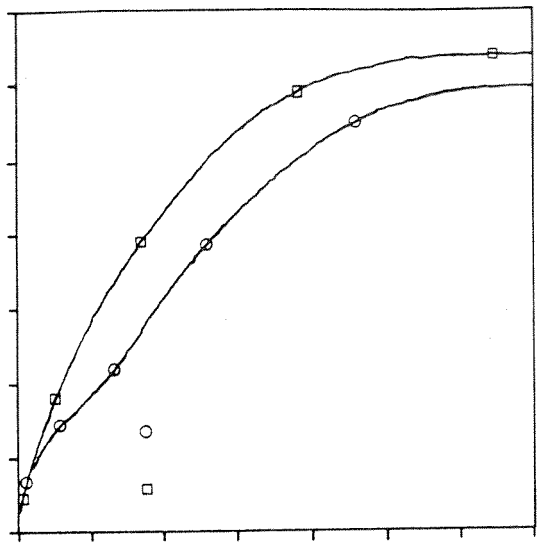

Figure 12A. Contact velocity comparisons of two cars in a weight group for unrestrained case at 30mph velocity change

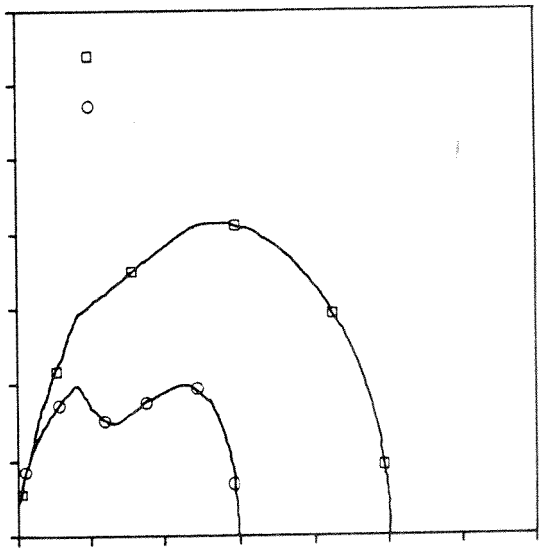

Figure 12B. Contact velocity comparisons of same two cars in Figure 12A for restrained case at 30 mph velocity change

intrusion characteristics, also in the 2,500 to 3,000 lb weight category.

The final step in the structural evaluation process is to determine the combined effect of intrusion and crash pulse throughout the accident scenario using the previously discussed SSI (structural severity index). This will be accomplished in the following manner. First, contact velocities will be established as previously discussed for all vehicles and all crash modes. Next, chest

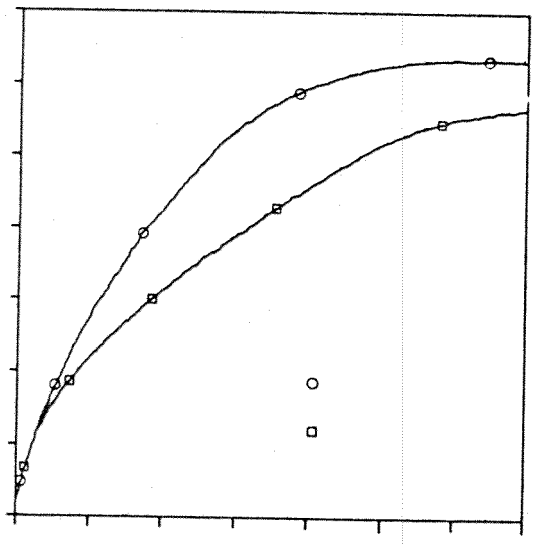

Figure 13. Contact velocity of best (large car) and worst (small car) for unrestrained case at 30 mph velocity change

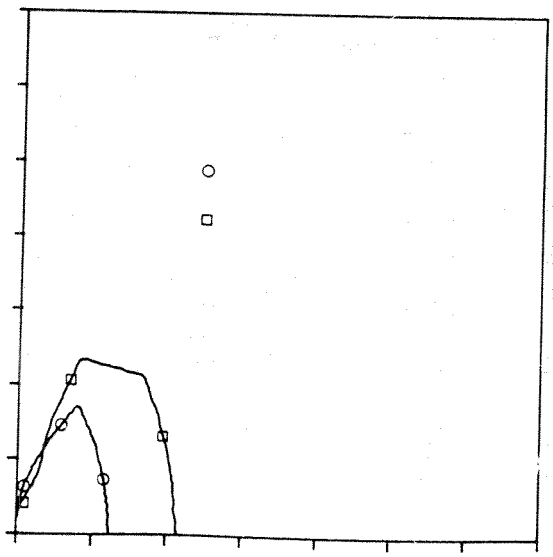

Figure 14B. Contact velocity comparison of same cars and crashmode shown in Figure 14A but with occupant restrained

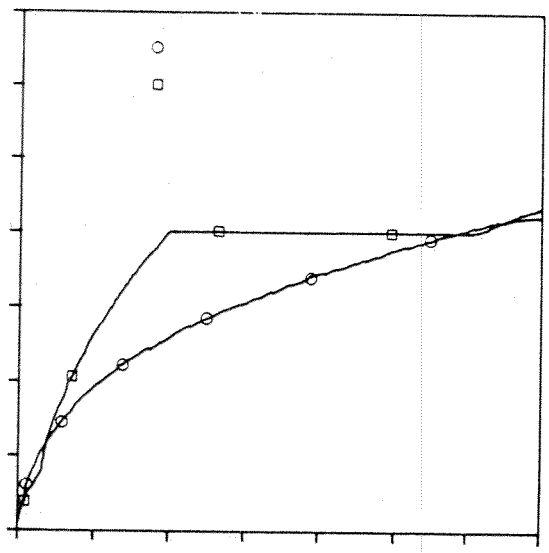

Figure 14A. Contact velocity comparison of two cars in a weight group with good and bad intrusion properties shown for a 20mph/-half offset crash mod and unrestrained

deflection and the corresponding crashworthiness potential, expressed as SSI, are computed from the previously described relationship. Then, for the 54 crash pulse/intrusion combinations for each vehicle, a probability of occurrence will be computed based on NCSS data for delta v distributions over each crash mode, fleet weight distributions, and fleet stiffness distributions. Finally, the overall relative structural attribute SSI will be computed for each vehicle to determine the best and worst performers within each weight group. An example of this approach, shown in Figure 15, compares the SSI versus change in velocity for the two vehicles compared in Figures 14A and 14B. The combined SSI for these two cars in the same weight class shows a relative difference of 40 percent. That is, the driver of car A has a 1.4 times greater potential for injury than the driver of car B based on structural attributes alone. Final results of these analyses are pending completion of ongoing work, which includes validation of the intrusion algorithm, completion and analysis of ongoing crash tests, and processing of all 27 vehicles through the described process.

Once the baseline fleet has been evaluated, changing fleet properties may next be assessed, along with various sensitivity studies of structural parameters. The primary purpose of this task, before proceeding to the PADS approach, is to evaluate the fleetwide effects of changing parameters on the previously identified best and worst performers. Parameters included in this study are stiffness distribution, weight distribution, and restraint usage rates. The last parameter, restraint usage rates, is least effectively analyzed by contact velocity due to large dummy kinematic differences caused by the restraints themselves. For example, a potential chest impact with the steering hub may change to a more lethal head impact with the hub. Once some understanding of the parameters is established, final analysis will rely on PADS on a more limited basis to reevaluate these best and worst structures. In addition, PADS will be used to combine the best and worst structures with the best and worst interiors to determine the overall potential for crashworthiness improvement.

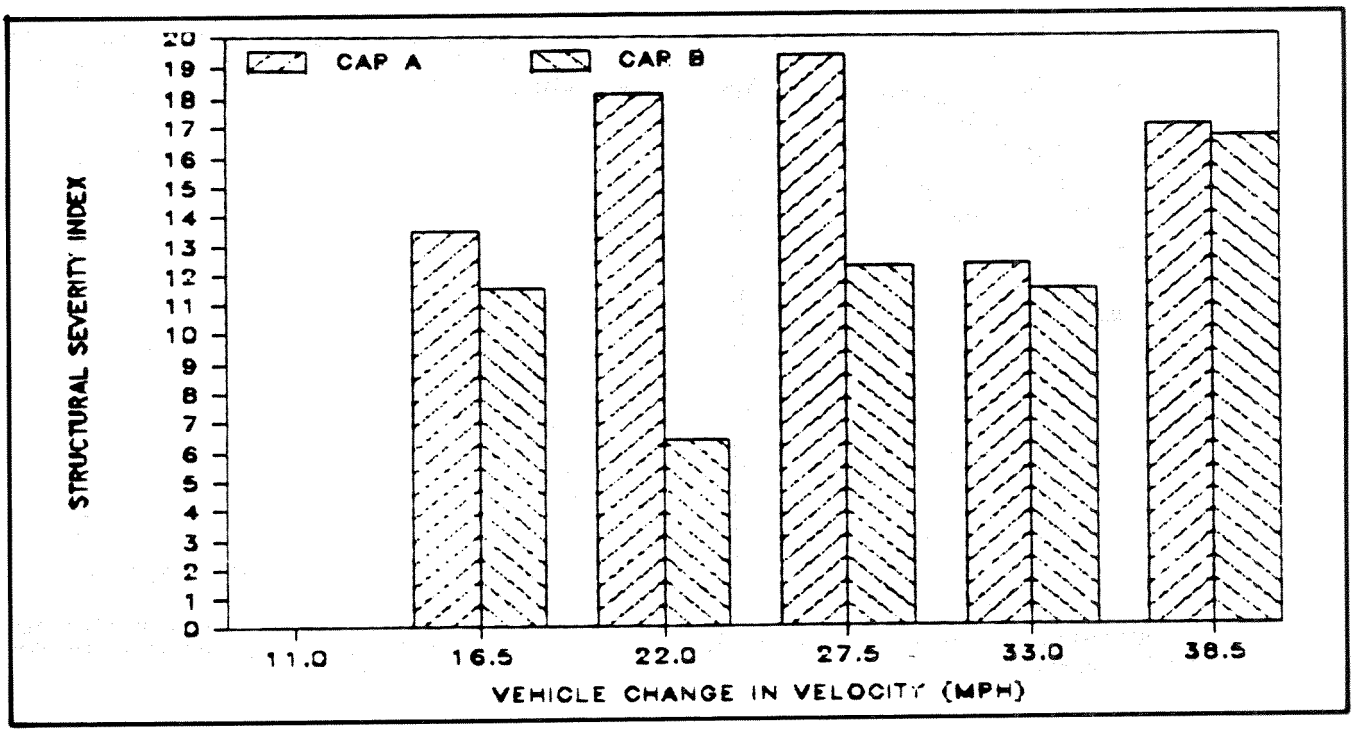

Figure 15. Relative injury potential expressed as structural severity index versus vehicle velocity change for two cars with different intrusion characteristics

Countermeasure Assessment for Driver

The objective of the countermeasure assessment is to determine improvements to the driver compartment, which can then be introduced into the 27-vehicle fleet to predict injury reductions over the baseline. The procedure consists of the following steps:

- Evaluation of contact surface properties and geometry for the 27 vehicles
- Ranking of vehicles by properties and defined parameters
- PADS simulations for comparisons of injury measures between high- and low-ranked vehicles
- Introduction of improved properties to lower ranked vehicles
- Determination of a group of best properties based on results of PADS runs, engineering evaluation, and biomechanical limits
- Selection of one vehicle with high baseline injuries, applying a best set of properties, and comparing simulation results with baseline

The goal of a countermeasure is to reduce injuries for the following body regions:

- Chest—Goal is to get minimum values for chest deflection and chest G's, i.e., lower the forces applied to the chest. Variables that directly influence the force level are—

		Good	Bad
(a)	EA characteristics of the column	high EA, relatively low force	low EA high force
(b)	EA friction	low	high
(c)	Hub recession	fairly deep	shallow or none
(d)	Hub padding	same as (a)	same as (a)
(e)	Wheel + column weight	low	high
(f)	Column damping	low	high

The deeper the hub is recessed, the more potential for abdomen penetration. The wheel/hub geometry should be designed for mitigating both chest and abdomen injuries. Load distribution affects the chest deflection but is not accounted for in the model, so, for the initial assessment, area will not be considered. Variables that indirectly influence the chest force are parameters that lower the impact velocity of the torso and/or alter body region/contact configuration. Geometry and force-deflection properties of the knee restraint and windshield, along with the crash pulse and intrusion, will affect the impact velocity and kinematics.

- Abdomen—Goal is to lower abdomen deflection by reducing the applied force. Since the abdomen is very soft, the force should be as low as possible within design limits. Variables that influence abdomen deflection are—

		Good	Bad
(a)	Hub recession	shallow	deep
(b)	Lower rim characteristics	low force long stroke	high force short stroke

Although a high EA rim would benefit chest injury by lowering chest impact velocity, preventing abdomen penetration is a more important role for the lower rim. Again, the same variables that influence contact velocity and kinematics for the chest also apply to the abdomen.

- Head—Goal is to reduce head G's and HIC's by lowering the force applied to the head. Important variables are—

		Good	Bad
(a)	Windshield characteristics	Low force but some EA	High force
(b)	Upper rim	low force	high force
(c)	Header	low force	high force

- Femur—Femurs can take a fairly high force without injury (about 2,500 lb). The lower instrument panel is the predominant contact. The main purpose of the knee contact is to be an energy absorber, but loads should remain below 2,500 lb. The location and stiffness of the knee contact also heavily influence the kinematics.

Evaluation of Baseline Contact Surface Properties

Data from PADS input sets were extracted to evaluate energy-absorption characteristics and force levels for the 27 vehicles. The objective of the evaluation is to assess characteristics that, from an engineering and biomechanical viewpoint, influence occupant injury. For each contact surface, parameters were either extracted from the force-deflection tables, computed, or developed. These include—

- Energy-absoption potential: the area under the force-deflection curve
- Average force: EA potential divided by the maximum stroke
- Maximum force
- Maximum stroke
- EA efficiency: a parameter defined as percent of the EA potential that lies below the average force level, i.e., a measure of how near the force-deflection curve is to a square wave response

A computer program was developed to extract the data from the PADS input files, compute parameters, and produce data files of these parameters for each contact surface of all 27 vehicles. The contact surfaces evaluated were: head/upper wheel rim (tangential and radial direction), abdomen/lower rim (tangential and radial), chest/wheel hub, whole wheel crush, steering column energy absorber, knee/lower instrument panel, chest/mid instrument panel (passenger), head/upper instrument panel (passenger), head/windshield, and head/header.

As discussed above, the injury potential of a surface is related to the amount of energy that can be absorbed by the surface and the maximum force that is applied to the body region. Obviously, these two parameters tend to contradict each other since a high energy-absorption potential is usually accompanied by high forces. A characteristic that combines these factors was needed to discriminate between the 27 vehicles. To accomplish this, the files were then read into another program that calculated a single parameter (which accounts for EA potential and efficiency, and maximum force) to better describe the injury potential of the contact surface. This defined parameter is equal to the ratio of EA potential to kinetic energy of the torso at 25mph times a force factor (equal to 1 if the maximum force is less than 1,200 lb and equal to the ratio of 1,200 divided by the maximum force if greater than 1,200 lb) times the EA efficiency. In addition, the ratio of the EA potential of the contact surface to the kinetic energy of the appropriate body part

is calculated for 25 and 30mph impacts. The final step in the evaluation is to combine the EA parameter and EA ratios for each contact surface into single values for the complete steering assembly and also for the complete driver compartment (defined as PARAM, EA25, and EA30 in Table 2). For all these parameters, the higher value, theoretically, represents better force-deflection properties.

parameter and EA ratio. The highest and lowest cars based on this criteria are—

	Steering Assembly		Total Compartment	
	Parameter	EA Ratio	Parameter	EA Ratio
High:	Granada	Mustang	Concord	Ford
Low:	Valiant	Valiant/ Fuego	Chevette/ Horizon	Chevette

Table 2. Summary of properties

	Energy Absorption Properties						Steering Assembly Properties			
	Total Compartment			Steering Assembly						Hub
Model	EA25	EA30	Param.	EA25	EA30	Param.	Weight	Frict.	Damp	Recess
Ford	0.91	0.63	1.24	0.94	0.65	0.31	15.60	0.49	0.00	0.50
Mustang	0.89	0.62	1.39	1.11	0.77	0.47	15.40	0.16	0.00	2.32
T-Bird	0.71	0.49	1.20	0.71	0.49	0.27	12.22	0.23	0.00	0.50
Fairmont	0.79	0.55	1.35	0.88	0.61	0.43	12.02	0.23	0.00	2.32
LeSabre	0.83	0.58	1.41	0.78	0.54	0.48	12.83	0.00	15.50	1.09
Electra	0.83	0.58	1.41	0.78	0.54	0.48	12.83	0.00	15.50	1.09
Camaro	0.81	0.56	1.22	0.56	0.39	0.31	12.86	0.00	9.10	1.03
Rabbit	0.55	0.38	1.12	0.73	0.50	0.38	5.44	0.36	9.10	0.00
Datsun	0.57	0.40	1.41	0.50	0.35	0.40	10.95	0.43	9.10	-0.57
Corolla	0.62	0.43	1.51	0.60	0.42	0.50	5.13	0.20	9.10	1.38
Subaru	0.62	0.43	1.51	0.60	0.42	0.50	5.13	0.20	9.10	1.38
Nova	0.76	0.53	1.12	0.46	0.32	0.21	10.55	0.00	9.10	1.03
Monza	0.77	0.54	1.14	0.46	0.32	0.21	12.00	0.00	9.10	-0.57
Malibu	0.79	0.55	1.57	0.44	0.30	0.30	13.54	0.34	9.10	-0.57
Volare	0.83	0.57	1.39	0.51	0.36	0.33	11.83	0.21	12.40	4.22
Cordoba	0.83	0.57	1.39	0.51	0.36	0.33	11.83	0.21	12.40	4.22
Citation	0.78	0.54	1.50	0.41	0.28	0.23	10.75	0.13	9.10	-0.57
Concord	0.86	0.59	1.67	0.58	0.40	0.40	11.14	0.62	9.10	3.18
Granada	0.79	0.55	1.48	0.69	0.48	0.56	18.40	0.33	0.00	1.65
Chevette	0.37	0.26	1.03	0.38	0.26	0.28	12.00	0.40	9.10	-0.57
Pinto	0.73	0.51	1.30	0.63	0.44	0.50	13.87	0.82	0.00	1.65
Celebrity	0.80	0.55	1.59	0.45	0.31	0.32	8.88	0.00	9.10	3.18
Accord	0.51	0.36	1.23	0.37	0.26	0.22	7.94	0.00	12.40	1.63
Valiant	0.74	0.51	1.23	0.32	0.22	0.17	9.95	0.00	12.40	1.86
Horizon	0.43	0.30	1.03	0.40	0.28	0.26	10.09	0.00	12.40	3.03
Civic	0.49	0.34	1.18	0.33	0.23	0.17	8.28	0.00	12.40	1.63
Fuego	0.49	0.34	1.24	0.32	0.22	0.23	9.39	0.59	9.10	-0.57

In addition, tables were constructed of geometric relationships and other driver parameters for the 27 vehicles. Geometry includes: knee to lower instrument panel distance, abdomen to rim distance, chest to hub distance, head to windshield distance, vertical distance from head to header, and head to upper rim. Other properties include: wheel + column weight, friction, damping hub recession (also in Table 2), and column angle.

Simulation Results

The 27 vehicles were ranked by steering assembly parameter and EA ratio and by total compartment

Comparison simulations between high- and low-valued cars were conducted using the PADS model. Comparison criteria were selected as HIC, chest deflection, and abdomen deflection. To minimize output data, runs were made with only the 50th percentile occupant, distributed crash pulse at 10, 15, 20, 25, 30, and 35mph, and no intrusion. In comparisons of the total compartment, the results are inconclusive. In these cases, the higher ranked cars had less chest deflection but generally higher HIC's and abdomen deflections. Since the cars with high EA ratio, also, have higher force levels, these results are not unexpected. However, in the case of the EA parameter for the total compartment (Concord versus Chevette), since force is accounted for, lower measures would be expected. It should be noted that the Concord was

highest ranked in this category predominantly because of superior knee restraint properties since it was ninth best for steering assembly alone (at this time only a few windshields had been tested, all with similar force-deflection properties, and therefore the windshield contribution to the EA parameter was similar for all cars). The contribution of the knee restraint may not be as important as the steering assembly and possibly shouldn©t have received equal weighting.

Comparisons based on steering assembly EA properties showed better distinction between high- and low-ranked cars. The Mustang showed significantly lower HIC and chest deflections than the Valiant, although abdomen deflections were higher in the Mustang (the Fuego results were not valid since the simulations aborted prior to significant occupant/compartment interaction). The Granada gave the lowest injury measures of all cars that were simulated. In comparisons with the Valiant, the HIC's in all cases were lower and chest deflections lower by 2in or more in all but the 10mph case, which only had about 1in deflection. The results of all simulations are shown in Table 3, and the comparison of Granada to Valiant is shown in Figure 16. To display HIC and chest deflection on the same graph, they are presented as AIS level. Formulas for chest and abdomen AIS are given in (5); head AIS based on HIC is given in (6).

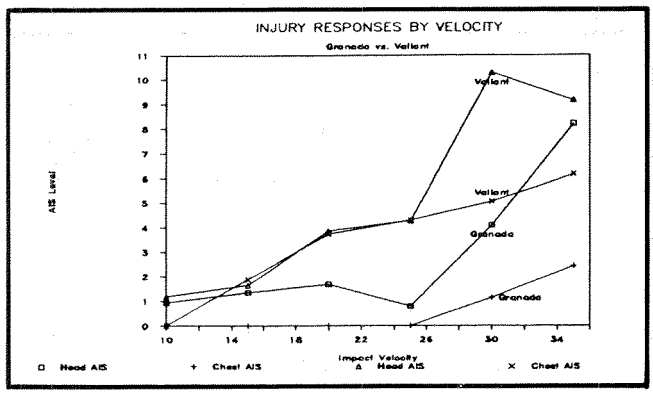

Figure 16. Granada and Valiant responses

Simulation of Other Properties

The Valiant was selected to introduce variations in other steering assembly properties. The same set of simulations, as discussed previously, was conducted for the following parameter variations: 4 lb wheel + column weight; 0 and 4in hub recessions; 0 friction and damping (Valiant has 0 friction as tested); 0 column and wheel angle; and improved column EA properties (LeSabre column). Table 4 shows the results for the runs.

Table 3. Simulation results for high- and low-ranked cars

		Velocity Change (mph)					
		10	15	20	25	30	35
Granada:	HIC	98	271	405	35*	1270	2469
	Chest Def.	1.0	1.9	2.1	1.0*	2.8	3.5
	Abdomen Def.	2.2	2.5	2.5	2.5*	2.5	2.1
Valiant:	HIC	202	387	1192	1331	7986	2722
	Chest Def.	0.8	3.2	4.2	4.5	4.9	5.5
	Abdomen Def.	1.6	1.9	2.0	2.0	2.1	2.1
Ford:	HIC	44	226	463	468	442	690
	Chest Def.	1.6	2.7	3.3	3.1	3.0	3.5
	Abdomen Def.	3.9	4.5	4.9	4.8	4.8	5.1
Chevette:	HIC	120	302	458*	441*	420*	793
	Chest Def.	1.8	2.8	2.7*	2.0*	1.8*	4.3
	Abdomen Def.	1.6	2.6	3.0*	3.1*	3.1*	3.4
Mustang:	HIC	73	174	413	712	831	675
	Chest Def.	1.1	2.3	3.6	3.9	4.1	4.2
	Abdomen Def.	2.1	3.2	3.6	3.7	3.7	3.6
Concord:	HIC	110	277	4330	2863	743	1022
	Chest Def.	1.0	2.3	2.3	2.7	3.2	3.7
	Abdomen Def.	1.9	2.9	3.4	3.5	3.6	3.6
Horizon:	HIC	89	243	356	438	556	852
	Chest Def.	0.5	2.4	3.6	4.1	4.4	4.5
	Abdomen Def.	1.9	2.1	2.6	2.6	2.6	2.6

* Indicates run shutoff before 110ms
NOTE: The HIC was cut off at 3,000 for graphics display

Table 4. Simulation results for variation of properties (Valiant as baseline)

Variation	Response	Velocity Change (mph) 10	15	20	25	30	35
	HIC	202	387	1192	1331	7986	2722
Valiant	Chest Def.	0.8	3.2	4.2	4.5	4.9	5.5
	Abdomen Def.	1.6	1.9	2.0	2.0	2.1	2.1
	HIC	222	384	902	1206	1601	9999
4# Column/	Chest Def.	1.4	3.3	4.2	4.4	4.5	4.9
Wheel Weight	Abdomen Def.	1.6	1.9	2.0	2.0	2.1	2.2
	HIC	133	430	1925	9999	7334	2191
0 Hub Recess	Chest Def.	1.9	3.9	4.3	4.5	4.6	4.7
	Abdomen Def.	1.5	1.9	2.0	2.0	2.2	2.1
	HIC	348	396	897	1416	1698	2091
4 Inch Hub	Chest Def.	0.5	2.1	2.9	3.4	3.7	4.2
	Abdomen Def.	1.5	1.9	2.0	2.0	2.0	2.1
	HIC	145	379	971	1083	1413	9999
0 Damping	Chest Def.	0.9	3.2	4.1	4.3	4.4	4.9
	Abdomen Def.	1.6	1.9	2.0	2.0	2.1	2.1
	HIC	211	459	364	390	567	1025
0 Column	Chest Def.	0.5	0.6	2.0	4.5	4.5	4.8
Angle	Abdomen Def.	0.0	0.0	0.0	0.0	0.0	0.0
	HIC	287	382	1481	1321	9999	2361
LeSabre	Chest Def.	0.9	3.3	4.2	4.5	4.8	4.9
Column	Abdomen Def.	1.6	1.9	2.0	2.0	2.1	2.1

All of the variations simulated produced lower chest deflections. The cases of 4 lb wheel/column weight, 0 hub recess, 0 damping, and addition of the LeSabre column did not improve (or worsen) the other injury measures. The case with the column angle at 0° eliminated abdomen deflection and substantially reduced the HIC. The 4in hub recession had the lowest chest deflections (over 1in reduction in most cases) and somewhat lower HIC values. It appears, at this point, that 0 column angle and 4in hub recession produced the highest reduction in injury measures of those evaluated.

Simulation With Improved Properties

The final set of simulations involved developing a set of driver compartment properties, which should result in the lowest injury measures for the PADS simulations, based on the previous countermeasure evaluation. All the improved properties are judged to be production feasible, since all improvements were similar to the characteristics of at least one of the 27 vehicles. The modifications to the baseline Valiant data set included the following:

Knee Panel		Lower Rim Tangent		Lower Rim Radial		Hub		EA Column	
Force (lb)	Defl. (in)	Force (lb)	Defl. (in)	Force (lb)	Defl. (in)	Force (lb)	Defl. (in)	Force (lb)	Defl. (in)
0.	0.	0.	0.	0.	0.	0.	0.	0.	0.
200.	0.75	250.	0.5	250.	1.0	300.0	1.0	800.	2.0.
500.	3.0	350.	10.0	500.	5.0	500.	5.0	1200.	3.0
1200.	5.0					2000.	5.5	1250.	8.0
3000.	12.0							1600.	8.5
								5000.	9.0

Other modifications include: 4in hub recession; 0 column friction and damping; and 4 lb wheel + column weight. Zero column angle was also tried but, due to occupant/compartment geometry, problems occurred in these runs. This will be resolved in the future.

The results of these simulations (shown below and in Figure 17) with the best properties showed substantial reductions over the baseline Valiant in the three injury measures evaluated.

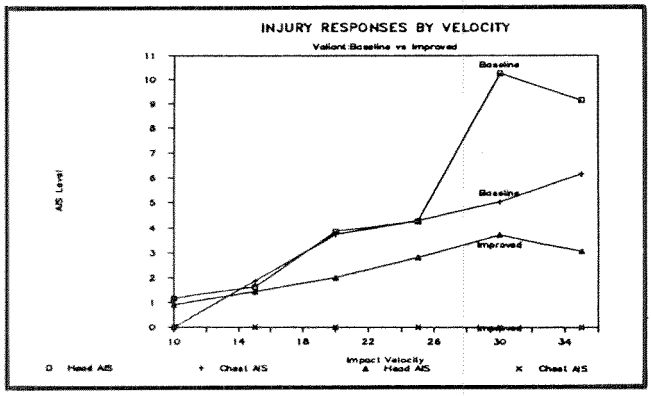

Figure 17. Comparison of baseline Valiant to Valiant with improved properties

frontal crashes. This baseline analytical characterization is being used to—

1. Identify possible relationships between vehicle attributes (structural, steering assembly, interior geometry, etc.) in the baseline fleet and injury causation
2. Test the effectiveness of the best countermeasures (such as those discussed in the previous sections related to the steering assembly and structure) in a fleetwide accident environment.

Baseline Simulation Data Base

The automated procedure for simulating the baseline fleet was implemented using the analytical tools discussed previously. Each of the 27 make/model vehicle groupings that compose the baseline fleet were simulated under varying crash conditions, including a range of velocities (10 to 35mph), damage locations (distributed, offset, and center), and object contacted (vehicle and tree/pole). Three occupant sizes (5th, 50th, and 95th) were considered. While not all combinations of these parameters are required (i.e., vehicle-to-vehicle center impacts), the various combinations resulted in 54 simulations for each make/model vehicle grouping (6 velocity categories, 3 crash distribution/object struck categories, and 3 occupant size categories). Thus, the total simulations amounted to 54 × 27 = 1,458 runs. Not all of the individual simulations successfully ran to completion. A judgment was made to reject any simulations that did not run at least 110ms. Out of the 1,458 possible simulations, 1,175 passed this criterion, which was felt to be extremely successful considering the wide range of environments in which the model was being exercised. Thus, the baseline simulation data base is composed of these 1,175 simulations and was used for all the analyses presented in this paper. As time permits, the simulations that did not meet the run time criteria will be examined to determine the cause of the problem and to determine whether not using these runs leads to any bias in the data when considering the aggregate results.

Case	Criteria	Velocity Change (mph) 10	15	20	25	30	35
Baseline Valiant	HIC	202	387	1192	1331	7986	2722
	Chest Def.	0.8	3.2	4.2	4.5	4.9	5.5
	Abdomen Def.	1.6	1.9	2.0	2.0	2.1	2.1
Valiant with Improvements	HIC	93	314	538	839	1149	925
	Chest Def.	0.5	1.1	1.2	1.3	1.7	1.6
	Abdomen Def.	1.1	1.4	1.4	1.5	1.5	1.5

These results show minimal injury, based on predicted AIS for deflection, for either the chest or abdomen. The HIC at 30mph may result in serious injury; however, in this series of countermeasure evaluations, attention was on chest and abdomen injury and no modifications were made to head impact areas.

Future countermeasure evaluation will be to apply an improved set of countermeasures to the 27 vehicles to predict injury reduction over the baseline.

Analysis of Accident and Simulation Data for Baseline Fleet

As mentioned in the introductory sections of this paper, a primary effort within the frontal crashworthiness research and development program is the analytical characterization of the in-use vehicle fleet involved in

Baseline Fleet Accident Data

Comparison of the results of the simulation data with accident data can provide additional support to the validity of the analytical modeling process and can provide a linking process to help in projecting changes in the accident environment from simulation results. This and the next several sections present results related to performing this comparison.

First, analyses were performed comparing NHTSA's complete accident files, including the NCSS and NASS, with subfiles consisting of accidents involving the vehicles in the 27-vehicle groupings. This was done to insure that the 27 make/model vehicle groupings selected as representative of fleetwide vehicle production are also representative of the accident environment. The 27-vehicle accident file is being compared to the complete files for crash, occupant, and vehicle factors and also as to injury consequences.

Figure 18 presents a comparison of the probability of receiving an AIS 3 or greater injury for the 27-Vehicle,

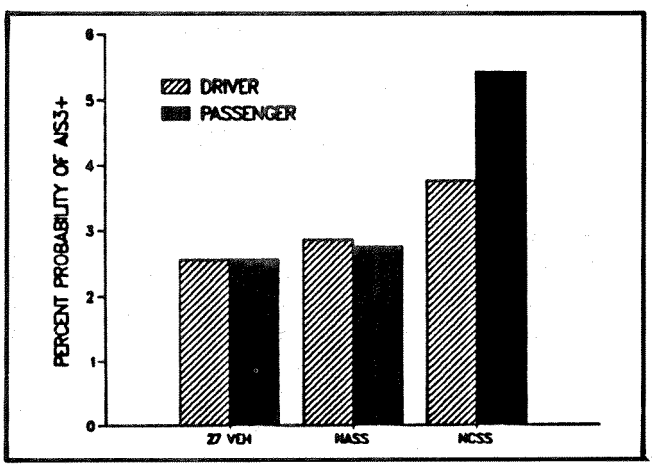

Figure 18. Probability of receiving an AIS injury of 3 or greater

NASS, and NCSS files. The 27-vehicle file was constructed from the NASS file, and thus better agreement can be expected between these files. Remaining comparisons focus on the driver seating position since this is the main focus of this effort. Table 5 compares the three files for body region injured for serious (AIS 3 or greater) injuries received by drivers. The distributions are based on a count of injuries and not occupants (i.e., one occupant could have received more than one injury at an AIS 3 or greater level). Table 6 compares the files for the source of serious injuries. The distributions in both figures show good agreement.

Figures 19 to 21 compare the delta v, damage location/distribution, and object-contacted distributions for the three files related to crashes in which a driver received a serious injury (AIS 3 to 6). As seen from these figures,

Table 5. Distribution of body regions injured (AIS 3+) for drivers

Body Region	27 Vehicle	NASS	NCSS
Chest	22%	27%	31%
Head	7	13	8
Lower Extremities	30	22	20
Upper Extremities	5	6	6
Abdomen	14	14	17

Table 6. Distribution of body regions injured (AIS 3+) for drivers

Injury Source	27 Vehicle	NASS	NCSS
Steering Assembly	42%	44%	54%
Windshield	9	5	4
Instrument Panel	22	18	18
A-Pillar	2	2	2
Header	1	2	2
Unknown	9	15	6

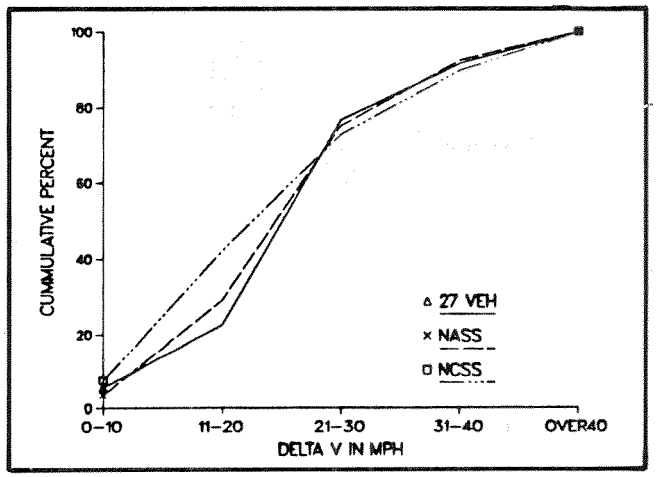

Figure 19. Distribution of delta v for seriously injured drivers

there is excellent agreement between all distributions. While additional comparisons between these files are continuing, it appears the 27 make/model vehicle groupings are representative of the accident environment.

For the remaining analyses between the simulation results and the accident data, the total NCSS and NASS files were utilized rather than the 27-vehicle accident file. Since the files appear to agree with each other on several variables, the use of the complete files offers a larger sample size, which, in turn, will permit more disaggregate analyses.

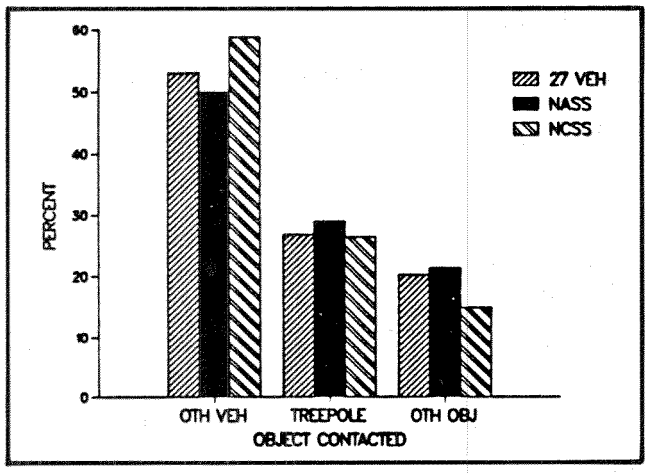

Figure 20. Distribution of object contacted for seriously injured drivers

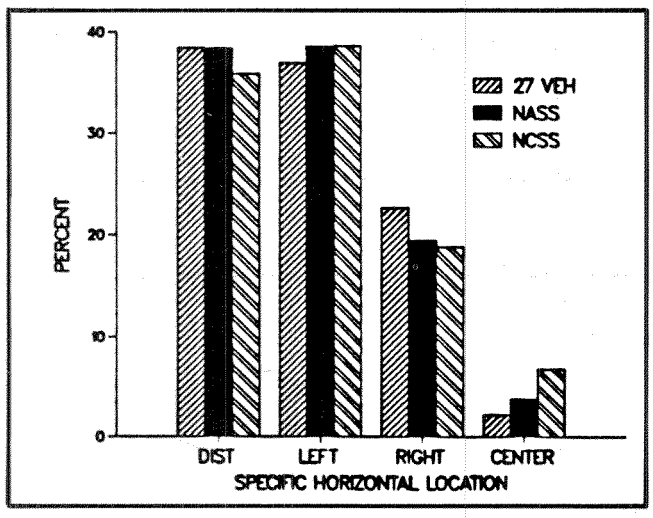

Figure 21. Distribution of location of vehicle damage for seriously injured drivers

Extrapolation of Simulated Runs To Reflect Accident Environment

As discussed, the PADS model was run for the 27 vehicles, several occupant sizes, different crash conditions, and different velocities. Each run represents a specific condition in the accident environment. Since each run does not represent equally occurring events in the environment, each run must be assigned a weighting or expansion factor to allow meaningful comparisons with accident files. The NASS file is being used to develop weighting factors associated with each simulation. The overall weighting factor is based on the specific make/model, the occupant size, the object struck, the location of damage, the delta v, and the weight of the vehicle. Many of these variables are interrelated, and the weighting factors were developed for combinations of the factors.

Comparison of Simulated Baseline With Accident Data

The focus of the comparisons presented in this section is on chest, abdominal, and head body regions, which account for the greatest harm to drivers in frontal crashes.

Initial comparisons focused on sources of injury predicted by the simulation data base and the accident files. For the chest and abdomen, as could be expected, the steering assembly was the primary area of injury. In comparing head contacts between the simulation results and the accident data, the following items must be considered:

1. PADS is limited to simulating contacts only with frontal surfaces and cannot consider contacts with A-pillars, side interiors, etc.
2. There are a large number of unknown contact sources in the accident data that need to be distributed.
3. For the PADS simulations, multiple contact sources are indicated for each body region impact. Thus, if the head contacts the header and windshield, the PADS simulation will indicate both sources as a possible injury source. For the accident data, only one contact source per injury is coded.

Table 7 indicates the source of serious head injuries (AIS 3 to 6) for drivers in frontal impacts as indicated by NCSS and NASS. Only the most serious head injury is considered. That is, if a driver received an AIS 3 and an AIS 4 head injury, only the source of the AIS 4 injury was considered. The first column in the table shows the distribution of sources including unknown sources. For NASS, this amounts to approximately 25 percent of the injuries. The second column presents the distribution of sources excluding the unknown category. The third column presents the distribution for only those sources of injury for the head that are modeled in the PADS simulations—the windshield, header, steering assembly, and upper instrument panel. Table 8 indicates the source of serious injury as predicted by the PADS simulations. As discussed above, multiple sources of injury are reported if the head contacts more than one interior surface. To compare these results with those of NCSS and NASS, the multiple sources had to be distributed among the steering assembly, windshield, and header. The second column shown in this table was constructed by equally distributing the multiple sources to each of the appropriate sources. Table 9 presents the distributions developed in the previous tables, which focus on the four contact sources. Considering the high percentage of unknown contact sources in the accident data and the subjective manner of dividing the multiple contact sources in the PADS simulations, the distributions for NCSS,

Table 10. Injury severity by delta v indicated by NASS and PADS

Injury Severity	Body Region Injured					
	Chest		Head		Abdomen	
	PADS	NASS	PADS	NASS	PADS	NASS
AIS 0	29%	63%	12%	73%	17%	91%
AIS 1-6	71%	37%	88%	27%	83%	9%

examine the probability of a serious injury given a contact occurred. Since the accident files do not indicate contacts unless an injury occurred, this type of analysis could not be accomplished. However, a reasonably close estimate of this can be obtained assuming that, if contact is made, at least an AIS 1 injury would have resulted. This would seem to be a reasonable assumption, especially at the higher delta v levels. Thus, the different files were compared on the basis of the probability of a serious injury given that an injury occurred (AIS 1 to 6).

Figure 23 presents the comparisons for the three files for the head, chest, and abdomen. The comparisons are for the probability of receiving an AIS 3 or greater injury. As can be seen, while there still exist fairly large differences in specific categories, the three files are in much closer agreement than in previous comparisons.

Figure 24 presents the results of an additional analysis related to explaining these differences. The accident files were rerun using filters that more closely matched the crash conditions being simulated by PADS. The crash pulses used in PADS tend to overrepresent the severe types of crashes (head-on). In addition to the filter of the general area of damage equal to front, filters were added to limit crash conditions to 12 o'clock direction of force, head-on car-to-car, and car-to-tree/pole conditions. The figure only presents the results for one delta v (26 to 35mph) and only for the NASS file. As can be seen, the probabilities for the chest and abdomen increase by approximately 40 percent, while the probability for head injuries decreases by about 10 percent. In general, the addition of these filters would further close the differences between PADS and the accident files.

Additional analyses are continuing in an attempt to understand the differences between PADS, NCSS, and NASS. Based on the results of the analyses presented, it is felt that the PADS automated runs scaled to the accident data can be considered a useful tool in developing information for predicting how vehicle modifications can affect the consequences of injury in the accident environment.

Future Analysis of PADS and Accident Data

Disaggregate Analyses

The previous sections examined the accident and simulation data at an aggregate level. It is planned to also examine the results at a disaggregate level (i.e., at a make/model vehicle group level).

For the accident data, it is not possible to use NASS and NCSS at this disaggregate level because of limitations in sample size. FARS and various State accident files will be examined for potential use in these analyses.

At the time of preparing this paper, these analyses have just been initiated, and results are not available. The analyses underway are using the injury severities predicted by PADS and accident files for the individual make/model groups and examining correlations with the vehicle attributes identified in the previous sections on structures and steering assemblies. The results of these analyses should help further in the identification of important attributes to consider in mitigating injuries.

Harm Reduction

The results presented above relate to the complete baseline PADS simulations. It is planned to make a number of complete simulations with a modified fleet that includes the best countermeasures as determined through the analyses described earlier relating to structures and steering assemblies. Total fleetwide harm reduction can be estimated by comparing the injury consequences of the baseline fleet to the modified fleet.

Conclusion

Structural Improvements

The findings in this research effort are preliminary since research is continuing. However, results to date show significant overall fleet safety improvements may

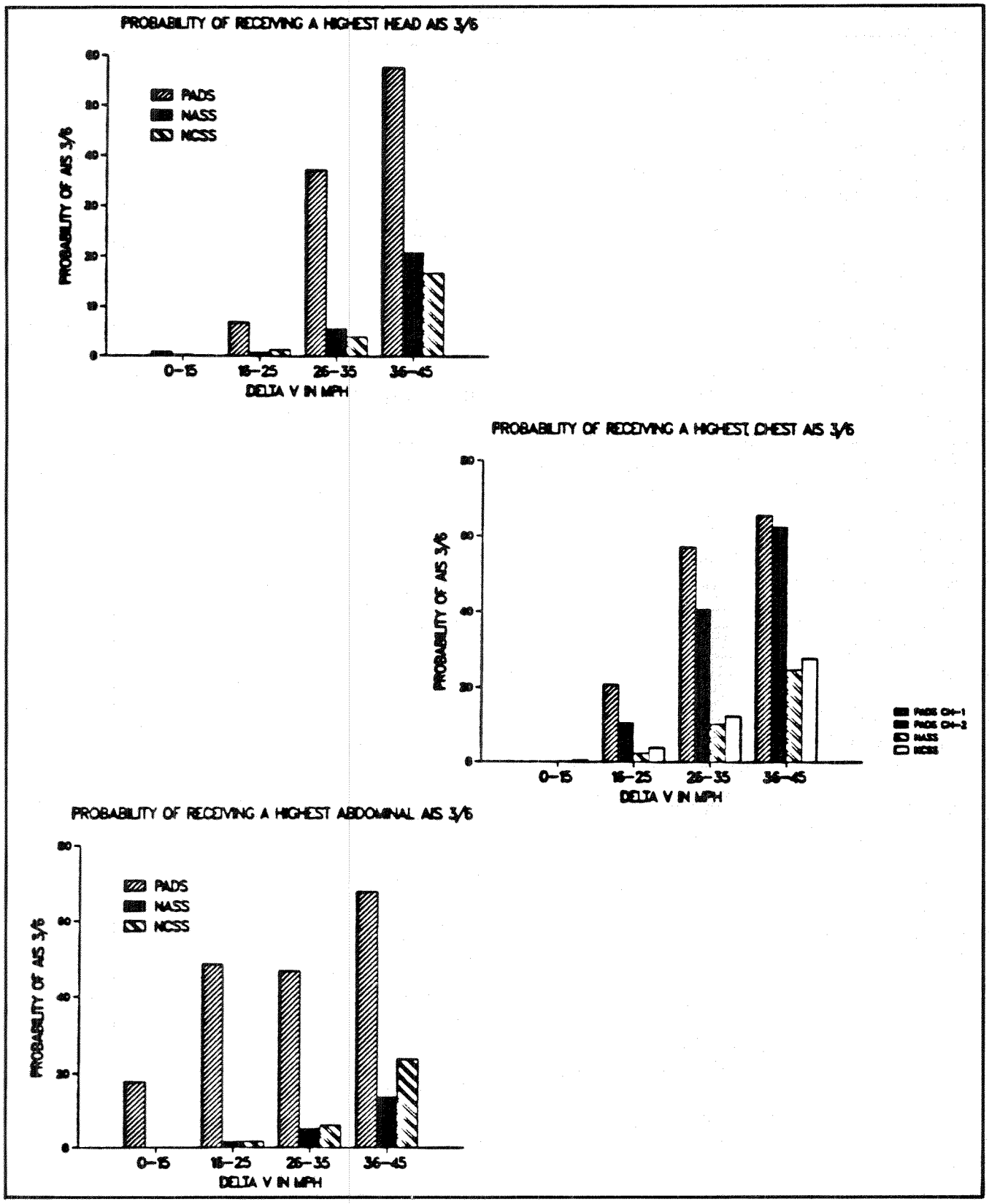

Figure 22. Probability of driver receiving a serious head, chest, or abdominal injury by delta v

Table 7. Sources of serious head injuries to drivers as indicatd by NASS and NCSS

	NASS			NCSS		
	All (1)	Excluding Unknown (2)	Four Sources (3)	All (1)	Excluding Unknown (2)	Four Sources (3)
Windshield	19%	26%	46%	25%	28%	40%
Steering Assembly	10	14	25	24	26	38
Header	9	12	21	10	11	15
Instrument Panel	3	4	8	5	5	8
Other Front	20	26	-	22	24	-
Other	14	19	-	6	7	-
Unknown	25	-	-	8	-	-

(1) All sources as reported in the accident files
(2) All sources excluding unknown sources
(3) The four sources modeled in PADS

Table 8. Sources of serious head injuries to drivers as indicated by PADS simulations

	All	Four Sources
Windshield	18%	47%
Steering Assembly	25	40
Header	0	13
Instrument Panel	0	0
Header/Windshield	26	-
Steering Assembly/Windshield	31	-

Table 9. Sources of serious head injuries to drivers as indicated by PADS, NASS, and NCSS

	PADS	NASS	NCSS
Windshield	47%	46%	40%
Steering Assembly	40	25	38
Header	13	21	15
Instrument Panel	0	8	8

NASS, and PADS appear fairly similar. (Differences in these distributions may be attributed to the planar representation used in PADS as discussed later.)

The next series of figures presents comparisons for the three files related to the probability of receiving serious injuries. Since PADS does not predict injuries for all body regions, the overall probability of receiving a serious injury to any body region could not be compared between PADS and the accident files. Thus, the comparisons analyzed were for the probability of receiving a serious injury to specific body regions. The body regions considered included the head, chest, and abdominal areas. The comparisons are shown in Figure 22. While the probability of being severely injured in crashes with high delta v's is high, the probability of getting a severe injury to any one specific body region is much lower. From the figure, it is noted that for all files the probability of serious injury increases with increasing delta v in a similar manner; however, the probabilities predicted by PADS are much larger than for NASS and NCSS.

A number of analyses are being undertaken to understand the differences in probabilities between PADS, NASS, and NCSS. Table 10 presents detailed data related to injury severity by delta v for the PADS and NASS files. The example given is for a delta v range of 26 to 35mph. As can be seen, NASS has a much higher percentage of occupants receiving no injury to a particular body region.

These differences could be attributed to differences in the probability that a certain body region contacts a specific interior component. PADS is a two-dimensional model with the occupant seated directly in front of the steering assembly, and the kinematics of the occupant represent those expected in a 12 o'clock, head-on type impact. The simulations almost always produce contact with the steering assembly. In the accident data bases, however, conditions exist in which the occupant might not contact the steering assembly directly. These conditions include—

- Direction of force at 11 or 1 o'clock
- Off-center impacts
- Occupant protective actions
- Submarining
- Out-of-position seating position

Thus, it was felt that a more appropriate comparison between PADS and the accident files would be to

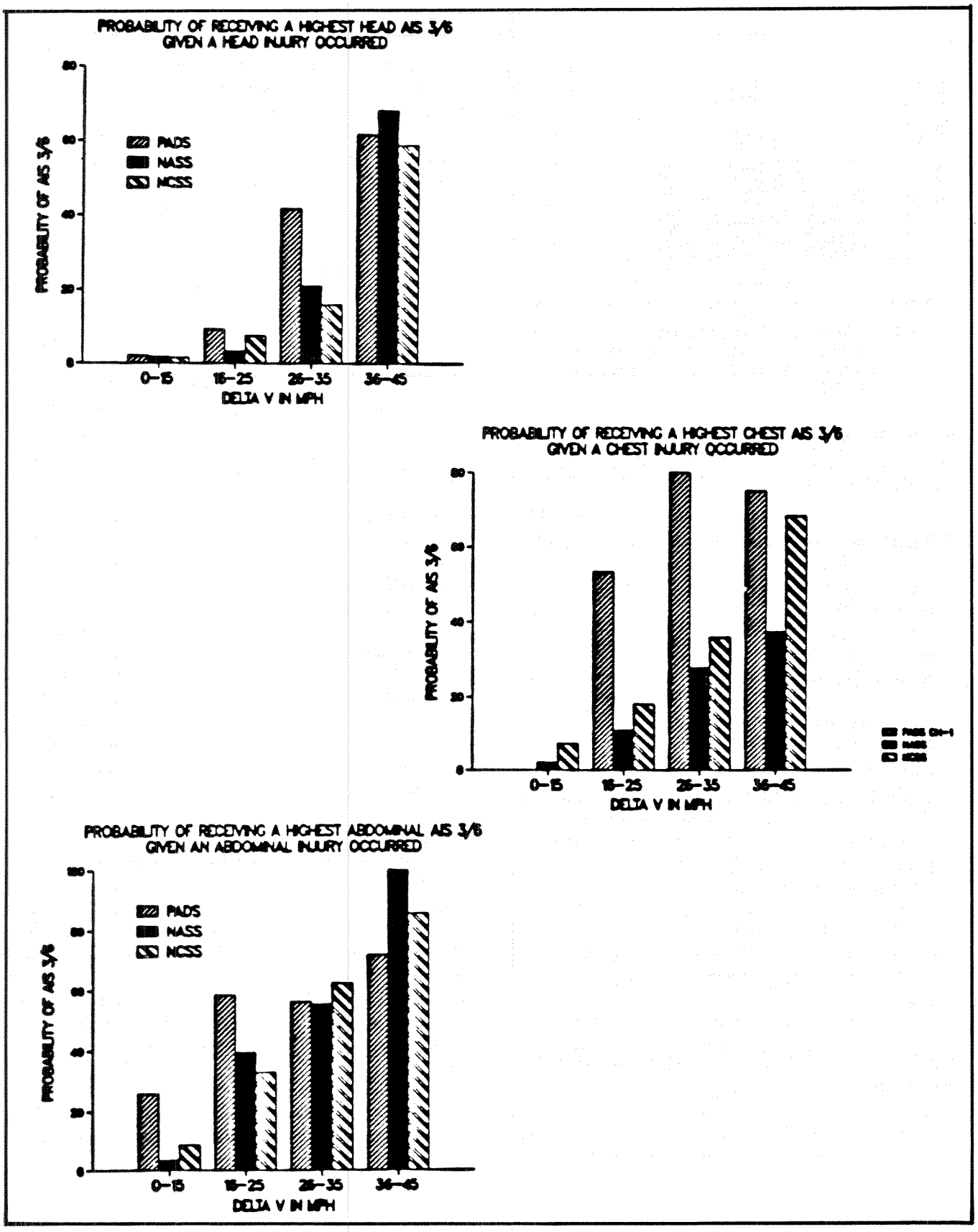

Figure 23. Probability of driver receiving a serious head, chest, or abdominal injury given a serious injury to that body region

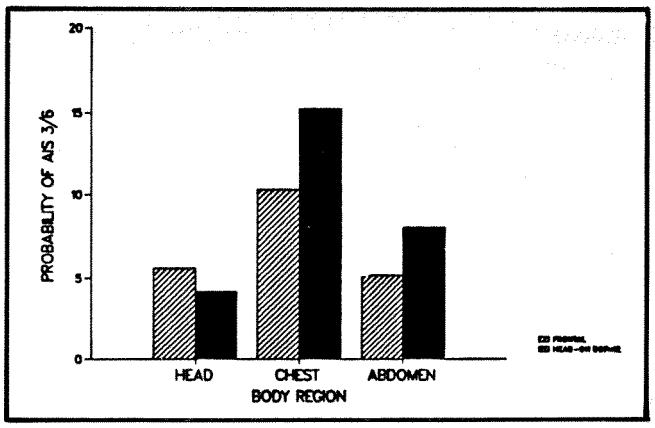

Figure 24. Probability of driver receiving a serious injury to the head, chest, or abdomen at a delta v of 26 to 35 mph for different crash conditions

be made by changes in structure. Furthermore, these potential structural changes are identified by vehicle properties in the fleet.

Accident and Simulated Data for the 27 Vehicles

1. The automated PADS simulation procedure was implemented. Eighty percent of the almost 1,500 runs that represent the vehicle and accident environment ran successfully.
2. Accident data related to the 27 make/model groupings appear to be representative of the complete NCSS and NASS files.
3. While there are differences between the simulated data and the accident data base as to injury severity predictions, it is felt that through the application of adjustment factors the PADS automated procedure is a useful tool in developing information for predicting how vehicle modifications can affect the consequences of injury in the accident environment.
4. Analyses are continuing using the simulation and accident data bases on a disaggregate level to correlate injury rates at a make/model level with vehicle attributes particularly related to structure and steering assembly.

Steering Assembly and Driver Compartment Improvements

1. Comparison of simulation results for high- and low-ranked vehicles, based on an analytically derived parameter for the steering assembly, showed significantly lower injury measures for the high- ranked car. This parameter was computed from the EA characteristics and force levels of potential impact surfaces.
2. PADS simulations with variations of other steering assembly properties (wheel/column weight, column angle, column friction and damping, and hub recession) produced the lowest injury measures for a column angle of 0° and a 4in hub recession.
3. Based on results of previous simulations and other factors, a best set of steering assembly and knee restraint properties was developed. Simulations of a baseline vehicle and the same vehicle with these improvements resulted in dramatic reductions in injury measures.

Based on computer simulations using PADS, the countermeasure evaluation has shown that by applying certain exterior structural and/or compartment interior improvements, injury measures can be reduced significantly. The next phase of this project is to apply these countermeasures to the entire 27-vehicle fleet to estimate fleetwide injury reductions.

References

1. Cohen, Daniel, Lee Stucki, and Carl Ragland, "Development of analytical procedures to characterize the vehicle environment in frontal impact accidents," SAE Paper 850251, February 1985.
2. "The development and use of PADS (Passenger/Driver Simulation) computer program," Final report, National Highway Traffic Safety Administration (NHTSA), Contract No. DTNH 22-82-R-07017, March 1984.
3. "Motor vehicle attributes—status report," Transportation Systems Center, Cambridge, Massachusetts, October 1983.
4. "Development of anthropometrically based design specifications for an advanced anthropomorphic dummy family," NHTSA Contract No. DTNH 22-80-C-07052.
5. "Steering assembly protection, T03 report: Human loading and tolerance" (Interim Report), Crashworthiness Research Division, National Highway Traffic Safety Administration, August 5, 1983.
6. Hackney, James, and Vincent Quarles, "The new car assessment program status and effect," Proceedings Ninth International Technical Conference on Experimental Safety Vehicles, November 1982.

Comparative Evaluation of the MVMA2D and the MADYMO2D Occupant Simulation Models With MADYMO-Test Comparisons

Priya Prasad
Ford Motor Company

Abstract

This paper compares and contrasts the modeling features present in the MVMA2D and the MADYM02D occupant simulation models. Simulations of a series of sled tests with a Hybrid II test dummy restrained with a 3-point belt system have been conducted using the MADYM02D model. The simulation results agree with the test results.

Introduction

Several mathematical models have been developed to simulate both vehicle occupants in crashes and pedestrian impacts. Over the years, the MVMA2D occupant simulation model(1) has been used extensively in the automobile industry for two-dimensional simulation of occupants or pedestrians involved in crashes. In recent years, a new two-dimensional model—the MADYM02D(2)—has been under development at TNO, Holland. Even in its current stage, it appears to be a powerful tool for simulation of vehicle occupants or pedestrians involved in crashes. Both these models contain some common features as well as some features that are unique.

This paper compares and contrasts the two models so further developments in these models may incorporate the features missing in one but present in the other. Additionally, simulations with the MADYM0 model of a series of sled tests have been carried out and compared to test results.

General Description and Comparison

Occupant Model

Both models treat the vehicle occupant as being made up of a collection of rigid bodies interacting with one another through hinged joints. Basically, the occupant is described as an open chain or tree. In the MVMA2D, the occupant is described by nine rigid bodies representing the head, neck, upper torso (chest, thoracic spine), mid-torso (abdomen and lumbar spine), lower torso (pelvis), upper leg (femur), lower leg (tibia and fibula), upper arm (humerus), and forearm (ulna and radius). The current formulation of the MVMA2D model does not permit the addition of any more rigid bodies to the occupant (e.g., the foot or a multi segment neck as in the Hybrid III dummy). Also, the MVMA2D model cannot be simplified to have less than nine rigid bodies.

In the MADYM0 model, the occupant can be described by one to any number of rigid bodies depending on the capacity of the computer, as long as the tree structure is maintained, i.e., no closed loops are allowed (Figure 1). Furthermore, in the MADYM0 model, several tree structures interacting with one another can be simulated.

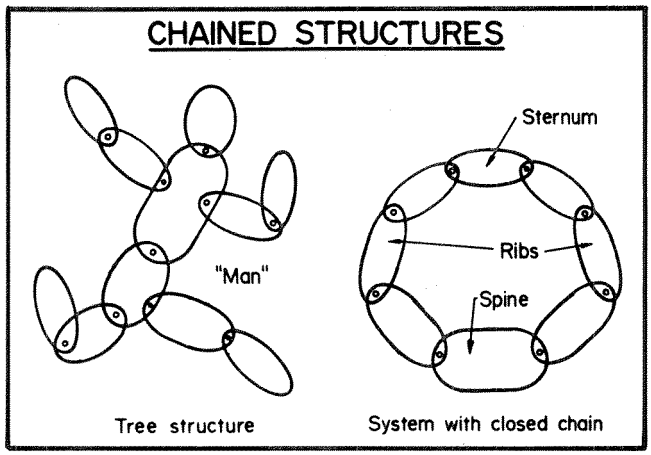

Figure 1. Pictorial representation of a tree structure and a closed loop system

The importance of this feature in the MADYM0 model is that collapsible (energy-absorbing) steering columns, children belted in child seats that in turn are belted in a car, etc.; can be simulated by proper definition of various trees. It should be noted that although the MVMA2D does have a collapsible steering column module, this module has not produced acceptable simulations and thus requires considerable debugging.

Two features used in the MVMA2D to describe the occupant are not currently in the MADYM0. The MVMA2D has extensible neck and shoulders, which are useful features for human and cadaver simulations. Additionally, active muscle tensions in the neck joints can be simulated in the MVMA2D(3). Although the MADYM0 manuals state that muscle tensions can be simulated by negative damping, its use has not been demonstrated in the literature.

Joint Model

Both the models treat the joints between the rigid bodies in similar ways. In both models, the joints can develop elastic, viscous, and frictional torques. The

elastic torque model in the MVMA2D is shown in Figure 2. As shown in the figure, the joint torques are described by a linear and nonlinear range by means of polynomials. Also in the nonlinear range, the joints can dissipate energy through hysteresis. The elastic joint torques in the MADYM0 model are described in tabular form. Therefore, complex shapes of joint torque versus relative angular deflections can be described. However, in the version available from TNO, there is no mechanism to dissipate the stored elastic energy as in the MVMA2D model. A simple algorithm to dissipate the elastic energy has been incorporated in the model at Ford.

The viscous and frictional torques in the joints are handled essentially the same in both models. Both models use ramps to avoid numerical instabilities in the frictional models.

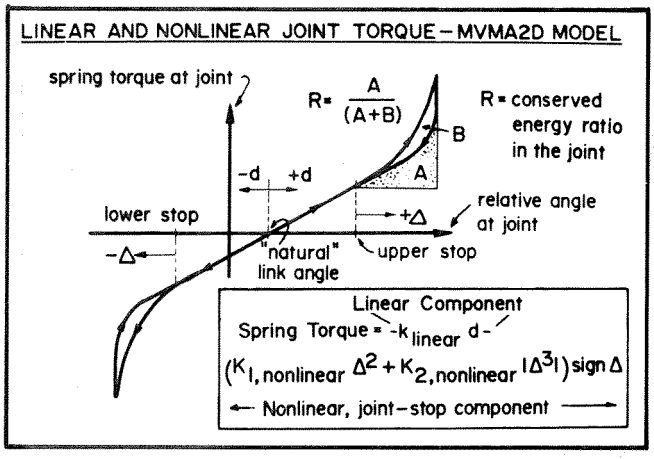

Figure 2. Joint torque description

Contact Model

The interaction between the occupant and the vehicle interior is detected by contact ellipses and planes. In the MVMA2D model, the vehicle interior is described by planes. Ellipses are attached to the occupant to sense and develop contact forces. When contact between the ellipses and planes takes place, reaction forces between the occupant and the vehicle are generated. These forces can be described by polynomials or in tabular form as a function of the depth of penetration of the occupant ellipses into the planes. Hysteresis can be simulated by assigning "R" and "G" factors as shown in Figure 3. There is no provision for rate-dependent reaction forces, such as viscous forces. Additionally, ellipse-to-ellipse contacts can also take place and reaction forces generated. This is useful for simulating chin/chest, head/knee, thigh/chest, etc., contact forces.

In the MADYM0 model, all the above features are present with the addition of a few other features. Perhaps the most useful additional feature is the ability to attach

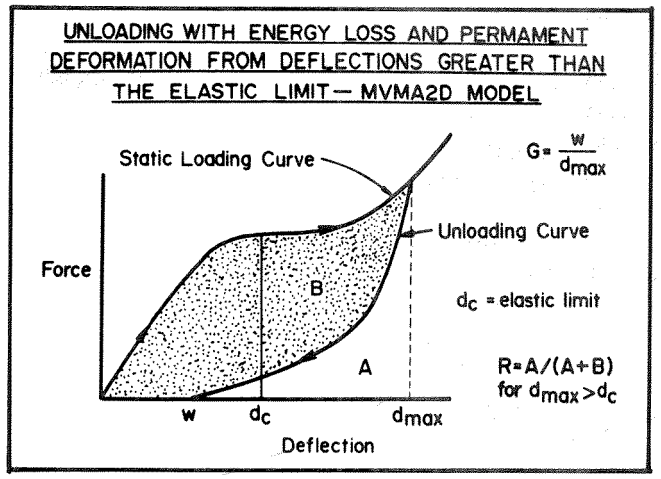

Figure 3. Description of hysteresis

ellipses or hyperellipses to the vehicle interior to simulate curved surfaces, and to attach planes (as well as ellipses) to the occupant. In addition to the linear or nonlinear contact forces, viscous forces also can be developed during contact. Hysteresis is simulated by unloading stiffnesses specified in the contact model.

Frictional forces can be developed in both models. The friction model in the MVMA2D is more general than that in the MADYM0. Whereas the coefficient of friction in the MADYM0 can be only a constant value, the coefficient of friction in the MVMA2D can be varied as a function of penetration. This feature of the MVMA2D has been used by many modelers to simulate the ploughing effect between the pelvis and the seat cushion as the pelvis moves with respect to the seat cushion in a crash.

The contact planes in the MVMA2D models can be moved as a function of time to simulate intrusion of vehicle components likely to be contacted by the occupant. This feature is not currently available in the version of the MADYM0 from TNO. However, this feature, along with the ability to prescribe motion to the contact ellipses, has been incorporated in the model at Ford.

Restraint Systems

Belt Restraint

The MVMA2D and the MADYM0 models have advanced belt subroutines that simulate the three-dimensional aspect of commonly used 3-point belt restraint systems. Inertia-locking retractors can be simulated in both models. However, neither can simulate pyrotechnic retractors, which tighten the belt during the crash sequence. Both can allow a user to study the effects of belt slack or pretension on occupant responses.

Both models can simulate continuous loop belt restraint systems. The MVMA2D belt system allows for the

simulation of the roof-mounted slings found in some cars and a buc le strap on the lower inboard side. The MADYM currently does not have these features. In the MADYMU, the inboard belt buckle is simulated, but the buckle is fixed to the vehicle. The general description of the belt systems and the data required for simulating the belt geometry are shown in Figures 4 and 5. It should be noted that in both models, the shoulder belt and lapbelt are prescribed to pass through fixed attachment points on the chest and pelvis. In both models, the belts can be attached to other body segments, if required.

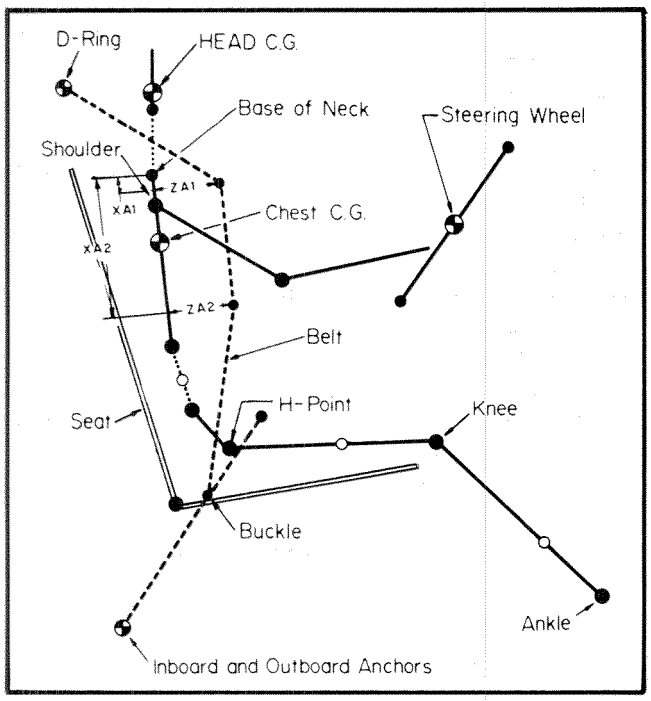

Figure 4. Initial geometry for a 5-segment belt simulation—side view

An important feature of the belt simulation not present in the MVMA2D is the incorporation of the film spool effect in the MADYM0 model. This feature is useful for simulating the effect of various amounts of webbing extension from the retractor under loading.

Airbag

The MVMA2D contains an airbag model originally described by Hammond(4). The airbag model can be used for the driver or the passenger, although the bag cannot be mounted on a collapsible column. An advanced airbag model is being developed for the MVMA2D.

The MADYM0 does not currently have an airbag model. Under contract with Ford, a driver-side airbag that can be mounted on a collapsible steering column is being developed at TNO, Holland. This model incorporates the features of DRACR(5)—an airbag/column model.

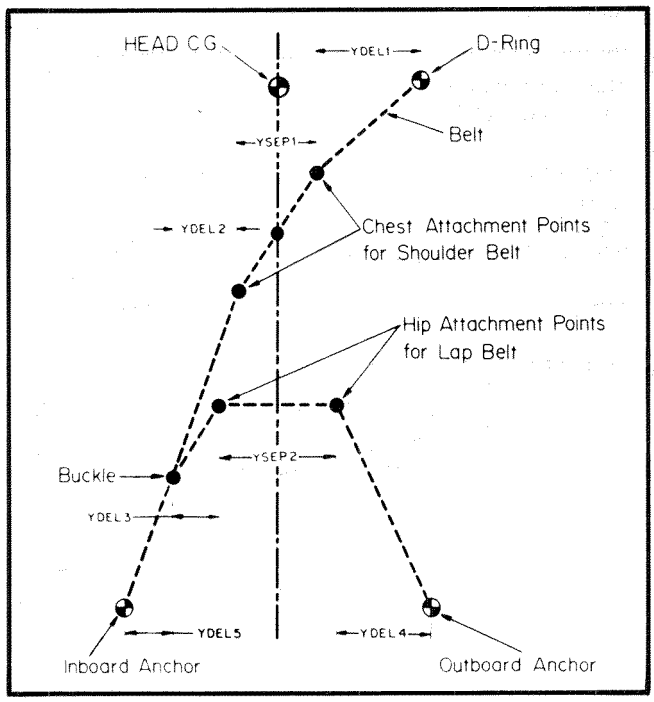

Figure 5. Initial geometry for a 5-segment belt simulation—front view

MADYM0 Simulations

Various studies utilizing the MADYM02D model have been reported in the literature(6,7,8). However, none has addressed the use of the MADYM0 for simulating the Hybrid II (Part 572) dummy in the automotive environment during sled or full-scale crash tests. A series of sled tests using the Hybrid II dummy and a production type 3-point harness system was conducted for comparing MADYM0 simulation results with actual tests. The goal of these tests was to provide restrained dummy responses to three levels of sled accelerations in a highly controlled laboratory environment.

The initial velocity of the sled was nominally 56km/h (35mph). The sled was brought to rest with a series of essentially trapezoidal acceleration pulses (Figure 6). The sled stopping distances were 915, 810, and 700mm (36, 32, and 27in). The restraint system geometry and the initial seated position of the Hybrid II dummy are shown in Figure 7. The lateral dimensions required for the simulations of the belt system geometry are shown in Table 1. A horizontal hard seat pan was used in the tests. The nominal elongation of the belt was 7.5 percent (i.e., 7.5 percent stretch at an applied load of 11.1kN (2,500 lb)).

Table 1. Lateral belt system dimensions.

Lateral Separation From Dummy Mid-Saggital Plane (mm)			
Retractor	399	Upper Chest Attachment	110
D-ring	254	Lower Chest Attachment	69
Inboard Anchor	229	Inboard Pelvis Attach.	140
Outboard Anchor	305	Outboard Pelvis Attach.	170

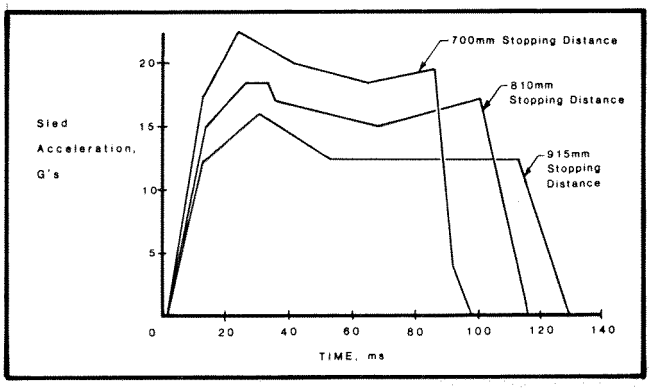

Figure 6. Sled acceleration pulses

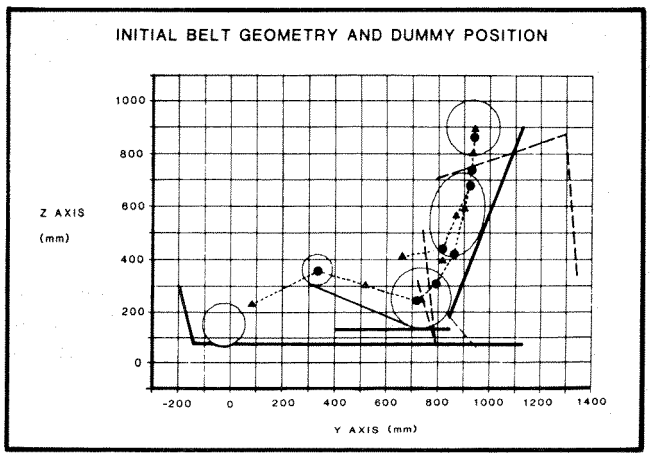

Figure 7. Dummy and restraint system test geometry

Modeling Assumptions

Dummy

To be compatible with the MVMA2D model, a nine rigid link representation of the dummy was used for this study. Thus, the feet of the dummy were not simulated. The inertial and joint torque characterization used for the dummy were those published in the literature(9). It should be noted that the neck and lumbar spine of the dummy are actually flexible elements. Their representation in the model by rigid links with two joints each is a simplification of the system. The dummy link lengths and joint torque characteristics used in the simulations were those determined by Calspan(9).

Restraint System

The anchor locations for the restraint system were simulated exactly as in the tests. However, the inboard strap used in the test was not simulated since the MADYM0 does not have this feature. As a result, the part of the shoulder belt leading from the chest to the inboard buckle was assumed in the model to extend from the chest to the inboard floor-tunnel anchor point. Similarly, the inboard portion of the lapbelt also was assumed to extend from the pelvis to the same inboard anchor point. These simplifications of the belt geometry are not expected to have a major effect on the model results since the inboard strap is made of an 8in piece of webbing that can stretch also.

The webbing stiffness of the shoulder portion of the belt from the retractor to the inboard anchor location was assumed to be 10 percent to account for the deflection of the chest. The retractor outlet function ("film spool effect") was measured in one test with a belt load cell and a string potentiometer. This function was assumed to be the same for all the tests and is shown in Figure 8.

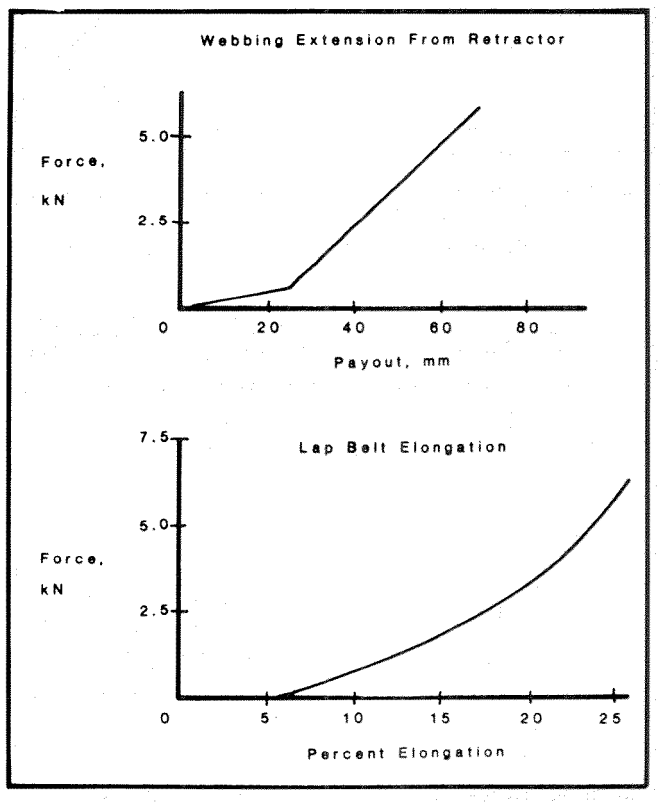

Figure 8. Belt system characteristics

Since there is considerable compression of the dummy pelvic flesh when loaded by the lapbelt, the effective lapbelt characteristics were determined by a static test. They are shown in Figure 8. Also, the effective points of application of the belt loads were assumed to be in the deformed position of the pelvic flesh.

New sets of belts and associated hardware (retractor and buckle) were used in all the tests. It is possible that the webbing stiffnesses and retractor characteristics were not identical in all the tests. Also, high-speed movies of the tests showed deformation of some of the anchor hardware. However, for the model exercises, the belt system characteristics were assumed constant in all the tests and hardware deformation was not simulated.

Seat

A hard seat pan without foam was used in the tests. Therefore, a high stiffness of 710N/mm (4,000 lb/in) was assumed for the seat material. The exact stiffness of the seat-pelvis system is not known.

Model Results and Comparison to Tests

The results of the simulations and their comparisons with test results are shown in Table 2 and Figures 9 through 20. It can be seen from the table that the peak head accelerations predicted by the model are within 5g's of those measured in the tests. The general shapes of the head acceleration-time histories agree well with the tests. The HIC's predicted by the model deviate by a maximum of 67 out of 595 when compared with the test results. The horizontal movement of the head center of gravity predicted by the model is within 20mm of those observed in the tests. However, the vertical movement of the head center of gravity predicted by the model appears to be 75 to 100mm more than those observed in the tests. Three main factors appear to explain the differences. Some out-of-plane movement of the dummy was observed in the tests but cannot be simulated with a two-dimensional model. Chin-chest contact appears to have occurred in the tests but has not been simulated by the model due to lack of chin-chest stiffness data. Also, the model predicts

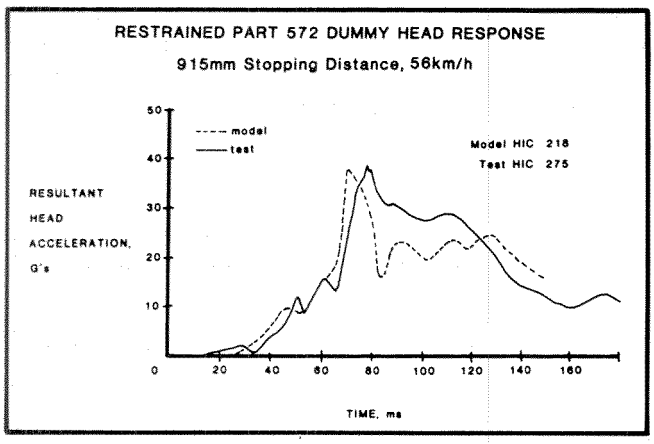

Figure 9. Model and test comparisons—head acceleration—low severity pulse

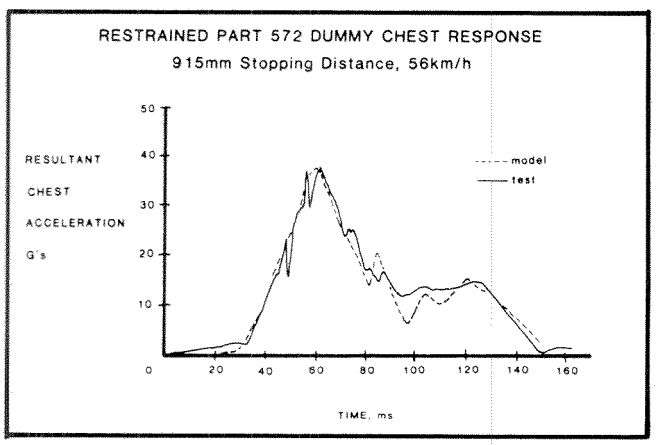

Figure 10. Model and test comparisons—chest acceleration—low severity pulse

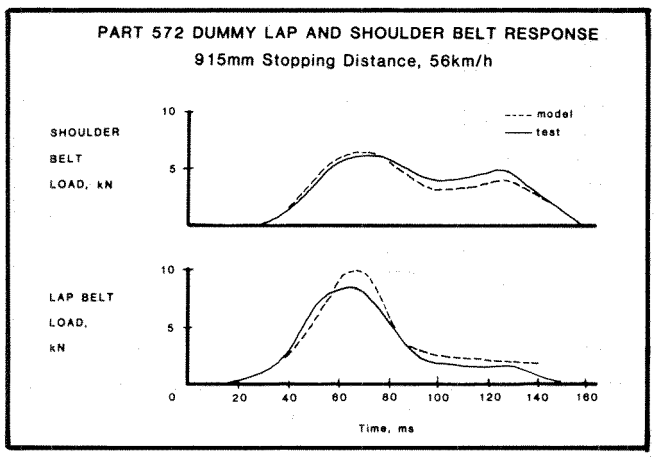

Figure 11. Model and test comparisons—belt loads—low severity pulse

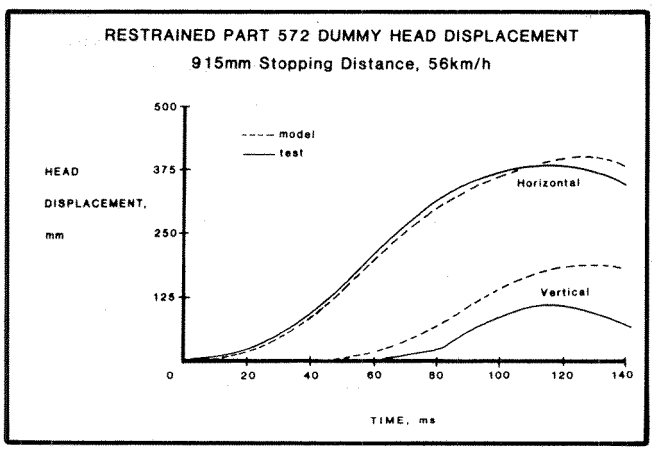

Figure 12. Model and test comparisons—head displacement—low severity pulse

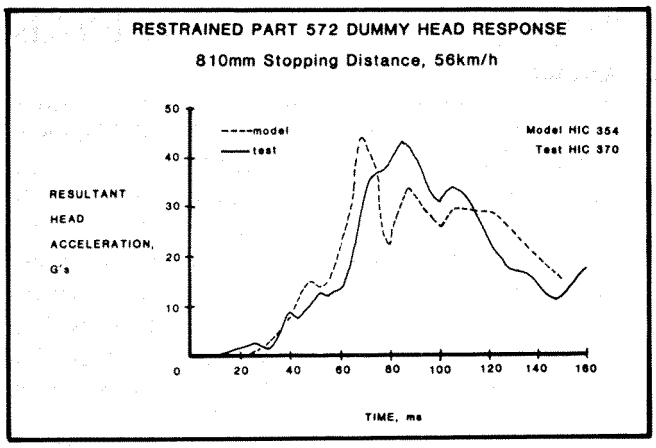

Figure 13. Model and test comparisons—head acceleration—medium severity pulse

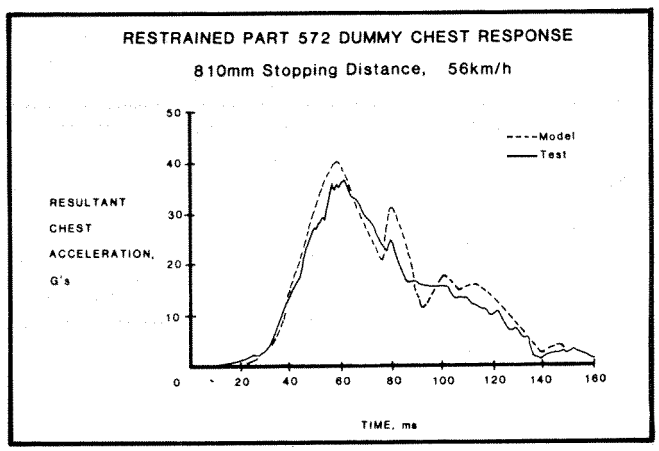

Figure 14. Model and test comparisons—chest acceleration—medium severity pulse

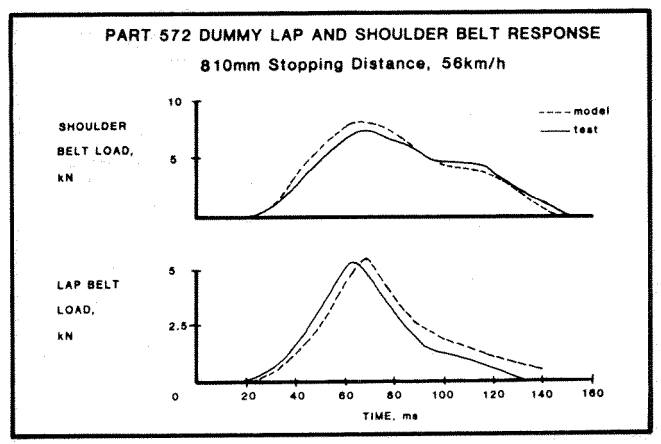

Figure 15. Model and test comparisons—belt loads--medium severity pulse

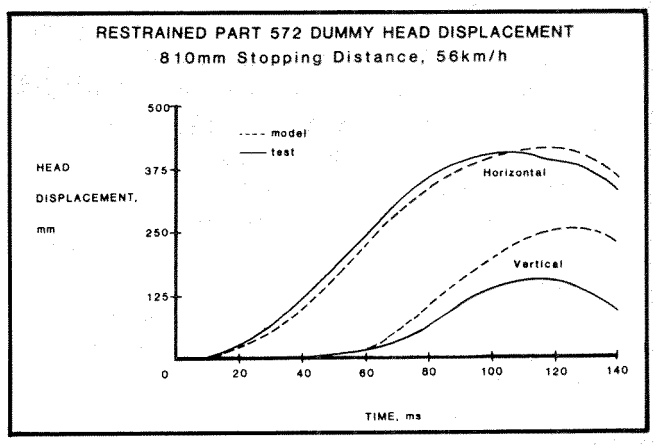

Figure 16. Model and test comparisons—head displacement—medium severity pulse

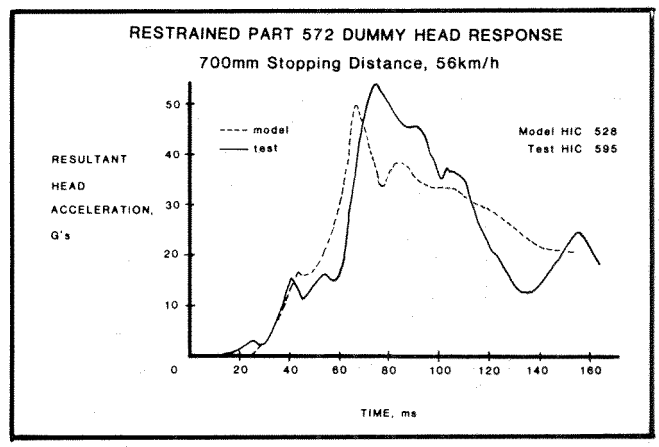

Figure 17. Model and test comparisons—head acceleration—high severity pulse

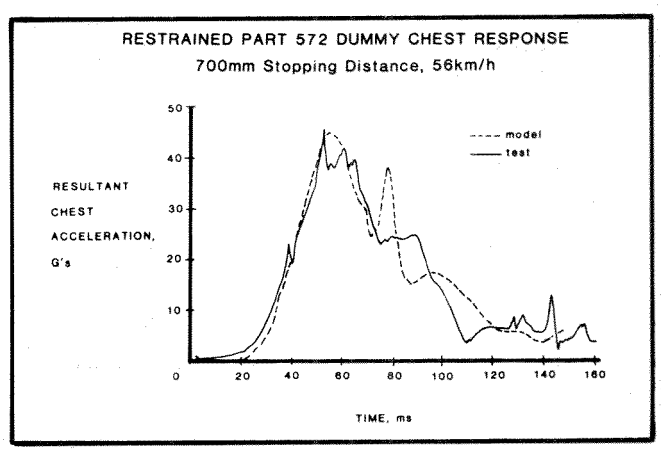

Figure 18. Model and test comparisons—chest acceleration—high severity pulse

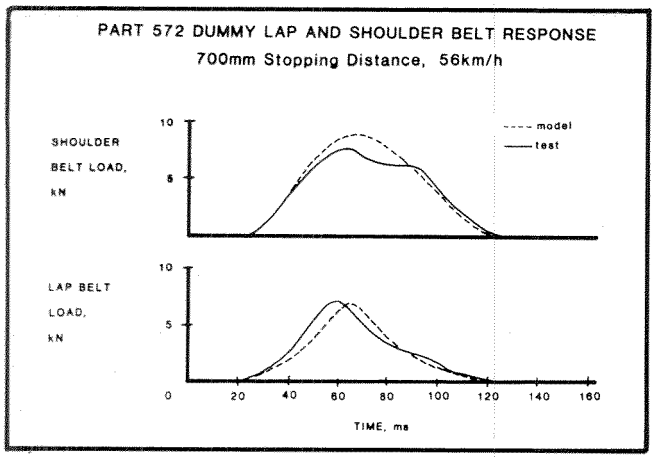

Figure 19. Model and test comparisons—belt loads—high severity pulse

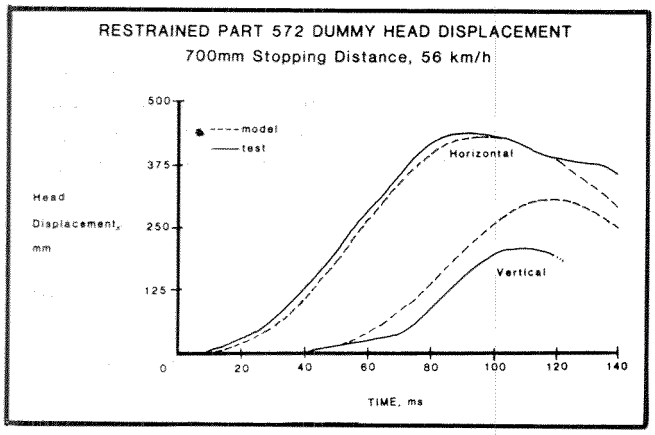

Figure 20. Model and test comparisons—head displacement—high severity pulse

approximately 20° greater rearward pelvic rotations than observed in the tests.

The chest accelerations predicted by the model are within 0.62g's in two tests and within 3.3g's in one test (810mm stopping distance). A calibration error might be present in the latter test since the peak test acceleration is 1g less than that observed in the 915mm stopping distance test, a less severe test. The shapes of the chest acceleration-time histories predicted by the model agree well with the test results.

As shown in Table 2 and in Figures 11, 15, and 19, the difference between the model-predicted and the test shoulder belt loads increases as the sled stopping distance decreases. It is felt that the differences are due to deformation in the belt attachment hardware in the tests, which deformation is not simulated in the model.

The lapbelt loads predicted by the model agree with the test results. The maximum variation from the test results is from only -180N to +785N (-40 to +176 lb) out of peak belt loads in the 6 to 8kN (1,350 to 1,800 lb) range.

Based on the above model and test result comparisons, it is felt that for the belt system geometry and the range of stopping distances tested, the model results agree with the test results.

Discussion and Recommendations

The current series of simulations with the MADYM02D model have shown that the model can be used for simulating dummy responses in frontal sled tests. Further modeling exercises and tests are required to determine the reasons for greater predicted head excursions in the vertical direction and pelvic rotations when compared

Table 2. Test and model dummy data

	915mm Stopping Distance		810mm Stopping Distance		700mm Stopping Distance	
	Test	Model	Test	Model	Test	Model
Peak Head Acceleration, G's	37.5	37.5	43.1	44.	54.9	50.0
Peak Chest Acceleration, G's	37.7	37.75	36.7	40.	45.62	44.0
Peak Shoulder Belt Load, kN	6.4	6.6	7.3	8.0	8.00	9.30
Peak Lap Belt Load, kN	4.2	5.0	5.3	5.5	7.1	6.9
Head C.G. Movement, mm						
Horizonal	387	409	409	412	445	442
Vertical	114	193	158	250	208	310
HIC	275	218	370	354	595	528

with test data. It is the experience of the author that both of the above dummy movements are very sensitive to the belt attachment points on the dummy. These attachment points are functions of the anchor locations. It should also be noted that the belt attachment points on the dummy are fixed in the simulations but can move in actual tests. Hence, a series of tests with a number of different anchor locations and their mathematical simulations is suggested for future studies.

Enough subtle differences between MADYM02D and the MVMA2D models exist that, at the time of writing, identical data sets for comparing the responses of the two models could not be prepared. Preliminary efforts indicate that the two models can yield comparable, but not identical, results. The differences between the two model results are due mainly to the differences in the restraint system models listed below:

1. No retractor outlet function ("film spool effect") is possible in the MVMA2D model.
2. No inboard strap simulation is possible in the MADYM0.
3. The MVMA2D treats the shoulder harness as one belt extending from the D-ring to the inboard buckle. The MADYM0 treats the shoulder harness as being made up of two belts—one between the D-ring and the upper chest attachment point and the other between the lower chest attachment point and the inboard buckle.
4. The inboard buckle can move in the MVMA2D but is fixed in the MADYM0.
5. The unloading function of the belt is described by "R" and "G" ratios in the MVMA2D, but it is described by tabular functions in the MADYM0.

Summary and Conclusion

The MVMA2D and the MADYM02D occupant simulation models have been compared to each other so that further developments in these models may incorporate the features missing in one but present in the other. A series of sled tests with the Hybrid II dummy and 3-point belt restraint systems was simulated using the MADYM02D model. The results of the simulations agree with the test results.

Acknowledgments

The author gratefully acknowledges the help provided by Mr. Roger Daniel in the discussions of the paper and preparation of the manuscript. Special thanks are due to Mr. Max Koga for his dedicated care in insuring that the sled tests were conducted in a highly controlled manner.

References

1. Robbins, D.H., B.M. Bowman, and R.O. Bennet, "The MVMA two-dimensional crash victim simulation," Proceedings 18th Stapp Car Crash Conference, SAE Paper 741195, Warrendale, Pennsylvania, December 1974.
2. Wismans, J., J. Maltha, J.J. van Wijk, and E.G. Janssen, "MADYM0—A crash victim simulation computer program for biomechanical research and optimization of designs for impact injury prevention," AGARD-meeting, Koln, Germany, April 1982.
3. Schneider, L.W., and B.M. Bowman, "Prediction of head-neck dynamic response of selected military subjects to $-G_x$ acceleration," *Aviation Space and Environmental Medicine,* Vol. 49, No. 1, January 1978.
4. Hammond, R.A., "Digital simulation of an inflatable safety restraint," SAE Paper 710019, Automotive Engineering Congress, Detroit, Michigan, January 1971.
5. Fitzpatrick, M., "DRACR computer program," Contract No. DTN22-80-C-07120, U.S. Department of Transportation, National Highway Traffic Safety Administration, Washington, D.C., 1981.
6. Wismans, J., and L.J.J. Wittebrood, "The MADYM0 crash victim package and its application in analyzing thoraxes of side impact dummies," Seminar on the Biomechanics of Impacts in Road Accidents, Commission of the European Communities, Brussels, March 21-23, 1983.
7. Van Wijk, J., J. Wismans, J. Maltha, and L. Wittebrood, "MADYM0 pedestrian simulations," SAE Paper 830060, Pedestrian Impact Injury and Assessment, p. 121, SAE, Warrendale, Pennsylvania, 1983.
8. Stalnaker, R.L., and J. Maltha, "MADYM0 used for computer aided design of a dynamic acting child restraint seat," Proceedings Fifth IRCOBI Conference on the Biomechanics of Impacts, Birmingham, England, 1980.
9. Fleck, J.T., and F.E. Butler, "Validation of the crash victim simulator," Vol. 1-4, Report No. ZS-5881-V-1, DOT-HS-6-01300, December 1981.

The Safe Transportation of Wheelchair Occupants in the United Kingdom

S.P.F. Petty
Transport and Road Research Laboratory

Abstract

In 1981, "The Year of Disabled People," the Department of Transport issued a Code of Practice and Special Provisions for the Carriage of Passengers in Wheelchairs on Public Service Vehicles. The safety aspects of the code are considered in this paper. Research has shown that the travelling space required for each wheelchair is 700mm wide and 1,200mm long.

Accident data have shown that the priority requirements for a wheelchair restraint are to hold the chair and occupant in place during normal driving and in 10g frontal impacts for full-sized public service coaches. The details are given of five different restraint designs and of the results from static and dynamic testing. The removal of one restraint design from the market as a result of testing to the Code of Practice highlights the need for a formal standard.

Introduction

Year 1981, "The Year of Disabled People," gave an increased incentive to both the transport industries and the organisations helping the handicapped to make transport more accessible to the wheelchair-bound disabled. British Rail has completed a study of restraint designs and is evaluating specific restraints for general use in trains. The Department of Transport proposed, and then contributed toward, the development of a new design of taxi, which it is evaluating. The number of Community Transport Operators and Local Authorities carrying wheelchairs in minibuses (9 to 16 seats) is increasing to form a nationwide network. Approximately 3,800 minibuses regularly carry passengers in wheelchairs(1). Certain bus and coach operators have introduced modified vehicles into their fleets. The Department of Transport has issued a Code of Practice and Special Provisions for the Carriage of Passengers in Wheelchairs on Public Service Vehicles(2) as an initial guide on access and safety. It is the safety aspects of that code that are considered in this paper.

Access

The dimensions for the entrance/exit, gangways, and designated positions for wheelchair accommodation are based on the British Standard BS 5568: 1978 for folding wheelchairs with principal dimensions of overall width 660mm and a maximum overall length of 1,065mm. Current anthropometric data are used. The space occupied by any wheelchair in its travelling position is defined as 700mm wide and 1,200mm long. This allows any wheelchair in a row to enter or leave without disturbing the others. In special cases, these dimensions have been changed. Under contract to the Transport and Road Research Laboratory (TRRL), Middlesex Polytechnic evaluated the dimensions using as subjects the wheelchair occupants who were visiting TRRL for an exhibition of Mobility Aids for the Disabled. The two main conclusions were: "Reducing the length to 1,150mm and 1,100mm did not reduce the time to enter but the wheelchair hit those in front and behind and this was not satisfactory"; "Also some certain types of wheelchair restraint were difficult to fit within the 1,200mm space and any reduction would only increase that difficulty".

Accident Data

The data related to Public Service Vehicle (PSV) passengers, excluding those injured while they were boarding or alighting, were obtained from the police STATS 19 form. This form gives nationwide coverage but cannot identify if the injured person was disabled. It relates the number of injured to the location of the first point of vehicle impact and is a guide to the main direction of deceleration. The breakdown for the year 1981 is typical and is given in Table 1, which highlights the two most important types of accident that should be covered by a code of practice.

Table 1. Injuries in 1981 to PSV passengers

First point of impact on vehicle	Severity of injury		
	Fatal	Serious	Total
Front	0	171	171
Back	1	6	7
Offside	0	16	16
Nearside	2	7	9
Rollover	2	60	62
MPD*	2	82	84
No impact	3	186	189
Total	10	528	538

* The Metropolitan Police Department data cannot be coded for direction of impact.

The first is an injury happening when no vehicle impact takes place, but emergency braking or sudden manoeuvres to avoid an accident cause passengers to be thrown against an unpadded part of the bus structure. Unrestrained wheelchairs would be free to roll and represent a

danger not only to their occupants but also to other users of the PSV. The second is the direct frontal impact. The restraint should be adequate in the frontal mode but still function at lower levels in side and rear loading. The restraint should also be designed so that the chair cannot rotate about an axle or revolve.

Restraint Systems and Tests

For a restraint system to be successful, it must not only be able to withstand the impact forces but also be easy to use. As such it should—

- Hold the wheelchair and occupant in place during normal driving
- Be simple to fit by untrained helpers who may not themselves be physically strong
- Be adaptable for use on different designs of wheelchair
- Be comfortable to use and wear
- Be so designed that it cannot be incorrectly assembled
- Be capable of being released quickly in abnormal conditions in a crashed vehicle

Restraint systems can be subdivided into three groups:

- Wheelchair restraints that are attached to the vehicle structure and hold only the wheelchair against forward, rearward, and sideway movements.
- Passenger restraints that are independent of the wheelchair and must withstand deceleration forces in a forward direction relative to the vehicle.
- Combined restraints that share some components for both wheelchair and passenger restraint. This will result in increased loads through the wheelchair restraint.

The Code of Practice that has been issued uses a rigid trolley to statically test the restraint anchorage strengths. The mass of the wheelchair is taken to be that of an electric chair weighing 90kg and the mass of the occupant as a slightly overweight adult also at 90kg. Previous work on coach seat safety(3) has shown that a deceleration of 10g from a speed of 30km/h using a 50th percentile dummy was required to reproduce the seat failures found in real impacts. Thus, the 10g deceleration level has been used acting through the centres of gravity of the two masses to give the test loading on the restraint in frontal impacts. For side and rear impacts, the level has been halved. Allowance has been made for the use of rearward facing wheelchairs held firmly against a bulkhead. Sideway-facing chairs are not recommended as the arm of the chair and any occupant webbing restraint will react on the soft tissues of the human body rather than on its skeleton.

Using a rigid trolley is useful for repeatability and is a low-cost test, but it can only test separately the wheelchair and occupant lapbelts. The trolley cannot be used to test combined restraints because it cannot measure the changing load due to movement of the occupant in relation to his seat. At present, such restraints are tested dynamically by the Department of Transport using a 50th percentile dummy in a standard Department of Health and Social Security (DHSS) type 8L wheelchair. Static testing with a dummy restrained in a wheelchair produces unrealistic modes of chair failure. Reinforcing the chair still does not overcome the problems. Further development of a static test is being examined.

Four types of restraint have been tested statically using the trolley. They are—

- A webbing belt system adapted from a cargo restraint design, strapping the wheelchair frame to steel rails bolted onto the floor and/or walls of the PSV. This is shown schematically in use on a wheelchair in Figure 1. The webbing is looped round the lower bar of this chair, clamped onto the rail, and then pulled tight.

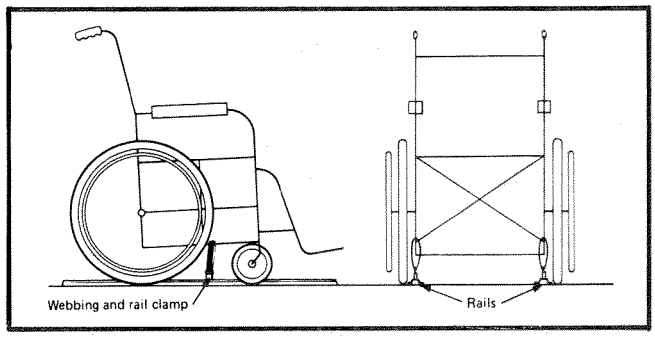

Figure 1. Type A restraint

- A system using a clamp on one side of the wheelchair and a separate webbing belt on the other side, anchored to the opposite corner of the wheelchair frame and mounted in the floor in an extruded aluminum alloy rail. This is shown schematically in Figure 2.

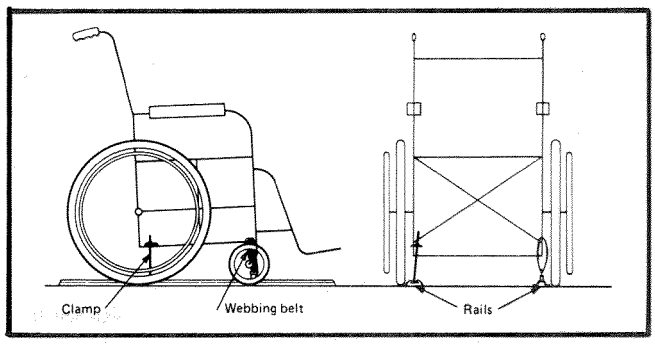

Figure 2. Type B restraint

- A system using a vertical clamp on each side of the wheelchair frame. The clamps could be attached to the floor either in their own special sockets, in the rails used for type A or B restraints, or in a modified aircraft seat rail extrusion. This is shown in Figure 3 using the special fixings and with one of the belt systems used in the dynamic tests.

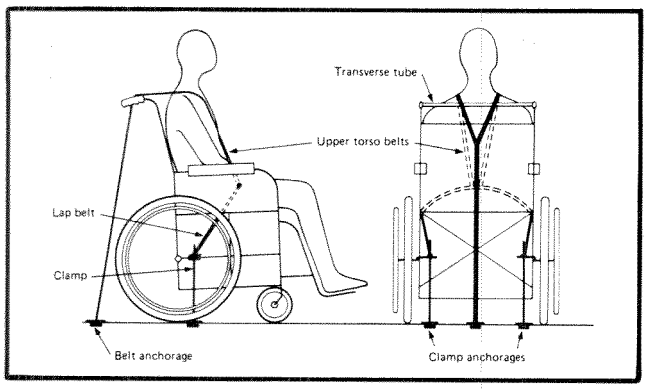

Figure 3. Type C restraint

- A system using type C restraints for the wheelchair but an independently designed lapbelt and anchorage.

As a result of the tests used to evaluate the new code, the type B restraint has been withdrawn from sale as it failed prematurely, and the other designs have been modified to improve their performance.

The two designs of restraint were tested dynamically. The type C restraint used the various anchorage rails with a lapbelt only and with a full harness. To prevent lumbar compression fractures, an adaptor was clipped onto the wheelchair handles. This adaptor can also be used to hold a headrest. A type E is a system using an adjustable A frame (Figure 4) that can be placed at the back of the wheelchair in sockets in the floor and roof of the vehicle. The wheelchair can then be held onto the A frame either by webbing or by clamps. This is shown schematically in Figure 4 with a belt system similar to those used in the dynamic tests.

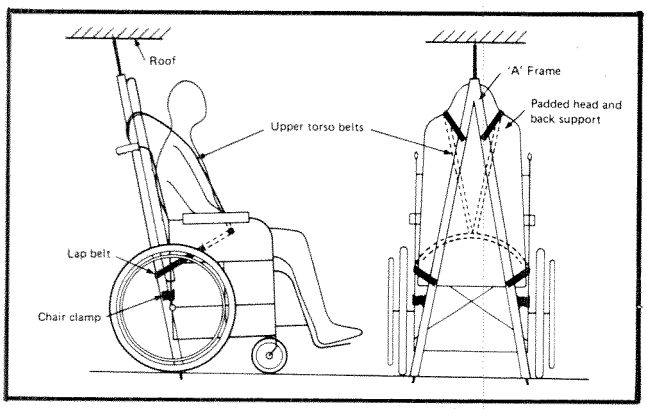

Figure 4. Type E restraint

The dynamic tests highlighted certain important aspects:

1. Using a lapbelt allows the upper torso to jacknife forward with the potential danger of the occupant hitting his head on the seat in front. The total forward movement allowed must relate to the 1,200mm seat spacing given in the Code of Practice.
2. When the upper torso is restrained by floor-mounted belts, care must be taken to insure that the lumbar spine is not damaged under compression loading.
3. Loads transmitted through the wheelchair can result in its frame collapsing. This started at a level of about 13g. As the frame failed, the loads on the wheelchair restraint changed with the possibility of sudden failure. Minor modifications to the wheelchair structure can delay the start of failure.
4. The floor structure must be sufficiently strong not only to hold the restraint anchorages but also to withstand the reaction forces through the wheelchair wheels.
5. During an impact, the vehicle structure will distort. The design of the anchorages must give a positive fixing and should not rely on the "peg in a hole" concept.
6. There is a need for continued quality control. In one test, a buckle made by a well-known car seatbelt manufacturer had been incorrectly modified by a third firm before it was presented for testing by a restraint manufacturer. It failed catastrophically.

Future Progress

It is recognised that the present Code of Practice requires updating and rewording to remove ambiguities. Also a static test method for combined restraints would be very convenient. The test levels using the 10g deceleration and the heavy electric wheelchair and the overweight occupant may be thought to be high for use on full-sized coaches but will not be so when applied to lighter vehicles with higher decelerations.

The continuing demand on manufacturers to make their restraints more user-friendly is resulting in a steady improvement in design. One design being developed for rapid wheelchair loading has a headrest and occupant restraint prefitted to the wheelchair. The whole assembly can be easily clipped to an arm mounted on the wall of the vehicle. In cold weather, this is particularly useful if a number of wheelchairs have to be loaded at one time.

In the longer term, the British Standards Institution is working with the Department of Transport, manufacturers, vehicle operators, and their passengers to make use of the experience gained from the Code of Practice to produce a formal wheelchair standard.

Acknowledgments

The work described in this paper forms part of the programme of the Transport and Road Research Laboratory, and the paper is published by permission of the Director.

References

1. Walmsley, D.A., "The use of minibuses in Great Britain," Research Report 6, Transport and Road Research Laboratory, Crowthorne, Berkshire, United Kingdom, 1985.
2. Department of Transport, *Code of Practice and Special Provisions for the Carriage of Passengers in Wheelchairs on Public Service Vehicles,* Publication VSE 518, Department of Transport, Vehicle Standards and Engineering Division, 2 Marsham Street, SW1, May 1982.
3. Petty, S.P.F., "Protection for public service vehicle occupants in frontal impacts," paper presented at the Conference on The Design Construction and Operation of Public Service Vehicles, The Cranfield Institute of Technology, Bedford, July 1977, I Mech E Conference Publications 1977-6 ISBNO 85298 373 5.

Discerning the State of Crashworthiness in the Accident Experience

A.C. Malliaris
Office of Vehicle Research, National Highway Traffic Safety Administration

Abstract

This paper addresses the risks of occupant casualties in highway accidents. Such risks are determined from U.S. accident experience in the past 10 years. Risks are analyzed as a function of vehicle type, car market class, make, nameplate, and model year for crashes of various impact types and various severities. Both absolute risks, per unit exposure, and relative risks are addressed. The influence of many exposure variables is examined and necessary adjustments, to a common set of exposure conditions, are made. The control variables for this purpose are: calendar year and car age; occupant's seating position, restraint status, and age; time and place of travel; and various roadway characteristics. Adjusted risks are reviewed versus major characteristics of cars as implied by make, nameplate, and model year. Occupant ejections and rollovers receive special attention due to their risk sensitivity to car class.

Introduction

In the past 10 years, the motor vehicle fleet in the United States has undergone significant changes in the mix of vehicle types on the road, the mix of car classes, the design and engineering of cars, and the introduction of new components and equipment. In addition, strong factors were at work in the early 1980's that individually or collectively had and have the potential to influence highway safety significantly. A depressed economy inhibited travel growth, especially for the higher risk discretionary travel. Highway safety programs, e.g., campaigns against drunken drivers and seatbelt use programs, were initiated and pursued vigorously. The questions we are addressing in this paper are whether or not and how all these changes affect occupant casualty risks, as determined from the accident experience of motor vehicles on U.S. roads in the past 10 years.

We treat occupant casualty risks as dependent variables where the independent variables are: calendar years, vehicle impact types, and severities; motor vehicle attributes such as vehicle types, market classes, makes, models, and model years; and occupant attributes such as seating position, restraint use, and age. Exposure attributes such as time and place of travel, roadway characteristics, etc., are also used in a supplemental fashion, especially as proxies for crash severity. A companion paper(12) addresses the risks of motor vehicle involvement in accidents as a function of accident type and severity; driver attributes, such as driver's age, sex, and alcohol involvement; and vehicle attributes as mentioned above.

Major Changes in the Motor Vehicle Fleet and Travel

Two car characteristics—weight and wheelbase—are given special consideration because they are frequently

discussed and analyzed in connection with casualty risks. A summary of changes in these characteristics for new cars retailed in the United States is given in Table 1 by market class. The changes refer to mean values of those characteristics between model years introduced in the early 1970's and model year 1983.

Table 1. Percent change in mean weight and mean wheelbase of model year 1983 cars by comparison to new cars of the early 1970's

Market Class	Percent Change Mean Weight	Mean Wheelbase
U.S. Subcompact	-18.0%	-2.5%
Compact	-23.5	-8.1
Intermediate	-22.8	-6.8
Standard	-11.5	-4.3
European Subcompact	+5.9	+1.9
Other	+9.9	+2.2
Japanese Subcompact	0.0	+1.6
Other	+5.8	0.0

Note in Table 1 that the domestically produced fleet shows substantial reductions of weight and wheelbase, all across the board, while this is not the case for the fleets of European or Japanese origin. Apparently, redesign practices and market shifts in the latter fleets, which consist of predominantly subcompact cars, led to modest increases in weight and wheelbase.

As a result of these developments, subcompact cars of U.S., European, or Japanese origin have become virtually indistinguishable when viewed in terms of the major characteristics discussed above. Moreover, the standard, intermediate, and compact U.S.-produced cars of model year 1983 have essentially assumed the weight and wheelbase characteristics of the intermediate, compact, and subcompact cars of the early 1970's, respectively.

Because of the prominence of car weight and wheelbase in safety reviews, we treat the changes summarized above with more detail and more quantitatively in Appendix A. In the same appendix, we also address changes that took place in the travel of motor vehicles and in the various aspects of exposure to casualty risks.

Occupant Risks and Risk Descriptors

Consider the definitions:

E_{jk} = Motor Vehicle Exposure (usually travel)

V_{ijk} = Accident-involved Vehicles

M_{ijkm} = Occupants in Accident-involved Vehicles

N_{ijkmn} = Occupant Casualties

where the subscripts are shorthand for groups of influential attributes.

- j designates vehicle attributes such as vehicle type (e.g., car, truck, etc.), market class, make, model, model year, etc.
- k designates travel attributes such as time and place, roadway characteristics, etc.
- i designates vehicle impact type (e.g., front, side, etc.) and impact severity
- m designates occupant attributes such as seating position, restraint status, age, etc.
- n designates occupant casualty attributes such as overall injury severity (e.g., fatal, major, minor, none) and, whenever the information is available, may designate an occupant's complete set of injuries by severity, body region, etc. Also, the same subscript may be used for certain intermediate outcomes such as ejection instead of the final outcome, which is an overall injury of certain severity.

Furthermore, consider the following additional definitions:

$$R_{ijk} = V_{ijk}/E_{jk} \quad (1)$$

$$S_{ijkm} = M_{ijkm}/V_{ijk} \quad (2)$$

$$T_{ijkmn} = N_{ijkmn}/M_{ijkm} \quad (3)$$

Equation (1) defines an absolute riskof accident involvement for motor vehicles. This type of risk is discussed extensively in (12). The occupancy, i.e., the number of occupants per accident-involved vehicle, is defined by Equation (2), according to occupant attributes represented by subscript m. Equation (3) defines the conditional risk of an occupant casualty with attribute n, given the occupant's inclusion in an accident-involved vehicle.

An overall occupant casualty risk may be defined by the product of Equations (1), (2), and (3), i.e.,

$$W_{ijkmn} = R_{ijk} * S_{ijkm} * T_{ijkmn} \quad (4)$$

or

$$W_{ijkmn} = N_{ijkmn}/E_{jk} \quad (5)$$

which is expressed in occupant casualties, with attributes implied by the subscripts, per unit travel exposure.

Equation (3) is one of the most commonly used descriptors of crashworthiness, and we shall apply it extensively in this paper for occupant risk determinations with as much resolution of subscribed attributes as the available data bases allow. We shall also apply extensively Equation (5) in determinations of overall occupant risk. As is evident in Equation (4), the overall occupant risk reflects in a composite fashion both the occupant casualty risk, given an accident-involved vehicle, and the accident involvement risk of the vehicle.

Occupant Fatality Risks by Vehicle Type

We address first the conditional risks of occupant fatality, i.e., the risks determined with the help of Equation (3).

A motor vehicle occupant's risk of fatality stood at about 2.41 ± .07 per 1,000 occupants involved in all police-reported accidents on U.S. highways.[2] This is the mean and standard error derived from six individual values, each obtained from the data for each of the 6 years 1979 to 1984. It refers to all accident, all vehicle, and all occupant attributes. It varies little within the specified time period (see Figure 1) in spite of the significant changes in the fleet and travel patterns discussed earlier.

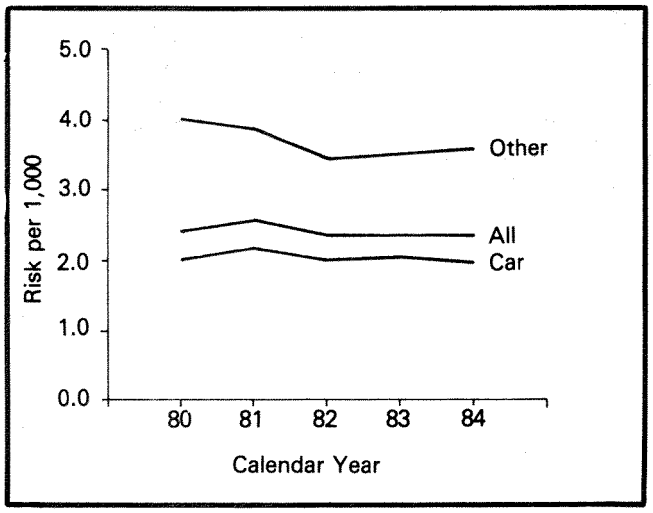

Figure 1. Risk of occupant fatality per 1,000 occupants involved in police-reported accidents of cars, other vehicles, and all vehicles

The data for the determination of this conditional risk are provided by two accident files of national scope, i.e., by FARS and NASS(1,2). Specifically, a total count of all occupant fatalities (national census) is obtained from FARS, and this is divided by a national estimate of all motor vehicle occupants involved in all police-reported accidents, as recorded in NASS. This process is repeated for each of the calendar years 1979 to 1984.

When resolved by vehicle type, the risk under consideration varies within a wide range as the data in Table 2 show. In this table, pickups and vans are vehicles with a gross vehicle weight rating under 10,000 lb. Straight trucks are nonarticulated trucks and vans over 10,000 lb.

Bus and motorcycle occupant risks are at the two extremes, lowest and highest, respectively, for obvious reasons. Car occupant risks are at about the middle of the range. Occupants of vans and straight trucks show substantially lower risks than car occupants, while the risks of pickup truck and especially of combination truck occupants are substantially higher than car occupant risks.

[2]The risk of fatality for all people, i.e., motor vehicle occupants, plus pedestrians and bicyclists, is higher: 2.93 ± .07.

Table 2. Fatality risk per 1,000 vehicle occupants involved in police-reported accidents as a function of vehicle type

Vehicle Type	Percent of Occupants*	Risk Per Thousand in Row
Cars	78.7 ± .08	2.01 ± .02
Pickups	12.1 .22	2.92 .06
Vans	3.29 .05	1.55 .03
Straight Trucks	1.53 .19	1.37 .11
Combination Trucks	1.46 .10	3.73 .42
Buses	1.53 .58	.27 .13
Motorcycles	1.42 .04	21.4 .77
Total	100.	2.41 .07

* In all police-reported accidents

It may sound ludicrous that occupants of pickups and especially occupants of such heavy commercial vehicles as combination trucks incur substantially higher fatality risks than car occupants, but there may be good reasons for it. Articulated trucks and pickups are likely to operate more on rural land and high-speed roadways. Consequently, they are likely to experience higher crash severities than cars, vans, or straight trucks. Nevertheless, on an aggregated basis, occupants of pickups and combination trucks incur higher fatality risks than cars. Furthermore, this pattern holds for all types of impacts, whether frontal, side, rear, or other.

Car Occupant Fatality Risks

Because of their overwhelming share of the vehicles in all police-reported accidents, cars are receiving further attention in this paper in connection with occupant fatality risks. According to Table 2, the fatality risk for car occupants is 2.01 ± .02 per 1,000 car occupants involved in all police-reported accidents. This is the mean and standard error for the 6 years 1979 to 1984. The smallness of the error indicates relatively little variation of the risk, whether random or systematic, in this period. This is also shown in Figure 1. However, the subject of risk variation versus calendar year will receive further attention in a later section.

Car occupant fatality risks are influenced by crash attributes, as well as by vehicle and occupant attributes. Crash severity is one of the most influential variables. However, the data we are dealing with do not allow an explicit and categorical description of this variable. The FARS data do not make any reference to crash severity, while the NASS data provide crash severity information

only for a small portion of the national sample. Accordingly, to characterize crash severity, we use as a rough proxy the time and location of the crash. It is well known that rural crashes are more severe than urban crashes and night crashes are more severe than daylight crashes. Rural night crashes are the most severe, while urban daytime crashes are the least severe.

Under these qualifications, we have resolved the overall fatality risk for car occupants as shown in Table 3. In addition, we have resolved the occupant's seating position into that of the driver, right-front passenger, and all other (primarily rear-seat) passengers. The risk values shown in this table are mean and standard errors over the early 1980's. For each calendar year, Equation (3) has been applied with numerator data provided by FARS and denominator data provided by NASS.

Most of the results and trends shown in Table 4 are intuitively expected, at least qualitatively. Fatality risks associated with side impacts or with rollover-type impacts (predominant component of "other") are substantially higher than the risk in frontal impacts, as shown in the last row of the table. The risk for rear impacts is much lower. This pattern holds for all car occupants regardless of seating position and restraint status, without significant exceptions.

The overall fatality risk for the right-front passenger, i.e., the passenger averaged over all restraint conditions and types of impact, is no different than that of the driver under the same aggregation conditions and within the reported error bounds. This is also what we concluded from Table 3. However, Table 4 shows several cases where the two risks might not be equal. For example, the

Table 3. Car occupant fatality risk per 1,000 involved in police-reported accidents resolved by accident attributes and occupant's seating position

Accident Attributes	Car Occupant's Seating Position: Driver	Front Passenger	Other	All
Urban				
Day	.57 ± .03	.68 ± .05	.43 ± .03	.56 ± .03
Night	1.89 .08	1.82 .14	1.42 .17	1.81 .10
All	1.00 .03	1.10 .07	.78 .06	.99 .04
Rural				
Day	5.33 ± .40	5.00 ± .36	3.34 ± .54	4.92 ± .33
Night	9.82 .43	7.85 .87	5.22 .61	8.48 .56
All	7.13 .18	6.16 .50	4.05 .38	6.37 .18
All				
Day	1.32 ± .04	1.57 ± .06	1.08 ± .08	1.35 ± .05
Night	3.59 .14	3.26 .26	2.48 .23	3.33 .18
All	2.10 .04	2.20 .08	1.59 .06	2.01 .02

The results in Table 3 show that car drivers run essentially the same risks as front passengers all across the spectrum of crash severities, or more precisely of exposure severities. This is so for all practical purposes if the shown error bounds are taken into account. Occupants in other seating positions, primarily rear-seat occupants, incur fatality risks that are substantially lower: about 30 percent lower in urban crashes and about 60 percent lower in the more severe rural crashes.

Risks for any one or all seating positions are very sensitive to exposure severity, i.e., to the shown accident attributes. This sensitivity is consistent across the board and shows differences by factors 10 to 20 between the least severe crashes, i.e., urban daylight crashes, and the most severe, i.e., rural night crashes. Next to impact severity, we address the type of impact, i.e., frontal, side, rear, or other, as an influencing factor. This is done in Table 4. In addition, we resolve two of the most important occupant attributes: seating position and restraint status. The entire table refers to car occupants, and the results have been obtained by the same procedure used in Table 3.

right-front passenger appears to incur higher risks in side impacts, whether restrained or not. Also, restrained front passengers appear to incur higher risks than restrained drivers. However, these differences are not large enough in view of the reported errors. Furthermore, their significance and a discussion of their possible origin requires further control and study beyond the scope of this paper.

As noted, the most striking feature of Table 4 is the much lower risk shown for restrained car occupants in comparison to unrestrained occupants, for any seating position and any type of impact. This trend is not only consistent all across rows and columns of the table but also implies generous values of restraint effectiveness. The great majority of the restraints under consideration here are manual seatbelts. Their effectiveness in casualty prevention is defined as the relative risk reduction, i.e., (unrestrained-restrained)/unrestrained. According to this definition, the effectiveness values implied by the data of Table 4 range from about 50 percent to over 80 percent.

However, a word of caution is appropriate. It has been recognized in the safety literature(13) that restrained car occupants traveling on U.S. roads are also occupants

Table 4. Car occupant fatality risk per 1,000 involved in police-reported accidents resolved by type of impact, occupant's seating position, and restraint status

Car Occupant's Seating Position and Restraint	Car's Type of Impact: Frontal	Side	Rear	Other	All
Driver					
Unrestrained	2.48 ± .06	3.08 ± .10	.55 ± .03	3.36 ± .25	2.54 ± .06
Restrained	.61 .03	.83 .08	.16 .03	.50 .07	.42 .01
All	2.24 .07	2.77 .07	.51 .05	2.96 .18	2.10 .04
Right Front Passenger					
Unrestrained	2.05 ± .07	3.39 ± .07	.54 ± .05	2.85 ± .16	2.35 ± .06
Restrained	.94 .02	1.37 .19	.19 .03	1.03 .21	.63 .08
All	1.95 .08	3.11 .05	.51 .06	2.65 .16	2.20 .08
All					
Unrestrained	2.24 ± .04	3.13 ± .09	.58 ± .03	3.14 ± .16	2.39 ± .03
Restrained	.64 .03	.92 .07	.20 .04	.60 .12	.45 .02
All	2.05 .06	2.83 .07	.54 .05	2.81 .14	2.01 .02

experiencing lower crash severities than unrestrained occupants. Thus, although the risk differentials shown in Table 4 between restrained and unrestrained occupants may be quite factual, part of these differentials may be due to lower crash severities, which would lower the risks of occupants even in the absence of the restraint. The issue under consideration would be clarified if the data of Table 4 could be controlled and adjusted for crash severity. However, although such control is possible and has been used in NASS data on several occasions, it is the lack of crash severity information in FARS that prevents the adjustment of the results in Table 4.

A person's age has been recognized as an attribute that influences significantly the person's risk of fatality. Table 5 resolves the overall fatality risk of car occupants in two major age slots for each of the seating positions and restraint conditions examined so far. Higher risks for the older occupants are evident across the board. Given that older occupants experience, in general, lower crash severities, the risk differentials under identical crash severities may be larger than those shown in Table 5.

Restraint Use Rates

This is one of the most timely subjects to address in a review of crash protection in the early 1980's because of the initiation and vigorous pursuit of seatbelt use programs in the United States during this period. The NASS and FARS raw data used for the risk determinations reported so far can also be used for straightforward determinations of restraint use rates for accident-involved car occupants.

Results for the overall restraint use rates are shown in Figure 2 as a function of the calendar year. The upper plot shows the rates observed for car occupants involved in all police-reported accidents, while the lower plot

Table 5. Car occupant fatality risk per 1,000 involved in police-reported accidents resolved by occupant's seating position, restraint status, and age

Car Occupant's Restraint and Age	Car Occupant's Seating Position: Driver	Front Passenger	Other	All
Unrestrained				
Under 45 Yrs.	2.34 ± .05	2.05 ± .07	1.67 ± .08	2.17 ± .03
45 Yrs. or Older	3.14 .11	4.06 .09	3.35 .11	3.31 .09
All	2.54 .06	2.35 .06	1.79 .08	2.39 .03
Restrained				
Under 45 Yrs.	.36 ± .01	.45 ± .06	.46 ± .13	.37 ± .02
45 Yrs. or Older	.59 .05	1.39 .26	1.73 .48	.74 .06
All	.42 .01	.63 .08	.49 .13	.45 .02
All				
Under 45 Yrs.	1.97 ± .06	1.89 ± .10	1.44 ± .04	1.89 ± .05
45 Yrs. or Older	2.53 .03	3.59 .09	2.95 .21	2.73 .03
All	2.10 .04	2.20 .08	1.59 .06	2.01 .02

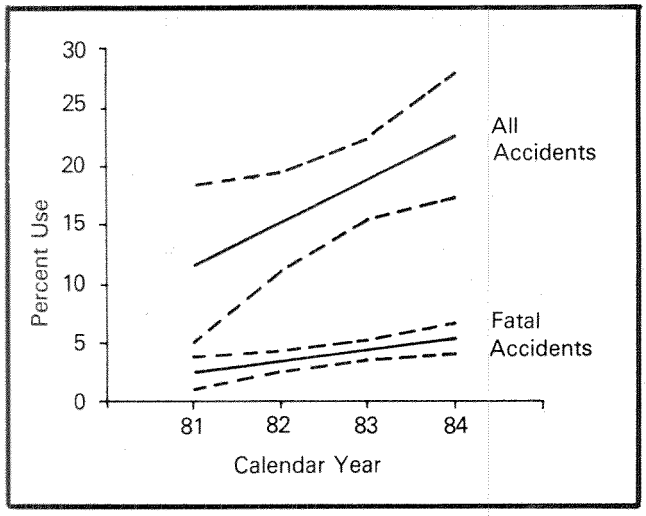

Figure 2. Safety belt use by accident-involved car occupants versus calendar year

refers to car occupants in fatal accidents. In each case, the rate is averaged over all other attributes and shown as the mean by the solid line, together with the 95 percent confidence bounds (dashed corridors).

The observed increase of the restraint use rate is both substantial and statistically significant. However, the reader should be aware that a potential bias is inherent in these data. The determination of restraint status, for the majority of car occupants, is made on the basis of answers given by occupants to investigating officers. Not only might there be an inherent bias in favor of a "yes" answer, but the bias may be increasing in recent years due to general publicity and awareness that seatbelt use may soon become mandatory. Note also the large difference between the upper and lower plots in Figure 2. There are at least two confounding factors that may contribute to this difference.

One confounding effect may arise from the possibility that restraint users are usually safety conscious and less likely to be involved in fatal accidents and appear as FARS statistics. The second confounding effect is the result of restraint effectiveness. Due to this effectiveness, restrained car occupants are underrepresented in a file with a fatal accident threshold, such as the FARS file.

Fatality Risk Variation in the Early 1980's

In spite of much change in influencing factors during the past 5 to 10 years, the overall fatality risk of all car occupants has not changed substantially. This is summarized in Figure 1. When the data of Figure 1, appropriately weighted for sample size, are fitted by a least square linear regression, the resulting slope is -.008 ± .032 per year for cars. This is zero for all practical purposes. An identical result has been reported(14).

To enhance resolution and relate the overall risk to post-1980 developments, we eliminated the 1979-1980 data and repeated our analysis for the 1981-1984 period. The elimination of the 1979-1980 data does not reduce much the overall sample of weighted data given that NASS in these years was only in partial implementation. A larger slope is obtained for this case, namely: -.056 ± .023, which is still marginally different than zero if one desires 95 percent confidence.

The year-by-year fitted values of the car occupant risk (car occupant fatalities per 1,000 involved in all accidents) and their standard error are—

1981	2.14 ± .05
1982	2.08 .03
1983	2.02 .03
1984	1.97 .04

A plot of this risk variation with the 95 percent confidence bounds is shown in Figure 3.

The nominal reduction of the risk in this period is about 8.5 percent, which is appreciable but also rather difficult to assign definitively to any single known influence, even if we disregard all questions of statistical significance. For example, we find this risk reduction entirely consistent with the rate increase of restraint use shown in Figure 2 for all accidents. However, other influences, some positive and some negative, were also in effect from 1981 to 1984. For example, an overall indicator of exposure severity (see Table A-7 in Appendix A) was declining during this period. On the other hand, travel speeds may have been increasing according to data shown in Table A-6 of Appendix A. A more extensive but equally frustrating discussion of crashworthiness and crash severity variations in the early 1980's is presented in (14).

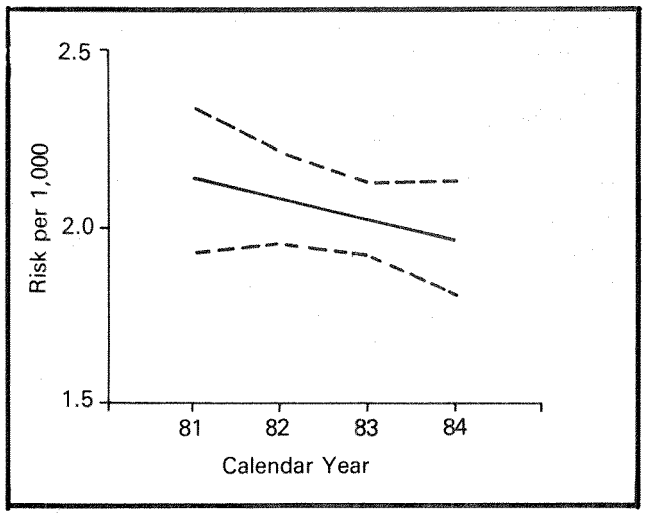

Figure 3. Risk of occupant fatality per 1,000 occupants of all cars involved in police-reported accidents—least-squares pitted mean and 95th percentile confidence rounds versus calendar year

Determination of Absolute Risks

To address the influence of car attributes on car occupant casualty experience, we focus our analysis on the new cars that traveled on U.S. roads from 1975 to 1984. This is also the period during which major changes took place in car attributes, as discussed earlier and as detailed further in Appendix A. For our analysis, we define new cars as those with an age (i.e., with a calendar year/model year difference) not exceeding 3 years. This is a compromise between retaining as much uniformity as possible in travel and exposure attributes while dealing with sufficiently large samples in the accident experience.

Under these constraints, we found it difficult to make the conditional risk determinations, by a combined examination of FARS and NASS data, as applied so far in the paper. This is so for several reasons: NASS data for car characterization (e.g., by make and model) are not available in a form compatible with FARS data until about 1981; NASS cell populations become rather small when the accident experience is subdivided by the many combinations of car market classes, makes, nameplates, and other specific attributes, especially when these subdivisions are made on new cars only. Furthermore, there are good reasons to suspect that NASS, as a sample of the national accident experience, may be biased in connection with car make/model content. For example, California and the West Coast in the United States are underrepresented in NASS, while the same regions are overrepresented in imported makes.

The conclusion is we may not apply Equation (3) for the task under consideration here because we have no means of obtaining reliable values for the denominator. This is another reason for using Equation (5), which is appropriate for the determination of absolute risks. In dealing, however, with the absolute risks of car occupant casualties, i.e., risks per car registration or per mile traveled, we must keep in mind these risks reflect in a composite fashion both the risk of casualty, given an accident-involved vehicle, and the accident involvement risk of the vehicle. We shall apply Equation (5) integrated over all attributes, except i and j. Thus, we write:

$$W_{ij} = N_{ij}/E_j \qquad (6)$$

where i and j represent impact type and vehicle-related attributes, respectively. Later we will examine the influence of other attributes.

The raw data necessary for the application of Equation (6) for car occupant fatality risks are provided by FARS(1) for the numerator and by (4) for the denominator. FARS contains records of about 60,000 occupant fatalities for new cars alone in the 10 years between 1975 and 1984. Car impact type and car nameplate are known for the great majority of these cases. Furthermore, their total count is generally adequate for analyses that demand disaggregation by several additional attributes of interest here.

Car registrations from (4) are used to quantify the denominator in Equation (6) by car descriptor j (nameplate and model year) for each of the calendar years included in the analysis. Although car exposure in general may not be characterized accurately by car registrations alone, our constraining the analysis to new cars only introduces a uniformity in the travel per car and other attributes sensitive to car age. Furthermore, a set of adjustments is made to the risks (determined for each model/calendar year) to bring them all under a common reference exposure.

The selected reference exposure is that experienced by 1-year-old cars in calendar year 1980. The adjustments, detailed in the first part of Appendix B, account for travel and exposure severity variations taking place in the 10 calendar years under consideration for new cars (i.e., 1-, 2-, and 3-year-old cars). Risk adjustment factors are shown in Table B-2 of Appendix B, as a function of calendar year and car age or model year. The most significant adjustment is that shown in column B of Table B-1. This covers the major decline in exposure severity (serious accidents per 100 million miles of travel) observed on U.S. highways in the early 1980's. There is little doubt that meaningful comparisons of car occupant risk for travel over the 1975 to 1983 period should incorporate an adjustment for exposure severity. Whether the adjustment applied here is the most appropriate is a matter that requires further consideration.

To achieve numerator/denominator compatibility in the application of Equation (6), we disaggregate both the occupant fatality car data (numerator) and the car registration data (denominator) by car nameplate, model year, and calendar year. We found nameplate, i.e., make and model, disaggregation more suitable than disaggregation by weight or wheelbase. Disaggregation by weight often introduces ambiguities due to weight variations on account of optional engine sizes and other optional equipment. Furthermore, when disaggregating by weight, borderline cases may fall in one weight slot for the numerator data but in a different weight slot for the denominator data. However, the main advantages of disaggregation by nameplate are that more information is potentially available about the car under consideration, even if this information is not always publicly available, and the number of unknowns is very small.

Risk determinations may be made at the nameplate, model year, and calendar year level by straightforward applications of Equation (6), with subsequent adjustments as discussed earlier. At this level, sample sizes are generally adequate for most purposes. Given that our analysis is focused on new cars, we calculate risks separately for the 1-, 2- and 3-year-old cars, all adjusted to the common reference exposure conditions, and form the mean of the three. In the process, we obtain the standard error of this mean.

In many instances, risks for new cars, whether by

nameplate or by higher levels of aggregation, are available for several calendar years within the 1975 to 1984 span. In such cases, we also calculate means and standard errors, in addition to reviewing the data for systematic variation versus calendar year. Thus, the standard errors we report are more conservative, given that they embrace not only purely statistical fluctuations but all other variations, whether random or systematic.

Results for levels of aggregation above nameplate are obtained as follows. The raw data, whether car occupant casualties or car registrations, are pooled together and the procedures described above are repeated. This leads to risk determinations for new cars aggregated by make, car body family designation, market class, origin of make, and the entire fleet of new cars. The market class designations used are those commonly used in the automotive trade literature. Furthermore, all traditional sports car nameplates and other low-volume specialty cars have been excluded from consideration because of possibly singular characteristics and circumstances.

Absolute Risks of Fatality for New Car Occupants

Results obtained according to the procedures described above are presented and discussed here for new cars. The absolute risk of fatality for new car occupants per 10,000 registrations is 2.36 ± .10 when averaged over all car market classes and all types of car impacts that occurred in the period 1975 to 1983. First we shall resolve this risk by car impact type and by car market class within each impact type. The results of this resolution are shown in Figures 4 to 8. Each figure refers to a type of impact: frontal, side, rear, other, and all types. Within each figure, the risk is resolved by market class of new cars.

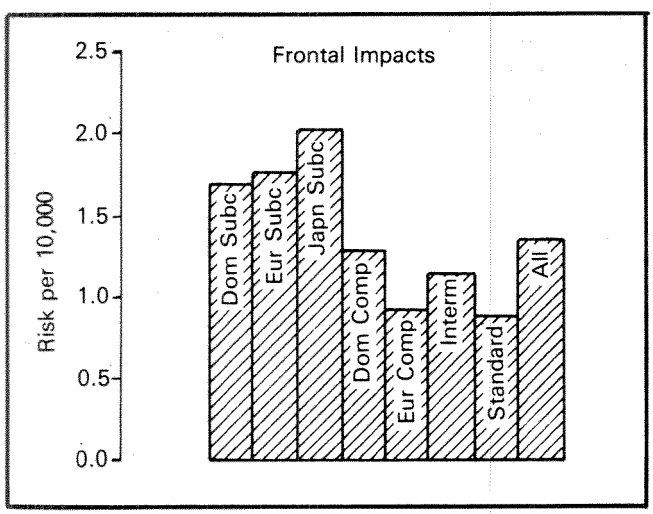

Figure 4. Fatality risk of new car occupants per 10,000 registrations by market class—frontal impacts

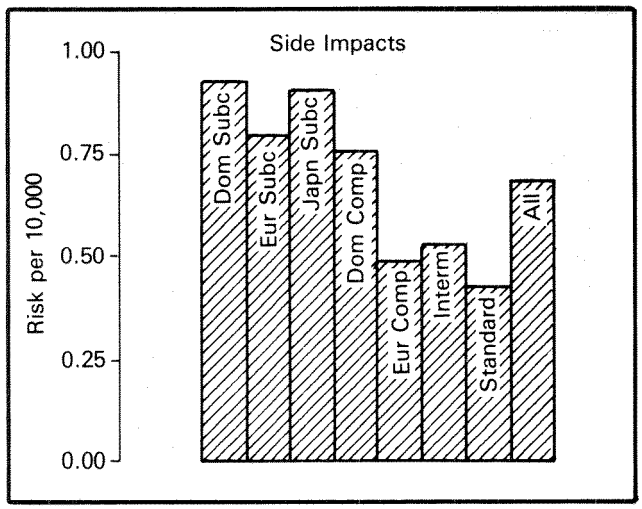

Figure 5. Fatality risk of new car occupants per 10,000 registrations by market class—side impacts

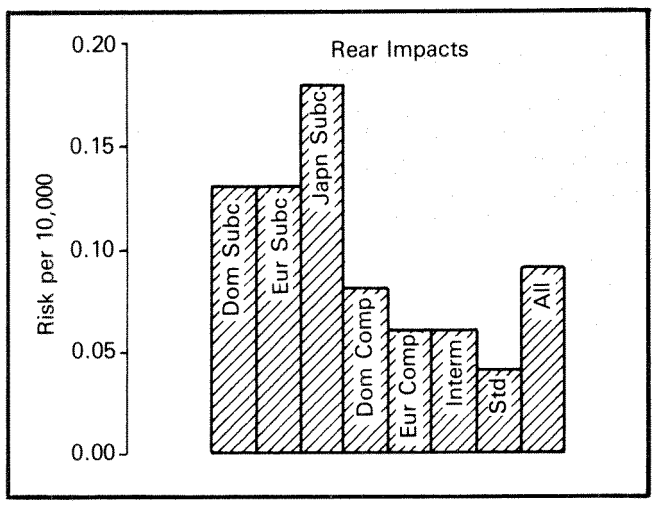

Figure 6. Fatality risk of new car occupants per 10,000 registrations by market class—rear impacts

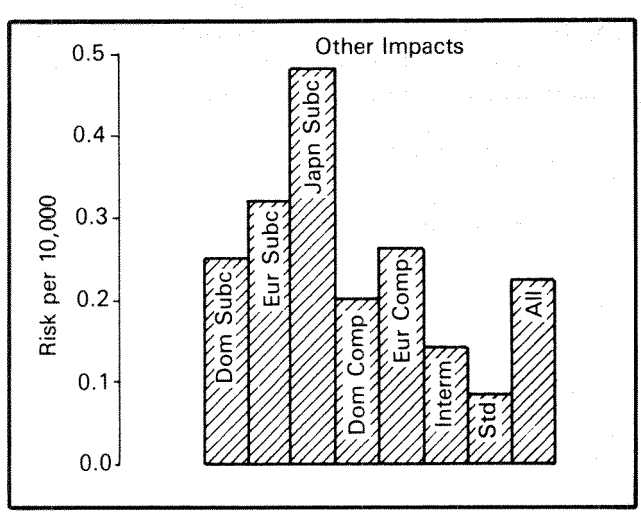

Figure 7. Fatality risk of new car occupants per 10,000 registrations by market class—other impacts (primarily rollover)

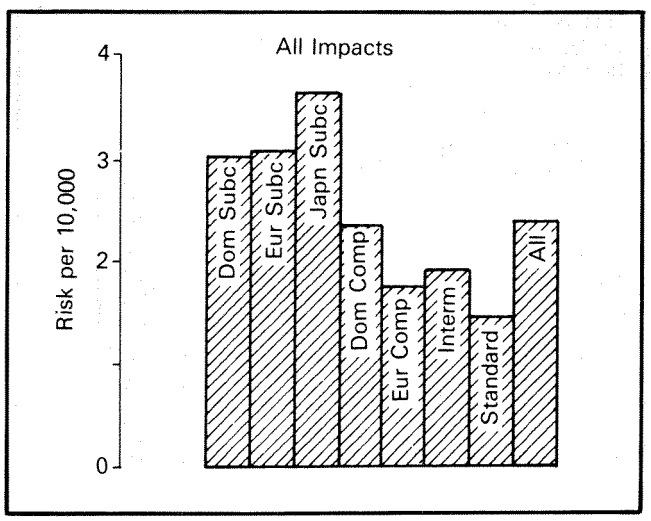

Figure 8. Fatality risk of new car occupants per 10,000 registrations by market class—all impacts

The last bar in each figure refers to all market classes together.

Keeping in mind the differences in the scales of these illustrations, we see that when all market classes are averaged (last bar), the principal contributions to the overall risk are made by frontal and side impacts. Smaller contributions are made by other impacts and rear impacts. Note that in other impacts, the principal component is rollover.

Each figure displays the sensitivity of the risk components mentioned above to the car market class. A general pattern is evident in all figures, namely higher risks for lighter cars and lower risks for heavier cars. This is not surprising; however, superimposed on this general pattern there are other sensitivities as is evident in Figure 6 and especially in Figure 7. Most of the risk differentials shown in Figures 4 to 8 may be established well beyond the statistical or other fluctuations that may be contained in the results. This is evident in the data shown in Table 6, which displays the risk values appearing in these figures together with their standard errors.

The data included in the overviews of Figures 4 to 8 and in Table 6 represent the national census of car occupant fatality experience of over 250 million new-car years. This total is subdivided into the market classes discussed above as shown in Table 7, which is formatted as Table 6 for reference convience. Table 7 also presents information about the major characteristics—weight and wheelbase—of new cars in each of the market classes under consideration. Keep in mind these are weighted means over the 1975 to 1983 period.

In addition to the sensitivity of fatality risks to car market class, there is a strong sensitivity to nameplates within each market class. This is especially true for the market classes of smaller new cars. Relevant results are given in Table 8, which displays fatality risks of new car occupants in the first column. These risks are in terms of occupant fatalities per 10,000 new car registrations. The second column tabulates occupant fatalities per occupant involved in the car. This descriptor is, in general, most appropriate for evaluating crashworthiness, based on the data of any file, except that a distorted scale is introduced when the descriptor is applied to the data of a file that records only fatal accidents, such as FARS.

The distortion comes as a result of the requirement that at least one fatality must occur in a crash before the data are entered into FARS. Usually this is an occupant fatality. An example will clarify further the shortcoming of applying the descriptor under consideration to FARS data. Consider the fatal accidents of single vehicles with the driver as the only occupant. This is not a very uncommon occurrence. In FARS, these vehicles appear

Table 6. Risk of occupant fatalities per 1,000 new car registrations by market class and type of impact. Shown values are means and std. errors over calendar years 1975 to 1983

New Car Market Class	Type of Impact Frontal	Side	Rear	Other*	All
Subcompact					
Domestic	1.68 ± .06	.93 ± .05	.18 ± .01	.25 ± .03	3.8 ± .09
European	1.76 .05	.80 .04	.13 .02	.32 .03	3.05 .07
Japanese	2.02 .09	.91 .05	.18 .02	.48 .02	3.63 .13
Compact					
Domestic	1.28 .08	.76 .06	.08 .01	.20 .02	2.34 .15
European	.91 .08	.49 .03	.06 .01	.26 .04	1.74 .11
Intermediate	1.14 .05	.53 .03	.06 .01	.14 .02	1.90 .08
Standard	.88 .07	.43 .03	.04 .01	.08 .01	1.44 .10
Entire Fleet	1.34 .06	.69 .03	.09 .01	.22 .36	2.36 .10

* Primarily Rollover

Table 7. Exposure (car-years) and major characteristics of new cars by market class for the combined calendar years 1975 to 1983

New Car Market Class	Car Years (millions)	Mean Weight (pounds)	Mean Wheelbase (inches)
Subcompact			
Domestic	28.5	2,422	96.3
European	10.5	2,014	94.3
Japanese	29.9	2,193	93.9
Compact			
Domestic	49.5	3,087	107.4
European	5.0	2,982	104.5
Intermediate	54.5	3,640	111.5
Standard	50.6	4,119	118.6
Entire Fleet*	250.5	3,208	106.9

* Includes about 8 percent of the total not classified in the above categories for various reasons.

always with a driver fatality, or else they would not be recorded in this file. However, at the same time these vehicles show a value (occupant fatalities per occupant) equal to one, always and regardless of any vehicle characteristic.

The above discussion explains why the data in the second column of Table 8 show a very limited sensitivity to car nameplates. However, in spite of this shortcoming, the information is still worth reviewing as it tends to supplement our evaluation. The third column in Table 8 displays the values of ejected occupants, fatal or not, per 10,000 new car registrations. As formulated, this rather important descriptor is free of file-imposed biases of the type discussed above.

To put into perspective the data shown in the first three columns of Table 8, dealing with car occupant outcomes, we provide the data in the fourth column showing the corresponding car involvement risks. This last descriptor has been discussed and analyzed in more detail(12). The last three columns of Table 8 display the exposure and the major car characteristics of new cars for each entry.

Rollovers, Ejections, and Fires

These events are some of all possible intermediate outcomes between the crash initiation and the final outcomes, which are occupant casualties. They are singled out here for special consideration due to the traumatic experiences associated with their occurrence in car crashes. Rollovers in the context of this discussion are postimpact events, i.e., events taking place following a car collision either with another motor vehicle or with an object. They are distinguished from overturns, which take place in the absence of a noticeable impact before the car overturn. Summary evaluations of these risks are shown in Figures 9, 10, and 11 for rollovers, ejections, and fires, respectively. The results are resolved by car market class and refer to new cars, Figures 9 and 11, or new car occupants, Figure 10, involved in fatal accidents in the 1975 to 1983 period, per 10,000 registrations.

All three risk descriptors are sensitive to car market class; the risks of rollover and ejections show high sensitivity. The risk of fire or explosion shows a lower but still noticeable sensitivity. As expected, the pattern of ejection risk sensitivity is well correlated with the pattern of rollover sensitivity. This is especially true when, in addition to the risk of rollover as a subsequent event, the risk of overturn is also considered. The data shown in Table 9 are relevant.

This table summarizes the risks of overturn in column 1, the risks of postimpact rollover in column 2, and the sum of (1) plus (2) in column 3. The occupant ejection risks are shown in column 4, while the ratio of ejection to total rollover risk is shown in column 5. It is evident that, although rollover and ejections have risks that show a high sensitivity to car market class, the ratio of these two risks is virtually invariant. The ratio under consideration here is not necessarily the number of ejectees per car rollover, because there are car impact types other than rollover that contribute to occupant ejections. However, not unexpectedly, the rollover mode appears to be the principal contributor to ejections since it accounts for most of the ejection risk variability.

Table 8. Casualty risks, exposure, and major characteristics of new cars by nameplate in the 1975 to 1983 period. (Risks are shown per 10,000 car registrations except in column 2 where they are given per FARS-involved occupant)

New Car Market Class and Nameplate	Risks		Exposure	Mean	Mean		
	Occupant Fatality*	Occupant Fatality**	Occupant Ejection	Car Involvement	Thousands Car-Years	Weight Lbs.	Wheelbase Inches
Domestic Subc.							
Nameplate 1	3.70 ± .15	.53 ± .01	.94 ± .10	4.06 ± .14	4,683	2,072	95.4
2	2.88 .09	.50 .01	.58 .08	3.42 .11	3,607	2,598	97.0
3	2.51 .17	.45 .02	.78 .09	3.49 .20	1,594	2,782	96.0
4	4.11 .14	.55 .02	1.03 .16	4.40 .14	1,422	2,172	98.3
5	3.59 .22	.48 .01	1.50 .07	4.24 .16	901	2,059	94.0
European Subc.							
Nameplate 1	2.68 ± .18	.51 ± .01	.86 ± .11	3.21 ± .18	3,075	1,973	94.6
2	3.27 .12	.53 .02	1.25 .19	3.98 .18	1,471	2,238	93.2
3	4.28 .34	.55 .01	1.41 .12	4.67 .30	814	1,768	90.0
4	2.04 .22	.50 .05	1.31 .46	2.39 .26	684	1,837	94.1
5	4.37 .32	.56 .02	1.78 .26	4.86 .24	359	1,925	95.5
Japanese Subc.							
Nameplate 1	4.35 ± .14	.51 ± .01	1.57 ± .10	4.87 ± .16	3,456	2,021	92.0
2	3.62 .22	.46 .01	1.50 .19	4.77 .24	2,800	2,591	98.0
3	3.72 .44	.50 .01	1.31 .12	4.35 .48	2,426	2,199	93.4
4	3.92 .19	.50 .01	1.54 .16	4.55 .17	2,281	2,239	94.3
5	2.77 .16	.49 .03	.68 .08	3.31 .19	2,009	2,152	94.3
Domestic Compact							
Nameplate 1	4.02 ± .24	.39 ± .01	1.35 ± .10	5.96 ± .26	4,058	3,451	107.6
2	2.55 .12	.44 .01	.54 .05	3.33 .19	3,452	2,806	106.0
3	1.94 .25	.38 .01	.33 .06	2.87 .31	3,022	3,396	111.8
4	2.81 .02	.45 .01	.67 .07	3.53 .05	2,500	2,522	105.0
5	2.46 .10	.47 .01	.50 .32	2.88 .06	509	2,388	100.0
European Compact							
Nameplate 1	1.33 ± .10	.36 ± .02	.79 ± .16	2.13 ± .12	1,351	2,980	104.1
2	1.45 .22	.37 .02	.45 .10	2.50 .45	1,177	3,606	109.4
3	1.95 .17	.42 .02	.74 .07	2.67 .17	950	2,474	102.2
4	3.08 .10	.50 .02	1.03 .10	3.93 .10	858	2,590	101.0
5	3.18 .41	.45 .01	1.61 .14	3.88 .47	696	2,797	101.9
Interm. and Std.							
Nameplate 1	1.92 ± .09	.37 ± .02	.41 ± .04	3.15 ± .06	6,925	3,441	110.1
2	2.47 .29	.34 .03	.65 .10	4.35 .29	3,021	3,999	112.9
3	1.98 .19	.33 .02	.52 .06	3.81 .21	2,006	3,990	114.8
4	1.70 .25	.31 .01	.32 .03	3.27 .51	7,478	4,224	117.7
5	1.16 .16	.32 .02	.25 .03	2.06 .25	3,646	3,852	117.3

* Occupant fatalities in new cars per 10,000 registrations
**Occupant fatalities in new cars per occupant involved in a fatal accident

Risk Changes Versus Model Year

The results discussed so far, especially those shown in Figures 4 to 11 and Tables 6 to 9, are averaged over all calendar years 1975 to 1983. In spite of the fact they address new cars only, they are essentially averaged over as many as 10 model years. Given that much change has taken place in new car design during this period, the question arises whether the risks under consideration are changing. To address this question, we examine the data as a function of calendar year and thus as a function of model year for new cars.

Figure 12 displays the variation of the total risk of occupant fatality for all types of impact and for all new cars, regardless of market class. The actual data, available by calendar year, have been treated here by a linear regression that yields the fit, shown by the solid line, and the 95 percent confidence bounds, shown by the dashed corridor. The slope is statistically significant and equal to .099 ± .019 per year. In a 10-year period, this amounts to .99 ± .19 occupant fatalities per 10,000 new car registrations. This is rather substantial when compared to the mean of the risk for the same period: 2.36 ± .10 shown in the last entry of Table 6.

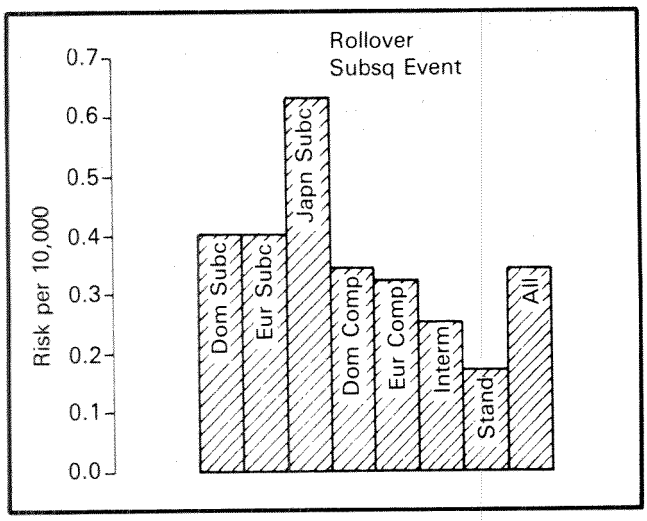

Figure 9. Fatal involvement risk of new cars in post-impact rollover per 10,000 registrations by market class

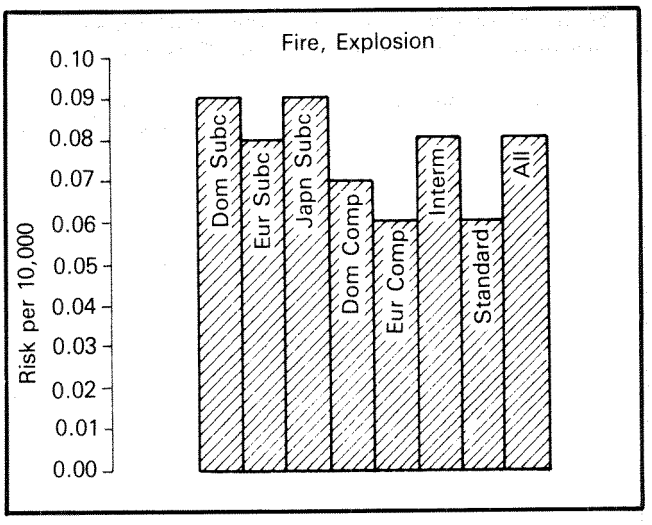

Figure 11. Risk of fire or explosion of new cars involved in fatal accidents per 10,000 registrations by market class

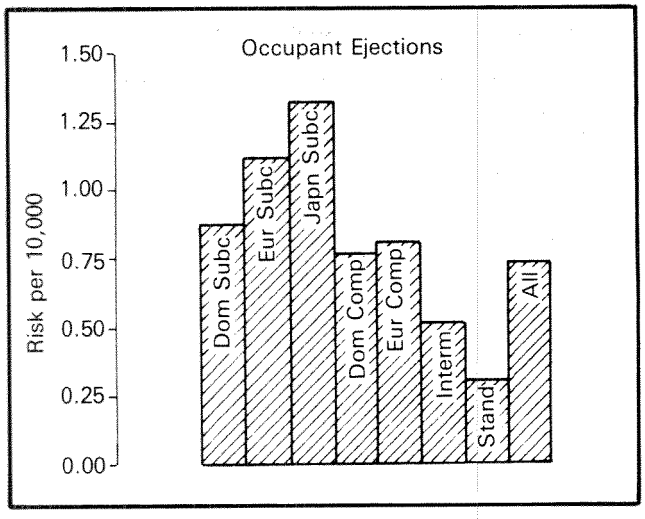

Figure 10. Ejection risk of new car occupants involved in fatal accidents per 10,000 registrations by market class

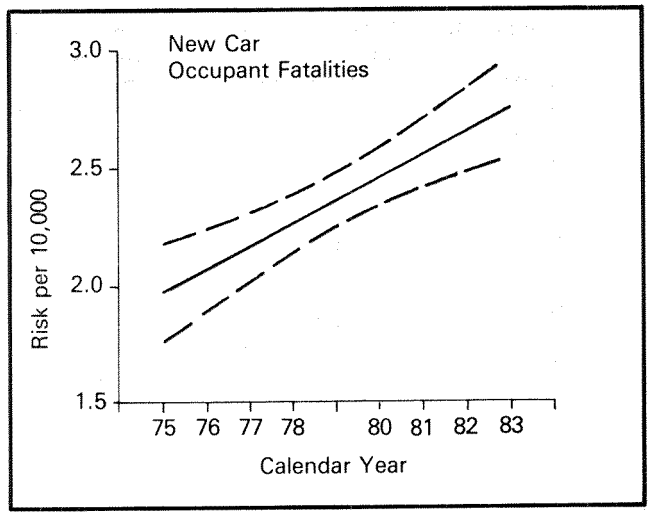

Figure 12. Fatality risk of new car occupants per 10,000 registrations—least-squares pitted mean and 95th percentile confidence rounds versus calendar year

In spite of the statistical significance of the above estimates, the reader should keep in mind that the risks under consideration, obtained from the raw data for each of the past 10 calendar years, have been adjusted for variations in travel and exposure severity. These adjustments, discussed earlier and detailed in the first part of Appendix B, are necessary to secure comparability of exposure and exposure severity for new cars in the period 1975 to 1983. There is no certainty these adjustments are the most appropriate or that they are free of error.

With full awareness of these uncertainties and for information purposes only, we have proceeded to examine the possible origins of the estimated risk increase by impact type and market class of new cars. For this purpose, we repeated the procedure discussed above in connection with Figure 12. The results are shown in Table 10 as estimates of the risk increase for a 10-year period. The units in this table are occupant fatalities per 10,000 new car registrations. Only cases with statistically significant (95 percent confidence) results are shown. All other cases are either omitted or show the entry "none." Note that Table 10 has an entry-by-entry correspondence with Table 6. The latter displays means, while the former displays change within the 10-year period under consideration.

The calendar year variation of the risk by market class is shown in Figure 13, which essentially resolves Figure 12 by market class. It also resolves the last column of

Table 9. Risks of overturns and rollovers for new cars and ejections for new car occupants

New Car Market Class	Risk Per 10,000 New Car Registrations 1 Car Overturns	2 Car Rollovers	3 Sum (1)+(2)	4 Occ. Ejection	5 Ratio (4)/(3)
Subcompact					
Domestic	.22	.40	.62	.88	1.42
European	.29	.40	.69	1.12	1.62
Japanese	.46	.63	1.09	1.32	1.21
Compact					
Domestic	.16	.34	.50	.77	1.54
European	.24	.32	.56	.81	1.45
Intermediate	.11	.25	.36	.51	1.42
Standard	.06	.17	.23	.30	1.30
Entire Fleet	.18	.34	.52	.73	1.40

Table 10. Estimates of fatality risk increase in the last 10 years for new car occupants involved in crashes of shown impact

New Car Market Class	Fatality Risk Increase by Type of Impact Frontal	Side	All Types
Subcompact			
Domestic	.49 ± .15	.35 ± .15	.79 ± .25
European	None	None	None
Japanese	None	None	None
Compact			
Domestic	.77 ± .17	.58 ± .09	1.46 ± .29
European	None	None	None
Intermediate	.39 ± .13	.22 ± .07	.57 ± .23
Standard	.64 ± .14	.35 ± .04	1.03 ± .14
Entire Fleet	.57 ± .13	.34 ± .04	.99 ± .19

Table 10 by calendar year. Note that the slope for the entire fleet of new cars, evident in Figure 13, is the result of two factors: (1) a contribution from individual market class slopes, most of which are significantly different than zero, and (2) market class shifts that took place between 1975 and 1983. For example, the share of fleet component 3, highest risk shown in Figure 13, increased by a factor about 2.5 between 1975 and 1983, while the share of fleet component 7 (lowest risk) was reduced by over 50 percent in the same period. Such market class shifts by themselves account for a significant part of the overall risk increase observed for new cars in Figure 12.

The risk increase observed in the past 10 years for new cars is not necessarily inconsistent with the observation made earlier that the risk for all cars remained unchanged, or changed very little, during this period. The difference between all cars and new cars, let us say the older cars, is a substantial fraction of all cars, accounting for about two-thirds of the exposure to risk. Although we have made no specific determinations yet, we have good reasons to believe that the older cars of calendar year 1983 may show lower risks than the older cars of 1975. Our reasons are based on the fact that the latter subfleet is dominated by cars produced in the 1960's and very early 1970's, i.e., before the manufacturers had the opportunity to fully implement an extensive set of safety improvements.

Occupant ejection risks for new cars have been examined by the same procedure, as a function of calendar year 1975 to 1983. The resulting slope is .036 ± .006 per year in occupant ejections per 10,000 new

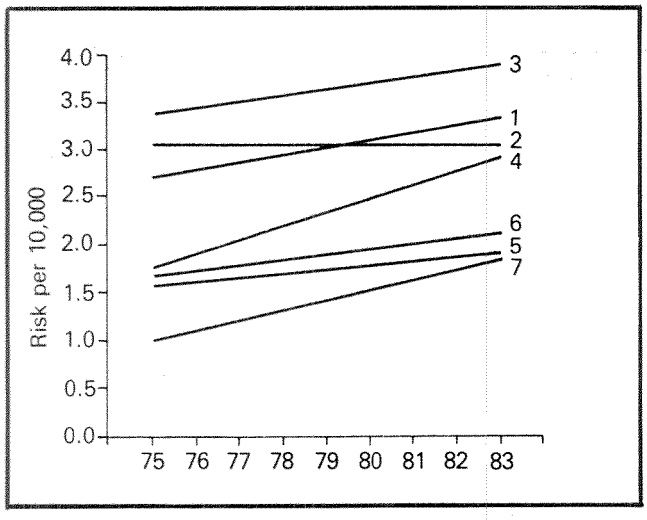

Figure 13. Fatality risk of new car occupants per 10,000 registrations by market class—linear least-squares fits to variation versus calendar year (plots 1, 2, and 3—domestic, European, and Japanese subcompact, respectively; plots 4 and 5—domestic and European compacts; plots 6 and 7—intermediate and standard cars)

car registrations. The risk increase for a 10-year period is .36 ± .06, which is also rather substantial when compared to the mean risk .73 ± .03 of occupant ejections for the same period. This increase appears to be as unevenly distributed among car market classes as the overall fatality risk is (see Table 10). A similar examination of the risk for crash events such as fire or explosion showed no statistically significant variation in the calendar years under consideration.

Influences of Car Weight and Wheelbase

An examination of Table 8 leads us to believe that market class and especially nameplate designations appear to influence the risk of fatal accident involvement as much, if not more, than weight and wheelbase. To quantify these notions, we have examined the data—risk versus car weight and/or car wheelbase—for over 500 nameplate model year combinations, each weighted with exposure (registered car years). We have applied log-linear regressions and have segregated the data by type of impact in addition to examining them for all accident types combined.

The results of these regressions are shown in Table 11 as regression coefficients and their standard errors. The upper part of the table shows the coefficients of separate regressions, i.e., the effect of weight with no control over wheelbase variation and vice versa. The striking similarity between the weight and wheelbase effects is no mystery, given these two variables are covariant in the fleet of cars. Accordingly, the question arises whether one and which one of the two effects is dominant. Thus the risk data were also regressed versus weight and wheelbase concurrently.

The coefficients of these regressions are given in the lower part of Table 11. They show the effect of car weight when the wheelbase variation is controlled and vice versa. It is evident in these results that the car weight influence is not only small in general and smaller than the wheelbase influence but also contrary to a popular notion that risk increases sharply with weight reduction. Note, in Table 11, negative coefficients indicate a risk reduction per unit weight reduction. This is what is observed for the car

Table 11. Occupant fatality risk variation for new cars by impact type as a function of car weight and wheelbase

Impact Type	Percent Risk Increase Per 500 Pounds of Car Weight Reduction	Per 5 Inches of Wheelbase Reduction
Frontal	16.6 ± 1.1	14.8 ± .9
Side	17.4 1.1	14.9 .9
Rear	24.6 2.0	21.8 1.7
Other	32.3 2.1	30.1 1.6
All Types	18.6 1.0	16.4 .8
	Per 500 Pounds of Car Weight Reduction at Fixed Wheelbase	**Per 5 Inches of Wheelbase Reduction at Fixed Weight**
Frontal	- .4 ± 3.2	15.1 ± 2.7
Side	5.3 3.4	10.7 2.8
Rear	1.6 6.1	20.5 5.2
Other	-14.6 5.9	41.8 5.0
All Types	.9 3.0	15.7 2.5

weight influence on occupant fatality risks for the (predominantly rollover) other impacts. Front, side, and rear impacts show a very small sensitivity, positive or negative, that is not easily distinguishable from zero within the stated standard error. Overall, the risk sensitivity to car weight, at fixed wheelbase, is zero for all practical purposes.

On physical grounds, lighter cars, colliding with heavier cars or other vehicles, experience a momentum disadvantage and thus a crash severity disadvantage by comparison to the heavier cars. On these grounds, a substantial risk sensitivity to car weight is expected, but it appears to be masked by other factors with a stronger influence. The influence of car wheelbase, at fixed car weight, appears to be substantial and quite sensitive to the type of impact. Although there may be certain physical reasons for expecting this influence, a much stronger influence may be attributed to nameplate or market class designations, as is evident in the results shown in Table 8.

The Possibility of Confounding Factors

The observed sensitivity of car occupant casualty risks to car class or nameplate is not immune from the confounding effects due to variations in the distribution of circumstantial but influential attributes among the car occupants and the car classes or nameplates under consideration. Included in these confounding factors is any attribute that: (1) has a substantial influence on the risk, and (2) has a significantly varying distribution among the car classes under examination.

A more detailed discussion of this subject is given in Appendix B in connection with Equations (B-1) to (B-8). In the same part of this appendix, we address what determinations are necessary to estimate the likelihood of confounding effects and what adjustments are appropriate to control their influence. We have applied these procedures in the examination of the data concerning sensitivity of car occupant risks to car class.

The number of circumstantial attributes that may influence the outcome of a car occupant involvement in fatal accidents is large, and their complexity is also large. Given that the occupant casualty risks under consideration here are on a per registered car basis, confounding effects may originate from attributes that influence car involvement in a crash, as well as from attributes that influence the casualty outcome, given a crash. The extent of the influence of the former type of attributes has been addressed (12), at least in connection with types of accidents showing a high sensitivity to market class. The adjustments necessitated by these considerations were found to be small in comparison to risk differentials between market classes.

We estimate the magnitude of the effects due to differences in the distribution of attributes that influence casualty outcome, given a crash. Among the most likely to be influential, we consider the time and place of the crash as proxies of crash severity, the restraint status of car occupants, and the age of car occupants. Table 12 shows the frequency of these attributes among car occupants involved in fatal crashes by car market class. Note that for brevity in this table, the shown circumstantial attributes have a binary categorization and the shown frequency values, in percent, concern the shown category. The percent value for the not-shown category is obviously 100 percent minus the shown percent.

It is evident in the data of Table 12 that the distribution of circumstantial attributes among car market classes shows no significant variation or any pattern conspiring to enhance an occupant's susceptibility to harm, given a crash. On this basis alone, we may expect no substantial

Table 12. Frequency of circumstantial attributes in fatal accidents of new cars, 1975-1983

Market Class	Percent by Circumstantial Attribute: Night Accident	Rural Accident	Occupant Age Over 45 Yrs.	Occupant Restrained
Subcompact				
Domestic	56.1 ± 1.1	60.5 ± 1.3	15.9 ± 1.1	6.6 ± 1.1
European	58.4 1.0	59 1.4	14.8 .9	9.7 .5
Japanese	58.6 .9	59 1.4	13.6 .4	8.3 1.1
Compact				
Domestic	55.5 ± 1.2	59.4 ± 1.3	24.3 ± .7	6.6 ± .9
European	60.5 2.0	53.3 2.5	18.4 1.9	11.7 1.0
Intermediate	55.5 ± 1.4	57.1 ± 1.3	25.6 ± 2.3	6.6 ± .9
Standard	49.2 ± .6	58.6 ± .9	41.2 ± .7	8.0 ± 1.0
Entire Fleet	55.1 ± .7	58.8 ± 1.2	24.2 ± .4	7.2 ± .8

confounding effects. However, we have proceeded to apply the estimation procedure, discussed in the second half of Appendix B, for arriving at risk values adjusted for the differences in the distribution of influential attributes shown in Table 12.

We computed the occupant risk adjustment factors shown in Table 13. These are ratios of the adjusted to unadjusted values of the risk by market class. An account is given for each influential attribute taken individually and for all attributes combined. As is evident in this table, the effects are noticeable but not very large.

Table 13. Occupant fatality risk adjustments accounting for differences in the frequency of influential attributes

Market Class	Risk Adjustment Factor by Attribute				
	Night Accident	Rural Accident	Occupant Age Over 45 Yrs	Occupant Restrained	All Combined
Subcompact					
Domestic	.992	.979	1.035	.995	.999
European	.974	.996	1.040	1.022	1.031
Japanese	.973	.995	1.045	1.010	1.021
Compact					
Domestic	.997	.992	.999	.995	.984
European	.958	1.076	1.024	1.040	1.099
Intermediate	.997	1.022	.994	.995	1.008
Standard	1.050	1.003	.936	1.007	.991
Entire Fleet	1.00	1.00	1.00	1.00	1.00

The above analysis leads to the conclusion that no major confounding influences are in effect in the determination of occupant casualty risks when cars are aggregated by market class. However, the reader should not generalize this conclusion. First, it should be kept in mind there is no automatic assurance that all potentially influential confounding factors have been examined. In addition to possible unsuspected factors recorded in the accident files, there may be influential factors not recorded.

Another equally important consideration is the degree of desired disaggregation of the data in relation to the magnitude of the risk differentials we are attempting to examine. When relatively small differentials must be examined for a large number of classes and subclasses, the procedure of controlling for confounding factors can be very frustrating.

References

1. "Fatal accident reporting system," Automated Files, National Highway Traffic Safety Administration, Annual Issues 1975-1984.
2. "National accident sampling system," Automated Files, National Highway Traffic Safety Administration, Annual Issues 1975-1984.
3. "National crash severity study," Automated Files, 1977-1979, National Highway Traffic Safety Administration.
4. "National vehicle population profiles," R.L. Polk, Annual Issues 1975-1983.
5. "Highway statistics," Federal Highway Administration, Annual Issues 1975-1983.
6. "Nationwide personal transportation study," conducted in 1976-1977 by the U.S. Bureau of the Census for the Federal Highway Administration.
7. "Consumption patterns of household vehicles," survey conducted by the U.S. Department of Energy in 1979-1982.
8. "Truck inventory and use survey," conducted in 1977 by the U.S. Bureau of the Census.
9. "On-road fuel economy and annual travel of cars and light trucks," survey conducted in the early 1980's by the National Highway Traffic Safety Administration.
10. a. Stewart, J.R., et al., "Annual mileage comparisons and accident rates in North Carolina," Final report to the National Highway Traffic Safety Administration, 1980.
    b. Dutt, A.K., et al., "Annual mileage comparisons and accident rates in North Carolina," Final report to the National Highway Traffic Safety Administration under Contract DOT HS-803041, January 1978; also under Contract DOT HS-802428, June 1977.
11. "Fatal and injury accident rates on public roads in the United States," Federal Highway Administration, Annual Issues 1975-1983.

12. Malliaris, A.C., "Discerning the state of accident avoidance in the accident experience," Proceedings Tenth International Technical Conference on Experimental Safety Vehicles, Oxford, England, July 1985.
13. O'Day, J., et al., "Alternative measures of restraint effectiveness and interaction with crash severity factors," SAE Paper 820798, June 1982.
14. Malliaris, A.C., et al., "Harm causation and ranking in car crashes," SAE Paper 850090, February 1985.

Appendix A

Major Changes in the Motor Vehicle Fleet and Travel

While the resident population in the United States grew at an average rate of 1.1 percent per year in the past 15 to 20 years, the number of licensed drivers grew faster, at an average rate of about 3 percent per year. An even faster growth took place in the number of registered motor vehicles and in the miles of travel of these vehicles each year. These grew at a rate of about 4.5 percent per year. In addition to growth, significant changes took place during this period in the composition and major characteristics of the motor vehicle fleet as discussed next.

Shifts in Fleet Shares by Vehicle Type

Between the early 1960's and 1980's, the mix of vehicle types in the fleet on the road changed significantly. In the early 1960's, vehicles other than cars were a relatively small fraction of the fleet. Since then, two fleet components, trucks and motorcycles, have grown and are growing faster, as shown below:

	Registration (Millions)		
	Cars	Trucks (All Types)	Motorcycles
Early 1960's	55-65	10-13	1.3
Early 1980's	105-110	35-39	5.8

It is evident that while car registrations have barely doubled in 20 years, truck registrations have easily tripled and motorcycle registrations have more than quadrupled. Furthermore, new truck sales as a percent of all motor vehicle sales have risen from about 12 percent in the early 1960's to about 22 percent in the early 1980's.

These two vehicle types have been and still are of concern in the safety community because they are, in general, substantially more involved in accidents than the average vehicle type (see Table 2 in the main text). They also present special problems that are size-related. Trucks are more aggressive and motorcycles more vulnerable than the average vehicle type.

Changes in Major Car Characteristics

Two car characteristics—weight and wheelbase—are singled out for general consideration because they are often discussed and analyzed in connection with accident and casualty risks. Significant changes have taken place in these characteristics in the past 10 years for most makes and market class categories, especially of the domestically produced new cars. Table A-1 shows car weight changes, and Table A-2 displays the wheelbase changes in an identical format.

For the market class characterization in these tables, we have followed the practice of the domestic car trade literature, i.e., a classification by nameplate or car line into market class categories. European makes are classified as subcompact except for makes with a wheelbase above 100in (e.g., Mercedes Benz, Audi, BMW, Volvo, and a few others). Also, the great majority of the Japanese makes are subcompacts with a few low volume exceptions. We have used the R.L. Polk registration counts by nameplate and model year for obtaining weighted means of car weight and wheelbase and for the percentages of front-wheel-drive cars.

Travel and Exposure Pattern Changes

Gasoline supply disruptions, the 55mph speed limit, the rising cost of highway travel, and various cycles in the economy have influenced travel and exposure patterns in the past 15 years. The resulting variations are noticeable but lesser than the changes in the motor vehicle fleet discussed above.

The average annual travel per vehicle has fluctuated by less than 5 percent in the period under consideration. However, larger fluctuations have been observed for specific vehicle categories as shown in Table A-3. The source of the data in this table is (5). The annual travel of cars, for example, shows a significant reduction between 1973 and 1974 and again between 1978 and 1981. Car travel is generally more responsive to and follows the pattern of major influencing factors.

In the late 1960's and early 1970's, car travel showed minor fluctuations around 10M/mi/yr. A significant decline occurred between 1973 and 1974 due to the oil embargo at that time. From 1974 to 1978, car travel per year increased slowly but steadily until 1979, when another oil crisis forced an abrupt reduction. This reduction was prolonged and deepened well into 1981 due to a depressed economy.

The increase of annual travel per car, starting in 1982, has coincided with the economic recovery that also started at that time. Note the annual travel for other

Table A-1. Mean car weight (pounds) for cars retailed in the United States by origin of make and market class

I. New Cars by Model Year

Market Class	1977	1978	1979	1980	1981	1982	1983
Domestic Subcomp.	2,597	2,453	2,425	2,393	2,118	2,211	2,125
Compact	3,415	3,231	3,047	2,756	2,651	2,708	2,612
Interm.	4,062	3,589	3,417	3,311	3,295	3,147	3,135
Standard	4,109	4,081	3,929	3,844	3,886	3,838	3,874
European Subcomp.	1,994	1,897	1,989	2,098	2,032	2,085	2,071
Other	2,990	2,955	3,056	2,997	2,988	3,023	3,057
Japanese Subcomp.	2,191	2,243	2,114	2,188	2,203	2,196	2,159
Other	2,673	2,740	2,834	2,849	2,887	2,886	2,851

II. All Model Years by Calendar Year

Market Class	1977	1978	1979	1980	1981	1982	1983
Domestic Subcomp.		2,592	2,573	2,545	2,512	2,468	2,432
Compact		3,184	3,176	3,139	3,103	3,071	3,042
Interm.		3,946	3,861	3,802	3,753	3,703	3,637
Standard		4,379	4,347	4,325	4,311	4,285	4,259
European Subcomp.		1,948	1,957	1,968	1,993	2,008	2,026
Other		2,755	2,801	2,827	2,860	2,891	2,924
Japanese Subcomp.		2,187	2,188	2,184	2,183	2,187	2,187
Other		2,699	2,735	2,773	2,798	2,831	2,842

Table A-2. Registrations weighted mean car wheelbase (in) for cars retailed in the United States by origin of make and market class

I. New Cars by Model Year

Market Class	1977	1978	1979	1980	1981	1982	1983
Domestic Subcomp.	95.7	96.9	96.5	96.6	95.7	96.4	95.3
Compact	110.0	108.9	106.5	105.4	103.9	102.8	101.1
Interm.	115.1	111.0	110.1	108.6	108.3	107.1	107.3
Standard	118.1	118.2	116.9	117.4	116.5	116.5	116.9
European Subcomp.	94.8	93.4	93.8	94.2	95.0	96.5	96.6
Other	104.0	104.3	105.4	104.8	105.2	105.3	105.7
Japanese Subcomp.	93.4	93.6	93.4	94.3	94.3	95.2	95.3
Other	104.0	104.0	104.0	100.4	103.6	103.3	103.1

II. All Model Years by Calendar Year

Market Class	1977	1978	1979	1980	1981	1982	1983
Domestic Subcomp.		97.7	97.4	97.3	96.9	96.6	96.4
Compact		109.0	108.8	108.5	108.1	107.7	107.3
Interm.		115.1	114.2	113.6	113.0	112.4	111.8
Standard		122.1	121.7	121.5	121.2	120.9	120.5
European Subcomp.		94.8	94.7	94.7	94.7	94.7	94.8
Other		103.4	103.7	103.9	104.0	104.2	104.4
Japanese Subcomp.		93.8	93.8	93.8	93.9	94.0	94.2
Other		104.0	104.0	103.5	103.3	103.3	103.3

Table A-3. Average annual travel per vehicle in thousand miles as a function of calendar year.

Year	Cars	Trucks		Motorcycles	All Motor Vehicles
		Single	Comb.		
1973	10.0	9.87	46.7	4.50	10.1
1974	9.45	8.98	49.1	4.50	9.53
1975	9.63	8.88	51.7	4.50	9.64
1976	9.76	9.37	48.3	4.50	9.84
1977	9.84	9.40	50.2	4.50	9.93
1978	10.0	9.25	49.3	4.50	10.1
1979	9.49	9.18	49.7	4.00	9.58
1980	9.14	10.1	42.7	3.14	9.41
1981	9.00	11.0	47.0	2.57	9.48
1982	9.53	9.81	50.1	2.09	9.64
1983	9.64	9.71	52.4	2.15	9.73

vehicles, especially trucks, is much less discretionary and does not necessarily follow the pattern of car travel. The pattern for all motor vehicles agrees with that of cars because car travel dominates.

Annual travel per car is known to vary substantially as a function of car age (or of model year in a fixed calendar year). Variations may also exist as a function of market class. The data for a detailed and systematic examination of these patterns and their variation in the past 10 to 15 years are not at hand. However, the available information is generally consistent with the summary shown in Table A-4, which addresses relatively new cars, i.e., of age 3 years or less.

Table A-4. Annual travel per car as a function of car age and car market class

Car Market Class	1st Yr. Travel Thousand Miles/Car	Travel Ratio 2nd Yr./1st Yr.	Travel Ratio 3rd Yr./1st Yr.
Subcompact	13.2 ± .47	1.00 ± .02	.95 ± .03
Compact	12.1 .51	.91 .05	.89 .07
Intermediate	13.3 .60	.89 .02	.82 .03
Standard	13.6 .36	.91 .03	.84 .02
All	13.0 .2	.94 .02	.87 .03

The data in each entry of this table are averages of corresponding values provided by a large number of sources(2,3,6,7,9,10) spread over several years between the mid-1970's and early 1980's. The raw data in these sources have very dissimilar origins. In spite of this, fair agreement is observed for car ages up to 3 years or with respect to car market classes. This is reflected in the relatively small errors that arise when data from all these sources are averaged, as shown in Table A-4. Furthermore, no significant or systematic trend has been found in the data with respect to calendar year variations, again for car travel categorized as in Table A-4.

Travel speed patterns have also changed substantially in the past 10 to 15 years. The 55mph speed limit went into effect nationwide early in 1974. Before that time, the prevailing average speed on interstate highways was about 65mph. This average speed dropped to about 57.5mph in 1974. In the following years, this speed increased steadily, slowly in the second half of the 1970's but faster in the early 1980's. Table A-5 shows the percentage of motor vehicles noncomplying with the 55mph speed limit while driving on U.S. highways. The source of these data is (5).

Travel speed is one of the factors that influence the severity of the exposure to accident and casualty risks. Many other factors, driver-, environment-, and vehicle-related, may also be influential with varying strengths. As an overall descriptor of exposure severity, we have considered the rate of accidents per unit travel for all vehicles on U.S. roads. Table A-6 shows how this rate has varied in the past 10 years. The source of these data is (11).

Table A-5. Percent of motor vehicles on U.S. highways exceeding shown speed in the early 1980's

Year	55 MPH	65 MPH	75 MPH
1980	49.3	16.8	4.1
1981	48.5	18.4	5.2
1982	52.6	24.2	7.9
1983	54.1	25.4	8.5

Table A-6. Fatal accidents and nonfatal injury accident rates per 100 million vehicle-miles traveled on U.S. roads, by calendar year

Year	Accidents Per 100 Million Miles Fatal	Nonfatal Injury
1975	2.85	133.0
1976	2.87	133.3
1977	2.91	129.8
1978	2.92	135.9
1979	2.97	137.5
1980	2.96	132.8
1981	2.84	130.1
1982	2.45	123.6
1983	2.30	121.6

Appendix B

Errors and Adjustments in Risk Determinations

The most common and serious source of error in the estimation of absolute risks, in any application of Equations (1) to (6), is the absence of coincidence in the categorization of vehicle attributes represented by subscript j between the numerator and denominator. The steps taken to minimize this type of error have been outlined in the main text in connection with absolute risk determinations.

A second, but separate, concern is the number of vehicle, accident, and occupant categories that must be introduced to obtain the desirable resolution in the computation of risks. It is desirable, although not always feasible, to resolve the entire data base into as many cells as necessary to obtain fairly uniform risks within each population. This, however, must be traded off against the statistically insignificant results obtained when a large number of cells yields populations that are too small.

Even after the concerns discussed above are satisfied, further adjustments may be appropriate to deal with nonuniformities in the exposure conditions relevant to risk determinations. This appendix discusses such adjustments.

We consider first a normalization procedure used for relatively new cars (1 to 3 years old) traveling on U.S. roads in any of the calendar years 1975 to 1983. The exposure variations experienced by these subfleets were discussed in the last section of Appendix A. Tables A-3, A-4, and A-6 display relevant data. When comparing or aggregating these subfleets, it is convenient and appropriate to normalize their accident experience to an arbitrary but common basis. For this purpose, we have selected the 1-year-old cars, under the travel and exposure severity conditions of calendar year 1980.

In practice, normalization is performed through factors that multiply the risks of accident involvement per vehicle registration to normalize them to the reference exposure conditions. Table B-1 shows normalizing factors A and B for annual travel per car by calendar year and for exposure severity, respectively. Factor A is obtained from the car travel data shown in the first column of Table A-3, by making 1980 the reference year. Similarly, Factor B is obtained from the data of Table A-6.

The product of Factors A and B is the composite normalization factor for 1-year-old cars. This product appears in the first column of Table B-2. The other two columns of this table show the composite normalization factors for 2- and 3-year-old cars, respectively. These factors have higher values, which reflect the travel reduction taking place as the car age increases. The relevant data for these transformations are shown in the last row of Table A-4.

Table B-1. Normalization factors by calendar year for annual travel per car (column A) and for exposure severity (column B)

Calendar Year	A	B
1975	.95	1.04
1976	.94	1.03
1977	.93	1.02
1978	.91	1.01
1979	.96	1.00
1980	1.00	1.00
1981	1.02	1.04
1982	.96	1.21
1983	.95	1.29

Table B-2. Normalization factors for travel and exposure by car age and calendar year

Calendar Year	Car Age 1 Year	2 Years	3 Years
1975	.99	1.05	1.14
1976	.97	1.03	1.11
1977	.95	1.01	1.09
1978	.92	.98	1.06
1979	.96	1.02	1.10
1980	1.00	1.06	1.15
1981	1.06	1.13	1.22
1982	1.16	1.23	1.33
1983	1.23	1.31	1.41

In addition to travel per vehicle and exposure severity in general that show variations from year to year, there are many exposure attributes that influence accident risks, even in the absence of calendar year or model year considerations. Accordingly, adjustments would be necessary to bring the determination of risks under

exposure conditions as comparable as possible, when such comparability is desired. When necessary, these adjustments are made according to the procedure discussed below. Consider first the risks R_1 and R_2 concerning two different vehicle classes 1 and 2, as determined from aggregated data of casualty counts C and exposure E:

$$R_1 = \text{Sum } C_{1q}/\text{Sum } E_{1q} \quad \text{(B-1)}$$
$$R_2 = \text{Sum } C_{2q}/\text{Sum } E_{2q} \quad \text{(B-2)}$$

The summations in these relations are over all exposure conditions designated by q. Note that in Equations (B-1) or (B-2) as well as in the following discussion, E, referred to as exposure, is not necessarily limited to travel or registrations but could be any variable used in the denominator of a risk determination. See, for example, the denominators in Equations (3) or (5). Furthermore, subscript q is a generalization representing any exposure attribute that may influence the risk. It is now helpful to introduce the exposure distribution frequencies:

$$F_{1q} = E_{1q}/\text{Sum } E_{1q} \quad \text{(B-3)}$$
$$F_{2q} = E_{2q}/\text{Sum } E_{2q} \quad \text{(B-4)}$$

Note that the sum of all F_{1q} or all F_{2q} values equals unity.

The use of these equations in (B-1) and (B-2) yields:

$$R_1 = \text{Sum } (F_{1q}R_{1q}) \quad \text{(B-5)}$$
$$R_2 = \text{Sum } (F_{2q}R_{2q}) \quad \text{(B-6)}$$

where the risks R_{1q} and R_{2q} are defined by $R_{1q} = (C_{1q}/E_{1q}$ and $R_{2q} = (C_{2q}/E_{2q})$. Equations (B-5) and (B-6), which are fully equivalent to (B-1) and (B-2), are more informative. They show that, in each case 1 or 2, the aggregated risk is the sum of risks corresponding to individual exposure conditions, with each such risk weighted by the frequency of occurrence of the corresponding exposure condition.

When risks R_1 and R_2 are determined under aggregated exposure conditions, i.e., by Equations (B-1) and (B-2), any difference between them may be not entirely due to risk differentials under specific exposure conditions. As shown in Equations (B-5) and (B-6), differences between R_1 and R_2 may arise from differences between R_{1q} and R_{2q}, or from differences between F_{1q} and F_{2q}, or from both sources.

A numerical example will clarify these points. Let subscripts 1 and 2 represent two different vehicle types and subscripts a and b represent two different exposure conditions, say urban and rural travel. Furthermore, suppose the data we are dealing with are:

$F_{1a} = 90\%$,
$F_{1b} = 10\%$;
$F_{2a} = 10\%$,
$F_{2b} = 90\%$

for the frequencies of occurrence of the exposure and:

$R_{1a} = 3$,
$R_{1b} = 1$;
$R_{2a} = 5$,
$R_{2b} = 2$

for the individual risks, in accidents per unit exposure. The risks R_1 and R_2, integrated over both exposure conditions for each vehicle type, are:

$R_1 = 2.8$ and $R_2 = 2.3$.

This answer may be fine if we wish to compare the risks of vehicle categories 1 and 2 under their recorded exposure conditions. However, this answer is absurd if it is meant to be a risk comparison under exposure conditions assumed to be fairly similar. It is absurd because R_{1a} is lower than R_{2a} and R_{1b} is lower than R_{2b} so R_1 is also expected to be lower than R_2, but it is not. This very substantial distortion is introduced because the frequencies of occurrence of exposure categories differ significantly between vehicle types 1 and 2.

Whenever risk calculations and comparisons, vehicle category 1 versus 2, are made over aggregated exposure conditions, it is essential as a minimum to determine and review the frequency distributions of exposure conditions for each of the vehicle categories 1 and 2. If these distributions are fairly similar, the possibility of distorted results is minimized. However, if the distributions differ substantially, then Equations (B-1) and (B-2) or their equivalent (B-5) and (B-6) as written are inappropriate for risk determinations.

Equations (B-5) and (B-6) may be used but only after an adjustment. The necessary adjustment requires that F_{1q} and F_{2q} must be made identical. This can be done either by retaining F_{1q} in (B-5) but also using the same in (B-6) instead of F_{2q}, or by retaining F_{2q} in (B-6) and also using the same in (B-5) instead of F_{1q}. These two alternatives correspond to risk comparisons either under the exposure conditions of vehicle category 1 all across the board or under those of vehicle category 2 also all across the board. A third alternative may be considered by pooling the exposure conditions of both vehicle categories together and determining a frequency distribution F_q for the pooled populations. For this alternative, the appropriate version of Equations (B-5) and (B-6) is:

$$R_{\bar{1}} \quad \text{Sum } (F_qR_{1q}) \quad \text{(B-7)}$$
$$R_{\bar{2}} \quad \text{Sum } (F_qR_{2q}) \quad \text{(B-8)}$$

Note that the risks R_{1q} and R_{2q} must be determined for each exposure category q and then used in conjunction with the common frequency distribution F_q for the determination of R_1 and R_2. Other alternatives are possible for introducing a common frequency distribution. Which alternative is selected depends on the terms under which we wish to compare risks.

Technical Session No. 4

Accident Investigation and Its Relevance to Legislation

R. Stamm, Chairman, Germany

The Causes of Injury in Car Accidents—An Overview of a Major Study Currently Underway in Britain

Margaret Galer and
Sue Clark
Accident Research Unit, Institute for Consumer Ergonomics, Loughborough, Leicestershire, United Kingdom

G.M. Mackay and
S.J. Ashton
Accident Research Unit, Birmingham University, West Midlands, U.K.

Abstract

A major study is currently underway in Britain, funded jointly by the Department of Transport, Ford, and BL Technology, to investigate the causes of injury to occupants in car accidents. The Accident Research Units at the Institute for Consumer Ergonomics, Loughborough, and at Birmingham University each have a team of researchers who, together with the Department of Transport Traffic Area teams, investigate approximately 700 accidents each year. The data are collected in a uniform manner by all investigators, and the data bases are compatible. The accidents are strictly sampled from a predominately urban (Birmingham) and a rural (Loughborough) catchment area.

High-quality data are collected on the performance of the vehicles in crashes by detailed investigations after the accident; occupant injury details are provided by hospital consultants and coroners, sometimes by the occupants; sources of injury are assigned by the ARU teams.

The computerised data can be structured in an analysis from the point of view of the vehicle's performance in the accident, to which occupant's details can be applied, or an occupant's performance, to which vehicle details can be applied.

This paper describes the organisation of the study and provides some preliminary data on accident circumstances, occupant injuries, and vehicle performance.

Introduction

The detailed, objective investigation of the causes and mechanisms of injuries in traffic crashes originated in the United States in the 1950's. The pioneering work of Hugh de Haven and the Automotive Crash Injury Research (ACIR) group at Cornell University illustrated the potential knowledge that can be gained from such studies. Similar work did not begin in Europe until the 1960's.

Following that work in the United States of ACIR, and of Huelke and Gikas on fatal crashes, Starkes and Miller at the Road Research Laboratory in Great Britain began detailed at-the-scene studies in 1961(1). In 1964, Mackay formed an interdisciplinary team working closely with Gissane and Bull at the Birmingham Accident Hospital, and throughout the 1960's those two groups conducted a number of specific investigations covering both accident causation and the relationships between vehicle design and injuries(2).

The funding structure operating in the 1960's resulted in such investigations being limited to some 200 to 300 cases per year. As the studies were broad in their approach, encompassing all types of environments, classes of road users and vehicles, and different severities of injury, the sample sizes were correspondingly small for any specific detailed analysis. Thus, those early projects mainly defined a range of topics, gave some insight into the frequencies of various crash characteristics, and the consequences in injury terms, but did not adequately address either the specifics of the detailed relationships between vehicle design and trauma or the sampling problems created by too broad an approach.

Consequently, in the early 1970's, the Accident Research Unit at Birmingham University and also TRRL introduced different procedures. Instead of going to the scene, the involved vehicles were examined retrospectively a few days after the accident. Furthermore, several relatively rigorous sampling procedures were introduced; for instance, limiting the criteria to current model cars, serious and fatal casualties, restraint use, or frontal impacts only.

In the 1970's, there was a general upsurge of interest in in-depth studies in Europe, in part generated by the North Atlantic Treaty Organisation's Committee on the Challenges of Modern Society (NATO-CCMS) programme. Teams began operating in Sweden at the Volvo and Saab corporations, in Germany at the Technical University in Berlin, in France at the Association Peugeot-Renault, and at the Organisme National de Securite Routiere (ONSER) in Lyon, as well as at the Transport and Road Research Laboratory (TRRL) and at Birmingham University in England. In addition, various car manufacturers ran their own in-house studies notably at Ford, Volkswagen, and Daimler-Benz. As part of the NATO-CCMS programme, attempts were made to unify crash investigation procedures but, although a lot of useful interchange took place, local and national practices worked against the introduction of completely uniform practices(3). What did emerge, however, was recognition of the need to agree to uniform definitions of crash characteristics and also the need to have standardised scales for the basic input and output variables of crash injury research.

The fundamental input variable is crash severity, and this has been defined variously in terms of degrees of vehicle damage. In the United States, the TAD scale was adopted by ACIR and then used in a modified form in an early in-depth study in Australia(4). The Society of Automotive Engineers (SAE) then took up the problem, and the Collision Deformation Code was developed. This is now SAE-recommended practice and is used throughout the world for describing vehicle damage. At the same time, the concept of Equivalent Test Speed (ETS) was developed(5). In France, the Peugeot-Renault Association introduced the concept of Delta V, i.e., the velocity change in the crash phase of the impact. This has subsequently been shown to be the most appropriate measure of crash severity and is now widely used(6).

The second fundamental variable required in detailed studies is an agreed method of assessing the output, i.e., injury severity. In the 1960's there were almost as many injury scales as there were crash investigation teams. Through the efforts of the American Association for Automotive Medicine, the Abbreviated Injury Scale (AIS) was evolved. The AIS is now the standard method for injury severity classification and is used in almost all detailed accident studies(7).

The 1980's have seen a decline in crash injury research in Europe, which is probably related to the economic recession. No European country has a systematic, long-term, in-depth programme similar to the U.S. National Accident Sampling System (NASS) and the Fatal Accident Reporting System (FARS). With the benefit of hindsight, the establishment of the NASS system and the continued commitment of resources to maintaining that programme must be ranked as one of the most enlightened and far-sighted acts of any safety research administration. By contrast, the European effort continues on an ad-hoc basis without any long-term structure that would allow the detailed evaluation of the effects of design changes and associated legislation with a satisfactory longitudinal experimental design.

It has become apparent from the various studies performed that there are a number of critical points to be considered in conducting in-depth studies.

First, the dependence of the research group on other organisations is great. Good relationships with police, hospitals, garage staff, and, indeed, the general public are vital, and therefore a diplomatic approach and careful use of the media for positive reinforcement are essential.

Second, training of research staff and establishing study procedures takes much longer than most people would expect. The techniques of photography, the recording of vehicle crush measurements, and the reconstruction of occupant-vehicle interactions are quite complex.

Third, given that the investigator is inspecting the crashed car in person, it is easy to be beguiled into collecting information on the general basis that somehow it will be useful someday.

Fourth, allied to the above, is almost total neglect in the formative stages of project planning of consideration of the need for control data. This often results in the limited usefulness of some of the conclusions from in-depth crash studies.

Fifth, it is normal to underestimate the time and effort to be devoted to analysing the data from an in-depth study. Sponsors often see the end point of a project as a sample of a specified number of cases of a particular collision sample, and arrange funding and targets accordingly. The reality is that for the sensible and thorough analysis of in-depth crash injury findings, the contract length should be doubled to allow for analysis and interpretation of the findings and the presentation of such findings in appropriate reports and publications.

In the following sections, the structure of current British in-depth studies is described. The primary aim of the current studies is the collection of data on injury causation and vehicle crashworthiness. These data are used for different purposes by the members of the sponsoring consortium. The Department of Transport Vehicle Standards and Engineering Division (VSE) requires information on the performance of injury-reducing features of vehicles controlled by legislation and information on the trends occurring to review and update the regulations for the construction and use of cars. This information is used both in a national context and internationally with the EEC and ECE organisations. The Vehicle Inspectorate (VI) monitors the data for possible problems and defects that may lead to changes in future vehicle design or recalls under the U.K. Code of Practice on action concerning vehicle safety defects. The Transport and Road Research Laboratory uses the data

for a variety of studies on human tolerance to injury. The two motor companies, Ford and BL Technology, who provide a service to Austin Rover Group, Freight Rover, Land Rover, Leyland vehicles, and Jaguar cars, require detailed information on the performance of current models in real-world collisions to supplement laboratory tests and for the development of their products.

Organisation of the Study

The sponsoring consortium has contracted the Accident Research Units (ARU) at the Institute for Consumer Ergonomics, Loughborough, and Birmingham University to investigate the causes of injury to occupants of cars involved in accidents. Together with the Department of Transport's vehicle examiners in four traffic areas, data will be collected on approximately 700 accidents each year. The team at Loughborough investigates accidents in Derbyshire, Nottinghamshire, and Leicestershire, and the team at Birmingham investigates accidents in the West Midlands. Two of the Department of Transport traffic area teams work with the ARU's, namely East Midlands with the Loughborough team and West Midlands with the Birmingham team. The Northern traffic area team investigates accidents in Durham, and the Western traffic area team investigates accidents in Avon, Somerset, and parts of Wiltshire. The work of the traffic area teams is coordinated by the ARU at Loughborough.

Disproportional stratified sampling of all crash severities is carried out by the Loughborough and Birmingham teams. The Northern and Western traffic area teams investigate a proportion of the serious and fatal accidents in their areas. The area covered by the teams at Loughborough is predominately rural and contains three major centres of population—Leicester, Derby, and Nottingham. There are 9,093 miles of public road comprising 79 miles of motorway, 417 miles of trunk road, 860 miles of A-class nontruck road, 2,820 miles of B-class road, and 4,917 miles of unclassified road. These roads comprise 5.6 percent of the total road mileage in Britain. In 1983, there were 124 car occupants killed and 5,880 injured. The area covered by the team at Birmingham is essentially an urban area with a small rural area separating Coventry from the rest of the conurbation made up of Wolverhampton, Walsall, West Bromwich, Dudley, Sandwell, Birmingham, and Solihull. There are 3,945 miles of public road comprising 43 miles of motorway, 60 miles of trunk road, 350 miles of A-class nontrunk road, 456 miles of B-class road, and 3,036 miles of unclassified road. These roads comprise 2.4 percent of the total road mileage of Britain. In 1983, there were 47 car occupants killed and 4,336 injured. The populations of the two areas are similar: 2.76 million in the Loughborough team area and 2.67 million in West Midlands. The car ownership rates are also similar: 733 thousand private cars and vans in the area covered by the Loughborough team and 776 thousand in the West Midlands area. The car occupant casualties in the area covered by the Loughborough team comprise 5.3 percent of the national total; those in the West Midlands comprise 3.8 percent. Compared with the figures for Great Britain, the areas covered by the two ARU's comprise 6 percent of the total road mileage.

The study is concerned only with cars up to 5 years old that are damaged sufficiently in the accident to be towed away from the scene. These are "case" vehicles. Accidents are notified to the teams by their local police forces. Accident cases are sampled according to police injury classifications of fatal, serious, slight, and noninjury. The disproportional stratified sampling scheme is structured so that each ARU team investigates approximately 300 accidents each year with a roughly equal split between serious/fatal accidents and slight/noninjury accidents. The two remote traffic area teams also investigate 50 accidents each. The local hospital consultants provide data on injuries sustained by those occupants who are taken to hospitals. The coroners provide injury data on fatally injured occupants. The teams also send questionnaires to the occupants in all cases except specified sensitive cases.

Data Collection and Analysis Procedures

The teams all follow standard procedures and record data in identical forms. Consistency between the teams is most important and is achieved by the use of a manual defining procedures and conventions, by regular team meetings, and by an updating newsletter.

Vehicle data are collected on case vehicles by systematic investigation of vehicle component performance carried out by the teams at recovery garages within a few days of the accident occurrence. The teams work in pairs, one person taking photographs and the other completing the form. Vehicle damage and occupant contact details are recorded on specially designed data collection forms used by all the teams. The forms allow information to be recorded in coded and descriptive formats. Certain coding is carried out at the time of the examination, and other coding is completed after the accident has been reconstructed. All aspects of the vehicle that could affect occupant injury are examined and the performance noted and recorded photographically. These include performance of vehicle structures, safety features such as seatbelts, and other aspects such as steering wheels and columns, seats, doors, and glass. The data collected are factual such as extent of crush, extent of steering column stroke, measurement of plastic transfer on seatbelt webbing, and damage to components. Other data are inferential, such as whether the occupant may have been ejected during

the accident, possible contacts, and whether seatbelts were likely to have been worn in the accident. In these cases, the conclusion is recorded and the evidence on which the conclusion is reached noted on the form. A report is generated for each case vehicle, which can be from 12 to 20 A4 pages in length depending on the complexity of the vehicle damage, with certain pages being completed only if there is damage to the component.

Occupant data are recorded on occupant injury forms, based on reports from the hospital consultants, coroners, and the questionnaires. Injury severity is scored and recorded using the Abbreviated Injury Scale (AIS) and the Treatment Period (TP) and Permanent Impairment (PI) scales of the Comprehensive Research Injury Scale. The occupant kinematics are estimated from the collision circumstances, from the occupant contact data recorded during vehicle examination, and from the occupant's injuries. The causes of the injuries are inferred from these sources. This is normally done by the accident teams in consultation with the medical advisers and those who examined the vehicle.

It is important that data of different types are differentiated. There are factual data comprising measurements, observed damage, injuries, and so on, and there are inferential data comprising conclusions drawn from evidence such as whether a seatbelt was worn or what was the source of an injury. The coded data are transferred to mainframe computers for analysis using the SPSS-X statistical analysis package. Both teams have access to Honeywell computers that use the Multics operating system and can be linked together allowing combined analyses. Each team also has a microcomputer for general office management, for keeping track of each accident case prior to completion, and for indexing basic data on vehicle damage and occupant injury severity.

The Data Base

An accident case comprises a detailed investigation and record of each case vehicle involved in the accident, a brief examination and record of the other vehicles, a detailed record of the injuries sustained by each occupant in the case vehicles, and a summary sheet describing the main points of interest for the accident as a whole. The data are recorded in a number of ways within the accident case record. Photographic records in the form of slides are taken for each vehicle. There are standard photographic shots of the vehicle exterior and interior and also photographs of damage detail and occupant contacts. On the vehicle form, the data are recorded in precoded form; wherever damage or other points of interest have occurred, detailed descriptions are written on the form. Information from other sources, such as the occupant questionnaires or causes of component faults or damage, are postcoded. Figure 1 is a section of the vehicle form and shows precoded, descriptive, and postcoded data.

Data are recorded on the injury forms for each occupant. The data are factual, such as occupant's date of birth; descriptive, where each injury is described in detail; and inferential, such as the probable cause of the injury or the contact observed in the vehicle investigation. In addition, the injuries are scored using the AIS, PI, and TP scales. Figure 2 shows an extract from the occupant injury form where the injuries are described, scored, and coded.

The sources of injury are assigned in discussion with the team's medical adviser and entered on the coding forms. The Maximum Abbreviated Injury Score (MAIS) and the Injury Severity Score (ISS) are also calculated. Figure 3 shows an extract from the Injury Coding sheet, which is used to encapsulate all the injury and correlational injury causation data.

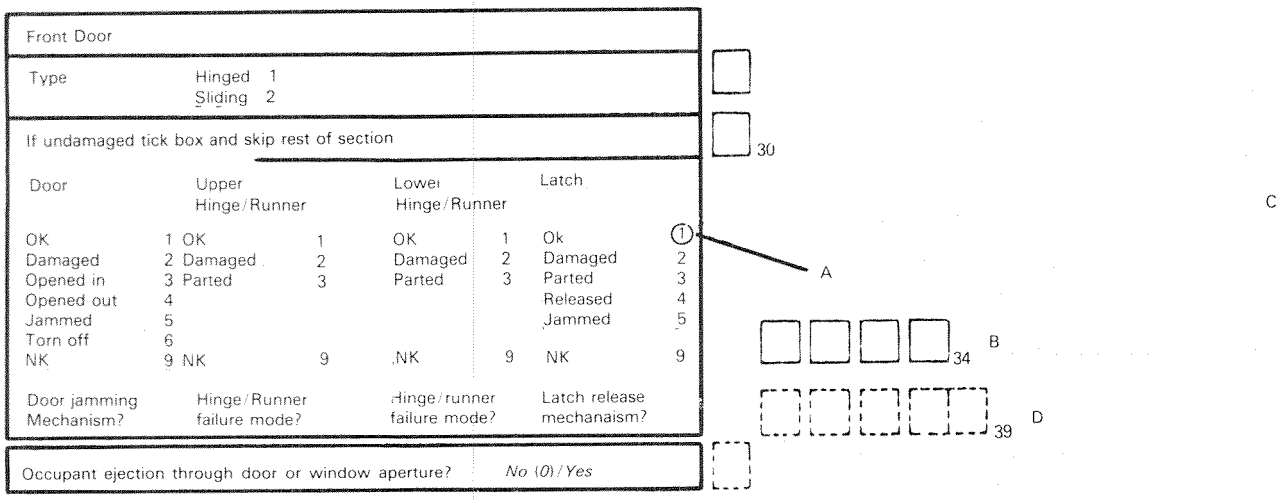

Figure 1. Extract from vehicle form

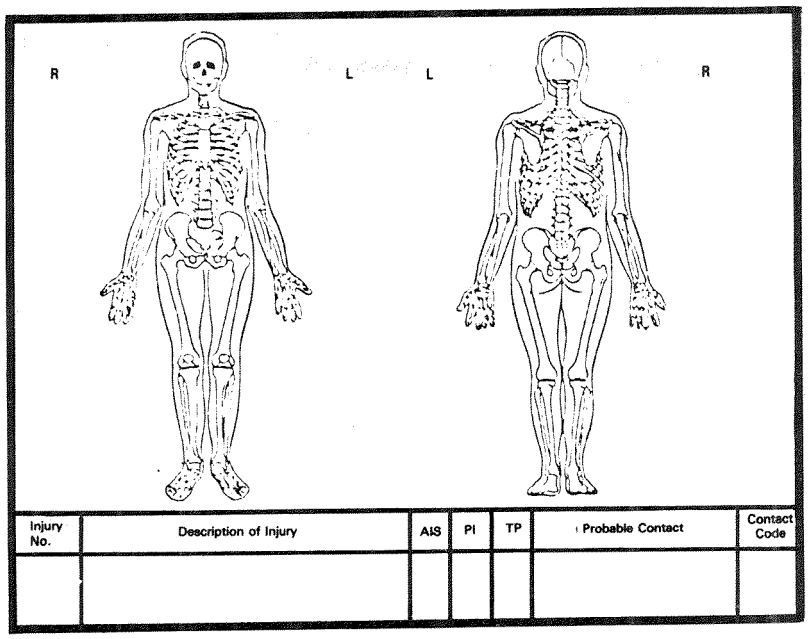

Figure 2. Extract from injury form

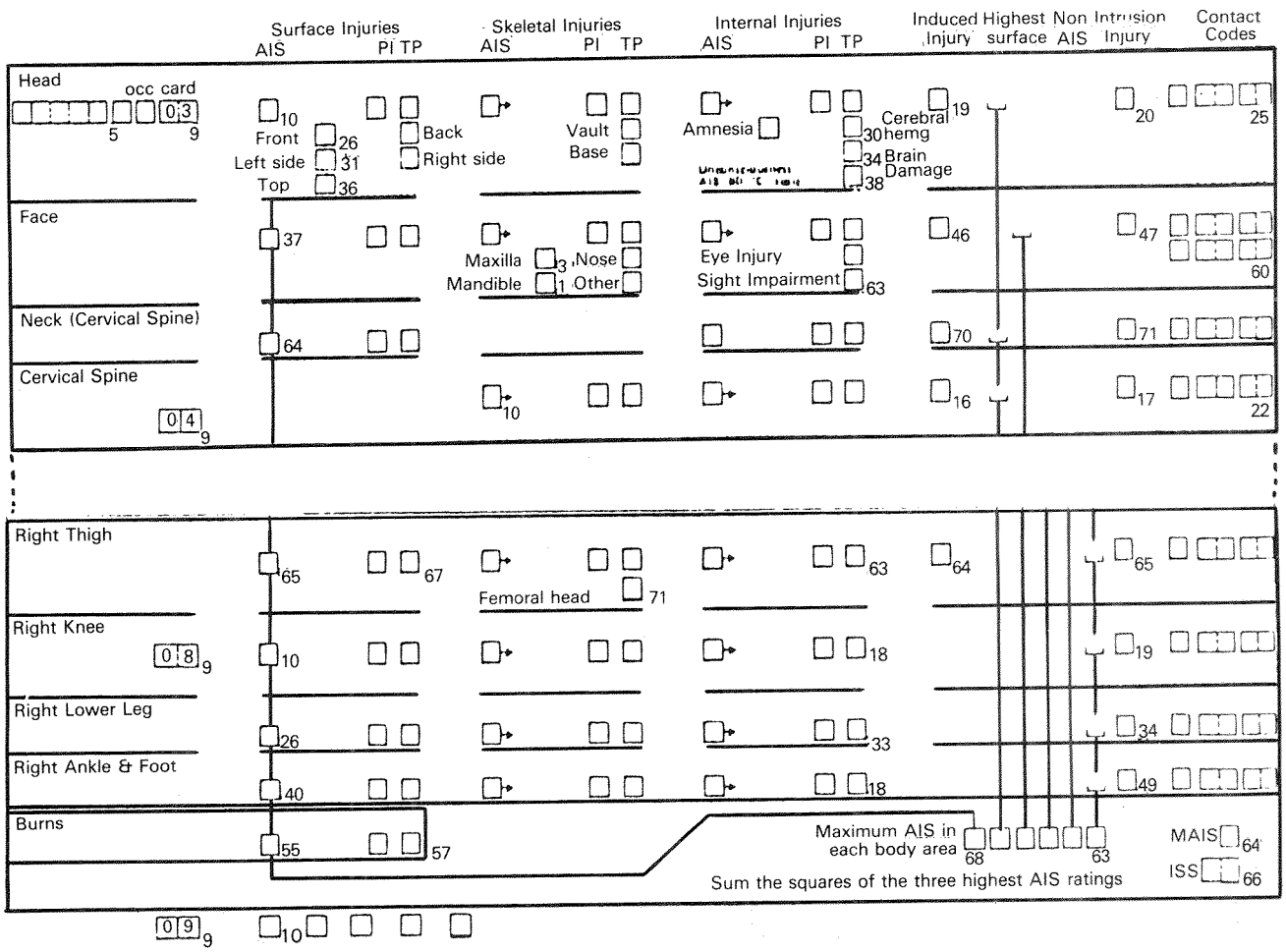

Figure 3. Extract from injury coding form

The data are organised in the computer data base such that all the coded variables are available for each vehicle and each occupant. Certain vehicle variables are also repeated and associated with the injury variables so the data for vehicles and occupants can be analysed together where appropriate.

Preliminary Findings

The study has been underway since 1983. The following preliminary findings are based on data collected by the ARU at the Institute for Consumer Ergonomics at Loughborough and the East Midlands traffic area (EMTA) team during the year 1984.

The accidents are sampled in such a way that the population comprises cars of all makes up to 5 years old involved in an accident in which the car is towed away. From this population, accidents are sampled for investigation in such a way as to include all cases in which an occupant is fatally injured, the majority of cases in which an occupant is seriously injured, and a proportional sample of accidents in which an occupant was slightly injured or not injured at all. To represent the occurrence of accidents generally, weighting factors are applied according to the sampling ratios employed in the accident case selection. Weighted data include injury accidents only, whereas the unweighted data include noninjury accidents that have been investigated.

Accidents

It can be seen from Table 1 that the ARU at Loughborough examined 261 accident cases in the year 1984. These accident cases comprised 297 case vehicles containing 506 occupants. There were on average 1.1 cars investigated per case containing on average two car occupants per case.

Table 1. The size of the data base.

Data Base	Unweighted	Weighted
Total no. of accidents	261	908
Total no. of cars	297	1,058
Total no. of occupants	506	2,558

The distribution of accidents by speed limit in Table 2 is bimodal with 29 percent of the accidents occurring in 30mph speed limits and 23 percent occurring in 60mph speed limits. The former result is not surprising as the greatest density of traffic is found in 30mph urban areas.

Table 2. The accident circumstances

Accident Circumstances		Unweighted freq.	Unweighted %	Weighted freq.	Weighted %
Speed limit mph	30	77	29	272	30
	40	12	5	13	1
	50	4	1	6	1
	60	59	23	250	28
	70	20	8	56	6
	Not known	89	34	312	34
	Total	261	100	908	100
Road class	Motorway	14	5	42	5
	A class	130	50	469	52
	B class	29	11	69	7
	Unclassified	54	21	194	21
	Private road	1	-[1]	2	-
	Not known	33	13	132	14
	Total	261	100	908	100
Time of day (hrs)	00.00-5.59	21	8	38	4
	06.00-11.59	57	22	238	26
	12.00-17.59	86	33	286	32
	18.00-23.59	90	34	318	35
	Not known	7	3	28	3
	Total	261	100	908	100

[1] Denotes percentage values less than 1.

However, the results showing a quarter of the accidents occurring in 60mph speed limits reflect the essentially rural nature of the Loughborough catchment area with more than twice the miles of road of the Birmingham catchment area. This is emphasised by the fact that half the accidents occurred on A-class roads (50 percent).

The majority of accidents occurred between 12 noon and midnight with 33 percent occurring between noon and 6 p.m. and 34 percent between 6 p.m. and midnight. Only 8 percent occurred in the early hours of the morning.

Table 3, a review of the vehicles that occur most frequently in the sample, shows that the Ford Cortina made up 41 of the 297 vehicles investigated during 1984. This was the most frequently occurring, followed by the Ford Escort Mark 3, of which 24 vehicles were included.

Table 3. The cars in the accident sample.

Make and Model of Vehicle	Unweighted freq.	%	Weighted freq.	%
Ford Cortina	41	13	152	17
Ford Escort 3	24	8	66	7
Vauxhall Cavalier 2	15	5	18	2
Ford Sierra	12	4	10	1
Austin Mini	12	4	33	4
Austin Metro	12	4	31	3
Vauxhall Cavalier 1	8	3	71	8
Ford Fiesta 1	7	2	25	3
BMW (all models)	6	2	11	1
Hillman Avenger 2	5	2	20	2
Vauxhall Astra	5	2	16	2
Audi 80	5	2	7	1
Volvo 240/260	5	2	11	1
Others	140	47	437	48
Total	297	100	908	100

This shows that in a sample of nearly 300 vehicles, very few occur in any reasonable numbers. The composition of the sample reflects the market share of each vehicle as well as the type of roads in the area, possibly indicating that the proportion of business cars in the sample is relatively high, travelling on main roads, with a low average number of occupants. Weighting the data makes a considerable difference in the ranking of vehicle type, causing the Vauxhall Cavalier 1 to appear second in the ranking.

Sixty-five percent of the vehicles involved in accidents in the sample experienced a single impact, as shown in Table 4. Twenty-nine percent experienced two impacts and only 5 percent more than two impacts. This may reflect the traffic density in the Loughborough sample as it is less likely that after an impact a vehicle will go on to strike anything else.

Table 5 shows that in 157 accidents (55 percent), the object struck in the most severe impact was another car. In 47 cases (17 percent), the object struck was an HGV/LGV or PSV, generally of considerably more mass than a car. In 54 cases (19 percent), an object other than another road user or vehicle was struck. These other objects included trees (3 percent), road furniture (4 percent), and a wall. In the second most severe impact,

Table 4. The total number of impacts seen by each case vehicle.

Total number of impacts	Unweighted freq.	%	Weighted freq.	%
1	197	67	701	66
2	84	28	328	31
3	15	5	29	3
Not known	1	-	-	-
Total	297	100	1,058	100

Table 5. The object struck on each impact.

Object Struck	Unweighted a) Most severe impact freq.	%	Unweighted b) 2nd most severe impact freq.	%	Weighted a) Most severe impact freq.	%	Weighted b) 2nd most severe impact freq.	%
Car	157	55	28	31	640	65	152	53
HGV/LGV/PSV	47	17	9	10	192	19	19	6
Rollover	15	5	14	16	43	4	46	16
Motorcycle & other vehicle	8	3	1	1	1	-	-	-
Other object	54	19	29	32	116	12	63	22
Not known	2	1	9	10	-	-	9	3
Total	283	100	90	100	992	100	289	100
Data missing	14		9		66		68	

Table 6. The part of the vehicle struck in the impact.

Struck Part of Vehicle	Unweighted a) Most severe impact freq.	%	b) 2nd most severe impact freq.	%	Weighted a) Most severe impact freq.	%	b) 2nd most severe impact freq.	%
Front	186	65	22	25	730	73	51	18
Right	34	12	28	32	99	10	105	36
Left	46	16	23	26	138	14	62	21
Back	10	3	10	11	6	-	60	21
Top	7	2	1	1	22	2	-	-
Unclassifiable	5	2	4	5	9	1	11	4
Total	288	100	88	100	1,004	100	289	100
Data missing	9				54		68	

the car was still most likely to strike another car (31 percent).

As indicated in Table 6, it is clear that frontal impacts were most common (63 percent) of the most severe impacts. Impacts on the right side were slightly more common for the second most severe impact. There is, however, very little difference between front and both side impacts for the second more severe impact. The main effect on impact type of weighting the data has been to increase the proportion of rear impacts in the second most severe impact.

As shown in Table 8 the proportion of persons fatally injured in each seating position was approximately the same (6 percent). The proportion of persons seriously injured in each seating position was similar (24 percent). Forty-seven percent of rear-seat passengers were slightly injured. The proportion of front-seat occupants, drivers, and passengers slightly injured was smaller (32 and 38 percent, respectively). This shows that the rear-seat occupants are more likely to receive injuries (77 percent) than the driver (61 percent) or the front-seat passenger (69 percent). The main difference is in the proportions slightly injured.

Occupants

The following tables provide information about the occupants, and the nature and causes of their injuries.

Table 7 shows that of the 506 occupants of vehicles investigated 293 (58 percent) were the drivers of the cars involved, 21 percent were front-seat passengers, and 20 percent were travelling in the rear seats. There are three less drivers than vehicles because some of the vehicles investigated were parked with occupants sitting in them.

Table 7. The seating position of occupants.

Seating position	Unweighted freq.	%	Weighted freq.	%
Drivers	293	58	1,402	55
Front seat passengers	107	21	571	22
Rear seat passengers	102	20	575	22
Not known/other	4	1	10	1
Total	506	100	2,558	100

Table 8. The distribution of injury severity [1] by seating position.

Seating position	Injury Severity: Fatal freq.	%	Serious freq.	%	Slight freq.	%	Noninjury freq.	%	Total
Driver	15	5	69	24	94	32	115	39	293
Front seat passenger	6	6	27	25	41	38	33	31	107
Rear	6	6	24	24	48	47	24	24	102
Not known/other	-	-	2	-	-	-	2		4
Total	27		122		183		174		506

[1] Injury severity in Tables 8 and 9 is based on the severity assigned by the police.

In Table 9, the distribution of injury severity for drivers in different age groups is shown. The drivers in the 1- to 19-year age group appear to be much more likely to be killed in this sample of accidents than drivers of other ages. Taking drivers of 29 years and younger, the table indicates they are more likely to receive injuries of all severities with only 21 percent uninjured. Because of the physical changes to the body associated with ageing, particularly in terms of bone structure, older drivers are generally more likely to be injured than younger drivers in an accident of similar severity. Taking the age group 50 years and over, 65 percent of the drivers received injuries compared with 35 percent of drivers age 30 to 49 years and 79 percent of drivers age 29 years and under. The majority of drivers in the sample (93 percent where the use of seatbelts could be established) were wearing seatbelts.

Causes of Injury

The causes of injury are established from a variety of sources including the evidence of occupant contact marks in the vehicle or elsewhere, from the nature of the injuries, and the likely injury mechanisms. Corroborative evidence may also be obtained from the occupants via the questionnaires.

In Tables 10 and 11, only the weighted data are presented so as to more effectively reflect the injury patterns occurring generally. The weighting takes account of the disproportional sampling procedures, which over-represent the serious and fatal injuries in the population.

Drivers' and Front-seat Passengers' Injuries

The injuries have been divided into minor (AIS 1) and nonminor (AIS 2 to 6) to highlight the differences in causes of injury. In most of the body areas, minor injuries (bruises and lacerations) are caused by objects that will give, such as seatbelt webbing, soft metal facias, and laminated windscreens. The nonminor injuries are caused by more solid objects such as the steering wheel, doors, or another vehicle. These injuries are often caused by an intruding contact—one of the main causes of nonminor leg injuries is an intruding footwell.

Many of the drivers' nonminor skull injuries are coded as noncontact. This is the movement of the brain within the skull due to the deceleration of the head, and is often an AIS 2 injury (loss of memory; a short period of unconciousness) that will result in a 1-night stay in a hospital.

Drivers received minor injuries (AIS 1) from seatbelt webbing and steering wheel and more severe (AIS 2 to 6) injuries from steering wheels, footwell intrusions, and a variety of other sources. Front-seat passengers also received minor injuries from their seatbelt webbing or from the facia. However, their more severe injuries often came from external objects such as the other vehicle, loose objects within the car, or footwell intrusion.

Only occupants known to have been wearing a seatbelt are included in Tables 10 and 11; other occupants were excluded, as the trajectories of unbelted occupants are quite different, resulting in different injury sources.

Vehicles

The vehicles involved in the accidents are examined in detail by the teams, and data on the performance of vehicle components are recorded. The following tables indicate how certain vehicle features performed.

Windscreens

As shown in Table 12, 31 percent of the vehicles in the sample had toughened windscreens and 61 percent had laminated windscreens. In 22 cases, it was not possible to establish the type of windscreen. The proportion of cars with laminated windscreens increases with later models.

Table 9. The age and injury severity of drivers.

Age (years)	Severity of Injury								Total
	Fatal freq.	%	Serious freq.	%	Slight freq.	%	Non-injury freq.	%	
17-19	4	17	7	30	9	39	3	13	23
20-29	4	5	22	29	31	41	18	24	75
30-39	4	8	13	21	20	33	24	39	61
40-49	1	3	9	29	9	29	12	39	31
50-59	0	-	10	29	9	26	15	44	34
60-69	2	12	7	41	5	29	3	18	17
70 and over	0	-	1	25	2	50	1	25	4
Not known	0	-	0	-	9	24	28	76	37
Total	15	5	69	24	94	33	104	37	282
Missing data									11

Table 10. The drivers—the main causes of injury.

Body region (1)	Injury severity (2)	Frequency of injury	Main causes of injury (frequency)
Skull	minor	55	Roof (19)
	nonminor	143	noncontact injury (42)
			Laminated windscreen (16)
			A-pillar (12)
Chest	minor	221	Seatbelt webbing (164)
			Steering wheel (93)
	nonminor	93	Door (22)
			Steering wheel (16)
Abdomen & Pelvis	minor	153	Seatbelt webbing (90)
			Door (18)
	nonminor	23	Steering wheel (7)
			Door (16)
Arms	minor	159	Knobs & switches (32)
			Steering wheel (18)
			Flying glass (18)
	nonminor	23	Facia (7)
			A-pillar (5)
Legs	minor	258	Facia (170)
			Steering column
			Cladding (57)
	nonminor	74	Footwell intrusion (96)
			Facia (70)
			Pedals & bracketry (17)

(1) Surface, skeletal and internal injuries have been combined. Face and neck injuries are not included in any of the table as there is an error in a computer program which would give rise to misleading results.

(2) Minor = AIS 1, Nonminor = AIS 2-6

Table 11. The front seat passengers—the main causes of injury.

Body region	Injury severity	Frequency of injury	Main causes of injury (frequency)
Skull	minor	10	Windscreen (3)
	nonminor	34	Side window glass (9)
			Other vehicle (9)
Chest	minor	95	Seatbelt webbing (77)
	nonminor	17	Other occupant (3)
			Other external object (3)
Abdomen & Pelvis	minor	64	Seatbelt webbing (58)
	nonminor	17	Door (9)
			Other vehicle (9)
Arms	minor	100	Side window glass (17)
			Door (12)
	nonminor	18	Loose object (8)
Legs	minor	92	Facia (44)
	nonminor	8	Footwell intrusion (7)

Table 12. Causes of windscreen breaks.

State of windscreen	Type of windscreen				
	Toughened		Laminated		Total
	freq.	%	freq.	%	
Broken	35	41	99	56	134
Cause of break:					
Occupant	2	6	9	9	11
Frame distortion	14	40	54	55	68
Other vehicle	3	9	6	6	9
Other intruding object	4	11	10	10	14
Internal object	0	0	1	1	1
Other	0	0	2	2	2
Not known	12	34	17	17	29
Not Broken	51	58	79	45	130
Not Known	-	-	-	-	22
Total	86		178		286
Data missing					11

Laminated windscreens are more likely to be broken than toughened windscreens. The majority of windscreen breaks to both toughened (41 percent) and laminated (56 percent) glass were caused by distortion of the frame. The next most common cause of break to both types of windscreen was an intruding object that was not the other vehicle. The former accounted for 11 percent of toughened screen breakages and 10 percent of laminated screen breakages. The latter accounted for only 9 percent and 6 percent, respectively. In only 2 cases did the occupant cause the windscreen break to toughened glass and in 9 cases for laminated glass. Occupant contacts on windscreens were noted in 27 cases and, in a further 50 cases, occupant contact was suspected but not established. Of these 27 cases, 16 of the contacts were onto a broken screen and 7 onto an unbroken screen. In 4 cases, the state of the windscreen at the time of contact was not known.

Hatchback/Estates

Damage to the tailgate is a fairly frequent occurrence—20 percent of the sample of 149 hatchbacks and estates had some damage to the tailgate. Approximately one-third of those that sustained damage opened in the accident. This can lead to ejection of any unrestrained occupants. There are several different modes of door opening—bodyshell distortion leading to misalignment of latches, latch overload, and component failures. Of these, bodyshell distortion was the most common method, accounting for five of the nine openings. Two rear-seat occupants were suspected of being ejected through an open tailgate. Five rear-seat occupants were ejected through the rear glass area. The rear-seat occupants were not using seatbelts.

Side Doors

Out of 297 vehicles, almost half had damage to the driver's door. Sixty-nine of the 140 damaged doors were jammed, 39 of these by compression of the door aperture. This reflects the predominance of frontal impacts in the sample. Twenty-two drivers were trapped in the vehicle by door jamming. Side doors opening during the accident is less frequent than tailgate opening on hatchbacks and estates, as might be expected, as side doors are fitted with antiburst locks, whereas only a few vehicle models have antiburst locks on tailgates. External crush causing linkage activation was the most common reason for doors opening.

Front passenger doors showed a similar pattern to drivers' doors, though rather more were totally undamaged (64 percent). This is consistent with the fact that more of the frontal impacts were offset toward the right than the left. Again, jamming was fairly frequent, and opening uncommon. Seven front left-seat occupants were trapped by door jamming.

There were 140 cars with rear side doors. More than half the rear doors were damaged, but there was no difference between the proportions damaged on the rear right (34 percent) and the rear left (35 percent) doors. Of those doors that were damaged, 24 percent were jammed by compression, with no difference between left and right sides. Eight occupants in rear seats were trapped by door jamming. Four occupants were ejected through an open side door, and these were all unrestrained rear-seat occupants. A further five occupants were partially ejected through a side window.

Seats

Of all front seats, 64 percent were fixed (i.e., did not tip forward to allow passengers into the rear), 24 percent had hinged backs, and only in 11 percent of cases did the whole seat tip forward (base-hinged). Nine out of 104 of the seat back hinge types and 7 out of 54 of the seat base hinge types failed. The most common cause was misalignment of components for the seat back hinge, and catch overload for the base hinge. If the antitilt lock did fail, there nearly always appeared to be the potential for extra loading being transmitted to the seat occupant.

Four cars had no rear seats, 137 (46 percent) had fixed seats, 102 (35 percent) had a folding single seat, and 52 (18 percent) had divided seats where one section could be folded and the other remain upright. Of the folding seats, there were 24 cases of latches releasing (out of 308 latches). Nearly all of these occurred on the single folding seats—only 5 released on divided folding seats. The explanation may be that the divided seats will distort on their inboard edge, thus dissipating loads, whereas the single folding seat is forced to take most of the weight of any loading on its latches. The most common cause of

latch failure is misalignment of the two parts of the latch (10 cases). There were 6 cases where both seat latches released, effectively leaving no restraint for any loads in the rear of the car. In the cases where the latches released, there appeared to be the potential for loading to be transmitted to any seat occupant in approximately half the cases. However, there were only three occupants in a rear seat when a latch failed—these people all sustained extra loading. None of these occupants were in a seat where both latches failed.

The questionnaires completed by the vehicle occupants provided information on the materials carried in the luggage compartments. Some of the items could seriously increase the loading on the seat backs and the seat occupants. Examples of the loads carried in a luggage compartment are advertising materials in boxes, tools and a tool box, suitcase, spare wheel, computer accessories, and a car gearbox.

Conclusion

The purpose of this paper has been to provide an overview of a major study of the causes of injury to car occupants currently underway in Britain. The establishment of a high-quality, reliable, and strictly sampled data base has been a very extensive exercise. It involves the cooperation of a large number of people outside the Accident Research Units: hospital consultants, coroners, police officers, recovery garage owners, and many more. It is important, therefore, that the data obtained in this study are consistently collected by the accident investigators, that the data from the two units are compatible, and that the computer programs are reliable.

This paper has described the organisation of the study and the ways in which data on vehicles and occupants are collected, recorded, and analysed. The data presented as examples of the preliminary findings are based on a single year, 1984, the first full calender year of the study in which both teams were investigating accidents. The data are presented to indicate the sort of information available from the study and the ways in which it can be used. The variety of vehicle makes and models found in a sample of nearly 300 means that very few vehicles are represented in any quantity. Only one vehicle occurred more frequently than 10 percent. This makes detailed analysis difficult due to the small numbers involved. Most vehicles saw only one impact, and most impacts were frontal and with another car. Rear-seat occupants are more likely to receive injuries than front-seat occupants. The majority of front-seat occupants were using seatbelts (93 percent); the majority of rear-seat occupants were not. The majority of minor injuries (AIS 1) to belted front-seat occupants were bruising from seatbelt webbing or from contact with the steering wheel (drivers). The steering wheel also caused more serious injuries (AIS 2 to 6) to drivers. The more serious injuries to front-seat passengers often came from external objects such as the other vehicle. With regard to vehicle components, damage to the tailgate of hatchbacks and estates was fairly frequent. Approximately one-third of those that sustained damage opened in the accident, usually due to compression of the door aperture. Four occupants were ejected through an open side door, and these were all unrestrained rear-seat occupants. In the future, further detailed analysis will be made on the increasing data base. The general crashworthiness of vehicles and the detailed performance of specific components will be studied. The specific causes of injury will be investigated, and the relative frequencies of different crash types and injuries will be documented. One of the first detailed analyses is the examination of seatbelt effectiveness in reducing injury to front-seat occupants. This is reported by Dr. S.J. Ashton et al., at this Conference.

Acknowledgments

In a study such as this, which relies on the cooperation of many different organisations and individuals, there are many people to acknowledge. The authors would like to thank all those who have made this work possible. In particular, they would like to thank:

1. The sponsoring consortium for their financial support and their representatives for their advice and guidance. They are: Department of Transport VSE and VI, TRRL, Ford, and BL Technology who coordinate Austin Rover Group, Freight Rover, Land Rover, Leyland vehicles, and Jaguar cars.
2. The Chief Constables and their officers in the study areas for their cooperation.
3. The consultants and other staff at all the hospitals in the study areas for their assistance.
4. The coroners in the study areas for their cooperation.
5. The Department of Transport vehicle examiners in the West and East Midlands, Northern and Western traffic areas of the Department of Transport.
6. The staff of the two Accident Research Units:

at ICE, Loughborough	Birmingham University
Geoff Hedges	Stephen Jowett
Ann Marshall	Andy Parkes
Abayomi Otobushin	Michael Twiss
Nigel Robertson	Meryl Knight
Carl Sutton	Wendy Phipps
Mo Symes	Colin Smith
Pete Thomas	Duncan Lander

References

1. D.S.I.R., "Research on road safety," H.M.S.O., London, pp. 464-477, 1963.
2. Mackay, G.M., "Some features of traffic accidents," *Brit. Med. J.*, Vol. 4, pp. 799-801, December 1969.
3. N.A.T.O., Proceedings of a Conference on Accident Investigation, Committee on the Challenges of Modern Society, Brussels, June 1973.

4. Robertson, J.S., A.J. Mclean, and G.A. Ryan, "Traffic accidents in Adelaide," Australian Road Research Board, Kew, Victoria, Special Report No. 1, July 1966.
5. Mackay, G.M., and S.J. Ashton, "Injuries in collisions involving small cars in Europe," SAE Transactions, Paper 730284, SAE, New York, 1973.
6. Hartmann, F., C. Henry, and C. Tarriere, "Respective effects of Delta V, mean gamma and intrusion on the severity of injuries," Proceedings Sixth International Technical Conference on Experimental Safety Vehicles, National Highway Traffic Safety Administration, Washington, D.C., pp. 574-579, October 1976.
7. AAAM, "The abbreviated injury scale—1980 version," American Association for Automotive Medicine, Arlington Heights, 1980.
8. Mackay, G.M., M.D. Galer, S.J. Ashton, and P.D. Thomas, "The methodology of in-depth car crashes in Britain," SAE Paper 850856, 1985.

Large Scale Data Collection Systems—The NASS Experience

Franklin G. Richardson and
Frances Bents Costello
National Center for Statistics and Analysis, National Highway Traffic Safety Administration

Abstract

The National Accident Sampling System (NASS) has grown from a pilot data collection system with 10 teams in 1978 to the current system of 50 teams using over 130 accident data researchers in 27 States. At the end of 1984, there were over 45,000 cases in the NASS files with each case including approximately 400 different data elements. This large system with widely separated collection sites requires that each team use specific operational procedures to assure the consistency, uniformity, and reliability of data. The overall goals of NASS are to create and maintain a network of collection teams that use specific operational procedures to assure consistency, validity, and reliability of the resultant data file. Since NASS attempts to serve statistical and clinical needs, both creativity and compromise have been employed in developing the field capabilities and in maintaining the system so that useful data are acquired. It is important for the users of any data file to be aware of the definitions and limitations of the data, but it is especially important in a system such as NASS where such a large amount of data is gathered and the collection occurs at such widely separated locations under varying local conditions and regulations. Current procedures for the selection of cases, collection of data, and quality control are described. Sampling revisions that will be introduced in 1985 to enhance the file usefulness and significant field operational changes are also discussed. The paper concludes with the argument that NASS, or any similar system, must be concerned as much with the qualifications, training, and motivation of field personnel as with statistical design.

Introduction

The National Accident Sampling System (NASS) was established by the U.S. Department of Transportation in 1978. It was designed to produce nationally representative estimates of the highway accident toll to provide a detailed accident data base that could be used to identify significant safety problems, to detect trends, and to evaluate motor vehicle safety countermeasures(1). Beginning with a pilot effort at 10 data collection sites, NASS increased the number of teams annually. By mid-1982, it had reached its current complement of 50 Primary Sampling Units (PSU's) in 27 States that produce data on 12,000 highway accidents each year. At the end of 1984, there were over 45,000 cases on the file. The NASS teams gather about 400 data items on accidents of every type (pedestrian, motorcycle, light truck and van, heavy truck, and passenger car) and on accidents of every severity (nontow property damage only, minor, moderate, and serious injury, and fatal).

The establishment of a multitier data collection and quality review system requires expertise in the subject area of interest; equally important are skills in planning, coordination, task identification, negotiation, and management. The administrative challenges are often greater than the technical difficulties that must be mastered to create and maintain a smoothly operating system. This paper examines some issues that the field operations staff considered in establishing, operating, and maintaining the NASS data collection system. Part of the discussion is specific to the accident investigation field, while much of it can be applied to any data collection effort.

Case Selection Procedures

An important first step in any data gathering scheme is to define what you want to examine. NASS begins by selecting as its universe all accidents that are reported to the police as documented on Police Accident Reports

(PAR's) and are submitted to the individual State traffic records agencies. Immediately this leads to an underrepresentation of very minor accidents that are: (1) never reported to police, or (2) are not subject to inclusion in State files. Statistically, these minor accidents are addressed outside of NASS and are of little general interest to clinical users(2).

Since PAR's from almost all jurisdictions include vehicle type and some measure of injury severity, it is feasible to stratify accidents in NASS with this information. Accidents are classified in a hierarchy of 22 strata that begin with the more rare accident types of pedestrian, motorcycle, and truck accidents and end with automobiles and all others. As a second stratification, the recorded injury severity is adapted from the various police codes. Experience has shown there is some over- or undergrading of injuries in this process, which will be discussed later, but the stratification system generally is useful in allowing statisticians to select a greater proportion of serious accidents. If such weighting schemes were not applied, the bulk of the NASS file would consist of very minor accidents. This would be satisfactory for national estimates but of little use to engineers responsible for improving vehicle crashworthiness and reducing occupant injuries. This hierarchical approach will be modified with the introduction of revised sampling procedures described later.

NASS teams record all accidents reported by designated police jurisdictions, either two or three times each week, and then execute a PSU-unique sampling algorithm that selects the specific cases to be investigated in that PSU for that day. There was uncertainty during the initial planning about the effectiveness of small team sizes and the ability of two or three investigators to manage a variable workload of cases, so each investigator is assigned a fixed caseload of two accidents per week. The fixed workload lends itself well to program planning and management. It creates difficulties for statisticians, however, when, for example, one motorcycle accident holds a case selection weight of 20 while a similar accident in the same site on a different day holds a selection weight of 360. Consistency in case selection is an important operational achievement.

Staff

The next major protocol is concerned with staff selection. In establishing NASS, it was decided data would be collected through contracts with firms that would hire technician-level staff who are trained and directed by NHTSA. Prior to NASS, contracts were awarded to those few organizations that had developed their own style of expertise in accident investigation. The NASS design required almost 200 investigators collecting data in precisely the same way. Significant attention during the pilot study was devoted to determining whether individuals who often had no related experience or expertise in accident research could be trained to become proficient in standardized data gathering methods. Experience has shown that about 6 months of formal training and careful oversight are required to train a novice. Training remains a key element in field operations.

A second level of expertise was established called Zone Centers. The Zone Centers consist of groups of several highly experienced accident researchers who not only assist in developing standardized protocol but provide all technical oversight and quality review to the data collection teams. These mid-level managers have been critical to the success of NASS through their involvement in training PSU investigators and in reviewing, monitoring, and controlling the information that becomes the data files.

Data Collection

Once the sample of police-reported accidents is selected, it becomes necessary to describe the various data gathered from numerous reports and field inspections in a consistent way. NASS uses a set of standard reporting forms that are modified every 2 to 3 years. The 400 data elements are arrayed according to the following scheme:

- Accident
- Pedestrian/Nonmotorist
- Vehicle
- Driver
- Occupant

The Accident Form is used to collect data on the first harmful event, ambient conditions, and case administrative information. The Vehicle Form guides the data collector in gathering specific vehicle information, and one form is completed for each involved vehicle. Separate forms are used for towaway or nontowaway vehicles. Included are vehicle make/model descriptions, some vehicle component conditions (e.g., tire condition), Collision Deformation Classification (CDC)(3), and Truck Deformation Classification (TDC)(4), and such postcrash data as the amount of intrusion, the amount of exterior crush, and steering column performance. Similarly, the Driver Form is used to acquire specific data on the driver's education and training, precrash maneuvers (if any), license status, alcohol involvement, and traffic violations. One form is completed for each involved driver, which permits the coding of any environmental data unique to the involved vehicles (roadway characteristics). The Pedestrian/Nonmotorist Form and the Occupant Form are identical in the nature and extent of injury information recorded, but the Pedestrian Form includes data on location and activity while the Occupant Form has provision for seating location and restraint type and use. NASS also uses special forms for CRASH III(5) reconstructions and schematics of scene data.

To make data collection consistent across all 50 collection sites, extensive documentation has been employed. The five basic data forms are accompanied by

a Coding and Editing Manual that currently includes a total of 780 pages of specific coding instructions. The Collision Deformation Classification (CDC), Abbreviated Injury Scale (AIS)(6), and Injury Severity Score (ISS)(7) systems have been incorporated. This extreme level of specificity is crucial for clinical use of the data. When field personnel enter data onto the Master File, there are 800 automated range and consistency checks applied to every NASS case before the data are accepted. These checks are identical to coding manual instructions and supplement Zone Center review by assuring that incorrect key strokes or out-of-range entries are flagged and corrected.

Other data collection aids are available and used. Most rural PSU's use a scene inspection jig that can be adjusted to simulate the wheelbase of vehicles and can be used to trace postcrash trajectories. In 1984, we also introduced the vehicle contour gauge, which not only facilitates taking crush measurements on passenger cars but also assists case review staff and data users in assessing vehicle damage.

Consistency of technique is further reinforced in NASS through training. In NASS, all investigators undergo up to 10 weeks of intensive training, which includes self-paced audiovisual modules, classroom training, and on-the-job supervision. This is followed by about 6 months of careful oversight by Zone Center staff. Even though we consider NASS to be technician level data, investigators still generally cannot assimilate the wide variety of data taking procedures for many months.

Limitations of Procedures

The use of these standardized procedures has both benefits and costs. They clearly contribute to the uniformity and reliability of data encoding. At the same time, unusual circumstances (which are very common in this field) can be difficult to categorize according to convention. When this occurs, data can be "force fit" into a specific coding attribute or a default to "other" or "unknown" codes can be used. Either way, the clinical user of the file may find it impossible to locate the specific accident circumstance that is of interest if he relies solely on the automated files for his information. Because of this, both automated files and the individual case reports are routinely reproduced and made available to users.

A good example of the difficulties encountered in standardization is the categorization of accidents into strata for case selection. This classification is based on police-reported information, but, unfortunately, the States do not all use a uniform code. Overall, NASS teams class about 28 percent of police-reported injuries as serious or incapacitating. There is a wide variation among States, however. Alabama, where two PSU's operate, instructs the police to class accidents at this severity level if the injured person is "carried from the scene." This means that in any accident when one occupant is transported to a medical facility, regardless of the true severity of the injury, the accident is classified as serious. As a result, 48.6 percent of the accidents in Alabama are initially classified as serious. At the other extreme, Pennsylvania, where six PSU's operate, classes injury severity as major, moderate, or minor, adds the type of apparent injury such as amputation, broken bones, concussion, burns, etc., and from this additional description the field investigator must determine the injury severity. In this State, only 4.1 percent of the accidents are initially classified as resulting in a serious or incapacitating injury. The practical effect is that a large number of cases in Alabama are selected for investigation as serious injury cases when in fact they are not, while in Pennsylvania teams are failing to select as many cases with serious injury because they are grouped together with a large number of truly minor injury cases. Under the present circumstances then, national estimates of injury severity based upon initial classification may be skewed, but individual case files are rich with injury data for the clinical users. Changes in case stratification are being studied that would go beyond the initial police-reported severity in these two States to make the initial injury severity classification. This improvement will serve both statistical and clinical users.

A second problem is the limitation that must be placed on data collection so files can be produced. Because of the sampling scheme employed, an accident is not selected for investigation until it is 3 to 4 days old. Given this late start, it is imperative the researchers locate and measure scene data and vehicle damage as quickly as possible before vehicles are repaired and scene evidence is scattered. These data must be gathered within 2 days of case selection. Likewise, drivers and occupants must be interviewed within 4 days so recollections are altered as little as possible. Researchers must also request and encode medical records, driver and vehicle registration information, and, when possible, execute a CRASH III reconstruction. All the above activities are scheduled to be completed and case data are to be entered onto the microcomputer data entry system within 2 weeks of case selection. Then the cases are to be submitted to the appropriate Zone Center for review no later than 35 days after selection. These deadlines guarantee that the data flow, from collection through quality review and to final file, occurs smoothly and rapidly. This allows the publication of statistical reports within a few months of accident occurrence. These deadlines also result in some loss of data, particularly in fatal accidents. The NASS system underreports fatalities because cases are selected based on police reports and are therefore limited to those fatalities that occur almost immediately after an accident. A small number of longer term fatal injuries are drawn from cases initially listed as involving serious injuries. The Fatal Accident Reporting System (FARS)(8) provides

a precise count of traffic fatalities that occur within 30 days of an accident and is a valuable complement to NASS.

The loss of medical data is accommodated somewhat through the use of an update protocol. Under this scheme, the completed portion of the case investigation must be submitted to the Zone Center according to the 35-day schedule. A notation is made that additional medical data will be forthcoming. The team then has 90 days to obtain copies of hospital emergency room reports and discharge summaries. When received, the medical information is encoded on update forms and submitted to the Zone Center, which appends the original case file, conducts a quality review, and approves the case for inclusion on the Master File.

Scheduling also creates challenges in the collection of data from the vehicle inspection. The interval between accident occurrence and case selection allows 4 days in which vehicles can be towed, transferred, and repaired. For truck tractor-trailer combinations, the vehicles are generally drivable and have left the study area. The data completion rates for truck inspections are often low compared to an overall vehicle inspection rate of about 75 percent.

Protocol Changes

It is important to understand the capabilities of the data collection system and concentrate on those things that are achievable. NASS data collection activities have been limited to those areas that lend themselves to objective measurements. It is impossible to insure consistent data collection methods if the coding is left to an investigator's judgment.

Most NASS data collection at the present time is focused on vehicle crashworthiness, i.e., extent of vehicle damage and resultant injuries. There are major reasons for this. First, NHTSA applies much of its resources to vehicle safety design and countermeasures. Second, the state-of-the-art in accident investigation is most advanced in the areas of damage measurement and reconstruction. Finally, given the importance of standardization and consistency, NASS can most effectively produce documentation of physical, measurable, and verifiable data sources. Several hundred researchers have been successfully trained to measure roadway dimensions and vehicle damage, and to report injury severity in the same consistent manner. Areas such as human factors and accident causation, which rely on extensive data interpretation and judgment by trained experts to reach conclusions that may not be otherwise substantiated, have been avoided.

It is difficult to make valid assessments of pre- or at-crash conditions. For instance, during the extrication of entrapped occupants, towing of the vehicles, or even handling at the crashed vehicle repair or impoundment facility, major modifications can occur to the vehicle crush profile, tire and wheel condition, restraint condition, etc. Because of the difficulties engendered in assessments of this kind, NASS has chosen to focus its resources on those data elements of major concern such as restraint use and vehicle damage. Extensive training is conducted to show how seatbelt webbing can be used to detect belt use and the differences between door beam crash damage and distortion of the door from emergency extrication tools. Some areas such as tire condition and performance would require a substantial commitment to extensive data collection if meaningful conclusions are to be reached. The perceived need for tire data is small at this time, however, so NASS has avoided both a major commitment to collecting tire data and the seduction of doing more limited data collection, which is easy but inconclusive.

In recent years, a beginning has been made in collecting precrash data by coding driver-related factors such as erratic driving or improper, if not illegal, actions. In 1985, the CALAX(9) system, which describes preimpact locations and actions, for one or two vehicles, was incorporated into NASS. These first attempts at encoding accident-related factors are the subject of considerable dispute at the quality review level because there is little substantive information such as measurements or slides that can be used as verification. The activity is useful for analysts who are interested in precrash conditions and is contributing to advancements in field protocol.

Quality Control

Almost 20 percent of NASS resources are devoted to quality control. The technical experts at the four Zone Centers are tasked with responsibility for monitoring the development and performance of PSU staff, serving as accident investigation specialists, conducting periodic visits to all field sites, maintaining and upgrading all supporting documents, training, performing elaborate reviews of case materials, and creating and analyzing an automated file on every aspect of data quality. The NHTSA staff also performs independent spot checks of the analysis file, conducts site visits to PSU and Zone Center installations, and monitors myriad status reports produced by the field. Until very recently, the Zone Centers spent an average of 4 hours reviewing every variable of every case submitted by PSU's. This appears to be too large an effort. When NASS began, there was no comprehensive quality control plan to accompany the data collection scheme. Since NASS was the first to attempt to implement such a specialized major system, there was little direct experience on which to draw. The expertise available was in field investigation, not data management and review. The roles of the Zone Centers have remained critical to NASS success but have shifted greatly with time. Through trial and error, education,

and budget constraints, the approach to file building has changed to one seeking only excellence, not perfection. NHTSA is concentrating on improving the quality of work at the lowest common denominator by selecting and training new investigators more carefully and removing nonperformance from the system more quickly. Case review has been reduced until only a portion of cases completed by competent investigators are examined, freeing Zone Center staff to focus on weak performance areas. Further review of the quality control activities is planned. A group of NASS experts representing statistical design, analysis, and data collection is working with a quality control expert to further streamline the review activities while maintaining the high quality of the data file. This task will take several years to fully implement but is necessary to improve NASS performance as Federal dollars become more limited.

NASS Sampling Revisions

As the NASS system has become stabilized at the 50-team size and the process of data collection and file building has become more routine, attention has turned to ways to modify the system to better meet user needs as to the type and injury severity of accidents sampled. Earlier adjustments to the accident sampling procedure had been made in 1982 to provide an increased number of "heavy truck" accidents, and in 1982 and 1983 the percentage of heavy truck accidents was increased, although many of these were low-injury-severity accidents.

Beginning in 1984, the concern was to increase the proportion of cases with a higher injury severity. This was accomplished primarily by reducing the number of low-injury-severity heavy truck accidents. More recently, work has begun on examination of means to increase the proportion of high-injury-severity cases even further, and to combine this with changes that would improve the accuracy of the national estimates and simplify the case weights. Obviously, the original NASS statistical design approach and the current team locations impose limits on how much change is possible without a significant expenditure of funds. Four team locations, for example, produce police reports for less than 50 serious injury accidents in a year and about one-third of the locations have less than 150 police-reported serious accidents. These sites provide valuable data representative of very rural accidents but present unique problems to the sample and design staff.

Three aspects of this change are being planned. First, a change already implemented is the accomodation of field staff personnel shortages (caused by illness, lack of training, or resignation) by reducing the workload. Whereas previously, if a team was understaffed or undertrained, the number of cases to be investigated was reduced, the number of cases is now maintained but less information is collected on some accidents with less serious injuries. Since teams are understaffed or undertrained about 20 percent of the time, this change has been important in keeping the number of cases up and thus improving the case weighting.

The second major change planned is a change from a "constant caseload assignment" to a "variable caseload assignment." From its inception, NASS has assigned each investigator a fixed number of cases each week—nominally two. By changing to a variable caseload, the ability to sample a greater number of serious cases is increased (more cases will be sampled when serious injury accidents occur) and the variation in case weights will be reduced. Both statisticians and clinical users will benefit. The shift will require more aggressive field management and increased quality control because the workload is largely determined at the PSU level rather than being dictated by sampling protocol.

The third major change is a revision of the Police Report stratification from 24 to 5. Accidents are now stratified on both vehicle type (e.g., motorcycle, heavy truck, pedestrian) and on police-reported injury severity, combined with the reported transportation of injured persons to a medical facility. The revised stratification would be based only on the injury severity and whether any injured persons were transported to a hospital; accident type will not be considered.

The anticipated effect of these changes will be to increase the number of serious injury cases (AIS 3+) that are investigated. It is anticipated that about 3,000 serious injury cases will be acquired annually with this system as compared with the current 1,800 cases at that injury severity.

Remaining Challenges

Experience in building and refining the National Accident Sampling System has proven one thing—it can be done and done very well. The greatest resource and most formidable obstacle is people. From the beginning, NASS concentrated on elaborate statistical design, consistent field protocol, extensive documentation, and creative administrative control. What was largely overlooked was that the backbone of this system would really be a sizable group of reasonably qualified, modestly paid technicians who would become experts in a field with an uncertain career path, little recognition, and even less job security. The NASS investigator turnover rate is about 30 percent each year because of poor initial candidate screening, contractual recompetition, and movement to related career fields. Federal procurement guidelines do not equip NHTSA well in providing incentives, upward mobility, and job security, and yet these gains would provide NASS with a greater proportion of highly experienced researchers while reducing the data and dollars lost to attrition and retraining.

Consideration is being given to alternative ways of awarding contracts for multiple PSU's, extending the interval between contract awards, and promoting highway safety as a career to address this problem.

The solution to these "people" problems may well be the most creative element in NASS and the most valuable contribution to meeting NASS goals.

References

1. O'Day, James, "A proposed new national system for collecting multipurpose accident data: SIR," Proceedings Fifth International Technical Conference on Experimental Safety Vehicles, National Highway Traffic Safety Administration, U.S. Department of Transportation, London, England, June 1974.
2. Greenblatt, Janet, Mary Beth Merrin, David Morganstein, and Sanford Schwartz, NASS Non-reported Accident Survey, DOT-HS-806-198, National Highway Traffic Safety Administration, U.S. Department of Transportation, Washington, D.C., November 1981.
3. Society of Automotive Engineers, Standard J 224 Mar 80, Collision Deformation Classification.
4. Society of Automotive Engineers, Standard 1301, Truck Deformation Classification.
5. National Highway Traffic Safety Administration, Crash III User's Guide and Technical Manual, U.S. Department of Transportation, Washington, D.C., revised April 1982.
6. American Association for Automated Medicine, "The abbreviated injury scale," Morton Grove, Illinois, 1980.
7. Baker, S.P., and B. O'Neill, "The injury severity score: an update," *Journal of Trauma* 16: 882 885, 1976.
8. National Highway Traffic Safety Administration, "Fatal accident reporting system," Data Tapes for 1981-1984, U.S. Department of Transportation, Transportation Systems Center (DTS-32), Kendall Square, Cambridge, Massachusetts.
9. Terhune, Kenneth W., "CALAX: a collision taxonomy for research and traffic records," *Journal of Safety Research*, Vol. 14, pp. 13-20, 1983.

Five Years of New Car Assessment Program: Balance and Current Conclusions

J. Provensal,
F. Hartemann, and
C. Tarriere
Regie National des Usines Renault

Introduction

Over 6 years have elapsed since the inception of activities devoted to crashworthiness ratings in the United States. A large number of vehicles, covering virtually the entire fleet of representative American vehicles of the early 1980's, have been subjected to tests whose conditions were established concurrently with devising what was destined to become the New Car Assessment Program.

However, as work progressed, a major controversy arose over the validity of methods employed by the National Highway Traffic Safety Administration (NHTSA). This controversy has not ceased. Now that a second type of test—one involving a deformable mobile barrier—seems to be in process of evaluation, it is deemed timely to complete the data acquired so far, summarize the state of progress, and examine—even propose—the orientations anticipated for the future.

Choice of a Rating Method

In 1972, the Motor Vehicle Information and Cost Savings Act assigned to the Department of Transportation the mission of evaluating methods designed to yield a determination of the following vehicle characteristics:

- Damage susceptibility
- Degree of crashworthiness
- Ease of diagnosis and repair

In this text, "crashworthiness" was defined as the protection a passenger vehicle affords its passengers against personal injury or death as a result of a motor vehicle accident(1).

In 1978(2), NHTSA resumed its work devoted to establishing a rating system for application to automobiles. The discussion was already underway on the relative feasibility and advantages of methods of rating based on the following:

- Historical data collected from information on vehicles already in service
- Predictive data collected from evaluation tests and yielded by new vehicles for which there were no available results based on the experience of utilization

This alternative presumes a choice that is not easy to make. In fact, if one does not generally contest an

indicator or a criterion based on the careful processing of statistical data, it can be assumed—in the particular case of automobiles where the rate of launching of new models is high—the time required for establishing such an indicator would make this indicator unusable in actual practice, since the model to which it was to apply would no longer be on the market by the time the indicator was available.

Conversely, a predictive method can supply the market with an indicator available immediately, concurrently with the release of a new model onto the market; however, it is vital to make sure, beforehand, that it is feasible and actually yields valid results corresponding to a vehicle's performance.

This fundamental point had not eluded the attention of NHTSA, which, in 1976, had reduced its research devoted to the development of a predictive method for crashworthiness, deeming the feasibility of such a method was mediocre at that time(2).

After examining various data bases (police reports, accident records compiled by insurance companies, and the accidentological data banks of NHTSA (NCSS, NASS, and FARS), NHTSA concluded that "specific make and model crashworthiness comparisons isolating the effects of the vehicle are not yet feasible from historic data files..."(2), and undertook a testing program aimed at developing a predictive method.

The testing work, based on 1979 model vehicles, consisted of subjecting these vehicles to impact tests under the conditions listed in FMVSS 208, 212, 219, and 301; one major difference was in the choice of impact velocity, which was fixed at 35mph, i.e., 5mi faster than the speed normally used for the aforesaid standards.

It is not without interest to recall and comment on the requirements compiled by NHTSA, which had formed the basis for the choice. These were contained in four points summarized as follows(2):

1. The system must supply the data sufficiently ahead of time before the market release of a given new model.
2. The results yielded by the predictive method must be readily accessible and usable by consumers.
3. The cost of obtaining data must be reasonable.
4. The test procedure must be repeatable and objective, capable of distinguishing significant differences in the safety performance of the cars, and carefully developed after wide review by the scientific and technical community.

This list of requirements shows the omission of a basic point that, in our opinion, should have been listed as the first entry in the conditions to be met by a predictive rating system.

The system of rating must accurately take into account the possible differences in behavior regarding the passive safety of the vehicles, this behavior being evaluated on the basis of historical data collected from, for example, accident investigation reports.

This requirement was in no way contested, either by the individuals who took part in the discussion from its outset(3,4) or by NHTSA itself(2,5). Finally, setting up a predictive rating method and a historical rating method in competition with each other implicitly amounts to acknowledging that the aim is to provide an accurate representation of the vehicles' real performances with regard to passive safety.

After 6 years of tests systematically performed by NHTSA on new models, a certain amount of data has been acquired and a few attempts have been devoted to correlating real-world accident data with the results of the predictive method. This paper summarizes the situation to date.

Global Statistical Approaches

Two global statistical approaches were made prior to NHTSA's deciding on its choice of predictive method(2). In fact, these approaches had been requested by the latter to evaluate the feasibility of a rating by a historical method. In 1980, Friedman(6) concluded, after a study of FARS data, "it is clear from the FARS data results that notable differences in fatality rates exist across make-models groups, while the analysis which controls for the crash severity (ΔV) shows little or no differences." This clearly shows that the differences between vehicles, all impact conditions combined, are due to the influence of the mass of the aforesaid vehicles; once the data are grouped on the basis of equivalent conditions of impact, i.e., of fixed speed variations, the differences shown by the FARS data are insignificant.

Similarly, after examining the data in police files and in FARS and NASS records, Carlson(7) stated: "...we conclude either that the present statistical techniques are not sensitive enough or that in general the overall injury severity differences between makes and models—except those differences associated with vehicle size—are very small. This result should not be ignored by NHTSA as it proceeds with its overall crashworthiness rating development."

The initial evaluations based on accidentological findings were hence negative and, logically, they should have led to the discontinuation of the investigation of a predictive method whose most foreseeable result was the absence of the detection of any difference whatsoever.

Actually, at that point, NHTSA's procedure was the complete reverse: "The principal goal (of the test program) was to determine if automobiles of similar mass exhibited significant performance differences..." and "if the data (of the test program) revealed significant differences in the performance of cars...a good basis to proceed with a permanent program would exist."(2)

The discontinuation, in 1982, of tests performed at 35mph against oblique barriers (30° angle) also illustrated this determination to use only a test that would reveal "significant differences." In fact, examination of the findings yielded after six oblique barrier impact tests performed in 1981 shows that the thoracic criteria (for both passengers and drivers) remained in the range of from 31 to 50g/3ms, and, most importantly, that, for the six vehicles involved, the head criterion remained below 1,032. Therefore, no further action was devoted to this test, preference being given to the tests performed against orthogonal barriers, and even if:

1. The conclusions of these tests were in agreement with the results anticipated obtained on the basis of the initial examinations of the accidentological investigations, i.e., the absence of significant differences between vehicles.
2. It was recognized that the most frequently occurring configuration of frontal impact in real-world accidents is distinctly more to be assimilated with impacts against oblique barriers (involving only part of the vehicle's front surface) than with impacts against orthogonal barriers. This is shown in Figure 1, which represents cases of frontal accidents sustained by Renault 5 cars recorded in the A.P.R. survey to date. References (8) and (9) are also clear in this respect.

In light of the initial investigations and in pace with the accumulation of NCAP data, six reports (10, 11, 12, 13, 14, 15) were published; they endeavor to connect NCAP findings properly so-called with those from the accidentological data banks. With only one exception (Report No.14), these reports concluded there was an absence of correlation between the accidentological results and those of the NCAP. It is not without significance to recall the latest of these reports(15), compiled at NHTSA's request, which clearly summarizes the general opinion: "With respect to the broader question of whether or not the NCAP crash test results are useful as a general measure of crashworthiness for both belted and unbelted drivers and passengers in all types of accidents, it seems quite clearly that they are not. This can be seen perhaps in variable injury distributions across a wide range of HIC scores."

Figure 2 contains diagram 3, based on (15), which summarizes the overall findings based on the analyses performed.

Investigation No. 14, which concludes as to the existence of a correlation between the FARS data and the NCAP findings, is of major interest in that it endeavors to restrict the accidentological sample to only those impacts whose configuration is close to the NCAP testing conditions (orthogonal frontal impact against a fixed barrier). However, a number of comments can be made concerning the methods used and the ensuing conclusions:

1. As the author of the investigation admits, the sample is very small. It is composed of 695 fatal casualties, representing a fraction of the percentage of the victims killed in front-seat positions in frontal impacts in the United States during the reference period. Basically, this ensues from the following:—
   - The rigorousness of the procedure in the selection of cases
   - The fact that the population from which the samples were taken is that of the FARS file, which—as its name indicates—includes only accidents that cause at least one death. Thus it is that, at the beginning of the selection, nearly 63 percent of the cases are eliminated of those that, since they did not involve collisions between vehicles in motion, are unsuitable for the analysis envisaged.

   In view of the foregoing, it is not possible to claim that the samples chosen are representative of the reality of front-frontal collisions. In particular, this sample excludes collisions against fixed rigid obstacles, which are theoretically covered by the NCAP. In addition, it is clear that vehicle/vehicle collisions—even those of vehicles of closely similar mass—have results influenced by the relative aggressiveness of the vehicle, which is an undeniable factor of skew.
2. The subsample pertaining to belted passengers is far too small for the statistical analysis applied thereto to have any value: 95 percent of the drivers in the sample were not belted; the number of belted individuals in the subsample is therefore only about 35. Finally, the level of significance ($p \leq 0{,}05$) (Table 5 of (14)) is not achieved for the SUM and RSUM parameters (indicators constructed on the basis of the NCAP results).

   Under these conditions, the finding of a relation (Figure 1, (14)) between the NCAP results and the probability of the decrease of a belted driver is of no validity whatsoever.
3. In addition, and most importantly, the application of the NCAP results to unbelted passengers (as noted above, the latter constituted virtually the entire sample) is technically inadequate. It suffices to examine the comparative trajectories and kinematics of a belted passenger and of an unbelted passenger in cases of frontal impacts to see they share absolutely no points in common, either as concerns the relative movements of the various parts of the body or, for example, the points of impact against the elements of the passenger compartment. There is no question of deducing from the results measured on a belted dummy the performances concerning unbelted

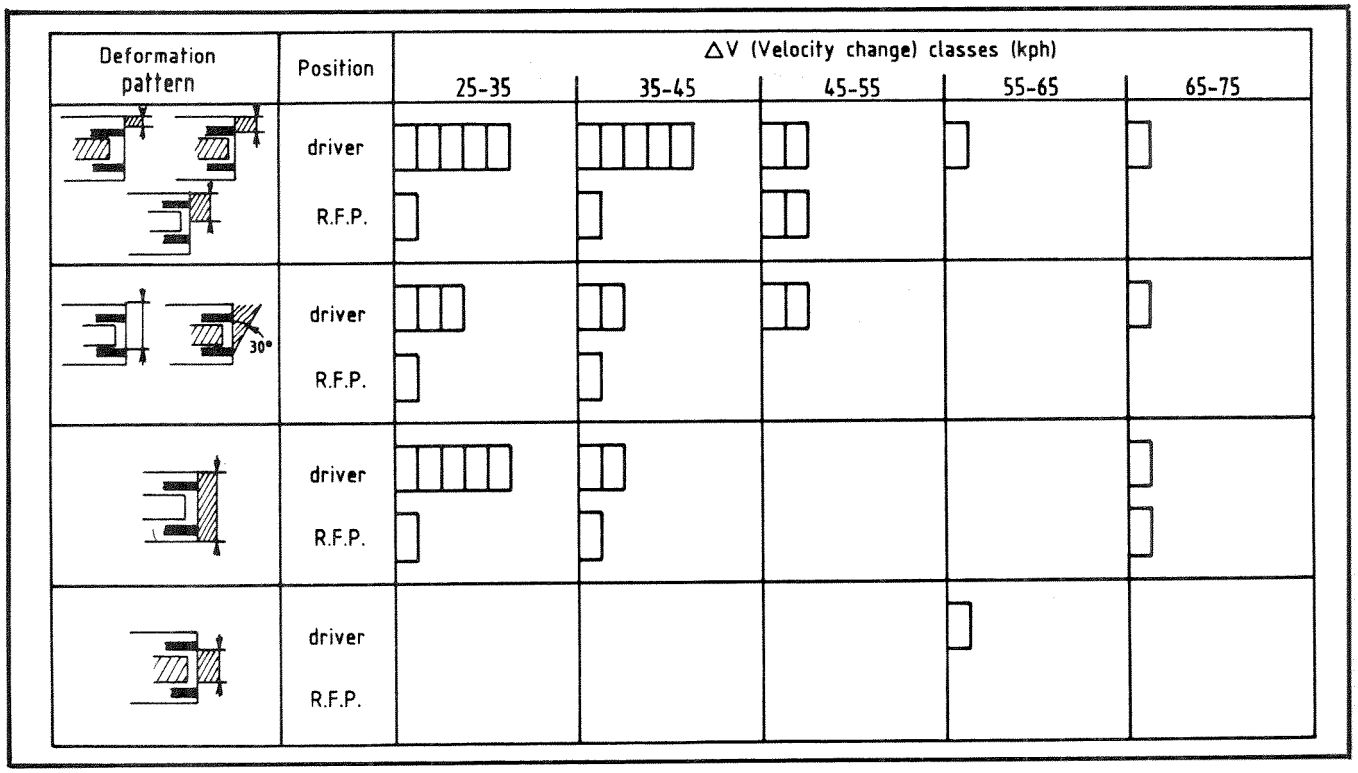

Figure 1. Number of belted occupants (Renault 5) involved in frontal impacts

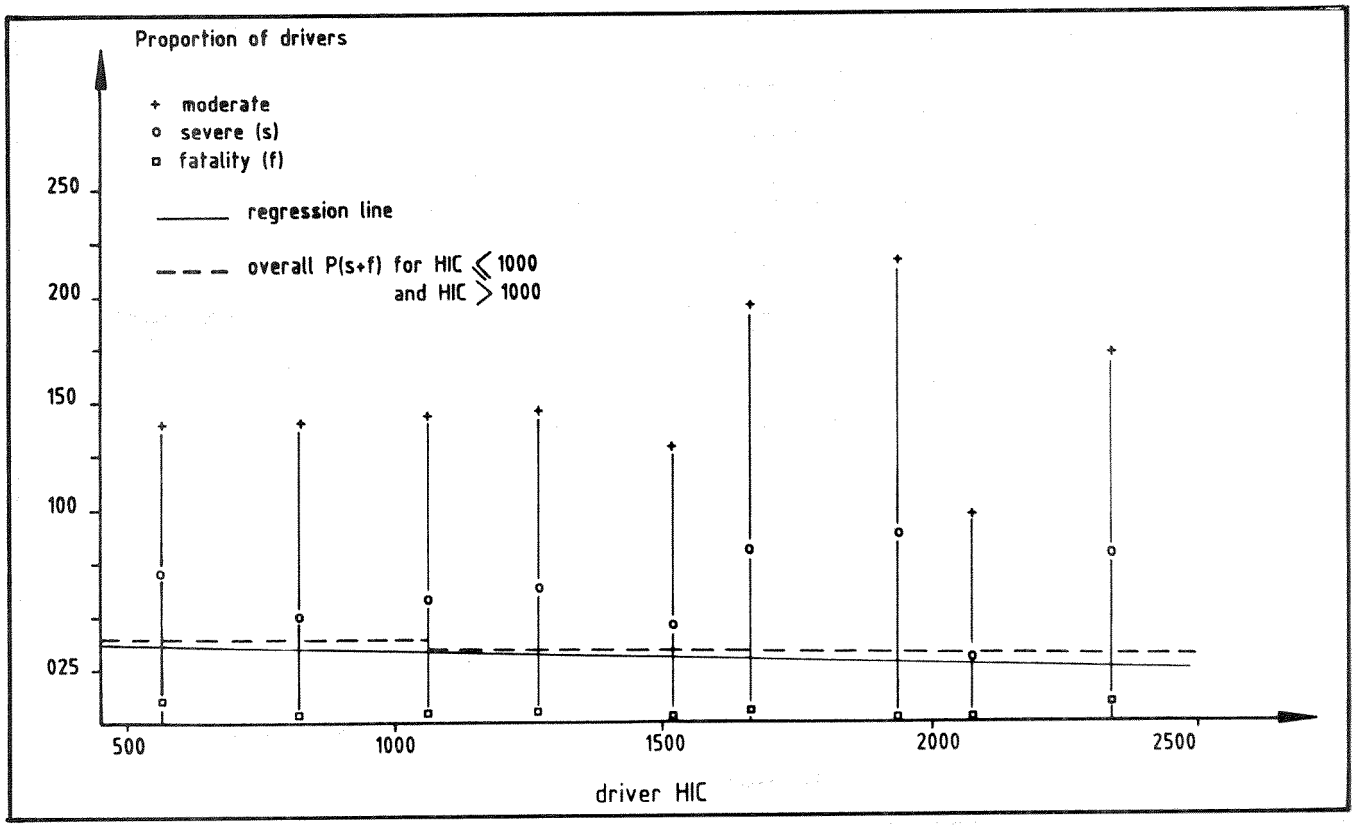

Figure 2. Driver injury distributions by driver HIC(15)

passengers. This fact is unanimously acknowledged both by NHTSA(16)—"The test results are indicative of relative crash protection provided to occupants wearing safety belts"—and by the ITHS itsel(17): "Recently, the Highway Loss Data Institute reported that among 1978 car models, small imports had the worst injury claim frequencies. The DOT results are based on injury severity to belted occupants in 35mph crash tests of 1979-1980 models, while the HLDI data are based on insurance claim frequencies for 1971 and 1978 models whose occupants were, for the most part, unbelted." This being stated, it is always possible to correlate the two factors. However, it emerges (Tables 2, 3, 4 of document 14) that when parameters such as velocities, vehicle-mass ratio, drivers' ages, and the wearing of safety belts have, as expected, a strong influence on the probability of death, with an excellent level of significance (Figure 3), the trend observed with the crashworthiness parameter is more than discrete, with a level of significance that drops below the usually recognized limit ($p \leq 0{,}05$) by a marginal value only $p = 0{,}045$) and in the one case in which HIC and chest deceleration are combined to obtain the term SUM.

4. Finally, examination of the previous publications (10, 11, 12, 13) by Zador(14) enables them to conclude: "An important conclusion that can be

Variable	Beta	Std Error	p	Mean	Comment
Intercept	-4.20	0.91	0.0001	1	
V	3.09	0.66	0.0001	1.00	V is speed limit /50
M	0.06	0.09	0.4989	6.37	M is sum of weights /1000
Ln M_1/M_2	-3.64	0.84	0.0001	0.005	Ln (case vehicle weight/other vehicle weight)
A_1	0.81	0.22	0.0003	0.22	A_1 is function of case vehicle driver age
A_2	-0.49	0.17	0.0029	0.42	A_2 is function of other driver age
RESTR 1	-1.78	0.62	0.0044	0.05	Indicator of case vehicle driver restraint use
RESTR 2	-1.04	0.79	0.1885	0.02	Indicator of other driver restraint use
PASS	-0.16	0.10	0.0909	1.60	Number of front seat occupants in case car
SUM	0.05	0.02	0.0454	6.85	SUM is case vehicle octile ranks for HIC and CD

Figure 3. Compared levels of significance for various parameters

drawn from this review is that there is evidence of a trend of decreasing injury risk with better NCAP results."

Zador(14) processes, for example, the data of document 13, grouping them differently to reach this conclusion.

It suffices, as we did in Figure 4, to carry over from document 13 the representative points of the couples (Gillis index, actual fatality rate) to see that it is wishful thinking to try to correlate these two factors. The trend noted by Zador(14), if it exists, has not so far been detectable and therefore cannot be considered as established.

To conclude this discussion of global statistical approaches, let us note that neither the automobile manufacturers nor the automobile users can be satisfied with a coherence that is only partial between the NCAP results and the real-world accident behaviors. If an indicator is set up, it must accurately reflect the real-world characteristics that are to be quantified.

Investigation of Certain Occurrences of Real-World Accidents

In the face of the failure of the global statistical methods, which for the time being do not allow us to reject the null hypothesis (no relation between NCAP results and real-world performances), we are led to adopt a different approach, i.e., a detailed case-by-case investigation of real-world collisions that are closely similar to NCAP impacts. Clearly, such a procedure inevitably brings about a loss of the concept of the statistical significance of the possible conclusions to be drawn from such an approach: It is difficult to generalize them.

Figure 4 lists the vehicles and occupants, both belted and unbelted, involved in collisions featuring conditions closely similar to those of the NCAP-type impacts. These vehicles were selected from the APR accidentological files, which now contain more than 6,000 thoroughly analyzed cases.

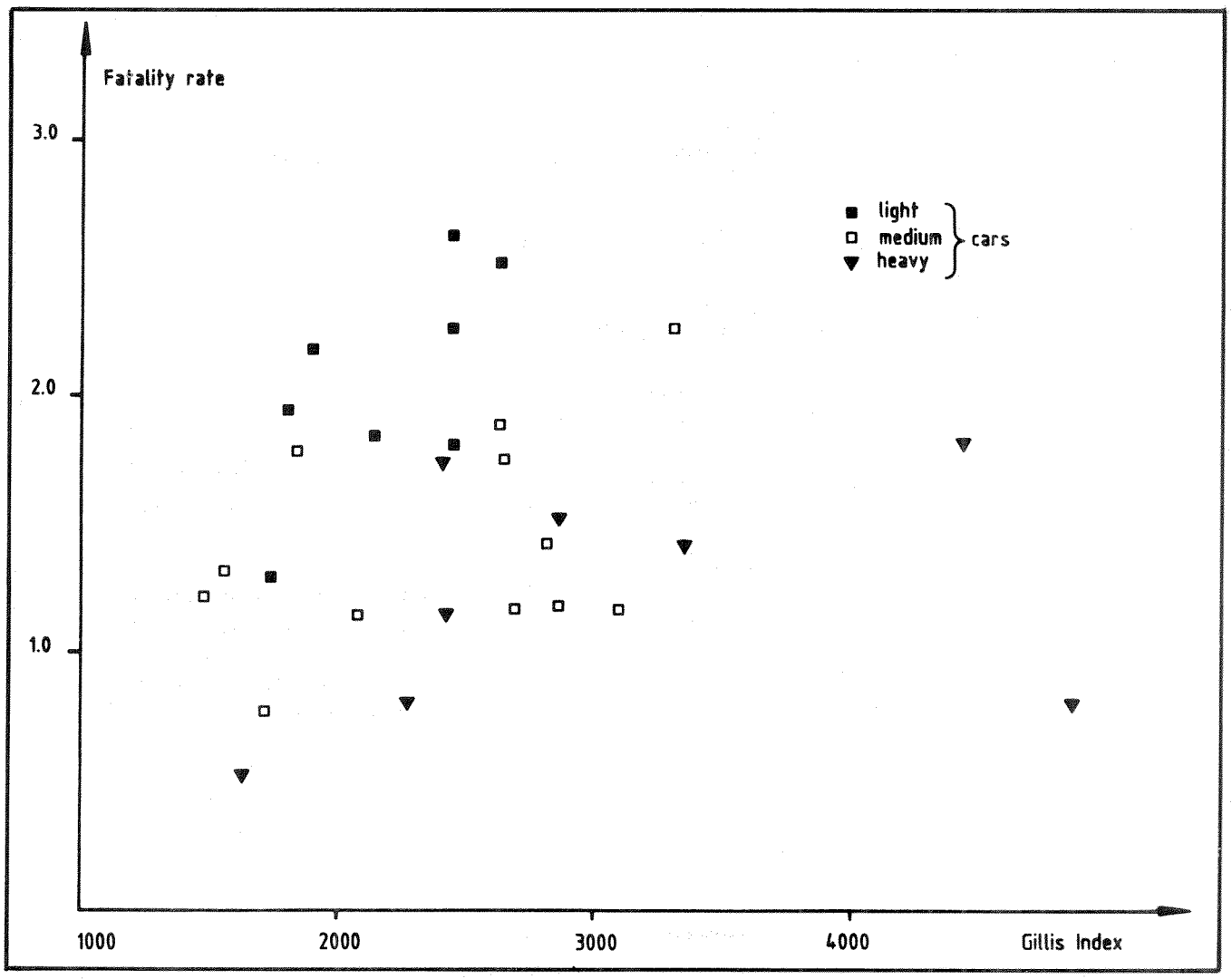

Figure 4. Fatality rate versus Gillis index(13)

The criteria of the choices were based on the following considerations:

- Extent of deformation of the vehicle's front surface. (This surface must have been involved in its entirety, and the intrusion points must have been distributed: appearance of deformation comparable to that of an impact against an orthogonal barrier.)
- Estimated value of the velocity change undergone at the time collision occurred ($\Delta V \geq 56$km/h)
- Estimated value of the vehicles' average deceleration ($\bar{\gamma} \geq 15$g).

Figure 5 compares the points representative of the real-world collisions selected (21 vehicles) with those of NCAP tests (fixed orthogonal barrier) at velocities ranging from 50 to 65km/h.

			TOTAL ↓
Nb of Vehicles	8	13	21
	BELTED OCCUPANTS	UNBELTED OCCUPANTS	
DRIVER	8	13	21
R.F.P.	6	6	12
TOTAL →	14	19	33

Figure 5. APR sample of occupants involved in severe frontal collisions

The degree of injury sustained by the 33 occupants in the sample is indicated in Figure 6. It is clear that these severe collisions involve a high rate of fatal casualties and serious injuries. Only 3 out of 14 belted occupants involved sustained moderate injuries, of a level lower than OAIS 3, with all the unbelted victims incurring injury levels far beyond this limit. Despite the smallness of the sample (due to the infrequent occurrence of this kind of collision identifiable with impacts against fixed orthogonal barriers), the effectiveness of the safety belt once again emerges.

Present-day vehicles offer a possibility of survival under these impact conditions, which are severe. In certain cases, unbelted occupants (with the age factor playing a preponderant role) sustained injuries of a level lower than the fatal level. However, beyond a certain severity ($\Delta V > 65$km/h, $\bar{\gamma} = 15$g), the 5 unbelted individuals in our sample met death; this was the case for only 2 belted subjects involved in collisions of similar violence.

Among the 14 belted occupants in our sample, 3 of the fatal casualties were not autopsied, so we have no record of the state of their injuries. A summary of the injuries sustained by the 11 other occupants is shown in Figure 7.

This latter figure, although based on a very small sample, shows that if the injuries to the body areas concerned by Regulation 208, and, consequently, by the NCAP (the head, chest, and lower limbs), recur with great frequency to the 11 belted occupants for whom we have records, two of the body areas not governed by this regulation,i.e., the pelvis and the abdomen, are also extensively involved. This is not surprising in view of the severity of the collisions investigated. It is therefore insufficient to attempt, in impacts of this same type, to describe, as does the NCAP, the protection afforded by the vehicle and its retention system while failing to investigate the fate of all the body parts and areas. In the final analysis, this can lead only to a result devoid of validity.

Before ending this analysis, we will devote special attention to two cases taken from the sample previously described, which are interesting in that they are comparable to tests performed by NCAP, the results of which are in our possession. The first case involved a Renault 5 and the second a Renault 18. A brief description of the accidents, an assessment of their severity, and the state of the injuries sustained by the occupants compared with the NCAP results are provided in Figures 8 and 9, respectively.

Although these results cannot be judged as statistically significant, the total incoherence between the NCAP values and the injuries actually sustained by the occupants do not incline us to optimism concerning the predictive character of the NCAP results. Yet the two cases investigated are similar in terms of configuration of collision to the tests performed within the NCAP.

Comparison Tests Performed With Human Subjects

Finally, it appeared interesting to use a third way for assessing the performances of NCAP's predictive method since, at present, the statistical approaches (whether global or focused on real-world accidents whose configurations are similar to those of the NCAP impacts) make it possible to reach only a negative conclusion with regard to the correlation between real results and predicted results.

We therefore decided to reproduce, at our testing site, only experimental collisions against fixed, rigid orthogonal obstacles at a velocity of 50km/h (35mph), the Part 572 dummies replaced by human subjects. These subjects, placed in vehicles that had been assigned different classifications in the NCAP tests, were to make it possible to confirm or infirm the classification emanating from the crashworthiness rating procedure.

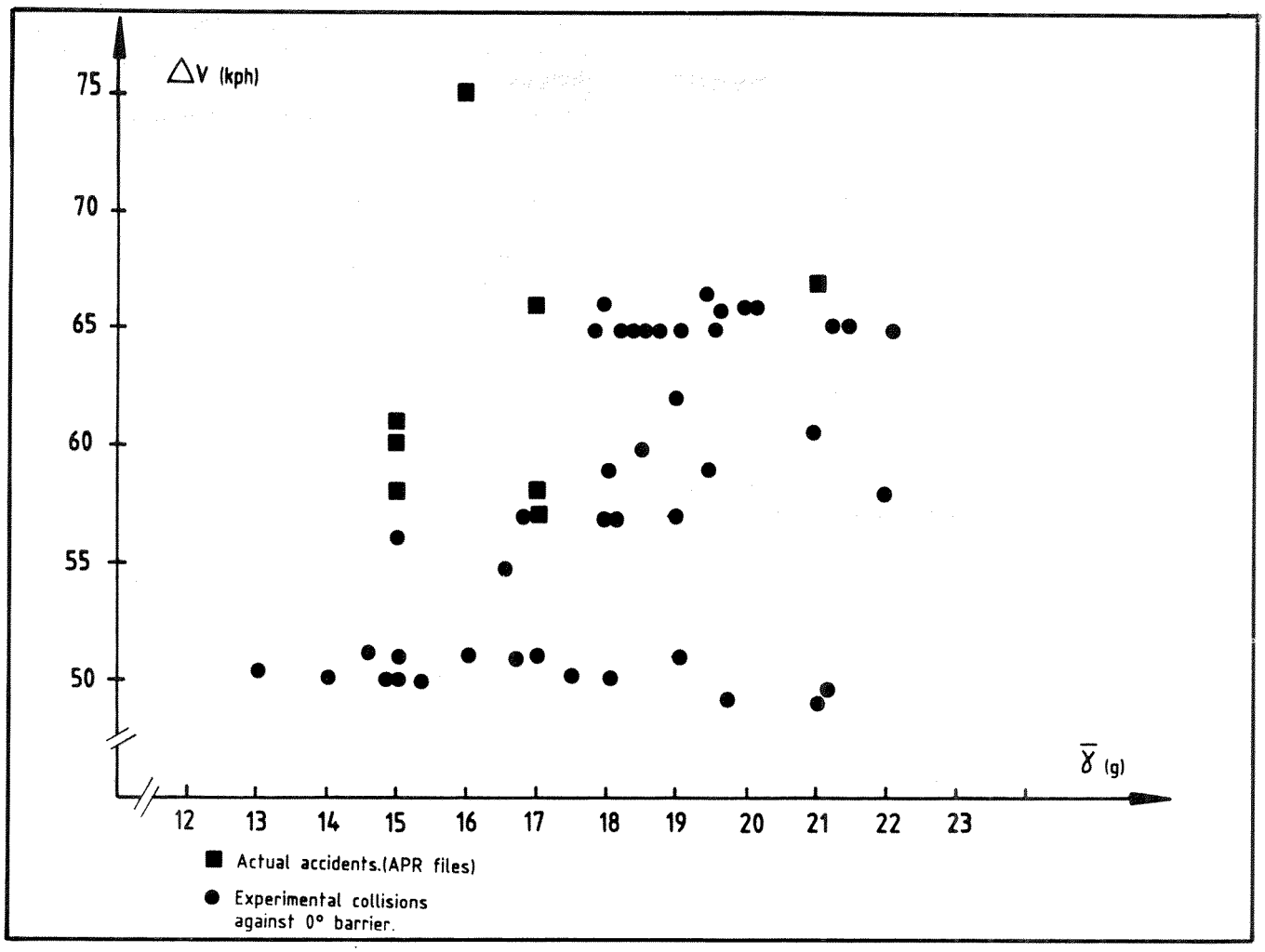

Figure 6. Compared severity between selected actual accidents (belted occupant) and experimental impacts against 0° barrier

	Collision severity classes								TOT
BELTED OCCUPANTS	55 < ΔV ≤ 65 (kph)	OAIS.	0	1	2	3	4	5	6	
	13 < γ̄ ≤ 17 (g)	Nb. of occupants	-	1	2	-	2	1	3	9
	65 < ΔV (kph)	OAIS.	0	1	2	3	4	5	6	
	15 < γ̄ (g)	Nb. of occupants	-	-	-	1	1	1	2	5
UNBELTED OCCUPANTS	55 < ΔV ≤ 65 (kph)	OAIS.	0	1	2	3	4	5	6	
	13 < γ̄ ≤ 17 (g)	Nb. of occupants	-	-	-	6	3	1	4	14
	65 < ΔV (kph)	OAIS.	0	1	2	3	4	5	6	
	15 < γ̄ (g)	Nb. of occupants	-	-	-	-	-	-	5	5
										33

Figure 7. OAIS distribution in APR sample of 33 occupants in severe frontal collisions—distributed deformation of vehicle front end ($\Delta V > 55$kph, $\bar{\gamma} < 13$g)

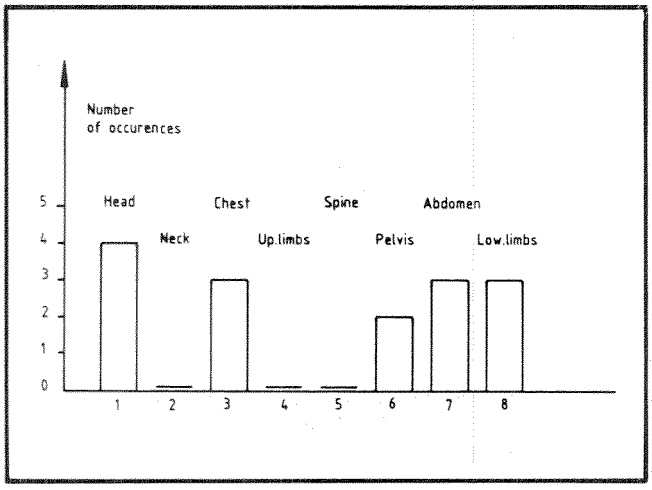

Figure 8. Number of severe injuries (AIS ≥ 3) observed on eight body segments (11 belted occupants)

Choice of Vehicles

The choice of vehicles was made on the basis of a single a priori consideration, that of the desire to have two cars that had yielded distinctly different results with regard to the HIC and chest deceleration in the NCAP tests. The only other selection criterion was the availability of these cars. It was necessary to get cars strictly similar to those used in the crashworthiness rating tests.

Figure 10 shows the table listing, for each of the A and B vehicles, the areas in which the NCAP results are located (HIC and chest deceleration).

Testing Procedure

The cadavers[1] were prepared and equipped with instruments in accordance with methods described in earlier reports (18, 19, 20, 21, 22):

- Pressurization of the vascular system
- Correct placing of the intrathoracic viscera
- Fitting of instruments to the head and spinal column

The purpose of the tests implied that the zones of the heads of the dummies and cadavers involved in the impacts should be the same, and that the localizations of these impacts—for example, against the steering wheel—should also be closely similar. These requirements were met through adjustments of the positions of the seats in their tracks on the basis of the anthropometry of the cadavers used (described in Figure 11).

After the tests, the cadavers were x-rayed and then autopsied. The heads, necks, and spinal columns were removed for a closer analysis of injuries that might possibly have occurred (notably, brain lesions).

Ribs were also collected for the purpose of characterizing the overall bone resistance of the thorax.

Findings

The findings are summarized and compared with the NCAP values in Figure 12.

In vehicle A, the central cushion of the steering wheel failed to provide sufficient protection for the face of the driver. In addition, there is doubt regarding the brain. In fact, the failure of the injection does not permit a conclusion as to the possible occurrence of microscopic injuries. However, no large macroscopic lesion was found.

The passenger sustained chest fractures (11 rib fractures and 1 sternal fracture, without the occurrence of flail chest or visceral lesions). These were moderate injuries classified at level 2 in the AIS scale. They were particularly moderated in view of the poor condition of the subject's bone structure (BCF = -0,54)(22).

In summary, it may be concluded there was adequate protection of the occupants in vehicle A under these impact conditions, except for protection of the driver's face.

In vehicle B, a rather late chest retention brought about impact of the cadaver's head (lower jaw) and neck against the center of the steering wheel and caused the injuries associated therewith, which were severe. It also permitted impact of the passenger's forehead against the dashboard. The chest injuries were quite severe for both occupants (AIS 4). Submarining occurred for both cadavers, with that of the passenger bringing about abdominal injury. Although the trajectories and the zones impacted of the various body areas were similar in the tests performed with cadavers and those performed with dummies, the latter tests completely failed to show the actual results from vehicle B in this specific type of collision.

Comment

Although the findings are presented only on the basis of a single test involving cadavers, obviously ruling out any statistical interpretation, the conclusions are clear. In this particular case (which was a case chosen at random only on the basis of the criterion of a difference with regard to the NCAP findings), the result obtained via the predictive rating method is manifestly reversed. At worst, and to take into account the unsuccessful injection of the brain mass, which prevented detection of the possible occurrence of microscopic injuries, we might deem as equivalent the findings for the drivers (fatal casualties in both cases), whereas the NCAP ratings classified "B" as better than "A" for the drivers, and the findings for the

[1] The cadavers were those of individuals who had bequeathed their bodies.

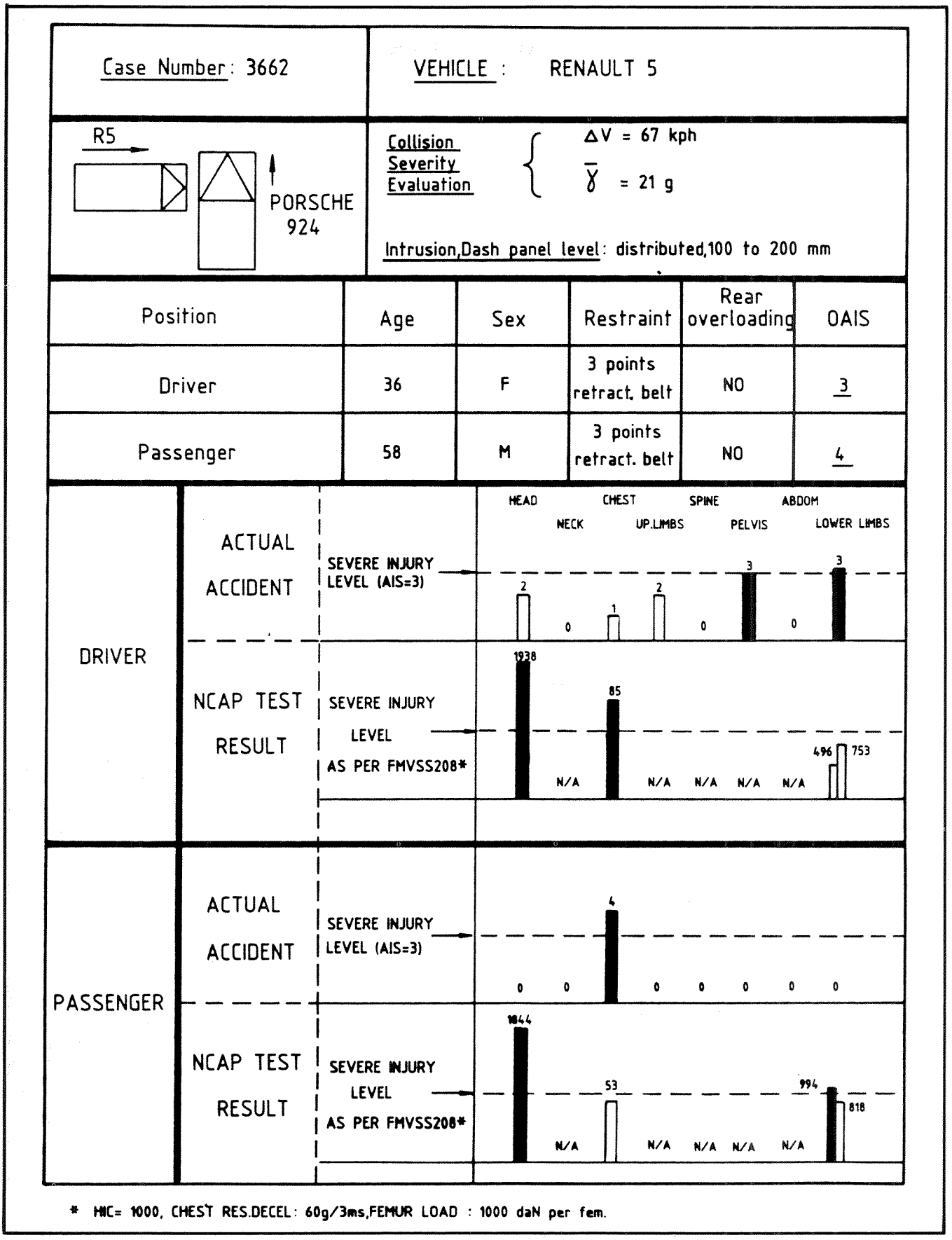

Figure 9. Comparison between NCAP and actual accident results—Renault 5

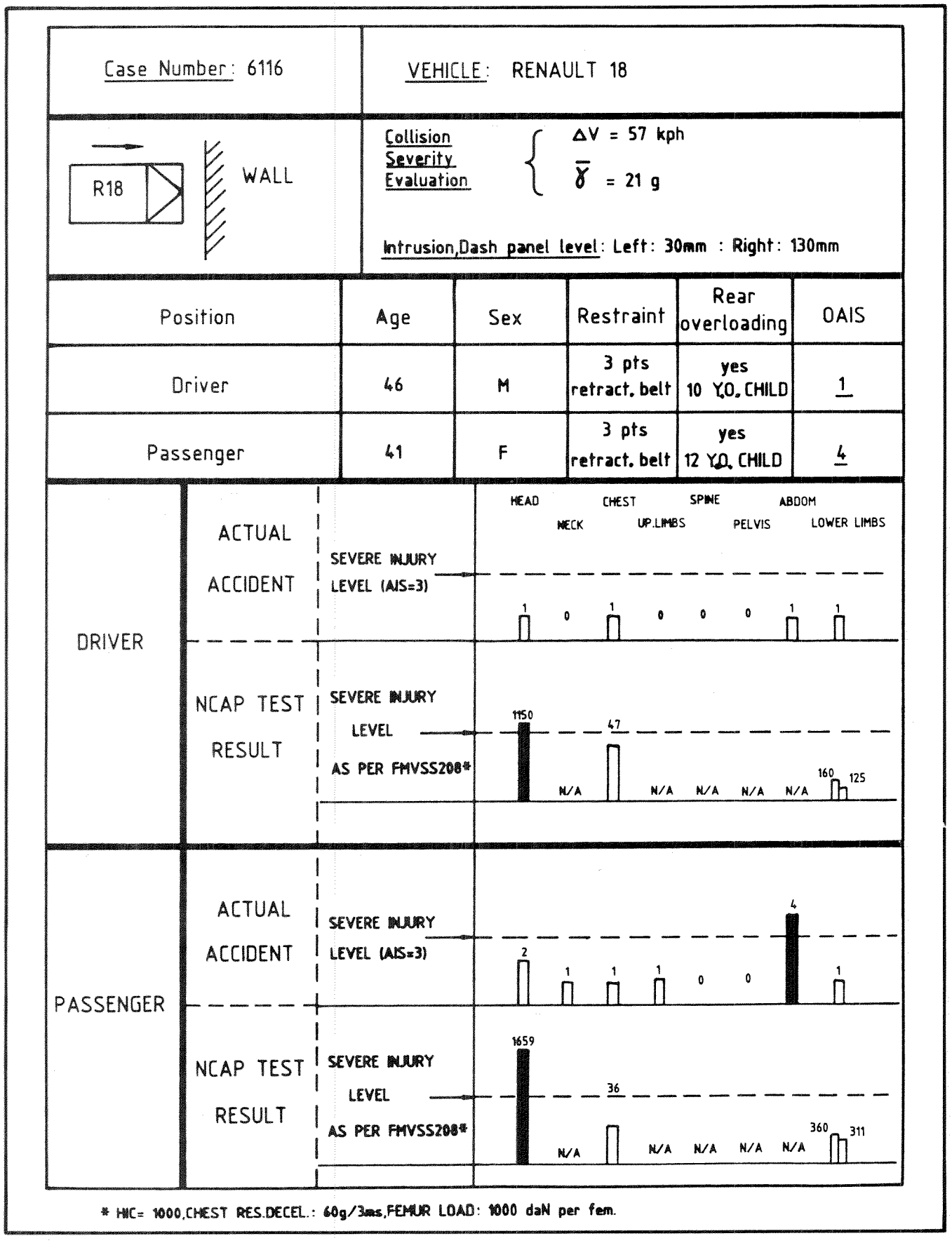

Figure 10. Comparison between NCAP and actual accident results—Renault 18

	POSITION	HIC	CD/3ms
CAR A	DRIVER	1400-1600	35-45
	PASSENGER	600-800	35-45
CAR B	DRIVER	300-1000	45-55
	PASSENGER	800-1000	35-45

Figure 11. Selected cars A and B for cadaver tests—NCAP results with Part 572 dummies

car	Position	Anthropometrical data Age/sex	Height,cm	Weight,kg	BCF *
A	Driver	49/M	167.5	83	-2
	R.F.P.	49/M	177	75	-0.54
B	Driver	54/M	160	55	-0.55
	R.F.P.	57/M	162	49	-0.56

* B.C.F. = Bone condition factor. (the smaller the algebric value,the better the bone strength [See ref 22])

Figure 12. Cadaver anthropometrical data and bone characterization

passengers as different ("A" > "B"), whereas NCAP predicted them as equivalent. However, this failure was obtained under circumstances that were the most favorable for the demonstration of the validity of NCAP, i.e., strict abidance by the conditions of the crashworthiness rating impact.

Conclusion

In this report, we have summarized certain research work that, since the onset of the New Car Assessment Program in 1979, has been geared to finding confirmation of the merits of the vehicle ratings ensuing from the application of the NCAP.

The analyses reveal the following:

1. It is vain to hope that the predictive method currently being implemented in NCAP can accurately represent the passive safety performances of vehicles in all types of accidents.
2. The general statistical studies that endeavor to correlate the predicted results with the real-world vehicle results do not at the present time make it possible to establish this correlation. This is likewise true for the studies that limit the samples investigated only in the cases of configurations similar to those performed within the framework of the NCAP.
3. There are clear technical reasons that account for this lack of correlation between the historical results, and the predictive results; we consider two of these reasons to be especially important:
   - The failure to take into account all the body areas that can be involved during the NCAP-type collisions, which are severe
   - The absence of representativeness of the Part 572 dummy, which does not allow any valid evaluation of the passenger protection performance of a given vehicle

   To date, there is nothing to support declarations of the following kind:
   - "NHTSA concludes that, generally, the car performing well (in the NCAP test) should be the vehicle of choice(2)."
   - "If a vehicle restraint system performs well in the NCAP tests, it is likely to perform well in a variety of accidents on public roads(23)."
   - "Changes made in restraints and vehicle crash characteristics as a result of weaknesses shown in NCAP tests have almost certainly improved their crash safety(23)."

   On the contrary, at the present time the following conclusion must be drawn: "We do not have any engineering reason to conclude that a 35mph barrier test is a reasonable predictor of car safety in the real world."

   In the last analysis, the above-quoted conclusion is in no way surprising. It ensures—quite logically—from the list of requirements that governed the compilation of NCAP: the search—we might almost say at any cost—for a difference whose reality still remains to be proven in relation to the real-world accidents, which are and will remain, inescapably, the reference.

In light of the foregoing, the following emerge as both vital and urgent necessities:

- Pinpointing the possible real differences between vehicles
- Identifying the causes of these differences
- After that—and only after that—devising a predictive method that will be able to take these differences into account both effectually and accurately

Moreover, it is entirely possible that such an approach would lead to one or the other of the following conclusions:

- The differences are not significant: uselessness of a rating program.
- The differences do actually exist, but no predictive method is feasible.

CAR	POSITION	HEAD INJURIES: SKULL	FACE	NECK	BRAIN	THORAX INJURIES	ABDOMEN INJURIES	COMMENTS
A	DRIVER CAD	NO	FRACTURE AIS=3	NO	NO Macroscopic injury	NO	NO	See ①
	DRIVER DUM	1400 < HIC < 1600				35 < CD 3ms < 45(g)	N/A	
	PASSENGER CAD	NO	NO	NO	NO Macroscopic injury	11 RF + SF } AIS=2	NO	
	PASSENGER DUM	600 < HIC < 800				35 < CD 3ms < 45(g)	N/A	
B	DRIVER CAD	NO	FRACTURE AIS=3	FRACTURE C2 (AIS=3)	NO Macroscopic injury	14 RF + SF } S.F.C. AIS=4	NO	See ② +Submarining
	DRIVER DUM	800 < HIC < 1000				45 < CD 3ms < 55(g)	N/A	
	PASSENGER CAD	NO	NO	NO	NO Macroscopic Microscopic injury	15 RF SF+CF } S.F.C. AIS=4	Rupture of Mesentery } AIS=3	Submarining
	PASSENGER DUM	800 < HIC < 1000				35 < CD 3ms < 45(g)	N/A	

Abbreviations : CD 3ms = Chest deceleration as per FMVSS 208.
RF = Rib fracture (11 RF = eleven rib fractures).
SF = Sternum fracture.
CF = Clavicle fracture.
S.F.C. = Severe flail chest.

① : facial impact against steering wheel hub.

② : face and neck impact against steering wheel.

Figure 13. Test results—comparison of dummy and cadaver data

Conversely, if the program were pursued along its current lines, it is probable the interest of the clients—and of the automobile manufacturers—in the aforesaid program would eventually vanish completely, if only as the result of their perusal of the precautions for the use of the rating that it has been necessary to include and that, in certain cases, goes so far as to point out "there is no guarantee that a car that passed the test will adequately protect you in an accident(24)"

References

1. Title II of the Motor Vehicle Information and Cost Saving Act (15 USC 1941 et seq.).
2. Brownlee, M.B., "Automotive ratings: past, present and future," International Automotive Ratings Symposium, December 1980.
3. Martin, D.E., "Automotive ratings: the technological challenge," International Automotive Ratings Symposium, December 1980.
4. Seiffert, U., "Crashworthiness ratings," International Automotive Ratings Symposium, December 1980.
5. Hackney, J., and V. Quarles, "The new car assessment program—status and effect," Proceedings Ninth International Technical Conference on Experimental Safety Vehicles, November 1982.
6. Friedman, K., and L.A. Klimlo, "Some considerations on automotive safety ratings," International Automotive Ratings Symposium, December 1980.
7. Carlson, W.L., "The use of accident data for crashworthiness ratings," International Automotive Ratings Symposium, December 1980.
8. Ventre, P., et al., "The behaviour of vehicles and occupants in asymetrical frontal collisions," Proceedings Sixth International Technical Conference on Experimental Vehicles.
9. "Results of comparative crash tests," CCMC, September 1975.
10. Campbell, B.J., "A comparison of NHTSA car safety ratings with injuries in highway crashes," *HSRC Highway Safety Highlights,* Vol. 15, No. 3, 1982.
11. Jones, I.S., "Injury severity related to crash severity," CMRSC II, Winnipeg, June 1983.
12. Grush, E.S., et al., "Comparison of high speed crash test results with fatality rates," 27th AAAM, October 1983.
13. Thomas, C., et al., "Crashworthiness rating system and accident data: convergences and divergences," SAE Congress, February 1984.

14. Zador, P.L., et al., "Fatal front to front car collisions and the results of 35mph frontal barrier impacts," 28th AAAM, October 1984.
15. Stewart, J.R., "Comparisons of NCAP crash test results with driver injury rates in highway crashes," Final report, Contract DTRS-57-83-C-00047, October 1985.
16. In *U.S. DOT News,* May 10, 1984.
17. In *HLDI (IIHS)*, Status report, Vol. 14, No. 16, October 29, 1979.
18. Got, C., et al., "Results of experimental head impacts on cadavers. The various data obtained and their relation to some measured physical parameters," Proceedings 22nd Stapp Car Crash Conference, October 1978.
19. Sacreste, J., et al., "Proposal for a thoracic tolerance level in side impacts based on 62 tests performed with cadavers having known bone characterization," Proceedings 26th Stapp Car Crash Conference, October 1982.
20. Walfisch, G., et al., "Les caracteristiques morphologiques des côtes et leurs relations avec la déflexion provoquée du thorax,"Proceedings Second International IRCOBI Conference, September 1975.
21. Walfisch, G., et al., "Tolerances and mechanical characteristics of the human thorax in frontal and side impacts, and their transposition into protection criteria," Proceedings Seventh International IRCOBI Conference, September 1982.
22. Walfisch, G., et al., "Predictive functions for thoracic injuries to belt wearers in frontal collisions, and their conversion into protection criteria," Proceedings 29th Stapp Car Crash Conference, October 1985.
23. Letter to Renault (Governmental Affairs) from Carl E. Nash (Chief, Accident Investigation Division, NHTSA), September 5, 1984.
24. *The Car Book*, DOT HS 80580, 1980.

An Aid for the Assessment of Biomechanical Values With High Scatter and Uncertain Limit Values

Dr. Walter Schmid
Daimler-Benz AG, Sindelfingen

Abstract

In the case of characteristic quantities with an unusually high scatter and remarkably high uncertainties in establishing limit values, it is often very problematic to determine a particular value as the development target. This value must keep a defined safety margin to a limit value that is probably set down by regulations. But often a certain safety margin to the requirements of reality has already been observed when establishing limit values. In the case of the values referred to here, this double safety might—on the one hand—lead to development targets that are technically not feasible or only at unacceptable expenditure. On the other hand, this might compel actual safety reserves that no sensible person would ever demand.

For this reason, the example of HIC, the head injury criterion, is used to demonstrate the possibility of finding development targets and limits for specifications and regulations without being forced to keep unrealistic safety margins. It becomes obvious that in the example of HIC, a limit of 1,500 is much more realistic than, for example, a limit of 1,000.

Introduction

The endeavor to make their vehicles as safe as possible during traffic accidents presents vehicle manufacturers with the still unsolved problem of how to measure safety with few accident tests. For this purpose, the mechanical stress on the human body is determined with the help of dummies.

It is attempted in other specific tests on the human body to deduce from the mechanical stress whether this stress will lead to injuries. If so, it should be possible to determine the degree of seriousness of such injuries.

Unfortunately, deterministic considerations are often made during such attempts, although it is generally

known today that a connection between mechanical stress and injury of human body depends on many statistically distributed influences and can thus be established only in the sense of statistical statements.

On the other hand, it is not usual to fix certain factors, e.g., vehicle characteristics, in regulations and guidelines on the basis of statistical information. Rather, the intention is to set up limit values, whereby it is possible to ascertain in as few tests as possible whether values lie below these limits.

Such limit values can, however, be deduced from statistical statements. It became obvious that it is necessary to define a development target first before the limit value suitable for the individual problem can be given. The application of the method proposed is demonstrated by the example of the head injury criterion.

A Method To Determine Problem-Specific Limit Values

When investigating the interdependency between a mechanical stress and an injury of the human body, it became apparent very quickly there is no clear-cut limit stress, in the sense that stresses below the limit would never and those above the limit would always lead to injuries.

Statistically distributed dimensions, physical properties, age, and condition of the human body (e.g., muscles flexed or not), as well as the scatter of important parameters in the test procedure, can be taken as the reason why statements on the probability of injury with a given mechanical stress in biomechanical systems are the right problem-specific standards.

At first sight, it seems easy to define limit values by seeking mechanical stresses that insure the probability of injury remains below a given value (e.g., 10 percent). But if such limit values were adopted in legal regulations or guidelines, one would be compelled to seek development targets at an appropriate distance, because this is the only way—as a result of the measurement scatter occurring during the test—to make the risk of failing the test go down to an acceptable level.

This method required a double safety margin—that for establishing the limit value and that for the development targets. In reality (on the road), the probability of injury is no longer 10 percent, as assumed in the regulations, but considerably lower.

The uncertainties in establishing the limit values and the measurement scatter for biomechanical quantities are unusually high. In addition to giving unrealistic information about the real probability of injury, the method—first limit value, then development target—would lead to conditions for the design of a vehicle that are at present neither feasible nor economically reasonable.

For this reason, the right way is to define the development targets first, taking into consideration the uncertainty of the biomechanical interdependencies and the measurement inaccuracy, and afterward determine limit values, which should be the only factors for checking whether or not the development targets have been achieved.

Development Target

In Figure 1, the probability of injury is plotted versus a mechanical stress parameter selected at will.

The larger the mechanical stress (MS), the higher the probability of injury of the human body. Usually this curve has the shape of a cumulative frequency curve.

The lower the influence of statistically distributed parameters, the steeper the curve. It can be regarded as the cumulative frequency curve of a normal (bell-shaped) distribution ($\overline{MS}$, S_{MS}), particularly if the influence parameters are normally distributed.

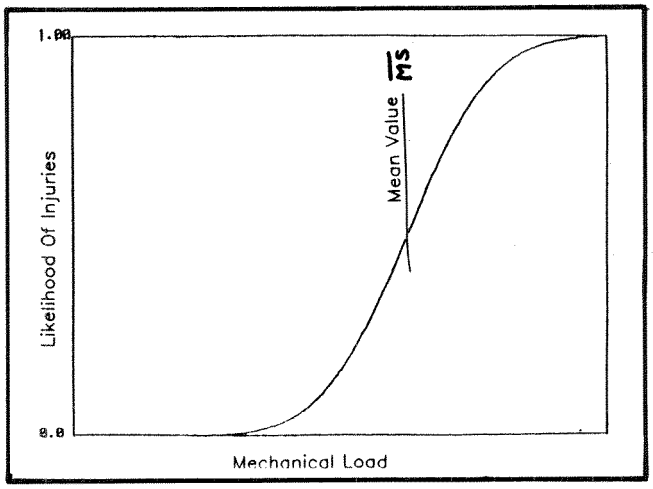

Figure 1. Interdependence between the probability of injury and a mechanical stress

Figure 2 shows the distribution of the measurement results, which, as a rule, are normally distributed as well ($\overline{M}$, S_M).

S_M comprises both the scatter of the vehicle characteristic varying from vehicle to vehicle and the scatter of the measurement results caused by measurement uncertainty.

In addition, the scatters S_M and S_{MS} depend upon the error probability, i.e., upon the size of the sample.

The probability of injury (P_V) in a vehicle is calculated from the product of the curve in Figure 1 and the curve in Figure 2 (Equation 1).

To insure that the probability of injury (P_V) in a vehicle is kept below a value to be specified (e.g., 10 percent), the development target ($\overline{M}$) should keep a specific distance (m) from the average ($\overline{MS}$) of the curve in Figure 1 (Figure 3).

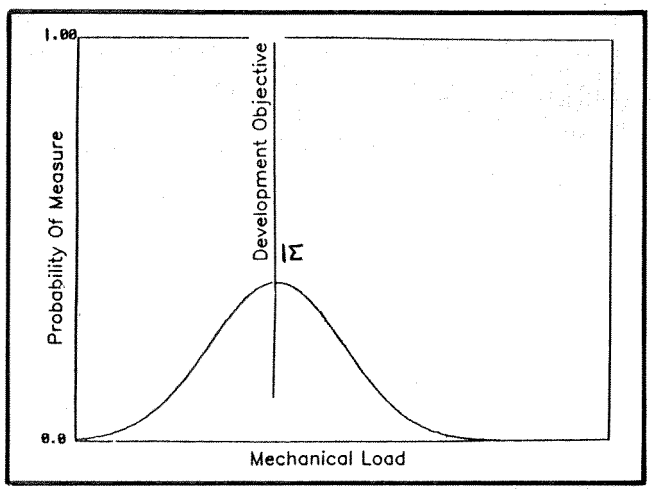

Figure 2. Scatter of the measuring results

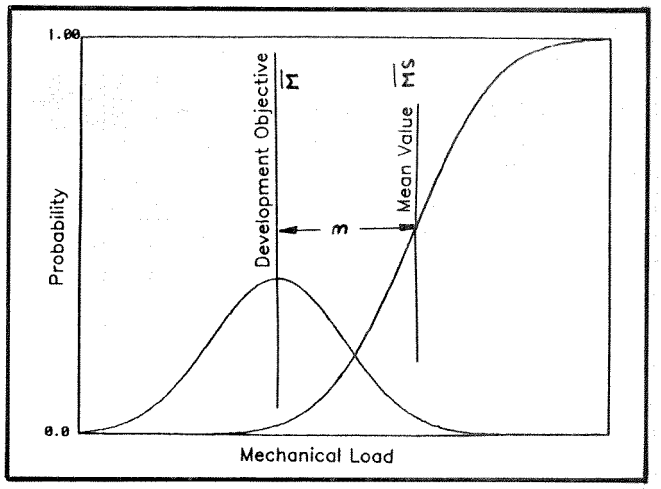

Figure 3. Determination of a development target

In general, this makes it possible to define a development target in accordance with the following proposition:

Proposition 1:"An article should be made so as to insure with a probability of more than (1-P) % that a desired property is actually provided. For this decision the error probability should be lower than α%."

Concerning safety on the road (1-P) = 90% and α = 5% are the usual values.

Limit Value

As by now the development target has been well defined and determined, a limit value to be set in regulations and guidelines need only allow for the probability with which an article (the vehicle) may fail a test.

The limit value is defined:

Proposition 2:"The limit value is to be determined so that an article whose development target is well defined and complied with will pass a test with a probability of (1-Q) %. For this decision the error probability should be lower than α% as well."

The probability mentioned here depends on the scatter occurring when measuring different samples of an article. This means that it comprises changes of the properties and the measurement uncertainty.

$$(1)\quad P_V(m) = \frac{1}{2\pi\, S_M \cdot S_{MS}} \int_{-\infty}^{\infty} e^{\frac{-1}{2}\frac{(MS-\overline{M})^2}{S_M}} \cdot \left[\int_{\infty}^{MS} e^{\frac{-1}{2}\frac{(u-\overline{MS})^2}{S_{MS}}}\, du \right] dMS$$

where $m = \overline{MS} - \overline{M}$

The Head Injury Criterion (HIC)

The method proposed for fixing the development targets and the limit values to be deduced shall now be explained by the example of the HIC.

The results of a large number of experimental investigations are shown in (2). For these investigations, cerebral injuries, given in AIS (Abbreviated Injury Scale), were compared with the "causing" HIC values (Figure 4). If the axes are exchanged, and the relationship AIS = f (HIC) determined with the help of a modern, non-parametric, statistical analysis method(3,4,5), it is possible to determine the probability with which the seriousness of the injury equals or exceeds 3 (AIS 3+) as a function of HIC. For the HIC (Figure 5), we obtain the values $\overline{MS} = \overline{HIC} = 1750$, the mean value, and $S_{MS} = S_{HIC} = 450$, the scatter value.

On the basis of the acceptable probability of injury (e.g., 10 percent), we obtain the development target for the HIC value. Additionally, this development target depends on the "measurement scatter" S_M. For this reason, Figure 6 shows the development targets for the HIC value for various probabilities of injury (1, 5, 10, 20, 30, 40, and 50 percent) plotted versus the ratio of the measurement scatter S_M and the scatter S_{MS}. As the vehicle characteristics themselves scatter, and because additional inaccuracies occur during measuring, the limit value should keep a certain margin to the development target in specifications and regulations, and this the more, the higher the scatter S_M. Moreover, this margin depends on the probability with which a test is to be passed. Figure 7 shows the test limits for different probabilities of erroneous rejections. The development target is chosen for a 10 percent likelihood of injuries AIS 3+. The HIC value has a standard deviation S_M = 225 (~20.5%), so that with S_{MS} = 450 the ratio S_M/S_{MS} = 0.5. If, for example, the limit is fixed at 1,500 for the HIC values, the probability of failing a test is still as high as 4

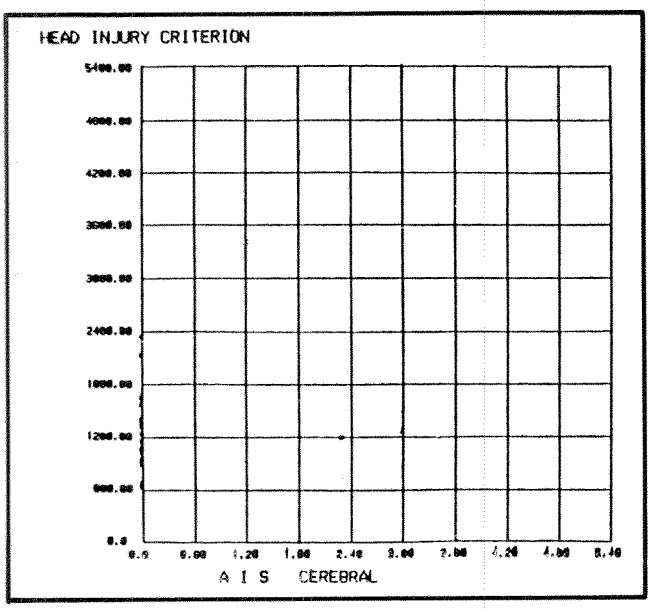

Figure 4. Biomechanical measurement results(2)

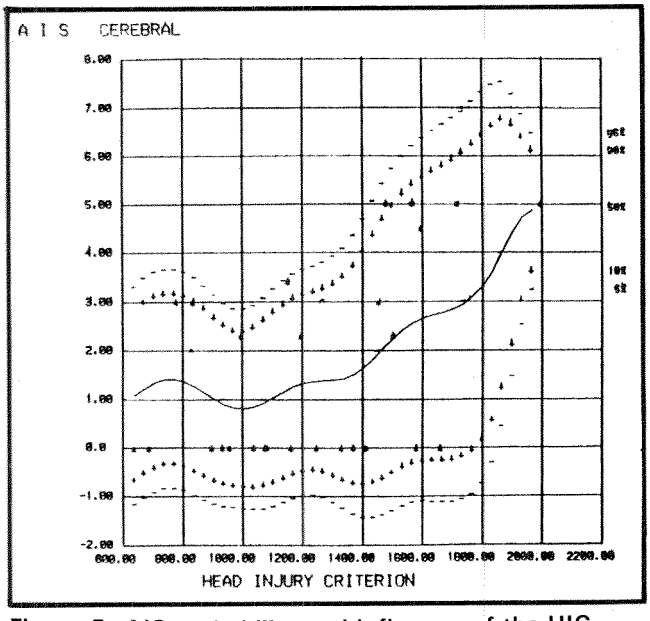

Figure 5. AIS probability and influence of the HIC

percent. The development target has been chosen correctly in relation to the problem, and the vehicle population represented by the vehicle under test was designed correctly with regard to the development target.

In addition, this example shows that the limit value 1,000 would be extremely unrealistic for the HIC whereas the value HIC_{limit} = 1,500 would be well defined.

Test Results and Real Accidents

Is the HIC value a quantity that gives information about the risk of injury in real road traffic? The vehicle

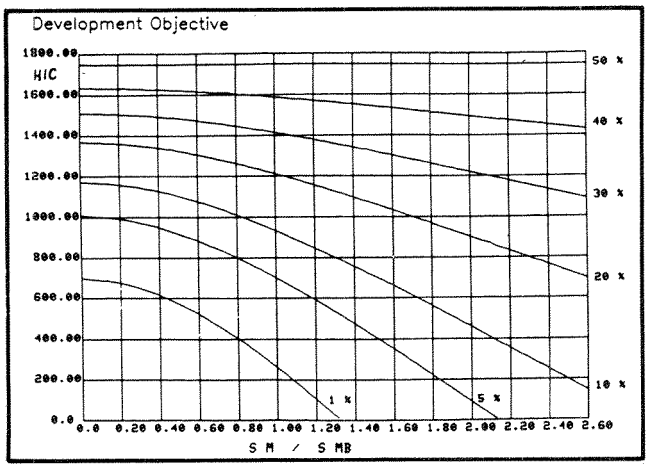

Figure 6. The development target HIC

developer must ask this fundamentally significant question in view of the high development costs caused by lowering the limit of the HIC value with given test conditions.

In the test program, New Car Assessment Program (NCAP), carried out by the National Highway Traffic Safety Administration (NHTSA), vehicles are driven into a rigid barrier at 35mph, and the HIC, the chest acceleration, and the femur load are measured on dummies(6).

The real accident is recorded in large-scale statistics of the vehicle insurers and published for the various vehicle models, e.g., in (7), in the form of information about the relative frequency of accidents involving injuries.

Figure 8 shows that the HIC seems not to be a sensitive standard for measuring safety on the road. This may be due to:

- The test method used in the NCAP is not problem-relevant.
- The test parameters in the NCAP are incorrectly chosen (e.g., v_0 = 35mph is too high(8,9).
- Head injuries are not the characteristic feature in road traffic.

References

1. Koch, M., and A. Nilson-Ehle, "A practical statistical approach to set specifications in car safety engineering," SAE Paper 830470.
2. Lestrelin, D., C. Tarriere, G. Walfish, A. Fayon, C. Got, A. Patel, and J. Hureau, "Proper use of HIC under different typical collision environments," Proceedings Ninth International Technical Conference on Experimental Safety Vehicles, Kyoto, 1982.
3. Watson, G.S. "Smooth regression analysis," Sankya, Series A, 26, pp. 359-372, 1964.
4. Nadaraya, E.A. "On estimating regression. Theory of probability and its applications," 9, pp. 141-142, 1964.

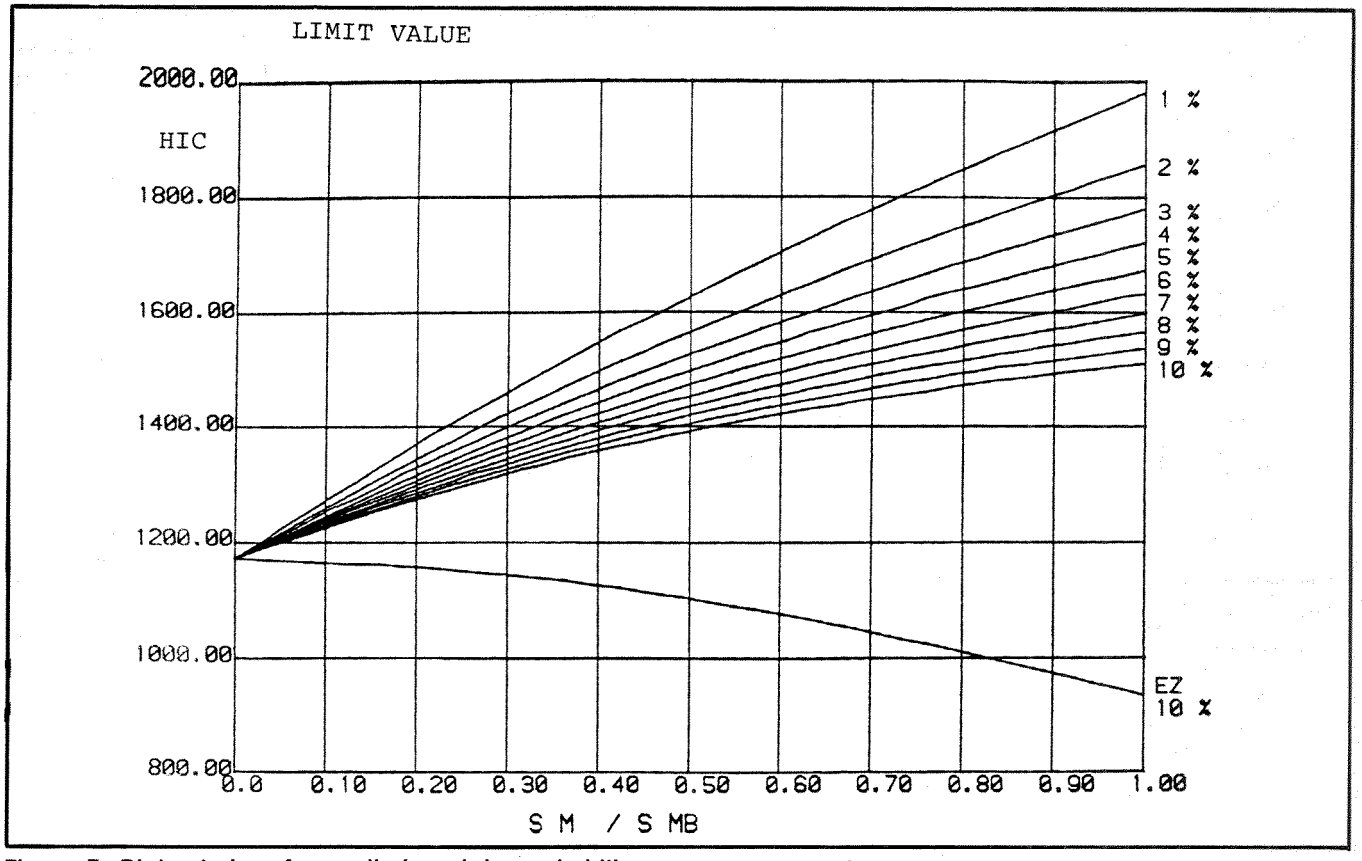

Figure 7. Right choice of a test limit and the probability of erroneously rejecting a correctly designed vehicle

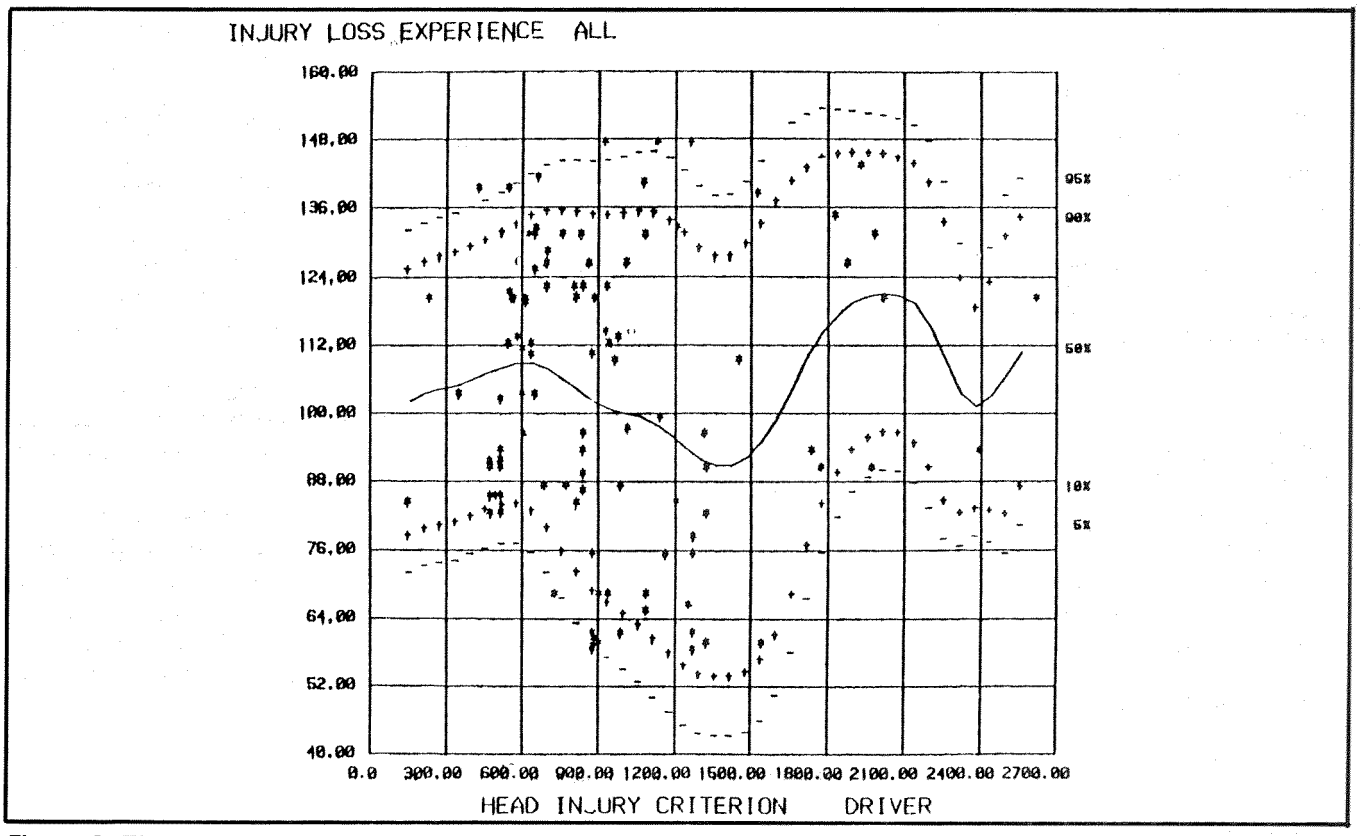

Figure 8. The problem of test results (NCAP) and their sensitivity in road traffic (HLDI)

5. Härdle, W. "Nichtparametrische robuste regressions analyse," diss. 1982, Universität Heidelberg.*
6. National Highway Traffic Safety Administration, "New car assessment program crash test results," September 17, 1984.
7. Highway Loss Data Institute, "Personal injury protection coverages," Research report HLDI 183-1, September 1984.
8. Schmid, W., "The increase in the risk of injury in traffic accidents as a result of higher test impact speeds," Proceedings Ninth International Technical Conference on Experimental Safety Vehicles, Kyoto, 1982.
9. Schmid, W., "A model to assess risk of injury in traffic accidents as a function of regularized test impact speed," SAE P 146, May 1984.

*"Nonparametric, robust regression analysis," diss. 1982, University of Heidelberg.

Car Size and Safety: Results From Analyzing U.S. Accident Data

Leonard Evans
Transportation Research Department, General Motors Research Laboratories

Abstract

The results of studies performed by the General Motors Research Laboratories to investigate the relationship between car size (indicated by car mass) and safety are presented. Most of the studies reviewed rely heavily on one data set that has uniquely useful features. This is the Fatal Accident Reporting System (FARS) data set maintained by the National Highway Traffic Safety Administration (NHTSA), which is part of the U.S. Department of Transportation. This file contains detailed information on every fatal traffic crash occurring in the United States since 1975. The studies find that given a single-car crash, the unbelted driver of a 900kg car is about 2.6 times as likely to be killed as is the unbelted driver of an 1,800kg car. The relative disadvantage of the smaller car is essentially the same when the corresponding comparison is made for belted drivers. For two-car crashes, it is found that the driver of a 900kg car crashing into another 900kg car is about 2.0 times as likely to be seriously or fatally injured as is the driver of an 1,800kg car crashing into another 1,800kg car. The above-mentioned results refer to what happens if a crash occurs. Relations between car size and accident involvement rates will also be discussed.

Introduction

This paper summarizes a number of studies performed by General Motors Research Laboratories to investigate relationships between car size and safety. The main thrust will be on the probability of driver death (or injury) given that a crash has occurred, as a function of the car size.

In all cases, we characterize car size by the physical variable mass as measured by the curb mass of the car. We then determine relation between probable driver death (or injury) and car mass. Such relations do not imply that car mass, as such, is the causative factor. Clearly, a wide variety of vehicular characteristics are strongly correlated with car mass (e.g., wheelbase, track, size in general, hood length, trunk size, engine displacement, etc.).

Most of the studies reviewed rely heavily on one data set that has uniquely useful features. This is the Fatal Accident Reporting System (FARS) data set maintained by the National Highway Traffic Safety Administration (NHTSA), which is part of the U.S. Department of Transportation. This data set contains detailed information on every fatal traffic crash in the United States since January 1, 1975. Thus, unlike most traffic crash data sets, it is not a sample but a census. Much of the focus of this paper is on fatal crashes because the uncertainties surrounding such crashes, especially as recorded in FARS, are so much less than those associated with other levels of injury. Some of the studies to be reviewed use other data sources, which will be described in the appropriate sections.

In this paper, the main findings from previously published studies are summarized. For full details, including raw data, specific derivations of results from raw data, references to other work, and detailed discussion of underlying assumptions, the reader is referred to the original paper cited. The topics discussed in this paper are—

Crashes involving one car
- Driver fatality likelihood versus car mass
- Belted compared to unbelted fatality risk versus car mass

Crashes involving two cars
- Effect of mass of each car on driver fatality likelihood
  - — Crashes in all directions

  - — Head-on crashes only
- Effect of mass on driver fatality likelihood when cars of similar mass crash into each other
  - — Crashes in all directions
  - — Head-on crashes only

Method

Exposure

A problem common to essentially all investigations using field accident data is that of exposure, or the opportunity to be involved in a crash(6). Although the FARS data give detailed information on the characteristics of the drivers and vehicles involved in particular types of crashes, information of the type often used to estimate exposure (for example, distance of travel, number of registered cars) is not available internal to the FARS file. Although such information might be available from an independent source, there are pitfalls associated with bringing together data sets with dissimilar origins and definitions(8).

Exposure for most of the studies reviewed here that use the FARS data will be estimated using the exposure approach introduced by (6), and more simply described in (8).

For simplicity, let us consider that we wish to estimate as a function of car mass the likelihood a driver is killed, given his car strikes a tree. The FARS data do not provide any information on the number of crashes with trees in general, because only crashes in which a car occupant is killed are coded. In the exposure approach(6), we, in essence, assume that the number of crashes with trees (most of which are nonfatal) is proportional to the number of crashes with pedestrians, and the number of crashes with pedestrians is in turn proportional to the number of crashes with pedestrians in which the pedestrian is killed, this latter quantity being coded in the FARS data because of the pedestrian fatality. This involves assuming that, given a car-pedestrian crash, the likelihood the pedestrian is killed is independent of the car mass. This is reasonable on physical grounds. Even the lightest car is generally much heavier than the heaviest pedestrian, so the pedestrian kinematics after the crash are essentially independent of car mass. That is, the car's speed is not appreciably altered by the pedestrian impact. Note that other factors being the same, the larger car, being wider, is more likely to strike a pedestrian. This does not bias the exposure measure because the larger car is equally more likely to strike the tree.

The results of many studies(1) do not refute the assumption that in car-pedestrian crashes, the probability of a pedestrian fatality is independent of car mass(6). There is at most a weak hint that the larger car is more likely to kill the pedestrian, given a crash.

In the exposure approach, it is also assumed the relative dependence on car mass of the likelihood of encountering a pedestrian is the same as the relative dependence on car mass of the likelihood of encountering a tree. Examining variations by time of day and by urban versus rural classification showed no large departures from this assumption(6).

Thus, in the exposure approach, the number of car drivers killed in some group of cars divided by the number of pedestrians killed in crashes involving cars from the same group is proportional to the likelihood of a driver fatality, given a crash. That is, to within a scaling factor, the probability of driver fatality, given a crash, is estimated by the number of drivers killed divided by the number of pedestrians killed.

The degree to which results derived using this exposure approach are independent of driver behavior, and agree with results from other methods, will substantiate its appropriateness. Other exposure estimates used in this paper will be discussed in the appropriate sections.

Analytical Relations

In most of the studies, relative driver fatality (or injury rate), y, and mass, m, are fitted using a least squares procedure to:

$$\ln y = A + bm \qquad (1)$$

The data are plotted in the figures in a linear rather than logarithmic form, so Equation 1 may be conceptualized more conveniently as:

$$\text{where:} \quad y = a \exp(bm), \quad a = \exp(A) \qquad (2)$$

The logarithmic relation (Equation 1 or Equation 2) was chosen in preference to a linear relationship between y and m for two reasons. First, the logarithmic relation generally provides a better fit to the data. Second, the logarithmic relation is a simpler and more effective way to compare relative rates for cars of different masses. Such comparison involves only the slope parameter, b. Hence the relative influence of car mass is immediately given by this one parameter. The other parameter, a, is merely a scaling factor that cancels when rates for cars of different masses are compared.

Rather than using the analytical relationship between rate y and car mass m (Equation 1 or Equation 2), it is often even simpler to focus on a comparison of rates for two cars of specific masses—one a small car and the other a large car. The specific illustrated masses we choose are 900kg and 1,800kg. Thus, we compare the rate for a 900kg car with the rate for an 1,800kg car, which, from Equation 2, is given by

$$y(m = 900\text{kg}) / y(m = 1{,}800\text{kg}) = \exp(900\, b) \qquad (3)$$

where b is in kg^{-1}. The simplicity of Equation 3, involving only b and the difference between the illustrative masses chosen, underlines the advantage of the logarithmic relation.

Results

Crashes Involving One Car

Driver Fatality Likelihood Versus Car Mass

The relationship between driver fatality likelihood and car mass was addressed by (6) applying the previously described pedestrian fatality exposure approach. All fatally injured drivers, independent of whether they were coded as using a restraint system, were included. As only a few percent of such drivers are coded as using any restraint system, the results apply essentially to a population of unrestrained drivers. Later we discuss the corresponding relationship for restrained drivers.

The ratio of drivers killed in single-car crashes to pedestrians killed is shown versus car mass in Figure 1; all crashes involved cars whose drivers were ages 16 to 24 years. This ability to focus on specific subsets (e.g., drivers of given age) is an important advantage of the pedestrian exposure approach over most traditional exposure approaches.

The data in Figure 1 show a clear reduction in fatality likelihood, given a crash, with increasing car mass.

Figures 2 and 3 show information similar to that in Figure 1, but for driver ages 25 to 34 and ≥35 years, respectively. Despite the large differences in accident involvement rate for drivers of different ages, observe that the ratios plotted in Figures 1 through 3 are essentially the same for each of the age groups. This supports the claim that the ratio is reflecting physical properties of the vehicle, essentially independent of driver behavior effects.

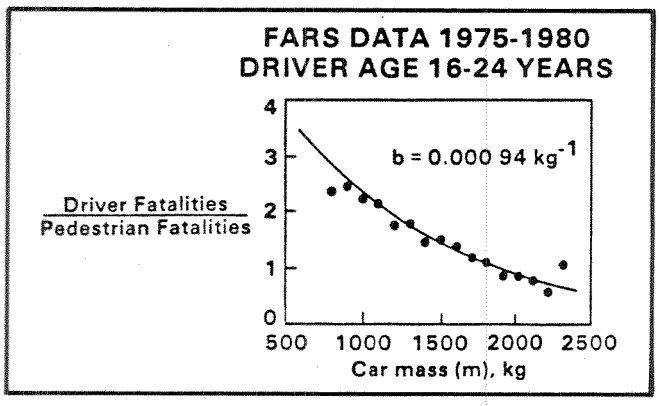

Figure 1. Ratio of drivers killed in single-car crashes involving no other vehicles to number of pedestrians killed in crashes involving cars of the same mass, versus car mass (driver age 16-24 years)

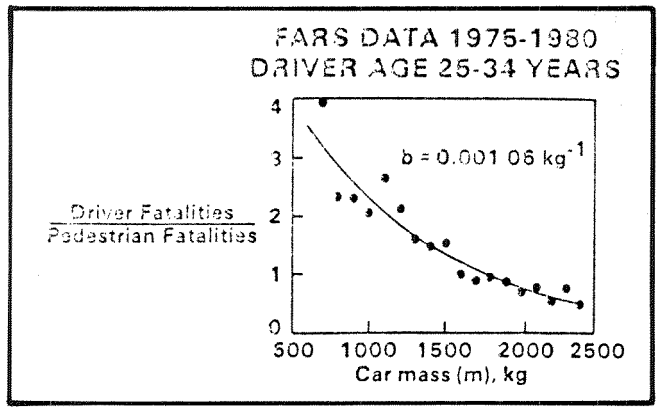

Figure 2. Ratio of drivers killed in single-car crashes involving no other vehicles to number of pedestrians killed in crashes involving cars of the same mass, versus car mass (driver age 25-34 years)

In addition to using pedestrian fatalities to estimate exposure, Evans also used motorcycle fatalities based on a parallel rationale(6). Furthermore, crashes in which car drivers were killed as a consequence of a crash with a truck are examined as another type of single-car crash. Thus, Evans(6) examined 12 relations (two types of driver fatalities × two types of exposure fatalities × three age categories) of which Figures 1 through 3 represent three. The results for all 12 cases are summarized as:

$$y(m) \propto \exp(-0.001\ 06m) \qquad (4)$$

where y is the relative likelihood of a driver fatality, given a crash, and m is the car mass in kg.

In terms of the specific example discussed earlier, Equation 4 implies that the driver in a 900kg car is 2.6 times as likely to be killed in a single-car crash as is the driver in an 1,800kg car.

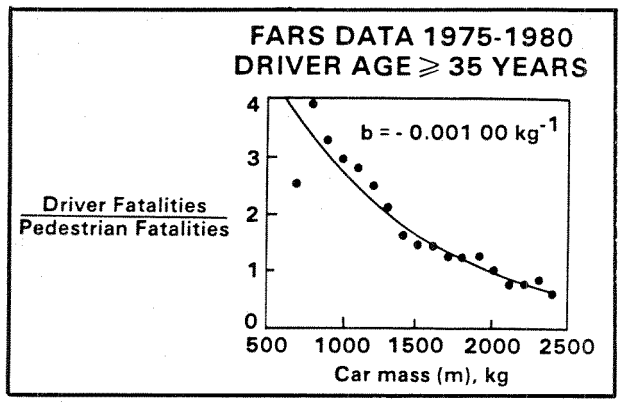

Figure 3. Ratio of drivers killed in single-car crashes involving no other vehicles to number of pedestrians killed in crashes involving cars of the same mass, versus car mass (driver age 35 years)

Belted Driver Compared to Unbelted Driver Fatality Risk Versus Car Mass

To determine the car mass relationship for belted drivers, a similar analysis was applied(9) to that small subset (less than 3 percent) of drivers coded in FARS as using some type of safety belt (lap, shoulder, or lap plus shoulder). Here the sample size is too small to disaggregate by driver age. To further increase the sample size, the numerator was taken to be the sum of all drivers killed in crashes involving one car (single-car crashes plus car drivers killed in crashes with trucks) divided by all nonoccupants killed (pedestrians plus motorcyclists).

This composite ratio of drivers killed per nonoccupant killed is shown versus car mass in Figure 4.

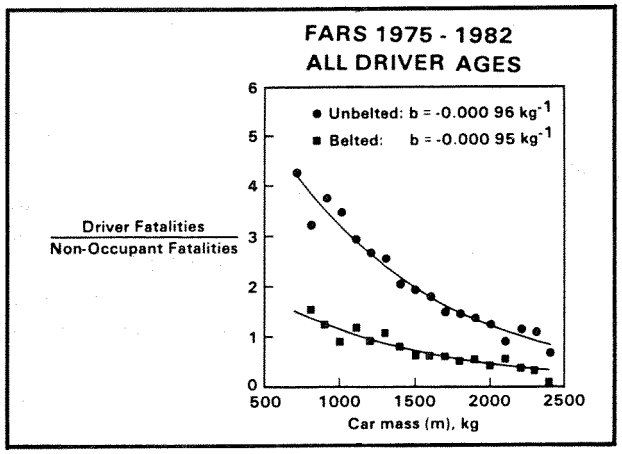

Figure 4. Ratio of car drivers killed in crashes involving only one car to nonoccupants (pedestrians and motorcyclists) killed involving cars in the same mass range

The data shown here should not be used to estimate safety belt effectiveness in preventing fatalities because of likely systematic bias in restraint use indications. Belt use indicated for fatally injured drivers is probably unbiased. However, for crashes in which nonoccupants are killed, the driver usually survives uninjured. The safety belt use information provided to the investigating officer is therefore, to a considerable extent, self-reported. Self-reporting, interview-type surveys invariably indicate belt use rates that exceed observed actual use rates by factors of two or more (compare, for example, the survey results of (14) or (13) with consistently observed U.S. use rates of 11 to 14 percent. Although the circumstances of such surveys have little in common with those at the scene of a crash in which a pedestrian or motorcyclist is killed, they nonetheless point out the possibility of a bias toward the more socially acceptable response; namely, to indicate a restraint system was used. Accordingly, the data should not be used to estimate safety belt effectiveness in preventing driver fatalities, given a crash. Any bias toward overestimating belt use for the crashes in which nonoccupants were killed will not affect the relations with car mass provided such bias is not also a function of car mass; we assume any such bias to be independent of car mass.

The curves shown in Figure 4 are:

$$y_{unbelted}(m) \propto \exp(-0.000\ 96m) \quad (5)$$

$$y_{belted}(m) \propto \exp(-0.000\ 94m) \quad (6)$$

Clearly, from Equations 5 and 6 there is no material difference in the relative effect of car mass for the belted and unbelted cases.

In terms of the example using specific car masses, we find the belted driver of a 900kg car is 2.3 times as likely to be killed in a crash as is the belted driver of an 1,800kg car.

From Equation 5, an unbelted driver in a 900kg car is 2.4 times as likely to be killed in a crash as is an unbelted driver in an 1,800kg car. Note this is not identical to the 2.6 ratio reported earlier because Equation 5 is not identical to Equation 4. The calculation that produced Equation 5 differs from that which produced Equation 4 by including unbelted drivers only rather than all drivers; by using 1975-1982 data rather than 1975-1980 data; by using a composite ratio rather than an average of individual ratios; by combining all ages rather than disaggregating into three driver age groups. These and other differences reflect either improvements over the earlier work or aggregation performed to increase the population size to obtain sufficient data for the belted case.

Thus, in conclusion, we find that in a single-car crash, a driver of a 900kg car is about 2.4 times as likely to be killed as is the driver of an 1,800kg car. This result is essentially the same for belted or unbelted drivers.

Crashes Involving Two Cars

Here we wish to examine how the mass of each car involved in a two-car crash affects the relative likelihood that the driver is killed. As the data must be disaggregated twice by car mass, coarser divisions than used in the single-car case are required. Accordingly, a number of analyses based on the six mass categories displayed in Table 1 have been performed.

Relative Driver Fatality Likelihood When Cars of Different Mass Crash Into Each Other

All Impact Directions—The data from FARS 1975 through 1980, given in (12) and based on (5), are reproduced in Table 1.

Each entry in the table shows the number of drivers in cars in the m_i mass category killed as a result of crashes with cars in the m_j category. For example, 35 drivers of

Table 1. Number of driver fatalities in cars of mass m_i in collisions with cars of mass m_j, all impact points

			Car j						
	Mass, kg		m_1	m_2	m_3	m_4	m_5	m_6	Total
Car i	500- 900	m_1	34	79	156	352	582	578	1,781
	900-1,100	m_2	33	86	165	396	679	693	2,052
	1,100-1,300	m_3	36	74	171	443	684	698	2,106
	1,300-1,500	m_4	47	79	226	604	1,088	1,132	3,176
	1,500-1,800	m_5	34	95	189	558	1,071	1,253	3,200
	1,800-2,400	m_6	35	70	139	415	753	878	2,290
	Total		219	483	1,046	2,768	4,857	5,232	1,4605

m_6 cars were killed as a consequence of crashes with m_1 cars. In these same crashes involving m_1 and m_6 cars, 578 drivers of m_1 cars were killed. Thus, we can infer immediately that in crashes involving m_1 and m_6 cars, for every driver killed in m_6 cars, there are 578/35 = 16.5 drivers killed in m_i cars. Note this result is exposure independent. If there were more crashes involving m_1 and m_6 cars, this would affect the quantity of data but not the 16.5 result in any obvious way.

The relative risk to the drivers in cars in any pair of masses may be compared in a similar exposure-free way. One may readily note, for example, how rapidly the ratio of drivers killed in the lighter car compared to in the heavier car increases as the mass disparity increases. Cerrelli presents data in a similar format to Table 1, but including a wider range of vehicles, from minicompact cars to heavy trucks; for the case of these vehicles crashing into each other, the driver fatality risk in the minicompact car was 36 times what it was in the heavy truck(4).

Estimates for arbitrary masses are best made by interpolation. For example, the data indicate that when 900kg and 1,800kg cars crash into each other, the driver in the 900kg car is about 13 times as likely to be killed as is the driver of the 1,800kg car. This is larger than the 8 times ratio, which was based on substantially fewer data, reported by Evans(5).

To proceed beyond pair-wise comparisons requires some estimate of exposure. The pedestrian exposure approach was used(12) to transform the data in Table 1 into that of Table 2. Each number in Table 1 was divided by the product of the number of pedestrians killed in crashes involving cars of mass m_i and the number of pedestrians killed in crashes involving cars of mass m_j. For convenience, all values were rescaled so the nominally safest case, a driver in a car in the heaviest mass category (m_6) crashing into a car in the lightest mass category (m_1) was assigned the value 1.00. Each value in that a driver in a car of mass m_i is killed in a crash with a car of mass m_j. This table is interpreted as the result sought. Efforts to summarize the information in bivariate analytical form were unsuccessful, so, again, estimates for arbitrary masses are best made by interpolation.

Head-on Crashes Only—Here the analysis is essentially as above, except the data are for head-on crashes, defined as follows. The head-on data are based on the variable "principal impact point," the position on the vehicle of the impact that produced the greatest personal injury or property damage. This variable is coded in 12 "clock points." Direction of impact force as such is not coded in FARS data. For FARS data, we define a head-on crash as one in which both cars are coded as having principal point of damage at the 12 o'clock position. That is, if either car is coded as, for example, left front (clock point 11), this crash is not included. Hence the data come as close as possible to representing head-on crashes, based on FARS data.

Table 3 shows the raw fatality data for the head-on case, which is to be compared to the all-directions case shown in Table 1. From these tables, we see that about 40 percent of all fatal two-car crashes are head-on crashes. Head-on crashes compose a much smaller percentage of two-car crashes with less severe injuries.

The data in Table 3 are converted into relative fatality rates using the pedestrian exposure method to generate Table 4. Again, it is rescaled so the bottom left value has the value of 1.00.

Generally, the car mass effect tends to be somewhat larger, though not consistently so, for the head-on than for the all-directions case. For example, the data indicate that when a 900kg car and an 1,800kg car crash head-on, the driver of the 900kg car is about 14 times as likely to be killed as is the driver of the 1,800kg car.

Cars of Similar Mass Crashing Into Each Other.

One type of a two-car crash of particular interest is when the two cars are of similar mass. In such crashes, the

Table 2. Relative likelihood of driver fatality in car mass m_i involved in a 2-car crash with car mass m_j, all impact points

			Car j					
	Mass, kg		m_1	m_2	m_3	m_4	m_5	m_6
Car i	500- 900	m_1	7.04	12.12	15.15	16.05	16.86	16.51
	900-1,100	m_2	5.06	9.78	11.88	13.38	14.58	14.68
	1,100-1,300	m_3	3.50	5.33	7.79	9.48	9.30	9.36
	1,300-1,500	m_4	2.14	2.67	4.83	6.06	6.94	7.12
	1,500-1,800	m_5	0.98	2.04	2.57	3.56	4.34	5.01
	1,800-2,400	m_6	1.00	1.48	1.86	2.61	3.01	3.46

Table 3. Number of driver fatalities in cars of mass m_i in collisions with cars of mass m_j, principal impact point "12 o'clock" for both cars.

			Car j						
	Mass, kg		m_1	m_2	m_3	m_4	m_5	m_6	Total
Car i	500- 900	m_1	14	38	68	136	218	207	681
	900-1,100	m_2	13	43	68	186	264	274	848
	1,100-1,300	m_3	17	34	65	168	253	268	805
	1,300-1,500	m_4	17	29	92	252	407	445	1,242
	1,500-1,800	m_5	10	44	73	222	450	573	1,372
	1,800-2,400	m_6	10	31	50	152	326	367	936
	Total		81	219	416	1,116	1,918	2,134	5,884

dynamical forces on each car are similar. Indeed, for the head-on case, such crashes are in some respects similar to barrier crashes.

All Impact Directions—The relative risk of fatality when a car in the m_i mass category crashes into another car in the same mass category is given in the highlighted diagonal elements in Table 3. These are shown plotted in Figure 5. The values, y, have been rescaled as follows. The data highlighted in the diagonal elements were fitted to Equation 1 using weighted least squares(12), and the value for M = 1,800kg assigned the rescaled value 1.00. Here we use M to denote the common mass of the two cars that crashed into each other, in contrast to m, the mass of one car.

The other two curves in Figure 5 show estimates of the probability of driver serious injury or fatality when cars of similar mass crash into each other based on two State data sources, New York(15) and North Carolina(2). The rates here are number of drivers injured divided by the number of crashes, rescaled in the same way so the value at M = 1,800kg corresponds to y = 1.

The results in Figure 5 are summarized in Table 5 in terms of the comparison between 900kg and 1,800kg cars.

Note the relatively good agreement (see Figure 5, Table 5) between the FARS results based on the pedestrian exposure approach and the State results calculated as drivers injured per crash. This agreement provides support that the pedestrian exposure approach is reasonable.

In summary, we find that a driver in a 900kg car crashing into another 900kg car is about 2.3 times as likely to be seriously injured or killed as is a driver in an 1,800kg car crashing into another 1,800kg car when all directions of impact are considered together.

Head-on Crashes Only—Here the analysis is as before, except that the starting point is the highlighted diagonal data in Table 3, which is used to generate the relative fatality data in Table 4. These data are shown plotted, after rescaling as before, in Figure 6, together with head-on only data for the States of New York and North Carolina.

Results from the data plotted in Figure 6 are summarized in Table 6 in terms of comparing a 900kg car

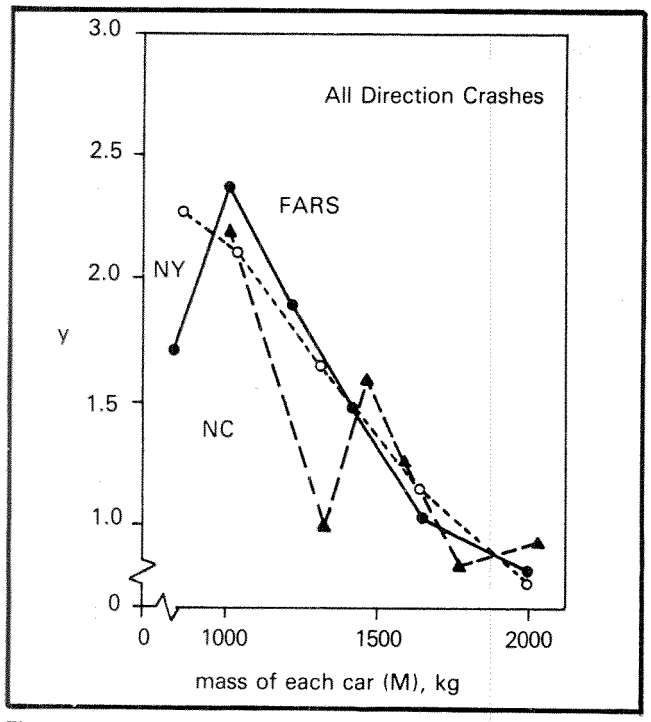

Figure 5. Relative likelihood, y, of driver injury (serious or fatal) when a car of mass M crashes into another car of similar mass (all directions) (values relative to a value one for two 1,800kg cars crashing into each other)

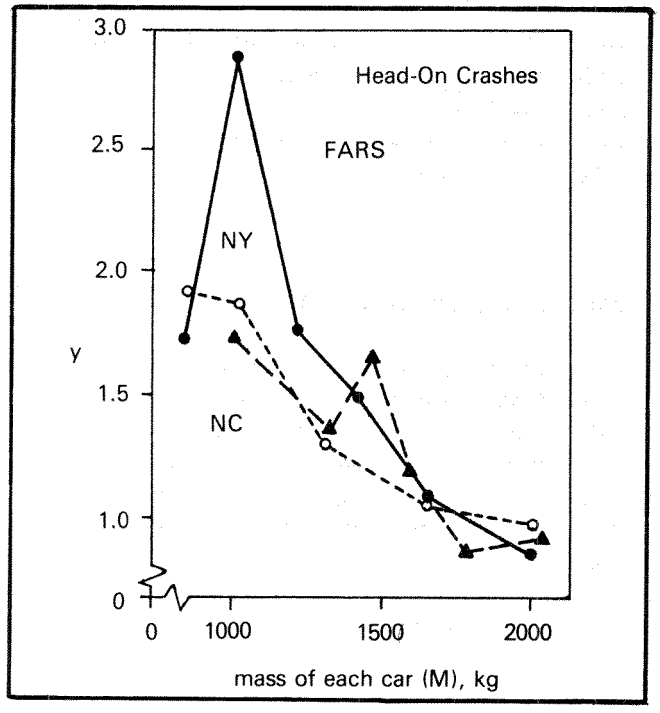

Figure 6. Relative likelihood, y, of driver injury (serious or fatal) when a car of mass M crashes into another car of similar mass (values relative to a value one for two 1,800kg cars crashing head-on into each other)

Table 4. Relative likelihood of driver fatality in car mass m_i involved in a 2-car crash with car mass m_j, principal impact point "12 o'clock" for both cars

Mass, kg		Car j					
		m_1	m_2	m_3	m_4	m_5	m_6
Car i 500- 900	m_1	10.14	20.41	23.12	21.70	22.10	20.70
900-1,100	m_2	6.98	17.12	17.14	22.00	19.84	20.31
1,100-1,300	m_3	5.78	8.57	10.37	12.58	12.03	12.58
1,300-1,500	m_4	2.71	3.43	6.89	8.85	9.09	9.80
1,500-1,800	m_5	1.01	3.31	3.47	4.96	6.38	8.02
1,800-2,400	m_6	1.00	2.30	2.35	3.35	4.56	5.07

Table 5. Summary of the ratios of driver injury (serious or fatal) when two 900kg cars crash into each other (all directions) to that when two 1,800kg cars crash into each other.

Data	Driver Injury	y(M=900kg) / y(M=1,800kg)
FARS	fatal	2.27
NY	serious or fatal	2.35
NC	serious or fatal	2.16
	mean	2.26
	standard deviation	0.10

Table 6. Summary of the ratios of driver injury (serious or fatal) when two 900kg cars crash head-on into each other to that when two 1,800kg cars crash into each other.

Data	Driver Injury	y(M=900kg) / y(M=1,800kg)
FARS	fatal	2.42
NY	serious or fatal	1.68
NC	serious or fatal	2.02
	mean	2.04
	standard deviation	0.37

crashing head-on into a 900kg car to an 1,800kg car crashing head-on into an 1,800kg car. In summary, it is found the likelihood of driver serious injury or fatality is about twice as great when two 900kg cars crash head-on as when two 1,800kg cars crash head-on.

Summary and Discussion

The results presented are summarized in Table 7. These reports support the overall conclusion that given a crash, the driver in a smaller car has a substantially higher probability of serious injury or fatality. In no case of comparing 900kg to 1,800kg cars was the disadvantage to the driver of the lighter car less than a factor of two.

The main focus of this paper has been on how car size affects the probability of driver death or injury, given a crash occurs. Although the effects found are of substantial magnitude, they are smaller than many influences due to driver behavior. For example, younger drivers have fatality rates that exceed those for older drivers by factors of four or five(3,16). Part of the physical disadvantage of the smaller car is mitigated by lower accident involvement rates being associated with smaller cars(8,7,9). Indeed, although when a 900kg car crashes into a 900kg car, the probability of driver serious injury (or fatality) is twice as great as when an 1,800kg car crashes into an 1,800kg car, the actual number of drivers seriously injured or killed in the small-small crashes is, paradoxically, less than for the large-large crashes when normalized for numbers of cars and driver age(10). This is one of a number of examples of "human behavior feedback"(11). Such feedback need not necessarily reduce the effectiveness of safety engineering improvements; these are indications(11) that in some specific cases, such feedback may further enhance such improvements. However, as stressed in (11), the question of how users react to safety engineering changes should always be addressed in any consideration of the potential net effects of such changes.

In overall conclusion, it is found that given a crash occurs, drivers of smaller cars are substantially more likely to be killed than are drivers of larger cars. For the example given of comparing driver fatality likelihood in a 900kg car to that in an 1,800kg car, in none of the crash types discussed in the paper was the disadvantage to the driver of the 900kg car less than a factor of two.

References

1. Ashton, S., A bibliography of pedestrian accident references with emphasis on vehicle design and pedestrian injury, included in SAE special publication P121, "Pedestrian injury and assessment," p. 265-275, SAE, Warrendale, Pennsylvania, 1983.
2. Campbell, B.J., and D.W. Reinfurt, "The relationship between driver crash injury and passenger car weight," Highway Safety Research Center, University of North Carolina, Chapel Hill, North Carolina, 1973.
3. Carsten, O., "Use of the nationwide personal transportation study to calculate exposure," University of Michigan, *The HSRI Research Review,* 11, 1-7, 1981.
4. Cerrelli, E.C., "Risk of fatal injury in vehicles of different size," U.S. Department of Transportation Report DOT-HS-806-653, November 1984.
5. Evans, L., "Car mass and likelihood of occupant fatality," SAE Paper 820897, June 1982.
6. Evans, L., "Driver fatalities versus car mass using a new exposure approach," *Accident Analysis and Prevention,stA1 16,* 19-36, 1984.
7. Evans, L., "Accident involvement rate and car size," *Accident Analysis and Prevention,stA1 16,* No. 5/6, pp. 387-405, 1984.

Table 7. Summary of results presented comparing small and large car safety

Crash type	Measure	Restriction	900kg to 1,800kg ratio
Single-car crashes	driver fatalities per crash	unbelted	2.4
		belted	2.3
Two-car crashes:- into each other	driver fatalities per crash	all directions	~13
		head-on	~14
into another car of similar mass	driver serious injuries (including fatality) per crash	all directions	2.3
		head-on	2.0

8. Evans, L., "Driver behavior revealed in relations involving car mass," in L. Evans and R.C. Schwing (Eds.), *Human Behavior and Traffic Safety,* New York: Plenum, 1985.
9. Evans, L., "Fatality risk for belted drivers versus car mass," *Accident Analysis and Prevention,* in press, 1985.
10. Evans, L., "Involvement rate in two-car crashes versus driver age and car mass of each involved car," *Accident Analysis and Prevention,* in press, 1985.
11. Evans, L., "Human behavior feedback and traffic safety," *Human Factors,* in press, 1985.
12. Evans, L., and P. Wasielewski, "Serious or fatal driver injury rate versus car mass in head-on crashes between cars of similar mass," Proceedings 28th Conference of the American Association for Automotive Medicine, 1984.
13. Lund, A.K., "Public opinion about automobile occupant restraint," Insurance Institute for Highway Safety, submission to Docket 74-14, No. 32, Occupant Crash Protection, December 19, 1983.
14. O'Day, J., and L.D. Filkins, "Attitudes towards wearing belts: a survey of Michigan drivers," *The UMTRI Research Review,stA1 14* (1), July-August, 1983.
15. Negri, D.B., and R.K. Riley, "Two car collision study II," Report No. DOT-HS-245-2-478-4, performed by State of New York Department of Motor Vehicles, June 1974.
16. Williams, A.F., "Nighttime driving and fatal crash involvement of teenagers," *Accident Analysis and Prevention, stA117,* No. 1, 1-5, 1985.

Rating System for Serious Consequences (RSC) Due to Traffic Accidents—Risk of Death or Permanent Disability

Hans Gustafsson
Folksam Research and Development Division, Stockholm, Sweden

Åke Nygren and
Claes Tingvall
Folksam Research and Development Division, Karolinska Hospital, Department of ENT, Stockholm, Sweden

Abstract

Injury rating is an important issue in the field of traffic safety. The injury pattern can be obtained either from the scene of the accident, including all severity grades, or from the frequency of those fatally injured. Less attention has been paid to the long-term consequences of an injury. Furthermore, the existing rating system is based on the medical status at the scene of the accident or immediately after and judges only the risk of death.

Nygren(6) showed that for many body regions the AIS values did not reflect the outcome of a trauma expressed in permanent medical disability.

In this study, 339,675 accidents with private cars were analyzed with respect to injuries to car occupants. In these accidents, 14,361 persons were injured. The risk of permanent disability due to different injuries is derived and linked to AIS values to different body regions.

A rating system for injuries based on the risk of death or permanent disability is proposed. The rating system called RSC, risk of serious consequences, used ISS and AIS for different body regions. RSC was used to describe differences in injuries to belted and unbelted car occupants.

Background

Much attention has been paid to the problem of injury rating, especially in the field of traffic accidents. Today the AIS (Abbreviated Injury Scale) is used all over the world and accepted as a sufficient tool for injury rating. There is a great number of empirical materials coded according to the AIS.

Several methods have been used to judge multiple injuries coded in the AIS such as OAIS and MAIS. The most widely used technique today seems to be the ISS (Injury Severity Score) where the highest AIS values for three body regions are squared and summed(1).

AIS and ISS, as well as other expressions of multiple injuries, have been treated with questionable statistical methods(2), although this is not very surprising as many normal and well-known statistical quantitative methods are not possible to use when analyzing AIS values. This is mainly due to the fact that AIS values as well as ISS values are not equidistant and the scale is qualitative.

Bull(3) and Baker(1,4) showed there is a high correlation between ISS and risk of death. Somers(2,5) has also shown this connection but proposed another score

system, PODS, with a mathematical expression for risk of death for a given combination of AIS values.

Bull(3) made an analysis of the relationship between ISS and permanent disability where he found rather good correlation.

Nygren(6) showed that injuries with low severity according to AIS (AIS 1 and 2) with no interaction of other injuries often lead to permanent disability. These results indicate that neither ISS nor AIS, not linked to body region, can fully explain the risk of permanent disability. This is not surprising as AIS and its outlines are not primarily derived to serve purposes other than estimating threat of death.

On the other hand, there is a certain need to be able to describe risks of disabling injuries and long-term consequences as such consequences are expensive to society and important to reduce.

Since many materials are coded in the AIS and most accident researchers are familiar with the AIS and its outlines, one should be cautious in proposing a new rating system. A better way to proceed is probably to derive new methods based on the AIS and ISS.

In this paper, a new way of using the AIS is presented, aimed at giving a tool for estimating the risk of medical disability. A new score is also presented where two highly unexpected consequences of traffic accidents are mixed together, namely fatalities and medical disability. The score is called RSC, risk of serious consequences.

The proposal to use the AIS, in this case linked to body region, to predict the risk of medical disability is also meant to be a system where the individual patient is not followed up but only observed immediately after the accident.

Material

A material consisting of 5,871 car occupants injured during the period July 1, 1976, to December 31, 1978, has been used to produce risks of permanent disability. All injuries have been coded according to the AIS.

The accidents in which the injuries occurred were reported to the Folksam Insurance Company, and a further description of the material was presented by Nygren(6). A small loss of data, consisting mainly of minor injuries, was shown to exist, but this was considered to affect the result only marginally. The same material was used to demonstrate the RSC. In this article, the difference between belted and unbelted occupants in accidents was shown.

Figures for death risks given by the ISS were taken from Bull(3) and Baker(4).

The definition of medical disability was described by Nygren(6) and is used by Swedish insurance companies. The basis for the medical disability should be an objective judgment based on functional loss and pain. No attention should be paid to occupation or other individual parameters. Most disability cases have fixed values or latitudes. The advantage of the Swedish system is not the scaling in itself, but the fact that cases of medical disability are judged by a committee consisting of members of all insurance companies. This guarantees a certain level of consistency.

Method

The risk of death or permanent disability is:

$$P(FUD) = P(F) + (I-P(F)) * P(D) \quad (1)$$

Expressed in this way, the probability also includes the risk of being both dead and medically disabled, although this is, of course, impossible in real life.

As the probability is not separated, this is of no practical meaning. If the probability of being medically disabled is based only on survival, separation is still possible if the expected number of deaths is calculated first and then the number of those surviving with medical disability.

The way used to express the probability of death or medical disability(1) in a way gives understanding of the above-mentioned idea.

The probability of death can be derived in two different ways from AIS data, either by empirical figures or by some sort of mathematical expression. Somers(2,5) proposed PODS, probability of death score, based on the AIS. Bull(3) and Baker(4) showed the correlation between the ISS and death. In this paper, empirical death risks have been used but mathematical expressions could be used as well. Data were taken from Bull(3) and Baker(4). The death risk was separated for different ISS intervals, and these figures are given in Table 1.

The risk of medical disablement for surviving injured car occupants has been separated in risks to different body regions for different AIS values.

The figures given in Table 2 are originally shown by Nygren(6). The figures here are slightly modified.

Table 1. Risk of death correlated to the ISS

ISS-intervals	Risk of death ($0 \leq r_f \leq 1$)
1- 3	0.00
4- 8	0.001
9-14	0.005
15-19	0.04
20-24	0.08
25-29	0.16
30-34	0.26
35-39	0.37
40-44	0.50
45-49	0.65
50-54	0.85
>54	1.00

Table 2. Risk of permanent disability for different body regions and AIS for those surviving

Body region	AIS 1	AIS 2	AIS 3	AIS 4	AIS 5
Skull/brain	0.01	0.02	0.15	0.25	0.50
Neck	*	0.10	0.50	0.50	0.75
Face	0.0001	0.005	0.10	0.10	-
Arm	0.0005	0.035	0.15	0.60	-
Leg	0.0005	0.15	0.25	0.60	-
Chest	0.0001	0.0005	0.01	0.03	0.05
Abdomen	0.0001	0.0001	0.0001	0.01	0.01
Pelvis	0.0001	0.075	0.075	0.075	-
Back	0.0001	0.05	0.20	0.75	-
External	0.0001	0.05	0.05	0.05	n.a

* 0.10 if rear-end collision
0.04 if other direction

The risk of being injured or medically disabled can be expressed as(2):

$$P(FUD) = P(F) + [(1 - P(F)) * (1 - \prod_{i} P(D_i^c))] \quad (2)$$

or expressed as a risk with empirical values:

$$RSC = r_f + [(1 - r_f) * (1 - \prod_{i} (1 - r_{id}))] \quad (3)$$

where r_{id} is the risk of medical disability for different body regions.

The expression $\pi (1-r_{id})$ is the risk of not having at least one medical disability for a specific body region. The risk, called RSC, is calculated for every single individual. The RSC value for a single injured person is treated as a single observation with fixed risk figures for death and disability.

The risk of death or medical disability for a certain group is called MRSC (Mean Risk of Serious Consequences). MRSC can be calculated because RSC values are equidistant. RSC and MRSC can also be treated with common statistical techniques.

The risk of death sometimes fails to be calculated by ISS. This occurs when there is only one very high AIS value (5 or 6). AIS 6 is by definition a fatal injury with rf = 1 though in studies of the interrelation between ISS and risk of death, ISS = 36 (from AIS = 6) only has $r_f \approx 0.4$. This problem is also present for AIS code 5. Baker(1) showed that an AIS = 5 together with a second low AIS code to another body area led to a mortality rate of more than 50 percent. In RSC, 50 percent is used as the lowest fatality risk for AIS = 5.

Example

Three persons had injuries as listed in the table below.

Injured person 1	Injured person 2	Injured person 3
AIS 3, Skull/brain AIS 2, lower extr.	AIS 1, neck (rear-end) AIS 2, upper extr.	AIS 4, chest AIS 3, abdomen
ISS = 13	ISS = 5	ISS = 25
Risk of death $r_f = 0.005$	$r_f = 0.001$	$r_f == 0.16$
Risk of permanent disability [1 - ($\prod$ (1 - r_{id})] (if surviving)		
$r_d = 0.278$	$r_d = 0.132$	$r_d = 0.030$
Σ RSC = 0.598 MRSC = 0.199		

Results

RSC was tested on accident material to describe the differences between belted and unbelted car occupants. Table 3 shows the distribution of injured persons in ISS groups for belted and unbelted front-seat occupants.

Table 3 shows clearly the positive effects due to seatbelt use. However, these values are not possible to translate into understandable figures on followings of seatbelt use apart from the number of fatalities. Let MRSC denote the estimation of MRSC in a sample.

Table 4 shows the difference between belted and unbelted expressed by MRSC for the same material as in Table 3.

Table 4 demonstrates clearly the difference between belted and unbelted car occupants when MRSC is used. The mean risk of serious consequences is reduced by 69 percent for drivers and by 60 percent for front-seat passengers when seatbelts are used compared to not-used. Apart from this effect, there is a reduction of the number of injured of about 30 to 40 percent(6), so the real effect on MRSC is larger.

If MRSC in big samples can be assumed to be asymptotically normally distributed, simple calculations can be used to give confidence limits for estimations of MRSC.

Discussion

This paper describes a technique to estimate the serious outcome of road traffic accidents. There is need for such techniques, especially when dealing with permanent medical disability. However, there are many questions that must be discussed before a technique based on the present suggestion can be accepted as a general tool for description of injury severity. In this paper, there is only one definition of permanent medical disability used. Of course, there are other definitions, as well as several other techniques, to describe the outcome of an injury.

Thorson(8) used a subjective but individually judged scale for the long-term consequences of injuries. In some respects, such a scale takes into account the social consequences due to a trauma, but since it is individually graded the demands for high-quality data require a long period of collecting data, etc. Thorson did not compare AIS values with the outcome.

Others have studied the relation between ISS and the risk of permanent disability(3).

Table 4. MRSC (mean risk of serious consequences) for injured, belted, and unbelted front seat occupants

	MRSC
Drivers	
Belted	0.079
Unbelted	0.257
Front seat occupants	
Belted	0.078
Unbelted	0.196

In this paper, it is proposed there should be a scale used on a common basis where there is no information required for the injured person other than AIS values for different body regions. A discussion should, therefore, also concentrate on such a scaling system. There are mainly three areas that are interesting:

1. Limits and criteria for medical disability or impairment
2. Age and sex factors influencing long-term consequences
3. Body areas and AIS

The limit for medical disability is subjective and can be set from 1 to 100 percent. In this paper, 10 percent was used due to technical and subjective reasons. The technical reasons are that only cases with at least 10 percent medical disability are judged systematically by a certain group of experts.

A subjective reason to use 10 percent as a limit is, among other things, that disability over this level is a long-term consequence of an accident that is unacceptable to most people. Other limits must, of course, be discussed. To use the disability level (1 to 100 percent) for weighing the seriousness of the outcome is on the other hand a method that can be questioned since the precision in the decision of different levels is subjective in many cases.

Table 3. Distribution of ISS among car occupants >15-years-old with and without seatbelt use (%)

	ISS 1-3	ISS 4-10	ISS 11-	Killed	N
Drivers					
Belted	61.7	29.1	5.7	3.4	3,173
Unbelted	33.3	30.8	14.8	21.1	522
Front seat passengers					
Belted	57.3	31.8	7.8	3.2	1,509
Unbelted	40.6	34.3	14.2	11.0	254

Age and sex have an influence on the risk of being both killed(3,4) and disabled(6). In some cases, it is necessary to take age and sex into consideration. The present material was not big enough to produce figures for subsets of injured.

AIS to body regions was used to generate disability risk figures. AIS to single body regions is the lowest level that can be reached in most accident materials. Nygren(6) showed that a higher level (e.g., AIS irrespective of body region or ISS) would be incorrect. Still, it is necessary to study the sufficiency of the level. For some AIS levels to certain body areas, e.g., lower extremities, it is still an open question if such a region should be divided into joint injuries and other injuries.

The relation between ISS and risk of death has been shown by several authors(3,4). Other techniques have been proposed to predict fatalities(2,5). In this paper, empirical values were used, but other techniques can be used as well with no other modification of RSC.

The figures used in this paper were taken from injured car occupants. It is important to have figures also for other road traffic categories.

Conclusion

By using ISS as a tool for describing death risks and AIS values to different body regions to calculate the risk of medical disability, it should be possible to use a technique to give figures on the risk of death or permanent disability by using only AIS data on a sufficient level. The relation between AIS and risk of permanent disability can be established by following injured persons over a period until the objective medical disability level is fixed.

Today there is no adequate system to judge serious consequences due to traffic accidents on a common basis, though there is a strong demand for such a system. ISS, as well as AIS not separated to body regions, cannot describe the risk of medical disability. RSC can describe both death risk and the risk of long-term consequences at the same time and can be used on most accident materials collected all over the world. It is, however, very important to discuss mainly the definition and limits for medical disability.

MRSC, used on seatbelt effectiveness, shows that the risk of death or medical disability is reduced (among injured car occupants) by 60 to 70 percent. The reduction is higher when injury frequency reducing factors are included.

References

1. Baker, S.P., B. O'Neill, W. Haddow, Jr., and W.D. Long, "Injury severity score: a method for describing patients with multiple injuries and evaluating emergency care," *Journal of Trauma* 14:187-96, 1974.
2. Somers, S.L., "The probability of death score: a measure of injury severity for use in planning and evaluating accident prevention," *Accident Analysis and Prevention*, 4:259-266, 1983.
3. Bull, J.P., "The injury severity score of road traffic casualties in relation to mortality, time of death, hospital treatment time and disability," *Accident Analysis and Prevention*, 7:249-255,1975.
4. Baker, S.O., and B. O'Neill, "The injury severity score: an update," *Journal of Trauma*, 11:882-885, 1976.
5. Somers, S.L., "The probability of death score. An improvement of the injury severity score," *Accident Analysis and Prevention*, 4:247-257, 1983.
6. Nygren, Å., "Injuries to car occupants—some aspects of the interior safety of cars," *Acta Oto-Laryngologica*, Suppl. 395, 164 p, 1984.
7. "Medical disability," Swedish Committee of Personal Injuries, FSAB 1981.
8. Thorson, J., "Long-term effects of traffic accidents," Karolinska Institutet Thesis, 1973.

Seatbelt Research and Legislation in The Netherlands

L.T.B. van Kampen
Institute for Road Safety Research SWOV, The Netherlands

Abstract

SWOV is the coordinating institute for scientific research on traffic safety in the Netherlands. A new international approach is being prepared for integrated road safety plans both in the field of the policymakers (on all levels) and in the field of research. This approach becomes necessary to further improve the safety of traffic on a large scale. Research projects such as detailed accident studies and seatbelt surveys have been carried out by SWOV and the results reported to the government and used to develop seatbelt legislation in the Netherlands. The layout of current seatbelt legislation and the compliance details are discussed.

Legislative developments are to be expected with respect to seatbelts on back seats. A comprehensive

report of SWOV on the pro's and contra's of new measures in this field has been published.

Mathematical crash models are being developed and used and may well be applied to predict changes in the population at risk with regard to injury severity levels. This will create a priority scale for proposed new measures.

Introduction

For more than 20 years, the Institute for Road Safety Research SWOV has been the coordinating institute for scientific research on traffic safety in the Netherlands. Though some 90 percent of its activities are carried out on behalf of or by order of the traffic safety departments of the Ministry of Transport, SWOV is an independent institute with regard to the scientific aspects of its work and publication of its reports.

The research program of SWOV is revised annually in consultation with the Ministry of Transport.

Typical research activities of SWOV are (Figure 1)—

- Design of new research projects with emphasis on the methodological aspects, such as accident studies, evaluation studies, surveys, etc.
- Carrying out research projects or supervising studies designed by SWOV and carried out by other institutes
- Analysis of traffic safety developments
- Acquisition of relevant data from external data sources and positively influencing their quality
- Acquisition of relevant literature, reports, articles, etc., and maintaining a national library and documentation data bank on traffic safety (IRRD)

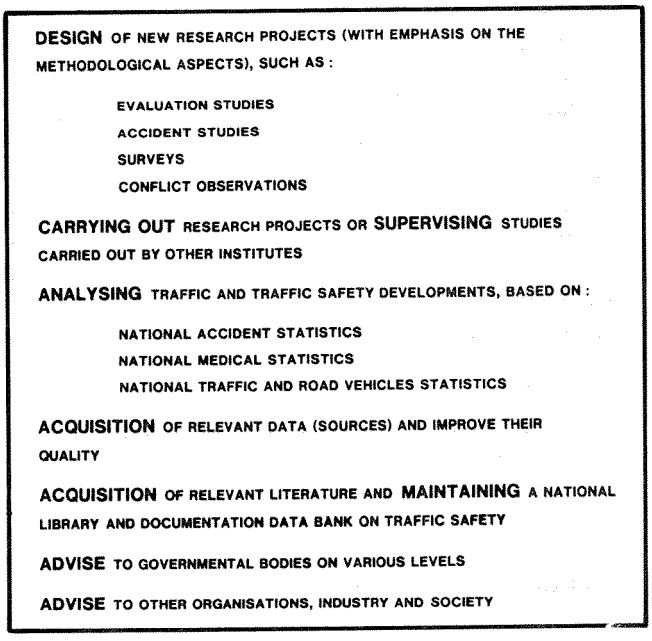

Figure 1. Typical examples of SWOV research activities

The knowledge acquired from the research activities is reported mainly to the government, either in written reports or as advice in various working and policy groups. This way, the investment of taxpayers is returned with profit for society. The results are then used by the authorities to develop and implement new legal measures to further reduce traffic unsafety.

Integrated Road Safety Programs

SWOV took a leading part in the OECD-S1 High Level Group on "Concepts and Methodologies for Integrated Road Safety Programmes" during 1983 and 1984.

The final report on this international research project gives conclusions and recommendations for further development of the dynamic systems approach as a tool toward far better integrated and cost-effective national and international policy and research programs. These are very much needed to (further) reduce the still too heavy toll of road casualties: fatalities, injured, and disabled(6).

As part of this program, SWOV developed the so-called "phase-model of the transport and traffic (unsafety) process" (Figure 2).

On the level of the individual road user, the model shows the various sequential steps starting from travel need, through the different phases, to the ultimate outcome of an accident. It shows at what phases in the traffic process disturbances may occur, leading to failures and, if not controlled, inevitably to the next phase where again failure may occur. It illustrates that no accident ever is the result of just one separate item, but always has a multicausal character.

At the moment, SWOV applies the theories by trying to integrate all types of research into an overall design of traffic safety research. This implicates that the outcome of studies should be checked against this integrated design and that proposed measures are also viewed in that much broader perspective.

With regard to seatbelts in cars, this means all different aspects of that problem have to be considered before a final conclusion or final measure can be derived. All interactions should be considered among those different aspects. To mention a few in the seatbelt area—

- Technical factors (such as design and testing of seatbelts and anchorage points)
- Biomechanical factors (such as effectiveness of seatbelts in crashes, measured in real accidents and simulated in crash tests and mathematical models)
- Behavioral factors (such as attitudes of road users toward the problem and actual use established by surveys; influence by campaigns)

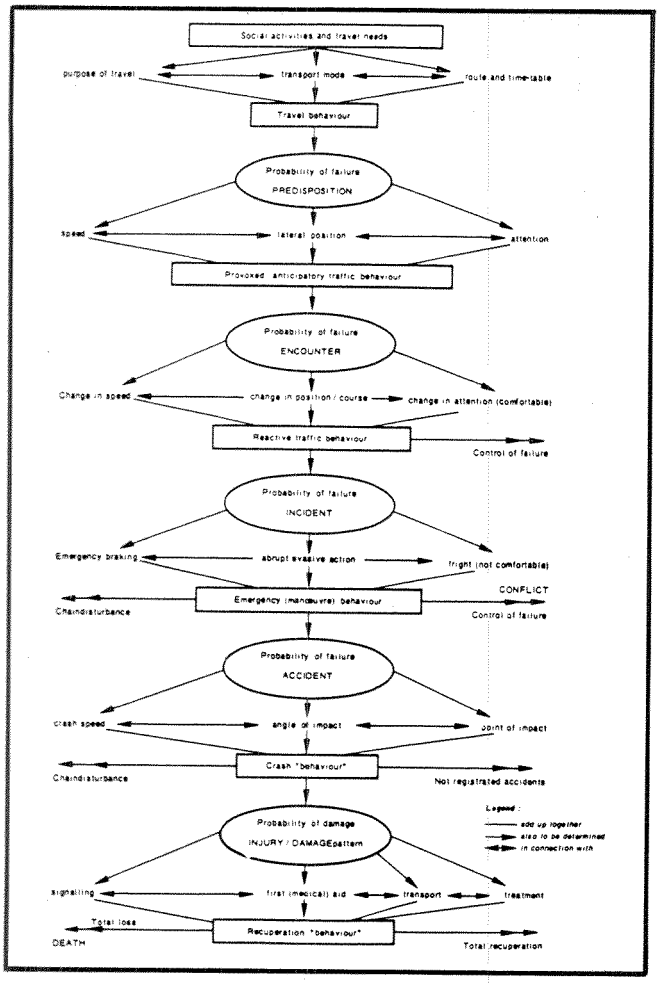

Figure 2. Phase-model of the transport and traffic (unsafety) process

- Legislation (design and implementation of legal measures)
- Law and enforcement (police motivation)

In all those fields, SWOV has to acquire scientific knowledge to maintain its coordinating functions. On the other hand, it can be understood that the efforts and cooperation of those many other institutes and organizations, authorities, and industry in the Netherlands working on specific fields of the problem are needed to influence traffic safety successfully.

Seatbelt Research

Before introducing the actual situation on seatbelt legislation and use in the Netherlands, this paper will give a summary of some research projects and their results that have influenced the development of those legislative measures.

SWOV research, of course, takes into account what other research on a specific subject area has already been carried out by other institutes in the world and what results can be used therefrom.

In 1969, when SWOV started with its first extensive accident study (aimed at seatbelt effectiveness), it certainly took into account what had already been done in other countries, such as Sweden (the Volvo-Bohlin study) and the United States. Results there were very promising. Since the Dutch traffic situation (road types, vehicle mix, etc.) differed considerably from other countries, it was decided to carry out a similar study in the Netherlands. This was a typical crash phase-oriented project, aiming at a representative sample of many thousands of cars in crashes from all over the Netherlands.

Without going into detail on that study, it brought enormous amounts of data on cars and car damage, on accidents, and on the occupants and their injuries. Self-evident, this material was processed and analyzed by means of the computer. Sophisticated analysis by multivariate techniques was applied. Results were given in the report called "Lap belts and three point belts"(7). This report gave other researchers something to think or to laugh about, since SWOV found no statistical difference in effectiveness between the two types. We are speaking about the years 1969 and 1970 when only a small part of the cars were supplied with belts and the overall use was less than 5 percent! It is therefore reasonable to suppose that the sample could not discriminate fully between the different types of belt. However, there was and still is more than enough scientific evidence that lapbelts do prevent fatalities and injuries by preventing ejection and reducing contact with the car interior, though in a different way than 3-point belts, leading to different injury patterns(2).

In the second SWOV accident study, carried out during 1976 and 1977, this result was confirmed, but now SWOV was also able to show that 3-point belts (with or without an automatic locking system) have a statistically significant greater effectiveness than lapbelts, both giving above 50 percent fatality-reducing capability. Practically, the matter is not very interesting now since it was internationally decided to apply only 3-point (automatic) seatbelts on front and back seats, except on middle seats where lapbelts are allowed under certain conditions.

Convincing and statistically significant results from that second SWOV accident study (which aimed more broadly at injury-causing parameters in car crashes) showed again the great benefits of seatbelts for both drivers and front-seat passengers (at least 60 percent less chance of being killed). Taking into account also the injury-reducing potential of seatbelts, SWOV used these results to show what would happen in the Netherlands if seatbelts were suddenly not used anymore (Figure 3).

With regard to victims in car crashes, this would—

- Almost double the number of fatalities
- Increase the hospitalized by some 30 percent
- Increase the less severely injured by some 20 percent

- Decrease the number of uninjured by some 10 percent

Although the absolute numbers of road casualties in the Netherlands may be low in comparison to other countries, the relative effect of this thought is terrifying. Important both for SWOV and for policymakers are the results of the annual seatbelt surveys. Since 1969, SWOV has carried out an annual nationwide survey into the availability and use of seatbelts in cars.

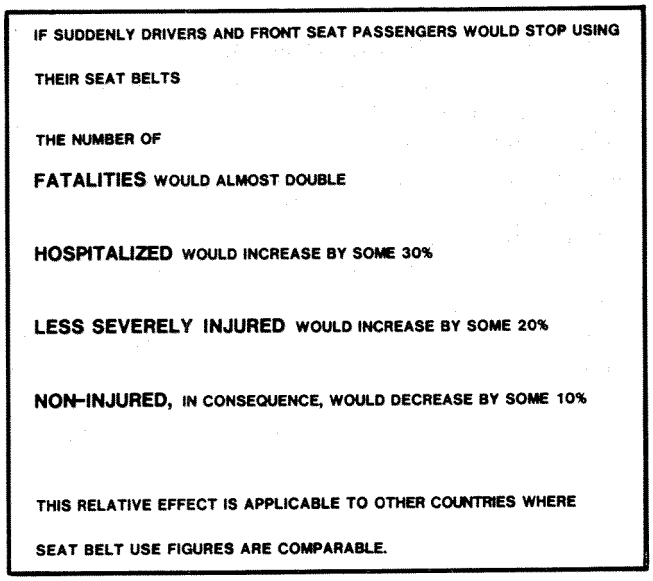

Figure 3. Illustration of seatbelt effectiveness in The Netherlands

In the first 10 years, SWOV used petrol stations for this purpose, where additional questions could be asked of drivers while there. Before the 3-point automatic belt became more or less a standard provision in cars, SWOV measured the slack in static seatbelts used at that particular moment. The average slack was very high, but this did not seem to prevent seatbelts from having a great effect as documented in the accident studies. Of course, the general recommendation to the public was to use the seatbelt properly without any slack.

After 1979, SWOV changed methods and the surveys were then carried out at traffic signals, where cars had to stop in the normal traffic situation and seatbelt use could be observed directly and beyond doubt. A few questions were asked just to have a final look at the seatbelt and its use.

The results of the surveys point out that the most important factors influencing the use of seatbelts by drivers and seat occupants are the length of the trip and whether use is compulsory or not. It was found that use inside city limits (shorter trips) was always considerably lower than that outside city limits. To determine this, trip length was asked. Another result was that women used seatbelts more often than men, and there was some age influence, though not systematically.

Before 1975, use levels were a maximal 35 percent; after 1975, use stabilized around 70 percent outside and 50 percent inside city limits (Figure 4). From June 1, 1975, occupants of front seats had to use their seatbelts, and it is undeniable this had a great influence on actual use as shown in the figure (see also next paragraph).

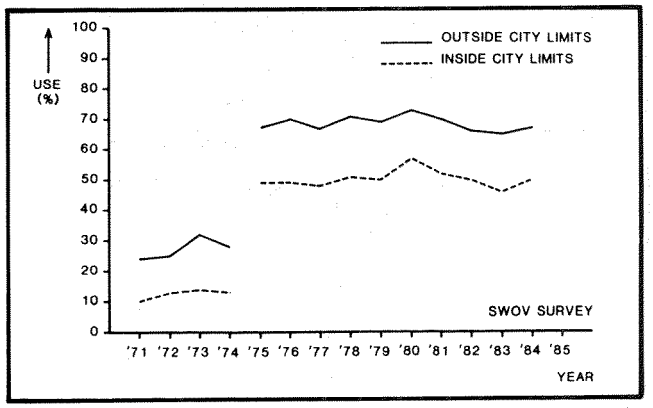

Figure 4. Use of seatbelts by drivers of cars in The Netherlands, from 1971

Legislative Situation on Seatbelts in The Netherlands and Its Relation to Research Results

On January 1, 1971, anchorage points and seatbelts became compulsory in new passenger cars, on both front-seat outboard positions. Exceptions were made for open cars and for all cars older than 1971. All existing types of seatbelts (3-point, lap, and diagonal) were allowed. Nationally, 3-point belts and lapbelts still are allowed.

After that period, a governmental working group in which SWOV had advisory capacity prepared compulsory use, taking into account results of the first SWOV accident study and other relevant research. There was a strong international movement toward compulsory use in Europe and outside Europe (Australia), so the political situation was clearly in favor of the measure.

Many technical and legal problems were solved in the group and the outcome was that on June 1, 1975, use of seatbelts became compulsory, both outside and inside city limits. Main items of the seatbelt law are:

Use is compulsory—

- For front-seat outboard occupants (driver and front-seat passenger)
- In cars from 1971 (not in older cars)
- For occupants over 1.5m length
- For occupants over 12 years of age (passenger)

Exceptions were made—

- For the driver in case of backward driving
- For the driver in case of short trips (delivery)
- For taxi drivers if passengers were transported

- For children under 12 (they should be seated in the back) unless they were over 4 years and could be properly restrained

Individual exemptions are possible on certain specific medical grounds only, considered by a special committee and approved by the Secretary of Transportation (see also Figure 5).

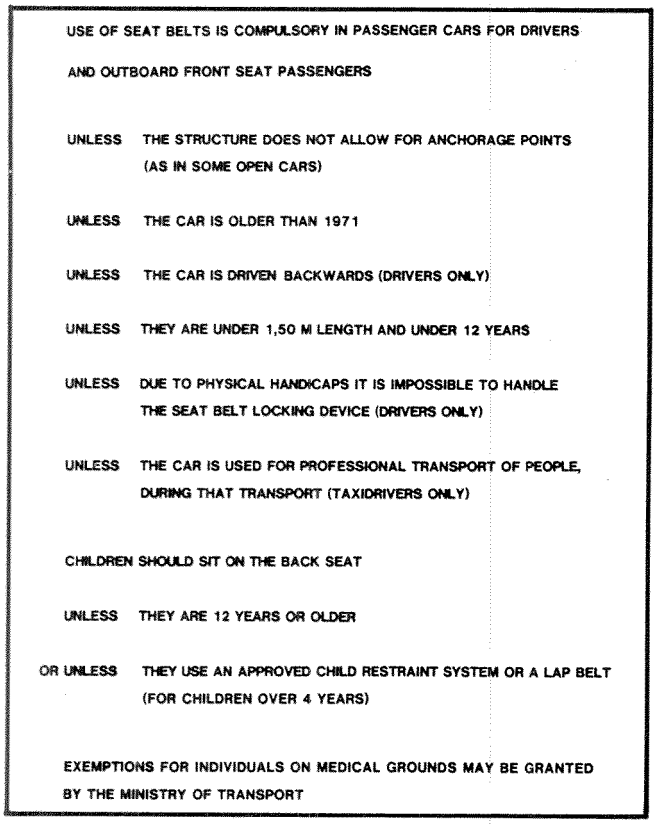

Figure 5. Details of seatbelt use legislation in The Netherlands, 1975 to 1977

The situation with regard to children was reviewed in 1977. Since then, children of all ages were allowed on front seats if use could be made of special and appropriate child restraint systems. Children over 4 years were allowed to use lapbelts on front seats. The reasoning behind this specific measure was that it was considered far better that children were restrained on front seats than unrestrained on back seats.

Since then, the seatbelt and child restraint industry developed various good child restraint systems for use on front seats as well as back seats. The latest developments in this field are two types of rear-facing infant restraint systems (for babies under 1 year) having approval of TNO-Delft and, therefore, they are legally allowed on front seats.

Approval under ECE 44 is still not possible since that particular age group is not present in the regulation. Changes are being prepared under leadership of the Netherlands. Both approved systems are restrained by means of available adult seatbelts.

There is some discussion about the fact that children over 4 years are allowed to be seated on front seats in lapbelts. Since in most cars only automatic 3-point belts are available, this seatbelt is sometimes used as a lapbelt by directing the shoulder strap behind the body or even behind the back of the front chair. By some experts, this is considered dangerous, since straps are located in the wrong direction and separation may occur in the edges of metal parts on the upper B-pillar or on the locking device.

Seatbelts on Back Seats of Cars

There is at the moment in Europe some international movement toward compulsory use of seatbelts on back seats. In most new cars, seatbelts are already available as a standard provision on two or three back-seat positions. A few countries already have made this use compulsory.

In the Netherlands, the Ministry of Transport asked SWOV to appraise the different aspects of seatbelts on back seats in order to prepare new legislation. SWOV reported on this subject in 1982(9), and the Ministry of Transport has announced that, as a first step, compulsory availability of seatbelts will be prepared.

In the SWOV report, the many aspects of the problem were singled out and assessed, leading to conclusions and recommendations on the different legislative options (no special measure; compulsory availability only; compulsory availability and use). Some aspects were—

- Effectiveness in crashes
- Type of seatbelt
- Anchorage points
- Definition of seating position
- Use of back seat for different purposes
- Use of back seat by different age groups (emphasis on children)
- Relation with existing seatbelt legislation on front seats
- Psychological aspects with respect to compulsory use
- Seatbelt campaigns

Starting points were the results of the previous SWOV accident studies with respect to effectiveness of seatbelts, occupancy of back seat, age distribution of back-seat passengers, etc. Additional information on the actual situation with regard to seatbelts and child restraint system availability and use was separately gathered by means of regular inquiries from a representative sample of Dutch households in 1983.

At that moment, seatbelts on back seats were available in 20 percent of all cars in the Netherlands. This percentage was 40 percent in cars of households with children under 4 years. Child restraint systems were available and used in about 15 percent of all cars. This percentage was also much higher in cars of households with small children(5).

Effectiveness of seatbelts in back seats had to be derived from front-seat effectiveness, since use of seatbelts on back seats is still very low, and accident studies, whatever their sample, will not produce any significant result due to lack of data.

It was reasoned in the report that the effectiveness of seatbelts on back seats would be less than on front seats, due to better protection capability of the back-seat environment in most collision modes. On the other hand, seatbelts would protect fully against ejection, although the data of the last SWOV accident study show that ejection from back seats occurs somewhat less often than ejection from front seats under comparable conditions. It was concluded that, given the Dutch accident situation, seatbelts on back seats, if used to the same degree as on front seats, would probably prevent less than 50 fatalities and, of course, reduce the injury severity of several hundreds of injured occupants to lower levels.

Typical aspects of the Dutch back-seat problem are (see also Figure 6)—

- Total occupancy is about 15 percent of all car occupants.
- 50 percent of back-seat occupants are under 15 years of age.
- Seating positions are not well defined, especially if children are present; this is primarily a legal aspect.
- If more than two or three passengers occupy the back seat, there will be confusion with regard to available seatbelts.

In view of the age distribution, SWOV concluded that very special attention in the legislative field as well as in the technical field should be given to the seating and restraining of children. Priority should be given to the implementation of ECE 44, the international regulation on child restraint systems, to prevent that new measures on back seats would interfere with the proper restraining of children according to this regulation.

SWOV expressed preference for the use of regular adult seatbelts for child restraint devices, as allowed in ECE 44. Since various good child restraint designs are already available using adult seatbelts, there seems no reason to seek other solutions. However, seatbelt legislation on back seats should also not prevent use of child restraints (already available) that need special straps, since it is unlikely that other use is made of seating positions where such special straps are fastened.

Final conclusions in the SWOV report were that compulsory use (and availability) of seatbelts on back seats would need many more exemptions and exceptions than the front-seat legislation has now, and would have to be designed very carefully to prevent misuse and interactions with those groups already using restraint systems (i.e., small children). Even if the government would decide to make only availability compulsory, some of those problems, and others with regard to seating position, should be solved first. It was felt, therefore, by SWOV that voluntary use was the best possible way, supported if feasible by well-designed and properly aimed campaigns.

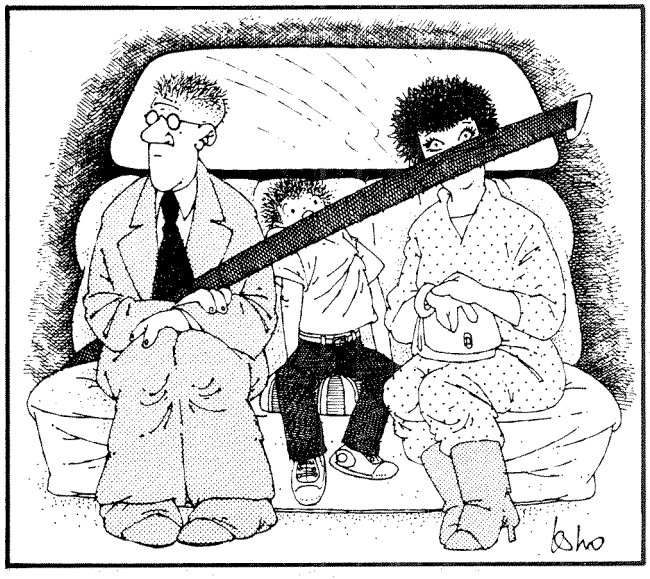

Figure 6.

Campaigns and Special Enforcement Programs

During part of 1984 and 1985, a national seatbelt campaign was carried out by the Dutch Organisation for Traffic Safety (VVN) using various ways of influencing car occupants, especially on short trips where use figures are low. The campaign was considered relevant, since use figures appeared to be decreasing.

As part of the current National Traffic Safety Plan from the Ministry of Transport, SWOV helped design a special seatbelt enforcement program, to be applied in one particular area of the Netherlands (Friesland), while another specific part was used as a control area. Police cooperation was the essential part of this enforcement program aimed at dramatically improving seatbelt use. Before-studies (survey) were organized by SWOV in 1984, and the special program was applied in September/October 1984. The first series of after-surveys have been performed, and others will follow this year. At first sight, a very substantial rise in use figures, far above the average national level of use, has been established, probably proving that special enforcement programs, combining campaigns with police enforcement activities, are successful. The long-term effects of this type of measure, however, have still to be assessed.

Mathematical Models and Seatbelts

As are many other institutes, SWOV is busily engaged in the field of mathematical modeling of road vehicles and their occupants in crashes. Together with others,

SWOV developed models such as MADYMO (with TNO) and VEDYAC (with S.P.A.T., Italy). VEDYAC is a very refined and flexible model simulating many types of vehicles moving in and interacting with all different kinds of environment (such as the road itself and roadside obstacles; also other vehicles, pedestrians, etc.)(3). The car occupant may be simulated either with or without seatbelt. (See Figure 7 for some plot-output examples.)

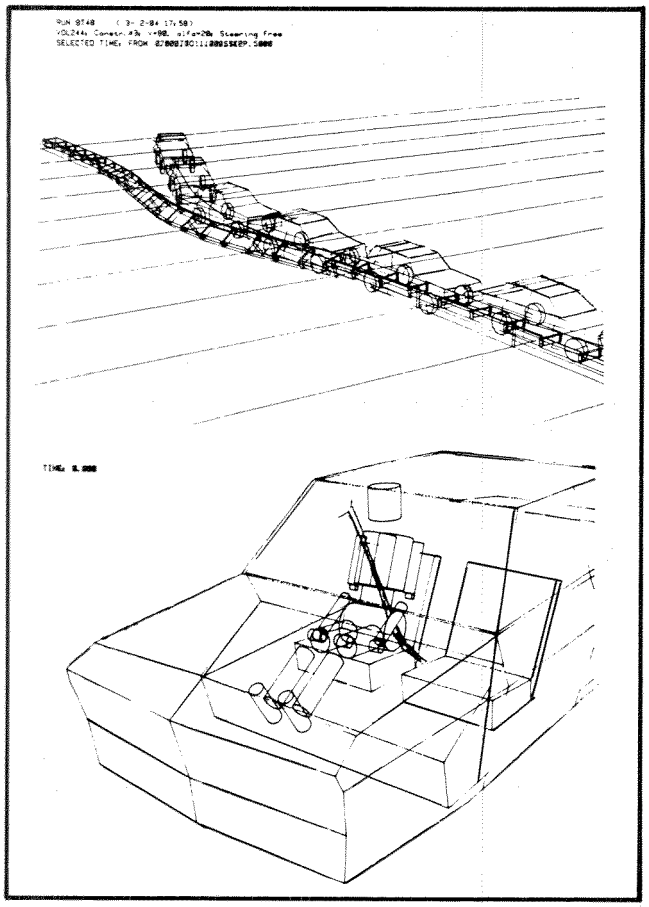

Figure 7. Examples of plot-output from VEDYAC

Quite another interesting development is that SWOV is working on chaining these models with another model representing the traffic population at risk (for instance, car occupants using belts). In such a chained model, proposed changes in policy, legislation, design, etc. (for instance, specific changes to the seatbelt stiffness, steering column, car design, or road obstacle design, etc.) may be applied by changing relevant parameters. The consequences on the population at risk may be predicted in terms of changes in injury pattern and injury severity levels. Such results may have (and should have) considerable influence on, for instance, priorities given by policymakers to different proposed new measures in the field of traffic safety. In view of the various and numerous data needed to carry out this research successfully and put it into practice, there is still much to be done(4).

Other Seatbelt Topics

To complete the list of relevant research, another SWOV report may be mentioned. Reacting on a specific industrial product, developed by a Dutch inventor, SWOV made an appraisal of the possible advantages and disadvantages of an automatic opening system for use in seatbelt locking devices—the Lassche system.

Here again, SWOV based its opinion primarily on accident data concerning the technical condition of seatbelts and locking device after accidents, data on the occurrence of fire, and cars getting into (deep) water. Also the problem of occupants being unconscious or unable to help themselves out of a car is discussed.

It was concluded that the device would not improve traffic safety figures on any great scale, but was undeniably useful for those fearing to be locked in by their seatbelts after collisions (which, in fact, does not often occur judging by the average good technical state of the seatbelts after collisions). There has been some international pressure to allow this and other devices to become legally acceptable by changing ECE Regulation 16 and the comparable Directive of the EC. The present situation is not clear.

Another more practical device, allowed under international and national legislation, is the adjustable upper anchorage point of the seatbelt on the B-pillar. Some car manufacturers already sell such systems as a standard provision. Though no research results are known to SWOV, this seems to be a proper solution for the adaption of the seatbelt to different postures and seating positions of the occupants.

On the other hand, SWOV would like to emphasize that an even more proper approach of the seatbelt case, especially on front seats, is an integral approach. In such an approach, the seatbelt system would be considered part of the total seat structure and fastened directly to it, as is already the case in some vehicles. At the same time, this integral approach should be expanded to the car as a whole, regarding the seating system as part of the car structure and designing and testing both toward optimization of the restraining function for different collision modes. Of course, this thought is not really new, and the drawback may occur when seatbelts are not used. Car safety designers, therefore, also have to allow for unprotected occupants. The point of a fully automatic restraint system such as airbags then comes into focus, and the world is still waiting for solid real-world accident studies on this subject.

Conclusion

Mention must be made again of those other institutes, organizations, industries, etc., working in the field of traffic safety in the Netherlands on various different aspects of this enormous problem for society. Without their efforts, the problem cannot be solved.

References

1. Arnoldus, J.G., and G.A. Varkevisser, "Aanwezigheid en gebruik van autogordels," 1979 t:m 1983, R-84-13, Institute for Road Safety Research SWOV, Leidschendam, 1984. (Availability and use of seatbelts 1979-1983)
2. Edelman, A., and L.T.B. van Kampen, "Practical and medical aspects of the use of car seat belts; tentative views from recent research by the Institute for Road Safety Research SWOV," *Arts en Auto*, 40, 19, pp. 1556-1559, 1974.
3. Giavotto, V., et al., "Vehicle dynamics and crash dynamics with minicomputer," *Computer & Structures*, Vol. 16, No. 1-4, pp. 381-393, Pergamon Press Ltd., Great Britain, 1983.
4. Heijer, T., "Development of an injury prediction model. A study of feasibility on the basis of literature data," R-83-31, Institute for Road Safety Research SWOV, Leidschendam, 1983.
5. Van Kampen, L.T.B., "De aanwezigheid en het gebruik van kinderbeveiligingsmiddelen en de aanwezigheid van autogordels op achterbanken van personenauto's. Beoordeling van de voornaamste resultaten van een NIPOenquête," R-84-48, Institute for Road Safety Research SWOV, Leidschendam, 1984. (Availability and use of child restraint systems and availability of seatbelts on back seats of passenger cars)
6. OECD, "Integrated road safety programmes," Report prepared by an OECD scientific expert group, Road Transport Research, Paris, 1984.
7. SWOV, "Lap belts and three-point belts. A comparison of effectiveness," Institute for Road Safety Research SWOV, Voorburg, The Netherlands, 1975.
8. SWOV, "Autogordelsluiting met automatische ontgrendeling. Consult in opdracht van de Rijksdienst voor het wegverkeer," R-81-33, Institute for Road Safety Research SWOV, 1981. (Automatic opening seatbelt locking device)
9. SWOV, "Autogordels op de achterbanken van personenauto's. Consult in opdracht van de Rijksdienst voor het wegverkeer," R-82-46, Institute for Road Safety Research SWOV, Leidschendam, 1982. (Seatbelts on the back seats of passenger cars)

The Effects of Mandatory Seatbelt Use in Great Britain

S.J. Ashton and
G.M. Mackay
Accident Research Unit, Department of Transportation and Highway Engineering, University of Birmingham, United Kingdom

P.D. Thomas and
M.D. Galer
Accident Research Unit, Institute for Consumer Ergonomics, Loughborough, United Kingdom

P. Harms
Transport and Road Research Laboratory, Crowthorne, Berkshire, United Kingdom

Abstract

Some of the factors influencing the introduction of mandatory seatbelt use in Great Britain are outlined. The effectiveness of seatbelts is considered. Pre- and postlaw seatbelt use rates are described. The reductions in front-seat car occupant casualties following the introduction of the law are reported, and it is noted the actual reduction in fatalities is in line with the expected reduction.

The results of the time series analyses of all road accident casualties are presented. These analyses indicate, with the data currently available, the changes in the numbers of other road users injured and killed cannot be attributed to the effects of the seatbelt legislation but are in line with normal seasonal and annual fluctuations.

A brief review is made of studies relevant to the debate on risk compensation, and it is concluded that available evidence indicates that risk compensation probably does not occur when drivers are compelled to wear seatbelts.

Some preliminary results of a study examining changes in injury frequency following the mandatory seatbelt use law are presented. Data from current in-depth studies of accidents are used to describe patterns of injury to restrained occupants. Consideration is given to some of the factors associated with accidents in which restrained occupants are fatally injured, and it is shown that the main characteristic of such accidents is they are high-energy accidents with gross intrusion into the occupant's seating position.

Factors limiting seatbelt performance are discussed, and some possible future developments in occupant protection are described.

Introduction

The Legislation

Although the mandatory use of seatbelts by car occupants was first recommended by crash injury research experts in the late 1960's, it was not until the success of Australian legislation, enacted in 1970, that serious attempts were made to enact such a law in Britain. The first Parliamentary Bill, introduced in 1973, was soundly defeated. Repeated attempts were made over the next 10 years, with the legislation almost being agreed in 1978, only failing to reach the statute book because of the dissolution of Parliament. During the passage of the 1981 Transport Bill through Parliament, a clause on seatbelts was inserted into the bill at committee stage. Members of Parliament were allowed to vote according to their own beliefs as it was recognised by the Government that there were strong feelings both for and against the mandatory use of seatbelts. Prior to the vote, there was considerable public debate about this issue and in this debate professional and specialist organisations, such as the police, the medical community, and in particular the British Medical Association, the Automobile Association, the Royal Society for the Prevention of Accidents, the Society of Motor Manufacturers and Traders, which represent the car industry, together with a number of professional engineering societies and a few individual academics with specialised expertise in transport safety, were almost unanimous in support of the mandatory use of seatbelts by the front-seat occupants of cars.

A further factor was that the general public was generally in favour of mandatory seatbelt use. The public forms its opinions by what it sees on television, hears on radio, and reads in the papers, and one of the key factors in forming public opinion was a television documentary on road accidents entitled The Greatest Epidemic of Our Time. That programme, which was screened twice, once on each of the BBC channels, at prime time, with the last screening shortly before one of the votes in Parliament, had an important role in educating the public about the road accident problem.

The vote was in favour of the mandatory use of seatbelts, and as a result the use of seatbelts by front-seat occupants of cars and light vans has been compulsory since January 31, 1983.

Seatbelt Effectiveness

There are a number of methods of determining seatbelt effectiveness; effectiveness being defined as the reduction in casualties when seatbelt use goes from 0 to 100 percent. One method is to look at a sample of crashes in which seatbelts have not been worn and to predict what would have happened had seatbelts been worn. A second method is to calculate the probability of injury as a function of crash severity and then to compare the probability of injury for restrained and unrestrained occupants at equivalent crash severities. A third method is to look in aggregate at the changes in frequency of different severities of injury as a result of a change in seatbelt use rates, usually as a result of legislation being introduced.

Accident studies have shown that seatbelt effectiveness is a function of collision type, the benefits being greatest in frontal impacts and rollovers and least in rear impacts and for struck side occupants in side impacts. Additionally, crash severity has been shown to have a significant influence on effectiveness. If the accident is of such severity that there is gross intrusion into the passenger compartment of the car, there is often insufficient space for the restraint system to work correctly and thus prevent high-energy occupant contacts with the interior.

Estimates of effectiveness vary greatly between different studies due to differences in samples considered. For instance, Huelke(1) reported that in frontal collisions, 77 percent of the fatalities would have been prevented had the occupants been restrained. However, in a later study, which considered only rural high-speed crashes, Huelke reported an effectiveness of only 32 percent in preventing occupant fatalities(2).

In a study on seatbelt effectiveness carried out in 1963 at the then Road Research Laboratory, Lister et al., reported an injury reduction of about 50 percent(3).
In 1976, from a study of 255 unrestrained car occupant fatalities in Great Britain, Griffiths reported that approximately 41 percent of the fatalities would not have occurred if all the front-seat occupants had been restrained(4).

Bohlin in 1967(5) reported that in two models of Volvo cars, the effectiveness of seatbelts in preventing nonfatal injuries varied from 57 to 63 percent at lower speeds and from 48 to 54 percent at higher speeds, while for the fatalities the seatbelt offered full protection up to 60mph. Although the total sample was large, over 28,780, a large proportion of the accidents occurred at relatively low speeds. The observation about effectiveness for fatalities was based on a very small sample, there being only three restrained occupant fatalities in the sample.

Hobbs and Mills, using data from a British study of towaway accidents(6), reported that seatbelt effectiveness is strongly related to the velocity change in the accident and to the severity of the injuries being considered. They found the effectiveness of seatbelts in preventing nonminor injuries (AIS $>$ 1) in frontal impacts varied from 76 percent when there was a 10mph velocity change, through 42 percent for a 20mph velocity change and 11 percent for a 30mph velocity change, to only 1 percent for a 40mph velocity change. This corresponds to an overall effectiveness of about 65 percent.

Trinca and Dooley(7) reported that 4 years after the introduction in 1970 of mandatory seatbelt use in Victoria, Australia, the first legislature to require the mandatory use of seatbelts, there had been a 37 percent reduction in occupant fatalities and a 41 percent reduction in occupant injuries based on predicted values trend line analysis. Prior to the introduction of the legislation, seatbelt use was around 25 percent, although not all cars had seatbelts fitted.

Mandatory seatbelt use by some or all of the occupants of cars is now required in approximately 33 jurisdictions throughout the world, and, although the effects of such laws are still being debated, the general result of the introduction of such laws has been an increase in the use of seatbelts and a decrease in the number of car occupants seriously injured or killed.

Seatbelt Use Rates

Prelaw Use Rates

In Great Britain, the compulsory fitting of seatbelts for the driver and outboard front-seat passenger has been required since 1967 with retrofit to 1965 model year cars. Consequently, by 1975 virtually all cars had lap and diagonal seatbelts fitted to the front outboard seats and overall use rates were about 30 percent, although there were substantial variations in use by road type. Observations conducted in and around Birmingham in 1975 showed that use rates varied substantially by environment, ranging from below 25 percent in the city centre to over 50 percent on motorways (Table 1)(8).

Table 1. Driver seatbelt use: Great Britain 1975

LOCATION	SAMPLE SIZE	USE RATE
City Centre	5,951	21.9%
Rural 'A' Road	5,742	30.1%
Motorway	7,040	56.7%

Other counts conducted between 1975 and 1981 indicated that overall use rates were essentially static at about 30 percent in spite of Government-sponsored advertising campaigns. Differences in use rates by environment were still evident in counts conducted in June 1982, shortly before the introduction of the law (Table 2)(9). These counts indicated that the average use rate shortly before the introduction of the law was 29 percent in built-up areas, 40 percent in non-built-up areas, and 52 percent on motorways, and the overall use rate was 37 percent.

As the date for the introduction of the law approached, there was a rise in belt use rates, particularly in urban areas, as people anticipated the legal requirement(10).

Table 2. Pre- and post-law driver daytime seatbelt use by road type: Great Britain

	Pre-law (June 1982)	Post-law (June 1983)
Motorways	52%	97%
Built-up roads		
Trunk roads	32%	97%
Principal roads	32%	95%
Secondary roads	26%	95%
Minor roads	27%	92%
Non-built-up roads		
Trunk roads	49%	95%
Principal roads	37%	94%
Secondary roads	47%	98%
Minor roads	34%	92%

Postlaw Use Rates

With the enactment of the law, there was a spectacular increase in seatbelt use to around 95 percent, and use rates have stayed around this level. Figure 1 adapted from official Department of Transport publications(11,12) shows the change in seatbelt use rates with time. There are, however, still slight variations in use by road type, use rates tending to be slightly lower on minor roads than on other roads (Table 2).

Predicted Influence on Casualties

Two parameters are often referred to when discussing the effects that seatbelts have on occupant casualties; these parameters being seatbelt effectiveness and reduction in casualties. These two parameters are not the same, and confusion between them has occasionally led to misunderstanding in the expected decrease in casualities following the introduction of a mandatory seatbelt use law. It should be noted the reduction in casualties will be less than seatbelt effectiveness except in the special case when seatbelt use goes from 0 to 100 percent. The relationship between seatbelt use rates, seatbelt effectiveness, and the reduction in casualties is considered in Appendix 1.

The average seatbelt use rate in Great Britain in 1982 was 37 percent, while in 1983, after the introduction of the law, the average use rate was about 95 percent. Griffiths(4) showed that approximately 41 percent of unrestrained front-seat occupant deaths could be prevented if all front-seat occupants were restrained. The expected reduction in front-seat occupant fatalities with the above use and effectiveness rates is 28 percent. In deriving estimates for pre- and postlaw belt use rate, it is necessary to take into account that occupant fatalities are more frequent on rural roads than on urban roads, and on rural roads prelaw belt use rates were higher than on urban roads. The effect of this is to reduce the expected fatality reduction to about 25 percent (Table 3).

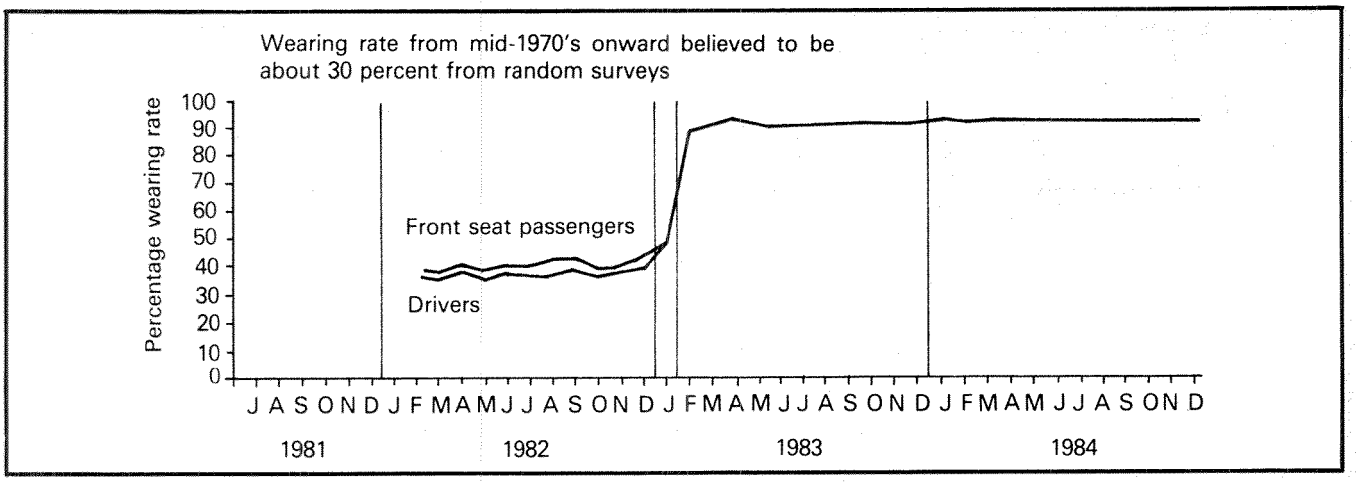

Figure 1. Car and light van front-seat occupant seatbelt use rates

Table 3. Expected reduction in front seat occupant fatalities for differing pre- and post-law seatbelt use rates

Pre-law Belt Use Rate	Post-law Belt Use		
	85%	90%	95%
35%	23.9%	26.3%	28.7%
40%	22.0%	24.5%	27.0%
45%	20.1%	22.6%	25.1%

Note: Assumed Seatbelt Effectiveness = 41%

Actual Influence on Casualties

Figure 2, based on figures in official Department of Transport publications(11,12), shows the monthly totals for front- and rear-seat car and van occupants, and also for other road users, seriously injured or killed in road accidents. Casualties with slight injuries have been excluded as their inclusion produces problems due to underreporting, particularly of bicycle accidents. It is clear from Figure 2 that a significant drop in front-seat car and van occupant casualties occurred coincident with the introduction of the seatbelt law.

Car and Light Van Drivers and Front-Seat Passengers

In describing the effects of mandatory seatbelt use laws, comparisons have often been made between the numbers of casualties in similar periods before and after the introduction of the law.

For example, early in 1984 it was provisionally reported that, in the period February to December 1983, there had been, for car and light van front-seat occupants, 475 (23 percent) fewer persons killed and 6,947 (26 percent) fewer persons seriously injured than in the corresponding 11-month period in 1982(11). Early in 1985, it was provisionally reported that, in the period February 1983 to December 1984, there had been, for car and light van front-seat occupants, 691 (17 percent) fewer persons killed and 12,153 (22 percent) fewer persons seriously injured than in the corresponding 23-month period February 1981 to December 1982(12). Superficially, the difference between these two sets of figures appears to suggest that the mandatory seatbelt use law is becoming less effective with time. This is not, in fact, the case; the difference between the figures for the two periods being due to an underlying upward trend in the number of casualties.

Consider for illustrative purposes the number of drivers and front-seat passengers killed each year between 1981 and 1984 (Table 4).

In 1983, there were 20 percent fewer fatalities compared with 1982; in 1983 and 1984 taken together, there were 15 percent fewer fatalities than in 1981 and 1982 taken together. There was, however, an increase of approximately 7 percent in fatalities between 1981 and 1982 and an increase of approximately 6 percent between 1983 and 1984. This suggests there might have been an underlying upward trend in car and light van front-seat occupant fatalities between 1981 and 1984. Assuming for purposes of this discussion that the annual upward trend was 6.5 percent, i.e., approximately equal to the annual increase from 1981 to 1982 and from 1983 to 1984, then had the seatbelt law not been introduced there would have been approximately 2,380 fatalities in 1983 and 2,530 fatalities in 1984, and the reduction in fatalities as a result of the introduction of the law would have been about 24 percent. This figure (24 percent) is greater than those obtained from simple year-on-year comparisons (20 percent and 15 percent).

The above illustrates that simple before-and-after comparisons can be misleading if there is an underlying trend. A further difficulty in making comparisons between yearly totals comes from the random year-to-year variations in the data. Time series analysis, however, can be used to separate the effects due to different factors.

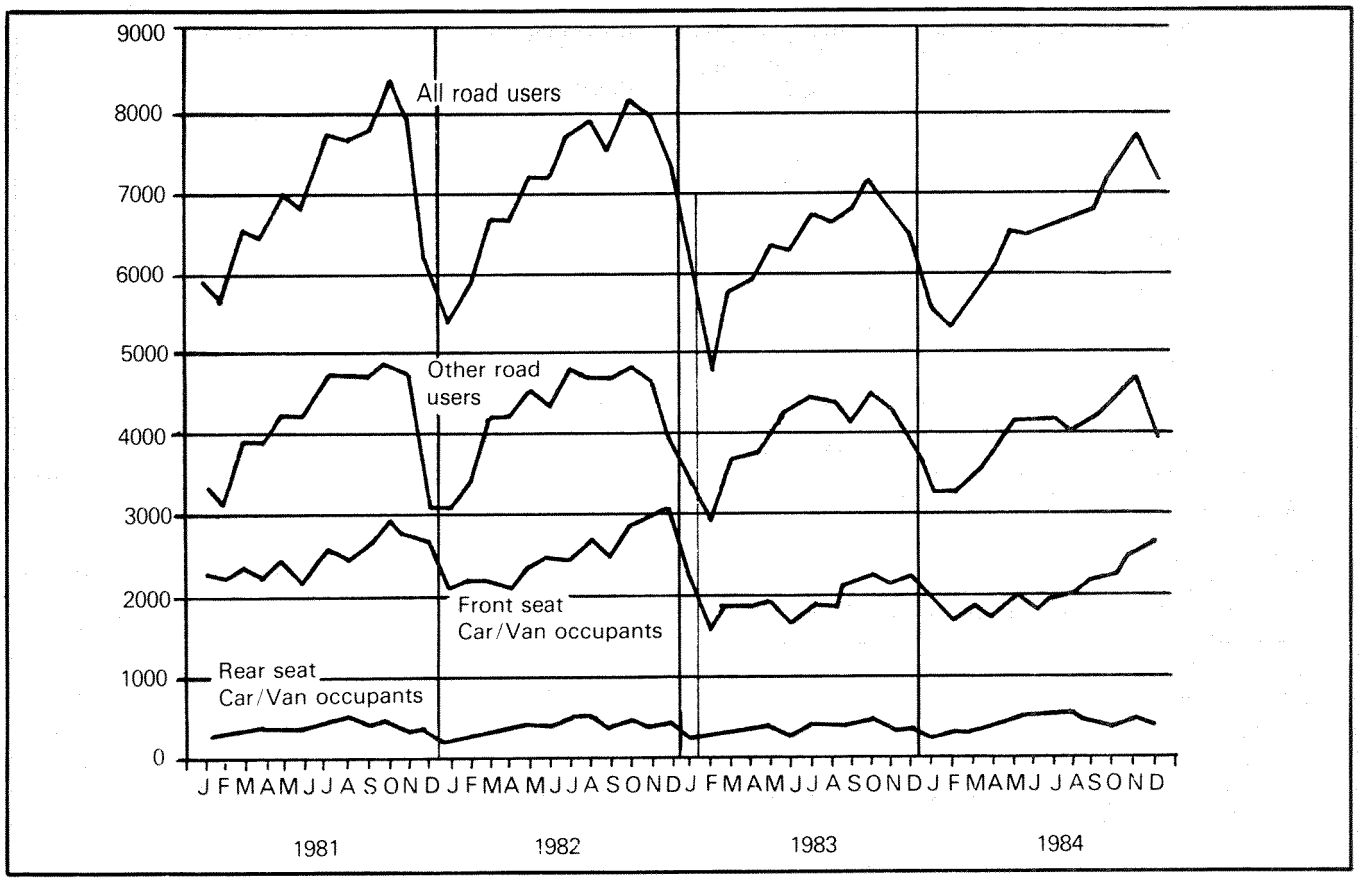

Figure 2. Fatal and serious casualties by month

Table 4. Car front seat occupant casualties: 1981 - 1984

Year	Slight	Serious	Fatal
1981	99,847	28,839	2,112
1982	103,738	28,993	2,260
1983	89,375	22,142	1,799
1984	97,178	23,347	1,901

Scott and Willis(9) have performed time series analyses in which monthly casualty data were fitted to a model that, among other features, allowed for changes in traffic. The model was of the form:

$$C = V^{v}.\exp(k + t.T + x.d_x + e)$$

where:

- C = the number of casualties
- V = the traffic volume for the vehicle type
- T = time in months since December 1978
- d_x = a dummy variable representing the presence or absence of the seatbelt legislation (i.e., $d_x = 0$ in the before period and $d_x = 1$ in the after period)

The parameters "v", "k", "t", "x", and "e" were estimated by the analysis; "x" measuring the change attributable to the seatbelt law. Some of the results of the analyses are given in Table 5.

The results of these time series analyses show that, overall, the reductions in serious and fatal casualties coincident with the introduction of mandatory seatbelt use were about 20 to 25 percent for drivers and about 30 percent for front-seat passengers. It was noted there has been a greater reduction in casualties in built-up areas than in non-built-up areas. This is most probably due to seatbelt use rates being lower in built-up areas than in non-built-up areas prior to the law, there being a greater potential for injury reduction in built-up areas, but may also be partly due to differences in crash severity between the two areas.

In numerical terms, approximately 7,000 fewer people have been killed or seriously injured and approximately 13,000 fewer people have been slightly injured while vehicle occupants as a result of the introduction of the mandatory seatbelt use law.

An examination of the casualty reductions by time of day showed that for car drivers only there was a greater reduction in casualties in the 2200h to 0400h time period than at other times of the day. While this may possibly be due to a greater percentage change in seatbelt use rates at night, it may also be partly due to a change in police procedures for testing drunken drivers that took place in 1983; this change possibly influencing nighttime accident rates.

Table 5. Reductions in car driver and front seat passenger casualties coincident with the introduction of mandatory seatbelt use: estimated from 1979 - 1983 data

		Built-up Areas		Non-built-up Areas		Overall	
	Change	Percent Limits	90% Confidence Change	Percent Limits	90% Confidence Change	Percent Limits	90% Confidence
Driver	Fatal	19%	3% - 32%	25%	16% - 33%	25%	18% - 31%
	Serious	25%	21% - 29%	18%	14% - 22%	21%	17% - 25%
	Slight	12%	7% - 17%	9%	4% - 14%	11%	7% - 15%
Passenger	Fatal	26%	9% - 40%	32%	22% - 41%	29%	20% - 38%
	Serious	33%	27% - 38%	27%	22% - 32%	30%	26% - 33%
	Slight	21%	15% - 27%	15%	9% - 20%	19%	15% - 24%

Car and Light Van Rear-Seat Occupants

Table 6 gives the number of rear-seat occupant casualties for the 4 years 1981 to 1984. It can be seen from these data there has been a general upward trend in the number of rear-seat casualties since 1982. A time series analysis using 1979 to 1983 data indicates there was an increase in the number of fatalities and slightly injured casualties and a decrease in the number of seriously injured casualties coincident with the introduction of mandatory seatbelt use. However, the wide variation in the 90 percent confidence limits stemming from the small numbers involved results in the changes being within the range of normal yearly variations. There is thus no statistically discernible indication that the seatbelt law has had an effect on car and light van rear-seat occupant casualties (Table 7)(9).

Table 6. Car rear seat occupant casualties: 1981 - 1984

Year	Slight	Serious	Fatal
1981	18,127	4,308	304
1982	18,663	4,409	297
1983	19,300	4,282	321
1984	21,084	4,690	372

Other Road Users

It has been suggested that the introduction of a mandatory seatbelt use law may encourage drivers to drive in a more dangerous way(13). This hypothesis, the "Risk Compensation" hypothesis, is discussed in more detail later in this paper. If that were the case, then an increase in the number of injured other road users, i.e., persons struck by cars, such as pedestrians, cyclists, and motorcyclists, would be expected.

To examine whether this has occurred, Scott and Willis(9) performed time series analyses for pedal cyclists, pedestrians, and motorcyclists struck by cars and light vans and by buses, coaches, and heavy goods vehicles; the latter group being considered as the number of unprotected road users struck by these vehicles form controls as the drivers of such vehicles would be unaffected by the seatbelt legislation. The model used for the unprotected road users was a modified form of that used for car occupants in which the respective traffic volumes of both parties were included and took the form:

Table 7. Changes in car rear seat occupant casualties coincident with the introduction of mandatory seatbelt use: estimated from 1979 - 1983 data

	Percent Change	90% Confidence Limits
Fatal	+14%	- 7% - +38%
Serious	- 5%	-11% - + 2%
Slight	+ 2%	- 3% - + 7%

$$C = V1^{v1}.V2^{v2}.\exp(k + t.T + x.d_x + e)$$

where:

- C = the number of casualties
- V1 = the traffic volume for the unprotected road user under investigation
- V2 = the traffic volume for the other vehicle, i.e., cars and light vans or buses, coaches, and heavy goods vehicles
- T = time in months since December 1978
- d_x = a dummy variable representing the presence or absence of the seatbelt legislation (i.e., $d_x = 0$ in the before period and $d_x = 1$ in the after period)

The parameters "v1", "v2", "k", "t", "x", and "e" are estimated by the analysis; "x" measures the change attributable to the seatbelt law.

In performing the time series analyses, only casualties in built-up areas were considered as pedestrian and cyclist accidents are essentially an urban problem. Table 8 details the change in the number of casualties that occurred coincident with the introduction of mandatory seatbelt use, together with the underlying in the number

Table 8. Changes in unprotected road user casualties in built-up areas: estimated from 1979 - 1983 data

		Possible seatbelt effect		Underlying annual trend	
		Percent Change	90% Confidence Limits	Percent Change	90% Confidence Limits
All Severities of Injury					
Pedestrians	Car/van	+ 4%	+ 1% / + 9%	-0.2%	- 2.2% / + 1.9%
	PSV/HGV	+ 1%	- 6% / + 8%	- 7.4%	- 9.1% / - 5.8%
Pedal Cyclists	Car/van	+ 3%	- 5% / +12%	+ 8.2%	+ 5.8% / +10.7%
	PSV/HGV	- 5%	-12% / + 3%	+4.5%	+ 2.3% / + 6.8%
Motor Cyclists	Car/van	- 4%	- 9% / + 1%	-0.1%	- 1.0% / +1.2%
	PSV/HGV	- 3%	-14% / + 9%	- 8.2%	-10.1% / - 6.3%
Fatal and Serious Injury					
Pedestrians	Car/van	+ 2%	- 3% / + 7%	+ 0.4%	+ 0.0% / + 0.7%
	PSV/HGV	+ 3%	-10% / +18%	- 7.7%	-10.7% / - 4.8%

of casualties, for three different road user groups—pedestrians, pedal cyclists, and motorcyclists—struck by vehicles in which drivers have to wear seatbelts, i.e., cars and light vans, and vehicles in which drivers do not have seatbelts fitted, i.e., PSV's and HGV's.

The use of PSV's and HGV's as a control group may not be entirely correct as it is likely that drivers of PSV's and HGV's also drive cars. It cannot, therefore, be stated that accidents involving PSV's and HGV's are unaffected by the seatbelt law.

The casualty series for pedestrians and motorcyclists involved in accidents with PSV's or HGV's shows downward trends, while that for pedestrians and motorcyclists struck by cars or vans shows virtually no trend. Pedal cyclist collisions with cars or vans and with PSV's or HGV's show upward trends; the upward trend for pedal cycle-car/van collisions being stronger than that for pedal cycle-PSV/HGV collisions.

The results of the analyses indicate there was a reduction in the number of motorcyclist casualties struck by both cars or vans and PSV's or HGV's coincident with the introduction of the seatbelt legislation. This reduction is likely to be due mainly to a change in the use of motorcycles following a lowering of the size of motorcycles that learners are permitted to ride; the change in the regulations taking place on February 1, 1983, i.e., almost coincidently with the seatbelt legislation.

For pedestrians, it was found there had been a slight increase in the number of casualties involved in collisions with both cars or light vans and with PSV's or HGV's. However, although the increase in the number of car or light van collisions was slightly greater than the number of PSV or HGV collisions, there was considerable overlap in the 90 percent confidence limits.

The changes in the number of pedal cyclists injured were in opposite directions for the two vehicle groups, there being an increase in the number of pedal cyclists struck by cars or light vans and a decrease in the number struck by PSV's or HGV's. Again, there was considerable overlap in the 90 percent confidence limits.

Scott and Willis(9) reported that although their analyses showed a slight increase in the number of pedestrian and pedal cycle casualties coincident with the introduction of the mandatory seatbelt use law, the changes were statistically insignificant. It was, therefore, concluded that the casualty figures did not support the hypothesis that risk compensation had occurred as a result of drivers being compelled to wear seatbelts but did not permit the suggestion to be entirely refuted.

Further time series analyses, which include 1984 casualty data, are proposed, the results of which will lead to a more accurate assessment of the effects of the mandatory seatbelt use law.

Pedal Cyclists

The greatest changes in the other road user casualties occurred with pedal cyclists. These will therefore be considered in more detail. In conducting their analysis, Scott and Willis grouped together all ages of pedal cyclists and all types of roads in built-up areas. An examination of the ages of pedal cyclists killed or seriously injured in 1982 and 1983 by type of striking vehicle shows considerable differences with age (Table 9). While overall there was a 10 percent increase in pedal cyclists struck by cars or vans compared to a decrease of 7 percent for those struck by PSV's or HGV's, the difference was greatest for children, i.e., those less than 14 years old,

Table 9. Fatal and serious pedal cycle casualties in two-party collisions: Great Britain, Feb. to Dec. 1982 and 1983

	Cyclists hit by cars or light vans			Cyclists hit by PSV's or HGV's		
	1982	1983	% Change	1982	1983	% Change
0 - 14 years	1,384	1,592	+15%	109	87	-20%
15-29 years	1,315	1,428	+9%	124	133	+7%
30 years and over	1,006	1,069	+6%	135	123	-9%
All ages (inc. NK)	3,716	4,104	+10%	368	344	-7%

there being a 15 percent increase in child cyclists struck by cars or vans and a 20 percent decrease in child cyclists struck by PSV's or HGV's. This difference was statistically significant; the changes for the other age groups were not statistically significant. This suggests that whatever occurred between 1982 and 1983 was predominantly due to a change in collisions between child pedal cyclists and cars or light vans. While this could be due to a change in the way cars and light vans were being driven, it could also be due to a change in the way pedal cycles were being used.

Concurrent with this rise in casualties was a change in the use of bicycles by young people: the BMX bicycle becoming popular among children at that time. The use of such bicycles is likely to be greatest in residential areas, and thus it would be expected that the increase in pedal cycle casualties would be greatest in such areas. This, in fact, was the case (Table 10).

Consideration of the location of pedal cycle accidents in built-up areas indicates that the majority occur in residential areas; just over half of all fatal and serious pedal cycle casualties in built-up areas occur on C roads and unclassified roads. Traffic on such roads consists predominantly of cars and light vans; the ratio of cars and light vans to PSV's and HGV's is approximately 22:1 on C and unclassified roads in built-up areas, whereas on other roads in built-up areas it is approximately 14:1.

Thus, an increased use of pedal cycles on C and unclassified roads would be expected to lead to a greater increase in car and van to pedal cycle collisions compared to PSV and HGV to pedal cycle collisions, all other things being equal. There was additionally a reduction of 11 percent in car or light van traffic, and a reduction of 20 percent of PSV and HGV traffic, on C and unclassified roads in built-up areas between 1982 and 1983. These changes in traffic would have the additional effect of reducing the number of pedal cycle to PSV/HGV accidents compared to pedal cycle to car/light van accidents. As this is what actually occurred, support is given to the hypothesis that the increase in the number of collisions between cars or light vans and pedal cycles is mainly due to a change in the use of pedal cycles in residential areas by young people.

Risk Compensation

Adams(13) has suggested that when mandatory seatbelt use is introduced, the actual reductions in fatalities are less than the expected reductions due to an increase in accidents as a result of people driving more dangerously when compelled to wear seatbelts. He has also suggested that, due to the increased risk-taking by drivers compelled to wear seatbelts, other road users, i.e., pedestrians, cyclists, and motorcyclists, are put at greater risk. This hypothesis is an example of the risk compensation theory put forward by Peltzman in the mid-70's(14).

Peltzman hypothesized the introduction of safety devices into cars results in drivers increasing their level of

Table 10. Fatal and serious pedal cycle casualties by location of accident: Great Britain, 1982 and 1983

	1982		1983		Change 1982 - 1983	
	N	%	N	%	N	%
Motorways	3	0.0%	3	0.0%	0	0.0%
Built-up roads						
A roads	1,908	29.2%	2,072	29.8%	+164	+ 8.6%
B roads	656	10.0%	648	9.3%	- 8	- 1.2%
Other roads	2,638	40.3%	2,898	41.8%	+260	+ 9.8%
Non-built-up roads						
A roads	676	10.3%	708	10.2%	+ 32	+ 4.7%
B roads	188	2.9%	187	2.7%	- 1	- 0.5%
Other roads	474	7.2%	423	6.1%	- 51	-10.7%
	6,543	100.0%	6,936	100.0%	+393	+ 6.0%

driving intensity, which, in turn, leads to an increase in the rate at which they will be involved in accidents. He argued, using time series regression analysis of traffic fatalities and injury statistics, that the vehicle safety regulations introduced into America in the 1960's had no net benefits. According to Peltzman, seatbelts, energy-absorbing steering columns, and other safety features do work, but the introduction of such measures compromises their injury-mitigating potential.

Peltzman's work, however, has been strongly criticized by Robertson(15) and by Joksch(16,17). Robertson noted that Peltzman took no account of increased motorcycle usage in the 1970's, although this was probably mainly responsible for the increase in nonvehicle occupant casualties during that period. Joksch reconstructed Peltzman's time series equations and found they were either unstable or had a high degree of time dependency, thus making them unsuitable for prediction.

Limited support for a risk compensation theory comes from a study conducted by Rumar(18) in Sweden. Rumar and his colleagues looked at the speeds at which drivers travelled around icy bends and compared the speeds of vehicles with and without studded tyres. It was found the drivers in cars with studded tyres travelled at a higher speed. There would thus appear to be some evidence for risk compensation. However, a comparison between vehicle travelling speeds and the critical speed for the bend, taking into account the tyre road friction, indicated that drivers of vehicles with studded tyres had a greater margin of safety than drivers of vehicles without studded tyres. Evans and Herman(19) found, in test track experiments, that drivers of vehicles with high acceleration capabilities accepted smaller gaps when crossing a traffic stream. However, it was also found the reduction in accepted gap was less than the increase in safety margin provided by the increase acceleration capabilities of the car. The Transport and Road Research Laboratory has reported that resurfacing of roads results in higher travel speeds(20)

There is thus some evidence that risk compensation occurs when there is direct feedback to the driver as a result of improved performance, ride, or handling of the vehicle.

Support for the risk compensation theory applying to a mandatory seatbelt use situation appears to come from Conybeare(21) in Australia. Like Peltzman, he used a regression model to predict expected casualties and reported that, while deaths and injuries to car occupants decreased after the introduction of compulsory seatbelt use laws, deaths and injuries to nonoccupants increased above predicted values. However, the criticisms applied to Peltzman's models may also apply to Conybeare's model.

A number of studies have examined driver behaviour as a function of seatbelt use. These studies, in the main, have been conducted in environments where seatbelt use has been voluntary. Von Busack(22) compared following headways between users and nonusers of seatbelts on a Detroit freeway and found that nonusers tended to follow other vehicles closer than did users. Deutsch(23) observed driver behaviour at intersections and found that nonusers of seatbelts jumped red lights more frequently than users. Mackay(24) reported on the speeds that drivers traverse sharp curves and noted that the mean speed for restrained drivers was slightly faster than the mean speed for unrestrained drivers. However, it was also noted that vehicle age and seatbelt use and vehicle age and vehicle speed were correlated: the newer the vehicle, the faster the curve speed and the higher the belt use. Ashton(10) reported on the difference in gap acceptance between restrained and unrestrained drivers turning right from a main road into a minor road. They found that unrestrained drivers accepted shorter gaps than restrained drivers.

There is thus strong evidence that users of seatbelts drive less dangerously than nonusers when seatbelt use is voluntary.

Evans(25) compared following headways in high-flow freeway traffic in Michigan, U.S.A., where seatbelt use is voluntary, with following headways on similar roads in Ontario, Canada, where seatbelt use is mandatory. It was found, in both areas, the percentage of drivers travelling at short headways was lower for drivers using seatbelts. It was therefore concluded that belt use laws did not appear to influence drivers to drive at closer and thus riskier headways.

There have been only two studies that have directly examined driver behaviour before and after the introduction of a mandatory seatbelt use law, one in this country(26,27) and one in Newfoundland(27,28). In the Newfoundland study, four measures of driving behaviour were studied, these being travel speed, response to amber at signalized intersections, gap acceptance when turning left in front of oncoming traffic, and following headways. It was reported that there was only one statistically significant change in driver behaviour and that was a reduction in travelling speed on four-lane roads in the period after the use of seatbelts became mandatory. The other changes in behaviour, which were all nonsignificant, were split evenly between increased and decreased risk-taking. In the British study, there were only two significant changes in driver behaviour, these being a significant reduction in speeds on bends and a significant increase in the speeds at which women travelled on straight two-lane single carriageways. There were no significant changes in the speeds at which males travelled on two-lane single carriageways or in the speeds on dual carriageways or in following headways.

Thus, the available evidence from studies of driver behaviour indicates that risk compensation probably does not occur as a result of drivers being compelled to wear seatbelts.

Influence on Patterns of Injury

Preliminary results from a study of the change in injury patterns as a result of the mandatory seatbelt use have been presented by Rutherford(29). In the first 6 months after the introduction of the law, there was, at the 15 hospitals included in the study, a 20 percent reduction in casualties attending hospital and a 35 percent reduction in admissions (Table 11). It was reported that for most body regions, there had been a decrease in the incidence of injury although for some regions—for instance, the neck—there had been an increase in reported injuries (Table 12).

Other hospital-based studies have reported similar findings. Christian(30), comparing 12-month periods before and after the introduction of the seatbelt use law, reported a 54 percent reduction in front-seat occupants killed or seriously injured (ISS > 12). Front-seat occupants requiring admission declined by 42 percent, while deaths fell by 27 percent.

Table 11. Casualties treated at a sample of hospitals

	Pre-law Feb-Jul 1982	Post-law Feb-Jul 1983	% Change
Not Admitted	18	11	-39%
Admitted - Survived	568	367	-35%
Admitted - Died	2,062	1,699	-16%
	2,612	2,077	-20%

Table 12. Changes in injury frequency

	Pre-law Feb-Jul 1982	Post-law Feb-Jul 1983	% Change
Concussion	434	237	-45%
Facial Wounds	479	173	-64%
Fractured Skull	26	14	-46%
Internal Chest Injuries	42	12	-71%
Neck Sprain	427	517	+21%

Results From Current In-Depth Accident Studies

The Data

In-depth studies of the causes of injuries to car occupants are currently being conducted by the Accident Research Units of the Department of Transportation and Highway Engineering at the University of Birmingham and the Institute for Consumer Ergonomics, Loughborough. A detailed description of the general methodology has been published elsewhere(31). Both groups investigate accidents in which cars less than 5 years old are towed away, using disproportionate stratified sampling schemes based on injury severity.

In this paper, weighted data are presented from a preliminary analysis of a sample of injury accidents that occurred in 1984 in Derbyshire, Leicestershire, Nottinghamshire, and Durham. In this area, a total of 240 accidents involving 275 cars less than 5 years old were investigated, and in these vehicles there were 539 occupants. Weighting the data to allow for the differing percentages of accidents of each injury severity investigated provided a weighted data base of 2,804 occupants. Unless otherwise stated, all quoted results are based on an analysis of the weighted data. It should be noted there may be small differences between the totals of the various tables. This arises from rounding errors in the calculation procedures used to produce the weighted totals.

Drivers accounted for 50 percent of the occupants, front-seat passengers for 23 percent, and rear-seat passengers for 27 percent (Table 13). The relatively high proportion of rear-seat occupants probably stems from the increased relative risk of a rear-seat occupant being injured compared to that for a front-seat occupant now that front-seat occupants are generally restrained by seatbelts.

Table 13. Occupancy and seatbelt use: weighted data

	Restraint Use			
	Used	Not Used	Not Known	Total
Driver	975	68	353	1,396
Front Seat Passenger	401	43	210	654
Rear	0	752	0	752
Not Known	0	2	0	2
	1,376	865	563	2,804

Seatbelt Use

Seatbelt use was determined from an examination of the seatbelt, from consideration of the injuries sustained by the occupant, and from the occupant's contacts with the interior of the car. Police reporting or self-reporting of seatbelt use was not used as a basis for determining seatbelt use.

In approximately three-quarters (73 percent) of the cases, it was possible to ascertain, with confidence, whether a seatbelt had been worn by a front-seat occupant. In the remaining cases (27 percent), it was not possible to determine if the seatbelt had been worn. Many of these cases were low-speed accidents, and in these accidents the forces are such that the characteristic use marks seen on seatbelt webbing and hardware do not occur, and, additionally, occupant contacts with the interior of the car, if they do occur, do not leave any

evidence. Thus, in a proportion of the cases where seatbelt use was not known, the seatbelt would have been used although there was no evidence to indicate this.

The overall seatbelt use rate for front-seat occupants, excluding those cases where seatbelt use was not positively established, was 93 percent. If it is assumed that all those for whom seatbelt use was not established were not wearing their seatbelt, then the use rate falls to 67 percent; if it is then assumed that all those for whom seatbelt use was not established were wearing their seatbelt, the use rate becomes 95 percent. Thus, the accident data indicate that the seatbelt use rate for front-seat occupants involved in accidents was between 67 and 95 percent. Use rates for drivers were generally slightly higher than for front-seat passengers (Table 14).

Table 14. Seatbelt use rates: weighted data

	Excluding Not Knowns	Including Not Knowns	
		Min	Max
Driver	94%	70%	95%
Front Seat Passenger	90%	62%	93%
All Front Seat Occupants	93%	67%	95%
Rear	0%	0%	0%

Front-Seat Occupant Injury Severity

Although the data base consists of injury accidents, approximately 21 percent of the front-seat occupants were uninjured. This stems from the fact that there can be, and frequently are, injured and uninjured people in the same vehicle. Table 15 gives details of the police assessment of the severity of the injuries sustained by the occupants, while Table 16 gives details of the maximum AIS rating (MAIS) of the occupants. A three-point injury classification system is used by the police. A fatality is a person who dies within 30 days of the accident. A slightly injured person is a person with injuries of a minor nature, these injuries being roughly equivalent to AIS 1 injuries. In each table, restraint use is also considered.

A comparison of the MAIS distributions for restrained and unrestrained front-seat occupants indicates that in towaway accidents, unrestrained occupants are approximately 2.6 times more likely to receive MAIS 4 to 6 injuries, 1.1 times more likely to receive MAIS 2 to 3 injuries, and 1.4 times less likely to receive MAIS 1 injuries, and 1.3 times less likely to receive no injuries than restrained occupants (Table 16). While these figures suggest restrained occupants are less likely to sustain serious injury than unrestrained occupants, the small number of unrestrained occupants (29 in the unweighted data base) means that the relative risk of injury between restrained and unrestrained occupants cannot be calculated with any degree of accuracy.

Table 15. Overall injury severity of restrained and unrestrained front seat occupants according to police classification: weighted data

Police Classification of Injury Severity	Restrained N	Restrained %	Unrestrained N	Unrestrained %
No Injury	281	20%	35	32%
Slight	667	49%	37	34%
Serious	343	25%	18	16%
Fatal	82	6%	20	18%
	1,373	100%	110	100%

Table 16. Maximum AIS of restrained and unrestrained front seat occupants: weighted data

MAIS	Restrained N	Restrained %	Unrestrained N	Unrestrained %
0	270	20%	17	16%
1	552	42%	31	30%
2	321	24%	32	30%
3	76	6%	3	3%
4	22	2%	10	10%
5	45	3%	9	9%
6	33	3%	3	3%
	1,319		105	
N.K.	52		6	
	1,371		111	

Interestingly, there were differences in the police assessment of injury severity and the investigating teams' assessment of the severity of the injuries. A comparison of the number uninjured between the police classification (Table 15) and the MAIS classification (Table 16), based on an examination of medical records and occupant questionnaire returns, indicates that a proportion of those classified as having no injury by the police were in fact injured. Likewise, it was found that a proportion of those classed as having slight injuries by the police did not have an injury assessable under the AIS system.

Pattern of Injury to Restrained Occupants

Table 17 shows the distribution of the injury severity for each of the five body areas for restrained occupants. It can be seen that, overall, the chest and legs were the most frequently injured body areas: 47 percent of restrained occupants sustained a chest injury and 47 percent a leg injury. Head injuries were sustained by only 26 percent. If, however, only nonminor injuries are considered, the head was the body area most frequently injured, followed by the chest and then the abdomen. AIS 4 to 6 injuries were sustained in roughly equal proportions by the head, chest, and abdomen.

Table 17. Pattern of injury by injury severity for restrained occupants: weighted data

AIS	Head		Chest		Abdomen		Arms		Legs	
	N	%	N	%	N	%	N	%	N	%
0	1,013	74%	730	53%	974	71%	926	67%	732	53%
1	107	8%	419	30%	324	24%	370	27%	513	37%
2	184	13%	133	10%	7	-	65	5%	81	6%
3	18	1%	38	3%	16	1%	14	1%	50	4%
4	7	-	28	2%	12	1%	0	-	0	-
5	18	1%	22	2%	43	3%	0	-	0	-
6	28	2%	5	-	0	-	0	-	0	-

All Severities of Injury

For each injured occupant, the most severely injured body area has been identified. Where there were several body areas with injuries of the same severity, each region has been counted. Table 18 shows the rank order of involvement of different body areas by impact type counting all severities of injury sustained by those with any severity of injury. It can be seen from this table there are considerable differences in the relative importance of different body regions between different impact types. Leg injuries were the most frequently sustained injury by occupants in frontal impacts and by nonstruck side occupants in side impacts. Chest injuries were the most frequently sustained injury by struck side occupants in side impacts. Abdominal injuries were less frequent in frontal impacts than in other impact types.

Nonminor Injuries

Over half those injured sustained MAIS 1 injuries. It is perhaps more useful to consider nonminor injuries (AIS 2+) sustained by only those with nonminor injuries (MAIS 2+) (Table 16). When this is done, the head emerges as the body area most frequently injured for all impact types except struck side occupants where torso injuries were more frequent (Table 19). Serious abdominal injuries were relatively infrequent in frontal impacts but were frequent in side impacts.

Seatbelt Effectiveness in Fatal Accidents

The Data

Data from two sources have been used to examine the circumstances of accidents in which restrained front-seat occupants are fatally injured. The first data set consisted of 48 accidents investigated by the various teams currently conducting in-depth studies of crash injury(31); the second data set consisted of 49 accidents for which details were obtained from police reports. In the 97 accidents available for analysis, there were 109 fatally injured front-seat occupants seated in 100 cars: 74 of these fatally injured occupants were drivers and 35 were front-seat passengers.

While the data from the in-depth studies contained detailed information on the extent of the damage to the vehicle, the location of occupant contacts with the interior, and the causes of injury to the occupants, the data obtained from police records lacked this information. Consequently, no attempt has been made to classify the accidents by impact speed nor have the specific causes of injury been considered.

The Representativeness of the Data

The age distribution of the drivers was similar to that occurring nationally for all fatally injured drivers, the most frequent age group being the 20 to 29 year age group and the second most frequent, the 30 to 39 year age group. A comparison of the age distribution for fatally injured passengers was not undertaken due to the small numbers in the sample. The ratio of males to females in the sample was similar to that occurring nationally. In the sample, 81 percent of the fatally injured restrained drivers were males, whereas nationally, in 1983, 83 percent of all fatally injured drivers were male. For front-seat passengers, the corresponding figures were 49 percent for the sample and 50 percent nationally. Table 20 gives details of the age distribution of the fatally injured restrained drivers and front-seat passengers in the sample, together with the age distribution for all fatally injured drivers nationally.

The Collision Circumstances

The majority of the accidents in which restrained front-seat occupants were killed occurred on high-speed roads. Only 12 percent of those accidents for which the speed limit was known occurred on roads subject to a 30mph speed limit, whereas 73 percent occurred on roads subject to a speed limit greater than or equal to 60mph.

Approximately two-thirds of the vehicles were involved in accidents with other vehicles. Just over half the collisions with other vehicles were head-on collisions. Heavy Goods Vehicles (HGV's), or Public Service Vehicles

Table 18. Most severely injured body area by impact type for injured restrained occupants - all severities of injury counted: weighted data

Frontal Impacts		Side Impacts (Occupant Location) Struck Side		Side Impacts (Occupant Location) Nonstruck side		Other Impacts	
Legs	28%	Chest	43%	Legs	31%	Head	26%
Chest	22%	Head	30%	Chest	25%	Chest	25%
Head	16%	Abdomen	22%	Abdomen	25%	Abdomen	17%
Arms	15%	Arms	4%	Arms	12%	Legs	17%
Abdomen	13%	Legs	2%	Head	11%	Chest	14%

Table 19. Most severely injured body area by impact type for restrained occupants with nonminor injuries - nonminor injuries counted: weighted data

Frontal Impacts		Side Impacts (Occupant Location) Struck side		Side Impacts (Occupant Location) Nonstruck side		Other Impacts	
Head	33%	Chest	34%	Head	50%	Head	50%
Chest	29%	Abdomen	34%	Abdomen	22%	Chest	27%
Legs	24%	Head	31%	Legs	22%	Abdomen	14%
Arms	10%	Arms	0%	Arms	6%	Arms	10%
Abdomen	5%	Legs	0%	Chest	0%	Legs	0%

Table 20. Age distribution of fatally injured restrained front seat occupants

Age Group	Sample Driver N	Driver %	F.S.P. N	F.S.P. %	National Data All Drivers*
<16			6	18%	
17-19	10	14%	2	6%	11%
20-29	16	22%	4	12%	29%
30-39	13	17%	4	12%	17%
40-49	12	16%	5	15%	13%
50-59	8	11%	4	12%	8%
60-69	10	14%	4	12%	11%
>70	5	7%	5	15%	11%
	73		34		
N.K.	1		1		
	74		35		

*Note: Irrespective of seatbelt status

(PSV's) were the other vehicle in just over a third of the cases where another vehicle was involved and in just under one-quarter of all the cases.

In three of the cases, the vehicle caught fire. However, in all these cases, the accidents were of such severity that the occupants would most probably have died from injuries sustained in the initial impact had there not been fire present.

The Vehicles

Table 22 gives details of the approximate ages of the involved vehicles. Age has been determined from the registration letter, which changes on August 1 each year. It will be noted there are no vehicles older than 5 years in the in-depth data. This is due to the fact that only vehicles less than 6 years old are examined in the current in-depth accident studies(31). The police data indicate that roughly half the restrained occupants killed are in vehicles more than 5 years old.

Gross intrusion was a characteristic of the accidents. Approximately three-quarters (74 percent) of the fatally injured restrained front-seat occupants were involved in accidents where there was gross intrusion, while a further 13 percent were involved in accidents where there was complete disintegration of the vehicle (Table 23). In the great majority (93 percent) of the cases where there was gross intrusion, the fatally injured restrained occupant was seated on that side of the car where the intrusion was greatest (Table 24).

Table 21. Principal collision type for accidents in which a restrained front seat occupant was fatally injured

Collision Type		N
Head-on impact	- with Car/LGV21	
	- with HGV/PSV	17
Side impact	- with Car/LGV	17
	- with HGV/PSV	7
Other	- with Car/LGV	5
	- with HGV/PSV	0
Collision with Roadside Object		
	- with Narrow Object	14
	- with Wide Object	3
	- Other	5
Rollover		5
Other		4
		100

Table 22. Vehicle age for vehicles in which a restrained occupant was fatally injured

	Vehicle Age (years)						
	<4	4-5	6-7	8-9	>9	N.K.	Total
In-depth Data	39	10	-	-	-	1	50
Police Data	19	5	9	9	8	-	50
	58	15	9	9	8	1	100

Table 23. Level of intrusion in accidents in which a restrained front seat occupant was fatally injured

Level of Intrusion	N	%
Negligible	14	13%
Gross	81	74%
Vehicle Disintegration	14	13%
	109	

The Occupants

Although there were 109 fatally injured restrained front-seat occupants in the 100 vehicles under consideration, these vehicles contained a total of 152 front-seat occupants. In addition to the 109 fatally injured restrained front-seat occupants, there was one fatally injured unrestrained front-seat passenger, 16 surviving injured restrained front-seat passengers, and 26 surviving restrained drivers. Table 25 gives details of status of the front-seat occupants by impact type. In approximately half the cases, the driver was the sole occupant, these accidents being predominantly distributed frontal or offside frontal impacts. In just over one-quarter of the cases, the vehicle was struck on the side and in the majority (74 percent) of these cases the fatally injured occupant was seated on the struck side.

The Injuries

Multiplicity of injury was a characteristic of restrained occupants fatally injured. The 99 fatally injured front-seat occupants for whom the number of fatal injuries could be established sustained a total of 182 fatal injuries, i.e., an average of 1.8 fatal injuries per fatality. Over half (60 percent) sustained more than one fatal injury (Table 26), while approximately one-fifth (21 percent) sustained more than two fatal injuries.

Just under half (46 percent) sustained maximal Injury Severity Scores (ISS = 75), most of these being associated with maximal AIS ratings (AIS = 6) (Table 27).

Discussion

In the preceding sections, some numerical aspects of seatbelt use, effectiveness, and the consequences of the seatbelt law on injury patterns have been considered. One advantage of detailed in-depth studies is that it allows the investigating team to make a thorough assessment of seatbelt performance on a case-by-case basis. It is difficult to quantify such experience because every collision is in some way unique. There are many ways of describing the impact conditions; crash severity and impact force direction being two of the relevant parameters. Other factors relate to vehicle design, which influences the kinematics of the occupants and their contacts. Finally there are parameters such as human tolerance, which influence the injuries sustained. However, the experience gained of seatbelt function in the real world of crashes examined by the various teams involved in in-depth crash injury studies(31) allows some comment to be made about the limits to seatbelt performance and about future developments that are likely to enhance the already good protection provided by seatbelts.

Intrusion

The most important limitation on the ability of the seatbelt to prevent death in a collision arises not from the functioning of the seatbelt itself, but from the destruction of the passenger compartment. This is particularly so in car/truck collisions, where there is geometrical and structural mismatch between the engaging vehicles(32). Approximately 25 percent of restrained occupant deaths in Britain now occur in car-to-HGV and car-to-PSV collisions. Single-vehicle, off-road crashes with hostile roadside furniture form another important part of this

Table 24. Seating position of fatally injured front seat occupant by location of intrusion for accidents in which there was gross intrusion

	Location of Intrusion					
	Frontal		Side		Other	
	Driver Side	F.S.P. Side	Driver Side	F.S.P. Side	Driver Side	F.S.P. Side
Driver	28	2	16	3	9	-
F.S.P.	1	9	-	7	-	6

Table 25. Front seat occupant injury severity by impact type

Status of Occupant		Frontal Impact			Side Impact		Other	Total
Driver	F.S.P.	All Front	Offside	Nearside	Right	Left		
Killed	None	13	12	3	8	5	7	48
Killed	Killed	4	2		1	1	2	10
Killed	Survived	4	3	2	5		2	16
Survived	Killed	8	3	3	1	6	5	26
		29	20	8	15	12	16	100

problem. In such crashes, the localised, unforgiving nature of structures such as trees, lamp posts, and sign supports produce levels of intrusion where seatbelt use becomes irrelevant to injury causation. While some reduction in occupant fatalities can probably be achieved by improvements in vehicle structural design, issues of compatability between vehicles of disparate mass, and policies on the design of roadside furniture, are of importance in reducing occupant fatalities.

Rear Loading

Serious injury to restrained front-seat occupants is more likely when the front-seat occupants are loaded from behind by unrestrained occupants or luggage. Great Britain, unlike many other motorised countries, has not yet required the mandatory fitting of rear seatbelts. In our in-depth studies, evidence of additional loading to the front seats by unrestrained rear-seat occupants is common when rear-seat occupants are present, and in severe frontal collisions this additional loading can cause injury to the restrained front-seat occupants. However, other objects besides rear-seat passengers load and injure correctly restrained front-seat occupants. This has been seen to occur in estate cars and hatchbacks where current designs of folding rear seats do not appear to be able to withstand the forces applied to them by luggage in accidents. Injury to restrained front-seat occupants as a result of rear loading by luggage has been seen in those exceptional accidents in which large, heavy objects have been carried in the luggage area. Thus, the design of rear seat backs with respect to load retention is of importance.

Rear Seatbelts

Currently, approximately 300 to 350 people are killed each year in Great Britain while rear-seat car occupants. Griffiths(4), from a study of fatally injured unrestrained car occupants, concluded that with 100 percent seatbelt use in the rear seats there would be a reduction of about 74 percent in the number of rear-seat occupants killed. This effectiveness rate is higher than for front-seat occupants as severe intrusion, which compromises an occupant's seating position, is relatively infrequent for rear-seat occupants. Thus, the mandatory fitting, and use, of rear seatbelts, assuming use rates similar to those for front-seat occupants, would result in a reduction of about 200 to 230 in the number of rear-seat occupants killed. Griffiths also reported that approximately 8 percent of fatally injured restrained front-seat occupants would not be killled if all rear-seat occupants were restrained. Since the introduction of mandatory seatbelt use, the number of front-seat car occupants killed has been about 1,800 per annum. Assuming that seatbelt use rates in the rear, with mandatory fitting and use, would be similar to those in the front, there would potentially be a reduction of approximately 100 to 120 in the number of restrained front-seat occupants killed if the fitting and use of rear seatbelts was made compulsory.

Overall, the mandatory fitting and use of rear seatbelts, assuming rear seatbelt use rates would be similar to those for front seatbelts, would potentially result in a further reduction of between 300 and 350 in the number of car occupants killed.

Occupant Kinematics and Contacts

During a frontal impact, a restrained occupant moves forward and is decelerated as a result of forces applied to the body by the seatbelt. As the seatbelt is loaded by the occupant, the belt stretches and contact with the interior can occur.

Injuries to the chest, from the forces applied to the chest by the seatbelt, have been seen. These injuries

Table 26. Number of fatal injuries sustained

Number of Injuries	Driver		F.S.P.		Total	
	N	%	N	%	N	%
1	27	39%	13	43%	40	40%
2	25	36%	13	43%	38	38%
3	15	22%	3	10%	18	18%
4	2	3%	1	3%	3	3%
	69		30		99	
N.K.	5		5		10	
	74		35		109	

Table 27. Injury severity score by posted speed limit

Speed Limit	Injury Severity Score					
	0-15	16-24	25-49	50-74	75	N.K.
30	-	-	6	1	3	1
40	-	-	8	1	8	1
50	-	-	-	-	2	-
60	1	3	14	7	17	7
70	-	1	4	5	10	-
N.K.	-	-	2	1	6	-
	1	4	34	15	46	9

normally only occurred in severe collisions, particularly if the restrained occupant was elderly or there was additional rear loading. The severity of these collisions was such that the occupant would most probably have been more severely injured if unrestrained.

A limit to the protection afforded by seatbelts comes from the restrained occupant running out of space and being injured as a result of contact with the interior of the passenger compartment. With current car designs, the interior geometry, crash pulse, and belt characteristics are such that a driver's face is likely to strike the steering wheel in that small proportion of frontal crash where the velocity change is greater than about 25mph. Such contacts do not normally result in fatal injuries, but they do generate significant soft tissue trauma, concussion, and occasionally facial bone fractures. Thus, consideration needs to be given to designing steering wheels for facial contact.

Knee contacts are also frequent for restrained occupants in severe frontal impacts, and thus the design of the knee contact zones is still of importance.

Seatbelt Design Features

A number of specific items of detailed design have emerged from these current studies and from previous in-depth studies carried out at Birmingham University. For example, the weakening of retraction springs has been seen to result in belt slack and consequent poor belt geometry; excessive slack and incorrect belt geometry have been noted when swinging arms, which have been used on two-door cars to improve rear-seat access by rotating the belt at the lower outboard mounting point, have failed to correctly align with the belt; poor belt geometry has also been noted for part of the car user population, particularly when the seat is at the extreme limit of its travel; damage to seatbelt webbing under crash conditions has been observed as a result of the belt catching on items such as seat back adjusters. All of these limitations to current seatbelt performance can be, and generally have been, improved by technical development.

Future Developments

In terms of improving seatbelt crash performance, the authors consider that the following will lead to a significant upgrading of the already good performance of current belt systems:

- Integration of the front-seat lower belt mounting points into the seat structure
- Matching the dynamic response of the seatbelt and the seat to the geometrical constraint of the compartment package for the actual population at risk, which may lead to knee contacts occurring by design as a means of controlling occupant kinematics for some segments of the population
- Preloading the belt system to remove slack and to couple the occupant dynamically to the crash characteristics of the front structure
- Changing steering wheel design to either diminish the frequency of driver face contacts or to make such contacts more benign through improvements in hub, spoke, and rim design or developing supplementary restraint systems such as the steering wheel airbag

In addition to the benefits that would come from the improvements in vehicle design outlined above, significant benefits would come from requiring that rear seatbelts be fitted in cars and by encouraging their use, possibly by legislation. In designing rear seatbelt installations, the characteristics of the population that use rear seatbelts need to be considered, a high proportion of rear-seat occupants being young children.

Conclusion

This paper has reported on some of the consequences of the mandatory seatbelt law in Britain. The main conclusions are—

1. The introduction of the mandatory seatbelt use law resulted in seatbelt use rates for front-seat occupants, rising from around 35 percent to around 95 percent.
2. There has been a reduction of approximately 25 percent in the number of car and light van front-seat occupants seriously injured or killed coincident with the introduction of the mandatory seatbelt use law.
3. The actual reduction in front-seat occupant fatalities is in line with the expected reduction.

4. While there have been increases in the number of pedestrians and pedal cyclists killed or injured as a result of being struck by a car or light van, the increases are not statistically significant.
5. The increase in the number of pedal cyclist casualties coincident with the introduction of the mandatory seatbelt use law is mainly due to an increase in accidents involving child cyclists on unclassified roads in residential areas and may reflect the increased use of BMX bicycles by children.
6. While the changes in the other classes of road casualties are statistically insignificant and are consistent with the random annual fluctuations and changes in traffic volumes and patterns, the reduction in front-seat car occupant deaths and serious injuries coincident with the seatbelt law is large, statistically significant, and not explainable in any other way than being related to the seatbelt law.
7. The data currently available do not support the hypothesis that risk compensation, well accepted for some developments in the field of active safety, applies to the mandatory use of seatbelts.
8. Accidents in which restrained occupants are killed are normally so severe there is gross intrusion into the passenger compartment with the result that the seatbelt has virtually no effect.

Acknowledgments

In a study such as this that relies on the cooperation of many different organisations and individuals, there are many people to acknowledge. The authors would like to express particular thanks to—

1. The Department of Transport, British Leyland, and Ford for providing financial support for the two University groups.
2. The Chief Constables and their officers in all the areas in which the investigation teams work for allowing access to accident data.
3. The consultants and other staff at the various hospitals in the study areas for their assistance in providing injury data.
4. The coroners in the study areas for their cooperation in providing copies of post-mortem reports.
5. The Department of Transport vehicle examiners in the West and East Midlands, Northern, and Western traffic areas for their assistance in collecting vehicle data.
6. The staff of the two Accident Research Units.

The opinions expressed in this paper are entirely those of the authors and are not necessarily the views of the sponsors.

Appendix 1

If

T = total deaths with zero belt use

D_B = number of deaths before the introduction of the law

D_A = number of deaths after the introduction of the law

U_B = seatbelt use rate before the introduction of the law

U_A = seatbelt use rate after the introduction of the law

e = seatbelt effectiveness rate

then

$$D_B = U_B.(1 - e).T + (1 - U_B).T$$
$$= (1 - U_B.e).T$$

and

$$D_A = U_A.(1 - e).T + (1 - U_A).T$$
$$= (1 - U_A.e).T$$

The expected reduction in fatalities R_F is thus:

$$R_F = (D_B - D_A)/D_B$$
$$= ((1 - U_B.e).T) - ((1 - U_A.e).T) / ((1 - U_B.e).T)$$
$$= ((U_A - U_B).e / (1 - U_B.e)$$

References

1. Huelke, D.F., T.E. Lawson, R. Scott, and J.C. Marsh, "The effectiveness of belt systems in frontal and rollover crashes," SAE Paper 770148, Warrendale, Pennsylvania, 1977.
2. Huelke, D.F., H.W. Sherman, and M.J. Murphy, "Effectiveness of current and future restraint systems in fatal and serious automobile crashes," SAE Paper 790323, Warrendale, Pennsylvania, 1979.
3. Lister, R.D., and B. Millsom, "Car seatbelts and analysis of injuries sustained by car occupants," *The Practitioner*, Vol. 191, pp. 332-340, 1963.
4. Griffiths, D.K., H.R.M. Hayes, P.F. Gloyns, S.J. Rattenbury, and G.M. Mackay, "Car occupant fatalities and the effects of future safety legislation," Proceedings 20th Stapp Car Crash Conference, SAE Paper 760811, Warrendale, Pennsylvania, 1976.
5. Bohlin, N.I., "A statistical analysis of 28,000 accident cases with emphasis on occupant restraint value," Proceedings 11th Stapp Car Crash Conference, SAE Paper 670925, New York, 1967.
6. Hobbs, C.A., and P.J. Mills, "Injury probability for car occupants in frontal and side impacts," TRRL Report LR1124, Transportation and Road Research Laboratory, Crowthorne, 1984.
7. Trinca, G.W., and B.J. Dooley, "The effects of seatbelt legislation on road traffic injuries," *Aust. N.Z. J. Surg.*, Vol. 47, No. 2, April 1977.
8. Mackay, G.M., "A review of seatbelt crash performance in the U.K.," Paper 12, Proceedings Seatbelt Seminar, Melbourne, 1976.

9. Scott, P.P., and P.A. Willis, "Road casualties in Great Britain during the first year with seatbelt legislation," TRRL Research Report 9, Transportation and Road Research Laboratory, Crowthorne, 1985.
10. Ashton, S.J., G.M. Mackay, and S. Camm, "Seat belt use in Britain under voluntary and mandatory conditions," Proceedings 27th Conference American Association for Automotive Medicine, AAAM, Illinois, pp. 65-75, 1983.
11. Road Accidents & Casualties GB: 4th Quarter 1983, Department of Transport Statistical Bulletin STC4(84)3, Department of Transport, London, 1984.
12. Road Accidents & Casualties GB: 4th Quarter 1984, Department of Transport Statistical Bulletin 85(10), Department of Transport, London, 1985.
13. Adams, J., "The efficacy of seat belt legislation: a comparative study of road accident fatality statistics from 18 countries," Occasional Paper No. 38, Department of Geography, University College, London, January 1981.
14. Peltzman, S., "The effects of automobile safety regulations," *J. Political Economy*, Vol. 85, No. 4, pp. 677-725, 1975.
15. Robertson, L.S., "A critical analysis of Peltzman's 'The effects of automobile safety regulations'," *Journal of Economic Issues*, Vol. 11, No. 3, pp. 586-600, 1977.
16. Joksch, H.C., "Critique of Sam Peltzman's study: 'The effects of automobile safety regulations'," *Accident Analysis and Prevention*, Vol. 8, pp. 129-137, 1976.
17. Joksch, H.C., "The effects of automobile safety regulations: comments on Peltzman's reply," *Accident Analysis and Prevention*, Vol. 8, pp. 213-214, 1976.
18. Rumar, K., U. Berggrund, P. Jernberg, and U. Ytterbom, "Driver reaction to a technical safety measure—studded tyres," *Human Factors*, Vol. 18, pp. 443-454, 1978.
19. Evans, L., and R. Herman, "Note on driver adaptation to modified vehicle starting acceleration," *Human Factors*, Vol. 16, pp. 235-240, 1976.
20. "Research on Road Traffic," H.M.S.O., London, p. 440, 1965.
21. Conybeare, J.A.C., "Evaluation of automobile safety regulations: the case of compulsory seat belt legislation in Australia," *J. Policy Sciences*, Vol. 12. No. 1, pp. 27-39, 1980.
22. Von Buseck, C.R., L. Evans, D.E. Schmidt, and P. Wasielewski, "Seat belt usage and risk taking in driving behaviour in 'Accident Causation'," SAE Publication SP461, Warrendale, Pennsylvania, 1980.
23. Deutsch, D., S. Sameth, and J. Akinyemi, "Seat belt usage and risk taking at two major traffic intersections," Proceedings 24th Conference American Association for Automotive Medicine, AAAM, Illinois, pp. 415-421, 1980.
24. Mackay, G.M., K.J. Dale, and A. White, "Seat belt use under a voluntary regime—some aspects of use related to occupant and vehicle characteristics and driving behaviour," Proceedings 7th International Conference on Biomechanics of Impact, IRCOBI, pp. 40-50, 1982.
25. Evans, L., P. Wasielewski, and C.R. Von Buseck, "Compulsory seat belt use and driver risk-taking behaviour," *Human Factors*, Vol. 24, No. 1, pp. 41-48, 1982.
26. Ashton, S.J., and G.M. Mackay, "Mandatory seat belt use and risk compensation," Proceedings PTRC Annual Meeting, Brighton, 1985.
27. O'Neill, B., A.K. Lund, P. Zador, and S.J. Ashton, "Mandatory belt use and driver risk taking: an empirical evaluation of the risk compensation hypothesis," Proceedings G.M. Symposium, 1985.
28. Lund, A.K., and P. Zador, "Mandatory belt use and driver risk taking," *Risk Analysis*, Vol. 4, No. 1, pp. 41-53, 1984.
29. Rutherford, W., A. Greenfield, H.R.M. Hayes, and J.K. Nelson, "Study of car occupant patients and their injuries before and after seat belt legislation," Casualty Surgeons Annual Conference, Edinburgh, 1984.
30. Christian, M.S., "Morbidity and mortality of car occupants: comparative survey over 24 months," *British Medical Journal*, Vol. 289, December 1984.
31. Mackay, G.M., M.D. Galer, S.J. Ashton, and P.D. Thomas, "The methodology of in-depth studies of car crashes in Britain," SAE Paper 850556, Warrendale, Pennsylvania, 1985.
32. Mackay, G.M., and A. Walton, "Heavy commercial vehicle design and other road users," Proceedings 28th Conference American Association for Automotive Medicine, AAAM, Illinois, pp. 1-14, 1984.

Collision Types and Characteristics of Bus Accidents—Their Consequences for the Bus Passengers and the Accident Opponent

K. Langwieder,
M. Danner, and
Th. Hummel
HUK-Verband, Automobile Engineering Department, German Association of Third Party, Accident, Motor Vehicle and Legal Protection Insurers

Abstract

The omnibus occupies an important position in the traffic scene in the Federal Republic of Germany; this paper furnishes statistical data on this fact. In the light of the national statistics, it is deduced that the risk of being killed or seriously injured as the occupant of a bus is low. This study covers 97 bus accidents with a collision in which occupants were injured; for the bus occupants, the risk of injury is given dependent on the accident opponent and kind of collision. For bus/car accidents, the risk to the car occupants, i.e., the passengers in the opposing vehicle, is also described. Moreover, this paper contains 142 accidents with injuries to the bus occupants without the bus being involved in a collision. These injuries resulted from the driving maneuvers of emergency braking, starting, and driving in a bend.

The majority of persons killed or seriously injured in this study met with their accident in long-distance coaches; rollover accidents are of particular significance. On the basis of this knowledge, measures are indicated that could achieve a further increase in the passive safety of buses.

As unfavorable road conditions played an essential part in the available accident material, an investigation was carried out to ascertain whether the accident would have been influenced by the use of an antilock brake system. These systems turned out to be of great advantage. About 4 percent of the bus accidents could certainly have been avoided, and probably even 15 percent.

The Bus Accident in the Federal Republic of Germany

The omnibus occupies an important place in the traffic scene in the Federal Republic of Germany. In 1983, 71,159 omnibuses were registered(1); thus, compared with 1970 (47,253 registered buses), the number has increased by more than 50 percent.

The safety of present-day bus transport is relatively high compared to other means of transport. On average, only 1.9 persons met with an accident per billion (10^9) passenger kilometers; the comparable figure with the car is 20 persons and with the motorcycle as high as 178(2) (Figure 1).

The high safety level of the bus, however, not only turns out to be relative, but the absolute accident figures also make this fact clear. In 1983, altogether 26 bus occupants (drivers and passengers) were killed, 523 seriously and 3,645 slightly injured(1) (Figure 2). For 1984, the figures were 34 killed, 563 seriously injured, and 3,638 slightly injured(3). Although the number of injured persons remains fairly constant each year, with such low accident figures one single serious bus accident can have considerable influence on the national accident statistics, as, for example, in 1966, when 68 bus occupants were killed or in 1980 when the comparable figure ws 43(1).

In view of the high mileage of buses and number of injured persons given above, the risk of being killed or seriously injured as a bus occupant is low, and today a very high level of safety has been achieved, but this study indicates even further possibilities for improvement.

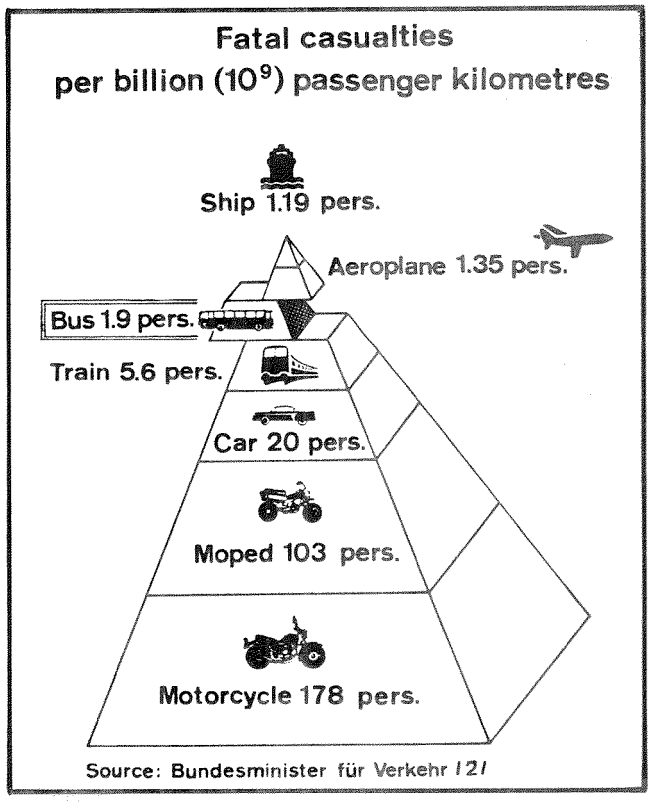

Figure 1. Relative risk to users of various means of transport

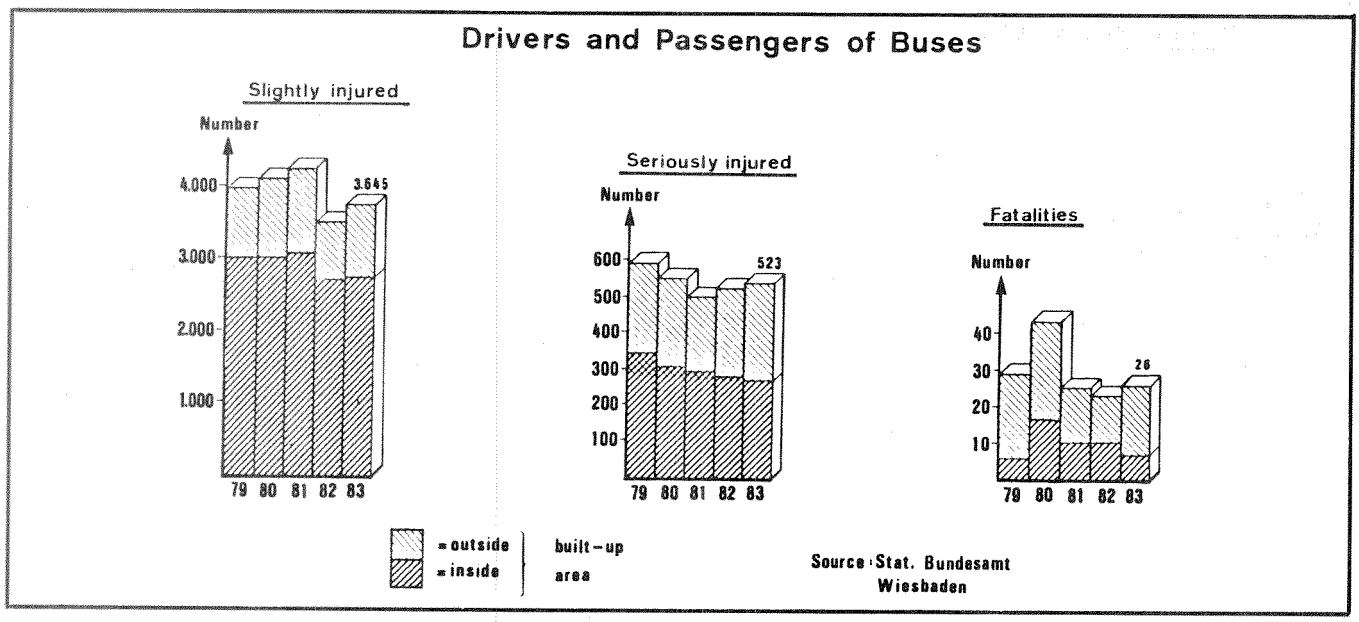

Figure 2. Bus occupant injured in accidents in the Federal Republic of Germany in 1979-83

Future considerations, however, will have to take into account traffic policies, economic aspects, and public acceptance to establish whether these measures—especially since extreme, isolated cases can never be avoided—can be justified with respect to cost/benefit rates and can be carried out uniformly on an international scale.

The Accident Studies of the German Motor Insurers

Since 1978, the accident research of the HUK-Verband has also included 239 bus accidents with injuries to persons. The selection of these accidents is based—with the exception of a few serious accidents—on the random principle. The bus accidents were recorded in the course of the continuous analysis of traffic accidents, which are made available by all the German motor insurers to the HUK-Verband for purposes of accident research. The condition for analyzing an accident is that at least one of the persons involved in the accident sustained injuries of AIS 1(4) or worse. The accidents were retrospectively evaluated by the HUK-Verband's own team of engineers in cooperation with doctors. The method of the HUK accident research is described in (5).

This study comprises only accidents of buses with a seating capacity of over 25; accidents with minibuses, bus collisions with two-wheeled vehicles or pedestrians, and accidents that occurred when bus occupants were boarding or alighting are not included.

The 239 bus accidents covered by this study are broken down into—

- 97 accidents with a collision
- 142 accidents without a collision

Altogether 100 buses were involved in the 97 accidents with a collision. The 142 accidents without a collision are accidents resulting from driving maneuvers, meaning emergency braking, starting, or driving in a bend.

Accident Characteristics With and Without a Collision

Bus Accidents Without a Collision

For the sake of completeness, bus accidents without a collision are mentioned here, as they also constitute a problem of bus safety, especially on a scheduled bus service. In these accidents, a dominant role (both with regard to frequency and to injury severity of the occupants) is played by emergency braking causing injuries, e.g., to standing passengers (Figure 3).

If all degrees of injury severity are included, in accidents without a collision head injuries dominate with 27.3 percent, followed by injuries to the chest with 19.2

Driving manoeuvre	Accidents caused by driving manoeuvres	Number of injured persons			
		MAIS*1	MAIS 2	MAIS 3	MAIS n.a.
Braking	120	47	5	5	93
Starting	13	7	-	3	3
Bend	9	4	1	-	4
Total	142	58	6	8	100

*MAIS = Maximum AIS /4/
n.a. = not ascertained

Figure 3. Frequency and severity of injuries in accidents without a collision caused by driving maneuvers by scheduled buses

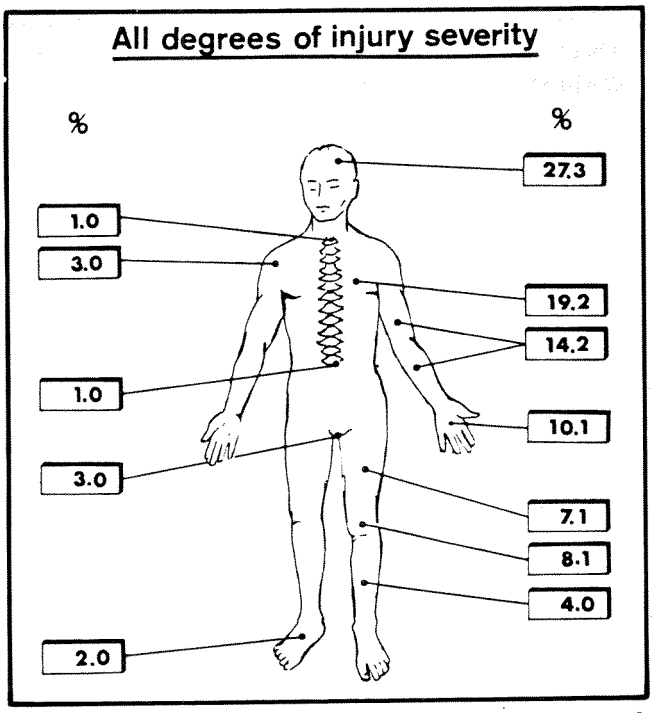

Figure 4. Frequency of injuries to the different parts of the body in accidents caused by driving maneuvers

percent and to the arm with 14.2 percent (Figure 4). Serious injuries (MAIS = 3) were observed in a total of only eight persons in 142 accidents, one case involving a serious head injury; injuries of MAIS 4 to 6 were not recorded in the 142 accidents without a collision.

In braking accidents, head injuries occurred with the greatest frequency. In accidents resulting from starting or driving in a bend, injuries to the chest were the most frequent. Most of these were chest bruises, although the available accident material does contain cases of multiple rib fractures. In general, only slight to moderate injuries result from driving maneuvers. When the occupants are standing in the regular scheduled bus, however, the long falling distances when the bus brakes may also cause serious injuries, such as fractured skulls, complicated

Bus Accidents With a Collision

Injury Risk Dependent on Operational Function of the Bus

Figure 5 shows the distribution of the bus accidents with a collision for the operational functions broken down according to scheduled bus, school bus, and long-distance coach.

fractures of the femur, or multiple rib fractures. Frequently, the occupants of the bus are old people who find it more difficult to hold tight or to support themselves than younger ones and who are exposed to a considerably higher injury risk simply by reason of their lower physical resistance.

Fifty percent of the buses concerned were involved in an accident on a scheduled service, about 35 percent on long-distance service, and about 15 percent on school bus service. To what extent this distribution agrees with the actual circumstances in the overall accident scene and national accident statistics cannot at present be ascertained for lack of comparative data. Figure 6 gives the number of accident victims according to the injury severity and the total number of bus occupants involved, again for the three operational functions of scheduled bus, school bus, and long-distance coach, in relationship to the four accident groups—bus/car, bus/truck, bus/bus, and single-bus accidents.

On a scheduled bus service, about one-third of the total of 1,990 bus occupants involved were recorded; of these 651 occupants involved in bus accidents on a scheduled service, no person was found to be killed, and the number of seriously and slightly injured persons is relatively low.

For long-distance coaches, the injury risk is, however, considerably higher: 38 of all 40 fatally injured persons were in long-distance coaches; the other two occupants were killed in school buses. This means the risk of being injured is altogether higher in school buses and coaches

Accident group	Buses involved								
	Scheduled buses		School buses		Long-distance coaches		Total		Operational function
	No.	%	No.	%	No.	%	No.	%	n.a.*
Bus/car	23	71.9	3	9.4	6	18.7	32	100.0	11
Bus/truck	18	48.6	6	16.2	13	35.2	37	100.0	3
Bus/bus	1	16.7	1	16.7	4	66.6	6	100.0	–
Single-bus	1	9.1	3	27.3	7	63.6	11	100.0	–
Total	43	50.0	13	15.1	30	34.9	86	100.0	14

*n.a. = not ascertained

Figure 5. Number of buses involved in the four accident groups independent of operational function

Accident group	Scheduled bus				School bus				Long-distance coach			
	sli. inj.	ser. inj.	fat.	Bus occupants involved	sli. inj.	ser. inj.	fat.	Bus occupants involved	sli. inj.	ser. inj.	fat.	Bus occupants involved
Bus/car	25	1	–	276	1	–	–	84	19	3	–	164
Bus/truck	62	10	–	328	60	13	–	127	106	43	5	367
Bus/bus	1	–	–	1	16	8	1	40	42	6	–	152
Single-bus	24	22	–	46	38	5	1	63	83	96	33	342
Total	112	33	–	651	115	26	2	314	250	148	38	1.025

sli. inj. = slightly injured
ser. inj. = seriously injured
fat. = fatalities

1.990
Bus occupants involved

Figure 6. Bus occupants involved and injured in the four accident groups depending on operational function

than in buses on a regular service. This statement, however, must take into account that much greater distances are covered by long-distance coaches and that long-distance coaches travel at higher speeds, and this generally results in a higher injury risk as well.

Apart from the higher risk of injury in long-distance travel, Figure 6 also shows another very important finding, namely that in the case of single-bus accidents there is indeed a higher risk of serious/fatal injuries compared with the general bus risk. This point is dealt with later.

Risk of Injury Dependent on Accident Opponent and the Kind of Collision

The effects of bus accidents, unrelated to the accident opponent or the kind of accident, are given in Figure 7. All data here refer to the maximum injury severity of the bus occupants in each case.

The central result in Figure 7 is that out of the altogether 40 persons killed in the accident material under consideration, as many as 34—that is, 85 percent—were killed in single-bus accidents—to be more precise, in single-bus accidents with rollover. In the other accident groups (bus/car, bus/truck, and bus/bus), not one single rollover occurred, not even as a secondary event after the collision with the accident opponent.

The high risk of injury in rollover accidents is further confirmed by the equally high number of seriously injured bus occupants: 114 out of a total of 208 persons who were seriously injured sustained their injuries in rollover accidents.

Insofar as one would like to increase bus safety even further, one has to start with accidents with a rollover, which in the available accident material accounted for 85 percent of the killed and more than 50 percent of the seriously injured bus occupants, although these rollover accidents amount to only 7 percent in the total material.

Very serious accidents also result from bus/truck and from the rare bus/bus collisions. In the 40 bus/truck collisions recorded, 5 persons were killed and 66 seriously injured.

In the case of a bus/truck collision, only those bus occupants whe are seated in the direct intrusion area are normally affected by the risk of serious or fatal injuries. In contrast to this, in rollover accidents there is risk of very serious injuries in every case for a relatively large number of occupants by impacting the interior side or roof or by being ejected out of the bus.

Figure 7 also shows that the risk of injury for the bus occupants in bus/car collisions is relatively low, and this corroborates the findings of the HUK study presented in 1981(6), in which this was also stated. Nor in the case of the 43 bus/car accidents now available was any person killed in the bus. Even in serious bus/car collisions, the strain on the bus occupants is not so great that substantial risks of injury exist.

The risk for the car occupants is, however, serious. Although the shape of a bus resulting from the lattice-work girder structure is less dangerous than that of a truck, the bus front is so rigid that if the car is totally deformed, the bus front is relatively only slightly damaged (Figure 8). In the accident in Figure 8, the car driver was killed, but the 36 bus occupants were only slightly injured

Accident group	Number of accidents				Number of persons			
	with sli. inj.	with ser. inj.	with fat.	Total	sli. inj.	ser. inj.	killed	Total
Bus/car	40	3	–	43	46	4	–	50
of these with roll-over	–	–	–	–	–	–	–	–
Bus/truck	24	14	2	40	229	66	5	300
of these with roll-over	–	–	–	–	–	–	–	–
Bus/bus *	3	2	1	6	59	14	1	74
of these with roll-over	–	–	–	–	–	–	–	–
Single-bus	1	2	1	4	20	10	–	30
without roll-over		3	4	7	123	114	34	271
with roll-over								
Total	68	24	8	100	477	208	40	725

* 3 bus/bus accidents with a total of 6 buses

sli. inj. = slightly injured
ser. inj. = seriously injured
fat. = fatalities

Figure 7. Number of bus accidents and of the bus occupants injured in them dependent on the accident opponent and the kind of accident

Figure 8. Bus/car frontal collision in which the car driver was killed and several bus occupants slightly injured

or not at all. There would therefore still seem to be room for improvement with regard to partner protection in the case of the omnibus.

In contrast to truck/car collisions, in bus/car collisions it is frequently possible to observe, however, that after the collision the car skids away from the bus, which reduces the strain on the car occupants. But the high-speed change remaining is clearly reflected in the risk of injury to the car occupants (Figure 9). In 43 bus/car accidents, 22 car occupants were fatally injured, 29 persons sustained serious injuries, and 21 slight injuries. In several of these cases, however, safety belts, if they had been used, would have resulted in decreasing the injuries to the car occupants.

The distribution of the collision types for bus/truck and bus/car accidents is shown in Figure 10. In the left-hand half of the bus diagram, the areas of impact in bus/car accidents are given, and in the right-hand half those in bus/truck accidents; the overall percentages refer in each case to the total front, rear, or side areas of the bus. Here no distinction has been made between left/right, partial offset, etc.

If all cases including every category of injury are counted, three collision types dominate: front/front (bus/truck 30.2 percent, bus/car 55.8 percent), front/side (bus/truck 16.3 percent, bus/car 18.6 percent), and side/front (bus/truck 11.6 percent, bus/car 20.9 percent), the first-mentioned impact area referring to the bus in all cases. Another noticeable feature is the relatively high number of rear-end collisions of trucks onto buses, which represent 20.9 percent of the bus/truck collisions.

As previously presented in Figures 6, 7, and 9, no bus occupant was killed in bus/car accidents in the available material. The total of four seriously injured bus occupants in bus/car collisions sustained their injuries in front/front collisions as a consequence of the deceleration resulting from the collision and not from intrusion, and the slight injuries, too, occurred mainly in frontal collisions (Figure 8).

In bus/truck accidents, over 50 percent of all seriously or slightly injured bus occupants sustained their injuries as a result of a bus being involved in a frontal collision in which the front of the bus ran into the front, side, or rear of a truck (Figure 11). The primary cause of injury here is the rapid deceleration in the longitudinal direction of the bus, which throws the occupants forward, and not the intruding bus structure.

The bus occupants who were killed were almost exclusively in the indirect intrusion area of the truck (Figure 12). The local structure loads are then so high that it seems difficult to provide any effective protection against intrusion. In contrast to this, in frontal collisions the bus occupants are usually not affected directly by the intruding bus structure and are thus injured less severely.

	Injured bus occupants Drivers and passengers			Injured car occupants Drivers and passengers		
	Slightly injured	Seriously injured	Fatalities	Slightly injured	Seriously injured	Fatalities
43 bus/car collisions	46	4	–	21	29	22

Figure 9. Number of injured bus and car occupants in 43 bus/car collisions

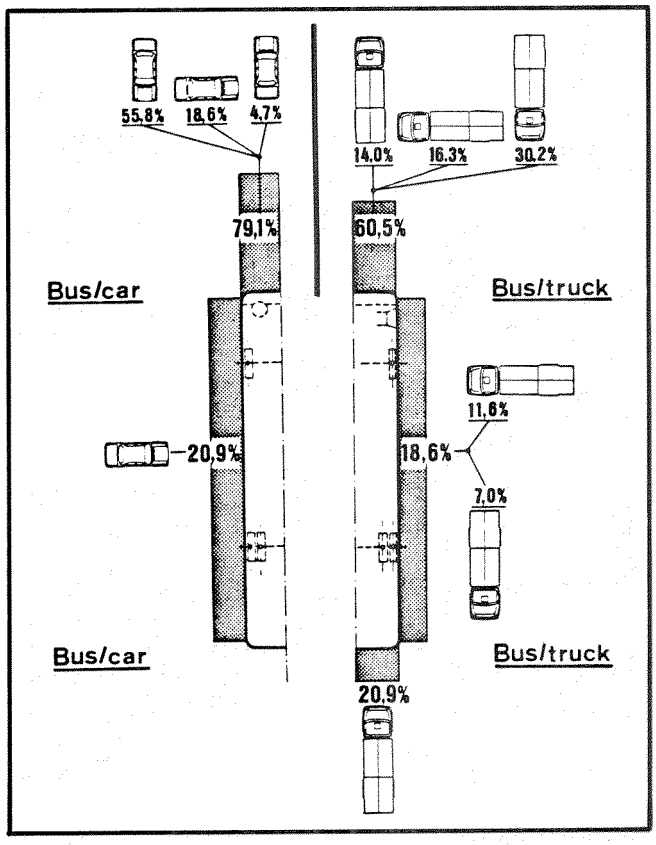

Figure 10. Distribution of the impact areas in bus/car and bus/truck collisions

Risk of Injury in Rollover Accidents

The extremely high risk of injury in bus accidents with a rollover has already been mentioned several times. In Figure 13, the consequences of the accident for the bus occupants are presented for all 7 rollover accidents based on the 97 bus accidents with a collision.

The following points of emphasis emerge:

- In 5 out of 7 rollover accidents, at least 1 bus occupant was fatally injured.
- The proportion of fatalities in rollover accidents related to the total number of bus occupants affected is above average.
- The risk of injury rises considerably in a rollover of half a turn or more.

- A large proportion of the fatally injured occupants were ejected out of the bus.
- The occupants who were ejected were also crushed to death by the bus in most cases.
- Even when they remained in the bus, there was an increased risk of serious/fatal injuries, as the interior was in most cases considerably restricted by the roof being crushed down sideward and by the bended roof posts (Figure 14).
- The chance of being involved in a rollover accident without being injured is relatively low.

Figure 11. Typical damage to a bus in a serious collision of a bus running into the rear of a truck, resulting in seriously and slightly injured bus occupants

In rollover accidents with fatalities, two injury mechanisms in particular can be ascertained:

- The occupant is ejected and crushed to death by the bus.
- The occupant remains in the bus and is hurled against the roof, while at the same time the interior is usually additionally restricted by the intrusion of the roof.

To further reduce the risk of injury in rollover accidents, the occupants in the bus would have to be prevented from being ejected or thrown around in the bus interior, but, in addition, it would have to be insured that the available interior space remains largely intact.

The Avoidability of Bus Accidents

Apart from increasing passive safety to avoid the results of accidents, avoiding the accident altogether is, of course, a better possibility of protecting the occupants of a vehicle. The analysis of bus accidents showed that one of the essential factors is the state of the road; critical road conditions, such as wet or icy surfaces, play a major role in bus accidents. The frequency distribution of the various road conditions presented in Figure 15 results from the available bus accident material (only collision cases and single-bus accidents). The road condition "dry" was registered in only 51.6 percent of all cases (by way of comparison, in car accidents with injury to persons(5) the condition "dry road" occurred in 60.9 percent of all cases). This means that unfavorable road conditions (damp, wet, snow, ice) play an important part in bus accidents. More than one-third of all accidents took place on a wet/damp road, and about one in seven on snow or ice. In the single-bus accidents, the road condition "ice" was recorded in even 4 out of 11 cases.

With regard to the avoidability of an accident, the available accident material was examined to see whether the accident would have been influenced by using an antilock brake system (in the material recorded, no bus was equipped with such a system).

The possible useful effects of the antilock brake system were divided into four categories, namely:

- None, for example when the brakes were not applied at all.
- Possible, but slight, for example when the intensity of the accident could have been decreased by reducing the braking distance, although the accident would have occurred all the same.
- Probable, if the accident could have been avoided as a consequence of external conditions, although this would have required a quick and appropriate reaction on the part of the driver.

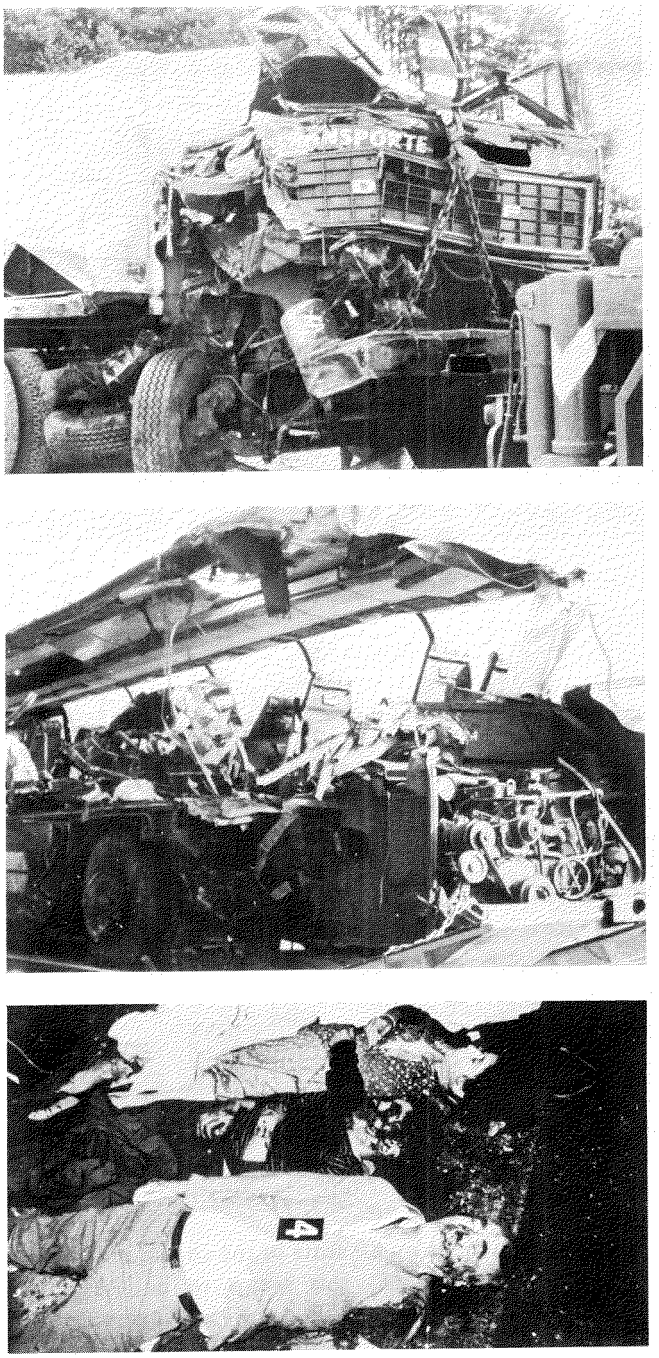

Figure 12. Typical damage to a bus caused by a very serious collision of a truck running into the rear of a bus, resulting in fatally injured bus occupants

Kind of roll-over	No. of buses	Total number of occupants	Uninjured	Slightly injured	Seriously injured	Fatalities: Total	Fatalities: number of these ejected	Fatalities: number of these ejected and crushed by bus
1/4 roll-over	3	54	17	35	1	1	1	1
		64	3	29	31	1	–	–
		12	–	5	2	5	5	5
1/2 roll-over	2	1) 54	–	3	37	14	–	–
		46	33	12	1	–	–	–
Single and multiple roll-over	2	48	–	15	20	13	ca. 10	ca. 10
		2) n.a.	n.a.	24	22	–	several*	–
			Σ	123	114	34		

*ejected but not killed
n. a. = not ascertained
1) damaged bus see fig. 14a
2) damaged bus see fig. 14b

Figure 13. Number of injured and uninjured bus occupants in the seven rollover accidents in the relevant HUK accident material

- Certain, if the emergency braking with an antilock brake system alone could have avoided the accident.

Figure 16 shows that in about 40 percent of the cases, an antilock brake device would have had an—at least slight—advantage, while it is certain that 4 percent and probable that even 15 percent of the accidents could have been avoided. Especially in the case of bus/truck and single-bus accidents, which represent a high risk for the bus occupants, there would have been an above-average advantage.

HUK-Verband, the association of all German motor insurers, has recommended, in view of the advantages to be expected from automatic antilock brake devices, that vehicles fitted with such a device should be given a 10 percent reduction in the fully comprehensive insurance. This recommendation was taken up by the insurance companies in 1984. The insurers thus want to take into account the lower accident risk of vehicles equipped with this system. But this reduction in the insurance premium is also meant to be an incentive to acquire vehicles thus equipped and so to make a contribution to increasing traffic safety.

Conclusions for Possible Safety Measures

In relation to the whole traffic scene, the risk of being injured as the occupant of an omnibus is very slight. In view of the total number of bus occupants involved in accidents in road traffic, it is not appropriate to demand additional cost-intensive safety measures. But the inquiries of this study have shown, nevertheless, there are risks for bus occupants that could be further reduced with the help of technical measures.

These measures would have to be concentrated mainly on long-distance coaches, as it is here that far more serious and fatal injuries occur compared with scheduled services; moreover, safety measures are also possible in the case of this operational function, since constantly changing bus occupants and standing passengers are not to be expected, as on scheduled services.

The injuries that occur in accidents without a collision, especially on scheduled services, could be further reduced by appropriate seat construction and making interior components less dangerous.

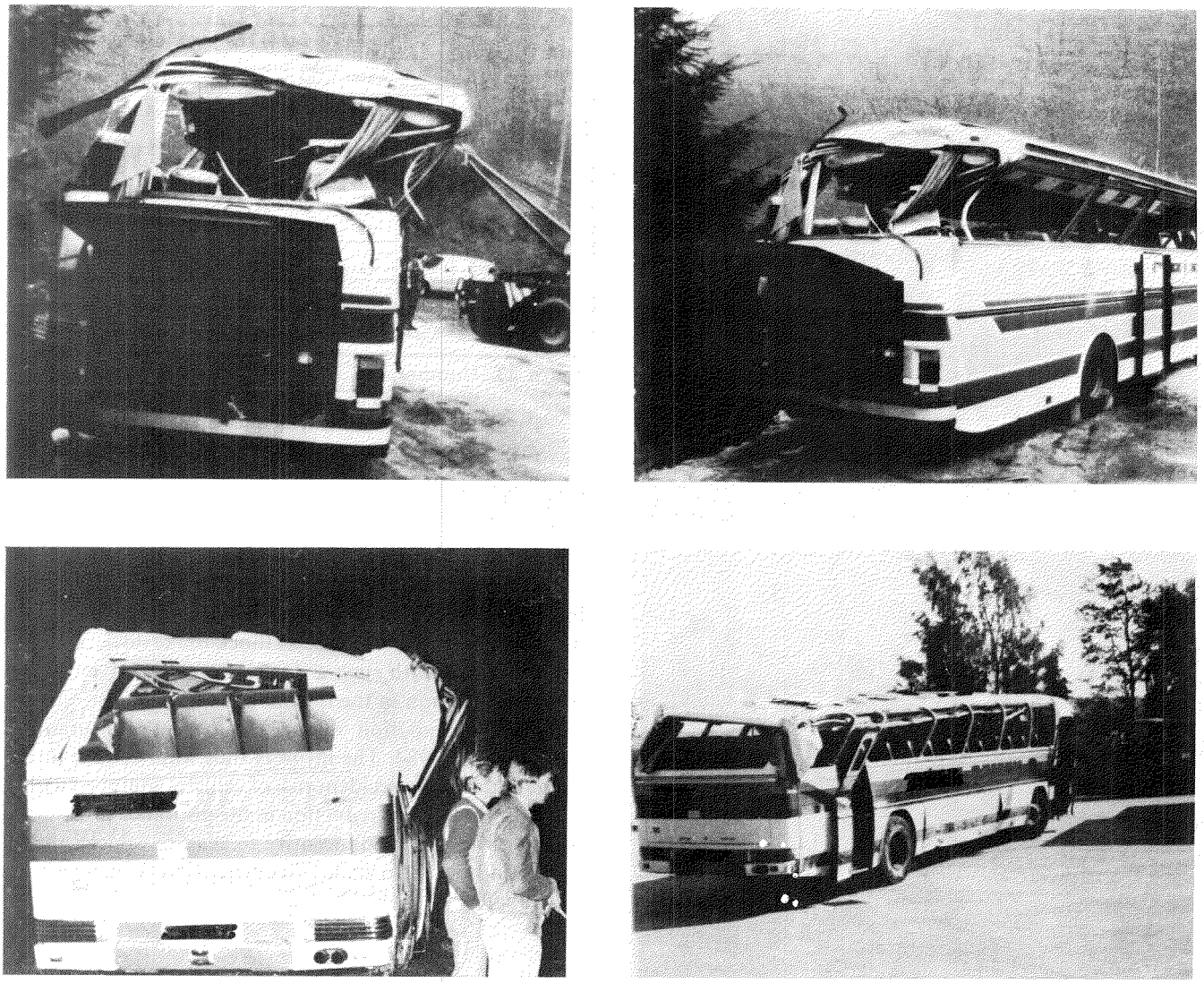

Figure 14. Typical damage to a bus caused by rollover accidents—roof bent sidewards, restricting the passenger space

Single-bus accidents with rollover have turned out particularly dangerous: 85 percent of all persons killed and 50 percent of those severely injured were found in a proportion of this kind of accident of only 7 percent. The serious/fatal injuries are caused, on the one hand, by the intrusion of the roof and, on the other hand, by ejection of the occupants. The intrusion in the roof area often arises by the roof being bent sideways when the bus rolls over, and this greatly restricts the passenger space (Figure 14).

If the aim is, therefore, to increase the safety of buses even further, the measures must be concentrated mainly on reducing the risk of injury in rollover accidents. In this case, the following two measures should be aimed at in conjunction with each other:

- A roof construction to prevent the roof bending away sideward and being deformed from above
- Safety belts on all seats of the coach, including driver's seat, as this seems to be the only possibility of avoiding the passengers being thrown around in the bus or being ejected out of the bus

Although the use of lapbelts would result in the occupants being restrained in their seats, an optimum protection would be provided here, too—as in the car—by the use of 3-point belts, which is technically feasible but, on account of the additional costs, appears to be only partially possible. The question has to be asked as to how far expenses are justified in view of the cost/benefit rate and with respect to acceptance by the bus occupants.

Serious injuries are frequently sustained by bus occupants as well when the bus is involved in a frontal collision and they are thrown forward and injure themselves on the seat backs in front of them, for example. By

Road conditions \ Accident group	Bus/car		Bus/truck		Bus/bus		Single-bus		Total	
	No.	%	No.	%	No.	%	No.	%	No.	%
dry	25	58.1	19	47.5	2	66.7	4	36.4	50	51.6
damp	4	9.3	3	7.5	–	–	1	9.1	8	8.2
wet	8	18.6	15	37.5	1	33.3	2	18.2	26	26.8
snow	3	7.0	3	7.5	–	–	–	–	6	6.2
ice	3	7.0	–	–	–	–	4	36.3	7	7.2
Σ	43	100.0	40	100.0	3	100.0	11	100.0	97	100.0

Figure 15. Road conditions in the four accident groups

Accident group	Advantages of the anti-lock brake system										
	none		possible, but slight		probable		certain		Σ		n.a.
	No.	%	No.	%	No.	%	No.	%	No.	%	No.
Bus/car	23	59.0	14	35.9	2	5.1	–	–	39	100.0	4
Bus/truck	20	58.8	8	23.5	4	11.8	2	5.9	34	100.0	6
Bus/bus	3	75.0	–	–	–	–	1	25.0	4	100.0	2
Single-bus	3	50.0	–	–	3	50.0	–	–	6	100.0	5
Total	49	59.0	22	26.5	9	10.8	3	3.6	83	100.0	17

n. a. = not ascertained

Figure 16. Estimated advantages of an antilock brake system in the four accident groups

constructing the seat backs so they absorb the fall of the occupants, a reduction in injury risk could be achieved, but here, too, better protection of the occupants from injuries could be expected from the use of 3-point safety belts.

Summary

In the area of omnibus safety, there are few data and studies that enable a detailed statement on the actual risk to bus occupants. The aim of this study is to identify focal points in the accident scene and possible technical countermeasures derived from them. The following emerged from our studies:

- The omnibus is the safest of all mean of road transport in the Federal Republic of Germany, and each year few bus occupants are injured in view of the large number of people conveyed by them.
- When discussing national statistics and bus accidents with injuries to persons, a careful distinction has to be made between accidents with and without a collision and the type of bus.
- Accidents without a collision caused by driving maneuvers occur chiefly in scheduled bus services; emergency braking plays an important part, head injuries being found most frequently. The injuries resulting from driving maneuvers are unfavorably influenced by the long distances standing passengers fall or by the seats being inadequately designed.
- In accidents with a collision, there are still substantial safety reserves for further bus development, above all in the area of active safety, although this also applies to passive safety to a limited extent.
- About 50 percent of the bus accidents in which occupants are injured occur when the road conditions are unfavorable.
- Considerable advantages are to be expected from the use of antilock brake devices in buses. About 40 percent of the collisions with injured passengers would be positively influenced by such a device. Most certainly 4 percent and probably as many as 15 percent of the accidents could be avoided.
- Although rollover accidents amount to only 7 percent of the bus accidents with a collision, they account for 85 percent of the persons killed and more than 50 percent of all seriously injured occupants. Most of the buses involved in this type of accident were long-distance coaches.
- A large proportion of the killed occupants were ejected out of the bus. If the risk of injury in rollover accidents is to be reduced below its present level, the occupant must be restrained in his seat by protective measures, such as a safety belt; in addition, it must be insured that the passenger space remains largely intact.
- The use of 3-point belts—in conjunction with an appropriate roof construction—would provide bus occupants with optimum protection, but this measure has to be discussed from the viewpoints of cost/benefits and acceptance.
- It has been observed that in rollovers with roof impact the interior is greatly restricted by the roof being bent away sideways; what is decisive is the diagonal loading of the roof posts, not the strictly vertical impact on the roof.
- In the case of technical innovations and their effect on bus safety, the fact that the life of buses is relatively long must, however, be considered, so it will take some time before technical improvements will begin to take effect on buses generally.

This study indicates possible ways of further improving the safety of omnibuses, but the economic costs and especially the need to coordinate safety standards on an international level will also have to be considered.

Acknowledgments

The authors are indebted to all the member insurance companies of the HUK-Verband, in particular, for

making their claims records readily available for this study, and to Messrs. Finkbeiner, Heider, and Zistler, members of the HUK staff who carried out accident analysis and evaluation work. The authors also owe a debt of gratitude to the various police departments whose active support made it possible to supplement the picture material already available.

References

1. Statistisches Bundesamt Wiesbaden, "Straßenverkehrsunfälle 1983," Fachserie 8, Reihe 3.3, Wiesbaden, September 1984.
2. Der Bundesminister für Verkehr, "Verkehrsnachrichten," Heft 1, Bonn, January 1985.
3. Statistisches Bundesamt Wiesbaden, "Straßenverkehrsunfälle Dezember und Jahr 1984," Fachserie 8, Reihe 3.3, Wiesbaden, March 1985.
4. States, J.D., et al., "The abbreviated injury scale, 1980 revision," American Association for Automotive Medicine.
5. HUK-Verband, "Facts on road traffic accidents and safety of automobiles," Munich, 1978.
6. Langwieder, K., and M. Danner, "Die Bedeutung von Busunfällen im gesamten Unfallgeschehen der Bundesrepublik Deutschland," XII, Beratung der Omnibus-Experten, Budapest, June 1981.

Fatality Rates in Toyota Cressidas With Automatic Belts

Carl E. Nash and
Barry Eisemann
National Center for Statistics and Analysis,
National Highway Traffic Safety Administration

Abstract

Automatic belts in Toyota Cressidas have increased belt usage by front-seat occupants of these cars to more than 95 percent. This paper compares the fatal accident experience of these cars with that of the fairly similar Datsun (Nissan) 810/Maxima automobiles (which are equipped with manual belts used by about 20 percent of their occupants). It shows the result of the increased belt usage is a decrease in fatalities among Toyota front-seat occupants. In fatal accidents where no front-seat occupants of the Toyotas or Datsuns are killed, the Toyotas have a higher involvement rate than the Datsuns. Also, on average, the fatally injured front-seat occupants of the Toyotas are 7 years older than those in the Datsuns.

Background

The concept of an automatic safety belt has been around since the late 1960's. A paper presented at the First International Technical Conference on Experimental Safety Vehicles in Paris on January 27, 1970, by Mr. R.D. Lister of the United Kingdom discussed the development of a 3-point passive belt whose upper and lower outboard anchors attached to the rear of the door of an automobile and whose inboard anchor was attached to a reel located between the seats. An alternative design put the reel at the lower door anchor. Dynamic tests of this system at the Transportation Road Research Laboratory showed it to be ".. comparable with that of the conventional belt ..."(1)

In 1973, Volkswagen showed a prototype passive belt system in a Beetle. For each front-seat occupant, the VW system had only a shoulder belt attached between the top rear of the door and a reel between the seats. For lower body restraint, VW provided an energy-absorbing knee bolster at the lower edge of the instrument panel.

This system was commercialized in 1975 on the Volkswagen Rabbit and was offered on this vehicle in the United States throughout its production run. The Volkswagen design has an emergency release buckle located at the door frame, and an ignition interlock to prevent starting the vehicle if the belt is detached. However, the ignition interlock can be disabled by disconnecting a wire under the seat, or the belt can be detached after starting the vehicle without affecting its operation.

Belt usage in the Rabbits with automatic belts has been observed to be 76.6 percent in NHTSA's most recent 19-city survey(2). By comparison, belt use was observed to be 28.4 percent for manual-belt Rabbits in the same survey. The overall fatality rate, per registered vehicle year, in the Rabbits with automatic belts was 18.2 per 100,000 vehicle-years compared with 22.6 for manual-belt models(3). The automatic-belt cars had a fatality rate 19 percent lower than in Rabbits with conventional lap/shoulder belts.

Toyota Automatic Belts

All 1981 and later Toyota Cressidas have automatic belts. Toyota uses a track over the front door frame, a motor, and a plastic strip to move the upper end of the shoulder belt forward, out of the way, when the front door is opened and in place when the door is closed. Cressidas have knee bolsters for lower body restraint and manual lapbelts. Thus, when the belts are in place, they are similar in configuration to the VW belts except for the added manual lapbelts.

Since the Toyota automatic belts are not detachable, we expect (and observe) higher use rates with them than with VW automatic belts. Furthermore, because they automatically move well forward of the seat for entry, they are very convenient. Finally, since all Cressidas have four doors, the mounting point of the upper end of the belt is sufficiently forward that it does not put much pressure on the shoulder of an average person (although it may cut across the neck of a person of shorter stature).

The purpose of this paper is to assess the front-seat fatality rates in automatic-belt-equipped 1981-1984 Toyota Cressidas. In earlier work, NHTSA compared fatalities in the automatic-belt Cressidas with fatalities in pre-1981 Cressidas that had manual belts. The automatic-belt cars were found to have a 21 percent lower fatality rate than the manual-belt cars(4).

For the present work, we used the Datsun (Nissan) 810/Maximas, which are similar cars with manual belts, as the control fleet for comparison. Except for differences in the restraint systems, Cressidas and 810/Maximas are similar in size, weight, pricing and market class, body styles (4-door sedan and 4-door station wagon only), seating configuration (two individual front seats), drive train (front mounted, in-line 6-cylinder engine driving the rear wheels), and performance. We have no direct information on the demographics of the people who drive either model.

Analysis

Belt usage in Toyota Cressidas, as measured in the 19-city survey, was 97.5 percent, up from 95 percent a year earlier. This was measured in 1984, a period when no State had a mandatory use law, and when overall belt use in the survey was 14.4 percent(5). The comparable belt usage in Datsuns was 20 percent.

We used car-years of operation as a measure of exposure. U.S. calendar year sales figures from *Automotive News*(6) are shown in Table 1. We assumed they approximate new car registrations for the same model year. Further, we assumed the cars of a given model year began to go into service on October 1 of the previous year and continued to do so at a constant rate for 1 year until all new cars of that year were sold and registered. While this is an oversimplification, using the same basis for both Cressidas and 810/Maximas should minimize any error. We also assumed the driving patterns for the two cars are similar, although we have no direct information on this. The total number of car-years of operation is 322,000 for the Toyota Cressidas and 491,000 for the Datsun 810/Maximas.

Accident data for this paper are from the Fatal Accident Reporting System files for calendar years 1981 through 1984(7). Front-seat occupant fatalities are shown in Table 2. The rate of fatalities per registered vehicle-year is found by taking the ratio of front-seat occupant fatalities to the number of car-years of operation. The results of this analysis are shown in Table 3.

To test whether these two vehicle populations are otherwise alike in their fatal accident experience, we compared fatal accidents in which no front-seat occupants of these models were killed. Table 4 shows the result.

There were 41 such accidents for the Cressidas and 34 for the 810/Maximas during accident years 1981 through 1984 when 810/Maxima exposure was 50 percent greater than that of the Cressidas. Thus, the Cressidas were involved at a much higher rate than the 810/Maximas in fatal accidents in which someone other than a front-seat occupant was killed.

To see if there were other differences between the two car models, we looked at the age and sex of people killed in them. The occupants of the Toyotas were, on average, 7 years older than the occupants of the Datsuns. But the difference was most pronounced for those involved in multivehicle accidents where the average age of fatally injured Toyota front-seat occupants was 12 years older than the average age of similar Datsun occupants. Figure 1 shows the spread of ages of front-seat occupants of the vehicles.

The age spread of those killed mirrored the age spread of drivers of vehicles involved in all fatal accidents. For the Cressidas, the average age of drivers was 44, while the average age of drivers of the 810/Maximas was 39. There was little difference in the ages of male and female drivers or in the ages of drivers killed versus those who survived.

Since it is well known that older people are more susceptible to accident injuries, the reduction in front-seat occupant fatalities in the Cressidas is more striking. However, since we do not have information on the demographics and driving patterns of either vehicle, we cannot draw more qualitative conclusions from these data. We found no particular differences in the ratio of male to female fatalities in the two car models.

Ejections occurred mostly in single-vehicle accidents in both models. In the Datsun 810/Maximas, 15 of the fatally injured front-seat occupants were ejected while four of the Toyota Cressida front-seat fatalities were ejected. Most, although not all, ejections occurred when the vehicle rolled over in the accident. We do not know whether the ejected Toyota occupants were restrained by the lap and shoulder belts.

Table 1. Sales of Toyota Cressida and Datsun 810/Maxima models

	Model Year			
Make and Model	1981	1982	1983	1984
Toyota Cressida	29,583	37,448	39,755	34,456
Datsun 810/Maxima	35,853	54,187	76,209	68,209

Table 2. Front seat occupant fatalities in Cressida and 810/Maxima models

Model	Vehicles Involved	Model Year	Accident Year 1981	1982	1983	1984
Toyota	one	1981	1	-	2	1
Cressida	multiple	1981	-	2	1	-
	one	1982	-	1	1	1
	multiple	1982	-	2	1	1
	one	1983	-	-	-	5
	multiple	1983	-	-	2	5
	one	1984	-	-	-	1
	multiple	1984	-	-	-	2
total single-vehicle accident fatalities: 13						
total multi-vehicle accident fatalities: 16						
Datsun	one	1981	4	3	1	1
810/Maxima	multiple	1981	2	3	1	3
	one	1982	-	5	-	2
	multiple	1982	-	2	3	3
	one	1983	-	-	4	1
	multiple	1983	-	-	6	4
	one	1984	-	-	1	2
	multiple	1984	-	-	2	8
total single-vehicle accident fatalities: 24						
total multi-vehicle accident fatalities: 37						

Table 3. Fatality rates for Cressida and 810/Maxima front seat occupants

Model	Single-Vehicle	Multi-Vehicle	Overall
Toyota Cressida	3.7	5.3	9.0
Datsun Maxima/810	4.9	7.5	12.4

(Rates are per 100,000 vehicle-years of operation)

Table 4. Fatal accidents in which all front seat occupants of Cressidas and 810/Maximas survived

Model		Accidents with Fatalities in: Rear Seat	Pedestrian	Other Vehicle	Total
Toyota	Number	6	16	19	41
Cressida	Rate	1.9	5.0	5.9	12.7
Datsun	Number	1	16	17	34
810/Maxima	Rate	0.2	3.3	3.5	6.9

(Rates are accidents per 100,000 car-years of operation of the Cressidas or 810/Maximas)

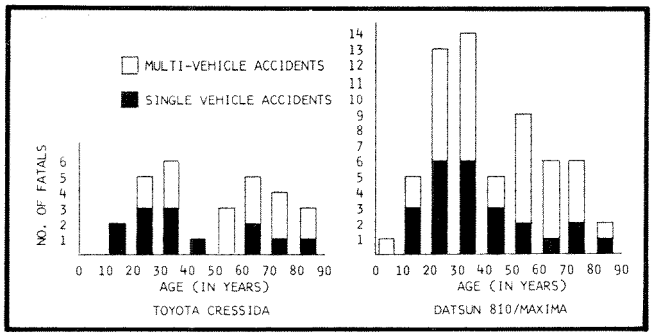

Figure 1. Numbers of front-seat occupants of Cressidas and 810/Maximas, by age groups, killed in accidents

Conclusion

We find the low fatality rates for front-seat occupants of the Toyota Cressidas with automatic belts to be generally consistent with the observed high belt use rate in them and the effectiveness estimated for automatic belt systems.

In short, the research demonstrated that belt use in the absence of belt use laws was significantly higher in the automatic-belt-equipped Cressidas than in the manual-belt-equipped Maximas. Consistent with the higher belt use, fatalities were significantly reduced.

References

1. Lister, R.D., "The U.K. technical presentations, investigations related to the design of safer vehicles," Proceedings First International Technical Conference on Experimental Safety Vehicles, National Highway Traffic Safety Administration, U.S. Department of Transportation, Paris, France, January 1970.
2. Perkins, David D., Michael J. Cynecki, and Michael E. Goryl, "Restraint system usage in the traffic population," DOT HS-806-582, National Highway Traffic Safety Administration, U.S. Department of Transportation, Washington, D.C., July 1983.
3. Van Dyke, John, "Volkswagen restraint systems and fatality rates," internal NHTSA report.
4. "Final regulatory impact analysis: amendment to federal motor vehicle safety standard 208, passenger car front seat occupant protection," NHTSA, DOT HS-806-572, p. IV 26-28, July 11, 1984.
5. Perkins, Op. Cit.
6. "Automotive News Market Data Book," Crain Communications, Inc., Detroit, April 24, 1985, p. 22; April 23, 1984, p. 30; April 27, 1983, p. 26; April 28, 1982, p. 46.
7. National Highway Traffic Safety Administration, "Fatal Accident Reporting System," Data tapes for 1981-1984, U.S. Department of Transportation, Transportation Systems Center (DTS-32), Kendall Square, Cambridge, Massachusetts 02142.

Trends and Forecasts of the Japanese Traffic Accident Situation

Keiko Takegawa
Traffic Safety Policy Office, Director-General's Secretariat, Management and Coordination Agency

Abstract

The number of people killed in road traffic accidents in Japan had increased from year to year until 1970 and the number of deaths and injuries recorded in the same year were 16,800 and 980,000, respectively, or a total of nearly 1 million casualties, resulting in the introduction of the phrase "traffic war." Under these circumstances, insuring traffic safety became a top priority social issue, and, as part of a national attempt to cope with this problem, the Fundamental Law Related to Traffic Safety Measures was enacted in 1970. Based on this law, the national and regional governments pursued comprehensive and powerful traffic safety policies and measures in various areas, including the improvement and provision of traffic safety facilities. As a result, the number of deaths and injuries from traffic accidents in 1979 was reduced to approximately 8,500 and 600,000, respectively, the former representing a decrease by nearly half that recorded in 1970.

Since 1980, however, the trend has reversed, and the number of deaths has followed an upward path; the death toll has exceeded 9,000 for 3 consecutive years from 1982 through 1984. A prediction study conducted by the Traffic Safety Policy Office of the Management and Coordination Agency in 1984 estimates the number of deaths will continue to rise and will reach approximately 10,600 in 1990. To suppress this increase in the number of deaths, legislation that reinforces the compulsory use of helmets for moped drivers and seatbelts is planned for enactment in the near future.

Trends in the Traffic Accident Situation in Japan From 1960 to 1984

As shown on Figure 1, the number of deaths from traffic accidents in Japan continued to increase until 1970, and the annual death toll recorded in the same year reached 16,765. This figure of 16,765 is from police

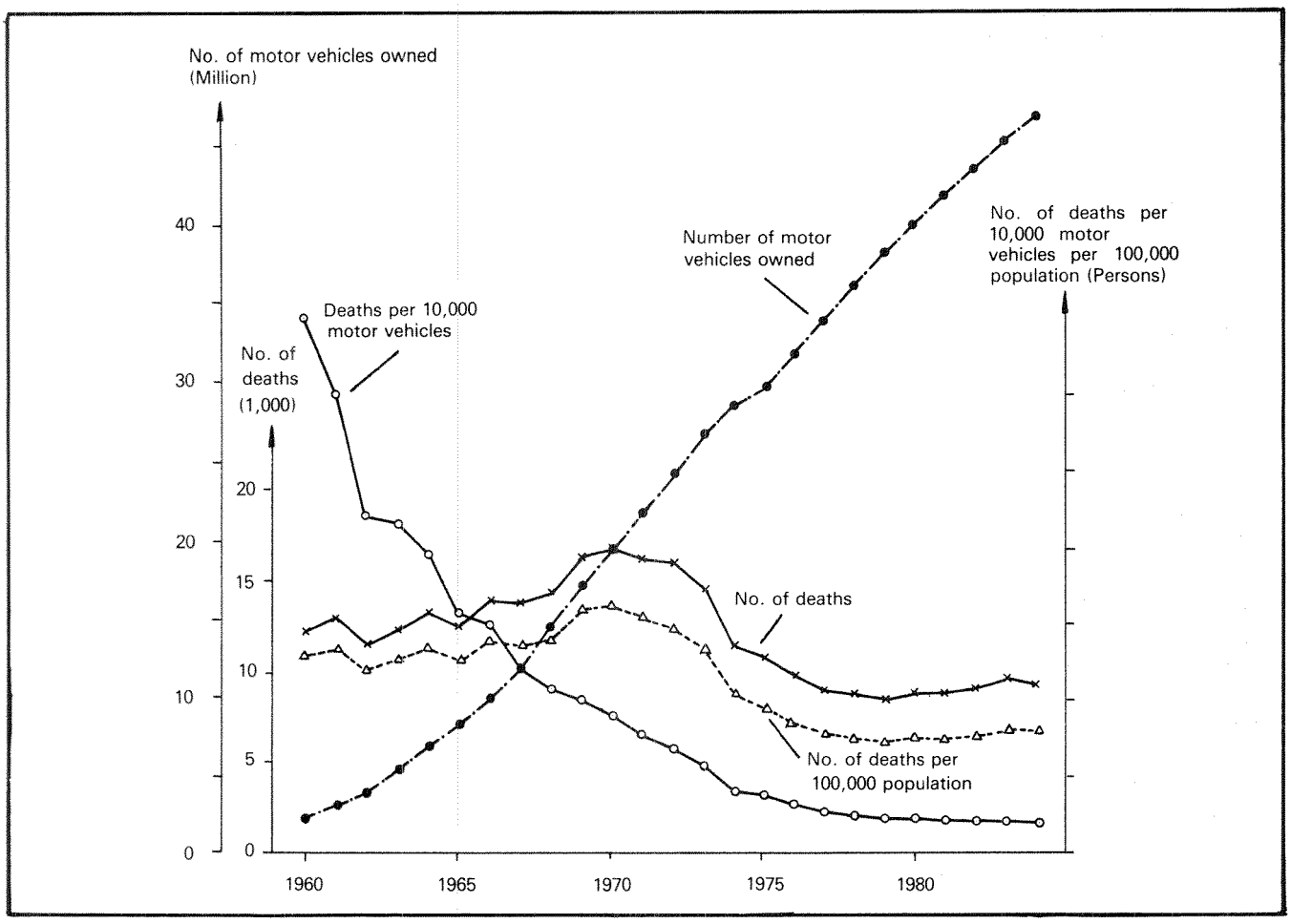

Figure 1. Traffic accident situation in Japan

statistics, for which prompt compilation is required, and refers to persons who die within 24 hours after the accident. The Ministry of Health and Welfare produces different statistics based on the number of all those who die as a direct result of the accident. According to these data, the death toll in 1970 was 21,101. In addition, the number of persons injured in the same year was 981,000, thus approximately 1 million people falling victim to traffic accidents in that year. It was during this time the phrase "traffic war" came to be widely used, and certainly the phrase was appropriate to describe a tragic situation producing an annual casualty toll of 1 million.

Under these circumstances, insuring traffic safety became a top priority social issue, and, as part of a national attempt to cope with this problem, the Fundamental Law Related to Traffic Safety Measures was enacted in 1970. Based on this law, the national and regional governments pursued comprehensive and powerful traffic safety policies and measures in various areas, including the improvement and provision of traffic safety facilities. As a result, the number of deaths from traffic accidents was reduced to 8,466 in 1979, or approximately half the number recorded in 1970. The number of injuries also decreased to 596,000.

However, the trend has reversed since 1980 and the death toll, which had continued to decrease for 10 years, began to show an upward curve. In particular, the death toll exceeded 9,000 for 3 consecutive years from 1982 through 1984, and the situation has been causing much concern. A slight decrease in the number of deaths has been recorded in 1984, but this may be attributed to the reduction in the amount of traffic due to heavy snow between January and March. Consequently, one should not hold an optimistic view that the trend in the death toll figure is headed downward. What has caused the trend of the number of deaths from traffic accidents to change from a downward to an upward curve?

Taking another look at Figure 1, one can see that though the number of those killed in traffic accidents has begun to increase since 1980, the number of deaths per 10,000 motor vehicles (excluding motorcycles) is stable. In Table 1, the figures corresponding to Japan not in parentheses have been taken from National Police Agency statistics; those in parentheses, from statistics by the Ministry of Health and Welfare. The figures corresponding to France and Italy represent deaths within 6 and 7 days, respectively, after the accident; the figures corresponding to the other countries refer to deaths within

Table 1. International comparison of traffic accident situations (1983)

Country	No. of deaths	Deaths per 100,000 population	Deaths per 10,000 motor vehicles
F.R.G.	11,732	19.1	4.2
France	11,946	21.9	5.0
Italy	7,685	13.5	3.6
Netherlands	1,756	12.2	3.4
U.K.	5,445	9.8	3.1
U.S.A.	44,600	19.0	2.7
Japan	9,520	8.0	2.1
	(12,919)	(10.8)	(3.0)

30 days after the accident. The table shows that Japan's traffic safety level ranks quite high in terms of both deaths per 10,000 motor vehicles and deaths per 100,000 population. Moreover, it can be seen from Figure 1 it would be quite difficult to substantially reduce the number of deaths per 10,000 vehicles from the current level. Meanwhile, the number of motor vehicles owned is expected to continue to climb. Will Japan have to experience another "traffic war"? A close look at the Japanese traffic situation follows.

Why Did the Number of Deaths From Traffic Accidents Begin To Follow an Upward Path Since 1980?

Figure 2 shows the trends in the number of deaths from traffic accidents by type of road user. It can be seen that though the total number of deaths has been on the increase since 1980, the tendency does not necessarily apply to all road user types. The frequency of deaths in pedestrian and bicyclist accidents has continued to follow a downward curve even after 1980. Figure 3 shows the total length of pedestrian/bicycle paths is presently five times that in 1970. The number of traffic signals has also increased by nearly six times. The decline in the number of pedestrian and bicyclist deaths can be attributed to such improvements in the provision of traffic safety facilities, promotion of traffic safety education for young children, etc.

As seen on Figure 1, the number of motor vehicles owned is now 2.4 times that in 1970 and is expected to continue to rise for some time. Meanwhile, as shown on Table 2, the number of motor vehicle occupant deaths per 10,000 motor vehicles had been decreasing since the 2.88 persons recorded in 1970 and has stabilized since 1979 at around 0.77 persons. Unless the number of motor vehicle occupant deaths per 10,000 vehicles is reduced, the death toll will continue to grow correspondingly with the number of motor vehicles owned.

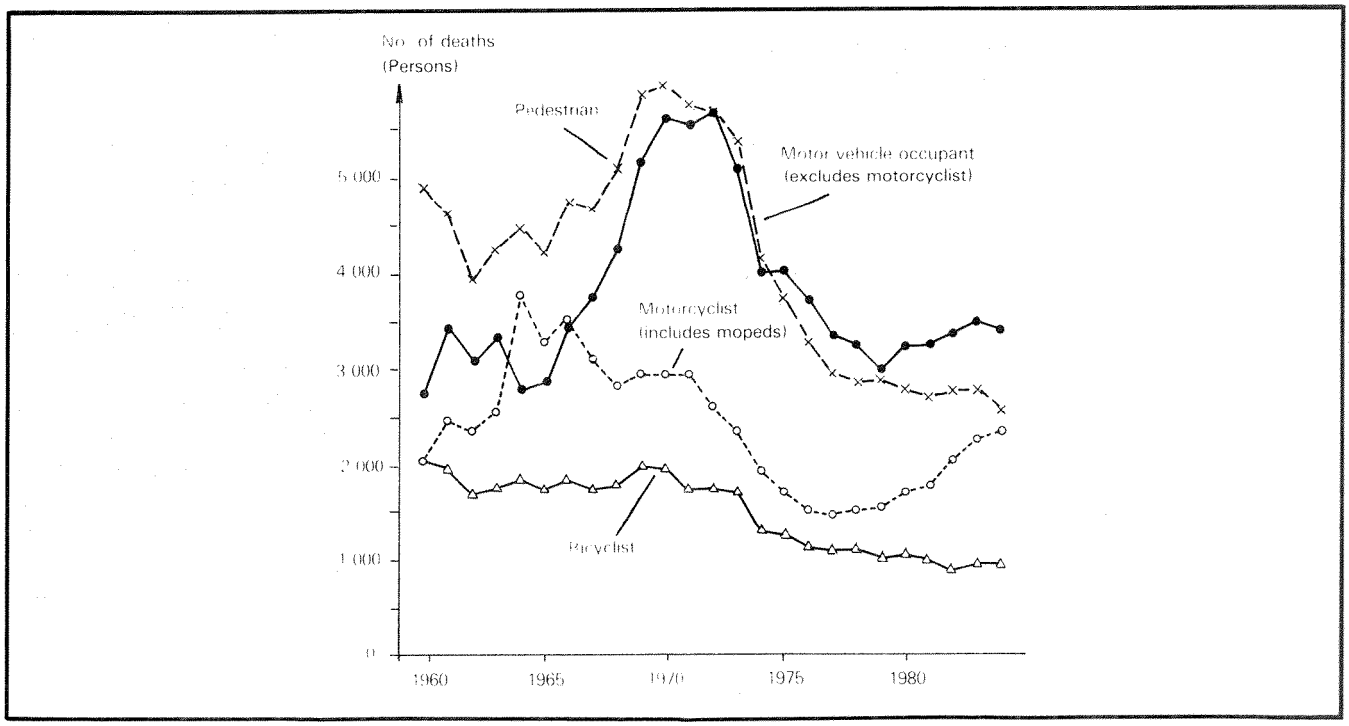

Figure 2. Trends in the number of deaths by type of road user

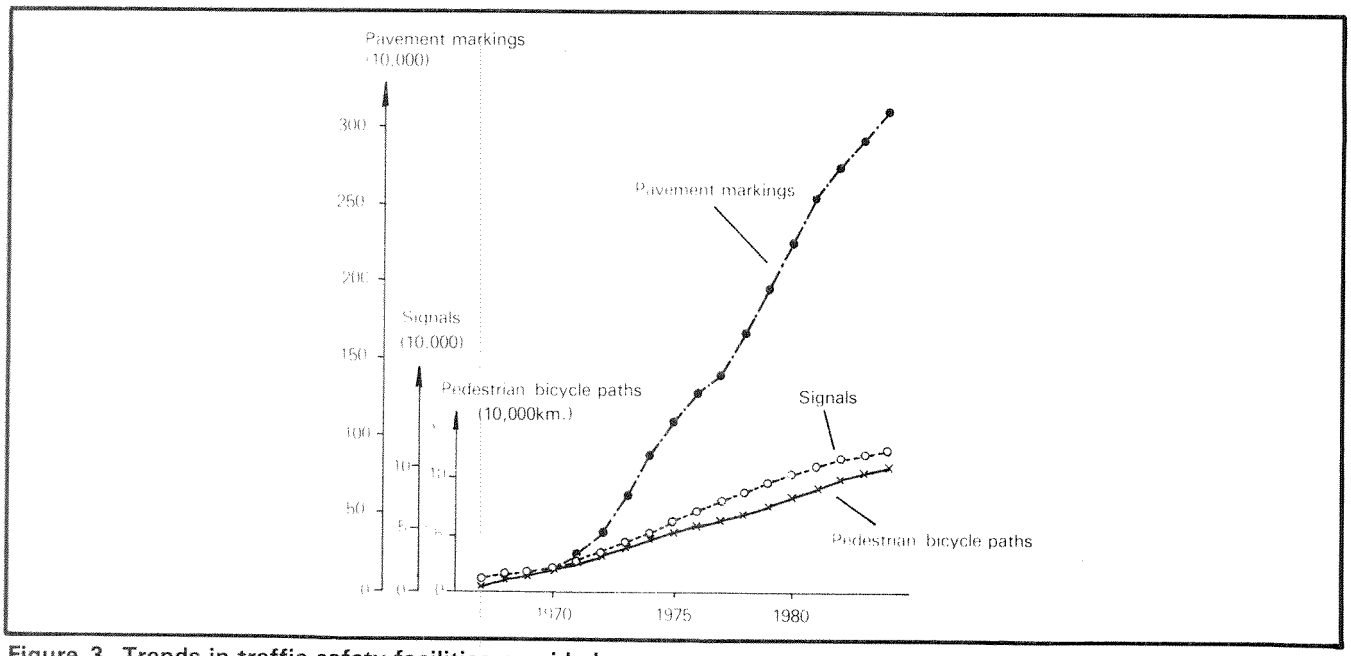

Figure 3. Trends in traffic safety facilities provided

The problem accumulating gravity in Japan in recent years is the growth in the number of motorcyclist (including moped) deaths. The trend of the number of those killed while riding motorcycles had already changed from a downward to an upward curve in 1978, and the death toll of 2,322 recorded in 1984 is 1.6 times the figure recorded in 1977, namely 1,467. Why has there been such an increase?

On Figure 4, one can see the number of motorcycles owned differs substantially among the four categories of motorcycles classified by engine capacity. It is further observed in Table 3 the number of those killed while riding the cycle per 10,000 cycles also varies considerably by cycle category. In the moped category of 50cc or less, the number of deaths per 10,000 cycles is low but the number of cycles owned is showing rapid growth; the number of cycles owned is decreasing but the number of deaths per 10,000 vehicles is low in the 2nd class moped of 51 to 125cc; the number of cycles owned in the light motorcycle category of 126 to 250cc is still relatively low but increasing in recent years and the number of deaths per 10,000 cycles is growing; in the motorcycle category of 251cc or more, the number of cycles owned is still low but climbing in recent years and the number of deaths per 10,000 cycles is dramatically high. These tendencies are reflected in the number of motorcyclist deaths shown on Figure 4. As in the case of motor vehicles, there is concern that the number of motorcyclist deaths will increase if nothing is done. Moreover, in addition to the rapid increase in the frequency of deaths, there are other factors that cause the motorcycle accidents to be viewed as a serious problem. The problem is further analyzed in the following section.

What Can Be Learned From the Number of Deaths in Various Road User Situations by Age Group?

Figure 5 represents the number of deaths in various road user situations by age group. With respect to motorcycles, distinction has been made between the motorcycles, whose engine capacity is more than 50cc, and the mopeds, which have a capacity of 50cc or less. It is observed that an overwhelming number of those killed while riding motorcycles are boys of upper secondary school age between 16 and 19. The same sex and age group also make up a large portion of those killed in moped accidents, but one sees a relatively large number of elderly as well as women are also killed in moped accidents. Hence it is the high number of deaths in youths, with long futures ahead, that adds to the gravity of the motorcycle accident problem. Concerned about this situation, a considerable number of Japanese upper secondary schools have implemented traffic safety campaigns, "Three-No-Movements," calling for the pro-

Table 2. Number of motor vehicle occupant deaths per 10,000 motor vehicles

1970	1971	1972	1973	1974	1975	1976	1977	1978	1979	1980	1981	1982	1983	1984
2.88	2.55	2.33	1.88	1.40	1.34	1.16	0.99	0.89	0.78	0.80	0.77	0.76	0.77	0.72

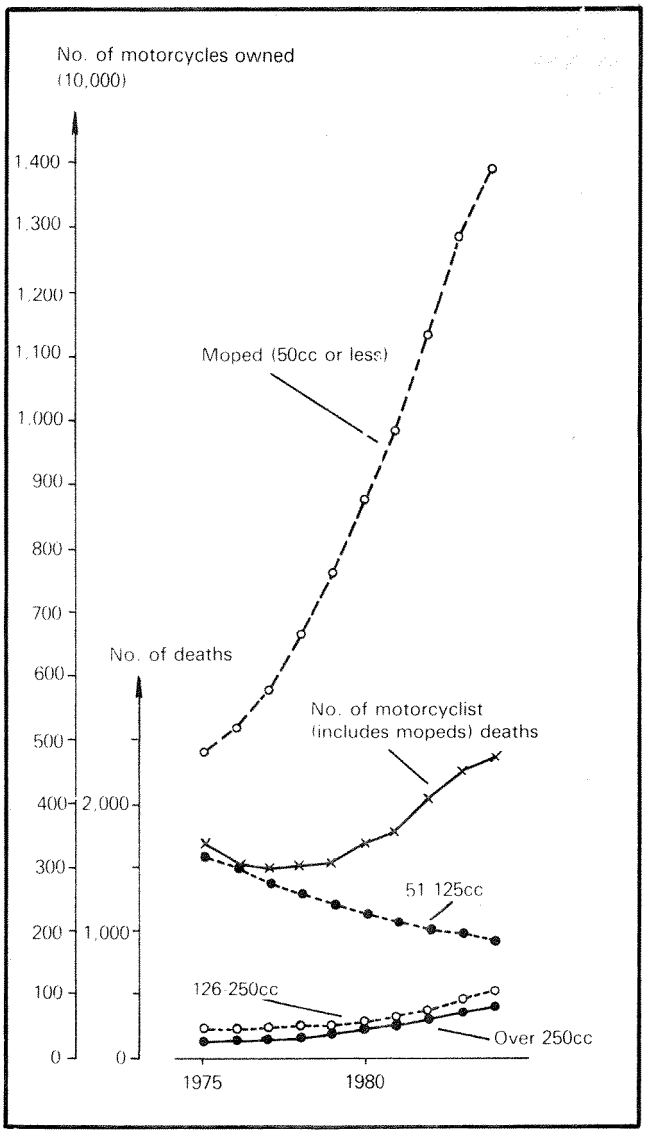

Figure 4. Number of motorcyclist deaths and number of motorcycles owned by cycle category

hibition of motorcycle purchase, motorcycle riding, and motorcycle license acquisition by their students.

The frequency of deaths in youths applies to motor vehicle accidents as well. In Japan, the legal age for riding motorcycles is 16 and that for driving motor vehicles is 18. Consequently, the peak in the death toll shifts between the two vehicle categories. In both cases, safety measures directed toward the young and beginner drivers are in urgent need.

With respect to bicyclists and pedestrians, the target populations are the children and the elderly. With the aged population, the problem seems to be not only the decline in their physical fitness but difficulty in adapting to the large amount of motor vehicle traffic, due to the relative delay of motorization in Japan. Thus, traffic safety education for senior citizens is more important today than ever before. With regard to children, the number of those killed in traffic accidents has steadily declined as a result of active efforts in traffic safety education through kindergartens and children's traffic safety clubs for preschool children between 0 and 6 and through elementary schools for children between 7 and 14. Nevertheless, the death toll is still high, and drivers are reminded through various traffic safety slogans to be particularly careful with children and elderly pedestrians.

Forecasting Traffic Accident Trends up to 1990

The Traffic Safety Policy Office of the Management and Coordination Agency has been issuing every 5 years since 1970 forecasts of traffic accident trends for the following 5 years. Accordingly, a forecast for the 5 years ending 1990 was undertaken in 1984 using the procedure described below. The procedure is also diagrammed in Figure 6.

First of all, in predicting the number of accidents, accidents were classified into five categories by the weaker party, namely, pedestrian accidents (all accidents involving pedestrians), bicycle accidents (all accidents involving bicycles but excluding pedestrian accidents), moped accidents (all accidents involving mopeds but excluding the preceding two), motorcycle (excluding mopeds) accidents (all accidents involving motorcycles but excluding the preceding three), and motor vehicle accidents (all accidents excluding the preceding four).

A multiple regression model that best describes the trends in the number of accidents in each prefecture by each accident category was produced, and the predicted numbers were substituted for the variables into the model to obtain the predicted number of accidents in each prefecture by accident category. The sum of the predicted figures for the 47 prefectures resulted in the national total of predicted number of accidents by accident category.

Table 3. Number of motorcyclist deaths per 10,000 cycles by cycle category

	1975	1976	1977	1978	1979	1980	1981	1982	1983	1984
Moped 50cc or less	1.51	1.38	1.30	1.14	1.03	0.97	0.87	0.82	0.79	0.76
51-125cc	1.34	1.14	1.13	1.04	1.01	0.98	0.83	0.94	1.03	1.06
126-250cc	1.73	1.55	1.55	1.24	1.61	1.85	2.31	3.38	3.96	3.64
Over 250cc	17.56	13.93	10.96	12.67	11.15	11.61	10.94	10.74	9.77	8.96

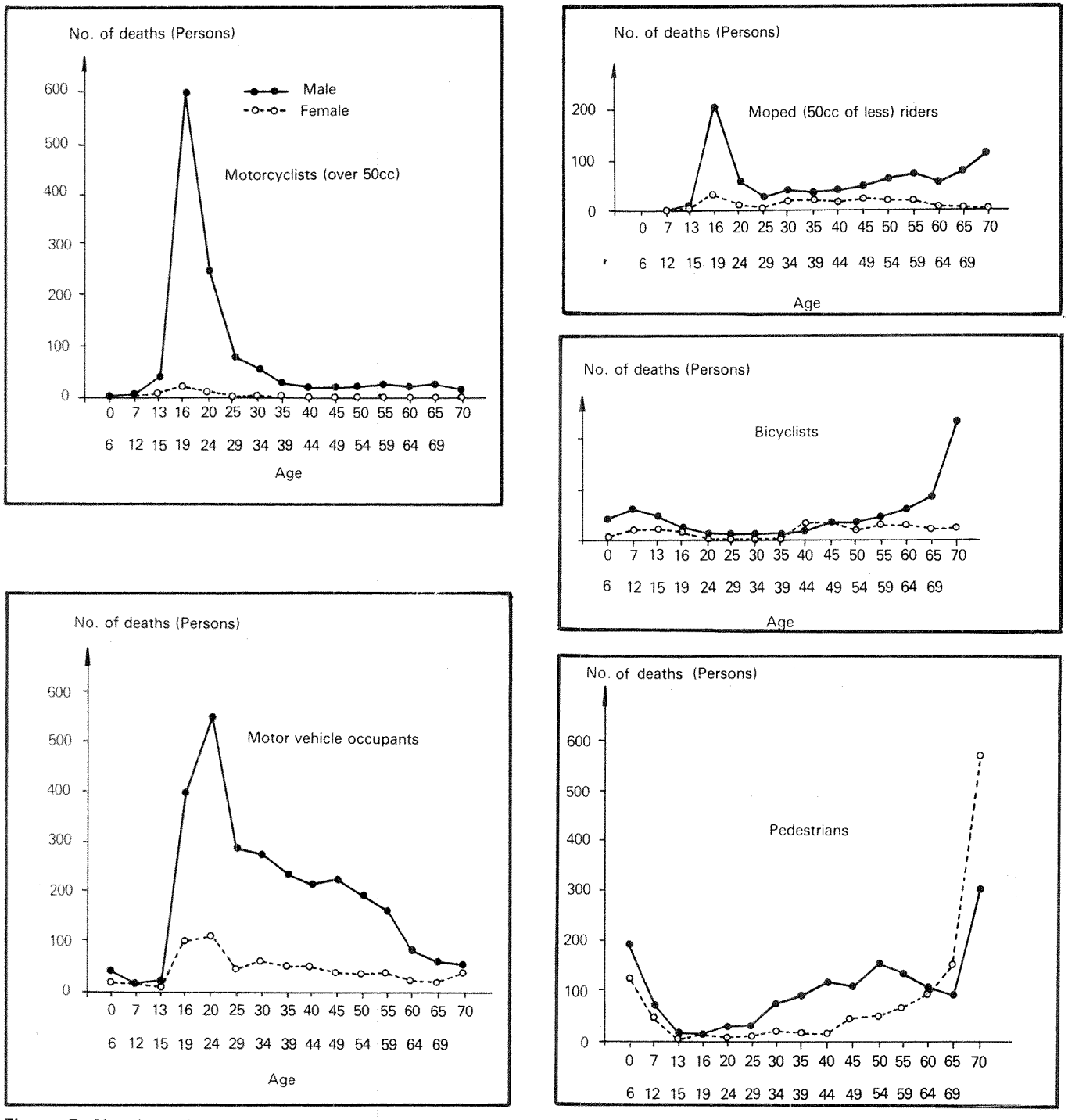

Figure 5. Number of deaths in various road user situations by age group (1983)

The forecast of the national death toll was calculated by first predicting the death rate by accident category (pedestrian death/pedestrian accident, etc.) in the same manner as that used for calculating the accident frequency above; then this death rate by accident category was weighted by the accident category structure ratio in each prefecture to produce the death rate in each prefecture. These prefectural death rates were then multiplied by the number of accidents in each prefecture to result in the prefectural death totals. The sum of these prefectural totals is the national death toll.

The national total of the predicted number of deaths by type of road user was obtained by multiplying the national total of the predicted number of accidents by accident category with the predicted death rate by accident category. In so doing, the predicted national death toll obtained above was established as the control total.

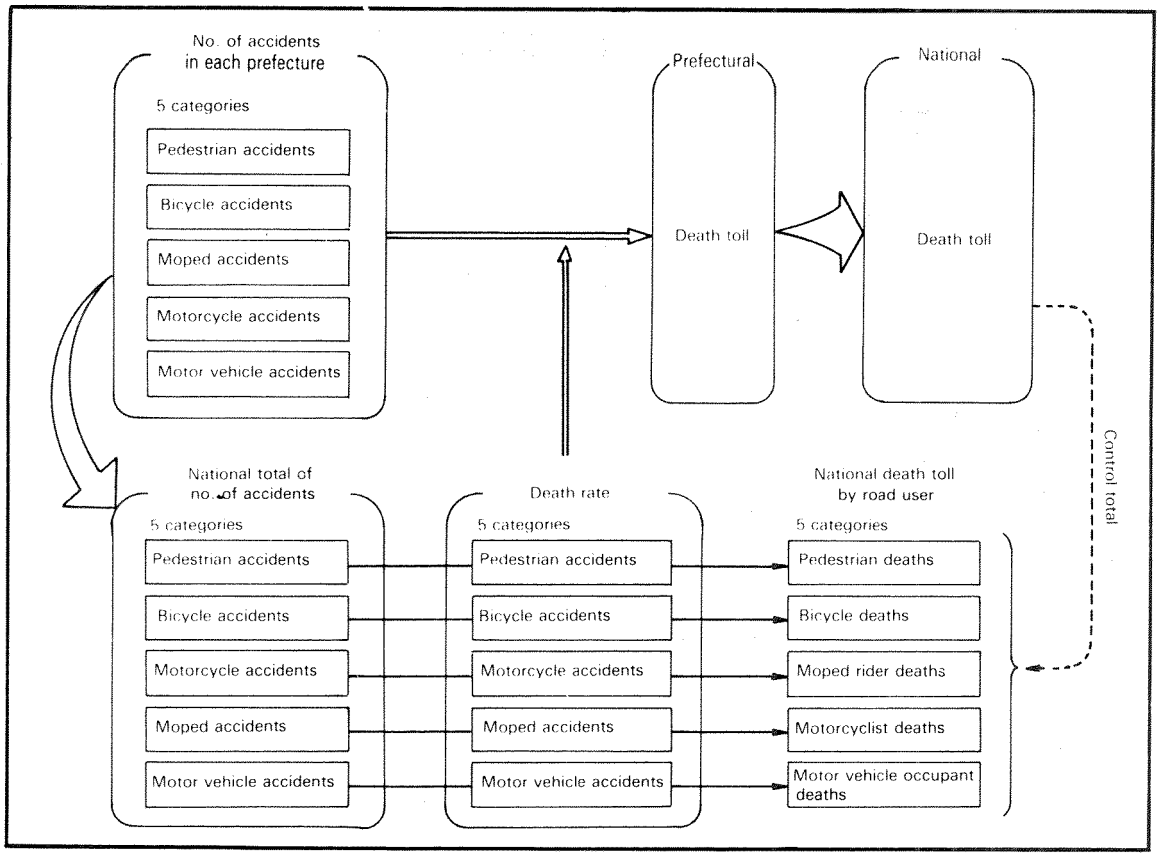

Figure 6. Traffic accident forecasting procedure

The result has been graphed in Figure 7. It estimates the total number of deaths at 10,600 in 1990. Taking a look at the figures by type of road user, one sees that the number of pedestrian or bicyclist deaths will be reduced to 2,600 and 700, respectively. On the other hand, however, the number of those killed while riding motor vehicles, motorcycles, and mopeds will each climb to 4,400, 1,500, and 1,400.

To cope with this anticipated increase, a legislation to reinforce the compulsory use of seatbelts for motor vehicles and helmets for mopeds will be enacted in the near future. The compulsory wearing of seatbelts and helmets is required in the existing law. However, the scope of application under the existing law is narrow, and no punitive measures accompany its violation. Consequently, the new law is designed to assign one penalty point upon its violation.

The Traffic Safety Policy Office of the Management and Coordination Agency has also conducted a prediction study of the effect of seatbelt and helmet-wearing. The study estimates that a seatbelt use rate of 90 percent will reduce the number of deaths by approximately 2,000, and a helmet wearing rate of 100 percent by moped riders will decrease the death toll by about 350, thus holding the total number of those killed at approximately 8,200 in 1990.

Furthermore, mopeds, as a rule, will be required to make right turns on roads with three lanes or more on one side by going through two traffic signals, just as bicycles and pedestrians, under this new legislation.

In addition, Tokyo has experimentally introduced double-stage right-turn signals (completely separate signal indications for vehicles proceeding straight and those making right turns), double stop lines at intersections (a separate stop line for motorcycles located ahead of the stop line for other vehicles, which is expected to reduce the number of accidents in which motor vehicles turning left entangle motorcycles, and collisions between motor vehicles making right turns and motorcycles proceeding straight), and installation of exclusive lanes for motorcycles as safety measures for motorcycles.

Future of the Motorized Society

Figure 8 shows that though the growth rate has recently declined a little, the number of passenger vehicles is still climbing at a rapid pace. The number of trucks in recent years shows a tendency of leveling off or a slight decrease. The number of light motor vehicles has started to rise rapidly since 5 years ago.

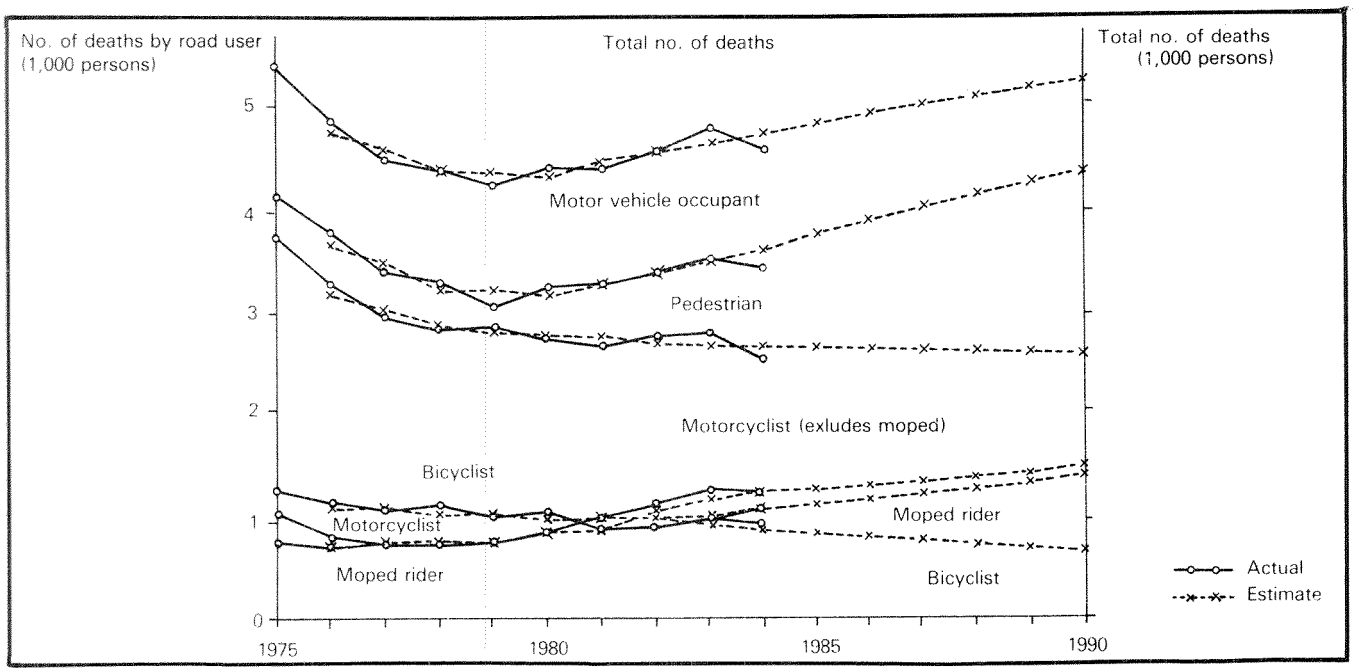

Figure 7. Forecast of traffic accident deaths up to 1990

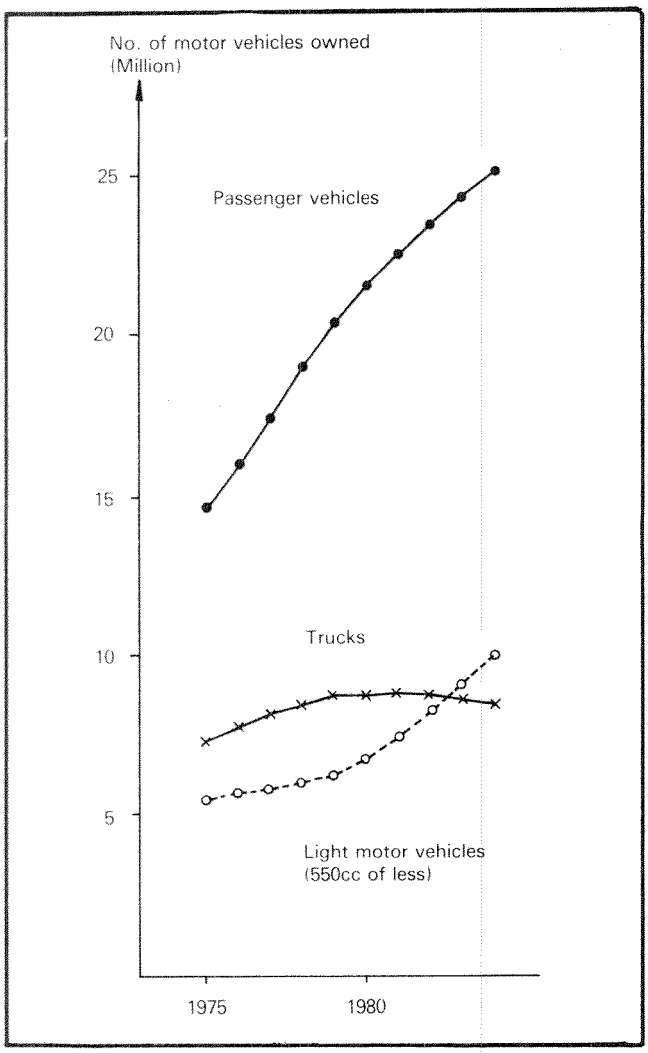

Figure 8. Trends in the number of motor vehicles owned

Motorization began relatively late in Japan, and, therefore, the number of driver license holders in the elderly age group is relatively low, as shown in Figure 9. However, the number of aged with a driver's license is expected to rise sharply in the future. Similarly, the number of women possessing driver's licenses had been relatively low hitherto but has been growing rapidly and is expected to continue to grow in the future.

In the past, it was mainly the young male population that shaped the motorized society. However, this society is expected to change into a diversified society participated in by a variety of population in terms of age group and sex. Accordingly, the types of vehicles in demand will also diversify.

With the coming of such a motorized society showing growth both in terms of size and diversification, it is absolutely necessary to reduce the number of those killed per 10,000 motor vehicles, which seems to have stabilized. This may not be easy, as seen above; however, unless this is accomplished, it is inevitable the number of those killed in traffic accidents will continue to rise correspondingly with the increase in the number of motor vehicles owned. In this context, it might be said that traffic safety measures must now make a new turn to meet this challenge. The reinforcement of compulsory use of helmets for moped riders and seatbelts for automobile occupants is one of such efforts. It is important that each motor vehicle is safe for its occupant and, of course, for the pedestrians and bicyclists. Furthermore, it is essential that parties concerned develop constructive ideas in the areas of traffic regulations, road structure, traffic safety education, etc., to pursue comprehensive traffic safety policies and measures.

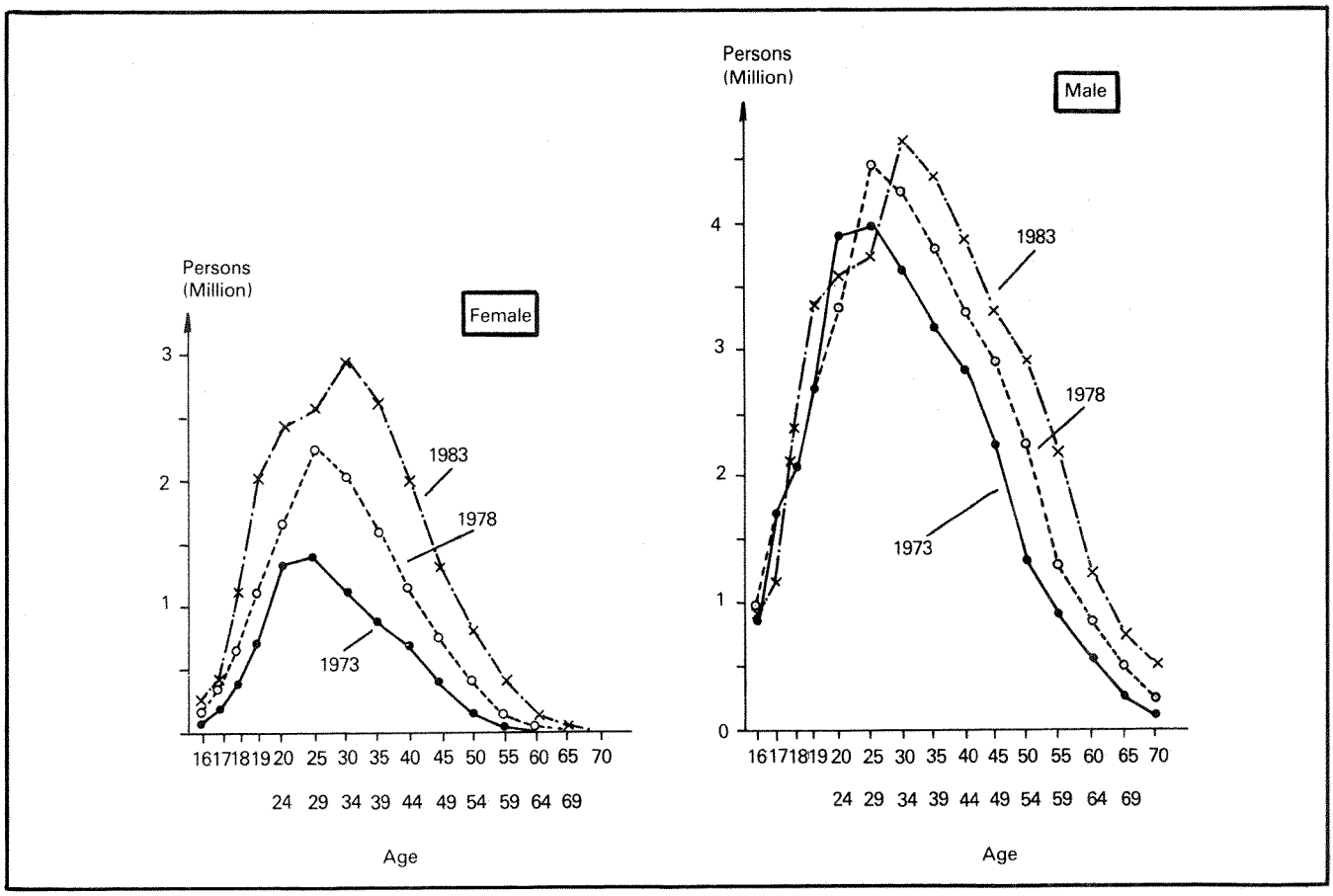

Figure 9. Number of driver's license holders by age group

Technical Session No. 5

Occupant Protection in Side Impact

I.D. Neilson, Chairman, United Kingdom

The Safety Performance of Production Vehicles in Side Impacts

Hampton C. Gabler III
Transportation Systems Center, Research and Special Programs Administration, U.S. Department of Transportation

James R. Hackney
National Highway Traffic Safety Administration, U.S. Department of Transportation

Abstract

The National Highway Traffic Safety Administration (NHTSA) has tested 12 current production cars in a series of controlled side impacts. As measured by the impact responses of NHTSA side impact dummies, the cars were found to vary dramatically in their capability to provide occupant protection. For the median-aged side-struck occupant, the potential for serious thoracic injury was found to range from a low of 9 percent for the 4-door AMC Concord to a high of 97 percent for the 2-door Nissan Sentra.

This paper investigates these differences in safety performance and reports those vehicle design parameters that are key to thoracic side impact protection. From the available data, the study concludes that the design parameter most crucial to occupant protection in side impacts is the Door Effective Padding THickness (DEPTH).

Problem Statement

NHTSA has undertaken a research project to characterize the safety performance of the vehicle fleet in side impacts and evaluate the feasibility of improving occupant protection in side impacts. The results of the NHTSA Thoracic Side Impact Protection Program are presented by Hackney(1). In that study, 10 current production passenger cars were tested in side impacts and found to vary dramatically in their capability to provide occupant protection.

The objective of this paper is to investigate these differences in safety performance and suggest design parameters that are key to thoracic side impact protection.

Background

This section presents an overview of those findings of the NHTSA Thoracic Side Impact Protection Program (TSIP) that bear on the safety performance of current production vehicles. Two additional tests not presented in (1), a Dodge 400 and a third Chevrolet Citation, are included in the discussion below.

Vehicle Crash Test Description

The accident configuration for the TSIP crash test series was designed to be representative of the side impact environment. The National Crash Severity Study (NCSS) accident files revealed that the most prevalent side impact angle was 90°. The NCSS files further showed the threshold for serious injuries occurs at a striking/struck vehicle velocity ratio of 30/15mph.

Based on the statistics presented above, the accident configuration chosen for actual crash testing was a 90° impact at a striking/struck vehicle velocity of 30/15mph. The striking vehicles in all cases were 3,000 lb movable deformable barriers with frontal force-crush characteristics near the upper bound of production vehicles. To represent the fleet, 12 production cars, listed in Table 1, were chosen for testing as a struck vehicle.

Table 1. Twelve production vehicles

1981	Chevrolet Citation	4 door	*
1982	Chevrolet Citation	2 door	
1981	Plymouth Horizon	4 door	
1981	Dodge Omni	2 door	
1981	Ford Granada	2 door	
1981	Ford Granada	4 door	
1980	AMC Concord	4 door	
1982	Nissan Sentra	2 door	
1981	Volkswagen Rabbit	2 door	
1982	Honda Civic	4 door	
1982	Dodge 400	2 door	

*Two tests were conducted on this model

All impacts were delivered to the occupant compartment on the driver's side of the struck vehicle approximately 37in forward of the centerline of the front and rear wheels as shown in Figure 1.

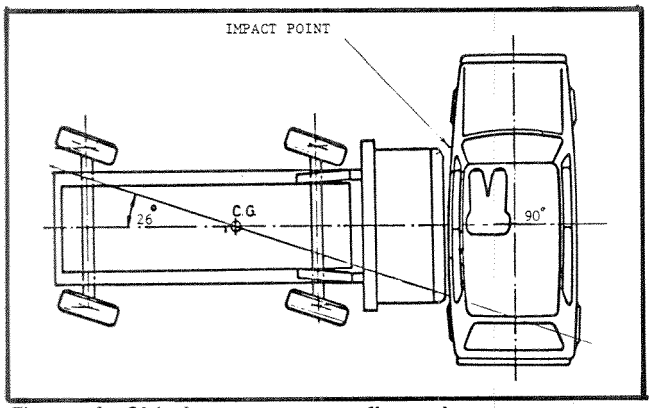

Figure 1. Side impact test configuration

Occupant Instrumentation

To measure the dynamic response of occupants, each crash test used two NHTSA Side Impact Dummies (SID). One SID was positioned in the driver's seat, and the second SID was positioned in the rear seat behind the driver. The dynamic impact lateral response of each SID was recorded by the following accelerometers:

- Lower left rib (primary)
- Lower left rib (redundant)
- Upper left rib (primary)
- Upper left rib (redundant)
- Lower spine (primary)
- Lower spine (redundant)
- Pelvis
- Head

In the results that follow, the primary and redundant channels for the rib and spine were averaged prior to use.

Occupant Responses

The peak occupant responses and the thoracic probability of injury are tabulated in Table 2 for each crash test. The peak rib and spine accelerations were used to predict the probability of thoracic injury for 23- and 41-year-old occupants. The 23-year-old occupant corresponds to the median age for side-struck occupants. The 41-year-old occupant corresponds to the median-aged side-struck occupant incurring thoracic injuries of AIS >= 3. Both ages are based on NCSS data.

By using the Thoracic Trauma Index developed by Eppinger(2), the SID responses can be related to the probability of thoracic injury. The Thoracic Trauma Index (TTI) is defined as follows for a 50-percentile human:

$$TTI = 1.4*Age + 0.5*(ribg + t12g)$$

where

Age= age of the occupant

ribg= max (lurg, llrg)

lurg= left upper rib peak acceleration

llrg = left lower rib peak acceleration

t12g= lower spine peak acceleration

Table 2. Twelve production vehicles: probability of injury

Test no.	Struck Vehicle	No. Doors	Occupant Position	Peak Occupant G's					TTI	Probability of AIS >= n					
				Rib		Spine		Pelvis		Age=23			Age=41		
				Upper	Lower	Upper	Lower	Center	Age=0	n=3	n=4	n=5	n=3	n=4	n=5
675	Chevrolet Citation	4	Driver	70.7	78.7	77.8	90.4	151.1	79.9	18	0	0	59	17	4
			Passenger	65.9	112.8	97.7	83.3	184.6	84.9	25	0	0	68	35	6
676	Chevrolet Citation (Repeat of Test 675)	4	Driver	91.2	88.0	77.6	102.4	170.3	89.0	31	0	0	76	54	7
			Passenger	82.0	119.3	101.3	87.8	157.5	88.7	31	0	0	76	53	7
677	Chevrolet Citation	2	Driver	74.1	71.9	82.5	114.7	185.2	90.9	34	0	0	80	63	8
			Passenger	54.8	73.7	58.6	58.7	105.0	62.8	5	0	0	29	0	0
678	Plymouth Horizon	4	Driver	126.4	104.9	80.7	100.0	184.9	96.6	44	2	2	89	85	10
			Passenger	83.7	86.2	57.5	69.1	131.1	71.1	10	0	0	44	2	2
679	Dodge Omni	2	Driver	130.2	121.3	105.2	109.1	174.4	102.1	54	9	3	96	95	12
			Passenger	98.4	104.2	74.5	100.2	121.5	91.2	35	0	0	80	64	8
683	Ford Granada	2	Driver	75.4	93.6	89.3	115.7	191.8	96.3	43	2	2	89	83	10
			Passenger	37.1	46.3	27.2	42.5	120.2	44.4	1	0	0	11	0	0
684	Ford Granada	4	Driver	93.6	135.3	89.2	104.1	166.1	100.9	52	7	3	95	93	11
			Passenger	38.4	70.3	45.7	61.0	203.6	63.1	5	0	0	30	0	0
702	AMC Concord	4	Driver	66.8	65.6	74.1	75.5	152.4	69.5	9	0	0	41	1	1
			Passenger	50.9	54.9	48.2	55.4	98.2	55.2	3	0	0	21	0	0
704	Nissan Sentra	2	Driver	121.7	149.3	110.5	150.3	213.1	127.5	97	96	12	100	100	22
			Passenger	56.2	61.9	76.6	73.1	144.0	67.0	7	0	0	36	1	1
710	Volkswagen Rabbit	2	Driver	93.6	114.2	120.5	120.0	188.2	103.6	57	12	4	97	97	12
			Passenger	97.0	109.1	53.7	80.1	161.7	82.3	21	0	0	63	24	5
719	Honda Civic	4	Driver	66.3	63.8	93.9	94.4	153.5	78.8	17	0	0	57	14	4
			Passenger	81.7	105.9	84.8	80.9	160.0	81.9	21	0	0	63	23	5
744	Dodge 400	2	Driver	90.4	124.5	112.6	115.0	201.7	103.6	57	13	4	97	97	12
			Passenger	93.6	134.4	92.3	95.6	156.1	96.4	44	2	2	89	84	10

For our study, the SID peak rib acceleration was first adjusted as shown below(1,2) to approximate the response that would be seen by a human:

ribg = SID ribg for SID ribg <= 60

ribg = (SID ribg)*0.5 + 30 for SID ribg > 60

The TTI was used to predict the probability of injury at the Abbreviated Injury Scale (AIS) levels of 3, 4, and 5. The relationship between the TTI and the probability of injury is shown in Figure 2.

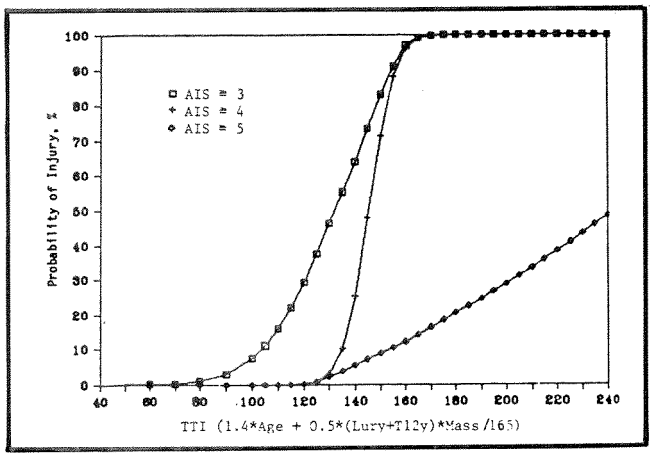

Figure 2. Thoracic trauma index

The probability of injury for each of the crash tests is given in Table 2 and ranked in Figures 3 and 4. The probability of injury varies widely among the tested struck vehicles. Injuries of AIS >= 3 for a 23-year-old driver vary from a low of 9 percent for the 4-door AMC Concord to a high of 97 percent for the 2-door Nissan Sentra. Injuries of AIS >= 4 fs4 for a 41-year-old driver vary from a low of 1 percent for the Concord to a high of 100 percent for the Sentra. These findings indicate that current production passenger vehicles vary substantially in their capability to provide occupant protection.

Other Aspects of Vehicle Safety Performance

In addition to the thoracic safety performance evaluation of the production vehicles, other safety-related performance aspects were noted during the crash test series. In two of the cars, the Honda Civic and the Plymouth Horizon, the right front passenger door opened during the crash event and allowed ejection of the driver from the vehicle. In the Plymouth Horizon test, the driver actually came to rest on the surface of the test track. In the Honda Civic test, the driver was not fully ejected.

In the test of the 4-door Ford Granada, the driver side B-pillar buckled significantly during the crash event. Post-test inspection showed that the spot welds at the base of the B-pillar had failed during the impact. This quality control problem with poor welds has been a common problem seen in other experimental side impact tests.

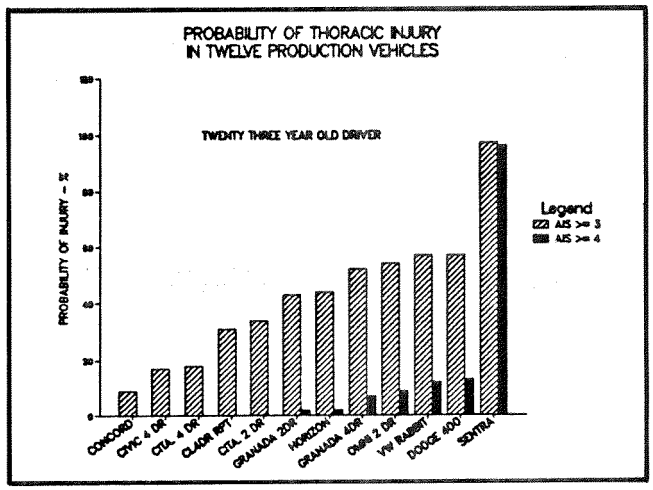

Figure 3. Probability of thoracic injury in 12 production vehicles for 23-year-old drivers

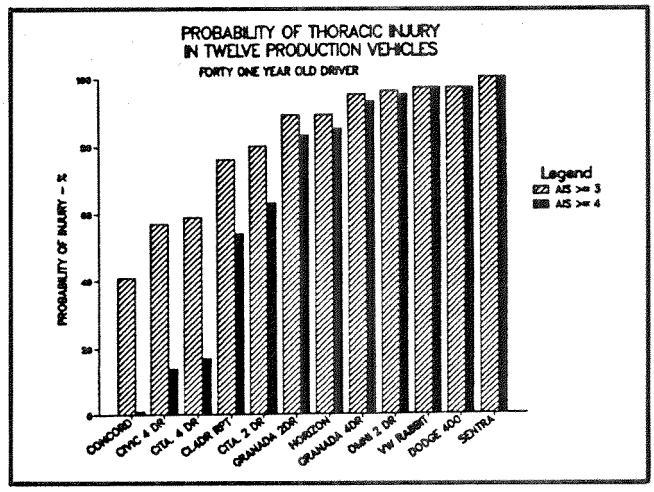

Figure 4. Probability of thoracic injury in 12 production vehicles for 41-year-old drivers

Occupant Responses vs. Vehicle Characteristics: Theory and Methodology

The objective of this paper is to determine what parameters of the struck vehicle design are most influential in affecting the occupant impact responses. The investigation will be limited to the responses of the driver.

In general, the occupant response to impact is a function of several parameters:

$$Rv = F(A, Di, Dv)$$

$$Ro = G(Rv, Dc)$$

where

Rv = response of the struck vehicle
Ro = response of the struck occupant
A = accident configuration
Di = structural design of the impactor
Dv = structural design of the struck vehicle
Dc = design of the struck vehicle occupant compartment

The response of the struck vehicle is a function of the accident configuration, the design of the impactor, and the design of the struck vehicle. The vehicle design includes both the energy-absorbing capability and the geometry of the structure. The accident configuration description includes the impact velocity, the impact angle, and the impact point. The response of the struck vehicle is described in terms of its acceleration profile upon impact and the intrusion of the door into the occupant compartment.

The response of the struck occupant is a function of the vehicle impact response and the design of the occupant compartment. In the case of side impact, the occupant compartment design includes both the energy-absorbing characteristics of the door and the initial occupant-to-door clearances.

In our study, the designs of the impactor and the accident configuration were held constant for each of the crash tests. With these constraints, the computation of the occupant responses becomes a simplified function of the energy-absorbing capability of the vehicle and the design of the occupant compartment. Symbolically, the relationship becomes:

$$Ro = G^*(Dv, Dc)$$

where G* represents a reduced form of the function G described above.

In this paper, we will mathematically search for the relationship between occupant impact responses and vehicle design parameters. First, we will characterize the design and response of each vehicle as a set of discrete parameters. Second, we will use a stepwise regression technique to determine occupant response as a function of the vehicle response. Finally, we will examine the results of the regression analysis to identify those design parameters most critical to occupant protection in side impact.

Vehicle Characteristics

For this study, the characteristics of the vehicle design and the occupant compartment design were divided into three categories:

- Vehicle geometry and mass
- Vehicle structural response
- Door structural response

Vehicle Geometry and Mass

For our investigation, the geometry and mass of each vehicle were described with the following 10 parameters:

- Number of doors
- Vehicle weight
- Wheel base
- Vehicle length
- Vehicle width
- Vehicle center of gravity
- Arm to door initial clearance
- H-point to door initial clearance
- Axle height
- H-point height

These parameters are tabulated in Table 3 for each vehicle—with the exception of the axle and H-point height. The axle height and the H-point height are tabulated in Table 4.

Table 3. Struck vehicle description

Test No.	Struck Vehicle	Number Doors	Vehicle Weight (lb)	Wheel Base (in)	Vehicle Length (in)	Vehicle Width (in)	Vehicle C.G. (in)	Arm-Door (in)	Hip-Door (in)
675	Citation	4	3045	104.8	176.8	68.8	46.0	4.9	6.7
676	Citation	4	3060	105.0	176.5	69.1	46.3	4.3	6.3
677	Citation	2	3100	104.9	176.7	68.1	43.3	5.4	7.1
678	Horizon	4	2600	99.1	162.5	66.5	45.8	3.6	5.5
679	Omni	2	2680	96.8	173.9	66.1	44.1	4.1	6.4
683	Granada	2	3380	105.4	195.3	71.1	49.3	4.8	7.3
684	Granada	4	3415	105.6	197.5	71.2	49.0	4.9	7.3
702	Concord	4	3558	108.5	180.0	70.4	53.8	3.2	6.4
704	Sentra	2	2340	94.6	167.1	63.9	44.5	3.9	6.2
710	Rabbit	2	2403	94.9	154.4	63.0	44.7	3.5	4.9
719	Civic	4	2488	91.3	161.4	62.2	43.8	3.4	5.8
744	Dodge 400	2	3028	100.0	180.8	68.6	41.3	4.5	5.7

Table 4. Struck vehicle impact responses

Test No.	Struck Vehicle	Number Doors	Delta V (mph)	Axle Height (in)	H-Point Height (in)	Static Crush* @Axle (in)	@H-Point (in)	Average (in)
675	Citation	4	15.2	10.0	20.5	11.3	15.1	13.2
676	Citation	4	14.8	10.0	20.0	11.2	13.1	2.2
677	Citation	2	15.3	11.0	22.0	10.3	15.7	13.0
678	Horizon	4	16.2	11.0	23.0	13.4	13.5	13.5
679	Omni	2	15.7	9.7	22.3	11.0	14.2	12.6
683	Granada	2	15.1	10.3	20.3	11.9	16.6	14.3
684	Granada	4		10.5	19.5	10.7	17.9	14.3
702	Concord	4	13.3	10.1	19.6	9.1	15.4	12.3
704	Sentra	2	14.8	11.0	20.0	14.6	18.0	16.3
710	Rabbit	2	17.2					
719	Civic	4	17.4	10.8	20.3	11.0	15.6	13.3
744	Dodge 400	2	13.6	11.0	18.0	15.5	20.0	17.8

*Static crush averaged over interval from 30" to 42" from impact target point

Struck Vehicle Impact Response

The struck vehicle impact response was described with the following three parameters:

- Lateral Delta-V
- Static Crush (axle height)
- Static Crush (H-point height)

These parameters are tabulated in Table 4 for each vehicle.

Delta-V, the change in struck car velocity, was computed from an accelerometer mounted on the front door sill on the undeformed side of the car. Static crush, tabulated at axle height and H-point height, is an average of post-test measurements taken over a range from 30in to 42in rearward of the targeted impact point. This area, on the side of the car, encompasses the location of the driver.

Door Impact Response

The door impact response was described with the following six parameters:

- Door-to-pelvis contact velocity
- Door-to-lower rib contact velocity
- Door-to-upper rib contact velocity
- Door effective padding thickness at the pelvis
- Door effective padding thickness at the lower rib
- Door effective padding thickness at the upper rib

The door structural parameters are tabulated in Table 5 for each vehicle. Door effective padding thickness measurements are unavailable for the Volkswagen Rabbit as all impactor accelerometer channels were lost during that crash test.

Table 5. Door impact responses

Test No.	Struck Vehicle	Number Doors	Arm-Door (in)	Hip-Door (in)	Contact Velocity LUR (mph)	LLR (mph)	Pelv (mph)	Thorax Defl (in)	Depth LUR (in)	LLR (in)	Pelv (in)	Avg (in)
675	Citation	4	4.9	6.7	25.8	26.4	27.8	1.77	4.9	5.7	7.0	5.9
676	Citation	4	4.3	6.3	25.6	26.7	27.7	1.78	4.7	6.3	7.0	6.0
677	Citation	2	5.4	7.1	25.2	26.3	27.0	1.80	4.2	5.8	5.5	5.2
678	Horizon	4	3.6	5.5	26.0	26.7	28.0	1.81	5.1	5.7	5.6	5.5
679	Omni	2	4.1	6.4	26.5	26.3	28.3	1.79	4.9	4.2	6.7	5.3
683	Granada	2	4.8	7.3	25.6	25.7	27.6	1.71	5.1	4.8	6.1	5.3
684	Granada	4	4.9	7.3	25.5	25.7	27.8	1.70	5.4	5.0	6.8	5.7
702	Concord	4	3.2	6.4	27.1	26.0	27.1	1.32	8.2	6.2	6.6	7.0
704	Sentra	2	3.9	6.2	26.2	26.8	28.2	1.80	3.6	4.0	5.0	4.2
710	Rabbit	2	3.5	4.9				1.72				
719	Civic	4	3.4	5.8	26.7	26.9	28.4	1.58	5.5	5.8	7.3	6.2
744	Dodge 400	2	4.5	5.7	25.3	25.2	27.5	1.62	4.8	3.8	4.8	4.5

Door Kinematics Model

The calculation of door contact velocity and effective padding thickness uses a variation of the method proposed by Strother and Morgan(3). In their idealized representation, the side impact is modeled as a one-dimensional system that can be readily analyzed from the velocity time traces of the system components.

The velocity time history of the impactor center of gravity, the door, and the occupant is shown in Figure 5. Door contact time, t3, is defined as the time at which the occupant velocity first becomes greater than zero. From the time of door contact, the contact velocity can be determined from the door velocity history. The relative displacement between the vehicle and the occupant can be determined by computing the area between the appropriate two velocity traces over the time interval of interest.

In this paper, we define a new parameter—the door effective padding thickness or DEPTH. DEPTH is defined as the relative displacement between the door and occupant from the time of contact, t3, until the time of separation, t4. From the crash observer's perspective, DEPTH is the amount the occupant crushes the door.

DEPTH is the maximum deflection measured between the occupant accelerometer and the door accelerometer. Depending on the location of occupant instrumentation, this will include a portion of the dummy compression as well as the crush of the door. As measured by the rib accelerometers, DEPTH includes compression of the dummy skin between the ribs and door surface. The effect of skin compression is considered negligible. Likewise, compression of the dummy at the pelvis contact point is considered insignificant as the pelvis is rigid.

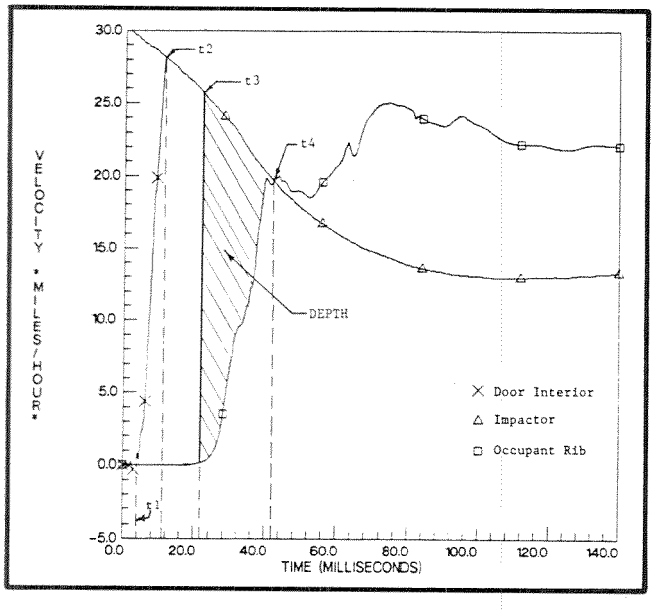

Figure 5. Door-occupant kinematics

Door Kinematics Model: An Example

Following is an example of a side impact event, as seen by the door kinematics model. This hypothetical scenario will demonstrate the physical nature of the DEPTH quantity and clarify the framework we have used to categorize our side impact tests. For our example, we will use one of the rib accelerometers to represent the occupant. However, the scenario applies equally to the pelvis. The door reference point, which we discuss below, physically refers to a hypothetical location within the door interior and not to either the door exterior or interior skin.

The side impact event can be separated into two sequences of events. The first is the deformation of the door interior as a result of the collision with the impactor. The second is the deformation of the door interior as a result of occupant impact. The deformation of the door exterior begins immediately upon impactor contact with the door exterior at t = 0. Although the door sheet metal begins to buckle immediately, the door reference point does not begin to accelerate until time t = t1 (typically about 3 to 4ms after impact). The door reference point ramps up quickly in velocity until such time, t = t2, as the door velocity and the impactor velocity are equal. Between time t = 0 and t = t2, the door exterior and impactor are crushing under the forces of impact. Using our model, we assume the deformation of the door exterior ends at t = t2.

At some time later, the occupant-to-door impact, the so-called second collision, begins. Initially, the door reference point and the occupant's rib are separated by the door-to-occupant clearance as well as the undeformed thickness of the door. Upon impactor contact with the car, the occupant begins to slide laterally across the seat toward the inside surface of the door. At time t3, the occupant collides with the door inside surface. By his own inertia, the occupant proceeds to intrude into the door—crushing the door interior structure and compressing the occupant's thorax in the process. Occupant intrusion into the door continues until t = t4 when the impact energy of the occupant is expended, and the occupant velocity equals the door velocity. The maximum intrusion of the occupant, reached at t = t4, is defined as DEPTH.

Analysis Using the Door Kinematics Model

In our crash tests, the inner panel of the driver's door was instrumented with 3 to 4 accelerometers. Because of the severity of the impact to the door, few of the door accelerometers survived the crash test or provided meaningful data throughout the entire event. Within 20ms of initial impact, the majority of the door accelerometers had either been physically damaged or had rotated in such a manner that their sensitive axis was no longer aligned with the direction of impact.

Examination of the door acceleration channels prior to accelerometer damage, however, does provide one important clue to the door behavior. In all cases, the velocity of the door inner panel ramps up quickly and appears to reach the impactor velocity very early in the event, i.e., t2 = 8-13ms. Beyond t = t2, the door acceleration measurements are of questionable validity. From t = t2 until the impactor and struck vehicle separate, the door (as opposed to the door inner panel) is assumed to move together at the same velocity. This assumption implies that all exterior vehicle crush and impactor crush have occurred by the time of occupant contact. It should be emphasized that while these assumptions are well suited to our study, i.e., for 30/15mph 90° side impacts, their applicability to other studies is not guaranteed—especially when extrapolated to alternate accident configurations.

For our study, the door contact was defined to have taken place once the occupant velocity exceeded a threshold velocity of 0.2mph. The time of door-to-occupant contact was computed for each of the cars and found to vary from 17 to 27ms for both the upper and lower rib, and from 12.5 to 20ms for the pelvis. For our study, the door is assumed to reach the impactor velocity prior to contacting the occupant, i.e., $t2 < t3$. Door contact velocity is then equal to the impactor velocity at the time of contact. The time of door/occupant contact, t3, and the time of door/occupant separation, t4, are tabulated in Table 6 for the 12 tested vehicles.

Door contact velocity was found to vary only slightly from car to car. Door contact velocity at the left upper rib varied from 25.2 to 27.1mph. Door contact velocity at the left lower rib varied from 25.2 to 26.8. Door contact velocity at the pelvis varied from 27.1 to 28.3.

DEPTH, at the pelvis and ribs accelerometers, was determined by computing the relative displacement between the door and occupant from the time of contact, t3, until the time of separation, t4. Once again, for $t > t3$, the door velocity is assumed to equal the impactor velocity.

Occupant Responses vs. Vehicle Characteristics: Regression Analysis

Comparison of the vehicle characteristics versus measured occupant responses suggests that lower peak occupant accelerations are observed in vehicles with a greater DEPTH. To statistically determine the relationship between the vehicle design and occupant injury, the vehicle structural characteristics and occupant responses were paired and examined through stepwise regression. The computed linear fits are shown below and presented in Figures 6a, 7a, 8a, 9a, and 10a.

PELG	=	318.3 + -18.1*Dpel + -5.6*Dlur	R**2 = .876
LLRG	=	238.3 + -26.6*Dllr	R**2 = .655
T12G	=	205.0 + -9.9*Dlur + -9.2*Dllr	R** = .783
T1G	=	163.9 + -14.1*Dllr	R**2 = .855
TTI	=	178.8 + -10.4*Dllr + -6.0*Dlur	R**2 = .794

where

PelG	= Pelvic peak acceleration (g's)
LLRG	= Left lower rib peak acceleration (g's)
LURG	= Left upper rib peak acceleration (g's)
T12G	= Lower spine peak acceleration (g's)
T1g	= Upper spine peak acceleration (g's)
TTI	= Thoracic Trauma Index (age = 0)
Dpel	= DEPTH at the Pelvis
Dllr	= DEPTH at the Lower Rib
Dlur	= DEPTH at the Upper Rib
R	= Statistical goodness of fit measure

Table 6. Door impact time history

Test No.	Struck Vehicle	Number Doors	Time of Door Contact* LUR (ms)	LLR (ms)	Pelv (ms)	Time of Door Separation** LUR (ms)	LLR (ms)	Pelv (ms)
675	Citation	4	23.0	20.4	13.9	44.9	41.8	33.9
676	Citation	4	22.4	17.8	13.4	42.3	39.0	33.3
677	Citation	2	26.1	21.5	18.5	45.3	44.3	34.8
678	Horizon	4	22.9	19.9	14.5	44.4	42.1	30.8
679	Omni	2	23.0	23.8	15.3	43.0	42.3	33.9
683	Granada	2	27.0	26.4	19.0	53.6	47.3	35.8
684	Granada	4	25.4	24.8	16.1	53.4	47.9	35.3
702	Concord	4	17.0	21.4	17.1	46.6	47.4	36.6
704	Sentra	2	25.8	23.0	16.3	42.0	41.0	30.0
710	Rabbit	2	23.5	22.4	14.8			
719	Civic	4	20.4	19.3	12.8	44.6	42.9	33.4
744	Dodge 400	2	26.9	27.5	19.8	45.0	44.4	33.8

*Occupant Velocity = 0.2mph
**Occupant Velocity = Door Velocity

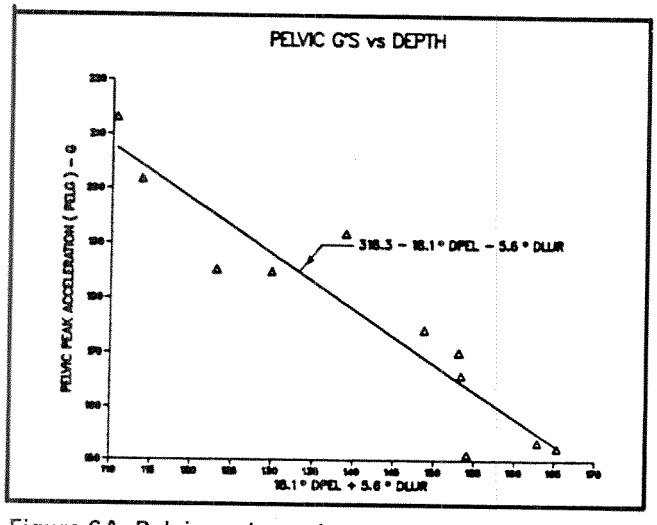

Figure 6A. Pelvic peak acceleration versus DEPTH at the pelvis and upper rib contact points (R^2 = .876)

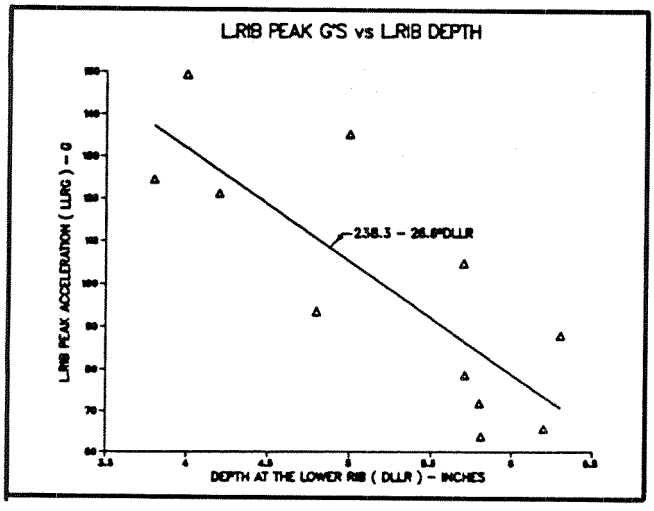

Figure 7A. Lower rib peak acceleration versus DEPTH at the lower rib contact point (R^2 = .655)

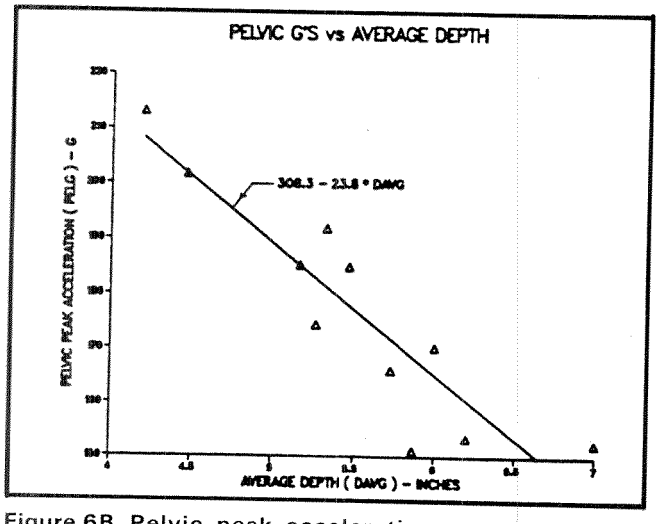

Figure 6B. Pelvic peak acceleration versus average DEPTH (R^2 = .817)

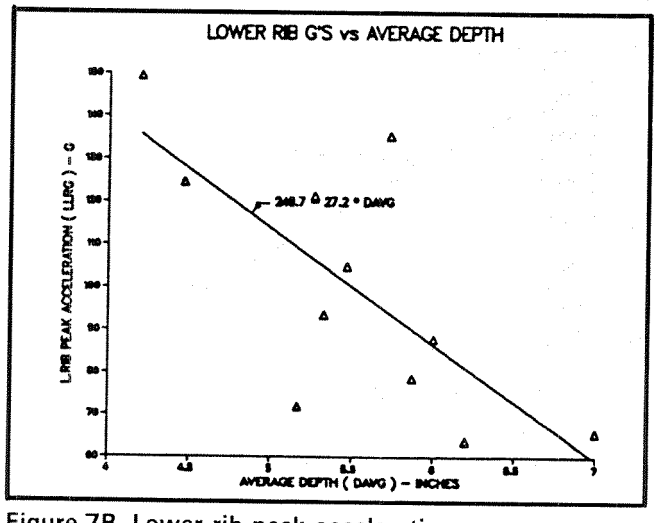

Figure 7B. Lower rib peak acceleration versus average DEPTH (R^2 = .522)

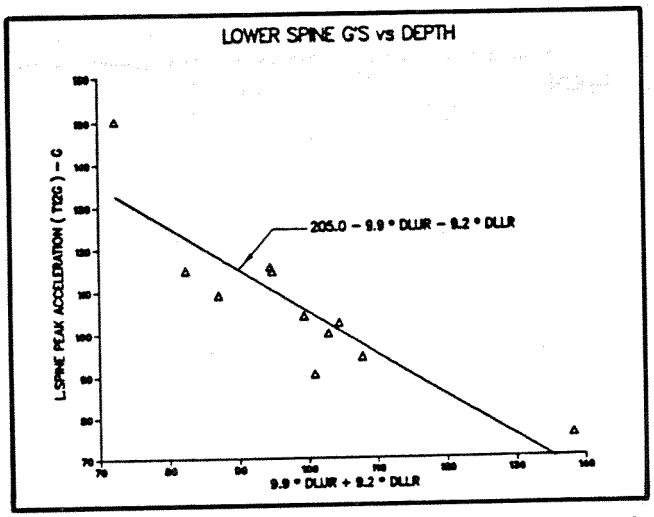

Figure 8A. Lower spine peak acceleration versus DEPTH at the upper rib and lower rib contact points (R^2 = .783)

After substituting the average DEPTH for the DEPTH at the individual body regions, the stepwise regression was completed a second time. The computed linear fits are shown below and presented in Figures 6b, 7b, 8b, 9b, and 10b.

The Importance of DEPTH

These mathematical fits indicate that sufficient DEPTH is crucial to providing the occupant with impact protection. Those vehicles with only a limited DEPTH, e.g., the Nissan Sentra, force the dummy to rapidly accelerate to the velocity of the intruding structure—resulting in high occupant responses. Those vehicles with a more generous DEPTH, e.g., the Honda Civic and AMC Concord, permit the occupant to ramp up to peak velocity more gently.

PELG	=	308.3 + -23.8*Davg	R**2 = .817
LLRG	=	249.7 + -27.2*Davg	R**2 = .522
T12G	=	227.1 + -21.8*Davg	R**2 = .817
T1g	=	164.8 + -13.5*Davg	R**2 = .595
TTI	=	191.7 + -17.7*Davg	R**2 = .796

where Davg = the average DEPTH
= (Dpel + Dllr + Dlur) / 3

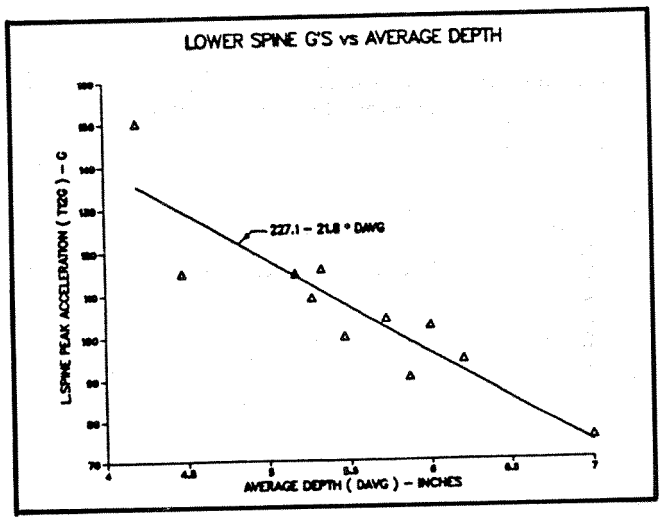

Figure 8B. Lower spine peak acceleration versus average DEPTH (R^2 = .817)

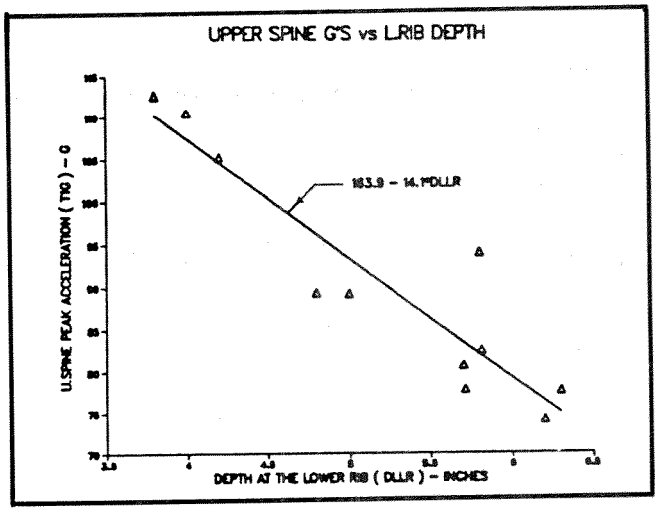

Figure 9A. Upper spine peak acceleration versus DEPTH at the lower rib contact point (R^2 = .855)

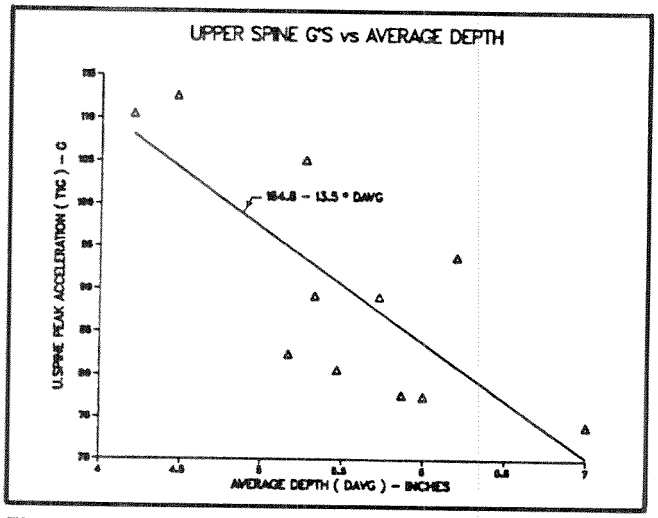

Figure 9B. Upper spine peak acceleration versus average DEPTH (R^2 = .595)

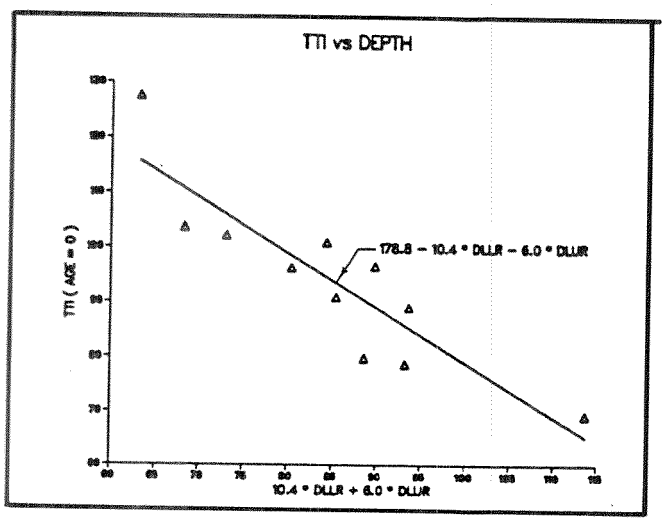

Figure 10A. TTI versus DEPTH at the lower rib and upper rib contact points (R^2 = .794)

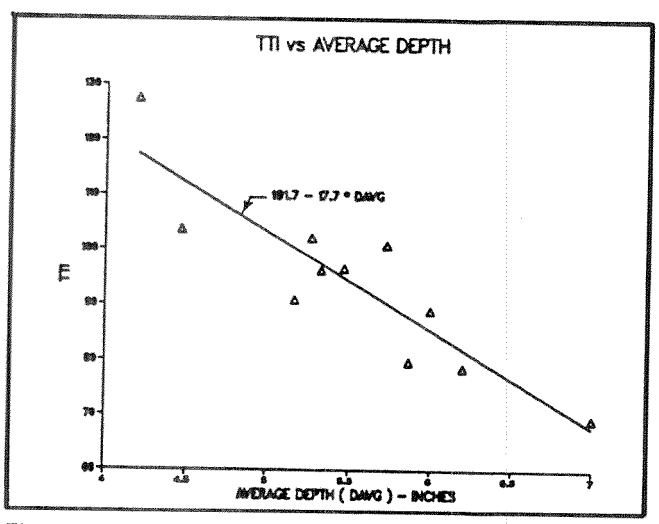

Figure 10B. TTI versus average DEPTH (R^2 = .796)

This finding is reinforced by an earlier study(1) that found that added door padding in production cars dramatically reduced the probability of injury in side impacts. In that study, several stock Volkswagen Rabbits were retrofitted with 3in of interior door padding and subjected to both high- and low-speed side impacts at both 90° and 60° impact angles. The supplemental padding was found to reduce thoracic injury by as much as 65 percent in high severity accidents(4).

From an impact energy perspective, peak occupant forces (and hence peak accelerations) would be expected to be proportional to the energy absorption in the door structure. This energy absorption is related directly to the stiffness (force-deflection properties) of the interior door structure and the interior door padding thickness. The fact that dummy peak g's and TTI are strongly correlated with the available DEPTH indicates that the force-deflection characteristics of the 12 doors are similar over the range of deflections observed in the tests.

This conclusion is reinforced by a study conducted by Willke and Monk(5), which measured the interior door stiffness of seven different vehicles. In this study, the door was crushed and backed by the same honeycomb impactor employed in our test series. The stiffness was reconstructed from the acceleration time history of a rigid thorax propelled into the crushed door assembly. Figure 11 shows the results of the experiment. With few exceptions, the force-deflection characteristics for the test group were quite similar over the range of crush. For comparison, Figure 11 also shows the stiffness of the honeycomb backing by itself.

Although this analysis appears to show that a certain minimum DEPTH is essential, this finding does not preclude the possibility that other vehicle design parameters may improve side impact protection. The manufacturer may choose vehicle designs that alter other

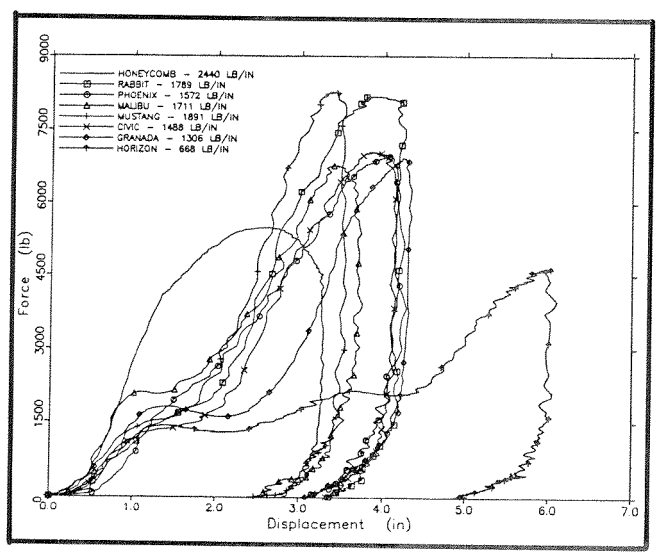

Figure 11. Interior door stiffness

factors that affect occupant protection. Two parameters that are potential candidates (and were reasonably constant in this study) are the occupant-to-door contact velocity and the inner door force-deflection characteristics. A significant reduction in the contact velocity and/or optimal force-deflection characteristics could be expected to improve side impact crashworthiness.

DEPTH vs. Vehicle Design Parameters

In the previous section, the peak occupant g's and TTI were shown to be strongly correlated with the DEPTH. The vehicle design parameters that influence the DEPTH remain to be determined. The candidate parameters include the total thickness of the door, the door attachments to the surrounding structures, the strength of these surrounding structures, the location and size of internal door hardware (window and window-operating mechanisms), and the location and size of the door beam.

The total thickness of the door, at the occupant contact locations, gives the maximum available DEPTH (unless outward bending of the door occurs during occupant impact). For crash events in which the door is not impacted, this total thickness, minus the space occupied by the internal door hardware and door beam, should be directly correlated to thoracic side protection.

The stiffness of the external sheet metal is insignificant. If exterior door stiffness were solely dependent on the external sheet metal, an almost total loss of DEPTH would be expected for even low-speed impacts into the occupant compartment. Therefore, it is very important that the side structural design provide load paths that maintain as much effective padding thickness as possible. This may be accomplished by efficient use of the door beam and the surrounding structures. The door beam should be located as close to the external sheet metal as possible and must carry some of the impact forces to the surrounding structures.

In our test, significant loading of the A- and B-pillars occurs. Similarly, the accident data show in most side impact events that the surrounding structure (A-pillar, B-pillar, sill, and roof header) is frequently impacted. To protect the side-struck occupants, the surrounding structures must provide adequate forces to maintain reasonable occupant compartment integrity and load paths for the forces that are transmitted from the door.

Some of the production vehicles in our tests, particularly the Honda and Concord, appear to perform this function very well. The designs for the modified vehicles in (1) included additional methods of load transmission between the door, sill, and A- and B-pillars. These simple changes also seemed to function very well.

In the ideal situation, the door would perform exclusively as an energy dissipation element: 100 percent of the door thickness would be maintained during impact, and the door would have optimum padding characteristics. Present vehicle designs do not have this luxury. The door must provide the required mechanical functions of housing the window, the window-operating mechanisms, and the door-opening mechanisms. Careful safety design considerations are required to minimize the loss of occupant protection due to these mechanical requirements. The hardware for these requirements should restrict the possible DEPTH as little as possible. Any hard points should be located away from the potential occupant contact zones.

Much of the design information discussed above has not been completely assembled and analyzed for the tested vehicles. Therefore, no definite conclusions can be drawn as to the scope of existing design parameters that provide better safety performance. However, data from this test series have been studied that may reflect the significance of the exterior door stiffness and the strength of the surrounding structure. These data include the static crush at the axle height and the number of doors on the subject vehicles.

The computed linear fit between the average DEPTH and these two parameters is shown below and presented in Figure 12.

Davg 7.2 + -0.242*AxleCrsh + 0.392*Ndoor
R**2 = .886

where

Davg	=	average DEPTH = Dpel + Dllr + Dlur)/3
AxleCrsh	=	static crush at the axle height
Ndoor	=	number of doors
R	=	statistical goodness of fit measure

The static crush at the axle height may be considered as directly proportional to the exterior door stiffness. The number of doors may have a direct relationship to the strength of the surrounding structure as well as exterior door stiffness.

Although this paper computes a single value of DEPTH for each vehicle, DEPTH may be dependent on the

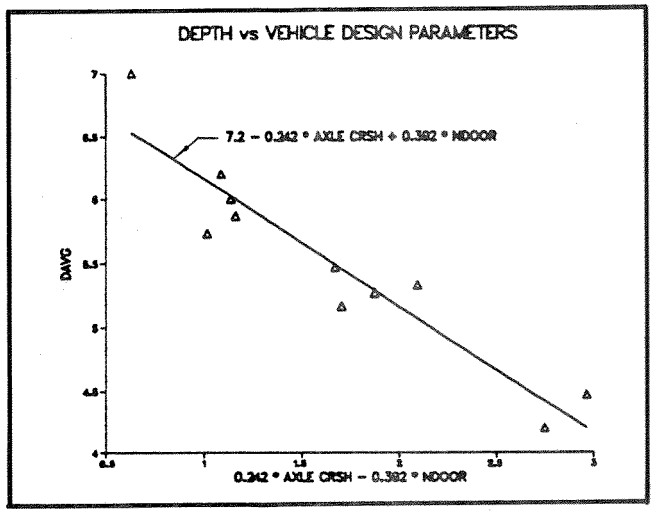

Figure 12. Average DEPTH versus vehicle design parameters (R_2 = .886)

location of occupant contact along the inner door width. It should be emphasized that the values of DEPTH presented here were computed for the contact regions experienced by a 50th percentile occupant. Different size occupants and/or different seating positions will result in correspondingly different contact points. It is important that the maximum possible DEPTH be maintained throughout the potential area of occupant impacts (the contact zone).

Implications of DEPTH on Component Testing Approaches

The use of component tests or full systems tests continues to be a subject of considerable interest and debate(6). The component test with its somewhat simpler, less expensive procedures and feasibility of application early in the vehicle design stage is very appealing. The full systems test with its closer relationship to the real accident event provides an easier transition to benefit calculations.

The findings presented in this paper have an important bearing on the design of a component test procedure. The regression analysis shows a strong correlation between—

- Occupant responses and DEPTH
- DEPTH and exterior door static crush (precrush)

The challenge of a component test is to design an experiment that avoids the expense of a full systems test but faithfully replicates the impact conditions seen by the struck driver. The two elements from the above analysis most relevant as input to a component test design are the contact velocity of the thorax to the interior door surface and the precrush of the exterior door.

From the presented data, the contact velocity is seen to be relatively constant for the tested production vehicles. Door-to-thorax contact velocity for the 30/15mph 90° impact condition is 26.1 +/- 1.0mph. This implies the impact velocity of a component test device should approximate this 26mph velocity to replicate a near real-world event. However, if a manufacturer chooses to make changes to the side structure of his vehicle that influence this velocity, the component test will not recognize these changes.

The second element, the precrush of the door, is the amount the door exterior must be crushed prior to a component test to repeat the conditions of a full systems test. The static crush of the exterior door as defined here is the permanent deformation of the door exterior measured at the end of the crash test. Recalling our door kinematics model, permanent deformation of the door is completed prior to occupant contact with the door. For our test configuration, the permanent deformation of the door and the required precrush are equivalent. For side impacts to the occupant compartment, a method for determining the correct door precrush for the component test approach will have to be developed if correlation to real-world events is to be obtained.

Based on the results presented above, we conclude the fidelity of door component test is greatly influenced by the fidelity of the door precrush and proper choice of the contact velocity. Until adequate methods are developed for determining these two elements, the economic justification for door component tests as an alternative to a full systems tests appears tenuous at best.

Future Studies

Several activities are planned by NHTSA to further evaluate the safety performance parameters of production vehicles in side impacts and to investigate potential improvements to side impact test procedures and side impact protection. These activities include—

1. Continued full systems testing of production vehicles. Additional production vehicles, including vans and light trucks, will be selected and tested in the 30/15mph, 90° condition. Resulting data will be used to supplement the above studies and more fully evaluate the importance of DEPTH across the complete vehicle fleet.
   Since the original group was tested, NHTSA has modified the SID dummy to improve the durability of the dummy leg. NHTSA has also finalized the side impact test procedure with significant refinements to the seating procedure for the SID. Based on two recent tests (May 1985), preliminary results suggest that, rather than mixing the pre- and postmodification SID tests, the two groups should be analyzed independently.
2. Collection of the vehicle parameters that are assumed to influence the DEPTH. Data collection efforts on the original 12 vehicles and all vehicles selected for testing will include these parameters as outlined earlier. These efforts will require some vehicle tear down and subsystem testing.
3. Component testing concurrently with the full systems tests of the selected vehicles. Component tests based on the forthcoming MVMA test procedure and utilizing the MVMA-designed thoracic test device will be conducted on all the selected vehicles. The results of these tests along with the results of ongoing MVMA tests will be used to assist in the evaluation of the relative elements between real-world side impact events and component test results.

Conclusion

This paper has examined the results of 12 side impact tests using current production cars with the objective of

determining the effect of vehicle design on the response of side-struck occupants. Our conclusions are—

- Current production cars vary widely in their capability to provide occupant protection in a side impact. For a 23-year-old driver, the probability of a thorax injury of AIS >= 3 was measured to range from a low of 9 percent for the AMC Concord to a high of 97 percent for the Nissan Sentra.
- For the vehicles tested, the door effective padding thickness (DEPTH) was found to be the single design parameter most crucial to occupant protection in side impacts.
- Four-door cars, in general, provide greater DEPTH than two-door cars.
- DEPTH is largely determined by the static crush of the vehicle at the door exterior—the more fully crushed the door, the lower the available DEPTH.
- The fidelity of door component tests is greatly influenced by the fidelity of the door precrush. Because accurate determination of the door precrush requires a full systems test, additional research is required to evaluate the feasibility of door component tests as a viable alternative to full car crash tests.

Our conclusion is that the wide variation in occupant side impact protection can be directly attributed to differences in the struck vehicle design. When the door and side structure provide adequate impact energy absorption, thoracic injuries are reduced. Furthermore, crashworthy doors and side structures do not appear to require exotic design modifications. The feasibility of enhanced side impact protection has been demonstrated by several of the current production cars tested in this study.

Acknowledgment

The authors wish to express a special word of thanks to Joseph Kanianthra for his expert and timely assistance in preparing much of the data in this paper for graphic presentation.

References

1. Hackney, J.R., M.W. Monk, W.T. Hollowell, L.K. Sullivan, and D.T. Willke, "Results of NHTSA's thoracic side impact protection research program," SAE Paper 840886, May 1984.
2. Eppinger, R.H., J.H. Marcus, and R.M. Morgan, "Development of dummy and injury index for NHTSA's thoracic side impact protection research program," SAE Paper 840885, May 1984.
3. Strother, C.E., and R.H. Morgan, "A fundamental look at side impact," Proceedings of the American Association for Automotive Medicine, Louisville, Kentucky, October 1979.
4. Gabler, H.C., K.P. White, and W.P. Pilkey, "Thoracic side impact protection research program: countermeasure effectiveness," University of Virginia Letter Report, September 1984.
5. Willke, D., and M.W. Monk, "Side interior stiffness measurement," DOT Report No. DOT-HS-806-708, September 1984.
6. MacLaughlin, T.F., and R.J. Wade, "Evaluation of full vehicle and component test procedures for improving side impact crash survivability," SAE Paper 830463, February 1983.

Load Transfer From the Striking Vehicle in Side and Pedestrian Impacts

Bertil Aldman and
Janusz Kajzer
Chalmers University of Technology

Torsten Anderlind
Saab Car Division

Merih Malmqvist
National Testing Institute of Sweden

Hugo Mellander
Volvo Car Corporation

Thomas Turbell
Swedish Road and Traffic Research Institute

Abstract

The level at which forces are transmitted from the striking vehicle in side impacts may influence the response of the struck car in several different ways. A better contact between the front bumper of the striking and the sill area of the struck car has been considered to be desirable in this respect.

In side impacts, the most frequent direction of the impact is from 3 and 9 o'clock, while the direction of the forces is usually from 2 and 10 o'clock due to the velocity of the struck car. A European car and the EEVC moving deformable barrier have, therefore, been used in a crabbed mode to study the problem of load transfer at different levels above the ground. Volvo and Saab cars were used as targets in 55km/h side impact with an APROD-81 side impact dummy placed on the struck side in the front seat. The results indicate that a difference in the level at which the loads were applied could influence the deformations, the kinematics of the struck cars, and the loading of the occupant.

Studies of the mechanisms of injury to pedestrians hit by cars have indicated that a reduction of the severity of the injuries to the lower extremity could probably be achieved by lowering the point of first impact. This would not necessarily influence the overall kinematics of the body in a negative way. An attempt has been made to assess the influence on different injury-related parameters by lowering the level of first contact and increasing the compliance of the car front structures. As tools for this study, a physical and a mathematical model of the pedestrian with particular emphasis on the lower extremity have been used. The results indicate a lowering of the level of load transfer would have more influence on some injury-related parameters and changing the compliance of these structures more influence on others.

The results of this combined project support the theory that a lower level aboveground of the leading force transmitting structures of the car front would be beneficial in both types of accident.

Introduction

Traffic safety research in Sweden is being discussed continuously and coordinated by representatives from the Swedish Road Safety Office (TSV), the Chalmers University of Technology (CTH), the Swedish Road and Traffic Research Institute (VTI), the Saab Car Division, and the Volvo Car Corporation.

The question of optimal bumper height related to side and pedestrian impact consequences has been debated; especially a risk of conserving the existing requirements governing bumper heights seemed to be impending.

This work, initiated by these discussions, has been a joint project between TSV, CTH, VTI, the Saab Car Division, and the Volvo Car Corporation.

In developing and testing the crashworthiness of passenger cars, the frontal fixed barrier testing at 30 and 35mph has been stressed for many years. Only recently have the side impact properties been discussed more. Together with the frontal impact protection, the bumper design and height have been regulated through low-speed impact performance requirements.

Often there is a conflict between the requirement for frontal protection and possible aggressiveness of the car front in impacts with the side of other cars and with pedestrians. Therefore, there is a need to optimize the car front both for frontal and for side and pedestrian impacts. The bumper height is an important part in this.

The objective of this investigation was to show that legal requirements leading to certain bumper heights may have to be reconsidered in view of their effect in side and pedestrian impacts.

The investigation had four phases. A literature study was made (see appendix), and the bumper level was measured for present cars under varying conditions. Side impact tests were made with a mobile deformable EEVC barrier in a crabbed mode at varying heights against Saab and Volvo cars. Finally, a new pedestrian dummy leg was impacted with a car front structure at varying heights, and several leg parameters were measured.

Traffic Environment and Bumper Heights for Stationary and Braking Vehicles

It is often said that guardrails are built to be compatible with the bumpers of passenger cars. As part of this project, an investigation was made of the traffic environment in Sweden and to some extent in the United States.

It became evident that guardrails in Sweden are positioned at the hub level of truck wheels. No evidence was found that lowering the bumper would be unpractical with the exception of loading ramps for cars on trucks and railroad cars. In the United States, the guardrails on the highways have been engineered to specific standards. The lowest horizontal rail is positioned level with car bumpers. However, due to movements in the ground, this level can vary ±75mm. A new type of guardrail is being installed in some States where the lowest nominal height is 250mm. New Jersey concrete barriers have been designed with the existing bumper heights in mind, and a lowered bumper may create forces that tend to lift up the front of the car and cause it to turn over. A number of people are being killed in the United States where guardrails have been involved. It is essential to investigate carefully any negative effect of a lowered bumper. This brief look into the U.S. traffic environment has not revealed any major problems for lowering bumper heights.

Ramp standards are considered to have very little influence on bumper heights as the bumper seldom is the lowest point of the car. Many modern cars have front air dams (spoilers) positioned considerably lower than the bumper, showing the potential to lower the bumper. The U.S. requirements in P581(1) set the impactor height at 406 to 508mm. The ECE R42(2) limits it to one value, 445mm. On a selection of current passenger car models, bumper (centerline) heights were within a range from 430 to 500mm. These values could, of course, be lower in real traffic conditions with loaded vehicles and possible dive motion due to braking. The height reductions due to brake diving were measured and found to be from 70 to 100mm.

In many accidents, the impacting car had started to brake before impact. According to a French investigation(3), this was the case in 54 percent of the investigated pedestrian impacts. It takes, however, a considerable time and distance for the full vehicle dive action. As shown in Figure 1, the dive motion has a frequency of approximately 1Hz, which means that the maximum amplitude is reached 0.25s after initiation. With time for the driver to react and apply the brakes, the vehicle will travel about 8m before the dive is completed at an initial speed of 57km/h. It seems probable, therefore, that a full dive is not reached in most cases.

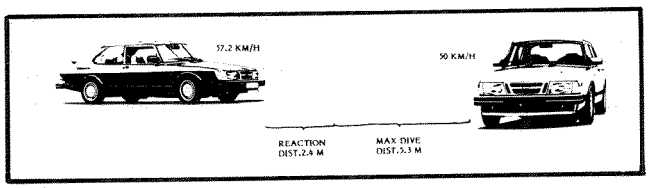

Figure 1. Front end dive (pitch) at braking with frequency of approximately 1Hz (maximum dive after 0.25s)

Side Impact Evaluation

Test Methods

A total of 10 dynamic tests were made according to the following description.

EEVC MDB

The Mobile Deformable Barrier (MDB) as specified by EEVC(4) was used in eight tests. Polyurethane foam blocks delivered by Fritzmeier GmbH (version II) were used as front elements (Figure 2).

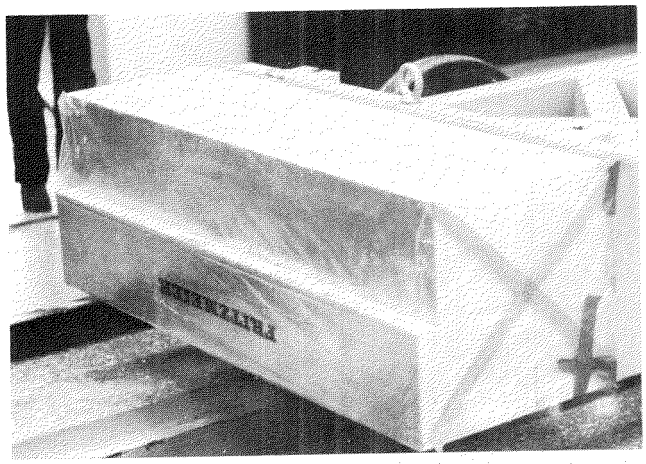

Figure 2. Front block of the MDB

Bullet Cars

In two tests, Peugeot 305 (1979) cars were used as striking vehicles (bullets). The reason for using this car was that its front construction was considered typical for the European car population. In all other tests, the EEVC MDB was used.

Crabbed Configuration

Although not specified by the EEVC, it was regarded as interesting(5) to find out how the EEVC MDB would perform in a crabbed configuration (Figure 3). The angle was 27° and the impact speed was 55km/h (34mph), resulting in a perpendicular speed of 48km/h (30mph) and a longitudinal speed of 24km/h (15mph). The Peugeot cars were also modified to this 27° crabbed configuration (Figure 4).

Ground Clearance

The MDB was made with an adjustable front plate, and the ground clearance was varied at the following

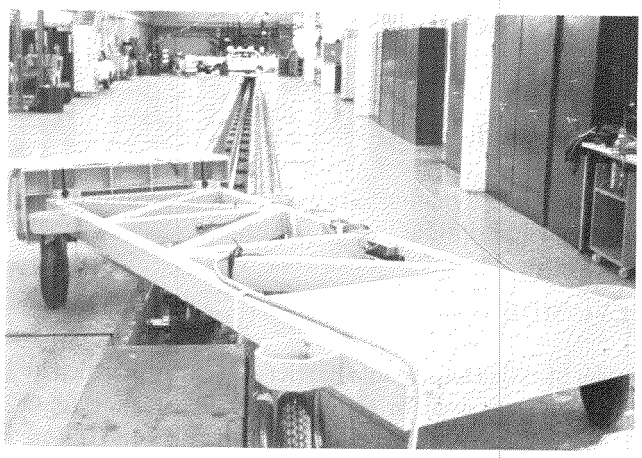

Figure 3. Crabbed EEVC MDB

Figure 4. Peugeot prepared for crabbed configuration

levels: 200, 250, 300, and 350mm. The Peugeot cars were used at their nominal ground clearance, which is hard to specify since there is no good definition of this value on the front of a real car. In one of the tests with the Peugeot cars, the impacted (target) car was lifted 100mm at its suspensions to simulate the effect of a lower ground clearance of the bullet car (Figure 5).

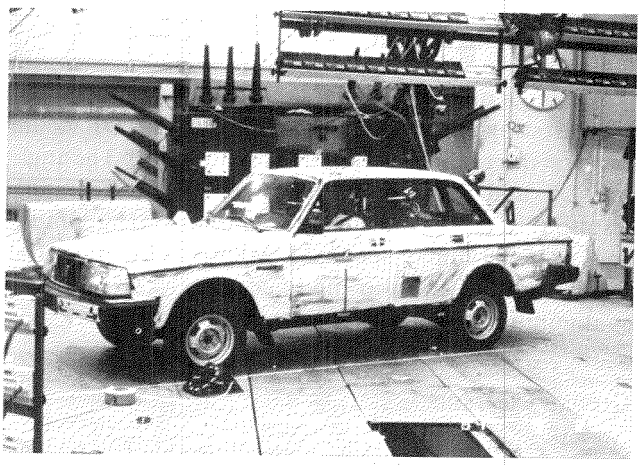

Figure 5. Elevated target car

Target Cars

Medium-size Volvo and Saab cars were used as targets. The impact point was such that the left corner of the bullet vehicle hit the target vehicle at a point 940mm (37in) in front of the centerline of the wheelbase. All impacts were made on the driver's side (Figure 6).

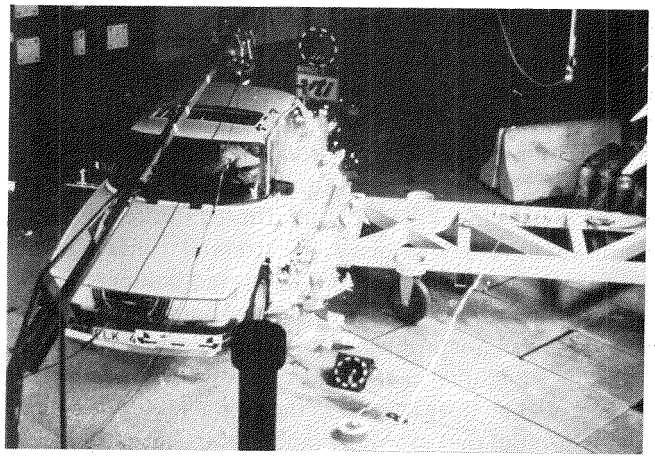

Figure 6. Impact configuration

Dummy

An APROD-81 dummy(6) was used in the driver's seat in all tests. The dummy was instrumented with 3-axial accelerometers in the head, chest, and pelvis. Lateral chest deflection was also measured at two levels (Figure 7).

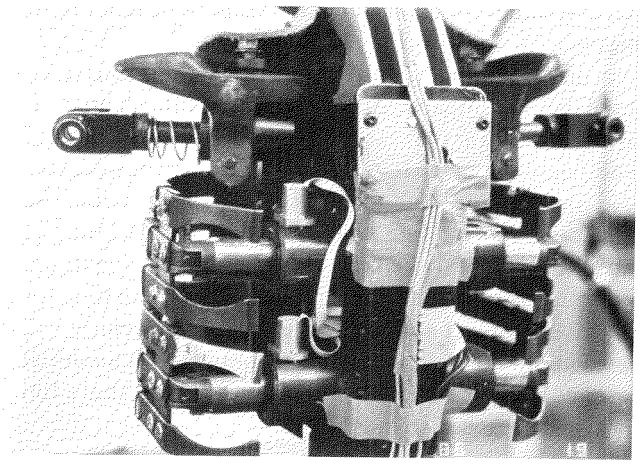

Figure 7. APROD-81 chest mounted on Part 572 dummy

Instrumentation

Apart from the dummy measurements mentioned above, the accelerations of the bullet vehicle and the target vehicle were recorded. The dynamics of the inside and outside door panels just behind the driver's seat were measured by steel rods installed transversely in the compartment. All measurements were made according to

ISO 6487(7)(Figure 8). Photographic coverage consisted of four high-speed 16mm cameras (Figure 9). To measure the permanent deformations of the impacted cars, a special measuring device was built (Figure 21).

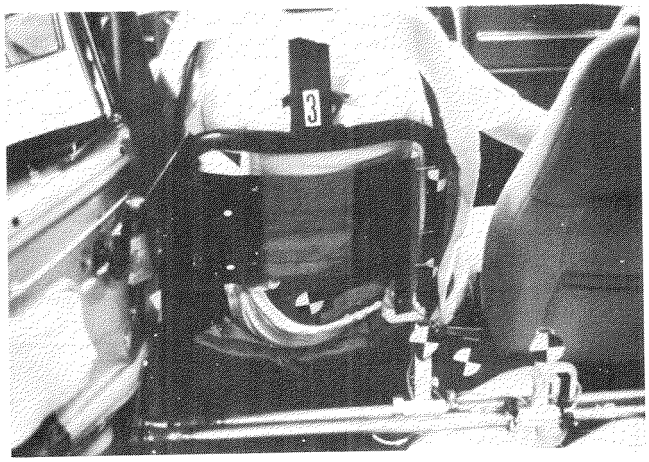

Figure 8. Inside view of target car (measuring rods for acceleration of outside and inside door panels visible at bottom of picture)

Figure 9. Target car in position for impact

Side Impact Test Results

The impact speed of the bullet vehicles was in the range of 55.0 to 56.1km/h. In the following diagrams, the peak values of some significant parameters are plotted against the ground clearance of the bullet vehicles. Several other parameters have been studied, but they have not given any additional information and are therefore not reported. Head accelerations, for instance, were of such a low magnitude, due to no head impact, that the HIC values were below 100. In the case of the MDB, the ground clearance is the nominal clearance to which the barrier front was installed. Because of the difficulty in determining the exact ground clearance for the Peugeots, when used as a bullet vehicle, the values for these tests are plotted at a ground clearance called normal and at a 100mm lower level.

The following symbols are used in Figures 10 to 12:

In the left part of the figures, △ and □ indicate values for the target cars, respectively, when impacted by the EEVC MDB.

In the right part of the figures, O indicates values for the target car when impacted by the Peugeot.

The chest measurements in Figures 10 to 13 indicate the loads on the chest decrease when the ground clearance is lowered.

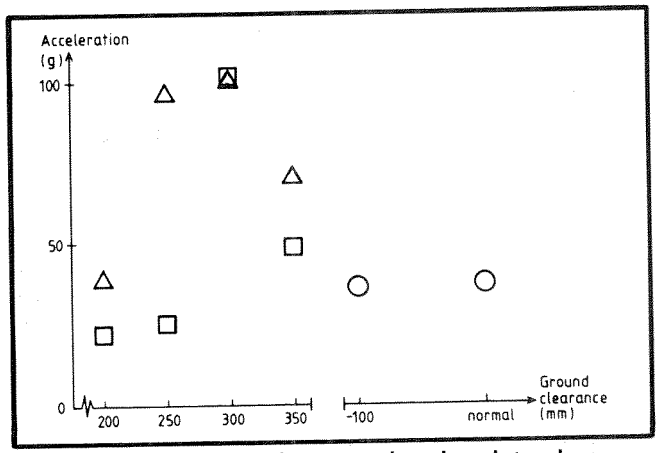

Figure 10. Maximum chest acceleration, lateral

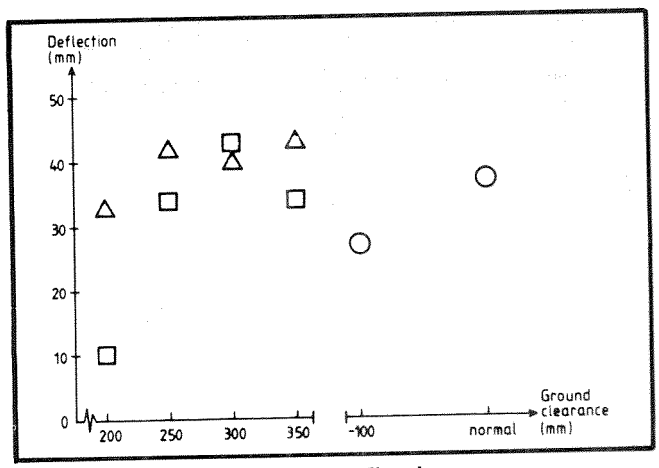

Figure 11. Maximum chest deflection, upper

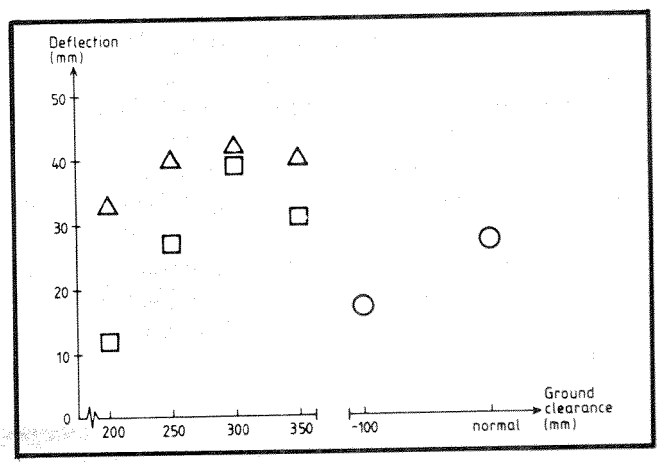

Figure 12. Maximum chest deflection, lower

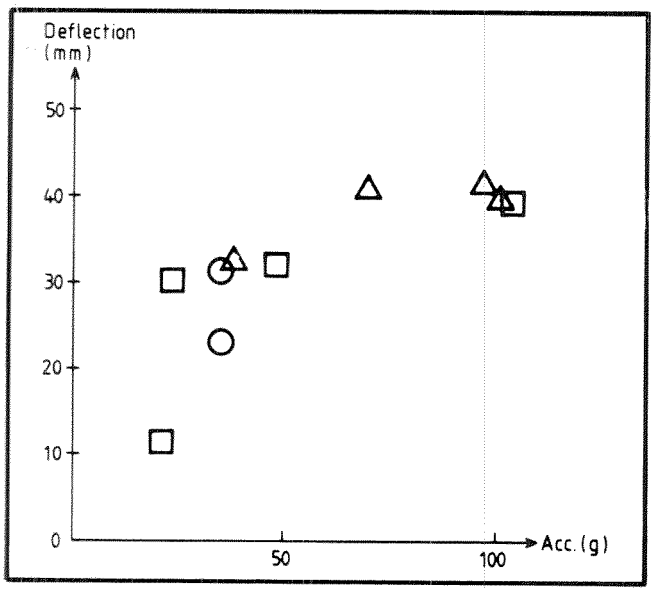

Figure 13. Relation between maximum chest acceleration lateral and maximum chest deflection (mean of upper and lower deflection values)

The maximum acceleration recorded in the pelvis of the dummy shows the same tendency as in the chest, i.e., a lower bumper level will result in lower accelerations in the pelvis (Figure 14).

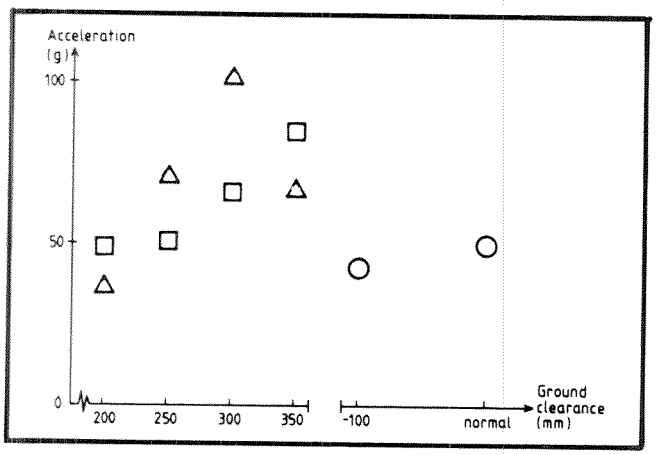

Figure 14. Maximum pelvis acceleration, lateral

The maximum velocity integrated from the acceleration measurements in the dummy is shown in Figures 15 and 16. The pelvis velocity is higher than the chest velocity, and the relationship between the ground clearance and these variables is more pronounced for the chest.

The permanent deformations of the side of the impacted vehicles were surveyed by a deformation measuring device (Figure 21). Deformations at the B-pillar at different levels are presented in Figures 17 to 20. The tendency of these deformations in relation to the ground clearance is as expected, and the magnitude of the deformation is approximately the same regardless of the type of bullet vehicle.

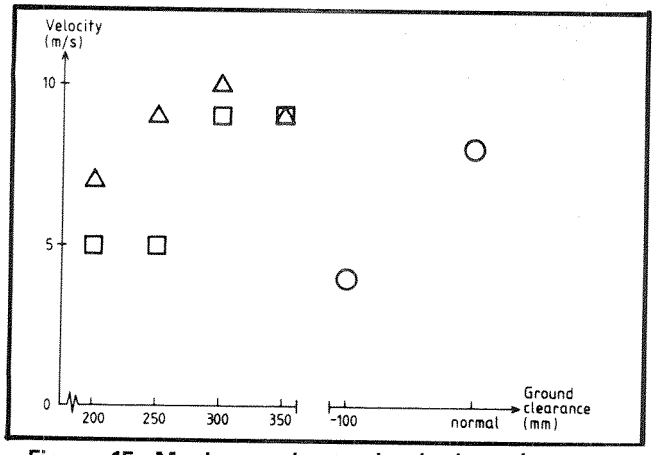

Figure 15. Maximum chest velocty, lateral

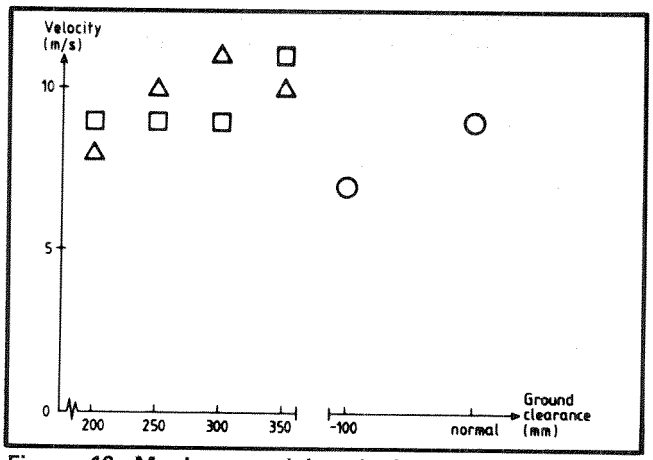

Figure 16. Maximum pelvis velocity, lateral

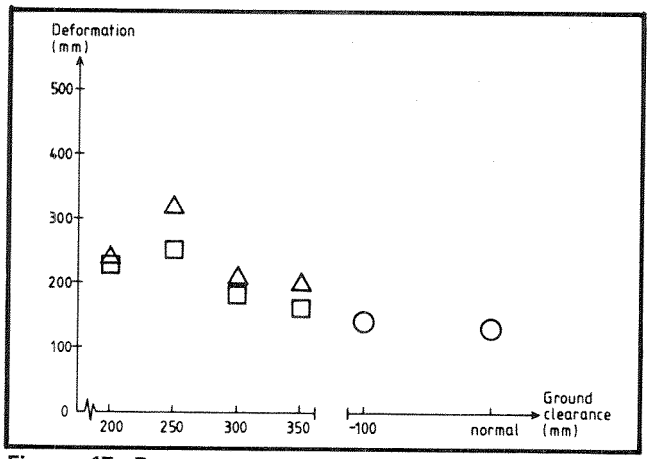

Figure 17. Permanent vehicle deformation at the B-pillar 300mm above ground level

In these figures, there is also a tendency that the deflection has a peak at the 250mm ground clearance level. This may be due to the fact that the EEVC front elements are not of a homogenous construction. There are calibration holes in the blocks, and in some circumstances these holes may coincide with strong parts of the target vehicle. This microscale phenomenon is not revealed in the macroscale verification tests in the specifications where the whole segment is evaluated. Further research about this problem is recommended.

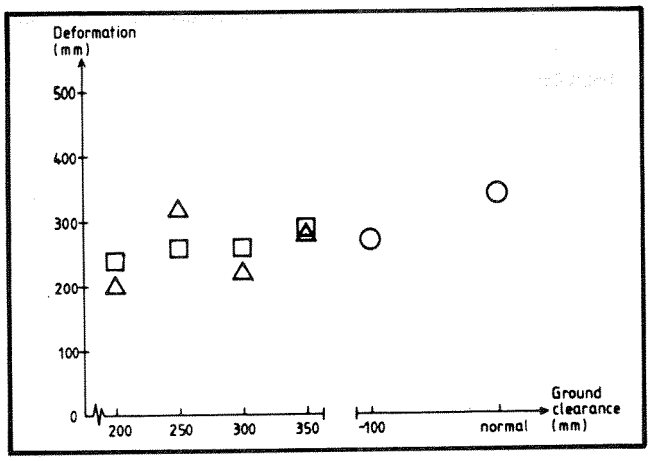

Figure 18. Permanent vehicle deformation at the B-pillar 500mm above ground level

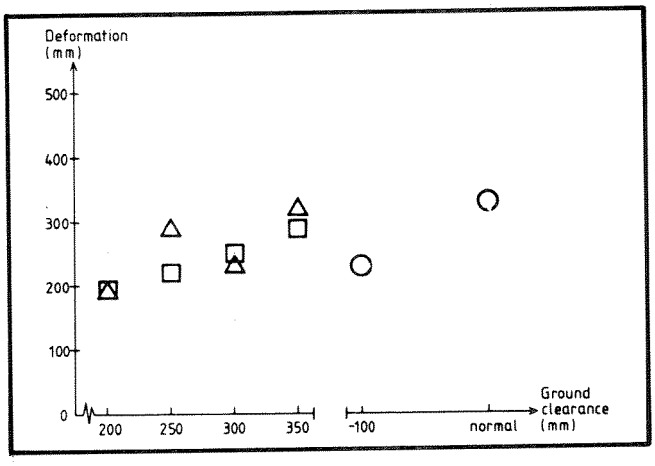

Figure 19. Permanent vehicle deformation at the B-pillar 700mm above ground level

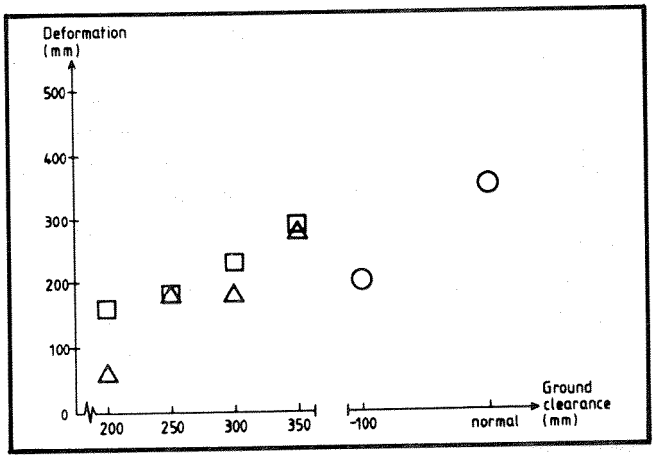

Figure 20. Permanent vehicle deformation at the B-pillar 900mm above ground level

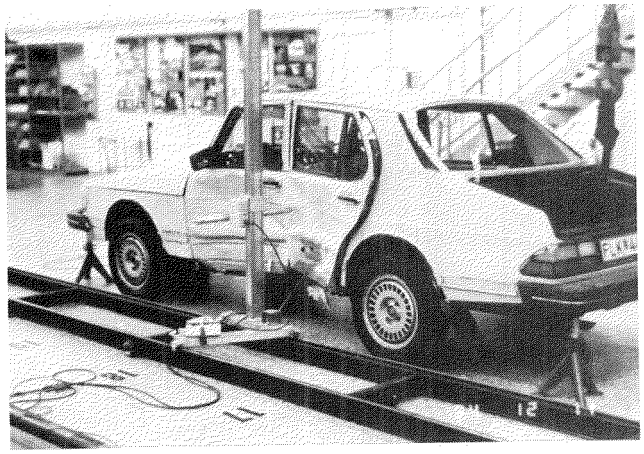

Figure 21. Deformation measuring device

Pedestrian Impact Evaluation

Mechanical Model

The dummy leg used in this project is a simplified version of the leg in a rotationally symmetrical adult pedestrian dummy developed to measure the aggressiveness of the car front in a collision(8).

The main purpose of this work was to measure the forces and torques in the lower extremities, especially at knee level in impacts at different bumper heights.

The dummy leg consists of two steel tubes simulating the long bones of the human upper and lower legs and a steel bar simulating the knee. To enable comparisons of results from previous experiments with cadaver legs, parameters such as mass, length, center of gravity, and moments of inertia were chosen in accordance with the real conditions in these experiments (Figure 22). The forces in the vicinity of the knee were measured with strain gauges mounted on steel tubes simulating the upper and lower legs. The bending moment, the shear force and, if necessary, the tensile force, and the torque about the longitudinal axis can be calculated from these data. The steel bar simulating the knee was designed to withstand the same lateral bending moment as a human knee. The bending strength of the knee in a lateral collision was calculated using strength data for the medial collateral ligaments, the cruciate ligaments, and the geometry of the knee(9,10).

The fact that the dummy was simplified to include only three elements is not believed to seriously affect the forces around the knee during the first part of the events(11).

Test Setup

The concentrated mass of the body was connected to the dummy leg by a universal joint. The dummy was

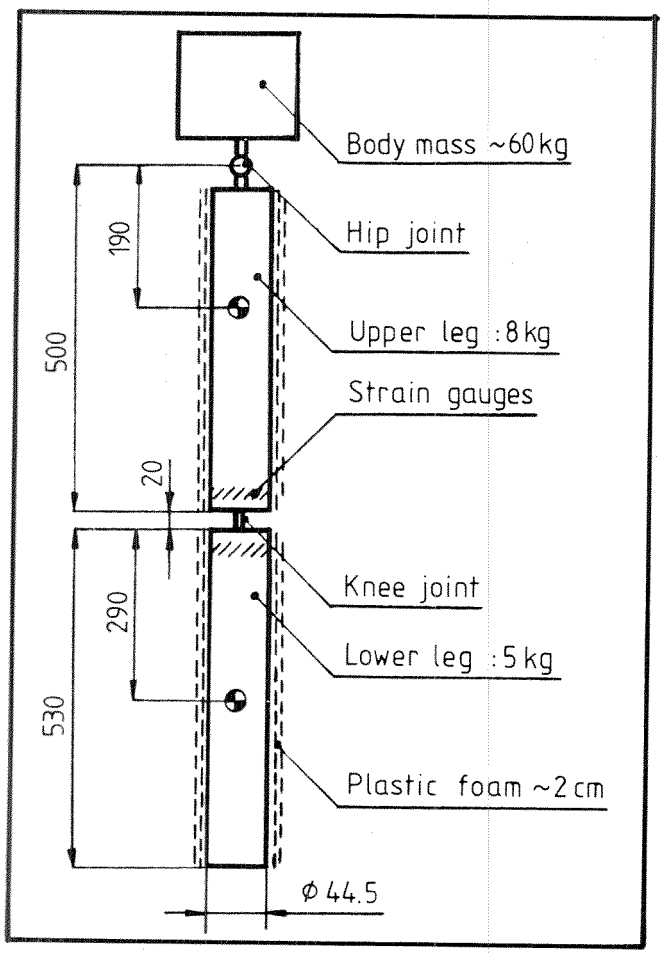

Figure 22. Mechanical model of rotationally symmetrical pedestrian leg dummy

balanced on a platform in an upright position by means of wires until a few milliseconds before collision. The impact height was varied by lowering or raising the platform supporting the dummy leg. The data from the strain gauges were registered according to SAE 32116, and the collisions were filmed with a 16mm high-speed camera at 500fps.

Two test series were made with the same dummy leg. During the first series of tests, only two types of bumpers were used:

- Rigid nondeformable steel bumper, 30mm high
- The same bumper with 150mm plastic foam

The tests were performed at a constant velocity of 26km/h at four different impact heights:

- Very close to the knee (h = 0.45m above the ground)
- Between the knee and the center of gravity of the lower leg (h = 0.28m)
- Near the center of gravity of the lower leg (h = 0.25m)
- Below the center of gravity of the lower leg (h = 0.18)

In the second series of tests, a complete car front from the National Highway Traffic Administration (NHTSA) of the U.S. Department of Transportation was used as shown in Figure 23. The point of impact was chosen very close to the knee (h = 0.45m). The velocity was varied from 30km/h down to 10km/h.

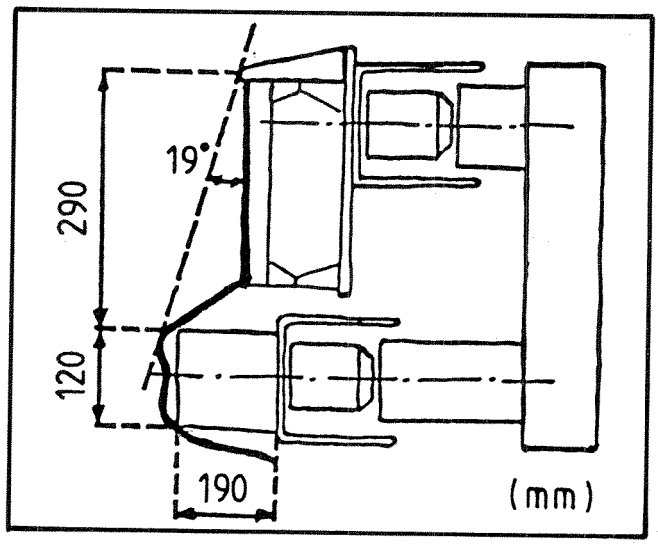

Figure 23. Section of impact zone of NHTSA car front

Mathematical Model

The MADYMO Crash Victim Simulation Programs were validated using the laboratory impact tests made on the rotationally symmetric dummy leg. The problem was to simulate a dummy leg with a knee joint consisting of a steel bar by means of a mathematical model intended primarily for ball-and-socket joints. The standard model in MADYMO describing the resistance in a joint against the relative movement of the two connected elements consists of a nonlinear spring, a viscous damper, and a dry friction component connected in parallel with each other. With this construction, it is not possible to simulate the elastic part of an elastic-plastic material having hysteresis in the unloading phase (Figure 24).

Such a simulation requires a series connection between a dry friction and a nonlinear spring or a differential description of the material. However, if the elastic region (Figure 24) is small compared with the total region used in the simulation, it may be sufficient to use the dry friction component of the total moment. In the simulations presented, the knee joint has been described using only the dry friction component of the resistive moment in the steel bar. The value of the dry friction component has been estimated both from material data for standard steel 2172 and empirically from test data from a statistic bending test. The characteristics of the soft parts of the leg, like the force-penetration function, were also determined by means of static tests. This should be kept in mind while comparing the results of the simulations with the results of the dynamic tests.

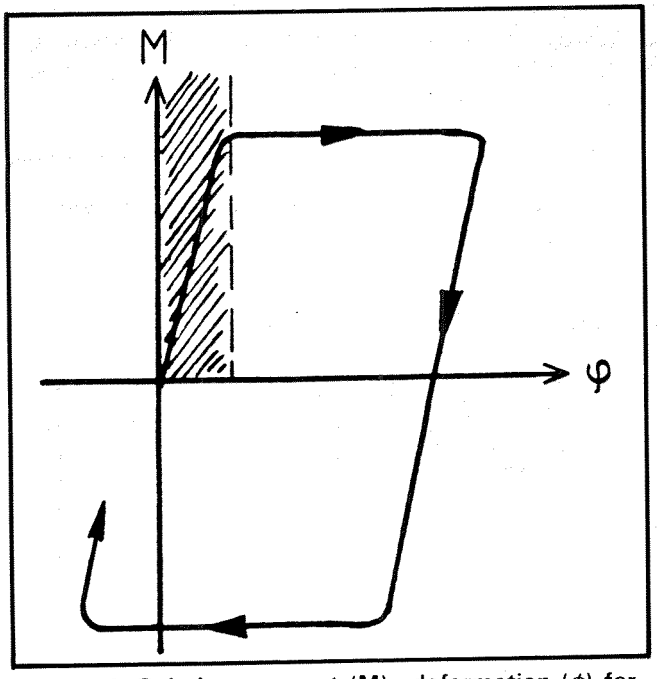

Figure 24. Relation moment (M)—deformation (ϕ) for an elastic-plastic material with hysteresis

Pedestrian Impact Test Results

Forty tests were made with the mechanical model in two series.

Figures 25 to 27 show the bumper force (at the point of impact), the shear force, and the bending moment about the knee for various impact heights in the first series of tests.

The bending moment about the knee in both series is expressed as a percentage of the maximum bending moment a living human knee can withstand without

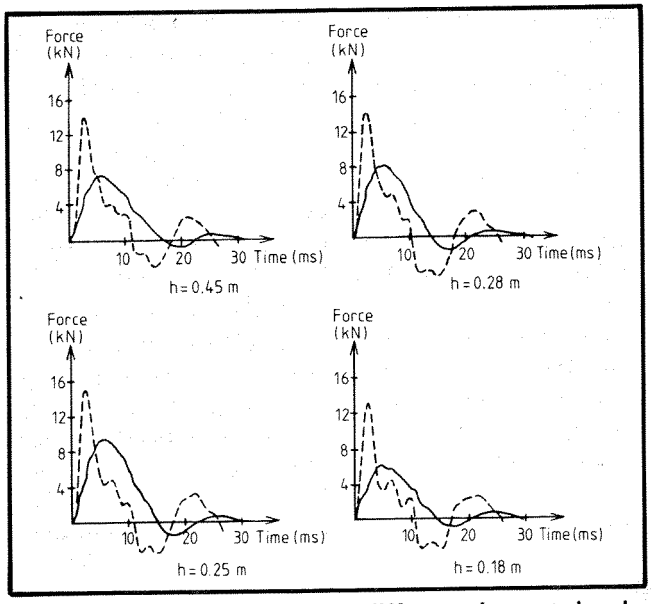

Figure 25. Bumper force for different impact levels (solid line—soft bumper; dashed line—rigid bumper)

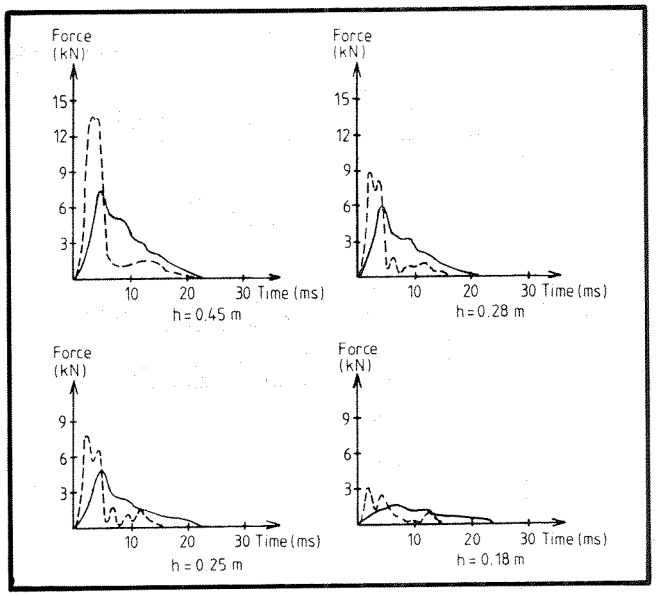

Figure 26. Shear force about the knee for different impact levels (solid line—soft bumper; dashed line—rigid bumper)

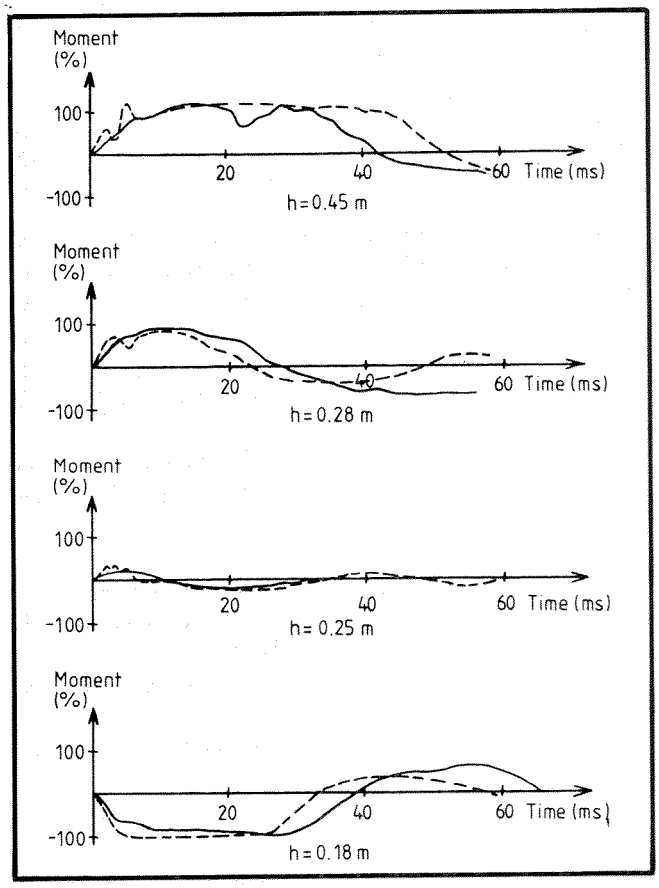

Figure 27. Bending moment about the knee for different impact levels (solid line—soft bumper; dashed line—rigid bumper)

being injured. Bending moments exceeding 100 percent can tear the ligaments and/or result in fractures, e.g., the tibial condyle.

Figure 28 shows the bending moment about the knee as a function of the impact velocity in the second series of tests.

The peak bumper force varied between 13.5 and 15.0kN for the rigid bumper and between 6.0 and 9.5kN for the soft bumper (Figure 25). The force pulses were somewhat more extended in time for the soft bumper. The time histories of the shear forces about the knee (Figure 26) were similar to those of the bumper forces. The peak values were 50 percent lower for the soft bumper. The bending moments (Figure 27) were 100 percent when the bumper levels were 0.45m and 0.18m above the ground. The bending moment is low (30 to 40 percent) only at impacts near the center of gravity of the lower leg.

The inertia of the lower leg and foot are probably the most important injury-causing factors when the impact point is high (h = 0.45m). The injury-producing effect of the inertia is seen even at low velocity (10km/h) (Figure 28).

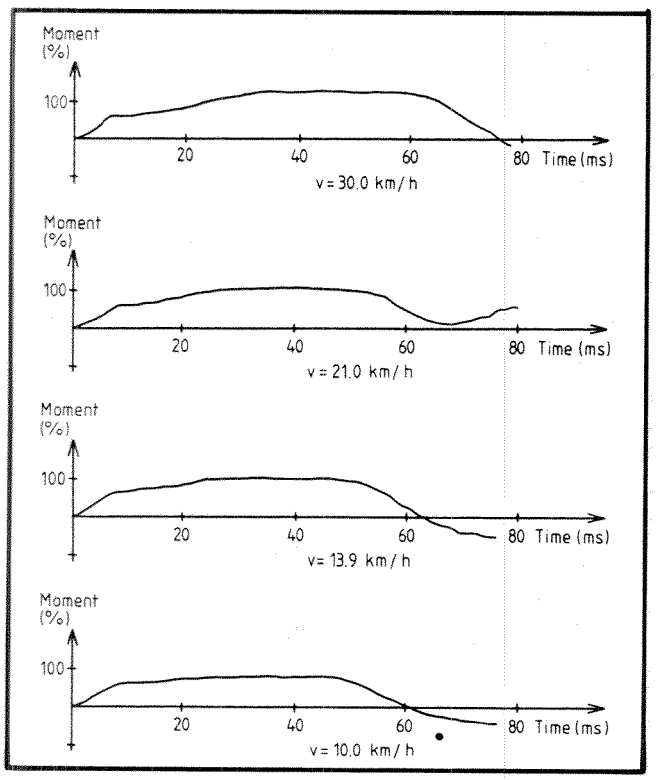

Figure 28. Bending moment about the knee for different velocity (h = 0.45m)

Figures 29 to 31 show the results of the mathematical simulations and the evaluation with the mechanical model. Despite the misleading graphics, the struck object does not represent the general shape of a complete dummy but only the simulated mass concentrated in a sphere, the upper, and lower leg. The concentrated mass of the body is connected to the leg by a ball joint. The foot and the ankle are integrated in the lower leg. There is no frictional force between the leg and the ground. The impactor represents a hard bumper without a car front, and the bumper is rigid. All three simulations (Figures 29 to 31) are made with a constant velocity of 26km/h. The impact heights were h = 0.45m (Figure 29), h = 0.25m (Figure 30), and h = 0.18m (Figure 31).

As expected, the best correlation between the experimental results and the mathematical simulations is obtained for the case where the deformation in the knee joint (steel bar) is plastic during the major part of the event, i.e., the case where h = 0.45m (Figure 29). In both of the other cases (Figures 30 and 31), the deformation is either elastic or in the vicinity of the elastic limit, thus

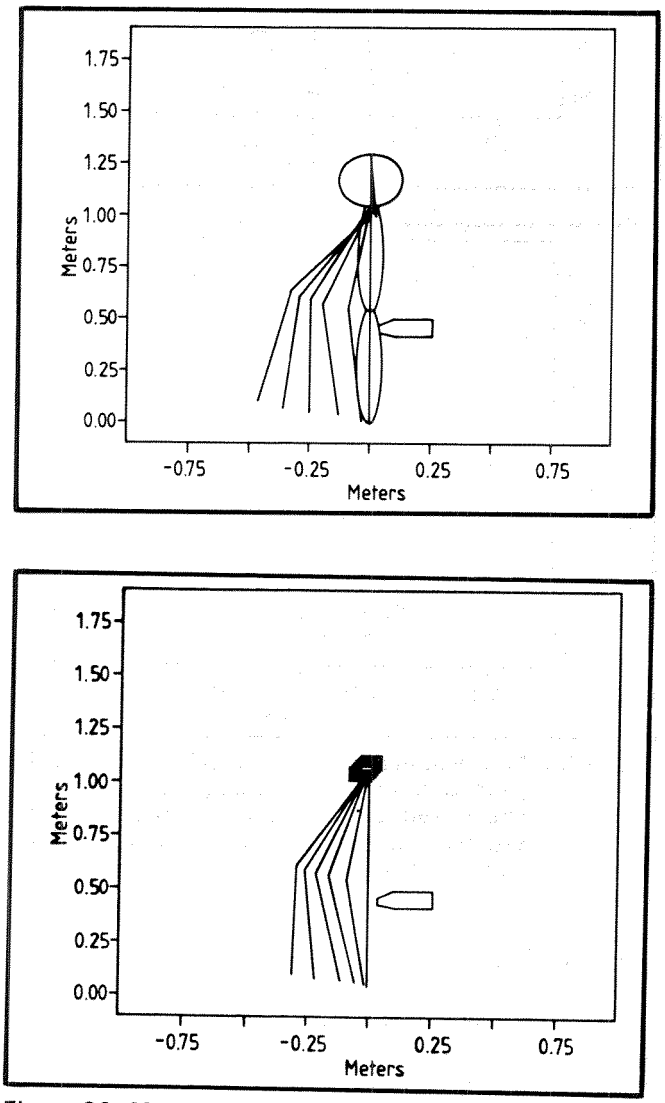

Figure 29. Mathematical and mechanical simulations of pedestrian impact—impact point h = 0.45m above ground (upper segment—body; middle segment—upper leg; lower segment—lower leg; Δt = 10ms)

falling in the region where the chosen approximation of the knee proves insufficient. However, the tendency is quite obvious, and deformation of the knee joint is in the same direction as that of the laboratory experiments. When the first point of impact was near the center of gravity of the lower leg, the knee deformation was low.

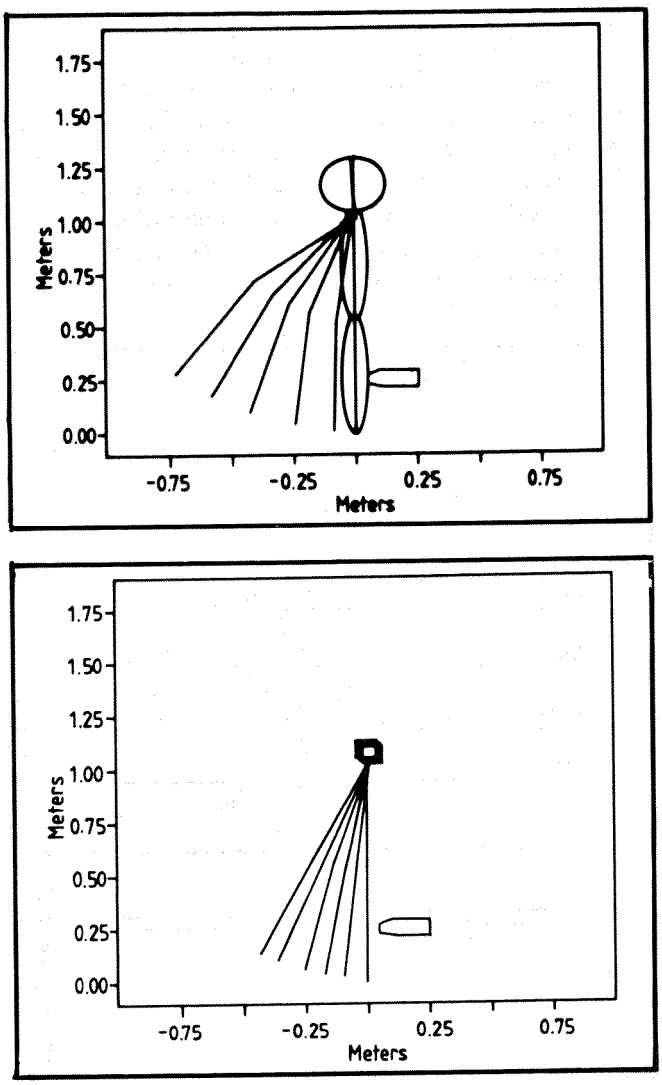

Figure 30. Mathematical and mechanical simulations of pedestrian impact—impact point h = 0.25m above ground (upper segment—body; middle segment—upper leg; lower segment—lower leg; Δt = 10ms)

Discussion

The intention of this project was to simulate the effect of lowering the bumper of a passenger car.

When the choice was made to use the EEVC MDB as a bullet vehicle in the side impact tests, it was obvious this would lead to some simplifications. As the face of the barrier has a defined height, the only way to simulate the different bumper levels was to move the entire block vertically. It is uncertain whether a future car with a lowered bumper will also lower its entire front face in the same magnitude. In spite of this problem, it was decided to use an MDB to enable general conclusions that would have been difficult if a specific car had been used as a bullet vehicle.

It is disappointing the APROD dummy did not discriminate to a higher degree between the different levels of violence. It is clear from the results that the lowest ground clearance produced significantly lower chest deflections than any of the other clearances. These results suggest that the lateral deflection characteristics of the dummy are extremely progressive in the upper half of the 50mm stroke. It could be questioned if this response is humanlike. Another possible explanation could be that the shoulder bottoms out and transfers much of the loading to the spine. This is, however, not

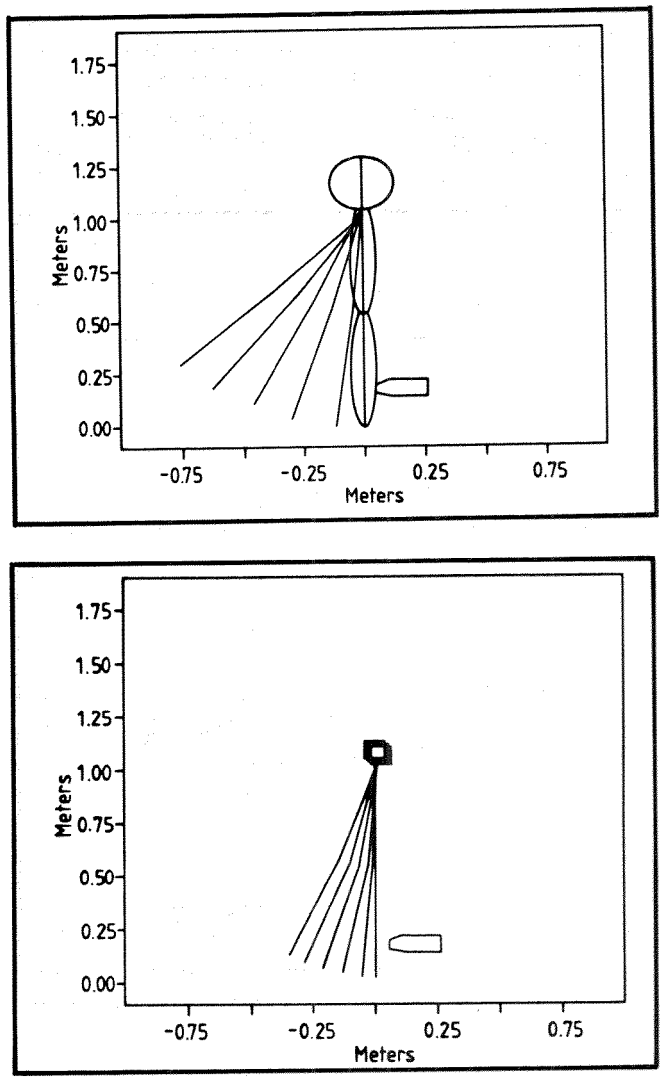

Figure 31. Mathematical and mechanical simulations of pedestrian impact—impact point h = 0.18m above ground (upper segment—body; middle segment—upper leg; lower segment—lower leg; Δt = 10ms)

very probable since the dummy was positioned so that contact between the B-pillar and the shoulder was prevented.

The accelerometer maximum readings in the pelvis show a clear trend toward a decreasing magnitude with decreasing ground clearance. This supports the theory the chest deflection should have had a larger variation for the different test heights.

The high-speed films show the roll angle of the impacted car is influenced by the ground clearance. From this project, it is not possible to quantify the effect of this phenomenon, but it points out the importance of further investigation of this matter.

The velocity profile of the intruding door is known to be an injury-explanatory parameter. The methods used in this project to assess this velocity were not satisfactory and, therefore, these results have been omitted. It is, however, recommended that feasible methods to record this velocity be developed.

This work has shown that changes in ground clearance of 50mm can influence the results. It is uncertain to what degree the nominal ground clearance could be kept at the time of impact in this type of testing. If the barrier is pitching up and down due to irregularities in the paving of the test track, the actual ground clearance at the time of impact may vary within a couple of centimeters. The target cars will also vary in height due to equipment, loading, tire pressure, etc. If entirely controlled test conditions are desired, the parameter that should be defined is the barrier location in relation to the car at impact.

This report shows experiments with a pedestrian dummy leg with sophisticated instrumentation can provide valuable insight into the effect of changing the impact point. It is planned to mount this leg on a complete pedestrian dummy(1). Further testing with this dummy may confirm the findings in this report and also demonstrate the influence of the bumper level on gross kinematics and head and chest impact violence. As pointed out above, the description of the knee in the MADYMO model is not suitable for simulation of the mechanical model of the leg used in this project. It is necessary to change the MADYMO model slightly to develop a versatile tool for engineering pedestrian leg injury mitigating car fronts.

Conclusion and Recommendations

It is evident from these test results there is a correlation between the collision load transfer height and the injury level of the struck occupant in side impacts. The new test methods used, and the limited number of tests that could be made, limit the confidence level of the results.

It is therefore recommended these findings be used to demonstrate the need for further development of test methods and equipment and evaluation of how much lower the optimum bumper or load transfer level should be.

Measurements of present car bumper levels showed that most are at about 450mm. At full braking at urban speeds, this level decreases approximately 90mm after a braking distance of 8m. Consequently, in most urban side collisions, a fully developed dive seems very unlikely.

A general comparison between the EEVC MDB and the Peugeot 305 used as bullet vehicles shows that the EEVC MDB can be used as an acceptable test device even in the crabbed configuration. The value of using the more complex crabbed mode should be investigated further.

Possible problems with the performance of the EEVC front elements at local loads have been observed, as well as problems with the deflection measurements in the chest of the APROD dummy. Further research in these areas is recommended.

The pedestrian impact evaluation part of this project indicates the following:

- For each impact velocity, the soft bumpers caused lower forces than the rigid ones. The bumper forces were highest at impact points near the center of gravity of the lower leg.
- The bending moment about the knee was lowest at impacts near the center of gravity of the lower leg. The use of soft or hard bumpers did not significantly change the maximum value of the bending moment about the knee.
- The shear force about the knee was diminished with decreasing impact height and was lower in collisions with soft bumpers.
- When the first point of impact was close to the knee, the bending moment exceeded the maximum tolerable level. This was true even at very low impact velocities.

The results from both series of tests confirm the previous clinical and experimental observations that there is a correlation between both the level and the compliance of the bumper and the seriousness of the injuries to the knee(12,13).

Problems with the use of conventional mathematical models for the simulation of an advanced leg model have been recognized.

References

1. *Federal Register,* 49 Transportation, NHTSA Part 581, Bumper Standard, 1981.

2. ECE Regulation 42, "Uniform provisions concerning the approval of vehicles with regard to their front and rear protective devices (bumpers, etc.)," 1980.

3. Thomas, et al., "A synthesis of data from a multipurpose survey on pedestrian accidents," Proceedings 3rd IRCOBI Conference, Amsterdam, 1979.

4. EEVC Working Group 6, "Structures," Final report, 1982.

5. Klaus, G., R. Sinnhuber, and G. Hoffmann, "Mobile deformable barrier for lateral collision testing—a contribution toward a harmonization of future side impact performance requirements," SAE Paper 840888, Washington, D.C., 1984.

6. Hue, B., Y.C. Leung, C. Tarrière, and A. Fayon, "Design of APROD-dummy," Seminar on the Biomechanics of Impacts in Road Accidents, Brussels, 1983.

7. ISO Standard 6487, "Road vehicles—techniques of measurements in impact tests—instrumentation," 1980.

8. Aldman, B., et al., "A new dummy for pedestrian tests," Proceedings Tenth International Technical Conference on Experimental Safety Vehicles, Oxford, 1985

9. Aldman, B., L. Thorngren, O. Bunketorp, and B. Romanus, "An experimental model system for the study of lower leg and knee injuries in car pedestrian accidents," Proceedings Eighth International Technical Conference on Experimental Safety Vehicles, pp. 841-849, Wolfsburg, 1980.

10. Kramer, M., K. Burow, and A. Heger, "Fracture mechanism of lower legs under impact load," Proceedings 17th Stapp Car Crash Conference, pp. 81-100, Oklahoma, 1973.

11. Wijk, I., J. Wismans, J. Maltha, and L. Wittebrood, "MADYMO pedestrian simulations," SAE Symposium Pedestrian Impact Injury and Assessment, Detroit, 1983.

12. Bunketorp, O., "Pedestrian leg protection in car accidents. An experimental and clinical study," Diss. Department of Orthopaedic Surgery II, University of Gothenburg, Gothenburg, 1983.

13. Aldman, B., O. Bunketorp, R. Eppinger, and J. Kajzer, "An experimental study of a modified compliant bumper," Tenth International Conference on Experimental Safety Vehicles, Oxford, 1985.

Appendix

Review of the Bibliography Concerning Vehicle Front Structure Characteristics and Their Consequences for Pedestrian Injury Mitigation and for Other Goals

Background and Objectives

This review was made by T.E.A. Benjamin from France during the period 1982-83 and includes 42 technical papers from a total of 72, of which reference is stored in the OECD/IRRD retrieval system.

The objectives of the review were to examine and collate information concerning the scientific methods used and the conclusions reached by the authors of these papers with particular focus on—

- The consequences, in terms of pedestrian injury frequency and severity of various vehicle (essentially passenger car) front structure configurations, special reference being made to bumper height
- The consequences for the occupants of passenger cars laterally impacted by various front structure configurations of the striking vehicle
- Information concerning the possible consequences, in terms of vehicle aerodynamics (with its influence on fuel consumption) of injury-mitigating changes to front structures

The conclusions drawn from this review can be used to improve the relevance of upgrading vehicle structural standards that will reflect the best compromise between requirements that may be conflicting—

- Between road user groups at risk: adult pedestrians versus child pedestrians; pedestrians as a whole versus laterally impacted vehicle occupants
- Between vehicle safety performance goals and other goals: energy conservation (via aerodynamic performance and weight reductions); considerations of production costs and of repair costs

Further, the conclusions can be used to increase the relevance of tests used in research and in vehicle or component type approval by rendering the test conditions maximally representative of real-world accident circumstances and injury mechanism and to establish baseline safety performance data on current vehicles so the consequences of future upgrading can be measured.

Even if one considers solely the problem raised, it can be seen that the range of conditions in which pedestrians are impacted and in which their injuries are produced includes combinations of all the following:

- Different vehicle front structure combinations (especially bumper height width shape deformability, bumper lead angle, bonnet height)
- Various impact speeds
- Various degrees of pitch
- Pedestrians having various (to some extent age-dependent) characteristics (life cycle stage and state of health, overall knee and hip height, mass and mass distribution, bone quality)
- Different postures in relation to the front structure
- Different weight distribution on each leg caused by walking or running
- Different shoe/roadway friction characteristics
- Different body segment kinematics in relation to vehicle zones of different stiffness

Review of Conclusions Concerning Pedestrian Injury Frequency and Severity

Bonnet Height, Leading Edge, and Other Characteristics

In the earliest paper(22), it is stated that the selection of an optimal bonnet height involves a dilemma: a high front may knock an adult under the car at low speeds and throw a child forward at most speeds with a high risk of head-ground impact. A low front reduces these risks but increases the possibility of head-windscreen surround impact (particularly for adults). A long bonnet—1,100mm or more—reduces this latter possibility. The bonnet leading edge should be made of an energy-absorbing material (yield: at least 150mm and preferably much more) that matches adult pelvis and child thoracic tolerance levels.

Optimal bonnet shape is very sensitive to bonnet parameters(40); the principal design problem being that of avoiding head contact (see also below: Devices: Induced Kinematics). Bonnet properties should associate appropriate stiffness with crush depth (idem). It is recalled that head injuries are the main cause of death (N:211), the windscreen frame being the main fatal contact point(8).

The same author(10) found that pelvic fractures were mostly likely to occur when the relative bonnet height was in the range 0.46 to 0.50, and suggested the interesting concept of bonnet effective height: the height acquired by the bonnet due to its deformation during impact. Acting in combination with the bumper, the bonnet leading edge should minimize rotational acceleration and head velocity(16). Bonnet edge height, in cases where bumper lead angle is below 60°, does not seem to influence adult leg injuries, but it may increase risk of injury to children's heads, necks, and torsos(14).

An important feature of the high leading edge profile—tested alongside medium and low variants(41)—is that adult and child head impact velocities are consistently below vehicle impact speed. The child thorax/pelvis contact problem this profile engenders can be reduced by increasing bumper lead. With various medium and high leading edges, further reductions in severity can probably be achieved, but this will call for further study of stiffness and geometry.

Bumpers: Energy-Absorbing; Force-Limiting

As early as 1974(26), it was stated that bumpers should be energy-absorbing, their softening up being agreed to be beneficial(32) but seeming to accentuate the influence of ground reaction in the injuries sustained (net result: injury severity seems not to be reduced). It is suggested(40) that bumper and grille padding significantly reduce lower body injury (pelvis acceleration and knee force) it being considered(2) that while bumper force can be reduced by a deformable bumper structure, not all the knee reaction forces can be so reduced.

One group of papers(17,19), Fifth ESV Conference (various authors)(25,30,33,34,35) is mostly concerned with the U.S. FMVSS 215 standard, that is to say, with very low (up to 8km/h) impacts.

Bumper Height

In the earliest paper(32), attention is drawn to what sometimes seems to be a difficulty. In experiments, the lowered bumper height (from 508 to 355.6mm) reduces adult knee injury and limits pelvic and abdominal involvement—head velocity for the lowered profile, however, being almost twice as high as for the standard profile. In other experiments(13), bumper heights of less than 400mm did not produce head impact more frequently than higher bumpers. The FMVSS 215 standard is stated(7) to require a minimum bumper height of 400mm; it is also being pointed out(36) that adult knee height (500mm) coincides with the top of bumper height standardized by FMVSS 215 and ISO. An upper edge at 400mm would, in that author's opinion, produce a gain of 25 percent.

Looking at Swedish work in sequence, we see(1) that the 450mm bumper caused significantly greater injury than the 250mm version and that injury would be reduced by a bumper lead angle of less than 60° and lowered static level from 450 to 350mm, such a bumper to be energy-absorbing and force-limiting and to strike the lower half of the tibia. This is corroborated(23): The bumper should strike near the tibia/fibula center and well above the ankle joint. There seem to be other advantages: When the

leg is struck at its center of percussion (approximately 317mm for adults and 203mm for a 6-year-old child dummy), negligible forces are generated in the hip but vehicle front and ground contact could still produce high values(11). The same author cites some effects of bumper height extremes: Intolerably large knee bending moments are generated by high (about 508mm) bumpers, and a height of about 254mm reduced this to zero.

The negative effects of high bumpers are cited elsewhere(10). In a subsample of knee injury victims (N:44), 70 percent were struck by bumpers in the height range 450 to 540mm; in only 11 percent of cases was it less than 400mm. The same author(9) reports that 92 percent of knee injuries were caused by bumpers in the relative bumper height range 0.26 to 0.33 (corresponding to 420 to 530mm, taking 1.6m as average pedestrian height) and raises another complicating factor: that lowered bumpers reduce fracture probability but, at a relative bumper height in the range 0.16 to 0.20, ankle injuries—especially at high speed—can occur.

Some of the proposals made are as follows. To reduce adult leg injury severity, a bumper lower than the 380mm knee height (60 percent of a British sample) would reduce leg impact forces and bending moments across the knee(23). A height in the range of 305 to 356mm has been proposed(11). Optimum static bumper height for adults should be 340mm(14). The last mentioned author also reports that in a follow-up of disability, six out of seven cases of walking impairment were due to bumper heights at or above 400mm. In an anthropometry-dependent proposal, it is suggested(26) that the bumper should be below the height of the adult knee and below that of the child's pelvis (6-year-old's height). This indicates the need for anthropometric data on the population at risk (Writer's note).

A height of 375mm from ground to top of bumper in semi-laden conditions is proposed(22). Such a bumper should have energy-absorbing characteristics with a yield of at least 100mm. The same author(24) later suggests, however, that the following configuration (bonnet height: 700mm, combined with either a bumper at 375mm or a bumper lead of about 150mm or more) may allow excessive torso rotation and increasing risk of head-ground impact. It is stated that, in experiments, the 500mm bumper always reduced risk of head-windscreen surround impact. The combination finally proposed is as follows: For thoracic/head impacts to the bonnet, both adults and children would seem to benefit from the 700mm bonnet height, a 50mm bumper lead, and, to reduce leg injuries, a crushable 500mm bumper (combined with a crushable secondary bumper mounted at 300 to 350mm and below and about 50mm behind the primary bumper).

From epidemiological research(13), it was established that the bumper level parameter has no effect on healing time.

Bumper Lead and Lead Angle

Bumper lead cannot be assessed in isolation. Reducing lead benefits the second leg struck, but there is a corresponding increase in the contact loads of the hip and femur with the front end. Bumper lead should mainly be considered as a means for reducing front end contact loads—typically, 127mm dependent on front end height(11).

Decreasing bumper lead (increasing bumper lead angle) is associated with decreased bumper contact fractures and increased leading edge contact fractures. All acetabulum fractures involved elderly adults and vehicles with relative leading edge height in the range 0.45 to 0.51 and short bumper leads(9).

Conflicting goals appear to exist from a reading of the following: While it is stated that risk of knee injury will be reduced if bumper lead angle is below 60° (that is, if bumper lead is long) and found in conjunction with a force-limiting and energy-absorbing bumper(14), it has also been concluded(28) that, independently from bumper height, increasing bumper distance brings head impact areas nearer to the windscreen.

Bumper Width and Shape

Broad, flat-faced, or slightly rounded surfaces with rounded top and bottom edges would reduce bumper leg forces, maximum bending and crushing stresses, and leg rebound velocity(22).

Devices: Head Injury Mitigation

It is stated(29) that pedestrian kinematics can be controlled so impact is as close as possible to the bonnet center, which has a built-in honeycomb structure for impact energy absorption. No results, however, are provided.

Devices: Induced Kinematics

A low-mounted energy-absorbing bumper (yield: at least 100mm) and bonnet leading edge (yield: at least 150mm; preferably much more) would help direct the pedestrian head toward a suitably designed energy-absorbing bonnet(23). A device has been developed to retain adult pedestrians on the bonnet and to help lift a child onto it(22). It is also suggested(40) that a hood with a high coefficient of friction of its surface could increase head protection when the pedestrian's arm or elbow interacted with it.

Epidemiology (Related to Test Conditions)

Impact Direction—Pedestrians are normally struck from the side (79 percent of a sample of 211 at ±22.5° to the vehicle's path(8); almost always laterally(5); laterally in 84 percent of cases (N:87)(39). NB Cadaver experiments indicate(15) that, when laterally impacted, pedestrian head impact speed is approximately the same as car impact speed; when impacted to their front, it is higher.
Pedestrian Pace at Impact—Two epidemiological studies(39,8) provide data: for the former, 42 percent walking, 47 percent running, and 8 percent standing. For the latter, 25 percent of adults less than 60 years old and 76 percent of children were running.
Average Vehicle Profile—In (39) this was unloaded bumper height 420mm, front face upper edge 730mm, and distance from front face to windscreen 1,110mm.

Impact Speeds

It is thought worthwhile to draw up these data in a collated form in spite of the fact the source documents reporting on experimental and epidemiological studies and the data are of different types (based on samples of different size and representativity for the accident data and on different test conditions for the experiments). The following has been noted:

Speed or speed b (km/h)	and Remarks and source
17	AIS 3 injuries occur at speeds as low as this(1)
20	No vehicle contact injuries (N:211) at less than this(8)
20-25	Risk of severe injury exists laterally and frontally(15)
20-35	Ligament strain noted(10)
24.8	Side impact leg fracture threshold(*)(18)
32	Frontal impact leg fracture threshold(*)(18) Speed arbitrarily selected for experiment as being the fatal impact speed threshold(40)
33	In a pedestrian accident sample (N.72) 50 percent were at impact speeds below this(37)
34	Mean impact speed in fatal and nonfatal accidents(5)
35-45	Complete ligament rupture noted(10)
36	Average impact speed(N:87): 29km/h for injured; 51km/h for killed(39)
40	Probable limit to pedestrian protection(24)
50	No adult life-threatening/fatal contact injury at less than this(8)

* No cadaver age or bone condition data were given.

The demographic/anthropometric scatter of the population at risk takes on its full meaning when one reads that at comparable impact speeds vehicle front contact injuries appear to be age-dependent(8). In a later study(9), the same author reported (N:211) assessed impact speeds as less than 20km/h: 12 percent; 21 to 40km/h: 57 percent; 41 to 60km/h: 25 percent; and above 60km/h: 4 percent.

Research Needs

Epidemiological—With so much attention directed at narrowly limited body segments and injury mechanisms, it is not surprising that there is a call(32) for close examination of overall injury potential. A part of this close examination should apparently be long-term effects: Leg injury effects are not well correlated with primary injury severity nor impact speed(13), and more research is needed. The same theme is cited(31) in relation to knee injuries that may lead to degenerative arthritis. He states that recognition and early treatment of extremity injuries should decrease long-term disability.

In another area, it is suggested(7) more data are needed to resolve areas of conflict (quantification of trade-off factors such as those in the field of bumper height optimization for adult versus child pedestrian protection).
Methodological—There is a call for more complex test procedures that take account of hip reaction forces and knee joint angulation(10) and for a more precisely defined injury-scaling method for bumper-leg contact(1).

Test Conditions (See Also Epidemiology)

Dummy/Cadaver Posture—The portion of the walking cycle that gives the most serious impact loading is with 90 percent of body weight on the fully extended leg closest to the vehicle(32). Dummies should be free-standing due to the influence on kinematics of foot friction(11); the reduction of ground contact forces increases angular rotation, which can sometimes lead to greater head impact velocities (idem).
Vehicle Pitch (Influence on Bumper, Etc., Dynamic Height)—The vehicle had started to brake in 54 percent of cases (N:87)(39); in 30 percent of cases (N:363)(10). Bumper mismatch, caused by vehicle pitch, can increase vehicle damage but may mitigate pedestrian injuries(7).
Other Points—In mathematical simulations, the method of modeling joint dynamic and static properties is critical(40).

Vehicle Aggressiveness: Ranking Methods

The mechanical leg model developed(2) can probably become an instrument for ranking bumper aggressiveness. The development is also reported(24) of a local impactor device for use horizontally (bumper-knee) or vertically (head-bonnet).

Vehicle Aggressiveness and Upgrading Priorities

While the bumper has been stated to be the most aggressive zone for adults and the bonnet for child injury(5), the point is made(13) that car front aggressiveness cannot finally be judged without noting long-term effects of injury. In accident samples, the bumper is reported on as follows: Among lower extremity/vehicle injuries, the bumper was responsible for 70 percent and the top part of the front end for 30 percent(N:87)(39). Also, 55 percent of nonminor leg injuries (N:211) were attributed to the bumper and a further 36 percent to the front structure above the bumper(9).

From an analysis (N:292) of accidents, the requirements of the age groups less than 15 years old and 15 years or more were stated(38) to be different and to suggest the need for two levels of reaction forces for some vehicle exterior elements (such as bumper contact stiffness). The same author(37,38) more generally suggests that vehicle features, including their deformation characteristics, should be adapted to the biomechanical load values of victims' body segments contacted and that vehicle layout upgrading priorities should be based on such capacities in an age-dependent way.

The problem is shown as being not only to upgrade vehicle features but also to combat the deleterious effects of some add-on items: Bullbars (as used in Australia)(16) amplify front end aggressiveness and negate the effects of positive design features.

Struck-Striking Car Compatibility in Side Impacts

Two not very recent references make up the sum of data. It is stated(7) that one aspect of the FMVSS 215 standard has been to increase front end aggressiveness, one aspect of this being a mismatch in side impacts between the striking car's bumper and the struck car's side beam. A different view comes from (27), which asserts that the 5mph energy-absorbing bumpers lower the aggressiveness of vehicles fitted with them and do not degrade the small benefits, for unrestrained struck-side occupants, achieved by side door reinforcement beams.

References

1. Aldman, B., B. Lundell, L. Thorngren, O. Bunketorp, and B. Romanus, "Physical simulation of human leg-bumper impacts," 1979.
2. Aldman, B., L. Thorngren, O. Bunketorp, and B. Romanus, "An experimental model for the study of lower leg and knee injuries in car-pedestrian accidents," Proceedings Fifth IRCOBI Conference, 1980.
3. Aldman, B., and O. Bunketorp, "Lower leg injury prevention by vehicle design," Chalmers Tekniska Högskola Göteborg, Transport Research Delegation Stockholm, Commission of the European Communities, Brussels, 1981.
4. Anonymous, One-page summary in "The voice of the pedestrian" (International Federation of Pedestrians) of: Fosser, Stein, "Under-run guards and lorries—an investigation into the feasibility of reducing the severity of injuries resulting from collisions between heavy vehicles and other road users," Institute of Transport Economics, Oslo, 1980.
5. Appel, H., G. Stuertz, and L. Gotzen, "Influence of impact speed and vehicle parameters on injuries of children and adults in pedestrian accidents," Proceedings Second IRCOBI Conference, 1975.
6. Appel, H., G. Stuertz, and S. Behrens, "Influence of front-end design of pasenger cars on injuries of pedestrians on car-to-pedestrian collisions," Proceedings Third IRCOBI Conference, 1976.
7. Appleby, Bintz L.J., "Real world relevance of bumper standards," Automobile Club of Southern California, SAE Paper 760063, 1976.
8. Ashton, S.J., J.B. Pedder, and G.M. Mackay, "Pedestrian injuries and the car exterior," SAE Paper 770092, 1977.
9. Ashton, S.J., J.B. Pedder, and G.M. Mackay, "Pedestrian leg injuries. The bumper and other front structures," Proceedings Third IRCOBI Conference, 1977.
10. Ashton, S.J., J.B. Pedder, and G.M. Mackay, "Influence of vehicle design on pedestrian leg injuries," Proceedings 22nd AAAM Conference, 1978.
11. Bacon, D.G., et al., "Bumper characteristics for improved pedestrian safety," Proceedings 20th Stapp Car Crash Conference, 1976.
12. Bourret, P., J. Farisse, B. Seriat-Gautier, R. Larousse, P. Billault, M. Ramet, D. Cesari, and C. Cavallero, "Experimental study of injuries observed in pedestrians," Proceedings Fourth IRCOBI Conference, 1979.
13. Bunketorp, O., and B. Romanus, "Clinical studies on leg injuries in car-pedestrian accidents," 1981.
14. Bunketorp, O., B. Aldman, R. Jonson, B. Romanus, and B. Roos, "Experimental studies on leg injuries in car-pedestrian accidents," Proceedings Sixth IRCOBI Conference, 1981.
15. Cesari, D., M. Ramet, C. Cavallero, P. Billault, J. Cambarelli, G. Guerinel, J. Farisse, B. Seriat-Gautier, and P. Bourret, "Experimental study of pedestrian kinematics and injuries," 1981.
16. Chiam, H.K. and J.A. Thomas, "Investigation of the effect of bull-bars on vehicle-pedestrian collision dynamics," Royal Melbourne Institute of Technology (Department of Mechanical and Production Engineering), Report CR 13, Office of Road Safety, Department of Transport, Melbourne, Australia, 1980.

17. Child, J.R. and G. Persicke, "A practical approach to the protection of motor vehicles by the absorption of impact energy," Proceedings Fifth International Technical Conference on Experimental Safety Vehicles, 1974.
18. Farisse, J., B. Seriat-Gautier, J. Dalmas, N. Daou, R. Bourret, C. Cavallero, C. Cesari, M. Ramet, P. Billault, and M. Berthommier, "Anatomical and biomechanical study of injuries observed during experimental pedestrian-car collisions," 1981.
19. Felzer, B., "Federal Republic of Germany technical presentation," Proceedings Fourth International Technical Conference on Experimental Safety Vehicles, 1973.
20. (1) Dutsch, K., M.G.J. Elson, and R.W. Moore; (2) Iida, T.; and (3) Newton, D.A., Proceedings Fifth International Technical Conference on Experimental Safety Vehicles, Part 3, "Vehicle structural properties."
21. Finch, P.M., and D. Gebbles, "Design of frontal structures of small cars," Proceedings Sixth International Technical Conference on Experimental Safety Vehicles, 1982.
22. Harris, J., "Research and development toward improved protection for pedestrians struck by cars," Proceedings Sixth International Technical Conference on Experimental Safety Vehicles, 1976.
23. Harris, J., "Research and development toward improved protection for pedestrian struck by cars," TRRL Supplementary Report, Department of the Environment, London, 1977.
24. Harris, J., and C.P. Radley, "Safer cars for pedestrians," Proceedings Seventh International Technical Conference on Experimental Safety Vehicles, 1979.
25. Hintzen, H., and R.A. Dunleavy, "An energy-absorber elastomeric bumper," SAE Paper 730027, 1973.
26. Jehu, V.J., "Towards pedestrian safety," Proceedings Fifth International Technical Conference on Experimental Safety Vehicles, 1974.
27. Jones, I.S., "The effect of side door reinforcement beams and 5mph energy-absorbing bumpers on injury severity," Proceedings 21st AAAM Conference, 1977.
28. Lucchini, E., and R. Weissner, "Influence of bumper adjustment on the kinematics of an impacted pedestrian," Proceedings Third IRCOBI Conference, 1978.
29. Marumo, N., T. Maeda, and A. Wada, "Japanese technical presentation," Proceedings Fourth International Technical Conference on Experimental Safety Vehicles, 1973.
30. Merz, E.J., and J.E. Greene, "Application and testing of an internal air cushion bumper on a structurally modified automobile," SAE Paper 750012, 1975.
31. Nagel, D.S., and J.D. States, "Dashboard and bumper knee—will arthritis develop?" Proceedings 21st AAAM Conference, 1977.
32. Pritz, H.B., C.R. Hassler, J.T. Herridge, and E. Weis, "Experimental study of pedestrian injury minimization through vehicle design," SAE Paper 751166, Proceedings 19th Stapp Car Crash Conference, 1975.
33. Schaefer, "Elastic bumpers made of bayflex 90," Published by Farbenfabriken Bayer in *Anwendung, Entwicklung und Trends*, Bayer Chemische Werkstoffe Fuer den Fahrzeugbau, 1974.
34. Scrivo, J., "1979 Firebird—and advanced (Part 581) soft bumper system," SAE Paper 790335, 1979.
35. Seiffert, U., and P. Krischner, Volkswagenwerk, 1974 VW, "Energy-absorbing bumper system," SAE Paper 730033, 1973.
36. Stcherbatcheff, G., "Protection des pietons caracteristiques particulieres du vehicule Renault epure," Proceedings Seventh International Technical Conference on Experimental Safety Vehicles, 1979.
37. Stuertz, G., and E.G. Suren, "Analysis of injury mechanics in the case of accidents to child pedestrians by investigations at the site of the accident," *Automobiltechnische Zeitschrift*, 1976-09.
38. Stuertz, G., "Main points of the endangering by different vehicle front contours. Their element/body region combinations as well as the type of injuries produced," Proceedings Fourth IRCOBI Conference, 1979.
39. Thomas, C., G. Stcherbatcheff, P. Duclos, C. Tarriere, Y. Foret-Bruno, C. Bot, and A. Patel, "A synthesis of data from a multi-purpose survey on pedestrian accidents," Proceedings Third IRCOBI Conference, 1976.
40. Twigg, D.W., J.L. Ticher, and R.H. Eppinger, "Optimal design of automobiles for pedestrian protection," SAE Paper 770094, 1977.
41. Fowler, J.E., R.K. Axford, and K.R. Butterfield, "Computer simulation of the pedestrian impact—development of the contact model," Proceedings Sixth International Technical Conference on Experimental Safety Vehicles, 1976.
42. Kuehnel, A., and H. Appel, "First step to a pedestrian safety car," Proceedings 22nd Stapp Car Crash Conference, 1978.
43. Leaver, A.D.W., "The use of rubber for impact protection in automobiles," Malaysian Rubber Producer's Research Association, 1976.
44. Martin, K., "Standardisation of car bumpers at a safe height," Department of the Environment (Vehicle Engineering Div.), preliminary draft, 1975.
45. Martin, J.K., "Standardisation of the heights of vehicle bumpers," Department of the Environment, London, 1975.
46. Neilson, I.D., "The way forward for car safety article in the motoring review," *Autocar*, 1972.

47. Ravani, B., D. Brougham, and R.T. Mason, "Pedestrian post-impact kinematics and injury patterns," Proceedings 25th Stapp Car Crash Conference.
48. Rosentahl, F., R.L. Bort, G.J. O'Hara, and E. Clements, "The mechanics of automobile collisions, Naval Research Laboratory, Washington, D.C., 1972.
49. Taylor, H., "Structural strength and compatibility of vehicles in the event of impact. Potential hazards to other means of transport and to pedestrians," Symposium Automobile European, EEC, 1975.
50. Timpner, F.F., "Vehicle impact analysis," SAE Paper 710540, 1971.
51. Wollert, W., "Structural design measures implemented on the uni-car research auto for improvement of passive safety with respect to cyclists," Technical University of Berlin, 1982.

Side Impact Aggressiveness Attributes

Michael W. Monk
U.S. Department of Transportation, National Highway Traffic Safety Administration

Donald T. Willke
The Transportation Research Center of Ohio

Abstract

Thoracic injury to the near side occupant in a side collision is normally caused from contact with the struck vehicle's crushed side structure engaged by the striking vehicle's front end. Extensive research has already been done to investigate the effect that strengthening and padding struck vehicle side structure has on occupant safety. This study investigated the effect that altering the striking vehicle front end characteristics has on occupant safety in a side impact.

The National Highway Traffic Safety Administration's (NHTSA) moving deformable barrier (MDB) was used to conduct 12 crash tests. Three different types of honeycomb barrier faces were used, each representing a front end characteristic change. These were a reduction in stiffness, a lowering and tapering of the hood profile, and a lowering of the bumper. The alterations were believed to represent achievable production vehicle changes.

Each of the altered frontal designs were tested four times, striking baseline and padded Volkswagen Rabbits at both 60° and 90° configurations. In each case, the simulated striking and struck velocities were 35 and 17.5mph, respectively. The occupant responses and relative benefits from each of these concepts are shown and discussed.

Introduction

In May 1984, NHTSA summarized the results of the near-term research toward improved side-impact thoracic protection(1). This near-term research effort consisted of problem definition, surrogate development, and demonstration of improved performance. The improved performance was achieved by strengthening the side structure and adding interior padding to the side interior.

The effort described here was a first step toward understanding potential alterations to the fronts of vehicles that would reduce the potential for occupant thoracic injury when these vehicles strike other vehicles in the side. It represents a recognition of the long-range nature of the front/side compatibility issue.

Three specific alterations to vehicle frontal characteristics were included for consideration in this research: reduction of the frontal crush strength; lowering the hood height; and lowering the bumper height to allow side sill engagement.

Objective

The objective was to identify which of the three candidate characteristics could provide the most benefit to occupants in side-impact collisions. The characteristic that, when altered a reasonable amount, caused the largest reduction in occupant thoracic injury potential was the one to be recommended for future research.

Background

The research described used a dynamic crash test to measure the level of safety of a vehicle. This type of testing is relatively complex and was performed in an attempt to simulate in the laboratory as many aspects of a highway accident as possible. The test involved the placement of two Side Impact Dummies (SID's) in the struck vehicle (one in the driver and the other in the left rear seated positions). The SID has been documented in other presentations(1,2). Measurements of acceleration and displacement were taken at the following locations in the SID:

- Lateral accelerations—left upper rib, left lower rib, upper spine, lower spine, head, and pelvis

- Longitudinal accelerations—upper spine, lower spine, head, and pelvis
- Vertical accelerations—upper spine, lower spine, head, and pelvis
- Lateral displacement—left ribs relative to spine

All of the lateral accelerations in the thorax were measured redundantly to assure capture of these data. The lateral accelerations of the ribs and lower spine were used to estimate the thoracic injury potential of the test environment using the Thoracic Trauma Index (TTI) criterion presented at the 1984 SAE Government/Industry Meeting(2).

The crash test mode and the severity level were the same as derived for Crash Test Matrix II(1) and will be reviewed briefly here. All conditions were derived from a study of thoracic injury-producing side-impact accidents in the National Crash Severity Study. It was found that for the serious-to-fatally injured cases, roughly the same numbers of oblique and near perpendicular impact orientation were present. Impact angles of 60° and 90° have been used to represent these two groups of impact orientations. An impact area was also derived from the file. Basically, the left edge of the striking vehicle was aligned with a vertical line on the left side of the struck vehicle. The vertical line was 37in forward of the midpoint of the wheel base. The severity level was derived in the form of traveling velocities for the striking and struck vehicle. A 35 and 17.5mph velocity combination was found to be an average among the serious-to-fatally injured cases.

The striking vehicle used for the study was the NHTSA MDB. The barrier design was reviewed in (1). The MDB was configured to a weight of 3,000 lb to represent a median weight of the striking vehicle for injury-producing side impacts in the United States. The wheels of the MDB were adjustable to allow the simulation of two-vehicle-moving collisions when, in fact, the struck vehicle is stationary. A wheel setting of 26° was used in the 90° impact orientation and a wheel angle of 19° for the 60° orientation.

The above test conditions, derived for the Matrix II tests, were used for testing in this effort. Most of the Matrix II tests and all of the tests for this research were performed at the Transportation Research Center of Ohio (TRCO). A test report (available upon request) documenting the conditions and results of each test was submitted by TRCO. These results are summarized in this report.

It was found from the Matrix II testing with VW Rabbits that interior padding alone resulted in a significant reduction of rib accelerations, but that both padding and structural reinforcement were required to significantly lower both rib and spinal accelerations. To allow the results of the previous work to be compared with the frontal modification work, the VW Rabbit was again used as a target vehicle. The relative improvement achieved through modifications to the struck vehicle will be compared with those achieved through changes to the striking vehicle in a later section.

Test Conditions

Selection of Test Conditions

In the previous section, the crash configuration was reviewed. Two angles, 60° and 90°, a speed combination of 35/17.5mph, and an impact area were derived. In formulating the project, it was further decided the testing would be conducted in both padded and unpadded interior conditions. The reason for this was to allow application of these test results as to whether or not future vehicles use interior padding such as that tested in earlier programs. This resulted in 12 tests being planned for the evaluation of frontal characteristics of striking vehicles. The test conditions are shown in Table 1. Note that each test at an alternate level has a corresponding test at the standard level for comparison. The comparison tests were conducted under earlier agency test programs, with the test number shown on Table 1.

Table 1. Test conditions for evaluation of frontal characteristics

MDB Front	60°		.90°	
	Padded	Unpadded	Padded	Unpadded
Reduced Stiffness	840905	840713	840913	840621
Lowered Hood	841008	841001	841015	840919
Lowered Bumper	841204	841109	841120	841026
Standard Matrix II	831013	830505	830930	3144-6

Derivation of Frontal Characteristics

This section describes how the improved levels of each of the three frontal characteristics were chosen and reviews the fabrication procedure used. As stated earlier, it was the intent of the project to use reasonable values for each of the alterations, that is, to attempt to select alternate levels that were believed to be within the present or near future state-of-the-art. It was decided the baseline for comparison of frontal characteristics would be the NHTSA MDB. The primary reasons for this decision were the ease and repeatability of testing. The various types of alterations were then accomplished by the use of various types of honeycomb fronts for the MDB.

The standard front for the MDB is documented in a series of drawings, which are in NHTSA Docket No. 79-04. Figure 1 gives most of the frontal geometry and the

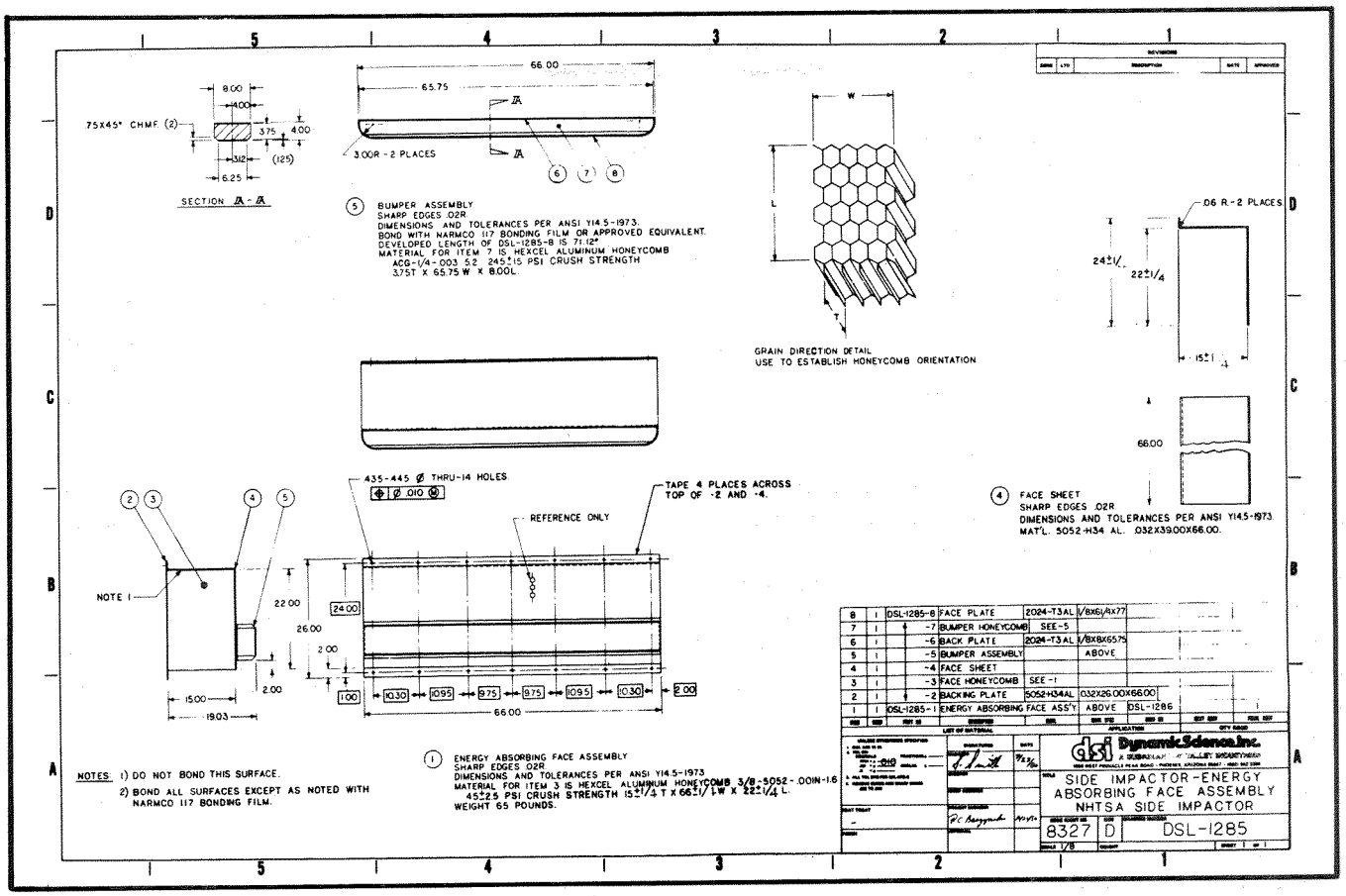

Figure 1. Standard MDB honeycomb face assembly

specified crush properties. The alterations of frontal characteristics will be presented relative to the standard geometry and crush properties.

Frontal Crush Strength

The core material of the MDB is made of aluminum honeycomb and has a specified level of crush strength of 45 ± 2.5psi. It should be pointed out that the term crush strength is used here in the same context that most of the honeycomb manufacturers use it, i.e., an average force level divided by the average area. Thus, it is given units of pressure or stress.

The present barrier face was shown in (1) to represent the stiffness of a vehicle such as the AMC Concord. The Concord was found to be relatively stiff in laboratory crash testing. The Chevrolet Celebrity was found to be one of the softest vehicles. It seemed reasonable, therefore, to select a barrier face stiffness that approximated the stiffness of the Celebrity. One simplified basis for making this selection was to use the energy equation and assume a square wave pulse shape. The average properties for an assumed ramp shape pulse were also computed. They were not used in the selection process but were of interest because the force versus deflection curves were somewhat ramp-like. The relationship used to derive the average "F" for an assumed square wave was as follows:

$$F = \frac{m(v_0^2 - v_1^2)}{2x}$$

x = amount of crush
m = test mass
v_0 = initial velocity
v_1 = velocity at crush x

The relationship used to derive the average "k" for an assumed ramp shape was as follows:

$$k = \frac{m(v_0^2 - v_1^2)}{x^2}$$

These equations were applied to crash test results of the Concord, MDB, and Celebrity. Since the MDB face "bottomed out" beyond 15in of crush, the values for each pulse shape were derived at 15in. The Concord and Celebrity values were also derived at maximum crush. Table 2 contains a summary of this analysis.

An approximation to honeycomb crush strength representative of the Celebrity was obtained by dividing the square wave force value by the surface area of the

Table 2. Front end stiffness analysis

Vehicle	Test Number	Force, based on Square Wave		Stiffness, based on Ramp	
		15″ (lb)	Max Crush (lb)	15″ (lb/ft)	Max Crush (lb/ft)
Concord	Cal-30829470	69,000	78,000	110,000	81,000
MDB	TRC-820528	69,000	N/A	110,000	N/A
Celebrity	DOT-HS-9-02274	27,000	47,000	44,000	31,000

MDB face (1,452in^2). The values obtained for 15in crush and maximum crush were 18.6 and 32.4psi, respectively. (Values representing the Concord, derived similarly, were 47.5psi and 53.7psi, which were close to the specified barrier face crush strength of 45 ± 2.5psi.) A value of 25psi was selected as the crush strength for the reduced stiffness barrier front.

Lowering the Hood Height

A sampling of the front end profiles of 20 passenger vehicles was done(3). The results are given in Table 3. From this, it was judged that a front edge hood height of 25in off the ground would be representative of one of the lowest hood profiles currently produced. In addition, as reported in (3), a striking vehicle with this hood height would contact the door of a VW Rabbit (the struck vehicle in this study) below the ribcage of a normally seated SID dummy.

Many of the vehicles sampled had hood profiles that sloped upward from the front to the rear. This was especially true for vehicles with relatively low front edge hood heights. For this reason, the lowered profile barrier fronts were also designed to slope upward. Over the 15in depth of the barrier fronts, the hood profile would rise from 25 to 29in.

Table 3. Hood profiles

Vehicles	Hood Height* (in)	Distance from Front of Bumper* (in)
Datsun 280 Z	22.7 (29.5)	6.3 (19.3)
Isuzu Impulse	25.9	5.5
Honda Prelude	25.9	6.5
Toyota Camry	28.6	5.4
Plymouth Turismo	28.8	10.0
Mitsubishi Starion	28.9	10.1
Nissan Sentra	29.4	8.0
Toyota Celica	29.4	10.0
Chevrolet Cavalier	29.8	6.5
Plymouth Horizon	30.1	7.0
Mercury Lynx	30.4	6.8
Dodge 600	30.6	6.8
Chevrolet Chevette	30.9	6.6
Buick Skylark	31.0	5.0
Ford Thunderbird	31.4	7.8
Datsun 810 Wagon	31.6	4.0
AMC Spirit	31.9	7.8
Ford LTD Wagon	32.4 (34.6)	4.5 (9.0)
Volvo GL	33.2	5.0
Ford Bronco	39.6 (42.5)	2.3 (5.8)
Average	30.1	6.6
Current MDB	33.0	4.0

*Measurements taken at major bend in front end of vehicle
()Measurements taken at second bend, if present

Lowering the Bumper

Federal Safety Standard 215 specifies a zone in which an impact surface will hit the front of a vehicle. This has the effect of regulating bumper heights. A sampling of bumper heights is shown in Table 4. This sample placed the center of the bumpers for passenger vehicles between 17 and 18in above the ground. The bottom of the bumpers ranged from 13 to 16in.

Table 4. Bumper profiles

Vehicles	Bumper Height (inches) Bottom	Center	Width
Datsun 280 Z	15.0	16.8	3.6
Isuzu Impulse	14.9	17.4	4.9
Honda Prelude	16.1	18.3	4.3
Toyota Camry	15.6	18.3	5.4
Plymouth Turismo	12.9	17.2	8.6
Mitsubishi Starion	14.3	17.9	7.1
Nissan Sentra	14.1	17.6	6.9
Toyota Celica	14.4	18.1	7.3
Chevrolet Cavalier	14.8	17.6	5.6
Plymouth Horizon	15.2	17.6	4.7
Mercury Lynx	15.3	18.0	5.3
Dodge 600	13.0	17.0	7.9
Chevrolet Chevette	13.8	16.8	6.0
Buick Skylark	14.5	17.0	5.0
Ford Thunderbird	13.9	17.7	7.6
Datsun 810 Wagon	14.4	17.0	5.1
AMC Spirit	13.6	16.9	6.5
Ford LTD Wagon	13.4	17.4	8.0
Volvo GL	14.4	17.2	5.5
Ford Bronco	18.5	21.6	6.1
Average	14.6	17.7	6.1
Current MDB	13.0	17.0	8.0

The centerline of the bumper of the MDB is 17in above the ground, which matched well with the vehicles measured. Since there was a 5in offset between the alignment of the MDB bumper and the side sill of the VW Rabbit, the alternate bumper height for the MDB was then set at 5in lower than the standard. The lower portion of the altered bumper was then 8in above the ground.

The hood height was kept the same for these fronts, so as not to confuse the results with the lowered hood height fronts. These fronts were thus larger in cross-sectional area than the standard fronts.

Simulation of Frontal Characteristics

Each of the frontal characteristic alterations mentioned in the previous section was incorporated into the design of an MDB honeycomb face. The surface area of the lowered hood and lowered bumper fronts was different than the standard. Because of this, either the localized unit crush strength or the overall crush force had to be different from the standard front. It was judged more important to maintain the unit crush strength (i.e., use 45psi core material) and let the total load on the struck car vary. The effect of this will be discussed later.

Reduced Crush Strength Barrier Faces

Four faces were constructed that had a crush strength of 25psi ± 10 percent. To accomplish this, the honeycomb material that comprised the main core of the face had this reduced stiffness. The bumper honeycomb material had the standard crush strength of 245psi. Finally, the geometry of these faces had the standard dimensions.

Lowered Hood Height Barrier Faces

The main core and bumper honeycomb materials for these four faces had the standard crush strength of 45psi and 245psi (±10 percent), respectively. Figure 2 shows the cross-sectional shape of these faces compared to those with the standard geometry. Note the bottom edge of the face and the bumper remained the same distance from the ground as the standard. The front hood edge, though, was lowered by 8in and the rear hood height was 4in lower than the standard.

Lowered Bumper Barrier Faces

As with the lowered hood height faces, the main core and bumper honeycomb materials had the standard crush strengths. As Figure 2 indicates, the hood height and profile were also standard. Note, though, that the bottom edge of the face was lowered by 4in while the bumper position was lowered by 5in. The actual dimensions of the bumper did not change.

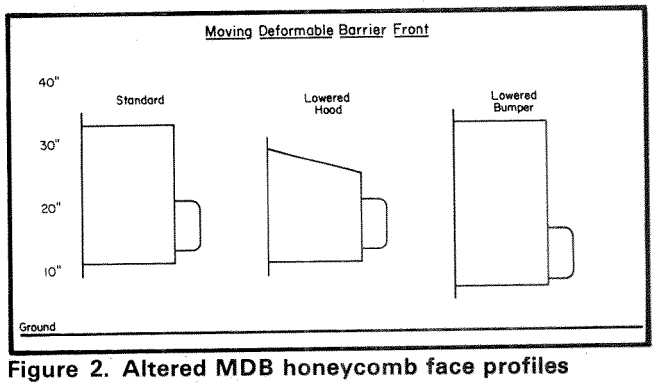

Figure 2. Altered MDB honeycomb face profiles

Crash Test Results

Twelve crash tests were performed to investigate the effect that altering striking vehicle front end characteristics has on struck vehicle occupant safety in side impacts. Each of the three different MDB front designs were involved in four different crash tests. For each test, two SID's were used: one as a driver, the other as a left rear passenger.

Tables 5 through 7 list the lateral rib, spinal, and pelvic accelerations (in g's) as well as the calculated HIC values

for each dummy of each test. Table 8 lists these same results obtained from similar Matrix II tests using the standard MDB fronts.

Table 5. Reduced crush strength barrier face

Driver	90° baseline	60° baseline	90° padded	60° padded
Up. Rib	110.1	165.9	91.9	132.6
Lo. Rib	118.0	202.7	81.9	117.2
Up. Spine	117.0	187.6	76.2	167.0
Lo. Spine	157.1	159.5	97.7	180.7
Pelvis	—*—	239.6	92.3	322.5
HIC	1220	3990	1067	3414
Passenger				
Up. Rib	63.2	131.0	46.7	68.9
Lo. Rib	83.4	162.8	54.5	79.1
Up. Spine	69.6	159.0	42.7	73.0
Lo. Spine	72.8	109.8	56.7	95.8
Pelvis	158.1	142.7	—*—	110.6
HIC	657	2545	477	1173

* Peak acceleration not available due to intermittent rattling of the accelerometer

All test simulate a 35/17.5mph collision

Table 6. Lowered hood barrier face

Driver	90° baseline	60° baseline	90° padded	60° padded
Up. Rib	74.1	84.6	54.4	87.0
Lo. Rib	93.5	72.7	55.2	67.1
Up. Spine	67.8	73.1	73.3	95.8
Lo. Spine	72.2	67.5	96.7	115.2
Pelvis	234.0	—*—	142.5	264.2
HIC	3008+	5147+	946+	3569+
Passenger				
Up. Rib	52.7	80.6	43.3	55.4
Lo. Rib	82.1	83.4	47.3	88.2
Up. Spine	56.1	72.8	53.4	68.7
Lo. Spine	52.2	98.5	65.2	103.1
Pelvis	171.6	189.5	126.9	198.4
HIC	484	2724+	855	590

* Peak acceleration not available due to intermittent rattling of the accelerometer

\+ Value artificially high due to the head impacting the MDB face mounting plate

All tests simulate a 35-17.5mph collision

Table 7. Lowered bumper barrier face

Driver	90° baseline	60° baseline	90° padded	60° padded
Up. Rib	132.6	241.3	102.7	83.4
Lo. Rib	168.1	258.6	91.1	103.1
Up. Spine	111.3	205.8	105.2	126.8
Lo. Spine	208.1	217.7	128.0	160.0
Pelvis	216.6	—*—	107.2	204.1
HIC	616	1831	852	1440
Passenger				
Up. Rib	77.7	144.3	75.5	122.9
Lo. Rib	67.6	135.4	72.5	94.5
Up. Spine	64.1	164.2	81.8	77.1
Lo. Spine	76.2	145.7	98.6	121.5
Pelvis	—*—	102.7	87.5#	89.4#
HIC	1583	1236	1066	745

* Peak acceleration not available due to intermittent rattling of the accelerometer

\# Peak acceleration is an estimate only, due to intermittent rattling of the accelerometer

All tests simulate a 35/17.5mph collision

Table 8. Standard barrier face

Driver	90° baseline	60° baseline	90° padded	60° padded
Up. Rib	185.6	185.7	102.3	93.9
Lo. Rib	171.8	241.3	114.6	117.6
Up. Spine	153.6	217.1	115.1	166.0
Lo. Spine	127.9	151.9	135.5	160.1
Pelvis	220.5	217.8	187.7	326.7
HIC	681	3322	944	3691
Passenger				
Up. Rib	128.4	149.4	57.0	79.0
Lo. Rib	179.1	188.2	67.0	99.2
Up. Spine	75.2	139.9	57.5	85.5
Lo. Spine	110.3	115.4	86.0	98.3
Pelvis	147.6	183.5	174.1	176.4
HIC	988	1810	1012	884

All tests simulate a 35/17.5mph collision

Several of the pelvic responses were not reported on these tables. The reason for this was that an unexplained rattling occurred on these acceleration signals. This problem was not new to this study for it appeared frequently in crash tests of previous projects. For most of these, it was not possible to estimate a pelvic response as the rattling occurred at the peak. An estimate was possible for a couple of them since the rattling occurred near, but not at, the peak. As can be seen in these tables, the reduced stiffness MDB faces produced peak driver pelvic accelerations that were 0.3 percent higher on average than those of the corresponding standard MDB

face tests. Similarly, the lowered hood fronts produced a 2.2 percent decrease while the lowered bumper fronts resulted in a 19.4 percent decrease.

It is also noted that the driver HIC values listed in Table 6 (lowered hood crash tests) are unusually high. These barrier faces had two effects. The first was that the striking vehicle front end penetrated the occupant compartment further than it did in the other crash tests. The second was that the submarining of the lowered profile front end caused the dummy to rotate, pelvis toward the roof, rather than just pushing the entire dummy across the arc. The result of these effects was that the dummy's head struck the barrier face mounting plate. Although no such structure is present in a real car, the rotation of the dummy did cause the head to contact the hood of the striking vehicle, which was an infrequent occurrence in tests using standard MDB faces. This may indicate that additional head protection would be required if future cars are built with lowered front end profiles.

As mentioned, Matrix II explored the possibility of reducing the thoracic injury to an occupant of a car struck in a side impact collision through structural and padding modifications to the side of the struck car. Figure 3 shows a summary of these tests, averaging 60° and 90° test results. As an average, a 23-year-old driver in the baseline vehicle (VW Rabbit) would have had a 97 percent chance of receiving an AIS 3 or greater thoracic injury. The introduction of door padding alone reduced this average possibility to 82 percent, while the combination of padding with side structural modifications reduced this to 61 percent. All these tests were performed using a standard honeycomb front on the MDB.

Presently, an upgrade to FMVSS 214 is under consideration. Based partially on the results of Matrix II, this upgrade would require a certain level of occupant safety to be maintained in a side impact crash test. Since the future of this upgrade is at this time undetermined, two separate cases are examined. In case A, it is assumed that no FMVSS 214 upgrade has been enacted. Consistent with that assumption, effects of the MDB front alterations have been determined on unpadded baseline cars. In case B, it is assumed that an upgrade to FMVSS 214 is in place. Accordingly, effects of barrier modifications have been determined on cars containing additional interior padding.

Again, averaging the results of the 60° and 90° tests, Figure 4 presents the results of the tests done with no additional padding (case A). In this and the following figure, the Matrix II results from structurally modified and padded struck cars are shown on the left of the figure, while the results of the frontal alterations are shown on the right. This provides a direct comparison of benefits

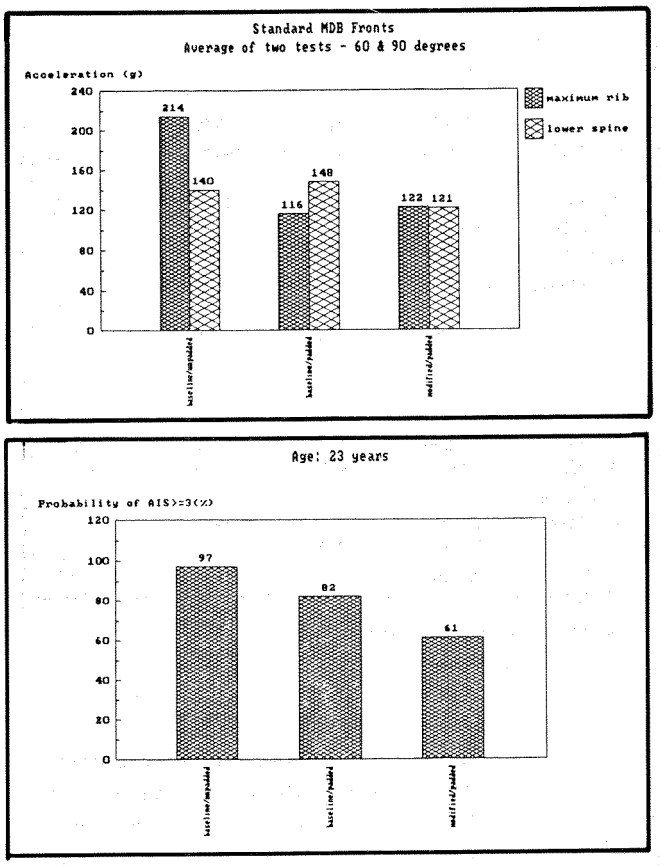

Figure 3. Struck vehicle study—matrix II results—driver

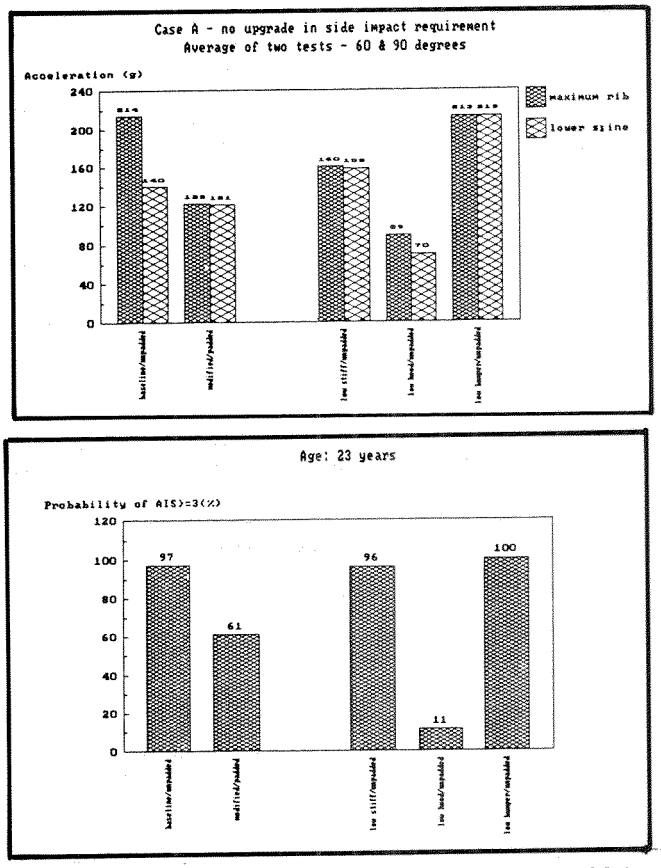

Figure 4. Comparison of striking and struck vehicle studies—driver—case A

derived from altering the front of the striking vehicle with those derived from modifying the struck vehicle. The reduced stiffness and lowered bumper tests showed little change in the thoracic injury probability from the baseline tests done with standard MDB fronts. However, the lowered hood tests produced a large reduction in injury probability. For a 23-year-old driver, the average chance of receiving an AIS 3 or greater thoracic injury went from 97 percent for the standard MDB front to 11 percent for the lowered hood MDB front. This was an even lower injury potential than that from the least severe tests of Matrix II (modified structure and additional padding—61 percent).

Case B is presented in Figure 5. The altered MDB front test results represented here are the average of the 60° and 90° padded tests of each type. Again, based on average thoracic injury probabilities, the reduced stiffness and lowered bumper tests did not perform as well as the modified vehicle tests of Matrix II (64 percent and 73 percent versus 61 percent). Although no vehicles with structural modifications were tested in this project, it is reasonable to assume that the addition of such modifications for the reduced stiffness and lowered bumper tests would further reduce the above injury potentials. The extent of this is not known.

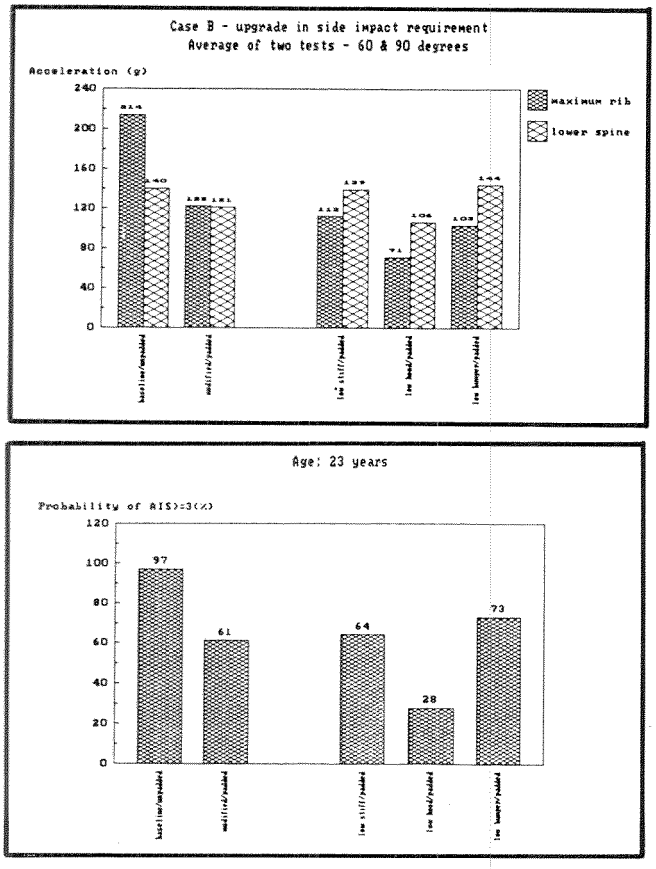

Figure 5. Comparison of striking and struck vehicle studies—driver—case B

The most important portion of Figure 5 deals with the lowered hood tests. Even without structural modifications, these tests produced a much lower thoracic injury potential than the fully modified vehicle tests of Matrix II. For a 23-year-old driver, the probability of an AIS 3 or greater thoracic injury fell from 61 percent to 28 percent. The effect of the addition of structural modifications, although not known, would probably be to reduce this injury potential further.

The appendix contains complete listings of the probabilities for receiving an AIS 3 or greater, 4 or greater, and 5 or greater thoracic injuries for both 23- and 41-year-old drivers and passengers.

From these results, it appears that since the lowering of the striking vehicle hood height reduced the dummy thoracic responses substantially, the injury an actual occupant receives should also be reduced. While it is likely this is true, there was an oddity in the data that merits discussion. The following addresses this point.

Table 9 lists the lateral chest deflections for the 12 crash tests performed for this investigation as well as for the 4 comparable tests from the Matrix II study. A standard deflection ranges from 1.8 to 2.0in. The reduced stiffness and lowered bumper tests resulted in chest deflections that were within this range. The lowered hood tests, though, had much lower values for this measurement. Particularly low was that from the 60° baseline test.

One explanation for this was that the thorax may not have been loaded directly due to the submarining action described previously. This could have reduced deflection and acceleration of the ribcage and spine. In this case, the actual thoracic injury an occupant would have received would indeed have been reduced.

Another possibility was that the lowered hood MDB fronts caused an unusually large amount of nonlateral loading on the SID ribcage and spine. Since the chest deflection potentiometer and rib accelerometers were not omnidirectional, they may not have measured a significant portion of the total responses.

Nonlateral accelerations were measured at the upper and lower spine locations. Table 9 lists the lateral and resultant peak accelerations (in g's) for the upper and lower spine of the driver dummy for each of the tests. As an indication of the magnitude of the effect of the nonlateral responses, the percentage increase of the resultant as compared to the lateral peak is also included.

This table would seem to indicate, with one exception, the effect of nonlateral loads on the spine was no greater for the lowered hood crash tests than they were for the others. This exception was the baseline 60° test, which, as mentioned previously, also had a very low chest deflection.

In the lowered hood crash tests, there was no structure immediately contacting the upper door as there was in the tests involving the other MDB fronts. Since the thorax of the dummy contacted this portion of the door, the door-to-thorax impact caused the door to indent around the

Table 9. Comparison of lateral and nonlateral responses

Test Type	Lateral Chest Deflection (in)	Driver Spinal Accelerations (g)					
		Upper result.			Lower result.		
		lateral		delta	lateral		delta
25psi							
bas,90	2.01	117	126	7.7%	157	161	2.5%
bas,60	1.82	187	203	8.6%	159	169	6.3%
pad,90	1.96	76	77	1.3%	98	99	1.0%
pad,60	1.92	167	172	3.0%	181	181	0%
Low Hood							
bas,90	0.91	68	73	7.4%	72	78	8.3%
bas,60	0.19	73	131	79.5%	68	69	1.5%
pad,90	1.07	73	74	1.4%	96	105	9.4%
pad,60	0.77	96	98	2.1%	115	116	0.9%
Low Bump							
bas,90	1.91	111	120	8.1%	208	224	7.7%
bas,60	1.92	206	209	1.5%	218	221	1.4%
pad,90	1.83	106	110	3.8%	128	130	1.6%
pad,60	—	127	128	0.8%	160	164	2.5%
Standard							
bas,90	1.88	154	157	1.9%	128	135	5.5%
bas,60	1.91	217	223	2.8%	152	160	5.3%
pad,90	1.80	115	116	0.9%	135	136	0.7%
pad,60	1.82	166	169	1.8%	160	161	0.6%

thorax. As is often the case for 60° impacts, the hinges tore away from the A-pillar in both the padded and unpadded 60° lowered hood tests. The combination of the door being bent around the thorax and the loose door being forced rearward may have caused the unusually high amount of nonlateral loading on the thorax for the unpadded test. Although the damage to the doors was similar in the two tests, the additional padding may have lessened the effect of this indentation to cause nonlateral loads on the thorax. If this was true, the lateral results of this test do not give the complete picture. Even if this were so, the overall findings of this study would not change.

It is also possible, however unlikely, that nonlateral loading occurred on the ribcage, not measured by the chest potentiometer or the rib accelerometers, that did not translate through to the spine. Since the ability of the SID to measure nonlateral loading on the ribcage is uncertain, no judgment was made as to which of the preceding explanations is correct. A further investigation would be necessary to make this determination.

Since the passenger dummy responses are generally used less frequently than those of the driver, these results are only summarized here. Complete responses are listed in Tables 5 through 8 and in the appendix.

Similar to Figures 4 and 5, Figure 6 shows the probability that a 23-year-old rear left seat occupant would receive an AIS 3 or greater thoracic injury in both this study and in the Matrix II study. As before, 60° and 90° tests are combined and two cases are considered. In case A, the lowered hood MDB fronts produced the most benefit to the occupant as compared to the other MDB faces. Thoracic injury probability was reduced from 82 percent for the standard front to 15 percent for the lowered hood front.

In case B, the reduced stiffness MDB faces produced the lowest chance of serious thoracic injury for the vehicles without structural modifications (13 percent). The lowered hood fronts were only slightly higher (17 percent). Both of these MDB fronts performed better than the standard front did under the same level of struck vehicle modification (22 percent). If these tests were repeated using structurally modified cars, it is reasonable to assume that these probabilities would be reduced further. The extent of this reduction is not known.

Finally, the results of the reduced stiffness tests helped to evaluate the decision to use 45psi honeycomb in the lowered hood and lowered bumper MDB faces (see previous section). The 25psi fronts used for the reduced stiffness tests represented a 44 percent reduction in both overall and localized (adjacent to occupant) stiffness. The response changes due to this reduction were minimal. The lowered hood profile tests and lowered bumper tests

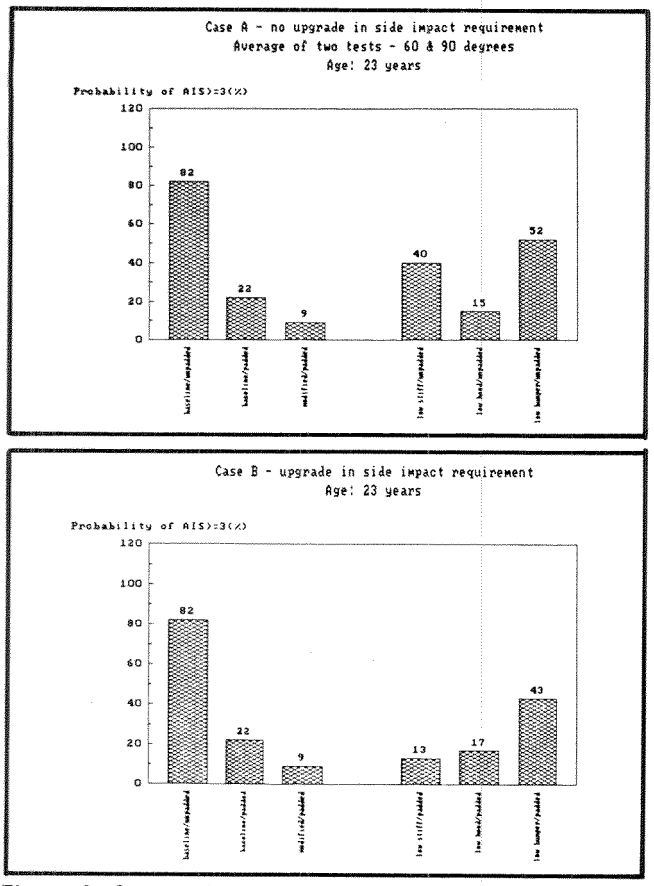

Figure 6. Comparison of striking and struck vehicle studies—passenger

resulted in a 36 percent decrease and an 18 percent increase in overall stiffness, respectively, due to the differences in impacting surface area. Since a 44 percent decrease in overall stiffness did not significantly reduce occupant responses, the large reduction in thoracic responses in the lowered hood tests was judged to be due primarily to the lack of localized external structure at the thoracic level. It was not believed to be caused by the reduction in overall stiffness. It was also judged that the 18 percent increase in overall stiffness for the lowered bumper tests did not significantly affect occupant response.

All aspects considered, the concept of lowering the striking vehicle's hood shows much promise as a means to reduce struck vehicle occupant thoracic injury in side impacts.

Conclusion and Recommendations

NHTSA has completed a preliminary study of the effects that altering the front end characteristics of striking vehicles has on the safety of an occupant of a vehicle struck in a side-impact collision. The following are conclusions from this investigation. Each injury potential listed here is the average probability of a 23-year-old occupant receiving an AIS 3 or greater thoracic injury from the 60° and 90° tests of each type.

1. When considering thoracic injury to a driver in a subcompact car, when struck in the left side, there appeared to be more potential benefit in altering the front end characteristics of the striking vehicle than in modifying the side of the struck vehicle. The best performing vehicle of the Matrix II tests, which had both structural and padding modifications, resulted in a thoracic injury potential of 61 percent. This compared to 11 percent for baseline vehicles struck by the MDB with lowered hood fronts.
2. For the three types of MDB fronts tested in this project and the standard fronts tested previously, the lowered hood MDB fronts produced the least severe thoracic injury environment for the driver of a subcompact vehicle struck in the left side. The injury potentials were as follows:

   For unpadded tests:
   - Standard—97 percent
   - Reduced stiffness—96 percent
   - Lowered hood—11 percent
   - Lowered bumper—100 percent

   For padded tests:
   - Standard—82 percent
   - Reduced stiffness—64 percent
   - Lowered hood—28 percent
   - Lowered bumper—73 percent

3. Of the three types of MDB fronts tested in this project, the lowered bumper fronts showed the largest improvement in the peak lateral driver pelvic responses as compared to the standard front. The average driver peak pelvic acceleration from three lowered bumper tests was 19.4 percent lower than that from the same three standard MDB front tests of Matrix II. Similarly, the reduced stiffness fronts showed a 0.3 percent increase, while the lowered hood fronts produced a 2.2 percent decrease.
4. If lowered front end profiles were required on vehicles, additional protection for the head may also be needed. The submarining of the lowered hood MDB fronts caused the driver dummy to rotate, pelvis toward the roof, much more than did the other three MDB fronts. This rotation caused the head to contact the hood of the striking vehicle, thereby increasing the risk of serious head injury.
5. The lowered hood MDB fronts produced the lowest thoracic injury potential for a left rear occupant in the unpadded tests, while the reduced stiffness fronts resulted in the lowest for the padded tests. These injury potentials were as follows:

For unpadded tests:
- Standard—82 percent
- Reduced stiffness—40 percent
- Lowered hood—15 percent
- Lowered bumper—52 percent

For padded tests:
- Standard—22 percent
- Reduced stiffness—13 percent
- Lowered hood—17 percent
- Lowered bumper—43 percent

Based on the results presented in this paper, it is recommended that future aggressiveness studies focus on the relative placement of the striking vehicle hood to the occupant thoracic region. This should include an investigation of the SID thorax dynamics in this type of testing as well as an attempt to determine an optimum hood design, considering all factors. Finally, an investigation should be done to determine whether the findings of this study apply to other vehicle size/weight categories.

References

1. Hackney, J.R., M.W. Monk, W.T. Hollowell, L.K. Sullivan, and D.T. Willke, "Results of the National Highway Traffic Safety Administration's thoracic side impact protection research program," SAE Paper 840886, May 1984.
2. Eppinger, R.H., R.M. Morgan, and J.H. Marcus, "Development of dummy and injury index for NHTSA's thoracic side impact protection research program," SAE Paper 840885, May 1984.
3. Monk, M.W., and D.T. Willke, "Side interior stiffness measurement," Report No. DOT-HS-806-708, available from the National Technical Information Service, September 1984.

Appendix

Thoracic Injury Probabilities From Analysis of Aggressiveness Factors Crash Testing

Table A-1. Aggressiveness factors crash testing—driver probability of AIS≥n

Driver	60°						90°					
	padded			unpadded			padded			unpadded		
Age: 23 yrs	n=3	n=4	n=5	n=3	n=4	n=5	n=3	n=4	n=5	n=3	n=4	n=5
Reduced Stiffness	100	100	17	100	100	19	28	0	0	91	88	10
Lowered Hood	40	1	1	9	0	0	15	0	0	13	0	0
Lowered Bumper	88	81	10	100	100	39	58	16	4	100	100	26
Age: 41 yrs												
Reduced Stiffness	100	100	27	100	100	30	72	44	7	100	100	21
Lowered Hood	86	77	9	42	2	1	54	9	4	50	6	3
Lowered Bumper	100	100	20	100	100	100	98	98	13	100	100	37

Table A.2. Aggressiveness factors crash testing—passenger probability of AIS ≥ n

Passenger	60°						90°					
	padded			unpadded			padded			unpadded		
Age: 23 yrs	n=3	n=4	n=5	n=3	n=4	n=5	n=3	n=4	n=5	n=3	n=4	n=5
Reduced Stiffness	22	0	0	69	38	6	3	0	0	11	0	0
Lowered Hood	30	0	0	25	0	0	4	0	0	5	0	0
Lowered Bumper	62	21	5	92	90	11	23	0	0	11	0	0
Age: 41 yrs												
Reduced Stiffness	64	26	5	100	100	15	21	0	0	46	3	2
Lowered Hood	75	53	7	69	36	6	25	0	0	28	0	0
Lowered Bumper	99	99	14	100	100	21	65	28	5	46	3	2

Table A.3. Matrix II crash testing probability of AIS ≥ n

Driver	60°						90°					
	padded			unpadded			padded			unpadded		
Age: 23 yrs	n=3	n=4	n=5	n=3	n=4	n=5	n=3	n==4	n=5	n=3	n=4	n=5
Baseline Structure	93	91	11	100	100	22	71	42	71	94	92	11
Modified Structure	85	74	9	98	98	13	37	1	1	100	100	24
Age: 41 yrs												
Baseline Structure	100	100	21	100	100	33	100	100	16	100	100	22
Modified Structure	100	100	19	100	100	24	83	72	9	100	100	35
Passenger	60°						90°					
	padded			unpadded			padded			unpadded		
Age: 23 yrs	n=3	n=4	n=5	n=3	n=4	n=5	n=3	n=4	n=5	n=3	n=4	n=5
Baseline Structure	31	0	0	86	78	9	13	0	0	78	58	8
Modified Structure	6	0	0	39	1	1	12	0	0	18	0	0
Age: 41 yrs												
Baseline Structure	76	54	7	100	100	19	50	6	3	100	100	17
Modified Structure	34	0	0	85	75	9	49	5	3	58	15	4

Volvo Side Impact Testing

Mats Nilsson,
Kjell Andersson,
Johnny Korner, and
Anna Nilsson-Ehle
Automotive Safety Centre, Volvo Car Corporation

Abstract

The improvement of side impact protection is today a major concern to the crashworthiness community. A prerequisite for making this development possible is the establishment of a common side impact test method, representative of several traffic environments.

Volvo has made a study aimed at determining the suitability of a moving barrier test as a tool for the development of side impact protection. Traffic accident data from car-to-car accidents have been used as references to full-scale tests. Certain test parameters have been varied to find out if an improved correlation is possible between real-world accidents and laboratory collisions. To further understand the interaction between the occupant and the car structure, sled testing has been used as a complement.

The conclusion of the study is that a suitable side impact test method is a moving deformable barrier (MDB) impacting in a 90° noncrabbed configuration. A good resemblance to real-life accidents is achieved with a CCMC MDB 76, mass 1,400kg, ground clearance 250mm, and impact speed 35mph.

Future work at Volvo will include further accident investigations, improvement of measurement techniques, development of subsystem testing, and evaluation of different MDB front faces in terms of force-crush characteristics.

Background

Volvo strives to continuously improve the crashworthiness of Volvo cars by a conscious development and design strategy, the Volvo Safety Design Philosophy(1,2).

In short, this means the experience from traffic accident studies is used as an important source for establishing crashworthiness requirements, which, in combination with other requirements, form the input to the establishment of laboratory test methods. Requirements on performance in these tests are established and further developed into requirements on systems and subsystems in the car. These requirements provide the basis for the actual design work of the car structure and the interior safety systems.

Side impact collisions have been focused on for several years, and a broad analysis of the Volvo accident material was published in 1982(3). Here the complexity of the problem was enlightened, for instance, the varying injury patterns due to different collision objects, and it was recommended, to cover different types of side impacts, that a car-to-car simulating full-scale test should be accompanied by complementary subsystem testing.

Since then, further in-depth studies of side impact accidents have been conducted to improve the input data for the development of test methods.

This paper focuses on the simulation of car-to-car accidents and the establishment of a corresponding test method. Irrespective of the severity of lateral collisions with poles and trucks, car-to-car side impacts still constitute an essential problem to be dealt with.

Volvo has followed the development of the CCMC moving deformable barrier, the MDB 76(4). This barrier is thought to be a good representative of modern cars, not only European but also American(5). It has a good repeatability and makes a suitable substitute for actual cars. However, comparisons with struck Volvo cars in real-life accidents have shown certain discrepancies that have initiated part of the Volvo study presented here.

The objective of the study has been to find the effect of variations of certain test parameters and to establish a test configuration corresponding to real-life experience.

Side Impact Accident Studies

The side impact test procedure described in this paper has partly been chosen on the basis of a comparative analysis of Volvo 240 field accidents and laboratory collisions in corresponding crash configurations.

Two different investigation levels were used in the accident sample. From Volvo's statistical accident material (large number of accidents, limited investigation depth), 645 car-to-car side impact cases were chosen for analysis, the selection criteria being that the occupant compartment was impacted and an occupant was seated nearside.

To these accidents were added 23 side impact cases investigated by Volvo's multidisciplinary in-depth study team and chosen to insure accident conditions comparable to the laboratory crash tests. The selection criteria were: Volvo 240 accidents where the compartment was run into by a medium-size car or a van at 60° to 120° (orientation angle) and with an occupant seated on the near side. The in-depth study cases were analyzed thoroughly with a view to the degree and shape of deformation (B-pillar intrusion) and the degree of injury severity (MAIS) to the near side occupant.

In spite of the absence of reliable crash severity calculation methods for side impacts, it has been possible

to establish a fairly reliable assessment of the connection between the degree of deformation, the impact speed (for a homogenous group of specified striking cars), and the resulting injury to occupants, since laboratory crash tests corresponding to the field accident conditions were available.

The results are shown in Figures 1, 2, and 3.

Both the accident statistics (Figure 1) and the analysis of the in-depth study cases (Figure 2) show that serious injuries (AIS 3+) start to occur more frequently at deformations corresponding to impact speeds exceeding 30 to 35mph. This does not mean that AIS 3 injuries necessarily occur in such collisions. Occupants sometimes escape with minor or moderate injuries (AIS 1 to 2) at B-pillar intrusions corresponding to approximately 35mph (see Figure 3).

It should be pointed out the deformation pattern analysis described here does not necessarily imply that a mere reinforcement of the side structure—and consequently a reduced deformation—would reduce the severity of injuries.

The deformation shape of a Volvo 240 run into by the CCMC barrier does not satisfactorily correspond to the deformation shape in the field accidents investigated. The barrier causes a considerably greater deformation at shoulder/head height, (see Figure 2).

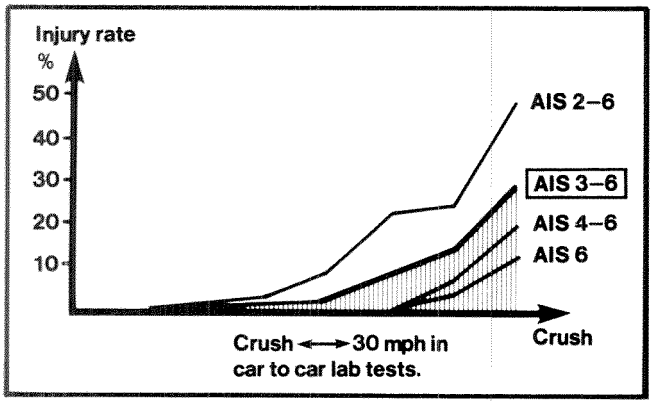

Figure 1. Injury rate as a function of deformation—Volvo 240 accidents from 1974 to 1976 (645 cases)

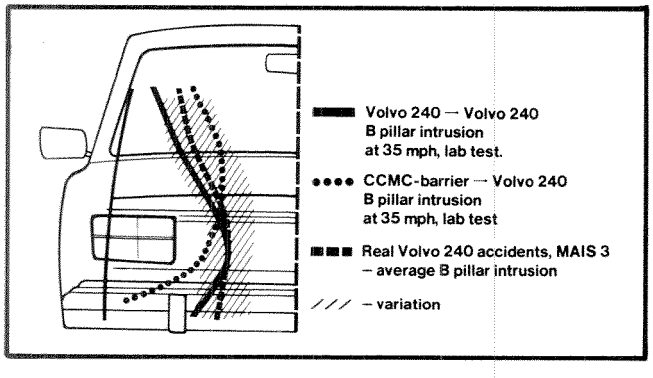

Figure 2. Comparison between laboratory tests at 35mph and real-life accidents—MAIS 3

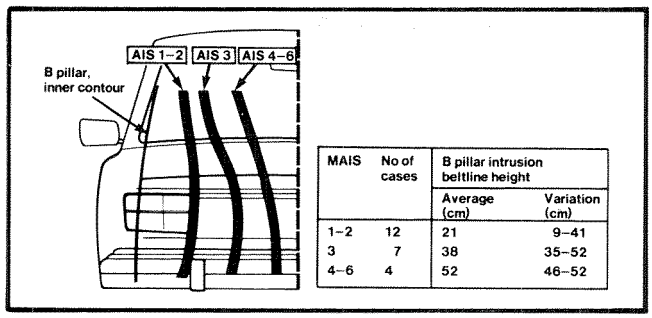

MAIS	No of cases	B pillar intrusion beltline height	
		Average (cm)	Variation (cm)
1–2	12	21	9–41
3	7	38	35–52
4–6	4	52	46–52

Figure 3. Injury severity as a function of B-pillar intrusion—summary of 23 in-depth study cases—Volvo 240

Full-Scale Tests

The traffic accident experience shows the necessity of improving the resemblance of today's laboratory tests to actual side impacts. The basis for this study has been the CCMC test method(4). At present, the CCMC test configuration and barrier are felt to be the most representative setup. Volvo cars have also been tested earlier according to this.

Test Matrix

Six full-scale tests were conducted in Volvo's crash testing facility, (see Table 1).

In all tests, the target was standing still and was run into by the bullet vehicle on the driver's side. In tests 1 to 5, the bullet hit the target perpendicularly with centerline in bullet at SRP-position in target. Test 6 was conducted in a 90°/27° crabbed configuration. The varied parameters were—

- Type of bullet
- Mass of bullet
- Ground clearance of barrier
- Structural reinforcements and padding
- Crash configuration

Based upon experience from a previous side impact study of the Volvo 240, the Volvo 760—the most recent production car—was chosen as the target vehicle in this study. In tests 5 and 6, the target was an experimentally reinforced Volvo 760 (see Table 1).

Choice of Varied Test Parameters

Type of Bullet

The comparison between cars and MDB's as bullets was made to give an idea of the difference between a mid-size car with US-bumper system, such as a Volvo

Table 1. List of conducted full-scale tests

Test No.	Bullet Type	Bullet Mass (kg)	Bullet Ground Clearance (mm)	Target Type	Target Mass (kg)	Test Type	Impact Velocity (mph)
1	Volvo 240	1400	—	Volvo 760	1690	90°	35
2	MDB 76	1400	300	Volvo 760	1690	90°	35
3	MDB 76	950	300	Volvo 760	1690	90°	35
4	MDB 76	1400	250	Volvo 760	1690	90°	35
5	MDB 76	1400	250	Volvo 760 reinforced	1690	90°	35
6	MDB 76	1400	250	Volvo 760 reinforced	1625	90°/27°	35 simul. 39 resulting

240, and an MDB 76(4) regarding intrusions, wall speeds, and dummy responses. The bullet had a mass of 1,400kg in both cases (tests 1 and 2 in Table 1). A comparison was also made with the previous study of the Volvo 240 as target and with field cases.

Mass of Bullet

The mass was varied to ascertain the effect on wall speeds and dummy responses. The levels chosen were 950kg in accordance with CCMC specifications and 1,400kg, a typical medium-size car mass close to the NHTSA barrier(6). Ground clearance in the compared tests was 300mm (tests 2 and 3 in Table 1).

Ground Clearance of Barrier

The barrier's ground clearance was reduced in test 4 to 250mm, as the basic MDB 76 ground clearance of 300mm turned out to give greater loads on the structure and the dummies at chest height as compared with the Volvo 240, and poor resemblance of intrusion profiles in the field cases. The bullet in the full-scale tests compared had a mass of 1,400kg (tests 1, 2, and 4 in Table 1). A comparison was also made with the earlier tests where the target was a Volvo 240.

Structural Reinforcements and Padding

The target was reinforced primarily to permit investigation into how an MDB 76 reacts, regarding its resistance to bottoming out when put up against a test object that is essentially stronger (test 5 in Table 1). The target vehicle was also equipped with padding.

Crash Configuration

It was also decided to study the effect of testing in crabbed configuration, as it is generally considered this type of test better simulates side impacts in the field. The same test configuration was chosen as is used in the joint NHTSA and VW(5) project MIV, i.e., a 90° / 27° crabbed configuration.

Nonvaried Test Parameters

MDB

No comparative testing was made on the different deformable fronts available. The CCMC MDB 76 was chosen as the bullet due to its force-crush characteristics and good repeatability.

Test Speed

The speed of the bullet at right angles to the target was, in all cases, 35mph. The reason for this is that severe injuries (AIS 3+) in the Volvo 240 field accidents start to occur more frequently at impact speeds exceeding 30 to 35mph. To improve side impact protection, the relevant test criteria, therefore, must be met at an impact speed of 35mph).

Choice of Structure-Related Evaluation Parameters

In the full-scale tests, a large number of parameters were measured with the aid of accelerometers and high-speed cameras. Some of the relevant structure-related

parameters were chosen for a comparative analysis of the various tests.

The injuries affecting the nearside occupant in a side impact depend to a large extent on the speed of the intruding side structure. It is therefore essential that intrusion speeds are correctly simulated. In traffic accidents, only postcrash data are available. A comparison between laboratory tests and traffic accidents must rely on such data, e.g., residual deformation. For the evaluation of the full-scale tests, comparison is made for—

- Wall speed at chest height
- Wall speed at pelvis height
- Residual internal deformation of B-pillar

A further indication of the fundamental side impact mechanisms is also the velocity increase to which the target is exposed in relation to the velocity increase of the side structure, i.e.—

- The target's rigid body movement pattern
- The movement pattern of the side structure
- The relation between these two

The velocity, in chest- and pelvis-level, of the intruding side structure is graphically established from high-speed film of the B-pillar at the time of dummy impact. This method of measuring the wall speed is more reliable than using accelerometer readings from the structure that actually impacts the dummy. The wall speed is looked upon as a structural parameter since its importance as an injury-producing parameter is reduced when padding is introduced. The time of dummy impact is assessed by using the chest acceleration resultant graph.

Since this is a comparative analysis, the different evaluation parameters are normalized so that values in one test are set to 1.0. The values in the tests to which the first test is compared are all in relation to this.

Comments

The wall speeds must be interpreted with care due to both the inaccuracy of the measuring method used and the fact that the dummy responses are not only dependent on wall speed at the time of contact, but also on the wall speed history during the total period of contact. Thus, wall speeds and dummy response in some cases may appear to be contradictory.

Choice of Dummy-Related Evaluation Parameters

The APROD-81 dummy has been used as a measuring device. This dummy is basically a Part 572 dummy with a special chest designed to measure chest deflection at two levels(7).

This dummy was preferred to the American SID dummy because the deflection and deflection rate are biomechanically better related to injury than acceleration is. However, during testing it was found that imperfect design of the chest, especially the shoulder part, has reduced the information from the chest deflection readings and the reliability of these measurements.

The following parameters are used for the evaluation of test results:

- Maximum head acceleration (>3ms)
- Maximum chest acceleration (>3ms), center of gravity
- Peak resultant chest acceleration
- Peak acceleration upper rib
- Peak acceleration lower rib
- Maximum hip acceleration (>3ms)

Sled Test Method

As a complement to full-scale testing, a test method is required for studying the interaction between the car side interior and the occupant. This test method must simulate the desired dummy contact speed and also provide further acceleration for the dummy as long as it is in contact with the wall.

In the sled test, a test rig is mounted on an HYGE crash simulator. Padding is fastened to two steel plates attached to the rig by six load transducers. Two bars project from the rig, and the seat with the APROD dummy moves along these (see Figure 4).

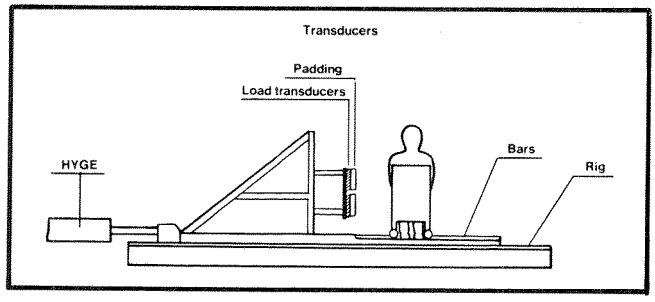

Figure 4. Side collision rig mounted on HYGE

The rig is geared to the desired impact speed and acceleration after dummy impact. The dummy seat remains still until the wall hits the dummy.

Three load transducers and an accelerometer are mounted on each steel plate to which chest padding and pelvis padding are fastened (Figure 5). They measure the load and rate of acceleration at pelvis and chest when the dummy is hit. Impact times for chest and pelvis padding are recorded by means of two zero triggers. The accelerometers on the steel plate and on the far side of the ribs record the intrusion in the padding after two integrations. As an extra check on the padding intrusion, a sliding potentiometer is also used. With a few additions, the rig can easily be adapted for simulation of B-pillar impact.

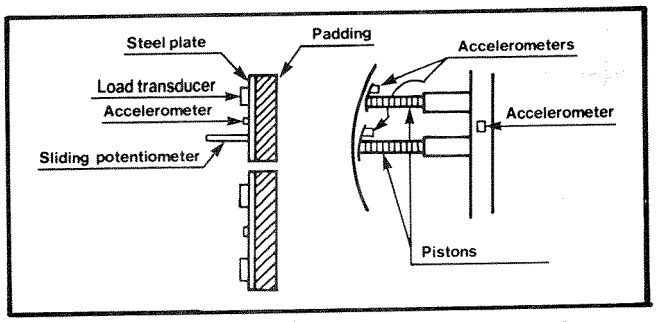

Figure 5. Transducer positioning in wall and dummy chest

Results of Full-Scale Tests

Type of Bullet

Structure

Tests 1 and 2, i.e., Volvo 240 versus Volvo 760 and MDB versus Volvo 760 (see Table 1), show the residual deformation is considerably greater at chest height in the case of an MDB 76 than in that of a Volvo 240. At pelvis height, on the other hand, the deformation is greater for the Volvo (Figure 6). The same results are obtained using

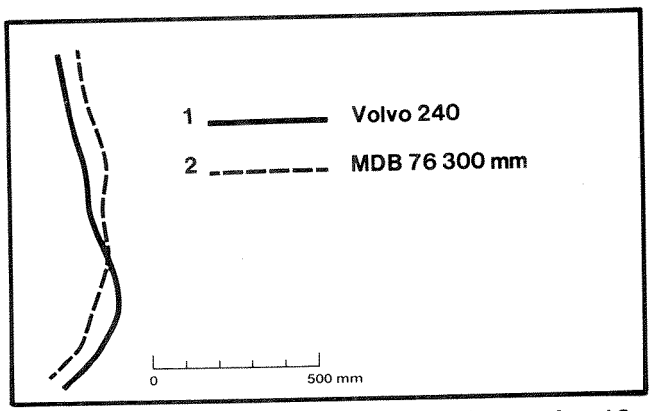

Figure 6. Internal deformation of B-pillar in tests 1 and 2

a Volvo 240 as target in the 90° test configuration (Figure 7). The Volvo 240, however, is relatively rigid in the bumper region compared with other car models, which can also be seen from the field accidents that have been analyzed.

The field cases (Figure 2) also show the residual deformation of the B-pillar caused by the MDB 76 is greater at chest height, the difference being equivalent to that in Figure 6.

Figure 8 shows the wall speed on impact with the dummy is the same both at chest and pelvis height in test 2. It can also be seen that vc (wall speed at chest height) and vp (wall speed at pelvis height) are somewhat lower in test 1, and also that vc $<$ vp. This suggests that the MDB

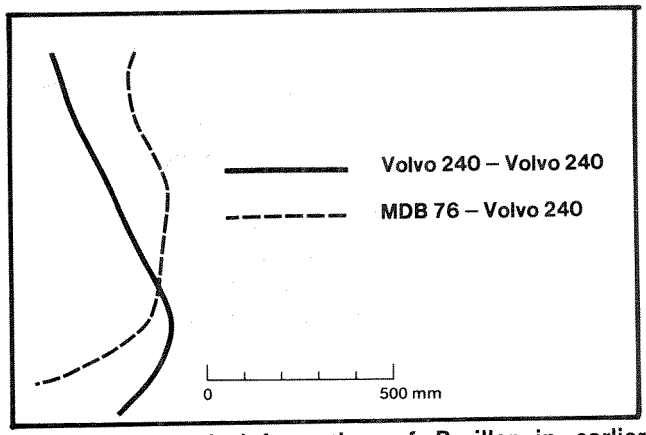

Figure 7. Internal deformation of B-pillar in earlier Volvo test series

76 loads the target's side structure more than the Volvo 240, and the load is more evenly distributed.

The dynamic intrusion process illustrated in Figure 8 shows there is no difference, at the time of dummy impact, between the Volvo 240 and MDB 76 at the point in the structure where measurement was made.

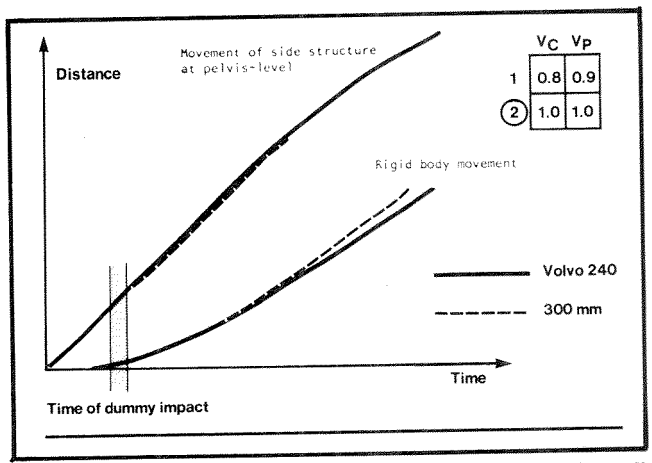

Figure 8. Comparison of intrusion patterns and wall speeds (v) in tests 1 and 2

Interior

The load on the dummy, like the residual deformations, varies greatly regarding chest and pelvis from test 1 to test 2 (see Figure 9).

The different evaluation parameters are for the comparative analysis normalized so that values in test 2 are set to 1.0, and the values for test 1 are given in relation to this.

The level of acceleration at the ribs depends on the impact speed, and maximum acceleration occurs soon after the dummy is hit. Max Cr occurs when the dummy's deflection pistons bottom out, since the dummy is relatively compressible to begin with before going too rigid. The Cr level is thus extremely dependent, at a later stage, on the intrusion speed.

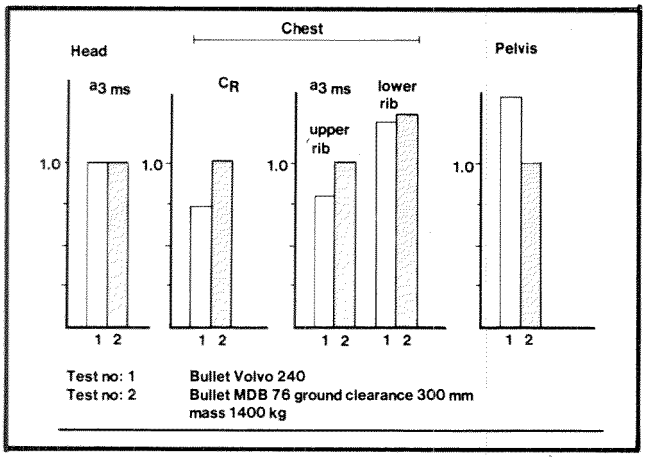

Figure 9. Dummy response in tests 1 and 2—normalized values

Figure 9 shows that the Cr in the dummy is higher with an MDB 76 with a ground clearance of 300mm as the bullet than for a Volvo 240, while the acceleration levels at pelvis height are lower.

Comments

It is clearly unsuitable to model a car's side impact protection on the basis of a specific car model as the bullet. The above results suggest, however, that the MDB 76, 300mm, does not satisfactorily represent either the Volvo 240 or the colliding vehicles in the field accident analysis. It is our opinion tests should be carried out with a bullet that, in respect of the decisive criteria, is more representative of the average car. Certain modifications to improve the resemblance of the CCMC barrier to the average car are discussed further on.

Mass of the Bullet

Structure

A reduction of 450kg in the mass turned out to have little effect on wall speed at chest and pelvis level on impact with the dummy (Figure 10).

Figure 10 shows that dynamic intrusion is not affected appreciably until after impact with the dummy, when the greater kinetic energy in test 2 results in a greater acceleration and, in the end, a greater residual deformation (Figure 11).

Interior

The speed of the intruding wall at chest and pelvis height at the time of impact is the same in both tests (see Figure 10). However, in the case of the lower barrier mass, the speed of the intruding wall at the time of head

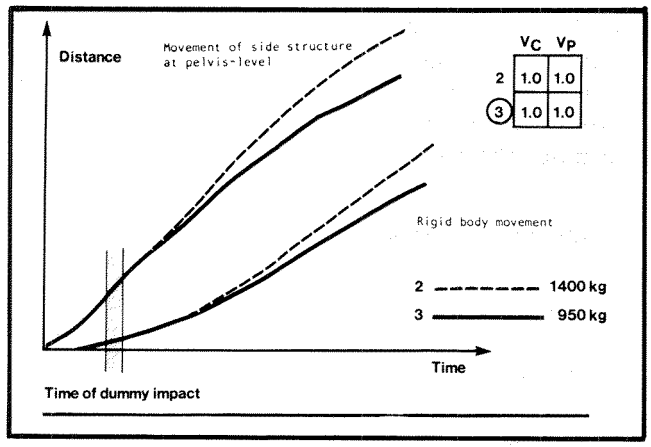

Figure 10. Comparison of intrusion pattern and wall speeds (v) in tests 2 and 3

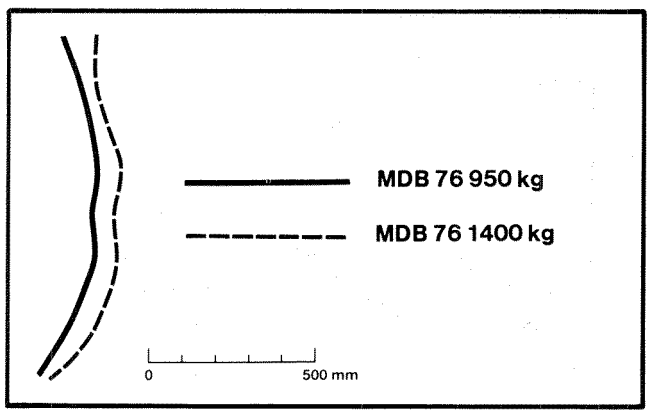

Figure 11. Internal deformation of B-pillar in tests 2 and 3

impact is lower, thus giving less severe head impact (see Figure 12).

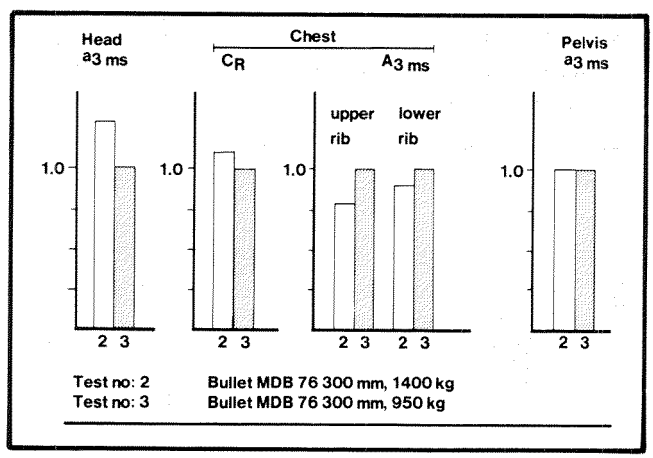

Figure 12. Dummy response in tests 2 and 3—normalized values

Comments

Greater mass means greater deformation of the target but no decisive difference in the loading of the dummy.

We find it preferable, for development reasons, to maintain a high mass in the bullet: first, to cause greater deformation in the target enabling us to pinpoint weaknesses in the structure, and, second, to take into consideration the heavier vehicles in the field.

Ground Clearance of the Bullet

Structure

Lowering the ground clearance from 300 to 250mm means the overlap of the deformable foam front over the door sill structure of the target is bigger. This, however, has little effect on the wall speeds at chest and pelvis height on impact with the dummy (see Figure 13).

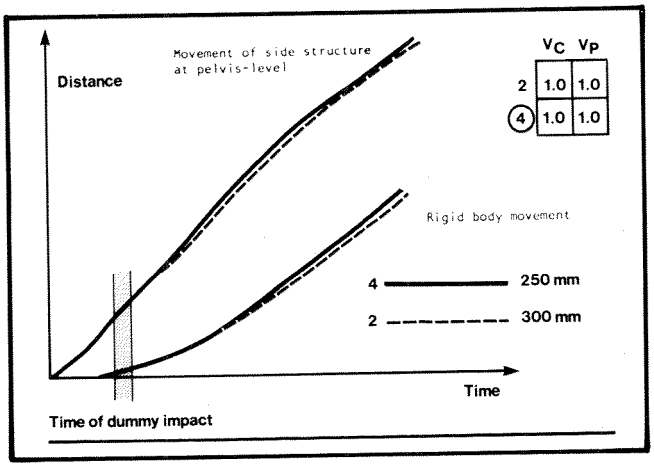

Figure 13. Comparison of intrusion pattern and wall speeds (v) in tests 2 and 4

The residual deformation of the B-pillar at chest height is less than the intrusion caused by a barrier height of 300mm. Thus, the 250mm barrier height better resembles the situation for a Volvo 240 (see Figure 14).

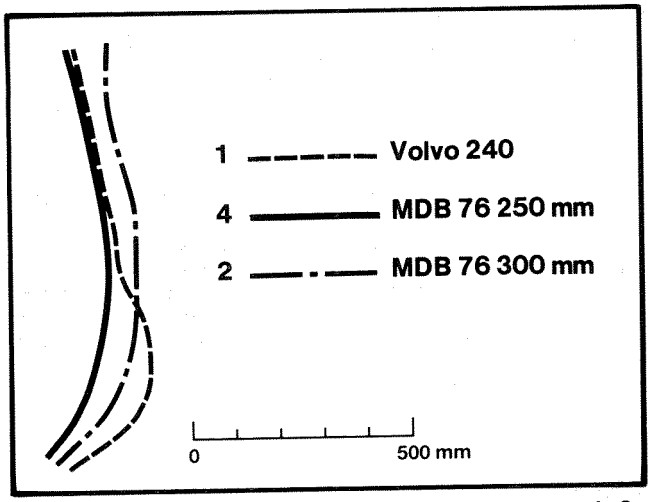

Figure 14. Internal deformation of B-pillar in tests 1, 2, and 4

Intrusion at pelvis height is, however, considerably greater with the Volvo 240. This car is stiffer than average in the bumper region, as was mentioned above, and this is also shown in Figure 15.

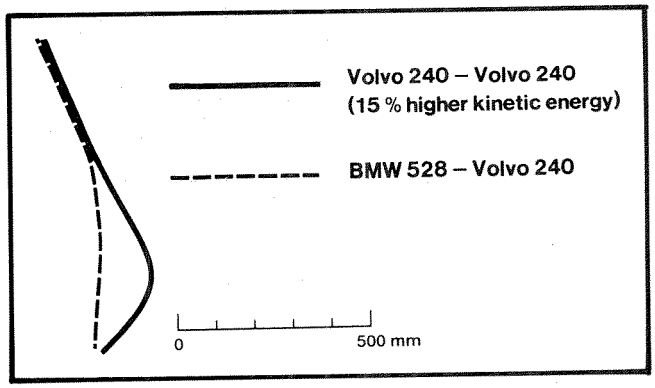

Figure 15. Internal deformation of B-pillar from Volvo test series in 1978

Interior

Lowering the ground clearance by 50mm resulted in a lower load on the chest. The load on the pelvis, however, was a little higher than with a 300mm barrier (see Figure 16). The chest value shows a good resemblance with the Volvo 240 as a test bullet, but the difference at pelvis height still remains. It should be pointed out the Volvo 240 is representative of the average car at chest height but is more stiff in the bumper region (see Figures 2 and 15).

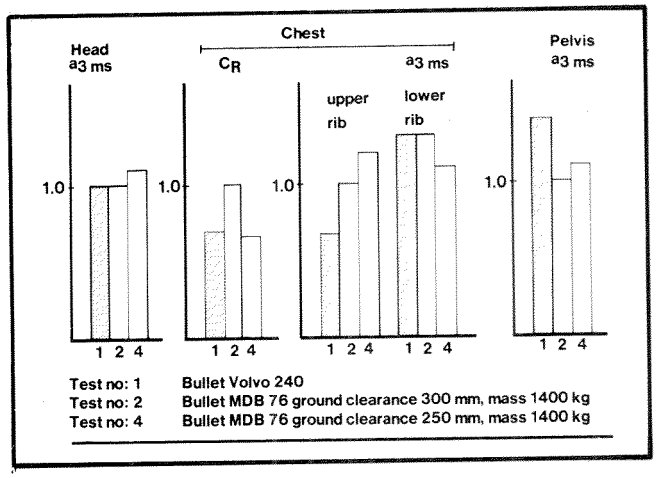

Figure 16. Dummy response in tests 1, 2, and 4— normalized values

Comments

Figures 2, 14, 15, and 16 together indicate that lowering the ground clearance to 250mm provides a more realistic load on the target's side structure and therefore a more realistic dummy response.

Structural Reinforcements and Padding

The residual deformation is appreciably less in test 5 than in test 4, which means the bullet must absorb more deformation energy (Figure 17). Despite this, the MDB 76 functions well and shows no tendency to bottom out. It should be mentioned that the target's mass, which amounts to 1,690kg with the two dummies, is considerably greater than that of many car models on the market.

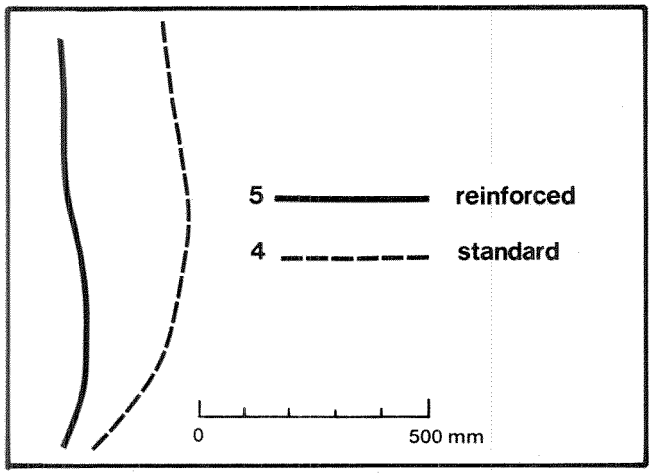

Figure 17. Internal deformation of B-pillar in tests 4 and 5

Comment

A structural reinforcement as extensive as that in test 5 considerably reduces wall speeds on impact with the dummy (Figure 18). This reinforcement leads to an increase of the velocity in the nondeformed parts of the target, which, in general, causes an increase in the relative velocity of the occupant's body as compared with that of the intruding side structure. The result of this could be a reduced effect of the reinforcement. However, this increase of velocity is very small at the moment the dummy is hit, and the reduction in velocity of the intruding side structure predominates, as can be seen from Figure 18.

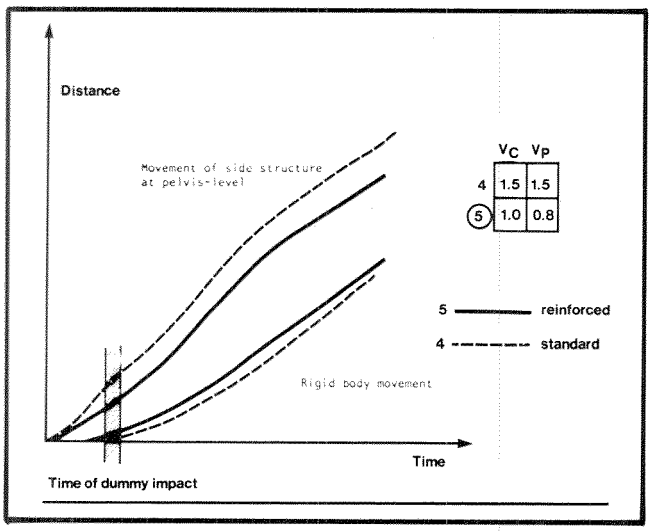

Figure 18. Comparison of intrusion pattern and wall speeds (v) in tests 4 and 5

The dummy response in Figure 19 shows the acceleration levels in the chest are considerably lower when padding is added together with a substantial reinforcement of the body structure.

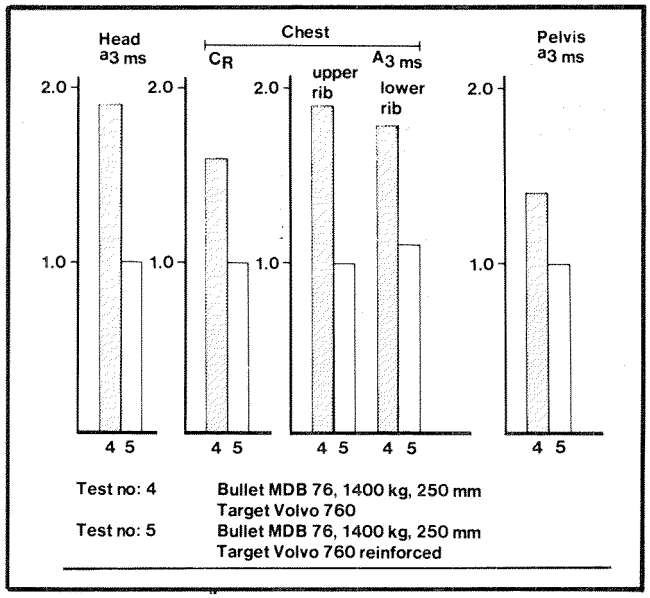

Figure 19. Dummy response in tests 4 and 5—normalized values

Crabbed Configuration

Test 6 was carried out in a 90°/27° crabbed configuration(5). Compared to test 5, the wall speeds with this configuration are affected to the extent that a small increase occurs at chest height and a slight decrease at pelvis height. Impact with the dummy takes place at about 20ms. Figure 20 shows no appreciable rotation of the target occurs until after about 40ms. However, the target is moved in parallel along a line about 10° from its lateral direction. This means that during the first 40ms, the target is exposed to a load that is almost the same as with a perpendicular configuration at 35mph.

The residual deformation of the B-pillar is slightly less than in the corresponding 90° collision, due to the fact that a large proportion of the bullet's kinetic energy is transformed into rotational energy throughout the system (see Figure 21).

Taking the cross sensitivity of the accelerometers into account, it is a very difficult task to plot the intrusion process and target acceleration laterally, since the target and the bullet do not move in the rectilinear manner throughout the process of deformation as in the case of the 90° configuration.

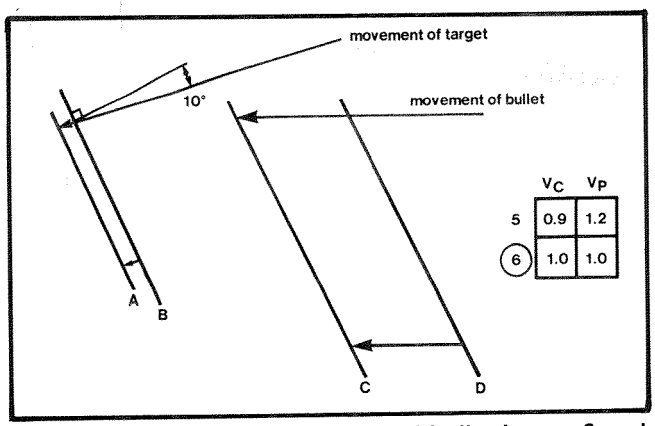

Figure 20. Movement of target and bullet in test 6 and wall speeds (v) in tests 5 and 6 (lines B and D—center line of target and rigid part of bullet at 0ms respectively; lines A and C—center line of target and rigid part of bullet respectively at around 40ms)

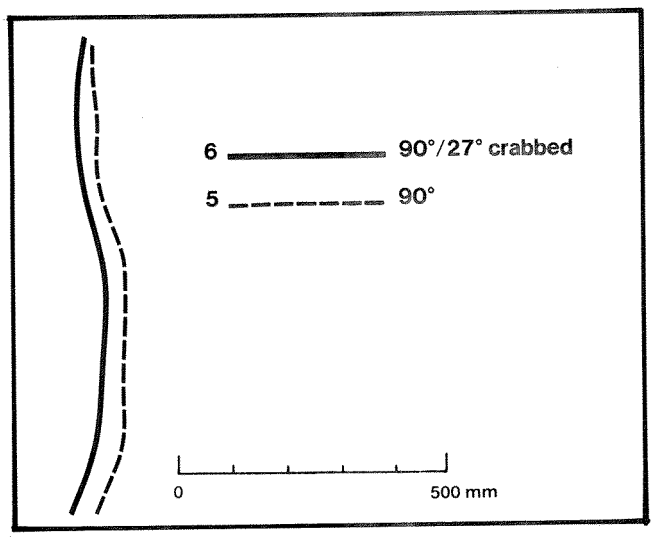

Figure 21. Internal deformation of B-pillar in tests 5 and 6

Interior

The effect of a 90° / 27° configuration on the response of the dummy is that the dummy does not impact the B-pillar of the Volvo 760. The head at 3ms is lower and the Cr increases, since no load is transferred through the shoulder part of the dummy but is entirely directed to the chest. The greatest difference concerns the load on the head, while the difference regarding chest and pelvis acceleration is fairly small (Figure 22).

Comments

The test in crabbed configuration showed the load on the car body is less severe laterally compared to the 90° configuration, and the dummy moves somewhat differently. The latter difference can, in development testing,

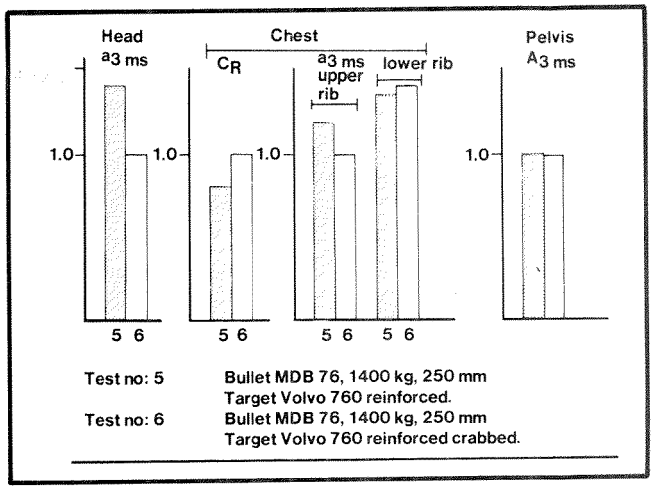

Figure 22. Dummy response in tests 5 and 6—normalized values

be obviated by altering the position of the seat so the dummy does not impact the B-pillar in case of a perpendicular configuration.

The perpendicular situation leads to greater lateral load on the structures added to improve side impact protection, as most of the kinetic energy is used for the deformation of the deformable front, deformation of the target's side structure, and acceleration of the target, without any significant amount transformed into rotation in the system. The perpendicular situation is thus more severe than the crabbed one, as far as the structure is concerned, when the impact speed normal to the side is the same. Even if the judgment is that field accidents are simulated more realistically by a crabbed configuration, there is, with the discussion above in view, still reason to let the main part of the development tests be conducted in the 90° perpendicular configuration.

Conclusion

The conclusion from this study is that a suitable side impact test method is a moving deformable barrier impacting in a 90° noncrabbed configuration. A good resemblance to real-life accidents is achieved with a CCMC MDB 76, mass 1,400kg, ground clearance 250mm, and impact speed 35mph. The motives for this are discussed above and briefly summed up below.

A moving deformable barrier was chosen as the bullet, since it is unsuitable to model a car's side impact protection on the basis of a specific car as the striking vehicle. The MDB 76 used with its standard ground clearance of 300mm did not satisfactorily represent the striking cars in the field accidents investigated, nor in the laboratory tests. Lowering the ground clearance by 50mm gave good results, however, in terms of car resemblance. Reduction of the mass to 950kg did not appreciably affect the dummy response, so the mass 1,400kg was chosen for development reasons to cover

also the American medium-size cars as striking vehicles and to pinpoint weaknesses in the side structure.

The chosen impact speed, 35mph, is in the upper range of the speed interval where severe and more serious injuries (AIS 3+) start to occur more frequently in Volvo 240 side impact accidents today. Therefore, this level must be kept if the object of future car designs is to improve side impact protection.

The differences, in terms of dummy response, between a crabbed configuration and a noncrabbed one were small. The advantage of a greater field accident realism, when conducting the tests in the crabbed configuration, were found to be overruled by the disadvantage of an increased test complexity. Thus, for development work, it is believed the noncrabbed configuration is more suitable. For the evaluation of certain design solutions, the performance in the crabbed situation must, of course, be checked at regular intervals.

Volvo will continue to work with the improvement of test methods for side impact testing. Some steps in this process will be—

- Further accident investigations and development of methods to assess side impact crash severity as a basis for improvement of the resemblance between real-life accidents and laboratory tests
- A complete evaluation of the different MDB's in terms of force-crush characteristics
- Testing with the NHTSA honeycomb MDB in different crabbed configurations
- Development of an MDB, based on the MDB 76, that measures deflection and force in several sections of the front
- Further development of the MDB front face based on experience from both field accidents and laboratory testing
- Extending the test methods with supplementary subsystem testing
- Further development work on side impact dummies
- Extending the test methods to cover accident types other than car-to-car impacts

References

1. Almqvist, R., H. Mellander, and M. Koch, "Frontal crash protection in a modern car concept," Proceedings Ninth International Technical Conference on Experimental Safety Vehicles, Kyoto, Japan, November 1982.
2. Norin, H., and J. Korner, "Volvo traffic accident research," Paper presented at SAE Conference, Detroit, Michigan, February 1985.
3. Norin, H., A. Nilsson-Ehle, and C. Gustafsson, "Volvo traffic accident research system as a tool for side impact protection evaluation and development," Proceedings Ninth International Technical Conference on Experimental Saftey Vehicles, Kyoto, Japan, November 1982.
4. Gebbels, D.R., "The CCMC mobile deformable barrier for lateral collision testing," to be published, Proceedings Tenth International Technical Conference on Experimental Safety Vehicles, Oxford, England, July 1985.
5. Klaus, G., R. Sinnhuber, and G. Hoffmann, "Mobile deformable barrier for lateral collision testing—a contribution toward a harmonization of future side impact performance requirements," SAE Paper 840888.
6. Hackney, J.R., et al., "Results of the National Highway Traffic Safety Administration's thoracic side impact protection research program," SAE Paper 840886.
7. Hue, B., et al., "Injury criteria in lateral collisions, when an APROD dummy is used," Proceedings Ninth International Technical Conference on Experimental Safety Vehicles, Kyoto, Japan, November 1982.

Side Impact Testing

J. Gratadour
P.S.A.

Abstract

Basic parameters that determine the occupant injury gravity, in a side crash are speed and the hit sidewall hardness. These two parameters are intimately linked together, and a full-scale reconstitution of a lateral collision does not permit their separation easily.

A method is presented in this paper that uses a subsystem-type test arrangement, reproducing the physical lateral shock sequence while having the two parameters separated. It then becomes possible to show the role played by different elements involved in a real-life impact:

- Impacting vehicle deformable front end part
- Impacted vehicle structure at the door inner panel, where deformability plays an energy-absorbing role

- Impacted vehicle structure at the body side, where side speed is rigidity-dependent

As a result of these tests, a subsystem test procedure should take into account the impacted vehicle side structure rigidity, and use a flexible prop fixed to the body, for the impact phase with a side impactor.

Introduction

Accident statistics generally show that lateral shock is the secondmost cause of injuries and fatalities, coming immediately after frontal shocks. The case of shock, vehicle against vehicle, is of great importance in side collisions. These well-established facts are acknowledged all over the world and will not be discussed further in this paper.

Due to its importance, side impact is the objective in numerous studies, be it at the level of accident study, biomechanics, representative dummies definition, or test methods.

As to vehicle evaluation test methods, three main directions are possible. In conformity with ISO-adopted terminology, they are—

1. Full-Scale Tests—Full-scale testing is a test or set of tests performed on the vehicle as a whole with anthropomorphic dummies, and chosen as a reference because of its representativity for a range of actual accidents (front or side collisions, for example).
2. Subsystem Tests—Subsystem testing consists of a test or set of tests sufficiently sophisticated to represent the important interactions between intervening parts. A test or set of tests will be qualified as subsystem testing if the following conditions are met:
   - The assembly includes a sufficient part of the complete vehicle tested to emphasize the interactions between various components of the vehicle.
   - The test equipment allows reproduction of those phenomena that contribute to injuring road users, in particular by taking into account interactions of body segments.
   - The test results are expressed in terms that can be correlated to the performance criteria of a given full-scale test, i.e., criteria based on human tolerance of impact (protection criteria).

   The fundamental basis of the subsystem concept is the concept of a system that permits a representation of the interaction between vehicle elements and the implicated road user. Only satisfactory representation of these interactions can lead to an optimization of the technical solutions.
3. Component Tests—Component testing is a test or set of tests of specific vehicle elements that provide a sufficient evaluation of the ability of these elements to provide road users protection without reproducing interaction of elements not included in the test.

Component tests are, in fact, used by all car builders for vehicle development and are obviously of primary importance for that purpose, while standard testing has to insure an effective level of passenger security and even to progress faster in it.

Component tests, however, used in the spirit of regulation, would not yield this true level of security. As a consequence, they would not permit whole vehicle optimization and could even block new and efficient systems applications if the latter do not enter in the regulation frame. This is not to the benefit of users and should be excluded.

The only regulation tests having some value are the full-scale and subsystem tests. The full-scale tests' advantage is due to their holding close to reality and thus they are easily justified; they are cumbersome, costly, and some improvement in their repeatability is desirable.

Hence the idea of defining the subsystem-type tests. Tests described in this paper bear the ambition to become, in their final definition, tests of the subsystem type. As of now, certain details need to be improved, and a more complete valuation must be achieved.

Notions of Wall Speed and Hardness

The basic idea of the work presented in this paper is that "the higher the speed of blow, the higher its hardness" and consequently "the greater one's injury." This is conducive both to the definition of wall speed and to body-side hardness, this being said for the case of lateral shock.

These are simple notions in appearance, but in reality they are very subtle to understand and should be handled with caution.

Wall Speed

Let us consider a collision of two objects, the following assumptions being accepted:

- The impact can be considered as a unidimensional phenomenon, forces and inertia forces being distributed well enough to ignore balance conditions in all but impact direction.
- Forces related to the masses located in the deformation zones are negligible in regard to deformation effects.
- Deformation effect laws in the zones where deformations occur are linear or at least, in all cases, equivalent in the two objects.

We consider the contact surface behavior of the two objects (Figure 1) at any time the following equation is true:

$$x_2 = x_o + l_o - v_o = x_o + l_o - \frac{F}{k_o}$$

$$x_2 = x_\Lambda - l_\Lambda + y_\Lambda = x_2 - l_\Lambda + \frac{F}{k_o}$$

$$x_2 = \frac{k_o}{k_o + k_\Lambda} x_o + \frac{k_\Lambda}{k_o + k_2} x_\Lambda + \frac{k_o l_o - k_\Lambda l_\Lambda}{k_o + k_\Lambda}$$

The speed of the contact surface is thus equal to:

$$V_\xi = \frac{k_o}{K_o + k_\Lambda} V_o + \frac{k_\Lambda}{k_o + k_\Lambda} V_\Lambda$$

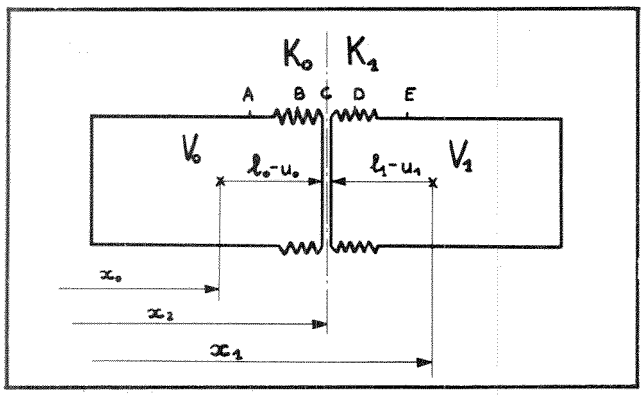

Figure 1.

This is conducive to the laws of velocity of the type illustrated in Figure 2.

The same theory is applicable to any other part of the contact zone (B or D). If the rigidity repartition in the impact zone is homogenous, the fact is conducive to the speed laws shown in Figure 2 relative to points B and D.

Now let us consider what is happening in a lateral crush where object 1 is the impacting vehicle and object 2 is the impacted. The occupant hits a sidewall, side of the body, the thickness of which is small and the speed practically uniform throughout the thickness. The speed is that of the body side, and its value can be evaluated using the above-described method.

Sidewall Hardness

The sidewall that is hit by the occupant is composed of the side of the vehicle body and also by the front face of the impacting vehicle in its crushing action. Its hardness will be a function of its building materials (influence of speed of shock on its rigidity) and also of its mass effect. To evaluate it realistically, it is necessary to come nearest to the true conditions of impact.

Test Method

The test method described in this paper consists of separating the analysis of the body-side speed, and consequently of the rigidity of the body side, from its hardness.

Body Side Rigidity

To study this rigidity, we use a rigid punch, the outer configuration of which reproduces that of a 205 front section after it has hit the side of a 205 body (Figure 3). More precisely, the shape is that of a 205 front section, carried out to fit the shape of a 205 panel after a lateral impact.

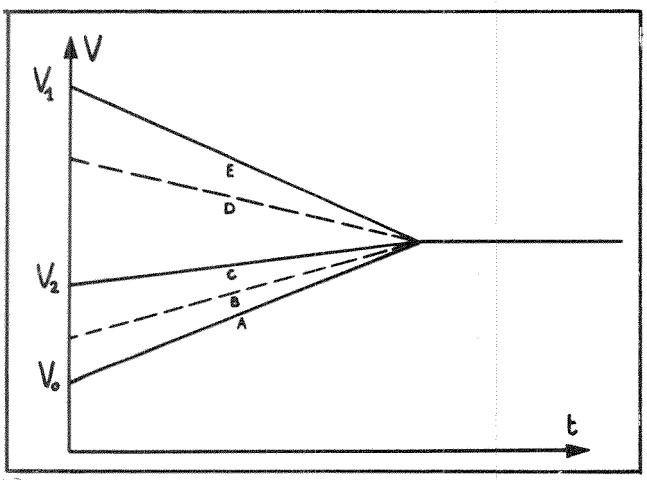

Figure 2.

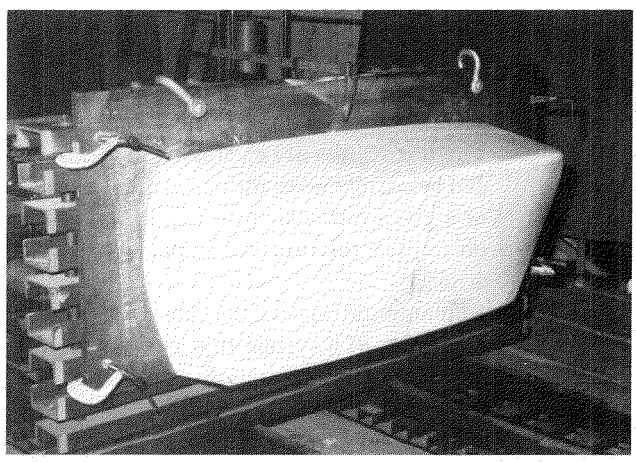

Figure 3.

This punch is fitted into a dynamometric movable wall (or barrier) facing the body being tested (Figure 4).

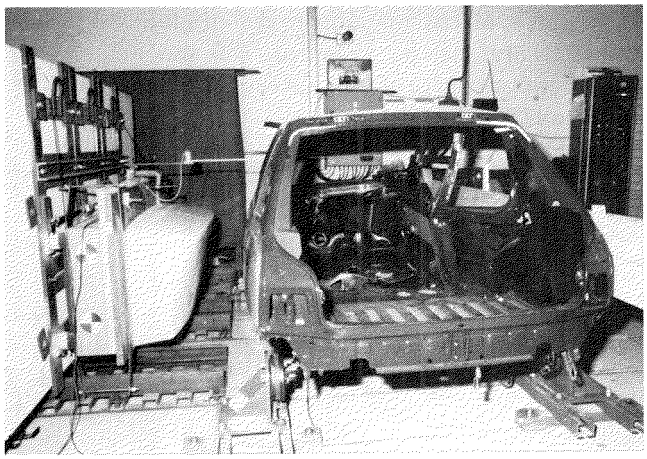

Figure 4.

The latter is fixed securely to the ground through its suspension system and moreover is buttressed on the opposite side by a prop. height; both the punch and side panel facing it are adjusted to the relative lateral post-impact positions 205 against 205 (Figure 5).

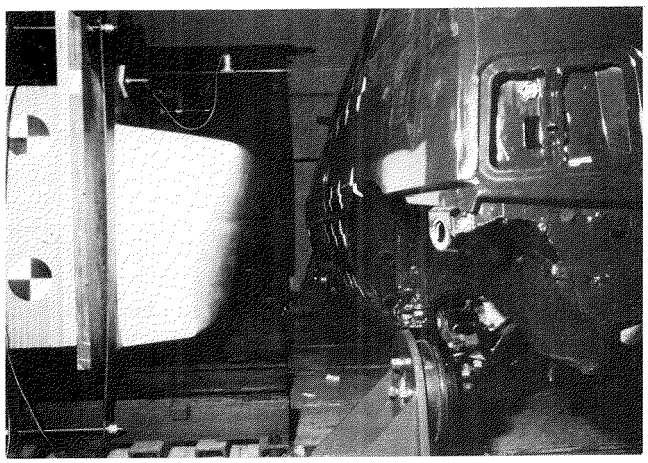

Figure 5.

This requires a slight engagement on a frame member. The punch is centered on point H of the driver as it is in a full-scale lateral impact test (Figure 6). The body is then crushed in a pseudo-static operation until the global shock deformation is obtained (Figure 7).

The applied force is measured and also the deformation of the body part facing the punch. The latter measurement is performed relative to the wall (to eliminate parasitic deformations of fixing bracings). Analysis of applied forces versus deformation curves permits the evaluation of the first parameter: speed of body sidewall.

This first operation being achieved, the crushed side of the body is recovered by cutting it out and will serve next for the second parameter evaluation, namely, the sidewall hardness.

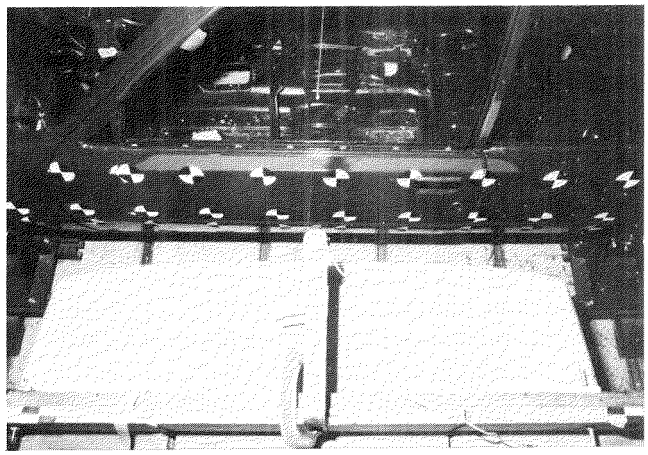

Figure 6.

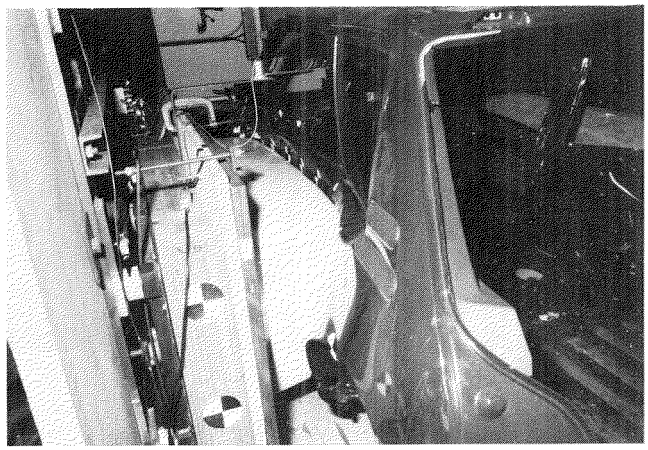

Figure 7.

Sidewall Hardness

The evaluation is performed dynamically (Figure 8). The impactor is a dummy APROD-82 (the same as used in full-scale reference tests).

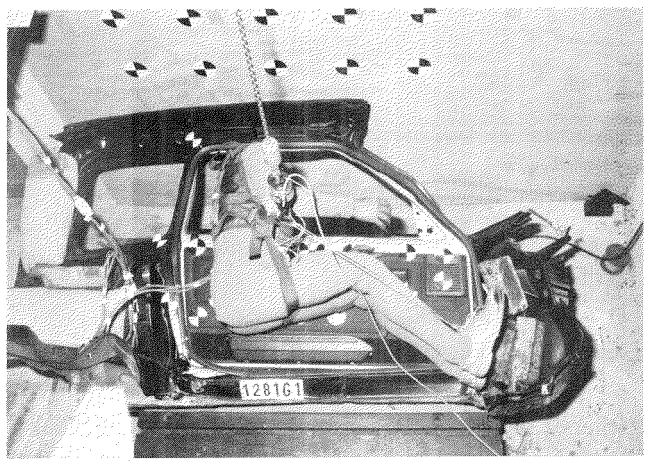

Figure 8.

Impactor (Figure 9) speed is obtained by dropping the dummy (free chute) from the height necessary to duplicate at arrival the body-side speed observed in the full-scale tests. In future tests, speed will be determined from the results of body-side crush tests. Impact configuration is selected to have different dummy body segments hit the same zones as in the full-scale test.

There will be no problem at this level if the dummy sensor wiring is correctly located so as not to interfere with anything during the drop, and if the dummy is kept motionless prior to its drop. Thus, it lands on the sidewall having the anticipated configuration.

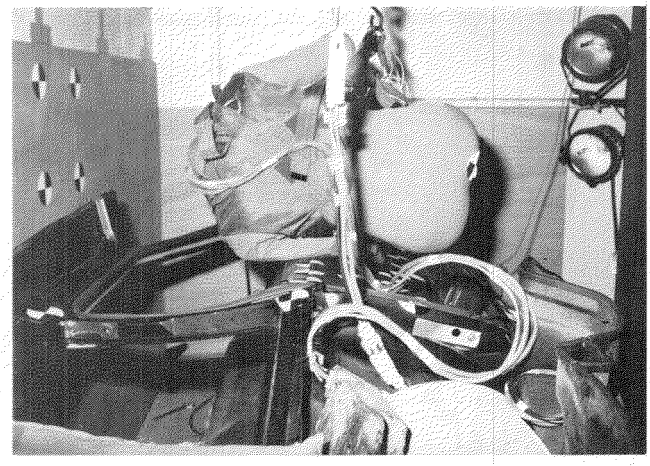

Figure 9.

Installation of the predeformed body-side panel requires a few precautions. It is installed on a foot base having the predeforming punds shape (Figure 10). This furnishes an excellent support to the body-side panel on the foot base: the body side bears on the entire impact zone of vehicle versus vehicle full-size collision.

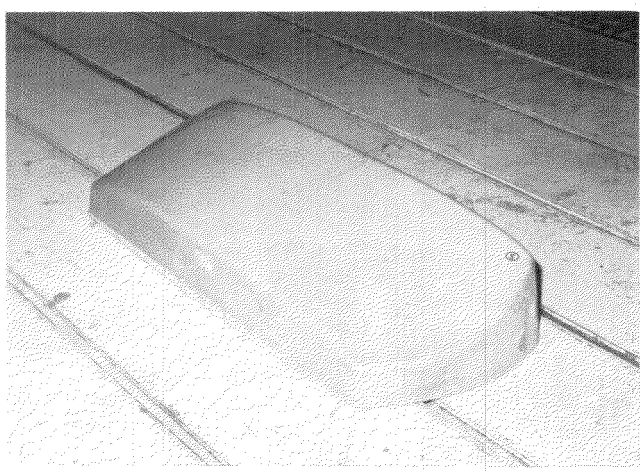

Figure 10.

The foot base used is constituted, according to the case, either by the punch itself or by polyurethane foam blocks. For future tests, the retained solution will be that of foam blocks.

In course of the impact dummy versus body-side panel, the contact effects between the body side and foot base may vary and even get inverted. To obtain a linear behavior, or at least one close to that of a full-scale test, a ballast charge has been applied. This was obtained by distributing a charge of 130kg at each end of the body side (Figure 11).

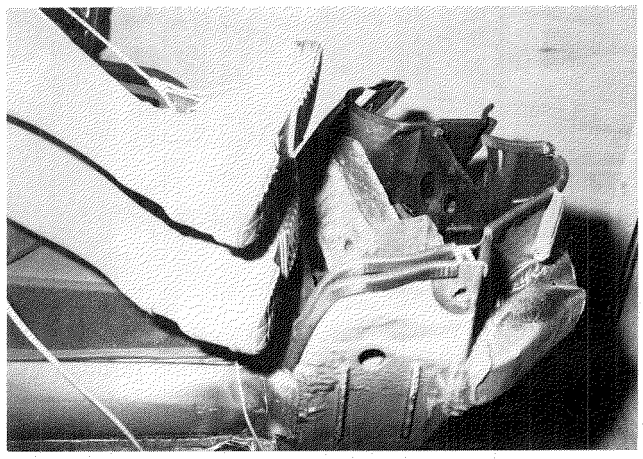

Figure 11.

Tests Performed

The above-described method has been applied in different configurations. The first aim was to validate the method relative to the full-scale testing.

Validation

The aim was to evaluate the correlation between this test and the full-scale test, in the case of the 205 car, for which a number of full-scale test results are available (3- and 5-door versions: car against car or with moving deformable barrier CCMC).

For dummy/sidewall impact, the chosen speed was that measured with the full-scale test, that is, 10m/s (corresponds to a fall from about 5m high). The only unknown parameter being the rigidity of the support simulating the full-scale test impactor, various configurations have been tested, either with a rigid support or a support made of polyurethane foam of various rigidities.

Although the speed of body side chosen was that of the full-scale test, its measurement is not immediate, and it was of interest to check the impact speed validity by means of some other parameter: the maximum ΔV of the occupant (Figure 12) for one.

At this level, an acceptable concordance has been observed. One can now examine the results (Figures 13 and 14). These figures represent the pelvis and thorax accelerations for different tested supports and full-scale collisions. What appears most clearly is the aberrant

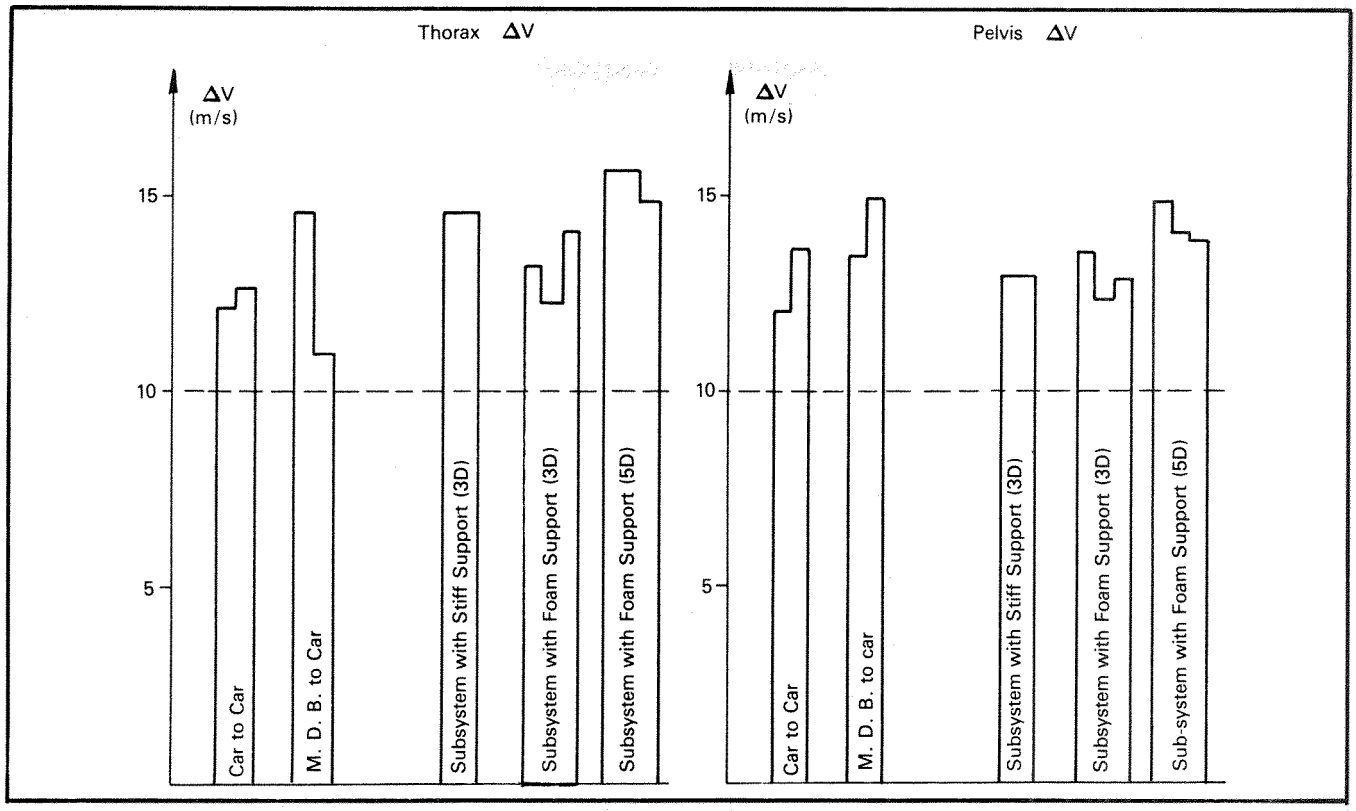

Figure 12.

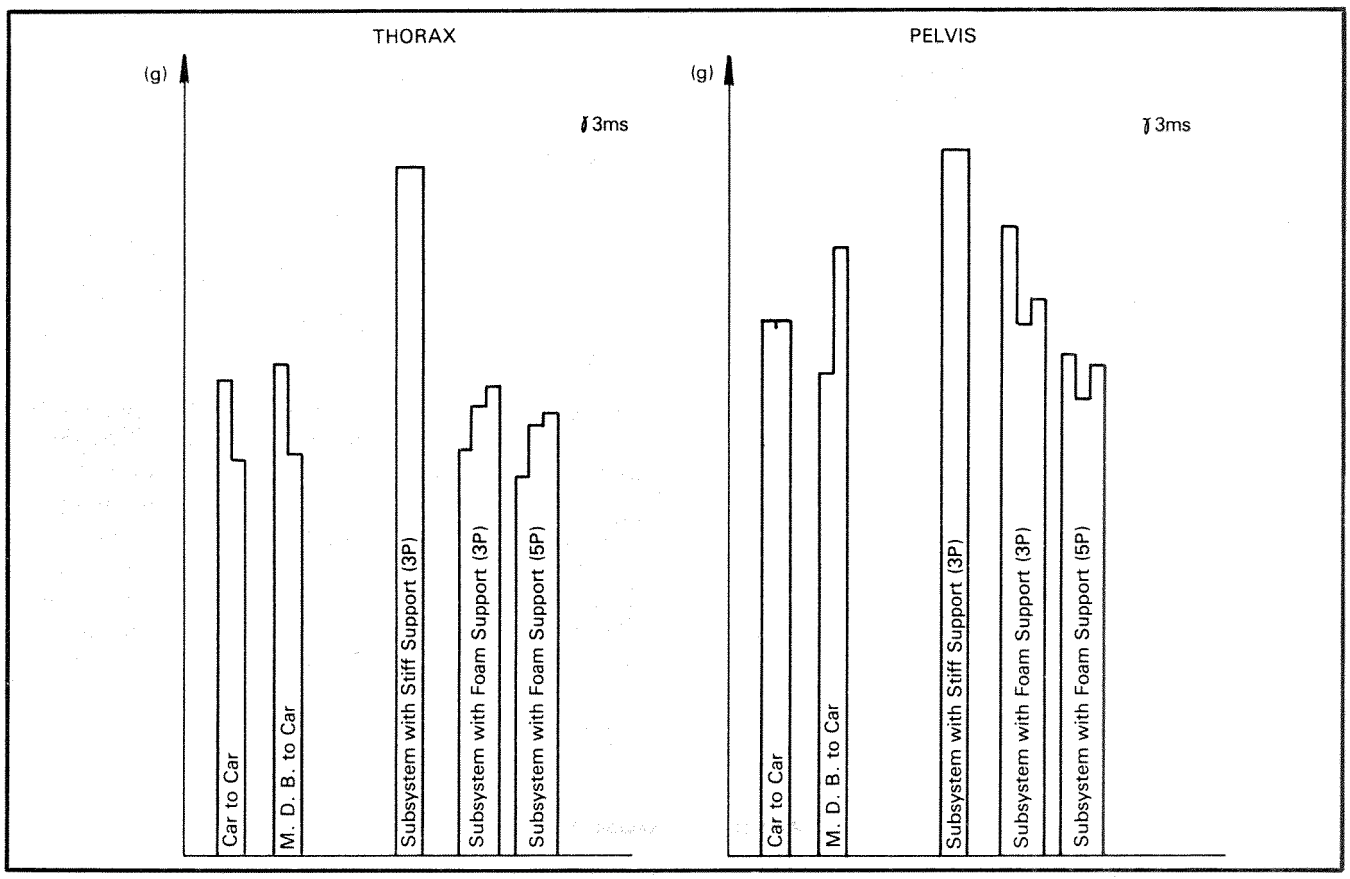

Figure 13.

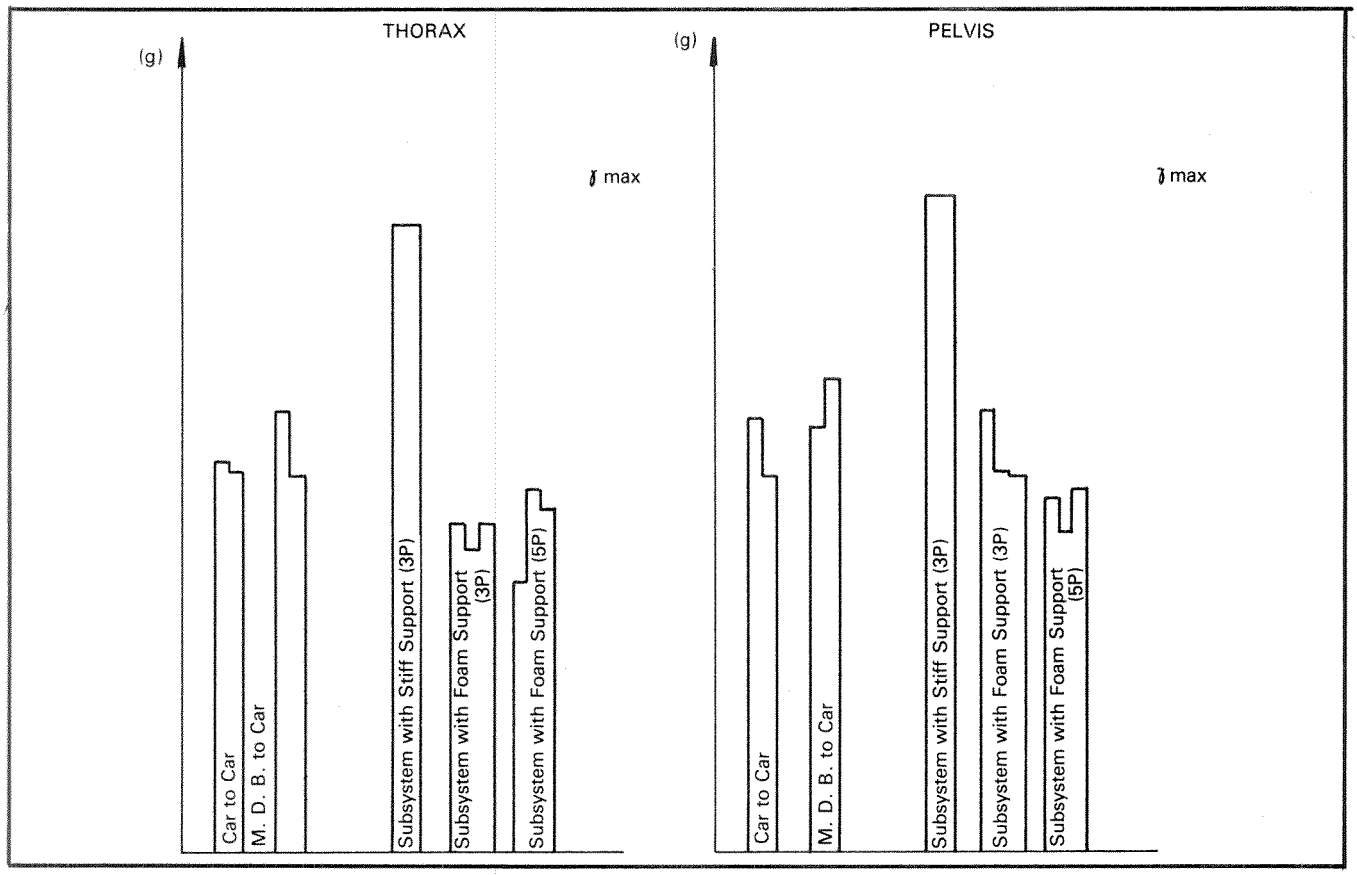

Figure 14.

characteristics of the test carried out with a rigid support. This test is of such violence that we have refused to reproduce it, so as to not destroy the dummy.

Values obtained with foam support are contained inside the full-scale test data dispersion.

At this stage of tests, the conclusions are as follows:

- In a test of the subsystem type, a rigid support against the body side does not permit a correct full-scale test simulation.
- A foam support of convenient rigidity permits an acceptable full-scale test simulation.

Influence of the Body-side Rigidity

The influence of body-side rigidity on occupant injury severity is a very controversial topic. This seems due to the fact that it is difficult to act on the wall speed without acting on its hardness, which generally reacts in opposite directions.

To clarify the problem, a reinforcement, which, in principle, should eliminate it, has been defined (Figure 15). To cope with this, no reinforcement has been added to the zones of impact with the dummy. Supplementary cross members were used—

- Behind the dashboard
- At the bottom of the A-pillar
- Under the seat
- On the rear floor

We also have reinforced the B-pillar and fixed a cross member between the two B-pillars at the height of body waistline, in order to have the opposite side work. It is to be underlined again that reinforcements are used only to demonstrate the principle of increasing body-side rigidity without increasing its hardness.

These reinforcements are absolutely not optimal, nor are all of them even useful. A body reinforced in this

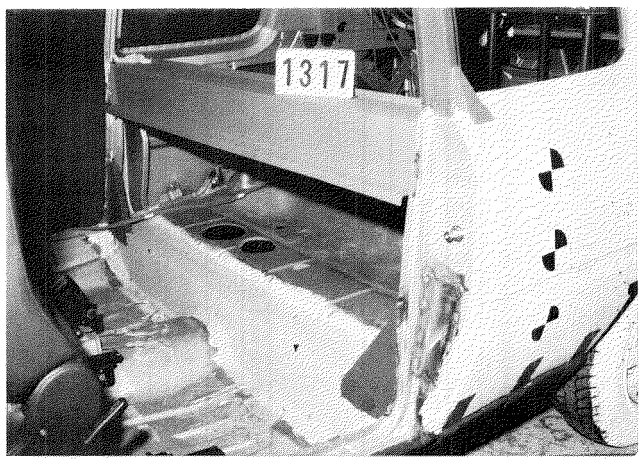

Figure 15.

manner has undergone a static crash test. The result is shown on Figure 16, compared with a vehicle from the production line. The maximum force level shows an increase (about 40 percent), but, more importantly, the mean rigidity at the start of crushing is practically doubled.

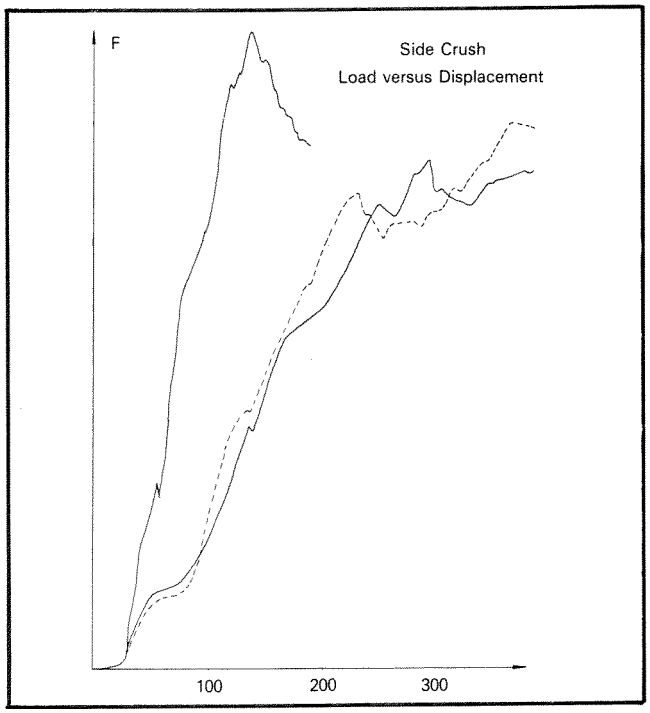

Figure 16.

A vehicle equipped with an identical reinforcement was submitted to the full-scale test with a CCMC mobile deformable barrier (Figure 17).

Figure 17.

Figures 18 and 19 show the results obtained at the thorax and pelvis levels. Thorax improvement is quite clear, on the order of 30 percent, but, for the pelvis, the improvement is less apparent. We feel two reasons clarify the phenomenon at the pelvis level. The CCMC mobile deformable barrier hardly hits the sill. Due to the great difference in rigidity between the body understructure and the door, the barrier overrides the sill, and the body understructure reinforcements do not perform their work. In spite of this, according to the measurement, the wall speed has notably diminished; consequently, it may seem that test dispersion played a false role here.

At this point of testing, the following conclusions have been made:

- Structural reinforcements are capable of having an important influence on the results, by means of wall speed.

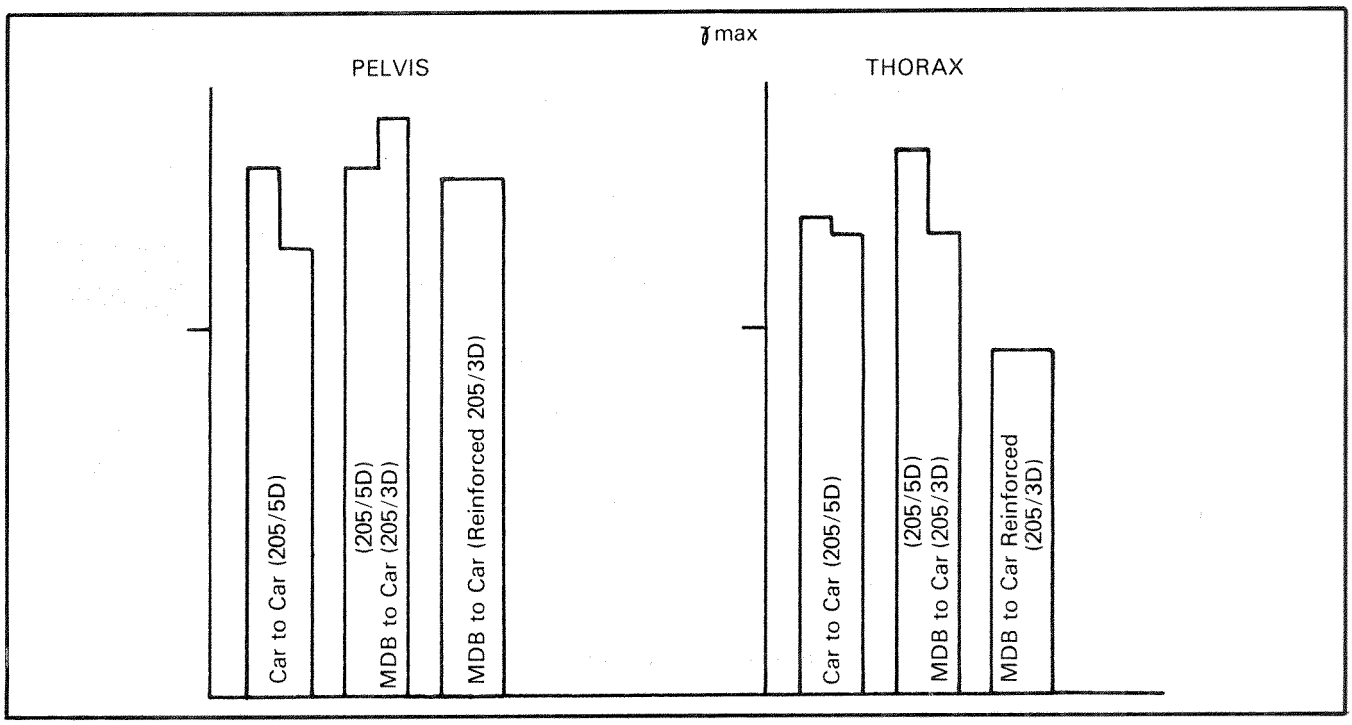

Figure 18.

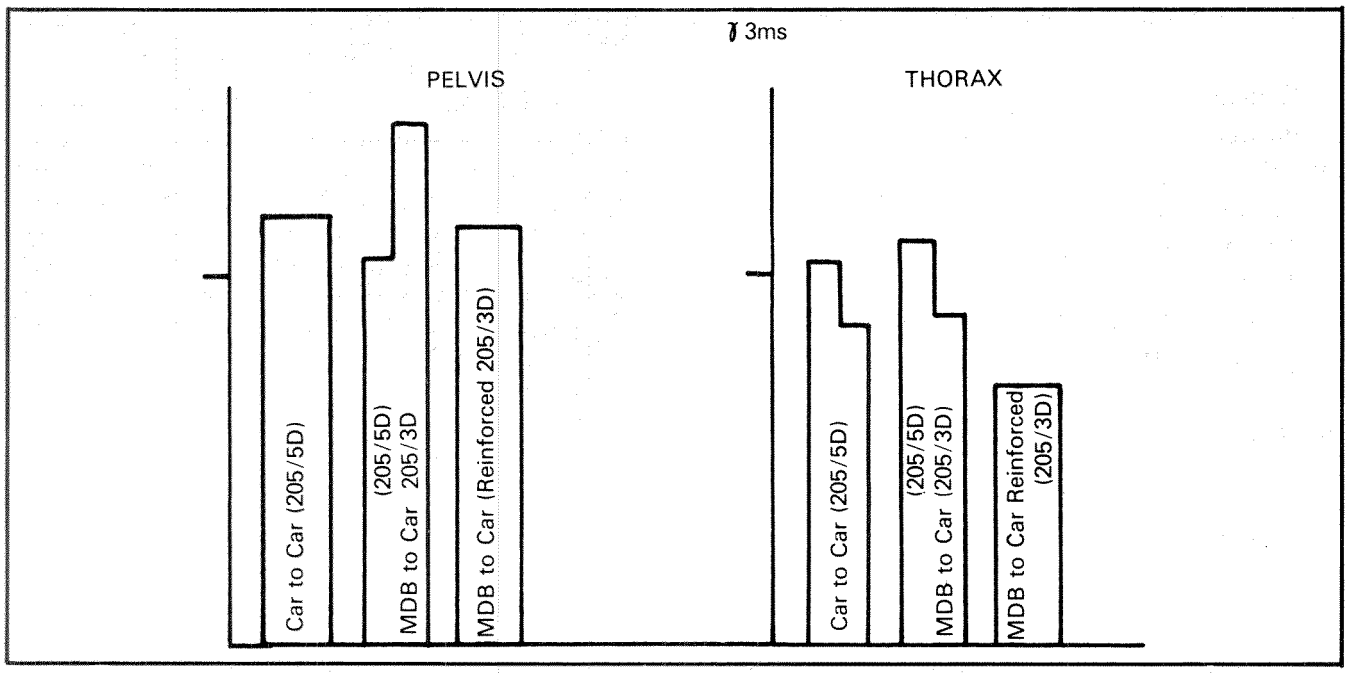

Figure 19.

- Interactions between elements (sill overridden by the barrier) are multiple, and for any simplified test it is hardly possible to take them all into account.

Conclusion

As stated in the introduction, component tests are not adapted for regulation purposes. The possibility of choice remains between full-scale tests and subsystem tests.

The above-described method is intended to enter the latter category. To become a true subsystem test method, it should be refined, particularly in what concerns the relationship between structure rigidity and wall speed. Once this is accomplished, the method will still remain cumbersome, and it is not clear whether it will have much to offer compared with a full-scale test.

One possible way to simplify it consists of a separate testing of different body segments. This has already been initiated by certain laboratories, but it is of absolute necessity to verify whether this method still permits body segment interactions. The problem of the abdomen, which has not been examined due to lack of adequate instrumentation, should not be forgotten.

Of some points brought to light in this paper, two at least are important:

- In a subsystem test, the support to be placed behind the body side for the test with an impactor must not be infinitely rigid.
- The influence of structural rigidity is an important factor and should not be neglected.

Testing the Side Impact Tests: Method and Some Initial Results

S.E. Henson,
M. Huang,
R.W. Hultman,
I.S. Parekh,
E.S. Grush, and
J.A. Pike
Ford Motor Company, Environmental and Safety Engineering Staff, Safety Research

Abstract

This paper addresses the general problems of selecting an impact test method. A test method must produce results that (a) are repeatable, (b) can distinguish between tested items that are of different design, and (c) predict real-world performance of the tested item.

The paradigm employed here is based on the notion that to identify the most appropriate test method among a set of candidate methods, one must compare the results of laboratory testing over a wide range of products with the results of actual field use of the various products.

This is difficult in a case where a new test procedure is to be evaluated and actual field data and laboratory data may not yet exist. This paper provides a methodology for assessing alternative test device concepts by means of simulation and applies it to the side impact test situation. This is done by (1) simulation of field accident experience of vehicles involved in side impacts, and (2) the simulation of test devices and procedures. Simulated test results can then be compared with simulated field accident data. This study shows some interim results for several impact test device design variations.

The principal tasks of this study were to: develop a vehicle occupant dynamics model suitable for estimating field results in side impacts; develop a test device dynamic model; select a range of alternative hardware configurations for both the simulated vehicle and the simulated test device; and develop random variable exposure distributions of accidents, vehicles, and occupants so the simulated "field" accidents cover a broad spectrum of exposure conditions. Approximately 90,000 simulations are run, using a Monte Carlo procedure, to estimate the distribution of outcome over the range of exposure conditions.

Introduction

This paper is the second in a series of side impact simulation papers. The first paper(1) given at the 1985 Government/Industry Meeting & Exposition described the project background and methodology. The current paper provides more detail.

Despite the exploratory nature of this study and the assumptions and simplifications embodied in the mathematical solutions, we believe the results show the substantial potential for test concept exploration this simulation methodology can provide. Two test procedures were chosen for simulation: the first, a simplified simulation of a mobile deformable barrier-type test; and the second, an early version of the MVMA Side Impact Test Development Component Procedure.

In the moving deformable barrier simulations, the results were not very sensitive to such things as the moving barrier weight, moving barrier face, or whether it was a SID or APR side impact dummy. While changes in the test parameters may make substantial differences in a single test, they did not seem to change the overall correlation of test results with simulated real-world performance.

The predictive power of the test procedure, in these results, was sensitive to impact severity. There appeared to be an optimal test severity, above or below which the predictive power of the test is diminished.

The comparisons between real performance and test performance on the component test procedures also showed a sensitivity to test severity. There was some small amount of variation in the predictive power of the test procedure as a function of the size of the test device (i.e., 40th percentile male, 50th percentile male, etc.). The results were somewhat similar among the model configurations that simulated the MVMA test device and variations thereon as well as the simulations of a rigid impact. The component test results were rather sensitive to car mass/stiffness, thus corroborating the frequently voiced expectation that such tests need to have an adjustable speed to account for variations in door gap and side structure stiffness.

In any case, the results presented are tentative and intended to serve as an exposition of the overall methodology. Future work will develop the speed compensation formula for the component test, expand the test parameters studied, and introduce the effect of test-to-test variability in test procedures into the model.

Correlation Coefficient Measures Test Performance

How do we measure the performance of a car safety test? We could draw a graph with the real-world injury rates of cars on the vertical axis and the test performance of cars on the horizontal axis as shown in Figure 1. For each car tested, we could plot a point on this graph representing the real-world injury rates and the test results of that car. We might expect to see a scatter of

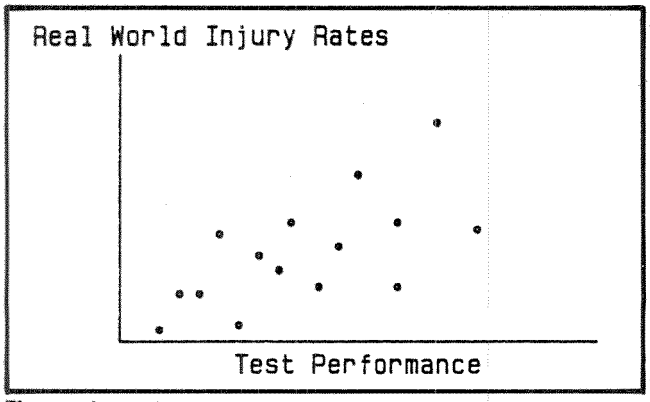

Figure 1. Validation plot—low correlation example

points if we plotted data for a number of different car designs. The scatter would come about because the test cannot possibly take into account all the different accident conditions represented in the real-world performance. If the test were a perfect linear predictor of real-world performance, then the points for different cars would all fall on a line (Figure 2). The correlation coefficient is a measure used by statisticians of how closely these points are to forming a line. If all the points fell on a straight line, the correlation coefficient would be one. If the points formed a completely random pattern, the correlation coefficient would be zero. So the correlation coefficient can be used as a measure of how well the test predicts the real-world performance—the higher the correlation coefficient, the better the test.

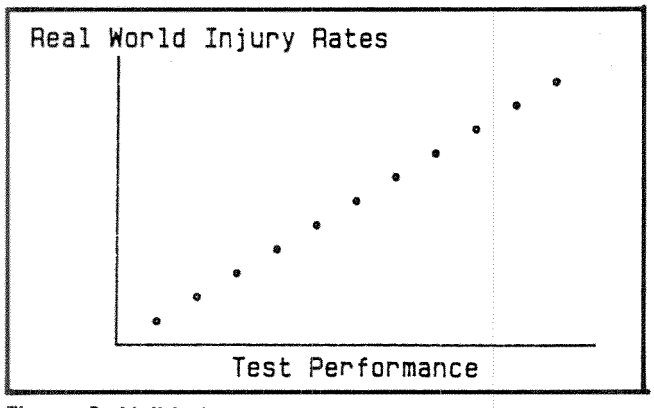

Figure 2. Validation plot—high correlation example

A Data Analysis Approach

How would one actually go about testing the predictability of a side impact test? One way might be through accident data analysis. Several vehicles could be chosen that are thought to have a range of side impact performance and have been in service long enough to have been in a large number of accidents. A measure of performance for these cars would have to be chosen, such as the total number of injuries, total number of fatalities, or some weighted measure such as harm. Because different vehicles experience different exposures to accidents, the measure of performance would have to be adjusted to take into account the different exposures. For example, the number of injuries or fatalities might have to be divided by the number of vehicles of each type in operation or by the number of miles driven annually by each vehicle. Also it may be necessary to adjust for demographic variables such as the age of the driver. The next step would be to test the individual vehicles with each proposed test. Plots of the injury measure versus the test performance could be made as shown in Figure 1. The calculated correlation coefficients would then be used to compare the tests—the closer the correlation coefficient is to one, the better is the test.

There are some problems with this procedure. Large variations in human tolerance and crash conditions will make it necessary to have a large number of accidents for each vehicle to show that the performance of one vehicle is actually different from that of another. Over the period of time needed to collect the number of accidents necessary, one or more of the vehicles may not remain in production unchanged from earlier models. Design changes could add to uncertainty in the results.

Another problem is in identifying and properly accounting for all the demographic factors such as driver age, which could influence the results. Many unaccounted-for demographic factors may be interpreted as a change in vehicle performance rather than a difference in accident involvement rates.

Also, it would be necessary to test several samples of each vehicle to account for test-to-test variability in test performance. The large number of tests required could economically limit the number of alternative candidate test procedures that could be included in the study.

Finally, there may not be vehicles currently in production with a wide enough range of side impact performance to allow discrimination among the vehicles in injury rates or in test performance. In that case, correlation coefficients for different tests would be effectively zero, and the performance of one test would be no different than another.

All things considered, the data analysis approach would be expensive, time-consuming, and would produce uncertain results. If vehicles are expected to be substantially changed by a new side impact standard, then results obtained from cars already on the road may not apply to these new vehicle designs.

Computer Simulation Is More Practical

Rather than actually performing the data analysis just described, we decided to simulate the data analysis approach on the computer. The computer simulation required four major steps:

1. Simulate a large sample of accidents for several different vehicle designs as if the accidents were randomly drawn from today's accident data.
2. Establish a measure of vehicle performance in the simulated accidents.
3. Test the different vehicle designs using a variety of computer-simulated tests.
4. Plot the scattergrams and calculate the correlation coefficients for the simulated real performance versus the simulated test performance for the individual vehicle designs.

A flow chart of the simulation is shown in Figure 3. We start with 105 distinctly different cars—15 cars in each of seven weight classes. Within each weight class, the 15 cars are made up of unique combinations of the following variables:

- Side structure strength
- Door interior padding thickness
- Door interior padding stiffness

The description of the hardware variables and the 15 experiments are presented in Appendix A.

For each of these 105 car designs, a crash model simulates a representative sample of 850 side impact collisions. The collisions differ in the following ways:

- Striking vehicle size and front structure stiffness

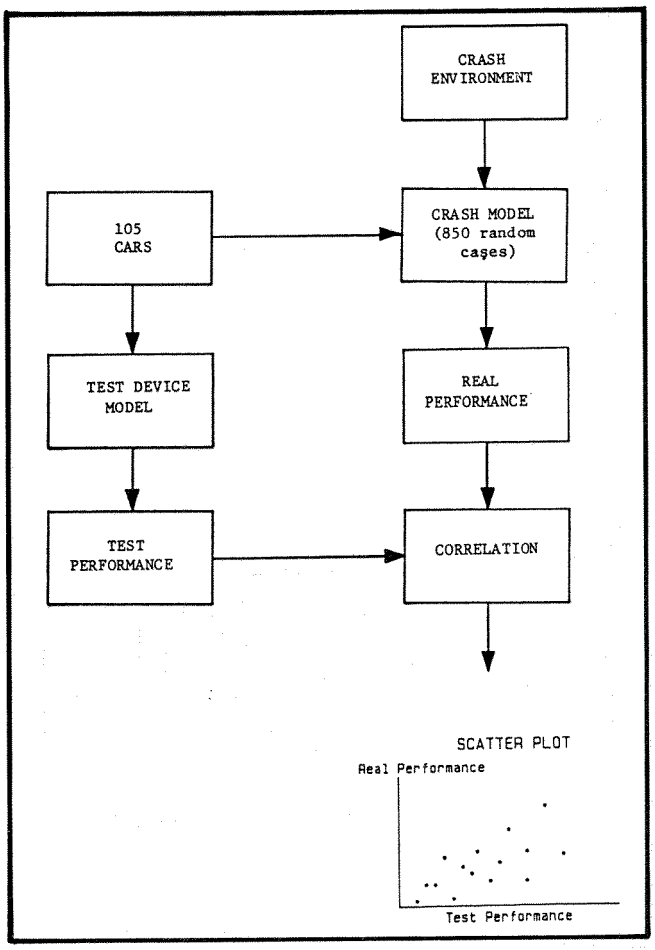

Figure 3. Flow chart of side impact simulation

- Striking vehicle speed and weight
- Driver size
- Driver gender
- Driver age

The crash model uses statistical distributions drawn from the National Accident Sampling System (NASS)(2) of these random collision variables.

In the real world, the safety performance of a vehicle is judged by the number of fatalities and injuries occurring to occupants of that vehicle. Since there are more of some vehicles on the road than others, the fatalities and injuries must be adjusted according to some measure of exposure to accidents. Common measures of exposure are the number of vehicles produced or the number of miles driven by a vehicle in a year.

There is an element of uncertainty in predicting fatalities and injuries from a computer model of crashes. The transformation to injury from the model output of such things as chest acceleration or chest deflection is not known with a great deal of accuracy. To avoid the extra complication of an uncertain biomechanical transformation, we decided to use the following outputs as measures of injury and accident severity for each of the 89,250 (105 $\times$ 850) side impact simulations:

- Rib acceleration
- Chest acceleration
- Chest force
- Chest deflection
- Thoracic Trauma Index, TTI(3)
- Bolster force
- Bolster deflection
- Door intrusion (for the full-vehicle tests)

Once the performance criterion levels were established, the performance of the 105 cars was calculated by finding the percentage of crash simulations for each car that was above the performance level. In this manner, the performance of the 105 cars was calculated for each of the six outputs of the crash model.

Each of the 105 cars was also tested using a test simulation model. The test simulation model simulated a component impactor-type test and a moving barrier full-vehicle-type test. For each of the 105 cars tested in the test model, five chest injury parameters were determined:

- Rib acceleration
- Chest acceleration (spinal acceleration)
- Chest deflection
- Thoracic Trauma Index

Since the study uses the Monte Carlo Method, the output of the model is a collection of 850 answers for each car design studied—a total of 89,250 results. Since we looked at four response measures, there was a total of 357,000 results. If the results are grouped into ranges and the count of the number of results falling into each range plotted as a bar chart for each vehicle design, the results form a statistical distribution as shown in Figure 4. We defined the measure of performance to be the number or

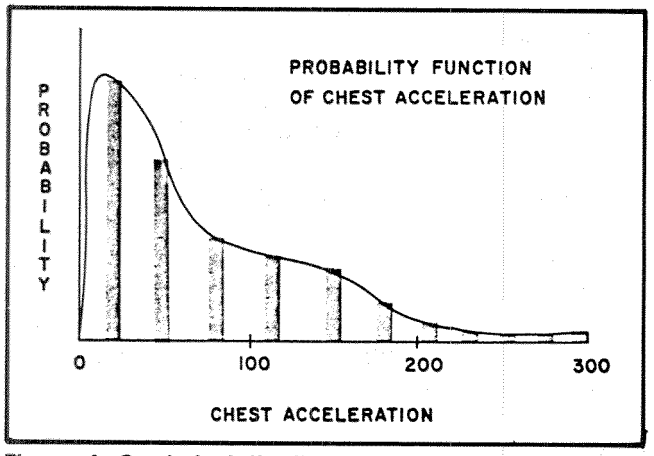

Figure 4. Statistical distribution—frequency counts

percentage of occupants who fell above an optimal cutoff value of the injury indicator. The performance measure is the area of the distribution curve above the cutoff limit. For example, the fewer the percentage of occupants receiving chest acceleration greater than 50, the better the performance of the vehicle.

The remaining question then is: "How do we pick the cutoff limit?" The cutoff limit was chosen to give the greatest difference in performance for a range of different vehicle designs. Choosing the cutoff limit in this way insures that the test procedure will have the best chance of discriminating among vehicle designs. For example, a different vehicle design might produce a different distribution of chest accelerations on the vehicle occupants when exposed to the same representative crashes (Figure 5). For any cutoff limit, the percentage of occupants above the cutoff level for Vehicle A will always be greater than the percentage of occupants above the cutoff for Vehicle B (Figure 6). However, as the cutoff limit increases from 1 to 2 to 3, the difference between Vehicles A and B becomes less and less clear (Figure 7). We chose the cutoff levels after the simulation results for all 105 vehicle designs were completed. We tried cutoff limits at small intervals across the whole range of occupant response until we identified the cutoff limit for each occupant response that made the standard deviation of the performance measure the greatest for the 105 vehicle designs simulated. The resulting cutoff limits are shown in Table 1.

The outputs of the test device model and the crash model, the test performance and the real performance,

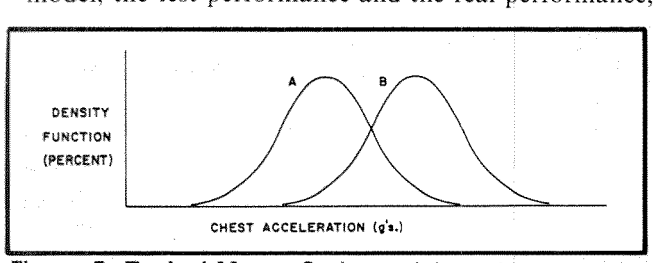

Figure 5. Typical Monte Carlo model results

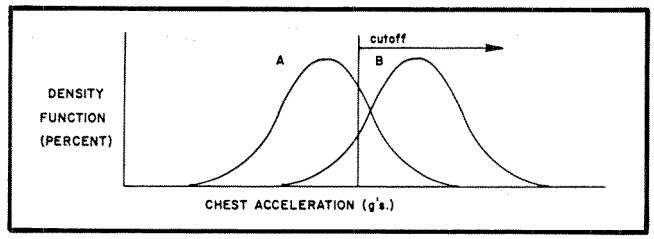

Figure 6. Monte Carlo model results—cutoff effect

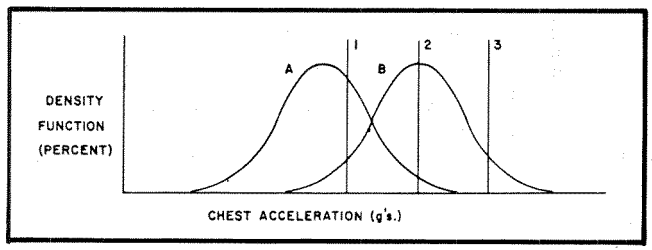

Figure 7. Monte Carlo model results—effects of various cutoffs

were compared for all combinations of responses by plotting the scatter plots of the real performance versus the test performance (Figure 3). Scatter plots and correlation coefficients were used to judge which test procedure and test readings best predicted the simulated real performance.

The individual elements of the model will now be discussed in detail.

A Computer Model of Side Crashes

The computer simulation used in this study was a lumped mass model very similar to others that appear in the literature(4). Six masses (Figure 8) and six energy absorbers are used to simulate a perpendicular car-to-car side impact. Table 2 lists the physical interpretation of each mass, energy absorber, and of the torso-to-pad clearance. Mass 1 represents the weight of the striking car, while energy absorbers 1 and 2 are used to simulate the striking car's crushable structure. The struck vehicle is represented by masses 2, 3, and 4, which are the door

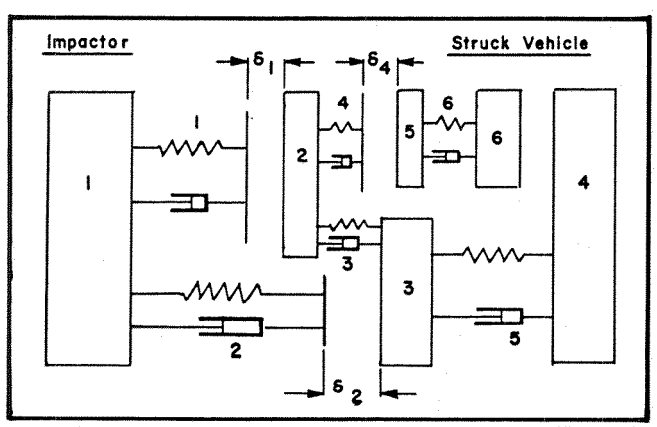

Figure 8. T-type side impact model schematic

Table 1. Optimal cutoff value, range and increments of side impact response variables

Variable	Range Lower	Range Upper	Increment	Optimal Cutoff
Rib Acceleration	0	290	10	90
Chest Acceleration	0	145	5	50
Thoracic Trauma Index	20	310	10	120
Chest Force, Kip	0	2.9	.1	1.4
Chest Deflection, in.	0	2.9	.1	0.6
Padding Force, Kip	0	5.8	.2	2.2
Padding Deflection, in.	0	5.8	.2	2.2
Door Intrusion, in.	0	8.7	.3	6.0

Table 2. Description of masses and energy absorbers used in the front-to-side impact model

Mass 1	—	Impactor Body
Mass 2	—	Door (Fender or Quarter Panel in L-Type)
Mass 3	—	Sill, A and B Pillars
Mass 4	—	Struck Vehicle
Mass 5	—	Rib Cage
Mass 6	—	Torso
EA 1	—	Impactor Front End
EA 2	—	Impactor-to-Sill
EA 3	—	Door-to-Sill (Side Panel-to-Sill in L-Type)
EA 4	—	Door Pad (Bolster)
EA 5	—	Sill-to-Struck Vehicle Compartment
EA 6	—	Torso-to-Rib Cage
δ 4	—	Torso-to-Pad Clearance

and side pillars, sill, and main car body, respectively. Energy absorber 3 represents the door-to-vehicle connection and the A- and B-pillars. Energy absorber 5 is the car underbody. A deformable occupant upper torso is represented by masses 5 and 6, with an initial gap, Delta 4, between the occupant and the energy-absorbing inner door surface, energy absorber 4.

In the study, masses 5 and 6 increase with occupant size. Energy absorber 6, the thorax stiffness, depends on occupant age and weight. The value of energy absorber 4, the energy-absorbing characteristics of the door inner surface, depends on the contact area of the occupant, which increases with increasing occupant size.

The occupant size being simulated affects many of the other variables in the simulation. It was found that chest stiffness is related to chest girth, so that larger occupants have stiffer chests. Since larger occupants are also wider, the gap between occupants and the door is smaller for larger occupants. These effects are accounted for in the model. The gap between the occupant and the door, Delta 4, depends on the car size as well as the occupant size. The relationships among all of these variables will be discussed more completely in the next section.

Input data for the model were gathered from crash test results of various size cars. Side impact models were defined for the seven car-size categories used in this study to represent the passenger car population. A set of baseline input data can be found in Appendix B.

The model was exercised over a range of collision speeds, and results were compared to side impact tests and the results of other computer model simulations. The model generally agreed with the trends and response levels found in the tests and other model results (Figure 9 and Appendix C).

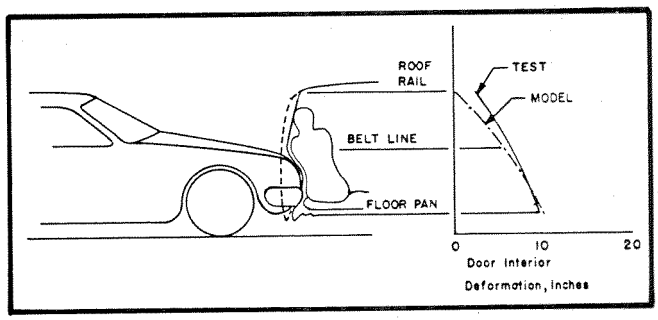

Figure 9. Comparison of side crushes between crash tests and the side impact model

The model was revised to simulate car-to-car collisions in which the impact point is near the front or the rear of the car (Figures 10 and 11). These collisions, called L-type, have little or no intrusion of the side structure into the occupant compartment and, due to the impact point, have a lower speed change at the center of gravity, and higher rotational velocity than the impacts to the occupant compartment, called T-type. The L-type collisions were modeled by exposing the occupant to the acceleration of the whole vehicle rather than the door and by softening the inner door stiffness since the door is not precrushed in the L-type collision. It was our judgment that the L-type model would produce a reasonably accurate simulation of the crash event while avoiding unnecessary complexities involved in a two-dimensional model with vehicle rotation. It is believed most of the occupant loading from the side structure in the L-type collision takes place before significant vehicle rotation has occurred. We also had to keep the models simple so it would be practical to run the tens of thousands of simulations necessary for this type of study.

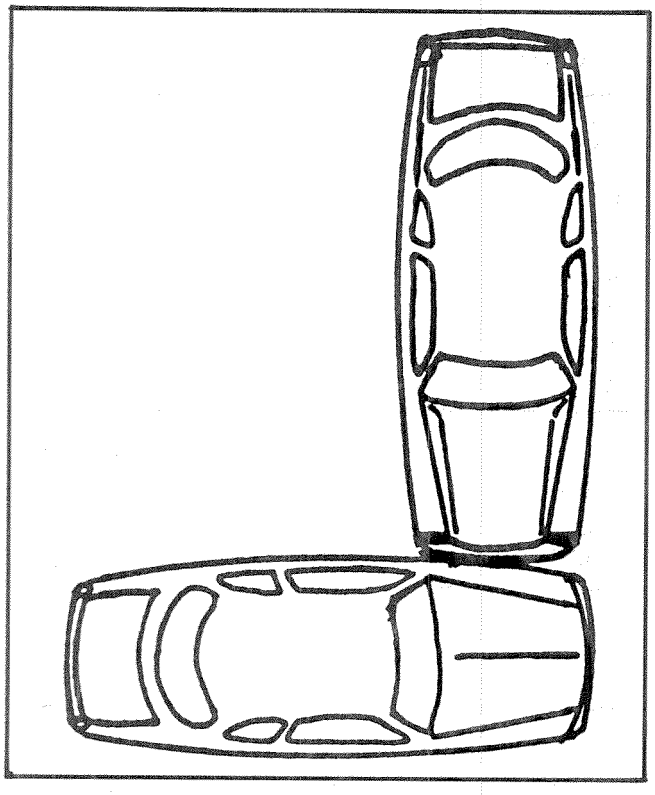

Figure 10. L-type collision

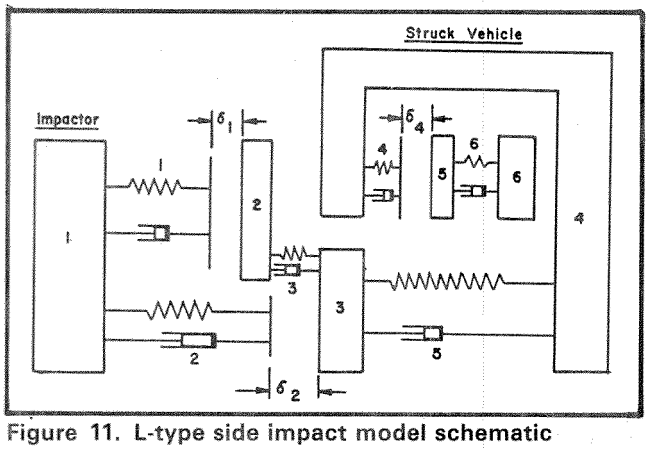

Figure 11. L-type side impact model schematic

Many Variables Considered

Car design can affect occupant dynamics in various ways. Our model considered cars with varying amounts and stiffnesses of energy-absorbing material on the inside of the door and several levels of side structure rigidity, which influences the speed of collision between the occupant and the side of the vehicle. A more detailed description of the study variables follows.

Injuries to occupants in car crashes can also vary widely from crash to crash because of the individual circumstances of each crash. The outcome of the collision is influenced by such randomly occurring variables as collision speed, car sizes, occupant size, occupant gender, and occupant age. There are many other variables that influence the outcome of a car crash, but the foregoing list was believed to be important enough to be included in this study. The effects of these random variables can be either direct or indirect. Variables such as vehicle speed and vehicle weight have an obvious direct effect on the severity of the collision. However, variables such as occupant size can have an indirect effect since larger occupants are closer to the door, and the occupant dynamics are known to be affected by the distance from the occupant to the door.

Door Gap

The definition of the door gap is shown schematically in Figure 12. The procedure used to determine this gap was based on the driver's elbow-to-elbow breadth, Society of Automotive Engineers (SAE) vehicle dimensions, and car size. The derivation of elbow-to-elbow breadth is discussed in a subsequent section, Occupant Size. Car size is defined as subcompact, compact, intermediate, and full size. The car size categories were determined based on wheelbases. These car size categories are discussed further in a subsequent section, Car Size. A range of cars was surveyed from 1978-82 model years to determine the Motor Vehicle Manufacturers Association (MVMA) shoulder room (W3) and centerline of driver (W20) for each car size. The cars used were not weighted for units in operation, UIO's (i.e., each car counted as a weighting factor of one). The space available between the interior of the door and the centerline of the driver for the cars surveyed was determined by—

space available = .5 * W3 - W20.

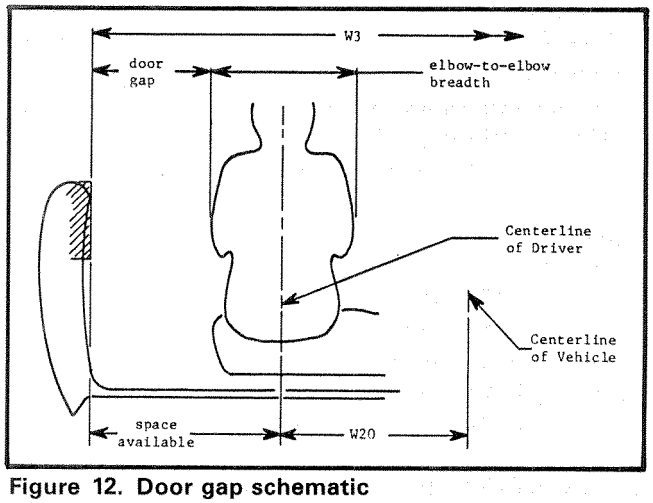

Figure 12. Door gap schematic

The means and standard deviations from the data were calculated. Table 3 presents the results of this analysis and the sample sizes used.

Using the statistical data from Table 3, the space available can be randomly determined from the following equation:

space available = mean + (number of standard deviations) * (standard deviation)

Table 3. Space available versus car size

Wheelbase (in)	Space Available (in) Mean	Standard Deviation	Sample Size
80-100	12.76	.44	11
101-111	14.00	.42	20
112-117	14.60	.68	12
118+	15.43	.77	8

No imports were included in the calculations with the exception of captive imports (e.g., Ford Fiesta).

The gap between the driver's torso and the interior door panel was determined for each car and driver combination.

gap = (space available) - .5 * (elbow-to-elbow breadth)

In the simulation, the struck car was widened or the occupants were moved closer together to account for the addition of the side bolster. Thus, the gap was kept the same as different size pads were simulated. However, no vehicle weight penalty was assessed for the side bolster or for widening the car.

Chest Stiffness

A stiffness parameter was calculated(5) from the thoracic force and deflection measurements made on 14 subjects reported by Tarriere(6) at the Seventh ESV Conference.

Linear correlations of this stiffness parameter with seven primary factors (age, sex, chest depth, chest circumference, subject weight, impact surface padding, and impact velocity) and the secondary factors, consisting of all two-at-a-time combinations of the primary factors, were calculated. These indicated that stiffness was most highly correlated with age and that the inclusion of chest circumference in the regression model improved the correlation (R^2 increased from 0.17 to 0.31 (while slightly improving the confidence level (85.2 to 87.2 percent).

To improve the correlation of the model without degrading its confidence level, a logarithmic transformation was tried. It resulted in a 3-term model, which, when compared to the 2-term model, had a greatly improved correlation (R^2 = 0.43, rather than 0.31) as well as a slightly improved confidence level (probability (of model being applicable) = 88.2 percent, rather than 87.2 percent). This regression accounts for about 43 percent of the variation of the data. The remainder, about 57 percent of the total variance of the data, is relegated to so-called unexplained variance.

This regression equation, relating the calculated chest stiffness (N/m) to the subject's age (years) and chest circumference (m) is given by:

$$\log_{10} \text{Stiffness} = K_1 * \text{Age} + K_2 * \text{Circumference} + K_4 + K_3 * \text{Circumference}^2$$

K_1 = -.014
K_2 = +33.4
K_3 = -18.4
K = - 9.1

The calculation of chest circumference will be discussed in the next section, Occupant Size.

Occupant Size

The driver's anthropometric data were based on the distribution of U.S. adult population age 18 to 79 as documented in the 1960-62 Health Examination Survey (HES)(7). The driver's age and weight were randomly determined using bivariate frequency distributions. The driver's gender was randomly chosen based on a 69/31 male/female mix. These characteristics were based on the 1979-82 NASS data base.

The anthropometric measurements used in developing the driver's profile are shown schematically in Figure 13.

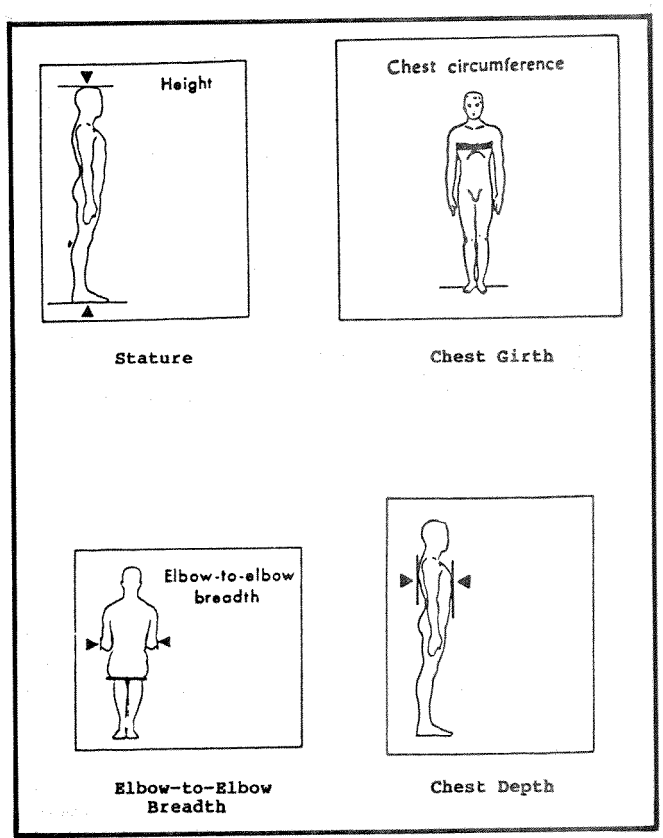

Figure 13. Anthropometric measurement definitions

Using the driver's age, weight, and gender, the driver's stature was based on bivariate data from HES(8). The height was randomly determined based on the distribution within each gender, age, and weight cell. Once the driver's height was determined, the chest girth and elbow-to-elbow breadth were determined. Multiple regression equations for these measurements as a function of height, weight, and age for men and women were derived from the HES data(9). The regression equations used are shown below.

Chest Girth (used to calculate chest stiffness):

- Male: chest girth = 33.206 - .201 * height + .114 * weight + .015 * age
- Female: chest girth = 30.321 - .150 * height + .094 * weight + .020 * age

Elbow-to-Elbow Breadth (used to calculate door gap):

- Male: breadth = 17.283 - .169 * height + .061 * weight + .017 * age
- Female: breadth = 14.060 - .148 * height + .060 * weight + .022 * age

where:

height in inches
weight in pounds
age in years
calculated quantities in inches

A correlation matrix is presented in Table 4. Eighty to 90 percent of the variation in these measurements are accounted for by the driver's weight.

Table 4. Anthropometric measurements correlation matrices

Male:

	Age	Height	Weight	Chest Girth	Elbow Breadth
Age	-				
Height	-.270	-			
Weight	-.058	.394	-		
Chest Girth	.062	.189	.885	-	
Elbow Breadth	.156	.069	.804	.833	-

Female:

	Age	Height	Weight	Chest Girth	Elbow Breadth
Age	-				
Height	-.270	-			
Weight	-.058	.394	-		
Chest Girth	.062	.189	.885	-	
Elbow Breadth	.156	.069	.804	.833	-

The driver's chest girth (chest circumference) and age were used as inputs to the chest stiffness regression model. This model was discussed in the section titled Chest Stiffness.

The last anthropomorphic measurement modeled was the driver's chest depth. Chest depth is used to estimate driver's contact area with door to calculate the interior door stiffness. The HES survey did not record this measurement. Since the correlation of chest girth with weight was high (approximately 90 percent), the assumption was made that the chest depth would be the same percentile as the weight. Using the data from HES(7) of percentiles versus weight, the driver's weight percentile was determined. This percentile was transformed into standard deviation. The data from the Henry Dreyfuss Human Scale Manual(10) for male and female chest depth gave means and standard deviations. The following equations present the chest depth data used.

Chest Depth (used to calculate driver contact area):

- Male: chest depth = 9.0 + .7653 * (standard deviation)
- Female: chest depth = 6.5 + .7143 * (standard deviation)

where the standard deviation is the same as for the driver's weight.

Car Size

The car size algorithm for determining struck car weight versus struck car size was based on the CRASH3 program(11). The algorithm had seven vehicle categories versus a range of wheelbases. These CRASH3 wheelbases were needed to allow using the National Vehicle Population Profile (NVPP) data for determining the frequency of vehicle size versus vehicle weight in the real world. The CRASH3 vehicle categories were also needed for obtaining basic structural characteristics of the struck car and striking vehicle during the side impact simulation. To facilitate using the NVPP data, the CRASH3 wheelbases were rounded to whole numbers. The CRASH3 categories were then combined into the more traditional car sizes to develop the gap between the driver's elbow and the interior door trim. The gap categories were based on an algorithm of car size used by NHTSA and MVMA for the MDAI (Multidisciplinary Accident Investigation Data File)(12). Table 5 shows the relationship of these categories.

Accident and Vehicle Exposure Variable Distributions

Data Base

NASS data files from 1979 to 1982 were used for the accident and vehicle crash exposure variables. The NASS data are a probability sample of each year's nationwide

Table 5. CRASH3 category wheelbase comparisons

CRASH3 Category	CRASH3 Wheelbase (in)	Rounded Wheelbase (in)	Traditional NHTSA & MVMA Category	Wheelbase (in)
1	80.9 - 94.8	81 - 95	Subcompact	80 - 93
2	94.8 - 101.6	96 - 102		94 - 100
3	101.6 - 110.4	103 - 110	Compact	101 - 111
4	110.4 - 117.5	111 - 117	Intermediate	112 - 117
5	117.5 - 123.2	118 - 123	Full Size	118+
6	123.2 - 150	124+		
7	109 - 130	Lt. Truck	Lt. Truck	Lt. Truck

motor vehicle accidents for which candidate accidents were chosen with varying probabilities. The selection of the final side impact data base was made by applying the following filters to NASS data files.

- Accidents involving two vehicles
- Struck cars—direction of force (highest) 2 to 4 o'clock or 8 to 10 o'clock
- Striking vehicles—either cars or light trucks

The detailed NASS vehicle selection criteria are given in Appendix D. Unless stated otherwise, the analysis of each NASS variable was performed on weighted data by using National Inflation Factors as weights. Background information on the NASS files is given in Appendix E.

NVPP data files from 1979 and 1980 were used to obtain the distribution of vehicles in use by weight and size (wheelbase). The NVPP data are compiled by R.L. Polk from State registration files as of July 1 of each calender year for model years back to 1966.

Exposure Variables

The following variables described the individual accident simulations:

- Weight of struck car
- Weight of striking vehicle
- Vehicle wheelbase
- Delta V of struck car and striking vehicle—used in estimating impact speed of striking vehicle
- Driver's age
- Driver's height
- Driver's weight

Method of Establishing the Collision Sample

The NASS and NVPP data were analyzed to establish the frequency distribution of each variable. Some of the variables were believed to be correlated, that is, certain combinations of their frequency distributions would occur more often than others. To determine the degree of their dependence on each other, the correlation coefficients between them were estimated and tested for their being different from zero. The analysis was performed by using the Statistical Analysis System (SAS), a highly flexible statistical package. SAS has been implemented for NASS files by storing each year's NASS file as a SAS data base. When the side impact study was launched in early February 1984, SAS was implemented for 1979 and 1980 NASS files only. So, the first estimates of the correlations were made from 1979 and 1980 NASS files. These estimates were twice updated since then, once in June when the NASS 1981 file was added and again in July when the NASS 1982 file was added.

The analysis of NASS 1979 and 1980 data was performed on the combined sample of male and female drivers. The results of their analysis are shown in Table 6 (raw data) and Table 7 (weighted data). They include the summary statistics and the correlation coefficients. When more data were added from NASS 1981 and 1982 files, the analysis was also performed by driver's gender, in addition to the analysis of the combined sample of male and female drivers. The results of the analyses by driver's gender are shown in Tables 8A-8B (raw data) and Tables 9A-9B (weighted data).

The results from NASS 1979 through 1982 weighted data showed some degree of dependency between driver's age and weight parameters. The correlation coefficients for male and female drivers were 0.13 and 0.30, respectively.

Bivariate Frequency Distributions

- Bivariate frequency distributions of driver's age*weight were generated separately for male and female drivers (Tables 10 and 11).
- Struck passenger cars' wheelbase*weight distribution (Table 12) was obtained from NVPP passenger car units in operation data. The data showed a high correlation between car weight and car wheelbase ($r = 0.93$).
- Striking vehicles' (cars + light trucks) wheelbase*weight distribution was developed by adjusting the Polk passenger car data distribution downward by an estimated truck portion of it. The truck portion for each weight group was estimated from NASS 1979-1980 data (Table 13). Truck portion for each weight group was then assigned to one category of wheelbase.

Table 6. Correlation matrix of variables from NASS—raw data

NASS7980 Data File
Raw Data

Variable	N	Mean	Std Dev	Sum	Minimum	Maximum
Age	327	37.13455657	19.29764278	12143.00000000	15.00000000	88.00000000
Height	327	67.16819572	3.98376661	21964.00000000	56.00000000	76.00000000
Weight	327	154.33333333	33.01406405	50467.00000000	85.00000000	320.00000000
Car-Wt	327	34.29969419	8.57064293	11216.00000000	16.00000000	53.00000000
Del-V	255	29.67450980	27.93397617	7567.00000000	4.00000000	96.00000000
Car-Wt1	309	35.48867314	8.14583201	10966.00000000	18.00000000	80.00000000
Del-V1	236	23.19915254	21.45967419	5475.00000000	2.00000000	96.00000000

Correlation coefficients/prob > IRI under H0:RHO=0/number of observations

	Age	Height	Weight	Car-Wt	Del-V	Car-Wt1	Del-V1
Age	1.00000	-0.03409	0.14467	0.15688	-0.00969	-0.06945	0.04489
Driver's Age	0.0000	0.5390	0.0088	0.0045	0.8776	0.2235	0.4926
	327	327	327	327	255	309	236
Height	-0.03409	1.00000	0.58928	0.00580	-0.07809	-0.01419	-0.04452
Driver's Height	0.5390	0.0000	0.0001	0.9168	0.2139	0.8038	0.4961
	327	327	327	327	255	309	236
Weight	0.14467	0.58928	1.00000	0.18047	-0.07253	-0.03838	-0.00236
Driver's Weight	0.0088	0.0001	0.0000	0.0010	0.2485	0.5014	0.9712
	327	327	327	327	255	309	236
Car-Wt	0.15688	0.00580	0.18047	1.00000	-0.07128	-0.05608	0.10180
Struck Car's Weight	0.0045	0.9168	0.0010	0.0000	0.2568	0.3258	0.1188
	327	327	327	327	255	309	236
Del-V	-0.00969	-0.07809	-0.07253	-0.07128	1.00000	0.15091	0.95399
Struck Car's Total Del-V	0.8776	0.2139	0.2485	0.2568	0.0000	0.0167	0.0001
	255	255	255	255	255	251	236
Car-Wt1	-0.06945	-0.01419	-0.03838	-0.05608	0.15091	1.00000	0.04963
Striking Car's Weight	0.2235	0.8038	0.5014	0.3258	0.0167	0.0000	0.4499
	309	309	309	309	251	309	234
Del-V1	0.04489	-0.04452	-0.00236	0.10180	0.95399	0.04963	1.00000
Striking Car's Total Del-V	0.4926	0.4961	0.9712	0.1188	0.0001	0.4499	0.0000
	236	236	236	236	236	234	236

Table 7. Correlation matrix of variables from NASS—weighted data

NASS7980 Data File
Weighted by National Inflation Factor

Variable	N	Mean	Std Dev	Sum	Minimum	Maximum
Age	426483	35.15600856	18.74201865	14993440.00000	15.00000000	88.00000000
Height	426483	67.33765707	3.97768909	28718366.00000	56.00000000	76.00000000
Weight	426483	157.98325138	39.25318825	67377171.00000	85.00000000	320.00000000
Car-Wt	426483	34.73136327	8.27240010	14812336.00000	16.00000000	53.00000000
Del-V	321317	26.33256566	26.91711887	8461101.00000	4.00000000	96.00000000
Car-Wt1	406353	34.18829687	8.06135624	13892517.00000	18.00000000	80.00000000
Del-V1	297123	19.96711799	18.24538129	5932690.00000	2.00000000	96.00000000

Correlation coefficients/prob > IRI under HO:RHO=0/number of observations/freq var=nat-wt

	Age	Height	Weight	Car-Wt	Del-V	Car-Wt1	Del-V1
Age	1.00000	-0.04764	0.07020	0.18266	-0.01654	-0.10543	0.01494
Driver's Age	0.0000	0.0001	0.0001	0.0001	0.0001	0.0001	0.0001
	426483	426483	426483	426483	321317	406353	297123
Height	-0.04764	1.00000	0.55211	0.10084	-0.07067	-0.03781	0.00762
Driver's Height	0.0001	0.0000	0.0001	0.0001	0.0001	0.0001	0.0001
	426483	426483	426483	426483	321317	406353	297123
Weight	0.07020	0.55211	1.00000	0.12044	-0.03167	-0.02709	0.05764
Driver's Weight	0.0001	0.0001	0.0000	0.0001	0.0001	0.0001	0.0001
	426483	426483	426483	426483	321317	406353	297123
Car-Wt	0.18266	0.10084	0.12044	1.00000	-0.04765	-0.05467	0.14267
Struck Car's Weight	0.0001	0.0001	0.0001	0.0000	0.0001	0.0001	0.0001
	426483	426483	426483	426483	321317	406353	297123
Del-V	-0.01654	-0.07067	-0.03167	-0.04765	1.00000	0.17518	0.95255
Struck Car's Total Del-V	0.0001	0.0001	0.0001	0.0001	0.0000	0.0001	0.0001
	321317	321317	321317	321317	321317	316123	297123
Car-Wt1	-0.10543	-0.03781	-0.02709	-0.05467	0.17518	1.00000	0.05841
Striking Car's Weight	0.0001	0.0001	0.0001	0.0001	0.0001	0.0000	0.0001
	406353	406353	406353	406353	316123	406353	295058
Del-V1	0.01494	-0.00762	0.05764	0.14267	0.95255	0.05841	1.00000
Striking Car's Total Del-V	0.0001	0.0001	0.0001	0.0001	0.0001	0.0001	0.0000
	297123	297123	297123	297123	297123	295058	297123

Table 8A. Correlation matrix for male sample from NASS—raw data

NASSDATA Data File
Raw Data
Occupant's Sex=Male

Variable	N	Mean	Std Dev	Sum	Minimum	Maximum
Occ-Age	612	33.98366013	16.60259660	20798.0000000	15.00000000	90.00000000
OHGT	612	70.01633987	2.74736493	42850.0000000	60.00000000	78.00000000
OWGT	612	170.09150327	29.40447865	104096.0000000	100.00000000	356.00000000
Curb-Wt	612	32.90032680	8.32256019	20135.0000000	16.00000000	53.00000000
Del-V	423	11.08983452	5.89613623	4691.0000000	2.00000000	42.00000000
Curb-Wt1	579	34.72193437	8.36559020	20104.0000000	17.00000000	80.00000000
Del-V1	416	10.29807692	5.12847906	4284.0000000	2.00000000	38.00000000

Correlation coefficients/prob > IRI under H0:RHO=0/number of observations

	Occ-Age	OHGT	OWGT	Curb-Wt	Del-V	Curb-Wt1	Del-V1
Occ-Age	1.00000	-0.14603	0.15935	0.04516	-0.06436	0.15860	-0.10303
Occupant's Age	0.0000	0.0003	0.0001	0.2646	0.1865	0.0001	0.0357
	612	612	612	612	423	579	416
OHGT	-0.14603	1.00000	0.42450	0.00472	-0.04591	0.00591	-0.01772
Occupant's Height	0.0003	0.0000	0.0001	0.9072	0.3462	0.8872	0.7186
	612	612	612	612	423	579	416
OWGT	0.15935	0.42450	1.00000	0.05746	-0.01618	0.10688	-0.00271
Occupant's Weight	0.0001	0.0001	0.0000	0.1557	0.7401	0.0101	0.9561
	612	612	612	612	423	579	416
Curb-Wt	0.04516	0.00472	0.05746	1.00000	-0.27550	-0.04860	0.21992
Vehicle Curb Weight	0.2646	0.9072	0.1557	0.0000	0.0001	0.2429	0.0001
	612	612	612	612	423	579	416
Del-V	-0.06436	-0.04591	-0.01618	-0.27550	1.00000	0.21983	0.74009
Total Delta V	0.1865	0.3462	0.7401	0.0001	0.0000	0.0001	0.0001
	423	423	423	423	423	416	411
Curb-Wt1	0.15860	0.00591	0.10688	-0.04860	0.21983	1.00000	-0.18173
Vehicle Curb Weight	0.0001	0.8872	0.0101	0.2429	0.0001	0.0000	0.0002
	579	579	579	579	416	579	411
Del-V1	-0.10303	-0.01772	-0.00271	0.21992	0.74009	-0.18173	1.00000
Total Delta V	0.0357	0.7186	0.9561	0.0001	0.0001	0.0002	0.0000
	416	416	416	416	411	411	416

Table 8B. Correlation matrix for female sample from NASS—raw data

NASSDATA Data File
Raw Data
Occupant's Sex=Female

Variable	N	Mean	Std Dev	Sum	Minimum	Maximum
Occ-Age	268	34.03358209	15.46588583	9121.00000000	15.00000000	81.00000000
OHGT	268	64.46641791	2.54303614	17277.00000000	57.00000000	72.00000000
OWGT	268	132.35074627	20.89917206	35470.00000000	92.00000000	215.00000000
Curb-Wt	268	33.0676418	8.33583282	8862.00000000	18.00000000	53.00000000
Del-V	177	10.18079096	5.07680481	1802.00000000	2.00000000	38.00000000
Curb-Wt1	265	32.82264151	7.98546600	8698.00000000	17.00000000	51.00000000
Del-V1	174	10.08620690	4.47711386	1755.00000000	1.00000000	32.00000000

Correlation coefficients/prob > IRI under HO:RHO=0/number of observations

	Occ-Age	OHGT	OWGT	Curb-Wt	Del-V	Curb-Wt1	Del-V1
Occ-Age Occupant's Age	1.00000 0.0000 268	-0.12105 0.0477 268	0.27445 0.0001 268	-0.05675 0.3547 268	0.01945 0.7973 177	0.13367 0.0296 265	-0.09301 0.2222 174
OHGT Occupant's Height	-0.12105 0.0477 268	1.00000 0.0000 268	0.24863 0.0001 268	-0.05449 0.3743 268	0.00238 0.9749 177	-0.02072 0.7370 265	-0.06050 0.4278 174
OWGT Occupant's Weight	0.27445 0.0001 268	0.24863 0.0001 268	1.00000 0.0000 268	-0.01955 0.7501 268	-0.05724 0.4492 177	0.17357 0.0046 265	-0.22131 0.0033 174
Curb-Wt Vehicle Curb Weight	-0.05675 0.3547 268	-0.05449 0.3743 268	-0.01955 0.7501 268	1.00000 0.0000 268	-0.30645 0.0001 177	0.06869 0.2652 265	0.13937 0.0666 174
Del-V Total Delta V	0.01945 0.7973 177	0.00238 0.9749 177	-0.05724 0.4492 177	-0.30645 0.0001 177	1.00000 0.0000 177	0.21478 0.0041 177	0.69740 0.0001 171
Curb-Wt1 Vehicle Curb Weight	0.13367 0.0296 265	-0.02072 0.7370 265	0.17357 0.0046 265	0.06869 0.2652 265	0.21478 0.0041 177	1.00000 0.0000 265	-0.22448 0.0029 174
Del-V1 Total Delta V	-0.09301 0.2222 174	-0.06050 0.4278 174	-0.22131 0.0033 174	0.13937 0.0666 174	0.69740 0.0001 171	-0.22448 0.0029 174	1.00000 0.0000 174

Table 9A. Correlation matrix for male sample from NASS—weighted data

NASSDATA Data File
Weighted by National Inflation Factor
Occupant's Sex=Male

Variable	N	Mean	Std Dev	Sum	Minimum	Maximum
Occ-Age	433866	32.33558518	15.68739293	14029311.00000	15.00000000	90.00000000
OHGT	433866	70.21085082	2.89626511	30462101.00000	30.00000000	78.00000000
OWGT	433866	169.63860501	26.92430734	73600423.00000	100.00000000	356.00000000
Curb-Wt	433866	33.46711888	8.44975993	14520245.00000	16.00000000	53.00000000
Del-V	321514	10.07904166	5.77047654	3240553.00000	2.00000000	42.00000000
Curb-Wt1	412024	34.35998388	7.96816880	14157138.00000	17.00000000	80.00000000
Del-V1	319466	9.48256152	4.48569613	3029356.00000	2.00000000	38.00000000

Correlation coefficients/prob > IRI under H0:RHO=0/number of observations/freq var=natwt

	Occ-Age	OHGT	OWGT	Curb-Wt	Del-V	Curb-Wt1	Del-V1
Occ-Age	1.00000	-0.18335	0.13068	0.05614	0.00390	0.20205	-0.02979
Occupant's Age	0.0000	0.0001	0.0001	0.0001	0.0270	0.0001	0.0001
	433866	433866	433866	433866	321514	412024	319466
OHGT	-0.18335	1.00000	0.39710	0.09035	-0.15197	-0.06622	-0.07314
Occupant's Height	0.0001	0.0000	0.0001	0.0001	0.0001	0.0001	0.0001
	433866	433866	433866	433866	321514	412024	319466
OWGT	0.13068	0.39710	1.00000	0.01760	0.06870	0.11137	0.03965
Occupant's Weight	0.0001	0.0001	0.0000	0.0001	0.0001	0.0001	0.0001
	433866	433866	433866	433866	321514	412024	319466
Curb-Wt	0.05614	0.09035	0.01760	1.00000	-0.34353	-0.04984	0.14376
Vehicle Curb Weight	0.0001	0.0001	0.0001	0.0000	0.0001	0.0001	0.0001
	433866	433866	433866	433866	321514	412024	319466
Del-V	0.00390	-0.15197	0.06870	-0.34353	1.00000	0.32116	0.75537
Total Delta V	0.0270	0.0001	0.0001	0.0001	0.0000	0.0001	0.0001
	321514	321514	321514	321514	321514	316202	317031
Curb-Wt1	0.20205	-0.06622	0.11137	-0.04984	0.32116	1.00000	-0.05138
Vehicle Curb Weight	0.0001	0.0001	0.0001	0.0001	0.0001	0.0000	0.0001
	412024	412024	412024	412024	316202	412024	315341
Del-V1	-0.02979	-0.07314	0.03965	0.14376	0.75537	-0.05138	1.00000
Total Delta V	0.0001	0.0001	0.0001	0.0001	0.0001	0.0001	0.0000
	319466	319466	319466	319466	317031	315341	319466

Table 9B. Correlation matrix for female sample from NASS—weighted data

NASSDATA Data File
Weighted by National Inflation Factor
Occupant's Sex=Female

Variable	N	Mean	Std Dev	Sum	Minimum	Maximum
Occ-Age	217851	33.26736164	17.34228006	7247328.00000	15.00000000	81.00000000
OHGT	217851	64.53405768	2.49745710	14058809.00000	57.00000000	72.00000000
OWGT	217851	134.63397001	22.30753922	29330145.00000	92.00000000	215.00000000
Curb-Wt	217851	33.61693543	7.73945057	7323483.00000	18.00000000	53.00000000
Del-V	151139	9.11122874	4.30389235	1377062.00000	2.00000000	38.00000000
Curb-Wt1	214573	32.97506210	8.12735164	7075558.00000	17.00000000	51.00000000
Del-V1	150613	9.05945038	4.01677597	1364471.00000	1.00000000	32.00000000

Correlation coefficients/prob > IRI under H0:RHO=0/number of observations/freq var=natwt

	Occ-Age	OHGT	OWGT	Curb-Wt	Del-V	Curb-Wt1	Del-V1
Occ-Age Occupant's Age	1.00000 0.0000 217851	-0.16300 0.0001 217851	0.30323 0.0001 217851	-0.00186 0.3858 217851	0.10399 0.0001 151139	0.31020 0.0001 214573	-0.04204 0.0001 150613
OHGT Occupant's Height	-0.16300 0.0001 217851	1.00000 0.0000 217851	0.34607 0.0001 217851	-0.02959 0.0001 217851	-0.18557 0.0001 151139	-0.12568 0.0001 214573	-0.18768 0.0001 150613
OWGT Occupant's Weight	0.30323 0.0001 217851	0.34607 0.0001 217851	1.00000 0.0000 217851	0.00912 0.0001 217851	-0.15405 0.0001 151139	0.17882 0.0001 214573	-0.28901 0.0001 150613
Curb-Wt Vehicle Curb Weight	-0.00186 0.3858 217851	-0.02959 0.0001 217851	0.00912 0.0001 217851	1.00000 0.0000 217851	-0.09949 0.0001 151139	0.11461 0.0001 214573	0.26589 0.0001 150613
Del-V Total Delta V	0.10399 0.0001 151139	-0.18557 0.0001 151139	-0.15405 0.0001 151139	-0.09949 0.0001 151139	1.00000 0.0000 151139	0.36117 0.0001 151139	0.76070 0.0001 148990
Curb-Wt1 Vehicle Curb Weight	0.31020 0.0001 214573	-0.12568 0.0001 214573	0.17882 0.0001 214573	0.11461 0.0001 214573	0.36117 0.0001 151139	1.00000 0.0000 214573	-0.00495 0.0548 150613
Del-V1 Total Delta V	-0.04204 0.0001 150613	-0.18768 0.0001 150613	-0.28901 0.0001 150613	0.26589 0.0001 150613	0.76070 0.0001 148990	-0.00495 0.0548 150613	1.00000 0.0000 150613

Vehicle Speed

The sum of CRASH3 delta V's for the striking vehicle and struck car were used as an estimate of impact speed for the striking vehicle. The speed distribution was obtained by type of vehicle damage: occupant compartment (T-type) and nonoccupant compartment (L-type). The T-type is defined as P + Y + Z + D, while the L-type is B + F using the Collision Deformation Classification (CDC)(13) Specific Horizontal Damage Area.

Collision theory shows that for pure one-dimensional impacts (no rotation), the sum of the speed changes of two vehicles is equal to the closing speed of the vehicles prior to the collision. Since the struck car in a side impact collision essentially has a zero velocity relative to the direction of travel of the striking vehicle, then the striking vehicle speed at impact should be equal to the sum of the speed changes of the two vehicles, provided the impact is at or near the center of gravity of both vehicles. Comparing the speed distributions of the T- and L-type collisions shows that the delta V sum for the L-type is less than the delta V sum for the T-type. This is consistent with collision theory, which indicates that for the same vehicle striking speeds, the delta V at the vehicle center of gravity will be less in the L-type collision than in the T-type collision due to vehicle rotation. The difference in the means of the two speed distributions was found to be consistent with collision theory when the amount of offset of the impact point from the center of gravity in the L-type collision was taken into consideration. Therefore, it was decided to use the 1979-82 NASS distributions for the T- and L-type impact speeds.

The cumulative percentage distribution of striking speed of NASS data (unweighted) were compared with that of Highway Safety Research Institute CPIR3 accident data files as of September 1974. The results were consistent (see Figure 14).

Table 10. Driver's age/weight bivariate frequency distribution—male sample

NASSDATA Data File
Weighted by National Inflation Factor

Occupant's Sex=Male
Table of Occ Age by OWGT

Occ Age Frequency Percent Row Pct Col Pct	Occupants Age OWGT Occupant's Weight -119	120-139	140-159	160-179	180-199	200-	Total
15-24	2726	15716	52613	72298	22545	15430	181328
	0.63	3.62	12.12	16.65	5.19	3.55	41.76
	1.50	8.67	29.02	39.87	12.43	8.51	
	49.34	70.76	47.58	44.88	25.90	32.33	
25-34	988	2819	28638	46758	29341	9935	118479
	0.23	0.65	6.60	10.77	6.76	2.29	27.29
	0.83	2.38	24.17	39.46	24.76	8.39	
	17.88	12.69	25.90	29.03	33.71	20.81	
35-44	0	3107	6810	14490	10512	7004	41924
	0.00	0.72	1.57	3.34	2.42	1.61	9.66
	0.00	7.41	16.24	34.56	25.07	16.71	
	0.00	13.99	6.16	9.00	12.08	14.68	
45-54	0	0	7074	14565	12674	7857	42170
	0.00	0.00	1.63	3.35	2.92	1.81	9.71
	0.00	0.00	16.78	34.54	30.05	18.63	
	0.00	0.00	6.40	9.04	14.56	16.46	
55-70	1811	312	7033	11776	10032	6333	37297
	0.42	0.07	1.62	2.71	2.31	1.46	8.59
	4.86	0.84	18.86	31.57	26.90	16.98	
	32.78	1.40	6.36	7.31	11.52	13.27	
71-	0	255	8400	1196	1943	1171	12965
	0.00	0.06	1.93	0.28	0.45	0.27	2.99
	0.00	1.97	64.79	9.23	14.98	9.03	
	0.00	1.15	7.60	0.74	2.23	2.45	
Total	5525	22210	110568	161083	87046	47730	434162
	1.27	5.12	25.47	37.10	20.05	10.99	100.00

Table 11. Driver's age/weight bivariate frequency distribution—female sample

NASSDATA Data File
Weighted by National Inflation Factor

Occupant's Sex=Female
Table of Occ-Age by OWGT

Occ-Age Frequency Percent Row Pct / Col Pct	Occupants Age -119	120-139	OWGT 140-159	160-179	Occupants Weight 180-199	200-	Total
15-24	32263	35404	19692	8446	3184	0	98989
	14.80	16.24	9.03	3.87	1.46	0.00	45.41
	32.59	35.77	19.89	8.53	3.22	0.00	
	58.31	44.83	44.06	32.30	27.95	0.00	
25-34	17307	18396	2828	3645	489	647	43312
	7.94	8.44	1.30	1.67	0.22	0.30	19.87
	39.96	42.47	6.53	8.42	1.13	1.49	
	31.28	23.30	6.33	13.94	4.29	44.47	
35-44	3222	10594	6089	2803	4861	0	27569
	1.48	4.86	2.79	1.29	2.23	0.00	12.65
	11.69	38.43	22.09	10.17	17.63	0.00	
	5.82	13.42	13.63	10.72	42.68	0.00	
45-54	698	5118	4278	6461	477	809	17840
	0.32	2.35	1.96	2.96	0.22	0.37	8.18
	3.91	28.69	23.98	36.22	2.67	4.53	
	1.26	6.48	9.57	24.71	4.18	55.53	
55-70	1250	6744	6382	1145	2380	0	17901
	0.57	3.09	2.93	0.53	1.09	0.00	8.21
	6.98	37.67	35.65	6.40	13.30	0.00	
	2.26	8.54	14.28	4.38	20.90	0.00	
71-	588	2709	5420	3651	0	0	12369
	0.27	1.24	2.49	1.68	0.00	0.00	5.67
	4.75	21.90	43.82	29.52	0.00	0.00	
	1.06	3.43	12.13	13.96	0.00	0.00	
Total	55327	78964	44690	26151	11390	1456	217979
	25.38	36.23	20.50	12.00	5.23	0.67	100.00

Sample Selection From Two Correlated Variables

A sample selection of pairs of two correlated variables can be made by using the matrix of random numbers constructed from the bivariate frequency distribution. A method of constructing such a matrix and its use in sampling procedure is outlined in Appendix F.

Sample Size To Validate Vehicle/Occupant Model

The exposure variable set developed above was input into the preprocessor computer program (discussed in section, Monte Carlo Method) to exercise the vehicle/occupant model of an impact test method. For bivariate variables, the sample selection of random pairs was made by employing the sampling method outlined in Appendix F. The preprocessor generated two sets of univariate and bivariate frequency distributions using sample sizes of 400, 600, 850, and 1,000 cases. The results of each sample were compared with those from the NASS data. The results of the chosen sample size were then compared with the second sample of the preprocessor output for the reliability, that is, the repeatability of the results based on the same sample size.

Method of Comparison

NASS Versus Preprocessor

The percents of cell frequencies of the driver's age*weight distribution generated by the preprocessor were compared with those of the NASS data. Table 14 shows the summary of these results. The results showed a

Table 12. Struck car wheelbase/weight bivariate frequency distribution

R.L. Polk, July 1, 1979 + 1980, model years 1966+
car units in operation—detailed long file

Table of PWB by PWT

Striking Vehicle[1]	PWB Frequency Percent Row Pct / Col Pct	PWT 15-19	20-24	25-29	30-34	35-39	40-44	45-57	Total
Struck Car	80- 95	7718765	12893944	3881826	32703	0	0	0	24527238
		4.54	7.59	2.29	0.02	0.00	0.00	0.00	14.44
		31.47	52.57	15.83	0.13	0.00	0.00	0.00	
		94.93	66.84	17.17	0.11	0.00	0.00	0.00	
	96-102	412041	6285805	9211799	1123131	411432	860	0	17445068
		0.24	3.70	5.42	0.66	0.24	0.00	0.00	10.27
		2.36	36.03	52.80	6.44	2.36	0.00	0.00	
		5.07	32.58	40.75	3.68	1.27	0.00	0.00	
	103-110	0	111919	8558831	15431201	4018098	14933	0	28134982
		0.00	0.07	5.04	9.08	2.37	0.01	0.00	16.56
		0.00	0.40	30.42	54.85	14.28	0.05	0.00	
		0.00	0.58	37.86	50.53	12.43	0.04	0.00	
	111-117	0	0	951833	13745896	21510544	13885313	493689	50587275
		0.00	0.00	0.56	8.09	12.66	8.17	0.29	29.78
		0.00	0.00	1.88	27.17	42.52	27.45	0.98	
		0.00	0.00	4.21	45.01	66.53	36.25	2.64	
	118-123	0	0	2516	204976	6393730	18516176	6833263	31950661
		0.00	0.00	0.00	0.12	3.76	10.90	4.02	18.81
		0.00	0.00	0.01	0.64	20.01	57.95	21.39	
		0.00	0.00	0.01	0.67	19.77	48.34	36.59	
	124-152	0	0	0	0	0	5885090	11348520	17233610
		0.00	0.00	0.00	0.00	0.00	3.46	6.68	10.14
		0.00	0.00	0.00	0.00	0.00	34.15	65.85	
		0.00	0.00	0.00	0.00	0.00	15.36	60.77	
	Total	8130806	19291668	22606805	30537907	32333804	38302372	18675472	1.7E+08
		4.79	11.36	13.31	17.98	19.03	22.55	10.99	100.00
	Car	100%	96%	92%	94%	73%	83%	87%	86%
	Lt.Trk.	—	4%	8%	6%	27%	17%	13%	14%

[1] Adjustment factors for striking vehicle to be applied to above struck car table. The distribution of striking car/lt. trk. is derived from NASS 79 and NASS 80 data weighted by national inflation factor(see Table 13)

Table 13. Vehicle type/weight bivariate frequency distribution

NS79 and NS80 striking car & lt truck weighted data (nat-factor)
Table of Veh-Typ by Veh-Wt

Veh-Typ Frequency Percent Row Pct / Col Pct	Vehicle Curb Weight 15-19	20-24	25-29	30-34	35-39	40-44	45-57	Total
Car	148596	446382	519085	802088	861706	725809	343425	3847092
	3.31	9.96	11.58	17.89	19.22	16.19	7.66	85.81
	3.86	11.60	13.49	20.85	22.40	18.87	8.93	
	100.00	95.73	91.67	93.63	73.12	83.37	86.63	
Lt Trk	0	19909	47144	54608	316802	144814	53000	636277
	0.00	0.44	1.05	1.22	7.07	3.23	1.18	14.19
	0.00	3.13	7.41	8.58	49.79	22.76	8.33	
	0.00	4.27	8.33	6.37	26.88	16.63	13.37	
Total	148596	466291	566230	856696	1178508	870623	396425	4483368
	3.31	10.40	12.63	19.11	26.29	19.42	8.84	100.00

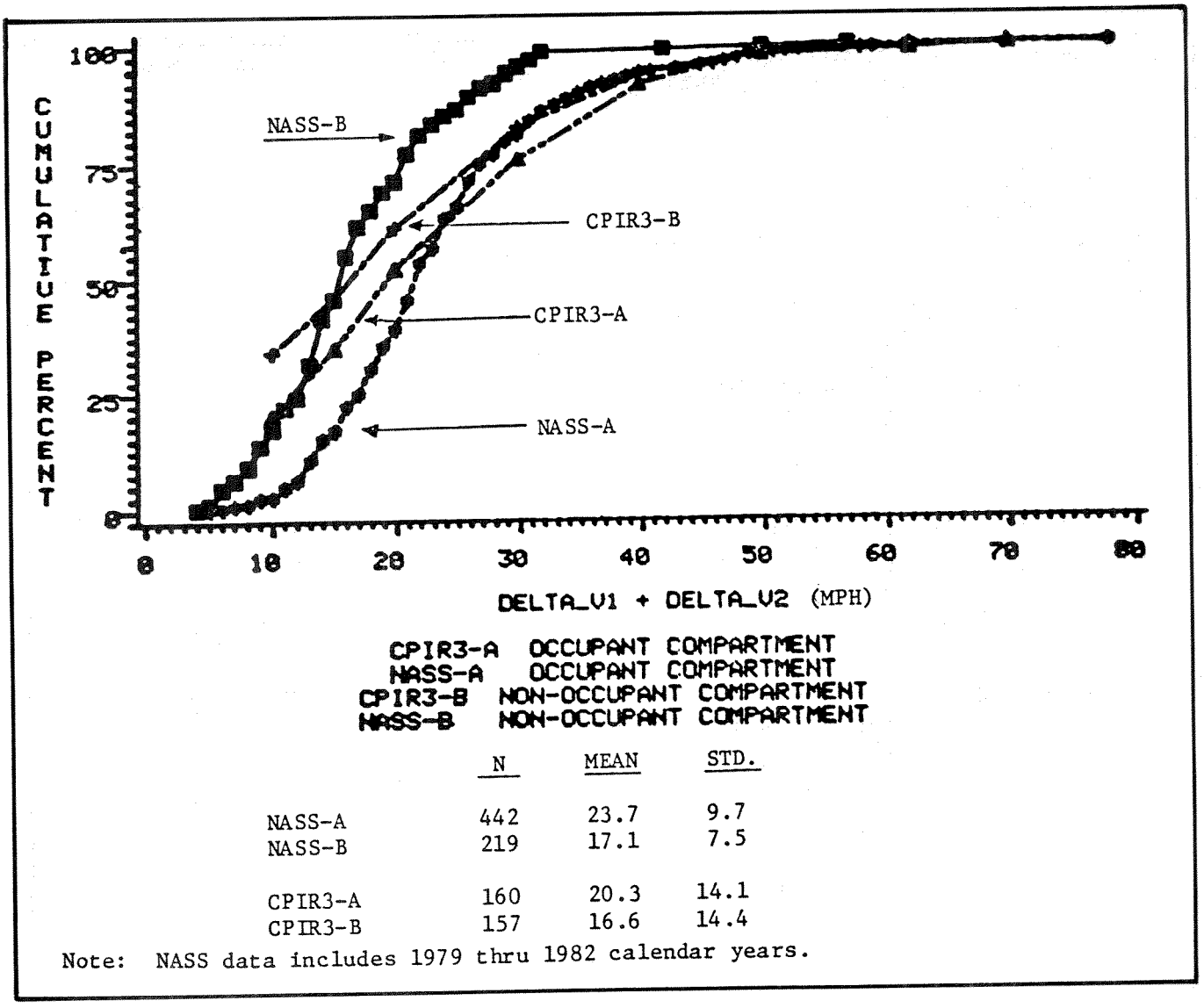

	N	MEAN	STD.
NASS-A	442	23.7	9.7
NASS-B	219	17.1	7.5
CPIR3-A	160	20.3	14.1
CPIR3-B	157	16.6	14.4

Note: NASS data includes 1979 thru 1982 calendar years.

Figure 14. Cumulative percentage distributions—striking speed by type of vehicle damage

good convergence for the samples of 850 cases and higher. For female drivers, 94 percent of the cell differences had a magnitude of 2 percent or less, and the maximum difference for any cell was 2.8 percent. For male drivers, the differences were even smaller, and the maximum difference was 1.2 percent. The comparison of 1,000 cases with NASS data showed only slight improvement, and, because of computer core limitations, a sample of 850 cases was considered adequate.

Preprocessor Sample 1 Versus Sample 2

Table 15 shows the comparison between two samples of preprocessor results based on 850 cases each. It shows that for female drivers, 86 percent of the differences were of magnitude 2 percent or smaller (maximum 2.9 percent). For male drivers, 97 percent of the differences were of magnitude 2 percent or less (maximum 2.2 percent).

Also, a nonparametric test procedure called a sign test was employed to the differences of the paired cell percents of driver's age*weight distributions of the two samples. If the two samples are similarly distributed, then the number of positive and negative differences are divided evenly. Table 16 shows the results of sign tests. No significant difference is found, that is, repeated samples of the same size produce similar results.

The Monte Carlo Method

The Monte Carlo Method was used in this study to select a sample of representative side impact accidents to simulate. Several of the key elements in our study vary randomly in accidents—collision speed, car sizes, occupant age, and occupant size, for example. In the Monte Carlo Method, information about the frequency of occurrence of values of the random variables is gathered,

Table 14. NASS versus preprocessor (sample)

Analysis of Occ Age * Occ Wt Percents
NASS vs. Sample 114
Gender = Female

Diff	Freq.	Cum. Freq.	Percent	Cum. Percent
0.00-0.50	16	16	44.4	44.4
0.51-1.00	3	19	8.3	52.8
1.01-2.00	11	30	30.6	83.3
2.01-4.84	6	36	16.7	100.0

Analysis of Occ Age * Occ Wt Percents
NASS vs. Sample 184
Gender = Female

Diff	Freq.	Cum. Freq.	Percent	Cum. Percent
0.00-0.50	20	20	55.6	55.6
0.51-1.00	9	29	25.0	80.6
1.01-2.00	3	32	8.3	89.9
2.01-4.64	4	36	11.1	100.0

Analysis of Occ Age * Occ Wt Percents
NASS vs. Sample 286
Gender = Male

Diff	Freq.	Cum. Freq.	Percent	Cum. Percent
0.00-0.50	22	22	61.1	61.1
0.51-1.00	9	31	25.0	86.1
1.01-2.00	15	36	13.9	100.0

Analysis of Occ Age * Occ Wt Percents
NASS vs. Sample 416
Gender = Male

Diff	Freq.	Cum. Freq.	Percent	Cum. Percent
0.00-0.50	23	23	63.9	63.9
0.51-1.00	6	29	16.7	80.6
1.01-1.71	7	36	19.4	100.0

Analysis of Occ Age * Occ Wt Percents
NASS vs. Sample 245
Gender = Female

Diff	Freq.	Cum. Freq.	Percent	Cum. Percent
0.00-0.50	23	23	63.9	63.9
0.51-1.00	5	28	13.9	77.8
1.01-2.00	.6	34	16.7	94.4
2.01-2.80	2	36	5.6	100.0

Analysis of Occ Age * Occ Wt Percents
NASS vs. Sample 296
Gender = Female

Diff	Freq.	Cum. Freq.	Percent	Cum. Percent
0.00-0.50	24	24	66.7	66.7
0.51-1.00	5	29	13.9	80.6
1.01-2.00	6	35	16.7	97.2
2.01-3.40	1	36	2.8	100.0

Analysis of Occ Age * Occ Wt Percents
NASS vs. Sample 605
Gender = Male

Diff	Freq.	Cum. Freq.	Percent	Cum. Percent
0.00-0.50	20	20	55.6	55.6
0.51-1.00	12	32	33.3	88.9
1.01-1.15	4	36	11.1	100.0

Analysis of Occ Age * Occ Wt Percents
NASS vs. Sample 704
Gender = Male

Diff	Freq.	Cum. Freq.	Percent	Cum. Percent
0.00-0.50	26	26	72.2	72.2
0.51-1.00	7	33	19.4	91.7
1.01-1.94	3	36	8.3	100.0

Notes: 1) Diff = | NASS %—Sample % |
2) Occ Age * Weight = Driver's Age * Weight distribution
3) Total sample size (male + female) are: 400, 600, 850, and 1,000 cases.

Table 15. Preprocessor sample 1 versus sample 2

Analysis of Occ Age * Occ Wt Percents
Sample 1 (245) vs. Sample 2 (273)
Gender = Female

Diff.	Freq.	Cum. Freq.	Percent	Cum. Percent
0.00-0.50	21	21	58.3	58.3
0.51-1.00	6	27	16.7	75.0
1.01-2.00	4	31	11.1	86.1
2.01-2.90	5	36	13.9	100.0

Analysis of Occ Age * Occ Wt Percents
Sample 1 (605) vs. Sample 2 (577)
Gender = Male

Diff.	Freq.	Cum. Freq.	Percent	Cum. Percent
0.00-0.50	25	25	69.4	69.4
0.51-1.00	5	30	13.9	83.3
1.01-2.00	5	35	13.9	97.2
2.01-2.20	1	36	2.8	100.0

Notes:
1. Diff = | Sample 1% — Sample 2% |
2. Occ Age * Weight = driver's age * weight distributions.
3. Total sample size (male + female) is 850 for each sample.
4. The number in the parentheses are subsample sizes.

Table 16. Preprocessor sample 1 versus preprocessor sample 2_1 sign test for repeatability

For a given cell of two bivariate frequency tables, define
difference = '+' if Sample I % > Sample II %
= '-' if Sample I % < Sample II %
= 0 for ties.

Let sum (+) = sum of '+' signs, sum (-) = sum of '-' signs.

Results of Driver's Age * Car Weight Percents

	Sum(+)	Sum(-)	Critical Values R^2 90%	95%
Male:	10	16	8	7
Female:	18	13	10	9

[1] Each sample of 850 cases. The male/female mix is 69/31 (average of two samples).

[2] Decision Rule:
Reject H_o: Pr {difference = '+' or '-'} = 1/2, if smaller of sum (+) and sum (-)≤R, at that level of significance.

and statistical distributions are constructed. Values of the variables are then randomly chosen according to each variable value's probability of occurring. A set of variables is randomly chosen for the first simulation, then another randomly chosen set is used for the second simulation, the third simulation, and so on. In the Monte Carlo Method, hundreds or even thousands of simulations are done in this manner, and the results of the simulations may be grouped into statistical distributions. So instead of saying that the outcome of a simulation is a chest acceleration of 60, one would say that the probability of a chest acceleration of less than 60 is, say, 35 percent.

One of the difficulties in using the Monte Carlo Method is in knowing how many simulations using random inputs need to be run for the results to be representative of the entire population of simulations that could have been run. For a number of practical reasons, we chose a sample of 850 simulations of side impact traffic encounters for one vehicle design.

Structure of Preprocessor Model

The side impact simulation model preprocessor was developed to provide the random inputs for the side impact simulation. The preprocessor program is run using a random seed for the random number generator or a set of previously determined uniform or normal random numbers. The random seed is based on the time and date of the program execution.

The uniform and normal random number routines are general computer system functions. The uniform random number distribution (integer values) ranges from 1 to 100 with equal probability. The normal random number distribution ranges from -6.0 to 6.0 with a mean of 0.0 and a variance of 1.0.

The preprocessor starts randomly determining driver's gender and whether the impact was a T- or L-type. A 61/39 mix of T- or L-type impacts was used, based on the 1979-82 NASS weighted data base. It then randomly determines driver's age versus driver's weight. The preprocessor model source code is written in Fortran 77 for the Ford Honeywell Multics operating system(14). The program can determine up to 1,000 random sets of side impact simulation inputs. Table 17 shows the output format of the preprocessor and briefly defines each variable. A sampling of the side impact Monte Carlo input data from the preprocessor is presented in Appendix G.

A Test Device Model

A simple component test device was modeled using two masses and energy absorbers (Figure 15). For validation purposes, the parameters of the model were adjusted to produce force-time responses that were within the response corridors developed by MVMA for a

Table 17. Preprocessor output format

Variable
Case number
Driver's gender [1=male; 2=female]
Driver's weight [lb]
Driver's age [yr]
Driver's height [in]
Driver's chest girth [in]
Driver's elbow-to-elbow breadth [in]
Driver's chest depth [in]
Driver's chest stiffness [N/m]
Striking vehicle weight [lb]
Striking vehicle size (CRASH3 wheelbase categories with 7 = Light Trucks
Impact type [1-T-type; 2=L-type]
Striking vehicle impact speed [mph]
Gap distance from driver's elbow to inside door interior [in] for each struck car weight category defined below:
i = 1 1,750 lb
2 2,200 lb
3 2,700 lb
4 3,200 lb
5 3,700 lb
6 4,200 lb
7 4,800 lb

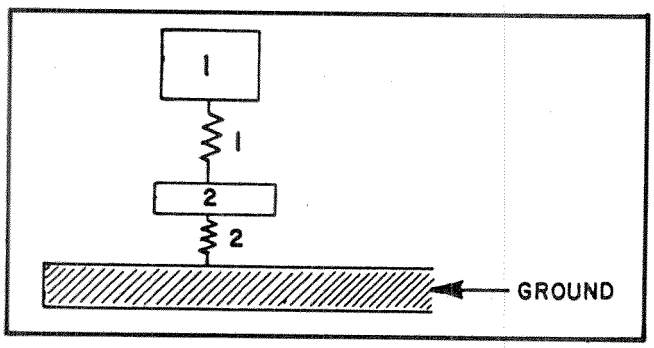

Figure 15. Test device model schematic

component test device(15,16). These corridors were developed from human cadaver drop test data(6) and are believed to be representative of living human dynamic response. The test device response fell within the MVMA corridors when the cadaver drop tests were simulated with the model. Figures 16 and 17 show the validation responses for a lateral rigid impact at 16km/h and a lateral padded impact at 22.5km/h, respectively.

The model of a full-vehicle test procedure was also developed from the computer model used to simulate car-to-car collisions. Since the test tries to duplicate a typical car-to-car crash, the model of the full-vehicle crash described earlier was altered to include the stiffness of the NHTSA and CCMC moving deformable barrier (MDB) face and the effect of mass and stiffness of the SID and APR side impact dummies.

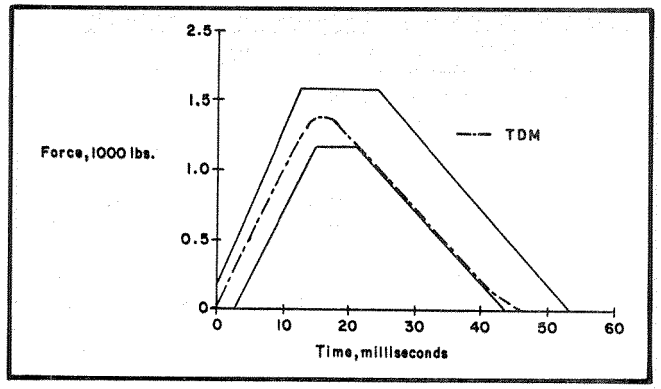

Figure 16. Lateral rigid impact test corridor with test device model response at 16km/h

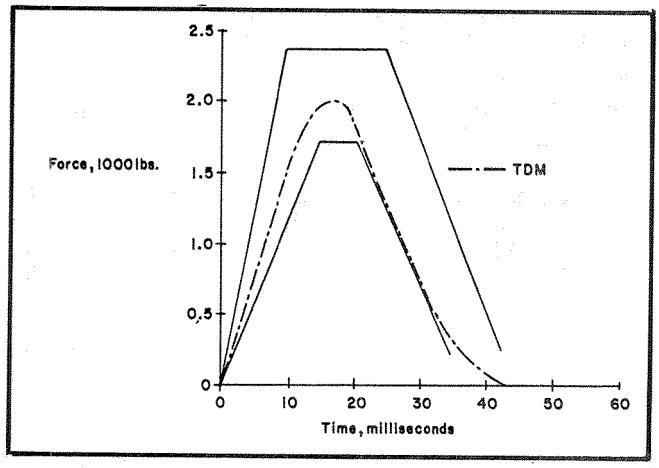

Figure 17. Lateral padded impact test corridor with test device model response at 22.5km/h

Initial Results

We simulated both component and full-vehicle type tests. The component tester was similar to the one developed for MVMA by MGA, Inc.(17), and the full-vehicle tests were patterned after those proposed by NHTSA and the Committee of Common Market Automobile Constructors (CCMC). In this initial study, we did not attempt to investigate fully the effect on test predictability of all the possible changes in test design parameters. Instead, we chose to look at a few plausible test procedure variations.

Component Tests

In the component test, we varied the size of the impactor from a 40th percentile male to a 60th percentile male, and we also varied the impact speeds from 16km/h to 32km/h to study the effect on test predictability of changes in these parameters. We also looked at the effect of using a rigid component test impactor rather than an impactor with realistic thorax stiffness. All component test simulations were run with the door precrushed. A table of the component test runs is shown in Table 18.

Table 18. Test procedure variations—component test runs (precrushed door)

Procedure	Impactor	Occupant	Impact Speed
1	MVMA	50% Male	22km/h
2	MVMA	40% Male	22km/h
3	MVMA	60% Male	22km/h
4	MVMA	50% Male	16km/h
5	MVMA	50% Male	32km/h
6	Rigid	50% Male	22km/h

For the component tests, we measured Thoracic Trauma Index (TTI), chest acceleration, chest deflection, and rib acceleration on both the component test device and the vehicle occupant. We also looked at how well TTI on the occupant is predicted by chest acceleration on the test device and how well chest acceleration on the occupant is predicted by TTI on the test device. Validation plots were made for each of these seven possibilities, and correlation coefficients between test results and real-world simulation results were calculated.

Generally, the component tests have relatively low correlations between real performance and test performance due to the following:

1. The component test model has only a 2-mass and 2-energy absorber.
2. The door gap is not taken into account following the precrushed door. However, the precrushed door stiffness of the struck vehicle was considered.
3. The component test speeds (16, 22, and 32km/h) are the contact speeds between the dummy and door interior.

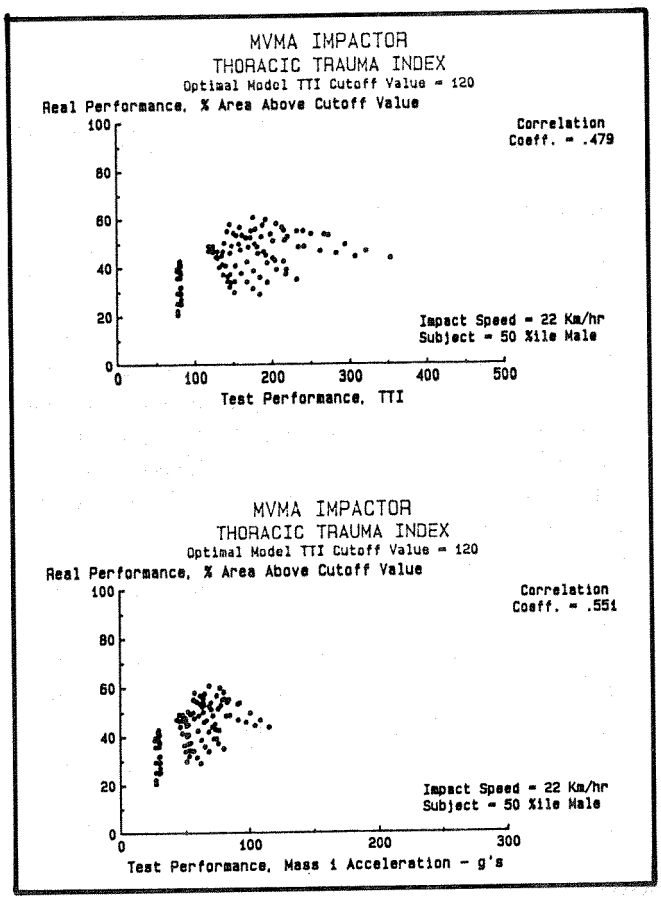

Figure 18. Validation plots—MVMA baseline impactor—thoracic trauma index

MVMA Baseline Impactor

Validation plots for the baseline impactor are shown in Figures 18 through 21. All of the seven response combinations show similar scatter and similar correlation. Note that there are 105 points (15 experiment designs × 7 vehicle sizes) in each validation plot. The highest correlation for the baseline impactor at 22km/h is found with chest acceleration. Note that TTI on the occupant is better predicted by chest acceleration on the impactor than by TTI on the impactor.

Size Variations

Different sizes of the MVMA impactor were also simulated. Validation plots for all of the responses are shown for the 40th percentile and 60th percentile male

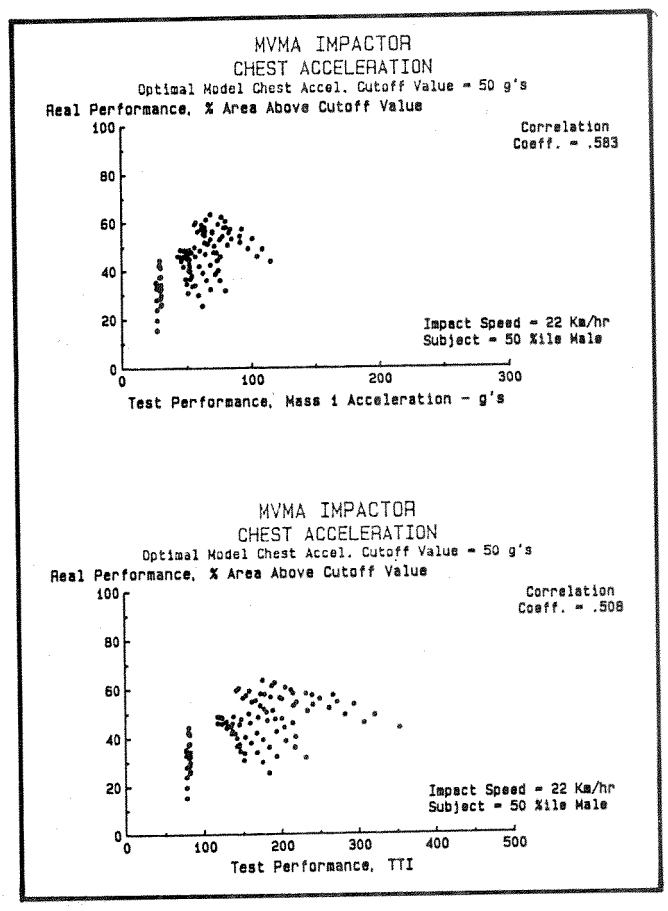

Figure 19. Validation plots—MVMA impactor—chest acceleration

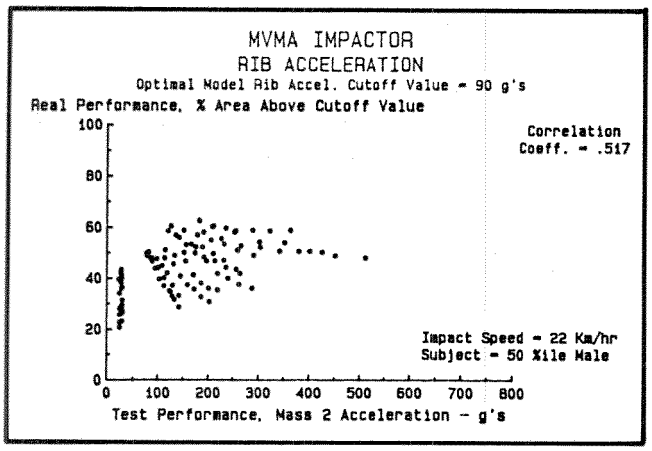

Figure 20. Validation plots—MVMA impactor—rib acceleration

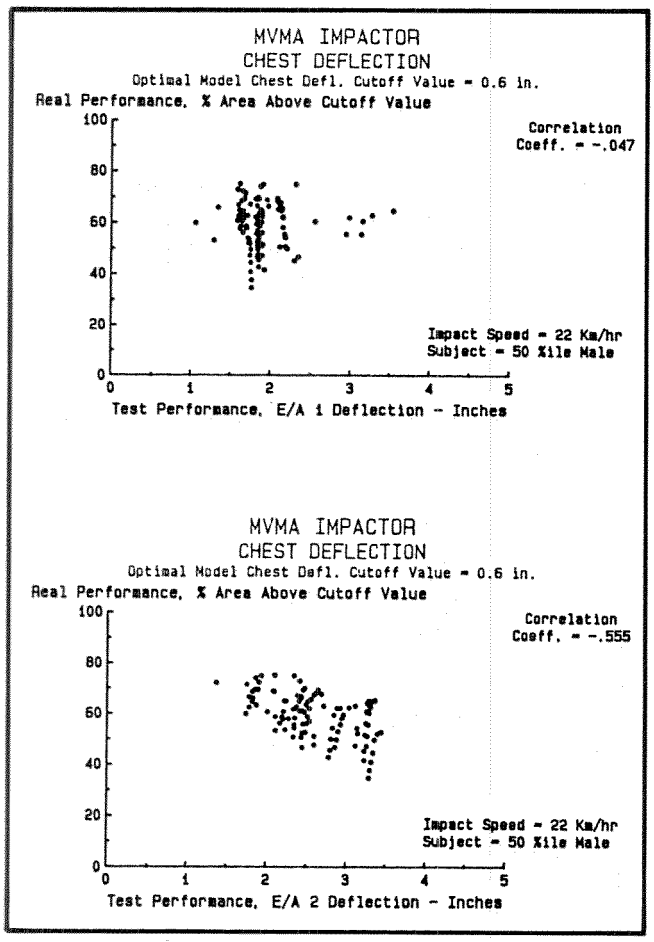

Figure 21. Validation plot—MVMA impactor—chest deflection

sizes in Figures 22 through 25. The different size impactors were simulated by scaling the weight and stiffness values of the 50th percentile impactor in proportion to the change in total body weight. In general, the 40th percentile size impactor correlates slightly better with all the responses than either the 50th or 60th percentile impactor sizes. The correlation coefficients are shown in Table 19.

Speed Variation

The 50th percentile MVMA impactor was also tested at 16 and 32km/h to investigate the effect of different test speeds on the correlation between test results and real-world performance. Validation plots for these tests are shown in Figures 26 through 29. The highest correlations of all the component tests resulted from the MVMA 50th percentile impactor run at 16km/h while the poorest correlations were with the MVMA 50th percentile male impactor at 32km/h. The correlation coefficients for these tests are shown in Table 19. At least in these simulations, the selection of test speed is a critical item in the predictability of a test procedure.

Rigid Impactor

Questions have arisen about just how biofidelic a test device needs to be. Does the impactor need to have exactly the same compliance as a human? To explore this notion of biofidelity, we simulated a component test device that had no compliance. In all other respects, it was the same as the 50th percentile male MVMA impactor simulation. The validation plots for the rigid impactor are shown in Figures 30 through 33. Note, there is very little difference in the validation plots between the rigid impactor and the MVMA 50th percentile male impactor. Does this mean a component test device does not need to be compliant like a human? This issue needs further research to answer the question. The correlation coefficient for the rigid impactor test simulations are shown in the last line of Table 19.

Full-Vehicle Tests

The full-vehicle test simulations investigated the NHTSA MDB(18) and SID dummy(19,20) combination, as well as the CCMC MDB barrier(21) and APR dummy(22,23) combination. We also looked at the effect of changing the weight of both barriers to 1,100kg, the effect of raising the impact speed from 32km/h to 40km/h, and the effect of using the SID dummy with the CCMC barrier. The full-vehicle test simulation plan is shown in Table 20.

Figures 34 and 35 show the force-deflection relationships of the NHTSA and CCMC barriers, respectively. The NHTSA MDB at 0° impact angle approximates the front end characteristics of a typical AMC Concord(18), while the CCMC MDB approximates that of a CCMC average European car(21). Note, a power curve has been used to fit each test curve.

The SID and APR dummy force-deflection characteristics are shown in Figure 36. The lateral stiffness of the HSRI SID is shown compared with that of the APR. The

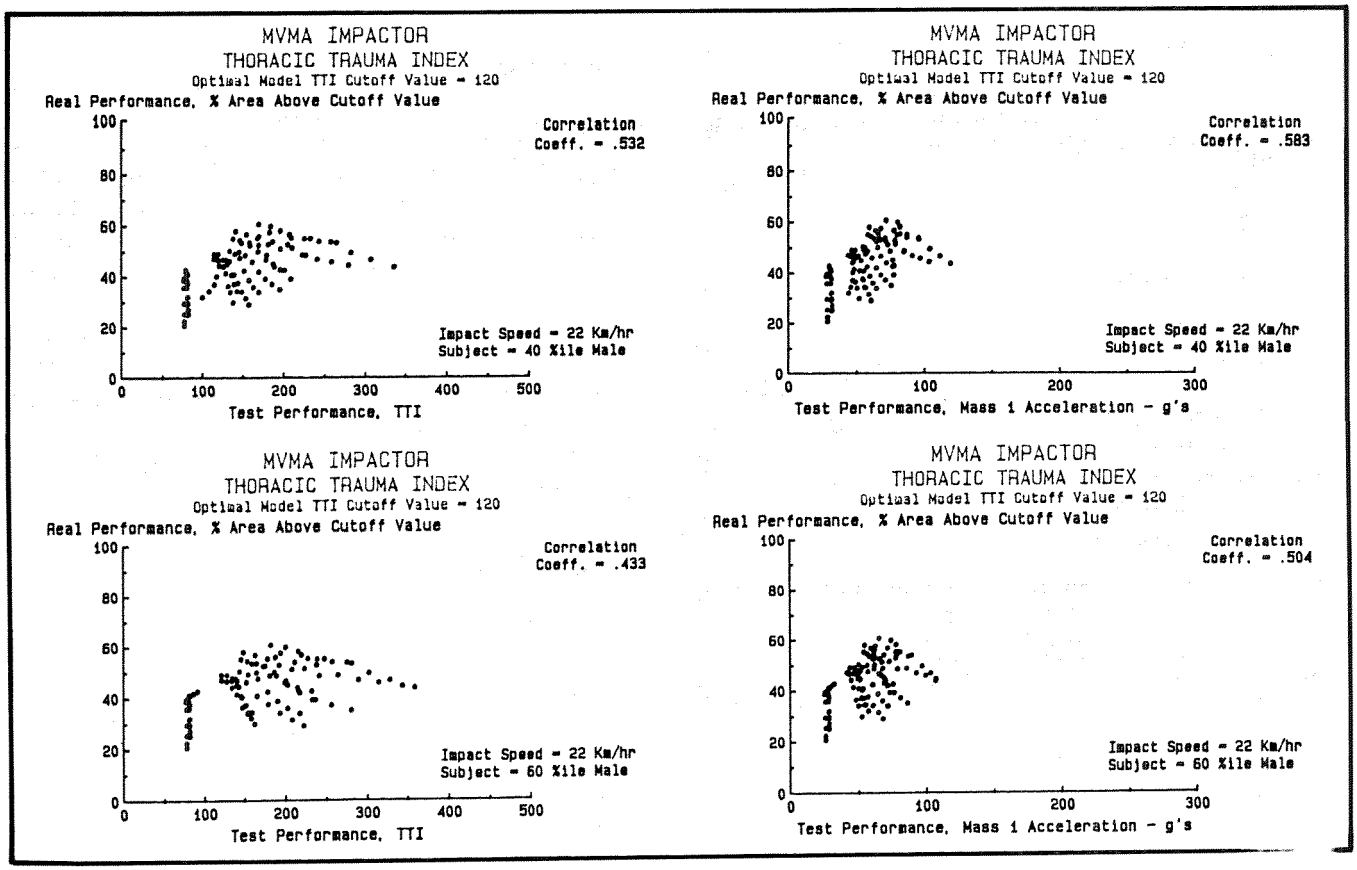

Figure 22. Validation plots—MVMA impactor, size variation—thoracic trauma index

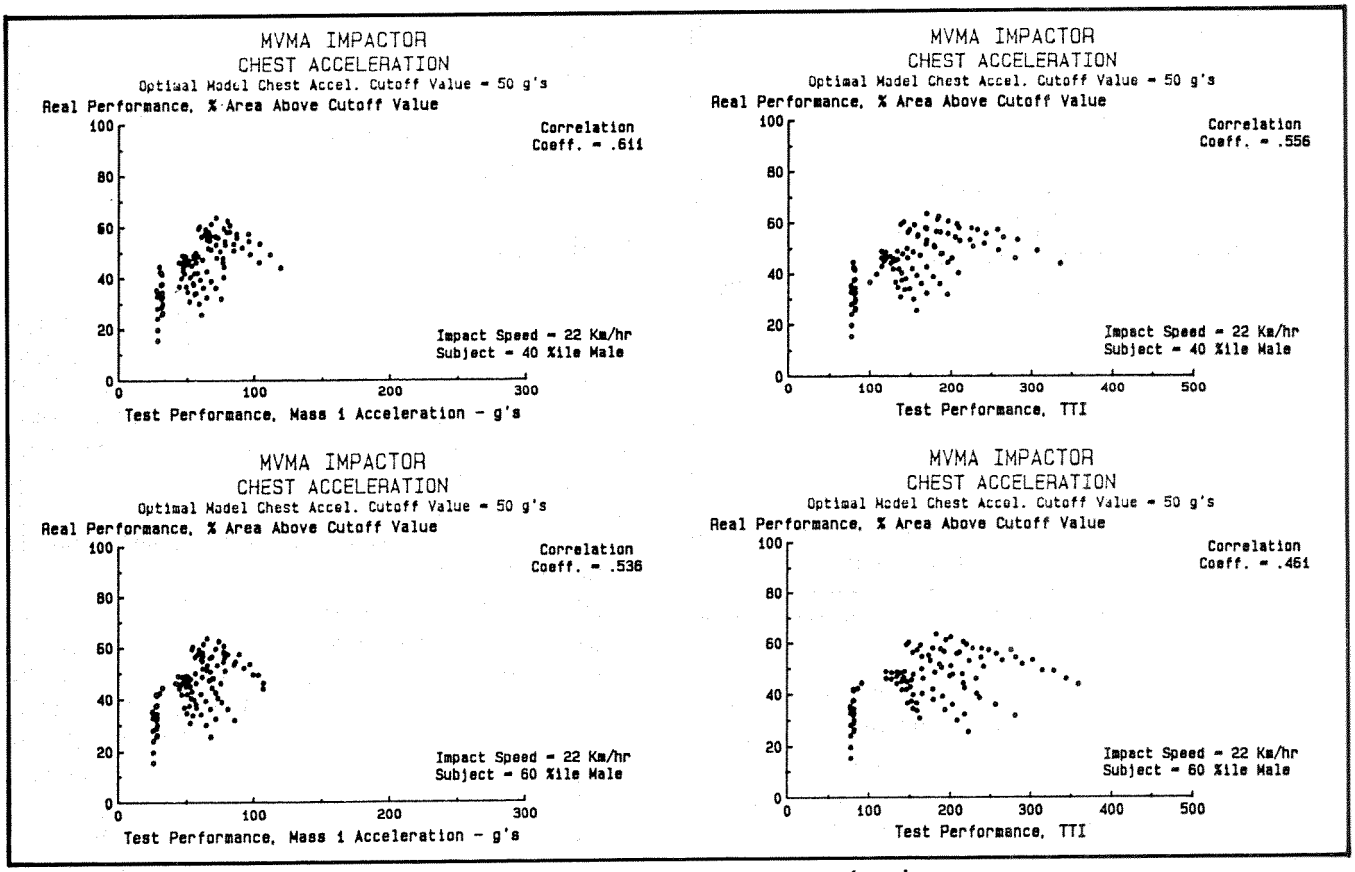

Figure 23. Validation plots—MVMA impactor, size variation—chest acceleration

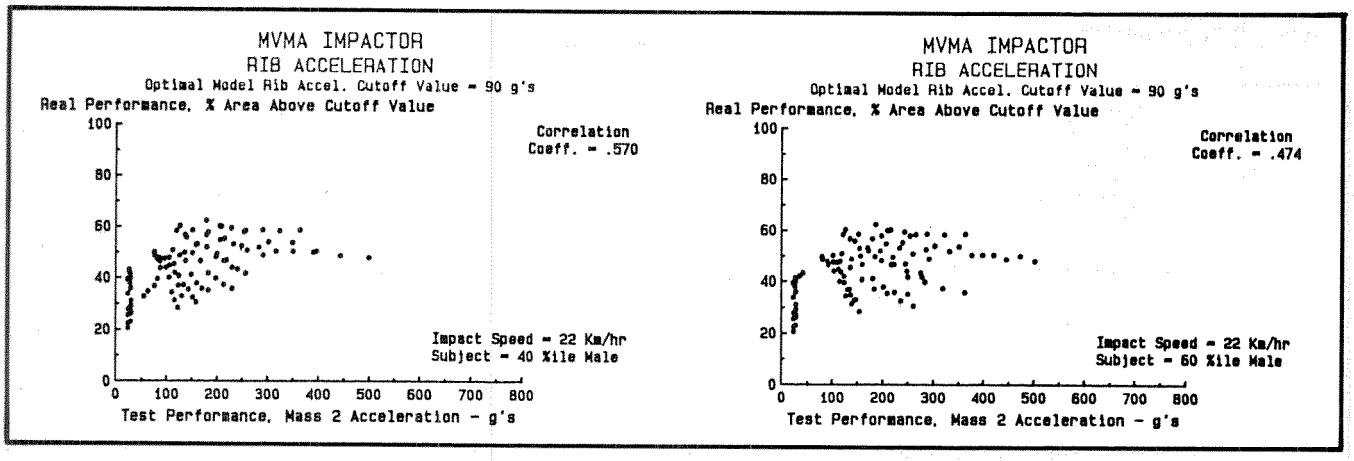

Figure 24. Validation plots—MVMA impactor, size variation—rib acceleration

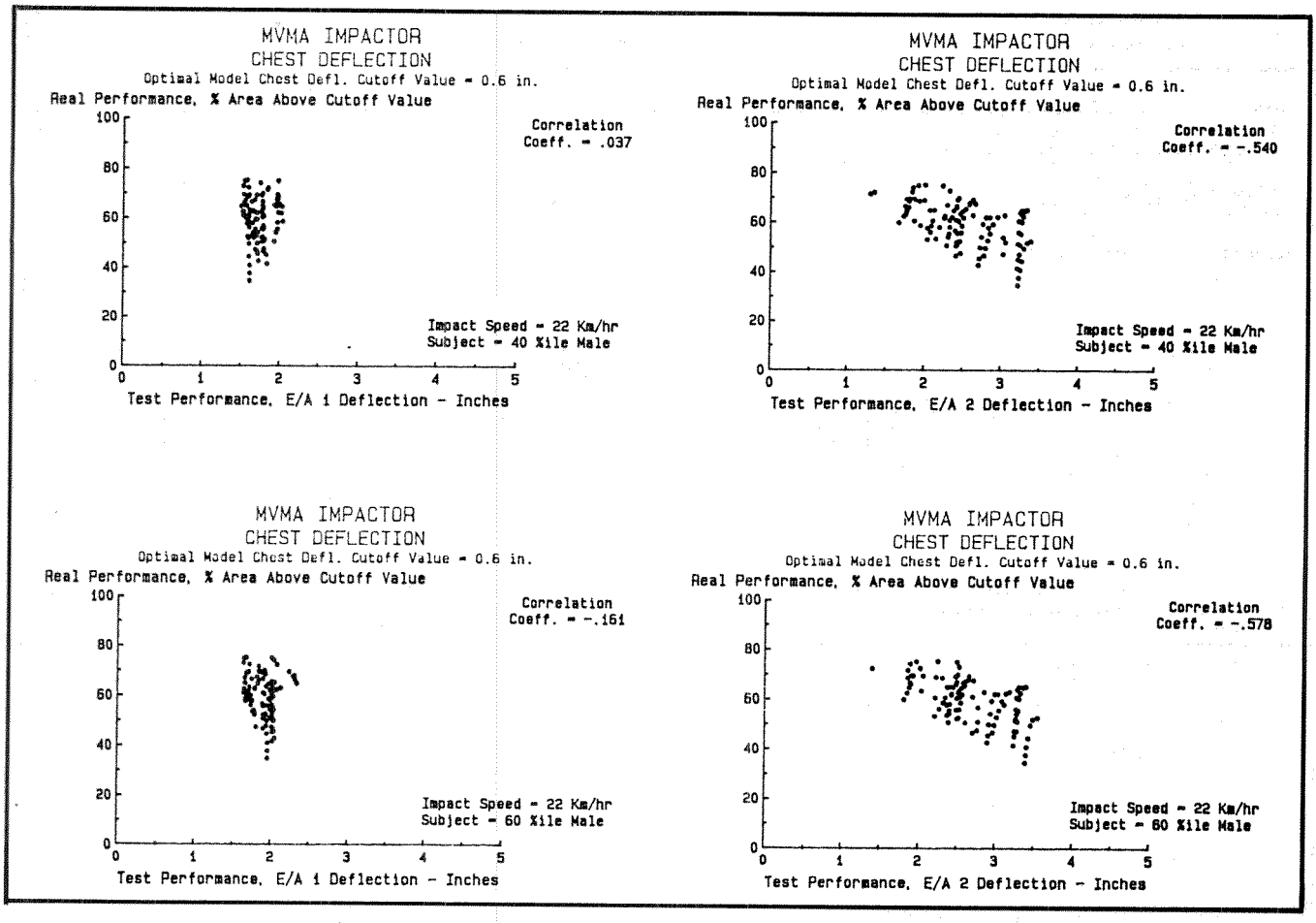

Figure 25. Validation plots—MVMA impactor, size variation—chest deflection

Table 19. Correlations between real performance and test performance (component test procedures)

Optimal Cutoff Real Performance	120 TTI	50 Chest G	90 Rib G	120 TTI	50 Chest G	0.6 in Chest Deflection	0.6 in Chest Deflection
Test Performance Test Procedure	TTI	Mass 1* G	Mass 2* G	Mass 1 G	TTI	Ea #1* Deflection	Ea #2 Door-Pad Deflection
1 (MVMA 50%) (Male, 22km/h)	.479	.583	.517	.551	.508	-.047	-.555
2 (MVMA 40%) (Male, 22km/h)	.532	.611	.570	.583	.556	.037	-.540
3 (MVMA 60%) (Male, 22km/h)	.433	.536	.474	.504	.461	-.161	-.578
4 (MVMA 50%) (Male, 16km/h)	.620	.699	.637	.650	.659	.188	-.432
5 (MVMA 50%) (Male, 32km/h)	.018	.076	.095	.040	.056	.207	-.643
6 (Rigid, 50%) (Male, 22km/h)	.517	.539	.564	.509	.548	N/A	-.441

* Mass 1: main mass in TDM (Test Device Model)
Mass 2: Striking Mass in TDM.
Ea #1 Deflection: Relative Deflection between Masses #1 and #2.

For Test proc. #6 (Rigid Impactor, with 1-mass model).
Mass 1 Acceleration = Mass 2 Acceleration.

Assumption in all cases: precrushed door.

Table 20. Monte Carlo model test procedure variations—full- vehicle test runs

Procedure	Barrier Face/Weight	Dummy	Impact Speed
1	NHTSA/1361 kg	SID	32km/h
2	NHTSA/1361 kg	SID	40km/h
3	CCMC/950 kg	APR	32km/h
4	CCMC/950 kg	APR	40km/h
5	CCMC/1100 kg	SID	32km/h
6	CCMC/1100 kg	APR	32km/h
7	NHTSA/1100 kg	SID	32km/h

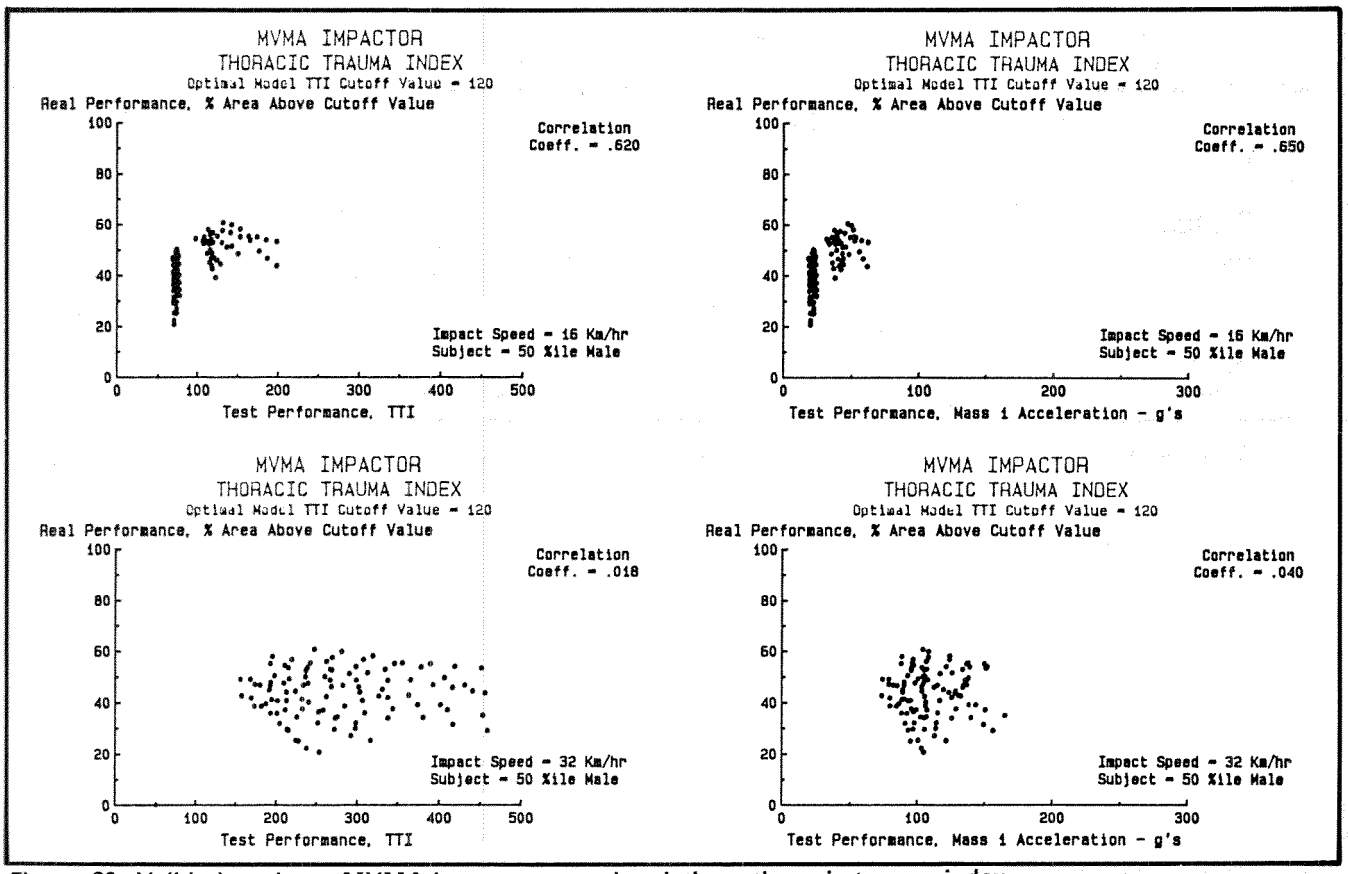

Figure 26. Validation plots—MVMA impactor, speed variation—thoracic trauma index

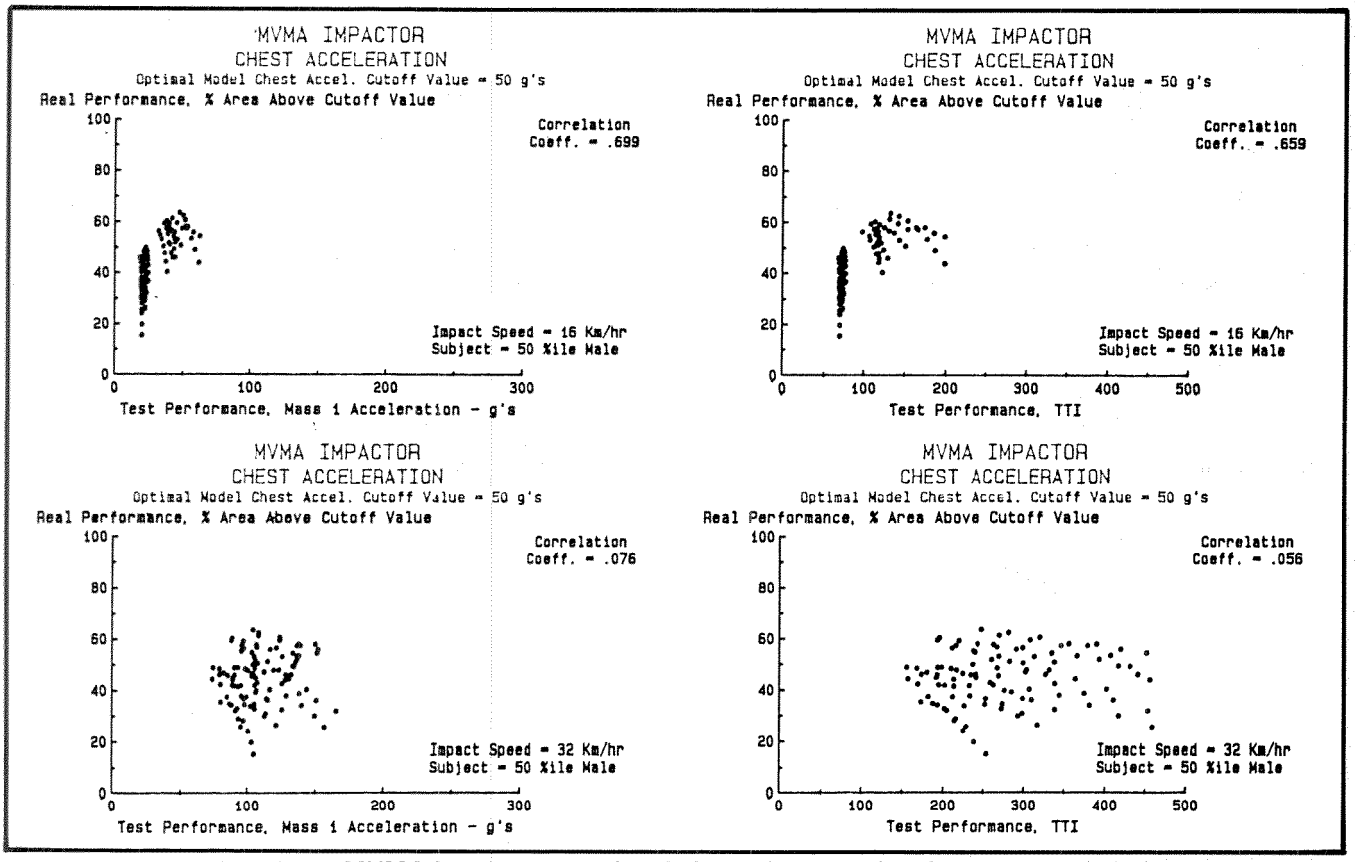

Figure 27. Validation plots—MVMA impactor, speed variation—chest acceleration

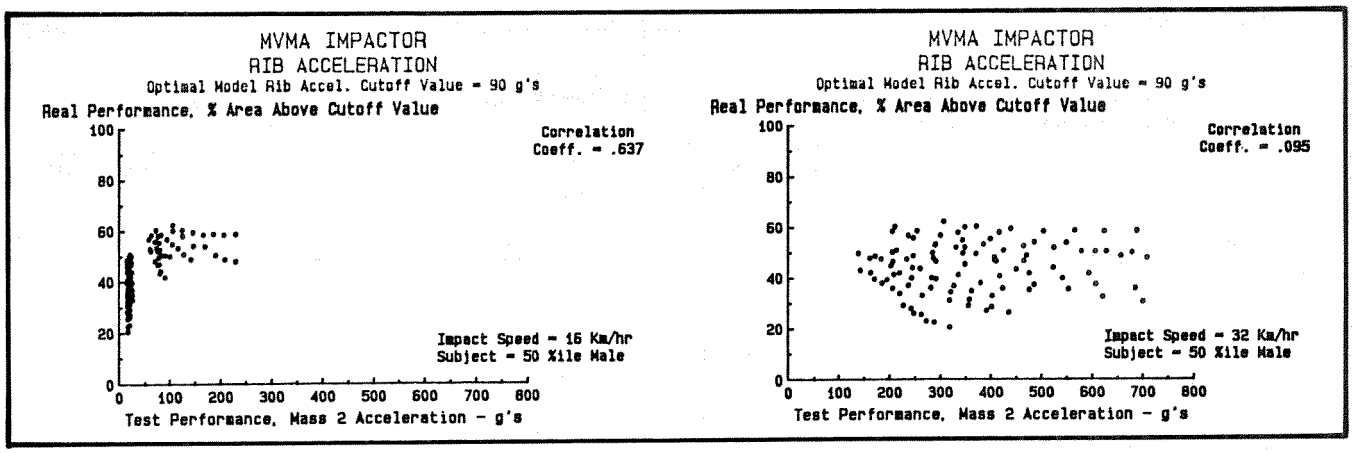

Figure 28. Validation plots—MVMA impactor, speed variation—rib acceleration

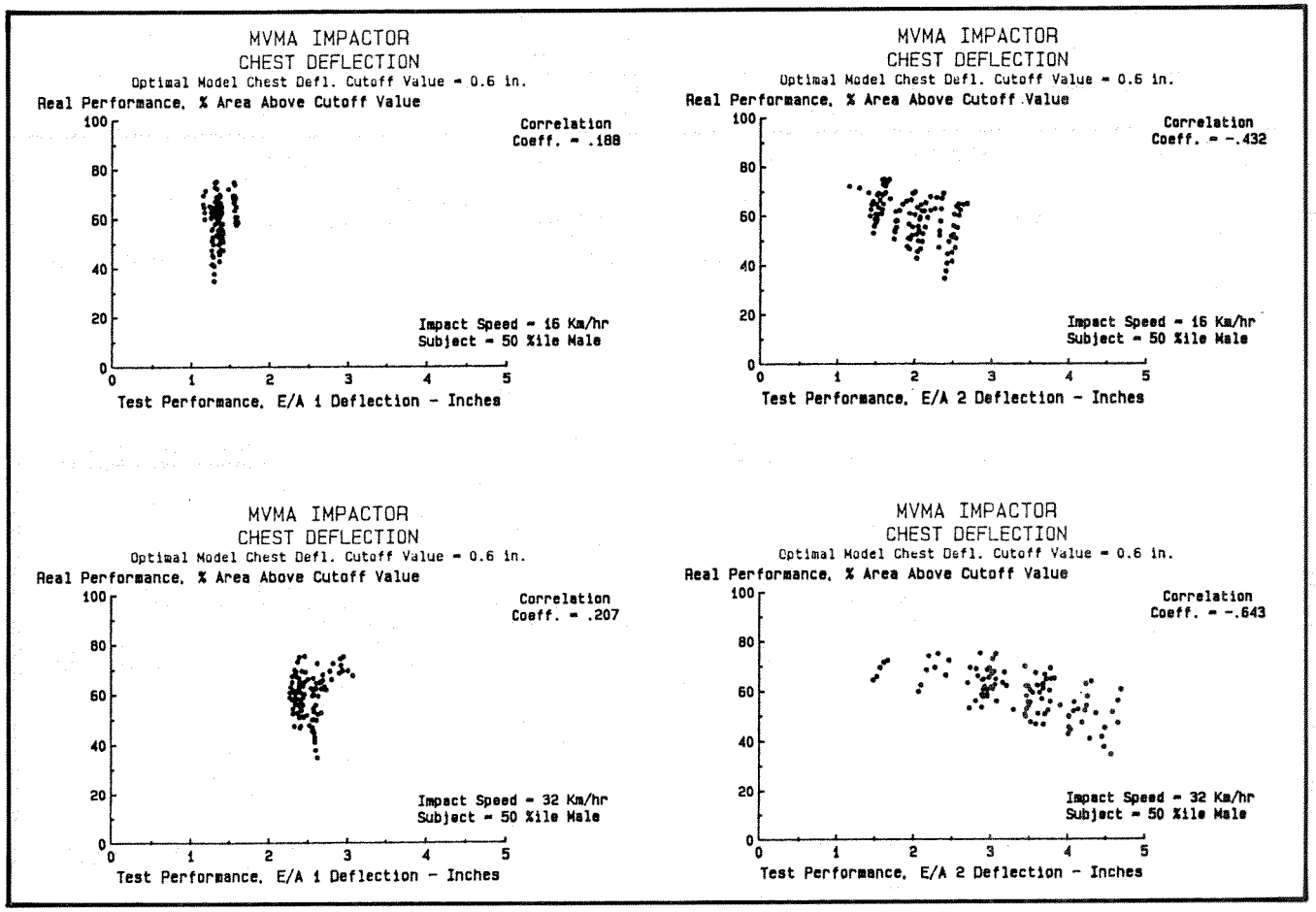

Figure 29. Validation plots—MVMA impactor, speed variation—chest deflection

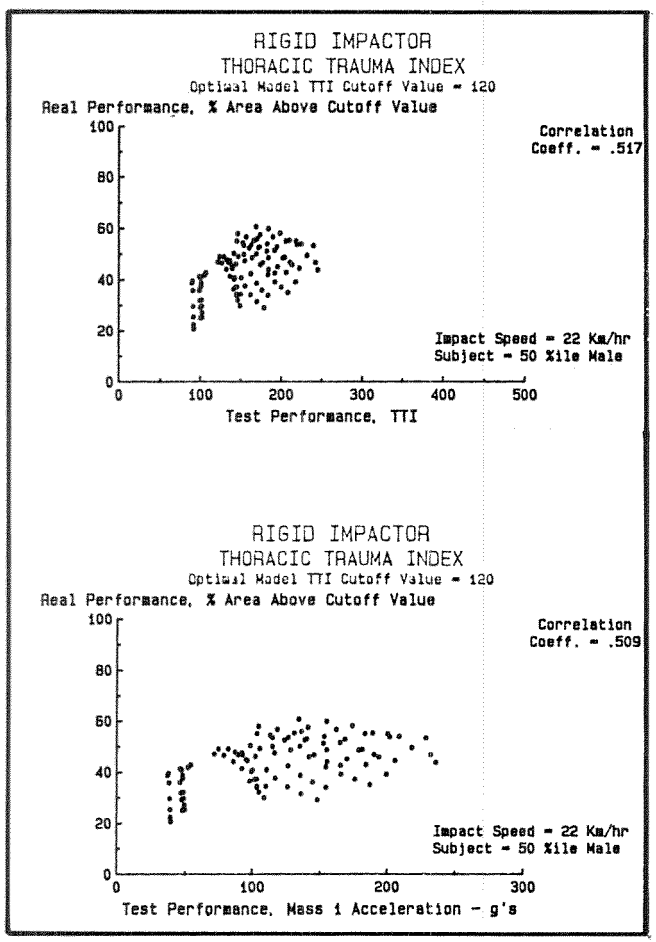

Figure 30. Validation plots—rigid impactor—thoracic trauma index

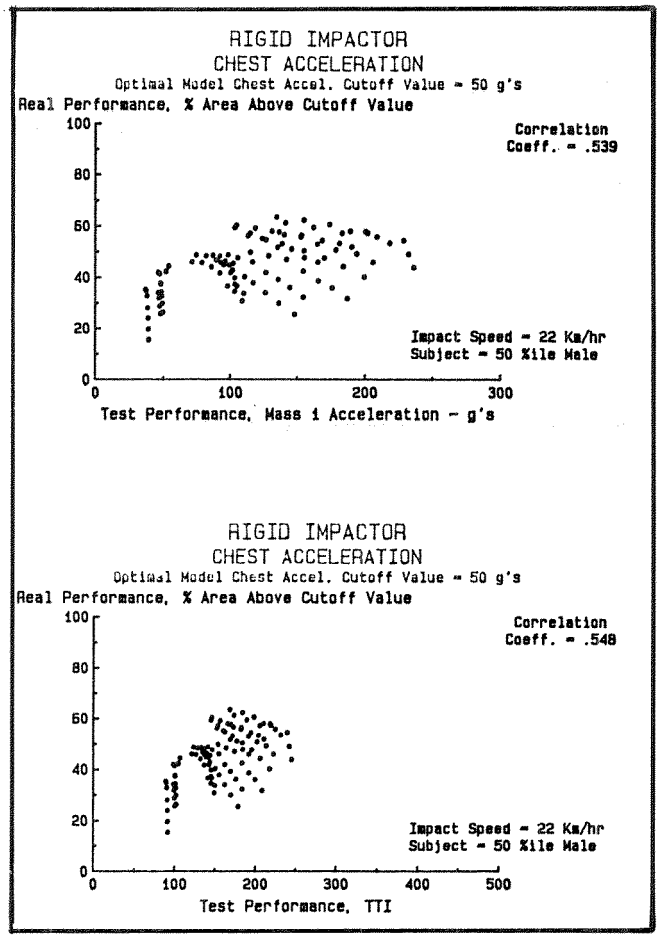

Figure 31. Validation plots—rigid impactor—chest acceleration

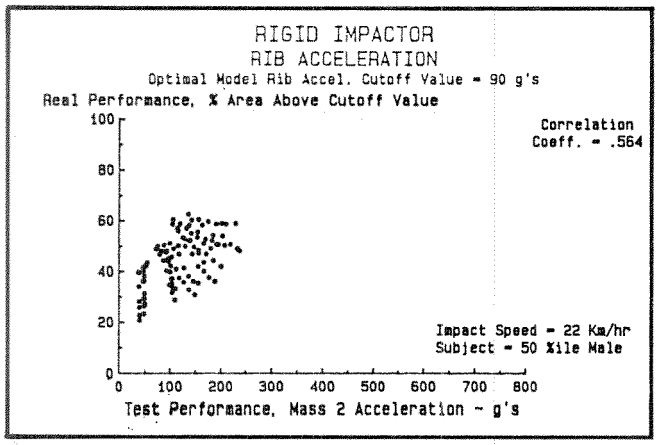

Figure 32. Validation plots—rigid impactor—rib acceleration

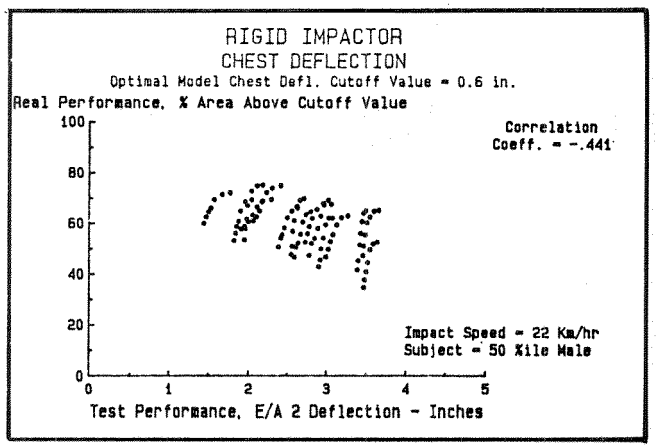

Figure 33. Validation plots—rigid impactor—chest deflection

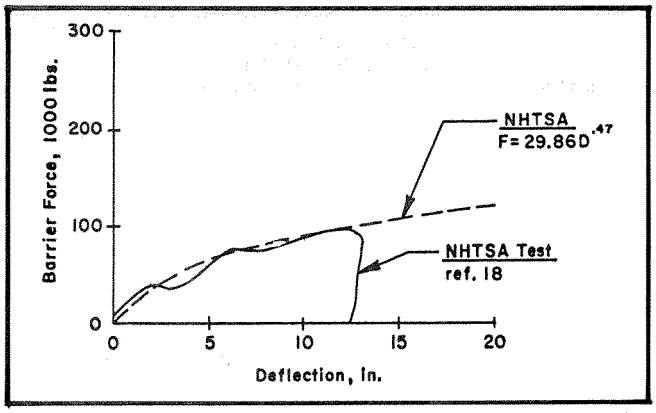

Figure 34. NHTSA moving deformable barrier force-deflection characteristics

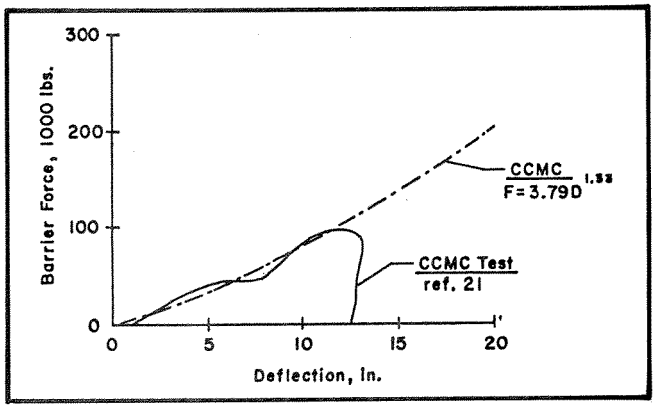

Figure 35. CCMC moving deformable barrier force-deflection characteristics

dummy weights used were 174 lb and 166 lb for the SID and APR dummies, respectively.

The T-type side impact model schematic shown in Figure 8 is used for the full-vehicle test procedure. Energy absorbers 1 and 2 of the impactor are assumed to represent the barrier front end structure and are equal in stiffness. Masses 6 and 5 represent the torso mass and the rib cage mass of the dummy, respectively; energy absorber 6 represents dummy chest stiffness. The door gap, delta 4, is between the 50th percentile dummy and the door interior of a given vehicle. The door gap values used are shown in Table 21.

The correlations between the real performance and the test performance for the seven full-vehicle test procedures are shown in Table 22. These seven test procedures have impact speeds of 32 and 40km/h (or 20 and 25mph). In

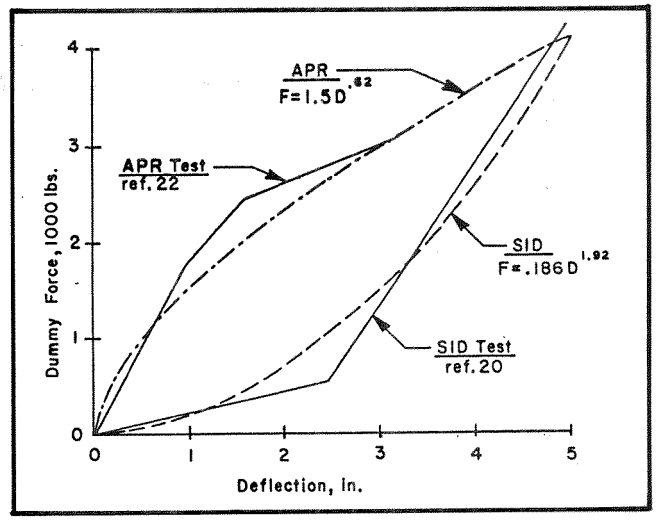

Figure 36. SID and APR dummy chest force-deflection characteristics

Table 22, masses 6 and 5 accelerations represent the torso and rib cage acceleration readings of the struck dummy in the full vehicle.

NHTSA Impactor Speed Variation

As shown in Table 22, test procedures 1 and 2 used the NHTSA MDB impactor weighing 1,361kg at 32 and 40km/h, respectively. Both procedures assume a SID test dummy in a struck vehicle. In general, test procedure 1 at lower speed exhibits higher correlations for most of the responses than those of test procedure 2 at the higher speed.

Figures 37 through 40 show the validation plots of real performance versus test performance for the seven major response correlations in the two test procedures.

Note that the real performance of TTI is predicted better by the mass 6 acceleration (torso acceleration) than by the TTI in the full-vehicle tests. This is true throughout the seven test procedures shown in Table 22.

CCMC Impactor Speed Variation

Test procedures 3 and 4 show the effect of test speed using the CCMC MDB weighing 950kg on the correlation

Table 21. Door gap for a 50th percentile dummy seated in a vehicle

Vehicle Category	1	2	3	4	5	6	7
Weight (lb)	1750	2200	2700	3200	3700	4200	4800
Door Gap (in)	4.45	4.45	4.98	5.93	6.39	6.83	7.09

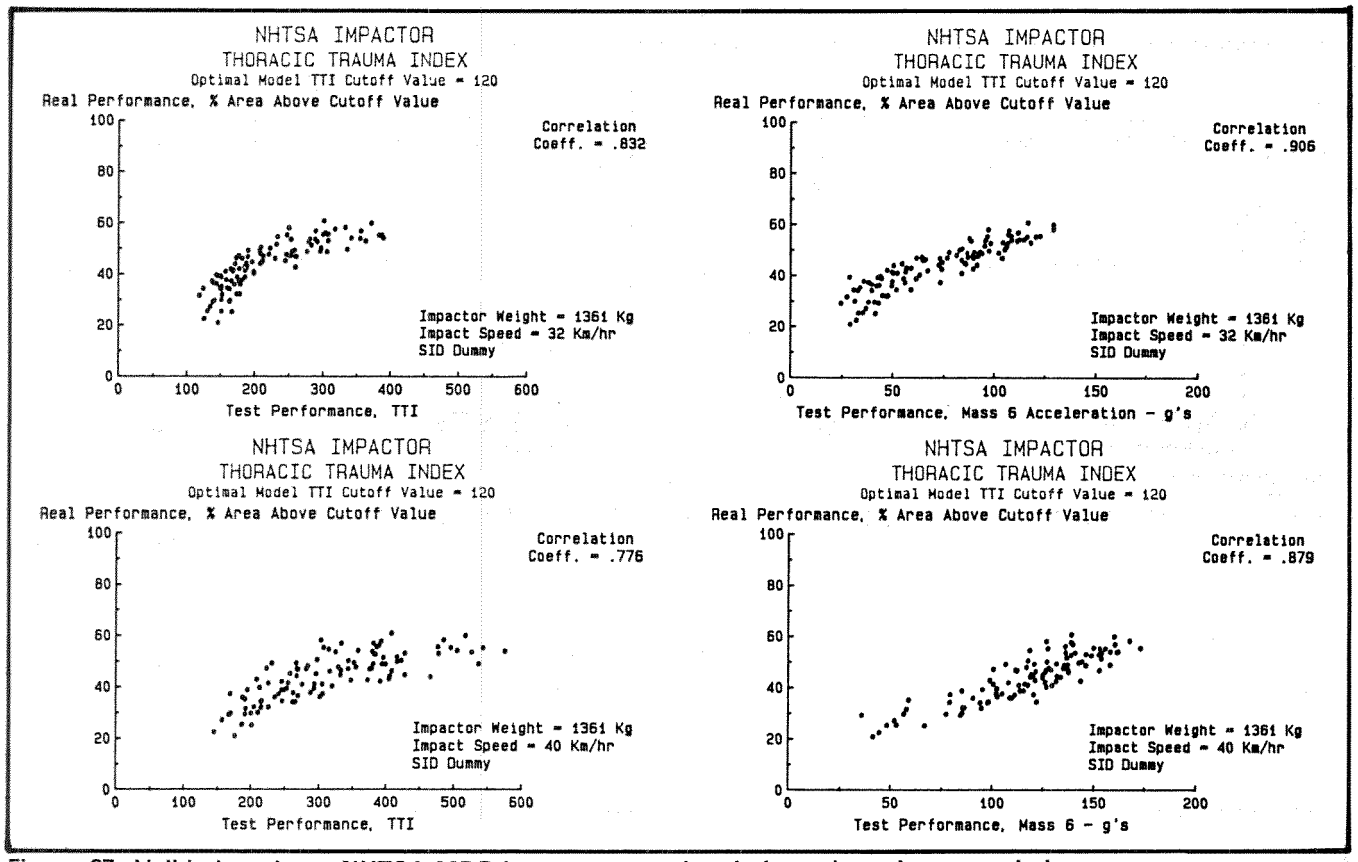

Figure 37. Validation plots—NHTSA MDB impactor, speed variation—thoracic trauma index

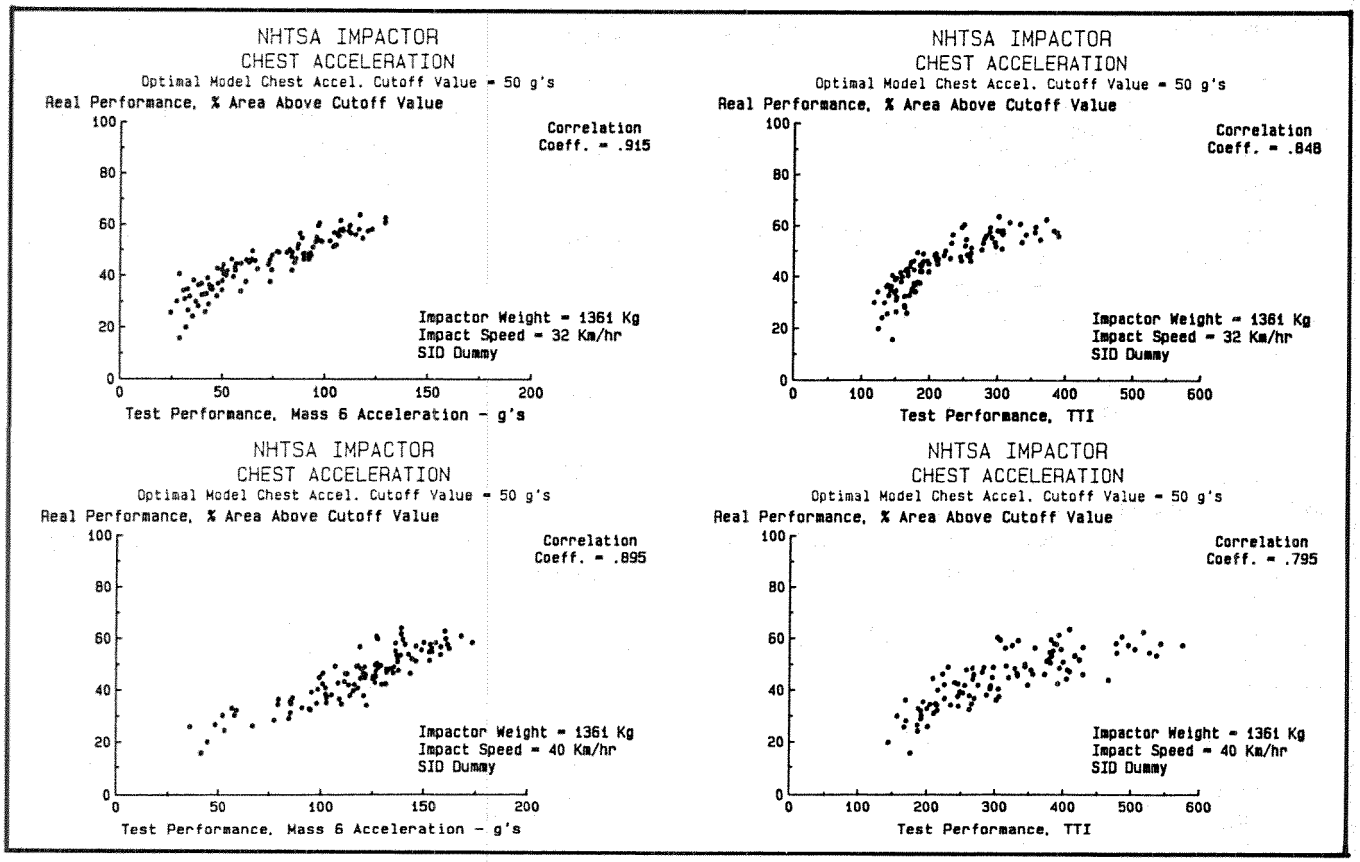

Figure 38. Validation plots—NHTSA MDB impactor, speed variation—chest acceleration

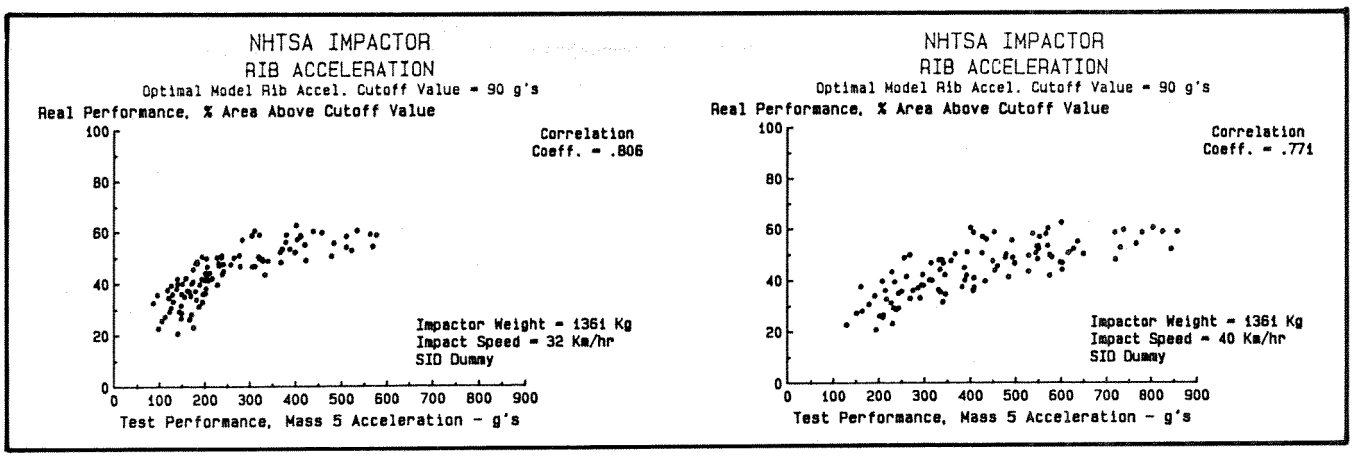

Figure 39. Validation plots—NHTSA MDB impactor, speed variation—rib acceleration

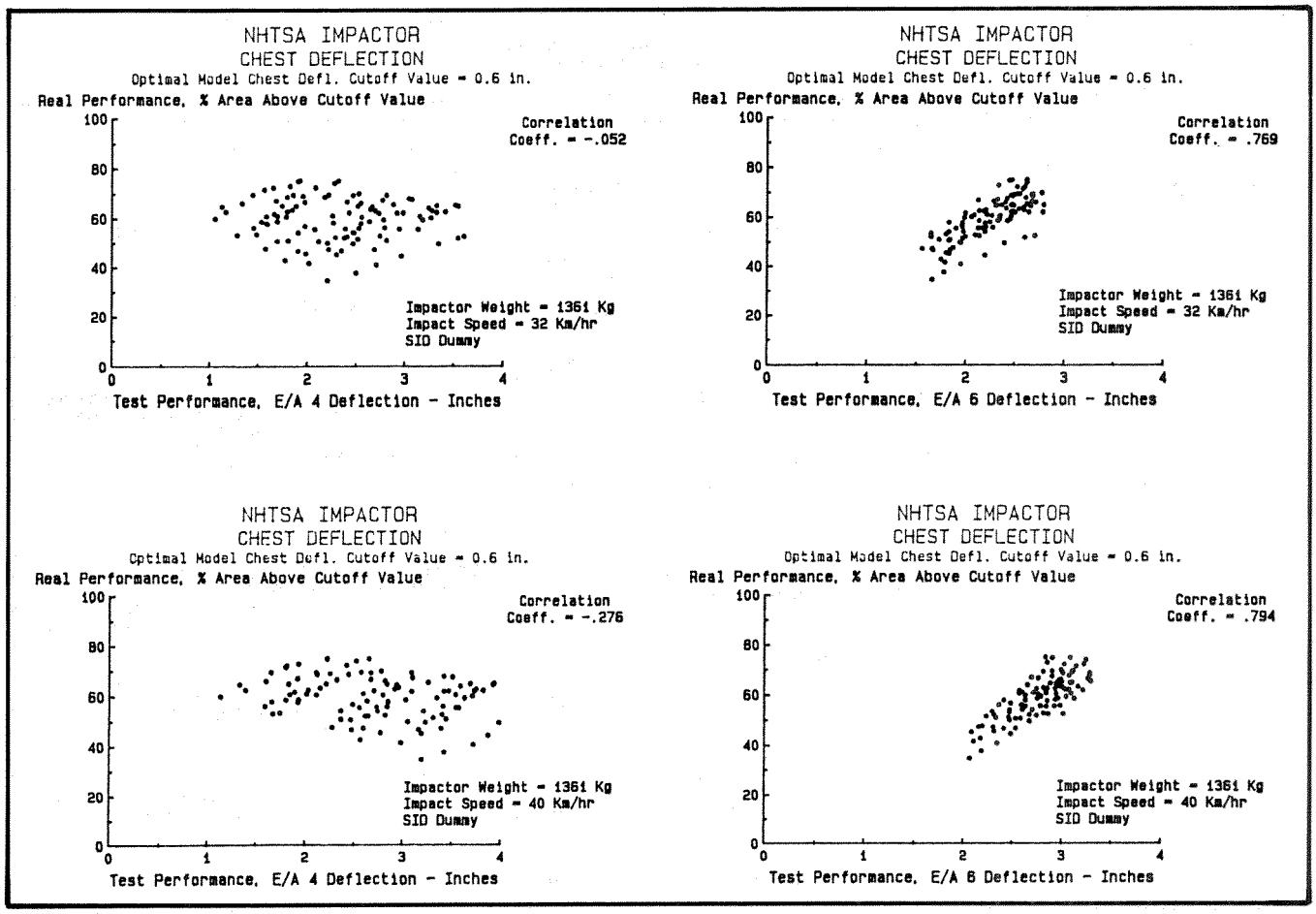

Figure 40. Validation plots—NHTSA MDB impactor, speed variation—chest deflection

Table 22. Correlations between real performance and test performance (full-vehicle test procedure)

Optimal Cutoff Real Performance	120 TTI	50 Chest G	90 Rib G	120 TTI	50 Chest G	0.6 in Chest Deflection	0.6 in Chest Deflection Ea #4 Door-Pad Deflection
Test Performance	TTI	Mass 6* G	Mass 5* G	Mass 6 G	TTI	Ea #6* Deflection	
Test Procedure MDB/Kg Dummy/Km/h							
1 NHTSA/ 1361/SID/32	.832	.915	.806	.906	.848	.769	-.052
2 NHTSA/ 1361/SID/40	.776	.895	.771	.879	.795	.794	-.276
3 CCMC/ 950/APR/32	.779	.864	.727	.860	.791	.858	.114
4 CCMC/ 950/APR/40	.821	.931	.807	.927	.826	.881	-.230
5 CCMC/ 1100/SID/32	.772	.849	.739	.841	.790	.722	.161
6 CCMC/ 1100/APR/32	.791	.866	.743	.861	.803	.854	.078
7 NHTSA/ 1100/SID/32	.831	.912	.805	.905	.843	.798	-.022

* Mass 6: torso mass in side impact model
Mass 5: rib cage mass in side impact model.
Ea #6: chest deflection between mass 6 and 5

	Mean Value of Full-Vehicle Test Reading						
	Test Procedure No.						
Response	1	2	3	4	5	6	7
TTI	218	315	162	246	168	163	211
Mass 6 G	73	117	60	109	50	62	70

between the real performance and test performance. The two test speeds are 32 and 40km/h, and the dummy used in the struck vehicle was the APR.

In the seven response correlations, test procedure 4 at 40km/h produces consistently higher correlation coefficients than test procedure 3. The main reason is that to produce the impact severity observed in the real world, the impactor speed would have to be higher, if the impactor weight is less than the mean striking vehicle weight, which is about 1,500kg.

Figures 41 through 44 illustrate the correlations between the real performance and the test performance for the seven responses in the two test procedures.

CCMC Impactor at 1,100kg—Dummy Variation

Test procedures 5 and 6 have the CCMC MDB impactor weighing 1,100kg at 32km/h with the SID and APR dummies, respectively. Test procedure 6 with the APR dummy yields a slightly higher correlation between real performance and test performance than procedure 5 using the SID dummy. However, the difference in correlation due to dummy type is not as significant as that due to speed, as shown by test procedures 3 and 4 in Table 22.

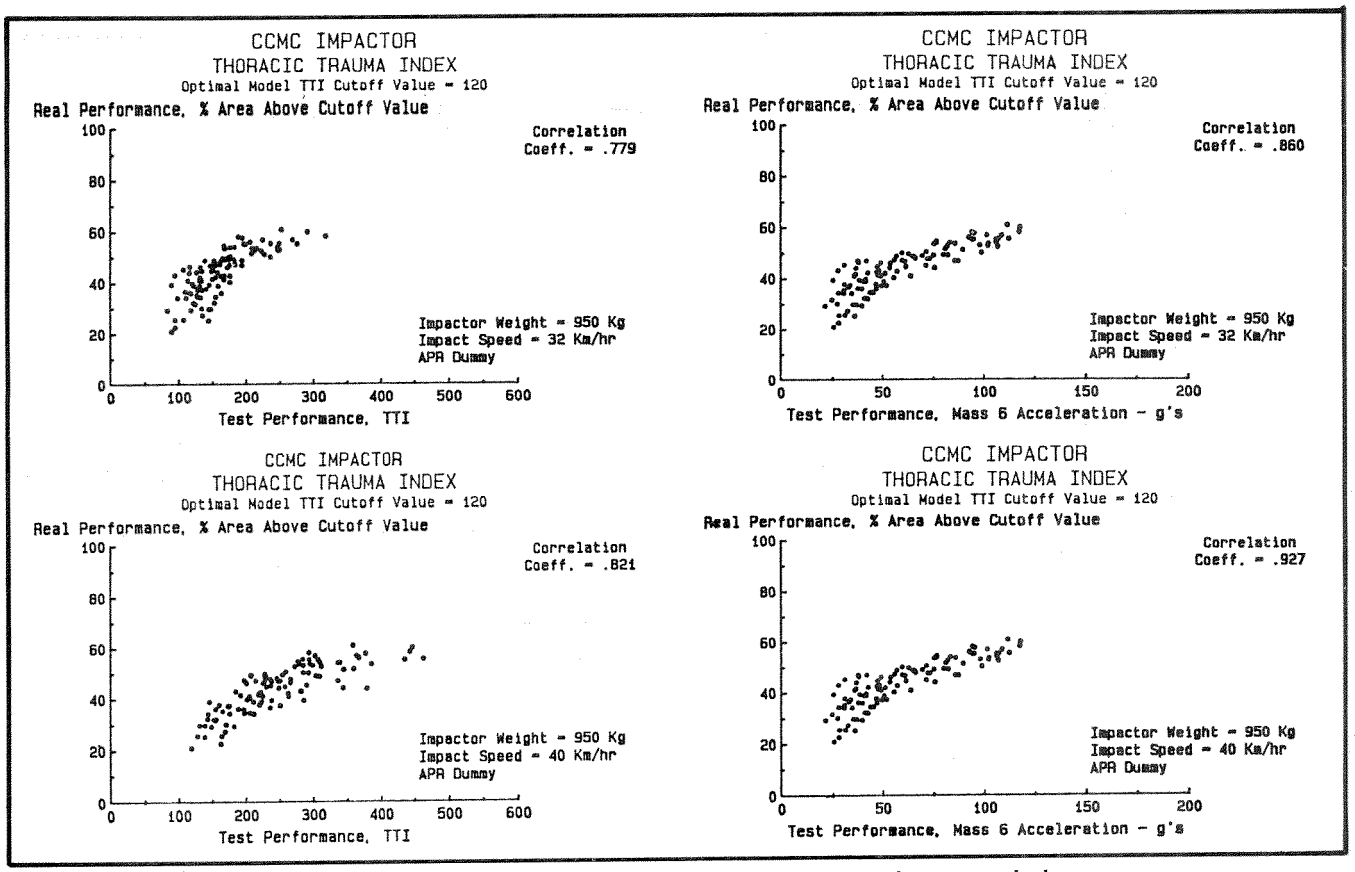

Figure 41. Validation plots—CCMC MDB impactor, speed variation—thoracic trauma index

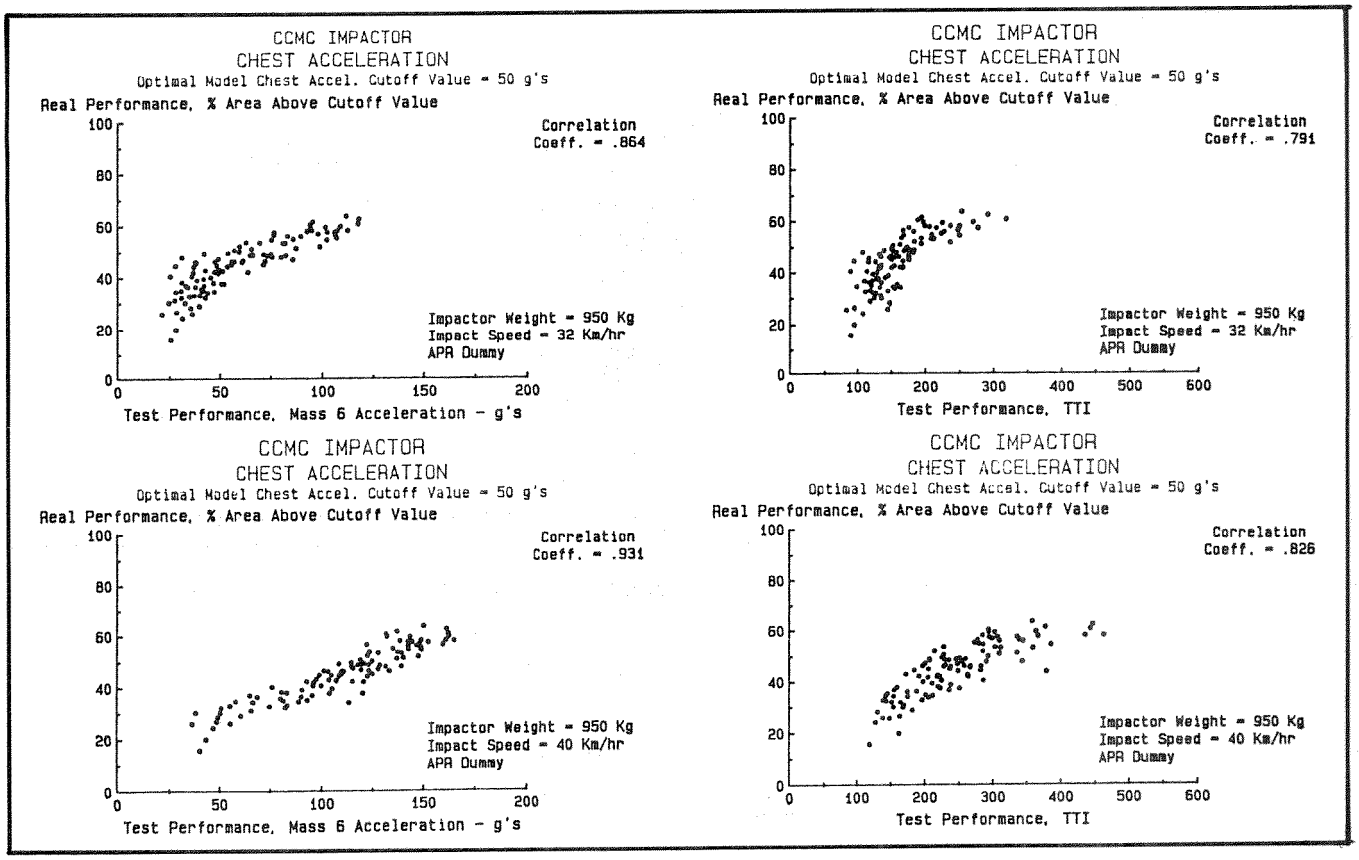

Figure 42. Validation plots—CCMC MDB impactor, speed variation—chest acceleration

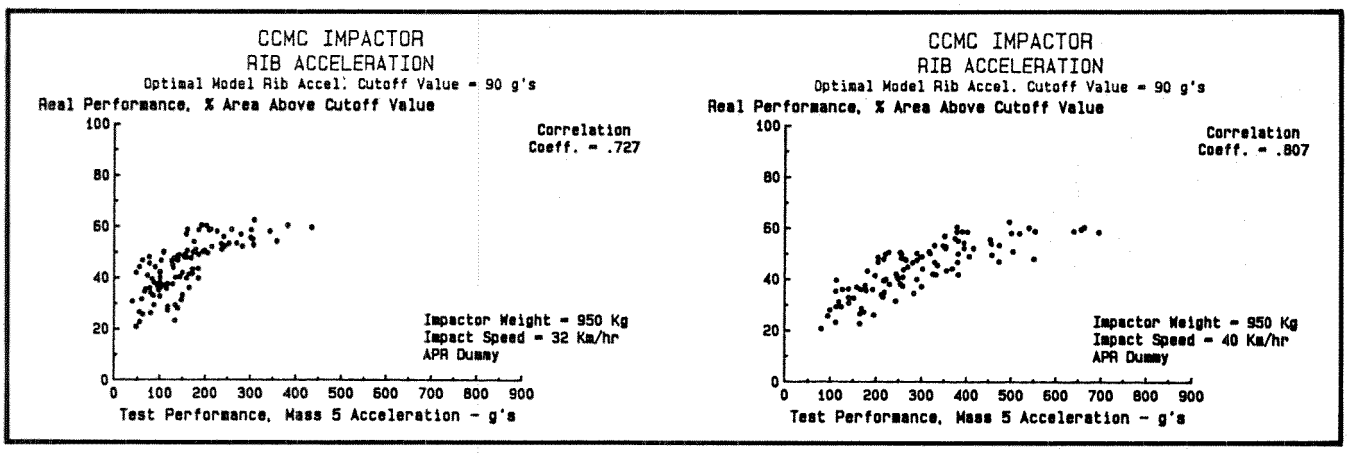

Figure 43. Validation plots—CCMC MDB impactor, speed variation—rib acceleration

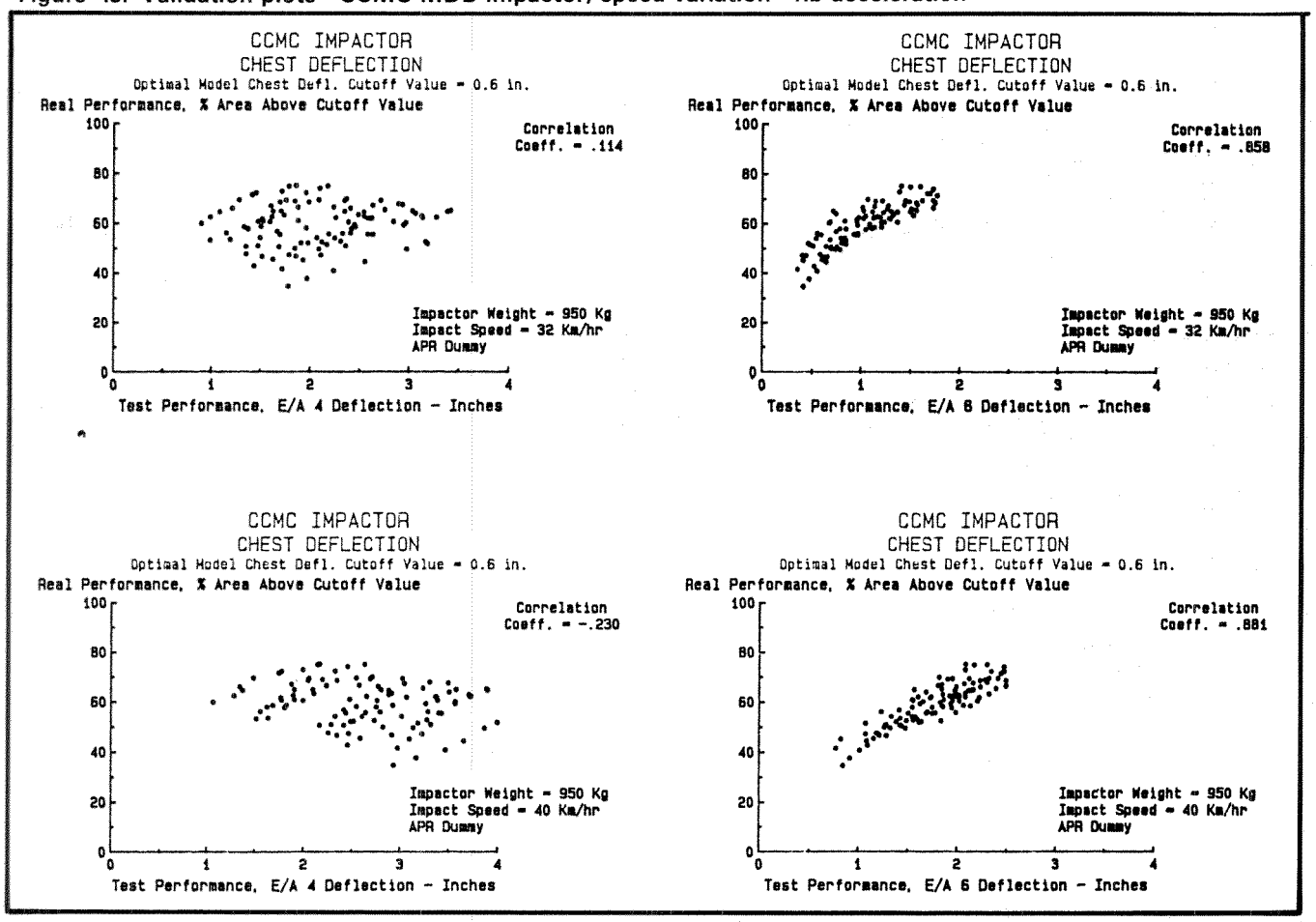

Figure 44. Validation plots—CCMC MDB impactor, speed variation—chest deflection

Figures 45 through 48 show the validation plots and correlation coefficients for the seven responses using test procedures 5 and 6.

NHTSA Impactor at 1,100kg

Test procedure 7 uses the NHTSA MDB impactor weighing 1,100kg at 32km/h with a SID dummy in the struck vehicle. This procedure, for practical purposes, produces the same correlation coefficients as test procedure 1, in which the NHTSA impactor weighs 1,361kg at the same speed. It is concluded that the weight of the NHTSA impactor is not statistically significant as far as predicting the real performance from the test performance.

Figures 49 through 52 show the validation plot and correlations of the seven performance responses for test procedure 7.

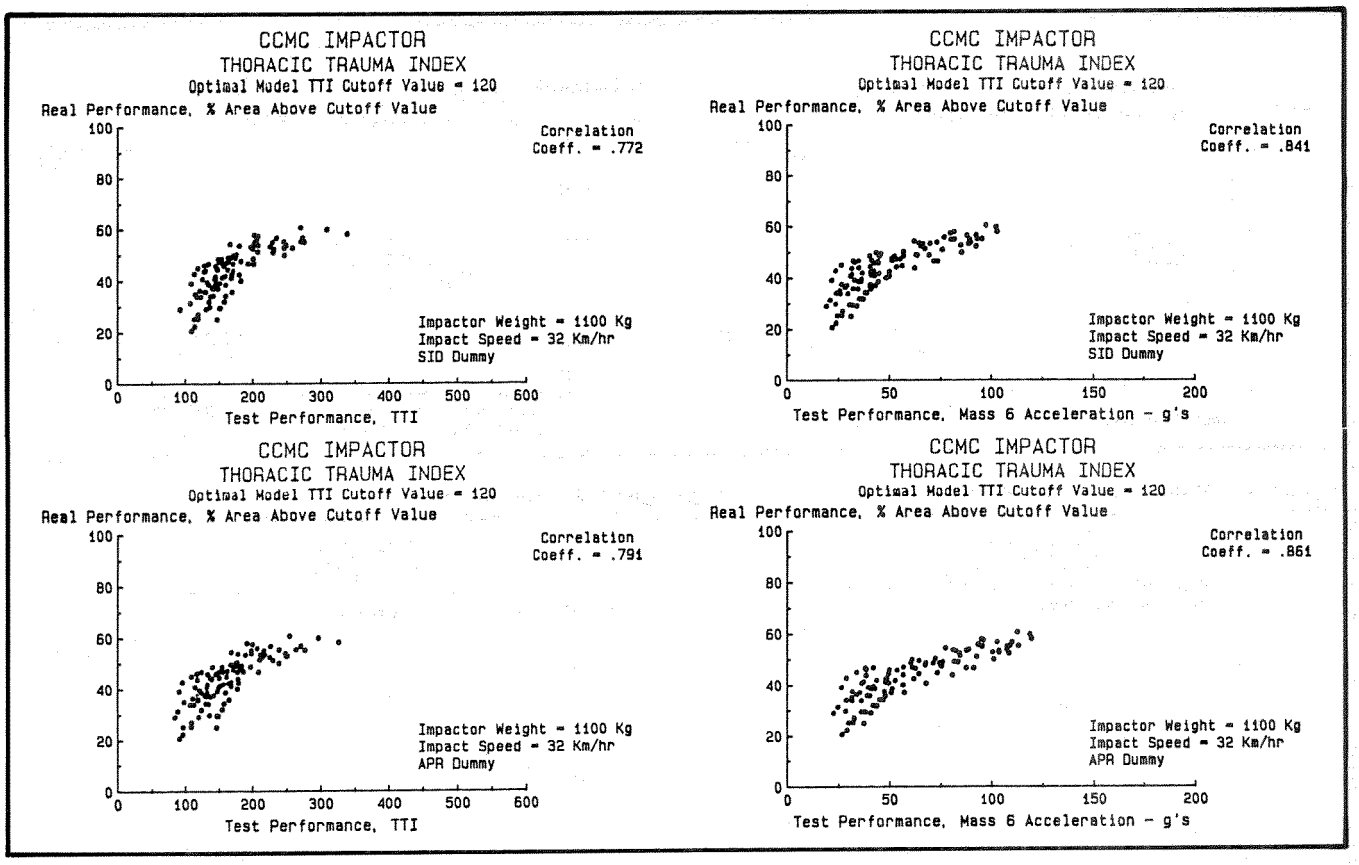

Figure 45. Validation plots—1,100kg CCMC MDB impactor, dummy variation—thoracic trauma index

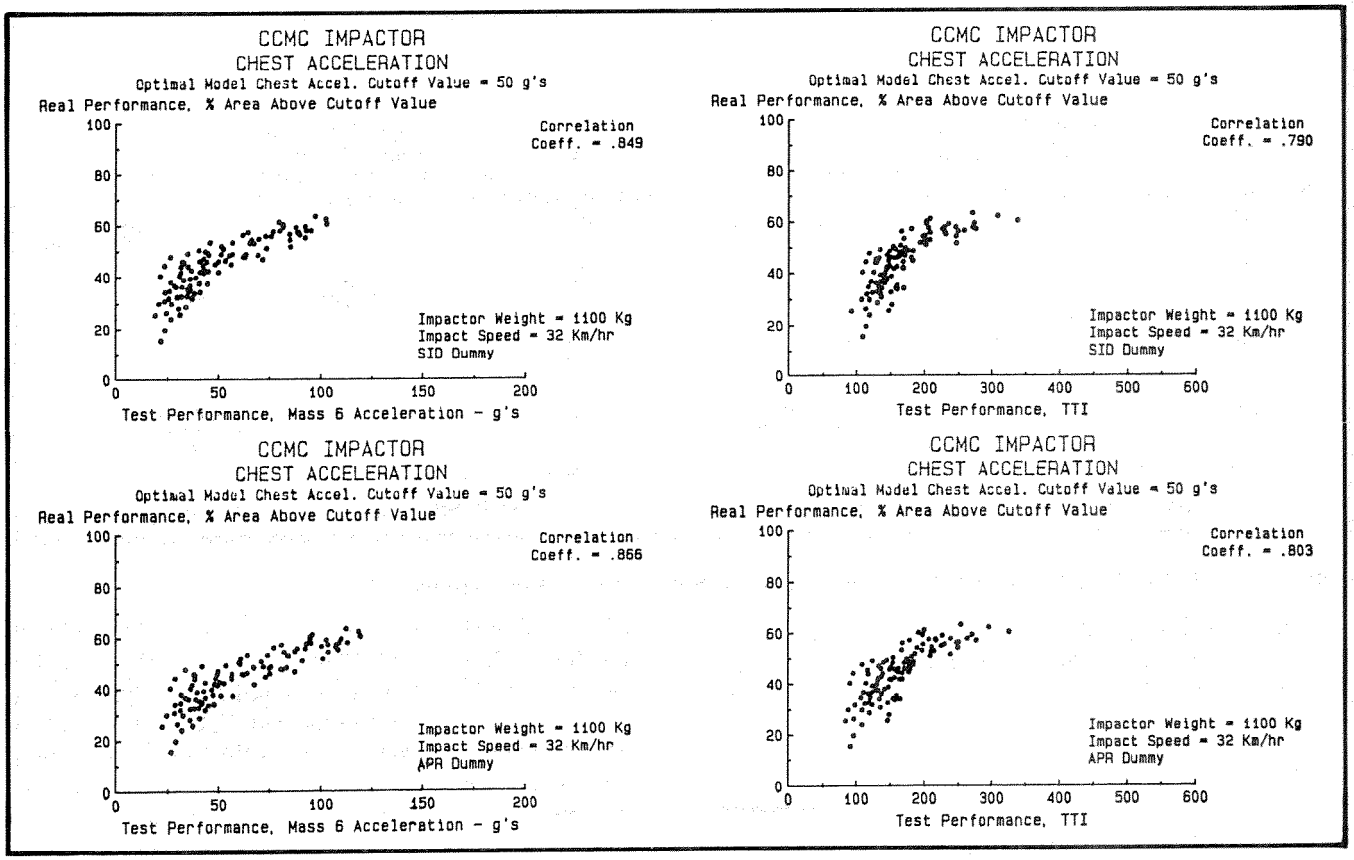

Figure 46. Validation plots—1,100kg CCMC MDB impactor, dummy variation—chest acceleration

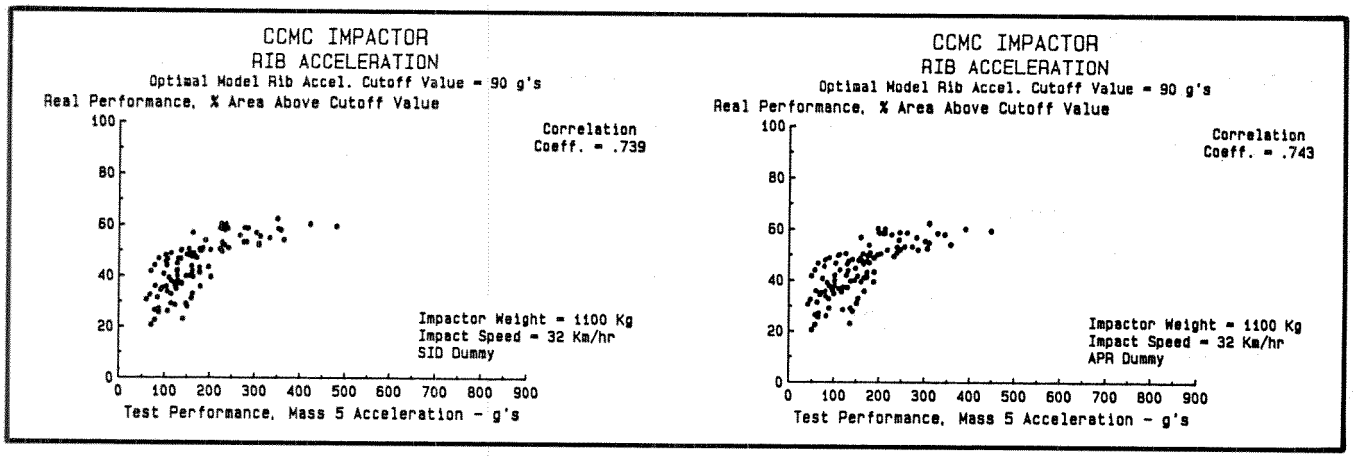

Figure 47. Validation plots—1,100kg CCMC MDB impactor, dummy variation—rib acceleration

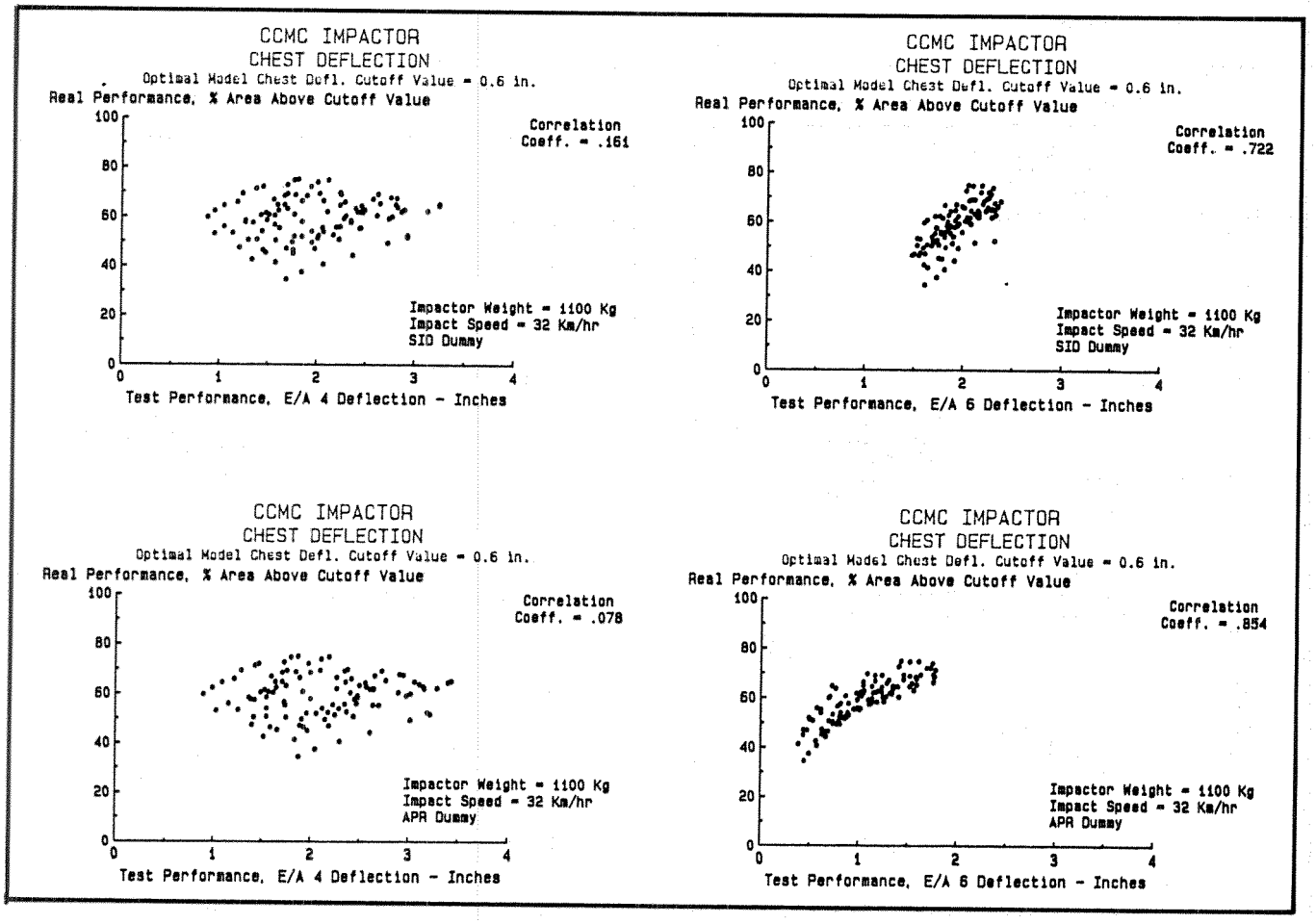

Figure 48. Validation plots—1,100kg CCMC MDB impactor, dummy variation—chest deflection

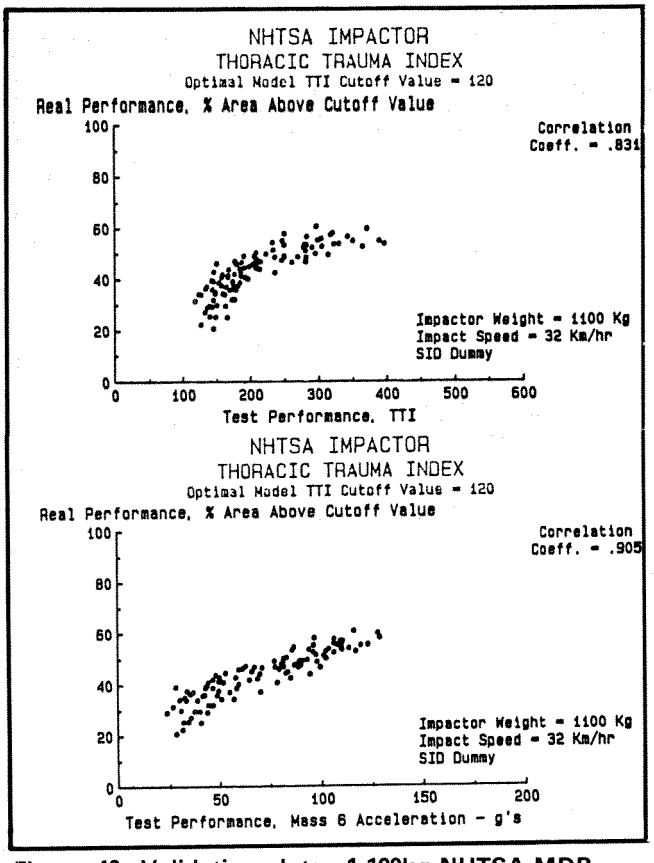

Figure 49. Validation plots—1,100kg NHTSA MDB impactor—thoracic trauma index

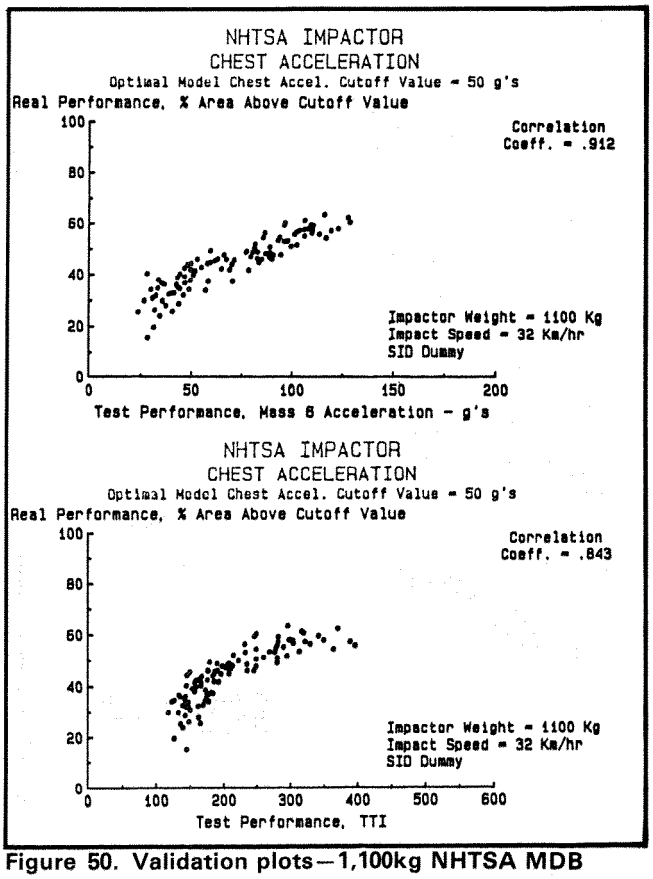

Figure 50. Validation plots—1,100kg NHTSA MDB impactor—chest acceleration

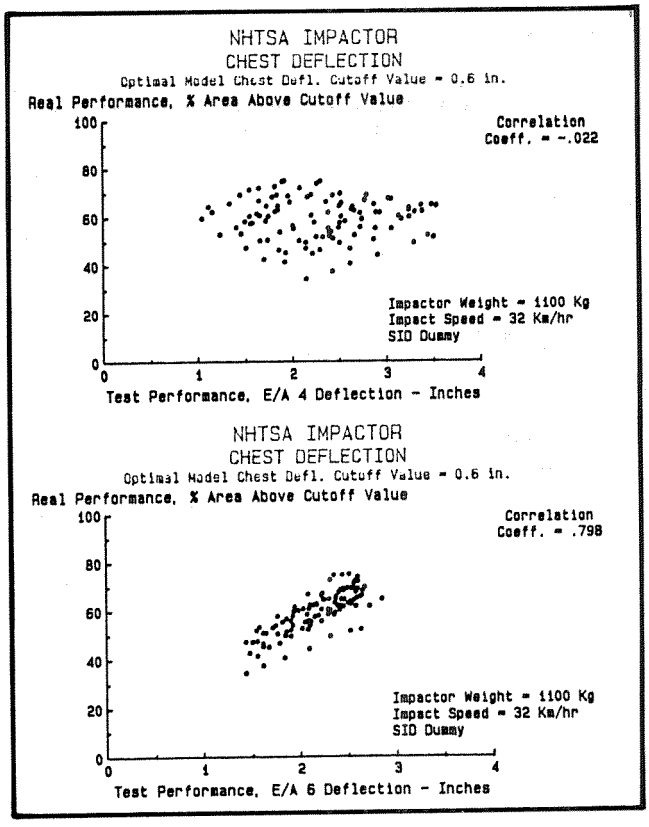

Figure 51. Validation plots—1,100kg NHTSA MDB impactor—rib acceleration

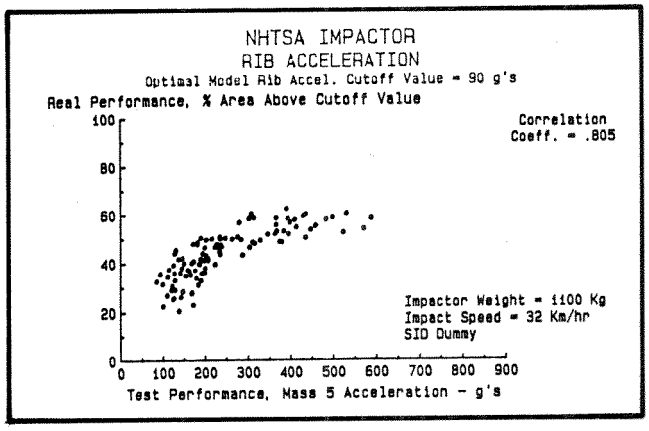

Figure 52. Validation plots—1,100kg NHTSA MDB impactor—chest deflection

Discussion

Although these simulations are in a relatively preliminary and somewhat undeveloped condition, they suggest certain kinds of conclusions. There are factors to which the results seem insensitive and others to which they seem sensitive.

One of the questions that this kind of research is oriented toward answering is whether it really makes much difference if some of the test details are biofidelic

and realistic or not. Particularly, there has been a continuing discussion and controversy as to the minute details of the crash test dummies and of the full-vehicle moving barriers. To the extent that the kind of simulation done in this study has tapped the principal phenomena, the results indicate that some things don't matter very much because the correlation of test results to population experience seems pretty much the same. It really did not much matter whether it was the NHTSA or CCMC barrier or what their weights were. Nor did it much matter if it was the SID or APR dummy used. Furthermore, the impactor used in the component test simulations produced a similar correlation to accident simulations, whether the impactor was biofidelic or if it was just a rigid mass. These kinds of results suggest that much of the discussion about the particulars of these kinds of tests may be far less important than other considerations. For example, the running of simulations at different test speeds shows there may be an optimum speed for such tests, and it is not very high. That is, if the purpose of the test is to predict what is going to happen in the field, then it may be self-defeating to run these tests at too high a speed, because such tests may not predict what goes on in the field.

There are certain sensitivities in the findings. Particularly, it was found the weight of the test car (and/or its stiffness, which in these simulations was set proportional to the weight) had a very noticeable effect on the correlation between component test and field simulations. The correlation plots for the component tests show a very distinct patterning of the data points. This came about because each point represents a particular vehicle design, and the vehicle designs were systematically configured according to their weight and other parameters. One must not jump too quickly to conclusions about the relative quality of the correlations found with the component test as opposed to the full-vehicle test by superficial comparison of the plots. For example, see Figures 53 and 54. These are repeats of the upper left plots in Figures 27 and 38, respectively, shown earlier in the report. The first one relates to the component tester, and the second relates to the full-vehicle test, both of them for chest g. The tested vehicles have been segregated according to their weight (and corresponding stiffness) in these plots. It is seen that once the data are segregated by weight of the test vehicle, the correlations were similarly high with either type of test. But it also shows the component test must be further developed. There had already been considerable discussion about the necessity of taking into account the twin factors of structural energy absorption and occupant nearness to the door to standardize side impact component tests. The results in this report verify the need to do that. In further phases of this investigation, we will be developing an adaptive component test procedure, i.e., the speed of impact in the component test will be set after appropriate consideration of the test vehicle's properties.

This study has not, to this point, attempted to get at injury, per se, and makes no attempt at establishing any kind of pass-fail criteria. An implied criterion may evolve by working backwards from the population results to the test results by picking a criterion population performance level and then finding the test result corresponding to it. For example, one might examine any of the graphs in this report and draw a horizontal line across the graph, say, at the 50 percent level, and then drop a vertical to the abscissa to identify what might be an appropriate test criterion. This may be more easily said than done, because the attempt to do that will immediately disclose that the horizontal criterion line intersects a large scatter of test results. That is true even for the largest correlations observed in this study. Although this study is trafficking in correlations, it must be understood that in a regulatory or in an NCAP environment, it is individual models that will be branded by the test results, and fairness then becomes much more of an issue than does correlation. Individual makes having the same population experience (they are all the points intersected by any horizontal iso-level) can really have quite a range of different test results.

There are other factors to be considered such as repeatability, reproducibility, and text complexity and cost, but, in the end, a test's ability to rank cars in order of safety performance is very important. The results of this study must be considered as mainly suggestive. It is our wish that those who have ideas about improving the simulations or trying other conditions would communicate with us so we might incorporate them into our continuing work.

Future Plans

We plan to continue the development and use of the model described here and report our findings in future papers. Future work will be initially concentrated in the following areas:

- The test parameters explored for the full-vehicle and component tests will be expanded to include all combinations of the parameters. This will allow an analysis of the effects of the individual test design parameters such as impact speed, barrier weight, etc., and possible interaction of those parameters.
- We will explore various proposals for improving the predictive power of the component test. It may be possible to improve the performance of the component test by adjusting the speed of the test to account for variations in door gap and side structure stiffness.
- The effect of test-to-test variability will be introduced into the model. Test variability will

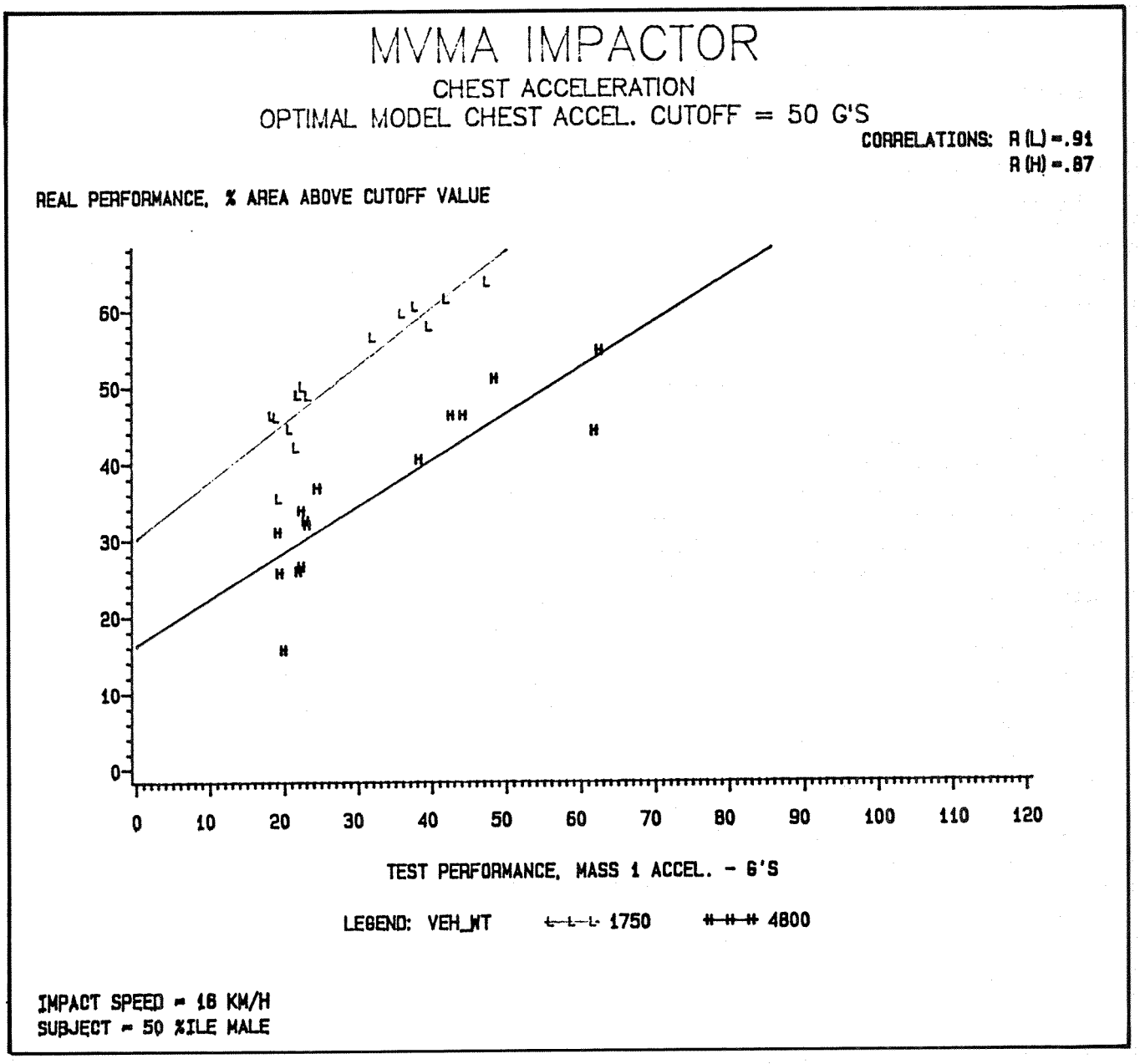

Figure 53. Vehicle weight effect on correlations—component tests

degrade the correlation between test results and real-world performance. The effect will be to either reduce or to accentuate the differences in predictability between the component and full-vehicle test.

- We will attempt injury prediction in the model rather than the current performance measure. The inclusion of injury prediction may or may not change the overall findings of the study.

References

1. Versace, J., and S.E. Henson, "Testing the side impact tests: criteria and strategy," SAE Paper 851248, Government/Industry Meeting & Exposition, Washington, D.C., May 20-23, 1985.
2. Edmonds, H.J., R.H. Hanson, D.R. Morganstein, and J. Waksberg, "National accident sampling system: sample design, phases 2 and 3," NHTSA, DOT-HS-805-274, November 1979.
3. Eppinger, R.H., J.H. Marcus, and R.M. Morgan, "Development of dummy and injury index for NHTSA's thoracic side impact protection research program," SAE Paper 840885, Government/Industry Meeting & Exposition, Washington, D.C., May 21-24, 1984.
4. Tomassoni, J.E., "Simulation of a two-car oblique side impact using a simple crash analysis model,"

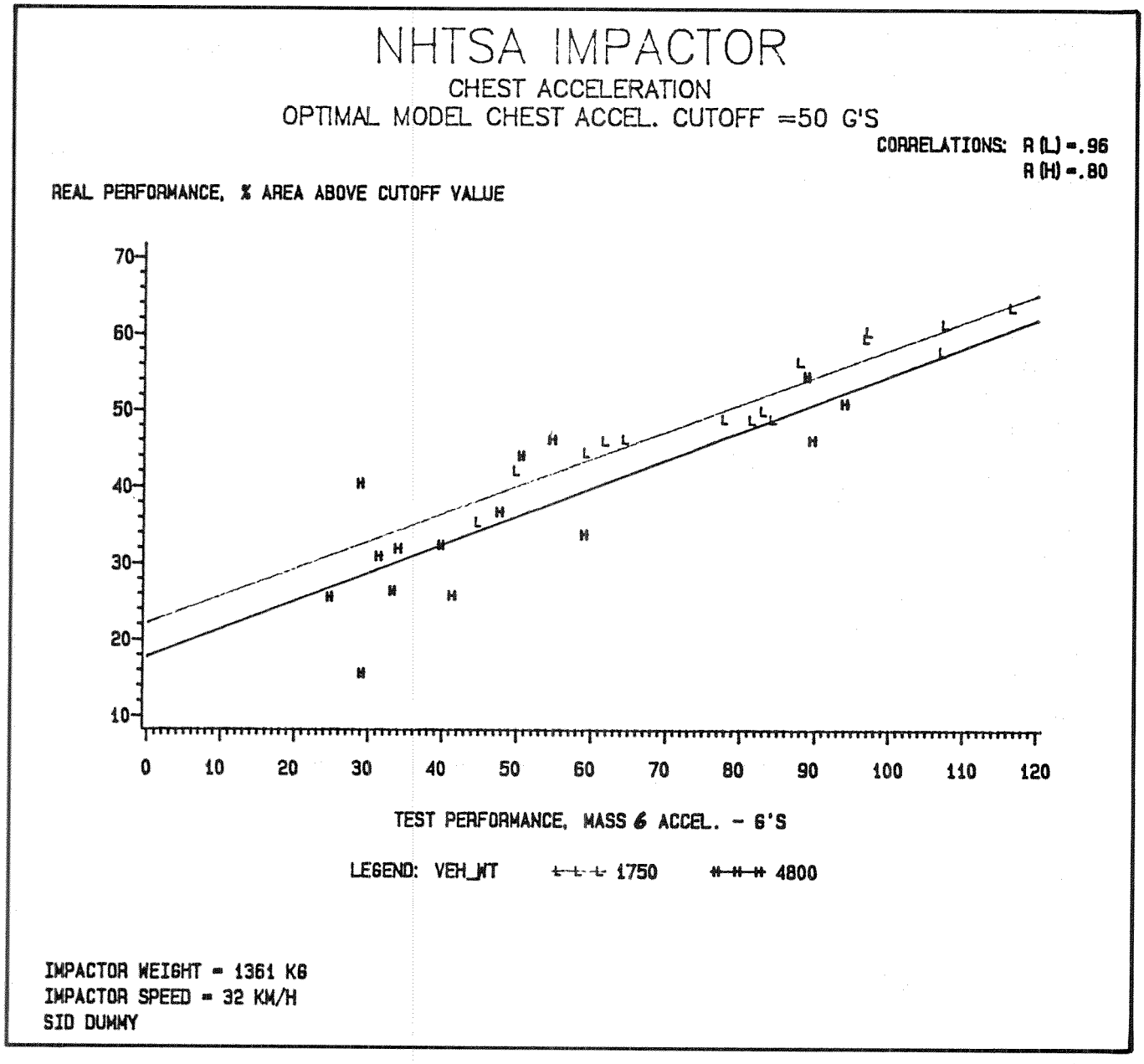

Figure 54. Vehicle weight effect on correlation—full vehicle tests

SAE Paper 840858, Government/Industry Meeting & Exposition, Washington, D.C., May 21-24, 1984.

5. Pike, J.A., "A biomechanical model for thoracic side impacts," Ford Motor Company, Report S-85-03, May 31, 1985.
6. Tarriere, C., G. Walfisch, A. Fayon, J.P. Rosey, C. Got, A. Patel, and A. Delmas, "Synthesis of human tolerances obtained from lateral simulations," Proceedings Seventh International Technical Conference on Experimental Safety Vehicles, DOT-HS-805-199, pp. 359-373, Paris, France, 1979.
7. Health Examination Survey, "Weight, height, and selected body dimensions of adults: U.S. 1960-62," U.S. Department of Health, Education and Welfare, Public Health Service Publication No. 1000, Series 11, Number 8, Washington, D.C., June 1965.
8. Health Examination Survey, "Weight by height and age of adults: U.S. 1960-62," U.S. Department of Health, Education and Welfare, Public Health Service Publication No. 1000, Series 11, Number 14, Washington, D.C., May 1966.
9. Health Examination Survey, "Skinfolds, body girths, biacromial diameter and selected anthropometric indices of adults: U.S. 1960-62," U.S. Department of Health, Education and Welfare, Public Health Service

Publication No. 1000, Series 11, Number 35, Washington, D.C., February 1970.
10. Diffrient, N., A.R. Tilley, and D. Harman, "Humanscale 7/8/9 manual," Henry Dreyfuss Associates, Massachusetts Institute of Technology, 1981
11. NHTSA, "CRASH3 user's guide and technical manual," DOT-HS-805-732, February 1981.
12. "Multidisciplinary accident investigation data file, editing manual and reference information, Volume II—1976 Reference Information," DOT-HS-802-412, Highway Safety Research Institute, June 1977.
13. SAE, "Collision deformation classification," SAE-J224 MAR80, SAE Handbook, 1985.
14. Hultman, R.W., "Side impact simulation model Monte Carlo preprocessor: source code," Ford Motor Company Report SR-85-02, May 31, 1985.
15. Krause, P.L., "Normalization of side impact cadaver dynamic response data utilizing regression techniques," SAE Paper 840883, Government/Industry Meeting & Exposition, Washington, D.C., May 21-24, 1984.
16. Mertz, H.J., "A procedure for normalizing impact response data," SAE Paper 840884, Government/Industry Meeting & Exposition, Washington, D.C., May 21-24, 1984.
17. Wasko, R.J., and R.A. Wilson, "Results of the Motor Vehicle Manufacturers Association component and full-vehicle side impact test procedure development program," Proceedings Tenth International Technical Conference on Experimental Safety Vehicles, Oxford, England, July 1985.
18. Hackney, J.R., M.W. Monk, W.T. Hollowell, L.K. Sullivan, and D.T. Willke, "Results of the National Highway Traffic Safety Administration's thoracic side impact protection research program," SAE Paper 840886, Government/Industry Meeting & Exposition, Washington, D.C., NHTSA, May 21-24, 1984.
19. Melvin, J.W., D.H. Robbins, and J.B. Benson, "Experimental application of advanced thoracic instrumentation techniques to anthropomorphic test devices," Proceedings Seventh International Technical Conference on Experimental Safety Vehicles, DOT-HS-805-199, pp. 416-427, Paris, France, 1979.
20. Padgaonkar, A.J., and P. Prasad, "A mathematical analysis of side impact using the CAL3D simulation model," Proceedings Ninth International Technical Conference on Experimental Safety Vehicles, pp. 578-585, Kyoto, Japan, 1982.
21. Klaus, G., R. Sinnhuber, and G. Hoffmann, "Mobile deformable barrier for lateral collision testing—a contribution toward a harmonization of future side impact performance requirements," SAE Paper 840888, Government/Industry Meeting & Exposition, Washington, D.C., May 21-24, 1984.
22. Fayon, A., Y.C. Leung, R.L. Stalnaker, G. Walfisch, M. Balthazard, and C. Tarriere, "Presentation of the frontal impact and side impact dummy, defined from human data and realized from a 'Part 572' basis," Proceedings Seventh International Technical Conference on Experimental Safety Vehicles, DOT-HS-805-199, NHTSA, pp. 407-416, Washington, D.C., 1979.
23. Fayon, A., C. Tarriere, G. Walfisch, M. Duprey, and M. Balthazard, "Development and performance of the APR dummy (APROD)," Proceedings Eighth International Technical Conference on Experimental Safety Vehicles, pp. 451-462, Wolfsburg, West Germany, October 1980.

Appendix A

Experiment Design

A three-dimensional star-cube design is used to establish the design matrix of the three side-struck controlled variables. A star-cube design is a rotatable design in which it has equal predictability in all directions from the center, and the points are at a constant distance from the center.

A pictorial representation of a three-dimensional star-cube design is shown in Table A-1. The number of design experiments in the star-cube design is fifteen. They are (1)

Table A-1. Dimensional star-cube design for the side impact model

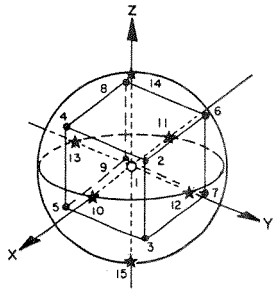

Point	Point No.	Normalized Variable x	y	z	Real Variable x	y	z
Center	1	0	0	0	2.5	110.	1.0
Corner Points	2	1	1	1	3.7	139.	1.3
	3	1	1	-1	3.7	139.	0.7
	4	1	-1	1	3.7	81.	1.3
	5	1	-1	-1	3.7	81.	0.7
	6	-1	1	1	1.3	139.	1.3
	7	-1	1	-1	1.3	139.	0.7
	8	-1	-1	1	1.3	81.	1.3
	9	-1	-1	-1	1.3	81.	0.7
Stars	10	$\sqrt{3}$	0	0	4.5	110.	1.0
	11	$-\sqrt{3}$	0	0	0.5	110.	1.0
	12	0	$\sqrt{3}$	0	2.5	160.	1.0
	13	0	$-\sqrt{3}$	0	2.5	60.	1.0
	14	0	0	$\sqrt{3}$	2.5	110.	1.5
	15	0	0	$-\sqrt{3}$	2.5	110.	0.5

X = Pad thickness
Y = Elasticity of pad, Young's modulus
Z = Non-precrushed door stiffness, kip/in

one at the center of the sphere (center point 1), (2) six at the intersections of the three mutually perpendicular coordinate axes and the spherical surface (star points 10-15), and (3) eight points on the corners of the cubes (corner points 2-9) that are inscribed in the sphere. Note that the eight corner points are also on the spherical surface.

Hardware Variables

The three side-struck variables are defined as follows:

X: padding thickness, in
Y: modulus of elasticity of padding (E), psi
Z: nonprecrushed door stiffness, kip/in

Using the axial loading relationship in the strength of material, one has:

$$\delta = \frac{PL}{AE}$$

where:
δ: axial deflection of a material
P: applied axial load
L: length (or depth) of a material
A: constant cross-sectional area
E: modulus of elasticity

Rearranging Equation (1), it becomes:

$$K = \frac{A}{L} E$$

where K: material stiffness $= \frac{P}{\delta}$

Equation (2) computes the equivalent stiffness of a padding provided that the padding thickness, the contact area between the side of the occupant and the pad, and the modulus of elasticity of the padding are given. It is assumed in the side impact model that the height of the padding on the interior of the door is 6in and the padding is wide enough that the impact load of the occupant on the pad is evenly distributed. The contact area is then computed as follows:

A = effective chest depth $\times$ padding height
= (.5 $\times$ chest depth) $\times$ (6) in^2

Note that due to the protrusion of the upper arm and shoulder, the effective chest depth that is in contact with the padding is assumed to be 50 percent of the chest depth

Appendix B

Baseline Energy-Absorbing Force Deflection Characteristics

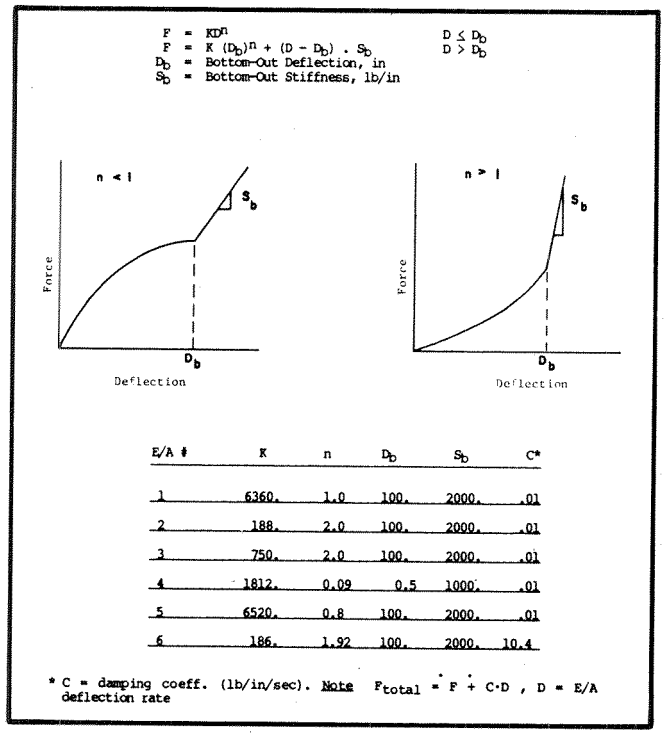

E/A #	K	n	D_b	S_b	C*
1	6360.	1.0	100.	2000.	.01
2	188.	2.0	100.	2000.	.01
3	750.	2.0	100.	2000.	.01
4	1812.	0.09	0.5	1000.	.01
5	6520.	0.8	100.	2000.	.01
6	186.	1.92	100.	2000.	10.4

* C = damping coeff. (lb/in/sec). Note $F_{total} = F + C \cdot \dot{D}$, $\dot{D}$ = E/A deflection rate

Appendix C

Side Impact Model Validation

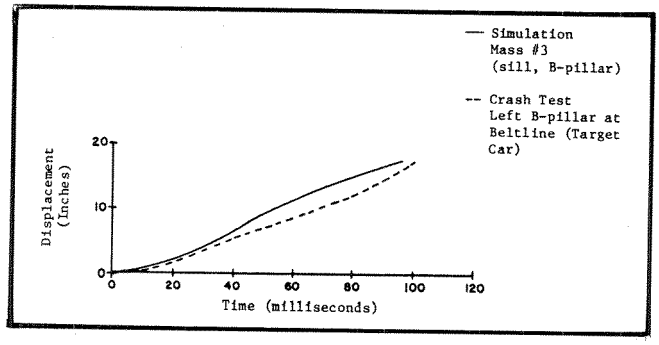

Figure C-1. Side impact model validation—mass #3

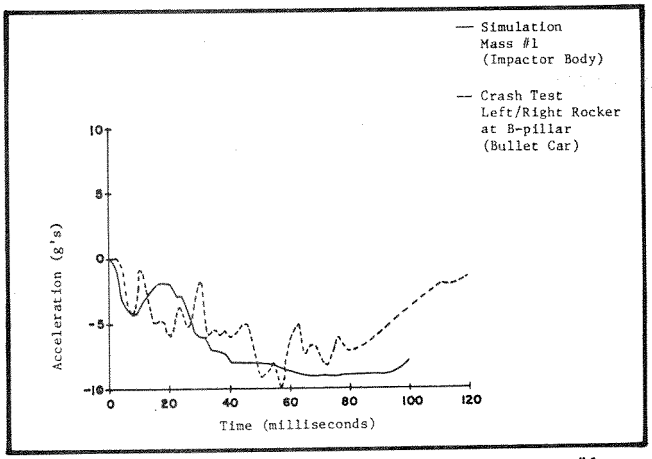

Figure C-2. Side impact model validation—mass #1

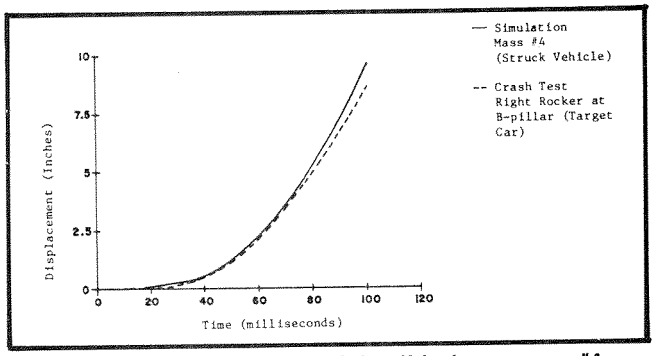

Figure C-3. Side impact model validation—mass #4

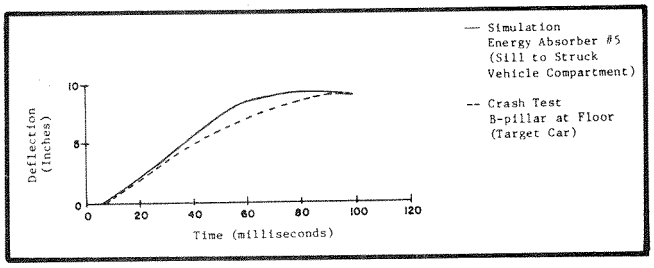

Figure C-4. Side impact model validation—energy absorber #5

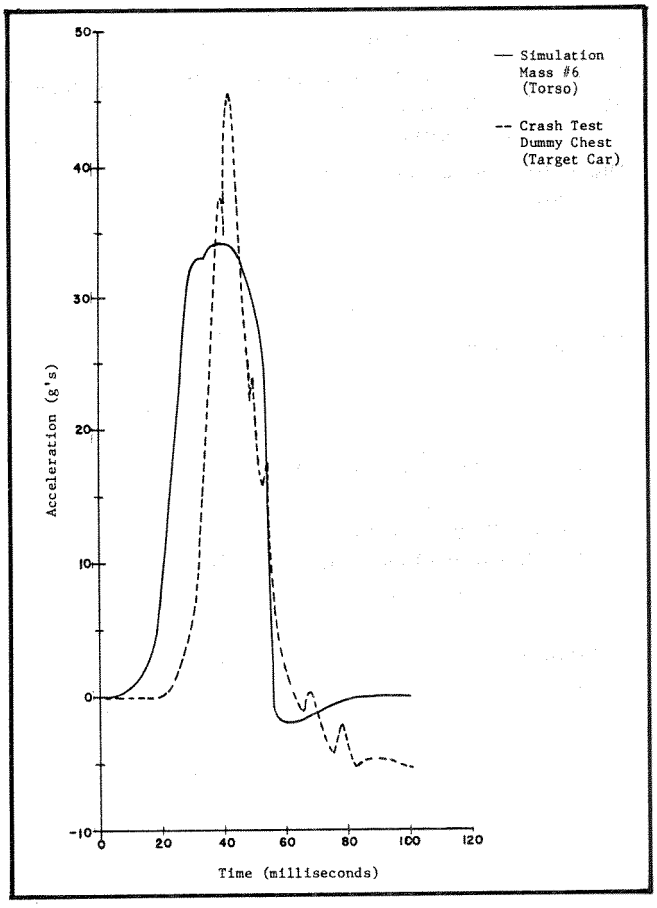

Figure C-5. Side impact model validation—mass #6

Appendix D

NASS Vehicle Selection Criteria

1979

Struck Cars

veh = 1 2-door passenger car
= 2 4-door passenger car
= 3 Station wagon (excludes van- or truck-based)
= 4 Convertible
= 6 Car—pickup body (e.g., El Camino)
= 8 Other automobile type
= 9 Unknown automobile type

Striking Vehicles

Includes struck cars plus:

veh = 5 On/off road vehicle (e.g., Jeep, Scout, Bronco, Blazer)
= 11 Pickup
= 12 Van (passenger, cargo van-based station wagon)
= 13 Station wagon, truck-based (e.g., IH Travelall)

1980

Struck Cars

veh = 1 Convertible

= 2 2-door sedan, hardtop, coupe
= 3 4-door sedan, hardtop
= 4 3-door or 5-door hatchback coupe
= 5 Auto with pickup body (e.g., El Camino, Ranchero)
= 6 Station wagon (not van- or truck-based)
= 8 Other automobile type
= 9 Unknown automobile type

Striking Vehicles

Includes struck cars plus:
veh = 50 Pickup (includes stake and small dump bodies and campers)
= 51 Van (VW bus, small Dodge van, van-based station wagon, but not moving van or horse van)
= 52 Station wagon, truck-based (e.g., IH Travelall)

1981

Struck Cars

veh = 1 Convertible
= 2 2-door sedan, hardtop, coupe
= 3 4-door sedan, hardtop
= 4 3-door or 5-door hatchback coupe
= 5 Auto with pickup body (e.g., El Camino, Ranchero)
= 6 Station wagon (not van- or truck-based)
= 8 Other automobile type
= 9 Unknown automobile type

Striking Vehicles

Includes struck cars plus:
veh = 50 Pickup (includes small stake and small dump bodies and campers)
= 51 Van (VW bus, small Dodge van, van-based station wagon, but not moving van or horse van)
= 52 Station wagon, truck-based (e.g., IH Travelall)

1982

Struck Cars

veh = 1 Convertible (excludes sun roof, t-bar)
= 2 2-door sedan, hardtop, coupe
= 3 3-door/2-door hatchback
= 4 4-door sedan, hardtop
= 5 5-door/4-door hatchback coupe
= 6 Station wagon (excludes van- and truck-based)
= 8 Other automobile type
= 9 Unknown automobile type
= 10 Auto-based pickup (includes El Camino, Cabellero, Ranchero, Brat)

Striking Vehicles

Includes struck cars plus:
veh = 40 Van (including VW bus, Vanagon, Kombi, Beauville, Chateau, Club Wagon, Sportman; excludes moving van)
= 41 Van-commercial cutaway (includes box van, multistop, parcel, van pickups)
= 50 Pickup (includes open box and caps)
= 53 Cab chassis-based (includes rescue vehicles, light stake, dump, and tow trucks)
= 54 Truck-based panel
= 55 Truck-based station wagon (4-door; includes Suburban, Travelall, Wagoneer)
= 56 Truck-based utility (2-door; includes Blazer, Bronco—78 on, Jimmy)

Appendix E

National Accident Sampling System

The National Accident Sampling System (NASS) is a continuous nationwide accident data collection program sponsored by the U.S. Department of Transportation. It is operated by the National Center for Statistics and Analysis (NCSA) of the National Highway Traffic Safety Administration (NHTSA).

NASS was developed to provide an automated, comprehensive national accident data base for use by regulatory agencies and accident researchers. The accidents investigated in NASS are a probability sample of all police-reported accidents in the United States. A NASS accident must fulfill the following requirements: must be police-reported, must involve a harmful event (property damage and/or personal injury) resulting from an accident, and must involve a motor vehicle in transport on a trafficway. Every accident that meets these conditions has a chance of being selected. This type of sample design makes it possible to compute not only national estimates but also probable errors associated with these estimates.

Sample Selection

The selection of sample accidents for NASS is accomplished in three stages: selection of primary sampling units (PSU's), selection of police jurisdictions, and selection of accidents. The three stages of sample selection are briefly discussed below. Greater detail can be obtained from the technical report on NASS sample design(2).

The first stage is selection of geographic areas called PSU's. Each PSU is composed of a large city, a county, or

a group of continuous counties. The Nation was divided into 1,279 PSU's. The PSU's were then grouped into 75 strata, and one PSU was then selected from each strata. It is not practical to investigate every accident in each sample PSU, so a second stage of sampling is performed on a list of police jurisdictions within each PSU. The final stage of sampling is the selection of accidents from all accidents recorded in the sample police jurisdiction. A probability of selection is assigned to each accident category so that high severity and rare vehicle type accidents are oversampled.

PSU and National Inflation Factor

The sample accidents from a PSU have a unique selection probability associated with them as a result of selecting a particular jurisdiction and accident. The reverse of this probability is called the PSU inflation factor. If sample accidents in a given PSU are multiplied by this factor, an unbiased estimate of the number of NASS accidents in the PSU is obtained. The inverse of the probability of selecting PSU (Stage I of sampling procedure) multiplied by the PSU inflation factor provides the National Inflation Factor. Using the National Inflation Factor, an unbiased estimate of the national frequency of the specific type of accident is obtained.

Appendix F

Outline of Sampling Procedure

Matrix of Random Numbers

A matrix of random numbers can be constructed from a bivariate frequency distribution (Table F-1). The

Table F-1. A sample bivariate frequency distribution

NASSDATA Data File
Weighted by National Inflation Factor

Occupant's Sex=Male
Table of Occ Age by OWGT

Occ Age Frequency Percent Row Pct	Occupants Age			OWGT	Occupants Weight		
Col Pct	-119	120-139	140-159	160-179	180-199	200-	Total
15-24	2726	15716	52613	72298	22545	15430	181328
	0.63	3.62	12.12	16.65	5.19	3.55	41.76
	1.50	8.67	29.02	39.87	12.43	8.51	
	49.34	70.76	47.58	44.88	25.90	32.33	
25-34	988	2819	28638	46758	29341	9935	118479
	0.23	0.65	6.60	10.77	6.76	2.29	27.29
	0.83	2.38	24.17	39.46	24.76	8.39	
	17.88	12.69	25.90	29.03	33.71	20.81	
35-44	0	3107	6810	14490	10512	7004	41924
	0.00	0.72	1.57	3.34	2.42	1.61	9.66
	0.00	7.41	16.24	34.56	25.07	16.71	
	0.00	13.99	6.16	9.00	12.08	14.68	
45-54	0	0	7074	14565	12674	7857	42170
	0.00	0.00	1.63	3.35	2.92	1.81	9.71
	0.00	0.00	16.78	34.54	30.05	18.63	
	0.00	0.00	6.40	9.04	14.56	16.46	
55-70	1811	312	7033	11776	10032	6333	37297
	0.42	0.07	1.62	2.71	2.31	1.46	8.59
	4.86	0.84	18.86	31.57	26.90	16.98	
	32.78	1.40	6.36	7.31	11.52	13.27	
71-	0	255	8400	1196	1943	1171	12965
	0.00	0.06	1.93	0.28	0.45	0.27	2.99
	0.00	1.97	64.79	9.23	14.98	9.03	
	0.00	1.15	7.60	0.74	2.23	2.45	
Total	5525	22210	110568	161083	87046	47730	434162
	1.27	5.12	25.47	37.10	20.05	10.99	100.00

matrix then can be conveniently used to locate the pairs of subgroups of two variables by selection of numbers. A method of constructing such a matrix is outlined below:

Let (R+1)*(C+1) be the matrix of bivariate frequency counts, where R represents the numbers of subgroups of one variable and C represents the other correlated variable. The (R+1)th row and (C+1)th column represent the marginal totals. The frequency counts of (R+1)*(C+1) can be expressed as row percents or column percents of their respective marginal totals. Similarly, the marginal totals can be expressed as percents of the grand total. Such a matrix is produced by the SAS Frequency Procedure. A matrix of random numbers then can be constructed by assigning each cell within each row a number from 1 to 100 based on row percents as weight (Table F-2). Similarly, a matrix from column percents can be constructed (Table F-3). An example of a matrix of random numbers is given below.

Sampling Method

A sample selection of pairs of two correlated variables can be made from the matrix of random numbers by following the three-step procedure described below:

(a) Select one of the two variables at random (variable 1) (e.g., driver's age). Then, select its subgroup by choosing a random number from 1 through 100 (e.g., 75) and locating it from the matrix of random numbers associated with the frequency distribution of its marginal totals (e.g., Table F-2).

(b) Select a subgroup of the second variable (variable 2) by choosing a random number (e.g., 49) and locating it from the matrix of random numbers associated with the frequency distribution (Table F-2) of the selected subgroup of variable 2.

(c) Select a subgroup of variable 1 by choosing a random number (e.g., 98) and locating it from the matrix of random numbers associated with the frequency distribution (Table F-3) of selected subgroup of variable 2.

The subgroups selected in (b) and (c) form a random pair of two variables. From the example given, the weight category would be 160 to 179 lb and the age category would be 55 to 70yr.

It should be noted that the selection of subgroup of variable in (a) is made independent of variable 2. Steps (b) and (c) make their selection dependent on each other.

Table F-2. A sample matrix of random numbers within each row

Example:

Matrix of Random Numbers
Driver's Weight (lb)
Sex: Male

Driver's Age	90-119	120-139	140-159	160-179	180-199	200-215	Total
15-24	1-2	3-11	12-40	41-80	81-92	93-100	1-42
25-34	1	2-3	4-27	28-67	68-92	93-100	43-69
35-44	—	1-7	8-23	24-58	59-83	84-100	70-79
45-54	—	—	1-17	18-51	52-81	82-100	80-89
55-70	1-5	6	7-25	26-56	57-83	84-100	90-97
71-85	—	1-2	3-67	68-76	77-91	92-100	98-100
Total	1	2-6	7-31	32-69	70-89	90-100	

Note: The entries are random numbers. They are constructed from row percents of male driver's age * weight distribution weighted by National Inflation Factors (NASS 1979 through 1982 data files).

Table F-3. A sample matrix of random numbers within each column

Example:

Matrix of Random Numbers
Driver's Weight (lb)
Sex: Male

Driver's Age	90-119	120-139	140-159	160-179	180-199	200-215	Total
15-24	1-49	1-71	1-48	1-45	1-26	1-32	1-42
25-34	50-67	72-84	49-74	46-74	27-60	33-53	43-69
35-44	—	85-98	75-80	75-83	61-72	54-68	70-79
45-54	—	—	81-86	84-92	73-87	67-85	80-89
55-70	68-100	99	87-92	93-99	88-98	86-98	90-97
71-85	—	100	93-100	100	99-100	99-100	98-100
Total	1	2-6	7-31	32-69	70-89	90-100	

Note: The entries are random numbers. They are constructed from column percents of male driver's age * weight distribution weighted by National Inflation Factors (NASS 1979 through 1982 data files).

Appendix G-1

Side Impact Monte Carlo Model Input Data

													Gap (in) Struck Car Weight Category (lb)						
case	sex	dwgt	age	hgt	circum	elbow	depth	ch stiff	sk wt	sk s	i type	speed	1750	2200	2700	3200	3700	4200	4800
1	2	110	19	63.5	31.5	11.7	5.5	393362.0	4200	7	2	13	7.33	6.94	7.29	9.35	9.85	8.86	9.03
2	2	110	29	62.5	31.9	12.0	5.5	307776.7	4200	7	1	23	7.67	7.19	8.07	8.56	8.15	9.43	8.94
3	1	150	20	65.5	37.4	15.7	8.5	568920.9	2200	2	1	38	4.39	4.75	6.54	7.91	6.77	9.04	6.78
4	1	150	29	70.5	36.6	15.0	8.5	452517.4	2200	1	1	18	5.85	5.02	5.46	6.36	7.49	8.52	7.31
5	1	170	29	71.5	38.6	16.1	9.1	364996.2	2700	2	1	18	4.91	4.14	6.41	4.94	7.28	6.37	8.65
6	1	170	20	71.5	38.5	15.9	9.1	498268.7	4800	5	1	8	5.32	4.52	6.39	6.41	6.68	6.22	7.09
7	2	130	29	64.5	33.4	13.0	6.3	400892.6	2700	3	1	23	6.71	6.46	6.06	7.61	8.96	7.94	9.65
8	1	170	29	68.5	39.3	16.6	9.1	328114.9	3200	4	2	13	4.12	3.99	4.42	5.73	6.12	7.46	7.84
9	1	170	20	72.5	38.3	15.7	9.1	513243.1	3200	4	1	18	5.81	5.09	5.85	7.17	8.01	6.17	7.66
10	1	220	49	66.5	45.7	20.3	10.4	16322.5	2200	1	1	13	2.69	3.05	2.11	3.71	4.19	5.61	5.62
11	1	150	20	67.5	37.0	15.4	8.5	588257.3	4200	5	2	13	4.99	5.75	5.55	5.57	7.13	6.71	8.31
12	1	150	39	69.5	36.9	15.4	8.5	321418.9	3700	5	2	31	4.39	5.07	4.87	6.64	6.99	6.82	8.65
13	2	130	29	66.5	33.1	12.7	6.3	385290.2	3700	4	1	28	5.67	5.60	7.82	7.62	7.34	9.02	9.81
14	2	110	19	62.5	31.7	11.8	5.5	406893.9	2200	1	1	23	6.35	6.78	8.43	8.90	9.71	7.87	10.07
15	1	190	29	68.5	41.5	17.8	9.6	183279.9	4200	6	1	8	4.51	3.73	3.87	5.03	6.19	6.85	5.65
834	1	220	20	72.5	44.0	18.8	10.4	94137.8	4200	5	1	18	4.04	3.11	2.87	4.94	6.36	5.70	5.93
835	1	190	49	70.5	41.4	17.8	9.6	99326.5	3200	4	2	22	3.99	3.03	5.40	3.49	7.01	7.00	7.00
836	1	190	29	70.5	41.1	17.5	9.6	207331.1	3700	4	1	18	3.24	2.99	4.91	6.99	6.26	6.28	6.25
837	2	150	62	58.5	36.9	15.8	6.8	153486.6	1750	1	1	18	5.05	3.86	4.67	6.99	7.70	6.11	6.28
838	2	110	19	66.5	31.1	11.2	5.5	352795.4	4800	6	1	23	6.72	7.26	6.82	7.94	8.81	10.19	8.38
839	1	150	29	69.5	36.8	15.2	8.5	447805.1	3200	3	1	13	5.58	5.17	5.89	6.66	7.02	7.76	7.44
840	1	220	20	68.5	44.8	19.5	10.4	64243.4	4200	5	2	13	1.75	2.78	3.27	4.88	5.15	4.61	4.05
841	1	170	29	73.8	38.2	15.7	9.1	390762.6	2200	1	1	13	4.52	5.14	4.80	5.07	7.45	8.25	7.35
842	2	170	19	65.5	36.9	15.0	7.2	615023.0	2200	1	1	23	4.81	4.67	6.72	7.18	7.76	6.18	7.09
843	2	110	29	64.5	31.6	11.8	5.5	288236.0	4200	6	2	13	7.80	6.88	7.46	8.16	8.59	8.53	9.56
844	1	170	62	68.5	39.7	17.1	9.1	102235.2	3200	3	1	18	4.09	4.46	4.16	5.58	5.32	5.85	8.27
845	1	170	29	69.5	39.1	16.4	9.1	340726.1	2700	3	1	13	4.60	4.11	4.44	6.91	6.22	7.59	8.07
846	1	150	62	67.5	37.7	16.1	8.5	143586.9	2700	3	2	13	4.71	4.47	5.22	6.08	6.69	7.43	7.93
847	1	170	20	70.5	38.7	16.1	9.1	482664.3	3700	7	2	22	4.44	5.53	5.60	5.92	6.15	6.94	8.26
848	1	170	20	67.5	39.3	16.6	9.1	432950.7	4200	6	1	23	4.77	3.85	4.59	6.33	5.42	5.46	7.96
849	1	170	20	64.5	39.9	17.1	9.1	380718.1	4200	7	2	7	4.93	4.63	3.50	5.49	5.75	7.04	8.40
850	1	130	29	63.5	35.7	15.0	7.9	461590.6	4800	6	1	23	3.84	5.36	5.47	6.89	6.71	8.41	8.29

Results of the Motor Vehicle Manufacturers Association Component and Full-Vehicle Side Impact Test Procedure Evaluation Program

Ronald J. Wasko
Motor Vehicle Manufacturers Association of the United States

Richard A. Wilson
General Motors Corporation (Chairman, MVMA Engineering Research Subcommittee)

Abstract

This paper presents an extensive research program undertaken to develop improved side impact test methods. The development of a component side impact test device along with an associated test procedure are reviewed. The results of accident data analysis techniques to define anatomical areas most likely to be injured during side impact and definition of test device response corridors based on human surrogate testing conducted by the Association Peugeot/Renault and the University of Heidelberg are discussed. The relationship of response corridors and accident data analyses in earlier phases of the project resulted in definition and development of a component side impact test device to represent the human thorax.

A test program to evaluate and compare component and full-vehicle test results is presented.

History

In 1982, the MVMA undertook a comprehensive, long-term research program to evaluate both full-vehicle and component side impact test procedures. This program was initially structured with seven tasks as shown in Figure 1.

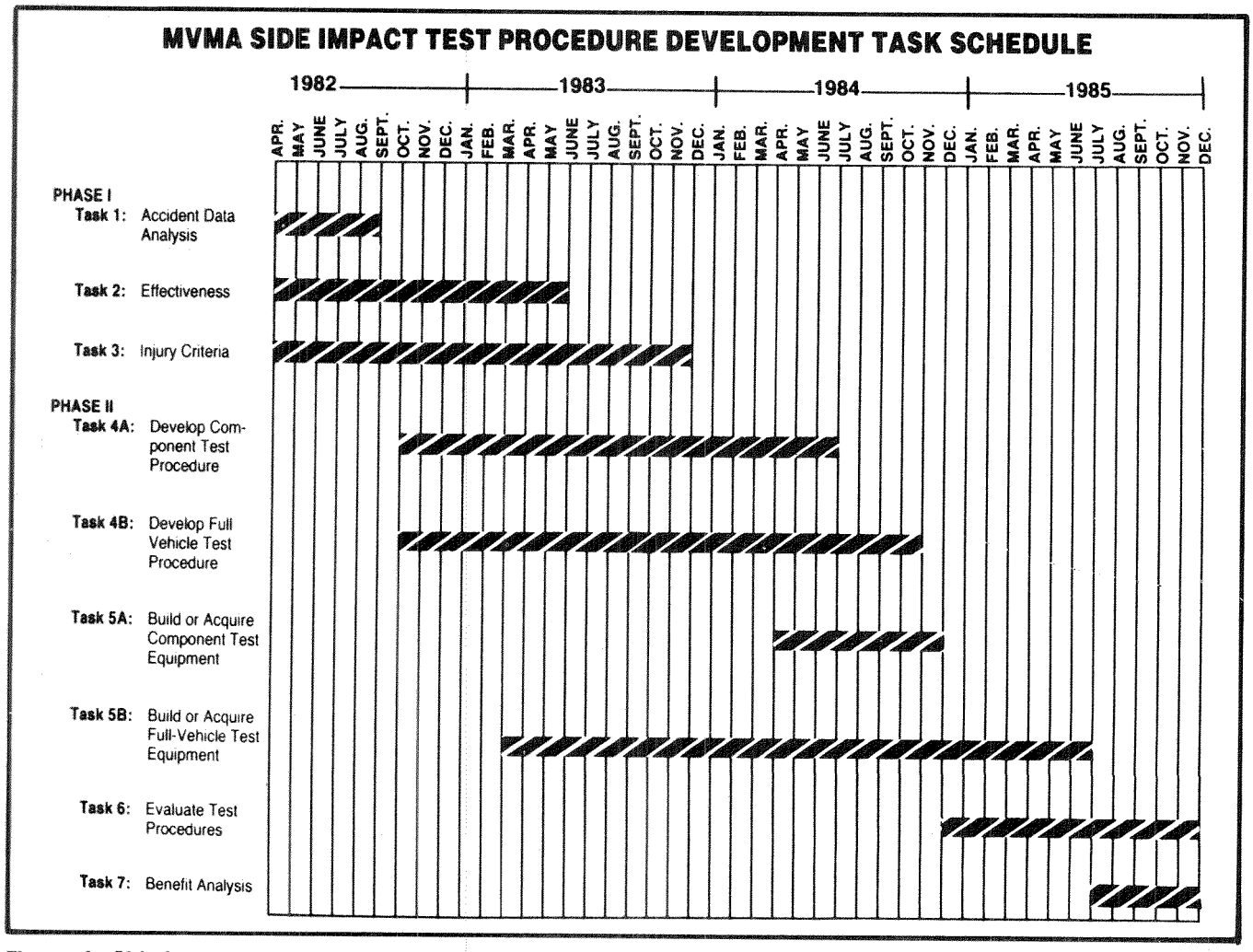

Figure 1. Side impact project task schedule

Side Impact Accident Data Analysis—Task 1

The primary objective of Task 1 was to analyze existing accident data to investigate the following aspects of injuries to occupants of side damaged passenger cars(1):

- Define and rank the predominant side impact injury categories, i.e., the body areas injured and the relation of these injuries to components of the vehicle that were contacted
- Quantify the relationship of injury to the mode and severity of the collision
- Determine the role of structural integrity with regard to occupant injury

Two accident data bases were used concurrently to develop the results of the task. The National Crash Severity Study (NCSS) was a major accident data collection program of the National Center for Statistics and Analysis of the U.S. Department of Transportation, National Highway Traffic Safety Administration (NHTSA). The NCSS file is a representative sample of passenger car towaway accidents, and it contains information on over 3,000 side impact accidents. The second is the Motors Insurance Company (MIC) Injury-Accident File, an accident data base maintained by General Motors Corporation. The MIC file contains information on accidents involving GM vehicles that were current models in the year the data were collected and in which there was an injury to at least one case-vehicle occupant. The MIC file has information on more than 5,000 side impact passenger car accidents. Whenever possible, the results from comparable analyses of both the NCSS and the MIC accident data files were presented, and the concurrence between the conclusions drawn from these separate accident data sources is discussed.

The serious-to-fatal injuries (AIS[1] 3 or greater) to nonejected occupants of side-damaged passenger cars in nonrollover accidents were grouped by body region injured and component of the vehicle contacted, each such pairing being considered as an injury category. Using both the NCSS and the MIC data files, the 10 leading injury categories were ranked for all side impact AIS 3+ injuries, and the results are presented in Figure 2. The rank orderings of the injury categories using both data files are in general agreement, but the percent of AIS 3 injuries in many of the injury categories varies considerably between the two data bases. The differences between the results from these files have two sources:

- The accident populations sampled by each file are different—NCSS represents towaway accidents to vehicles of all ages and makes on the road in the 1977 to 1979 period of data collection, while the accidents in the MIC file involve GM cars that were current models in the year the data were collected and in which there was an injury to at least one case-vehicle occupant.
- The methods used to determine and define body region injured and object contacted differ between the two files—for example, NCSS uses a restrictive procedure to obtain injury information, which may bias its large category of unknown contact data, while MIC data were completed with an expert's "best estimate" when the contact code was unknown.

A Ranking of Injury Categories for All Non-Ejected Occupants Of Side Damaged Passenger Cars in Non-Rollover Accidents

– Serious-to-Fatal Injuries –

	Accident Data File			
	NCSS		MIC	
Injury Category	Rank	Percent (%)	Rank	Percent (%)
Upper Torso/Side Surface	1	30.9	1	23.0
Abdomen/Side Surface	2	12.5	3	5.7
Upper Torso/Steering Assembly	3	8.6	2	7.9
Upper Torso/Instrument Panel	4	6.7	9	3.0
Pelvis/Side Surface	5	6.0	7	3.9
Head/Upper Side Structures	6	5.4	6	4.5
Neck-Spine/Non-Contact	7	3.8	8	3.2
Abdomen/Steering Assembly	8	3.6	11	2.4
Lower Extremities/Side Surface	9	2.7	Not Ranked	
Abdomen/Instrument Panel	10	2.4	Not Ranked	
Head/Side Surface	Not Ranked		4	5.7
Head/Windshield	Not Ranked		5	5.2
Other	-	17.4	-	35.5
Total Injury Count				
Sampled		826		823
Weighted		923		923

Figure 2. Ranking of side impact injury causes

The effects of several variables commonly used to characterize the mode and severity of side impact collisions on the ranking of the side impact injury categories were investigated using only the NCSS accident data file. The results indicate the injury category rankings differ by accident type (single-vehicle impacts versus all other side impacts) and struck vehicle Delta V (Delta V $\geq$ 20mph versus Delta V $\leq$ 20mph). The four distinct injury category rankings defined by the combinations of these two side impact categorization variables are presented in Figure 3.

The order of the injury categories changes only slightly across the four injury category rankings presented in Figure 3, but the percent of serious-to-fatal (AIS 3+) injuries to nonejected occupants of side-damaged passenger cars in nonrollover accidents contained within each injury category is distinctly different for each of the four injury category rankings. Because of their close correspondence in injury category ranking, AIS 3+ injuries in side impacts with unknown Delta V were

[1] Abbreviated Injury Scale—1980 Revision, American Association for Automotive Medicine.

Injury Category Rankings for Selected Groups of Non-Ejected Occupants of Side Damaged Passenger Cars in Non-Rollover Accidents

– Serious-to-Fatal Injuries –

Group A: Vehicle-to-Vehicle Side Impacts
Side Struck Vehicle Delta V $\leq$ 20 mph*
(Based on 456 NCSS AIS 3+ Injuries)

Rank	Injury Category	NCSS Percent
1	Upper Torso - Side Surface	40.8
2	Abdomen - Side Surface	12.5
3	Upper Torso - Steering Column	7.5
4	Pelvis - Side Surface	6.1
5	Upper Torso - Instrument Panel	5.5
-	Other	27.6

Group B: Vehicle-to-Vehicle Side Impacts
Side Struck Vehicle Delta V $>$ 20 mph
(Based on 203 NCSS AIS 3+ Injuries)

Rank	Injury Category	NCSS Percent
1	Upper Torso - Side Surface	20.7
2	Abdomen - Side Surface	14.8
3	Upper Torso - Steering Column	8.9
4	Upper Torso - Instrument Panel	7.4
5	Head - Upper Side Surfaces	6.4
-	Other	41.8

Group C: Single Vehicle Side Impacts
Vehicle Delta V $<$ 20 mph*
(Based on 76 NCSS AIS 3+ Injuries)

Rank	Injury Category	NCSS Percent
1	Upper Torso - Side Surface	22.4
2	Abdomen - Side Surface	13.2
3	Upper Torso - Steering Column	11.8
4	Head - Upper Side Structures	7.9
-	Other	44.7

Group D: Single Vehicle Side Impacts
Vehicle Delta V $\geq$ 20 mph
(Based on 81 NCSS AIS 3+ Injuries)

Rank	Injury Category	NCSS Percent
1	Upper Torso - Side Surface	12.3
2	Upper Torso - Steering Column	12.3
3	Upper Torso - Instrument Panel	12.3
4	Head - Upper Side Structure	7.4
5	Abdomen - Side Surface	7.4
-	Other	48.3

* NOTE: The AIS 3+ injuries which occurred in NCSS side impacts grouped with unknown Delta V were grouped with those from NCSS side impacts with Delta V $\leq$ 20 mph.

Figure 3. Injury category rankings for side impacts

grouped with the Delta V $\leq$ 20mph serious-to-fatal injuries.

The number of injury categories ranked for each side impact subset was limited to those with more than 5 percent of their respective totals so the rankings presented for each category of side impact would be based on enough serious/fatal injuries to be reasonably reliable. As seen in Figures 2 and 3, the injury categories with less than 5 percent of their respective totals cumulate to a substantial percent of the total NCSS serious/fatal injuries. However, due to the small number of cases within each injury category, a meaningful ranking of these categories with less than 5 percent of the NCSS side impact injuries could not be constructed.

The major injury mechanisms associated with each of the five most frequent injury categories were investigated using both the MIC and the NCSS data files, and the results of this investigation are presented in Figure 4.

The data analysis of Task 1 concludes that the upper torso to side surface is the predominant injury category. The major injury mechanisms result in fractured bones and internal organ damage. A comprehensive analysis of

the data is provided in the referenced report developed by Task 1.

Injury Mechanisms for Predominant Side Impact Injury Categories

– Serious-to-Fatal Injuries –

Upper Torso - Side Surface	% NCSS	% MIC
Fractured Bones	50	62
Lung Damage	35	18
Other	15	20
Abdomen - Side Surface	**% NCSS**	**% MIC**
Kidney Damage (contusion)	25	27
Spleen Damage (rupture)	22	29
Liver Damage (laceration)	17	16
Other	36	28
Upper Torso - Instrument Panel/Glovebox	**% NCSS**	**% MIC**
Fractured Bones	53	58
Lung Damage	35	27
Other	13	15
Upper Torso - Steering Assembly	**% NCSS**	**% MIC**
Fractured Bones	53	75
Lung Damage	31	16
Other	16	9
Head - Upper Side Structure	**% NCSS**	**% MIC**
Brain Concussion	36	49
Brain Contusion	24	9
Skull Fracture	22	26
Other	18	16

Figure 4. Injury mechanisms for side impacts

Side Impact Test Effectiveness—Task 2

After accident data were analyzed in Task 1, a second task on Test Effectiveness(2) was undertaken utilizing the output of Task 1. Factors to evaluate side impact candidate tests were developed and ranked according to relative importance. The purpose of this task was to identify specific tests that would be able to discriminate among vehicle designs that should have a significant effect on side impact injuries.

In an Advanced Notice of Proposed Rulemaking on side impact protection, NHTSA had proposed a moving barrier side impact test procedure using crash test dummies. Comments by several U.S. manufacturers urged NHTSA to take a broader approach and consider component test procedures as well, which may be simpler and a more practicable alternative than the procedure proposed in the Notice. Both component tests and the full-vehicle test using crash dummies may have unique advantages when compared with one another.

During the deliberations of Task 2, two important philosophical issues were discussed extensively. The first dealt with the Task Group's perceptions of the fundamental advantages and disadvantages of full-vehicle crash testing as compared with component testing. As a consequence of this comparison, a list of evaluation factors for different tests (both full-vehicle and component) were developed and prioritized, and the advantages and disadvantages of the tests were discussed in detail.

The second issue involved the basic approach taken toward accomplishing safety improvements to vehicles. Task 2 recognized two fundamental approaches to safety advancement. The incremental approach takes into account the spectrum of existing performance within a given safety area as observed among the various vehicle designs in current production. This range of performance can be observed by testing the various vehicles. Then, an appropriate minimum performance level can be established, relative to the group performance, to eliminate outliers. In contrast, the idealized approach uses reference values derived from field accident data and human tolerance data to set an absolute goal for minimum performance in a given safety area. This second approach may or may not affect only the outliers. It could require large changes to be made to a significant portion of the whole group, all in a single step. Historically, the incremental approach has tended to involve mainly component testing procedures, while the idealized approach has been associated mainly with full-vehicle testing. These associations, however, are not necessarily tied to any particular type of test.

A key question to be answered when choosing between the two approaches is: which approach will provide the motoring public the larger overall benefit? This, of course, will be greatly dependent on performance criteria that have yet to be established. Importantly, this evaluation must take into account both the degree of improvement and the absence of delay in getting the improvements actually on the road. Thus, simplicity of a safety test procedure can be an important factor in the election of the approach taken to move ahead in vehicle safety advancement.

The deliberations included a review of past and current side impact research. For the full-vehicle tests, the NHTSA and Committee of Common Market Automobile Constructors (CCMC) Mobile Deformable Barrier procedures were reviewed. The review of the test procedures also included a comprehensive review of the anthropomorphic test devices. Component testing included an analysis of the following devices and methods:

- Ford's Side Impact Body Block (SIBB)
- NHTSA's head and thorax impactors
- GM's head area impactor
- GM's thorax area impactor
- External crush
- Hinge and lock component tests

Advantages and disadvantages of both the component and full-vehicle tests were developed, as well as areas

requiring further scientific research to support side impact test procedure development.

Items addressed by Task 2 include—

- Definition of test conditions
- Sufficient correlation to field data cover adequate spectrum of accident conditions
- Evaluate an appropriate area of the interior
- Allow an assessment of potential ejection paths
- Allow evaluation of components under impact conditions
- Exhibit injury category in question
- Validity of test output
- Employ a valid injury criteria
- Exhibit a relationship to field injury characteristics
- Discriminate levels of performance
- Detection of synergistic effects
- Allow interaction between interior energy absorption and structure
- Allow interaction between various structural components
- Allow interaction between striking object and struck vehicle
- Allow interaction among occupant body segments
- Acceptable degree of complexity
- Acceptable degree of reproducibility and repeatability
- Permit simultaneous evaluation of multiple elements in the chosen accident condition
- Evaluate a variety of loading conditions

The Task 2 need to develop side impact tests included a variety of applications such as establishing compliance with possible future rulemaking, establishing crashworthiness ratings, and improving product safety through voluntary industry efforts.

Rankings of the relative importance evaluation factors resulted in the conclusion that for any given thorax to side interior surface test procedure, three parameters are important:

- A high level of repeatability and reproducibility plus low level of test complexity
- Ability to discriminate levels of safety performance in different vehicle designs
- Ability to accurately represent the injury category and injury severity occurring in the real world under a variety of conditions that reflect real-world occurrences

The conclusion reached as a result of Task 2 was that a full-vehicle test may represent a single field accident condition because real-world crash conditions and synergism may be more accurately duplicated in a full-vehicle test than in a component test. However, the full-vehicle test involves considerable equipment, facilities, and manpower to conduct; therefore, it is extremely complicated. For an equivalent level of effort, a number of component tests can be conducted under a variety of test conditions to simulate a variety of accident conditions.

MVMA did not choose one test type (i.e., full-vehicle versus component) over the other, since both have merit.

Task 2 identified important areas for near-term research, to support both full-vehicle and component test procedure development. These areas are—

A. Full-vehicle tests:
   1. Determining the validity of extrapolating results from one test condition to other conditions
   2. Establishing repeatability and reproducibility of test results
   3. Developing dummy improvements

B. Component tests:
   1. Establishing correlation between test results and field data
   2. Determining the effects of parameters such as side stiffness and occupant seating position on test conditions
   3. Determining importance of synergistic effects between interior energy-absorbing panels and structure, or among various structural components

Component Side Impact Test Device—Task 4 and Task 5

As shown by the conclusions of Task 1, accident data analysis, the thorax to side surface was the predominant injury source. Therefore, in the development of a component test device, it was deemed essential that the thorax be the initial part of the anatomy to be evaluated by any component test device. It is anticipated that after a thorax-type test device has been developed, other parts of the body would then be investigated for side impact injury mitigations. As noted earlier, desirable characteristics for a component test device should include a high level of repeatability and reproducibility. Also, a low level of test complexity is desirable. It was also a condition of the program that any component test device have the ability to discriminate levels of safety performance for various vehicle safety designs. Also, a variety of conditions that reflect real-world occurrences should be represented in terms of the injury category and injury severity by a component test.

With knowledge of these constraints and the fact that correlation between component test results and actual field data need to be developed, the development of a component test device was undertaken.

MVMA contracted the development of a component side impact test device with MGA Research Corporation of Akron, New York, U.S.A. The project was to address the validity of developing a component side impact test procedure by designing, fabricating, testing, and delivering

a side impact component test device that would be used to simulate a human thorax impact to interior side components of a motor vehicle.

The objective of the contract with MGA was to achieve a test device capable of evaluating the energy absorption of vehicle interior side components. Initial thoughts in defining the physical profile of the impactor for the component test device was to have it physically duplicate a human thorax. Since the test device was to represent a human thorax, a decision was made to use the curvature dimensions based on an approximation of the horizontal curvature of a semicompressed human thorax. For simplicity, the vertical section of the test device was chosen, after much deliberation, to be the same curvature as the horizontal section. The component test device impact face physical parameters chosen by MVMA are—

- Diameter 190mm
- Radius of curvature 305mm

These were chosen because (1) the dimensions are representative of areas on the human thorax that are loaded in side impacts, and (2) being circular helps eliminate test device positioning error in the vehicle, permitting a variety of test conditions without increasing test complexities. By specifying a rounded face to represent the thorax, some biofidelity was sacrificed, but this loss was more than offset by reductions in test interference from armrests, door handles, etc. Also, test complexity is reduced because orientation of the test device is not as critical as in the case of a more faithful representation of the thorax.

MVMA also deemed it important that the impactor be a two-mass, constrained device. The impact face represents the ribs and outer surfaces of the human thorax, whereas the main mass represents the inertia of the spinal column and major organs. The two masses are separated by a spring and damper system to represent the biomechanic coupling within the human thorax. Figure 5 shows the two-mass impactor as finally developed by the contractor. Again, to enhance the usability and decrease the complexity of the device plus simplify the test procedure, a decision was made to constrain the movement of the two-mass impactor to a uniaxial relative motion along the impact direction.

For realistic test speeds of the device, MVMA specified that the component impactor be capable of being accelerated to an impact speed of 40km/h (24mph). Based on the accident data analysis of Task 1 and cadaver tests, this velocity is representative of impact velocities that will cause serious to fatal injuries to humans from side impacts.

Provisions were also required to prevent relative displacement errors between the two masses while the unit is accelerated to test velocity. This was accomplished by means of a mechanical locking system that holds the two masses in relative position when accelerating. At an acceleration of 30g's, a maximum relative displacement of not more than 1mm in any direction is achievable.

One of the purposes in developing a component test device is to permit a number of tests to be conducted at various velocities, impact angles, and occupant positions. Therefore, the propulsion and guidance system were specified by MVMA to be capable of delivering the impactor to an impact location within 5mm of the desired center of the test location at speeds up to 22km/h (14mph).

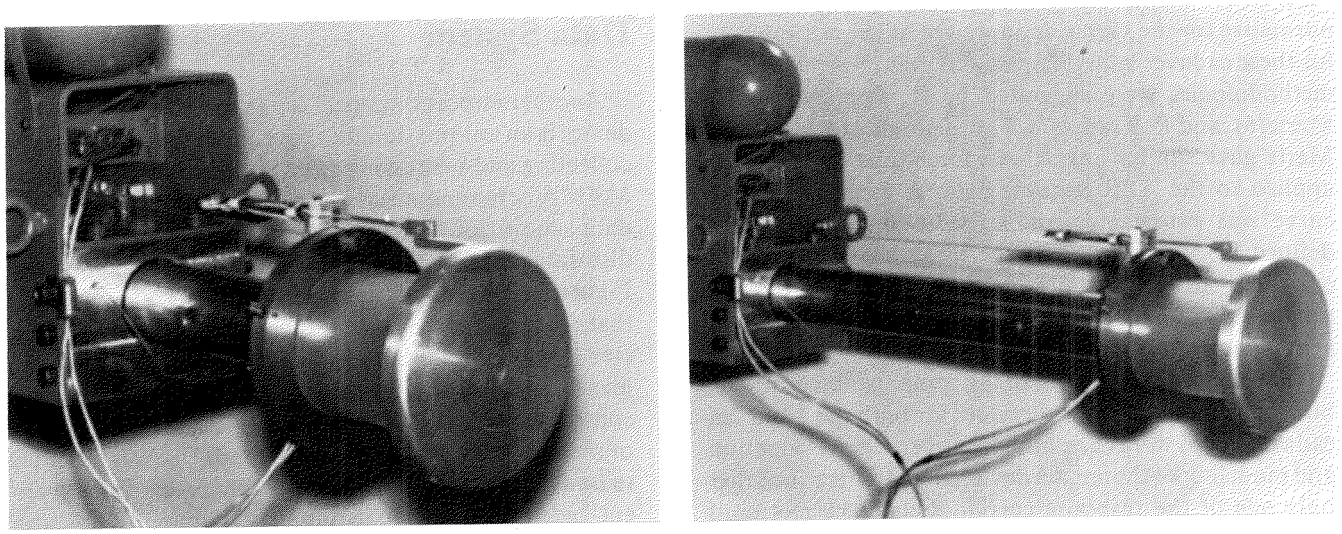

Figure 5. Two mass impactor

A prefiring interlock to prevent inadvertent actuation of the test device was deemed necessary and is incorporated in the device. Over-travel control, in case there is no test specimen in front of the test device when it is actuated, is a necessity, as well as rebound control, to absorb the energy from the test device after striking a test subject. It was also deemed appropriate that a working depth for at least 300mm of target crush would be required to provide information relatable to real-world accidents.

The mechanical design includes the ability to adapt the test device to other propulsion means to permit universal use of the device. The design of the alignment system provides capabilities for the device to withstand off-center and off-angle loads.

The following measurements can be made in each component test:

- Displacement between the outer (simulated rib) mass and main (spine and internal organs) body mass
- Force on the outer mass produced from impact with the tested structure
- Velocity of the impactor prior to impact and rebound velocity (provide energy dissipated in the test)
- Velocity of the impactor at impact

Based on the parameters that are available to measure, it should be possible to evaluate injury criteria related to the human thorax. Changes in energy dissipation from various structural modifications can be obtained easily with the component test device.

The most difficult part of the test device to define and develop was the human biomechanical response corridor. To obtain a realistic representative response corridor, the worldwide cadaver data bases for side impact were reviewed and analyzed. Two main sources of side impact cadaver tests were available—the Association Peugeot/Renault(3) and the University of Heidelberg(4) data. Considerable analysis was expended by the U.S. motor vehicle biomechanics community to develop a method to normalize for the variation in weight of the test subjects for these cadaver lateral impact test data. Normalization methodologies were suggested by R. Eppinger(5), H. Mertz(6), and P. Krause(7). The methods of Krause and Mertz gave similar normalized force-time curves when applied to the APR cadaver data. A mean force-time curve was constructed and corridor boundaries were defined as ±15 percent of the mean curve. Response corridors for both the 1 and 2m cadaver drop data as shown in Figure 6 were taken from Krause's paper(7) and are similar to those proposed by Mertz(6).

During the development of the component test device. biomechanical response corridors for both the 1 and 2m cadaver drops were to be met. However, upon evaluation and modeling of the impact device, it was determined that only one of the response corridors could be met until further comprehensive modeling and testing were undertaken. The nonlinearity of the response corridor and coupling effects of the two simulated masses for both corridors were beyond the scope of the initial effort. A decision was made by MVMA to initially have the test device meet the 2m lateral drop response corridor because it provided a more severe response and better relates to serious injuries in vehicle accidents.

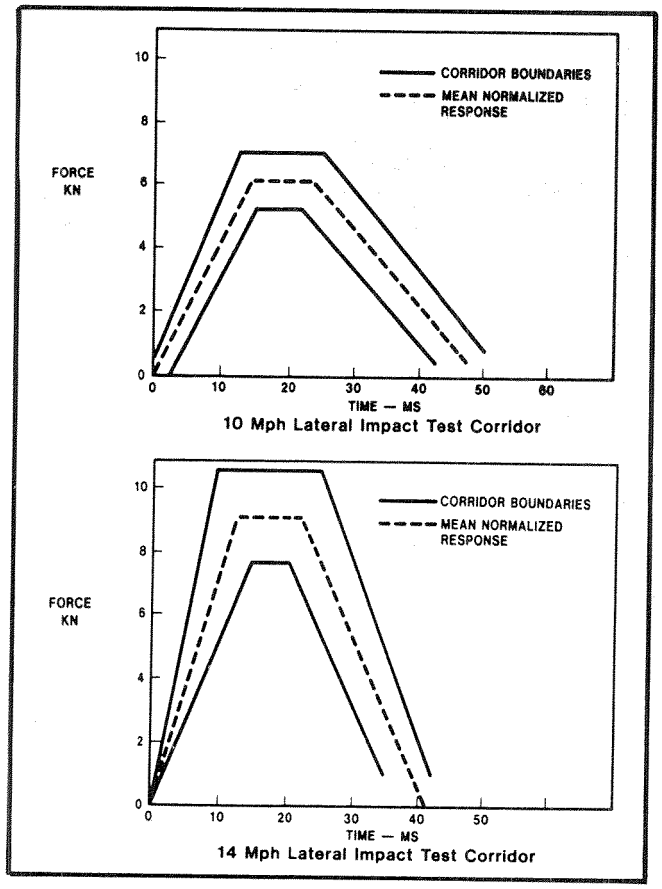

Figure 6. Normalized response corridors

Data System

Another important aspect for a usable component test device is an automatic data acquisition system capable of collecting and processing dynamic impact test data. The MVMA component test device includes a "stand-alone" data acquisition system consisting of a digital computer, disc data storage, digital plotter, and printer as shown in Figure 7. The data acquisition system has many features that make the component test device unique. All parameter changes and inputs such as test velocities and measurements of parameters can be done via computer control from the data acquisition system control console or manually. The actual firing of the device was specified to be a manual two-hand operation to preclude inadvertent activation due to equipment failure or operator inattention.

Figure 7. Component test system data acquisition

Operator selectable programmable gains and variable filter frequency responses from 60 to 1,000Hz are programmable from the computer keyboard. The frequency response can be stepped as per SAE J211, June 1980, Instrumentation of Side Impact Tests.

The computer calibrates data channels and initiates the collection of test data, then the measured test data are transferred from the data acquisition system to the digital computer. The collection portion of the data measurement sequence is performed with data acquisition software control and, after the data have been transferred into the computer, a second processing program processes and outputs the test data.

Control software was developed to provide an interactive sequence for test personnel to set up the data acquisition system and collect test data. The software program is menu-driven, and options such as determining and selecting gain, bandwidth, and the amplitude calibration of conversion of measured voltage data into physical units for each channel are provided. The data acquisition system is capable of digitizing 10,000 samples per second for each of the eight data channels provided in the test device. To insure a complete test sequence is captured on the digital data format, the system is capable of accessing and storing data for a test sequence time of at least 300ms per channel.

The processing and analysis software include menu-driven functions such as filtering, scaling, integration, addition, and subtraction. The control software allows various plotting routines such as cross-plotting and over-plotting of test results.

Data from a test can be printed immediately or plotted. As an alternative, several tests can be conducted and the data stored on computer disc. These stored data can then be over-plotted showing the results of several different tests on the plot. In this manner, changes to the test subject can be evaluated by referencing the original and subsequent test runs with various modifications made to the tested article to help in the engineering analysis.

The data system has the capability of storing at least 15 tests in archival (floppy disc) form. This storage feature permits a number of tests to be conducted, and the analysis can be done at a later date or more convenient time. Conversely, test sequence results can be compared even if a considerable real time period elapses between the tests.

Repeatability

Repeatability requirements were specified by MVMA to consist of five consecutive impact tests at 22km/h (14mph) into APR foam padding.[2] This test condition is comparable to the 2m cadaver drop onto APR foam padding. The coefficient of variation was specified to be less than 5 percent for each of these series of five consecutive tests. The test device met this requirement, and the repeatability results are shown in Figure 8. The prototype component test device also has the capability of discriminating between several energy-absorbing materials as shown by Figure 9.

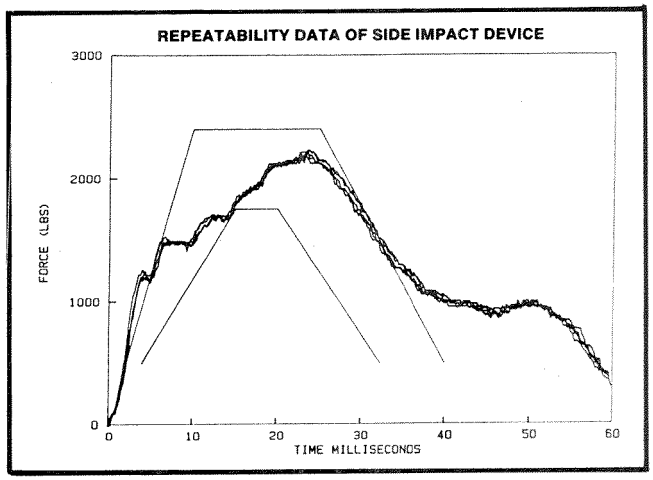

Figure 8. Force-time repeatability measures

Conclusions reached by Task 2 (Test Effectiveness) members recognized that a side impact test may be used for a variety of applications, but three major considerations are extremely important for any test device. These considerations are—

1. High level of repeatability and reproducibility plus a low level of test complexity
2. Ability to discriminate levels of safety performance in different vehicle designs
3. Accurate representation of the injury category and injury severity occurring in the real world under a variety of conditions that reflect real-world occurrences

[2]The padding was as close as could be obtained to that used for the lateral cadaver impacts in (3).

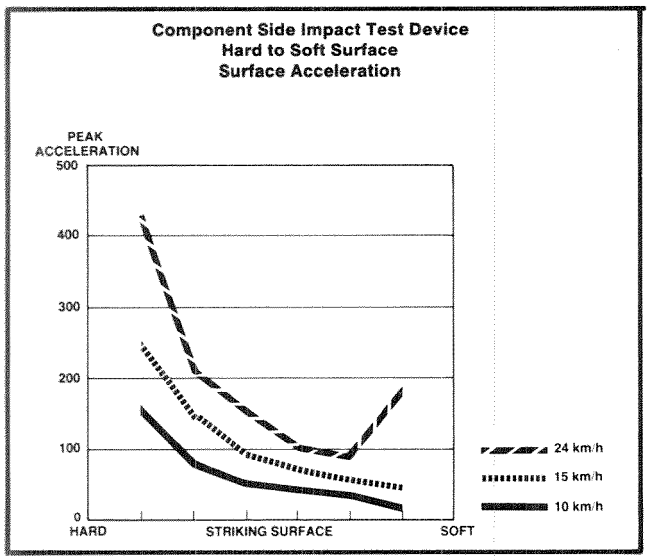

Figure 9. Discrimination characteristics of component test device

Using existing cadaver data as the reference, the component prototype test device developed under the MVMA side impact test procedure program has begun to meet the first two requirements. The third consideration will be addressed in future research.

Future Research

Enhancement to Component Test Device

To increase the biofidelity of the component test device, several enhancements will be made to the system to improve its functionality. These include—

- A specified deflection for both the 22km/h force-time corridor and the 16km/h force-time corridor
- Development of a monotonically increasing curve of peak force versus peak deflection from minimum speed to maximum test speed
- A provision to allow maximum relative deflection of 55mm between the main (spine and organs) and small (rib) mass to better represent cadaver data

A contract will be issued to incorporate these changes into the device, and these modifications are scheduled to be complete within the next few months.

Test Procedure Evaluation

MVMA is continuing the evaluation of test procedures for both the full-vehicle and component testing. Efforts to develop a full-vehicle side impact test have been underway in the United States and Europe for some time. NHTSA is in the process of developing a full-vehicle test procedure and has recently submitted a procedure to the public record.

MVMA plans to use a full-vehicle side impact procedure that is nearly identical to the procedure being considered by NHTSA. The MVMA procedure specifies a crabbed moving barrier to simulate a side intrusion obtained with a moving test vehicle. The impactor characteristics are identical to those proposed by NHTSA. The dimensions of the energy-absorbing impactor face are—

Width	1,676mm
Height	559mm
Depth	482mm
Ground Clearance	280mm
Surface Located	200mm High Bumper 330mm aboveground

The total mass of the impactor face, carriage, and ballast, as necessary, is 1,360kg ± 9kg to be consistent with the NHTSA-selected 1985 vehicle average mass of 1,224kg + 136kg to represent two occupants.

The MVMA full-vehicle test will simulate a 90° side impact with simulated speeds of 24km/h for the struck vehicle and 48km/h for the striking vehicle. Figure 10 represents the test conditions for the simulation in which the struck vehicle remains stationary and the crabbed moving barrier travels at 54km/h.

The NHTSA Side Impact Dummy (SID) will be used as the human surrogate in the full-vehicle test. The NHTSA SID was selected as the dummy to be used since it has been specified by NHTSA in their proposed full-vehicle side impact test procedure. (Selection of the NHTSA SID should not be construed as endorsement of this test device by MVMA.)

The parameters to be measured in the MVMA full-vehicle test are—

Required Measurements	Direction	Range
Accelerations		
Test Vehicle Sill	3 Axis	50G
Lower Thoracic Spine, Vertebra 1	3 Axis	200G
Lower Thoracic Spine, Vertebra 12	3 Axis	200G
Upper Rib (Near Side)	Y Axis	200G
Lower Rib (Near Side)	Y Axis	200G
Pelvis Sacrum	3 Axis	130G
Dummy Clearance to Side Interior	mm	
Velocity of Impactor	km/h	
Lateral Deflection of Impacted Ribs Relative to Spine	Y Axis	75mm

Optional Measurements	Direction	Range
Accelerations		
Sternum Acceleration	X & Y Axis	150G
Head Acceleration	X, Y & Z Axis	100G
Belt Load	Tension	10kn
Intrusion of the Interior Side Panel	mm	250mm

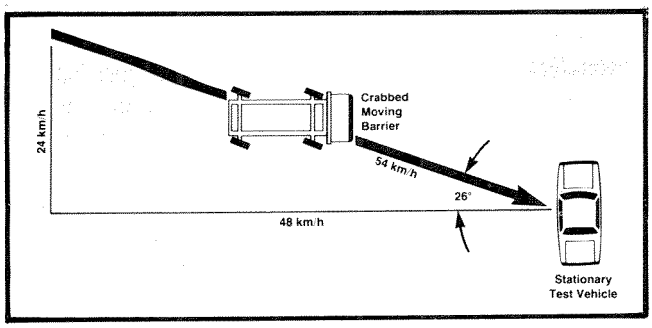

Figure 10. Full-vehicle test procedure representation

Full-Vehicle/Component Tests

Over the next several months, MVMA will undertake a comprehensive side impact test project for comparing full-vehicle and component tests. The objective of the full-vehicle portion of the project is to—

- Determine the repeatability of the full-vehicle test procedure
- Investigate the ability of the full-vehicle test to discriminate between changes in vehicle occupant protection
- Evaluate the effects of dummy position, energy-absorbing padding, and changes to vehicle structure

The objective of the component test portion of the project will be to investigate the ability of the component test procedure to evaluate changes in the vehicle and to determine if these changes are reflected by the component test in a similar manner as in a full-vehicle test.

The full-vehicle portion of the project will consist of side impact tests of 16 full-size 1985 model year vehicles under a variety of conditions including spacing of the dummy from the door, changes in the energy-absorbing characteristics of the interior of the door, and changes in the structural stiffness of the door. Two tests with each variable are scheduled.

A matrix of the tests and conditions to be investigated is shown in Figure 11.

	Baseline Door		Padded Door	
Dummy Spacing	Near	Far	Near	Far
Baseline Structure	2	2	2	2
Stiffened Side Structure	2	2	2	2

Figure 11. Full-vehicle test matrix

The test procedure to be used is the MVMA full-vehicle test. Test conditions, dummy placement, and vehicle speeds will be those specified in the MVMA procedure. The data from the tests will be placed in the NHTSA public docket for general public review.

For the component portion of the tests, the MVMA-developed component side impact test device will be used to conduct tests on doors that are identical to the doors used in the full-vehicle test portion of the project, that is, doors that are—

- Standard production
- Modified with energy-absorbing material
- Modified through increased structural stiffness

The test velocities for the component test will be determined from measurements and observations made during the full-vehicle test portion of the program. The velocity the SID dummy striking the door inner panel shall be determined and utilized as the velocity the component impactor. By using a striking velocity identical to the SID dummy, the component test can be compared to the full-vehicle test. The component test procedure specifies precrushing the door utilizing an MVMA specified ram to represent the front of the striking vehicle. The door to be tested will be precrushed and held in the crushed condition by the ram for the component test.

Three component tests are scheduled for each test condition. A matrix of the proposed component tests is shown in Figure 12.

	Speed* (MPH)	Body Buck
Baseline Door	TBD	3
	TBD	3
Padded Door	TBD	3
	TBD	3

*Test speeds to be determined based on full vehicle tests.

Figure 12. Component test matrix

After the component and full-vehicle tests are complete, an analysis is scheduled to be undertaken to compare the repeatability and reproducibility of the two types of tests.

The component test results will be compared with the full-vehicle test results for each of the conditions tested, and a comprehensive analysis shall be undertaken to determine the relationship of the two tests.

The component and full-vehicle tests are currently scheduled to be complete in the late fall of 1985. The statistical analysis of the two procedures should be complete and reported in the summer of 1986.

The complete prototype side impact test system is shown in Figure 13.

Acknowledgments

The authors would like to thank all the people who provided the time and expertise to make this project successful. Without their continuing support, it would not have been possible to perform this comprehensive analysis and development.

Task Group 1 and 2 members have been identified in the final reports issued by them and referenced herewith.

The following people have contributed to the development of the program:

F. Peters AMC
T. Hayek AMC

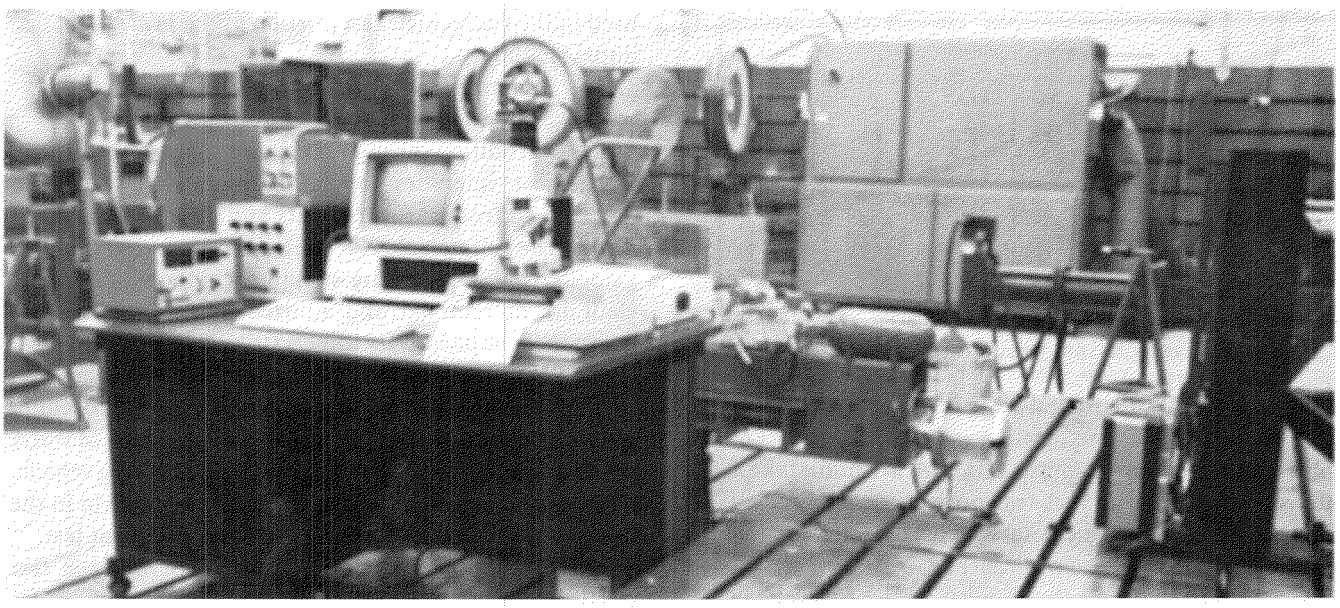

Figure 13. Prototype component test system.

J. Brinn	Chrysler
H. Rolueau	Chrysler
W. Koebnick	Chrysler
S. Henson	Ford
R. Daniel	Ford
P. Prasad	Ford
R. MacLean	Ford
P. Krause	Ford
C. Griswold	General Motors
H. Mertz	General Motors
L. Baker	Volkswagen of

References

1. Report of the Accident Data Analysis Task Force, Task 1, Side Impact Test Procedure Development, NHTSA/MVMA Coordinated Research, September 1982.
2. Report of the Test Effectiveness Task Force, Task 2, Side Impact Test Procedure Development, NHTSA/MVMA Coordinated Research, June 1983.
3. Tarriere, C., G. Walfisch, A. Fayon, and J.P. Rosey, "Synthesis of human tolerances obtained from lateral impact simulations," Proceedings Seventh International Technical Conference on Experimental Safety Vehicles, Paris, France, June 1979.
4. Marcus, J.H., R.M. Morgan, R.H. Eppinger, D. Kallieris, R. Mattern, and G. Schmidt, "Human response to and injury from lateral impact," Proceedings 27th Stapp Car Crash Conference, San Diego, California, October 1983.
5. Eppinger, R.H., J.H. Marcus, and R.M. Morgan, "Development of dummy and injury index for NHTSA's thoracic side impact protection research program," SAE Government/Industry Meeting and Exposition, SAE Paper 840885, Washington, D.C., May 21-24, 1984.
6. Mertz, H.J., "Procedure for normalizing impact response data," SAE Government/Industry Meeting and Exposition, SAE Paper 840884, Washington, D.C., May 21-24, 1984.
7. Krause, P.L., "Normalization of side impact cadaver dynamic response data utilizing regression techniques," SAE Government/Industry Meeting and Exposition, SAE Paper 840883, Washington, D.C., May 21-24, 1984.

A Comparison of European and American Test Devices and Test Parameters for Lateral Impacts

G. Klaus,
R. Sinnhuber, and
G. Hoffmann
Volkswagenwerk AG, Wolfsburg, West Germany

Abstract

European and American side impact research efforts are directed toward the realization of further increases in existing levels of passive safety. Because side impact accident experience here and abroad exhibits many similarities, governments of the European community and the United States should cooperate and agree on a common test procedure including common test devices and test parameters.

Within this context, Volkswagen studied the deformable side impact barriers presently under discussion in the United States and Europe. The results of this comparative study are presented. In addition to this comparison, the comparative evaluations of dummies and human subjects by the German Research Association for Automobile Technology (Forschungsvereinigung Automobiltechnik—(FAT) as well as the Thoracic Trauma Index (TTI) developed by NHTSA are discussed.

With these investigations, Volkswagen demonstrates that the European CCMC deformable element mounted on the chassis of the NHTSA crabbed barrier constitutes a valuable basis for further research efforts with respect to a common European and American test device for 90° lateral impact testing that cannot be ignored.

The comparison of loads and kinematics of human subjects and dummies examined demonstrates that the biofidelity of dummies must be improved to be suitable as a test device for lateral impact testing. Because of the present lack of a suitable side impact dummy and absence of correlation between dummy loadings and occupant injury, research activities must continue so as to be able to assess the effectiveness of vehicle measures in real-world impacts.

Introduction

This paper presents and discusses results of Volkswagenwerk's extensive research effort in the field of lateral impacts to increase further the existing levels of occupant protection. It demonstrates the feasibility of developing a universally acceptable common moving deformable barrier for lateral collision testing in Europe and the United States. It discusses the suitability of side impact dummies as test devices and, in this connection, the correlation of dummy loads and occupant injuries to establish occupant protection criteria for the matching of dummy results with real-world accidents.

The behavior of human subjects and HSRI, APROD, and Hybrid II dummies is compared in 90° lateral impacts at a 50km/h impact velocity. The test subjects are seated in an Opel Kadett car body struck by the European CCMC barrier.

Volkswagen investigated and compared 90° lateral impacts with the struck Rabbit vehicles and five different striking vehicles to determine which of the most commonly discussed European and American barriers could be selected within the context of the recognized need for harmonization of future side impact performance requirements for the United States and Europe.

The striking vehicles used were the average European passenger car (VW Passat), the average American car (Chevrolet Citation), the European CCMC and EEVC barriers, and the American NHTSA barrier.

Objectives

The objectives of the Volkswagen research effort presented are to develop a meaningful scientific statement regarding the suitability of commonly discussed European and American Moving Deformable Barriers (MDB) and Side Impact Dummies (SID) for experimental simulation of 90° vehicle-to-vehicle side impacts through comparison of kinematics and loads of colliding vehicles and dummies examined. The results of this study are intended to contribute to the development of test devices and a test procedure that should be used all over the world within the context of performance standard harmonization and simulation of real-world accidents.

Test Procedure for Lateral Impact Testing

Within the scope of its investigation into suitable test procedures and test devices for simulation of lateral collisions, Volkswagen took European and American accident experience into account to establish a test configuration and meaningful test parameters.

The important parameters in this context such as—

- Impact angle
- Impact force direction
- Point of impact
- Impact velocity

- Barrier mass
- Stiffness of the deformable element
- Impactor geometry
- Ground clearance

are described in detail in a previously published SAE paper(1). In the present paper, the parameters that represent the basis for the simulation of actual side impacts are restated.

Crabbed Test Configuration

Analysis of European(2) and American(3) accident statistics demonstrates a necessity to distinguish between impact angle and the impact force direction (Figure 1).

This analysis demonstrates that the struck vehicle generally also has a forward velocity in lateral impacts. Therefore, during the M.I.V. side impact project(4), Volkswagen performed side impact tests with a crabbed barrier and crabbed Citations. Under this test configuration, it was possible to simulate both the impact angle (90°) and the impact force (crabbed angle 27°) along the direction of the resultant impact velocity of both vehicles (Figure 2) with a stationary struck and a moving striking vehicle. This impact configuration is intended to simulate the velocity of the struck vehicle, which is half that of the striking vehicle.

With the context of the goal of harmonization of future side impact performance requirements and considering available U.S. and European accident statistics, this crabbed test configuration should constitute an important part of a joint European and American research program designed to develop a common test device for lateral collision testing.

Point of Impact

Within the M.I.V, project, the defined point of impact of the left edge of the striking vehicles was selected by NHTSA based on American accident statistics(3). The point of impact is 37in forward the center of the wheelbase of the struck vehicle.

Impact Velocity

European committees CCMC (Committee of Common Market Automobile Constructors) and EEVC (European Experimental Vehicles Committee) selected a 50km/h impact velocity for 90° lateral impacts. According to HUK statistics(5) this test velocity covers more than 95 percent of the impact velocities of striking vehicles(1).

Simulating the velocity of the struck vehicle, which may amount to half that of the striking vehicle, by taking into account the main impact force direction (Figure 1), the velocity of the crabbed striking vehicle is increased to 34mph. This velocity was also selected by NHTSA for the M.I.V. project, Phase II. The new Phase II test conditions resulted from a review by NHTSA of the completed National Crash Severity Study (NCSS) accident file. NHTSA noted that these test parameters constitute a life-threatening environment. This view was also supported by the side impact project carried out by FAT(6).

The FAT side impact study at the Institute for Forensic Medicine, University of Heidelberg, sponsored by the Arbeitsgemeinschaft Industrieller Forschungsvereinigung e. V., "AiF", with the CCMC barrier as a striking and a car body mounted on a movable platform as a struck vehicle, demonstrates that this 90° impact with 50km/h impact velocity constitutes a very severe impact environment. Virtually independent of the test subject age, severe injuries (up to AIS 5) consistently result.

These findings constitute a further basis for the development of a common European and American test procedure for 90° lateral impact testing as presented in (1).

Test Devices for Lateral Impact Testing and Protection Criteria

During the discussion of test devices and procedures for the evaluation of the effectiveness of engineering measures for the further increase of present levels of occupant protection during side impact, the deformable barriers from CCMC, EEVC, and NHTSA will be compared. These barriers are intended to simulate the deformation characteristics of the average European and American striking vehicle, respectively, in simulated side impacts.

Presently available side impact dummies, HSRI SID in the United States and APROD SID in Europe, were extensively tested and evaluated by FAT. Kinematics and loadings of the dummies were compared with those of human subjects under comparable and reproducible test conditions(6). One of the purposes of this research project was to generally determine the suitability of dummies as test devices for lateral impact testing. In this context, the correlation of dummy loads and occupant injuries was also to be examined to establish meaningful occupant protection criteria.

Moving Deformable Barriers

Various studies on the development of deformable barriers have been carried out recently. They principally concern the CCMC, Fiat, NHTSA, TRRL (Transport and Road Research Laboratory (GB)), UTAC (Union Technique de l'Automobile du Motorcycle et du Cycle (F)), and EEVC barriers. The CCMC research effort on the deformable element served as a basis for the development of the EEVC element.

The main features of the CCMC, EEVC, and NHTSA barriers discussed here are presented in Figure 3.

Harmonization of side impact test procedures will require compromises acceptable to the regulatory bodies that will ultimately establish performance parameters and standards.

Mass

The CCMC and EEVC barriers have the same mass, 950kg, while the mass of the NHTSA barrier is 1,360kg. A compromise of 1,100kg has been proposed as discussed in the MVMA/NHTSA project, Side Impact Test Procedure Development, and the ISO document(7), Figure 3.

Stiffness

Figure 4 shows the force/deflection (F/D) characteristics of the three deformable elements examined. The characteristics were established in fixed barrier impact testing at a velocity of 35km/h, Figures 5 to 7.

Although the relatively sensitive NHTSA deformable element did not withstand shipping without damage and was thus already deformed at the time of the test (Figure 8), its F/D characteristic evidences a high level of stiffness. Because the first deformation phase is a very important determinant of intrusion velocity, it is very aggressive in lateral impacts as demonstrated in (1) (see also the section on Harmonization of Future Side Impact Performance Requirements). Although static deformation of the struck Rabbit was nearly identical with the CCMC and NHTSA barrier as well as with the Citation as striking vehicles, the dummy loads are substantially higher with the NHTSA barrier (Figures 25 to 31, 36, 38, 40, and 42).

Figure 9 shows the F/D characteristics of the average European sedan (VW Passat) and the average American passenger car (Chevrolet Citation). It also contains the characteristics of the CCMC element and those of the average 1976 European vehicle as calculated by CCMC.

The F/D characteristics specified for the CCMC MDB were determined by applying the test results obtained from dynamometric barrier impacts with 15 different European passenger cars at 30mph. The 15 different car models represented approximately 1.5 million vehicle registrations for the calender year 1976. Characteristics from individual cars were then weighted according to 1976 sales figures and subsequently averaged.

The characteristics depicted in Figures 4 and 9 provide a meaningful and acceptable basis for the joint development of a deformable element for the United States and Europe within the context of the desirable harmonization effort. The knowledge gained in the MDB/Rabbit side collisions demonstrates that the CCMC element provides a sound basis for the harmonization of future requirements with respect to vehicle performance in simulated side impacts.

Ground Clearance

The ground clearance of the barriers as depicted in Figure 3 lies in the range of 250 to 279mm. A reassessment of the ground clearance of the CCMC barrier was contemplated within the context of real-world accident experience and the comparative 90° side impacts with passenger cars and the CCMC barrier as striking vehicles.

According to the APR sample (2), bumper/sill engagement occurs in more than two-thirds of all side impacts (Figure 10). The final determination of the ground clearance of a joint barrier should follow out of a joint American and European research project.

Side Impact Dummies

The effectiveness of engineering measures is examined by means of experimental simulation using dummies. One of the purposes of the FAT research projects was to determine the suitability of available dummies as test devices for lateral impact testing.

The FAT research project was initiated with the goal of assessing the suitability of existing HSRI, APROD, Hybrid II, and the new Euro SID for experimental simulation of lateral impacts through comparison of dummy loading and kinematics with those of human subjects. The ultimate goal of determining the biofidelity of the new European dummy could not be achieved by FAT because of the availability of the dummy for testing. The first prototype will be presented at this ESV conference.

Comparison of the acceleration/time (a/t) histories for the three different dummies examined and the human subject group approximated by a 50th percentile male was based on mean values.

For example, the a/t histories of the 4th and 8th rib, impacted side, as well as the 1st and 12th thoracic vertebrae and the sacrum are compared in Figures 11 to 15.

Analyses of these five parameters, based on lateral impact results of 15 dummy and 35 human subject tests, clearly show there is a substantial and, therefore, unacceptable variance between data measured on dummies and actual data obtained with human subjects. Despite the fact that the HSRI and Hybrid II dummies have quite different chest structures, they demonstrate a nearly identical a/t history at the 4th rib. Because of these findings, it is questionable whether this parameter can be used as injury indicator as discussed in (9), measured at dummies examined.

Despite identical pelvis structures, the dummies provide different response data at the sacrum. This is probably caused by the interaction of the thorax and pelvis during lateral impact.

These results will contribute significantly to the development of a side impact dummy with improved biofidelity. This new dummy should be used throughout the world within the context of the recognized need for harmonization of future side impact performance requirements. During development, particular care should be taken to insure the resulting dummy will not only be suitable for the standardized side impact testing but also for existing frontal impact requirements.

Protection Criteria

Knowledge of load limits and injury mechanisms of occupants is mandatory for the definition and assessment of measures to further increase existing levels of vehicle occupant protection. Therefore, FAT performed a total of 35 lateral impact tests with human subjects at different velocities (40 to 60km/h) and in left and right side impact modes to establish by iteration the loading limits on human subjects. The test series further sought to examine the relationship between injury severity and the measured acceleration values. This constitutes a sound basis for the determination of future protection criteria. Suitable dummies and the relationship between protection criteria and occupant protection are, of course, a prerequisite for the application of dummy loads measured during tests to the real-world accident scene. Without such a correlation, those responsible for the establishment of meaningful standards will not have fulfilled their mandate.

The results of this FAT study are described in (6). They will be summarized here.

In accordance with our presentation(8), and as also noted during the continuation of the test series, the most serious injuries were observed at the abdomen. These generally consist of liver ruptures, which predominantly occur during 50km/h lateral collisions and where occupant impact occurs on the right side. In the three tests with a collision velocity of 60km/h, abdominal injuries occurred during left-side impacts, consisting principally of injuries to the spleen, the left kidney, and the liver. No abdominal injuries occurred at a velocity of 40km/h during right-side impacts. Even during left-side impacts at a velocity of 45km/h, no abdominal injuries were observed (Figures 16 and 17).

The high frequency of abdominal injuries indicates that side impact dummies must be developed to simulate these injuries.

Again, it should be noted that the simulated 90° lateral impact test performed in this study represents a very severe accident exposure, which overemphasizes the frequency of severe abdominal injury in relation to overall accident experience.

The evaluation of the severity of thoracic injuries was based principally on the number of fractured ribs. In a few cases, perforations of the pleura occurred. Figures 18 and 19 depict the correlation between the number of rib fractures and accelerations measured at the 4th rib and 1st thoracic vertebra by means of linear regression analysis. The correlation coefficients do not indicate the existence of a strong correlation. Injuries to the head and extremities were rarely observed.

Two-dimensional Spearman correlation results have been evaluated to examine the correlation of loads and injury severity. Comparison of these coefficients and significant levels of all parameters examined indicates there may well be a relationship between 4th rib or 1st thoracic vertebra accelerations and rib fractures as there is between 12th thoracic vertebra or sacrum acceleration and abdominal injury severity. Figure 20, however, depicts no such correlation between sacrum acceleration and abdominal injury. These findings will be analyzed within the scope of a further study by performing a multiple, nonlinear regression analysis. The two-dimensional Spearman correlations should be viewed only as an initial effort for assessment and evaluation of the extensive data collective.

The relationship between loads and injury is also discussed in (9). A relationship, called the Thoracic Trauma Index (TTI), has been developed by NHTSA that is intended to indicate the injury to the thoracic cage and the organs within it.

$$TTI = 1.4\ Age + 0.5\ (T12Y + LURY) * Mass/165$$

Subject age and mass (lb) and lateral peak acceleration of struck side 4th rib and 12th thoracic vertebra are parameters of the equation for the calculation of TTI.

Figures 21 to 24 depict the relationship between TTI and thoracic and abdominal injuries. Because of the lack of correlation and the great variance between data measured with HSRI dummy and human subjects, at present the algorithm is not suitable for calculation of the theoretical TTI from data measured with this dummy.

Harmonization of Future Side Impact Performance Requirements

To effectively realize further meaningful increases in existing levels of passive safety, the common goal of all concerned must be to promote uniform vehicle performance requirements on a worldwide basis. The governments in Europe and of the United States must demonstrate a willingness to cooperate and compromise with respect to appropriate test procedure, configuration, devices, and parameters.

To investigate the merits of this concept, Volkswagen evaluated and compared the behavior of five striking vehicles in 90° lateral impact tests with the crabbed test configuration and struck Rabbits (Figure 25):

- Chevrolet Citation (average American car)

- NHTSA barrier
- VW Passat (average European car)
- CCMC barrier
- EEVC barrier

Comparison Between the CCMC Barrier and the Average American Car

The side impact test with the Citation (Figures 26 and 27) was part of the M.I.V. research project performed by Volkswagen(4) under NHTSA sponsorship. The Citation was selected because it is said to represent the average American car in terms of dimensions, structure, and mass. In addition, it was selected by NHTSA for the M.I.V. project, Phase II, because, according to NHTSA test results, the deformable barrier, developed by NHTSA only for 60° side impacts, is too stiff in 90° impact configurations. This characteristic was also demonstrated by Volkswagen in a further test with this barrier, (Figures 25, 30, and 31).

The essential characteristics of the deformable element of the CCMC barrier have been matched as closely as possible to those of an average, current production European-type passenger car in terms of mass, F/D characteristics, geometry, etc.(1).

To evaluate the suitability of the CCMC barrier as a test device for lateral collision testing (Figures 28 and 29), HRSI dummy response data and the overall deformation of the struck vehicles, as well as that occurring at specific levels, are compared (Figures 36, 38, 40, and 42).

It can be seen that the CCMC deformable element, which is in part stiffer than the average European car, closely simulates the deformation behavior of the front structure of the average American car, the Chevrolet Citation, as defined by NHTSA.

The driver dummy loads are nearly identical in the thoracic area when side impacts with the Citation and the CCMC barrier are compared (Figures 25 and 36). Loads are higher in the head and pelvic region for the Citation/Rabbit side impact test. Because thoracic injuries dominate according to U.S. and European statistics(2,3), mainly thoracic loads should be taken into account.

The higher pelvic loads were caused by the 5mph bumper layout of the Citation. The CCMC deformable elements closely simulate the 2.5mph bumper layout. Here the negative effect of the more aggressive 5mph layout on occupant protection in lateral impacts is clearly evident.

With the exception of the bumper region, deformation of the struck vehicles is similar when lateral impacts with the Citation and the CCMC barrier are compared. They are, however, equal in the thoracic area (Figures 38, 40, and 42).

Comparison Between the NHTSA Barrier and the Average American Car

Comparing dummy response data from lateral impacts with the NHTSA barrier with the NHTSA deformable element and the Citation as striking vehicles, it is obvious the barrier does not simulate the deformation behavior of the average American car as defined in any region (Figures 25 and 36). The barrier is substantially more aggressive than the Citation and will thus lead to false assumptions and unrealistic measures to reduce dummy loads. The NHTSA barrier does not accurately reflect the effects and consequences of real accidents.

The static crush of Rabbits struck by the Citation and the NHTSA barrier is similar (Figures 27, 31, 38, 40, and 42). Because the difference in dummy loads of these two tests is so immense, the deformation/time history of the side structure of the struck vehicles, caused by the two different striking vehicles, disclose substantial disparities.

Comparison Between the CCMC and EEVC Barriers and the Average European Car

The design of the EEVC barrier and its deformable element is described in (10). Design parameters are compared in Figure 3.

Comparison tests with the average European vehicle (VW Passat) and the CCMC and EEVC barriers (Figures 28, 29, and 32 to 35) clearly show that the CCMC barrier represents a significant and acceptable compromise for the harmonization of future vehicle performance requirements in defined side collisions.

The F/D characteristics of the CCMC element are in some areas stiffer than those of the average European car. The F/D characteristics of the EEVC element are softer as demonstrated by a comparison of the dummy values (Figures 25 and 37) and characteristics (Figure 9). A stiffening of the element has been discussed(10), thus the characteristics of the updated CCMC and EEVC elements will ultimately be quite similar.

The side impact test with the crabbed chassis of the NHTSA barrier and the EEVC elements (Figures 34 and 35) demonstrates this element can also be used for the crabbed test configuration that is intended to simulate real-world side impacts.

Comparison of driver dummy loads (Figures 25 and 37) demonstrates that the CCMC deformable element mounted on the crabbed chassis of the NHTSA barrier appears to represent an excellent and most realistic compromise for the harmonization of future side impact performance requirements intended to further increase existing levels of passive safety. This combination should constitute the basis for further research efforts with respect to a common European and American test device for 90° lateral impact testing.

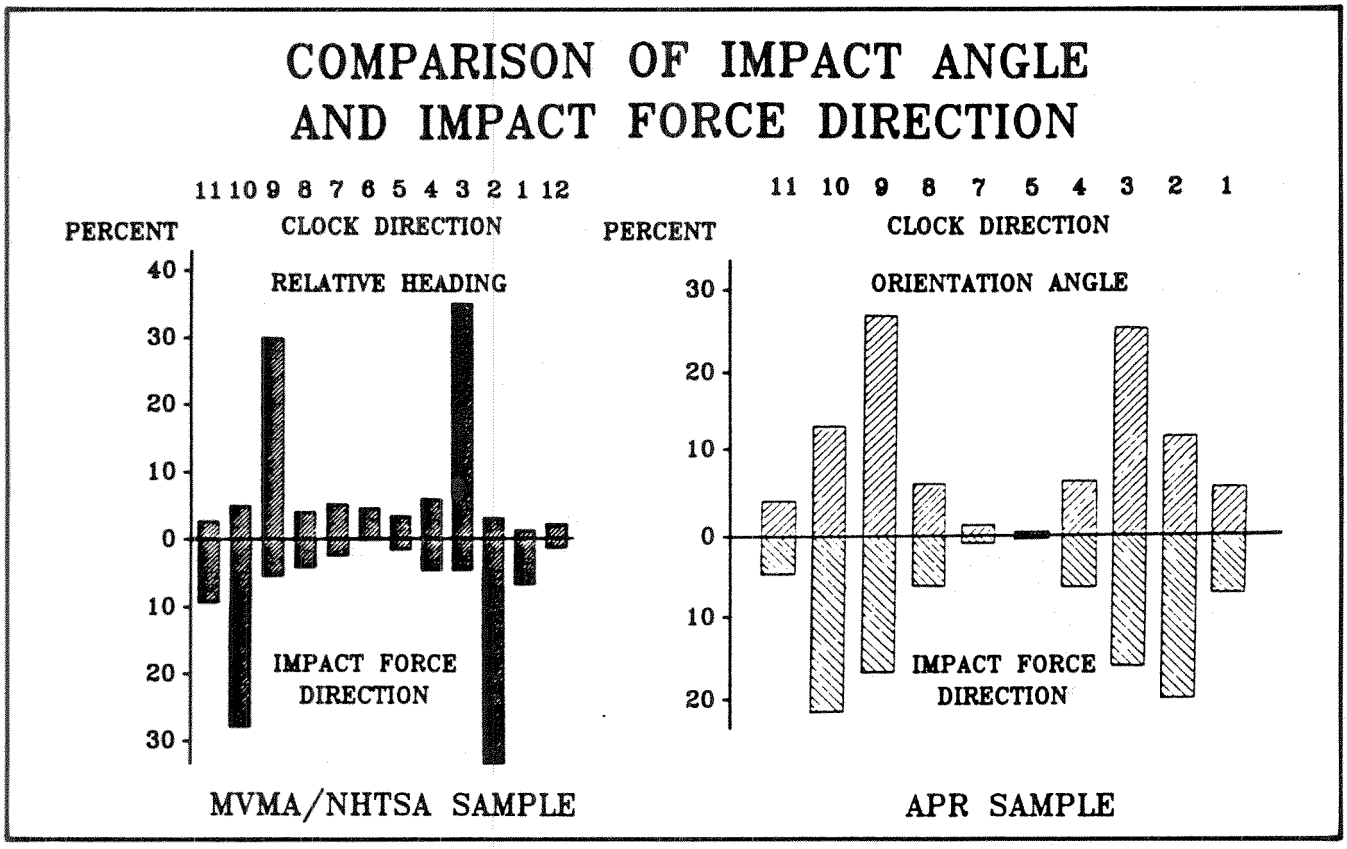

Figure 1.

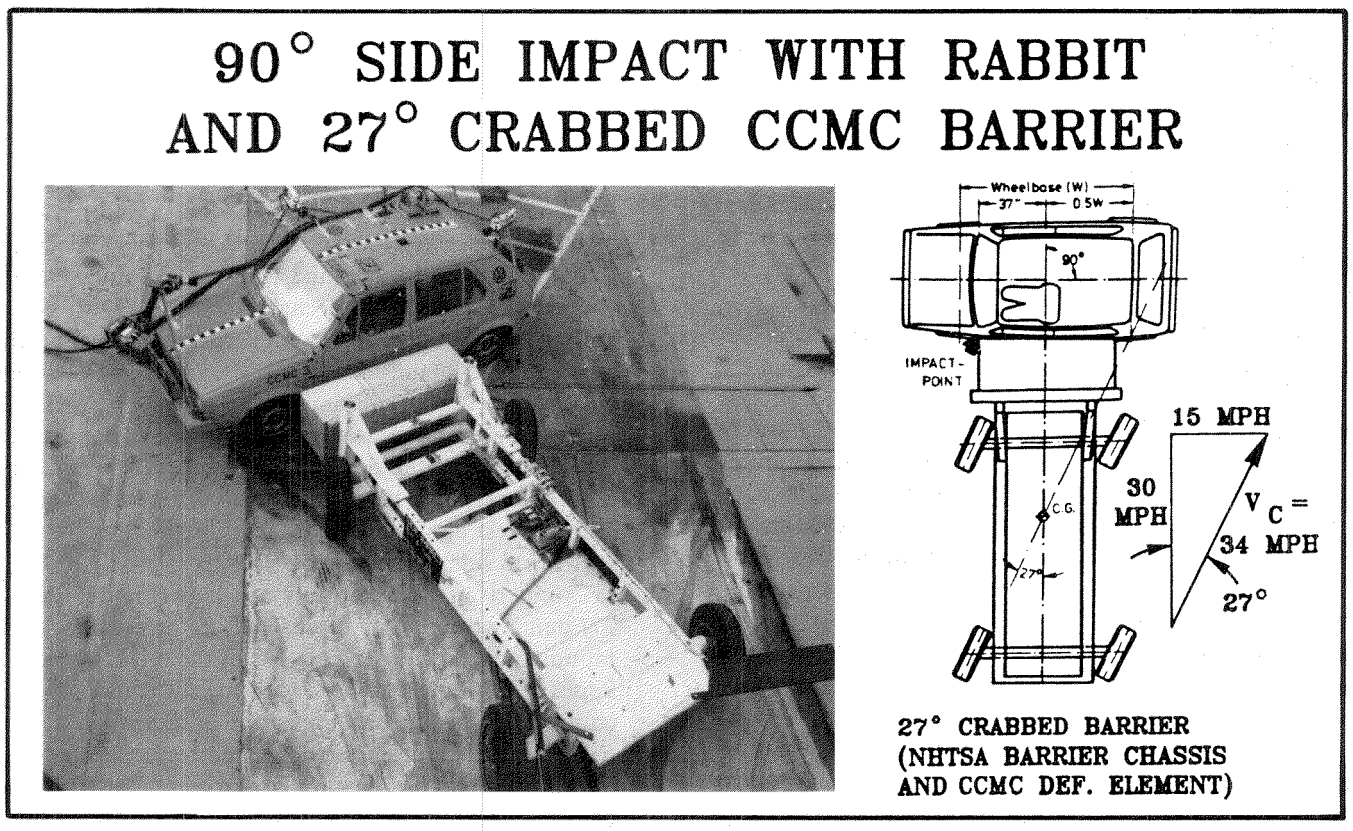

Figure 2.

COMPARISON OF MOBILE DEFORMABLE BARRIERS

	CCMC	EEVC	NHTSA	ISO (7)
MASS (KG)	950	950	1360 (3000 LB)	1100
SHAPE	FLAT	FLAT + BUMPER	FLAT + BUMPER	FLAT
NUMBER OF BLOCKS	8	6	1 + BUMPER	
GROUND CLEARANCE (MM)	250	250	279	260 $\pm$ 10
HEIGHT (MM)	490	500	559	500 $\pm$ 10
WIDTH (MM)	1550	1500	1679	1550 $\pm$ 20
THICKNESS (MM)	430	500	483	450
MATERIAL	PU FOAM	PU FOAM	ALUMINIUM HONEYCOMB	

Figure 3.

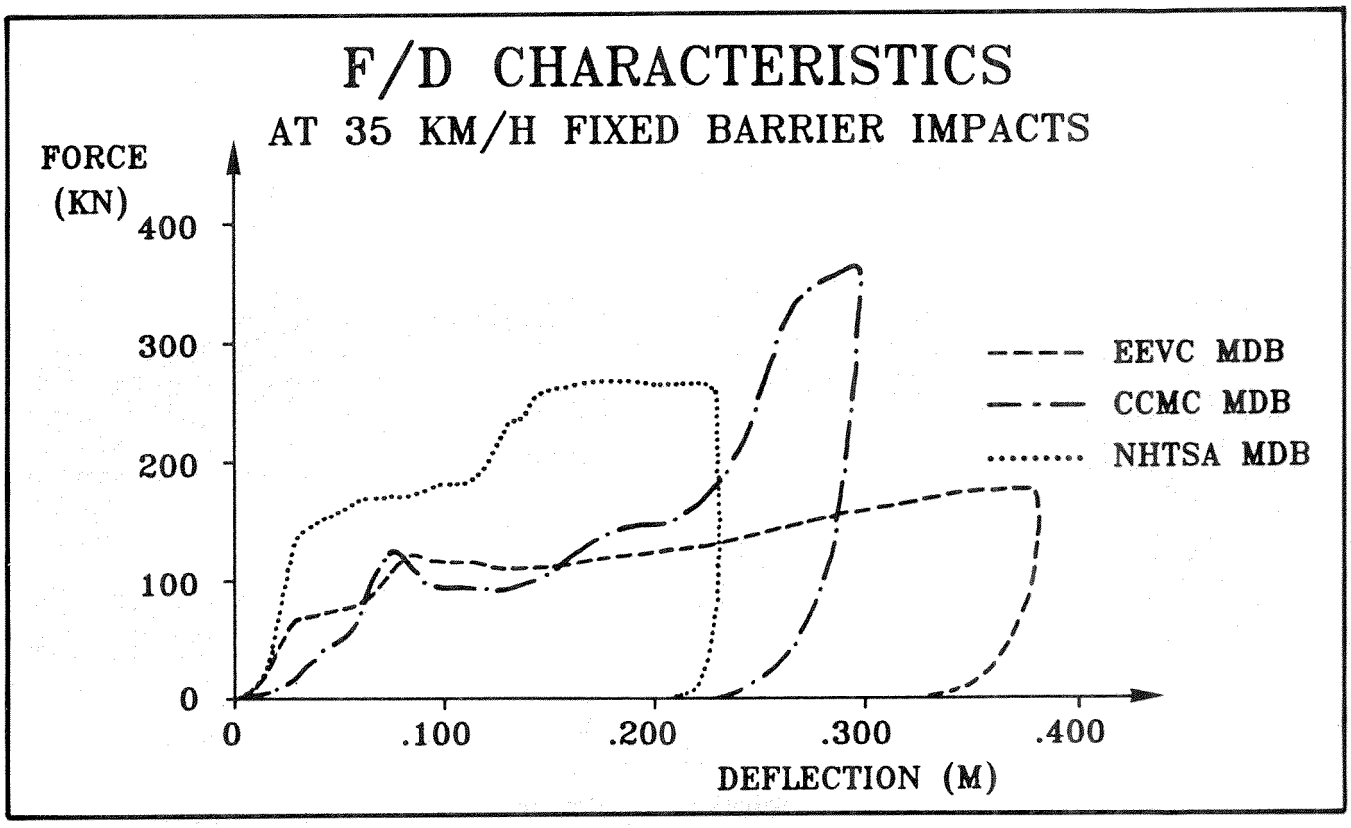

Figure 4.

CCMC MDB ELEMENT

FIXED BARRIER IMPACT AT 35 KM/H

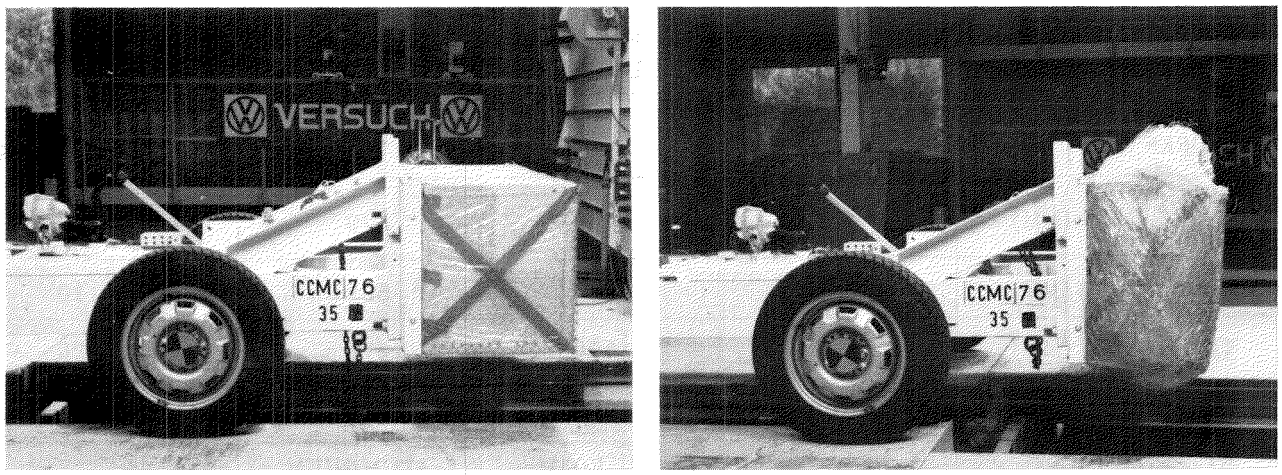

PRE–CRASH POST–CRASH

Figure 5.

EEVC MDB ELEMENT

FIXED BARRIER IMPACT AT 35 KM/H

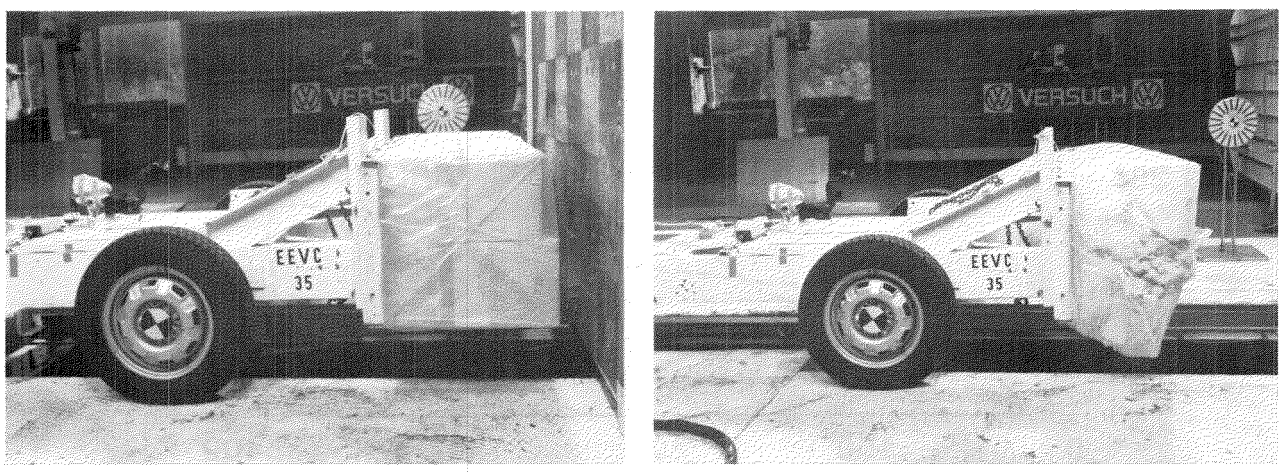

PRE–CRASH POST–CRASH

Figure 6.

NHTSA MDB ELEMENT

FIXED BARRIER IMPACT AT 35 KM/H

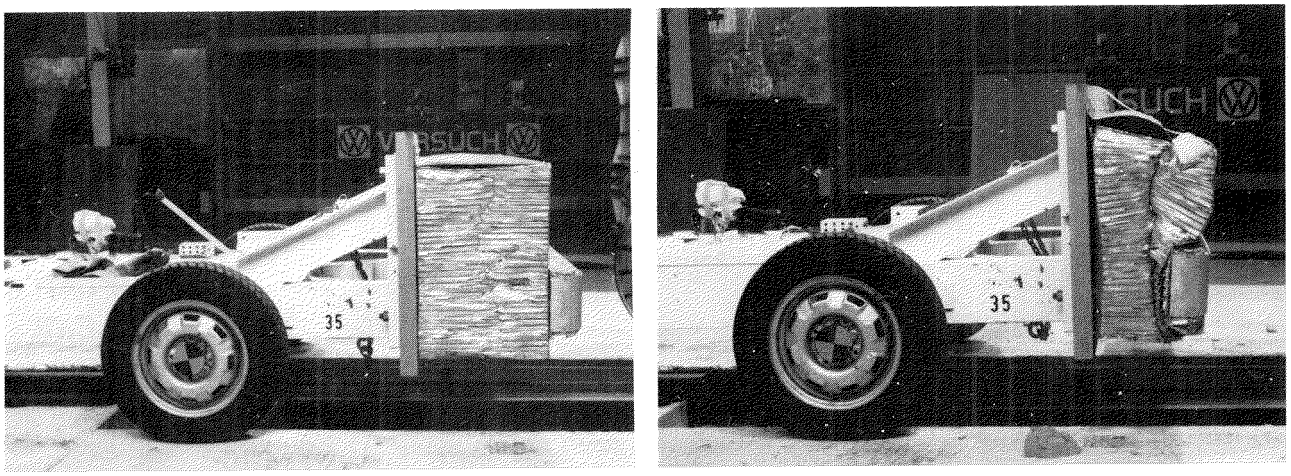

PRE–CRASH POST–CRASH

Figure 7.

NHTSA ELEMENT

PRE–TEST CONDITION, DEFORMATION CAUSED BY SHIPPING

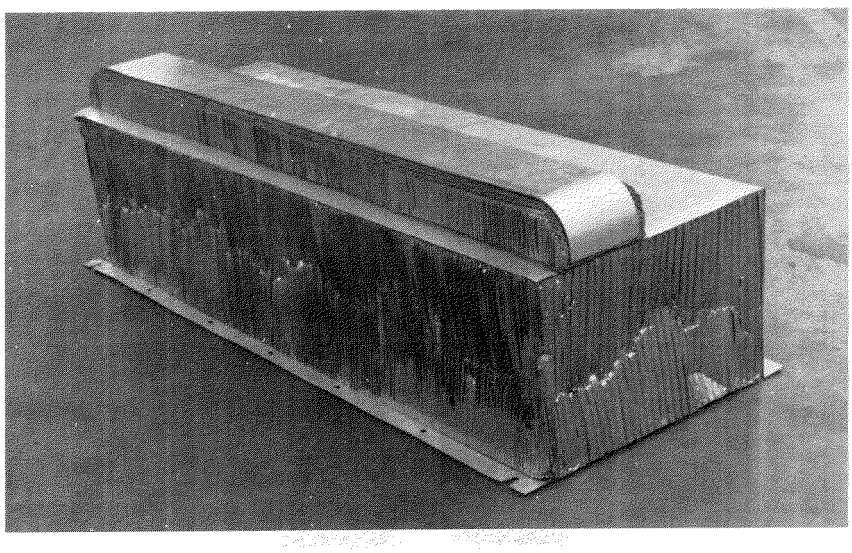

Figure 8.

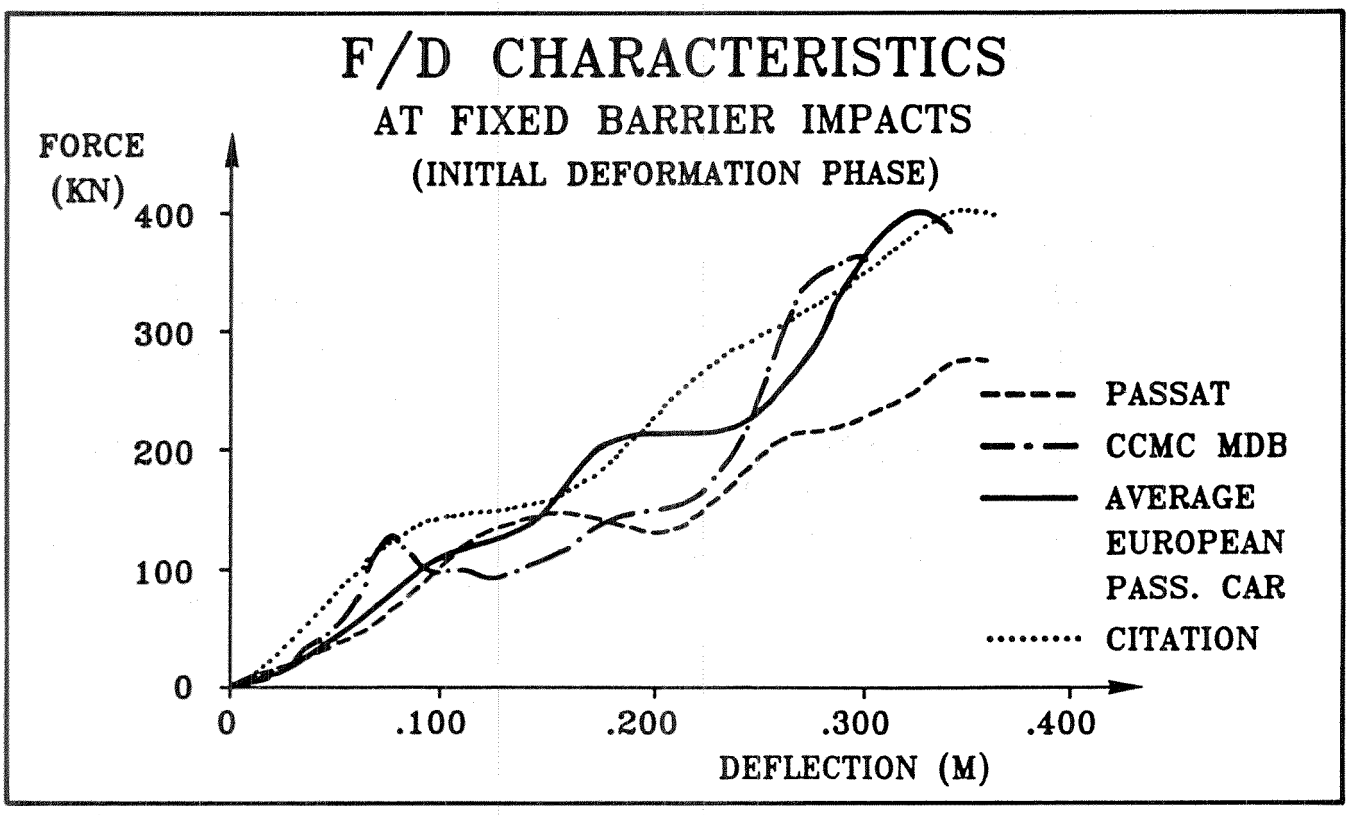

Figure 9.

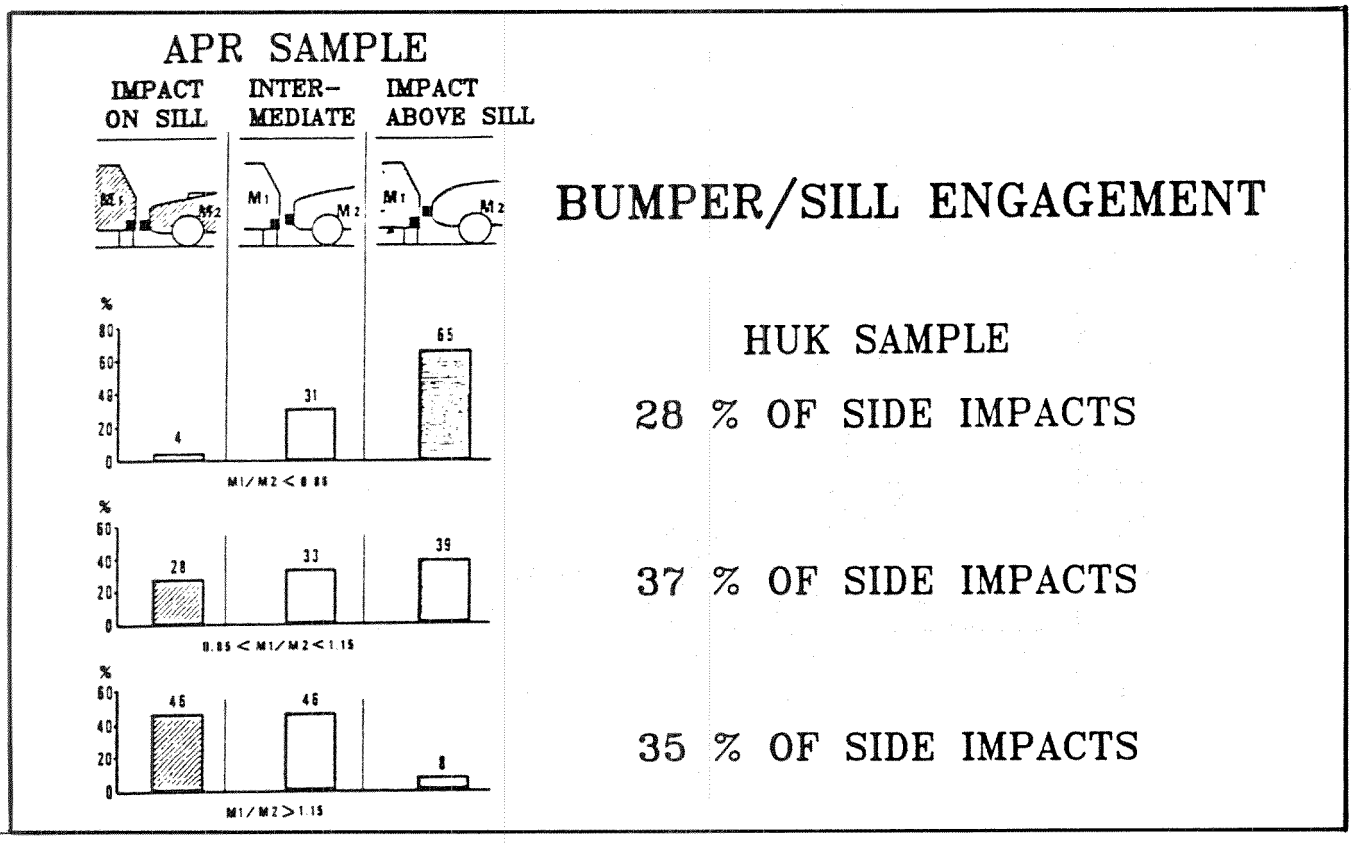

Figure 10.

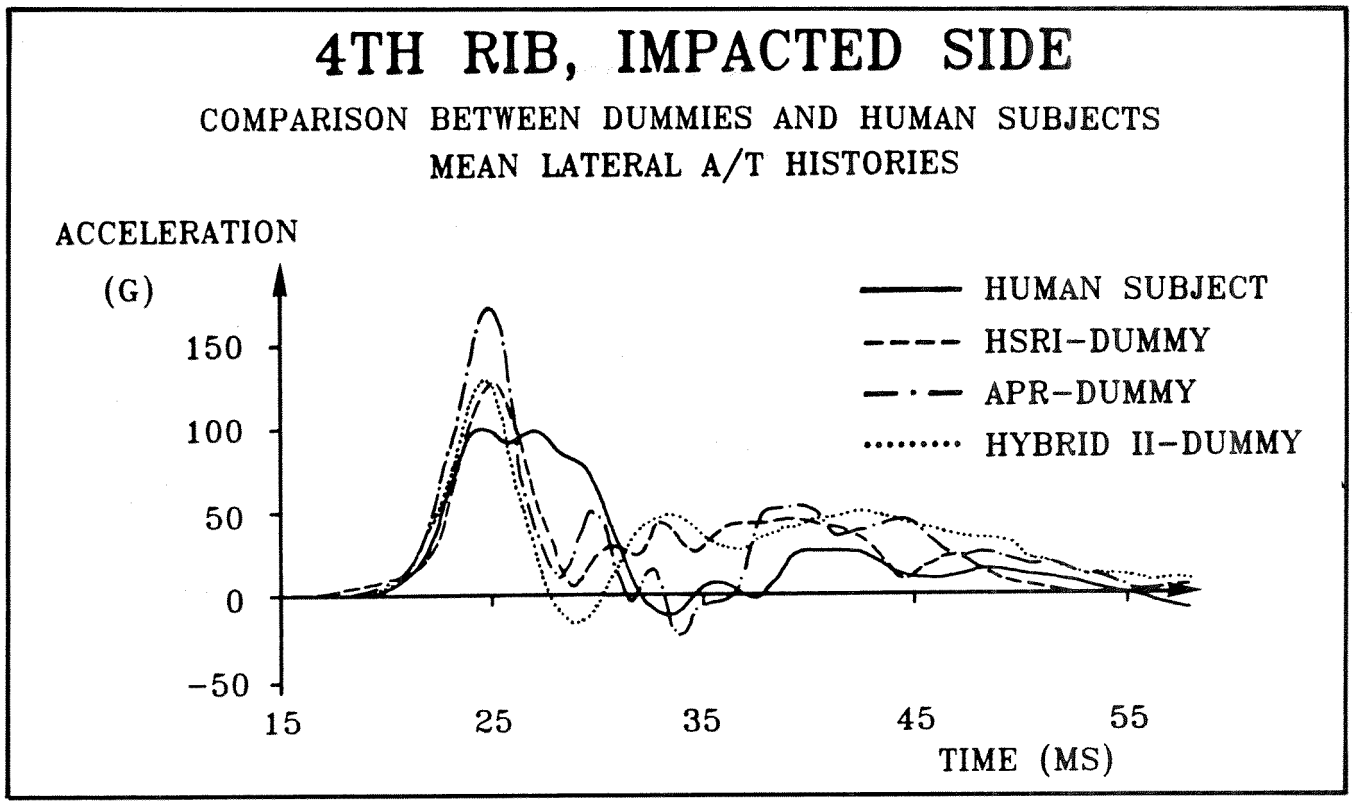

Figure 11.

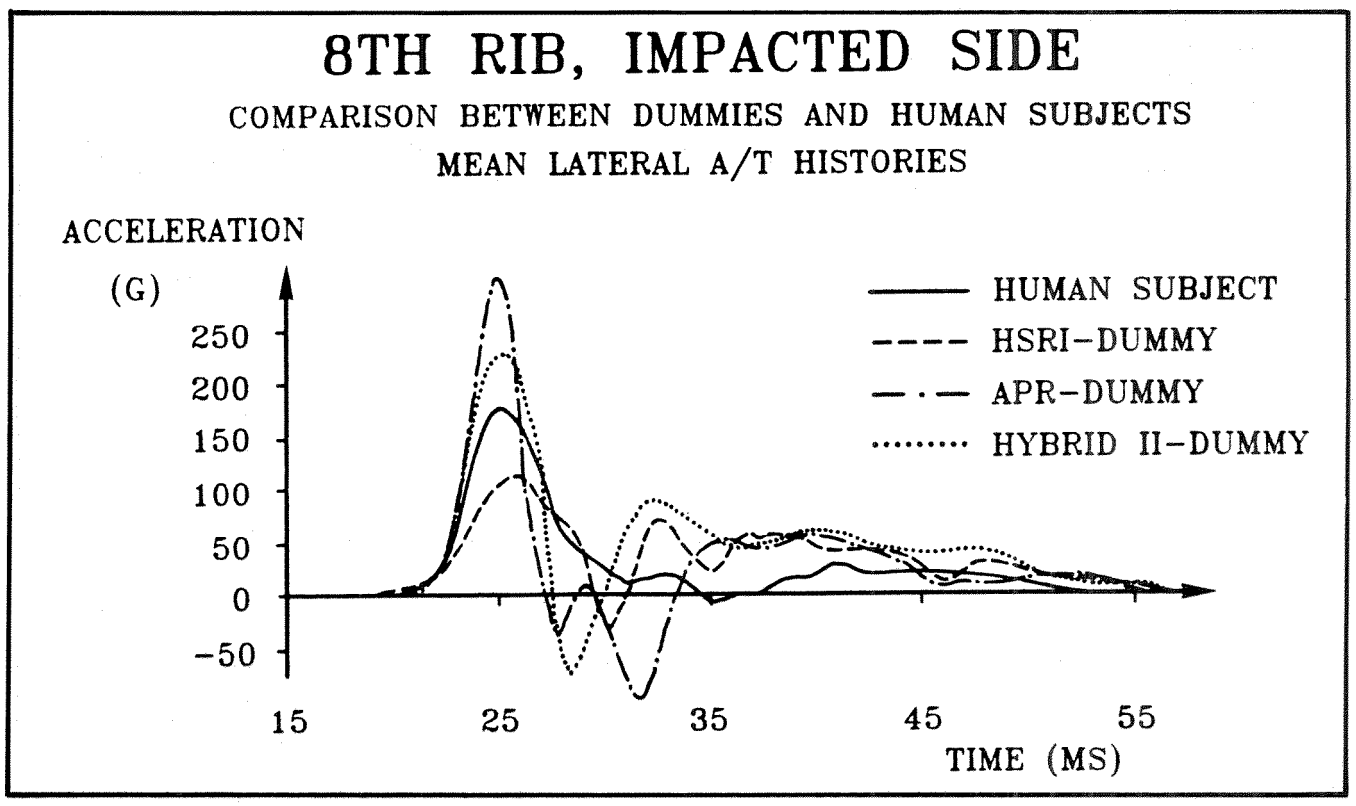

Figure 12.

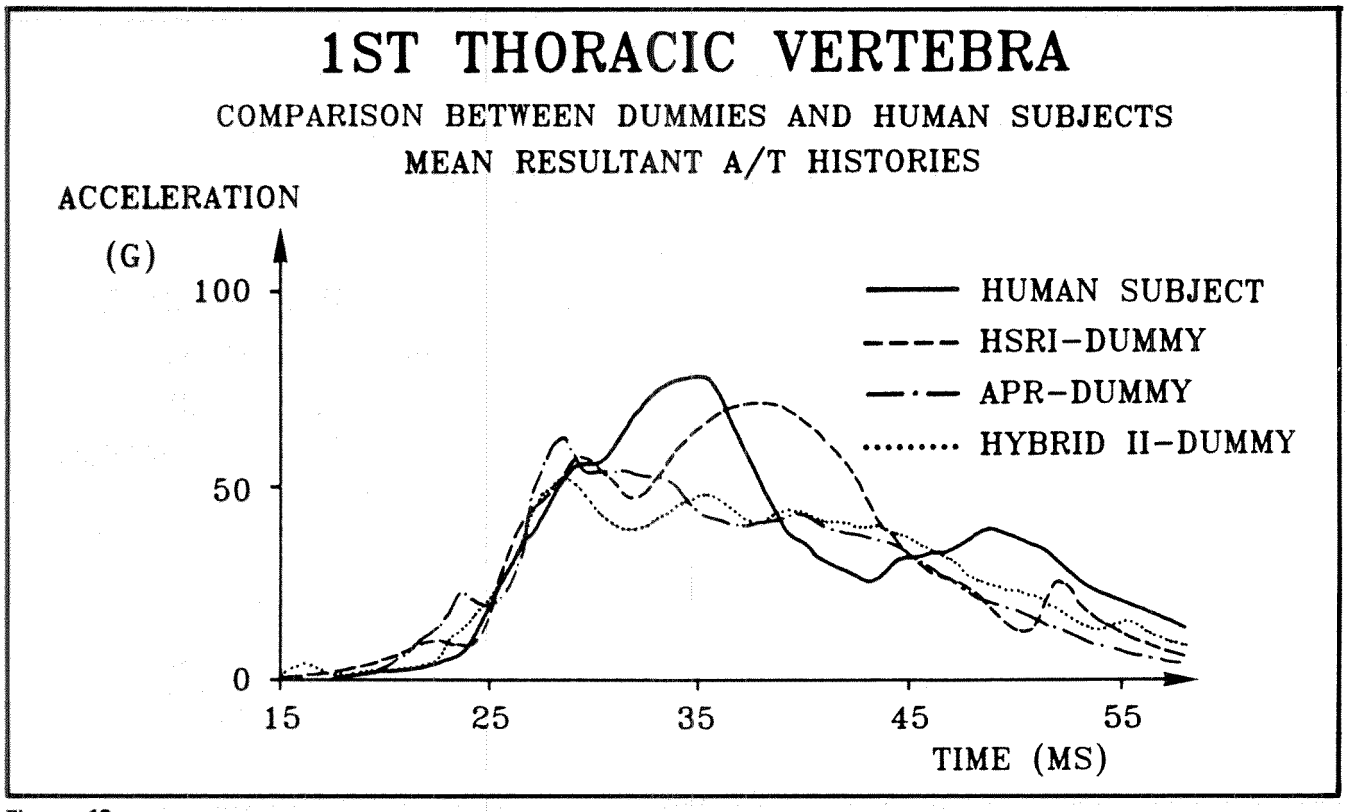

Figure 13.

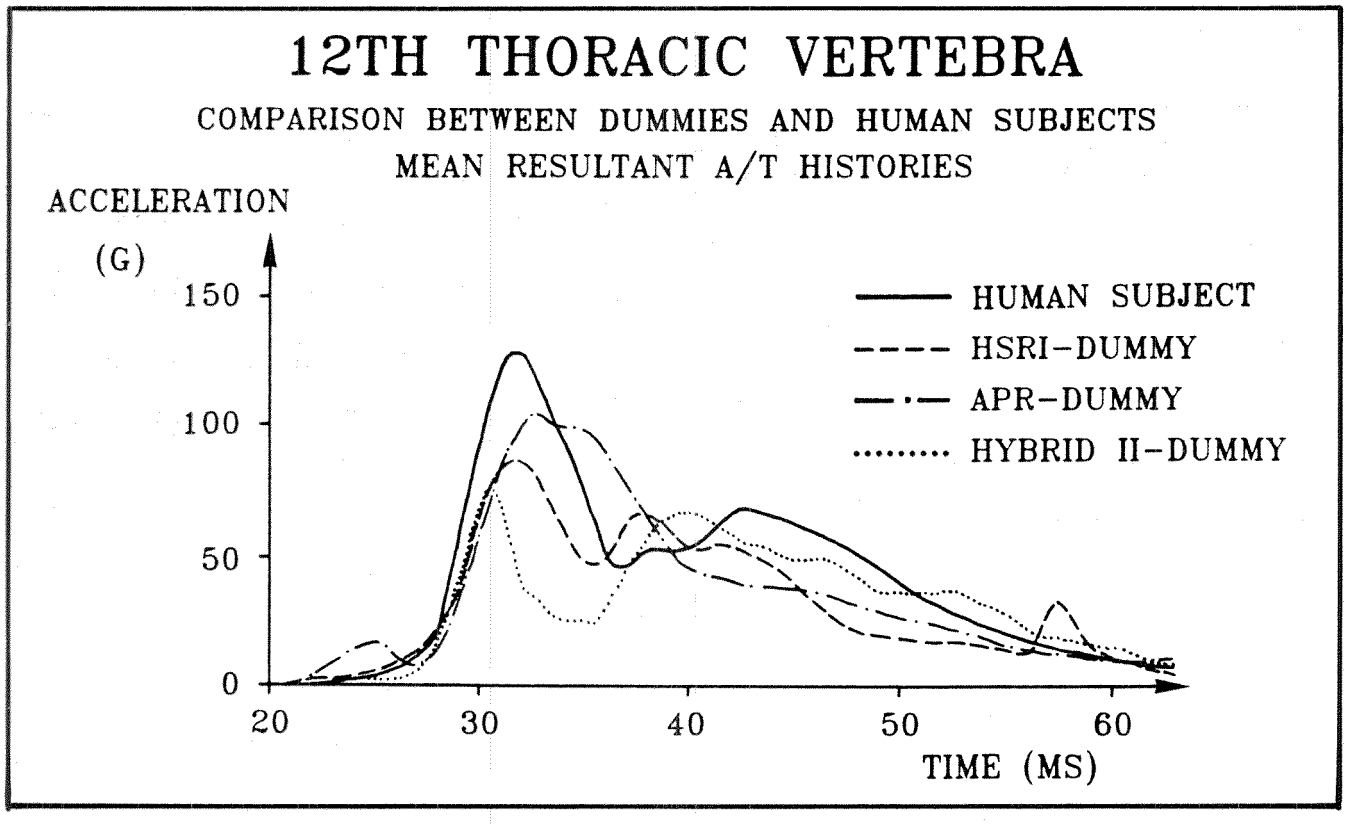

Figure 14.

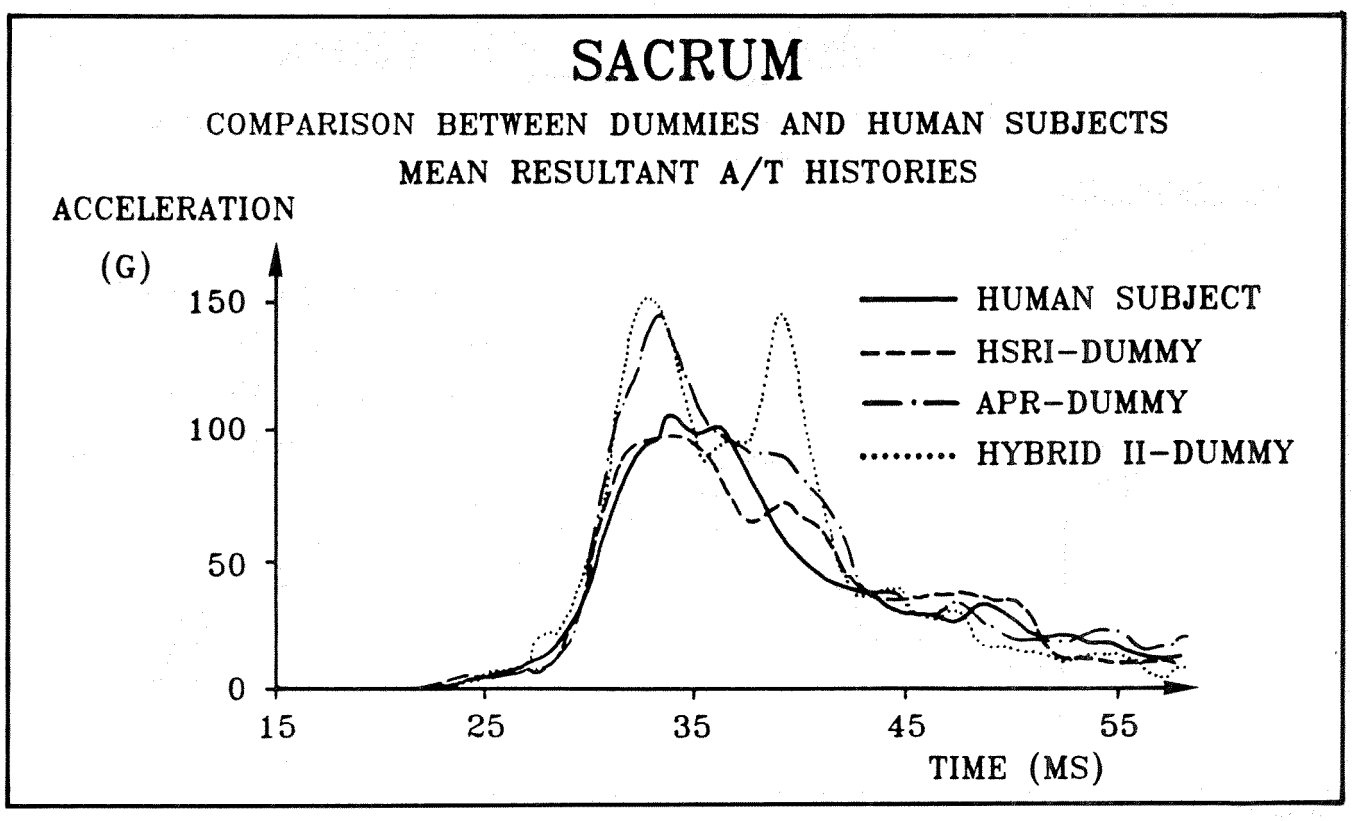

Figure 15.

FAT-PROJECT "SIDE IMPACT"

Test No.	Impact Side	Impact Velocity (km/h)	Test Subject Sex	Age (years)	Body Mass (kg)	Body Lenght (cm)	Sitting Height (cm)	Chest Circumfer. (cm)	Number of Rib Fracture	Head	Thorax	Spinal Column	Abdomen	Pelvis	MAIS	a_{max}* 4th Rib	T12Y	TTI
812?	right	50	M	22	71	178	92	85	0	0	0	2	0	0	2	45	85	92.5
820?	right	50	M	21	68	173	93	87	0	0	0	2	5	0	5	137	120	146.3
820-	left	50	F	40	60	158	80	74	18	0	4	1	0	0	4	109	112	144.6
820?	left	50	M	43	77	178	93	94	23	3	4	1	0	0	4	217	116	231.7
820?	right	50	M	23	63	175	97	81	14	0	3	1	4	0	4	74	94	101.9
820?	left	50	M	56	66	165	89	98	19	0	4	1	0	0	4	162	103	201.6
821?	right	50	M	29	70	184	100	87	6	0	2	0	5	0	5	56	69	99.0
821-	left	50	M	29	59	177	95	83	14	0	3	0	0	0	3	122	120	136.0
822?	right	50	M	47	90	170	90	104	27	0	4	2	5	0	5	69	81	158.4
830?	left	50	F	39	57	173	81	86	19	3	4	1	0	0	4	144	126	177.3
830?	right	50	M	22	65	175	94	90	0	0	0	0	5	0	5	128	148	148.0
830?	right	50	M	52	68	172	91	94	22	0	4	1	5	0	5	147	114	191.4
830-	left	50	M	26	61	172	91	86	18	1	4	1	3	0	4	145	151	159.8
830?	left	50	F	42	60	162	87	83	26	0	4	2	4	0	4	193	117	181.5
830?	right	50	M	59	60	169	87	88	26	0	4	2	4	2	4	213	140	224.1
832?	right	50	M	32	85	171	96	95	5	0	2	0	5	0	5	70	83	128.6
832?	left	50	M	53	65	171	92	83	4	0	2	2	0	0	2	141	115	181.9
832?	left	50	M	44	86	186	100	91	19	0	4	1	0	0	4	101	117	190.1
832?	right	50	M	36	77	178	94	92	16	0	4	0	5	0	5	89	94	147.5
840?	right	50	M	36	91	176	90	102	6	0	2	0	4	0	4	60	70	129.4
840?	left	50	M	33	73	187	98	87	17	0	4	1	0	0	4	93	120	150.1

HUMAN SUBJECT
INJURY SEVERITY
RESULTS FROM
LATERAL IMPACTS
AT
50 KM/H

* 100 HZ
DIGITAL FILTERED

Figure 16.

FAT-Project "SIDE IMPACT"

Test No.	Impact Side	Impact Velocity (km/h)	Test Subject						Number of Rib Fracture	Injury Severity (AIS)						a_{max}*		TTI
			Sex	Age	Body Mass (kg)	Body Length (cm)	Sitting Height (cm)	Chest Circumfer. (cm)		Head	Thorax	Spinal Column	Abdomen	Pelvis	MAIS	4th Rib	T12Y	
8813	right	40	F	28	51	159	90	72	0	0	0	1	0	0	1	125	113	120.3
8815	right	40	F	38	60	164	87	77	4	0	2	0	0	0	2	110	72	126.2
8818	right	40	M	28	63	184	99	90	0	0	0	1	0	0	1	33	52	75.0
8804	left	40	M	51	80	168	90	93	17	0	4	2	0	0	4	44	64	114.7
8805	right	40	M	60	64	170	91	91	16	0	4	1	0	0	4	80	71	148.6
8806	right	45	M	30	60	175	99	85	0	0	0	0	0	0	0	49	92	98.5
8807	left	45	F	27	61	160	86	94	11	0	3	0	0	0	3	93	85	110.3
8809	left	45	M	25	95	188	101	99	7	0	3	0	0	0	3	105	100	165.1
8810	right	45	M	53	74	172	92	92	17	0	4	0	5	0	5	116	71	166.6
8811	right	45	M	64	76	172	89	85	18	0	4	0	4	0	4	79	58	159.1
8812	left	45	M	54	68	177	95	98	12	0	3	0	0	3	3	66	97	149.6
8814	left	60	M	27	80	190	100	94	16	0	4	2	5	0	5	126	232	223.6
8817	left	60	M	50	85	173	88	101	21	3	4	2	4	0	4	182	167	268.2
8819	left	60	M	40	85	175	90	102	20	1	4	5	5	0	5	167	150	229.7

HUMAN SUBJECT INJURY SEVERITY RESULTS FROM LATERAL IMPACTS AT 40, 45 AND 60 KM/H

* 100 HZ DIGITAL FILTERED

Figure 17.

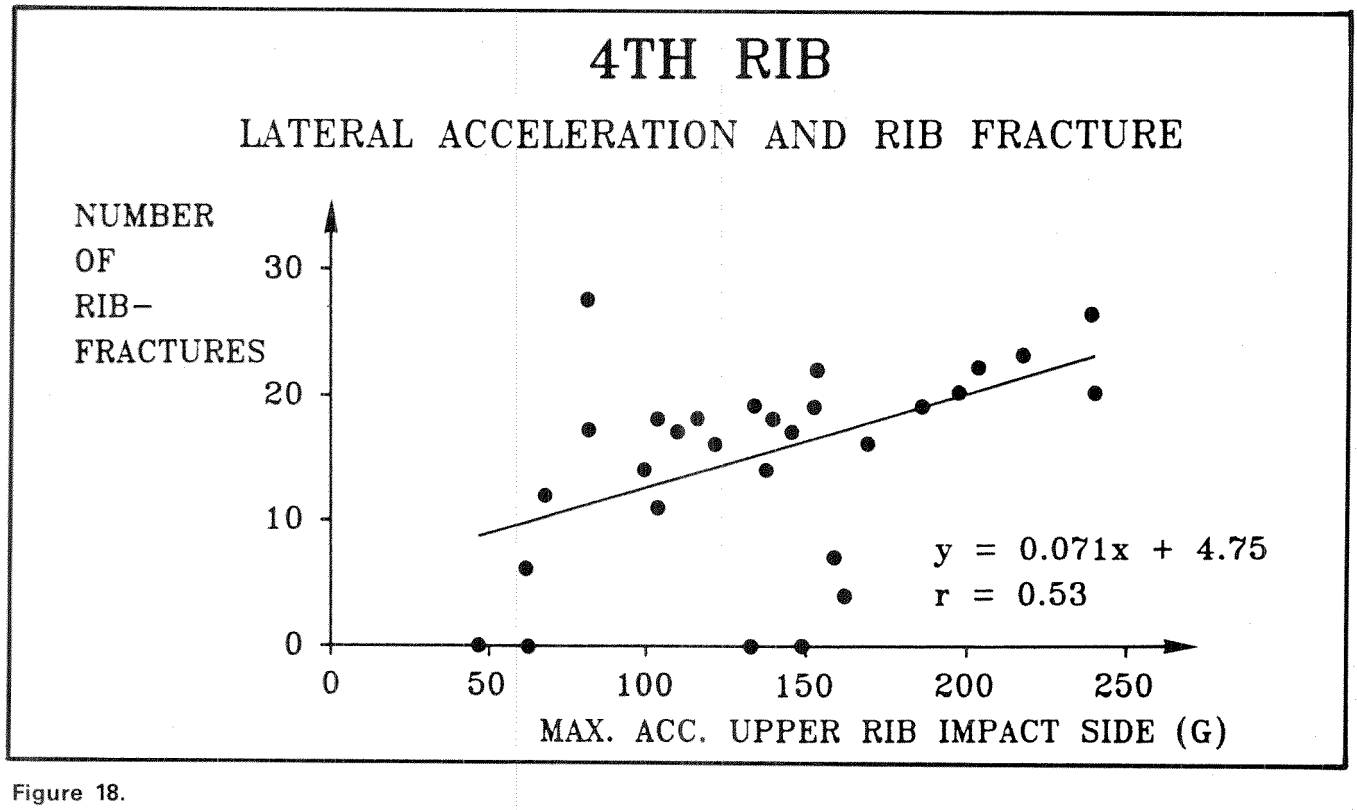

Figure 18.

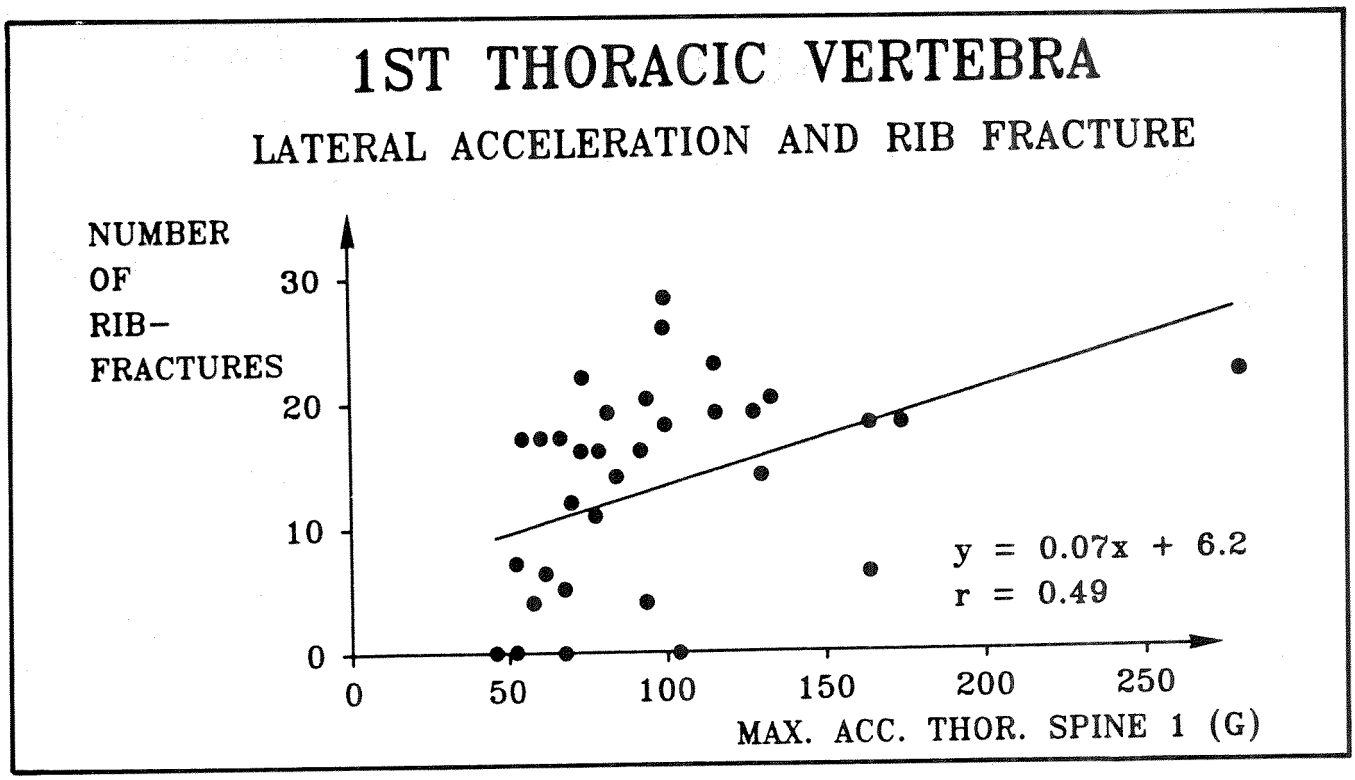

Figure 19.

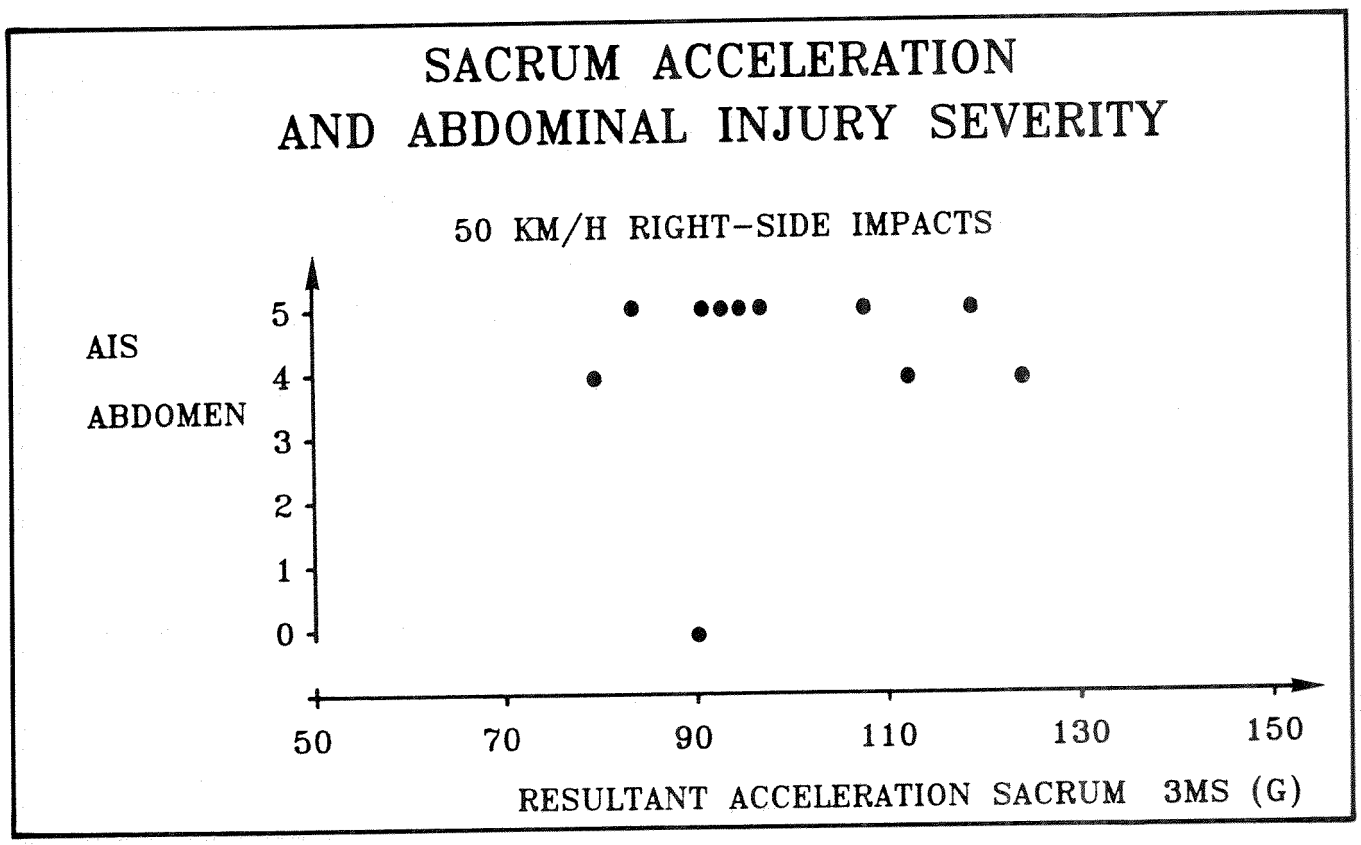

Figure 20.

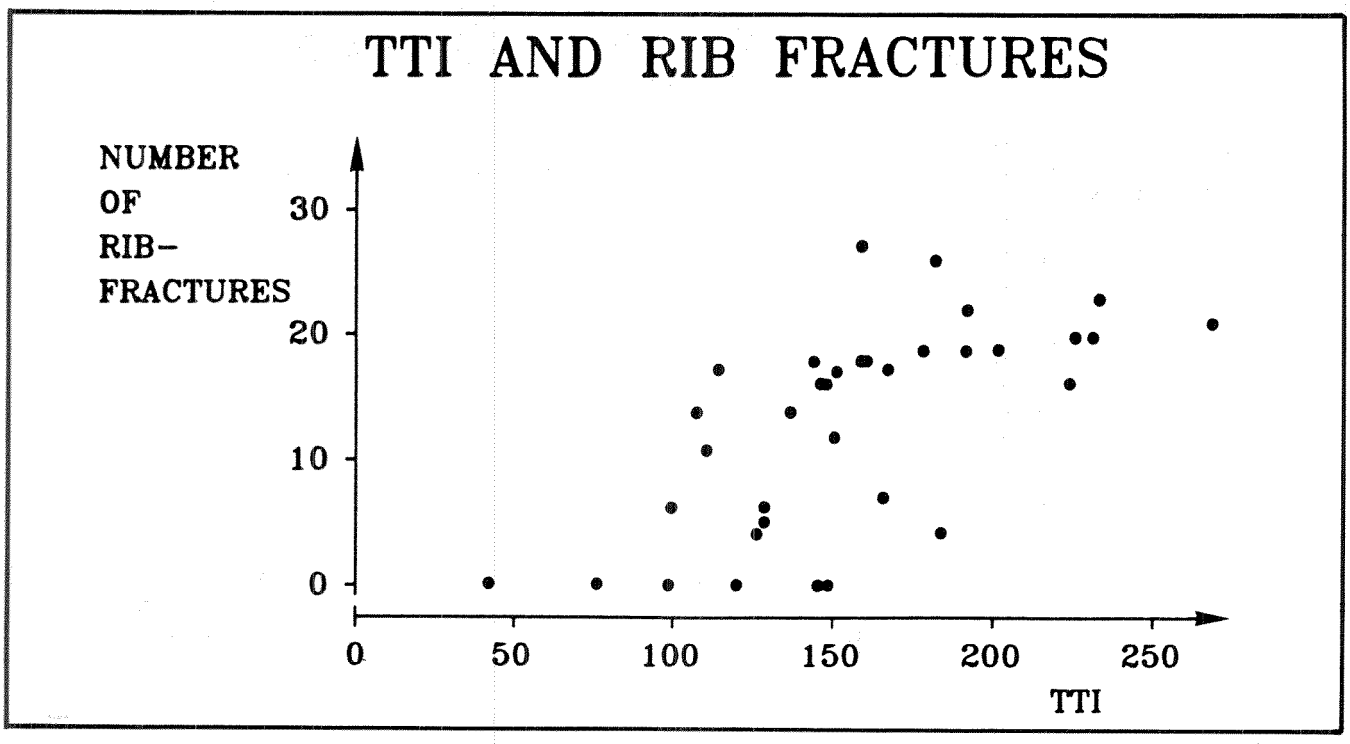

Figure 21.

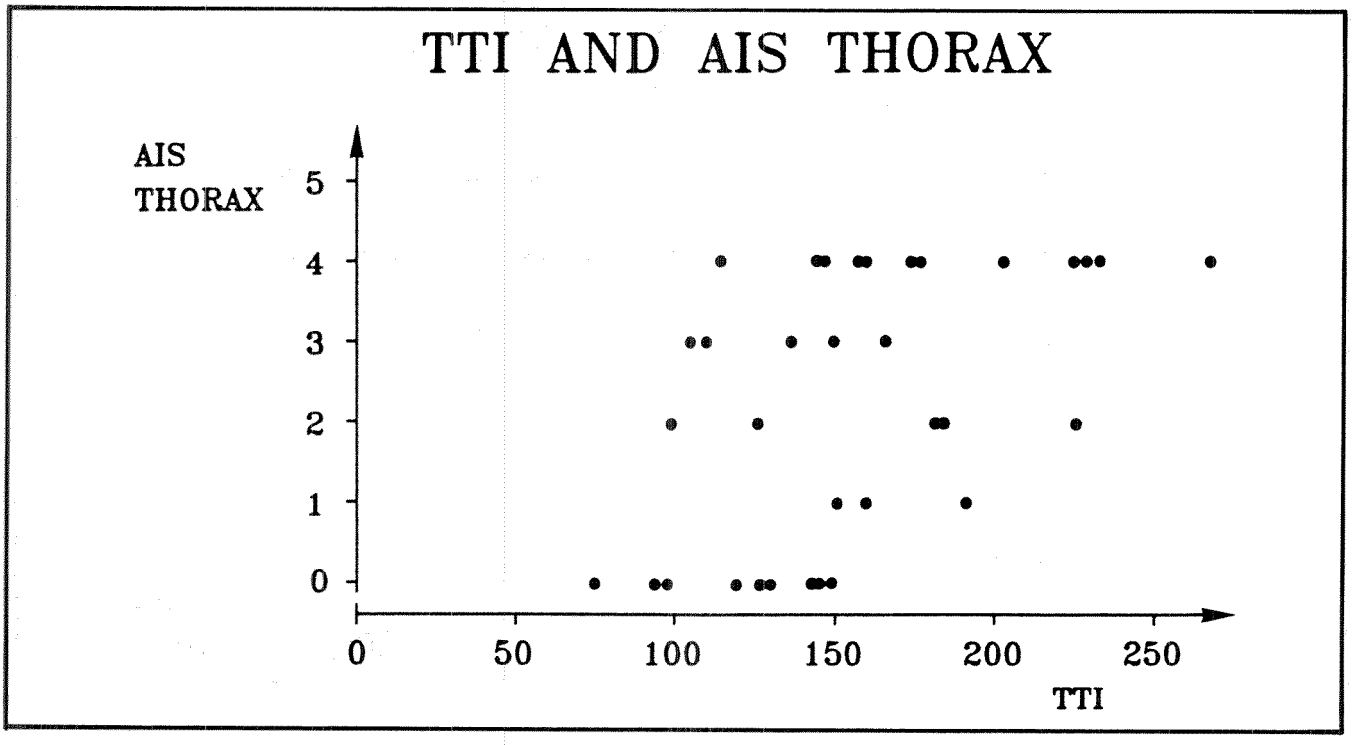

Figure 22.

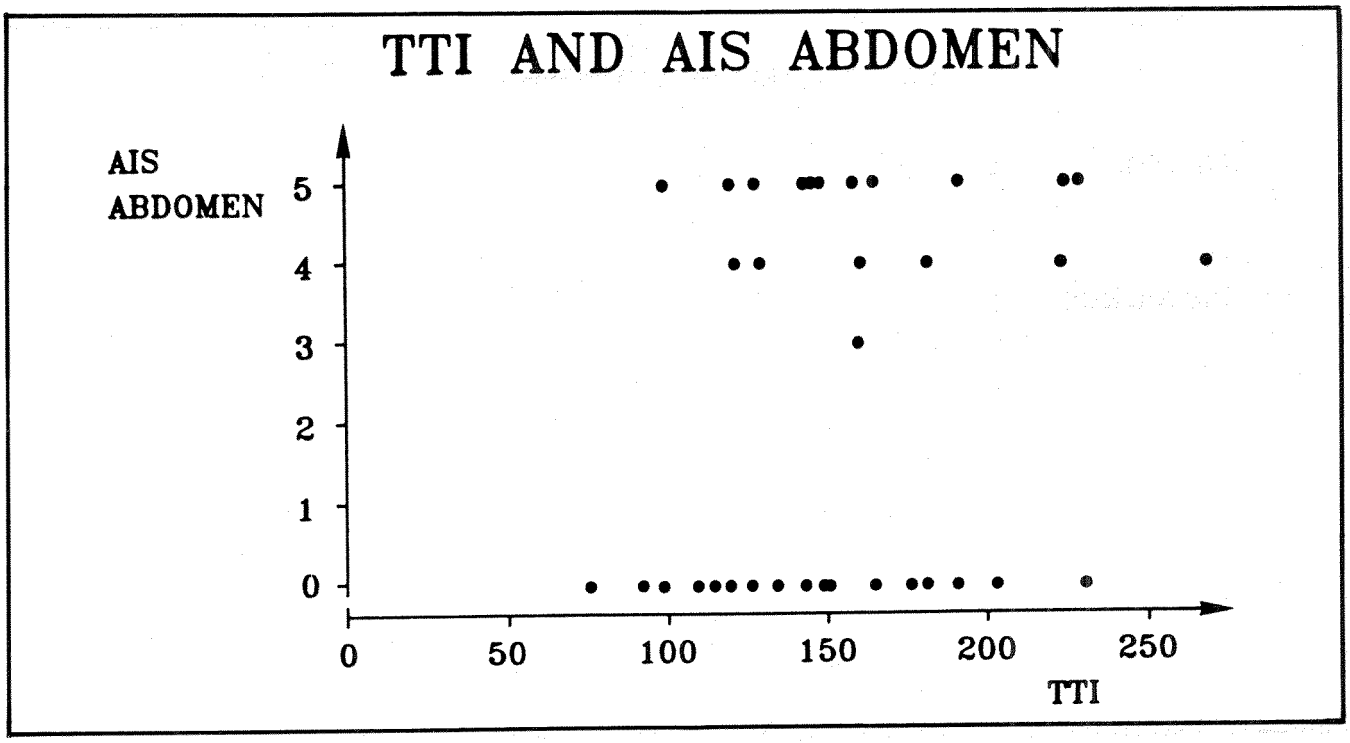

Figure 23.

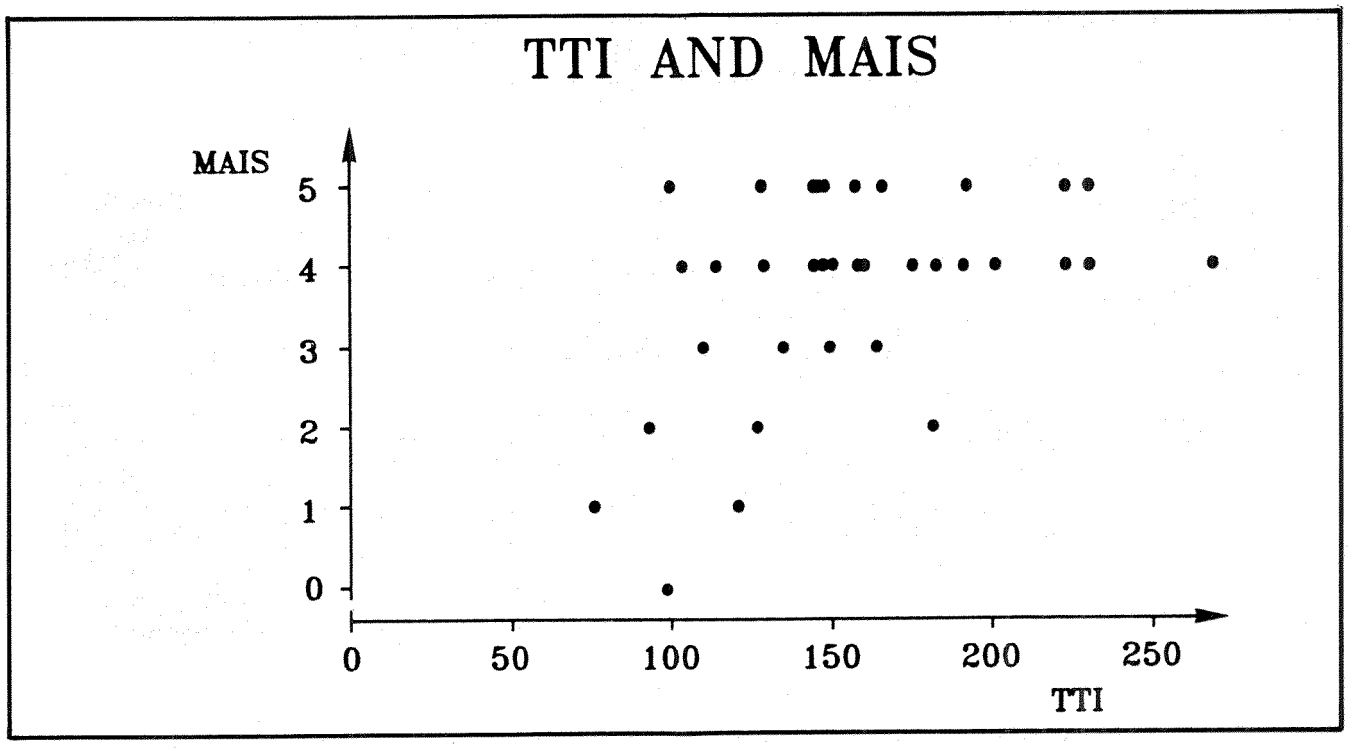

Figure 24.

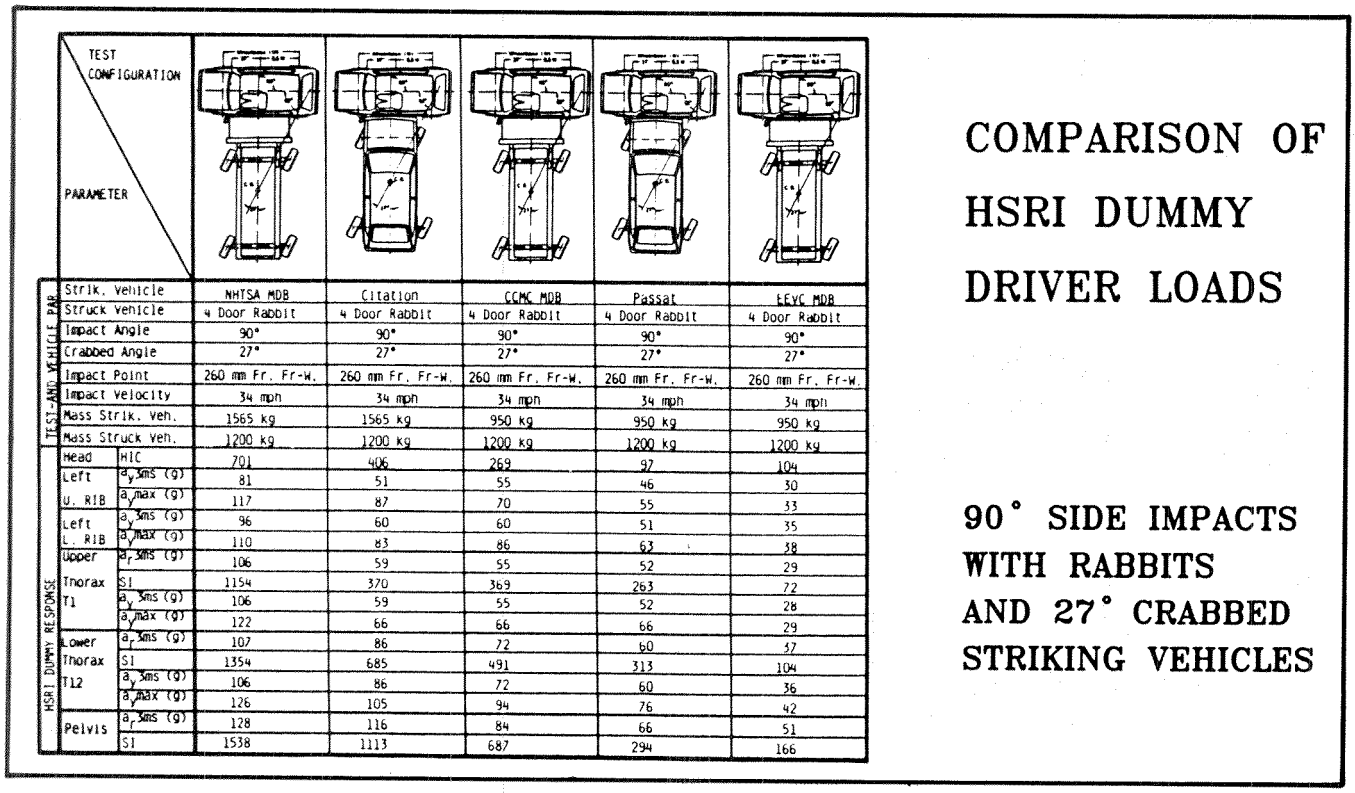

	TEST CONFIGURATION / PARAMETER						
TEST AND VEHICLE PAR	Strik. Vehicle		NHTSA MDB	Citation	CCMC MDB	Passat	EEVC MDB
	Struck Vehicle		4 Door Rabbit	4 Door Rabbit	4 Door Rabbit	4 Door Rabbit	4 Door Rabbit
	Impact Angle		90°	90°	90°	90°	90°
	Crabbed Angle		27°	27°	27°	27°	27°
	Impact Point		260 mm Fr. Fr-W.	260 mm Fr. Fr-W.	260 mm Fr. Fr-W.	260 mm Fr. Fr-W.	260 mm Fr. Fr-W.
	Impact Velocity		34 mph	34 mph	34 mph	34 mph	34 mph
	Mass Strik. Veh.		1565 kg	1565 kg	950 kg	950 kg	950 kg
	Mass Struck Veh.		1200 kg	1200 kg	1200 kg	1200 kg	1200 kg
HSRI DUMMY RESPONSE	Head	HIC	701	406	269	97	104
	Left U. RIB	a_y 3ms (g)	81	51	55	46	30
		a_y max (g)	117	87	70	55	33
	Left L. RIB	a_y 3ms (g)	96	60	60	51	35
		a_y max (g)	110	83	86	63	38
	Upper Thorax T1	a_r 3ms (g)	106	59	55	52	29
		SI	1154	370	369	263	72
		a_y 3ms (g)	106	59	55	52	28
		a_y max (g)	122	66	66	66	29
	Lower Thorax T12	a_r 3ms (g)	107	86	72	60	37
		SI	1354	685	491	313	104
		a_y 3ms (g)	106	86	72	60	36
		a_y max (g)	126	105	94	76	42
	Pelvis	a_r 3ms (g)	128	116	84	66	51
		SI	1538	1113	687	294	166

Figure 25.

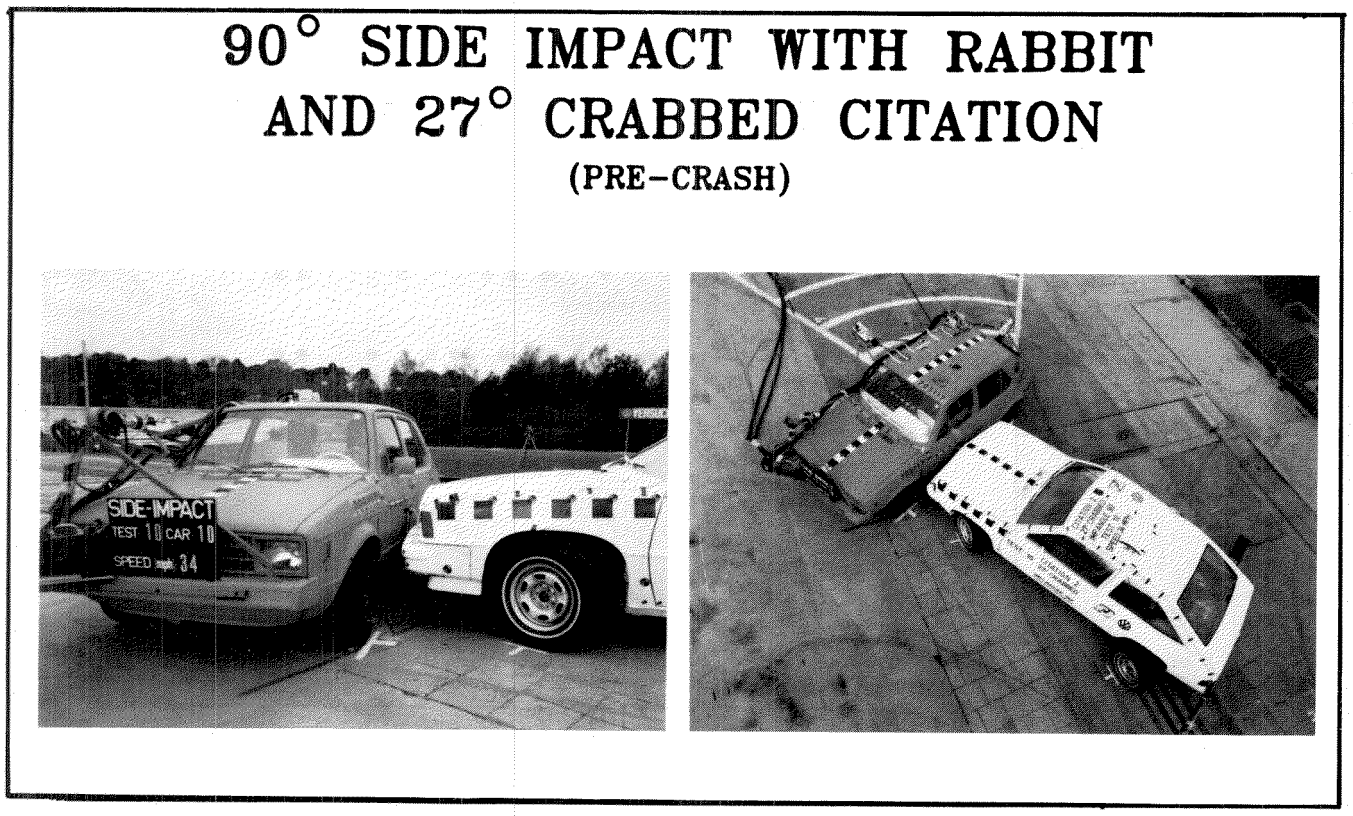

Figure 26.

90° SIDE IMPACT WITH RABBIT AND 27° CRABBED CITATION

(POST-CRASH)

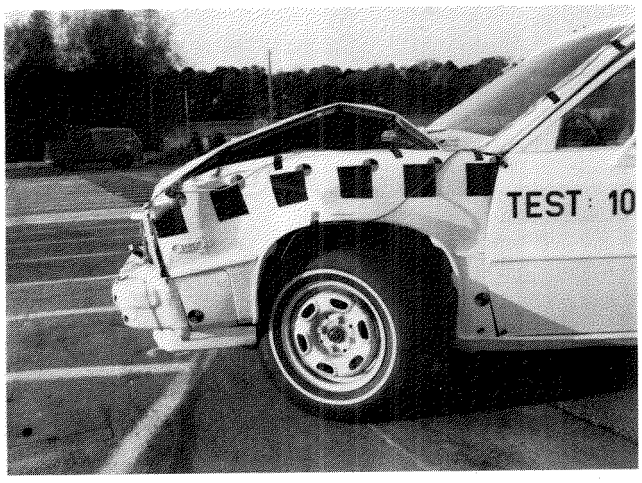

Figure 27.

90° SIDE IMPACT WITH RABBIT AND 27° CRABBED CCMC BARRIER

(PRE-CRASH)

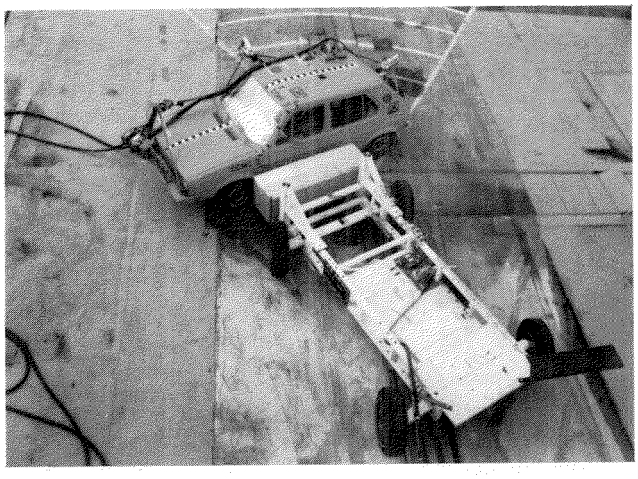

(NHTSA BARRIER CHASSIS AND CCMC DEFORMABLE ELEMENT)

Figure 28.

90° SIDE IMPACT WITH RABBIT AND 27° CRABBED CCMC BARRIER

(POST-CRASH)

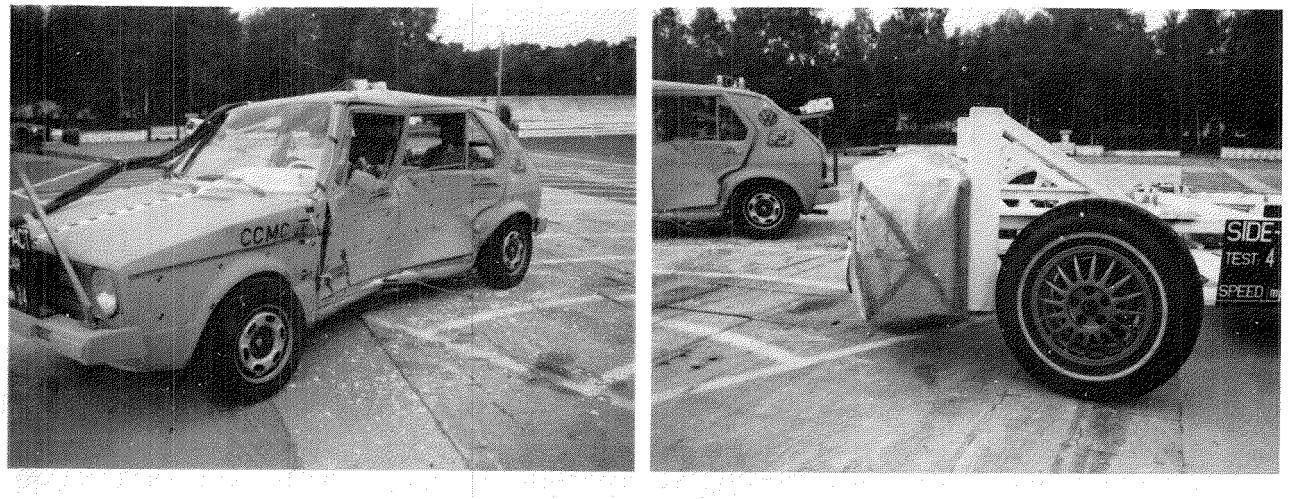

(NHTSA BARRIER CHASSIS AND CCMC DEFORMABLE ELEMENT)

Figure 29.

90° SIDE IMPACT WITH RABBIT AND 27° CRABBED NHTSA BARRIER

(PRE-CRASH)

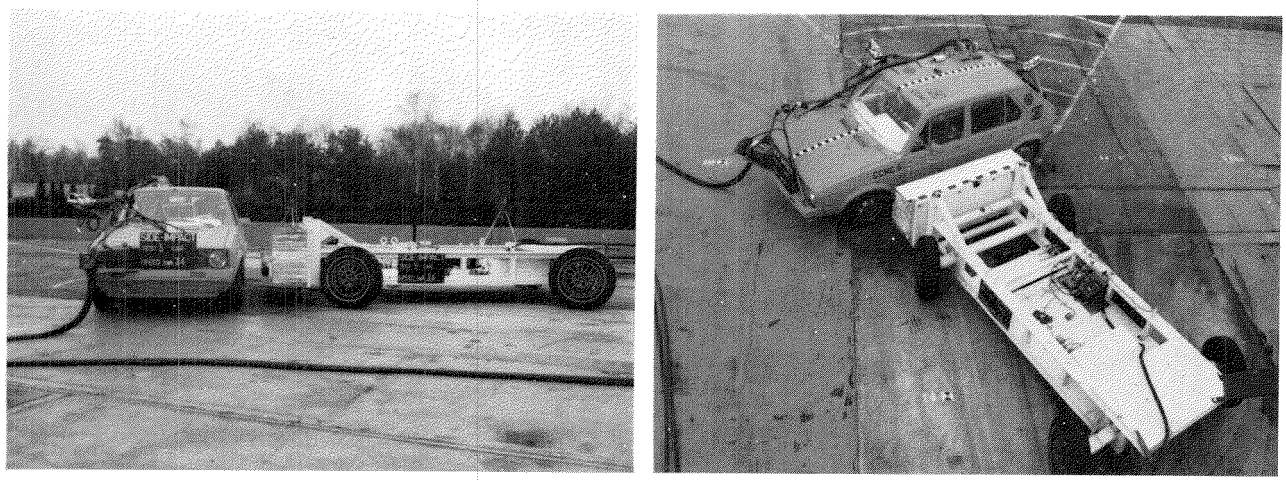

Figure 30.

90° SIDE IMPACT WITH RABBIT AND 27° CRABBED NHTSA BARRIER

(POST-CRASH)

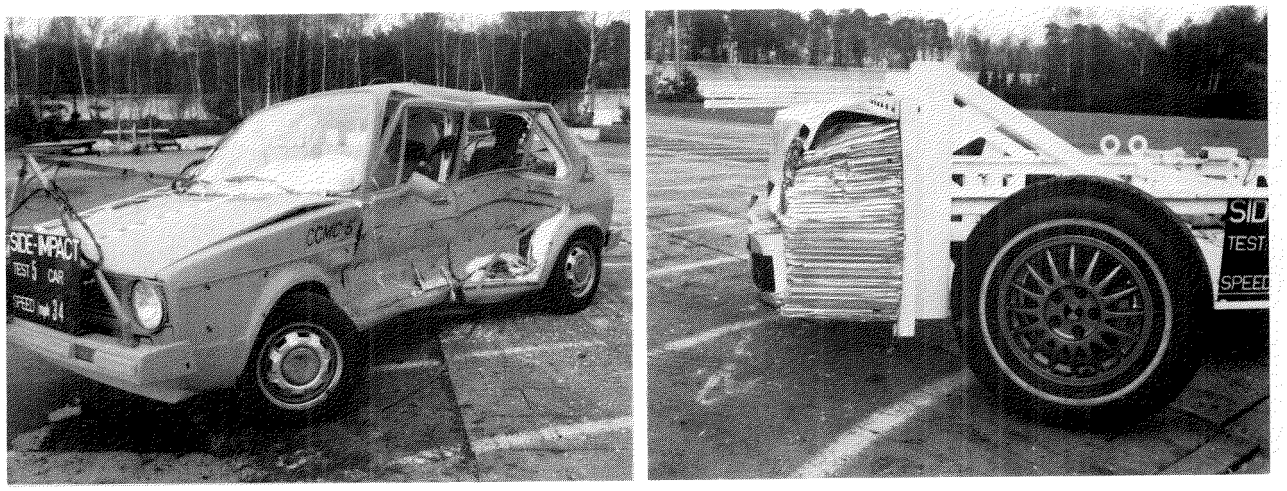

Figure 31.

90° SIDE IMPACT WITH RABBIT AND 27° CRABBED PASSAT

(PRE-CRASH)

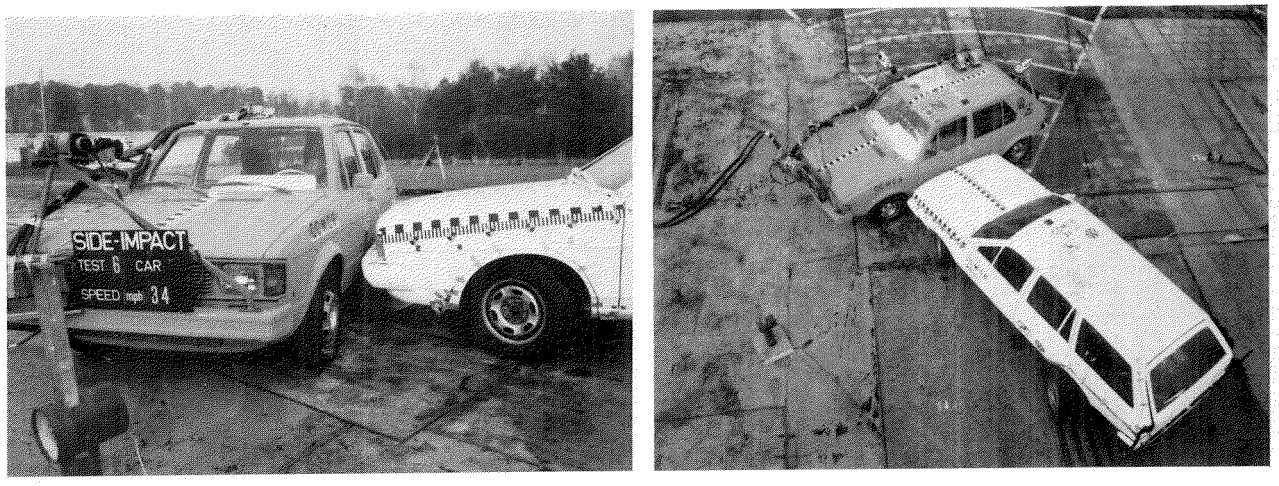

Figure 32.

90° SIDE IMPACT WITH RABBIT AND 27° CRABBED PASSAT

(POST-CRASH)

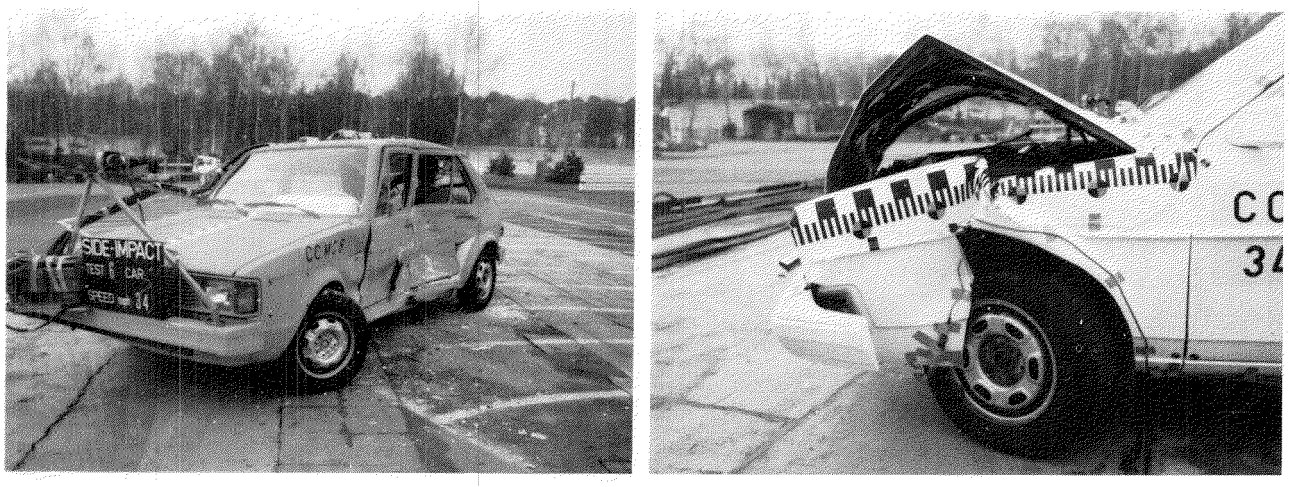

Figure 33.

90° SIDE IMPACT WITH RABBIT AND 27° CRABBED EEVC BARRIER

(PRE-CRASH)

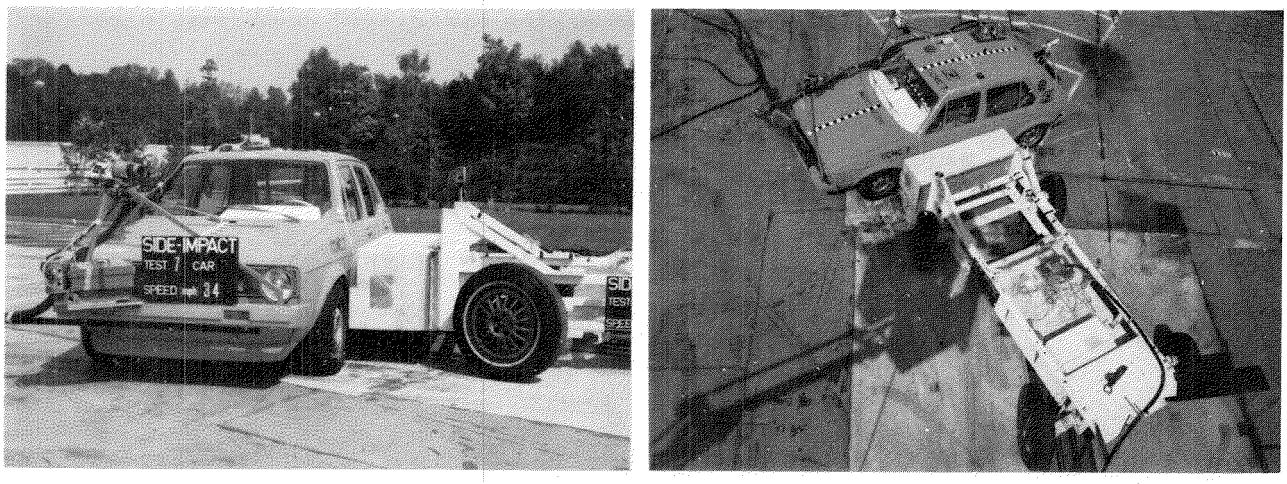

(NHTSA BARRIER CHASSIS AND EEVC DEFORMABLE ELEMENT)

Figure 34.

90° SIDE IMPACT WITH RABBIT AND 27° CRABBED EEVC BARRIER

(POST–CRASH)

(NHTSA BARRIER CHASSIS AND EEVC DEFORMABLE ELEMENT)

Figure 35.

COMPARISON OF HSRI DUMMY DRIVER LOADS

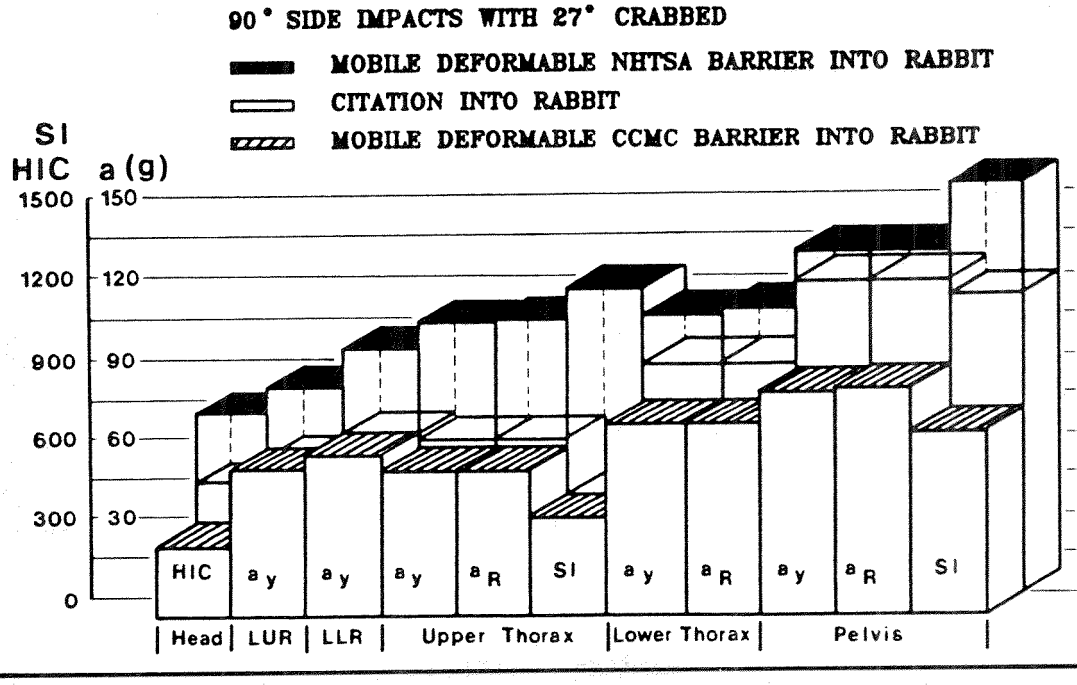

Figure 36.

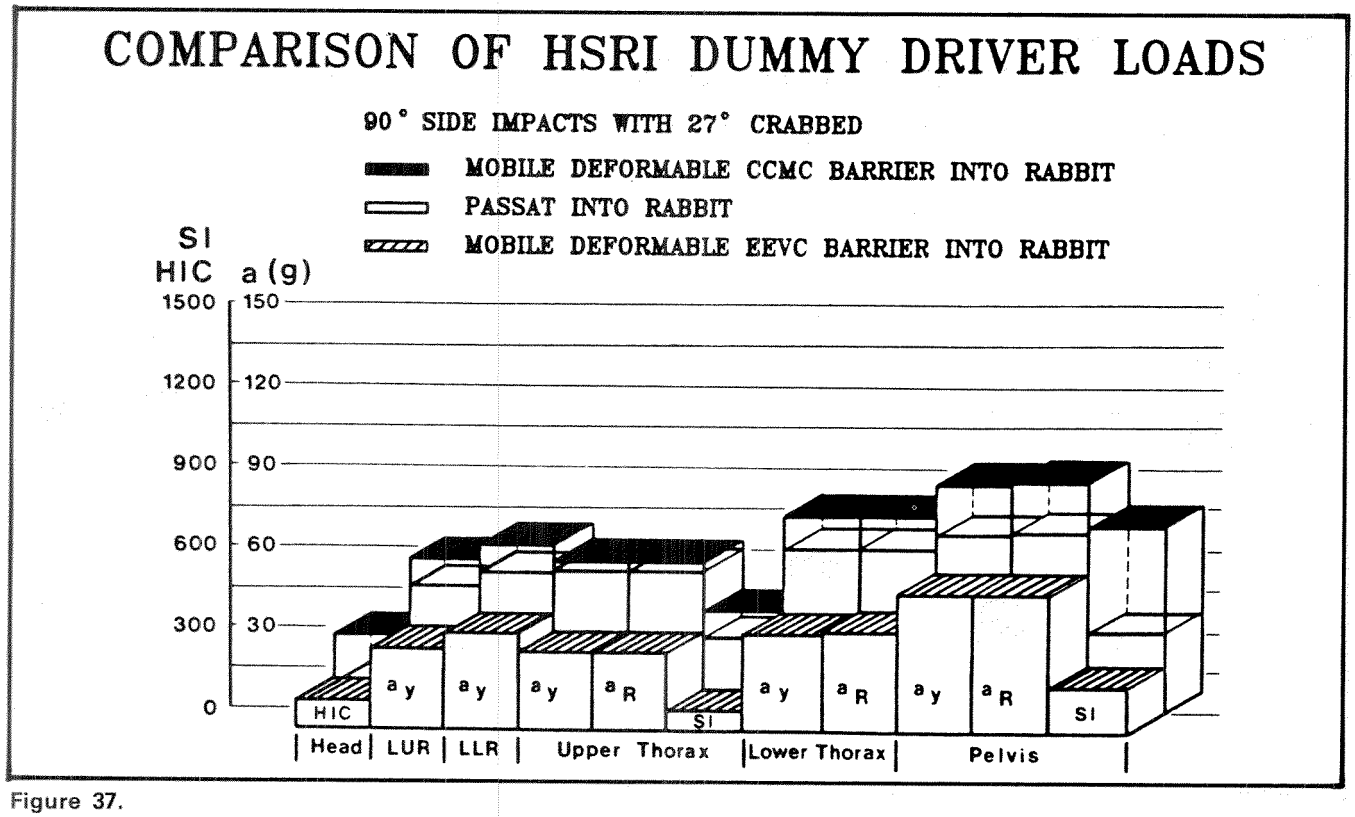

Figure 37.

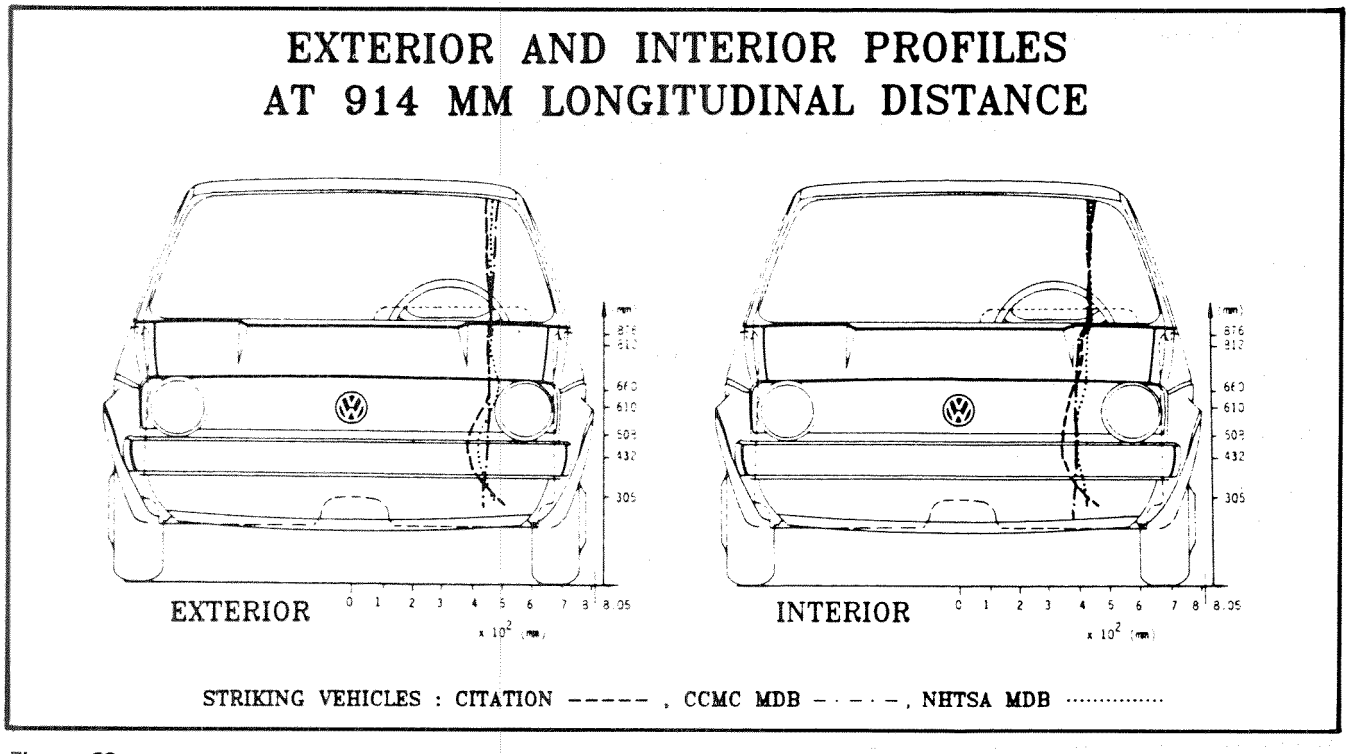

Figure 38.

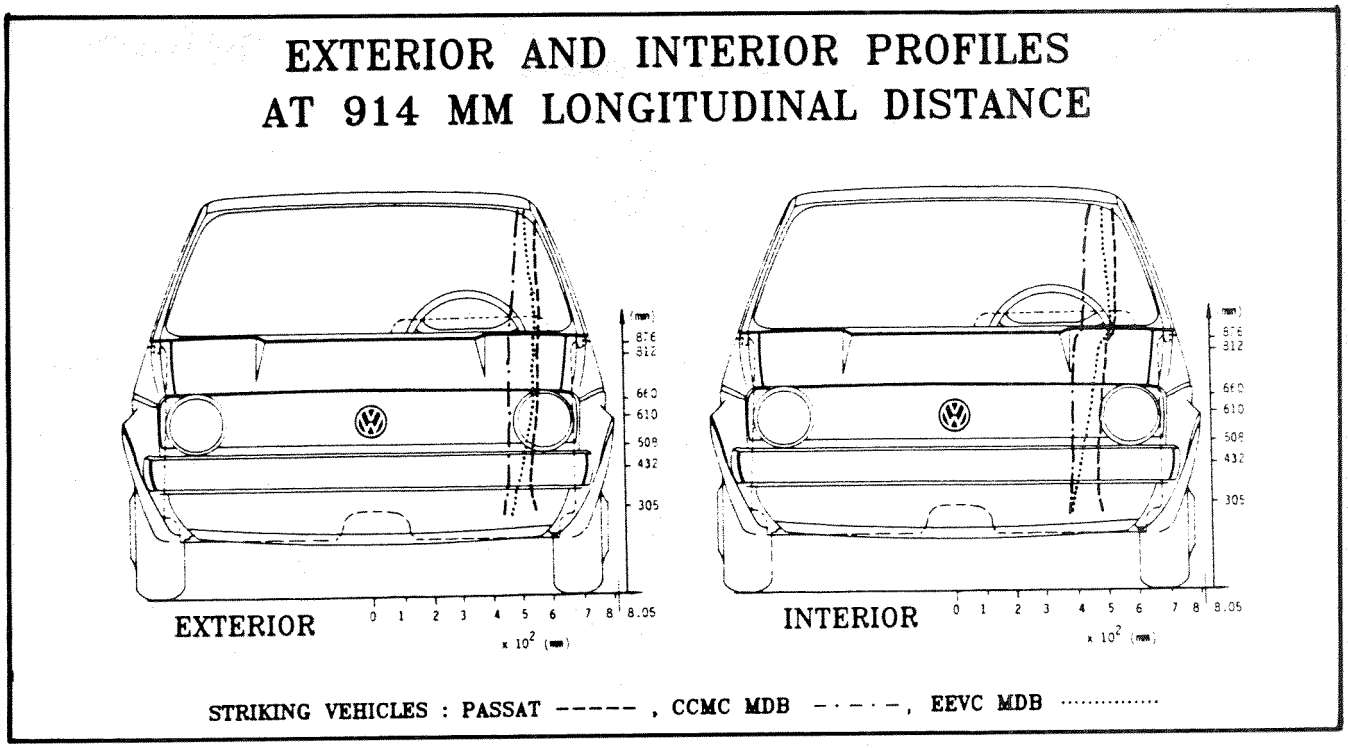

Figure 39.

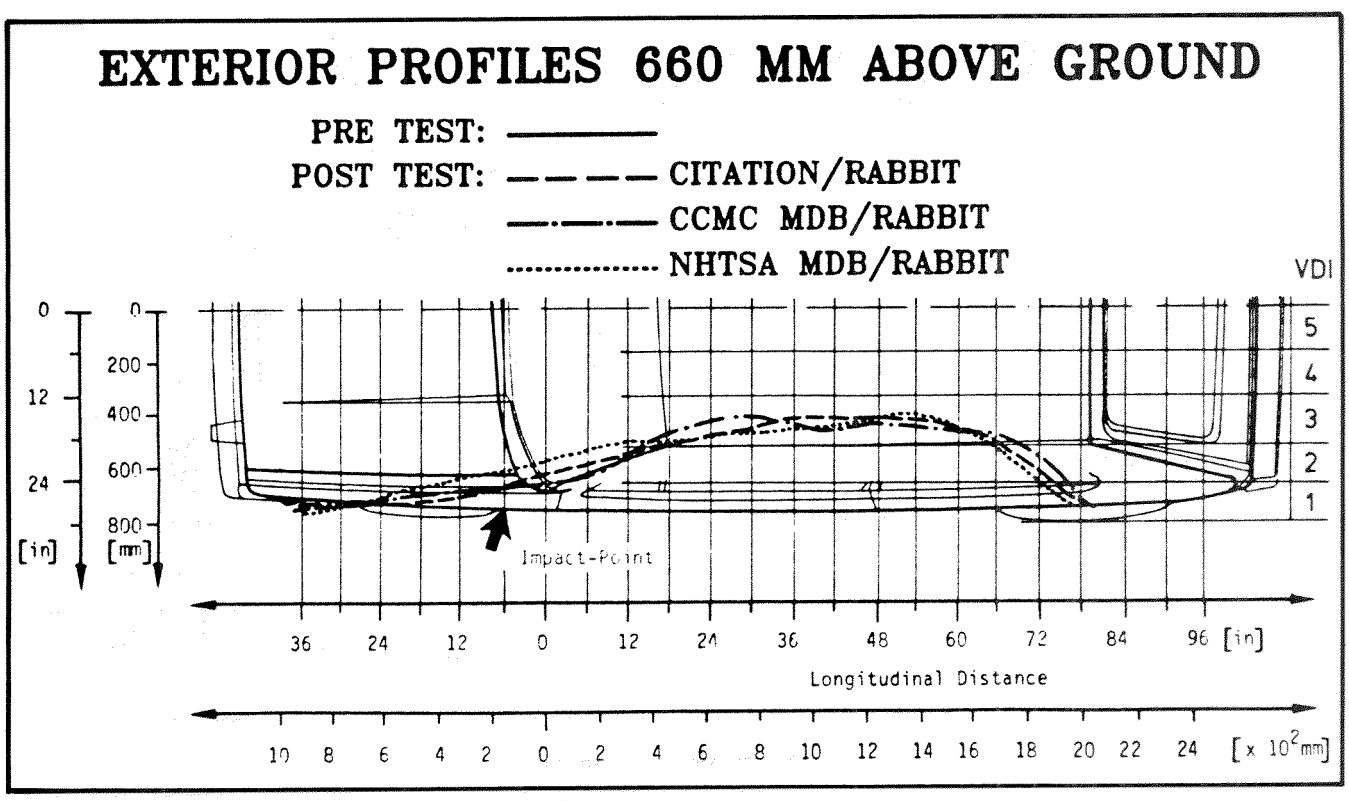

Figure 40.

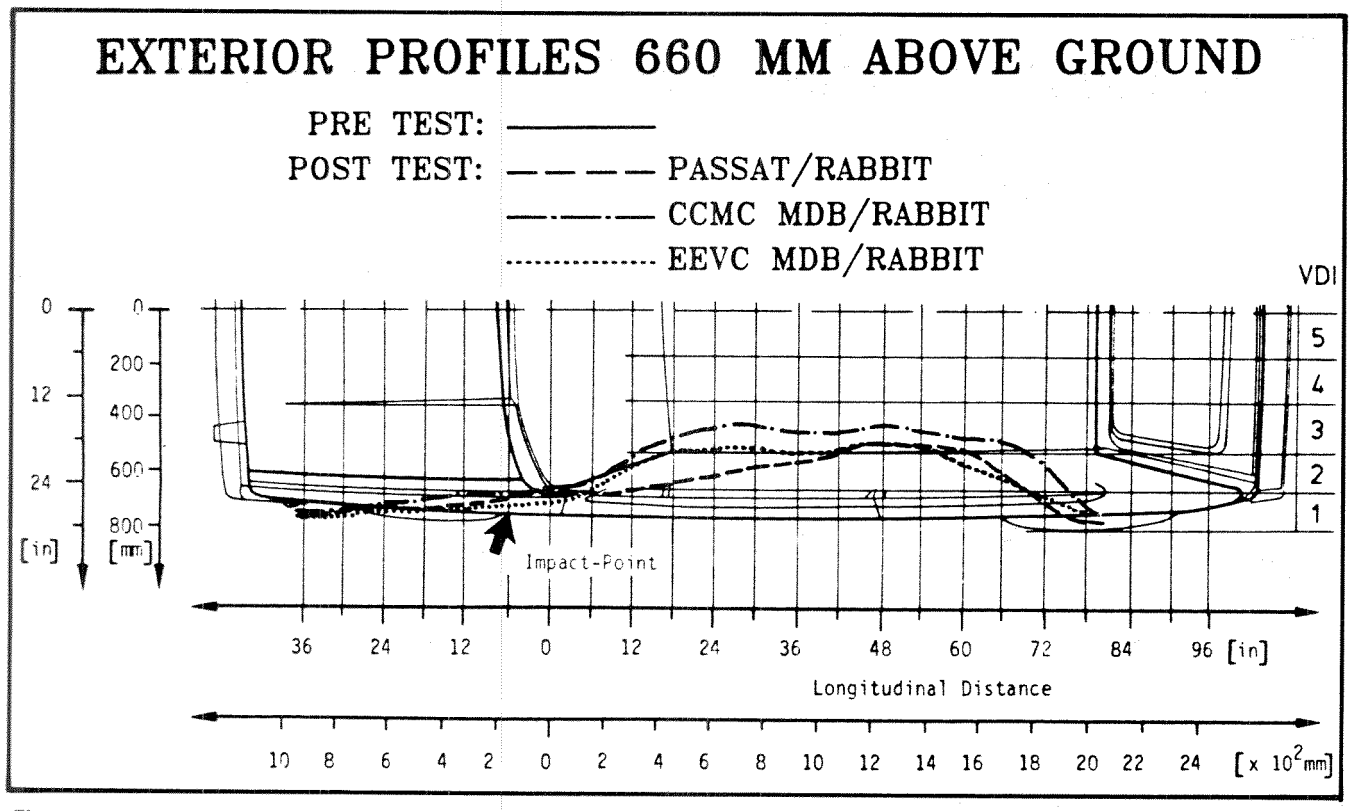

Figure 41.

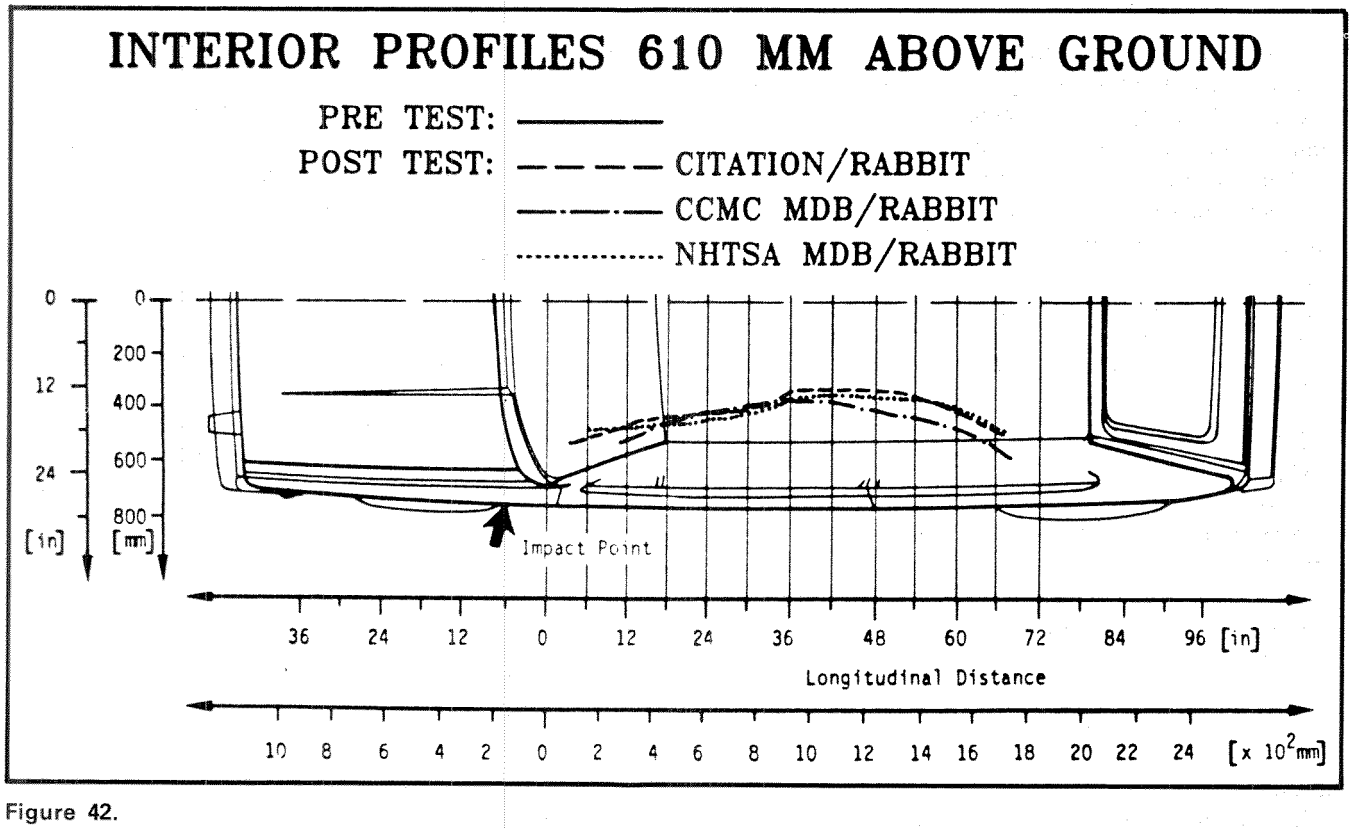

Figure 42.

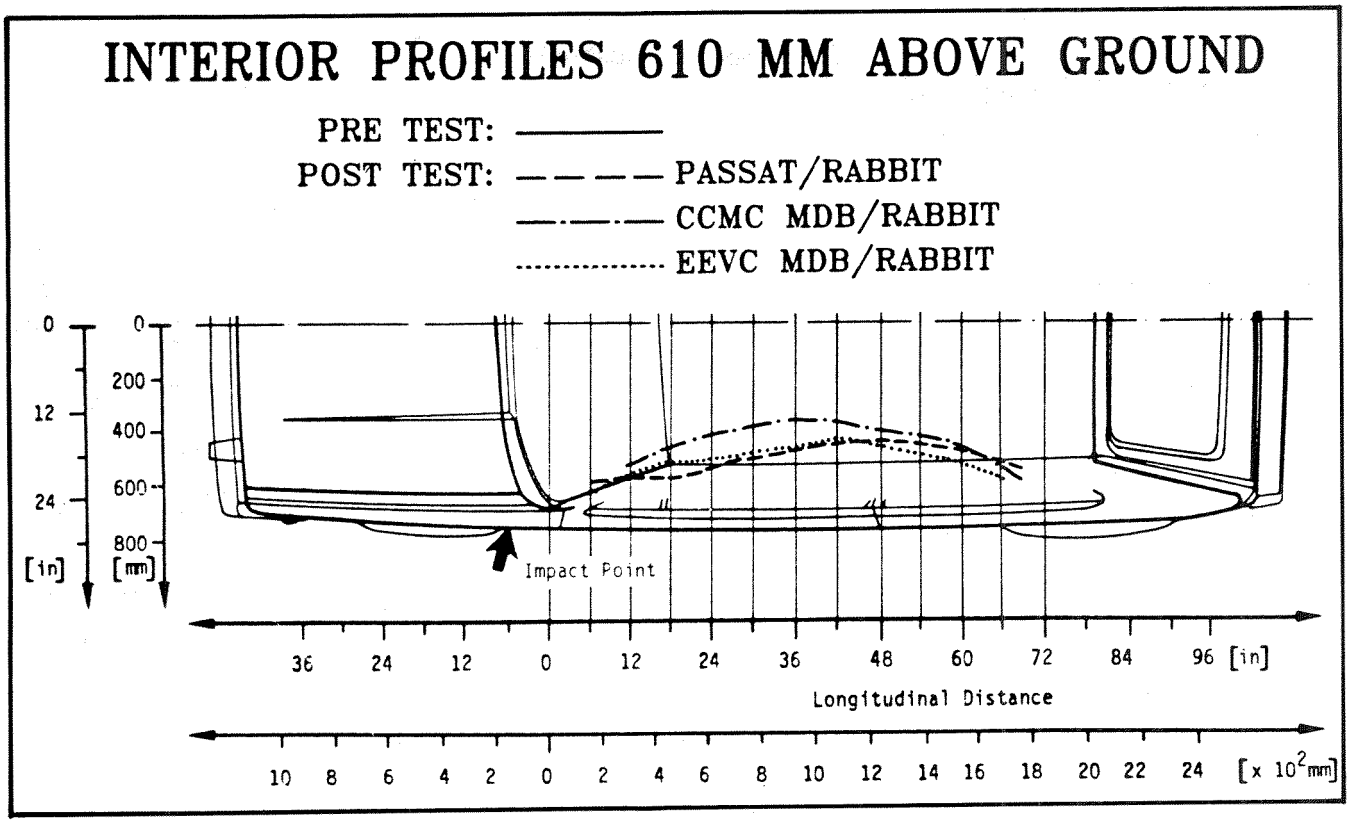

Figure 43.

Conclusion

This report discusses the suitability of deformable barriers and dummies as test devices for the standardized side impact. Comparative evaluation demonstrates that while the available test devices also constitute a basis for further research activities for the development of side impact test procedures, the comprehensive and necessary research activities cannot be viewed as having been completed.

So that the effectiveness of measures for the further increase of occupant protection in side impacts will not be jeopardized and can be appropriately applied to real-world accidents, biofidelity of dummies must be greatly improved and the correlation of dummy loadings and occupant injuries must be reliably established. The FAT project(6) provides a useful foundation for these efforts.

An important further goal must be the development of omnidirectional dummies capable of being used throughout the world. Such a development effort must include a computer simulation and mathematical description of the very complex spring-damper-mass system to analyze fully the complex interactions of individual body parts and other relevant parameters. The FAT project also provides a basis for the validation of the mathematical dummy model.

The extent to which the newly developed European side impact dummy correlates with respect to kinematics and loadings with human subject behavior requires evaluation within the scope of the FAT project as soon as a sufficient number of prototypes becomes available.

The comparative evaluations with the CCMC, EEVC, and NHTSA barriers as well as with average European and American passenger cars, combined with the experience gained during repeatability testing at the Dutch Research Institute TNO and tests at BASt (German "Bundesanstalt für Straßenwesen"), Ford, FAT, and CCMC, indicate that the deformable element developed by CCMC constitutes a good compromise for a model of the front structure deformation behavior of the average European and American passenger car. As noted, a joint European and American research program, as already initiated between MVMA and CCMC, is warranted and needed to develop a common test device based on the crabbed NHTSA barrier chassis and the CCMC deformable element for lateral collision testing.

Dummy response data in lateral impacts with the NHTSA barrier and NHTSA deformable element differ substantially in all regions from data obtained in tests with the average American car, the Citation, as defined by NHTSA.

The EEVC deformable element is similar in design to the CCMC element. It is manufactured by the same firm (Fritzmeier) and consists of the same PU foam material. As previously discussed(10), the F/D characteristics of the EEVC element are softer than those of the average

European passenger car and those of the CCMC barrier. Because of the common features of both elements, a joint research effort by CCMC and EEVC will result in a European element that, with respect to deformation characteristics and design, will more closely resemble the CCMC element.

This finding, together with the knowledge that the European and American lateral accident experiences are largely similar, should constitute the basis for further research efforts with respect to a common European and American test device for 90° lateral impact testing. A reasonable and acceptable compromise appears to be represented by the 27° crabbed chassis of the NHTSA barrier with a total mass of 1,100kg in combination with the CCMC deformable element, with a ground clearance of 250mm. This element will cost less than DM1,000 in mass production. In contrast to the NHTSA element(4), the CCMC element is not shipping-sensitive, not sensitive to slight exterior cracks, and constitutes representation of the front structure deformation behavior of the average European and American passenger cars.

This approach should be viewed as a step toward a harmonization of future side impact performance requirements.

References

1. Klaus, G., R. Sinnhuber, and G. Hoffmann, "Mobile deformable barrier for lateral collision testing—a contribution toward a harmonization of future side impact performance requirements," SAE Paper 840888, Government/Industry Meeting, Washington, D.C., 1984.
2. Peugeot SA-Renault Laboratory of Physiology and Biomechanics Accidentology Section, "Side impact collisions, accidentological summary report," June 1983.
3. NHTSA/MVMA Coordinated Research, "Side impact test procedure development," Task 1, September 1982.
4. Seiffert, U., Volkswagen Research Division, "Research M.I.V., modified integrated vehicle," NHTSA Contract DTNH 22-81-C-17085, September 1983.
5. HUK, TU Berlin, Volkswagenwerk AG, "Entwicklung kompatibler Fahrzeuge," Research project sponsored by the German Federal Government, Ministerium für Forschung und Technologie, February 1980.
6. Klaus, G., R. Sinnhuber, G. Hoffmann, D. Kallieris, and R. Mattern, "Side impact—a comparison between dummies and cadavers, correlations between cadaver loads and injury severity," SAE Paper 841655, Proceedings 28th Stapp Car Crash Conference, Chicago, 1984.
7. Resolutions Taken at the 14th Meeting of ISO/TC 22/SC 10, Impact Test Procedures, M 191 E, AFNOR La Defense, Paris, 1984.
8. Klaus, G., and D. Kallieris, "Side impact—A comparison between HSRI, APROD and Hybrid II dummies and cadavers," SAE Paper 831630, Proceedings 27th Stapp Car Crash Conference, San Diego, 1983.
9. Eppinger, R.H., J.H. Marcus, and R.M. Morgan, "Development of dummy and injury index for NHTSA's thoracic side impact protection research program," Government/Industry Meeting, SAE Paper 840885, Washington, D.C., 1984.
10. Pullwitt, E., and W. Sievert, Bundesanstalt für Straßenwesen, "Feasibility of the side impact test procedure proposed by EEVC," Final report, Contract A0/83/394, Bergisch Gladbach, June 1984

Occupant Response Sensitivity Analyses Using a Lumped Mass Model in Simulation of Car-to-Car Side Impacts

Thomas J. Trella
Transportation Systems Center, Research and Special Programs Administration

Joseph N. Kanianthra
U.S. Department of Transportation, National Highway Traffic Safety Administration

Abstract

Results of a sensitivity study, based on lumped spring/mass modeling approaches for the characterization of structural and occupant responses in 60° and 90° side impacts, are presented in this paper. Test data from collisions between a moving deformable barrier (MDB) and the side of a Volkswagen Rabbit in two crash configurations, simulating 60° and 90° impacts, are used to derive the force-deflection characteristics of the non-linear springs in the model.

The mathematical model is used to investigate the sensitivity of occupant responses to parametric changes in the striking and struck car characteristics. The variables included in this parametric study are striking vehicle and struck vehicle stiffnesses, crash configuration, impact velocity, occupant-to-door clearances, and padding characteristics. The striking car and struck car side stiffnesses are varied in the range of ±40 percent and ±30 percent, respectively, from the nominals. The effects of padding material characteristics and padding thicknesses up to 6in are evaluated. The effects of the above parametric changes on predicted thoracic probability of injury using the National Highway Traffic Safety Administration (NHTSA) Thoracic Trauma Index (TTI)(1) are also presented.

The results showed that the rib, spine, and pelvis peak accelerations generally increased with increases in striking vehicle stiffness and impact velocity. Increases in struck car side stiffness and the addition of door padding reduced the peak rib, pelvis, and spine accelerations. The results indicate padding is very effective in reducing the thoracic probability of injury. It is observed that the probability of injury at Abbreviated Injury Scale (AIS) levels of 3 or greater in a 30-year-old male will be reduced from 50 to 20 percent by adding a 3in-thick padding in a 90° collision with the striking car moving at 26mph and the struck car moving at 13mph, respectively. It is also observed that the relative effectiveness of the above changes in vehicle characteristics is a function of impact speed.

Introduction

Results of side impact sensitivity analyses based on lumped mass collision modeling studies that characterize parametrically the lateral acceleration response levels of a normally seated driver dummy in the struck vehicle are discussed. The crash configuration studied for the characterization of driver and structural responses was a stationary target vehicle (2-door, VW Rabbit) that was struck by a crabbed MDB simulating a two-car collision when both vehicles are moving. The impacts were on the driver's side door and surrounding structures (A- and B-pillars) at 90° and 60° as shown in Figure 1. These

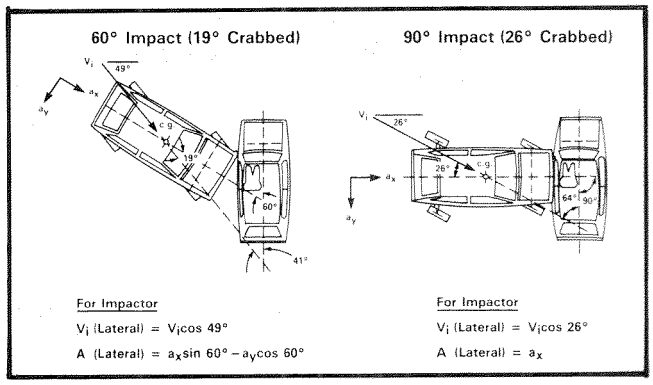

Figure 1. Crash configuration

configurations simulate side impacts where the striking and struck vehicles moved at 26 and 13mph (low-speed condition), and 35 and 17.5mph (high-speed condition). This corresponds to MDB closing speeds of approximately 29 and 39mph (26 and 35mph lateral velocity) for the 90° low- and high-speed conditions, respectively. The 60° impact MDB closing speeds were approximately 34 and 46mph (22 and 30mph lateral velocity) for the low- and high-speed conditions, respectively. In this study, the influence of striking vehicle stiffness, struck vehicle side stiffness, impact angle, impact velocity, and padding thickness and stiffness were parametrically investigated.

The characterization effort was performed in three parts. First, the dummy's pelvic and upper thorax (rib and spine) peak acceleration levels were determined from simulations in which the parameters listed above were varied. Based on these results, the sensitivities of the dummy's peak accelerations (G's) to changes in those parameters were derived. Last, thoracic probability of injuries were computed, based on the NHTSA TTI.

Validations were carried out comparing the simulation and test results. In this paper, special emphasis is given to defining driver dummy response trends.

Side Impact Model and Characteristics

The sensitivity results were derived from the one-dimensional lumped parameter nonlinear spring mass model(2) shown in Figure 2. Basically, this model is a modified version of the CRUSH model (Crash Reproduction Using Static History)(3) with a lumped mass representation of the upper thoracic as well as the pelvic regions of an unrestrained occupant. The crush of the struck vehicle's side structure is represented in this model as a nonlinear spring connecting the side door structure and compartment. The occupant simulation is based on a simple model, mainly to predict the thoracic response and probability of injury, and, therefore, does not include the head-to-interior surface contact elements. Model validations were performed by simulating three different crash conditions. These involved a baseline VW Rabbit in a 90° impact (BL-90°), a structurally modified VW Rabbit in a 90° impact (MOD-90°), and a baseline VW Rabbit in a 60° impact (BL-60°).

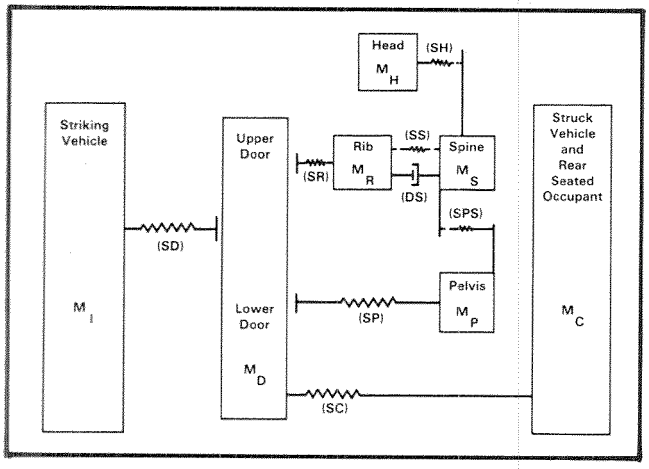

Figure 2. Side impact lumped spring/mass model

Four masses (rib, pelvis, spine, and head) with three nonlinear interconnecting springs and a damping element were used to model the occupant. The rib- and pelvis-to-door contacts were represented by two nonlinear springs. Padding was introduced as a spring between the dummy and the door. A ¾in bottomed-out thickness was assumed for all pad thicknesses considered in this study. In this investigation, the connection between the spine and pelvis was neglected. The pelvis was positioned 4in from the inner surface of the door for the sensitivity calculations. The rib-to-door clearance was composed of the pelvis-to-door clearance and the rib-to-pelvis spacing derived from accelerometer data in side impact tests using Side Impact Dummies (SID's). Rib-to-spine damping was provided by means of a viscous damper. In this model, head motions were assumed coupled directly to the spine by means of a nonlinear spring. Head contact with the side structure was not modeled.

The force-deflection properties for the modified CRUSH model were derived from acceleration traces obtained from the side impact tests in (4). Experimental accelerometer time histories of the inner surface of the door were used for this purpose. The MDB's longitudinal and lateral responses were resolved in the direction perpendicular to the side of the struck vehicle, since only the lateral motions were of concern in this collision-modeling effort. The force-deflection characteristics were based on the low impact speed (26/13mph[1]) crash test results since the force versus deflection traces derived from other speed conditions indicated that the dynamic rate effects were small. For the simulations, the force-deflection diagrams were approximated by segmented straight line elements to (a) eliminate higher order oscillations, (b) eliminate multivalued forces due to instrumentation system inaccuracies and incompleteness of the choice of the lumped mass model used in the derivation of the force-deflection characteristics, and (c) extend the range of applicability of the model to other speed conditions. Figure 3 shows the force-deflection diagrams for impactor-to-door spring (SD) and door-to-compartment spring (SC) for the three crash conditions.

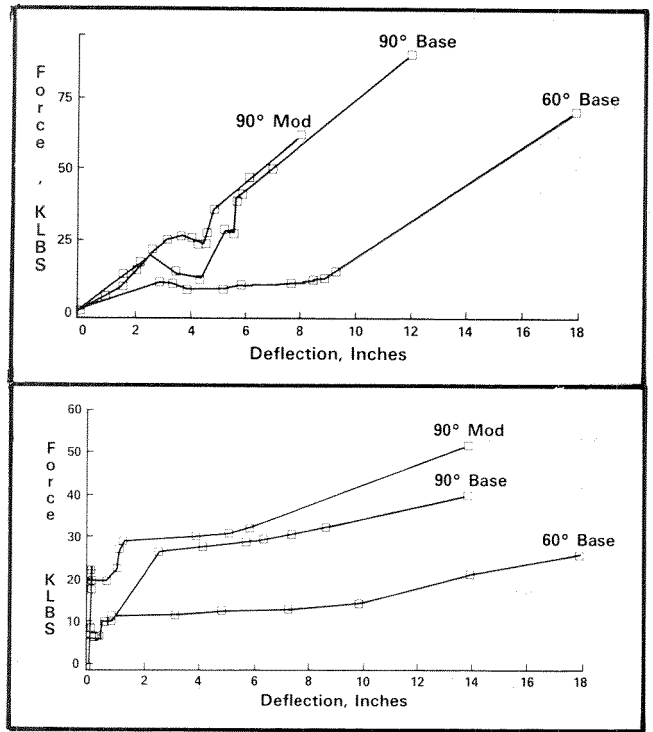

Figure 3. Assumed force versus deflection for springs SD and SC in CRUSH

The MOD-90° force versus deflection traces shown in these diagrams were obtained from the VW Rabbit MOD-90° impact padded door crash test time histories. Door padding force-deflection characteristics were based on a nonlinear expression developed from the measured

[1] Denotes the striking and struck vehicle collision speeds, respectively.

force-deflection characteristics of a General Tire and Rubber (GTR) pad used in the side impact car crash tests(4,5). This expression provided the GTR pad force level as a function of its bottomed-out thickness, a force level coefficient, a padding displacement, and a shape coefficient(2). Figure 4 shows the analytically derived GTR pad force-deflection trace for a 4.0in-thick sample.

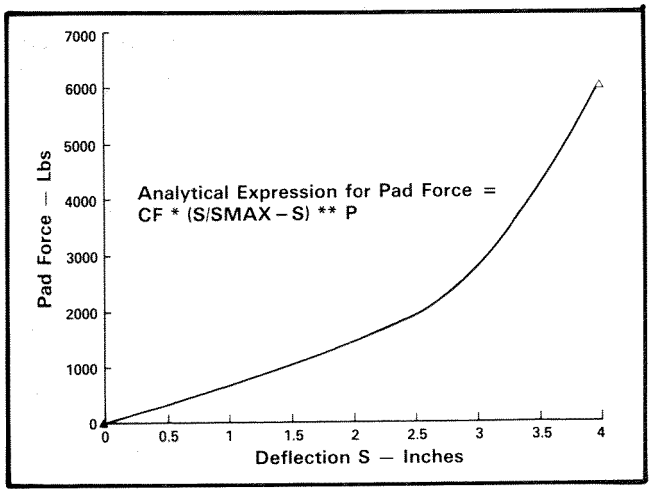

Figure 4. Analytically derived force versus deflection for the GTR pad

26/13mph and 35/17.5mph speed conditions. The calculated responses appear to show reasonable levels of agreement in terms of peak G levels for the rib, pelvis, and spine for the test conditions simulated. These simulated dummy peak G levels are based on the acceleration-derived pelvis-to-door and rib-to-door clearances derived from the dynamic crash tests. (For the 90° impact simulations, 5.20in was assumed for the pelvis-to-door clearance and 8.02in was assumed for the rib-to-door

Table 1. Weight data

	Weight (lb)		
Impact Angle	90°	90°	60°
Configuration	BL	MOD	BL
Impactor	3006.0	2990.0	2990.0
VW-Rabbit			
Door	30.0	30.0	30.0
PX-Compartment	2276.0	2224.0	2459.0
Driver Dummy			
Rib	20.0	20.0	20.0
Pelvis	79.0	79.0	79.0
Spine	32.0	32.0	32.0
Head	10.0	10.0	10.0
VW-Vehicle-Test Weight	2447.0	2395.0	2630.0

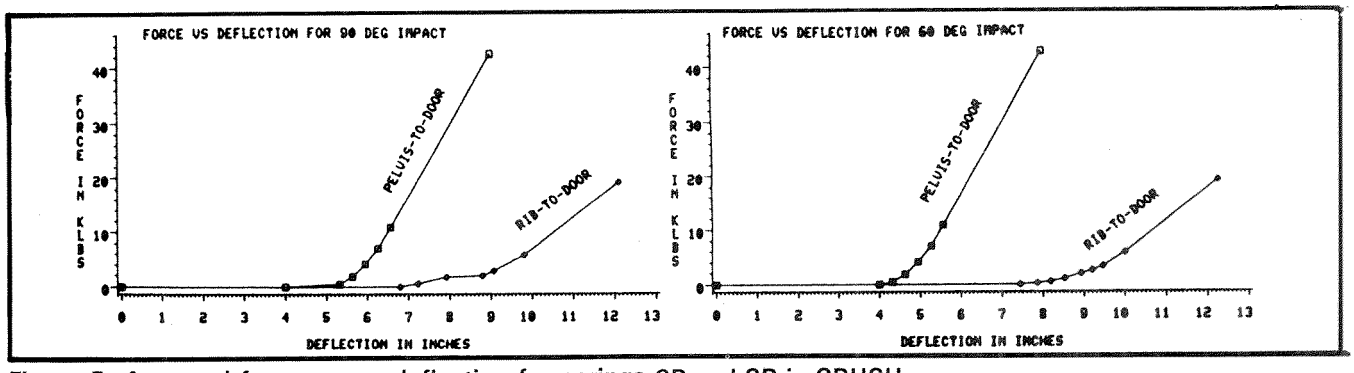

Figure 5. Assumed force versus deflection for springs SP and SR in CRUSH

Force-deflection traces are also illustrated in Figure 5 for the rib-to-door (SR) and pelvis-to-door (SP) contact. The rib-to-spine spring (SS) force-deflection characteristics, the head-to-spine spring (SH) characteristics, and all other model inputs are as shown in (2). Table 1 summarizes the component weights used for the three crash conditions that represent the best estimates for the purpose of this lumped mass modeling.

Model Validations With Characterization Test Data

Before conducting the sensitivity studies, the lumped mass model was validated with experimental data over two impact speeds. The results are shown in Figure 6, which compares the simulated peak acceleration responses of the three body components in the 90° test at the

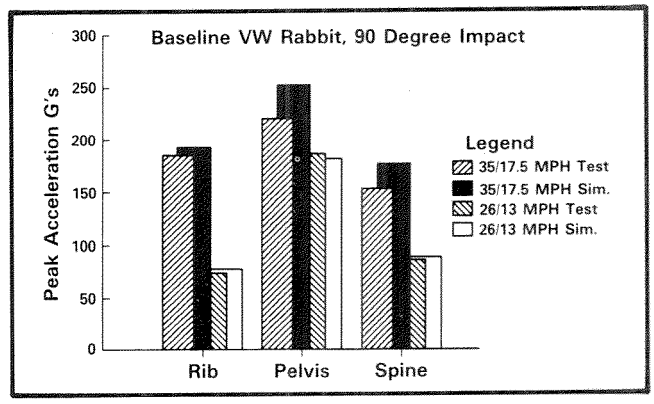

Figure 6. Comparison of simulated responses and test results at two impact speeds

clearance in the BL-90° impact.) Note, these clearances are different from the clearances used to calculate the

sensitivities discussed in the following sections where the pelvis was positioned 4in from the door.

Model Considerations

The sensitivity results discussed in this paper are influenced by the weight assumed for the door structure, the rib and pelvis-to-door clearances, the pelvis-to-rib spacings, and the bottomed-out thickness assumed for the pad. Deviations from values assigned to these parameters will yield different dummy peak G levels and trends for the parametric changes investigated. For example, a different door structure and weight will produce phase shifts and response level differences. Decreasing the clearance between dummy and door to a certain clearance value will generally increase the rib and pelvis peak G levels. Further decreases in clearance from this value will reduce the occupant peak G levels since the side structure velocities increase and then decrease in time during the collision phase in response to the colliding striking vehicle. For rib response, this occupant-to-door clearance value was estimated to be about 2in(2).

Sensitivity Investigations

Parametric investigations were conducted at two impact speeds of 26/13mph and 35/17.5mph, respectively. The parameters considered included—

- Door padding (thickness and force levels)
- Struck vehicle stiffness (VW Rabbit door-to-compartment stiffness)
- Striking MDB stiffness (MDB-to-struck VW Rabbit door stiffness)

The striking MDB and struck VW Rabbit door stiffnesses were varied in the range of ±40 percent and ±30 percent, respectively, from the nominal. Three- and six-inch door padding thicknesses were investigated with the same thickness at the rib and pelvis striking points. The range of stiffness values used for the door padding varied from -20 percent to +20 percent from the nominal in increments of 10 percent. These stiffness changes were reflected in the forces obtained by multiplying the nominal force levels in the spring force-deflection diagram by factors corresponding to the percent changes described above. Note that the striking and struck car side stiffness changes obtained in this manner do not necessarily imply that the baseline (BL) VW Rabbit door structure force-deflection characteristics, when changed by a stiffness factor, should exactly reproduce the force-deflection characteristics of the structurally modified (MOD) VW Rabbit. Typical force-deflection characteristics for the striking and struck vehicles and door interior padding to occupant body component interactions are given in (2).

Finally, as a special case, some occupant peak G level trends are discussed as a result of changes to the GTR-pad shape factor (P). These trends are based on preliminary investigations of a pad analytically tailored to dissipate the impact energy more linearly as a function of its thickness. This padding characteristic is shown in Figure 7, which compares the baseline (P = 0.8) with the analytical pad (P = 0.2).

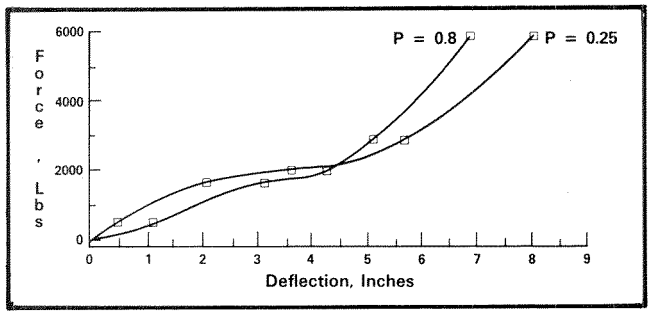

Figure 7. Combined padding and rib contact element characteristics for two different shape factors for the GTR pad

Dummy's Acceleration Response Trends

Tables 2 through 4 summarize the dummy's (rib, pelvis, spine, and head) peak G levels as a function of: (1) door padding thickness changes, (2) door-to-compartment stiffness changes, (3) MDB-to-struck-door stiffness changes, (4) padding thickness changes plus VW Rabbit door-to-compartment stiffness changes, and (5) padding thickness changes plus MDB-to-struck-door stiffness changes. These simulated responses correspond to the BL-90° and MOD-90° crash conditions for impact speeds of 26/13mph and 35/17.5mph, respectively, and the BL-60° crash conditions for an impact speed of 26/13mph.

In general, for the range of variables considered, the simulated results indicate that—

Dummy (rib, pelvis, and spine) peak G levels decreased when—

(1) The thickness of the GTR door padding was increased; and

(2) The VW Rabbit door-to-compartment stiffness levels were increased.

Dummy (rib, pelvis, and spine) peak G levels increased when—

(1) The collision speed was increased; and

(2) The MDB stiffness levels were increased.

Dummy (pelvis) peak G levels increased when—

(1) The stiffness of the GTR door padding was increased.

Dummy (rib and spine) peak G levels increased when—

(1) The stiffness of the GTR door padding was decreased.

Furthermore the results presented in Tables 2 through 4 indicate that door padding thickness changes were

Table 2. Driver dummy peak acceleration levels due to padding thickness variations, VW-Rabbit door to compartment and MDB to VW-Rabbit door stiffness variations (baseline VW-Rabbit, 90° impact)*

		Rib		Pelvis		Spine		Head	
		26/13mph	35/17.5mph	26/13mph	35/17.5mph	26/13mph	35/17.5mph	26/13mph	35/17.5mph
Baseline VW-Rabbit		112.6G	239.3G	205.0G	266.1G	104.8G	200.8G	99.7G	102.6G
Baseline VW-Rabbit	3 in Gtr Pad	61.9	122.3	145.2	222.4	80.1	144.4	98.8	98.0
	6 in Gtr Pad	55.2	97.5	82.4	153.4	76.1	99.9	102.2	102.1
Nominal MDB Stiffness	Door to Compartment Stiffness								
	1.1 Nom	105.5	243.0	188.7	252.4	99.3	197.8	100.3	95.3
	1.2 Nom	99.3	245.6	172.6	241.8	92.8	194.5	103.0	100.8
	1.3 Nom	91.2	244.5	156.3	231.8	86.9	190.4	100.1	96.9
Nominal VW-Rabbit Door to Compartment Stiffness	MDB Stiffness								
	0.8 Nom	119.6	265.0	163.9	238.4	106.7	206.1	101.8	99.3
	0.6 Nom	112.7	258.7	105.3	199.0	103.7	205.5	101.0	97.3
Nominal 3 in MDB Gtr Pad Stiffness	Door to Compartment Stiffness								
	1.1 Nom	55.8	113.6	127.2	209.3	76.8	137.3	99.5	98.7
	1.2 Nom	55.1	105.7	114.0	193.6	73.7	131.7	102.8	100.2
	1.3 Nom	55.7	97.0	95.4	182.6	71.5	127.3	100.8	96.5
Nominal 6 in MDB Gtr Pad Stiffness	Door to Compartment Stiffness								
	1.1 Nom	53.4	87.3	76.8	131.5	72.2	94.0	99.8	98.6
	1.2 Nom	47.2	69.6	65.6	115.7	68.3	88.2	102.1	102.4
	1.3 Nom	41.3	67.2	51.7	102.1	64.7	84.2	103.0	97.8
Nominal VW-Rabbit Door 3 in to Gtr Pad Compartment Stiffness	MDB Stiffness								
	0.8 Nom	55.5	103.3	107.2	192.9	76.8	134.9	103.0	99.9
	0.6 Nom	59.4	118.6	60.9	130.1	77.8	139.0	100.0	98.9
Nominal VW-Rabbit Door 6 in to Gtr Pad Compartment Stiffness	MDB Stiffness								
	0.8 Nom	43.6	88.4	60.4	113.6	67.7	85.8	102.8	98.5
	0.6 Nom	45.4	74.2	48.4	84.3	68.2	79.0	100.8	99.0

* Note: Simulation results based on force versus deflection curves derived from the BL-90° crash condition.

Table 3. Driver dummy peak acceleration levels due to padding thickness variations, VW-Rabbit door to compartment and MDB to VW-Rabbit door stiffness variations (modified VW-Rabbit, 90° impact)*

		Rib		Pelvis		Spine		Head	
		26/13mph	35/17.5mph	26/13mph	35/17.5mph	26/13mph	35/17.5mph	26/13mph	35/17.5mph
Modified VW-Rabbit		112.6G	246.3G	157.8G	240.7G	101.3G	194.5G	100.9G	96.4G
Modified VW-Rabbit	3 in Gtr Pad	56.3	100.8	101.9	182.4	76.5	130.7	102.9	100.2
	6 in Gtr Pad	44.3	68.5	56.5	93.4	68.4	83.7	100.7	100.2
Nominal MDB Stiffness	Door to Compartment Stiffness								
	1.1 Nom	100.4	236.8	162.2	235.5	93.1	187.0	102.6	94.3
	1.2 Nom	87.6	231.6	155.4	227.2	84.5	181.9	99.9	97.7
	1.3 Nom	75.5	221.8	137.2	212.6	77.6	176.6	102.2	96.1
Nominal VW-Rabbit Door to Compartment Stiffness	MDB Stiffness								
	0.8 Nom	109.6	249.8	154.8	226.0	99.9	195.0	102.1	96.4
	0.6 Nom	103.1	237.7	113.4	202.5	96.5	190.0	99.5	96.1
Nominal 3 in MDB Gtr Pad Stiffness	Door to Compartment Stiffness								
	1.1 Nom	55.5	99.1	103.0	176.9	73.7	126.1	100.7	102.1
	1.2 Nom	55.7	95.8	95.2	165.0	70.5	123.1	100.6	96.2
	1.3 Nom	56.0	95.0	80.9	143.2	70.0	120.1	100.3	102.2
Nominal 6 in MDB Gtr Pad Stiffness	Door to Compartment Stiffness								
	1.1 Nom	41.7	65.3	52.9	88.8	65.6	81.3	101.5	100.9
	1.2 Nom	41.2	60.6	50.6	84.0	64.6	79.6	100.7	101.5
	1.3 Nom	41.2	45.4	48.9	69.0	64.0	20.2	101.3	29.5
Nominal VW-Rabbit Door 3 in to Gtr Pad Compartment Stiffness	MDB Stiffness								
	0.8 Nom	56.4	100.2	92.3	167.0	75.5	129.1	102.0	101.7
	0.6 Nom	58.3	94.6	64.4	131.6	75.0	121.9	102.4	99.6
Nominal VW-Rabbit Door 6 in to Gtr Pad Compartment Stiffness	MDB Stiffness								
	0.8 Nom	42.2	68.4	49.3	84.4	65.5	79.2	101.6	98.5
	0.6 Nom	43.4	66.7	45.4	79.3	65.9	75.5	102.8	101.4

* Note: Simulation results based on force versus deflection curves derived from the MOD-90° crash condition.

Table 4. Driver dummy peak acceleration levels due to padding thickness variations, VW-Rabbit door to compartment and MDB to VW-Rabbit door stiffness variations (baseline VW-Rabbit, 60° impact)*

		Rib 26/13mph	Pelvis 26/13mph	Spine 26/13mph	Head 26/13mph
Baseline VW-Rabbit		146.1G	163.9G	111.9G	102.3G
Baseline VW-Rabbit	3 in Gtr Pad	76.7	116.6	91.2	100.7
	6 in Gtr Pad	55.2	73.6	76.8	102.3
	Door to Compartment Stiffness				
Nominal MDB Stiffness	1.1 Nom	141.5	144.3	109.1	101.9
	1.2 Nom	139.2	133.0	105.9	100.5
	1.3 Nom	134.7	128.9	102.4	99.0
Nominal VW-Rabbit Door to Compartment Stiffness	MDB Stiffness				
	0.8 Nom	149.9	139.6	115.1	98.2
	0.6 Nom	152.2	130.3	116.6	99.0
	Door to Compartment Stiffness				
Nominal 3 in MDB Gtr Pad Stiffness	1.1 Nom	77.2	96.7	89.2	100.9
	1.2 Nom	76.4	84.9	86.9	101.3
	1.3 Nom	75.0	80.6	84.5	100.4
	Door to Compartment Stiffness				
Nominal 6 in MDB Gtr Pad Stiffness	1.1 Nom	48.9	63.8	72.4	101.8
	1.2 Nom	48.6	56.4	71.3	101.6
	1.3 Nom	48.2	51.8	70.4	101.2
Nominal VW-Rabbit Door 3 in to Gtr Pad Compartment Stiffness	MDB Stiffness				
	0.8 Nom	80.0	90.0	93.3	101.9
	0.6 Nom	82.5	81.9	94.8	102.0
Nominal VW-Rabbit Door 6 in to Gtr Pad Compartment Stiffness	MDB Stiffness				
	0.8 Nom	49.5	60.3	72.7	102.1
	0.6 Nom	48.9	53.3	71.9	100.2

* Note: Simulation results based on force versus deflection curves derived from the BL-60° crash condition.

especially beneficial as a countermeasure in reducing the thorax and pelvis peak G levels. The thorax G level reductions through increased door-to-compartment stiffnesses (up to 1.3 nominal), generally, were small. The model indicated that the reductions obtained as a result of stiffened door-to-compartment structure could also be achieved through increase in padding thickness. For example, in the case of the 26/13mph, BL-90° impact, a 3in GTR pad reduced the rib peak G levels from 112.6G to 61.9G, a 3in GTR pad plus a 20 percent increase in struck vehicle side stiffness yielded a rib peak G level of 55.1G, whereas a 6in-thick GTR pad alone reduced the rib peak G level to 55.2G. It must be pointed out, however, that space limitations and other considerations

limit the thickness of the padding that can be used as a countermeasure. Struck VW Rabbit side stiffness changes affected all three dummy body components' peak G levels, while changes to the striking MDB stiffness principally affected the pelvis response.

Door Padding Thickness Effects

Driver Dummy Peak G Response Trends

GTR padding was very effective in reducing the dummy peak G levels, particularly for the rib. For example, at an impact speed of 26/13mph and an impact angle of 90°, a 3in-thick door padding in the baseline and structurally modified VW Rabbit reduced the rib peak G level from 112.6G to within 61.9G for the baseline and 112.6G to 56.3G for the modified vehicle. Much smaller reductions were achieved with an additional 3in-thick pad where rib peak G levels were further lowered to 44.3G for the modified and 55.2G for the baseline vehicle. At an impact angle of 60°, a 3in-thick pad lowered the rib peak G level from 146.1G to 76.7G for the baseline vehicle and a 6in-thick pad lowered the rib peak acceleration levels to 55.2G. The GTR padding was also quite effective in reducing the rib peak G levels at the higher speed even for padding thicknesses less than 3in. For example, at the 26/13mph speed, a 3in GTR pad reduced the BL-90° rib peak G levels by 45 percent and the MOD-90° by 50 percent. At the higher speed of 35/17.5mph, rib peak G level reductions of 49 and 59 percent were calculated for the BL-90° and MOD-90° configurations, respectively. The baseline VW Rabbit's rib peak G level percentage reductions for a 3in GTR pad did not appear to be largely affected by the collision angle. Rib peak G level percentage reductions were slightly higher for the structurally modified VW Rabbit than for the baseline VW Rabbit.

For the padding thicknesses considered herein, the spine peak G levels dropped off linearly with increase in the GTR pad thickness. The spine peak G level reductions were also lower by approximately one-half the value obtained in rib responses.

The pelvis peak G level reductions, on the other hand, were somewhat similar to those calculated for the rib. Here the pelvis peak G percentage reductions were about 30 percent for the 3in GTR pad and 60 percent for the 6in GTR pad for all three impact models at the lower impact speed. Due to the higher impact force encountered at the 35/17.5mph impact speed, the BL-90° pelvis peak G level percentage reductions were lower, since the GTR pad bottomed out. For example, for the 6in-thick GTR pad, the pelvis peak G level was reduced from 205G to 82.4G (60 percent) at the lower 26/13mph impact speed, while for the same pad thickness at the 35/17.5mph impact speed, the pelvis peak G level was reduced from 266.1G to 153.4G (42 percent). Pelvis peak G level percentage reductions for the MOD-90° at the 35/17.5mph impact speed were slightly higher than the peak G level percentage reductions obtained at the lower impact speed (26/13mph).

These results showed that 3in of GTR padding added to the door significantly reduced the rib peak G levels. Moreover, the GTR padding seemed more effective in reducing the thorax peak G levels even at lower padding thicknesses than in reducing the heavier pelvis mass peak G levels, especially at the higher impact speed. To further illustrate this point, the rib, pelvis, and spine peak G levels were computed using smaller padding thickness increments up to a thickness of 8in. The results are shown in Figure 8. Here, the rib peak G levels drop off sharply at the lower GTR padding thicknesses where they are largely affected by the interaction of the pelvis with the padded door. On the other hand, at the higher GTR padding thicknesses, the thorax peak G levels seem to level off with increase in the GTR padding thickness. This

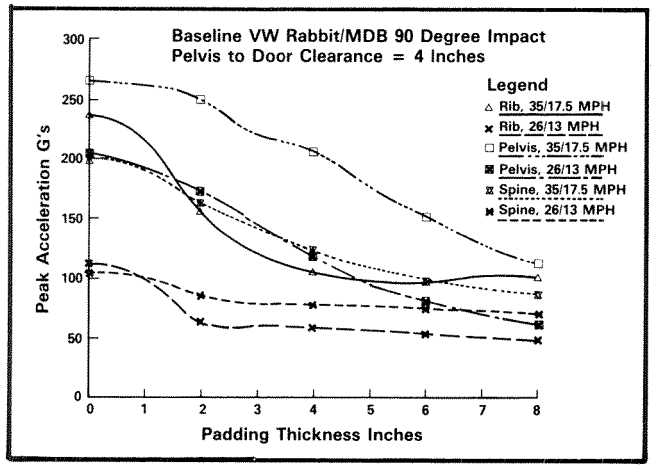

Figure 8. Effect of GTR pad thickness at rib and pelvis on dummy peak G levels

trend is due to the phasing difference between the rib and pelvis peak G levels when different padding thicknesses were applied to the door and to secondary impacts of the thorax mass. Door velocity time histories are also shown in Figure 9 for an unpadded door and a door with a 3 and 6in GTR pad, respectively, which further explains these differences. These histories show that the pelvis-to-door contact lowered the velocity of the door and, therefore, the velocity of impact of the rib in the case of the unpadded door and door with the smaller padding thicknesses (up to 3in). At the higher door padding thicknesses (beyond 3in), the influence of the pelvis on rib peak G levels diminished and the rib responded as if the pelvis never made contact with the padded door. In this case, the further reductions in rib peak G are due to the cushioning effect provided by the thicker padding in reducing the secondary impacts.

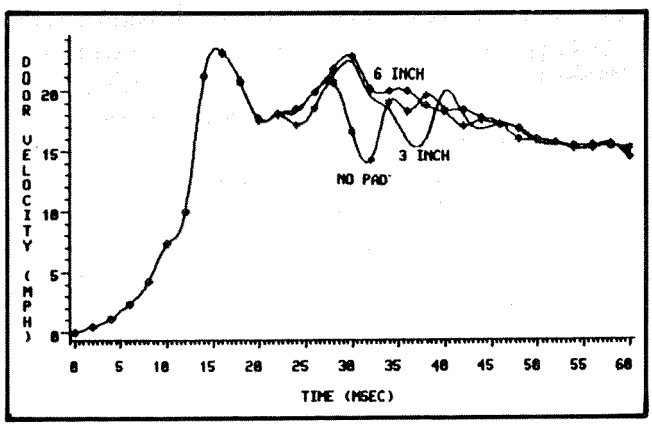

Figure 9. Door velocity time histories

Sensitivities Due to GTR Padding Thickness Changes

Sensitivities relating the change in the dummy peak G levels to the change in the GTR padding thickness (G/in of added padding) were also calculated. For sensitivity calculations, the slope between adjacent pairs of the parametrically changed padding thickness was used to denote the rate of expected peak G reduction/in of added padding.

The peak G level reductions for the rib, pelvis, and spine/in of the added GTR padding for the three mean thicknesses are given in Table 5. Additional sensitivities as a function of padding thickness for the BL-90° crash conditions are shown in Figures 10 and 11 for the 26/13 and 35/17.5mph striking speed, respectively.

In general, these results indicate that the dummy's rib, pelvis, and spine body components exhibit different sensitivity values for the different GTR padding thicknesses. Typically, these sensitivities increase, reach a maximum value, and then decrease with increasing thickness. The maximum values also occur at different GTR padding thicknesses for all three body components. In the case of the dummy normally seated 4in from the door, the maximum sensitivities related to the rib and spine occur at a lower pad thickness (the same thickness at rib and pelvis striking locations) than that for the pelvis. Generally, the pelvis peak G levels appear to be more sensitive to padding thickness changes than the rib and spine peak G levels over the range of GTR padding thicknesses investigated. At the smaller thicknesses (0 to 3in) where the pelvis-to-door interaction influenced the thorax contact velocity, the rib and spine peak G levels were highly sensitive to changes in the GTR padding thickness. The rib, pelvis, and spine exhibited roughly the same levels of sensitivity for the three simulated crash conditions, which suggests that padding effectiveness as a first approximation could be evaluated independent of the crash angle and the door strength of the struck vehicle.

As noted above, the thorax region exhibited the largest variation in the sensitivity with increase in the GTR

Table 5. GTR Padding Sensitivity Coefficients

	Impact Speed, MPH/MPH In	GTR Padding Thickness,	Sensitivity Coefficient* GTR Padding Thickness Variations, G/in		
			90° Baseline	90° Modified	60° Baseline
Rib	26/13	1.5	16.9	18.7	23.1
		3.0	9.5	11.4	15.2
		4.5	3.4	4.0	7.2
	35/17.5	1.5	39.0	48.5	
		3.0	23.6	29.6	
		4.5	8.3	10.7	
Pelvis	26/13	1.5	19.9	18.6	15.8
		3.0	20.4	16.9	15.1
		4.5	20.9	15.2	14.3
	35/17.5	1.5	14.6	19.4	
		3.0	18.8	24.6	
		4.5	23.0	29.6	
Spine	26/13	1.5	8.2	8.2	6.9
		3.0	4.8	5.5	5.9
		4.5	1.8	2.7	4.8
	35/17.5	1.5	18.8	21.2	
		3.0	16.8	18.5	
		4.5	14.8	15.6	

* Based on three points (non-padding, 3in padding and 6in padding)

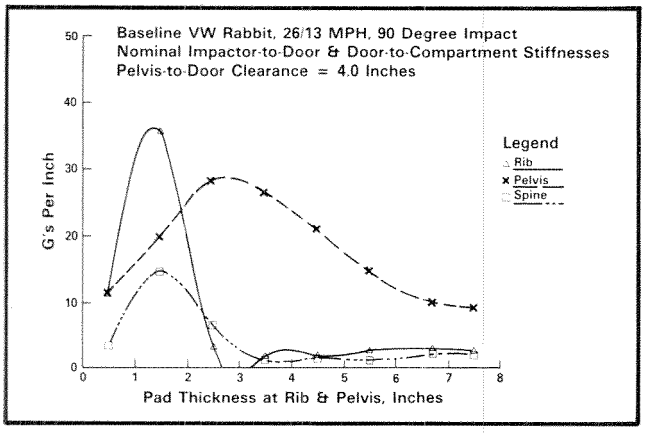

Figure 10. Sensitivities of dummy response as a function of GTR pad thickness at the low speed condition

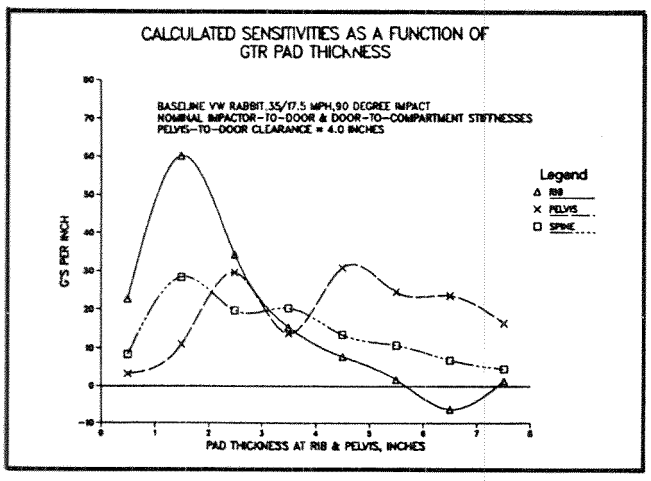

Figure 11. Sensitivities of dummy response as a function of GTR pad thickness at the high speed condition

padding thickness, whereas the variations in the pelvis sensitivity were less. The rib showed the largest variation in the thorax region. Moreover, the sensitivities related to the thoracic region showed, characteristically, different patterns where at the smaller thicknesses the thoracic accelerations are highly sensitive to the GTR padding thickness changes and the thoracic accelerations are much less sensitive at the higher thicknesses. These sensitivities also exhibited the largest changes as a function of impact speed. For example, in the case of the 26/13mph, BL-90° impact, the rib sensitivities ranged from 16.9G reduction/in of padding added to a 1.5in GTR pad to 3.4G reduction/in of padding added to a 4.5in GTR pad. In addition, in the first region, the thorax peak G levels were less sensitive at the lower 26/13mph impact speed to the GTR padding thickness changes than at the higher 35/17.5mph impact speed. Also at both speeds, the rib peak G levels were approximately twice as sensitive as were the spine peak G levels to the GTR padding thickness changes. It is of interest to note, in the first region, the pelvis peak G levels seemed as sensitive to GTR padding thickness changes at the lower impact speed as the rib and less sensitive at the higher speed. In this case, the sensitivities at the lower impact speed ranged from 17.0G to 23.0G reduction for the pelvis, compared to the 39.0G to 49.0G reduction/in of padding added to the 1.5in GTR pad for the rib, and 15.0G to 20.0G reduction for the pelvis at the higher impact speed. At the higher pad thicknesses, as the collision speed was increased from 26/13mph to 35/17.5mph, the spine peak G levels showed a higher sensitivity than the rib peak G levels to increases in the GTR padding thickness.

As a further consideration, the percentage reduction in G levels achieved by the various GTR padding thicknesses relative to the unpadded door case for the BL-90° crash condition at the low and high collision speeds (26/13mph and 37/17.5mph, respectively) indicate that—

1. Increase in the rib peak G reduction with increase in the impact speed (45.0 percent and 48.9 percent for the low and high collision speeds, respectively, for the 3in pad)
2. Decrease in the pelvis peak G reduction with increase in the impact speed (29.2 percent and 16.5 percent for the low and high collision speeds, respectively, for the 3in pad)
3. Increase in the spine peak G reduction with increase in the impact speed (23.6 percent and 28.1 percent for the low and high collision speeds, respectively, for the 3in pad)

Note here that the pelvis peak G percentage reductions appear less at the higher speed than the lower striking speed since the GTR pad bottomed out as previously noted.

Struck VW Rabbit Stiffness Effects

Dummy Peak G Response Trends

Much smaller dummy peak G reduction levels were achieved through increase in the VW Rabbit door-to-compartment stiffness ranging from the 1.0 to 1.3 nominal stiffness value than through the addition of door padding (see Tables 2 through 4). The peak G reduction levels were most sensitive to the three different crash conditions considered. In the case of the rib, the largest reduction was achieved by the MOD-90° crash condition, from 112.6G to 75.5G, followed by the BL-90° crash condition, from 112.6G to 91.2G, and finally by the BL-60° crash condition, from 146.0G to 134.7G, at the lower speed when the VW Rabbit door-to-compartment stiffness was increased to 1.3 nominal stiffness. The primary reason for the larger reduction in the modified vehicle is that the 1.3 nominal stiffness reflected a much larger change in the structurally modified VW Rabbit's door than a similar 1.3 nominal stiffness change in the baseline

compartment stiffness in either the 60° or 90° impact. Lower rib peak G reduction levels were indicated at the higher impact speed when the struck vehicle stiffness was increased from 1.0 to 1.3 nominal due to the increased force of impact. Also under this condition, no benefits were indicated for the BL-90° crash condition because of the lower strength of the VW Rabbit door-to-compartment interconnecting spring. The modified VW Rabbit design indicated marginal peak G reduction levels for the rib of 4 to 10 percent at the higher speed, where the driver dummy rib peak G levels were reduced from 246.4G to 236.8G, 231.0G, and 221.8G for VW Rabbit door-to-compartment stiffness levels of 1.1, 1.2, and 1.3 nominal, respectively.

The spine reductions through increased struck side vehicle stiffness changes were similar to those obtained for the rib. The pelvis peak G level reductions, however, were higher than those obtained for the rib. Generally, the pelvis percentage reductions were higher for the BL-90° crash condition than for the MOD-90° crash condition. These reductions were also lower when the collision speed was increased from 26/13mph to 35/17.5mph. For example, the BL-90° crash condition indicated pelvis reductions of 23 and 12 percent for the 26/13mph and 35/17.5mph impact speeds, respectively, when the compartment stiffness was increased from 1.0 to 1.3 nominal. Likewise, reductions of 13.0 and 11.6 percent were indicated for the MOD-90° crash conditions when the collision speed was increased from 26/13mph to 35/17.5mph, respectively.

Sensitivities Due to Struck VW Rabbit Stiffness Changes

The response curves describing the trends in dummy peak G levels with changes in struck vehicle stiffness were most irregular (particularly for the pelvis) exhibiting spikes due to the nonlinearities in the striking and struck vehicles' force-deflection characteristics. Because of this, the response curves were recalculated using a smaller grid to define more precisely the peak G level trends for sensitivity calculations. These response curves (peak G versus log-normalized stiffness) are shown in Figure 12 for the BL-90° and MOD-90° crash conditions at the 26/13mph impact speed, Figure 13 for the BL-90° and MOD-90° crash conditions at the 35/17.5 mph impact speed, and Figure 14 for the BL-60° crash conditions at the 26/13mph impact speed. The general rate of decrease in the dummy peak G levels with increase in the struck vehicle stiffness for log-normalized stiffnesses greater than the nominal were also calculated from straight lines connecting the extremums of the peak G levels. The results are shown in Table 6. (Note, since the sensitivities defined in this manner are mean values, they are expected to yield in some circumstances reduction trends that may

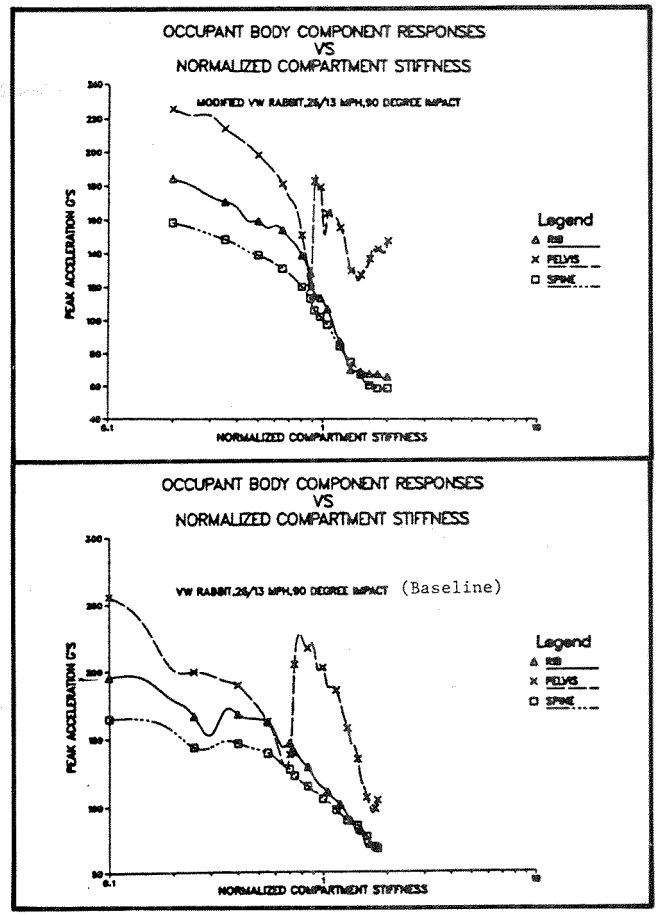

Figure 12. Dummy response as a function of normalized compartment stiffness for the baseline and modified vehicle at the low speed condition

differ from those trends discussed in the previous section.)

In general terms, these results indicate, for normalized stiffness values greater than the nominal, that the mean rate of decrease of the dummy peak G levels with stiffness depends to a large extent on the crash condition. For example, these results show that the mean rib peak G levels generally decrease with log-normalized stiffness at rates of about 80G for each doubling of stiffness for the MOD-90° crash condition, 57.0G for each doubling of stiffness for the BL-90° crash condition, and 32.0G for each doubling of stiffness for the BL-60° crash condition. Moreover, the mean peak G reductions for each doubling of stiffness are inherently higher for the pelvis than the rib and the spine. For example, in the BL-90° crash condition, the mean pelvis peak G levels are reduced by approximately 104.0G for each doubling of normalized stiffness, for the rib by approximately 57.0G, and for the spine by 42.0G, respectively. It should be further noted that when larger mean peak G level reductions were brought about through the struck vehicle stiffness changes for the pelvis, generally lower mean peak G level reduction resulted for the thorax and vice versa. This is best illustrated by the stiffness changes included in the BL-90° and MOD-90°

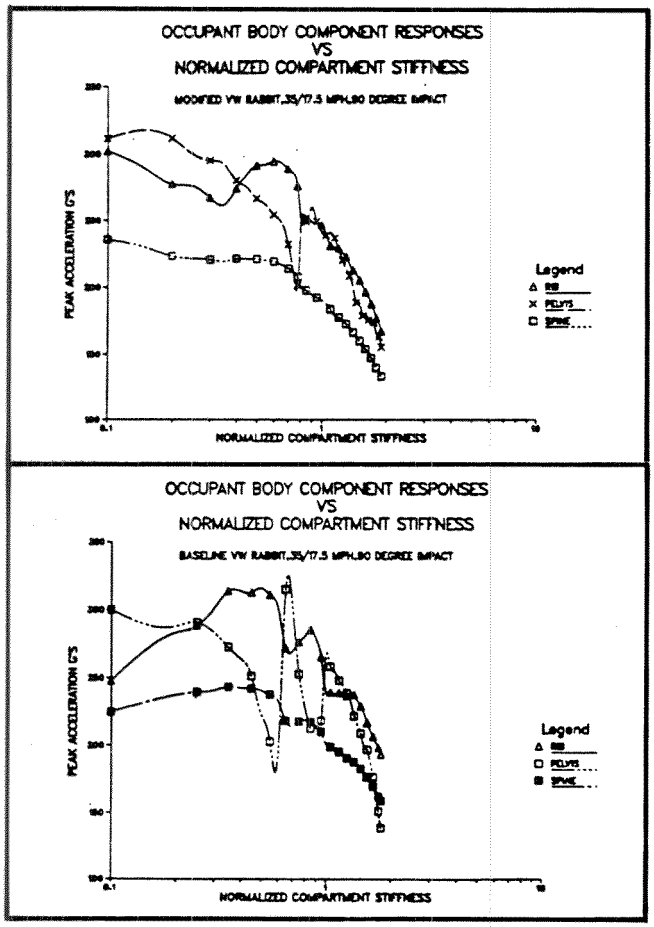

Figure 13. Dummy response as a function of normalized compartment stiffness for the baseline and modified vehicle at the high speed condition

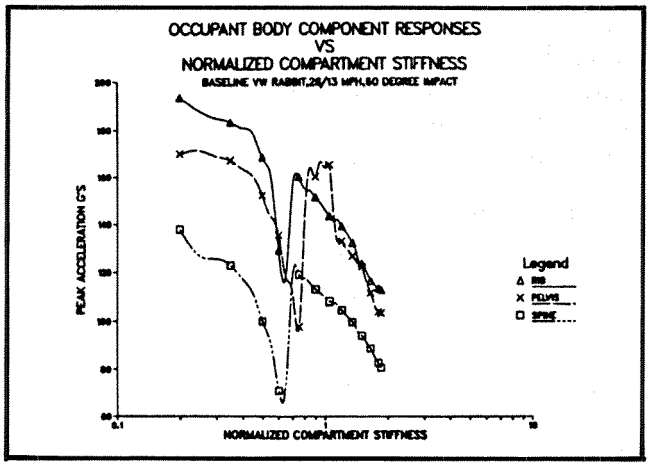

Figure 14. Dummy response as a function of normalized compartment stiffness for the baseline vehicle at a low speed 60° impact condition

crash conditions where the mean pelvis and rib peak G levels at the 26/13mph impact speed decrease with log-normalized stiffness at rates of about 104.0G and 57.0G for each doubling of stiffness for the BL-90° crash condition, respectively, and 87.0G and 80.0G for each doubling of stiffness for the MOD-90° crash condition, respectively. The thoracic mean sensitivity did not seem to change substantially with impact speed nor did the pelvis mean sensitivities.

In general, the rib and spine showed a higher rate of sensitivity with stiffness for the stiffer MOD-90° crash condition than for the softer BL-60° crash condition. The spine rates (although slightly lower) were of approximately the same order of magnitude as were the rib rates for the

Table 6. Compartment stiffness sensitivity coefficients (1.0 nominal impactor to door stiffness)

	Impact Speed MPH/MPH	GTR Padding Thickness	Estimated Mean Sensitivities* for Door to Compartment Stiffness Variations 90° Baseline	90° Modified	60° Baseline
Rib	26/13	no padding	57.0	80.0	32.0
	35/17.5	no padding	58.0	83.0	—
Pelvis	26/13	no padding	104.0	87.0	not able to define
	35/17.5	no padding	104.0	97.0	—
Spine	26/13	no padding	42.0	58.0	23.0
	35/17.5	no padding	40.0	52.0	—

* G reductions for each doubling of log-normalized stiffness.

two softer VW Rabbit door-to-passenger-compartment spring configurations (BL-90° and BL-60° crash conditions). However, this was not true for the stiffer MOD-90° crash condition where the spine rates were much lower than those simulated for the rib. Characteristically, the sensitivities increased (starting at low struck vehicle stiffness), reached a maximum value, and then decreased asymptotically to zero at the higher struck vehicle side stiffnesses where the door contacts the unrestrained driver dummy at the common velocity.

Striking Vehicle Stiffness Effects

Dummy Peak G Response Trends

Pelvis peak G levels were influenced the most through the MDB stiffness changes ranging from 0.6 nominal to 1.4 nominal stiffness (see Tables 2 through 4). Moreover, the BL-90° pelvis peak G levels were reduced more than the MOD-90° (stiffer side door) pelvis peak G levels at both impact speeds. For example, the results show that when the MDB-to-struck-door stiffness was reduced from 1.0 to 0.6 nominal, the baseline VW Rabbit's pelvis peak G level was reduced from 205.0G to 105.3G (49 percent) whereas, under identical conditions, the structurally modified VW Rabbit pelvis peak G level was reduced from 157.3G to 113.4G (28 percent). Futhermore, the pelvis peak G levels seemed as sensitive to the MDB-to-struck-door normalized stiffness changes as they were for the VW Rabbit door-to-compartment normalized stiffness changes for comparable changes in stiffness. Based on the local change in stiffness, for example, a decrease in the MDB-to-struck-door normalized stiffness from 1.0 to 0.8 nominal stiffness reduced the pelvis peak G levels by 41.1G for the BL-90° crash condition, by 3.06G for the MOD-90° crash condition, and by 24.3G for the BL-60° crash condition at the 26/13mph collision speed. An increase in the struck door-to-compartment normalized stiffness from 1.0 to 1.2 nominal reduced the pelvis G levels by 32.4G for the BL-90° crash condition, by 2.4G for the MOD-90° crash condition, and by 30.9G for the BL-60° crash condition.

Changes in the rib and spine peak G levels were small for the baseline VW Rabbit at impact angles of 60° and 90° due to pelvis interaction with a softer door-to-compartment interconnecting spring.

Sensitivities Due to Striking Vehicle Stiffness Changes

In general, for normalized striking vehicle stiffnesses less than the nominal, the mean rib and spine sensitivities (defined here as the mean rate of decrease in the dummy G level with decrease in striking vehicle stiffness) as expected are much lower in magnitude than those computed for the pelvis. The estimated rates indicate that the dummy peak G levels appear to decrease for the MOD-90° crash condition with log-normalized stiffness of about 86.0G for each halving of stiffness for the pelvis, 18.0G for each halving of stiffness for the rib, and 8.0G for each halving of stiffness for the spine at the 26/13mph impact speed. These rates also changed as the impact speed was increased from 26/13mph to 35/17.5mph. In this case, a lower mean rate of about 52.0G for each halving of stiffness was estimated for the pelvis, and higher rates were estimated for the rib and spine, 26.0G and 12.0G for each halving of stiffness, respectively.

Effect of Door Padding Thickness and Struck Vehicle Stiffness Changes

Dummy Peak G Response Trends

With the same door padding thicknesses at the rib and pelvis locations, an increase in the struck vehicle stiffness showed small benefits in reducing the rib peak G levels at the 26/13mph impact speed. Reductions were slightly higher when the struck vehicle stiffness was increased with a thicker door padding of 6in than with a thinner door padding of 3in. For example, the following rib peak G level reductions shown in Table 7 were calculated when the struck vehicle's stiffness was increased from 1.0 to 1.3 nominal. Also, at the higher impact speed, these reductions increased with increase in padding thickness.

With a padded door, the pelvis benefited most through increase in the struck vehicle stiffness. With no door padding, the pelvis peak G reductions were higher for the BL-90° than for the MOD-90°, and likewise at the higher impact speed of 35/17.5mph. For the BL-90° crash conditions with door padding, when the struck vehicle's stiffness was increased from 1.0 to 1.3 nominal, the pelvis G level reductions were approximately the same as with no padding on the door at the 26/13mph impact speed (see Table 8A). Note that at the lower impact speed of 26/13mph, the BL-90° pelvis peak G levels generally decreased with increase in the padding thickness when the struck vehicle's stiffness was increased from 1.0 to 1.3 nominal, whereas, at the higher speed of 35/17.5mph, the opposite trend was evident. For the MOD-90° crash condition, on the other hand, the pelvis peak G level reductions decreased with the increase in padding thickness at both impact speeds for padded door thicknesses greater than 3in (see Table 8B). Finally, these trends shown here indicate an increase in stiffness of a soft side structure plus the addition of door padding through thickness changes yields higher benefits in reducing the dummy peak G levels than padding thickness changes

Table 7. Occupant peak G level reductions as a function of GTR-pad thickness and crash condition due to increase in side stiffness from 1.0 to 1.3 nominal

	No Door Padding (Rib)	3in Padded Door (Rib)	6in Padded Door (Rib)
BL-90°	21.4G (reduction)[a]	6.2G (reduction)[b]	14.0G (reduction)[b]
MOD-90°	37.1G (reduction)	0.3G (reduction)	3.1G (reduction)
BL-60°	11.4G (reduction)	1.7G (reduction)	7.2G (reduction)

[a] Reduction due to increase in struck vehicle stiffness only.

[b] Reduction denotes, G(pad) - G(pad + struck vehicle stiffness)

alone. In addition, these benefits appear to increase through these two parametric changes with increase in the striking vehicle's speed.

Table 8. Pelvis peak G level reductions due to increased side stiffness from 1.0 to 1.3 nominal as a function of impact speed and GTR pad thickness

	(26/13mph) Pelvis, BL-90°	(35/17.5mph) Pelvis, BL-90°
	(A) BL-90° Crash Condition	
No Pad	48.7G (reduction)	34.3G (reduction)
	(Reductions relative to padded door)	
3in Pad	49.8G (reduction)	40.8G (reduction)
6in Pad	30.7G (reduction)	51.3G (reduction)
	(B) MOD-90° Crash Condition	
	(26/13mph) Pelvis, MOD-90°	(35/17.5mph) Pelvis, MOD-90°
No pad	10.6G (reduction)	28.1G (reduction)
	(Reductions relative to padded door)	
3in Pad	21.0G (reduction)	39.2G (reduction)
6in Pad	7.6G (reduction)	24.4G (reduction)

Effect of Door Padding Thickness and Striking Vehicle Stiffness Changes

Dummy Peak G Response Trends

Changes reflecting reductions in the MDB stiffness affected both the thorax and pelvis peak G levels when the VW Rabbit door included the GTR pad. In general, the added GTR door padding through thickness changes and a softer MDB frontal structure combined together resulted in lowering the pelvis and upper thorax peak G levels. With a padded door, the peak G reduction levels were less for the pelvis and slightly higher for the rib when the MDB frontal structure was softened in comparison to an unpadded door. These decreasing pelvis and increasing rib reduction trends continued for doors with thicker GTR padding. This is actually due to the longer duration of time that both body components are in contact with the padded door and to the impact velocities of the rib and pelvis. As the GTR pad thickness was increased, the contact time became longer, and the pelvis G levels were less affected than the thorax peak G levels when the striking vehicle stiffness was reduced. This is illustrated in Table 9 where rib and pelvis peak G level reductions are shown for the case when the BL-90°, 26/13mph, MDB normalized stiffness was reduced from 1.0 to 0.8 and 0.6 nominal for three padded doors.

The sensitivity results shown in Tables 2 and 3 also show that with door padding included, the rib peak G levels were less affected when the MDB normalized stiffness was reduced from 1.0 to 0.8 and 0.6 nominal in the stiffer MOD-90° crash condition than in the BL-90° crash condition. For example, for the 6in-thick padded door, the rib peak G levels were reduced from 55.2G to 43.6G (21 percent reduction) and 45.4G (18 percent reduction), when the BL-90°, 26/13mph, MDB normalized stiffness was reduced from 1.0 to 0.8 and 0.6 nominal, respectively, and from 44.3G to 42.2G (5 percent reduction) and 43.4 (2 percent reduction) when

Table 9. Occupant peak G level reduction as a function of GTR pad thicknessw and striking vehicle stiffness changes (BL-90°, 26/13mph)

	MDB-Normalized Stiffness Reductions	No Padding Rib G-Reduction	No Padding Pelvis G-Reduction	3in Padding Rib G-Reduction	3in Padding Pelvis G-Reduction	6in Padding Rib G-Reduction	6in Padding Pelvis G-Reduction
				(Reductions relative to padded door)			
from	1.0 to 0.8	7.0	41.1	6.4	38.6	11.6	22.0
from	1.0 to 0.6	0.1	99.7	2.5	84.3	9.8	34.0

the MOD-90°, 26/13mph, MDB normalized stiffness was reduced from 1.0 to 0.8 and 0.6 nominal, respectively.

Larger dummy peak G level changes were also observed for the BL-90° configuration as the collision speed was increased. For example, when the MDB normalized stiffness was reduced from 1.0 to 0.6 nominal with a 6in-thick pad on the VW Rabbit door, the dummy rib peak G levels were reduced from 55.2G to 45.4G (18 percent reduction) at 26/13mph and from 97.5G to 74.2G (24 percent reduction) at 35/17.5mph. On the other hand, the rib peak G level changes were insignificant for the MOD-90° configuration as the impact speed was increased (0.9G reduction at 26/13mph and 1.8G reduction at 35/17.5mph, respectively).

Effect of GTR Padding Force Level and Shape Factor Change

Dummy Peak G Response Trends

The pelvis, rib, and spine peak G levels were not significantly affected by the GTR padding force level changes (0.8 nominal to 1.2 nominal strength) for the two GTR padding thicknesses of 3.0 and 6.0in. investigated. Actually, the GTR pad strength changes considered accounted for only marginal differences in the dummy-to-door contact spring force levels. Based on the results of the BL-90° crash condition at the 26/13mph impact speed where the VW Rabbit's side and MDB stiffnesses were varied, generally, an increase in GTR pad stiffness reduced the pelvis peak G levels and increased the rib and spine peak G levels. Other trends indicated are—

- Larger changes in the dummy component peak G levels at the lower GTR padding thicknesses than at the higher padding thicknesses
- Larger changes in the dummy component peak G levels at the lower normalized VW Rabbit door-to-compartment stiffnessess
- Very little to no change in the dummy component peak G levels for the 0.6 through 1.4 nominal stiffnesses considered for the MDB-to-struck-door spring

Based on limited calculations performed for the BL-90° crash condition, a change in the GTR-pad shape factor from 0.8 to 0.2 indicated—

- Further reductions in the pelvis peak G levels of the order of 10 to 20G's (The higher G level reductions were achieved with the thicker 6in pad.)
- Further reduction in rib peak G levels for normalized side structure stiffnesses less than the nominal and normalized MDB stiffnesses ranging from 0.8 to 1.2 nominal with a 3in-thick pad
- General trend toward increase in rib peak G levels when the VW Rabbit's side and MDB stiffness were varied with the 6in-thick pad

Thoracic Probability of Injuries

The results presented below are based on NHTSA-developed relationships that indicate the thoracic probability of injury as a function of the TTI for various AIS values.

Here, the thoracic probability of injuries in a 30-year-old for an AIS greater than or equal to 3 are considered. This probability of injuries is based on the rib and spine peak G levels predicted for the BL-90°, MOD-90°, and BL-60° crash conditions as a function of GTR padding thickness changes, striking and struck vehicle stiffness changes, and impact speed. These results indicate that—

1. At the lower impact speed of 26/13mph, the 6in-thick GTR pad effectively reduced the thoracic probability of injury below 14 percent in both 60° and 90° impacts. The lowest thoracic probability of injury (6.6 percent) resulted for the MOD-90° crash condition with a 6in-thick padded door.
   6.6 percent for MOD-90° crash condition
   13.6 percent for BL-90° crash condition
   12.5 percent for BL-60° crash condition
2. Side stiffness plus door padding rendered additional benefits above those already achieved with door padding alone in lowering further the thoracic probability of injury. However, these benefits were small, particularly for the strengthened side (MOD-90°) crash condition, which showed only a marginal change in thoracic probability of injury. For example, for the 26/13mph impact condition, the thoracic probability of injuries was reduced to—
   4.9 percent compared to 6.6 percent (padding only) for MOD-90°
   5.1 percent compared to 13.6 percent (padding only) for BL-90°
   6.3 percent compared to 12.5 percent (padding only) for BL-60°
   by increasing the side stiffness by 1.3 nominal of a 6in-thick GTR padded door.
3. As expected, higher thoracic probability of injuries resulted when the collision speed was increased from 26/13mph to 35/17.5mph. As far as the side structure of the VW Rabbit vehicle was concerned, much larger increases in the thoracic probability of injuries were indicated for the BL-90° than for the MOD-90° crash conditions. As an example, the following thoracic probability of injuries resulted for the 35/17.5mph impact speed for a door with a 6in-thick GTR pad:

26.5 percent for MOD-90° crash condition
65.2 percent for BL-90° crash condition

Both side stiffness and door padding clearly showed some advantage.

4. The thoracic probability of injuries was not substantially reduced at the higher impact speed through increase in the struck VW Rabbit stiffness from 1.0 to 1.3 nominal alone or through decrease in the striking MDB stiffness from 1.0 to 0.6 nominal alone.

Conclusion

An investigation was undertaken characterizing, parametrically, the thoracic and pelvic acceleration response levels of a driver dummy during side impacts from a lumped nonlinear spring/mass model. Force-deflection characteristics were derived from three different crash conditions where the striking vehicle engaged the struck vehicle's door during the collision. Padding force-eflection characteristics were based on a GTR pad used in car crash tests. The parameters considered included striking vehicle stiffness, struck vehicle stiffness, impact angle, impact speed, and door padding thickness and stiffness. Based on these results, sensitivities and thoracic probability of injuries were computed. The following conclusions are based on the driver dummy in a normal seated position located 4in from the door.

Model Features and Capabilities

1. The response of the dummy is a dynamically coupled process related to the interactions of the dummy with the door. The time of impact of the dummy's body components with the door, the duration of the contact of these body parts with the door, and the corresponding door velocities and accelerations influence the outcome of their peak G levels.
2. The lumped mass model was validated with experimental data over a range of impact speeds and shows reasonable agreement for the rib, pelvis, and spine. No attempt was made to verify the parametric changes investigated in this study with tests. However, they show trends consistent with some of the findings from dynamic tests in (4). The model in its present form is incapable of predicting the head response, since the model did not include the appropriate head-to-neck spring compliance or the head-to-contact-surface spring resistance.

General Observations

1. The driver dummy's peak upper thorax (rib and spine) and pelvis G levels were reduced through (1) increased padding thickness, (2) increased door-to-compartment stiffness, (3) decreased MDB-to-struck-door stiffness, and (4) decreased impact speeds.
2. Much larger G level reductions appeared for the pelvis than for the thorax through all of the above parameter changes explored in this study.
3. Different degrees of sensitivities were observed among rib, pelvis, and spine peak G levels for the parametric changes in padding thickness, MDB, and struck vehicle stiffness.

Effect of Door Padding

1. Door padding of various thicknesses, in general, was found to be a very effective countermeasure explored in this study in reducing the dummy thorax and pelvis peak G levels. (This is based on the GTR door padding used in car crash tests.)
2. For upper thorax peak G level reductions, the relative effect of padding is more pronounced at the higher than at the lower impact speeds.
3. The reduction/in of added GTR padding seemed generally to be independent of the impact angle and stiffness changes to the side structure or the MDB frontal structure.
4. The rate of reduction of the peak thoracic acceleration is high up to a certain thickness of padding. The effectiveness is reduced as the padding thickness is further increased. This padding thickness varies depending on the impact speed.
5. The upper thorax (rib and spine) peak G levels seem to be less sensitive to padding thickness changes at the lower (26/13mph) impact speed than at the higher (35/17.5mph) impact speed, and the rib peak G levels seem to be more sensitive than the spine peak G levels to the GTR padding thickness changes examined. The pelvis peak G levels, on the other hand, seem to be as sensitive as the rib peak G levels were to the GTR padding thickness changes at the lower speed and less sensitive than the rib peak G levels were to padding thickness changes at the higher speed. These sensitivities ranged for the smaller size GTR pad anywhere from 17G to 23G reduction/in of added padding for the rib, 16G to 20G reduction/in of added padding for the pelvis, and 7G to 8G reduction/in of added padding for the spine at the 26/13mph impact speed and 40G to 49G reduction/in of added

padding for the rib, 15G to 20G reduction/in of added padding for the pelvis, and 19G to 21G reduction/in of added padding for the spine at the high 35/17.5mph impact speed. The thorax exhibited a wider variation in the sensitivity with increase in the GTR pad thickness.

6. Altering the force levels of the general force-deflection shape of the pad did not significantly affect the upper thorax and pelvis peak G levels. However, a general change in shape could potentially produce beneficial differences.

Effect of Side Structure and Striking Vehicle Stiffness

1. Increased side structure stiffness reduced the dummy peak G levels. The increased side structure stiffness affected the pelvis peak G levels more than the upper thorax peak G levels.
2. A softer striking vehicle frontal structure offered small benefits in reducing the upper thorax G levels. Pelvic responses, on the other hand, were found to be reduced by decreases in stiffness of the MDB.
3. The rate of decrease of the driver dummy peak G levels with increases of the side structure stiffness seems dependent on the crash condition. The mean rib peak G levels decreased with log-normalized stiffness at rates of about 80.0G for each doubling of stiffness for the MOD-90° crash condition, 57.0G for each doubling of stiffness for the BL-90° crash condition, and 32.0G for each doubling of stiffness for the BL-60° crash condition. Moreover, the G level reductions for each doubling of stiffness were higher for the pelvis, followed by the rib and spine in that order (for example, for the BL-90° crash condition, the mean pelvis peak G levels were reduced by about 104.0G for each doubling of stiffness, the mean rib peak G levels were reduced by 57.0G for each doubling of stiffness, and the mean spine peak G levels were reduced by about 42.0G for each doubling of stiffness).
4. Substantially lower sensitivities were indicated for the rib and spine for MDB-to-struck-door stiffness changes less than the nominal. For example, for the MOD-90° crash condition, the mean of the dummy G levels decreased with log-normalized stiffness at a rate of about 86.0G for each halving of stiffness for pelvis, 18.0G for each halving of stiffness for rib, and 8.0G for each halving of stiffness for spine at the 26/13mph impact speed. These sensitivities increased with impact speed for rib and spine.

Effect of Door Padding Plus Side Structure and Striking Vehicle Stiffness

1. The combination of padding and increased side structure stiffness seems to provide the best reduction for the G-level magnitudes investigated for soft side structures. However, the reductions achieved because of the increased side structure stiffness are proportionately less and generally could be achieved through further increases in the GTR padding thickness. (It is clearly obvious that padding thickness is limited by space and other considerations in cars.)
2. For a padded door, increasing the side structure stiffness or decreasing the struck vehicle stiffness seems to have more of an effect in reducing the thorax G level than in reducing the pelvis G levels. Generally, as more door padding is added, the pelvis peak G level reductions decreased and the thorax G level reductions increased through these two stiffness changes.

Acknowledgments

The authors wish to express their sincere appreciation for the many suggestions offered throughout the course of this work to Mr. James R. Hackney (DOT-NHTSA/NRD), Mr. John E. Tomassoni (DOT-NHTSA/NRM), and Mr. Herbert H. Gould (DOT-RSPA/TSC). Special thanks is also extended to Mr. John D. Guglielmi (DOT-RSPA/TSC) for his many valuable contributions.

References

1. Eppinger, R.H., et al., "Development of dummy and injury index for NHTSA's thoracic side impact protection research program," SAE Paper 840885.
2. Trella, T.J., and J.N. Kanianthra, "Application of derived characteristics from dynamic test data for simulation of car to car side impacts using a lumped mass approach," SAE Paper 851187.
3. Pilkey, W.D., et al., "Proceedings of safety system optimization model workshop," University of Virginia, Charlottesville, Virginia, pp. 73-155, October 1981.
4. Hackney, J.R., et al., "Results of the National Highway Traffic Safety Administration's thoracic side impact protection research program," SAE Paper 840886.
5. Monk, M., and L. Sullivan, "Side impact padding integration study," NHTSA-Vehicle Research Center, East Liberty, Ohio, NHTSA DOT HS-805-957, March 1981.

Inclusion of Crashworthiness in Concept Design

G.D. Suthurst and
P. Ng
Ford Motor Company, United Kingdom

Dr. M. Sadeghi
Cranfield Impact Centre, United Kingdom

Abstract

A side impact study carried out on a particular vehicle has been described and used as a case study to represent a methodology for incorporating side crashworthiness in a new vehicle concept design. In the automotive design environment, it has proved difficult to include side crashworthiness satisfactorily in the initial stages of the passenger car design. Lack of vehicle data at such a stage does not allow detailed finite element analysis. It is, however, possible to suggest the required collapse properties for individual components within the structure so that, through a coarse finite element idealization, a design for crashworthiness can be carried out. The crash properties of the structure can be arrived at by parametric studies of individual components that are absorbing the major portion of the crash energy.

This paper describes a methodology that, as a tool, can be used at the start of a vehicle program enabling the side impact performance to be monitored continuously and thus the structure to be designed in the most efficient way for a specified level of side crashworthiness. This has major advantages over current methods where a late finite element analysis or a late crash test is the first indication of how well a vehicle meets a specified standard and, if unsatisfactory, the necessary structural modifications are normally costly and result in inefficiencies in design and manufacturing processing.

Introduction

The inclusion of a good crashworthiness performance is a prime objective in any new vehicle concept development. It would be ideal if the implications of a good performance could be evaluated at the same early stage when marketing studies, alternate packages/clay models, legislative reviews, and manufacturing process decisions are taking place. Such an ideal system must be capable of assessing concept changes quickly and producing structural guidelines for an acceptable performance in return.

In the absence of any physical systems to test for performance at this stage, side crashworthiness assessments must depend on past experience or the development of a nonlinear finite element analysis that takes into account the nonlinear behaviour and large-scale deformations associated with crash conditions. The current state of the art of such nonlinear finite element codes, combined with a lack of essential detailed structural data for the analysis at the concept stage, makes a crashworthiness prediction difficult. This paper describes a test methodology for side collisions that overcomes many of these difficulties by combining known structural data with a coarse finite element model based on the new vehicle package.

It allows a continuous assessment to be made of side impact performance including structural collapse, energy absorption, impacted vehicle trajectory and occupant kinematics, and injury levels. The continuous interchange of data between the finite element model and the new vehicle design is an essential feature of the methodology providing broad guidelines initially and becoming more detailed as the structure develops. This results in minimum crash testing since the first crash test is more to confirm a performance level that has been continuously monitored than to determine a level that normally then requires modifications to achieve the desired standard.

This paper shows its application in relation to the development cycle of a new model and how it substitutes for a detailed finite element model initially and subsequently complements it in the later stages. Validation of the methodology is also discussed, and a typical case study is included that demonstrates the procedure from the initial concept stage.

The Side Impact Methodology

The basic problem with finite element analysis is well known and is demonstrated in Figure 1.

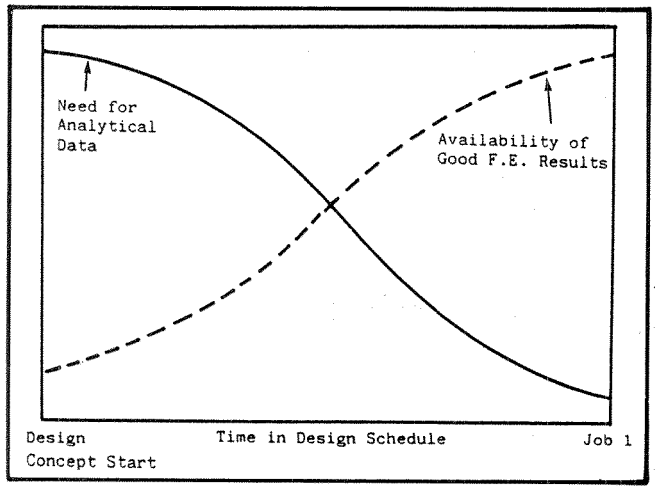

Figure 1. The problem with finite element analysis

This problem is compounded when considering nonlinear finite element codes where the state of the art is such that programs are large, complex, and costly, and meaningful results are usually only available late in the design cycle when their results are too late to influence the design. The methodology adopted for side impact crashworthiness studies is shown in graphical form in Figure 2.

The concept here is to use the previous vehicle component data—established by tests—assembled into the new vehicle package and the performance assessed initially relative to the new vehicle. Shortfalls in performance due to the new package can be established and, using parametric studies, guidelines can be produced to obtain a specific performance. As shown in the figure, as more detailed structural data become available, a detailed finite element model can be developed, eventually taking over from the initial coarse beam model, but the initial model is still available for a quick assessment of major vehicle modifications.

The methodology consists of a suite of programs:

- SimSim 1—a nonlinear large deformation beam element structural finite element method
- SimSim 2—a vehicle rigid body and dynamic deformation program
- Calspan 3D—a crash victim simulation program

The most important part of the methodology is the SimSim 1 program as the vehicle structural integrity largely determines the side impact occupant protection performance, assuming a standard crash test procedure. Due to its hybrid nature, this program can be used in the concept stage of a new vehicle. It uses test-derived data on the nonlinear behaviour of beams and joints, and analyses the overall collapse behaviour of the assembled structure. The contribution of each individual element in the structure can also be quantified.

The SimSim 1 structural result is then used in the SimSim 2 program, which is able to simulate a 90° side impact test. This program will predict the vehicle trajectory as well as the dynamic side structure deformation of the impacted vehicle in the collision.

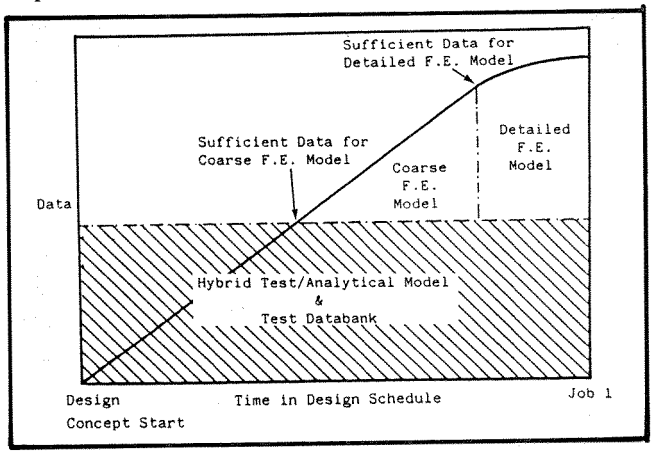

Figure 2. Crashworthiness model

Finally, the effects of such structural and vehicle dynamic behaviour on the occupant can be assessed by utilising the SimSim 2 results into an occupant simulation program, e.g., Calspan 3D CVS program.

The methodology is well suited for early crashworthiness parametric studies as a typical analysis turnaround time is an hour and the analysis costs are in the order of pounds sterling per run. A detailed description of the programs is to be found in the Appendix.

Application of the Methodology

The application of the methodology in a design environment is envisaged as follows (Figure 3):

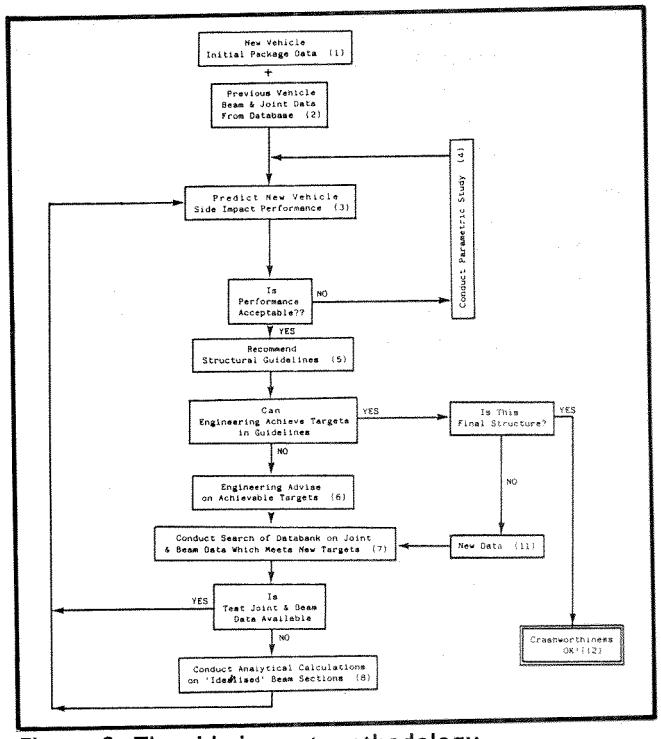

Figure 3. The side impact methodology

- Step 1—The new vehicle package data are obtained, and a beam model is assembled using the SimSim 1 program.
- Step 2—The beam and joint data required by the SimSim 1 program are initially assumed to be similar to the previous vehicle; a valid assumption as the design of new vehicles is generally evolutionary. New structural configurations (e.g., a new 5-door variant) can be analysed using existing structural element data (e.g., B-pillar) from other vehicles, which are stored in a computerised databank.
- Step 3—The initial side impact performance for the new vehicle is established by the SimSim 1, SimSim 2, and Calspan programs. Redundant or overstressed structural elements can be highlighted.

- Step 4—If the performance is not acceptable in relation to legislative or corporate standards, a parametric study can be conducted to optimise the side impact performance.
- Step 5—When the performance is acceptable, design guidelines on the side structure can be recommended, e.g., cross-section area.
- Step 6—Engineering/manufacturing advice on the achievable structural targets.
- Step 7—A search of the databank for suitable beam and joint data to meet the new structural targets.
- Step 8—If the data are unavailable, analytical calculations can be made to derive the required beam and joint nonlinear data using idealised cross-section shapes for the particular element(1).
- Step 9—Repeat Steps 3-8 updated with achievable engineering targets until a satisfactory and workable set of design guidelines can be established.
- Step 10—Initiate detailed finite element techniques for identified problem areas, e.g., weak joints if appropriate.
- Step 11—Return to methodology as more data are available due to hard points approval or design changes.
- Step 12—Achieve specified crashworthiness targets.

Validation of the Methodology

The validation of the methodology was conducted using crash test results in which a European hatchback was subjected to a 90° side impact with a CCMC (Committee of Common Market Automobile Constructors) mobile deformable barrier as the impactor. The impact velocity of the barrier was 50km/h, as currently under discussion in Europe for side impact test procedures.

Figure 4 shows a good comparison of the impacted vehicle centre-of-gravity velocity of simulation (SimSim 2) versus the test result.

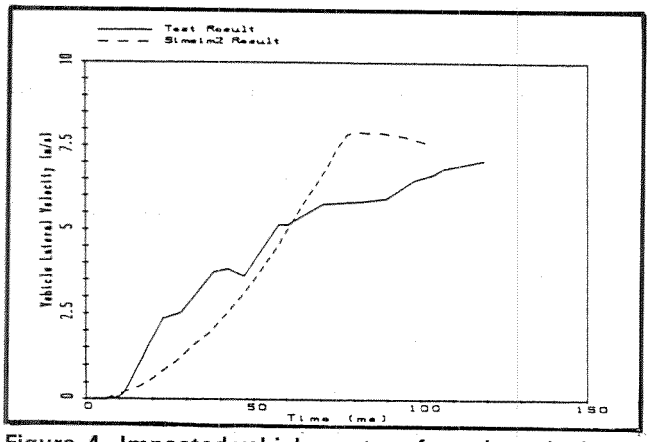

Figure 4. Impacted vehicle centre-of-gravity velocity of SimSim 2 simulation and test result

Figure 5 shows a better comparison of the B-pillar velocity of the impacted vehicle. This result is more important as it determines the injury levels inflicted on the occupants.

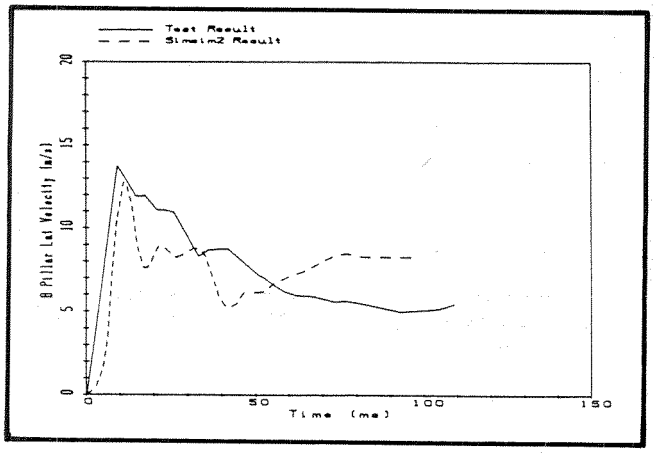

Figure 5. Impacted vehicle B-pillar velocity of SimSim 2 simulation and test result

Figures 6 and 7 are comparisons of velocities of the chest and pelvis of the impact dummy for the simulation and test results. In view of the simple structural models analysed and the low computer resource usage, the comparison of the simulation with the test result is very good.

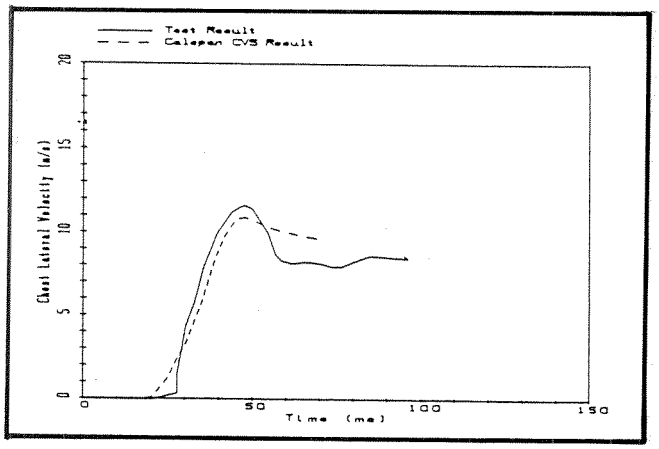

Figure 6. Driver chest velocity of Calspan CVS simulation and test result

Case Study of the Methodology

A case study was conducted to test the capabilities of the methodology. The vehicles selected were concept studies for a new European 3/5-door hatchback for which only package information was available. Suitable beam and joint data from the previous vehicle were used except for the 5-door vehicle whose B-pillar data were assumed from a similar vehicle.

Structural models for the 3- and 5-door vehicles were assembled using the geometric data from the new vehicle package information but using the previous vehicle beam

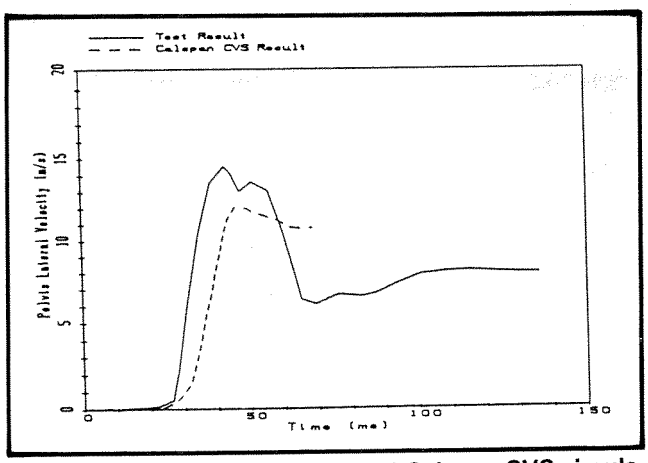

Figure 7. Driver pelvis velocity of Calspan CVS simulation and test result

or joint data. The SimSim 1 program was able to simulate the collapse mechanism of the structure when impacted in the side by the CCMC mobile deformable barrier (Figures 8a and 8b). It was also able to quantify the

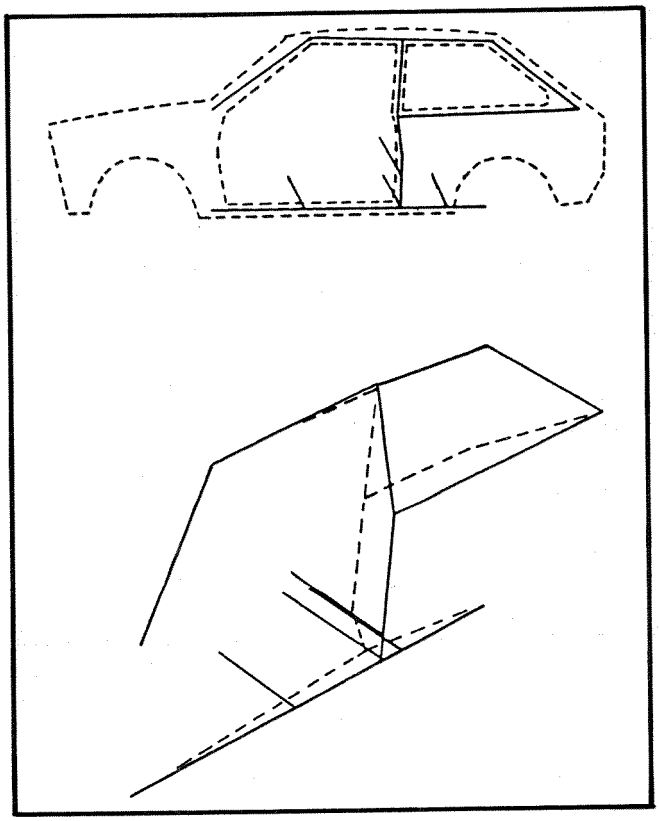

Figure 8a. Initial 3-door vehicle and structural model

structural contribution of each failed beam element by calculating the crash energy absorbed (Figure 9). The results showed the bottom of the B-pillar (A) in the 3- and 5-door initial vehicle designs absorbed up to 25 percent of the crash energy. This will result in excessive deformation in the B-pillar assembly. The structural integrity of the B-pillar is important in preserving the occupant survival

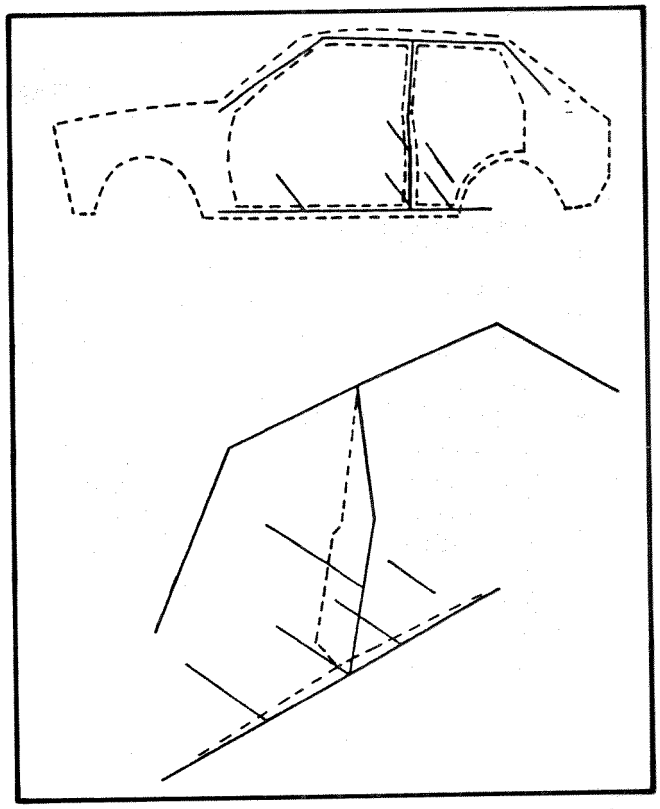

Figure 8b. Initial 5-door vehicle and structural model

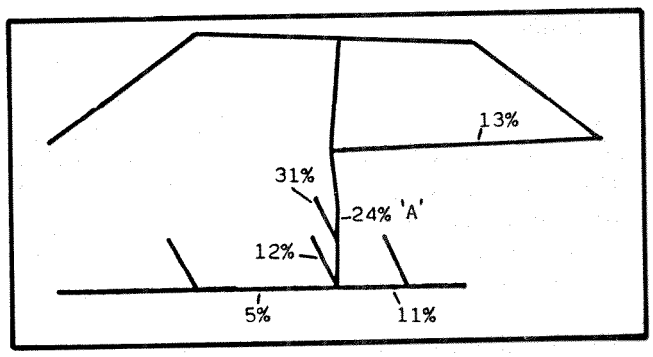

Figure 9a. Initial 3-door vehicle

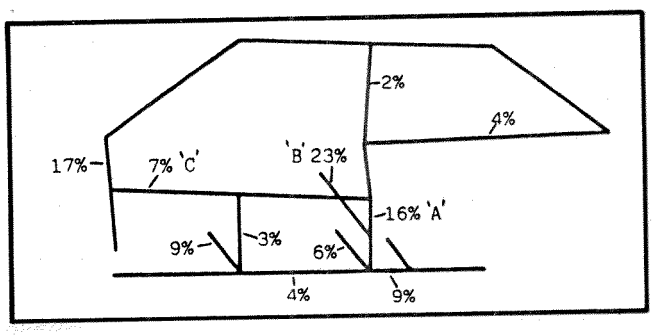

Figure 9b. Optimised 3-door vehicle

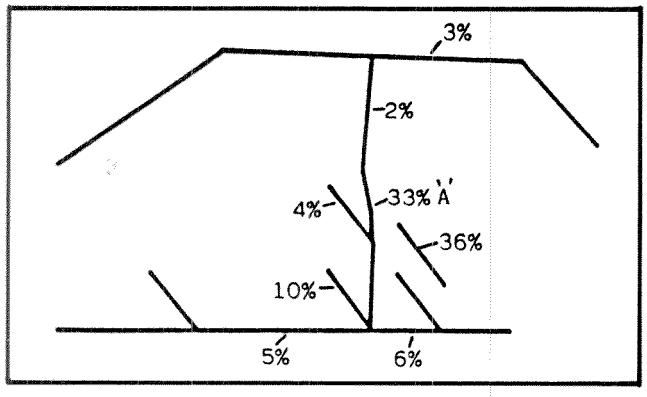

Figure 9c. Initial 5-door vehicle

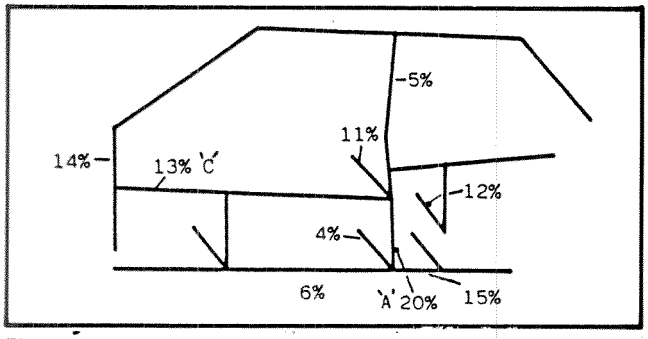

Figure 9d. Optimised 5-door vehicle

space. A weak B-pillar assembly will tend to pull the door toward the seated occupants. SimSim 2 and Calspan occupant simulations were also conducted to establish the initial side impact protection for both vehicles. These results will be presented later for comparisons.

Having established the initial performance, a parametric study was conducted to achieve the required performance. The structural criterion used was to limit the side structural collapse by distributing more evenly the loading by the impacting vehicle into as many beam elements as possible, preventing large local structural deformations.

Various structural configurations were investigated by including additional structural elements in the initial vehicle designs and modifying the beam or joint properties in these configurations. Only the results of the initial and optimised vehicles are presented here, for clarity.

The methodology showed the best results were achieved by structural compatibility through additional structural elements (e.g., door intrusion beams) and increasing the beam or joint properties of the structure. The optimised structural configurations studied were as follows: (Figures 9b and 9d)

- An increase in the B-pillar properties (A), significant increase in the rear-seat pan property (B), and the addition of a door intrusion beam (C) for the 3-door vehicle
- Increases in the B-pillar and rocker panel properties (A) and the addition of a door intrusion beam (C) for the 5-door vehicle

Note: The increases in the B-pillar and rocker panel properties are increases in the joint linear and nonlinear properties in these areas and not the beams themselves. This is because joints are normally the weak areas in the side structure and will fail before the beams.

Figure 9 shows the distribution of the crash energy absorbed throughout the structures in both the initial and optimised vehicles. The consequence of this optimisation is that there will be a reduction in the deformation of the B-pillar assembly in the optimised vehicles. Figure 10 shows a significant increase in the B-pillar strength over the initial vehicles. Using a standard 3kJ crash energy input, the deformation predicted by SimSim 1 showed a significant reduction in the B-pillar deformation in the optimised initial vehicles (e.g., 147 to 70mm for a 3-door and 175 to 67mm for the 5-door variant).

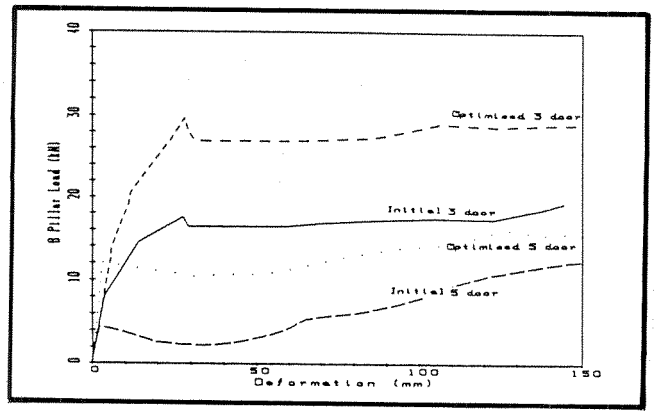

Figure 10. B-pillar stiffness characteristic for 3- and 5-door SimSim 1 structural models

These trends were also seen in the SimSim 2 results in Figure 11 where there is a significant reduction in the B-pillar deformation in the optimised vehicles.

Finally, the effects of the improvements were seen in the Calspan results (Table 1). The effect of reducing the side structure velocities resulted in the reduction of injuries sustained by the occupants (e.g., lower HSI and CSI induces) and dummy accelerations.

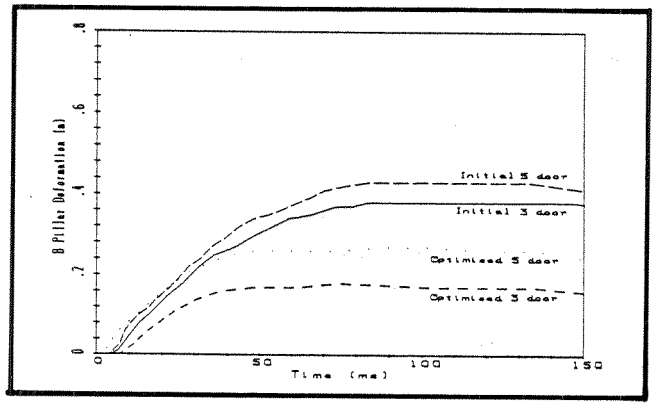

Figure 11. SimSim 2 results of B-pillar deformation at waist height for 3- and 5-door structural models

Table 1. Calspan CVS results

CVS Analysis	Initial 3 door Vehicle	Optimized 3 door Vehicle	Initial 5 door Vehicle	Optimized 5 door Vehicle
Max Velocity of Side Structure (m/s)	12.5	10.7	15.2	12.7
Velocity of Side Structure on Contact with Dummy (m/s)	12.5	10.2	15.1	12.2
Velocity of Side Structure at Chest Velocity of 0.1 m/s (m/s)	7.9	4.7	9.9	7.2
Head Injury Criteria (HIC)	138.0	67.0	224.0	94.0
Max Lateral Head Acceleration (g)	29.5	21.2	31.8	22.7
Chest Severity Index (CSI)	375.0	154.0	497.0	229.0
Max Lateral Chest Acceleration (g)	67.3	49.5	76.2	51.8
Max Lateral Chest Velocity (m/s)	10.5	7.8	12.5	8.9
Max Lateral Pelvis Acceleration (g)	110.0	80.6	117.5	83.9
Max Lateral Pelvis Velocity (m/s)	12.0	8.5	14.4	9.8

An example of the Calspan results output is shown in Figure 12. When the methodology has been established in an engineering environment, it should be possible to conduct a similar parametric study in a man-month analysis time.

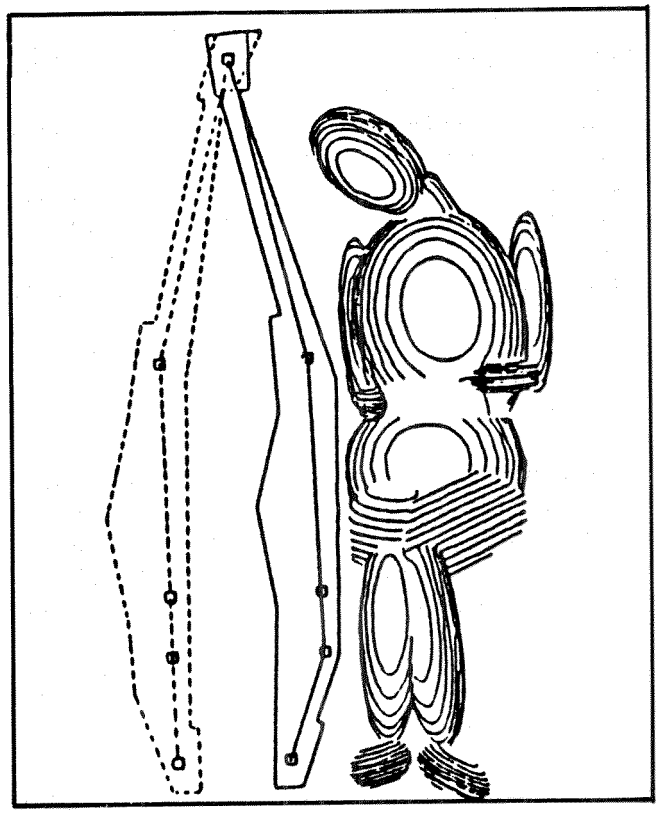

Figure 12. Calspan result showing dummy kinematics and impacted door deformation

Conclusion

- It has been shown that the described methodology can be used, at the early concept design stage of a new vehicle development, to achieve a specified side impact performance.
- Guidance at this early stage in the vehicle development will result in a more efficient design/structure and a more efficient manufacturing process. This will have benefits in the cost and weight of the vehicle and with additional development savings through the reduction in the number of crash tests that are currently necessary to achieve a specified crashworthiness performance.
- This type of hybrid prediction method has a short analysis turnaround time compared to other nonlinear finite element codes and has the additional benefit of improved accuracy through the inclusion of empirical data.

- The short analysis turnaround time and the low computer running costs enable the structural model to be up to date with the latest design update in the vehicle program, thus allowing a continuous interchange of data between the finite element model and the vehicle design.
- Finally, with its ability to predict the effects of a side collision on the structure, vehicle trajectory, and the occupants in the impacted vehicle, the methodology is ideal to use to assess and influence impending side impact legislation so that practical and achievable requirements are specified.

Further Developments

Developments are underway to reduce the reliance on test beam and joint data, i.e., to refine the methodology toward a more analytical approach. Investigations will be made to see if it is possible to develop a computer code to predict the linear and nonlinear properties of any given cross section of a beam. This will enable elastic buckling failure of the cross section of a beam to be examined as this mode of failure limits its theoretical load-carrying capability. This analytical capability will enable optimisation of the cross section of the beam elements and assess the influence of access holes, flanges, etc. The SimSim 1 structural analyses can then begin with optimised beam sections.

Acknowledgments

The authors would like to express their thanks to K. Stone of the Ford Motor Company and R. Hardy of the Cranfield Impact Centre for their valuable contributions during the development of this methodology.

Appendix

SimSim 1 Program

The SimSim 1 program is a customised coarse mesh beam element nonlinear finite element code. It is well suited to analysing vehicle structures in side collisions as these structures are essentially beams in bending. Other modes, e.g., compression and torsion, can also be simulated. It is a hybrid program that analyses elastic behaviour from traditional beam theory but requires test-derived nonlinear material behaviour to determine the nonlinear behaviour of the structure.

The program is based on a matrix method of structural analysis that is able to simulate large deformations plus the local and global collapse mechanism in a side structure of a vehicle. The stiffness matrix of the structure is assembled, and the loading increment (force or displacement) is applied. After each loading cycle, the beam element's internal loads are compared with its failure load derived from beam and joint tests in a yield criterion check. The program can simulate nonlinear behaviour such as perfectly plastic (i.e., the beam can maintain its load-bearing capability after failure) or moment drop off (i.e., the load that the beam can support before failure falls off rapidly after it has failed).

The program takes into account the deformations in the structure and any remaining beam strength before failure in the previous load cycle. The loading of the structure continues until either the structure collapses or the load limit is reached.

The program incorporates some useful features such as—

- The crash energy absorbed by each element due to plastic deformation can be analysed and quantified in relation to the input energy.
- A restart option allows any changes to be made to the structural model during the analysis due to changes in the boundary conditions, etc.
- The loading increments can be automatically scaled to insure the beam or joint yield failure behaviour determined by tests will be accurately modelled in the analysis.
- The finite stiffness of joints can be taken into account as they can significantly degrade the analysis result.

The application of this analysis method will lead to a better understanding of the behaviour of structures under side collision conditions and provide input to the SimSim 2 program to analyse the impacted vehicle motions.

SimSim 2 Program

SimSim 2 is a computer code developed to predict the rigid body motions and vehicle side deformations experienced in a 90° side collision.

The side collision dynamics are simulated by a series of unidirectional spring-mass systems representing the impacting and impacted vehicles while in contact with one another. The spring elements represent the impacting vehicle front end stiffness characteristics and impacted vehicle side structure stiffness characteristics. The mass elements represent the mass of both impacting and impacted vehicles, assuming the proportion of the mass of the impacted vehicle side structure is negligible compared with its overall mass. The impacting vehicle or mobile barrier front-end stiffness characteristics are obtained from vehicle crash tests, and the impacted vehicle side structure stiffness characteristics are derived from the SimSim 1 nonlinear analyses. The program can then predict the side structure dynamic deformations experienced in the side collision.

General equations of motions, together with the impacted vehicle tyre and suspension data, are utilised to predict the whole vehicle motions (e.g., centre-of-gravity velocity, yaw, and pitch).

The vehicle centre-of-gravity velocity and the side structure deformation data are used in an occupant simulation program to assess the effects of the collisions on the occupants. When these data are unavailable for a new vehicle due to lack of tyre and suspension data, the impacted vehicle rigid body motions can be calculated from crash test data of similar vehicles, taking into account the new vehicle mass and side structure stiffness characteristics.

The use of the SimSim 2 program, together with the occupant simulation program, will help to understand fully the effects of the collision on the occupants. The Calspan program is not described here as it is well documented in past conference papers.

References

1. Kecman, D., and G.D. Suthurst, "Theoretical determination of the maximum bending strength in the car body components," Vehicle Structures Conference, Cranfield, July 16-18, 1984.
2. Hardy, R.N., and G.D. Suthurst, "Simulations to assess the influence of car lateral impact characteristics on occupant kinematics," Vehicle Structures Conference, Cranfield, July 16-18, 1984.

Development and Testing of Optimized Deformation Structures

Florian Kramer and
Alfred Heger
Institut für Fahrzeugtechnik, Technische Universität Berlin

Abstract

To improve occupant protection in side collisions, it is not sufficient to consider only lateral structures deformation characteristics. It is also necessary to modify frontal structures, which are generally designed for rigid barrier frontal impacts.

In the following study, an analytical simulation model is used to optimize lateral as well as frontal deformation structures of passenger cars. The aim of the optimization is to minimize the risk of injuries of passenger car occupants, considering all relevant types of car-to-car and car-to-obstacle accidents.

Structures built according to the analytical results are likely to show differences in their dynamic behavior compared with the calculated characteristics. As the analytical optimization yields optimum reduction of occupant loadings, differences of actual structures do not lead to optimally low loadings. Restrictions have to be considered as to what extent nonoptimal reductions in safety can be accepted.

In full-scale tests and component tests, the performance of the structures has to be demonstrated.

The Analytical Optimization of Vehicle Structures

The aim of the research project "Occupant protection"[1] was the optimization of deformation structure characteristics of the front and lateral areas in vehicles of various weights, as seen from the economic aspect (Figure 1).

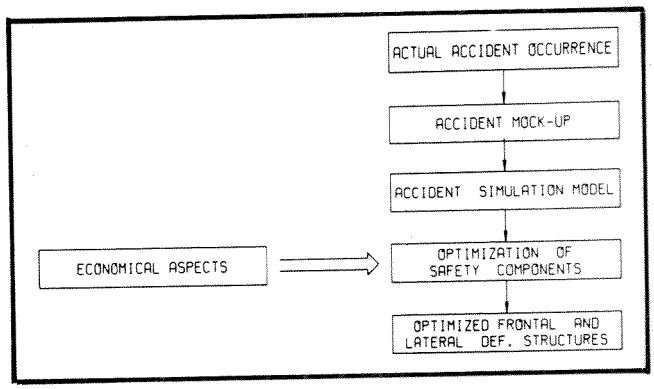

Figure 1. Aspects of development of passenger cars considering economically optimal occupant protection

[1] "Development of passenger cars with regard to optimum occupant protection from an economical aspect," promoted by the Federal Ministry of Research and Technology and carried out by the parties working in cooperation: Volkswagenwerk AG (project management), Institut für Fahrzeugtechnik der Technischen Universität Berlin, Dr. Ing.h.c. F. Porsche AG and HUK-Verband.

Accident Occurrence

The complexity of the actual accident occurrence was taken into consideration by condensing the essential factors influencing the injuries of the vehicle occupants, such as type of collision (frontal and lateral collisions for vehicle/vehicle accidents and for single-vehicle accidents), mass distribution and impact speeds, to one accident mock-up with the aid of a relevant analysis. The accident mock-up consists of 57 different individual accidents: vehicle/vehicle accidents, 18 frontal and 27 lateral; vehicle/obstacle accidents, 6 frontal and 6 lateral; with three reference vehicles of various weights and 3- and 2-speed classes, respectively(1).

Simulation Model

A mathematical simulation model was developed on the basis of extensive accident data analysis and detailed evaluation of crash tests. Despite the necessary simplifications, this model clearly illustrates the manifold interrelationships between the deformation structures of the vehicles involved in collisions and their effect on the severity of injuries incurred by the occupants(2). The translation of mathematically determined occupant loading values into corresponding grades of injury severity and the ensuing costs of injury resulting from these is made possible by the procedure of so-called statistical biomechanics(3).

National Economic Aspect

The monetary evaluation of the occupant injuries alone is not sufficient, however, because a complete assessment of the national economic aspect and assessment of costs for all design measures involved had to be provided. The evaluation of these so-called effective field costs not only includes the sale price of the vehicles but also the fuel consumption, which is influenced by the weight and geometry of the vehicle(4).

Optimization

A process based on the principle of biological evolution was used in optimizing the deformation behavior of the vehicles in the substitute accident occurrence(5).

In the above-mentioned research project, three optimization runs were carried out, each being different in the formulation of their aims and the restrictions imposed, and each of which led to a different interpretation of the deformation structure characteristic(6). All the optimization runs had in common that the occupants were connected to the vehicles by safety belt systems. The choice of the restraint system (3-point automatic belt, with and without preloading) led to vehicle structures that were especially suited to these.

In addition, in all three optimization runs it could be determined that the desired protection, especially for the laterally struck occupant, could be achieved to a considerable extent by matching the design of the front structures of the colliding vehicles (30 to 70 percent, depending on the formulation of the object function). From this it ensues that the isolated examination of the frontal barrier crash tests as carried out and prescribed—at least by American law—at the moment may possibly lead to an improvement of self-protection in frontal collisions, but the important aspect of partner protection, in particular in frontal collisions but also in lateral collisions, is neglected.

The Deformation Structures of the Laterally Crashed Car as the Result of Optimization

In the two-dimensional modeling of the lateral car collision, the characteristic curves door/roof frame, door/floor group, door/occupant thorax, and door/occupant pelvis were made variable (Figure 2). The door

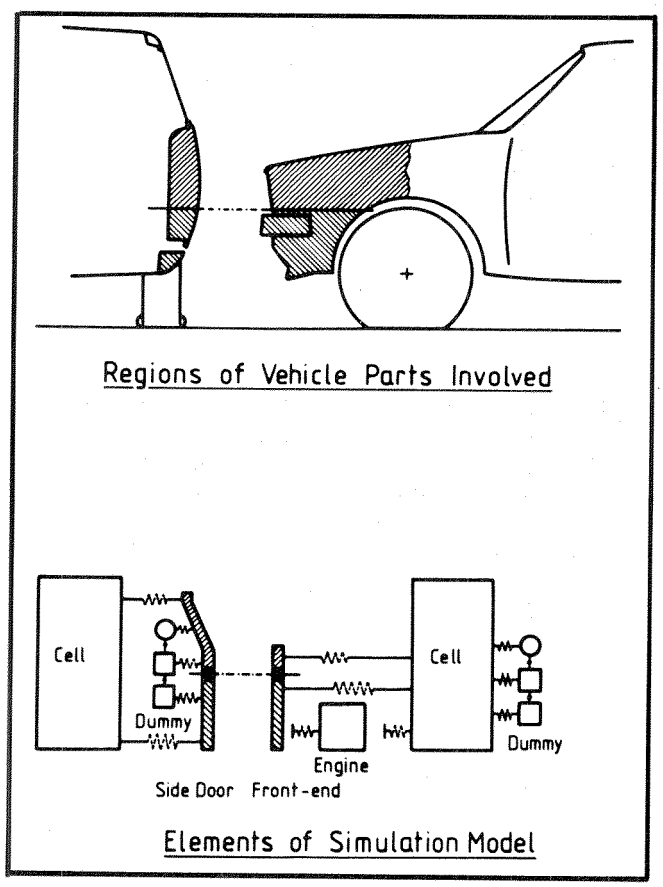

Figure 2. Structure characteristics of lateral accident simulation model

has to be subdivided due to the different loadings on the thorax and the pelvis of the laterally hit vehicle occupant; the permitted relative movement was not varied once it had been predetermined. Head impact was not considered due to the fact that Hybrid II dummies were used in the test, and the lateral impact characteristics determined here were unrealistic.

In the optimization runs, the following four characteristic curves were determined in accordance with the model:

- Upper side/cell
- Lower side/cell
- Door paneling at thorax height (inner door panel, inside padding, rigidity of thorax)
- Door paneling in pelvis area (inner door panel, inside padding, rigidity of pelvis)

As an example of characteristics of curves optimized in this way, the results of an optimization run are shown in Figure 3(6).

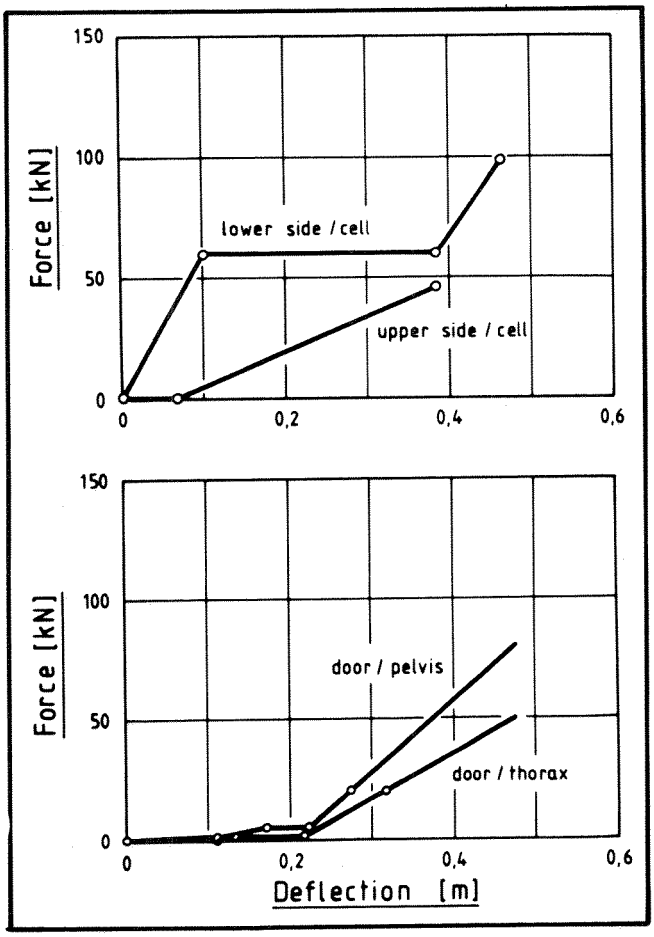

Figure 3. Optimised lateral deformation structures

Concept of the Experimental Examination of the Lateral Structures of Cars

Using the analytical determination of the structure characteristics as shown above, the following necessary requirements for deriving a test concept(7) can be formulated (Figure 4):

- Reliability of accident mock-ups
- Accuracy of reproduction of the simulation model
- Validity of the object-system limits in the formulation of the object function

Once these basic requirements have been fulfilled, the objectives of the tests are reduced to the question of—

- Extent to which the structure modifications can be checked
- Comparison between the characteristic curves as determined in the analysis and their realization in design
- Measures to be taken when there are discrepancies

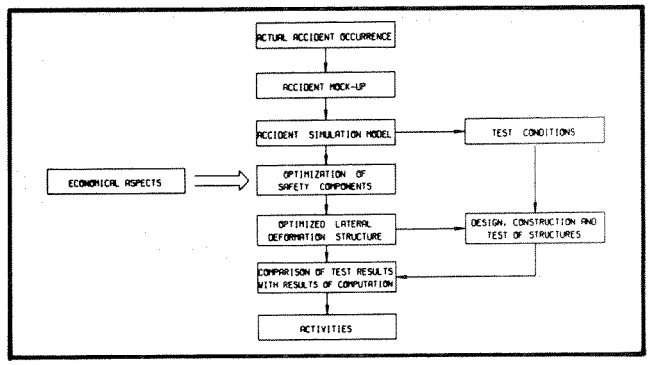

Figure 4. Conception for experimental verification of analytically designed side structures of passenger cars

Connection Between Mathematical and Experimental Simulation

The close interlinkage of simulation and experiment is prescribed by the fact the vehicle lateral structure is determined by analysis and it is necessary to examine the structure characteristic curves realized in the design experimentally. Compared with previous tests on lateral collisions, the test conditions that determine the test object, test procedures, measured variables, and the evaluation criteria are oriented less toward the accident occurrence than to the structuring of the simulation model. One must be able to check the parameters introduced in the model experimentally.

Apart from this, in the experiment, one can leave out areas for examination that have already been taken into consideration in the course of optimization, e.g., the accident constellation, the characteristics of the collision opponents, the loading of the occupants and their biomechanical effects, as well as the effects of the structure modifications from an economic aspect. The experiment thus merely serves to examine the structures for their deformation characteristics and to provide measured results for comparison to the mathematically obtained results; for this, component tests, which are

noted for providing considerably better reproducibility in the test results, are adequate. Integral vehicle tests, in which dummies serve only to check and validate the simulation model, can be made outside of the strict time limits involved in preparing an automobile for series production.

Extent to Which the Deformation Characteristic Curves Can Be Checked

In the optimization model, the front and lateral structures of colliding vehicles were matched to one another, but, as opposed to this, the mutual interaction of the front and lateral structures of one and the same vehicle was ignored. This corresponds to the accident mock-ups and, to a large extent, to the actual accident occurrence; also to a large extent because the structure elements set out for the lateral impact only take effect in frontal collisions when there is considerable deformation of the cell. Such serious deformation only takes place, however, at a speed range that, from a statistical point of view, occurs far less often than the range at which the frontal structure can absorb the whole of the deformation energy.

In lateral collisions, no effects of the front structure, which acts in a longitudinal direction, on the deformation behavior of the vehicle hit side-on could be established. Therefore, tests can be used for lateral structures separately.

The structure characteristic curves introduced into the optimization as initial values are derived from characteristic curves determined by means of static and dynamic test procedures. As opposed to these, the optimized characteristic curves are the result of the optimization calculation in which they act dynamically as part of a complex spring-mass system.

The dynamic definition, however, is the result of the vehicle model-structuring and the distribution of mass in the simulation model. In the experiment, therefore, both the static and dynamic deformation behavior had to be examined. If one assumes a suitable vehicle modeling as a precondition, however, the dynamic behavior is characterized merely by velocity- (damping) and acceleration-dependent (mass moment of inertia) influences(8). These characteristic quantities of the material are introduced into the optimization as constants and are not subject to any changes. Therefore, if these conditions are retained in the realization of the design, the dynamic checking can be omitted in the test. As already mentioned, dynamic tests are merely necessary for validating the simulation model.

Another range of problems arises from the fact the optimization calculation determines individual structure characteristic curves that can be realized in the design but cannot be examined separately, e.g., the characteristic curves upper side/cell and lower side/cell since it cannot be excluded that these support and, therefore, influence each other. Examination of the lateral structure, which consists of several individual characteristic curves, has to be carried out while, at the same time, insuring that several characteristic curves correspond with the respective predetermined results obtained from calculation. The experimental proof is, therefore, necessary since the injury mechanics depend to a large extent on the definition of the characteristic curves.

In view of the demand for reduction of the development costs in automobile construction and, at the same time, for improvement of occupant protection, one can conclude that an examination of the lateral structure with quasi-static component tests is possible and can be carried out with a relatively small amount of effort regarding time and costs. This procedure requires, however, that the simulation model must be continuously checked with the aid of integral vehicle crash tests and, if necessary, be adapted accordingly.

Agreement Between Calculations and Tests, and Considerations To Be Taken in the Case of Deviations

In the optimization calculation, a total of four characteristic curves are prescribed for the lateral structure of cars. These are:—

- Upper side/cell
- Lower side/cell
- Upper door padding
- Lower door padding

It is not probable that the mechanical structures were to achieve an exact reproduction of the calculated characteristic curves, so deviations must be allowed for from the start and must be tolerated within firmly established limits. Since these deviations lead to the vehicle showing a different behavior in an accident situation compared to the precisely calculated occurrence, they have to be estimated.

The accident simulation model was subjected to great simplifications in favor of the shortest possible calculating times. For this reason, a more detailed simulation model in which a subsequent calculation of the individual accident is carried out on the basis of the characteristic curves determined by measurement is used for the estimation (Figure 5). In this, the evaluation algorithms used for the optimization are utilized for assessing the injury-dependent costs and the effective field costs. Of course, only the calculated results and test results can be compared for agreement; this only leads, however, to a yes/no statement. The effects on the ensuing costs situation cannot be predicted in this way.

An agreement between the structural characteristics as set out in the design and the mathematically predetermined characteristic curves leads to the structure being accepted.

If an acceptance agreement between these two cannot be obtained, the design must be adapted to suit the appropriate requirements, either in part or as a whole. In an iterative process "design-construction-testing-comparison," the design realization of the mathematically established deformation structure within a tolerable permitted range is retained.

At the same time, when these test results are made available, the simulation models used can be examined and validated and can thus be subjected to a continuous process of adaptation (Figure 5).

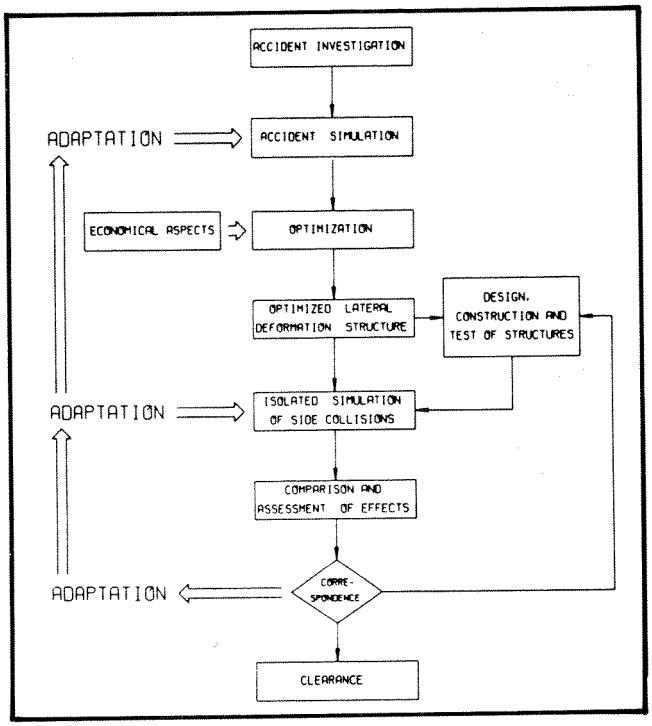

Figure 5. Conception for verification of constructed side structures of passenger cars and following consequences

Test Conditions for Checking Analytically Determined Lateral Structure Characteristic Curves

If one follows the concept of closely linking the simulation calculation and the test technology as explained above, this simplifies experimental examination of the design realization of the mathematically determined lateral structure characteristic curves in the following areas:

- Test objects
- Test procedures
- Measured variables
- Evaluation criteria

Test Objects

In accordance with the structuring carried out in the simulation model, the test objects to be examined are the door paddings and the door connection to the passenger cell.

From the characteristic curves of the door paneling at the thorax and pelvis levels, the rigidity of the dummy can be eliminated so the combined characteristic curve comprising the padding and the inside door panel rigidity can be examined in a single test setup. Here, the form of the test body corresponds to the respective part of the occupant's body. In the examination of the characteristic curves upper side/cell and lower side/cell in the two-dimensional simulation model, the complete occupant cell serves as a test object, and a front-contoured ram serves as a test body.

Test Procedures

The experimental examination of the structure characteristic curves is static. In this, the door paneling or the occupant cell has to be fixed in such a way that it cannot evade the quasi-static penetration process. On the other hand, the mounting must not influence the rigidity characteristics of the test object.

Measured Variables

In the examination of the padding characteristic curves, it is no problem to measure the deformation force and the deflection. More effort is involved, however, in determining the characteristic curves for the door/cell structure by measurement. On the one hand, it is necessary to establish the force-deflection curve of the examined body, which is suitably subdivided. On the other hand, the three-dimensional penetration movement of the inner door panel must be determined using displacement transducers to obtain a correlation for the distribution for the upper and lower structure characteristic curves. A distribution statement can be deduced from the relative position of the displacement transducers and, in this way, the upper and lower force-deflection curve for the door/cell system can be determined.

Evaluation Criteria

First of all, relative deviation is the decisive quality criterion for an agreement between the mathematically predetermined and the measured characteristic curve.

The relative deviation, however, provides no assistance in deciding whether to retain an existing structure or whether a modification and reexamination of the structure is necessary. To do this, it is necessary to enter the measured results as a set of data for the single-case simulation models and to calculate the effects on the ensuing costs of injury and effective field costs.

Summary

In the close connections between mathematical and experimental simulation, which are desirable objectives, a wide range of aims such as the determination of the dummy loading, as well as the selection of relevant accident constellations, can be set for the mathematical calculation. This method may not necessarily reduce the total effort involved in vehicle and component tests, but the tests during the strictly time-limited phase of preparing for series production can be carried out more simply and quickly, so that necessary adaptations of the structure characteristic curves are easier to introduce and check. A higher degree of reproducibility of the test results can be achieved by the more simple construction of the test setup. Deviations in the objective/actual-state comparison can be clearly allocated. Integral vehicle crash experiments for adaptation and validation of the simulation models or as acceptance tests to prove that legal requirements are being met can be carried out in accompaniment to the model and thus lie outside of the critical path of an automobile development project.

References

1. Langwieder, K., and W. Schmelzing, Kollisionen von Personenwagen unterschiedlicher Masse. XI. Statusseminar "Kraftfahrzeuge und Straßenverkehr" des BMFT, Münster, 1984.
2. Zimmermann, P., B. Richter, H.-C. Wille, and R. Zobel, "Impact—integrated multiple program for accident crash trauma," SEA, Technical Paper Series 840868, 1984.
3. Zobel, R., "Economically justified passenger protection results of simulation," SEA, Technical Paper Series 850517, 1985.
4. Hoefs, R., L. Hamm, and H. Brandsch, "Vehicle analysis with respect to passive safety and economic effects," SEA, Technical Paper Series 850517, 1985.
5. Oberdieck, W., B. Richter, and P. Zimmermann, Evolutionsstrategie—Ein Hilfsmittel bei der Lösung fahrzeugtechnischer Aufgaben, Automobiltechnische Zeitschrift (ATZ) L, 1982.
6. Richter, B., H. Appel, R. Hoefs, and K. Langwieder, Entwicklung von PKW im Hinblick auf einen volkswirtschaftlich optimalen Insassenschutz, Abschlußbericht, Wolfsburg, 1984.
7. Kramer, F., A. Heger, and H. Appel, Konsequenzen aus der Optimierung von PKW-Deformationsstrukturen, XI, Statusseminar "Kraftfahrzeuge und Straßenverkehr" des BMFT, Münster, 1984.
8. Hoffman, J., Rechnerische Untersuchung zur optimalen Seitenstruktur von Personenkraftwagen, Dissertation an der Technischen Universität Berlin, 1980.

Status of the MADYMO Crash Victim Simulation Package 1985

J. Wismans
T. Hoen, and
L. Wittebrood
Research Institute for Road Vehicles TNO, Delft, The Netherlands

Abstract

MADYMO is a compact, general purpose, computer program package for two- or three-dimensional crash victim simulations. The program predicts the kinematics and dynamical behavior of the victim during the crash, based on data of the victim, environment, safety devices, and crash conditions. The package differs from most of the existing CVS programs by its flexibility in choice of number of linkages and number of elements in each linkage. Great flexibility in the modeling of force interactions between elements and environment is assured by the fact that user-defined submodels can be incorporated readily.

This paper summarizes the most important features of the current MADYMO 2D and 3D versions and reviews a number of applications. Topics covered include side impacts, pedestrian safety, human body segment models, and computer-aided design. An attempt to identify areas of future developments and general trends in the field of crash victim simulations concludes this paper.

Introduction

In the field of automotive research, simulation of crashes is of vital importance to evaluate and improve safety devices and occupant environment. Most of this

work is done by experiments, using instrumented dummies, cadavers, and occasionally animals or volunteers. During the past years, a strong increase could be observed in the use of computer simulations in this area due to the fast developments both in computer hardware and simulation software. Similar trends could be observed in other engineering disciplines where mathematical modeling has been an accepted tool for many years.

The behavior of dynamical systems in a crash environment appears to be of a very complex nature where, in general, a large number of system parameters will influence the system's dynamic response. Due to this, a strong emphasis should be placed on experimental verification. As soon as an adequate level of reliability is obtained for a specific application, an effective economic tool will be available for further analyses or optimization of that system.

This paper describes the most important features and reviews of various applications of the MADYMO Crash Victim Simulation program. The program is of the type gross-motion simulators, which describe the human body (or other structures) by means of a number of connected rigid bodies. A review of several programs of this type, including the CALSPAN CVS model and the MVMA model, is given by (1,2,3).

Theoretical background of the MADYMO package will not be discussed here. Readers interested in this subject are referred to (4) for a general treatment of rigid body dynamics theories and to (5) for a brief summary of the specific MADYMO equations of motion.

Current MADYMO Features

General

MADYMO is a compact, general purpose, computer program package for two- or three-dimensional simulations of human body gross-motions. The program, which is based on rigid body dynamics using Lagrange equations, can be used to simulate one or more linkage systems without closed loops. Such systems are also known as tree-structures(3). However, MADYMO allows the behavior of a closed loop system to be approximated by connecting the end segment of a tree to any other segment by means of a massless element. The number of elements (rigid bodies) in each linkage system can be selected freely. The connections (joints) between the elements in a linkage system are of the hinge type for the two-dimensional and of the ball and socket type for the three-dimensional simulations.

Motion of the tree-structure of joint-connected elements is caused by external forces. MADYMO offers the user a set of standard force-interaction models, e.g., for belts, joints, and contacts of segments with each other or with the environment. The program is organized in such a way that the user can modify these routines in a relatively simple way while, in addition, user-defined submodels can be incorporated readily.

The standard solution technique to solve the equations of motion is a fourth order Runge-Kutta-Merson method with a fixed time step. In MADYMO 3D optional, a fifth order Runge-Kutta-Merson method with variable time step is available. A restart option in MADYMO 3D allows restart of a simulation at any point of time on the basis of calculation results in a preceding simulation.

The description of MADYMO to be presented here relates to MADYMO 2D version 3.0, which has been available for several years for external users, and MADYMO 3D, which will become available later this year. A number of features described for MADYMO 3D and not yet incorporated in the current MADYMO 2D version will be included in the next MADYMO 2D release. Both the 2D and 3D versions have been applied extensively in various research programs in the past years as described later. Based on the experience in these research applications, the MADYMO 3D version has gone through considerable debugging and optimizations with particular emphasis on the user convenience of the package.

In the next section, some of the current features of MADYMO 2D and 3D will be discussed in more detail. Among other things, attention will be given to joint, contact, and belt models.

Joint Loads

In MADYMO 2D, elements are connected by pin joints with 1° of freedom (Figure 1a). A nonlinear joint torque can be specified, consisting of elastic, viscous damping, and coulomb friction components. The standard features of MADYMO 2D allow in addition the simulation of a 3° of freedom planar joint, i.e., with 1 rotational and 2 translational degrees of freedom by specification of the joint segments as elements of different systems. Interaction between the two elements can be represented, for instance, by spring-damper models and contact models. A hypothetical example simulating the human knee joint is illustrated in Figure 1b.

The standard joint connecting two segments in the MADYMO 3D version is of the ball and socket type with 3° of freedom. Three methods are currently available to apply joint loads (Figure 2):

- Option I—The cardan joint model
- Option II—The flexion-torsion joint model
- Option III—Spring-damper and/or contact models

In the cardan joint model (option I), the relative position between the joint segments is considered to be the result of three successive rotations. The first rotation is around an axis fixed to segment i, the second rotation around a floating axis, and the third rotation around an axis fixed to segment j (Figure 2a). The centers of

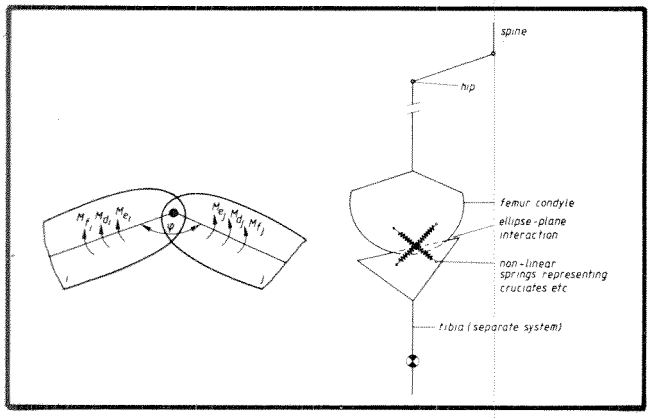

Figure 1. Methods to apply joint loads in MADYMO 2D (a. pin joint; b. hypothetical example of a joint with 3 degrees of freedom)

rotation for the three hinge joints are assumed to coincide in one point. Joint torques can be specified for each rotation separately by means of nonlinar elastic, viscous damping, and friction torque components similar to the MADYMO 2D version. One or more rotations can be locked by defining relatively stiff elastic torque characteristics. This joint model is suitable to describe, for instance, some of the joints in the Part 572 dummy such as the shoulder, elbow, and knee joints.

In the flexion-torsion model (option II), the relative rotation is thought to be the result of a flexion α and a torsion β (Figure 2b). Similar to the cardan joint model, nonlinear elastic joint torques can be specified as a function of these angles. In addition, a damping and friction torque can be applied as a function of the relative rotational velocity between both segments. This joint model can be used, for instance, to approximate the behavior of the rubber cylinders representing the spine and neck in the Part 572 dummy.

For each joint in a MADYMO 3D linkage system, it is possible to define the cardan joint model or flexion-torsion joint model. Both joint models can also be defined in combination for the same joint, which allows the user additional flexibility in modeling a more complicated joint type. In some situations, the application of spring-damper systems or contact models (option III) might also offer realistic additional possibilities for joint modeling (Figure 2c).

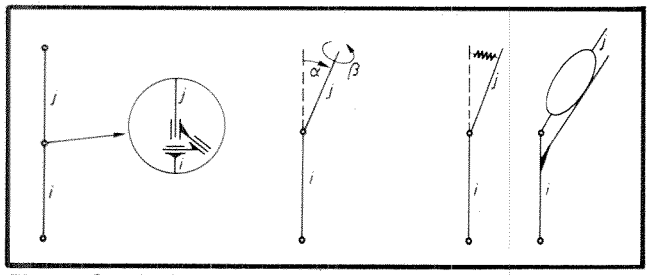

Figure 2. Methods to apply joint loads in MADYMO 3D (a. cardan joint model; b. flexion-torsion joint model; c. spring-damper and/or contact models)

Joints with 6° of freedom can be represented in MADYMO 3D by assigning the two joint segments to separate linkage systems similar to the 3° of freedom joint in MADYMO 2D (Figure 1b).

Contact Loads

In MADYMO 2D, contact lines and hyperellipses can be attached to any element of any system or to the laboratory reference frame. A hyperellipse is defined as follows:

$$\left(\frac{|x|}{a}\right)^n + \left(\frac{|y|}{b}\right)^n = 1$$

where a and b are the semi-axes of the hyperellipse and n is the degree (Figure 3). If n = 2, this equation describes a standard ellipse; if n increases, the hyperellipse approximates more and more a rectangle as illustrated in Figure 3. In this way, edge contacts can be described quite realistically. In a similar way in MADYMO 3D, contact planes and hyperellipsoids can be specified.

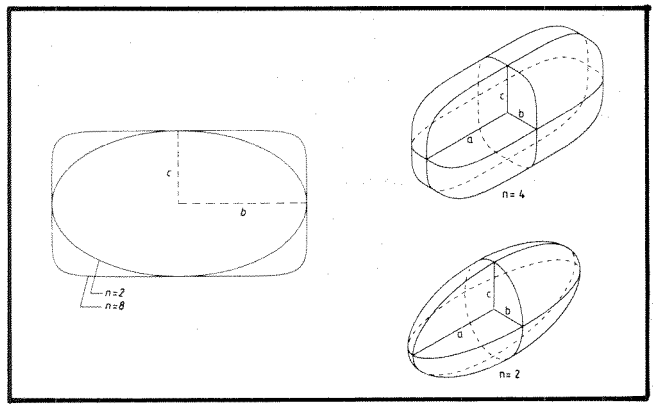

Figure 3. Hyperellipses (left) and hyperellipsoids (right)

The contact lines (planes) and hyperellipses (hyperellipsoids) describe the occupant interaction with vehicle interior surfaces. Two contact models are available, namely for contact lines (planes) interacting with ellipses (ellipsoids) and for hyperellipses (hyperellipsoids) interacting with each other. The reaction forces on the system segments are generated as a function of the penetration between these contact contours. More details on the penetration algorithms are provided in (6). Nonlinear elastic damping, as well as friction forces, can be applied.

Additional features of these contact models are—

- Simulation of Intrusion, etc.—A user-defined subroutine (standard in MADYMO 3D) allows specification of the position of contact contours as a function of time. In this way, for instance, intrusion of the car-side structure into the compartment can be simulated.

- Initial Penetration Correction—The penetration used to calculate contact forces can be taken relative to the initial penetration. In a relatively simple way, a state of equilibrium can be obtained at the start of the simulation, provided the effect of gravity can be neglected.
- Hysteresis—The effect of energy absorption in material can be simulated by defining the unloading slope of the force-deflection characteristic.

Belt Loads

Two force-interaction routines are available to represent belt restraint systems:

1. A simple massless spring-damper element, which can be used to simulate a lapbelt or the upper or lower part of a torso strap.
2. An advanced belt system model. This model is basically the same in MADYMO 2D and 3D and describes the real spatial belt geometry (Figure 4). The model consists of five segments and can account for slip between the belt segments and initial belt slack (or penetration). For the belt material, energy dissipation and permanent elongation can be specified. An option called "film spool effect" is available for belt systems with a retractor.

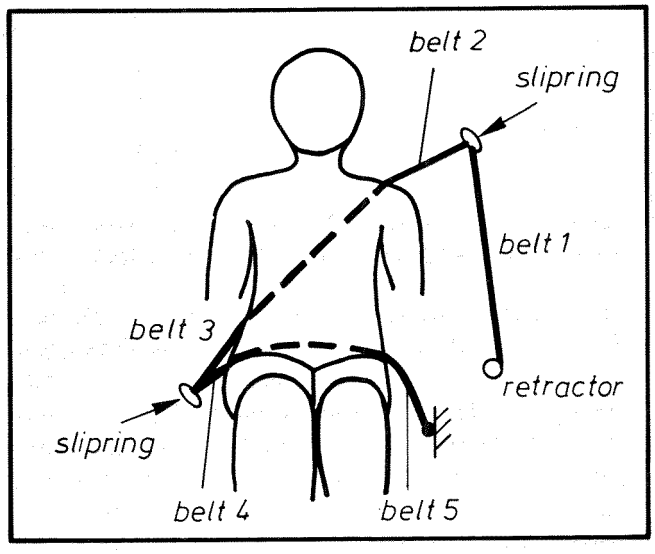

Figure 4. Advanced belt model

Point-Constraint Model

This routine constrains the position of one point of a segment relative to an arbitrary point fixed to another segment (or the environment). Both elastic and damping constraint loads can be specified in three mutually perpendicular directions (MADYMO 3D). Application of this model is useful to constrain the motion of a separate rib cage segment(7) or to simulate a deformable steering column.

Deformable Steering Column

MADYMO does not have a separate force-interaction routine for a deformable steering column since the standard features of MADYMO specify such a system directly in a simple way. Figure 6 illustrates a realization of such a model as it was successfully implemented by several MADYMO users. A two-segment linkage system is used here where one segment represents the steering column and one segment the steering wheel. The column is connected to the vehicle by means of two point constraints describing the column deformation characteristics.

Airbag

The current MADYMO versions do not include a standard force-interaction model for an airbag. A user-defined subroutine has been developed recently for the driver-airbag interaction where the airbag can be connected to a deformable steering column. This routine is expected to be available as an option in the next MADYMO 2D release.

Software Characteristics

MADYMO is a compact modular program package written in FORTRAN 77. Due to the limited size of the program, the MADYMO package can be implemented even on small computer systems, which is illustrated by the following figures.

A simulation of an occupant in a frontal collision with MADYMO 2D requires 100k byte memory and 3.5min CPU time, whereas a complicated simulation of a cyclist impacted by a car with MADYMO 3D needs only 200k byte memory and 12min CPU time (above data relate to a VAX 11/750).

Pre- and Postprocessing

The input for the current MADYMO versions is contained in a single formatted input file, which can be changed simply by the user's editor. A special user-convenient subroutine has been developed in MADYMO 3D for specifying the initial position of the occupant and the various local coordinate systems that define inertia axes, joint rotation axes, hyperellipsoids orientations, and point-constraint directions.

Special attention has been paid to user-convenient postprocessing in MADYMO 3D. In the input dataset,

the user has to define which parameters must be calculated for output purposes, such as—

- Kinematics
- Linear displacements, velocities, and accelerations of specified points
- Angular velocities and accelerations of specified elements
- Forces of specified force models
- Torques of specified joints

For additional output, a user-defined subroutine can be incorporated in the program to generate the model data in a format similar to experimental test data to apply user's standard experimental analysis software for further data processing.

For postprocessing of the kinematics, a three-dimensional graphics package is available that can be used in conjunction with both MADYMO 2D and MADYMO 3D. Features of this package include—

- Isometric projections of ellipsoids and planes
- User-defined viewpoint
- Intersecting ellipsoids
- Countour lines on the surface of the ellipsoids
- Hidden lines elimination
- Self-contained; only simple plot routines are used

Some of the features of this graphics package are illustrated in Figures 5, 6, 7, 9, and 12.

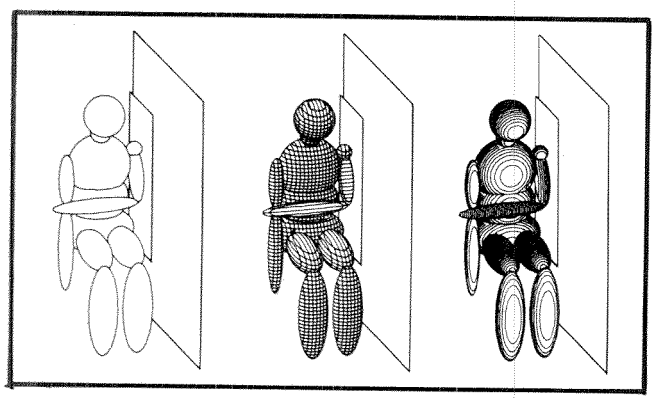

Figure 5. Examples of output from the MADYMO 3D graphics package

Applications

The versatility of the MADYMO program package will be demonstrated here by means of a number of simulations conducted in the past years. For most of these examples, a detailed experimental verification was performed. The applications will be divided into six categories:

- Frontal collisions
- Side collisions
- Pedestrian and cyclist impacts
- Child in a child restraint system

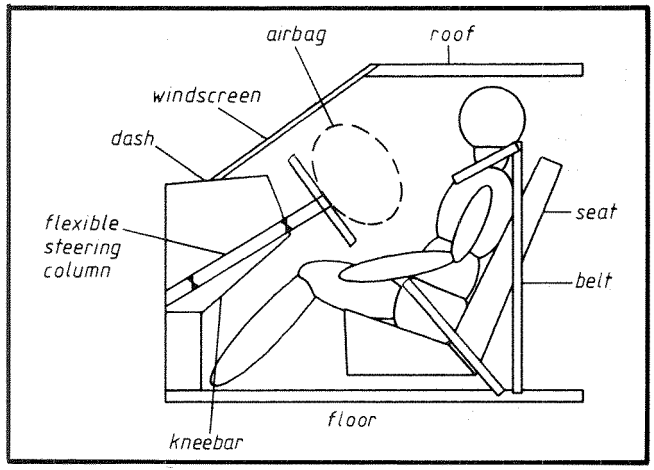

Figure 6. General model setup for an occupant in a frontal collision

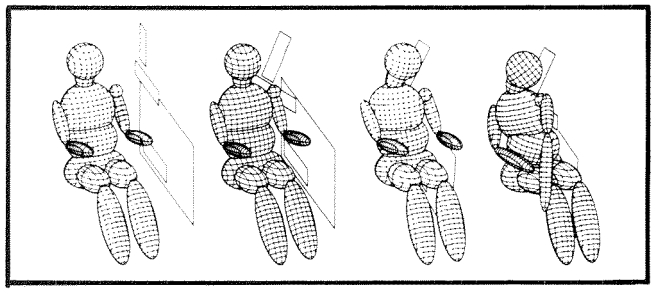

Figure 7. Mathematical simulation of a Part 572 dummy in a Peugeot 504 during a lateral collision (75km/h)

- Human body segment models
- Computer-aided design studies

Frontal Collisions

The general model setup of an occupant in a frontal collision most often used today is illustrated in Figure 6. The first experimental verification of the MADYMO 2D model was for a sled test with the simple five-segment TNO adult test dummy. This verification was followed by several studies with the (much more complicated) Part 572 dummy under various test conditions.

In a research program started in 1979 in cooperation with the Organisme National de Securité Routiere (ONSER), an attempt was made to simulate a real accident(8,9). This accident had been experimentally reconstructed before with dummies and human cadavers, which allowed a detailed validation of the MADYMO model for this specific accident situation. For both the dummy and cadaver tests, quite realistic results were obtained from the mathematical simulations. Based on these results, a mathematical reconstruction could be made for the real accident by simulating the real occupant anthropometry.

Side Collisions

The first side impact simulations conducted in our laboratory were rigid wall sled tests and drop tests with the Part 572 and APROD 80 dummies(10). The 3D option of MADYMO was used. Model predictions such as contact loads and dummy accelerations were found to agree quite well with experimental results.

Side Impact Accident Reconstruction

The model of the Part 572 dummy was also used in a simulation of a more complicated impact: a real collision between a Peugeot 504 (stationary) impacted on the side (impact angle 70°) by another Peugeot 504 having a velocity of approximately 75km/h(11). For this accident, several experimental reconstructions were conducted by the Lab. of Phys. and Biom. Peugeot S.A./Renault. The mathematical simulation was limited to the interaction between the occupant in the struck vehicle (a Part 572 dummy) and the inside structure of the vehicle. The displacement of the struck door was used as model input. The stiffness characteristics of door padding and of the armrest were determined with a hydraulic tester. The predicted dummy kinematics in this accident are illustrated in Figure 7.

Dummy Thorax Models

Another side impact application of MADYMO presented here is the analysis of the dynamical behavior of the thorax section in four different side impact dummies: the DOT/SID, MIRA, APROD 82, and ONSER. The basic design characteristics of the four thorax sections are completely different. Several models with varying complexity were formulated during this project. In these models, the complete dummy was simulated in a rigid pendulum impact as illustrated in Figure 8. Dependent on the complexity of the thorax design, the rib cage was simulated by zero, one or two segments in case of two-dimensional simulations, and seven segments in the three-dimensional model setup. The mathematical simulations offered a very good insight into the dynamical behavior of the four thorax designs. In the ONSER as well as the MIRA dummies, the thorax behavior appeared to be determined mainly by the elasticity of the rib cage structure. In the DOT dummy, elasticity as well as damping (due to the viscous damper in this design) and inertia effects were found to play a significant role. These effects were of such a complex nature that a detailed three-dimensional representation had to be used for adequate simulation. A decisive judgment of the reliability of the APROD mathematical simulation could not be given due to inadequate functioning (jamming) of this thorax design. More details of this study are presented in (7) and (12).

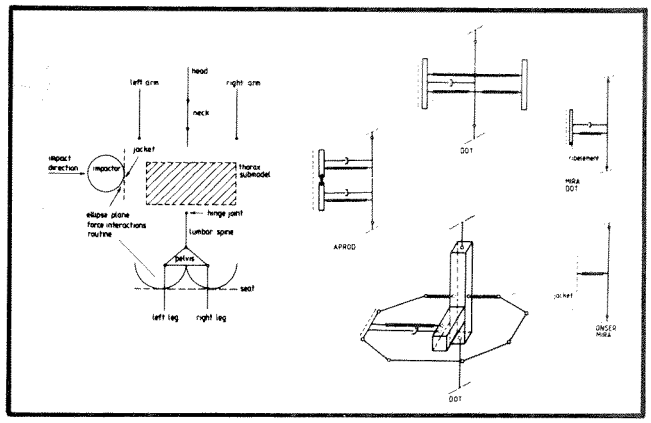

Figure 8. Simulation of thorax pendulum impact tests with four different side impact dummies

Pedestrian and Cyclist Impacts

In the past, the Research Institute for Road Vehicles TNO has been involved intensively in research in the field of pedestrian and cyclist safety. As part of this research program, four pedestrian models with varying complexity were formulated with MADYMO: three two-dimensional models with two, five, and seven segments, respectively, and one three-dimensional model with fifteen segments (Figure 9). Model results were compared with experimental results of a Part 572 dummy impacted laterally by an Audi 100 vehicle at two velocities (30 and 40km/h). In general, all models appeared to provide values for the body segment accelerations within or close to the experimental range of responses. A slight improvement of the model results could be observed in the more complex models. For instance, due to the lower head impact velocity in the three-dimensional model, a lower and much more realistic peak head acceleration during the hood impact could be observed. More details of this study are presented in (6) and (13).

More recently, research in this area in our laboratory has focused primarily on the integration of pedestrian and cyclist safety(14). As part of this study, a model of a cyclist has been formulated where the bicycle is represented by a separate one-segment system (Figure 9). The cyclist

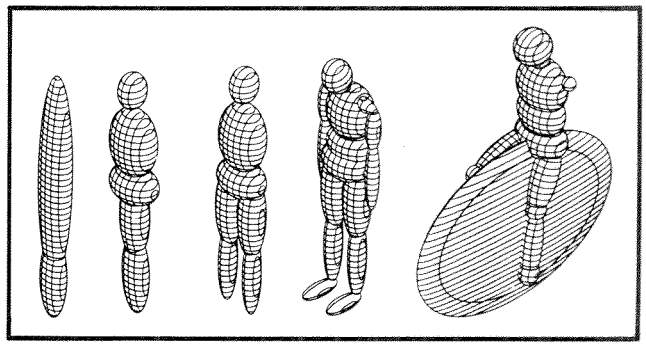

Figure 9. Geometry and contact ellipses of 2-, 5-, and 7-segment 2D pedestrian, a 15-segment 3D pedestrian, and a 9-segment 3D cyclist model

is simulated by a nine-segment system without arms to avoid the complex interaction of the arms with the hood in this type of impact. Experimental verification for several test conditions with a simulated vehicle front is incorporated in a separate contribution to this Conference(15).

Child in a Child Restraint System

The next example is the simulation of an impact sled test with a child in a harness-type child restraint system (Figure 10). Details of this study were presented at the 23rd Stapp Conference(16). The child restraint system is represented by a separate one-segment system connected to the sled by a lapbelt and back strap. Because of the 2D nature of the motions, the 2D option of MADYMO was used for this analysis. Model results were compared with two sled tests conducted at the Highway Safety Research Institute in Michigan: one sled test with a 3-year-old Part 572 dummy and the other with a child cadaver. In general, a satisfactory agreement could be obtained between model and experimental results. Model predictions of the dummy behavior were, however, found to be more realistic than for the cadaver, which may be due mainly to the great number of estimations that had to be made for the mass distribution and joint properties of the child cadaver.

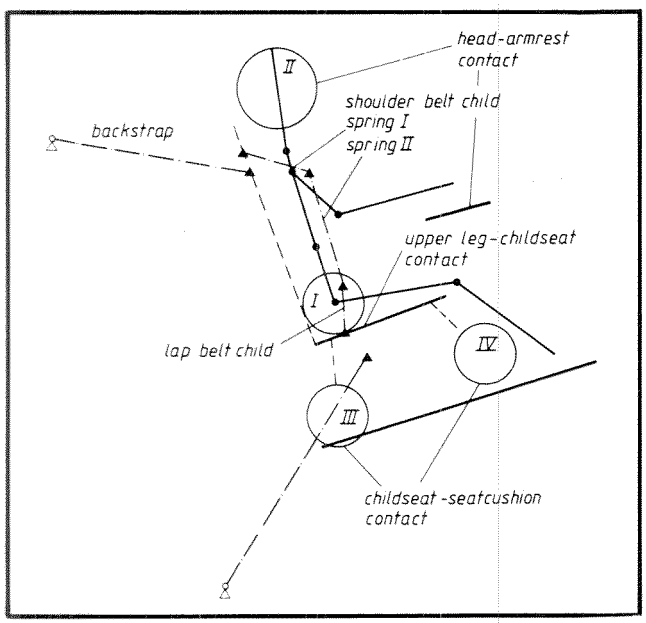

Figure 10. Mathematical representation of a child in a child restraint system

Human Body Segment Models

Applications in the preceding sections all relate to the simulation of the whole body response. MADYMO has also been applied to study the behavior of specific body structures. Two examples will be presented here: a model for the head-neck kinematics of human volunteers and a model for the thorax behavior in human cadavers.

Head-Neck Model

The model describing the head-neck kinematics was formulated with MADYMO 3D and consists of three segments: a torso link, a neck link, and a head link, which are connected by means of a pivot in the head near the occipital condyles and a pivot close to the T1 vertebral body in the torso (Figure 11). A detailed description of

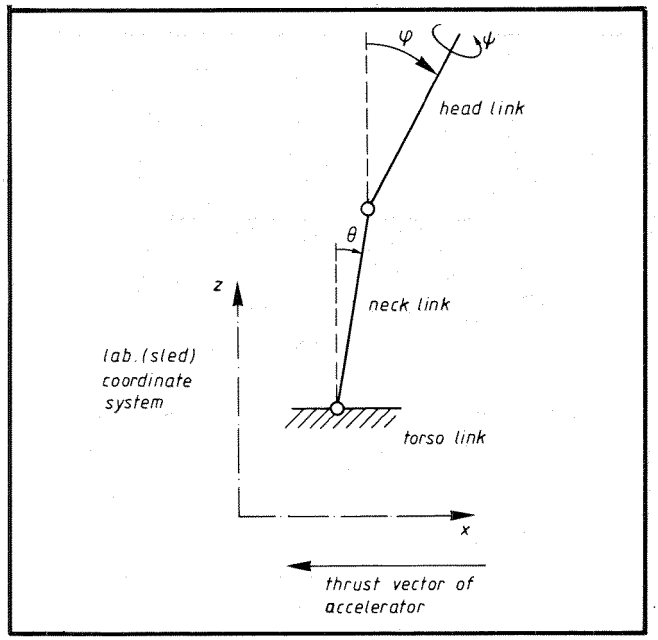

Figure 11. Mathematical model for head-neck motion of human volunteers in frontal, lateral, and oblique impacts

this model and the experimental verification by means of lateral, oblique, and frontal human volunteer tests is given in (17-20). Figure 12 illustrates model predictions in a lateral human volunteer test.

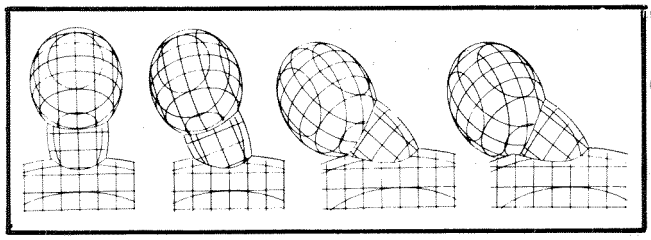

Figure 12. Prediction of the head-neck kinematics of a volunteer in lateral flexion

Thorax Model.

The thorax model was developed at the Ohio State University using the MADYMO 2D program(21). The model, which represents the rib cage, including sternum,

consists of a series of 17 elements (Figure 13). A special user-defined subroutine was developed that accounts for pressure changes within the chest cavity during simulation. The model was used to study some of the thorax impact tests with human cadavers conducted during the mid-1970's at the Highway Safety Research Institute. Thoracic accelerations in these tests were collected using a 12-accelerometer array(22). The general shape of the acceleration time histories and force-deflection characteristics predicted by the model showed good agreement with the tests. Predictions for the thorax pressure, however, showed significant deviations.

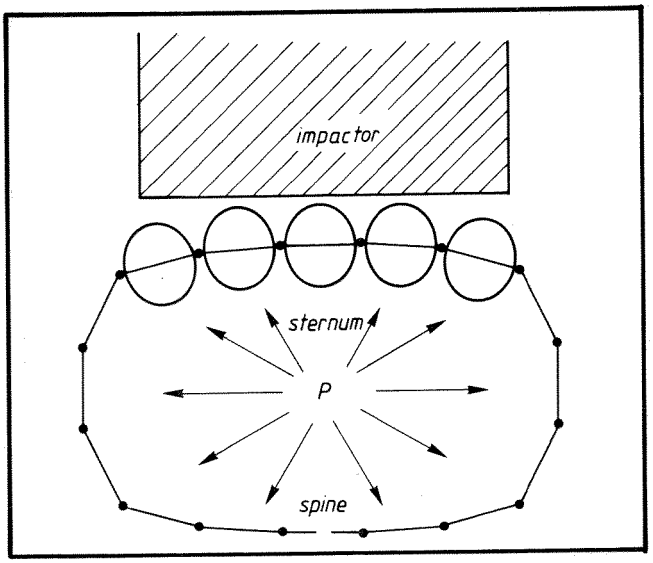

Figure 13. Thorax mathematical model

Computer-Aided Design Studies

In the preceding sections, a number of examples have been presented illustrating the use of MADYMO as a basic biomechanical crash research tool. Another interesting application of this type of program is the development and optimization of crash safety devices such as seatbelts, child seats, and vehicle paddings. One example presented here illustrates this, namely, the design of a dynamic-acting child restraint system. Two other examples relate to the computer-aided design of dummy components, namely, a dummy abdomen section and a dummy neck.

A Dynamic-Acting Child Restraint System

This new child restraint system features a moving impact shield, which is horizontal during normal use. The shield rotates upward during a frontal collision to restrict the forward motion of the child's head and thorax. The 2D option of MADYMO was first used to design and optimize the actuating mechanism for the shield and, second, to optimize the performance of the whole system in a standard ECE 44 50km/h sled test with a 3-year-old child dummy (Figure 14). The shield-actuating mechanism consists of a lever arm on the pivoting shield to which a rod with a mass is connected. During the car crash, the shield moves into an upright position due to deceleration forces acting on the mass. The downward motion of the shield caused by loadings from head and chest is prevented by a locking device. Several calculations, together with only a limited number of sled tests, finally led to an optimized child restraint system, which is commercially available today. Details of this study are provided in (23).

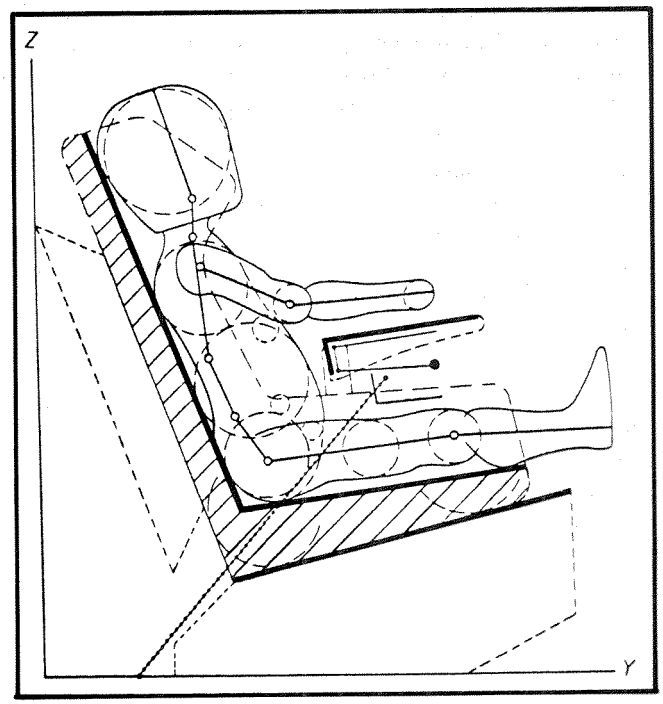

Figure 14. Mathematical model of child restraint system with dynamic-acting impact shield

A Dummy Abdomen Section for Side Impacts

The principle of this design is a rigid drum placed at the critical penetration tolerance level around the lumbar spine, with pressure-threshold contact switches on its surface. This drum is covered by a composite material that should have a dynamic stiffness identical to the human abdomen. The outside layer of the abdomen is made of a relatively heavy but flexible material. To avoid preparing and testing a large number of specimens necessary to obtain the correct response empirically, it was decided to use computer simulations to find the design parameters. MADYMO was utilized to formulate a dynamical nonlinear finite segment model of the cross section through a half abdomen (Figure 15). This model was exercised with a wide variety of mass distributions and for different impact velocities. A few specimens of the most promising combinations were made and tested

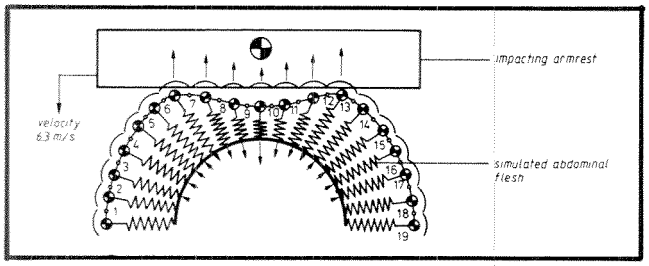

Figure 15. Mathematical model of dummy abdomen section

and were used for validation of the model. A prototype abdomen section has been built, based on the optimal parameters found with the simulation model, and will be incorporated in the future Eurosid side impact dummy. More details of this study are provided in (24).

A Dummy Neck With Improved Biofidelity

Experimental evaluation of the Part 572 neck system with respect to the volunteer behavior showed that this neck is much too stiff(20). Mathematical simulations have been conducted to optimize the design of this neck(18). A model of the Part 572 head-neck assembly was used for this purpose where the neck is represented by a seven-segment linkage system. Experimental verification of this model was conducted for a calibration pendulum test and a more severe sled test. The first results of the computer-aided design efforts that include simulation of longer and softer necks were quite promising. The best results were obtained by a design that consists of a soft neck reinforced by a relatively stiff structure in the front and back sections (Figure 16). A possible realization of such a design principle is a soft rubber cylinder imbedded in strong fibers or provided with one or more separate stiff rubber segments. Based on these findings, several prototypes have been built that are currently tested at the Vehicle Research and Test Center under test conditions representative for the human volunteer tests.

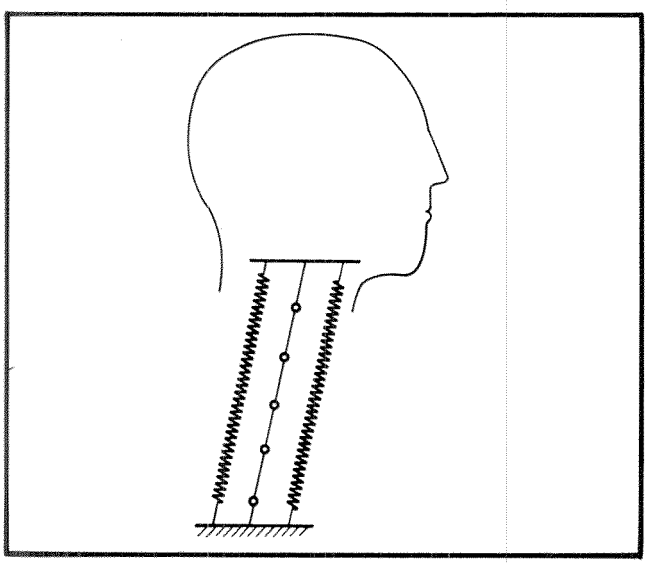

Figure 16. Mathematical model of a dummy neck with improved frontal biofidelity

Discussion: Future Trends and Developments

In the past, the MADYMO package has gone through a continuous process of optimizations, refinements, and extensions. It is expected that such developments will proceed. In fact, the rapid growth and progress in computer technology will open new directions and perspectives, particularly in the field of data base management and postprocessing. Another trend will be that further progress in vehicle structural crash models can lead to an integrated computer analysis approach for the vehicle-occupant interaction in a crash situation.

One of the most critical areas in current crash victim simulation programs is the description of contact between occupant and environment. Present algorithms applied for contact interaction of occupant with vehicle interior or between pedestrian and vehicle cannot account in a realistic way for the effect of strain rate and shape of the contact geometries. As a consequence, a large number of impactor tests is often required with varying impactor velocities and impactor shapes to obtain realistic model input data. The need for such elaborate input data experiments can be reduced considerably if more realistic contact models become available. Beside improvements in contact-interaction models, further developments can also be expected in the area of restraint system modeling, for instance with respect to the description of the belt-occupant interaction or the development of advanced three-dimensional airbag models capable of simulating the complex occupant interaction with passenger and driver airbag systems.

Human body data bases used today in crash victim simulation programs relate mostly to a representation of crash test dummies. A comparison of the data bases for the description of the standard Part 572 test dummy by various researchers showed differences, particularly with respect to the joint characteristics. Therefore, a strong emphasis should be placed on future standardization of this type of data base.

Experimental validation of the whole body response predicted by mathematical models is related mostly to dummy experiments. Studies reporting model verification for human volunteer or human cadaver tests appear to be limited. In most cases they are related to the behavior of certain body segments such as the thorax or neck, as was illustrated in the application section in this paper. Development of well-validated human body data bases describing different size real vehicle occupants and pedestrians is considered to be a challenge in the near

future for the biomechanical community. If the status of mathematical models becomes such that they offer a more realistic representation for the human body than current crash test dummies, a major step forward in the field of automotive safety modeling will have been made. Further program extensions with respect to flexible elements might be necessary to achieve an adequate level of validation.

Further acceptance of this type of model can also improve by an increasing user convenience. A MADYMO 2D version is expected to become available in 1986 as a special-purpose program for the simulation of frontal collisions. This program will be installed on a microcomputer system and could be used as a local computer-aided design work station in design departments. Although detailed specifications are not available at the present time, features expected to be included are menu-driven modules to generate data bases, interactive graphical-supported positioning of the occupant, and extensive output display capabilities with animation facilities.

A final trend, which will be mentioned briefly here, is found in the area of computer graphics. The MADYMO 3D graphics package used to visualize the complex occupant kinematics appears to be of invaluable importance for the analysis of three-dimensional motions. An even more realistic representation, however, can be obtained with a color graphics package developed in the field of solid modeling. Figure 17 illustrates the use of such a program for the visualization of the MADYMO Part 572 dummy model. This graphics program was developed at the Department of Industrial Design Engineering of the University of Technology in Delft and is still in an experimental stage. A relatively large CPU time is required for this type of visualization, which at the moment prevents applications on a large scale.

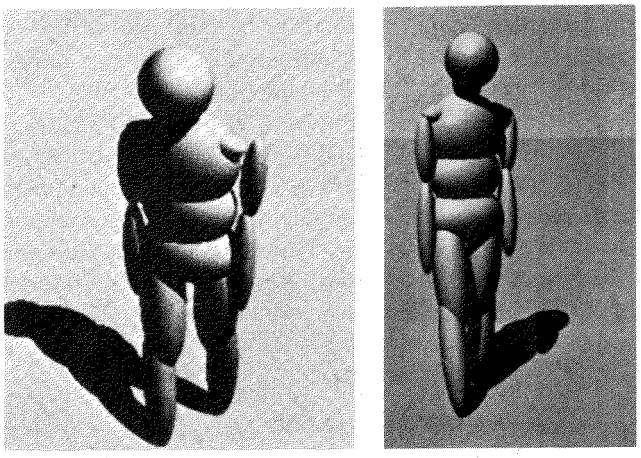

Figure 17. Part 572 dummy represented by the new generation 3D graphics package

Acknowledgments

MADYMO has been developed at the Research Institute for Road Vehicles TNO in cooperation with The Netherlands Institute for Road Safety Research SWOV. Development has been supported by the Dutch Government and the European Communities.

References

1. Robbins, D.H., "Simulation of human body response to crash loads," Shock and Vibration Computer Programs, Monograph No. SVM-10, Shock and Vibration Computer Center, U.S. Department of Defense, 1975.
2. King, A.I., and C.C. Chou, "Mathematical modeling, simulation and experimental testing of biomechanical system crash response," *J. Biomechanics*, Vol. 9, pp. 301-317, 1976.
3. Prasad, P., "An overview of major occupant simulation models," SAE Paper 840055, Warrendale, Pennsylvania, 1984.
4. Wittenburg, J., "Dynamics of systems of rigid bodies," G.B. Teubner, Stuttgart, 1977.
5. Maltha, J., and J. Wismans, "MADYMO-crash victim simulations, a computerized research and design tool," Proceedings 5th IRCOBI Conference on the Biomechanics of Impacts, Birmingham, 1980.
6. Wismans, J., and J.J. van Wijk, "Mathematical models for the assessment of pedestrian protection provided by a car contour," Proceedings Ninth International Technical Conference on Experimental Safety Vehicles, Kyoto, 1982.
7. Wismans, J., and L.J.J. Wittebrood, "The MADYMO crash victim simulation package and its application in analysing thoraxes of side impact dummies," EEC Seminar: Biomechanics of Impacts in Road Accidents, Brussels, 1983.
8. Cesari, D., and M. Ramet, "Comparison between in-the-field accidents and reconstructed accidents with dummies and cadavers," Proceedings 19th Stapp Car Crash Conference, 1975.
9. Wismans, J., D. Cesari, J. Maltha, and M. Ramet, "Evaluation of the experimental reconstruction of a real frontal collision with a mathematical model," Proceedings 5th IRCOBI Conference on the Biomechanics of Impacts, Birmingham, 1980.
10. Wismans, J., and J. Maltha, "Application of a three-dimensional mathematical model for the evaluation of side impacts," Proceedings of the 6th IRCOBI Conference on the Biomechanics of Impacts, Salon de Provence, 1981.
11. Wismans, J., J. Maltha, J.J. van Wijk, and E.G. Janssen, "MADYMO—a crash victim simulation computer program for biomechanical research and optimization of designs for impact injury prevention," AGARD Meeting, Cologne, Germany, 1982.
12. Wismans, J., and L. Wittebrood, "Lateral dummy comparison: theoretical analyses," Final report, phase

4, EEC Biomechanics Programme, Contract NL8, IW-TNO, 1982.
13. van Wijk J., J. Wismans, J. Maltha, and L. Wittebrood, "MADYMO pedestrian simulations," SAE P-121, Pedestrian Impact Injury and Assessment, Detroit, 1983.
14. Janssen, E.G., and C.G. Huijskens, "Cyclists impacted by simulated vehicle fronts," Proceedings 10th IRCOBI Conference on the Biomechanics of Impacts, Delft, 1984.
15. Janssen, E.G., and J. Wismans, "Experimental and mathematical simulation of pedestrian-vehicle and cyclist-vehicle accidents," Proceedings Tenth International Technical Conference on Experimental Safety Vehicles, Oxford, 1985.
16. Wismans, J., J. Maltha, J.W. Melvin, and R.L. Stalnaker, "Child restraint evaluation by experimental and mathematical simulation," Proceedings 23rd Stapp Car Crash Conference, San Diego, 1979.
17. "Preliminary development head-neck simulator," Vol. 1: Analysis volunteer tests, Final report, Phase I, Project SRL-59, Vehicle Research and Test Center, East Liberty, Ohio, 1985.
18. "Preliminary development head-neck simulator," Vol. 2: Mathematical simulations, Final report, Phase I, Project SRL-59, Vehicle Research and Test Center, East Liberty, Ohio, 1985.
19. Wismans, J., and C.H. Spenny, "Performance requirements for mechanical necks in lateral flexion," Proceedings 27th Stapp Car Crash Conference, SAE Paper 831613, 1985.
20. Wismans, J., and C.H. Spenny, "Head neck response in frontal flexion," Proceedings 28th Stapp Car Crash Conference, 1984.
21. Wiechel, J.F., "The development of a bidirectional multi-speed impact model of the adult human thorax," Dissertation, Ohio State University, 1983.
22. Robbins, D.H., R.J. Lehman, and K. Augustijn, "Prediction of thoracic injuries as a function of occupant kinematics," Proceedings Seventh International Technical Conference on Experimental Safety Vehicles, Paris, 1979.
23. Stalnaker, R.L., and J. Maltha, "MADYMO used for computer aided design of a dynamic acting child restraint seat," Proceedings 5th IRCOBI Conference on the Biomechanics of Impacts, Birmingham, 1980.
24. Maltha, J., and R.L. Stalnaker, "Development of a dummy abdomen capable of injury detection in side impacts," Proceedings 25th Stapp Car Crash Conference, San Francisco, 1981.

Validation of the EEVC Mobile Deformable Barrier for Side Impact Testing

D. Cesari and
J. Bloch
O.N.S.E.R. Laboratoire des Chocs et de Biomécanique

W. Sievert and
E. Pulwitt
Federal Highway Research Institute (BASt), Traffic Safety and Accident Research Department

I.D. Neilson and
A. Hobbs
Transport and Road Research Laboratory, Vehicle Safety Division

Abstract

Following the European Experimental Vehicles Committee's definitions(1), the mobile barrier frame was built by several partners and rigid polyurethane foam selected as the material for the front deformable face. A validation process consisted of different tests distributed among ONSER, BASt, and TRRL. ONSER, UTAC, and TRRL conducted impact tests on individual blocks, total tests against a dynamometric wall, and lateral impact tests against the Renault 14 as struck cars.

The validation was completed by performing barrier-to-car tests at the BASt facility according to the proposed EEVC impact test procedure. The basis for comparison was given by car/car tests under the same conditions and with cars of the same type. These cars were the Golf and Daimler Benz (W 123 series). Results from this test series show the barrier face has a very useful crash simulation fidelity and repeatability.

Introduction and Aim

In 1982, Working Group 6 of the European Experimental Vehicle Committee proposed a side impact standard test procedure(1). To perform this test, it is necessary to use a mobile deformable barrier, the characteristics of which were determined by the group and based on characteristics of European cars.

To validate the test procedure proposed by EEVC and especially the force-deflection characteristics of the barrier, four European research groups—BASt in the Federal Republic of Germany, ONSER and UTAC in France, and TRRL in the United Kingdom—decided to work together in a coordinated research program.

This work is done under an EEC contract, for which ONSER is the project leader. Its aim is to validate the proposed solution, which is rigid polyurethane foam for the front deformable face. Different validation tests were conducted such as individual block tests, barrier against a dynamometric wall tests, and barrier-to-car tests.

Proposed Solution for the Front Deformable Face

The front deformable face studied and built by Fritzmeier GmbH is described in Figure 1. Each block is constituted with two elements of different rigid polyurethane foam densities. Six different densities are useful:

- 28kg/m^3 for 4a, 5a, and 6a elements
- 30kg/m^3 for 5b and 6b elements
- 35kg/m^3 for 4a elements
- 42kg/m^3 for 1a and 3a elements
- 50kg/m^3 for 2a and 2b elements
- 60kg/m^3 for 1b and 3b elements

The real densities must take place in ±5 percent around the theoretical values. Figure 2 shows the design of the EEVC barrier.

Work Done by ONSER, UTAC, and TRRL

This section describes and gives results of part of the research performed in France and England. UTAC performed a frontal impact of the barrier against a dynamometric barrier and a barrier-to-car test. ONSER made the evaluation of force-deflection characteristics of each block of the barrier and also conducted two barrier-to-car side impact tests under the same conditions as the test performed by UTAC. TRRL conducted individual block tests and two impact tests of the mobile barrier against a dynamometric wall.

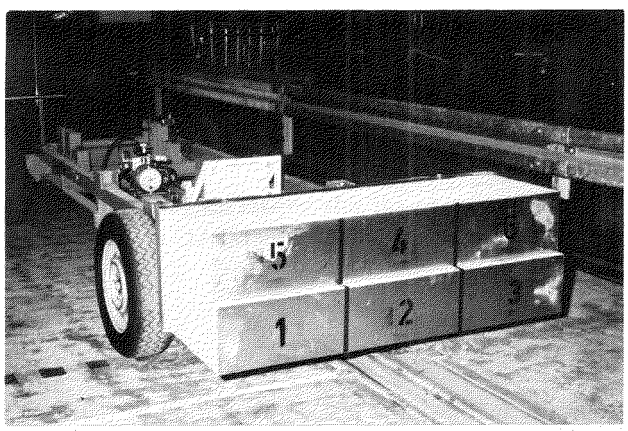

Figure 1. Front deformable face in polyurethane foam

Tests of Individual Blocks (ONSER and TRRL)

These tests were conducted first to determine the behavior of each block when tested separately.

The force-deflection characteristics of individual blocks tested separately show that the curves are closed to the corridor but partly under them. This relatively low stiffness can be explained by the absence of edge effect when one block is separated from the others. In a complete front force, the blocks cannot extend on interfaces with other blocks. The tests show a breaking down of the foam, which in some of them is associated with a high force peak at the maximum of deformation.

Test Against Dynamometric Barrier (UTAC and TRRL)

One frontal test with the mobile deformable barrier was conducted by UTAC. This test is necessary to check if the force deformation characteristics fulfill the specifications.

Test Conditions

The weight and sizes of the mobile deformable barrier used in this test were in agreement with the values decided by Working Group 6 of EEVC. The dynamometric barrier allowed the measurement of impact forces on each block of the barrier front end. The test impact speeds were 31.8km/h in the UTAC test, which is a little lower than the specification (35 ± 2km/h), and 35.1km/h in the TRRL tests. Longitudinal, transverse, and vertical accelerations were recorded in two points (one on each side) and the longitudinal acceleration at the center of gravity of the barrier. The dynamic deformation of the barrier front end was calculated by double integration of the longitudinal acceleration. High-speed movies and post-test pictures were taken.

Test Results

From data recorded during the test, we were able to draw the following curves

- Longitudinal acceleration, speed, and crush for each side of the barrier frame as a function of time

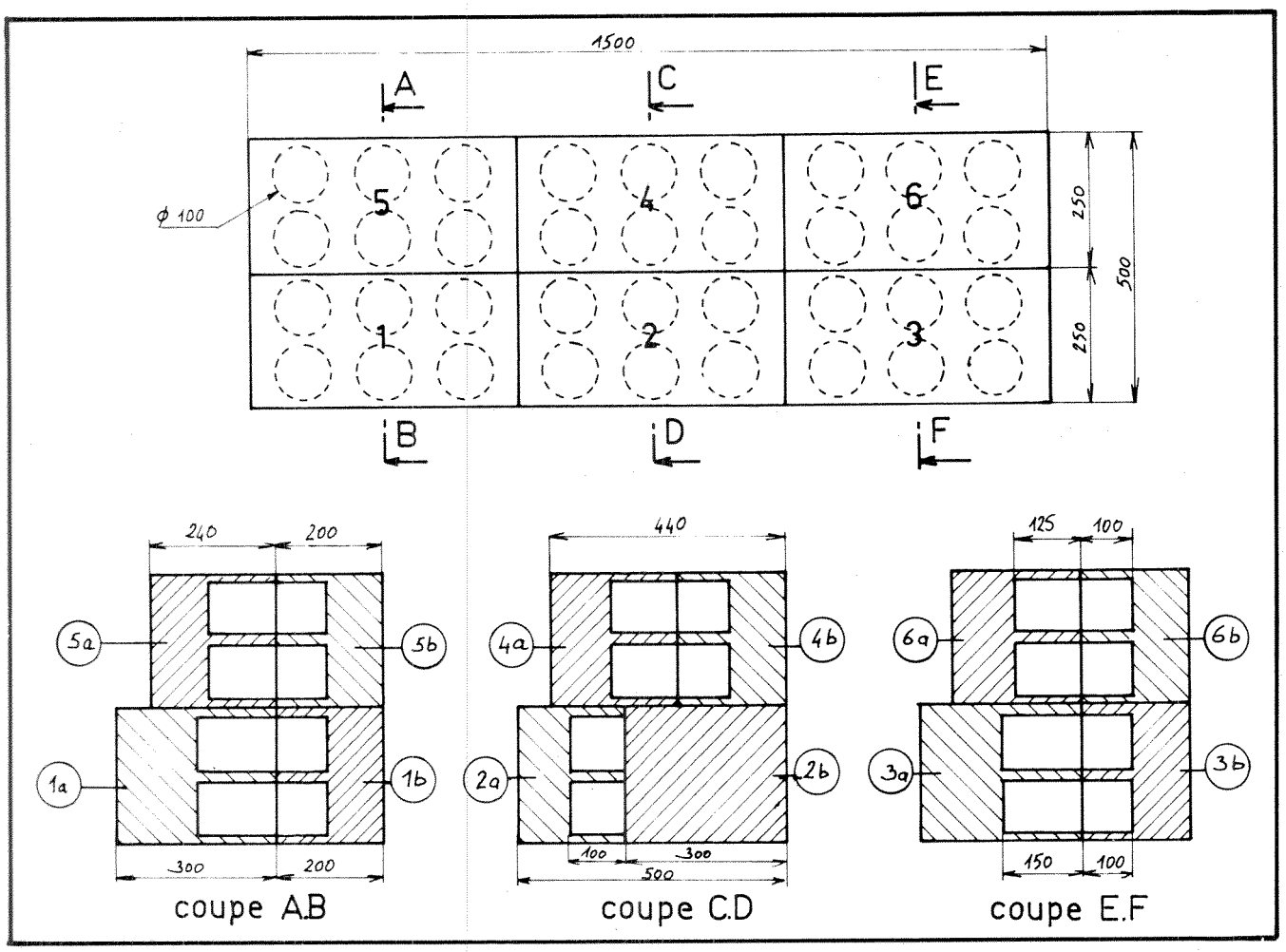

Figure 2. The EEVC mobile deformable barrier

- Transverse and vertical accelerations at the same locations versus time
- Longitudinal acceleration of the center of gravity versus time
- Impact force on each plate and total impact force as a function of time and crush
- Comparison of the total force/time curve with the mass acceleration versus time curve.

Figures 3 to 5 are the force-deflection characteristics of each block and the total force-deflection variation of the mobile deformable barrier during the UTAC test. Analysis of these figures shows that the blocks of the upper row give results almost included inside the specification corridor whereas the impact force of the lower row blocks is partly under the corridor. For blocks 1 and 3, this occurs for the second half of the deformation; on block 2, the curve was below the corridor in the second third of the deformation.

These figures show a good symmetry of barrier front elements: the force-deflection curve of block 1 can be almost superimposed on the block 3 one, and it is the same for blocks 5 and 6.

The maximum crush of each block is slightly lower than the specifications, but this can be related to the lower impact speed. According to kinetic energy difference at the correct impact speed, the dynamic crush would be 34/35cm instead of 31cm, and this corrected value is inside the specified bracket.

Barrier-to-Car Side Impact Tests (ONSER and UTAC)

Three barrier-to-car side impact tests were conducted, one in the crash test facility of UTAC and two in the facility of ONSER.

Test Procedure

Figure 6 shows the test configuration of the barrier tests, which was laid down in the report of EEVC's Working Group 6, "Structures"(1).

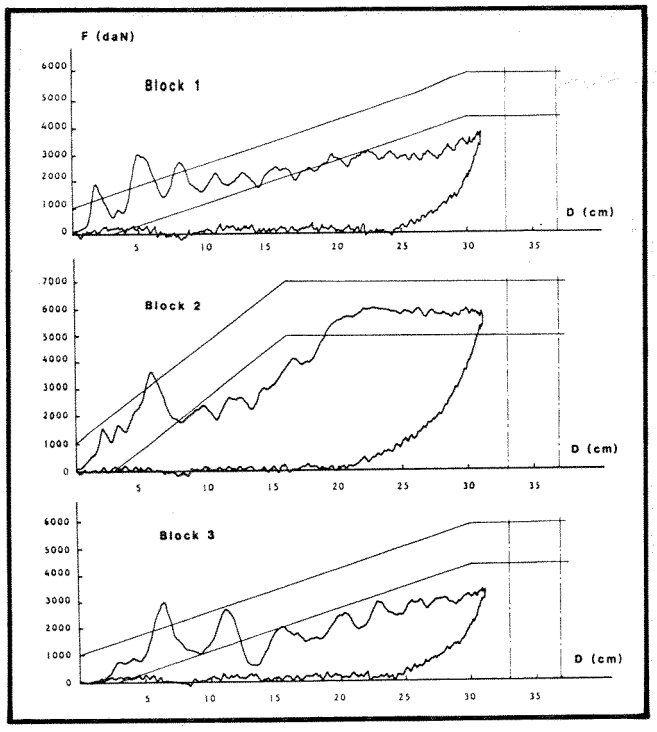

Figure 3. Force-deflection characteristics of the lower deformable part of the EEVC barrier

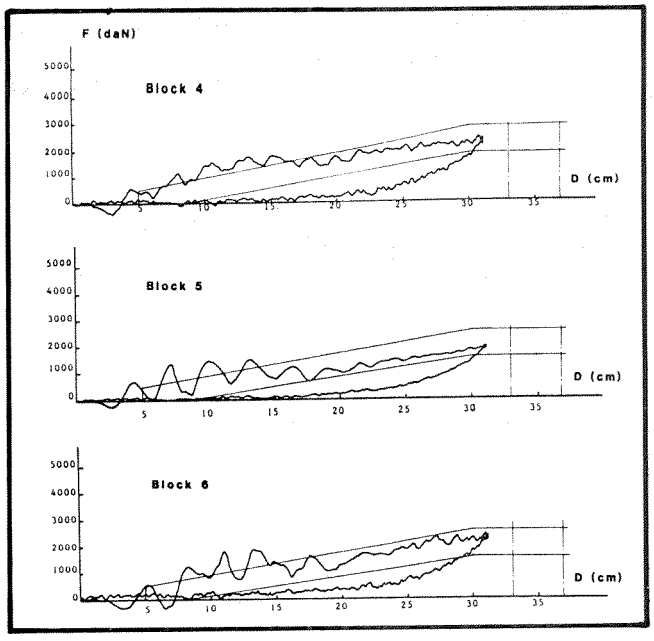

Figure 4. Force-deflection characteristics of the upper deformable part of the EEVC barrier

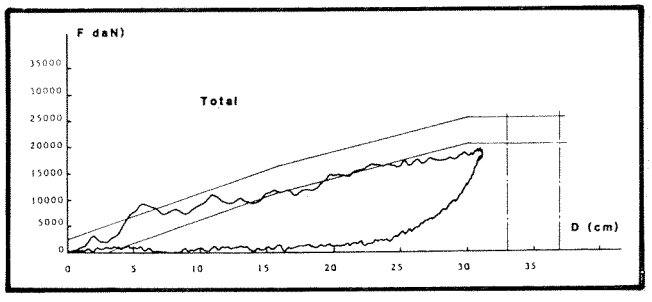

Figure 5. Force-deflection characteristics of the EEVC barrier

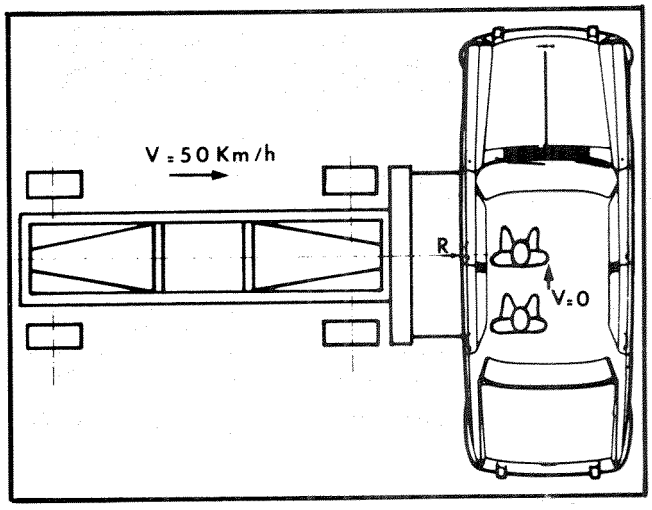

Figure 6. Collision situation in the barrier tests

The main features of this procedure are—

- Barrier impact speed: 50km/h
- Stationary struck car
- Impact angle: 90°
- Impacted side: driver (left side)
- Barrier symmetrical plane passing through R point of driver struck car

Two tests were performed with two Part 572 dummies in the impacted car at the driver and the rear left occupant seats. The third test, conducted by ONSER, was performed with the following dummies (the European dummy planned for lateral collision tests not yet available):

- Left rear sit: a Hybrid II dummy on which we note the triaxial accelerations on the head, the thorax, and the pelvis
- Driver sit: the dummy is compounded with various elements which are—
  - — Hybrid III head on which we measure triaxial accelerations (same head as the EUROSID)
  - — EUROSID neck
  - — APROD thorax on which we measure two deflections and three accelerations
  - — TNO (EUROSID) abdomen, which is able to detect a penetration

— EUROSID pelvis on which we measure three accelerations, one force at the pubic symphysis level and one force on the left iliac wing
— APROD arms

The main differences between this dummy and the EUROSID concern the thorax and arms.

The mobile deformable barrier is equipped with two triaxial accelerometers, one at the center of gravity and the other at the center of the sustaining sheet of the polyurethane foam front face.

A camera is also fixed on the mobile barrier to visualize possible shocks of the dummy heads against the struck car structure. The vehicle kinematic is studied from accelerations noted on the longitudinal and transverse axes on the A- and B-pillars at the opposite side of impact. The left front door (at the impact side) is equipped with accelerometers at the shoulder and at R point levels. Two on-board cameras help to study the passenger kinematic during impact.

Figure 7. EEVC barrier/Renault 14 lateral impact test

Test Results

Test results were analyzed to see if the barrier reproduced correctly the car deformations, vehicle kinematics, and dummy loadings.

Car Deformations

Figure 8 represents the deformations of the Renault 14 at the upper, medium, and lower levels. This figure shows a greater deformation of the car for the test conducted at UTAC. Figure 9 shows the deformations of the Renault 14 in three conditions: when impacted by the mobile deformable barrier (average value), struck by another car (average value of 10 tests with different cars), and hit by a Peugeot 305. This test was selected because the Peugeot 305 has characteristics closest to those of the barrier.

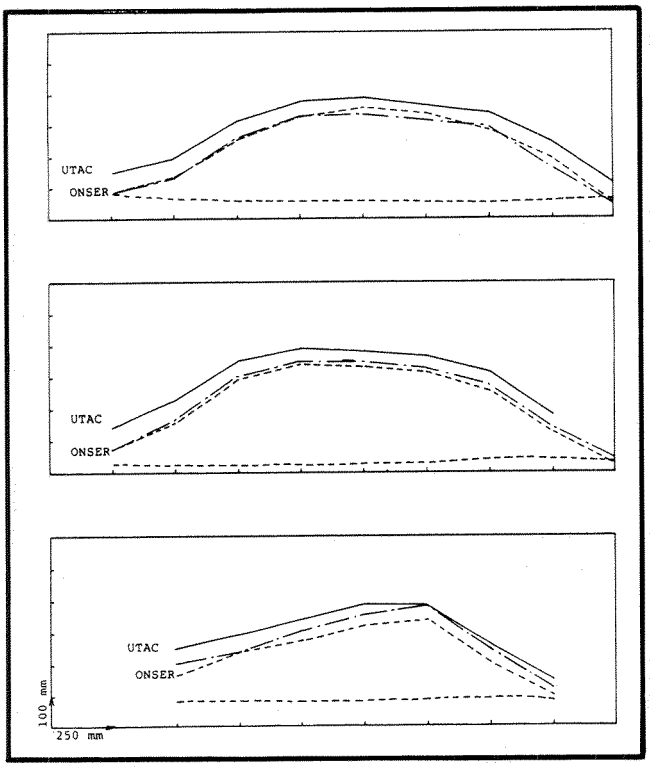

Figure 8. Deformation of the Renault 14 side when struck by the mobile deformable barrier

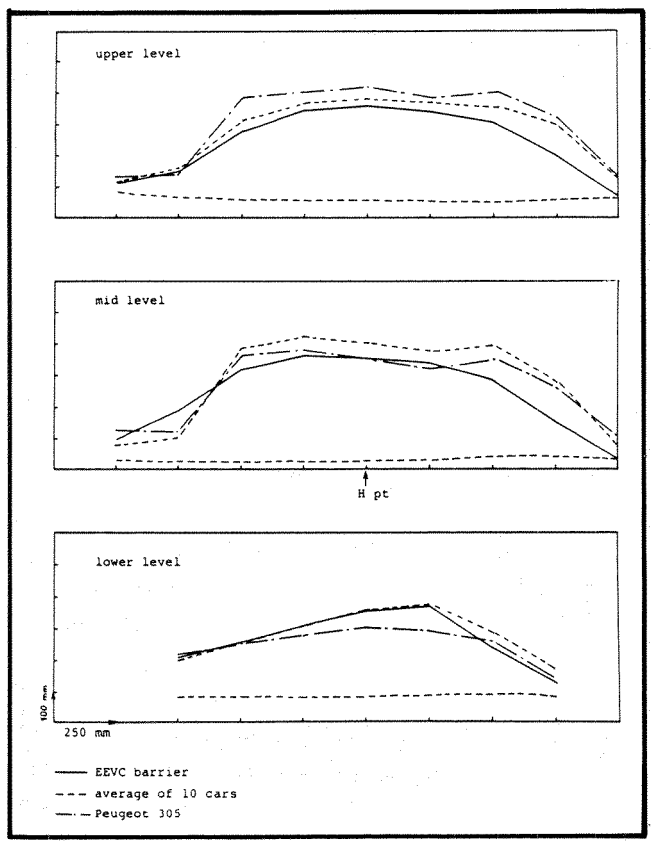

Figure 9. Deformation of the Renault 14 after side impact tests

Compared to other tests, the barrier gives correct deformations at the lower level and slightly lower at the upper level. However, differences are very low, especially in front of the driver. Figures 10 and 11 picture the struck Renault 14 in tests with the barrier and a Peugeot 305.

Vehicle Kinematics

From vehicle accelerations, it is possible to draw the speed variations versus time. The speed variation is an important factor, especially for the impacted door as it is correlated to the risk of injuries in side impact(2). Figure 12 shows the speed variation of the striking car, the struck car, and the impacted door of the struck car in the three tests with the mobile deformable barrier (the two tests conducted by ONSER give similar results) and in the test with the Peugeot 305. This figure does not show any big differences between these four tests, as indicated in Table 1. The speed ratios are in the same order of magnitude for the three tests.

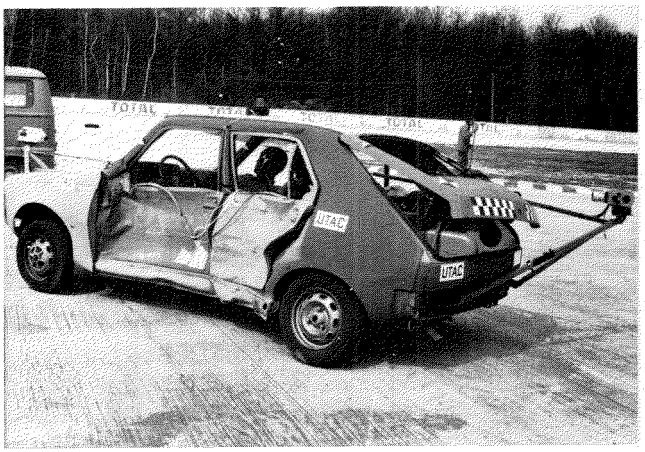

Figure 10. Renault 14 hit by a Peugeot 305

Figure 11. Renault 14 hit by the mobile deformable barrier

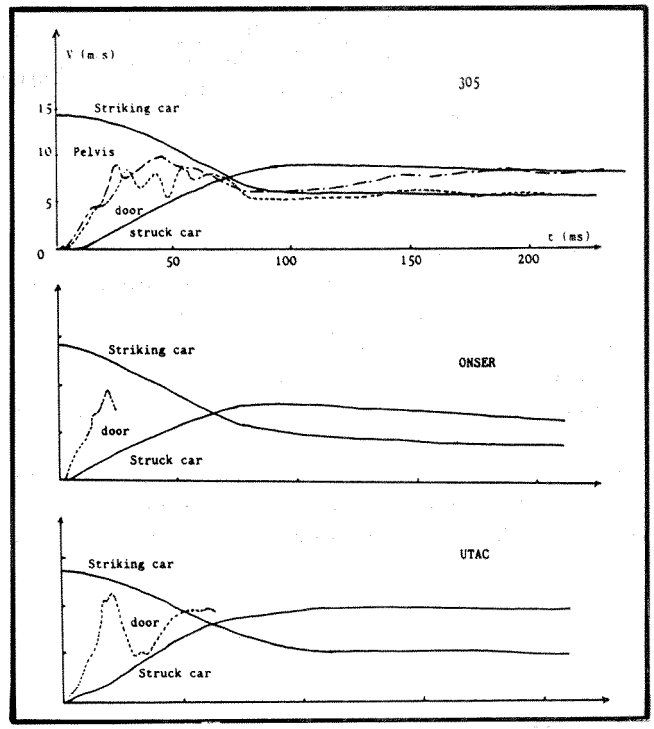

Figure 12. Speed varations in side impact tests

The distribution of deformation energy between the struck car and the impactor seems satisfactory in the car-to-car tests as in the barrier-to-car tests. If we consider the variation of the door speed, the barrier seems to give a higher slope and a higher maximum value.

Table 1. Speed ratios in side impact tests

Test	V2/Vo (%)	V1/Vo (%)	V1/V2 (%)
305/R.14	61	35	57
barrier/R.14	57	27	48
barrier/R.14	70	37	52

Vo = impact speed
V1 = striking vehicle speed at the end of impact
V2 = struck vehicle speed at the end of impact

Dummy Loadings

In each test, the dummy acceleration was recorded on the head, thorax, and pelvis. We are considering only the driver, who is more involved by the vehicle deformations than the rear passenger. Results of dummy loadings are listed in Table 2, which shows there are few variations in dummy loadings for the thorax and pelvis.

The barrier test results are closer to the Peugeot 305 test result than the average of the results of 10 tests performed with 10 different European cars.

Compared to average values, the barrier seems to increase the thoracic acceleration and decrease the pelvic one. However, the values recorded in barrier tests are in

Table 2. Dummy loadings

	Average 10 Tests	Weighted Average	P. 305 Impacting	Barrier UTAC	Barrier ONSER
Head HIC	304	241	511	141	408
Thorax 3ms accel. (g)	72	69	100	85	96
Pelvis 3ms accel. (g)	106	106	85	78	84

line with those recorded in the test with the Peugeot 305, the car whose characteristics are closest to those of the barrier.

Work Done by BASt

Concept for the Full-scale Tests of BASt

The tests were carried out in the crash test facility of BASt. The measuring technique used was described fully in (3).

Figure 13 shows the test configuration of the barrier tests, which was laid down in the report of EEVC Working Group 6, "Structures"(1).

The collision speed in all tests was 50km/h. The results of the barrier tests, were compared with those of the vehicle/vehicle tests. Table 3 lists all the important test parameters. To date, two tests have been conducted with the EEVC barrier for each test configuration.

In this phase of the validation tests for the EEVC barrier, Hybrid II dummies were used since the European dummy planned for lateral collision tests was not yet available.

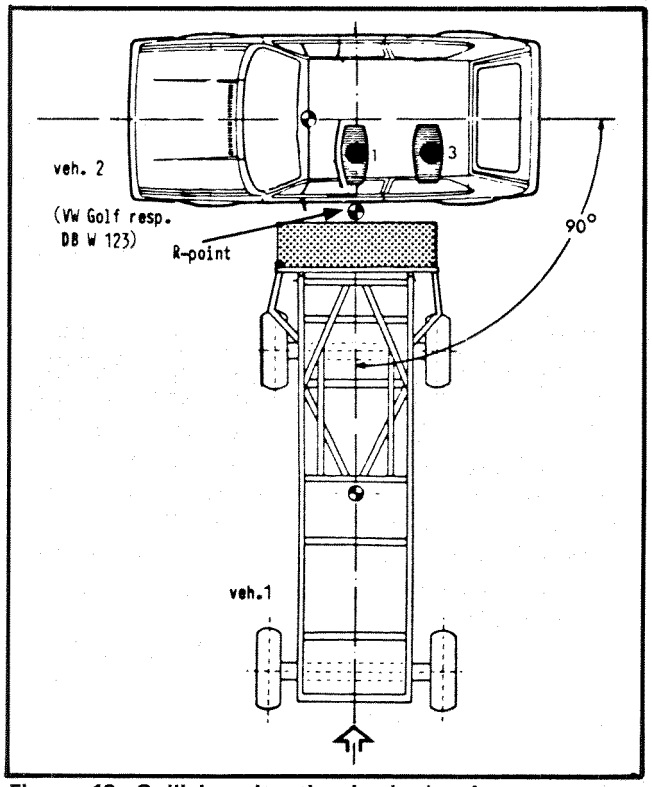

Figure 13. Collision situation in the barrier tests

Table 3. Important test parameters

test parameter					
collision partners	veh. 1	EEVC and CCMC-barrier	VW Golf	DB W 123	EEVC-barrier
	veh. 2	vs. VW Golf	vs. VW Golf	vs. DB W 123	vs. DB W 123
collision speed	(km/h)	50	50	50	50
impact point		R-point	R-point	R-point	R-point
impact angle		90° left	90° left	90° left	90° left
car mass					
test weight*(kg)					
	veh. 1	950	800	1460	950
	veh. 2	800	800	1460	1460
mass ratio m_1/m_2		1.19	1	1	0.65
place of accelerometer mounting	veh. 1	centre of gravity 2 × tunnel	centre of gravity 2 × tunnel	centre of gravity 2 × tunnel	centre of gravity 2 × tunnel
	veh. 2	2 × left side door	2 × left side door	2 × left side door	2 × left side door

* test weight = curb weight + measuring equipment, without dummies

Standard measuring equipment, supplemented by six high-speed cameras, was used to measure the loads on dummies and vehicles. To determine the residual vehicle deformations, the vehicle was measured before and after each test; the points of deformation measurement are shown in Figure 14. The target points for the deformation measurements were adjusted to the R point, doorsill, and lower side window rail. The horizontal distance between the target points was 200mm. The target points on the DB 123 were located analogously.

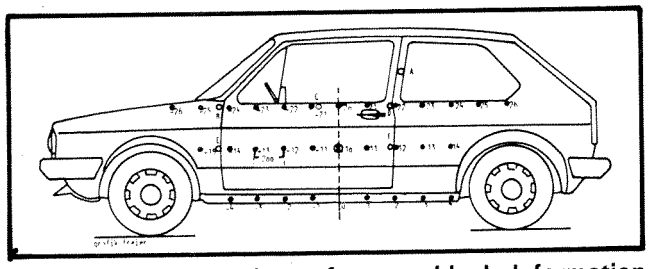

Figure 14. Target points of car residual deformation measurements

Results

The results will be used to demonstrate the differences in the vehicle and dummy loads between the vehicle/vehicle and barrier/vehicle tests. Below, the results of the barrier tests will be compared with the vehicle/vehicle tests; the mean values, particularly for the deformations of the VW Golf tests, can be regarded as the lower limit values that a test tool should achieve for a standardized test procedure for lateral collision testing.

For further comparison of different barrier designs, the results of a test series with the CCMC barrier are shown in the tables. These tests were conducted by BASt in 1982(4). The most important vehicle load values are the deformations, particularly the intrusion of the left front door of the struck vehicle into the passenger compartment, the acceleration of car body and side door, and the velocity changes thus caused.

Deformations and Vehicle Loads

In the tests with two VW Golfs, the striking car suffered a higher mean acceleration (a) and a greater velocity change (Δv) than the struck car (see Table 4). The accelerations of the side door, which are the primary determinants of the passenger load, are high (150g) and display only a small scatter.

The mean frontal deformation of the striking VW Golf was approximately 100mm, with obvious damage to the longitudinal members and outer body members (see Figure 15). On the laterally struck car, deep intrusions occurred in which the A-pillar and doorsill were ruptured and bent. The rupture of the A-pillar in the area of the windscreen frame and the deformation of the doorsill are

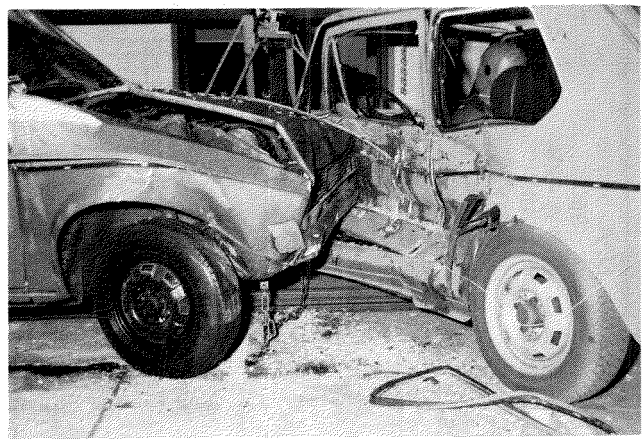

Figure 15. Deformation of the VW Golf

shown in Figure 16. The measuring rod in this illustration shows the approximate line of the original vehicle contours at the height of the doorsill.

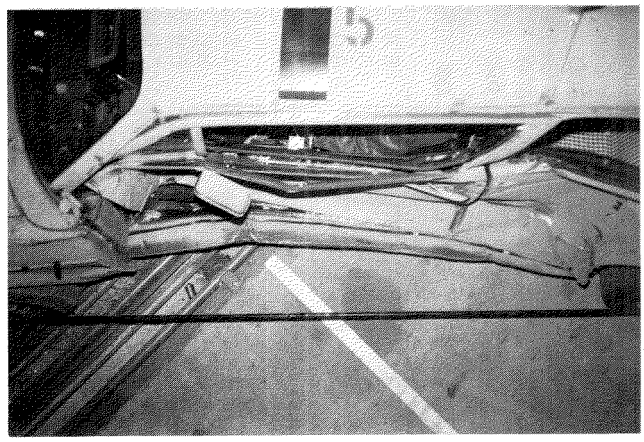

Figure 16. Rupture of the A-pillar and deformation of the doorsill of the VW Golf

The lateral deformation in the three tests with the VW Golf differed in both profile and depth. Figure 17 shows the depth of the deformation and the scatter for the three tests (in the area of maximum penetration).

These differences in lateral deformation were partly caused by the differing prior damage (corrosion) to the

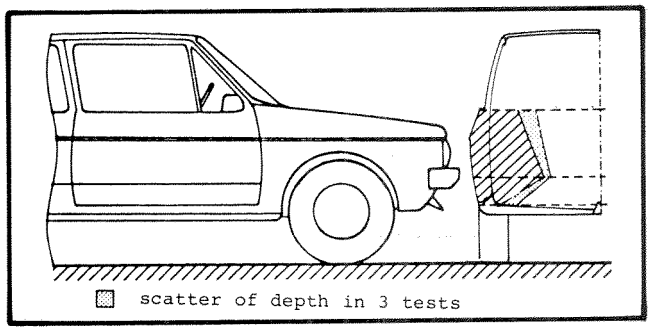

Figure 17. Deformation profile in tests with VW Golf—values for measuring line -2 (in the vertical plane of measuring points -22, -12, -2 shown in Figure 14)

Table 4. Comparison of the vehicle accelerations and the derived values

striking vehicle			veh. 1		CCMC-barrier		EEVC-barrier		VW Golf			DB W 123		EEVC-barrier	
car mass (test weight)*			(kg)		950		950		800			1460		950	
struck vehicle			veh. 2		VW Golf		VW Golf		VW Golf			DB W 123		DB W 123	
car mass (test weight)*			(kg)		800		800		800			1460		1460	
impact speed			(km/h)		50		50		50			50		50	
test no.				21	22	01	02	03	05	06	07	08	09	04	10
vehicle 1															
car acceleration	a_{max}	(g)		14.4	14.3	15.6	15.9	15.1	16.8	18.4	16.0	14.6	12.2	17.0	17.0
car mean acceleration	$\bar{a}$	(g)		9.3	9.3	10.5	10.2	9.8	10.9	10.5	9.3	8.2	9.1	12.3	11.8
velocity change	Δv	(m/s)		7.0	7.1	6.7	6.4	8.0	8.0	7.4	7.1	6.8	7.1	8.1	8.2
period of time for vehicle 2	$t_{\Delta v}$	(m/s)		76	77	65	64	83	75	72	76	84	80	67	71
car acceleration	a_{max}	(g)		15.2	14.9	26.5	32.8	19.6	31.6	34.3	22.0	26.0	23.2	28.5	25.0
car mean acceleration	$\bar{a}$	(g)		9.3	9.0	11.3	12.0	7.3	8.0	9.2	9.1	8.7	8.7	8.8	8.2
velocity change	Δv	(m/s)		6.9	6.8	7.2	7.5	5.9	5.9	6.5	6.8	7.1	6.8	5.8	5.7
left side door acceleration	a_{max}	(g)		265.0	206.0	170.0	163.0	154.0	145.0	153.0	64.0	71.0	73.0	83.0	91.0
velocity of side door left	v_{max}	(m/s)		12.0	11.5	12.9	11.9	12.5	11.4	13.4	8.2	9.1	8.5	8.3	10.3
moment for v_{max}	door	(m/s)		23.0	18.0	22.0	23.0	22.0	25.0	28.0	45.0	53.0	29.0	21.0	26.0

* without dummies

Table 5. Comparison of cumulative deformation values

Test type	Cumulative Deformation Measurements									total of 27 points	mean depth of one measuring point
	line-4	line-3	line-2	line-1	line-0	line-1	line-2	line-3	line-4		
VW Golf/VW Golf	750	918	898	800	720	639	602	419	169*	5925**	227
VW Golf/VW Golf	460	804	834	745	674	617	604	496	214*	5448**	210
VW Golf/VW Golf	640	986	985	928	841	741	698	567	302*	6688**	257
DBW 123/DBW 123	366	614	759	850	873	877	890	729	540	6498	241
DBW 123/DBW 123	420	663	834	915	859	957	917	780	565	6910	256
DBW 123/DBW 123	499	698	862	921	963	949	898	712	452	6954	258
EEVC-barrier/VW Golf	409	809	948	874	831	776	644	391	118*	5800**	223
EEVC-barrier/VW Golf	609	930	901	833	770	668	645	392	110*	5858**	225
EEVC/DB	227	509	716	816	832	742	694	503	253	5292	196
EEVC/DB	299	537	755	836	847	732	654	487	251	5398	200

* only two values

** total of 26 points

□ maximum of deformation

vehicles in the area of the A-pillar. The mean intrusion on the side door—measured in the inner passenger compartment at chest height of the occupants—reached a maximum of 216mm (dynamic value); the residual intrusion was 152mm. The lateral intrusion of the A-pillar and side door led to a displacement of the steering column of approximately 90mm toward the center of the vehicle.

In the tests with two Daimler Benz W 123's, the mean car accelerations ($\bar{a}$) and velocity change (Δv) were roughly equal for both vehicles (see Table 4). With a relatively large deformation depth, the side door acceleration is unexpectedly low. This can be attributed to the greater deformation contingency of the door structure—due to the greater door thickness—and the installation point of the acceleration transducers—distance from the B-pillar.

The mean depth of front deformation on the striking vehicle was 140mm with clear damage to the lateral members caused by the hard areas of the A-pillar and rear wheel housing (see Figure 18).

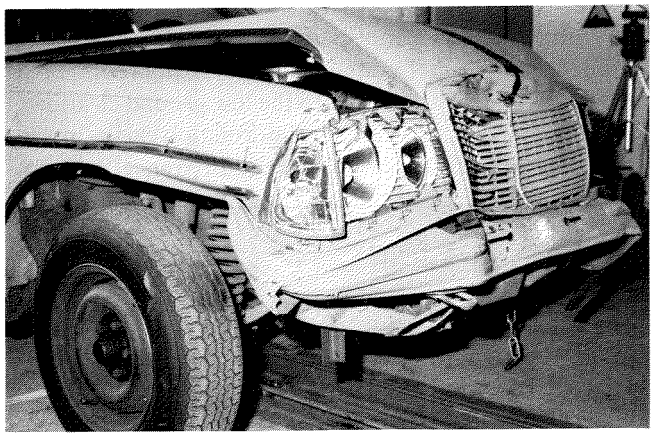

Figure 18. Frontal deformation of the striking DB W 123

The lateral intrusion in these tests displays a smaller zone of scatter than in the tests with the VW Golf (Figures 19 and 20). This can be explained by the high stability of the A- and B-pillars of the DB W 123. No complete rupture of these members occurred.

The mean dynamic intrusion of the side door reached a maximum of 299mm, and a residual intrusion of 220mm was measured (approximately 30 percent more than in the tests with the Golf). The lateral displacement of the steering wheel was, however, only 45mm.

In the tests with the deformable EEVC barrier, the struck Golf sustained higher car accelerations than in the Golf/Golf tests. The mean car load (a) was, for example, approximately 30 percent higher (Table 4). The higher vehicle loads corresponded to the considerably higher door accelerations.

The lateral deformation (measuring line -2) of the VW Golf in the impact with the barrier was of a more uniform distribution than in the Golf/Golf tests. The deformation in the area of the doorsill is considerably greater than that

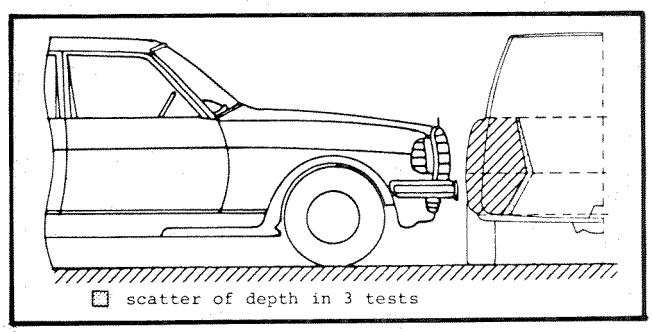

Figure 19. Deformation profile in tests with two DB W 123's from the measuring line -2 (definition in Figure 18)

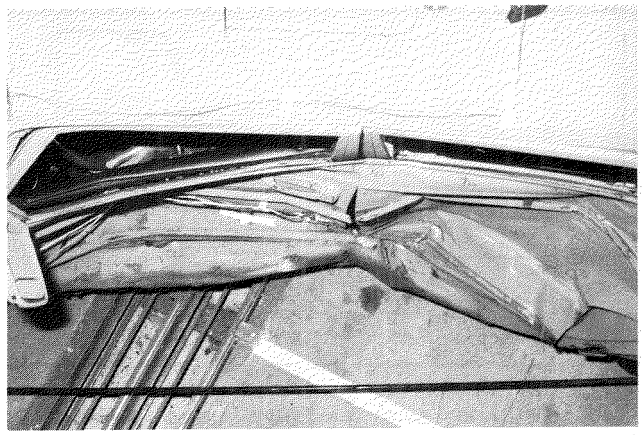

Figure 20. Lateral deformation of the struck vehicle in tests with two DB W 123's

produced in the Golf/Golf tests; the difference in penetration depths in the two tests was less in the area of the sill. The rigidities of the individual barrier elements and their ground clearance are influencing factors in these vertical deformation characteristics. Figure 21 shows the deformation profile for measuring line -2.

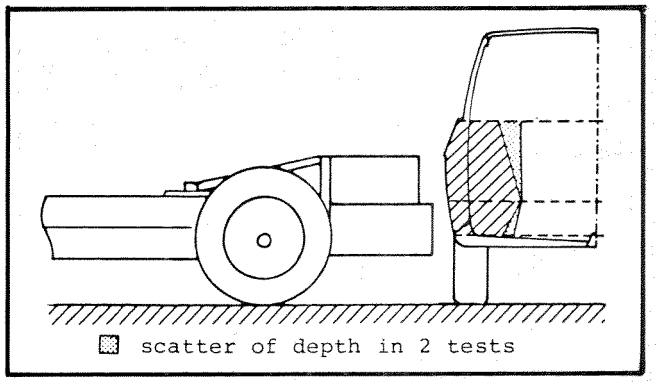

Figure 21. Deformation profile of a VW Golf after impact with the EEVC barrier for measuring line -2 (definition in Figure 14)

In the tests with the EEVC barrier and the DB W 123, a smaller scatter was also observed than is generally the case in the car/car tests. In view of the considerable difference in weight, the barrier was subjected to a greater change in speed.

The loads are therefore lower than in the tests with two DB W 123's—they correspond roughly to the level of the loads occurring during a collision between two VW Golfs, (see Table 4). The acceleration of the left-hand driver's door is low, although slightly higher than in the tests with the two DB W 123's. When the differences in weight are taken into consideration, this indicates that the foam block of the barrier is more easily deformed by the B-pillar than is the front structure of the DB W 123. The vertical deformation profile (Figure 22) during the barrier tests is very similar to that achieved in tests with two DB W 123's (see Figure 19). In these tests, the scatter of the measured deformations is low, particularly in the area of the doorsill.

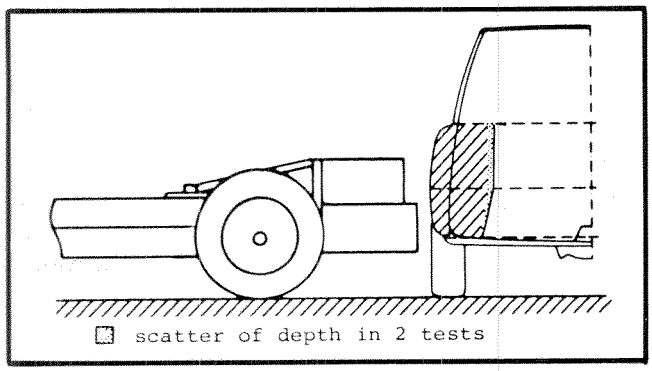

Figure 22. Deformation profile of a DB W 123 after impact with the EEVC barrier (definition in Figure 14)

For a qualitative evaluation of the differences in lateral deformation, Table 5, with a list of cumulative deformation measurements for the individual measuring points, can be used (definition in (6)). In a comparison between the Golf/Golf tests and the EEVC barrier/Golf tests, it is apparent that the mean depths of the measuring points are very similar. Also similar are the lines of maximum deformation, which, in the case of the two-door VW Golf, are approximately in the middle of the driver's door. The edge of the barrier strikes the door rabbet and hinges in front of the A-pillar and rips these out of the pillar. Whereas the VW Golf is a two-door car with a relatively rigid sidewall between B- and C-pillars, the side sectional stability of the four-door DB W 123 is relatively lower.

The low rigidity of the doors and, therefore, the only slight involvement of the A-pillar and the rear wheel housing in the distribution of the forces lead to maximum deformation in the area of the B-pillar. Furthermore, the distance between the A-pillar and the rear wheel housing on the DB W 123 is approximately 100mm greater than on the VW Golf; with the same width of barrier, this leads to a less favorable distribution of forces. The deep deformations in the tests with two DB W 123's, particularly in the area of the B-pillar at measuring line -4, are caused by the greater impact energy of the striking vehicle and by the width of the front structure. This is made particularly clear when compared with the tests using the EEVC barrier.

A comparison of the measured deformations in Table 5 shows the EEVC barrier causes the same horizontal deformation characteristics as a corresponding vehicle. The limits to this correspondence are determined by the excessive differences in mass and geometrical differences (vehicle width).

To clarify this, Figure 23 shows the horizontal deformation patterns of the struck VW Golf compared with the tests between the EEVC barrier and the VW Golf. In the upper door area, the deformation in the Golf/Golf tests is higher than in the barrier/Golf tests.

It is not possible to determine whether this phenomenon is due to the low rigidity of the upper part of the EEVC barrier or to the effect of the greater sill deformation. If the EEVC elements have a greater ground clearance, a smaller sill deformation and a greater deformation in the upper door area would be produced with otherwise constant parameters.

The deformation depth in the area of the R point important for the dummy load is equal in both test series. The deformation in the doorsill area is too high compared with the Golf/Golf tests due to the low ground clearance of the barrier. To represent the deformation curves, mean values were plotted to emphasize the differences between

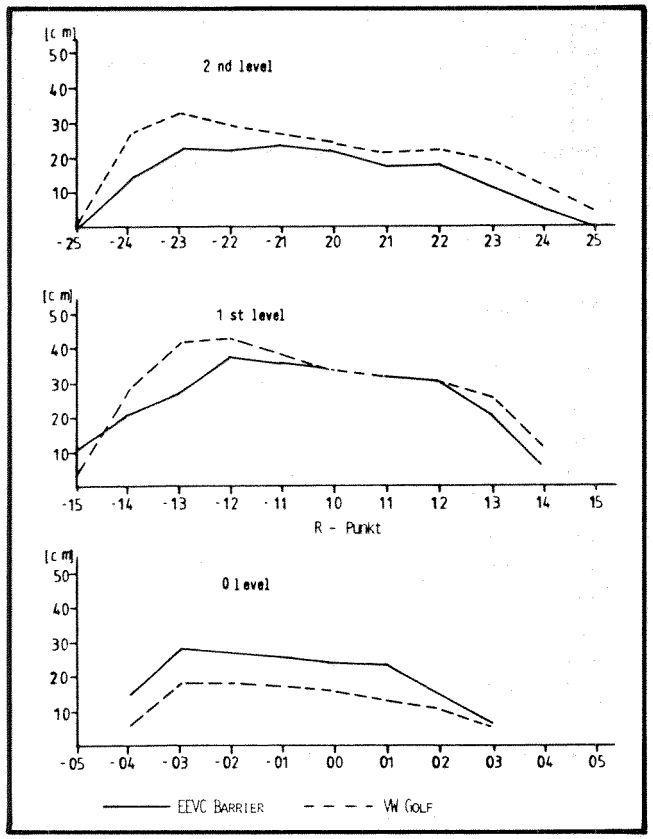

Figure 23. Mean deformation values in tests—EEVC barrier/Golf (n = 2) and Golf/Golf (n = 3)

the test series. With the exception of a few points, the conformity between the barrier tests was high in the upper door area (see also Table 5).

If one compares the horizontal deformation curves of the test series with the middle class vehicles (DB W 123), Figure 24, it can be seen that here, too, the EEVC barrier reproduces well the deformation characteristics of an impact with the same type of vehicle. As was to be expected in view of the greater vehicle mass and the consequent greater front rigidity of the DB W 123, the overall deformation caused by the DB W 123 is greater. What is unexpected is the very good conformity of the doorsill deformation, which can be attributed to the fact that the height of the sill of the DB W 123 is higher than that of the Golf and, in the event of a lateral collision, is also deformed by vehicles with greater ground clearance than the EEVC barrier. The good conformity of the sill deformation also indicates the rigidity of the lower barrier elements corresponds well with the rigidity of the average front structure of a DB W 123. The depth of deformation in the area of the middle door height shows wide deviations since the rigidities of the front of the vehicle and the front of the barrier are too dissimilar—the reason for this is probably the ground clearance of the barrier (see Figure 14). The deformation in the upper door area during a lateral collision is not normally caused by direct contact with the striking vehicle but is usually a consequence of the deformation of the door lower down. The deformation in the upper door area is therefore greater if the intrusion in the middle door area is deeper.

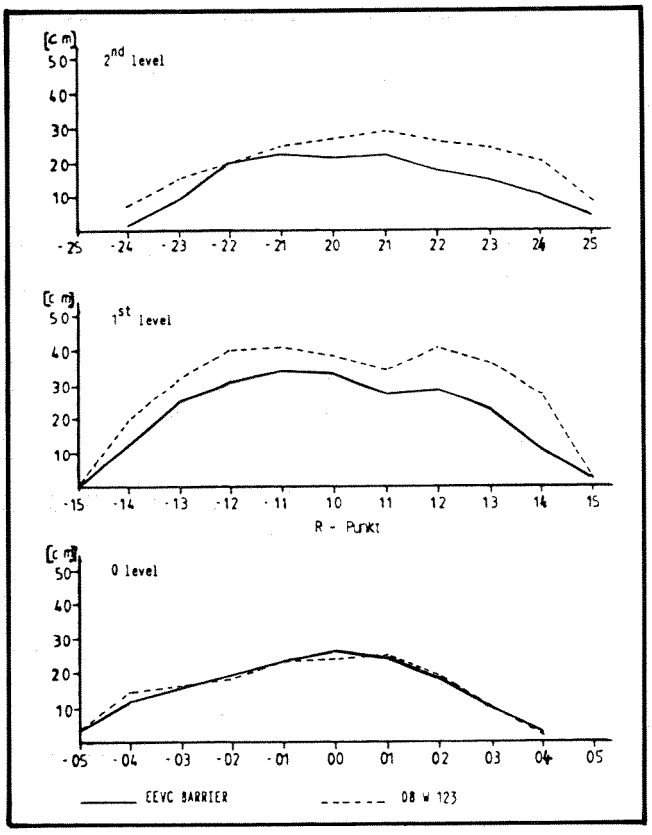

Figure 24. Mean deformation curves in tests—EEVC barrier/DB W 123 (n = 2) and DB W 123/DB W 123 (n = 3)

Deviations between the deformation values of the barrier tests are only very slight, and the reproducibility of the deformation with the EEVC barrier is, in this test configuration, very good—even better than in the VW Golf tests.

The differences in the vehicle loads during tests with the EEVC barrier and with two VW Golfs are caused primarily by the lower ground clearance of the barrier elements. This applies unreservedly to the deformation in the area of the doorsill—with additional influences of the greater mass of the barrier and the greater mean acceleration and velocity change—and probably also to the smaller deformation in the upper area of the door.

The differences in the vehicle loads during tests with two DB W 123's compared with the tests between the barrier and the DB W 123 are also large for the parameters a and Δv due to the large mass-related energy differences. The deformation characteristics are, however, very similar to those occurring during impact with a similar type of vehicle (although with a lesser depth in the middle and upper areas of the door).

The test results with the two tested vehicle types indicate clearly that the ground clearance of the deformation elements is too small:

- On the Golf, due to excessive doorsill deformation
- On the DB W 123, due to insufficient deformation in the upper area of the door

With this adaptation, the EEVC barrier has a very good simulation characteristic.

Occupant Loads

The vehicle loads described above result in the acceleration values listed in Table 6.

As can be seen from Figures 23 and 24, the deepest lateral intrusion of the side occurs in the area of the passenger's pelvis, both in the vehicle tests and barrier tests.

The highest load values were consequently also measured in the pelvis area of the driver dummy.

The obvious differences in the level of pelvis load are clearly attributable to the different depths of deformation.

Dummy kinematics and loads will generally be influenced by:

- The mean vehicle acceleration (a) and velocity change (Δv) of the struck vehicle
- The depth and speed of the intruding side
- The initial distance between the dummy and the inner panel, which affects the time of contact and thus the different speeds of side structure and dummy

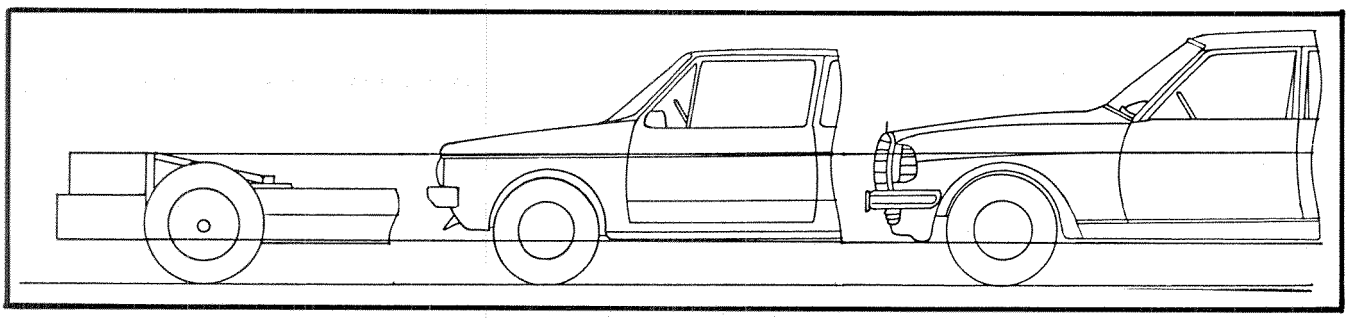

Figure 25. Comparison of heights of vehicle fronts

• The construction of side structure and paneling

When considering both test series, barrier and vehicle tests with VW Golf, only the first two parameters mentioned above can influence the differences in these tests. The sequence of the dummy kinematics is as follows: When one VW Golf is struck by another VW Golf or the EEVC barrier from the side, the intruding side first strikes the driver's seat and pushes it against the passenger seat. During this period, the dummy remains in its initial position and, after approximately 24ms (after start of crash, average for all VW Golf tests), is then struck by the intruding side. The chest and pelvis are struck almost simultaneously. The times and accelerations for the impact between the side of the vehicle and these parts of the dummy are almost identical in all tests. A slight difference was evident in the impact times for the chest with the intruding side door. During the vehicle tests, the dummy was struck by the door before it reached its maximum intrusion speed; during the barrier tests, the door reached its maximum speed before impact with the dummy (see Table 7 and Figure 26). During the barrier tests, the maximum chest acceleration of the driver dummy was reached after 35ms, in the car tests after 33ms. A greater difference in the acceleration peaks was measured for the pelvis—for barrier tests 33ms, for car tests 40ms.

These differences are associated with the deformation behavior of the door. The loads have a lesser effect on the chest than on the pelvis. The side door area at the height of the pelvis was not fitted with accelerometers. The sharp rise in the velocity curve can, however, be recognized in Figure 26 from the acceleration measured on the pelvis of the dummy. The speed in the barrier test is considerably higher.

As a result of the impact between the driver dummy and side door, the head of the dummy rotates toward the point of contact and hits its own shoulder and/or the safety belt directly behind the mounting. The resulting

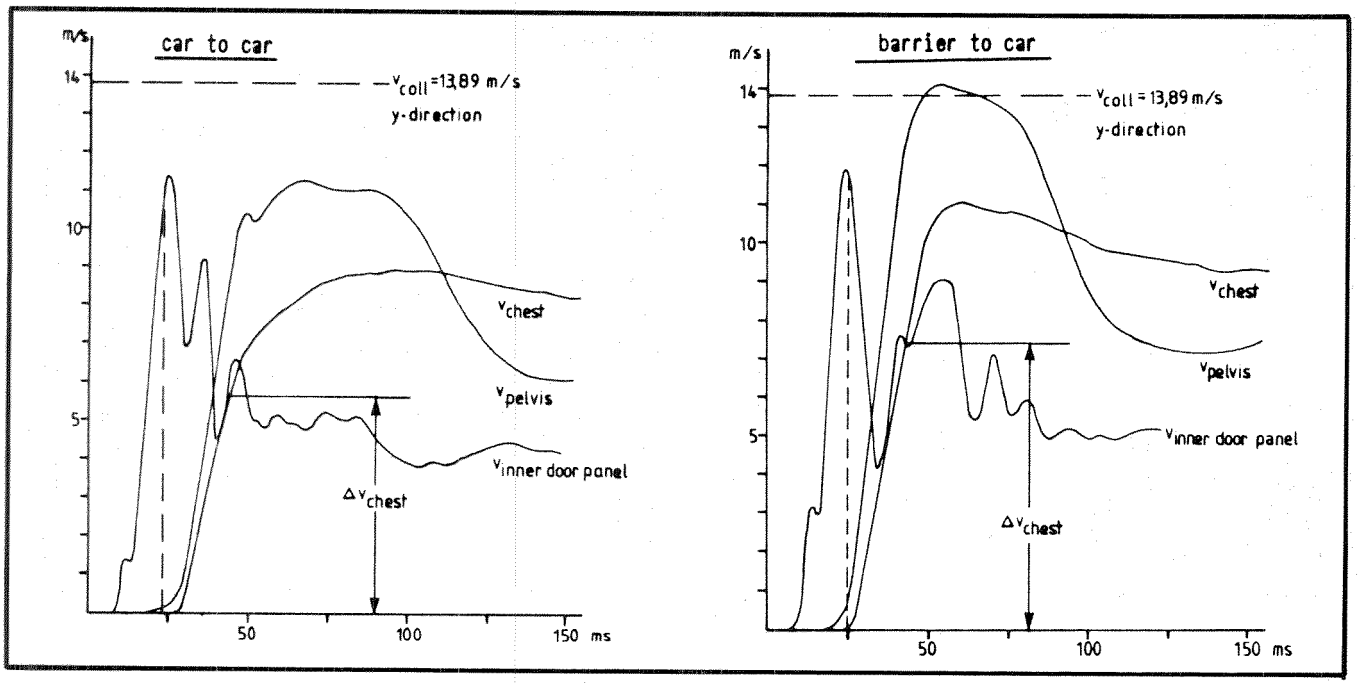

Figure 26. Velocity/time graphs of inner door panel and driver dummy in tests with EEVC barrier and VW Golf

Table 6. Comparison of the measured accelerations of the dummies in barrier and vehicle tests

striking vehicle		veh. 1	CCMC-barrier		EEVC-barrier			VW Golf			DB W 123			EEVC-barrier	
car mass (test weight)*		(kg)	950		950			800			1460			950	
struck vehicle		veh. 2	VW Golf		VW Golf			VW Golf			DB W 123			DB W 123	
car mass (test weight)*		(kg)	800		800			800			1460			1460	
impact speed		(km/h)	50		50			50			50			50	
test no.			21	22	01	02	03	05	06	07	08	09	04	10	
front passenger-nearside															
Head	a_{max}/a_{3ms}	(g)	55/46	80/65	51/42	65/45	42/40	31/30	42/40	67/62	67/64	64/60			
	HIC		407	388	245	255	110	105	151	333	429	272	127	155	
Chest	a_{max}/a_{3ms}	(g)	75/59	60/59	55/49	67/55	68/56	48/42	59/52	113/94	110/98	104/82	95/75	90/84	
	SI		672	482	278	405	270	169	330	663	687	590	404	450	
Pelvis	a_{max}/a_{3ms}	(g)	204/169	195/170	115/105	98/91	85/76	80/72	107/98	110/100	102/98	104/101	99/97	79/73	
rear passenger-nearside															
Head	a_{max}/a_{3ms}	(g)	75/70	88/85	94/78	90/69	68/58	87/75	104/65	64/53	116/78	68/59	93/69	23/22	
	HIC		431	543	420	345	148	284	237	122	423	151	232	64	
Chest	a_{max}/a_{3ms}	(g)	36/34	36/35	44/43	46/42	21/21	25/24	35/20	51/48	41/42	42/37	57/47	36/36	
	SI		161	158	228	209	78	72	61	168	124	83	—	94	
Pelvis	$a_{max}/a/_{3ms}$	(g)	54/48	64/48	68/62	83/76	79/63	62/53	70/63	105/87	117/98	67/51	55/35	52/38	

without dummies
Comparison of dummy load

Table 7. Values related to the collision between dummy and inner door

striking vehicle	veh. 1	CCMC-Barrier		EEVC—Barrier			VW Golf			DB W 123		EEVC-barrier	
car mass (test weight)*	(kg)	950		950			800			1460		950	
struck vehicle	veh. 2	VW Golf		VW Golf			VW Golf			DB W 123		DB W 123	
car mass (test weight)*	(kg)	800		800			800			1460		1460	
impact speed	(km/h)	50		50			50			50		50	
test no.		21	22	01	02	03	05	06	07	08	09	04	10
front passenger—nearside													
contact of chest and	t (ms)	17	17	24	24	21	24	26	22	24	19	21	20
inner door panel	v (ms)	7.2	8.6	12.7	11.7	12.3	11.2	13.2	7.8	7.9	6.8	9.3	9.0
chest velocity change													
caused by inner door	t (ms)	33	37	43	48	48	45	49	42	43	48	30	30
panel impact	Δv (ms)	4.8	7.0	7.3	7.2	8.2	5.6	7.4	7.6	7.9	8.2	5.6	6.0
maximum chest acceleration													
caused by primary impact	t (ms)	26	27	35	34	34	32	33	30	33	27	30	26
in y-direction	a_{max} (g)	71.9	55.8	52.8	64.3	65.2	46.7	57.5	110.7	103.8	101.4	92	86
maximum pelvis acceleration													
caused by primary impact	t (ms)	30	29	34	32	36	43	42	42	44	42	41	35
in y-direction	a_{max} (g)	182.9	182.0	114.7	96.7	83.8	79.3	106.5	104.3	98.5	100.1	96	77.3

* without dummies

head load was low and depended on the chest acceleration. The behavior of the chest and the head during lateral impact is determined by the design of the Hybrid II dummy; the chest and shoulder area as well as the vertebral column are too stiff for the lateral impact. In lateral collision tests with the newly developed lateral dummies, which demonstrate a more realistic behavior, the head moved through the plane of the side window(5). The load criteria for the various regions of the body were exceeded for the pelvis area (80g/3ms) in all barrier tests and one Golf/Golf test.

Due to the collision configuration (e.g., impact points), the loads on the rear passengers were less affected by the lateral intrusion. In addition, a longitudinal component was included in the direction of movement. These factors lead to markedly lower loads on the chests of the rear passengers. Due to the direction of movement toward the point of impact and also the shifting of the driver's seat because of deformations of the car floor, the knees of the rear dummy collided with the driver's seat. The loads thus caused could be measured in the chest and pelvis of the driver dummy and in the femur and pelvis of the rear seat dummy.

In the event of a head impact, the rigid, practically unpadded C-pillar and the lateral roof rail lead to high accelerations, although these do not exceed the protection criterion (HIC $\leqq$ 1,000). The kinematics and loads on the rear seat dummy were practically identical in the test series with the barrier and with the VW Golf—the slightly higher loads in the barrier tests correlated with the higher collision energy as a result of the greater vehicle mass.

In the tests with the intermediate size cars DB W 123, the characteristics of the car construction and the greater car mass of the striking vehicle produced significantly higher loads on the driver dummy (80g/3ms and 60g/3ms were exceeded in all tests for pelvis and chest, respectively). The dummy kinematic load was generally the same as in the other tests. The main difference was in the pelvis region. Whereas chest and pelvis were struck by the intruding door at the same time in all the Golf tests, the intruding door in the DB W 123 tests accelerated the chest earlier (approximately 10ms). This was caused by the seat, the side door geometry, and the resulting seating position.

A further difference involved the driver's seat, which, together with the dummy, was pushed against the passenger seat. In tests where a VW Golf was struck from the side, on the other hand, the seat displacement was almost complete before the dummy was struck by the intruding door. This means the load on the dummy during the tests with a VW Golf was not affected by the behavior of the driver's seat but was affected in the tests with the DB W 123. The effects of the impact site for chest and pelvis relative to the speed curve of the side door are shown in Figure 27.

The loads on the head of the driver dummy follow the same pattern of movements as in the other series of tests, although the head loads are higher due to the higher chest acceleration.

The loads on the rear seat passengers were also significantly lower than those for the driver dummy in these tests. The acceleration level was roughly similar to that in other test series. This may be the result of better door padding; here again, no clear interactive contact is made between the driver's seat and driver dummy. The more stable floor and the maximum side deformation

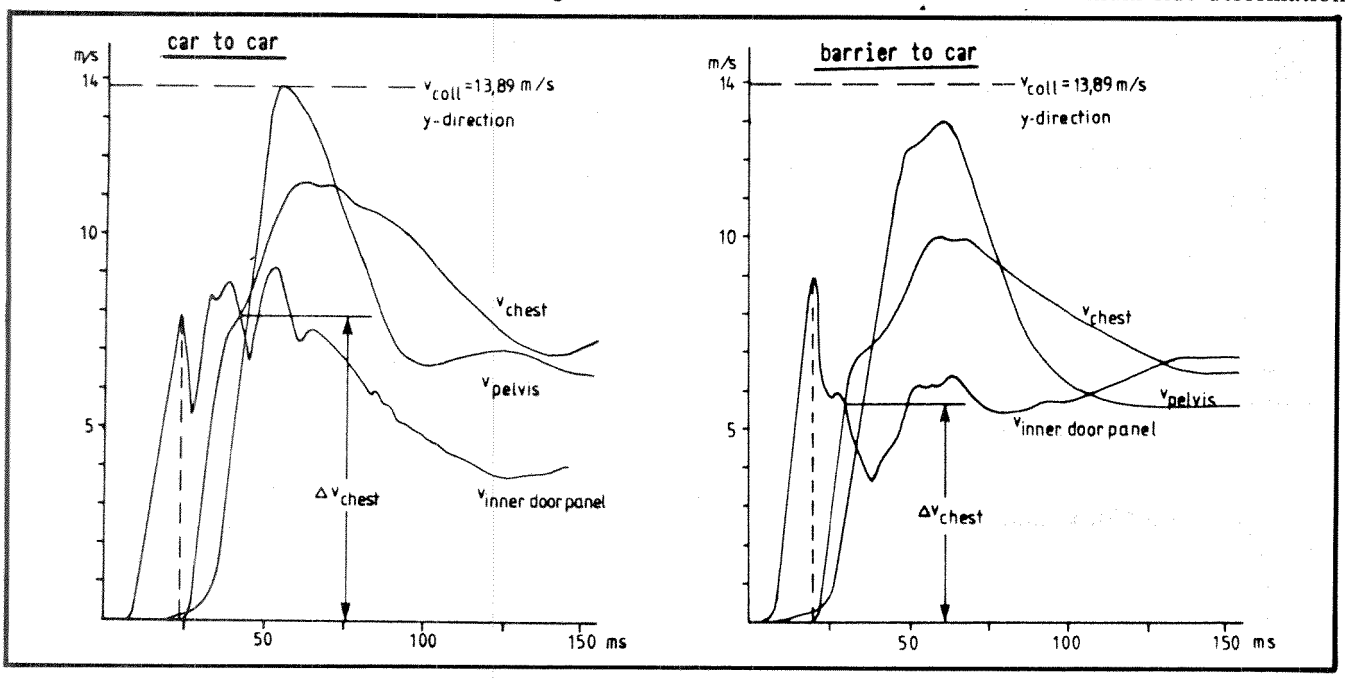

Figure 27. Velocity/time graphs for chest and pelvis relative to intruding door in test DB W 123 and EEVC barrier/DB W 123

lying further to the rear of the vehicle prevent impacts between the rear seat dummy and the driver seat.

During lateral impact of the EEVC barrier with the DB W 123, the dummy kinematics are similar to those occurring during car/car collisions, and the curve characteristic for the pelvis loads is also similar. Only the acceleration of the various parts of the dummy body is lower, and other contact times are the result of the lesser deformation depths with roughly similar deformation speeds (see Tables 6 and 7 and Figure 27).

In the following, the distribution of the accelerations over different parts of the body is compared; acceleration values with an effective duration of 3ms will be compared. Figure 28 shows the mean values from the various series of tests.

The expected distribution of the loads from head to pelvis with ascending values could be observed in all tests. The loads produced by a striking VW Golf were lower for all body parts than in the EEVC barrier tests. In contrast to the corresponding CCMC barrier tests, the EEVC barrier does not produce unrealistically high loads on the pelvis region. The greater weight and associated rigidity of the front of the DB W 123 caused high dummy accelerations not achieved in the tests with the lighter EEVC barrier. Nevertheless, the dummy loads were so high that the injury criteria for chest and pelvis were exceeded.

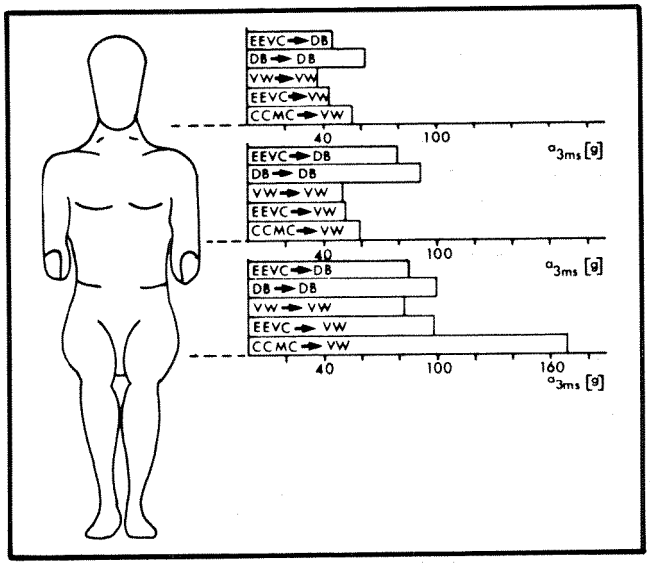

Figure 28. Comparison of acceleration mean values (a_{3ms}) for various regions of body of driver dummy

Summary and Conclusion

The development of a test regulation for lateral collisions as part of a type approval test is currently being promoted by ECE. Before a joint regulation can be accepted by the governments of the participating states, a more suitable anthropometric test dummy (lateral dummy) must be developed for lateral collisions and a suitable test tool selected as a standard vehicle from the existing proposals. This study was to prove the validity of a mobile deformable barrier whose parameters (e.g., rigidity and deformation behavior) were specified by EEVC, regarding its suitability in comparison with collisions between real vehicles. In this project, two tests were carried out with the EEVC barrier against the VW Golf. The results of the vehicle and dummy loads were compared with those from another test series, VW Golf versus VW Golf. In addition, a similar series of tests was carried out with the DB W 123, results of which were used to demonstrate differences in vehicle and dummy behavior. Furthermore, data from a test series with the CCMC barrier against the VW Golf are shown in comparison tables to assess the suitability of the EEVC barrier in comparison with other solutions. The most important results from the three series of tests are summarized below:

Golf/Golf Tests

- During the tests, the deepest deformation was measured in the front door area. The deformation of the doorsill on the struck vehicle was low due to the relatively high ground clearance of the striking Golf. The A-pillar was ruptured at the transition to the sill.
- The distribution of the impact speed did not produce equally high ratios to the change in velocity—the striking VW Golf sustained greater velocity changes.
- The dummy loads were comparatively low. The protection criteria were exceeded in only one test for the dummy (driver) pelvis.

EEVC Barrier/VW Golf Tests

- The barrier produced a very deep intrusion in the doorsill of the struck Golf; the profile of the deformation in the upper door area was similar but less deep. The maximum deformation was also in the front door area.
- The vehicle acceleration was greater than in the car tests. The velocity change of the struck Golf was slightly higher than that of the barrier.
- As a result of the slightly higher mass of the barrier, the dummy loads were also greater than in tests with the VW Golf. The pelvis protection criterion was exceeded in all tests.

Compared with the Golf/Golf tests, the following conclusions can be drawn as to the suitability of the EEVC barrier:

- The distribution of the various rigidity zones in the horizontal plane of the EEVC barrier conforms well to the front face of the VW Golf.

- The ground clearance of the EEVC barrier elements, designed to be compatible with future vehicle development, is too low to produce deformations comparable with those caused during a VW Golf/VW Golf collision.
- The dummy loads for head and chest in the EEVC barrier tests were of approximately the same level as in tests with the VW Golf. The pelvis was subjected to greater loads in the barrier tests, and the protection criterion (80g/3ms) was exceeded.

DB W 123/DB W 123 Tests

- In the tests, deformations in the upper door area were large and approximately the same depth as in the tests with the VW Golf. The maximum side deformation in this case, however, was in the area of the B-pillar. The doorsill deformation was significantly higher than in the Golf tests.
- The car acceleration and velocity changes were greater than in the Golf tests. The distribution of the velocity change of the striking and struck DB W 123 was the same.
- The protection criteria were exceeded in all tests for the chest (60g over 3ms) and the pelvis (80g over 3ms).

EEVC Barrier/DB W 123 Tests

- The deformations in the area of the doorsill were very similar—the areas in the middle and upper side door were deformed considerably less than in the DB W 123/DB W 123 tests. The area of maximum deformation was again in the area of the B-pillar.
- The mean vehicle acceleration of the struck DB W 123 was slightly lower than during the car tests. The mean deceleration of the EEVC barrier was approximately 1.5 times higher. The velocity change of the struck DB W 123 was considerably lower than in the car tests. On the other hand, a higher acceleration of the side door was measured that did not, however, have any major effect on the door intrusion speed.
- The similarity of the loading by the EEVC barrier compared with the DB W 123 is also indicated by the dummy loads; they are in a similar proportion for parts of the body but, as a result of the lower vehicle acceleration and deformation depth, are lower overall. The protection criteria for chest and pelvis were also exceeded during the barrier tests.

Compared with the tests using two DB W 123's, the following conclusions can be drawn regarding the suitability of the EEVC barrier:

- The distribution of the rigidity zones in the horizontal plane of the barrier conforms as well as with the Golf with the front face of the DB W 123, e.g., it leads to similar deformation profiles.
- To cause similar deformations in the vertical plane, however, the upper edge of the barrier must be raised and cause a greater deformation of the upper door area. In the critical R point area, however, it conforms satisfactorily.
- The dummy loads in the barrier tests correspond to those in the tests DB W 123/DB W 123 when the difference in the kinetic energy is regarded; e.g., they are appropriately lower. Chest and pelvis loading exceed the protection criteria.

In conclusion, the following comments can be made regarding the suitability of the EEVC barrier:

- The distribution of the rigidity zones in the horizontal plane of the EEVC barrier conforms well with the demands of such a wide spectrum as that of the VW Golf and DB W 123 as shown by comparisons of the deformation profiles.
- The ground clearance of the EEVC barrier elements is too low to produce deformations similar to those produced by cars currently on the road in small vehicles, e.g., the VW Golf tested here. If the position of the doorsill, e.g., on the DB W 123, is so high that even vehicles currently on the road cause a deep deformation of the doorsill during lateral collisions, the area of the barrier that is superfluous for sill deformation appears to be lacking in the upper door area; i.e., for a better simulation for this type of vehicle, the ground clearance of the deformation elements must be raised.
- The dummy loads in the EEVC barrier tests were, in all cases, similar to the loads caused by real vehicles and demonstrated only higher or lower values through the differences in impact energy. During the EEVC barrier/VW Golf tests, the pelvis was overloaded and the protection criterion (80g over 3ms) was exceeded. In the tests between the EEVC barrier and the DB W 123, chest (60g over 3ms) and pelvis (80g over 3ms) were overloaded.
- The EEVC barrier is capable of simulating well the specific deformation characteristics even with widely differing vehicles. The rigidity of the hard foam elements combined with the aluminum panels is a good approximation of the average vehicle structure. In view of the test results shown here, a correction of the ground clearance of the deformation elements appears to be

necessary for it to conform with vehicles currently on the road.

General Conclusions

This research involves four different European laboratories: BASt in the Federal Republic of Germany, ONSER and UTAC in France, and TRRL in the United Kingdom, under the project leadership of ONSER.

This work was split into two phases. The first phase is achieved, whereas the second phase is in progress. The main conclusions of the part of the work that is finished are—

- The force-deflection characteristics of the front element in polyurethane foam developed by Fritzmeier are close to the specification corridors. Keeping the values of foam density inside a scatter of ±5 percent and taking care of manufacturing would allow almost all the force-deflection curves to stay within the corridor.
- The frontal tests with these elements show a force peak at the beginning of the deformation. However, this force peak probably has small effect on struck car deformations and dummy loadings, as it occurs very early compared to the time of maximum crush and maximum dummy loadings.
- Investigation on alternative material showed that reusable components would be very complicated, heavy, and often damaged by the tests. They would not comply with the proposed specifications.
- The problem of the disintegration of foam was solved by covering the deformable elements with a glued fiberglass net.
- Barrier-to-car side impact tests, compared to car-to-car tests, showed that the barrier correctly reproduces car deformations as well as dummy loadings.
- The validation of the EEVC barrier is near completion, especially in tests using the EUROSID dummy as it is prescribed in the EEVC side impact test procedure. At the same time, the repeatability of the barrier is evaluated, as well as the possibility of using it to check compatability between front and side structures.

References

1. European Experimental Vehicle Committee (EEVC), "Structures improved side impact protection in Europe," Proceedings Ninth International Technical Conference on Experimental Safety Vehicles, Kyoto, 1982.
2. Cesari, D., M. Ramet, and D. Herry-Martin, "Injury mechanisms in side impact," Proceedings 22nd Stapp Car Crash Conference, October 1978.
3. Faerber, E., D. Cichos, and W. Sievert, "Aufzeichnung von Messdaten der Aufprallversuchsanlage der Bundesanstalt für Strassenwesen," (Results from the crash test facility of the Federal Highway Research Institute), ATZ 80 (1978) 9, pp. 401-403.
4. Sievert, W., and E. Pulwitt, "Lateral protection of passenger cars. Comparison tests by means of different barrier configurations," Proceedings 27th Stapp Car Crash Conference, San Diego, 1983.
5. Glaeser, K.P., "Lateral dummy testing," Proceedings Ninth International Technical Conference on Experimental Safety Vehicles, Kyoto, 1982.
6. Pulwitt, E., et al., "Validation of the EEVC mobile deformable barrier," Final report of the 1st phase, EEC Contract No. A0/83/394.

The CCMC Mobile Deformable Barrier for Lateral Collision Testing

D.R. Gebbels
Pilot CCMC Working Group Crashworthiness
(Ad Hoc Group Barriers)

Abstract

As reported at the Seventh ESV Conference, Paris, 1979, the European car manufacturers associated with the Committee of Common Market Automobile Constructors (CCMC) carried out a large program of lateral collision tests. From this data base, CCMC proceeded to develop a mobile deformable barrier (MDB) to investigate its use as a test tool. This paper describes the criteria used in MDB definition, MDB construction, and the assessment testing undertaken to date and reviews and discusses the possibilities for further harmonization of test standards.

Introduction

From 1979, CCMC has been developing an MDB to investigate its use as a realistic test tool for lateral collisions.

Importantly, it must be restated that during its early investigations into the use of side impact barriers, CCMC concluded dummies such as the Part 572 do not adequately represent the performance of human beings in lateral collisions. Therefore, MDB development will be of limited advantage until suitable progress has been made in the development of dummies for lateral collisions.

Phase I—Design Objective

The objective was to match the essential characteristics of the MDB as closely as possible to those of an average European car running on European roads in the late 1970's. A regular check was to be made, say every 2 years, to detect any trends in these characteristics so that changes could be considered. The first reevaluation of the MDB is now taking place and is discussed under Further Research. The original version was based on 1976 vehicle data and is designated CCMC-MDB76.

The essential parameters and development criteria for the MDB were—

- Mass
- Force-deflection characteristics
- Deformation zone structure (geometry)
- Deformation length
- Energy-absorbing material

The deformable part was to be designed for the most severe 90° lateral impact of the MDB against a vehicle.

Mass (CCMC76)

From 1976 sales figures, frequency distribution for unladen car masses were determined for the automobile industries in individual European countries. Weighting the basic vehicle masses with available frequencies for the vehicle types produced an unladen weight of 850kg as the average value. Allowing for vehicle occupancy of 1.5 to 1.7 (average) and the estimated shift in mass from 1976 to the date of the MDB specification, a specification for the MDB was established at 950kg.

Force-Deflection Characteristics

The force-deflection characteristics specified for 300mm deformation were determined from the test results obtained from 15 different cars into 0° full frontal dynamometric barrier at 48km/h. The dynamometric barrier information was supplied by CCMC member companies, and the 15 different car models represented some 1.5 million cars registered for the road in 1976. With consideration of geometric data, the barrier face was split into eight separate segments. The characteristics from the individual cars were weighted according to the 1976 sales figures and then averaged.

Deformation Zone Geometry

To obtain representative geometric dimensions for the deformable element, the essential geometric data of approximately 45 cars, weighted according to frequency, were determined. Figure 1 shows the representative geometry (mean value) of the front of an average European car circa 1978. Based on these findings and in conjunction with the force deflections, segmentation of the deformation zone and design dimensions were defined (Figure 2).

The front face of the barrier was specified flat, vertical, and normal to the barrier's longitudinal axis, without simulation of a bumper. The distance of the lower edge of the impact surface from the ground was set at the maximum of 300mm to allow the barrier to slide over the side doorsills of most cars.

Deformation Length

Based on the finding concerning maximum deformation values for the colliding vehicles in (1), a deformation length of 300mm was considered adequate—the MDB being originally envisaged as a test instrument for perpendicular lateral collision only. Its use under a crabbed test configuration is discussed under Harmonization of Side Impact Test Procedures.

Energy-Absorbing Material

Steel tubes, hydraulics, aluminum honeycomb, and rigid urethane foam were all considered for the energy-absorbing element. Both the hydraulics and tubes were discarded because they would require a heavy rigid front plate and such a plate would have adverse mass effects in a side collision.

After preliminary investigations and testing of aluminum honeycomb, this too was abandoned because the barrier segmentation and load deflection curves required could not be readily achieved without significant developments in the technology. Also, the source of supply for such material was limited and, with it being at a basic cost and weight disadvantage when compared to foam, rigid urethane foam was finally adopted for the energy-absorbing elements.

Material Testing

Deflection Characteristics

Quasi-static pressure tests with foams of different densities were performed to quantify the relationship

	A	B	C	D	E	F	G	H	J	K	β	α	L	M_1	M_2	P	R
CURB WEIGHT	285.2	390.4	390.8	109.0	816.4	53.5	731.9	1539.7	1433.9	746.6	5.27°	3.0°	361.7	577.1	692.0	232.3	521.5
2 FRONT OCCUPANTS	260.6	367.3	368.1	/	792.3	/	/	/	/	/	/	3.15	336.5	556.5	671.3	/	496.7

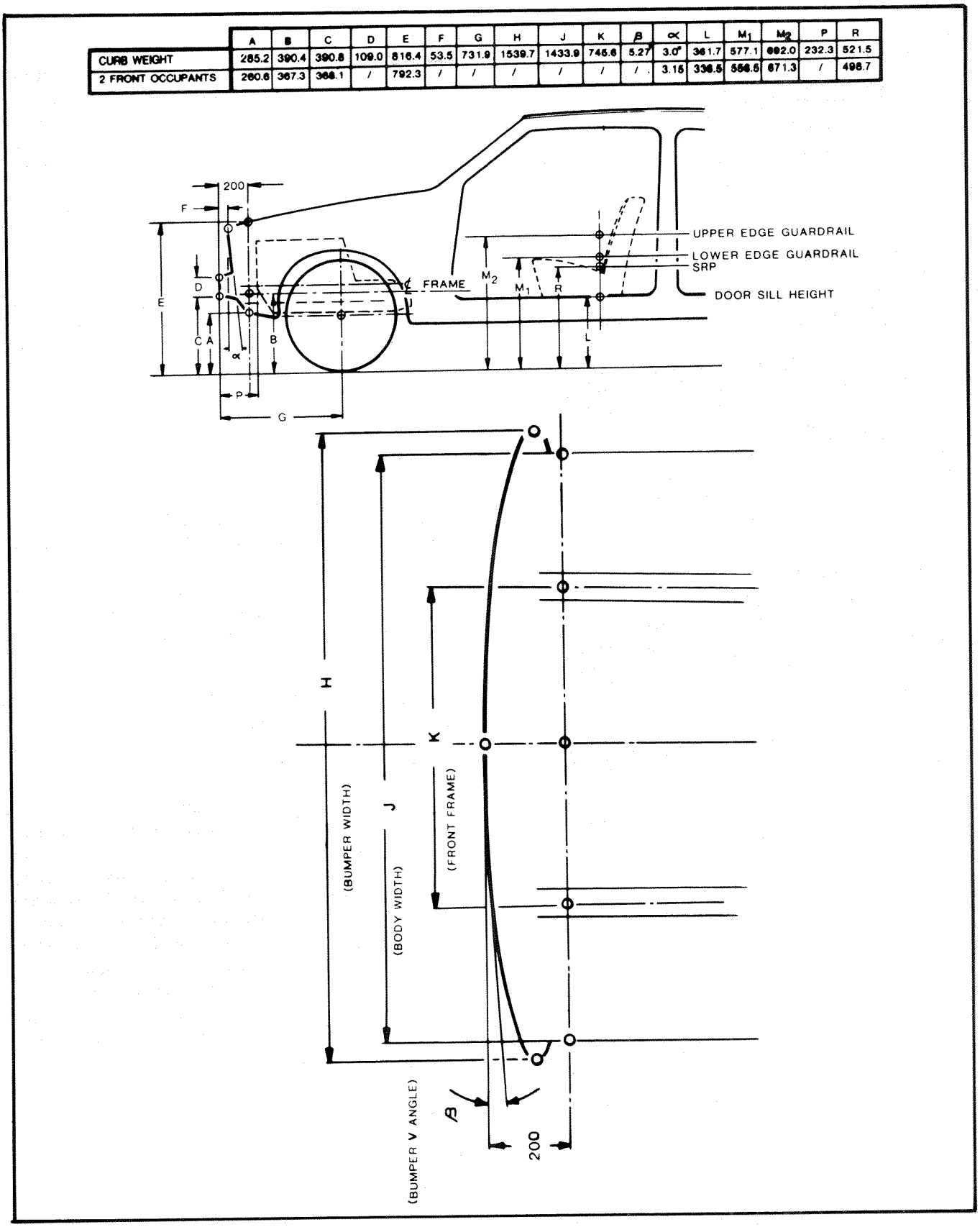

Figure 1. Geometrical car dimensions—European mean values

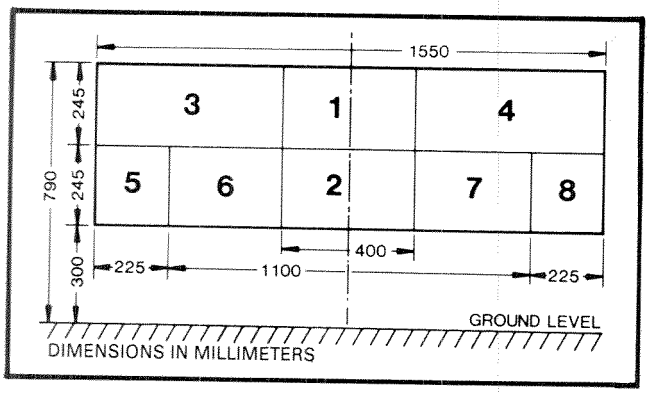

Figure 2. MDB segmented front face

between collapse force and the respective density. To obtain the necessary force-deflection, test specimens with internal sculpturing for some of the depth were made. For production reasons, the internal cavities were bored parallel to the direction of force. To adapt the foam material to the given force-deflection characteristic, each individual segment of the barrier had to comprise separate layers of different density foam with different internal cavity arrangements.

Temperature Influence

Foam samples of different density and core temperature were submitted to static and dynamic testing. The densities were 30, 70, and 96kg/m^3, and the tests performed at temperatures of 0°, +20°, and +40°C. With a density of 30kg/m^3, temperature did not have any significant influence on the force, whereas the more dense foams produced reduced forces of around 15 percent as the temperature was raised +40°C (Figures 3 and 4).

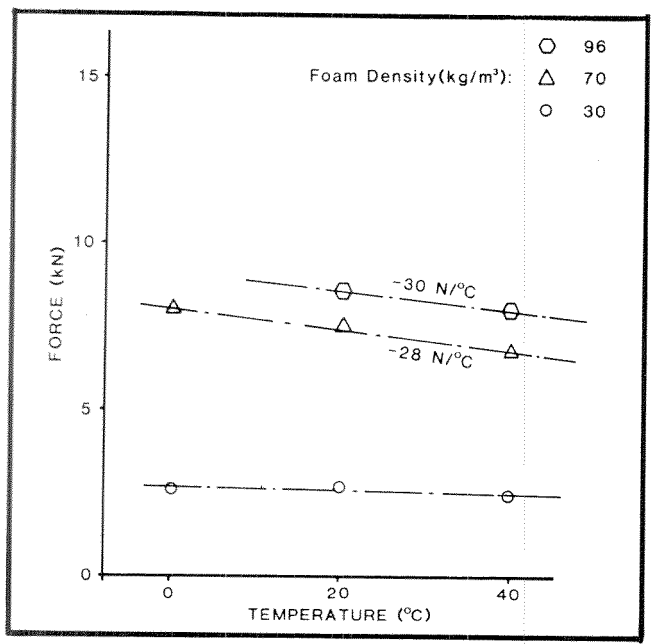

Figure 3. Temperature effects (PU foam) in static tests

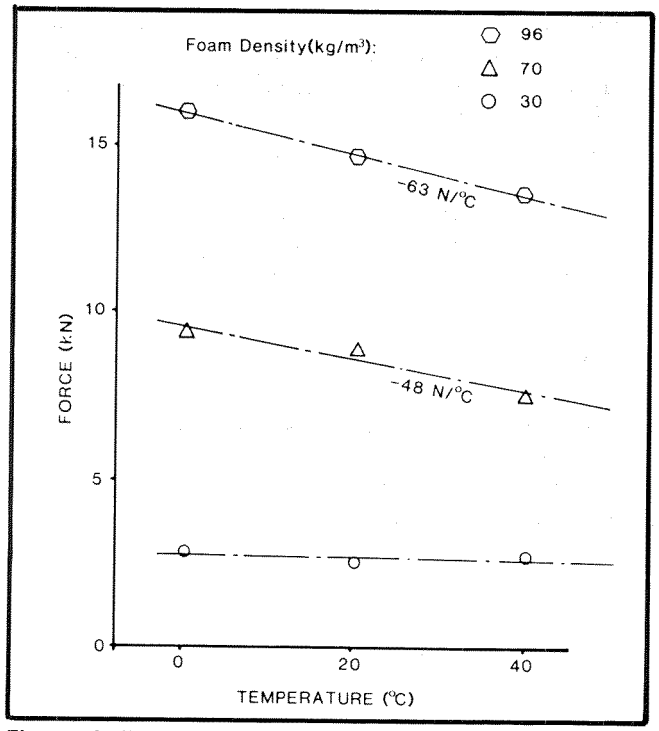

Figure 4. Temperature effects (PU foam) in dynamic tests

Consequently, to limit the effect of temperature variation to below 5 percent, a temperature range of +18°C to +25°C would be specified for the deformable zone of the MDB during a lateral collision. (This requirement is similar to that required for the anthropomorphic dummy in U.S. legislation.)

Speed Influence

Although polyurethane foam was found to be velocity-sensitive in that the collapse load was higher under dynamic loading than quasi-static, this particular criterion was not pursued in depth. Since the speed variation allowable in any test procedure would not be greater than, say, ±5 percent, it was not considered a problem. Fixed barrier tests at 35 and 50km/h impact velocities showed no differences in the force/deflection characteristics up to 300mm deformation.

Preliminary Testing of MDB Deformable Element

For the preliminary verification of the force-deflection characteristics, two differently structured MDB deformable parts were manufactured; one with three layers of foam giving a five-step characteristic, and one with four layers giving a seven-step characteristic. The constituents of the individual segments were cut from freely expanded polyurethane blocks and provided with the required

cavities by mechanical means. Tests with the two prototypes into a dynamometric barrier at 50km/h showed a good approximation to the required force-deflection curve by the three-layer variant with the four-layer version being less satisfactory. The three-layer polyurethane part was chosen for further development. Because the MDB deformable element absorbs only the energy of a 33km/h fixed barrier impact, it was mounted on an additional foam block with high stiffness.

Front Cover Plate

A flexible front cover plate was necessary to allow a continuous deformation process with different lateral stiffnesses of the impacted vehicle—to spread the forces and mitigate local penetrations. Various covering plates were tested with a 2mm aluminum plate being finally chosen.

Barrier Construction

Deformable Zone

Each segment was made from two blocks of foam glued together with internal cavities for part of their depth. Over the entire face of the MDB was glued a thin (30mm) layer of low-density foam. Onto this was stuck the 2mm aluminum plate.

To insure the temperature of the elements could be maintained between 18° C and 25° C at the time of test (as would be necessary for an outside facility in winter), the entire unit was designed so it could be installed onto the rigid chassis at the last moment before test. This was achieved by having an aluminum plate glued to the back of the foam elements so the entire assembly could be mounted easily to the rigid part of the barrier by quick-release pit pins. The entire assembly was wrapped in a thin plastic sheet to prevent foam scatter on impact. Weight of the deformable unit was 25kg.

Rigid Chassis

The frame configuration was adapted from that proposed by ISO for its barrier for side impact testing. It consists of welded steel profiles and has a front covering plate to support the deformable unit and react the deformation forces.

The chassis is equipped with two Porsche 924 rear axles so the overall height may be adjusted via the torsion bars. The suspension of both axles can be locked. The chassis is also equipped with a hydraulic brake system acting on all four wheels. The basic chassis weighs 744kg. With the deformable zone attached, the minimum barrier weight would be 770kg.

Ballast at the back of the chassis produces the specified barrier mass with a center-of-gravity height of approximately 500mm and an inertia moment between 1,500 and 2,000kgm^2 about the yaw axis.

MDB Testing

Whole Vehicle Side Impact

Since the essential characteristics of the MDB were matched as closely as possible to those of an average European-type car, circa the late 1970's, the first tests involved impacting the MDB into a car close to the established average condition. Two subject vehicles were chosen, namely the Renault 14 and VW Passat. These vehicles had characteristics closest to the European average defined in Design Objectives. Two deformable parts were manufactured. The components of the individual segments were still cut from freely expanded blocks and provided with mechanically drilled cavities.

Although CCMC members agreed that the U.S. Part 572 dummy was not designed to evaluate lateral impact protection, it was used since it was the only measurement device available at that time.

In both cases, the struck car was stationary. The impact angle was 90°, and the speed was 50km/h. The front seats of the struck car were in the 50th percentile seating position. The median axis of the impacting barrier passed through the lateral projection of the SRP point onto the outside surface of the car. Dummies were placed in both the front and rear seats on the impact side.

For brevity, only the results from the Renault 14 tests are presented here (Figures 5, 6, and 7). From these tests, it was concluded that the MDB, as designed, was capable of simulating a car-to-car side collision and that development should proceed.

Repeatability—MDB Solely

As with all crash tests that are developed to assess a vehicle's capability of protecting its occupants in accidents, it is imperative that the test procedure, inter alia, gives repeatable results. Test tools and procedures that do not provide repeatability cannot be used.

Five separate tests were run into a fixed dynamometric barrier at 48km/h (to insure complete collapse). These parts had to be manufactured under the same conditions as eventual series parts would be. For that reason, expansion moulds were prepared to maintain identical production conditions. Initially, the production of the

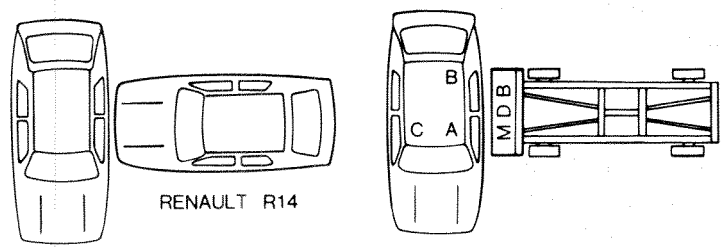

RESULTS OF CARS α 90° V 50kph			STRUCK CAR					STRIKING CAR	STRUCK CAR					M.D.B
Curb weight/Test weight		kg	865/1100					865/1025	865/1100					950
Impact velocity		kph	0					49.0	0					50.99
Impact angle		degree	90					0	90					0
Max. deformation outside		mm	385					165	466					–
Max. deformation inside		mm	310					–	416					–
Max. deformation inside at SRP		mm	354					–	–					–
RESULTS OF DUMMIES			A'	A*	A	B	C		A'	A*	A	B	C	
Head	HIC		106	–	106	123	105		354	–	354	155	210	
	a max /a 3 ms	9.81m/s²	41/32	–	41/32	53/51	42/40		58/56	–	58/56	39/38	53/52	
Chest	SI		132	54	186	45	301		390	150	540	110	540	
	a max /a 3 ms	9.81m/s²	40/37	52/35	52/39	21/20	85/72		77/56	130/40	130/56	27/26	185/73	
Pelvis	SI		760	97	857	239	123		990	160	1150	183	37	
	a max /a 3 ms	9.81m/s²	99/93	41/35	99/93	96/55	45/38		111/105	51/48	114/105	40/37	24/22	

Figure 5. Comparison of test results—MDB/Renault 14 and Renault R14/Renault R14

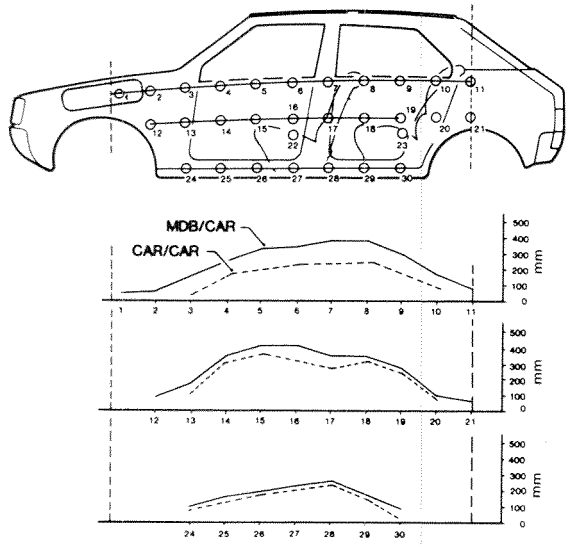

Deformation Outside (Horizontal) (mm)

POINT	MDB/CAR	CAR/CAR
1	45	-
2	60	-
3	152	24
4	265	170
5	356	200
6	378	216
7	413	256
8	413	250
9	307	170
10	158	60
11	77	-
12	118	-
13	205	112
14	392	330
15	466	360
16	455	320
17	398	300
18	399	340
19	292	256
20	93	56
21	68	-
22	438	-
23	245	-
24	138	128
25	202	160
26	242	212
27	280	260
28	312	295
29	209	168
30	102	56

Figure 6. Outside deformation pattern—MDB/R14 and R14/R14

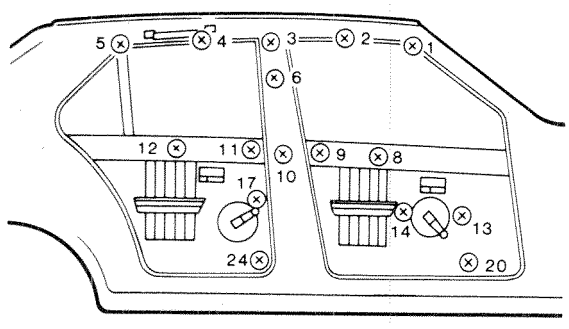

POINT	CAR/MDB	CAR/CAR
1	101	35
2	124	35
3	171	50
4	124	55
5	111	110
6	253	110
7	-	-
8	328	160
9	362	194
10	407	260
11	416	240
12	298	175
13	262	180
14	346	228
15	-	-
16	-	-
17	360	264
18	-	-
19	-	-
20	280	175
21	-	-
22	-	-
23	-	-
24	323	300

Figure 7. Inside deformation MDB/R14—R14/R14

cavities was tried by the addition of inserts within the expansion mould.

Unfortunately, this procedure had to be abandoned for technical reasons—the foam density increasing in the area of the inserts with a resultant increase in the force level. With certain refinements to the tools later, insert-type bores were used in segments having a density of more than 50kg/m^3, which meant a considerable reduction in the mechanical treatment during production.

characteristics were specified to be made symmetrical about the centerline of the barrier. In addition, certain refinements were proposed to the separate force-deflection characteristics to make them more representative of the average European car specification.

The final specification for the deformable part as used in subsequent MDB76-to-car testing is shown in Figures 9 and 10 and Table 1.

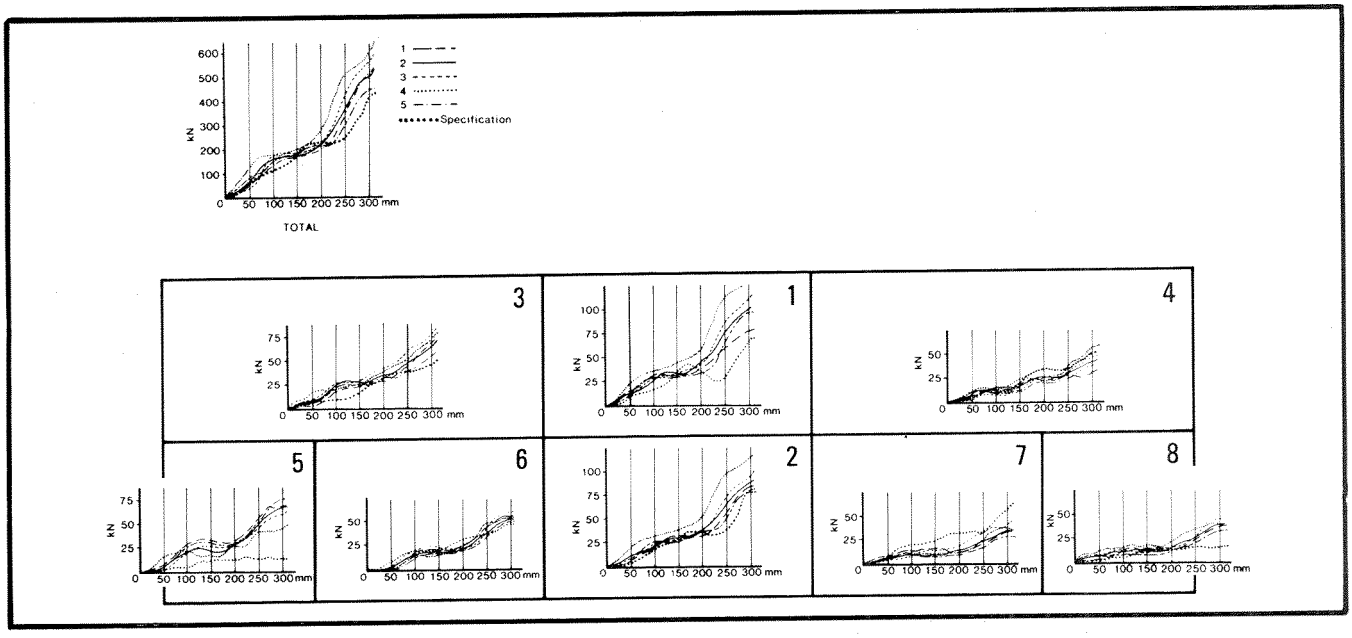

Figure 8. Segment load deflections—repeatability tests

When the five tests were evaluated, it was noted that while some segments showed deviations of as much as ±20 percent, the scatter of the overall (total) force was less than ±10 percent at 300mm (Figure 8).

After these tests, to make the barrier construction simpler and, therefore, more acceptable, the segment

Table 1. Foam densities and dimensions of segments for one CCMC deformable part

Number	Dimensions (mm^3)	Foam Density (kg/m^3)	Cell Number
2	575×245×200	20	3.1; 4.1
2	225×245×200	20	5.1; 8.1
2	225×245×200	30	5.2; 8.2
2	350×245×200	40	6.1; 7.1
1	400×245×200	40	1.1
2	575×245×200	50	3.2; 4.2
1	400×245×200	60	2.1
1	400×245×200	100	1.2
2	350×245×200	100	7.2; 6.2
1	400×245×200	140	2.2
2	775×490×30	10	Frontplate

Foams Used (I.C.I.):—"Daltolack K129"—"Suprasec Dnr"

Repeatability—MDB/Car Testing

To assess the repeatability of the MDB when impacted into a car, six strictly identical tests were performed with the Renault 14 as the subject car. The test protocol for

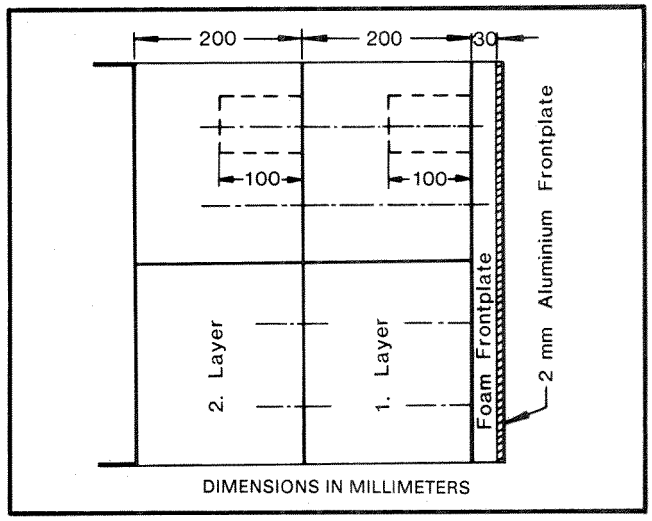

Figure 9. Final specification of MDB76 deformable part

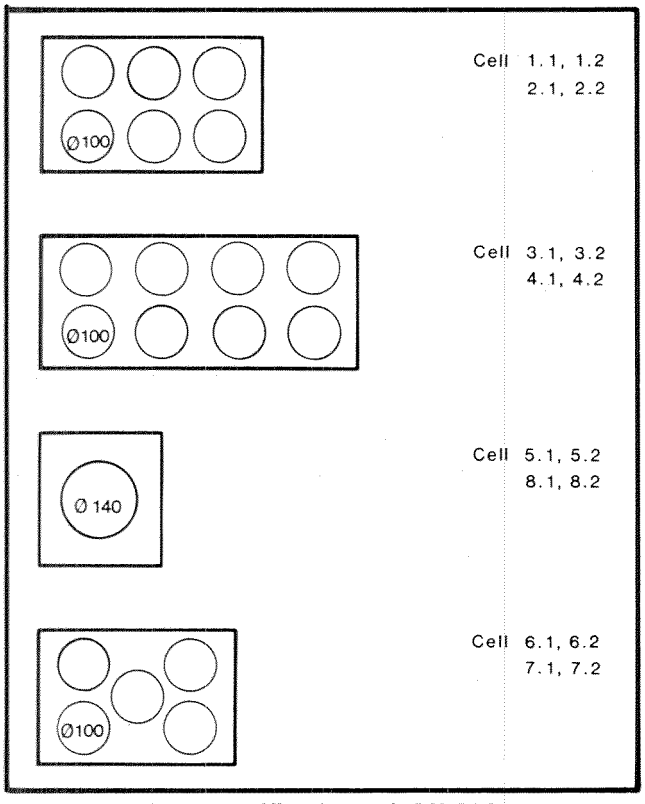

Figure 10. Final specification of MDB76 deformable part

these impacts was the same as described in MDB Testing. All impact speeds were within the range 50.2 to 50.3km/h with the subject car weight between 1,036 and 1,042kg.

As previously stated, the Part 572 dummy is not suitable for lateral collision evaluations, and so, for this part of the test program, the cars were fitted with two APROD 81 side impact dummies for simulation of driver and back-seat occupant. Since, for this exercise, the repeatability of the MDB and subsequent car deformations were the important parameters, the dummy results are not included in this report. A summary of the dummy results are, however, contained in the CCMC paper(2).

Figure 11 shows—

- The outside deformation measurement points
- Outside deformation values recorded

Figure 12 shows—

- Variations in interior intrusion at strategic points

Regarding the outside deformation of the vehicles, the damage was very similar in the six tests. Analysis of the results produced a standard deviation for maximum inside deformation of 3.14 percent and deformation at the front SRP of 1.42 percent.

These results indicated the repeatability of the MDB was satisfactory when samples from the same batch of deformable elements were used.

MDB Round Robin Testing

The MDB was then assessed by the CCMC member companies in a series of round robin tests against their

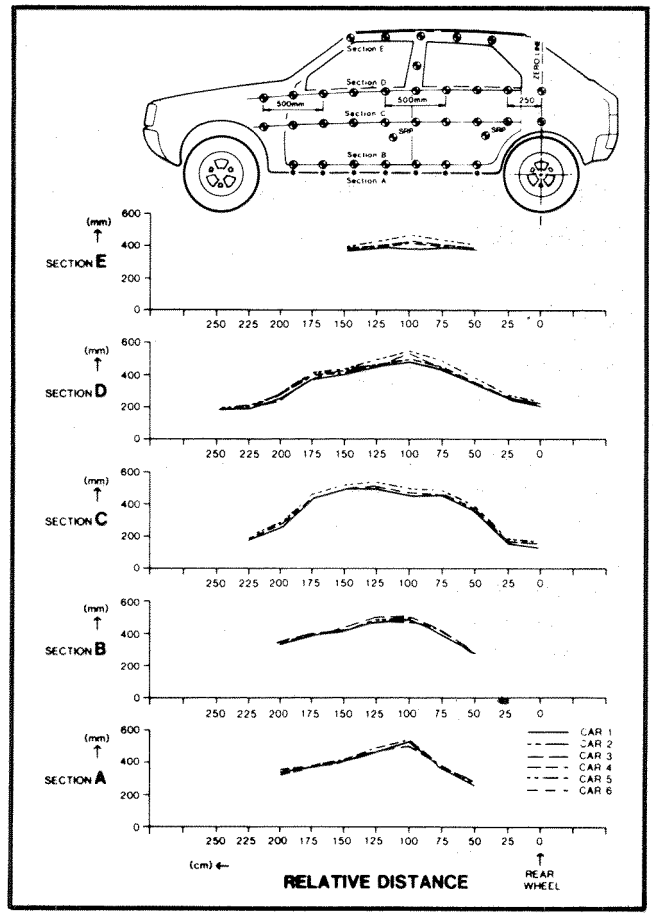

Figure 11. Outside deformations—MDB/R14 repeatability tests

own vehicle models, previously used in the earlier car-to-car and rigid barrier testing phase of their program(1). A total of 12 MDB-to-car tests were conducted, according to the test protocol of MDB Testing, but at each manufacturer's own test site. The appendix gives an analysis of these tests and compares the results with the previously conducted car-to-car tests(1).

A major conclusion from these individual assessments was that despite a lower impact energy with the MDB, the car deformation and main dummy recordings were higher than with the car-to-car tests. To improve this situation required reduction in the stiffness of the MDB deformable element. Consequently, the decision was made in 1982 to reevaluate the main MDB characteristics and attempt to get the actual values closer to the required specification.

Further Research

The testing of the barrier into European cars has shown it to need some modifications to come closer to the specification derived from 1976 data. The opportunity is being taken to establish any changes that have occurred in vehicle design characteristics during the initial evaluation period so this latest information can be considered. The member companies of CCMC have supplied data on their newer models, and a similar weighting procedure is

being used as in Phase I. Research indicates some changes have occurred, but only minor modifications will be required.

Harmonization of Side Impact Test Procedure

During the time of CCMC MDB development, both NHTSA and EEVC have been pursuing their own proposals, which vary with respect to test procedure, configuration, and MDB design itself.

The requirements of the EEVC barrier were established in the final report of Working Group 6 in March 1982 with the European community financing an evaluation program based on these requirements. NHTSA started their research program in 1977 with testing and development continuing.

Since each investigation has the same aim of improving the passive safety of motor vehicles, a proliferation of such devices and procedures is clearly not desirable or necessary, especially with the similarity in the European and the U.S. side collision accident scenes(3). The ultimate assessment criteria should be based on internationally accepted standards.

The main characteristics of the three barriers are presented in Table 2.

Mass

CCMC and EEVC have the same mass at 950kg, while NHTSA is 1,360kg. A compromise should be found, and 1,100kg is proposed.

Ground Clearance

The CCMC ground clearance will be reassessed to account for real accidents. Tests at 250mm will be undertaken during the summer of 1985.

Stiffness

With the minor modification proposed by CCMC, and the discussed stiffening of the EEVC barrier(4), the stiffness of the EEVC and CCMC element will align closely.

Test Procedure Comparisons

Configuration

CCMC and EEVC have chosen a 90° impact with a velocity direction perpendicular to the impacted car. Although it is not the most frequent impact force direction, it is the most frequent impact angle(3). NHTSA simulates the velocities of the striking and struck vehicles by having a crabbed barrier. The CCMC barrier has been assessed in this latter mode and has proved satisfactory in performance(3).

Test Velocity

Both CCMC and EEVC have used a test velocity of 50km/h. NHTSA generally uses 54km/h, taking the crabbed motion into account. This simulates the velocity of the striking (48km/h) and the struck (24km/h) vehicles in a 90° lateral impact.

Impact Point

For CCMC, the centerline of the barrier passes through the lateral projection of the SRP onto the outside surface of the car. Whereas EEVC is similar, the NHTSA point is related to the subject vehicle's wheelbase.

This brief resume of the research proposals to date shows there is a basis on which harmonization can be advanced.

Europe should consider the adoption of the crabbed impact at 90°, while the United States should consider the 90° impact for its crabbed test proposition. The repeatability and reproducibility of the CCMC MDB is such that a joint European and American research program is warranted to develop a common test procedure.

Table 2. Comparison of mobile deformable barriers

		CCMC	EEVC	NHTSA
Mass	(kg)	950	950	1360 (3,000 lb)
Shape		flat	flat + bumper	flat + bumper
Number of Blocks		8	6	1 + bumper
Ground Clearance	(mm)	300 (250) (harmonised)	250	279
Height	(mm)	490	500	559
Width	(mm)	1550	1500	1679
Thickness	(mm)	430	500	483

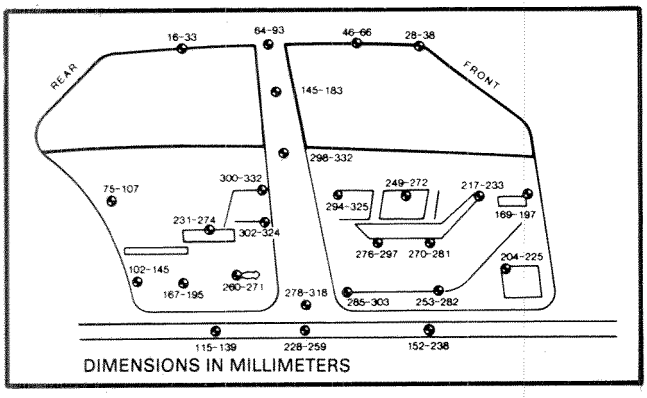

Figure 12. Inside deformations—MDB/14 repeatability tests (minimum-maximum values—six tests

The conformity and batch repeatability of the CCMC MDB have been demonstrated. Should the barrier be adopted as a homologation device, it will be very important that all deformable elements perform in a similar manner. Since a number of parameters can modify the characteristics (e.g., batch changes, transportation, storage), it is fundamental these criteria are precisely known and defined. It will be necessary to define tests that should be performed so conformity with specification is guaranteed. CCMC continues to work on these aspects.

Conclusion

1. CCMC has developed an MDB for lateral collision testing. The MDB76 version has been used by many research organizations and has proved suitable as an evaluation tool.
2. The specification is being upgraded to reflect the latest vehicle characteristics. Work on MDB calibration will continue.
3. European and U.S. researchers should collaborate more to achieve the harmonization of side impact test procedures and so avoid a proliferation of requirements. CCMC proposes to amend the mass and ground clearance of their barrier and suggests joint research should be undertaken into the use of the CCMC deformable element mounted to the U.S. crabbed chassis in a 90° impact.

References

1. Report on Lateral Collision Tests, CCMC-WGCW ESV Conference, Paris, 1979.
2. Report on the Results of Tests Performed by CCMC on the APROD Dummy, AHD/9/83, EEC Biomechanics Seminar, Brussels, March 1983.
3. Klaus, Gunter, et al., "Mobile deformable barrier for lateral collision testing—a contribution toward a harmonization of future side impact performance requirements," SAE Paper 840888.
4. Pullwitt, E., and W. Sievert, "Feasibility of the side impact test procedure proposed by EEVC," Final report, Bundesanstalt Ever Strassewesen, Contract A0/83/394, Bergishe Gladbach, June 1984.

Appendix

MDB Round Robin Test Results Compared With Car-to-Car and ECE Barrier-to-Car Impacts Tested in (1)

In the following diagrams, a comparison of 12 MDB tests is made with the 60 car-to-car impacts and 10 ECE rigid barrier-to-car impacts conducted earlier, all at 90°.

Analysis is restricted to the main parameters, notably:

Car		—maximum external and internal deformations —maximum internal deformation at the front SRP (Seating Reference Point)
Dummy A	Head	—3ms (milliseconds) resultant acceleration
(Part 572)	Thorax	—SI (Severity Index):3ms:contact time car door/thorax
	Pelvis	—SI:3ms:contact time car door/pelvis

Dummy A is the front-seat dummy on the impact side. This was the most critical seating position in terms of high dummy loading.

Dummy results are split:

(A*) — first impact with intruding structure
(A**) — second impact with adjacent dummy
(A) — total result

Since all the rigid barrier (ECE) tests were run at 35km/h and all MDB tests at 50km/h, only the mean values and the standard deviation have been computed for these. For the car-to-car tests, however, the speed range lay between 34 and 64km/h so the influence of impact velocity for this test type could be obtained.

Figures A-1 through A-4 show the graphical results.

The black line always shows the predicted mean value versus impact velocity from the car-to-car tests. On either side are dotted lines at a distance of one standard deviation.

The mean value of the ECE test is marked with a circle, with a vertical line showing the standard deviation.

The MDB results are shown as ellipses with the diameters giving the standard deviations measured in the two directions.

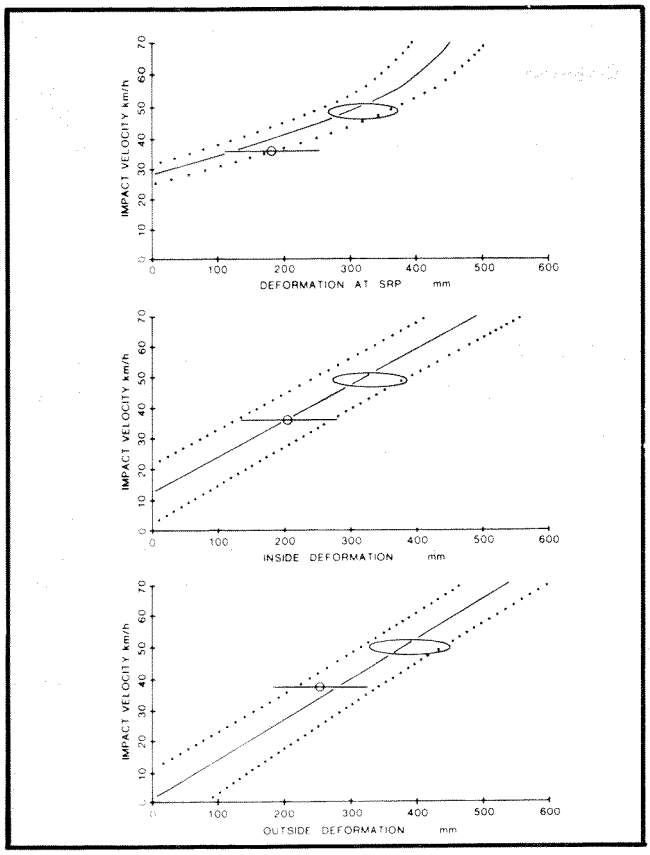

Figure A1. Car deformations

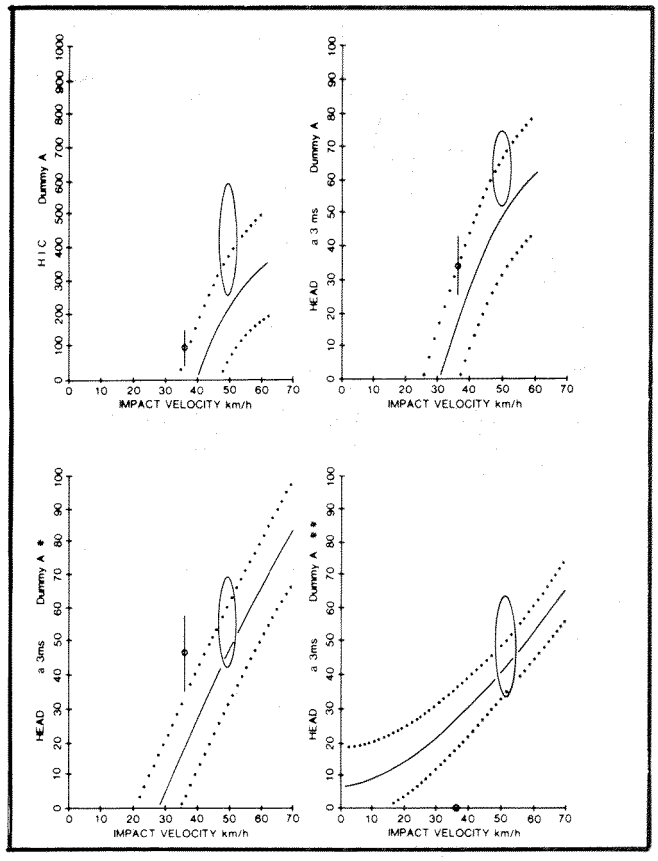

Figure A2. Front impact side dummy—head results

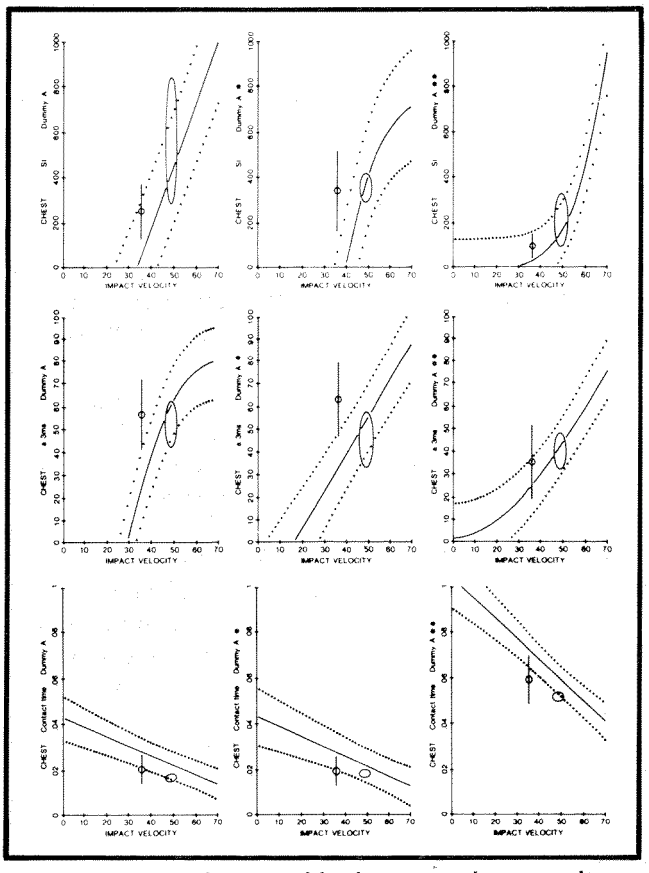

Figure A3. Front impact side dummy—chest results

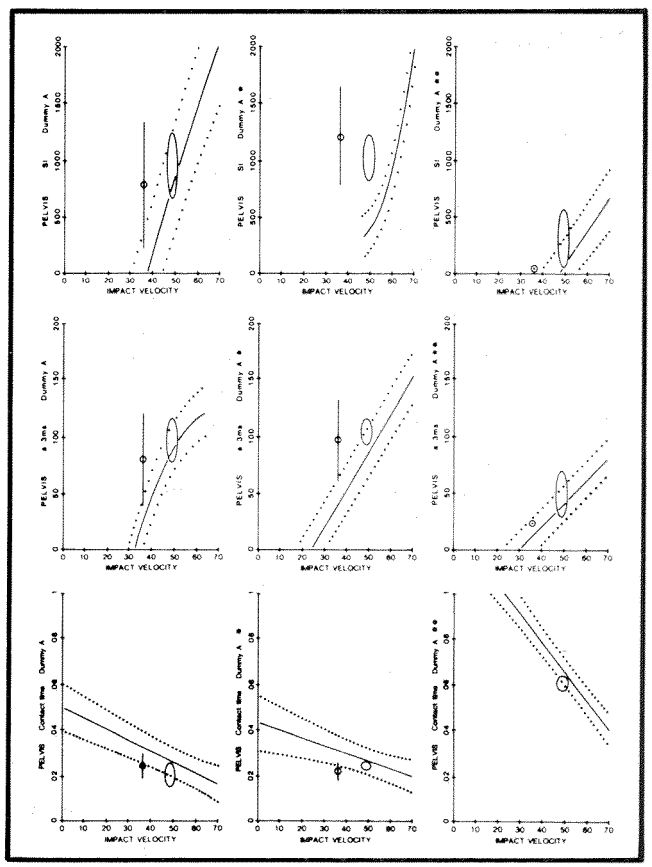

Figure A4. Front impact side dummy—pelvis results

Fabrication and Validation of a Mobile Deformable Barrier for Side Impact

H. Le Guen,
R. Dargaud, and
T. Bourdillon
Union Technique de L'Automobile, du Motorcycle, et du Cycle (UTAC)

Abstract

At the last ESV conference in Kyoto, the Laboratory of UTAC had proposed a work that has permitted the characteristics of a mobile deformable barrier to be defined.

After discussion at the European Experimental Vehicles Committee (EEVC) and study of proposals from different members of the Group of Rapporteurs on Crashworthiness (GRCS) of Geneva, a design of a mobile deformable barrier has been defined.

To obtain the prescribed force-deflection curves of each part of the front impactor, the use of honeycomb materials has been studied by the Laboratory of UTAC. This material was chosen because—

- The force-deflection curve is linear and constant.
- The repeatability of compression tests is good.
- The restored energy after impact is very low.
- The implementation to build the front face is very easy.
- The stiffness of the whole front impact surface is uniform.
- The visible print of the struck vehicle in the front face shows the different stiff sections of the lateral structure of the struck vehicle.

Many tests have been carried out, as part of a study contract for the "Direction de la Sécurité et de la Circulation Routières (DSCR)," against a load cell fixed barrier to verify the repeatability of deflection and effort measurements of the whole impactor. Moreover, this barrier has been evaluated during lateral impacts against vehicles.

These tests have shown that, using honeycomb to construct the front face, it is possible—

- To meet the requirements of the draft specifications established by EEVC and accepted by GRCS, especially with regard to—
  - The effort-deflection curves with an excellent repeatability
  - The amounts of energy dissipated by the different parts and the whole front face
  - The deformations of this front face
- To simulate the energy absorption of the front part of a striking vehicle

Moreover, the material permits a print in the front face, making it easier to study the lateral structure resistance of the struck vehicle.

Introduction

At the Ninth ESV Conference, the Laboratory of UTAC presented a study(1) that defined the specifications for a mobile deformable barrier. Such a barrier should be used as a striking mobile, in a test procedure, to evaluate the protection brought to the occupants of a passenger car in a lateral collision.

These specifications have been established at the request of the French Administration and are supported by French car manufacturers. The specifications of the front face of the barrier were defined after studying the frontal structures of 20 vehicles considered as performant toward frontal impact.

The characteristics of the mobile deformable barrier were defined after examining the characteristics of the vehicles. The dimensions and mass of this barrier were determined by calculating the weighted average value from the parameters measured on the 20 vehicles.

A weighted coefficient, taking into account the number of the vehicle-type registered in France in 1980, has been assigned to each parameter.

To define the stiffness of the impactor, the front structures of the 20 representative vehicles were studied in frontal collisions at 35 ± 2km/h against a load cell fixed barrier, designed to measure the contact loads during impact.

For each value of the crush, the value of the corresponding weighted average effort has been calculated. Force-deflection characteristics have been established from data provided by each of the six plates of the load cell wall. The weighted total force is defined with the same calculation.

The dimensions of the impactor of the barrier have been defined from measurements of the front parts of the vehicles.

The barrier front face was composed of six independent parts to allow the validation of the barrier against the load cell fixed barrier and to verify the stiffness of each part (Figures 1 and 2).

In the same way, European car manufacturers carried out such a study, which was presented by the Committee of Common Market Automobile Constructors (CCMC)(4). A mobile deformable barrier is defined later in this paper.

Both designs and studies carried out in Italy(5) and by TRRL(6) have been compared.

EEVC, which has been responsible for the study of a global lateral test procedure for a vehicle-type approval

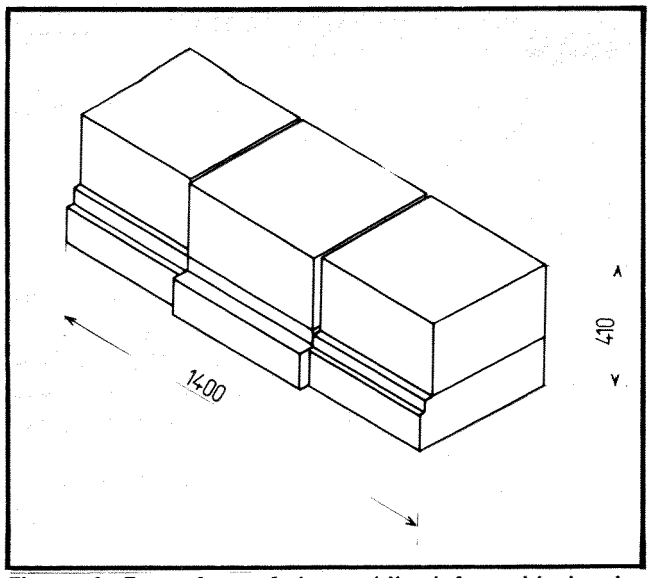

Figure 1. Front face of the mobile deformable barrier developed by UTAC

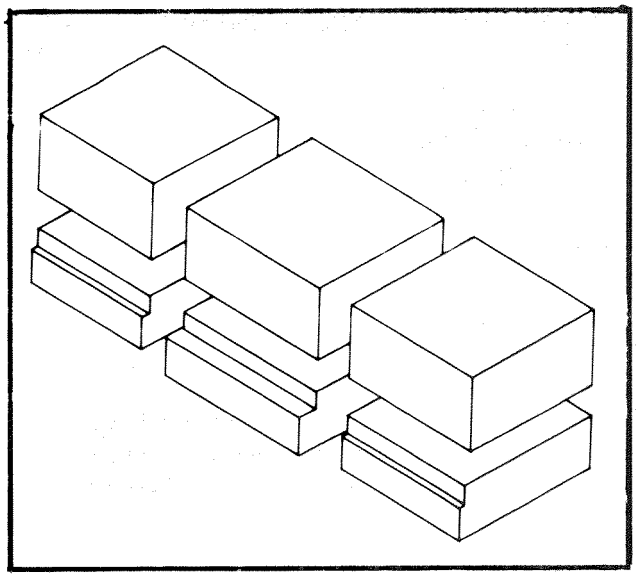

Figure 2. Front face of the mobile deformable barrier developed by UTAC

similar to the procedure proposed for front impact, has defined draft specifications for such a barrier(3).

This proposal was presented to GRCS at Geneva and has been accepted as the definition of the future European mobile deformable barrier used as a striking mobile in a vehicle-type approval test procedure for lateral impact(2).

This document summarizes the work carried out by the Laboratory of UTAC to—

- Choose a material likely to be suitable for the construction of the front face of the barrier
- Build the mobile deformable barrier according to the specifications
- Validate the front face of the barrier in frontal collisions against a load cell fixed barrier to verify its stiffness
- Validate the mobile deformable barrier in lateral collisions against a type of vehicle

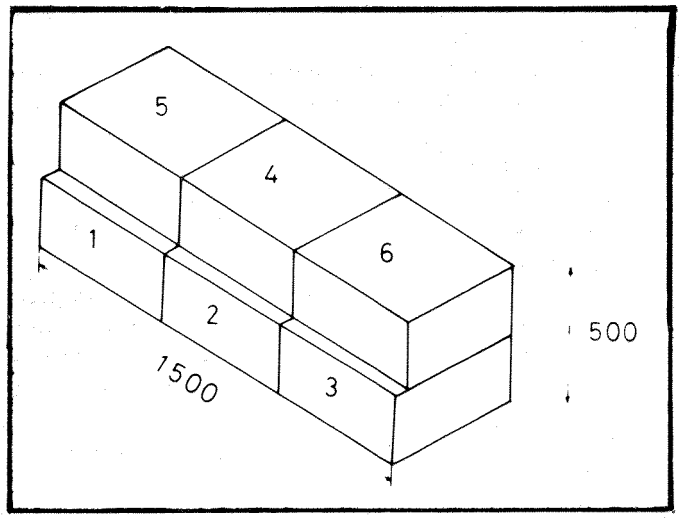

Figure 3. Dimensions of the specified front face of the mobile deformable barrier

Specifications of the Mobile Deformable Barrier

The characteristics of the mobile deformable barrier are as follows(2):

- Mass: 950 ± 20kg
- Front and rear wheel gauges: 1,500 ± 10mm
- Wheel base: 3,000 ± 10mm
- Position of the center of gravity: in the longitudinal median plan, 1,000 ± 10mm behind the front axle and 500 ± 10mm above the ground
- Distance between the front surface of the impactor and the center of gravity of the barrier: 1,800 ± 20mm

The front face consists of six independent parts. The shape and dimensions of this front face are given in Figures 3 and 4.

The front face has a ground clearance of 250mm to take into account further developments in the design of vehicles to solve the problem of compatibility between frontal and lateral structures.

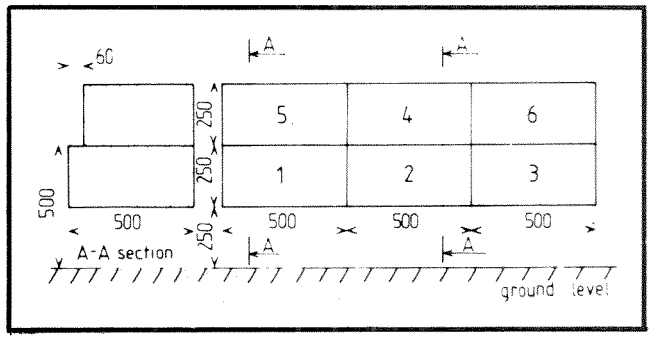

Figure 4. Dimensions of the specified front face of the mobile deformable barrier

The stiffness of the front face must meet the following requirements:

- Parts 1 and 2 on the one hand, and 5 and 6 on the other hand, must be identical.
- The force-deflection curves must be drawn in the hatched regions defined in Figure 5.
- The total force-deflection curve must also be drawn in the prescribed zone of Figure 5.

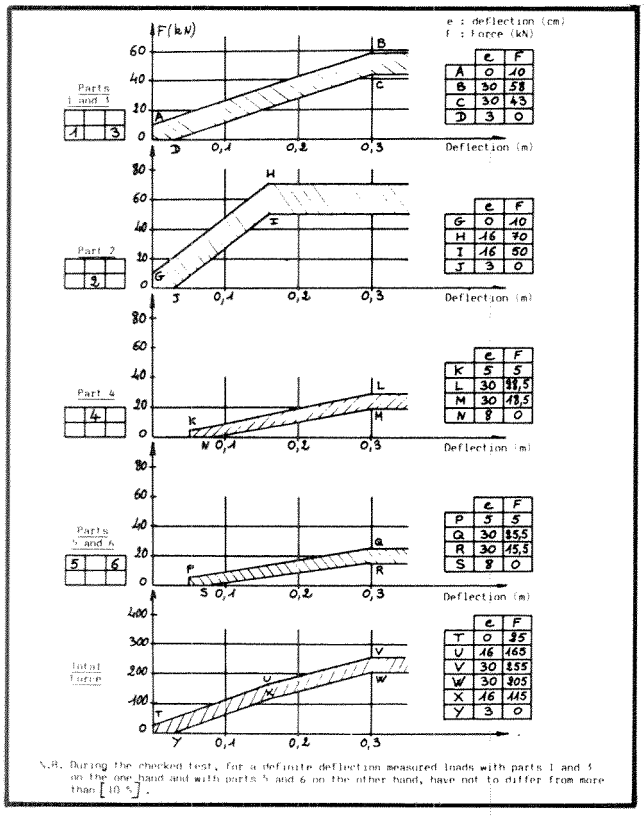

Figure 5. Specified deflection curves

The stiffness of the front face must be verified in a frontal impact of the barrier at 35 ± 2km/h against a load cell fixed barrier. The quantities of energy dissipated by each part and by the whole front face during the impact must meet the requirements prescribed in Table 1.

The deformation of the front face, measured after the impact at the level of point B (Figure 4) must be equal to 350 ± 20mm.

Comments

Meanwhile, an examination of the specifications and a study of preliminary tests show that these specifications should be modified as follows:

- The distance between the front surface of the deformable part and the center of gravity of the barrier is specified as 1,800 ± 20mm. This distance cannot be actually respected because of the dimensions of the front face and the position of the front wheels. This dimension should be raised to 2,000 ± 50mm.
- The conditions for measuring the efforts during the validation of the front face of the barrier against a load cell fixed barrier should be clearly defined. The data channel of the efforts should meet the requirements of ISO Standard 6487, and the data channel class of frequency (CFC) should be equal to 60.
- The specification relative to the deformation of the front face of the barrier is not in accordance with the nominal value of the kinetic energy (m = 950kg, V = 35km/h) and with the required effort levels. The nominal value of this deformation should be adjusted to correspond to the distance required to stop a mobile, the kinetic energy of which is equal to the nominal kinetic energy with an average effort level.

Considering the values indicated in the specifications, a value of 330mm should be adapted further.

Determination of a Material for Construction of the Front Face

The Laboratory of UTAC has studied different materials likely to be used for building the barrier front face(17).

Such a material must have the following essential characteristics:

- Its mechanical characteristics must stay constant in relation with time.
- Tests of compression with the material must show a good repeatability.
- Its force-deflection variation must be such that the specified levels of the curves may be reached. Crush force should increase linearly with deflection up to a limit, beyond which the force should be constant.
- The restored quantity of energy after crush must be low.

A first inventory examined some materials (Figure 6):

- Cardboard and structures made of cardboard
- Metallic cylindrical tubes
- Different types of foam
- Honeycombs

Table 1. Amounts of dissipated energy (kJ)

Part 1	Part 2	Part 3	Part 4	Part 5	Part 6	Total
10 ± 2	14 ± 2	10 ± 2	4 ± 1	3.5 ± 1	3.5 ± 1	45 ± 5

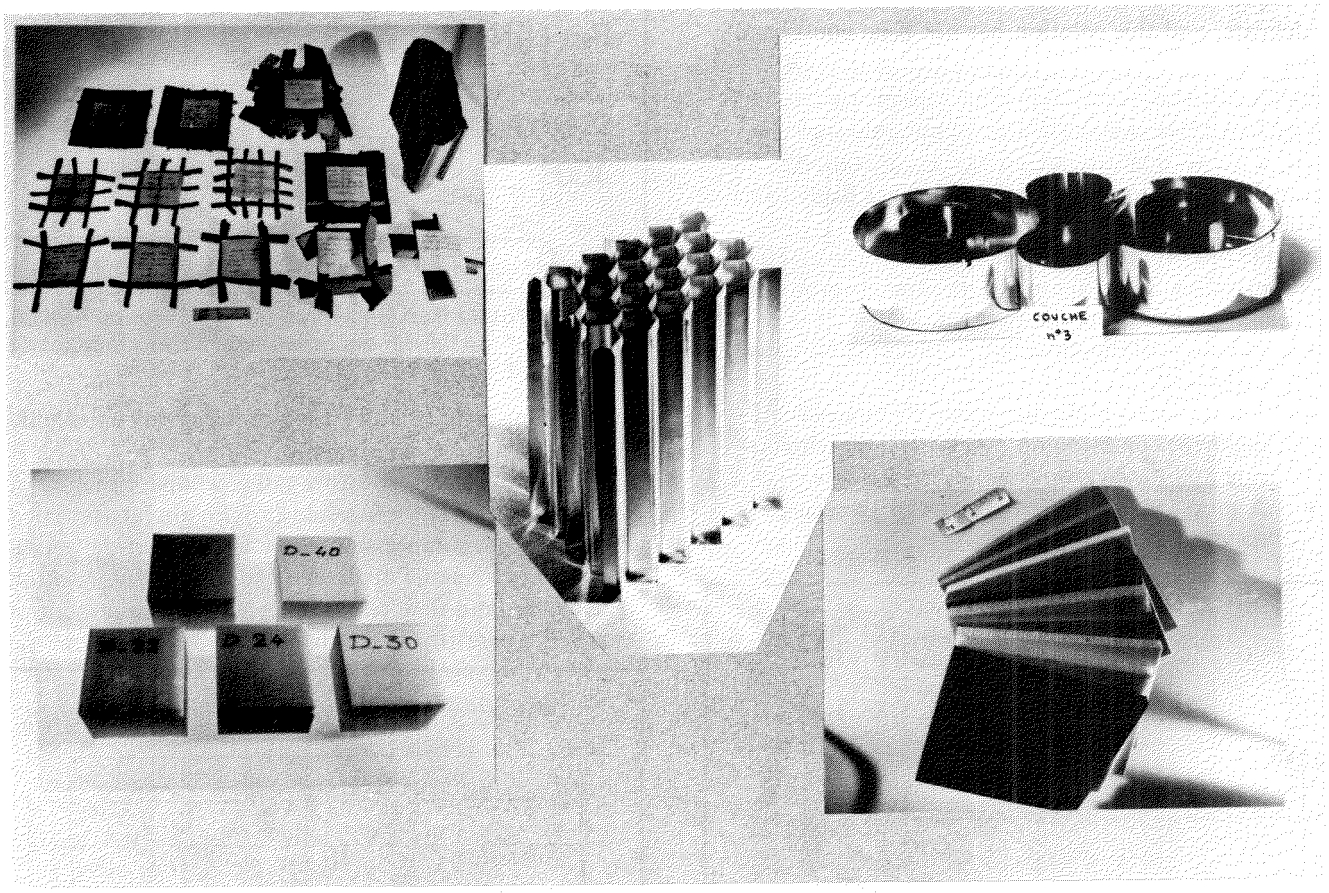

Figure 6. Various tested materials

Quasi-static crush tests of samples consisting of a stack of corrugated cardboard were carried out with a tensile-testing machine. These tests show that (Figure 7) the effort-deflection curves do not show any plateau force level, and the stiffness greatly decreases as soon as humidity increases.

Tests carried out with assemblies of structures made of cardboard showed the same failures and made this material unlikely to be worth pursuing.

Repeated crush tests with cylindrical tubes showed that the compression efforts oscillate around a mean value. However, these curves show a series of picks due to the formation of pleats during the crushing of tubes. So, the compression efforts vary to a large extent (Figure 7b). The tubes have been cut in order to weaken them and obtain the prescribed stiffness.

Some assemblies, consisting of layers of tubes and reproducing different parts of the front face, have been tested with the tensile-testing machine. It was attempted to advance with successive steps to obtain the first parts of the force-deflection curves by adjusting the stiffness of the tubes of the different layers that constitute the parts of the front face.

Some tests carried out with a tensile-testing machine showed that the force-deflection curves of an assembly, corresponding to the lower lateral parts, were inside the prescribed limits. Unfortunately, some dynamic tests showed that the measured efforts were definitely higher than the efforts obtained during the static tests, certainly because of the relative displacement of the tubes during impact. These materials are not suitable to obtain a uniformity of each part of the impactor. Moreover, the

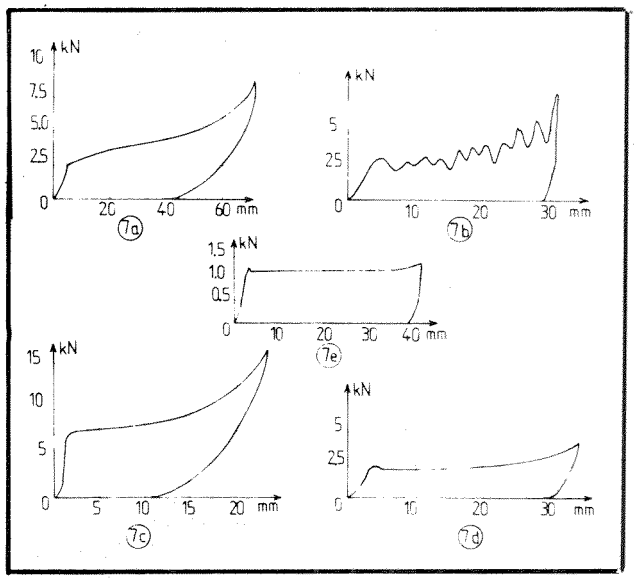

Figure 7. Force-deflection characteristics of the tested materials

labor required to build the whole front face is significant and delicate, and this solution has not been considered further.

Some quasi-static tests of flexible or semi-rigid foams showed that these materials are not suitable since they restore a large quantity of energy after compression (Figure 7c). Rigid foams were the only ones likely to be suitable (Figure 7d).

Samples of 11 types of different foams have been tested in compression after temperature and hygrometric conditioning. These tests showed that—

- The slope of the curve may vary according to the deflection.
- The mechanical characteristics fluctuate according to the conditioning, especially if the temperature and the hygrometric degree increase.
- A more or less important part of the energy is restored after impact (Figure 8).

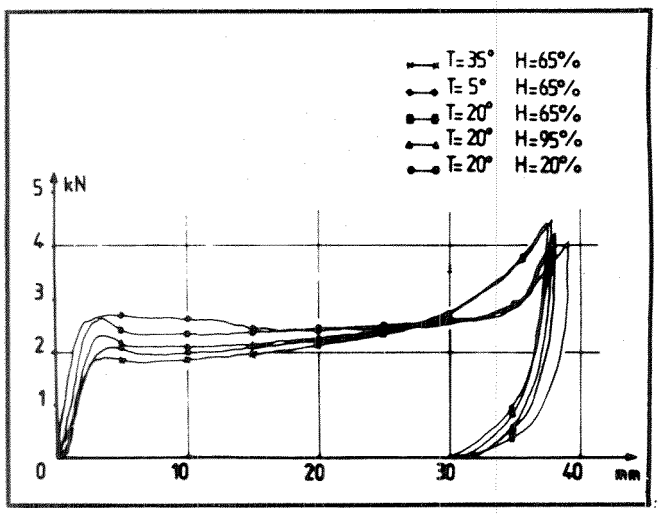

Figure 8. Crush tests of samples made of rigid foam after temperature and hygrometric conditioning

A dynamic frontal impact at 35km/h against a load cell wall of a barrier, equipped with a complete front face made of rigid foam, showed that the front face blew out and cut itself into small pieces during the impact. The collapse of the material induces a fall of the efforts, which cannot stay inside the prescribed area (Figure 9). The pieces, issuing from the burst of the front face, do not take enough part in the kinetic energy dissipation of the barrier. Therefore, a large amount of this energy was restored after impact as shown by the rebound distance of the sled, which was about 15m for the test. This was confirmed by the shape of the total force-deflection curve.

The foams also have a major disadvantage in that the makers cannot guarantee constant mechanical characteristics. These characteristics can vary about 20 percent for ordinary foams. The variations may be high, even with special foams. Considering the situation of the foam

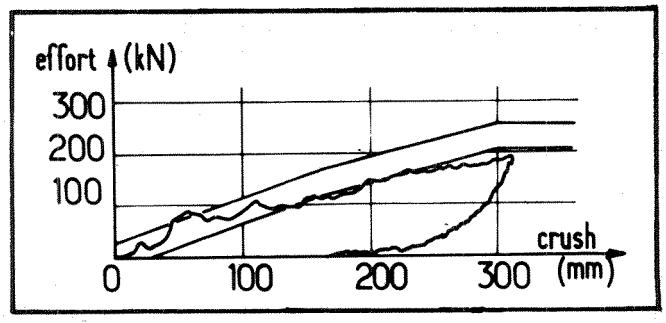

Figure 9. Total effort measured during a frontal impact of the barrier equipped with a front face made of rigid foam

manufacturing techniques, these materials are not wholly suitable as part of our study.

The honeycombs, consisting of a cellular structure of aluminim foils, have been tested also (Figure 7e). Repeated static tests of compression show their effort-deflection curves have a clean, flat plateau, their law of deformation is constant, and they restore only a very low amount of energy (Figure 10). It had been proposed to obtain the

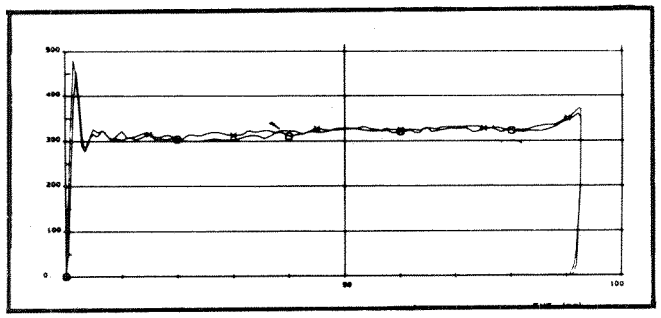

Figure 10. Quasi-static crush tests of sample of the same honeycomb type

ascending part of the curves, in making the efforts increase, by stacking honeycombs of different rates of stiffness. Unfortunately, the range of available varieties of this material is relatively limited, especially for honeycombs with low stiffness. It was decided to cut honeycomb blocks so that the sections vary according to the crush (Figure 11).

Many quasi-static and dynamic tests have been carried out with stacks of honeycombs of the same stiffness. These stacks consisted of two layers, one with a section that varied according to the crush degree. These tests showed it was possible to make some parts with honeycombs according to the prescriptions of stiffness and energy-absorption capacity and showing a good repeatability. Therefore, UTAC has decided to develop a mobile deformable barrier equipped with a front face made of this material.

Construction of the Mobile Deformable Barrier

The sled consists of a tubular steel 3,655mm × 1,065mm frame. Tubular cross members have been welded in the

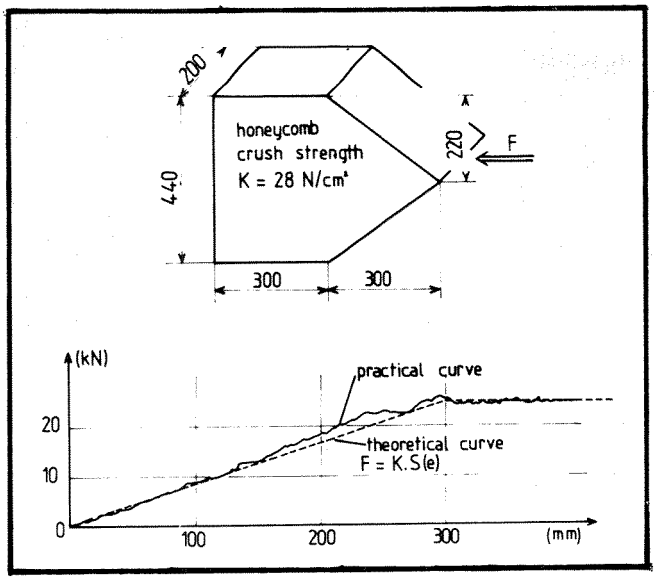

Figure 11. Crush characteristics of honeycomb with variable section

frame to strengthen it.

A 1,500mm × 500mm aluminum plate, 30mm thick, is fixed in front of the frame to support the front face. The dimensions for positioning the center of gravity have been adjusted by fixing added masses on the frame. The other specified dimensions have been respected (Figure 12). The mass is equal to 950kg when equipped.

The front face consists of six independent parts made of honeycomb. The dimensions of these parts are given in Figure 13. Steel sheets, 4mm thick, are fixed at the rear of the front face and between the different parts. The characteristics of honeycombs used for the fabrication of the front face are specified in Figure 14.

Figure 15 shows the UTAC mobile deformable barrier.

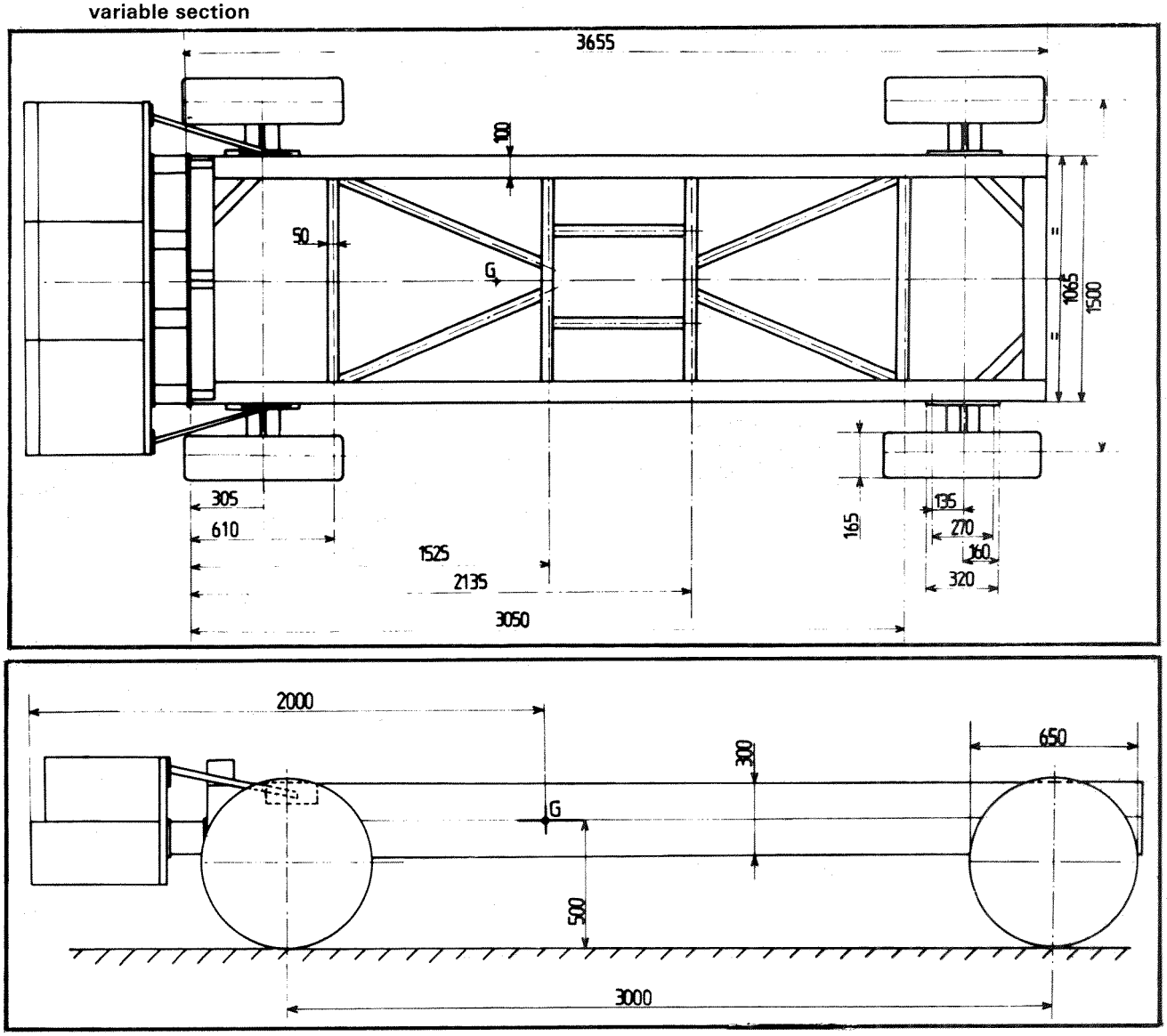

Figure 12. Characteristics of the UTAC mobile deformable barrier

Validation of the Mobile Deformable Barrier Against a Load Cell Fixed Barrier

Three tests of frontal collisions at 35 ± 2km/h of the total barrier have been carried out against a load cell fixed barrier studied and built by UTAC. Comments concerning the draft specifications were taken into account to carry out these tests.

This equipment consists of six independent plates for measuring the efforts of contact during an impact (Figure 16). Each dynamometric plate is equipped with four load cells. The signals emitted by the transducers of one plate are added through an electronic totalizer. The total effort is obtained by calculating the value of the result of these efforts.

The accelerations of the mobile barrier have been measured on the longitudinal beams of the frame, at the level of the center of gravity.

The force-deflection curves of the barrier front face have been obtained with a double integration of accelerations measured on the sled frame.

The curve is shown in Figure 17, and it is possible to compare the amount of acceleration ($m\Sigma\ell i$) of the barrier with the total effort measured by the load cell fixed barrier for one of the tests.

Figure 18 shows the force-deflection curves of the six parts of the front face obtained for the three tests. The variation of the total efforts corresponding to the various tests are also shown in Figure 19.

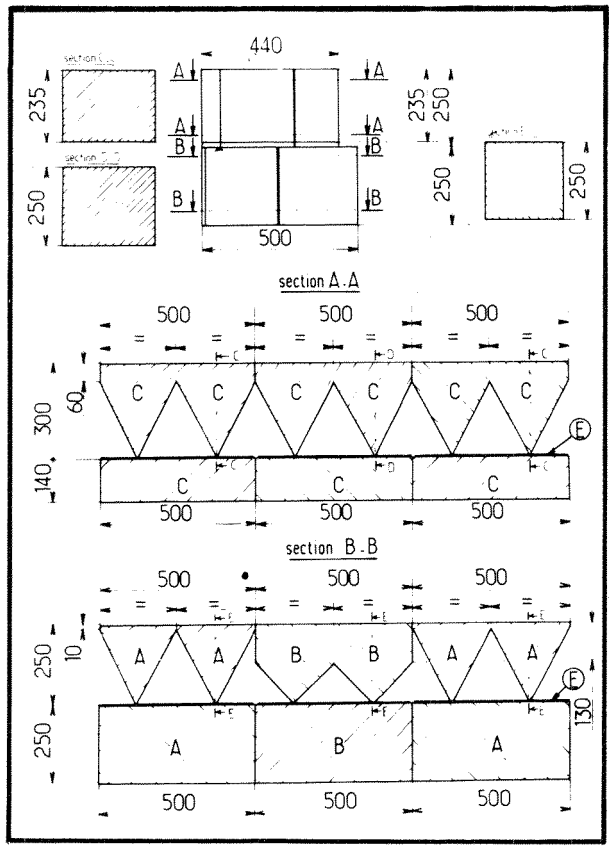

Figure 13. Detailed drawing of the front face of the UTAC mobile deformable barrier

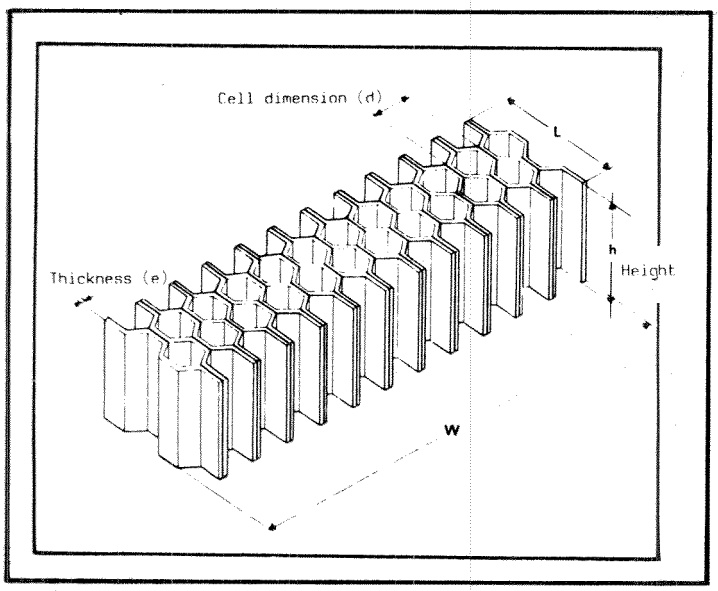

	d (in)	e (10^{-3} in)	Crush strength (psi)
A	1/4	0,7	50
B	1/16	0,7	60
C	1/8	0,7	25

Figure 14. Characteristics of honeycombs used for the construction of UTAC barrier front face

The measurements of the different parameters have been carried out according to ISO standard 6487.

The data channel classes of frequency were—

- 60 for the efforts
- 180 for the accelerations

Figure 20 shows that the front face was uniformly crushed and the behavior of the parts with variable section was quite acceptable. The barrier impactor has not disintegrated during impact, and it was possible to verify the deformations at the level of point B, as required by the specifications.

Table 2 summarizes the main results of these tests:

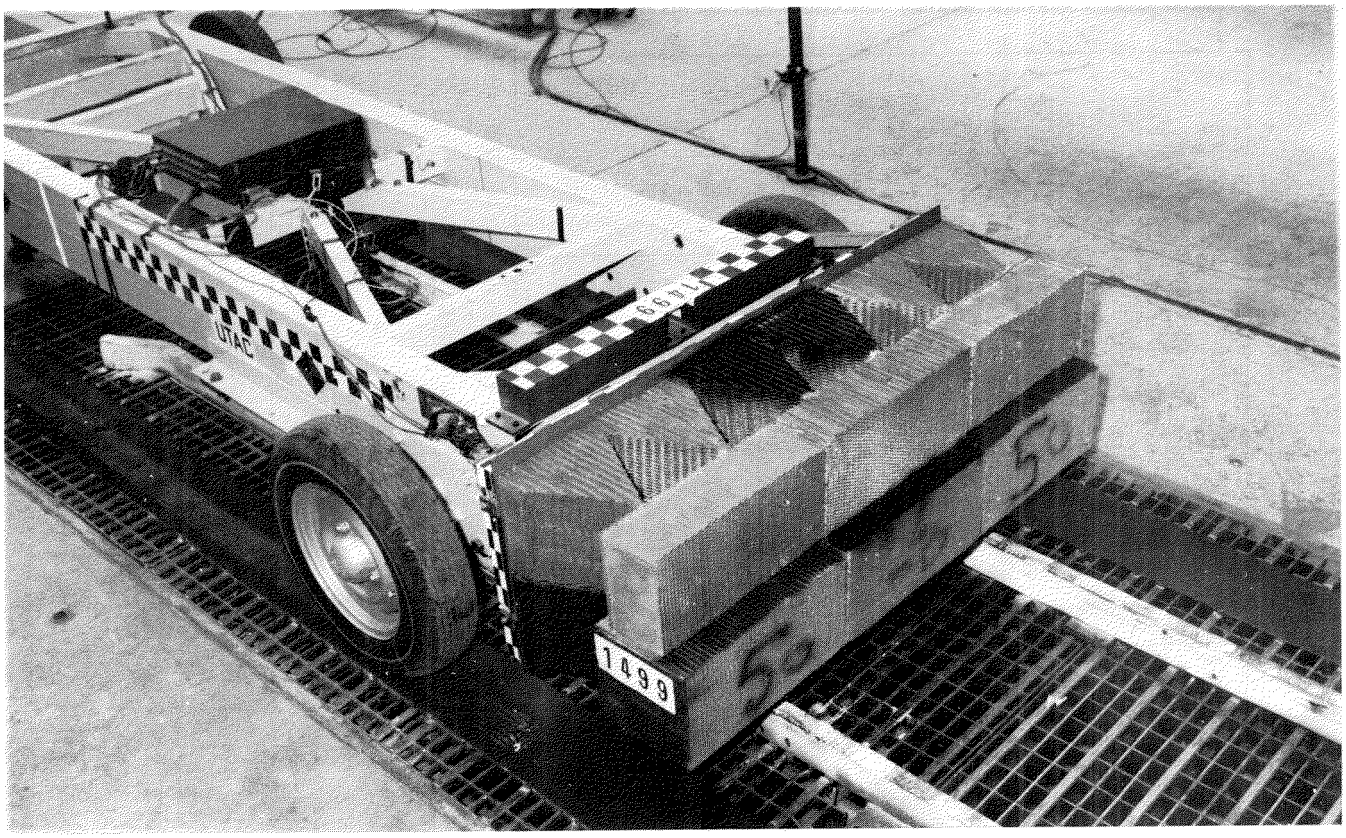

Figure 15. UTAC mobile deformable barrier

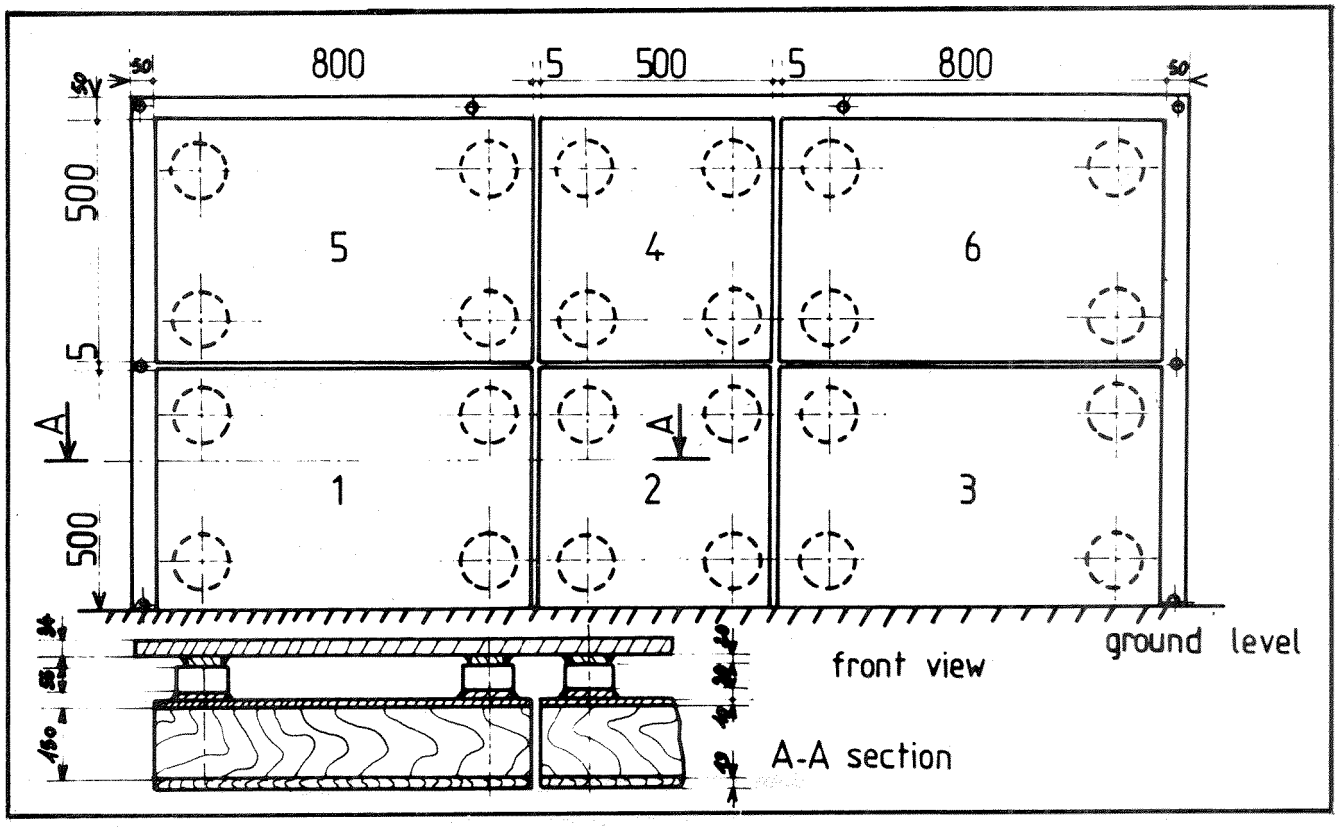

Figure 16. UTAC load cell fixed barrier

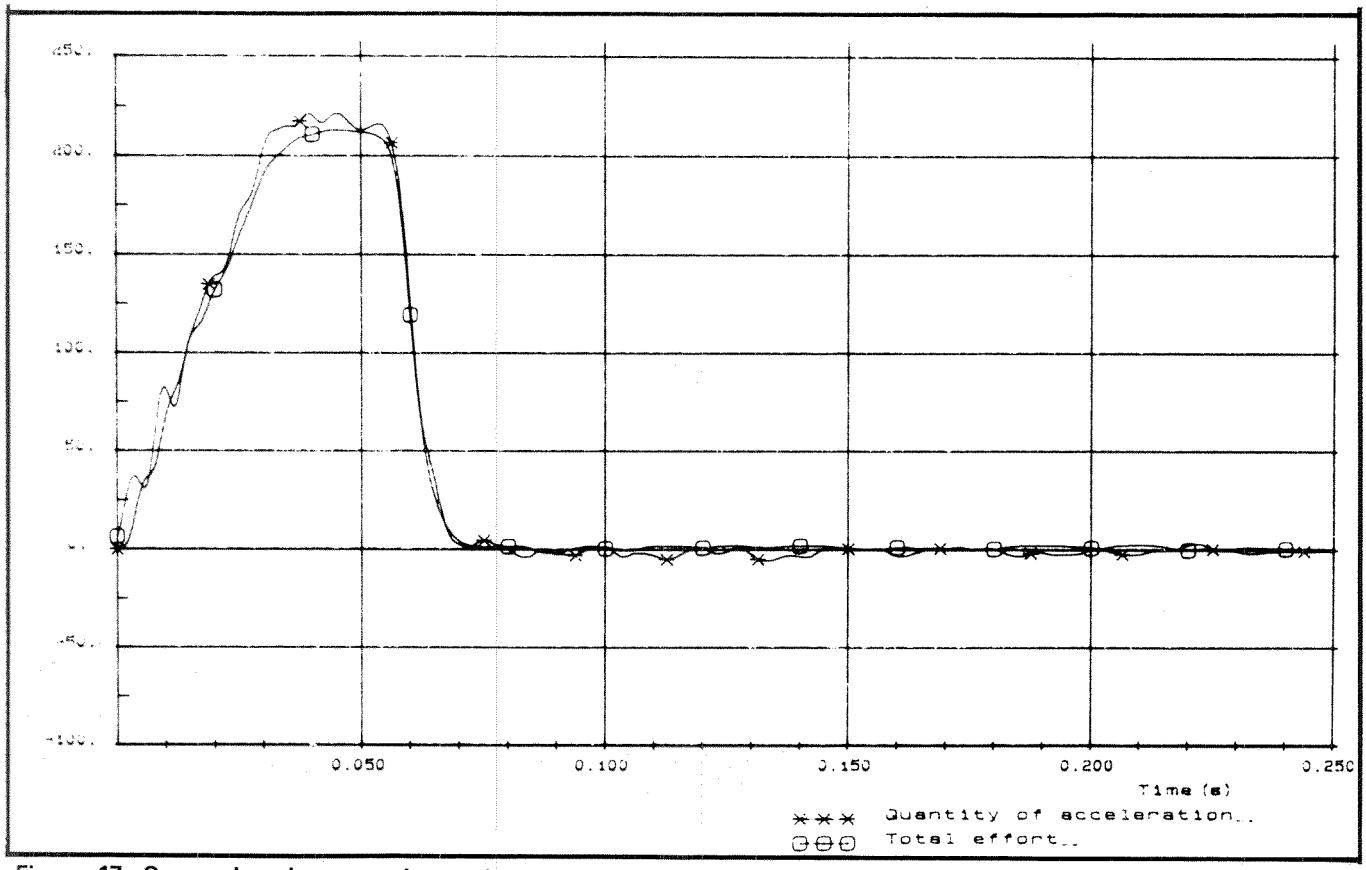

Figure 17. Comparison between the total measured force and the amount of acceleration of the barrier for one test against the load cell fixed barrier

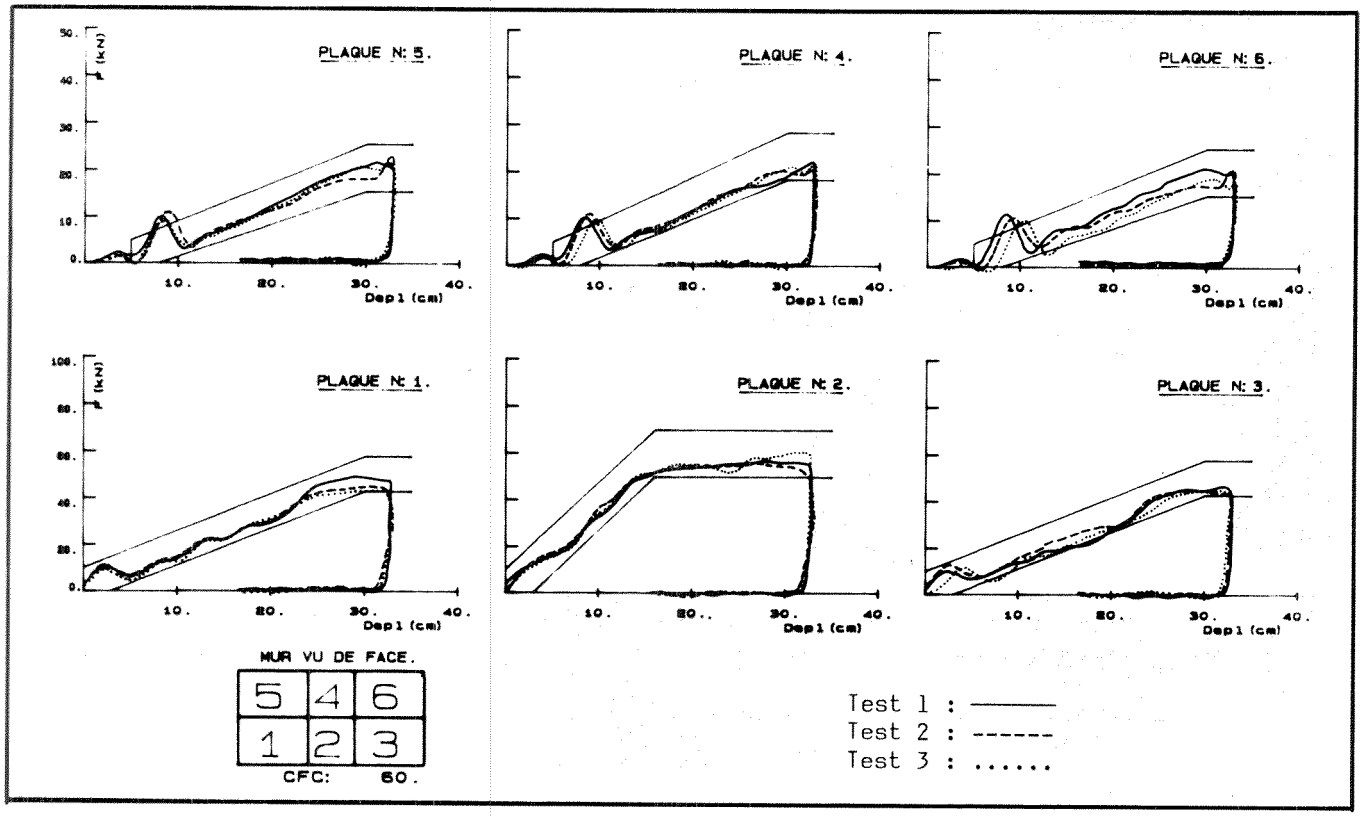

Figure 18. Effort-deflection curves of the six parts of the barrier front face obtained from the load cell fixed barrier for three tests

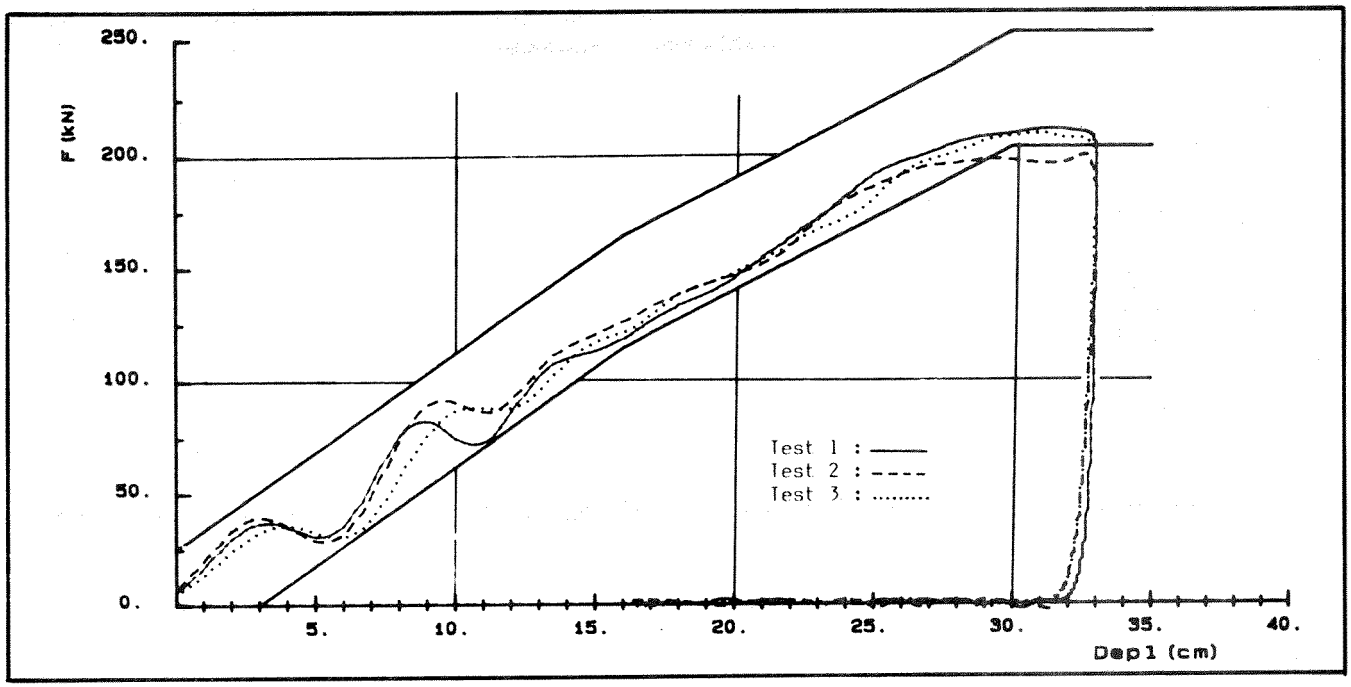

Figure 19. Force-deflection curves of the whole barrier front face obtained from the load cell fixed barrier for three tests

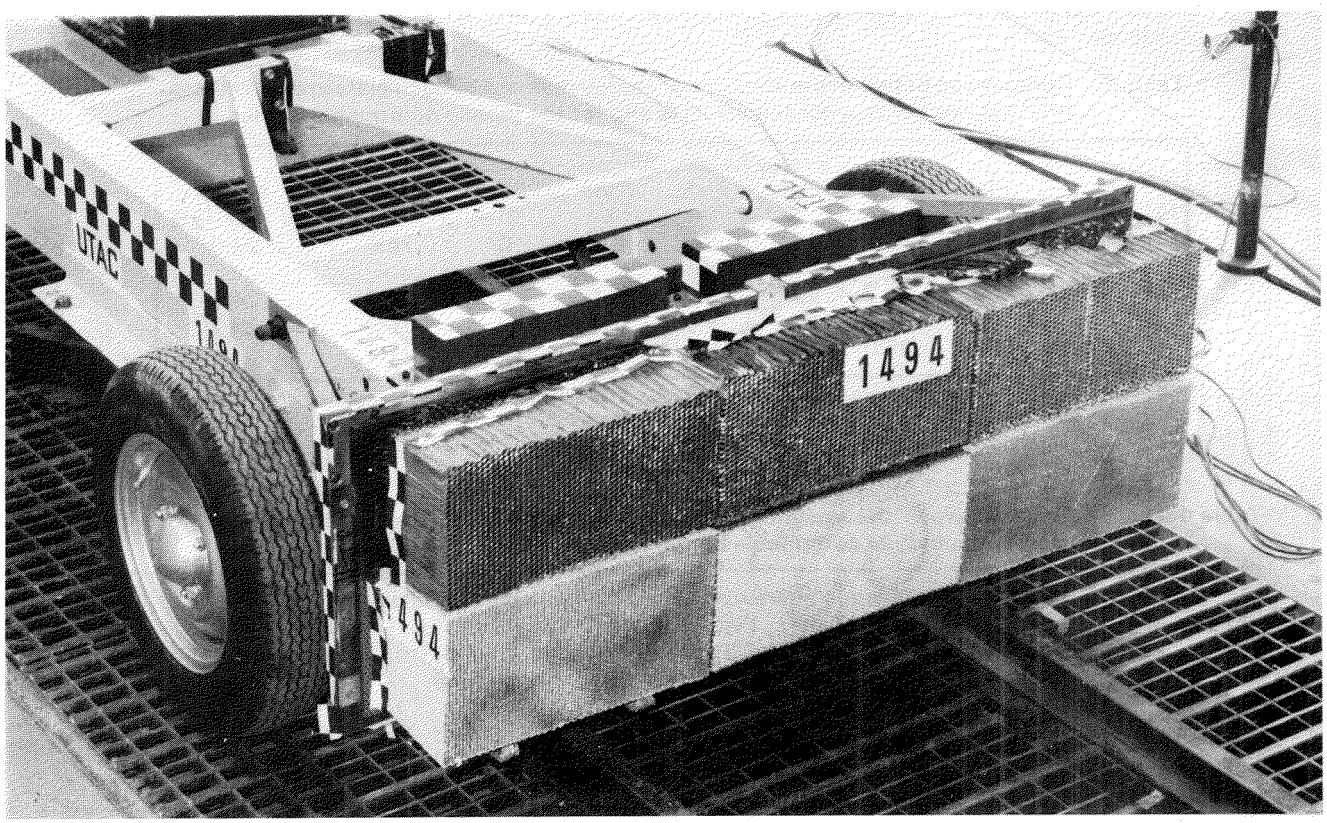

Figure 20. Barrier front face after one of the tests against the load cell fixed barrier

- The force-deflection curves of the different parts may be drawn within the prescribed zones, with the exception of the initial pick for the upper parts.
- The variation curves of the total efforts are also inside the zone while being near the lower limit.
- All the maxima of the dynamic deflections are equal to 330mm.
- The permanent deformations, measured at point B, are comprised between 290 and 315mm and are symmetrical.[1]
- The different parts have absorbed the required amounts of energy for the three tests.
- The behaviors of the front face were similar during the three tests, which confirms the excellent repeatability of crush tests carried out on structures made of honeycombs.
- The tolerances indicated for the total dissipated energy may be too close.

Table 3 shows the following:

- The amounts of energy dissipated at the level of each dynamometric plate are very close to the average weighted values obtained from the tests of 20 vehicles against a load cell fixed barrier.
- Symmetrical and identical parts absorb equivalent amounts of energy.
- During the three tests, one part absorbs the same amount of energy.

The results mentioned in Table 4 indicate—

- The average efforts, calculated for the impact duration, are constant for the three tests, for a given part.
- The average efforts obtained with the barrier are slightly lower than the average weighted values of the vehicles as shown by the force-deflection curves.

Table 2. Test results of three frontal collisions of the barrier against a load cell fixed barrier

	Impact speed (km/h)	Maximal dynamic crush (mm)	Deformation at points B (mm) left	right	Amounts of energy absorbed by each part (kJ) Part 1	Part 2	Part 3	Part 4	Part 5	Part 6	Total dissipated energy (kJ)
Specifications	35 ± 2	—	330 ± 20		10 ± 2	14 ± 2	10 ± 2	4 ± 1	3.5 ± 1	3.5 ± 1	45 ± 5
Essai 1	33,4	330	300	290	8.6	13.5	8.2	3.3	3.2	3.2	40.0
Essai 2	34.8	330	310	310	8,6	13.5	8.4	3.3	3.0	2.9	39.7
Essai 3	34.9	330	315	295	8.4	13.6	7.9	3.1	3.1	2.7	38.8

N.B. The mentioned energy amounts correspond to the energy absorbed for the deformation of the barrier front face.

Table 3. Comparison between the amounts of energy restored by each plate in relation to the total restored energy for the vehicles and for the mobile deformable barrier

		Energy for each plate/Total energy (%) Plate 1	Plate 2	Plate 3	Plate 4	Plate 5	Plate 6	Plates 1 + 2 + 3	Plates 4 + 5 + 6
Vehicles		23.7	33.1	19.2	8.9	8.1	7.0	76.0	24.0
M	Test 1	21.5	33.7	20.5	8.2	8.1	8.0	75.7	24.3
B	Test 2	21.7	34.0	21.2	8.3	7.5	7.3	76.9	23.1
D	Test 3	21.6	35.0	20.4	8.0	8.1	6.9	77.0	23.0

N.B. The amounts of energy have been calculated in relation to the total energy restored either by the front part of the vehicle or by the barrier front face.

Table 4. Comparison between the weighted average efforts for the 20 vehicles and the efforts obtained with the mobile deformable barrier

		Average efforts calculated for the impact duration (kN) Plate 1	Plate 2	Plate 3	Plate 4	Plate 5	Plate 6	Total
Vehicles		11.5	14.5	9.9	4.5	3.9	3.6	47.9
M	Test 1	8.5	11.3	7.5	3.4	3.9	4.0	38.6
D	Test 2	8.7	11.9	8.3	3.4	3.5	3.4	39.2
B	Test 3	8.3	12.9	8.2	3.5	3.4	3.2	39.5

[1] The barrier arrived with a slight angle against the load cell fixed barrier for test no. 3.

These tests against a load cell fixed barrier show—

- The front face meets the requirements of the specifications.
- The behavior of the barrier is repetitive.
- The behaviors of symmetrical parts are the same.

Validation of the Mobile Deformable Barrier in Lateral Collision

Car-to-Car Lateral Collisions

Ten car-to-car lateral collisions have been carried out at the Laboratory of UTAC. For these tests, the struck vehicle, a Renault 14, was standing.

The striking vehicle impacted the tested vehicle at 50 ± 2km/h. At the moment of impact, the longitudinal median plane of this vehicle passed through the R point of the driver seat, situated on the impacted side (Figure 21).

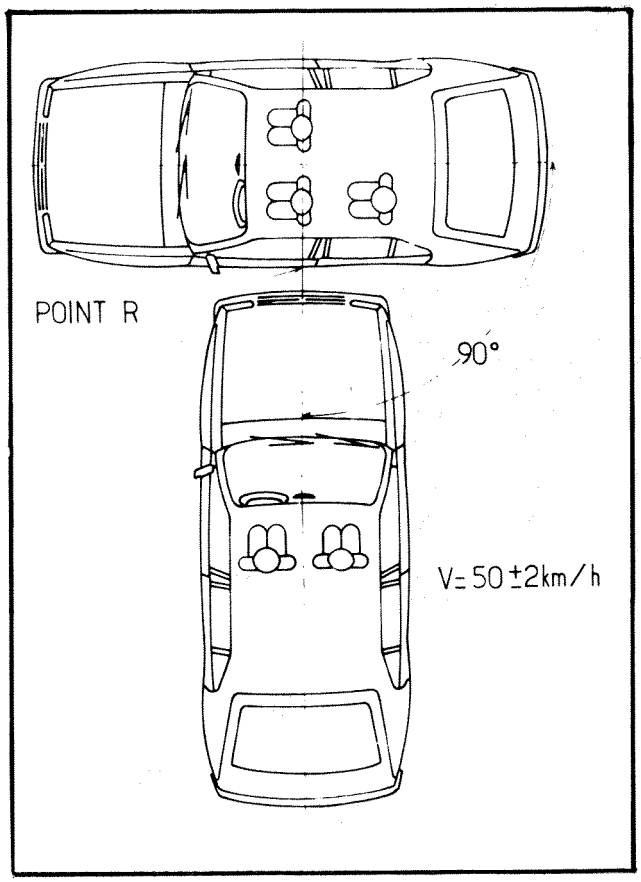

Figure 21. Lateral car-to-car impact test conditions

The front seats of the struck vehicle were positioned 50mm forward of the rearmost position. The seat backs were inclined at 25°.

Hybrid II dummies—50th percentile, calibrated according to the prescriptions of Part 572—have been positioned in the vehicles as follows:

- Striking Vehicle—Two dummies restrained by automatic 3-point belts at the front seats
- Struck Vehicle—At the front seats, two dummies restrained by automatic 3-point belts; at the rear seats, on the struck side, a nonbelted dummy

The longitudinal accelerations of the striking vehicle have been measured—

- On the engine
- On the front axle assembly
- On the structure at the level of B-pillars

The longitudinal and transversal accelerations of the struck vehicle have been measured at the level of the right A-pillar and the right B-pillar, opposed to the impact. The transversal accelerations of the inner door panel of this vehicle have been measured at the level of the shoulder and the H-point of the dummy. The accelerations of the head, the torso, and the pelvis of the dummy, situated at the front left seat of the struck vehicle, have been measured in the longitudinal, transversal, and vertical directions.

The biomechanical criteria have been calculated for this dummy.

The results of these tests are summarized in Table 5, and the deformations of the struck vehicle side during the different tests are shown in Figure 22.

Tests With Mobile Deformable Barrier

Two tests (8501 and 8502) also were carried out under the same conditions with the mobile deformable barrier (Figure 23).

The accelerations of the struck vehicle and the dummy have been recorded under the same conditions. The accelerations of the barrier have been measured on the frame of the sled.

Vehicle No. 9 had the highest coefficient (21.5 percent) for the design of the UTAC proposal.

Figure 24 shows the deformations of the side of the vehicle struck by the barrier after one of these tests.

The deformations measured after both tests have been superimposed on those obtained with the different vehicles in Figure 25.

The results of these tests are summarized in Table 6, which shows the results obtained with three striking vehicles with masses similar to the barrier mass.

Figures 26, 27, 28, and 29 show the speed variations of—

- The driver dummy chest and pelvis
- The inner door panel situated near this dummy

The curves have been superimposed on the curves obtained from the car-to-car tests.

These two lateral collisions show—

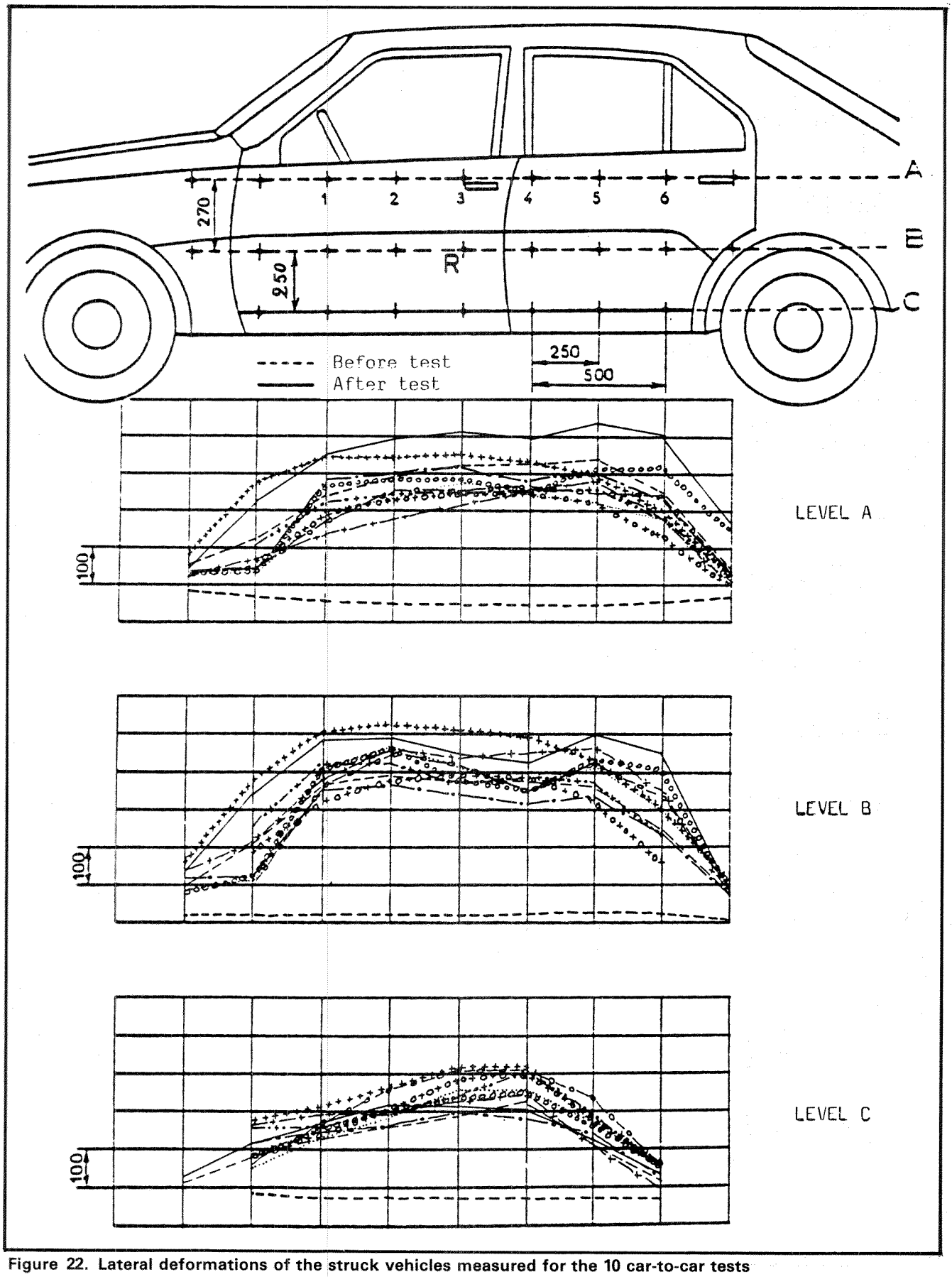

Figure 22. Lateral deformations of the struck vehicles measured for the 10 car-to-car tests

Table 5. Car-to-car lateral impact test results

	Lateral Impact Test		Vehicle 1	Vehicle 2	Vehicle 3	Vehicle 4	Vehicle 5	Vehicle 6	Vehicle 7	Vehicle 8	Vehicle 9	Vehicle 10
Striking Vehicle	Impact speed	km/h	51.3	48.8	50.7	50.5	50.6	51.3	50.5	49.9	48.6	49.0
	Vehicle mass	kg	1210	1295	1340	1320	1045	1090	1470	885	1025	1025
	ΔV	km/h	30	25	25	27	33	31	30	35	32	30
	Vehicle maxi acceleration	g	18.0	11.0	15.5	18.0	18.0	18.5	14.0	19.0	16.0	14.0
	Duration of deceleration	ms	125	135	135	155	155	115	150	150	125	120
	Vehicle mean acceleration	g	6.7	5.3	5.3	5.0	6.1	7.8	5.8	6.5	7.3	7.2
	Backward movement of bonnet	mm	100	110	0	175	65	85	215	90	105	65
	Total deformation — Right	mm	70	250	10	100	50	245	70	100	115	150
	Total deformation — Left	mm	110	230	10	80	20	205	170	35	180	150
	ΔV — A pillar	km/h	26	26	27	27	25	25	32	—	22	25
	ΔV — B pillar	km/h	31	27	—	34	29	31	32	24	25	27
	Outer deformation at level of — Thorax	mm	455	365	395	335	330	360	265	310	245	215
	Outer deformation at level of — Pelvis	mm	430	355	490	360	400	325	420	405	370	355
	Head — γ_R(3ms)	g	69 (27ms	75 (29ms	48 (33ms	48 (32ms	37 (31ms	72 (32ms	25 (38ms	50 (27ms	42 (29ms	32 (33ms
	Head — HIC		536 (80ms	645 (73ms	333 (96ms	237 (85ms	168 (92ms	511 (73ms	125 (110ms	184 (94ms	198 (67ms	106 (89ms
	Head (*) — γ_R(3ms)	g	28	—	—	—	30	—	22	—	—	—
	Head (*) — HIC	—	—	—	—	—	—	—	—	—	—	—
Struck Vehicle	Thorax — γ_R(3ms)	g	100	80	70	60	75	100	55	85	60	35
	Thorax — γ_T(3ms)	g	100	80	70	60	75	100	55	80	60	35
	Thorax — SI (1)	—	914	884	740	606	487	850	257	716	345	186
	Thorax — SI (2)	—	768	569	540	283	442	719	191	628	—	—
	Thorax (*) — γ_R(3ms)	g	30	35	45	35	30	45	35	35	35	35
	Thorax (*) — γ_T(3ms)	g	30	35	40	25	30	45	35	35	35	35
	Thorax — ΔV transversal	km/h	40	37	43	36	36	38	30	36	32	29
	Thorax — Maximal velocity of panel door.	km/h	24	37	32	31	35	31	28	29	38	23
	Thorax — Begining of impact side door/thorax.	ms	20	19	27	29	24	26	27	22	26	27
	Pelvis — γ_R(3ms)	g	105	80	145	95	135	85	110	105	105	95
	Pelvis — γ_T(3ms)	g	95	75	135	95	120	85	100	105	105	90
	Pelvis — SI (1)	—	2344	935	3218	1343	2165	1355	1033	1380	1293	857
	Pelvis — SI (2)	—	1306	698	2170	923	1700	1099	842	1008	—	—
	Pelvis (*) — γ_R(3ms)	g	120	60	90	65	75	60	45	70	50	35
	Pelvis (*) — γ_T(3ms)	g	110	60	90	65	75	55	40	70	50	35
	Pelvis — ΔV transversal	km/h	56	48	56	49	51	49	43	42	50	45
	Pelvis — Maximal velocity of panel door.	km/h	49	36	47	34	41	31	34	—	41	27
	Pelvis — Beginning of impact side door/pelvis.	ms	25	22	26	23	23	30	23	—	30	24

SI (1): Criteria calculated on the whole duration of the impact.
SI (2): Criteria calculated without taking dummies' interaction into consideration.
(*) Values obtained when dummies impact each other.

Table 6. MDB to car lateral impact test results

	Lateral Impact Test			8,008	1,314	1,339	8,501	8,502
	Type		—	Vehicle 6	Vehicle 9	Vehicle 10	MDB	MDB
	Impact Speed		km/h	51.3	48.6	49.0	51.3	49.5
	Vehicle mass		kg	1,090	1,025	1,025	950	950
Striking vehicle	Variation of speed		km/h	31	32	30	30	29
	Vehicle maxi acceleration		g	18.5	16.0	14.0	12.5	12.5
	Duration of deceleration		ms	115	125	120	125	130
	Vehicle mean acceleration		g	7.8	7.3	7.2	6.8	6.3
	ΔV struck vehicle	A pillar	km/h	25	22	25	25	22
		B pillar	km/h	31	25	27	26	24
	Outer deformation at level of	Thorax	mm	360	245	215	300	355
		Pelvis	mm	325	370	355	380	415
	Head	γ_R(3ms)	g	72	42	32	26	33
				32ms	29ms	33ms	31ms	32ms
		HIC	—	511	198	106	80	115
				73ms	67ms	89ms	79ms	87ms
		γR(3ms)	g	100	60	35	73	60
		γT(3ms)	g	100	55	35	70	58
		SI (1)	—	850	345	186	605	769
		SI (2)	—	719	—	—	505	444
Struck vehicle	Thorax	* γR(3ms)	g	45	35	35	34	50
		* γT(3ms)	g	45	35	35	31	48
		Transversal speed variation	km/h	38	32	29	42	47
		Maximal velocity of side door	km/h	31	38	23	34	37
		Beginning of impact side door/thorax	ms	26	26	27	24	24
		γR(3ms)	g	85	105	95	98	120
		γT(3ms)	g	85	105	90	96	115
		SI (1)	—	1,355	1,293	857	1,485	1 692
		SI (2)	—	1,099	—	—	1,146	1,358
	Pelvis	* γR(3ms)	g	60	50	35	64	62
		* γT(3ms)	g	55	50	35	60	60
		Transversal speed variation	km/h	49	50	45	49	49
		Maximal velocity of side panel door	km/h	31	41	27	—	37
		Beginning of impact side door/pelvis	ms	30	30	24	25	28

SI (1) Criteria calculated on the whole duration of the impact.
SI (2) Criteria calculated without taking dummies interaction into consideration.
(*) Values obtained when dummies' impact each other - γR and γT(3ms) calculated on duration of impact.

- The results of both tests are very similar, especially with regard to—
  - — The deformations of the struck vehicle side
  - — The parameters measured in the dummies
  - — The speed variation of the inner door panel
- These results are very close to the results obtained for the lateral impacts with the 10 vehicles, mainly with those having rather the same mass and stiffness.
- However, the deformations are higher at the level of the beams.[2]
- The movements of the dummies in the struck vehicle are very similar.
- The parameters measured in the dummies are very close to those recorded for the car-to-car tests; the head is less involved, however. Meanwhile, the speed variations of the thorax are higher.
- The inner door panel speed variation is quite significant and very close to the variation obtained when the vehicle is struck by another vehicle.

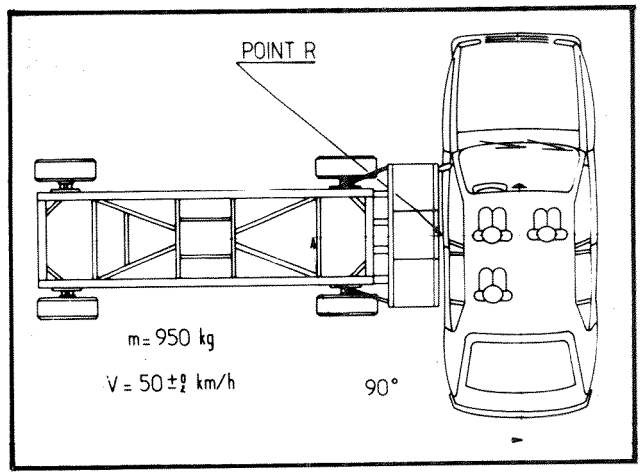

Figure 23. Lateral collision at 90°, on the driver side, with the mobile deformable barrier

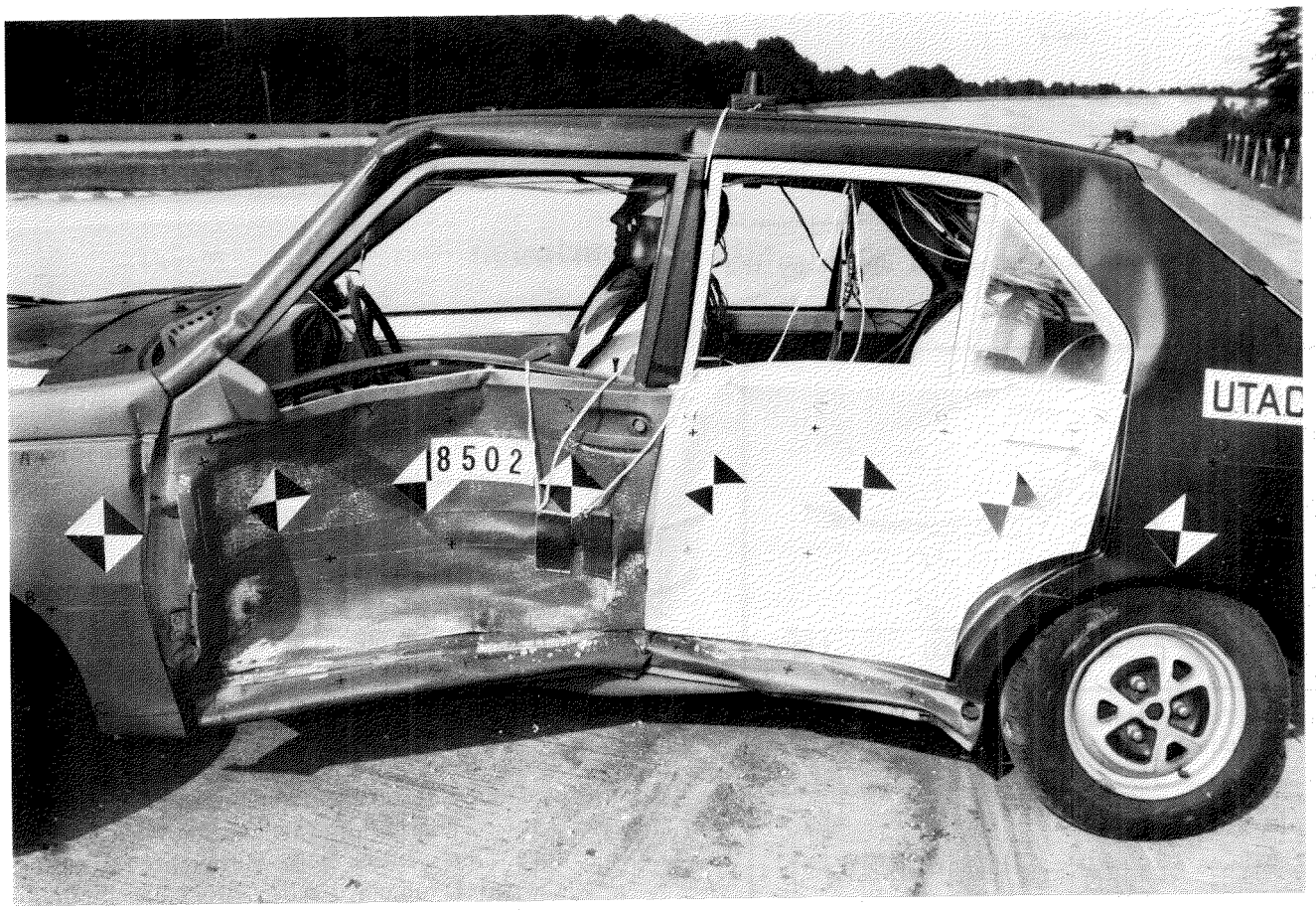

Figure 24. Lateral deformations of the struck vehicle for one of these tests

- The print of the struck vehicle, in the front face, is quite visible after test.

[2] It has been decided to reduce the height of the barrier front face from the ground to take account of future evolution in vehicle conception, which explains the downward displacement of the efforts

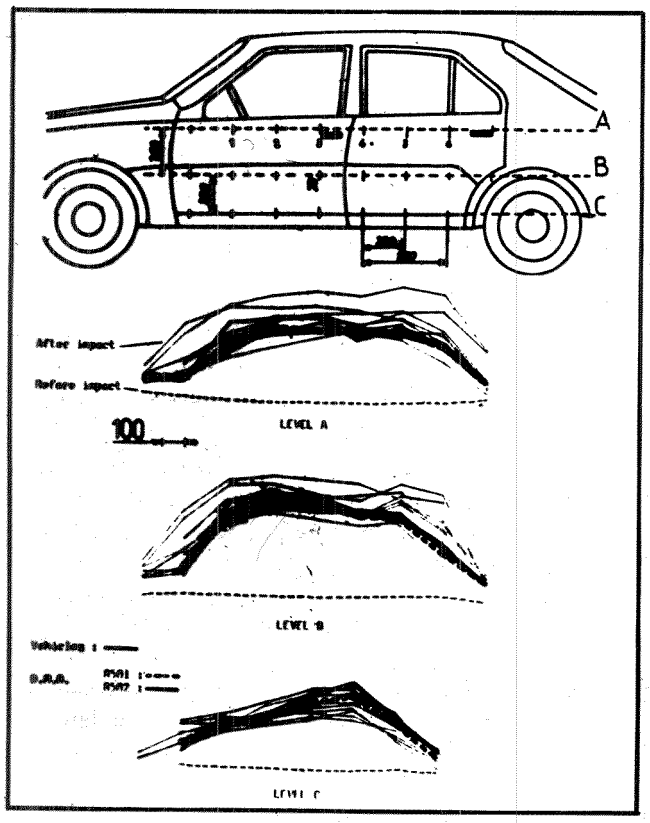

Figure 25. Deformations of a vehicle struck by the barrier for two tests

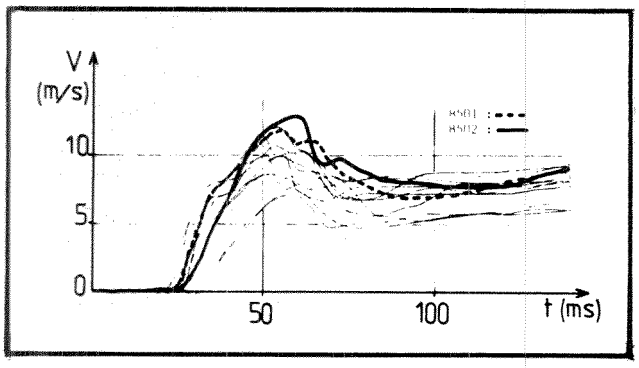

Figure 26. Transversal speed variations of the dummy chest

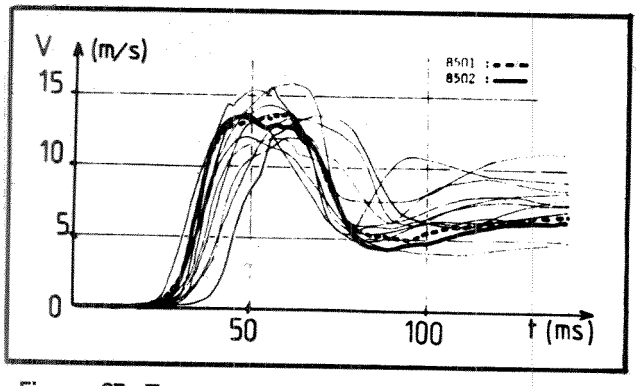

Figure 27. Transversal speed variations of the dummy pelvis

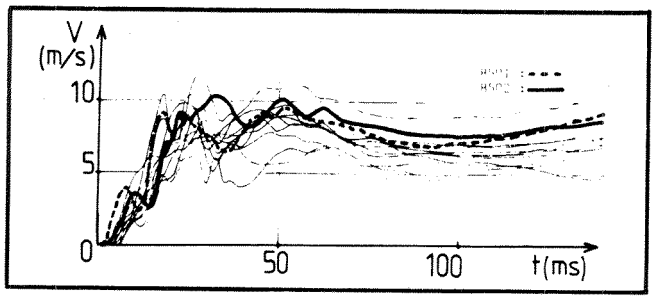

Figure 28. Inner door panel speed variations at the dummy thorax

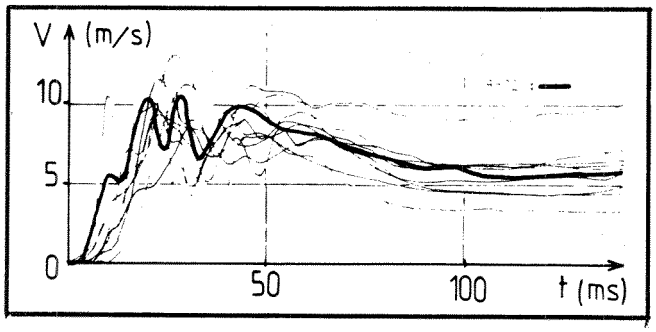

Figure 29. Inner door panel speed variations at the dummy pelvis

Conclusion

The results of the validation tests carried out against a load cell fixed barrier and against the side of a given vehicle type permit the following conclusions:

- The mobile deformable barrier meets the requirements defined in the specifications, especially with regard to—
  - — The force-deflection curves of the different parts and of the whole front face
  - — The amounts of energy restored during impact
  - — The deformations of the front face
- Tests performed with the barrier equipped with a front face made of honeycomb are very repetitive.
- The effort distribution is perfectly symmetrical.
- The front face does not disintegrate during tests and allows the deformation measurements.
- The accelerations and deformations measured on a vehicle, struck by the barrier, are very near the values obtained when struck by another vehicle. The height of the front face from the ground induces the low part of the vehicle to be more loaded.
- The behavior of occupants situated in this vehicle is also very similar.
- The print of the struck vehicle, in the front face, is quite visible.
- The mechanical characteristics of the material for the front face are insensitive to aging and atmospheric conditions.

- The fabrication and modification of the front face are easy and need no specific industrial means, especially if the force-deflection curves had to be modified.
- The barrier behavior will have to be verified during other lateral collisions against other vehicle types.

Therefore, a mobile deformable barrier equipped with a front face, made of honeycomb according to the barrier developed by the Laboratory of UTAC, meets the imperative requirements specified in the draft lateral test procedure studied by GRCS.

Taking account of these performances, this barrier will contribute to the improvement and evolution of test procedures for evaluating the protection of the occupants of a vehicle struck in a frontal impact and a rear collision.

References

1. Chapoux, E., J.C. Jolys, and R. Dargaud (UTAC), "An approach for the design of a deformable mobile barrier," Proceedings Ninth International Technical Conference on Experimental Safety Vehicles, Kyoto, November 1982.
2. Group of Rapporteurs on Crashworthiness (GRCS), Draft test procedure to evaluate the protection of passenger car occupants in the event of a lateral collision, December 1984.
3. European Experimental Vehicles Committee (EEVC), "Structures improved side impact protection in Europe," Proceedings Ninth International Technical Conference on Experimental Safety Vehicles, Kyoto, November 1982.
4. Committee of Common Market Automobile Constructors (CCMC), "Development of the CCMC mobile deformable barrier for lateral collision testing," Ref. AHB/29/81, Brussels, November 1981.
5. Franchini, E., Fiat Technical Presentation, "Side collision," Proceedings Seventh International Technical Conference on Experimental Safety Vehicles, Paris, 1979.
6. Chinn, B.P., Department of the Environment and Department of Transport, "The feasibility of a crushable barrier face constructed from tins," Transport Road and Research Laboratory, August 1981.
7. European Experimental Vehicles Committee (EEVC), "Validation of the EEVC movable deformable barrier," Final report of the first phase.
8. Provensal, J., M. Balthazard, and M. Petiot (RNUR), "Simulation of an automobile front end with a movable deformable barrier," Proceedings Ninth International Technical Conference on Experimental Safety Vehicles, Kyoto, November 1982.
9. Davis, Sol, "Development of a deformable side impact moving barrier," National Highway Traffic Safety Administration, October 1980.
10. Cesari, D., and R. Zac, "Evaluation of side impact protection in barrier to car tests," Proceedings 27th Stapp Car Crash Conference, San Diego, October 1983.
11. Sievert, W., and E. Pullwitt, "Lateral protection of passenger cars—comparison tests by means of different barrier configurations," Proceedings 27th Stapp Car Crash Conference, San Diego, October 1983.
12. Neilson, I.D., and P.M. Watson, "Compatibility between car front and side structures to improve side impact protection," Proceedings Ninth International Technical Conference on Experimental Safety Vehicles, Kyoto, 1982.
13. Kitamura, O., K. Watanabe, and K. Matsushita (Nissan), "An experimental study of the lateral impact protection," Proceedings Eighth International Technical Conference on Experimental Safety Vehicles, Wolfsburg, October 1980.
14. Hofmann, J., and H. Appel, "Mathematical simulation of side impact. A contribution to the problem of rigid deformable barriers," Proceedings Eighth International Technical Conference on Experimental Safety Vehicles, Wolfsburg, October 1980.
15. Seifert, V., and R. Weissner, "Development of a movable deformable crash barrier," Automobile Engineering Meeting, Dearborn, October 1976.
16. Le Guen, H., J.C. Jolys, and R. Dargaud, "Etude des structures frontales de vingt vehicles contre un mur dynamométrique et exécution de dix chocs latéraux."
17. Jolys, J.C., and T. Bourdillon, "Etude de matériaux absorbant l'énergie pour simuler la déformation de la partie avant d'un véhicule moyen," UTAC Test Report No. 84.13.83.522/3080.
18. Jolys, J.C., R. Dargaud, and T. Bourdillon, "Construction d'une barrière mobile deformable et essais de répétabilité contre mur dynamométriqe," UTAC Internal Report No. 84.13.83.522/3081 (not published yet).
19. Jolys, J.C., R. Dargaud, and T. Bourdillon, "Etude du choc latéral sur véhicule de milieu de gamme," UTAC Internal Report No. 84.13.83.522/3082 (not published yet).

Technical Session No. 6

Safety Developments of Goods Vechicles and Buses

L. Strandberg, Chairman, Sweden

Improved Commercial Vehicle Conspicuity and Signalling Systems

Russell L. Smith,
William J. Burger,
Kenneth Ziedman, and
Mark Mulholland
Vector Enterprises, Inc.

Abstract

Vehicle-into-large-truck accidents produce a disproportionately large number of fatalities. It is hypothesized that increasing a truck's visibility or conspicuity will reduce the number of vehicles colliding with trucks. The purpose of this project was to analyze thoroughly this specific accident problem, establish information requirements of other drivers, review the state of the art of conspicuity techniques, design and conduct a series of conspicuity experiments, design a new integrated lighting and marking system, design an augmented, low-cost reflectorized system for retrofitting on large trucks, and field test the augmented system on fleets of trucks. Approximately 2,000 trucks were fitted with the augmented system, and accident rates are currently being monitored and compared with those of a matched control group of 2,000 trucks. At the time of this writing, the 2-year field study is nearing completion. About 70 percent of the total accidents expected have been analyzed, and the results thus far indicate that the trucks treated with the reflectorized systems are being hit at a lower rate than are control trucks. Increasing conspicuity, therefore, appears to be an effective method of reducing vehicle-into-truck accidents.

Introduction

Purpose

Large trucks equal to or in excess of 26,000 lb constitute less than 2 percent of the total population of vehicles in the United States but are nevertheless involved in accidents yielding nearly 9 percent of all traffic fatalities. The great majority of these fatalities are occupants of passenger cars that collide with such trucks. It would seem, therefore, that countermeasures aimed at a small percentage of vehicles could lead to a significant reduction in a relatively large percentage of fatalities. One obvious countermeasure would be the improved visibility or conspicuity of large trucks.

This paper summarizes a 3-½year project, funded by the U.S. Department of Transportation and designed to develop and evaluate improved conspicuity systems for large trucks.

Rationale

Imposing new Federal lighting and reflector system requirements would clearly impact directly on the trucking industry and indirectly on every driver. Thus, prior to the development and test of proposed new conspicuity systems, every effort was made to provide a thorough statement of the problem.

The project was composed of the following tasks and subtasks:

1. Task 1: Define and analyze the vehicle-into-truck collision problem.
   - Review relevant literature
   - Interview trucking companies
   - Analyze accident data
   - Develop functional requirements of drivers
   - Analyze retroreflective and fluorescent materials
   - Evaluate current Federal Motor Vehicle Safety Standards
2. Task 2: Design and evaluate augmented (retrofit) and new integrated lighting and reflector systems.
   - Design various conspicuity systems and conduct laboratory/field experiments
   - Design a specific low-cost augmented system for field testing on truck fleets
   - Prepare a detailed plan for conducting the field test of the augmented system
   - Design a new, integrated conspicuity system for original equipment manufacture
3. Task 3: Conduct field test of the augmented system on selected truck fleets.
   - Select conspicuity materials
   - Select truck fleets
   - Install conspicuity materials
   - Collect and analyze accident data

The following sections emphasize major findings, analyses, and considerations with respect to the above three tasks. Vastly more detailed accounts can be found in (3) and (12). As of this writing, the project is not quite completed, there being a few months remaining in Task 3 field testing. The results reported for Task 3 represent approximately 70 percent of the total accident data expected in the field test.

Task 1: Define and Analyze the Vehicle-Into-Truck Collision Problem

Analyze Accident Data

Reviews of extensive analyses of a number of accident data bases reveal that large trucks are struck about equally often in the rear and side, the latter including both sideswipes and perpendicular impacts. They are also equally often struck at night or in dimly lit environments as during the day and are struck about equally often on rural and urban roads that are both level and graded.

Rear impacts tend to occur when the truck is traveling straight ahead and moving slowly or stopping or stopped on the roadway. The following driver either (1) does not see the truck at all, (2) sees the truck but misjudges its motion and/or distance, or (3) correctly perceives the truck's dynamics and distance but not within sufficient time to avoid a collision.

Trucks are struck perpendicularly in the side most often when turning or being astride lanes, e.g., backing, making U-turns, etc., but are often sideswiped when traveling straight ahead.

In view of the foregoing, therefore, it would appear the conspicuity problem with large trucks is not restricted to nighttime conditions or specific lighting and marking systems. Trucks are apparently inadequately conspicuous during the day, and both their sides and rear ends seem in need of increased conspicuity.

Develop Functional Requirements

Based on the analyses of accidents, 19 scenarios were established that encompassed nearly every situation in which trucks are hit by cars. Each scenario was analyzed at a level of detail necessary to identify the functional requirements of truck communication systems. These scenarios included vehicle locations, directions of movement, and varying speeds. Stopping distances were computed that indicated the distances at which the driver of the striking vehicle would have to apply the brakes to stop or slow sufficiently to avoid a collision. Dynamics of both vehicles and system reaction times were included in the computations.

Scenario analysis demonstrated that a truck conspicuity system communicated general rather than specific information with respect to its dynamics. For example, the current system for indicating changes in velocity has only two states: the brake light is either on or off. The vehicle can either be stopped, accelerating, maintaining a constant speed, or decelerating, and, with regard to acceleration and deceleration, the rate of change can vary substantially. Thus, the current system relies on the driver to perceive changes in rate of closure, an extremely difficult perceptual task, particularly at night where much of the visual input is severely reduced.

The analyses of vehicle-into-truck accidents and associated scenarios clearly indicated a need for improved truck conspicuity systems that would provide drivers with the following specific information on the truck's position and dynamics:

- Presence of a vehicle
- Indication of a truck
- Distance
- Speed
- Whether it is maintaining a constant speed
- Whether is it accelerating
- Whether it is decelerating
- Whether it is stopping
- Whether it is stopped
- Whether it is backing up
- Whether it is maintaining a constant direction
- Whether it is turning

A number of techniques exist for satisfying the above functional requirements. Unfortunately, most of them would be too costly to be considered seriously at this time. Thus, less than optimal solutions must be sought that are, nevertheless, significant improvements over current systems. Such solutions must derive from an understanding of how drivers detect and identify the presence of a truck and acquire knowledge of its dynamics.

It has often been said that most accidents are wholly or principally caused by inattentive behavior. Thus, detection performance depends, at least partially, on the ability or conspicuity of a target (e.g., trucks) to compensate for inattention and penetrate a driver's field of view.

It is generally believed that luminance contrast is the major cue for detection(4). However, while luminous contrast is certainly necessary for detection, a stimulus may not attract a driver's attention in a cluttered environment. Burg and Hulbert(2) and Burg and Beers(1) demonstrated that the unique shape of a stimulus is of considerable importance in attracting attention and establishing recognition. For example, reflectors completely outlining wheels attract far more attention than do nondistinct reflectors arbitrarily located on bicycles and motorcycles.

Drivers employ subjective judgments in determining distances and dynamics of other vehicles. Carefully controlled laboratory experiments indicate that size

changes of an object moving in depth constitute the dominant cue in judging motion in depth(9,10). Apparently, the larger the object appears to an observer, the smaller the change in size necessary to detect motion(11).

The speed differences in vehicle following become increasingly important the closer the following vehicle approaches the leading vehicle. Ittleson (1951) noted that while size changes in an object provide motion cues, the judgment of distance of an object depends on a priori known characteristics of the object. Thus, if an object projects characteristics that provide no cues or ambiguous cues, no basis exists for estimating its distance. An example would be the rear end of a truck. Most drivers are knowledgeable of truck sizes and can estimate distances of trucks by virtue of that knowledge when such vehicles are well illuminated. On the other hand, when trucks are poorly illuminated at night, size cues are degraded and estimations of distance would be expected to be degraded as well.

In a laboratory setting, Jannsen(6) found that changes in size and brightness of taillights were ineffective cues in the detection of relative motion in depth. His results indicated that changes in the angular separation between taillights constituted the primary cues for such judgments. Such findings were confirmed in on-the-road studies(7,8).

In extrapolating from the foregoing, it seems apparent that the perception of movement in depth would be enhanced even more by presenting a larger target to drivers than that inherent in two taillights. In fact, Fisher and Hall(5) presented evidence that outlining the entire rear end of a truck was more effective than the simple angle generated by two taillights. As noted previously, one must assume driver inattention undoubtedly contributes substantially to degradations in the perceptual process. It seems clear, therefore, that attention and subjective judgments can be enhanced by improving perceptual cues.

Analyze Retroreflective and Fluorescent Materials

Reflective materials are obviously far less costly than lighting systems and far more easily retrofitted to trucks to improve conspicuity. Therefore, a thorough analysis of reflective materials was performed to determine their characteristics, particularly their effectiveness and durability.

Retroreflective Materials

A retroreflector directs most of the light it reflects back along the line of incidence, i.e., back toward the light source. Thus, the reflector is seen as brightest when the observer's eye is close to the light source. Retroreflectors inherently have very narrow beam patterns with respect to observation angles. At an observation angle of 1.0°, relative intensity may typically be only one-tenth that of 0.1°.

The retroreflective devices relevant to trucks include materials containing (1) spherical glass bead elements, or (2) cube corner or prismatic elements. In each case, it is the elements that reflect the incident light. The glass bead materials include those having beads partially imbedded within a supporting surface such as paint and partially exposed to the atmosphere and those having beads that are completely imbedded within a transparent material. The exposed bead designs generate greater brightnesses but are more easily damaged by abrasion and completely lose their reflectivity when wet. Newer versions of enclosed bead materials, referred to as encapsulated lens sheeting, have provided higher brightnesses while retaining protective characteristics.

With regard to prismatic-based materials, the corner of a cube forms three mutually perpendicular surfaces that will reflect light back in the direction of incidence. This principle is used in two types of reflector materials: rigid plastic and sheeting of vinyl, polycarbonate, or other plastic materials. These reflectors are typically brighter than beaded glass materials at small observation angles but exhibit a sharper decrease in brightness as that angle increases.

A number of conditions reduce the life expectancy of retroreflective materials. The top layer of reflective sheeting can be damaged by abrasion due to dust, sand, etc. Oxidation and other chemical reactions can affect the top coat, internal layers, and adhesive backing. Ultraviolet exposure can cause hazing discolor and affect properties of plastics, resins, and the adhesive backing. Physical impact (and any flexing or bending) and extreme temperatures can cause cracking. Moisture can also affect the adhesive backing and, if it penetrates inner layers, can degrade retroreflectivity.

Weather conditions can severely degrade retroreflector materials. Rain, fog, blowing dust and sand, snow, dew, and frost reduce brightness by (1) attenuating and scattering of the light paths to and from the reflector, and (2) forming a degrading optical surface on the reflector.

Empirical data regarding the durability of retroreflective materials is severely limited. It is therefore difficult to predict reflector lifetime in truck operations from available data. It would appear, however, that 5 years may be a reasonable expectation.

Fluorescent Materials

Fluorescent pigments are organic substances containing dyes capable of fluorescing in solid solution, e.g., in a paint pigment or resin binder. Such pigments convert light from the shorter wavelengths (violet, blue, green, and yellow) to longer wavelengths. The fluorescent

energy is added to normally reflected light, resulting in an effective reflection factor of 200 to 300 percent, compared to 90 percent for a bright, nonreflective color. Several manufacturers produce sheeting materials that are both fluorescent and retroreflective.

Studies on visibility and conspicuity of fluorescent colors agree that such colors are much more easily seen than are nonfluorescent colors. Fluorescent orange appears to be the most conspicuous. Of particular interest, especially when considering application to daytime truck conspicuity, is the fact that fluorescent colors are found to be more attention getting in peripheral vision than are ordinary pigments.

The most serious drawback to the use of fluorescent materials is their limited lifetime with ultraviolet exposure. Two years is a practical maximum in most outdoor situations, and useful lifetime can be as short as 3 to 6 months. Therefore, applications to truck conspicuity appear generally impractical.

Task 2: Design and Evaluate Augmented (Retrofit) and New Integrated Lighting and Reflector Systems

Task 1 demonstrated that the range of possibilities for improved conspicuity systems was very large and available empirical data were inadequate for selecting the best of the most cost-effective designs. Therefore, Task 2 consisted of a series of experiments for resolving important issues and screening out most of the possible design configurations. Prior to conducting the experiments, the following design guidelines were established for the augmented and integrated conspicuity systems:

- Truck marking and signaling systems should be standardized as much as possible across all truck body types.
- The augmented system should be restricted to reflectorization treatments to maintain low cost for retrofitting.
- Designs should have acceptable implementation costs and life expectancies.

Only 6 months were allocated to the design phase, which limited the number and types of experiments that could be conducted and the number and types of issues that could be addressed.

Design Systems and Conduct Experiments

All experiments were concerned with reflectorization designs, as little could have been added to the large body of experimental data on vehicle lighting systems within the current program scope. Thus, all recommendations concerning lighting and signaling aspects of the integrated system were based on previous research.

Six experiments were conducted. In some cases, subjects directly observed conspicuity treatments on an actual truck. In other cases, slides were taken of an actual truck and subsequently used in a laboratory setting. In still other cases, slides were taken of miniature vehicles on a 1/25 scale roadway and subsequently used in a laboratory setting.

The first experiment evaluated 45 rear end reflector treatments and compared them to conventional configurations specified by the U.S. Federal Motor Vehicle Safety Standards. Designs outlining the entire rear perimeter and mudflaps were found to be superior to all other designs with respect to conspicuity and ease of detection.

In the second experiment, 12 different patterns involving style and color were presented in pairs on a test truck to subjects at night. Alternating white/colored rectangles were found to be superior in terms of conspicuity, detail, and visible detail. The actual color was less important.

The third experiment replicated the second experiment during the day. Again, the alternating white/colored rectangle design was superior to the other designs. The actual color was again of lesser importance except when fluorescent materials were used.

The fourth experiment studied the effect of reflectorized rear end patterns on distance judgments. Seven patterns were employed. The design having the perimeter of the rear end and the mudflaps reflectorized were judged to be closest to subjects than the other designs. It was also found that the lower the reflectorized area, the closer the truck appeared.

The fifth experiment evaluated partial-to-complete perimeter outlines of the rear and side of trucks and compared them to the conventional configuration during day and nighttime illumination levels. For nighttime conditions, the complete perimeter outlines were found best for the side and rear of trucks. Essentially no differences were found between designs during daytime.

Finally, the sixth experiment evaluated partial-to-complete outlines in terms of their ability to provide rate of closure information to subjects. All experimental designs were found superior to the conventional configuration, particularly the complete rear and side outline design.

Design a Specific Low-cost Augmented System for Field Testing on Truck Fleets

The recommended augmented system design was based on the results of Task 1, the experiments described above, previous research by others, and the guidelines discussed earlier. The recommended system consisted of outlining the entire rear end and sides of trucks. The reflector pattern was a 4in-wide stripe of alternating red/white rectangles. In the case of flatbeds, a continuous stripe

around the rear and side rails was recommended. A U-shaped outline of the mudflaps was also recommended, using a 2in-wide stripe of white retroreflective material.

A variety of retroreflective and reflective materials and devices can be used, including glass bead and prismatic-type sheetings and reflex reflectors. It is considered essential, however, that retroreflector materials be hermetically sealed. Also, reflex reflectors should be of a dispersed angle prism design so that a wide angular characteristic is obtained.

Minimum and maximum SIA (Specific Intensity per unit Area) values were recommended, based on considerations of minimum intensity necessary for adequate conspicuity, the effects of temporary degradation due to dirt and grime and long-term weathering, and of glare potential. These were 250 to 300 $cd/lx/m^2$ and 500 $cd/lx/m^2$, respectively, for the stripe outlining the truck, and 200 $cd/lx/m^2$ and 300 $cd/lx/m^2$, respectively, for the mudflap stripe.

Detailed materials and installation cost analyses were performed for the recommended retroreflective design and partial configurations such as rail only, partial rail, and broken whole outline. The 1981 estimated costs ranged from a low of $34 for the partial rail treatment to a high of $416 for the complete outline treatment.

Design a New Integrated Conspicuity System for Original/Equipment Manufacture

The perimeter outline reflectorization design for the augmented system described above was also recommended for the integrated system.

Two pairs of four lights each were recommended for the rear lighting system of trucks. Each set of lights could be positioned horizontally or vertically on the lower corners of the truck. The outer (horizontal) or lower (vertical) lights represented red presence indicators. The next light represented amber turn signals. The inner (horizontal) or upper (vertical) two lights comprised red brake lights. Thus, this design not only provides separation of functions, color and size coding are also involved.

In addition to the two conventionally placed amber turn signals at the front of truck cabs, two additional turn signals were recommended on each side of the truck, one mounted on the truck's cab and one mounted midway along the body or trailer.

Amber (except for rearmost lights) side clearance lights evenly spaced every 6 to 8ft, including the corners, were recommended along each side of a truck bed or trailer. The rearmost lights were recommended to be red.

All of the lights were along or close to a truck's railing. Because of the high-mounted reflectorization, no justification was seen for high-mounted lights, including the currently required conventional three-light truck identification bar. It was believed the recommended design amply described and identified vehicles as large trucks.

The currently required intensity levels for truck signals and identification lighting appear adequate. However, a minimum area requirement of $12in^2$ should be retained for rear signals, and consideration should be given toward increasing the minimum area requirements for front and side turn signals. In addition, consideration should be given to a dual intensity system to adjust brake, presence, and turn signals to different ambient conditions, such as day, night, and fog.

Prepare a Detailed Field Test Plan for the Augmented System

A detailed test plan was prepared for field testing the recommended augmented system. Sample sizes, fleet compositions, candidate fleets, exposure data, accident rates, existing truck markings, short- versus long-haul operations, experimental and control group matching, and materials and installation costs were discussed and evaluated in detail. Two thousand trucks were recommended for the augmented system treatment, and a matched like number was recommended for a control group. A 24-month data collection period was considered adequate to demonstrate significance between the groups at appropriate alpha and beta error levels.

As will be noted in the following section, funding was insufficient for field testing the complete augmented system, i.e., full side and rear outline.

Task 3: Conduct Field Test of the Augmented System on Selected Truck Fleets

Select Conspicuity Materials

Prismatic sheeting known as Durabrite and manufactured by Avery International was selected for the field test. This selection was based on four criteria: brightness, ease of installation, durability, and cost. Durabrite more closely satisfied all four criteria than other materials. However, the cost to purchase and install this material on 2,000 trucks according to the recommended design specifications presented in Task 2 still exceeded budget. Therefore, the design specifications were modified as follows.

The recommended design was a 4in-wide stripe outlining the entire rear and sides of truck trailers. This stripe was reduced to a 2in width. And, while outlining the entire rear of trucks remained essential, only the side rail was to be treated with the prismatic sheeting. The materials cost for each vehicle was $35.

As can be seen in Table 1, the actual photometric characteristics of the Durabrite material closely approached the values recommended in Task 2. It will also

Table 1. Recommended maximum and minimum SIA values (upper) and durabrite actual values (tabled entries are in candelas/1x/m^2)

Entrance Angle	Observation Angle			
	0.2°	0.5°	0.2°	0.5°
-4°	330-500 475	150-400 325	75-125 90	38-100 62
30°	150- 220	75- 82	38- 42	19- 16
45°	75- 61	38- 42	19- 12	9- 8
	White		Red/Blue	

be noted that the colored material is labeled "Red/Blue" in Table 1. This term is explained in the following section.

Select Truck Fleets

The selection of trucking fleets for this study was a difficult and time-consuming task. Many fleets were not able to participate for a variety of reasons. Of those that wanted to participate, many had already installed reflectorized materials on their vehicles. Few fleets remained for which matched groups of control and experimental trucks could be generated. However, 4,162 trucks were ultimately obtained from three trucking fleets: Overnite Transportation, Paul's Trucking, and Ruan Trucking. These fleets included short- and long-haul, 40 to 45ft trailers. The experimental and control groups were matched as closely as possible, based on a number of variables such as exposure or mileage.

Because one trucking fleet employed a logo that included the color blue, an alternating blue/white stripe was permitted along the side rail instead of the recommended red/white stripe. However, the fleet agreed to have the recommended red/white stripe on the rear of their trucks.

The trucking fleets installed the prismatic sheeting themselves. In addition to receiving the reflector material at no cost, the fleets also received $26 per truck to cover installation costs.

Collect and Analyze Truck Accident Data

The planned data collection period was 24 months and was initiated in the middle of 1983. Approximately 3 months remain as of this writing. The 24-month period and 2,000 vehicles per group (actually 2,081 per group) were selected to provide a sample size/exposure sufficient to detect a 15 percent reduction in other vehicle-into-truck collisions in the reflectorized group with alpha and beta errors of .10 and .50, respectively.

During the data collection period, accident reports were obtained from fleet records on a quarterly basis. At the end of each quarter, the fleets' master accident logs were reviewed to identify all trailers for which accidents were reported in that period. Reports for trailers in both the reflectorized and control groups were obtained.

Each accident was coded with respect to identifying information, precrash factors, and, very importantly, the degree to which conspicuity was a likely contributing or causative factor. The conspicuity rating coding was conducted in a double-blind situation by two highly experienced motor vehicle safety professionals.

All accidents were placed in one of six classifications. The first three classifications were other-vehicle-into-truck accidents and represented high, moderate, and low likelihood that the accidents were conspicuity-related. The fourth classification comprised accidents in which the experimental and control trucks struck other vehicles. This classification permitted a test of the assumption that experimental and control groups were matched, e.g., each group should demonstrate approximately the same number of truck-into-other-vehicle accidents.

The fifth and sixth classifications were composed of accidents completely irrelevant to the study.

As of this writing, about 30 percent of the total expected accident reports have yet to be received. Therefore, only preliminary analyses of the data are presented here. The total number of relevant accidents (i.e., trucks struck by other vehicles) in the control and reflectorized groups thus far are 113 and 86, respectively. Figure 1 presents the cumulative number of relevant accidents by yearly quarter for daylight and nighttime driving. As can be seen, strong trends are in evidence, with reflectorized

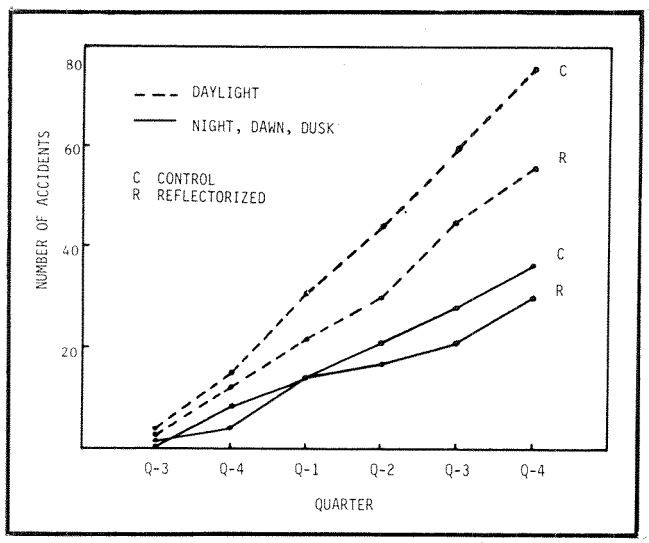

Figure 1. Cumulative number of struck trucks by quarter for daylight and nighttime driving

trucks consistently being hit at a lower rate than control trucks. Data for two additional quarters will ultimately be included in this graph, but it appears unlikely that the current trends will be altered significantly.

The relatively large difference in accident rates between daytime and nighttime driving is easily explained by the fact that the trucks were driven to a much greater extent during the day than at night. However, the difference between the control and reflectorized groups during the day is not easily explained because the reflectorization's effectiveness is primarily dependent on the light projected from other vehicles' headlights. On the other hand, the red/white and red/blue patterns do increase the conspicuity of trucks somewhat. Further analyses will be required to explain this finding more fully.

In conclusion, the field test appears strongly to be demonstrating that increasing the conspicuity of large trucks will reduce substantially the number of other-vehicle-into-truck accidents. This finding is particularly significant in view of the fact that the conspicuity treatments employed in this field test are considerably less emphatic than was recommended. Two-inch rather than 4in-wide stripes effectively reduced the recommended SIA values by 50 percent. In addition, the use of rail-only reflectorization of trailer sides equally reduced the recommended conspicuity. Thus, there is strong likelihood that even greater reductions of other-vehicle-into-truck accidents will occur with the recommended reflectorization treatment.

References

1. Burg, A., and J. Beers, "Motorcycle reflectorization for nighttime conspicuity," University of California School of Engineering and Applied Science Report, Los Angeles, California, 1976.
2. Burg, A., and S.F. Hulbert, "Bicycle wheel reflectorization as an aid to detection and recognition," Los Angeles, California, 1976.
3. Burger, W.J., R.L. Smith, K. Ziedman, M.U. Mulholland, M.C. Bardales, and T.J. Sharkey, "Improved commercial vehicle conspicuity and signalling systems, Task I: interim report," Vector Enterprises, Inc., Santa Monica, California, March 1981.
4. Cole, B.L., "Visual aspects of road engineering," Proceedings 6th Conference of the Australian Road Research Board, pp. 102-148, 1972.
5. Fisher, A.J., and R.R. Hall, "The effect of presence light on the detection of change of vehicle headway," Australian Road Research, 8, pp. 13-16, 1978.
6. Jannsen, W.H., "The perception of maneuvers of moving vehicles: perceptability of relative sagittal motion on the basis of changes in apparent size or brightness of taillights," Institute for Perception, Holland, 1972.
7. Jannsen, W.H., "The perception of maneuvers of moving vehicles: thresholds for relative motion in depth," Institute for Perception, Holland, 1973.
8. Jannsen, W.H., J.A. Michon, and L.O. Harvey, "The perception of lead vehicle movement in darkness," *Accident Prevention and Analysis*, *8*, pp. 151-166, 1976.
9. Smith, W.M., "Sensitivity to apparent movement in depth as a function of stimulus dimensionality," *Journal of Experimental Psychology*, *43*, pp. 149-155, 1952.
10. Smith, W.M., "Effect of monocular and binocular vision on the sensitivity to apparent movement in depth," *Journal of Experimental Psychology*, *49*, pp. 357-363, 1955.
11. Steedman, W.C., and C.A. Baker, "Perceived movement in depth as a function of stimulus size," Aerospace Medical Research Laboratory, Wright-Patterson Air Force Base, Ohio, 1961.
12. Ziedman, K., W.J. Burger, R.L. Smith, M.U. Mulholland, and T.J. Sharkey, "Improved commercial vehicle conspicuity and signalling systems. Task II: analyses, experiments and design recommendation," Vector Enterprises, Inc., Santa Monica, California, October 1981.

The MVMA Investigation Into the Complexities of Heavy Truck Splash and Spray Problem

Clarke B. Gorte
Ford Motor Company

Ronald C. Joyner
General Motors Corporation

Kjell Pedersen
International Harvester Company

Carl C. McConnell
Motor Vehicle Manufacturers Association

Abstract

Splash and spray conditions created by tractor-trailer combinations operating on the Federal highway system have been studied and tested for many years with mixed results. Past events are reviewed briefly in this paper. In additional testing during 1983, using new state-of-the-art splash/spray suppressant devices, some encouragement was provided that these devices could work.

The 1984 Motor Vehicle Manufacturers Association (MVMA) test program was designed to develop practicable and reliable test procedures to measure effectiveness of splash and spray reduction methods applied to tractor-trailer combination vehicles.

Over 40 different combinations of splash/spray suppression devices on five different tractors and three van-trailer types were tested. The spray-cloud densities for some 400 test runs were measured by laser transmissometers and also recorded by still photography, motion pictures, and videotape. On-site observers made subjective ratings of spray density. In general, this research demonstrated that improved visibility can be achieved; however, performance varied by vehicle configuration and could not be quantitatively predicted.

This paper explores the complex relationship that exists between the amount of spray generated and various vehicle aerodynamic characteristics. Ambient conditions such as wind direction and velocity and their effect on repeatability are discussed in detail.

Background

Splash and spray generated by heavy trucks and tractor-trailer combinations on wet road surfaces have long been a source of irritation to highway users. The motor carrier industry and vehicle manufacturers recognize the condition as a major element in the public perception of trucks and the trucking industry. There is little doubt that reductions in driver visibility, regardless of reason (snow, rain, fog, smoke, or vehicle splash and spray), are important to the safe operation of a motor vehicle.

Splash and spray is not a new problem. Long before motor-driven vehicles, pedestrians and other vehicular and equestrian traffic were confronted with the splash and spray annoyance factor. Motor vehicles compounded the public irritation in the early days of soft road surfaces. Over a period of several years, driver vision was aided by windshield wipers, fender designs, and vehicle mudflaps. Mudflaps, evolving from road surface debris deflectors to mostly splash deflectors today, have been effective to a degree in reducing the total spray from the rear of trucks.

In the late 1940's, the move toward building multilane highways around the country was the beginning of road building that led into the Interstate Highway system. The advent of more and more multilane highways brought on increased traffic densities and higher vehicle speeds. Vehicle manufacturers designed new products to meet increased performance demands for the new highway system. Increased speeds, exceeding the critical speed at which splash and spray becomes an appreciable visibility problem, resulted in a more vocal public irritated by the splash and spray problem. Since the late 1960's, organizations such as the Western Highway Institute, vehicle manufacturers, equipment suppliers, MVMA, and others have tested generic concepts to reduce splash and spray. The U.S. Department of Transportation National Highway Traffic Safety Administration (DOT/NHTSA) early on proposed rulemaking with the purpose of reducing the annoyance and possible dangers of splash and spray produced by heavy trucks. However, until the relatively recent introduction of textured spray suppressing materials for flaps and skirting, no potentially practical, effective solution to the problem has been identified.

The U.S. Congress, in the Surface Transportation Assistance Act of 1982, included requirements for the installation of splash and spray suppressant devices on all new tractors, semitrailers, and trailers by January 1, 1985, and for retrofitting all such vehicles in use by January 1, 1988. Minimum performance standards for such installations were to have been established by January 1984. A Congressional amendment adopted in 1984 removed the effective dates, which are now to be determined as part of DOT/NHTSA final rules.

Prior to developing proposed rulemaking, DOT/NHTSA ran a limited number of full-scale spray reduction tests at the Transportation Research Center (East Liberty, Ohio) in which test observers visually evaluated and rated the effectiveness of reduction devices tested. The rating

results of these tests indicated that reduction device combinations previously considered effective did not consistently make a discriminate difference in subjective evaluations. Subsequent tests conducted by MVMA at the same site also failed to find consistent improvements.

In January 1984, DOT/NHTSA began another series of tests with Systems Technology, Inc., as contractor at a test site at Fort Stockton, Texas.

The methodology used was substantially that developed earlier by David Weir(1), using objective laser measurements. These full-scale tests were designed to correlate laboratory test ranking of various types of spray suppression devices on various vehicles with objective laser measurements. The results of this test project are being statistically analyzed under MVMA sponsorship.

In addition, MVMA has conducted supplementary tests duplicating the Fort Stockton approach as closely as possible. Data from these tests are useful in filling gaps in the NHTSA data and are considered important to insure that the devices requirements adopted in future DOT/NHTSA rulemaking would be practicable and effective. The balance of this paper describes the 1984 MVMA splash and spray project and the test conclusions in detail.

Project Objectives

The purpose of this project was to develop quantitative and subjective data on the splash and spray attenuation performance of different aerodynamic devices and spray reduction devices applied to heavy tractor-trailer combination vehicles. The data collected through this testing project would supplement the results of similar testing conducted under the auspices of DOT/NHTSA.

Objectives of this project were to—

1. Validate the testing performed under DOT/NHTSA auspices of several spray attenuation treatments, using the same instrumentation and test setup, and identical vehicle combinations. (Note: The DOT/NHTSA data were not available for statistical analysis for inclusion in this report. These comparative studies will be available at a later date.)
2. Test vehicle combinations not included in the DOT/NHTSA test project to determine to a greater extent than would otherwise be possible whether different types have an effect on the efficacy of spray attenuation devices.
3. Develop new and/or more extensive instrumentation that can provide more comprehensive, cost-effective, objective measures of spray from heavy tractor-trailer combination vehicles.
4. Perform statistical analyses of collected test data for the purpose of evaluating heavy truck splash and spray attenuation devices.

Test Preparation

The testing was carried out at the Texas A&M University Texas Transportation Institute (TTI)[1] Proving Grounds at Bryan, Texas. The Proving Grounds, located at an abandoned air base, provided the necessary 7,000ft runway for testing combination vehicles at 55mph. The test area (Figure 1) included a new 400ft section of asphalt surface, constructed on top of existing pavement, to duplicate the Fort Stockton surface. The asphalt mix was developed to provide a final average texture depth of 0.33in. During construction, extra care was taken to produce as level a surface as possible to eliminate water

[1] Principal investigators: D.L. Ivey, R.J. Koppa, O. Pendleton, and R.A. Zimmer.

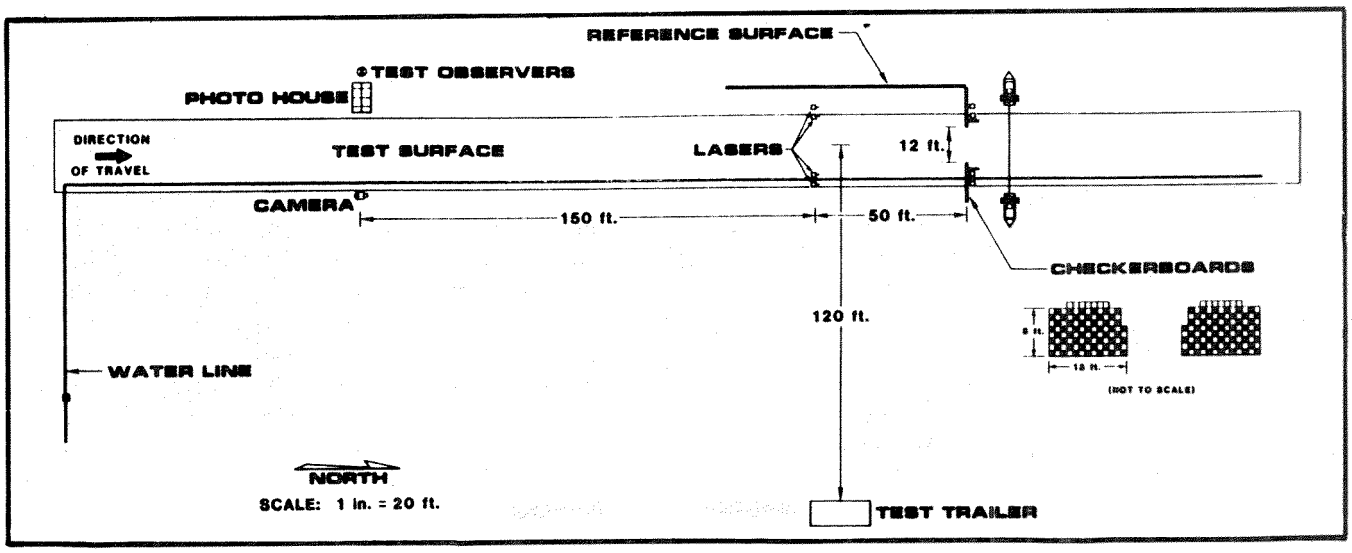

Figure 1. Test area

puddling. The new asphalt pavement was designed to have a 1 percent cross slope over its entire 400ft length. The width was 18ft to allow for a 12ft vehicle lane and 6ft for the water to stabilize.

Surface water was distributed to the pavement by a 400ft-long, 4in-diameter pipe. Water was directed to the road surface through DIN holes spaced 12in apart to provide uniform wetting. The water supply pressure was adjusted through a manifold and valve system to maintain the proper surface water depth throughout testing. Water depth measurements were recorded between each test run at 10 locations spaced along 300ft of test surface in the wheel paths by the use of NASA-type water depth gauges. The water depth throughout the entire test program was nominally 0.050 to 0.060in.

The major differences in this test project, as compared to prior tests, were the use of eight lasers for taking light transmissivity measurements and 35mm photos simultaneously on both sides of each combination vehicle as it went through the test area (Figure 2). An 8ft × 12ft black and white checkerboard target was positioned on each side of the vehicle lane.

Perpendicular to the track, 120ft from the center of the vehicle lane, a 35mm still camera was focused at a point on an 80ft × 4ft black backboard 50ft down the vehicle path from the checkerboard. The three still cameras were fired simultaneously, by means of a pneumatic trip switch as the vehicle combination entered the test area. All runs were recorded on video tape, and select runs were recorded on high-speed 16mm film.

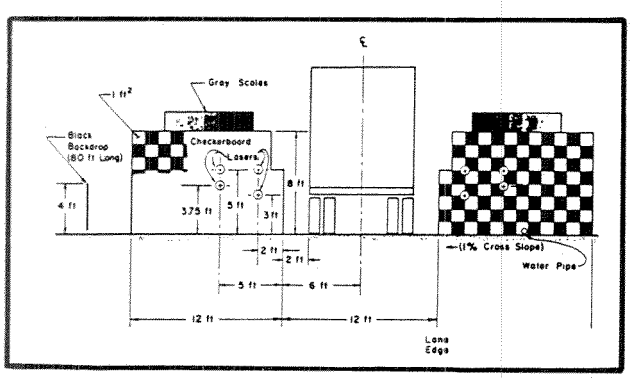

Figure 2. Test setup looking downrange

Eight low power lasers (5mw), located 50ft from the photo detectors or light meters in the checkerboard target, were used to measure quantitative spray density data. To account for crosswind, four lasers were located symmetrically on each side of the vehicle lane. The lateral and vertical placement is shown in Figure 2. The two lower positions are representative of eye levels in passenger cars, while the two higher positions are representative of eye levels in pickups and vans. The lower inboard laser positions (numbers 4 and 7) duplicate the positions used in previous test studies.

All lasers and detectors were mounted in waterproof enclosures with stable mounts (Figure 3). The sturdy mounts did not permit any motion of the laser beam due to air blast or pavement vibration, which could produce flawed data. Trial tests were run to determine effectiveness. An innovative lens system was developed to focus the 0.75in spot at the detector back to a pinpoint on the 10mm photocell. This technique eliminated the signal noise experienced in prior studies as a result of nonuniformity across the beam in addition to beam motion due to air density changes.

Signals from the detector were displayed on meters for alignment purposes and then transmitted to the telemetry system in the control trailer. These signals were then relayed via radio to the base station (Figure 4). These data were then filtered through a 5Hz, 4th order low pass filter (Butterworth), which approximates the reaction of the human eye to rapidly changing densities (Figure 5). After filtering, these data were recorded on magnetic tape, a strip chart, and the digital computer. The strip

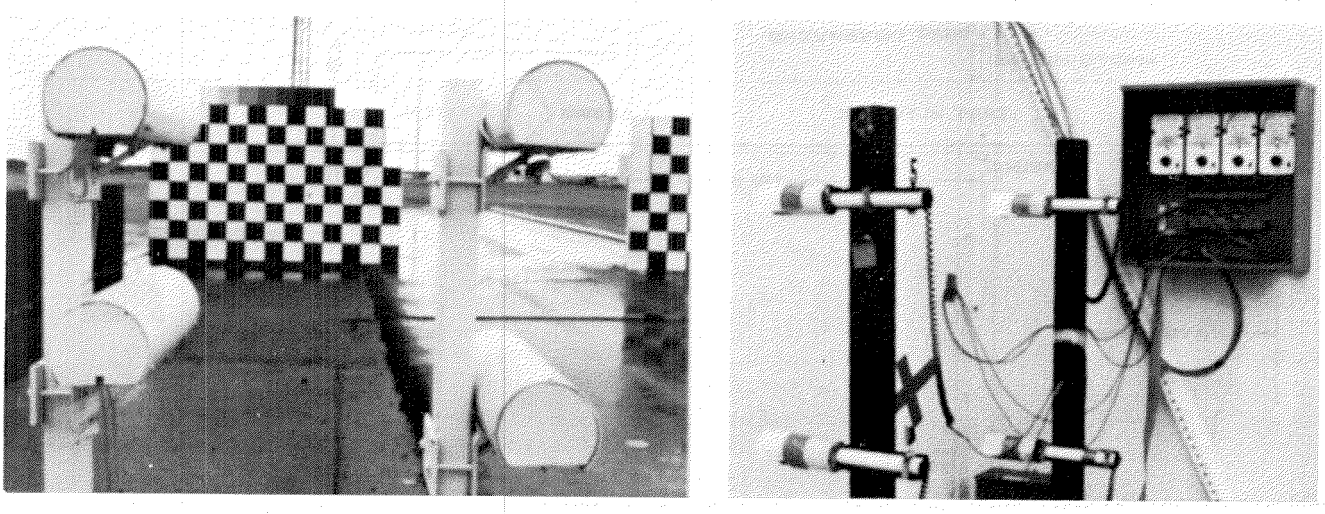

Figure 3. Laser housings and photocell detectors

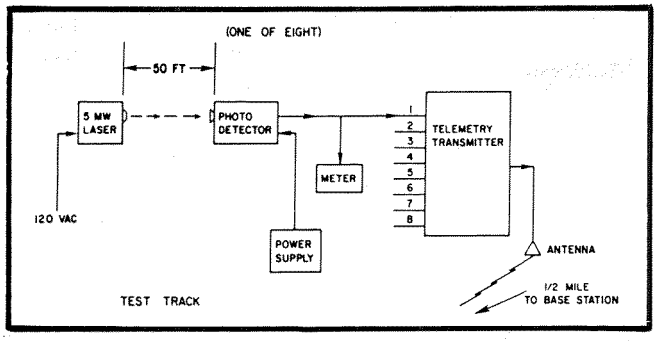

Figure 4.

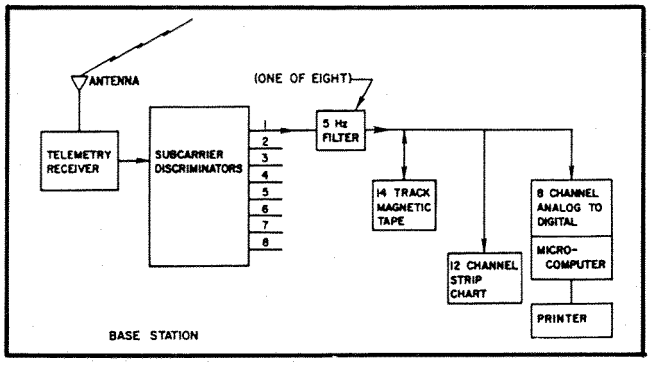

Figure 5.

chart provided instantaneous analysis of data quality, and the digital computer provided a summary printout of the minimum light transmission (based on 0 to 100 percent calibrations) from each laser. A typical strip chart trace of one transmissometer channel is shown in Figure 6, and a typical computer printout is shown in Figure 7.

End-to-end laser calibration (nominally within 2 percent of the true filter values) was achieved by inserting precision neutral density filters of 12, 25, and 50 percent in each beam and observing the digital output values.

To accommodate the greater length of the combination vehicle, the number 6 laser was relocated at a height 6in above number 7 laser and at a distance of 80ft from the detector. Thirty-six runs were made with a correlation coefficient of 0.91 between the 50 and 80ft laser positions.

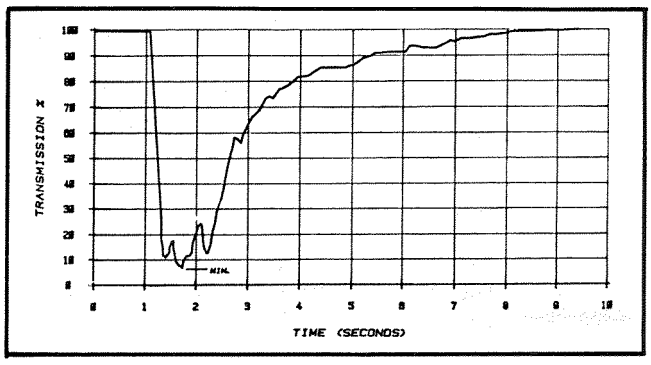

Figure 6. Typical strip chart trace

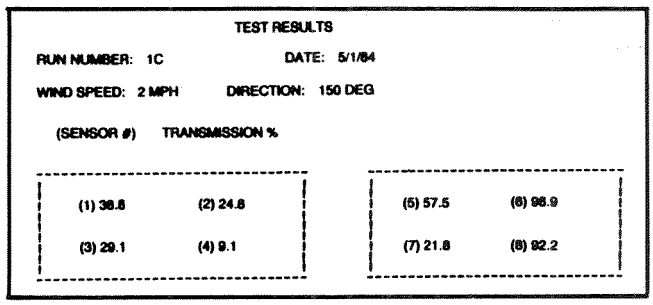

Figure 7. Typical computer printout

Therefore, in this type of testing, either a 50 or 80ft laser and detector separation could be used (Figure 8).

The effects of wind, believed to be the most significant uncontrollable variable, were minimized by taking identical measurements on both sides of the test area and by running the comparative tests within 4 to 5min. Wind speed and direction were measured prior to each test using a precision anamometer and recorded on a strip chart. Testing limits were set at a maximum wind speed of 10mph allowing for gusts up to 12mph. Ambient air temperature and relative humidity were also recorded; however, no data corrections were deemed necessary.

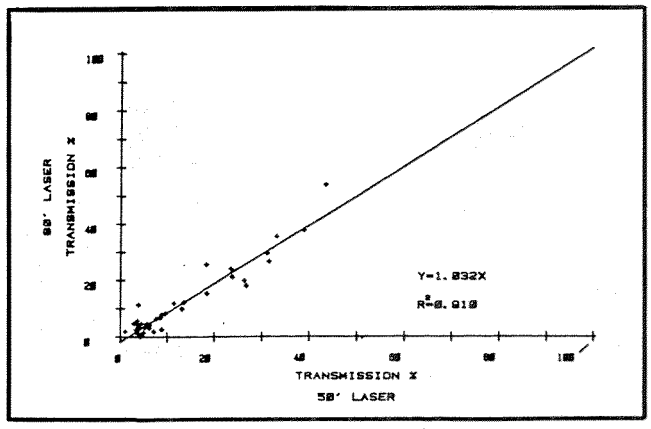

Figure 8.

As stated previously, all test runs were made at 55mph with the same driver for all runs. Vehicle speed was measured and recorded for each run by means of a standard law enforcement radar unit mounted in a vehicle positioned behind the checkerboard. The vehicle speed did not vary by more than ±1mph.

Test Plan

To assure that objective laser test measurements were repeatable from one site and one work crew to another, several DOT/NHTSA tests were duplicated using two of the actual vehicles tested by DOT/NHTSA. Refer to Figure 9 for 6×4-long nose conventional cab and single van trailer.

For this test study, the contractor was required to use three different cab types (COE, long and short conventional cabs), three van trailer types (96in-wide single, 102in-wide single, and one set of 96in-wide doubles), and two spray suppressant type devices (rear of axle-mounted flaps and vehicle side-mounted skirts). See Figures 10, 11, and 12.

Out of the series of vehicle combinations there were 47 configurations. These configurations included combinations of side-mounted skirts, treated (suppressant) flaps, and various aerodynamic devices. Each of these configurations was repeated three times for a total of 141 runs. Each run consisted of a calibration vehicle combination, an untreated baseline combination (identical to the test vehicle), and the treated test vehicle combination (Figure 13). The total number of runs for this program was 396.

Figure 9. Long nose conventional

Figure 10. COE with single van trailer

Figure 11. Short nose conventional

The calibration vehicle combination was equipped with new, plain, masticated rubber flaps (at the trailer rear only) mounted in the same location as the suppressant flaps. The baseline vehicle combination (identical to the test vehicle) was also equipped with new, plain masticated flaps (at the trailer rear only). The test vehicle combination received varying levels of suppressant devices as required by the test matrix.

The project contractor considered skirts and suppressant flaps (manufactured by Schlegel Corp. and Monsanto Co.) to be representative of the current state-of-the-art devices. These devices were installed in locations recommended by the device manufacturer. No attempts were made during this test program to vary the locations of the skirts or treated flaps. Figure 14 shows a typical front steering axle skirting and treated flap installation. Figure 15 shows a typical tractor drive axle installation (treated flap behind last axle and skirt nose of trailer mounted). Figure 16 shows a typical trailer rear installation.

Figure 12. COE with doubles

Figure 13. Calibration, baseline, and test vehicles

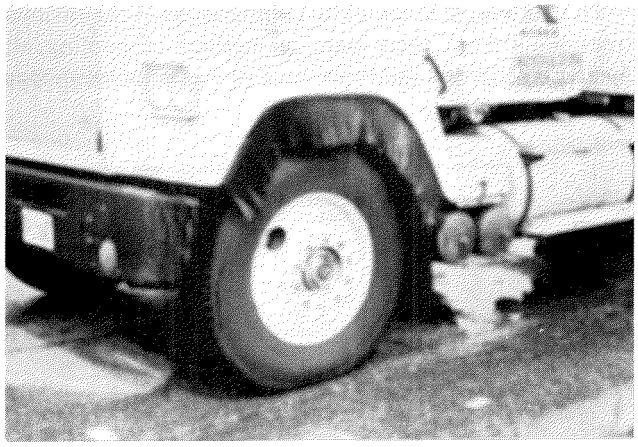

Figure 14. Steer axle installation

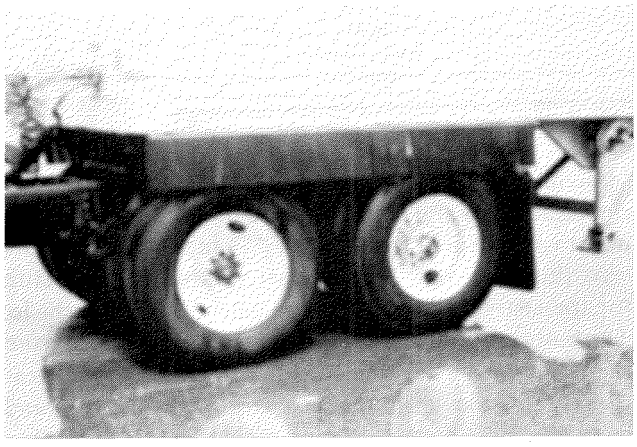

Figure 15. Drive axle installation

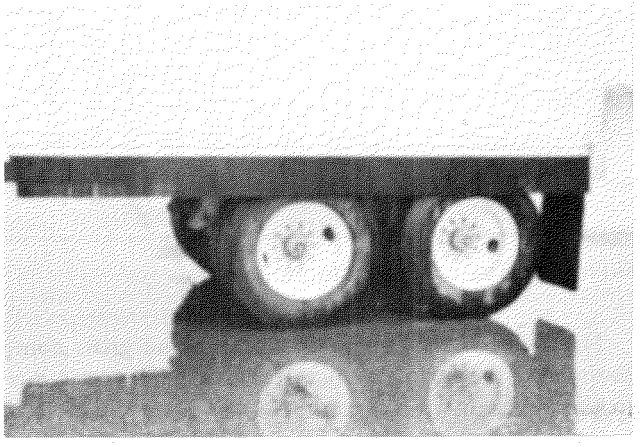

Figure 16. Trailer rear installation

The specific objectives of this test plan were designed to produce the following direct comparisons:

1. Compare the effect of aerodynamic devices
   a. Between cab configurations
   b. With various levels of suppressant devices
2. Compare the effect of suppressant devices
   a. Between cab configurations
   b. With various levels of aero devices
   c. With plain masticated flaps
   d. With varying levels of valances

TEST MATRIX

Tractor Type	Trailer Type-Width	Aeroaid	Flaps T	Flaps D	Flaps S	Side Skirts Tr	Side Skirts Tf	Side Skirts SL
COE, 6x4	SV - 96"	X*	X	X	X	X	X	X
COE, 6x4	SV - 96"	X*	X	X	X	X	X	
COE, 6x4	SV - 96"	X*	X	X	X	X		
COE, 6x4	SV - 96"	X*	X	X	X			
COE, 6x4	SV - 96"	X*	X					
COE, 6x4	SV - 96"	X	X	X	X	X	X	X
COE, 6x4	SV - 96"	X	X	X	X	X	X	
COE, 6x4	SV - 96"	X	X	X	X	X		
COE, 6x4	SV - 96"	X	X	X	X			
COE, 6x4	SV - 96"		X	X	X	X	X	X
COE, 6x4	SV - 96"		X	X	X			
COE, 6x4	SV - 102"	X*	X	X	X	X	X	X
COE, 6x4	SV - 102"	X*	X	X	X			
COE, 6x4	SV - 102"	X	X	X	X	X	X	X
COE, 6x4	SV - 102"	X	X	X	X			
COE, 4x2	DV - 96"	X	X	X	X	X	X	X
COE, 4x2	DV - 96"	X	X	X	X			
COE, 4x2	DV - 96"		X	X	X	X	X	X
COE, 4x2	DV - 96"		X	X	X			
LNC, 6x4	SV - 96"	X	X	X	X	X	X	X
LNC, 6x4	SV - 96"	X	X	X	X	X	X	
LNC, 6x4	SV - 96"	X	X	X	X	X		
LNC, 6x4	SV - 96"	X	X	X	X			
LNC, 6x4	SV - 102"	X	X	X	X	X	X	X
LNC, 6x4	SV - 102"	X	X	X	X			
LNC, 6x4	SV - 96"		X	X	X	X	X	X
LNC, 6x4	SV - 96"		X	X	X			
SNC, 6x4	SV - 96"	X*	X	X	X	X	X	X
SNC, 6x4	SV - 96"	X*	X	X	X	X	X	
SNC, 6x4	SV - 96"	X*	X	X	X	X		
SNC, 6x4	SV - 96"	X*	X	X	X			
SNC, 6x4	SV - 96"	X	X	X	X	X	X	X
SNC, 6x4	SV - 96"	X	X	X	X	X	X	
SNC, 6x4	SV - 96"	X	X	X	X	X		
SNC, 6x4	SV - 96"	X	X	X	X			
SNC, 6x4	SV - 96"		X	X	X	X	X	X
SNC, 6x4	SV - 96"		X	X	X			

Legend

Vehicle Type:

- COE = Cab-Over-Engine Tractor
- LNC = Long Nose Conventional Tractor
- SNC = Short Nose Conventional Tractor
- SV = Smooth Side Singles, Van Semi-trailer
- DV = Smooth Side Doubles, Van Trailer

Aeroaid:

- X* = Cab Roof and Side Fairings
- X = Cab Roof Only

Flaps:

- T = Trailer, behind rearmost axle
- D = Tractor, behind rearmost axle
- S = Tractor, behind front steering axle

Skirts:

- Tr = Trailer, rear axles (8')
- Tf = Trailer, nose area over tractor drive axles (8')
- SL = Tractor, front steering axle.

Figure 17.

Test Results

The still photographic records of each test run as the vehicle reached the checkerboard reference surfaces provide only a qualitative feel for the differences between the many vehicle treatments. The spray density measurements obtained during testing provided the primary basis for evaluating the effectiveness of the various spray attenuation treatments. The results of these spray density measurements are discussed in two parts as described below.

The first part of this section will discuss the results of the digitized minimum light transmission data for each sensor for the test plan as follows:

1. Data reduction and analysis
2. Correlation of sensor measurements with one another and with wind
   - Pairwise correlation analysis
   - Principal component analysis
   - Variance attributable to test conditions
3. Comparisons of conditions by grouping of setups
4. Analysis of variance and other tests of significance
   - Difference analysis of variance
   - Regression or covariate analysis of variance
   - Analysis of cases taken as treatments

The second part will discuss the results of the following special evaluations:

1. The relationship between heavy vehicle speed and the amount of spray generated
2. Observer ratings of spray clouds and correlation with spray density measurements

Data Reduction and Analysis

The actual data recorded included eight readings of minimum percent laser light transmission, wind velocity, and direction for each run; the test (T) and baseline (B) vehicles are identified and the setup number that identifies the specific spray suppressant treatment being evaluated (see Figure 18).

Note there are three runs per unique setup, that is, a combination of aeroaid, skirts, and spray flaps on the front steering axle and the tractor and trailer rear axles.

OBS	RUN	VEHICLE	SETUP	WIND	DIRECT	SENSOR1	SENSOR2	SENSOR3	SENSOR4	SENSOR5	SENSOR6	SENSOR7	SENSOR8	TRUCK
1	001	B	44	5	115	22.9	23.6	13.6	3.3	82.8	83.8	26.0	88.9	LNC
2	002	B	44	4	120	26.9	23.7	14.8	7.0	48.2	91.6	9.1	86.1	LNC
3	003	B	44	6	110	26.6	25.2	11.7	3.9	50.3	87.6	8.0	71.6	LNC
4	004	B	45	7	310	80.7	77.5	57.1	22.9	19.5	13.4	4.1	4.3	LNC
5	005	B	45	8	320	58.3	63.2	40.9	9.5	21.1	12.5	2.7	5.6	LNC
6	006	B	45	8	320	80.9	78.4	51.5	26.6	19.1	14.8	0.6	9.1	LNC
7	007	B	46	6	120	19.0	37.9	8.5	2.5	84.3	95.7	71.0	89.4	LNC
8	008	B	46	4	100	18.4	22.5	8.1	3.0	79.9	96.6	31.4	89.3	LNC

Figure 18. Typical data sheet

To make some meaningful comparisons of the various treatments from these data, a method of pooling all measurements for the three runs of a unique setup was used (see Figure 19).

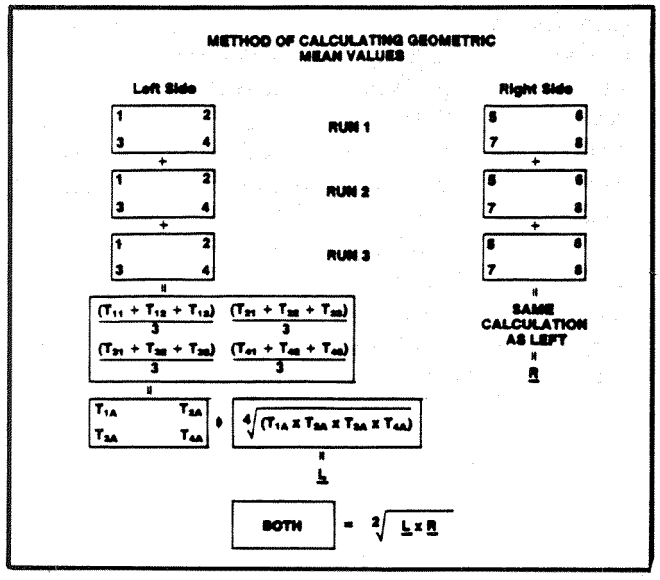

Figure 19.

Geometric mean values were calculated for left and right side lasers and then combined into a third geometric mean value expressed as "Both." Pooled measurements were thus determined for each set of three runs per setup for the test vehicle and the equivalent baseline vehicle. The baseline pooled measurements are subtracted from the test pooled measurements to provide the first indication of how the various vehicle treatments perform and compare. These data are presented in a typical bar histogram form showing the difference rank ordered from left to right in ascending magnitude for each type of vehicle (see Figure 20).

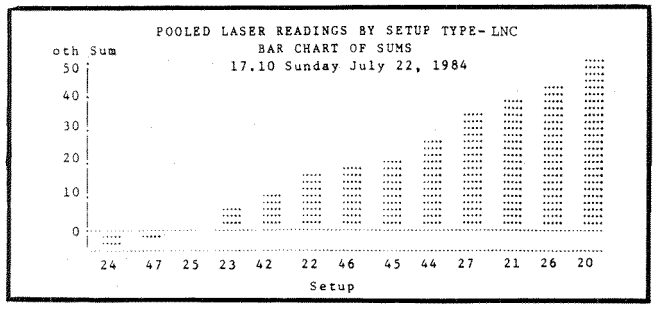

Figure 20. Typical bar histogram chart

The pooled measurements permit some gross comparisons of the various vehicle treatments. However, due to the effect of wind directions and velocity as well as limited data points, the contribution of each level of treatment could not be evaluated accurately.

Correlation of Sensor Measurements

To further study the effect of wind direction and velocity on the spray density, the use of eight different sensors in this test project permitted comparisons of various sensor measurements to determine correlation with one another in addition to wind effect.

Earlier work by Weir suggests that sensors located outboard of the "NHTSA Locations," i.e., sensors 4 and 7 in this test project, provided little additional information about the spray cloud. As shown in Figure 21, a series of correlations of sensor 4 versus sensors 1, 2, and 3 and sensor 7 versus sensors 5, 6, and 8 were computed based on data gathered on the calibration vehicle in which all eight lasers were operating. From this simple statistical analysis, it can be concluded that for comparison purposes of one treatment versus another, sensors 4 and 7 are sufficient.

Comparison	Correlation	Adjustment	MN Value*
SENSOR 4 vs.			
Sensor 1	0.796	3.48	49.81%
Sensor 2	0.89	2.56	36.64%
Sensor 3	0.86	2.37	33.95%
Sensor 4	1.00	1.00	14.33%
SENSOR 7 vs.			
Sensor 5	0.93	1.77	63.46%
Sensor 6	0.75	2.17	77.92%
Sensor 8	0.82	1.96	70.56%
Sensor 7	1.00	1.00	35.89%

Figure 21. Correlation of sensors 4 and 7 with other sensors

A more in-depth investigation and analysis of the interrelationships among the eight sensors and wind effect were conducted using the following statistical methods.

Pairwise Correlation Analysis

Pairwise correlation analysis is a bivariate statistical procedure that provides a two-dimensional description of sensor and wind relationship. Wind was selected as a single response variable representing both direction and speed.

Pairwise correlations were run among all eight sensor readings, the wind component for the calibration vehicle and the baseline vehicle separately. The results of this analysis are shown in diagrammatic form in Figure 22. Typical data plots for all sensor pairs are given in Figures 23, 24, 25, and 26.

The following observations can be made concerning these results:

1. Sensor correlation patterns are distinctly different for the right sensor (5-8) versus the left sensor (1-4). Sensors 1 to 4 have significant positive linear correlations. Sensors 5 to 8 are nonlinearly related (see scatter plots shown in Figures 23 through 26).

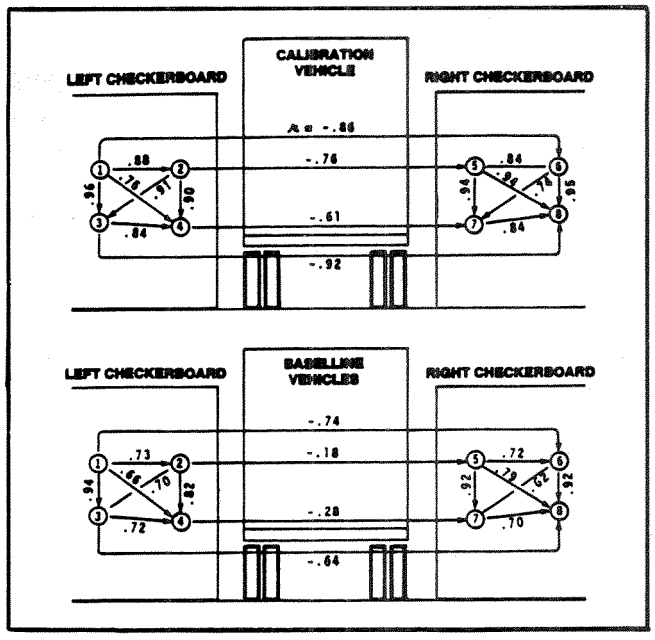

Figure 22. Pairwise correlations among sensors

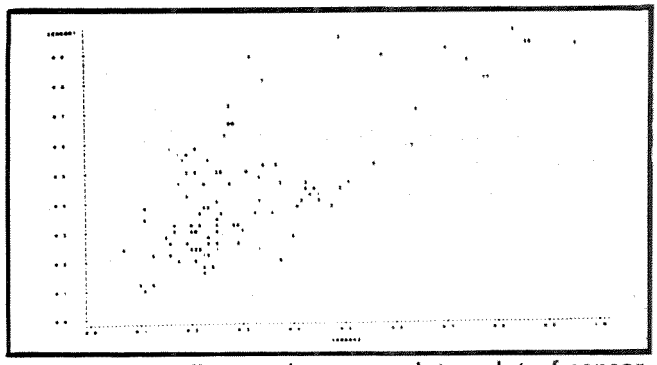

Figure 23. Baseline truck scatter plots—plot of sensor 1—sensor 2 symbol is vehicle type

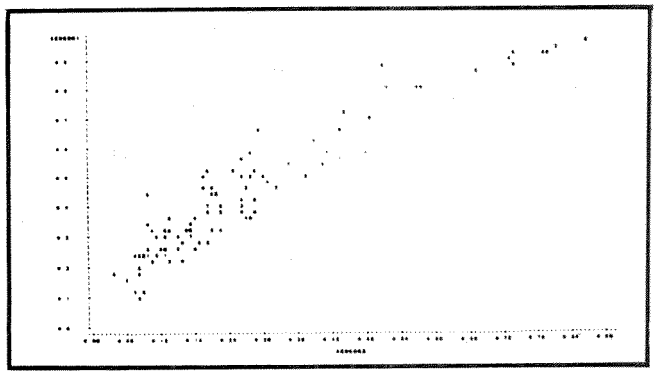

Figure 24. Baseline truck scatter plots—plot of sensor 1—sensor 3 symbol is vehicle type

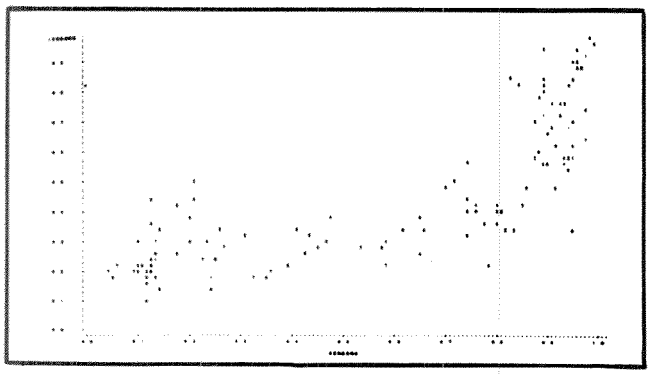

Figure 25. Baseline truck scatter plots—plot of sensor 5—sensor 6 symbol is vehicle type

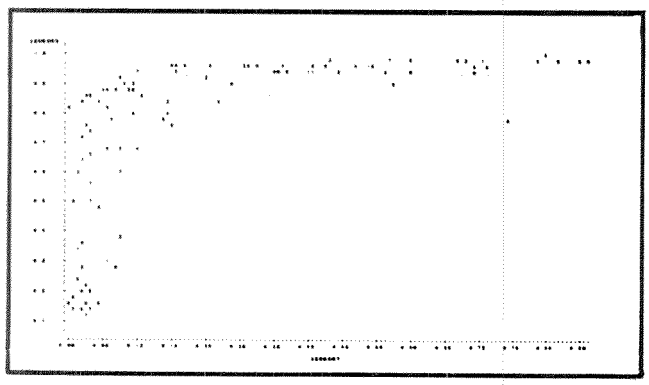

Figure 26. Baseline truck scatter plots—plot of sensor 6—sensor 7 symbol is vehicle type

2. Left sensors (1 to 4) correlate positively with the wind component and right sensors (5 to 8) correlate negatively. However, these correlations are generally lower for the inside sensors (2, 4, 5, 7). Thus, wind has the strongest effect on the outer sensors.

Principal Component Analysis

This statistical analysis is a multivariate procedure that provides a multidimensional description of sensor and wind relationships. Sensor readings and wind components are weighted and summed to provide a single response. This response reflects a significant proportion of the total variability among sensor readings and wind component variables. The magnitude and direction of these factor loadings provide information on how these variables interrelate in a multivariate setting.

Figure 27 lists the weighting factor (or factor loadings) for the standardized sensor readings and wind component for the calibration and baseline vehicles.

From the results of the correlation of sensor measurements with one another and with wind, it can be concluded that—

LOADINGS

	S_1	S_2	S_3	S_4	S_5	S_6	S_7	S_8	Wind	Prop. Var.
Calibration Vehicle										
Both	.35	.34	.35	.31	-.34	-.33	-.33	.35	.29	.83
Left	-.46	-.46	-.47	-.43					-.41	.86
Right					-.47	-.44	-.45	-.46	.42	.86
Baseline Vehicle										
Both	.38	.24	.36	.26	-.34	-.36	-.32	-.37	.33	.65
Left	-.47	-.44	-.47	-.43					-.42	.78
Right					-.46	-.46	-.44	-.48	.40	.78

Figure 27. Vehicle principal component results

1. Right and left sensors behave oppositely as evidenced by the equal but opposite signed factor loadings when all sensors are analyzed together.
2. The sensors behave oppositely with regard to wind; the left sensors are positively correlated with wind and the right sensors negatively correlated.
3. For the purposes of comparing treatments, sensors 4 and 7 are sufficient.
4. The baseline vehicle data did not reflect this behavior as clearly as the calibration vehicle data. Loadings on sensors 2 and 4 were high for the second largest factor.

Variance Attributable to Test Conditions

Throughout the test program, a third vehicle, the "Calibration" vehicle, was run with every pair of evaluation vehicles. This vehicle was equipped with plain mudflaps behind the trailer rear axle as the only spray control device, and it was left unchanged for the duration of the testing. Figure 28 presents summary statistics on this vehicle, spatially arranged to reflect sensor arrangement on the checkerboards, as seen down range (north). Wind velocity and percentage transmission level standard deviations are comparable to those for baseline and test vehicles. The summary statistics of two categories of

MN WIND VELOCITY = 7.24 MPH
STANDARD DEVIATION = 6.50 MPH (SKEWED)
RANGE = 0 - 14

LEFT			RIGHT		
49.81	MN	39.93	60.67	MN	77.92
22.10	SD	21.52	25.77	SD	24.25
6.8	MIN	10.50	17.70	MIN	26.8
94.6	MAX	98.20	98.70	MAX	99.5
37.99		14.33	35.89		66.18
25.07		16.86	30.77		32.41
0.20		0.10	0		8.10
94.60		88.10	97.70		99.20

Figure 28. Summary statistics on all calibration vehicle runs

vehicles are given in Figures 29 and 30, respectively. The dispersion in relationship to each mean transmittance, which is expressed as the standard deviation, is indicative of the problem facing all testers of splash and spray devices: very large variation.

The large amount of variability in measurements for any given sensor is explained, at least in part, by wind velocity and direction, plus inherent variability in measurements of a complex aerodynamic phenomenon such as spray from a speeding vehicle. This variability far exceeds that acceptable for normal engineering test protocol. It is this variance that makes interpretation of limited runs on a given configuration difficult.

MN WIND VELOCITY = 6.55 MPH
STANDARD DEVIATION = 3.20 MPH
RANGE = 0-20

		LEFT		RIGHT
43.7%	MN	32.0	45.5 MN	72.6
21.0%	SD	18.5	25.3 SD	28.4
9.5%	MIN	6.4	5.1 MIN	12.5
95.8%	MAX	95.7	97.9 MAX	99.1
27.5		10.4	22.3	57.0
19.3		13.8	25.3	33.4
3.9		0	0	4.3
91.2		88.0	91.2	91.2
				99.0

MN RATING = 5.0
STANDARD DEVIATION = 1.0
RANGE 1-7

Figure 29. Summary statistics on all baseline vehicle runs

MN WIND VELOCITY = 6.65 MPH
STANDARD DEVIATION = 3.12 MPH
RANGE = 0-15

		LEFT		RIGHT
66.1%	MN	51.8	72.3 MN	85.5
24.2%	SD	25.9	25.0 SD	21.4
18.1%	MIN	6.3	9.6 MIN	21.8
97.3%	MAX	98.4	98.7 MAX	99.6
50.2		25.3	50.6	74.0
27.2		22.5	31.8	27.3
4.9		0.1	00.1	5.8
93.8		84.5	97.6	99.3

MN RATING = 3.6
STD DEV. = 1.0
[illegible]

Figure 30. Summary statistics on all treated vehicle runs

Comparison of Conditions by Grouping of Setups

To determine in a general overall sense if those spray reduction devices evaluated really work or are of benefit, a statistical analysis was made using the t-test of independent means. This approach to inferential statistical analysis allows a gross kind of comparison setup. The t-test for most of the sample sizes of this test project approximates a Z-distribution-test. The reader is referred to any standard text on statistics for a further explanation of inferential tests, and the t-test or Z-test in particular.

The results of the t-test of mean differences between all treated vehicles (T) and their baseline (B) vehicles are shown in Figure 31.

COMPARISON	N	SENSOR	MN VALUE	t VALUES	PROB >|t|
B	143	4	10.38%	-6.73	.0001**
T	140	4	25.33%		
B	143	7	22.28%	-8.30	.0001**
T	140	7	50.61%		
AERO	97	4	29.10%	4.72	.0001**
NO AERO	28	4	13.76%		
AERO	97	7	32.65%	1.89	.06
NO AERO	28	7	30.90%		
102" TRAILER	30	4	21.5%	-1.132	.26
96" TRAILER	95	4	27.0%		
102" TRAILER	30	7	56.2%	1.22	.22
96" TRAILER	95	7	47.8%		

*Significant Difference (Pr<0.05)
**Highly Significant Difference (Pr<0.001)

Figure 31. T-test—sensors 4 and 7

For both DOT/NHTSA sensors (and the others as well), a significant difference was observed. Overall, transmittance was more than twice as large for treated vehicles as compared to baseline. Sensor 4 had a mean value of 10.38 percent versus 25.33 percent for treated trucks. That this great a mean value difference could occur, and yet there was no difference between treated and baseline vehicles as measured by sensor 4, is associated with a probability of less than 0.0001. These spray reduction devices, taken overall, do indeed work.

For the purpose of evaluating the effect of the cab roof-mounted aerodynamic shield on spray reduction, the setups shown in Figure 32 were used. The t-test results

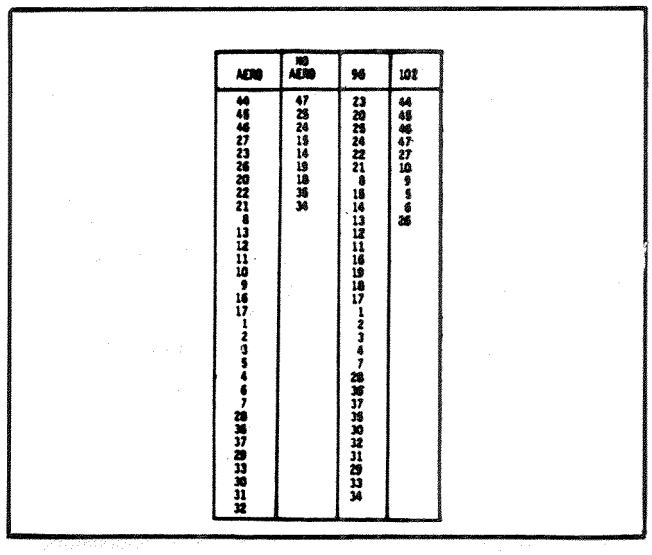

Figure 32. Setup partitioning for comparison of conditions

as shown in Figure 31, AERO versus NO AERO, indicate the differences on the left side (sensor 4) were significant, but less so on the right side. If pooled, these differences would remain significant beyond the 0.05 level; hence, it can be concluded that the cab-mounted aeroaid has a measurable effect on reducing spray. Figure 32 also provides the results of the comparison of spray levels between 96in-wide and 102in-wide trailers and indicates no significant measurable difference.

The above findings merely scratch the surface so far as making definitive statements about the many treatment strategies tested. T-tests between different individual treatments with only three runs per treatment or setup would be unproductive, and, in any case, multiple t-tests for data that could be analyzed by more sophisticated methods can be very misleading.

Therefore, analysis of covariance using several different models was performed on all the data gathered for B and T vehicles in this research project. This analysis is explained and interpreted in the following section.

Analysis of Variance and Other Tests of Significance

Individual setups were tested only three times; therefore, meaningful statistical comparison of transmissometer data is difficult. A strategy was developed to make inferences concerning the effects of different treatment combinations of flaps, skirts, and aeroaid. This strategy required the sacrifice of certain variables, namely, trailer type (which has been found to produce no significant difference) and tractor type (five different tractors). These data were simply collapsed over these two variables. Once this was accomplished, a variable called Aero can be identified as having three levels:

No aeroaid installed	= 0
Standard aeroaid	= 1
Special (Gelco) aeroaid	= S

Another variable is the treatment on the steering axle of the test vehicle, which can be called Steer:

Flaps only	= F
Flaps and skirts	= FS

A third variable is the treatment on the drive axle(s) of the tractor, which has two levels, just as the Steer variable does. This third variable is called Drive.

A final variable is Rear, which is the rear (trailer) axle treatment. Since all setups specified special flaps on the rear of the trailer, the two levels of this variable are—

Flaps only	= 0
Skirts and flaps	= S

Figure 33 identifies 10 different combinations of these variables that were tested in the setups of the test matrix. Each setup, in other words, can be classified as being one of these two cases. In Figure 33, each of the 10 cases is related to the setups that match that case.

CASE	SETUPS	AERO	STEER	DRIVE	REAR
1	3, 37	S	F	F	S
2	4, 5, 29	S	F	F	0
3	2, 36	S	F	FS	S
4	1, 6, 28	S	FS	FS	S
5	14,18,24,34,47	0	F	F	0
6	15,19,25,35	0	FS	FS	S
7	12,22,32,45	1	F	F	S
8	10,13,17,23,27,33,46	1	F	F	0
9	11,21,31,44	1	F	FS	S
10	8,9,16,20,26,30	1	FS	FS	S

Figure 33. Setups classified into 10 cases

Since, as Figure 33 shows, the few cases of flaps only at the rear covaried with the presence or absence of an aeroaid and combinations of Steer and Drive, this factor could not be extracted independently. Thus, this analysis concentrates on differences among the various combinations of Aero, Steer, and Drive. Two approaches were used. In the first, the difference between test and baseline vehicle sensor readings on equivalent runs was the dependent or criterion variable. The other involved a more direct approach for controlling the troublesome intervening variable of wind. The first analysis is referred to as the difference analysis.

Difference Analysis of Variance

A two-factor interaction analysis of variance model was used with Aero and Steer/Drive being the main effects with three levels each. This resulted in a missing cell design, since no Aero = U and Steer/Drive = (F-S) combination or levels were observed. The assumption in this experimental design is that the test and base vehicle experienced similar wind conditions. Since this was precisely the purpose of running baseline and test vehicles in close sequence, this may not be an unreasonable assumption.

Based on the considerations of relationships among the eight sensors previously discussed, four different criterion variables were developed. Each variable required a separate analysis of variance. These variables were as follows (each observation is a difference between a sensor's readings on a baseline truck pass and the equivalent test truck pass moments later):

- Variable 1—The geometric mean of all eight sensors
- Variable 2—The geometric mean of sensors 4 and 7 only
- Variable 3—The geometric mean of left sensors only (1 to 4)
- Variable 4—The geometric mean of right sensors only (5 to 8)

The geometric mean is frequency used as the measure of central tendency when the random variable of interest is a portion or percent since the population frequency distribution of such random variable tends to be skewed. The frequency distribution of the sensor arithmetic mean did show a definite skewness. The frequency distribution of the geometric mean, on the other hand, appeared to be nearly normally distributed. To further support the use of geometric mean, analyses were run using both measures, arithmetic and geometric, and there were no differences in results concerning treatment effects.

Figure 34 provides a summary of the results of this difference analysis of variance for all four criterion variables. In this table, an asterisk (*) indicates a level of significance of 0.05 under a null hypothesis of "no difference." This signifies that means that are as far apart in value as those observed, among the various levels of the factors being analyzed, have a chance of 5 in 100 of being just that—chance—rather than reflecting a real difference between treatments or combinations of treatments.

		Criterion Variable			
Factor		1	2	3	4
Aero		*[1]	*	*	*
Steer/Drive		*	*	N.S.	*
Aero X Steer/Drive		N.S.[2]	N.S.	N.S.	N.S.
Aero:	1	27.1%[3]	21.3	24.7	26.4
	S	14.3%	9.5	18.5	16.5
	0	11.6%	8.8	7.5	8.3
Steer/Drive	FS-FS	26.0	20.8	20.4	26.3
	F-FS	19.2	15.4	16.6	22.0
	F-F	17.1	12.1	19.2	15.3

NOTES:
1. $\alpha = 0.05$
2. N.S. = NOT SIGNIFICANT
3. Geometric mean difference in percent transmittance, Test vs Baseline Vehicle

Figure 34. Results of difference analysis of variance on aero and drive steer comparisons

The rows under the significance matrix help the reader understand the meaning of these findings. For criterion variable 1, in which all eight sensors are pooled, a standard aeroaid, across the board, produces consistently better results (a higher mean transmittance difference of 27.1 percent) than either the special aeroaid or no aeroaid.

The Steer/Drive combinations are consistent for all but variable 3, as can be seen in Figure 34. The most effective combination is both flaps and skirts for all axles, and it is significantly better than just flaps alone on these same axles. Note in this table that the interaction between the levels of aeroaid treatment and axle treatments is uniformly nonsignificant. This means that whether or not an aeroaid is installed has no differential effect on the efficacy of the wheel treatments; the percentage change (in this case improvement), associated with the use of an aeroaid, works as a constant on whether wheel treatment is installed. It should be noted that the standard aeroaid condition occurred with greater frequency in this data set; i.e., there were 63 standard aeroaid runs as compared to 30 special and 27 nonaero conditions.

Regression or Covariate Analysis of Variance

To address more directly the effects of wind, a second method of analysis was undertaken, with the dependent or criterion variables being the transmissometer readings for baseline and test vehicles considered separately. In this analysis, the crosswind vector component of wind is entered as an independent variable just like treatments on the test vehicles. Other independent variables in the model were, as before, Aero and Steer/Drive axle combinations. This model essentially fits separate linear regression lines for the four ways of pooling sensor data used in the difference analysis for each factor level combination and tests for the equality of slopes and intercepts. Since baseline vehicles had no treatments, these lines should be equal in slope and intercept. If the slopes are equal for test vehicles, this implies that treatment combinations shown in Figure 33 can be compared at any wind value and result in the same conclusions. If, however, slopes are not equal, this finding would suggest that a treatment was better under some wind conditions than under others. Inequality of intercepts means that the treatments were not equal with regard to the amount of spray recorded, and thus different treatments can be rank ordered with respect to the extent of spray control.

Figure 35 summarizes the findings of these analyses, organized as before with respect to the four different

		Criterion Variable							
FACTOR		1		2		3		4	
Aero		*[1]		*		*		*	
Steer/Drive		*		*		N.S.		N.S.	
Aero X Steer/Drive		N.S.[2]		N.S.		*		*	
Wind		N.S.		N.S.		*		*	
Aero X Wind		N.S.		N.S.		N.S.		N.S.	
Steer/Drive X Wind		N.S.		N.S.		N.S.		N.S.	
Aero X Steer/Drive X Wind		N.S.		N.S.		N.S.		N.S.	
NOTES: 1. * = 0.05 2. N.S. = Not Significant									
		Test[3]	Baseline	Test	Baseline	Test	Baseline	Test	Baseline
Aero	1	51.4%	24.4	30.1	8.7	51.6	26.9	71.2	44.8
	S	45.9	31.7	22.1	13.4	46.3	27.8	73.4	57.0
	0	37.0	25.4	19.3	9.8	33.8	26.3	58.9	50.6
Steer/Drive	FS-FS	51.8	25.6	30.1	9.3	46.8	26.4	72	45.7
	F-FS	48.3	29.0	26.0	10.6	42.6	26.0	77.8	55.9
	F-F	43.4	26.2	23.0	10.5	46.8	27.6	64.4	49.1

NOTES: 1. * = 0.05
2. N.S. = Not Significant
3. This mean transmittance pooled as denoted by Criterion Variable Designation

Figure 35. Results of regression analysis of variance on aero and drive steer combination

methods of pooling sensor observations. Baseline vehicle geometric mean readings are also included in this table for comparison with test vehicle geometric means.

In this analysis, wind is not a significant covariate either by itself or in interaction with other factors for criterion variable 1 or for variable 2. These, it will be remembered, are (1) laser readings pooled over all eight sensors, and (2) sensors 4 and 7 only pooled by taking their geometric mean. In the section Correlation of Sensor Measurements, the correlational analysis of sensor readings with wind for the baseline and calibration vehicle runs, it was determined that sensors on the left and right correlated oppositely with wind; hence, the fact that wind is not a significant covariate for sensor readings pooled on both sides of the vehicle should not be surprising. That wind (really the crosswind vector) should be a significant variable for criterion variables 3 and 4 is also not surprising, since these are left-only and right-only sensors, respectively. These geometric means were greatly influenced by wind velocities and directions from one period of time to another, and thus wind is a significant covariate. This relationship was, however, the same for all factor levels as evidenced by the lack of interaction of wind with any of these factors.

The slopes and intercepts of the lines for all factor level combinations of the baseline vehicles were equal, indicating that the baseline vehicles' pooled laser readings were essentially equivalent for all runs.

The results for the test vehicle responses, as summarized in Figure 35, show that wind was a significant covariate for the right and left responses, criterion variables 3 and 4, but the slopes of the regression lines were the same for all factor levels. Thus, equivalent conclusions regarding treatment effectiveness will result at any wind condition. This figure again shows that for criterion variables 1 and 2, the standard aeroaid was superior to either the special aero or no aeroaid.

When left-only sensor 3 and right-only sensor 4 are used as the dependent variable, the results are not as straightforward. For the right-only sensors, there was a significant interaction between the kind of aeroaid treatment that was used and the wheel treatment used. The main effects of wheel treatment closely parallel the findings of the difference analysis of variance; the fuller the treatment of tractor axles, the better the results.

As a supplementary analysis, the single factor of rear axle (on the trailer) with two levels—flaps only versus skirts and flaps—was studied, using test vehicle data only. The results show a significant difference between these two conditions for all but the right-only sensors, with skirts and flaps superior to flaps only on the rear axles (see Figure 36).

	Criterion Variables			
	1	2	3	4
Rear: Flaps & Skirts	49.9	27.6	50.4	89.5
Flaps ONLY	37.0	21.4	36.9	87.4

Figure 36. Results of regression analysis of variance on effects of skirts on rear axles

Analysis of Cases Taken as Treatments

A difference approach can be taken for the data of this study, if each of the 10 cases identified in Figure 33 can be taken as an individual treatment. Through analysis of variance methods and criterion variables identical to those described in the previous section, it should be possible to make some overall statements concerning the relative efficacy of these generic installations on vehicles. In addition, an analysis of covariance was performed on these data.

Figure 37 summarizes pooled laser readings for the 10 cases, plus pooled case readings for their equivalent baseline vehicle runs. The pooled transmissometer variables are (1) the geometric means of all eight sensors, and (2) the geometric mean of sensors 4 and 7 only, just as before. A study of this table will show some differences among the various cases, and a quite evident overall superiority of test vehicles over their equivalent baselines.

	Conditions				Variables			
					1		2	
CASE	Aero	Steer	Drive	Rear	T	B	T	B
1	S	F	F	S	39.6%	29.7	17.2	13.9
2	S	F	F	0	49.9	31.2	24.9	13.3
3	S	F	FS	S	36.4	34.6	14.2	14.5
4	S	FS	FS	FS	53.3	31.4	28.8	12.3
5	0	F	F	0	33.1	26.5	16.1	11.1
6	0	FS	FS	S	42.1	24.0	23.5	13.9
7	1	F	F	S	52.0	23.5	28.1	8.8
8	1	F	F	0	44.5	24.2	25.4	8.9
9	1	F	FS	S	54.3	26.3	31.9	8.6
10	1	FS	FS	S	57.1	24.0	35.0	8.8

Figure 37. Summary of pooled laser readings by cases

The following methods of analysis were used to determine treatment effects:

1. Analysis of Differences—In which the dependent variable was the difference in laser readings, sensor by sensor, between the test and the baseline vehicle on a given run. A one-way analysis of variance and a duncan multiple range test were run using 10 cases as the independent variable (each case is a level in this fixed model). Data were analyzed by separate wind directions defined as either a positive or negative value according to the crosswind vector. Another

analysis was performed with only those observations in which a crosswind component of equal to or less than ±2mph was recorded ("no wind").

2. Regression Analysis—Which is similar in approach to the differences analyses discussed earlier and yields little more definitive information. A separate regression line was developed for each of the 10 treatment combinations (cases). These regression lines were then compared for equality of slope and intercept.
3. Analysis of Covariance—In the analysis of covariance regression, model wind was considered by fitting lines for pooled laser readings versus wind (crosswind vector) for 10 test cases and their equivalent baseline runs. Hence, 20 lines of regression were fitted simultaneously and then tested by equality of slopes and intercepts. Since this procedure involved multiple hypothesis testing (40 parameters being estimated), in order to have an overall significance (α) level of 0.05 for rejecting the null hypothesis of "no significant difference," individual slopes and intercepts were tested at the level of 0.001.

Criterion variables used in these analyses were the usual four described previously, plus a special category consisting of each sensor taken individually (no summary by pooling). Duncan multiple range tests were then used to evaluate the significant differences found among many of the 10 cases in the difference analysis.

Figure 38 identifies cases in rank order of efficacy in attenuating spray from left to right for criterion variables 1, 2, 3, and 4. Those cases identified in each row corresponding to an analysis such as "All Winds (considered)" are cases significantly better than their baseline equivalents but not differing significantly among themselves. Case numbers in parenthesis are cases that mark the threshold from significantly better than base to no better than base (in some instances worse).

Geometric Mean of All Sensors		Geometric Mean of Sensors(4&7)	
All Winds:	10 9 4 7 2 8 6 1 3 (5)	All Winds:	10 9 7 4 8 2 6 1 5 (3)
No Sig. Wind:	10 4 9 6 7 8 2 1 5 (3)	No Sig. Wind:	10 9 6 4 8 7 2 1 5 (3)
Sig. Wind:	9 2 10 7 4 1 8 6 3 (5)	Sig. Wind:	9 2 10 7 4 1 8 6 3 (5)
Geometric Mean of Left Sensors(1-4)		Geometric Mean of Right Sensors(5-8)	
All Winds:	2 7 10 9 8 1 4 6 3 (5)	All Winds:	4 9 10 7 8 1 6 2 5 (3)

Figure 38. Rank order of cases

In Figure 38, first results are shown for all data (all winds) for variables 1 and 2. Then results by comparing data generated under low or no wind versus significant wind are given. For left-only and right-only sensor data, where directionality is obviously of interest, rankings of cases are shown for the all winds considered analysis (all winds) and for only those observations in which wind is significant (greater than ±2mph, crosswind vector).

These findings can be interpreted as follows. Cases 10, 9, and 7 were uniformly superior across all wind directions and types of pooling of laser readings. Cases 3 and 5 were generally least effective in attenuating spray.

Turning to an analysis of individual sensor data, Figure 39 provides rank order information. Treatment difference responses that are underlined are significantly different than those that are not underlined and are significantly greater than zero. Cases 10 and 7 again were consistently selected, although case 2 was ranked as one of the best treatments by sensors 1 through 4 but not by sensors 5 through 8. Conversely, case 4 was ranked very highly by sensors 5 through 8 but not by sensors 1 through 4.

(Individual Sensors:)										
S1	10	8	2	9	7	1	4	3	6	5
S2	2	7	10	6	9	8	4	1	5	3
S3	7	2	10	9	8	4	3	1	6	5
S4	7	2	10	6	9	8	1	5	4	3
S5	4	9	7	8	10	6	1	2	3	5
S6	7	10	9	1	4	8	6	2	5	3
S7	9	4	8	10	7	6	1	3	2	5
S8	7	9	10	4	8	6	1	2	5	3

Figure 39. Rank order of cases by individual sensors

In summary, a standard full treatment of flaps and skirts on every axle, together with a standard aeroaid (case 10), provided the best overall results in spray attenuation. Leaving the steering axle without skirts but installing everything else (case 9) is next most efficacious, followed by a treatment in which skirts are retained only on the rear of the trailer. Case 2, which has no skirts but does have cab side fairings in addition to a special cab roof-mounted aeroaid, produces highly wind-dependent effects. The aeroaid is very critical, since the cases without it perform erratically to poorly (cases 5 and 6).

Relationship Between Speed and Spray Generated

Special speed tests (in increments of 5mph from 35 to 60mph) were conducted using various levels of suppressant devices and plain rubber flaps. It can be concluded that speed and spray generation are linear and that combination vehicle speeds over 60mph will produce unacceptably high levels of spray.

Observer Ratings and Correlation to Objective Measurements

To better correlate observer ratings and objective laser measurements, the relationship between spray density and observer contrast sensitivity was investigated. To this

end, a vision contrast test system marketed by Vistech Consultants, Inc., was used along with an artificial rainmaker. Observers, plus a single laser beam, were used to rate four levels of transmission: 100 percent (no water), 60 percent, 40 percent, and 20 percent. Predictably, contrast discrimination falls off rapidly with increased density of spray or as the fineness of the target patterns increases. An evaluation of the computed percent change in contrast sensitivity of the laser compared to observer ratings demonstrated a high degree of correlation (.92). Based on these findings when a condition of 40 percent laser transmittance was reached, observer contrast discrimination had fallen off by a factor approaching two.

It can be concluded that when spray obscures light to below 40 percent transmissivity, loss of observer contrast sensitivity results. Such a controlled test does not reproduce the dynamic situation of a driver attempting to pass a truck with all of the variables of wind, speed, aerodynamic effects, windshield, windshield wipers, etc. Therefore, a conclusion that treated vehicles must achieve a threshold level of 40 percent or above for the motoring public to perceive improvement cannot be substantiated.

Innovative Instrumentation

Within the scope of the research objectives of this project, the University of Michigan Transportation Research Institute (UMTRI) conducted a limited study of advance instrumentation for measuring the effectiveness of heavy truck splash and spray suppression devices.

Visibility is a subjective measure that can vary greatly between observers. Thus, to measure the effectiveness of spray suppression devices, it is desirable to select a quantity that can be objectively measured, preferably with simple instrumentation, and that exhibits a reasonable correlation with visibility. The transmissivity of the spray cloud along the side of the vehicle is the quantity that has been measured in several previous studies. The rationale for selecting this measurement, together with a general discussion of the problems involved in measuring the effectiveness of spray suppressors, follows.

Two schemes were considered practical for potential field implementation:

- The use of expanded collimated laser beams (2in diameter or larger) to obtain spatial averaging over a larger area of the spray field than obtained with the raw laser beam
- Photometric measurement of laser light scattered or reflected by the spray field

Because eight laser transmissometers were implemented at the start of the field test program, no further consideration was given to the multiple laser transmissometer scheme. Laboratory experiments were performed relating to the expanded laser beam and the light-scattering measurement schemes. These experiments were intended to define the hardware requirements for potential field implementation.

The generation and use of an expanded laser beam up to 6in in diameter were shown to be simple and straightforward. Beams 12 to 15in in diameter could also be easy to generate and apply. By virtue of averaging over a larger area of the spray field, the expanded laser beam arrangement may provide a useful enhancement of the laser transmissometer scheme. Thus, field evaluation of the expanded laser beam transmissometer appears worthwhile.

Photometer measurements of the light scattered as a beam of light passes through the spray field do not appear to have practical application for measuring the visibility through the entire spray field along the side of a vehicle. A photometer focused on the beam would receive power from only a small area of the spray field. However, such methods could provide a useful measurement of local spray density.

In a scattered light-measuring system, the light level received by the photometer is several orders of magnitude less than received in a transmissivity-measuring system. Consequently, a modulated light source and a sensitive bandpass-tuned photometer must be used to detect the scattered light separately from the ambient light. Using a 10mW laser light source, with 100 percent modulation, a tuned photometer with a sensitivity of at least 50pW is required. Of course, a less sensitive photometer would be adequate with a proportionately higher powered light source, and the light source does not have to be a laser. A search of literature indicated that bandpass-tuned photometers are not readily available as standard test instruments. Although the design of such a photometer is straightforward, such a task was not included in this research project.

Summary of Findings

Based on the analyses of the extensive data collected in this test study and the results previously discussed, the following seem warranted.

Vehicle Performance

- When equipped with an aeroaid, skirts, and treated flaps at each axle, most tractor-trailer combinations demonstrated improved mean light transmissivity over the equivalent baseline (untreated) vehicles, by a factor that can approach two. The prime contributor in reducing spray is the cab roof-mounted aeroaid.
- Flaps alone are insufficient to reduce spray reliably, although they can help. Skirts on the trailer rear axle are more important than skirts on the axles farther forward on the vehicle.

- Any improvement varied with vehicle/trailer configuration and, depending on baseline performance, improvement can be expected but not quantitatively predicted.
- The relationship between vehicle speed and spray density is an approximately linear one. Above 60mph, the effectiveness of any treatment was totally negated.
- Insufficient replications of treatment combinations were made to permit adequate statistical analysis of the relative contribution of specific treatments at various locations or the effect of wind condition on treatment effects.

Equipment/Procedure

- Computer image digitization of spray cloud density appears to be a viable alternative to costly and stationary laser instrumentation.
- Use of eight lasers versus two provided little additional information about the spray cloud.
- Expanded laser beam transmissometers, up to 15in in diameter, appear feasible and allow spatial averaging that will reduce received output fluctuations caused by large water droplets.
- Photometer measurements of scattered light are feasible for measuring localized spray density but not throughout the entire spray field.
- No correlation methodology or procedure exists to relate the improvement in light transmissivity to improved visibility as perceived by the motoring public.
- Under controlled conditions, the contrast sensitivity of an observer is substantially impaired when a laser transmissivity of below 40 percent through a spray cloud is reached.

References

1. Weir, D.H., et al., "Reduction of adverse aerodynamic effects of large trucks," U.S. Department of Transportation Report, FHWA-RD-79-84, September 1978.

An Evaluation of the Obstacle-Avoidance Capabilities of Articulated Commercial Vehicles

Paul S. Fancher
The University of Michigan Transportation Research Institute

Abstract

Analytical methods are used to evaluate the braking and steering performance of tractor-semitrailer, truck-full trailer, double, and triple combinations that have mechnical properties corresponding to current design and usage practices in the United States.

Introduction

Drivers of articulated commercial vehicles are expected to stabilize directional response, avoid rollover, and judge stopping capabilities under various operating conditions. This paper examines the extent to which the design and configuration of combination vehicles influence (1) the nature of the driver's control tasks, and (2) the fraction of the tire-road friction that can be used in successfully avoiding obstacles and resolving traffic conflicts.

The purpose of this paper is to describe analytical approaches used for evaluating the steering and braking performance of heavy trucks in a current project sponsored by the National Highway Traffic Safety Administration (NHTSA)(1) in the United States. In that project, the sensitivity of vehicle performance to parametric changes in component characteristics will be evaluated. An ultimate goal of the NHTSA project is a vehicle dynamics handbook for straight and articulated heavy trucks. The approach described will be used in formulating the vehicle dynamics handbook.

Description of the Methodology

The results presented are based on models developed during studies supported by the Motor Vehicle Manufacturers Association (MVMA), the Federal Highway Administration (FHWA), the State of Michigan, and NHTSA. Table 1 provides correspondence between open-loop vehicle maneuvers, computerized models, and published references. Simulated vehicle maneuvers have been used to make design evaluations similar to those that might have been obtained from typical vehicle tests.(19,20,21).

Table 1. Correspondence between models, references, and maneuvers

	Models	Background References*
Equilibrium Analyses	1. Static Roll	(2, 3)
	2. High-speed Tracking	(4, 5, 6)
	3. Steady Turning (Handling)	(7, 8, 9, 6)
	4. Constant Deceleration Braking	(10)
Simulations	5. Low-speed Tracking (Tractrix)	(11, 12, 13)
	6. Linear Yaw Plane Analysis	(14, 15, 5)
	7. Yaw and Roll (Constant Velocity)	(2, 10)
	8. Comprehensive Braking and Steering	(16, 17, 18)

* Simplified versions of models 1 through 5 have been developed in (1).

	Model Number							
Maneuvers	1	2	3	4	5	6	7	8
Steady Turning								
a. Roll	X						X	X
b. Tracking		X					X	X
c. Handling			X				X	X
Straight-Line Braking (Constant Deceleration Braking)				X				X
Low-Speed Cornering (In-Town Corner)					X		X	X
Transient Turning (Ramp-Step Steer)						X	X	X
Obstacle Evasion						X	X	X
Response to External Disturbances							X	X
Braking in a Turn								X

For most of the maneuvers employed here, a performance signature is obtained for each type of vehicle. Then, performance measures are evaluated at safety-relevant levels of the performance signatures of the various vehicles. For example, in a steady-turning maneuver, the roll angles of the vehicle's unit increase as the lateral acceleration of the turn increases. At the limit of performance, one of the vehicle's units rolls over at a level of lateral acceleration called the rollover threshold. In this case, the roll angle versus lateral acceleration graph is the performance signature and the rollover threshold is the safety-relevant performance measure.

A family of maneuvers and associated performance measures (see Table 2) has been selected for assessing the influences of changes in vehicle properties on steering and braking performance(1). The steady-turning maneuver is used to examine three aspects of performance, namely, roll, tracking, and handling. Constant deceleration braking is used to evaluate friction utilization and braking efficiency. The other maneuvers are transient in nature in that they involve changing from one path to another.

Some of the maneuvers are open loop such that a test driver would perform predetermined control actions

Table 2. Performance signatures and measures for various maneuvers

Maneuvers	Performance Signatures (or Operating Condition)	Performance Measures
Steady Turning		
a. Roll	Lateral acceleration versus roll angle	Rollover threshold
b. Tracking	(360m radius at 88kph)	Offtracking
c. Handling	Handling diagram (22,6) and critical speed versus lateral acceleration (23)	1. Steering gain at 80kph 2. Critical speed at 0.3g
Constant Deceleration Stopping	Friction utilization and deceleration versus pressure	Braking efficiency at 0.4g
Low-speed Cornering (In-Town Corner)	(12.3m radius, 90° corner)	Maximum offtracking
Transient Turning (Ramp-Step Steer)	Steering wheel angle (200°/s to 28°)	Lateral acceleration response times (50% steering to 90% of steady state)
Obstacle Evasion (Rearward Amplification)	Transfer function: lateral acceleration of last unit to that of the first unit	Maximum rearward amplification (steering frequency < 0.5Hz
Responding to External Disturbances	Transfer function: steering control to equivalent disturbance input	Maximum closed-loop steering gain
Braking in a Turn	(2s braking pulse while following a 360m turn at 80kph)	Open-loop: maximum changes in yaw rate and sideslip Closed-loop: deviation from a reference yaw rate

independent of the instantaneous position or path of the vehicle. Constant acceleration maneuvers are inherently of this type. Transient maneuvers may have either open- or closed-loop versions. In this case, the ramp-step and low-speed cornering maneuvers are treated in an open-loop fashion. Obstacle evasion and braking in a turn are investigated using both open- and closed-loop analyses, and the response to external disturbances is studied through closed-loop calculations.

Open-loop results serve to define the accident-avoidance capabilities of the vehicles. In this study, a driver representation(24) is used to steer the vehicles to attempt to follow preselected paths in simulated closed-loop situations. These closed-loop analyses aid in understanding the influences of open-loop vehicle properties on the predicted performance of the driver/vehicle system.

Performance Signatures and Measures

Steady Turning

Roll

Equilibrium values of roll angle are a function of lateral acceleration, as illustrated in Figure 1. This performance signature has a discontinuity in slope at the point (0.36g) where the semitrailer's inside wheels lift off the ground. The maximum value of lateral acceleration, the rollover threshold, occurs at 0.39g when the tractor's inside rear wheels lift. Above 0.08rad of roll angle, the slope of the curve (lateral acceleration versus roll angle) becomes negative, indicating points of unstable equilibrium.

The roll performance signatures of vehicles with full trailers include additional acceleration versus roll angle curves for each full trailer. Nonlinear spring characteristics

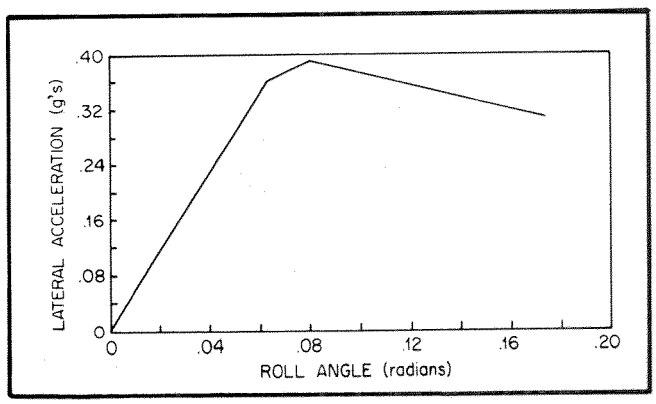

Figure 1. Roll performance signature

and free play when leaf springs go into tension cause more complicated-looking characteristics than those shown in Figure 1. Nevertheless, the rollover threshold is readily identified as the maximum attainable level of lateral acceleration before rollover of any unit of the vehicle.

The first row of Table 3 provides first-order estimates of the rollover thresholds of fully laden versions of various types of articulated commercial vehicles commonly employed in the United States. (Table 4 presents prototypical values of fundamental parameters describing the basic vehicles.) In addition to the ratio of center of gravity (c.g.) height to track width, these estimates are influenced by those conditions that allow the c.g. of the sprung mass to translate laterally—specifically, low suspension roll rates, free play, and low roll center heights(9). Accident data have been used to show that small changes in rollover threshold can have a large influence on the number of rollover accidents for heavy vehicles having values of rollover thresholds in the vicinity of those given in Table 3(10).

Tracking

Ideally, the trailing units in an articulated vehicle would be expected to follow exactly the path of the front axle of the towing unit. Practical vehicles come close to achieving this type of performance at highway speeds on highway curves. However, small deviations from the path of the front axle have caused trailer wheels to strike curbs and other roadside obstacles and thereby precipitated rollovers or control difficulties. Recognition of this danger has prompted the recommendation of a tracking test(21).

For a given length of vehicle, low-speed maneuverability is enhanced by adding articulation points. The addition of articulation points will greatly reduce low-speed offtracking. However, this improvement in low-speed offtracking contributes directly to the amount of outboard offtracking at high speed.

A specific turn has been selected as being representative of a high-speed exit ramp. The simulated maneuver is performed at a velocity of 88km/h (55mph) on a flat turn with a radius of 360m (1,200ft). The outboard offtracking attained by the end of the last trailer has been selected as the performance measure.

Figure 2 is a parameter sensitivity diagram showing the influences of (a) the cornering stiffnesses of the tires, and (b) the wheelbase of the third trailer on the high-speed offtracking of a typical triple combination employing 8.1m (27ft) trailers. The abscissa values of +1 and -1 represent deviations from the baseline values of wheelbase and cornering stiffness. These deviations are equal to ±½ of their baseline values. At low speed, the offtracking on a

Table 3. Summary of performance measures for basic vehicles

	Tractor-Semi 3-S2	Truck-Full Trailer 3-2	Double 2-S1-2	Triple 2-S1-2-2
1. Rollover Threshold (g's)	0.385	0.410	0.404	0.404
2. High-speed Offtracking (m)	0.22	0.411	0.411	0.582
3. Critical Speed at 0.3g (kph)	Nonexistent	Nonexistent	130	130
4. G-Level at Neutral Steer. 50mph	Axle lifts first	0.388	0.328	0.328
5. Braking Efficiency at 0.4g (Loaded)	0.88	0.77	0.78	0.80
(Empty)	0.59	0.50	0.55	0.61
6. Maximum Transient Offtracking (m)	4.29	2.88	3.48	4.74
7. Lateral Acceleration Response Time (sec)	0.80	0.79	0.98	0.98
8. Maximum Rearward Amplification	1.08	2.03	2.07	2.96

Table 4. Fundamental parameters for the basic vehicles

	Tractor-Semitrailer	Truck-Full Trailer	Doubles
Tractor or Truck	3-S2	3-2	2-S1-2
weight (Newtons, N)	69,000	187,000	59,000
c.g. height (meters, m)	0.88	1.62	0.95
front axle to c.g., m	1.54	4.48	1.08
c.g. to rear suspension center	2.11	1.44	2.28
c.g. to hitch (5th wheel)	1.75	4.14	2.3
total cornering stiffness, N/deg	21,300	20,200	12,900
brake gain per front brake, Nm/Pa	779.	779.	779.
brake gain per rear brake, Nm/KPa	1169.	1169.	1169.
Semitrailer			
weight, N	287,000		141,000
c.g. height, m	1.99		1.99
5th wheel to c.g., m	5.78		3.52
c.g. to rear suspension center, m	5.19		2.88
c.g. to rear hitch, m	6.10		3.79
total cornering stiffness, N deg	16,700		8,500
brake gain per brake, Nm/KPa	1169.		1169.
Full Trailer			
weight, N		169,000	156,000
c.g. height, m		1.87	1.92
front axle to c.g.		2.82	3.20
c.g. to rear axle, m		2.82	3.20
c.g. to rear hitch		3.74	4.11
total cornering stiffness, N.deg		17,500	16,900
brake gain per brake, Nm/KPa		1169.	1169.

Note: The triple (2-S1-2-2) is the same as the double except that it has another full trailer

360m (1,200ft) radius turn would be 0.19m (0.62ft) toward the inside of the turn. As speed is increased, the offtracking decreases to zero and then increases toward the outside. The basic triple is predicted to track more than .57m (1.9ft) outboard in a maneuver requiring 0.17g at 88km/h (55mph).

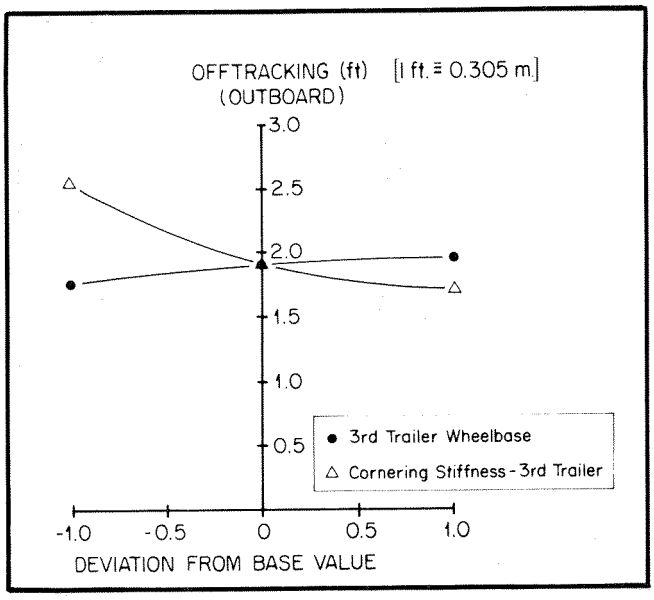

Figure 2. High-speed offtracking, parameter sensitivity diagram

The +1 value of deviation represents the cornering stiffness typical of radial tires, the 0 value corresponds to bias-ply tires, and -1 represents lug-type tires. Although lug tires are not usually used on trailers, the parameter sensitivity diagram shows the adverse effect of low cornering stiffness.

The triple tracks outboard of the double by an amount equal to the contribution of a full trailer since the double and triple are made up of identical units. The triple has by far the largest offtracking among the basic vehicles (see the second row of Table 3).

Handling

In this context (i.e., steady turning), handling refers to the response of the towing unit to steering inputs. Handling diagrams(22) (see Figure 3a) have been constructed at 80km/h (50mph) to obtain performance signatures. The handling diagram contains a handling curve that displays steady-turning properties as a function of lateral acceleration, yaw rate, forward velocity, and a reference front-wheel angle (in this case, steering-wheel angle divided by steering-gear ratio).

Vehicles with tandem axles on the tractor or the first semitrailer do not have a unique handling curve applicable at all speeds(6). However, vehicles without tandem axles do have special handling diagrams analogous to those

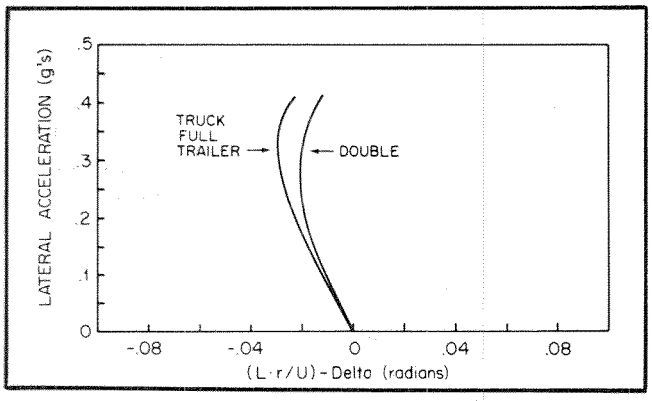

Figure 3a. Handling diagram

used in the study of passenger cars. Figure 3a contains handling curves for a truck-full trailer and a double combination. The handling curve for the double is applicable to all speeds since this double has single-axle suspensions. The truck in the truck-full trailer combination has tandem axles at the rear of the truck. For the truck-full trailer, the handling curve only applies at 80km/h (50mph) because, due to the tandem axles, the effective wheelbase changes with velocity(6). The wheelbase used in Figure 3a is the distance from the front axle to the center of the rear suspension of the towing unit (i.e., the truck).

In the handling diagram, an oversteer condition is indicated by a positive slope of the handling curve. For vehicles that become oversteer at lateral acceleration levels below their rollover thresholds, critical speeds have been computed. For these vehicles, a stability boundary can be plotted in a space defined by critical speed and lateral acceleration (see Figure 3b). This stability boundary is a special type of performance signature that provides an indication of the conditions under which the driver has to control an unstable vehicle.

For the baseline vehicles, the results indicate that all of them remain stable at speeds up to 88km/h (55mph) and lateral acceleration levels below 0.3g. The third row of Table 3 lists the critical speeds obtained at 0.3g of lateral acceleration. The fourth row indicates the lateral acceleration levels at which the vehicles become neutral steer while traveling at 80km/h (50mph).

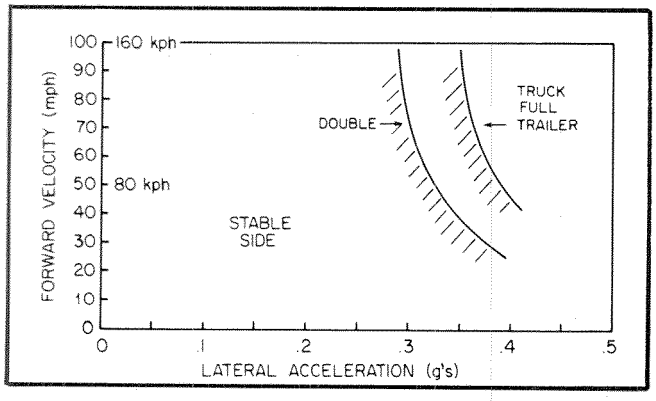

Figure 3b. Critical speed versus acceleration

For vehicles with full trailers, the handling results are similar to those that would have been obtained if the full trailers had been removed. That is, conventional dollies nearly decouple the full trailer from the unit towing it because the lateral force at the pintle hitch is very small compared to the tire forces acting on the towing unit(14). For example, the handling results for the double and triple are practically identical to those obtained if only the tractor-semitrailer portion of these vehicles were to be analyzed. (The handling results for the double and triple are also identical to each other since these vehicles employ the same tractor-semitrailer as their towing unit.)

At turning levels above 0.15g, lateral load transfer has an important influence on truck tire characteristics. The curvature of tire cornering stiffness with respect to vertical load becomes especially important for the drive axles of the lead unit since a large portion of the lateral load transfer takes place at these axles on typically suspended heavy vehicles in the United States. Given a bias in roll stiffness distribution, the level of oversteer at high g levels depends to a large extent on the curvature of the tire characteristics. The results presented here are for vehicles with typical bias-ply truck tires, having a moderate amount of curvature in their characteristics. However, sudden transitions to large oversteer may take place for tires with considerable curvature in the relationship between cornering stiffness and vertical load.

Constant Deceleration Braking

The performance signature selected for constant deceleration braking is a family of curves (one for each axle) showing the friction, required to avoid wheel lock, displayed as a function of treadle pressure (see Figure 4). Also superimposed on this plot is a graph of deceleration

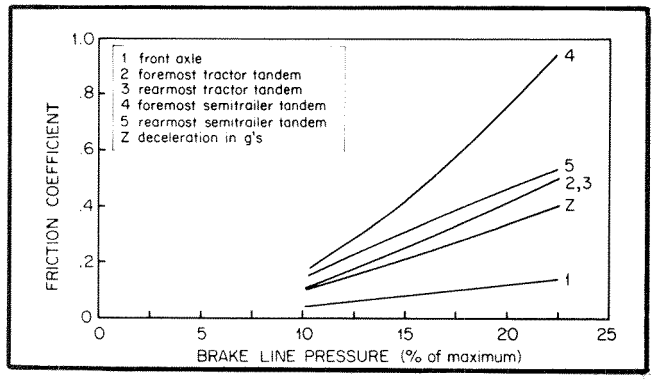

Figure 4. Friction utilization and deceleration, empty tractor-semitrailer (interaxle load transfer for the semitrailer's tandem equal to 20 percent of the braking torque divided by the tandem spread

in g's versus treadle pressure. Braking efficiency is the ratio of deceleration divided by the highest required friction coefficient (i.e., the results for axle 4 in Figure 4). The braking efficiency at 0.4g has been used to provide the performance measures listed in row 5 of Table 3. These results indicate that empty heavy vehicles have braking efficiencies that are less than 0.6.

In the example shown in Figure 4, the brake torque acting on the tandem suspension of the tractor does not cause interaxle load transfer. Hence, the curves labeled 2 and 3 coincide in Figure 4. Curves 4 and 5 do not coincide because, in this example, a significant amount of load is transferred from axle 4 to axle 5 during braking. The effect of this interaxle load transfer is to reduce the braking efficiency at 0.4g from 0.59 for a vehicle without interaxle load transfer to 0.43 for a vehicle with a semitrailer whose tandem suspension has a large amount of interaxle load transfer (for American suspensions).

Transient Maneuvers

Tractrix

The term tractrix pertains to the path of the axles of a semitrailer while it is turning a corner at low speed. To evaluate transient offtracking at low speed, articulated heavy vehicles are treated as a train of semitrailers in which the path of each hitch is the general curve followed by the attached semitrailer.

The trajectories (tractrices) of the various axle sets of a truck-full trailer are shown in Figure 5. The center of the steering axle is assumed to follow a 90° turn with a radius of 12.3m (41ft). The rear axles of the truck are treated as a single axle. The dolly axle does not offtrack far from the path of the truck's rear axle (see Figure 5). The rear axle

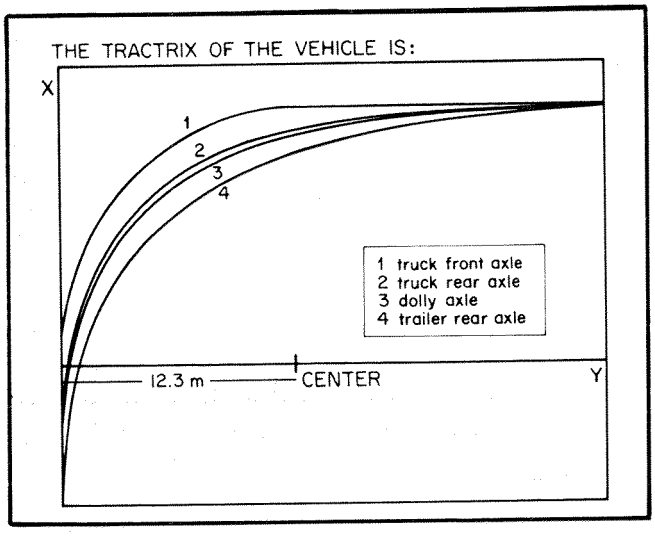

Figure 5. Tractrices for a truck-full trailer

of the trailer has a maximum inboard offtracking of 2.9m (9.6ft), which occurs when the rear axle has turned through 59°.

The maximum offtracking of the rear of the last unit has been used to quantify low-speed turning performance of the prototypical vehicles (see Table 3, row 6).

Ramp Step Steer

This maneuver is used to establish the quickness of the lateral acceleration response of the first unit in a combination vehicle. Response times are measured between the time when a rapid steering input reaches 50 percent of its final value and the time when the lateral acceleration response reaches 90 percent of its steady-state value. The magnitude of this response time depends on vehicle loading, speed, and the amplitude of the steering input. The results given in Table 3, row 7, are for low-amplitude steering-wheel inputs (28°) applied to fully laden vehicles traveling at 80km/h (50mph) on high-friction surfaces. The response times of the basic vehicles range from 0.79 to 0.98s.

The lateral acceleration response time is believed to relate to the manner in which drivers correct for external disturbances. A computational method, similar to one used in vehicle testing(25), has been developed by MacAdam(26) for assessing closed-loop response to external disturbances. Results from these computations for the basic vehicles indicate that drivers, represented by a delay time of 0.25s and a preview time of 1.5s, will increase the magnitude of the influences of external disturbances, occurring at approximately 3rad/s, by a factor of approximately 2. These results are sensitive to driver-control characteristics (delay time and preview time). Shorter delay times and/or longer preview times will reduce the gain of the closed-loop response.

Obstacle Evasion

The obstacle-evasion maneuver is based on traffic conflicts in which another vehicle stops or suddenly pulls out in the path of a heavy truck. The truck driver is assumed to attempt to avoid a collision by suddenly swerving into another lane. Vehicle performance in this type of situation depends on the period of the maneuver and the forward velocity of the vehicle. Quick maneuvers, in which the major steering activity occurs within 2s, have been found to excite amplified responses at the last units of combination vehicles with full trailers(15).

These amplified responses, referred to as rearward amplification, have been studied in both time and frequency domains. The frequency domain approach has been found to be effective because (1) the worst frequency, the one causing maximum amplification, can be readily observed, and (2) the magnitude of the amplification

determined by linear methods has proven to be a good indicator of the magnitude of amplification predicted by nonlinear analyses(15).

Rearward amplification not only has tracking or swept-path implications, it also indicates situations in which full trailers with high c.g. loads are likely to roll over. Since the rollover threshold is expressed in terms of lateral acceleration, the ratio of the lateral acceleration of the last unit divided by the lateral acceleration of the first unit of a combination vehicle has been used to quantify rearward amplification. In the frequency domain, this ratio is displayed as the amplitude of the transfer function between the motion of the c.g. of the towing unit and the motion of the c.g. of the last unit (see Figure 6). The maximum value of this transfer function has been selected as a performance measure for this maneuver.

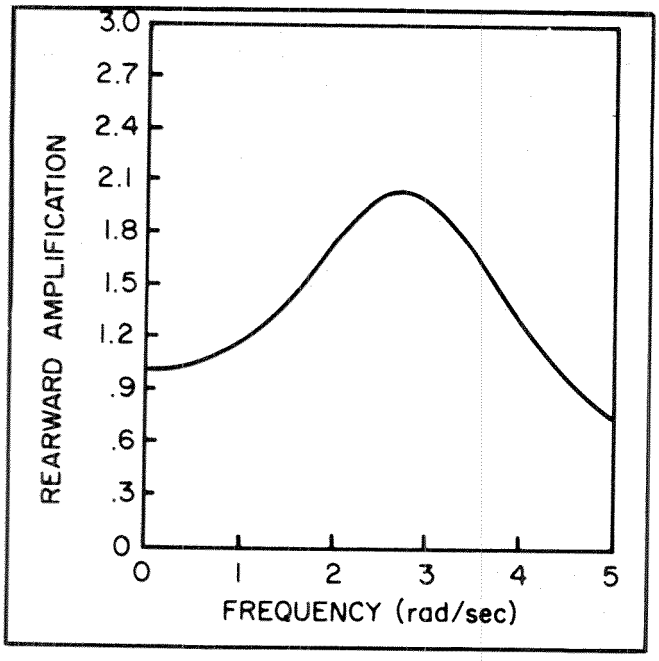

Figure 6. Rearward amplification for a basic U.S. double

The results, given in row 8 of Table 3, indicate that tractor-semitrailers have small amounts of rearward amplification compared to vehicles with full trailers. To first approximation, rearward amplification is a cumulative property consisting of the product of transfer functions between (a) unit c.g.'s and hitch points, and (b) hitch points and unit c.g.'s from the front to the rear of the vehicle(27,5). Hence, vehicles with more units tend to have higher amplifications.

For example, the basic triple is obtained by adding a full trailer to the basic double. The rearward amplification of the triple is approximately equal to the rearward amplification of the double multiplied by (a) the transfer function from the c.g. of the first full trailer to the pintle hitch between the first and second full trailers, and (b) the transfer function from that pintle hitch to the c.g. of the last full trailer(5). The rearward amplification of the triple exceeds that of the double by a multiplicative factor that depends primarily on where the last pintle hitch is located, the length of the last trailer, and the ratio of the weight of the last trailer divided by the sum of the cornering stiffnesses of all of the tires installed on the last trailer(5).

Sensitivity analyses have shown that rearward amplification may be reduced significantly by (a) reducing speed (the results given here are at 80km/h (50mph)), (b) increasing the wheelbases of full trailers, (c) reducing the distance from the center of gravity of a unit to the pintle hitch installed at the rear of that unit, and (d) increasing the cornering stiffnesses of the tires.

To produce a closed-loop version of the obstacle-evasion maneuver, a path is selected to represent the choice made by the driver in an attempt to avoid the obstacle. Driver-controlled path following is then used in the simulations(24). Preliminary results for a maneuver in which the driver attempts to suddenly translate the basic double by a lateral distance of 1.2m (4ft) while traveling at 80km/h (50mph) show a rearward amplification of approximately 1.5 if the driver has a 2s preview and is allowed an additional 2s (a total of 4s) for completing the 1.2m (4ft) displacement. However, the last unit will not experience more than 0.1g of lateral acceleration in this case where the driver can use a long preview time. If the preview is shortened to 1.0s and the total time for clearing the obstacle is 1.6s, corresponding to a maximum lateral acceleration at the tractor of 0.27g, the lateral acceleration of the last unit exceeds 0.7g during the rollover of the last trailer. These closed-loop results are interpreted to mean that rearward amplification is not a problem if the driver can foresee the obstacle to be avoided. However, if drivers are forced to take emergency evasive actions to resolve traffic conflicts at highway speeds, fully laden (high c.g.) full trailers are likely to roll over.

Braking in a Turn

Combined braking and steering maneuvers are difficult to control on a poor, wet road. When braking is applied while turning, the driver may lose directional control momentarily or wheels on individual axles may lock up, leading to jackknifes or trailer swings.

From an analytical point of view, braking in a turn is difficult to treat because it involves all the dynamic modes of vehicle motion. The tires are required to produce both longitudinal and lateral force. On even moderately slippery surfaces, demand for high deceleration may result in a lack of side force. The critical levels of performance, where loss of control may occur, are significantly altered by many vehicle characteristics. The interaction between longitudinal and lateral tire forces is

clearly critical, but data describing the influences of longitudinal slip on lateral force and slip angle are not generally available.

Not only are the basic results difficult to predict, but suitable performance signatures and performance measures are difficult to select. In open-loop testing, the disturbances in yaw rate and sideslip shortly after braking have been used to quantify the magnitude of the directional control problem presented to the driver(28,29).

Closed-loop results have been predicted for vehicles equipped with antilock brakes(30). In that situation, the simulated driver does not need to modulate brake pressure. However, information is not available to use in predicting how drivers will modulate brake pressure when the vehicle does not have an antilock system.

Currently, our plans are to perform open-loop calculations for empty and fully laden vehicles turning at 0.11g at 80km/h (50mph) on poor, wet roads (skid number at 65km/h is 28). (See (30) for a discussion of tire properties applicable to turning and braking on a poor, wet road.) The maximum deviations in yaw rate, sideslip angle, and articulation angles (where appropriate) will be used to quantify the influences of the disturbances caused by braking. The brakes will be applied suddenly and fully. At the end of 2s from the initiation of braking, the brake pressure will be released. The maximum deviations occurring (a) when the brakes are applied and (b) after the brakes are released will be used as performance measures.

Given the above braking disturbance, closed-loop simulations will also be run to study driver/vehicle system performance during braking in a turn. If the results of these calculations (both open- and closed-loop) are significant, they will be included in the previously mentioned vehicle dynamics handbook.

Conclusion

The constraints that vehicle characteristics place on the obstacle-avoidance capabilities of the driver/vehicle system have been evaluated using performance measures derived from computations based on open-loop maneuvers (see Table 2). Closed-loop calculations are now being used to examine control difficulties that may develop in obstacle-avoidance situations.

These results provide information that should necessarily be considered by persons specifying and assembling articulated commercial vehicles. However, these results are not sufficient in themselves to provide the guidance needed to assemble a satisfactory combination vehicle.

In particular, two further steps need to be taken. First, a synthesis procedure is needed to define the sequence of choices (priorities) so the vehicle will satisfy its functional requirements—for example, low-speed maneuverability in small areas. Second, guidance is needed to aid in deciding the tradeoffs between conflicting performance requirements.

The two main areas in which tradeoffs are required are (1) compromises between high- and low-speed tracking, and (2) the choice between longitudinal and lateral force capability in combined braking and steering maneuvers. With regard to tracking, the addition of articulations within a given overall length can increase overall maneuverability, but it also increases high-speed offtracking and rearward amplification. In combined braking and turning, truck brakes in the United States have traditionally been able to override the lateral force potential of all tires except those on the front axle. The driver is expected to steer out of difficulties although it may be difficult or nearly impossible to avoid jackknifing on slippery surfaces.

Adjustable or adaptive components are being developed to resolve situations that currently require compromises and tradeoffs. For example, antilock braking systems have been and are being perfected. Also, new types of dollies are being considered. Ideally, these dollies would change their characteristics depending on vehicle speed and the type of maneuver the driver wants to perform. If properly developed, these automatic systems will aid the driver in avoiding control difficulties while, at the same time, not limiting the driver's abilities and responsibilities for safe vehicle operation.

References

1. NHTSA Contract DTNH-22-83-C-07187, "An evaluation of the factors influencing heavy truck dynamic performance," Contract Technical Manager: W. Leasure.
2. Maillikarjunarao, C., "Road tank design: its influence on the risk and economic aspects of transporting gasoline in Michigan," Ph.D. Thesis, The University of Michigan, 1982.
3. Mallikarjunarao, C., R.D. Ervin, and L. Segel, "Roll response of articulated motor trucks during steady-turning maneuvers," ASME Winter Annual Meeting, November 1982.
4. Bernard, J.E., and M. Vanderploeg, "Static and dynamic offtracking of articulated vehicles," SAE Paper 800151, 1980.
5. Fancher, P.S., et al., "Tracking and stability of multi-unit truck combinations," University of Michigan Transportation Research Institute, Report No. UMTRI-84-25, July 1984.
6. Fancher, P.S., "The static stability of articulated commercial vehicles," *Vehicle System Dynamics*, Vol. 14, 1985.
7. Ervin, R.D., et al., "Effects of tire properties on truck and bus handling," Final report, Contract No. DOT-HS-4-00943, Highway Safety Research Institute,

University of Michigan, Report No. UM-HSRI-76-11, December 1976.
8. Ervin, R.D., et al., "The yaw stability of tractor-semitrailers during cornering," Final report, Contract No. DOT-HS-7-01602, Highway Safety Research Institute, University of Michigan, Report No. UM-HSRI-79-21, June 1979.
9. Winkler, C.B., P.S. Fancher, and C.C. MacAdam, "Parametric analysis of heavy duty truck dynamic stability," Final report, Contract No. DTNH-22-80-C-07344, University of Michigan Transportation Research Institute, Report No. UMTRI-83-13, March 1983.
10. Ervin, R.D., et al., "Influence of size and weight variables on the stability and control properties of heavy trucks," Final report, Contract No. FH-11-9577, University of Michigan Transportation Research Institute, Report No. UMTRI-83-10, May 1983.
11. Segel, L., et al., "Mechanics of heavy-duty trucks and truck combinations," University of Michigan Engineering Summer Conference, June 13-17, 1983.
12. Morrison, W.R.B., "A swept path model which includes tyre mechanics," Proceedings 6th Conference of the Australian Road Research Board, Vol. 6, Part 1, Canberra, 1972.
13. Sayers, M.W., "Vehicle off-tracking models," Symposium on Geometric Design for Large Trucks, Transportation Research Board, Denver, Colorado, August 1985.
14. Ervin, R.D., et al., "Ad hoc study of certain safety-related aspects of double-bottom tankers," Final report to Michigan State Office of Highway Safety Planning, Report No. UM-HSRI-78-18, May 7, 1978.
15. Mallikarjunarao, C., and P. Fancher, "Analysis of the directional response characteristics of double tankers," SAE Paper 781064, December 1978.
16. MacAdam, C.C., et al., "A computerized model for simulating the braking and steering dynamics of trucks, tractor-semitrailers, doubles, and triples combinations—users' manual," Final Report MVMA Proj. 1197, Highway Safety Research Institute, University of Michigan, Report No. UM-HSRI-80-58, September 1, 1980.
17. Gillespie, T.D., et al., "Truck and tractor-trailer dynamic response simulation—T3DRS," Final report, Contract No. FH-11-9330, Highway Safety Research Institute, University of Michigan, Report No. UM-HSRI-79-38, March 1979.
18. Bernard, J.E., C.B. Winkler, and P.S. Fancher, "A computer-based method for predicting the directional response of trucks and tractor-trailers," Phase II report, Highway Safety Research Institute, University of Michigan, Report No. UM-HSRI-PF-73-1, June 1, 1973.
19. Mischke, et al., "Contribution to the development of a concept of driving mechanics for commercial vehicles," Daimler Benz AG, SAE Paper 830643, 1983.
20. Rompe, K., and B. Heissing, "Methods of objective description of the handling characteristics of heavy commercial vehicles," XXth FISITA Congress, May 1984.
21. Nordstrom, O., and S. Nordmark, "Test procedures for the evaluation of the lateral dynamics of commercial vehicle combinations," *Automobil-Industrie*, Edition 2, June 1978.
22. Pacejka, H.B., "Simplified analysis of steady-state turning behaviour of motor vehicles," *Vehicle System Dynamics*, 2pp. 161-183, pp. 185-204, 1973.
23. MacAdam, C.C., "A computer-based study of the yaw/roll stability of heavy trucks characterized by high centers of gravity," SAE Transactions, Vol. 91, SAE No. 821260, 1983.
24. MacAdam, C.C., "Application of an optimal preview control for simulation of closed-loop automobile driving," *IEEE Transportation on Systems, Man, and Cybernetics*, Vol. SMC-11, No. 6, pp. 393-399, 1981.
25. McRuer, D.T., et al., "Measurement of driver/vehicle multiloop response properties with a single disturbance input," *IEEE Transportation on Systems, Man, and Cybernetics*, Vol. 5, No. 5, 1975.
26. MacAdam, C.C., "Frequency domain methods for analyzing the closed-loop directional stability and maneuverability of driver/vehicle systems," International Conference on Modern Vehicle Design Analysis, London, 1983.
27. Fancher, P.S., "The transient directional response of full trailers," SAE Paper 821259, 1982.
28. Uffelmann, F., "Steering behaviour of motor vehicles under braking," 2nd Course on Advanced Vehicle System Dynamics, International Center for Transportation Studies, Amalfi, Italy, May 28-June 1, 1984.
29. Rompe, K., "Vehicle handling characteristics during braking in a turn," Proceedings Eighth International Technical Conference on Experimental Safety Vehicles, Wolfsburg, October 1980.
30. Fancher, P.S., "Integrating antilock braking systems with the directional control properties of heavy trucks," International Conference on Antilock Braking Systems for Road Vehicles, Institute of Mechanical Engineers, Oxford, England, September 1985.

Test Procedures and Evaluation Criteria for the Handling Characteristics of Heavy Commercial Vehicles

Klaus Rompe and
Bernd Heißing
Institute for Traffic Safety, TÜV Rheinland e.V., Cologne, Federal Republic of Germany

Abstract

In the years past, quite a number of relevant test procedures, including appropriate criteria of description, have been conceived to describe objectively the handling characteristics of passenger cars and passenger car-trailer combinations. Because of the various design principles of commercial vehicles and the ever-increasing advances of vehicle combinations insuring optimum utilization of space, i.e., single trucks or buses, truck-trailer combinations, semitrailer combinations, articulated buses, platform road trains, and short coupling truck combinations, the handling characteristics of these vehicles are definitely more distinct from each other. A description of the handling characteristics as compared with existing designs will be of great importance to the classification of new vehicle combinations. This paper gives a survey of the measuring procedures applied so far and the findings as published on the handling characteristics of heavy commercial vehicles. This approach is compared with measurements taken by the authors for a 16t truck[1], a 38t truck-trailer combination, and a special type 38t semitrailer combination. Against this background, the transferability of the test procedures, which have previously been applied to passenger cars only, and the required restrictions under their application to heavy commercial vehicles is illustrated and evaluated on the basis of the measurement results obtained. Any measuring variables and criteria of description that are of significance to this particular class of vehicles are detailed.

Current Status of Test Procedures

The registration regulations as applicable to commercial vehicles are specifying requirements to be accommodated by mainly two areas of the handling characteristics complex, viz., straight line braking and mobility in turning. Since these procedures have been applied for quite a long time, they will not be treated further in this paper. The examples detailed in the sections to follow are rather related to the lateral dynamics and the combined lateral and longitudinal dynamics of heavy commercial vehicles.

[1] In charge of the German Federal Minister of Transport

Table 1 is a survey of the measurement results available in the literature on the driving behavior of heavy commercial vehicles throughout the past decade. From this, it can be gathered there are basically five eligible test procedures:

1. Steady state turning to determine the understeer/oversteer behavior as a function of lateral acceleration or driving speed.
2. Braking during steady state turning to determine the yaw stability and steerability.
3. Lane change to determine the steering effort and the effect of a lane change as an excitation function for yaw angle oscillations.
4. Step steering input to determine the promptness of vehicle response.
5. Frequency response measurement to determine the extent and promptness of vehicle response as a function of the steering angle input.

Figure 1 shows the required measuring variables illustrated by the example of a truck-trailer combination. There is evidence that the standard variables referring to the towing vehicle such as steering angle, driving speed, lateral and longitudinal acceleration, and yaw velocity are needed and so are corresponding measuring variables referring to further elements of the combination and the relative yaw angles at the different joints or couplings.

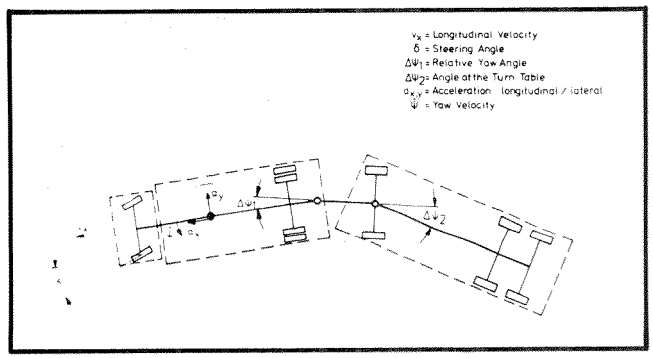

Figure 1. Commercial vehicle measuring variables

Steady State Turning

Steady state turning is to provide data on the steering tendency, i.e., on the driving course as a function of steering angle and lateral acceleration. The conditions for implementation relating to passenger cars are specified in an ISO standard(22).

Figure 2 illustrates the characteristic curves of a steering angle increase over the lateral acceleration

Table 1. Measurements of driving behavior of heavy commercial vehicles

Test Procedure	Vehicle, Mass		Author			
	Double Decker Bus	13t	Rompe		1971	[1]
	Truck-Trailer Comb.		Nordström		1977	[2]
	Bus	11t, 16t	Benedek	et al.	1978	[3]
Steady State	Truck	16t-22t	Falkner	et al.	1978	[4]
	Special-Type Tank Truck Comb.		Winkler	et al.	1978	[5]
	Semitrailer Comb.	26t, 38t	Emery		1980	[6]
Turning	Truck	8t-19t	Krisper	et al.	1981	[7]
	Semitrailer Comb.	10t, 36t	Burg		1981	[8]
	Truck-Trailer Comb.	8t-38t	Gauß	et al.	1982	[9]
	Truck-Trailer Comb.	8t-38t	Heißing	et al.	1982	[10]
	Special-Type Semi-trailer Comb.	40t	Heißing		1982	[11]
	Truck-Trailer Comb.	8t, 12t	Alberti		1983	[12]
	Semitrailer Comb.	38t	Helber	et al.	1984	[18]
	Semitrailer Comb.	10t, 25t	Itami	et al.	1974	[13]
Braking during	Semitrailer Comb.		Fancher		1975	[14]
Steady State	Semitrailer Comb.	10t, 36t	Burg		1981	[8]
	Truck-Trailer Comb.	8t-38t	Heißing		1982	[10]
Turning	Special-Type Semi-trailer Comb.	40t	Heißing		1982	[11]
	Articulated Bus	16t-27t	Bruns	et al.	1984	[19]
	Semitrailer Comb.	38t	Gauß	et al.	1973	[15]
	Truck-Trailer Comb.		Nordström		1977	[2]
Lane	Special-Type Tank Truck Comb.		Winkler	et al.	1978	[5]
	Truck	16t-22t	Falkner	et al.	1978	[4]
Change	Truck	8t-19t	Pilz	et al.	1981	[16]
	Truck	8t-38t	Gauß	et al.	1982	[9]
	Special-Type Semi-trailer	40t	Heißing		1982	[11]
	Articulated Bus	16t-27t	Bruns	et al.	1984	[19]
	Bus, Truck		Weir	et al.	1974	[20]
Step Steering	Bus		Bisimis		1978	[17]
	Bus	11t, 16t	Benedek	et al.	1978	[3]
	Truck	8t-19t	Pilz	et al.	1981	[16]
Input	Truck-Trailer Comb.	12t	Alberti		1983	[12]
	Semitrailer Comb.	38t	Helber	et al.	1984	[18]
	Semitrailer Comb.	38t	Gauß	et al.	1973	[15]
Frequency	Bus		Bisimis		1978	[17]
	Bus	11t, 16t	Benedek	et al.	1978	[3]
Response	Semitrailer Comb.	38t	Helber	et al.	1984	[18]
Measurement	Truck-Trailer Comb.	8t-38t	Hamann		1984	

expressed as the difference between the steering angle δ_H minus the steering angle needed to drive on a circular path at the smallest lateral acceleration $\delta_{H,Ack}$. This variable, also known as understeering index, permits turning maneuvers on different but constant radii to be illustrated together. While the understeering tendency is distinct for all the loaded single vehicles illustrated in the upper part of the figure, it was found to be comparatively small for individual trucks. Besides, Figure 2 shows that a trailer will not always bring about a significant change in steering characteristics. The handling characteristics are rather governed by both the steering characteristics and the yaw angles acting at the single joints.

Figure 3 illustrates the steering angle and side slip angle of the towing vehicle of a loaded 16 to 22t truck. Also illustrated are the yaw angles at the coupling point $\Delta_{\psi 1}$ and at the turn table $\Delta_{\psi 2}$. While the side slip angle of the towing vehicle increases with the lateral acceleration, the two yaw angles and hence the trailer's position to the towing vehicle remain almost constant. A deviation of

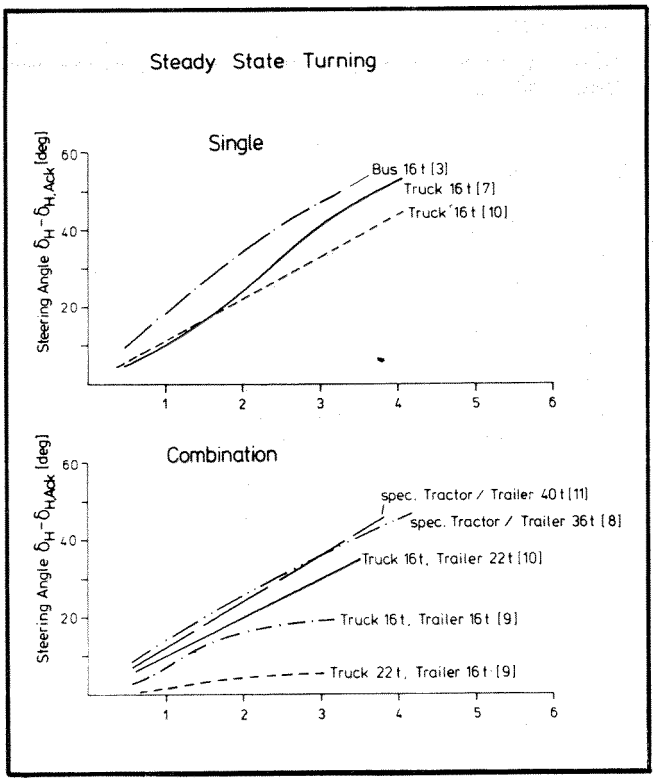

Figure 2. Steering angle increase — $\delta H - \delta H,Ack$ as a function of lateral acceleration a_y during steady state turning (all vehicles with maximum permissible weight)

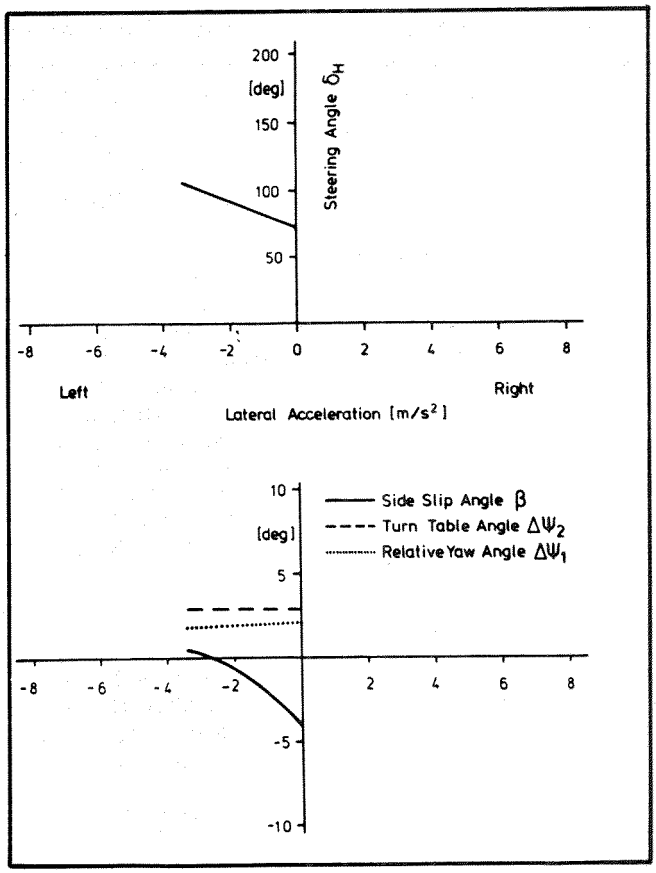

Figure 3. Steering angle, slide slip angle, yaw angle, and ring mount angle of a truck-trailer combination (38t) during steady state turning (truck with trailer), R = 105m, maximum permissible weight, dry road surface)(10)

the trailer from the circular path or a lateral displacement of the trailer was observed. This phenomenon is stated to be a criterion for the evaluation of steady state turning, e.g.,(2).

Another important criterion is the maximum physically obtainable lateral acceleration during turning. It is naturally highly dependent on the respective center-of-gravity height. Table 2 is a listing of maximum values, as measured by the various authors, for the vehicle types when driving on a dry road surface.

As loading in driving tests is generally of a low center-of-gravity height, for more practical purposes, the actual values are assumed to be slightly lower. One will see that the values obtained for single vehicles and combinations are in reasonable agreement and that the maximum physically obtainable lateral acceleration will in an average decrease under loading conditions by about $1 m/s^2$. When comparing these values with the values of modern passenger cars, one will find a lateral acceleration of 6.1 through $8.2 m/s^2$, which will decrease only slightly with increasing load(27).

Braking During Steady State Turning

The test procedure of braking during steady state turning was designed to yield information about the extent to which a vehicle's steering behavior is influenced by the simultaneous acting of braking forces. The criteria for evaluation are measuring variables that describe the

Table 2. Maximum lateral acceleration during turning on a dry road surface (7, 8, 9, 10, 20)

Maximum Physically Obtainable Lateral Acceleration			
Vehicle Type		unloaded	loaded
Bus		$4.7 m/s^2$	
Truck	16-22t	$4.4\text{-}4.5 m/s^2$	$3.6\text{-}4.2 m/s^2$
Truck-trailer Comb.	38t	$4.1\text{-}4.5 m/s^2$	$2.9\text{-}3.4 m/s^2$
Semitrailer Comb.	38t	$5.5 m/s^2$	$3.9\text{-}4.2 m/s^2$

capacity to keep the course, yaw stability, and steerability with distinct decelerations. The draft standard provided for passenger car braking during turning(23) has to be adapted for heavy commercial vehicles, especially in terms of starting conditions, because the physically obtainable lateral accelerations are lower during turning and deceleration takes more time to set in.

The time functions plotted in Figure 4 relating to yaw velocity Ψ, lateral acceleration a_y, side slip angle β, braking pressure p, and deceleration a_x were determined for a 16t truck with permissible total weight(10). With a mean deceleration, hardly any deviations were observed in comparison with a passenger car. Unlike this, the vibration of lateral acceleration was found to be distinct with great decelerations. This can be attributed to pronounced pitching motions resulting from the initiation of braking forces. This behavior of the truck tested persisted when it was coupled to a trailer.

The evaluation functions are established by deriving reference values from the time functions, which were measured in single tests at the respective deceleration levels. Such reference values are synchronous values obtained from the single tests, e.g., 1 or 2s after brake application over the respective deceleration. For minor variations in the starting conditions to be equalized, the yaw velocity and lateral acceleration are related to the original values, and the variation of the side slip angle as compared with the initial state is plotted. A reference curve is used for evaluation purposes. The underlying principle is that a vehicle will continue to travel exactly along the initial radius even after brake application and that deceleration and side slip angle will remain constant during the braking maneuver.

Figure 5 shows the evaluation function of the lateral acceleration for an unloaded 16t single truck, a loaded 16t and a 22t truck, and a special type 40t semitrailer combination with antilock system (ABS)(10,11). Experience has shown that an initial lateral acceleration of $2 m/s^2$ and an evaluation instant of 2s after brake application at an adequately high initial driving velocity are fit for the purpose. The lower half of the figure illustrates also the yaw angles at the coupling point $\Delta_{\psi 1}$ and the turn table $\Delta_{\psi 2}$ of the combination truck. The increasing locking tendency of the truck with increasing deceleration will result in growing yaw angles. With the towing vehicle nearing the limit of steerability, the decreasing yaw angles point to the almost straight position of the unit. In the ABS vehicle a control device will preclude this limit from being reached. This will lead to a minor increase of yaw angles between the elements of the combination when coming under the influence of

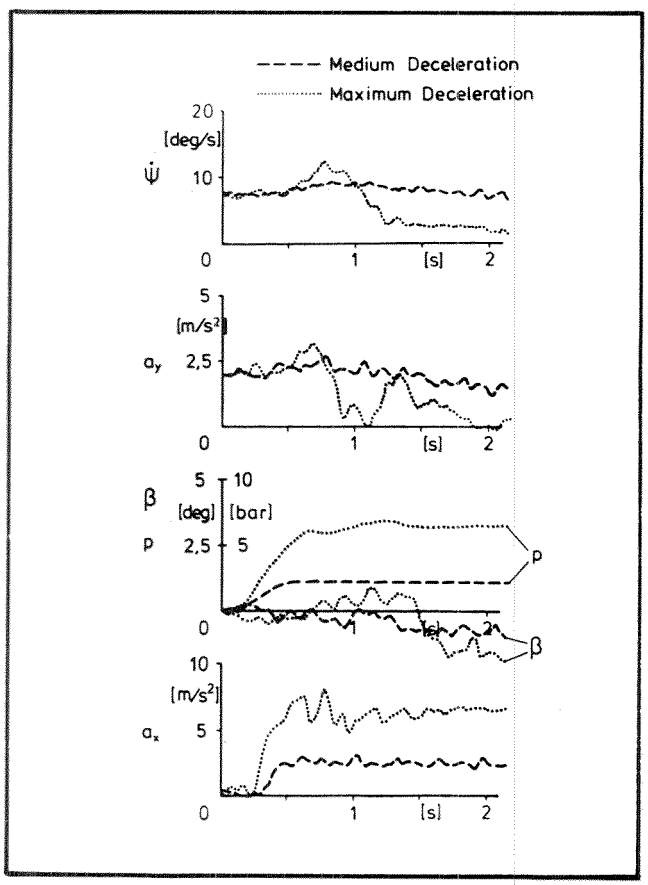

Figure 4. Time functions of characteristics measuring variables for braking during steady state turning ($a^{y,o}2m/s_2$, R = 105m, truck, drive road surface, maximum permissible weight)(10)

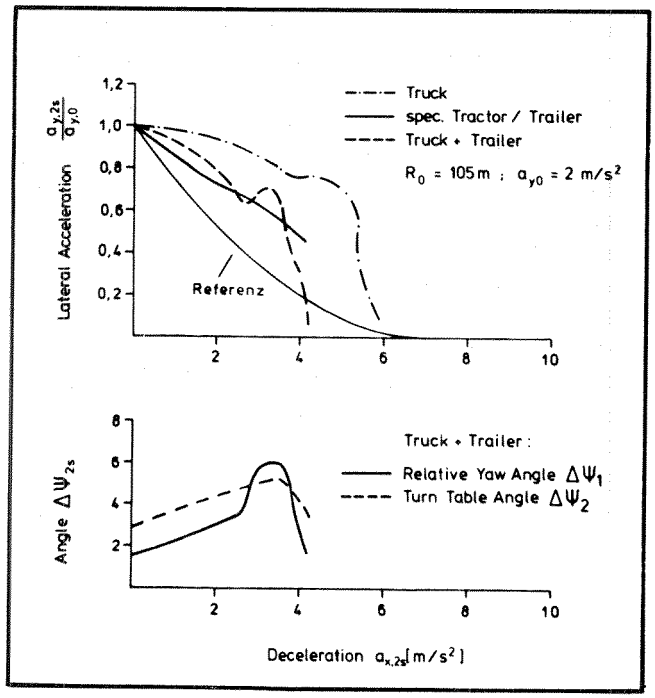

Figure 5. Comparison reference values for braking during steady state turning for a single truck, a truck-trailer combination (38t), and a special type semitrailer combination (40t) ($a^{y,o}$-2m/s_2, R = 105m, maximum permissible weight) (10,11)

great decelerations(11). Comparable trends of the evaluation function were established by (8) also. Although comparative tests have rarely been published so far, it can be assumed that Figure 5 is representing the likely range of evaluation criteria as valid for the vehicle category in question.

In view of the different response behavior of towing vehicles and trailers, it will be reasonable to incorporate in the analysis not only the evaluation functions but also the variation with time of the measuring variables 2s after initiation of braking.

Lane Change

This test procedure is applied to serve a dual purpose in the evaluation of handling characteristics of heavy commercial vehicles.

Evaluation of Transient Steering Behavior

The driving course chosen, e.g., by (4,16), is the dual ISO lane change(24), which is to be understood as a lane displacement of 3.5m over a distance of 30m. With this, the evaluation will cover the steering activity especially, i.e., the amount of required steering movements to be made by the driver to first keep to the lane and then to stabilize the vehicle.

Evaluation of the Damping Behavior of Combination Elements

In this test, which is based on a course similar to the ISO lane change, e.g., in the form of a single(9,11) or dual(2) lane change, the lane change will mainly serve to excite the combination's oscillation. The aim of the test procedure is to determine the damping of the yaw angles and the oscillation paths at the end of the trailer.

The measured values will therefore be recorded only after the lane has been changed and the vehicle is driven straight ahead again. A short steering angle impulse as applied for passenger car-trailer combinations will not suffice to generate an adequate oscillation energy in commercial vehicles(11).

Table 3 summarizes the maximum values obtained for different truck-trailer combinations, both loaded and unloaded, when driving on two road surfaces(9). The lane displacement was intended to be 3m over a distance of 40m. With no load or uniformly distributed load, the lateral movements of the trailer were established to be 1.5m on wet, antiskid asphalt pavement at a driving velocity of about 80km/h and on a less skidding blue basalt surface (moistened) at about 70km/h. When changing the lane at the highest possible velocity trailer oscillation, paths of 3m and over can be observed for both surface types. The vibration paths established for the unloaded truck-trailer combinations were on an average slightly shorter as compared with the loaded combinations. With the trailer unfavorably loaded, e.g., only in the back third, the driving conditions, in some cases, turned out to be much more critical.

To eliminate the driver influence on the measured results, it will be a meaningful approach to evaluate the results as a function of the actual vehicle excitation as represented by the yaw movement or the lateral acceleration in the coupling points(21).

Figure 6 shows the position of the elements of a special type 40t semitrailer combination after having passed the single lane displacement of 3m over a distance of 40m on a wet, hardly skidding surface at a 1s interval(11). This clearly proves the validity of the procedure for the application of new vehicle combinations also.

Transient Steering Behavior

The evaluation of the steering activity during lane change has proven to be a suitable tool to determine the handling characteristics during rapid steering motions, i.e., transient steering behavior.

Table 3. Maximum values reached during single lane change for driving velocity v_{max}, yaw angle in the coupling point ψ_{1max}, and at the turn table ψ_{2max} and for the lateral displacement at the trailer end s_{max}(9)

Truck-trailer combinations 32t and 38t		v_{max} (km/h)	ψ_{1max} (degree)	ψ_{2max} (degree)	s_{max} (m)
μ = 0.8	unloaded	85-75			0.6-1.0
	loaded	75-85		25-35	1.6-2.8
μ = 0.3	unloaded	70-75	28-45	24-35	1.0-2.8
	loaded	72-80		15-35	1.7-3.8

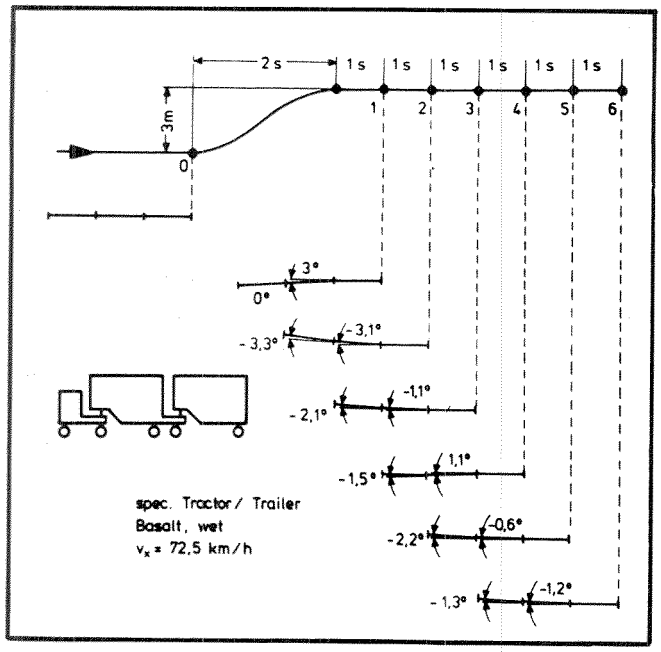

Figure 6. Positions after an extreme change of lane for a special type semmitrailer combination; (loading condition—maximum permissible weight; road surface—wet blue basalt)(11)

Step Steering Input

The step steering input as applied to commercial vehicles is comparable to that applied to passenger cars. A draft standard on this subject has been prepared(25). The driving velocities range from 50 to 80km/h with transient obtainable lateral accelerations of 2.5 to 5m/s^2. The steering wheel's rotational speed may reach from 300 to 500°/s. Because of the different, and in part not exactly stated, definitions of the delay periods between steering input and yaw velocity or lateral acceleration being used as an evaluation criterion, and because of the different starting conditions, the results obtained by different authors can hardly be compared. As a basic fact, the essentially higher inertia moments alone of the commercial vehicles will naturally cause essentially longer delay periods increasing with loading, as compared with passenger cars. For a 16t bus with permissible load, the deceleration is 0.05 to 0.10s as compared with an unloaded vehicle(3).

Figure 7 illustrates the basically different tendency in vehicle response between a bus(17) and a modern passenger car(27) exemplified by the yaw velocity. While the passenger cars reach a maximum value about 0.2 to 0.5s after steering input (50 percent rating), the motional variables referring to the bus change over into the steady state value aperiodically. In addition, the figure shows the distinctly decelerated response behavior of the bus compared with the passenger car. Measurements taken for semitrailer combinations(12,18) indicate a similar behavior with no reaching of the maximum yaw velocity or without excessive overswing.

Detailed comparisons on a literature basis cannot be made because there is no information available on series of measurements with different driving velocities and lateral accelerations. This will surely be due to the comparatively large space needed to conduct this test.

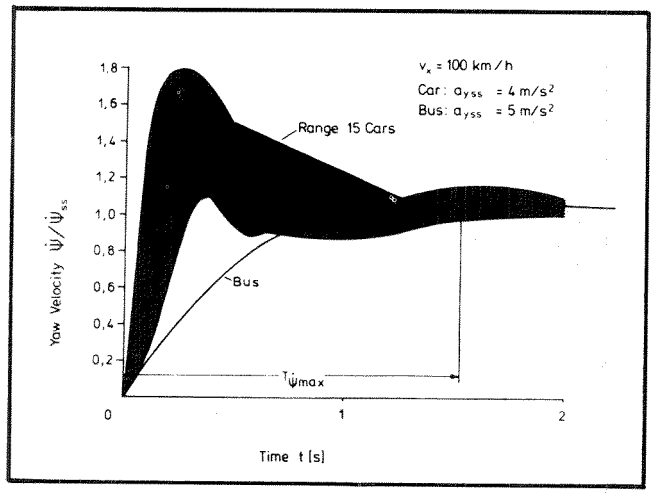

Figure 7. Comparison of vehicle response in the step steering input test for 1 bus(17) and 14 passenger cars(25)

Table 4. Test conditions and some results for the test procedure step steering input

Vehicle		v (km/h)	$a_{y,oo}$ (m/s^2)	$T_{\delta 50\% \psi 90\%}$ (s)	$T_{\delta 50\% a_y 90\%}$ (s)
Bus, Truck (17,20)		80	5	≈1	
Semitrailer comb. (12) 32t unloaded		68-72	3.5-3.8	0.4-0.5	0.7-0.75
Semitrailer comb. (10) 38t loaded	towing vehicle	54-59	3	0.2-0.3	
	trailer			0.7-1.0	

Frequency Response Characteristic

The determination of the frequency response characteristic of yaw velocity, lateral acceleration, and yaw angle with periodic steering input as described in the ISO/DIS(26) permits a more extensive evaluation of the transient steering behavior. The amplitude frequency characteristics of this variable related to the steering input are illustrated in Figure 8 for a loaded 38t container semitrailer combination at a driving velocity of 50km/h(15). The rapid decrease of the measuring variables with increasing steering frequency is indeed striking. Given a steering frequency of 0.5Hz, the obtainable lateral acceleration has dropped to about 50 percent of the value produced by the very same steering input under transient steering conditions.

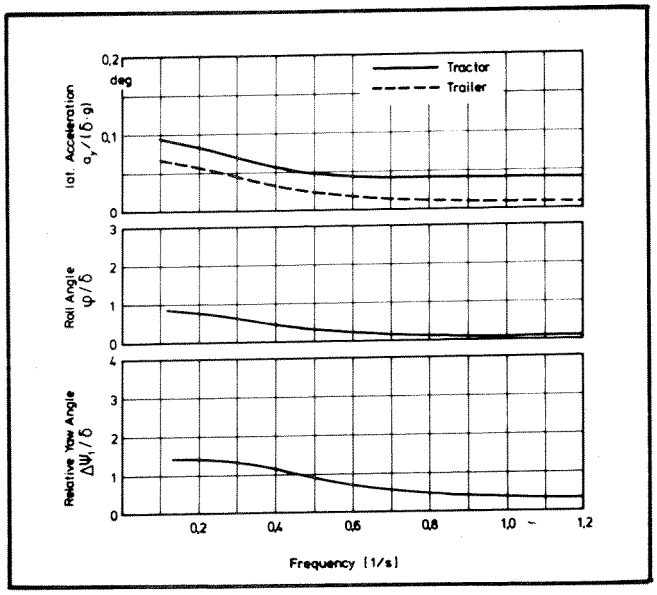

Figure 8. Frequency response characteristics of a fully loaded 38t container-carrying semitrailer combination at 50km/h(15)

Under comparable conditions, passenger cars are likely to reach this value only with frequencies above 1Hz. The large yaw inertia inherent in the commercial vehicles finds expression in this phenomenon. Unlike this, the yaw angle between the towing vehicle and the trailer decreases distinctly slower with the steering frequency but does not show a pronounced resonance point. Other measurements taken do, however, show such a resonance point in the range of 0.3Hz for a truck-trailer combination(18) and 0.3 through 0.6Hz for an articulated bus(19). The amplitude frequency characteristic of the yaw angle can be considered an index of the damping properties of the truck-trailer combination. Comparable findings on the oscillation behavior of a combination as derived from the lane change test can be derived equally for combinations with only one joint, i.e., semitrailer combinations, from the frequency response characteristics.

Measurements of amplitude frequency characteristics of the yaw velocity of a bus also show a rapid decline in yaw response without any distinct resonance point(17). To insure an all-inclusive evaluation, the phase angle characteristic, too, describing the promptness of a vehicle response has to be taken into account. Hardly anything is known about such measurements. To identify the phase angle characteristic of the yaw velocity, one can use the equivalent response time of the frequency at a -45° phase angle. According to (21), the result will be about 0.2s for an unloaded truck at v = 80km/h, and about 0.3s for an unloaded truck-trailer combination. The value obtained for passenger cars is ranging from 0.1 to 0.2s(28).

Summary and Conclusion

When analyzing the pertinent literature available on measurements taken on the handling characteristics of heavy commercial vehicles, one will easily find that results are on hand for buses, truck-trailer, and semitrailer combinations that were obtained from a good many test procedures. Since the authors working on this subject use different starting conditions, the findings cannot always be compared.

The test procedures applied to determine the handling characteristics of passenger cars are basically applicable to commercial vehicles and combinations as well. In doing so, one should bear in mind there is a need for adapting either the starting conditions or the criteria of description accordingly.

With regard to relevant test procedures such as steady state turning, braking during turning, and lane change, as well as transient steering behavior, it is possible, in some cases, to indicate measuring ranges or at least tendencies for the behavior of heavy commercial vehicles that will provide a sound capability, e.g., in comparing new vehicle combinations.

References

1. Rompe, K., Die Kippgrenze von Doppeldeck-Omnibussen, DKF-Heft 214, 1971, VDI-Verlag.
2. Nordström, Ole, "Test procedure for the evaluation of the lateral dynamics of commercial vehicle combinations," Kolloquium TÜV Rheinland, 1977, S. 168-193.
3. Benedek, A., I. Geller, J. Geller, and F. Robinek, "Ein Beitrag zur Frage der Fahrstabilität von Autobussen mit besonderer Rücksicht auf die Gummireifen," FISITA, 1978, S. 877-892.
4. Falkner, W., and K. Feitzelmayer, "Lenkkräfte und Fahrzeughandling," FISITA, 1978, S. 245-255.

5. Winkler, C.B., R.L. Nisonger, and R.D. Ervin, "Testing the Michigan double-bottom tanker," SAE Paper 781066.
6. Emery, L.H., "Limited yaw stability of trucks and tractors," Proceedings Eighth International Technical Conference on Experimental Safety Vehicles, 1980.
7. Krisper, G., P. Reichweger, and P. Pühringer, "Einfluß von Fahrzeugparametern auf die Fahrdynamik von Lastkraftwagen," FISITA, 1980, 1.2.3.
8. Burg, H., "Untersuchung des Fahr- und Bremsverhaltens bei einem Sattelzug," DEKRA Symposium, 1981.
9. Gauß, F., H.-D. Hamann, and H.-Chr. Pflug, Fahrverhalten von Lastzügen und hierbei insbesondere von Anhängern. FAT Schriftenreihe Nr. 30, 1982.
10. Heißing, B., and J. Ehlich, Fahrverhalten von schweren Nutzfahrzeugen und Zügen beim Bremsen in der Kurve, DKF-Heft Nr. 281, 1983, VDI-Verlag.
11. Heißing, B., "Untersuchung eines speziellen Sattelzuges," Bericht Nr. 954/82003 TÜV Rheinland (not published), 1982.
12. Alberti, V., "Messungen der TU Braunschweig," (not published), 1983.
13. Itami, S., and M. Oda, "Directional stability of tractor and semi-trailer combination in braking," *Bulletin of JSAE* No. 7, 1976.
14. Fancher, P.S., "Prediction of braking and directional responses of commercial vehicles," HSRI, University of Michigan, 1975.
15. Gauß, F., and H. Isermann, Wankbewegungen, Radlastschwankungen und Kippgrenzen von Sattelkraftfahrzeugen bei zeitlich veränderlichen Querkräften, DKF-Heft Nr. 232, 1973, VDI-Verlag.
16. Pilz, H., and H. Stumpf, "Lenkverhalten von Lkw-Reifen im Labor und auf der Straße," FISITA, 1980, 1.3.4.
17. Bisimis, E., "Fahrverhaltensvergleich zwischen Omnibus und Personenkraftwagen," FISITA, 1978, S. 173-179.
18. Helber, R. u.a., Sicherheitstankfahrzeug für brennbare und explosible Flüssigkeiten, Phase I, Daimler-Benz im Auftrage des BMFT, 1984.
19. Bruns, H., G. Matyssek, and G. Stangl, Fahrdynamische Untersuchungen an einem Schubgelenkbus, ATZ, 1984, S. 551-554.
20. Weir, D.H. u.a., "Analysis of truck and bus handling," Final report, DOT-HS-801-153, 1974, STI.
21. Hamann, H.-D., "Versuche zum Grenzfahrverhalten von schweren Lastzügen," Diss. Universität Hannover, 1984.
22. ISO 4138-1982, "Road vehicles—steady state circular test procedure"
23. ISO/DIS 7975, "Road vehicles— braking in a turn—open loop test procedure."
24. ISO TR 3888, "Road vehicles—double lane change," 1975.
25. ISO/DIS 7401, "Road vehicles—transient response test procedures (step/ramp input)," 1982.
26. ISO TC 22 SC 9, "Road vehicles—lateral transient response test procedures," Doc., 1983.
27. Rompe, K., and E. Donges, "Variation ranges for the handling characteristics of today's passenger cars," SAE Paper 841187, 1984.

Tractor Semitrailer Unit for the Future

Pierre Soret
Renault Véhicules Industriels

Abstract

For the truck maker, safety is a major component of the general specifications. However important this component may be, it is only one item among others:

- The goods transport vehicle for 2000 induces a break in all fields of performance.
- Particularly for safety, we have deepened major locking areas as the rollover phenomena.
- We have elaborated, with other related industries, in a complete program named V.I.R.A.G.E.S., an experimental tractor-semitrailer unit, providing substantial improvements in all fields.
- We show here specific elements related to safety in all its aspects but under constraints of other heavy components of the general specifications.

It must be seen as the global approach and response of the makers.

Introduction—Safety and Truck

For the truck maker, safety is but an element of the general truck specifications, however important this element may be. The designer's choices come under a global compromise between a set of often conflicting obligations. The cost of the product compared to the market price is a major limit to the evolution of performance. Furthermore, different specific constraints (safety, environment, energy, etc.) often induced side evolution processes of vehicles that, to instantly meet a

requirement (either legal or regular), have hampered the development of other features of the transport vehicle.

For instance, the taking of an under-run structure or a retarder is surely an efficient factor of traffic safety, but it is an extra cost and extra weight that appreciably and directly affects the economy of transportation. In Europe, this step-by-step evolution of the transport vehicle has been the main feature of the past 20 years.

The margin answers then brought lead nowadays to a technical and economical compromise difficult to improve, especially when we want to use the new technologies for the most satisfactory economical conditions. Furthermore, the vehicle is not the responsibility of only one maker. Custom has separated two types of industry:

- The power vehicle
- The towed vehicle, trailer, or semitrailer

This distribution of activities has substantial consequences on safety since in this field, more than in others, the performance of the convoy has to be considered rather than that of the separate vehicles.

Also, we must notice that weight and dimension regulations do not take into account the capital elements of the transversal stability of the units. It is true that, on this point, different influences oppose each other and compromises are needed: for instance, motor vehicle/ railer vehicle mass ratio, and the ability to turn within the regulated swept circle.

To sum up, the analytic and margin approach that has prevailed in the evolution of safety of goods transport vehicles has reached its limits. It has to be replaced by a more synthetic approach that (1) associates truck and trailer makers, and (2) integrates the demand for safety into other strong demands related to the general evolution of road transport—energy, environment, driving and use conditions, and productivity.

Renault Véhicules Industriels undertook to answer this type of demand, along with related industries under the aegis of the authorities (Ministère de l'Urbanisme, du Logement et des Transports and Agence Française pour la Maîtrise de l'Energie) according to a program called V.I.R.A.G.E.S. (Experimental and Research Transport Vehicle Improving Energy and Safety Performances).

We present the outline of this program, especially as it relates to safety, but still keeping in mind we have integrated the need for a global approach to satisfy a compromise in appreciable evolution in all directions.

The project is backed by general specifications of the high-range road vehicle, 38/40 and 44t, a tractor-semitrailer unit. It does not systematically comply with existing regulations, and the choices made may allow valorization and quotation of certain trends in regulations and standards.

An experimental vehicle, the first step toward the aims of the general specification, is undergoing tests. Another, aiming at a substantial break in performance, is in the study phase and planned for testing in late 1987.

V.I.R.A.G.E.S.—General Specifications

General specifications of this vehicle aim substantially higher than the present industrial practice in the fields of energy, environment, comfort, and safety, but of reasonable access, at least from an experimental point of view, by means of new technologies.

As for safety, the aims were worked out with the help of the National Office for Road Safety (ONSER).

Primary Safety

Ride, Handling, and Rollover

The following prone factors were defined and numerically aimed:

- Driveability in evasive motion
- Road handling in curves
- Rollover resistance

To sum up, the main line is an improvement of the maximum transverse acceleration within the behavior of the vehicle is satisfying from $3.5ms^{-2}$ to $5ms^{-2}$.

Braking

The following accident-prone factors have been selected:

- Stability of the trajectory during braking
- Braking power
- Action delay
- Nonlocking of wheels
- Tightness of the circuits

Visibility and Lights

- Quantified improvement of forward, side, and back visibility field
- Modulation of lights according to luminosity
- Lowering splash and spray

Note: The detection of proximity of the vehicle running ahead or behind was not included in this study. It has been considered as relevant to auxiliary techniques, which are relatively easy to integrate, and having little influence on the architecture of the vehicle.

Secondary Safety

Three accident-prone factors were concerned:

- In priority, non-under-running on the front for passenger vehicle, in case of front-to-front shock
- Side guard against two-wheelers and, if possible, passenger cars
- Rear under-ride device as an improvement of regulations in force

Safety in Use

Nonquantified lines were defined for the driver's safety that related to work around the vehicle:

- Access to the cab
- Room for life aboard
- Coupling/uncoupling operations
- Loading/unloading operations

Last, considerations related to driving comfort but with positive return on safety are included in the program, such as control automatisms or driving aids.

Related Analytic Works

This project has led to increasing knowledge of physical phenomena for—

- Front-to-front shocks for passenger cars versus heavy vehicles
- Rollover of articulated units

The first are under development and will be presented with the second experimental vehicle. The second has been completed and the results have been communicated to the 1984 FISITA Congress in Vienna. They confirm the work of other researchers in the United States, Europe, and Australia.

The program has been carried out through four steps:

1. Test campaign on a standard tractor-semitrailer equipped for measuring the rollover limits in quasi-stationary conditions, circular, eight shaped trajectories, and in transient conditions (sharp bend and evasive motion).
2. Working out of mathematical models of transverse stability allowing the forecast of quasi-stationary and dynamic behaviors.
3. Making a more stable experimental convoy by modifying a standard tractor and designing a very torsion-resistant, three-axle semitrailer with axle-by-axle adjustable rolling stiffness.
4. Test campaign on this unit for measurements as in step 1.

The conclusions helpful to a designer can thus be resumed.

The sensitivity to rollover of articulated convoys is due mainly to the bad coherence of load transfers in rolling motion.

The rollover limit can be appreciably improved by making a stiffer chassis and by a rolling stiffness according to the suspended load per axle. It is thus possible to come closer to the theoretical rollover limit. This last depends on simple geometrical dimensions such as the gauge and altitude of the center of gravity. To improve it, the following will have to be considered: outlines that use for the best as much of the gauge as possible (regulations' limit); development of low, large tires; and suspension with trim correction to lower as much as possible the semitrailer floor and the center of gravity.

In transient motion, roll and yaw are dynamically stable. However, it is useful, in order to take the best advantage of good geometry and coherent stiffnesses, to adjust the other parameters of the vehicle so the transient response is correctly damped while keeping good driving comfort.

For the biggest limit values ($> 4ms^{-2}$), the fifth wheel backlash induces modifications in the mass transfers that it would be better to eliminate.

It still remains that, in limit conditions, the driver does not perceive the state of the vehicle and so cannot attempt corrective maneuvers. But the risk of this situation

Table 1. Primary safety

	Handling	Roll-Over	Braking	Splash and Spray	Visibility Field
Outline Tractor 6×4 Semitrailer 2 Axles 5 - 17.5 - 17.5 = 40T	X	X	X		
Single tire = Maxi Gauge	X	X			
Disc Brake and A.B.S.			X		
Same Wheel 19"5 on all axles Low Large Tire	X	X			
High Torsion Stiffness of chassis		X			
Rolling Stiffness —nonlinear		X			
—proportional loads					
High Cab Large Windshield reaching cab floor					X
Six Sided Stream Lining including twin axles				X	

Table 2. Secondary safety

	Agressivity PV/IV Shock	Cab Access	Room and Comfort	Driving Aids
Forwarded Front Axle	X	X		
Front Low Rigid Structure	X			
Possible Front Asborbing Shock Area	X			
Six Sided Stream Lining	X			
Single Door Right Hand Sliding Roof Safety Exit		X	X	
Inner Stairs Fixed Cubic Cab (2.5m)3			X	
Rotative Lateral Plastics Remove Controlled Window			X	
Automated Gear—Box				X
Air Suspension for Cab			X	

Note: For all tests, bicycle wheels were 600mm from edge of the platform and overtaking speed was 10km/h.

decreases if the convoy is built according to the rules above-mentioned, and if, in consequence, limit transverse acceleration is appreciably increased.

Experimental Vehicle—V.I.R.A.G.E.S.

Let us not forget this is a multicriteria experimental vehicle that does not emphasize safety but improves it, along with other needs of the general and global specifications.

It is the maker's answer, necessarily related to compromises, not the safety specialist's.

To simplify, we present in the shape of a matrix the technical and technological choices made and their effects on safety criteria selected (see Tables 1 and 2).

These choices concern the first experimental vehicle. The second takes into account the same fundamental outline choices but covers the case of the 44t convoy and presents much improved technological devices, mainly in the field of the structure and chassis concept, having an important impact on secondary safety.

Conclusion

This global approach and the different related fundamental works bring new knowledge to the designers of truck and trailer industries.

The program V.I.R.A.G.E.S. allows evaluation of the capabilities of making other technical and economical compromises. It also permits a real break in all fields of the general specifications: fuel consumption, safety, environment, driving and service, reliability, and productivity. It is a difficult, new, and expansive experience, but it allows the goods transport vehicle to be developed in a satisfactory manner after 2000.

Protecting Car Occupants, Pedestrians, and Cyclists in Accidents Involving Heavy Goods Vehicles by Using Front Underrun Bumpers and Sideguards

B.S. Riley,
S. Penoyre, and
H.J. Bates
Transport and Road Research Laboratory, Department of Transport, United Kingdom

Abstract

This paper starts with a review of accident situations requiring underrun bumpers and sideguards. Bumper design features discussed include height aboveground, strength, travel, and force-deflection characteristics. A joint programme between the Transport and Road Research Laboratory (TRRL) and TI Tube Products Ltd. is described for the design and development of a front underrun bumper using the plastic deformation of mild steel tubes to absorb energy, and results of car-to-truck front impact are summarised. The final design is able to protect seatbelted car occupants from intrusion from a frontal collision at a closing speed of 65km/h, for a total bumper weight of approximately 60kg. It is

recommended that any future legislation for front underrun guards require an energy-absorption capability, and a possible legislative test procedure is outlined.

Tests carried out on sideguards fitted to an articulated goods vehicle, using a simulated pedal cycle accident, are described. It was found that the incidence of running over of the cyclist could be reduced to 40 percent of the test runs by using a guard that just met the United Kingdom legal requirements. An improved guard with lower ground clearance reduced the incidence to near zero. Better performance in other respects was obtained by making the guard flush with the side of the semitrailer and by extending the sideguard longitudinally, nearer to the trailer wheels and closer to the tractor.

Introduction

Although the overall involvement rate of Heavy Goods Vehicles (HVG's) in injury accidents in Great Britain is about the same as that of cars, their rate of involvement in fatal accidents is about twice as great(1). The fatal casualties in these accidents are usually road users other than the HGV occupants. An analysis of all the fatal road accidents in Great Britain in 1976(1,2) involving HGV's found that, of the 844 fatalities, 391 were car occupants. About 250 of these were killed when their cars collided with the fronts of HGV's and about 50 in collisions into the rears of HGV's. There were also 47 pedal cyclists, 112 motorcyclists, and 159 pedestrians killed in these accidents. One of the most frequent causes of death for these unprotected road users was by being run over by the rear wheels of the HGV's. About 100 of the two-wheeler users and pedestrians suffered this fate, mostly after impact with the sides of the goods vehicles.

It was estimated in (2) that about 40 car occupant lives could be saved each year by directly preventing front underrun. There are probably as many again in these accidents into the fronts of HGV's who might also be saved where underrun is not the primary cause of injury but where a more controlled use of the existing energy absorption of the front of the car might save casualties. Energy absorption built into the HGV front underrun guard should increase the survivable speed of impact in these accidents and is more necessary in frontal than in rear impacts because of the higher closing speeds involved. This estimated saving of car occupant lives relies on seatbelts being worn.

It has also been estimated(2) that nearly 60 two-wheeler user and pedestrian lives could be saved annually by lightweight sideguards fitted to HGV's.

More recent figures obtained from the U.K. National Road Accident Statistics (Stats 19) suggest that the number of car occupants likely to be saved by front underrun guards is now nearer to 60 (compared with 80 in 1976), and the number of two-wheeler users and pedestrians likely to be saved by sideguards is about 50 (compared with 60 in 1976).

This paper presents first the results of impact tests carried out on one type of front underrun guard fitted to a rigid lorry, and then the results from testing a sideguard fitted to an articulated lorry.

Front Underrun Guards

Design Principles

There are three basic features of an HGV that combine to make it so aggressive to car occupants: mass, which can be from about 3 to 50 times that of a car; the great stiffness of its structure; and the height of this structure above the road.

The large ratio of truck mass to car mass and the principle of conservation of momentum insure that in a car-to-truck collision the velocity change of the car is much greater than that of the truck. For example, in a head-on collision between a 30,000kg truck and a 1,000kg car travelling in opposite directions with both vehicles initially moving at 30km/h, the velocity change of the car is about 58km/h and that of the truck is about 2km/h (that is, the car is finally being pushed backward at about 28km/h).

The strength and stiffness of the truck structure mean that very little of the kinetic energy dissipated in the collision is used in deforming the truck. Nearly all of the deformation occurs in the car's structure. The allowable limit is reached when the car structure collapses far enough for there to be severe intrusion of damage into the occupant compartment. This intrusion is made even more serious by the difference in height between the strong chassis members of the truck and the strong parts of the car front. The truck structure may be so high that it passes above the car engine and meets no resistance until it hits the windscreen pillars, and gives very severe intrusion into the car passenger compartment and its occupants.

It is not realistic to expect the design of car structures to be altered to reduce this height mismatch problem, since this would require either mounting car engines higher or providing strong structures high above the road at the level of the truck chassis. These changes would be unacceptable for many reasons. Therefore, the main contribution to protecting car occupants in car-to-truck collisions must be made by changing truck rather than car structure with respect to both bumper positioning and stiffness.

The truck underrun guard must clearly be low enough to meet the strong part of a car's front structure, so a ground clearance of not more than about 300mm is preferable. Truck front to car side impacts are also a

significant source of car occupant injuries, and to reduce these injuries the bumper should be low enough to hit the strong doorsill rather than the weak door. This will reduce intrusion and will also insure that the bulge into the car will be mainly below the occupant rather than level with his hips or ribs. If the bumper face is about 150mm deep, a maximum ground clearance of approximately 250mm would be desirable for this side impact case. The need to negotiate ramps may demand a slightly higher figure, but fortunately the bumper is usually close to the front wheels of the truck and little increase should be necessary.

A rigid underrun guard of suitable dimensions would overcome the structural misalignment problem and so would allow the car's strength and energy-absorbing capability to be used to help protect its occupants. Current cars are designed to provide protection for occupants wearing seatbelts in a head-on frontal impact into a rigid wall at up to 50km/h. It is therefore probable that a rigid truck underrun guard would prevent serious injuries in truck-to-car collisions up to this closing speed for a heavy truck, and this would protect to a slightly higher speed for a lighter truck.

However, in car front to truck front collisions, the vehicles are usually moving in opposite directions so the closing speeds in this type of accident are frequently well above 50km/h. To protect car occupants at these higher speeds, it is essential that the truck bumper is not a rigid structure but designed to yield in a controlled way to absorb part of the crash energy.

The energy absorbed by the bumper as it yields is, of course, given by the area of its force-deflection curve, and, for maximum absorption, as long a horizontal stroking distance as possible should be used. It is unlikely under current legislation controlling vehicle length that operators could accept a bumper that initially projects beyond the truck structure, while it must not move back so far when hit that the car windscreen pillars meet the truck chassis. Thus, the total crush of both the bonnet of the car and the bumper of the truck must not be greater than the original length of the car's bonnet. Small bonnets (e.g., Mini, Metro) frequently extend only about 900mm ahead of the base of the screen pillars and can crush approximately 500 to 600mm without giving serious intrusion into the passenger compartment. The maximum allowable stroke for the energy-absorbing truck bumper is, therefore, about 300 to 400mm. In practice, of course, lack of space below the truck front structure may require a shorter stroke than this for a front underrun bumper.

For a given allowable stroke, the maximum energy-absorption capability of the bumper would be obtained by designing it to deflect at a constant horizontal force chosen to be the greatest that can be applied to the car without producing serious intrusion or too violent a deceleration. In other words, the bumper force must match the force at which the car front collapses so that, at the end of a severe impact, both have crushed. The difficulty is that car frontal stiffnesses differ greatly between large and small cars, so a truck bumper optimised for collisions with small cars may be too soft for large ones. Since the proportion of small, light cars is increasing, and since these vehicles give less protection than bigger cars to their occupants in a collision at any particular speed, it is suggested that a small car (e.g., 750kg unladen) should be the most important design case chosen for the underrun guard. However, it is essential that the guard can also handle a collision with a heavy car without catastrophic failure.

Tests with a large number of recent European cars(3) show that on average a frontal force of about 230kN is developed when the crush reaches 300mm, while local peak forces of about twice this size are measured briefly as the engine is decelerated. These high forces suggest that the bumper should be designed to stroke at a force of approximately 200kN, which with a stroke of 300mm would give an energy absorption of 60kJ. This is equal to the kinetic energy of a lt-car moving at nearly 40km/h.

In reality, achieving this high constant force will be difficult in a bumper that must be both light and cheap. Its desirability is questionable, too, because it may not stroke at all when hit by a small, weak car at up to about 50km/h relative speed, and damage and intrusion may then be becoming critical for the occupants of such a car. Also, lower speed impacts occur more often than high-speed ones. It is likely, therefore, that a force-deflection characteristic that starts at a comparatively low level (possibly 100kN or rather less) and then increases as the bumper strokes is preferable to the constant force one, despite its lower energy-absorption capability.

Design Details

A cheap and light method of dissipating energy is to use plastic deformation of steel on the invertube principle. After discussion with several possible manufacturing partners, a joint programme of work between TRRL and TI Tube Products Ltd. was agreed to using this approach. The bumper bar, a rectangular hollow steel section 150mm × 75mm × 6mm wall thickness, was welded to two vertical drop arms about 260mm long, which were pivoted from brackets bolted below the end of the truck chassis member. Two invertube cartridges initially 450mm long and able to be compressed by 200mm joined the lower ends of the drop arms to additional brackets bolted below the chassis member 300 to 400mm from the other brackets (Figure 1).

These invertubes consisted of two steel tubes of different diameters (100 and 80mm), the smaller of which was turned back on itself at one end and was then peripherally welded to the open end of the larger tube.

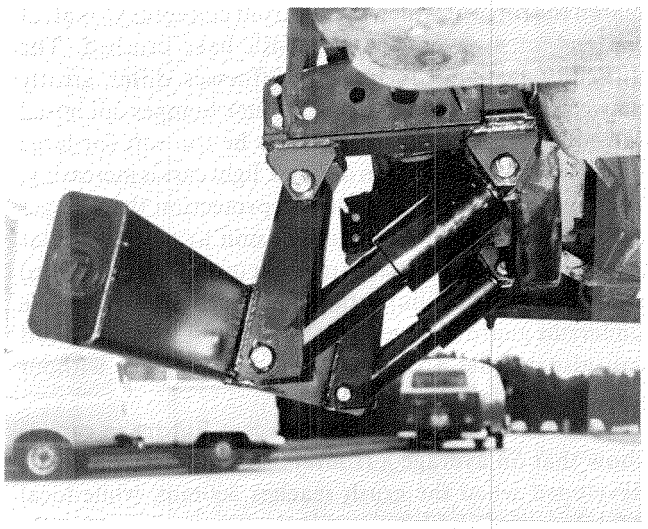

Figure 1. Invertube underrun guard

When a compression load is applied, the smaller tube progressively turns itself inside out as it is forced inside the larger tube ("like taking a sock off"). After an impact, the invertube units have to be replaced.

The invertube struts telescope at nearly a constant load over their 200mm stroke, but the geometry of the underrun guard means the horizontal force on the bumper approximately doubles as the bumper bar moves through its stroke of 220mm. This is advantageous as discussed above.

It is estimated that an underrun guard to this design would retail for approximately £150 plus VAT and fitting and that the invertube energy-absorbing cartridges would cost about £35 per pair to replace. The total weight of the guard is about 60kg.

Test and Development Programme

The original plan was to build an energy-absorbing front or rear underrun bumper that would pass the strength requirements of Construction and Use (C&U) Regulation 46B for rear underrun guards(4) before the invertubes started to stroke. For this, it should start to stroke at a load above the 100kN (approximately 10t) force required by that regulation.

Invertubes made from 14swg (2.03mm) steel tube were therefore used, with the two parts having diameters of 100 and 80mm. Dynamic tests carried out by TI Tube Products Ltd. using a falling weight rig at speeds up to 65km/h showed that these tubes each had a collapse load of 102kN, and, with a working stroke of 200mm, the bumper's total theoretical energy-absorbing capacity would be $2 \times 102 \times 0.2 = 40.8$kJ, equivalent to a lt mass falling through about 4m or moving at 32km/h. The geometrical design used would give a horizontal load on the bumper bar when stroking started of about 146kN, well below the figures measured for car frontal strengths described above but comfortably higher than the 100kN required by the C&U Regulation 46B.

However, tests in which BL Marina cars (1,000kg) were impacted centrally into the bumper mounted on a stationary Ford truck (5,100kg) showed that this bumper failed to stroke completely even in impacts severe enough to break the seatbelts of the dummy car occupants. In two tests with angled/offset and perpendicular/offset Marina impacts at 50 and 64km/h, the bumper did not stroke fully but still proved effective in preventing underrun and passenger compartment intrusion. A perpendicular central test with a 1,550kg Volvo car at 56km/h also failed to stroke the bumper fully but bent the truck chassis seriously behind the bumper rear mounting brackets.

It was therefore agreed that a major reduction in the strengths of the invertubes was required, and this was obtained by using 16swg (1.63mm) thickness tubes instead of 14swg (2.03mm). These have a load when stroking of approximately 47kN each instead of 102kN and require a total horizontal bumper force of about 68kN to start stroking. The maximum energy-absorbing capability of the invertubes is reduced proportionally to about 20kJ. It is no longer possible to withstand the 100kN loads of Regulation 46B before stroking, but the geometry of the bumper is such that this load is developed when it strokes about 175mm. Since the regulation requires that the distance of the bumper inside the rest of the vehicle's structure must not exceed 400mm, this regulation is passed by the modified energy-absorbing bumper, although most of its working stroke is used up during the test procedure.

The weaker bumper was tested in another Marina head-on central impact at 65km/h. It performed well, stroking fully and protecting the dummy occupants by leaving the passenger compartment almost undamaged (Figure 2) while developing only moderate seatbelt loads.

The latest test carried out so far in this development programme used the weaker (16swg) invertubes in a 65km/h head-on impact to assess the protection given to occupants of a small, light car with a short bonnet (Mini, 680kg loaded). This gave very satisfactory results as far as the behaviour of the bumper and the car structure were concerned, with the bumper stroking fully and only very minor damage intrusion into the passenger compartment. The present truck bumper design, therefore, appears to be reasonably satisfactory, although further tests are planned for offset and angled impacts with both the truck and the car moving. The feasibility of installing this bumper on modern trucks is also being studied.

Protection for car occupants at a closing speed of 65km/h does, of course, assume seatbelts are worn. If seatbelts are not worn, protection cannot be provided at relative speeds much above 40km/h.

The bumper developed in this programme is, of course, not the only way of producing an energy-absorbing truck

Figure 2. Damage to Marina car from impact at 65km/h into front underrun bumper

underrun guard, and it is to be hoped other design teams will be able to produce cheaper and lighter alternatives, possibly by using hydraulic systems. However, the programme has clearly demonstrated it is feasible to make such a device that need not be significantly heavier or more expensive than an adequately strong rigid (that is, non-energy-absorbing) bumper. The theoretical benefits in improved car occupant protection resulting from the use of an energy-absorbing design have been confirmed in practical car-to-truck impact tests.

A Possible Legislative Test Procedure for Energy-absorbing Front Underrun Guards

Widespread use of energy-absorbing underrun guards for trucks, in conjunction with compulsory seatbelt wearing for car occupants, would produce significant reductions in deaths and injuries, However, these benefits will be felt by the car occupants, while the cost of the bumpers will fall on the HGV owners. It therefore seems unlikely that many truck operators will voluntarily fit front underrun guards, and legislation will be needed. This should be drafted to require use of energy-absorbing bumpers rather than rigid ones for the fronts of trucks, as explained above. The test specification should probably use a rigid-faced impactor to hit the bumper, thus avoiding the cost and repeatability problems of deformable impactors. Since some designs of bumper may be very speed-sensitive (especially if they use hydraulic energy absorbers), an impact test rather than a quasi-static loading test is essential, and this should be carried out at a fairly high speed representative of the maximum survivable car-truck collisions, for example, 50 or 60km/h. The programme described above shows that the bumper can readily be designed to absorb 20kJ of energy, which would require an impactor mass about 200kg moving at 50km/h or 140kg at 60km/h. The moving mass could either be a trolley or a pendulum, which would have to fall through nearly 10m to reach 50km/h.

It is suggested that to pass this test would require (a) the maximum force acting on the impactor not to exceed 200kN (102g on a 200kg impactor) at any time, (b) the maximum force acting on the impactor not to exceed 100kN during the first 100mm of its movement after contact with the bumper, and (c) the maximum allowable horizontal movement of the impactor in the direction of impact not to exceed 400mm. The bumper would also have to meet the strength and dimensional requirements of C&U Regulation 46B.

The width of the impactor face used in the energy-absorption tests should represent a narrow car engine block of, say, 200mm. Its height should be approximately 200mm and its ground clearance also 200mm, so the height of the top edge of the impactor would be 400mm above ground level. The face edges should be curved to a radius of about 5mm.

The test impact would be carried out both at the centre of the bumper and offset to opposite the truck chassis members; new energy absorbers (or a new bumper) could be used for each impact. The truck would be butted up against a rigid heavy block during the test impacts to prevent its mass affecting the result and to insure that the impact energy is mostly absorbed by the bumper system.

The offset impact test should insure that the torsional strength of the bumper bar and its joints to the drop arms is high enough for the drop arms to remain parallel during stroking, so the bumper's total energy-absorbing capability will be utilised even in an offset collision.

Sideguards

An amendment to the United Kingdom C&U Regulations(4) came into operation on May 1, 1983. Two of the new regulations (46C and 46D) require the fitment from various dates of lightweight sideguards to new goods vehicles and trailers over certain weights and to some of the larger existing semitrailers.

The main purpose of the sideguards is to prevent pedal cyclists, motorcyclists, and pedestrians from being run over by the rear wheels of lorries. Because of their light weight, it was not intended, nor is it likely, that the sideguards will protect car occupants other than in accidents where the car strikes the side of the lorry at a shallow angle.

The programme of work described in this paper was initiated to determine how effective such sideguards would be, in preparation for European discussions to harmonise sideguard requirements. It was therefore decided to test what was considered to be a minimum legal sideguard and then to make changes to that guard to improve its performance.

The specification of the sideguard when fitted to a semitrailer tends to give it different characteristics compared with guards fitted to rigid vehicles and other types of trailer. The main difference is the distance from the bottom of the guard to the ground. Although, in common with other vehicles and trailers, the maximum ground clearance is 550mm, it is defined as such when the platform is horizontal. This means that when the semi-trailer is connected to a tractor unit, the actual ground clearance may be considerably greater than 550mm, particularly at the front of the guard.

It was mainly for the above reason that a maximum length, articulated HGV was chosen as the test vehicle. It was considered that a sideguard fitted to this type of vehicle, and just meeting the regulations, would represent the worst guard likely to be found in practice.

The accident situation chosen to test the effectiveness of the sideguard was a pedal cycle accident such as occurs in urban areas at low speed when a cyclist is overtaken by an HGV. As the lorry passes the cyclist, he or she may be nudged by the side of the vehicle or become unstable for some reason and topple toward the lorry, falling into the path of the rear wheels.

The accident data show that this is a relatively common cause of death for cyclists. Pedestrians are also run over by falling toward and under the side of HGV's.

It is hoped recommendations for sideguard design obtained from the cycle test will also help protect pedestrians.

Sideguards Used in the Tests

The Basic Sideguard

The sideguard used as the starting point in the tests is shown in Figure 3. It was of a tubular construction as illustrated in Figure 5a and was fitted to a 12.2m platform semitrailer, which was coupled to a Leyland 16-28 Roadtrain tractor unit. The guard was made so that it just met the specification described in paragraph 5 of C&U Regulation 46D(4).

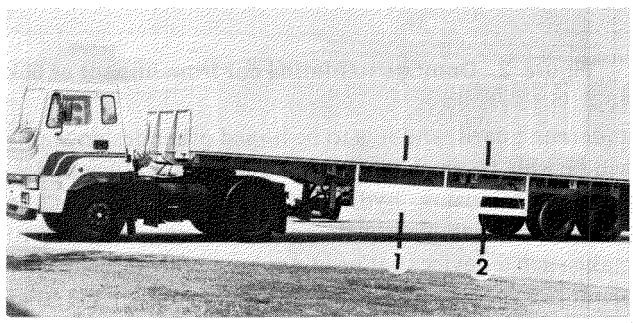

Figure 3. Basic sideguard showing dummy impact positions 1 and 2

The ground clearance was set to 550mm, the maximum allowed, with the platform horizontal. With the semitrailer coupled to the Roadtrain tractor unit, the actual ground clearance was 695 and 575mm at the front and rear of the sideguard, respectively.

The sideguard was set in from the face of the tyres by the maximum allowable 30mm, which for this particular semitrailer resulted in the face of the guard being 75mm inboard from the edge of the platform.

The overall length of the sideguard was the minimum allowed in that it was to the rear of the landing leg centreline by the maximum 250mm and forward of the front of the trailer tyres by the maximum 300mm.

The gaps between the rails of the guard were the maximum allowed consistent with the width of the rails themselves, which was the minimum allowable 100mm.

The number of uprights used to support the rails of the guard was the minimum needed to allow the sideguard to meet the strength requirement consistent with the

particular uprights and rails used. The sideguard in this form weighed approximately 45kg.

The Extended Sideguard

After analysing the results from tests on the basic guard, changes were made in an attempt to improve its performance, both to reduce the incidence of running over and to reduce the severity of injury due to other causes.

An overall view of the extended guard is illustrated in Figure 4, where it is shown with an actual ground clearance of 300mm. Other ground clearances of 400 and 450mm were also tested.

The guard was extended rearward to be as close as possible to the semitrailer tyres (Figure 5c) and forward as far as possible toward the tractor wheels.

The sideguard in its extended form weighed about 80kg, an increase of 35kg over the basic sideguard. It would be difficult to justify this extra weight and cost unless the extended guard proved to be much more effective.

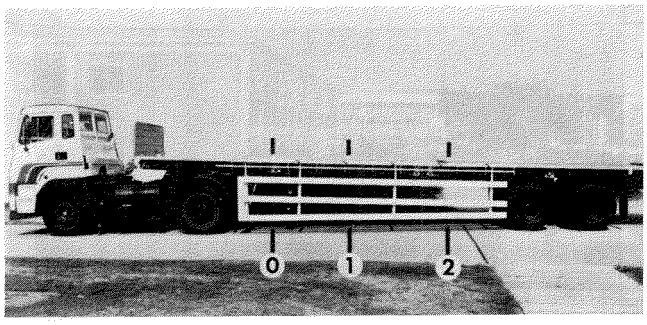

Figure 4. Extended sideguard showing dummy impact positions 0, 1, and 2

The Simulated Accident

The test consisted of driving the articulated lorry at low speed past a dummy mounted on a stationary bicycle. The dummy and cycle were released from their support and allowed to fall onto specific points along the sideguard.

The general arrangement is shown in Figure 6. The dummy was an RAE Mk5 and sat on the bicycle in the same way a normal rider would. The dummy and bicycle were prevented from falling over by a cable attached, via a magnetic release device, to a shoulder harness fixed to the dummy. The cable was, in turn, attached to a small mobile crane that enabled the dummy and bicycle to be placed leaning slightly toward the vehicle at an angle of about 5° and, for the majority of the tests, with the bottom of the bicycle wheels approximately 600mm from the vertical plane passing through the edge of the trailer platform. A couple of tests were also carried out at a distance of 1,000mm.

Most of the test runs were carried out with the vehicle being driven past the bicycle at 10km/h. Some runs were also carried out at 15 and 20km/h.

Tests were done with the dummy falling against the sideguard at two positions (1 and 2) along the basic sideguard and at three positions (0, 1, and 2) along the extended guard, as shown in Figures 3 and 4. This was achieved by driving the vehicle over a rubber tube laid across the test track. The tube was connected to an electrical air pressure switch, which released the magnetic device holding the dummy and bicycle.

The speed of the vehicle was controlled by using a fifth wheel measuring device attached to the tractor unit.

Ten runs were carried out for each condition because of the variability with which the dummy could fall. In this way, a more meaningful result was obtained in that a probability of effectiveness could be evaluated.

Each test run was recorded using two video cameras and recorders. One was so placed as to give a three-quarter view from the front of the dummy and bicycle, and the other, a narrow angle from the front.

Test Results

Tables 1 and 2 list the configurations of sideguard tested at the various conditions of overtaking speed, position of impact along the guard, and distance of the bicycle wheels from the semitrailer platform.

About 10 runs were carried out for each test condition. Information such as whether the dummy cyclist was run over or struck by the trailer tyres was in part obtained by observation at the time of the test, but it was confirmed, and more detailed information obtained, by analysis of the video recordings.

A typical test run is illustrated in Figure 7. The first photograph shows the dummy and bicycle just after the magnetic device had released the dummy (time t = .08s). The succeeding photographs are at about 0.57s intervals and show the dummy cyclist falling against the sideguard and then to the ground. It is important to note that the dummy is not attached to the bicycle in any way. The only differences between the test cycle and an ordinary bicycle are that the former has a specially shaped saddle to help keep the dummy and bicycle in a straight line and there are fittings that allow the dummy hands to rest on the handlebars without slipping off during the time between release and impact with the sideguard. The elbow joints of the dummy were tightened just enough to prevent the upper torso of the dummy slumping forward after release from the supporting cable. All other joints were loose.

Basic Sideguard Results

Before starting on the main tests, two runs were carried out without the sideguard in place. In both these runs, the

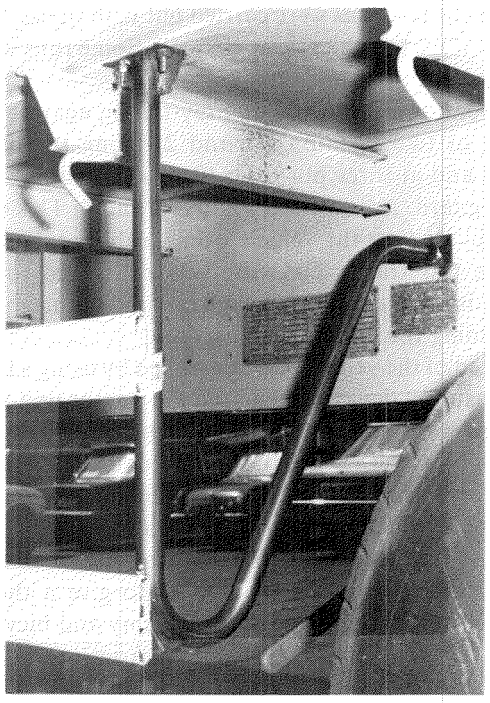

(a)

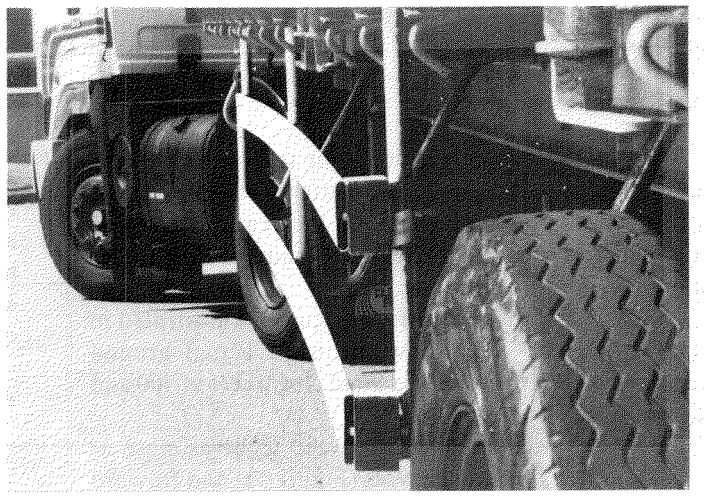

(b)

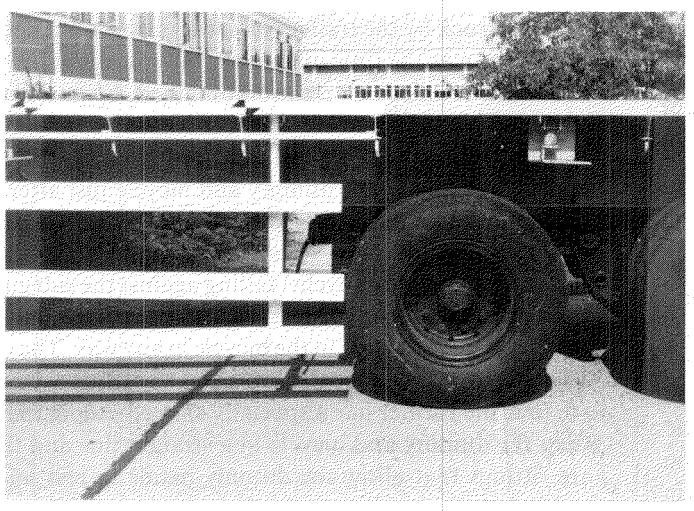

(c)

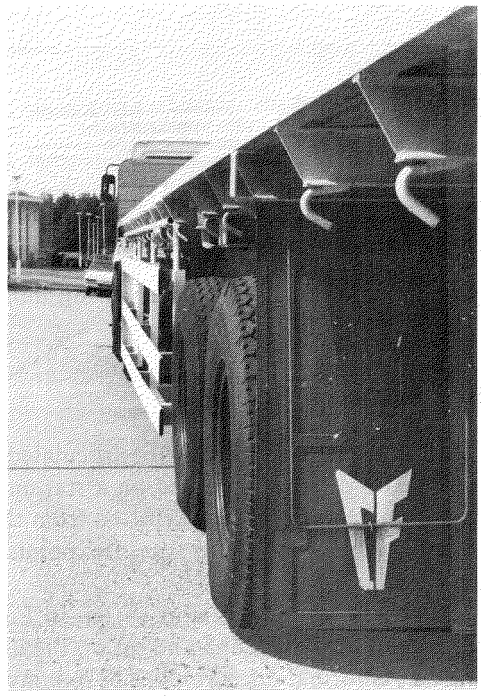

(d)

Figure 5. Details of sideguards

Figure 6. Dummy and bicycle before impact

dummy fell straight to the ground in the path of the semitrailer wheels and was run over.

The first six tests with the basic sideguard fitted, as listed in Table 1, were carried out with the sideguard set in from the edge of the trailer platform by the maximum allowable distance.

Four of the tests were at 10km/h and the other two at 15km/h. Two tests were carried out with the bicycle wheels 1,000mm from the platform edge and the rest at 600mm.

It was found that when the dummy impacted at position 1, at the lower speed, there was time for the dummy to slide down the guard and, having reached the bottom of the guard, there was sufficient ground clearance for the dummy to roll under the sideguard. It was largely a matter of chance whether it rolled far enough toward the trailer wheels to be run over. Table 3 shows that in Test 1, the dummy was run over in four of the nine runs, giving about a 40 percent probability of being run over.

When the dummy impacted at position 2, at either speed, it had less time to slide down the guard and fall

Table 1. Basic sideguard test conditions

Test	Sideguard configuration						Test conditions		
	Whole guard inset by maximum allowed	Rear of guard flared out from half way point, level with edge of platform	Rear of guard flared out from three quarter point level with edge of platform	Protective tube at junction of load hooks and I-sections	Uprights inset from guard rails	Guard rails flush with edge of platform	Impact position	Overtaking speed (km/h)	Distance of bicycle wheels from platform edge (mm)
1	X						1	10	600
2	X						2	10	600
3	X						1	10	1000
4	X						2	10	1000
5	X						2	15	600
6	X						1	15	600
7		X					1	15	600
8		X					2	15	600
9		X					2	10	600
10			X				2	15	600
11			X				2	10	600
12	X			X			1	10	600
13	X			X			2	10	600
14					X	X	1	10	600
15					X	X	2	10	600

Note: For all tests, sideguard ground clearance 550mm when semitrailer platform horizontal. Actual ground clearance 695mm at front of sideguard and 575 mm at rear.

Table 2. Extended sideguard test conditions

	Sideguard configuration				
Test	Ground clearance constant along length of guard (mm)	Distance in of guard rails from edge of platform (mm)	Uprights inset from guard rails	Protective tube at junctions of load hooks and I-sections	Impact Position
16	300	Flush	X	X	1
17	300	Flush	X		1
18	300	75			1
19	300	75			0
20	300	Flush			0
21	300	50	X		0
22	300	25	X		0
23	400	75			0
24	450	75			0

Note: For all tests, bicycle wheels were 600mm from edge of the platform and overtaking speed was 10km/h.

t= .08 secs

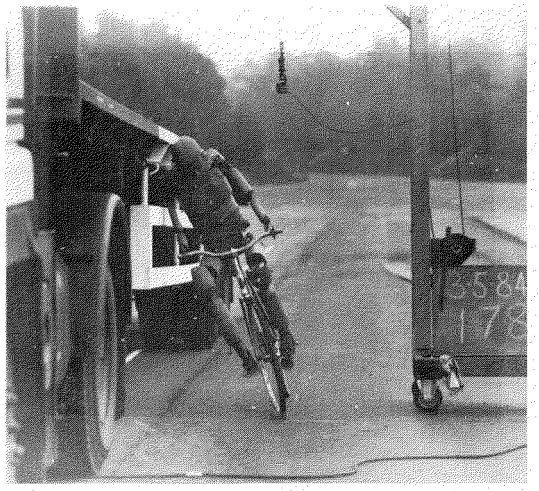

t= .65 secs

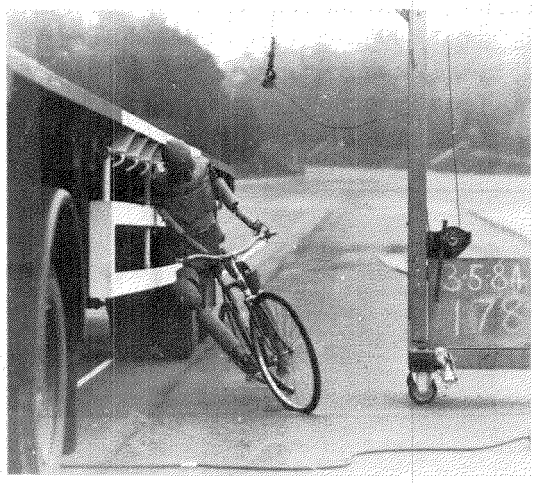

t= 1.22 secs

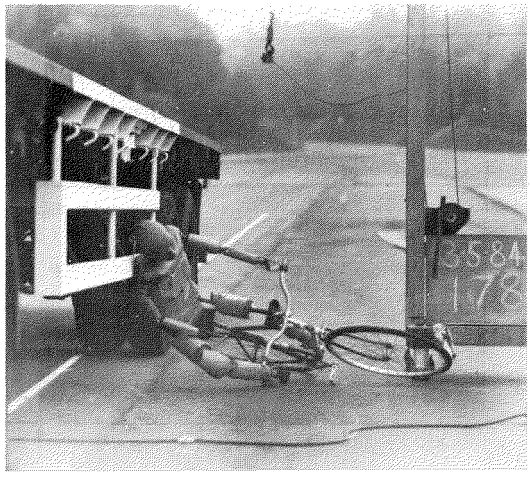

t= 1.80 secs

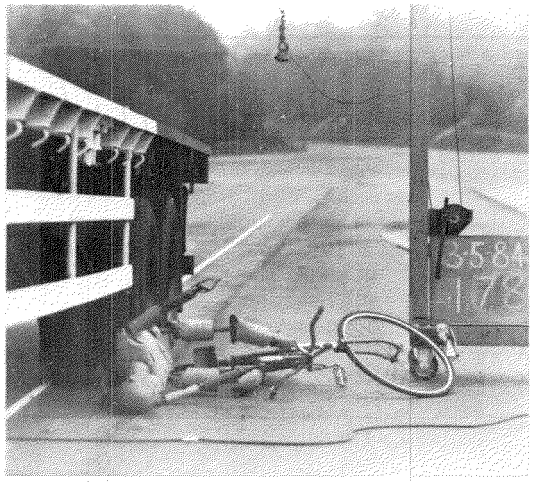

t= 2.37 secs

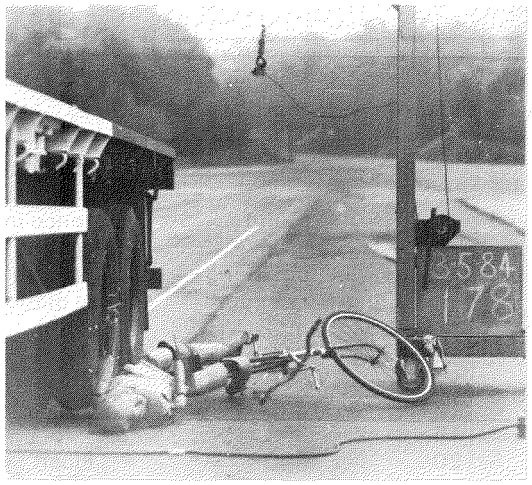

t= 2.77 secs

Figure 7. Impact of dummy at position 1 on basic sideguard at increasing time (t) after release of the dummy

Table 3. Comparable tests to show the effects of ground clearance on running over

Ground clearance (mm)	Test	Number of runs	Numbers run over	Numbers probably fatal	Comments
"550"	1	9	4	3	Dummy able to roll under guard into path of wheels after falling
"550"	12	11	3	3	Dummy fell off guard later than Test 1.
300	18	10	0	0	Dummy held away from path of wheels by bottom rail.
300	19	6	0	0	Similar to Test 18 but earlier impact point on guard.
400	23	10	4	0	Dummy body restrained by bottom rail but limbs run over occasionally.
450	24	10	2	2	Dummy able to roll under guard as Test 1, but had less time to do so.

For all these tests the guard was inset by 75mm, test speed was 10km/h and bicycle wheels were 600mm from edge of platform.

below it. The tendency instead was for the dummy to slide off the end of the guard and be struck by the edge of the leading tyre. The impact was made more severe by the fact that the dummy could fall into the 300mm gap between the end of the guard and the front of the tyre. In Test 2, at 600mm, 10km/h, and position 2, the dummy was struck by the leading edge of the tyre in about 40 percent of the cases.

The overall effect of speed was such that at the higher speed of 15km/h, there was less time for the dummy to slide down to the ground and be run over, even when impact was at position 1. However, the impact with projections such as load restraint hooks and lateral I-sections beneath the platform and the tyres was considerably more severe at the higher speed. A few runs were made at 20km/h, but the dummy was damaged too frequently and it was considered impracticable to continue testing at this speed.

At this stage of the testing, some modifications were made to the basic sideguard to help decide which features should be incorporated in the extended guard.

Throughout all the test runs, the shoulder had tended to go between the top rail of the sideguard and the platform, the head striking the platform edge itself. In about a third of the cases, the shoulder was then struck by either the load restraint hooks or the lateral I-sections to which they are attached. To try and reduce the incidence of striking these projections, a steel tube was positioned longitudinally at the junctions of the hooks and I-sections (Figure 5d). The tests (12 and 13) showed that this worked well and prevented the shoulder striking the projections. This also resulted in the dummy not being brought to the ground quite so quickly with a consequently slightly reduced incidence of running over as shown in Table 3, Test 12.

In an attempt to reduce the incidence and severity of impact with the tyre, as found when testing at position 2, three modifications were tested.

The first modification was to curve the sideguard so that a smooth flare was produced bringing the rear edge of the guard level with the edge of the platform, as shown in Figure 5b. The second was a more abrupt flaring of the guard, from about a metre from the rear edge of the guard, again so that it was level with the platform edge. Neither of these changes, when tested at impact position 2 (Tests 8, 9, 10, and 11) reduced the incidence of hitting the protecting edge of the tyre. It was hoped that the flaring out of the guard would give an outward push to the dummy to prevent impact with the tyre, but, because of the 300mm gap between the end of the guard and the tyre, it still tended to fall back onto the tyre.

The third modification was to bring the whole guard out level with the edge of the platform (Tests 14 and 15). The incidence of hitting the edge of the tyre was reduced from the original 40 percent to about 10 percent when tested at position 2, but it was not clear why this modification was more effective than just bringing out the rear end of the guard.

It was obvious from all the tests of the three modifications that further improvements would be obtained by reducing the gap of 300mm between the rear of the sideguard and the front edge of the semitrailer tyre.

It was noted that in Tests 14 and 15 with the whole guard flush with the platform edge, the impact of the head with the platform edge was not as severe as with the inset guard, as well as reducing the incidence of the dummy hitting the tyre. This was because the shoulder did not travel as far under the trailer platform.

Wooden blocks were used to make the sideguard flush with the platform edge (Figure 5d), resulting in the

uprights supporting the sideguard being inset by 95mm from the face of the guard. This prevented the dummy from being struck by the uprights. The earlier tests had shown that the dummy's hip was struck occasionally by the uprights, which led to the dummy being thrown off the guard soon after the initial impact.

Tests 14 and 15 with the inset uprights and rails flush with the platform edge showed that the dummy remained in contact with the guard for a longer period, which lessened the probability of it being run over.

From the results of the tests on the basic sideguard and its modifications, an extended guard was constructed with the following features.

Distance of the Sideguard From the Ground.

One extra rail was added to the guard, parallel to the ground with the semitrailer coupled to the tractor unit. The ground clearance was adjustable to 300, 400, or 450mm. The lowest of these was roughly equivalent to the minimum allowed on coaches. The other two distances were just less and just greater than the dummy shoulder width. It was hoped that if the ground clearance was less than the shoulder width, it might prevent the dummy from rolling under the sideguard once it had fallen to the ground.

Length of the Sideguard

The guard was extended forward as near as possible to the rear of the tractor unit. This was done not only to fill in the obvious gap through which cyclists or pedestrians might fall but also to give a point of impact that was further forward than those used in the tests with the basic sideguard. The earlier tests had shown that when the dummy impacted at the more forward position on the guard, it was more likely to be run over. Thus, an even more forward position of impact would be a better test of the effectiveness of the sideguard. The forward extension should also help prevent impact with the hard front edge of the guard, which is otherwise difficult to make less injurious.

The rear of the sideguard was extended to be as close as possible to the trailer tyre to test whether it would prevent the dummy striking the forward edge of the tyre.

Distance of the Sideguard From the Edge of the Platform

Three of the nine tests on the extended guard were carried out with the guard flush with the platform edge as this was shown to be beneficial in the earlier tests. The remaining tests were done with the guard inset at various distances from the edge.

Sideguard Uprights Inset From the Rails.

The extended guard was constructed so that the uprights would be inset by 95mm from the face of the rails when the guard was flush with the edge of the platform.

Extended Sideguard Results

Test conditions 16 to 22, as shown in Table 2, were carried out with the sideguard ground clearance at 300mm.

In the tests where the sideguard was flush with the edge of the platform, the dummy tended to remain upright and came off the end of the guard onto the tyre sidewall, even at impact position 0. It had been noted in the earlier tests with the basic sideguard that the dummy was knocked more easily to the ground when the guard was inset. Therefore, some tests (18, 19, 21, and 22) were carried out with the sideguard inset from the platform edge. In these runs, which were directly comparable with the tests carried out on the basic sideguard, as detailed in Table 3, the incidence of running over was reduced to zero.

When the dummy fell to the ground and rolled toward the vehicle, it was prevented from rolling into the path of the wheels by the bottom rail.

When the sideguard was flush with the platform edge (Tests 16, 17, and 20), the results confirmed the earlier findings from the basic sideguard tests in that the incidence of the dummy striking the trailer tyre was negligible. In addition, impact with the load restraint hooks and lateral I-sections was less severe, as was impact of the dummy head with the platform edge. In these three tests, running over occurred in only three instances. In each case, the dummy was run over by the rear trailer tyre after coming off the rear end of the sideguard and onto the sidewall of the front trailer tyre.

Test 20, in particular, with the guard flush and the uprights not inset, confirmed the earlier findings of Tests 14 and 15 with regard to the dummy being knocked to the ground by the uprights.

In Test 23, with the ground clearance at 400mm, the dummy was run over in 4 of the 10 runs, as shown in Table 3, but 3 of these cases were relatively less serious in nature, involving either an arm or a leg.

With the ground clearance at 450mm (Table 3, Test 24), running over occurred twice, and these cases involved either the dummy head or trunk.

Acceptable Ground Clearances for Sideguards

The results shown in this paper indicate that if the ground clearance of the sideguard could be reduced to about 300mm, the incidence of running over would be negligible. It no doubt will be argued that such a low clearance is not acceptable to operators of HGV's even

though an equivalent ground clearance does appear to be acceptable to coach operators. Increasing the clearance to 400mm gives nearly as good results, and it is interesting to note that, since 1980, goods vehicles in Japan(5) have required sideguards with a maximum ground clearance of 450mm. From observation of the vehicles in Japan, even the largest articulated vehicles often have clearances of 380 to 400mm without obvious operating difficulties.

Severity of Injury to Two-Wheeler Users and Pedestrians

No attempt has been made in this paper to estimate severity of injury except to distinguish between obviously fatal injuries when the head or trunk of the dummy was run over by the trailer wheels and the relatively less serious injuries caused by running over limbs.

Qualitatively, some of the impacts of the dummy with the leading trailer tyre and the head with the platform edge appeared to be very severe. This was particularly true with the inset guard. It is hoped in the near future to carry out some tests with an instrumented OPAT dummy to estimate the severity of likely injury caused by such impacts.

Alternative Sideguards

The present paper deals only with sideguards made up of uprights supporting longitudinal rails. Where access beneath or to the side of the vehicle or trailer is necessary, this may be a sensible choice of construction. However, on trailers or semitrailers where this access is less important, other types of construction could be used. An obvious alternative is a skinned sideguard using a lightweight frame covered with aluminum or a glass-reinforced plastic sheet. On platform-type trailers, some ingenuity could be required to overcome the problem of access to restraint hooks, but this form of construction would present a smoother surface for the cyclist or pedestrian to fall against.

From work done on HGV aerodynamics, it has been shown this type of sideguard would also give reduced aerodynamic drag, a definite bonus for the vehicle operator. It might also reduce spray and should make the side of the trailer more conspicuous, especially if treated with bright paint and reflective strips.

Conclusion

Front Underrun Guards

1. An energy-absorbing underrun bumper for trucks has been developed that should protect the occupants of a car hitting it from death or serious injuries at closing speeds up to about 65km/h provided they are wearing seatbelts to the latest specifications and the car interior is sufficiently spacious forward of the front occupants.
2. The bumper absorbs approximately 20kJ of impact energy by deforming steel tubes using the invertube principle. The bumper weighs about 60kg and would probably cost about £150 retail. This is only slightly more than the estimated cost of an adequate rigid (that is, non-energy-absorbing) guard.
3. In view of the benefits in reduced car occupant deaths and injuries that would result from the use of energy-absorbing front underrun bumpers on trucks, it is suggested that any future legislation for these guards be based on requiring an agreed capability to absorb energy rather than specifying a minimum strength. A possible legislative test procedure for energy-absorbing bumpers has been outlined using an impactor with a rigid face perhaps 200mm square, weighing 200kg, and hitting the bumper at 50km/h. The maximum allowable deformation of the bumper and the maximum force experienced by it would be limited, provisionally to 400mm and 200kN, respectively.
4. The almost universal wearing of seatbelts in the United Kingdom makes it worthwhile to fit underrun bumpers giving this performance. In countries where seatbelts are rarely worn, there may be little justification for underrun bumpers to prevent intrusion into occupants at relative speeds much above 40km/h.
5. Further tests are planned with both the truck and car moving to confirm that the underrun guard is effective in these conditions.
6. Work is in hand to investigate the feasibility of fitting guards to modern HGV's.

Sideguards

Tests have been carried out on sideguards fitted to the semitrailer of an articulated HGV by simulating an accident where the lorry overtook a pedal cyclist at low speed. From these tests, it was found that—

1. With a sideguard fitted that just meets the UK C&U regulation, the pedal cyclist was run over by the wheels of the semitrailer in about 40 percent of the test runs. This compares with the near certainty of being run over every time without a sideguard fitted.

   Because the whole sideguard was inset from the face of the tyres and also because of the 300mm gap between the rear end of the guard

and the leading trailer tyre, the pedal cyclist could be struck severely by the leading edge of the front trailer tyre.

Due also to the guard being inset, the head of the cyclist could severely strike the platform edge.

The pedal cyclist was more likely to be run over by the trailer wheels at the lowest test speed used of 10km/h than at higher speeds.

2. With a sideguard extended rearward to be closer to the trailer tyre and brought out flush with the platform edge and having a reduced ground clearance, the performance of the guard was improved as follows.

   With a uniform ground clearance of 300mm, the incidence of running over was reduced to zero. At ground clearances of 400 and 450mm, the incidence of running over increased slightly.

   The incidence of the pedal cyclist being struck by the edge of the leading trailer tyre was considerably reduced.

   The severity with which the dummy head struck the platform edge appeared also to be reduced.

   Insetting the uprights from the rails of the guard prevented the dummy from being knocked to the ground by the uprights.

   The forward extension of the sideguard would reduce the possibility of falling in front of the guard or onto the hard front edge.

3. The procedure described in this paper could form the basis for the development of a standard test to evaluate the effectiveness of future sideguards.

Acknowledgments

The work described in this paper forms part of the programme of the Transport and Road Research Laboratory, and the paper is published by permission of the Director. Thanks are due to Mr. M. Page of TI Tube Products Ltd. for his cooperation in the programme of work presented in this paper.

References

1. Riley, B.S., and H.J. Bates, "Fatal accidents in Great Britain in 1976 involving heavy goods vehicles," Department of the Environment, Department of Transport, TRRL Supplementary Report SR 586, Crowthorne, Transport and Road Research Laboratory, 1980.
2. Riley, B.S., B.P. Chinn, and H.J. Bates, "An analysis of fatalities in heavy goods vehicle accidents," Department of the Environment, Department of Transport, TRRL Report LR 1033, Crowthorne, Transport and Road Research Laboratory, 1981.
3. EEVC Working Group 6, "Structures, improved side impact protection in Europe," Proceedings Ninth International Technical Conference on Experimental Safety Vehicles, Kyoto, NHTSA, U.S. Department of Transportation, 1982.
4. Motor Vehicles (Construction and Use) (Amendment) (No. 7) Regulations 1982, Regulations 46B (incorporating Council Directive 70/221/EEC), 46C, and 46D.
5. Automobile Type Approval Handbook for Japanese Certification, Effective Date: August 20, 1980.

Load Restraint for the Protection of Occupants in Light Vans Including Car Derivatives

D.G.C. Bacon and
I. Gazeley
The Motor Industry Research Association

Abstract

The problems of restraining miscellaneous loads in light vans and passenger cars derivates were quantified with a view to developing specifications for strong anchorage points, bulkheads, racking, and restraint systems. The project brought together the main organisations involved: the fleet operators, vehicle manufacturers, restraint manufacturers, and racking manufacturers.

In an information gathering phase, the type of accidents were defined against which the restraint system would be required to provide protection. The specified accidents were simulated using barrier crash tests and dynamic sled tests. The test vehicles were equipped with bulkheads and storage bin systems. Various schemes of loads were held down with webbing restraints attached to anchorage points. This test work, as well as providing the loading information for the restraint specification, also indicated the performance given by existing systems. Specifications for cargo restraint systems were drawn up and prototype designs engineered to this standard for evaluation. Performance tests were carried out on the overall systems

to cover the different conditions and types of load experienced in service.

The final stage of the project involved preparation of the detailed specifications for the anchorage points, bulkheads, racking systems, and restraints that would form part of a Recommended Practice.

Introduction

The light van is one of the most widespread vehicles on the roads today. Passenger car derivatives and the forward control vans, which form the two main groups, are used by the thousands for carrying light loads.

It is, of course, often necessary to restrain the load within the van. This is needed for the protection of the front-seat occupants and sometimes for the prevention of damage to the load itself. Indeed, sometimes it is necessary just to prevent the load from becoming mixed by the motion of the vehicle. For all these reasons, a variety of load restraint systems has been developed. The main ones are—

- Bulkheads, intended to provide occupant protection by holding back the load
- Racks, used with containers into which loose tools and other small items can be gathered
- Webbing restraints, used to anchor heavy loads of a variable nature
- Clamps, used to hold down heavy items of a predetermined kind, such as trolley jacks

The need for such systems is felt particularly by the major national organisations who operate large fleets. Such organisations operate in a more systematic way than the small operator and place a greater emphasis on safe operation.

In fitting out their vans for various purposes, the major national fleets found they faced a common problem. There were no established fixing points within the back of the van to which the fleet engineers could attach their systems. All sorts of methods were improvised for overcoming this difficulty, and pickup points were devised on an ad hoc basis. It was considerably more difficult to add strong anchorage points after the vehicle was completed than it would have been in the course of manufacture. Furthermore, the engineers of the vehicle manufacturer would have been far better placed to decide suitable locations and designs. Finally, there was no control over the strength of these anchorages. If they were designed into the vehicle, instead of being added on an ad hoc basis, they could have had a specified strength.

The project described in this paper brought together the main organisations involved, that is, the fleet operators, vehicle manufacturers, restraint manufacturers, and racking manufacturers. They steered a programme of test work, analysis, and assessment to provide a consensus specification for light van restraint systems.

Survey of Fleet Operators' Accident Reports

A search was made through the records of four fleet operators to determine the number of accidents involving frontal impacts and the range of impact speeds. The combined number of vehicles operated by the organisations amounted to approximately 15,000, and the search covered a 5-year period. Side and rear impacts were not considered since it was felt these types of impacts would not propel unrestrained loads toward the occupant compartment. The accident reports studied did not refer to displacement of cargo. The investigations looked at a total of 303 vehicles that were in motion when the accidents occurred.

The obstacles that the vehicles collided with were categorised and are shown in Table 1.

Table 1. Obstacles encountered by vans from a survey of fleet accidents

Cars	:	218
Roadside furniture	:	33
Heavy commercials	:	23
Motorcycles and cyclists	:	11
Farm machinery	:	8
Buildings	:	4
Others	:	6

The distribution of the number of vehicles relative to impact speed is shown in Figure 1. Taking into account that the majority of impacts involved another car and 95 percent of the accidents were at speeds less than 64km/h (40mph), then this information provided the guidance for the speed to be used in the crash tests with a rigid nondeformable barrier carried out in this project. In vehicle-to-vehicle impacts, the equivalent barrier impact speed can be considered to be approximately half the vehicle speed. Therefore, in this work an impact speed of 32km/h (20mph) was employed to cover the majority of accident circumstances in frontal impacts.

Test Procedures

Crash Simulation Testing on the HYGE

To carry out a typical test series, a van floorpan or bodyshell was secured to the HYGE sled through its suspension mounting points by a purpose-built rigid frame. Particular attention was paid to making certain that it was well secured in view of the number of dynamic tests to which it would be subjected. The van would then be kitted out with the appropriate load of equipment for a test. Cameras required for filming movement of objects

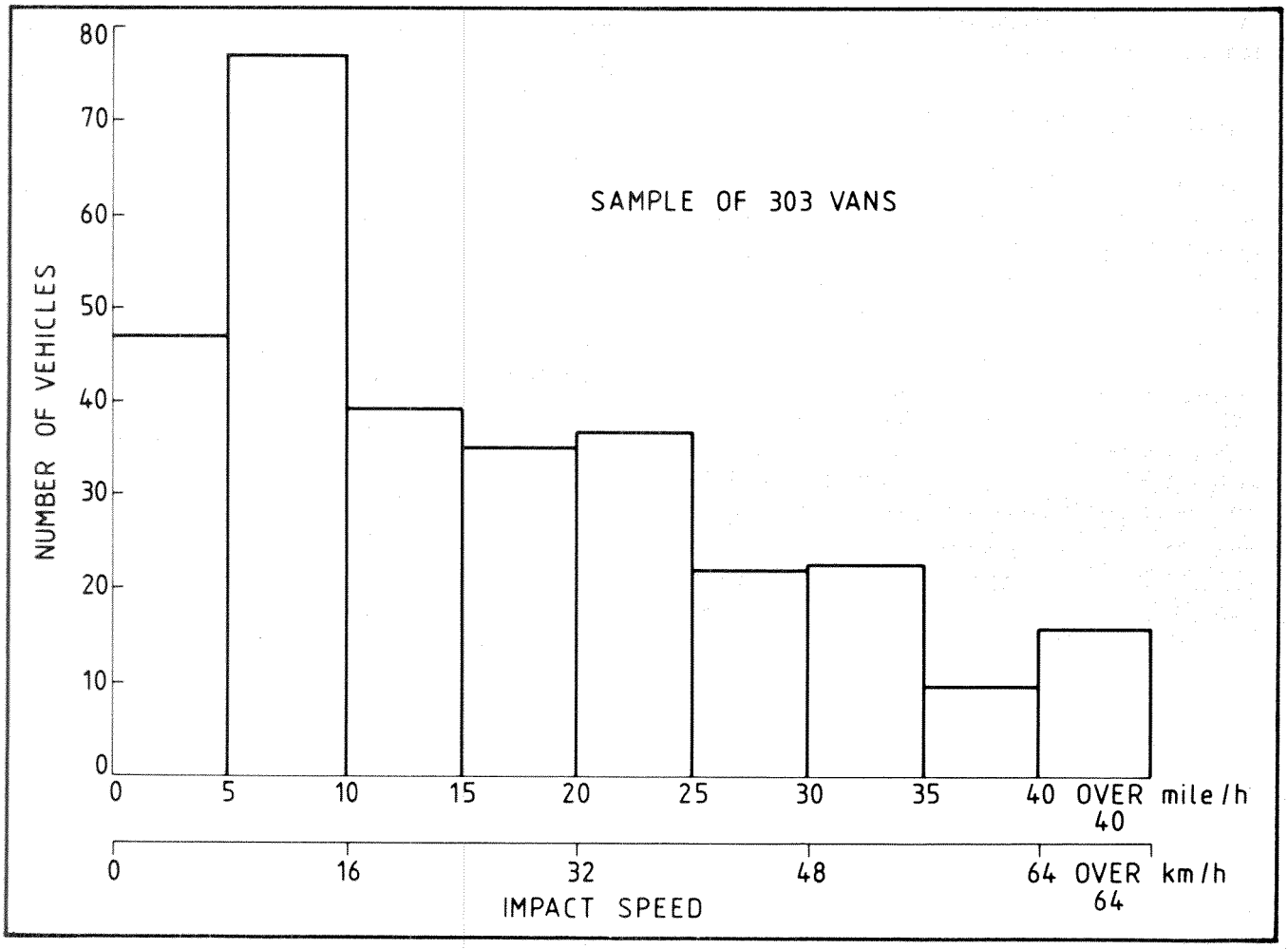

Figure 1. Number of vehicles involved in accidents in specified speed ranges

during the test were positioned on the sled and instrumentation transducers attached to record forces and accelerations. The sled with the bodyshell mounted on it was then accelerated backward by firing the HYGE, thus simulating a forward deceleration impact. Instrumentation and film analysis were then carried out to assess the results of the test.

Figures 2 and 3 show views of typical floorpan and bodyshell installations before a test.

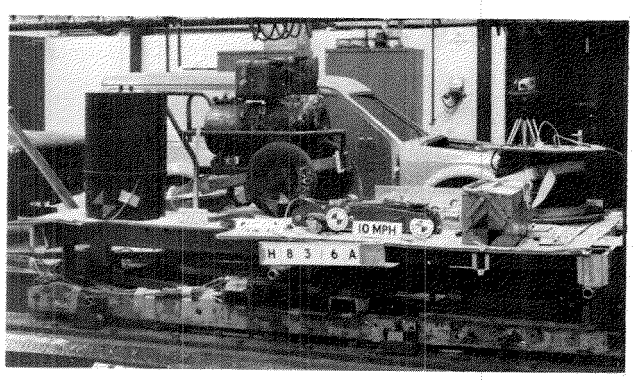

Figure 2. Van floorplan test on the HYGE, showing equipment carried and webbing restraints

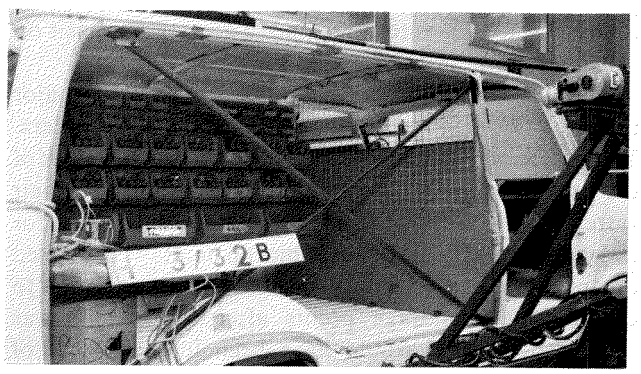

Figure 3. Van bodyshell test on the HYGE, showing equipment carried and storage bin system on vehicle side

Barrier Crash Testing

In preparation of a van for a typical load restraint test, large apertures were cut in the van side to give good photographic coverage of the movement of the cargo inside. Usually some light cross-bracing was welded across the apertures to maintain the stiffness of the body.

Any racking or storage bin system would be fitted to the opposite side that had not been cut.

Static Load Testing

Tests were carried out with a floorplan of the vehicle bolted to a channel section subframe. Shackles were installed into the floor anchorage, and then a load was applied at a specific angle by means of a hydraulic ram and a chain. A view after one of the tests can be seen in Figure 4.

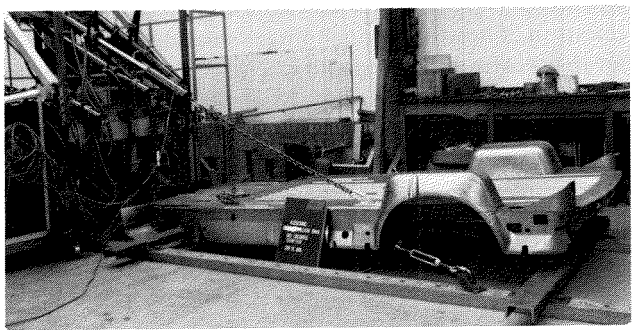

Figure 4. Static load anchorage test using van floorplan

Road Manoeuvre Testing

A series of braking tests were performed to evaluate the retention of storage bin systems. This work was followed by cornering tests that involved driving the van at various speeds around a constant radius to induce lateral accelerations.

Test Programme

An outline description of the test programme is given in Table 2. Full details of the tests and their results have been published in a MIRA report(1).

Bulkheads

Bulkheads provide a division between the load-carrying area of the van and the occupant compartment. Their main function is to prevent loose objects sliding or flying forward to cause damage or injury. Existing bulkheads are constructed from various sheet or mesh materials and are attached to the van sides, roof, and floor by a variety of means. Figure 3 shows a typical ad hoc timber and mesh bulkhead.

The existing Swedish regulation for bulkheads, SS2562, provided an immediately available specification, which was assessed to see if it matched the requirements of these investigations.

Bulkhead Test Programme

The majority of bulkhead tests were carried out in vehicle bodyshells in the "body in white" condition on the HYGE. Various items of cargo were left loose in the back, which then moved forward to strike the bulkhead. Small items of high mass, such as a trolley jack, were used to give a concentrated load that could cause problems with some designs of bulkhead.

In addition, bulkheads were assessed in the programme of full-scale crash tests that involved impact from similar items of cargo.

Bulkheads—Summary of Findings

It was not practicable to view the bulkhead as a restraint device capable of stopping all loads carried up to the maximum capacity of the van and at all possible impact speeds. A maximum load would have to be specified that could be allowed to come loose in an impact and also a maximum velocity at which the bulkhead was capable of stopping such a load. This load and velocity would be relatively small compared with the maximum payload and the maximum speed the van could reach. This meant the remaining cargo of the van should be adequately restrained to floor anchorage points. Information from other parts of the project were brought in to provide guidelines for the loose load and impact velocity.

In a survey of typical storage bin contents of vans, load values of about 110kg were found for a 900kg payload vehicle. The accident survey showed that an equivalent

Table 2. Load restraint test programme

Type of Test	No. of Tests	Speed km/h	Vehicle State	Evaluating			
				Bulk-heads	Anchor-ages	Storage Bins	Restraint
Barrier Impact	4	32	Whole van	*	*	*	*
Hyge Sled	23	16-40	Bodyshell	*		*	
Hyge Sled	8	16-40	Floorpan		*		*
Static Pull	14	—	Floorpan		*		*
Braking	6	20-60	Whole van			*	
Cornering	9	20-90	Whole van			*	

barrier impact speed of about 32km/h (20mph) covered most of the crashes seen on the roads.

These figures of 110kg at 32km/h seemed a reasonable target for the performance of a bulkhead for that size van, and the sled and crash tests indicated some current designs of bulkheads were capable of withstanding that type of impact. It also seemed reasonable that vans with higher payloads should have stronger bulkheads and smaller vans less strong bulkheads.

This philosophy was part of the Swedish regulation on bulkheads which specified a range of impact energy for bulkheads to withstand, based on vehicle maximum payload. This energy specification has been interpreted in terms of loose payload and impact velocity in Table 3. It can be seen that for the 900kg van, the unrestrained payload is 90kg at 32km/h.

Table 3. Permissible unrestrained payloads impacting bulkheads at different velocities in accordance with Swedish standard SS2562 for various size vehicles

Size of Vehicle Payload	Unrestrained Payload Permissible Energy Level (Joules)	Unrestrained Payloads Impact at 16km/h 10mph	Impact at 24km/h 15mph	Impact at 32km/h 20mph	Impact at 40km/h 25mph	Impact at 48km/h 30mph
250kg	1000	100kg	45kg	25kg	16kg	11kg
400kg	1600	160kg	71kg	40kg	26kg	18kg
900kg	3600	360kg	160kg	90kg	58kg	40kg
2,000kg	8000	800kg	356kg	200kg	128kg	88kg

The main requirements of the Swedish regulation in relation to bulkheads were adopted as the specification or Recommended Practice resulting from this project. This had the considerable benefit of a common requirement for vehicle manufacturers to meet.

However, attention was drawn to a desirable addition to the standard relating to the prevention of small objects passing through mesh-type bulkheads in the vicinity of the driver's head.

Load Anchorages

A load anchorage is a strong point on the van floor or sides to which items of cargo can be attached. The load anchorage will have a defined capacity under certain loading conditions, which will mean the item of cargo can be restrained up to a specified level of impact severity.

The problem for the fleet operators had been that until recently most vans did not have established anchorage points. To attach restraints or racking systems required the improvisation of drilled holes and attachment of reinforcing plates. The strength of these arrangements was often in doubt, and in most cases it was not known how strong they should be anyway.

It was considered more difficult to add anchorage points after the vehicle had been manufactured, and it was more appropriate for them to be incorporated during vehicle build. Also the manufacturers' designers would have more information to engineer the required strengths. However, the positions and number of these anchorages would be very much influenced by the experience of the fleet operators in their day-to-day usage of the vans.

The main task was to decide what was expected of a load anchorage, in terms of where they would be located within the van, and what would be attached to them. The question of how many anchorages should be provided in a van was also addressed and whether this number varied with the size of the van.

Load Anchorages—Purposes and Locations

The fleet operators' experience showed there was a dual function requirement for floor anchorages and there was also a need for anchorages at a high level in the van.

The floor anchorages had to be sufficiently numerous to allow convenient lashing of cargo at most positions on the load-carrying area, though it was considered more probable that this lashing would take place at the rear end of the vehicle because it was more accessible to the operator. Therefore, in defining an arrangement of anchorage points for the larger vans, more points have been put at the vehicle rear. It was also evident that a large proportion of these fleet vehicles have installed side-mounted racking systems with storage bins. These systems require attachment for the feet of the louvred panels to the vehicle floor. To keep the number of anchorages down, it was decided that those along the sides of the floor should have a dual function of lashing point and rack-mounting point.

The side-mounted racks require an upper fixing point, which is usually the vehicle cant rail (or similar structure) to attach the top of the rack. As the racking system is

vertical (or nearly vertical), this upper fixing point defines the lateral location of the floor anchorages along the side of the floor.

In summary, the anchorage locations in the floor were planned as a row on each side at a lateral spacing dictated by the upper fixing points and a row on the vehicle centreline biassed toward the vehicle rear. The upper anchorage points consisted of a row on each side in the cant rail.

Types of Load Anchorage

Various designs for a single-load anchorage or attachment point were examined. Some of these were simple but difficult to use, and others were complex in design with useful features but quite costly to incorporate. The intention was to find a suitable design that was acceptable to both the fleet operator and van manufacturer while still meeting a specified load condition.

The variants based on the 7/16in UNF-threaded hole were more attractive for several reasons. The concept of an anchorage being a reinforced 7/16in UNF-threaded hole is widely accepted in the field of vehicle safety belts. Also this design allows the addition of, say, the attachment of a bracket for racking systems as well as the link for the load restraint. The 7/16in UNF-threaded hole as an anchorage was adopted for floor anchorages.

The van manufacturers found this type of anchorage could be incorporated in the vehicle build without extensive tooling changes. Consequently, these anchorages were fairly inexpensive and had a high probability of actually being offered as an option (or as standard equipment).

It was decided that the upper fixing points could be a simple hole or any other connection detail at the discretion of the manufacturer as long as it met the strength criterion. However, to avoid any element of doubt about reinforcement details, it was preferred that this upper fixing point should again be a threaded hole but of a smaller diameter than the floor anchorages (and seatbelt anchorages). In this case, a metric thread of 8mm was chosen as the standard.

Floor Load Anchorages—Test Programme

Dynamic Tests

The aim of this programme was to establish the dynamic loading of floor anchorages under typical conditions of payload and impact severity. These data would provide the guidelines for the specification of anchorage strength in terms of a static pull test.

A series of sled tests were performed using van floorpans on the HYGE sled. A range of items of cargo to be restrained in these simulated impacts was provided by the fleet operators. Electronic force transducers were attached to the webbing restraints to record the tensile loads in each run of webbing. Figure 5 shows typical loads measured. From these records, it was possible to establish the load variation on each anchorage during the test and also the maximum value that occurred.

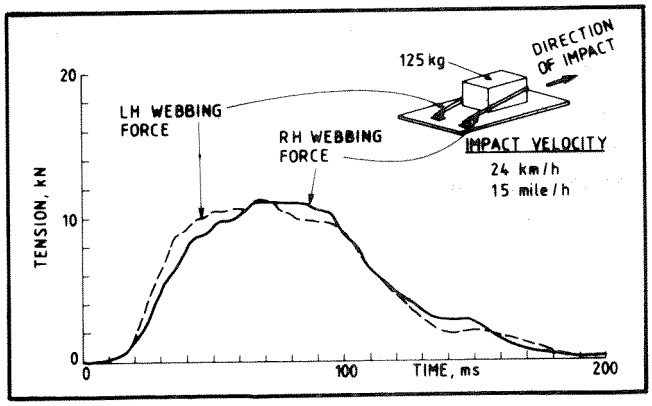

Figure 5. Loads measured in webbing restraint

Static Tests

The aims of the programme were to achieve similar anchorage deformations in the static pull test and the equivalent dynamic test to discover the static force that would destroy the anchorages and to establish a standard static test of force against a time period for testing anchorages without having to rely on dynamic testing.

Dynamic/Static Comparison

The greatest loads of about 20kN were measured in restraining a 125kg generator in simulated 40km/h (25mph) crashes. This payload was considered to be typical of some of the heavier items used by the fleet operators in their vans, and, if it could be restrained successfully by the anchorage system, it would represent a suitable standard to achieve.

The floor distortion caused by dynamic loads of 20kN was reproduced in static tests by loads of about 15kN that were of much longer duration. This observation follows other experiences in impact studies on steel structures, which show a dynamic amplification factor with higher velocities.

The outcome of this exercise was the establishment of the strength requirement of floor anchorages at 15kN. The angle of load application was specified to be 30°, which was consistent with typical lashing angles for cargo. A minimum load application time of 0.2s was also specified to be consistent with similar tests on seatbelt anchorages (Figure 6).

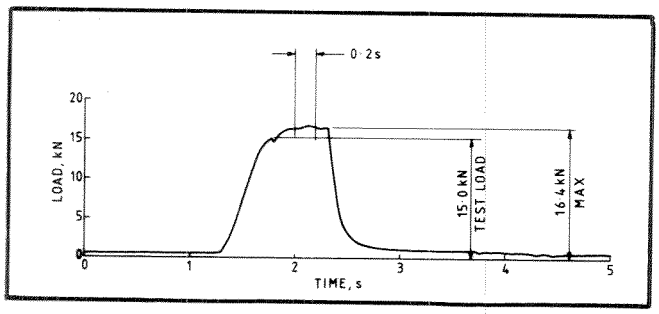

Figure 6. Typical static loads applied to floor anchorages meeting strength requirement

Upper Fixing Points—Test Evaluation and Results

The attachment of storage bin systems was usually straight onto the upper fixing points, and the measurement of forces acting at these points could not be measured directly. The method used was to take a value for the deceleration of the van in an impact, which, with knowledge of the mass of the storage bin system, would give a value to the force acting.

This information led to consideration of the strength of the upper anchorage fixing points as a function of the van maximum payload. Rounded values of upper fixing point load for both sides of the van were calculated as follows:

250 to 400kg payload	4.0kN
900kg payload	9.0kN
2t payload	20.0kN

A formulation based on payload was put forward for the strength of the upper fixing points.

Floor Anchorage Locations

The anchorage point layout for a light van (short wheelbase) was designed to suit fleet operators' needs and is shown in Figure 7. For longer vehicles, it could be seen that an additional anchorage would be required on each side and in the middle. This aspect is covered by the Recommended Practice as a function of loading area length.

The anchorage point layout for car derivative vans followed similar principles.

Storage Bin Systems

Racking systems in vans provide storage bins of various capacities (usually 5, 10, and 15kg) that are

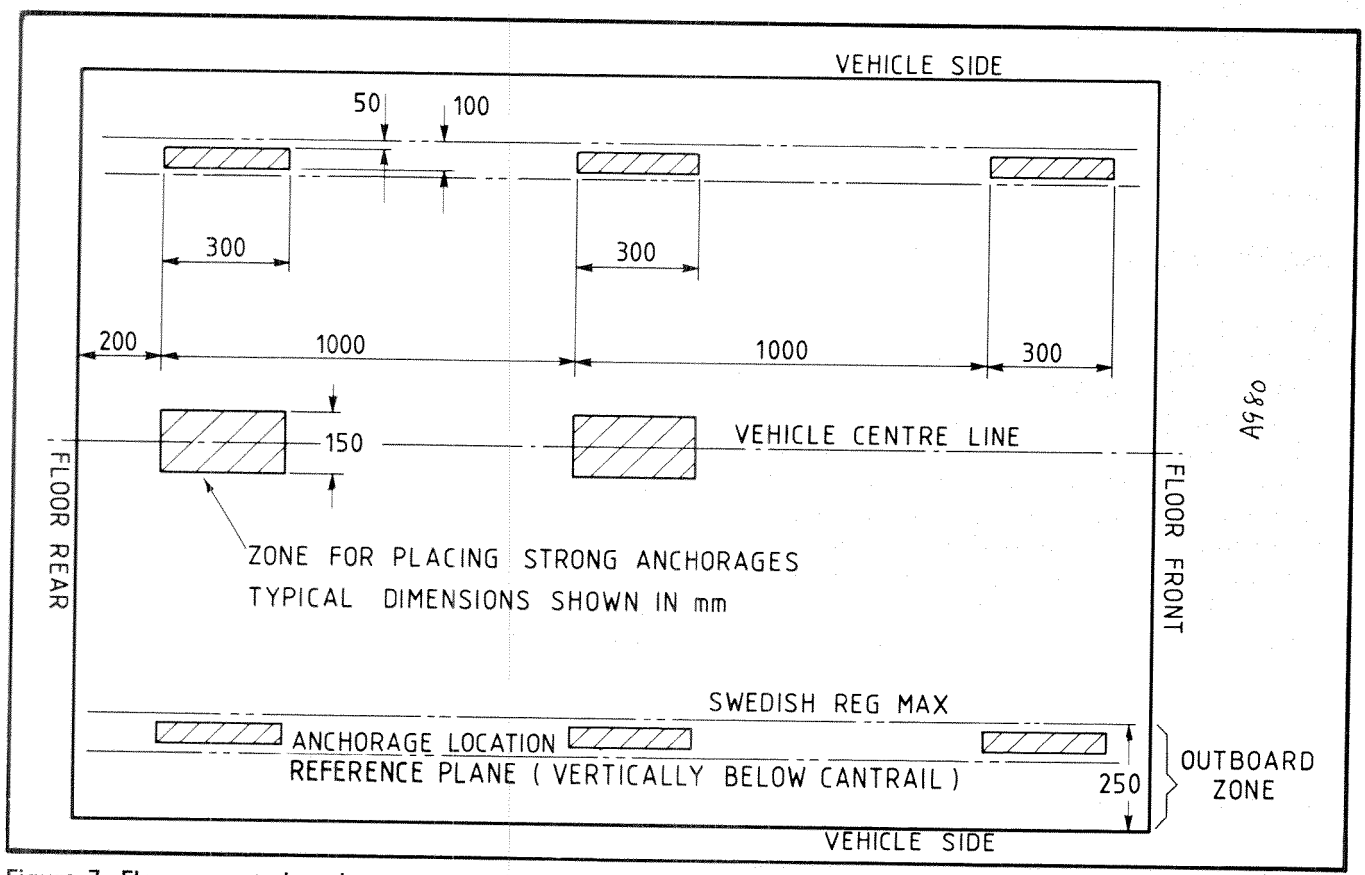

Figure 7. Floor-mounted anchorage zones for 1t payload vans

hooked onto pressed steel-louvred panels. Two systems made by different manufacturers were assessed in this project. Both were based on wall-mounted assemblies that were used mainly in workshops for storage of small items such as nuts and bolts. The louvred panels offered flexibility in the position that a bin could be attached, and it was common practice to unhook a bin of necessary components and take it to where a job was being done. Figure 3 shows a typical storage bin system.

Although this project concentrated mainly on the storage bin/louvred panel system, racking and shelving constructed from slotted angle is also widely used by fleet operators. The main requirement for this type of racking is strong attachment points, and it would be the intention that the anchorages specified in this work would be employed for these fittings as well.

Storage Bin Systems—Test Programme

Impact Tests

The majority of sled tests employing van bodyshells and all full-scale van crash tests carried storage bin systems fitted out with a variety of bins and bin-loading schemes.

It was apparent from the very first test carried out with fully loaded bins at 16km/h that they become detached from the louvred panels. A repeat test with partially loaded bins (about 50 percent) still showed bin separation from the panels.

Once it was realised that in almost every impact circumstance the bins would leave the panels, most of the tests assessing the strength of bulkheads also included some loaded bins.

Road Manoeuvre Tests

A small test programme was initiated with a van fitted out with a storage bin system and involved standard hard braking and cornering tests.

Under braking, it could be concluded that despite some small forward movement, all bins remained on the panels and retained their contents. Average accelerations during these tests did not exceed 1.0g. The value, 1.0g, was used in specifying the longitudinal load test for bins.

During cornering, the tests showed that all bins were retained by the louvred panels up to the maximum lateral acceleration of 0.7g. Only small items were displaced from a small bin at accelerations of 0.54g and above. In this work, the value of 1.0g was adopted for the lateral load test specification for bins.

Storage Bin Systems—Summary of Findings

In almost every impact test of racking systems fitted with bins, loaded to a variety of schemes, the bins became detached from the louvred panels and flew forward to strike the van bulkhead.

A major concern was that even if a method was devised to retain the bins, the bin contents may come out and still become a hazard.

It was concluded that if bins and contents would come loose in an impact, the bulkhead would have to be the prime protective device. However, bulkheads will only withstand a specified range of impact energy based on vehicle maximum payload. This meant the maximum unrestrained payloads for different impact speeds would be as given in Table 3. Therefore, the maximum weight of unrestrained bins and contents that could be carried in a van would be given by the 32km/h column, e.g., 90kg for a 900kg payload vehicle. This became the basis for the maximum permissible loading of a storage bin system.

Restraint Systems

This section relates to the various fittings such as shackles and D-links, together with webbing harnesses, ropes, or chains that connect the cargo to the anchorages in the load floor.

Every test carried out in this project with a restrained item of cargo employed some type of restraint system. Therefore, many restraint components were proved in the assessment of other systems.

Having decided on a strength specification of 15kN for the load anchorage, this automatically set the minimum standard for all other components in the load path. However, in line with working practices for these systems, a percentage overload was desirable—this was set at 33 percent giving a restraint test load of 20kN.

This criteria can be met by chains, wire ropes, rope, or synthetic webbing. The latter was the material used in the tests and proved very suitable. It is easy to use, absorbs much of the dynamic force, and does not cause secondary damage to the cargo.

Exercises were also carried out in lashing items of cargo to the anchorage layout specified for a variety of van floors. In an early vehicle test, it was most noticeable that, in a forward collision or severe braking condition, the cargo attempts to move vertically and, if insufficient vertical restraint is applied, it is possible for the cargo to rise and roll over the horizontal restraint.

Conclusion

This project brought together the main organisations involved in the problems of the transportation of cargo in vans.

Information was gathered from the fleet operators to provide background data for the performance of the bulkheads, load anchorages, and storage bin systems. This not only established the range of items carried in

vans but also involved the definition of the type of incident against which the systems must hold the fitted equipment.

Simulation of the incidents, which included vehicle collision, emergency braking, and cornering, formed a major part of the test programme that provided the data to quantify the problems of restraining miscellaneous loads. This enabled specifications to be drawn up and assessed against a background of realistic information.

Some of the more important conclusions of the work are as follows:

- Injury from loose objects may be prevented by fitting an impact-resistant bulkhead between the load-carrying area of the van and the occupant compartment. Typically, such a bulkhead fitted in a 900kg payload van will stop unrestrained objects of 90kg moving at 32km/h (20mph).
- Fleet operators require strong anchorage points to be installed in the floor of the van so cargo can be restrained. A static load criterion has been specified for these anchorages as a result of the tests in this work. The strength required is a load of 15kN at an angle of 30°. Anchorages should consist of 7/16 UNF-threaded holes in an arrangement that is a function of load floor length.
- Strong anchorages are also required at a higher level in the van for the attachment of the top of racking systems. The preferred form of these anchorages is an 8mm threaded hole.
- The performance of side-mounted storage bins was assessed and, as a result, it was recommended they not be used without a bulkhead being fitted to the van. The capacity of the storage bin system should be limited to what the bulkhead can contain in an accident.
- Restraint systems such as chains, ropes, or synthetic webbing can be used to connect the cargo to the strong anchorages in the load floor. It is a requirement that all components in the load path should withstand a load of 20kN.

As a conclusion to the project, the various specifications developed in the course of the work were brought together in a Recommended Practice(2).

Acknowledgments

The authors would like to thank the following organisations for their contributions to this work: U.K. Department of Trade and Industry, Austin Rover, Automobile Association, British Gas Council, British Rail, Dexion, Electricity Council, Ford Motor Company, Linvar, Spanset, and Tyrite. Additional financial support was given from the MIRA General Fund.

References

1. Bacon, D.G.C., J.A. Searle, and I. Gazeley, "The restraint of loads in light vans," MIRA Report, November 1984.
2. MIRA Project Group, "Recommended practice for restraining loads in light vans," MIRA Publication, April 1985.

Severe Coach Accident Survey

C. Thomas,
F. Hartemann, and
C. Tarriere
Laboratory of Physiology and Biomechanics of Peugeot SA/Renault (France)

P. Botto,
C. Got, and
A. Patel
Orthopaedic Research Institute,
Hospital Raymond Poincare (France)

Abstract

Data about severe coach accidents are still limited. More knowledge in this field is required to define safety priorities that designers and manufacturers need to consider in future vehicles. Despite the good safety level of coaches, some spectacular accidents nevertheless occur causing serious injuries and death to the users, and these are often brought to the public's attention by the media.

This survey is based on all the fatal coach accidents that occurred in France between 1978 and 1984. The paper describes the causes and accident configurations and analyzes the injury mechanisms. Countermeasures are discussed, and possible ways of minimizing occupant injuries, related to strength of front end structures, seat back improvements, window retention, and fire protection, are suggested.

Introduction

During each of the past 10 years in France, 32 people were killed and 162 seriously injured on average in

coaches and buses. Coach accident victims represent only 0.2 percent of the total of road accident victims.

Table 1 shows for 1984 the number of deaths and serious injuries among motorized road users, together with an estimate of user kilometers and the fatality rate for each mode.

Table 1. Road transport casualties in France in 1984

	Killed	Seriously Injured	Deaths Per Thousand Million User kms
Bus and coach	18	452	0.5
Truck	165	712	6
Car	7,111	39,930	16
Moped and motorcycle	1,684	15,238	100

It is clear that the fatality rate of coach and bus users is very much lower than that of any other means of traveling by road.

However, action to minimize future similar occurrences, where possible, is in the hands either of designers and manufacturers or legislators. Real-life accident data overviews are needed to help them rationalize new improvements for coach safety. Few studies have been published on this matter.

Baxter(1) discussed some of the problems associated with coaches involved in rollover-type accidents and proposed a minimum standard for the strength of coach structures.

Stansifer and Romberg(2) conducted a cost-benefit analysis of safety belts based on 66 intercity bus accidents. They concluded that a requirement to fit safety belts at all seats in coaches should not be recommended. This conclusion is also supported by frontal impact test findings(3) that demonstrated lapbelts could do more harm than good due to harder head impacts against seat backs.

Davies(4) analyzed 11 school bus crashes in Ontario. The author mentioned that padded seat backs designed to yield under impact loading would be better than voluntary seatbelt usage. It was recommended that emergency exit windows be required as well as an emergency exit door.

Due to the small number of severe cases recorded in each country, efforts to analyze coach accidents must be intensified, and the comparison of independent studies must be encouraged.

The Sample

Characteristics

The study concerns 48 accidents in which at least one coach occupant was killed. They include all fatal coach accidents occurring on the road network where the Gendarmerie Nationale operate (the entire French network except major conurbations and suburban motorways) during a 7-year period (January 1, 1978, to December 31, 1984).

All vehicles were large buses (empty weight: >8,000kg and 40 passengers or more) except six were busettes (empty weight: >4,000kg and 30 to 39 passengers). Cases involving small buses or city buses were eliminated from the sample.

The accident reports were collated and studied at the Paris Headquarters of the Gendarmerie by two accident analysts. These documents, in particular, provide information concerning the general circumstances of the accident, the site plan, interviews with those involved, the seriousness of victims' injuries, as well as photographs of vehicles involved.

In the case of 14 accidents, a much deeper analysis performed by our laboratory enabled the police-based information to be complemented.

Active Safety Aspects

According to the police data(5), the extent of coach driver blameworthiness in all personal injury accidents is fortunately very low (only 30 percent). But, in the fatal accident sample, this rate is 2.5 times higher (73 percent) than the former. This highlights the importance of the coach driver in accidents where there is at least one occupant death. This high degree of presumed blameworthiness should be related to the fact that, in 18 cases out of 48 (38 percent), the coach is the only vehicle involved.

Accidents often have many causes. The distribution of main apparent causes of the 35 accidents in which the blameworthiness of the driver seems clear-cut is shown below:

Loss of control on a bend	—	6
Loss of control on black ice	—	5
Slowing down	—	5
Other cases of loss of control	—	4
Driver's drowsiness	—	4
Dangerous overtaking	—	3
Alcohol	—	2
Driver feeling unwell	—	2
Mechanical failure	—	2
Inattention	—	1
Unknown	—	1

Moreover, in 13 out of 35 cases, the drivers were exceeding the speed limit for the type of road.

Main Impact Types and Distribution of Victims

In two-thirds of the cases, coaches sustained more than one impact during the accident. This should be related to

the fact that glancing blows are frequent. It is noticeable that the stopping distance of the coach after the first impact is less than 10m in only two cases but above 40m in half the cases. Thus, for multiple impacts, the main one is taken to be that producing the fatal injury.

Three types can be distinguished:

- Frontal impacts: 42 percent (20/48)
- Rollover or tipping-over accidents: 33 percent (16/48)
- Other cases: 25 percent (12/48) (including fire, falling into water or a ravine, side impacts)

In accidents in which at least one coach occupant is killed, the distribution of injury severity among victims (Table 2) in frontal impacts and in rollover and tipping-over accidents is somewhat comparable.

The high proportion of those killed in the impact type classified as "Others" is due to the inclusion of the 48 persons burned to death in a single fire accident, as well as accidents in which the coach fell into a ravine or into water (32 killed out of 73 involved).

It will be observed that even in a sample of accidents in which a coach occupant was killed, approximately three-quarters of those involved were uninjured or only slightly injured.

Table 2. Distribution of victims by impact type

		Impact Types							
		Frontal	Overturning Accidents	Others					Total
				Fire	Falls into a ravine	Side impacts	Falls into water	Miscel-laneous	
(number of case)		(20)	(16)	(1)	(2)	(4)	(2)	(3)	(48)
Injury Severity	Killed	46	30	48	25	11	7	3	170
	Severely Injured	135	104	0	12	25	1	0	277
	Slightly Injured	290	262	0	13	30	12	35	642
	Uninjured	253	161	16	0	38	3	88	559
Total		724	557	64	50	104	23	126	1,648

Frontal Impacts

The 20 frontal collisions resulted in 46 fatalities (about one-quarter of the total) and 135 seriously injured (half of the total of seriously injured) out of 724 passengers involved.

Front End Damage Area and Severity of Victims

Frontal impacts have been broken down according to the degree of overlap of the coach front with the struck obstacle (which in 15 out of 20 cases is a truck, and in the others a high, stiff, fixed object). The degree of severity of injuries according to the extent of overlap is given in Figure 1.

Less Than 1/3 Overlap Impacts

They represent half of all fatal frontal impacts. Respectively, 44 percent and 48 percent are killed and severely injured in this collision type. Seven out of the 10 cases are offset to the left (Figure 2).

1/3 to 3/4 Overlap Impacts

These represent 41 percent of killed and 22 percent of severely injured. They occur mainly in slowing-down situations. Due to the driver's reaction, the right front is concerned in 3 out of the 5 cases.

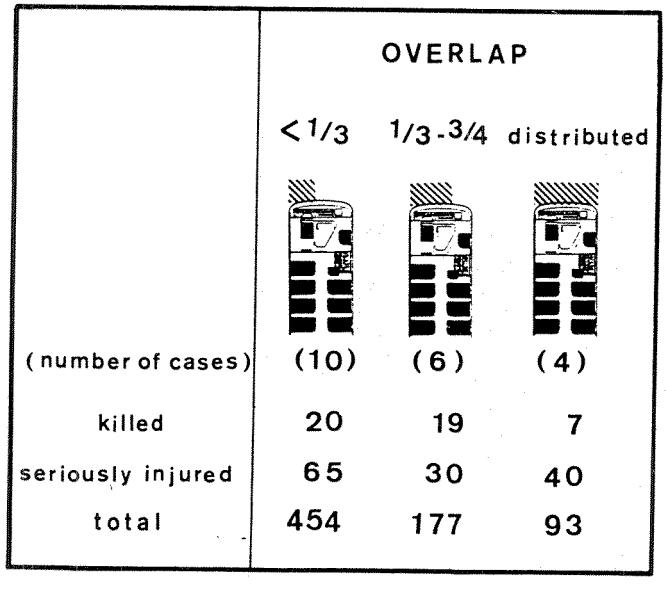

Figure 1. Distribution of injury severity of victims by overlap in frontal impacts

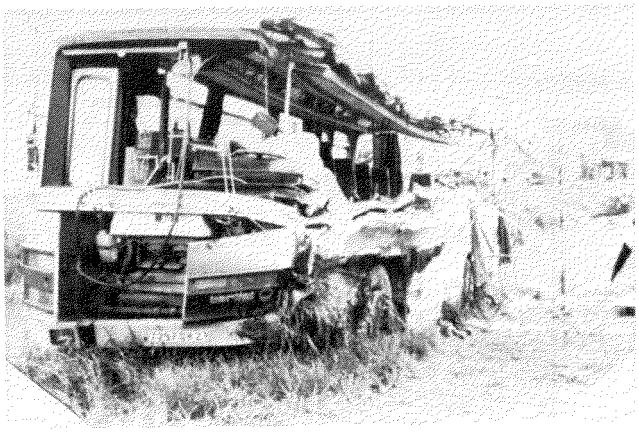

Figure 2. 1/4 offset impact against a truck—8 killed, 2 seriously injured for 27 involved

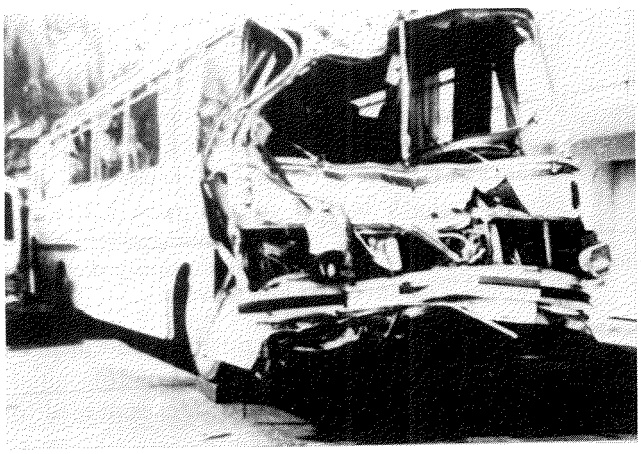

Figure 3. 1/2 offset impact against the rear of a truck—1 killed, 10 seriously injured for 28 involved

Distributed Frontal Impacts

Only 4 out of 20 fatal frontal impacts show deformations spread across the whole of the front of the coaches involved. They result in few killed (15 percent), but the seriously injured are relatively numerous (30 percent).

All in all, in fatal frontal impacts, offset cases cause 82 percent of all deaths and 59 percent of serious injuries.

Intrusion and projection are, respectively, the main mechanisms of injuries for those killed (91 percent) and for the seriously injured (61 percent). The two fatalities by projection took place in particular circumstances (one child standing up in the gangway and an elderly person involved in a multiple frontal impact accident).

Among frontal projection victims, the body areas of face and knee/leg are injured in 36 and 30 percent of the cases, respectively.

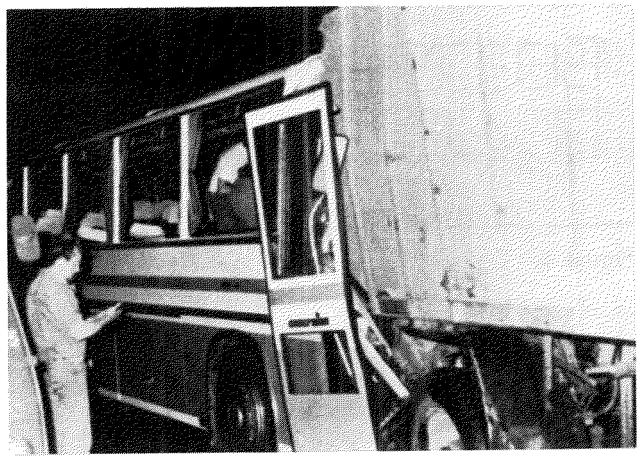

Figure 4. Distributed front impact against a truck—1 killed, 24 seriously injured for 51 involved

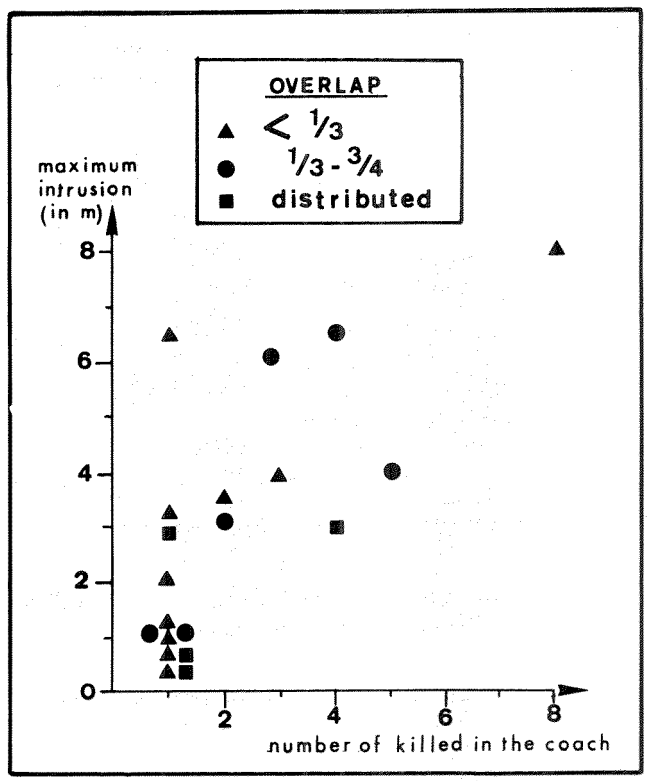

Figure 5. Number of killed in the coach

Rollover and Tipping-Over Accidents

In 14 out of 16 cases, rollovers occurred after the coach had left the road beside which was a shallow embankment of at least 1m in depth. An initial impact against a heavy vehicle and loss of control on a motorway without the vehicle leaving the road were the two remaining events precipitating rollovers. Estimation of the vehicle speed at the first moment of loss of control is given in 10 cases by the tachygraph and 6 by the driver or witnesses (Figure 8).

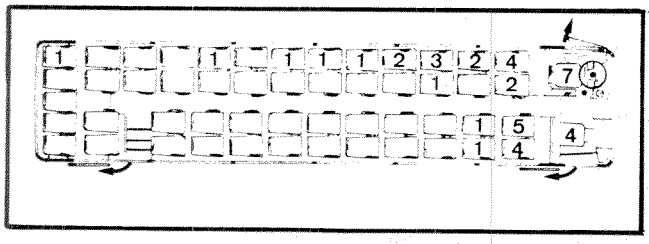

Figure 6.

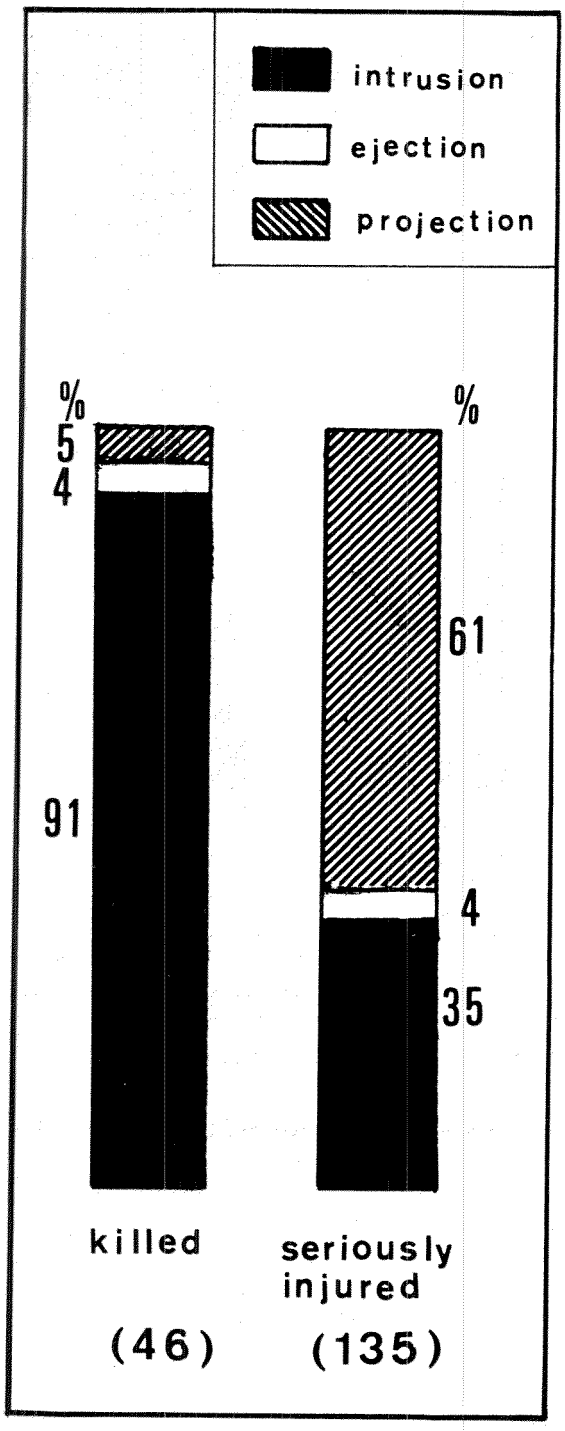

Figure 7. Injury mechanisms in frontal impacts

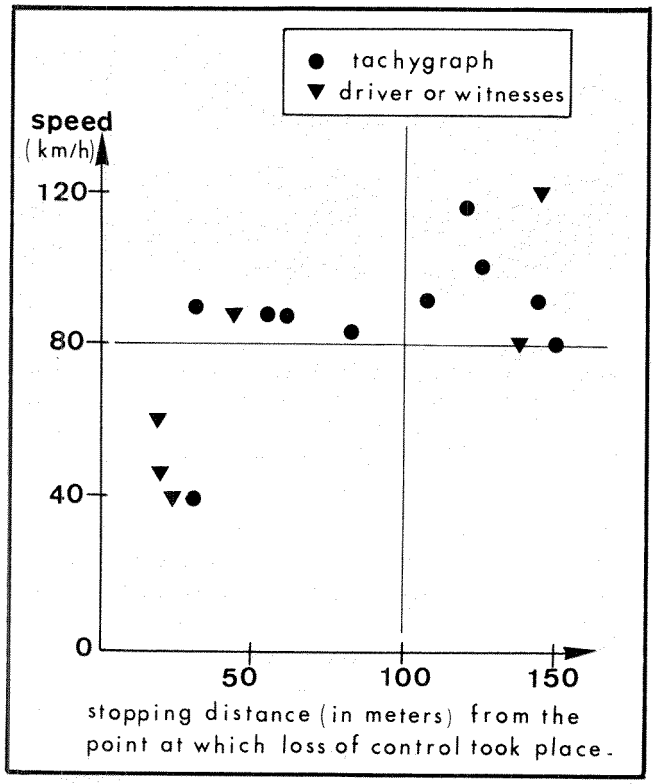

Figure 8. Estimated initial speed and stopping distance of coaches involved in rollovers

The forward motion of coaches during the accident is obvious. In about half the cases (7 out of 16), initial speeds were 80km/h or more with distances needed to stop not less than 100m.

Rolls (180° or more) with at least one contact "roof-ground" occurred in 10 cases, making 18 killed and 66 severely injured among the 329 involved. Tipping-over accidents (90° only) were observed in 6 cases—12 killed and 38 seriously injured were recorded among the 228 involved in such configurations. Thus, the importance of tipping-over accidents must not be underestimated. While there is no collapse of the body in tipping-over accidents, it must be mentioned that, in fatal coach accidents, distributions of the severity of injuries are rather similar between those involved in rollover and tipping-over accidents.

Coach Body Deformation and Severity for Occupants

The collapse of coach body was nil in 9 cases, partial in 3 cases (the crush did not exceed the upper quarter of the side window), and substantial in 4 cases (the cant rail reached the top of the seats).

The 7 cases with collapse of the body superstructure have been divided according to whether the tipping over or the rollover occurred on a flat surface or against an aggressive localized obstacle (an embankment or a highway guardrail—Figure 9).

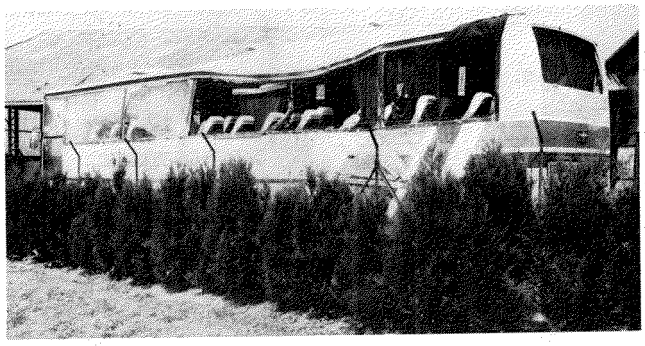

Figure 9. Localised coach body deformation after tipping over on a motorway against a median highway guardrail—5 killed, 14 seriously injured among 46 involved

It will be observed in Table 3 that the side collapse after a rollover on a flat surface occurred in only 3 out of the 16 overturned fatal coach accidents, representing 19 percent of all seriously injured persons. While coach deformations are spectacular in such cases, this configuration is not representative of the majority of seriously injured persons in coach-overturning accidents.

It is noticeable that 22 out of the 26 killed (exact place unknown for 3, and 1 standing up in the gangway) were sitting alongside the side windows (Figure 11).

Partial ejection occurred in rollovers inducing a collapse of one side of the coach body structure. On the impact side, the cant rail and also the luggage racks are crushed toward the gangway area (Figure 12).

It is noticeable that none killed and only a few seriously injured were observed in the rows offside the impact in spite of the reduction, there also, of the passenger space. In this configuration, all killed and most of the seriously injured were sitting alongside the windows on the impact side. In the collapse, people are partially ejected through broken tempered window glass and crushed between the ground and the exterior of the coach.

These victims represent 45 percent of those killed and 30 percent of seriously injured persons.

Last, the nonejected occupants have sustained serious injuries due to their projection against upper interior fittings or the side part of seat frames.

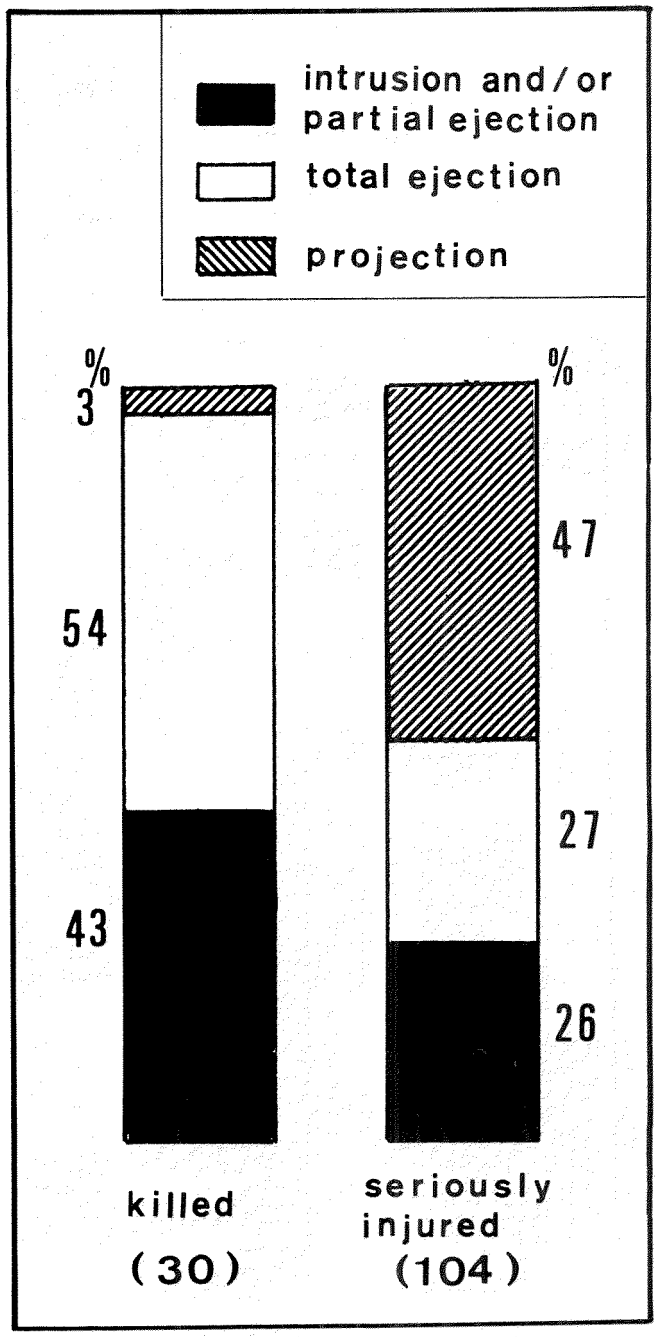

Figure 10.

Table 3. Distribution of victims by type of body deformation in coach-overturning accidents

Body Deformation	Obstacle Surface	Rollover (R) or Tipping-over (T) Accidents	Killed	Seriously Injured	All Involved
Nil or slight	Flat	4(R) + 5(T)	11	47	288
Side collapse	Flat	3(R)	9	16	121
Local collapse	Narrow and Stiff	3(R) + 1(T)	10	41	148
	Total	10(R)+ 6(T)	30	104	557

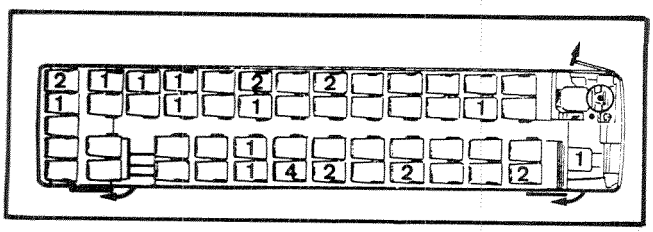

Figure 11. Distribution of 26 killed involved in overturning accidents by seat location

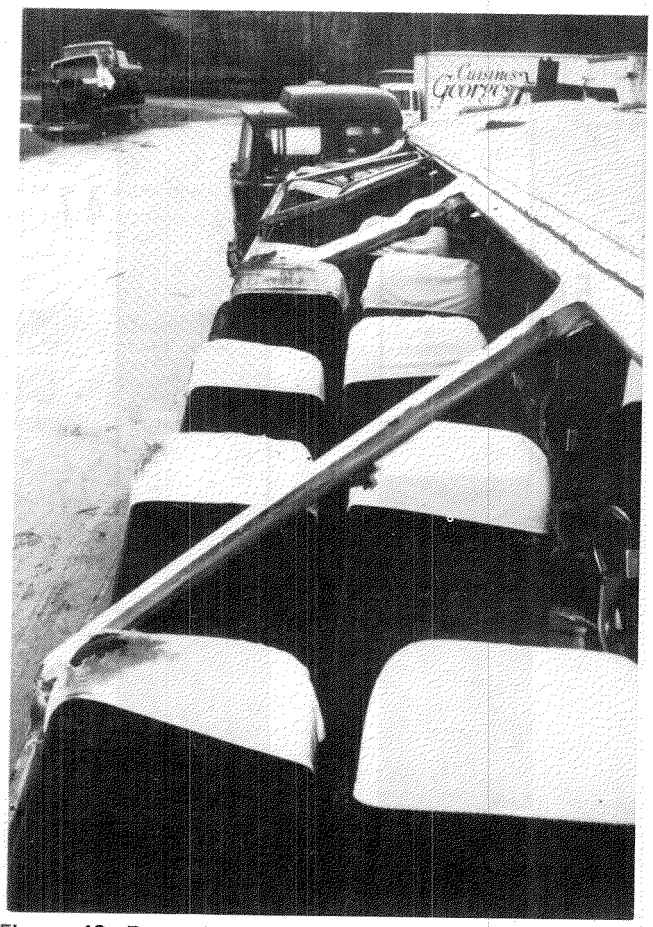

Figure 12. Example of side roof collapse—3 killed, 11 seriously injured for 42 involved

Other Accident Types

The 12 remaining accidents generated 55 percent (94 out of 170) of all killed but only 14 percent (38 out of 277) of all seriously injured studied in the sample.

The wide scatter of accident types (fire, falls into a ravine, side impacts, falls into water) and their respective severity has been previously given (see Table 2).

The coach fire problem was dramatically highlighted by the motorway accident that occurred at night in July 1982 in Beaune (Figure 13).

The coach was running at about 100km/h and, due to the slowing down of the preceding vehicles and despite braking by the coach, it hit the rear of four cars causing

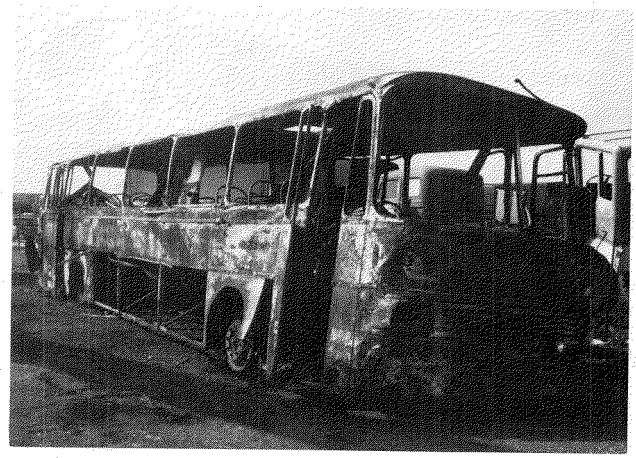

Figure 13. Fire accident—48 killed out of 64 involved

fuel tank damage with leakage for three of them. A fire immediately broke out, especially involving the front of the coach, which was only slightly damaged by actual impact.

Only 15 out of the 59 children and 1 of the 5 adults were able to escape by the rear door during a period not exceeding 2min. All of them were uninjured. The investigation showed that the victims were probably asphyxiated before being burned.

Falls into water were observed in 2 cases, generating 7 fatalities by drowning out of the 23 involved in the 2 slightly damaged coaches.

It appears from the survivors' statements that the main difficulty is to find and reach coach exits quickly. As far as fire accidents are concerned, it must be pointed out that the problem of emergency exits must not be underestimated since one-third of all fatalities (55/170) in the studied sample were related to this important point.

Only falls into ravines more than 30m deep are considered. As excepted, the severity is high since half of the involved (25 out of 50) were killed in the 2 recorded cases. The analysis pointed out that 16 fatalities have been crushed by the important collapse of the front end and roof structures. For the remaining 9 deaths, the absence of damage in their seat compartment areas indicated that projections of occupants were too severe and exceeded the human tolerance limits.

As far as side impacts are concerned, the obstacle was a truck in 3 cases and a tree in another. Passive safety in such collisions is not currently feasible. For example, in one truck-to-coach accident, the truck driver lost control on a bend and impacted the middle side of a coach coming from the other way. Despite the small degree of residual crush ($\leq$140mm), the 6 persons sitting alongside the windows in the impact area were killed.

The remaining 3 fatal accidents classified as "Others" were due to the death of the driver (driver feeling unwell two times, and hit by an external projectile lost by a truck in another).

Injury Mechanisms

Many different kinds of injury mechanisms leading to death were observed (Figure 14).

The importance of fire/asphyxia, intrusion, and projection against the occupant compartment walls will be especially noted. These three mechanisms together account here for virtually all the cases of death and serious injury.

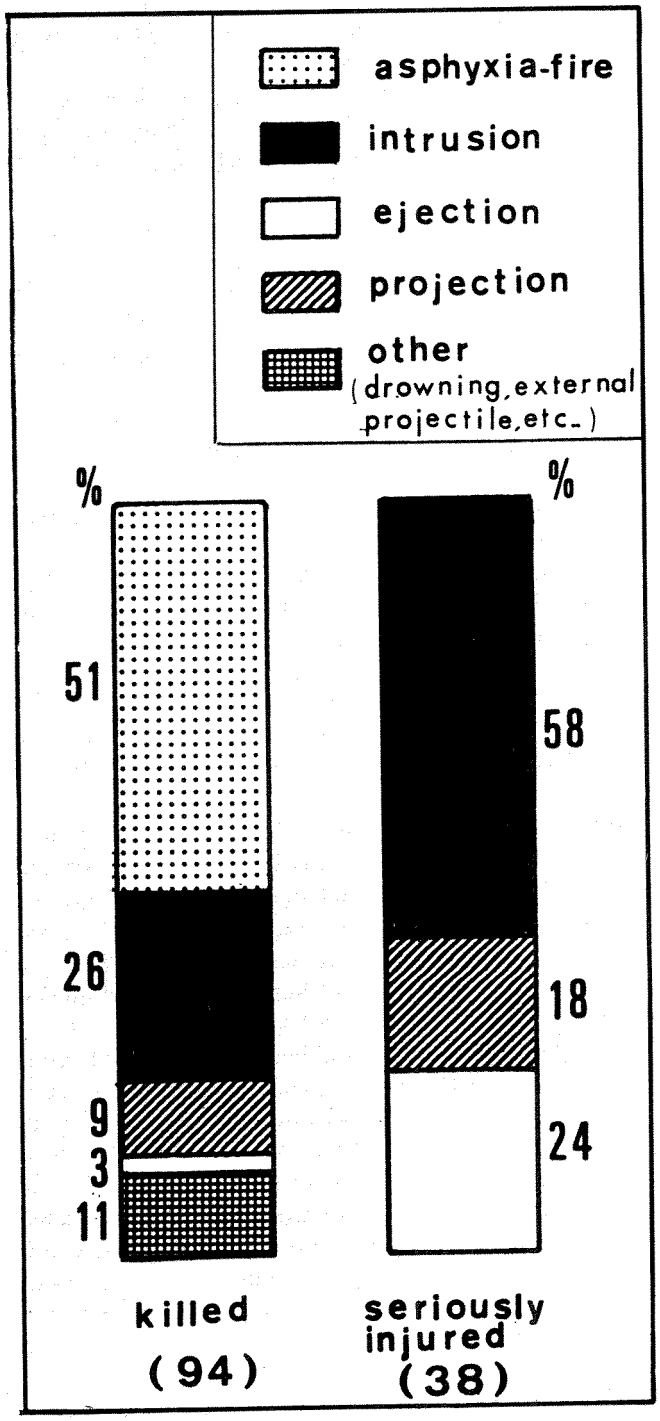

Figure 14. Injury mechanisms in accidents classified as "others"

Discussion

How can the safety of passenger coaches be improved?

One answer could be by action on active safety, primarily on braking, and by action in the field of passive safety—body strength, seat design, and better protection against the consequences of fire.

Braking Improvements

The kinetic energy reduction at the instant of impact can be determinant on the accident's seriousness. It is thus necessary to use to the maximum the potential possibilities of improvements in braking performance. These improvements should include—

- Improvements of speed reduction performance without brake overheating, especially in long descents
- Reduction of minimum stopping distances when the normal brakes are used
- Maintenance of directional stability during braking

It must be remembered that in 12 out of the 48 cases studied it was considered that better braking performance would have avoided the collision, or, at least, reduced the collision severity.

Mandatory retarders are recommended as a countermeasure in one case, but, as it is well known, most coaches today are not equipped with such a device.

Stopping distance reduction is concerned in 7 cases. A shorter stopping distance cannot always avoid the collision, but it permits a reduction in its seriousness, provided, of course, that the driver is not tempted to drive at constant risk.

Thus, the minimum stopping distance using normal brakes could be reduced by 12 to 15 percent and should not tend to increase the risk of wheel-locking.

The fitting of an antilock braking system would have been favorable in 4 out of the 48 cases in our study (loss of control during braking on slippery surfaces). The advantage is increased for vehicles with powerful brakes reaching wheel-locking limits even on dry asphalt.

Thus, these two measures—minimum stopping distance of braking and fitting of an antilock braking device—should be applied simultaneously.

Passive Safety

How can the passive safety of coaches be improved?

To answer this question, the injury mechanisms leading to death and serious injury must be borne in mind (Table 4).

Intrusion is the leading cause of fatalities in coaches. In frontal impacts, it would be desirable to increase front

Table 4. Summary of injury mechanisms

	Killed (n = 170)	Seriously injured (n = 277)
Intrusion	47%	35%
Asphyxia-Fire	28%	0%
Total ejection	12%	15%
Projection	7%	50%
Other	6%	0%
	100%	100%

structure resistance, especially in highly offset impacts, but the feasibility of this is doubtful. Reinforced coach stiffness aimed at avoiding intrusion from the front row of seats could be an objective. The problem of protecting the driver and the occupant of the hostess seat remains. In tipping-over and rollover accidents, proposed standards(1) aimed at avoiding crushing of the superstructure concern only a maximum of 6 to 15 percent of all severely injured victims in the sample. In the light of our analysis, it may be feared that, even if one managed to eliminate superstructure collapse sufficiently, the number of seriously injured victims would not be reduced significantly because of the high risk of ejection.

Ejection is the cause of 12 of 15 percent of serious injuries and occurs mainly in overturning accidents. Ejection occurs via side windows (71 percent), the windscreen (22 percent), and the rear window (7 percent). A simple lapbelt would provide effective protection against the risks related to total ejection. A 100 percent wearing rate would eliminate 12 percent of all deaths and many serious injuries also. To combat ejection, the other alternative is that of restraining uncontrolled kinematics by the windows themselves (acting as a net). This could be achieved by adding glued laminated glass. This totally passive safety characteristic could in addition improve coach structural resistance. Such an approach, however, has the disadvantage of militating against rapid passenger evacuation (except, if satisfactory solutions in terms of emergency exits—whatever the coach's final position after impact—can be developed).

Last, it seems that lowering the height of the bottom of the side windows increases ejection risk. In the absence of either making the window act as a net or of restraint system use, the bottom of the side window should not be lower than the shoulder of an average adult passenger.

Projection of a passenger against internal panels of the coach compartment was the cause of half the serious injuries, but only of 7 percent of deaths. It is only really possible to envisage two countermeasures, that is wearing a restraint system or modifications to seat backs:

- Restraint System—Case-by-case analysis shows that wearing a seatbelt, even a 3-point type, would not have avoided with certainty any of the few cases of deaths due to projection that occurred mainly in falls into a ravine

  The countermeasure of universal wearing of 3-point belts among all the seriously injured in our sample would, according to our estimate, have lessened the injuries of 43 percent (120/277) of such nonfatally injured people, taking all impact types together. This percentage contains a wide range of conditions of very different presumed effectiveness and type of protection achieved (Table 5).

  The countermeasure of universal wearing of a lapbelt among those seriously injured in our sample would have forestalled 25 percent (70/277) of such injuries, taking all impact types together. The difference in the preceding estimates is due to the fact the wearing of a lapbelt would not provide a cranio-cervical protection in frontal impacts. This evaluation does not take into account the possible adverse effect mentioned by recent reports(3) in frontal cases.

  However, these are estimates of maximum benefits, and it is believed such devices would be less than universally used in coaches. Thus, the only efficient action, without compulsion for coach users, consists of improving the restraint effect of seat backs.
- Seat-back Improvements—These modifications would aim at achieving the following objectives, especially in frontal impacts:
  - Limiting the forward movement of the occupant to the back seat without overloading to the occupant seated in front of him.
  - Reducing the seriousness of lower limb impacts (for example, by knee bolsters) and of cranio-facial injuries (for example, by appropriate padding). Such modifications should take into account the simultaneous need to protect both children and adults, especially the elderly.

  Compared to 3-point belt-wearing, the effectiveness of this purely passive protective device is less pronounced because it only concerns occupants seated behind a seat back; and such a device cannot, in case of very oblique frontal impacts, prevent all risks for occupants seated near the central gangway.

  All in all, this countermeasure could, in our view, eliminate 20 percent of all those seriously injured.

The last point related to passive safety is the consequences of fire. Fire as a cause of death is rare. Nevertheless, we should mention that the fire case studied highlights the problem of being able to get occupants clear of coaches quickly. The same would be true for

Table 5. Presumed effectiveness of 3-point belts for all seriously, but not fatally, injured occupants

Impact types	Number of seriously injured avoided by prevention of		Presumed 3-point belt effectiveness
	...projection	... ejection	
Frontal	50	5	41% (55/135)
Overturning	36	24	57% (60/104)
Others	1	4	13% (5/38)

coaches falling into water. Apart from such cases, the problem does not arise.

One may note that the means of achieving the two aims of reducing ejection and facilitating evacuation are currently contradictory. Can the frequency of ejection be reduced by increasing the number of emergency exits, especially through the side windows?

In this context, doors seem to be the emergency exits that are the most rational and involve the fewest problems. In case of tipping-over accidents, the possibilities of transforming the rear window and roof windows into emergency exits cannot be neglected. In all cases, the rapidity of evacuation must be a priority, and everything must be done to maintain clear and free gangways, door approaches, and emergency exits.

The effort to obtain better flammability characteristics of vehicle interior materials must be pursued, but it is also necessary to consider the effects of smoke emission and toxic gas, which may accompany such fires. The fact that smoke is opaque is an important cause of panic, and carbon monoxide induces paralysis, particularly of the lower limbs. Measures aimed at improving smoke emission evacuation will reduce the risk of asphyxia and facilitate the rapid escape of coach users.

Conclusion

Travel by coach is by far the safest means of road travel, but seeking ways to prevent coach accidents or to lessen their effects is still necessary.

This survey, based on 48 fatal coach accidents, shows it is clearly preferable that accidents be avoided by greater care being taken by coach drivers, since 73 percent of these were blameworthy in the studied sample. But because an exceptionally large number of people are at risk in such accidents, improvements in the construction of coaches must also be developed if some of the causes of death and serious injuries are to be minimized.

Shortening stopping distances by increasing braking performances could avoid or reduce in severity about 15 percent of the cases studied.

Intrusion in frontal impacts is the main cause of death in coaches. Increasing coach front structure resistance, especially for highly offset impacts, would be desirable, but the feasibility of this is questionable.

In the sample analyzed, death by being thrown forward against a seat back has not been observed, but this accounted for half of those accidents involving serious injuries. Particular attention should be given to improving seat backs to insure adequate passive restraint for head and lower limbs in frontal impacts.

Total and partial ejection are frequent and severe in rollover and tipping-over accidents. Window retention using glass plastic products mounted so as to act as a net could prevent ejection without any restraint usage. But such a device is in conflict with the need to be able to use all glass-covered apertures as potential emergency exits, particularly in cases of falling into water or the outbreak of fire. Improvements in escape routes for the last two cases must be considered.

In case of fire, measures aimed at evacuating smoke emission will reduce risk of asphyxia and increase the time available to leave the vehicle.

To provide a chance of assessing more precisely the effect of feasible and necessary safety measures, doing so on the basis of very severe coach accident data, the comparison of independent studies has to be intensified through the auspices of international organizations.

Acknowledgments

The authors wish to thank the Gendarmerie Nationale for their cooperation; without it, this study would not have been possible.

References

1. Baxter, W.L., "Coach accidents—a perspective," International Congress of FISITA, Hamburg, 1980, VDI Berichte N. 367, 1980.
2. Stansifer, R.L., and R.A. Romberg, "An analysis of accidents involving buses and an assessment of the need for safety belt requirements in such vehicles," Proceedings 22nd AAAM Conference and the IAATM VII Conference, Ann Arbor, Michigan, July 10-14, 1978.

3. Farr, G.N. "School bus safety study," Crashworthiness section of *Transport CANADA*, 1985.
4. Davis, M.M., "A study of some schoolbus crashes," Proceedings 21st AAAM Conference, Vancouver, British Columbia, September 15-17, 1977.
5. Gendarmerie Nationale, "Statistique annuelle des accidents de la circulation routière," Année 1984.

Optimisation of a Bus Superstructure from the Rollover Safety Point of View

D. Kecman
Faculty of Mechanical Engineering, Belgrade
Consultant to Cranfield Impact Centre

G.H. Tidbury
Cranfield Impact Centre, Cranfield, United Kingdom

Abstract

Bus superstructures may soon be subject to new rollover safety requirements. Increased rollover safety must be achieved with minimum weight or cost penalty; hence, optimisation has a significant practical relevance.

This paper demonstrates the possibility of predicting the collapse performance of a bus superstructure by a completely theoretical model. The work described also created a basis for the option offered by the new regulations that allows type approval by calculation combined with some component tests. It also shows how a safety structure can be optimised from the weight or cost point of view by means of a special computer program.

Introduction

The importance of adequate bus rollover safety has been recognised for many years. Bus superstructures may soon be subject to new rollover safety requirements, which are currently being discussed by Working Party 29 of the ECE.

The regulations are likely to offer the following choice of methods for obtaining type approval:

- A standard full-scale rollover test
- Pendulum tests on individual structural segments (bays)
- A calculation method, combined with some component testing

The standard full-scale test implies rolling a complete vehicle from a tilting platform onto a horizontal plane 800mm below. The superstructure must not intrude into a residual (survival) space defined with reference to the H-point and centreline of the seats. Such a test is very expensive and unsuitable for development purposes.

The pendulum test on structural bays is carried out by an oblique impact at the cant rail level. The speed of impact is 3 to 8ms, while the impact energy represents a fraction of the total energy for the complete bus. The energy is proportional to the mass of the vehicle and the vertical fall of the centre of gravity between the maximum level of the fitting platform and the position corresponding to the first contact of the body with the ground. The energy declared for each pillar of the bay must meet five constraints specified by regulation.

The introduction of the calculation method was based mainly on the work carried out at the Cranfield Impact Centre(1-6), although such an option was in the original Hungarian submission to the Working Party. It will almost certainly be a requirement that the calculation must include effects arising when the structure undergoes large plastic deformations. Separate component tests may be required to verify the assumptions for the collapse behaviour of components.

A calculation method offers not only the chance to obtain type approval without large-scale testing, but it is also suitable for bus body development and optimisation in terms of both safety and economy.

Theoretical Prediction of the Collapse Behaviour of a Complete Bus

Bus bodies under impact develop localised bending failures—hinges, which absorb most of the impact energy. Investigation of almost 30 bus rollover accidents(5) identified a variety of collapse modes (Figure 1). Mode A with hinges at the waist and cant rail levels was most common. Hinges at the floor level (B,C) occurred mainly near door apertures, while roof members also collapsed (D,E) in some cases. Control of the overall collapse mode is very important because it affects the amount of deformation prior to the intrusion into the survival space. Mode A usually provides the greatest angles of hinge rotation.

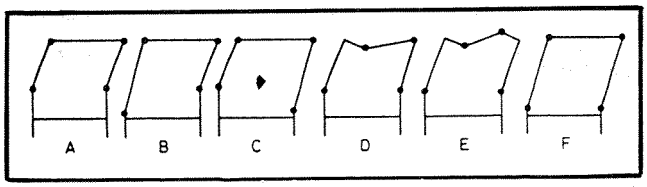

Figure 1. Collapse modes of bus rings

Isolated rings collapse in mode F, which demonstrates the effect of the surrounding structure (cladding, longitudinal beams, seats, floor) in altering the collapse mode of any ring in a bus body. These effects were studied within the elastic range(6), and it was demonstrated they can be modelled successfully by springs C and C, attached as shown in Figure 2. The impact load P is applied obliquely to one of the cant rails.

Spring C has an axial and bending stiffness selected in such a way that the bending moments of the floor, waist, and cant rail levels of the simplified model correspond to those obtained by a much more detailed elastic analysis of a segment of the body.

It was also demonstrated that rings with an incomplete floor member (i.e., without the dotted line in Figure 2) are much more flexible than the complete ones. However, the typical restraining effect of the surrounding structure in the vertical direction (simulated by spring C) is sufficient to eliminate the effect of the central gap on the collapse mode.

A collapse analysis of a complete, all-metal body of a coach was carried out(3,4,6). The skeleton was made of rectangular and square section tubes clad with aluminium sheets. A quasi-static analysis of a standard rollover test situation is possible because of a relatively low impact speed (less than 10ms) and because the mass of the deforming structure is much less than the mass that is being retarded.

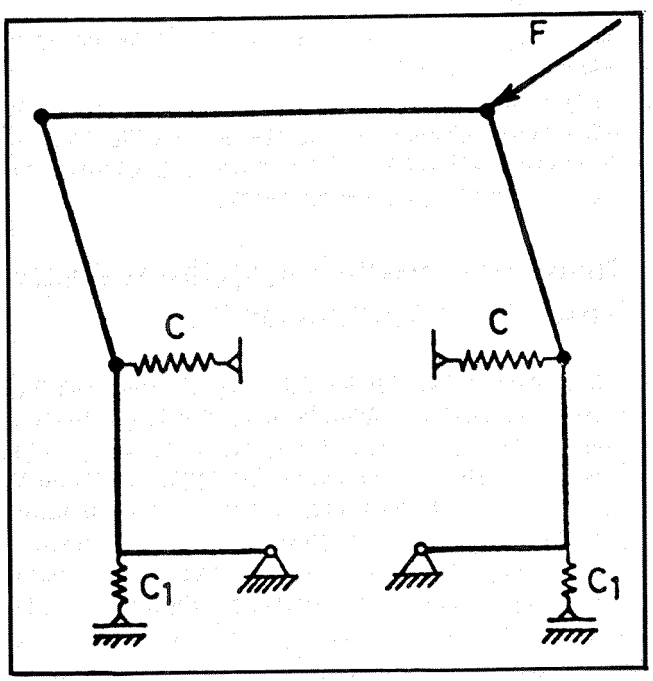

Figure 2. Collapse mode of bus ring with springs simulating the connecting structure

Collapse analyses were performed using the Cranfield Structural High Deformation program CRASH-D, which allows for the highly nonlinear effects of large deformations, hinge occurrence, and variable hinge moment-rotation curves.

The analysis started with the elastic finite element model in Figure 3a, which included all the main beam and plate elements. Loads were applied obliquely along the cant rail and the main load paths determined. It was shown theoretically(3) that the collapse mode can be controlled by careful selection of the side components below the waist rail. The model for collapse analysis was much simpler (Figure 3b) and included only those main elements that would form the main collapse mechanism. Fictitious beams were attached laterally to the pillars at

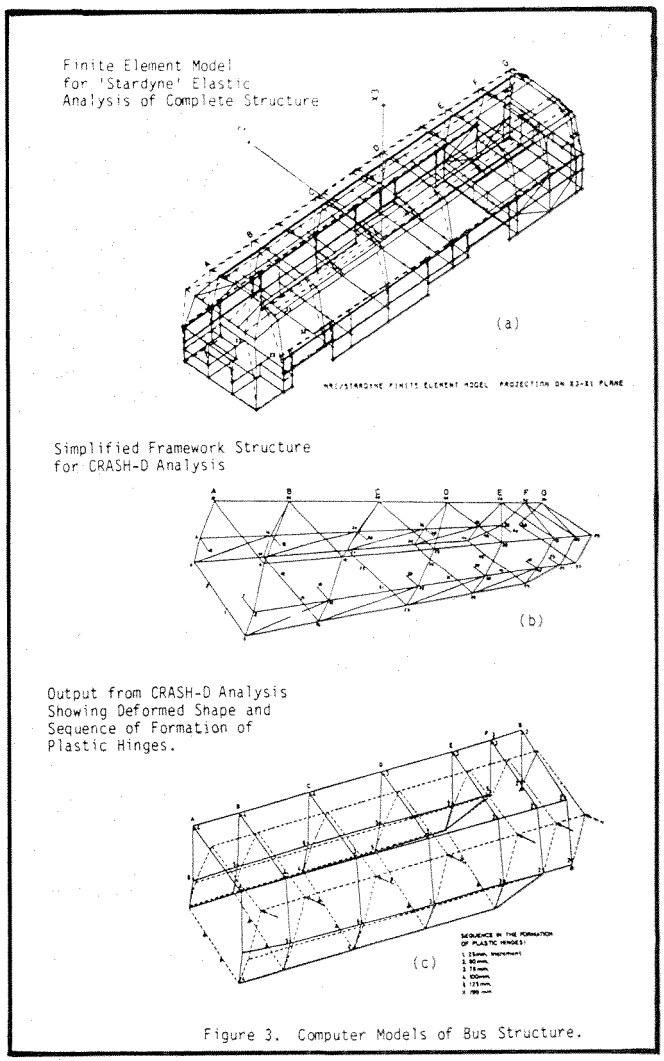

Figure 3. Computer models of bus structure

the waist rail level to simulate the effect of those elements in the side structure that were eliminated from the first model.

The theoretical collapse mode (Figure 3c) predicted hinges at the cant rail and waist rail level in all rings except the front door, where the hinge occurred below the waist rail. Secondary hinges, which did not take part in the main collapse mechanism, were also predicted at the floor level of all rings. The full-scale test of the vehicle (performed after the analysis) gave an excellent agreement with the predicted location and character (primary or secondary) of all hinges.

To predict the final deformations of the structure, it was necessary to determine the energies absorbed by each ring and compare the sum with the total energy input. At the time of analysis, variable hinge moment-rotation curves could be modelled in two-dimensional structures only. The theoretical load-deflection curves of all rings were, therefore, produced by separate analyses. Rings A and G (Figure 3c) included two normal rings, but they collapsed differently. The elastic stiffness of all rings was obtained from the model in Figure 3a, and the theoretical collapse phase was common to all normal rings. Theoretical moment-rotation curves, including the calculated strain-rate effect, were used in the model.

The energy input per ring was equated to the area under the load-deflection diagram, and hence the maximum ring deflections were calculated. Comparative results are summarised in Table 1, where δ_m represents the maximum deflection of the cant rail when it is impacted along a line at 30° to the floor cross-member. The difference is less than 15 percent except in ring F (21 percent), to which displacements could not be applied directly. The agreement is, in fact, better than is shown in Table 1 because experimental displacements were measured after the test when some springback from the maximum deflections had already taken place.

Section Optimisation From the Safety Point of View

The bending moment that can be carried by a thin-walled rectangular section tube drops off rapidly after the onset of collapse. Repeatability of collapse modes produced by uniaxial bending enabled a definition of the theoretical hinge collapse mechanism to be made(6,7). The bending and rolling deformation along the concentrated yield lines (Figure 4) was related to the hinge rotation angle θ, as was the energy absorbed by plastic

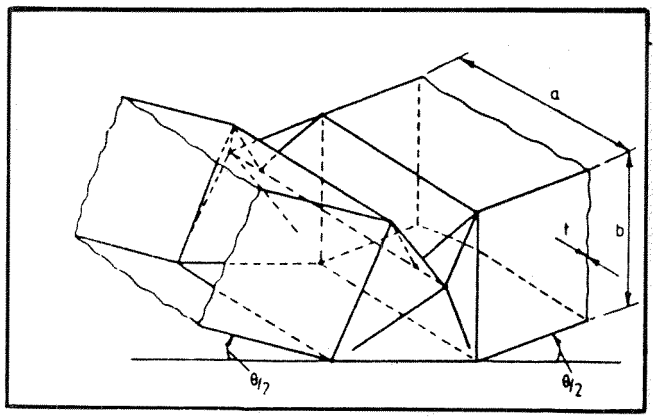

Figure 4. Theoretical model of hinge collapse mechanism

deformation. In such a way, it was also possible to derive the theoretical M-θ curves (Figure 5c) in terms of the section dimensions a, b, t (Figure 5a) and the yield stress o and maximum nominal flow stress of the material (Figure 5b). The theory was verified by very extensive experimental work on tubes with a/t ratios between 9 and 128 and a/b ratios between 0.33 and 3. The agreement with experimental data was excellent (examples are shown in Figure 6).

The theory provided a basis for the development of a section optimisation program WEST(8) for the selection of the lightest or cheapest standard or nonstandard section tubes meeting the following safety criteria: maximum bending strength, energy absorbed, and remaining strength after a given hinge rotation angle. It

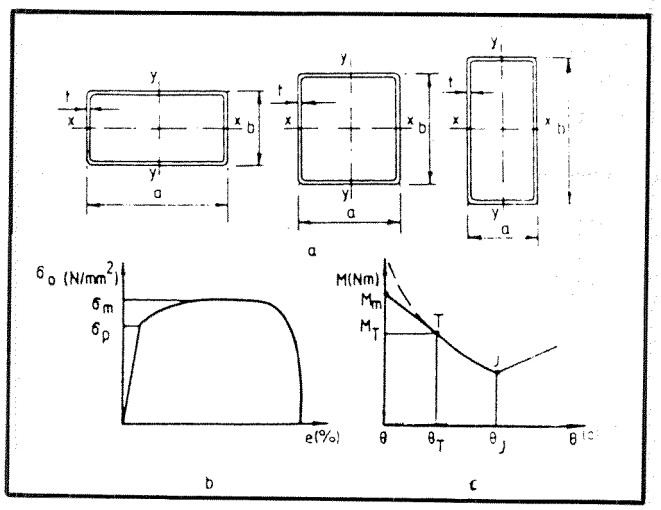

Figure 5. Input parameters for calculation of theoretical hinge moment-rotation curves

Table 1.

Ring	A	B	C	D	E	F	G
δ_m(theoretical)(mm)	536	555	505	491	488	488	430
δ_m(experimental)(mm)	577	550	508	466	424	402	385

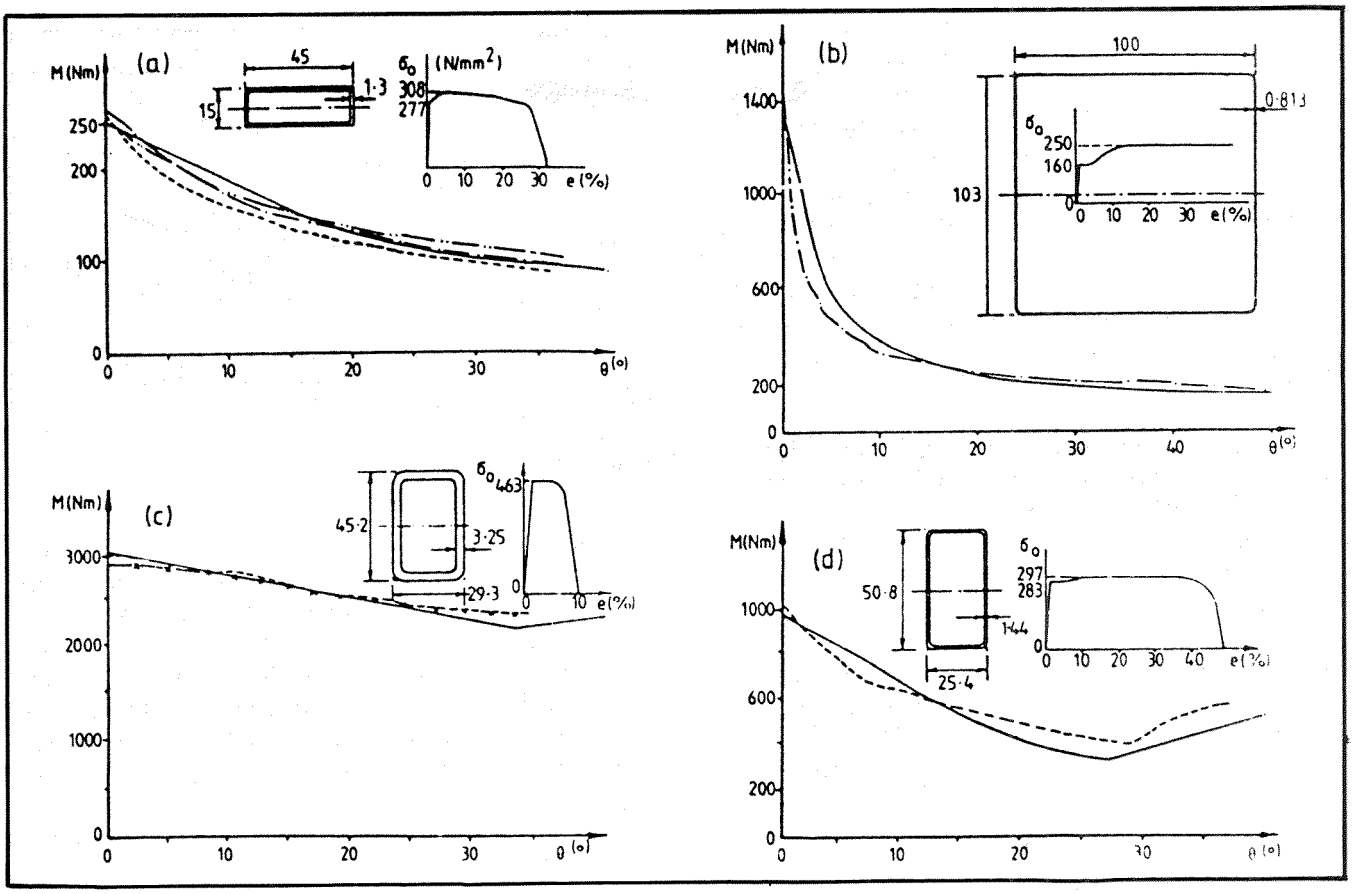

Figure 6. Theoretical (solid) and experimental (dotted) curves for a range of tube dimensions

also enables selection of minimum material properties if section dimensions and the target safety performance are specified. The program can also produce the bending collapse properties of given sections, which may be used further, either directly in design or as input data to finite element programs for collapse analysis.

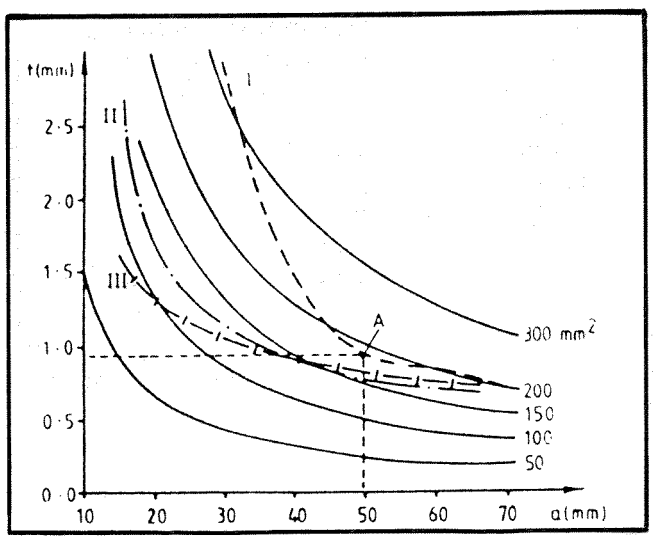

Figure 7. Diagram illustrating operation of optimisation program WEST

The most general case corresponds to the selection of a minimum weight theoretical section made of a given material and meeting one, two, or all three of the safety constraints. By specifying the ratio of the properties about the two principal axes, it is possible to determine the aspect ratio a/b of the section and reduce the number of variables to two, say a and t (Figure 5). Each of the constraints can then be solved for the wall thickness t starting from a range of values of the width a. Three curves are thus obtained (I, II, and III in Figure 7). The section with minimum area, i.e., weight, corresponds to the point A that is lowest on the complex surface defined by constant area curves (shown solid in Figure 7) but that does not fall below any of the three curves I, II, and III.

Procedure for Optimisation of a Bus Structure From the Rollover Safety Point of View

Optimisation of a bus structure from the rollover safety point of view is performed in the following stages:

(a) Choice of the general concept (e.g., two safety rings at the front and back, or no special rings). Subsequent steps allow a parallel estimate of both options.

(b) Assume starting section dimensions and perform an elastic analysis of the complete body or the segment as if it were going to be subject to a pendulum test (main load paths are determined and information on the effects of noncollapsing members is estimated).
(c) Perform collapse analysis of a simplified model, using collapse properties calculated by the program WEST and allowing for the full range of deformations required to absorb the energy required.
(d) Analyse the results of step c and determine the hinge rotation angles and energies required. Use these as input data to the program WEST to determine new section dimensions or material properties, depending on which of the four program options is considered most significant (lightest standard or nonstandard tube, cheapest standard section, or material for given dimensions).
(e) Repeat steps (c) and (d) until the best solution is found.
(f) Repeat steps (b) to (d) to check that the alterations do not introduce important new effects on load redistribution, elastic stiffness, etc.
(g) Design and produce components (beams and joints) based on the theoretical analysis and test them to collapse statically and dynamically (by a small pendulum). This exercise should prove that the assumptions concerning beam and joint stiffness, strength, and energy-absorbing properties are correct.
(h) Accept the solution, or repeat the same procedure with appropriate corrections if results of step (g) require it.

Conclusion

A design procedure has been outlined that involves the use of three computer codes:

- A standard structural finite element code working in the elastic range, e.g., Stardyne
- A special large deflection framework code that includes collapse hinges—CRASH-D
- An optimisation program for the choice of tubular framework members—WEST

The time involved in carrying out the procedure is short enough to become part of the early design process for a new vehicle. It provides the most rational and cost-effective method for the design of structures to comply with the new strength of superstructure regulation.

Acknowledgments

While the optimisation code is solely the work of the first author, the general method of analysing the whole structure was developed at the Cranfield Impact Centre under the sponsorship of the Department of Transport.

References

1. Kecman, D., "Analysis of framework-type safety structures in road vehicles," *Structural Crashworthiness,* edited by N. Jones and T. Wierzbicki, Butterworths, 1983.
2. Miles, J.C., "The determination of collapse load and energy absorbing properties of thin walled beam structures using matrix methods of analysis," *Int. Journal of Mechanical Science,* 18, 1976.
3. Wardill, G.A., and D. Kecman, "Theoretical prediction of the overall collapse mode and maximum strength of a bus structure in a roll over situation," Congress FISITA, Hamburg, 1980.
4. Kecman, D., and G.H. Tidbury, "Theoretical predictions of the complete collapse behaviour of a coach subject to the proposed standard roll over test," Congress FISITA, Melbourne, 1982.
5. Structural Design Group (Cranfield Impact Centre), "Bus rollover accident investigations 1976-1979," Report to the Department of Transport (London) No. DRG/463/139, Cranfield Institute of Technology, United Kingdom, 1979.
6. Kecman, D., "Bending collapse of rectangular and square section tubes in relation to the bus roll over problem," Ph.D Thesis, Cranfield Institute of Technology, 1979.
7. Kecman, D., "Bending collapse of rectangular and square section tubes," *Int. Journal of Mechanical Science,* 25, No. 9-10, 1983.
8. Kecman, D., "Program WEST for optimisation of rectangular and square section tubes from the safety point of view," International Conference on Vehicle Structural Mechanics, SAE Paper 811312, 1981.

Improvements for Bus Safety

Klaus Rompe and
Hans Joachim Krüger
Institute for Traffic Safety, TÜV Rheinland e.V., Cologne

Abstract

Today about 14 percent of passenger transport on the roads is accounted for by buses. For bus occupants, the risk of being killed as a result of a bus collision is about 40 times lower than in passenger car accidents. Therefore, buses can be classified as road vehicles with the most upgraded safety. Nonetheless there are some aspects of safety still to be developed in the future:

- There is still a lack of objective criteria designed to assess the driving behavior of the new type generation of high-capacity buses.
- Underfloor cockpits restrict the driver's field of vision and expose the driver and, hence, the occupants to additional risk of injury in accidents. Bus driver cockpits could be adequately improved at low cost.
- The anchorage of seats and the capacity of deformation energy of backrests can be exploited to incorporate an advanced passenger restraint system.
- There is need for specifying criteria of effectiveness applicable to emergency exit systems.

Safety of Buses

Today approximately 14 percent of the total passenger transport on the roads of the Federal Republic of Germany is accounted for by buses(1). It is obvious the safety of these vehicles is a reason for their attractiveness. The risk of being injured in an accident by bus is 10 times lower than in a passenger car accident. Referring to the number of kilometers per person, the risk of being killed is even 40 times lower. There are, however, three essential arguments for a further increase of bus safety in the future:

1. Along with the technical development of safety components in buses, e.g., antiskid devices, retarders, headlight range adjustment, and passenger protection devices, there has also been a change in the construction concept of buses. In modern bus construction, the permissible limiting values for the outer dimensions—18m long, 4m high, 2.5m wide, and weight 28t—today are fully exploited (Figure 1). For long-distance travel, high- and double-decker buses—even in an articulated form—have become more popular, and, as a result of their increasing number, they also play a role in the overall accident occurrence. There is, however, especially for these vehicle types, very little knowledge concerning the driving properties, particularly in critical driving situations(2).
   Recently, for reasons of cost, more and more lorry chassis parts are used for bus construction. This raises the question as to whether this will change the design strength of the bodywork in a collision and the structural aggressivity of the vehicle toward other vehicles.
2. Due to the heightened seating position of bus occupants, the consequences of collisions with other traffic participants are generally not severe. The construction of high- and double-decker buses, however, could favor the frequency of the accident type "running off the road." The danger arises of overturning and, at the same time, up to 150 passengers are subjected to a hazardous

Figure 1. Modern high-capacity coach dimensions (above—18 x 2.5 x 4m, seats100-144; below—18 x 2.5 x 3.2m, seats 68-80)

situation, e.g., individual survival space is not granted by the structural strength.

3. Children and elderly persons figure significantly in the number of injured bus passengers(3). Since these persons are more or less dependent on bus transport, their protection should be particularly considered.

By order of the Federal Ministry of Transport, the Institute for Traffic Safety of TÜV Rheinland has conducted several investigations to find new possibilities to improve bus safety.

Safety is based on the ergonomic design of the bus driver's workplace. The driver obtains essential information for driving by his vision. Therefore, the sight from the vehicle to the front, to the side, and via the mirrors to the rear is of particular importance (Figure 2).

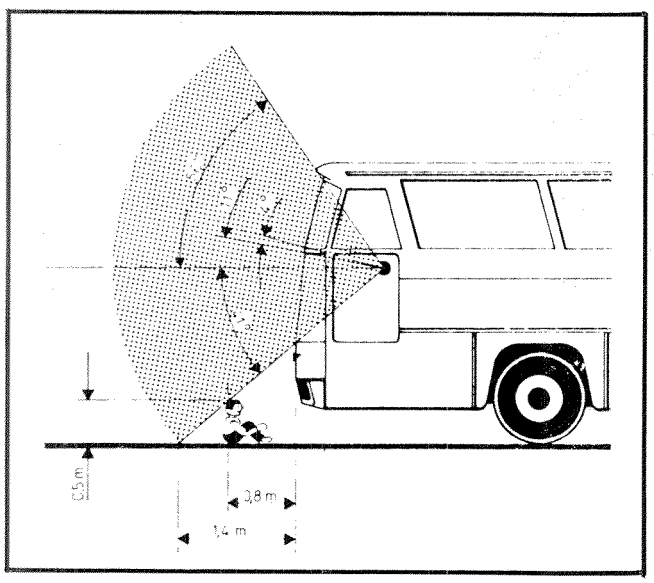

Figure 2. E-point level and frontal direct field of vision

For high-decker buses, an average height of the driver's eyes of 2.2m above the road was calculated. Together with the extremely large surface of the windscreen, this means perfect vision to the front. For underfloor cockpits, coming more and more into use, the eye level 0.5m lower than usual causes problems concerning safety. The all-round vision of the driver is limited, and the danger of the driver being injured in an accident with a passenger car (the most frequent participant in a collision) is increased (Figure 3).

If the sight conditions to the right and to the rear are taken into consideration, problems are caused by the conflict between structural strength and the required unhindered all-round vision (Figure 4)(4). Nonmisting, heated side windows, additional mirrors, and a television system at the rear of the vehicle could be technical solutions. A comparative assessment of the different possible systems is being effected at present.

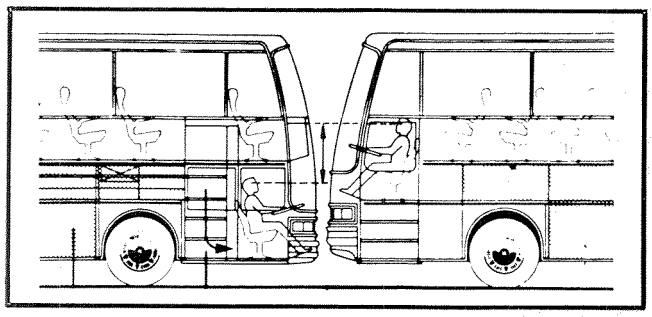

Figure 3. Eye level in underfloor cockpits

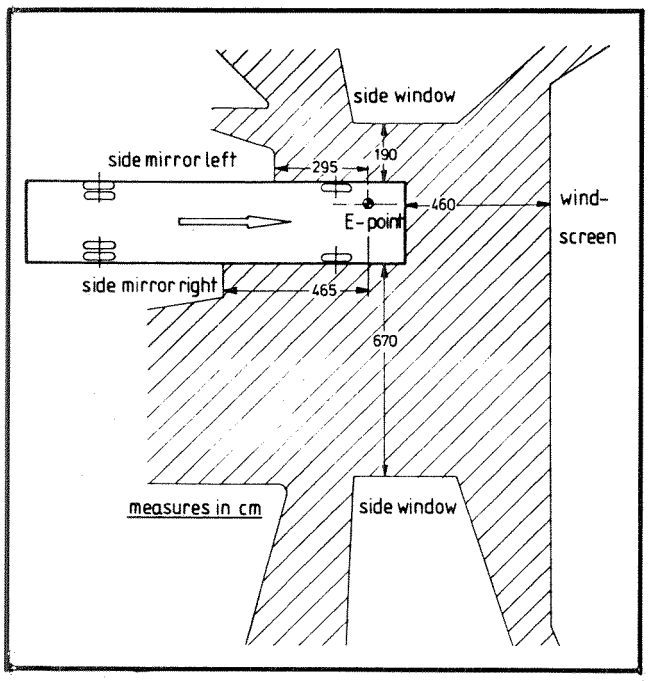

Figure 4. All-round field of vision

Also, control switches and monitoring instruments must be arranged favorably within the driver's field of vision. It is, however, questionable whether he is able to observe up to 84 displays besides his actual task of driving (Figure 5).

Based on our measurements and driver interviews, further improvements are required, especially for the ergonomic design of control devices at the driver's workplace(5). One example is a suitable resting place for the left foot in a rest position. The slope of the accelerator frequently does not meet comfort requirements. To reduce the time of change from the accelerator to the brake pedal, the half-loaded accelerator should be positioned approximately to the same height as the unoperated brake pedal.

Within the driver's reach, all control devices should be arranged within a radius of approximately 700mm around the shoulder joints. This requirement is not yet fulfilled in all cases. The movements of the gear level,

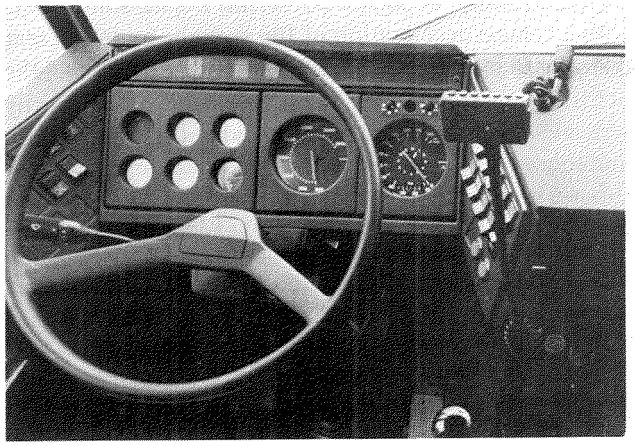

Figure 5. Instrument panel with 84 controls and displays

which are still necessary, exceed this range by far (Figure 6).

The example given in Figure 7 shows that one hand must leave the steering wheel to activate the windscreen wiper. To maintain continuous two-handed steering, all controls operated frequently should be located within finger reach around the steering wheel.

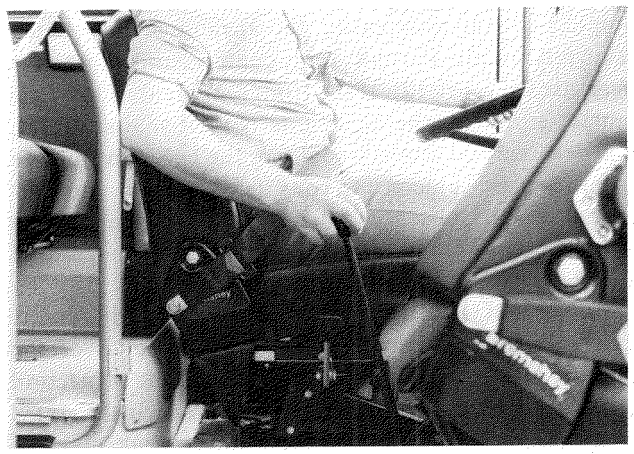

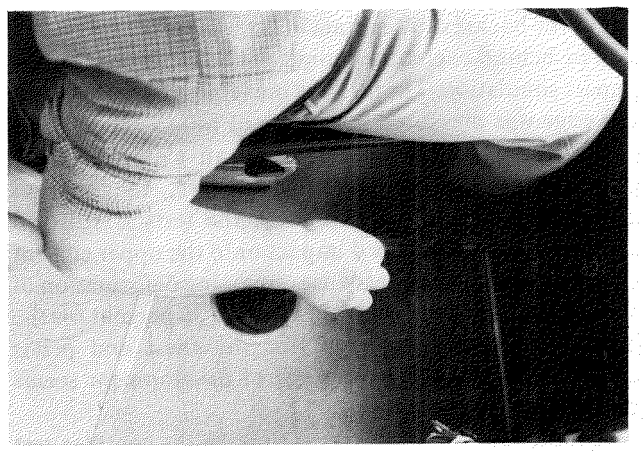

Figure 6. Nonergonomic gear level position

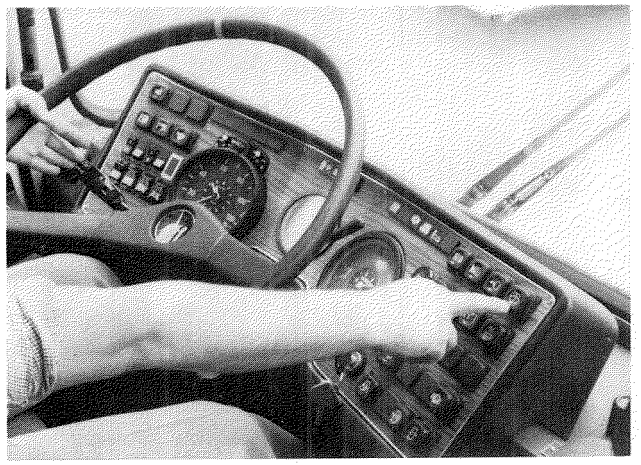

Figure 7. Interruption of two-handed steering for switching on the wiper/washer system

Although the driver's workplace conditions in buses are sufficient in general, these examples show that further improvements are possible without great effort.

Fifty to 60 percent of all bus accidents are head-on collisions, more than half of which are collisions with passenger cars. Because the passenger seats are located about 1.2m above the road, the risk of bus occupants being injured is relatively low. However, the risk is considerably higher in overturning vehicles. The risk of the occupants being injured or killed occurs particularly when the vehicle deformation does not maintain necessary survival room for the passenger seats. If the passengers are thrown out of the vehicle, the risk of being killed is about six times higher than in similar accidents with passenger cars(6,7). In about 50 percent of all overturning accidents, passengers are thrown out. Therefore, the accident type "overturning of vehicle" must be given more attention in the future.

In the Federal Republic of Germany, long-distance buses with a permissible travelling speed of 100km/h for motorways must be equipped with lapbelts for those seating positions that do not have a similar seat in front of them—the so-called risk seats. However, the systems available at present with uncomfortable locks, long belt straps, and even with automatic locking retractors are not accepted voluntarily by the passengers (Figure 8). Moreover, automatically locking lapbelts, such as those currently in use, restrict the occupants and it has proven difficult to have them fasten their belts. It has, therefore, been investigated in comprehensive studies how to improve the restraining effect of seat systems to add to occupants' safety(8,9).

During the first stage of the investigation, we varied the distance between the seat rows from 700 to 1,000mm. In simulated head-on collisions with vehicle decelerations of 5g, we measured the strain of different size dummies in sled tests. Figure 9 illustrates the movement paths of an adult dummy for head, chest, and pelvis. On the left part

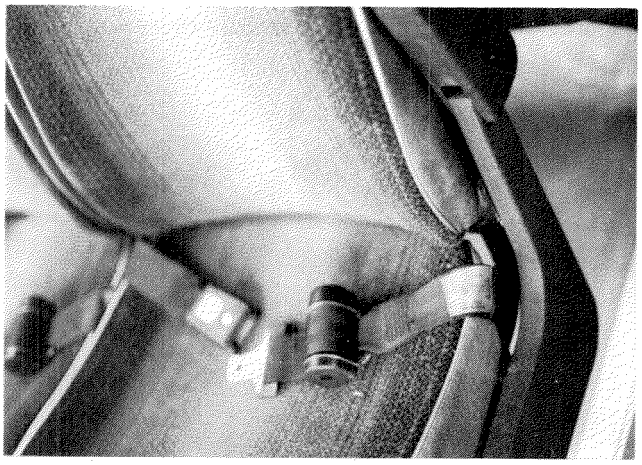

Figure 8. Lapbelts on exposed seating positions in 100km/h limit coaches

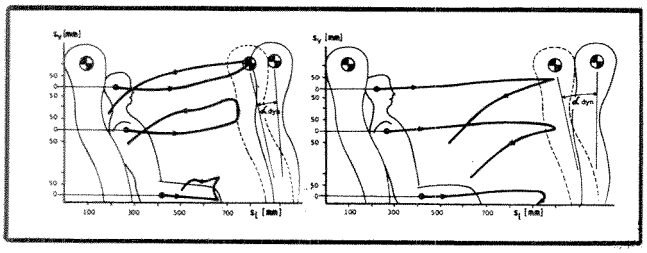

Figure 9. Trajectories of child-dummy movements at 5g deceleration in different distances between two forward-faced double seats (left—70mm; right 900mm)

of the figure, the distance between the seats is 700mm; on the right, it is 900mm. The test results showed that, for child as well as adult dummies, a minimum of injuries may occur with a distance between the seats of 800 and 850mm (Figure 10). This figure illustrates the resulting head acceleration in a head-on collision for an adult dummy as a function of the distance between seats. Due to different impact conditions of the head onto the backrest of the front seat, the strain of the occupants is increased for small and long distances between the seats.

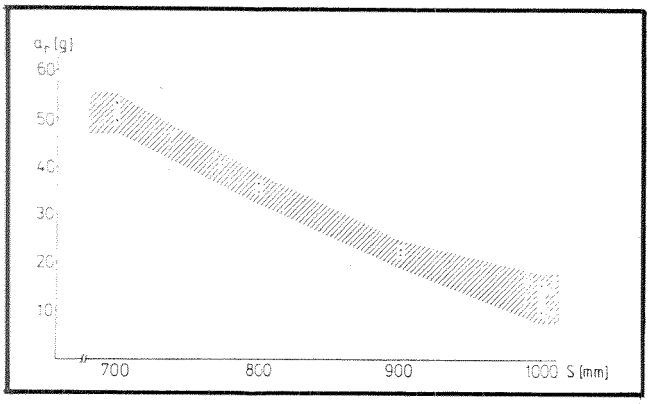

Figure 10. Resultant head deceleration of child-dummy as a function of distance S to the next impact

Subsequently, we carried out further impact simulations with a vehicle deceleration of 10g with the optimum seat distance to investigate the strain on the dummies and the deformation behavior of the front backrests. Primarily we stated that the seat anchorage did not stand the strain and loosened. Figure 11 shows a construction drawing of this anchorage on the left outer wall of the vehicle and on the bottom of the right side of the vehicle. To change the

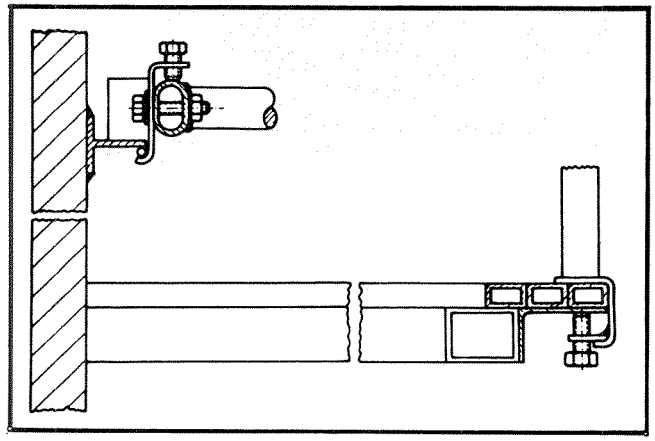

Figure 11. Lateral and inside elements of seat anchorage

number of seat rows easily, the anchorage is executed relatively simply. Partially, only compression joints have been used (Figure 12). If the front seat breaks loose, the impact strain on the occupants is relatively small. If, however, several seat rows loosen, the occupants on the front rows are subjected to considerable strain. Furthermore, partially loosened or displaced seats will hinder the work of emergency helpers considerably in case of accidents.

For further tests, the seat rows were fixed additionally. The measured strain on the chest and pelvis of the dummy was relatively low compared to the protection criteria to be considered concerning the survival chances of the passengers. For the head, however, peak values of 150g were measured, caused by impact of the head on the top of the backrest. A contact of occupants sitting side by side or behind each other could not be observed for this impact simulation. The forward movement of the backrest top edge was measured in a range of 140 to 180mm.

If the seat is considered to be an element of the occupant-restraining system in buses, the energy-absorption capacity measured in the tests is still too small. Especially the head impact onto the upper edge of the backrest does not yet cause remaining deformation of the seat. A reduction of strain of about 30 percent for the head and about 15 percent for the chest and pelvis compared with the actual stage of development seems possible.

Another aim of the tests was to leave the complex test procedure using dummies with complete instrumentation

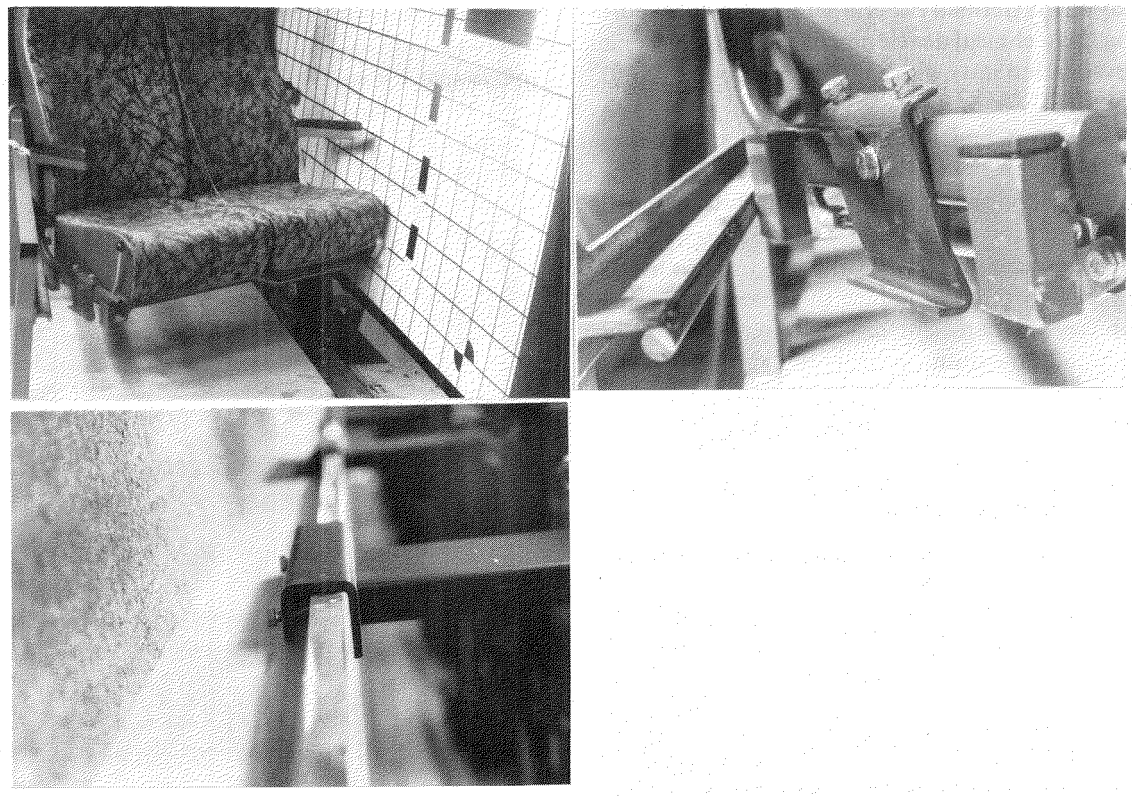

Figure 12. Failure of anchorage elements in a simulated 10g frontal impact

and develop a simplified test procedure. In several stages, the required masses were reduced accordingly without considerably changing at the same time the kinetical and kinematical ratios during the impact (Figure 13). Such a test procedure will give much help to the manufacturers of bus seats concerning increased safety for passenger room. If the resistance of the seat anchorage on the vehicle bottom is guaranteed, it will define individual survival room for each passenger, considering also the required backrest deformation (Figure 14).

At least for two accident types, the severity of the accident results is considerably dependent on the bus emergency evacuation system. After a collision, single exits may be blocked within the collision range. In general, there are sufficient evacuation possibilities in the residual compartment.

In case of the vehicle overturning, however, more than half the exits may be blocked. Escaping from the compartment to the top requires enormous physical strength. Compared to the normal escape direction to the back or through the roof, this way seems to be a detour. The most important requirement for an emergency evacuation system is caused by a burning vehicle in a lateral position.

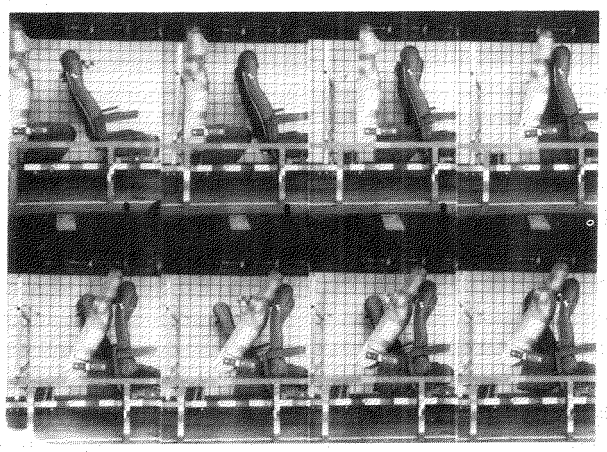

Figure 13. Simplified test with reduced dummy masses

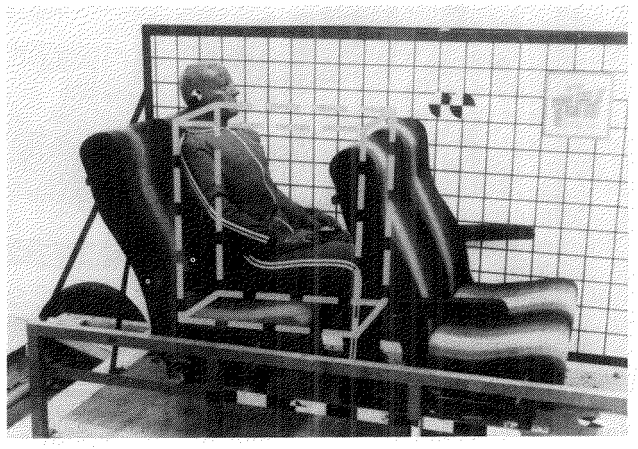

Figure 14. Individual survival room for each passenger

In a study by the German Federal Ministry of Transport concerning the technical development of emergency exit systems, evacuation tests with a children's group (8 to 10 years) and an adult group were carried out in a long-distance travel bus and a short-distance bus. During several test runs, the following main escape directions were prescribed: doors (Figures 15 and 16), as well as two emergency windows on the left side (Figure 17). A platform was erected in front of the windows to avoid injuries caused by jumping. Since the emergency scene shown for the compartment discourages hesitation in front of a free evacuation opening, the platform was a protection measure(10).

The evacuation tests showed the following results:

- .Escape route: doors

  For each vehicle type, the evacuation was finished after about half a minute (children, long-distance travel bus: 40s). Two-thirds of the passengers escaped through the rear door.
- Escape route: two emergency windows, left side (2 and 4 side window)

Figure 15 Evacuation test through the doors with an adult group and a short-distance bus

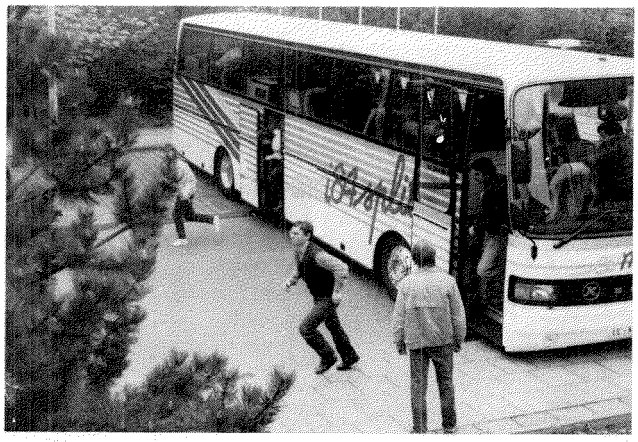

Figure 16. Evacuation test through the doors with an adult group and a long-distance travel bus

Figure 17. Evacuation through an emergency window

Destroying the window glass and removing approximately 90 percent of the window surface required 15s, equally for single- or double-glassed windows. Half the adult group left the vehicle by each window within less than 1min (52s).

It seems important that, in case of alternative escape routes, the doors—especially the rear door—are preferred. As a result, a stoppage is caused in front of the rear door, whereas the capacity of the other exits is not fully exploited. Improvements will be possible for the ergonomic design of the exit aids, for children in the door area and for adults with access to emergency windows. As the most effective measure, the internal door access areas should be kept free (ticket barriers, folding seats, etc.).

For a normal position of the vehicle and an escape route to one side, the evacuation time is less than 1min. The relative requirement for airplanes is 90s. This is based on the toxic effect of fumes, which determines the escape time of possibly injured passengers. Up to now, accident analysis has not yet brought secured time values for vehicle evacuation.

A comparison of international construction regulations concerning bus emergency exit systems shows that, besides the minimum requirements for vehicle construction, there exist alternatives for a great number of other

technical solutions. The position of the individual emergency exits and the necessary opening by folding out, removing, and destroying (tool!) require detailed knowledge and ability of the bus passengers, which, in general, is not given. In contrast to construction regulations for airplanes, there is need of an effectiveness requirement for the bus emergency exit system, based on the required evacuation time.

From the frequent use of doors, these must range equally as an element of the emergency exit system. The mounting position of the emergency door-activating device must be determined on a standard basis within a limited area for vision and handling by the standing bus occupant. This device must be secured against unauthorized use (threshold of shrinking from an impulse for action). An emergency door at the vehicle's rear could be an additional main escape route.

The rigid side windows consist of single security glass and guarantee also the structural rigidity of the vehicle compartment. As a result, opening each of these windows by destroying it is given as a technical solution and could mean a most important capacity increase for the emergency exit system. The necessary emergency hammer—available only within vision and handling range—raises a reasonable expectancy of effectiveness, also for nonspecialists.

Emergency holes in the roof could be an efficient escape route with a minimum climbing height, especially from vehicles in a lateral position.

The improvement of passenger safety must be proved with an efficiency test of the emergency exit system. Subject to test methods still to be determined, a limiting value of 45s seems possible for evacuating a completely occupied, upright-standing vehicle.

It is required also for developed bus emergency exit systems that the passengers have good knowledge of the details. Therefore, it seems important to instruct bus passengers regarding the emergency equipment of each vehicle, its use, and passenger behavior.

This study has made it clear that improvements of bus safety are necessary and possible.

References

1. Statistisches Bundesamt, Wiesbaden: Statistisches Jahrbuch, 1982.
2. Rompe, K., and B. Heißing, "Test procedures and evaluation criteria for the handling characteristics of heavy commercial vehicles."
3. Statisticsches Bundesamt, Wiesbaden: Straßenverkehrsunfälle, Fachserie 8, Reihe 3.3.
4. Rompe, K., and H.J. Krüger, "Possibilities of development in bus safety," 1st IAVD-Congress, Geneva, February 22-24, 1984.
5. Krüger, H.J., Gestaltung des Bus-Fahrerarbeitsplatzes. BMV, FP 7816/2, Bericht des Instituts für Verkehrssicherheit, TÜV Rheinland, 1979.
6. Krüger, H.J., Bestandsaufnahme der Inneren Sicherheit von Bussen, BMV, FP 7816/1, Bericht des Instituts für Verkehrssicherheit, TÜV Rheinland, 1979.
7. Krüger, H.J., Prüfverfahren für KOM-Fahrgastsitze als Rückhaltesysteme, BMV, FP 1.8001, Bericht des Instituts für Verkehrssicherheit, TÜV Rheinland, 1983.
8. Rickey, Stansifer, "An analysis of accidents involving busses and an assessment of the need for safety belt requirements in such vehicles," Proceedings 22nd AAAM Conference.
9. Walz, F., "Aus der Unfall- und Verkehrsmedizin," *Automobil-Revue*, Nr. 48, 1978.
10. Krüger, H.J., Notausstiege in Kraftomnibussen, BMV/BASt, FP 1.8306, Statusseminar, Münster, 1984.

Heavy Truck Safety—What We Know

Henry E. Seiff
Motor Vehicle Manufacturers Association

Abstract

The overall highway fatality rate has dropped almost continuously since 1925, from 20 to 2.5 per 100 million miles of travel in 1984. Still, the almost 44,000 fatalities in 1984 can and will be decreased. In 1983, 5,475 of the 42,584 highway fatalities were in accidents involving medium or heavy trucks. Only 18 percent of these were occupants of the trucks themselves; 82 percent were pedestrians or occupants of the other vehicle. The greatest number of combination truck accidents takes place on two-lane rural roads. Single-vehicle accidents are responsible for 70 percent of heavy truck occupant fatalities. Doubles and heavier trucks appear to be as safe as other heavy trucks. Rollover and ejection are responsible for the greatest number of truck occupant fatalities.

When asked about her top priority as the new Secretary of Transportation, Mrs. Dole replied, "There's no higher mandate for the Department than to promote safety. . . ."

The Secretary is particularly concerned with heavy truck safety.

Several years ago, the Motor Vehicle Manufacturers Association (MVMA) summarized the state of heavy truck safety research in its presentation, "Heavy Truck Safety—The Need to Know." It emphasized the urgent need for adequate safety research as a foundation for improving heavy truck safety. It is appropriate now to follow up with a summary of the things we have learned since that time and to place the heavy truck safety problems in perspective.

In reviewing highway fatalities and fatality rates for all motor vehicles, we see the extraordinary safety gains that have been made over the past 60 years (Figure 1). The fatality rate (persons killed per 100 million vehicle-miles of travel) has dropped almost continuously from 1925 to the present—from nearly 20 to 2.5 in 1984. Although vehicle-miles traveled have constantly increased, with the exception of World War II and a short time after the 1973 and 1978 oil shortages, the total number of highway deaths peaked in the late 1960's and early 1970's. The year 1984 marked a 22 percent decrease in deaths from the high year of 1972, despite a 36 percent increase in vehicle-miles traveled(1).

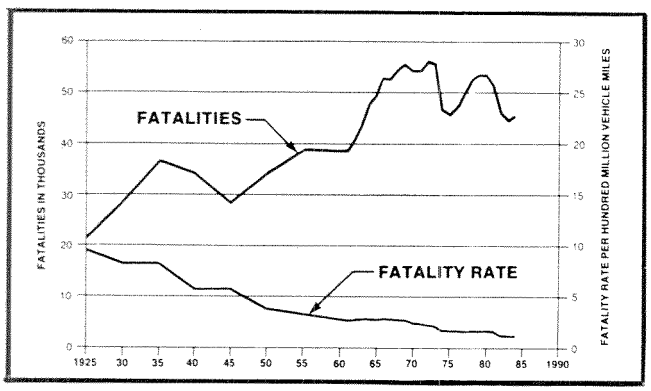

Figure 1. U.S. motor vehicle accident fatalities, 1925-1984

Although we can be justly proud of these figures, we still had almost 44,000 fatalities on our highways in 1984. We believe we can and will lower this number in future years.

The reasons for decreases in both the fatality rate and total fatalities include safer vehicles, safety belts, highway safety improvements, child restraints, better medical care, the 55mph speed limit, the imposition of the Federal Motor Vehicle Safety Standards, improved driver skills and attitudes, and the antidrunk driving campaign of recent years. We are doing better and can be especially proud to see fatalities continue to drop at a time when Americans are switching to smaller, lighter cars, and truck size and weight are increasing.

Of the 42,584 highway fatalities in 1983, the latest year for which we have detailed data, 5,475 were in accidents involving medium or larger trucks, that is, all trucks over 10,000 lb gross vehicle weight rating.

Of these 5,475 fatalities, only 18 percent were drivers and passengers in the trucks themselves; 82 percent were pedestrians or occupants of the other vehicle—the passenger car or light truck—in a multivehicle accident.

Among the truck occupant fatalities, 735 were occupants of combination vehicles, usually a tractor-semitrailer combination. Two-hundred and forty-four were occupants of straight trucks(2).

Since 1979, fatalities in medium and heavy truck accidents have generally been decreasing as have all highway fatalities (Figure 2). From 1976 through 1979, the increase in truck accident fatalities paralleled the increase for all highway vehicles (the quality of the National Highway Traffic Safety Administration's Fatal Accident Reporting System data on truck accidents in those early years was questionable, so we have reason to believe the relatively low numbers of fatalities in 1976 and 1977 may be understated).

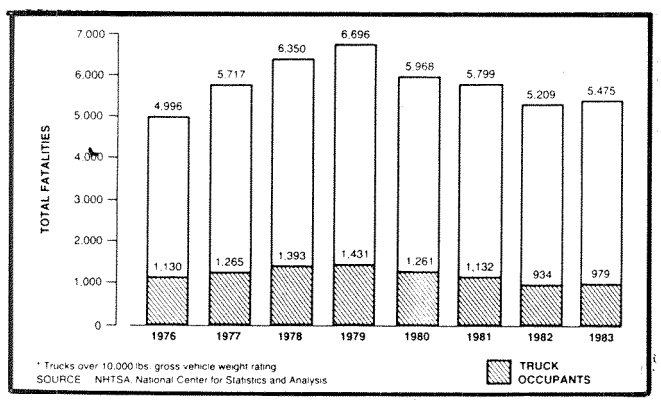

Figure 2. U.S. fatalities—medium and heavy truck accidents

Part of the recent decrease in truck-related fatalities was certainly due to the business downturn of the past few years and the consequent decrease in truck mileage. However, combination vehicle-miles dropped less than 1 percent from 1979 to 1983 while fatalities dropped 15 percent, so there has been a real drop in truck-related fatalities these past few years.

The vast majority of the medium and heavy trucks involved in fatal accidents are tractor-semitrailer combinations(3) (Figure 3). Although doubles were allowed in 36 States in 1981, for example, doubles and triples together were involved in only 3 percent of the fatal accidents for that year.

Combination vehicles as a group have a slightly lower accident rate than do passenger cars, but a substantially higher fatality rate (Figure 4). Although we have a lot more to learn about why this is true, some things we do know.

Because of the wide difference in mass between a heavy truck and a car or pickup truck, a multivehicle accident

	Number	Percent
Single Unit	3,632	24
Tractor-Semi	9,917	66
Doubles/Triples	455	3
Bobtails	383	3
Other, Unknown	631	4
Total	15,018	100

SOURCE: *Trucks Involved in Fatal Accidents*, 1980-82, Carsten and Pettis, UMTRI, Variable 1063

Figure 3. Types of trucks involved in U.S. fatal accidents, 1980-1982

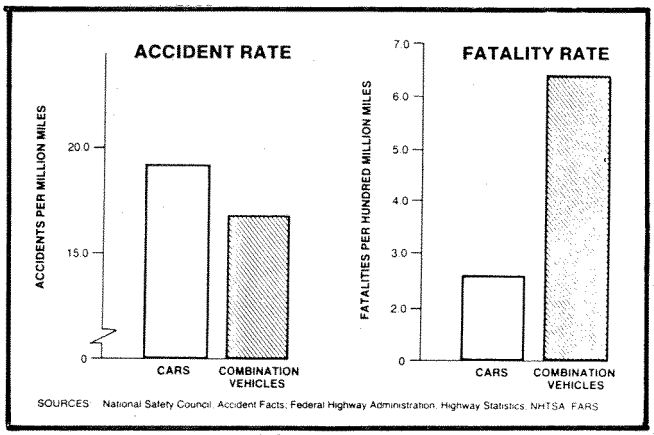

Figure 4. U.S. accident and fatality rates for passenger cars and combination vehicles, 1983

involving those vehicles is especially dangerous to the light vehicle occupants.

Although combination trucks operate more miles on the Interstate highways than on any other kind of highway, Figure 5 shows the greatest number of fatal accidents takes place on two-lane rural roads. Because vehicles are traveling at high speeds in opposite directions on these undivided highways, accidents can be more frequent and more serious than on Interstates or other divided multilane roads.

Combination vehicles travel 63 percent of their miles on rural highways(4), being used primarily to haul goods between cities or from farm or factory to city. This accounts for both a low accident rate and a high fatality rate. Because there is less congestion on rural than on urban roads, there generally are fewer accidents. But, because of higher speeds on rural roads, each accident tends to be more serious than in the city, leading to a higher fatality rate.

Single-vehicle accidents, involving such things as a truck running off a high-speed highway, rolling over, or hitting a stationary object like a tree, are responsible for 70 percent of the heavy truck occupant fatalities, even though they represent only 30 percent of the fatal accidents.

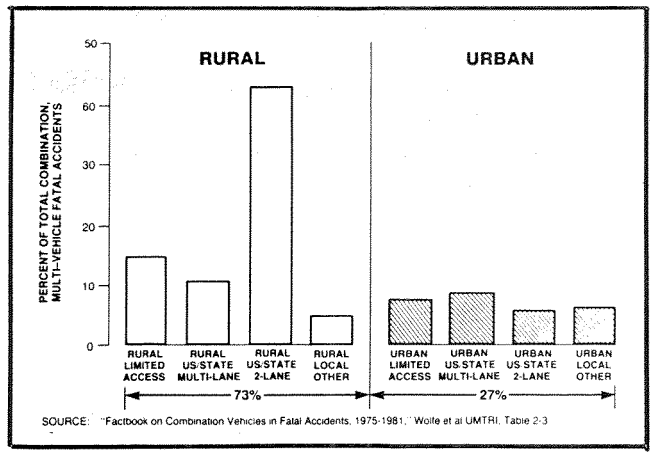

Figure 5. Where do combination multivehicle fatal accidents take place? (1976-1980)

Multivehicle accidents represent 70 percent of the fatal heavy truck accidents, but only 30 percent of the truck occupant fatalities(5). Truck accidents are most dangerous to the occupants of the other vehicles involved.

We mentioned earlier that doubles and triples combined were involved in only 3 percent of medium and heavy truck fatal accidents. Unfortunately, information is not available yet to allow a definitive safety comparison of tractor-semis and doubles operated under identical conditions. The studies that have been done produced inconsistent findings. Four studies found the doubles accident rate lower, two studies found it higher, and three found no significant difference between the two kinds of trucks.

After evaluating studies done by others and all existing data, the University of Michigan Transportation Research Institute has concluded that the involvement rate of the two types of trucks is nearly the same(6).

The Supreme Court agreed with the University of Michigan in cases involving the operation of doubles in Wisconsin and Iowa. The Court found, "The evidence convincingly, if not overwhelmingly, establishes that the 65-foot twin trailer combination is as safe or safer than the. . .55-foot semi."(7)

The use of larger and heavier trucks to increase productivity has raised questions about their safety. As with doubles, studies have produced conflicting conclusions. Reviewing existing studies on the subject, the Ontario Commission on Truck Safety found that an overall increase in safety cannot be effectively achieved by limiting, within acceptable bounds, the weight or size of trucks. The Commission noted that once trucks had reached a weight of from 15 to 20 times that of passenger cars, increasing the weight further did not seem to have any effect on accident severity(8).

Clearly, heavier and larger trucks can move freight in fewer vehicles, reducing fuel usage, costs to consumers,

and the total miles of operation during which the vehicle is exposed to traffic hazards.

Where the truck, the truck driver, or the truck's operating environment were seen as contributing factors to a fatal accident, the University of Michigan found 64 percent were driver-related, 27 percent were environment- or highway-related, and 9 percent were vehicle-related(9).

When the truck driver contributed to the accident, driving too fast was identified 27 percent of the time; failure to keep in lane or driving on the wrong side, 19 percent; carelessness or inattention, 17 percent; failure to yield or to obey traffic controls, 13 percent; and improper following or passing, 7 percent. Drowsiness and fatigue were cited only 6 percent of the time.

The combination vehicle driver in a fatal accident is involved with alcohol only 4.5 percent of the time, compared to a 46 percent involvement in all fatal accidents(10).

When highway or environmental conditions contribute to the fatal combination vehicle accident, obscured vision and swerves, due to weather conditions, highway design problems, etc., are identified as the major factors(11).

When vehicle condition was identified as contributing to a fatal accident, the brake system and tire and wheel problems accounted for nearly 80 percent of the contributing factors(12). Although only 9 percent of the combination vehicle fatal accidents were identified as involving vehicle-related factors, there is no doubt that in many instances good vehicle design and maintenance can allow a driver to safely compensate for his mistakes and avoid an accident.

The experience of the Bureau of Motor Carrier Safety is important in evaluating the role of vehicle condition. The Bureau inspected over 33,000 interstate trucks in 1982. It put 37 percent of those vehicles "out of service" for "imminently hazardous" mechanical problems. The Bureau finds that almost half the maintenance problems that led to putting vehicles out of service were related to brakes, followed closely by lighting or electrical problems, tires, and wheels(13). While the Bureau selects vehicles for inspection based on its estimation that they are in greatest need of inspection, "out-of-service" percentages were not that much lower when vehicles were selected at random.

The Bureau of Motor Carrier Safety's new State grant program, (Motor Carrier Safety Assistance Program), combined with the State and Provincial reciprocal inspection program of the Commercial Vehicle Safety Alliance, will insure that many more vehicles are inspected on the highway from now on. The Bureau found, in a four-State pilot study of increased truck inspections, a 25 to 52 percent reduction in truck accidents from 1979 to 1981(14). If these initial results can be projected to a nationwide program, we can expect a substantial decrease in truck accidents in the future.

The National Transportation Safety Board (NTSB) conducts detailed investigations of individual traffic accidents. From 50 heavy truck investigations, NTSB has isolated these accident causation factors:

- The driver
- Vehicle-braking capability
- Vehicle mechanical condition
- Steering or directional control
- Coupling devices
- Fuel systems
- Truck cab environment

In three-fourths of these investigations, NTSB identified the truck as the primary cause of the accident and, in virtually all 50 accidents, the size and weight of the truck contributed to the severity of the injuries and the number of fatalities. Driver behavior was either a primary or secondary causal factor. This led to NTSB concern about licensing, training, experience, alertness, understanding of vehicle systems, physical health, and the driver's environment in the cab(15).

Earlier we showed that 82 percent of the fatalities in medium and heavy truck accidents were not the occupants of the large truck. They were generally occupants of passenger cars and other light vehicles that collided with the large truck. In summary—

- The fatalities take place in the 70 percent of fatal accidents involving large trucks that are multi-vehicle accidents.
- The accidents are especially serious because of the large disparity in mass between a large truck and the other vehicle involved, usually a passenger car.
- Almost half of the multivehicle accident fatalities occur on rural, two-lane roads where 90 percent are in head-on, angle, and sideswipe accidents(16)

This suggests that further separation of vehicles traveling in opposite directions, especially vehicles of such disparate masses as passenger cars and large trucks, should be investigated. As proof of the effectiveness of separating traffic directions, one has only to look at the divided, limited-access Interstate system, which is credited with having saved approximately 4,600 lives in 1983 alone by cutting the fatality rate in half compared with all U.S. highways(17).

Rollover is involved in 50 percent of combination vehicle driver fatalities, with ejection found in 34.4 percent (Figure 6). Extrication accidents (22.4 percent) are those in which the victim must be physically removed from the damaged vehicle. In some cases, the victim was crushed within the truck cab. Fire is found in few truck accidents overall but is present in about 16 percent of accidents that prove fatal to the combination vehicle occupant—about 125 cases annually(18).

The percentages given add up to more than 100 percent. In many accidents, more than one event is involved, such as a rollover and ejection or a fire and extrication.

	Percent
Rollover	59.0%
Ejection	34.4
Extrication	22.4
Fire	16.1
None of the Above	15.1
Total Number of Fatalities	1964

SOURCE: University of Michigan Transportation Research Institute - from NHTSA Fatal Accident Reporting Systems data.

Figure 6. Combination Vehicle Driver Fatalities, 1980-1982

Research has provided substantial information on the types of accidents that prove fatal to truck occupants and pointed out a number of ways in which lives can be saved. Foremost among them are safety belts. Safety belts are tailor-made for the rollover and ejection accidents, which cause the majority of truck occupant fatalities. Research suggests safety belts could save perhaps 40 percent of the combination vehicle occupants who die each year and reduce injury severity in perhaps 70 percent of the serious-injury accidents(19). Since 1970, the use of safety belts has been required in interstate trucks by the Bureau of Motor Carrier Safety; yet today, only about 6 percent of the drivers wear them—less than half the use rate in passenger cars(20). So, if we can get truck drivers to buckle up, a significant number of lives can be saved.

We now know far more about highway accidents than we did just a few years ago. But there are many problems still to investigate. For example, we have little detail on accident exposure by type of vehicle. A wide range of trucks, having specialized vocational uses, travel on different kinds of roads, with varying loads, at various times of day, under all kinds of environmental conditions. Until we can analyze this exposure information, it is impossible to pinpoint exactly how to identify and break the accident causation chain for specific kinds of vehicles and accidents. We need more detailed information on drivers, highways, vehicles, accident forces, handling, braking, and stability in crisis maneuvers, and specifics of the accidents themselves to consider potential accident countermeasures intelligently.

Research is underway on a wide variety of subjects to get these answers, including continuing accident data collection and analysis; combination truck braking, coupling, and handling; vehicle crashworthiness; and ways of encouraging safety belt use.

Research is being conducted or sponsored by virtually everyone involved in the trucking industry, including insurance companies, motor carriers, various government agencies, organized labor, industry trade associations, vehicle manufacturers, suppliers, and universities.

Our challenge is to use better data and better analysis to find innovative and constructive solutions.

References

1. National Safety Council, *Accident Facts* (Chicago, 1984), p. 59, and U.S. Department of Transportation, Federal Highway Administration, *Highway Statistics* (Washington, D.C.: U.S. Government Printing Office, 1983, and earlier editions), Table VM-1.
2. Interview with Grace Hazzard, National Center for Statistics and Analysis, National Highway Traffic Safety Administration, Washington, D.C., January 24, 1985.
3. Carsten, Oliver, and Leslie C. Pettis, *Trucks Involved in Fatal Accidents, 1980-82*, Ann Arbor, MI: University of Michigan Transportation Research Institute, 1985, variable 1063.
4. Federal Highway Administration, *Highway Statistics*, Table VM-1.
5. Clarke, Robert M., and Joseph Mergel, "Heavy truck occupant crash protection—a plan for investigating ways to improve it," SAE Paper 821270, Indianapolis, Indiana, November 1982.
6. Chirachavala, Thipatai, and James O'Day, *A Combination of Accident Characteristics and Rates for Combination Vehicles with One or Two Trailers,* Ann Arbor, MI: University of Michigan Transportation Research Institute, p.7, 1981.
7. Kassel, et al., vs. Consolidated Freightways, *450 U.S. 662,* 1981.
8. Uffen, Robert J., "Report of the Ontario Commission on Truck Safety," Ontario Ministry of Transportation and Communications, p. 159, 1983.
9. Wolfe, A.C., L.D. Filkins, and J. O'Day, *Factbook on Combina-Vehicles in Fatal Accidents, 1975-1981,* Ann Arbor, MI: University of Michigan Transportation Research Institute, 1983, Tables 2.10, 2.17, and 3.6.
10. Ibid, Table 3.7, and U.S. Department of Transportation, National Highway Traffic Safety Administration, "National accident sampling system 1982," Washington, D.C., 1984, Table 6.
11. Wolfe, et al., *Factbook,* Table 2.10.
12. Ibid, Table 2.17.
13. U.S. Department of Transportation, Federal Highway Administration, Bureau of Motor Carrier Safety, "1982 roadside vehicle inspection report," Washington, D.C., pp. 6,10, 1984.
14. U.S. Department of Transportation, Federal Highway Administration, Bureau of Motor Carrier Safety, "Commercial motor carrier safety inspection and weighing demonstration program, interim report," Washington, D.C., pp. 3,4, 1981.

15. Kissinger, J. Peter, National Transportation Safety Board, to author, April 26, 1984, MVMA files, Washington, D.C.
16. O'Day, James, "Commercial vehicle safety issues," National Highway Safety Symposium paper, Williamsburg, Virginia, February 28-March 1, 1984, Table 1.
17. National Safety Council, *Accident Facts*, p. 44.
18. Computer run of University of Michigan Transportation Research Institute data files of heavy truck fatal accidents, MVMA files, Washington, D.C.
19. Ranney, Thomas A., "A study of heavy truck occupant protection: accident data analyses," Calspan Field Services, Inc., Buffalo, New York, p. 60, 1983.
20. Clarke and Mergel, *Heavy Truck Occupant Crash Protection,* p. 17.

Heavy Trucks Aggressivity for Road Users— In Search of Improved Safety

Maryvonne Dejeammes
ONSER—Laboratoire des Chocs et de Biomécanique

Abstract

For many years, heavy trucks have accounted for a large part of the damaging road traffic in France. To determine ways of improving heavy vehicles so as to diminish the severe score of accidents, the national statistic file of injurious accidents in 1982 and the ONSER bidisciplinary investigation file have been analyzed. The most important risks affect pedestrians, two-wheelers, and car passengers.

It appears research on heavy vehicles should be undertaken at first for—

- Improving lateral vision
- Fitting up of heavy vehicle flanks to avoid falls under rear wheels and to limit underrun
- Fitting up of heavy vehicle front structure to reduce its aggressivity against passenger cars

The purpose of safety measures complementary with energy savings necessity should bring about realizable solutions.

Introduction

For many years, heavy vehicles have been considered a factor of dangerous road traffic in France. Because of their large mass, these vehicles contribute to the severe harm inflicted on their opponent road users. Upon action of the French Department of Transport, the Committee named "For a better safety of heavy vehicle traffic" has recommended research themes to improve the safety of heavy vehicle occupants and other road users.

It is then necessary to define the most dangerous accident situations with respect to the different categories of road users—pedestrians, two-wheel riders, and car occupants. Research axes to diminish the aggressivity of heavy vehicles will emerge from the analysis of national statistics (1982 files) as well as from the detailed study of accident cases (ONSER bidisciplinary investigation). The first lines of an evaluation methodology will be presented in the case of a front crash heavy vehicle/car.

General Traffic Conditions

Heavy vehicles are different from cars by their assignment to goods transportation or people transportation, and consequently by their larger mass. They are divided into three categories: light trucks or delivery vans of less than 3.5t, heavy trucks of 3.5 to 38t, and public service vehicles (transporting more than nine people).

The following table shows the number of vehicles and covered distances:

Category	Number	Covered distance/year in kilometers
Passenger car	20,420,000	13,000
light truck		
1.5t to 3.5t	1,060,000	25,000
heavy truck >3.5t	450,000	15,000 to 70,000
public service vehicle	76,000	25,000 to 62,000

Risks related to the traffic of heavy vehicles can be defined by the involvement of vehicles and the number of fatalities related to the number of vehicles × covered distance in kilometers:

1980	HT (>3.5t)	Car
Vehicles × km	$20\ 10^9$	$250\ 10^9$
Involvement / 10^6km	0.85	1.12
Fatalities / 10^8 veh/km	11.0	4.0

So, the rate of involvement of cars is higher than that of heavy trucks, but the number of fatalities related to

vehicle kilometers is 2.75 higher in accidents involving a heavy truck.

Analysis of General Accidental Statistics

To take into account the types of heavy vehicles involved (different by their design and mass), the categories of road user opponents, and even the type of traffic network, an analysis of the statistical file RESUME, worked out from the basis data of the National Constabulary and the National Police, has been conducted. This combined file has been drawn up from the forms on injurious accidents occurring each year, and it has some limits from its homogenous coding and simplification:

- A maximum of three vehicles is reported in a same accident (1 percent of accidents involve more than three vehicles).
- A maximum of two roads is described for an accident.
- A maximum of four occupants is reported in an accident. Registered occupants are those whose injury severity is the highest.

These limitations may be accepted to analyze the problem of heavy truck opponents. Some reserves must be made for analyzing accidents involving a public service vehicle because of the number of occupants registered.

General Presentation

The analysis of the file RESUME has been made for 1982, which shows 222,047 injurious accidents, among which a heavy vehicle was involved in 21,957 cases.

We take into account heavy vehicles (HV) classified in three categories:

- Light truck (1.5 to 3.5t) noted L.T.
- Heavy truck (lorry and tractor-trailer) noted H.T.
- Public service vehicle (motorbus and motorcoach) noted P.S.V.

The road user opponents are:

- Pedestrians noted Ped.
- Two-wheelers noted 2-Wh.
- Passenger cars noted Cars

The traffic network is divided into three types:

- Highway
- Nonurban road
- Urban area

Data on collision configurations are more difficult to analyze, and the combination of impact zone of vehicle and impact direction is not considered reliable enough in this file to insure a good description. It was then decided to address the parameter "vehicle impacted zone" with the following distinctions:

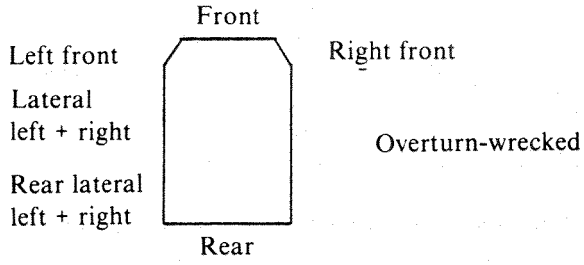

Front = Front + Left and Right Front
Lateral = Lateral Left + Right and Rear Left + Right

Accident severity can be determined by the percentage of fatal accidents in relation to the total of injurious accidents. Aggressivity will be given by the rate of external killed and severely injured (other than heavy vehicle occupants) per accident.

The overall distribution of accidents in which at least one heavy vehicle was involved for 1982 is shown in Figure 1.

Accidents Involving Heavy Vehicles/Pedestrians

In this category, 2,620 accidents resulted in 297 fatalities and 765 severely injured pedestrians. The overall external aggressivity is then of 0.40.

The implication is related mainly to the road network:

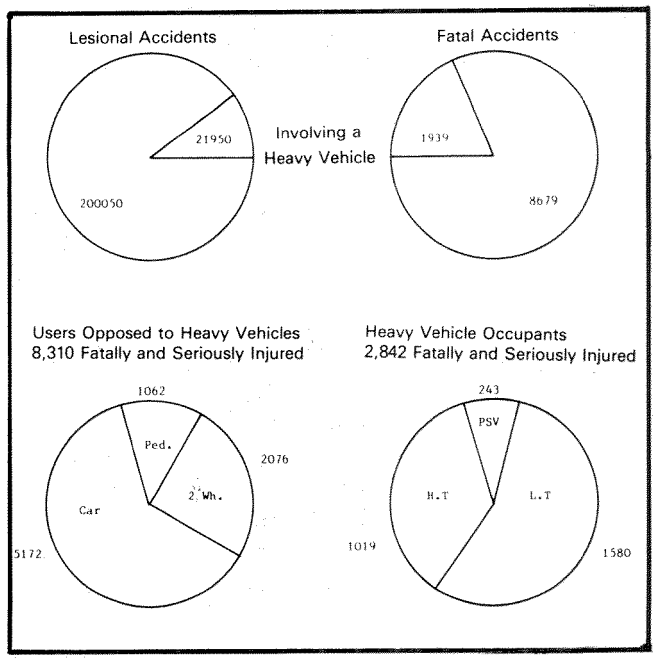

Figure 1. Accidents involving heavy vehicles

1982	No. of acc.	Fatal acc.	Pedestrians Killed	Severely injured	Aggressivity
Highway	17	10	10	6	0.94
Nonurban road	251	74	74	102	0.70
Urban area	2,371	213	213	657	0.37

Urban collisions represent 90 percent of accidents. While they show a not too high aggressivity (0.37 external killed and severely injured people per accident), they total 82 percent of killed and severely injured pedestrians.

As for the category of heavy vehicles, even if public service vehicles run a lot in urban areas, light trucks and heavy trucks are those that cause the most pedestrian victims.

1982	No. of acc.	Fatal acc.	Pedestrians Killed	Severely injured	Aggressivity
Light truck	1,087	100	100	318	0.38
Heavy truck	824	155	155	270	0.52
Pub.serv.veh.	729	42	42	177	0.30

Note the higher aggressivity of heavy trucks, a figure derived from numerous and severe collisions on connection roads passing through an urban area.

Accidents Involving Heavy Vehicles/Two-Wheelers

A total of 4,499 collisions resulted in 394 fatalities and 1,682 severely injured two-wheel passengers. Consequently, the overall external aggressivity is 0.46, which is a slightly higher rate than for pedestrian opponents.

The implication depends on the road network with a large frequency in urban areas:

1982	No. of acc.	Fatal acc.	Two-wheeler Killed	Severely injured	Aggressivity
Highway	27	6	6	8	0.52
Nonurban roads	887	143	146	484	0.71
Urban area	3,585	241	242	1,190	0.40

The aggressivity related to the vehicle category is roughly comparable to the one for accidents against pedestrians, but it has to be noted that severe accidents involving a heavy truck prevail.

1982	No. of acc.	Fatal acc.	Two-wheeler Killed	Severely injured	Aggressivity
Light truck	1,773	90	90	678	0.43
Heavy truck	2,150	271	275	830	0.51
Pub.serv.veh.	576	29	29	174	0.35

The analysis of the heavy vehicle zone impacted by the two-wheeler shows an unquestionable difference between the categories of vehicles:

% 2-wh Fat.sev jured	Impacted Zone Front	Rear	Lat.Front	Lat.Rear	Total
Light truck	59	6	19	16	100%
Heavy truck	43	9	23	25	100%
Pub.serv.veh.	57	8	20	15	100%

Table 1 gives a detailed description of accidents involving heavy trucks/two-wheelers.

The highest frequency and the highest severity of impacts against heavy truck flanks in comparison with light trucks and public service vehicles can certainly be explained by the design of their structures (presence of side fairings flush with axles).

Accidents Involving Heavy Vehicles/Passenger Cars

A total of 11,473 accidents resulted in 1,139 fatalities and 4,033 severely injured car passengers. The external aggressivity is 0.45, similar to the one for two-wheeler opponents, but car passenger victims are 2.5 times more numerous.

The implication is more frequent in urban areas, but the gravity is much more important in nonurban roads as shown below:

1982	No. of acc.	Fatal acc.	Car passengers Killed	Severely injured	Aggressivity
Highway	409	56	69	138	0.51
Nonurban roads	4,564	660	776	2,240	0.66
Urban area	6,500	262	294	1,655	0.30

Heavy trucks are more frequently involved and exhibit the highest aggressivity:

1982	No. of acc.	Fatal acc.	Car passengers Killed	Severely injured	Aggressivity
Light truck	3,453	153	147	1,007	0.33
Heavy truck	6,675	752	857	2,684	0.54
Pub.serv.veh.	1,345	73	95	342	0.32

The analysis of the accident configuration has been made by distinguishing between the various parts of the passenger car that were impacted—front, side left and right, rear. The impacted parts of the heavy vehicle were detailed in the computerized sorting according to the above presentation. Table 2 summarizes registered figures according to the category of heavy vehicles.

The fronto-frontal collision accounts for more than 40 percent of killed and injured car passengers for the three categories of heavy vehicles. Collisions between passenger

Table 1. Heavy truck/two-wheeler collisions

1982		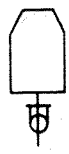	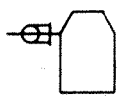	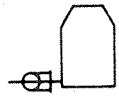
No. of acc.	765	192	473	469
Fatal acc.	111	12	65	65
Killed 2-Wh	113	13	65	65
Sev.Inj. 2-Wh	322	74	167	188
Killed = Sev. Inj. 2-Wh*	435	87	232	253
%	39	8	21	23
Killed = Sev. Inj.2-Wh per acc.	0.57	0.45	0.49	0.54

* 9% are not determined

Table 2. Heavy vehicle/passenger car collisions

	1982			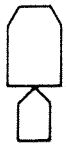	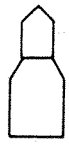	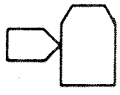	Others
L.T.	Accidents	1,502	590	177	202	720	262
	Fat. + Sev. Inj. car	624	224	38	22	173	73
Car	%	54	19	3	2	15	6
	Ext.Agg.	0.40	0.38	0.21	0.11	0.24	0.28
H.T.	Accidents	2,273	1,046	514	363	1,689	790
	Fat. + Sev. Inj. car	1,455	612	225	88	848	353
Car	%	41	17	6	2	24	10
	Ext.Agg.	0.64	0.59	0.44	0.24	0.50	0.45
P.S.V.	Accidents	555	273	83	84	243	107
	Fat. + Sev. Inj. car	224	81	28	5	70	29
Car	%	51	19	6	1	16	7
	Ext.Agg.	0.40	0.30	0.34	0.06	0.29	0.27

car and heavy vehicle flanks and between heavy vehicles and passenger car flanks represent nearly 20 percent of killed and severely injured car passengers in each case. However, it has to be noted that heavy trucks differ from light trucks and public service vehicles because accidents against their flanks are more severe. As previously stated for two-wheelers, explanation must be found in the chassis structures that stand high and are recessed from the loading frame and make underrun possible.

Detailed Study of Accident Cases

To illustrate the problem of the aggressivity of heavy vehicles toward passenger cars, we have sorted out the accidents from the files of ONSER bidisciplinary survey where heavy trucks of more than 3.5t and public service vehicles (motorcoach and motorbus) were involved from 1975 to 1984. The term "passenger car" is used for any vehicle equipped as a limousine, break, or coupé.

Since it is difficult to get precise data on material damage to heavy vehicles, whose occupants are rarely injured, it has been found in the files:

- 25 accidents front car/front HV
- 13 accidents front car/side HV
- 18 accidents front car/rear HV

Given the priorities that could be drawn from general statistics, the analysis of fronto-frontal collisions is presented. These collisions involve front parts of each vehicle, and impacts are directed at 11, 12, and 01h on a clock dial.

The accident severity noticed in the files of the bidisciplinary survey is higher than that found at the national level. This is even more enhanced for the fronto-frontal configuration between a passenger car and heavy vehicle: 12 out of the 25 accidents are fatal.

The lesional score is given on Table 3, where a distinction is made between front and rear occupants and where belt-wearing by car passengers is mentioned:

Table 3. Car passengers injury severity

	Killed AIS 6	Severely Injured AIS ≥3	Lightly Injured AIS 1-2	Uninjured
Belted front occupant	3	5	6	1
Unbelted front occupant	7	4	4	1
Front occupant belt-wearing unknown	4	1	0	0
Rear occupant	5	1	1	0
Total	19	11	11	2

It is then shown there are more killed occupants among unbelted ones. The severity of this collision type for rear occupants has to be noted also.

These collisions are characterized by the well-known risk of the passenger car to underrun the heavy vehicle structure, which means a limitation of the protective effect of the 3-point belt due to the reduction of the deceleration zone in the compartment. Impact directions and underrun cases are drawn out by analyzing passenger car deformations. Underrun is defined as the case when the car is impacted above its rigid structures, i.e., side-members, motor, and gear-box unit.

Impacts to the left are the more numerous:

- Front left impact: 12 cases
- Center impact: 8 cases
- Front right impact: 5 cases

Cases of underrun are more numerous (13 cases); 6 accidents occurred without underrun. In the 6 remaining cases, the underrun criterion has not been asserted because of the important lateral deformations of the car.

The relationship between deformations of the vehicle and its compartment and injuries to its occupants is shown in the table below:

This table emphasizes the violence of impact with a complete intrusion of the compartment in 10 cases, along with the increasing injury severity according to the level of compartment intrusion.

The description of lesions, which is available except in the 10 cases of fatality (no autopsy), gives evidence of the impact violence against compartment parts such as steering column, dashboard, windscreen frame, pedals, and even an outer object (heavy truck structure). Any body part is then likely to be severely injured.

On the other hand, heavy vehicle occupants are very seldom exposed. In our sample, it appears the injured people found in three heavy vehicles sustained lesions either on ejection (one slightly injured) or during an impact subsequent to the one against the passenger car. During an impact against a tree, 2 front passengers of a motorcoach sustained severe injuries; during an impact against a pole, 12 passengers of a motorcoach were lightly injured.

There are also various categories of heavy vehicles in this sample to draw out behavior tendencies. It can merely be said that trucks of more than 10t and tractor-trailers do not show a very different behavior, which is explained by their similar front profile.

So, the fact that front structures of heavy vehicles are not compatible with passenger cars, as well as the ratio of their masses, explains the severe tribute paid by car occupants. However, speeds and severity levels of these collisions cannot be assessed in a reliable way, either from available data or from present knowledge. As a matter of fact, it is not possible to compare the deformations observed on the passenger car with those found after

Deformed area	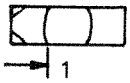	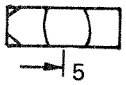	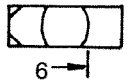	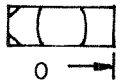
Left front	1	5	6	0
Center	3	2	1	2
Right front	4	0	1	0
Killed	0	3	8	4
Severely injured AIS ≥3	3	4	2	0
Lightly injured AIS 1-2	7	1	2	0

impacts against a rigid barrier. Calibrated tests thatwould give a set of data on car deformations and decelerations are lacking up to now, and the estimation of speeds before the impact and of braking distances are not unquestionable factors.

This accident case study, however, bears out the severity and frequency of left frontal collisions (on drivers' side); the analysis of injuries to car passengers points out that factors liable to improve safety are the limitations of underrun and intrusion into the car passenger compartment.

Countermeasure Proposals

The analysis of circumstances of accidents involving heavy vehicles has been carried out to find effective measures applicable to heavy vehicles and likely to limit this dramatic tribute. These measures can be examined in relation to the heavy vehicle opponent:

- Accidents involving pedestrians with very severe consequences occur in urban areas most of the time. It is difficult to think of equipment on heavy vehicles that will prove to be absolutely efficient with the pedestrian looking so small and weak next to a heavy vehicle. It can be recommended that the lateral visual field of the truck driver be improved. Otherwise, primary safety measures need to be worked out, especially concerning road equipment and traffic.
- Two-wheelers are involved in accidents occurring in urban areas and on nonurban roads as well. Often they are victims of impact against heavy vehicle fronts. It would be interesting to estimate how the front structure could be modified to limit underrun, but the closing speeds are often high and do not enable one to think of specific and well-adapted measures. Concerning impacts against heavy vehicle flanks, lateral fairings such as those equipping public service vehicles or light trucks (for most of them) undoubtedly can limit the consequences of this accident type. In France, to further the study made by Favero(1), a first step has been taken that provides for fitting heavy trucks with "protective devices against the risk of falling of two-wheelers on the trajectory of rear wheels" (Decree of June 16, 1979-Art.1). It is now necessary to estimate their effectiveness and even to consider other equipment such as more complete fairings. Would not improving heavy truck aerodynamics contribute to a better safety?
- Car passengers are the most numerous victims. It seems impacts against the heavy truck rear no longer constitute an important risk as in past years. The rear underrun guards provide a certain efficiency, which could be still improved by energy-absorbing devices(2,3).

The work to be done now is to limit the aggressivity of heavy vehicle fronts. The collision severity is in direct relationship with the geometry and the masses of the involved vehicles. As mentioned by Franchini(4), the heavy vehicle does not behave like a rigid barrier since the opponent car often runs under its strong structures. The design of the heavy vehicle front should meet two requirements:

- Compatibility of its structure by lowering the rigid structures of the heavy vehicle, especially the bumpers. And yet recent studies have shown that this design is still not sufficient since the whole collision energy is absorbed by the passenger car(5).
- Energy dissipation by a deformable part. The problem is to know if the energy dissipation is possible only by adding a material of particular size and increasing the vehicle length, even if the compartment design of future heavy trucks is completely thought over. Johnson(6) proposes a deformable part 500mm long.

Some drafts whose credit is to verify the feasibility of devices able to absorb part of the energy have been proposed(7,3). Another research field could focus on the shape of heavy trucks. Having in mind that frontal impacts offset to the left are the most severe, and most frequent as well, it could consider a round-shaped compartment that enables the car to slip aside during such a collision.

The question, then, is to know up to which collision severity level is fair to require heavy vehicle fronts to be less aggressive toward passenger cars. Accident analysis shows that in France, from our study, as well as in the Federal Republic of Germany(7) and in the United Kingdom(8), the more frequent configuration is the one with an angular incidence or an offset on the driver's side. It is more difficult to estimate the closing speed of the vehicles since there are no reference collisions available.

With some tests of fronto-frontal impacts carried out with closing speeds of 40 to 65km/h, it is quite fair to believe that a modification of the heavy truck front can be designed to dissipate part of the energy released during a collision with a closing speed of 60km/h. This would enable belted car occupants to sustain forces that remain within the limits of biomechanical criteria currently admitted.

The second priority lies in the improvement of heavy truck flanks; the risk of underrunning their loading platforms is quite similar to that incurred by two-wheelers. It could then be recommended that lateral protective devices or fairings offer a minimal resistance to act as an underrun guard toward passenger cars.

Conclusion

In France in 1982, 21,950 accidents involving a heavy vehicle resulted in at least 8,310 killed and severely injured among pedestrian, two-wheeler, and car opponents, whereas more than 2,800 truck occupants were killed or severely injured.

The analysis of the circumstances and the consequences of these accidents has produced measures likely to limit this heavy tribute:

- Improve the side visual field offered to the truck driver
- Modify heavy vehicle flanks to limit falls of two-wheelers on the trajectory of rear wheels and also to avoid car underrun under loading platforms
- Modify the heavy vehicle front to make it less aggressive toward passengers cars, especially by avoiding the underrun under rigid structures of the chassis and by providing an energy-absorbing area

Heavy vehicle traffic has been considered a factor of unsafeness for many years. Several countries, like France, admit it is most desirable that solutions to the aggressivity of heavy vehicle fronts and flanks be found. These safety measures can be complementary to current priorities concerning road traffic, such as energy savings. We believe actual outcomes will emerge from international research being carried out at present. Evaluation procedures need to be determined, which necessitates a better knowledge of collision severities to give a more realistic picture of traffic accidents.

References

1. Favero, J.L., Sécurité et conception des poids-lourds, Cahier d'études ONSER No. 47, March 1979.
2. Beermann, H.J., "Behaviour of passenger cars on impact with underride guards," *Int. J. of Veh. Design*, Vol. 5, No. 1.2, pp. 86-103, 1984.
3. Penoyre, S., B.S. Riley, and M. Page, "Desirable structural features for the design of front and rear underrun bumpers for heavy goods vehicles," International Conference on Vehicle Structures, *I Mech E* Pub., pp. 139-146, 1984-7.
4. Franchini, E., "Truck crash testing," International Congress FISITA, pp. 901-912, 1970.
5. Document UTAC, "Diminution de l'agressivité des véhicules utilitaires en cas de collision avec des voitures particulières," ATP Sécurité des véhicules, Contrat 77114, Rapport final, 1979.
6. Johnson, W., and A.C. Walton, "Protection of car occupants in frontal impacts with heavy lorries: frontal structures," *Int. J. Impact Design*, Vol. 1, No. 2, pp. 111-123, 1983.
7. Danner, M., and K. Langweider, "Results of an analysis of truck accidents and possibilities of reducing their consequences discussed on the basis of car to truck crash tests," Proceedings 25th Stapp Car Crash Conference, pp. 903-950, 1981.
8. Riley, B.S., B.P. Chinn, and H.J. Bates, "An analysis of fatalities in heavy goods vehicle accident," TRRL Laboratory Report 1033, 1981.

P.S.V. Rollover Stability

D.M. White
Cranfield Impact Centre, United Kingdom

Abstract

Nine buses and coaches were tested to experimentally determine various parameters considered to affect rollover stability—principally, spring stiffness, position of centre of gravity, and roll moment of inertia. Utilising these data, a computer simulation of a typical rollover accident was used to compare the relative performance of the different vehicles and investigate the effect of each parameter on the rollover threshold. Height of the centre of gravity and, to a lesser extent, roll centre height were found to have the greatest effect.

Introduction

To get from safe, normal driving in a bus or coach to a fatal rollover accident requires a sequence of events similar to those outlined in Figure 1. It can be seen there are two stages where governmental efforts may be made to reduce rollover accidents, and two further areas in which the severity of an accident, if it does occur, may be reduced. Already significant legislation exists to minimise loss of control. Other factors, such as careful road design and layout, and treating icy road surfaces, may also be added to the measures listed in Figure 1.

However, coaches will not usually roll over without certain other circumstances. These are typically—

- Travelling off the road onto a significantly inclined bank

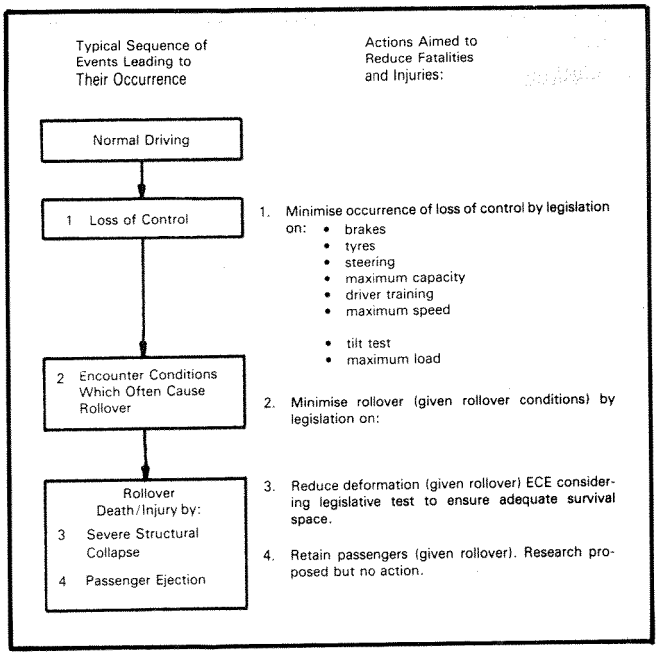

Figure 1. Components of typical bus rollover accident

- Sliding sideways into some form of roadside tripping obstacle (such as a curb, low wall, or soft verge)

Whether or not a coach rolls on an inclined bank would be almost solely dependent on its static tilt limit, as measured on a tilt test. The factors affecting whether a given vehicle would roll if it struck a curb with a given lateral velocity are less apparent and are the subject of this paper.

Description of Computer Program

The Rollover Accident Simulation Program (RASP) was developed to study in detail the design factors that the propensity of a vehicle to roll over when it strikes a curb, low wall, soft verge, or similar roadside obstacle while sliding sideways. As such, it assumes the driver has already lost directional control and, therefore, the program does not include vehicle dynamics routines to model steering, braking, or acceleration modes. Instead, the simulation begins with an initial lateral velocity perpendicular to the curb. Impact between tyres and curb occurs, and the ensuing motion may or may not result in rollover.

Mathematical Model

The vehicle is defined by its mass distribution, inertial properties, spring and damping constants, and dimensions as indicated in Figures 2 and 3.

The equations of motion were formulated by considering the sprung mass as a rigid body with 6° of freedom (that is, longitudinal, lateral, vertical, roll, pitch, and yaw). Each axle was considered to be a beam axle, free to roll or displace vertically or laterally with respect to the body. For a two-axle vehicle, this results in a 12° of freedom model. Simple modifications to the program created a 15° of freedom version for three-axle double-deckers.

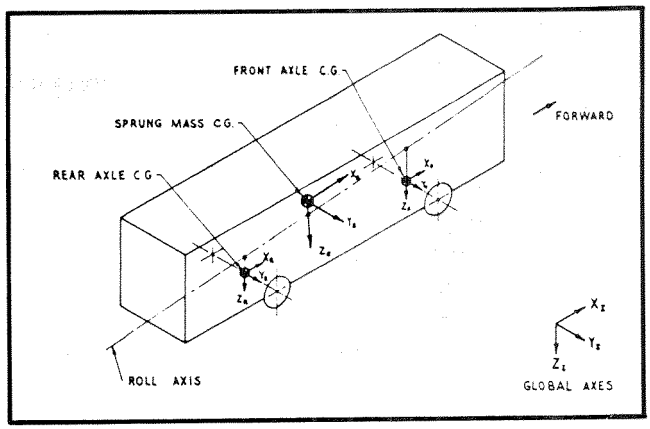

Figure 2. Mathematical model (12 degrees of freedom)

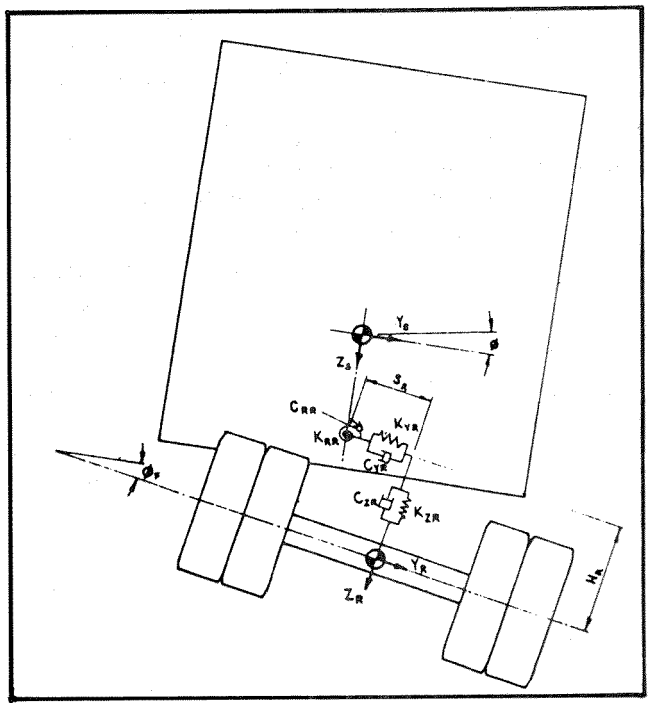

Figure 3. Suspension layout of mathematical model

Assumptions and Features of Model

The features incorporated in the model and assumptions made in deriving the equations of motion are as follows:

1. The road surface is assumed to be uniform and horizontal.

2. The curb is positioned perpendicular to the vehicle's initial velocity.
3. Pitch angle of the sprung mass is assumed to be small (that is, small angle approximations are used: $\sin\theta \doteqdot \theta$ and $\cos\theta \doteqdot 1$).
4. Axle roll angles relative to the sprung mass are also assumed to be small.
5. The relative roll motion of the sprung mass and axles is assumed to take place about a roll axis that is fixed with respect to the sprung mass. It is defined by specifying the initial values of the roll centre heights at the front and rear axles. The roll axis is taken as the line joining these two points. Weir(1) in the bus version of a vehicle dynamics program assumed that the vehicle centre of gravity (CG) must lie on this roll axis. This program, however, enables the CG position to be defined independently of the roll axis.
6. Spring/damper units act at the tyre contact points where the forces from the road and curb are applied, and also between the sprung mass and each axle, simulating the suspension components. Figure 3 shows in greater detail the connection between the sprung mass and an axle. Note that only one vertical spring is employed (with an axle rate stiffness) and the roll stiffness is provided using a separate torsional spring.
7. Linear characteristics are used for every spring with two exceptions: the roll stiffnesses and tyre/curb stiffnesses are as shown in Figures 4 and 5, respectively. The secondary roll stiffness models the effect of bump stops when the relative roll angle exceeds 15°. Similarly, the curb stiffness takes into account the limited tyre lateral stiffness and attempts to account for the increased stiffness when the curb contacts a more solid part of the vehicle, such as a wheel rim.
8. Provision is also made for energy losses at the tyre/curb contact (due perhaps to ground or bus deformation) by allowing plastic behaviour. This is evident in Figure 5, where the deflection increases with constant force and is not recovered when the spring is unloaded (shown as the dashed line).

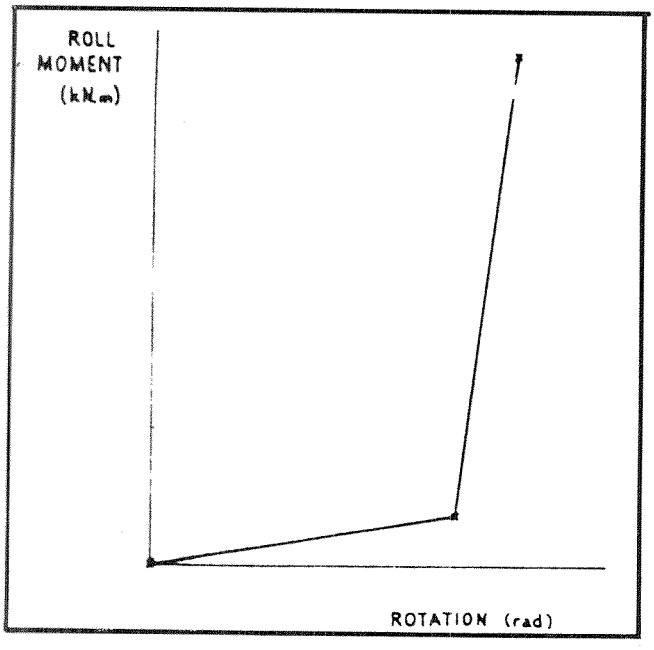

Figure 4. Representation of roll stiffness nonlinearities

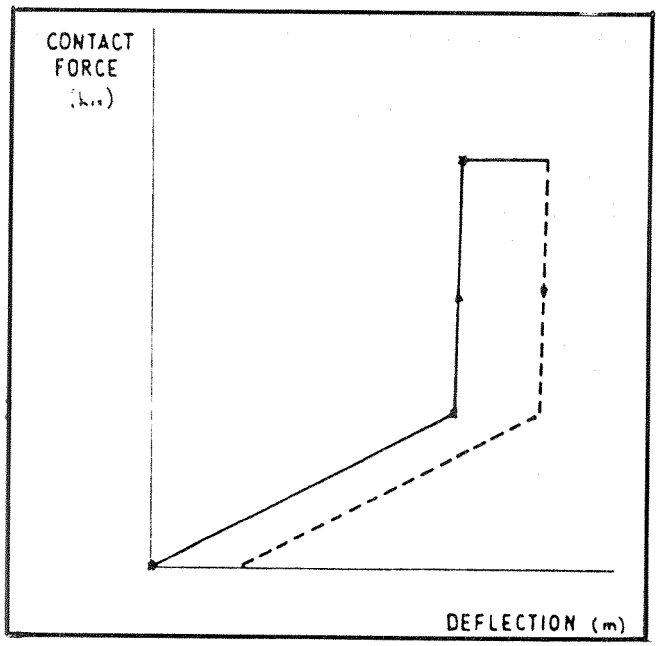

Figure 5. Representation of tyre/curb stiffness nonlinearities

Validity of Model

A full-scale instrumented rollover test was not feasible due to resource limitations, so the simulation could not be checked directly. However, similar earlier work on the dynamic behaviour of buses during superstructure strength tests showed reasonable correlation between measurements of actual tests from high-speed cine film and results predicted by a 6° of freedom model(2). Since RASP contains many routines derived from the earlier model, and an energy checksum insures that the total energy variation is minimal, the results of RASP are considered to be of value, particularly for comparing one vehicle with another.

Data Measurement

Nine different vehicles were tested to determine by experiment the values of the parameters required for the

simulation program. Most were considered to be potentially significant factors affecting rollover performance.

Height of Centre of Gravity

The same method and equipment used for determining CG height as described in "The SDG Bus Roll Moment of Inertia Test Rig"(3) was adopted. To summarise the technique, the vehicle is positioned with each axle supported from a transverse steel beam that has a central roller bearing, allowing the bus to roll if unrestrained. By measuring the reaction force (R in Figure 6) for a range of roll angles from 0° to 3° and plotting a graph of these two variables, the CG height may be calculated from the equation for static equilibrium of moments about the pivot.

The vertical distance from the top of the beam to the pivot is subtracted to give the unladen CG height above the ground. Note that the suspension and tyres are prevented from deflecting by suitable use of jacks or blocks, effectively converting the bus into a rigid body.

The bus rollover simulations were conducted for vehicles in the laden condition defined by current tilt test regulations, as this is intended to be the worst case situation for rollover stability. This means that 63.5kg per passenger must be added at the correct position for each seated or standing passenger, plus the driver. Double-deckers only require the driver (and conductor) plus passengers on the upper deck.

Knowing the average seat height on each deck and given the regulation height for the CG of standing passengers is 2'8" (0.813m), the overall CG height for the laden vehicle can be determined.

Roll Moment of Inertia

With the vehicle on the same test rig as for the CG height measurement, and the suspensions and tyres blocked to effectively insure rigid body motion, the method of determining the roll moment of inertia as outlined in (3) was used. Figure 7 illustrates the important feature, namely, the air springs, which provide a restoring moment when the bus is oscillated about an axis joining the two beam pivots. The moment of inertia about the pivot axis is given by:

$$I_P = (2kl^2 + mgh)\left(\frac{T}{2\pi}\right)^2$$

where

k = combined spring stiffness on one beam
l = distance from spring to pivot
m = total oscillating mass
h = height of combined CG above pivot
T = period of free oscillation

The roll moment of inertia of the vehicle about its CG is obtained using:

$$I = I_P - I_B - mh^2$$

where I_B = moment of inertia of support beams about pivot

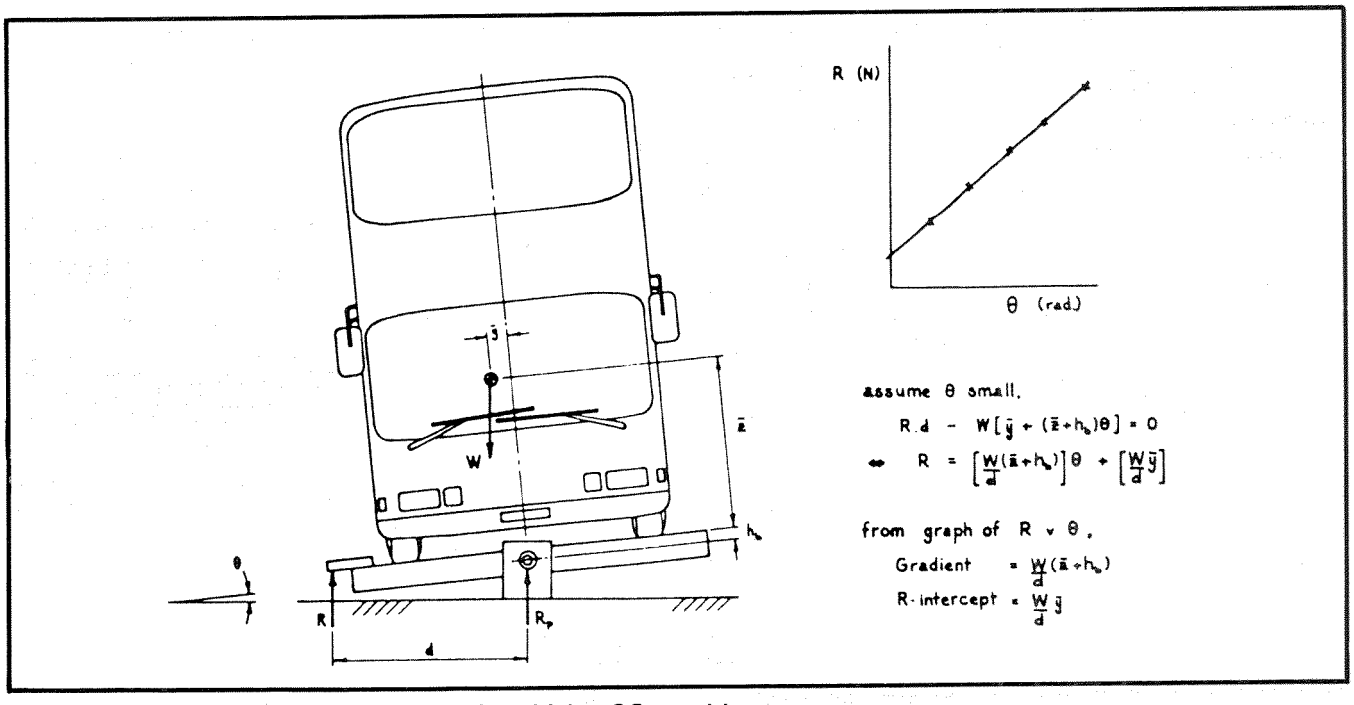

Figure 6. Method of measurement of vehicle CG position

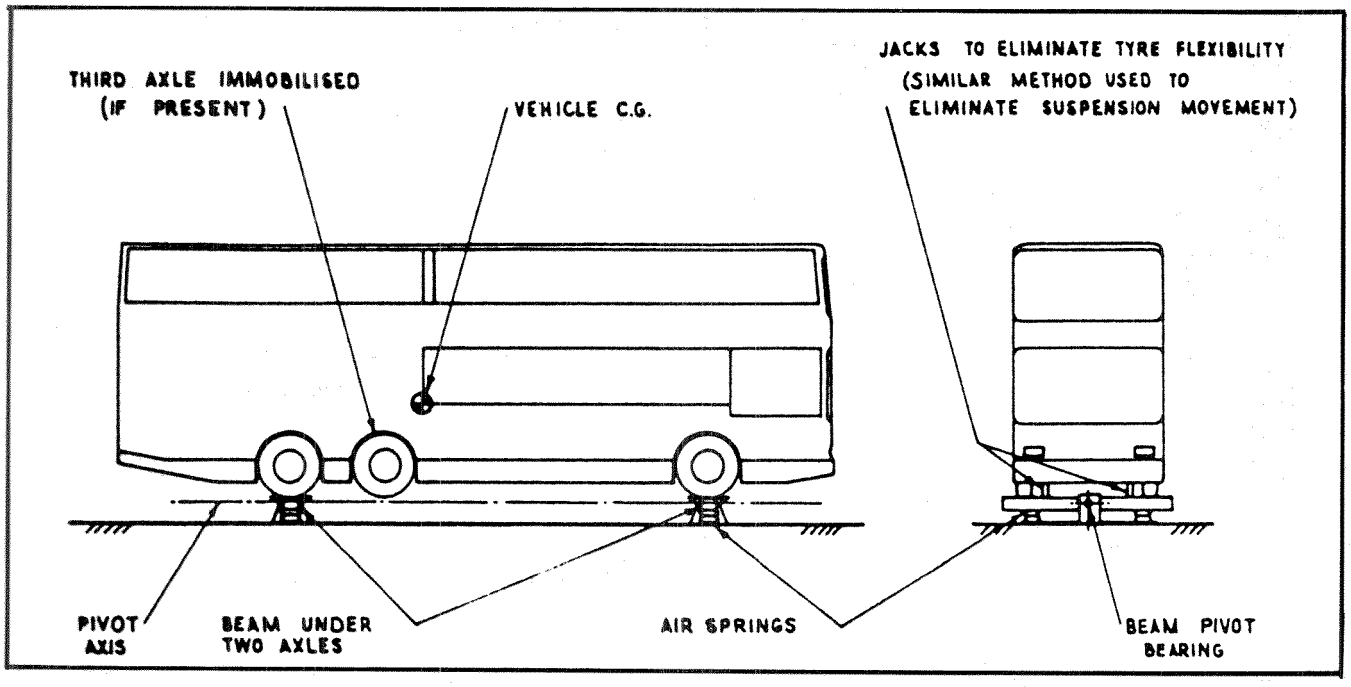

Figure 7. General layout of vehicle on roll moment of inertia rig

The time for several oscillations was recorded and the average calculated from several such measurements. This process was repeated for three different air spring pressures.

Stiffnesses

Vertical, lateral, and roll stiffnesses were obtained for the suspension and tyres of each axle of a vehicle by applying a force in a particular direction, and measuring both the force and the associated deflection in the same direction. Vertical force was applied by loading sandbags and was measured with weighpads—one for each wheel. Roll moment was obtained by shifting the sandbags from one side of the bus to the other. By calculating the difference between weighpad readings and measuring the distance between wheels on one axle, the actual applied roll moment was determined. Gravity supplied the lateral component of force during a tilt test (Figure 8), which was recorded using loadcells to measure the force between the tyre sidewall and the tilt table restraint. Linear bearings under the weighpads minimised friction losses from the lateral force.

By mounting three transducers in the configuration shown in Figure 8 and measuring their initial positions in space, it was possible, using geometric relationships, to extract separately the vertical, lateral, and roll displacements of one body relative to another. Graphs of force v displacement give an indication of linearity. Figure 9 contains typical graphs for each stiffness obtained at one axle.

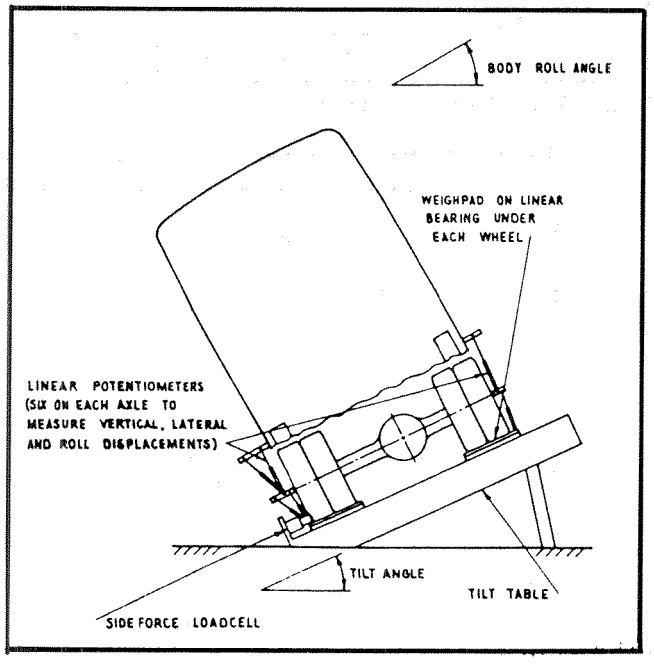

Figure 8. Cutaway view of instrumentation layout for tilt test

Roll Centre Heights

It was possible to also calculate the position of the instantaneous roll centre at each axle, using the successive position of the displacement transducers during the roll moment test.

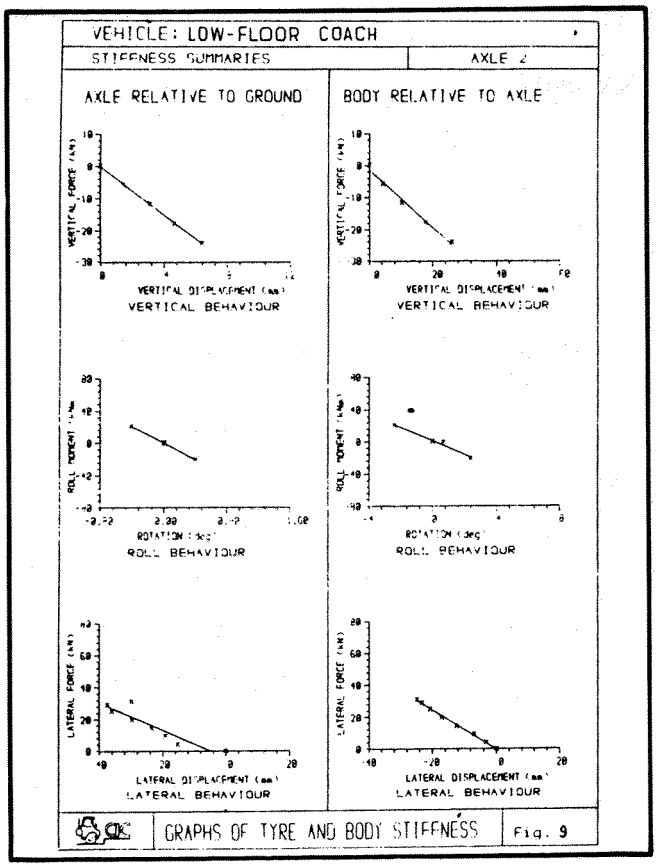

Figure 9. Stiffnesses measured at one axle

Experimental Results

Table 1 summarises the experimental results obtained from tests of nine buses and coaches into the parameters that are typical of three categories of vehicle.

Sample Rollover Simulation

The data from Table 1 were used to determine the threshold impact velocity (that is, the lateral curb-impact velocity that, if exceeded, would cause the vehicle in question to roll over) for each generalised vehicle.

Simulation Results

The rollover accident simulation program was run using the data for the three typical coach categories given in Table 1. By running the simulation with different values for the curb impact velocity, it was possible to determine the threshold impact velocity for each vehicle configuration and these are given (along with the maximum roll angle attained without overturning) in Table 2.

Parametric Study

To determine the factors that most affect the rollover propensity, a parametric study was undertaken. The

Table 1. Experimental data generalised for three typical coach configurations

Parameter		Low-Floor Coach or Bus	High-Floor Touring Coach	3-Axle 2-Decker
Mass (kg)		13,000	16,000	21,000
CG Height (m)		1.25	1.60	1.70
Moment of Inertia ($kg \cdot m^2$)		12,000	18,000	26,000
Vert Stif.(kN/m)				
springs	front	600	600	800
	mid	—	—	1,800
	rear	1,000	1,000	3,000
tyres	front	1,900	1,900	1,900
	mid	—	—	1,900
	rear	3,500	3,500	3,500
Roll Stif.(kNm/r)				
springs	front	200	120	200
	mid	—	—	800
	rear	500	500	600
Lat. Stif.(kN/m)				
springs	front	500	1,300	1,400
	mid	—	—	400
	rear	1,000	1,400	1,300
tyres	front	700	700	600
	mid	—	—	1,000
	rear	1,000	1,000	1,200
Roll. Ctr. Height (m)	front	1.00	0.80	0.90
	rear	1.30	0.95	0.80
Wheelbase (m)		5.80	5.95	6.30
Axle Wt. F:R(%)		42:58	36:64	34:66

Table 2. Rollover simulation results for three typical coach configurations

Parameter	Low-Floor Coach or Bus	High-Floor Touring Coach	3-Axle 2-Decker
Threshold Impact Velocity (m/s)	3.15	2.89	2.95
Maximum Roll. Angle (deg)	38.00	33.70	31.50

magnitudes of the various parameters (mass, moment of inertia, stiffnesses, and dimensions) for the Low-Floor Bus were taken as baseline values. Keeping the other variables at these base levels, each parameter in turn was varied to assess directly its effect on the threshold impact velocity. The preliminary results for the more significant factors are displayed in Figure 10, which uses a normalised horizontal scale, obtained by dividing the parameter in question by its baseline magnitude.

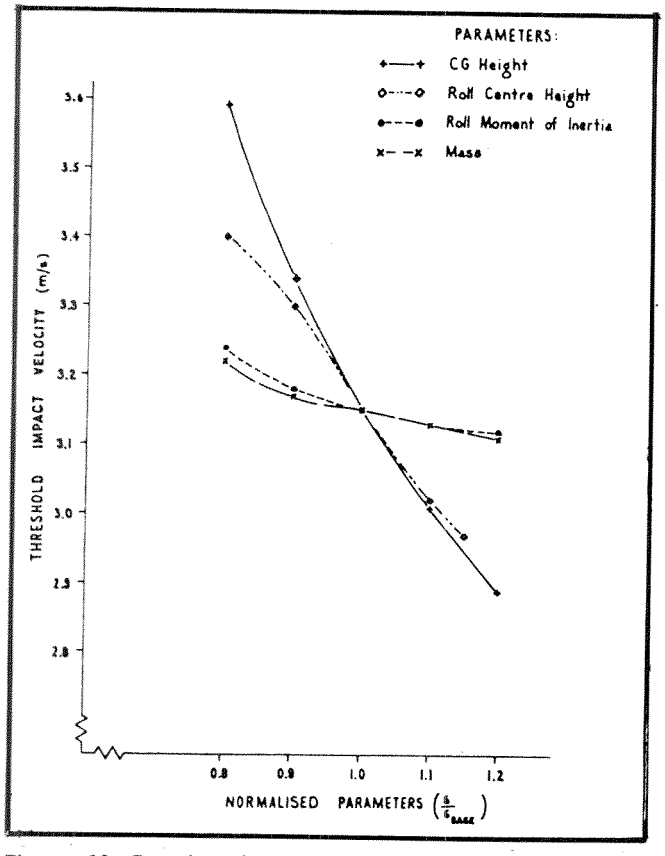

Figure 10. Results of parametric study

Discussion

It is apparent from Figure 10 that the most critical factor affecting rollover propensity is the CG height. Minimising this should, therefore, be the primary goal of vehicle designers who wish to improve rollover safety. The dimensions and mass-related properties would be unlikely to vary more than 20 percent from the baseline values as shown in Figure 10. Other parameters were examined but found to have little influence on rollover behaviour.

The stiffnesses were varied by a factor of two, but early indications reveal only minor effects, with the roll stiffness having the greatest effect.

Applications of This Research

The Rollover Accident Simulation Program is currently being used to investigate bus and coach rollover safety and, in particular, to assess the suitability of UK stability legislation for modern coach designs and travel patterns.

Acknowledgments

The author would like to thank the Department of Transport, London, for permission to publish this paper, and the New Zealand government who provided the doctorate scholarship. Cranfield Impact Centre, and particularly the retiring Director, Guy Tidbury, has been invaluable in coordinating and assisting technically on the experimental phase.

References

1. Weir, D.H., et al., "Analysis of truck and bus handling," Vol. 2, Report No. DOT-HS-801-153, June 1974.
2. Openshaw, M., G. Tidbury, and D. White, "Simulation of dynamics of a bus rollover test," XV Meeting of Bus and Coach Experts, Scientific Society of Mechanical Engineers, Hungary, September 1984.
3. Knight and Tidbury, "The SDG (Cranfield) bus roll moment of inertia test rig," Conference of Bus Experts, Hungarian Scientific Society of Mechanical Engineers, Budapest, 1981.

Technical Session No. 7

Pedestrian Protection

Franco R. Rossi, Chairman, Italy

General Problems Concerning Car-Pedestrian Collision

Andrea Costanzo

Associate Professor of Traumatology, School of Medicine and Surgery, Rome University, La Sapienza

Abstract

This study was to analyze road accident epidemiology of pedestrians by stressing the age of the injured, vehicle speed, possible trajectories of the impact, location of traumatic lesions on the human body, and environment of accidents.

At the conclusion of the study, recommendations were made to acquire methods aimed at using data in a more rational way, as well as seeking more complete sources.

Introduction

This study outlines accident epidemiology with particular reference to pedestrians. It also describes the most noteworthy aspects of the subject, as well as suggested methods for gathering data.

Problem Analysis

We will concentrate mainly on the following:

- Age of the injured
- Vehicle speed
- Type of vehicle
- Location of traumatic injuries

Another key aspect is to be added; that is, in a given town, find the ratio existing between the number of accidents occurring in certain areas and the total to determine the factors that influence the nature of the accidents.

As far as age is concerned, research carried out so far shows that children (under 18) and old people (over 60) are the most exposed in road accidents (see Figure 1). A logical explanation is that in the case of children, the accident rate is connected with their irresponsible attitude toward danger; the elderly, on the other hand, seem to be unaware of danger. Generally speaking, the solutions found in the past were aimed at better security measures for crossings, stops, signals, etc.

Regarding the influence of speed on accidents, it must be remembered that a higher accident rate occurs at a rather reduced speed.

Figure 2 shows that about 50 percent of the accidents occur at 15km/h while 90 percent occur at 45km/h. It shows also that most of the accidents occur in city traffic within these speed limits. From this standpoint, it would appear a gradual reduction of speed limits is the only way to prevent road accidents.

In a study carried out in Zurich in two stages, where the speed limits ranged from 50 to 60km/h, the number of accidents underwent a 20 percent drop when the 60km/h speed limit was reduced to 50km/h. The 20 percent drop of accidents also brought about a 50 percent decrease in the death toll.

When the driver races at a lower speed, he has enough time to brake.

As for the influence of the type of vehicle and its design, we can sum up the problem by stressing some peculiar features. For example, one category is called V form, a second is called Pontoon form, and a third is called Box form including lorries and buses that represent a wall against pedestrians.

Accordingly, we can say a pedestrian would be hit in his lower body parts by vehicles of the first category. The higher parts would be hit by vehicles of the second category, while the whole pedestrian's body would be endangered by vehicles of the third category.

In Figure 3, we see a subdivision of the types of vehicles mentioned above. The individual's height is also important. More accurate indications are found in Figure 4

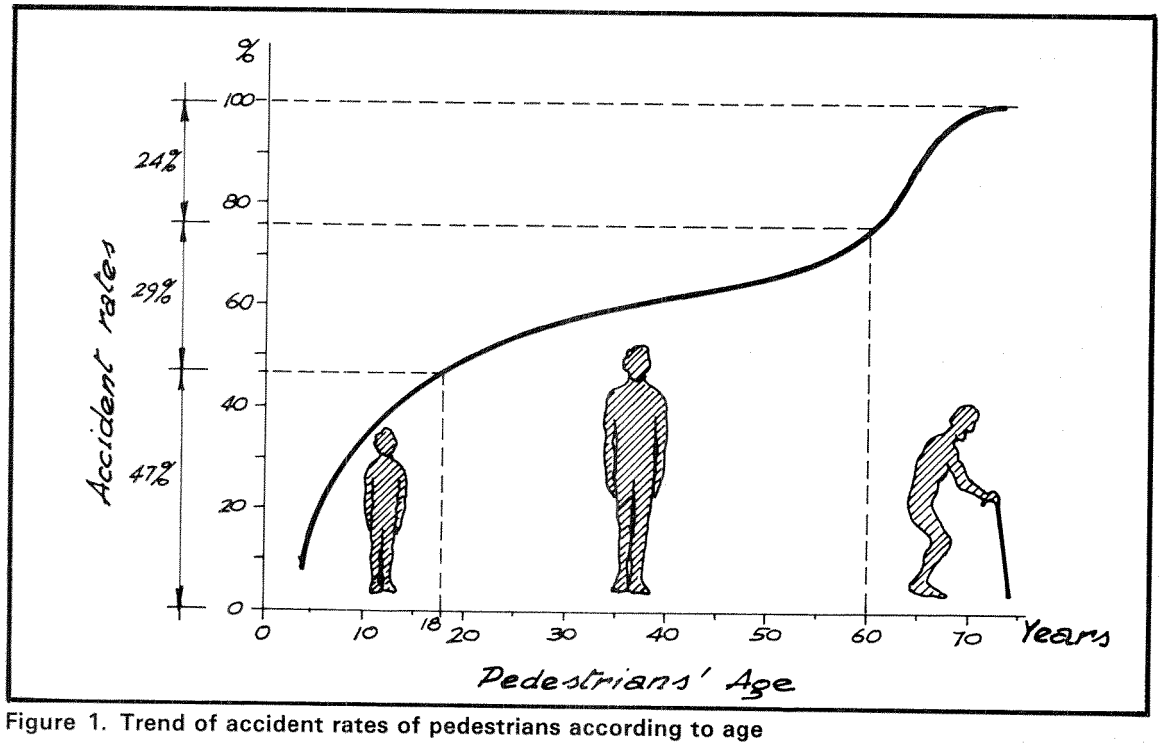

Figure 1. Trend of accident rates of pedestrians according to age

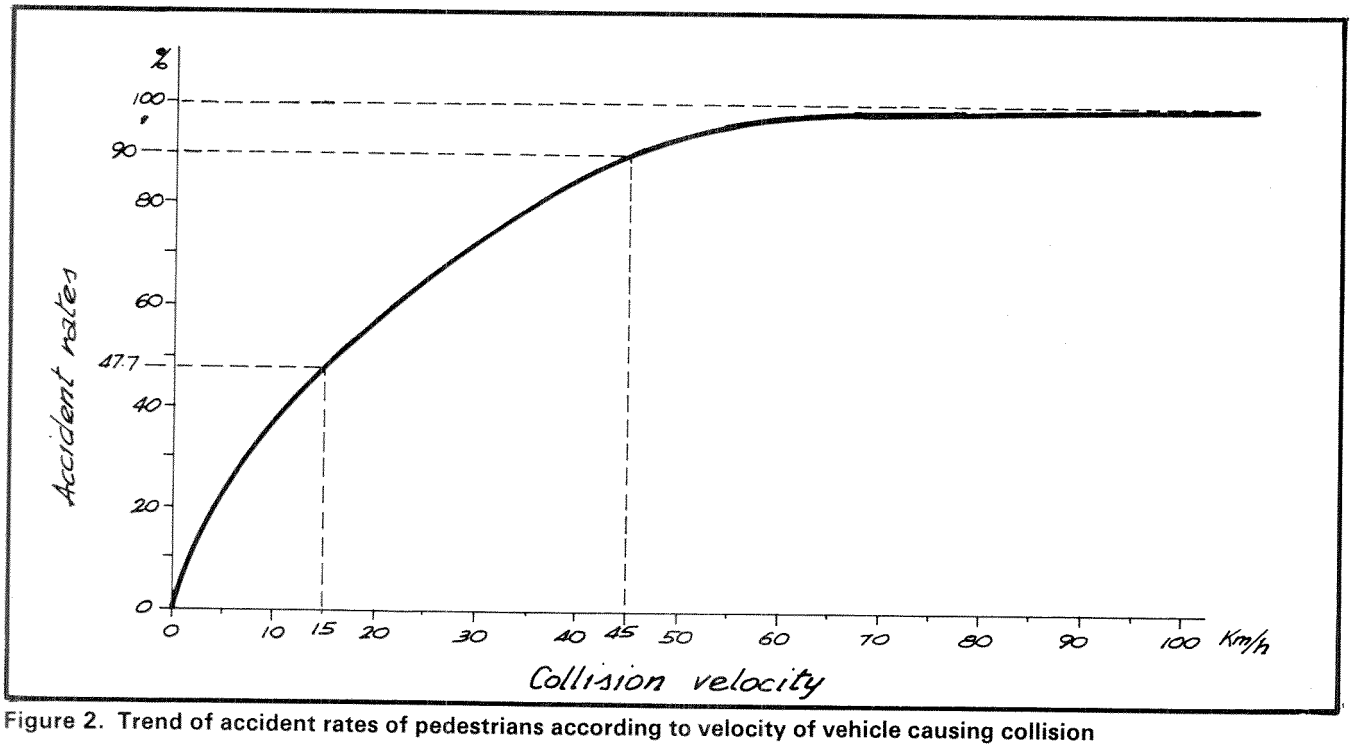

Figure 2. Trend of accident rates of pedestrians according to velocity of vehicle causing collision

where, in a given situation, an adult (Figures 4a and 4b) and a child (Figure 4c) are hit by a Pontoon form vehicle. The comparison between an adult's and a child's height is described in Figure 5.

If we want to foretell the impact result as far as the vehicle is concerned, location of masses on the human body must be taken into account by imagining the human body divided into some areas and indicating their centers. In Figure 6, a chart roughly analyzes this point; however, this should be studied with respect to the possible trajectories shown in Figure 4. It is possible to foretell the impact results by following the chart.

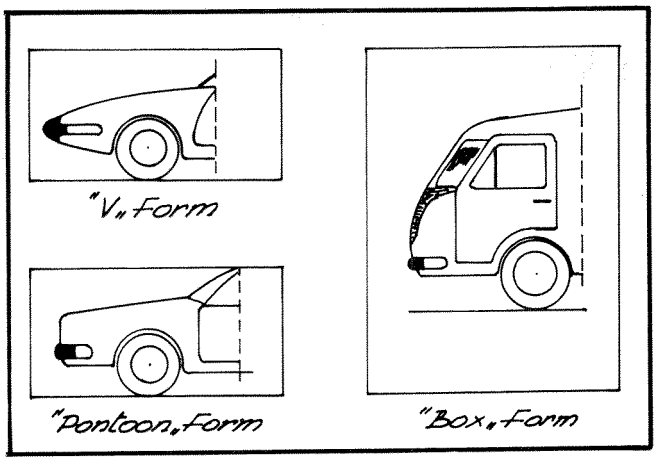

Figure 3. Classification of three types of vehicles causing collision

As far as location of traumatic injuries is concerned, many studies have proved that the gravity of an accident is often ascribed to the part of the vehicle causing the accident.

It is possible to locate some particular areas of the human body where seriousness of the accident relates to different conditions; this fact helps to get information for the survey.

A brief comment of these aspects would include a percentage of the injuries on a person connected with the impact area on the vehicle; the most serious accidents obviously occur in the front area (about 70 percent).

In Figure 7, the accident rate of pedestrians connected with the impact area on a vehicle is shown. Many studies have concentrated on the injured rate, and a case referring to a survey of 2,582 injured is described in Figure 8. From this figure, we see that the rate of injuries to the head is particularly impressive compared to other cases; the same is true of the most serious accidents, which involved head shock. Other cases concerning accidents involving one or more parts of the body have been included; therefore, the total percentage is higher than 100 percent (227.2).

Such an accurate subdivision describes the organic parts of the human body, but it demands a particular effort to obtain further data. Otherwise it would lend itself to errors of interpretation. We will give only a broad picture of the subject; we will describe the 15 subdivision parts of the human body.

As previously outlined, the purpose of this study is to examine accident epidemiology of pedestrians, as well as to work out other concepts that will enable us to complete

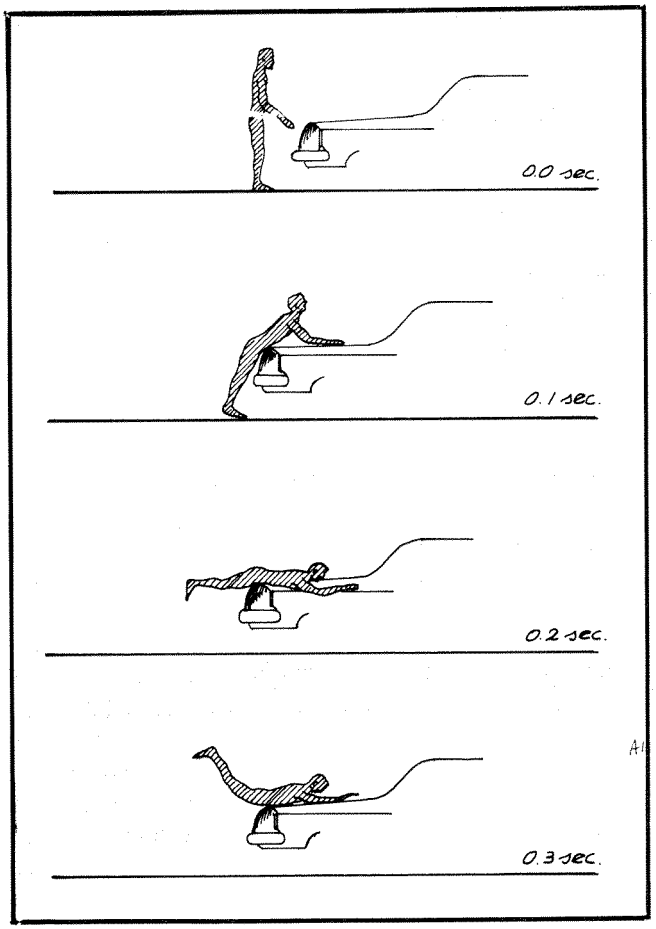

Figure 4a. Sequence of events referring to a standard situation of collision between an adult and a Pontoon form vehicle

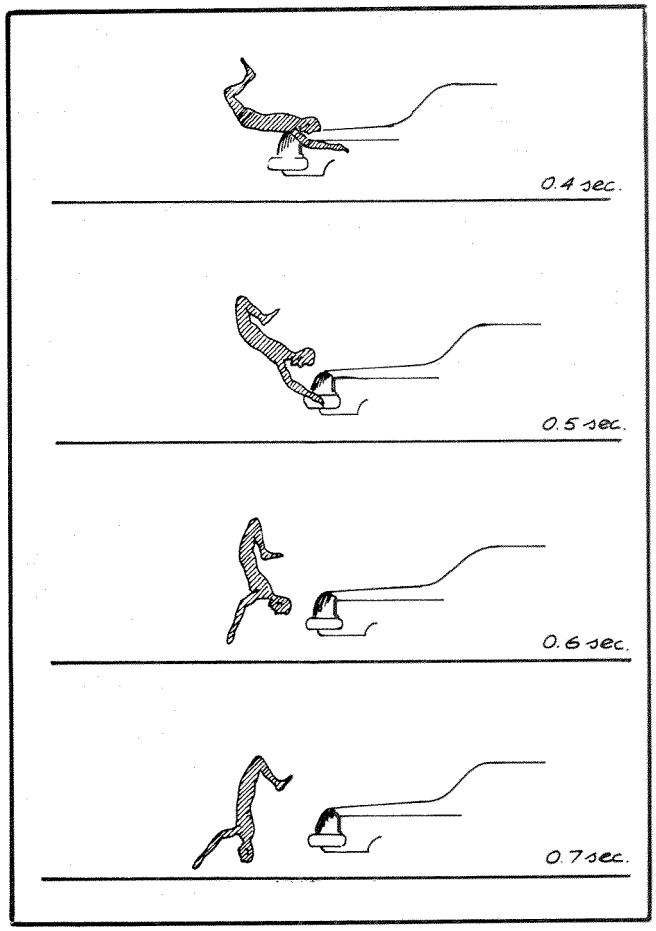

Figure 4b. Sequence of events referring to a standard situation of collision between an adult and a Pontoon form vehicle

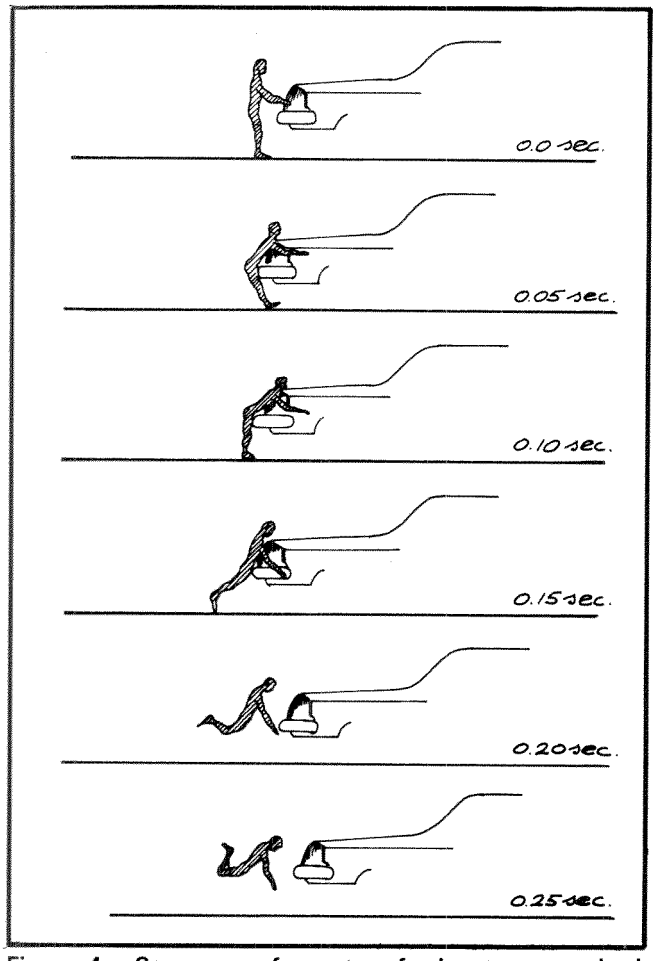

Figure 4c. Sequence of events referring to a standard situation of collision between a child and a Pontoon form vehicle

a thorough picture of accidents involving pedestrians. This can also give indications on the procedure followed.

So far we have examined the solutions found in three points: age of pedestrian, speed and vehicle distribution, and location of traumatic injuries in the human body. It is pointless to obtain information and data on subjects already studied; on the other hand, location of the accident environment is also very important.

To give a clearer picture, we will examine certain situations that are similar to those already set forth as far as children and old people are concerned. For example, we will examine an accident occurring in an urban area where certain social services, such as schools, bus stops, hospitals, and shopping centers, can be found. We will focus on two particular areas:

- Central area near school buildings, bus stops, hospitals, shopping centers, and railway stations
- Suburban areas close to highway exits

In the first area, we see data showing a higher percentage of accidents involving access to social facilities; therefore, regulations must be adapted for vehicles and road crossings that will considerably reduce the number of hazards. It is advisable to build overbridges or subways linking the school entrance to the road; furthermore, what is needed also is a responsible policeman at work!

In the second area, estimates show a higher percentage of serious accidents; therefore, we need a series of laws enforcing speed reduction of vehicles, especially those coming up from the outskirts to the town and v.v., and racing at speed levels higher than the average security level.

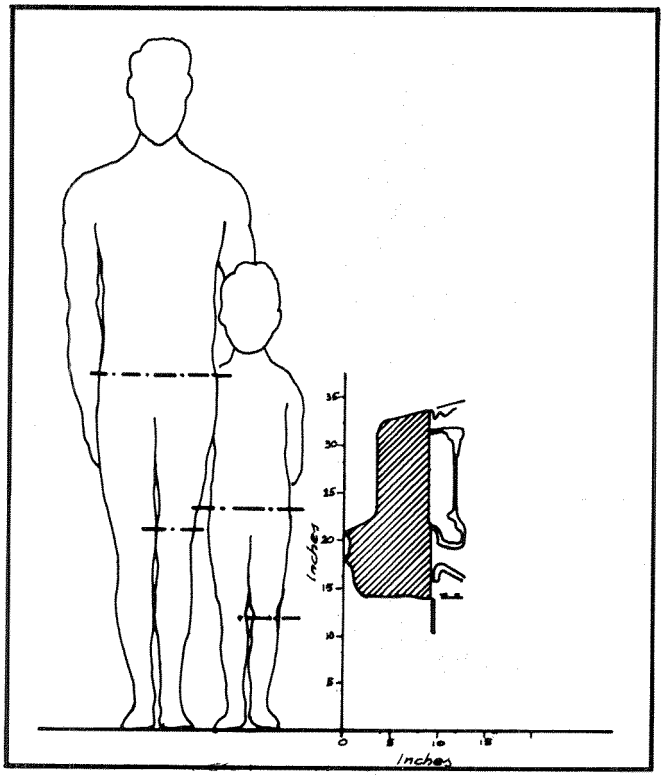

Figure 5. Rough comparison between an adult's average height and a child's average height with respect to a Pontoon form vehicle

Methodology of Data Acquisition

As has already been stated, the aim of such an analysis is to examine first those problems arising from pedestrian accidents and work out conclusions to outline a methodology of data acquisition. This methodology should make the information more reliable and give a thorough picture of all centers acquiring and providing data.

It is to be stressed that in the analysis previously carried out, we pointed out certain concepts such as environment that have not been mentioned in other studies. They should be taken into account. We have carried out an analysis including the most significant yardsticks that characterize accident collision to sum up what has already been set forth. Once a certain amount of information following our methodology is gathered, a publication containing the basic elements of this study will be issued.

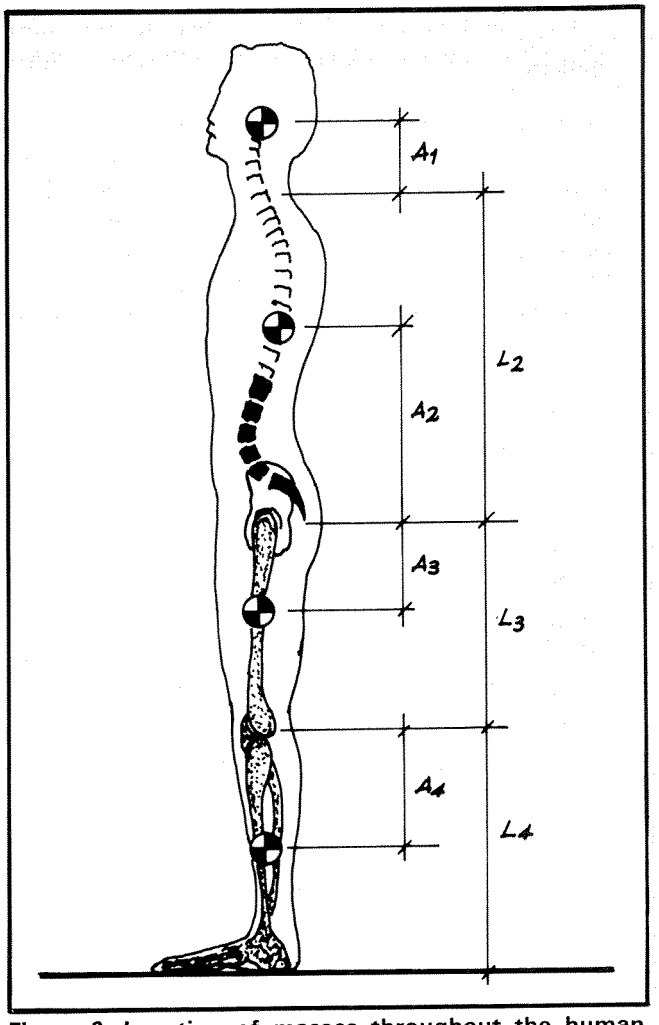

Figure 6. Location of masses throughout the human body

Conclusion

A reduced number of accidents is directly connected with a good number of laws aimed at establishing a deeper respect for the highway code, a strict application of speed limit regulations, and improved service capacity (especially crossings in traffic-impacted areas).

A more rigid enforcement of speed limits in the suburban areas is to be envisaged.

Furthermore, the analysis and considerations concerning the influence that the vehicle type exerts on the severity of an accident involving a pedestrian cannot be modified. In fact, suggestions for technical changes with no supporting grounds cannot be made to motor companies. Some slight changes are instead envisaged without affecting the technical elements of an automobile design; they certainly might reduce some hazardous situations.

While stressing the seriousness and importance of such a problem, we need to go on gathering reliable data from different sources to concentrate more on the elements of accident epidemiology of pedestrians.

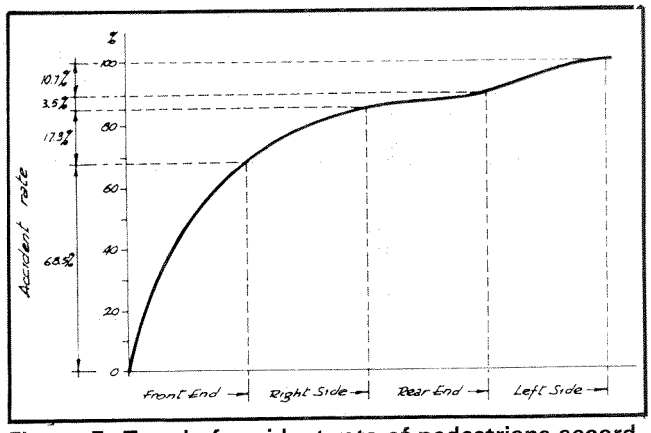

Figure 7. Trend of accident rate of pedestrians according to the impact area of a standard vehicle

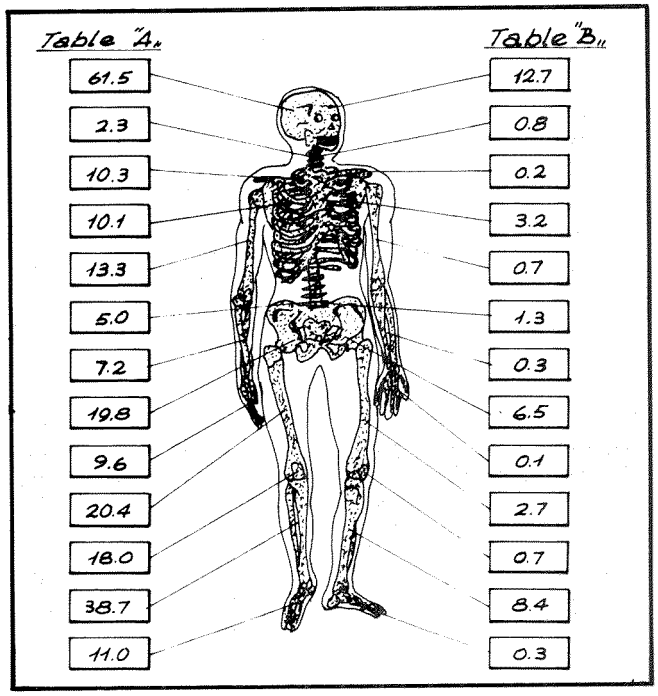

Figure 8. Percentage of hazards (Table "A") and serious hazards (Table "B") based on a survey of 2,500 accidents

References

1. Aldman, B., et al., "Physical simulation of human leg-bumper impacts," Proceedings Fourth IRCOBI Conference on the Biomechanics of Trauma, pp. 232-242, 1979.
2. Aldman, B., et al., "An experimental model system for the study of lower leg and knee injuries in car pedestrian accidents," Proceedings Eighth International Technical Conference on Experimental Safety Vehicles, October 1980.
3. Aldman, B., and D. Bunketorp, "Experimental study on human adult pedestrians in frontal impacts," Proceedings of Seminar on the Biomechanics of Impacts in Road Accidents, Commission of the European Communities, Brussels, March 1983.

4. Appel, H., et al., "Influence of impact speed and vehicle parameters on injuries of children and adults in pedestrian accidents," Proceedings IRCOBI Conference, 1975.
5. Ashton, S.J., "A preliminary assessment of the potential for pedestrian injury reduction through vehicle design," Proceedings 24th Stapp Car Crash Conference, pp. 607-633, 1980.
6. Ashton, S.J., A bibliography of pedestrian accident reference with emphasis on vehicle design and pedestrian injuries in *Pedestrian Impact Injury and Assessment*, SAE, Warrendale, Pennsylvania, Book Nr. P-121, 1983.
7. Baker, S.P., et al., "The injury severity score. A method of describing patients with multiple injuries and evaluating emergency care," *J. Trauma*, 14, pp. 187-196, 1974.
8. Brun, F., et al., "A synthesis of available data for improvement of pedestrian protection," Proceedings Seventh International Technical Conference on Experimental Safety Vehicles, 1979.
9. Bunketorp, O., et al., "Experimental study of a compliant bumper system," SAE Paper 831623, 1983.
10. Costanzo, A., F. Amici, and G. Gigante, Contributo ortopedico-traumatologico per una "auto sicura," *Minerva Ortopedica*, Vol. 25, N. 4, 1974.
11. Costanzo, A., L'incidente della strada (Analisi, prevenzione, soccorso), Atti 3° Conv. Naz. del Collegio dei Medici Italiani dei Trasporti Pugnochiuso, 10-14 Ottobre, 1984.
12. Daniel, S., Jr., "The role of the vehicle front and in pedestrian impact protection," SAE Paper 820246, 1982.
13. Danner, M., L. Klaus, and W. Wilhelm, "Injuries to pedestrians in real accidents and their relation to collision and car characteristics," SAE Paper 791008, 1979.
14. Eppinger, R., and V. Kulkarni, "Relationship between vehicle front structure and injury to the adult pedestrian hip area," Proceedings Eighth International Technical Conference on Experimental Safety Vehicles, October 1980.
15. Harris, J., and C.P. Radley, "Safer cars for pedestrians," Proceedings Seventh International Technical Conference on Experimental Safety Vehicles, June 1979.
16. Iton, M., "Analysis of pedestrian accidents taken from a road traffic accident investigation," Proceedings Seventh International Technical Conference on Experimental Safety Vehicles, 1979.
17. Kamiyama, S., and G. Schmidt, "Relations between collision speed, car damage, fractures and distance of projection in fifty cases of pedestrian-car accidents," *J. Legal Med.* 67, 282, 1970.
18. Lenz, K.H., "Speed limit experiments in the Federal Republic of Germany," in *Traffic Speed and Casualties*, Odense University Press, 1975.
19. Lucchini, E., and R. Weissner, "Difference between the kinematics and loadings of impacted adults and children; results from dummy tests," Proceedings Seventh International Technical Conference on Experimental Safety Vehicles, June 1979.
20. Monticelli, G., La Traumatologia del Traffico, I° corso di Medicina Sociale, Ist. Ital. Med. Soc., 1965.
21. Monticelli, G., Aspetti della Traumatologia del Traffico, Relaz. XVI Congr. Medico Interreg. Accad. Med. del Piceno—Jesi, 1965.
22. Pritz, H.B., "Vehicle design for pedestrian protection," Proceedings Seventh International Technical Conference on Experimental Safety Vehicles, pp. 699-703, U.S. Department of Transportation, Washington, D.C., 1979.
23. Ravani, B., D. Brougham, and R.T. Mason, "Pedestrian post-impact kinematics and injury patterns," SAE Paper 811024, 1982.
24. Romanini, L., S. Becelli, and A. Costanzo, Inchiesta campione sul numero, tipo, entità e cause delle lesioni traumatiche, Relaz. LVIII Congr. SIOT, Roma, 30 Nov. - 1,2 Dicembre, 1973.
25. Schmidt, D.N., B. Ravani, and D. Brougham, "Pedestrian injury causation study," Final report to NHTSA under contract No. DOT-HS-7-01581, August 1980
26. Searle, J.A., and A. Searle, "The trajectories of pedestrians, motorcycles, motorcyclists, etc., following a road accident," SAE Paper 831622, 1983.
27. Sturtz, G., et al., "Biomechanics of real child pedestrian accidents," SAE Paper 760814, 1976.
28. Svensson, A., "Experiences of speed restrictions in Sweden," in *Traffic Speed and Casualties*, Odense University Press, 1975.
29. Tharp, F.J., and N.G. Tsongos, "Injury severity factors—traffic pedestrian collision," SAE Paper 770093, 1977.
30. "The Abbreviated Injury Scale (AIS)—1976 Revision," American Association for Automotive Safety.
31. Walz, F.H., M. Hoefliger, and W. Fehlmann, "Speed limit reduction from 60 to 50km/h and pedestrian injuries," SAE Paper 831625, 1983.
32. Young, R.D., H.D. Ross, Jr., and W.F. Lammert, "Simulation of the pedestrian during vehicle impact," Proceedings Third International Congress on Automotive Safety, 1974.

Vehicle Pedestrian Head Impacts: A Computer Method for Rating a Profile Without Previous Mathematical Modelization

D. Lestrelin,
F. Brun-Cassan,
A. Fayon, and
C. Tarriere
Laboratory of Physiology and Biomechanics,
Peugeot SA/Renault

Abstract

No method based on experiments is convenient for evaluating globally the potential risk of a given vehicle for the whole population of pedestrians at risk, which encompasses the smallest children and the tallest adults simultaneously, when a large range of impact speeds has to be considered.

Mathematical models are also inadequate, due to the large number of runs required for obtaining the probability of impact on each section of the front end profile.

This paper describes first a recently improved mathematical method for defining the head trajectories yielded by experimental simulations or by a validated mathematical model. Then, a computer program is presented that simultaneously uses this method and statistical data concerning real accidents. The output of this program is a distribution of the impact probabilities for a given profile. The head impact velocities can be utilized for weighing the results.

Possible improvements and application of this method are discussed.

Accidentological Review

1. Between 1970 and 1980, the number of pedestrians killed in France decreased by 28 percent, stabilizing in 1980 at 2,277 killed and 42,490 injured, including 14,000 seriously injured(1).

   Between 1980 and 1984, the number of pedestrians killed on the road continued to fall, reaching a total of 1,760 in 1984 (Figure 1). This drop can be explained by a number of different simultaneous developments:

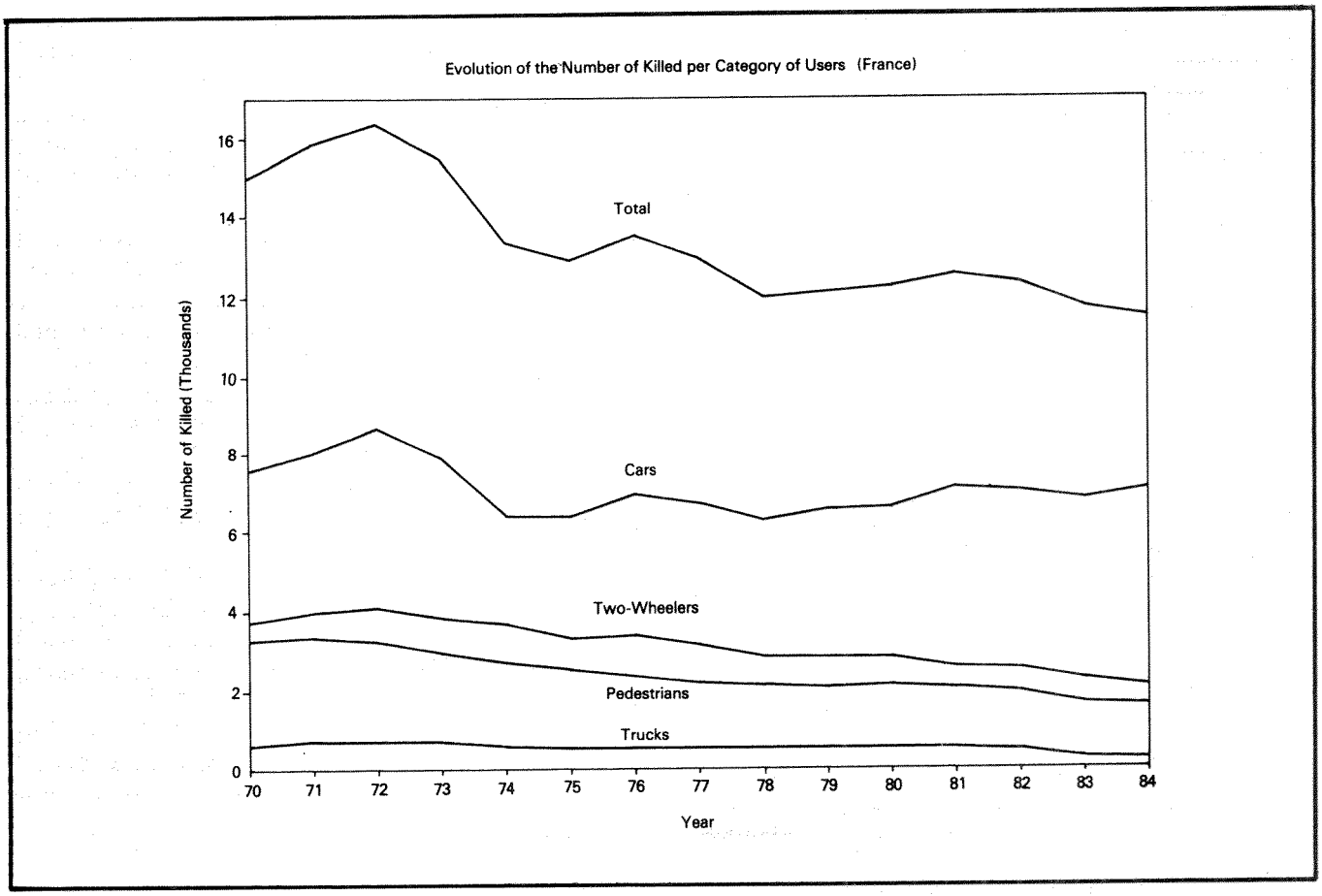

Figure 1. Evolution of the number killed per category of users (France)

- Extension of school bus services in the country
- Fewer pedestrians and more cars
- Increased separation between pedestrians and motor vehicles
- Less aggressive modern vehicles in terms of their more streamlined design and their greater deformability, etc.

This favorable evolution has also been observed in other industrialized countries (West Germany, Great Britain, and the United States).

2. The body segment most frequently and most severely affected is the head (see Figures 2 and 3).

Moreover, at speeds lower than 25 or 30km/h, the lesions due to secondary impact with the ground are more severe than those inflicted by the vehicle (primary impact), but the opposite applies at higher speeds. The head-vehicle impact is, therefore, the predominant feature of pedestrian accidentology, for the speeds at which severe or fatal injuries can be observed.

3. The great majority of pedestrian accident victims are adults with a maximum density height of 1.64m (Figure 4). However, it should not be forgotten that 16 percent of the pedestrian accident victims are children.
4. The size of the pedestrian and speed of the vehicle are the essential determining factors in the site of impact of the head with the vehicle and the relative speed between the head and the vehicle just prior to the impact.
5. Two age groups are at high risk in a pedestrian accident, in relation to the general population (Figure 5) (frequency of involvement greater than the demographic distribution).

It is concluded that priority must be given to a child's and an adult's head, which justifies this presentation.

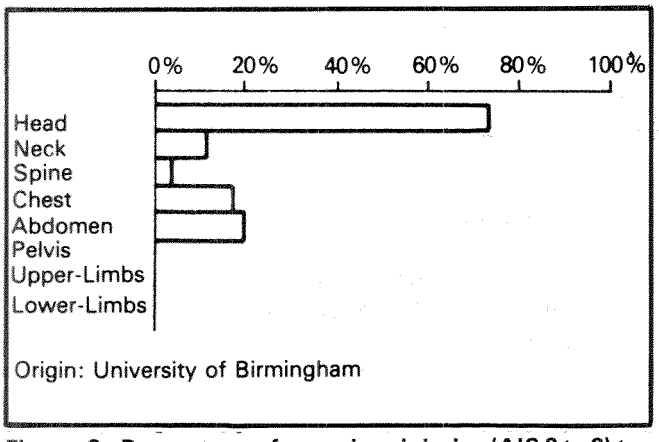

Figure 2. Percentage of nonminor injuries (AIS 2 to 3) to the different parts of the body of 739 pedestrians sustaining injuries of a moderate degree (OAIS 2 to 3)

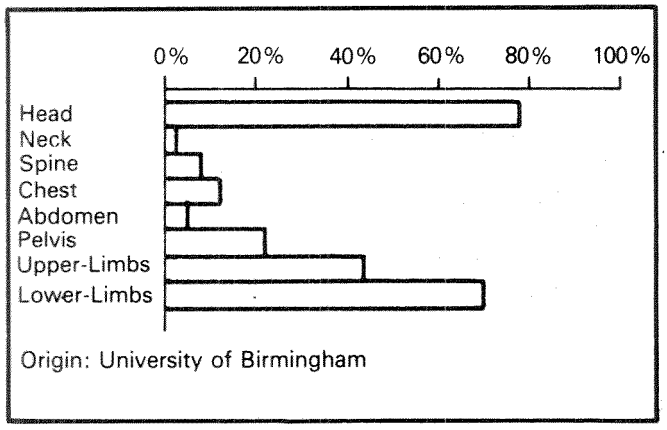

Figure 3. Percentage of very serious and fatal injuries (AIS 4) to the different parts of the body of 253 pedestrians seriously injured or killed (OAIS ≥ 4)

Scatter of the Results of Experimental Trials

The scatter of sites of impact of the head obtained during experimental simulations with dummies and performed under identical conditions, i.e., with the same

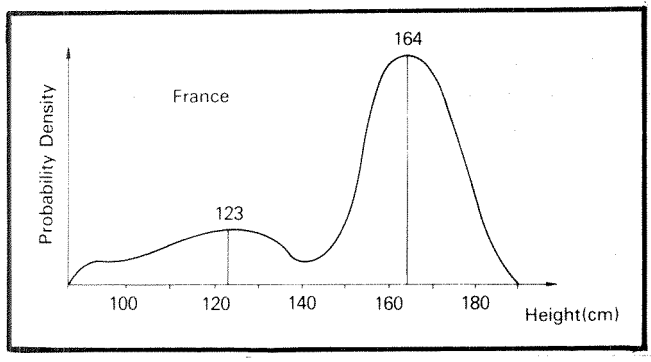

Figure 4. Distribution of pedestrians involved in accidents according to their size

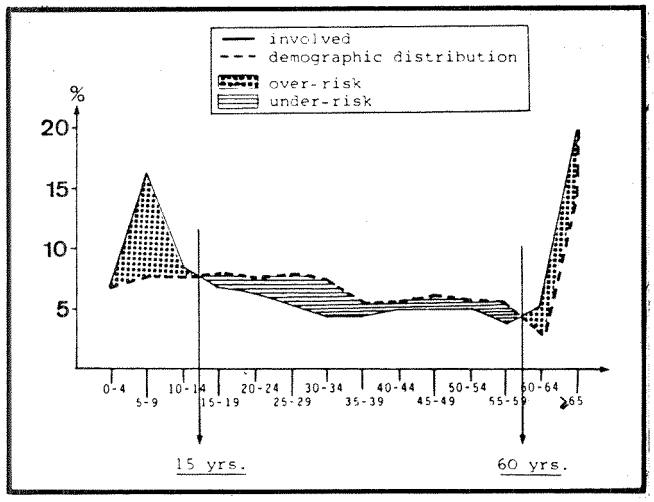

Figure 5. Risk of accident according to age of pedestrian

dummy and the same vehicle traveling at the same speed at the moment of first impact and with the dummy in the same position in relation to the vehicle (in particular, the position of the feet) and without any risk of interposition of elbow, cannot be neglected: in the order of 10cm for a sample of five trials.

The scatter of the velocities of head/vehicle impact is even greater. Under the same test conditions, the ratio of the velocity of head/vehicle impact to the initial velocity of the vehicle, which is in the order of 1, can vary within a range of 0.5 or even 1.

In the case of real accidents, it is obvious that the scatter of the sites and the velocities of head/vehicle impact for the same vehicle at the same initial velocity and the same height of the pedestrian will also be very wide.

One should not, therefore, be excessively demanding about the accuracy of the results provided by a mathematical model of simulated shock or by a system of equations of trajectory of the center of the head, such as the one described in this paper. The essential point is that these results lie within a scatter of experimental results.

System of Equations of the Trajectory of the Head: TRAJ Program

In a previous paper, we explained how we validated the two-dimensional PRAKIMOD mathematical model in the context of pedestrian shock on the basis of experimental tests (some of which were reconstructions of real accidents). These tests involved the use of vehicles of various sizes and shapes traveling at a wide range of velocities—from 16 to 48km/h(2). We investigated a mathematical form of CG kinematics of the head, obtained by means of PRAKIMOD, for 24 simulations consisting of those performed during the phase of validation of the model and the complementary simulations with 6-year-old pedestrians or pedestrians with a height between that of a 6-year-old and a 50th percentile adult(4).

The form initially selected(3) consisted of 18 terms adjusted by least squares for each coordinate:

$$\frac{X}{T} = \frac{Xo}{T} + \frac{Vot}{T} = A_{1,1}t^2 + A_{1,2}t^3$$

$$\frac{Z}{T} = \frac{Zo}{T} + A_{2,1}t^2 + A_{2,s}t^3$$

or, in polar coordinates:

$$x = x_o + \rho \cos \vartheta$$

$$z = \rho \sin \vartheta$$

with

$$\frac{\rho}{T} = \frac{\rho o}{T} = A_{3,1}t^2 + A_{3,2}t^3$$

$$\vartheta = \frac{\pi}{2} - \frac{Vot}{Po} + A_{4,1}t^2 + A_{4,2}t^3$$

where the constants A (two per coordinates X, Z or ρ or) were functions of V, T and G:

$$A_{i,1} = B_{i,1,1}\frac{V^2}{T^2} + B_{i,2,1}\frac{g}{T} + B_{i,3,1}\frac{V}{T}\sqrt{\frac{g}{T}}$$

$$A_{i,2} = B_{i,1,2}\frac{V^3}{T^3} + B_{i,2,2}\frac{V}{T}\frac{g}{T} + B_{i,3,2}\frac{V^2}{T^2}\sqrt{\frac{g}{T}}$$

the constants B (2 x 3 = 6 per coordinate) were functions of H and T:

$$B_{i,j,k} = C_{i,j,k,1} + C_{i,j,k,2}\frac{H}{T} + C_{i,j,k,3}\left(\frac{H^2}{T}\right)$$

and the constants C (18 per coordinate) were determined by a least squares method on the basis of the coordinates of CG of the head with a time interval of 10ms from the output data of the 24 PRAKIMOD simulations.

A form of equation was then obtained using fewer terms (12 instead of 18 per coordinate), but remaining close to the given points(4) by replacing T by Po in all of the denominators and by eliminating the terms containing G.

Simultaneously, for the polar coordinates, the center of the system, initially at ground level, was raised to the level of the front of the hood.

The pole of the polar coordinates was displaced because, if we consider that on first approximation the part of the pedestrian situated above the hood of the car would pivot around the anterior border of the hood, it seemed preferable to make the pole of the polar coordinates coincide with the center of rotation than to place it at ground level.

When the pole was placed at the level of the anterior border of the hood, the description of the movement by polar coordinates generally gave better results than the description by means of cartesian (rectangular) coordinates for all the forms tested.

A further improvement has recently been added to this form:

- By further reducing the number of degrees of freedom of the model from 12 to 8 per coordinate (suppression of the terms involving $(H/P)^2$)
- By replacing H/P with its inverse Po/H

- By replacing the height of the edge of the hood (H) with an equivalent hood height equal to H decreased by the projection (Dx) of the bumper bar over the anterior edge of the hood

(A detailed description of the calculations will be in the final paper.)

Most of the original trajectories were well fitted by these equations (Figure 6), except for those that involved vehicles with a high and angular hood border (Figure 7). This demonstrates that the present form of the equations is not optimal. They can certainly be improved while retaining the general principle of a statistical, nonlinear model for all of the trajectories used in the input data.

Application: The Program PROF for the Determination of the Sites and Velocities of Impact Between the Pedestrian's Head and Any Vehicle Profile

These new equations can be used by the PROF program simulating the bombardment of the front profile of any vehicle by spheres with a given radius simulating the heads of pedestrians. The kinematics of the center of these spheres are controlled by the equations, in which the coefficients have been determined by the TRAJ program and which involve the height of the pedestrian, the projection of the bumper bar, the height of the anterior edge of the hood, the initial velocity of the vehicle, and the time.

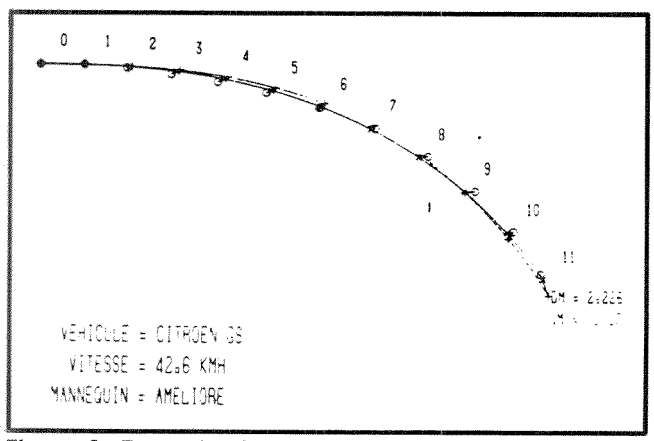

Figure 6. Example of good adjustment of the trajectory by the TRAJ equations

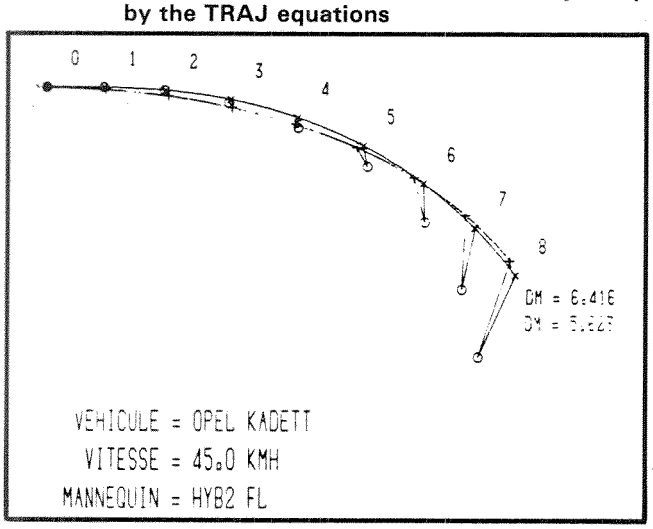

Figure 7. Example of poor adjustment of the trajectory by the TRAJ equations

The immediate typical applications for use with the PROF program are—

1. Determination of the site and velocity of head/vehicle impact for a particular impact characterized by—
   - A vehicle profile
   - The height of the pedestrian
   - The velocity of collision (Figure 8)
2. The same operation for—
   - A given vehicle profile
   - A series of pedestrian heights defined by the user at the beginning of the program
   - A series of velocities of collision defined in the same way

   The program determines the head impacts for all sets (height of the pedestrian and velocity of collision) obtained by combination of the elements of the two series (Figure 9).
3. The computerized statistical data can be used as input data for the heights of the pedestrians and the velocities of collision so as to attribute to a density distribution of the probability of impact of the head of a pedestrian belonging to the population described by the statistical data (Figures 10 and 11).

At the stage of conception of a vehicle, the attention of the constructor's research department can, therefore, be drawn to the zones with the highest risk of impact to make them less rigid.

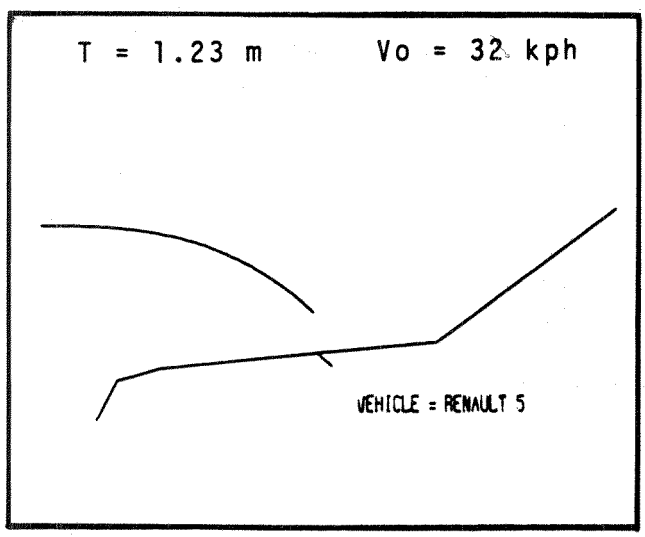

Figure 8. PROF output examples—determination of the site and velocity of head/vehicle impact in different cases

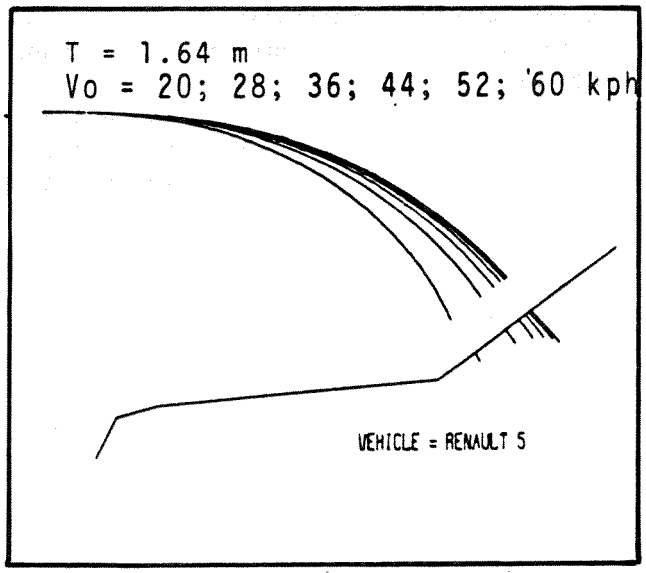

Figure 9. Determination of the site and velocity of head/vehicle impact in different cases

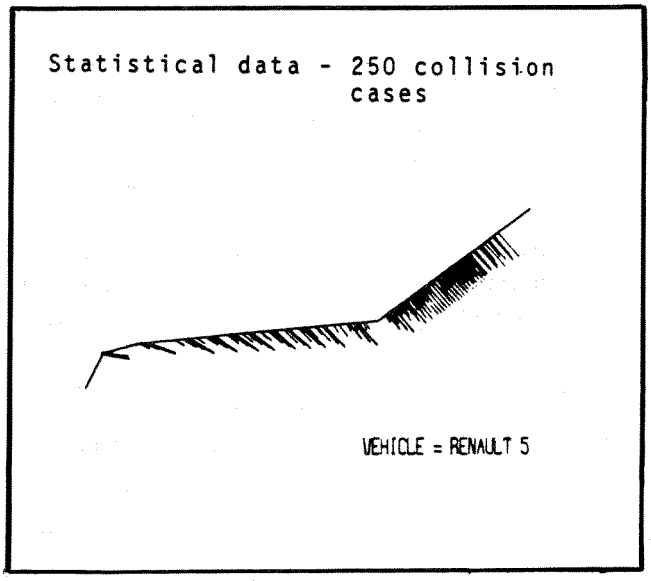

Figure 10. Determination of the site and velocity of head/vehicle impact in different cases

Validation of the TRAJ and PROF Programs

A validation of these programs has been attempted by using them to determine the site and velocity of head/vehicle impact in cases of collision between a Volvo 244 and a 50th percentile adult in the middle zone of the front of the vehicle at a velocity of 40km/h. Figure 12 shows the impact obtained—

- By the PROF program (using the coefficients previously determined by TRAJ)
- By mathematical simulation by means of PRAKIMOD
- In five experimental collisions with mannequins

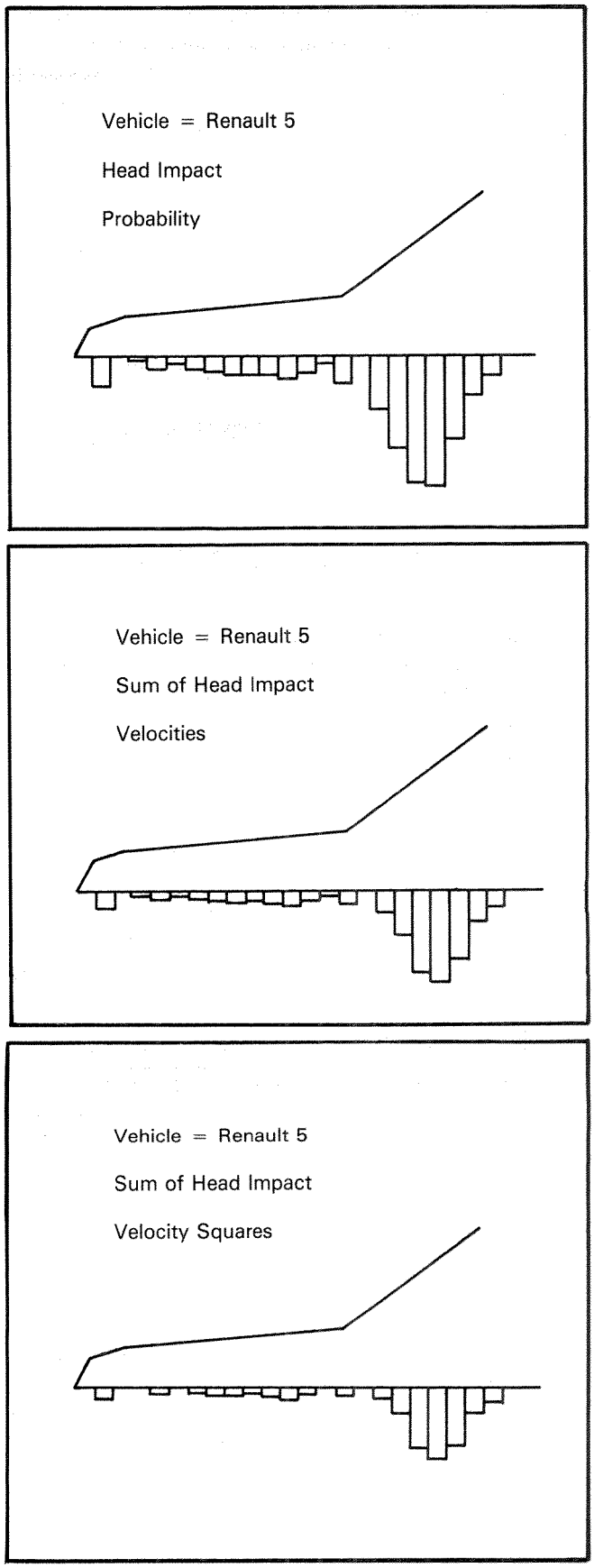

Figure 11. Weighting of the results shown on Figure 10 by the impact velocity

The site and the velocity of impact predicted by PROF were within the scatter of the values obtained by PRAKIMOD and by the experimental trials.

This attempted validation can be considered to be successful.

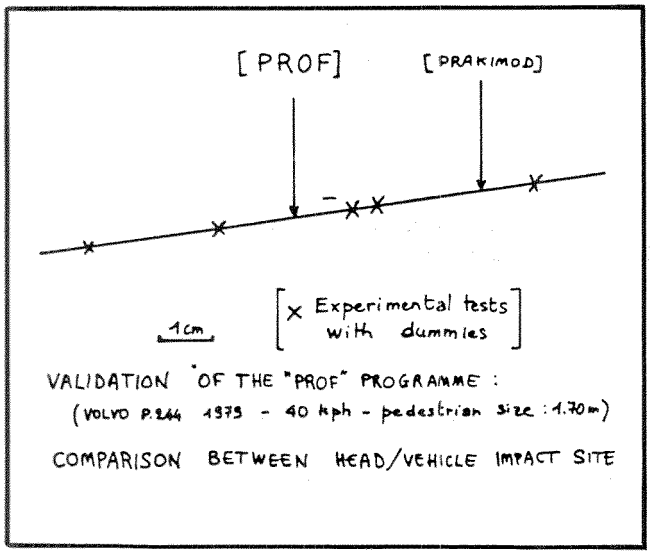

Figure 12. Comparison between head/vehicle impact site

Discussion

To obtain a better reproduction of the kinematics of the pedestrian's head induced by high or angular vehicle profiles, as described above, we need to find a better statistical model.

However, it is true this type of profile is tending to disappear and is being replaced by more aerodynamic profiles, which are well simulated by our model.

To be able to supply research departments with the means of associating each part of a planned vehicle (or at least those parts most frequently involved in accidents) with the optimal rigidity and a depth associated with deformability, we would need to have a value for the mass equivalent of the head in relation to the position of the body of the victim at the time of head/vehicle impact, as well as the height and age of the victim. We also need to have a better understanding of the tolerance of the human head to such impact, as a function of age.

The Mass Equivalent

The PRAKIMOD model allows the mean mass equivalent of the head to be determined during impacts conducted under well-defined conditions.

Unfortunately, in this model, the neck is reduced to a simple articulation. The simplicity of this model of the neck does not prevent good simulation of the kinematics of the head up until head/vehicle impact, but it does not allow good simulation of the behavior of the head and neck unit during the head/vehicle impact if the trunk exerts a force in the axis of the neck.

Until more detailed data are available, we can recommend that the mass of the head alone or that of the head and neck together be used as the mass equivalent of impact.

Tolerance of the Head to Impact

Although the tolerance of the head of a middle-aged adult is beginning to be defined, the tolerance of children and elderly people is less well known. The tolerance to linear acceleration is probably greater in children than in adults and less in elderly people.

In the absence of any precise information, we could adopt the criterion of adult head protection for all the pedestrian population.

Conclusion

Following a more detailed validation and, if necessary, an improvement in the statistical model used, the TRAJ and PROF programs described in this paper may constitute a very valuable computerized tool to determine the zones of a vehicle at greatest risk of impact with the head of a pedestrian.

The relative potential dangers of the corresponding impacts can be rated by means of an experimental procedure using a model of the head.

References

1. Thomas, Ch., and H. Vallee, "An accidentological reminder concerning the pedestrians involved in road accidents," in SIA Conference—Secondary Safety and the Automobile of Today Facing New Constraints, Paris, March 18-19, 1982, published in *Ingénieurs de l'Automobile,* No. 83-2.
2. Lestrelin, D., F. Brun-Cassan, A. Fayon, C. Tarriere, and F. Castan, "Mathematical simulation of accident victims—validation and application to car pedestrian collisions," Proceedings Eighth International Technical Conference on Experimental Safety Vehicles, Wolfsburg (R.F.A.).
3. Lestrelin, D., "Mathematical simulation of pedestrian behaviour—an application of the prediction of head impact localizations," in SIA No. 83-2.
4. Lestrelin, D., F. Brun-Cassan, A. Fayon, and C. Tarriere, "Mathematical evaluation of the head impact risk on a linear part of a vehicle, as regards pedestrians," SAE Paper 830059.

Computer Simulations of a Range of Car-Pedestrian Collisions

G.D. Suthurst
Ford Motor Company, United Kingdom

R.N. Hardy
Cranfield Impact Centre, United Kingdom

Abstract

Realistically, the only way to significantly improve the pedestrian injury situation is by separation of the vehicle and pedestrian population to prevent collision occurring, since injury to a pedestrian is inevitable if hit by a car travelling at even low speeds.

However, it is important to assess the contribution that vehicle design characteristics can make to minimise the consequences of such collisions for a variety of pedestrian types, and to establish the various vehicle parameters that can influence pedestrian injury.

This paper describes the initial stages of an investigation into these parameters by means of computer simulation.

First, the joint, inertia, and contact characteristics of a 50th percentile adult dummy and a 6-year-old child dummy were established by tests. The contact characteristics of a range of car fronts were also determined from pendulum tests at speeds of 24 and 40km/h. A vehicle-pedestrian interaction model was then established, and simulations of previously staged tests were carried out by means of the Calspan Crash Victim Simulation (CVS) program. This paper shows the comparison between tests and simulations for adult and child representations with a range of front end parameters. The particular effects of the various parameters are also discussed.

Introduction

Accident statistics relating to traffic accidents involving pedestrians are well documented in many countries(1,2,3,4,5,6,7). In these accidents, approximately 80 percent of the pedestrians are struck by cars, representing 25 percent of all fatalities in road traffic accidents and 16 percent of all those seriously injured. These statistics show the need to reduce the number and severity of car-pedestrian collisions. In the future, the pedestrian percentage figures are likely to increase as safety measures currently implemented for vehicle occupant safety begin to be reflected more in the accident data.

It is self-evident that injury is inevitable if a pedestrian is hit by a car even at low speeds and that major improvements can only be achieved through accident avoidance measures. It is, however, worthwhile to determine whether any realistic action can be taken in car design to reduce the severity of the injury that the pedestrian is likely to sustain.

Examining the car-pedestrian accident data further, several features can be highlighted:

- 60 to 70 percent of the pedestrian fatalities are inflicted by the car(8).
- 70 to 75 percent of pedestrian injuries are due to primary contact with the front of the car(1,4,5,10).
- 60 to 75 percent of AIS 4 and 5 injuries are due to head impact against the car(3,9).
- Age groups 6 to 9 years (40 percent) and over 65 years (20 percent) are most at risk(3,4,10).

It is, therefore, necessary that pedestrian studies should concentrate on the car front end and its effect in collisions with both adult and child pedestrians.

The car front end has been receiving increased attention in recent years due to the influence of front impact legislation and/or company policy on frontal impact performance. The need to reduce weight and the cost of ownership has also influenced front end design.

Reviewing the list of constraints on the front end, we have—

- Aesthetic appearance
- Engine and accessory packaging
- High-speed front impact performance for occupant protection
- Low-speed front end damageability performance—low cost of ownership
- Reduced overall weight
- Pedestrian impact performance—6-year-old child and adult
- Aerodynamics

The final design will need to be a compromise as some of these factors work for each other while others work against.

With such a list of constraints, a design and test exercise to achieve the compromise would be a mammoth task as each item would need to be optimised and then its effect on each of the other constraints would have to be checked, modified, and rechecked for an acceptable overall effect.

Mathematical modelling of the impact situation is the obvious solution to such a problem. Parametric studies can be conducted rapidly, and each optimised item can then be assessed relative to the other criteria prior to a build-and-test program.

This paper describes the initial stages of an investigation into these parameters by means of a computer simulation. Included are descriptions of a test program simulating car-pedestrian collisions, necessary for the validation of the prediction program details of dummy and car contact characteristic tests, and the development of a vehicle-pedestrian interaction model using the Calspan CVS program. Comparisons are shown between tests and simulations for adult and child representations with a range of car front end parameters. The particular effects of the various parameters are also discussed.

Technical Approach

To provide an experimental data base for the development and validation of the simulation model, a test program was conducted using four different cars in collision with pedestrian dummies of a 6-year-old child and 50th percentile male.

Previous studies of pedestrian impacts have shown there are normally two impacts in the typical car-pedestrian collision that can cause injury: first, the vehicle impacting the pedestrian, and then the pedestrian impacting the ground. Ashton(11) shows that contact with the vehicle is the main cause of nonminor injury and that severity is dependent on vehicle speed whereas ground contact severity is independent of speed. Other studies have shown that the majority of serious/fatal injuries are caused by head impact against the car. In tests using the present generation of pedestrian dummies, it is unlikely the response of the dummy would be accurate enough to reproduce the actions of a pedestrian for kinematics of the duration and complexity necessary to include the ground contact.

For these reasons, the analysis of the tests was concentrated on the car-dummy contact period, i.e., from initial dummy contact up to head contact with the upper surfaces of the car exterior. This is the period in which car design, size, and stiffness characteristics provide the major influences on dummy kinematics and eventual head-to-car contact.

The Calspan 3D CVS program was selected for the development of the vehicle-pedestrian interaction model. This choice was based mainly on its three-dimensional capability, which was considered essential to allow for a rotation about the vertical axis of the dummy, and on previous experience gained using Calspan CVS for another crash simulation investigation.

Input to the Calspan CVS program includes dummy and vehicle data; therefore, tests were conducted to establish the joint, inertia, and contact characteristics of the 50th percentile adult and the 6-year-old child dummy. The contact characteristics of the selected car fronts were also determined from pendulum tests at speeds of 24 and 40km/h.

Previous vehicle-pedestrian interaction models have utilised planes to represent the profile of the vehicle. Some researchers have used 5 or 6 planes to represent the front of the vehicle(12,13,14), while others have used up to 10 planes to achieve the correct geometry of the vehicle front(15). As an alternative, TNO has written a hyper-ellipse contact model(16) that eliminates some of the problems inherent in ellipsoid-plane contacts. Ellipsoids were selected to represent the front of the vehicle for this interaction model as the authors had a relatively short time scale available for this stage of their research—too short to allow a new contact model to be written, implemented, and debugged—and to avoid the problems associated with ellipsoid-plane contact models that have previously been reported(17).

Car-Pedestrian Test Program

Test Vehicles

The vehicles were selected primarily to include differences in front end design, stiffness, materials, etc. Figure 1 shows the main dimensions of the models. The model identifications A to D are in descending order of front end stiffness.

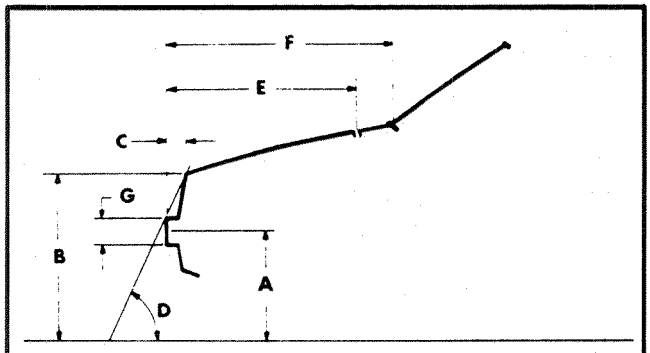

DIMENSIONS	MODELS A	B	C	D
A	450	444	423	435
B	667	682	702	760
C	70	59	196	205
D	73°	73°	56°	65°
E	923	1028	1157	1200
F	1042	1128	1275	1330
G	45	35	120	40

Figure 1. Vehicle dimensions

Data Analysis Criteria

To assist in the evaluation of the car front ends, dummy data from the primary contact up to the time immediately prior to head contact with the car were compared. Head velocity (a function of front end design/stiffness) immediately prior to head contact with the car was compared rather than head acceleration at head contact. The head velocity was considered to be a more valid comparison than acceleration data because of the considerable differences in stiffness of possible head contact areas in close proximity to each other; for instance, due to the location, at some point on one car, of an engine component beneath but close to the hood surface or in areas where joints occur, e.g., fender/hood opening lines. The influence of these variables on the head acceleration data could give quite a false assessment of a particular front end parameter, such as bumper stiffness, on pedestrian injury.

Dummies

As the age group 6 to 9 years accounts for 40 percent of the injured pedestrian population, it was necessary for the test program to assess impacts on a child, as well as on an adult, to enable areas of possible conflict in design to be determined. The dummies currently available for pedestrian impact tests have been criticised for several reasons, but mainly due to a lack of compliance in the segments and joints. As dummy development was outside the scope of this investigation, a 50th percentile standing adult male dummy (Part 572) and a 6-year-old child dummy, both manufactured by Humanoid, USA were selected.

Impact Speeds

In European countries, collisions between vehicles and pedestrians occur in built-up areas at speeds below 50km/h. Of cases involving serious injury, 50 percent occur at speeds less than 35km/h and 85 percent at speeds below 40km/h.

Two impact speeds were selected for the test program, a lower speed of 24km/h—typical of the below 35km/h range—and a higher speed of 40km/h. This was considered a suitable range to include up to 85 percent of accidents where serious and fatal injuries occur and also to provide a means of validating the mathematical model prior to parametric studies.

Dummy Stance

Seventy percent of pedestrians injured in collision with a car are struck by the front of the car(1,3,4,5,10); the majority are struck on the side of their body by the inner or outer third of the car front(1,3,4). The dummies in this test program were positioned for impact essentially on the side of the body but with the dummy rotated toward the car by 30° and with the legs in a walking stance with the impacted leg in the rearmost position (Figures 2 and 3). This position was selected for the following reasons:

- Impact on the side represents the major directional frequency in the real accident situation, and this position also gives the most severe leg impact condition as there is no natural rotation in the knee joint in that direction. However, in a collision using dummies, it gives an unrepresentative level of protection to the head due to shoulder and/or elbow impact with the hood as these parts of the dummy are far more rigid than on a human.
- The rotation of 30° gives representative loading on the legs while allowing the dummy to rotate during the impact to insure head contact without prior shoulder contact.

Figure 2. Initial adult dummy stance

- To eliminate the elbow influence, the dummy arm nearest to the car was lightly attached to the torso.
- The car centre line of car considered to be preferable for repeatability reasons.

Vehicle Attitude

To insure comparable and repeatable test conditions, a brake dive attitude was simulated with braking of 0.7g at impact with the pedestrian. The brake dive position was constant throughout the impact test as the procedure involved bodyshells mounted on a trolley. This eliminated any rapid change of ride heights that might occur at impact and enabled a consistent impact velocity to be achieved.

Dummy Test Program

The characteristics of the adult (Part 572, 50th percentile) and child (Part 572, 6-year-old) dummies were measured by a series of tests to establish—

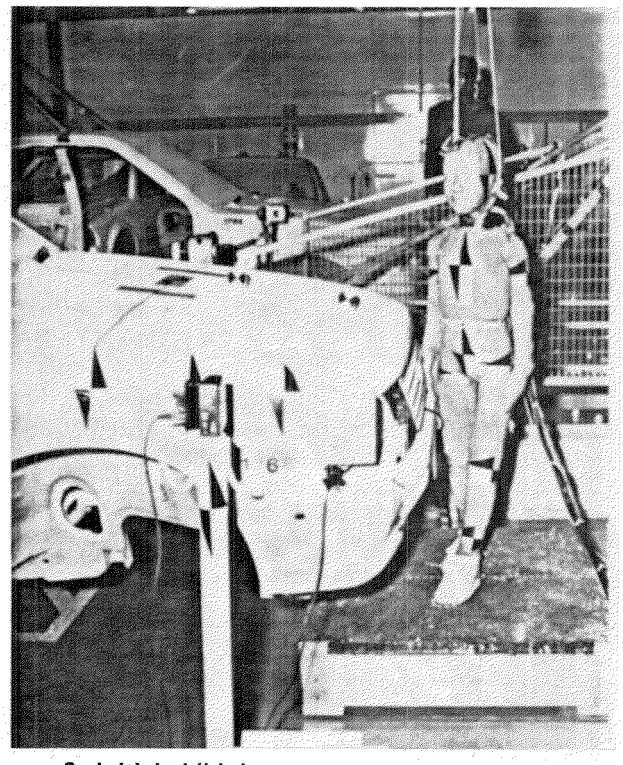

Figure 3. Initial child dummy stance

- Mass and moment of inertia of each limb
- Link dimensions and external limb sizes
- Joint characteristics at 1g settings
- Skin and limb compliance characteristics

Principal moments of inertia were measured for some body segments (e.g., lower torso, head, upper legs, and arms).

Car Front Contact Test Program

Dynamic force-deflection characteristics of the bumper, hood top, and hood edge of each of the cars were determined experimentally using a pendulum. To allow tests to be carried out at both 24 and 40km/h, the pendulum consisted of a centralised mass and shaped wooden former hung on a wire suspension. An accelerometer was mounted on the pendulum to determine the forces on the car, and deflections were measured with a linear potentiometer. The mass of the pendulum and shape of the wooden former were varied to determine characteristics for both dummies at the two speeds. Typical setups prior to testing are shown in Figures 4 and 5. An after-test situation is shown in Figure 6.

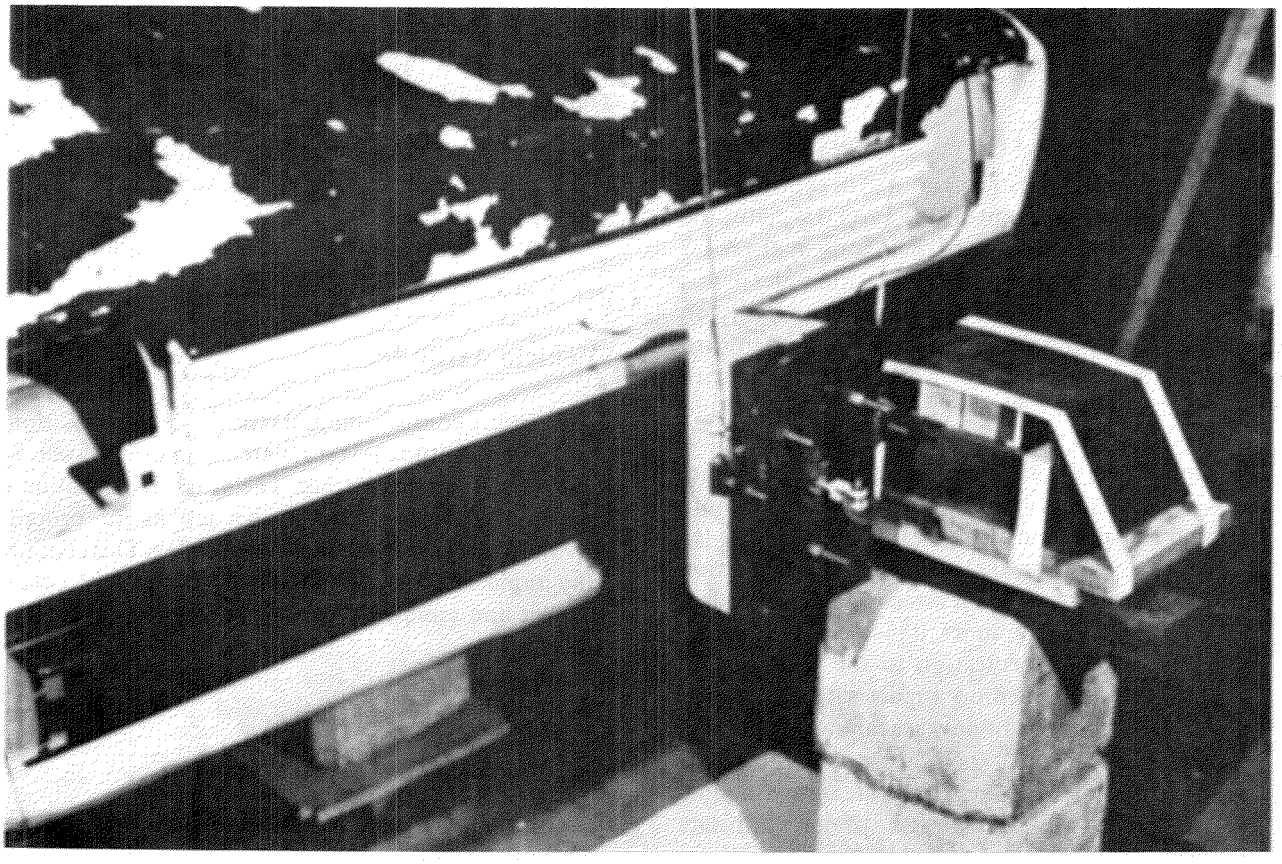

Figure 4. Bumper prior to pendulum test

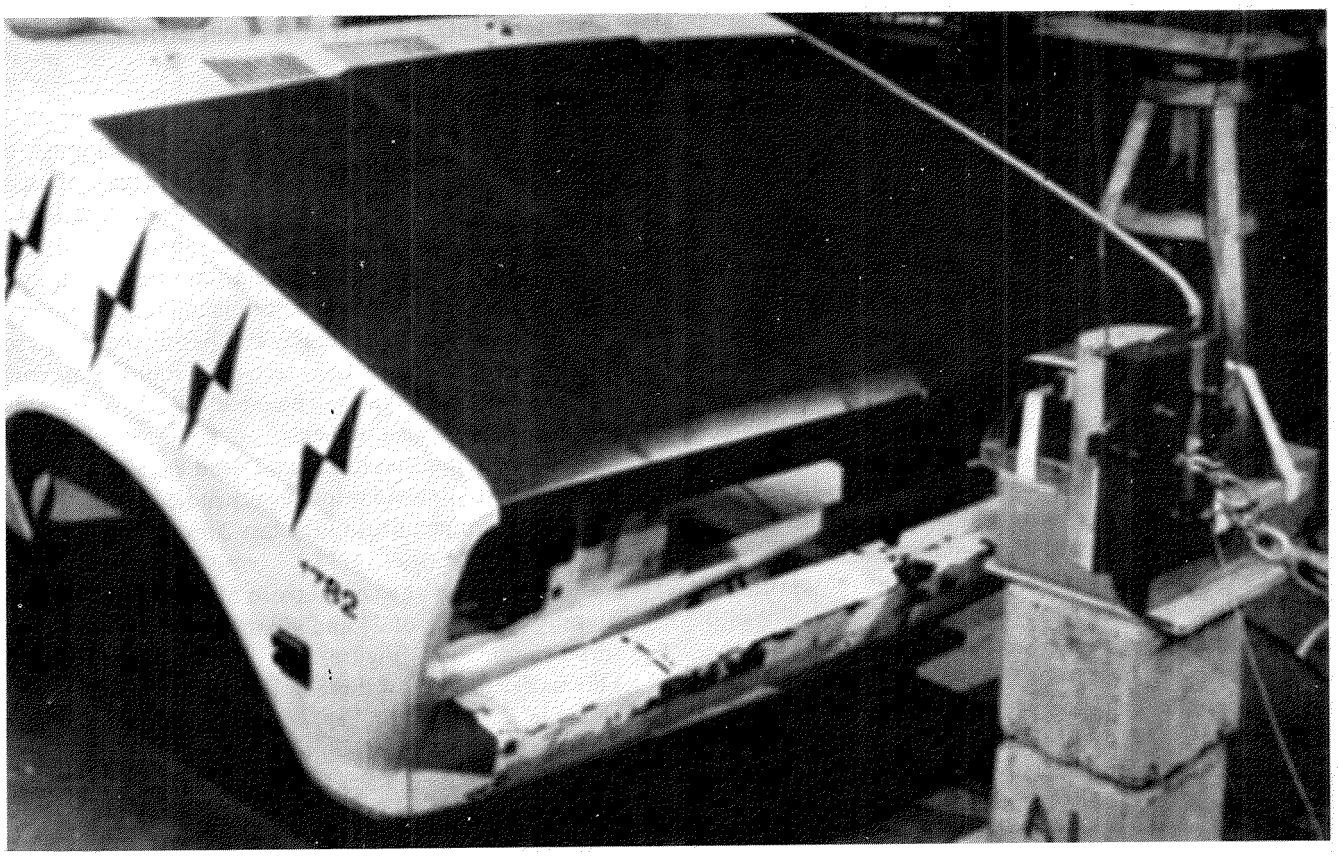

Figure 5. Hood edge prior to pendulum test

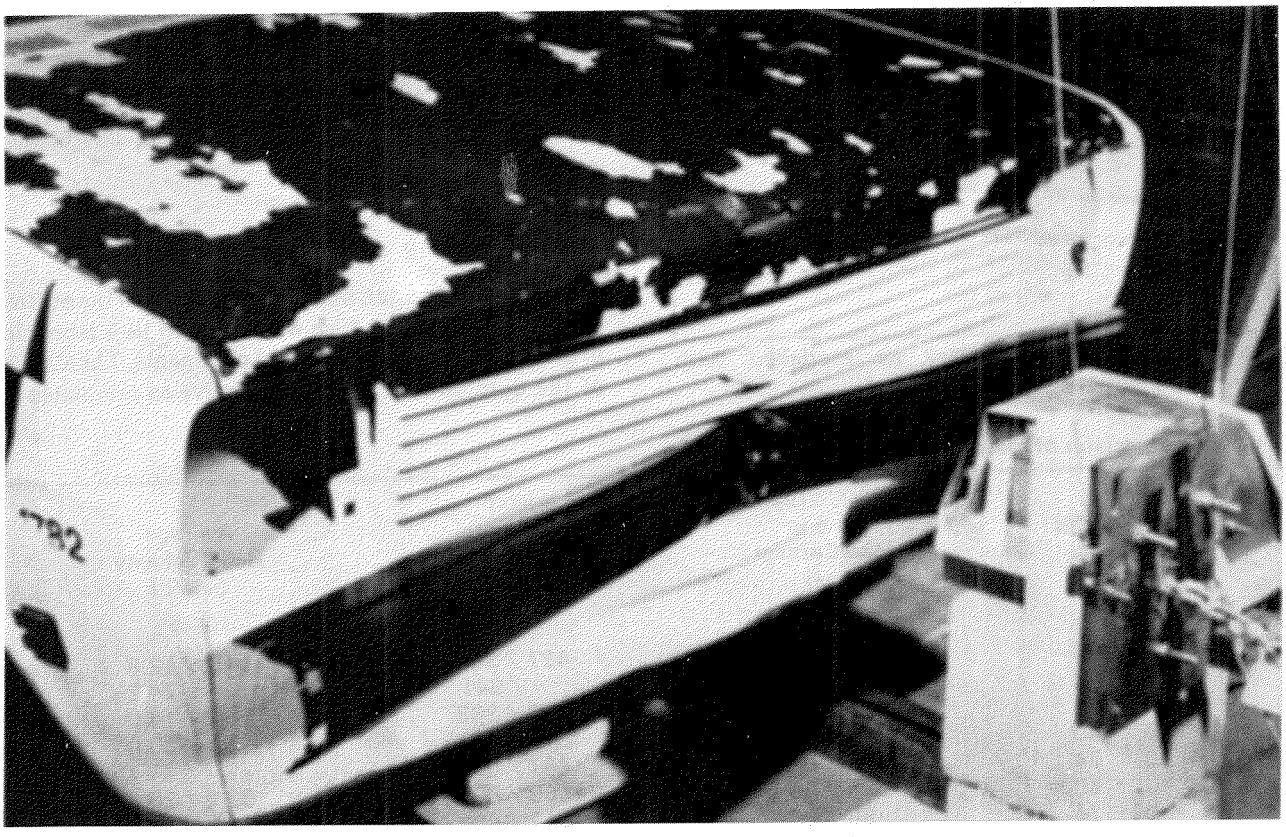

Figure 6. Bumper after test

Car-Pedestrian Interaction Model

The use of ellipsoids to model to the front of the vehicle has worked well. Where there have been problems, they often related to contacts at the end of the elongated segments, such as arms or legs, and especially when the penetration was a high proportion of the semi-axes of the two contacting ellipsoids. The most severe was most obvious during the leg-to-bumper contact for both the child—due to the small limb size—and the adult—due to the penetration. At one stage, artificially large leg segments were defined for the bumper-leg contact phase. The final solution adopted was to use the correct leg geometry and have a bumper ellipsoid having a longitudinal semi-axis up to an order of magnitude greater than the semi-axes of the leg. The curvature of the foremost edge of the ellipsoid was adjusted to the geometry of the front of the car bumper by having a lateral semi-axis that projected beyond the side of the car. In a similar manner, the semi-axes of the ellipsoid representing the hood top were chosen to reproduce the correct geometry over the full width of the car but were of necessity greater than the width of the car (Figure 7).

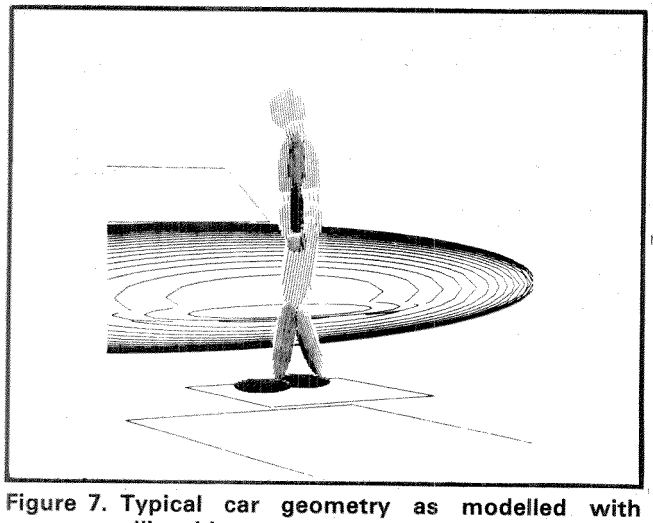

Figure 7. Typical car geometry as modelled with ellipsoids

Comparison Between Test and Simulation

Prior to this work, it was difficult to quantify by experimental tests the gains, for a pedestrian, of small variations in vehicle geometry, due in part to problems of repeatability. To assess these changes, it was essential to establish that a computer simulation could accurately reproduce the results from experimental tests. The simulation method was validated by comparing the results for several parameters between tests and simulations for a range of dummy impacts. These parameters were—

- Time to head impact
- Longitudinal horizontal head excursion
- Average head velocity perpendicular to the point of contact during the last 20ms prior to contact
- Kinematics

Table 1 shows the comparison of results for the child dummy at speeds of 24 and 40km/h and covers the first three parameters. Figure 8 shows the comparison of kinematics for one of these impacts.

Table 2 shows similar comparisons for the adult dummy. At this time, the adult simulations have not been completed, but Figure 9 shows the comparison of kinematics for one of the completed simulations.

It was concluded that, in general, there was good correlation between the simulation results and experimental tests. The repeatability of the experimental tests was an important consideration here, and until a more repeatable test could be devised it was sufficient for the computer prediction to be within the order of variation normally associated with the equivalent dummy test.

Discussion

Dummy Setup

Setting up the adult and child dummies in the attitudes specified in the procedure was found to be a labourious process and is worthy of several comments. The attitudes of the dummies are specified relative to templates that

Table 1. Comparison of child test and simulation results

Model & Speed (km/h)	Test/Simulation Comparison: Time to Head Contact (ms)	Horizontal Head Excursion (mm)	Average Head Velocity (km/h)
A 24	84 / 87	427 / 384	14.2 / 12.8
A 40	- / 56	- / 341	- / 24.2
B 24	89 / 88	413 / 383	16.2 / 14.0
B 40	- / 52	- / 431	- / 30.0
C 24	76 / 81	487 / 551	21.7 / 21.7
C 40	55 / 55	569 / 579	33.9 / 28.6
D 24	88 / 85	517 / 459	19.2 / 18.0
D 40	56 / 60	512 / 433	23.9 / 24.2

Table 2. Comparison of adult test and simulation results

Model & Speed (km/h)	Test/Simulation Comparison Time to Head Contact (ms)	Horizontal Head Excursion (mm)	Average Head Velocity (km/h)
A 24	189 / 202	938 / 963	18.2 / 20.2
A 40	- / 126	- / 1090	- / 30.2
B 24	208 / 212	931 / 882	21.1 / 17.6
B 40	- / 138	- / 1116	- / 29.3
C 24	185 /	1181 /	24.5 /
C 40	112 /	1251 /	47.9 /
D 24	179 / 178	1031 / 925	22.5 / 21.3
D 40	108 / 110	1097 / 1050	46.9 / 39.7

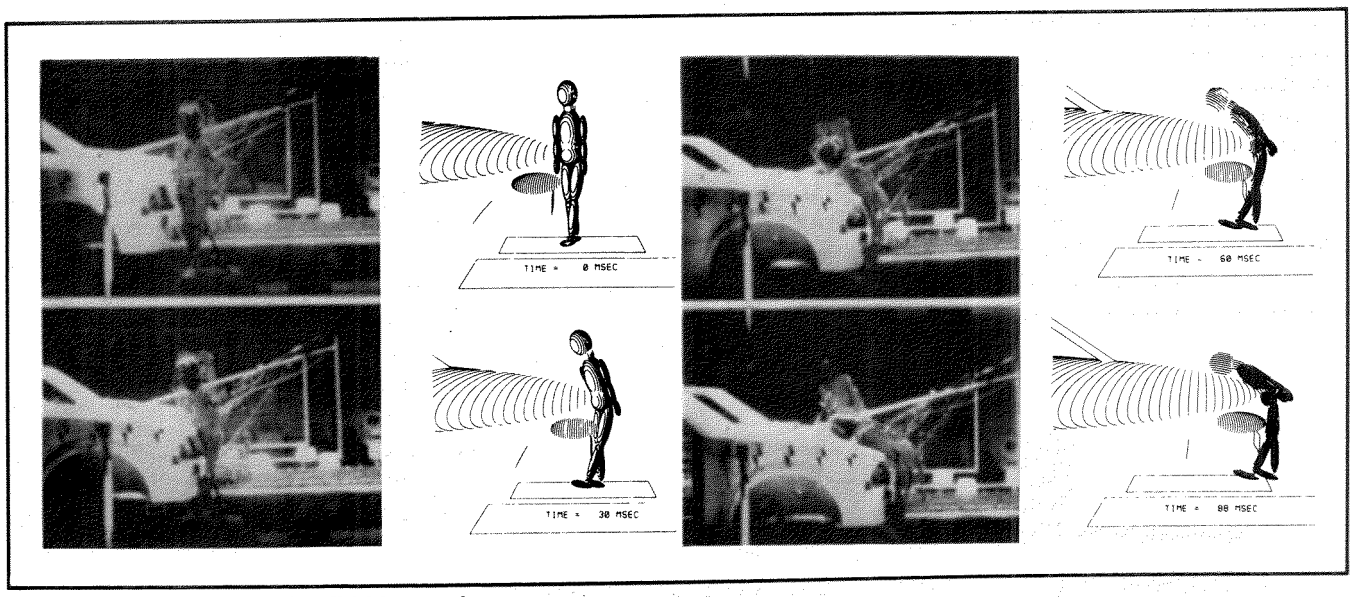

Figure 8. Comparison of child kinematics

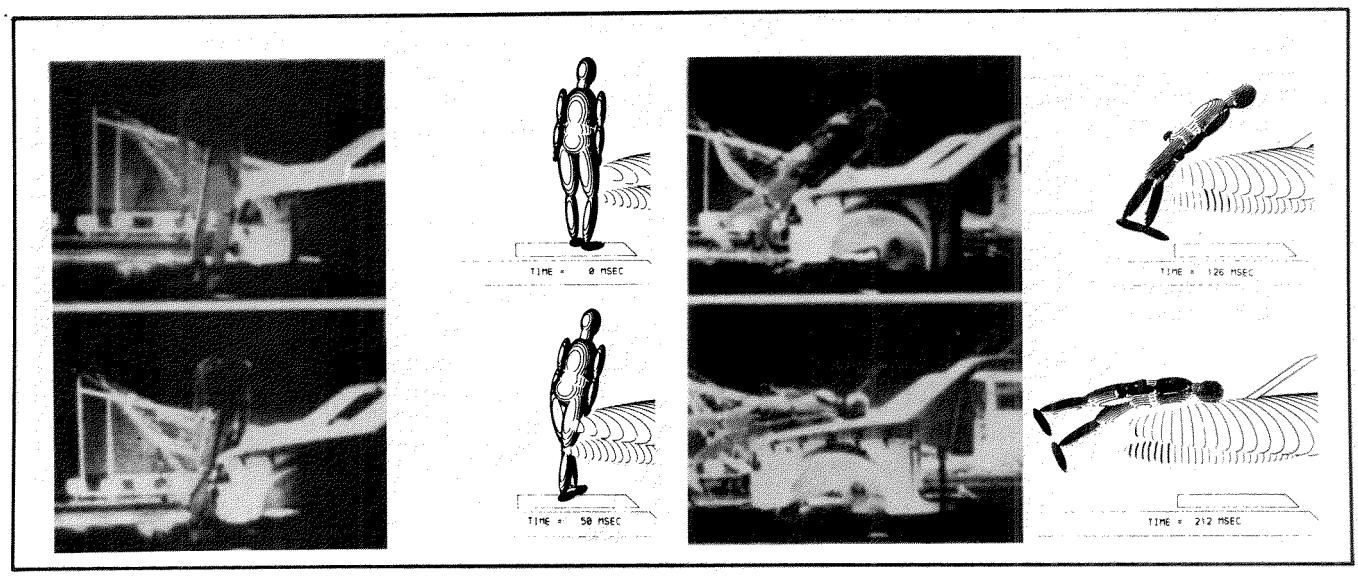

Figure 9. Comparison of adult kinematics

show the feet location, the lateral axis of the pelvis, the axial plane of the dummy, the Z-point, and the direction of impact. The accuracy with which the lateral axis of the pelvis—the axis passing through the centre of the femur heads—can be positioned so that its orthogonal projection on the template is correct must be open to question, as is the ability to position the shoulder axis parallel to the lateral pelvis axis and to locate the orthogonal projection of the head's hook hole Z as specified on the template. In addition, weight distribution between the feet is not specified, and the dummy joints can be tightened beyond the standard lg settings should the dummy fail to stand of its own accord in the specified attitude. While it is appreciated that measuring the weight distribution as part of the setup would be extremely awkward, it is possible that it could vary quite considerably between various test houses. Indeed, even within one test house, variations of upward of 10 percent have been recorded despite best efforts to achieve repeatable attitudes.

With these variations, the repeatability of the whole setup procedure is in doubt, and this has been confirmed by the results from supposedly identical tests. One improvement would be the use of a body jig to locate the key features of a dummy (e.g., lateral axes of pelvis and shoulders, head hook hole, etc.). This may well enable weight distribution, as well as attitude, to be controlled more accurately.

Adult Dummy Attitude at Head Contact

During all the tests with the adult dummy, a shoulder-hood top contact was noted. The extent of this contact varied from model B at 24km/h, where the dummy almost achieved a face-down attitude at head contact (Figure 9), to model D at 40km/h, where the shoulder-shoulder axis was 45° to the lateral axis of the car with the left shoulder raised (Figure 10).

However, the initial stance of the dummy was specifically chosen to eliminate shoulder and elbow impact with the hood top. This was because these parts of the dummy are far more rigid than on a human and would otherwise give an unrepresentative level of protection to the head.

Consequently, the initial stance recommended in the test procedure was not achieving its desired aim. One of the reasons for this seems likely to be connected with the position of the right (leading) leg. To achieve the correct positioning of the dummy features as on the template the right knee is forward of the hip (i.e., right upper leg

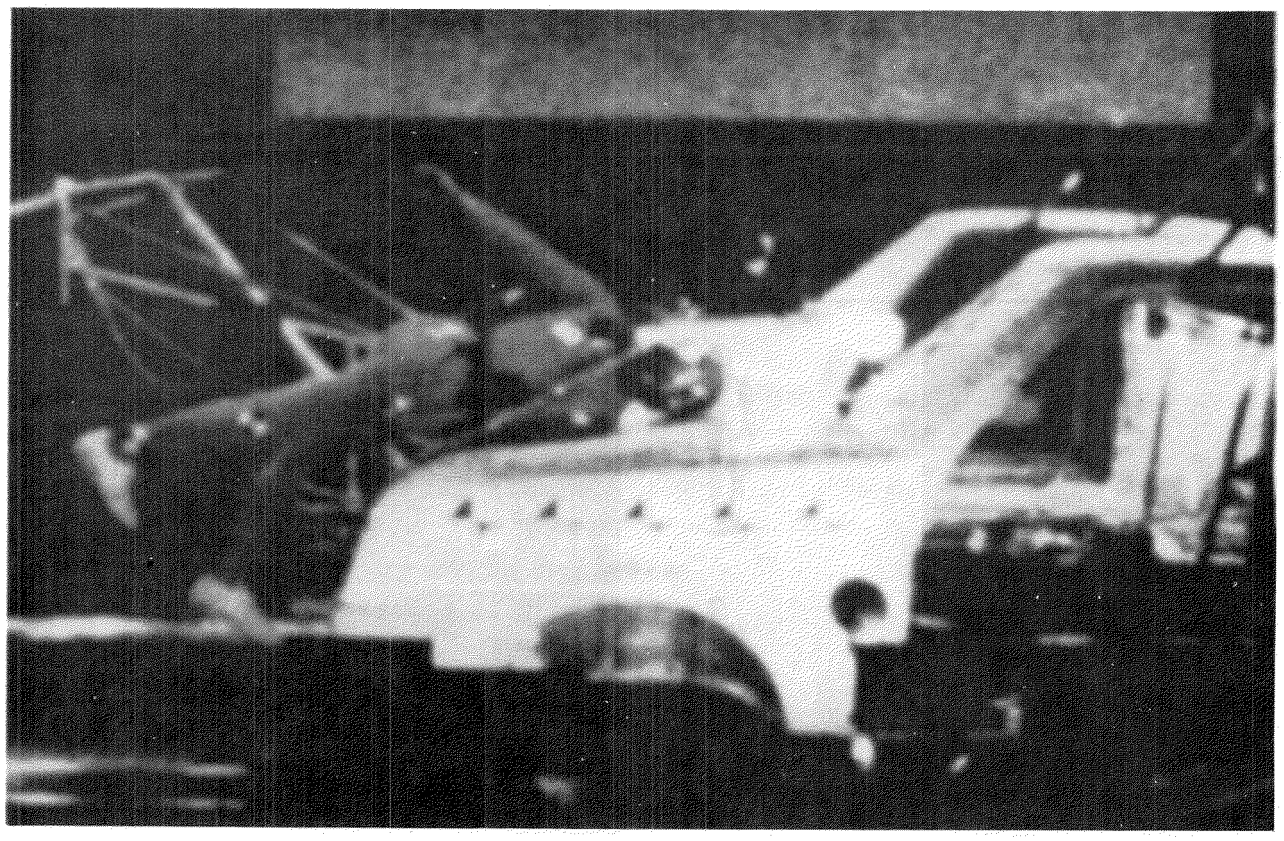

Figure 10. Adult attitude at head contact—model D

rotated forward). The right ankle is behind the knee (i.e., right lower leg rotated backward) (Figure 7). During the initial period of leg-bumper contact, this causes the right leg to rotate at the hip, about an axis parallel to the right upper leg, in an anticlockwise direction (lateral rotation). This rotation is eventually checked and reversed as happens during a test. However, this initial lateral rotation may help maintain the torso of the adult dummy in its initial attitude.

An alternative leg position could be with both left and right legs straight, while maintaining the footprints on the template, which would probably cause the full weight of the dummy to be more evenly distributed. In this stance, the right knee would be behind the right hip and may well cause a face-down attitude at head contact.

Front End Parameters

The severity of the initial impact and the resulting kinematics are influenced by the car front end design and the stiffness of the contacted car components.

The initial car-dummy impact location is nearly identical, that is, at the knee of the adult dummy and the femur of the child. However, there are considerable differences in the actual contact depth, ranging from 72 to 165mm.

Tests at 40km/h were restricted to the models with softer front ends, i.e., models C and D, to validate the computer simulations at the higher speeds. Simulations have been completed for most models.

24km/h Impact—Adult

The cars with softer front ends, models C and D, had definite beneficial effects with respect to the major areas of the dummies. The softer, deeper bumper faces reduce initial leg contact acceleration and more effectively spread the impact load.

The position of the front edge of the hood is a major influence on the dummy kinematics after initial impact. The more vertical front ends of models A and B produce a pronounced knock forward effect due to the distinct leading edge of the hood. This produces high pelvis accelerations but minimises head velocity and the horizontal excursion of the head relative to the front of the car.

The models with a lower or less distinct hood leading edge—models C and D—produce a wraparound effect, which tends to result in lower pelvis accelerations but higher head velocities and greater horizontal head excursions.

24km/h Impacts—Child

As with the adult, head velocities show the same upward trend for models C and D. Dummy kinematics were also similar, with models C and D producing the wraparound effect and consequent reductions in accelerations in the secondary impact areas.

40km/h Impacts—Adult

Head velocities did not show a significant variation between models. They were considerably higher than the vehicle velocity at impact. Dummy kinematics were similar to those of 24km/h except that events occurred earlier.

40km/h Impacts—Child

The benefits of the softer front end models were reflected in the head velocities, with only modest increases from these at 24km/h. However, the models with distinct hood leading edges caused head velocity increases of around 100 percent. As with the adult, kinematics were similar but events occurred earlier.

Head Velocity

Generally, the head velocities from the computer simulations were lower than those from the practical tests. The reasons for this are not clear, especially as the times to head impact show good correlation, but this has been reported elsewhere when three-dimensional dummy representations are used(16).

At the higher impact speeds, head velocity tends to approach or exceed 30km/h, and it is necessary to examine whether realistic vehicle design can prevent serious or fatal injury at such speeds.

If a half sine wave deceleration pulse shape is assumed with decelerations not to exceed 80g, then the contacting surface will need to deflect approximately 65mm for a head impact velocity of 30km/h (8m/s). It is debatable if this amount of deflection is realistic without some underhood component being contacted. Consequently serious head injury is inevitable. An upper limit for the head velocity for which vehicle designs can realistically be expected to prevent serious or fatal injuries must be less than 30km/h.

Conclusion

The trend toward the use of more resilient bumper materials with larger contact areas will have a significant part to play in reducing the initial impact severity to the lower limbs of adult and child pedestrians involved in collisions with automobiles.

Cars with lower, less distinct hood leading edges, while giving benefits with respect to injuries due to the wraparound effect, may not produce the same benefits in

reducing the head velocity at the time of head contact with the car.

Lower, less distinct hood leading edges and the use of more resilient bumper materials should, overall, make significant reductions in pedestrian injury levels at speeds that are considered to be survivable.

At collision speeds of more than 30km/h, the velocity of the pedestrian's head, irrespective of the car front end characteristics, tends to approach or exceed 30km/h; hence, it is unlikely head injuries can be reduced to an acceptable level by realistic changes to the head contact areas of the car.

This confirms the need to concentrate attention to avoid the car-pedestrian collision occurring. This is best achieved by segregation of the vehicle and pedestrian populations wherever possible. This, combined with realistic contributions from vehicle designs, will produce an improvement in the overall pedestrian injury problem.

Ellipsoids have been used successfully to represent the geometry of the front of the car and provide a smooth, continuous surface.

A more repeatable method of setting up the dummies is needed if changes in vehicle parameters are to be assessed by means of practical tests. The use of a body jig to locate key features of the dummies would be of great benefit.

An alternative initial dummy stance with both legs straight would cause a face-down attitude at the time of head/hood top contact and minimise or eliminate shoulder and elbow contacts with the hood top.

Acknowledgments

The authors would like to express their thanks to colleagues at the Ford Motor Company and Cranfield Impact Centre for their assistance and support.

References

1. Danner, M., and K. Langweider, "Collision characteristics and injuries to pedestrians in real accidents," Proceedings Seventh International Technical Conference on Experimental Safety Vehicles, Paris, 1979.
2. Braun, F., et al., "A synthesis of available data for improvement of pedestrian protection," Proceedings Seventh International Technical Conference on Experimental Safety Vehicles, Paris, 1979.
3. Thomas, C., and H. Valle, "Accident report covering pedestrian involvement in real accidents," tabled at WP29/GESG Special Meeting.
4. WP29/GRCS/R33, "ECE draft proposal on protection of pedestrians," 1981.
5. National Highway Traffic Safety Administration, "Pedestrian impact protection," Notice of Proposed Rule Making.
6. Daniel, S., et al., "Considerations in the development of a pedestrian safety standard," U.S. Department of Transportation, National Highway Traffic Safety Administration.
7. Office of Plans and Programs, National Highway Traffic Safety Administration, "Regulatory evaluation-pedestrian initial impact protection, a new MVSS."
8. Stcherbatcheff, et al., "Simulation of collisions between pedestrians and vehicles using adult and child dummies," Proceedings 19th Stapp Car Crash Conference, Warrendale, Pennsylvania, 1975.
9. Boulaire, J.P., et al., "Severity of head to car and head to ground impacts of pedestrians."
10. Langweider, K., M. Danner, et al., "Patterns of multi-traumatisation in pedestrian accidents in relation to injury combinations and car shape," Proceedings Eighth International Technical Conference on Experimental Safety Vehicles, Wolfsburg, 1980.
11. Ashton, S.J., and M. Mackay, "Car design for pedestrian injury minimisation," Proceedings Seventh International Technical Conference on Experimental Safety Vehicles, Paris, 1979.
12. Backaitis, S., S. Daniel, D. Cesari, and C. Cavallero, "Comparison of pedestrian kinematics and injuries in staged impact tests with cadavers and mathematical 2D simulations," Proceedings Symposium on Pedestrian Impact Injury and Assessment, SAE International Congress, 830186, Detroit, 1983.
13. Pereira, J.M., and D.A. Guenther, "A graphic computer simulation of the pedestrian vehicle impact," SAE International Congress, 820170, Detroit, 1982.
14. Hou, C., and D.A. Guenther, "A comparison between two different computer simulations in measuring the vehicle/pedestrian impact," SAE International Congress, 820171, Detroit, 1982.
15. Fowler, J.E., and K.F. Newman, "The use of computer simulations for the design of safer vehicles," Proceedings of the Conference on Progress Towards Safer Passenger Cars in the United Kingdom, Paper C180/80, Institution of Mechanical Engineers, London, 1980.
16. van Wijk, J.J., J. Wismans, J. Maltha, and L. Wittebrod, "MADYMO pedestrian simulations," Proceedings of Symposium on Pedestrian Impact Injury and Assessment, SAE International Congress, 830060, Detroit, 1983.
17. Fowler, J.E., R.K. Axford, and K.R. Butterfield, "Computer simulation of the pedestrian impact—development of the contact model," Proceedings Sixth International Technical Conference on Experimental Safety Vehicles, Washington, D.C.,1979.

Pedestrian Injury Protection by Car Design

Report by an ad hoc group of the European Experimental Vehicle Committee

Abstract

Remaining concerned with the problem of pedestrians hit by cars, the European Experimental Vehicle Committee (EEVC) has set up an ad hoc group on pedestrian accidents, with the following tasks: formulation of appropriate recommendations with regard to car design, survey and coordination of European research projects and activities, and cooperation with the National Highway Traffic Safety Administration (NHTSA).

The report will present the conclusions of this group:

1. Progress that has been made in the relevant knowledge since EEVC Working Group 7 published its report (presented at the Ninth ESV Conference):
   - Accident analysis, injury mechanisms, and tolerance levels
   - Development of tools for protection assessment: mathematical models, pedestrian dummies, and component impact devices
2. Means and prospects for improving pedestrian protection:
   - Guidelines to be considered for protection policies and future regulations
   - Short-term recommendations
   - Priorities for future research

Introduction

In the European countries that are taking part in the work of EEVC, pedestrians account for a major proportion of road accident victims: ranging from 13 to 33 percent of those killed. Even accidents that are not fatal are often serious, and, because of the cost of treatment and rehabilitation and the permanent disabilities they engender, their consequences are extremely severe.

This is why EEVC was anxious to examine specific problems involved in protecting pedestrians struck by cars to determine what conceptual improvements might be applied to such vehicles to reduce the number and severity of the injuries resulting from such accidents.

Thinking has focused on those features that play a role during the intracrash phase of the accident. In fact, those countermeasures that have to do with avoiding pedestrian accidents either do not concern vehicle design characteristics (for example, speed limits in built-up areas) or, when they do concern the vehicle, are not specific to this type of accident (braking capacity, handling characteristics, field of vision).

In 1980, therefore, EEVC set up Working Group 7 to review pedestrian accident data in Europe and to make recommendations and decide priorities. The report produced by this working group was approved by EEVC's Main Committee in 1982 and presented at the Ninth ESV Conference (Kyoto, Japan, November 1982).

To pursue still further the making of concrete proposals, EEVC then set up an ad hoc group to fix the main avenues where progress in improving protection levels might be achieved, such progress being based on the report from Working Group 7 and other gains in knowledge.

Participation of NHTSA in this ad hoc group was agreed on, but unfortunately the NHTSA representative was not able to attend the group meetings.

In parallel with this, EEVC had set up Working Group 8 to deal with the problem of the safety of cyclists and lightweight motorized two-wheelers. The ad hoc group was, therefore, asked to insure the countermeasures recommended for pedestrian protection would have no unfavorable consequences for cyclists and lightweight two-wheeler riders.

The work of the ad hoc group had two main facets: an inventory of advances in knowledge achieved since the 1982 report and proposals for safety improvements. Before setting these out in detail, it may be helpful to recall the salient features of the report by Working Group 7.

Report of Working Group 7

After setting out an overview of the statistics showing the share of pedestrian victims among road accident casualties as a whole in the six EEVC participant countries (Federal Republic of Germany, France, Italy, Netherlands, Sweden, and United Kingdom), the report gave a profile of pedestrian accidents: especially those involving children between 5 and 15 years (who make up the greater part of the injured) and elderly persons over 60 years (who make up the majority of those killed). In order of frequency, the injuries concern the head, the legs, the arms, the thorax, and the pelvis. It is difficult to determine accurately the role played by impact against the ground. As far as impact against the vehicle is concerned, the contact zones are, in particular, the bumper and leading edge of the bonnet for lower limb injuries and the bonnet and windscreen area for head injuries. Secondary impacts against the ground are difficult to clarify but can be the prime determinant of injury severity in relatively low-speed impacts. Last, a complex subject but an important one to study in depth is the influence of vehicle-front configuration on overall pedestrian kinematics, which determines the kind and

speed of impacts against various body segments, whether these are against the vehicle or at the time of falling to the ground.

The report then examined knowledge in the field of human tolerances and the protection criteria to be considered for the head, lower limbs, thorax, and pelvis. A fourth chapter listed the vehicle design features where improvement could be envisaged: the overall configuration and local dynamic stiffness of the zones likely to be impacted by a pedestrian's body. The wide range of pedestrian heights and the inadequacy of knowledge of the impacted pedestrian's kinematics did not, however, permit making definitive recommendations concerning the best configurations and dimensions. Progress is, however, possible in reducing aggressivity of the vehicle zones struck by isolating the stiff structural members and by using new plastic materials that absorb energy. Last, the report analyzed test and evaluation methods suitable for dealing with the problem of protecting struck pedestrians and bringing out the complementary role of global tests, vehicle component tests, and mathematical models.

A Summary of Pedestrian Protection Research Reported Since 1981

General

This chapter summarizes the advances made in research on pedestrian protection since the first EEVC Group 7 report was prepared in 1981(1).

Generally the research has been based on accident investigation, accident reconstruction, accident damage reproduction, and mathematical computer simulation studies to gain further knowledge on the many detailed aspects of the problem.

This chapter has been compiled with respect to the following of these aspects: accident investigation, the performance of dummies, human tolerance, test methods, component tests, design recommendations, mathematical simulation, and other unprotected road users.

Accident Investigation

Accident studies have given added emphasis to the need to design cars with improved safety for pedestrians and have also provided more information on the cause of head injury and the severity of leg injury.

Traffic Schemes

In South Australia after a widespread increase in the use of pedestrian controlled road crossings, a study(2) suggested that traffic schemes have a significant effect but on their own are not capable of reducing the pedestrian casualty rate to a tolerable level. In the survey area, the number of pedestrian casualties per 100,000 of population who suffered fatal injury fell by 30 percent after implementation of the traffic scheme, with an 18.8 percent reduction in the rate for all casualties.

Head Injury

An analysis of the U.S. Pedestrian Injury Causation File (PICS)(3) gives the distribution of causes of head injury, as shown in Table 1. Contact with either the vehicle or ground were both judged to be major causes of head injury. This compares with the first report of Working Group 7(1), which reported that in early studies head injuries were thought to result from secondary impact with the ground, but more recent studies show a different result. The changes in the importance of the different causes of head injury in all these studies may illustrate the difficulty of determining the true source of head injury.

It was also observed from the data that, as a pedestrian's age increases, a stiff structure becomes increasingly more dangerous to the head than a soft structure.

Table 1. Percentage cause of head injury (PICS) file

Injury Source	Head Injury	
	AIS 2-3	AIS 4-6
Car structure	33	55
Ground	60	42
Other or unknown	7	3
Total	100	100

Leg Injuries

Leg injuries are a major feature of pedestrian accidents and a frequent cause of pedestrian disability.

A study of 463 pedestrian accident cases(4) reported that bumper shape has an important influence on leg injury.

Multiple fragmentation fractures were seen from higher speed contacts with wedge-shaped but not rounded bumpers. Wedge-shaped bumpers were also found to cause fractures at lower impact speeds than rounded shapes.

As we know, the AIS scale is designed for evaluating threat to life, and a clinical study of typical accidents to the lower limbs(5) suggested that the existing AIS scale has poor correlation with respect to resulting working days lost and percentage permanent disability.

Dummies

In general, present dummies have shown some unacceptable limitations in performance, which are most

clearly demonstrated by bonnet leading edge impact conditions.

Dummies are reported to cause considerably more damage to the bonnet leading edge than occurs in road accidents, while cadavers in contrast cause slightly less. This difference has been attributed to the cadaver showing a greater tendency to slip over the leading edge(6,7) compared to a dummy, which has more of a rolling action. The resulting difference of input energy between the two at this stage influences both the location and severity of subsequent head impact to the rear of the bonnet.

It has been suggested that the different kinematic characteristics result from the excessive lateral stiffness of dummies and, consequently, the thorax and legs have been modified in an attempt to improve the performance.

Thorax

Dummies with the thorax developed for an impact to the side have been assessed in three sets of full-scale tests.

In one, the performance of dummies developed by ONSER, MIRA, and HSRI were compared with that of cadavers and Part 572 dummies(8). It was observed that all the side impact dummies have a better response in a pedestrian impact than a Part 572 dummy, but they are still too rigid in lateral bending of the spine. The neck of the ONSER dummy was reported as too stiff, and the collapse force of the MIRA shoulder was too high.

The second set of tests assessing HSRI and APROD 82 side impact dummies(7) initially noted that the hip of a standard Hybrid II dummy rolled around the bonnet leading edge, whereas the cadaver showed a greater tendency to slip over it, as mentioned previously. This difference was attributed to the lateral bending of the cadaver's knees and also to its more flexible hip.

To improve lateral flexibility, laterally compliant knees, as described below, were fitted to the side impact dummies for all subsequent tests(9).

With the modified knees fitted, the side impact dummies were reported as having a more cadaver-like behavior.

A summary of the dynamic performances is shown in Table 2.

The third set of tests(10) at 40km/h, using cadavers and ONSER APROD and Hybrid II dummies all struck on their sides, showed that the head trajectory was more horizontal for the cadavers than for the dummies, particularly at head impact.

The head impact velocities of the Hybrid II and APROD dummies were significantly lower than those of the ONSER dummy and the cadavers. These variations may result from the arms of the dummies, which frequently became interposed between the thorax and the bonnet, thus modifying the head and thorax impact characteristics.

Similar accelerations were recorded from all the dummies and cadavers at head, thorax, and pelvis, but differing values were obtained from the knee and ankle as shown in Table 3.

Table 3. Comparison of cadaver and dummy accelerations for tests at 40km/h

Body Region	Cadaver	Dummy		
		Hybrid II	APROD	ONSER
Head*	61	65	74	84
Thorax*	31	38	28	35
Pelvis*	39	42	42	49
Knee#	104	58	53	98
Ankle#	71	181	169	95

* 3ms acceleration
\# maximum acceleration

Legs

A need for lateral compliance at the knee was given in the first report of Working Group 7(1), and two examples have been produced.

One of these referred to above (9) allowed ±30° of rotation and utilized a rubber block to simulate knee ligaments. With this configuration, a deformed knee will return to its normal orientation when the impact forces return to zero.

Table 2. Head impact location and velocity for comparative tests at 40km/h

Car		Cadaver			Dummy Hybrid II		HSRI		APROD 82	
Citroen	V(km/h)	53	58	40	43	47	52	53	65	58
	L/H (m)	1.09	1.11	1.0	.97	.89	1.11	1.17	1.07	1.08
Audi	V(km/h)	33	35	36	40	40	35	39	43	59
	L/H (m)	1.14	1.17	.84	.85	.86	1.07	1.06	1.02	1.08

V — Head impact velocity normal to surface contacted
L/H — Wraparound distance from ground to head impact point/surrogate height

The second example allowed ±20° of lateral rotation with the ligaments simulated by a friction pad, which was set to give a friction torque of 200Nm(11). When the impact forces return to zero, the maximum angular displacement is maintained and its amplitude may be used to assess the severity of the simulated injury. In some instances with this arrangement, subsequent ground impact will alter the angular displacement resulting from vehicle impact.

To further improve the lateral compliance in the pelvic region of this dummy, the hip joint was also modified to allow up to 28° of adduction. In standard dummies, hip adduction is normally 5 to 10°, but for the human body it is approximately 40°.

Human Tolerance

It was noted in the first report that the aged have lower tolerance levels, and investigations have continued (to find representative values) for the head, thorax, pelvis, and legs.

Head

The head studies have concentrated primarily on a reassessment of acceptance values for HIC. The results of work with cadavers(12) suggested that an HIV tolerance level of 1,000 is appropriate when striking a rigid structure, but a value of 1,500 is acceptable when striking a compliant structure. This proposal has caused some disagreement internationally. The value of HIC 1,000 has been widely used in the past for automobile research, and HIV 1,500 is in accordance with tests for motorcycle helmets, which can result in peak headform acceleration of up to 250g. The difficulty arises with structures that have a rapidly changing stiffness, which may give very high localized loadings. This situation is potentially injurious and exists at the bonnet and wings of existing cars.

Comparative HIC and injury values have been reported from reconstructions of actual accidents and also from accident damage reproductions using headform component tests.

A report of component tests using a Part 572 headform weighted to 4.5kg to reproduce accident head impact damage(13) gives the result shown in Table 4.

Results from a similar series of tests(6) are shown in Table 5 for comparison.

Table 4. Accident head injury AIS compared with HIC's from damage reproduction tests

Accident AIS	Accident Damage Reproduction Test HIC		
	<1000	1000-1500	>1500
0	764		
1	538		
2	107	1082	2278
5		1191	1919
		1392	2578

Table 5. Accident head injury AIS compared with ranges of HIC's from damage reproduction tests

Accident AIS	Accident Damage Reproduction Tests HIC
2	2278-2596
5	1392-1648
	4890-7630

Similar comparisons were reported from accident reconstruction tests(14) using a Part 572 dummy and from damage reproduction component tests, again using a Part 572 headform of 4.5kg weight. The results of both these sets of tests are shown in Table 6.

In an accident reconstruction, it is difficult to insure that the simulation headform strikes the vehicle in exactly the same location as a victim's head, although it is important because of changing stiffnesses that it should do so. Nevertheless, the accident reconstruction results do not support the suggestion that the tolerance level for the head should be higher than HIC 1,000, when measured by existing dummy headforms striking bonnet structures.

Table 6. Headform HIC from damage reproduction and accident reconstruction tests, compared with AIS from head injuries in accidents

Accident AIS	HIC Values	
	Dummy Test Accident Reconsruction	Component Test Damage Reconsruction
2	—	1400
3	443	1257
4	1367	670
5	1371	890
	2136	779
	1934	775

The poor relationship between AIS and HIC in the tests to reproduce accident damage illustrates the difficulties currently experienced in setting up and assessing the results of components tests. It is possible that the difficulties may in part result from the use of headforms with unrepresentative effective masses, and a possible method of driving an appropriate mass is outlined later.

Thorax

Lateral impact tests on the thorax of cadavers(15) to determine suitable tolerance values for the ribcage suggested that the degree of lateral deflection of the ribs with respect to the spine gives the most satisfactory correlation with injury. A half thorax deflection of 30 percent is reported as corresponding to an injury of eight rib fractures, having a rating of AIS 3. The report proposed a tolerance level of 35 percent deflection.

A tolerance method of this type is, of course, only relevant to a pedestrian dummy if the impact between the dummy and the bonnet top is essentially to the side of the thorax and not to its front or rear.

Pelvis

A further series of cadaver tests(16) to study tolerance values for lateral impacts to the pelvis suggested the severity of injury is best assessed by force measurements. In the tests, the 3ms force on the pelvis to cause skeletal injury ranged from 3.24 to 12.92kN and showed a correlation between fracture force and cadaver weight. The average force value for female cadavers was 5.6kN and about 8.6kN for males.

Based on weight variations, the appropriate tolerance value for the 50th percentile male was reported as 10kN and a value of 4kN for the 5th percentile female, which gives a tolerance force of approximately 5.0kN for the average pedestrian casualty.

Legs

Femur samples have been subjected to static lateral bending tests(17). The femurs are reported to have been mounted on supports 0.126m apart and loaded at midspan. The bending, breaking loads ranged between 276 and 1,131kg f, which gives, by calculation, bending moments of failure of 82 to 347Nm.

Test Methods

Recommendations for test methods generally agreed on a combination of full-scale simulations allied with component tests(6,7).

The simulation may be full-scale testing or mathematical computer simulation, both having the objective of determining the directions, locations, velocities, and effective masses of surrogate impact at each stage of the impact. This information is to be used to provide a sound basis for defining the requirements of the associated component tests.

To overcome the difficulty of establishing the effective mass of the part of a dummy instantaneously in contact with a car, it has been suggested(6) that accidents may be reproduced by a successive interaction between mathematical computer modeling and component impact testing.

The process would initially involve a component test to the bumper of a car under assessment to determine leg forces and bumper deflection characteristics.

These values are to be used in the mathematical simulation to determine the impact velocity to the bonnet leading edge and this velocity will be used for a component test to obtain the force and deflection characteristics of the bonnet edge. These values, in turn, will be used in the mathematical simulation to calculate velocity, location, and direction of head impact for defining head component tests.

Component Tests

Further studies have been made of component tests representing the pelvic and head impact stages of a full-scale test.

Pelvis

Analysis of cadaver tests(18) suggested that the effective mass of the hip or upper leg when striking bonnet leading edge ranges between 5 and 9kg. From this, an impactor was designed having a mass of 7.3kg and a contact face of 152 by 203mm.

The velocity of the upper leg or hip when striking the bonnet leading edge varied in the tests from 100 to 36 percent of the initial impact velocity, depending on the location of the leading edge with respect to the bumper.

Headform

Headform to bonnet top component tests to reproduce accident damage(6) were reported as showing that accident dents may be reproduced, but that each case could be achieved by a range of combinations of effective mass and velocity of the headform impactor.

This difficulty has already been mentioned, and a method of overcoming it is suggested in the Test Methods section.

Vehicle Design

Research into the design of cars for pedestrian safety includes studies of idealized shapes and stiffnesses by

mathematical modeling simulations, an investigation of the design of the bonnet for head impact and of the bumper for improved safety for the legs, plus an experimental safety car study.

Vehicle Shape

Car shape or localized stiffness can influence the severity of pedestrian injury. In 50 tests in which cadavers were struck by five different types of car(19), it was noted that all the cars tested—Citroens 2 CV, VISA, GSA, and BX, plus a Peugeot 505—were equally injury-producing, but the location of the major injury varied with respect to the different car types. It was deduced that improvements for the pedestrian necessitate making innovative changes to either small areas, in which case only localized improvements in injury will result, or major alterations that could give overall improvement.

Mathematical three-dimensional simulations of different idealized shapes and stiffnesses of vehicles(11) studied the importance of the location and stiffness of the bonnet leading edge. In general, a low bonnet leading edge, 600mm aboveground, showed high loading in the region of the knees of adults. The medium height profile at 720mm indicated severe direct loading to the femur and indirect loading to the knee of adults and to the pelvis of children.

For the high bonnet at 850mm, severe loadings were noted for both the pelvis and the thorax of children. The profile height also influenced the nature of head impact. As the height increased, the location of head impact moved further forward and the velocity of head impact decreased. This change was particularly significant in the range 720 to 850mm high.

A similar study involving dummy and cadaver tests and mathematical simulations(20) showed similar characteristics. It was concluded that, since accident studies suggest severe injury occurs more frequently to the head than to the pelvis, a relatively high and near vertical compliant front would be an advantage in reducing head injury.

Head Protection

In a study of head-to-bonnet impacts, the distribution of heights of pedestrians struck by cars in France were divided into 50 groups and related in a mathematical computer simulation to five representative impact velocities to give a range of 250 accident conditions(21).

The simulation demonstrated the probable distribution of head impacts to the bonnet and windscreen of a car type, also showing the direction of motion and the velocity of the head at impact. For the typical car profile studied, the impacts were shown to be uniformly distributed over the length of the bonnet and particularly concentrated in the lower half of the windscreen.

The performance of current bonnet tops was assessed by head impact component tests to eight different types of bonnet tops at eight locations on each bonnet(22). The impactor was a Part 572 headform of 4.45kg mass and accelerated by a pneumatic gun to strike the bonnet tops at 40.25km/h.

The resulting levels of HIC were strongly influenced by the amplitude of dynamic deformation, and typical values are shown in Table 7.

Table 7. Comparison of headform HIC and bonnet deformations in headform component tests

HIC	Bonnet Displacement (mm)
1000	84
2000	60
4000	42
6000	33
8000	23

The stiff wing-to-bonnet seam gave HIC's of 4,000 to 6,000 and most central regions of the bonnet produced values of 1,000 to 2,000, but this rose at times to 6,000 when the bonnet top bottomed out on rigid understructures.

It was noted in cadaver tests(23) that impacting either laminated or toughened windscreens resulted in only moderate head injury, whatever the collision speed, except for one impact close to the A-pillar. Head injuries were seen, however, to become more serious as the speed increased for impacts against dashboards or steering wheel systems after windscreen failure.

Leg Protection

An experimental study of the causes of leg injury using ordinary human leg specimens(24) gives some insight into the influence of the bumper on the severity of leg injury. Test specimens were impacted by a sled fitted with bumpers of rigid and compliant construction mounted at heights of 450 and 325mm above the ground. Five tests were conducted at each condition and a summary of the results is shown in Table 8. The lowest overall frequency and lowest severity of leg injury occurred with a low deformable bumper, but the low rigid bumper caused less injury to the knee.

Safety Structures

Studies on an experimental pedestrian safety car were reported as giving the following conclusions(25). A flexible polyurethane integral skin foam, backed by energy-absorbing foam, may be designed to give good impact characteristics that overcome the stiff sections

Table 8. Frequency of injury AIS ≥2/bumper height and stiffness

Bumper Height mm Stiffness		Summation of Injuries for 5 Tests (AIS ≥2)				Peak Force kN	
		Long Bone	Ankle	Knee	Total	Bumper	Bonnet
450	(R	4	2	10	16	7.9	2.6
	(C	4	—	6	10	2.6	2.7
325	(R	9	2	2	13	5.3	1.6
	(C	1	1	5	7	2.4	1.6

R — Rigid
C — Compliant

that develop in a collapsing conventional steel-skinned structure. There are still, however, impact stiffness problems where a rigid support structure extends to or close to the outer surface.

For soft fronts made of the above polyurethane construction, difficulties may be experienced in reaching a suitable compromise between flexibility to insure safety and stability to give a durable product. There may also be difficulty achieving a suitable finish free from distortion.

The experimental bonnet top consisted of a 30 to 50mm-thick energy-absorbing panel, sandwiched between an aluminum under skin and an upper skin made of glass fiber-reinforced synthetic resin. The upper surface was covered by a thin integral foam polyurethane skin to contain glass fibers in an impact.

A headform component test with a mass of 5kg and at a velocity of 13.2m/s gave peak decelerations of about 100g and approximately 95g at 3ms duration.

Safety Benefit

Various attempts have been made to quantify the possible reduction of injury to pedestrians that will result from changes in car design.

A study (26) of the experimental pedestrian safety car, described above, estimated that the reduction of injuries at speeds up to 45km/h would result in a 40 percent reduction in fatalities to pedestrians struck by cars.

A different study(27) that considered designs giving protection at speeds up to 40km/h estimated a 33 percent reduction in serious injury.

A manufacturer(28), however, reported that the upper head velocity limit at which it might be realistic to expect design measures to prevent severe or fatal injuries certainly falls short of 30km/h, which would give benefits significantly lower than those quoted above.

These estimates will be influenced by the percentage of head injuries resulting from impact with the ground, and this is not clearly understood, as previously stated.

Mathematical Simulation

A simulation model MADYMO(29), which is based on hyperellipsoid contact models, was used to study its relative accuracy with respect to the number of segments that represent the dummy and also with regard to the option of two- or three-dimensional operation.

The simulations of 2-, 5-, and 7-segment 2D models and a 15-segment 3D model were compared with the results of tests with a Part 572 dummy. The comparisons in Table 9 show that at least a 7-segment model giving separately represented legs is necessary to give realistic leg accelerations.

The head impact locations were closest for the 7-segment 2D and the 15-segment 3D models, but the 2-segment model gave the most realistic head impact velocities. The velocities of the 5- and 7-segment models were too high and the 15-segment too low.

In a further study(30) including the MVMA 2D model and also MACDAN, a simplistic representation, correlation with head and thorax impact velocities was reported as poor. It was suggested that, to reduce excessive stiffness in the lateral direction, the modeling should be improved to simulate lateral flexure at the knee and include displacement due to fractured leg bones.

Other Unprotected Road User

Cyclists are frequently involved in accidents with cars, and concern has been expressed that improvements in the design of car fronts for the benefit of pedestrians should not be to the disadvantage of cyclists.

The accident characteristics of cyclists were considered in an EEVC study(31) that reviewed accident data for two-wheeled vehicles and made recommendations, including priorities for action on the vehicle to reduce the severities of such accidents and injuries.

Simulations of car-to-cycle frontal impacts suggest, however, that any improvements for pedestrians will also be to the benefit of cyclists(32). A further study that

Table 9. Head impact velocity and head impact point for four models, along with experimental results

	2D-Model			3D-Model	Experimental
	2-Segment	5-Segment	7-Segment		Test-Range
v = 30km/h Resultant head-impact velocity (m/s)	9.1	12.3	11.4	6.1	6.7-9.2
Distance head-impact point/ hood-edge (m)	0.91	0.90	1.02	0.96	0.82-1.00
v = 40km/h Resultant head-impact velocity (m/s)	12.7	16.6	15.6	9.9	11.2-12.5
Distance head-impact point/ hood-edge (m)	0.96	0.95	1.08	1.03	1.00-1.07

simulated impacts by cars into the sides of stationary bicycles(33) reported that the distance between the leading edge of the bonnet and the location of head impact is 300mm greater for the cyclist, which was attributed to the higher center of gravity of cyclists.

Proposals for Improving Pedestrian Protection

Guidelines To Be Considered for a Pedestrian Protection Policy

Analysis of pedestrian accidents (see EEVC Working Group 7 report) helps find the guidelines to improve pedestrian safety. The passenger car is the vehicle most frequently involved in pedestrian accidents, and it is therefore appropriate to give priority to the study of car-to-pedestrian collisions.

The age distribution of pedestrian casualties is important. Children between 5 and 10 and elderly people constitute a great majority of pedestrians involved in accidents, the children involved mainly in nonfatal accidents.

Moreover, pedestrian accidents can cause injuries with long-term consequences. Proposals to improve pedestrian safety should give special attention to the requirements of both children and old people whose tolerance levels and, to some extent, injury mechanisms are different from those of the normal adult.

With regard to injury distribution, it is clear that injuries to the head and to the lower limbs must be considered as priorities in pedestrian protection measures.

Generally, lower limb injuries are associated directly with impact against the front of the car (bumper, bonnet edge, head lamps, etc.). Several head injuries are often related to impacts against the windshield frame for adults, whereas head injuries of children are due mostly to head impact against the bonnet edge or the front of the bumper.

Long-term Recommendations

The aims of long-term recommendations should be the protection of pedestrians from severe and fatal injuries. The protection against injuries of AIS 3 and over occurring in pedestrian accidents with an impact speed up to 40km/h seems a reasonable goal. These recommendations would consider first the injuries of AIS 3 and over that are the most frequent in pedestrian accidents—mainly injuries to the head and injuries to the legs.

Long-term Recommendations for Head Protection

As the mechanisms of head injuries are not well established, it is not possible to make precise long-term recommendations for head injury protection. Head injuries concerned with this protection level are mainly head trauma with unconsciousness, skull fractures, and some face fractures. However, facial fractures are less frequent than other head injuries.

The presently used injury criterion is the HIC with a limit of 1,000 to 1,500. To give better head protection to pedestrians in car-to-pedestrian collisions, it is important

to consider the areas of the car that could be hit by the pedestrian's head and produce head injuries. These areas are mainly around the windshield, especially the A-pillar, lower windshield frame, and the scuttle area for adult pedestrians, and in the front end of the bonnet for children. It has been shown in experimental safety vehicle studies that it is possible to reduce considerably the value of HIC by changing the design of these areas(25,34,35,36). In these cases, HIC values seem to remain below 1,000 in car-to-pedestrian dummy tests at an impact speed up to 40km/h, whereas this value was clearly exceeded in many tests conducted with mass production cars. However, the value of HIC recorded during a pedestrian test depends on the type of dummy used. Present dummies have a bad repeatability and are generally too stiff, especially in the neck and shoulder areas. Redesigning a dummy for use in pedestrian tests seems, then, of great importance. Although the HIC is still under review, there is at present no other validated criterion for head injuries. Besides the HIC itself, there is a general uncertainty of head injury mechanisms and human tolerance to head injuries. Biomechanical programs aiming to increase the knowledge in this field are to be encouraged.

A series of experimental car-to-pedestrian collisions at impact speeds of 30 to 40km/h gave head impact velocities (normal to the surface contacted) that ranged from 1 to 1.2 times the vehicle impact speed(37).

However, the values published vary considerably; for example, values of 0.5 to 1.0 times the car speed have been found on American cars(22). As an alternative, the dynamic response of the area hit by the head may be assessed by a headform drop test at the range of speeds shown above, during which an HIC value (or a maximum acceleration value) is not exceeded.

Long-term Recommendations for Lower Limb Protection

Most leg injuries have an AIS value equal to or less than 3; moreover, several leg injuries with the same AIS value could have completely different long-term consequences. Permanent disability appears, therefore, to be more important than AIS as a factor for assessing leg injury protection.

Several mechanisms can induce leg injuries. The impact point between the car front and the pedestrian legs, as well as the mechanical properties of the car element that hits the pedestrian legs, are of great importance in pedestrian injury causation.

It has been found experimentally that lowering the bumper close to the center of gravity of the lower leg would minimize the bending moment applied at the knee level(38). Such a measure would then decrease the risk of knee ligament rupture and other knee articular injuries, which are severe injuries for their long-term consequences. The corresponding value seems close to a height of 350mm above the ground. Lowering of the bumper seems effective for adult pedestrians but is not yet proved for children with respect to their injuries.

To decrease the bending moment and the shearing force applied to the leg and thereby reduce the number of tibia, fibula, and/or knee fractures, it seems desirable to use a compliant bumper. However, the preferred stiffness is dependent on the height of the bumper above the ground and its vertical depth. The bonnet leading edge also has an important influence on the severity of femur and/or pelvic injuries to adults and, in some cases, to child pedestrian thorax and/or head injuries.

However, there is an interaction between the bumper and bonnet leading edge characteristics, and it is important that the influence of these elements on pedestrian behavior is taken into consideration.

Short-term Recommendations

It is important that short-term improvements go in the same direction as long-term recommendations, even if the long-term goal cannot be completely reached.

Many improvements for pedestrian protection could be included in the design of new cars, with particular attention given to avoiding, wherever possible, localized areas of the bonnet and the top of the wings, which are too rigid.

The design of a front bumper is also of great importance, and, even if it does not seem possible to lower it for a short-term improvement, fitting an air dam that limits the leg-bending process by impacting the leg below the knee would decrease the risk of knee injuries. A softer and deeper bumper that decreases the impact force and gives a better distribution of the impact force could also improve the situation for pedestrian injuries.

It is possible, however, to give general performance recommendations for the bumper/air dam.

A mathematical analysis of pedestrian accidents proposes maximum forces as listed in Table 10 when the bumper is hit by a 50mm diameter cylindrical rigid impactor of 10kg mass at a velocity of 11m/s(25).

Table 10. Maximum bumper impactor force

	Vertical depth of bumper	
	100mm	300mm
Max force (kN)	5	7

If the forces shown in Table 10 are not exceeded, serious leg injuries will probably be avoided. Typical values of energy that the bumper would absorb are approximately 380J in 32km/h impact and 600J at 40km/h.

In addition to shearing forces, other criteria such as bending moment at knee level are to be considered.

The stiffness characteristics of the leading edge of the bonnet are dependent on its location with respect to the ground and to the bumper. From the same mathematical analysis, it seems the stiffness is suitable if an impact force of 5kN is not exceeded when the leading edge is deformed to absorb the energy values shown in Table 2.

The impact energy shown in Table 11 is dependent on bonnet leading edge height, the distance that the bumper is in front of the bonnet leading edge (bumper/bonnet lead), and impact velocity.

Table 11. Impact energy of bonnet leading edge for different edge locations and impact speeds

Impact Velocity (km/h)	Bumper Bonnet Lead (mm)	Height of Bonnet Edge Aboveground (mm)	Impact Energy (J)
32	0	600	200
		720	450
		850	650
	250	720	80
		850	270
40	0	600	310
		720	700
		850	1020
	250	720	130
		800	420

Need for Further Research

To be able to define precise long-term recommendationa and procedures and to determine the resulting improvements, it is important to continue research, especially in the field of injury mechanisms, human tolerance, and test methods.

Prospective in Pedestrian Biomechanical Research

Experimental and computer simulation methods to evaluate pedestrian protection standards are based on the results of research studies of human tolerance and injury mechanisms. So it is of great importance that an extensive and well-validated bank of biomechanical data is compiled, especially for the most severe and most frequent injuries occurring in pedestrian accidents.

The problem of head injuries is of great importance, not only for pedestrians but also for other road users. It is also a very difficult matter, and to improve the knowledge in this field it seems advisable to propose a harmonized program of research. This program would include detailed analysis of injuries sustained by traffic accident victims, evaluation of injury mechanisms, especially the relative importance of linear and rotational accelerations, in order to propose and validate head injury protection criteria.

Long-term consequences of some injuries sustained by pedestrians are considered to be of great importance and need further investigation to be quantified more precisely.

Most pedestrian accidents involve children and the elderly, and it is clear there is a change in human tolerance according to age. Existing studies are concerned mainly with bone strengths; it is, therefore, of great importance to clarify the effect of age on human tolerance for both bones and internal organs.

Validation of test procedures would be aided by an investigation into the influence of pedestrian posture on the risk of leg injuries, particularly with respect to standing with all the body weight supported by one leg. Walking pedestrians spend almost all the time on one leg whereas, until now, tests are generally performed with a pedestrian model standing on both legs.

Further Research Needed To Improve Test Procedure

Validated test procedures should first consider a biomechanical analysis of pedestrian accidents. Other important parameters include the specification of dummy characteristics and the interactive effects of car components, all of which have a great influence in the choice—and the results—of pedestrian test procedures.

Dummies currently used to reconstruct pedestrian impacts have been criticized for their lack of realism and poor repeatability. Clearly, there is a need for a pedestrian dummy having good repeatability, acceptable reproducibility, and a high sensitivity. This dummy should include the measurement of parameters directly associated with important injury mechanisms, especially the legs and the head. It is hoped that work in progress in Sweden and France(40) will contribute toward the design of such a pedestrian dummy.

One alternative to a full-scale test is a range of component tests. However, on their own, component tests do not consider the overall behavior of the pedestrian; therefore, it is also of great importance to assess the effect of the interaction between car component characteristics on pedestrian kinematics.

Prospectives in Mathematical Modeling

Mathematical models have gained acceptance as a research tool and as a possible method for the approval of passenger cars regarding pedestrian safety.

The accident process of the pedestrian (and two-wheeler rider) in collision with a passenger car is very complex. One must therefore use all available research methods to obtain comprehensive and reliable information that may be used as a basis for the formulation of

proposals leading to the reduction of injuries to pedestrians (and two-wheeler riders). This is even more important as all research methods deal with approximations of the accident process.

It is important that all research methods are rigorously validated. Mathematical models should be validated against all other appropriate research studies, including tests with dummies, cadaver tests, and accident studies, even though they yield only approximate values. Besides validating the model, it is important that input data defining the performance characteristics of the dummy and vehicle structure are accurate and complete.

When further developed models can be used to give better approximations of accident investigation data, it is hoped to obtain a statistically significant relationship between accident parameters and the probability of certain groups of road users being injured. Models can also be used to examine cars with novel and untested design features.

In general, models generate mechanically defined output such as acceleration. Information about internal forces, e.g., bending moments in bone structure (legs of a pedestrian), can be found by introducing, for instance, a simplified kind of finite element structure.

The mathematical models currently in use simulate single events in which vehicles and victims are each characterized by a specific selection of properties. The results are valid only for that single event and cannot be as a general assessment of risks of a population of pedestrians. e.g., in accidents. Therefore, a method to combine the results of a sequence of single victim predictions into a valid general prediction (injury prediction model) is required in the near future.

Mathematical models, in combination with subsystem tests, can be used for the approval of passenger cars. Disadvantages and advantages have been summed up in the report of EEVC Working Group 7.

One of the main advantages is the test results can be determined when the car is in the drawing board stage, and testing the full population at risk can be performed quite cheaply and easily and incorporated in a CAD/CAM procedure.

References

1. EEVC Committee, "Pedestrian injury accidents," Proceedings Ninth International Technical Conference on Experimental Safety Vehicles, Kyoto, Japan, November 1982.
2. McLean, A.J., and A.J. Woodward, "Pedestrian accidents in South Australia over two decades," Proceedings Pedestrian Impact and Injury Assessment, Detroit, March 1983.
3. Greetham, T.A., and D.A. Guenther, "An analysis of head injuries in real world pedestrian accidents," Proceedings Pedestrian Impact and Injury Assessment, Detroit, March 1983.
4. Otte, D., and E.G. Suren, "Pedestrian accidents from the viewpoint of statistics and traffic medicine," Symposium on Pedestrian Safety, Cologne, Germany, March 1984.
5. Farisse, J., et al., "A detailed injury severity scale for lower limbs based on analysis of injuries sustained," Proceedings 27th Stapp Car Crash Conference, San Diego, October 1983.
6. Ashton, S.J., et al., "Experimental reconstruction and mathematical modelling of real world pedestrian accidents," Proceedings Pedestrian Impact and Injury Assessment, Detroit, March 1983.
7. Faerber, E., "Synthesis report of Phase 3 Project G6. Proposed pedestrian test methodology," Proceedings Biomechanics of Impacts in Road Accidents, Brussels, Belgium, March 1983.
8. Cesari, D., et al., "Behaviour of side impact dummies used as pedestrians in accident reconstruction," Proceedings IRCOBI Conference, Cologne, Germany, September 1982.
9. Glaeser, K.P., "Step to step approach to a standardised full-scale pedestrian test," Proceedings Pedestrian Impact and Injury Assessment, Detroit, March 1983.
10. Brun-Cassan, F., et al., "Comparison of experimental car-pedestrian collisions performed with various modified side impact dummies and cadavers," Proceedings 28th Stapp Car Crash Conference, Chicago, November 1984.
11. Fowler, J.E., and J. Harris, "Practical vehicle design for pedestrian protection," Proceedings Ninth International Technical Conference on Experimental Safety Vehicles, Kyoto, Japan, November 1982.
12. Lestrelin, D., et al., "Proper use of HIC under different typical collision environments," Proceedings Ninth International Technical Conference on Experimental Safety Vehicles, Kyoto, Japan, November 1982.
13. Pereira, J., and S.J. Ashton, "Experimental development of pedestrian head injury tolerance data," Proceedings Pedestrian Impact and Injury Assessment, Detroit, March 1983.
14. Brun-Cassan, F., et al., "Tolerance of the human head at impact: reconstruction of head impacts observed in true-life accidents," Proceedings Biomechanics of Impacts in Road Accidents, Brussels, Belgium, March 1983.
15. Sacreste, J., et al., "Proposal for a thorax tolerance level in side impacts based on 62 tests performed with cadavers having known bone condition," Proceedings 26th Stapp Car Crash Conference, Ann Arbor, October 1982.
16. Cesari, D., and M. Ramet, "Pelvic tolerance and protection criteria in side impact," Proceedings 26th Stapp Car Crash Conference, Ann Arbor, October 1982.

17. Leung, Y.C., et al., "Study of knee-thigh-hip protection criterion," Proceedings 27th Stapp Car Crash Conference, San Diego, October 1983.
18. Pritz, H.B., and J.M. Pereira, "Pedestrian hip impactor simulator development and hood edge location consideration on injury severity," Proceedings 27th Stapp Car Crash Conference, San Diego, October 1983.
19. Cavallero, C., et al., "Improvement of pedestrian safety: Influence of shape of passenger car-front structures upon pedestrian kinematics and injuries: Evaluation based on 50 cadaver tests," Proceedings Pedestrian Impact and Injury Assessment, Detroit, March 1983.
20. Niederer, P.F., and M.R. Schlumpf, "Influence of vehicle front geometry on impacted pedestrian kinematics," Proceedings 28th Stapp Car Crash Conference, Chicago, November 1984.
21. Lestrelin, D., et al., "Mathematical evaluation of the head impact risk on a given part of a vehicle as regards pedestrians," Proceedings Pedestrian Impact and Injury Assessment, Detroit, March 1983.
22. Pritz, H.B., "Experimental investigation of pedestrian head impacts on hoods and fenders of production vehicles," Proceedings Pedestrian Impact and Injury Assessment, Detroit, March 1983.
23. Brun-Cassan, F., et al., "Reconstruction of actual car pedestrian collisions with dummy and cadavers," Proceedings Pedestrian Impact and Injury Assessment, Detroit, March 1983.
24. Bunketorp, O., et al., "Experimental study of a compliant bumper system," Proceedings 27th Stapp Car Crash Conference, San Diego, October 1983.
25. Wollert, W., et al., "Realisation of pedestrian protection measures on cars," Proceedings Pedestrian Impact and Injury Assessment, Detroit, March 1983.
26. Appel, H., et al., "Exterior safety and side protection with the Uni-Car," Proceedings Ninth International Technical Conference on Experimental Safety Vehicles, Kyoto, Japan, November 1982.
27. Ashton, S.J., and G.M. Mackay, "Benefits from changes in vehicle exterior design: field accident and experimental work in Europe," Proceedings Pedestrian Impact and Injury Assessment, Detroit, March 1983.
28. Suthurst, G.D., and W. Egglestone, "Pedestrian protection: can it be developed further?" Symposium on Pedestrian Safety, Cologne, Germany, March 1984.
29. van Wijk, J., et al., "MADYMO pedestrian simulations," Proceedings Pedestrian Impact and Injury Assessment, Detroit, March 1983.
30. Backaitis, S., et al., "Comparison of pedestrian kinematics and injuries in staged impact tests with cadaver and mathematical 2D simulations," Proceedings Pedestrian Impact and Injury Assessment, Detroit, March 1983.
31. EEVC Working Group 8, "Cycle and light-powered two-wheeler accidents," Summarized: IRCOBI, Delft, Netherlands, September 1984.
32. Brun-Cassan, F., et al., "Investigation of a series of representative experimental collisions between automobiles and two-wheeled vehicles, with specific analysis of severity of head impacts," IRCOBI, Delft, Netherlands, September, 1984.
33. Janssen, E.G., and C.G. Hujskens, "Cyclists impacted by simulated vehicle fronts," IRCOBI, Delft, Netherlands, September 1984.
34. Stcherbatcheff, G., "Pedestrian protection: special features of the Renault EPURE," Proceedings Seventh International Technical Conference on Experimental Safety Vehicles, Paris, June 1979.
35. Echavidre, J.P., and J. Gratadour, "Peugeot VLS 104 and pedestrian protection,", Proceedings Seventh International Technical Conference on Experimental Safety Vehicles, Paris, June 1979.
36. Appel, H., Fussgangersicherheit, Beispiele fur Technische Massnahmen in Einzfallen FAT, Schriftenreihe nr 42, 1984.
37. Césari, D., C. Cavallero, P. Billault, M. Berthommier, J. Farisse, J. Bonnoit, B. Sériat-Gautier, and B. Castera, "Analysis of pedestrian head kinematics based on car-pedestrian test results," 1985 IRCOBI Conference (to be published).
38. Aldman, B., et al., "An experimental model system for the study of lower leg and knee injuries in car pedestrian accidents," Proceedings Eighth International Technical Conference on Experimental Safety Vehicles, Wolfsburg, Germany, October 1980.
39. Harris, J., and N. Grew, "The influence of car design on pedestrian protection," Proceedings Tenth International Technical Conference on Experimental Safety Vehicles, Oxford, July 1985.
40. Aldman, B., and D. Césari, "A new dummy for pedestrian tests," Proceedings 10th International Technical Conference on Experimental Safety Vehicles, Oxford, July 1985.

Experimental and Mathematical Simulation of Pedestrian-Vehicle and Cyclist-Vehicle Accidents

E.G. Janssen and
J.S.H.M. Wismans
Research Institute for Road Vehicles TNO, Delft, The Netherlands

Abstract

In several European countries, unprotected road users form a significant proportion of road accident casualties. The Research Institute for Road Vehicles TNO has started a long-term research program on pedestrian and cyclist safety. Up to now, 38 full-scale dummy tests with simulated vehicle fronts and real passenger cars were performed. Furthermore, 3D mathematical model simulations were conducted with the MADYMO Crash Victim Simulation (CVS) package. A part of the program is presented in this paper. The influence of vehicle geometry and speed on pedestrian and cyclist kinematics in a lateral impact is shown, as well as the influence of bicycle mass and speed. The results of cyclist and pedestrian tests will be compared with each other.

Introduction

In several European countries, unprotected road users form a significant proportion of road accident casualties. In almost every country, the pedestrian is the most frequently involved unprotected road user. In The Netherlands, however, the bicycle is very popular, and more cyclists than pedestrians are killed or severely injured. In the past years, international research has focused mainly on pedestrian safety. Based on this research, various recommendations for the front structure design of passenger cars were developed. Discussions about future international regulations in this field have also started. Cyclist safety, however, should be included to avoid development of regulations concerned only with pedestrian safety.

The Research Institute for Road Vehicles TNO has started a long-term research program on this topic. The final objective of the study is to reduce the number and severity of injuries sustained by unprotected road users in a vehicle impact, by decreasing the aggressiveness of vehicle fronts. A research program is developed in which several research methods, including full-scale tests, body segment impactor tests, and mathematical model simulations, are integrated. A relatively simple experimental test setup, based on accident analysis studies, is defined, and the influence of several test parameters has been analyzed. The tests were performed with simulated vehicle fronts to improve the repeatability. Some tests with real passenger cars were performed to validate these tests. Simple standard dummies were used to simulate child and adult unprotected road users. Furthermore, 3D mathematical pedestrian and cyclist models were formulated with the MADYMO CVS program and verified experimentally to support the analysis and to extrapolate to situations that are not experimentally evaluated. In the near future, the program will be extended to human cadaver tests under similar test conditions as the dummy tests. The mathematical models will be refined by simulating the cadaver tests. The influence of the victims' anthropometry will be analyzed in detail. All test methods will be evaluated with respect to future regulations in this field. Comparison of pedestrian and cyclist accidents is an important objective in all phases of the research program.

This paper presents the results of experimental and mathematical simulations of a number of cyclist and pedestrian impacts. The influence of vehicle geometry and speed will be illustrated and the results of cyclist and pedestrian tests compared with each other.

Accident Statistics

Table 1 shows that approximately 20 to 30 percent of the killed road users are pedestrians and cyclists. The percentage of killed cyclists among all killed road users is high in The Netherlands compared to other countries. International studies show that, in most cases (60 to 85 percent), passenger cars are the opponent in the pedestrian and cyclist casualties(1,2). The pedestrian is struck by the of the car in 70 to 80 percent of the reported car-pedestrian accidents. In almost all these cases (90 percent), the pedestrian was hit from the side. Most of the cyclists (50 to 65 percent) were also hit in the side by the front of a car.

In The Netherlands, most car-pedestrian and car-cyclist accidents occur within built-up areas where a speed limit of 50km/h or less exists. From accident analysis, it is known that many cars were braking before hitting the pedestrian; the impact speed in 90 percent of pedestrian accidents was in the range of up to 60km/h(1). The speed variety is larger for bicycle accidents, and it is always clear if car speed or relative car/bicycle speed is The safety benefits to be expected from improvements in vehicle design, however, seem to be most important for the speed range up to 40km/h.

The legs and head are the most frequently injured body areas of pedestrians as well as cyclists. Head injuries are more serious and life threatening at short term; leg

Table 1. Percentage of pedal cyclists and pedestrians killed in road traffic

Countries	Percentage of Killed Pedal Cyclists in Traffic in 1981(2)	Percentage of Killed Pedestrians in Traffic in 1979(1)
Federal Republic of Germany	9.2	23.9
France	4.8	17.1
Great Britain	5.3	33.3
Italy	7.6	21.5
The Netherlands	19.7	13.3
Sweden	9.7	22.7

injuries, however, can also lead to serious injuries at long term (disability). The age distribution of the victims shows two peaks; children and elderly people are often involved in pedestrian and cyclist accidents. Elderly people are more frequently killed, and children are more frequently injured(1,2).

Experimental Simulations

Test Method

Introduction

The general test setup has been described earlier(3) and will be reviewed briefly in the next sections. Most of the conditions were selected on the basis of analysis of real vehicle-cyclist and vehicle-pedestrian accidents. The test program to be analyzed here is summarized in Table 2.

Vehicle Front

To determine the influence of test parameters, the best approach is to keep all test parameters constant and to vary only the parameter of interest. Therefore, it was decided to define one standard test (test number 8303/8306) and to change parameters with respect to this test. Each variation was tested twice. With regard to the vehicle, important parameters are the geometry and dynamical stiffness of the vehicle front. To vary these parameters and increase the repeatability of the tests, a moving barrier with simulated vehicle fronts was used. The vehicle front consists of three sections simulating the bumper, the grill, and the hood (see Figure 1) and is made

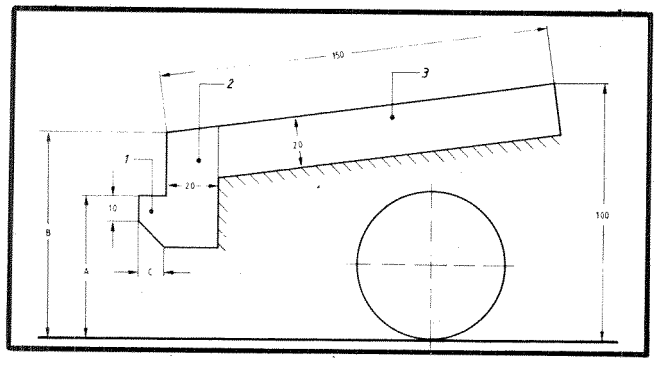

Figure 1. Simulated vehicle front consisting of bumper (1), grill (2), and hood (3)—geometry changed by variation of bumper height (A), hood-edge height (B), and bumper protrusion (C) (see Table 2)

Table 2. Variations of test parameters (see also Figure 1)

Test Number	Test Code	Dummy	Vehicle Impact Speed (km/h)	Vehicle Front Geometry (cm) A	B	C
8303	C30H	Cyclist	30	55	80	10
8306	C30H	Cyclist	30	55	80	10
8311	C40H	Cyclist	40	55	80	10
8312	C40H	Cyclist	40	55	80	10
8317	C30L	Cyclist	30	35	60	10
8318	C30L	Cyclist	30	35	60	10
8401	P30L	Pedestrian	30	35	60	10
8402	P30L	Pedestrian	30	35	60	10
8403	P30H	Pedestrian	30	55	80	10
8404	P30H	Pedestrian	30	55	80	10
8404R	P30H	Pedestrian	30	55	80	10
8407	P40H	Pedestrian	40	55	80	10
8408	P40H	Pedestrian	40	55	80	10

of homogenous polyurethane foam (density of 50kg/m^3 in tests presented here). The bumper height, hood-edge height, and bumper protrusion are varied in the test program. Only two geometric variations are included in this paper: a high vehicle front with a bumper height of 55cm and a hood-edge height of 80cm, and a low vehicle front with a bumper height of 35cm and a hood-edge height of 60cm.

Dummies and Bicycles

In these tests, the cyclist and pedestrian are represented by a 50th percentile anthropomorphic adult male dummy. The standard Part 572 dummy was chosen because it is a well-defined dummy and often used as a research dummy, in spite of its disadvantages, such as limited lateral flexibility. Other, more representative dummies are not available yet. To use this dummy as a cyclist dummy, some modifications were necessary. The range of motion in the hip joint was increased by cutting away some buttocks flesh. The knees, lower legs, and feet of the standard Part 572 dummy were replaced by special pedestrian body parts, supplied by Humanoid Systems. These body parts are reinforced and easily replaceable. Furthermore, the ankles have a lateral flexion possibility, and accelerometers can be mounted into the knees and feet. For the pedestrian, additionally, the pelvis of the Part 572 dummy was replaced by a special pedestrian pelvis, which allows a standing position. The neck bracket of the Part 572 dummy was also replaced by a special bracket to hold the pedestrian head in a vertical position. The pedestrian dummy was standing in a prescribed position (see Figure 2) with the impacted leg (left) slightly backwards and the body weight equally distributed over both legs (controlled by femur force transducers). The lower arm at impact side (left) was removed, and the upper arm fixed to the thorax to avoid disturbance of the dummy kinematics by elbow/hood impact. The cyclist dummy was sitting in a prescribed standard position on the stationary bicycle (see Figure 2). The pedal cranks were fixed in a vertical position, and the leg on impact side was stretched downward. The bicycles are standard Dutch men's bicycles (frame height 58cm, wheel diameter 28in) but without chain, mudguards, lighting, etc. The remaining bicycle mass was 12.5kg.

Impact Direction and Speed

As most pedestrians and cyclists are laterally impacted by the front of a car, the impact direction selected for the standard tests is therefore 90° to the longitudinal bicycle axis (left side). The vehicle impact speed in these tests was 30 or 40km/h, in accordance with the findings of accident analysis. The moving barrier with the simulated vehicle

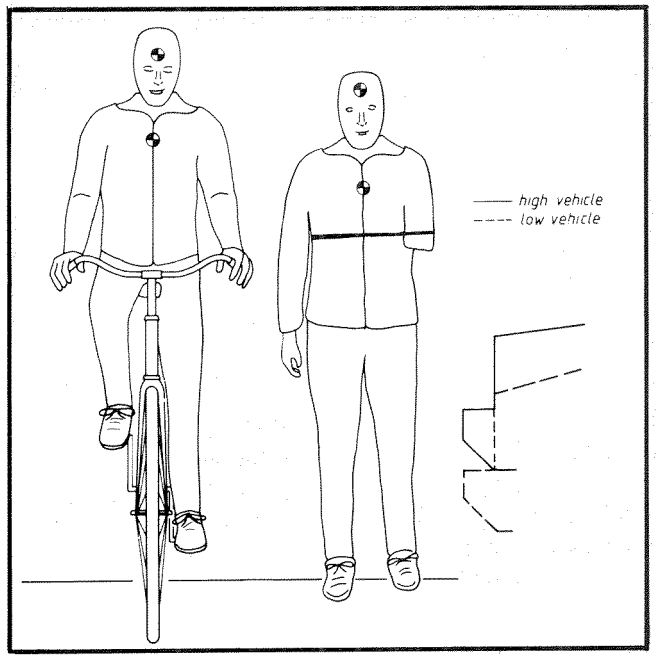

Figure 2. Initial position of pedestrian and cyclist compared to vehicle front height

front (total mass 930kg) started braking at vehicle-dummy contact. The moving barrier does not dive during braking because it is constructed without any suspension. Therefore, the vehicle front height is maintained during the complete test. To simplify the test setup in this phase of the research program, the initial bicycle speed was taken zero km/h. The influence of this will be analyzed in this paper by means of mathematical simulations.

Instrumentation and Measurements

The dummy was instrumented with triaxial accelerometers in the center of gravity of the head, thorax, and pelvis. Additionally, triaxial accelerometers were mounted into the knees and uniaxial accelerometers into the feet (lateral direction). The pedestrian dummy was also instrumented with femur force transducers to measure the body weight distribution at impact. The throwing distance of the (c.g. of the) dummy and bicycle were measured, as well as the permanent deformations of vehicle components. Eight high-speed film cameras were used to measure and analyze the motions of the dummy and bicycle during the impact. To extend the analysis of the tests, an imaginary windshield, consisting of a target-plane for high-speed film analysis, was added to the vehicle front (see Figure 3). The chosen length of the hood (dimension D is 100cm) leads to a head impact approximately on the center of the imaginary windshield in the cyclist tests with the high vehicle front. Therefore, the hood length is typical for vehicles with a short hood.

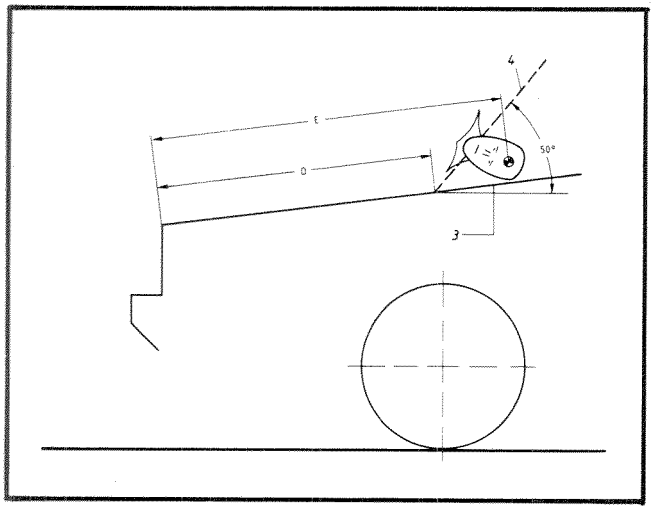

Figure 3. An imaginary windshield (4) added to the vehicle front for film analysis (hood length (D)—100cm; distance (E)—impact location of head on hood)

Test Results

General

The permanent deformations of the vehicle front and the bicycle, and the location of these deformations,as well as the throwing distance of the dummy and bicycle, were all found to reproduce very well. The overall kinematics of the dummy and the acceleration-time histories of the head, chest, and pelvis also reproduced very well. Due to dummy construction (e.g., joint-stops) and due to the contact with stiff bicycle parts, the acceleration-time histories of the knees and feet showed more differences in identical tests. In one pedestrian test (8403), the left knee was broken due to direct bumper impact. Table 3 summarizes some important test results.

Influence of Vehicle Geometry on Dummy Kinematics

The motion of a cyclist or a pedestrian as a result of a vehicle impact is above all dependent on the position of the victim relative to the vehicle. In this lateral test setup, the motion is influenced by the position of the legs of the pedestrian or the cyclist. In the cyclist tests presented in this paper, the bicycle pedal cranks were fixed in a vertical position and the impacted leg was stretched downward (see also Figure 2). This means the impact locations of the bumper and grill on the cyclist's legs are located in or close to a vertical plane through the dummy's c.g. and parallel to the vehicle direction of motion. Therefore, the motion of the dummy is an almost purely latera! one in this vertical plane, without rotation around the dummy's longitudinal axis. The vehicle front impacts the left leg, which is compressed between bicycle and vehicle front. Then the bicycle starts rotating and strikes the right leg. The cyclist rotates around the hood edge, and successively the left side of the hip, the left arm, the left shoulder, and finally the left upper side of the head strike the hood. When the legs are horizontal, the bicycle starts moving away from the dummy and vehicle. In the pedestrian tests, the leg on the impact side was positioned a little backward. Therefore, a forward rotation around a longitudinal axis could be observed, resulting in a frontal-lateral impact of the head on the hood. Furthermore, the whole (left) upper arm of the pedestrian is compressed between chest and hood, instead of only the shoulder in the cyclist tests.

The vehicle front height appears to have a predominant influence on the kinematics of the cyclist and the pedestrian. Figures 4 and 5 show the trajectories of the head, chest, and ankles of a cyclist and a pedestrian, struck by a high and low vehicle front. It can be seen that the distance between hood edge and head impact location strongly increases if the hood-edge height and bumper height are decreased. In this test setup, the head impact on the hood is located approximately 30cm closer to the windshield, for both pedestrian and cyclist, if the vehicle front height is 20cm lower.

The acceleration-time histories are also influenced by the vehicle geometry. The increase of the dummy's rotational velocity, caused by a decrease of the vehicle front height, leads to an increase of the maximum head and chest accelerations, as well as HIC and SI, for both pedestrian and cyclist. The HIC, for instance, is doubled

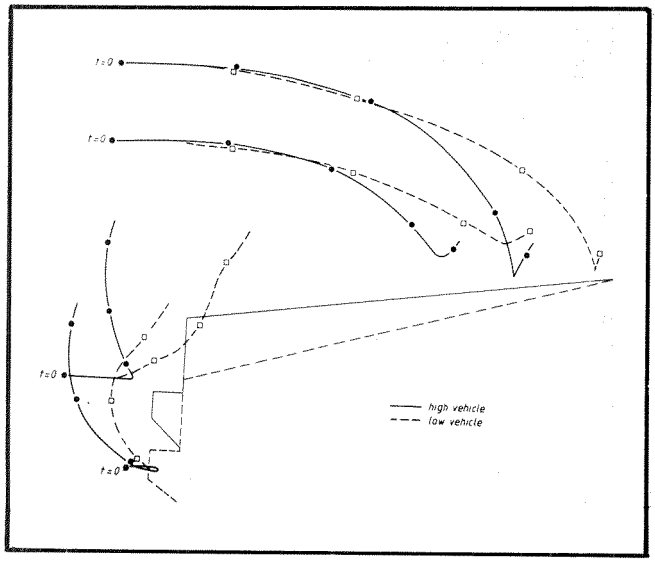

Figure 4. Influence of vehicle front height on trajectories of head, chest, and ankles of cyclist (vehicle speed 30km/h); time intervals—50ms

Table 3. Results of full-scale cyclist and pedestrian tests

Test Number		8303	8306	8311	8312	8317	8318	8401	8402	8403	8404	8404R	8407	8408
Accelerations:														
— Head:														
max. result. acc.	(m/s^2)	1061	990	1701	2365	1190	1460	775	876	835	709	769	1508	1066
time	(ms)	180	169	140	137	187	185	167	162	163	159	162	118	121
HIC		581	515	1840	3271	1003	1267	652	843	302	232	282	1190	592
— Chest:														
max. result. acc.	(m/s^2)	286	328	356	523	550	526	460	498	282	392	283	520	397
time	(ms)	167	155	145	128	167	170	152	141	156	152	159	125	126
SI		77	89	130	176	201	193	154	176	67	93	73	249	190
— Pelvis:														
max. result. acc.	(m/s^2)	673	888	861	995	343	406	325	422	595	734	782	815	998
time	(ms)	20	19	17	17	9	11	48	22	27	19	21	12	10
— Left knee:														
max. result. acc.	(m/s^2)	1252	1570	1432	1876	893	(1100)*	1217	1047	2383**	1178	—	1535	1610
time	(ms)	15	30	13	14	12	(14)*	12	27	23	5	—	19	16
— Right knee:														
max. result. acc.	(m/s^2)	1658	1182	1555	2311	476	454	970	1451	1687	1960	1536	2202	2315
time	(ms)	34	31	28	27	25	31	27	27	23	24	26	19	17
— Left foot:														
max. lat. result. acc.	(m/s^2)	2459	1036	3647	3108	1234	1210	1947	2163	2345	2499	2237	2139	2352
time	(ms)	14	21	13	13	10	9	12	12	16	16	18	15	14
— Right foot:														
max. lat. result. acc.	(m/s^2)	2178	3390	3611	3809	958	1072	2206	2213	1822	2230	1595	2218	2225
time	(ms)	31	30	25	25	24	30	27	29	38	29	33	29	26
Head Windshield Impact Velocity	(km/h)	42	40	61	62	44	44	48	48	—	—	—	—	—
Head Hood Impact Location Distance E	(cm)	114	112	124	124	145	145	112	112	86	77	82	84	84
Throwing Distance C.G. Dummy	(m)	6.4	6.8	10.8	10.6	6.3	5.9	6.7	6.4	6.6	7.7	7.2	13.4	13.5

* Unrealistic peak value of 2147m/s^2 after 79ms (joint-stop)

** Knee broken due to direct bumper impact

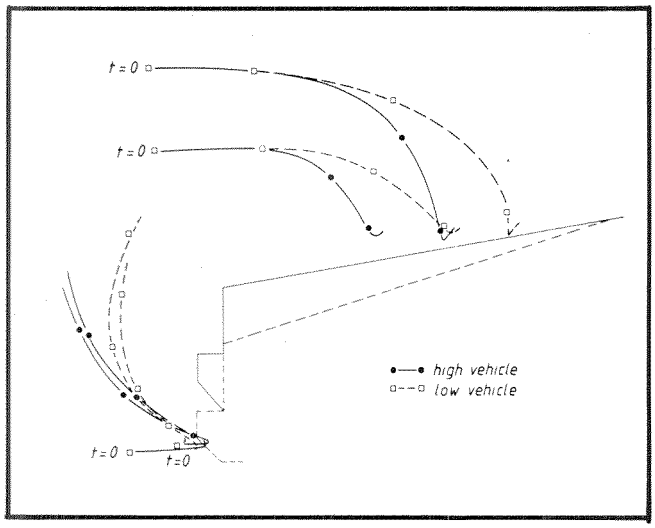

Figure 5. Influence of vehicle front height on trajectories of head, chest, and ankles of pedestrian (vehicle speed—30m/h; time intervals—50ms)

if the vehicle front height is decreased by 20cm. However, the maximum pelvis accelerations of the cyclist and pedestrian are reduced by approximately 50 percent if the vehicle front height is decreased. The vehicle geometry does not have much influence on the maximum knee and foot accelerations of the pedestrian. In the cyclist tests, however, these accelerations are lower in the tests with the low vehicle front (especially for the right leg).

Table 3 shows the head impact velocities on the imaginary windshield. In the pedestrian tests with the high vehicle front, no contact occurred. If the front height is decreased, the rotational dummy velocity increases, resulting in a higher head/windshield impact velocity and a lower throwing distance (see also Table 3). The throwing distance of the pedestrians appears to be somewhat higher than that of the cyclists.

Influence of Vehicle Speed on Dummy Kinematics

An increase of the vehicle impact speed from 30 to 40km/h also influences the head impact location on the hood. However, the influence is smaller than described before in the geometry variation tests (an increase of 11cm for the cyclist and only 2cm for the pedestrian). Table 3 shows that the throwing distance of the dummy and the head/windshield impact speed of the cyclist strongly increase if the vehicle impact speed is increased.

Accelerations and injury prediction parameters of pedestrian and cyclist are increased if the vehicle impact speed is increased. The HIC and SI are (sometimes more than) doubled if the vehicle speed increases from 30 to 40km/h. However, the maximum foot accelerations of the pedestrian seem to not be influenced by the vehicle impact speed.

Comparison of Pedestrian and Cyclist Tests

The trajectories of the pedestrian and the cyclist look quite similar (except for the right cyclist's leg in the low vehicle test). However, the head impact on the hood is located approximately 30cm closer to the windshield for the cyclist (see section Parameter Variations for the influence of the bicycle speed!). In the 40km/h tests, the difference was even 40cm. This is caused by the slightly higher position of the cyclist's head and the higher position of the cyclist's center of gravity (see also Figure 2). Therefore, in real road accidents, a head impact on the windshield (or roof) is more likely for cyclists than for pedestrians. The results show that increasing the victims's (c.g.) height has the same influence on the head impact location as decreasing the vehicle front height. This is illustrated in Figure 6, which shows that the head impact location of a cyclist impacted by a high vehicle front almost coincides with the head impact location of a pedestrian impacted by a low vehicle.

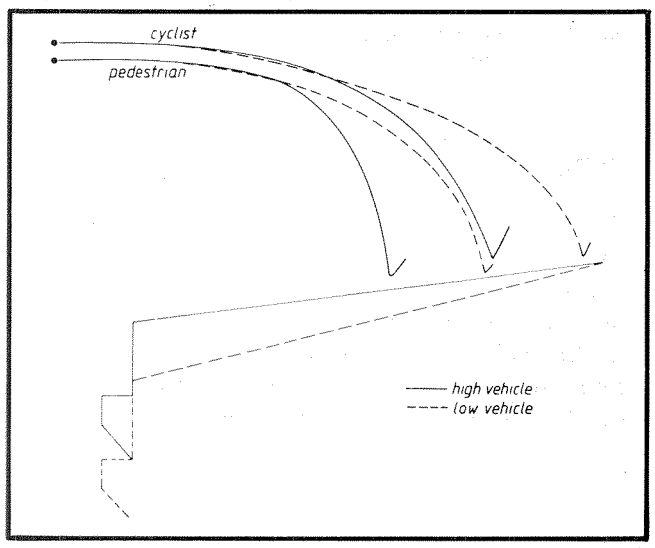

Figure 6. Influence of vehicle front height on head trajectories of pedestrian and cyclist (vehicle speed—30km/h)

In identical test conditions, the maximum head accelerations (and HIC) of the cyclist were always higher than those of the pedestrian. However, maximum chest accelerations of cyclist and pedestrian were almost equal in the tests with the high vehicle front and only slightly higher for the cyclist in the low vehicle tests. Chest SI appears to be equal (30km/h test) or slghtly lower (40km/h) for the cyclist in the tests with the high vehicle front and slightly higher in the low vehicle front tests. Maximum pelvis accelerations were also of the same magnitude in identical tests. The maximum knee and foot accelerations were lower for the cyclist in the low vehicle tests.

Mathematical Simulations

Model Setup

The model to be formulated here represents a pedestrian or cyclist impacted from the side by a vehicle front (Figure 7). Due to the three-dimensional nature of the dummy kinematics observed in some of the tests, simulations will be conducted with the MADYMO 3D version(4). The model can be divided into three separate systems: one for the dummy, one for the bicycle, and one for the vehicle.

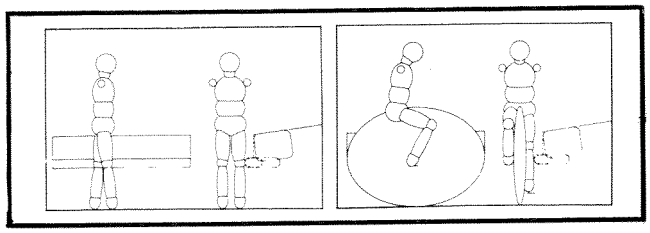

Figure 7. Pedestrian and cyclist mathematical model setup

Dummy Model

The same dummy model will be used to represent the dummy in the pedestrian and cyclist tests, except for the position of the head-neck assembly relative to the torso, since a special neck bracket with parallel interfaces for the connection to head and torso was used in the pedestrian tests. From earlier mathematical and experimental studies, it could be observed that small changes in the initial arm position can have a relatively large effect on the test results. Based on this, it was decided not to incorporate the arms in the mathematical model and to assign the arm mass for 50 percent to the upper torso mass. As a consequence, the dummy model will have nine segments: head, neck, upper torso, central torso, lower torso, and four elements for the legs. The mass distribution will be based on a recommended dataset of the Part 572 dummy prepared for the SAE Human Biomechanics and Simulation Subcommittee based on measurements by three different laboratories(5). Joint characteristics including joint stops, free range of motion, friction, and damping characteristics in this model have also been selected on the basis of measurements or estimations in various laboratories. Ellipsoids are attached to the model segments to describe the outer body geometry. Besides the standard ellipsoid as used in the Part 572 dummy model, two additional ellipsoids were attached to the upper torso to represent the shoulders. One ellipsoid was also connected to the right hip to account for initial contact beween cyclist and the right side of the saddle. The position of the dummy before impact was reconstructed in the model using detailed measurements of a number of dummy segment targets. Figure 7 illustrates the resulting initial model position.

Bicycle Model

Although the bicycle consists of several segments, it was decided to represent the bicycle in the present model by only one element. Mass distribution data for the bicycle, as far as center-of-gravity location and total mass (12.5kg) are concerned, were based on actual measurements, while moments of inertia were estimated. The external geometry of the bicycle is represented by an ellipsoid cylinder and two finite planes to represent the pedals (Figure 7). In addition, a plane is defined to represent the saddle (not shown in Figure 7).

Vehicle Model

The vehicle is represented in the model by one segment. The vehicle mass (i.e., moving barrier + simulated front) was measured (930kg) and assigned to the element. Due to the one-dimensional nature of the vehicle motion in the tests, moments of inertia and center-of-gravity location do not have to be specified accurately. The standard test defined earlier (i.e., 8303/8306) will be used here as the reference simulation. The mathematical representation of the vehicle front is illustrated in Figure 7; two hyperellipsoids are used for the bumper and the grill/hood-edge, respectively, while the hood is represented by a plane.[1] Input for the simulation is the initial velocity of the vehicle while a 0.7g acceleration field is applied to simulate braking.

Contact Interactions

Force-deflection characteristics of the foam used for the vehicle front were determined using a rigid spherical impactor(3). On the basis of these data, model parameters for the dummy-vehicle interactions were determined. Since no local stiffness data were available for the bicycle, model parameters for these contacts were roughly estimated taking into account the gross bicycle deformation during the crash. A coulomb friction coefficient of 0.7 was specified for all contacts with the vehicle and 0.5 for all contacts with bicycle and the bicycle-ground interaction.

[1] The present version of MADYMO 3D graphics does not have an option for hyperellipsoids and, as a consequence, contact surfaces in the vehicle model differ slightly from the approximation used in the graphics program (compare Figures 7 and 8).

Model Validation

Six test conditions from the cyclist-pedestrian test program have been selected for an initial judgment of the model's reliability (C3OH, C3OL, C4OH, P3OH, P3OL, P4OH in Table 2). For the standard test condition specified earlier, i.e., a 30km/h crash with a high vehicle front (C30H and P30H in Table 2), a detailed model verification will be presented here. The other test conditions will be discussed only briefly here. Figure 8 shows a comparison between the cyclist and pedestrian kinematics predicted by the model for this standard test condition. Gross kinematics appear to be very well in agreement with observations from the high-speed films. For instance, the differences in rotational motion between cyclist and pedestrian around the longitudinal body axis is well illustrated by the model. Model predictions for the head impact location on the hood appear to be quite realistic (see Table 4). The pedestrian model results are very close to the range of experimental variability, while the cyclist model shows a slight overestimation for this parameter (8 to 10cm).

Figure 9 shows a comparison between mathematical and experimental acceleration-time histories. Results are presented for the head, chest, pelvis, and left knee of the dummy and, in addition, for the acceleration of the vehicle. A quite good agreement between model predictions and experimental results can be observed, although, in general, the deviations between model and experiments are larger than the deviations between two experiments. One striking difference, for instance, between model and experiment is in the peak dummy accelerations, which show differences up to 50 percent. A sensitivity study showed these deviations are due mainly to the limited accuracy and reliability of the present contact-interaction models. Model input parameters are based on tests with a standard spherical impactor, while in reality the shape of the interacting geometries is much more complicated.

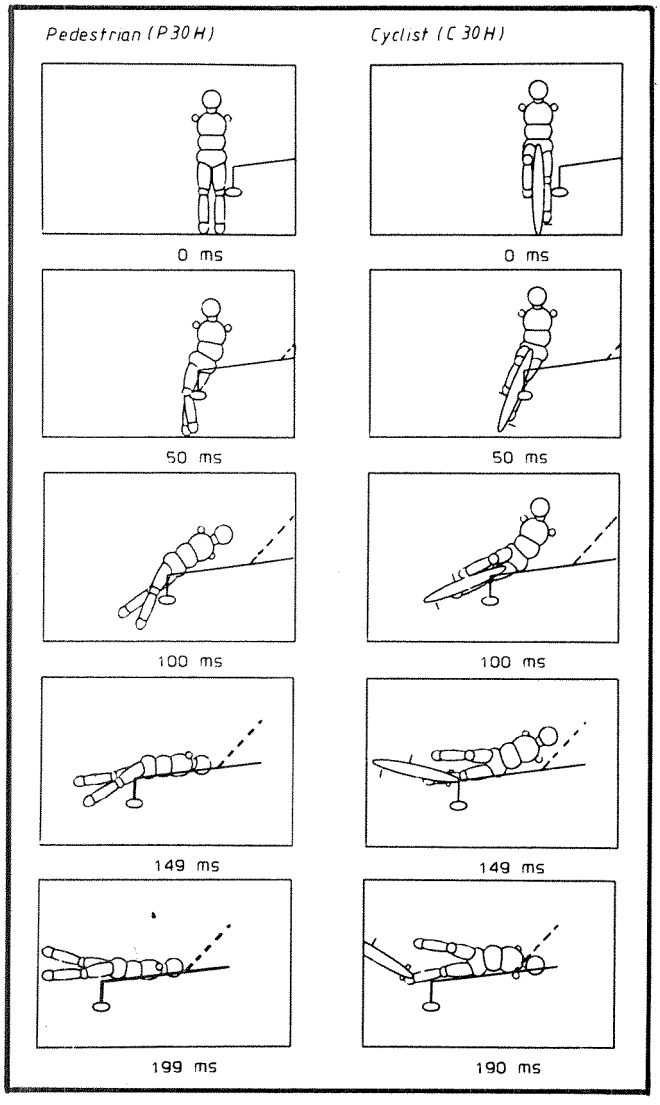

Figure 8. Comparison of kinematics in cyclist (C30H in Tables 2 and 4) and pedestrian (P30H in Tables 2 and 4) mathematical simulation

Table 4. Comparison of head impact location on the hood and the head impact velocity with an imaginary windshield

Test Condition	Head Impact Location on the Hood		Windshield Impact Velocity	
	Model (m)	(Experiment) (m)	Model (m/s)	(Experiment) (m/s)
C30H	1.22	(1.12-1.14)	11.7	(11.1-11.7)
C30L	1.40	(1.45)	15.4	(12.2)
C40H	1.33	(1.24)	16.7	(16.9)
P30H	0.76	(0.77-0.86)	10.5*	(*)
P30L	1.23	(1.12)	15.6	(13.3)
P40H	0.79	(0.84)	18.7*	(*)

* The imaginary windshield is connected to the hood at 1m from the hood-edge so no imaginary windshield impact velocity can be detected in this experiment. For the model, the head impact velocity with the hood is incorporated.

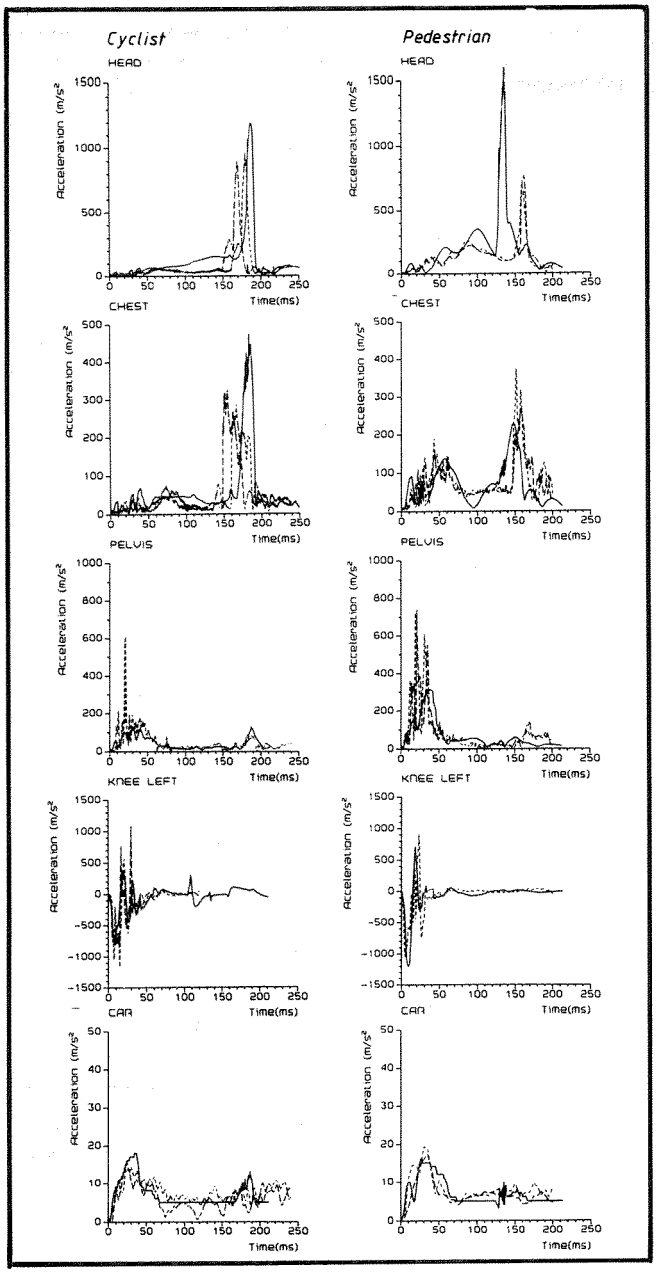

Figure 9. Comparison of acceleration-time histories from cyclist (C30H) and pedestrian (P30H) mathematical simulation (solid line) with the experimental results (dashed line)

Future contact models should account for such geometrical effects.

Deviations between model and experimental accelerations for the other test conditions incorporated in Table 2 are found to be in the same order of magnitude as in the standard test condition. Two parameters that characterize the impact of the head with the hood or windshield are presented here for both the experimental and mathematical simulations (see Table 4):

- The head impact locations on the hood
- The head velocity at the time of contact with the imaginary windshield

It follows that the deviations between model and test results for the head impact location are all less than 0.11m. For the head impact velocity, model predictions for the high vehicle front are very close to the experimental results. For the low vehicle front, they are overestimated by 20 to 25 percent.

Parameter Variations

In addition to the preceding simulations, various calculations were conducted without experimental verification. The reliability of the model is considered to be of such a level that the model results to be presented here are expected to be realistic, at least in a qualitative sense. The following types of simulation will be presented in this paper:

- The influence of an initial velocity of the cyclist
- Variations in bicycle mass
- The behavior of a pedestrian and cyclist in a simulation with a low vehicle front and a 40km/h vehicle velocity

Results of these simulations, together with the validated simulations, are summarized in Table 5. The effective head impact mass in this table is defined as peak head load during head impact, divided by peak head acceleration.

The Influence of the Initial Velocity of a Cyclist

In the cyclist impact tests, the initial velocity of bicycle and cyclist is zero. To study the influence of this velocity, a mathematical simulation has been conducted with an initial velocity for the bicycle-cyclist combination of 15km/h perpendicular to the vehicle velocity. Results for the kinematics in two planes are shown in Figure 10. The most important effect is a shift in head impact location on the hood of 67cm to the lateral side of the vehicle. Another effect is that the dummy model rotates forward around its longitudinal axis, while in the reference simulation (i.e., zero bicycle-cyclist velocity) almost no rotation could be observed. The distance of the head impact location on the hood to the hood edge is hardly affected, namely an increase by only 1cm (Table 5). The effect on other response parameters such as dummy acceleration-time histories appears to be small.

Variations in Bicycle Mass

The cyclist impact tests were conducted with a standard Dutch men's bicycle with a mass of 12.5kg. Two simulations were conducted with a varied bicycle mass. In the first simulation (light bicycle), the mass is decreased by 90 percent; in the second simulation (light-powered two-wheeler), the mass is increased to 5 times the original bike

Table 5. The influence of some parameter variations

Validated Simulations	Head Impact Location on Hood (m)	Head Impact Velocity on Windshield (m/s)	(ms)	Peak Bumper Load (N)	Effective Head Impact Mass (kg)
C30H	1.22	11.7	159	9753	5.2
C30L	1.40	15.4	155	7057	3.4
C40H	1.33	16.7	124	12685	5.2
P30H	0.76	10.5*	125*	8690	5.5
P30L	1.23	15.6	145	7087	4.1
P40H	0.79	18.7*	93*	12725	5.3
Variations					
C40L	1.49	18.2	122	8789	3.6
P40L	1.36	18.1	117	8910	4.1
Light bicycle	1.18	13.6	153	7681	4.7
Light-powered two-wheeler	1.23	8.5	177	24423	4.8
Initial velocity bicycle	1.23	10.8	160	9789	5.7

* Head impact velocity on hood

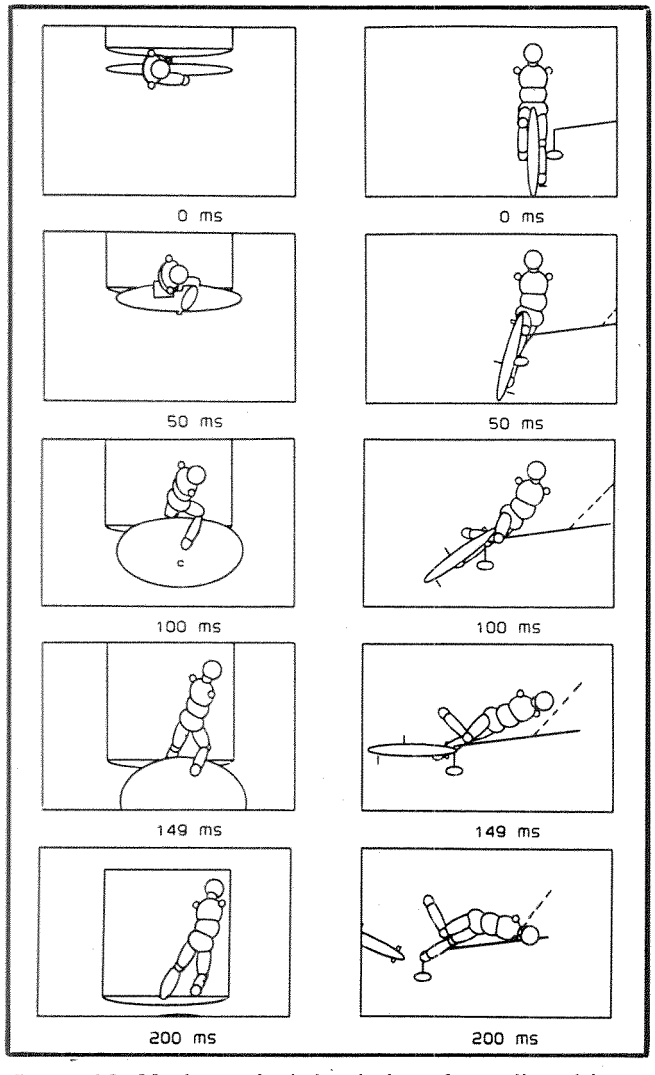

Figure 10. Mathematical simulation of a cyclist with an initial velocity of 15km/h (vehicle speed 30 km/h; high vehicle front)

mass. Results of these simulations, together with the reference simulation, are summarized in Table 5. It follows that the head impact location on the hood is hardly affected by these parameter variations. In case of a light bicycle, the head impact velocity slightly increases, while the bumper load decreases. In case of the light-powered two-wheeler, the opposite can be observed: a decrease in head impact velocity but a much larger bumper load.

The Influence of a Low Front in Combination With a High Vehicle Velocity (40km/h)

In the tests in the experimental verification program, only one test parameter was changed with respect to the standard test conditions (standard = 30km/h and high front). Here the effect of two variations at the same time will be considered, namely, a 40km/h vehicle velocity and a low vehicle front. The effect of this for a pedestrian and cyclist on head impact location, head impact velocity, and peak bumper load is included in Table 5. For both the pedestrian and the cyclist, a strong increase can be observed in the windshield head impact velocity and in the head impact location on the hood relative to the hood edge. The bumper load is not affected much because the effects of speed increase and lower front height compensate each other.

Discussion and Conclusion

Injury prevention research concerned with pedestrian safety has focused mainly on leg and head injuries, since these body areas are most frequently injured in road accidents. Accident analysis studies show for cyclist

accidents a similar trend in the injury distribution over the body. A major objective of the present study was to analyze, in detail, similarities and differences between pedestrian and cyclist accidents. A large number of experimental reconstructions of pedestrian and cyclist impacts have been conducted for this purpose, while additional mathematical simulations were performed to extend the analysis to conditions for which no experimental data were available. These models were formulated for both pedestrian and cyclist impacts. Experimental verification was conducted for three different test conditions, and, in general, very realistic model results were obtained. The experimental and mathematical simulation results offered a good insight in a large number of aspects of this rather complex impact behavior. Some major trends will be summarized in this section.

Figure 11 shows in eight different conditions the head impact location on the hood or windshield, and the corresponding head impact velocity. Results are based on mathematical simulations, since no expermental data were available for some of the test conditions. Incorporation of experimental findings in this figure, however, would not affect the general trends that can be observed:

- If the vehicle impact speed increases, a strong influence on the head impact velocity can be observed while the head impact location is hardly affected (Figure 11a).
- If the pedestrian is replaced by a cyclist, the opposite effect can be seen: a large shift in head impact location, with only a slight change in impact velocity (Figure 11b).
- Replacement of the high front by a low one influences both the head impact location and the head impact velocity (Figure 11c).

From the head acceleration-time histories and the contact load-time histories resulting from the mathematical models, effective head mass values can be determined (see Table 5). Significant differences could be observed between a high and a low vehicle front, while the effective masses for cyclists and pedestrians in similar test conditions are quite close to each other.

The above findings relate to the secondary impact, i.e., the impact with the vehicle hood. The impact with the vehicle front (i.e., primary impact) can be characterized by the peak bumper load, which has been included in Table 5. It follows that the differences in peak bumper load between pedestrian and cyclist impacts are relatively small, in spite of the fact that the cyclist mass distribution relative to the vehicle significantly differs from that of the pedestrian due to the higher body c.g. location and the upward position of the cyclist's right leg. The bicycle mass probably compensates for these differences.

The preceding results indicate important similarities between pedestrian- and cyclist-vehicle impacts for the test conditions evaluated in this study, namely, almost identical bumper impact loads and head impact velocities

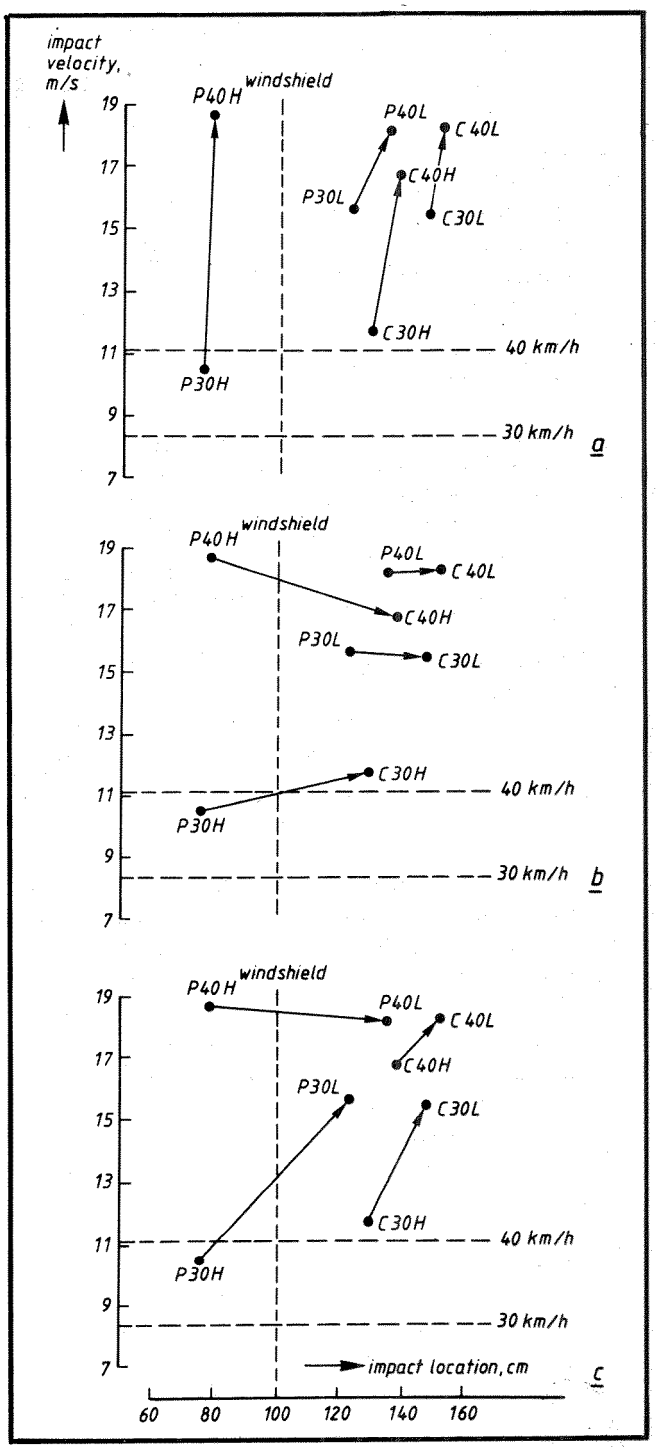

Figure 11. Head impact location and velocity on the hood or windshield from mathematical simulations (influence of vehicle speed (a), pedestrian versus cyclist (b), and vehicle geometry (c))

and only small differences in effective head masses. A major difference is found in the head impact locations and, as a consequence, impact of a cyclist's head with the windshield or even with the roof is much more likely than for a pedestrian. Mathematical simulations showed the effect of an initial cyclist velocity is small, except for the

shift of the head impact location to the lateral side of the vehicle, which could lead eventually to an absence of head/hood contact. This longitudinal and lateral shift of the cyclist's head impact compared with the pedestrian's head impact can also be obtained in a test with a large pedestrian initially impacted more lateral on the car front. Another difference between a moving and non-moving cyclist is the rotation around the longitudinal dummy axis; this rotation is absent in the stationary cyclist. For the moving cyclist, this rotation appears to be close to that observed in the pedestrian simulations.

If impactor tests are selected in future international regulations for the evaluation of vehicle fronts, the above data indicate that similar impactor masses and velocities can be selected to account for cyclist as well as pedestrian safety. However, other impact locations should be selected for the cyclist. The mathematical model results obtained here indicate the capabilities offered by mathematical simulations for specification of the initial conditions for these impactor tests (impact location, velocity, and effective mass). If accident analysis studies or human cadaver tests show that typical bicycle-induced injuries occur that are not observed in pedestrian accidents, special recommendations could be made in this respect.

It should be noted here that the results obtained up to now are mainly based on tests with a (modified) Part 572 dummy, which is not a realistic human substitute for this type of impact. Deficiencies of this dummy are, among other things, the limited flexibility of the shoulder-thorax and knee areas, and the limited instrumentation possibilities. Spine accelerations, for instance, are not well correlated with typical dummy response; they normalize direct rigid or padded impacts on the chest(6). Furthermore, leg injuries cannot be assessed by knee and foot accelerations but should be replaced, for instance, by long bone and knee torques. In this respect, the research program will be extended with human cadaver tests, with special emphasis on integration of cyclist and pedestrian safety.

Acknowledgments

The research program is sponsored by the Dutch Government in the framework of the Dutch National Road Safety Program. The authors wholeheartedly thank E. van Oorschot for conducting the mathematical simulations.

References

1. European Experimental Safety Vehicle Committee, "Pedestrian injury accidents," Proceedings Ninth International Technical Conference on Experimental Vehicles, Kyoto, November 1982.
2. European Experimental Vehicles Committee, "Cycle and light-powered two-wheeler accidents," Proceedings 9th IRCOBI Conference, Delft, September 1984.
3. Janssen, E.G., and C.G. Huijskens, "Cyclists impacted by simulated vehicle fronts," Proceedings 9th IRCOBI Conference, Delft, September 1984.
4. Wismans, J., T. Hoen, and L. Wittebrood, "Status of the MADYMO crash victim simulation package Proceedings Tenth International Technical Conference on Experimental Safety Vehicles, Oxford, July 1985.
5. Wismans, J., "Comparison of mass distribution data of the Part 572 dummy and recommendations for a standard dataset for CVS modelling," document prepared for the Analytical Human Simulation Task Force of the SAE Human Biomechanics and Simulation Subcommittee, August 1983.
6. Maltha, J., and E.G. Janssen, "EEC comparison testing of four side impact dummies," Proceedings of Biomechanics of Impacts in Road Accidents, Brussels, March 1983.

Experimental Research on Pedestrian Protection Using a Mobile Deformable Barrier

L. Maestripieri
Alfa Romeo Auto S.p.A., Safety Laboratory

Abstract

A test device has been built that consists of a mobile deformable barrier with the capacity to simulate different configurations and structural behaviors of various car front ends, using foam shapes of various density and moulding (Figure 1). With this barrier, a series of tests were carried out using a standing adult dummy as a pedestrian. The tests were aimed at generally reviewing and identifying the main factors contributing to an effective reduction in pedestrian injuries. As manufacturers, we have obtained information on how to improve both the structures and shapes of striking cars. In testing, research is not restricted to pedestrian car

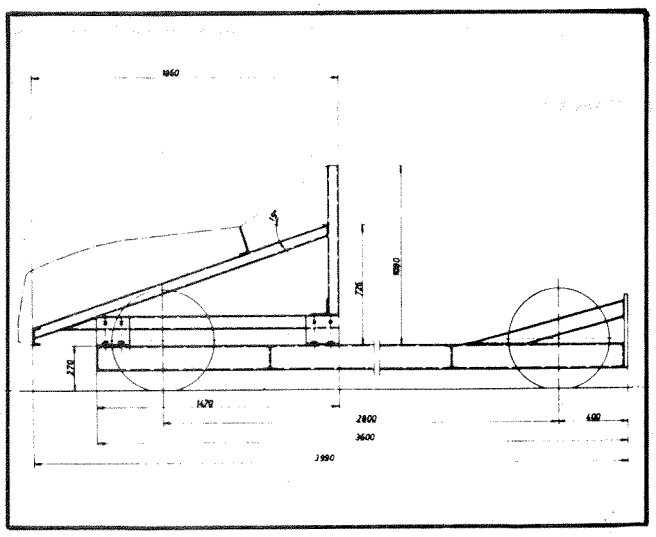

Figure 1. Mobile deformable barrier specifications

contacts but includes pedestrian/ground impacts to identify a possible correlation between car architecture and pedestrian injury levels in impacts against the ground.

Introduction

Vehicle manufacturers have felt a particular need to obtain information as soon as possible on vehicle configuration and structural aspects capable of limiting and reducing injury to pedestrians involved in road accidents. This has pushed the industry to use theoretical as well as experimental research to obtain a maximum amount of valid information and indications for organs in charge of defining future products. In the experimental research field, this need has induced Alfa Romeo to make, in addition to simulation by means of mathematical use of models, a mobile deformable barrier. This barrier has made it possible, during a short period of time and at fairly low cost, to simulate a considerable number of external configurations of vehicles, as well as structural solutions, with the purpose of obtaining a series of chosen elements for the designers before final experimentation takes place with definitive prototypes. To date this has usually been carried out with complete vehicles.

Description of the Equipment

The low cost and speedy achievement aspects have led us to define a simplified equipment solution. It consists essentially of a platform-truck with four braking wheels without suspension. A further framework can be mounted on the platform-truck, which supports the various configurations or mock-ups of previously chosen vehicle fronts (see Figure 1). Both vertical and transverse adjustments of the mock-ups are clearly possible. The global mass of the barrier can be varied starting from a minimum weight of 700kg.

For the deformable part, which simulates the front configuration of the vehicles, we chose polyurethane foam shapes after having considered various alternative material solutions (honeycomb, simplified steel structures, etc.). This foam shape offers the following advantages:

- Possibility of making practically any external configuration in a short time and with simple processes (cutting with a belt saw or a heated steel wire)
- Good homogeneity and constancy by the force/deformation (F/D) characteristics
- Ease in varying the F/D characteristics themselves
- Moderate constancy and repeatability of the physical characteristics of the product
- Low cost, approximately \$50/m3 (machined product)
- Easy traceableness on the national market

Characterization of the Deformable Barrier

When passing to the characterization of both the external configuration and the structure of the deformable part of the barrier, bearing in mind that improving vehicles to reduce injury to pedestrians involves both structural and configuration aspects, it was thought opportune to seek significant and optimal design values in the first phase, privileging only the external front configuration of the vehicle. This has been done bearing in mind a preestablished and constant determined structural characterization that appeared to be optimal and consistent with present mass-produced production possibilities.

Influencing Factors Linked With the External Configuration

Consistent with the abundant and in-depth bibliography available, it is possible to individuate and catalogue, within the global collision phenomenon, three distinct contact phases for the pedestrian; the first two are linked with pedestrian/vehicle contacts, whereas the third involves the successive pedestrian/ground contact.

During the first phase, usually defined as primary contact, the zones and parts of the pedestrian body involved are the legs and pelvis, whereas the vehicle bumpers and front structures are involved. The principal factors, linked with the vehicle configuration, that influence this first contact, are—

- Contour of the bumpers
- Height of the bumpers
- Height of the engine bonnet
- Bumpers/bonnet tangent angle

During the second contact of the pedestrian/vehicle, the involved parts of the pedestrian body are the pelvis, thorax, and head; the vehicle parts are the bonnet/mudguard zone and, according to speed, the windscreen and surrounding structures.

The following principal influence factors, linked with the vehicle configuration, should be mentioned:

- Curve of the pointed low V-shaped engine bonnets and the pontoon shapes
- Length of the bonnet where the initial positioning of the windscreen is particularly important
- Friction characteristic on the surface of the bonnet, which particularly influences the W.A.D. (Wrap Around Distance)

For the third and last phase regarding the pedestrian/ground contact, particular indications do not appear from studies and works already carried out, which demonstrate that a certain aspect of the vehicle particularly influences same. We have, nevertheless, also considered this phase of the phenomenon in the hope that significant data would emerge due to the particular simplification and schematization obtainable in the configuration of our deformable barrier.

Basic Prechosen Configurations

Because of the substantial number of influencing factors linked with the configuration alone, we soon realized the need to circumscribe the number of variables examined with the precise purpose of not increasing greatly the number of necessary tests.

In carrying out a first indicative inquiry into the influence of the front external configuration of the vehicle during a pedestrian collision, we have chosen three basic configurations (see Figure 2), of which (A) and (C) represent the two extremes of the shape. (A) is a low, rounded contour; (C) is a squared (pontoon) contour; and (B) is, instead, an intermediate configuration that approaches the average contours presently used on our vehicles.

Consistent with a need to limit a part of the influencing factors, the three configurations present identical solutions for some fundamental parameters, such as—

- Contour of bumpers
- Height of the bumpers from the ground, kept at a value of about 350mm
- Tangent angle of the bumpers—the beginning of the bonnet, kept constant at 80°

The common preestablished values for the above parameters reflect, in their values, optimization indications traceable in the many relative studies.

In short, only the height of the beginning of the bonnet and the characteristics of same have been introduced as influencing factors linked with the configuration and kept differentiated among the three configurations.

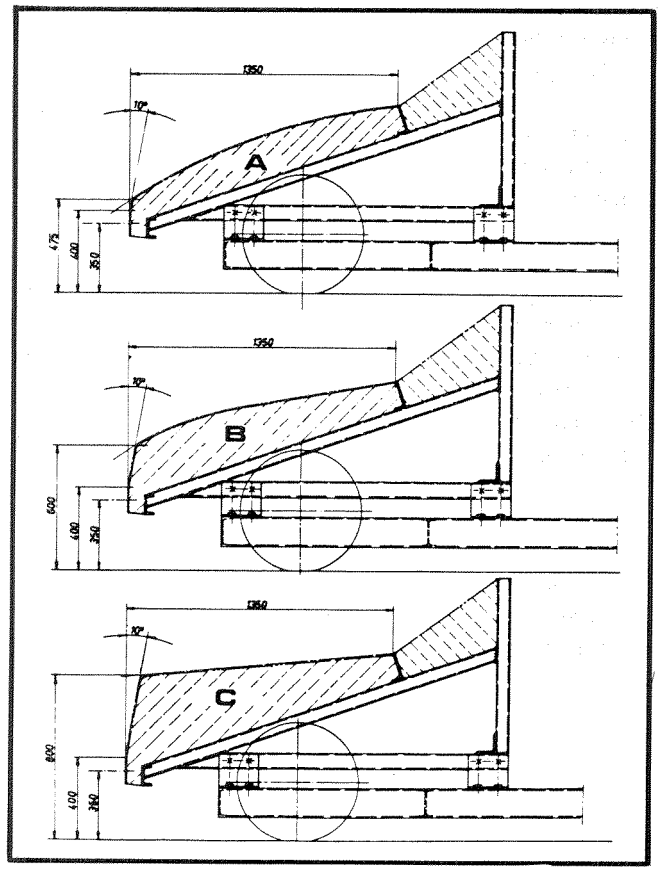

Figure 2. Different PU foam shapes

It was decided to obtain a bonnet contour length to guarantee that the pedestrian's head comes in contact with the bonnet structure, even at a speed of approximately 40km/h, to avoid, for the time being, dealing with the ulterior problem of the head coming in contact with the windscreen.

Structural Characterization

Our decision to begin an inquiry, limited only to the possible influence that the external configuration may have, forced us to choose and define a very precise structural definition to maintain constant behavior on the part of the various configurations and during various repeated tests. Such a configuration has been simulated with elevated-thickness polyurethane elements, taking care to verify by means of static and dynamic calibration tests a constant and homogenous behavior in all contour zones.

Tests for Defining the Structural Characteristics

The preliminary tests for defining and characterizing the materials to be used in the global collision tests have been chosen from those that help us establish a good

correlation between replacement materials and the front parts of mass-produced vehicles made of steel sheets.

In light of this, we have adopted both a simple static test, carried out by compressing samples of the material under examination with a spheric head (ø 165mm) to obtain some F/D values, and a dynamic test, using the head of the pedestrian dummy destined for the tests, opportunely equipped with accelerometers and dropped onto an analogous sample from a height that varies according to the speed adopted. In this latter test, the data available for analyses are represented by the acceleration values and the HIC. To obtain reference values with these two types of tests, we have also carried out a series of trials on the front parts of our vehicles presently manufactured in the zones foreseeably involved in pedestrian/car collisions (see Figures 3, 4, 5, and 6).

This type of inquiry and, in particular, that carried out by means of the test alone, unfortunately has revealed how the constructive solutions adopted at the present time and relating to certain front zones of the car do not permit acceptable results in contacts at a certain speed,

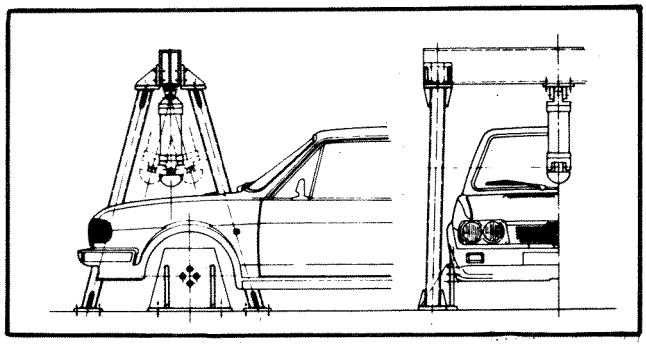

Figure 3. Equipment used for static body F/D characteristics

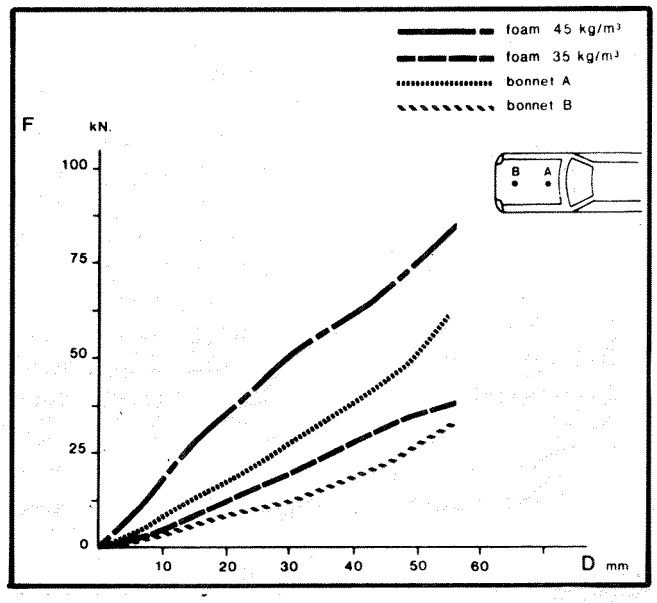

Figure 4. Various static F/D characteristics

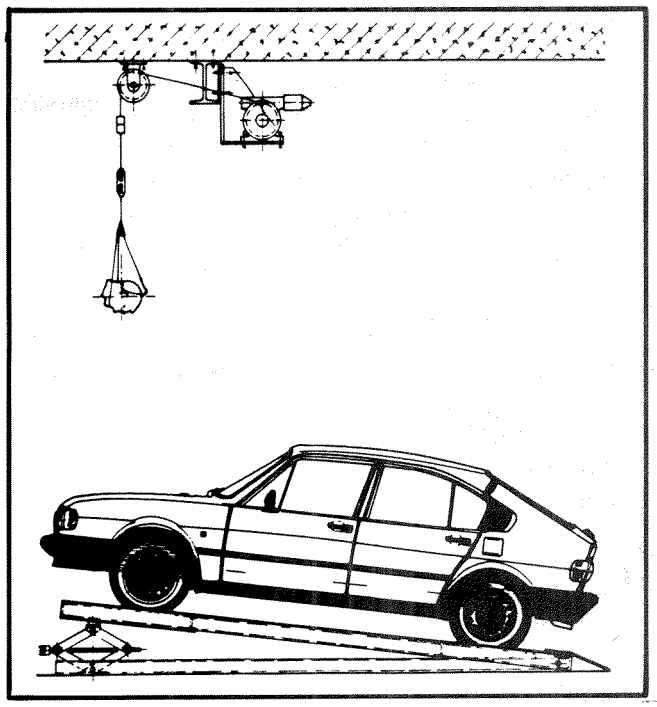

Figure 5. Equipment used for head drop tests

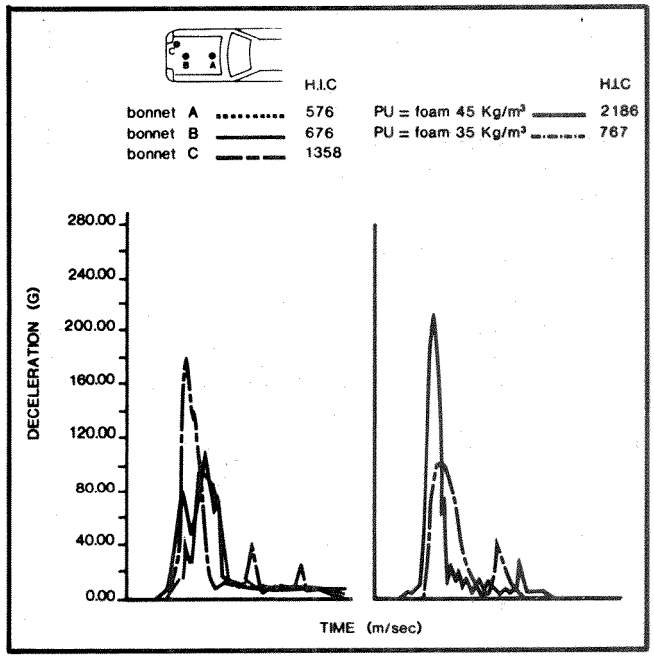

Figure 6. HIC and head acceleration values for different bonnet points and PU foams

when compared with presently accepted biomechanics criteria (see Figure 6). Nevertheless, these experimental data demonstrate that the structures presently used in relation to fairly vast engine bonnet and vehicle front zones seem to have 600 to 800 HIC values at a speed of about 30km/h and are therefore acceptable because these HIC values, obtained with the test alone, must definitely be considered more critical when compared with data

obtained from the same zones hit by complete dummies at the same speed and, therefore, by a greater mass.

Bearing in mind these latter data, it was decided to adopt as a structural reference characteristic, in the correlation sought between foam shapes and real vehicles, that characteristic obtained in the engine bonnet central zones. It was thought that such structural behavior could really be adopted and extended to the whole zone involved in the pedestrian/vehicle contact, at the same time guaranteeing good fulfillment of and respect for all other functions of the front part of a vehicle and fully consistent with production knowledge and techniques presently used when mass-producing vehicles.

Having defined as structural reference behavior that of the engine bonnet structure, we then passed to the selection of the polyurethane foams by means of the static and dynamic tests adopted, correlating F/D and HIC values.

The mechanical characteristics of the foam shapes are easily modified both by acting on the density and by making holes of variable diameters. The inquiry carried out regarding the various samples and using exclusively density variations has enabled us to individuate a 35kg/m3 density value. For both the F/D and maximum acceleration values as well as the HIC values obtained, 600 to 800 to be very similar to the behavior of the engine bonnet metallic structure (see Figure 6).

Experimentation

Barrier Test Speed

In defining and choosing the speed at which to carry out the tests, the results of the available statistical data have been borne in mind, i.e., that 50 percent of the accidents produce grave injuries to pedestrians at a speed of less than 35km/h, whereas the percentage of grave injury increases to 90 percent at speeds around 50km/h.

Since we are also interested in the influence of speed, together with the influencing factors linked with the configuration, we have chosen some test speed levels on the colliding barrier above and below 35km/h. Such chosen levels were 30 and 40km/h. The barrier begins braking at the first moment of collision with a 0.7 ± 1g deceleration.

Pedestrian Involved in the Accident

The 572-50P Pedestrian Dummy Model has been used simulate the pedestrian involved in the accident, equipped with the following instrumentation:

- Head: three right-angled accelerometers at the center of gravity (Fh = 1,000Hz)
- Thorax: three right-angled accelerometers (Fh = 180Hz)
- Pelvis: three right-angled accelerometers (Fh = 180Hz)
- Leg involved: one accelerometer in the knee and one accelerometer in the ankle (positioned on opposite side to the impact)

To reduce the influence of the pedestrian dummy's when the head is hit, a 60° angulation of the dummy's axial body plan with the direction of the impact has been adopted.

Experimental Tests

A total of 24 tests has been carried out with the three configurations (A, B, and C) previously chosen (see Figure 2), 12 at 40km/h, submitting each foam element to two tests in two symmetrical zones in relation to the central line; this was possible due to the constancy of the section and the good homogeneity of the material. In this way, four tests have been carried out with each configuration at 30km/h and four at 40km/h (see Photos 1, 2, and 3). At the end of each test and with regard to all contours, some tests have been carried out to check the characteristics of the foam shapes when only the head fell at 30km/h (see Photo 4).

Analysis of the Results

When analyzing the results (see tables in Figures 7 and 8), we thought it opportune to analyze the values obtained by each individual part of the dummy (head, pelvis, etc.) during the two phases, which can be traditionally distinguished as—

(a) Pedestrian/vehicle impact phase during its two primary and secondary contacts
(b) Pedestrian/ground impact phase

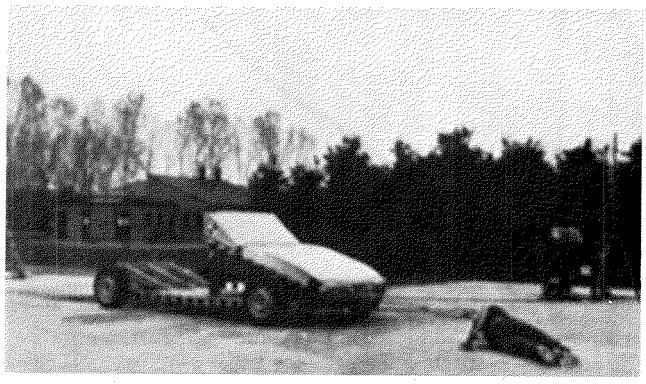

Photo 1.

Photo 2.

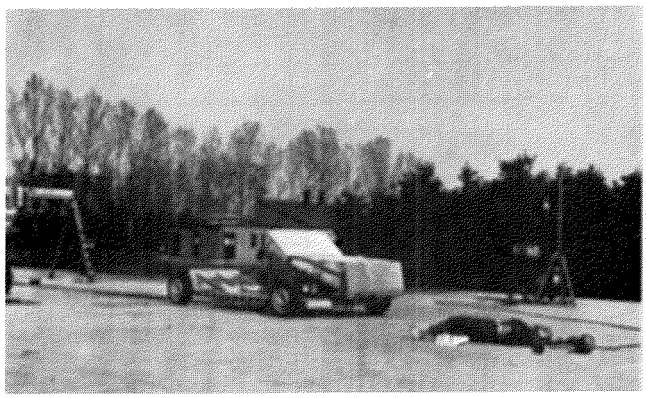

Photo 3.

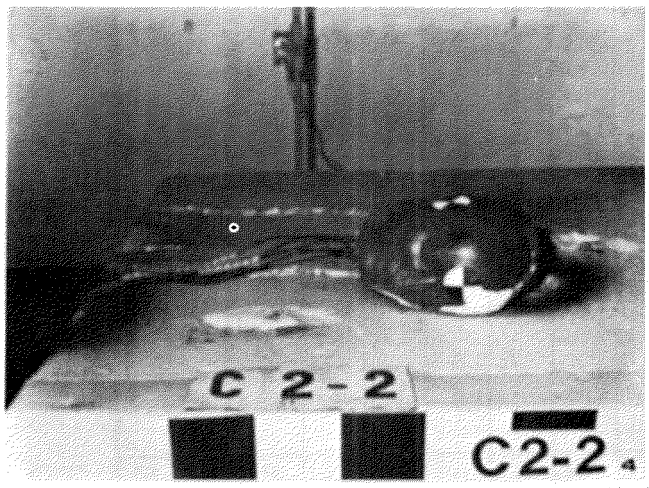

Photo 4.

Ankle (A Max)

Pedestrian/Vehicle Contact

This part of the dummy pedestrian in contact with the part of the contours and which had intentionally been defined as constant for the three types (A), (B), and (C) (H = 350, constant bumper section, 80° bumpers and bonnet angle) has supplied acceleration values which have been kept moderately constant at all speeds, increasing consistently with the increase in same.

It should be noted how these values, obtained with a 35km/m3 foam shape uniformly adopted in all its contours, must be considered slightly elevated on an average if compared with those obtained during analogous tests regarding a real Alfa Sud-type vehicle (see Figure 9).

Pedestrian/Ground Contact

This contains values that are aleatory and independent of the contour (Figure 9).

Knee (A Max)

Pedestrian/Vehicle Contact

The fact that all contours were made uniform, both with regard to the bumper height and the angle (bumper/bonnet tangent), brings about constancy of values in the three configurations with a moderate increase that can be appreciated only by passing from 30 to 40km/h (Figure 10).

Pedestrian/Ground Contact

These values are also aleatory and independent of the contour (Figure 10).

Pelvis (A Max)

Pedestrian/Vehicle Contact

This part of the pedestrian is involved differently according to the deformable barrier configurations, which present different heights from the beginning of the engine bonnet and a different bonnet curve. From data gathered during the tests, it is, in fact, possible to individuate an increase in accelerations consistent with the increase in the engine bonnet height itself.

PU-Foam Shape	Impact Speed (km/h)	IMPACT AGAINST VEHICLE: Ankle-Max.Accel.(g)	Knee-Max.Accel.(g)	Pelvis-Max.Accel.(g)	Thorax-Max.Accel.(g)	Head-Max.Accel.(g)	H.I.C	Head Speed	W.A.D Wrap around distance	L.O.I Impact location	IMPACT AGAINST GROUND: Ankle-Max.Accel.(g)	Knee-Max.Accel.(g)	Pelvis-Max.Accel.(g)	Thorax-Max.Accel.(g)	Head-Max.Accel.(g)	H.I.C	Head Speed
A1	29,5	105	81	41	35	78	350	8,7	1750	1170	-	-	98	31	224	804	5,6
A2	30,1	99	84	39	43	98	800	9,3	1760	1190	42	30	94	24	30	97	1,3
A3	29,6	117	77	34	26	32	119	6,2	1780	1210	84	146	64	37	255	957	7,4
A4	30,9	111	85	57	39	92	625	11	1775	1200	24	82	100	42	298	1277	6,7
B1	30	107	66	32	44	74	388	7,3	1690	1020	14	36	70	23	28	18	-
B2	30,5	132	83	40	54	77	516	7,6	1710	1045	26	80	88	13	24	19	2,5
B3	30,1	133	89	37	44	78	449	9,7	1625	955	50	40	96	18	188	599	6,4
B4	28,1	106	80	55	42	84	486	8,8	1620	950	48	24	110	36	201	438	4,3
C1	30,1	123	82	50	35	65	181	5,7	1580	825	86	101	82	28	225	857	4,9
C2	30,5	104	86	60	44	74	276	6,1	1595	820	26	20	116	25	197	820	5,2
C3	29,2	88	76	47	30	58	159	5,8	1540	725	44	88	68	35	259	1120	9,8
C4	30,2	94	93	55	31	77	323	8,3	1610	810	8	26	16	30	216	913	9,4
Alfasud	28	80	52	25	31	70	302	8,3	1610	1075	13	17	35	24	30	25	3

Figure 7. 30km/h test results

PU-Foam Shape	Impact Speed (km/h)	IMPACT AGAINST VEHICLE: Ankle-Max.Accel.(g)	Knee-Max.Accel.(g)	Pelvis-Max.Accel.(g)	Thorax-Max.Accel.(g)	Head-Max.Accel.(g)	H.I.C	Head Speed	W.A.D Wrap around distance	L.O.I Impact location	IMPACT AGAINST GROUND: Ankle-Max.Accel.(g)	Knee-Max.Accel.(g)	Pelvis-Max.Accel.(g)	Thorax-Max.Accel.(g)	Head-Max.Accel.(g)	H.I.C	Head Speed
A5	40,4	137	90	40	48	105	628	11,3	1900	1325	200	80	66	80	354	1221	-
A6	40,1	128	90	41	42	51	331	7,5	1920	1310	-	28	-	128	291	1221	6,8
A7	40,1	112	87	39	46	113	920	12,1	1903	1315	73	98	53	93	120	608	13,3
A8	39,9	130	85	42	41	101	570	11,1	1916	1321	-	152	42	84	88	302	10,1
B5	40	139	94	51	35	117	1052	13,2	1735	1030	-	50	40	58	345	1584	14,6
B6	40,2	134	-	58	50	141	1377	13,4	1720	1050	-	132	65	34	90	238	11,9
B7	39,8	141	98	53	38	107	980	12,8	1728	1034	180	148	72	76	302	1110	14,1
B8	40,5	138	102	49	44	113	1020	13,3	1731	1046	30	22	56	81	243	1031	12,7
C5	39,6	156	142	62	45	72	712	11,1	1605	790	52	184	75	70	243	1065	11,1
C6	39	128	65	42	42	110	1141	13,2	1645	855	-	102	69	56	207	679	9,6
C7	39,3	150	133	68	47	93	840	11,8	1623	800	160	18	71	68	298	1201	12,1
C8	40,6	148	131	61	51	103	1040	12,3	1631	814	-	-	73	77	237	1041	11,7
Alfasud	40	90	70	32	40	140	806	14	-	1226	55	53	61	54	88	155	7,9

Figure 8. 40km/h test results

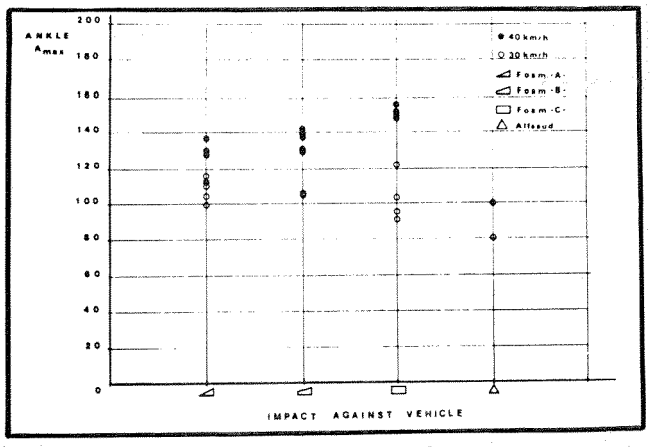

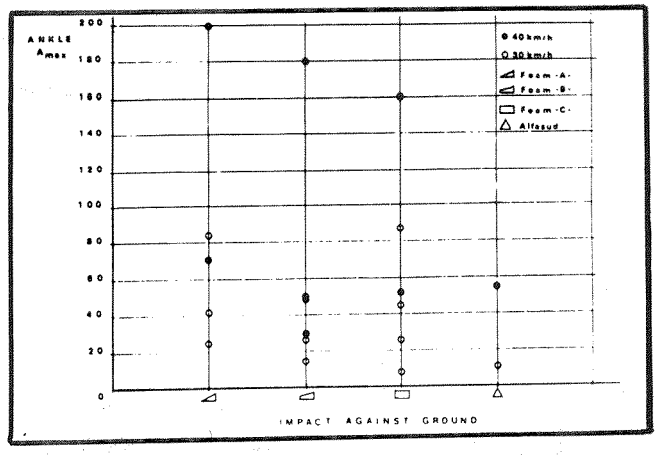

Figure 9. Ankle A Max for different shapes

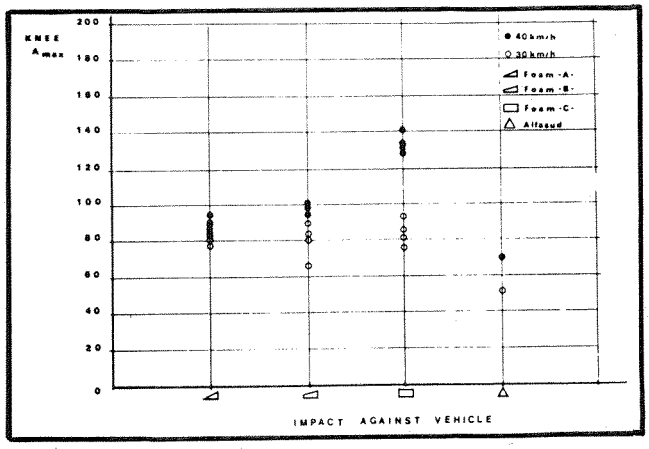

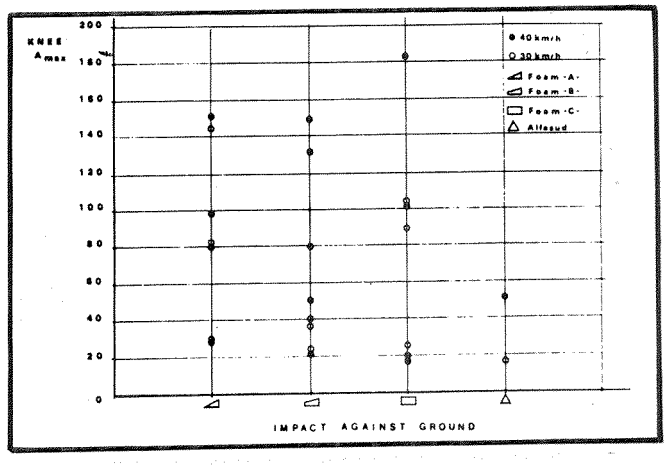

Figure 10. Knee A Max for different shapes

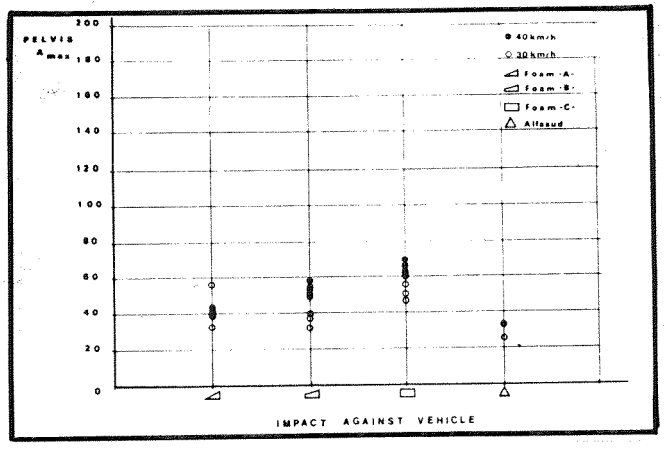

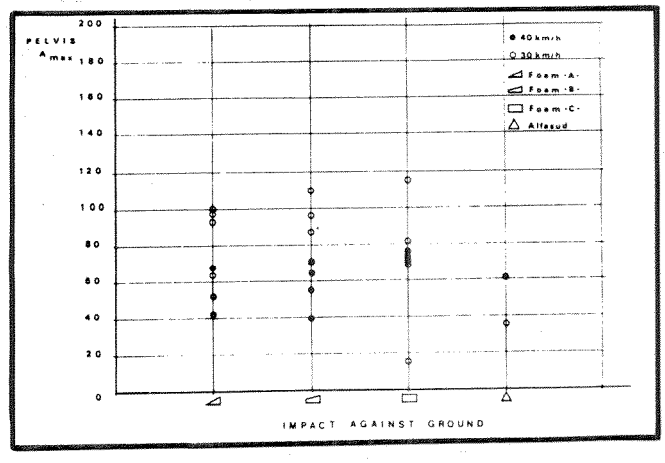

Figure 11. Pelvis A Max for different shapes

An analogous increase is also traceable when the impact speed is increased (Figure 11).

Pedestrian/Ground Contact

These values are aleatory and independent of the type of contour and the speed (Figure 11).

Thorax (A Max)

Pedestrian/Vehicle Contact

The acceleration values obtained show a certain insensitivity toward the barrier configuration variation as well toward the collision speed variation (Figure 12).

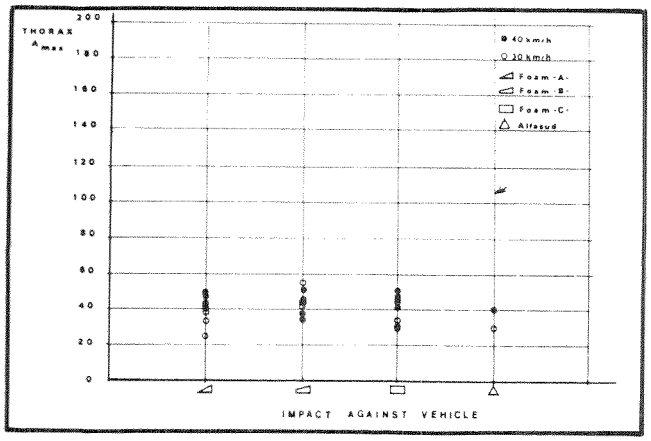

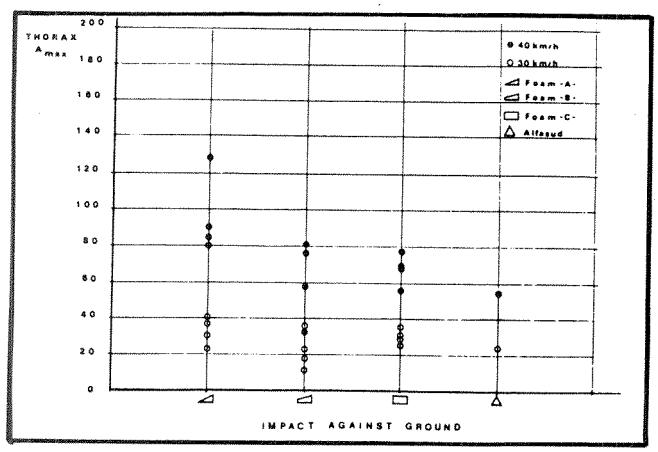

Figure 12. Thorax A Max for different shapes

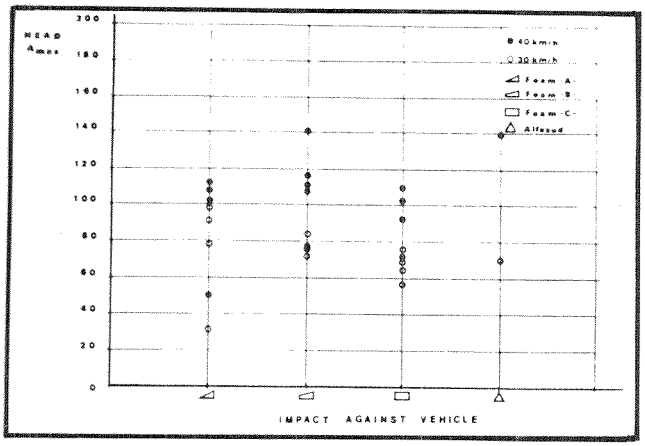

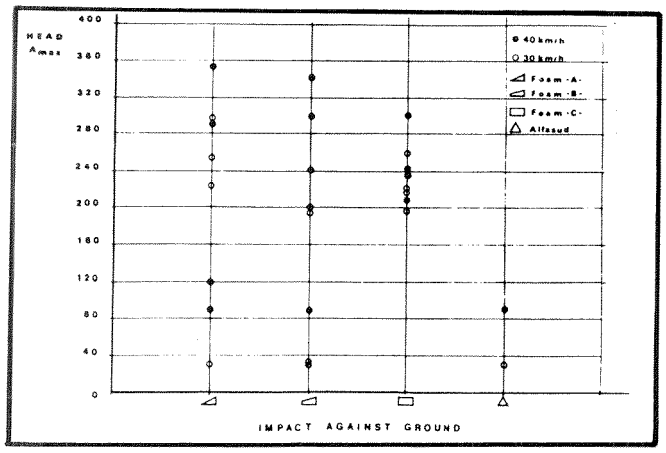

Figure 13. Head A Max for different shapes

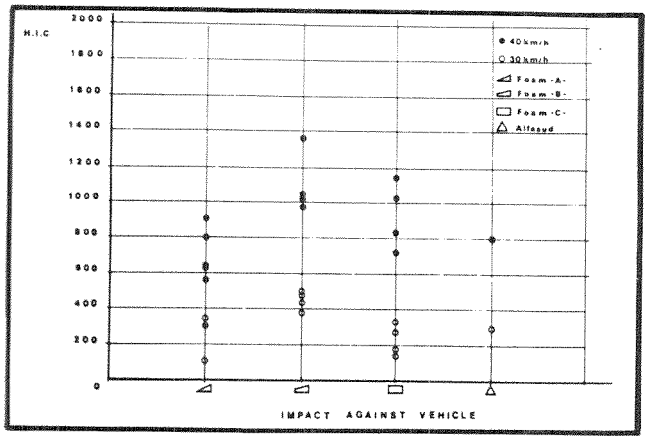

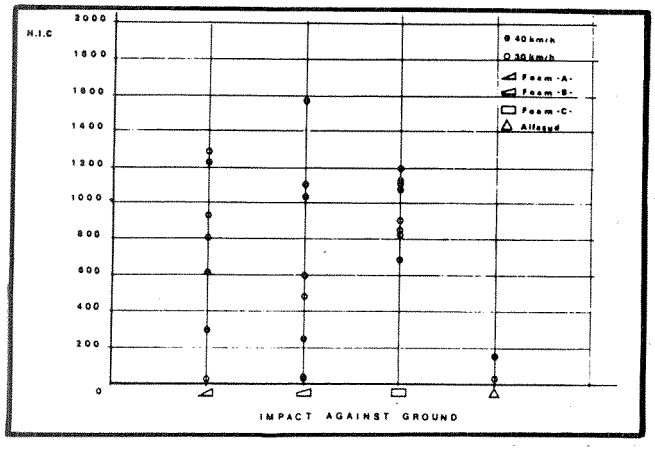

Figure 14. HIC for different shapes

Pedestrian/Ground Contact

Though a certain dispersion of data and the usual independence from the type of contour occurs, it is possible to individuate a certain increase in average value in accordance with the impact speed increase and, consistently, the speed with which the dummy's body hits the ground (see Figure 12).

Head (A Max, HIC)

Pedestrian/Vehicle Contact

This part of the pedestrian behaves differently in the case of the two speed values:

- During the 30km/h tests, the speed of the head and, consistently, the maximum acceleration

HIC seem to decrease when the bonnet is higher, provided a considerable dispersion of contour values is accepted due to a different way in which the arm rests on the contours.

- During the 40km/h tests, the differences are less noticeable and tend, however, to disappear, the lowered (A) contour on an average due to a greater possibility of the arm resting on it before impact with the dummy's head (Figures 13 and 14).

Pedestrian/Ground Contact

Also in the case of the head, it is not possible to individuate the degree to which the gravity of injuries depends on the vehicle's configuration. As in the case of other body parts, there is a certain tendency toward an average increase in gravity when the speed increases (Figures 13 and 14).

General Considerations

Considerations Regarding the Various Configurations

We have intentionally destined the first series of tests for research into the eventual influence of the external configuration alone in relation to injuries suffered by pedestrians involved in collisions.

If we carry out a reconstruction action regarding injuries suffered by various parts of the pedestrian's body, it is possible to individuate a series of information that reconfirms many of the conclusions reached by other researchers.

In fact, as far as injuries to the head are concerned, the lowered type (A) and (B) external configurations seem to induce impact speeds that are slightly greater on average and, consequently, of greater stress in relation to more squared-off (C) type solutions within a collision speed band that is relatively low. The increase in the latter, on the other hand, seems to lead to a certain leveling out among the various solutions, even if much higher levels of injury can be traced.

With regard to all other parts of the pedestrian's body, the stress seems to increase when passing from the lowered (A) type configuration to those of the squared-off (C) type.

Nevertheless, when limiting the slight global prevalence of the (A) type contours, some aspects linked with general modern vehicle architecture should be pointed out.

In fact, if we examine the W.A.D. (Wrap Around Distance) and the L.O.I. (Location of Impact) in Figures 7, 8, 15, and 16, it becomes evident that the head impact zone is always further away from the tangent surface and

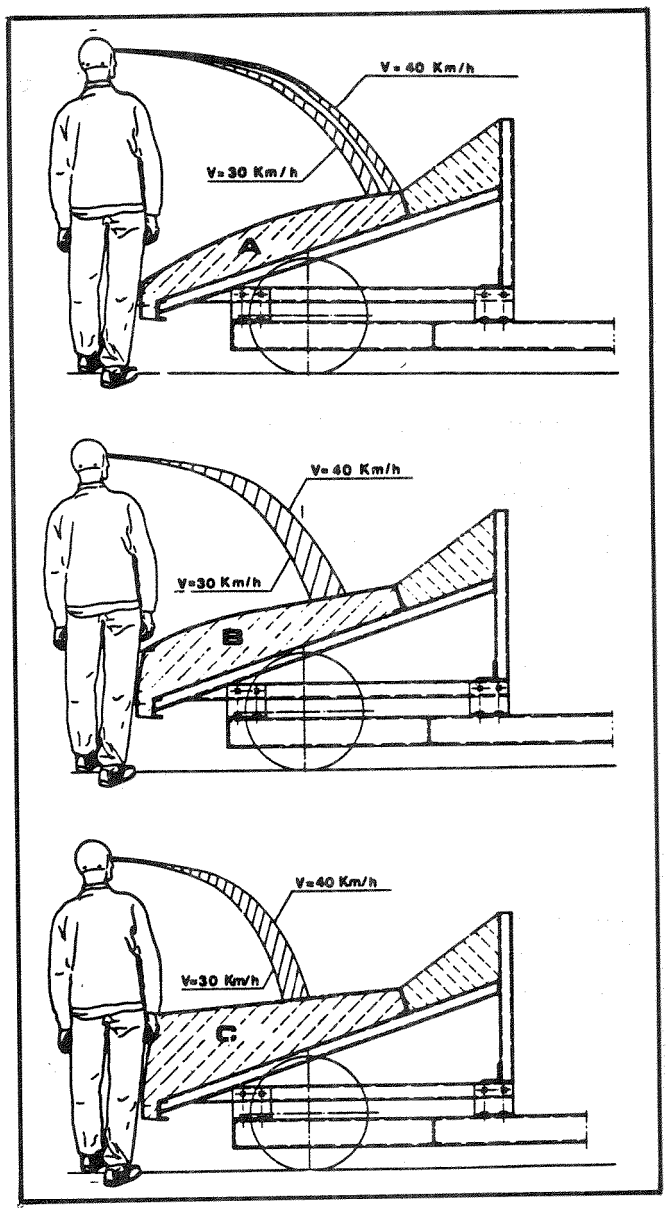

Figure 15. Movement of head relative to various shapes

nearer to the bumpers, both under the influence of speed as well as type of contour. At 40km/h, L.O.I. values vary from about 800mm for the (C) profile to more than 1,300mm for the (A) type contour.

Such a characteristic on the part of the lowered (A) contours means that, whenever you want to limit the contact between the head and the windscreen zone, a bonnet length (Lw) of around 1,400mm must necessarily be foreseen—and a value acceptable only in the case of vehicles in the superior or sports segments (see Figure 17).

In the case of vehicles in the medium-small segments, if you want to keep the Lw/Lt (total length) ratio at an approximate acceptable value of about 0.30m, a need clearly arises for more squared-off type (C) contours, which require lower L.O.I. values.

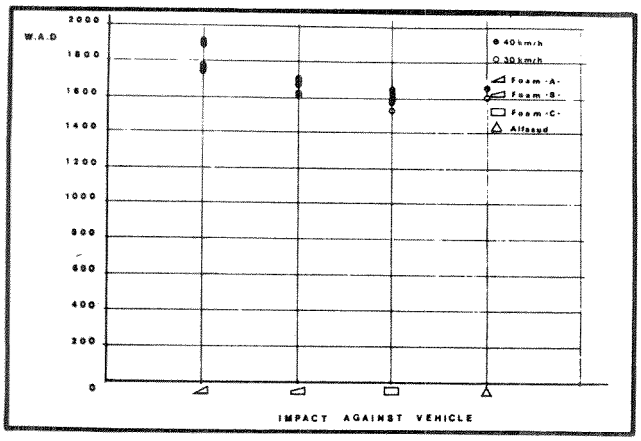

Figure 16. W.A.D. (wrap around distance) and L.O.I. (location of impact) for different shapes

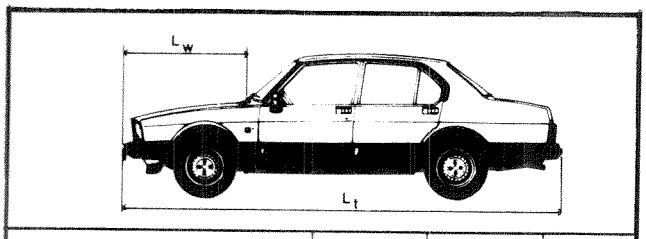

Make	L_w	L_t	L_w/L_t
ALFA ROMEO "ALFETTA"	1344	4800	0,28
AUDI "100"	1316	4373	0,30
FORD "SIERRA"	1307	4394	0,298
LANCIA "THEMA"	1235	4590	0,27
PORSCHE "944"	1460	4447	0,328
SAAB "900"	1380	4620	0,298
VOLVO "760	1390	4785	0,29

Figure 17. Comparison of various Lw/Lt values for some compact/large cars

Structural Considerations

As already mentioned, this series of tests was intended mainly to review and confirm the optimal design characteristics for the front external configurations of the vehicles in view of improving the eventual pedestrian/colliding vehicle contact.

The behavior of the 35kg/m3 polyurethane foam shapes as structural elements simulating the real structures has proved satisfactory, easily repeatable, and homogenous. This can be reconfirmed by the final calibration tests carried out by the test alone at 30km/h, which presented HIC values ranging from 650 to 800 for the various foam shapes points (see Photo 4).

As far as the optimal characteristics of the structures are concerned, the fact that a type of structure similar to of the engine bonnet has been adopted for all the

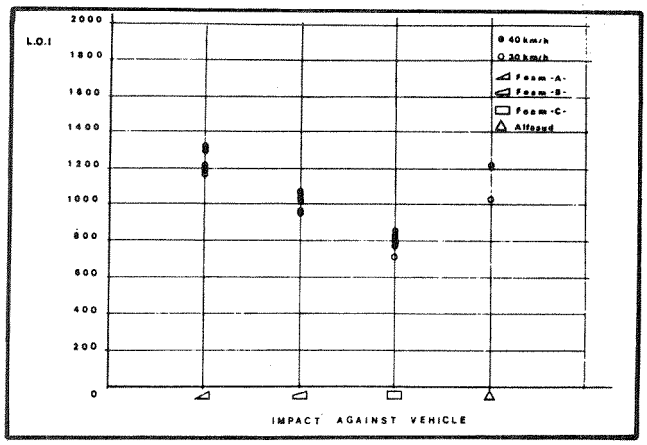

configurations demonstrated some limits linked with the greater speed.

In particular, the data obtained during the 40km/h tests (see the table in Figure 7) demonstrate that, even in the absence of contact of the head with the windscreen zone, no guarantees exist sufficient for obtaining acceptable head injury values.

Conclusion

We have carried out a simplified means of experimental research to obtain the greatest amount of information and data to forward to those in charge of defining and designing our vehicles, encouraging them to install therein all that is presently available to reduce injuries suffered by pedestrians involved in collisions with vehicles.

The first series of experimental tests has been aimed mainly at an inquiry into the most suitable configuration for new vehicles. The performance and fundamental characteristics we have sought in the equipment have been the capacity to rapidly assume the desired configuration with certain structural simulations, all at costs and times that justify its alternative use in place of real structures. The series of experimental tests carried out, in addition to demonstrating the good homogeneity and structural constancy qualities of the polyurethane foam shapes, has supplied a series of indications consistently in line with many conclusions offered by studies already carried out in this specific research area.

In fact, from the point of view of the optimal configuration to be assigned to the front parts of a vehicle, carrying out a global evaluation of the injuries suffered by the pedestrian involved, it would seem that slight preference should be given, in substance, to the lowered type (A) contours or the intermediate (B) type contours, bearing in mind, however, the considerable bonnet length necessary for reducing the possibility of the head hitting the windscreen zone.

Among the ulterior research themes set at the beginning of this experimental cycle, there was also the eventual

individuation of a possible correlation between vehicle architecture and pedestrian injury levels during the final impact-with-the-ground phase. The dispersion of the values in the traced data, consistent with other bibliographical data available, seems to make this final collision phase rather aleatory. The only consistent aspect traceable is a certain general tendency to increase injuries to all parts of the body when the speed increases.

As far as suggestions connected with the choice of suitable structures are concerned, it should be pointed out that the generalized adoption of structures, however good and feasible they may be, such as those regarding the engine bonnet, does not guarantee adequate protection at speeds of around 40km/h. Future use of a simplified piece of equipment, such as the deformable barrier, will undoubtedly be of great help in rapid definition of the structural characteristics to be achieved and suitable for future vehicles.

The really important problem will clearly be that of achieving these new structurally optimized solutions for reducing injury to pedestrians, bearing in mind the surrounding design and production limits existing.

Research Concentrated on an Experimental Method for Protecting Pedestrians

Kouzo Maeda,
Hisaaki Isobe,
Yuuichi Sakuma, and
Yuuki Kurihara
Nissan Motor Co., Ltd.

Abstract

This paper describes a test procedure in which a dummy and a sled impact tester are used to simulate vehicle-pedestrian accidents for the purpose of investigating pedestrian protection. In the series of tests conducted, the bumper height, hood-edge height, bumper lead, front-end compliance of the vehicle, impact velocity, and other factors were varied in an effort to clarify to what extent modifications to the vehicle front end would contribute to enhanced pedestrian protection.

Preliminary test findings obtained with this test procedure are also presented regarding the effects of the front-end shape of the vehicle and the stance of the dummy at the moment of impact.

Introduction

There has been a substantial increase in motor vehicle ownership in Japan since 1970. Yet the number of pedestrians killed in traffic accidents dropped significantly during the second half of the 1970's after having peaked in 1970 (Figure 1). In recent years, the number of fatalities has remained at virtually the same level, and the current figure is actually less than half the 1970 level.

A comparison of pedestrian fatalities by age group shows that children under 6 and elderly people over 70 make up a large proportion of the total number. Recently, the number of fatalities among children under 6 has dropped greatly(1,2).

Various factors can be cited for this rapid decrease in pedestrian fatalities in Japan, including an improved traffic environment, more extensive traffic safety education, and protective modifications[1] made to motor vehicles. In particular, improvements made to the traffic environment and to traffic safety education programs are presumed to have contributed greatly to the reduction in pedestrian fatalities.

To investigate to what extent modifications made to the shape and compliance of the vehicle front end would contribute to pedestrian protection, a study was conducted to find a suitable test procedure for simulating vehicle-pedestrian accidents. This paper presents the results of

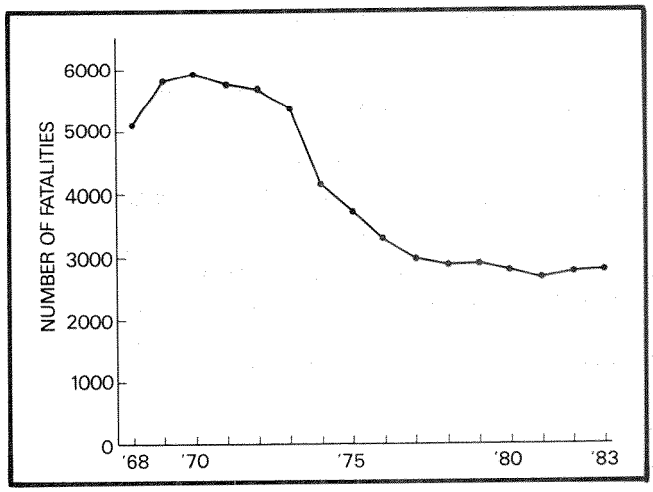

Figure 1. Change in number of pedestrian fatalities

1 An example of a vehicle modification is the addition of side bars to large trucks prevent people from being dragged under the wheels when the vehicle makes a turn.

that study, together with preliminary test findings obtained with the test procedure that was devised.

Test Procedure Study

The following objectives were set for the test procedure simulating vehicle-pedestrian accidents using a dummy and a sled impact tester(3,4):

- It must be possible to evaluate the primary impact characteristics at the moment of impact between the dummy's legs and the vehicle front end as well as the secondary impact characteristics at the moment of impact between the dummy's head and the top of the hood. Tertiary impact characteristics at the moment the dummy strikes the ground are excluded from the analysis.
- It must be possible to vary such factors as the shape and compliance of the vehicle front end and impact velocity to examine their respective influence on pedestrian protection.

Test Buck Simulating Vehicle Front End and Dummies Used

Test Buck Simulating Vehicle Front End

A test buck used to simulate the shape of a vehicle front end was installed on a sled as illustrated in Figure 2. This test buck was utilized in place of actual vehicles in investigating the influence of the shape and compliance of the front end. The buck was designed so that the

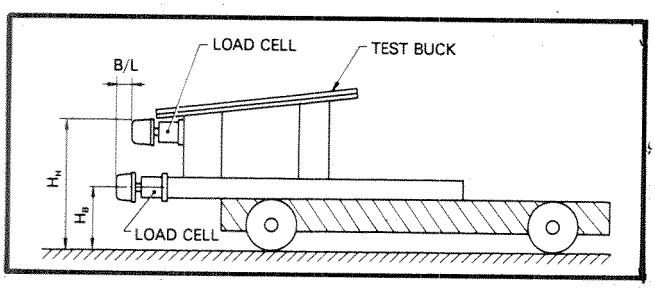

Figure 2. Test buck configuration simulating shape of vehicle front end

bumper height (H_B), hood-edge height (H_H), and bumper lead (B/L) as well as the compliance of the bumper and hood edge could be varied as desired. Load cells were installed where the bumper and hood edge were attached to measure the force input to the bumper and hood edge at the moment of impact between the dummy's legs and the vehicle front end.

Dummies Used

A Hybrid II 50P dummy made by the Alderson Co. was used as the adult dummy in a frontal stance impact, and a Hybrid II 50P dummy manufactured by the Humanoid Co. was used in a lateral stance impact. The rubber neck attachment of the Alderson-made dummy was replaced so the dummy's head would be in a perpendicular condition. A Humanoid-made Hybrid II 6C dummy representing a 6-year-old child was used as the child dummy.

Preliminary Study

Items Measured

Impact Forces of Bumper and Hood Edge—The load cells illustrated in Figure 2 were adopted to measure the forces input to the bumper and hood edge at the moment of impact between the dummy and the vehicle front end. These measurements were used to determine the impact forces sustained by the dummy's legs and pelvis.

Head Impact Velocity—A high-speed camera was employed to photograph the behavior of the dummy's head. The head impact velocity at the moment of impact between the dummy's head and the top of the hood was found by analyzing the photographs. As illustrated in Figure 3, the head impact velocity was divided into the horizontal component V_Y and the vertical component V_H and the maximum vertical velocity V_{HM} and vertical velocity V_{HO} were found.

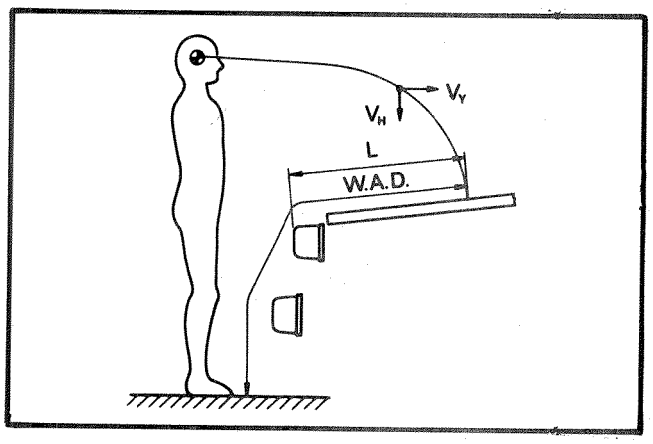

Figure 3. Head impact point

Head Impact Point—The point of impact between the dummy's head and the top of the hood was also found by analyzing the photographs taken with the high-speed camera. The point where the dummy's head struck the hood was indicated by using the Wrap Around Distance (W.A.D.) and the distance from the edge of the hood.

Acceleration (g) Waveforms—

- Head g Waveform—In the case of the Hybrid II dummy, acceleration is generated on the dummy's head both at the moment of impact between the

bumper and the knees and at the time of impact between the hood edge and the thighs. The time of impact between the dummy's legs and the vehicle front end differs greatly from the time of impact between the dummy's head and the top of the hood. Consequently, the acceleration on the dummy's head can be accurately measured when the dummy's head strikes the hood.

However, since the stiffness of the test buck used in this study was higher than that of an actual hood, the acceleration generated on the dummy's head was larger than what would be true for a production vehicle. Therefore, the head g waveform was treated simply as reference data.

- Pelvis g Waveform—The impact between the bumper and the knees generates acceleration on the dummy's pelvis, similar to the situation for the dummy's head. When there is a large bumper lead of 300mm, the impact between the hood edge and the thighs produces a g waveform with two peaks (Figure 4). However, when the bumper lead is 100mm, the two peaks overlap and the acceleration generated by the impact between the hood edge and the thighs cannot be measured accurately.

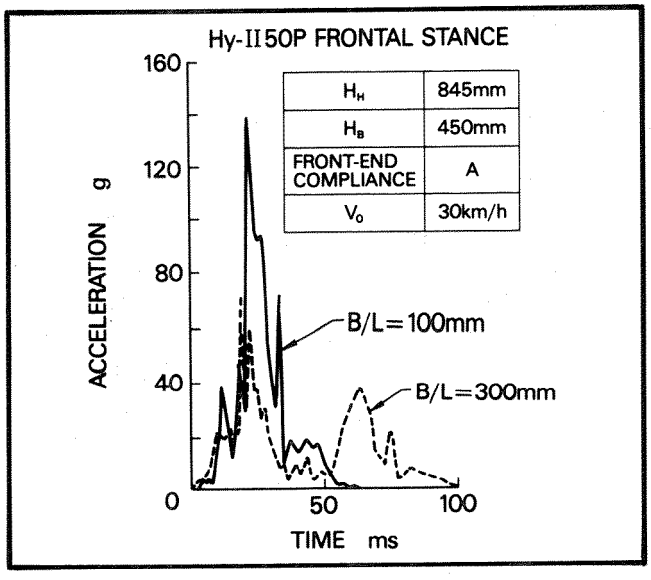

Note: Front-end compliance A represents a semi-hard urethane foam (density of 0.1 g/cm^3) to which a urethane fascia is attached.

Figure 4. Resultant pelvis acceleration

- Knee g Waveform—The waveform for the acceleration generated on the dummy's knees by the impact between the bumper and the knees shows a certain correlation with the impact force of the bumper. Thus it can be regarded as one index for comparing the severity of an impact.

In this study, the primary impact characteristics were evaluated on the basis of the impact forces of the bumper and hard edge and the secondary impact characteristics on the basis of the head impact velocity and head impact point.

Dummy Release Timing

To improve test accuracy and repeatability, the dummy's posture must be uniform at the moment of impact. Changes in the dummy's posture following release were investigated by analyzing photographs taken with a high-speed camera. The results indicated that the dummy retained its posture for about 200ms following release and that it was necessary to keep the force suspending the dummy constant. Thus, in each test, dummy release timing was set so impact would occur within 200ms following release of the dummy. Further, a load cell was employed to keep the force suspending the dummy constant.

Measures To Prevent Dummy Knee Damage

Results of experimental tests indicated that the knees and shoulders of the current Hybrid II dummy suffered damage even at an impact velocity of 20km/h. To prevent such damage, the adult dummy was made with steel clavicles, and the femur link rod was designed to allow shape changes (Figure 5). The shape of the link rod yielded before the kneecap was damaged, and the link rods were replaced after every test.

The same type of flexible femur link rod was adopted for the child dummy, and, in addition, the kneecap was modified.

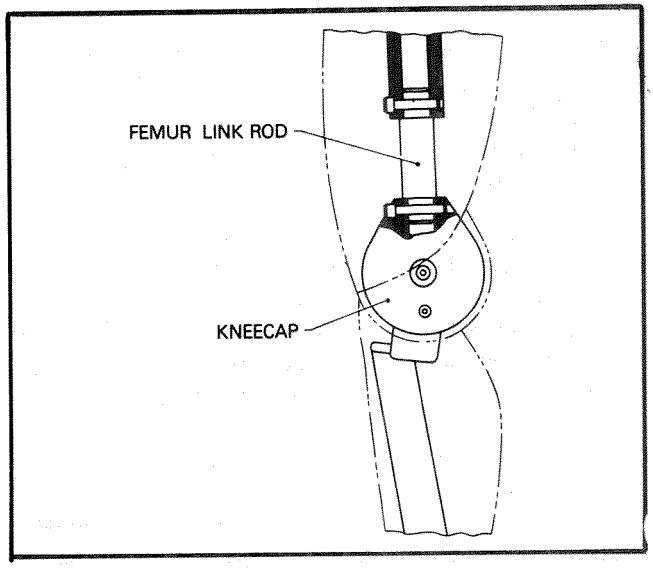

Figure 5. Leg profile of Hybrid II pedestrian dummy

Effects of Ground Friction Coefficient

The effects of the ground friction coefficient on impact characteristics at the moments of impact between the dummy's legs and the vehicle front end and between the dummy's head and the top of the hood were investigated to determine at what value the ground friction coefficient should be set during the tests.

Tests were conducted under the conditions given in Figure 6, and the results obtained are shown in Figures 7 and 8. Because the number of tests was limited and there was considerable variability among the data, no definite conclusions can be drawn. However, it would appear there is no clear-cut difference in bumper impact force, hood-edge impact force, and head impact point (W.A.D.) for various ground friction coefficients.

As far as the head impact velocity is concerned, there was only one test result. Considering the possibility of variability in the data, nothing definite can be concluded.

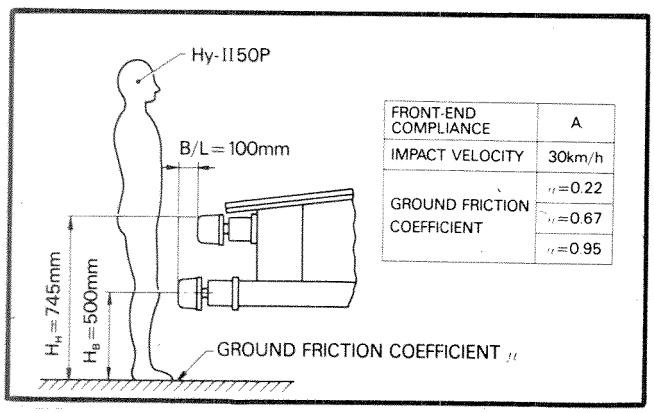

Figure 6. Test conditions

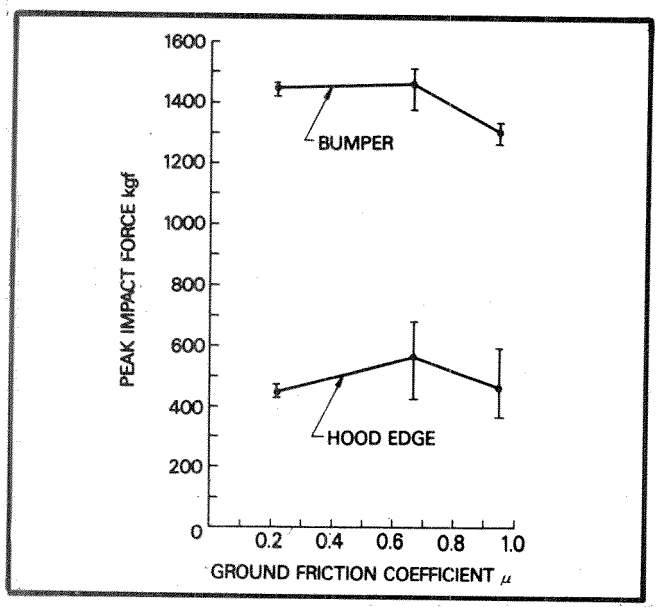

Figure 7. The effects of ground friction coefficient on peak impact forces of bumper and hood edge

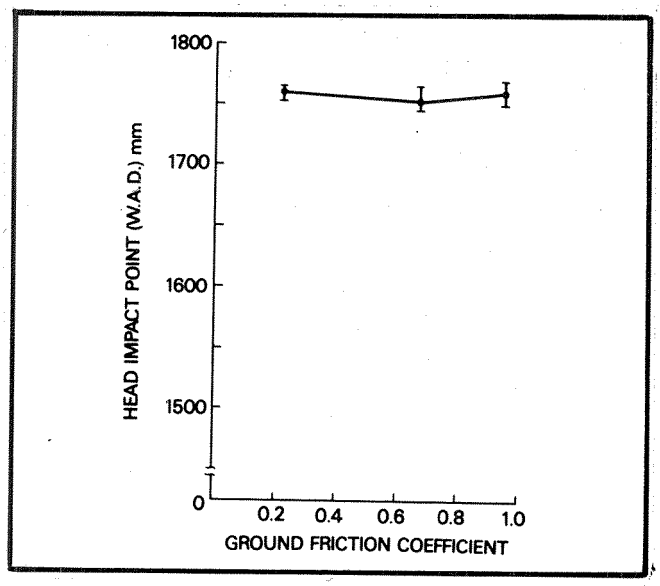

Figure 8. The effects of ground friction coefficient on head impact point (W.A.D.)

Based on the foregoing results, it was decided to conduct the tests with the ground friction coefficient set at a constant μ = 0.67, which is close to the actual value. Additional studies need to determine whether the effects of the ground friction coefficient can be accurately grasped with just the evaluation index used in this work.

Effects of Dummy's Femur Joint Torque

Tests were conducted under the conditions shown in Table 1 to investigate the effects of the dummy's femur joint torque on the impact characteristics and dummy's behavior at the moment of impact between the dummy's legs and the vehicle front end. In these tests, the dummy's femur joint torque was varied between 1 and 2g.

The test results are presented in Figures 9, 10, and 11. There is a great deal of variability in the data, and no definite conclusions can be drawn. However, it would appear there is no appreciable difference even when the femur joint torque is increased to 2g.

Table 1. Test conditions

Hood Edge Height (H_H)	780mm
Bumper Height (H_B)	450mm
Bumper Lead (B/L)	100mm
Front-End Compliance	A
Impact Velocity (V_o)	30km/h
Dummy	Hy-II 50P
Dummy Stance	Frontal

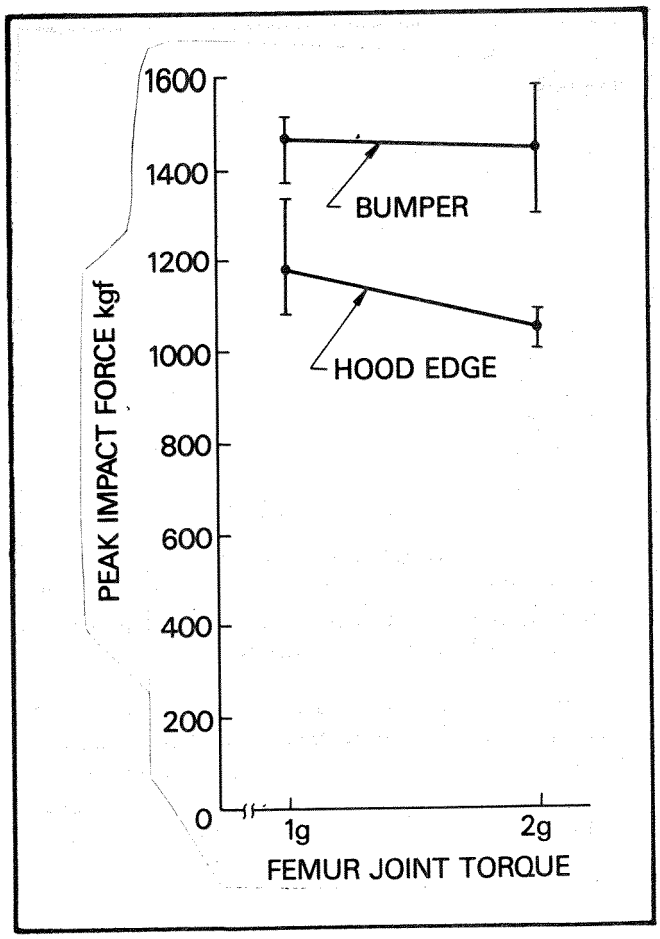

Figure 9. The relationship between dummy femur joint torque and peak impact forces of bumper and hood edge

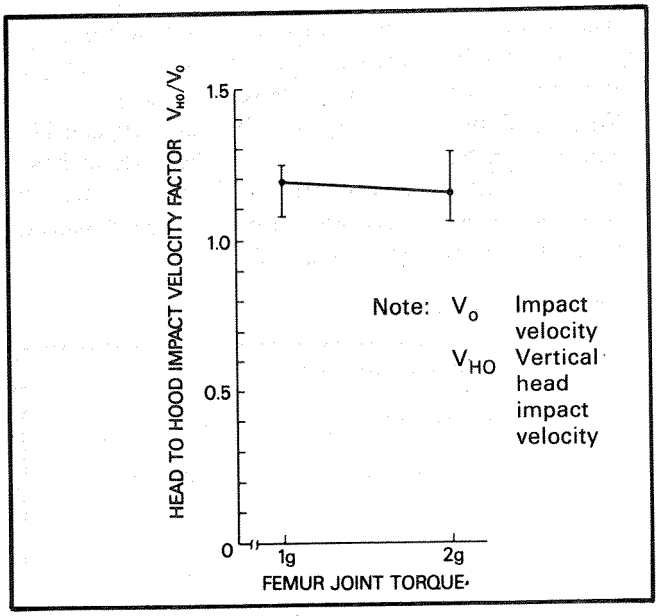

Figure 10. The relationship between dummy femur joint torque and head-to-hood impact velocity

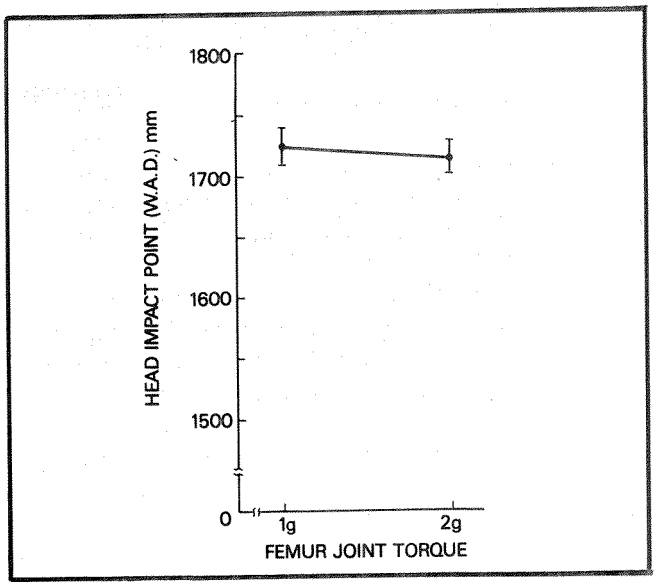

Figure 11. The relationship between dummy femur joint torque and head impact point

Based on these results, it was decided to set the femur joint torque at 1.5g, which would make it easier to keep the dummy's posture uniform during testing.

Summary of the Test Procedure

A diagram illustrating the specific configuration of the dummy and test apparatus used to simulate vehicle-pedestrian accidents is shown in Figure 12. The various elements are: (A) dummy, (B) dummy release mechanism, (C) load cell for measuring the force suspending the dummy, (D) sled, (E) test buck simulating the front end of a vehicle, (F) load cell for measuring the force input to the hood edge, and (G) load cell for measuring the force input to the bumper.

The prominent features of this test apparatus are as follows:

- The factors noted below can be varied in a simulated impact between a pedestrian and the vehicle front end.

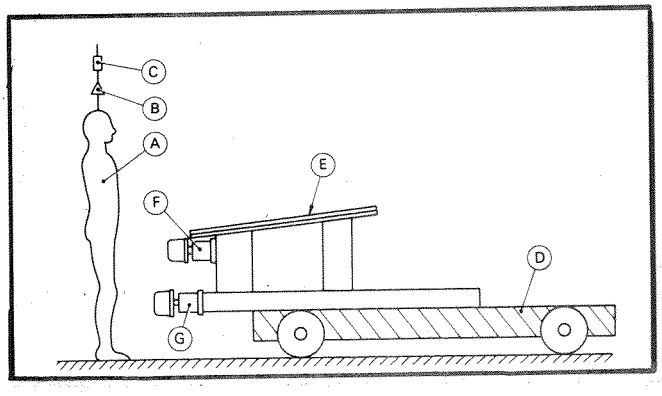

Figure 12. Test apparatus for simulating vehicle-pedestrian accidents

— Impact velocity between pedestrian and vehicle front end
— Front-end shape (bumper height, hood-edge height, bumper lead, hood slant)
— Front-end compliance (compliance of bumper and of hood edge)
— Dummy stance at time of impact (lateral stance, frontal stance, and oblique stance impacts)
— Dummy size (adult or child dummy)

- The dummy knee has been modified to prevent damage to the kneecap.

The following items were measured during the tests:

- Measurements were made of the bumper impact force and the hood-edge impact force to determine the impact forces applied to the legs and pelvis at the moment of primary impact.
- The dummy's behavior at the time of secondary impact was photographed using a high-speed camera. The head impact velocity and impact point were then found by analyzing the photographs.
- Measurements were made of the acceleration generated on the dummy's head, thorax, pelvis, and knees.

In this series of tests, the primary impact characteristics were evaluated on the basis of the bumper impact force and the hood-edge impact force and the secondary impact characteristics on the basis of the head impact velocity and impact point.

The following preset values were employed:

- The dummy's femur joint torque is set at a constant 1.5g.
- The ground friction coefficient is set at a constant 0.67.
- The apparatus can be set so impact occurs at all impact velocities within 200ms following dummy release.

Test Results

Using the test procedure described in the previous section, a fundamental study was done on the following items:

- Effects of the front-end shape of the vehicle
- Effects of the dummy's stance at the moment of impact
- Effective mass of the legs in tests using dummies

The Effects of the Front-end Shape of the Vehicle

Four types of front-end shapes were assumed (Table 2) to investigate what effects the shape of the vehicle front end has on pedestrian protection with respect to a pedestrian's legs and head. Preliminary tests were conducted with an adult dummy in a frontal stance and at an impact velocity of 30km/h.

Table 2. Front end specifications

Item / Type	H_B	H_H	B/L	Front End Compliance
A	350mm	695mm	100mm	A
B	↑	795mm	↑	↑
C	450mm	695mm	↑	↑
D	↑	795mm	↑	↑

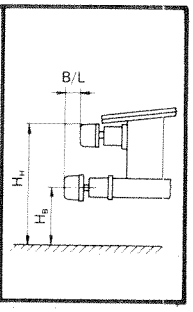

Bumper Impact Force

The relationship between the shape of the front end and the bumper impact force is illustrated in Figure 13. The peak bumper impact force tends to be larger at a bumper height of 350mm than at a height of 450mm. Moreover, the peak bumper impact force does not appear to change significantly when the hood-edge height is varied from 695 to 795mm, although a definite conclusion cannot be drawn on the basis of these tests alone.

In other papers, it has been reported that a lower bumper height tends to mitigate injury to a pedestrian's lower limbs, a finding contrary to the results obtained in these tests. This suggests there are certain aspects about lower limb protection that cannot be evaluated with just

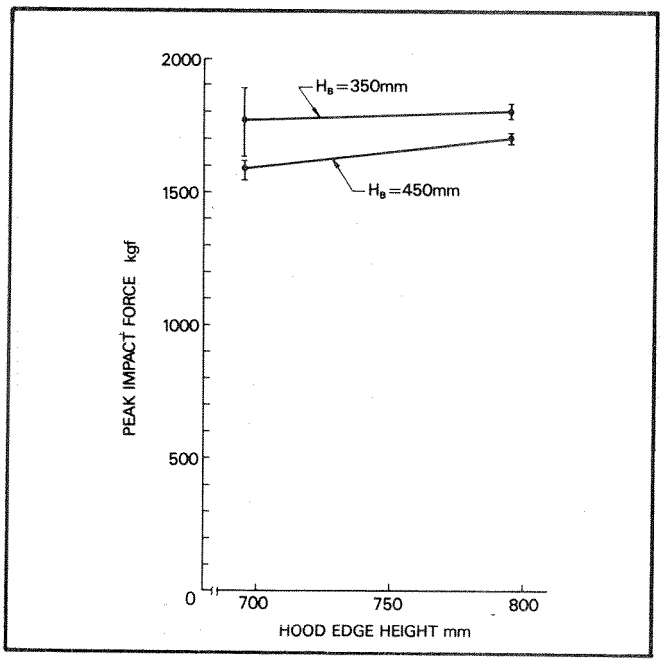

Figure 13. The relationship between front-end shape and bumper impact force

the criteria of the peak bumper impact force and the acceleration generated on the dummy's legs(5,6,7).

Hood-edge Impact Force

The relationship between the shape of the front end and the impact force of the hood edge is illustrated in Figure 14. In this series of tests, the peak impact force of the hood edge was smaller than the peak bumper impact force. The peak impact force of the hood edge tends to increase in proportion to increasing hood-edge height and is higher with a lower bumper height. On the whole, the peak impact force of the hood edge seems to be more strongly influenced by the shape of the front end than the peak bumper impact force.

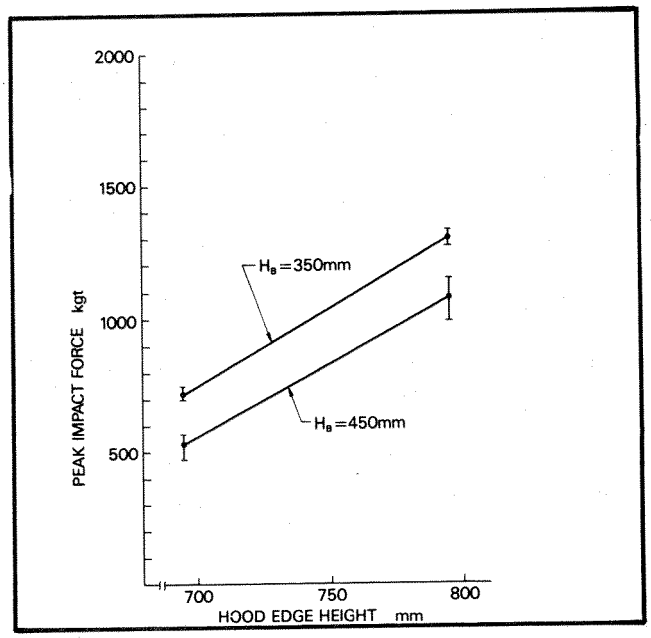

Figure 14. The relationship between front-end shape and impact force of hood edge

Head Impact Velocity

The relationship between the shape of the front end and the head impact velocity is illustrated in Figure 15. The head impact velocity shows different tendencies depending on the bumper height. With a bumper height of 350mm, the head impact velocity tends to increase as the hood-edge height increases.

With a bumper height of 450mm, the head impact velocity tends to decrease slightly as the hood-edge height increases. These results suggest that the head impact velocity changes in a complex fashion depending on the shape of the front end. Thus more detailed studies are needed to elucidate the factors involved.

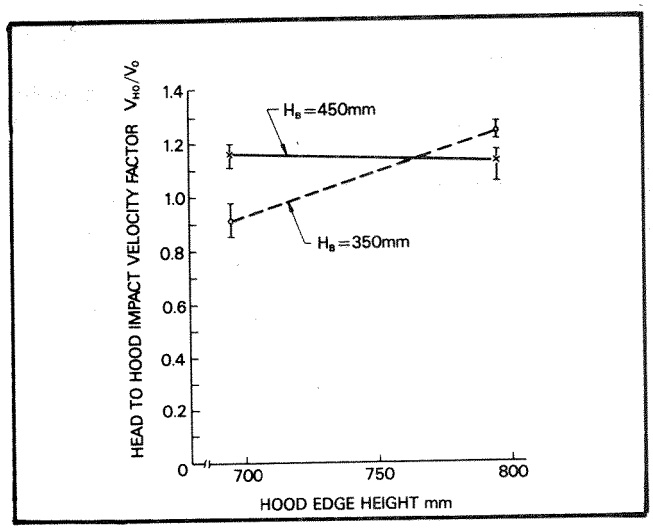

Figure 15. The relationship between front-end shape and head impact velocity

Head Impact Point

The relationship between the shape of the front end and the head impact point is shown in Figures 16a and 16b. In Figure 16a, the head impact point is expressed in terms of W.A.D. and in Figure 16b in terms of the distance (L) from the front of the hood edge. Both W.A.D. and L tend to become smaller as the height of the hood edge increases. Although the change in W.A.D. is less than 50mm, L shows a change of more than 100mm (Figure 16b), which suggests it is strongly influenced by the hood-edge height. The same tendencies are also observed for various bumper heights.

Results obtained in these tests show good correlation with the findings reported by other researchers with

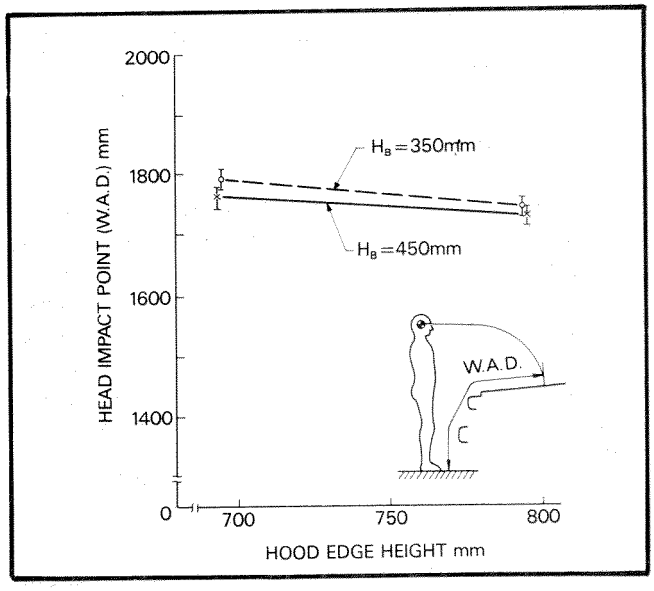

Figure 16a. The relationship between front-end shape and head impact point (W.A.D.)

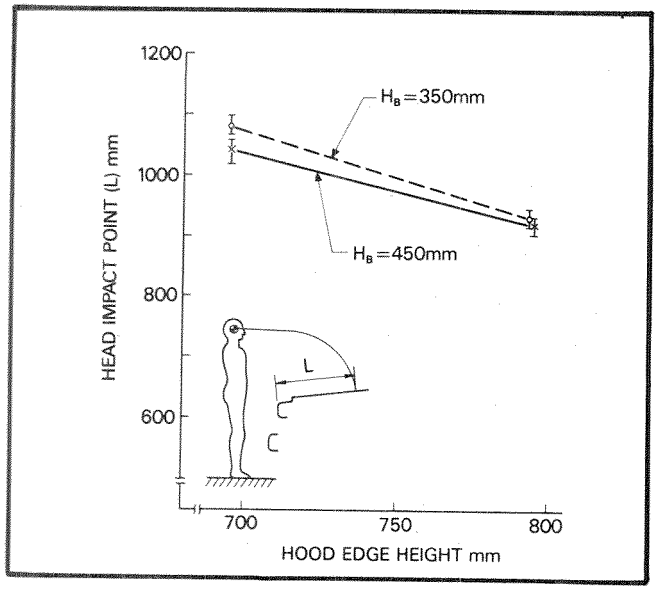

Figure 16b. The relationship between front-end shape and head impact point (L)

respect to tendencies for the peak impact force of the hood edge to increase and the head impact point to shift forward as the hood-edge height increases(8,9,10). As was noted, the head impact velocity shows opposite tendencies depending on the bumper height. Few detailed analyses have been reported regarding this point, and it is difficult to affirm whether this result is valid or not. However, since this factor has an important bearing on pedestrian protection, more detailed investigations should be done in the future.

It has been seen that the hood-edge impact force, head impact velocity, and head impact point undergo complex changes by simply varying the front-end shape as was done in these tests. Therefore, comprehensive investigations should be undertaken to clarify what effects the front-end shape and compliance, impact velocity, and other factors have on pedestrian protection.

Dummy Stance at the Moment of Impact

Preliminary tests were conducted using an adult dummy, an impact velocity of 30km/h, and the front-end specifications listed in Table 3 to investigate possible differences between frontal and lateral stance impacts. Particular attention was focused on the variation that occurred in the impact forces of the bumper and hood edge at the moment of primary impact and in the head impact velocity and impact point at the time of secondary impact.

Impact Forces of Bumper and Hood Edge

The relationship between dummy stance and the impact forces of the bumper and hood edge is shown in Figure 17.

Table 3. Front end specifications

Hood Edge Height	(H_H)	845mm
Bumper Height	(H_B)	450mm
Bumper Lead	(B/L)	100mm
Front-End Compliance		A

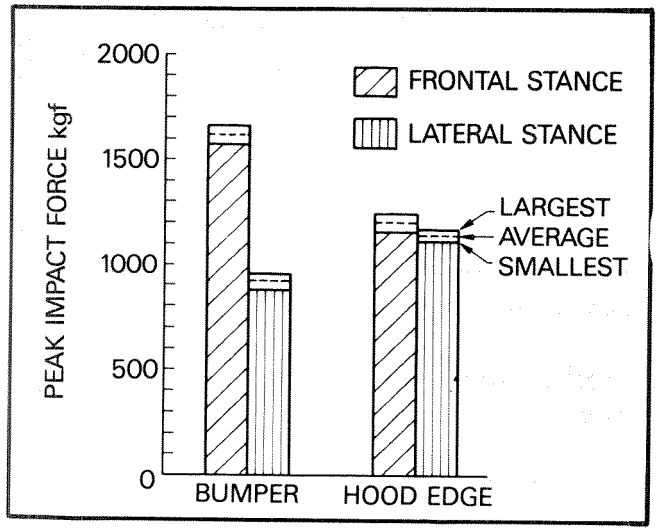

Figure 17. The relationship between dummy stance at moment of impact and impact forces of bumper and hood edge

The bumper impact force is smaller in a lateral stance impact than in a frontal stance impact. The impact force of the hood edge is virtually the same in both types of impacts. One reason for the difference in bumper impact force between the frontal stance impact and the lateral stance impact can be found in the difference in bumper impact force waveforms. As illustrated in Figure 18, the impact force waveform of a frontal stance impact has one peak, whereas that of a lateral stance impact has two peaks.

Head Impact Velocity and Impact Point

The dummy's head inevitably strikes the top of the hood in a frontal stance impact. However, in a lateral stance impact, the dummy's head is not likely to strike the top of the hood because its shoulder or arm strikes the hood first. For this reason, a comparison of the head impact velocity and impact point at the moment of secondary impact could not be made between the frontal stance and lateral stance impacts.

Dummies used to simulate pedestrians should be improved to incorporate the features of side impact dummies when used to test lateral impact.

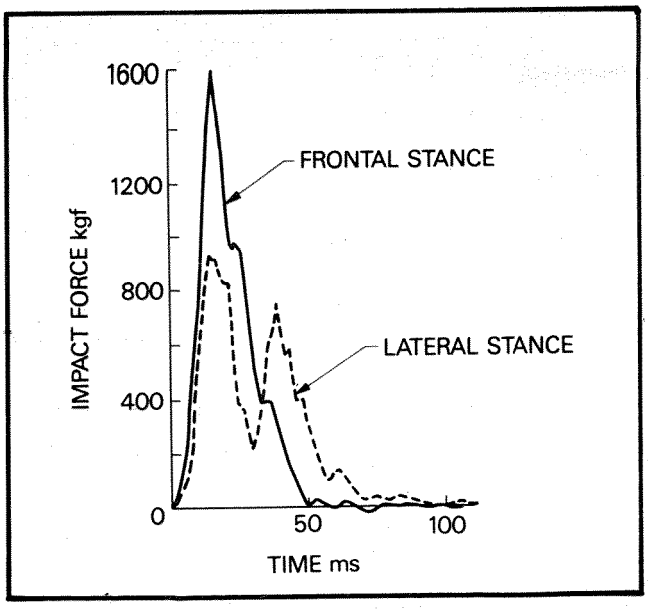

Figure 18. Bumper impact force as a function of time

Effective Mass of the Legs in Tests Using Dummies

In tests in which adult dummies were used, the effective mass applied on the bumper and that applied on the hood edge at the moment of impact were estimated.

Effective Mass Applied on the Bumpers

The effective mass applied on the bumper at the moment of impact was estimated at 6.7kgf from the bumper impact force obtained in a lateral stance impact using the front-end specifications listed in Table 4. This result is approximately double the figure of 3.2kgf given in (3) for cadavers. However, a precise comparison cannot be made because the test conditions were different.

Table 4. Front end specifications

Hood Edge Height	(H_H)	845mm
Bumper Height	(H_B)	450mm
Bumper Lead	(B/L)	100mm
Front-End Compliance		A

Effective Mass Applied on the Hood Edge

The effective mass applied on the hood edge was estimated from the impact force of the hood edge in the same manner as for the effective mass applied on the bumper. The results are given in Table 5.

The effective mass applied on the hood edge is little affected by the dummy stance, but it changes greatly according to the bumper height and the hood-edge height. The values for the effective mass applied on the hood edge in these tests in which dummies were used compare favorably with the findings given in (11) for the effective mass applied on the hood edge in tests using cadavers.

In summary, the effective mass applied on the hood edge in these tests using dummies was close to that of the cadaver tests, but the effective mass applied on the bumper was approximately twice the value reported for the latter. It is assumed that the reason for this difference is that the bumper impact force in the dummy tests was larger than the bumper impact force in the cadaver tests.

Conclusion

This study on a test procedure for investigating pedestrian protection by using dummies has brought out the following results:

- The ground friction coefficient did not have a significant effect on the bumper impact force, hood-edge impact force, or the head impact point within a friction coefficient range of 0.22 to 0.95.
- The dummy's femur joint torque did not have a significant effect on the bumper impact force, hood-edge impact force, head impact velocity, or head impact point within a torque range of 1 to 2g.
- To assure a uniform dummy posture at the moment of impact, the force suspending the dummy must be constant and the impact must take place within 200ms following dummy release.

Table 5. Effective mass applied on hood edge

Dummy Stance / Item	Frontal Stance		Lateral Stance	
Hood Edge Height ($H_H$mm)	745	845	745	845
Bumper Height ($H_B$mm)	450	450	500	450
Bumper Lead (B/L mm)	100	100	100	100
Effective Mass (kgf)	5.8	10.4	5.1	13.8

The results of this study suggest that the following points are the main issues remaining to be resolved with respect to the test procedure for investigating pedestrian protection by utilizing dummies.

- A dummy should be developed that is designed exclusively for use in pedestrian tests. Such a dummy would help to overcome the following problems with the Hybrid II dummy:
  - In lateral stance tests, the head of the Hybrid II dummy is not likely to strike the top of the hood.
  - The impact between the bumper and the dummy's knees also generates acceleration on the dummy's pelvis, which overlaps with the acceleration generated by the impact between the hood edge and the dummy's thighs. As a result, accurate measurements cannot always be made of just the acceleration generated by the impact between the hood edge and the dummy's thighs.
- A new evaluation method should be studied and devised because the characteristics of the impact between the pedestrian's lower limbs and the bumper cannot be fully evaluated with only the criteria of the bumper impact force and the acceleration generated on the dummy's knees.

The primary and secondary impact characteristics tend to change in complex ways by simply varying the shape of the front end. This result was brought out in preliminary tests that were conducted with the test procedure for examining pedestrian protection and in which various front-end shapes were used. However, since the number and types of tests were limited, this conclusion is not regarded as definitive. In future work, therefore, a comprehensive analysis should be done to determine what effects the front-end shape and compliance, impact velocity, and other factors have on pedestrian leg and head protection.

References

1. *Traffic Statistics for 1983,* compiled by the Japan National Traffic Safety Society.
2. *Legal System of Japan on Motor Vehicles,* published by the Road Transport Bureau, Ministry of Transport, October 1983.
3. Eppinger, Rolf H., and Howard B. Pritz, "Development of a simplified vehicle performance requirement for pedestrian injury mitigation," Proceedings Seventh International Technical Conference on Experimental Safety Vehicles, Paris, France, June 1979.
4. Harris, J., and C.P. Radely, "Safer cars for pedestrians," Proceedings Seventh International Technical Conference on Experimental Safety Vehicles, Paris, France, June 1979.
5. Bunketorp, O., B. Aldman, L. Thorngren, and B. Romanus, "Clinical and experimental studies on leg injuries in car-pedestrian accidents," Proceedings Ninth International Technical Conference on Experimental Safety Vehicles, Kyoto, Japan, November 1982.
6. Daniel, Samuel, Jr., Rolf H. Eppinger, and Daniel Cohen, "Considerations in the development of a pedestrian safety standard," Proceedings Seventh International Technical Conference on Experimental Safety Vehicles, Paris, France, June 1979.
7. Pritz, H.B., C.R. Hassler, J.T. Herridge, and E.B. Weis, Jr., "Experimental study of pedestrian injury minimization through vehicle design," Proceedings 19th Stapp Car Crash Conference, SAE Paper 751166, San Diego, November 1975.
8. Niederer, Peter F., and Max R. Schlumpf, "Influence of vehicle front geometry on impacted pedestrian kinematics," Proceedings 28th Stapp Car Crash Conference, SAE Paper 841663, Chicago, November 1984.
9. Cavallero, C., D. Cesari, M. Ramet, P. Billault, J. Farisse, B. Seriat-Gautier, and J. Bonnoit, "Improvement of pedestrian safety: influence of shape of passenger car-front structures upon pedestrian kinematics and injuries: evaluation based on 50 cadaver tests," SAE Paper 830624.
10. Daniel, Samuel, Jr., "The role of the vehicle front end in pedestrian impact protection," SAE Paper 820246.
11. Pritz, H.B., and J.M. Pereira, "Pedestrian hip impact simulator development and hood edge location consideration on injury severity," SAE Paper 831627.

The Influence of Car Design on Pedestrian Protection

J. Harris
Transport and Road Research Laboratory

N.D. Grew
Austin Rover Group Ltd. B.L. Cars PLC

Abstract

In pedestrian accidents, the many differences that occur in the impact location and size of pedestrians and design of vehicles produce wide variations in the severity and location of the resulting injuries.

To obtain a better understanding of the mechanisms influencing the variability of these injuries, B.L. Cars PLC and the Transport and Road Research Laboratory have conducted a collaborative project using highly developed computer simulation techniques(1), matched to experimental test results, to study the relationship of vehicle shape and stiffness with the resulting forces and accelerations acting on pedestrian dummies.

Changes to the spoiler, bumper, and bonnet leading edge for simulated impacts to adult pedestrians at a speed of 40km/h show the following results:

1. A low front profile concentrates most of its input energy well below the centre of gravity of an adult, inducing high angular rotation onto the bonnet resulting in high head impact velocities.
2. Increasing the height of the bonnet leading edge increases the energy it absorbs resulting in higher accelerations to the regions of the adult and child that it contacts, but this is combined with reduced head impact velocities.
3. In a 40km/h impact, the energy absorbed by the bumper or bumper plus spoiler is generally between 1,000 and 1,200J.

   A bumper mounted at 450mm above the causes high bending moments and shear forces adult knees. If the bumper stiffness is above 3kN, child pelvic accelerations may also be high.

   Lowering the bumper reduces the risk to the adult knee and child pelvis. Introducing a suitable spoiler (air dam) reduces the risk of adult knee and lower leg injury and gives the most satisfactory conditions, providing the bumper component of the bumper/spoiler stiffness is approximately 3kN.
4. The input energy of the bonnet edge and grille varies widely with respect to its location, increasing as the bumper lead decreases or as the bonnet leading edge height increases.

   For adult impact at 40km/h, energy input values for the bonnet front ranged from 150J for a low bonnet with a bumper lead of 150mm, increasing to 1,700J for an 850mm-high vertical front profile and reducing to 600J for a high profile and 350mm lead. For some car profiles, a stiffness of 7kN, typical of some current small cars, produces high child pelvic accelerations and high adult femur bending moments. Reducing the stiffness to 5kN gives acceptable child pelvic accelerations and reduces the magnitude of leg bending moment by about 20 percent.
5. Within the range of shapes studied, the adult head impact velocity may be reduced by up to 40 percent of the worst case by increasing the bonnet height from 600 to 850mm. It may also be reduced by 30 percent by reducing the bumper lead from 350mm to zero, but only for a medium-height bonnet. Extreme values of head impact velocity range from 40 percent above car impact velocity to 25 percent below.

   For the child, head impact velocities are more consistently just below car impact speed, reducing by 60 percent for a high vertical front profile.
6. The most significant changes noted in the simulations of different dummy sizes are that head impact velocity increases in magnitude and the location of head impact point moves further rearward with increasing dummy height.

   The severity of pelvic acceleration is increased as the pedestrian's height is reduced because the bonnet leading edge strikes closer to the pelvis.
7. The relationships determined in these studies have been utilised to give guidelines for modifying a small saloon car to give improved pedestrian protection(2).

Introduction

In pedestrian accidents, the many differences that occur in the impact location and design of vehicles and the size of pedestrians produce wide variations in the severity and location of the resulting injuries.

To obtain a better understanding of the mechanisms influencing the variability of these injuries, B.L. Cars PLC and the Transport and Road Research Laboratory have conducted a collaborative project using computer simulation techniques matched to full-scale dummy impact tests to study the relationship of vehicle shape and stiffness with the resulting forces and accelerations acting on pedestrian dummies.

This paper summarizes the results of this work and gives examples of simulations that represent changes to the spoiler (air dam) bumper and bonnet for adult and 6-year-old child pedestrians at impact speeds of 40km/h.

Only the impact between the pedestrian and the vehicle is considered because this is the most predictable period and is claimed to be more injury-producing(3) than the final stage when the pedestrian falls to the ground. In the simulations, the model of the adult leg is based on modified dummy legs having lateral compliance at the knee and increased adduction at the hip joint.

Computer Simulation

The computer model used was developed by B.L. Cars from the Calspan Corporation 3D Crash Victims Simulation Program version (CVS 111 version 20).

This development(4) has been extensively validated and includes improved vehicle-to-dummy contact models.

Forces and torques may be output for any joint in the geometric reference system of a segment as seen at any point within that segment. The data are also output in the same reference system as the vehicle, which with vehicle panel contact data allows an investigation of segment bending moments.

Dummy Model

The simulation model of the pedestrian is based on a dummy of Ogle design representing a 50th percentile adult male, 1.76m tall, and a 6-year-old child, 1.19m tall.

The simulation of the child dummy depicted standard, current joint movements and torques. The adult embodied modifications that were fitted to the Ogle dummy at the hip and knee to give a more realistic performance. These dummies have been used in representative tests to check the accuracy of the simulations discussed in this paper. The hip joint of the leg on the impacted side only was modified to increase the maximum possible angle of adduction to 28° with a corresponding reduction in adduction.

With the leg on the nonimpacted side unmodified, both legs are able to swing up to 25° in the direction of impact.

Both the knee joints were modified to allow lateral rotation in either direction, with friction pads added to give an adjustable but constant level of friction torque. With this arrangement, the severity of the impact to the knee is a function of the amount of lateral angular rotation that occurs. The acceptance level is judged to be 6° of rotation, with the friction torque set at 200Nm, representing the onset of an injury of severity AIS 3(4).

Simulated Impact Conditions

Since the simulations are based on the characteristics of a dummy, the majority of the posture conditions chosen are those that have been shown by full-scale tests to compensate most successfully for the limitations in the performance of a dummy and yet represent a typical car-pedestrian accident.

Pedestrian

The pretest condition simulates a pedestrian in a walking stance with the right leg backward and the left leg forward. Both legs are straight and the full body weight evenly distributed between the two legs. Impact is to the right-hand side at an angle of 30° forward of truly sideways.

This stance gives a near lateral impact to the lower limbs that represents typical accident conditions and improves the probability of head-to-vehicle contact, without the shoulder striking in such a manner that it gives an unrealistically high level of protection to the head.

Two different postures were also simulated. In one case, the dummy was represented as having all its weight on the struck leg; in the second case, the dummy was struck squarely on the side.

Vehicle

Most simulations represent a 40km/h impact on the centreline of the car. This speed is considered to be the maximum at which pedestrian protection could be practically achieved. One additional case is simulated at 32km/h to study the influence of speed.

The vehicle is represented as having a fixed suspension with the brakes applied at the instant of impact to simulate a deceleration of 0.7g.

Vehicle Simulation

Vehicle Components

The vehicle front is modelled by using six flat planes or groups of planes, which is the minimum number required to represent the important shapes and features for pedestrian impact. The planes are given idealised stiffness functions that are initially based on those for current production vehicles.

The panels are shown in Figure 1 and represent the under-bumper region, bumper, grille, bonnet leading edge, bonnet top, and windscreen. The dimensions of the car shapes that are simulated are given in Table 1.

To increase the amount of information gained from each run of the program, three bonnet lengths are modelled simultaneously, each having the same leading and trailing edge heights. Associated with each bonnet length is a group of three windscreens that are given negligible stiffnesses. This allows the head impact velocity

Table 1. Vehicle parametric variables

Vehicle Dimensions (See Figure 1)

Run No.	Height mm A Bonnet	Height mm B Bumper	Height mm C Spoiler	Bumper Lead mm D Bonnet	Bumper Lead mm E Spoiler	Leading Edge Shape
L 1			—	150	—	
L 3		450	—	150	—	
L 4	600		—	0	—	S
L 2		350	—	150	—	
M 1			—	150	—	S
M 3			—	150	—	S
M 4			—	250	—	S
M 5		450	—	350	—	S
M 6	720		—	150	—	R
M 8			262	150	50	R
M 9*			262	350	50	S
M 10			—	0	—	S
M 11*			262	250	50	S
M 7		350	—	150	—	R
I 1*				350	50	
I 2*				200	50	
I 3*	750	450	262	200	50	S
I 4*				200	0	
I 10*		350				
I 11*		250				
I 12*	—	450	—	—	—	—
I 13		450				
I 14 to I 16	770	—	—	150	—	S
I 17 to I 23	770	450	232	200	0	S
H 1			—	150	—	S
H 4			—	250	—	S
H 5			—	350	—	S
H 6		450	—	150	—	R
H 8	850		—	0	—	S
H 9*			262	350	50	S
H 2		350	—	150	—	S
H 7			—	150	—	R

R — Radiused
S — Square
Bumper generally 100mm deep
* Narrow Bumper 30mm deep

with the windscreen to be determined for nine different locations of windscreen.

Two forms of leading edge are examined, one approximating to a square edge and the second to a radiused front.

When a radiused front is simulated, a slightly more complex model is used (Figure 1). The three panels used to model the curvature operate in a dependent manner, and, for each body segment, only the panel with the greatest contact is assumed to generate a reactive force at any instant.

The leading edge vertical plane, panel 4, is utilised to supplement the lower panel of the rounded front to give the increased stiffness often present in this location.

Stiffness Characteristics

The planes are given idealised stiffness functions, which are shown in Figure 2 and Table 2, and describe forces that are normal to the vehicle panels. All reach a force plateau at which there is no limit of deflection and no allowance made for the stiffness of understructure

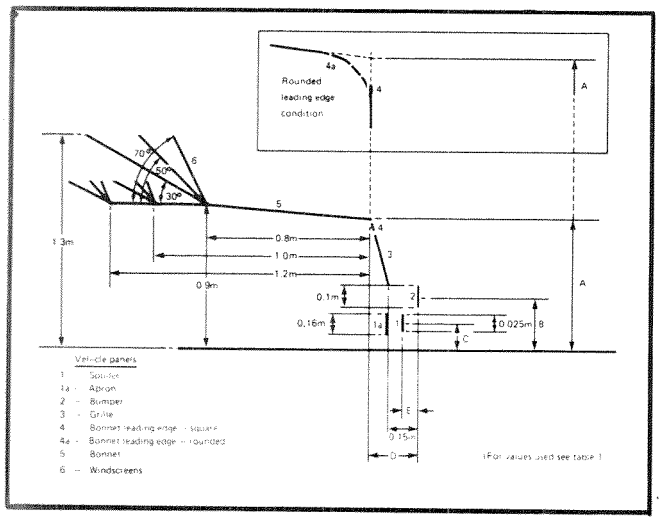

Figure 1. Vehicle simulation panels

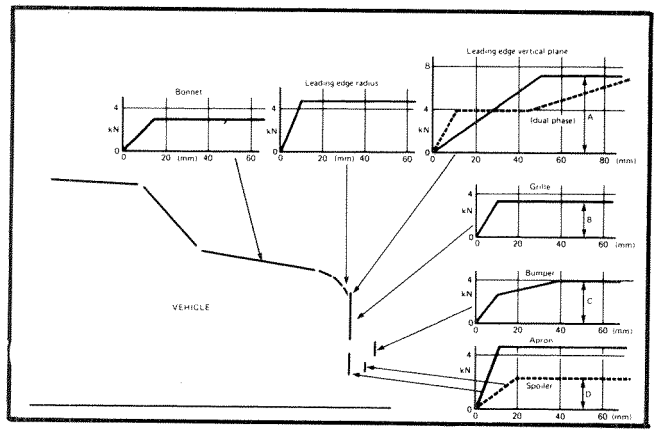

Figure 2. Simulation panel stiffness

Table 2. Vehicle panel stiffness

Run No.	Panel Stiffness kN (Max Force) (see Figure 2) A Leading Edge Vertical	B Grille	C Bumper	D Spoiler
L1-L2	7	3.5	4	—
L3	4/7*	1	4	—
L4	7	2.5	4	—
M1	7	3.5	4	—
M3	4/7*	1	4	—
M4-M5	7	3.5	4	—
M6-M7	5	3.5	4	—
M8	5	3.5	4	2.5
M9	5	1	3	2.5
M10	7	2.5	4	—
M11	5	1	3	2.5
I1	5	1	3	2.5
I2	3.5/5*	1	3	1.5
I3-I4	3.5/5*	1	2.25	2.25
I10-I13	—	—	4	—
I14	7	2.5	8	—
I15	7	2.5	4	—
I16	7	2.5	6	—
I17-I23	5	1	2.25	1.75
H1-H7	7	3.5	4	—
H8	7	2.5	4	—
H9	5	1	3	2.5

* Dual phase leading edge

(engine, etc.). By this means, necessary material crush depths can be assessed for each condition. The maximum stiffnesses used are based on values determined by dynamic impact tests on current small production cars.

For the round front, the stiffness of the leading edge vertical plane is utilised to supplement the lower panel of the rounded front to give the increased stiffness often present in this location.

Results

The impact loadings and responses calculated for the pedestrians in the simulated tests are shown in the appendix.

In these results, the location of head impact is the distance behind the bumper front face that the path of the centre of gravity of the head intersects the bonnet top or windscreen 2A, as appropriate.

The head impact velocity is the average of the head velocities, normal to each of the three windscreens that form the most forward group of three windscreens.

Pelvic and thoracic accelerations are the peak calculated values while the pedestrian is struck by the front or bonnet of the car.

Knee lateral angular rotation is given for two phases of the impact. Phase A spans the first part of the impact up to the instant the bumper forces start to reduce. These angles will, therefore, give an indication of the influence of the bumper and spoiler on knee bending forces.

Phase B gives the total angular displacement of the knee. The difference between the values of phases A and B is the influence of the cantilevering of the femur around the bonnet leading edge, causing a loading across the knee to accelerate the lower leg.

If the femur were to fracture from the action of these forces, the loading across the knee would be relieved. In these simulations, the femur is not programmed to fracture.

Knee shear force is the maximum value across the joint of the impacted leg. Leg bending moments are calculated for the instant when the applied forces are a maximum on the upper and lower legs, respectively.

For the adult, the upper leg bending moments derive from contact with the bonnet leading edge and the lower leg moments from either bumper or spoiler contact. For the child, the upper leg moments derive from bumper contacts and the lower leg from striking the spoiler.

Comments on Results

In general, all features of the shape of a vehicle combine to influence the characteristics of an impact, but the following broad trends could be attributed to respective vehicle components for the cases studied. The influence on the overall kinematics has already been reported(4).

Adult Pedestrian (Impact Speed 40km/h)

Bumper Stiffness

Bumper stiffnesses of 4, 6, and 8kN were simulated at a height of 450mm, and the resulting lower leg and knee forces are compared in Table 3.

Table 3. Adult lower leg and knee forces with respect to bumper stiffness

Run No.	Bumper Stiffness kN	Lower Leg Bending Moment Nm	Lateral Knee Angle Degrees	Knee Shear Force kN
I15	4	390	6.8	1.5
I16	6	478	6.9	2.1
I14	8	560	6.8	2.7

The results show that lower leg bending moment and knee shear forces both increase with bumper stiffness: a 100 percent increase in stiffness giving a 43 percent increase in leg bending moment and an 80 percent increase in knee shear force.

The angle of lateral displacement of the knee is constant because its magnitude is related to the total rotational energy input resulting from torque loadings, and the energy required to accelerate a leg to a given velocity is approximately constant.

Bumper Height and Spoiler

Three heights of bumper were simulated, centred at 250, 350, and 450mm above the ground. These are compared in Table 4 with cases that include spoilers mounted at 262.5mm above the ground.

In selected cases for this comparison, the bumper was the only part of the car simulated so that its effect could be isolated.

For the cases shown, lower leg bending moments are approximately constant except for a high value resulting from the narrow 30mm deep bumper at 450mm and low values from the more compliant bumper plus spoiler combinations. Both the shear forces and the lateral angular displacements of the knee reduce with lower bumper heights and reduced bumper-to-spoiler lead.

Table 4. Adult lower leg and knee forces with respect to bumper height and spoiler

Run No.	Bumper Height mm	Bumper to Spoiler Lead mm	Bumper Plus Spoiler Stiffness kN	Lower Leg Bending Moment Nm	Lateral Knee Angles Degrees	Knee Shear Force kN
I11	250*+	—	4	399	0.1	0.9
I10	350*+	—	4	347	0.3	1.4
I13	450 +	—	4	389	6.1	3.1
I12	450*+	—	4	525	11.7	3.0
I4	450*	0	4.5	308	1.7	1.0
I3	450*	50	4.5	329	4.2	1.4
M11	450*	50	5.5	298	3.9	2.0
M8	450	50	6.5	379	3.7	2.2

Bumper generally 100mm deep

* Narrow bumper 30mm deep

\+ Only bumper simulated

Bonnet Leading Edge

The position of the bonnet leading edge directly influences pelvic accelerations and upper leg bending moments and also affects the location and severity of subsequent impacts of the head to the car.

Pelvic Accelerations—Pelvic accelerations vary with respect to bonnet leading edge height and bumper-to-bonnet lead (see Table 5).

The accelerations range from 18 to 64g and increase in magnitude with increased bonnet height and also with reduced bumper lead.

Table 5. Adult pelvic accelerations relative to bonnet leading edge location

Bumper to Bonnet Lead mm	Pelvic Accelerations g for Bonnet Leading Edge Heights mm		
	600	720	850
0	24	43	63
150	18	34	64
250	—	30	54
350	—	21	52

Upper Leg Bending Moment—For the leg arrangement simulated, the upper leg bending moments (see Table 6) were a maximum for impacts to the midsection of the upper leg and were associated with bonnet leading edge heights of 720 and 750mm. The 600mm- and 850mm-high bonnets struck near the ends of the upper leg and the adjacent hip joint and friction-loaded knee joints limited the magnitude of the bending moments generated.

Table 6. Adult upper leg bending moments relative to bonnet leading edge location and stiffness

Bumper to Bonnet Lead mm	Upper Leg Bending Moments Nm for Bonnet Leading Edge Heights mm		
	600	720	850
0	397	581	226
150	307	495	218
250	—	451 (388)	202
350	—	303 (241)	276

Location and Velocity of Head Impact—The location of the bonnet leading edge influences both the position and the velocity of head impact. The location of head impact may affect its severity. For example, an impact to traditionally soft bonnet top will probably cause less injury than an impact to a rigid scuttle or windscreen frame. Table 7 shows that the head impact point ranges from 0.84 to 1.4m behind the bumper and moves further rearward as the height of the bonnet is reduced and also as the bumper-to-bonnet lead is increased.

Table 7. Distance of adult head impact point from bumper, relative to location of bonnet leading edge

Bumper to Bonnet Lead mm	Distance of Head Impact Point Behind Bumper m for Bonnet Leading Edge Height mm		
	600	720	850
0	1.33	1.15	0.84
150	1.4	1.25	1.05
250	—	1.4	1.25
350	—	1.4	1.35

With a bumper height of 450mm, the velocity of head impact (see Table 8) ranges from 73 to 142 percent of car impact speed. It increases as the height of the bonnet is reduced and also for a medium height bonnet as bumper-to-bonnet lead increases.

Table 8. Impact velocity of adult head with forward windscreen group relative to location of bonnet leading edge

Bumper to Bonnet Lead mm	Head Impact Velocity m/s for Bonnet Leading Edge Height mm		
	600	720	850
0	13.3	9.75	8.3
150	14.3	11.4	8.1
250		13.0 [13.9]	8.5
350		14.2 [15.8]	9.1 [10.0]

Note: Velocities shown generally relate to bumper height of 450mm without spoiler. Numbers in brackets refer to bumper combined with spoiler.

These velocities are increased by approximately 10 percent with the inclusion of a spoiler, which effectively lowers the height of leg contact.

Energy Distribution

The energy absorbed by the front panels is shown in Table 9 for cases having a 450mm-high bumper with no spoiler. The total energy absorbed by all the front panels, the bonnet leading edge, the grille, the bumper, and the bumper panels is shown together with the energy absorbed by the bumper and bumper under-panels only.

The total energy absorbed increases significantly with increased bonnet height and less significantly with reduced bumper lead. The energy absorbed by the bumper ranges between 970 and 1,170J for all configurations except for zero bumper lead where values range from 280 to 500J.

The results shown in the appendix indicate that, for the shapes studied, the energy absorbed by a bumper plus spoiler is approximately the same as that absorbed by a 450mm-high bumper without spoiler.

Changes to Dummy and to the Impact Speed

In nearly all the simulations, the impact speed and the characteristics of the dummy are held constant. In Table 10, the results of changes to these characteristics are compared with those from a run with the standard dummy arrangement described in an earlier section.

The variations studied are for a 5th percentile female and a 95th percentile male of 1.53 and 1.85m height, respectively; a test at the standard dummy arrangement, but with all the weight on the impacted leg; an impact with the dummy turned so it is struck squarely on the side; and, finally, a simulation of a 32km/h impact with the dummy again simulated as described previously.

Some significant differences are noted in these runs. The head strikes nearer the front and at a lower velocity for the 5th percentile female, and this is coupled with higher pelvic accelerations. A more rearward head impact occurs at a higher velocity for the 95th percentile male, and there is a reduced head velocity for the side-impacted case. Accelerations were not significantly reduced for the 32km/h run because, with a constant crush force stiffness characteristic for each panel, the contact forces generated were the same for both velocities.

Child Pedestrian (Impact Speed 40km/h)

Bumper Height and Spoiler

Bumpers were simulated at heights of 350 and 450mm, and their influence on forces to child legs is compared in Table 11 with cases that include spoilers mounted 262mm above the ground.

The combination of spoiler and 450mm bumper gives low leg bending moments of approximately 150Nm and low knee shear forces of 0.5kN. Removal of the spoiler increases the shear force to 0.9kN, and lowering the

Table 9. Energy absorbed by car front relative to location of bonnet leading edge

Bumper to Bonnet Lead mm	Total Energy Absorbed by All Front Members J			Total Energy Absorbed by Bumper Plus Bumper Under Panel J		
	Bonnet Height mm			Bonnet Height mm		
	600	720	850	600	720	850
0	1046	1207	2198	438	281	505
150	1199	1611	1989	1042	967	1011
250	—	1439	1891	—	1172	1114
350	—	1314	1756	—	1170	1150

Table 10. Results of adult simulations with respect to changes in the impact speed or dummy characteristics

		Standard Simulation Condition	5th Percentile Female	95th Percentile Male	All Dummy Weight on Impacted Leg	90° Side on Impact	Standard Test at Speed of 32km/h
Run number		I 17	I 21	I 20	I 22	I 23	I 18
Distance of head impact from leading face of bumper m		1.23	1.0	1.4	1.23	1.22	1.22
Average impact velocity of head to forward group windscreens (m/s)		11.32	8.3	13.1	11.2	9.6	7.9
Peak Thoracic Acceleration		23	27	13	26	20	9
Peak Pelvic Acceleration g		25	55	21	25	26	21
Right knee lateral angular displacements* degrees	A	1.8	1.0	4.0	1.9	4.5	0.4
	B	5.8	1.4	16.9	5.3	10.2	1.4
Peak upper leg bending moment (Nm)		228	204	247	193	284	217
Peak lower leg bending moment (Nm)		245	224	275	245	243	224

*A Angular displacement of knee at end of maximum bumper force

*B Maximum angular displacement of knee

Table 11. Child leg bending moment and shear forces and pelvic accelerations with respect to bumper height and spoiler

Run No.	Bumper Height (mm)	Bumper to Spoiler Lead (mm)	Bumper plus Spoiler Stiff-ness (kN)	Lower Leg Bending Moment (Nm)	Knee Bending Moment (Nm)	Upper Leg Bending Moment (Nm)	Knee Shear Force (kN)	Pelvic Accel (g)
L 2	350	—	4	—	239	323	1.24	65
L 3	450	—	4	—	189	147	.91	98
I 4	450	0	4.5	192	165	122	.58	56
I 2	450	50	4.5	157	152	153	.52	62

bumper to 350mm raises the upper leg and knee bending moments and the knee shear force.

Bending moments have been calculated only where direct contact occurs, and consequently no values are given for the lower leg in cases where spoilers have been omitted.

Bumper/Bonnet Leading Edge

For the child, the location of the bonnet leading edge directly influences thoracic accelerations and the subsequent impacts of the head to car. It also interacts with the bumper to affect pelvic accelerations.

Pelvic Accelerations—In these simulations, the magnitude of child pelvic accelerations is influenced primarily by the stiffness of the car front, particularly the and also by the height of the bonnet.

The effect of stiffness is shown in Table 12, in which the pelvic accelerations given, ranging from 52 to 99g, are the averages for all the shapes studied.

Table 13 shows that the effect of changes in shape is less pronounced. The only direct pelvic impact with the

Table 12. Average child pelvic acceleration with respect to the bumper and bonnet edge stiffness

Front Structural Stiffness kN			Pelvic Acceleration. Averaged for All Car Shapes (g)	
Bumper Plus Bonnet kN	Bumper kN	Bonnet Edge kN	Average	Standard Deviations
7.25	2.25	5	52	10
8	3	5	69	12
11	4	7	99	23

Table 13. Child pelvic accelerations relative to location of bonnet leading edge

Bumper to Bonnet Lead (mm)	Pelvic Acceleration (g) for Bonnet Leading Edge Height mm		
	600	720	850
150	73	115	107
250	—	95	95
350	—	100	100

bonnet leading edge resulted in the highest acceleration of 115g; for the lowest acceleration of 73g, the bonnet edge struck below the pelvis.

In other cases, pelvic impact was essentially to the softer front grille.

In these cases, the effect of car shape was partly masked because a level force plateau was used to describe the stiffness function and the maximum force was reached in each run.

Thoracic Accelerations—Thoracic acceleration is most affected by car shape and structural stiffness, and results are shown in Table 14. The 150mm bumper lead clearly demonstrates the influence of shape. With the lower 600 and 720mm bonnets, the leading edge strikes below the thorax giving low thoracic acceleration of 50g. Conversely, for the 850mm bonnet, direct leading edge to thorax contact occurs giving a higher acceleration of 85g.

For increased bumper-to-bonnet leads, the thoracic acceleration increased for the 720mm high bonnet and decreased for the 850mm bonnet.

Table 14. Child thoracic acceleration relative to location and stiffness of bonnet lead edge of 7kN, but with values in brackets for 5kN stiffness

Bumper to Bonnet Lead (mm)	Thoracic Accelerations (g) for Bonnet Leading Edge Heights (mm)		
	600	720	850
150	50	47	85
250	—	56 (37)	68
350	—	59 (34)	59 (45)

Reduction of leading edge stiffness from 7 to 5kN gave corresponding reductions in accelerations ranging from 21 to 42 percent.

Location and Velocity of Head Impact—The location of the bonnet edge also influences the location and velocity of head impact for the child. Generally the location of head impact was between 300 and 800mm behind the front face of the bumper with impact being more rearward with reducing bonnet height.

The head impact velocities given in Table 15 are generally in the range of 8.5 to 10.5m/s, but values of 4.0 to 6.5m/s occur with the 850mm-high bonnet and more vertical front. The velocity of the head striking the bonnet top is significantly influenced in the simulations and tests by neck flexure.

Table 15. Child head impact velocity relative to location of bonnet leading edge

Bumper to Bonnet Lead (mm)	Head Impact Velocity m/s for Bonnet Leading Edge Heights (mm)		
	600	720	850
150	10.3	10.2	4.0
250	—	9.7	6.5
350	—	10.4	8.6

Conclusion

This study of the influence of car shape and stiffness on the protection offered to pedestrians in an accident is based on the presumption from previous studies that the highly developed mathematical model used gives a good simulation of the characteristics of a car-to-pedestrian impact.

It has been extensively validated by comparison with selected dummy impact tests and includes improved vehicle-to-dummy contact models and the output of additional joint force data allowing the evaluation of segment bending moments.

The adult dummy simulation has improved hip and

knee joint flexure to give more realistic bumper and bonnet leading edge contacts.

1. The studies show the following general relationship between vehicle design and the resulting severity of impact to pedestrians at speeds of 40km/h:
   - A low-front profile concentrates most of its input energy well below the centre of gravity of an adult, inducing higher angular rotation onto the bonnet resulting in high head impact velocities. Distribution of energy input is closer to the centre of gravity of the simulated child, resulting in lower head impact velocities.
   - A medium-height profile results in similar energy inputs at the bumper but increased energy input at the bonnet leading edge giving higher accelerations to the regions of the child and adult contacted by the leading edge, but this is combined with lower head impact velocities.
   - A high profile further increases the energy input of the bonnet edge, giving increased accelerations to the adult pelvis and child thorax, but gives a further reduction in head impact velocity.
2. Changes to individual components give the following trends. Specific values relate only to the size of pedestrians that are simulated: a 50th percentile adult male and a 6-year-old child.
   - Bumper—A bumper mounted at 450mm causes excessive lateral bending to the adult knee but low loadings to a child knee. Lowering the bumper improved conditions for the adult but gave increased loading to the child knee and femur. The introduction of a suitable spoiler with the 450mm bumper gave improvement to both adult and child.

     If a leg bending tolerance value of 200Nm is assumed(4), then adult lateral knee bending is excessive from a bumper mounted at 450mm and having a stiffness of 4kN. Lowering the bumper to 350mm or introducing a spoiler giving total bumper/spoiler stiffness of up to 6.5kN gave acceptable conditions.

     For the child, the 450mm-high bumper influences pelvic acceleration, and a simulated stiffness of 4kN is associated with pelvic accelerations of about 100g. Lowering the bumper to 350mm reduces these accelerations to 65g.

     A bumper/spoiler combination gives acceptable values for both child leg and pelvis providing the stiffness of the bumper component is 3kN or less.

     When struck by an adult, a bumper or bumper plus spoiler absorbs between 1,000 and 1,200J of energy when the bumper lead is 150mm or more. In the cases with zero bumper lead, only 280 to 500J are absorbed.

     When assessing the safety of a bumper/spoiler combination, the spoiler may reduce the bending and shear forces across the knee, but it will not give adequate protection when added to a bumper that is so hard it causes crushing injuries.
   - Bonnet Leading Edge—The input energy of the bonnet edge and grille varies widely with respect to its location, increasing as the bonnet is raised or as the bumper lead decreases. Energy input values range from 150J for a low bonnet with a bumper lead of 150mm, increasing to 1,700J for a high vertical profile and reducing to 600J for a high profile and 350mm bumper lead.

     Child pelvic accelerations and bending moments on the adult upper leg are too high in nearly all cases when the leading edge stiffness is 7kN. Reducing the stiffness to 5kN gives acceptable values for the child pelvis and reduces the magnitude of leg bending moments by about 20 percent. The stiffness of the leading edge of some current small cars is about 7kN.
   - Bonnet Top Impact—The location of head impact is between 0.3 and 0.8m behind the bumper for the child and from 0.4 to 1.4m behind the bumper for the adult. Within the range of shapes studied, the adult head impact velocity may be reduced by up to 40 percent of the worst case by increasing the bonnet height from 600 to 850mm.

     It may also be reduced by 30 percent by reducing the bumper lead from 350mm to zero, but only for a medium-height bonnet. Extreme values of head impact velocity range from 40 percent above car impact velocity to 25 percent below. For the child, head impact velocities are more consistently just below car impact speed, reducing by 60 percent for a high vertical front profile.
3. Dummy characteristics. The most significant changes in responses noted in the simulations of different dummy sizes are that head impact velocity increases in magnitude and the location of head impact point moves further rearward with increasing dummy height.

   The bonnet leading edge strikes closer to the pelvis of the 5th percentile female giving higher pelvic accelerations than for a taller dummy.

   Changes to the standing arrangement of the dummy do not produce major changes in the

impact conditions. Striking on the side at right angles gives a 15 percent reduction in head impact velocity, but changing the weight distribution from evenly spread over two feet to all the weight on the impacted leg causes no notable change.

4. The relationships determined in these studies have been utilised to give guidelines for modifying a small saloon car to give improved pedestrian protection(5).

References

1. Fowler, J.E., and J. Harris, "Practical vehicle design for pedestrian protection," Proceedings Ninth International Technical Conference on Experimental Safety Vehicles, Kyoto, Japan, November 1982.
2. Hobbs, C.A., G.J.L. Lawrence, and C.S. Clarke, "PSC1— demonstration car with improvements for pedestrian protection," Proceedings Tenth International Technical Conference on Experimental Safety Vehicles, Oxford, Great Britain, July 1985.
3. Ashton, S.J., and G.M. Mackay, "Car design for pedestrian injury minimisation," Proceedings Seventh International Technical Conference on Experimental Safety Vehicles, Paris, France, June 1979.
4. Fowler, J.E., and J. Harris, "Practical vehicle design for pedestrian protection," Proceedings Ninth International Technical Conference on Experimental Safety Vehicles, Kyoto, Japan, November 1982.
5. Hobbs, C.A., G.J.L. Lawrence, and C.S. Clarke, "PSC1—a demonstration car with improvements for pedestrian protection," Proceedings Tenth International Technical Conference on Experimental Safety Vehicles, Oxford, Great Britain, July 1985.

Appendix A

Results With Simulated Pedestrians

Table A-1. Results with simulated adult pedestrians

Run No. (See Table 1)		L1	L2	L3	L4	M1	M3	M4	M5	M6	M7	M8	M9	M10	M11	I1	I2	I3	I4
Distance of head impact from leading face of bumper (m)		1.39	1.42	1.4	1.33	1.26	1.25	1.42	1.39	1.36	1.38	1.31	1.39	1.15	1.39	1.38	1.25	1.27	1.27
Average impact velocity of head to forward windscreens (m s)		14.3	14.1	14.1	14.1	13.7	11.3	13.0	14.2	12.7	12.7	14.2	15.8	9.75	13.9	13.5	11.5	11.6	11.7
Peak thoracic accelerations (g)		19	15	11	14	19	15	21	25	21	19	24	25	15	21	22	24	23	22
Peak pelvic accelerations (g)		17	18	19	24	34	34	30	21	34	33	26	18	43	25	28	26	26	24
Knee peak shear force kN		1.55	1.37	1.56	1.66	1.51	1.51	1.96	2.88	1.53	1.23	2.22	2.57	2.00	1.98	2.38	1.4	1.46	1.01
Right knee lateral angular displacement degrees	A*	6.2	2.5	7.6	5.3	19	8.7	5.6	5.9	8.5	4.6	3.7	3.8	14.8	3.9	3.8	6.9	4.2	1.7
	B*	23	19	26	34	48	38	26	10	39	31	20	5.0	67	6.8	5.1	14	10	3.5
Peak upper leg bending moment (Nm)		307	361	273	397	518	495	451	303	334	427	379	241	581	388	464	304	215	258
Peak lower leg bending moment (Nm)		408	404	408	519	393	391	448	500	403	352	459	361	394	398	362	361	362	308
Energy absorbed by bonnet leading edge (J)		64	80	164	312	341	468	134	115	301	598	172	83	700	180	210	407	420	402
Energy absorbed by bumper (J)		1042	1023	1037	217	967	993	1172	1170	1014	980	806	788	281	777	792	853	686	601
Energy absorbed by spoiler (J)												283	346		338	346	278	377	485

A Angular displacement of knee at end of maximum bumper force
B Maximum angular displacement of knee

Table A-1. Continued

		I10	I11	I12	I13	I14	I15	I16	I19	H1	H2	H4	H5	H6	H7	H8	H9
Distance of head impact from leading face of bumper (m)		—	—	—	—	1.19	1.15	1.18	1.20	1.04	1.05	1.25	1.35	1.22	1.23	0.84	1.35
Average impact velocity of head to forward windscreen (m/s)		—	—	—	—	9.9	9.95	9.6	10.9	8.1	8.3	8.5	9.1	9.0	10.4	8.3	10.0
Peak thoracic accelerations (g)		—	—	—	—	16	16	16	21	21	21	15	15	15	13	24	13
Peak pelvic accelerations (g)		—	—	—	—	45	39	44	25	64	61	54	52	42	42	63	44
Peak knee shear force(kN)		1.40	.90	3.04	3.12	2.73	1.51	2.12	1.34	1.39	1.20	2.57	2.31	1.40	1.05	.94	2.16
Right knee lateral angular displacement degrees	A	0.3	0.1	11.7	6.1	6.8	6.8	6.9	0.5	3.1	0.3	6.9	5.8	7.2	5.3	2.4	3.9
	B	—				26	28	27	5.8	3.9	0.9	9.0	11.0	48	39	8.0	3.9
Peak upper leg bending moment (Nm)		—	—	—	—	486	529	490	222	218	212	180	276	528	560	226	157
Peak lower leg bending moment (Nm)		347	399	525	389	560	390	476	239	377	242	550	484	384	378	319	400
Energy absorbed by bonnet leading edge (J)		—	—	—	—	446	594	498	531	564	584	425	269	610	612	1025	311
Energy absorbed by bumper (J)		1.09	810	1173	1188	1048	988	1053	648	1011	966	1114	1156	938	912	505	788
Energy absorbed by spoiler (J)		—	—	—	—	—	—	—	408	—	—	—	—	—	—	—	345

Note: For runs I17, I18, I20, I21, I22 and I23, see Table 10.

Table A-2. Results with simulated child pedestrians

(see Table 1)	L1	L2	L3	M1	M3	M4	M5	M6	M7	M8	M9	M10	M11	I1	I2	I4
Distance of head impact from leading face of bumper (m)	.65	.89	.77	.55	.52	.6	.61	.57	.65	.6	.7	.41	.65	.65	.53	.53
Average impact velocity of head to forward windscreen (m/s)	10.3	10.5	9.5	10.2	11.9	9.66	10.4	9.1	9.3	9.8	9.9	11.1	10.7	9.7	8.7	9.1
Peak thoracic accelerations (g)	50	51	60	47	44	53	59	62	39	47	34	56	37	36	40	42
Peak pelvic accelerations (g)	73	65	98	115	100	95	100	96	135	75	60	152	78	60	62	56
Peak knee shear force (kN)	.95	1.24	.91	.95	.89	.91	.91	.93	1.25	.52	.51	2.22	.48	.51	.52	.58
Peak upper leg bending moment (Nm)	—	323	147	—	147	146	148	147	326	174	150	85	142	150	153	122
Peak knee bending moment (Nm)	163	239	189	239	145	161	163	164	263	250	195	155	268	237	152	165
Peak lower leg bending moment (Nm)	—	—	—	—	—	—	—	—	—	293	224	—	213	223	157	192

Table A-2. Continued

Run No. (see Table 1)	I15	I17	I18	I19	H1	H2	H4	H5	H6	H7	H9
Distance of head impact from face of bumper (m)	.43	.59	.55	.59	.34	.39	.43	.49	.47	.52	.57
Average impact velocity of head to forward windscreen (m/s)	9.6	7.6	6.4	7.6	4.0	1.6	6.5	8.6	4.3	5.4	6.1
Peak thoracic accelerations (g)	63	53	43	53	85	75	68	59	84	63	45
Peak pelvic accelerations (g)	99	59	36	59	107	157	95	100	98	218	60
Peak knee shear force (kN)	1.93	.44	.44	.44	.75	1.24	.94	.92	.95	1.22	.51
Peak upper leg bending moment (Nm)	147	112	112	112	—	316	145	148	147	315	150
Peak knee bending moment (Nm)	204	138	134	138	145	227	157	158	155	228	232
Peak lower leg bending moment (Nm)	—	135	142	134	—	—	—	—	—		218

Evaluation of a Pedestrian-Compatible Bumper

B.J. Kelleher and
M.J. Walsh
Calspan Corporation

R.D. Vergara and
J.T. Herridge
Battelle

R.H. Eppinger
U.S. Department of Transportation, National Highway Traffic Safety Administration

Abstract

As part of an ongoing NHTSA/Battelle/Calspan research program, 16 experimental vehicle-to-pedestrian impacts at 25mph are being performed using the Calspan sled facility. The instrumented vehicle test buck represents a vehicle front end that can be equipped with either an unmodified hard production-type bumper or a modified compliant pedestrian-compatible bumper. The instrumented pedestrian surrogates are unembalmed whole body anatomic specimens. The test matrix involves carefully paired subjects for comparison of the modified and unmodified configurations. Individual results are reported regarding pedestrian kinematics, measured forces and accelerations, physiological trauma incurred, and estimates of associated impairment, as well as an overall evaluation of injury-mitigating potential of the bumper system modifications.

Background

Each year, thousands of pedestrians are struck by motor vehicles. Data from the National Highway Traffic Safety Administration (NHTSA) Fatal Accident Reporting System (FARS) and Pedestrian Injury Causation Study (PICS) indicate that an excess of 135,000 pedestrians are injured annually. Approximately 72 percent of these pedestrian accidents involve passenger cars, and 74 percent of these passenger car accidents involve impact with the front structure of the vehicle. Translated into numbers, approximately 73,000 pedestrians are struck by the front structures of passenger cars annually. Ninety-one percent of these accidents occur at or below 20mph. Most of the accidents at these velocities are not fatal; however, many people suffer serious and often permanent impairment, especially to the lower extremities due to knee contact with the bumper and pelvic contact with the hood leading edge areas of the vehicle. Through the use of statistical techniques, NHTSA has predicted that over 140,000 pedestrians will be struck in 1994 with a total number of projected fatalities of 8,700(1). Assuming the same percentage of passenger car frontal impacts, approximately 77,000 pedestrians will be injured in 1994 if the design of passenger car front structures remains essentially unchanged. The purpose of the study discussed in this paper is the evaluation of injury reduction benefits achieved when the lower extremities of pedestrian victims are struck by a front bumper that is more compliant than those currently produced.

In January 1981, NHTSA published a notice proposing a new safety standard applicable to passenger cars that would require modification of front structures to reduce knee injuries sustained by pedestrians when struck by a vehicle. Since 1974, Battelle's Columbus Laboratories have been performing research on trauma-producing and trauma-mitigating mechanisms in pedestrian impacts by vehicles. This research utilized both instrumented Anthropomorphic Test Devices (ATD) and human cadavers(2-7) in support of this proposed safety standard. From 1974 through 1977, these impact experiments using human cadavers were performed at the Transportation Research Center (TRC) of Ohio. Since 1982, research using human cadavers and ATD's has been performed at the Calspan Advanced Technology Center (ATC). During the past year, Calspan has conducted eight pedestrian experiments using fresh, unembalmed cadaver subjects to evaluate the effects of production and modified bumper impacts.

Bumper Design

Early Battelle experiments resulted in the selection of a 1978 Pontiac LeMans as a representative test vehicle. All subsequent testing performed at Calspan has used the LeMans as the impacting vehicle. The results of these Battelle tests indicated that a bumper that limited the acceleration to less than 100g when impacted with a 7 lb mass (i.e., a representative knee mass) at 20mph would result in significant reductions to lower extremity injuries in pedestrian accidents. The proposed regulation has specified a bumper design that demonstrates a 90g acceleration level when impacted at 20mph with the 7 lb mass to achieve the maximum benefit to pedestrian accident victims. To accomplish the desired impact conditions of not over 90g, Battelle and NHTSA selected an open-cell polyurethane foam material. This particular energy-absorbing foam used in the bumper modification has a density of 4.8 lb/ft^3 and a modulus at 50 percent strain of 16 lb/in^2. This foam was cut into several layers and stacked into the C section of the LeMans bumper after the face plate had been removed. Figure 1 is a drawing of the foam insert indicating the size and shape. The corresponding acceleration (deceleration) time history

of a 20mph impact with the 7 lb impactor is presented in Figure 2. Also included in Figure 2 is the acceleration-time history of a similar impact at a velocity of 25mph. It should be noted that, in addition to satisfying the knee acceleration criteria just discussed, the design criteria for the modified LeMans bumper included a need to (1) satisfy the then existing 5mph no-damage performance requirement, and (2) stay within the space envelope provided by the production vehicle.

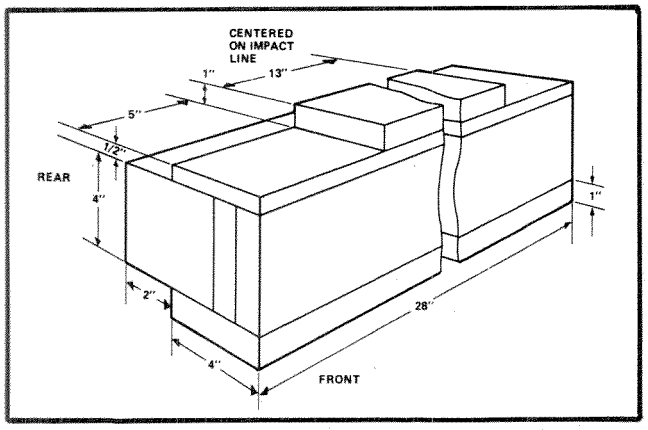

Figure 1. Foam bumper configuration

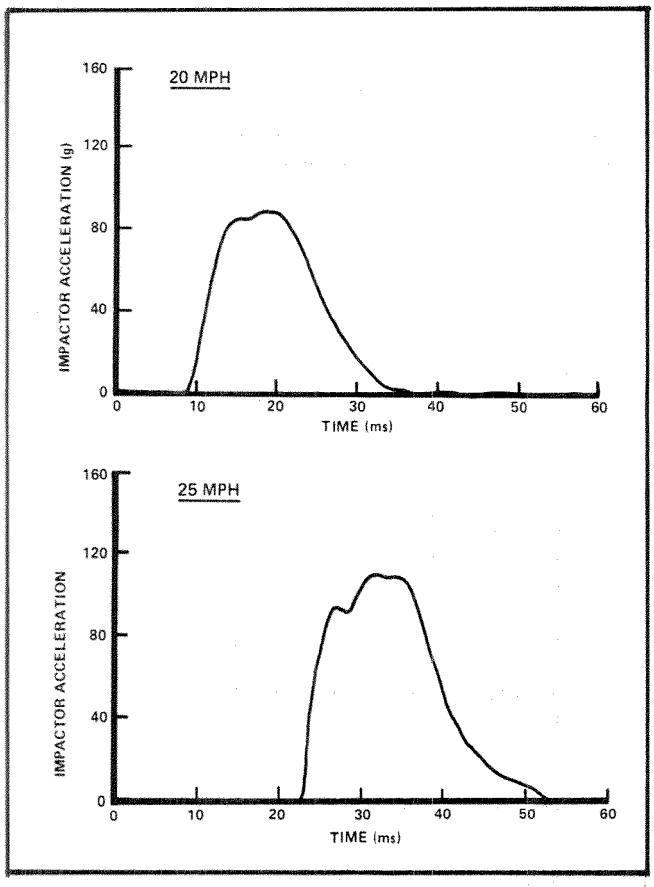

Figure 2. Seven lb impactor acceleration versus time history

Load cell balance systems were designed into the structure of the LeMans test buck at the bumper and hood leading edge (HLE) locations to record the longitudinal impact forces imparted to the knee and hip regions of the test subjects. The expression hood leading edge is used for convenience. The load cell balance at this location measures the forces applied to the forwardmost portion of the upper fascia and grille work of the vehicle. This area is approximately 6in in front of the forwardmost edge of the hood.

Cadaver Selection

Cadavers used in this research program were supplied by the Department of Anatomical Sciences of the State University of New York at Buffalo (SUNYAB). The subjects had been willed to the university for use in scientific research. A personal interview with the next of kin was conducted by representatives of Calspan and SUNYAB. During this interview, the objectives and techniques of the program were explained briefly and an informed consent release document for use of the body was signed and witnessed. After the experiment, the subject was returned to SUNYAB for disposition according to the willing document. Strict adherence to NHTSA Order 700-4 was observed in all instances.

Pretest full body x-rays were taken, and the femur x-rays were used to determine a Percent Cortical Area (PCA) measurement. This PCA was used to assess the acceptability of the subject with respect to bone quality. All accepted subjects were within one sigma of the average normal PCA as defined by Garn(8), and extended by Calspan(9). One subject was rejected during this study due to an obvious osteoporotic condition. Cadavers that had been confined to bed for more than 1 week's duration prior to death were also determined to be not acceptable. Cadaver anthropometry is presented in Table 1, and the averaged PCA values of the femurs are displayed in Figure 3. Human cadavers are referred to as Calman XX during this study. Calman is a generic form used by Calspan to designate a cadaver. The number is a serial number that provides a means of reference while maintaining anonymity of the donor.

To assess the benefit received from impact with the modified (MOD) bumper versus the production (PROD) bumper, an attempt was made to match the cadavers as closely as possible. The parameters used for matching cadavers are presented in Table 2. Table 3 indicates the modified versus production matched experiments selected for comparison. This table presents matched experiments wherein the sex remains constant, and age, height, and weight are displayed according to the degree of parameter match based on the criteria of Table 2. Comparison numbers 1 through 4 show the highest degree of parameter match. A good match for Calman 24 in age (46yr) and

Table 1. Cadaver anthropometry

Calman	Sex	Age	Stature (in)	Weight (lb)	Tibia height
20	M	72	72	161	20
21	F	77	59.5	127	17.5
22	F	71	62	156	17
23	M	77	68.5	155	18.5
24	M	46	70	132	21
26	M	77	68	157	19.5
27	M	63	71	194	21
28	F	79	62	121	19

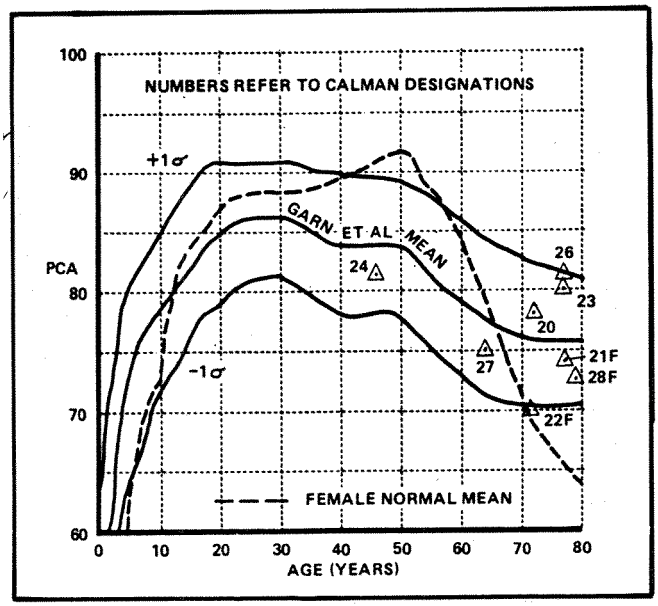

Figure 3. Femur PCA graph

Table 2. Parameters used for cadaver matching

Parameter of Comparison, P	Degree of Parameter Matching	Range of Departure from Exact Match*
Subject Height; Weight	Match	$Z<2$ Percent
	Excellent	$2 \leq Z < 10$
	Good	$10 \leq Z < 20$
	Fair	$20 \leq Z < 30$
	Poor	$Z > 30$
Subject Age	Match	$\Delta P < 2$ Years
	Excellent	$2 \leq \Delta P < 5$
	Good	$5 \leq \Delta P < 10$
	Fair	$10 \leq \Delta P < 15$
	Poor	$\Delta P \leq 15$

*Z = Absolute value of $[1 - (P_A/P_B)]$

P = Absolute Value of Age Difference

Table 3. Matched cadaver experiments

Comparison	Calman		Bumper	Degree of Parameter Match			
				Age	Sex	Height (in)	Weight (lb)
Number	A	B	(A/B)	(A/B)	(A/B)	(A/B)	(A/B)
1	20	23	(Mod/Prod)	Excellent (72/77)	Match (M/M)	Excellent (72/68.5)	Excellent (161/155)
2	21	28	(Mod/Prod)	Excellent (77/79)	Match (F/F)	Excellent (60/62)	Excellent (123/121)
3	21	22	(Mod/Prod)	Good (77/71)	Match (F/F)	Excellent (60/62)	Fair (123/156)
4	26	23	(Mod/Prod)	Match (77/77)	Match (M/M)	Match (68/68.5)	Match (157/155)
5	20	27	(Mod/Prod)	Good (72/63)	Match (M/M)	Match (72/71)	Good (161/194)
6	26	27	(Mod/Prod)	Fair (77/63)	Match (M/M)	Excellent (68/71)	Good (157/194)
7	24	23	(Mod/Prod)	Poor (46/77)	Match (M/M)	Excellent (70/68.5)	Good (132/155)
8	24	27	(Mod/Prod)	Poor (46/63)	Match (M/M)	Excellent (70/71)	Poor (132/194)

height/weight ratio (70in, 132 lb) was not found among the male subjects available for this program. Comparisons 7 and 8 show excellent matches in height between Calman 24 and both Calman 23 and 27, but poor matches in age and only good-to-poor matches in weight.

Test Procedures

When a suitable cadaver subject was selected and instrumented, the impact test was performed. Whole body x-rays were exposed and examined by a radiologist, a full autopsy examination was performed by a forensic pathologist, and the lower extremities were dissected. The results of these examinations were sent to Dr. John D. States at the Department of Orthopedics of the University of Rochester for evaluation of potential temporary and permanent impairment.

Equipment and Setup

All pedestrian impact experiments were performed using the Calspan 12in HYGE sled facility as a velocity generator for the 1978 Pontiac LeMans sled buck supplied by Battelle. Some structural modifications to the sled buck were required to insure compatibility with the Calspan sled facility since it had originally been fabricated for experiments performed on the larger TRC of Ohio sled. A photograph of the experimental setup is shown in Figure 4.

Each pedestrian subject was positioned in a walking posture with the struck leg placed 18in to the right of the centerline of the vehicle (midway between the center and outside edge of the bumper) with a minimum of 50 percent of the body weight on the struck leg. This percentage increases to approximately 80 percent between the time the pedestrian support quick release mechanism is triggered and initial impact. The subject was standing on a load cell platform to monitor this weight distribution. The struck side arm was secured behind the subject's back to preclude arm contact with the hood leading edge, and the subject was tethered to the sled buck to preclude secondary contact with the ground. A quick release mechanism attached to the body harness was electronically fired at a predetermined time in the testing sequence, allowing the subject to be freestanding at the time of contact.

Contact occurred at a velocity of 25mph with the sled brakes set to simulate a 3/4g braking deceleration. The impact velocity of 25mph was chosen to demonstrate the residual benefits of a higher velocity impact using the 20mph pedestrian-compatible bumper design according to the specifications of the Notice of Proposed Rule Making(1).

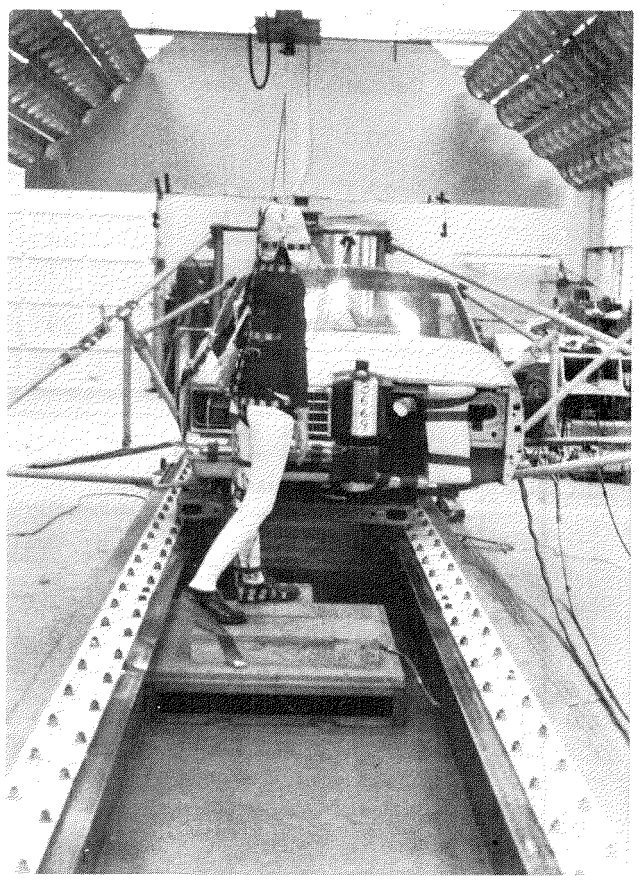

Figure 4. Experimental setup

A strobe-flash unit was mounted in the field of view of the cameras to indicate initial contact between the bumper and the subject's legs. Six high-speed cameras were used to document the impact tests. They included a full view of the event from the center of the sled track and an overhead view from off-board cameras. The four on-board cameras provided the rear view of the struck extremity, front view of the whole body, front view of the upper body, and upper body view through the windshield.

Subject Instrumentation

The human cadavers selected for use in this program were stored under refrigeration from the date of death until the morning of the test. The subjects were unembalmed with the exception of selective light embalming of the prevertebral muscles bilaterally done on Calman 27 and 28. This light embalming was to help stabilize the head/neck complex since no external cervical support was used.

The cadavers were clothed in tight-fitting, stretch, long underwear. Accelerometers were attached in the following locations:

Head	9-accelerometer head mount, angular accelerometer, triaxial mouth mount
Sternum	Upper Anterior-Posterior (A-P), Lower A-P
Ribs	#4 Medial-Lateral (M-L), #8 A-P, bilaterally
Thoracic Vertebrae	Triaxial mounts at T-1, T-12
Sacrum	S-2 triaxial
Knee	External triaxial
Ankle	External triaxial

The angular head accelerometer was attached to the 9-accelerometer head mount. The head and mouth mounts were attached to the subjects, and stereotaxic measurements were taken using a Kapf sterotaxic unit modified for a human head. Several dummy tests were conducted with full cadaver instrumentation to check out the system prior to any cadaver impact tests.

Experimental Results

Although electronic data were recorded for the head and thoracic regions of all subjects, only lower extremity data are presented in this paper. Table 4 contains a data summary of the peak accelerations on the struck knee and pelvis (sacrum) and load measurements from the vehicle bumper and hood leading edge for each test.

It is observed from Table 4 that the accelerations experienced by the struck knees are significantly lowered when the subject is impacted with the modified bumper as compared to impacts with the production bumper. Likewise, the peak longitudinal forces measured by the bumper load cell balance are also significantly lower (approximately one-third of the production bumper values). Figures 5 and 6 display comparative data from one of the matched experiments (Calman 20 and 23)

Figures 7 and 8 illustrate pelvic resultant acceleration and hood leading edge load data measured during a matched experiment (Calman 21 and 22). The resultant accelerations and hood leading edge loads are close in both magnitude and profile. These data indicate there is no significant effect in the pelvis/hood leading edge contact as a result of bumper design.

The averaged peak data from all modified and production impacts are displayed in Figure 9. This figure shows a significant decrease in knee accelerations and bumper

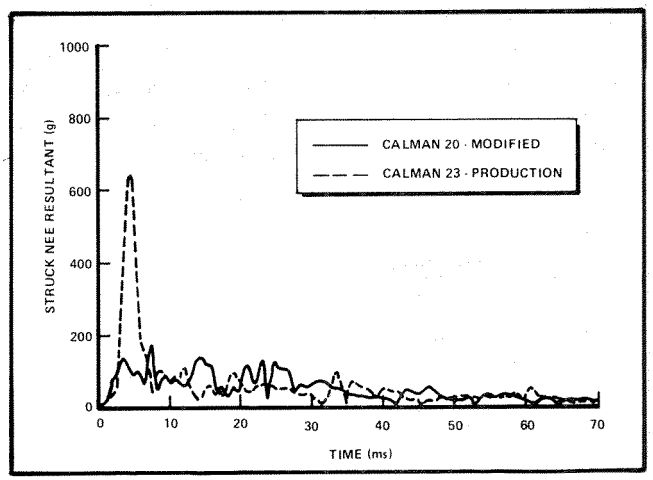

Figure 5. Knee acceleration time versus time—modified and production bumper comparison

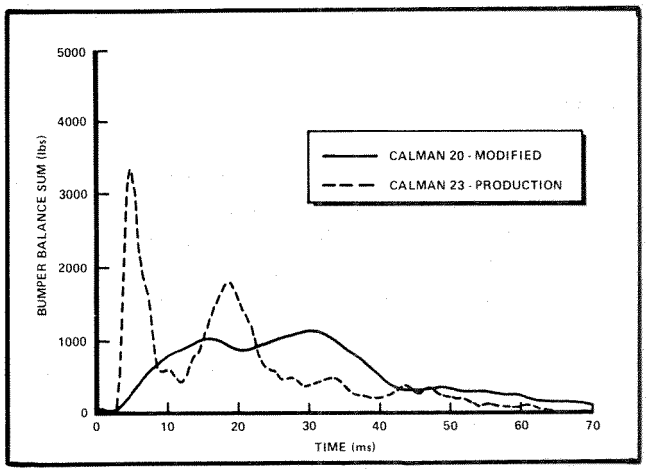

Figure 6. Bumper load versus time—modified and production bumper comparison

Table 4. Electronic data summary

Calman	Bumper	Knee R (g)	Bumper Load (lb)	Pelvis R (g)	HLE Load (lb)
20	Mod	160	1100	63	2200
21	Mod	180	1150	105	2950
24	Mod	200	950	48	1920
26	Mod	180	1000	80	2998
22*	Prod	680	2700	82	2400
23	Prod	630	3350	78	2100
27	Prod	680	3425	74	2219
28	Prod	687	2600	107	1927

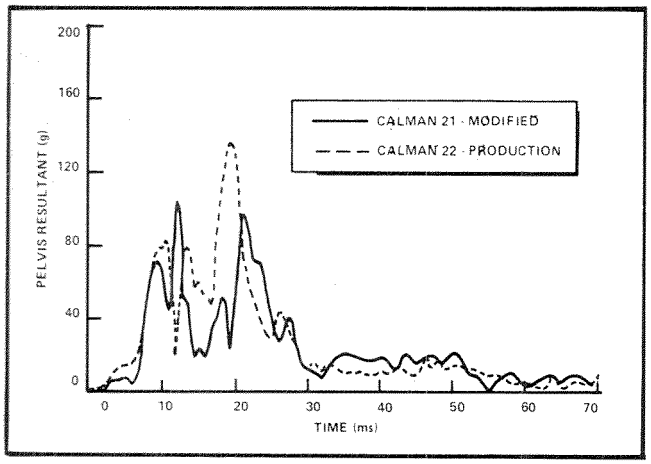

Figure 7. Pelvis acceleration versus time—modified and production bumper comparison

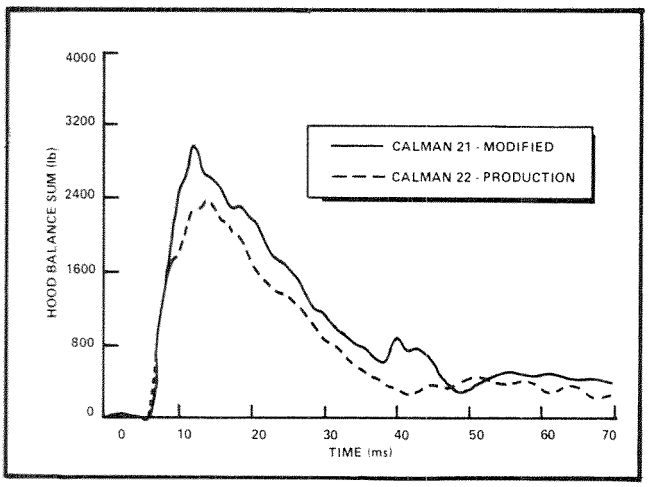

Figure 8. Hood leading edge load versus time—modified and production bumper comparison

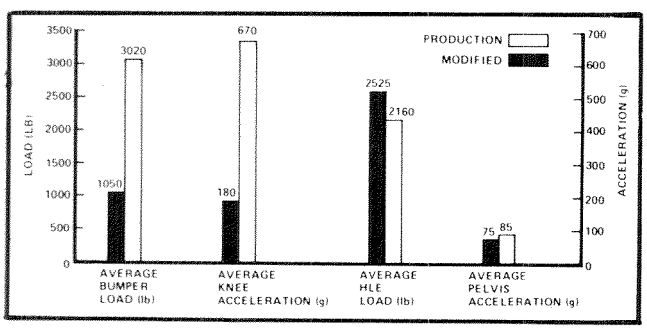

Figure 9. Average load acceleration data

loads as a result of bumper modification. Pelvis resultant accelerations and hood leading edge loads are close in magnitude; however, the average of the modified bumper hood leading edge loads is slightly higher (approximately 15 percent). This may be due to the different kinematic responses of the cadavers to impact using the modified and production bumpers. The modified bumper crushes over a 15 to 20ms timespan from time of contact with the pedestrian knee. The pedestrian is still in a standing position when his pelvic area is struck by the hood leading edge (about 10ms after knee contact). Impact with the rigid production bumper forces the pedestrian's lower extremities upward on contact, and the pelvic area contacts the hood leading edge when the subject's feet are lifted off the ground, thus causing a possible difference in the contact velocity and/or the effective mass of the hip at the time of impact with the hood leading edge.

The test that was performed using Calman 26 requires some discussion, due to two apparent data anomalies. The first is the resultant acceleration of the struck knee at approximately 22ms. During this experiment, the right knee (shielded) was contacted by the left knee (struck), thereby subjecting the left knee to increased loading as compared to the other subjects impacted by the modified bumper. This additional contact can be seen in the acceleration versus time history presented in Figure 10.

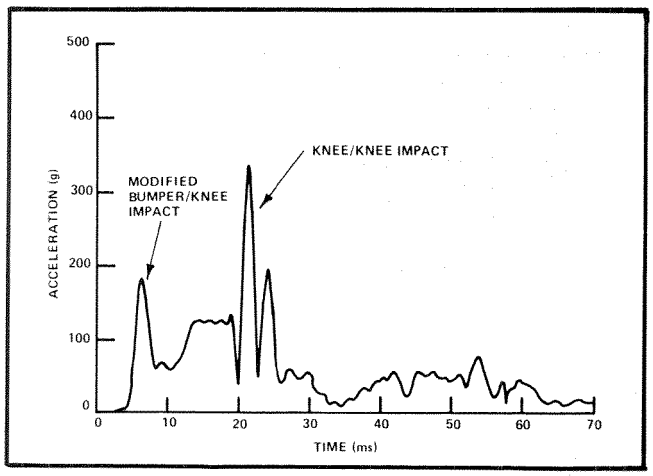

Figure 10. Calman 26 struck knee acceleration

The initial acceleration of approximately 175g at 6 to 7ms is typical of accelerations and times of the other modified bumper-struck knees. However, the second (and larger—335g) peak acceleration at approximately 22ms is not typical. Furthermore, the major contribution to the resultant acceleration value was from the X (A-P) direction, indicating that the struck knee had been turned somewhat prior to contacting the right knee. Second, the original hood leading edge load that was reported was 4,774 lb. This value is considerably higher than the other loads reported both for modified and production bumper combinations. Upon reevaluation of the load cell balance data, it was noted the inboard load cell (toward the center of the vehicle) was recording a load that was essentially a factor of two higher than the seven other inboard load cell recordings from all other impact tests, while the outboard load cell output was consistent with the other seven tests. It is believed that a shunt calibration resistor

of one-half the correct value was inadvertently installed in the load cell circuit for this test and that the sum of the hood leading edge load cells should be 2,998 as shown in Table 4.

Clinical Results

As stated earlier, an attempt was made to match, as closely as possible, the subjects used in the modified and production bumper tests. This effort was undertaken to assure that, within a reasonable range of age, stature, and weight, the outcome of the experiments would not be biased toward one or the other of the systems. Therefore, based on the criteria of Table 2 and holding the sex of the subjects as a match, comparisons of the clinical results are presented below. Tables 5 and 6 present a description of the injuries to the struck knees, as determined by a complete dissection, for the modified and production bumper impacts, respectively. The injuries to the struck knee of Calman 26, as noted in Table 5, are more severe than the injuries sustained by any of the other cadavers struck by the modified bumper. It is believed these injuries were due to contact between the right (shielded) knee and the left (struck) knee as previously described in Experimental Results. Table 7 displays comparisons of the knee injuries for modified and production bumper impacts in the format of the test matrix of the matched Calman experiments presented in Table 3. Note that comparison numbers 1 through 4 are the highest level matches that could be obtained for the maximum number of parameters. Comparison numbers 5 through 8 are presented for completeness even though the degree of parameter match is less than in comparison numbers 1 through 4.

The clinical results for injuries to the hip and thigh for both the hood leading edge/modified bumper and the hood leading edge/production bumper impacts are presented in Table 8.

Table 5. Injuries to struck knee—modified bumper impacts

Calman	Knee Injuries
20	Undisplaced vertical fracture of the lateral tibial plateau
21	None
24	None
26	Lateral tibial plateau fracture; medial collateral ligament avulsed from tibia; posterior cruciate ligament avulsed from femur; posteromedial side of joint capsule and lateral meniscus ruptured

Table 6. Injuries to the struck knee—production bumper impacts

Calman	Knee Injuries
22	Anterior cruciate ligament avulsed; posterior cruciate ligament partially avulsed; medial collateral ligament avulsed; popliteal vein ruptured
23	Anterior and posterior cruciate ligaments avulsed; superficial and deep fibers of medial collateral ligament avulsed; rupture of medial portion of knee capsule, deep fascia of knee joint and semimembranosus muscle
27	Posterior cruciate ligament avulsed from femur; posteromedial side of joint capsule ruptured; medial collateral ligament avulsed from femur
28	Tibia fractured in 2 places; complete fracture of fibula; medial collateral ligament laceration; cartilage and bone fracture of medial condyle

Clinical Evaluation

A clinical evaluation was performed(10) for each test based on the results obtained from the post-test x-rays and the complete knee and hip dissections as noted in the previous section, Clinical Results. For purposes of continuity (from previous work) and consistency (minimization of cadaver variability), the clinical results were treated as though the trauma reported had been determined on a 50-year-old person of the same sex as that of the subject cadaver. In the sections on Experimental Results and Clinical Results, information was presented only with regard to the struck leg (only the struck leg was instrumented) and hips. Both legs and hips were dissected. The clinical evaluations presented in this section include both knees as well as both hips.

Temporary impairment was defined as impairment lasting up to 365 days. The clinical evaluations of temporary impairment (in days) for the knees and lower extremities are presented in Table 9. This table includes an estimate of the requirement for surgery in treatment of the injury in the last column. It should be noted the requirement for surgery includes, but is not limited to, surgical reduction of fractures, avulsions, etc.

Table 10 presents the clinical evaluation of each subject for residual (over 1 year) and long-term (over 5 years) impairment. The same body areas and categories are addressed in Table 10 as were addressed in Table 9, with the addition of a sensory category. Calman 22 suffered a lacerated common peroneal nerve in the unstruck leg. Since this was the only sensory injury observed for any of the subjects, the category was not included in Table 9. Also included in these tables are the average days at the four levels of impairment for each category, for the

Table 7. Comparison of struck knee injuries—modified and production bumper impacts

Comparison No.	Calman Mod/Prod	Knee Injuries	
		Modified	Production
1	20/23	Tibial plateau fracture	Ant. and post. cruciate lig. avulsed; laceration of deep fascia, knee capsule and semimem branosus muscle; med. coll. ligament avulsed
2	21/28	None	Tibia and fibula fracture; med. coll. ligament laceration, med. condyle of femur fracture
3	21/22	None	Ant. and post. cruciate lig. avulsed; med. coll. ligament avulsed; popliteal vein ruptured
4	26/23	Tibia plateau fracture post. cruciate and med. coll. ligament avulsed; joint capsule and lateral meniscus ruptured	Ant. and post. cruciate lig. avulsed; laceration of deep fascia, knee capsule and semimembranosus muscle; med. coll. ligament avulsed
5	20/27	Tibia plateau fracture	Post. cruciate and med. collateral ligaments avulsed; rupture of joint capsule
6	26/27	Tibial plateau fracture; post. cruciate and med. coll. ligament avulsed; joint capsule and lateral meniscus ruptured	Post. cruciate and med. collateral ligaments avulsed; rupture of joint capsule
7	24/23	None	Ant. and post. cruciate lig. avulsed; laceration of deep fascia, knee capsule and semimem branosus muscle; med. coll. ligament avulsed
8	24/27	None	Post. cruciate and med. collateral ligaments avulsed; rupture of joint capsule

modified and production bumpers, the reduction in days attributable to the bumper modification (Table 9), the average level of residual and long-term impairment for each category, for the modified and production bumpers, and the reduction attributed to the bumper modification (Table 10). The results of the clinical evaluations for the knees, as presented in Table 9, are graphically displayed in Figure 11 and that information for the lower extremities is presented in Figure 12. The reduction in the average severity level for residual and long-term knee impairment, as listed in Table 10, is displayed in Figure 13.

The two body areas reported in these tables are knees and lower extremities. The lower extremities include the hip and everything below the hip. Therefore, the temporary impairment days for the knees and lower extremities are not always the same for the level of impairment for each category, nor for the total number of days in each category. The categories used for clinical

Table 8. Injuries to the hip and thigh—modified and production bumper impacts

Calman	Bumper	Hip-Thigh Injuries
20	Mod	Superior and inferior pubic rami fractured bilaterally; comminuted femur fracture; cartilage fracture to head of femur
21	Mod	Superior and inferior pubic rami fractured bilaterally; subcapital femur fracture; laceration of the lateral and medial femoral circumflex arteries and the superior gluteal vessels; left sacroiliac joint fracture
24	Mod	Spiral femur fracture; vastus lateralis laceration
26	Mod	Left superior and inferior pubic rami fractured; left acetabulum fracture
22*	Prod	Superior and inferior pubic rami fracture bilaterally; iliotibial band lacerated—right side; wing of ilium fractured—left side
23	Prod	left inferior pubic ramus fractured; left acetabulum fracture
27	Prod	None
28	Prod	Superior and inferior pubic rami fractured bilaterally; femur fracture; vastus lateralis and medialis lacerated

Table 9. Temporary impairment (days)

			Mobility				Cosmetic/Disfig				Pain				Daily Living				
Test No.	Veh. Type	Body Area	4	3	2	1	4	3	2	1	4	3	2	1	4	3	2	1	Surgery
Cm20	M	Knees	7	14	21	328	42			318	7	7	30	316	7	30	90	230	N
		lower ex	14	14	150	180	42			318	14	14	14		21	30	90	219	Y
CM21	M	Knees	4	4	90	180	42			300		7	7	346	4	14	14		Y
		lower ex	14	90	270		42			300		14	14	330	14	90	90	180	Y
CM24	M	Knees																	
		lower ex	7		49	120			60		7	7	14	60	7		21	150	Y
CM26	M	Knees	21	21	120	198	42		30		7	21	30	302	30	60	90	180	Y
		lower ex	90	42	230		42		120		14	14	30	302	30	60	270		Y
CM22	P	Knees	14	50	270		42		300			14	14	330	14	90	256		Y
		lower ex	14	90	270		42		300			14	14	330	14	90	256		Y
CM23	P	Knees	21	21	120	198	42		330		7	21	30	302	30	60	90	180	Y
		lower ex	90	42	230		42		330		14	14	30	302	30	60	270		Y
CM27	P	Knees	14	14	30	306	42		150		7	7	14	332		7	21	332	Y
		lower ex	14	14	30	306	42		150		7	7	14	332		7	21	332	Y
CM28	P	Knees	14	14	30	306	42		150		7	7	14	332		7	21	150	Y
		lower ex	21	21	120	198	42		300		14	14	30	300	14	30	120	196	Y
Average	Knees	M	8	10	58	177	32	0	8	155	4	9	17	241	10	26	49	103	
		P	16	35	113	203	42	0	233	0	5	12	18	324	11	41	97	166	
	Reduction due to Mod		-8	-25	-55	-26	-11	0	-225	155	-2	-4	-1	-83	-1	-15	-49	-63	
	Lower ex	M	31	37	175	75	32	0	45	155	9	12	18	173	18	45	118	137	
		P	35	42	163	126	42	0	270	0	9	12	22	316	15	47	167	132	
	Reduction due to Mod		-4	-5	12	-51	-10	0	-225	155	0	0	-4	-143	4	-2	-49	5	

Table 10. Level of residual and long-term impairment

			Residual Impairment					Long Term Impairment				
Test No.	Veh. Type	Body Area	Mob	Cos	Sen	Pain	D.L.	Mob	Cos	Sen	Pain	D.L.
CM20	M	Knees	1	1		1	1	2			2	1
		lower ex	1	1		2	1	2			2	2
CM21	M	Knees		1		1		2	1		1	1
		lower ex	2	2		2	2	2	1		3	3
CM24	M	Knees										
		lower ex										
CM26	M	Knees	1			1	1	2			2	2
		lower ex	2			1	2	3			2	2
CM22	P	Knees	2	2	1	1	2	2	2	1	1	2
		lower ex	2	2	1	1	2	2	2	1	1	2
CM23	P	Knees	1			1	1	2			2	2
		lower ex	2			1	2	3			2	2
CM27	P	Knees	1			1	1	2			2	2
		lower ex	1			1	1	2			2	2
CM28	P	Knees	1			1	1	2			2	2
		lower ex	1			1	1	2			2	2
Average	Knees	M	0.5	0.5	0	0.75	0.5	1.5	0.25	0	1.25	1
		P	1.25	0.5	0.25	1	1	2	0.5	0.25	1.75	2
		Reduction due to Modification	-0.75	0	-0.25	-0.25	-0.5	-0.5	-0.25	-0.25	-0.5	-1
	Lower ex	M	1.25	0.5	0	1.25	1.25	1.75	0.25	0	1.75	1.75
		P	1.5	0.5	0.25	1	1.5	2.25	0.5	0.25	1.75	2
		Reduction due to Modification	-0.25	0	-0.25	0.25	-0.25	-0.5	-0.25	-0.25	0	-0.25

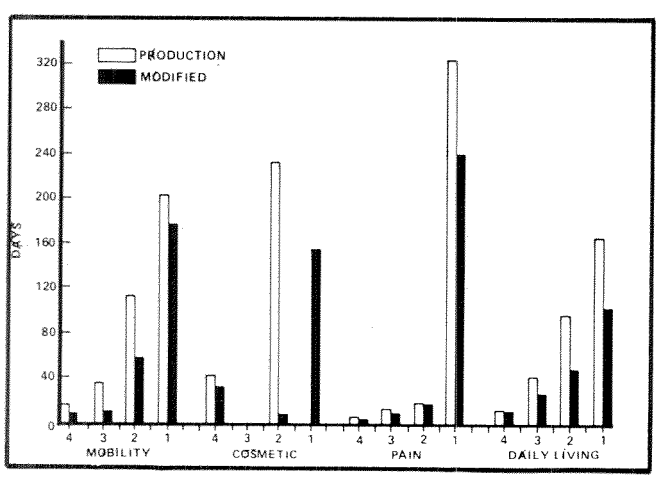

Figure 11. Temporary impairment—knees

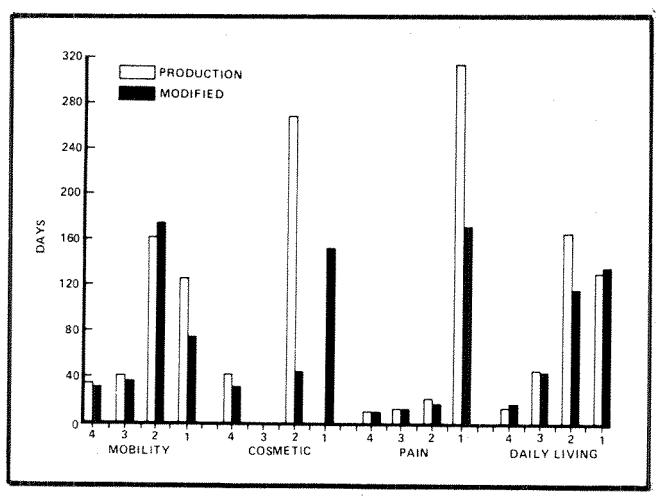

Figure 12. Temporary impairment—lower extremities

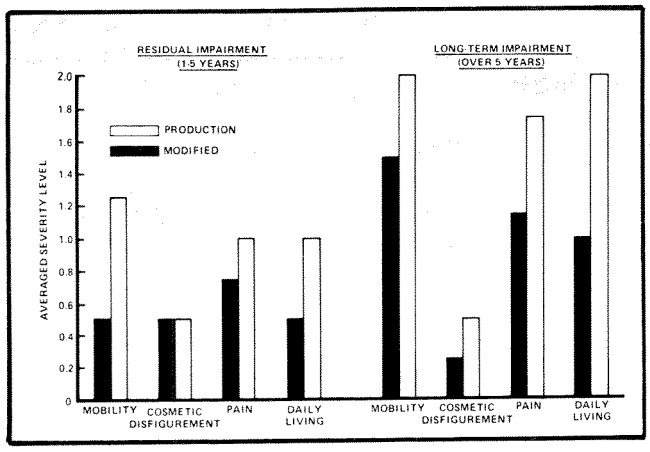

Figure 13. Reduction in average residual and long-term impairment severity levels due to bumper modification

evaluations were: Mobility, Cosmetic Disfigurement, Pain, and Daily Living. The levels (1 through 4) of each category are defined by the following guidelines:

Mobility

1. Impaired mobility with intact functional ability.
2. Impaired mobility with mildly abnormal function. Partially dependent on mechanical assistance. Unable to lift reasonable size objects. Needs crutches, walker, etc.
3. Severely impaired mobility with abnormal function. Dependent on mechanical assistance and wheelchair, occasionally needs attendant.
4. Entirely dependent on attendant or otherwise confined to bed.

Cosmetic Disfigurement

1. Mild—normally covered, amenable to cosmetic cover-up. Readily covered orthosis.
2. Moderate—can be effectively covered by cosmetics and/or forces a change in dress habits. May require orthosis but does not require prosthesis.
3. Severe—prosthesis or cover-up required.
4. Severe—readily observable, not amenable to cosmetic, prosthetic, or clothing cover-up.

Sensory

1. Slight—10 to 25 percent loss to special senses or limbs.
2. Moderate—26 to 50 percent loss to special senses or limbs.
3. Severe—greater than 50 percent loss to special senses or limbs.
4. Maximum—total loss to special senses or limbs.

Pain

1. Normal function with no or occasional nonnarcotic drugs and/or other noninvasive therapy.
2. Normal function only with the use of nonnarcotic drugs and/or other noninvasive therapy.
3. Can function normally only with narcotic drugs and/or invasive therapy.
4. Cannot function normally even with narcotic drugs and/or invasive therapy.

Daily Living

1. Inability to do some nonessential activities.
2. Inability to do most nonessential and/or some essential activities.
3. Partially dependent on assistance for essential functions.
4. Totally dependent on assistance for most activities and functions.

Concluding Remarks and Future Work

This effort has demonstrated a benefit to the struck knees of these pedestrian cadaver subjects at impact velocities of 25mph. This velocity is 5mph above the velocity specified in the NHTSA-proposed safety standard. The results of eight sled tests, four using the Pontiac LeMans production bumper and four using the bumper configuration modified to comply with the specifications of NHTSA's proposed safety standard, showed significant decreases in the days of temporary impairment of the lower extremities, particularly the knees, which can be expected from pedestrian accidents. Decreases in the severity levels of residual (1 to 5yr) and long-term (over 5yr) impairment was also demonstrated.

During this part of the program, the injuries observed in the hip and thigh areas of all subjects, regardless of the bumper design, were similar in severity level. These injuries were caused by contact with the hood leading edge of the 1978 Pontiac LeMans. NHTSA has conducted a study that indicates the frontal geometry of the Pontiac LeMans used for this program is not representative of post-1982 vehicles. Results of this study show that the location of the hood leading edge of more current vehicles is approximately 2in rearward and 4in lower than the LeMans hood leading edge.

Analytical modeling was performed that duplicated the results generated during the LeMans pedestrian impact experiments. Once the model was validated by reproducing these results, the effects of contemporary vehicle front geometry were examined. This was accomplished by maintaining the current production bumper characteristics in the model while changing the vehicle geometry to simulate a contemporary vehicle.

Results predicted that peak forces applied to the leg were identical to the baseline LeMans results, but the maximum hood leading edge forces were significantly lower. When the modified bumper characteristics were incorporated into the model with the new front end geometry, a drop in the peak bumper force and a corresponding increase in the peak hood leading edge force were noted (as was seen in the LeMans modified bumper experiments). This predicted peak hood leading

edge force, while being equal to the LeMans/production bumper hood leading edge force, was less than the force of the LeMans/modified bumper configuration. This indicates the contemporary hood design is less injurious to a pedestrian than the LeMans.

Based on the results of this study, it is planned that a sled buck will be fabricated using a representative contemporary vehicle. A similar 90g modified bumper will be developed and installed. Four cadaver impacts are planned with this modified bumper configuration. A determination will then be made, based on the level of injury associated with hood leading edge contact during these four tests, whether the remaining impacts will be performed using the contemporary front end/production bumper or (if the injury level is unacceptable) a contemporary vehicle with the modified bumper and a modified hood leading edge.

Acknowledgments

The authors would like to acknowledge the contributions of the following: Dr. Charles M. Severin, State University of New York at Buffalo, for subject selection, instrumentation implantation, and lower extremity dissection; Dr. George Alker, Erie County Medical Center, for radiologic examinations; Dr. Justine Uku, Erie County Morgue, for full-body pathologic examinations; and Dr. John D. States, University of Rochester, for clinical evaluations.

References

1. Federal Motor Vehicle Safety Standards; Pedestrian Impact Protection, *Federal Register*, Vol. 46, No. 14, January 22, 1981.
2. Pritz, H.B., E.B. Weis, and J.T. Herridge, "Body vehicle interaction experimental study," Contract No. DOT-HS-361-3-745, Report No. DOT-HS-801-747, March 1975.
3. Pritz, H.B., C.R. Hassler, and E.B. Weis, "Pedestrian impact: baseline and preliminary concepts evaluation," Contract No. DOT-HS-4-00961, Report No. DOT-HS-803-816, May 1978.
4. Vergara, R.D., H.B. Pritz, J.T. Herridge, T.W. Goodnight, and C.R. Hassler, "Compliance techniques for pedestrian protection; feasibility study," Contract No. DOT-HS-5-01218, Final report, January 30, 1981.
5. Pritz, H.B., C.R. Hassler, J.T. Herridge, and E.B. Weis, "Experimental study of pedestrian injury minimization through vehicle design," Proceedings 19th Stapp Car Crash Conference, 1975.
6. Eppinger, R.H., and H.B. Pritz, "Development of a simplified vehicle performance requirement for pedestrian injury mitigation," Proceedings Seventh International Technical Conference on Experimental Safety Vehicles, 1979.
7. Pritz, H.B., "Vehicle design for pedestrian protection," Proceedings Seventh International Technical Conference on Experimental Safety Vehicles, 1979.
8. Garn, S.M.A.K. Poznanski, and J.M. Nagy, "Bone measurement in the differential diagnosis of osteopenia and osteoporosis," *Radiology,* September 1971.
9. Walsh, M.J., and B.J. Kelleher, "Pre-test osteologic studies for determining cadaver skeletal quality," Proceedings Eighth International Technical Conference on Experimental Safety Vehicles, 1980.
10. Hirsch, A.E., R.H. Eppinger, et al., "Impairment scaling from the abbreviated injury scale," Final report, Contract No. DTNH22-80-C-07455 (T.O. No. 8), June 1983.

An Experimental Study of a Modified Compliant Bumper

B. Aldman and
J. Kajzer
Department of Traffic Safety, Chalmers University of Technology

O. Bunketorp
Department of Traffic Safety, Chalmers University of Technology, and Department of Orthopaedic Surgery, University of Göteborg

R. Eppinger
U.S. Department of Transportation, National Highway Traffic Safety Administration

Abstract

In a previous experimental study, a comparison was made between a 1978 Pontiac LeMans car front with a standard bumper and the same front with a more compliant bumper developed by the National Highway Traffic Safety Administration (NHTSA). The tests were made with the two car front and bumper systems mounted at the normal bumper level 45cm and with a lower front configuration with the bumper level 32.5cm above the ground. The experimental biological model system developed at Chalmers University of Technology for detailed kinetic analysis of car front to leg impact sequences was used for this comparison. The tests were carried out at 30 to 32km/h impact speed. A significant difference was found only between the standard bumper in the higher position and the compliant bumper in the lower position.

A still more compliant bumper than that used in the previous test series was produced by NHTSA and tested with the front and bumper system in the normal position 45cm above the ground. Ten impacts to the biological model were made at 32km/h with loaded and unloaded specimens, and five impacts were made at 20km/h with unloaded specimens.

Damage to the knee was seen, including fractures of the knee condyles, in two tests with the loaded specimens. Knee ligament tears were observed in all the tests, indicating the importance of the inertia of the lower leg and foot when the impacts occur at knee level. The modified, more compliant bumper in this test series caused equally serious damage to the knee as did the slightly stiffer bumper in the previous series.

Introduction

In the research program for improved pedestrian safety, NHTSA has developed a compliant bumper system for pedestrian protection(1). One prototype of this bumper system was tested previously at the Department of Traffic Safety, Chalmers University of Technology(2). An experimental model system, developed for detailed kinetic analysis of car front-leg impact sequences, has been used for this purpose(3). In the first test series, 20 human leg specimens were struck with a 1978 Pontiac LeMans car front using the standard rigid and a compliant bumper system. Collisions were made with a normal front configuration with the bumper structure impacting at the 45cm level and a 12.5cm lower front configuration with these structures impacting at the 32.5cm level. The impact velocity was 30 to 32km/h. Serious leg damage was noted with both front configurations and bumper types. The compliant bumper impacting at the 32.5cm level caused less serious damage than the rigid one impacting at the 45cm level. This bumper also seemed to cause less serious damage than the more rigid one at both the 45 and 32.5cm levels, but the difference was not statistically significant.

To try to reduce the risk of injuries to the lower extremity in impacts at the 45cm level, a modified, even more compliant bumper system was developed by NHTSA and tested in the same way as in the previous study.

Scope

The purpose of this study was to investigate the protective effect of the modified, more compliant bumper system developed by NHTSA. The tests were carried out at the 45cm impact level and comparison made with the rigid bumper and the less compliant bumper investigated in the earlier test series.

Method and Material

The experimental setup and the test procedure have been described earlier(3,4,5). The simulated car front was the same as in the previous series with the rigid and the moderately compliant bumper(2) (Figures 1 and 2). In the actual series, all tests were made with the car front mounted in such a way that the middle of the bumper was at the 45cm level. This bumper level was kept during the impact, and the test cart was not braked until 120 to 140ms after impact.

The material properties of the deformable polyurethane block of the compliant bumper and the flexible plastic cover were the same in the two series.

The force-deflexion relationship of the three bumper types was measured statically by pressing a 60mm iron tube at right angles against the impact area with and without the plastic cover (Figure 3).

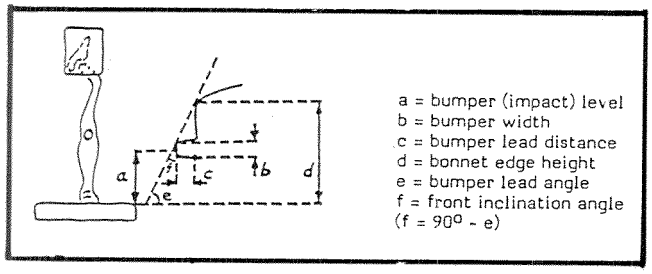

Figure 1. The experimental setup

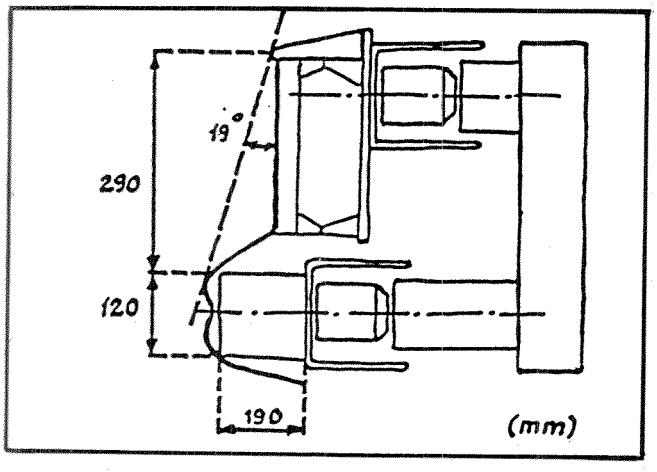

Figure 2. Section of the impact zone

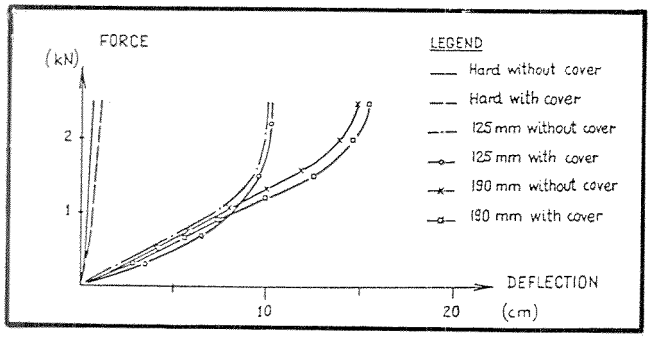

Figure 3. The force-deflexion relationship of the three bumper types with and without the plastic cover (static test)

Unembalmed human leg specimens with the hip joint included were used. These originated from individuals 63 to 87 years of age without skeletal abnormalities. Each specimen was radiographed, and the stability of the knee joint was measured before the test. The bone mineral content was not measured in this series since equipment for this was not available at the time.

The specimen was kept in a standing posture with the foot covered by a shoe on a foot plate before the impact with the toes turned 15° toward the car front from a pure lateral impact. It was balanced with the knee extended and struck on its anterolateral aspect. A simulated, 50kg body mass was connected to the iliac bone. This mass consisted of two equal metal blocks connected with steel wires and separated by plastic foam. The specimen and the body mass were supported by stabilizing cords released by the test cart just before impact.

Five tests were made at 32km/h with the full load (50kg) on the specimen. Five tests were made at the same velocity with the specimen unloaded, i.e., with the body mass supported by cords and the specimen hanging with the foot just above the foot plate. Another five tests at 20 to 21km/h impact velocity were made with the specimen unloaded in the same way.

The impact sequence was covered by high-speed cinematography. Accelerometers were strapped on the specimen opposite the impact side at the ankle, the impact level, and the knee. The impact forces were recorded from two horizontal force transducers in the bumper and two in the bonnet. All channel classes signals were stored on magnetic tape (filters used).

The specimens were radiographed after the test, and the knee stability was measured as in the previous study(2). A complete dissection was made after the test. The severity of the damage to the specimen was classified according to the ADS system, similar to the AIS system for living human bodies.

Results

Fifteen tests were made in this series. All experiments provided a complete set of data. The specimen data are shown in Table 1, the kinetic data in Table 2, and the damage in Table 3.

Damage to the Specimen

Knee damage was noted in all experiments. There was no damage in other parts of the specimens. The knee damage included fractures of the tibial condyles and stretch or rupture of the ligaments and the knee capsule. Fractures of the tibial condyle were noted in two of five experiments with loaded specimens at 32km/h. One of these was an intraarticular fracture (No. 4). There was also a complete rupture of at least one of the knee ligaments in the fractured specimens. At this velocity, the fact that the leg was loaded by a simulated body mass did not seem to influence the damage to the collateral or cruciate ligaments. Complete (ADS = 3) or almost complete (ADS = 3-) ruptures were noted in two or more of these ligaments or in the capsule in all tests with loaded specimens at 32km/h. The same type of ligament damage was noted in four of five tests with unloaded specimens at this velocity. In the fifth test, there was only a partial rupture (ADS = 2) of the medial collateral ligament. The specimen in that case was from the youngest individual (63yr) in the series. At the lower speed (20km/h), the ligament damages were complete in two and partial in three of the five tests.

Table 1. Specimen data

Test Conditions	Test No.	Age/Sex	Weight kg	Specimen Tibia Length mm	Condyle Width mm	Constitution
	1	83M	6.0	370	80	Ordinary
A:	2	71M	7.0	360	78	Ordinary
loaded:	3	91F	5.5	330	73	Ordinary
= 32km/h	4	67M	6.0	360	81	Sturdy
	5	78M	6.0	340	80	Ordinary
	6	74M	8.0	350	85	Sturdy
B:	7	84F	7.0	360	75	Ordinary
unloaded:	8	75M	8.0	380	81	Sturdy
= 32km/h	9	63M	6.0	360	80	Ordinary
	10	84F	7.0	330	73	Ordinary
	11	67F	6.5	330	74	Ordinary
C:	12	75F	9.0	380	86	Sturdy
unloaded:	13	81M	8.5	360	88	Ordinary
= 20km/h	14	86M	7.5	360	86	Ordinary
	15	70F	6.5	350	77	Ordinary

Table 2. Kinetic data

Test Conditions	Test No.	Peak Impact Force Bonnet Edge kN	Peak Impact Force Bumper kN	Peak Acceleration Ankle Joint g	Peak Acceleration Impact Level g	Peak Acceleration Knee Joint g
	1	0.9	2.6	45	78	72
A:	2	0.8	2.8	40	65	70
loaded:	3	2.0	2.6	35	67	65
= 32km/h	4	1.2	2.5	40	65	65
	5	1.2	2.6	27	63	68
	6	0.8	3.1	50	78	54
B:	7	1.5	2.5	40	74	65
unloaded:	8	1.3	2.7	30	62	66
= 32km/h	9	1.4	2.5	38	62	68
	10	3.0	3.1	20	98*	102*
	11	1.4	1.7	30	50	46
C:	12	0.8	2.4	40	44	34
unloaded:	13	0.8	2.4	36	43	35
= 20km/h	14	1.0	2.0	26	60	34
	15	0.7	2.0	28	42	43

* Some play was noted in the accelerometer mounting.

The medial collateral ligament was damaged in all tests. The ligament was completely ruptured in nine tests at 32km/h and in two tests at 20km/h. In nine cases, there was a complete rupture of the ligament at the femoral attachment point with a bone fragment in five and without a bone fragment in four cases. In two cases, there was a complete rupture of the superficial part of the ligament quite near the tibial attachment point. The deeper part of the ligament and the capsule were completely ruptured in one and partially ruptured in the other (No. 11) of these cases.

One or both of the cruciate ligaments were completely or almost completely ruptured in seven of ten experiments at 32km/h. Complete ruptures of the cruciate ligaments were not seen at 20km/h. However, almost complete and partial ruptures of the cruciates were noted in two experiments at this lower velocity. The cruciates were ruptured at the femural attachments in all except two cases.

Table 3. Nonminor damage (ADS≥2) and knee instability parameters

Test Conditions	Test No.	Fracture of the Tibia Condyle (ADS)	Rupture of the Knee Ligaments[1] and Capsule (ADS)				Instability Parameters[2]					Maximum ADS
			M	A	P	C	e deg	v deg	r deg	KAI deg	s cm	
	1	3	3	0	0	3	11	24	20	55	0.7	3
A:	2	0	3	0	3	3	3	29	41	73	0.3	3
loaded:	3	0	3	3	3	3	28	34	68	130	2.1	3
V = 32km/h	4	3	3	3-	0	0	7	33	32	72	0.6	3
	5	0	3	3	3-	3	18	30	44	92	0.7	3
	6	0	3	0	0	3	0	13	14	27	0.3	3
B:	7	0	3	3	3-	3	8	22	27	57	0.7	3
unloaded:	8	0	3	3-	0	3	14	11	26	41	0.2	3
V = 32km/h	9	0	2	0	0	0	2	6	15	23	0.2	2
	10	0	3	3	3-	3	13	22	33	68	0.8	3
	11	0	3	0	0	2	0	13	13	26	0.3	3
C:	12	0	2	0	0	0	4	5	5	14	0.2	2
unloaded:	13	0	2	2	0	0	1	1	0	2	0.1	2
V = 20km/h	14	0	2	0	0	2	1	6	11	18	0.0	2
	15	0	3	3-	3-	2	2	32	41	75	0.5	3

[1] M = the medial collateral ligament; A = the anterior cruciate ligament; P = the posterior cruciate ligament; C = the capsule of the knee (A - behind the ADS number indicates that there was slightly less severe damage than the number itself defines).

[2] e = hyperextension increment; v = (vargus+) algus bending increment (20° flexion); r = inward + outward lower leg rotation increment (20° flexion); s = sagittal translation increment (20° flexion); KAI == e+v+r = the total Knee Angular Instability increment.

Impact Forces

The time histories of the bumper forces were similar for the loaded and unloaded specimens at 32km/h (Figures 4a, 4b, and 4c). The peak force varied between 2.5 and 3.1kN. The force pulses were somewhat broader for the unloaded specimens (Figure 4b). This probably corresponds to the somewhat higher specimen weights in these tests (Table 1). The force pulses were somewhat more extended at the lower velocity (Figure 4c), and the peak forces were about 2.0kN in these tests. The velocity (Figure 4c) and the peak forces were about 2.0kN in these tests. The bonnet edge peak forces were low (less than 3kN in all cases) and approximately the same in tests with loaded and unloaded specimens at 32km/h (Figures 5a, 5b, and 5c).

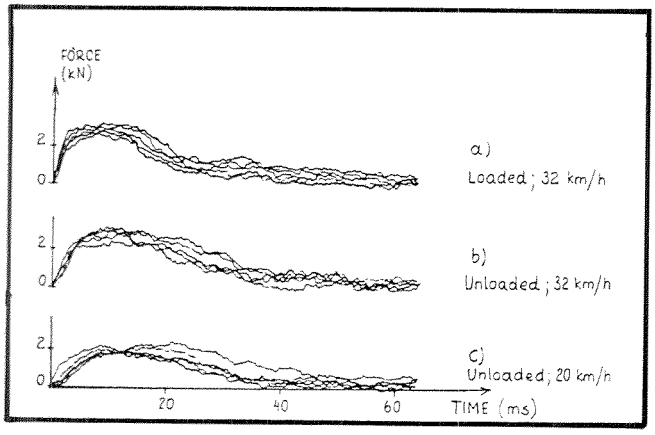

Figure 4. Time histories of bumper forces for (a) loaded and (b) unloaded specimens at 32km/h for (c) unloaded specimens at 20km/h impact velocity

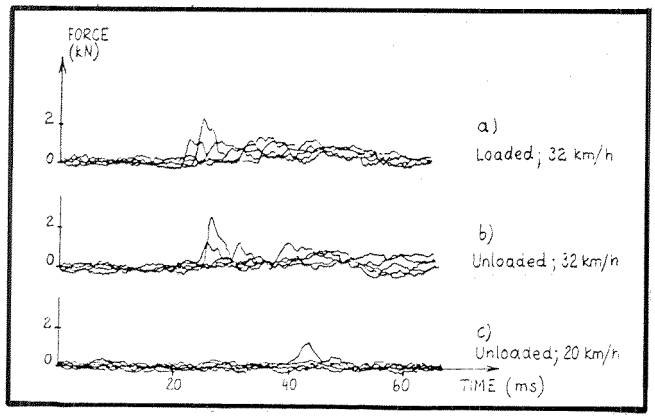

Figure 5. Time histories of bonnet edge forces for (a) loaded and (b) unloaded specimens at 32km/h and for (c) unloaded specimens at 20km/h impact velocity

Accelerations

The magnitude of the accelerations of the leg specimens with loaded and unloaded specimens was the same (Table 2). At 32km/h, the accelerations at the knee level and at the impact level varied between 50 and 100g in both test configurations. The accelerations at the ankle joint varied between 20 and 50g. The accelerations of the leg specimens in impact test with the less compliant bumper at the 45cm level in the previous series(2) were almost the same as in this series.

Discussion

According to the results of this and the previous studies(2,3,4,5), the risk of injuries to the ankle joint, the lower leg, the femur, and the hip joint seems to be low at or below 32km/h if the bumper strikes 45cm above the ground level. No damage was noted in these parts of the specimens in this series, and isolated damage was noted in only a few cases the previous series with the rigid and the less compliant bumper at the 45cm level(2). There may be a higher risk of moderate (ADS = 2) damage to the ankle joint with the rigid bumper at the 45cm impact level due to the somewhat greater accelerations in these cases. Two such damages were noted in five tests in the previous series with that bumper(2). No damage has been noted in the ankle joints in 15 tests with the two compliant bumpers. The bumper type does not seem to influence the risk of damage to the other parts of the specimens except for the knee if the bumper strikes at the 45cm level.

On the other hand, there is a high risk of injury to the knee joint if the bumper strikes at this level. There was a high incidence of serious (ADS = 3) knee damage in this test series as in the previous one with the two bumper types at the 45cm level(2). In this series with the modified, more compliant bumper, serious (ADS = 3) knee damage was noted in all tests with loaded specimens and in four of five tests with unloaded specimens at 32km/h. The type of damage and the ADS damage severity was the same as in the previous series with the less compliant bumper at the 45cm level.

The vertical load on the specimen does not seem to influence the ADS damage severity significantly. However, the load may influence the type of damage. Fractures of the tibial condyle were noted only if the specimens were loaded with the body weight. This type of damage was also noted in the previous series with loaded specimens(2). There is quite a high risk of such a "bumper fracture" if the pedestrian is struck when walking because the vertical load on the knee exceeds the static body weight during approximately 50 percent of the walking cycle(6,7).

The inertia of the lower leg and foot is probably the most important injury-causing factor if the bumper strikes at the 45cm level at 32km/h. This injury mechanism explains the high incidence of ligament damage in this and the previous series for 45cm bumper level. The injury-producing effect of the inertia exists even at 20km/h. Serious ligament damage (ADS = 3) was noted in two collisions at this lower velocity. The damage was moderate (ADS = 2) in the other three tests.

The knee ligaments are very vulnerable to impact forces near the knee if the leg is struck on its fronto-lateral aspect 10 to 20° from a pure lateral impact.

The degree of damage to the knee joint was estimated by the Knee Angular Instability Increment (KAI) and the sagittal translation increment (s) (Table 3). There seems to be a limit between isolated serious (ADS = 3) and combined serious damage to the cruciate and collateral ligaments for a KAI-value approximately equal to 40°. A complete rupture of the medial collateral ligament corresponds to a valgus instability increment exceeding 10°. A sagittal translation increment exceeding 0.3cm seems to be associated with a rupture of the anterior cruciate ligament. In test number 15, the two cruciates were ruptured macroscopically in 70 percent of the cross-section area. However, the instability parameters indicate a considerable elongation of the rest of the ligament tissue corresponding to serious knee ligament damage in that case.

The risk of knee ligament damage appears to be the same for the two compliant bumpers for a 45cm impact level. This might be explained by the force-deflexion relationship of the two bumpers(Figure 3). This relationship does not differ significantly below 70mm compression. The 70mm compression corresponds to a bumper force equal to 1kN in a static test. This is approximately the ultimate tensile strength of the medial collateral ligament(8,9). Thus, theoretically the more compliant bumper will cause a ligament injury of the knee as easily as the less compliant one. There might even be a higher risk of knee ligament injuries with the 19cm more compliant bumper as the front inclination is less steep in this case and might give less support against the femur and thus less protection against knee bending during the impact compared to the 12cm less compliant bumper (Figure 2). On the other hand, there might be less risk for injuries due to direct impact forces with the modified, more compliant bumper according to these deformation characteristics. However, dynamic deformation tests should be made to clarify this.

In all tests with this biomechanical leg impact model, the test cart was accelerated to reach a constant speed before the collision and did not brake during impact. Furthermore, the bumper impact level was equal to the static bumper level. In some real accidents, the car front may pitch down due to braking before the impact. The less compliant bumper tested in the previous series(2) was investigated at the 45cm impact level as well as the 32.5cm level. The risk of serious (ADS = 3) damage seemed to be

lower with the compliant bumper at the 32.5cm level compared with the ordinary rigid one. However, the number of tests was small, and the difference was not statistically significant. According to the results of our earlier test series(3,4,5), the risk of serious lower leg and knee injuries is reduced significantly if the bumper impacts at the mid-tibia level. The risk of lower leg fractures is further reduced with a compliant bumper impacting at the mid-tibia level. However, there may be a risk of such fractures even if the impact force is low if the leg is loaded with the body weight during impact(4).

Conclusion

If the injury mechanisms and tolerance levels can be assumed to be the same for living people as for the specimens, the following conclusions can be drawn from these experiments:

- The risk of serious (AIS = 3) knee ligament injuries is at its maximum for a bumper impact at the knee level.
- At 32km/h, serious (AIS = 3) knee ligament injuries will be caused practically always if the leg is struck at the knee level on its anterolateral side with an extended knee.
- For a bumper impact at the knee level at 20km/h, the risk of serious (AIS = 3) knee ligament injuries is reduced but it cannot be neglected.
- The inertia of the lower leg and foot is the most important injury-producing factor for a bumper impact at the knee level.
- Compared to the rigid bumper, the less compliant and the modified, more compliant bumpers tested in these series do not reduce the risk of serious (AIS = 3) knee ligament injuries if the bumper strikes at the 45cm level.
- The primary, less compliant bumper and the modified, more compliant bumper will cause injuries of equal severity if the bumpers strike at the 45cm level.
- The less compliant and the modified, more compliant bumper will both probably reduce the risk of serious injuries to the lower leg and ankle joint compared to the rigid bumper.

References

1. Daniel, S., Jr., R.H. Eppinger, and D. Cohen, "Considerations in the development of a pedestrian safety standard," Proceedings Seventh International Technical Conference on Experimental Safety Vehicles, Washington, D.C., U.S. Department of Transportation, pp. 724-738, 1979.
2. Bunketorp, O., B. Aldman, R.H. Eppinger, B. Romanus, L. Thorngren, and T. Hansson, "Experimental study of a compliant bumper system," Proceedings of the Joint IRCOBI-Stapp Conference, San Diego, October 17-19, 1983, pp. 287-297.
3. Aldman, B., L. Thorngren, O. Bunketorp, and B. Romanus, "An experimental model for the study of lower leg and knee injuries in car-pedestrian impacts," Proceedings 5th IRCOBI Conference on the Biomechanics of Impacts, Bron: IRCOBI Secretariate, pp. 180-193, 1980.
4. Bunketorp, O., B. Aldman, R. Johnson, B. Romanus, B. Roos, and L. Thorngren, "Experimental studies on leg injuries in car-pedestrian accidents," Proceedings 6th IRCOBI Conference on the Biomechanics of Impacts, Bron: IRCOBI Secretariate, pp. 243-255, 1981.
5. Aldman, B., B. Lundell, L. Thorngren, O. Bunketorp, and B. Romanus, "Physical simulation of human leg-bumper impacts," Proceedings 4th IRCOBI Conference on the Biomechanics of Trauma, Bron: IRCOBI Secretariate, pp. 232-242, 1979.
6. Morrisson, J.B., "The mechanics of the knee joint in relation of normal walking," *J. Biomechanics,* 3:51, 1970.
7. Strandberg, L., "On accident analysis and slip-resistance measurement," *Ergonomics,* Vol. 26, No. 1, pp. 11-32, 1983.
8. Aldman, B., L. Thorngren, O. Bunketorp, and B. Romanus, "An experimental model system for the study of lower leg and knee injuries in car-pedestrian accidents," Proceedings Eighth International Technical Conference on Experimental Safety Vehicles, U.S. Department of Transportation, Washington, D.C., pp. 841-849, 1980.
9. Kennedy, J.C., R.J. Hawkins, R.B. Willis, and K.D. Danylchuk, "Tension studies on human knee ligaments," *J. Bone and Joint Surgery,* Vol. 58-A, No. 3, pp. 350-355, April 1976.

Simplified Test Recommendations for Pedestrian Protection

J. Harris
Transport and Road Research Laboratory, Department of Transport, Crowthorne, United Kingdom

Abstract

Pedestrian accidents are a serious problem in many countries, and some form of vehicle design recommendations to improve pedestrian protection are urgently required.

Research has shown that in an accident the severity of injury is influenced mainly by impact speed, shape of the car, stiffness of the car components struck by the pedestrian, and the stature and strength of the pedestrian (young or old, frail or strong). A measure of the importance of these variables has now been demonstrated, but limitations, in the performance of dummies and gaps in existing knowledge, particularly a human tolerance, have also been identified. These limitations reduce the precision with which car design requirements for pedestrian safety may be specified. Obtaining further information and proving a test dummy to overcome these limitations may be a lengthy process.

Sufficient information is available to allow generalised recommendations to be compiled that could be used as guidelines until more precise requirements may be determined.

This paper proposes a set of simple guidelines for the depth and stiffness of protection to be built into the various components of the car front, which are determined by the shape chosen for the front profile. Meeting these guidelines should insure a good level of protection but, although necessary, they may not be entirely sufficient, and further experience may eventually suggest some fine tuning of the proposals.

This paper shows that for the areas of a car that are important for pedestrian safety (bumper, bonnet leading edge, and bonnet top), the protection requirements may vary considerably according to the overall shape of the front of the car.

It can be shown that the major safe characteristics of these areas may be isolated and examined (with due regard to the overall shape of the car) to assess their potential for causing injury.

Methods of testing each of these areas are being proposed and performance criteria are suggested, which are based on a maximum safe impact speed of 40km/h and an acceptable injury level of severity of AIS 2.

These test criteria are—

- Bumper—Assessed by impact test using a 10kg legform. The maximum recommended impact force is adjusted with respect to the height aboveground and the vertical depth of the bumper.
- Bonnet Leading Edge—Assessed by an impact test using a 16kg hipform. The impact velocity is adjusted with respect to the height of the bonnet edge and the bumper-to-bonnet lead. The recommended maximum impact force is 5kN.
- Bonnet Top—Assessed by a conventional headform impact test using adult and child headforms. The impact velocity is adjusted with respect to the height of the bonnet edge, the bumper-to-bonnet lead, and also the location of the impact point.

It is suggested that these performance criteria may be used as the basis of recommendations for the pedestrian safety performance of cars and used as preliminary guidelines before final recommendations are made for regulatory tests.

These proposals formed the basis of the U.K. contribution to the EEVC ad hoc group on pedestrian protection.

Basis of Recommendations

Accident investigations and tests simulating accidents(1) have shown the regions of a car that most frequently cause injury are the bumper, the leading edge of the bonnet and wing, and the top of the bonnet, wing, and windscreen frame. Some measure of protection may be built into each of these areas, but the appropriate stiffness characteristic will depend on the overall shape of the front of the vehicle, the designed maximum safe impact speed, and the severity of injury considered to be acceptable.

In these proposals, the aim is to give a high probability that the severity of injuries from contacting these areas of a car will be limited to AIS 2 or less, for accidents at speeds up to 40km/h.

These levels have been chosen to reduce the risk of permanent disability, particularly to the legs, and because at least 30 percent of fatalities are reported to occur from accidents at speeds of 40km/h or less(1).

The stiffness recommendations and design performances are derived from the results of a series of computer simulations(2) studying the influence of vehicle shape and stiffness on the severity of an impact to a pedestrian.

These investigations showed clearly that in an accident all features of the shape of the front part of a car interact to influence the severity of an impact, but the following broad trends could be clearly identified for the bumper and bonnet leading edge and also for head impact to the bonnet top and surrounding structures.

Bumper and Spoiler

Current bumpers mounted at approximately 450mm above the ground can cause severe loading to the knee and lower leg of an adult and to the pelvis and upper leg of a child, with knee injury possibly the most likely to cause permanent disability. These injuries result from bending moments and shear forces required to accelerate the lower leg and also from crush forces at the point of impact.

Lowering the bumper gives an improvement for the adult, moving the impact away from the knee to the less vulnerable lower leg. For the child, the impact moves away from the pelvis and closer to the knee. Although serious knee injury to the child has not been a feature of accidents in the past, a change of this nature may put knees slightly more at risk for some age groups.

The introduction of a spoiler (air dam) mounted less than 50mm behind a 450mm bumper (in effect, a deep bumper) reduces knee bending moments and shear forces, and, if the upper part of the bumper is compliant, this then gives improvements similar to those obtained with a low bumper.

This suggests that the injury potential of a bumper or bumper/spoiler combination is influenced by its height above the ground and its effective vertical depth.

Typical simulation results are shown in Table 1.

The 40km/h simulations also show that the total energy absorbed by the bumper and spoiler is 1,000 to 1,200J (approximately 600J per leg) for all car shapes except those with zero bumper lead, and the effective mass of the adult leg striking the bumper ranges from 8 to 10kg.

If the onset of serious knee injury is set at 6° angular rotation of the knee joint(3), then serious injury from bumper contact would probably be avoided by bumpers meeting the following recommendations.

Bumper Recommendations

It is recommended that the appropriate impact force shown in Table 2 is not exceeded when a bumper is struck at any point at a velocity of 40km/h (11m/s) by a leg impactor of 10kg mass that spans the total effective depth of the bumper. In Table 2, the recommended force varies with respect to the height of the centre of the bumper above the ground and the effective vertical depth of the bumper.

A spoiler will only effectively help to reduce knee injury if it is mounted less than 50mm behind the bumper.

Typical safety bumpers (spoilers) absorb approximately 500 to 600J of energy from each adult leg in a 40km/h impact.

Leading Edge of Bonnet and Wing

The bonnet leading edge is the single most important area controlling the characteristics of an impact to a pedestrian.

Table 1. Results of child and adult leg impact simulations for different bumper arrangements

Bumper Plus Spoiler			Adult		Child	
Height of Centre Above Ground (mm)	Total Vertical Depth (mm)	Total Stiffness (kN)	Lateral Angular Rotation of Knee Joint (degrees)	Knee Shear Force (kN)	Knee Bending Moment (Nm)	Pelvic Acceleration (g)
350	100	4	0.3	1.4	239	65
450	100	4	6.1	3.4	189	98
450	30	4	11.7	3.0	—	—
350	280	6.5	3.7	2.2	250	75

Table 2. Recommended leg impactor to bumper loads for different bumper arrangements

Height of Centre of Bumper (and Spoiler) above ground (mm)	Recommended Safe Loads (kN) For Vertical Depths of Bumper (and Spoiler) of	
	100mm	300m
350	5	7
450	3	—

Increasing the bonnet height and reducing the bumper-to-bonnet-edge lead causes a progressive increase in the energy of the bonnet edge contact and a consequent reduction in head impact velocity.

In the simulations, the energy absorbed by the bonnet leading edge in a 40km/h impact with an adult ranges from 64 to 1,025J as shown in Table 3.

Table 3. Energy absorbed by the bonnet leading edge with respect to bonnet height and bumper lead in simulations of a 40km/h impact with an adult

Bumper to Bonnet Lead (mm)	Energy Absorbed by Bonnet Edge (J) for Bonnet Height of		
	600mm	720mm	850mm
0	312	700	1025
150	64	341	564
250	—	134	425
350	—	115	269

The effective mass striking the bonnet edge ranges from 5kg for a 600mm-high bonnet to 16kg for one 850mm high.

Adult and child tolerance levels are generally not exceeded if the leading edge stiffness does not exceed 5kN.

Serious injury from contact with the bonnet leading edge would probably be avoided if the following recommendations are satisfied.

Bonnet and Wing Leading Edge Recommendations

It is recommended that the impact force not exceed 5kN when a 16kg hip impactor strikes the leading edge of a bonnet, wing, or head lamp surround in a fore and aft direction at the velocities shown in Table 4. These velocities are appropriate for the bonnet edge arrangements shown with respect to a vehicle impact of 40km/h (11m/s).

Table 4. Hip impactor velocity m/s with respect to position of bonnet leading edge

Bumper to Bonnet Lead (mm)	Hip Impactor Velocity m/s for Bonnet Heights of		
	600mm	720mm	850mm
0	6	9	11
150	3	7	8
250	—	4	7
350	—	4	6

The effective vertical depth of the leading edge is important. Essentially the deeper it is, the safer it is.

Although it may be possible to design a nearly vertical high car front with an acceptable stiffness characteristic, this shape is inherently dangerous because it is likely to knock a small child forward to the ground. This increases the risk of being run over.

Bonnet Top

This section considers head impact with the top of the bonnet or wings, the scuttle, and windscreen lower edge.

In the simulations, child head impact is confined to the forward region of the bonnet up to 800mm behind the bumper. Impact velocities are about 10m/s for all but the 850mm-high bonnets, which are generally closer to 7m/s.

Adult head impact is, with one exception, more than 1,000mm behind the bumper with impact velocities, at right angles to the bonnet, ranging from 8 to 14m/s.

From the simulations, typical adult head impact velocities normal to the bonnet are shown in Table 5.

Table 5. Simulation results showing impact velocity of adult head normal to bonnet top, in relation to bonnet height and bumper lead

Bumper to Bonnet Lead (mm)	Head Impact Velocity (m/s) for Bonnet Heights of		
	600mm	720mm	850mm
0	12	9	8
150	13	11	8
250		13	8
350		14	9

On the basis of these simulation results, current head protection standards would be met if the structures under consideration satisfy headform impact at the velocities specified in the following section.

The simulation results are based on the performance of a dummy that, although improved at the knee and hip joint, still has a torso that is too stiff. The headform impact velocities would, therefore, be more representative if they were based on the results of a large number of cadaver tests.

Bonnet Top Recommendations

The top of the bonnet and wings, scuttle, and windscreen lower edge would meet current safety standards for the head if existing HIC or acceleration acceptance levels are not exceeded when struck by headform impactors at velocities in accordance with those recommended in Table 6. These impact velocities, at right angles to the

Table 6. Recommended headform impact velocity with respect to car shape and position of impact point

Distance of Test Point Behind Bumper (mm)	Bumper to Bonnet Lead (mm)	Recommended Head Impact Velocity (m/s) for Bonnet Heights of 600mm	720mm	850mm
Under 800	All	10	10	7
Over 800	0	12	9	8
	150	13	11	8
	250	—	13	8
	350	—	14	9

surface of the bonnet and wings, are appropriate for the bonnet edge arrangements shown with respect to a vehicle impact of 40km/h (11m/s).

Two sizes of impactor are proposed, one representing a child headform for tests on the forward section of bonnet within 800mm of the bumper and an adult headform for the rear section more than 800mm behind the bumper.

Conclusion

It has been shown in various simulations and tests that, for the areas of a car important for pedestrian safety (the bumper, bonnet leading edge, and bonnet top), the protection requirements may vary considerably according to the overall shape of the front of the car.

It can be shown the major safety characteristics of these areas may be isolated and examined (with due regard to the overall shape of the car) to assess their potential for causing injury. Methods of testing each of these areas are proposed, and performance criteria are suggested based on a maximum safe impact speed of 40km/h and an acceptable injury level of severity AIS 2.

These test criteria are—

- Bumper—Assessed by impact test using a 10kg legform. The maximum recommended impact force is adjusted with respect to the height aboveground and the vertical depth of the bumper.
- Bonnet Leading Edge—Assessed by an impact test using a 16kg hipform. The impact velocity is adjusted with respect to the height of the bonnet edge and the bumper-to-bonnet lead. The recommended maximum impact force is 5kN.
- Bonnet Top—Assessed by a conventional headform impact test using adult and child headforms. The impact velocity is adjusted with respect to the height of the bonnet edge, the bumper-to-bonnet lead, and also the location of the impact point.

It is suggested these performance criteria may be used as the basis of recommendations for the pedestrian safety performance of cars and used as preliminary guidelines before final recommendations are made for regulatory tests. These proposals formed the basis of the U.K. contribution to the EEVC ad hoc group on pedestrian protection.

References

1. Ashton, S.J., J.B. Pedder, and G.M. Mackay, "Pedestrian injuries and car exterior," Proceedings International Automobile Engineering Congress, Detroit, February 1977.
2. Harris, J., and N.D. Grew, "The influence of car design on pedestrian protection," Proceedings Tenth International Technical Conference on Experimental Safety Vehicles, Oxford, England, July 1985.
3. Fowler, J.E., and J. Harris, "Practical vehicle design for pedestrian protection," Proceedings Ninth International Technical Conference on Experimental Safety Vehicles, Kyoto, Japan, November 1982.

Experimental Simulation of the Pedestrian Impact

G. Stürtz
Daimler-Benz AG, Sindelfingen, Federal Republic of Germany

Abstract

Higher complexity of accident events makes it more difficult to analyze the efficiency of protection measures for pedestrians than for vehicle occupants. Considering the quality of transformation of the results found (dummy quality) as well as their statistical reliability (reproducibility), it is necessary to find a methodically clear solution.

The special problem of pedestrian accident simulation will be explained by examples showing the complexity of accident events, by valuation of protection measures, and by the reproducibility and transmissibility of results.

Advantages and disadvantages of experimental methods (integrated or component tests) to valuate the vehicle exterior will be shown, using our own test results, as well as results taken from literature. Following this, a procedure is derived.

Finally, car design characteristics are described that improve the protection of exterior road users.

Introduction

In the Federal Republic of Germany in 1983, 70 percent of the pedestrians and two-wheel riders—exterior road users—were impacted by a passenger car. Exterior road users have a rate of 46 percent among fatally injured traffic participants(1).

Among exterior road users, the protection of pedestrians has priority since they show a higher rate and absolute term of fatalities. Contrary to passenger car occupants, the distance of deformation for impact pulses is considerably shortened and the ratio of mass differs extremely. Vehicle impact as the main cause of trauma is overlapped by an additional trauma caused by the road surface.

Mitigation of accident trauma can be achieved by measures concerning hardness and plasticity of the impact, as well as accident kinematics. These are in conflict with other design characteristics.

Valuation of protection measures is more difficult for vehicle exterior safety than for passenger occupant safety. This is caused by the higher complexity of accident events. Considering the quality of transformation of the results found, as well as their statistical reliability, it is necessary to find a solution to the problem, at least for qualitative statements.

Problem of Accident Simulation

The main problem of pedestrian accident simulation will be explained by statements regarding the complexity of accident events, the efficiency of protection measures, and the reproducibility and transmissibility of results.

Simulation of Accidents With Occupants and Pedestrians

Principal differences exist between the simulation of accidents with passenger car occupants and pedestrians with regard to accident and traffic participant parameters (Figure 1).

		Occupants	Pedestrians
Accident Frequency (p.c.)		60[1]	77[2,3]
Braking of Vehicle		Yes	Yes[4]
Velocity of Traffic Participant Perpendicular to Impact Direction		No	Yes
Impact Direction of the Traffic Participant		Frontal	Divers
Physiological Data			
• stature[3,5]	$\bar{x}$ (cm)	173	160
	R: 5 - 95% (cm)	157-179	101-176
• age[3,5]	$\bar{x}$ (years)	24	31
	R: 5 - 95% (years)	15-64	3-80
• male sex (p.c.)			

1 Daimler-Benz accident data
2 60 percent for the six most frequent types of collision
3 Diversion by literature (1,2,3)
4 Lowering of contact zones
5 Severe or lethal injured traffic participants(1)

Figure 1. Selected parameters of accidents with traffic participant in the case of passenger car frontal impacts

In accidents involving pedestrians, the individual types of collision represent smaller percentages of the accident events than in accidents involving passenger car occupants (a maximum of 20 percent).

In contrast to occupant accidents, the motion sequence in pedestrian accidents is mostly three-dimensional, and the head impact of adults occurs later.

The simulation of pedestrian speed at impact $v_{ç}$ = 9km/h(2) and the resulting favorable increase of the contact zone has to be omitted, otherwise reproducibility would be drastically reduced.

In case of pedestrians, a higher range of stature and age of traffic participants has to be considered. This means also a greater range of different biomechanical load capacities, and it requires a stronger differentiation in the

anthropometry and characteristics of the dummies. Sex-specific signs have to be considered more intensely.

The selected parameters show a higher complexity of the pedestrian accident and of its simulation.

Valuation of Protection Measures

The behavior of a dummy is different from that of a living human being. This results in different kinematics, position of contact zones, and accident loads. Protection measures, therefore, can only be valuated qualitatively (with reference to the type of dummy). Efficient points of application for protection measures can be found by correlation of trauma and cause of injury (accident research)(2,4).

Transmissibility of Results

Dummies are at present insufficient substitutes for living human beings. Only in individual cases(2) can results of simulation be transferred to real cases by derived correlation. The low simulation quality of dummies is contradictory to the required highly sophisticated accident simulation.

For analyses of exterior passive safety of passenger cars, dummies require an extensive revision. For instance, the adult pedestrian dummy (Hybrid II P ≙ 95 percent pedestrian) developed for occupant safety analyses in frontal impacts was only modified by replacing the pelvis/thigh region. At present, there exists no typical adult dummy. Regarding the different body regions, the situation is as follows(5,6):

neck-/lumbar vertebra	too stiff; differences between ante-, retro- and lateral flexion are not considered
thorax/shoulders	too stiff
pelvis	geometrically incomplete (child)
thighs/shanks	not fracturable
knees	no lateral flexion possible

Figure 2. Restrictions of the simulation quality of dummies in the case of pedestrian accident loads

It is especially unfavorable that for some significant traumatized body regions—spine and lower extremities—no relevant mechanical loads are measured. On the other hand, some mechanical loads—thorax acceleration—have no biomechanical correlation.

Injury criteria that are found by biomechanical research and transferred as protection criteria to dummies are mostly known for sagittal load directions. For lateral loads, which are typical for pedestrians, they cannot be transferred. The little knowledge in the field of the biomechanical load capacity of children involves basic problems for the main group of pedestrians.

Reproducibility of Results

Reproducibility of accident loads in the case of pedestrians colliding with passenger cars—especially with adults—is not insured. This applies to a lesser degree to vehicle contact zones and to a greater degree to contact regions on the body as well as to accident loads. The main reasons for this are that accident kinematics are mostly three-dimensional; there is a high lag in time between the first contact and head impact, and there is a scatter of measured dummy values within the limits specified for dummy element tests (Part 572, *Federal Register* NHTSA).

Integrated and Component Tests

To find a starting point for the determination of the traumatic effect of vehicle elements and also as a basis for accident simulation, data of "in depth, at scene" individual case analyses of traffic accidents should be used (Federal Highway Research Institute, BASt/Daimler-Benz AG).

The correlation of injuries and their causes, using specific accident data of vehicle manufacturers, results in efficient points of application(7).

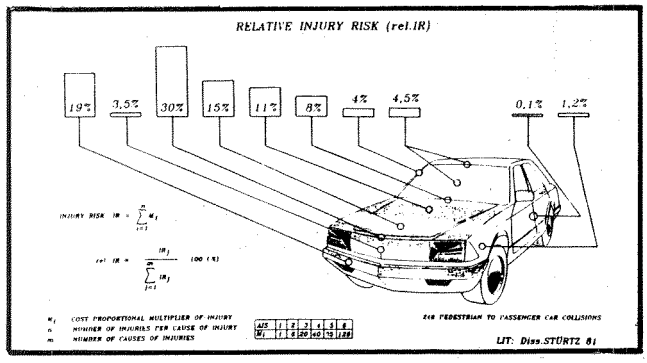

Figure 3. Points of application for pedestrian protection measures

In addition to the fundamental problems of accident simulation, the advantages and disadvantages of different present-day experimental methods are shown in detail. They are used to valuate the vehicle exterior. This aims at the definition of a procedure to reach maximim efficiency of protection measures.

Integrated Tests

An integrated test or full-scale test means a complete simulation of vehicle/pedestrian collisions, considering relevant accident parameters.

Analyzed in the following are the influence of the type of vehicle, the stature of the pedestrian, and the vehicle impact speed on the reproducibility of vehicle impact points, kinematic values, and accident loads. For this, the CCMC/AHP-type of collision is used.

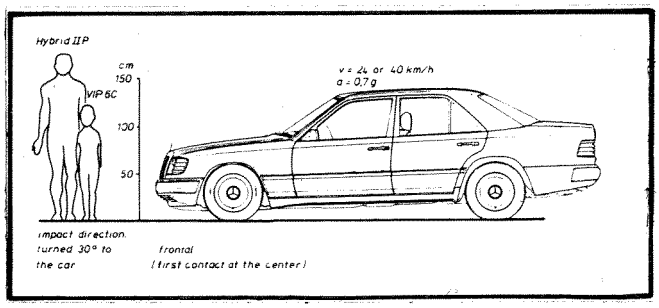

Figure 4. Full-scale simulation of vehicle/pedestrian collision

When using the coefficient of variation (V) as a measure of reproducibility, the following findings can be derived from Figures 5 and 6:

- In the case of accident load, V depends on the type of pedestrian, type of vehicle, and sometimes on the vehicle impact speed.
- For velocity and direction of head impact, as well as for the wrap around distance, V has low values.

The reproducibility of accident loads for collisions between passenger cars and pedestrians is not sufficient for kinematic values; on the other hand, it is.

Component Tests

A component test or subsystem test means an impactor/vehicle collision where the impactor with different quality simulates body regions. The test concerns kinematic accident parameters.

The following examples are shown for the three vehicle areas causing the highest trauma. The endangered body regions of adult pedestrians are simulated by the impactor.

Front Bumper

Tests with translatoric horizontally guided impactor: The latter is of wood and has a semicylindrical shape. Defined are impactor mass, impact and rebound speed, protection criteria, and test zone.

Unrealistic is the lack of simulated soft tissue and the high radius of curvature of the contact zone. The latter will reduce the normal depth of deformation. The adaption of the adult pedestrian is traumatically significant and, in principle, also possible for children. The advantage of a low, induced impact force and, therefore, also a low contact mass cannot be measured, but simulated by mass correction. The reproducibility is classified as good.

	Vehicle			Head					Thorax	Pelvis
Type	n (-)	v (km/h)	v (%)	a_{3ms} (%)	HIC (%)	v_{-20ms} (%)	α (%)	WD (%)	a_{3ms} (%)	a_{3ms} (%)
A	6	24	14(I)	49	68	—	—	—	39	37
	6	40	1	17	21	5	6	2	23	14
B	6	24	2	21	19	11	9	1	16	18
	6	40	1	23	38	21	3	2	7	4
C	6	24	2	41	50	24	46	2	26	65
	6	40	7	43	48	9	6	2	15	9

v_{-20ms}	head velocity relative to the vehicle 20ms before impact
α	Angle between head vector of velocity—just before impact—and contact surface
WD	Wraparound distance
(-)	Without head impact

Figure 5. Coefficient of variation for impact points, kinematic values, and accident loads in collisions between passenger cars and Hybrid II P

Type	Vehicle n (-)	v (km/h)	v (%)	a_{3ms} (%)	Head HIC (%)	v_{-20ms} (%)	α (%)	WD (%)	Thorax a_{3ms} (%)	Pelvis a_{3ms} (%)
A	6	24	2	6	26	—	—	—	19	12
	5	40	1	4	10	—	—	—	22	8
B	5	24	2	13	20	4	21	6	17	10
	5	40	1	15	34	10	22	2	7	5
C	6	24	5	7	11	10	18	1	12	9
	5	40	1	21	36	7	10	2	10	5

v_{-20ms} Head velocity relative to the vehicle 20ms before impact

α Angle between head vector of velocity—just before impact—and contact surface

WD Wraparound distance

(-) Without head impact

Figure 6. Coefficient of variation for impact points, kinematic values and accident loads in collisions between passenger cars and VIP 6 C.

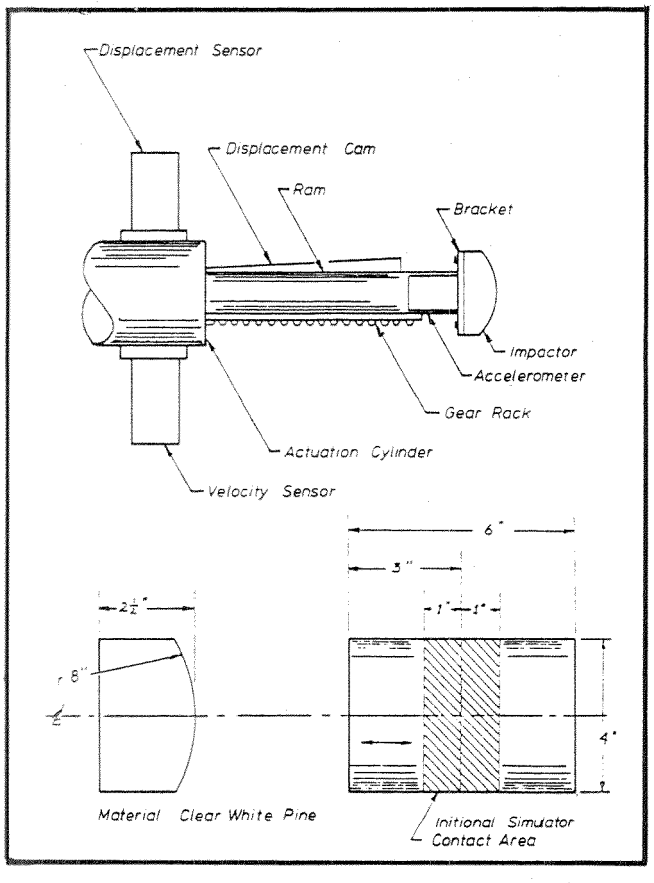

Figure 7. Simulator for shank impact(8)

Upper Front End

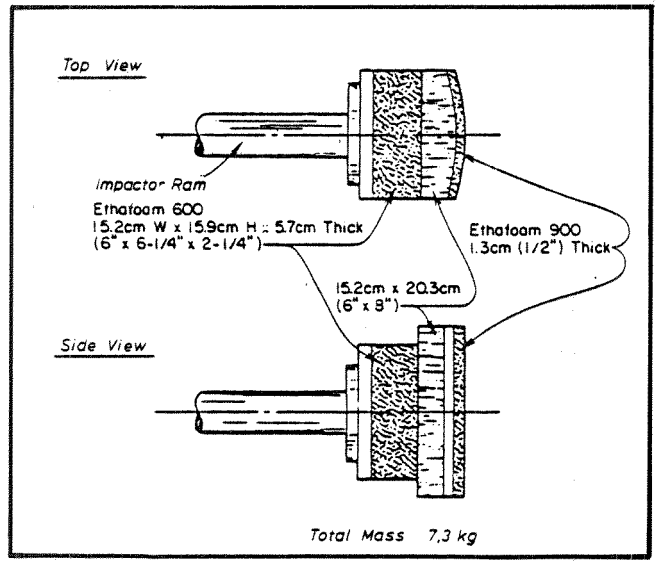

Figure 8. Simulator for hip/thigh impact(9)

Tests with translatoric horizontally guided impactor: The latter has a semicylindrical shape. The material is wood, in the contact zone, covered with foam. Defined is the impactor mass. The impact velocity has to be varied depending on the bumper position.

The adaption to the hip/thigh impact of adult pedestrians is traumatically significant but not described for the child's thorax and head impact. The reproducibility is declared as good.

Bonnet and Fenders

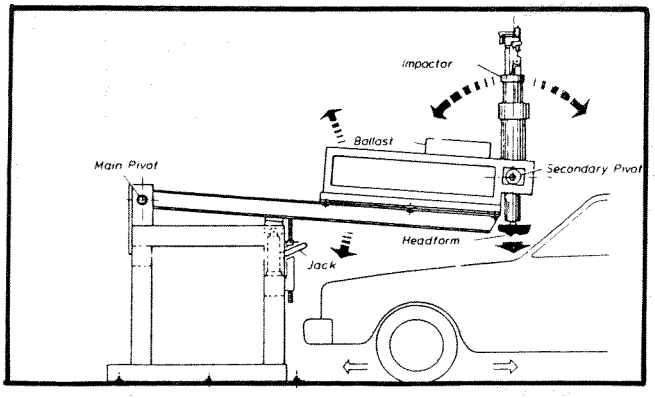

Figure 9. Simulator for head impact(10)

Tests with translatoric vertically guided impactor: The latter is a modified Part 572 dummy head with frontal orientation. Defined are impactor mass, impact speed, protection criteria, and test zone.

The adaption to the adult pedestrian is traumatically significant and, in principle, also possible for children. The reproducibility is declared for the HIC with a variation smaller than 25 percent and is very good in general.

In General

Component tests can basically be classified as simple and having a good reproducibility, also of accident loads. They allow large-area qualitative valuation of vehicle areas. To reach a higher level of simulation quality, the impactors have to be developed more realistically. The kinematic input values should be derived by mathematical or experimental simulations of the vehicle/pedestrian collision. Existing test devices—head impact pendulum-have to be considered.

Consequences

Integrated tests should be used only to find contact zones on the vehicle, as well as kinematic values of the loaded body region, because of the poor reproducibility of accident loads. They are also suitable to adjust mathematical models.

Contact zones are specific to each vehicle. Therefore, they can best be determined by the car manufacturer. Valuation of contact zones should be carried out at present and in the near future by component tests only. The latter, however, have to be better adjusted to the living human being.

Measures to protect pedestrians are in conflict with other design characteristics. Diversity and range of influencing factors cause various and partially contrasting requirements for the protection of pedestrians.

Evolutionary design characteristics to improve the protection of exterior road users are shown in the following, based on Mercedes-Benz Series 201 and 124.

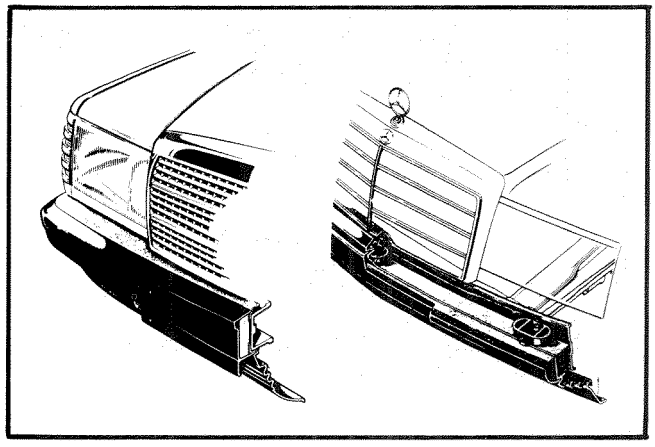

Figure 10. Front end

The front end has a smooth surface causing large-area initiation of the impact force (mitigating soft tissue injuries). The protective strip and the flashing of the bumper are made of visco-elastic material. In front of the bumper bending support there is an energy-absorbing foam, which is getting thicker to the vehicle sides. Taking the Mercedes-Benz Series 123 as a basis, the maximum force is reduced for the 201 and the 124. The point of first contact is lowered up to 50mm in the case of the 124, which reduces in addition the bending load in the lower extremities. The radiator grille is of thin sheet metal that has been reduced in thickness to 0.8mm. Thereby it has become a deformation zone.

The front end of the bonnet is rounded off, and its frame is deformable by using a Z-profile and punching. The headlamp units can, in the case of the 124, shift backward under load. Taking the 123 as a basis, the maximum force is reduced by 10 percent for the 124.

Vertical rigidity is reduced by using punched fenders and increasing the clearance between the wheel arch and the top of the fender. Taking the 123 as a basis, the maximum force is reduced by 30 percent for the 124.

The single axis of the wiper system and the cross member is covered. In contrast to the 123, the sheet metal of the 124 bonnet has a 10mm higher clearance to the bonnet cross member. Taking the 123 as a basis, the maximum force is reduced by 20 percent for the 124.

The external shell of the pillar is made of thin sheet metal. Taking the 123 as a basis, the maximum force is reduced at low impact speeds for the 124.

The large volume lateral roof frame has a smooth surface and can be well deformed under the impact of two-wheel riders. There is only one external shell, which

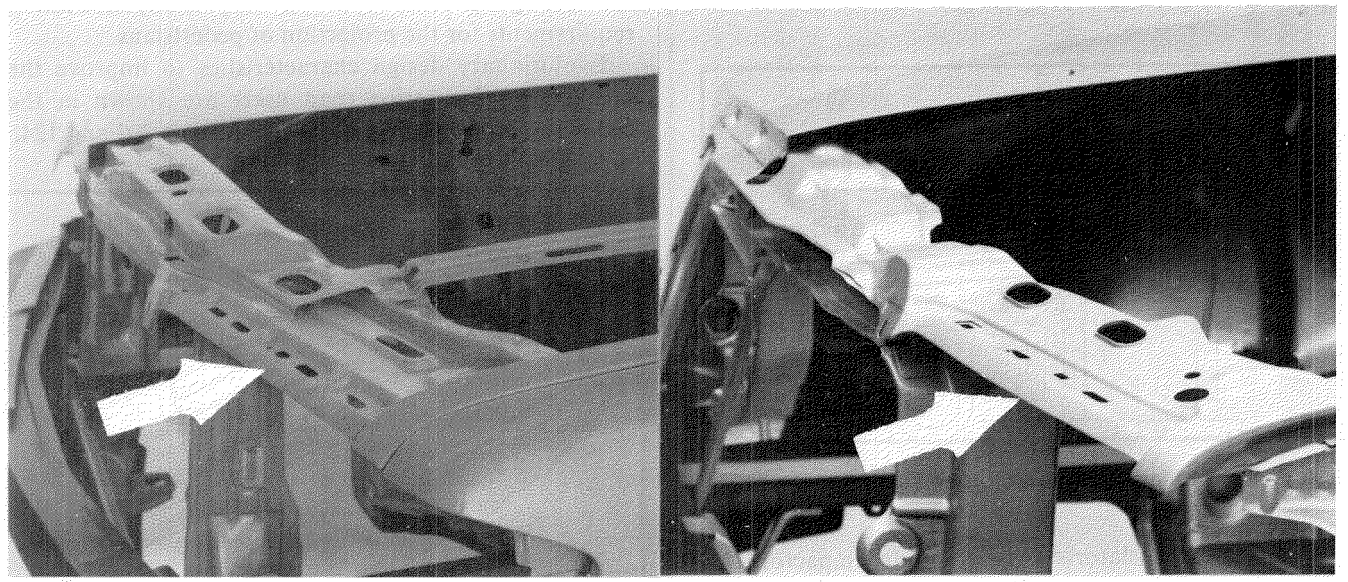

Figure 11. Substructure of upper front end

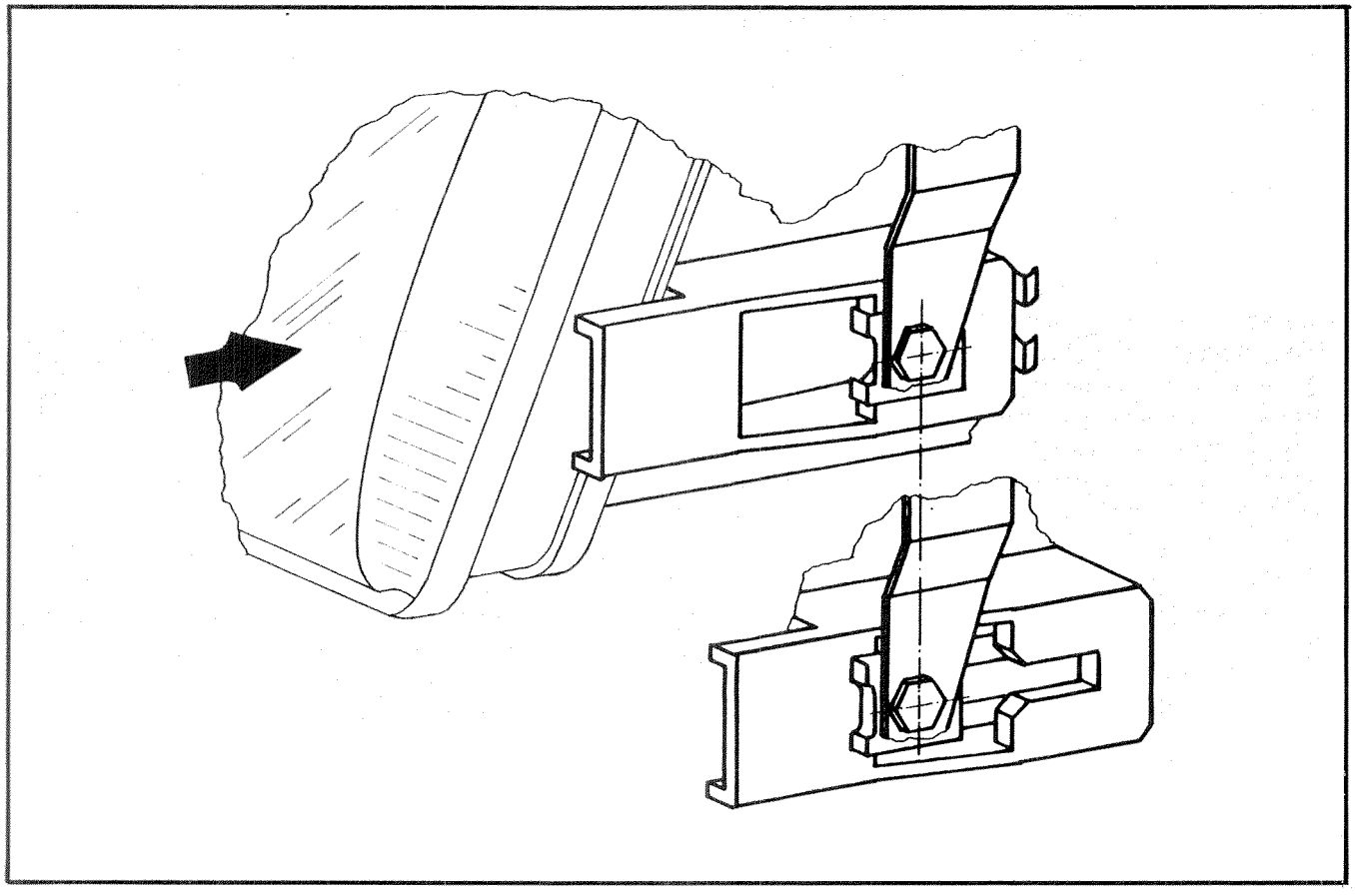

Figure 12. Kinematics of the headlamp under impact load

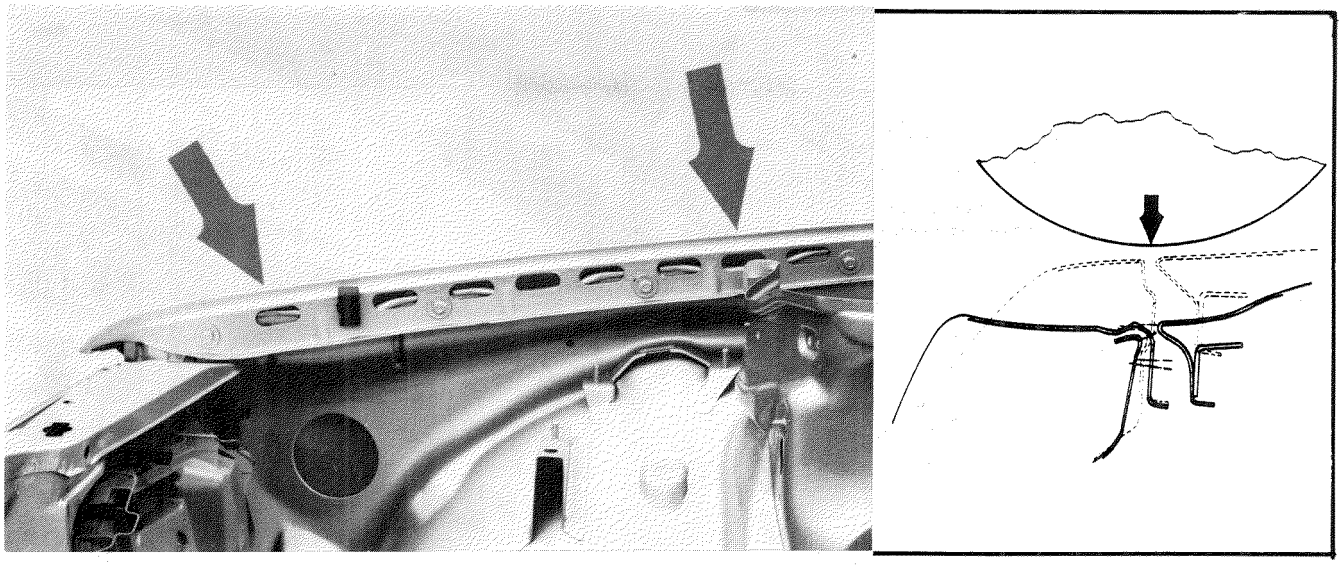

Figure 13. Transition from bonnet to fenders

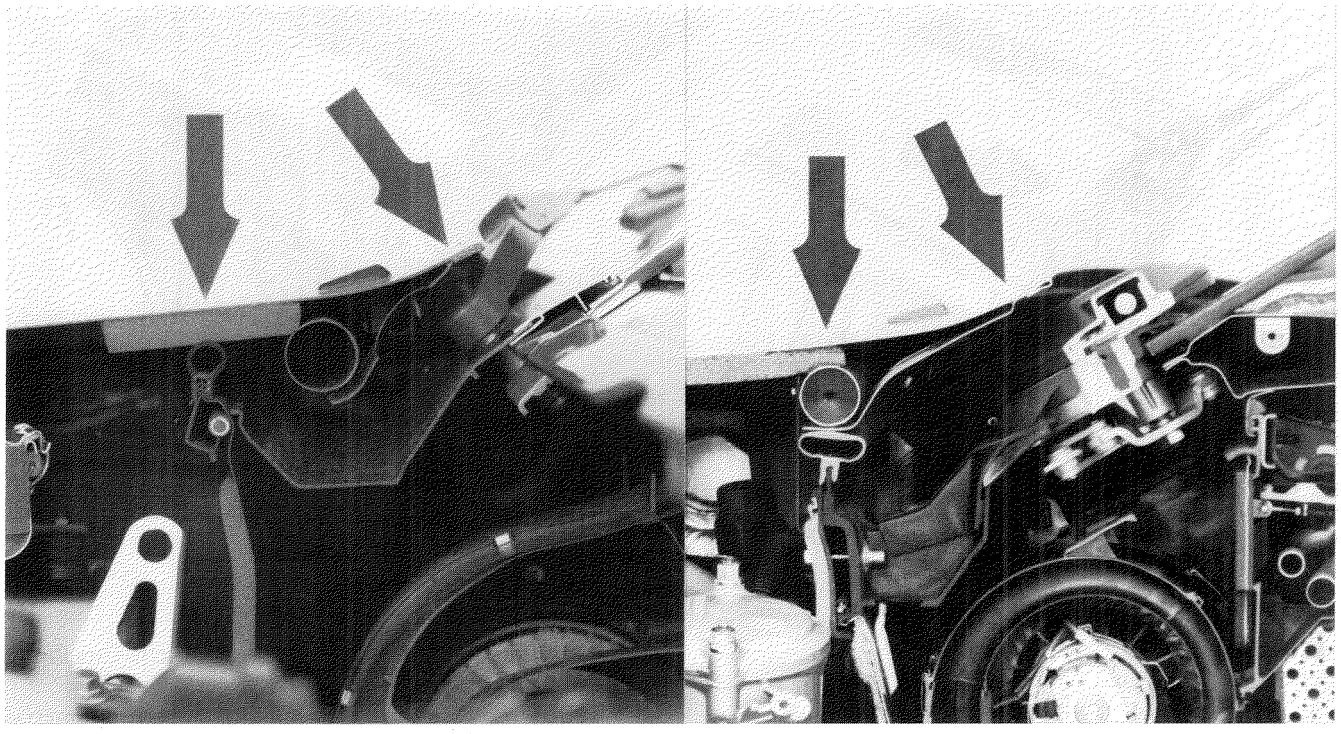

Figure 14. Upper end of bonnet

is made of thin sheet metal. Taking the 123 as a basis, the maximum force is reduced by 10 percent for the 124.

The high exposure of pedestrians to trauma, mostly a result of basically different impact partners, shows that vehicle-specific measures will have only limited efficiency in the future. A substantial reduction of the number of severely or fatally injured pedestrians will only be possible if, in addition, other measures are enforced. These are traffic education, separation of traffic areas, as well as improvement of visibility.

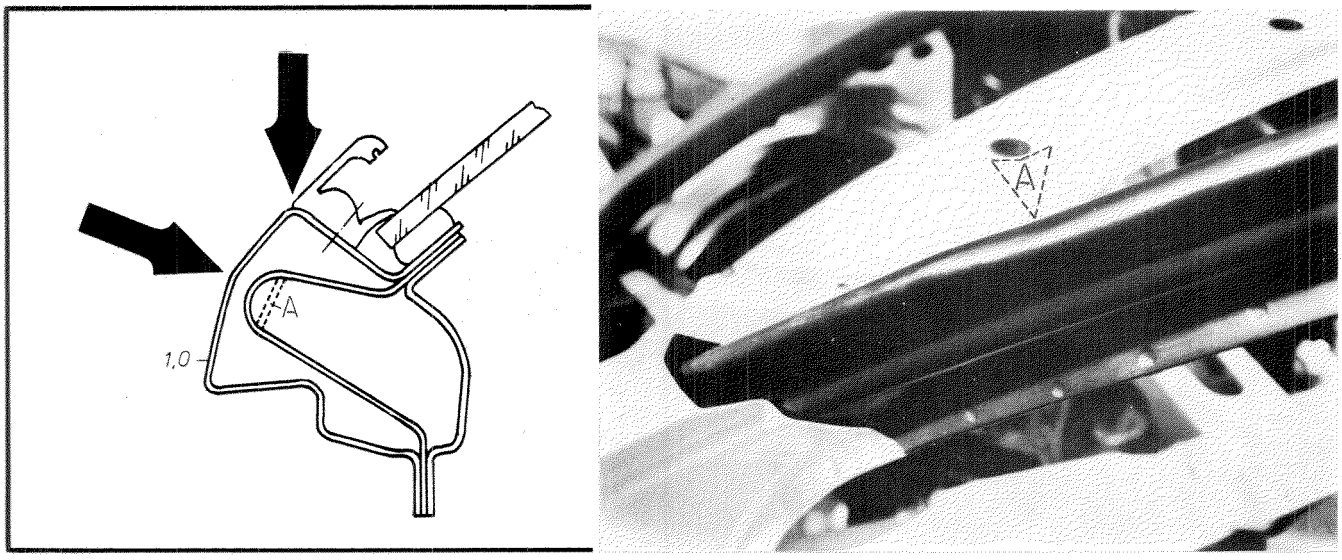

Figure 15. Windscreen side pillar

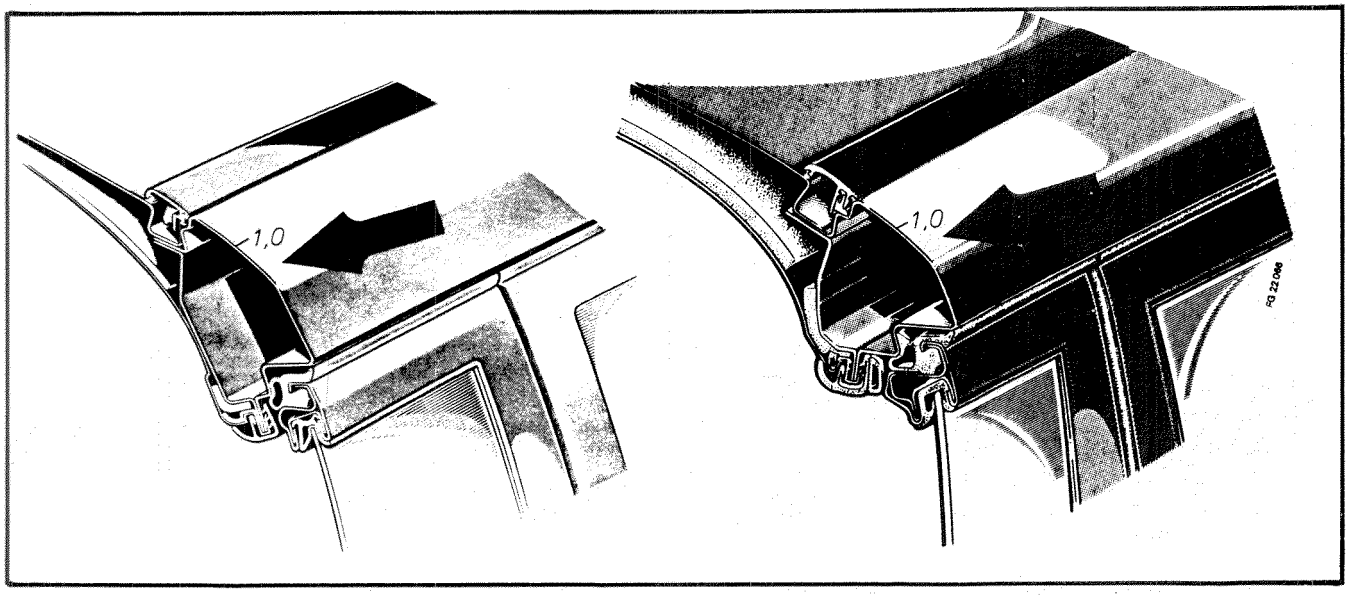

Figure 16. Lateral roof frame

References

1. Statistical Federal Office Weisbaden, "Straßenverkehrsunfälle 1983," Fachserie 8, Vol. 3.3, 1984.
2. Stürtz, G., "Das Kind im Verkehrsunfall: Biomechanik, Anforderungen an die äußere und innere Sicherheit von Kraftwagen," Fortschr.-Ber. VDI-Z., Vol. 17, No. 8, 1981.
3. "Verkehrsunfallentwicklung 1974 ohne BAB in Hannover," Verkehrs-Unfall-Dienst, Polizeidirektion Hannover, 1975.
4. Zeidler, F., "Möglichkeiten zum Schutz äußerer Verkehrsteilnehmer durch kraftfahrzeugtechnische Maßnahmen," Unfall-und Sicherheits-forschung Straßenverkehr, Vol. 41, 1983.
5. Niederer, P., et al., "The reliability of anthropometric test devices, cadavers, and mathematical models as pedestrian surrogates," Proceedings International Congress Exposition, Detroit, February - March, 1983.
6. Aldman, B., et al., "An experimental model for the study of lower leg and knee injuries in car pedestrian accidents," Proceedings Eighth International Technical Conference on Experimental Safety Vehicles, Wolfsburg, October 1980.
7. Huber, G., "Aspects of passive safety in the Mercedes-Benz research car," Proceedings Ninth International

Technical Conference on Experimental Safety Vehicles, Kyoto, Japan, November 1982.
8. U.S. Department of Transportation, *Federal Register*., Vol. 46, No. 14, Docket No. 78-19, Notice 1, 1981.
9. Pritz, H., and J. Pereira, "Pedestrian hip impact simulator development and hood edge location consideration on injury severity," Proceedings 27th Stapp Car Crash Conference, San Diego, October 1983.
10. Pritz, H., "Experimental investigation of pedestrian head impacts on hoods and fenders of production vehicles," Proceedings International Congress Exposition, Detroit, February - March 1983.

Technical Session No. 8

Safety Design of 2-Wheeled Vehicles

Y. Nakamura, Chairman, Japan

Leg Protection for Riders of Motorcycles

B.P. Chinn and
P. Hopes
Transport and Road Research Laboratory, Department of Transport, Crowthorne, United Kingdom

M.A. Macaulay
Brunel University, Uxbridge, United Kingdom

Abstract

A major cause of serious injury in motorcycle accidents is the rider's leg being trapped between the motorcycle and a car. This paper gives results from a number of full-scale impact tests of motorcycles with and without leg-protecting fairings. Motorcycles were crashed into a flat, rigid barrier inclined at 30° to their direction of travel. Three basic configurations were studied: motorcycles with no leg protection, with hard leg protection that absorbed negligible amounts of energy, and with soft leg protectors that absorbed 5 to 10 percent of the kinetic energy on impact. The use of a leg-protecting fairing substantially reduced damage to a dummy rider's legs in crash tests, and a protector that absorbs some energy seems preferable to one that does not. These results were achieved without increasing the risk of other types of injury.

Introduction

A major cause of serious injury in motorcycle accidents is trapping the leg of a rider between the motorcycle and a car(1). It has been suggested that a suitable fairing attached to the motorcycle could prevent this happening. Few tests of such fairings have been reported, but from these it appears a fairing could alter the dynamic behaviour of the rider during impact in such a way that he might be more likely to receive some other type of injury(2,3).

This paper gives results from a series of full-scale impact tests of motorcycles with and without leg-protecting fairings. As well as damage to the leg of the dummy rider, the dynamics of rider and motorcycle during impact were studied to check that the leg protectors used did not increase the risk of other types of injury.

Test Programme

The initial series of tests involved medium-sized motorcycles of 175cc engine size running into a flat, rigid barrier similar to those used in conventional motor car impact tests but only 1.23m high to simulate the height of a car roof. The barrier was inclined at 30° to the direction of travel of the motorcycle, as shown in Figure 1, and was faced with a sheet of 15mm plywood. The speed at impact was 48km/h. Subsequent tests were performed with light stepthrough motorcycles of less than 100cc engine size, heavy motorcycles of 800cc engine size running into the rigid barrier, and a heavy motorcycle running into the side of a stationary Morris Marina car at the same angle as the rigid barrier.

Three basic configurations were studied: a motorcycle with no leg protection, one with a hard leg protector that

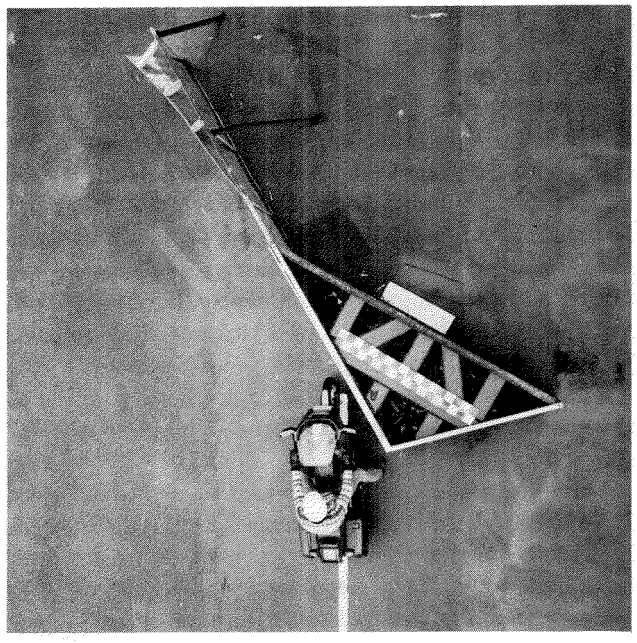

Figure 1. Overhead view of oblique barrier impact test of a motorcycle

absorbed a negligible amount of energy on impact, and one with a soft leg protector that absorbed about 5 to 10 percent of the total kinetic energy on impact. This energy absorption took place within the protector, and no energy-absorbing padding was used in front of the leg except with the heavy machines where padding had to be used because the protector was situated well forward of the rider's leg. This padding contributed very little to the total energy absorption and has been ignored.

Hard protectors were tested only on the medium-size machines. Some development tests of soft protectors were also made on these machines, but no attempt was made to optimise the energy absorption of the protectors.

The dummy rider was a 50th percentile male OPAT with the standard legs replaced by damage-indicating legs using aluminum honeycomb glued to thick flat plates. Two estimates of damage were used; the energy absorbed was related to the likelihood of bone fracture, and an estimate was made of the surface area of the leg that would have been lacerated. These legs are described more fully in (1).

Results

The energy absorbed by the leg of the dummy rider is shown in Figure 2. Also shown is a tentative limit of 20J suggested for the maximum energy that can be absorbed by the leg in (1). Mean values that break the upper and lower leg bones in bending are also given. A range of one standard deviation is shown about the mean of each set of measurements. This would include about 70 percent of the population, assuming a Gaussian distribution at breaking loads. These values are estimated from results given in (4) and (5).

Only the results for the final version of the soft protector are given. For the medium-size motorcycle, there is a consistent reduction from the damage with no protection for the leg, to some with a hard protector, and more with a softer one. The behaviour of the heavy motorcycles is anomalous. The machines used had horizontally opposed flat twin engines, and a cylinder head made contact with the barrier and altered the behaviour of the motorcycle completely. It did not rotate, and the impact was similar to a violent frontal impact. The leg damage was fairly low.

The addition of a soft protector produced rotation of the motorcycle and increased the damage to the leg slightly.

Estimates of lacerated surface area are shown in Figure 3. They follow the same pattern as the energy absorbed. Details of damage estimation are given in (6) for both bone breakage and lacerated surface area.

Leg protectors changed the dynamics of motorcycle and rider during the impact. Two simple parameters are used to summarise these changes: the forward velocity of

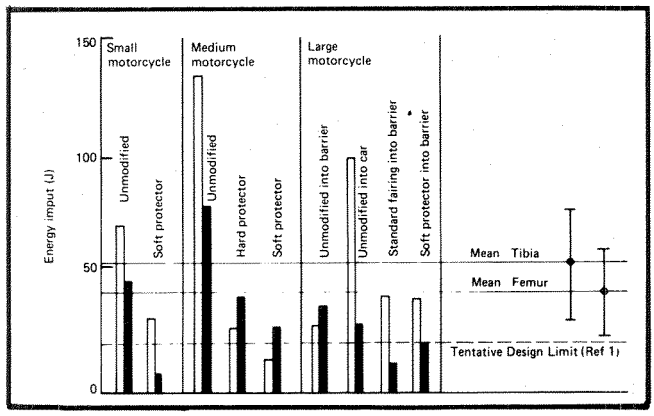

Figure 2. Energy absorbed by leg in tests of motorcycles into oblique barrier at 48km/h (one test into car)

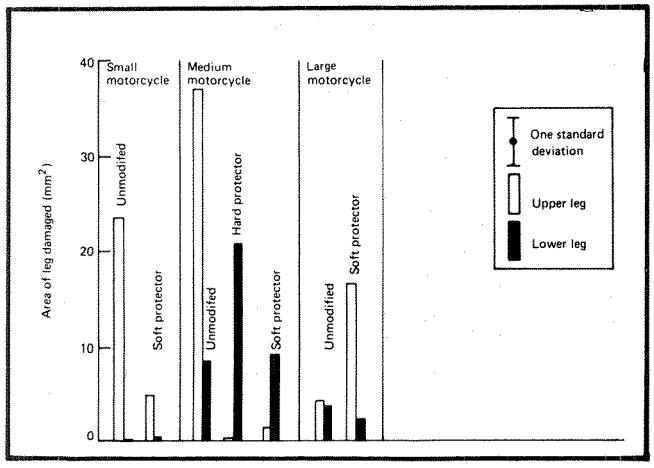

Figure 3. Areas of legs damaged in tests of motorcycles into oblique barriers at 48km/h

the dummy's head as it crosses the plane of the barrier, and the mean angular velocity of the motorcycle in the horizontal plane over the first 100ms of the impact. These are shown in Figures 4 and 5. Note that the forward velocity of the rider's head can be greater than the velocity of the motorcycle because he pivots about his hips and his torso can have rotational as well as translational velocity.

With the medium-size motorcycles, there is a consistent reduction in the forward velocity of the rider's head from that for no protector, for a hard protector, and for a soft protector. With the light motorcycles, there is no difference in forward head velocity, but, with the heavy motorcycles, the addition of a soft leg protector reduces the forward head velocity by about 35 percent.

The average angular velocity of the motorcycle during the first 100ms of the impact shows a reduction with the light and medium motorcycles and an increase with the heavy motorcycles when soft leg protectors are fitted.

When a heavy motorcycle with no leg protectors was run into a motor car, the protruding cylinder head deformed the car structure, which absorbed some of the kinetic energy. The behaviour of the motorcycle and rider

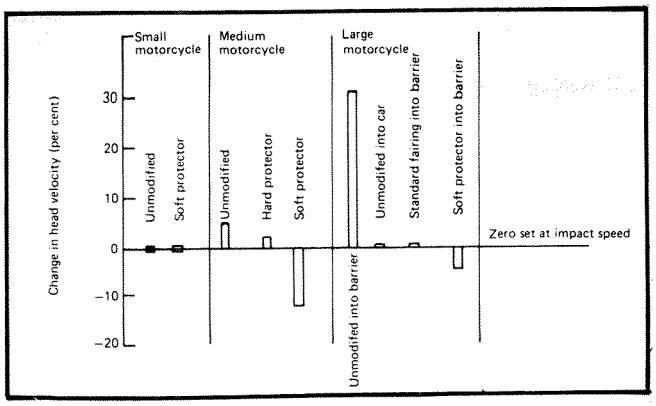

Figure 4. Change in forward velocity of head in tests of motorcycles

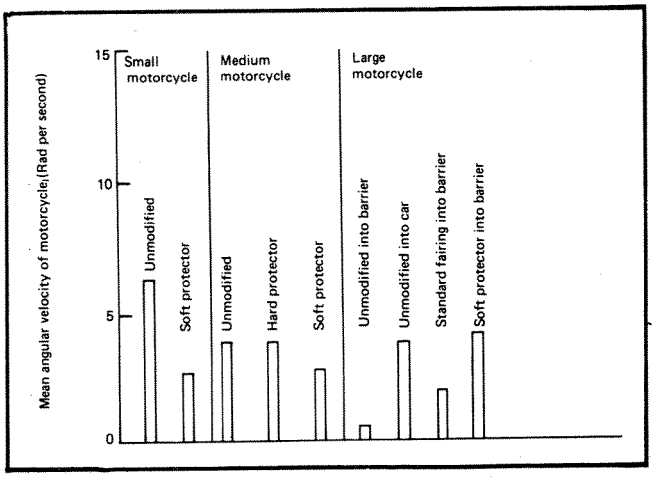

Figure 5. Mean angular velocity of motorcycle during first 100ms

was then similar to that of the unmodified medium-size machine and its rider.

Discussion

The main test programme used a flat, rigid barrier because it is generally found with motor cars that tests with a rigid barrier are easier to perform and the results are more consistent and easier to analyse than tests with a deformable barrier. In the rigid barrier test reported here, the use of a leg-protecting fairing on the motorcycle substantially reduced damage to the dummy rider's leg except for the heavy motorcycles. Leg damage was already fairly low on these machines, and it increased damage to the upper leg in these test circumstances. The cylinder head on the horizontally opposed engine of the heavy motorcycles prevented rotation of the motorcycle and stopped it violently, increasing the forward velocity of the rider's head. The addition of a soft fairing reduced this velocity appreciably. This indicates a greatly reduced chance of head injury, which more than compensates for slightly greater damage to the leg.

When a heavy motorcycle was run into a stationary car instead of a rigid barrier, it rotated and trapped the rider's leg causing severe damage.

A leg protector that absorbs some energy on impact appears to be preferable to a hard one that does not. The soft leg protectors used absorbed about 5 to 10 percent of the kinetic energy of the motorcycle plus rider, but no attempt was made to optimise the amount of energy absorption. Leg protectors reduced the forward velocity of the dummy rider's head. They also reduced the average angular velocity of the motorcycle in a horizontal plane except for the heavy motorcycle where a protector increased this velocity. They also effectively eliminated pitching of the motorcycle in a vertical plane.

In the initial tests using medium-size motorcycles of conventional design, the soft protectors absorbed about 10 percent of the kinetic energy of the motorcycle plus rider. The protectors used on the small and large motorcycles were modified so they should again have absorbed about 10 percent of the kinetic energy, but, in each case, they absorbed only about 5 percent. With the heavy machine, this is almost certainly because of the interaction of the engine cylinder head with the barrier; with the smaller machine, the reason is unclear. It may be because the rider sits in a different way with legs together instead of straddling the petrol tank. At present there is no theoretical basis for 10 percent energy absorption, which should be taken as a tentative empirical value.

When the heavy motorcycles were run into stationary motor cars, the effect of the protruding cylinder heads were less marked because the car deformed to absorb some of the motorcycle's energy. This machine can therefore be regarded as inherently aggressive, and it seems likely that the addition of suitably designed soft leg protectors would make it less aggressive.

Conclusion

The impacts of motorcycles into a rigid barrier inclined at 30° to their direction of travel reproduced the trapping of the rider's leg that has been reported from accident studies. This simulation was less successful for the heavy motorcycles tested, where protruding cylinder heads prevented rotation of the motorcycles. When a heavy motorcycle crashed into a stationary motor car, trapping of the leg occurred.

The leg protectors tested reduced the energy input into the leg of the dummy rider appreciably from a level at which severe damage is certain to one below the level needed to break the leg bones of 50 percent of the population. Leg protectors that absorb some energy on impact also reduce the forward velocity of the rider's head.

References

1. Chinn, B.P., and M.A. Macaulay, "Leg protection for motorcycles," Proceedings International IRCOBI Conference on the Biomechanics of Impact, p. 265, 1984.
2. Bartol, J.A., and G.D. Liners, "Development of side impact protection for an ESM," U.S. Department of Transportation, Technical Paper No. 73014, Washington, D.C.
3. Taneda, K., "Experimental investigation of motorcycle safety," Japan Automobile Research Institute, Proceedings IRCOBI Conference on Biomechanics of Injury to Pedestrians, Cyclists and Motorcyclists, pp. 270-282, 1976.
4. Mather, B. Sherwood, "Observations on the effects of static and impact loading on the human femur," *Journal of Biomechanics,* Vol. 1, p. 331, 1968.
5. Yamada, H., *Strength of Biological Materials,* Baltimore, Maryland: Williams and Wilkins, 1970.
6. Chinn, B.P., "Injuries to motorcyclists legs: testing procedures and protection," PhD Thesis, Brunel University, Uxbridge, 1985.

Application of Fluidics Technology to the Development of Antilock Brakes for Motorcycles

Robert R. Purves
Jet Propulsion Laboratory, California Institute of Technology

Abstract

This work was undertaken to develop antilock brakes for motorcycles utilizing the advantages of fluidics technology. Fluidic components are immune to electromagnetic interference, resistant to severe vibration, and potentially low in cost. The vehicle and brake control components were modeled. Using a system approach to the design, a nonlinear computer analysis was performed to determine acceptable delays and frequency functions for rapid and stable response. Emphasis was given to examining the transient characteristics of two functions of angular motion (acceleration and jerk) at the onset of wheel lock. Based on results of computer analyses and instrumented braking tests, angular acceleration was selected to initiate brake control. The control system components being developed are comprised of a unique pneumatic/fluidic velocimeter, a fluidic differentiation circuit, a fluidic amplifier, and a fluidic/electric threshold detector for toggle control of brake pressure. The development status of these components is discussed. The brake-pressure modulator is not being developed for this phase of the work. Results indicate a fluidic control system is feasible if the design focuses on minimizing the time response of the pneumatic/fluidic components.

Introduction

Safe braking of a two-wheeled vehicle depends on the existence of sufficient lateral force at the tire/road contact to maintain control and balance. If the wheels lock during braking, steerability of the front wheel and in-line travel of the rear wheel are lost. Capsizing of the vehicle following loss of control during braking accounts for a large number of motorcycle accidents. A solution to this problem is the use of an automatic antilock brake system.

A number of prototype antilock brakes are in existence, but to date none have appeared on production vehicles. These prototypes can be classified according to whether they are electronically or mechanically controlled. Although designs using electronic control are potentially more capable of adapting to road conditions than a simple all-mechanical type, they also tend to be more expensive to manufacture, subject to electromagnetic interference, and generally more sensitive to the harsh environment of the motorcycle. This work was undertaken to determine the feasibility of applying fluidics technology to a design that would be low-cost yet have most of the advantages of both the electronic and all-mechanical types.

Fluidic devices amplify pressure of a fluid such as air in much the same way that electronic devices amplify voltage. Fluid flow is analogous to current flow; there are components in fluidics equivalent to resistors, capacitors, and diodes. Amplifiers, filters, and logic circuits are feasible.

Although fluidic circuits do not have the frequency response and gain possible with their electronic counterparts, they do have characteristics advantageous for some applications. Fluidic circuits are not affected by nearby radio transmissions or by the electrical noise that exists near a motor's ignition system. Fluidic devices are not as sensitive to damage in a high vibration or extreme temperature environment as most electronic devices. In some applications, fluidic designs have proven to be less costly than their electronic equivalent.

Because of these advantages, fluidic technology has been used in a variety of applications. A computer using fluidic components has been designed for a Grumman fighter aircraft control. DC-10 and L-1011 aircraft depend on fluidic circuitry for operation of thrust-reverser and environmental-control systems. A military tank navigation system utilizes a fluidic motion sensor instead of a gyroscope. Fluidic components are also used for a variety of industrial controls where severe environments preclude the use of electric devices.

Fluidic antilock brakes have been designed by Boeing for commercial aircraft and by the Army's Harry Diamond Laboratories for military trucks. Efforts toward the design of fluidic antilock brakes for motorcycles were begun by Harry Diamond Laboratories in 1975. Two studies of control system concepts resulted(1,2). In 1978, Garrett Corporation continued the previous work and developed a fluidic/mechanical angular jerk (rate-of-change of acceleration) sensor for use in sensing the onset of wheel lock(3).

Scope

The work described here is a continuation of that started by Harry Diamond Laboratories and Garrett Corporation, with emphasis on system analysis and motorcycle braking tests to determine design requirements for control system components. The status of the component design effort is included. Design details and test results are given for development models of a fluidic angular velocimeter, fluidic amplifiers and differentiator, and fluidic control logic. These constitute the major components of the control system, except the brake-pressure modulator, which was not developed for this task. This latter component, therefore, was treated conceptually for system design purposes.

Approach

Past studies for applying fluidic technology to motorcycle antilock brake design focused primarily on sensors. Little consideration was given to the response requirements for other components that made up the control system. No analyses were made regarding the stability of the overall system, which includes control components and the nonlinear dynamics of the motorcycle with its tire/road interface.

The approach of this study was to analyze antilock brakes as a closed-loop, nonlinear control system with parameters chosen for stable operation and a reasonable stopping distance. The analysis objectives were to justify which variable of wheel motion (acceleration or jerk) to use for feedback and to identify the response requirements of the system components. These objectives were achieved by computer analyses and by motorcycle braking tests that provided data for determining computer model constants. These tests also supplied data for studying the wheel dynamics during braking as wheel lock occurs.

System Design

The system approach to antilock design and development is a departure from traditional approaches. Historically, antilock brakes have been developed by a combination of qualitative and trial-and-error methods. An alternate approach using classical control principles was used here in an attempt to characterize the components more accurately before fabricating them.

Basically, an antilock brake system is a device installed in the hydraulic brake line between the master cylinder and the wheel's brake assembly. It functions to prevent the braked wheel from locking up while the vehicle is in motion. The antilock system does this by automatically modulating the applied brake pressure so the braked wheel never has a tangential speed that is much less than the vehicle's forward speed. By doing this, the tires are able to retain most of their lateral force capability, allowing the vehicle to remain steerable and under the operator's control. In most cases, the stopping distance is shortened in comparison to a locked wheel stop.

As shown schematically in Figure 1, the antilock system consists of three key components:

- Modulator
- Controller
- Sensor

Together, these elements provide the antilock system function. Referring to Figure 1, the operator initiates the force command to the system. This action causes the vehicle and braked wheel to decelerate. A transducer senses the rotational action of the wheel and communicates this information to the controller. When a preset threshold of some function of wheel speed (usually deceleration) is exceeded, the controller unit, which is an on-off toggle, initiates a rapid command to the modulator, which

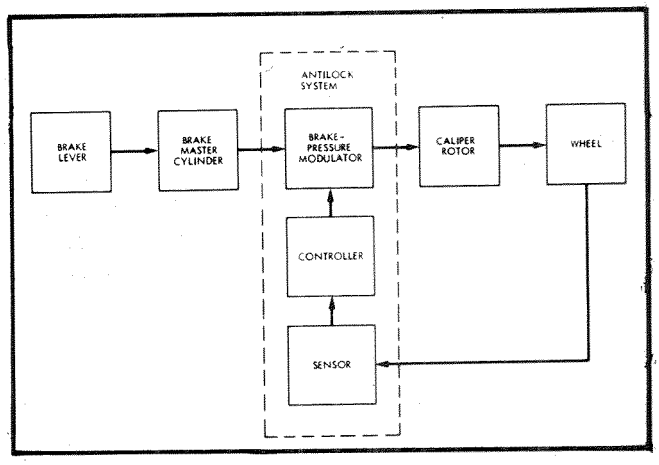

Figure 1. Basic antilock brake system

causes reduction of hydraulic pressure. As the wheel begins to recover speed, a second threshold is crossed, and the brake pressure is reapplied. The system continues cycling until the vehicle is near rest, or the brake command is reduced below the first threshold. This nonlinear cyclic action is called the limit cycle.

Antilock system requirements include such parameters as response, performance, operation, and reliability. These have been reviewed elsewhere in some detail(4). For this work, however, the main focus was on response-centered requirements.

Summary of Analysis Results

In the analysis,[1] the simplest feedback system that would result in a feasible, minimal-cost control system was sought. Results presented here pertain to the particular analysis model assumed, that is—

- Suzuki GS1000 SN (1979) with a rider weighing 165 lb
- Dry and wet asphalt road conditions
- Wheel angular-acceleration feedback
- Single-loop control, as illustrated in Figure 1
- Sudden and sustained application of front brakes by the rider

Under these conditions, several parameters were varied to achieve stable antilock brake action with reasonable stopping distances. These were—

- The magnitudes of wheel acceleration (toggle thresholds) at which brake pressure is released to prevent lockup and then reapplied to continue stopping (α_1,α_2)
- The rates at which brake pressure is dumped and reapplied by the modulator upon receiving commands by the controller (P_d,P_r)
- Total delay of control system components including brakes (τ_T)

An optimum design was computed as follows:

α_1 = -97rad/s^2
α_2 = 0rad/s^2
P_d = -3,600psi/s
P_r = 2,000psi/s
τ_T = 20-30ms

These values gave low-mu stops of -0.23g and high-mu stops of -0.54g at a limit cycle rate of 13Hz.

Perturbations of ±50 percent in each of these design parameters gave little change in performance and stability. This indicates a desirable level of insensitivity to controller variations. Perturbations somewhat beyond 50 percent gave sharp changes in stability and performance in most cases.

[1] Analysis work related to the system design was performed by Dynamics Research, Inc., of Torrance, California, under contract to JPL. Details of this work are given in (5), which is a companion paper to this paper.

Analysis of toggle width ($\alpha_2 - \alpha_1$) and bias ($\frac{\alpha_2 + \alpha_1}{2}$) values showed the effects of these parameters on limit-cycle stability. In particular, a wider toggle gives more lag and ultimately lockup, whereas a narrower toggle gives less lag and no reapply (no stopping). A more negative toggle bias lenghtens the dump well time, resulting in lockup. More positive biases reduce the dump dwell time, resulting in poor stopping performance.

For acceleration feedback and the type of controller and modulator assumed, stability of the control system operation was easily achieved. However, stopping performance was very sensitive to the net time delay in the system. A delay of 110ms was clearly unacceptable, while a 20 to 30ms delay gave reasonably good results.

Analysis of pressure dump and reapply rates showed that dump rates primarily affect the stability of the system, while reapply rates mainly affect stopping performance. In particular, higher dump rates give higher limit-cycle frequencies and higher stability, and higher reapply rates (within some limits) give shorter stops.

Sensing the Onset of Wheel Lock

Wheel lockup must be anticipated by sensing some function of wheel rotational motion such as angular velocity, acceleration, or the rate-of-change of acceleration (jerk). In a limit-cycle type of control, this function would be monitored for a predetermined threshold level, which, when reached, would start the release/apply cycle of brake pressure. Clearly, angular velocity is not an appropriate function for threshold detection. However, acceleration and jerk are feasible candidates for consideration since either changes rapidly as wheel lock occurs, regardless of vehicle speed.

The purpose of the following section is to compare acceleration and jerk as suitable feedback parameters for brake control.

Three methods of comparison have been used here:

1. Computer model analysis, where a model of a braking motorcycle has produced time domain plots of acceleration and jerk for several types of road surfaces
2. Braking tests, where wheel motion parameters at lockup were recorded during road testing of a motorcycle and the acceleration and jerk responses were compared
3. Control system analysis, where the stability of a closed-loop brake control system was compared for acceleration and jerk feedback

Computer Model Analysis

Analyses of the computer model indicate there are no apparent advantages to using jerk rather than acceleration for brake control. In fact, for some surfaces such as gravel

and glare ice where the maximum tire/road stopping force occurs with the wheel locked, jerk does not give a usable signal, while acceleration does.

Figures 2 through 5 illustrate the computer analysis. These plots show, as a function of time, torque on the wheel due to the brake (T_B), which represents the input function; torque on the wheel due to the tire/road interface (T_R), which is a function of the mu/slip curve; wheel angular acceleration, which is a function of the net torque on the wheel or $T_R - T_B$; wheel angular jerk, which is the first derivative of angular acceleration; and angular velocity. Each plot is for a particular road surface characterized by its mu/slip curve. Only that period of time prior to lockup is significant.

Accompanying each set of wheel transient curves is a mu-slip curve for the road surface considered. To make them more amenable for computer entry, these mu-slip curves are simplified versions of data in (6).

These plots show that jerk does not cross zero at maximum road torque, as concluded in a previous study. Figures 2 and 3, dry and slippery asphalt, show a sudden decrease in jerk and acceleration very near the maximum road torque. However, Figures 4 and 5, gravel and glare ice, show that acceleration produces a much stronger response. If system noise is taken into consideration, as discussed in the following section, it is unlikely the jerk signal would be strong enough to be useful.

Braking Tests

The real braking situation differs from computer simulation in significant ways. The computer simulation assumes a constant tire/road interface during braking, represented by a mu/slip curve. It does not take into account sudden variations in road surface, such as thin patches of dirt, bits of debris, painted lines, oil spots, etc. Such variations in the coefficient of friction can significantly affect the motion of the wheel when it is on the verge of locking. These perturbations in acceleration and jerk constitute a noise level that the control logic must contend with. It is clear that consideration of the signal-to-noise ratio is of primary importance in designing a threshold-sensing control system if false triggering of brake-pressure release or application is to be minimized.

A jerk sensor, since it differentiates angular acceleration, will amplify acceleration noise in direct proportion to its frequency. This means that noise levels, whether the result of road surface variations, brake, frame, or suspension vibrations, or background noise present in the sensor/controller system, can be many times greater if jerk rather than acceleration is sensed. Unfortunately, reduction of this noise by filtering is generally not an acceptable solution because filters introduce a delay in response that seriously degrades control system performance.

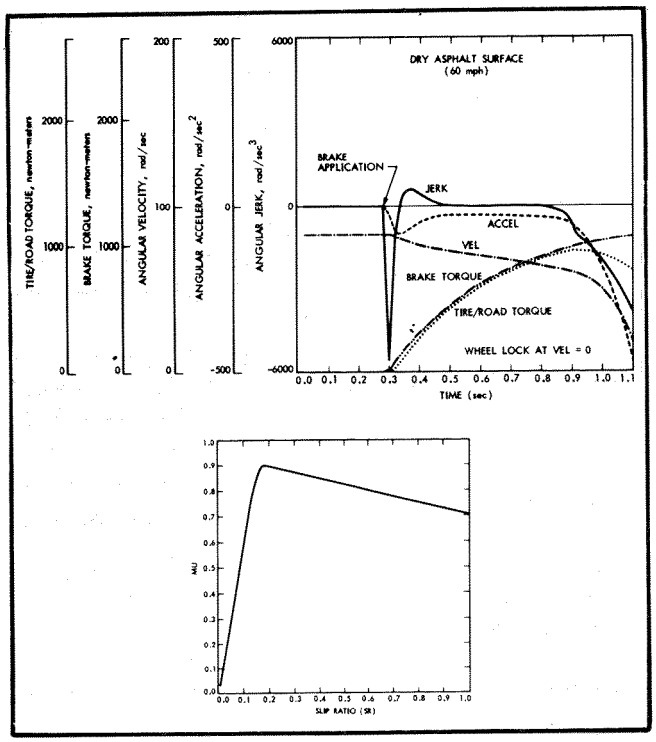

Figure 2. Braking wheel dynamics—dry surface

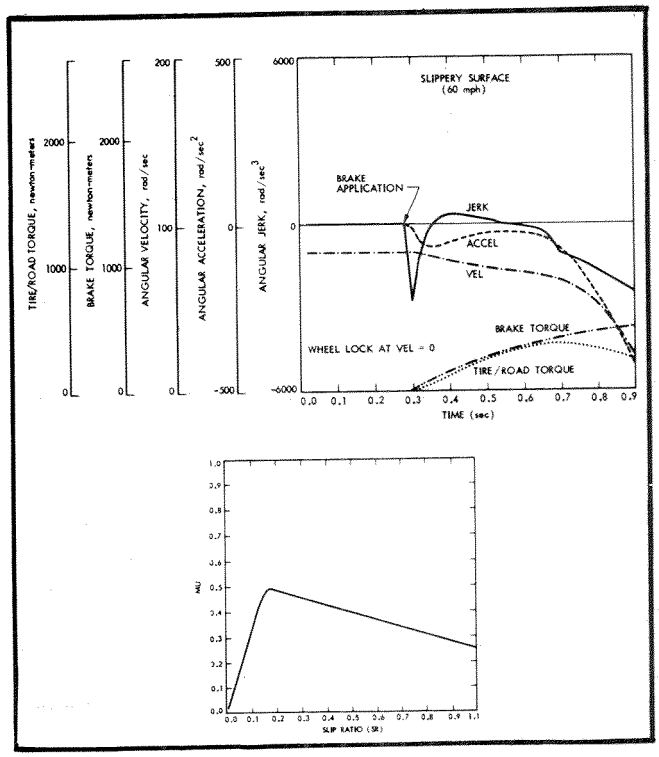

Figure 3. Braking wheel dynamics—slippery surface

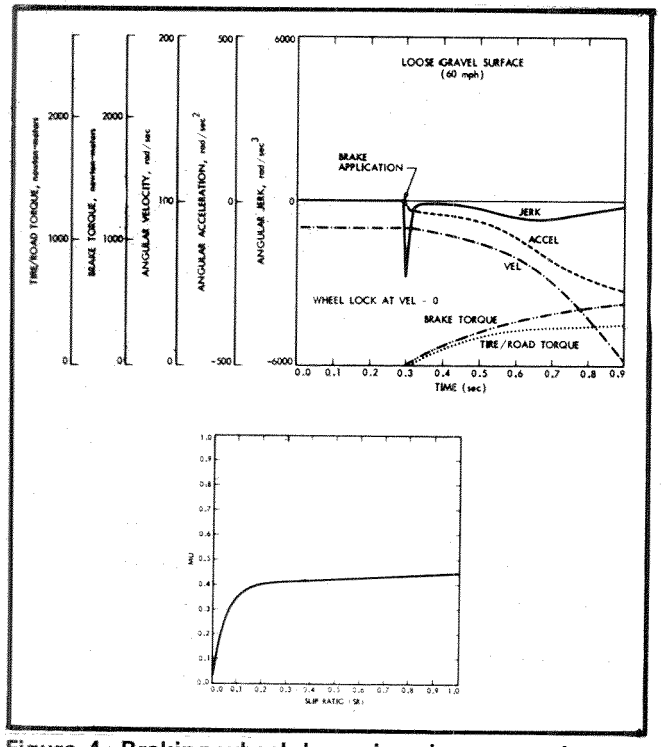

Figure 4. Braking wheel dynamics—loose gravel

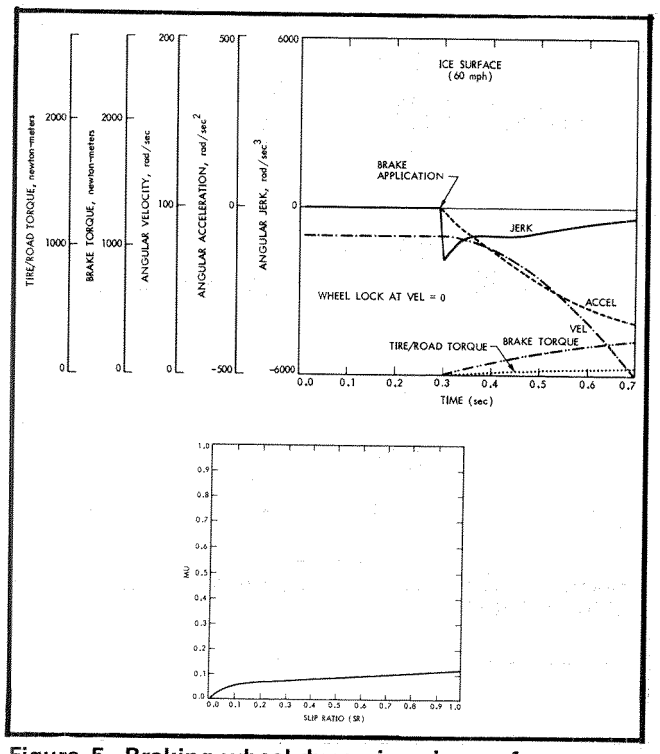

Figure 5. Braking wheel dynamics—ice surface

A series of braking tests were run using a motorcycle (Suzuki GS 1000) instrumented to record wheel dynamics. To simplify the analysis and instrumentation, braking was done on the front wheel only. The road surface was dry asphaltic concrete, a commonly used material. In each test, the front brakes were applied suddenly and hard enough to cause the wheel to lock and skid. Parameters recorded on a magnetic tape recorder included wheel angular velocity and angular acceleration. Upon playback of the tape, acceleration was electronically differentiated to produce jerk. For visual comparison, all signals were then recorded on an oscillograph, from which Figures 6 to 11 were produced. These figures illustrate what is happening to the wheel as it approaches and achieves a locked condition.

Brake pressure, which represents the input to the brake system, was not measured during these tests because of the tape recorder's limited channel capacity. The rider was instructed to apply the brakes suddenly and hard until lockup occurred and then release them for a normal stop. Although he may not have applied the brakes at the same rate each time, each test run does represent a braking situation that could occur in reality. To be usable, jerk and acceleration signals must show good characteristics regardless of how lockup is approached and how much noise is present.

In playing back the data, each channel was filtered to reduce noise. To identify the effect of filtering, four-pole low-pass filters with cutoff frequencies of 4, 8, 16, and 32Hz were compared. The effects on the same data for three cutoff frequencies are shown in Figures 6, 7, and 8.

The 8Hz filter was judged best, considering the compromise between low noise and rapid response. To show the delay effect of each filter on the acceleration and jerk, the filter for the velocity channel was fixed at 20Hz.

Referring to the figures, three traces that represent the motion of the braked wheel (angular acceleration, angular jerk, and angular velocity) are shown. The point at which the wheel velocity suddenly rises is when the motorcycle rider released the brakes enough to resume normal braking.

Starting with Figure 8, each figure is for a different stopping event (run). The velocity trace indicates where wheel lock and release occurred. It also shows several instances of impending lock before actual lockup occurred. In each case, acceleration and jerk traces show a response to these events as well as to the noise. These records are typical of all the runs (25) and show acceleration signal level at impending lock is greater, relative to the noise level, than the jerk signal level. In fact, in Figures 9 and 11, the jerk signal has no distinctive characteristics and would not be useful for initiating brake-pressure release.

Control System Analysis

The closed-loop analysis presented in (5) was made for each of the feedback parameters being considered. The results indicated that acceleration would give stable operation and jerk would not. Jerk feedback would be stable if the proper network were added, but this would be equivalent to making the jerk transducer an accelerometer.

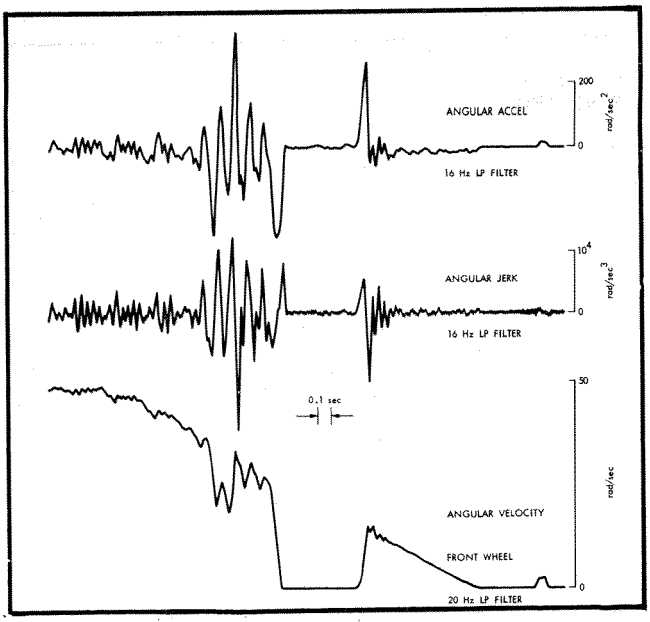

Figure 6. Run 6, 16Hz filter

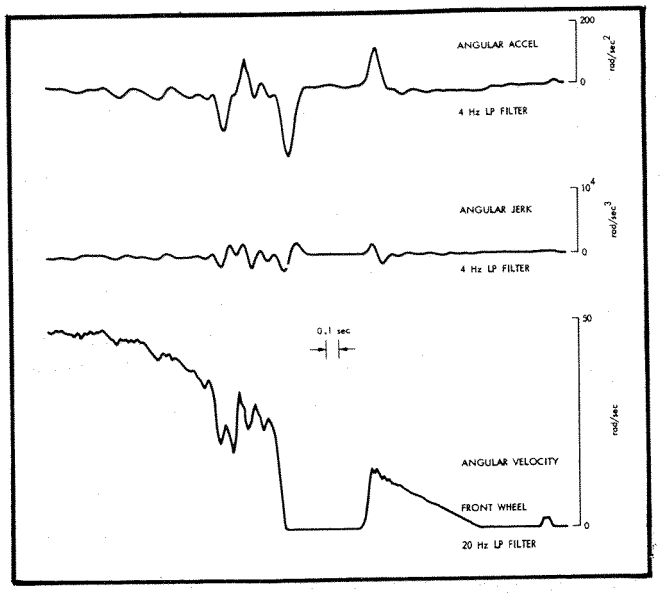

Figure 7. Run 6, 4Hz filter

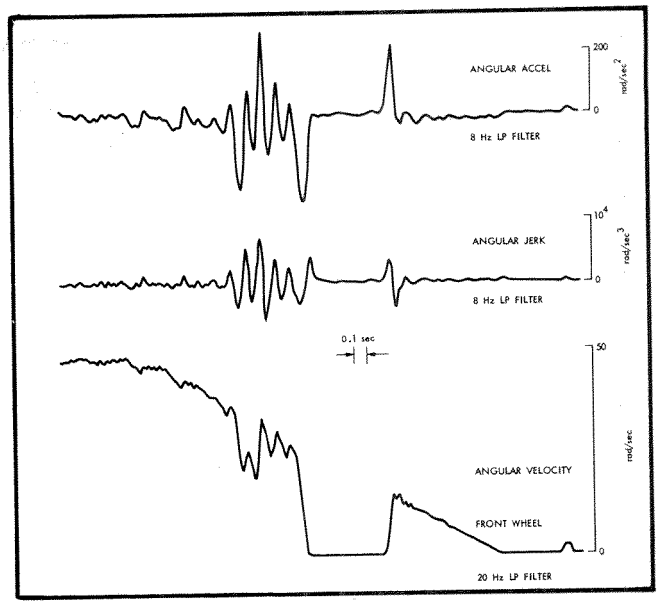

Figure 8. Run 6, 8Hz filter

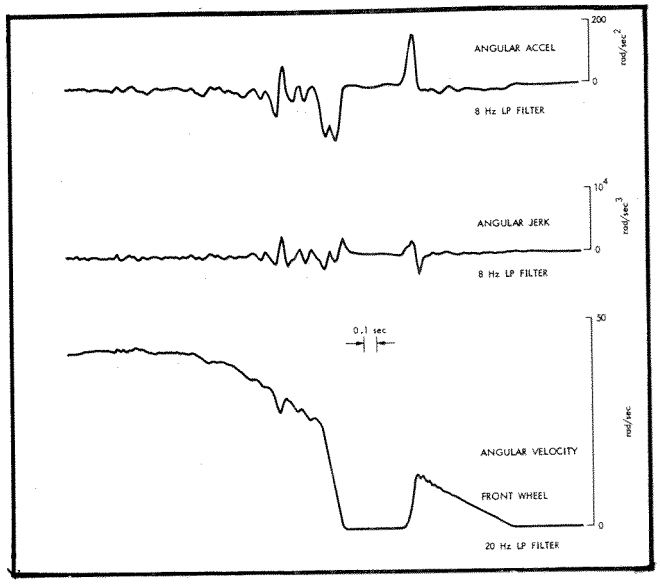

Figure 9. Run 7, 8Hz filter

Comparison Summary

When wheel lock begins, a pulse occurs in both the jerk and acceleration signals; however, if the pulse were used to initiate control action, the two signals compare as follows:

1. At impending lock, the acceleration signal is consistently greater in magnitude relative to the noise level.
2. For gravel or glare ice road surfaces (or other surfaces where the maximum stopping force occurs at lockup), the jerk signal has poor characteristics near lockup and is of such low magnitude that in the presence of noise it would be useless.
3. Closed-loop analysis shows that, for the control system concept proposed for this task, jerk feedback does not produce a stable control cycle, whereas acceleration does.

Component Design

The overriding physical requirements for a motorcycle antilock brake control are that it be small and resistant to the environment. It also must be inexpensive. Preferably it should be a single unit mounted near the wheel's brake caliper and coupled to the wheel to operate the sensor and the modulator. An example of how the unit could be mounted on the front fork is shown in Figure 12.

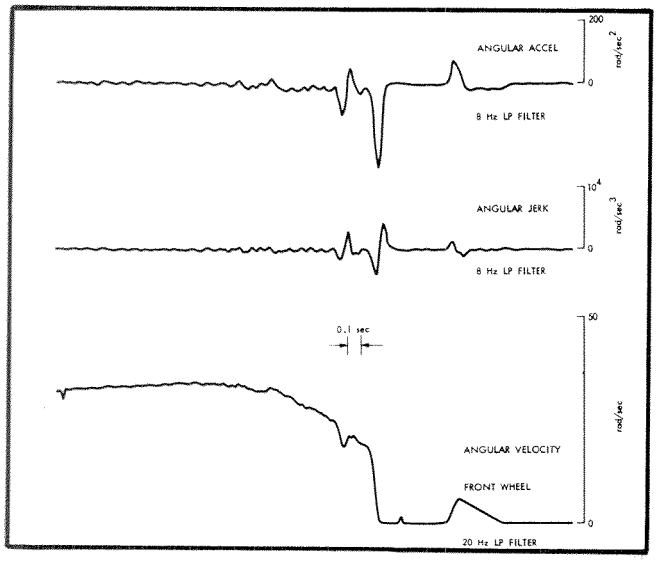

Figure 10. Run 8, 8Hz filter

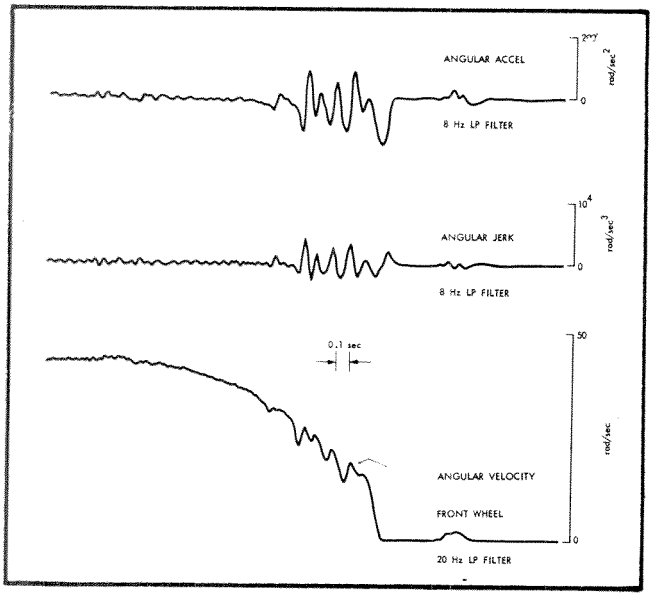

Figure 11. Run 10, 8Hz filter

For an experimental model, coupling to the wheel would be by belt and pulleys. The hydraulic line from the brake master cylinder would terminate at the modulator, with a short line connecting the modulator to the wheel cylinder. Also connected to the unit would be two hoses, one to the intake manifold vacuum and one to the carburetor air-filter housing (for clean air). One wire to the vehicle's battery would be required to operate the modulator's control solenoid.

The complete brake-control unit would be configured as shown in Figure 13, with the components combined in a cylindrical shape about 100mm in diameter and 90mm long. The final dimensions would depend on the size of the modulator. As presently conceived, the modulator would be close to the size shown.

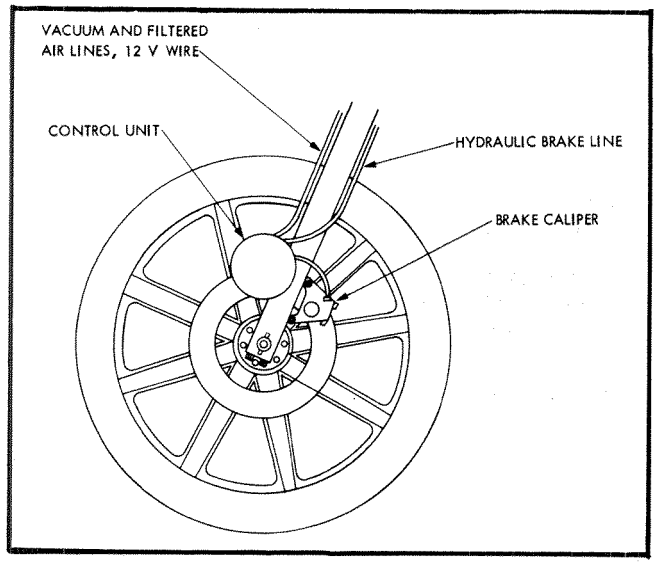

Figure 12. Control unit mounting concept

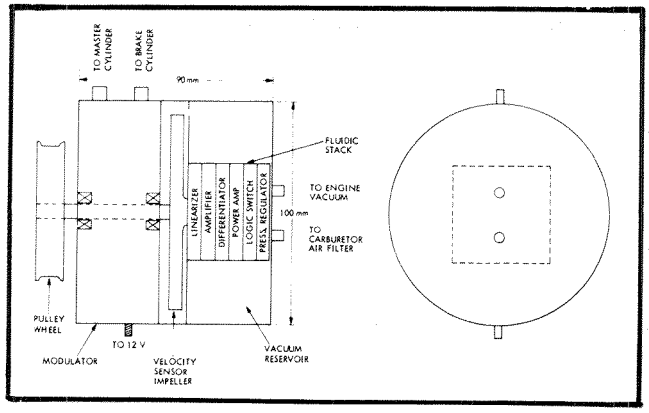

Figure 13. Control system packaging concept

Sensor

It was concluded by analyses and tests that wheel angular acceleration best indicates impending lockup. This variable can be sensed directly with an accelerometer or indirectly with a velocity sensor and a differentiating circuit. The latter approach was taken here because of the simplicity of the velocity sensor as compared with accelerometers. Past fluidic/pneumatic sensor designs, based on principles of inertia or centrifugal force(7), have involved moving weights and other moving parts with points of friction. Reducing friction to acceptable levels is a major design problem. Also the rotating, fluid-filled toroidal-type sensor(1) requires a rotating pneumatic coupling to transmit pressure changes to fluidic amplifiers. This rotating coupling presents a significant design problem to minimize leakage and noise on the pressure signal.

The sensor developed here has several advantages over past fluidic concepts and designs:

- One rotating part
- No rotating pneumatic coupler
- No friction problem
- Less expensive to fabricate
- More compact

This sensor, as shown in Figure 14, is basically a centrifugal pump with pressure sensed at the input rather than the output. Sensing the pressure at the input eliminates the problem of pressure pulses, or noise, that appear on the pump output. In addition, a fluidic circuit applied in a unique way is used to linearize the pressure signal.[2] Linearization is necessary to make the acceleration signal amplitude independent of velocity when the velocity signal is differentiated.

Referring to Figure 14, the impeller is a disk with six air ducts connected to a common opening in the center. Rotation of the disc causes air to flow from the center to the perimeter, in the manner of a centrifugal pump. The case is fixed. The air inlet is through a fluidic resistor and two orifices that function to linearize the relationship between the pressure across the resistor, or output, and the impeller angular velocity. Two small capacitances are formed by the volumes following the orifices.

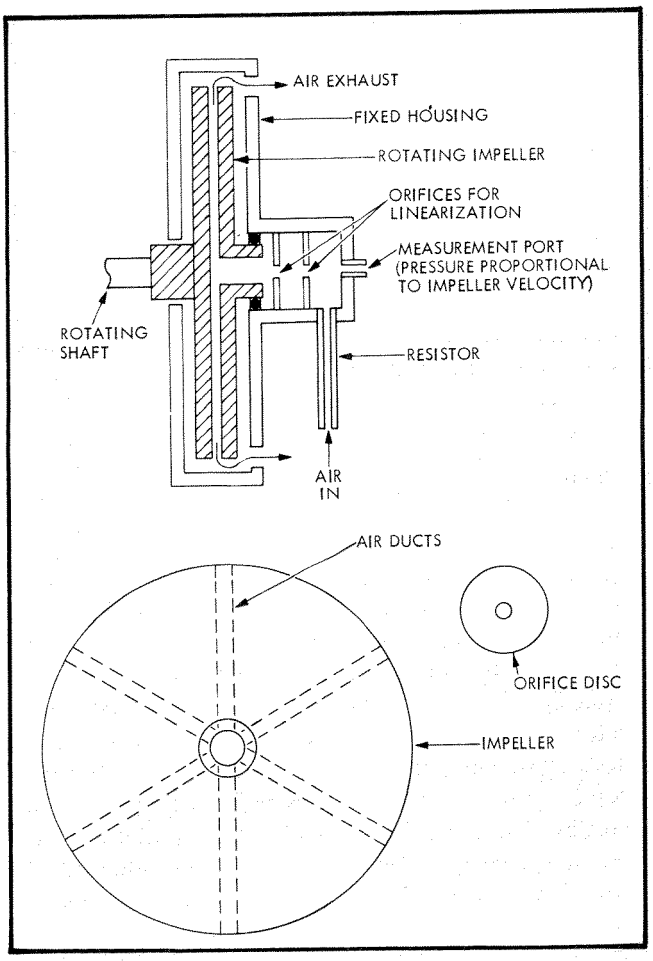

Figure 14. Angular velocity sensor—functional representation

The output pressure developed by a centrifugal-type pump, pumping fluid through a resistance load, varies as the square of the angular velocity or shaft speed. Thus,

$P_1 = K_1\omega^2$

where

P_1 = Pressure drop across the pump
K_1 = Constant of proportionality
ω = Pump speed in radians per second

Assuming the load resistance to be a linear element such as a tube or a pipe whose length-to-diameter ratio is sufficient to establish laminar flow (flow in which laminar shear forces reach from the pipe inside walls to the centerline), the flow through the device would be directly proportional to the pressure drop across it. In the case of the nonlinear pump applied to the linear (capillary) load resistance, a flow rate, Q, that is proportional to the pump pressure, or proportional to ω^2, would result. However, if a nonlinear resistance, such as an orifice, were substituted for the linear load resistance, a flow that is influenced by the nonlinear characteristics of the new load resistance would be established.

Referring to Figures 15 and 16, an orifice, Ro, which allows a fluid (in this case, air) to flow through it to a lower pressure region on the output side establishes a flow rate, Q, that is proportional to the square root of the pressure drop across it, P_2. This is true regardless of the ratio of orifice to pipe diameter in which the orifice plate is inserted. Since $P_1 = P_2$:

$$K_1\omega^2 = K_2q^2, \text{ so } Q = \sqrt{\frac{K_1}{K_2}}\,\omega,$$

which states that the circuit flow rate is proportional to speed.

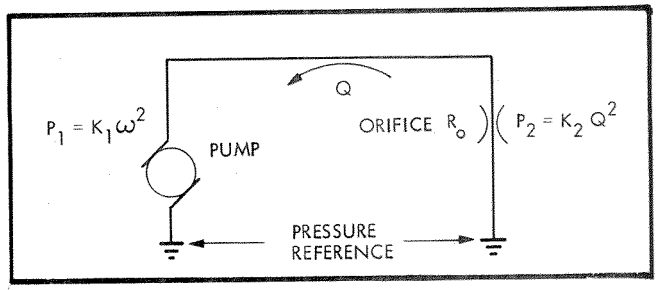

Figure 15. Pump and orifice circuit

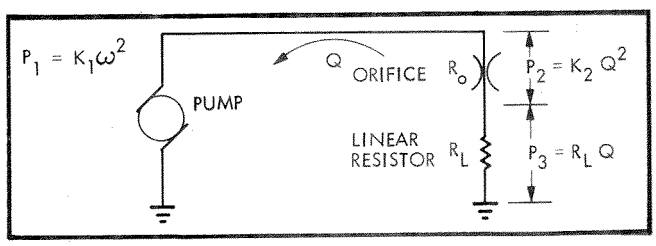

Figure 16. Circuit with linear resistor added to measure flow rate

[2] Patent applied for

The addition of R_L, however, introduces a nonlinearity as follows:

Now $$P_1 = P_2 + P_3$$

or $$K_1\omega^2 = K_2Q^2 + R_LQ$$

or $$Q^2 + \frac{R_{LQ}}{K_2} - \frac{K_1}{K_2}\omega^2 = 0$$

Solving for Q, $$Q = \frac{-R_L}{2K_2} \pm \sqrt{\frac{R_L^2}{4K_2}^2 + \frac{K_1\omega^2}{K_2}}$$

Q is no longer a linear function of ω. However, if, by design, R_L is an insignificant part of the total load, or $R_L << K_2$, Q will be proportional to speed, or, as before:

$$Q = \sqrt{\frac{K_1}{K_2}}\,\omega$$

However, when R_L is small, the pressure P_3 is small; therefore, a tradeoff of linearity for signal sensitivity must be made.

It can be shown that the addition of orifices may be used to linearize flow (see Figure 17). An analysis similar to that above shows that adding orifices diminishes the nonlinear effect of R_L by making R_L a smaller part of the total load.

For the experimental model of the sensor, two orifices, of a size determined by test, gave the desired degree of linearity. The linearization effect is shown in Figure 18. Without linearization, the pressure output versus velocity closely follows a square-law curve, as expected. With the linearizer, the curve is linear to within ±1.5 percent, if the portion below 1,000rpm is not used. One-thousand rpm is equivalent to 16km/h, which is below the required operating range of the antilock control.

Since the velocity output must be differentiated to get acceleration, the slope of the velocity curve is the significant characteristic. Over the range of interest, the slope variation of the nonlinearized curve is ±300 percent, while that of the linearized curve is ±15 percent, a twentyfold improvement.

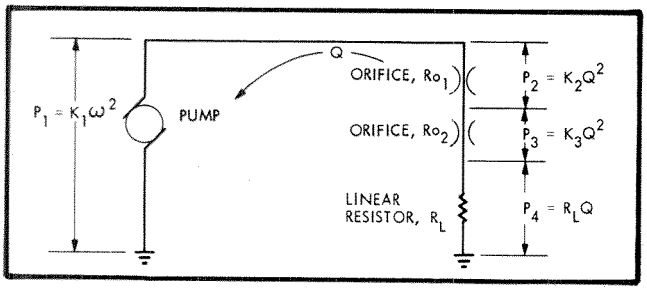

Figure 17. Multiorifice linearizer

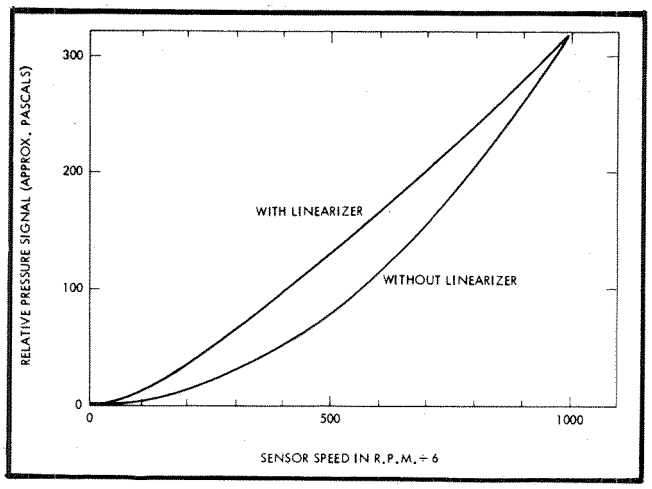

Figure 18. Effect of linearizer

Testing the sensor was done by using an electric motor with closed-loop speed control (Figure 19). The speed was varied with a DC voltage input. By using a linear-ramp voltage generator, the motor speed was accurately programmed to produce a known acceleration. Also, a sine-wave voltage generator was used to produce the frequency and phase response curves shown in Figure 20. For this test, the motor ran at 3,000rpm, and its speed modulated with a sine-wave. The results show the transducer has a flat attenuation response to 12Hz, the frequency limit of the test apparatus. Phase shift is about 9° at 12Hz. Assuming the sensor has a transfer function similar to a single-pole low-pass filter, the measured phase response is that of a filter with a cutoff frequency of 76Hz and a time delay of 2ms. This delay is well within our requirements for a total system delay of 20 to 30ms.

The experimental model of the transducer with the fluidic stack is shown in Figure 21. The case and impeller are made of acrylic resin. Details of the impeller and orifice disks are shown in Figure 22. The two disks, which are metal with 0.6mm orifices, are shown with two spacer-cavities.

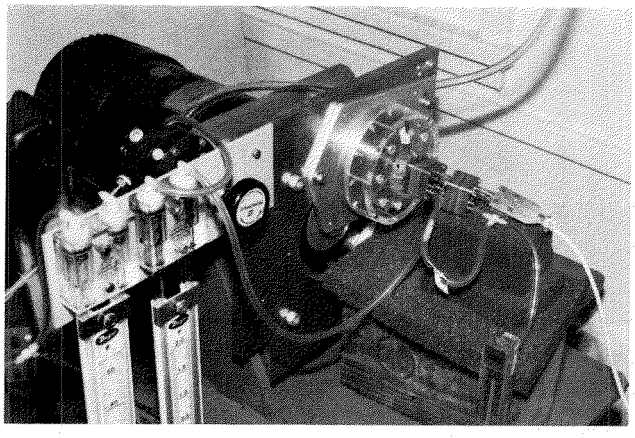

Figure 19. Sensor test apparatus

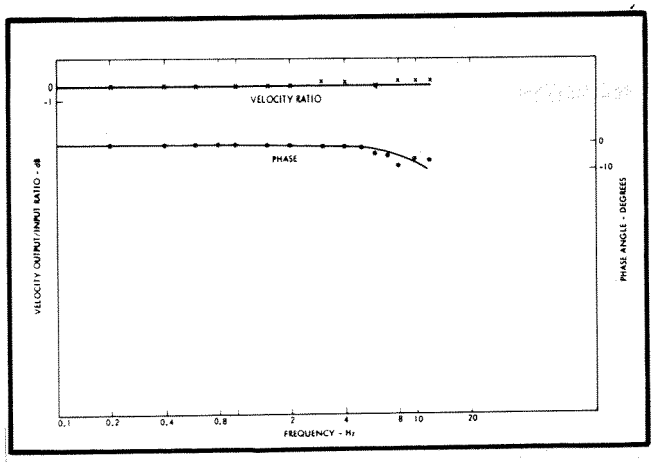

Figure 20. Sensor frequency response

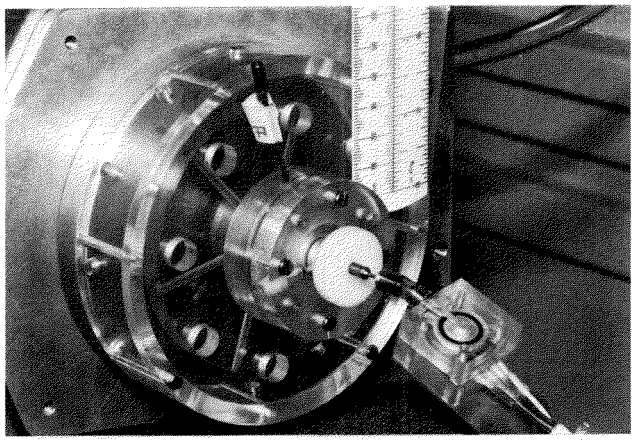

Figure 21. Velocity sensor

Fluidic Circuits

Referring to Figure 23, the fluidic circuitry following the velocity transducer is comprised of a preamplifier, a differentiator, a driver amplifier, and a power amplifier

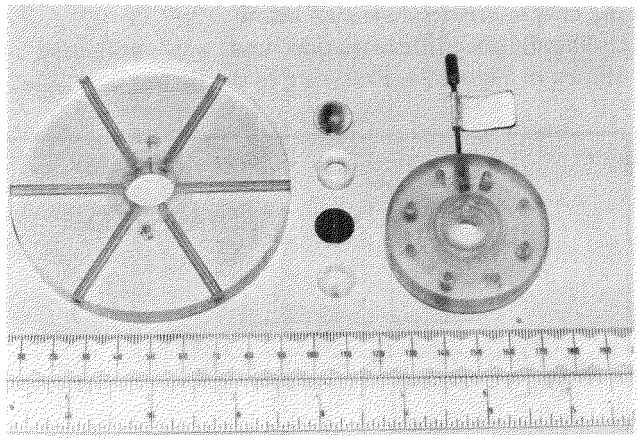

Figure 22. Sensor impeller and orifice disks

to operate the logic switch. This diagram represents the experimental setup, which operated from a positive pressure source. The final version would operate from engine vacuum and would include a vacuum reservoir and a pressure regulator to control the operating pressure to about 11kPa. The fluidic elements would be stacked and attached to the sensor, as shown in Figure 13.

Differentiator

In order to have a simple, low-cost sensor, a velocity type was designed. Since an acceleration signal is required, the velocity signal must be differentiated. While several approaches may be taken, the circuit shown in Figure 23 was fabricated and evaluated first because of its simplicity. It consists of diaphragm capacitors and resistors, equivalent to a single-pole RC high-pass electrical network. This approach to differentiation is valid over a limited range of frequency, being most effective at low frequencies. The design goal was to select component values that

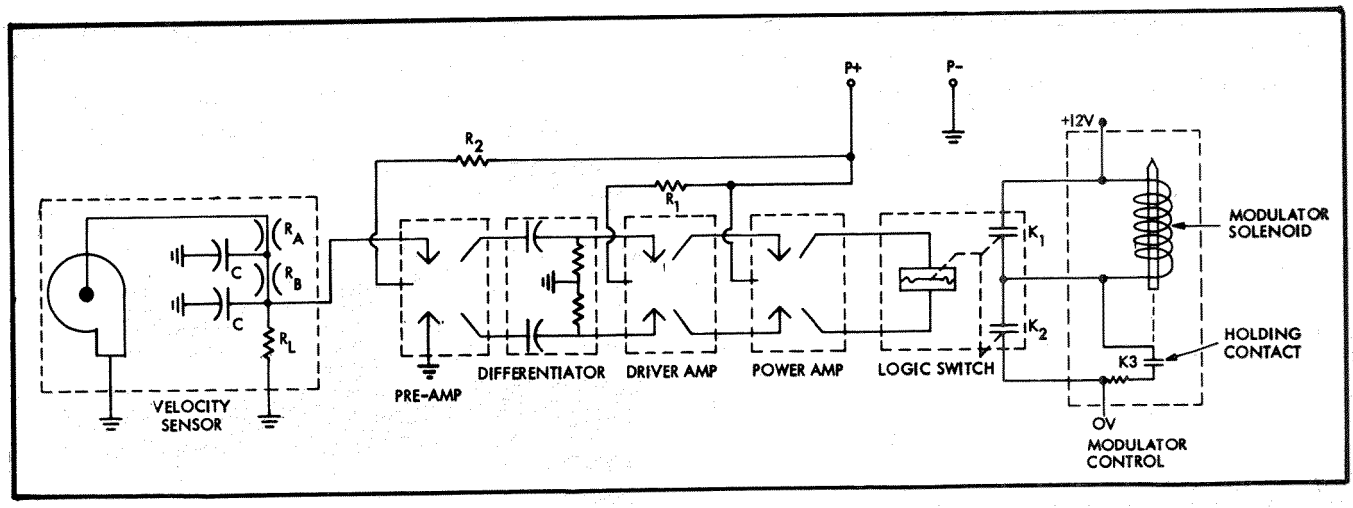

Figure 23. Schematic diagram of control system

would result in an acceptable compromise of the competing characteristics discussed below.

The fluidic differentiation unit was configured as shown in Figure 24. Referring to the figure:

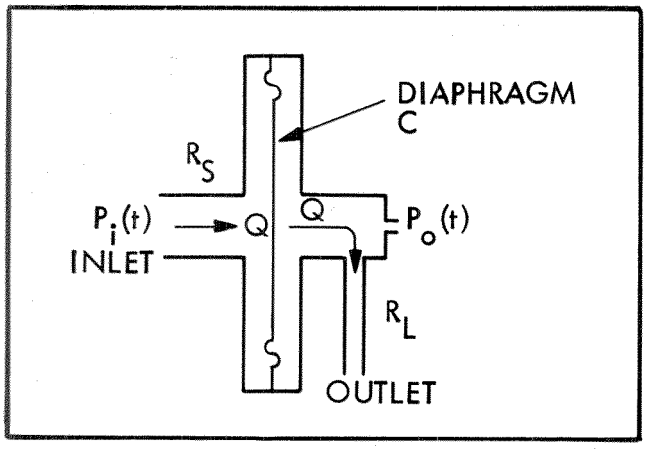

Figure 24. Fluidic differentiator

R_L = load resistance

R_S = input source resistance

$Q(t)$ = volume flow rate

$P_i(t)$ = input pressure

$P_o(t) = Q(t)R_L$ = output pressure

where P_i, P_o, and Q are a function of time, t.

C = diaphragm capacitance

$$= \frac{A^2}{K_D}$$

A = diaphragm area

K_D = diaphragm spring constant

Summing the pressure drops across each element,

$$Pi(t) = R_s\, Q(t) + \frac{1}{C}\int Q(t)\,dt + R_2\, Q(t)$$

$$Pi(s) = Q(S)\left[(R_L + R_s) + \frac{1}{SC}\right]$$

where S = Laplace variable

$$\frac{P_o(s)}{P_i(s)} = \frac{Q(S)R_L}{Q(S)\left[R_L + R_S + \frac{1}{SC}\right]} =$$

$$\left(\frac{R_L}{R_L + R_S}\right)\left(\frac{ST}{ST + 1}\right)$$

where $T = (R_L + R_S)C$

Since R_L is significantly larger than R_S, by design,

$$\frac{P_o(S)}{P_i(S)} = \frac{ST}{ST + 1}$$

This equation is the transfer function of a true differentiator, S, with a gain of T, combined with a simple one-pole low-pass filter, $\frac{1}{ST + 1}$, having a time-constant T, and a cutoff frequency $F = \frac{1}{2\pi T}$ Hz.

For this device to be an acceptable differentiator, the low-pass filter must have a small T to reduce the effects of phase shift and attenuation on the control loop, and reduce the lag in response. However, as shown by the transfer function, reducing T also reduces the differentiator's sensitivity, producing an undesirable effect on the signal-to-noise ratio. Since excessive noise on the acceleration signal will cause erratic operation of the control logic, careful attention must be given to minimize noise generated before the differentiator.

Results of evaluation tests are shown in Figures 25 and 26. Figure 25 is the frequency response in terms of attenuation and phase shift of the sensor/differentiator combination (hereafter referred to as accelerometer). These curves represent the relationship between input angular acceleration of the sensor and the pressure output of the fluidic driver amplifier (see Figure 23). The following conclusions may be drawn from these results:

- The cutoff frequency (-3db) of about 1.5Hz is much too low for use in the control loop. It should be about 10 times higher to reduce the effect of phase lag on the closed-loop limit-cycle frequency. As the limit-cycle frequency becomes lower, the stopping time increases to an unacceptable duration.
- The time-constant equivalent of a 1.5Hz cutoff frequency is about 100ms. This delay, added to other delays in the system, is too long to prevent wheel lockup in a panic stop.

Figure 26 shows the results of a transient test where a sudden acceleration (velocity ramp) was applied to the accelerometer. Preliminary analysis (see System Design) concluded that the threshold of wheel acceleration for triggering the reduction of brake pressure should be -97rad/s^2. Accordingly, for test purposes, the acceleration input was adjusted to a somewhat higher level of about ±130rad/s^2. The transient response of the accelerometer shows an unacceptable time constant of about 100ms (time to reach 63 percent of final value), which was predictable from the frequency response results.

To get satisfactory performance from the differentiator, the RC time-constant must be decreased by about a factor of 10, and the gain must be increased by adding another stage of fluidic amplification.

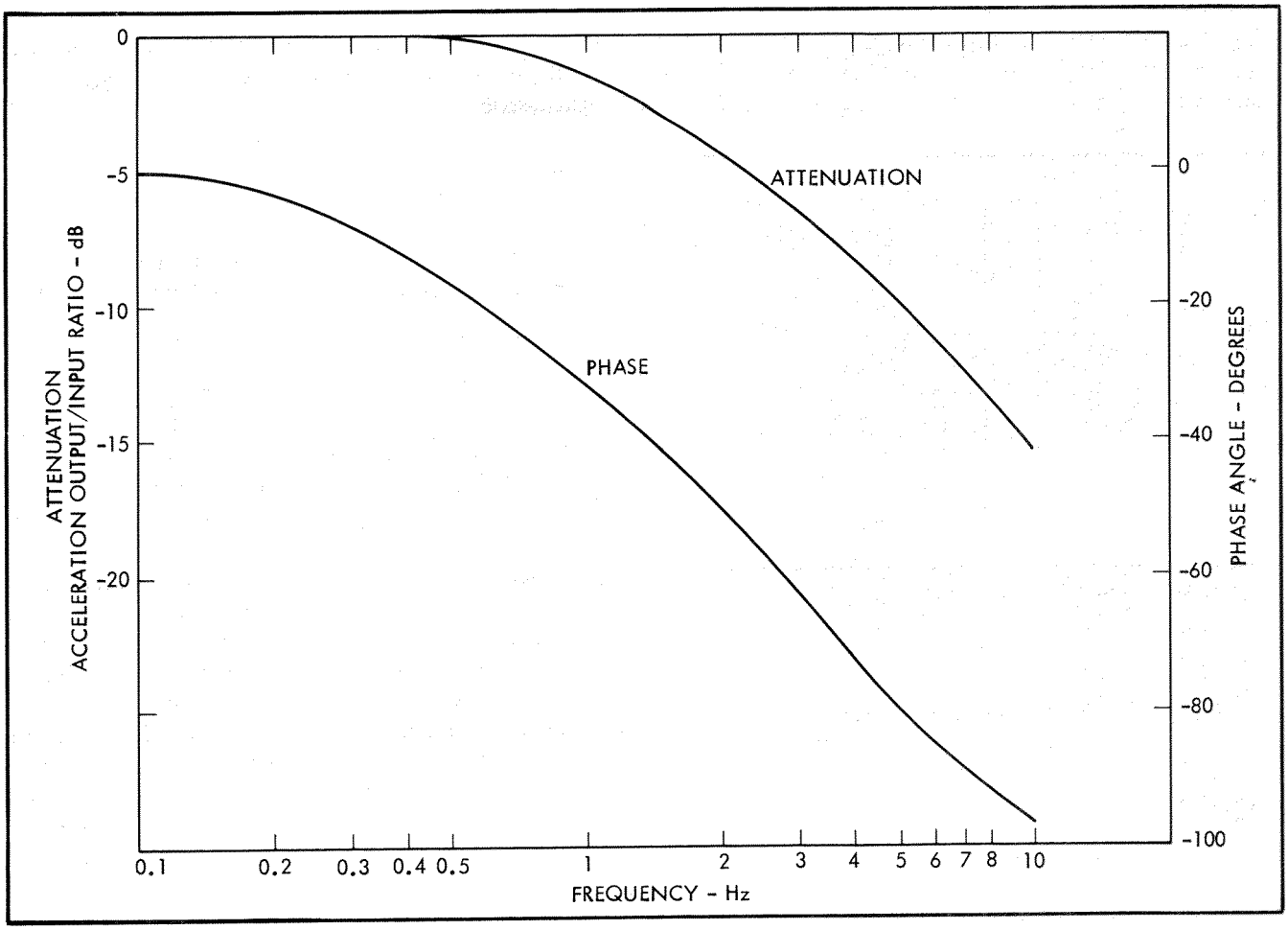

Figure 25. Combined sensor/differentiator frequency response

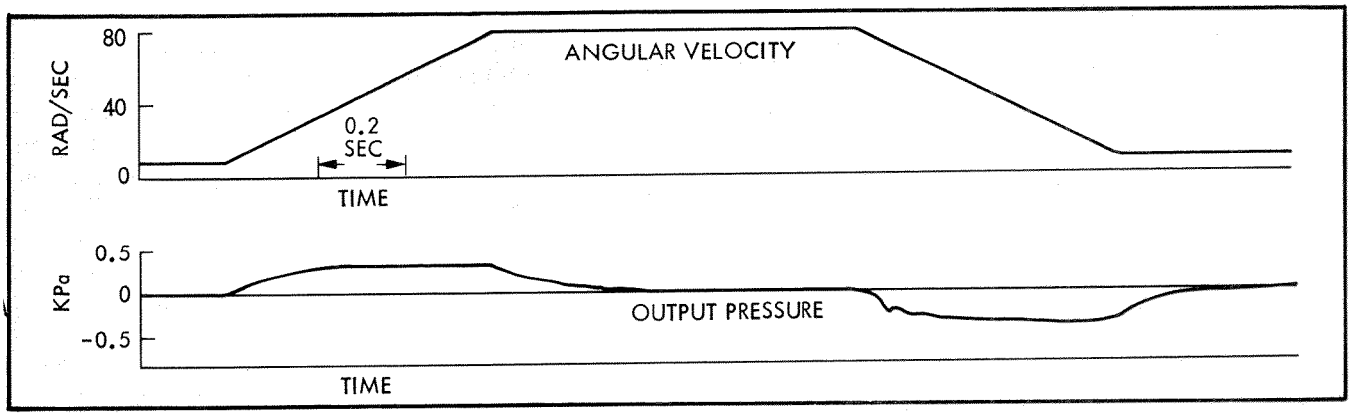

Figure 26. Sensor/differentiator response to acceleration step

Figure 27 shows the fluidic stack attached to the sensor. For convenience, the stacks were divided into two parts, one for the preamp and differentiator and another for the succeeding amplifier stages. The first stack is made up of the laminates shown in Figure 28. Most are standard C-format laminates from Harry Diamond Laboratories. The exceptions are those in the second row with large round holes. These are the differentiator capacitors, which, for the experimented model, have latex diaphragms of 0.15mm thickness, rather than metal diaphragms.

Control Logic

The function of the control logic is to initiate reduction of brake pressure at the correct level of wheel deceleration, and then to initiate increased pressure at the correct level of wheel acceleration. It does this by switching the modulator solenoid on or off in response to the acceleration pressure signal from the fluidic power amplifier (Figure 23).

An adjustable differential-pressure switch and a solenoid-controlled switch comprise the control logic.

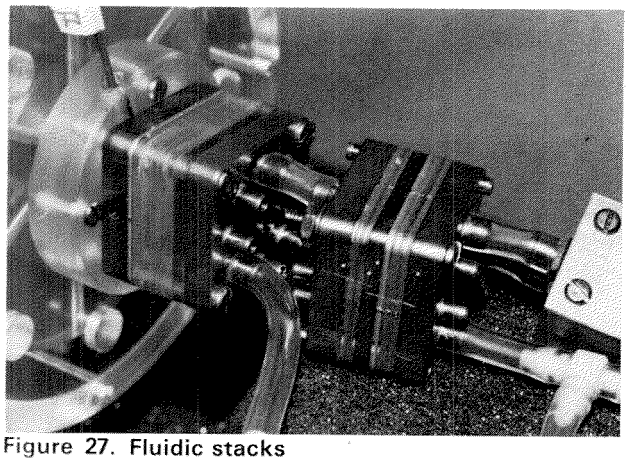

Figure 27. Fluidic stacks

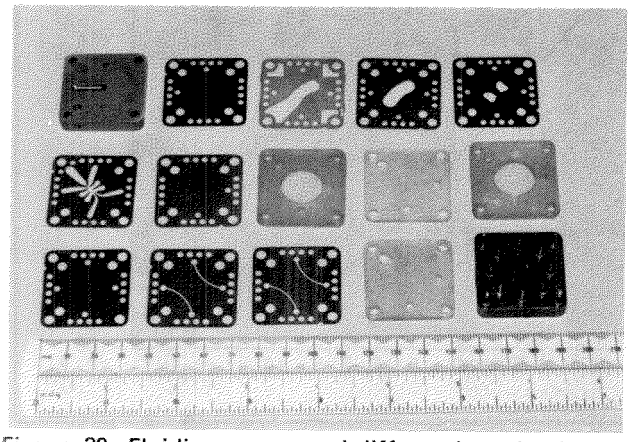

Figure 28. Fluidic preamp and differentiator laminates

The logic switch shown in Figure 29 has adjustable contact spacing, which permits an independent adjustment for deceleration and acceleration logic levels. The solenoid switch, which is closed when the solenoid is energized, is needed to hold the solenoid energized while the logic switch is changing direction between contacting positions.

The relationship between the switch action (control command) and the resulting braking dynamics is shown by the computed data in Figure 30. The cyclic action shown is the intentional result of the nonlinear form of control. The smoothly changing frequency of the limit-cycle rate indicates a stable control system.

Because the sensitivity of the logic switch developed was not compatible with the pressure levels produced by the fluidic circuits, an overall test that included the logic switch could not be run. To do so will require more fluidic amplification ahead of the switch. This modification is in progress.

Modulator

The function of the modulator is to reduce hydraulic pressure rapidly on command from the logic switch and then rapidly apply pressure on another command. The result should be a quick stop without wheel lockup. It is also necessary that the modulator not interfere with normal braking and the antilock action stops when the vehicle operator releases the brake lever.

Since the modulator was not developed as part of this work, the analysis model of the control system assumed a hydraulic type rather than the slower acting pneumatic type, which is probably not capable of operating with delays less than 20ms.

To explain the modulator's operation, the configuration shown in Figure 31 was chosen. It is simple and similar in concept to one developed by Mullard Research and TRRL in England(8).

Referring to Figure 31, normal braking occurs when the solenoid valve is closed. If the wheel is about to lock

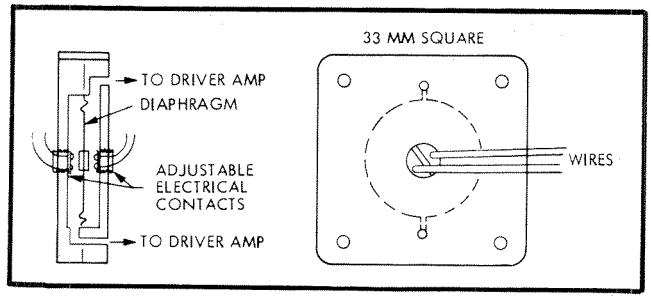

Figure 29. Pressure-operated logic switch

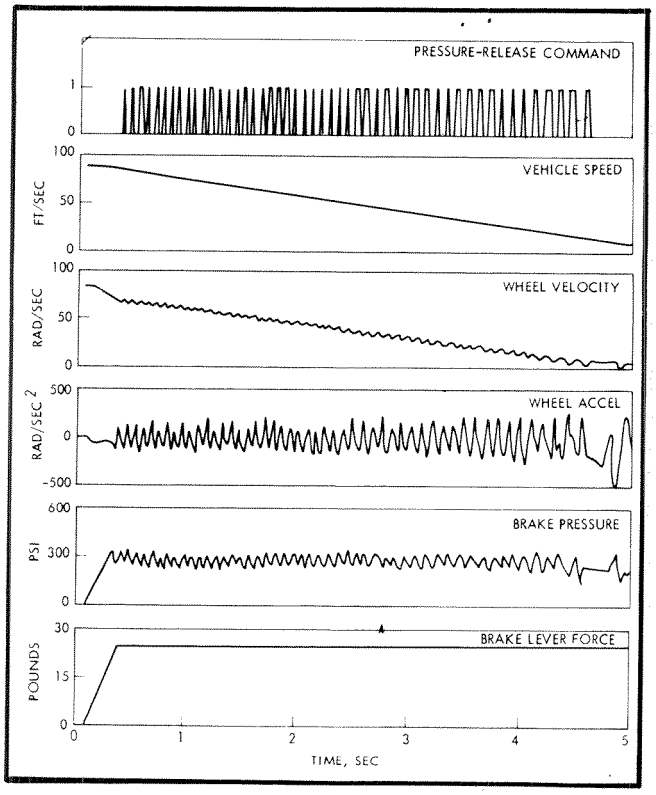

Figure 30. Brake control action

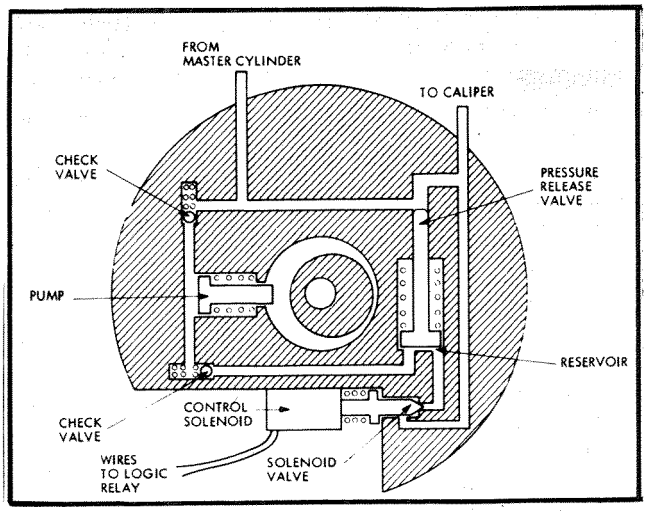

Figure 31. Modulator concept

because of high brake pressure, the solenoid will open the valve, allowing pressure to move the reservoir piston to block the connection between the master cylinder and the caliper and to provide a volume for pressure reduction in the caliper line. The pressure in the caliper line also forces the pump piston against the cam, and some fluid is forced back into the line. When the solenoid is deenergized, the valve closes, causing the reservoir piston to move back, opening the line to the caliper, and causing the pump to force excess fluid back into the line.

Design requirements dictate a fast-acting solenoid and rates of pressure change to match those specified in the System Design section.

Conclusion

The fluidic velocity sensor developed for this application met requirements for simplicity, compactness, and functional capabilities. It adapts well to the fluidic stack concept of fluidic circuitry, and its response time is negligible.

The differentiator must be modified to reduce its time-constant. This should present no particular problem if attention is paid to low-noise component design. Other types of differentiators that would not require moving parts, such as diaphragm capacitors, should be investigated. Also, more signal amplification must be included in the design modifications to operate the logic switch.

Analysis concludes that an acceleration feedback loop will give reasonable stopping distances for the road surfaces considered. Optimization of performance for a greater variety of surfaces would require adaptive techniques using more sophisticated logic involving other parameters, such as wheel slip. Such techniques are within the capabilities of fluidic technology but may be too complex for an inexpensive and compact brake-control system.

Although more work is needed for verification, it appears that a fluidic control system is feasible. The design challenge is to achieve fast response in the fluidic components.

Acknowledgments

This research was carried out by the Jet Propulsion Laboratory, California Institute of Technology, Pasadena, California, for the National Highway Traffic Safety Administration, Department of Transportation, under contract with Harry Diamond Laboratories.

References

1. Tenney, Stephen M., "Towards a low cost highly reliable antilock brake system for small motorcycles," Contract No. DOT-HS-802-288, February 1977.
2. Tenney, Stephen M., and John M. Goto, "Development of a low cost antilock brake system for small motorcycles," Contract No. DOT-HS-803-861, December 1978.
3. Thurston, John F., "Development of fluidic antilock system for motorcycles, Phase III," Final report, N000 19-78-G-0288 WY31, Garrett Pneumatic Systems Division, Phoenix, Arizona, June 1982.
4. Zellner, J., and M. White, "Advanced motorcycle brake systems," Final report, Contract No. DOT-HS-806-095, November 1981.
5. Zellner, J.W., and D.P. Chiang, "A feedback control method for antilock brake design," Proceedings Tenth International Technical Conference on Experimental Safety Vehicles, July 1985.
6. Harned, J.L., et al., "Measurement of tire brake force characteristics as related to wheel slip (antilock) control system design," SAE Paper 690214.
7. Scheer, Lawrence E., and Mel M. Steele, "Fluidic antilock braking/traction transfer system (FAB TRAC) sensor development," DAAK-30-78-C-0081.
8. Zellner, J., and D. Weir, "Evaluation of the Mullard/TRRL antilock brake system," Contract No. DOT-HS-804-192, May 1979.

Accidents of Motorcyclists — Increase of Safety by Technical Measures on the Basis of Knowledge Derived From Real-Life Accidents

M. Danner,
K. Langwieder, and
A. Sporner
HUK-Verband, Automobile Engineering Department

Abstract

Technical safety measures call for detailed knowledge of how accidents occur. Accidents involving two-wheel vehicles pose particular problems in describing the course of the accident and injury severity as well as ascertaining the causes.

Using material covering approximately 3,500 accidents with motorized two-wheelers, a realistic classification system is explained and problems of the different two-wheel categories are shown in this paper.

Experimental and mathematical simulations of the main accident type lead to some suggestions on how to change the motorcycle by adding some safety elements to reduce the injury risk of the driver.

A safety motorcycle is introduced that can improve, in a positive way, the flight path of the driver after an impact without being unrealistic.

Introduction

Safety research for motorcycles, compared with motorcar research, has only begun. Therefore, it is important not to aim at general solutions but to find the main causes of accidents after analyzing the characteristic features of accidents. Only then will it be possible to search for improvements, i.e., new safety elements to reduce the motorcyclists' risk of being injured and to make motorcycling safer in the future.

In the early 1970's, one of the first institutions to record and evaluate motorcycle accidents systematically was the HUK association. This started when the number of motorcycles was lower than ever; for example, in 1972 there were 198,221 motorcycles and, in 1984, 946,572. This early research made it possible to utilize a fundamental basis of accident analysis and experimental simulation that put us in a position to introduce sensible technological measures concerning the decrease of injuries.

To date, more than 3,500 motorcycle accidents have been evaluated and recorded in EDP data files by HUK engineers. These accidents mark the starting position for further experimentation and mathematical models. The study of accidents in which motorcycles were involved shows a continuous downward trend after 1982 (Figure 1). The number of accidents with motor-assisted bicycles and motor-assisted bikes with kick-starters has been decreasing also. Only the accidents with light motorcycles have increased in the past few years. This is due mainly to the conduct of beginner adolescent cyclists.

Nevertheless, there were still 1,548 fatally and 30,544 seriously injured cyclists in 1984, so we need to keep trying to achieve more safety.

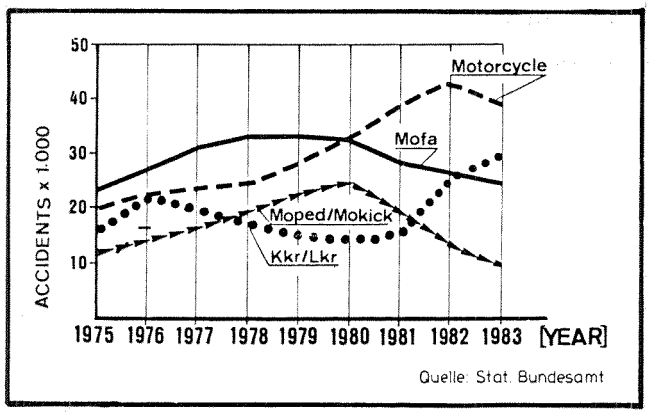

Figure 1. Accident with motorized two-wheelers

Technological Status Quo

Demonstration of accident numbers clearly shows it is not very sensible to evaluate motorcycle accidents invariably and generally. The main distinguishing features are summarized in Figure 2.

At present, there are four different types of motorcycles in the Federal Republic of Germany:

- 15-year-olds can drive a motor-assisted bicycle no faster than 25km/h.
- 16-year-olds can choose between the motor-assisted bicycle with kick-starter (no faster than 40km/h) or the Leichtkraftrad (80km/h).
- From 18 on, one can drive any motorcycle without any limits to the power, apart from the producer's voluntary limitation to 100hp.

The planned introduction of a graded driving license will place motorcycles in the following categories:

- Beginners' motorcycles up to 20kW power
- Motorcycles with unlimited power

There are characteristic accidents in each group of cycles. One has to make differences, especially between the light-powered motorcycles and the heavy ones. It is the exact knowledge of these sequences of motion that is the requirement for acquisition of realistic safety conceptions.

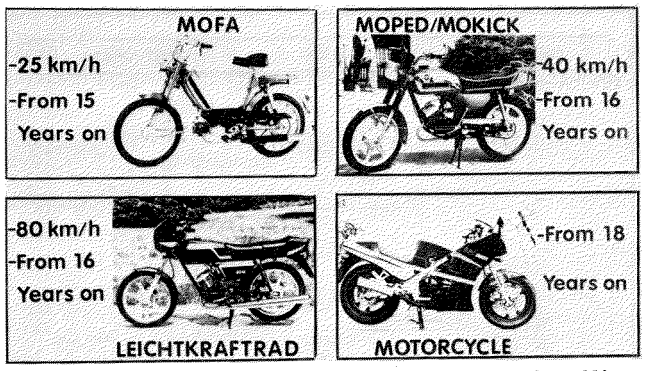

Figure 2. Motorized two-wheel vehicles in West Germany

Problems With Light-powered Motorcycles

From an extensive study of 1,700 accidents with motor-assisted bicycles(1) and from a special analysis of 1,000 accidents with Leichtkrafträdern(2), it can be seen that a main factor is found in the adolescent driver and his conduct. Lack of experience and a high readiness to take risks lead to driving maneuvers often resulting in an accident. Adolescent beginner drivers often recognize critical situations too late.

A further aspect limits the possible technological improvements. The design of motor-assisted bicycles and motor-assisted bikes with kick-starters (Mofa, Moped, Mokicks) hardly permits additional parts on the cycle because they are constructed with the lowest possible weight to achieve competitive power. Furthermore, if safety devices are to fulfill their function, they must have a certain solidity that is difficult to obtain on a light frame.

As we will show, this is especially true for side collisions, which are predominant with smaller motorcycles. This result leads to the conclusion there will be only limited success in technological safety measures for light motorcycles.

On the other hand, not all safety reserves known have been realized so far. Improvements can be found concerning the pedals of the motor-assisted bicycle, which have proved to lead to a higher risk of falling than footrests. Further improvements might be made in the lighting equipment and frame stability of cycles. Also, antimanipulation measures, which make it impossible to increase the power and speed, are among the desirable technological measures known but not yet fulfilled.

Accident Characteristics of Motorcycles

The analysis of all motorcycle accidents reveals sensible starting points, especially for heavy motorcycles, to influence the risk of injuries by technological measures. But first, the main characteristics have to be described that are typical of the motorcycle accident. Generally one can distinguish between single-vehicle accidents and collisions. The single-vehicle accident is being examined presently in research, and some possibilities can be seen already how to technologically influence the single-vehicle accident and the mechanism of injuries during the fall.

As far as collisions are concerned, there are, apart from the rare glance-off collisions, two completely different accident sequences (Figure 3):

- Collision of the vehicle involved against the motorcycle
- Collision of the motorcycle against the other vehicle

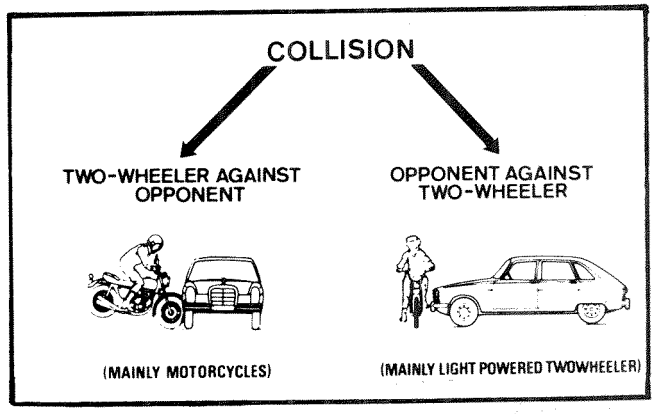

Figure 3. Collisions with two-wheelers

In the first case, the motorcyclist is impacted and run over by the other vehicle. The cyclist's kinetic energy is of less importance, and the sequence of motion is, in some respects, similar to that of an accident with pedestrians. In most cases, the casualty is caught by the other vehicle, hurled onto the bonnet, and eventually dropped. The injuries result mainly from contact with the other vehicle and are in first approximation proportional to its kinetic energy and shape aggressiveness. In other words, the faster and more edged the other vehicle, the more serious the cyclist's injuries. This type of collision happens most often with lighter motorcycles, such as the motor-assisted bicycle and the Moped/Mokick. As already mentioned, effective protective devices are difficult to realize, particularly as the light construction of these cycles does not permit a heavy protective bar in the area of the lower extremities.

In the second case of a collision of the cyclist with another vehicle, the accident sequence is completely different. Here the cyclist's speed and thus his kinetic energy is the central parameter for the motion path and the severity and kind of injuries. In addition, motorcycles and light motorcycles can be found in this group, and thus the requirements for the realization of technological measures are fulfilled.

The expensive and heavy touring motorcycles are ideally suitable for safety elements without giving up the characteristics of a motorcycle. Besides the promising prospects concerning technology, the relative frequency of this accident type—motorcycle against other vehicle—was a reason to deal more thoroughly with these problems. Figure 4, from another research project of the HUK association(3), shows it clearly.

About 60 percent of all accidents with motorcycles and Leichtkrafträdern belong to the category of motorcycle bumps against other vehicles. As for motor-assisted bicycles and Mokicks, this accident type is only 33 percent.

There are two reasons for a closer examination of this accident sequence: the frequency and the promising prospects for technological measures.

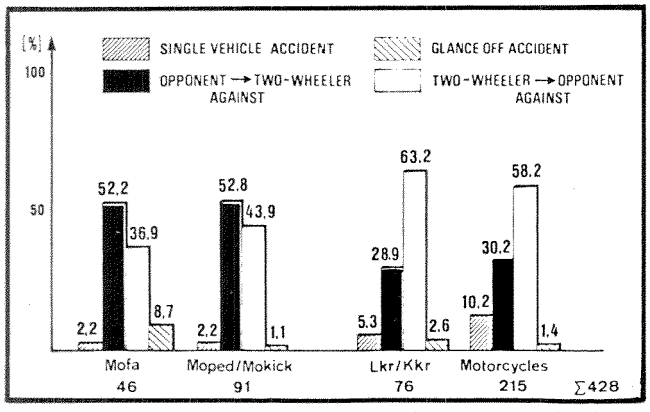

Figure 4. Distribution of motorcycles by main accident types

Accident Sequence

To find starting points for future safety elements, this collision sequence—the bump of a motorcycle against another vehicle—has to be divided into its single phases (Figure 5).

In the first phase—the precollision phase—the preconditions are determined for the kinds of motion in the second phase. The cycle, for reasons of its single-track construction, drive into the collision phase already in a falling way, and thus produce completely different motion sequences that do not occur with motorcar accidents(4).

During the collision phase, main differences can be seen in the direct bump of the cyclist against the other vehicle and in the overflight. This phase is decisive for the seriousness of injuries to the cyclist since the energy is reduced either by the cyclist's hard bump against the other vehicle or by the overflight.

The post-collision phase then shows the results, that is, whether the cyclist has suffered a bump or if he was able to destroy his energy by rolling onto the street.

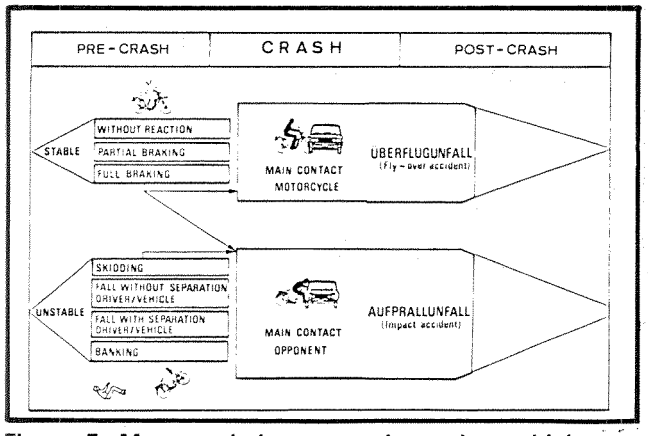

Figure 5. Motorcycle bumps against other vehicles

Motion Sequences and Injury Patterns

Starting points for developing protective measures are of greatest use during the precollision and the collision phase since the course is set here for the decision: bump or overflight.

How decisive this difference is shows the severity of injuries suffered by cyclists, divided into bump and overflight. The real accident sequence shows clearly that safety measures are possible only if they influence the cyclist concerning an overflight with its reduced strain (Figure 6). The seriousness of injuries increases according to an increase in speed, but the rate of seriousness after a bump in any speed range exceeds the rate resulting from overflight.

Which causes can be found for these different motion sequences?

The analysis of the real accident sequence(5) shows that cyclists on special types of motorcycles were more often able to start an overflight. These types were mainly enduros and cross-country motorcycles (Figure 7).

With similar collision speeds and similar vehicles, the cyclists were much more often able to overfly the other vehicle than the cyclists of normal motorcycles and light motorcycles. This result shows there are technological parameters that influence the path of motion. The knowledge of this then led to experimental and mathematical simulations of the possible influencing parameters. Possible parameters might be points that result on the one hand from the geometrical measurements of the motorcycle and on the other hand from defense reactions of the motorcyclist himself. If we first ignore the second point, then there is a variation of the parameters that determine the essential measurements and characteristic features of a motorcycle:

- Height of seat
- Seating position, influenced by the position and form of bench-seat, handlebar, and footrest
- Shape of contact surfaces: tank, handlebar, baffle-pad

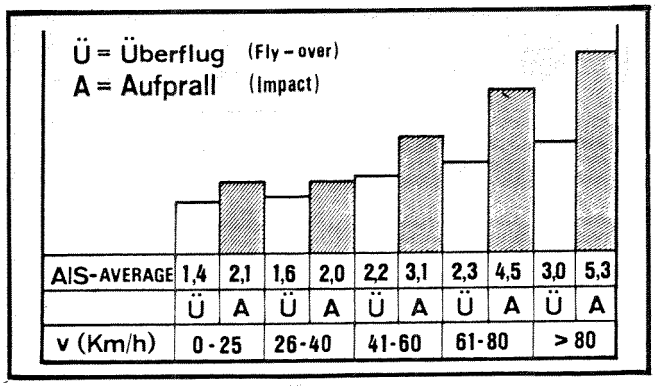

Figure 6. Injury severity with reference to collision speed

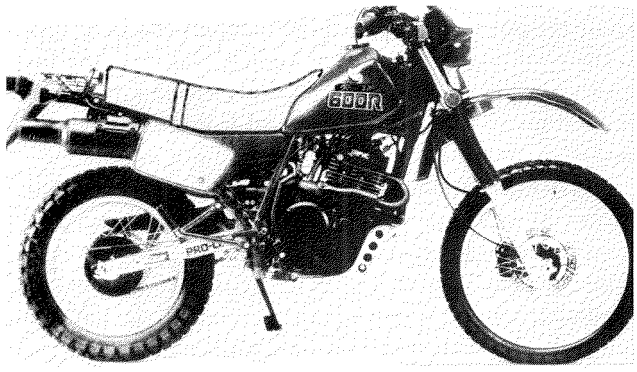

Figure 7. Cross-country motorcycle

Experimental Results

In the experimental part of the research, two series of crash experiments were carried out, which on the one hand very well complemented one another, and, on the other hand, led to important individual results—the real crash and the sledge-test.

In the real test, motorcycles of the same type were driven against different surfaces of a stationary vehicle (Figure 8).

Besides the decelerations of the motorcycle, the decelerations of the head and the chest of a 50th percentile Sierra dummy were measured; by means of high-speed film, a chronological description of all incidents in the first 200ms was made. The measured decelerations of the motorcycle permit the following conclusions (Figure 9):

- The form of deceleration sequence of the motorcycle can be varied theoretically by technological measures because it is determined essentially by the parts—tire, fork, and rim.
- Such a measure would not be successful with regard to the cyclist, since—
  - The cyclist is connected with the motorcycle only by sitting friction; therefore, a soft deceleration cannot be passed on to this body.

The deceleration of the motorcycle is strongly dependent on the geometry and rigidity of the impact point as the deceleration sequence with the rear crash shows.

Here, tire, fork, and rim could not deform themselves in the desired way because the motorcycle has driven under the rear of the car with its front wheel and has been decelerated only by the very hard contact between steering head and bumper. But there was no reaction to this different deceleration to be seen in the dummy's motion sequence.

The deceleration has a neglectable influence on the cyclist's motion path. Yet the chronological description of the single phases provides important hints (Figure 10). In the upper part of the figure, the dummy's activities are noted; in the lower part, the deformations and motions of the motorcycle. Both systems can be related to each other. If you take the case of a collision against the passenger compartment of a motorcar with a collision speed of 50km/h, the most important incidents happen during the first 100ms after t_0. This is a very short time for measures to have an effect, but there is a possibility to influence the cyclist's motion path in this time by varying some of the construction elements. The aim of a safety

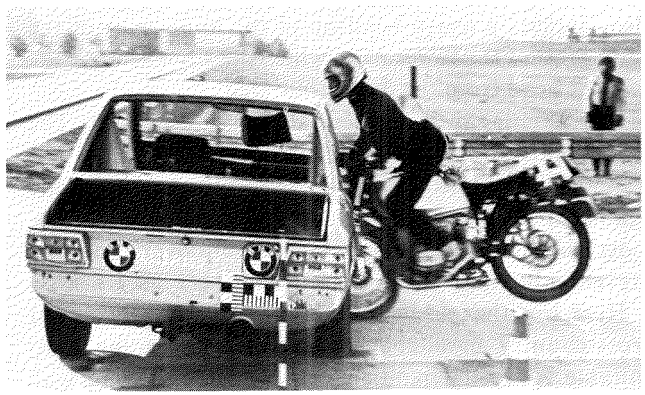

Figure 8. Motorcycle driven against stationary vehicle

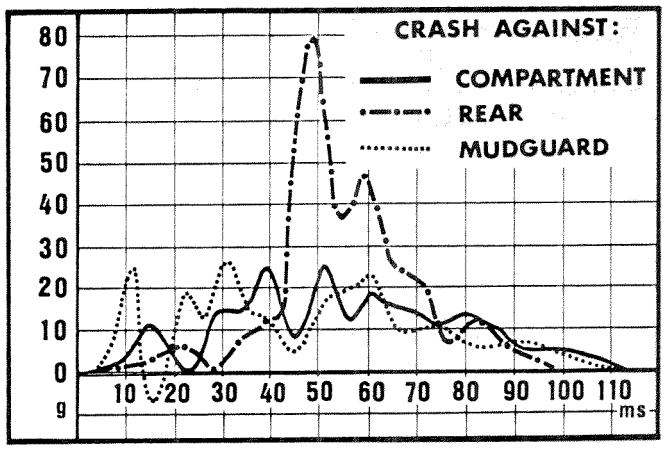

Figure 9. Measured decelerations of motorcycle

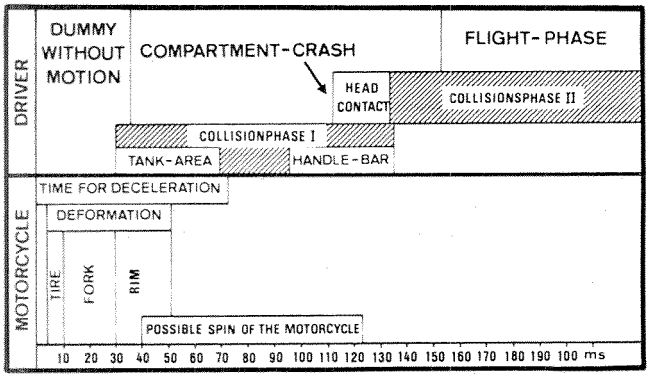

Figure 10. Chronological description of a 50km/h test

conception was to start an overflight and avoid the dangerous area roof edge for the cyclist's head(4).

The first contact after t_0 between dummy and motorcycle takes place after about 30ms. The lower part of the body bumps against the tank. On varying the shape of the tank, it has been shown that a tank-rising angle of about 40° to 45° is the best compromise (Figure 11).

First, a too-flat tank does not exercise any reactive power on the cyclist to raise the center of gravity; second, with a too-flat tank, the impact of the thighs against the handlebar is very hard because there is no speed reduction. A steep tank does raise the cyclist's center of gravity but also involves a heavy rotation of the upper part of the body around the lower part, which does not remove the cyclist's head from the dangerous area.

The handlebar is influential in two respects. The seating position is determined by its shape, and it is responsible for serious thigh injuries if there is an impact against it. The improvement must, therefore, find the most suitable seating position for an overflight and prevent a bump of the lower extremities (Figure 12).

Here, too, the middle course in the form of a touring or cross-country handlebar has proven to be the most suitable. A too-flat handlebar, as can often be found with sporting cycles, makes the cyclist sit in a very low position

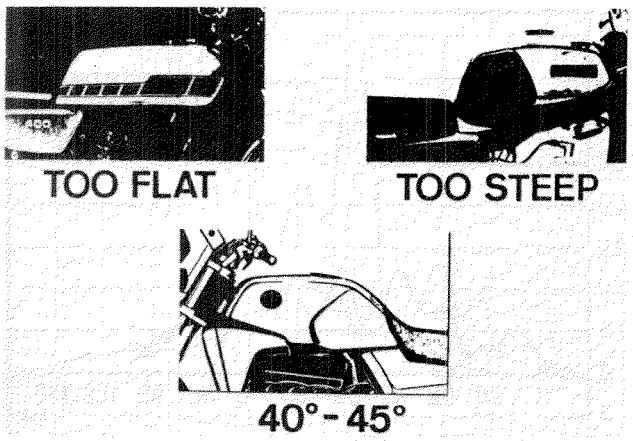

Figure 11. Shapes of fuel tanks

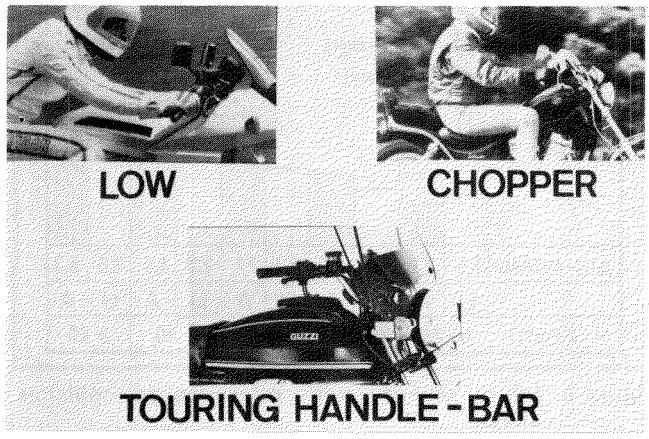

Figure 12. Handlebars

where the position of the head is relatively low in relation to the roof edge of the other vehicle. To raise the low position of the head by technological measures during the first 100ms so the head is removed from the dangerous roof edge area is extremely difficult, if not impossible.

A very high handlebar, also called a chopper handlebar, creates an optimal seating position but unfortunately develops characteristic features during the collision sequence that lead to the body getting caught on the handlebar, thus preventing the desired flight path. In addition, the seating height on chopper motorcycles is very low.

Mathematical Description of the Motion Sequence

All variations described so far have been carried out on a sledge installation with which it was possible to control the effects of the single parameters easily. At the same time, the motion sequence was calculated in a mathematical simulation program to obtain the rising powers and decelerations(5). By means of a converted passenger model with 10 degrees of freedom, it was possible to simulate the powers and motions of a cyclist who bumps against a stationary obstacle—a motorcar (Figure 13).

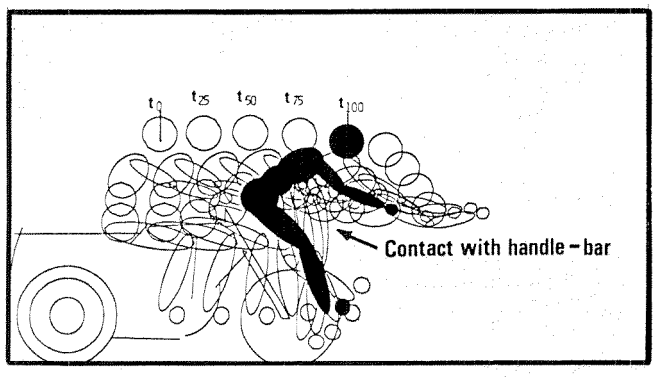

Figure 13. Simulation without leg-pad

Results

The first positive influence on the cyclist's path turned out arithmetically and experimentally after the introduction of baffle-pads in front of the cyclist's legs. Because of these, the bad impact of the legs against the handlebar could be prevented. Not only is the danger of thigh injuries averted, but also the danger of the body being caught on the handlebar—the so-called "flick-knife-effect",—can be eliminated in this way. An optimal function of this pad also includes absolutely necessary support of the entire lower leg. The full effect of the leg-pad could be observed afterward with the combination of a touring handlebar, as in this case the flight path was also influenced (Figures 14 and 15).

The dummy's body stretched and the bumping point of the head was some centimeters higher than it had been in the experiments without pad and with a sporting handlebar.

The possibility of influencing the flight path through the search for safety elements will continue within the HUK accident research.

In the past few years, there was no lack of suggestions on how to fix the cyclist by hold-back devices to the vehicle to minimize the risk of being caught on the bar. Looking at the patent applications, one can find constructions that try, some in a futuristic and others in an amateurish way, to force safety on the motorcycle. The probability of realizing these inventions is very low, as the effect of the new safety element is uncertain or the

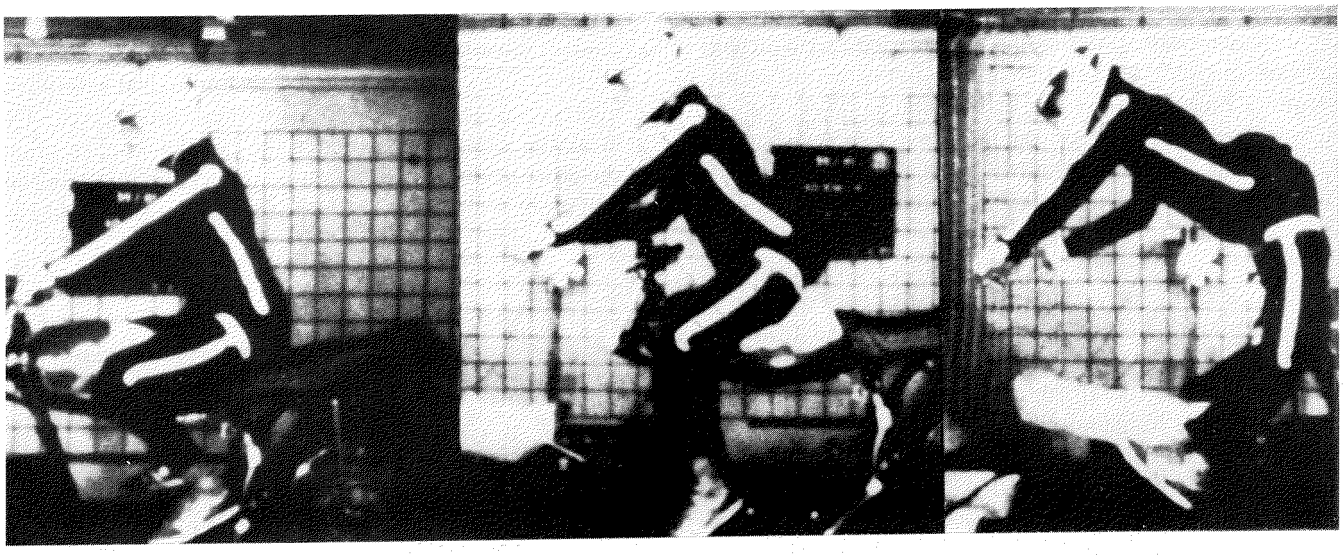

Figure 14. Test without baffle-pad

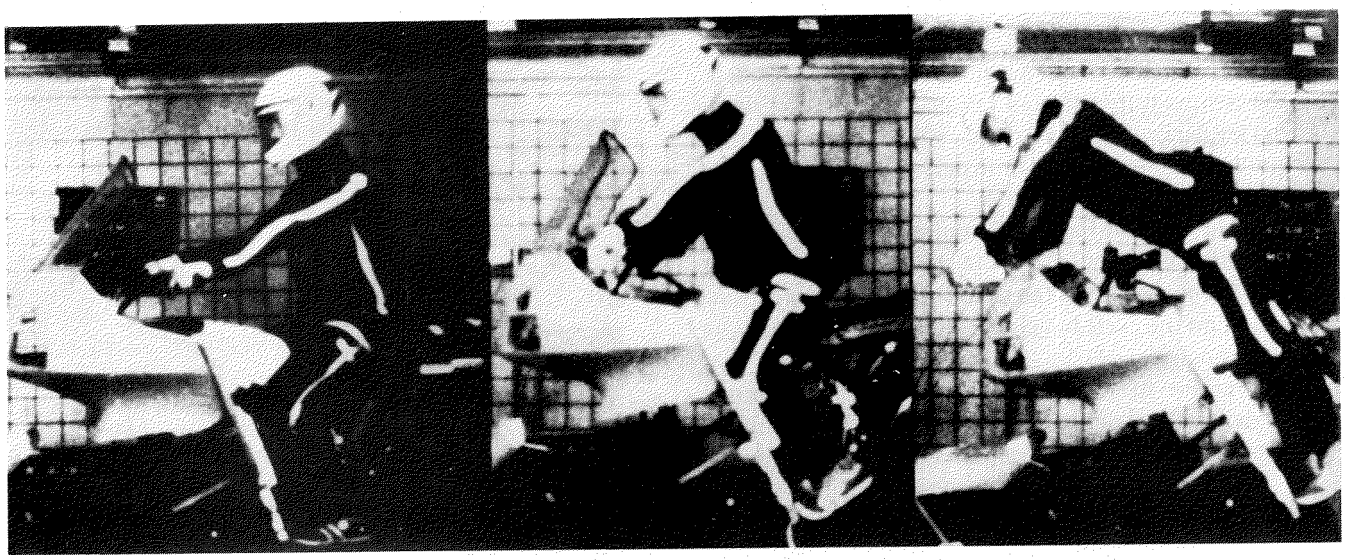

Figure 15. Test with baffle-pad (leg-pad)

conception of the entire motorcycle would have to be changed. The situation might be different with an additional safety element that has actually been applied for the car, namely, the airbag. At present, the airbag is one of the few car-safety elements that could also have an effect on motorcycles, but only if it is used additionally on the basis of the measures discussed and if it does not alter the characteristic features of the motorcycle. To fulfill these requirements, the effect of the airbag has to be extended. Concerning the motorcycle, apart from cushioning the impact, an influence on the flight path might be possible by means of the airbag. Compared to the car airbag, there are other priorities for the motorcycle airbag:

- Influence on the flight path and the driver movement
- Cushioning the impact between driver and other vehicle

Ten years ago, experiments were made(6) with airbags on motorcycles, at that time mainly to protect the cyclist from a bump against the other vehicle. They did not consider an influence on the flight path, so the shape of the airbag at that time had to be oriented to a support. Furthermore, this airbag had a volume of 200:1 and was very difficult to fill.

A further development of those ideas has not become known, except for an inflatable protective suit for the cyclist himself. This has never been able to fulfill its function entirely, since the filling was done with compressed air and therefore took longer than 150ms. This time period is long enough to protect the cyclist in a fall but not in a collision during which the decisive incidents take place during the first 100ms.

Fortunately, airbag technology has developed further because of activities in the motorcar sector and the basic knowledge can be taken over. Today filling the airbag (in its third generation) is done by burning solid fuel and no longer by compressed air (first generation) or by hybrid liquid gas (second generation). This defined burn-up with controlled expansion enables inflating times, dependent on the temperature, of about 30ms(7). As the chronological sequence of a motorcycle collision is known from previous experiments, this time period is long enough to realize a protective effect.

The volume of the bag, in the motorcar about 60:1, will not be sufficient for the motorcycle. Further points of improvement are also in the shape of the airbag and how to pack it on the cycle to achieve the two priority aims as much as possible.

The release of the fuel and the electronic control equipment have deliberately not been mentioned in this list. These partial system components are not yet important. First, it must be shown how the best influence on the cyclist can be achieved by coordinating all measures, and only then can the solution of these partial problems be tackled, which do not seem to cause substantial problems.

On the basis of these theoretical considerations and preparatory work already done, a first series of experiments has been started to observe the effect of the airbag experimentally. Figures 16 and 17 show the simulation of a collision with the sledge facility mentioned previously. The dummy is raised slightly by the airbag and thus is also removed from the dangerous area of the roof edge. In the further course, the airbag can soften the impact as it moves together with the body toward the vehicle.

Further research must show which of the designs mentioned above is most effective for the motorcycle and if there is a realistic chance to influence the flight path. Other problems, such as economical aspects or questions concerning bag activation safety, will have to be examined in following phases. Another future prerequisite would be that airbag system costs are reduced, since prices of about DM2,000 charged for a motorcar airbag are, of course, illusory for motorcycles.

Nevertheless, the search for technological safety elements must not fail because of these hindrances. The more the airbag is accepted in the car, the more certainly the costs of the system might be reduced in the long run, and it is not unrealistic to hope the motorcycle could also gain from this.

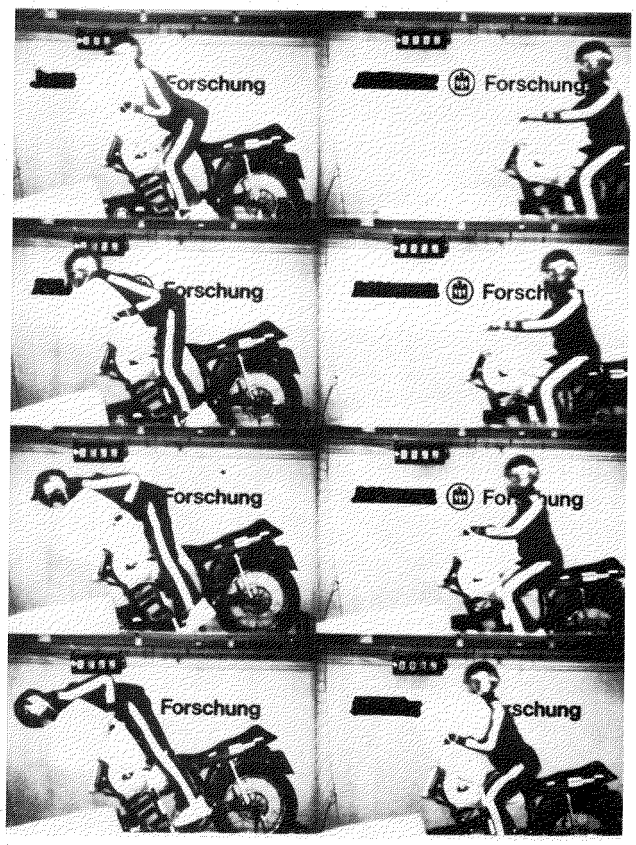

Figure 16. Simulation of collision with sledge facility

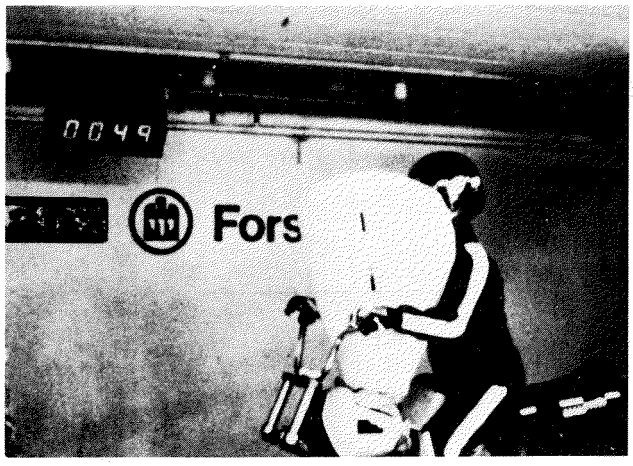

Figure 17. Simulation of collision with sledge facility

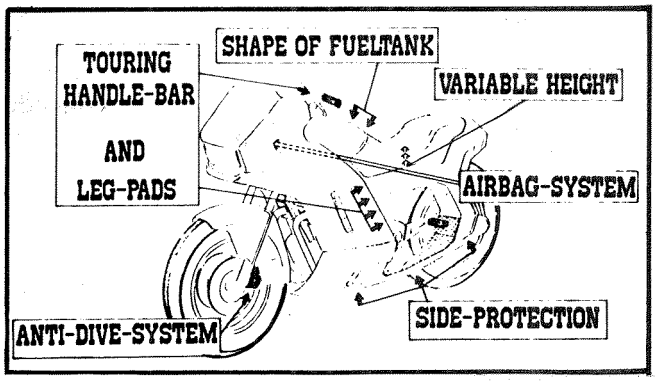

Figure 18. Summary of safety measures

Summary

The complex nature of motorcycle accidents requires an exact knowledge of motion sequences and accident characteristics in the search for technological measures aiming at increased safety. With some types of motorcycles, such as the light-powered motorcycles (Mofa, Moped, and Mokick), there seem to be only limited possibilities to influence safety by technological measures. This depends on their design and frame stability and on the collision mechanism since these motorcycles are impacted mostly by another vehicle.

Concerning heavy motorcycles, the prospects seem more positive, even if there cannot be total protection. Here, the collision of the motorcycle against the other vehicle is dominant and the design of the motorcycle permits additional technological measures that can increase safety.

On the basis of the analysis of real accidents and experimental and mathematical simulations, the following requirements have been worked out.

An effective safety element for the cyclist has to influence his motion path. The risk of being injured can only be reduced if the direct impact against the other vehicle is avoided. The sum of all possible measures is summarized once again in Figure 18. When bumping against a motorcar, the risk of suffering serious or fatal injuries can be reduced essentially by—

- A seating position as high as possible
- A touring handlebar combined with a baffle-pad in front of the legs
- An optimized tank
- An antidive system that does not make the cyclist's body dive during an emergency braking
- Perhaps an additional airbag system

Furthermore, the cyclist's legs can be protected additionally by integrated protective bars in side collisions and falls.

How realistic and easily carried out the discussed technological measures are can be seen in the latest models of some motorcycle producers who have already realized some safety elements. But since an improved protective effect is guaranteed only by the combination of all elements suggested, more developmental work remains to be done. It is to be hoped it won't be long before all technological safety measures already known will be realized.

Conclusion

The authors are indebted to all the member insurance companies of the HUK-Verband, in particular, for making their claims records readily available for this study; to the staff of the AZT for their help with the tests; and to the HUK staff who carried out accident analysis and evaluation work. The authors also owe a debt of gratitude to all the companies whose support made it possible to execute the various tests.

References

1. HUK-Verband, Unfallcharakteristik und Verletzungsfolgen bei Mofa-Unfällen, HUK-Verband, Büro für Kfz-Technik, März 1983.
2. Langwieder, K., H. Klein, and H.D. Zipfel, Untersuchung von 1000 Leichtkraftradunfällen in Bayern, Noch nicht veröffentlichte Untersuchung.
3. Danner, M., K. Langwieder, J. Polauke, and A. Sporner, Schutzkleidung für motorisierte Zweiradfahrer, Bundesanstalt für Straßenwesen, December 1984.
4. Langwieder, K., "Collision characteristics and injuries to motorcyclists and moped drivers," Proceedings 21st Stapp Car Crash Conference, 1977.
5. Sporner, A., Experimentelle und Mathematische Simulation von Motor-radkollisionen im Vergleich zum realen Unfallgeschehen, Dissertation, TU München, 1982.

6. Hirsch, A.E., and P. Bothwell, "Air bag crash protection for motorcycle application," U.S. Department of Transportation, National Highway Traffic Safety Administration, Washington, D.C., 1973.

7. Daimler-Benz AG, Luftsack und Gurtstrammer für Mercedes-Benz Pkw., Technische Information.

Analysis of Straight Running Stability of Motorcycles

Tomoo Nishimi,
Akira Aoki, and
Tsuyoshi Katayama
Japan Automobile Research Institute, Inc.

Abstract

In this paper, straight running stability without controlling behavior of the rider is analyzed with regard to a mathematical model of 12 degrees of freedom. This model has 2 degrees of freedom concerning leaning movement of upper body and lateral movement of lower body of the rider as well as 4 degrees of freedom of sideslip, yawing, rolling of motorcycle, and rotation of steering handlebar, and 6 degrees of freedom of frame rigidities.

Vibration characteristics of the rider's body influence both weave and wobble modes. Theoretical calculation results by using a mathematical model of 12 degrees of freedom are relatively and qualitatively similar to the results obtained by full-scale running experiments. The extent of quantitative coincidence between theory and experiment, however, varies with types of motorcycles. Parameters concerning vibration characteristics of rider's upper body influence weave mode, and those of rider's lower body influence mainly wobble mode.

Introduction

The studies on handling and stability of rider-motorcycle combinations have recently made remarkable progress. Particularly since the publication of Sharp's study report(1) on the straight-running stability of the rider-motorcycle combination, researchers in several countries have energetically participated in the analysis of the theme by adopting mathematical models(2,3,4,5). It is, however, still not experimentally ascertained fully that the theoretical calculation results using mathematical models can, or to what extent, represent the actual behaviors of the rider-motorcycle combination qualitatively and quantitatively. Furthermore, in addition to the dynamic characteristics of motorcycles, the vibration characteristics of the rider's body influence the straight-running stability of the rider-motorcycle combination, but the work to establish a rider model is still being gathered.

In this paper, a mathematical model of 12 degrees of freedom is introduced in consideration of the degrees of freedom concerning the frame rigidities and the rider's vibration characteristics, and the straight-running stability is studied without considering the controlling behavior of the rider. Six kinds of frame rigidities are adopted for this study as follows: torsional and lateral bending rigidities of the front fork, the main frame, and the rear swing arm. As to the vibration characteristics of the rider's body, leaning movement of the rider's upper body and the lateral movement of the rider's lower body are adopted. These characteristics are measured by means of an excitation bench experiment. Furthermore, a comparison is also made between the results of the theoretical calculation employing a 12 degrees of freedom model and those of the full-scale running experiments.

Vibration Characteristics of Rider's Body

Rider Model

Prior to the measurement of the rider's vibration characteristics, it is necessary to determine the degree of freedom of rider model. Observation of rider's movement on the running motorcycle indicates that leaning movement, lateral movement, yawing movement, and pitching movement are among the degrees of freedom. It is considered that, among them, the former two movements have primary influence on the straight-running stability, while the latter two have only secondary influence.

For the establishment of rider model, a 2 degrees of freedom model is adopted as the first step as shown in Figure 1. In this rider model, the rider's body is divided into two portions—upper and lower bodies. Then, it is assumed the upper body has a degree of freedom to lean with reference to the center of gravity of the lower body, and the lower body has a degree of freedom to make lateral movement only. Both upper and lower bodies are assumed to have concentrated mass, linear spring, and linear damper, respectively, and the moment of inertia of the upper body having the degree of freedom of rotation

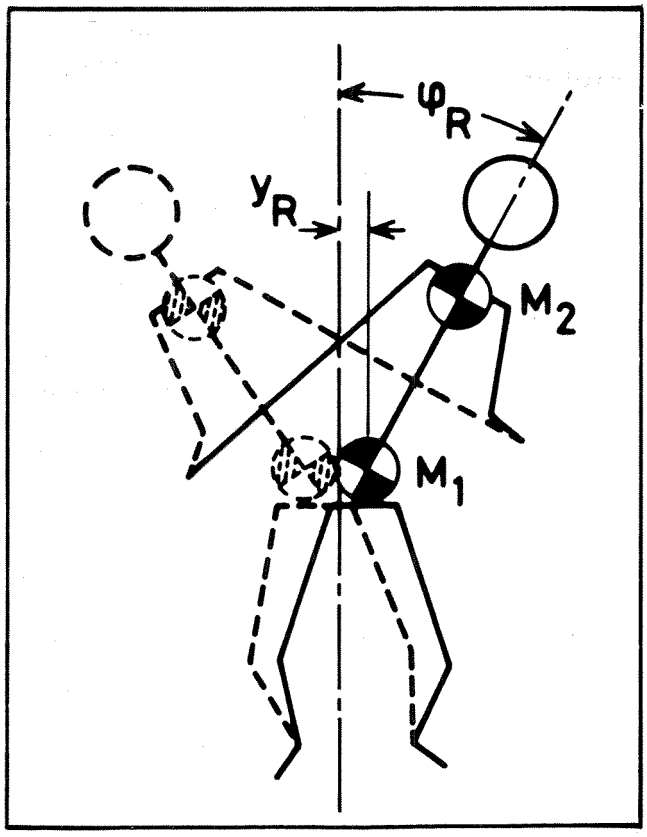

Figure 1. Rider model of vibration characteristics

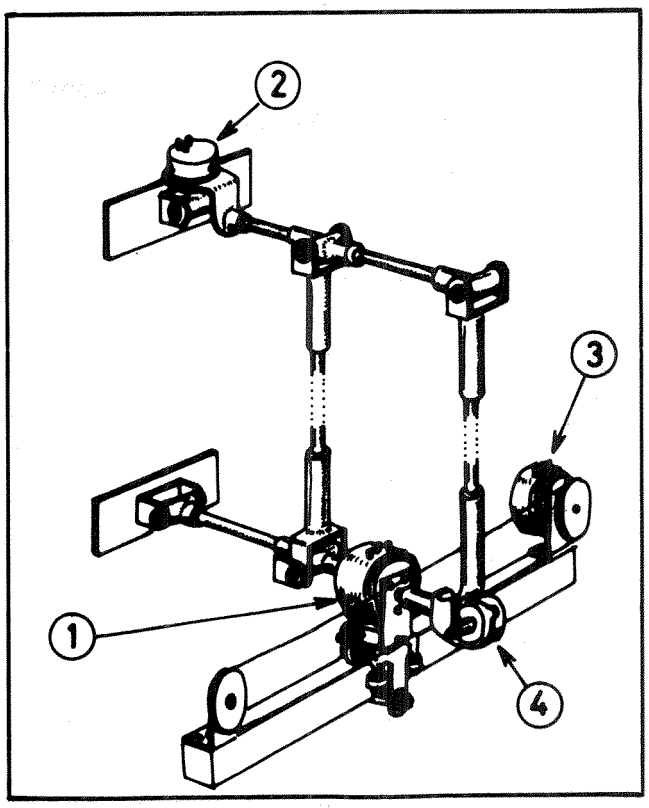

Figure 2. Rider's behavior measurement device

movement shall be represented as the product of squared radius of gyration and mass.

Experimental Method

As mentioned before, a rider on a motorcycle behaves with 4 degrees of freedom. Accordingly, a rider on a motorcycle placed on an excitation bench is also assumed to behave similarly, having these degrees of freedom. Hence, a rider's behavior measurement device as shown in Figure 2 was prepared, and the excitation experiment was performed with it. 1 , 2 , 3 , and 4 in Figure 2 are sensors (potentiometer) for the measurement of leaning angle, yawing angle, lateral movement, and pitching angle. Figure 3 shows a scene of excitation experiment with the device shown in Figure 2 being installed on a motorcycle and a rider.

The experimental method is that, as shown in Figure 4, a motorcycle is excited in rolling movement in reference to the axis through the centers of tire contact of front and rear wheels. The handlebar of the motorcycle was fixed in a straight-running position to restrict the movement of the motorcycle to rolling movement only. The Japan Automobile Research Institute (JARI) hydraulic excitation device(6) is used as an excitation source. The rider subjected to the excitation experiment was not given any special instructions and was allowed to behave freely.

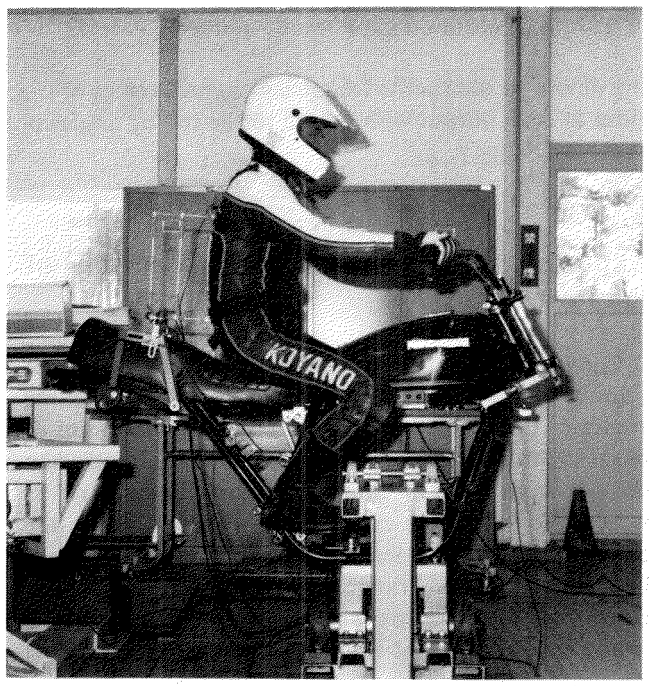

Figure 3. Scene of excitation experiment

Excitation method was a frequency sweep. The range of excitation frequencies was from 0.1 to 10Hz, and the amplitude of excitation was about 0.5°. The data collected from this experiment were processed by the data process-

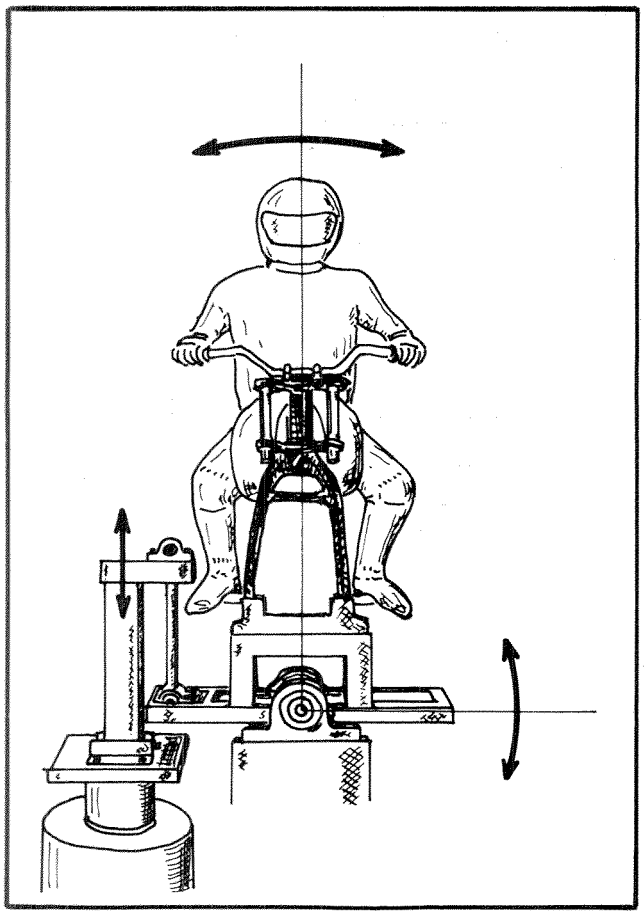

Figure 4. Excitation experiment method

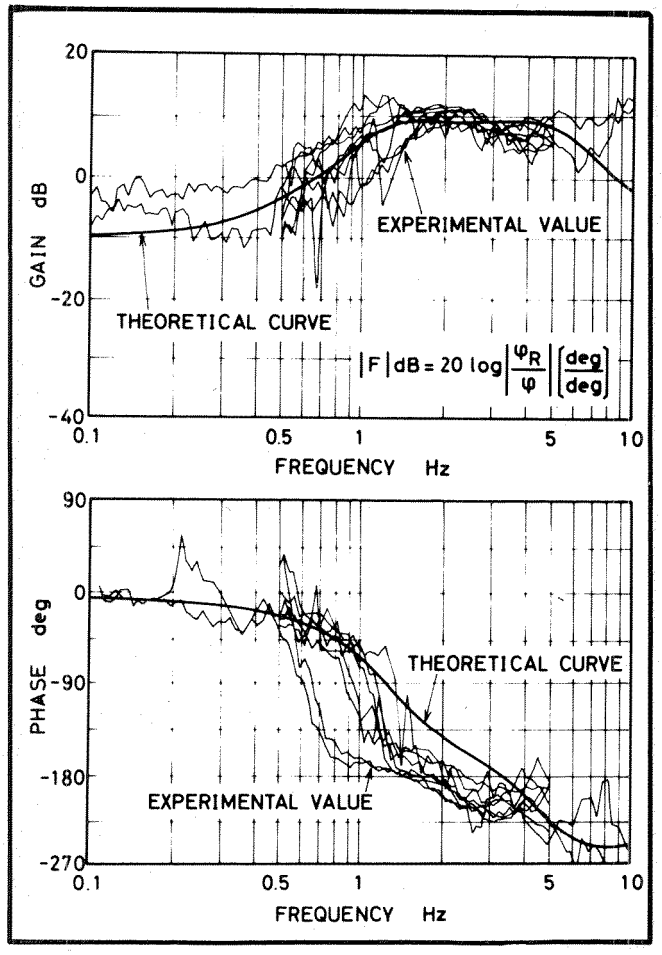

Figure 5. Measurement results of rider's vibration characteristics (without control of lean angle by rider)

ing device to obtain the frequency characteristics of the rider at each output with regard to the rolling angles of motorcycle body.

Experimental Results and Estimation of Parameters

Figures 5 and 6 show the measurement results of leaning angles of the rider with regard to the rolling angles of the motorcycle frame. From the viewpoint of phase characteristics, Figure 5 shows the condition when the rider conducted no controlling behavior (eight riders were subjected to the experiment). Figure 6 shows the condition that the rider behaved to control his upper body in a frequency range between 0.1 and 1.5Hz (six riders were subjected to the experiment). For this study, it is decided that straight-running stability is to be studied without considering the controlling behavior of the rider, and, therefore, values of parameters concerning the vibration characteristics of the rider's body were estimated, based on the measurement results indicated in Figure 5 and those of corresponding lateral movements (see Figure 7).

The estimation of values of these parameters are explained in the following. In the rider model (Figure 1), it is assumed that mass, position of center of gravity and moment of inertia of upper body, and mass and position of center of gravity of lower body are known, and that rigidities and damping of upper and lower bodies are unknown. Values of mass, position of center of gravity, and moment of inertia of upper and lower bodies are obtained by calculation using the data collected by JARI from living bodies and the data concerning individual portions of bodies collected by Chandler(7) from cadavers.

Figure 8 shows mass distribution in human bodies. Percentage value of each portion indicated in Figure 8 is a mean value of the data collected from six human bodies. Using this figure, the upper body comprises four portions, namely, head, chest, upper arms, and lower arms. Total mass of these portions amounts to 32.7 percent of total mass of human body. The lower body comprises three portions, namely, hips, upper limbs, and lower limbs. Their total mass amounts to 63.5 percent of total mass of human body. Here, it is considered that as hands or feet are rested on the handlebar or the footrest, respectively, these are not included in upper or lower bodies.

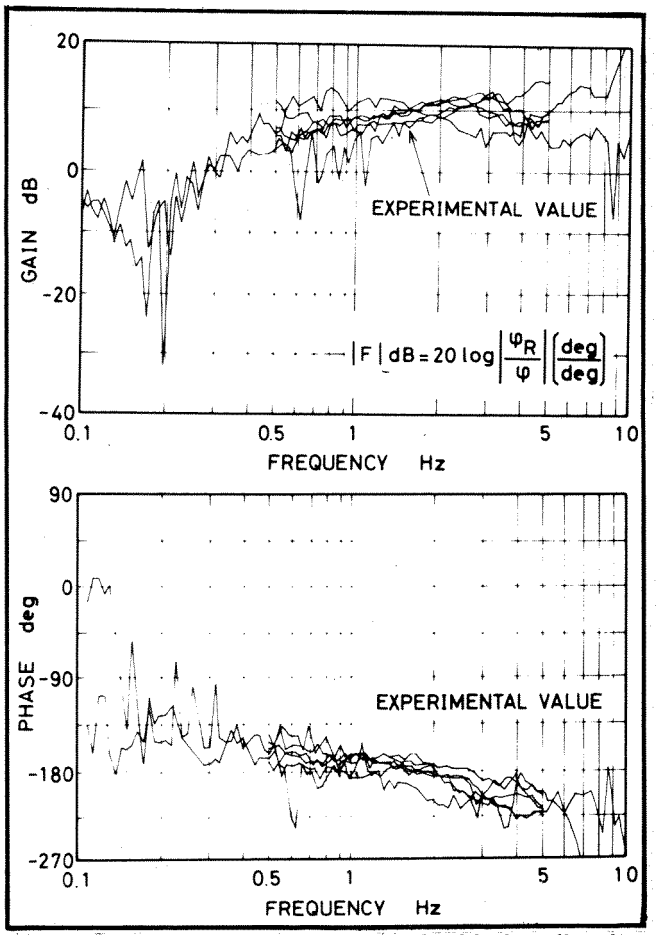

Figure 6. Measurement results of rider's vibration characteristics (with control of lean angle by rider)

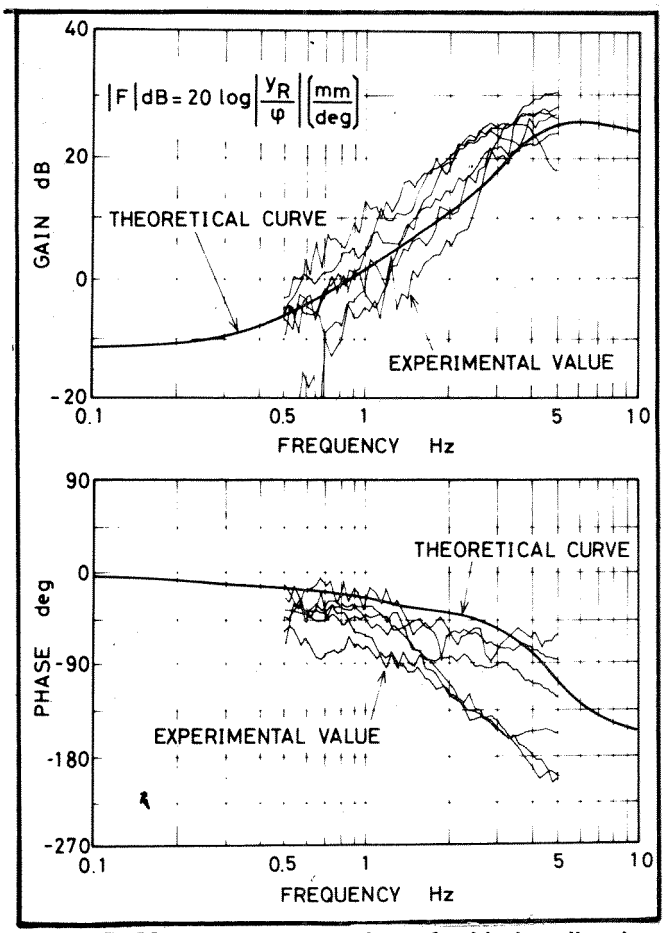

Figure 7. Measurement results of rider's vibration characteristics (without control of lateral movement by rider)

Centers of gravity of upper and lower bodies and moment of inertia of upper body are obtained through the process shown in Figure 9 from the rider's riding position determined by means of photographic measurement; centers of gravity are located at the one-third point from the top end regarding head and at the middle points regarding chest, upper arm, lower arm, hips, upper limb, and lower limb. From these values, centers of gravity of upper and lower bodies and moment of inertia of upper body can be calculated.

By using the above-mentioned data and applying transfer function of Equations (1) and (2), fixed curves in Figures 5 and 7 were obtained. In this case, each parameter value is indicated in Table 1. Parameter values of rigidities and damping of upper and lower bodies were selected from among those obtained by calculation by changing parameters step by step to make theoretical curves coincide with experimental results.

$$F_{y_R}(s) = \frac{y_R(s)}{\Phi(s)} =$$

$$K_R \frac{1 + A_{R1}s + A_{R2}s^2 + A_{R3}s^3 + A_{R4}s^4}{1 + B_1 s + B_2 s^2 + B_3 s^3 + B_4 s^4}$$

$$F_{\Phi_R}(s) = \frac{\Phi_R(s)}{\Phi(s)} =$$

$$K_\Phi \frac{1 + A_{\Phi 1}s + A_{\Phi 2}s^2 + A_{\Phi 3}s^3 + A_{\Phi 4}s^4}{1 + B_1 s + B_2 s^2 + B_3 s^3 + B_4 s^4}$$

$K_R = 17.45(M_1+M_2)g/K_1$

$A_{R1} = C_2/\{+(K_2-M_2h_2g)g\}$

$A_{R2} = -h_1/g+\{M_1M_2(h_2^2+e_2^2)+M_2^2e_2^2/\{(M_1+M_2)(K_2-M_2h_2g)\}$

$A_{R3} = -C_2h_2/\{(K_2-M_2h_2g)g\}$

$A_{R4} = -\{+M_1M_2h_1(h_2^2+e_2^2)+M_2^2(h_1-h_2)e_2^2\}/\{(M_1+M_2)\{(K_2-M_2h_2g)g\}$

$K_\phi = M_2h_2g/(K_2-M_2h_2g)$

$A_{\phi 1} = C_1/K_1$

$A_{\phi 2} = -(h_1h_2+e_2^2)/h_2g)$

$A_{\phi 3} = -(h_1h_2+e_2^2)C_1/(h_2gK_1)$

$A_{\phi 4} = -(M_1+M_2)e_2^2/(h_2gK_1)$

$B_1 = C_1/K_1 + C_2/(K_2-M_2h_2g)$

$B_2 = M_2(h_2^2+e_2^2)/(K_2-M_2h_2g) + (M_1+M_2)/K_1 + C_1C_2/\{(K_2-M_2h_2g)\}$

$B_3 = C_2(M_1+M_2)/\{K_1(K_2-M_2h_2g)\}+ M_2(h_2^2+e_2^2)C_1/\{K_1(K_2-M_2h_2g)\}$

$B_4 = M_2\{(M_1+M_2)e_2^2+M_1h_2^2\}/\{K_1(K_2-M_2h_2g)\}$

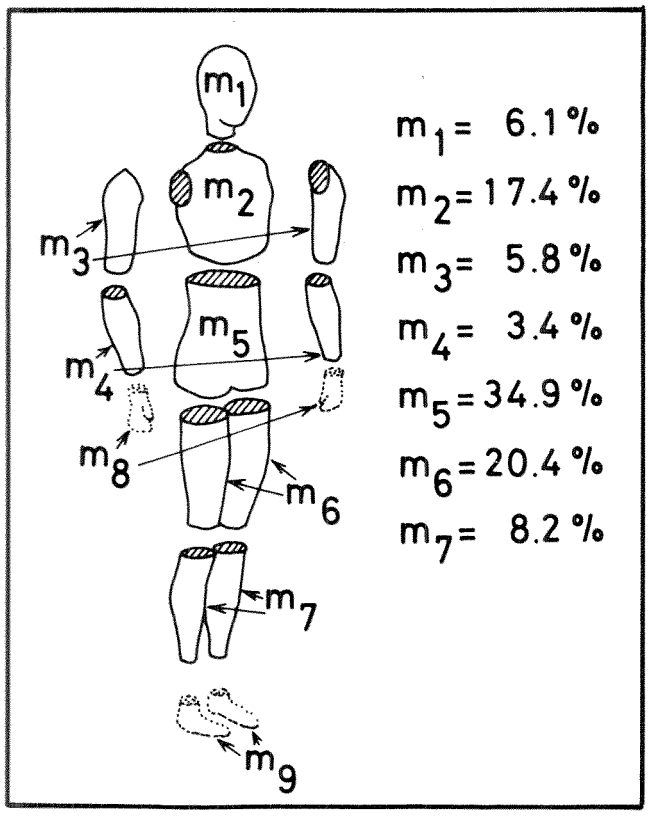

Figure 8. Rider's mass distribution(7)

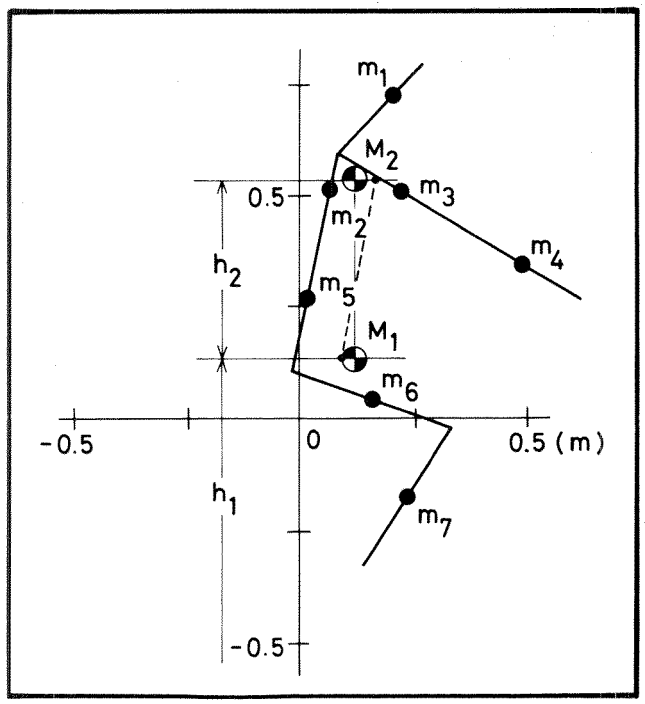

Figure 9. Mass centers (centers of gravity) of rider's upper body, lower body, and other portions

Table 1. Data of rider's vibration characteristics

M_1	4.2	kgs^2m^{-1}
M_2	2.0	kgs^2m^{-1}
e_2^2	0.041	m^2
h_1	0.87	m
h_2	0.39	m
K_1	3916.	kgm^{-1}
C_1	100.	$kgsm^{-1}$
K_2	32.0	$kgmrad^{-1}$
C_2	3.0	$kgmsrad^{-1}$

Then, natural frequencies and damping ratios in the directions of leaning and lateral movements are obtained by using these parameter values as follows:

- Natural frequency (leaning movement)—1.27Hz
- Natural frequency (lateral movement)—4.0Hz
- Damping ratio (leaning movement)—0.489
- Damping ratio (lateral movement)—0.321

For the analysis of straight-running stability, parameter values concerning rider's vibration characteristics obtained by calculation in accordance with these data are to be used hereafter.

Analysis of Straight-Running Stability

Mathematical Model

The mathematical models treated in this paper are based on some assumptions and simplifications as explained below.

The rider-motorcycle combination shall be composed of six masses as follows: (i) front wheel, (ii) front frame (excluding front wheel), (iii) rear wheel, (iv) main frame (motorcycle complete excluding (i), (ii), and (iii)), (v) upper body of the rider, and (vi) lower body of the rider.

The mathematical models shall be of 12 degrees of freedom that comprises: 4 degrees of freedom of sideslip, yawing, and rolling of motorcycle, and rotation of steering handlebar; 6 degrees of freedom of frame rigidities, i.e., torsional and lateral bending rigidities of front fork, main frame, and rear swing arm; and 2 degrees of freedom of leaning movement of upper body and lateral movement of lower body of the rider as mentioned before.

The controlling force inputted by the rider to the motorcycle shall be steer torque only. The controlling behavior of the rider shall not exist. Therefore, the rider-motorcycle combination, during running, is treated as one-input open-loop system.

The range of movement treated in this paper is limited within linear domain, and, therefore, each displacement is very small. The sine of angular displacement equals angular displacement itself, and the cosine of angular displacement equals 1. The product of each displacement and its differential shall be so small as to be negligible.

The motorcycle shall run on a flat and level road surface at a steady speed. The influence of pitching and vertical movement of motorcycle shall be negligible.

The front and rear wheels are represented as circular discs contacting the ground at a point, and no longitudinal slip shall exist. Forces and moments applied to the tires shall be lateral forces due to sideslip angle and camber angle, aligning moment, and overturning moment only. The transient characteristics of the tires shall be represented in the relaxation length (first-order lag element).

When steer angle is zero and motorcycle is in the upright position, all centers of gravity of six masses in the rider-motorcycle combination shall be located within plane XZ, a longitudinal plane of symmetry.

The rotating shaft of the flywheel of the engine shall be mounted on the motorcycle transversely to the longitudinal plane.

The rider-motorcycle combination shall run through stationary air. The change in load distributions on front and rear wheels during running shall be influenced by aerodynamic drag, lift, and pitching moment only. The change in tire characteristics due to change of loads on front and rear wheels shall be taken into consideration.

Aerodynamic force and moment that influence lateral movement of the rider-motorcycle combination shall be only the lateral force and the yawing moment due to air sideslip angle (sign is in reverse to frame sideslip angle) corresponding to frame sideslip angle.

Disturbance forces due to crosswind, uneven road surface, and driving and braking forces shall not be considered.

Torsional axis of the front fork, as shown in Figure 10, shall be in parallel with the steering axis and through the center of the front wheel axle. The front frame is composed of handlebar, steering head, steering stem, and front fork, which are considered to be connected with the front wheel through torsional springs.

The lateral bending of the front fork is in such a way as shown in Figure 10. The relation between bending deflection and deflection angle is assumed as follows:

$$\phi'_f = -C_{\phi f} s_f$$

Torsional axis of the main frame, as shown in Figure 10, shall be through the pivot of the rear swing arm, and torsion shall take place in reference to an axis perpen-

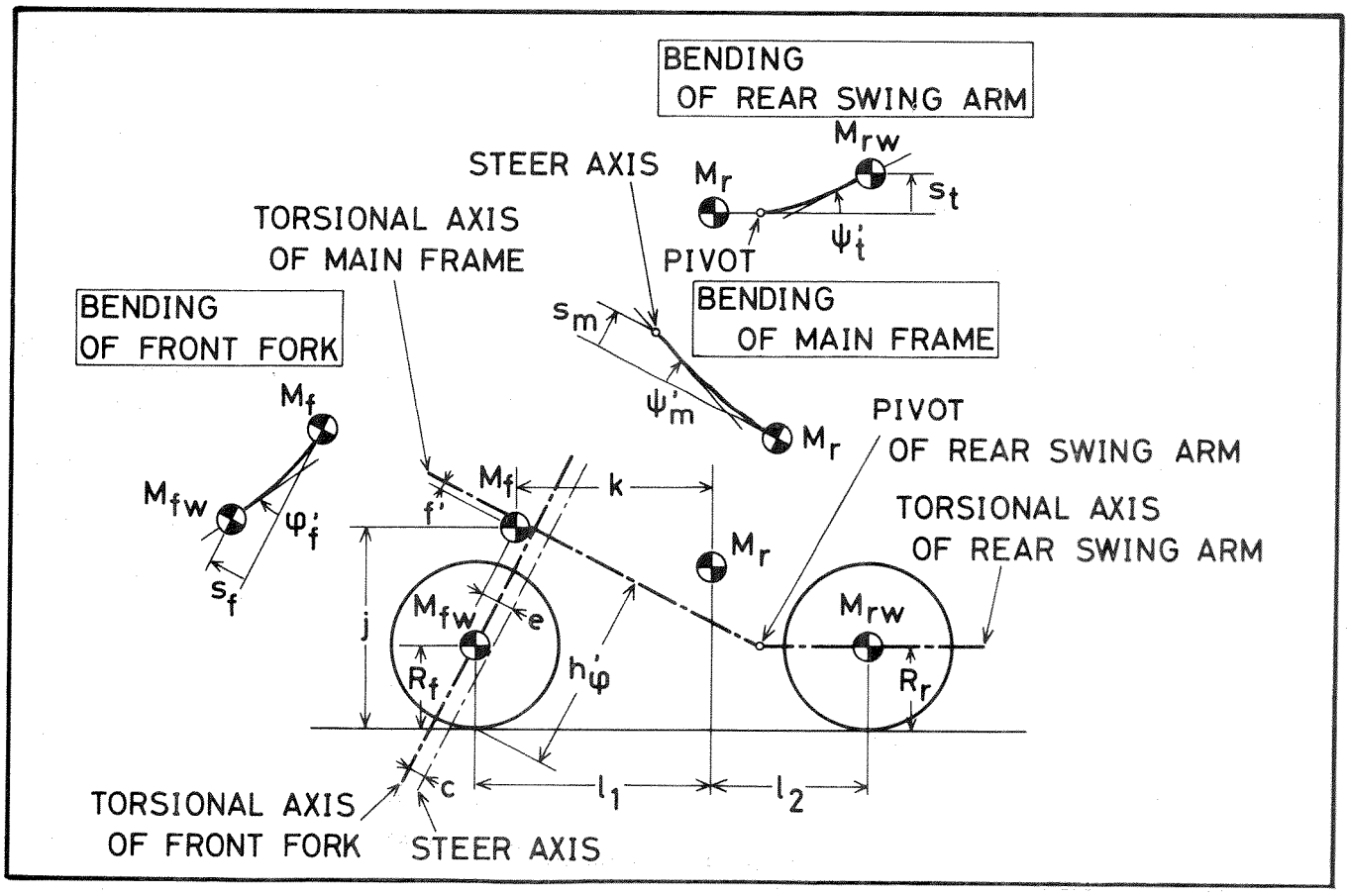

Figure 10. Motorcycle model in consideration of frame rigidities

dicular to the steering axis. The actual torsional axis, however, is slightly deviated upward from the said axis, but the said axis is adopted in this paper as an assumption for convenience.

The lateral bending of the main frame shall occur within a plane perpendicular to the steering axis as shown in Figure 10. The deflection angle, as in the front fork, shall be proportional to the deflection.

$(\psi'_m C_{\psi'_m} s_m)$

Torsional axis of the rear swing arm, as shown in Figure 10, shall be through the center of gravity of the rear wheel and in parallel with the road surface.

Bending of the rear swing arm shall take place within a plane perpendicular to the rear wheel including the torsional axis of the rear swing arm. As in the front fork and the main frame, the deflection angle shall be proportional to the displacement.

$(\psi'_t = -C_{\psi'_t} s_t)$

Rider model shall be as mentioned before.

The right-hand orthogonal axis system is adopted. Origin of the coordinate system can be represented as the projection point A of the center of gravity of the main frame on the road surface when the motorcycle is in an upright position as shown in Figure 11. The movement of the rider-motorcycle combination shall be represented in relation to the coordinate system mentioned below with point A as origin.

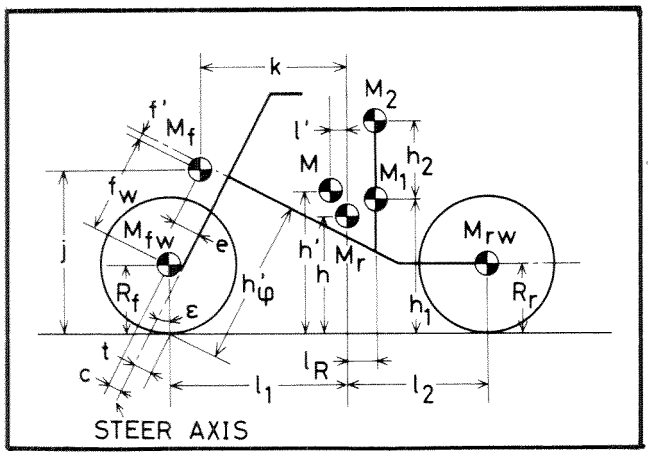

Figure 11. Motorcycle model in consideration of frame rigidities and rider's vibration characteristics

First, a coordinate system of $OX_0Y_0Z_0$, which is fixed to the road surface, shall be adopted. Here, X_0 means forward direction coordinate, Y_0 sideward direction coordinate, and Z_0 downward direction coordinate. Next, a coordinate system of $OX_1Y_1Z_1$ shall be obtained by rotating the frame by yaw angle ψ in reference to OZ_0 axis. Subsequently, a coordinate system of $OX_2Y_2Z_2$ shall be obtained by rotating the above coordinate system by roll angle ϕ in reference to OX_1 axis. Thus obtained coordinate system is fixed to the main frame. Further, rotation by caster angle ε in reference to OY_2 axis obtains a coordinate system of $OX_3Y_3Z_3$, rotation by angle ϕ'_m in reference to the torsional axis of the main frame obtains a coordinate system of $OX_4Y_4Z_4$, deflection by s_m perpendicular to the torsional axis of the main frame (i.e., rotation by the deflection angle ψ'_m) obtains a coordinate system of $OX_5Y_5Z_5$, and rotation by steer angle δ obtains a coordinate system of $OX_6Y_6Z_6$. This coordinate system is fixed to the front frame (excluding front wheel). When this coordinate system is rotated by ψ'_f in reference to the torsional axis of the front fork, which is in parallel with the steering axis and through the center of the front wheel axle, a coordinate system of $OX_7Y_7Z_7$ is obtained. In addition to the above, deflection by s_f perpendicular to the torsional axis (i.e., rotation by deflection angle ϕ'_f) obtains a coordinate system of $OX_8Y_8Z_8$. This coordinate system is fixed to the front wheel axle.

Meanwhile, rotation of coordinate system of $OX_2Y_2Z_2$ by ϕ'_t in reference to the assumed torsional axis of the rear swing arm to be in parallel with the road surface and through the rear wheel axle obtains a coordinate system of $OX_9Y_9Z_9$, and, in addition to this, deflection by s_t perpendicular to the said torsional axis (i.e., rotation by deflection angle ψ'_t) obtains a coordinate system of $OX_{10}Y_{10}Z_{10}$. This coordinate system is fixed to the rear wheel axle.

When the coordinate system of $OX_2Y_2Z_2$ is moved in the direction of Y_2-axis by lateral displacement y_R of rider's lower body, a coordinate system of $OX_{11}Y_{11}Z_{11}$ is obtained. In addition to the above, rotation by lean angle ϕ_R of rider's upper body in reference to X_{11} axis obtains a coordinate system of $OX_{12}Y_{12}Z_{12}$.

Equations of motion have been introduced by using Lagrange's equation as shown in Appendix I.

Measurement of Parameters

All the values of parameters used in the equations of motion, except for polar moment of inertia of engine flywheel, are based on the actually measured values. (Polar moment of inertia of the flywheel was calculated by assuming it to be 150 percent of the moment of inertia of the rear wheel in reference to its axle.) Individual values of parameters used for calculations in this paper are shown in Appendix II (see (8) through (12) for the measurement methods and results.).

Results and Discussion

It has been known that the vibration modes that govern the straight-running stability of the rider-motorcycle combination are three modes, namely, capsize, weave, and wobble modes. Capsize mode is an aperiodical rolling motion of the frame construction that occurs at a speed of about 50km/h or more causing slight instability. Weave mode is a coupled motion between yawing and

rolling motions of the frame construction. This is a vibration mode (1-4Hz) whose natural frequency increases in accordance with the increase of vehicle speed. Wobble mode is a high frequency vibration mode (6-10Hz) of the steering system, and its natural frequency does not vary with vehicle speed. In this paper, weave and wobble modes are studied as important modes that have influence on straight-running stability, and the influence of rider's vibration characteristics on straight-running stability is explained and compared with experimental results.

Figures 12 through 15 are comparisons between theoretical calculation results of 10 degrees of freedom and 12 degrees of freedom models and running experiment results with regard to four motorcycles. 10 degrees of freedom model means addition of 6 degrees of freedom concerning the frame rigidities to 4 degrees of freedom model, and 12 degrees of freedom model means addition of 2 degrees of freedom concerning rider's vibration characteristics to 10 degrees of freedom model. The running experiment results show damped natural frequencies and damping ratios of weave and wobble modes obtained from the frequency response characteristics of yaw angular velocity in accordance with the steer torque input measured by the pulse response method(13) (see Appendix III). The piston displacement

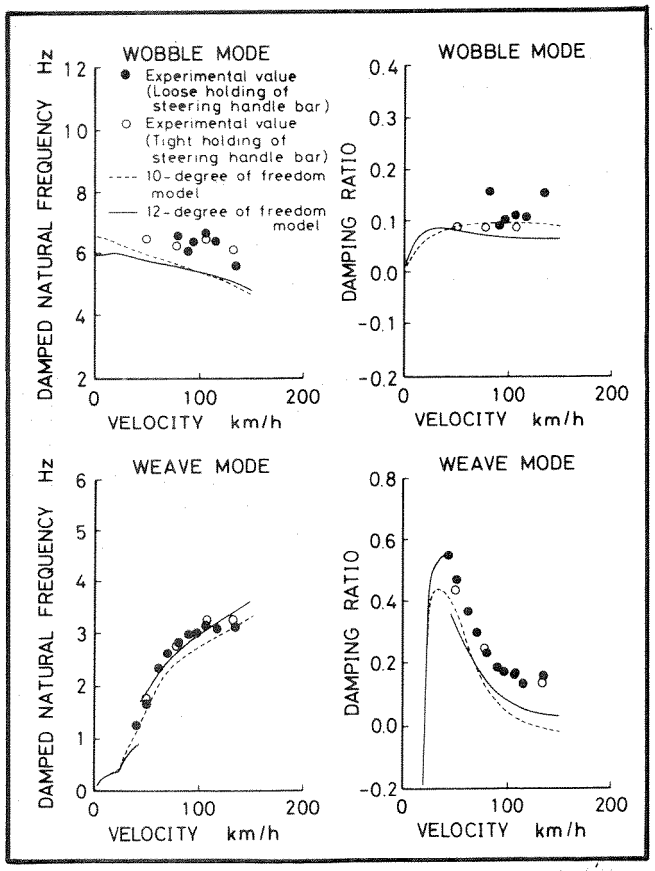

Figure 12. Comparison between theoretical calculation results and experimental results (experiment motorcycle A)

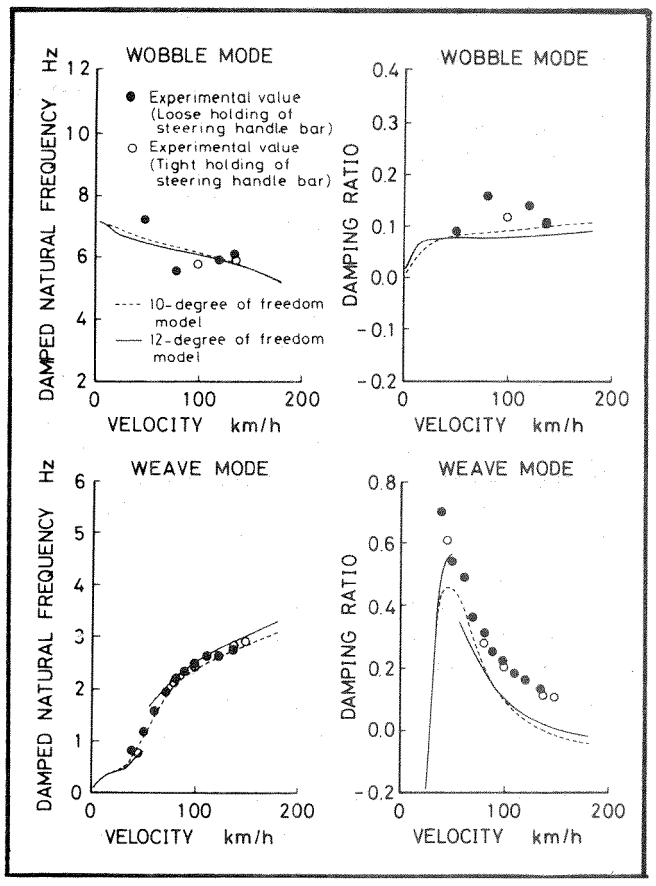

Figure 13. Comparison between theoretical calculation results and experimental results (experiment motorcycle B)

of four motorcycles A, B, C, and D are 400cc, 750cc, 250cc, and 1,100cc, respectively.

First of all, influence of rider's vibration characteristics is studied. Among the theoretical calculation results concerning 12 degrees of freedom model where rider's vibration characteristics are considered, the particularly notable matter is that weave mode shows discontinuity in a vehicle speed range between 40 and 60km/h. This is supposedly because, in this vehicle speed range, damped natural frequencies and damping ratios of weave mode are close to those of rider's lean mode causing interference between them. Weave mode and lean mode shall be determined by eigenvectors in the said range of vehicle speed.

Upon comparison between 10 degrees of freedom model and 12 degrees of freedom model with regard to the theoretical calculation results, it is recognized that rider's vibration characteristics have influence on weave and wobble modes; in weave mode, damped natural frequencies are increased in upper medium vehicle speed range, and damping ratios are decreased in medium vehicle speed range and increased in upper vehicle speed range. As to the damping ratios of the weave mode, the influence of rider's vibration characteristics given to medium- or small-size motorcycles such as A or C is

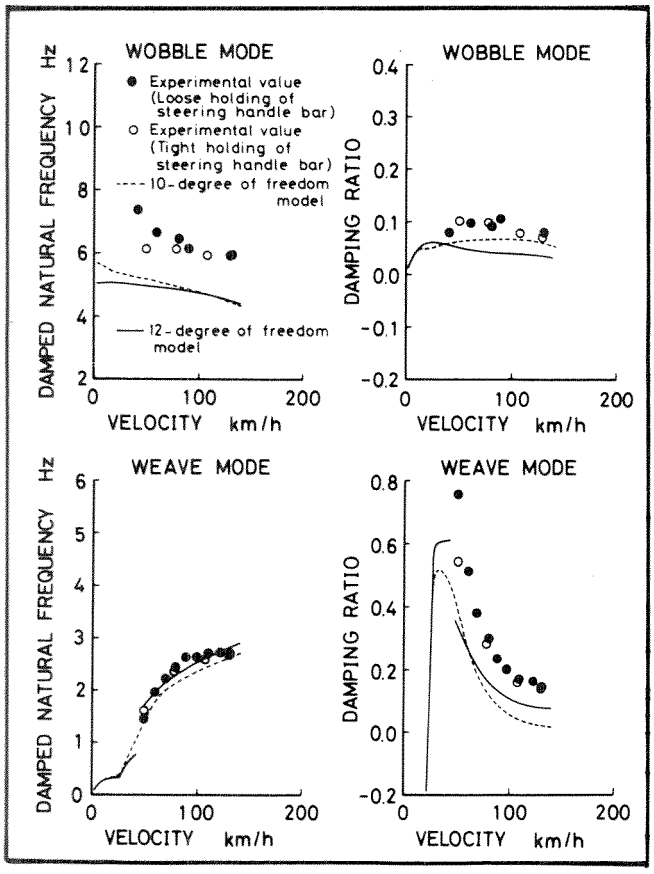

Figure 14. Comparison between theoretical calculation results and experimental results (experiment motorcycle C)

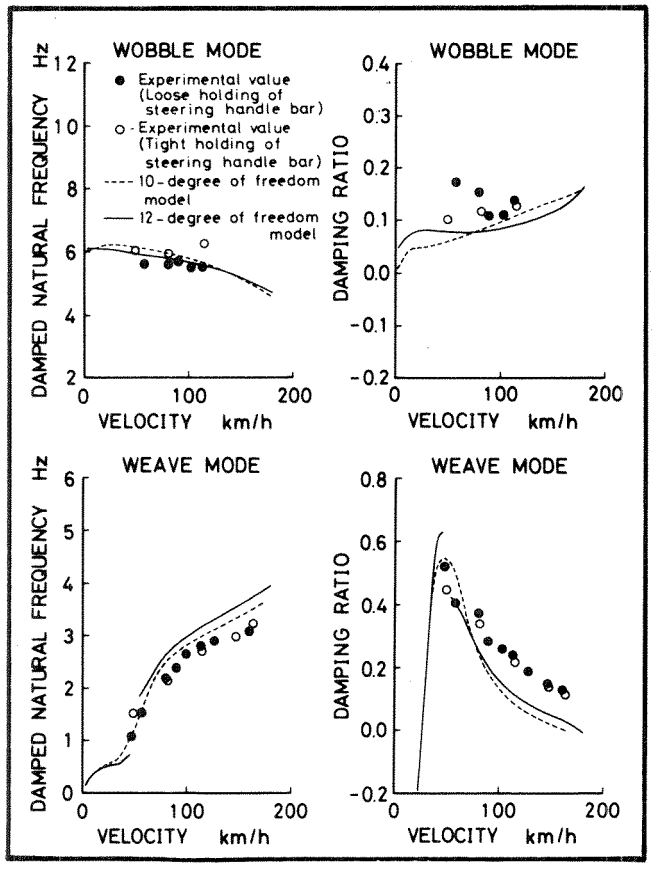

Figure 15. Comparison between theoretical calculation results and experimental results (experiment motorcycle D)

larger than that given to big motorcycles such as B or D. However, in the wobble mode, damped natural frequencies are decreased in lower medium vehicle speed range and damping ratios are increased in lower vehicle speed range and decreased in upper medium vehicle speed range.

When theoretical calculation results are composed with experimental results, the theoretical calculation results of the damped natural frequencies of weave mode in 12 degrees of freedom model coincide with the experimental results in medium- or small-size motorcycle A or C or in big-size motorcycle B, while the theoretical calculation results in motorcycle D, which is bigger than B in dimensions, show larger values than the experimental results in both 10 degrees of freedom and 12 degrees of freedom models. As to the damping ratio of weave mode, the theoretical calculation results of 12 degrees of freedom model show better coincidence with the experimental results of each motorcycle in the upper medium vehicle speed range than those of 10 degrees of freedom model. The discontinuity of weave mode in the lower medium vehicle speed range that was found in the theoretical calculation results has not been proved by the experimental results yet. As to the damped natural frequency of wobble mode, the experimental results show some scattering in their values, but the theoretical calculation results in big-size motorcycles B and D coincide with the experimental results very well, while the theoretical calculation results are somewhat smaller than the experimental results in medium- or small-size motorcycles A and C. As to the damping ratio of wobble mode, like in the damped natural frequency, the experimental results show some scattering in their values, but the theoretical calculation results in each motorcycle are regarded to coincide with many of the experimental results. As mentioned above, in each motorcycle, the theoretical calculation results of 12 degrees of freedom model coincide comparatively and qualitatively with the experimental results.

Finally, the influences of individual parameters on the rider's vibration characteristics are stated below. Table 2 shows the extent of influences of individual parameters concerning the rider's vibration characteristics in 12 degrees of freedom model on weave and wobble modes.

In this table, circle-marked items mean "large influence," triangle-marked items mean "noticeable influence," and hyphen-marked items mean "negligible influence." Table 2 is made with the theoretical calculation results obtained from four experiment motorcycles by changing parameters used for the calculations by ±10 percent, ±20 percent, and ±50 percent from their standard

Table 2. Influences of individual parameters on rider's vibration characteristics

	Weave Mode	Wobble Mode
Mass and moment of inertia	○	○
Rigidity of upper body	○	—
Damping ratio of upper body	○	—
Rigidity of lower body	△	△
Damping ratio of lower body	—	△
Height of center of gravity of upper body	○	—
Longitudinal location of rider's center of gravity	○	○

values within a vehicle speed range from 40 to 160km/h. From this table, it is understandable that the parameters concerning rider's upper body influence weave mode, and those concerning rider's lower body influence mainly wobble mode.

Conclusion

Straight-running stability of the rider-motorcycle combination with 12 degrees of freedom mathematical model was analyzed in consideration of rider's vibration characteristics and rigidities of frame. Before the analysis, rider's vibration characteristics were measured first by the excitation experiment, and the parameter values of 2 degrees of freedom concerning the leaning of rider's upper body and lateral movement of rider's lower body were obtained. Then, the theoretical calculation results of the said 12 degrees of freedom model were compared with the running experiment results. Next, the influences of individual parameters concerning the rider's vibration characteristics on the straight-running stability were studied.

Main conclusions reached in this research are as follows:

- Rider's vibration characteristics influence weave and wobble modes.
- Theoretical calculation results of 12 degrees of freedom model coincide comparatively and qualitatively with running experiment results, but the extents of quantitative coincidence vary with the types of motorcycle.
- Parameters concerning vibration characteristics of rider's upper body influence weave mode, and those of rider's lower body mainly influence wobble mode.

Acknowledgments

This paper is a part of the results of the research conducted by JARI for a long period of time under commission and financed by the Japan Automobile Manufacturers Association Inc. (JAMA). We would like to express our appreciation to the Motorcycle Handling and Stability Working Group of JAMA, which supplied experiment motorcycles and test riders for the running experiments of this research. We, also, are deeply thankful to the staff of JARI, Messrs. Motomiya, Sato, Okayama, Mogi, and Kobayashi, for the great cooperation extended to us for this research in the measurements of frame characteristics, tire characteristics, aerodynamic characteristics, etc.

This research was conducted independently by JARI, which is responsible for all results, knowledge, and other contents of this paper.

References

1. Sharp, R.S., "The stability and control of motorcycles," *J. Mech. Engr. Science*, Vol. 13, No. 5, pp. 316-329, 1971.
2. Sharp, R.S., and C.J. Alstead, "The influence of structural flexibilities on the straight-running stability of motorcycles," *Vehicle System Dynamics 9*, pp. 327-357, 1980.
3. Spierings, P.T.J., "The effects of lateral front fork flexibility on the vibrational modes of straight-running single-track vehicles," *Vehicle System Dynamics 10*, pp. 21-35, 1981.
4. Koch, J., "Experimentelle und Analytische Untersuchungen des Motorrad-Fahrer-Systems," VDI Zeitschriften, Reihe 12, Nr. 40 (1980-5).
5. Koenen, C., and H.B. Pacejka, "The influence of frame elasticity, simple rider body dynamics and tyre moments of free vibrations of motorcycles in curves," Proceedings 7th IAVSD-Symposium held at Cambridge University, Cambridge, United Kingdom, pp. 53-64, September 7-11, 1981.
6. Mochizuki, T., "Electric hydraulic vibration testing machines," *Journal of JARI*, Vol. 1, No. 6, pp. 196-197, 1979.
7. Chandler, R.F., G.E. Clauser, J.T. McConville, H.M. Reynolds, and J.W. Young, "Investigation of inertial properties of the human body," U.S. Department of Transportation, HS-801430, 1975.
8. Aoki, A., S. Motomiya, and K. Sato, "Inertial properties of motorcycles," *JARI TM*, No. 62, 1977.
9. Aoki, A., S. Motomiya, and K. Sato, "Aerodynamic characteristics of motorcycles," *JARI TM*, No. 63, 1977.

10. Aoki, A., T. Nishimi, and K. Sato, "Dynamic steering characteristics of motorcycle tires," *Journal of JARI*, Vol. 2, No. 6, pp. 167-171, 1980.
11. Study Report on Motorcycle Dynamics, JAMA Report, prepared by JARI under the auspices of JAMA, 1979-7, 1981-5, 1982-9.
12. Study Report on Handling and Stability of Motorcycle, JAMA Report, prepared by JARI under the auspices of JAMA, 1983-7, 1985-1.
13. Aoki, A., "Experimental study on motorcycle steering performance," *SAE Transactions*, Vol. 88, Paper 790265, pp. 946-961, 1979.

Appendix I

Symbols and Equations of Motion

Symbols

c, e, f', f_w, h, h', h_ϕ', h_1, h_2, j, k, l_1, l_2, l', l_R, R_f, R_r, t	Dimensions (see Figure 10 and Figure 11)
C_1, C_2	Damping constants of rider's body (1:Lower body, 2:Upper body)
C_{rxz}	Product of inertia about X_2 and Z_2 axes of main frame
C_{YS1}, C_{YS2}	Cornering stiffnesses (1:Front wheel, 2:Rear wheel)
C_{YC1}, C_{YC2}	Camber stiffnesses (1:Front wheel, 2:Rear wheel)
C_{ZS1}, C_{ZS2}	Aligning torque coefficients due to sideslip angle
C_{ZC1}, C_{ZC2}	Camber torque coefficients due to camber angle
C_{XS1}, C_{XS2}	Overturning moment coefficients due to sideslip angle
C_{XC1}, C_{XC2}	Overturning moment coefficients due to camber angle
C_δ	Damping constant of steering
$C_{\psi'm}$, $C_{\phi'f}$, $C_{\psi't}$	Transformation constants of deflection (>0)
$C_{\phi'm}$, C_{sm}, $C_{\psi'f}$, C_{sf}, $C_{\phi't}$, C_{st}	Damping constants of frame
g	Gravitational acceleration
I_{fx}, I_{fz}	Moments of inertia of front fork about X_6 and Z_6 axes
I_{rx}, I_{rz}	Moments of inertia of main frame about X_2 and Z_2 axes
i	Polar moment of inertia of engine flywheel
i_{1x}, i_{1z}	Moments of inertia of rider's lower body
i_{2x}, i_{2z}	Moments of inertia of rider's upper body
$i_z = i_{1z} + i_{2z}$	
i_{fx}, i_{fy}, i_{fz}	Moments of inertia of front wheel
i_{rx}, i_{ry}, i_{rz}	Moments of inertia of rear wheel
K_1, K_2	Rigidities of rider's body (1:Lower body, 2:Upper body)
$K_{\phi'm}$, K_{sm}, $K_{\psi'f}$, K_{sf}, $K_{\phi't}$, K_{st}	Rigidities of frame
M_1, M_2	Masses of rider
M_f, M_{fw}, M_r, M_{rw}	Masses
T_a	Aerodynamic yawing moment acting on center of gravity
T_{xf}, T_{xr}	Overturning moments on front and rear wheels
T_{zf}, T_{zr}	Aligning torques on front and rear wheels
Y_a	Aerodynamic lateral force acting on center of gravity
Y_f, Y_r	Lateral forces on front and rear wheels
Z_f, Z_r	Loads on front and rear wheels
α_f, α_r	Sideslip angles of front and rear wheels
ε	Caster angle
λ	Gear ratio between rear wheel and engine flywheel
σ_f, σ_r	Relaxation lengths of front and rear wheels
τ	Steer torque applied by rider
ϕ_f, ϕ_r	Camber angles of front and rear wheels
δ, ϕ, ϕ_m', ϕ_R, ϕ_t', ψ, ψ_f'	Angular displacements
s_f, s_m, s_t	Bending displacements
y_R	Lateral displacement of rider's lower body

Equations of Motion

Equation of Equilibrium of Lateral Forces

$$(M_f + M_{fw} + M_r + M_{rw} + M_1 + M_2)\ddot{y}_1 + \{M_f k + M_{fw} l_1 - M_{rw} l_2 - (M_1 + M_2) l_R\}\ddot{\psi} + (M_f + M_{fw} + M_r + M_{rw} + M_1 + M_2)\dot{x}_1\dot{\psi} + \{M_f j + M_{fw} R_f + M_r h + M_{rw} R_r + M_1 h_1 + M_2(h_1 + h_2)\}\ddot{\phi} - \{M_f f' + M_{fw}(f' + f_w)\}\ddot{\phi}_m' + \{M_f(1 + eC_{\psi'm}) + M_{fw}(1 + cC_{\psi'm})\}\ddot{s}_m + (M_f e + M_{fw} c)\ddot{\delta} + M_{fw}\ddot{s}_f + M_{rw}\ddot{s}_t + (M_1 + M_2)\ddot{y}_R + M_2 h_2 \ddot{\phi}_R - Y_f - Y_r - Y_a = 0$$

Equation of Equilibrium of Yawing Moments

$$\{M_f k + M_{fw} l_1 - M_{rw} l_2 - (M_1 + M_2) l_R\}\ddot{y}_1 + \{M_f k^2 + M_{fw} l_1^2 + M_{rw} l_2^2 + (M_1 + M_2) l_R^2 + (I_{fx} + i_{fx})\sin^2\varepsilon + (I_{fz} + i_{fz})\cos^2\varepsilon + I_{rz} + i_{rz} + i_z\}\ddot{\psi} + \{M_f k + M_{fw} l_1 - M_{rw} l_2 - (M_1 + M_2) l_R\}\dot{x}_1\dot{\psi} + \{M_f j k + M_{fw} l_1 R_f - M_{rw} l_2 R_r - M_1 h_1 l_R - M_2(h_1 + h_2) l_R + (I_{fz} - I_{fx} + i_{fz} - i_{fx})\sin\varepsilon\cos\varepsilon - C_{rxz}\}\dot{\phi} - \{i_{fy}/R_f + (i_{ry} + i\lambda)/R_r\}\dot{x}_1\phi - \{M_f f' k + M_{fw}(f' + f_w) l_1 + (I_{fx} + i_{fx})\sin\varepsilon\}\dot{\phi}_{m'} - (i_{fy}/R_f)\cos\varepsilon\dot{x}_1\phi_{m'} + \{M_f k(1 + eC_{\psi'm}) + M_{fw} l_1(1 + cC_{\psi'm}) + (I_{fz} + i_{fz})C_{\psi'm}\cos\varepsilon\}\ddot{s}_m - (i_{fy}/R_f)C_{\psi'm}\sin\varepsilon\dot{x}_1\dot{s}_m + \{M_f e k + M_{fw} c l_1 + (I_{fz} + i_{fz})\cos\varepsilon\}\delta - (i_{fy}/R_f)\sin\varepsilon x_1\delta + i_{fz}\cos\varepsilon\ddot{\psi}_{f'} - (i_{fy}/R_f\sin\varepsilon\dot{x}_1\psi_{f'} + (M_{fw} l_1 + i_{fx} C_{\phi'f}\sin\varepsilon)\ddot{s}_f + (i_{fy}/R_f)C_{\phi'f}\cos\varepsilon\dot{x}_1\dot{s}_f - (i_{ry}/R_r)\dot{x}_1\phi_{t'} - (M_{rw} l_2 + i_{rz} C_{\psi't})\ddot{s}_t - (M_1 + M_2) l_R\ddot{y}_R - M_2 h_2 l_R\phi_R - l_1 Y_f + l_2 Y_r - T_{zf} - T_{zr} - l' Y_a - T_a = 0$$

Equation of Equilibrium of Rolling Moments

$$\{M_f j + M_{fw} R_f + M_r h + M_{rw} R_r + M_1 h_1 + M_2(h_1 + h_2)\}\ddot{y}_1 + \{M_f j k + M_{fw} l_1 R_f - M_{rw} l_2 R_r - M_1 h_1 l_R - M_2(h_1 + h_2) l_R + (I_{fz} - I_{fx} + i_{fz} - i_{fx})\sin\varepsilon\cos\varepsilon - C_{rxz}\}\ddot{\psi} + \{M_f j + M_{fw} R_f + M_r h + M_{rw} R_r + i_{fy}/R_f + (i_{ry} + i\lambda)/R_r + M_1 h_1 + M_2(h_1 + h_2)\}\dot{x}_1\dot{\psi} + \{M_f j^2 + M_{fw} R_f^2 + M_r h^2 + M_{rw} R_r^2 + M_1 h_1^2 + M_2(h_1 + h_2)^2 + (I_{fx} + i_{fx})\cos^2\varepsilon + (I_{fz} + i_{fz})\sin^2\varepsilon + I_{rx} + i_{rx} + i_{1x} + i_{2x}\}\dot{\phi} - \{M_f j + M_{fw} R_f + M_r h + M_{rw} R_r + (M_1 + M_2) h_1 + M_2 h_2\} g\phi - \{M_f f' j + M_{fw}(f' + f_w) R_f - (I_{fx} + i_{fx})\cos\varepsilon\}\dot{\phi}_{m'} - (i_{fy}/R_f)\sin\varepsilon\dot{x}_1\phi_{m'} + \{h_\phi' Z_f + M_f f' g + M_{fw}(f' + f_w) g\}\phi_{m'} + \{M_f j(1 + eC_{\psi'm}) + M_{fw} R_f(1 + cC_{\psi'm}) + (I_{fz} + i_{fz})C_{\psi'm}\sin\varepsilon\}\ddot{s}_m + (i_{fy}/R_f)C_{\psi'm}\cos\varepsilon\dot{x}_1\dot{s}_m - \{Z_f(1 - tC_{\psi'm}) + M_f g(1 + eC_{\psi'm}) + M_{fw} g(1 + cC_{\psi'm})\}s_m + \{M_f e j + M_{fw} c R_f + (I_{fz} + i_{fz})\sin\varepsilon\}\delta + (i_{fy}/R_f)\cos\varepsilon\dot{x}_1\delta + (tZ_f - M_f eg - M_{fw} cg)\delta + i_{fz}\sin\varepsilon\ddot{\psi}_{f'} + (i_{fy}/R_f)\cos\varepsilon\dot{x}_1\psi_{f'} + R_f Z_f\sin\varepsilon\psi_{f'} + (M_{fw} R_f - i_{fx} C_{\phi'f}\cos\varepsilon)\ddot{s}_f + (i_{fy}/R_f)C_{\phi'f}\sin\varepsilon\dot{x}_1\dot{s}_f - \{Z_f(1 + R_f C_{\phi'f}\cos\varepsilon) + M_{fw} g\}s_f + i_{rx}\phi_{t'} + R_r Z_r\phi_{t'} + M_{rw} R_r\ddot{s}_t - (i_{ry}/R_r)C_{\psi't}\dot{x}_1\dot{s}_t - (Z_r + M_{rw} g)s_t + \{M_1 h_1 + M_2(h_1 + h_2)\}\ddot{y}_R - (M_1 + M_2) g y_R + \}M_2(h_1 + h_2) h_2 + i_{2x}\}\phi_R - M_2 h_2 g\phi_R - T_{xf} - T_{xr} - h' Y_a = 0$$

Equation of Equilibrium of Moments About Torsional Axis of Main Frame

$$-\{M_f f' + M_{fw}(f' + f_w)\}\ddot{y}_1 - \{M_f f' k + M_{fw}(f' + f_w) l_1 + (I_{fx} + i_{fx})\sin\varepsilon\}\ddot{\psi} - \{M_f f' + M_{fw}(f + f_w) - (i_{fy}/R_f)\cos\varepsilon\}\dot{x}_1\dot{\psi} - \{M_f f' j + M_{fw}(f' + f_w) R_f - (I_{fx} + i_{fx})\cos\varepsilon\}\dot{\phi} + (i_{fy}/R_f)\sin\varepsilon\dot{x}_1\dot{\phi} + \{h_\phi' Z_f + M_f f' g + M_{fw}(f' + f_w) g\}\phi + \}M_f f'^2 + M_{fw}(f' + f_w)^2 + I_{fx} + i_{fx}\{\phi_{m'} + C_{\phi'm}\phi_{m'} + \{h_\phi' Z_f\cos\varepsilon + M_f f' g\cos\varepsilon + M_{fw}(f' + f_w) g\cos\varepsilon + K_{\phi'm}\}\phi_{m'} - \{M_f f'(1 + eC_{\psi'm}) + M_{fw}(f' + f_w)(1 + cC_{\psi'm})\}\ddot{s}_m + (i_{fy}/R_f)C_{\psi'm}\dot{x}_1\dot{s}_m - \{Z_f(1 - tC_{\psi'm}) + M_f g(1 + eC_{\psi'm}) + M_{fw} g(1 + cC_{\psi'm})\}\cos\varepsilon s_m - \{M_f e f' + M_{fw} c(f' + f_w)\}\delta + (i_{fy}/R_f)\dot{x}_1\delta + (tZ_f - M_f eg - M_{fw} cg)\cos\varepsilon\delta + (i_{fy}/R_f)x_1\psi_{f'} + R_f Z_f\sin\varepsilon\cos\varepsilon\psi_{f'} - \{M_{fw}(f' + f_w) + i_{fx} C_{\phi'f}\}\ddot{s}_f - \{Z_f(1 + R_f C_{\phi'f}\cos\varepsilon) + M_{fw} g\}\cos\varepsilon s_f + h_\phi' y_f - T_{xf}\cos\varepsilon + T_{zf}\sin\varepsilon = 0$$

Equation of Equilibrium of Lateral Forces in Main Frame

$$\{M_f(1 + eC_{\psi'm}) + M_{fw}(1 + cC_{\psi'm})\}\ddot{y}_1 + \{M_f k(1 + eC_{\psi'm}) + M_{fw} l_1(1 + cC_{\psi'm}) + (I_{fz} + i_{fz})C_{\psi'm}\cos\varepsilon\}\ddot{\psi} + \{M_f(1 + eC_{\psi'm}) + M_{fw}(1 + cC_{\psi'm} + (i_{fy}/R_f)C_{\psi'm}\sin\varepsilon\}x_1\psi + \{M_f j(1 + eC_{\psi'm}) + M_{fw} R_f(1 + cC_{\psi'm}) + (I_{fz} + i_{fz})C_{\psi'm}\sin\varepsilon\}\ddot{\phi} - (i_{fy}/R_f)C_{\psi'm}\cos\varepsilon\dot{x}_1\dot{\phi} - \{Z_f + M_f g(1 + eC_{\psi'm}) + M_{fw} g(1 + cC_{\psi'm})\}\phi - \{M_f f'(1 + eC_{\psi'm}) + M_{fw}(f' + f_w)(1 + cC_{\psi'm})\}\phi_{m'} - (i_{fy}/R_f)C_{\psi'm}\dot{x}_1\phi_{m'} - \{Z_f + M_f g(1 + eC_{\psi'm}) + M_{fw} g(1 + cC_{\psi'm})\}\cos\varepsilon\phi_{m'} + \{M_f(1 + eC_{\psi'm})^2 + M_{fw}(1 + cC_{\psi'm})^2 + (I_{fz} + i_{fz})C_{\psi'm}^2\}\ddot{s}_m + C_{sm}\dot{s}_m + \{K_{sm} - (M_f e + M_{fw} c) g C_{\psi'm}^2\sin\varepsilon\}s_m + \{M_f e(1 + eC_{\psi'm}) + M_{fw} c(1 + cC_{\psi'm}) + (I_{fz} + i_{fz})C_{\psi'm}\}\delta - (M_f eg + M_{fw} cg)C_{\psi'm}\sin\varepsilon\delta + i_{fz} C_{\psi'm}\ddot{\psi}_{f'} + M_{fw}(1 + cC_{\psi'm})\ddot{s}f + (i_{fy}/R_f)C_{\psi'm} C_{\phi'f}\dot{x}_1\dot{s}_f - M_{fw} g C_{\psi'm}\sin\varepsilon\varepsilon s_f - Y_f = 0$$

Equation of Equilibrium of Moments About Steering Axis

$$(M_f e + M_{fw} c)\ddot{y}_1 + \{M_f e k + M_{fw} c l_1 + (I_{fz} + i_{fz})\cos\varepsilon\}\ddot{\psi} + \{M_f e + M_{fw} c + (i_{fy}/R_f)\sin\varepsilon\}\dot{x}_1\dot{\psi} + \{M_f e j + M_{fw} c R_f + (I_{fz} + i_{fz})\sin\varepsilon\}\ddot{\phi} - (i_{fy}/R_f)\cos\varepsilon\dot{x}_1\dot{\phi} + (tZ_f - M_f eg - M_{fw} cg)\phi - \{M_f e f' + M_{fw} c(f' + f_w)\}\phi_{m'} - (i_{fy}/R_f)\dot{x}_1\phi_{m'} + (tZ_f - M_f eg - M_{fw} cg)\cos\varepsilon\phi_{m'} + \{M_f e(1 + eC_{\psi'm}) + M_{fw} c(1 + cC_{\psi'm}) + (I_{fz} + i_{fz})C_{\psi'm}\}\ddot{s} (tZ_f - M_f eg - M_{fw} cg)\sin\varepsilon\delta + i_{fz}\ddot{\psi}_{f'} + R_f Z_f\sin^2\varepsilon\psi_{f'} + M_{fw} c\ddot{s}_f + (i_{fy}/R_f)C_{\phi'f}\dot{x}_1\dot{s}_f - (Z_f + M_{fw} g + R_f Z_f C_{\phi'f}\cos\varepsilon)\sin\varepsilon s_f + tY_f - T_{xf}\sin\varepsilon - T_{zf}\cos\varepsilon = \tau$$

Equation of Equilibrium of Moments About Torsional Axis of Front Fork

$$i_{fz}\cos\varepsilon\ddot{\psi} + (i_{fy}/R_f)\sin\varepsilon\dot{x}_1\dot{\psi} + i_{fz}\sin\varepsilon\ddot{\phi} - (i_{fy}/R_f)\cos\varepsilon\dot{x}_1\dot{\phi} + R_f Z_f\sin\varepsilon\phi - (i_{fy}/R_f)\dot{x}_1\phi_m' + R_f Z_f\sin\varepsilon\cos\varepsilon\phi_m' + i_{fz} C_{\psi'm}\ddot{s}_m + R_f Z_f C_{\psi'm}\sin^2\varepsilon s_m + i_{fz}\delta + R_f Z_f\sin^2\varepsilon\delta + i_{fz}\psi_f' + C_{\psi'f}\psi_f' + (K_{\psi'f} + R_f Z_f\sin^2\varepsilon)\psi_f' + (i_{fy}/R_f)C_{\phi'f}\dot{x}_1\dot{s}_f - (Z_f + M_{fw} g + R_f Z_f C_{\phi'f}\cos\varepsilon\sin\varepsilon s_f + R_f Y_f\sin\varepsilon - T_{xf}\sin\varepsilon - T_{zf}\cos\varepsilon = 0$$

Equation of Equilibrium of Lateral Forces in Front Fork

$$M_{fw}\ddot{y}_1 + (M_{fw}l_1 + i_{fx}C_{\phi'f}\sin\varepsilon)\dot{\psi} + \{M_{fw} - (i_{fy}/R_f)C_{\phi'f}\cos\varepsilon\}\dot{x}_1\psi + (M_{fw}R_f - i_{fx}C_{\phi'f}\cos\varepsilon)\dot{\phi} - (i_{fy}/R_f)C_{\phi'f}\sin\varepsilon\dot{x}_1\phi - (Z_f + M_{fw}g)\phi - \{M_{fw}(f' + f_w) + i_{fx}C_{\phi'f}\}\phi_m' - (Z_f + M_{fw}g)\cos\varepsilon\phi_m' + M_{fw}(l + cC_{\psi'm})\ddot{s}_m - (i_{fy}/R_f)C_{\psi'm}C_{\phi'f}\dot{x}_1\dot{s}_m - (Z_f + M_{fw}g)C_{\psi'm}\sin\varepsilon s_m + M_{fw}c\ddot{\delta} - (i_{fy}/R_f)C_{\phi'f}\dot{x}_1\dot{\delta} - (Z_f + M_{fw}g)\sin\varepsilon\delta - (i_{fy}/R_f)C_{\phi'f}\dot{x}_1\psi_f' - (Z_f + M_{fw}g)\sin\varepsilon\psi_f' + (M_{fw} + i_{fx}C_{\phi'f}^2)\ddot{s}_f + C_{sf}\dot{s}_f + K_{sf}s_f - Y_f = 0$$

Equation of Equilibrium of Moments About Torsional Axis of Rear Swing Arm

$$(i_{ry}/R_r)\dot{x}_1\psi + i_{rx}\dot{\phi} + R_rZ_r\phi + i_{rx}\dot{\phi}_t' + C_{\phi't}\phi_t' + (K_{\phi't} + R_rZ_r)\phi_t' - (i_{ry}/R_r)C_{\psi't}\dot{x}_1\dot{s}_t - (Z_r + M_{rw}g)s_t + R_rY_r - T_{xr} = 0$$

Equation of Equilibrium of Lateral Forces in Rear Swing Arm

$$M_{rw}\ddot{y}_1 - (M_{rw}l_2 + i_{rz}C_{\psi't})\dot{\psi} + M_{rw}\dot{x}_1\psi + M_{rw}R_r\dot{\phi} + (i_{ry}/R_r)C_{\psi't}\dot{x}_1\phi - (Z_r + M_{rw}g)\phi + (i_{ry}/R_r)C_{\psi't}\dot{x}_1\phi_t' - (Z_r + M_{rw}g)\phi_t' + (M_{rw} + i_{rz}C_{\psi't}^2)\ddot{s}_t + C_{st}\dot{s}_t + K_{st}s_t - Y_r = 0$$

Equation of Equilibrium of Lateral Forces in Rider

$$(M_1 + M_2)\ddot{y}_1 - (M_1 + M_2)l_R\dot{\psi} + (M_1 + M_2)\dot{x}_1\psi + \{M_1h_1 + M_2(h_1 + h_2)\}\dot{\phi} - (M_1 + M_2)g\phi + (M_1 + M_2)\ddot{y}_R + C_1\dot{y}_R + K_1y_R + M_2h_2\ddot{\phi}_R = 0$$

Equation of Equilibrium of Leaning Moments of Rider

$$M_2h_2\ddot{y}_1 - M_2h_2l_R\ddot{\psi} + M_2h_2\dot{x}_1\psi + \{M_2(h_1 + h_2 + i_{2x}\}\dot{\phi} - M_2h_2g\phi + M_2h_2\ddot{y}_R + (M_2h_2^2 + i_{2x})\ddot{\phi}_R + C_2\dot{\phi}_R + (K_2 - M_2h_2g)\phi_R = 0$$

Equation of Side Force on Tire of Front Wheel

$$(\sigma_f/\dot{x}_1)\dot{Y}_f + Y_f = -C_{YS1}\alpha_f + C_{YC1}\phi_f$$

Equation of Side Force on Tire of Rear Wheel

$$(\sigma_r/\dot{x}_1)\dot{Y}_r + Y_r = -C_{YS2}\alpha_r + C_{YC2}\phi_r$$

Equation of Aligning Torque and Camber Torque on Front Wheel

$$(\sigma_f/\dot{x}_1)\dot{T}_{zf} + T_{zf} = C_{ZS1}\alpha_f + C_{ZC1}\phi_f$$

Equation of Aligning Torque and Camber Torque on Rear Wheel

$$(\sigma_r/\dot{x}_1)\dot{T}_{zr} + T_{zr} = C_{ZS2}\alpha_r + C_{ZC2}\phi_r$$

Equation of Overturning Moments on Front Wheel

$$(\sigma_f/\dot{x}_1)\dot{T}_{xf} + T_{xf} = C_{XS1}\alpha_f - C_{XC1}\phi_f$$

Equation of Overturning Moments on Rear Wheel

$$(\sigma_r/\dot{x}_1)\dot{T}_{xr} + T_{xr} = C_{XS2}\alpha_r - C_{XC2}\phi_r$$

Sideslip Angle of Front Wheel

$$\alpha_f = \{\dot{y}_1 + l_1\psi - h_\phi'\phi_m' + (1 - tC_{\psi'm})\dot{s}_m - t\dot{\delta} - R_f\sin\varepsilon\psi_f' + (1 + R_fC_{\phi'f}\cos\varepsilon)s_f\}/\dot{x}_1 + \phi_m'\sin\varepsilon - s_mC_{\psi'm}\cos\varepsilon - \delta\cos\varepsilon - s_fC_{\phi'f}\sin\varepsilon - \psi_f'\cos\varepsilon$$

Sideslip Angle of Rear Wheel

$$\alpha_r = (\dot{y}_1 - l_2\psi - R_r\dot{\phi} + s_t)/X_1 + s_tC_{\psi't}$$

Camber Angle of Front Wheel

$$\phi_f = \phi + \phi_m'\cos\varepsilon + s_mC_{\psi'm}\sin\varepsilon + \delta\sin\varepsilon + \psi_f'\sin\varepsilon - s_fC_{\phi't}\cos\varepsilon$$

Camber Angle of Rear Wheel

$$\phi_r = \phi + \phi_t'$$

Appendix II

Parameters

Table 2-1. Masses, moments of inertia, dimensions and geometrical data used in theoretical calculation

		A	B	C	D
M_f	kgs^2m^{-1}	2.249	2.57	2.109	2.833
M_r	kgs^2m^{-1}	15.23	19.55	15.93	23.65
M_{fw}	kgs^2m^{-1}	1.20	1.43	1.04	1.81
M_{rw}	kgs^2m^{-1}	1.51	2.01	1.34	2.00
I_{fx}	$kgms^2$	0.048	0.025	0.063	0.074
I_{fz}	$kgms^2$	0.048	0.025	0.063	0.074
I_{rx}	$kgms^2$	0.826	1.635	0.981	1.843
I_{rz}	$kgms^2$	1.450	2.826	2.232	2.531
C_{rxz}	$kgms^2$	0.0	0.0	0.0	0.0
i_{fy}	$kgms^2$	0.053	0.059	0.045	0.076
i_{ry}	$kgms^2$	0.062	0.076	0.061	0.087
i_{fx}	$kgms^2$	0.027	0.031	0.023	0.041
i_{rx}	$kgms^2$	0.033	0.043	0.032	0.047
i	$kgms^2$	0.093	0.114	0.092	0.130
λ		1.0	1.0	1.0	1.0
Z_f	kg	-107.5	-129.5	-115.5	-176.9
c	m	0.065	0.050	0.050	0.047
e	m	0.065	0.160	0.049	0.042
j	m	0.727	0.728	0.692	0.696
k	m	0.593	0.634	0.556	0.602
t	m	0.079	0.095	0.086	0.111
h	m	0.531	0.566	0.530	0.510
1_1	m	0.828	0.860	0.759	0.913
1_2	m	0.561	0.561	0.594	0.636
h'	m	0.620	0.633	0.633	0.599
1'	m	0.026	0.026	0.008	0.021
f'	m	-0.049	0.033	0.045	0.118
f_w	m	0.438	0.402	0.443	0.434
R_f	m	0.311	0.320	0.299	0.321
R_r	m	0.313	0.323	0.312	0.317
ε	deg	27.5	27.0	27.0	29.5

Table 2-2. Data concerning frame rigidities used in theoretical calculation

		A	B	C	D
$K_{\phi'm}$	$kgmdeg^{-1}$	72.13	238.49	78.66	150.91
$C_{\phi'm}$	$kgmsdeg^{-1}$	0.0	0.0	0.0	0.0
K_{sm}	kgm^{-1}	60170.	62950.	33540.	33050.
C_{sm}	$kgsm^{-1}$	0.0	0.0	0.0	0.0
$C_{\psi'm}$	$radm^{-g}$	2.714	2.379	2.667	2.238
$K_{\psi'f}$	$kgmdeg^{-1}$	2.67	3.65	2.95	3.47
$C_{\psi'f}$	$kgmsdeg^{-1}$	0.0	0.0	0.0	0.0
K_{sf}	kgm^{-1}	31120.	25890.	25930.	24880.
C_{sf}	$kgsm^{-1}$	0.0	0.0	0.0	0.0
$C_{\phi'f}$	$radm^{-1}$	3.09	3.41	3.30	3.40
$K_{\phi't}$	$kgmdeg^{-1}$	15.39	24.11	13.91	90.08
$C_{\psi't}$	$kgmsdeg^{-1}$	0.0	0.0	0.0	0.0
K_{st}	kgm^{-1}	57290.	86830.	52500.	156050.
C_{st}	$kgsm^{-1}$	0.0	0.0	0.0	0.0
$C_{\psi't}$	$radm^{-1}$	3.125	3.226	3.226	3.529

Table 2-3. Tire characteristics data used in theoretical calculation

		A	B	C	D
C_{YS1}	$kgdeg^{-1}$	26.90	35.70	23.70	36.00
		6.10	13.20	6.20	7.50
C_{YS2}	$kgdeg^{-1}$	25.70	36.60	19.80	47.50
		9.60	11.10	7.90	10.05
C_{YC1}	$kgdeg^{-1}$	2.86	3.96	2.26	3.64
		-0.33	0.19	-0.49	-0.81
C_{YC2}	$kgdeg^{-1}$	2.53	4.05	2.96	5.27
		-0.59	-0.66	0.13	-0.17
C_{ZS1}	$kgmdeg^{-1}$	0.23	0.46	0.28	0.33
		-0.24	-0.39	-0.188	-0.208
C_{ZS2}	$kgmdeg^{-1}$	0.29	0.34	0.26	0.34
		-0.206	-0.538	-0.247	0.813
C_{ZC1}	$kgmdeg^{-1}$	0.019	0.044	0.016	0.032
		-0.0134	-0.0055	-0.0109	-0.0071
C_{ZC2}	$kgmdeg^{-1}$	0.034	0.044	0.033	0.065
		0.0005	-0.0318	-0.003	-0.0242
C_{XS1}	$kgmdeg^{-1}$	0.09	0.12	0.10	0.02
		-0.297	-0.391	-0.246	-0.332
C_{XS2}	$kgmdeg^{-1}$	0.032	0.13	0.08	0.12
		-0.523	-0.702	-0.308	-0.937
C_{XC1}	$kgmdeg^{-1}$	0.120	0.162	0.106	0.175
		-0.026	-0.031	-0.026	-0.041
C_{XC2}	$kgmdeg^{-1}$	0.161	0.248	0.160	0.298
		-0.052	-0.092	-0.060	-0.083
σ_f	m	0.176	0.179	0.157	0.158
		0.052	0.092	0.029	0.040
σ_r	m	0.147	0.162	0.134	0.185
		0.060	0.034	0.082	0.081
$\|Z_f\|$	kg	110.0	140.0	110.0	150.0
$\|Z_r\|$	kg	140.0	190.0	140.0	200.0

Notes: When two figures are indicated in a box, the upper figure shows differential coefficient and relaxation length of tire component force corresponding to values of $|Z_f|$ and $|Z_r|$ listed in the table, and the lower figure shows differential coefficient and relaxation length of tire component force when values of $|Z_f|$ and $|Z_r|$ are zero. IndividD2†Z_f s in their using ranges, in linear relations to $|Z_f\Delta 2|Z_f$ s in their using ranges, in linear relations to Z_f and Z_r.

Table 2-4. Zerodynamic characteristic data used in theoretical calculation

		A	B	C	D
C_{FX}	kg	-0.281	-0.267	-0.284	-0.240
$C_{FY\beta}$	$kgdeg^{-1}$	-0.00985	-0.0064	-0.00975	-0.00735
C_{FZ}	kg	-0.035	-0.0313	-0.0336	-0.0290
C_{MY}	kgm	0.0290	0.0450	0.0428	0.0580
$C_{MZ\beta}$	$kgmdeg^{-1}$	-0.00150	-0.00085	-0.00127	-0.00135

Table 2-5. Rider's vibration characteristic data used in theoretical calculation

		A	B	C	D
M_1	kgs^2m^{-1}	3.80	4.24	4.01	4.48
M_2	kgs^2m^{-1}	1.96	2.19	2.06	2.30
i_{1x}	$kgms^2$	0.252	0.281	0.265	0.296
i_{2x}	$kgms^2$	0.081	0.090	0.085	0.095
i_z	$kgms^2$	0.249	0.271	0.270	0.256
h_1	m	0.843	0.844	0.873	0.899
h_2	m	0.386	0.385	0.397	0.396
1_R	m	0.139	0.138	0.157	0.192
K_1	kgm^{-1}	3638.	4062.	3834.	4283.
C_1	$kgsm^{-1}$	92.9	103.8	97.9	109.4
K_2	$kgmrad^{-1}$	32.1	35.8	35.2	39.1
C_2	$kgmsrad^{-1}$	3.02	3.36	3.32	3.69

Appendix III

Running Experiments

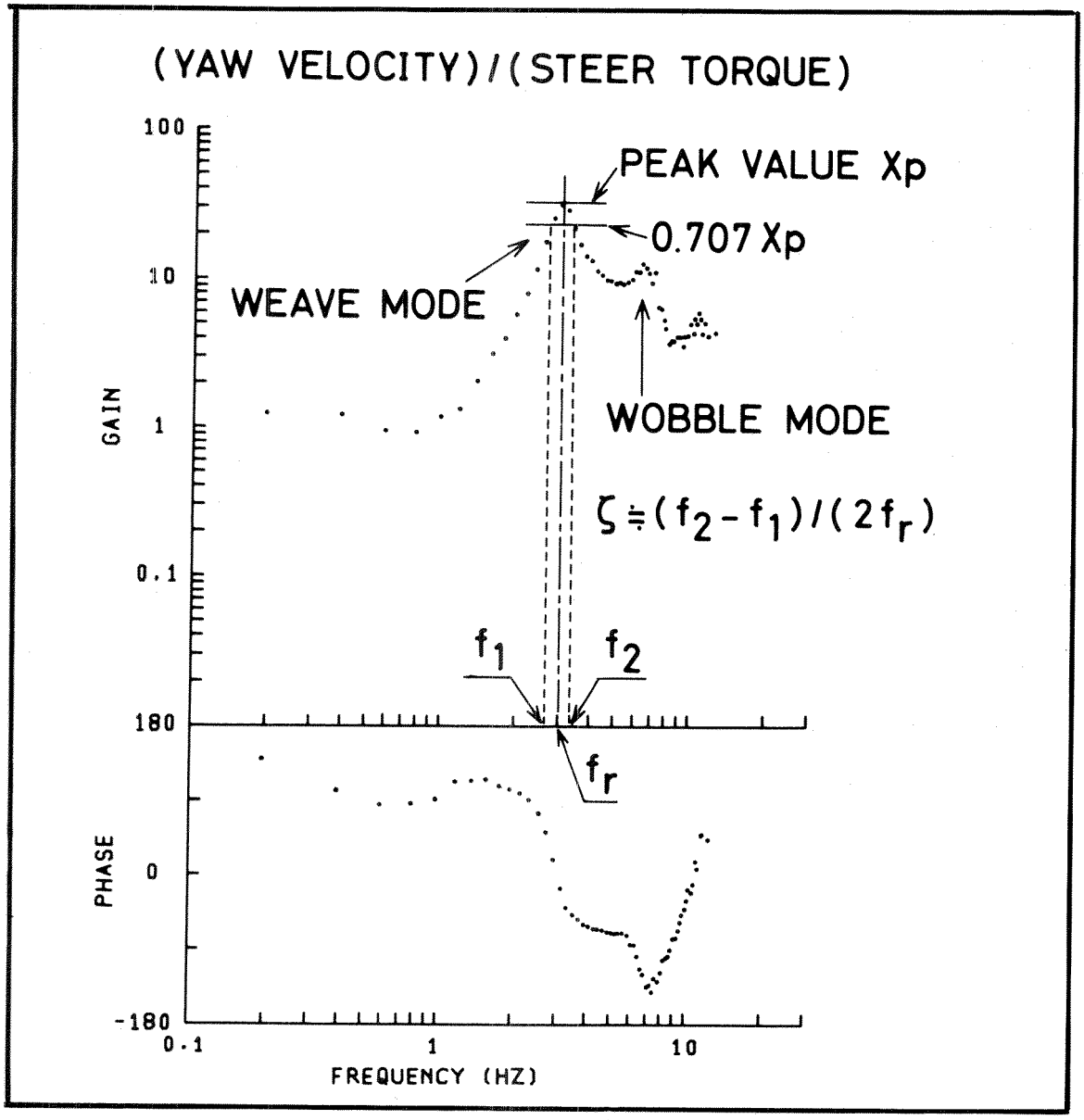

Figure A-1 Experimental data processing method

The Protective Effect of a Specially Designed Suit for Motorcyclists

Bertil Aldman and Janusz Kajzer
Chalmers University of Technology, Gothenburg, Sweden

Hans Gustafsson
Folksam Traffic Safety Group, Stockholm, Sweden

Åke Nygren and Claes Tingvall
Folksam Traffic Safety Group, Karolinska Hospital, Stockholm, Sweden

Abstract

Injuries to motorcyclists lead to permanent disability more often than injuries to car occupants (10 percent versus 6 percent). The use of helmets has decreased the risk of head injuries. Other injuries leading to permanent disability are currently concentrated on the extremities (about 70 percent). Almost all are due to fractures located in joints where knees, elbows, shoulders, and ankles are the most common spots.

In a study based on 200 motorcycle accidents, it was shown the existing protective clothing had no effect on the incidence of fractures to knees, elbows, and shoulders. Based on that knowledge, a new motorcycle suit was constructed. The main goal was to find a shock-absorbing material to protect knees, elbows, and shoulders in an accident. Confor Foam, a medium-density urethane foam, was tested and found to possess relevant characteristics. The material was tested under experimental conditions and found to be sensitive to dampness and temperature with an optimal shock-absorbing effect of +10° to +30°C. Experimental studies on the protective effect of different kinds of leather indicated the importance of continuous tests of leather when manufacturing motorcycle suits. The protective effects of the safety suit have been studied in real-life accidents during a 2-year period. A preliminary study showed the number of fractures decreased significantly.

Background

Driving a motorcycle is one of the most dangerous modes of travel. Efforts to reduce the injury risk must concern both active and passive safety. Until recently, passive safety development was concentrated on head protection and motorcycle design. It has, however, been shown that leather clothing has some effect on the incidence and severity of soft tissue injuries among motorcyclists. Feldkamp and Junghans(1) showed severe injuries were reduced by protective clothing. The reduction of soft tissue injuries was also shown by Aldman(2) and Engström(3).

A motorcycle helmet consists of a shell and an inner shock-absorbing layer to prevent injurious forces from reaching the head(1). A motorcycle suit is to some extent constructed in the same way. It consists of a covering layer of leather and a shock-absorbing material on vulnerable spots of the body, knees, elbows, and shoulders(2). To be comfortable, the suit must have special properties to allow necessary movements. This concerns especially the shock-absorbing material covering the joints. The leather must be supple and also strong.

The insurance company Folksam, together with the Department of Traffic Safety at Chalmers University of Technology, has constructed a suit based on the knowledge from real accidents. This suit will be presented in this study, which consists of the following:

- Evaluation of the properties of the leather and shock-absorbing material
- Evaluation of the effect of the constructed suit on bodily injuries

Evaluation of the Properties of the Leather and Shock-absorbing Material

Objectives

The objectives of this study were to evaluate the following:

- Movements of the body in case of an accident
- Essential differences between different types of leather and between samples of the same type of leather
- Influence of temperature on the shock-absorbing material
- Influence of dampness on the shock-absorbing material
- Shock-absorbing ability in different suits with and without shock-absorbing material

Material and Method

The movements of the motorcyclist when meeting with an accident were studied by viewing films of real accidents in motorcycle races.

Goatskin and bovine leather were studied in laboratory conditions regarding wear and tear, strength, and firmness.

The shock-absorbing material Confor Foam, which is a polyurethane foam, was tested in real traffic at different

temperatures and under laboratory conditions. The temperature was measured inside the material and on the inner and outer surfaces.

The shock-absorbing ability was tested under laboratory conditions at different temperatures and with varying degrees of dampness.

Result

In single motorcycle accidents, the motorcyclist normally skids on the road. During that time, the motorcyclist will normally be in the same position. The moment the motorcyclist reaches the verge of the road, he/she will start to roll over or roll around. The vertical fall is normally low, but the horizontal speed can be very fast. This type of accident causes no dangerous injuries unless the victim hits something or the protective clothes are torn into pieces, which may result in contaminated wounds.

In a collision, the impact on the body can be hard and produce fractures to unprotected limbs. To protect the body from injuries, leather and Confor Foam should be used.

Test of Leather

Leather from goats and oxen was tested as to wear and tear. Pieces of leather were mounted on dummies that simulated an elbow or shoulder, e.g., a sharp and a round part of the body. The leather was subjected to a rotating road surface. The thickness of the different test pieces was measured (see Table 1). On an average, bovine leather was thinner than goatskin.

Table 1. Thickness of different test pieces of leather

Type of Leather	Thickness					
	Micrometer with Point			Micrometer with Plate		
	C_1 Min.	C_1 Max.	C_1 Mean	C_2 Min.	C_2 Max.	C_2 Mean
Bovine	0.75	1.05	0.91	1.10	1.50	1.35
Goat	0.85	1.15	0.98	1.10	1.50	1.39

Table 2 shows the score for damage to leather. Table 3 shows the sum of the scores for 12 tests on the elbow dummy and 7 tests on the shoulder. It can be seen that the difference in resistance to grinding and tearing between goatskin and bovine leather is small.

Wear and tear strength of different test pieces of leather was also tested as to penetration. The results of this test can be seen in Figure 1. The worse the wear and tear strength, the larger the diameter of the hole. Bovine leather Type I had a mean thickness of 0.64mm, Type II, 0.90mm, and Type IV, 1.14mm, measured with a pointed micrometer. Corresponding values measured with a

Table 2. Scores for different types of grinding and tearing damages to test pieces of leather

Type of Damage	Score	Description of Damage
Grinding damage	1	Superficial damage, superficial scratches
	2	Superficial damage, deep scratches
	3	Deep scratches, small scratch holes
	4	Deep scratches, long scratch holes
	5	Large scratch holes
Tearing damage	0	No damage
	1	Small damage
	2	Extensive damage

Table 3. Grinding and tearing damage on different pieces of leather

Body Area	Type of Leather	Grinding Damage	Tearing Damage
Elbow (12)	Goat	26	4
	Bovine	34	2
Shoulder (7)	Goat	13	0
	Bovine	15	2

micrometer with a plate were 1.03, 1.36, and 1.60mm. Goat leather had a mean thickness of 0.98mm measured with a pointed micrometer and 1.37mm with a micrometer with a plate.

Figure 1 shows that bovine leather Types I and IV had a lower resistance to penetration compared with Type II and goatskin. This means it is possible to distinguish between good and bad quality by using a penetration test.

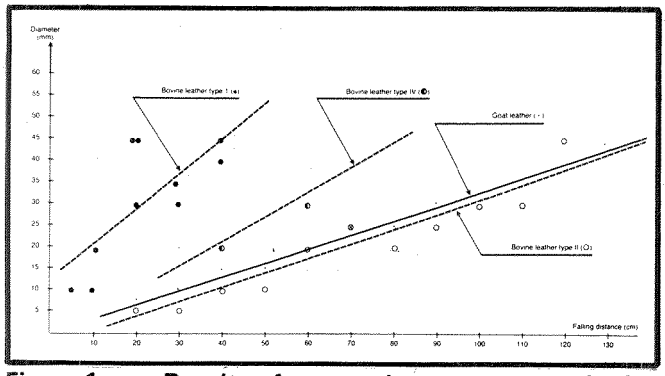

Figure 1. Results of penetration tests summarized by linear regression

Test of Shock-absorbing Material

Table 4 shows the temperature inside and on the inner and outer surface of the Confor Foam, measured in a real traffic situation for different air temperatures.

The mean temperature measured over the shock-absorbing material varies between +11.1° C and +26.3° C in the test situation at a temperature in the air of 0° C and +21° C when driving in urban traffic and at 110km/h. It is

Table 4. Temperature inside, on outer and inner surface of the shock-absorbing material measured in real traffic situations

	Air Temperature 0°C		21°C	
	Urban Traffic	110km/h	Urban Traffic	110km/h
Outer surface	9.4	5.4	24.3	22.6
Inside the confor foam	13.5	10.3	26.1	25.0
Inner surface	21.1	17.7	28.6	28.3
Mean	14.7	11.1	26.3	25.3

thus desirable that the shock-absorbing material keep its shock-absorbing ability between +10° C and +.30° C.

Figure 2 shows the shock-absorbing ability for Confor Foam at different temperatures inside the material. One plate of Confor Foam (15mm) was exposed to falling weights of 5kg and plane impact area (177cm^2). It can be seen that Confor Foam has good shock-absorbing properties between +.20° C and +30° C at which temperature a motorcycle is normally driven.

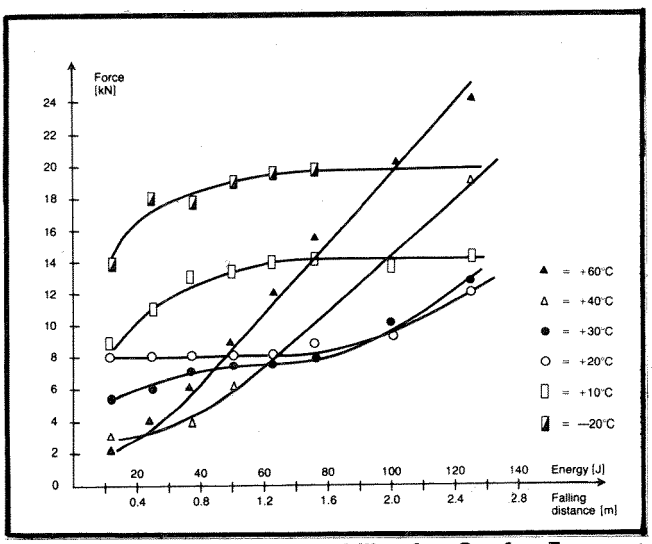

Figure 2. Shock-absorbing ability for Confor Foam at different temperatures

Figure 3 shows the shock-absorbing ability at different concentrations of water. Confor Foam loses its shock-absorbing ability at a low concentration of water.

Testing of the Shock-absorbing Ability in Different Motorcycle Suits

A suit with Confor Foam on knees, elbows, and shoulders was compared with a suit without any shock-absorbing material. The test was made on the knee area as to shock-absorbing ability.

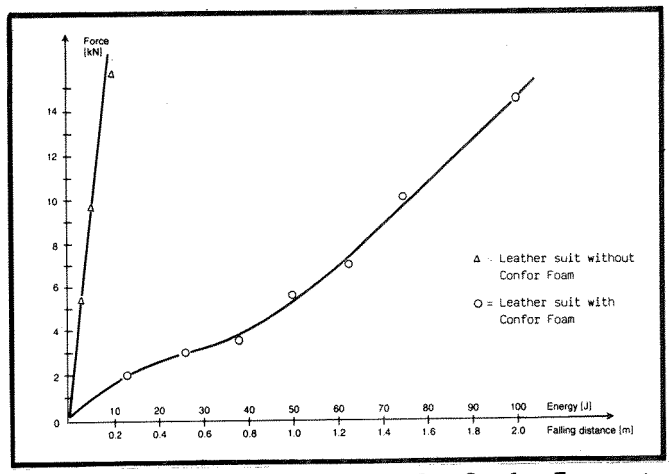

Figure 3. Shock-absorbing ability for Confor Foam at different concentrations of water

The knee areas of the two suits were exposed to two falling weights of 5kg of different shapes: one with a spherical impact area with a diameter of 45mm and the other with a plane surface with a diameter of 40mm. These two weights were dropped at different heights. The force directed toward the underlying surface was measured. The temperature was +20°, and the relative air humidity was 60 percent.

Figure 4 shows the force curves for a plane impact area and Figure 5 for a spherical one. It can be seen that a suit without shock-absorbing material has a linear force curve. The protective effect is thus very low (<5.0J) and cannot be measured in this study.

The suit with shock-absorbing material, on the other hand, can absorb energy. At energy levels between 10 and 30J, the curves are not linear, which means the shock-absorbing material will absorb energy until it touches the bottom and the relation between force and energy becomes linear.

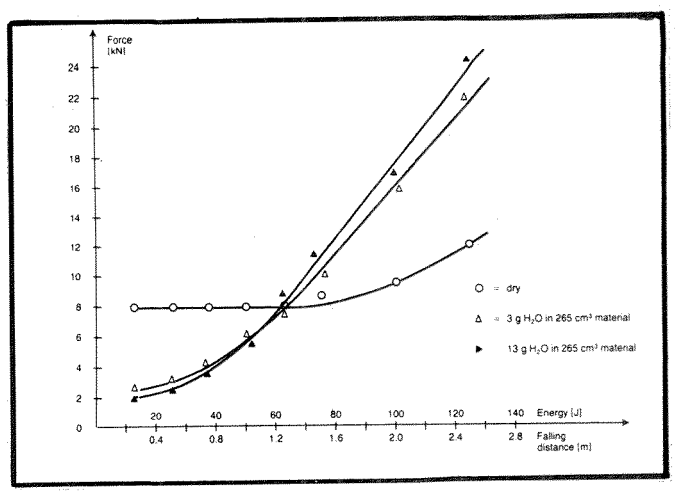

Figure 4. Force as a function of falling distance for two different suits with and without Confor Foam—plane impact area

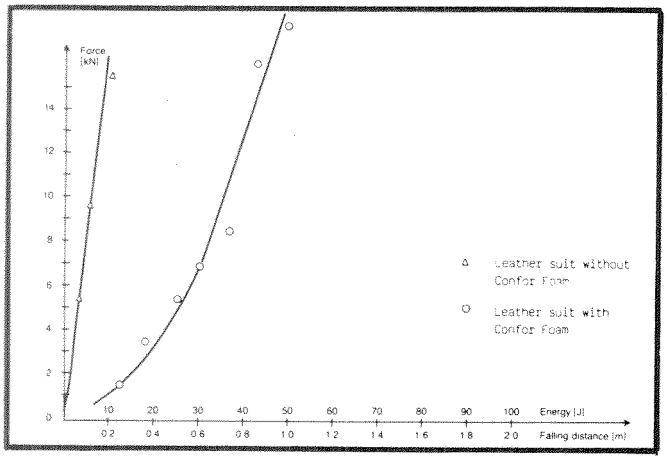

Figure 5. Force as a function of falling distance for two different suits with and without Confor Foam—spherical impact area

Evaluation of the Effect of the Constructed Suit on Bodily Injuries

Method and Material

Among policyholders having a motorcycle insured with the Folksam Group (about 35,000), several studies have been conducted.

- A sample of 1,001 motorcyclists, irrespective of their being involved in an accident or not
- A sample of motorcyclists injured in 1983 and 1984
- All motorcyclists that received a medical disability >10 percent from 1976 to 1982

Insurance records were completed with questionnaires on how the motorcyclists were dressed.

Results

Table 5 shows that 10.3 percent of the injured motorcyclists suffered a medical disability of >10 percent. The corresponding figure for car occupants was 6.2 percent.

Table 5. Relative frequency of permanent disability >10 percent for motorcyclists compared with car occupants

Type of Road User	Relative Frequency of Permanent Disability >10%
Motorcyclist	10.3%
Car occupant	6.2%

Table 6 shows contact areas for motorcyclists involved in accidents. Contact areas are defined as areas that came into contact with different surfaces during the accident and were recognized by the motorcyclist or could be seen on the clothing after the accident.

Table 6. Soft tissue injuries per contact area related to body region and type of clothing among motorcyclists involved in accidents for both injured and uninjured, head injuries omitted

Body Region	Not Covered by Leather	Covered by Leather	N
Knee, elbow shoulder	77.9%	24.4%	203
Other body regions	(4/17)	(5/21)	38

In Table 6, it can be seen that soft tissue injuries are less common among those wearing leather clothing compared to those wearing other types (significant). It is also shown that contact areas are concentrated on the joints of the extremities, e.g., knees, elbows, and shoulders.

Table 7 shows that contamination of soft tissue injuries is more uncommon to areas covered by leather compared to uncovered areas (significant). Table 8 shows 46 percent of all injuries that led to medical disability were located at shoulders, elbows, and knees. The most common location was the knee (32 percent).

Table 7. Soft tissue injuries; contaminated and not contaminated for areas covered and not covered by leather

Type of Clothing	Contaminated	Not Contaminated	All
Leather	4	34	38
Not leather	28	29	57
All	32	63	95

Table 8. Number of injuries causing medical disability >10 percent) among motorcyclists injured in 1976-1983. N = 93

Localization	Number	Localization	Number
Shoulder	7	Head (incl. face)	10
Elbow	5	Vertebrae	6
Soft tissue, leg	1	Spinal cord, nerves	4
Knee	30	Hands (incl. joints)	12
		Viscera	1
		Pelvis	2
		Ankle	14
Total	43		50

The suit with Confor Foam was introduced in 1983. During 1983 and 1984, about 12,000 safety suits were sold in Sweden. These suits fulfilled certain regulations according to Folksam specifications, built on the experimental studies described earlier.

Two studies in 1984 analyzed the injury-reducing effects of the safety suit. One was a sample among those wearing safety suits whether they were involved in an accident or not.

Table 9 shows a comparison between all kinds of clothing except safety suits. Contact areas were defined as described in Table 5. It can be seen there is a big difference between safety suits and other types of clothing. The difference is highly significant.

Table 9. Number of contacts between driver and any surface in an accident to areas protected by safety suit (knees, elbows, shoulders) and number of fractures to these areas

	No Safety Suits	Safety Suit
Number of contacts	187	78
Number of fractures	25 (13.4%)	1 (1.3%)

In the other study, a sample of injured motorcyclists was examined. All fractures were divided into two groups: fractures located in areas protected by the suit with shock-absorbing material and fractures located in other areas (except the head).

Table 10 shows the ratio between protected and unprotected areas is different for those wearing a safety suit compared to those not wearing one. The difference in distribution is highly significant.

Table 10. Number of fractures to areas protected by safety suit and other areas for injured motorcyclists wearing and not wearing a safety suit in an accident

Body Region	No Safety Suit	Safety Suit
Knees, elbows, shoulders	26	2
Other areas	22	15
Total	48	17

From Tables 9 and 10, it can be calculated the injury reduction to knees, elbows, and shoulders is more than 50 percent. To calculate with a higher precision, the research must be extended since the technique of relating different kinds of injuries to each other (affected versus unaffected injuries) requires further study.

Discussion

The number of motorcycles is increasing all over the world, and this results in an increase in the number of injured and killed. Efforts must be made to reduce this trend. Motorcycle helmets are compulsory in many countries, and this has decreased head injuries considerably. By studying disabling injuries, it is obvious that fractures near joints are important injuries to prevent.

In this study, the effects and properties of a specially designed suit have been evaluated in real-life situations as well as under laboratory conditions. When the movements of the motorcyclist involved in an accident are taken into consideration, it is obvious a layer of strong material should cover the body. During this type of sliding movement, there is great risk of wounds and contamination of these wounds. Contaminated wounds near a fracture lead to longer treatment periods and increase the risk of long-term consequences.

Leather is considered to be the best protective material. Prime and Woods(5) showed that synthetic materials cannot offer efficient protection.

What magnitude of forces produces fractures? Patric, Kroell, and Mertz(6) showed that a force of 6kN was the level for injuries to the knee. Injuries to patellae can occur at lower levels. A force of 5kN was chosen as a reference level for minor patella injuries. Powell(7) showed 80 percent patella fractures and 33 percent fractures of the condyles at a force of 10.5kN, and FMVSS 208 (1977) suggests a force of 10kN as a realistic limit for the risk of femur fractures.

Confor Foam protects from fractures. Experimentally it was shown that Confor Foam accumulates energy between 10 to 30J. The energy absorption for a suit with Confor Foam was 14.1 times higher than for a suit with no shock-absorbing material at a force of 10kN and with a plane impact area. The corresponding value for a spherical area was 6.5.

Tests on the suit with shock-absorbing material show that the suit seems to give satisfactory protection, and experimental tests appear useful to test the effect of different materials and suits.

Conclusion

Studies made in an insurance study have led to the following conclusions:

- Leather clothing diminishes the risk of wounds at least 50 percent in an impact between the body and the ground or other hard objects.
- Leather clothing diminishes the risk of the wounds becoming contaminated by at least 50 percent.
- Shock-absorbing material on knees, elbows, and shoulders diminishes the risk of fractures by at least 50 percent.
- Almost 50 percent of all disabling injuries were concentrated at knees, elbows, and shoulders.

The following conclusions could be drawn from the experimental studies made:

- The quality of leather varies, and it is important to have continuous tests when manufacturing motorcycle suits.
- A number of different shock-absorbing materials can probably be used.

- Confor Foam has been tested, used, and seems suitable.
- The quality of Confor Foam varies and must be tested at the manufacturer's facility before its use.
- Confor Foam is sensitive to dampness and should, therefore, be protected from water.
- Confor Foam is sensitive to temperature and has its optimal shock-absorbing effect at +10°C to +30°C, that is, at the temperature reigning during the motorcycle season in Sweden.

References

1. Feldkamp, G., and K. Junghans, "The typical traffic accident in adolescents: the motorcycle accident—some epidemiological features and the effectiveness of safety helmets and clothing," Proceedings of Conference on Biomechanics of Injury to Pedestrians, Cyclists and Motorcyclists, Amsterdam, pp. 75-80, 1976.
2. Aldman, B., I. Cacciola, H. Gustafsson, Å. Nygren, and J. Wersäll, "The protective effect of different kinds of protective clothing worn by motorcyclists," Proceedings 6th IRCOBI Conference, 1984.
3. Engström, A., "Causes and consequences of moped and motorcycle accidents," *Scandinavian Journal of Social Medicine*, Suppl. 15, 1979.
4. Aldman, B., L. Thorngren, H. Gustafsson, Å. Nygren, and J. Wersäll, "The protective effect of crash helmets. A study of 96 motorcycle accidents," Proceedings 4th IRCOBI Conference on Biomechanics of Trauma, Bron, France, pp. 63-74, 1979.
5. Prime, D.M., and R.I. Woods, "Tests on the protection afforded by various fabrics and leathers in a simulated impact of a motorcyclist on a road surface," Proceedings International IRCOBI Conference, 1984.
6. Patric, L.M., C.K. Croell, and M.J. Mertz, "Forces on the human body in simulated crashes," Proceedings 9th Stapp Car Crash Conference, University of Minnesota, 1966.
7. Powell, W.R., S.S. Ojala, S.M. Advani, and R.B. Martin, "Cadaver femur responses to longitudinal impacts," Proceedings 19th Stapp Car Crash Conference, SAE Paper 751160, San Diego, 1975.

A Study of Motorcycle Leg Protection

Hidetoshi Tadokoro
Motorcycle Rider Protection Subcommittee,
Japan Automobile Manufacturers Association

Shigehisa Fukuda and
Kyoichi Miyazaki
Japan Automobile Research Institute

Abstract

Researchers concerned with motorcycle occupant protection have attempted to develop ways to protect the motorcycle occupant from injury. In the hope of finding a means to protect the motorcycle occupant's lower extremities, the authors have investigated past research, designed a device that incorporates an energy-absorbing component, tested the device in a series of collisions with automobiles, and performed an analysis of the test results to assess the merits of the new device. Results show that although the device may under certain circumstances reduce lower leg injuries, there may be increased potential for upper leg, chest, and head injuries.

Introduction

It has been generally recognized the most frequent injury, although not the most serious, to the motorcycle occupant involved in a multivehicle collision is injury to the lower extremities(1).

The inherent design of the motorcycle leaves the occupant exposed to the environment, in contrast with an automobile that fully encloses the occupant within a substantial structure. Such inherent characteristics present the researcher with a formidable task in attempting to increase motorcycle occupant protection from injury during vehicle collisions.

In the area of leg protection, studies by various organizations were begun in the 1960's and have continued to the present(2). The studies sought a means to preserve sufficient leg space for the motorcycle occupant when impacted by an automobile. However, all of the numerous devices tested to date, including those previously examined by the Japan Automobile Manufacturers Association (JAMA) during the mid-1970's(3), were found to be unsatisfactory. Such devices were either structurally inadequate to preserve the leg space(2) or, when of sufficient structural strength to preserve leg space during the collision, were found to pose a significant potential to

increase injury to the head and chest of the motorcycle occupant(4).

In the hope of finding a solution to this problem, JAMA developed a device possessing energy-absorbing properties. In conjunction with the Japan Automobile Research Institute (JARI), the effectiveness of the new device was analyzed by a series of vehicle collision tests.

Review of Past Studies Concerning Motorcycle Leg Protection Devices

The study of motorcycle occupant leg protection originated from the intent to prevent the legs from being trapped and crushed between the opposing automobile and the motorcycle. Initially, crash tests were performed in the late 1960's and early 1970's with tubular steel structures to determine their ability to preserve the necessary leg space(2). However, the studies concluded that such devices then available did not possess sufficient strength and failed, due to the loads placed on them by the opposing automobile.

Subsequently, greatly strengthened and variously configured devices were designed, fabricated, and tested during the mid-1970's by various researchers in Great Britain, the United States, and Japan(3,4,5,6).

Although the more substantial of the reinforced structures did at times succeed in preserving the necessary leg space when struck by automobiles at speeds up to 48km/h, the reported conclusions stated such a device could not be recommended for use because of the following findings:

- When the leg space is sufficiently preserved so that no leg trap occurred, the motorcycle occupant seemed to be more readily ejected from the motorcycle at the time of the impact, resulting in the potential of causing significant injury to the motorcycle occupant's head and chest. Since head and chest injuries present a danger to life, such potential was identified as a primary concern(3,4).
- Although the lower portion of the leg was generally protected from injury, it was found that at times even the reinforced device did not eliminate all leg injury. For example, serious upper leg injury occurred when the upper leg was subjected to a torsional moment, which may have been sufficient to cause injury to the pelvic joint. Such is an undesirable result(3).
- Other injury-producing causes were identified, such as leg fracture due to the leg impacting the leg protection structure itself(5).

In summary, although the substantial leg protection structures did at times preserve necessary leg space, such a device was identified as being the cause of potentially more serious injuries.

Considerations and Proposed Requirements for the Design of a Leg Protection Device

Due to the problems identified above and in the hope of discovering a solution, basic principles were first reassessed and in doing so the following considerations resulted:

- To reduce or eliminate head and chest injury caused by ejection into the opposing automobile, energy absorption was considered as an element in the design of the new leg protection device. A new crushable component was incorporated with the hope that such a device would sufficiently reduce the initial motorcycle acceleration, occupant ejection, and chest and head injury caused by preservation of the leg space.

  As alternatives, motorcycle occupant ejection prevention by utilizing restraint systems such as seatbelts or airbags were considered. However, such alternatives had been previously considered, tested, and rejected by other researchers for various reasons(7).
- To preserve necessary leg space, the leg protection device should possess sufficient strength so it would not permit the opposing automobile to intrude to the extent of causing the leg to be trapped and crushed between the automobile and motorcycle.

Table 1 sets forth the details of the application of these considerations.

Table 1. Considerations and requirements for the design of a leg protection device

Element	Proposed Requirements	Remarks
Energy-absorbing component	Energy-absorbing component is to be provided.	The energy-absorbing component is to be provided to reduce the acceleration of the motorcycle on impact. The size of the energy-absorbing component is such that its outer dimension is not so large as to create other safety problems.
Preservation of leg space	The leg space is to be preserved with the reinforced structure.	A reinforced structure which does not deform and thereby preserves leg space is to be installed as an inner portion of the device. The reinforced structure should be strong enough to endure a broadside collision at 48km/h with an automobile.
	The leg space is to be the minimum required.	Excessive leg space is not desirable because the occupant will be more readily ejected, resulting in greater injury.
Restraint of occupant	Restraining the occupant with restraint device is not recommended.	When restrained with the motorcycle, the occupant may be caught between motorcycle and opposing vehicle or road surface, resulting in greater injury(7).

The following items were also to be considered to reduce injury-inflicting potential:

- Direct leg impact against the reinforced structure
- Hyperextension of the knee
- Trapping of the leg by the reinforced structure
- Highsiding of the motorcycle

In the design of this device, the maximization of the protective effect of the Crushable Leg Protector (CLP) was sought; therefore, no consideration was given to aerodynamic effects, braking, lean angle, or other performance requirements.

Test Procedures

Currently, there are no formal standards that apply to motorcycle crash tests as there are for automobiles. For the purposes of this test program, the following requirements were considered appropriate for evaluation of the CLP:

- The program should permit an evaluation of the effects of the device on the occupant during an accident.
- The program should permit kinematic analysis of various collision modes.

Test Motorcycle

In view of the above, a Yamaha XS 400 SP motorcycle was selected for all tests. It is a medium-size motorcycle. The basis for the selection was, first, that accident statistical reports(1) have indicated the 50th percentile size is a medium-size motorcycle; second, to permit the kinematic analysis it was determined that the medium-sized motorcycle would be appropriate. Test motorcycle specifications are given in Table 2.

Table 2. Specifications of test motorcycle

Manufacturer	:	Yamaha
Model	:	XS400SP
Overall length	:	2,070mm
Overall width	:	870mm
Overall height	:	1,140mm
Weight	:	170kg (210kg for the CLP type)
Appearance	:	Figures 1 and 2

Crushable Leg Protector (CLP)

The CLP used in this test program consisted of a rigid understructure made of steel tubing covered by an energy-absorbing component constructed of aluminum honeycomb and urethane foam. The specifications for these materials can be found in Table 3 and Figure 3. The CLP was attached to the motorcycle as shown in Figure 4.

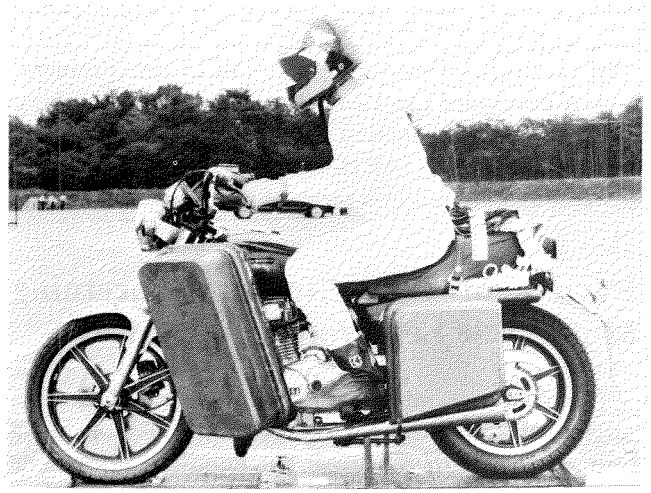

Figure 1. Side view of motorcycle with CLP

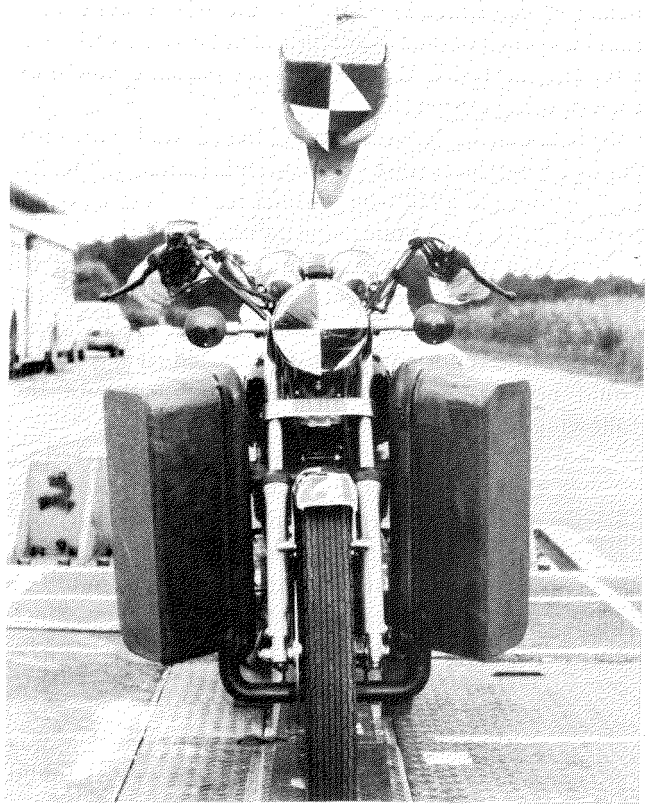

Figure 2. Front view of motorcycle with CLP

Opposing Automobile

The Toyota Crown automobile was selected for the test program. The basis for this selection was accident statistical studies that show that when motorcycles collide with opposing vehicles, approximately 80 percent of the opposing vehicles are identified as passenger automobiles(1). The Toyota Crown, which is representative of a medium-size automobile when viewed from a worldwide perspective, was believed to be appropriate

Table 3. Specifications of CLP

Energy-Absorbing Component			
Construction	:	Foamed urethane and aluminum honeycomb on steel sheet	
Energy-absorbing component size	:	Thickness 150mm	
Aluminum honeycomb	:	Manufacturer:	Hexcel & Showa
		Model No.:	AL ⅜-5052-001
		Compaction characteristic:	5kg/cm^2
		Density:	0.026 gr/cm^3
Urethane foam	:	Manufacturer:	Sekisui Chemical
		Model No.:	High-density poly urethane
		Expansion ratio:	33
		Density:	0.03 gr/cm^3
Steel Sheet	:	SPCC, 1.0mm (JIS G 3141)	
Leg space structure			
Composition	:	Steel tube structure	
Steel tube used	:	SGP (JIS G3452)	
Tube outer diameter	:	42.7mm	
Thickness	:	3.5mm	

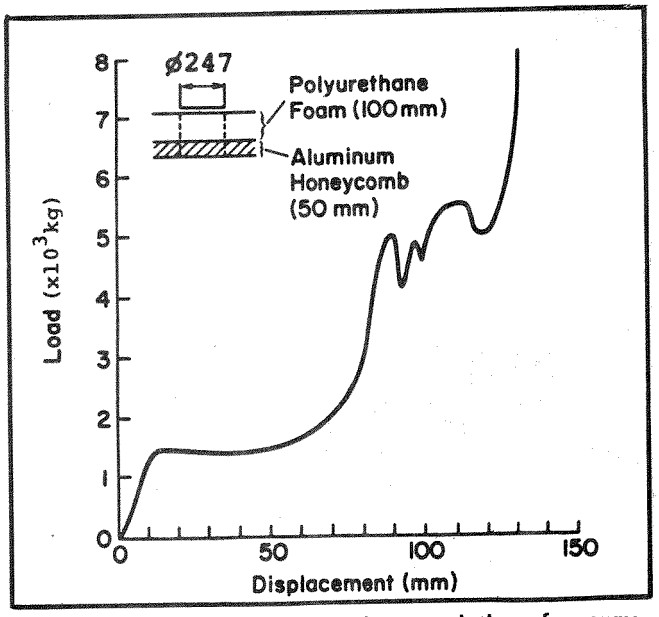

Figure 3. Load-displacement characteristics of energy-absorbing component

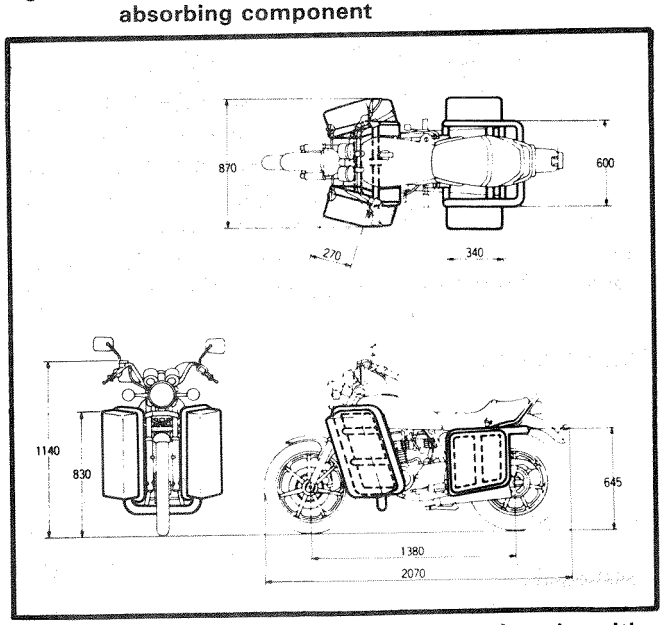

Figure 4. Drawing of motorcycle equipped with crushable leg protector

for the kinematic analysis. Its specifications are given in Table 4.

Collision Speed

To determine the effects of the device, the speeds for the collisions included 0, 24, 32, and 48km/h. It is notable that this speed range encompasses the speed of 34.4km/h, which one accident study found to be the mean collision speed(1).

Collision Configuration

In essence, three collision geometries were selected that the authors believed would satisfy the criteria. The three collision geometries are as follows:

- Angled Collision—The opposing automobile and motorcycle both in a moving configuration collide at a 45° angle with the motorcycle striking the front of the automobile.
- Broadside Collision—The opposing automobile strikes the motorcycle at a 90° angle.
- Offset Frontal Collision—The motorcycle traveling at a speed of 48km/h collides with the front corner of the opposing automobile in an offset mode.

Table 4. Specifications of opposing automobile

Manufacturer	:	Toyota
Model	:	Crown
Overall length	:	4,680mm
Overall width	:	1,690mm
Overall height	:	1,445mm
Weight	:	1,330kg
Appearance	:	Figures 5 and 6

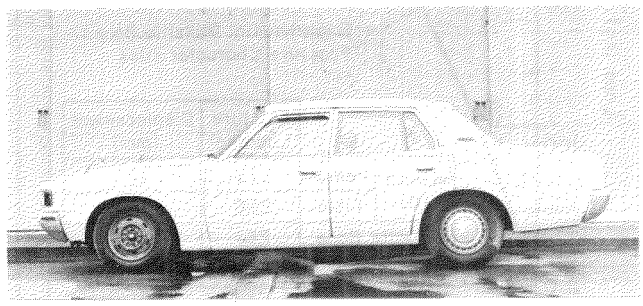

Figure 5. Side view of opposing automobile

Dummy Selection

A Humanoid, Hybrid II dummy was selected for the test program. Its characteristics are given in Table 5.

To permit analysis of leg injuries, the dummy was modified in that a breakable bakelite bone was used in

Figure 6. Front view of opposing automobile

Table 5. Specifications of dummy

Manufacturer:	Humanoid
Model:	Hybrid II with standing kit
Hands:	Able to grip
Legs:	Breakable bakelite bone with urethane foamed muscle
Fracture Characteristics:	See Figure 7 for bending characteristics

both the upper and lower leg. The bending properties of the bakelite bone as compared with human bone are shown in Figure 7(8). The dummy wore a helmet, shirt, pants, and boots during all of the collision tests.

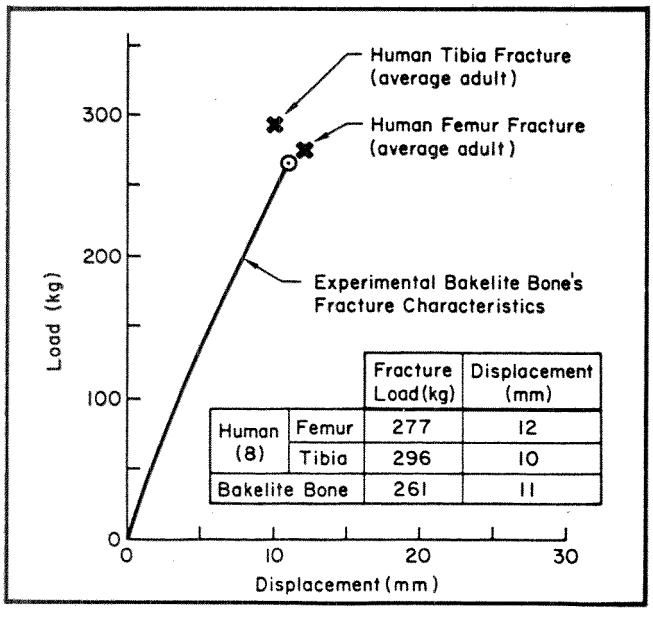

Figure 7. Bending fracture characteristics of bakelite and human leg bone

Test Conditions

Based on the above stated test purposes, the tests run are described in Table 6 as follows:

Table 6. Test conditions

Collision Configuration	No.	Motorcycle Speed(km/h)	Automobile Speed(km/h)	Motorcycle Configuration
Angled collision	A-1	32	32	STD*
	A-2	32	32	CLP**
	A-3	48	48	STD
	A-4	48	48	CLP
Broadside collision	B-1	0	48	STD
	B-2	0	48	CLP
	B-3	24	48	STD
	B-4	24	48	CLP
Offset frontal collision	C-1	48	0	STD
	C-2	48	0	CLP

* STD—Denotes the standard motorcycle
** CLP—Denotes the motorcycle equipped with the crushable leg protector

Collision Test Facilities

The collision tests were performed at JARI's collision test facility. This is shown in Figure 8 wherein the facility specifications in terms of towing speeds, propulsion drive, tow system, and test capabilities are set forth.

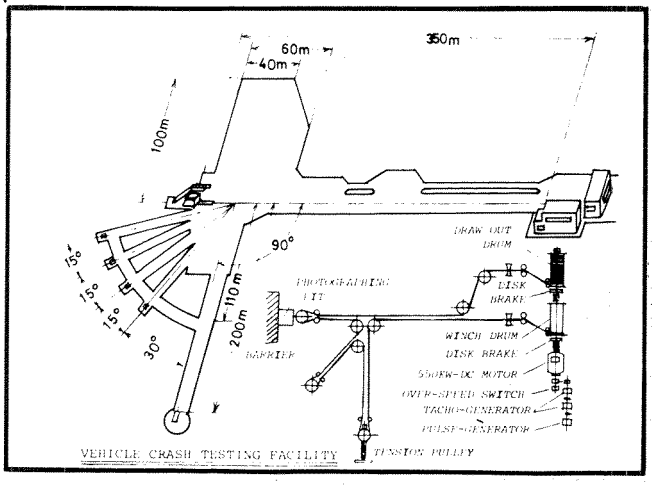

Figure 8. Specifications of JARI vehicle crash testing facility

The motorcycle was transported to the point of impact by the utilization of a four-wheeled trolley. The motorcycle was held in place by attachments at the handlebar, the lower section of the wheels, and the upper rear section of the motorcycle until its release just prior to impact. Figures 9 and 10 show from a frontal and side view the four-wheeled trolley used and the motorcycle mount system.

Measured Items

Leg Space and Fracture

The crushable leg protector device was evaluated for leg protection effectiveness by analyzing leg space preservation and leg fractures.

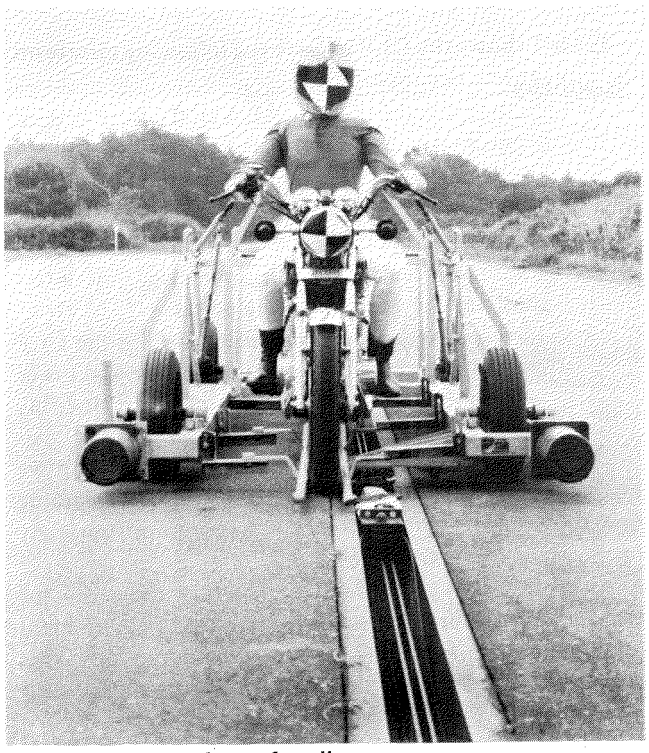

Figure 9. Front view of trolley

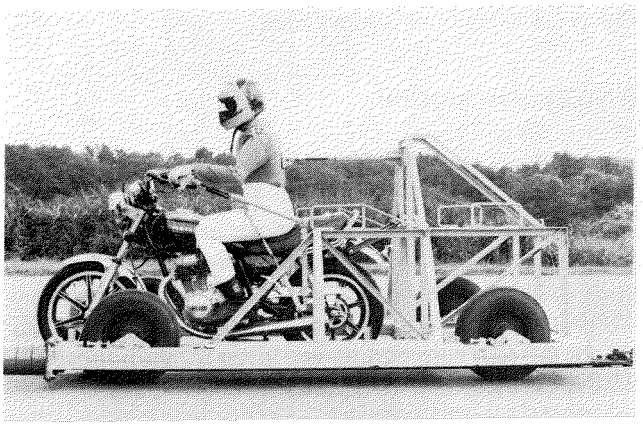

Figure 10. Side view of trolley

Energy Absorption

A triaxial accelerator was placed in the motorcycle at the point of its center of gravity. This was used to monitor the motorcycle acceleration and evaluate the effectiveness of the energy-absorbing component.

Head Velocity

As past studies indicated that reinforced-type leg protection structures possessed a potential to increase injury to the head and chest, the subject device was analyzed for such resultant effects. To evaluate these effects, a detailed head velocity and head travel analysis were performed, using photographic data.

Occupant Motion

In addition to the above, the dummy was further modified in that an accelerometer was placed at the hip. The lift of the hip was also measured to determine the tendency of the occupant to eject from the motorcycle.

Motorcycle Motion

Using film analysis, the motion of the motorcycle itself was observed.

Test Results

Leg Protection Effect

Leg Space

It was difficult to measure directly how much space existed around the leg at the time of the collision. Accordingly, the leg space was estimated on the basis of how near a reference mark on the opposing automobile came to a reference mark on the motorcycle.

Figure 11 shows the comparison between CLP and STD. In all cases, the motorcycle with CLP did preserve the leg space better than STD. The leg space in this design seems to be the minimum required for the prevention of bone fracture for a broadside collision at 48km/h, as discussed below.

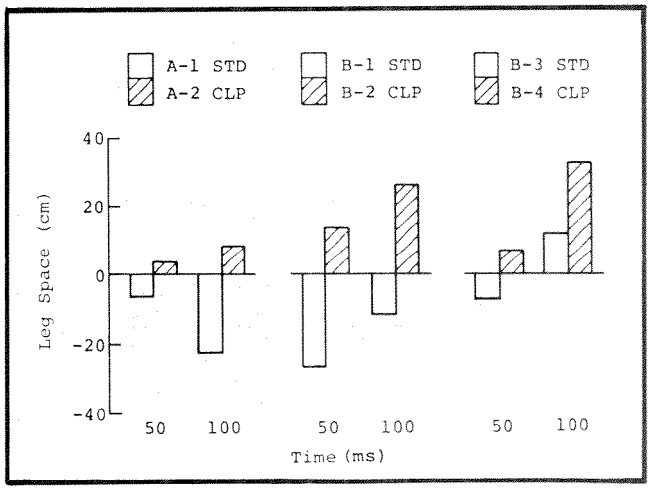

Note: Measurements were not obtained for A-3 and A-4 because of excessive deformation of vehicles

Figure 11. Comparison of estimated leg space

Leg Fracture

The state of the art of dummy technology for human injury analysis imposes some limits on the findings. The analysis of leg injuries was limited in scope because of the

lack of means of identifying the actual human injuries. Although it is believed the bakelite bone was a representative available means of identifying fracture modes in dummy analysis, it is also recognized there are limitations therein. Further research concerning the mechanisms of leg fractures is necessary.

For example, in the current test case, B-2, the bakelite bone did not fracture. It was found that the bakelite bone end experienced slippage at its connector; this was interpreted as a potential torsional fracture of the femur. To verify this, film analysis was used, and this showed that the enormous inertial loading would surely fracture the femur(9). Nevertheless, such experimental factors had to be addressed in interpreting the test results.

Note that in all tests, the leg of the dummy impacted against the front of the opposing automobile. Impacting of the leg resulted from the leg being caught between the motorcycle and opposing automobile or from the inertial force of the unrestrained leg itself. Figures 12 and 13 show examples of the bakelite leg bone fractures for tests A-3 and A-4, respectively.

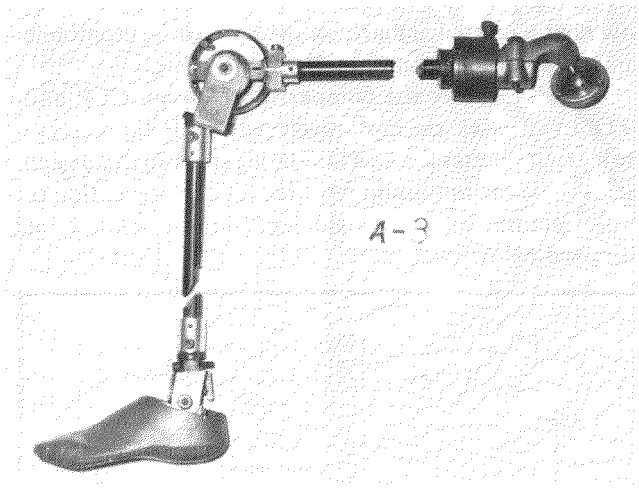

Figure 12. Example of bakelite leg fracture (test A-3)

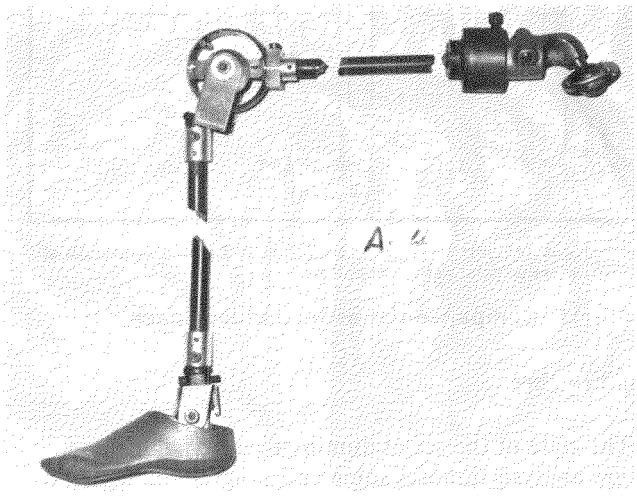

Figure 13. Example of bakelite leg fracture (test A-4)

Table 7 shows the CLP to have the following effects on the motorcycle occupant:

- In the angled collision (A1-A2), the CLP caused compression fracture in the upper leg that, in turn, may possibly extend to the pelvis.
- In the broadside collision (B1-B2), the CLP does reduce fracture of the lower leg and could cause a torsional fracture in the upper leg. The latter may possibly extend to the pelvis.
- In the offset frontal collision (C1-C2), the CLP caused transfer of bone fracture from the lower leg to the upper leg and such may possibly extend to the pelvis.

The fracture terminology shown is for descriptive purposes. It is recognized that generally both the bending and the compression fractures are more appropriately termed transverse fractures.

As used herein, the bending fracture describes the transverse fracture resulting from a bending moment applied to the bone. The compression fracture describes the transverse fracture that results from axial loading applied along the longitudinal axis of the bone.

Experimentally, such was determined by an examination of the shape of fracture point and film analysis of the motorcycle occupant's movement.

Energy Absorption

The object of the CLP was to reduce the motorcycle's acceleration due to impact by means of the energy-absorbing component. Therefore, the impact acceleration was measured for the broadside collision, which allows more accurate evaluation of the effect of the absorbing component. From the measurement, it was evident that the motorcycle acceleration was lower for the motorcycle with CLP than STD by approximately 10 percent.

Potential Head Injury

Head Velocity

The analysis of injury to the head and chest is necessarily incomplete. Not only is there lack of agreement in the medical field concerning injury criteria, but, in addition, appropriate dummy technology is lacking.

The potential for head and chest injury was evaluated by comparison of resultant head velocities relative to the opposing automobile after impact. A higher resultant head velocity indicated a higher potential for injury due to subsequent impact with the engine compartment, automobile roof, windshield, etc. For this study, velocity was chosen rather than acceleration because the latter is overly sensitive to impact angle, impact location, rigidity of objects, etc.

Table 7. Leg fracture data

STD	Test No.	A-1	A-3	B-1	B-3	C-1
	Upper Leg	Bending	Compression	Bending	Compression	None
	Lower Leg	Bending	Bending	Bending	Bending	Bending
CLP	Test No.	A-2	A-4	B-2	B-4	C-2
	Upper Leg	Compression	Compression	Torsional	Compression	Compression
	Lower Leg	Bending	Bending	None	None	None

Figure 14 shows the effect of CLP on resultant head velocity. In most cases, the motorcycle equipped with the CLP showed higher resultant head velocity than did the STD motorcycle. This shows potential for increased head and chest injuries due to CLP.

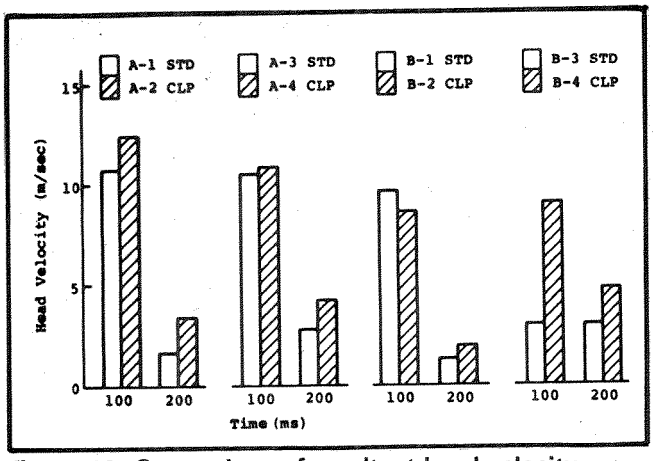

Figure 14. Comparison of resultant head velocity

Head Travel

Figure 15 shows the effect of CLP on horizontal head travel relative to the opposing automobile. More travel indicates more tendency for ejection. Ejection may result in the increased likelihood of impacting other vehicle structures.

In almost all cases, the CLP causes more travel across the opposing automotive engine compartment, meaning more ejection tendency.

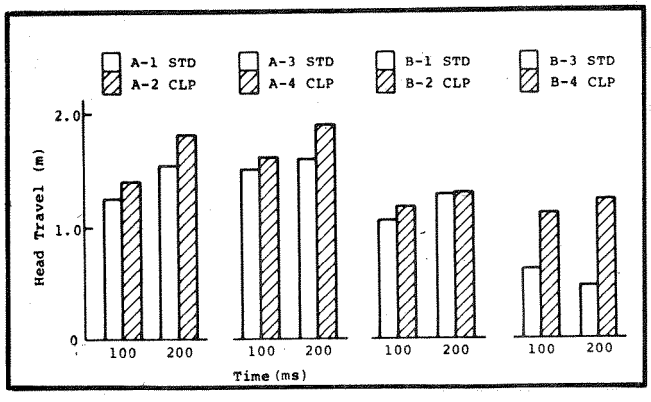

Figure 15. Comparison of horizontal head travel

Occupant Motion

To determine the tendency of the occupant to eject from the motorcycle, the lift of the hip was measured.

The results in Figure 16 show that the motorcycle with the CLP has higher hip lift than STD, showing that the CLP allows ejection more readily.

In performing the overall evaluation of leg space, energy absorption, and occupant motion, it appears the effect of leg space is so great in contributing to increased velocity of the motorcycle occupant's ejection that the benefits of the energy-absorbing component are overcome. In other words, the CLP-equipped motorcycle possesses the potential for increased injury.

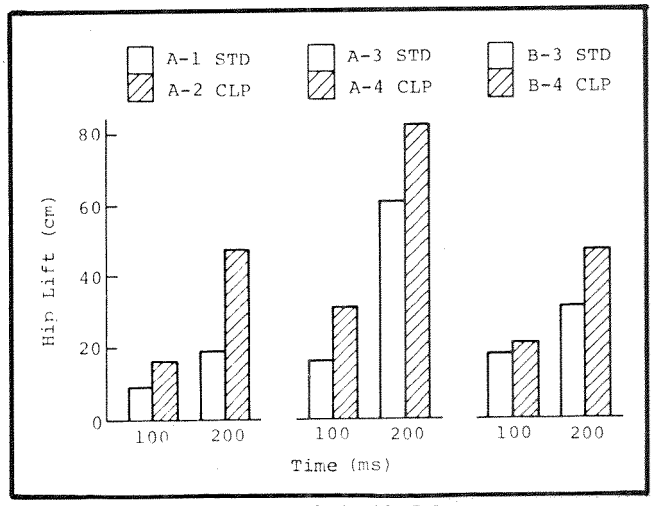

Note: Measurements were not obtained for B-2

Figure 16. Comparison of hip lift

Motorcycle Motion

An analysis of the film data showed that, at the time of collision, the STD overturns and comes to a halt after sliding for a short distance. The CLP exhibits a tumbling motion after impact, which may possibly involve third parties in the accident. In some conditions, this tumbling means the so-called highside phenomenon occurs.

Conclusion and Recommendations

The CLP was shown to be of generally sufficient structural strength for typical collision speeds and geo-

metries. In some cases, it did preserve leg space so the opposing automobile did not cause the leg to be trapped between the automobile and the motorcycle. In particular, the CLP prevented fracture to the lower leg in three of five cases. However, in at least one collision geometry, the CLP does seem to cause a torsional fracture of the upper leg, while with the standard motorcycle no torsional fracture circumstances were observed. This is a concern because it is believed the torsional fracture is a more serious injury. In summary, the CLP did not prevent injury to the motorcycle occupant's legs, but rather tended to move the site up into the upper leg and hip region.

Also, the energy-absorbing component appeared to function so the motorcycle's acceleration on impact was decreased to a degree.

However, the potential may still exist that the CLP may increase injury to the motorcycle occupant including the head and chest. As the velocity analysis shows, the motorcycle occupant in general had a higher ejection velocity when the motorcycle was equipped with the CLP. In one case, the velocity was significantly higher. This higher velocity produces a potential for more severe subsequent impact.

The motorcycle equipped with the CLP also tended to tumble for a long distance following the collision, while the standard motorcycle did not do so. The tumble condition could cause an accident or injury to third parties who were initially uninvolved in the motorcycle-automobile collision.

Based on the limited data, a fundamental problem appears to be the effectiveness of the CLP in preserving leg space may produce an undesirable increased velocity on ejection.

As there is a potential for the CLP that was presently tested to cause increased injury, the CLP device cannot be recommended for use on a motorcycle. Further study of human injuries in motorcycle collisions and of leg protection devices may be indicated.

References

1. Hurt, H.H., Jr., J.U. Ouellet, and D.R. Thom, "Motorcycle accident cause factors and identification of countermeasures," Contract No. DOT-HS-5-01160, Traffic Safety Center, University of Southern California, Los Angeles, California, 1981.
2. Bothwell, P.W., R.E. Knight, and H.C. Peterson, "Dynamics of motorcycle impact," Volume II, Motorcycle Crash Test Program, University of Denver, Denver Research Institute, Denver, Colorado, July 1971, NTIS PB-204-998, HS-800-587 (DOT), Contract No. F11-11-7307.
3. Uto, T., "Side collision test of motorcycles equipped with side protection devices," Rider Protection Working Group, Japan Automobile Manufacturers Association, Proceedings International Motorcycle Safety Conference, pp. 267-307, December 1975.
4. Bartol, J.A., G.D. Livers, and R. Miennert, "Near term safety improvements for motorcycles, Phase II," AMF Incorporated, NTIS PB-244-604, Report No. DOT-HS-801-653, Contract No. HS-4-00815, July 1975.
5. Bothwell, P.W., R.E. Knight, and H.C. Peterson, "Dynamics of motorcycle impact," Volume II,- Motorcycle Crash Test Program, University of Denver, Denver Research Institute, Denver, Colorado, NTIS PB-225-710, Contract No. DOT-HS-126-1-186, September 1973.
6. Bartol, J.A., G.D. Livers, and N.R. Hirsch, "Near term safety improvements for motorcycles," AMF Incorporated, Report No. B24-101-73, Report No. DOT-HS-800-971, Contract No. DOT-HS-257-3-584, November 1973.
7. Yamamoto, T. (1981), "Some basic considerations on occupant restraint systems for motorcycles," Rompe, K. (ed.), Sicherheit bei motorisierten Zweiradern, TUV-Akademie Rheinland, Koln, pp. 257-278, December 1980.
8. Motoshima, T., "Studies on the strength for bending of human long extremity bones," *Magazine of Kyoto Prefectural*, University of Medicine, Vol. 68, No. 6, pp. 1377-1397, September 14, 1960.
9. Sonoda, T., T. Zeniya, and S. Ibuki, "A study on the strength for torsion of human extremity long bones," *Magazine of Kyoto Prefectural*, University of Medicine, Vol. 71, No. 8, pp. 710-714, September 1962.

Aspects of Motorcycle Braking

G.L. Donne and
P.M.F. Watson
Transport and Road Research Laboratory, Department of Transport, Crowthorne, Berkshire, United Kingdom

Abstract

This paper discusses the problems inherent in the braking of motorcycles and other powered two-wheeled vehicles and suggests ways in which antilock brake systems and other engineering measures can assist riders. Evidence is presented of the failure of many motorcyclists to brake effectively, and it is suggested that advances in engineering will lead eventually to an improvement in braking behaviour. Results obtained by the antilock system installed in ESM-2 are compared with those obtained by a variety of riders.

Introduction

For many types of vehicle, incorrect or inappropriate brake application is not critical under most circumstances. With powered two-wheeled vehicles (PTWV), however, the situation is different. A mistake by the rider that leads to either wheel being overbraked will cause the machine to skid, become unstable, and capsize. The consequences can be serious, depending on surrounding traffic conditions and nearby obstacles. The incidence of skidding in personal-injury accidents has been higher for PTWV than other vehicles(1) for many years, and more recent data show no sign of this decreasing (Table 1).

The high incidence of skidding in PTWV accidents is an illustration of the difficulties faced by riders in braking such machines effectively. Motorcycles are inherently difficult to brake safely and efficiently because of a number of factors: a large load transfer from rear wheel to front wheel during braking, separate controls for front and rear brakes, and a wide variation in the proportion of front and rear brake effort required on different surfaces to give optimum performance.

The rider is faced with the almost impossible task of assessing these factors and applying correctly the necessary control inputs. Failure to do so is manifest in two main ways: simple misjudgment of brake application leading to the high incidence of skidding already mentioned and reluctance to apply high brake efforts because of the known skidding risk, which leads to unnecessarily long stopping distances. In addition, there are problems related to the design of particular machines, such as inadequate provision of brake power and susceptibility to the effects of water on the brake friction surfaces.

As in all aspects of riding a motorcycle, the experience and skill of the rider must play a considerable part in the effective and safe application of braking. Nevertheless, the task is so complex that it is beyond the abilities of the majority of riders, however experienced or well trained they are. Although training has a part to play, engineering measures applied to the machine appear to offer the greatest possibility of bringing about an improvement in PTWV braking generally. ESM-2 is equipped with antilock brakes that probably offer the greatest potential benefit of any such measures. The various factors involved in PTWV braking and the ways in which antilock systems and other measures can improve matters are now discussed.

Load Transfer During Braking

All vehicles are subject to the transfer of load from rear to front wheels as a result of the deceleration produced during braking. This effect produces changes in the levels of brake effort that can be safely applied, generally increasing those on front wheels and reducing those on rear wheels. In the case of cars and most commercial vehicles, which have wheelbases that are long in relation to the heights of their centres of gravity, the effect is less severe. A motorcycle with its rider has a centre of gravity that is very high in comparison with its wheelbase. This leads to considerable load transfer and produces a wide range of optimum brake distributions, which depend on the deceleration required and the road surface type. With PTWV, this effect is significant. For instance, it is

Table 1. Incidence of skidding in injury accidents in Great Britain—1983

	Dry			Wet			Ice/Snow			All Conditions		
	Skidded	Total	%	Skidded	Total	%	Skidded	Total	%	Skidded	Total	%
PTWV	6338	47375	13	5162	17471	34	695	1113	62	12195	65959	18
Other Vehicles	19024	197930	10	17976	106058	17	3650	7330	50	40650	311318	13

estimated that load transfer prevents a deceleration of more than about 0.36g when the rear wheel only is braked, even on a surface with a high friction coefficient(2). Simple measures such as a fixed relation between the brake efforts of the two wheels or valves that reduce rear brake effort are not sufficient to counter the difficulties caused. Because almost all PTWV have separate means of application for front and rear wheel brakes, it would be possible for the rider to make continuous adjustments to the levels of each. However, as already illustrated, the task is too difficult to permit even an approximation to optimum braking, particularly under adverse road surface conditions.

A braking system in which the brake effort is related to the behaviour of the braked wheel would overcome the problems caused by load transfer. The antilock system that is fitted to both brakes of ESM-2 does just this.

Each wheel is continuously monitored during braking, and brake effort is reduced if the level of wheel deceleration reaches a value at which the wheel locks. In this way, the maximum braking effort obtainable on any surface can be reached without danger of instability caused by wheels locking.

Braking While Cornering

It is not uncommon for a PTWV to brake while it is also changing direction. This situation can arise not only when it is necessary to reduce speed unexpectedly while negotiating a bend, but also during attempts to avoid an obstacle in an emergency. When a two-wheeled vehicle changes direction, the angle of inclination of the machine is adjusted to take account of the centrifugal force that is induced.

A reaction, in the form of a sideway force at the tyre contact area, is developed. This force is related to the mass of the machine and rider, the square of their tangential speed, and inversely to the radius of the curve traversed. Depending on the magnitude of these factors, it can be shown(1) is a minimum coefficient of friction that must exist to enable the cornering manoeuvre to be accomplished without braking. The frictional force between tyre and road must be divided between components for the sideways force required for cornering and the braking force. If grip is low and the cornering force requirement is high, there may be little left for braking.

This situation adds another variable to the rider's problems in achieving a balance between safe and effective braking. It means that instability will occur if either the cornering radius is reduced while hard braking is being undertaken or if brake force is increased while traversing a curve of fixed radius. However, if the level of braking applied to a wheel is controlled by a system that continuously monitors wheel behaviour, whatever component of the overall coefficient of friction between tyre and surface that remains after sideway force has been generated will be available for braking.

If, for instance, a rider has to make an abrupt change of direction while braking hard, there is no danger of wheel lock because the brake effort will be reduced to accommodate the side force requirement. The antilock system fitted to ESM-2 works in this way.

Braking in Wet Conditions

In addition to causing problems by acting as a lubricant between tyres and road surfaces, rainwater can affect the frictional properties of motorcycle brakes. It has been recognised for several years that disc brakes have been prone to problems in some wet weather conditions(3). Under these conditions, a laminar film of water exists between the brake pads and the disc and prevents dry contact. In extreme cases, it appears the only braking force generated between disc and pads is that due to the sheer strength of the water film(4). The motorcycle rider is thus faced with the possibility of extremely low brake power being available in wet conditions. The effect is, however, unpredictable and variable in its extent, which leads to considerable difficulty for the rider in judging the correct control input to give the required vehicle deceleration. It is reasonable to assume this effect has contributed to a considerable number of motorcycle accidents and is another factor that leads to the high incidence of skidding in two-wheeled vehicles.

An investigation of the factors involved in the performance of motorcycle disc brakes in wet conditions has been made by TRRL(5,6). This took the form of measuring the braking distance of an experimental motorcycle under controlled conditions.

The results obtained with a completely dry brake system were compared with those obtained when the brake friction surfaces were wetted at various rates from a supply of water carried on the machine. Many hundreds of test runs were made, using a variety of brake disc and pad materials with water applied over a considerable range of flow rates. As a method of quantifying the performance of a particular brake system, the term "wet retention" was used. This is the ratio of dry brake to wet brake stopping distances from the same test speed, expressed as a percentage. It was found in some cases that brake systems using standard pad materials were capable of a wet retention of only 15 to 20 percent, and it was uncommon to obtain a figure in excess of 60 to 70 percent even at very high levels of braking. (It is important to bear in mind that wet brake problems are most likely to occur under circumstances in which the available tyre/road adhesion is low and high braking forces are not appropriate.)

Although variations were found in the performance of brake systems depending on disc material, the most

significant factor was the selection of the pad material; sintered metal compositions were found to exhibit very little deterioration when wet, whereas some conventional organic materials were very poor and could not reach an acceptable standard. As a result of this work, a type approval test for wet brake performance has been incorporated into ECE Regulation 13. This specifies a minimum wet retention of 60 percent, based on a dry brake deceleration of $3m/S^2$ with water applied to the brake at 15 litre/h. Although the conditions are not particularly stringent, the advent of the type approval test and the interest generated by the research programme results have led to the use of friction materials that are better than those of recent years, and a range of sintered metal pads is commercially available for the majority of motorcycles. It is hoped this use of suitable friction materials will, in due course, eliminate the problems of inconsistent braking in wet conditions.

Antilock systems have a secondary role in overcoming wet brake inconsistency. Clearly they can do nothing to restore normal friction between brake discs and pads that are wet. They can, however, prevent wheel lock that might result from excessive brake torque becoming suddenly available when the water film is penetrated during a braking stop. However, the prime requirement is that motorcycles be equipped with brake systems that offer a consistent performance whether or not the friction surfaces are wet, thereby presenting riders with a less complex task. There seems to be scope to increase the requirements of the ECE test eventually, for example, either by increasing the wet retention requirement or by reducing the dry brake deceleration on which the test is based. This latter change would be an additional step toward consistency.

Antilock Braking

The high incidence of skidding in accidents that involve motorcycles has been mentioned already along with some of the factors that lead to it. This problem has been recognised for many years, and an experimental antilock installation on the front wheel of a motorcycle was produced at TRRL more than 20 years ago. This demonstrated the effectiveness of the principle of antilock on a two-wheeled vehicle in that riders were able to retain control of the machine in adverse conditions and, in some cases, braking distances were shorter using the system than when riders braked without it. A version of the Dunlop Maxaret system, which was used on aircraft, formed the basis of this experimental installation. This employed a flywheel overrun device to control the brake effort applied to the roadwheel. A system that could have been developed into a commercially acceptable unit was fitted to the first TRRL experimental safety motorcycle, ESM-1(1,7). This sensed wheel behaviour electronically and produced excellent results on machines ranging from a $200cm^3$ lightweight to one of the largest and heaviest motorcycles produced.

ESM-2 is fitted with an antilock system developed by Lucas Girling to both front and rear wheels. Wheel behaviour is sensed by a small flywheel driven via a toothed belt from the roadwheel hub. Under braking, the flywheel follows the deceleration of the roadwheel unless the latter reaches an unsafe level (equivalent to a vehicle deceleration of about 1.2g). At this point, the inertia of the flywheel is such that it cannot respond to the roadwheel deceleration, and it overruns. As it does so, it operates a valve that reduces the hydraulic pressure applied to the brake and allows the wheel to regain a safe level of deceleration. This causes the control flywheel to return to the state of following the roadwheel acceleration, and full braking is reapplied. This cycle of events continues until the vehicle comes to rest. The system on ESM-2 is similar to the Lucas Girling Stop Control System, which is to be made available for cars(8,9)

Many hundreds of experimental braking distance measurements have been made with the various antilock systems that have been developed for motorcycle use. In this way, considerable experience has been gained in the ways in which such systems might be of benefit and their performance relative to that of test riders. Limited results have also been obtained with a small number of riders with a range of limited experience(1). However, there are no data available either on the performance of antilock systems on motorcycles that are in service or from performance measurements obtained with a large number of riders. To provide this information, two trials have been conducted.

The Field Trial

A number of machines have been equipped with the Lucas Girling system, as on ESM-2, and issued to police forces to be used in their patrol vehicle fleets. The first of these, a BMW K100, was handed over to Gwent police in May 1985. During the course of 2 to 3 years' use, the performance of the system from the point of view of effectiveness, reliability, and rider reaction will be monitored.

Each machine will be fitted with counters that will record the number of cycles of operation of the antilock installations. The information obtained from this trial is of great importance. For instance, little is known about the question of reliability in a system likely to operate only very infrequently. In experimental use, there has been no reliability problem, but in these circumstances the frequency of operation of the system is high. It will also be of interest to note the reaction of riders, particularly with regard to the amount of use they make of its braking capability.

Comparison Between Riders

In terms of system performance, comparison of braking distances achieved with the system operating with those obtained by riders with the system immobilised is valid. Twenty-one riders, ranging widely in experience and ability, were asked to achieve, using their normal technique, braking distances shorter than those obtained with the antilock system working. (Although the experimental machine was equipped with skids to prevent capsize, the locking of the rear wheel can cause a sideway skid, which could throw the rider from the machine. As a safety measure, the rear wheel antilock system was left operative throughout these tests.) The tests were conducted at the TRRL track on a wet, slippery surface (Bridport gravel macadam). Note was taken of the number of occasions on which riders locked the front wheel and caused the machine to fall onto the safety skid and any obvious cycling of the rear wheel antilock system.

Measurements were made from a nominal speed of 50km/h (30mi/h), and five runs were made by each rider using both brakes. In addition, a sixth measurement was obtained with the rider using only the front brake. Table 2 presents the complete results. As there was some variation in test speed between riders and within each rider's set of runs, the braking performance is expressed as average deceleration.

The results show that five riders were able to consistently equal or exceed the deceleration obtained by the antilock system. Of these, one is familiar with the characteristics of the TRRL surfaces and has been involved in the development of antilock systems. Two others are regular riders with long experience and two are occasional riders. Five riders achieved average decelerations that were at least 80 percent of those obtained by the antilock system. However, one of these, with over 30 years' experience, lost and regained control during three runs and two others had at least one run that resulted in the motorcycle falling on a skid. The remaining eleven riders comprised three who were unable to achieve decelerations of 50 percent of that reached by the antilock system and eight who obtained values between 50 percent and 80 percent. In the former group was a rider of 30 years' experience who locked the front wheel in four of his runs and lost control.

Under the conditions of this trial where riders brake in a situation of no danger from losing control of the machine or of striking an obstacle, it is to be expected that those with skill and a degree of familiarity with the test surface will achieve results comparable with those of the antilock system. However, a number of riders were consistently unable to avoid losing control because they misjudged braking effort and locked a wheel. This failing seemed not to be related to experience. It is interesting that a number of riders were successful in completing five runs using both brakes but failed when asked to use only the front brake. This suggests they were unable to adjust quickly to the greatly reduced deceleration that was

Table 2. Average decelerations obtained by 21 riders braking without front wheel antilock compared with average deceleration using antilock (wet, slippery surface)

Rider No.	Average Deceleration % g	Remarks	Rider No.	Average Deceleration % g	Remarks
1 Regular rider with knowledge of test surface	47) 48) 46 Both 39) brakes 52) 46) 27 Front brake only		5 31 Year's experience	22) 42) 31 Both 30) brakes 32) 31) 19 Front brake only	Slight wheel lock—front Slight wheel lock—front Slight wheel lock—front
2 38 Year's experience	34) 36) 38 Both 40) brakes 39) 42) 28 Front brake only		6 25 Year's experience	25) 29) 34 Both Fail) brakes 40) 42) Fail front brake only	
3 Motorcycling writer	23) 27) 24 Both 23) Brakes 24) 30) 14) Front brake only		7 30 Year's experience	32) 26) 25 Both 29) brakes 20) 17) 15 Front brake only	
4 31 Year's experience	Fail) Fail) 19 See Fail) Remarks Fail) 19)	Rider chose to use only front brakes—his normal method	8 Regular rider	31) 31) 33 Both 30) brakes 38) 36) 23) Front brake only	Slight wheel lock—front

Table 2, continued

Rider No.	Average Deceleration % g	Remarks	Rider no.	Average Deceleration % g	Remarks
9 15 Year's experience	27) 37) 36 Both 36) brakes 43) 38) 27 Front brake only		13 13 Year's experience	25) 23) 23 Both 20) brakes 23) 26) Fail front brake only	Slight wheel lock—front
10 15 Year's experience	41) 38) 39 Both 39) brakes 39) 39) 29 Front brake only		14 4 Year's experience	Fail) Fail) 30 Both Fail) brakes 29) 31) Fail front brake only	Wheel lock—front Wheel lock—front Wheel lock—front
11 12 Year's occasional	34) 34) 35 Both 34) brakes Fail) 38) 18 Front brake only		15 10 Year's occasional	27) 26) 24 Both 31) brakes 29) 35) Fail front brake only	Slight wheel lock—front
12 2 Year's experience	17) 16) 17 Both Fail) brakes 17) Fail) Fail front brake only		16 6 Year's experience	16) 27) 22 Both 24) brakes 21) Fail) Fail front brake only	Several slight wheel locks—front Slight wheel lock
17 4 Year's experience	40) 45) 43 Both 47) brakes 36) 47) Fail front brake only	Slight wheel lock—front	21 Not ridden for 25 years	14) 16) 15 Both 13) brakes 16) 18) 11 Front brake only	
18 Occasional rider	46) 40) 41 Both 41) brakes 37) 39) Fail front brake only		Antilock operating on both wheels	36) 41) 38	
19 6 Year's experience	36) 26) 29 Both 27) brakes 26) Fail) Fail front brake only	Several slight wheel locks—front			
20 7 Year's experience	22) Fail) 24 Both 26) brakes Fail) Fail) Fail front brake only	Rear wheel lock Front wheel lock Front wheel lock			

possible and indicates that, when confronted with a strange situation, many riders commit errors. As mentioned, attempts were made to record cycling of the rear brake antilock system so that runs in which it was present could be counted as rider failures. It is likely there were occasions on which riders were able to obtain more braking from the rear wheel because of the antilock system than they would have if the system had been immobilised.

While the antilock system produced shorter braking distances than did many of the riders in this trial, it is the stability that it confers, particularly in an emergency, that is more likely to lead to a reduction in skidding accidents than any improvement in overall braking distances. However, if reliable and effective systems become common in the motorcycle population, there will undoubtedly be such an improvement as riders gain confidence in their operation and brake accordingly.

Antilock Systems for Small Machines

All the antilock systems mentioned above are applicable only to machines equipped with hydraulically actuated brakes. Disc brakes actuated by this means are now common on motorcycles. However, in the United Kingdom about 60 percent of the PTWV are lightweight machines with a capacity of 150cm^3 or less and mopeds. Many of these are fitted with mechanically operated disc brakes or drum brakes. It is, of course, technically impossible to equip such machines with the Lucas Girling antilock system unless their brake systems are redesigned and, additionally, such cheap machines would be unlikely to stand the cost imposed by such an addition.

A purely mechanical system has been devised and is under development for machines fitted with any type of brake that acts on the roadwheel hub. This system is illustrated schematically in Figure 1, and its method of operation is as follows.

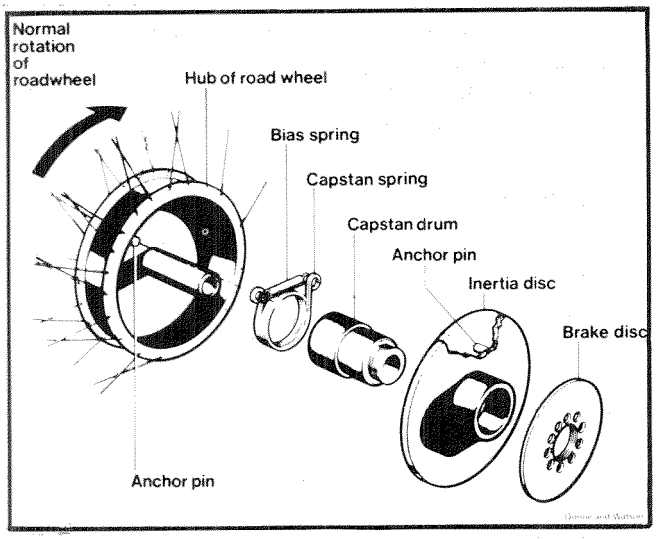

Figure 1. Capstan antilock brake system

The hub of the roadwheel carries a capstan drum that is free to rotate independently. Around the drum is wrapped a spring, one end of which is pinned to the roadwheel and the other is attached by a pin to a flywheel, itself free to rotate through a limited angle independently of all other components. A brake disc (or drum) is attached to the capstan drum. The flywheel is held at one end of its rotational travel by a light spring. In normal conditions, all parts of the device rotate together and, under braking, the wrapped spring connects the brake disc to the roadwheel. If, however, the wheel decelerates at a high rate, the flywheel overruns against the force of its bias spring and partially unwraps the spring from the capstan drum via the end that is pinned to it. This disconnects the brake disc and roadwheel, thus removing the brake torque and allowing the wheel to regain speed. When it reaches the speed of the flywheel, the spring is again tightly wrapped and brake torque is reapplied to the wheel. This sequence is repeated until the vehicle comes to rest.

It is unlikely this system will have the finesse of those with electronic wheel speed sensing or those that employ overrunning flywheels for sensing alone. (The flywheel in the capstan spring system provides the modulating force in addition to sensing wheel deceleration, hence it needs relatively high inertia.) However, if a satisfactory overall performance is attainable, this system should be relatively cheap to produce and could be fitted to almost any cycle, moped, or motorcycle, whatever the mode of brake operation.

Effect of Suspension Movement on Operation of Antilock Systems

Telescopic front forks are fitted to the majority of motorcycles for several reasons. They are simple and economical to manufacture, keep unsprung weight to a minimum, are aesthetically acceptable, and may be replaced as a unit in the event of minor machine damage. However, there is evidence(10) that such a suspension arrangement can not only lead to instability but is mechanically inadequate in some circumstances, particularly if antilock braking is applied to the front wheel. This is brought about by the cyclic behaviour of the antilock installation and the fact that such systems operate at a level of brake force near the maximum available. Study of high-speed cine film of a BMW R100, similar to ESM-2, braking using the Lucas Girling antilock system has revealed several aspects of suspension behaviour, which need more study to assess their implications. For instance, when using the front brake (either alone or with the rear) on a high-grip surface, the initial effect is for the front suspension travel to be fully used followed by considerable rearward bending of the fork legs. This reaches a maximum as wheel lock approaches. As brake force is reduced by the antilock system, a partial recovery of the forks occurs, and this cycle continues until the machine comes to rest. Perhaps the most important effect is the modification of the behaviour of the front wheel caused by fork flexing and suspension movement. In both circumstances, the wheelbase of the motorcycle changes, generally becoming shorter than in the static state. The result is that an acceleration is imparted to the front wheel in addition to that caused by braking torque alone. In the case of the R100, a rearward deflection of 65mm at the wheel spindle was noted when braking from a speed of 50km/h with the antilock system operative. This alone produces an apparent wheel acceleration of nearly 10 percent of the deceleration due to braking. This lasts for about 80ms; during shorter time periods, it is possible that larger accelerations occur. A film speed higher than the 200 frame/s used would be necessary to obtain

sufficient resolution to estimate these effects. The superimposed acceleration of the wheel could, depending on its sign, inhibit a necessary operating cycle of an antilock system or lead to an unnecessary one. In either case, the antilock system would operate in a less than fully effective manner.

TRRL is examining front suspension systems other than those based on telescopic forks and is fitting a centre hub-steered design to a BMW R80, similar to ESM-2, for evaluation. Such suspension designs are inherently stiffer than telescopic forks and should result in less interference to the operation of antilock systems.

Rider Behaviour

It is clear from the above there are many aspects of the PTWV that make safe and effective braking difficult to achieve even if the rider is aware of the problems and behaves accordingly. There is evidence to suggest that, in addition to the practical difficulties, riders do not even attempt to brake in an effective manner in many cases(11).

To obtain short braking distances, it is essential that both brakes be used; this is the method advocated officially(12). However, Sheppard(11) suggests that among many motorcyclists there is the view that the front brake should not be used at all, almost certainly based on fear of a skid caused by locking a front wheel. In Sheppard's study, driving test records were examined, roadside observations of braking behaviour were made, and riders were interviewed regarding their braking technique. It was found in about one-quarter of the driving test reports studied mention was made of a fault of some severity during the emergency stop, particularly "omits use of front brake." A similar incidence of poor braking technique was not found in car test candidates(13). From roadside observation of braking behaviour, it was noted that only in about half of the 5,410 cases did riders use both brakes under normal conditions, and even in emergency conditions only about one-third did so.

Clearly there is a considerable amount of incorrect and potentially ineffective braking by motorcyclists. There is obvious scope for improvement in rider training with more emphasis placed on braking technique in the driving test than at present. However, entrenched attitudes and beliefs are difficult to change. It is possible that machine improvements such as the widespread fitting of antilock brakes eventually will produce a motorcyclist population that will have less fear of locking a wheel than is the case at present. It will then be likely that brakes will be used correctly. One control to apply both brakes would prevent riders from using only one brake; this would be most effective when used in conjunction with antilock systems on both wheels.

Conclusion

Accident statistics show that PTWV's are more prone to skidding than are other vehicles, particularly in adverse conditions. This is a result of features of the vehicles themselves and of incorrect techniques applied by riders. It is likely the former have led to the latter during the history of motorcycling and produced, for instance, a widespread fear of the use of the front brake.

Education and rider training have a part to play in leading to improvement in rider techniques, but the most direct approach to the PTWV braking problem is to adopt engineering measures that simplify the demands placed on riders.

The availability of effective wet-weather brake pads has reduced the problems of wet fade, but most other adverse features are inherent in the design of motorcycles. The effects of load transfer, cornering, and road surface coefficient on brake effort proportioning can be overcome only by the use of antilock systems that respond to the behaviour of the wheel as it is braked. Widespread use of such systems will eventually eliminate the effects of poor rider technique and will lead to an overall improvement in motorcycle braking performance generally.

Acknowledgments

The work described in this paper forms part of the programme of the Transport and Road Research Laboratory and is published by permission of the Director.

References

1. Watson, P.M.F., "Features of the experimental safety motorcycle—ESM-1," Proceedings Seventh International Conference on Experimental Safety Vehicles, U.S. Department of Transportation, NHTSA, Paris, 1979.
2. Newcomb, T.P., and R.T. Spurr, *Braking of Road Vehicles*, Chapman and Hall Ltd., London, p. 24, 1967.
3. "Braking in the rain with motorcycles fitted with disc brakes," LF 697, Transport and Road Research Laboratory, Crowthorne, August 1978.
4. Davis, J., and N.D. Woodcock, "Dynamometer investigation of the effect of water on motorcycle disc brake pad materials," SAE Paper 810409, Warrendale, Pennsylvania, 1981.
5. Donne, G.L., "The performance of motorcycle disc brakes when wet," Department of Transport, TRRL Report LR 1121, Crowthorne, 1984.
6. Donne, G.L., and P.M.F. Watson, "The influence of brake system properties on motorcycle braking performance," SAE Paper 810406, Warrendale, Pennsylvania, 1981.

7. Watson, P.M.F., F.T.W. Lander, and J. Miles, "Motorcycle braking," International Conference on Automobile Electronics, I.E.E., London, 1976.
8. Scarlett, M., oq'Braking ground," *Autocar*, February 27, 1985, pp. 30-31, Haymarket Publishing Ltd., Teddington
9. Ward, D., "Brake through," *Motor*, February 27, 1985, pp. 18-19, Business Press International Ltd., Sutton.
10. Wilkins, H.A., "Tests on a motorcycle with an anti-locking braking system fitted to the front wheel," Department of Scientific and Industrial Research, Road Research Laboratory, Laboratory Note No. LN/659/HAW, Harmondsworth, 1964 (unpublished).
11. Sheppard, D., B.A.K. Hester, Sonya Gatfield, and Monica Martin, "Motorcyclists' use of their front brakes," Department of Transport, TRRL Report, Crowthorne (in course of publication).
12. Department of Transport, "Your driving test," Leaflet DL 68, 1980.
13. Jenkins, D., "Car driving before and after passing the driving test," Department of the Environment, Department of Transport, TRRL Report LR 869, Crowthorne, 1979.

Motorcycle Rider Protection in Frontal Impacts

B.P. Chinn,
G.L. Donne, and
P.D. Hopes
Transport and Road Research Laboratory, Crowthorne, Berkshire, United Kingdom

Abstract

The problem of motorcycle rider injuries in frontal impacts is discussed in relation to the trajectory of the rider. Possible methods for reducing injury severity are also considered. A system is described that provides partial restraint to the rider in frontal impact and is combined with devices intended to reduce rider injury in other accident situations. Results are given of checks on this system by means of tests on a dynamic impact rig and in controlled vehicle-to-vehicle impacts.

Introduction

It is well established that powered two-wheel vehicles suffer an accident rate that is disproportionately high when compared with that for other vehicles on any basis. The results from general and detailed(1,2) investigations of accidents that involve motorcycles indicate that by far the most common vehicle conflict causing injury to motorcyclists is the frontal collision. About two-thirds of all collisions occur at an angle within 15° of head-on for the motorcycle. In many cases, the motorcycle is travelling at a normal traffic speed at the time of impact, and injuries are caused to the rider when he hits obstacles after being thrown from the machine. Studies of simulated impacts show that as little as 15 percent of a rider's kinetic energy is absorbed during the vehicle impact, leaving considerable potential for serious injury when an object is struck by his body. Clearly some form of energy-absorbing system must be incorporated into the motorcycle if any reduction is to be achieved in the injuries caused by frontal impact.

Various investigations into the mechanics of frontal impacts and possible rider restraint methods have been made. Severy(3) described a series of controlled impacts of motorcycles into stationary cars and concluded that the space between the rider and the impacted obstacle is wasted from the point of view of the absorption of rider energy, the characteristics of the motorcycle front provide a deceleration pulse for use with a rider-restraint system, and the rider moves forward in his seated position after impact until an obstacle is struck. Bothwell(4) examined a number of variables in a series of frontal impact experiments, including various restraint systems. Several researchers(5,6) commented on the problem of pitching of the motorcycle and suggested a rigid projection at a level above the centre of gravity to counteract this. Whitaker(7) investigated the trajectory of riders after frontal impact and examined the effects of a number of possible restraint devices. These were a chest pad, an airbag, and a block of energy-absorbing foam mounted on the fuel tank. TRRL produced prototype chest pad installations(7,8), but the acceptability problems of such devices are considerable.

Airbag installations can be envisaged that would intrude little into the traditional character of the motorcycle. Considerable research into the use of airbags for car occupant restraint systems has been conducted in the United States and elsewhere, and it appears possible that such devices will be used widely, at least in North America. Problems posed by the use of airbags in cars (sudden inflation in confined space, spurious inflation) either do not exist or may be easily overcome in motorcycle applications. The installation of an airbag

restraint system in conjunction with measures to protect against leg injuries(9,10) in the TRRL experimental safety motorcycle ESM-2 is described in this paper. The effectiveness of this system has been assessed in a programme of controlled impacts both on a dynamic test rig and with a free-running motorcycle into cars and barriers. In both cases, instrumented dummy riders are used and provide data on the decelerations and loads likely to be applied to critical areas of the human body. Results obtained with the restraint system in use are compared with those from tests using similar but unmodified motorcycles.

The Restraint System

In the form exhibited on ESM-2, this consists of a strengthened and modified version of the BMW RT fairing as fitted to twin-cylinder BMW motorcycles of 850 and 1,000cm^3 capacity. In addition, an energy-absorbing knee restraint is provided, and an airbag is mounted above the steering head on a bracket attached to the front fork assembly (Figure 1).

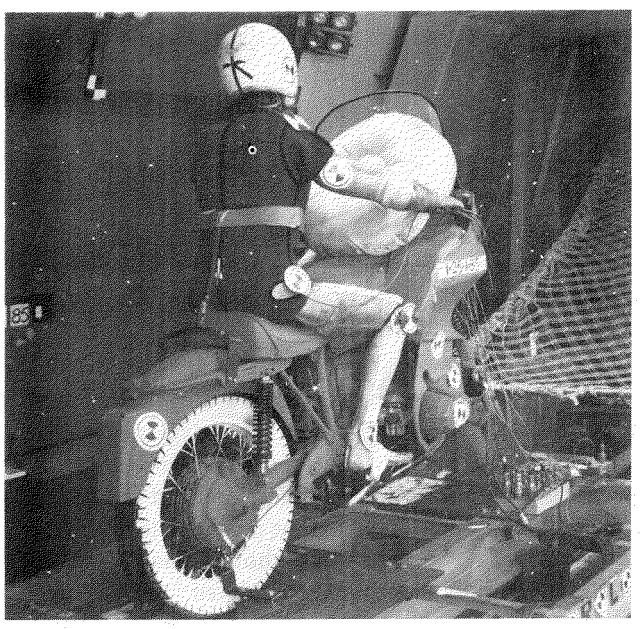

Figure 1. Airbag installed on impact rig test frame

The modifications to the fairing are a strengthened and extended bracket in the nose surrounding the headlamp to prevent pitching, a sheet metal instrument panel below the windscreen to provide increased stiffness and a reaction surface for the airbag, and a tubular steel internal structure to support the outer shell and provide lower limb protection in oblique impact(9,10). This last supports energy-absorbing knee restraints, which are present both to reduce knee injury and to modify the trajectory of the rider to induce rotation of the torso so load is applied to the inflated airbag in a substantially vertical direction.

The airbag itself is a prototype unit manufactured by Talley Industries in the United States and is of disc form, approximately 700mm in diameter and 250mm thick, with a volume of 70 litres when inflated. A pyrotechnic inflator assembly, 100mm in diameter and 50mm thick, is mounted on the front fork assembly and discharges directly into the bag, which is folded around it when not deployed. On inflation, the bag is at an angle of approximately 45° to the horizontal in side elevation and is supported by the handlebars, the front of the fuel tank, and the upper surface of the fairing with its strengthened areas.

One of the major problems with airbag installations in cars has been spurious deployment due to various causes such as high-intensity electromagnetic radiation from radar stations. This affects the deceleration-sensitive switches used to fire the bag inflators. In the ESM-2 installation, the bag inflator is fired by a switch activated by the seat of the motorcycle. This is mounted in such a way that it is able to slide forward under the effects of vehicle deceleration in an impact. In normal use, the seat is held in place by a section of aluminum honeycomb material, the dimensions of which determine the load at which the seat will move. Obviously it is essential that the actuating load level is set sufficiently high to prevent bag deployment in normal conditions of use. In calculating the dimensions of the seat assembly, it was assumed there would be at least some interaction between rider and seat during the bag initiation phase of the impact. Results from simulated impacts on the dynamic test rig(11) show it is possible to achieve reliable bag actuation with this system while maintaining sufficiently high seat sliding loads to prevent the possibility of accidental bag deployment.

As already stated, it is generally accepted by those in the field of motorcycle impact testing that a rider continues in his seated position after impact until an obstacle is struck. This does not provide the ideal situation for a practical airbag installation. It is essential the bag be well supported to withstand the loads applied to it by the rider. On a standard motorcycle, there is little possibility of providing this support for withstanding horizontally applied loads; in the ESM-2 installation, the rider trajectory is modified to cause rotation of the torso so a large proportion of the load is applied vertically. In this case, it is possible to provide support for the bag by means of the upper surface of the fairing, the instrument panel, and the fuel tank without markedly changing the character of the motorcycle. Rotation of the rider's torso is induced by the provision of energy-absorbing knee restraints attached to the rear of the fairing structure. After impact and as the rider moves forward in the sliding seat, his knees make contact with these restraints. The lower body is then decelerated, causing rotation about

the pelvis, which leads to his torso striking the inflated airbag.

Performance Tests

Two main methods of testing have been used to develop and assess the restraint system. First is the dynamic test rig(11) in which either a complete motorcycle or a simulation frame is mounted on a trolley that is subjected to an appropriate controlled deceleration from the test speed. The level of deceleration is chosen to simulate an impact. The second is controlled impacts on a test track, in which a complete motorcycle collides with a fixed barrier or part of another vehicle(10). In both cases, the motorcycle carries an anthropometric dummy to represent its rider. This carries instruments to record accelerations in the head, chest, and pelvis, and loads applied to the femur. In addition, all tests were recorded using high-speed cine cameras to enable analyses to be made of vehicle and rider trajectory and velocity.

Results

In the case of simulated impact on the test rig, there is no crushing of the motorcycle, such as would occur in a real vehicle-to-vehicle collision. Consequently, a Hypothetical Vertical Barrier (HVB) was used as a datum to enable comparisons to be made of rider velocity and energy between the various test conditions. The HVB was placed ahead of the test motorcycle by a distance that depended on the recorded deceleration achieved. In the analysis of high-speed film records, the dummy rider was assumed to have struck the HVB, which simulated an obstacle struck by the motorcycle. Figure 2 gives the kinetic energy of the rider on striking the HVB in three tests: using an unmodified motorcycle, with two pre-inflated airbags, and with one impact-actuated airbag. The energies were calculated using the rider linear and angular velocity and the mass and inertia of the torso. The test with two airbags (one mounted on the steering head and one on the petrol tank) was conducted to assess the effects of a large airbag installation.

It is clear that modifications to the motorcycle impart more rotational energy but greatly reduced linear energy to the rider compared with the standard machine. In the case of the double airbag installation, the rider's linear kinetic energy was zero at the HVB and reduced by 30 percent with the single impact-actuated airbag. The total kinetic energy of the rider was reduced by 78 percent for the double airbag and by 30 percent with the single airbag in comparison with the standard machine.

Discussion and Conclusion

The work described is at an early stage. The airbags used were standard items, and no attempt was made to optimise their size or shape. Despite this, a 30 percent reduction in kinetic energy of the rider has been obtained when using one airbag. The use of an airbag designed specifically for motorcycle applications and the careful design of other components of the motorcycle to provide suitable crush characteristics should enable greater reductions in rider energy to be achieved.

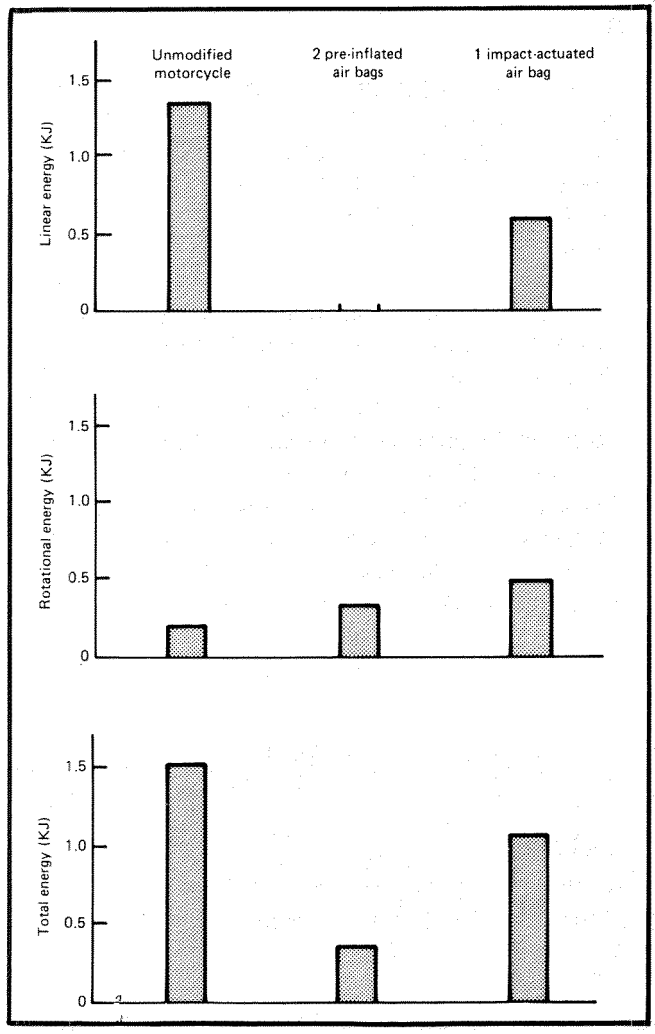

Figure 2. Rider torso kinetic energy at hypothetical vertical barrier

Preliminary analysis of a vehicle-to-vehicle impact indicates that a machine equipped with a single airbag provides a reduction in rider energy of 55 percent in comparison with a standard machine as he reaches a hypothetical point of impact of the motorcycle (the HVB).

Acknowledgments

The work described in this paper forms part of the programme of the Transport and Road Research Laboratory and is published by permission of the Director.

References

1. "Road accidents Great Britain 1983," H.M. Stationery Office, London.
2. Whitaker, J., "A survey of motorcycle accidents," Department of the Environment, Department of Transport, TRRL Report LR 913, Crowthorne, 1980.
3. Severy, D.M., H.M. Brink, and D.M. Blaisdell, "Motorcycle collision experiments," Proceedings 14th Stapp Car Crash Conference, SAE, 1970.
4. Bothwell, P.W., R.E. Knight, and H.C. Peterson, "Motorcycle crash safety research," Vehicle Safety Research Integration Symposium, U.S. Department of Transportation, May 1973.
5. Westcott, J.S., "Safety motorcycle," I. Mech. E. Automobile Division Proceedings, Vol. 189/75, 1975.
6. Hight, P.V., A.W. Siegel, and A.N. Nahum, "Injury mechanisms and motorcycle design," Proceedings IRCOBI Conference on Biomechanics of Injury to Pedestrians, Cyclists and Motorcyclists, Amsterdam, 1976.
7. Whitaker, J., "Motorcycle rider dynamics in frontal collisions," M. Phil. thesis, Brunel University, Uxbridge, November 1978.
8. Watson, P.M.F., "Features of the experimental safety motorcycle, ESM1," Proceedings Seventh International Technical Conference on Experimental Safety Vehicles, Paris, June 1979.
9. Chinn, B.P., M. Macaulay, and P.D. Hopes, "Leg protection for riders of motorcycles," Proceedings Tenth International Conference on Experimental Safety Vehicles, Oxford, July 1985.
10. Chinn, B.P., and M. Macaulay, "Leg protection for motorcycles," Proceedings IRCOBI Conference on the Biomechanics of Impacts, Delft, 1984.
11. "The impact test rig," LF 535, Transport and Road Research Laboratory, Crowthorne, 1975.

Motorcycle Conspicuity in Daylight

G.L. Donne
Transport and Road Research Laboratory, Crowthorne, United Kingdom

E.J. Fulton
Institute for Consumer Ergonomics, United Kingdom

P.G. Stroud
Loughborough University of Technology, United Kingdom

Abstract

In recent years, a series of studies has been conducted by the Institute for Consumer Ergonomics for the Transport and Road Research Laboratory concerned with finding effective and acceptable ways of improving the conspicuity of motorcycles in daylight. The relative effectiveness of clothing for riders, lighting, and other treatments for motorcycles was examined. Results from these studies have shown there are ways of effectively increasing motorcycle conspicuity in a wide range of daylight situations. Pairs of daytime running lamps, large dipped headlamps, or clothing displaying a large fluorescent area are all effective. Small headlamps on low-powered machines or small areas of fluorescent treatment are not effective.

Introduction

Detailed investigation conducted by the Transport and Road Research Laboratory into accidents between motorcycles and other vehicles concluded that, in almost one-third of the accidents, another vehicle driver had not seen the motorcycle prior to the collision(1,2). The accidents occurred principally at junctions in urban areas, and many involved manoeuvres in which other vehicles infringed on the motorcycle's right-of-way. Using 1983 data, it is estimated that approximately 18,000 motorcycle accidents are of this type each year in Great Britain(3). There appeared to be several reasons why people might fail to see motorcycles. Because of their small size, they can be obscured easily and are able to travel in positions on the road where other road users do not expect or search for traffic. Also, because of their irregular outline and the dark colour of much specialist motorcycle clothing, they do not readily stand out. Some of these qualities are inherent in the nature of motorcycles themselves, but it seemed likely that accident numbers could be reduced if the conspicuity (i.e., ability to attract attention) of motorcycles was improved.

A programme of work was conducted(4,5) to examine ways of achieving this. Treatments to the motorcycle, such as the use of various types of lights and fluorescent materials, and the use of special clothing for riders were considered.

There were thought to be advantages in machine-based options over those affecting riders because they are

permanent features and the motorcycle itself is already subject to vehicle legislation that could be readily adapted if necessary.

Options Assessed

Several different types of aids to conspicuity were examined.

Fluorescent Materials

These were applied to both rider and machine-based items, such as legshields, headlamp cover, sleeves, waistcoat, jacket, and helmet. The items of clothing conformed to BS 4610:1970, specification for high-visibility clothing.

Headlamps

Standard headlamps with a dipped beam were used and ranged in size from 100 to 180mm in diameter and in power from 18 to 55W. The effects of modulating the output of such lamps and the use of high-intensity bulbs in the parking light position were also assessed.

Running Lamps

These are specially designed lamps, measuring 100 by 80mm, fitted with a multiprism lens. They were used either in pairs, mounted on the motorcycle handlebar approximately 1000mm above the ground and 410mm apart, or singly, centrally mounted below the headlamp (Figure 1). They were assessed with a variety of bulbs, ranging in power from 6W tungsten to 15W glass-halogen. Luminous intensity along the central axis of each lamp varied from less than 100 to 825cd depending on the bulb fitted.

Methods

Several assessment methods were used at different stages in the investigation to compare the effectiveness of the proposed conspicuity aids. The measure of effectiveness used by all methods was based on judgments by numbers of people about the presence or otherwise of motorcycles with and without the test options. In all cases, the control condition comprised a motorcyclist in dark clothing on a motorcycle with its lights switched off and with no special conspicuity treatment. This type of measure was used because conspicuity is not only a matter of physically measured properties of an object but also of the physiological and psychological characteristics of observers.

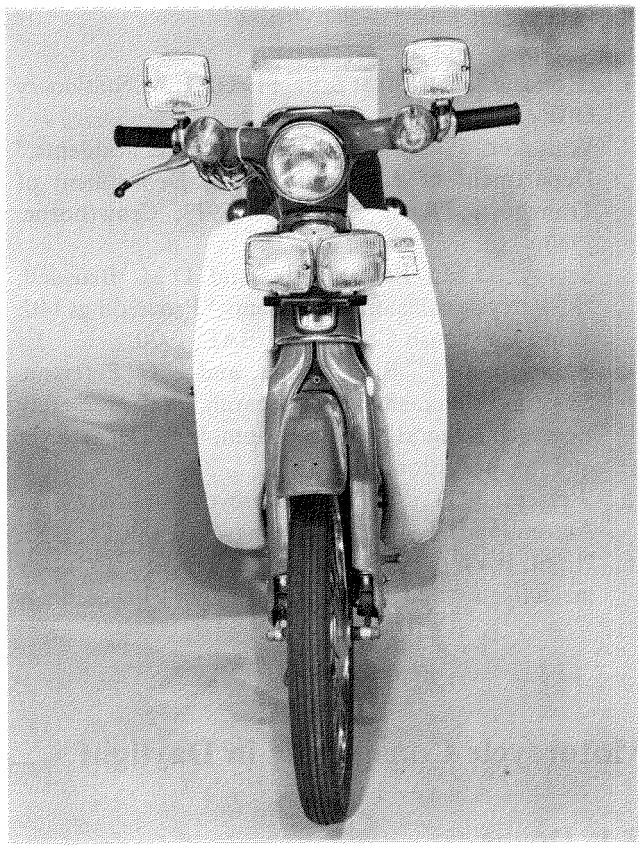

Figure 1. Experimental motorcycle fitted with a pair of running lamps and double running lamps

First, as a rough sorting procedure, a laboratory-based tachistoscopic experiment was conducted using slides of street scenes that included motorcycles. The mean time taken by subjects to detect the motorcycle using each of the test options was used as a measure of its effectiveness compared with the control condition. A short detection time indicates a conspicuous option.

Second, using those options that had offered improvements over the control condition in the first experiment, a field trial was conducted. A motorcycle and rider were positioned in a side street, and pedestrians who crossed the street at its junction with the main road were questioned to determine whether or not they had seen the motorcycle. This method enabled data to be collected from a large number of people. To avoid influencing subjects' responses, it was found to be essential they were unaware of the nature of the experiment. In this case, the percentage of subjects who detected the motorcycle was used as the measure of the effectiveness of each option as a conspicuity aid. The higher the percentage of detection, the more effective the option. This method has the advantage that large amounts of data can be gathered economically and from people who are unaware of the purpose of the experiment and their own part in it. However, it differs from the driving situation in important respects: subjects are pedestrians, and the motorcycle is stationary.

A third method was developed that used drivers as subjects and in which the test motorcycle was moving. Subjects, seated in the driving position in a car, were allowed brief glimpses through a shutter along the road ahead of them. The road might not contain any traffic or there might be just the vehicles that were incidentally present, but sometimes there would be the test motorcycle. The measure of conspicuity was based on the frequency with which experimental options were detected, compared with the control condition of the motorcycle.

Results

Results for the three methods are presented separately below.

Method 1—Laboratory Trial

Table 1 shows the mean detection times for 100 subjects. It was apparent that small areas of fluorescent material (e.g., sleeves and headlamp covers) provided no significant improvement over the control.

Table 1. Mean detection times for options using fluorescent material—laboratory method

Experimental Option	Mean Detection Time (seconds)
Control-not fluorescent	1.090
Legshields-fluorescent from front	1.048
Jacket-completely fluorescent	0.896*
Headlamp Cover-fluorescent from front	1.070
Helmet-covered in fluorescent material	1.008
Waistcoat-completely fluorescent	0.880*
Sleeves-completely fluorescent	1.116

* Denotes significantly better than control ($p < 0.05$)

Large areas of fluorescent material (e.g., jackets and waistcoats) were detected more quickly than the control condition.

Method 2—Pedestrian Field Trials

Pedestrian field trials were conducted at several sites on many separate occasions. There was a wide range of overall detection rates between sites, and Table 2 shows the range of detection rates for each option. In all, 18,596 subjects were involved.

Table 3. Mean values of ranks—road glimpse trials

Experimental Option	Mean Values of Ranks †
Control	2.68
40W, 180mm diameter headlamp	3.22*
1x15W Daytime running lamp-glass-halogen	2.90
2x15W Daytime running lamp-tungsten	3.11*
Fluorescent Jacket	2.99*

* Denotes significantly better than control ($p < 0.05$)

† Denotes always seen, 0 denotes never seen

Method 3—Road Glimpse Trials

For each subject, five sets of data were collected in the form of a seen (designated 1) or not seen (designated 0) response for each of the five motorcycle conditions. The five conspicuity aids were put into a rank order on a scale of 5 to 0 with 5 denoting the most seen. Table 3 shows the means of these scores obtained with 197 subjects at three experimental sites.

Table 2. Summary of results from pedestrian field trials

Experimental option	Range of Detection Rate %	Level of Performance Compared with Control
Control	7.1—26.5	—
Fluorescent helmet	15.2	No significant benefit
Fluorescent jacket/waistcoat	22.5	Significantly better
Small dipped headlamp. 100mm dia. 18W tungsten	17.3	No significant benefit
Small dipped headlamp. 100mm dia. 40W tungsten	3.9—29.5	No significant benefit
Small dipped headlamp. 100mm dia. 40W tungsten (flashing)	11.2—20.7	No significant benefit
Large dipped headlamp. 180mm dia. 24W and 40W tungsten	21.5—29.7	Significantly better in some trials
Large dipped headlamp. 180mm dia. 40W tungsten (flashing)	13.2—26.0	Significantly better at 1 site only
Large dipped headlamp. 180mm dia. 55W halogen	8.1—34.2	Significantly better at 2 sites only
1 x daytime running lamp. 10W tungsten	21.0—28.4	Significantly better in some trials
1 x daytime running lamp. 15W halogen	12.1—33.3	Significantly better at 1 site only
2 x daytime running lamp. 6W tungsten	30.8—38.0	Significantly better
2 x daytime running lamp. 10W tungsten	14.2—31.9	Significantly better
2 x daytime running lamp. 15W tungsten	18.7—44.7	Significantly better
Double daytime running lamp. 15W tungsten (2 running lamps mounted centrally, side by side)	11.5—37.7	Significantly better at 2 sites only
Small parking lamp—100mm dia. 15W halogen	12.5—28.8	No significant benefit
Large parking lamp—180mm dia. 15W halogen (high-intensity halogen bulb in parking light position of headlamp).	15.5—30.5	Significantly better at 1 site only

The results from field trials show that the use of small single lamps (including headlamps) provided no improvement in detection compared with the control condition.

All pairs of daytime running lamps, fluorescent jackets, and waistcoats performed significantly better than the control condition.

Results for large headlamps (i.e., those of 180mm diameter and 40W, or greater, power) were inconsistent but, in most cases, were an effective improvement over the control condition.

Conclusion and Discussion

The major conclusion from this work is that it is possible to improve the conspicuity of motorcyclists. Results show the most effective machine-based option assessed was a pair of daytime running lamps.

The use of headlamps has considerable appeal because they are machine-based and fitted to all machines. However, whereas the use of large, powerful headlamps was shown to confer benefits in some circumstances, small headlamps had no beneficial effect. In the motorcycle population of Great Britain, over 50 percent of machines have a capacity of $150cm^3$ or less(6) and are neither required to nor likely to have headlamps of adequate dimensions to be an aid to daytime conspicuity. Consequently, a requirement to use headlamps in daylight would be unlikely to be of benefit to machines of all sizes. It would enhance the conspicuity of large machines but would be of no benefit to the riders of the majority of motorcycles in use.

Of all the rider-based options assessed, a fluorescent jacket or waistcoat was found to be more conspicuous than the control condition. This conspicuity aid is available to all motorcyclists but has two disadvantages when compared with running lamps. Its effectiveness depends on riders' choosing to wear it, and fluorescence decays with exposure to light. So, to be effective, jackets must be stored away from light and replaced every few months if in frequent use.

The experimental safety motorcycle ESM-2 is equipped with a pair of running lamps of the type assessed in this work.

Acknowledgments

The work described in this paper forms part of the programme of the Transport and Road Research Laboratory and is published by permission of the Director.

References

1. Watson, P.M.F., and F.T.W. Lander, "Motorcycle accidents and injuries," Conference on Vehicle Safety Legislation—Its Engineering and Social Implications, I. Mech. E., London, 1973.
2. Whitaker, J., "A survey of motorcycle accidents," Department of the Environment, Department of Transport, TRRL Report No. LR 913, Crowthorne, 1980.
3. "Road accidents Great Britain 1983," Her Majesty's Stationery Office, London, 1984.
4. Fulton, E.J., C. Kirkby, and P.G. Stroud, "Daytime motorcycle conspicuity," Department of the Environment, Department of Transport, TRRL Supplementary Report SR 625, Crowthorne, 1980
5. Donne, G.L., and E.J. Fulton, "The evaluation of aids to the daytime conspicuity of motorcycles," Department of Transport, TRRL Report No. LR 1137, Crowthorne, 1985.
6. "Transport statistics Great Britain 1983," Her Majesty's Stationery Office, London, 1984.

A Feedback Control Method for Antilock Brake Design

John W. Zellner and
Dean P. Chiang
Dynamic Research, Inc.

Abstract

An analysis of antilock brake system dynamics—based on nonlinear control theory—was performed. Results were used to define initial performance and design requirements for a prototype fluidic motorcycle antilock system. The analysis emphasized the frequency response of system components and effects on stopping performance and stability. Results showed wheel angular acceleration provides a feasible single loop feedback for antilock control; wheel angular jerk is probably not a desirable primary feedback variable; nominal design requirements for modulator and controller exist that represent a compromise among high and low μ performance, stability, roughness, and signal-to-noise ratio; net time delay between modulator and brake caliper is a key design parameter and should be investigated more thoroughly.

Introduction

Since the 1930's, antilock brake technology has been developed and applied to a variety of vehicles, including railcars, aircraft, automobiles, commercial vehicles, and more recently motorcycles(1). The advantages of antilock for each vehicle category tend to be different: reduction of damage to wheels and tires has been a main goal for rail and aircraft systems; improved steerability and yaw stability are the goals of automotive systems. Motorcycle antilock examples—all in prototype versions only—have attempted to reduce the capsize tendencies of two-wheelers encountered under limit braking conditions. So, over the years, the antilock trend has been increasingly toward the role of stability and control augmentation and also toward applications involving smaller, lighter, more quickly responding vehicles. For motorcycles, these factors have combined to produce challenging prospects for antilock developers.

Motorcycle antilock prototypes have included perhaps a dozen well-known examples since the 1960's, as reviewed in (1). Many of these evolved from Experimental Safety Vehicle (ESV) programs in the United States, Europe, and Japan, begun in the 1970's, as well as proprietary development efforts. To date, all of the documented versions would have required additional development to make them viable, practical, and reliable production brake systems.

Historically, antilocks are usually developed empirically, supported by conventional design and test techniques. This process is made especially challenging by the complexities of tire/roadway friction and dynamic behavior of vehicles and brake systems. To date, not much insight has been provided by theoretical approaches, and the development process remains mostly empirical, with accompanying costs, time, and risks.

Recently, other technologies are being brought to bear in the antilock area. These include, to mention a few, digital- and microprocessor-based systems, all mechanical antilock systems, and fluidic sensing and control. As these new technologies join the several dozen antilock systems in various stages of development and use, the need for analytical input continues.

As part of such development—specifically of a fluidic antilock system for motorcycles(2,3)—an effort to treat antilock analytically was undertaken and is reported here in part.

The objective of this portion of the development was to analyze antilock dynamics in a preliminary way and to determine desirable and feasible feedback control structures (i.e., which variable to use as a feedback). A complementary goal was to identify antilock component response requirements and an initial configuration. The approach used was largely analytical, based on nonlinear control systems analysis.

This paper focuses on the analysis method used. An example preliminary design for a motorcycle antilock is used to illustrate the approach and typical results.

Analytical Approach

The antilock design task involves sensing the rotational motion of the braked wheel or wheels and using this information to modulate the brake fluid pressure applied to the wheel to avoid overbraking and lockup. The main motion variables, as shown in Figure 1, are the wheel angular velocity and acceleration, the linear velocity and acceleration of the vehicle itself, and the relative velocity or slip ratio at the tire/road interface. The design goal is to keep the wheel tangential velocity somewhat less than the vehicle velocity. This does two things. It retains most of the sideforce capability of the tire needed for vehicle stability and control, and it allows the vehicle to be decelerated at near the limit of available tire/road friction. Generally speaking, this involves a design tradeoff between maximizing wheel rotational stability versus stopping performance.

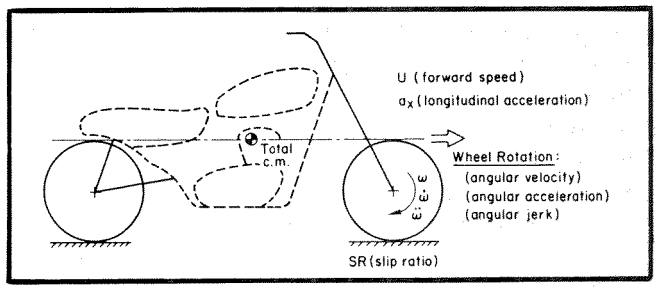

Figure 1. Primary motion variables for antilock dynamics

The interaction between stability and stopping performance is shown schematically in Figure 2. During normal forward operation, the rider uses steer torque to control motorcycle roll angle, thereby also effecting heading and path control(4). Brake force is used to control stopping distance (i.e., forward velocity). With conventional brakes, if a wheel is overbraked and locked, the motorcycle can be rapidly destabilized in roll, resulting in a potential capsize. A goal of motorcycle antilock is to automatically sense wheel speed and control brake force to maintain both stopping performance and attitude stability.

Past analytical studies of antilock have commonly involved developing a mathematical model of the vehicle and antilock components. Such models are typically analyzed in the time domain to produce time responses of the system. Once constructed, such models can be used as paper prototypes, where the antilock design can be modified and adjusted—much like a real vehicle—until satisfactory results are obtained. Such an approach was used in (5), for example.

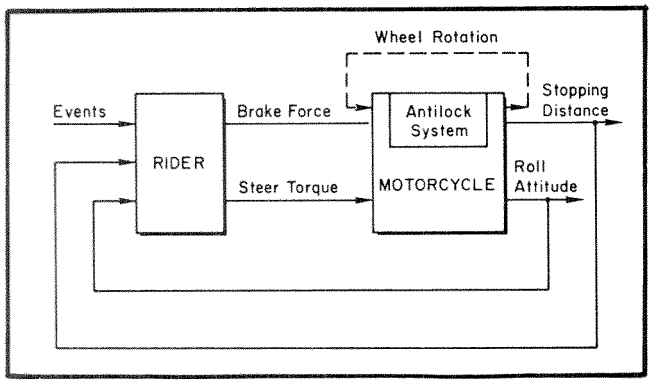

Figure 2. Schematic of rider/motorcycle/antilock control system

The next step could involve using control theory methods to determine the antilock design analytically (i.e., as opposed to by trial and error). Two methods are generally available: time domain and frequency domain.

A fundamental aspect of antilock that must be addressed by such theoretical methods is the nonlinear behavior of the vehicle and candidate antilock components. Such nonlinearities (e.g., tire/road friction) limit the range of analytical tools available to the designer.

In the time domain, antilock has been examined using external (or nonlinear optimal) control techniques, as, for example, GM used in the 1960's(6). Such approaches typically involve assuming a fixed form of control and numerical solution.

A somewhat more general approach is available in the frequency domain, involving describing functions and gain-phase techniques(7,8). Applying these methods to antilock design is described in the balance of this paper.

Feedback Control Formulation

Feedback control theory suggests that the controller and controlled element of a system be tailored to one another in order to result in a system that has a balance among such things as—

- Stability
- Rapid, well-damped response to commands
- Insensitivity to disturbances
- Insensitivity to small changes in controlled element or controller parameters.

For linear systems, a crossover model of a feedback control system includes the above considerations and can be used to determine requirements for feedback design. Zellner(9) provides an example of the crossover method applied to antilock design. One difficulty, as mentioned above, is the presence of amplitude nonlinearities. This can be partially handled with families of describing functions (i.e., frequency response curves). From a practical standpoint, the multidimensional nature of such curves makes a conventional graphical solution inconvenient.

An alternative technique also used in linear servo analysis(7,8) is the gain-phase plot method. The gain-phase plot provides a convenient tool for determining conditions for limit cycles in quasi-linear systems. If the linear portion of the transfer function is plotted on the gain-phase plot, together with the negative inverse describing function of the nonlinear portion, intersections of the two curves will illustrate the conditions for sustained oscillation. The frequency and amplitude of the limit cycle, if any, will appear directly; the plot can also be used to determine whether the limit cycle is stable, that is, whether the limit cycle will sustain itself in the face of disturbances.

Formally, in a manner similar to the basic stability condition that underlies the theory of constant-coefficient linear systems, the basic condition for stationary oscillations in quasi-linear closed-loop systems can be expressed as follows (see Figure 3):

$$1 + \mu\beta = 0$$

or

$$\mu\beta = -1 \qquad (1)$$

where

μ = forward path transfer function
β = feedback path transfer function

If any part of either μ or β is the describing function of a nonlinearity, N, and the remainder of the open-loop frequency response function is the linear term $G(j\omega)$, the stability condition is:

$$NG(j\omega) = -1$$

or

$$G(j\omega) = -1/N \qquad (2)$$

The solution of Equation (2) can be carried out graphically. Equation (2) indicates that, if $G(j\omega)$ and $-1/N$ are plotted together on the gain-phase plane, intersections of the two curves will satisfy the equation. Intersections, therefore, will show the conditions for neutral oscillatory stability, where the describing function, N, is a function of amplitude only, as it is for all simple nonlinearities in first approximation quasi-linear systems, the construction is especially convenient. $-1/N$ is then an amplitude variant function, and $G(j\omega)$ is a frequency variant function. Each curve can be plotted as a function of a single parameter.

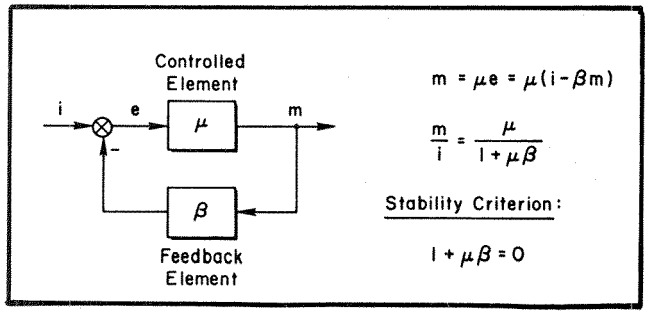

Figure 3. Generalized stability condition for single closed-loop control system

The gain-phase design method can be summarized as follows:

- Determine the time responses of system components (i.e., measure actual hardware or use a computer simulation)
- Calculate the corresponding component describing functions (i.e., Fourier transform the time histories) at a range of frequencies and amplitudes
- Identify the frequency dependent (linear) components and the amplitude dependent (quasi-linear) components, from the describing function data
- Plot the gain-phase characteristics of the frequency and amplitude dependent parts of the system
- Note characteristics of the intersection point (i.e., the limit cycle point)
- Modify the response curves to adjust the quality of the intersection

The quality of the gain-phase intersection (i.e., limit cycle) is determined by several criteria, including—

- Limit cycle existence is indicated by intersection existence.
- Limit cycle stability is indicated by the direction of the intersection (amplitude dependent curve crossing the frequency dependent curve from left to right is stable).
- Sensitivity to parameter changes is indicated by the angle of intersection (90° is least sensitive).
- Stability margin is indicated by the intersection's proximity to the end points of either the frequency or amplitude dependent curve.

Examples of the gain-phase approach are discussed next.

Example: Antilock Gain-Phase Analysis

For purpose of control system analysis, antilock systems can be broken down into four main components, as shown in Figure 4. These are the—

- Vehicle dynamics
- Sensor
- Controller
- Modulator

In general, each of these contain potentially significant nonlinearities. Yet, dynamic measurement of typical components, as well as simulation results, reported in (9) and elsewhere have shown that, to a first approximation, only the controller is fundamentally nonlinear (the other components are essentially linear). This means the frequency responses of the modulator, vehicle, and sensor can be combined and plotted and then compared to the response curve of the controller.

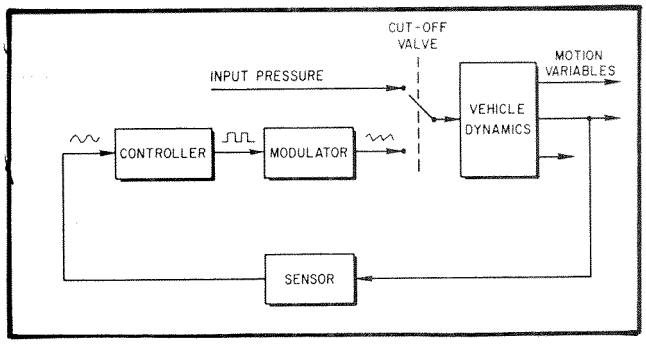

Figure 4. Generalized schematic of antilock control system

Figure 5 shows an example gain-phase plot. This is for an idealized acceleration sensor, a typical dump/reapply modulator (including time delay), and a dump/reapply switch controller. The latter can be referred to as a toggle, and in this case the toggle trigger values are 2g (i.e., ±1g) apart. Figure 5 shows that a limit cycle—

- Exists, at a frequency of 5Hz
- Is stable (left to right crossover)
- Is fairly insensitive to changes in vehicle or modulator gain (nonparallel curves)
- Has a fair stability margin (i.e., the limit cycle must decrease to less than 1g amplitude at 90° phase lag to destabilize the antilock)

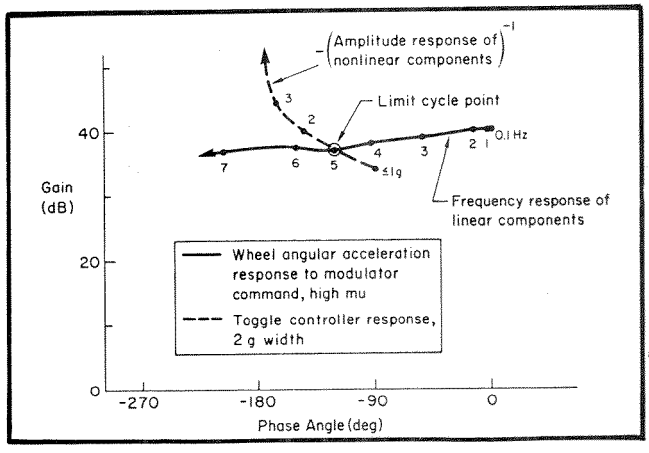

Figure 5. Example gain-phase plot for angular acceleration feedback, with 2g toggle

Another example is shown in Figure 6. The only difference from Figure 5 is that the toggle is set at ±2g, resulting in an unstable system (i.e., the wheel never decelerates enough to trigger the 2g dump condition; therefore, the wheel locks up).

Some of the fundamental difficulties inherent in using angular jerk as a feedback are shown in Figure 7. Since the linear and nonlinear response curves are fairly parallel (above 7Hz), small changes in any component will result in relatively large changes in limit cycle stability and stopping performance (i.e., it is an overly sensitive system). In particular, the potential limit cycle

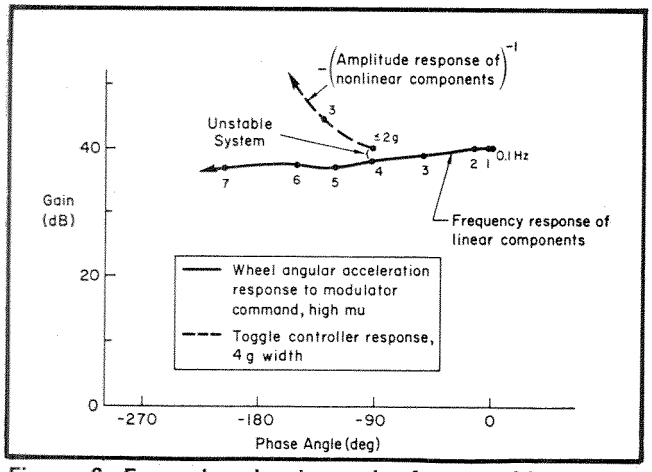

Figure 6. Example gain-phase plot for unstable system, angular acceleration feedback, with 4g toggle

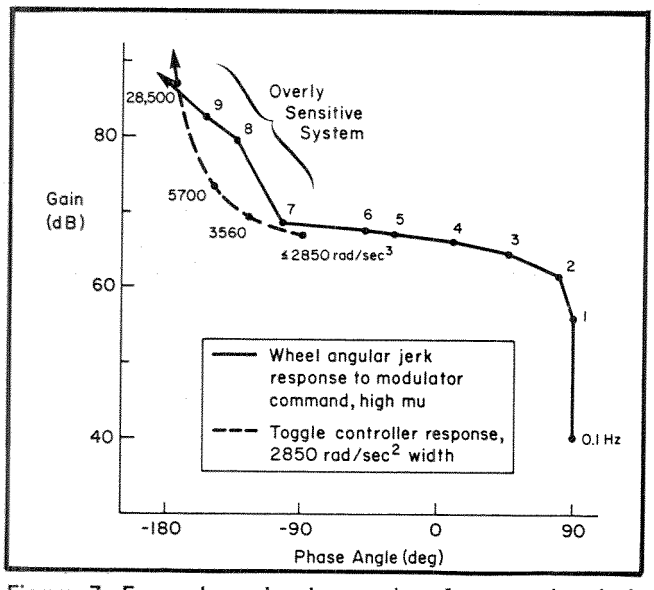

Figure 7. Example gain-phase plot for angular jerk feedback

near 7Hz is very close to the lockup boundary (i.e., 90° phase lag, as above), and the limit cycle near 10Hz is near the no-brake boundary where the system merely chatters, with little deceleration (i.e., 180° phase lag). Both of these adverse conditions can exist with jerk feedback, and a relatively small reduction in vehicle gain (e.g., about 10dB) could result in a completely unstable system. For these and other reasons, angular jerk feedback cannot be recommended.

An overall summary plot of antilock gain-phase results for acceleration feedback is shown in Figure 8. As can be seen, a feasible region of stable designs exists, bounded by a lockup region (at lower phase lags) and a no-braking region (at higher phase lags). Within the feasible region, higher intersections (or crossovers) result in rougher antilock cycling (the gain is logrhythmically related to limit cycle amplitude), while excessively low ones suggest oscillations so small they might become confused with

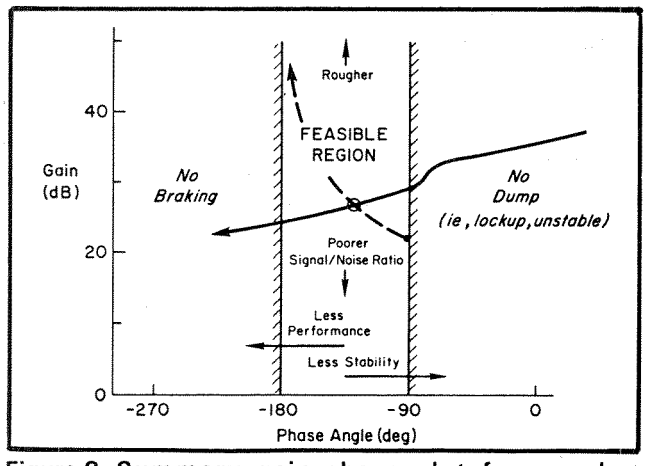

Figure 8. Summary gain-phase plot for angular acceleration feedback, with toggle controller

noise sources in the system. Again, stability decreases toward the right, and braking decreases toward the left.

Figure 8 is also significant in that it illustrates the relationships among antilock stability, performance, roughness, and noise, as well as the relative contributions of the controller's other system components. As an evaluation or design tool, it seems applicable to most single loop (and, with extension, possibly multiloop) antilock systems.

Preliminary Antilock Design

A combination of simulation, full-scale measurement, and gain-phase analyses was used to help define an initial feedback design and component requirements for the motorcycle fluidic antilock system. The analyses considered the effects of—

- Various feedback structures
- Controller (toggle) characteristics
- Modulator and vehicle responses
- High and low μ road friction characteristics

The basic design parameters are shown in Figure 9. Primarily these were modulator dump and reapply pressure rates, toggle (trigger) width and bias, and modulator-to-caliper net time delay.

A feasible front wheel antilock design for an example touring motorcycle (for both high and low μ surfaces) was defined as follows:

Feedback:	Wheel angular acceleration (assumed to have no sensor dynamics)
Dump rate:	-3600 psi/s
Reapply rate:	2000 psi/s
Toggle width:	3.0g
Toggle bias:	-1.5g
Modulator to caliper delay:	20ms

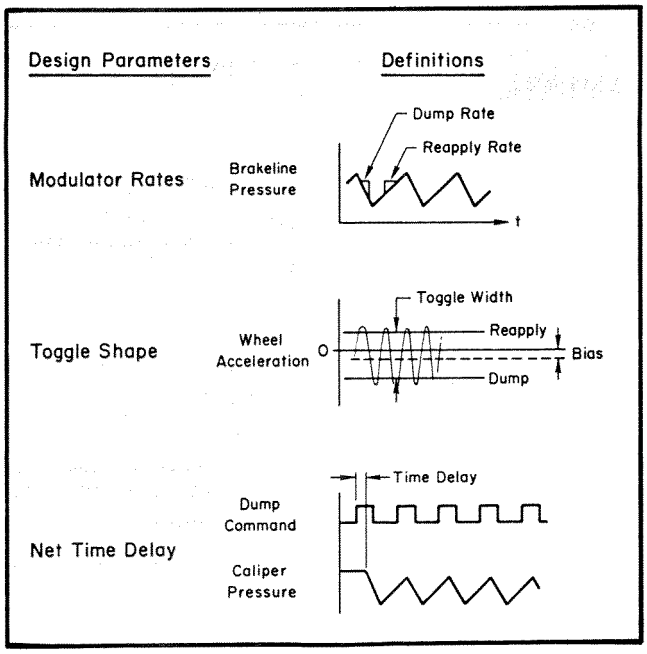

Figure 9. Design parameters varied in sensitivity analysis

This gave low μ stops of -0.23g at 13Hz, and high μ stops of -0.54g at 13Hz (subjectively, these were felt to be reasonable performance levels for an initial design; these are not intended to imply minimum acceptable levels or maximum attainable levels).

In addition, the initial design parameter values were perturbed ±50 percent to confirm that the design was not overly sensitive. Results are shown in Figures 10 and 11.

Effects of modulator pressure rates on vehicle deceleration and wheel speed roughness (peak to peak) are shown in Figure 10. The effects on high and low μ are seen to be quite different; not surprisingly, low μ is more sensitive to modulator response properties. For low μ, smaller reapply rates are better, as has been reported in the industry, while for high μ, higher reapply rates are better. The opposite preferences seem to apply to dump rates.

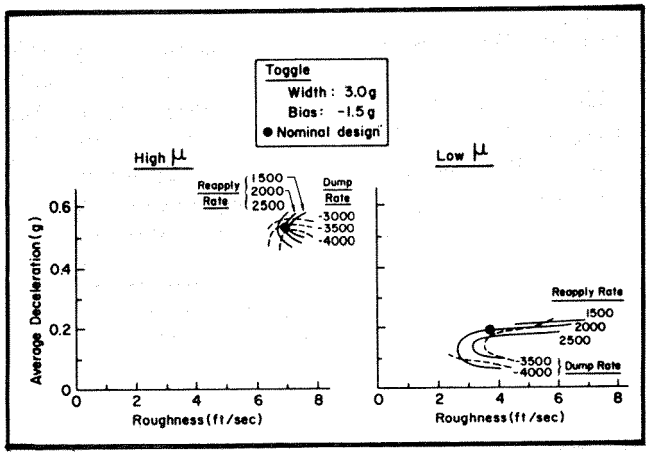

Figure 10. Effects of modulator dump and reapply rates on antilock performance

Effects of toggle (i.e., trigger) shape are shown in Figure 11. Here, fairly large effects are seen in both high and low μ performance. Greater toggle width, within limits, improves both high and low μ performance. On the other hand, greater toggle bias improves high μ performance but can considerably degrade low μ performance.

Of course, in general, somewhat larger changes in modulator or toggle design values than those listed here can result in exceeding the feasible design region or the subjectively acceptable region (related to roughness and noise).

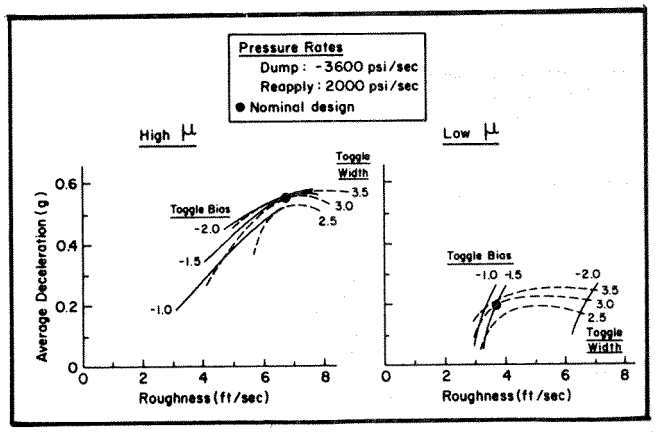

Figure 11. Effects of toggle width and bias on antilock performance

Preliminary results of the effects of time delay on high μ performance are shown in Figure 12. This shows a fairly high level of performance (-0.52g) at 20ms and considerably less performance (-0.36g) at 120ms. Currently it is unknown how the intermediate ranges of time delay compare to these more extreme values (i.e., whether there is a sharp or gradual reduction above 20ms). This seems to be a key design parameter variation for future antilock development, and a more complete analysis would be useful.

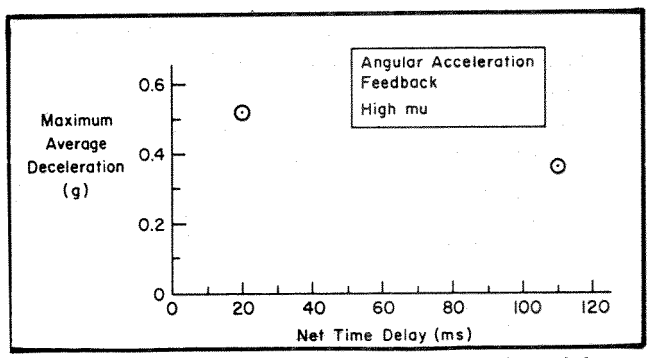

Figure 12. Effect of modulator-to-caliper time delay on antilock performance

Examples of resultant antilock time responses are shown in Figures 13 and 14 for 110 and 20ms delay times, respectively. Note that in these cases, the toggle and modulator parameters have been adjusted to give a balance among stability, performance, and roughness for

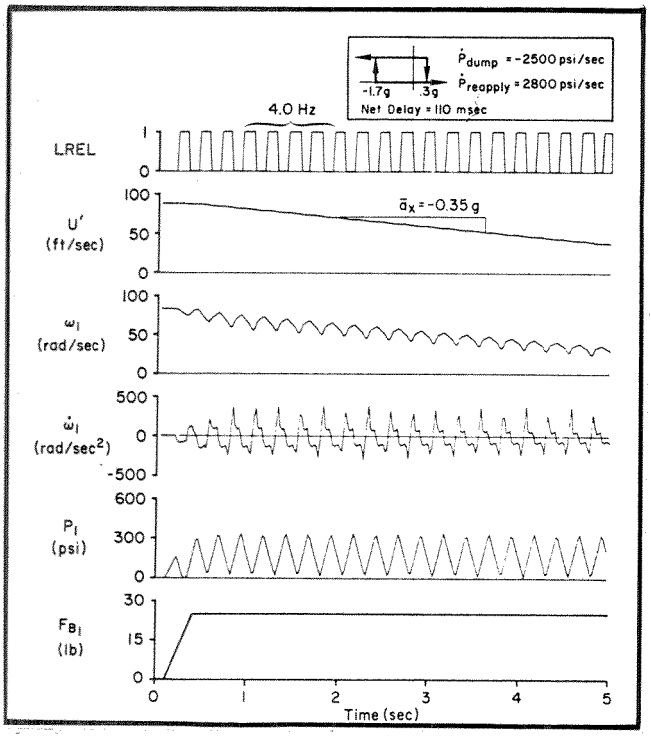

Figure 13. Example simulated antilock closed-loop response, 110ms time delay

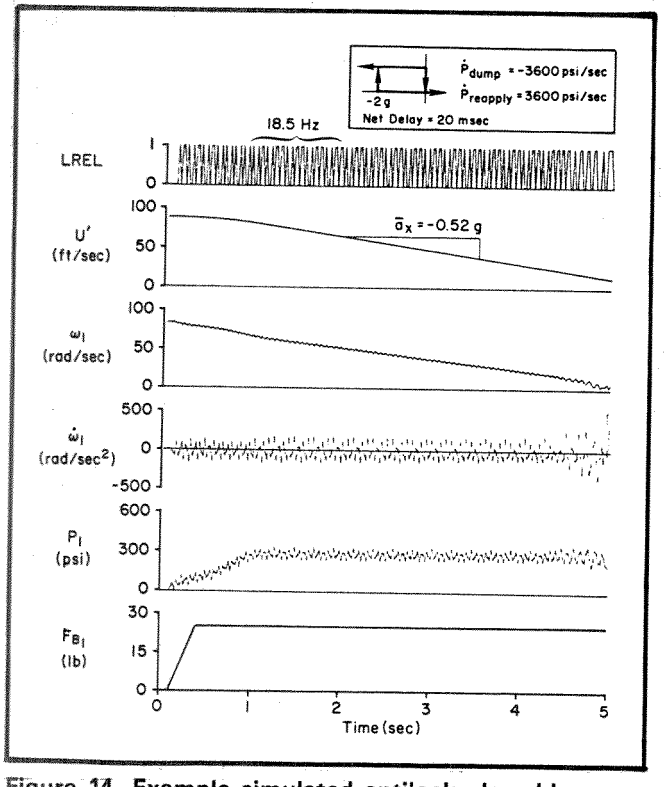

Figure 14. Example simulated antilock closed-loop response, 20ms time delay

high μ limit braking. Figure 13 (110ms delay) shows a relatively low (4Hz) cycling rate and deceleration level, with a fair amount of wheel speed roughness. Figure 14 shows a very smooth, high (18.5Hz) cycling rate similar to some aircraft systems and also a fairly high deceleration rate. Again, this suggests the importance of net time delay to overall antilock performance.

Conclusion and Recommendations

A generalized analysis of motorcycle antilock brake system dynamics—based on nonlinear control theory—was performed. Overall, the gain-phase analysis approach involved transforming antilock time responses to frequency responses and determining conditions necessary for existence of a stable limit cycle. The method was found to provide a generalized method for antilock analysis and to provide some possible insight into antilock dynamics and design effects and requirements.

In particular, preliminary design requirements were determined for example modulator, toggle, and sensor components. These indicated that—

- Wheel angular acceleration feedback provides a feasible single loop feedback design.
- Wheel angular jerk feedback is not desirable as a primary feedback control variable, in part because it results in excessive sensitivity to small variations in vehicle and systems parameters.
- A set of controller and modulator characteristics was found that gave a reasonable balance among performance, stability, and stability margin on both high and low μ surfaces.
- One way to achieve potentially higher performance stability levels on both high and low μ surfaces could involve use of μ dependent, adaptive controller or modulator, as may be found on some existing antilock systems.
- Net time delay between the modulator and caliper seems to be a key design parameter affecting performance and stability and should be evaluated more completely to assess fluidic and other antilock design requirements.

Acknowledgments

The work reported in this paper was accomplished under subcontract to the Jet Propulsion Laboratory, under prime contract to the U.S. Army Harry Diamond Laboratories, in cooperation with the National Highway Traffic Safety Administration. The opinions expressed are those of the authors and not necessarily those of JPL, the U.S. Army, or NHTSA.

References

1. Zellner, J., and M. White, "Advanced motorcycle brake systems," Final report, DOT-HS-806-095, November 1981.

2. "Development of fluidic antilock brake system for motorcycles," Contract RE 182-0230, between U.S. Army Harry Diamond Laboratories and the Jet Propulsion Laboratory for the National Highway Traffic Safety Administration, 1982
3. Purves, R.R., "Application of fluidics technology to the development of antilock brakes for motorcycles," Proceedings Tenth International Technical Conference on Experimental Safety Vehicles, Oxford, England, July 1985.
4. Weir, D.H., and J.W. Zellner, "Lateral-directional motorcycle dynamics and rider control," SAE Paper 78030-4, presented at the SAE Congress and Exposition, Detroit, February 1978.
5. Guntur, R.R., "Design considerations of adaptive brake control systems," SAE Paper 741082, presented at the Automobile Engineering Meeting, Toronto, Canada, October 1974.
6. Harned, J.L., and L.E. Johnston, "Antilock brakes," General Motors Safety Seminar Paper No. 21, July 1969.
7. Truxal, J.G., *Automatic Feedback Control System Synthesis*, New York, New York: McGraw-Hill Book Co., 1955.
8. Graham, D., and D. McRuer, *Analysis of Nonlinear Control Systems*, New York, New York: Dover Publications, Inc., 1961.
9. Zellner J., "An analytical approach to antilock brake system design," SAE Paper 840249, presented at the SAE Congress and Exposition, Detroit, February 1984.

Measurement of Motorcycle Riders' Eye Locations

Masanori Motoki and
Tsutomu Asah
Japan Automobile Research Institute, Inc.

Abstract

In this study, with a final objective of obtaining such data necessary for the international standardization of eye ranges of motorcycle riders in the future, we selected five different models of motorcycles (with engine capacities ranging from 250cc class to 1,000cc class) comprising four typical motorcycle types and measured the eye locations and riding positions of 456 Japanese and American motorcycle riders mounted on those motorcycles.

As a result, we found that when the shoulder location is adopted as the origin, four items—namely, distances between shoulder and handle grip, shoulder and hip, shoulder and eye, and the angle formed by the locations of eye, shoulder, and hip—are nearly constant, regardless of differences in vehicle frame dimensions. Therefore, the eye range of motorcycle riders can be located from the relative positions between the handle grip and hip point.

Furthermore, through comparison of anthropometric data between Europeans and Americans, the actually measured eye locations of American riders can be used as representing European riders' eye locations.

Introduction

The statistical distribution (eye range) and the representative point (eye point) of motorcycle riders' eye locations are not only indispensable as reference points for the study of the indirect field of view by means of rear view mirrors, but also those data will be useful as reference points for the study of the direct field of view.

The eye locations of automobile (four-wheeled motor vehicle) drivers have been standardized internationally by ISO 4513(1), while, as for the eye locations of motorcycle riders, only the reference eye point is specified in VDTUV Leaflet 736(2) and no standard exists that specifies eye ranges indicating statistical distribution of eye locations.

This study, with a final objective of obtaining data necessary for the international standardization of eye ranges of motorcycle riders, was started in 1981 as a 2-year program. In the study program, three research items were adopted: comparing anthropometric data among Japanese, American, and European riders; establishing eye ranges of Japanese, American, and European riders; and obtaining the correct formula for eye locations.

Mopeds were excluded from this study because moped riders were clearly different in category from the riders of such motorcycles as were used for this study, and their riding positions were also quite different from those of motorcycle riders.

Comparisons of Anthropometric Data Among Japanese, American, and European Riders

Purpose

The purpose of this portion of the study was to obtain statistical anthropometric data of Japanese and American

riders through actual measurement of their physical members and to gather the necessary data for the estimation of eye locations of European riders by comparing the anthropometric data with those collected from studies concerning Japanese, American, and European people.

Method

Anthropometry

(1) Anthropometric instruments: Anthropometers and a sliding caliper were used for the measurement.

(2) Measurement points: Before the measurement, well-trained measuring staff manually located such measurement points as were difficult to locate visually—namely, cervical, left, and right acromions, right radiale, left and right trochanterions, and sphyrion, as illustrated in Figure 1—and marked them.

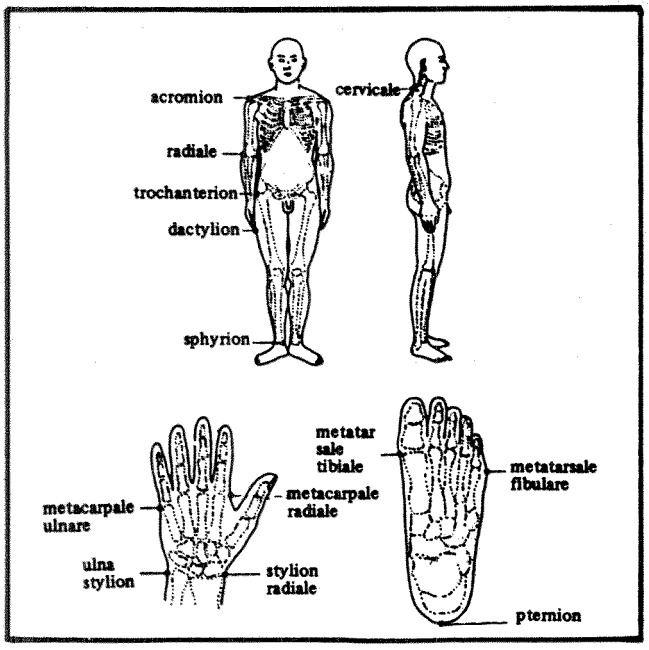

Figure 1. Measurement points

(3) Anthropometry items and physical members for measurement: The anthropometry items and physical members for the measurement are shown in Figure 2.

For the measurement in a standing posture, the riders took a natural standing posture with straight-ahead viewing so both left and right tragions and right orbitale were kept in a horizontal plane, and both arms were hanging down with their hand palms lightly contacting the side surfaces of the body except for the measurement of armreach from back.

For the measurement in a sitting posture, the riders took a natural sitting posture so that by adjusting the height of the chair, both thighs were nearly horizontal and both knees were about at a right angle to the thighs, both hands were placed on the thighs, and the head position was similar to that in a standing posture.

The riders measured wore jogging trunks only.

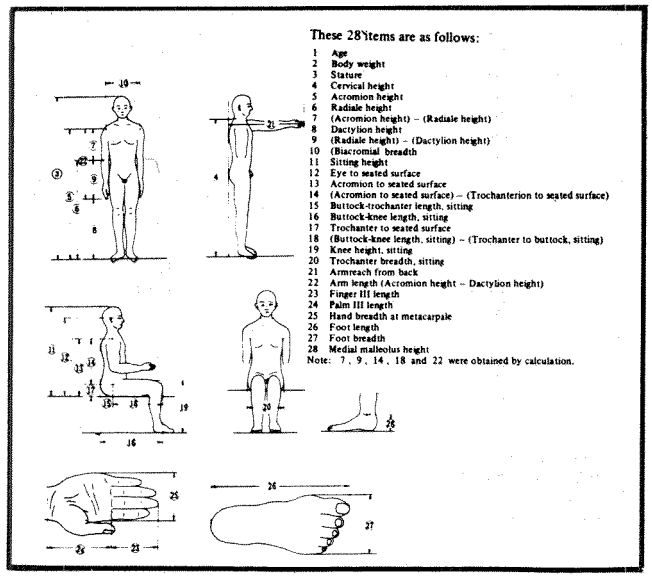

Figure 2. Anthropometry items and physical members for measurement

References Concerning Anthropometric Data

A Handbook of Anthropometric Data (3) published by the National Aeronautics and Space Administration (NASA) as the data to be used for the human engineering designs of space shuttles, space suits, and other space equipment contains rearranged data of anthropometry of various nations collected from 91 sources. In this handbook, 26 kinds of anthropometric data of male Americans and 5 kinds of those concerning Frenchmen, male Germans, and Englishmen, respectively, are included. NASA adopted one kind of data for the people of each nation from the above-mentioned data to determine the size of space suits(4).

In this study, the NASA-adopted data were used for the estimation of eye location of European riders.

Results

Anthropometric Data of Japanese and American Riders

The anthropometric data of Japanese riders are listed in Table 1 and those of American riders in Table 2. In these tables, statistical data of 28 items consisting of percentile values, maximum value, minimum value, mean value, and standard deviation are included as a result of calculation, although actual measurements were made with regard to 23 items.

Table 1. Anthropometric data of Japanese riders

Percentile	(1) Age	(2) Body Weight	(3) Stature	(4) Cervical Height	(5) Acromion Height	(6) Radiale Height	(7) (Acromion Height)—(Radiale Height)	(8) Dactylion Height	(9) (Radiale Height)—(Dactylion Height)	(10) Biacromial Breadth
5	17.3	49.8	1595	1363	1271	995	271	592	388	384
10	17.8	52.8	1613	1375	1287	1007	275	604	395	389
15	18.4	54.8	1623	1386	1299	1017	279	611	399	393
20	18.9	56.4	1634	1397	1309	1025	281	617	402	396
25	20.1	57.6	1648	1408	1317	1032	284	623	405	399
30	21.3	58.9	1657	1418	1325	1037	286	627	407	402
35	22.5	60.0	1665	1424	1332	1043	288	630	410	405
40	23.7	61.0	1672	1429	1338	1047	290	633	412	407
45	24.9	62.0	1678	1435	1345	1051	291	637	414	410
50	25.5	62.9	1683	1441	1350	1056	293	640	416	412
55	26.1	63.9	1688	1446	1356	1061	295	644	418	414
60	26.7	65.0	1695	1452	1361	1066	297	647	420	416
65	27.5	66.1	1704	1460	1368	1070	300	652	422	418
70	28.4	67.2	1713	1467	1377	1077	302	657	426	421
75	29.3	68.7	1722	1475	1385	1085	304	661	429	424
80	30.6	70.4	1732	1484	1353	1091	307	666	432	426
85	32.1	72.3	1744	1494	1401	1098	310	671	436	430
90	34.4	74.7	1756	1508	1417	1110	314	678	441	434
95	38.4	81.7	1780	1522	1436	1126	319	694	449	440
Mean value	25.3	63.7	1684	1441	1351	1058	293	641	417	411
Standard deviation	6.8	9.2	55.3	49.6	49.1	38.3	15.6	28.7	18.1	17.6
Max. value	51.0	104.0	1841	1578	1495	1162	339	713	478	472
Min. value	16.0	40.7	1525	1310	1212	947	225	567	373	368

Table 1, continued

Percentile	(11) Sitting Height	(12) Eye to Seated Surface	(13) Acromion to Seated Surface	(14) (Acromion to seated Surface)-(Trochanter to Seated) Surface)	(15) Trochanterion to Buttock, Sitting	(16) Buttock-Knee Length, Sitting	(17) Trochanterion to Seated Surface	(18) (Buttock-Knee Length sitting)-(Trochanter to Buttock, Sitting)	(19) Knee Height, Sitting	(20) Trochanterion Breadth Sitting
5	852	719	530	453	113	530	62	403	469	317
10	865	731	536	460	118	537	66	411	477	323
15	873	740	542	467	120	543	68	415	482	327
20	879	748	546	472	123	547	70	418	486	330
25	884	753	552	477	124	550	71	421	491	333
30	889	757	557	483	126	552	72	424	495	336
35	893	762	561	487	127	555	73	427	498	338
40	897	766	565	490	129	558	74	430	500	341
45	901	771	568	493	130	561	75	433	502	344
50	905	775	571	496	131	565	76	435	504	346
55	909	780	575	499	132	568	77	438	507	349
60	913	783	578	502	133	571	78	440	510	352
65	917	786	581	506	135	574	79	442	513	354
70	921	790	584	510	136	577	80	445	516	356
75	925	794	588	514	138	580	81	447	519	359
80	930	800	592	518	140	583	82	450	523	362
85	936	807	598	523	142	589	84	455	527	367
90	943	818	605	528	144	593	85	461	532	375
95	954	831	614	538	149	604	89	470	545	384
Mean value	904	774	571	495	130	565	75	434	505	347
Standard deviation	30.1	32.8	25.6	25.5	10.4	22.2	7.8	19.7	21.6	19.8
Max. value	998	881	635	558	164	633	94	501	568	403
Min. value	817	667	494	422	103	511	50	378	449	298

Table 1, continued

Percentile	(21) Armreach from Back	(22) Arm Length	(23) Finger III Length	(24) Palm III Length	(25) Hand Breadth at Metacar-pale	(26) Foot Length	(27) Foot Breadth	(28) Medial Mallelus Height
5	764	679	73	97	79	235	98	65
10	774	683	74	98	80	238	99	67
15	782	688	75	99	81	240	100	68
20	789	692	76	100	82	241	101	69
25	794	694	76	100	83	242	102	70
30	799	698	77	101	83	243	103	71
35	804	701	78	102	84	245	103	72
40	809	705	78	102	84	246	104	72
45	812	708	79	103	85	247	105	73
50	816	710	79	104	85	249	105	74
55	820	712	80	104	86	250	106	74
60	824	714	80	105	86	251	107	75
65	828	716	81	105	87	252	107	75
70	832	720	81	106	87	254	108	76
75	837	724	82	107	88	256	108	77
80	842	687	83	107	88	258	109	77
85	849	730	84	108	89	260	110	78
90	857	739	85	110	90	263	112	79
95	867	742	87	112	92	266	114	82
Mean value	816	710	79	103	85	249	105	73
Standard deviation	32.6	25.8	4.1	4.5	3.7	9.6	4.7	5.0
Max. value	917	782	97	116	99	274	116	85
Min. value	737	645	69	92	75	223	91	58

Table 2. Anthropometric data of American riders

Percentile	(1) Age	(2) Body Weight	(3) Stature	(4) Cervical Height	(5) Acromion Height	(6) Radiale Height	(7) (Acromion Height)— (Radiale Height)	(8) Dactylion Height	(9) (Radiale Height)— (Dactylion Height)	(10) Biacromial Breadth
5	20.0	62.1	1669	1431	1350	1037	298	616	404	388
10	21.1	64.6	1688	1448	1375	1060	307	630	420	392
15	21.9	67.5	1703	1463	1390	1069	313	638	424	398
20	22.7	70.3	1724	1478	1399	1079	317	645	428	401
25	23.6	71.6	1734	1489	1409	1088	320	651	431	404
30	24.7	73.0	1744	1500	1419	1096	323	656	434	408
35	25.8	74.4	1753	1512	1429	1104	326	660	438	410
40	27.0	76.1	1763	1526	1440	1111	328	665	441	412
45	28.1	77.8	1772	1533	1452	1116	330	669	444	414
50	29.2	79.7	1779	1540	1459	1121	332	673	448	416
55	30.0	81.6	1786	1547	1465	1127	335	677	451	418
60	30.9	83.2	1793	1555	1472	1133	337	681	455	420
65	32.7	84.7	1802	1562	1480	1141	339	685	458	422
70	33.7	86.1	1810	1569	1489	1149	343	690	462	425
75	34.5	88.1	1819	1577	1498	1157	348	697	465	428
80	35.5	90.6	1831	1586	1508	1165	353	704	471	432
85	36.8	92.9	1843	1595	1518	1173	358	713	477	436
90	38.2	95.5	1858	1611	1535	1181	363	721	484	441
95	40.6	102.7	1887	1642	1559	1202	370	737	494	445
Mean value	29.0	80.1	1775	1533	1454	1122	333	674	447	416
Standard deviation	6.7	12.1	66.5	64.4	62.9	49.6	21.4	38.2	31.3	17.5
Max. value	48.0	112.0	1939	1691	1629	1277	387	779	499	464
Min. value	16.0	49.0	1580	1343	1299	1004	269	580	376	368

Table 2 , continued

Percentile	(11) Sitting Height	(12) Eye to Seated Surface	(13) Acromion to Seated Surface	(14) (Acromion to Seated Surface)-(Trochanter to Seated) Surface)	(15) Trochanterion to Buttock, Sitting	(16) Buttock-Knee Length, Sitting	(17) Trochanterion to Seated Surface	(18) (Buttock-Knee Length sitting)-(Trochanter to Buttock, Sitting)	(19) Knee Height, Sitting	(20) Trochanterion Breadth Sitting
5	858	730	552	471	107	563	74	456	506	335
10	869	743	560	476	111	576	77	464	519	347
15	879	753	566	481	113	583	81	470	526	352
20	889	761	573	486	115	587	83	472	531	355
25	893	766	580	491	117	591	84	474	536	358
30	898	770	584	496	119	597	85	478	540	361
35	902	773	588	500	120	602	87	482	545	363
40	907	777	592	503	122	607	88	485	549	365
45	912	782	595	507	123	612	89	489	553	369
50	916	786	599	510	125	616	90	491	557	373
55	921	791	603	514	126	619	91	493	560	377
60	926	796	607	517	127	622	92	495	563	380
65	931	801	611	520	129	625	93	496	566	384
70	936	805	616	524	130	629	94	499	571	387
75	941	809	621	530	132	633	95	501	576	391
80	946	814	626	537	135	639	97	504	581	395
85	951	819	632	543	138	646	100	588	584	400
90	962	825	637	550	141	653	102	511	591	408
95	976	839	654	565	146	661	104	515	602	425
Mean value	914	786	601	512	125	613	89	488	555	375
Standard deviation	44.8	33.1	40.0	38.8	11.8	29.7	8.8	23.6	28.2	26.3
Max. value	1021	879	688	580	165	676	110	531	633	462
Min. value	537	693	526	444	101	538	65	451	488	323

Table 2 , continued

Percentile	(21) Armreach from Back	(22) Arm Length	(23) Finger III Length	(24) Palm III Length	(25) Hand Breadth at Metacarpale	(26) Foot Length	(27) Foot Breadth	(28) Medial Mallelus Height
5	820	733	75	101	83	244	99	65
10	838	445	76	103	85	252	101	67
15	850	752	78	105	86	255	102	69
20	863	754	79	105	87	258	103	70
25	872	758	80	106	87	261	104	73
30	876	763	80	107	88	264	105	74
35	880	769	81	108	88	266	105	75
40	885	775	82	109	89	267	106	75
45	890	782	83	109	89	268	107	76
50	894	785	83	110	90	270	107	77
55	899	788	84	111	90	271	108	78
60	906	791	84	112	91	272	109	79
65	913	795	85	113	92	274	109	79
70	918	799	86	113	92	275	110	80
75	923	801	86	114	92	277	111	82
80	928	804	87	115	93	279	112	83
85	939	805	88	116	94	281	113	84
90	954	813	89	117	95	284	114	85
95	975	822	91	118	96	287	116	88
Mean value	895	780	83	109	89	268	107	76
Standard deviation	43.7	33.8	5.0	5.5	4.0	12.5	5.3	6.7
Max. value	1010	880	98	123	100	298	125	92
Min. value	780	719	70	91	78	230	90	61

Comparisons Among Dimensions and Proportions of Physical Members

The anthropometric data are apt to differ from one another according to the reference sources even within a nation. In Tables 3 and 4, three kinds of representative data published in each nation are shown for the purpose of comparison. These data were published in 1965 or later, and measurements were made with regard to the male.

The NASA-adopted data are printed in thick line numerals in the tables and used chiefly for comparison with Japanese riders.

(1) Stature: Japanese riders are 90mm lower in stature than American riders, 71mm lower than Frenchmen, 82mm lower than Germans, and 89mm lower than Englishmen. The statures of American riders are nearly equal to the data adopted by NASA. The difference between the maximum and the minimum data in a nation is about 30mm.

(2) Arm length: Japanese riders are 70mm shorter in arm length than American riders and ordinary Americans' reference literature data, 66mm shorter than Frenchmen, and about 90mm shorter than Germans and Englishmen. American and European people are generally long in arm length and large in the ratio of arm length to stature.

(3) Armreach from back: There are few actual measurement data concerning armreach from back of American and European people. From the few actual measurement data, it was found the differences between armreach from back and arm length are 49mm in Englishmen, 73mm in Germans, and 115mm in American riders. The large deviations in armreach from back data are supposed to be caused by the differences in the measuring positions or arm-stretching positions which differ remarkably from one another among these nations. In the case of arm length, on the contrary, as it was measured in such a position that both arms are drawn downward, this measuring position resulted in smaller errors due to measuring position or arm-stretching position.

Accordingly, actual measurement data of arm length are adopted instead of armreach from back for the estimation of eye locations for European riders because the data of armreach from back are larger in errors and, in addition, few data can be obtained.

(4) Sitting height: As for the ratio of sitting height to stature, riders are about 1 percent smaller than ordinary people in Japanese and Americans. This is considered to

Table 3. Comparisons of stature, arm length and armreach from back among various nations (mean value)

Nation	Japanese		American				
Item	Rider	JSDF Member	Rider	Literature	French	German	English
Stature	1,685	1,678	1,775	1,773	1,756 (0.999)	1,767 (0.997)	1,774 (1.001)
				1,753	1,724	1,752	1,770
				1,746	1,716	1,745	1,741
Arm length	710	720	780	780	776 (0.995)	801 (1.027)	*802 (1.028)
				*771	776	*794	*800
				*768	773	*791	*787
Arm length/ stature (%)	42.1	42.9	43.9	44.0	44.2	45.3	*45.2
				*44.0	45.0	*45.3	*45.2
				*44.0	45.0	*45.3	*45.2
Armreach from back	816	816	895	*876	—	*874	*851
				*866	—	*866	849
				*863	—	863	*835
Armreach from back/ stature (%)	48.4	48.6	50.4	*49.4	—	49.5	*48.0
				*49.4	—	49.4	48.0
				*49.4	—	49.5	*48.0
Armreach from back— arm length	106	96	115	*96	—	*73	*49
				*97	—	*72	*49
				*97	—	*72	*48

Table 4. Comparison of sitting height, eye to seated surface, and acromion to seated surface among various nations (mean values)

Nation	Japanese		American				
Item	Rider	JSDF Member	Rider	Literature	French	German	English
Sitting height	904	914	914	932	932	913	936
					(1.000)	(0.980)	(1.004)
				916	913	916	927
				909	910	919	913
Eye to seated surface	774	795	786	810	834	800	*820
					(1.030)	(0.988)	(1.012)
				799	814	*803	*818
				788	810	802	*804
Acromion to seated surface	570	595	601	610	617	*613	612
					(1.011)	(1.005)	(1.003)
				*600	600	615	*606
				*595	602	*617	588
Eye to seated surface— Acromion to seated surface	204	200	185	200	217	*187	*208
				(1.085)	(0.935)	(1.040)	
				*199	214	*188	*212
				*193	208	*185	*216
Sitting height/ stature (%)	53.6	54.5	51.5	52.6	53.1	51.7	52.8
				52.3	53.0	52.3	52.4
				52.1	53.0	52.7	52.4
Eye to seated surface/ Sitting height (%)	85.6	87.0	86.0	86.9	89.5	87.6	*87.6
				87.2	89.2	*87.7	*88.2
				86.7	89.0	87.3	*88.1

Unit: mm

* : Estimated values
— : Data not available
() : Ratios against data of ordinary Americans

be due to the difference in physical positions in the measurement; in the measurement of sitting height, riders were somewhat relaxed.

(5) Eye to seated surface: American riders are 12mm longer in eye to seated surface than Japanese riders, while ordinary Americans as reported in reference literature are 36mm longer than Japanese riders.

Frenchmen are 60mm longer, Germans are 26mm longer, and Englishmen are 46mm longer in eye to seated surface than Japanese riders. Frenchmen especially show the longest eye to seated surface for all their shortest statures among European people, and the ratio of eye to seated surface to sitting height is about 2 percent larger than that of other European people.

(6) Acromion to seated surface: American riders are 31mm longer in acromion to seated surface than Japanese riders, ordinary Americans are 40mm longer than Japanese riders, and European people are 42 ~ 47mm longer than Japanese riders.

(7) Difference between eye to seated surface and acromion to seated surface: American riders are 19mm smaller in this value than Japanese riders, ordinary Americans are 4mm smaller than Japanese riders, and Germans are 17mm smaller than Japanese riders; Frenchmen are 13mm larger than Japanese riders, and Englishmen are 4mm larger than Japanese riders.

Deviation Range of Anthropometric Data

As an index to indicate the deviations in the measurement values in each nation, the ratios between the

measurement data of various physical members and statures are obtained. These ratios deviate by 1.0 percent in sitting height in Germans, 0.8 percent in arm length in Frenchmen, and about 0.5 percent in other items. Regarding sitting height, a 0.9 percent difference is found between Japanese riders and JASDF (Japanese Air Self Defense Force) members and a 1.1 percent difference between American riders and ordinary Americans.

These deviations found among the measured values within a nation are supposed to be caused by the differences in the positions taken for the measurement or the inaccuracy in making the measurement points and not by the variety in the specimens. Consequently, it is necessary to consider deviations of about 1 percent (18mm) of the values of statures for adopting anthropometric data.

Eye Ranges of Japanese, American, and European Riders

Purpose

The purpose of this segment of the study was to obtain the statistical distribution of eye locations (eye ranges) by means of the measurement of Japanese and American riders' eye locations and also to study the relation between the reference points on the test motorcycles (seat, handle grip, and footrest) and the eye range centroids after obtaining their riding positions from the locations of their eyes, shoulders, and hips.

An additional objective was to estimate the eye ranges of European riders from the anthropometric data of European and American peoples found in reference literature as well as the measurement data on eye locations of American riders.

Method

Measurement of Eye Locations of Japanese and American Riders

(1) Coordinates system: Three-dimensional indications of data in this paper are made in accordance with the orthogonal coordinates system with the seat reference point (a point located on the upper surface of the seat, and 200mm backward from the seat front end, and on the vehicle median plane) as the origin (Figure 3). When it is stated that the handle grip or footrest is adopted as the origin of the coordinates system, the center point of the upper surface of handle grip or footrest is to be the origin, respectively.

(2) Test motorcycles: Test motorcycles included five kinds of motorcycles whose engine capacities ranged

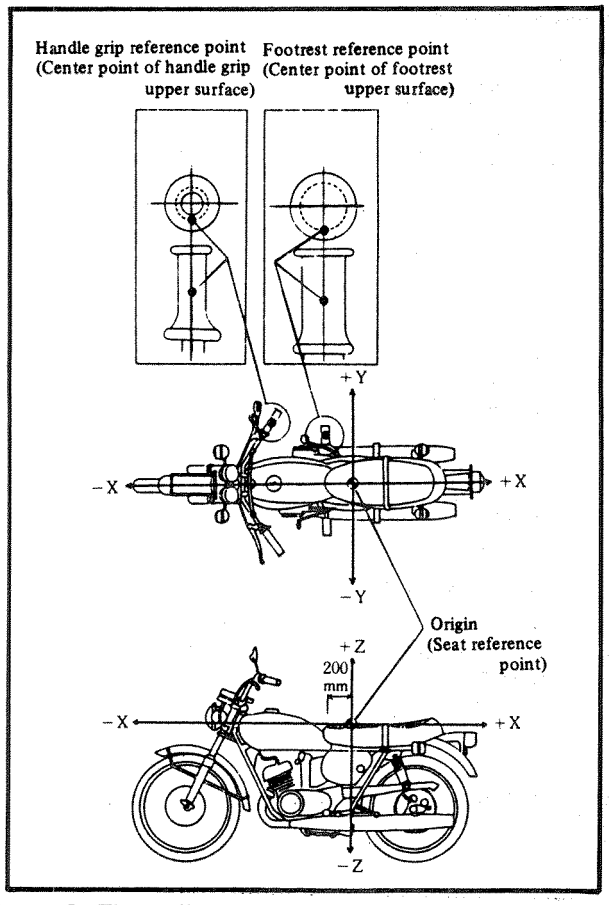

Figure 3. Three-dimensional orthogonal system and reference points

from 250cc class to 1,000cc class. They were divided into four types as follows:

- European-type motorcycles (handlebars located at the most forward position)—Yamaha RZ350, Honda CB750F
- Standard-type motorcycle (handlebar located at medium position)—Kawasaki Z1000J
- On-off-road-type motorcycle (bar-type handle, flat seat)—Suzuki TS250
- American-type motorcycle (chopper-type handlebar, stepped shape seat)—Honda CB750K

Dimensions of the test motorcycles regarding the seat reference point, shown in Figure 4, suggest that the test motorcycles can be divided into the following two groups:

- No. 1 Group: Distance between seat reference point and handle grip is long, thus the riding positions are inclined forward. (Hereinafter referred to as forward-inclined type. An example is shown in Figure 5.)
- No. 2 Group: Distance between seat reference point and handle grip is short, thus the riding positions are upright. (Hereinafter referred to as upright type. An example is shown in Figure 6.)

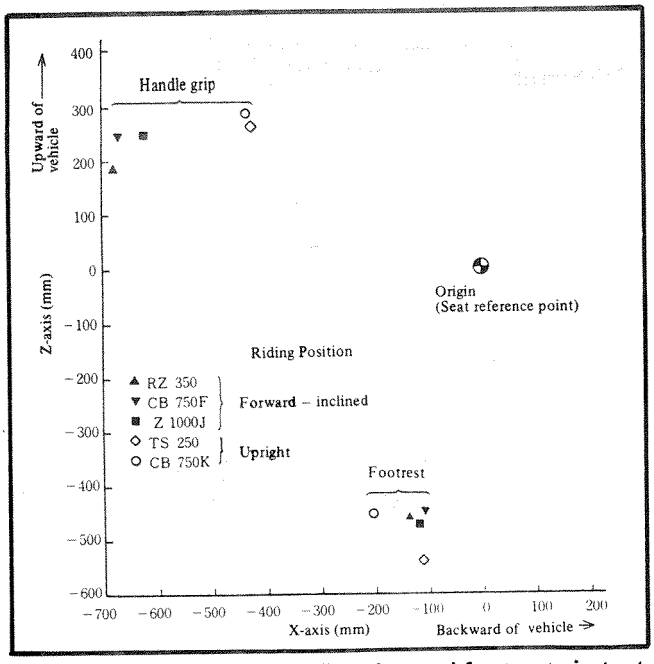

Figure 4. Locations of handle grips and footrests in test motorcycles

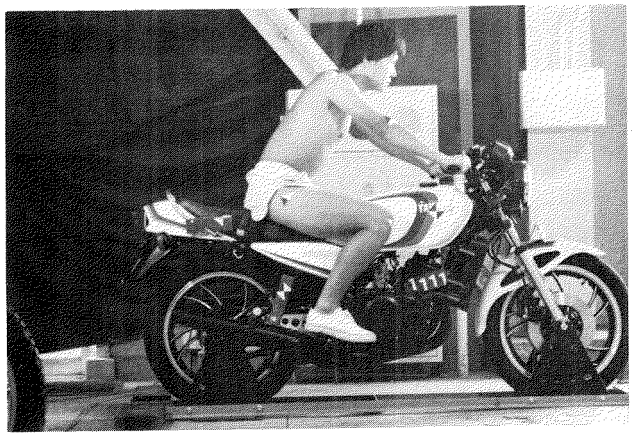

Figure 5. Example of test motorcycle showing forward-inclined riding position (RZ350)

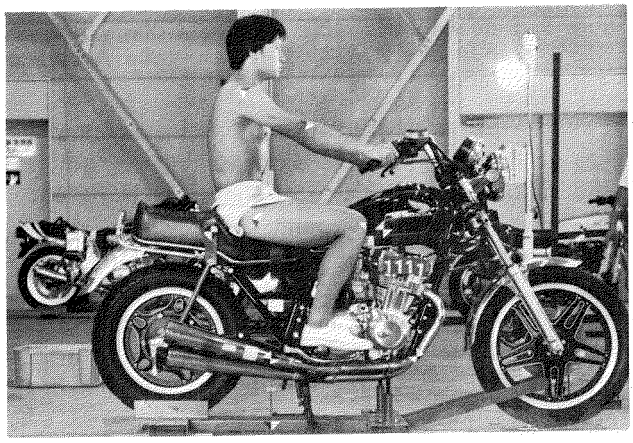

Figure 6. Example of test motorcycle showing upright riding position (CB750K)

(3) Locations of test motorcycle and cameras: The relative locations between the test motorcycle and cameras are illustrated in Figure 7. The test motorcycles were equipped with fixing jigs at the design attitude when one rider was mounting. The cameras were set at the same height as the seat reference point of the test motorcycle and located at 7.0m from the seat reference point.

(4) Measurement procedures: After the anthropometry was finished, the riders were affixed with the marks required for the data analysis at their shoulders and hips. The mark points (acromion and trochanterion) were located by means of manipulation of riders' shoulders and hips in nearly ordinary driving positions (both arms stretched horizontally and forward in a sitting position) and used as shoulder and hip reference points.

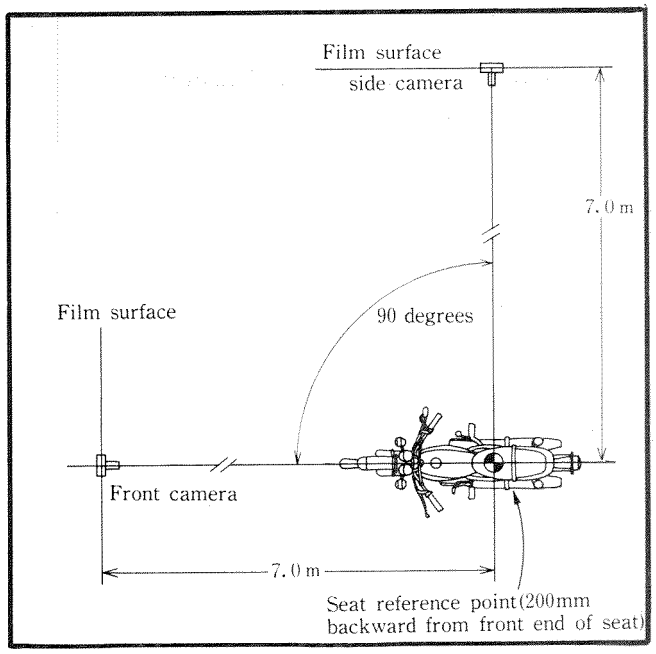

Figure 7. Locations of test motorcycle and cameras

As the next procedure, the riders taking such driving positions on the test motorcycles that correspond to ordinary driving at 50km/h were photographed synchronously by the front and side cameras.

(5) Data processing: The photographed 35mm films were read by a film analyzer with regard to the following items, and the data were collected as an output:

- Side view film (X and Z coordinates): Right eye, right shoulder, right hip, and frame marks for analysis
- Front view film (Y and Z coordinates): Right eye, left eye, and frame marks for analysis

The film analysis data were input into a computer to obtain the actual location of eyes, shoulders, and hips of the riders as well as their statistical distributions. As the locations in Y direction of the riders' acromion and trochanterion could not be photographed by the front camera, half values of biacromial breadth and tro-

chanterion breadth in a sitting position obtained by the anthropometry were used as substitutes for the calculation.

(6) Riders measured: A total of 456 motorcycle riders, comprising 301 Japanese riders and 155 American riders, were measured. All of them possessed motorcycle operation licenses and used motorcycles every day.

Estimation of European Riders' Eye Locations

Estimation was performed with the drawing method. Factors necessary for drawing were obtained by proportional calculations using the anthropometric data (ratios against the data of ordinary Americans listed in Tables 3 and 4) and the data of American riders' riding positions, assuming that the distance between shoulder and handle grip, shoulder and hip, and shoulder and eye are proportional to arm length, acromion to seated surface, and the difference between acromion to seated surface and eye to seated surface, respectively, in each nation.

In this estimation, the angles formed by eye-shoulder-hip and the location of hips of European riders were assumed to be the same as those of American riders.

Results and Consideration

Eye Range, Shoulder Range, and Hip Range of Japanese and American Riders

Eye ranges, shoulder ranges, and hip ranges of American riders on each test motorcycle, as well as the differences between those of American riders and Japanese riders, are shown in Table 5.

(1) Eye range: The sizes of side view eye ranges of American riders are similar for most test motorcycles. Eye ranges of 95th percentile values are ellipses with the major axes about 170mm long and the minor axes about 100mm long.

The inclination angles of the major axes in these eye range ellipses are about 30° in European-type motorcycles (Figure 8, for example) and 25° in standard-type motorcycles. No particular difference is found between these two types, while the inclination angles in on-off-road-type motorcycles and American-type motorcycles (Figure 9) are 14° and 8°, respectively, and are comparatively smaller than those in European- and standard-type motorcycles. When correcting by reducing the forward-inclined angles (the angles formed by the straight lines—one is drawn between the hip and shoulder, and the other is vertical) in riding positions, the inclination angles of the major axes of eye range ellipses, however, are nearly the same (10° ~ 13°) for all test motorcycles.

When compared with the side view eye ranges of Japanese riders, those of American riders are similar in

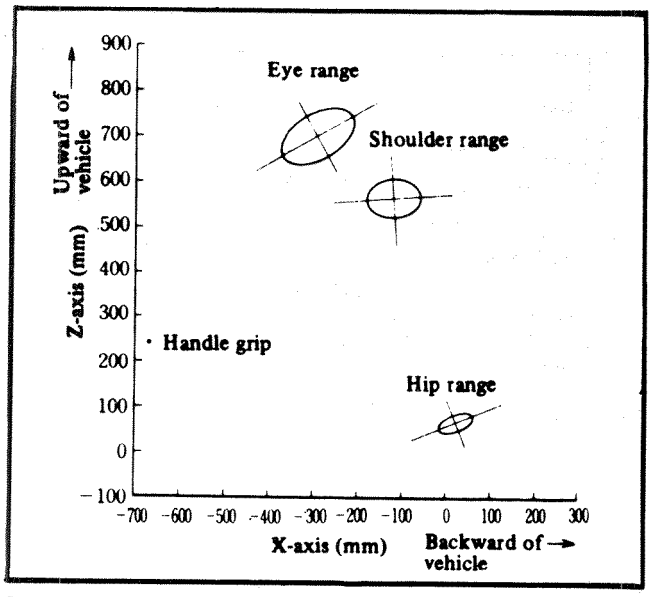

Figure 8. Side view eye range, shoulder range, and hip range of CB750F (95th percentile American riders)

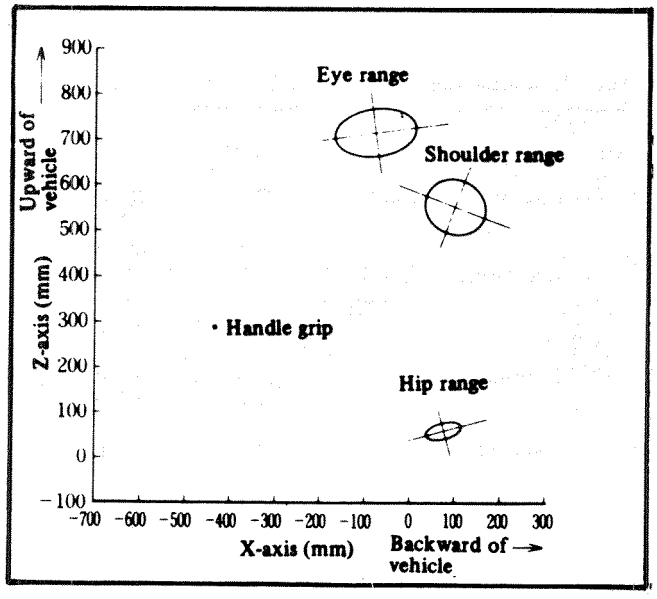

Figure 9. Side view eye range, shoulder range, and hip range of CB750K (95th percentile American riders)

the shape (the major axes of the ellipses are about 1.09 times as large as those of Japanese riders), but the inclination angles are smaller by about 20°.

The sizes of plan view eye ranges of American riders, in 95th percentile values, are a little larger and the major axes are 178mm long in American-type motorcycles (Figure 11) but nearly the same at about 160mm long in motorcycles of other types. (An example is shown in Figure 10.) The minor axes are about 35mm long in all test motorcycles.

The major axes of the plan view ellipses in American riders are somewhat larger (1.23 times) than those in

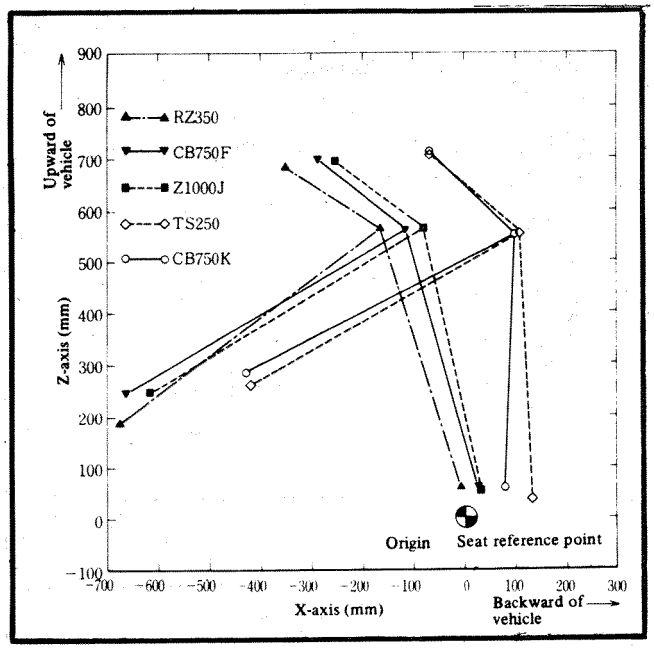

Figure 12. Locations of centroids with seat reference point as origin (American riders)

The differences in the locations of centroids between American and Japanese riders are—

- — Eye range centroids: 65 ~ 70mm in the longitudinal direction in the forward-inclined riding positions and 34 ~ 46mm in the upright riding positions, while 30 ~ 53mm in the vertical direction in the forward-inclined riding positions and 15 ~ 19mm in the upright riding positions
- — Shoulder range centroids: About 40mm in both directions
- — Hip range centroids: About 40mm in the longitudinal direction in most test motorcycles except for on-off-road-type motorcycles where the difference is 73mm owing to ample freedom in selecting seating positions on the seat

- With footrest reference point as origin: With the footrest reference point as the origin, centroids of eye ranges, shoulder ranges, and hip ranges of American riders are distributed in wide areas. (In the longitudinal direction, eye range centroids

Table 6. Locations of centroids of eye range, shoulder range and hip range of American riders

Origin	Centroid location		Type	European		Standard	On-Off-Road	American
			Model name	RZ 350	CB 750F	Z 1000J	TS 250	CB 750K
Seat	Eye range	Right eye	X	-357 (+70)	-293 (+67	-256 (+65)	-77 (+46)	-78 (+34)
			Y	36	35	25	33	27
		Left eye	Y	-28	-29	-39	-31	-36
			Z	682 (+53)	698 (+37)	695 (+30)	707 (+19)	713 (+15)
	Shoulder range		X	-170 (+43)	-122 (+41)	-82 (+42)	106 (+40)	99 (+35)
			Z	562 (+44)	563 (+32)	563 (+36)	557 (+43)	552 (+38)
	Hip range		X	-11 (+30)	25 (+30)	28 (+36)	126 (+73)	77 (+44)
			Z	62 (+17)	63 (+17)	54 (+19)	36 (+22)	58 (+20)
Footrest	Eye range		X	-219 (+70)	-185 (+67)	-136 (+65)	-36 (+46)	-127 (+34)
			Z	1,143 (+53)	1,149 (+37)	1,167 (+30)	1,246 (+19)	1,166 (+15)
	Shoulder range		X	-32 (+43)	-14 (+41)	38 (+42)	219 (+40)	304 (+35)
			Z	1,023 (+44)	1,014 (+32)	1,035 (+36)	1,096 (+43)	1,005 (+38)
	Hip range		X	127 (+30)	133 (+30)	148 (+36)	239 (+72)	282 (+44)
			Z	523 (+17)	514 (+17)	526 (+19)	575 (+22)	511 (+20)
Handle Grip	Eye range		X	321 (+70)	377 (+67)	366 (+65)	344 (+46)	355 (+34)
			Z	496 (+53)	452 (+37)	449 (+30)	443 (+19)	424 (+15)
	Shoulder range		X	508 (+43)	548 (+41)	540 (+42)	527 (+40)	532 (+35)
			Z	376 (+44)	317 (+32)	317 (+36)	293 (+43)	263 (+38)
	Hip range		X	667 (+30)	695 (+30)	650 (+36)	547 (+72)	510 (+44)
			Z	-124 (+17)	-183 (+17)	-192 (+19)	-228 (+22)	-231 (+20)

Unit: mm

(): Difference between American and Japanese riders
On X-axis, "+" means American riders are located backward than Japanese riders.
On Z-axis, "+" means American riders are located upward than Japanese riders

are distributed for 183mm range, shoulder range centroids for 336mm range, and hip range centroids for 155mm range.)

With hande grip reference point as origin: With the handle grip reference point as the origin, the distribution of centroids of eye ranges, shoulder ranges, and hip ranges show different tendencies from those in other cases where the seat reference point or the footrest reference point is adopted to be the origin.

Namely, the hip range centroids of American riders are distributed in a wider area (185mm range in longitudinal direction), and their eye range and shoulder range centroids are distributed in a relatively narrow area. (Eye range centroid distribution is 56mm range in longitudinal direction and 72mm range in vertical direction. Shoulder range centroid distribution is 40mm range in longitudinal direction and 113mm range in vertical direction.)

Accordingly, the handle grip reference point is more suitable as a frame reference point than the seat or footrest reference points.

With shoulder range centroid as origin: With the shoulder range centroid as the origin, the locations of eye range centroids, hip range centroids, and handle grip reference points are shown in Figure 13.

In every test motorcycle, the distances from the shoulder range centroid to the handle grip reference point, to the hip range centroid, and to the eye range centroid are nearly constant, and the angles formed with the locations of eye-shoulder-hip also scarcely differ from one another.

Therefore, as illustrated in Figure 14, with the shoulder range centroid as the origin, the following items are obtained and compared among various types and models (Table 7).

Distance (A)	Distance between the shoulder range centroid and the handle grip reference point
Distance (B)	Distance between the shoulder range centroid and the hip range centroid
Distance (C)	Distance between the shoulder range centroid and the eye range centroid
Angle (α)	Angle formed with the locations of handle-shoulder-hip
Angle (β)	Angle formed between the straight line (shoulder-hip) and the vertical line
Angle (γ)	Angle formed with the locations of eye-shoulder-hip

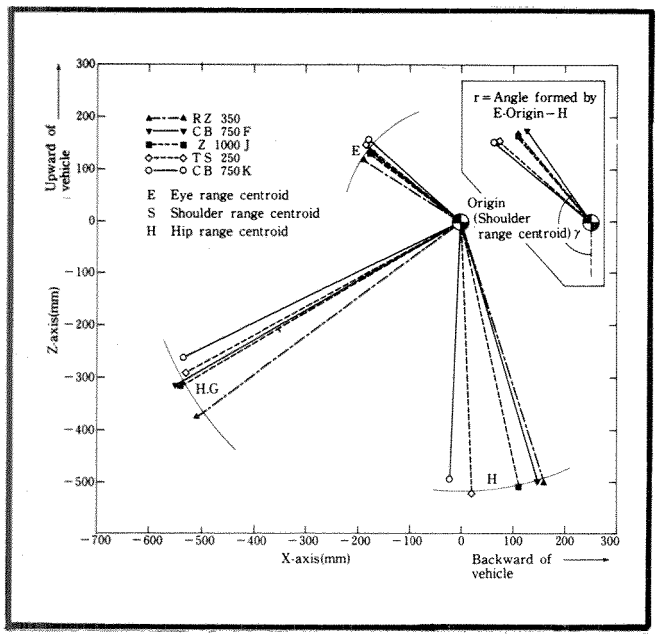

Figure 13. Locations of centroids with shoulder range centroid as origin (American riders)

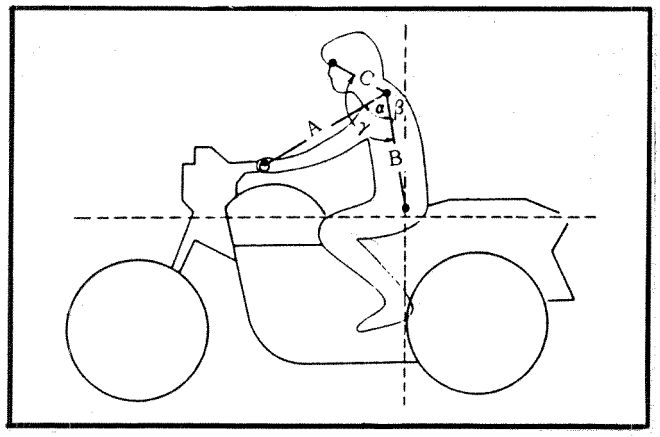

Figure 14. Indication of riding position with shoulder range centroid as origin

Distance (A) is about 630mm in European-type and standard-type motorcycles, 603mm in on-off-road-type motorcycles, and 593mm in American-type motorcycles. European-type and standard-type motorcycles are 30 ~ 40mm longer in distance (A) than on-off-road-type or American-type motorcycles.

Distance (B) is about 520mm and nearly the same in motorcycles of all types, except for American-type motorcycles in which distance (B) is 494mm.

Distance (C) in the forward-inclined-type motorcycles (European-type and standard-type motorcycles) is about 20mm shorter than that of the upright-type motorcycles (on-off-road-type and American-type motorcycles).

Table 5. Eye range, shoulder range and hip range of American riders

Plane		Type		European		Standard	On-Off-Road	American
	Percentile	Item	Model Name	Rz 350	CB 750F	Z 1000J	TS 250	CB 750K
Side View (X-Z Plane) Eye Range	90th	Major axis		145 (+11)	137 (+15)	130 (+8)	130 (+6)	140 (+16)
		Minor axis		74 (-4)	73 (+5)	74 (+6)	79 (+5)	78 (-8)
	95th	Major axis		186 (+14)	176 (+19)	167 (+11)	167 (+8)	180 (+21)
		Minor axis		95 (-5)	94 (+7)	95 (+8)	101 (+6)	100 (-11)
	99th	Major axis		263 (+20)	248 (+26)	236 (+16)	236 (+11)	254 (+29)
		Minor axis		134 (-7)	132 (+9)	134 (+11)	143 (+9)	141 (-16)
		Inclination angle		30.4(-21.5)	29.0(-20.9)	25.3(-21.7)	13.5(-21.5)	7.7(-13.4)
		Inclination angle—forward inclined angle		12.8(-19.1)	12.6(-19.2)	13.0(-20.7)	11.3(-25.3)	10.2(-14.7)
Shoulder Range	90th	Major axis		97 (+21)	93 (+22)	94 (+24)	97 (+13)	103 (+17)
		Minor axis		74 (0)	73 (+9)	77 (+9)	84 (+7)	89 (+14)
	95th	Major axis		124 (+26)	119 (+28)	121 (+32)	124 (+17)	132 (+21)
		Minor axis		95 (0)	94 (+12)	99 (+12)	108 (+9)	114 (+18)
	99th	Major axis		176 (+37)	169 (+40)	170 (+47)	176 (+25)	187 (+30)
		Minor axis		134 (0)	132 (+16)	140 (+17)	152 (+12)	161 (+25)
		Inclination angle		0.8(-19.9)	3.4(-13.3)	-7.3(-4.3)	-27.0(-69.0)	-20.5(-16.4)
Hip Range	90th	Major axis		79 (-11)	70 (+3)	76 (0)	119 (-3)	61 (-17)
		Minor axis		28 (-1)	31 (+2)	29 (0)	28 (-1)	31 (+3)
	95th	Major axis		101 (-15)	90 (+4)	98 (+1)	153 (-4)	78 (-22-)
		Minor axis		36 (-1)	40 (+2)	37 (0)	36 (-1)	40 (+4)
	99th	Major axis		143 (-20)	127 (+5)	138 (+1)	216 (-6)	111 (-30)
		Minor axis		51 (-1)	56 (+2)	53 (+1)	51 (-1)	56 (+5)
		Inclination angle		18.4(+1.7)	20.9(+4.2)	19.5(+1.2)	9.5(-1.2)	14.8(+3.6)
Plan View (X-Y Plane) Eye Range	90th	Major axis		131 (+28)	125 (+31)	122 (+25)	128 (+17)	139 (+20)
		Minor axis		27 (-2)	27 (-2)	27 (-1)	25 (-5)	29 (+1)
	95th	Major axis		168 (+36)	160 (+39)	157 (+33)	164 (+23)	178 (+25)
		Minor axis		35 (-2)	35 (-2)	35 (-2)	32 (-7)	37 (0)
	99th	Major axis		238 (+51)	227 (+56)	221 (+46)	232 (+33)	252 (+36)
		Minor axis		49 (-3)	49 (-3)	49 (-3)	45 (-10)	53 (+1)
		Inclination angle		1.6(-1.4)	1.7(-1.1)	-1.1(-2.7)	0.8(-1.4)	-0.8(-1.4)

Unit: Major and minor axes: mm
Inclination angle: degree

(): Difference between American and Japanese riders "+" means American riders are larger than Japanese in an item. "-" means American riders are smaller than Japanese in an item.

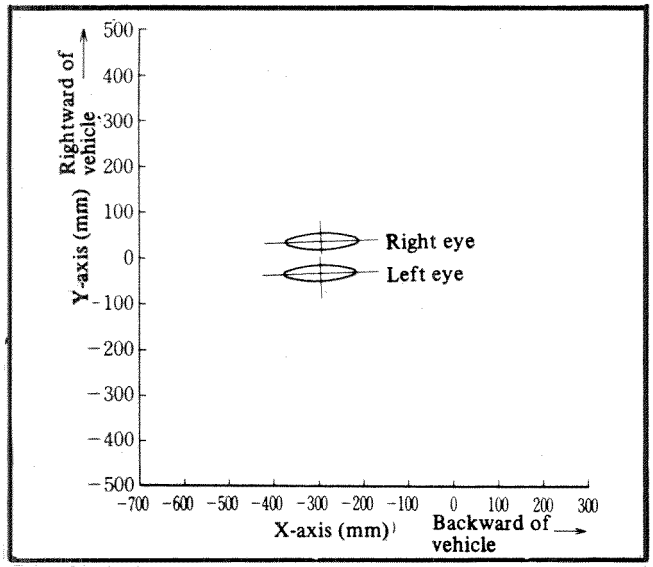

Figure 10. Plan view eye range of CB750F (95th percentile American riders)

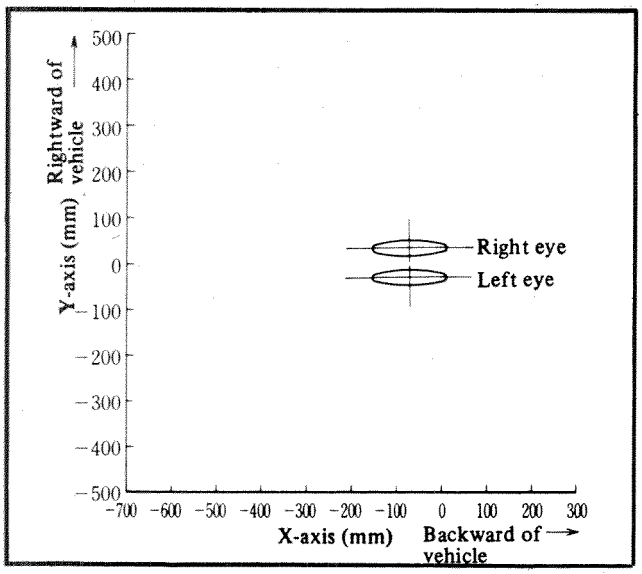

Figure 11. Plan view eye range of CB750K (95th percentile American riders)

Japanese riders. This is because the side view eye ranges of American riders are somewhat larger than those of Japanese riders, and the inclination angles of the major axes in the side view ranges are about 20° smaller than those of Japanese riders.

(2) Shoulder range: The sizes of shoulder ranges of American riders are nearly the same for all test motorcycles, and, in 95th percentile values, the shoulder ranges are ellipses with the major axes about 120mm long and the minor axes about 100mm long. The shapes of shoulder ranges are nearly circles.

The shoulder ranges in American riders are somewhat larger than those in Japanese riders. (The major axes are about 1.25 times as large as those in Japanese riders and the minor axes are 1.11 times.)

(3) Hip range: The sizes of hip ranges of American riders, in 95th percentile values, are nearly the same with the major axes about 95mm long in most European- and standard-type motorcycles, but are large (153mm in the major axes length) in American-type motorcycles and small (78mm in the major axes lengths) in American-type motorcycles. The minor axes are about 38mm long for all test motorcycles, and the inclination angles (of the major axes) are about 20° in European and standard types, 10° in on-off-road-type, and 15° in American-type motorcycles.

As for the sizes of hip ranges, American riders are similar to Japanese riders in all test motorcycles except for American-type motorcycles where American riders are a little smaller (0.78 times as large as Japanese riders).

(4) Relation between dimensions of test motorcycles and locations of eyes, shoulders, and hips of riders: The locations of eye range centroids, shoulder range centroids, and hip range centroids of American riders, as well as the differences between those of American riders and Japanese riders, are shown in Table 6, where the locations of those centroids are shown relatively in each test motorcycle with the seat reference point, the footrest reference point, and the handle grip reference point as the origins, respectively.

- With seat reference point as origin: The location of eyes, shoulders, and hips (eye range centroids, shoulder range centroids, and hip range centroids) of American riders on all test motorcycles with the seat reference point as the origin and the riding positions indicated by the lines drawn between these three centroids are shown in Figure 12.

  With the seat reference point as the origin, the locations of centroids of eye ranges, shoulder ranges, and hip ranges are distributed in wide areas. (In the longitudinal direction, eye range centroids are distributed for 280mm range, shoulder range centroids for 276mm range, and hip range centroids for 137mm range.)

  As the locations of hip range centroids of riders do not coincide with the seat reference points and are distributed in wide longitudinal ranges of 137mm, it is inappropriate that the seat reference point is adopted for setting H-point (hip point) or R-point (a design reference point corresponding to H-point). Accordingly, the actual measurements using a three-dimensional or two-dimensional manikin for motorcycles are considered necessary.

  When compared with Japanese riders, the locations of centroids of eye ranges, shoulder ranges, and hip ranges of American riders are more upward and rearward by a few centimeters than those of Japanese riders (Table 6).

Table 7. Relations among locations of eyes, shoulders, hips and handlegrip in American riders (factors for drawing)

Type			Forward-inclined				Upright		
			European		Standard	Mean Value	On-Off-Road	American	Mean Value
Centroid	Distance / Angle	Model Name	RZ 350	CB 750F	Z 1000J		TS 250	CB 750K	
s	d A		632 (+61)	633 (+49)	626 (+55)	630 (+55)	603 (+55)	593 (+47)	598 (+51)
H	a α		71.1 (-3.4)	76.4 (-2.4)	70.9 (-3.0)	72.8 (-2.9)	63.1 (+1.8)	61.2 (-0.6)	62.2 (+0.6)
s	d B		525 (+22)	521 (+11)	521 (+15)	522 (+16)	521 (+22)	494 (+17)	508 (+20)
hi	a β		17.6 (-2.4)	16.4 (-1.7)	12.3 (-1.0)	15.4 (-1.7)	2.2 (+3.8)	-2.5 (+1.3)	-0.2 (+2.5)
s	d C		222 (-19)	218 (-19)	218 (-22)	219 (-20)	237 (-21)	239 (-16)	238 (-19)
e	a γ		140.3 (+2.8)	144.7 (+3.2)	139.4 (+0.9)	141.5 (+2.3)	131.5 (+0.5)	129.8 (-2.6)	130.7 (-1.0)

Unit: Distance: mm

() Shows difference between American and Japanese riders.
"+" Means American riders are larger than Japanese in an item.
"-" Means American riders are smaller than Japanese in an item.

s = Shoulder hi = Hip H = Handle grip
e = Eye d = Distance a = Angle

Angle (α) of the forward-inclined-type motorcycles is larger than that of the upright-type motorcycles, and the angle formed with arm and back are closer to a right angle in the former type motorcycles than the latter.

Angle (β), which indicates the extent of the forward inclination in riding positions, is largest in European-type motorcycles. The average forward-inclination angle in European and standard types is 15.4°. On the contrary, in the upright-type motorcycles, this angle is 2.2° ~ -2.5°, which means nearly upright riding positions.

Angle (γ), formed with the location of eyes, shoulders, and hips, in the forward-inclined-type motorcycle is about 11° larger than that in the upright-type motorcycle, but the deviation of its value from the mean value in each type of test motorcycle is 3.1° maximum and in a stable condition.

It is found that riders adjust their riding positions to the differences in the dimensions of motorcycle frames chiefly by changing the angle (α) formed with arm and back and the forward-inclination angle (β).

It is also found that, with the increase in the forward-inclined angle, they would raise their head.

Distance (A) of American riders is about 50mm longer and distance (B) is 10 ~ 20mm longer than Japanese riders, while distance (C) of American riders is 20mm shorter than Japanese riders.

This tendency agrees with the fact that American riders are 70mm longer in arm length, 31mm longer in acromion to seated surface, and 19mm shorter in the distance between eye to seated surface—acromion to seated surface than Japanese riders (see Tables 3 and 4).

Angle (β), the forward-inclination angle of riders' torsos, of American riders on European-type motorcycles is about 2° smaller and on standard-type motorcycles 1° smaller than Japanese riders. This is because American riders have physical margins for the distance between shoulder and handle, which enables them to assume slightly forward-inclined riding positions.

Angle (γ), formed with the locations of eye-shoulder-hip, is about 3° larger in American riders on European-type motorcycles and is 2.6° smaller in American riders on American-type motorcycles than Japanese riders.

- Correction of eye locations in accordance with test motorcycle dimensions: As stated in the foregoing, with the shoulder range centroid as the origin, four factors—namely, distances (A), (B), (C), and angle (γ)—hardly vary with the dimensions of test motorcycles within each riding position type. (But distance (B) in on-off-road-type motorcycles is similar to that in the forward-inclined riding position types.)

  Therefore, for an American rider, eye location can be determined with regard to any motorcycle by describing a drawing with these four factors, if the positional relations between the handle grip reference point and H-point of the rider are known (see Figure 14).

Estimation of European Riders' Eye Locations

With the handle grip reference point and the hip range centroid as the origin, the locations of eye range centroids of European riders were estimated by the drawing method as shown in Figure 14, and the differences in eye range centroid locations between American and European riders are shown in Figure 15. In this figure, arrow marks show the differences in eye range centroid locations from

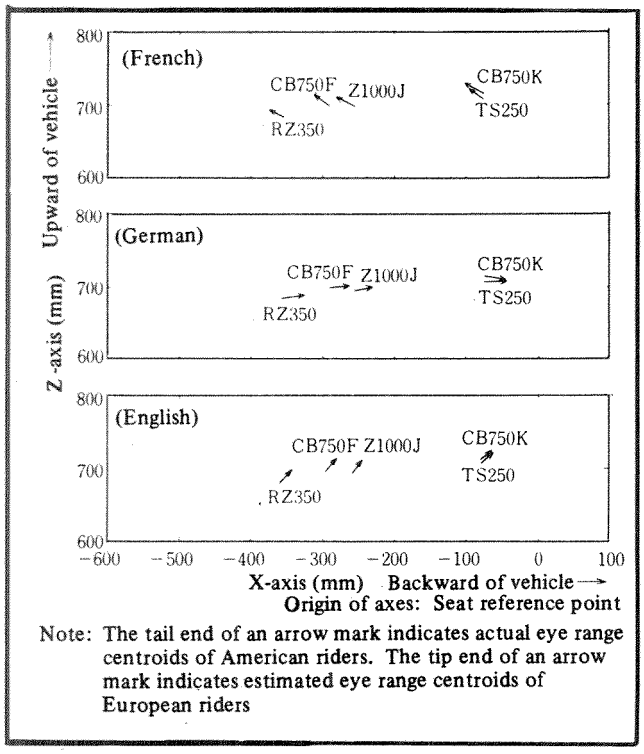

Note: The tail end of an arrow mark indicates actual eye range centroids of American riders. The tip end of an arrow mark indicates estimated eye range centroids of European riders

Figure 15. Differences between estimated eye range centroids of European riders and actual measured eye range centroids of American riders

those of American riders. (Base end points of arrow marks show actually measured locations of eye range centroids of American riders, and front end points indicate the estimated eye range centroid locations of European riders.)

The locations of French riders' eye range centroids are estimated to be 20 ~ 25mm forward and 15mm upward more than those in American riders. This is because French riders are somewhat longer in acromion to seated surface than American riders (acromion to seated surface in French riders is 7mm longer than in American riders), and they are also larger in the difference between eye to seated surface and acromion to seated surface than American riders. (This difference in French riders is 17mm larger than in ordinary Americans.)

The location of German riders' eye range centroids are estimated to be 24 ~ 30mm more backward than those of American riders. This is because German riders are longer in arm length (21mm longer than American riders) and the difference between eye to seated surface and acromion to seated surface in German riders is shorter (by 13mm) than in American riders.

The locations of English riders' eye range centroids are estimated to be 15 ~ 20mm backward and 10 ~ 20mm upward more than those of American riders. This is because English riders are longer in arm length (by 22mm)than American riders and are also somewhat larger in the difference between eye to seated surface and acromion to seated surface (by 8mm) than American riders.

As stated above, the differences between the estimated location of eye range centroids for European riders and the location of eye range centroids in American riders are not so large and are about 30mm maximum. The differences in anthropometric data used for the estimation of eye range centroid locations between Europeans and Americans are maximum 22mm and are nearly the similar values to the tolerances on the anthropometric literature references (18mm maximum).

Accordingly, until such time when actually measured data of eye ranges in European riders are obtained, eye ranges of actual measurement in American riders should be adopted instead of the estimated locations of eye range centroids for European riders as the representative eye range for European riders. Figure 16 shows an example of comparison in eye ranges, shoulder ranges, and hip ranges among Japanese, American, and German riders.

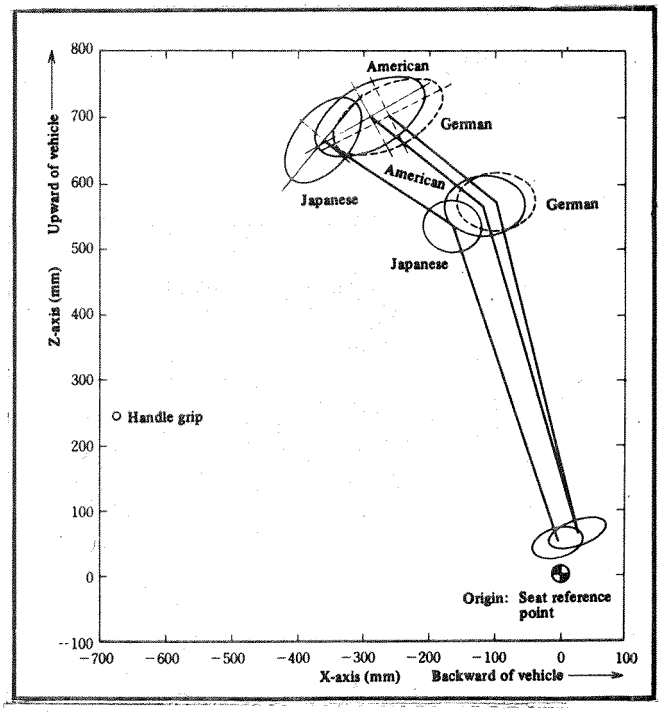

Figure 16. Comparisons of eye ranges, shoulder ranges, and hip ranges among Japanese, American, and German riders (CB750F)

Correction Formula for Eye Locations

Purpose

The purpose of this portion of the study was to establish a correction formula for eye ranges in consideration of vehicle dimensions and running speeds that affect riders' eye locations.

Method

Measurement of Variation in Eye Locations in Accordance With Vehicle Dimensions

(1) Mock-up: A mock-up for motorcycles was used. The locations of its handlebar and footrests could be changed in both longitudinal and vertical directions. In this study, the mock-up could cover the specifications of three types of test motorcycles (CB750F, TS250, and CB750K, Figure 17). In the mock-up, the standard locations of handle grip and footrest with the seat reference point as the origin coincided with those of each test motorcycle (see Figure 4).

(2) Measurement conditions: In each test motorcycle, either handle grip or footrest was fixed at the standard location and the location of the other was changed.

(3) Riders measured: Eleven motorcycle riders from Japanese manufacturers were measured. Their statures were averaged to be 1,679mm, which was nearly equal to the average of all Japanese riders' statures (1,685mm). The locations of test motorcycles and cameras, the measurement procedures, and the data processing were the same as stated before.

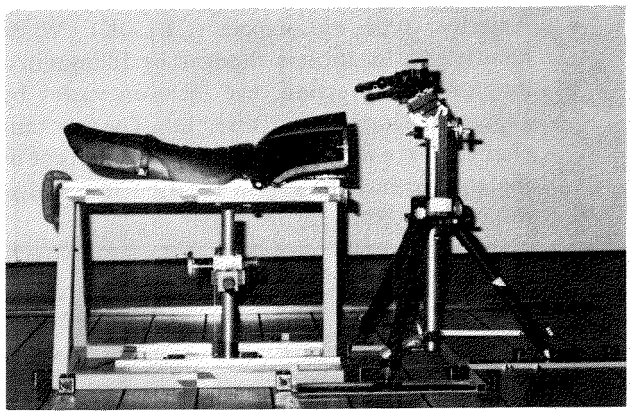

Figure 17. Motorcycle mock-up (European type)

Measurement of Variation in Eye Locations in Accordance With Vehicle Running Speed

(1) Test motorcycles: Two European-type motorcycles (Honda CB750F) with engines of 750cc piston displacement were used as the test motorcycles. One was equipped with a fairing and the other was not. The location of the fairing upper edge was 868mm forward and 534mm upward on the longitudinal median plane with the seat reference point as the origin.

(2) Photographing method: Side views of motorcycle riders running on a test course were photographed with a high-speed camera. The photographing rate was 500 frames/s, and the photographing distance was 15m.

As the riders wore full-face protective helmets, the locations of eyes were not photographed directly; therefore, the analysis marks for the indications of eye location were affixed on the surface of the helmets. (Intersections of those marks represent eye locations.)

Furthermore, the analysis marks representing locations of shoulder and hip were affixed on the riding wears for the identification of locations of acromion and trochanterion of the riders when they took riding positions adequate to various driving speeds.

(3) Running speed: Six running speeds in a range between 50 and 180km/h were selected for the testing. Each rider ran at a speed checked by a calibrated speedometer and passed through the front of the camera maintaining a steady and specified speed by assuming a natural riding position (Figure 18). The difference between the actual running speed obtained from the timing marks of the photographed films and the specified running speed was within about 2km/h in every running condition.

(4) Riders measured: Twelve riders from Japanese manufacturers participated in this test. Their statures were averaged to be 1,692mm, which was nearly equal to the averaged stature of all Japanese riders (1,685mm). The data obtained were processed in the same procedures as stated before.

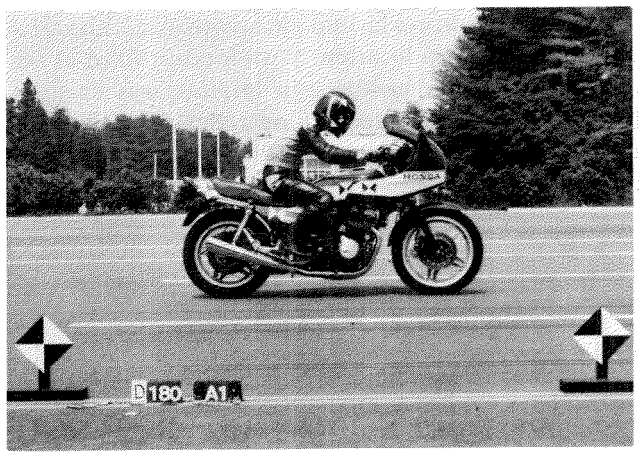

Figure 18. Riding position in actual running

Results and Considerations

Variation in Eye Locations in Accordance With Variation in Vehicle Dimensions

(1) Variation in eye locations in accordance with variation in footrest location: With handle grip fixed at the standard location, footrest location was changed from its standard location. Under this condition, the mean values of eye locations of 11 riders were obtained and studied.

- European-type motorcycle (CB750F): When footrest location is changed by 100mm in a

longitudinal direction, eye location varies by 18mm maximum in a longitudinal direction. When footrest location is changed backward, eye location shows a tendency to move somewhat forward. When footrest location is changed by 115mm in a vertical direction, eye location varies by 13mm maximum in a longitudinal direction, but no generally acceptable tendency is found.

- On-off-road-type motorcycle (TS250): When footrest location is changed by 100mm in a longitudinal direction, eye location varies by 10mm maximum in a longitudinal direction. When footrest location is changed by 115mm in a vertical direction, eye location varies by 19mm maximum in a longitudinal direction, but no generally acceptable tendency is found.
- American-type motorcycle (CB750K): Even if footrest location is changed by 100mm in a longitudinal direction, eye location hardly varies. When footrest location is changed by 75mm in a vertical direction, eye location varies by 11mm maximum in a longitudinal direction, but no generally acceptable tendency is found. It has become clear that the rider's eye location is scarcely influenced by the change in footrest location.

(2) Variation in eye location in accordance with variation in handle grip location: With footrest fixed at the standard location, handle grip location was changed from its standard location. Under this condition, the mean values of eye locations of all 11 riders were obtained and studied.

- European-type motorcycle (CB750F): When handle grip location is changed by 200mm in a longitudinal direction, eye location varies by 173mm in a longitudinal direction. The resultant change in eye location (179mm) is 90 percent of the change in handle grip location in a longitudinal direction (Figure 19).

  When handle grip location is changed by 125mm in a vertical direction, eye location varies by 89mm in a longitudinal direction. The resultant change in eye location (99mm) is 79 percent of the change in handle grip location in a vertical direction (Figure 20).
- On-off-road-type motorcycle (TS250): When handle grip location is changed by 125mm in a longitudinal direction, eye location varies by 82mm in a longitudinal direction. The resultant change in eye location (83mm) is 66 percent of the change in handle grip location in a longitudinal direction (Figure 21).

  When handle grip location is changed by 100mm in a vertical direction, eye location varies by 24mm in a longitudinal direction. The resultant change in eye location (25mm) is 25 percent of the change in handle grip location in a vertical direction (Figure 22).
- American-type motorcycle (CB750K): When handle grip location is changed by 187mm in a longitudinal direction, eye location varies by 145mm in a longitudinal direction. The resultant change in eye location (146mm) is 78 percent of the change in handle grip location in a longitudinal direction (Figure 23).

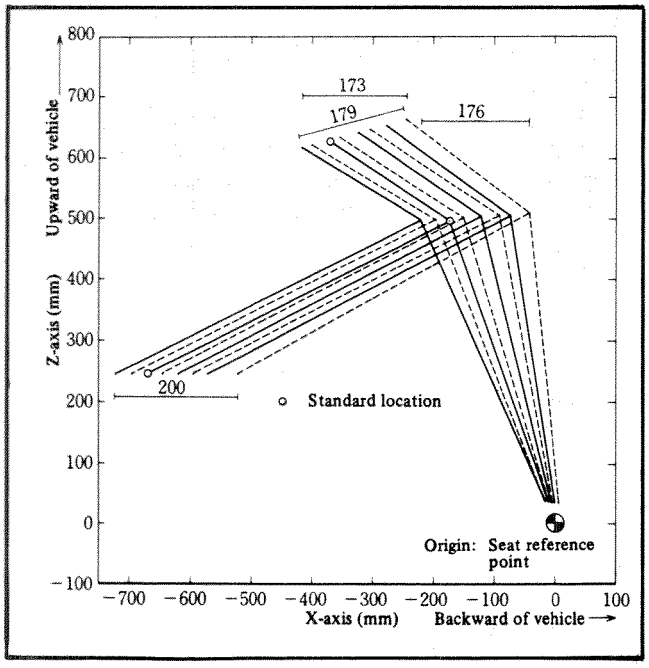

Figure 19. Riding position variation according to variation in handle grip location in longitudinal direction (European type)

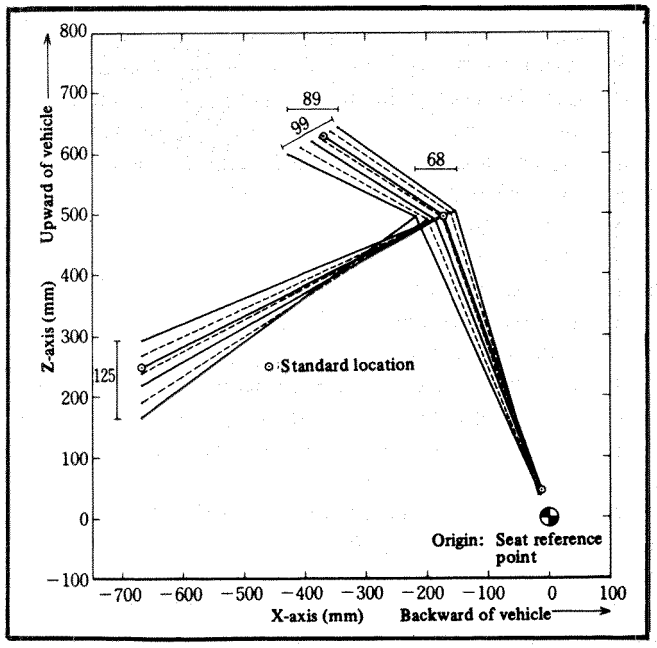

Figure 20. Riding position variation according to variation in handle grip location in vertical direction (European type)

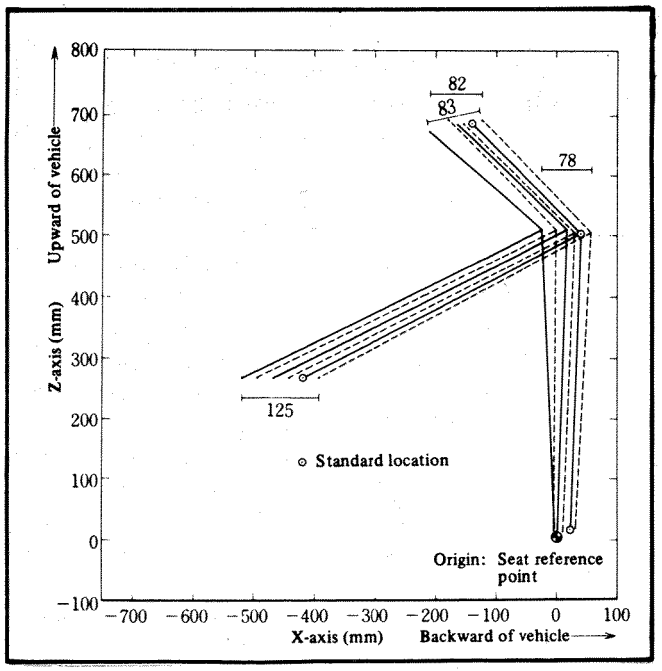

Figure 21. Riding position variation according to variation in handle grip location in longitudinal direction (on-off-road type)

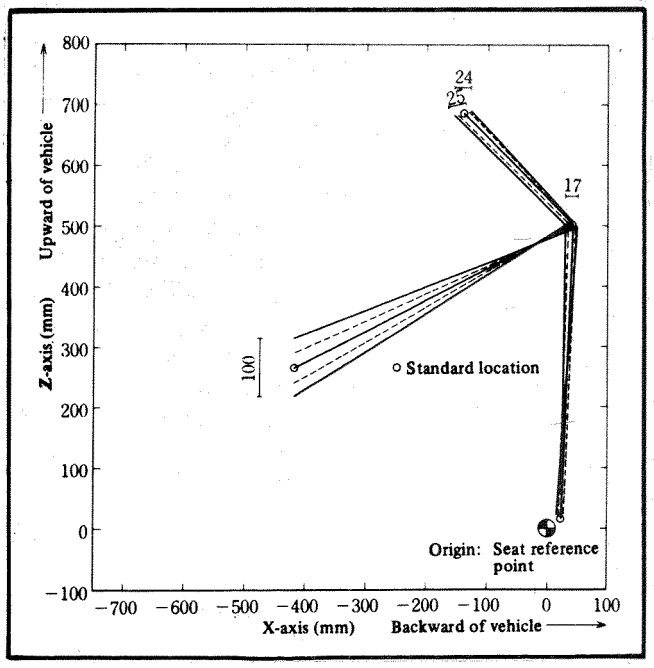

Figure 22. Riding position variation according to variation in handle grip location in vertical direction (on-off-road type)

When handle grip location is changed by 75mm in a vertical direction, eye location varies by 25mm in a longitudinal direction. The resultant change in eye location (26mm) is 35 percent of the change in handle grip location in a vertical direction (Figure 24).

As stated above, it is found that in any type of motorcycle with variation in handle grip location in a forward or downward direction, riding position is changed to forward inclined and eye location changes forward and downward.

The resultant change in eye location depends on the conditions. The longer the distance between the seat and the handle grip, the larger the variation in eye location. However, the variation in handle grip location in a longitudinal direction exerts a larger effect on the change in eye location than that in a vertical direction.

(3) Relation between handle grip location and riding position: The relation between the rider's forward-inclination angle (β) and four factors—namely, distance (A) (distance from shoulder to handle grip), distance (B) (distance from shoulder to hip), distance (C) (distance from shoulder to eye), and angle (γ) (formed with location of eyes, shoulders, and hips)—are shown in Figure 25.

Distance (A) is constant when angle (β) is 5° or more but is reduced when angle (β) is less than 5°, where riding position is near an upright position. (Distance (A) is reduced at a rate of about 30mm per 5° in the variation of angle (β).) This shows that the rider's arm is extended in a common manner in motorcycles of a forward-inclined riding position type irrespective of vehicle dimensions and that the arm-bending angle is increased with the decrease of angle (β) in an upright riding position type.

Distance (B) is a little decreased with the decrease of angle (β) in any type of motorcycle (about 6mm per 5° of variation in angle (β)) except for on-off-road type. In on-off-road-type motorcycles, distance (B) is constant irrespective of the forward-inclination angle. The value of distance (B) in on-off-road type is more similar to that in a European type than in an American type.

Distance (C), on the contrary, has a tendency to increase with the decrease of angle (β) (about 4mm per 5° of the variation in angle (β)).

Angle (γ) varies for some range even though angle (β) is constant, owing to other conditions, and shows a tendency to vary in such a manner as to be proportional to angle (β) (about 2.5° per 5° of the variation in angle (β) corresponding to about 10mm of the variation in eye location).

Variation in Eye Location in Accordance With Vehicle Running Speed

The riding positions at various running speeds are shown in Figures 26 and 27 by using mean values of 12 riders.

When a fairing was not equipped on the test motorcycle, with the increase in running speed, the forward-inclination angle in a riding position increased (hip location changed backward and shoulder location changed forward and downward), and eye location changed forward and downward (Figure 26).

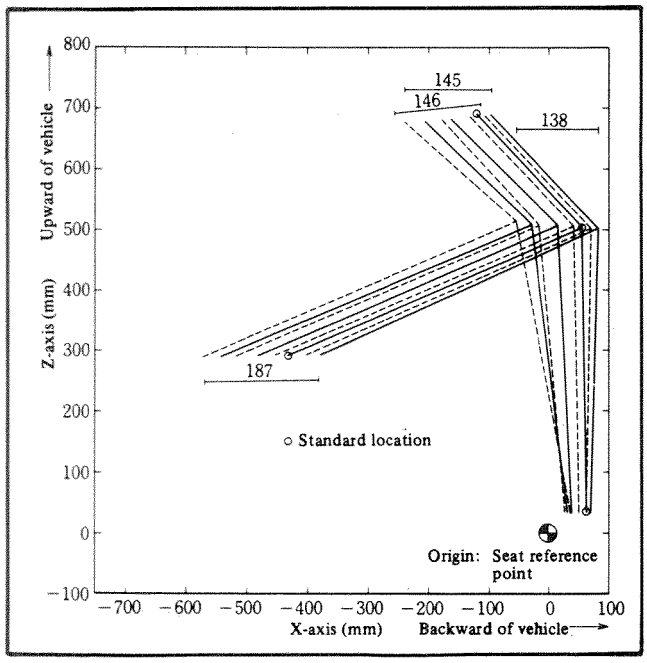

Figure 23. Riding position variation according to variation in handle grip location in longitudinal direction (American type)

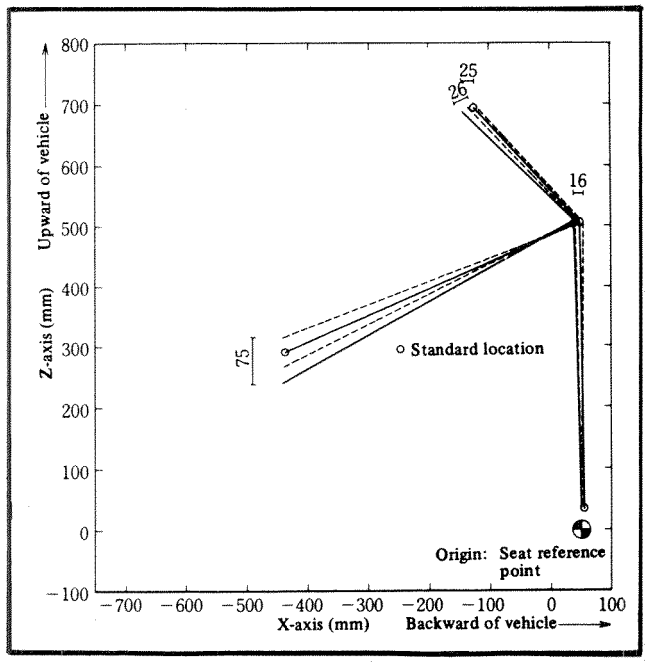

Figure 24. Riding position variation according to variation in handle grip location in vertical direction (American type)

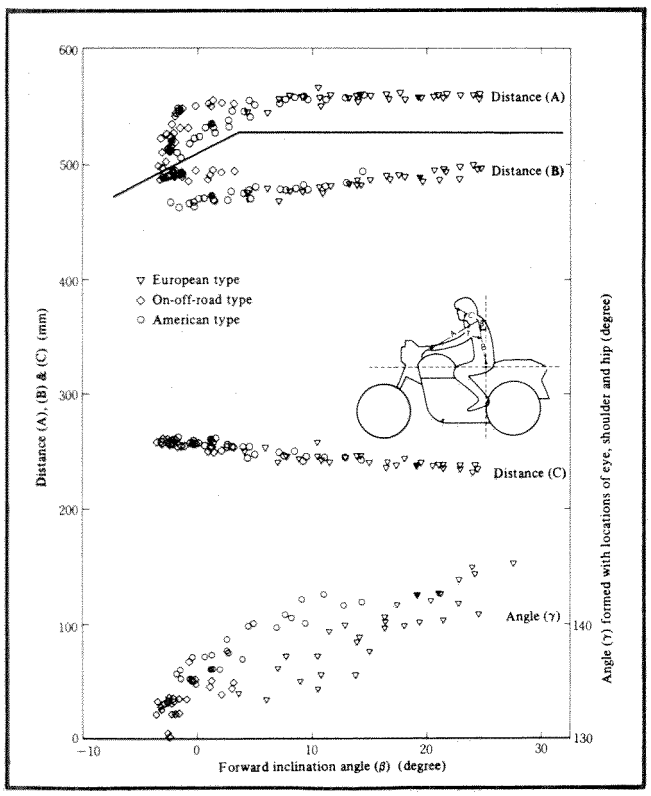

Figure 25. Factors (A), (B), (C), and (γ) for drawing in reference to forward-inclination angle (β)

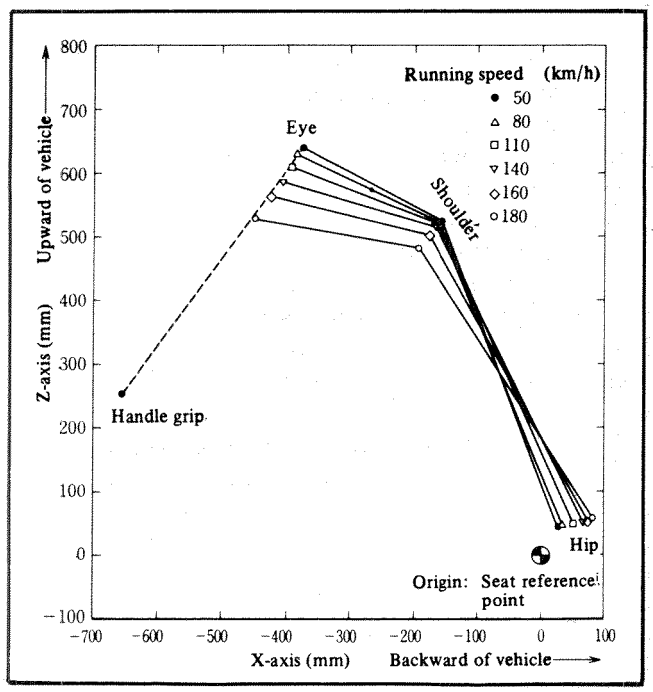

Figure 26. Variation of eye location according to running speed (without fairing)

When a fairing was equipped on the test motorcycle, the forward-inclination angle in a riding position also increased, and eye location changed forward and downward with the increase in running speed (Figure 27).

In addition to these tendencies, when eye location changed forward and downward, the downward view angle formed with a straight line drawn through the eye and the upper edge of fairing and the horizontal line

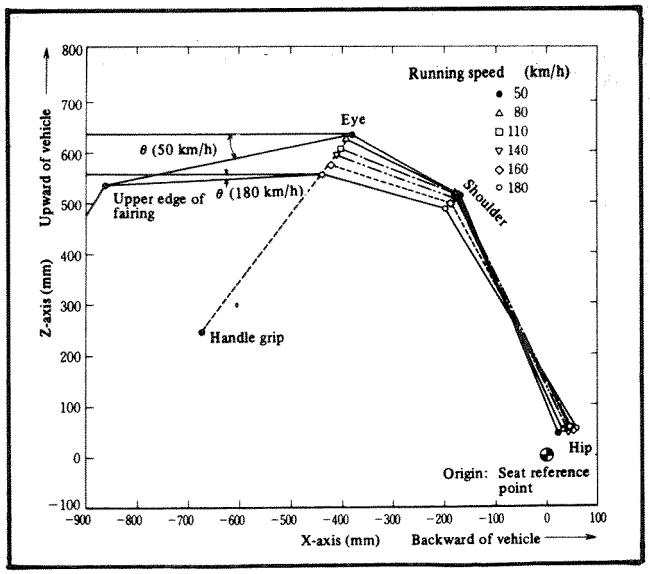

Figure 27. Variation of eye location according to running speed (with fairing)

(angle θ in Figure 27) decreased and was at a speed of 180km/h, about one-fourth of that at 50km/h.

In any case, with the change in running speed, eye location moved on a straight line drawn through the eye location at a running speed of 50km/h and the handle grip reference point. With location of eyes at a running speed of 50km/h as the standard location, resultant changes (distances) in eye location at various running speeds are shown in Figure 28.

If fairings are not equipped, the resultant changes in eye location are 37mm at a running speed of 110km/h and 65mm at a running speed of 140km/h. If fairings are equipped, the resultant change in eye location is 35mm at a running speed of 110km/h and 52mm at a running speed of 140km/h.

When compared with the former case, the difference is found to be negligible in change of eye locations between

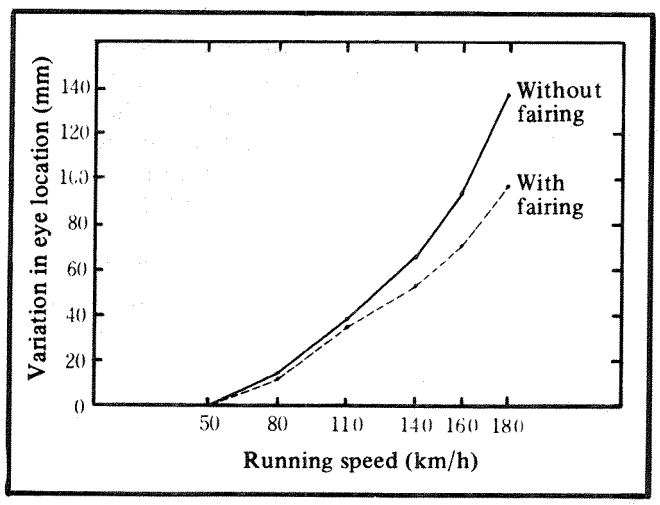

Figure 28. Resultant change of eye location according to running speed

this and the former cases until reaching a running speed of 110km/h, but, when reaching 140km/h or more, the eye location change in this case is smaller than that in the former case.

This shows that fairings will have no effect on the riding position until reaching high running speeds.

Method for Establishment of Eye Ranges

The Working Group for Motorcycle Rider's Eye Range of the Society of Automotive Engineers of Japan, Inc. (JSAE) worked to develop a standard based on the data obtained by this study and completed its work in establishing JASO T005(5), "Motorcycle Rider's Eye Range" under the approval of the Japan Automobile Standard Organization in March 1984.

The purpose of this standard is to specify the method for determining the rider's eye range that will be used as the origin in the study of the indirect field of view in motorcycles. Accordingly, this standard specifies the eye range of a motorcycle rider when seated on the motorcycle in the ordinary riding position and the method to determine it.

For assessment of the direct field of view in the motorcycle equipped with a fairing, this standard recommends considering also the eye location (estimated from the anthropometric data) of the rider taking a stretched riding position as the origin in addition to that of the ordinary riding position.

The factors for drawing prescribed in the standard for establishing eye range have been standardized in accordance with data of the ISO manikin and by using data of American riders obtained in this study. This method for the establishment of eye range of the motorcycle rider specified in JASO T005 is outlined in the following.

Selection of Factors for Drawing

Select the following items from Tables 8 and 9 corresponding to the design position angle β. (This angle corresponds to the forward-inclination angle β as shown in Figure 14. Plus-minus mark is in reverse between this angle and the forward-inclination angle β.):

- Factors for drawing
- Major and minor axes lengths of eyellipse
- Inclination angle of eyellipse

(Note: Eyellipse has nearly the same meaning as eye range. Eyellipse is the plan view and side view of eye range ellipse.)

Establishment of Eyellipse in Side View Drawing

Eyellipse is established by the side view drawing as follows (see Figures 29 and 30):

1. Describe a circle of radius A with G-point (center of the upper surface of handle grip) as the

Table 8. Factors for drawing

Design Position Angle β(°)		-45	-7	5
Item	Riding Position	Inclined Forward		Upright
	Distance A (mm)	630		598
	Distance B (mm)	514		486 (514)
	Distance C (mm)	219		238
	Angle γ (°)		131-0.67 β	

Remark: Use the value in parentheses in the case of on-off-road type motorcycles. (The value of distance B is corrected by 8mm in accordance with the difference between the height of "H-point to seated surface" in the three-dimensional manikin for motorcyles and that of "trochanterion to seated surface" in American riders, see Table 7.)

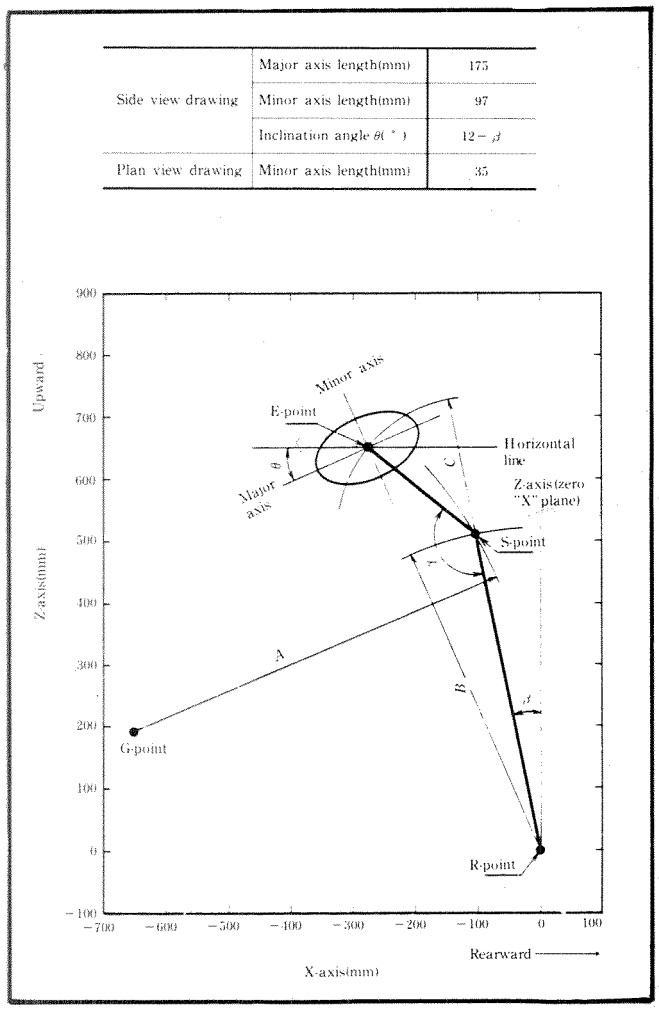

Figure 29. Method for the establishment of eyellipse

Table 9. Major and minor axis length and inclination angle of eyellipse

Side view drawing	Major axis length(mm)	175
	Minor axis length(mm)	97
	Inclination angle θ(°)	12-β
Plan view drawing	Minor axis length(mm)	35

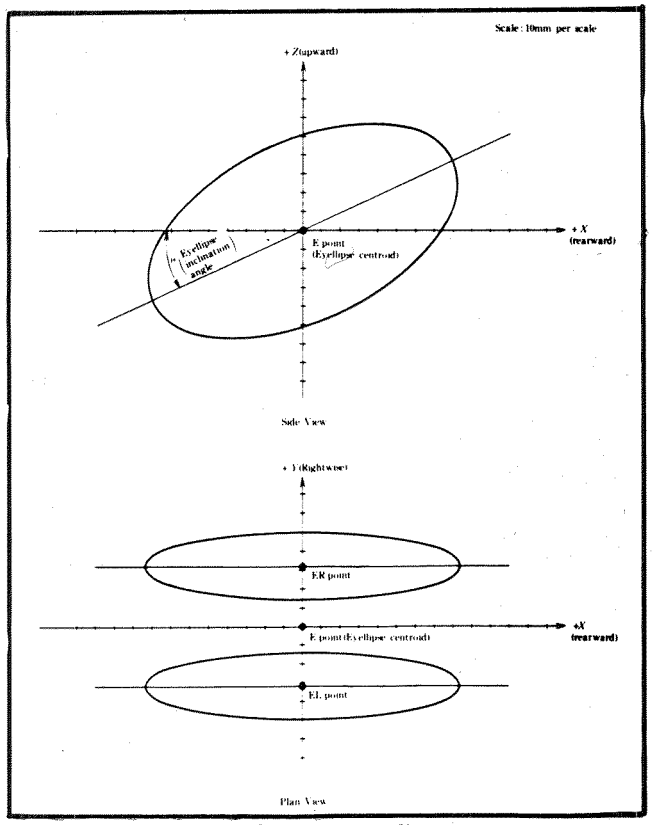

Figure 30. Eyellipse (95th percentile)

center. Describe a circle of radius B with R-point (a design reference point indicating H-point—hip location) as the center. Designate the intersection of these two circles as S-point.

2. Describe a circle of radius C with S-point as the center. The intersection between this circle and a straight line forming an angle (γ) with a straight line drawn through S-point and R-point is designated to be E-point.
3. Draw a straight line through E-point forming an angle θ with the horizontal line as the major axis of the eyellipse.
4. Draw a straight line through E-point and perpendicular to the straight line drawn in (3) as the minor axis of the eyellipse.
5. Make the major and minor axes of the eyellipse shown in Figure 31 coincide with the major and minor axes described in (3) and (4) above.

Thus, side view eyellipse is established.

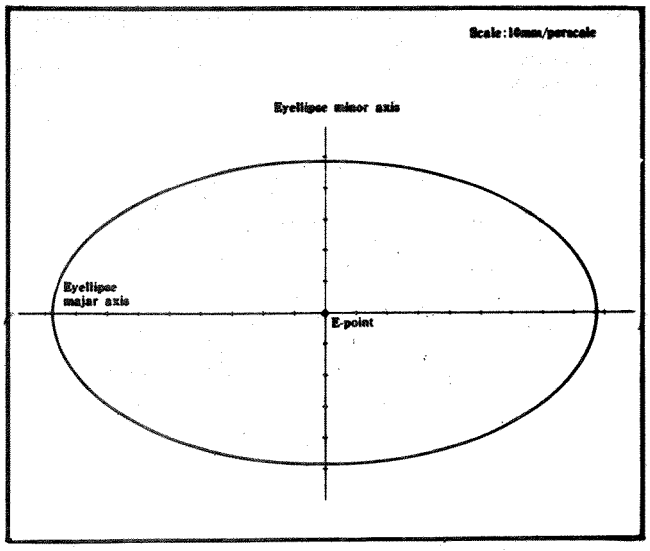

Figure 31. Eyellipse (95th percentile)

Establishment of Eyellipse in Plan View Drawing

Eyellipse is established in the plan view drawing as follows (see Figure 30):

1. Draw a straight line through the projection point of E-point on the plan view drawing and perpendicular to X-axis.
2. Draw two parallel lines at a distance of 32mm from X-axis, respectively.
3. The projection of the eyellipse in the side view drawing on the plan view drawing produces the major axis of eyellipse in the plan view drawing.
4. With two intersections (EL,ER) produced by the straight lines drawn by the procedures stated in (1) and (2) as the centers, two ellipses (eyellipses) can be described, whose minor axes are on the straight line drawn by the procedure stated in (1) and whose major axes are on the parallel lines drawn by the procedure stated in (2) (see Table 9).

Thus, eyellipses by plan view drawing can be established.

Reference Eye-point

Reference eye-point can be used as the representative location of the rider's eye. There are two cases, namely monocular reference point and binocular reference points (see Figure 30).

(1) In the case of monocular reference point: Projection of E-point on either side view drawing or plan view drawing is the reference eye-point.

(2) In the case of binocular reference points: In the plan view drawing, centers of two eyellipses (EL for left eye and ER for right eye) are the reference eye-points.

The Working Group of Motorcycle Rider's H-point of the Society of Automotive Engineers of Japan, Inc., completed its work in establishing JASO T006(6), "Procedure for Motorcycle Rider's H-point Determination," under the approval of the Japan Automobile Standard Organization in March 1985.

This standard specifies procedures for the determination of motorcycle rider's H-point as well as the construction of the manikin for motorcycles. The weight of each construction member, center of gravity, shape of seat pan, and so on in the three-dimensional manikin for motorcycles are basically corresponding to the three-dimensional manikin for automobiles in ISO 6549(7), but the manikin for motorcycles is not equipped with the back pan while having arm-hand (see Figure 32). The two-dimensional manikin for motorcycles is a template based on the side view of the three-dimensional manikin for motorcycles (see Figure 33).

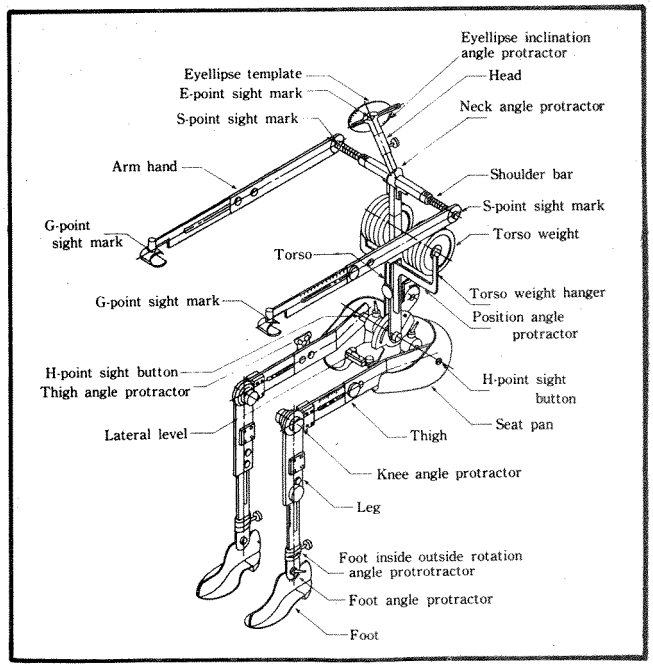

Figure 32. Three-dimensional manikin for motorcycle

Conclusion

It has been found that a motorcycle rider's eye range can be obtained from the relative position between handle grip and H-point.

Acknowledgments

The authors wish to express their appreciation to Mr. Sadahito Aramaki, Aero-Medical Laboratory, JASDF, for his helpful guidance in anthropometry; to LTC D.D. Erickson and MSGT R.G. Jacob, Mr. Noboru Horikoshi,

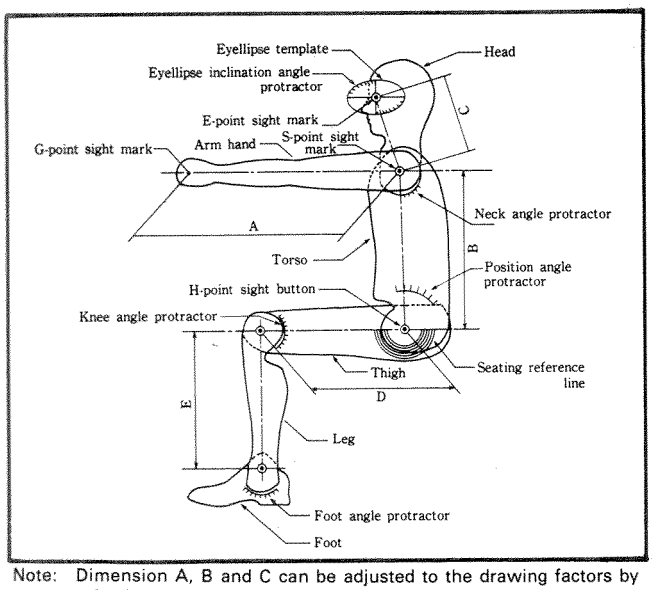

Note: Dimension A, B and C can be adjusted to the drawing factors by selecting the pivots respectively

Figure 33. Two-dimensional manikin for motorcycle

and Mr. Shozo Takamiya, Safety Department, Yokota Air Base, U.S. Air Force; members of the Working Group for Motorcycle Safety Structure and the Working Group for Motorcycle Steering and Stability of the Japan Automobile Manufacturers Association, Inc.; members of the Working Group for Motorcycle Rider's Eye Range and the Working Group for Motorcycle Rider's H-point of the Society of Automotive Engineers of Japan, Inc.; and members of the 1st Laboratory, 4th Research Department of Japan Automobile Research Institute, Inc., for their great assistance in carrying out this study, and to the many motorcycle riders for their willing cooperation as subjects for measurements.

References

1. ISO 4513, *Road Vehicle-Visibility-Method for Establishment of Eyellipses for Driver's Eye Location*, 1978.
2. VDTUV Leaflet 736 (Fairing Requirements).
3. National Aeronautics and Space Administration (NASA), "Anthropometric source book,", Vol. II, *A Handbook of Anthropometric Data*, NASA Reference Pub. 1024, 1978.
4. National Aeronautics and Space Administration (NASA), "Anthropometric source book," Vol. I, *Anthropometry for Designers*, NASA Reference Pub. 1024, 1978.
5. JASO T005, *Motorcycle Rider's Eye Range*, 1984.
6. JASO T006, *Procedure for Motorcycle Rider's H-point Determination*, 1985.
7. ISO 6549, *Road Vehicle-Procedure for H-point Determination*, 1980.

Cycle and Light-Powered Two-Wheeler Accidents

European Experimental Vehicles Committee

Summary

Importance of the Problem (Chapter 1)

In the various member countries of the European Experimental Vehicles Committee (EEVC), it was concluded that over the past decade much attention was paid to problems related to accidents with cars and the people using them; in recent years, attention shifted to other traffic participants and especially to pedestrians, for two reasons mainly:

- At present they are largely unprotected and therefore vulnerable in today's very complex traffic scene.
- Statistics show pedestrians actually form a large group of casualties.

Considering the scientific work already done for those groups in many countries, the public, Parliament, researchers, and authorities became aware of the growing importance of traffic safety problems for two-wheelers, relatively speaking, but to some extent also in absolute terms. The accident statistics as described in Chapter 1 indicate the following figures for bicyclists and moped riders (studied together because their position in traffic is comparable in many ways):

- In some countries, this group is the second largest after car users in terms of killed and severely injured; in other countries, it ranks third after car users and pedestrians.
- The percentage of killed (light-powered) two-wheeler users ranges from 6.7 percent (United Kingdom) to 28.4 percent (The Netherlands), with an average value of 15.8 percent for the participating countries (for pedestrians: from 13.3 percent in The Netherlands to 33.3 percent in the United Kingdon; an average of roughly 22 percent in 1979).

Chapter 1 gives a detailed description of those and other figures: number of injured, of vehicles in use, etc. It relates those figures to indicate some reasons for the variance between countries (number of casualties per

100,000 vehicles and per 100,000 inhabitants in various age groups). Work presented indicates the important influence on possible conclusions of differences in definitions and requirements (differences in accident registration systems and the related problem of under-reporting; differences in the technicalities of the vehicles). A separate paragraph describes the importance of economic assessment of these accidents, remedial measures, and some problems related to the available methods.

Description of Bicycle and Light-powered Two-wheeler Accidents (Chapter 2)

Chapter 2 gives details on typical types of accidents: accident, collision, and maneuver types are defined, and related (in-depth) studies are cited, indicating at the same time available knowledge on resulting injuries and speed at impact. All material available shows that cars most frequently are the collision partners (50 to 99 percent). There is no single category of road users ranking second; it ranges from other two-wheelers to heavy goods vehicles (HGV's), depending on various factors. Single-vehicle, light-powered, two-wheeler accidents occur so frequently they deserve special attention.

It is shown the frequency of an accident type is not the only relevant parameter; some indication of the seriousness is considered important too. A definition of lethality is suggested, indicating its influence on priorities. This approach gives more weight to collisions with HGV's. By describing collision types and to some extent maneuver types, it is shown which parts of the vehicles are mostly involved. Some similarity exists with pedestrian accidents, but additionally the sides of cars and the sides and rear ends of HGV's are involved (especially in crashes with light-powered two-wheelers), as well as some parts of the two-wheeler.

The kinematics of a rider during a collision is indicated as one of the important factors. Due to the range of accident and collision types for two-wheelers, a much wider variety of kinematics is seen for riders when compared with pedestrians; the presence of a two-wheeler and its speed can especially be a contributing factor.

As for injuries, literature gives a variety of distributions; most studies are hard to compare, for reasons indicated later, but some conclusions and tendencies are noted. The limited number of studies available indicates that the frequency of injuries to various body parts and their ranking depends on the injury severity level considered and on the type of two-wheeler involved. Most studies conclude the head has the highest frequency, especially when considering more severe injuries (and bicyclists have even higher frequencies than do riders of light-powered two-wheelers); arms and legs come in second and third, respectively.

The injury-scaling problem associated with long-term impairment, as mentioned in the report of EEVC-WG7 on pedestrian accidents, seems relevant for some two-wheeler accident types also.

The relative speed at impact is considered a very important factor. The limited number of studies indicating vehicle speeds show higher values than for pedestrian accidents: 50th percentile speed between 10 and 50km/h, 90th percentile between 37 and 72km/h (EEVC-WG7: 50th percentile between 16 and 36km/h, 90th percentile between 44 and 58km/h).

Injury-influencing Parameters (Chapter 3)

Contrary to the situation for car accidents, very little is known about the parameters for two-wheeler accidents. Therefore, only a short description is given, mainly of a theoretical and inferential nature and based on general knowledge from studies of various accident types, indicating probably the most important factors for each of the collision types that seemed important from Chapter 2.

Research Methods and Results (Chapter 4)

A global presentation of various research principles is given, indicating the advantages and disadvantages and especially indicating the usefulness of combining two or more methods. The following division is made:

- Accident studies
  - Accident statistics (police data level)
  - Intermediate (hospital/insurance data)
  - In-depth studies
- Experimental research methods
  - Full-scale tests
  - Component (or body segment) tests
  - Mathematical models

Until recently, little research was done specifically relating to bicycles and mopeds (and then mainly accident statistics). What has been done and can be used to some extent here was usually directed at pedestrians or motorcyclists. Nevertheless, a few bicycle-related studies are cited (accident studies of various levels as well as development work on mathematical models, together with the necessary related full-scale and component tests).

Current Knowledge on Human Tolerance (Chapter 5)

The accident situation for two-wheelers is different from the situation for other groups of road users, as mentioned before. This may influence typical injury-influencing parameters (kinematics, loading place, direction, and level); therefore, one would have to look for

typical cyclist and moped rider information regarding human tolerance. Very few studies have been performed, especially for cyclists and moped riders, and those were related mainly to helmets and head tolerance. For other elements, one has to rely on work for pedestrians, motorcyclists, and car users. For various body parts, parameters and tolerance values are given. Their relevance for two-wheeler users must be studied further.

Injury-prevention Measures (Chapter 6)

Starting from the basic philosophy of an integral approach to a safe vehicle (integration of requirements to benefit various groups of road users), three aspects were noted:

- Proposals for the benefit of two-wheeler users
- Consequences of these proposals for other road users
- Consequences of requirements for the benefit of other road users on two-wheeler users

Ad 1—Proposals for Two-wheeler Users

As research work in this area started only recently, availability of literature is limited, especially regarding concrete proposals. Based on information from earlier chapters, work concentrated on the car, the HGV, the two-wheeler, and its rider

Regarding cars, as for the pedestrian-to-car accidents, interest is focused on the stiffness of frontal parts. Some differences may exist: the generally somewhat higher seating position and a difference in the population (fewer younger children involved) may cause a different influence of various car components on the kinematics and loading of the human body in a crash. For two-wheeler users, the windshield and the higher parts of its frame become important, too. Considerations regarding vehicle shape follow the same lines as for pedestrians.

Regarding HGV's, two approaches exist:

- Improvement of shape and stiffness would be beneficial at the vehicle front, as for cars.
- For the HGV sides and rear, concrete proposals are indicated regarding underrun protection devices and improved rear view mirror systems and requirements (accident avoidance).

Regarding the two-wheeler itself, various protection devices are discussed, for both frontal and lateral collisions. Various types have been developed for motorcycles; whether they can be used practically on lighter two-wheelers and even whether they are advantageous on such vehicles is still unclear. This concerns side protection devices (e.g., knee bars) as well as knee padding for frontal collisions. Avoiding sharp protrusions on two-wheelers will help against minor injuries; examples introduced to some extent are sunken filler caps and handlebar expander pins.

For the passenger, especially the younger one, dress guards at the rear wheel and, up to a certain age, child seats are considered important against spoke injuries.

Regarding the rider, various well-known possibilities are described, such as safety helmets and protective clothing. Although they are widely accepted (and helmets even mandatory) in many countries for motorcyclists, this is not the same for all riders of light-powered two-wheelers and certainly not for cyclists (the use of special types of cyclist helmets has been introduced in some countries, nevertheless).

Ad 2—Consequences for Other Road Users

Little influence for others is expected from the above proposals regarding cars. Underrun guards should not create any negative effects for other road users. Rear view mirrors on HGV's might be dangerous for pedestrians and bicyclists during overtaking maneuvers, if they are not properly designed. Some doubt is expressed as to whether knee paddings may cause a rider to fly into a car's compartment; helmets may be dangerous for unprotected road users.

Ad 3—Consequences of Measures for the Benefit of Other Road Users

Bumper height is determined in SAE and ECE prescriptions, mainly for the car-to-car situation. Serious doubts are expressed on the appropriateness of these values for pedestrians and two-wheeler riders. Other requirements for car-to-car crashes are not expected to have much effect on two-wheeler riders.

Test Procedures (Chapter 7)

Test procedures, aiming at insuring conformity of a vehicle or component with relevant requirements, are discussed. The chapter was kept short because there are few concrete proposed measures to evaluate during type approval (Chapter 6), and much development work needs to be done on the methods themselves (e.g., integration of integral tests, component tests, and/or mathematical models; development of a dummy).

Accident Prevention (Chapter 8)

Injury prevention or minimization is clearly not the only and possibly not the best way to protect road users. Accident prevention would be far more preferable, but it is not expected to be effective enough for many years to come. The chapter describes various elements of the

vehicle system that may cause (or contribute to) accidents. Research work to improve these elements is described: active lighting systems, reflectors, spacers, braking systems, stability, and maneuverability. As a special aspect, the influence of the state of maintenance is discussed. Various proposals are described; some might be feasible for many countries because relevant technology has already been introduced in other countries.

Priorities and Recommendations

Introduction

Based on discussions in the group, the working group has pointed out priorities for action, general recommendations, and recommendations for future research. One conclusion is that the injury prevention research for two-wheeler riders received even less attention than injury prevention for pedestrians (Working Group 7). More attention is necessary, especially since the accident process of the two-wheeler rider is even more complex than that of the pedestrian because of the contribution of the two-wheeler itself to the injury-producing process. Also, the speed of the two-wheeler rider and his position in traffic situations leads to other collision types and speeds at impact.

Priorities for Action

1. The use of energy-absorbing materials in the front structure of the car will be beneficial for the two-wheeler rider, similar to that found for pedestrians by WG7. Whether other locations on the car should also be padded cannot be decided now. Preliminary results of experiments using dummies indicate that impact location of the two-wheeler rider's head on the car is somewhat higher than in the case with pedestrian heads in similar frontal collisions. Second priority should be given to the side of the car due to the relatively frequent side collisions with light-powered two-wheelers.
2. The use of well-dimensioned side underrun guards on HGV's will reduce the effect of the serious and relative numerous collisions of mopeds and bicycles with the sides of heavy vehicles. The risk of getting run over by the wheels will also be reduced.
3. Modern standards should be developed for lighting equipment, including reflectors, and braking performance (especially under wet conditions) of bicycles. The introduction of a high-standard retroflector at the rear end of the bicycle will probably reduce the effect of the frontal car collision with the rear end of bicycles, which is a serious type of collision. At the sides of bicycles, spoke reflectors and/or reflecting tires are recommended.

General Recommendations

- More attention should be given to accidents of bicycles and light-powered two-wheelers, especially—
  - Accident registration systems, e.g., underreporting of these accidents by police.
  - Standardization of definitions for a better comparison of the results of national accident statistics and research projects of the different countries. Especially needed is a more uniform definition of the different classes of light-powered two-wheelers.
- When introducing a new legal measure, a proper before-and-after evaluation study is necessary. Some reasons are—
  - Optimizing the measure
  - Giving arguments for possible introduction elsewhere
- In view of the differences in the proportion of head injuries between cyclists (not helmeted) and helmet-wearing motorized two-wheeler riders, it seems preferable that cyclists wear a specially designed helmet, too. Padding of certain parts of the car might have a beneficial result, depending on whether the car or the ground is the leading cause of injury. This question has to be answered yet by research.
- The use of better or additional side mirrors on HGV's will give better overview to the truck driver. Even the present EEC directive is not sufficient (an amendment is underway).
- Riders of bicycles and light-powered two-wheelers should wear conspicuous clothing. For daytime, a jacket of fluorescent material is recommended. Smaller areas of such material, e.g., on armbands or shoulderbands, are less effective. The brightest materials (highest luminance factor) should be used. Bands of reflective material applied to the jacket will help other road users recognize the presence of a rider. Spacers (i.e., devices attached to the side of a bicycle to discourage drivers passing too close when overtaking) are useful and should be promoted as a low-cost safety accessory. However, it should be noted the wearing of a conspicuous jacket has an effect on the gaps left by overtaking vehicles similar to that produced by the most effective spacer. The last recommendation is based on research and

theoretical considerations. In part, it is supported by accident studies.

Recommendations for Future Research

Real Accident Studies

Information of real accidents is needed to get better insight on injury-influencing parameters.

The first important question is: What is the leading cause of injury (taking into account speed at impact and collision type): the car, the two-wheeler, or the ground? From this, it may follow that for some collision types severe injuries occur mainly due to very high impact speeds regardless of other influences (for instance, outside built-up areas). In those cases, accident avoidance measures seem more suitable than injury-reducing ones. The next important question is: What is the influence of car shape and car stiffness on kinematics, on short- and long-term injury, and on injury severity of the two-wheeler rider (again taking into account impact speed and collision type but also human parameters such as age, length, and mass distributions)? Whether accident avoidance or injury-prevention measures should be taken may be decided with the help of cost-effective considerations.

Human Tolerance

Further research is needed on injury-producing mechanisms to develop more precise ranges of values of human tolerance criteria as a function of age, mass, height, and impact speed (visco-elastic behavior). Special attention should be given to the influence of translational and rotational accelerations of the head-on-head (brain) injury.

Mathematical Models

Computer models should be further developed and validated. This validation should be based on real accident information together with the results of cadaver or dummy experiments. Development of a simple mathematical model, capable of detecting the kinematics of the rider versus the shape and stiffness of the car, could be useful for standard test procedures in the near future.

Dummies

The dummies presently available for pedestrian research are not quite suitable. For two-wheeler rider purposes, this deficit is analog. Further development is needed to obtain dummies that give more realistic representations of two-wheeler riders.

General

- The recommendations above must be seen as complementary as they strengthen each other. A trend must be set to use as many tools as possible to solve this complex problem. This is an important argument for international cooperation and coordination of research facilities in the various countries.
- Because two-wheeler riders collide with passenger cars and HGV's in more different collision types than pedestrians do and because of the different parts of the body of the two-wheeler rider impacted in the different collision types, injury-prevention research should focus on the following collision types:

  Passenger car
  - Front of car to (left) side of bicycle/light-powered two-wheeler
  - Front of car to rear end of bicycle
  - Front of car to front of light-powered two-wheeler
  - Side of car to front of light-powered two-wheeler

  Heavy goods vehicle
  - Front of HGV to side of bicycle/light-powered two-wheeler
  - Front of HGV to front of bicycle/light-powered two-wheeler
  - Side of HGV to side of bicycle/front of light-powered two-wheeler
  - Side of HGV to front of bicycle/side of light-powered two-wheeler

  Single vehicle light-powered two-wheeler rider accidents
- Research should be undertaken into long-term consequences of injuries. Little is known about these consequences, especially their severity. This is considered a deficiency of existing injury-scaling systems.
- When using humans or human substitutes for two-wheeler rider protection research, the choice should be such that they represent the age of the real accident victims, e.g., for cyclists 5 to 25 and older than 65. For light-powered two-wheeler riders, this age group is 15 to 25.
- Research is needed for more reliable bicycle lighting equipment.
- Optimization of crash helmets should be undertaken:
  - Legal standards should be based on appropriate biochemical criteria.
  - Influence of the surface of the outer shell of the helmet on rotational acceleration of the brain and its resulting injuries should be studied.

— Research should be undertaken into the problem of losing crash helmets during accidents (although suggestions for improvements have been tabled in the relevant UN-ECE group of rapporteurs).

Introduction

In 1981 and 1982, the EEVC Working Group 7, "Pedestrian Injury Accidents," was preparing its report. At that time, the Dutch delegation suggested attention be given to bicycle-car accidents because in The Netherlands this accident type happened more frequently than pedestrian-car accidents. In 1982, EEVC accepted the task of setting up a new working group to deal with bicycle accidents and, as far as possible, light-powered two-wheeler accidents. The Dutch members of EEVC were invited to prepare a discussion paper for this group. The intention of this working group, described in the paper, was agreed to by EEVC, and the group was set up. This intention is focused on number of accidents, integrated safety approach, and international coordination. From this discussion paper, the following is cited:

- Concerning the number of accidents: "Compared to other European countries the relative proportion of bicycle casualties in The Netherlands is considerably higher, though the absolute numbers of those killed and those injured as reported from the different European countries also seem quite high. They indicate that proper measures in this field may save thousands of lives and injured, while reducing the severity of injuries."
- Concerning an integral safety approach: "Some conclusions with regard to changes of the car drawn from studies of pedestrian-car accidents may be useful for the bicycle-car situation, too; others may be indifferent, but some may be contrary to the bicycle case. For an integral approach to car safety, changes made (or to be made) for the benefit of one group of road users have to be checked carefully against knowledge about the characteristics of other groups. This can be illustrated by bumper height, for example, for which a SAE recommendation exists, as well as a UN/ECE regulation. From research on lateral car collisions, a recommendation for a lower bumper height may follow. From pedestrian accident research follows considerable doubt whether the SAE recommendation is an advantage for pedestrians. Considering two-wheeler accidents, the effects are even less predictable as yet."
- Concerning international coordination: "It seems the study of car-bicycle accidents ultimately may contribute a great deal to improvement of traffic safety. There is a need for accident data: there also seems to be a need for more experimental and human-tolerance data, as well as for better tools to gather those data. Investigations on crash protection for two-wheelers are starting in several countries. Research on crash protection for pedestrians started more than 10 years ago, which was followed some years later by international coordination. Now it seems to be the right moment for similar actions concerning bicyclists, while coordination of research is possible from an earlier stage."

As a result, EEVC gave the working group the following terms of reference:

- Review the available accident data concerning fatal accidents and injuries to bicyclists of different ages involved in road accidents in Europe and examine the accident data of light-powered two-wheelers. (The exact definition belongs to the task of the group.)
- Make recommendations including priorities for action on the vehicle to reduce the severity of such accidents and injuries. Recommendation may include direct measures to change bicycles and cars, as well as specified proposals for research.

Priority will be given to possible influences of certain proposed measures on the safety of bicyclists; changes to the car should be considered with respect to the benefit of nonoccupant road users (see also WG7).

During the first meeting of the working group, it was decided to deal also with light-powered two-wheelers because in some participating countries the number of light-powered two-wheeler casualties is higher than that of bicyclists and because it was the group's opinion there were great similarities between the two categories of road users. The group was aware of the difficulties that could arise because of differences in definitions of light-powered two-wheelers between countries. Therefore, the group decided to include a list of requirements (including definitions) for light-powered two-wheelers for the different countries. During the first meeting, the group decided to deal also with accident avoidance aspects related to vehicles.

The aim of accident avoidance is obvious, and many efforts have already been made by improving the construction of passenger cars and HGV's (brakes, tires, etc.) and by changes in infrastructure (bicycle lanes). However, there is considerable scope for improving the lighting devices and retroreflectors fitted to many bicycles and for improving the braking performance in the wet, especially of rim brakes. The decision of the group was that only specific two-wheeler, car, and HGV aspects in relation to two-wheeler accidents will be described in this report.

It is unrealistic to expect (on a short term) measures or solutions that will prevent accidents from happening at all. Some elusive elements will always remain. This is the main reason for injury-prevention work. The aim of injury prevention is either to prevent injuries or to minimize injury severity by influencing the kinematics of the victim and to minimize loads to the struck body parts, for instance, by minimizing the relative impact speeds between victim and struck object.

History of Bicycle and Light-powered Two-wheeler

Bicycle

The question of whether the first bicycle was designed by the Frenchman De Sivrac or by the German Kessler in ± 1790(2) is irrelevant since it appeared some years ago that the first drawing of a bicycle was made by Leonardo da Vinci or one of his pupils in ± 1450(3). This bicycle was already chain driven (Figure 1) contrary to the bicycles made by De Sivrac and Kessler that had to be pushed forward.

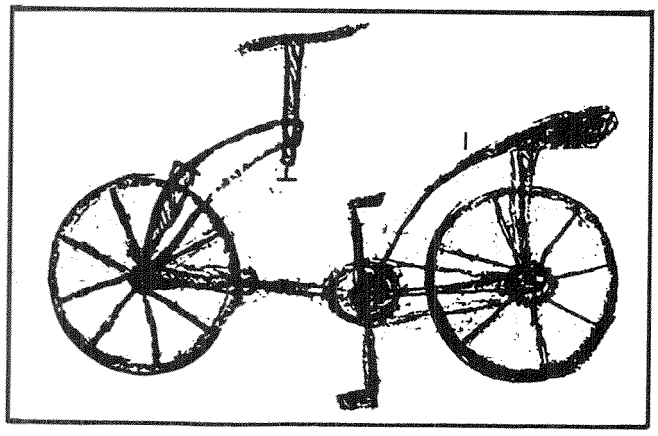

Figure 1. Bicycle designed by Leonardo Da Vinci (±1450)

The first bicycles driven by means of pedals had a front-wheel drive. To reach a higher speed, the front wheel was enlarged (Figure 2), to such an extent that it became dangerous when drivers fell off. Therefore, the first "safety bicycle" was designed by H.J. Lawson in 1874. It had front and rear wheels of equal diameter, and the rear wheel was chain driven. The first practical production machine, the Rover Safety, was made in 1885 by John Starley (Figure 3). When later (1888) it was equipped with pneumatic tires, invented by the Irish veterinary surgeon John Dunlop, the safety bicycle caused a bicycle boom in Europe and America(1). The safety bicycle had a design similar to the present vehicle,

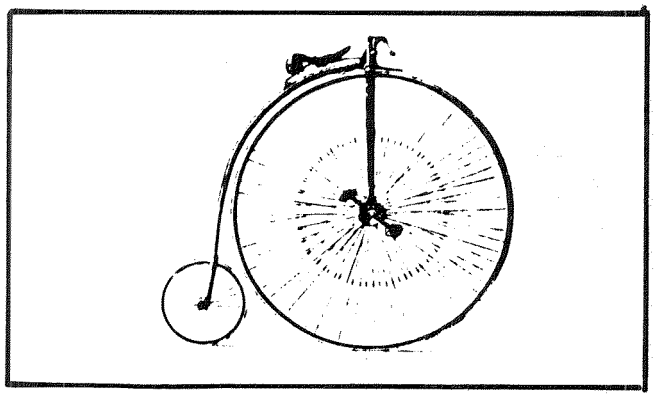

Figure 2. Bicycle with enlarged front-wheel (± 1880)

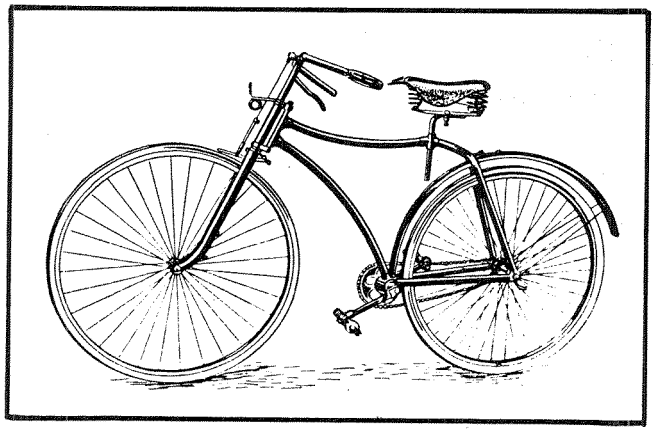

Figure 3. Rover "safety bicycle" (± 1885)

though it lacked the seat tube as a part of the frame structure.

Bicycle use in some countries became enormous and will probably grow even more due to rising energy prices, more spare time, and health care. At this moment, many alternative bicycle designs and prototypes are produced. They have in common the bicyclist lying backwards, and in some designs he or she is protected against weather conditions(5).

Light-powered Two-wheeler

According to Raucke(6) and Schneider(7), the first powered two-wheeler was constructed by Wolfmüller and Hildebrandt in 1894 (Figure 4). According to Elsevier(4) the first attempt to construct a light-powered two-wheeler dates from 1920; it is named the "Briggs and Stratton" (1894-1920: a matter of definition?). The engine was connected directly to a wheel next to the rear wheel. In later years, the engine could be found almost anywhere on the two-wheeler, but today the engine is normally placed under the frame, between front and rear wheel, driving the rear wheel. Use of the moped in The Netherlands increased strongly after 1960 but decreased after 1975 and is still decreasing.

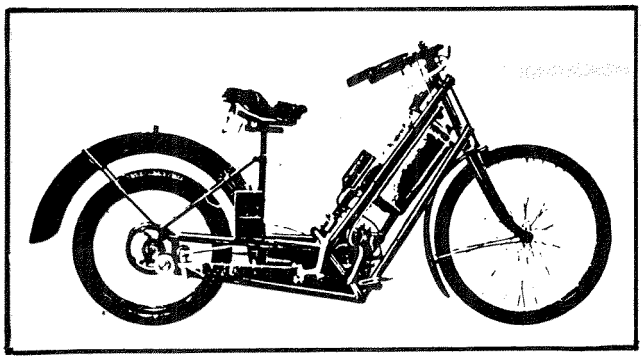

Figure 4. First patented, serially produced motorcycle by Hildebrandt and Wolfmüller (München, 1894)

1.Description of Two-wheeler Accident Statistics

This section deals with a comparative survey of the situation of vehicle numbers and number of persons involved in accidents in general. Special emphasis is placed on describing the situation of pedal cyclists and riders of light-powered two-wheelers in the member countries participating in the working group: France, Federal Republic of Germany, Great Britain, Italy, The Netherlands, and Sweden. The interpretation of the data will have to be undertaken with great caution since the definitions of a light-powered two-wheeler differ in the participating countries. The definition of a fatally (or severely or slightly) injured accident victim can also differ considerably, as well as the associated parameter definitions in the national accident statistics. Beyond that, other influencing parameters should be included in a comparative assessment as well, such as mileage (vehicle-kilometers per annum), road network, land use, topography, and climatic conditions of the countries under study.

This is to show that a statistical analysis based only on a one-dimensional way of looking at things (e.g., the number of accidents in a population of a defined age group) can easily lead to wrong conclusions. For this reason, only the tendencies of developments will be pointed out in this chapter.

Definitions of Bicycle, Light-powered Two-wheeler, Road Accident, Killed, Severely Injured, and Slightly Injured

The definitions of bicycle, light-powered two-wheeler, road accident, killed, severely injured, and slightly injured, enabling a better classification of the numbers of accident victims within the overall context, are summarized in Tables 1 to 5. The definitions of a bicycle found in Table 1 are based largely on the characteristics laid down in the

Table 1. Definition of a bicycle

France:	A vehicle which has at least 2 wheels and is propelled only by muscular force
Federal Republic of Germany	Bicycle means any vehicle which has at least two wheels and is propelled solely by the muscular energy of the persons on that vehicle, in particular by means of pedals or handcranks
Italy	Bicycle is a vehicle with two or more wheels, propelled by muscular power through pedals or similar mechanism
The Netherlands	No exact legal definition—a carriage or vehicle that is not a motor vehicle (WVR art. 1.1)
Sweden	1. A vehicle designed to be propelled by pedals which is not a toy vehicle 2. Electrical wheelchair designed for a maximum speed of 15km/h
Great Britain	Has no power assistance and includes toy cycles ridden on the carriageway, tandems and tricycles. (from Sept. 1983 the definition of pedal cycles for the purpose of regulations has been changed to include "Electrically assisted pedal cycles"; 0.2kW, 24km/h

Table 2. Some of the relevant legal requirements for bicycles(10)

Requirement for Bicycles	Federal Republic of Germany	France	Italy	The Netherlands	Great Britain	Sweden
Brakes						
— One front and one rear	X	X	X	—	X	—
— One brake	—	—	—	X	—	X
Lighting						
— Headlamp white	X	X	X	X	X	X
— Rearlamp red						
— By day and night	X	—	X	—	—	X
— By night or poor visibility	—	X	—	X	X	—
Reflectors	X(1)					
— On pedals						
— Obligatory	X	X	X	X	—	—
— Admitted	—	—	—	—	X	X
— Red rear	X	X	X	X(3)	X	X
— White front	—	—	—	—	—	—
White rear mudguard	—	—	—	X(2)	—	—
Reflecting tires Admitted	X(1)	—	X	X	X	X
Bell	X	X	X	X	—	X
Other construction Requirements	X	—	—	X(4)	—	—

1) In 1983 all new bicycles must have reflectors in the spokes or reflecting tires
2) Yellow reflecting is admitted
3) Additional high-performance reflector (min1000mcd/lx) required, seperate from the rearlamp (reflector)
4) Some requirements onthe seating position of child-passengers under age 10

Vehicle Codes(8). In some countries, bicycles are additionally subject to certain legal regulations, as listed by Horn(9) and in Table 2.

Defining a light-powered two-wheeler, and thus its description, is more difficult. In Table 3, the spectrum of the principal characteristics of a two-wheeler is represented on which a definition can be based. Taking the Federal Republic of Germany as an example, it can readily be seen the moped is only one of three classes of light-powered two-wheelers. According to the definitions given for mopeds and mokicks, the only difference between these vehicles appears to be the presence or absence of pedals or footrests. In contrast to that, the

Table 3 Definitions and requirements for a light-powered two-wheeler

	Federal Republic of Germany			France	Great Britain	Italy	The Netherlands		Sweden
Name of Class	Mofa	Moped	Mokick	Cyclomoteur	Moped	Ciclomotori	Snorfiets[4]	Bromfiets (1)[4A]	Moped[17]
Class Introduced in	1965	1954	1967	1970	1977	1959	21.4.1976	Since 21.11.1966 with pedals	July 1, 1952
Speed limit (km/h)	25	40	40	45	48[10]	40	20[5]	30/40[5A]	30
Piston displacement (cc)	≤50	≤50	≤50	≤50	≤50	≤50	≤50[6]	≤50[6]	≤50
Minimal Age (years)	15	16	16	16[1)]	16	14	16	16	15
Helmet obligatory since	No	24.7.78	24.7.78	1979	1973	Not yet obligatory	No	Yrs. since 1.2.1975	Sept. 1,1978
Driving licence	Only theor. test certificate	Yes	Yes	No	Yes	Not necessary	No	No	No
Driving on bicycle tracks allowed/mandatory	Mandation	Not allowed	Not allowed	Mandation	Permitted[11]	Not allowed	Mandation[7]	Mandation[7]	Allowed
Pedal or footrest	Pedal	Pedal	Footrest	Pedal	Pedal[12]	Not specified	Pedal	Pedal	No requirements
Min. and max. diameter of the wheels	B.T.[3] Min. 580	Not specified	Not specified	Not specified	No[13]	Not specified	254mm≤305mm	≥405mm	No requirements
Maximum mass (kg)	Not specified	Not specified	Not specified	Not specified	250[14]	16 (Engine)	No limdit[8]	No limit	2 Wheels: No limit 3 Wheels: 400
Admitted number of passengers	0	1	1	1[2]	1[15]	0	1	1	0
Brakes	2	2	2	2	2[16]	2	2[9]	2	2

1 14 years old with a special school training
2 Plus passenger if less than 14 years old
3 Minimum outer diameter of the back tyre
4 "Buzzle Bike"
4A Moped
5 IM "Woonerven" not faster than "walking speed"
5A 30km/h in built-up areas: 40km/h outside built up areas (and 5)
6 ≤50cc or approved electromotor
7 Some tracks mandated, other tracks allowed with engine off
8 50kg for "empty" vehicle, fully ready for use
9 $\geq 5 m/s^2$ (both brakes together)
10 Must have a design speed not greater than 48km/h if registered later than August 1977
11 Permitted in some cases but never mandatory
12 If registered before August 1977 must be equipped with pedals by means of which the moped is capable of being propelled
13 No requirements for pneumatic tyres, 670mm min. diameter for nonpneumatic tyres
14 250kg if registered later than August 1977
15 One passenger if proper seat fitted
16 Either must have a single system with two means of operation or two systems operating independently
17 Since January 1984 mopeds are divided into class 1 and class 2: class 1: moped old definition class 2: vehicle kerb mass ≤60kg and a transmission including maximum two gears or an automatic transmission without steps

definition of a mofa as for the legal speed limit, minimum age of rider, and driving license regulations are basically different. Legal speed limits for light-powered two-wheelers vary from 20km/h (NL, snorfiets) to 48km/h (GB, moped). The lowest possible first-time user age varies from 14 (Italy) to 16 (in most other countries).

Compulsory helmet use also does not apply in all countries to all categories of light-powered two-wheelers. Furthermore, regulations relating to the use of cycle lanes in the various countries have led to different forms of integrating the light-powered two-wheeler into road traffic as a whole. In some countries, for light-powered two-wheelers it is mandatory to use cycle tracks; in others, they may use them.

There are countries where light-powered two-wheelers are banned from cycle tracks and others where they are tolerated with the engine off. Applicable definitions of a road accident in the various countries, which are summarized in Table 4, differ only slightly. It can be assumed these are definitions of characteristic features. However, for the inclusion of accidents in the national accident statistics, the following additional information will generally be required:

- Event site and time
- Road users and vehicles involved
- Direct causation factors and accident circumstances as recorded by the police
- Accident injury consequences

The definitions of accident consequences applying to casualties in the various countries are summarized in Table 5. The definition of a person killed in an accident varies in terms of the time period applied in each country within which a victim dies, i.e., between 6 and 30 days. A period of 30 days is used in the majority of the countries. The definitions of severely or slightly injured accident victims also differ considerably, the extreme case being the Italian statistics where such difference is not made at all. In most cases, severely and slightly injured accident victims are distinguished by the kind of medical treatment required—hospitalization or outpatient treatment.

Table 4. Definition of a road accident for national statistics for casualties

Federal Republic of Germany	Accidents in road traffic with killed or injured persons on public roads and places (registered in official statistics; STVUNFG, BGBL. 1982, 2069
France	Accident in road traffic which generates at least one victim occurring on a public open road and involving at least one vehicle or ridden animals
Great Britain	One involving personal injury occurring on the public highway (incl. footways) in which a vehicle is concerned, and which becomes known to the police
Italy	Road accident is a collision involving vehicles or animals on public roads, which generates personal injuries
The Netherlands	Accidents included are those • that occurred or originated on a highway or street open to public traffic • that resulted in one or more persons being killed or injured • in which at least one moving vehicle was involved
Sweden	Accidents included are those • that occurred or originated on a way or street open to public traffic • that resulted in one or more persons being killed or injured • in which at least one moving vehicle was involved

Table 5. Definition of casualties; distinction between persons killed, severely, or slightly injured in road accidents.

Federal Republic of Germany	Killed	See ECE*
	Severely injured	An injury for which a person is detained in hospital as an in-patient
	Slightly injured	An injury for which a person is not hospitalized
France	Killed	Victim died immediately or during 6 days after the accident
	Severely injured	Accident victim who has sustained a traumatism needing medical treatment with at least a 6 days stay in the hospital
	Slightly injured	Accident victim who has sustained a trauma needing medical treatment with less than a 6 days stay in the hospital
Great Britain	Killed	See ECE*
	Severely injured	An injury for which a person is detained in hospital as an in-patient, or any of the following injuries whether or not he is detained in hospital; fractures, concussions, internal injuries, crushings, severe cuts and lacerations, severe general shock requiring medical treatment, injuries causing death 30 or more days after the accident
	Slightly injured	An injury of a minor character such as a sprain, bruise or cut not judged to be severe, or slight shock requiring roadside attention
Italy	Killed	All persons who die within the next 7 days after the accident
	Severely/ slightly injured	Are not distinguished in Italian statistics
The Netherlands	Killed	See ECE*
	Severely injured	Victims who are hospitalized for more than one day
	Slightly injured	Other injured victims
Sweden	Killed	See ECE*
	Severely injured	Fracture, concussion, internal lesions, crushing, severe cuts and laceration, severe general shock requiring medical treatment and any other serious lesions entailing detention in hospital
	Slightly injured	All injured not belonging to killed or severely injured

* ECE definition of killed: Any person who was killed outright or who died within 30 days as a result of the accident (for further definitions see ECE (26)).

Total Vehicle Numbers (Vehicle Population)

The vehicle numbers grouped in vehicle categories are found in Table 6 for all the countries participating in the working group. It should be pointed out that these populations, being subject to dynamic development processes, cannot be regarded as stable quantities. The development of mofas in the Federal Republic of Germany is a good example.

Table 6. Vehicle population in 1981 (in 1,000's)

	Cars	Goods Vehicles	Motor-cycles	Mopeds	Mofas/ Snorfiets	Pedal cycles*
France	19,725	2,568	645	4,900	—	19,000
Federal Republic of Germany	23,730	1,307	690	652	1,224	38,500
Italy	17,686 (1980)	1,338 (1980)	828 (1980)	3,461 (1980)	—	17,500
The Netherlands	4,594	339	114	700	10	10,800
Sweden	2,893	186	16	205	—	6,000
Great Britain	14,796	2,286	973	398	—	13,000

* Rough estimated data

Mofas were introduced in 1966; in 1974, the mofa population exceeded 1 million and reached a peak in 1980 with 1.4 million vehicles. In 1981, there was a slump in the number of mofas down to 1.2 million. Development of the mofa population from 1981 must be assessed in light of another development, namely, the introduction of the newly developed Leichtkraftrad in 1980 (80cc, 80km/h, minimum age 16 years).

Table 7 shows the number of vehicles in each vehicle category per 100,000 inhabitants. The peak value in the passenger car category, with a figure of 38,000, is displayed for the Federal Republic of Germany. Great Britain, with 27,000, shows the lowest figure in this category. The bicycle peak value is displayed for The Netherlands (76,000); here again, the lowest number is found in Great Britain (24,000). France has the highest number of light-powered two-wheelers (9,100) and Great Britain once more the lowest (700).

Table 7. Vehicle numbers (in 1,000s) per 100,000 inhabitants in 1981

	(1,000s)			
	Cars	Pedal cycles	Light-powered two-wheelers	Inhabitants 1981
France	36	35	9.1	53,960
Federal Republic of Germany	38	64	3.0	61,680
Great Britain	27	24	0.7	55,830
Italy	31	31	6.1	57,200
The Netherlands	32	76	5.0	14,250
Sweden	35	72	2.5	8,320

Statistical Records on Persons Killed and Injured in Road Accidents

The total number of casualties with a breakdown in light-powered two-wheeler victims and users of bicycles are represented in diagrammatic form below for the years 1977-81. The development of the number of accidents in the various countries in the same time period is found in Figures 5 to 10. Compared with the overall development of number of accident victims, a striking decline in fatalities in the Federal Republic of Germany, The Netherlands, and Sweden is noticed.

The group of severely injured also displays a slight downward trend with the exception of The Netherlands where a pronounced decline can be noticed in this group. In all the countries under study, the number of slightly injured also continued to decline. Great Britain, Italy, and France, however, display a quite different development of the overall number of road accident victims. In Great Britain, all three categories display a slight downward trend. In Italy, the number of persons killed in accidents remained nearly constant, whereas the number of injured accident victims displayed an upward trend. Casualty numbers in France, apart from the absence of

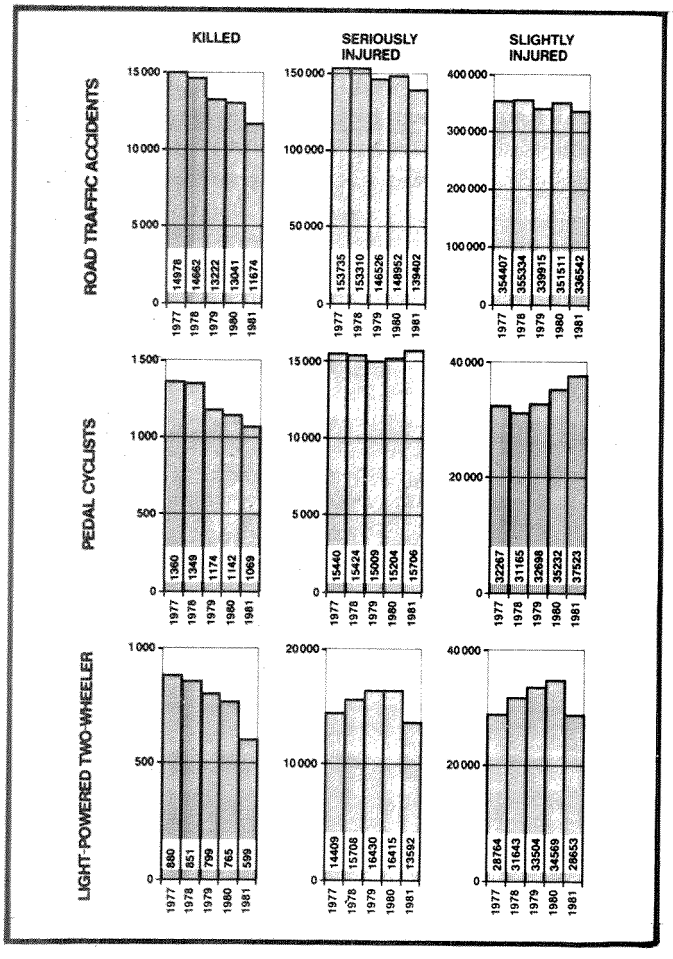

Figure 5. Number of accidents—Federal Republic of Germany (1977-1981)

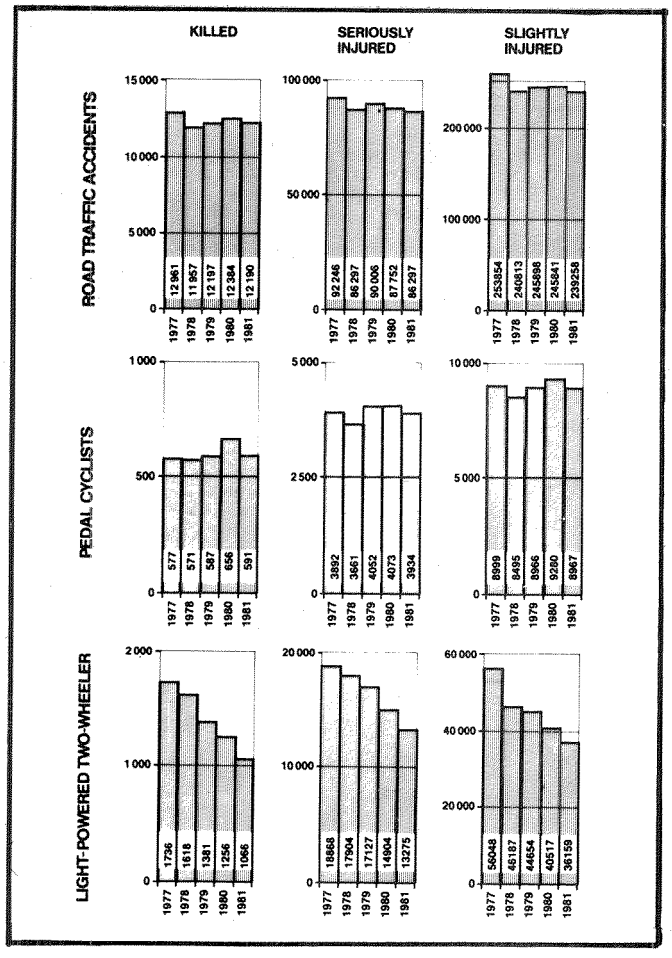

Figure 6. Number of accidents—France (1977-1981)

extremely low values and clear peaks, remained more or less constant.

The development of casualty numbers in the group of bicycle riders in participating countries also displays considerable variations in the three casualty groups. In the Federal Republic of Germany, the number of killed bicycle riders displayed a clear decline; the number of severely injured remained at a nearly constant level, whereas the number of slightly injured increased considerably. The development of the number of casualties in France appears to be balanced in all three categories in the years 1977-81.

In Great Britain, although the number of bicycle riders killed in accidents remained nearly constant during this period, the number of severely and slightly injured accident victims displayed upward trends. The Italian statistics show a slight decline in the number of accident victims in both injury categories. In The Netherlands, the number of killed bicycle riders dropped continuously (an exception being 1980) but is still on a high level.

The number of severely injured victims remained at a nearly constant level whereas the number of slightly injured displayed increasing rates. In Sweden, too, with the exception of 1980, the statistics show a clear decline in the number of killed riders of bicycles, whereas an overall rising trend is displayed by the overall number of severely and slightly injured accident victims.

In the group of light-powered two-wheeler riders involved in accidents, the statistics display a clear downward trend in the number of casualties in France, Great Britain, The Netherlands, and Sweden. The reductions in this category in France and Sweden even appear disproportionally high. In the German statistics, the absolute number of riders and passengers of light-powered two-wheelers involved in fatal accidents displayed clearly downward sloping curves. The number of severely and slightly injured increased until 1980. In 1981, a reverse trend took place, and the number again reached the values recorded in 1977. In Italy, the number of persons killed remained nearly constant during the time period considered, whereas slight increases were found in the number of injured accident victims.

The magnitude of the number of pedal cycle and light-powered two-wheeler accidents in the various countries is

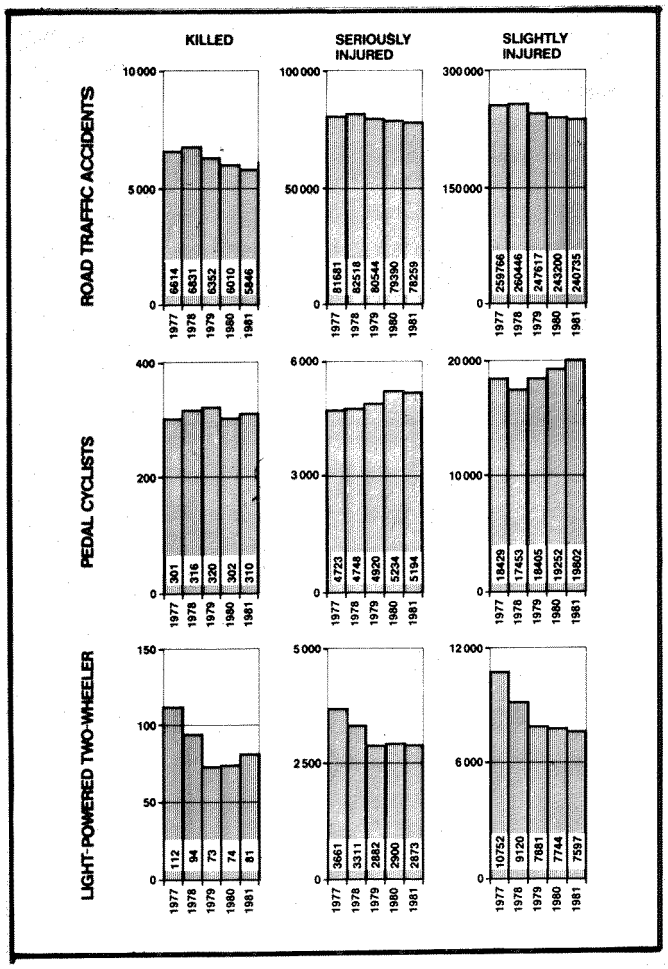

Figure 7. Number of accidents—Great Britain (1977-1981)

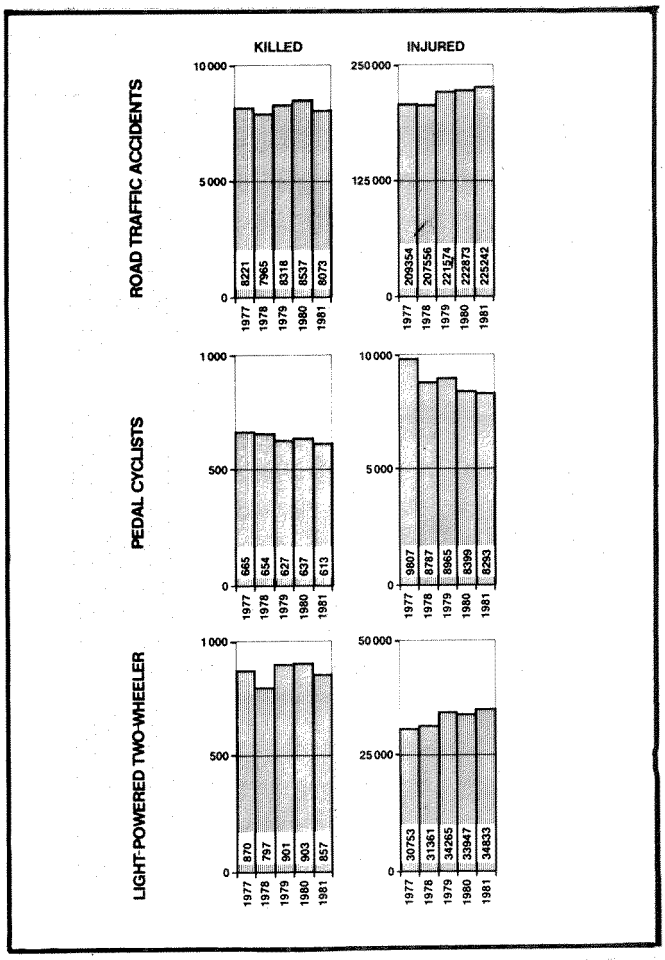

Figure 8. Number of accidents—Italy (1977-1981)

seen clearly when relating them to the total number of road casualties. The percentage of killed pedal cyclists and users of light-powered two-wheelers in 1981 is given in Table 8. The table shows in particular the importance of the accident involvement of this category of two-wheeler users in The Netherlands. As an example, the percentage of killed pedal cyclists is from two to four times as high as in other countries.

Great Britain, with an overall rate of about 7 percent, is the only country clearly remaining below the 10 percent level.

Table 8. Percentage of pedal cyclists and users of light-powered two-wheelers killed in road traffic

1981	Percentage of Killed Pedal Cyclists in Traffic	Percentage of Killed users of Light-Powered Two-Wheeler in Traffic	Total
Federal Republic of Germany	9.2	5.1	14.3
France	4.8	8.7	13.5
Great Britain	5.3	1.4	6.7
Italy	7.6	10.6	18.2
The Netherlands	19.7	8.7	28.4
Sweden	9.7	4.1	13.8

When the vehicle population is changing, the casualty rate in terms of the number of casualties per 100,000 vehicles shows the trend more clearly. The rates for killed pedal cyclists and users of light-powered two-wheelers for 1981 are found in Table 9. The table shows that, if calculations are performed on this basis, The Netherlands no longer is outside of the accident patterns displayed by the other countries participating in the study. In this case,

Table 9. Number of killed pedal cyclists and users of light-powered vehicles per 100,000 vehicles

	Number of Killed/100,000 Vehicles	
1981	Bicyclists	Light-Powered Two-Wheelers
Federal Republic of Germany	2.8	31.5
France	3.1	21.8
Italy	3.5	25.2
The Netherlands	3.4	22.6
Sweden	1.3	16.0
Great Britain	2.4	20.3

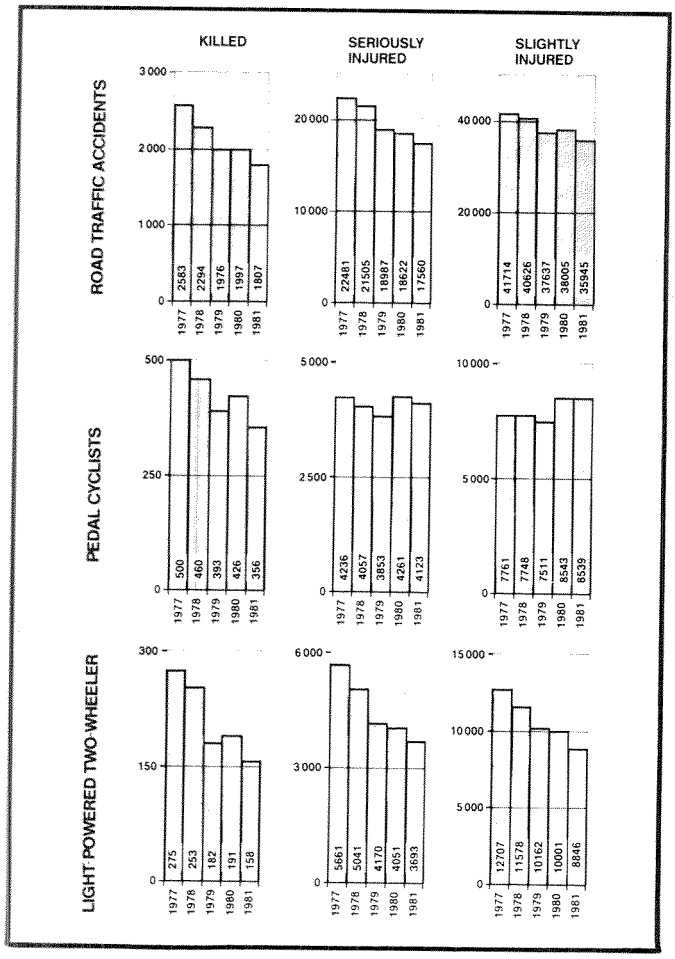

Figure 9. Number of accidents—The Netherlands (1977-1981)

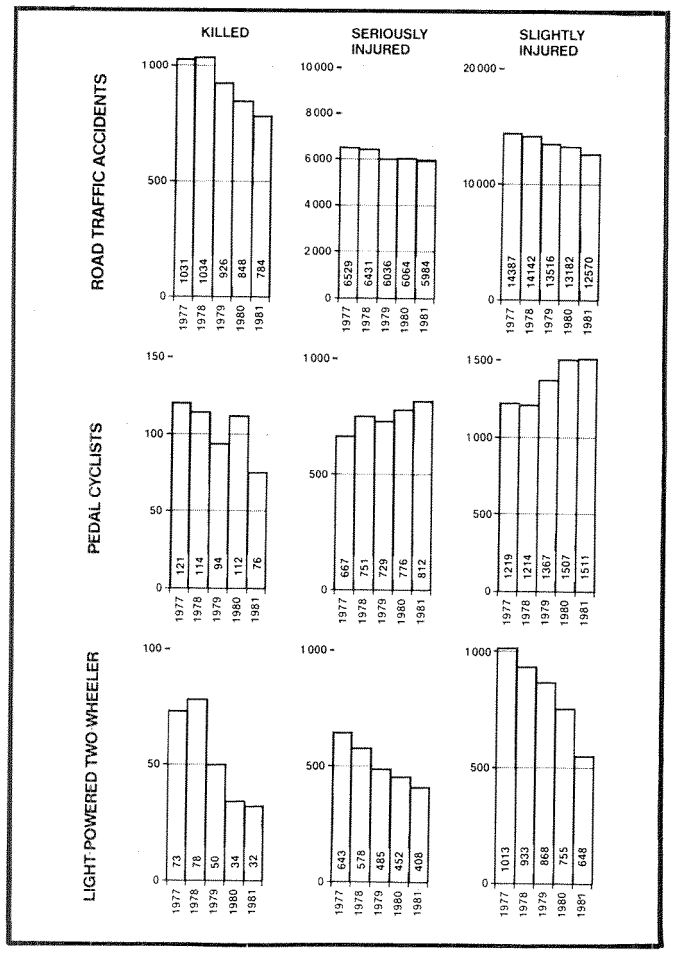

Figure 10. Number of accidents—Sweden (1977-1981)

it is Sweden that shows up as a positive example with its low rates, both for fatal pedal cycle and fatal light-powered two-wheeler accidents. The Federal Republic of Germany shows up as the leading country in the group of fatal light-powered two-wheeler accidents.

The absolute number of killed and injured users of bicycles and riders or passengers of light-powered two-wheelers, classified into age groups, is shown in Tables 10 to 15.

In all countries, fatal, severe, and slight injury peak values are reached in the age group of 10- to 14-year-old users of bicycles. The age group of 65 and over also displays a high frequency of fatalities. In the Federal Republic of Germany, fatalities in the age group of 65

Table 10. Federal Republic of Germany (1981)

	Age Groups	0-5	6-9	10-14	15-17	18-20	21-24	25-34	35-44	45-54	55-64	≥65	Ukn	Total
Pedal Cyclists	Killed	10	69	137	54	21	16	43	67	118	118	416	—	1061
		(2)	(3)	(3)	(-)	(-)	(-)	(-)	(-)	(-)	(-)	(-)	(-)	8
	Severely Injured	308	1710	3908	1708	722	573	906	1231	1381	1247	1990	28	15554
		(57)	(28)	(42)	(17)	(3)	(2)	(2)	(1)	(-)	(-)	(-)	(-)	(152)
	Slightly Injured	724	3206	9788	4828	2223	1845	3162	3593	3177	2176	2709	92	36929
		(327)	(103)	(93)	(39)	(15)	(8)	(5)	(2)	(2)	(-)	(-)	(-)	(594)
Light-Powered Two-Wheelers	Killed	—	—	14	221	67	21	31	47	53	41	104	—	557
		(-)	(-)	(11)	(21)	(6)	(3)	(-)	(-)	(-)	(-)	(1)	(-)	(42)
	Severely Injured	4	10	259	7289	188	592	789	869	906	498	531	8	13592
		(4)	(9)	(146)	(633)	(135)	(26)	(25)	(10)	(13)	(7)	(8)	(-)	(1016)
	Slightly Injured	22	22	341	16119	4040	1338	1737	1861	1605	785	126	57	28653
		(22)	(21)	(229)	(1449)	(375)	(64)	(51)	(35)	(17)	(11)	(3)	(-)	(2277)

Table 11. France (1980)

	Age Groups	0-4	5-9	10-13	14-15	16-17	18-19	20-24	25-34	35-44	45-54	55-64	≥65	Total
Pedal Cyclists	Killed	2	46	85	30	22	13	29	68	66	74	66	149	656
	Severely Injured	14	424	773	395	252	136	186	371	325	370	322	467	4073
	Slightly Injured	26	622	1718	1049	840	463	658	935	794	835	645	720	9360
Light-Powered Two-Wheelers	Killed	0	5	10	93	186	114	108	129	95	180	136	191	1256
	Severely Injured	4	22	171	2036	3662	1966	1531	1457	1014	1275	940	761	14905
	Slightly Injured	31	59	420	5472	10910	5898	4765	4403	2755	2855	1690	1116	40513

Table 12. Great Britain (1981)

	Age Groups	0-4	5-9	10-14	15	16	17-19	20-29	30-39	40-49	50-59	60-69	≥70	Total
Pedal Cyclists	Killed	5	13	68	18	15	29	19	17	18	32	23	53	310
	Severely Injured	19	547	1444	343	285	491	651	378	292	327	234	168	5179
	Slightly Injured	131	2216	7011	1775	1614	2577	3527	1890	1377	1302	908	600	24928
Light-Powered Two-Wheelers	Killed	0	0	1	2	29	14	9	3	7	4	7	5	81
	Severely Injured	0	0	26	24	1139	679	316	177	191	184	94	37	2867
	Slightly Injured	0	1	31	25	2987	1885	968	521	456	446	168	67	7555

Table 13. Italy (1981)

	Age Groups	- 5	6-9	10-14	15-17	18-20	21-24	25-29	30-44	45-54	55-59	60-64	≥65	Total
Pedal Cyclists	Killed	—	20	48	18	6	8	12	33	65	43	59	275	608
		(1)	(-)	(3)	(-)	(-)	(-)	(-)	(-)	(1)	(-)	(-)	(-)	(5)
	Injured	40	368	1378	623	311	261	228	929	874	572	1797	154	8087
		(30)	(27)	(38)	(39)	(7)	(4)	(3)	(5)	(2)	(1)	(3)	(4)	(206)
Light-Powered Two-Wheelers	Killed	—	—	48	181	49	25	13	70	97	68	47	183	800
		3	4	8	21	6	3	—	2	2	—	—	2	57
	Injured	1	—	2452	10870	4733	2078	1282	3028	2321	1080	780	1760	30889
		(65)	(93)	(726)	(1726)	(625)	(213)	(75)	(95)	(39)	(16)	(11)	(15)	(3944)

Table 14. The Netherlands (1981)

	Age Groups	0-4	5-9	10-14	15-19	20-24	25-34	35-44	45-54	55-64	65-69	70-74	≥75	Total
Pedal Cyclists	Killed	1	18	52	28	17	21	21	14	39	34	39	61	345
		(1)	(3)	(1)	(-)	(1)	(1)	(-)	(-)	(1)	(-)	(1)	(2)	(11)
	Severely Injured	18	323	830	638	266	325	279	287	364	209	227	260	4033
		(20)	(21)	(16)	(15)	(6)	(5)	(3)	(2)	(2)	(-)	(-)	(-)	(90)
	Slightly Injured	22	431	1686	1595	782	981	693	607	631	260	258	267	8252
		(58)	(64)	(52)	(69)	(14)	(12)	(4)	(3)	(2)	(-)	(-)	(1)	(287)
Light-Powered Two-Wheelers	Killed	—	—	2	89	6	7	1	8	15	7	4	9	148
		(-)	(-)	(1)	(6)	(-)	(-)	(-)	(-)	(1)	(1)	(1)	(-)	(10)
	Severely Injured	—	—	48	2398	280	176	115	129	110	56	30	36	3381
		(-)	(8)	(39)	(203)	(22)	(10)	(2)	(7)	(7)	(7)	(1)	(2)	(312)
	Slightly Injured	1	—	44	5750	770	413	300	253	212	70	44	33	7914
		(2)	(10)	(122)	(594)	(69)	(32)	(16)	(23)	(20)	(6)	(2)	(1)	(932)

Table 15. Sweden (1981)

	Age Groups	0-2	3-6	7-14	15-17	18-19	20-24	25-34	35-44	45-54	55-64	≥65	Ukn	Total
Pedal Cyclists	Killed	—	—	5	3	2	3	1	5	6	7	44	—	76
	Severely Injured	—	19	147	68	26	49	80	85	84	107	147	—	812
	Slightly Injured	1	24	288	150	72	121	223	166	146	147	167	6	1511
Light-Powered Two-Wheelers	Killed	—	—	5	13	2	1	—	1	2	—	—	—	32
	Severely Injured	—	—	46	254	11	9	6	11	17	17	—	—	408
	Slightly Injured	—	—	48	441	18	12	18	14	17	30	3	—	648

and over are three times more frequent than in the age group of 10- to 14-year-old riders of bicycles, the ratio for severely injured accident victims being 1:2. Similar ratios were found in The Netherlands. In Sweden and Italy, the comparison revealed still more unfavorable figures for the elderly.

The number of accident victims among riders and passengers of light-powered two-wheelers reach peak values at a later age—the group of 15- to 17-year-olds. Compared with the bicycle riders age 10 to 14, the fatalities displayed numbers that, on average, were two or three times as high.

With the exception of Italy, the number of fatalities in the age group of 65 and over is generally much lower than in the case of cyclists.

Tables 16 to 21 show the number of accident victims per 100,000 inhabitants of each age group. High frequencies and peak values are similar to those found in the absolute number (with the exception of Sweden where fatality and injury peak values are reached in the higher age groups of bicycle users). A striking fact, revealed by Italian and Swedish statistics, is the fairly low fatality rate in the group of 10- to 14-year-old juveniles, generally considered to be a particularly high-risk group.

Table 16. Federal Republic of Germany (1981)

	Age Groups	0-5	6-9	10-14	15-17	18-20	21-24	25-34	35-44	45-54	55-64	≥65	Total
Pedal Cyclists	Killed 100,000	0.283	2.76	2.74	1.7	0.695	0.435	0.52	0.73	1.55	2.00	4.36	1.72
	Severely/ 100,000	8.73	68.4	78.16	53.71	23.91	15.57	10.95	13.41	18.19	21.10	20.84	25.25
	Slightly/ 100,000	20.51	128.24	195.76	151.82	73.61	50.13	382.3	39.14	41.86	36.82	28.37	59.95
Light-Powered Two-Wheelers	Killed/ 100,000	—	—	0.28	6.95	2.22	0.57	0.375	0.512	0.698	0.694	1.09	0.904
	Severely/ Injured	0.113	0.4	5.18	229.21	60.86	16.09	9.54	9.47	11.94	8.43	5.56	22.06
	Slightly/ 100,000	0.623	0.88	6.82	506.89	133.77	36.36	21.00	20.27	21.15	13.28	7.60	46.51

Table 17. France (1980)

	Age Groups	0-4	5-9	10-13	14-15	16-17	18-19	20-24	25-34	35-44	45-54	55-64	≥65	Total
Pedal Cyclists	Killed/ 100,000	0.1	1.1	2.6	1.9	1.3	0.8	0.7	0.8	1.1	1.2	1.3	2.0	1.2
	Severely/ 100,000	0.4	10.4	23.3	24.6	14.5	8.0	4.4	4.3	5.4	5.8	6.5	6.2	7.6
	Slightly/ 100,000	0.7	15.3	51.8	65.2	48.3	27.3	15.6	10.9	13.2	13.0	13.1	9.6	17.4
Light-Powered Two-Wheelers	Killed/ 100,000	—	0.1	0.3	5.8	10.7	6.7	2.6	1.5	1.6	2.8	2.8	2.6	2.3
	Severely/ 100,000	0.1	0.5	5.2	126.6	210.6	115.9	36.3	17.0	16.8	19.9	19.1	10.2	27.7
	Slightly/ 100,000	0.8	1.5	12.7	340.3	627.4	347.8	113.0	51.3	45.7	44.6	34.3	14.9	75.2

Table 18. Great Britain (1981)

	Age Groups	0-4	5-9	10-14	15	16	17-19	20-29	30-39	40-49	50-59	60-69	≥70	Total
Pedal Cyclists	Killed/ 100,000	0.2	0.3	1.6	2.0	1.6	1.1	0.3	0.2	0.3	0.5	0.4	1.0	0.6
	Severely/ 100,000	0.6	14.4	33.3	37.4	31.1	18.6	8.4	5.1	4.8	5.1	4.3	3.1	9.5
	Slightly/ 100,000	4.0	58.5	161.5	193.8	176.4	97.6	45.7	25.7	22.4	20.3	16.5	11.1	45.8
Light-Powered Two-Wheelers	Killed/ 100,000	0	0	<0.1	0.2	3.2	0.5	0.1	<0.1	0.1	0.1	0.1	0.1	0.1
	Severely/ 100,000	0	0	0.6	2.6	124.5	25.7	4.1	2.4	3.1	2.9	1.7	0.7	5.3
	Slightly/ 100,000	0	<0.1	0.7	2.7	326.4	71.4	12.5	7.1	7.4	7.0	3.0	1.2	13.9

Table 19. Italy (1980)

	Age Groups	0-5	6-9	10-14	15-17	18-20	21-24	25-29	30-44	45-54	55-59	60-64	≥65	Total
Pedal Cyclists	Killed/ 100,000	0.1	0.6	0.9	0.5	0.3	0.5	0.1	0.3	0.9	1.2	2.1	4.2	1.1
	Injured/ 100,000	1.2	13.1	29.2	21.2	12.3	7.3	5.8	7.9	13.1	18.1	28.1	23.2	14.3
Light-Powered Two-Wheelers	Killed/ 100,000	0.05	0.1	1.1	5.4	2.8	0.9	0.4	0.6	1.4	2.0	2.6	2.7	1.5
	Injured/ 100,000	0.09	0.1	49.1	374.4	175.7	57.1	32.3	27.6	32.7	35.1	32.7	22.0	52.8

Table 20. The Netherlands (1981)

	Age Groups	0-4	5-9	10-14	15-19	20-24	25-34	35-44	45-54	55-64	65-69	70-74	≥75	Total
Pedal Cyclists	Killed/ 100,000	0.23	2.16	4.36	2.23	1.47	0.94	1.09	0.93	3.03	6.22	8.87	9.40	2.49
	Severely/ 100,000	4.27	35.41	69.66	51.92	22.13	14.03	15.28	19.18	27.60	38.23	50.31	38.79	28.86
	Slightly/ 100,000	8.99	50.95	143.12	132.3	62.67	42.25	37.70	40.46	47.69	47.56	57.18	39.98	59.76
Light-Powered Two-Wheelers	Killed/ 100,000	—	—	0.25	7.55	0.49	0.30	0.12	0.53	1.20	1.46	1.11	1.34	1.11
	Severely/ 100,000	—	0.82	7.16	206.8	24.58	7.92	6.38	9.00	8.72	11.52	6.78	5.67	25.85
	Slightly/ 100,000	0.33	10.29	13.66	504.5	68.29	18.94	17.03	17.30	17.26	13.90	10.19	5.06	61.91

Table 21. Sweden (1981)

	Age Groups	0-2	3-6	7-14	15-17	18-19	20-24	25-34	35-44	45-54	55-64	≥65	Total
Pedal Cyclists	Killed/ 100,000	—	—	0.55	0.81	0.91	0.55	0.08	0.43	0.68	0.72	4.69	0.91
	Severely/ 100,000	—	4.81	16.30	18.38	11.60	8.94	6.59	7.42	9.52	11.03	15.67	9.76
	Slightly/ 100,000	0.35	6.08	31.93	40.54	32.14	22.08	18.37	14.49	16.55	15.15	17.80	18.15
Light-Powered Two-Wheelers	Killed/ 100,000	—	—	0.55	3.51	0.89	0.18	—	0.08	0.22	—	—	0.32
	Severely/ 100,000	—	—	5.10	68.65	4.91	1.64	0.49	0.96	1.93	1.75	—	4.90
	Slightly/ 100,000	—	—	5.32	119.2	8.04	2.19	1.48	1.22	1.93	3.09	0.32	7.79

Compared with these numbers, the increased fatality rate for the elderly, especially in the age group of 65 and over, should be noted in particular.

Figures 11 and 12 show population-based numbers of casualties enabling a comparison between the participating countries. The number of killed and injured pedal cyclists is given in Figure 11 and the number of killed and injured users of light-powered two-wheelers in Figure 12.

Extremely high casualty figures for pedal cyclists are displayed by The Netherlands and the Federal Republic of Germany. This applies to all degrees of injury severity but particularly to the group of severe injuries. Once more, the diagrams are evidence that the proportion of persons age 65 and over increases disproportionally with increasing injury severity, Great Britain being the exception.

The variation in the number of casualties per 100,000 inhabitants for users of light-powered two-wheelers is not as large as for pedal cyclists. They are narrowly concentrated around the age group of the 16-year-olds.

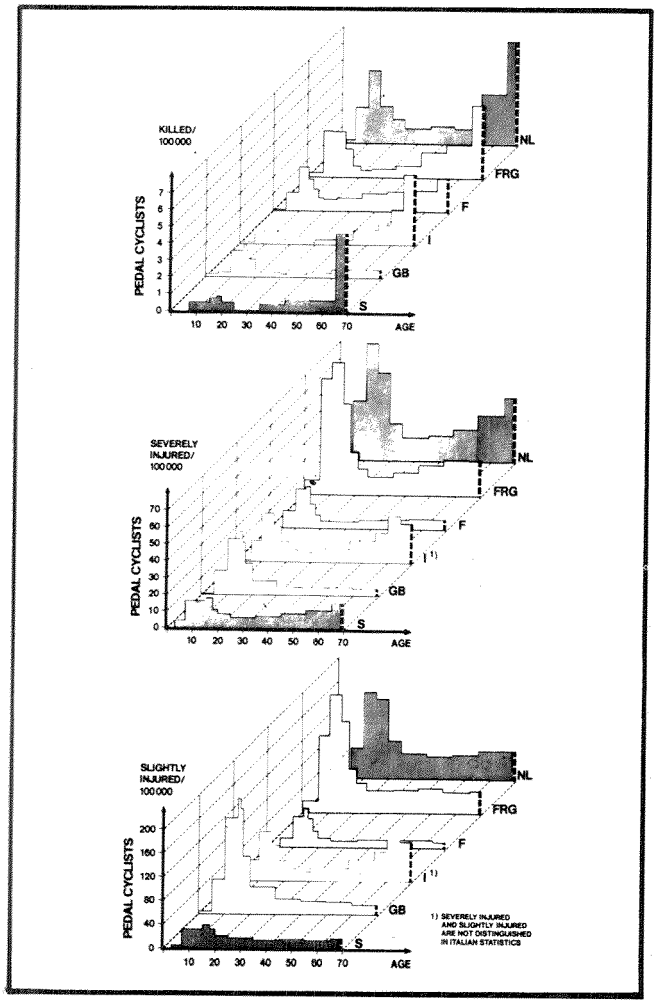

Figure 11. Killed and injured pedal cyclists per 100,000 inhabitants/age group (dotted line for age 70 stands for age group 65 and over)

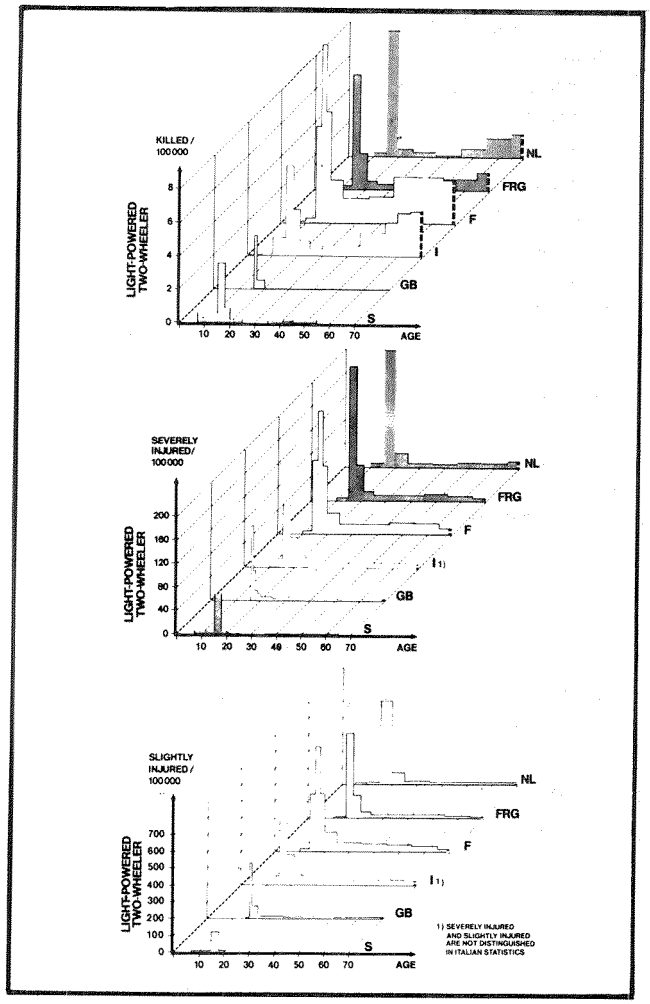

Figure 12. Killed and injured users of light-powered two-wheelers per 100,000 inhabitants/age group (dotted line for age 70 stands for age group 65 and over)

France, The Netherlands, and the Federal Republic of Germany display the highest figures in all these accidents. France, in particular, displays a remarkable death rate for the age group of over 40.

Unreported Accidents

The most important systematic error in all national accident statistics results from the material damage and injury accidents not reported. These so-called unreported accidents can reach considerable values, particularly with decreasing accident severity. Various studies have been consulted.

Sweden

Roosmark/Fraki(11) and Thorson/Sande(12) concluded that on the whole not more than half of the traffic casualties are reported in the national accident statistics.

In the case of material damage, unreported numbers are estimated at 85 percent even.

Based on a regional study in Göteburg, Bunketorp(18) determined a correction factor to describe the relationship between the overall number of accidents and those recorded by the police. For fatal accidents, a factor of 1.0 was found; for severe injury accidents, 1.4; and for light injury cases, 1.8. This corresponds to unreported rates of 0 percent for fatal accidents, 29 percent for severe injury cases, and 45 percent for light injury accidents.

Denmark

Nordentoft(13) revealed in 1972 in the Odense area an estimation of unreported injured accident victims of more than 60 percent. Unreported numbers are reportedly particularly high in single-vehicle injury accidents.

Switzerland

Hehlen(14) reports a high percentage inside urban areas at 70 percent and outside urban areas at 63 percent. The unreported accidents of cyclists were estimated at 81 percent, and for mofa riders at 74 percent.

The Netherlands

A study on unreported numbers, published in 1982, was conducted in The Netherlands(16). This study was based on the period 1977-79 and revealed the proportion of unreported numbers appeared to have remained unchanged over the entire period. A comparison with police accident records for 1979 showed that, in the case of accident victims hospitalized as a consequence of their accidents, only 17 percent appear to remain unreported. The underreporting seems to be a function of the mode of transport. The CBS/SMR ratio of reported accidents (police information/hospital information) is in vehicle categories and pedestrians:

Car occupants	Mopeds	Bicycles	Pedestrians
98 percent	97 percent	82 percent	78 percent

Germany

A study conducted by Lenhardt(17) in 1982 (still unpublished) was based on approximately 4,000 accidents and arrived at an estimated percentage of unreported numbers of about 54 percent. The number of unreported cases drops with increasing severity. The proportion of unreported fatalities is estimated at 4.8 percent; in the case of severely injured accident victims, 22.3 percent; and in that of slightly injured victims, 37.5 percent. The global estimate of 54 percent comprises material damage accidents. A breakdown in vehicle categories and pedestrians has not been undertaken.

Great Britain

Pedder(19) revealed the number of unreported accidents shown in Table 22. The figures are based on data collected by Pedder (1977-78) and Bull (1973) at Birmingham Accident Hospital and by Hobbs at a hospital in Berkshire.

Table 22. Casualties in nonreported accidents

	Two-wheeled Motor Vehicles			Pedal Cycle		
	Slightly Injured %	Seriously Injured %	Total Sample Size[1]	Slightly Injured %	Seriously Injured %	Total Sample Size[1]
Pedder(12)	58	29	540	91	83	459
Bull(13)	37	28	145	81	65	145
Hobbs(8)	45	27	754	71	59	488

[1] Fatalities have been excluded

The comparison shows how difficult it is for a regional study of this nature to arrive at a conclusive result of general validity. The year of data collection (Pedder: 1977-78; Bull: 1973) and the legal framework and social conditions applying therewith certainly would also affect an interpretation of the large differences found in the estimates, but also differences in sample sizes of the studies may contribute.

Injury Severity and Hospitalization of Users of Two-wheelers (Including an Approach to an Overall Economic Assessment)

It has generally been found that data are not collected on a national scale in any of the participating countries on the various degrees of injury severity and length of in-patient treatment. The research findings available are results of regional studies and thus involve the problem of translation to be of value at a national level.

A thorough analysis would have to consider also the economic significance of human accident costs, which, apart from hospital costs (during the period of a victim's hospitalization), also include the production loss during the period of a victim's inability to work (involving a much larger time and cost factor than the period of treatment as an in-patient). However, these are aspects that would be outside the scope of a regional study on a medical treatment facility concentrating on the classification of injuries into appropriate categories (e.g., AIS, OAIS, MAIS).

For the Federal Republic of Germany, first hints for an analysis of the time and cost factors involved in treating accident victims are found in studies conducted by Otte(21) and in the comparison of Otte's findings with the results obtained by Willeke(22). In Table 23, the periods of hospitalization relating to various degrees of injury severity (OAIS) are shown (on average in terms of days).

Note that Willeke's study is based on an all-road-user sample, whereas Otte concentrated on the users of two-wheelers only. The term "sum total of days of in-patient treatment" may include readmittance to the hospital, where necessary. The number of cases studied here was 123. Based on 282 case studies, Otte arrived at average periods of in-patient treatment (including complications or not) as stated on the last line in Table 23.

For calculating costs of treatment, the average length of hospitalization in each AIS group was linked with the hospital cost per day charged currently by the Medical University of Hanover (DM 310). The cost of medical treatment for users of motorized two-wheelers involved in injury accidents with resulting injuries of the OAIS 2 category (without complications) are thus estimated at DM 3,950. If complications have to be considered in addition, the costs rise to DM 10,000 (base: 123 cases).

A survey concerning the length of hospitalization in relation to the severity of injuries (MAIS) can be found in a study by Danner(23). One remarkable result of the study is that the high number of leg injuries with long treatment periods are dominating at the injury scale MAIS 3, whereas, at MAIS 4 and 5, head injuries determine the injury pattern (Table 24).

A study conducted by Krupp(24) describes the periods of hospitalization and resulting costs for severely injured riders of bicycles and motorized two-wheelers. The medical treatment costs and the costs with a breakdown into categories accounting for the absence and presence of effects on earning capacity, as estimated by health insurance companies or insurance companies for occupational accidents, are found in Table 25.

Table 23. Length of hospitalization in days related to OAIS

	OAIS	1	2	3	4	5	6
All Road users	According to Willeke	3	16	42	59	53	5
	According to Otte (without complications)	—	13	31	32	—	—
Users of Two-Wheelers	According to Otte (with complications)	—	33	80	58	—	6
Σ = 123 cases	According to Otte (Sum total of Days of in-patient treatment)	—	35	83	87	—	—
Users of two-Wheelers Σ = 282 cases	According to Otte on average	3	16	32	39	29	1

Table 24. Length of hospitalization of injured motorcyclists (base: 275 cases) (23)

Time in Hospital	MAIS 1	MAIS 2	MAIS 3	MAIS 4	MAIS 5	MAIS 6
Up to 2 weeks	29	36	9	—	1	2
Up to 2 months	4	55	60	10	9	—
Up to 1 year	1	5	37	10	5	—
Over 1 year	—	—	—	2	—	—

Table 25. Time and cost factors involved in hospitalization with and without effect on earning capacity (24)

	Users of bicycles		Motorized Two-Wheelers	
	Without effects on earning capacity	With effects on earning capacity	Without	With
Length of In-patient Treatment*	11	34	11	43
Costs (DM)	1,800	5,900	1,900	7,800

* Days

A survey among nearly all hospitals in The Netherlands(25) shows as a result the following average number of days in hospital for bicyclists and users of powered two-wheelers: bicyclists, 18 days; moped riders, 20 days; motorcyclists, 20 days. The average total costs per patient do not differ as much: bicyclists, 6,200 HFL; moped riders, 6,900 HFL; motorcyclists, 6,800 HFL.

In the TRRL study by Hobbs(15), the period of hospitalization and degrees of accident severity are considered separately for cyclists and users of motorized two-wheelers. In the case of cyclists, the degrees of injury severity fall primarily into the AIS 2 and 3 categories. On account of the limited number of case studies, the periods of hospitalization were classified into those of less or greater than 2 days. The group of accident victims with injuries in the AIS 2 category mainly involved periods of in-patient treatment of ≤ 2 days (57 out of 83 cases). In the case of injuries of the AIS 3 category, the period of hospitalization is clearly greater than 2 days (in 22 out of 29 cases). In 57 out of 85 cases, accident victims in the user group of motorized two-wheelers, whose injuries had been classified as corresponding to AIS 2, had to undergo hospital treatments of ≤ 2 days. The peak value reached by the injury cases of the AIS 3 category also exceeds 2 days of hospitalization by far: between 11 and 20 days in 27 out of 100 cases. Injury cases corresponding to AIS categories other than 2 or 3 were so few that statistically significant information was not obtained.

Summary

This chapter presents a survey of the national accident statistics of the countries represented in the working group. The frequencies of injuries of cyclists and users of light-powered two-wheelers are considered at greater depth. At the beginning, the numbers of registered vehicles are presented and the definitions of a bicycle and a light-powered two-wheeler, as applicable in the various countries, are summarized. In the case of the numbers of injured accident victims, given as overall figures and with a breakdown by vehicle categories, the distributions are fairly heterogeneous and often also display falling trends, in particular in the case of fatalities.

A consideration of the development of vehicle numbers in each vehicle category needs to be included in the study. In addition, the number of vehicles per 100,000 inhabitants needs to be considered both in the evaluation of the number of accidents and in the assessment of relative accident numbers. Due to the complex nature of the relationships and the basically different definitions given, e.g., of light-powered two-wheelers, a ranking of the countries by their rates of injured accident victims was refrained from in this conjunction.

With respect to the number of unreported accidents, there is still the problem of translating the results of regional studies to the conditions at a national level. On the whole, it was found that the percentages of unreported accidents tend to increase with decreasing injury severity.

No statistically supported findings on a national level can be given on the correlation between injury severity and periods of hospitalization. Only initial data material is available from regional studies.

National Statistical Data—Sources

- Federal Republic of Germany: Strassenverkehrsunfälle; Verkehr, Fachserie 8, Reihe 3.3, 1982, Statistisches Bundesambt Wiesbaden
- The Netherlands: Statistiek van de verkeersongevallen op de openbare weg—1981, Centraal Bureau voor de Statistiek, 1983
- Sweden: Road traffic accidents with personal injury, 1981 Statistics, Sweden, Stockholm, 1982
- Italy: Statistica degli incidenti stradali edizione 1981, Instituto Centrale di Statistica, Roma, 1982
- Great Britain: "Accidents in Great Britain 1981," Department of Transport, 1982

2. Detailed Description of Bicycle and Light-powered Two-wheeler Accidents

This section deals with more detailed data of bicycle and light-powered two-wheeler accidents, such as collision partners, collision types, resulting injuries, and speed at impact. These data are in general not available from national statistics. Therefore, most of the information is obtained through special accident studies.

Nevertheless, as is the case in The Netherlands, useful and more detailed information is gathered on a national base by the police and computerized at the Road Accident Record Office (VOR). To give direction to the injury-prevention research of bicyclists and moped riders, some priorities in the distribution of accident and collision types are made in The Netherlands(34). Many criteria may be used for this, but for some practical reasons magnitude and severity were used.

For magnitude, the number of killed and severely injured road users is used. Severity of road accidents is a

very complex term. Many dimensions are involved, such as damage, injury, cost of delays, etc. In injury-prevention research, the injury dimension of accident severity is used. But injury can also be distinguished in place, nature, and severity.

Injury severity is also complex and can be defined by threat to life, disability, etc. Scaling with the Abbreviated Injury Scale (AIS) seems to be the most appropriate, although there is some concern about the influence of long-term effects on the scaling(30). For the Dutch accident situation, only the number of killed or severely injured road users for the accident and collision types were available. Therefore, as a criterion for injury severity, lethality was used. (Lethality = 100 × number of killed / (number of killed + number of severely injured.)

There is a general problem concerning the accident data of different countries with regard to motorized two-wheelers. In most cases, this group cannot be divided into motorcycles and mopeds; the latter may even contain several types. This is needed for a proper comparison of the data since the distribution of these two groups differs considerably for the different countries.

Another more general problem in comparing the results of the different accident studies is caused by sample differences, e.g., the large differences in under-reporting figures for the different countries as shown earlier. In The Netherlands, the reporting of killed and severely injured road users is complete enough information to indicate priorities in injury-prevention research.

This section starts with a description of collision opponents of the two-wheeler riders, with respect to kind of opponent (accident type) and with respect to collision direction (collision type), with some information about the maneuver of the collision opponents just before the accident.

The resulting injuries (injury pattern) will be described, followed by a review of the impact speed, as mentioned in a number of accident studies. Information about braking (of the collision partners) before, during, or after the collision, as described in the report of EEVC Working Group 7 about pedestrian injury accidents, was not found in literature.

Accident Type

The particular combination of a two-wheeler and its collision opponent is called accident type (for instance, bicycle-car, moped-car, moped-HGV vehicle). The distribution of collision opponents will depend on the severity class of injuries considered; therefore, a large variety of distributions in the various studies may be noticed.

Great Britain

The distribution of collision opponents (motor vehicles only) for bicyclists according to (33) is:

Car and taxi	75%
Light goods vehicle	9%
Heavy goods vehicle	3%
Medium goods vehicle	1.5%
Others	11.5%

The group consists of accidents in 1974, reported by the police. There is no information about the collision partners of mopeds.

More recent information (1980) from national statistics(42) about accident types of two-wheeler casualties reported to the police, excluding accidents with three or more vehicles, is given in Table 26. The car is the most frequent collision partner in bicycle and two-wheeled motor vehicle accidents (73.1 percent; 60.3 percent) followed by the light goods vehicle and two-wheeled motor vehicle for the bicyclist (6.1 percent; 6.1 percent) and the light goods vehicle for the two-wheeled motor vehicle rider (4.8 percent).

The share of single-vehicle accidents (no pedestrian involved) for two-wheeled motor vehicle users is much

Table 26. Number of two-wheeler casualties (all severities) reported to police for different accident types in Great Britain (1980), Department of Transport (42)

	Single Vehicle				Two Vehicle				
	No Pedestrian	With Pedestrian	Pedal Cycle	Two-Wheeled Motor Vehicle	Car	Bus or Coach	Light Goods Vehicle	Heavy Goods Vehicle	Total
Pedal Cycle User	1794 (7.7%)	140 (0.6)	229 (1.0)	1,411 (6.1)	17013 (73.1)	457 (2.0)	1,433 (6.1)	807 (3.5)	23,284
Two-Wheeled Motor Vehicle User	15,522 (23.7%)	1950 (3.0)	765 (1.2)	2,434 (3.7)	39,428 (60.3)	615 (0.0)	3,146 (4.8)	1,504 (2.3)	65,364

* Excludes three or more vehicle accidents and accidents where details are not known.

higher (23.7 percent) than for the pedal cycle users (7.7 percent). In fact, these shares will probably be much larger due to the already mentioned underreporting.

Germany

A distribution of collision partners in Germany for 1982 is given in Table 27.

The group consists of killed road users in a single-vehicle accident or in collision with a car or an HGV. The table shows that, in collisions with another road user, the car in most cases is the collision partner (55 percent for bicyclists and 57 percent for motorized two-wheeler riders). Single-vehicle accidents occur more often with motorized two-wheeler riders (13 percent) than with bicyclists (11 percent).

(A)	Killed	Severely Injured
Bicyclist	89%	79%
Moped rider	72%	78%

(B1) The shares for bicyclists and moped riders are identical:

	Killed	Severely Injured
	4%	8%

(B2)	Killed	Severely Injured
Bicyclists	1%	3%
Moped Rider	17%	7%

(C) 5 to 10% The group defined in A will be considered for the distribution of collision partners.
The results for 1979 are shown in Table 28 and visualized in Figures 1 and 2.

Table 27. Number of killed bicyclists and light powered two-wheeler riders for different accident types in Germany (1982)

	Accidents with Two Participants		Single Vehicle Accidents	Total Number of Killed
1982	Car	Vans and HGV's		
Bicycle	598	127	116	1,085
Mofa/Moped	305	57	71	543

Source: BASt

The Netherlands

The Dutch data of the distribution of accident and collision types based on police information for 1978 and 1979 are available separately for fatal two-wheeler accidents and for accidents in which the two-wheeler riders were taken into hospitals for at least 1 day.

The data were coded by the Dienst Verkeersongevallen Registratie (VOR), manipulated by SWOV, and reported by Huijbers(34). These accidents are very well reported as already stated; almost 100 percent of the two-wheeler fatalities and 80 percent of the hospitalized casualties are reported by the police(35).

The bicycle and moped accidents can be divided into the following groups:

(A) Accidents with a pedestrian or a parked or moving vehicle
(B) Accidents with no other vehicle or pedestrian involved, divided into (1) collision without obstacle (tree, pole, animal, etc.), and (2) collision with an obstacle
(C) Multi- (> 2) vehicle accidents

For 1979, the total number of killed and severely injured bicyclists and moped riders is divided over these groups:

Fatalities—The car is the most frequent collision partner for bicyclists (62 percent) and moped riders (48 percent). The second most frequent collision partner is the HGV: 23 percent for bicyclists and 21 percent for moped riders.
Severely Injured—For the severely injured, the car is also the most frequent collision partner for bicyclists (69 percent) and for moped riders (74 percent). The second most frequent collision partner is the moped for bicyclists (10 percent) and for moped riders themselves (7 percent), together with the HGV (7 percent) for moped riders.

When lethality is used as a severity criterion, the collision with a tram or train has a high severity because there are few registered severely injured patients. But the number of these accidents is small. For bicyclists, the collision with an HGV has the next priority, followed by the collision with a delivery van. The collision with a car does not seem to be as severe. For moped riders, the collision with a motorcycle (or a scooter) has the next priority, followed by HGV's and delivery vans. The collision with the car does not seem to be relatively as severe (Figures 13 and 14).

United States of America

In Cross(28), a distribution from the United States is given. This group consists of bicycle casualties. In 87

Table 28. Distribution of accident types resulting in killed and severely injured cyclists and moped riders; lethality of the various accident types (34)

Casualties In Collision With	Bicyclist % Killed	Bicyclist % In-Patients	Bicyclist "Lethality"	Moped Rider % Killed	Moped Rider % In-Patients	Moped Rider "Lethality"
Car	62	69	9.2	48	74	2.6
Delivery Van	5	4	12.1	8	4	7.3
Heavy Goods Vehicle	23	5	34.2	21	7	11.2
Motor/Scooter	3	3	9.8	5	1	17.9
Train or Tram	2	—	54.5	10	—	56.5
Bicycle	—	6	0.0	—	3	0.0
Moped	3	10	3.1	4	7	2.2
Other 2 Wheelers	—	—	—	—	—	—
Pedestrians	—	1	0.0	—	2	7.4
Others	2	2	10.1	4	2	—
Total	100%	100%	—	100%	100%	—
N Total	349	3.082	—	131	3.169	—

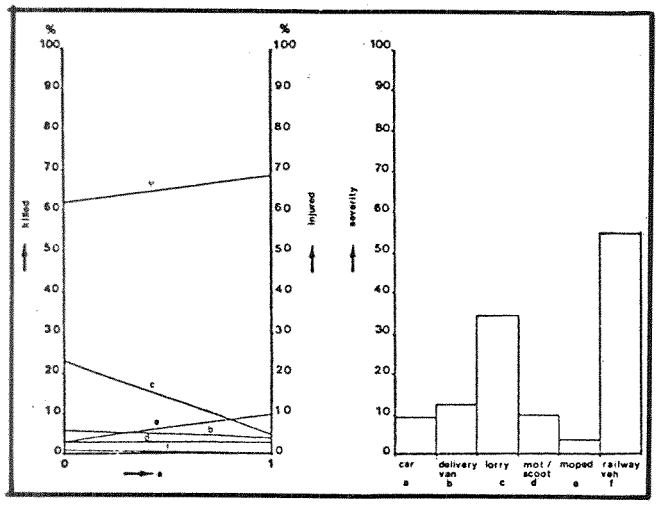

Figure 13. Priorities within the various accident types resulting in killed and severly injured bicyclists(34)

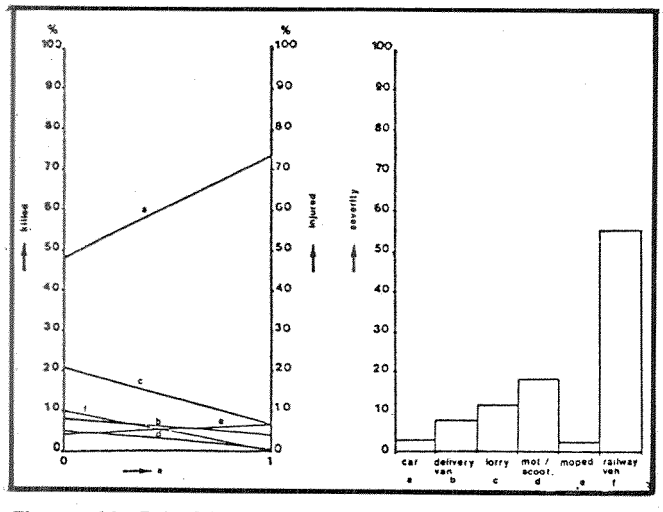

Figure 14. Priorities within the various accident types resulting in killed and severely injured moped riders(34)

percent of the cases, the car was the collision opponent; in 9 percent, it was a pick-up or van.

Collision Type

A collision type is a particular combination of impact sites of the two-wheeler and its collision opponent (for instance, front of a two-wheeler against the side of a car). The different collision types will probably result in different impact places on the body; for some types caused by the car and for others by the two-wheeler. This may cause different injury patterns.

This paragraph deals mainly with the car-to-bicycle, car-to-moped, HGV-to-bicycle, and HGV-to-moped accident types. As far as possible, collision type or impacted sites of two-wheelers and opponents are given, as specified in the different accident studies. Comparison of the results of these different studies is clearly limited due to sampling differences, as mentioned earlier.

Great Britain

Whitaker(40) gives a summary of impact sites on motorized two-wheelers. Frontal impacts occur in 59 percent, followed by lateral impacts in 38 percent of the cases. More left-side than right-side impacts were found. No information is given on the impacted sites of the collision opponent.

Riley(42) studies fatal accidents involving HGV's: 37 percent of the bicyclists hit the front of an HGV, 57 percent the side, and only 2 percent the rear end. There is no information about the impacted site of the bicycle.

Germany

Otte(37) states that in bicycle-to-car accidents 46 percent of all casualties occur with collision type front of

car-side of bicyclist, followed by the collision type front of car-rear end of bicyclist (20 percent) (Figures 15 and 16).

In a frontal collision (front of car-front of bicyclist), 17 percent of the persons were killed or injured; in side collisions (side of car-front of bicyclist), 15 percent of the casualties occurred. The distribution of some collision types causing casualties for motorized two-wheelers is 28 percent in collision type front of car-side of motorized two-wheeler, 24 percent in collision type front of car-front of motorized two-wheeler, and 21 percent in collision type side of car-front of motorized two-wheeler.

collision type		I	II	III	IV	V	other types
number of accidents		(37) (29%)	29 (23%)	22 (17%)	25 (20%)	11 (9%)	3 (2%)
persons involved		43 (28%)	36 (24%)	28 (18%)	32 (21%)	11 (7%)	3 (2%)
VERLETZUNGSSCHWERE GRAD-VERTEILUNG overall AIS [%] Injury severity	0	0	2,8	(7,1)	0	9,0	
	1	16,7	27,8	17,9	(37,3)	27,3	
	2	23,8	13,9	28,6	(31,3)	18,2	
	3	(35,7)	25,0	17,9	18,8	18,2	
	4	(11,9)	8,3	1,79	6,2	0	
	5	(4,8)	2,8	0	0	0	
	6	7,1	19,4	10,7	6,2	(27,3)	

Figure 15. Distribution of two-wheeler collision types in motorized crashes(37)

collision type		I	II	III	IV	V	other types
number of accidents		62 (45,6%)	22 (16,2%)	21 (15,4%)		28 (20,6%)	3 (2,2%)
person involved		63 (45,7%)	23 (16,6%)	21 (15,2%)		26 (20,3%)	3 (2,2%)
VERLETZUNGSSCHWERE GRAD-VERTEILUNG overall AIS [%] Injury severity	0	1,6	4,4	——		——	
	1	12,7	13,0	14,3		21,4	
	2	34,9	30,4	28,6		42,8	
	3	27,0	26,1	19,0		17,9	
	4	4,8	4,4	9,5		3,6	
	5	12,7	21,7	23,8		3,6	
	6	6,3	——	4,8		10,7	

Figure 16. Distribution of two-wheeler collision types in bicycle crashes(37)

From this information, it seems the distribution of the collision types for the motorized two-wheeler-to-car accidents is much more homogeneous than the distribution of the bicycle-to-car accidents. The collision type front of car-rear of two-wheeler occurs relatively often for the bicyclist but not for the motorized two-wheeler. The distribution of collision types for HGV's can be seen in a study of the HUK-Verband, Büro für Kfz-Technik, which treats the problem of truck accidents(44).

In almost 80 percent of all bicycle accidents, the contact area on the truck was the front or the right side in

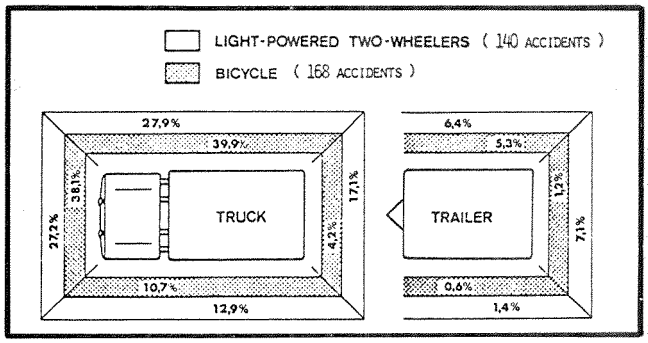

Figure 17. Heavy goods vehicle region contracted by bicycle or light-powered two-wheelers(44)

nearly equal proportions. For the light-powered two-wheelers, the contribution is a little more homogeneous (Figure 17).

The Netherlands

For the Dutch accident situation, priorities for injury-prevention research within the distribution of collision types (1978/1979) were based on the criteria of magnitude and severity (lethality). The collisions were categorized in some collision types (Figure 18)

Bicycle-to-car Accidents (Figure 19)—Most of the cyclists were hit in the side by the front of the car (type F1): 65 percent of those killed and 60 percent of the severely injured. The left side of the bicycle was hit twice as much as the right side. The other collision types did not occur as much; of these, the types F2 and F3 were most important. The collision with the side of the car happened most of the time with the front of the bicycle (type S1): in 10 percent of the cases with severely injured cyclists. With lethality as a criterion, collision type F3 (front of car-rear end of bicycle) was the most severe.

Moped-to-car Accidents (Figure 20)—In moped-to-car accidents, the collision type F1 (front of car-side of moped) dominated, too: 62 percent of the killed moped riders. The severely injured moped riders were hit nearly

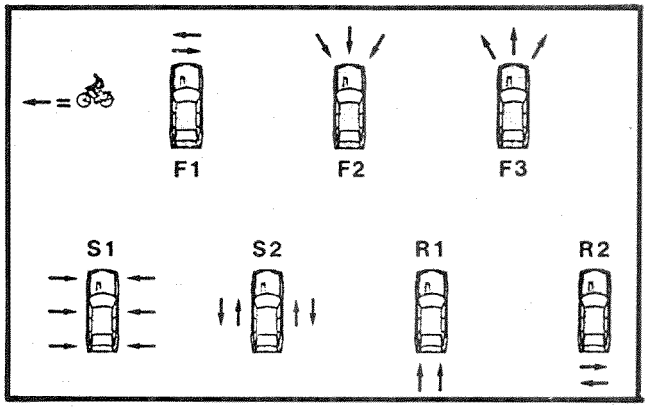

Figure 18. Definition of specific collision types(34)

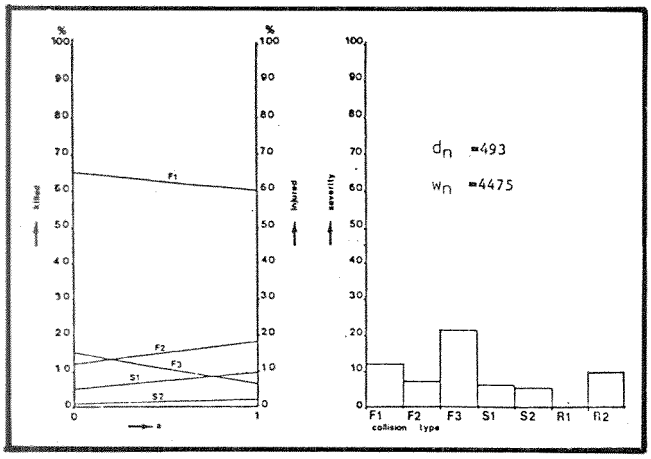

Figure 19. Priorities within the various collision types for bicycle-to-car collisions(34)

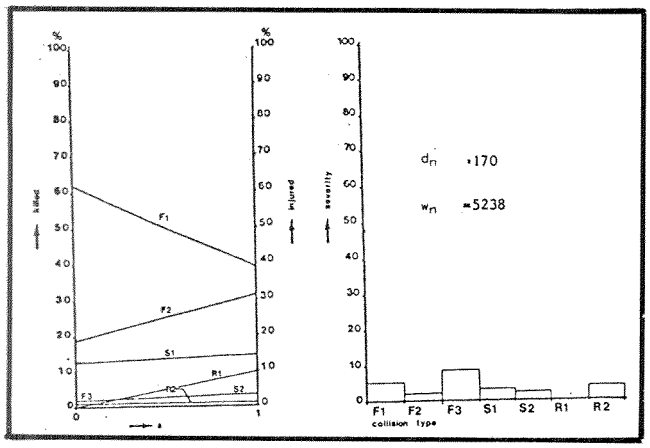

d_n = number of people killed w_n = number of people injured

Figure 20. Priorities within the various collision types for moped-to-car collisions(34)

as often sideways (F1) as frontal (F2) by the front of the car (39 percent; 31 percent). Frontal collisions with the side of the car happened nearly as frequently for the killed moped rider (13 percent) as for the severely injured. The collision type F3, where the front of the car hit the rear end of the moped, did not occur as much as for cyclists (3 percent killed; 1 percent severely injured), although this collision type had the highest lethality in analogy with the bicycle-to-car accident. The opposite rear-end collision (R1) happened for 10 percent of the severely injured moped riders. The lethality from this type was minimal because there were no killed moped riders registered in this collision type.

Bicycle-to-HGV Accidents (Figure 21)—The collision front of HGV-to-side of bicycle (F1) happened most frequently (42 percent for killed and severely injured cyclists). The second most frequent collision type was F2 (front of HGV-to-front of bicycle) for killed (19 percent) and S1 (side of HGV-to-front of bicycle) for severely injured cyclists (18 percent). The frontal collision with the rear end of the HGV (R1) happened relatively often with

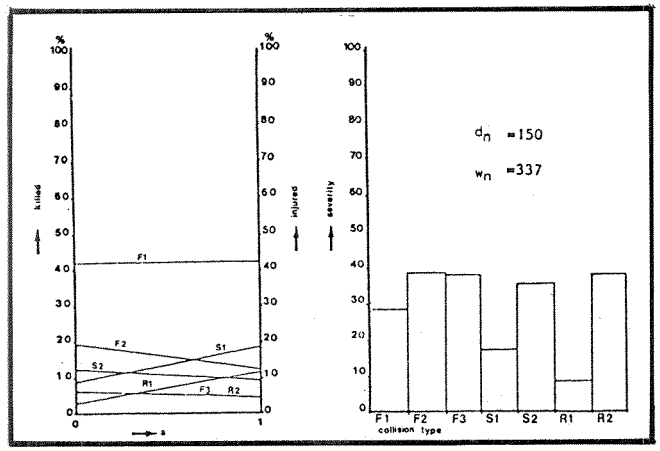

Figure 21. Priorities within the various collision types for cycle-to-HGV collisions(34)

severely injured cyclists (11 percent). The collision types F2, F3, S2, and R2 have nearly the same and highest lethality.

Moped-to-HGV Accidents (Figure 22)—The collision type distribution for this accident type is more or less homogeneous. Collision type F1 dominated for killed moped riders, but the collisions with the front of HGV's (F1 and F2) happen nearly as frequently as the collision with the rear end (R1) for the severely injured moped riders (28 percent), followed by the collision with the side of the HGV (S1).

The collision type side of moped-side of HGV (S2) seems to be the most severe, followed by F1.

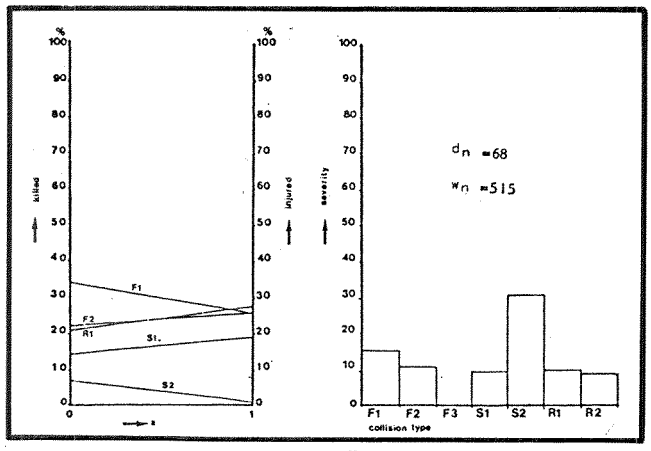

d_n = number of people killed w_n = number of people injured

Figure 22. Proirities within the various collision types for moped-to-HGV collisions(34)

United States of America

Data from the United States about impact points from car-to-bicycle crashes in Roland(39) show nearly the same pattern as in The Netherlands:

	Car	Bicycle
Front	63.2%	25.6%
Left side	10.7%	49.6%
Right side	23.4%	21.2%
Rear	1.9%	3.6%

The sides of the car are struck more frequently than in The Netherlands. This may be due to differences in injury severity in the samples. There is no information about collision types.

Maneuvers

The majority of accidents involving cyclists and light-powered two-wheeler riders in urban areas take place at road junctions(45). In Great Britain, accident statistics show that nearly two-thirds of injury accidents involving a pedal cycle occur at junctions(46).

In a study of accidents occurring at intersections, the Danish Council of Road Safety Research(47) found that, for urban accidents involving a bicycle and another vehicle, the most frequent maneuver type was where each was traveling on a different road before the collision. This was also the finding in a British study of national accident statistics. According to Gauss(44), nearly 45 percent of the HGV-to-two-wheeler accidents happened when one of the vehicles was changing direction.

Injuries

For injury-prevention research, injury is the most important output variable in the accident system. Injury can be described in terms of place, nature, and severity. These three dimensions are described in literature, mostly separately.

The place of the injury is reported in most of the studies, sometimes in relation to severity. Severity is mostly scored with the Abbreviated Injury Scale (AIS) system. Injury severity is a complex term. Probability of death but also temporal or permanent impairment will influence severity. The role of these long-term consequences in the AIS is under discussion, in particular for pedestrian injuries(30).

Whether this is also important for bicyclist or light-powered two-wheeler rider injuries cannot be answered now, but, for outcome variable injury severity, the scaling with the AIS seems to be the most suitable for injury-prevention research at this moment.

There is a wide variety of injury distributions in literature. As stated in (30), it is hardly possible to compare the results of accident studies because of some major differences, for instance—

- Differences in levels of injury severity in the sample (e.g., fatalities only, fatalities + hospitalized)

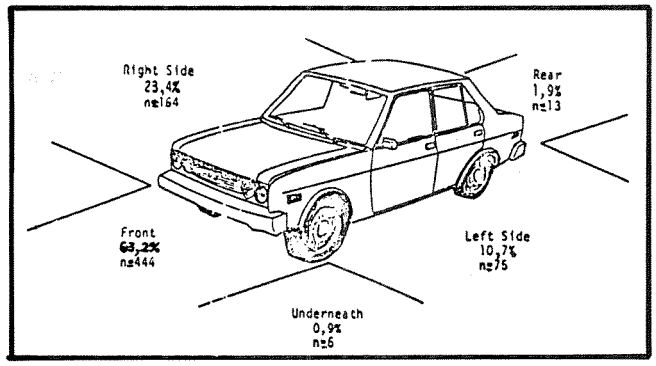

Figure 23. Motor vehicle region contacted by bicycle/-bicyclist (702 cases)(39)

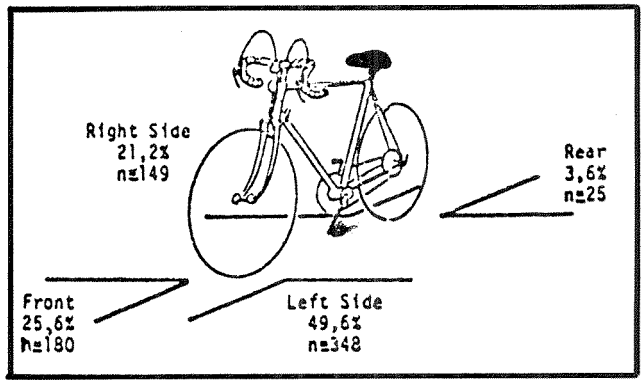

Figure 24. Bicycle region contacted by motor vehicle (702 cases)(39)

- Differences with respect to accident type (some studies contain all accident types, some only collisions with cars, some only specific collision types)

What matters are the main tendencies, common for all studies, and the differences and similarities within separate studies between injuries of bicyclists and moped riders (motorized two-wheeler riders). It seems obvious that injury distributions are dependent on accident and collision types because of differences in relative impact speed and impacted body areas. Therefore, as already stated, comparisons have to be made carefully.

When all injuries are considered, Pedder(38), Whitaker(40), Otte(37), and Grattan(31) state that arms and legs are the most frequently injured body areas, followed by the head.

Pedder(38) finds more arm injuries for bicyclists than leg injuries, and the opposite for the motorized two-wheeler riders. The other studies mentioned do not support this finding.

From Huijbers(34) and Nicholl(36), it follows that the head is the most frequently injured body area. Data from the first study are available from the Stichting Medische Registratie (SMR), containing information on 95 percent of all Dutch hospitalized casualties. Data of the second study are from a British hospital.

When the more severe injuries (AIS > 2) are taken into consideration in the studies of Pedder, Whitaker, Otte, and Grattan, the head is the body area most frequently injured.

Speed at Impact

As with the pedestrian-to-car accident, speed at impact seems one of the more important parameters. It is better to speak of relative impact speed since not only the impact speed of the car but also the impact speed of the two-wheeler and the direction of impact (collision type) have a big influence on the relative impact speed.

In this section, data on impact speed from the different studies are presented as in the report of Working Group 7 of EEVC(30). In some studies, it is not quite clear what is meant by impact speed. There were no impact speed data related to specific collision types. Therefore, the results must be looked at with great care.

Some results follow (Figure 25):

- Otte(37) indicates that, at impact, speeds of cars in collisions with motorized two-wheelers are, in general, lower than those in collisions with bicyclists.
- There is a wide variety in impact speeds of cars for the various studies:
  - 50th percentile speed varies from 10 to 50km/h.
  - 90th percentile speed varies from 37 to 72km/h.
  - This variety is larger than for pedestrian accidents(30).
- Gauss(44) found that speeds at impact depend on the collision types, but, in general, the speed at impact of the two-wheeler was remarkably higher than the speed of the HGV. Nearly two out of three two-wheelers collided with a speed between 31 and 60km/h.

Summary

In all the studies mentioned, cars are the most frequent collision opponents, rating from 50 to 90 percent of all opponents in bicycle and light-powered two-wheeler accidents. This is more or less similar to the situation for pedestrians as mentioned in EEVC(30). Second are vans and HGV's. In The Netherlands, mopeds are the second most frequent collision partner for injured bicyclists and moped riders. With motorized two-wheelers, single-vehicle accidents (in collision with an obstacle) happen relatively often. If a criterion such as lethality is used for accident severity, collisions with HGV's seem to be the most severe accident type for bicyclists and the second most severe for moped riders. An accident between a moped and a motorcycle or scooter seems to be the most severe for moped riders. The collision with a car does not seem to be very severe in relation to the other accident types.

From this, it seems obvious injury-prevention research for bicyclists and light-powered two-wheeler riders should focus on a confrontation with cars (magnitude) and

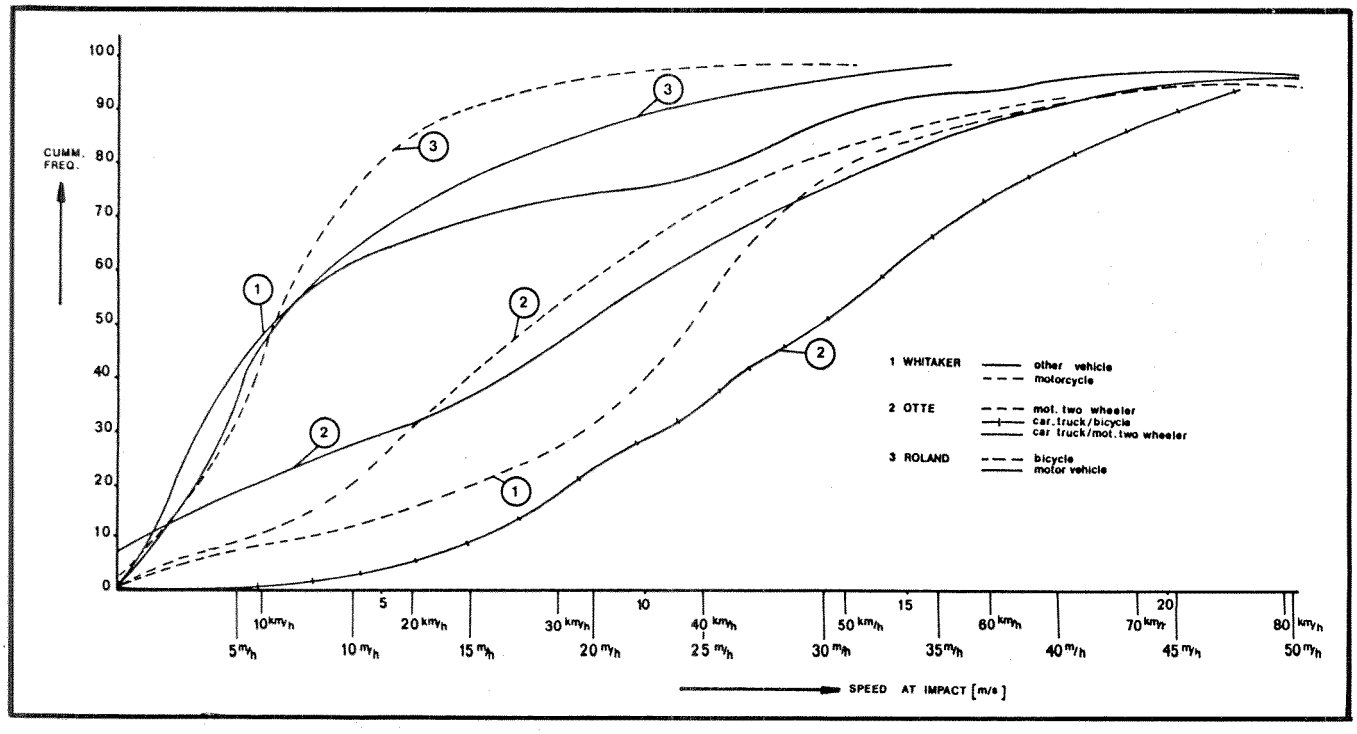

Figure 25. Cumulative distribution of vehicle speeds at impact in two-wheeler-to-car accidents by several studies

HVG's (severity). The single-vehicle motorized two-wheeler accidents happen so often that this accident type must be considered also.

For determining the collision types to be studied in the next section, a distribution of the collision types for the various countries was made. This information indicates also which parts of the motor vehicle need to be considered in injury-prevention work for bicyclists and moped riders. There are some differences in the results of the presented studies. These differences may be caused partly by sample differences, especially levels of injury severity. Other differences, such as infrastructure, modal split, etc., may also be present and influence the outcome. Also some similarities between the results of the various studies were noticed.

In most bicycle-to-car accidents, the bicycle is impacted at the left side by the front of the car. The collision type front of car-rear of bicycle occurs more often in accidents where the bicyclist was killed than when he was hospitalized. Collision types involving the side of the car did not occur often in the more severe bicycle accidents.

In light-powered two-wheeler-to-car collisions, the two major collision types are front of car-left side of light-powered two-wheeler and front of car-front of light-powered two-wheeler, followed by side of car-front of light-powered two-wheeler. The front of the light-powered two-wheeler therefore plays a more important role than the front of the bicycle. When lethality was taken into consideration, the collision type of front car-rear of bicycle (light-powered two-wheeler) seems to be the most severe, followed by the most frequent occurring type front of car-side of bicycle (or light-powered two-wheeler).

It seems obvious, therefore, the attention of injury prevention should be directed both toward the front of the car (as for pedestrian accidents) and to the side, particularly with respect to light-powered two-wheeler accidents.

Data of HGV accidents with bicyclists and light-powered two-wheeler riders from The Netherlands and Germany suggest that bicycle collisions with the front of HGV's happen most often. But collisions with the side of HGV's are also relatively frequent. Accidents with light-powered two-wheelers happen nearly as often with the front and the side as with the rear end of HGV's. Therefore, it seems obvious the attention of injury prevention should be given to all sides of HGV's.

Literature gives a wide distribution of injuries as a result of bicycle and light-powered two-wheeler accidents. These results can hardly be compared due to differences in injury severity or collision types under study. The various results indicate that the head has the highest frequency, especially when considering the more severe injuries. Arms and legs are the second and third most injured body areas.

Relative speed at impact depends not only on the speed of the collision partners at impact but also on collision type. The speeds at impact found in literature have a wider variety than for pedestrian-to-car accidents. The 50th percentile values range from 10 to 50km/h, the 90th percentile values from 37 to 72km/h. In HGV-to-two-wheeler accidents, it was found the speed of the two-wheeler was remarkably higher than the speed of the HGV.

3.Injury-influencing Parameters

Knowledge of injury-influencing parameters in different types of road traffic accidents is gained through in-depth investigation at the scene of the accidents, combined with detailed reconstruction and experimental studies. A large number of reports from this kind of investigation are found in the literature regarding cars colliding with fixed obstacles, other cars, motorcycles, or pedestrians. Very little is known about light (motorized) two-wheeler accidents. The following account of injury-influencing parameters in such accidents is, therefore, mainly inferential and rests on deductions from what is generally known in this field of research. This section deals mainly with comparisons of other accident types, and the conclusions drawn from these can, of course, be disputed.

Nevertheless, it was considered desirable to have this kind of a résumé of factors thought to be of importance for the production of injuries to two-wheeler riders colliding with cars and HGV's.

The rider here, if not otherwise stated, is generally supposed to be a teenager or an adult person, and the two-wheeler a bicycle or a moped with an internal combustion engine but otherwise essentially of the same basic construction as a bicycle. The car is considered to be an average size European-type sedan. For children on smaller bicycles, the kinematics may be similar to those of adults although the front structures of the car may hit the child's trunk rather than the lower extremities. In some cases, the child may have a more upright posture than an adult rider and the kinematics may then be more like that of a child pedestrian.

The kinematics of the two-wheeler rider in this kind of accident depend on the type of collision, velocities of the two vehicles, rider's posture at the moment of impact, and construction of the two-wheeler.

While a pedestrian hit by a car is usually upright at the moment of first contact, the rider of a two-wheeler is thought to be in a more or less seated position. This implies that his feet are usually some distance off the ground; the head may be at about the same level as that of an upright pedestrian, but this depends very much on the posture of the rider. The center of gravity of the rider's body may well be at approximately the same level above the ground as that of a standing adult pedestrian. While the velocity of a pedestrian is often negligible in relation to that of the car, the two-wheeler travels much faster.

This velocity may sometimes be as high as 50 to 70km/h and has, therefore, to be taken into account in many accident situations. However, the parameter of importance for injury production is, of course, not the speed of travel but the relative velocity between the rider's body, and that of the car at the time of impact and for each body part.

Another important difference between pedestrians and riders of two-wheelers is the presence of the two-wheeled vehicle; this presence may influence the kinematics of the rider. The inertia of its mass may in some collision types place an extra load on the rider's body, and his extremities may get entangled in the main structure of the vehicle during the accident sequence. A two-wheeler with an engine may also have parts that are hot enough to cause burns if the rider contacts them during the accident sequence.

Collision Types

The collision types referred to below are those depicted previously in Figure 18. Due to existing knowledge and the priorities indicated earlier, this paragraph will deal mainly with collisions with passenger cars.

Passenger Car

Type F1—In this type of accident, the front of the car impacts the left or right side of the two-wheeler traveling in a direction perpendicular to that of the car.

This collision type is similar to the most frequent type of car-pedestrian impacts. In both cases, the adult victim is hit below the center of gravity and comes into contact first with the bonnet or windscreen and then with the ground. One obvious difference is the usually higher speed of the two-wheeler at impact. This implies the rider's upper body will often hit the bonnet at a point further in the direction of his travel than a pedestrian would. The ratio between the speeds of the two vehicles will be decisive for where the rider's head and trunk will impact the car structures. In some cases, this ratio may, of course, be such that the upper body of the rider does not impact the car structure at all, but instead he falls directly to the ground.

The seated position of the rider at impact may sometimes induce a rotation of his body about its longitudinal axis. This is particularly the case when the car structure is low relative to the rider's torso and the thigh on the struck side is at about a right angle with the rider's torso. The lower leg and, to some extent, the arms are then accelerated by the car at an earlier moment than the rest of the body. The direction of rotation, therefore, is such that the back of the rider's trunk and head are turned against the car.

The rider's legs will thus be accelerated by the front structure of the car and may then be loaded also by the inertia of the two-wheeled vehicle's main structure. His torso will usually impact the bonnet or the upper parts of the wings. Where the head impact will take place will depend on the speed of the car and the car configuration parameters (e.g., bumper height, bumper lead angle, and length of its bonnet). It may be either on the bonnet, the upper parts of the wings, the windscreen, or the windscreen frame. The compliance of these car structures varies considerably and, as has been pointed out in connection with pedestrian-to-car accidents, is an important injury-influencing parameter. The speed of the car and the weight and construction of the two-wheeler are also important parameters.

Type F2—The two-wheeler is traveling in the opposite direction to that of the car and the impact occurs front to front; the closing speed is the sum of the speeds of the two vehicles. The mass of the two-wheeler is small compared to that of the car. This may, therefore, be the most violent accident situation. It is also a situation where the rider's body may be traveling with the head as the leading part of the body. Even if the trunk is not stooped forward before impact, the legs may get caught by the handlebar of the two-wheeler during the accident sequence, and this may induce a forward rotation of the trunk. Should the impact then be headfirst into the windscreen area, the axial load of the body would often lead to severe fractures at the base of the skull and in the cervical spine. These kinds of injury are usually lethal even at low velocities. In this situation, the total velocity change is the most important parameter, and the compliance of the impacted structures—or the use of a helmet by the rider—can probably influence the outcome only to a minor degree.

Type F3—The direction of travel is the same for both the car and the two-wheeler; the difference between the speeds of the two vehicles is a decisive factor. The position of the rider's upper body then governs his kinematics. He may more or less remain in his original position, slide over the bonnet, and impact the windscreen area with the lower part at his back. Severe back injuries can result from this type of accident. The main injury-influencing parameter is again the velocity, and the compliance of the structures is of secondary importance.

Type S1—In this type of accident, the two vehicles move perpendicularly to each other or the car may be stationary but the two-wheeler impacts either side of the car. Due to the higher speed of the two-wheeler, this type of accident has more similarities with the corresponding type of motorcycle accident than when a pedestrian walks into the side of a car.

If both vehicles are moving in this configuration, the front of the two-wheeler will be influenced by the moving car in such a way that the two-wheeler will rotate during the sequence and the rider will impact the car side in an oblique way. Usually the rider's head will be at or above the roof area of the car.

If the impact occurs at the passenger compartment in the middle of the car, the rider's body generally will be stopped by the car's side structure. The velocity of the two-wheeler and the compliance of the car's side structure will be the injury-influencing parameters and to some extent the structure of the two-wheeler.

If the impact occurs at the front or the rear of the car, where the car structures are lower, there is a possibility that the rider of the two-wheeler will pass over the car and fall to the ground on the other side. While airborne, the rider may tumble and it is therefore difficult to predict his attitude when impacting the ground.

Types S2 and R2—In the case of a near miss or side sweep, only one leg and possibly one arm and shoulder of the rider may impact a front corner of the car. Axial or near-axial loading of the femur is then possible. Severe leg injuries and even traumatic amputations at high-speed impacts are seen in this type of accident. Compliant car structures may be of some help, but the relative impact speed is probably more important. The arm and shoulder may be injured in a similar way, but the direction of force is probably more favorable.

Type R1—The two-wheeler impacts the rear of a car, and the relative velocity is likely to be less than in most of the other accident types. The car structures, other than vertical ones, are therefore probably less important, but attention should be drawn to the possible existence of spoilers, which should for this reason be as compliant as possible.

Oblique Impacts

Oblique impact directions may produce a combination of the injury mechanisms mentioned above. When a rider's upper body impacts the top of the bonnet, a higher relative velocity may result in a more oblique head impact than is the case for pedestrians. It is not possible to state on the basis of present knowledge whether this may lead to more severe head injuries due to angular acceleration of the head.

Accidents Involving Buses and Lorries

In the case of the frontal collision types (F_1, F_2, F_3), the configuration parameters do not seem to have as much influence on the kinematics and injuries of the two-wheeler rider. Compliance seems to be important. The configuration of the sides of HGV's seems to be important for the injuries of the colliding two-wheeler rider, due to the large gaps between the truck wheels. The two-wheeler rider will be hit at the head or neck level by the relatively stiff parts of the HGV. The risk of being run over seems to be important, too, just as the speed of impact of the two-wheeler rider.

The Structure of the Two-Wheeler

When the two-wheeler is hit from the side, there is a possibility for the rider's leg to be squeezed between the two vehicles. The construction and inertia of the two-wheeler is then of importance for injury production. If the two-wheeler collides in a frontal or oblique direction with another vehicle or an obstacle, it is possible the rider may be caught by the handlebar in the groin area. This may lead to vascular and/or nerve injuries and may change the kinematics of the rider. Any other protruding detail on the two-wheeler may cause injuries if the rider hits it during the accident sequence.

A special type of injury occurs when children are carried as passengers on two-wheelers without adequate protection for the child's legs. If the child's foot gets caught in the wheel, it will be squeezed between a spoke and the frame, and the resulting injury usually requires hospitalization.

The Ground

For pedestrians, it is now believed the ground is of little importance in relation to the car for injury production. The same is probably true for two-wheelers. At higher speeds, there may be a more substantial influence by the ground. The oblique impact of the head to the ground and possible kerbstone impacts may then become important for the severity of brain injuries. Another important factor is the dirt on the road surface. Open wounds caused by the primary impact to the car or resulting from the sliding of the rider on the ground after impact may be smeared with dirt. This prolongs the healing process and may lead to complicating infections. Normal clothes are of little use for protection since they are easily torn under these circumstances.

Obstacles

In the streets, there are several obstacles that a two-wheeler can contact violently after loss of control. Street appurtenances are sometimes designed to break away or yield when hit by cars to minimize the risk of injuries to car occupants. Because of their low mass, two-wheelers will normally not be capable of deforming these structures to any appreciable degree. Hence, the risk of having an injury is much greater for these categories. On country roads, trees and fences can also cause injuries if violently contacted by the rider of a two-wheeler.

Children particularly, and sometimes teenagers, also use their vehicles in playing grounds, parks, and other places outside the roads where there are several possibilities for contacting fixed obstacles. The types and severities of the resulting injuries from such contacts depend on many variables, such as type of accident,

which determines the kinematics and attitude of the body at impact, the velocity, the object struck, etc.

Children seem more prone than adults in overturning to fall on the end of the handlebar in such a way that abdominal injuries occur. Due to the very low tolerance of the child's abdomen to the high level of loading resulting from this kind of impact, very little can be done with the bicycle to prevent these injuries.

4.Research Methods and Results

Injury-prevention research for two-wheeler riders got less attention than injury-prevention research for pedestrians. The accident process of the two-wheeler rider is even more complex than that of the pedestrian because of the contribution of the two-wheeler itself to the injury-producing process. Also the speed of the two-wheeler and its position in traffic situations lead to other collision types and speeds at impact. There are several ways to study two-wheeler injury protection. One is analysis of accident data and another is experimental research.

Accident Studies

Accident studies give samples of reality to estimate the size of the problem, defining priorities within the problem and developing hypotheses in which relations between injury-influencing parameters and injury severity are postulated. Accident studies also give results with regard to the quantification of these relations. The study of the effect of a specific (legal) measure is a special application of this type of accident investigation.

One might distinguish at least three levels of depth of accident studies:

1. Accident statistics (police data level)
2. Intermediate level studies
3. In-depth studies

To describe the size of the problem, the relative proportions of collision types, etc., levels 1 and 2 are needed. These data may also form the basis for experimental studies under laboratory conditions.

The difference between level 2 and level 3 data is normally that, in level 3, far more detailed data are gathered including data on scene for each accident. Emphasis with level 2 data is on the statistical side, which means the sample size, sampling method, and detail of information are balanced with respect to representativeness and statistical analysis. For both levels, investigators of more than one discipline are often used (i.e., technical, medical, etc.).

Since accidents involving two-wheelers are complicated with respect to the exact cause of injury (for instance, contribution of vehicle and road factors), the in-depth level of data gathering is often used.

Level 3 in-depth data may provide the following for each case:

- Data from observation on scene, soon after the accident, helping to understand the sequences of the collision phases
- Data on the vehicles or obstacles involved, with emphasis on vehicle types, damage, marks for reconstructing the collision type, collision severity, and, if possible, injury mechanisms
- General data on two-wheeler riders, especially their position on the two-wheeler, their means of protection, etc.
- Detailed injury description for every casualty, if possible by direct observation or through hospital records

Level 2 data may also contain valuable information on injuries and the accident in general, and, since emphasis is on representativeness, a far more reliable picture of all occurring crashes is acquired than by means of police data (level 1).

Level 2 studies may be based on insurance data, hospital data (though these will be restricted to only part of the injury population), towaway accidents, or any other starting point. As in level 3 studies, damage, accident, and injury information will be gathered, often on a statistical basis (e.g., by a written inquiry to car owners, occupants, hospitals, or police). Visiting the scene of the accident is not part of this method since this would take too much time and effort.

For two-wheeler accidents, a visit to the scene and a full investigation of the surroundings and vehicles involved seems necessary if all injury-causing factors are to be known. However, the in-depth approach limits the quantity of cases to be studied in a given period. Therefore, level 2 data are needed to get a view of the problem and its relevant distributions as part of reality, especially if level 1 data are not available or are incomplete, as is the case in many countries.

Some Results

Cross(51) studied 753 nonfatal and 166 fatal bicycle casualties in collisions with motor vehicles (level 3). From the nonfatal group, only 17.5 percent remained in the hospital longer than 1 day. Contact with the road surface seemed to be the cause of injury in 60 percent of the cases, contact with the motor vehicle in 23 percent, and contact with the bicycle in 6.2 percent.

The conclusion from Roland(52), after examining 700 motor vehicle-to-bicycle accidents (level 3), is an agreement with this last statement as far as the injury causation of the bicycle is concerned. Roland concluded the bicycle did not seem to be a major source of severe injuries.

There were only four injuries resulting from a contact with the bicycle that produced an AIS rating greater than 1. There is a significant overrepresentation of the motor vehicle as the source of injury rather than the environment. For all the defined speed categories, more severe injuries

tend to result when the contact source was the motor vehicle as opposed to the bicycle or the environment. This does indicate the injuries are being produced in the initial contact rather than from secondary contacts with the environment. No significant influence on injury severity was found for estimated speed of bicycle prior to impact, bicyclist's age, handlebar type, and bicycle region contacted. Significant influence of motor vehicle variables was found for estimated speed at impact and vehicle maneuver prior to impact.

Some studies described specific injuries:

- The influence of the bicycle on intra-abdominal injuries(68,66). These injuries are usually caused by falling on the free end of the handlebar.
- Bicycle spoke injuries(67). These lesions occur if a child passenger's foot is caught in the wheel of the bicycle.

Some advantages and disadvantages of accident studies in relation to experimental research are the following:

- Advantages
  - — The only way to establish the size of the problem
  - — The only method that gives insight into the injury-influencing parameters in the real accident situation
- Disadvantages
  - — Approximation of some of the accident data (e.g., speed at impact, contact places)
  - — Only the influence of the values of the parameters, as they exist in real traffic, can be studied

Experimental Research Methods

In a collision between a two-wheeler and a car, type and severity of injuries sustained by the two-wheeler user may depend on its kinematics but also on the relative speeds of the two vehicles. The two-wheeled vehicle may have an important speed. Moreover, the crash configuration can differ from one case to another in a large range.

The main collision types are F1, F2, and S1. Experimental research on bicycle and moped collisions is mostly focused on type F1. Type S1 is dealt with in motorcycle collision experiments. The posture seems to have a small influence on the kinematics, and one can imagine that differences in height would also have a minor influence, as most of the two-wheeler users are adults.

Three main methods are available for research in two-wheeler safety:

1. Full-scale tests between a two-wheeler and a car (or a mobile barrier), the two-wheeler rider being a dummy or a cadaver. Even if they have the advantage of being realistic, for car-to-two-wheeler collisions they will have to be performed in a large number of configurations as the potential collision types are numerous and the impact speed can vary in a large range. The problem of impact with escape may be difficult to reconstruct.
2. Body segment tests (or component tests) in which the safety problems involving a specific body area are investigated. They would not be fundamentally different from research made on pedestrian safety since the same body segments are concerned. Moreover, specific research dealing with two-wheeler safety concerns head injury protection with crash helmets, as well as some other parts of cars, trucks, etc.
3. Mathemetical model. This can be used as a general tool to evaluate and predict two-wheeler rider kinematics and dynamics. Mathematical models are especially useful in parameter variation studies. As a result, mathematical modeling has the advantage (and may be the only practical tool capable) of determining generalized output for complete populations. The use of mathematical models in two-wheeler safety research is relatively recent. The method is promising for the near future. Mathematical models have to be validated with test results and/or accident investigation output.

Full-scale Approach of Two-wheeler Safety Research

This approach generally consists in reconstructing a collision between a car and a two-wheeler vehicle on which a model of a human being is seated. The impacts sustained by the two-wheeler rider ejected from his vehicle can be analyzed in relation to car-to-two-wheeler collisions or to impacts against objects in the surroundings(57). Two main research projects used this car-to-two-wheeler full-scale approach to study two-wheeler protection.

In the first tests(49), 22 collisions between a passenger car and a moped were reconstructed. These tests were made in six different configurations, most of the tests representing a road crossing collision, the moped either striking or being struck. All the tests except two were performed with a 50th percentile dummy; the other two used cadavers. In 13 tests, the two-wheeler user was helmeted; in the other 9, his head was not protected.

This research found, in the case of the struck moped, the two-wheeler user kinematics can be compared with pedestrian kinematics. The car modifications made to protect a pedestrian can be favorable for two-wheeler users also. The head-ground impact gave higher HIC values than the head-car impact. The helmet insures a certain measure of head protection; it is less effective in the temporo-parietal area. Finally, an interaction between the moped and the dummy pelvis has been found in several cases.

The second study(56) was made in Japan. For this research, 10 collisions were performed, in which a standing motorcycle was struck laterally by a car or a rigid mobile barrier. The aim of this research is to study lower limb protection of motorcyclists, so the tests were made with a 50th percentile dummy equipped with frangible legs.

The research found the modification of cars to optimize energy absorption would insure a better protection of the rider against leg injuries. It seems possible to protect from leg injuries at a speed up to 40km/h, and the authors think the other injuries are acceptable in this range of speed. The protecting device tested in lateral collisions would have a beneficial effect in other crash configurations, especially avoiding leg crush under the motorcycle in case of rollover and underride of the motorcycle under a car. The effect of the rider ejected from his motorcycle and impacting a guardrail has been studied experimentally(57) with tests in which a dummy is laid down on the back, the head forward, on a mobile platform that is suddenly stopped; the dummy is projected forward and hits a guardrail, the head first and under a chosen angle. This research has shown it is possible to design deformable shields avoiding the direct impact between the two-wheeler rider and the rigid and sharp parts of the guardrail (posts and rails).

The third study was done at TNO(64). Dummy tests were executed (type F1) as a first step to validate the MADYMO mathematical model. The first results indicate the kinematics of the bicyclists resemble that of a pedestrian but that the impact places of the bicyclist head on the car are somewhat higher.

There are advantages and disadvantages of the full-scale approach for two-wheeler protection research. This approach would give generally a realistic view of the two-wheeler vehicle-to-car collision, but the realism of the reconstruction is limited by the behavior of the dummies and by the selection of crash configurations. Making tests with a standing vehicle decreases the interest of this approach. These tests do not have a good repeatability, and each test can only allow a safety evaluation in one specific configuration, whereas the accidentology shows an important diversity of real crash configurations. The two-wheeler vehicle type has a big influence on the results of the tests; thus these results cannot be applied to all two-wheeler vehicles (e.g., mopeds versus motorcycles).

Component Tests Used in Research for Two-wheeler Safety

Many studies using the component test approach and dealing with two-wheeler protection have been performed; most of them concerned head protection, i.e., study of crash helmet protection. Some of these studies are limited to the verification of helmet performance in tests similar to standard tests(56,57).

Other more fundamental studies allow us to know better the mechanisms that govern the head protected with a helmet and then to increase the performance of these devices. One biomechanical research project (60) investigated injury mechanisms and head protection possibilities on the basis of drop tests. Eleven tests have been performed with cadavers. Nine of them were helmeted: the drop height was 1.83m or 2.50m. The subject was inclined at 30° downward, the head first hitting a rigid flat surface. These tests were completed by some tests using only the helmeted head of a Hybrid II dummy or a helmeted metallic head model. In this study, the HIC values are very high even in tests performed at 1.83m, but the measurements were not obtained at the center of gravity of the head. Tests performed with a head only (dummy head or metal form) gave HIC values lower than those obtained in tests using whole bodies.

Another research(61) studied the influence of horizontal velocity of the head when it hit the ground, the kinematics, and the linear and angular accelerations sustained by the head. Helmeted head and neck of a dummy, attached by a lever arm to a rail-guided carriage, sustained free falls on a ring simulating the road surface. The horizontal ring rotated to simulate the horizontal component of the head speed related to the ground. These tests showed that in these conditions the head sustained important angular accelerations and speeds while the HIC value, which takes into account only the linear acceleration components, remained generally below 1,000. This study concludes that some helmets have a shell made of material that is too soft to provide a desirable low friction between helmet and road surface.

Another study(62) compared the energy-absorption characteristics of a protective helmet and a coconut shell and showed on the basis of experimental tests that the coconut has greater energy-absorption capacity than the foam used for helmets. The author proposed to design helmets without a rigid external shell.

There are advantages and disadvantages of component tests as a basis of two-wheeler rider protection research. Component test methods allow research based on a large number of tests, having a good repeatability at a relatively low cost. But these tests give only a global view of the two-wheeler accidents as they reproduce just one phase of the accident. Moreover, the conditions in which they are performed are simplified (2D motions) and their realism is limited. From this point of view, the conclusions found in research using the component tests approach should be validated through full-scale tests.

Mathematical Models for Research in Two-wheeler Protection

It seems there is no mathematical model that is especially designed for bicycle and light-powered two-wheeler safety research. Existing models of car occupants

or pedestrians could be used for two-wheelers, but their adaptation and validation would need a sufficient number of test results.

The three-dimensional CVS 3 Calspan model has been adapted by the Denver Research Institute to study the behavior of crash victims in motorcycle accidents(63). In The Netherlands, SWOV and IW-TNO are working on a program to produce a validated mathematical model for two-wheeler accidents with cars. At this moment, dummy tests have taken place as a first step to validation(64). In Germany, a mathematical model exists that simulates the impact of a motorcycle in the side of a standing car(65). In fact, it seems that up to now there are practically no results of light-powered two-wheeler safety research using mathematical modeling.

There are also advantages and disadvantages of mathematical models. Potentially they have many advantages as they allow investigation of a large number of situations in a short period at low cost, without repeating experimental tests. For that reason, they can generalize output (complete) populations involved in certain (or all) crash configurations. The accuracy of the results of mathematical model studies are largely dependent on the quality of the validation of the model. For validation, not only full-scale test results must be used, but results from in-depth accident investigations and specially developed validation test results can be used. Compared with full-scale tests, the results of mathematical models can be stated to be at least as realistic. The condition of the representation of the real situation with dummies or cadavers is somewhat questionable.

5.Current Knowledge on Human Tolerance

Accidents involving bicyclists and moped users can occur in various situations, and, contrary to pedestrians, mechanisms producing two-wheeler user injuries are numerous and can be very different from one case to the other.

For this reason, it is not possible to describe a typical kinematic of a two-wheeler user involved in a traffic accident. The human tolerance can also vary according to the loading process (age, diseases, conditions, anthropometry, impact speed) and may, therefore, be different for cyclists and riders of light-powered two-wheelers.

Tolerance can be considered in terms of severity. Injuries sustained in real-world accidents can have several degrees of severity, as simple bone fractures or severe internal organ contusions corresponding to AIS 2 or 3 are considered tolerable.

There are few studies conducted to determine human tolerance of two-wheeler users involved in traffic accidents. Nevertheless, some of the studies dealing with pedestrians or car occupants can be taken into account.

Head Tolerance

Concerning head tolerance, it is necessary to investigate cranial and/or facial head injuries and brain injuries separately.

Bone Injuries

The tolerance of a skull to fracture depends mainly on the dimensions of the impacting structure. The main values published by the literature are shown as:

Impacted Area	Small		Large	
Frontal	5	(69)	7	(70)
Temporal	1,8	(71)	8,3	(72)
Partietal	3,4	(69)	8,5	(70)
Occipital	?		9,6	(72)

The tolerance of the facial bones is lower than the tolerance of the skull.

The main results found in the literature are summarized:

	Tolerance Force	
Zygoma	800 to 1800	(73)
Maxilla	650 to 1000	(72,73)
Mandible	800 to 3000*	(73)
Nose	1300	(74)

* Depending on impact direction

These two tables show the potential effect of helmets in avoiding small impacts that correspond to the lowest skull tolerance and in protecting facial bones from direct impact.

Tolerance of the Brain (Brain Concussion)

Brain tolerance is not well established, and brain injuries have no evident correlation with skull fractures. Tolerance of the head as a function of pulse duration has been established by Lissner(75) and is called Wayne State Curve. The corresponding parameter to this curve is the GSI (Gadd Severity Index), which is defined by:

$$GSI = \int_{o}^{t} a^{2,5} .dt$$

in which a is head acceleration in g's and the value of 1,000 is considered the tolerable limit.

A more recent index called HIC has been developed and is used for car occupant frontal impacts. The HIC is defined by:

$$HIC = \left[\frac{1}{t2 - t1} \int_{t1}^{t2} a(t).dt \right]^{2.5} \cdot (t2 - t1) \Bigg|_{max}$$

The proposed limit of tolerance for HIC is 1,000 or 1,500, but recent studies have shown this criterion is not very pertinent to predict head injuries. Some other criteria have been proposed, but none were widely accepted. However, in the absence of a pertinent criterion, the HIC can be accepted in dummy tests.

Two-wheeler accidents can correspond to large body motion, and the wearing of a safety helmet could increase the amplitude of head motion. For these reasons, the rotational acceleration that has been proposed to be correlated with brain injury would be considered a tolerance parameter.

Theoretical analysis using the mechanics of similitude seems to indicate children have a higher brain tolerance than adults(76), either if we consider translational or rotational acceleration; this is confirmed by the higher breaking strength of arterial tissues of children found by Yamada(77).

Thoracic Tolerance

Recent studies on thoracic tolerance indicate the tolerance to rib fractures is more correlated to thoracic deflection than to thoracic acceleration either in frontal or in lateral impact(78,79). However, the tolerance is not the same for frontal and lateral loadings. The proposed value of tolerance is 30 to 35 percent of the half thorax width in lateral impact.

Comparison of rib characteristics between children and adults seems to indicate children can sustain higher thoracic deflection without rib fracture, but in this case internal thoracic injuries can occur. In a general way, increasing the number of rib fractures enlarges the risk of thoracic internal organ injuries.

Abdominal Tolerance

The tolerance of the abdomen has been studied with cadaver free falls hitting an armrest model laterally(80). This study proposes a limit of 28 percent of abdomen width corresponding to 4.5N impact force as a human tolerance. These tolerance data mainly concern liver injuries.

Pelvis Tolerance

The tolerance of the pelvic bones has been studied for car occupants either in frontal or in lateral impacts. In frontal impacts the pelvis is loaded through the femur, when knees are impacted. This mechanism can be found as well in car occupants as in some two-wheeler accidents. The proposed tolerance in this case is close to 10kN(81).

In side impacts the pelvis can be loaded either through the hip or directly on the iliac wing. These mechanisms can occur in some two-wheeler accidents, as for example when a two-wheeler is hit laterally by the front of another vehicle. The proposed tolerance in this case is 10 to 12kN impact force(82).

Lower Limb Tolerance to Fracture

Several studies dealing with leg tolerance have been made either for car occupants or for pedestrians. The tolerance of the femur in a bending fracture depends on the point of impact, the lower tolerance corresponding to the mid-shaft impact. In this case, the tolerance seems to be close to 10kN.

Tibia tolerance to horizontal loading seems to be between 3,000N and 9,800N depending on the impacted area, with an average value of 5,000N(83).

However, a recent study conducted in Sweden dealing with pedestrian safety(84) has found a much lower value of lower limb tolerance. The value of the momentum corresponding to the fracture is about 200Nm(85). However, these values are related to a small surface impact, and the tolerance in a bumper-like impact is probably higher. In general, the child seems to have a tolerable bone strength higher than an adult(76).

6.Injury Prevention Measures for Bicyclists and Riders of Light-powered Two-wheelers

This section will deal with—

- Proposals for injury prevention of two-wheeler riders
- Consequences of these proposals for other groups of road users
- Consequences of (proposed) legal requirements for injury reduction of other groups of road users to the injuries of bicyclists and light-powered two-wheeler riders. The philosophy of the integral approach of the safety vehicle will take a central place; at the same time, it will be quite obvious that the amount of concrete proposals is limited due to just starting research activities in this area.

This section will deal also with the proposals as a function of the different relevant collision types. The proposals made are based mainly on information from literature.

Proposals for Injury Prevention of Two-wheeler Riders

Contact with a car is the leading cause of injury. Therefore, efforts concerning injury prevention should be directed to these contacts.

The proposals can be distinguished concerning—

- The car
- The HGV
- The two-wheeler
- The two-wheeler rider

In general, the aim of these proposals is to influence kinematics and minimize the loads to the struck body parts.

Car-to-Two-wheeler Collision

Car—The collision types F1, F2, and F3 (Figure 18) for bicyclist collisions and F1 and F2 for moped rider collisions seem to be the most important; in these collisions, the front of the car is hit.

Changing the stiffness of some parts of the car will probably have the same positive effect on the injury minimization for two-wheeler riders and pedestrians. The optimum values for the stiffness from a viewpoint of biomechanical tolerance cannot be measured at this moment. The parts of the car to be considered depend on the collision types but vary from bumper to the upper side of the windshield frame.

For shape, the same variables as for pedestrian impacts seem to be important, but no concrete proposals can be made at this moment; it seems obvious sharp protrusions and popping-up headlamps would probably have a negative effect.

Two-wheeler—For F1, side protection devices for motorcycles are proposed by Bourret(88), Rau(91), and Taneda(94) (Figures 26 and 27). According to Bourret, the leg injury severity in an F1 type of collision is strongly related to the mass of the two-wheeler. Whether these side protection devices are realistic for mopeds (or even bicycles) cannot be answered at this moment.

For F2, the question of whether the two-wheeler has to be ejected over the colliding object (if possible) or has to

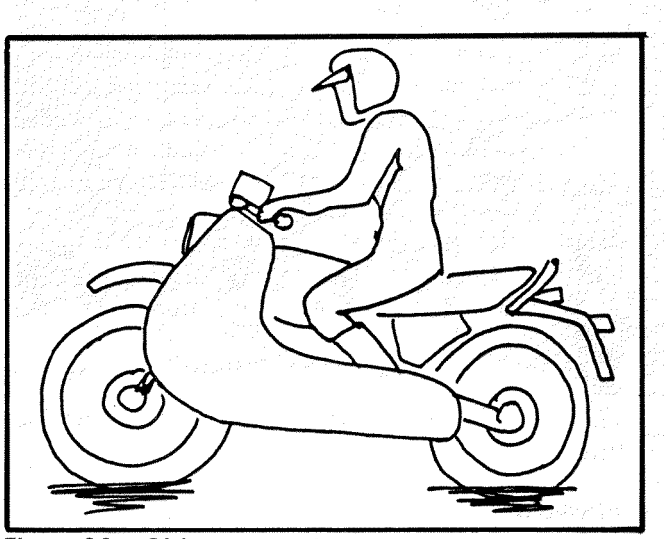

Figure 26. Side protection device proposed by Bourret(88)

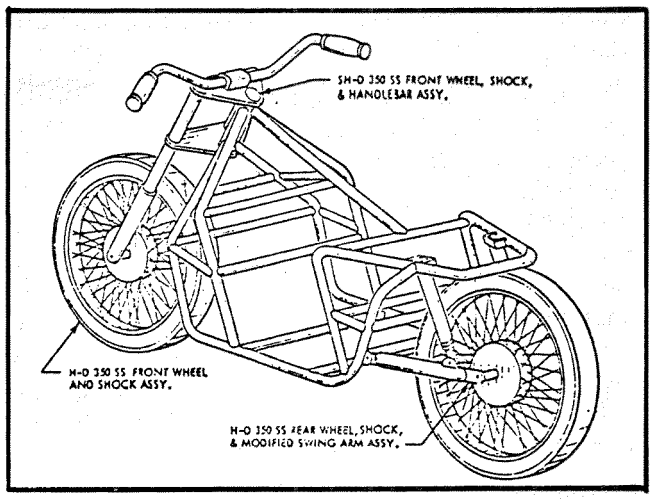

Figure 27. Side protection device proposed by Rau(91)

to be tightened to his two-wheeler also cannot be answered at this moment. Knee paddings were first proposed by Langwieder(97) (Figure 28). The aim is to avoid contact with the colliding object. Whether this can

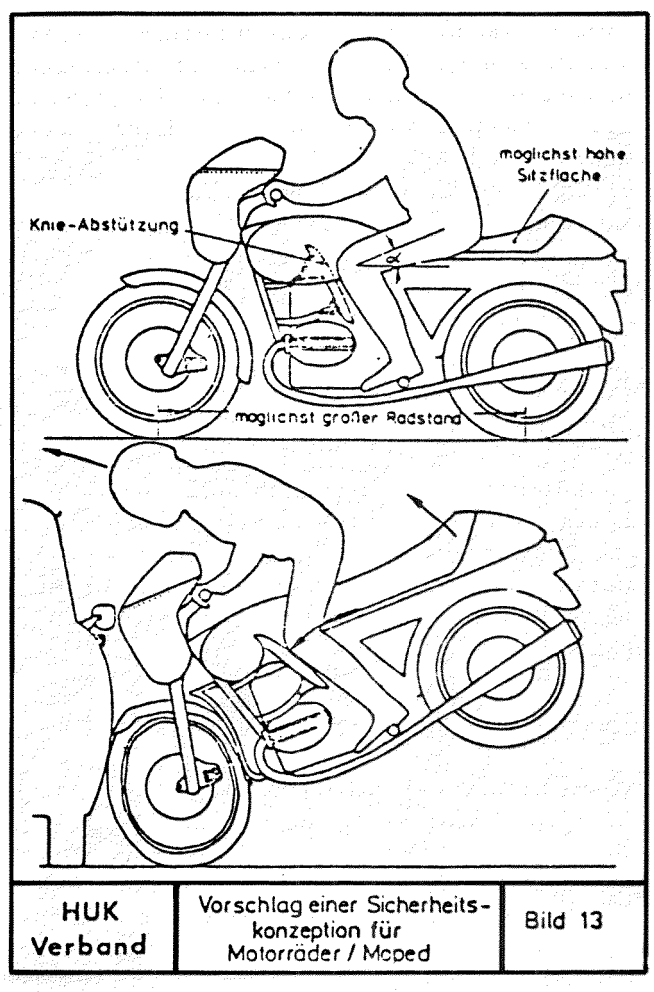

Figure 28. "Knee-padding" ejection device proposed by Langwieder(97)

be effective in a frontal impact (F2) is doubtful. If a rider is launched headfirst and contacts the motor vehicle, this will probably lead to brain stem injuries. The helmet cannot protect against this kind of injury. Filler caps or expander pins on handlebars cause minor injuries. Therefore, sunken caps are applied on motorcycles and sunken pins on bicycles.

HGV-to-Two-wheeler

It is later indicated that collision types F1, F2, S1, S2, and R1 are most important.

HGV—For F1 and F2, the same remarks as for the passenger car about stiffness and shape apply. For S1, S2, and R1, side and rear-end underrun guards seem to be the most concrete proposals at this moment (Volvo(96); Riley(92); Gauss(98); Figures 29,30, and 31). The use of better or additional side mirrors will be beneficial to give the truck driver a better overview.

Two-wheeler—For F1, S1, and R1, the knee padding proposal made by Langwieder(97) does not seem to be as effective due to the dimensions of the HGV.

For F2, whether the suggested side protection will be effective is an open question because the first impact point will probably take place at a higher level than for collisions with passenger cars.

For S2, no protection proposals are known.

Two-wheeler Injuries

Adequately designed child seats and/or a simple dress-guard can prevent bicycle spoke injuries.

Two-wheeler Riders

Helmets and protective clothing can prevent injuries. The positive effect of crash helmets in motorcycle accidents is well documented. The effect of moped helmets is not as well known. In a Dutch study made by SWOV, it is described as "a decrease in the chance of getting fatally injured of 40 percent and a saving of 500-600 lives for the years 1975 until 1977" (SWOV(93)). The proportional share of head injuries differs considerably for the bicyclists (not helmeted) and the helmet-wearing moped riders for the different studies:

		Bicyclists	Moped Riders
Grattan	(99)	48%	26%*
Huijbers	(100)	51%	36%
Nicholl	(101)	75%	52%*
Otte	(102)	85%	60%*

* Including motorcycle riders

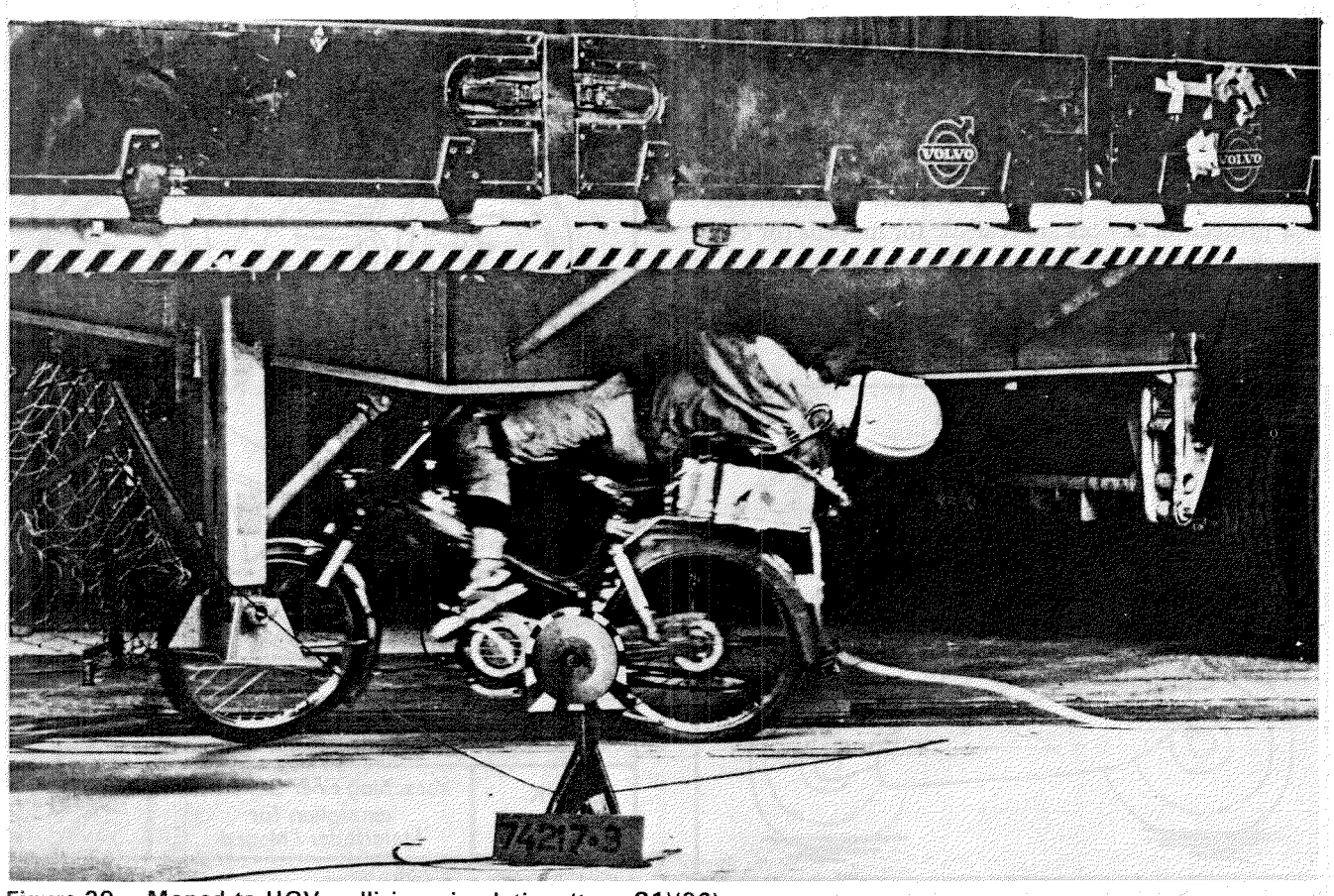

Figure 29. Moped-to-HGV collision simulation (type S1)(96)

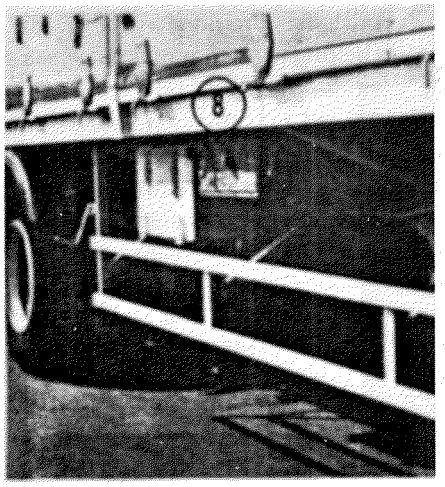

Figure 30. Side protection device for HGV(96)

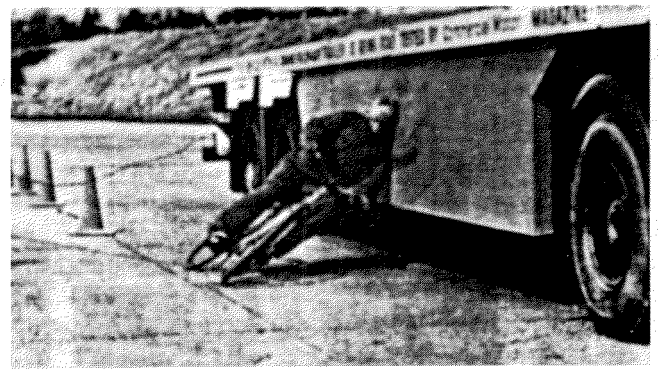

Figure 31. Side protection device for HGV(87)

Wearing helmets seems to be an obvious explanation for these differences, but differences in accident and collision types for bicycles and mopeds may also contribute. Adequate protection against head injuries may be achieved by the use of helmets. For bicyclists, this kind of protection is still not very widely accepted because, to some extent, existing bicycle helmets tend to become uncomfortable due to inadequate ventilation. For moped or motorcycle helmets, there is, among others, a European set of requirements (ECE Regulation 22); some countries already have requirements for bicycle rider helmets(98,99).

According to the studies of Otte(102), Appel(104), Pedder(105), and Ramet(106), some of the crash helmets came off during accidents. The wearing of protective clothing by motorcyclists has some positive effect on the minimization of injury severity, according to Hurt(90) and Aldman(86). The question is whether this is a practical solution for riders of light two-wheelers.

Speed at Impact

Speed at impact will probably be strongly related to injury severity, especially for the impacts with the fronts of motor vehicles. Lowering the speeds at impact in any way will therefore be favorable.

Consequences of These Proposals for Other Groups of Road Users

Car

As far as stiffness is concerned, the consequences may be a small reduction of the decelerations for car-to-car collisions. Because there are no concrete proposals for shape at the moment, there are no consequences either, but contradictions may occur.

HGV

If dimensions of the side and rear-end underrun guard are properly chosen, a positive effect for other accident types may be expected. Rear view mirrors mounted on the sides of vans and small trucks may extend beyond the sides of the vehicles and pose a hazard to other road users, e.g., two-wheeler riders(103).

Two-wheeler

The proposed knee paddings may have a negative effect. If the attempt is not successful, the two-wheeler rider might fly into the interior of the car and hit the driver or a passenger, just as in other cases without knee padding.

Two-wheeler Rider

Contact between a helmeted two-wheeler rider and a nonhelmeted victim may be a hazard for the one unprotected.

Consequences of Proposed Legal Requirements for Injury Reduction of Other Groups of Road Users to the Injuries of Bicyclists and Riders of Light-powered Two-wheelers

As far as bumper height is concerned, there is some doubt whether the required value is beneficial for pedestrians (e.g., ECE Regulation 42). Considering two-wheeler accidents, the effects are even less predictable as yet. The other requirements, e.g., for front-front or front-side impacts, do not seem to have as much effect on the

injuries of two-wheeler riders due to the differences in the amount of energy to be dissipated.

7. Test Procedures

The test procedures examined here are aimed at insuring conformity of the vehicle (bicycle, moped, car, and truck) and/or safety device (helmet, underride protection, etc.) to bicycle and moped rider protection requirements. As stated previously, accident case history for bicycle and moped riders is ample and cannot be reduced to a single standard situation. Doubts also exist about the possibility of considering the bicycle and moped together for studying any countermeasures. It seems, in fact, the two vehicles give rise to two different types of accidents.

Because of this complexity, proposals on test procedures for bicycle and moped rider safety are practically nonexistent or incomplete. To conclude, it is evident that, as far as test procedures for the protection of bicycle and moped riders are concerned, there are no exhaustive proposals. It is therefore necessary to draw from the experience acquired in other areas of safety and to extrapolate the methods that must obviously be verified experimentally to make sure they are feasible and meet the objectives.

Discussion on Possible Test Methods

The test methods that can be adopted are—

- Component tests
- Full-scale tests
- Subsystem tests
- Validation tests by mathematical models

Each of these methods has advantages and disadvantages, and, depending on the situation, it may be more convenient to adopt one method rather than another, or even to use them together. However, it is important to point out that the degree of knowledge of the phenomenon and the devices available determine the test method to be developed. For example, it is impossible to develop a test method based on a full-scale test if the accident mode is unknown (impossibility of obtaining the test conditions scientifically) or if a reliable dummy is not available (impossibility of having a reliable conformity response).

Component Tests

Component tests are tests performed on a single component or on a single safety device. Requirements are either design (geometrical and/or stiffness) or, in the more sophisticated cases, biomechanical. Included in this category are some of the first regulations developed for vehicle safety; it is, in general, a primitive approach whereby the result on a single component is often taken to represent overall safety provided by the vehicle. When component tests belong to a series of tests whose scope is to cover the various aspects of safety, there is a shift toward methods based on subsystem tests. Component tests are still valid today in those cases where it is demonstrated the objective is attained with a specific solution (e.g., if the objective is protection of the cyclist's head wherever it will strike, the helmet solution can be accepted and this component can be submitted to various tests).

By applying the above to the specific case of the bicycle and moped rider, it is possible that a method based on component tests has the following advantages and drawbacks:

- It is relatively easy to define, in the sense that a single aspect of the phenomenon can be examined (e.g., impact of the head) and requirements can be provided even with very little knowledge of the overall phenomenon.
- Method efficiency is low, and the method itself can prove to be inadequate because influence of the vehicle shape on the bicycle and moped rider is not taken into account. In this case, design requirements would prove particularly detrimental because they would be applied to all vehicles (even where not needed) and limit design. The result would be a poor quality product and a high cost for the user, but upgrading of safety would not be insured (e.g., when a bonnet is specified).
- This method can be applied correctly only to tests on particular safety devices developed for a specific purpose, such as helmets.

Full-scale Tests

A full-scale test reproduces the conditions of a typical road accident. This method poses many problems, the most important point being, however, the definition of test conditions. In fact, it is necessary that the full-scale test be equivalent to the actual accident. In the case of the bicycle and moped rider, more than one test condition must be defined, and this poses a few serious economic problems when a new model is developed and approved.

The situation with regard to the test equipment to be set up is more complicated. In particular, no reliable dummies, representative of cyclists, are available today, and it may be that the physical parameters traditionally recorded on dummies are inadequate for this type of accident. Moreover, for full-scale tests aimed at evaluating the effectiveness of a modification to the bicycle or moped, there would also be the problem of designing one or more standard impactors. As for this method, it is possible to conclude that its adoption for rider protection is more difficult than for other types of accidents. Because of the need to conduct more than one full-scale

test and the lack of reliable dummies, other methods should be adopted.

Subsystem Tests

Subsystem tests are those series of tests on different components whose results permit an assessment of the overall degree of protection provided to the rider in a specific accident. The difficulty of developing subsystem tests as defined is due to the need to know the phenomenon perfectly and the required capability to shear it into many single tests, taking into account the interaction between the impacts of the various components and body segments. (For example, for a given impact speed, the shape of a vehicle can determine particular data on speed, area, and direction of impact of the cyclist's pelvis against the bonnet; the type of impact of the pelvis and vehicle shape affect the head speed, area, and direction of impact; etc.)

Validation Tests by Mathematical Models

Development of a test method based on mathematical models will not be feasible for many years because the use of mathematical models in two-wheeler safety research is relatively recent.

It should also be noted the use of mathematical models for type approval on different computers and at different test centers poses the problem of issuing such procedure standards as to insure response identity. This is a field of activity for which the existing technical services are probably not yet prepared, but it enables a simulated vehicle to be assessed before it is actually produced.

Summary

None of the methods examined is capable today of verifying the degree of protection that can be provided to a struck cycle or moped rider. There are no proper, validated mathematical models of cyclists colliding with cars or HVG's at this moment and, above all, problems for transforming a model in a type approval instrument would arise. The full-scale test approach is likewise not feasible. There is no single equivalent test. Several full-scale tests would have to be carried out, and the test device (dummy) is not reliable. Component tests neglect the effect of vehicle shape on the kinematics of the cycle and moped rider.

Knowledge of rider collision is insufficient to permit the development of a method based on subsystem tests. The only feasible approach, in which it is desirable to carry out research, studies, and design of adequate devices, is the development of a mathematical model based on the use of a bicycle and moped rider elementary mathematical model to determine the impact conditions of each body segment and on tests of the corresponding elements. The elementary model is not used to evaluate impact severity but only to determine the initial conditions for testing the parts struck by the pelvis, chest, and head. Moreover, this model defines the angle, direction, and impact velocity for each body segment. It is, in practice, a subsystem test method integrated with an elementary mathematical model. An approach of this type can only be feasible when the approach for protection of the pedestrian is also of the same type. In fact, both pedestrians and cyclists are unprotected road users for which similar countermeasures should be developed.

8. Accident Prevention

Accident prevention or primary safety measures can make important contributions to the safety of the cyclist or moped rider. Accident studies suggest that conspicuity is a factor in accidents involving the two-wheeler and another vehicle. The parameters influencing conspicuity are related to the two-wheeler and its rider (active lighting, retroreflective materials, and the rider's clothing), to the other vehicle (optimal headlamps, good view), and to the surroundings (other light sources). In the overtaking situation, the gap left by the driver when overtaking the two-wheeler is critical, and experiments show the percentage of vehicles passing very close can be substantially reduced by spacers and conspicuity aids. Better brakes will reduce injuries by avoiding accidents or reducing speed at impact, especially in rainy conditions. Test results show that, with the correct combination of rim and brake blocks, significant improvements are possible. The state of maintenance of the two-wheeler was found to be an important factor in many accidents, and results of a survey are given. Studies on bicycle stability and maneuverability are also reported that show significant differences between styles of bicycles and mopeds.

Conspicuity

The conspicuity of bicycles and mopeds is an important factor for the prevention of accidents. The conspicuity presupposes an observer for which the different objects must be conspicuous: this observer obviously in many cases is the driver of a car. A number of factors may influence, hamper, or even obstruct the visual observations to be made by those drivers. Conspicuity will be described for daytime and nighttime.

Daytime Conspicuity

Accident Studies—From accident studies described previously, it follows that two-thirds of the injury accidents involving a pedal cyclist occur at junctions,

when in most cases the collision partners were traveling on a different road before collision. In another study, interviews with involved drivers who had not given way when emerging from junctions into the major road indicated a lack of awareness of the presence or movement of the cyclist(114). Cyclists often wear dark clothing; in one survey, only about 10 percent of the cyclists were wearing high-visibility aids. In addition, a two-wheeler rider presents a relatively small area to other road users, the frontal area being only one-third that of an average size car. The rider is also readily obscured by roadside objects, other vehicles, windscreen pillars, etc. The rider is often near the edge of the road and may be overlooked if a driver carelessly directs his attention only at heavier faster vehicles closer to the center of the road.

In cases where the driver fails to give way, the conspicuity of the frontal aspect of the rider is likely to be most important; since most accidents occur during daytime, initial studies at TRRL concentrated on comparisons of frontal conspicuity in daylight. From previous accident analysis, it is not possible to determine the number of cases where the driver failed to give way to the cyclist or moped rider. Where the rider is at fault, the importance of conspicuity may be less, although in instances where he is highly visible, the driver may see the rider sooner and appreciate his speed and direction more accurately, thus allowing more effective avoidance action to be taken.

Tests and Surveys—In a TRRL study, it was decided to use a peripheral detection technique similar to that used by Horberg and Rumar(115) to evaluate high-visibility aids for cyclists because the experimental conditions resembled a cycle accident situation common at junctions.

The test conditions are shown in Figure 32. Under constraint of an operational task (subjects were required to fixate a visual display and repeat random numbers that appeared), the driver had to signal when he first became aware of the cyclist. The detection distances were used as a measure of conspicuity. Initial tests(116) indicated that bicycle attachments were not as effective as clothing items in making the cyclists detectable and that the brightest materials (highest luminance factor) performed best against commonly encountered backgrounds. Color was found to be a less significant factor than brightness.

Further tests(117) were therefore aimed at establishing the most effective clothing styles (see Table 29), all made from one type of bright material. This was a fluorescent greenish-yellow woven nylon material with a luminance factor of 74 percent. The average detection distances for each each option are given in Table 29. Testing between

Table 29. Average detection distance of clothing options

Option	Detection Distance (m)
Jacket	63.2
Waistcoat	55.8
Hat	53.9
Armbands	49.8
Black Jacket (control)	49.6
Shoulder and Waist Belt	47.1

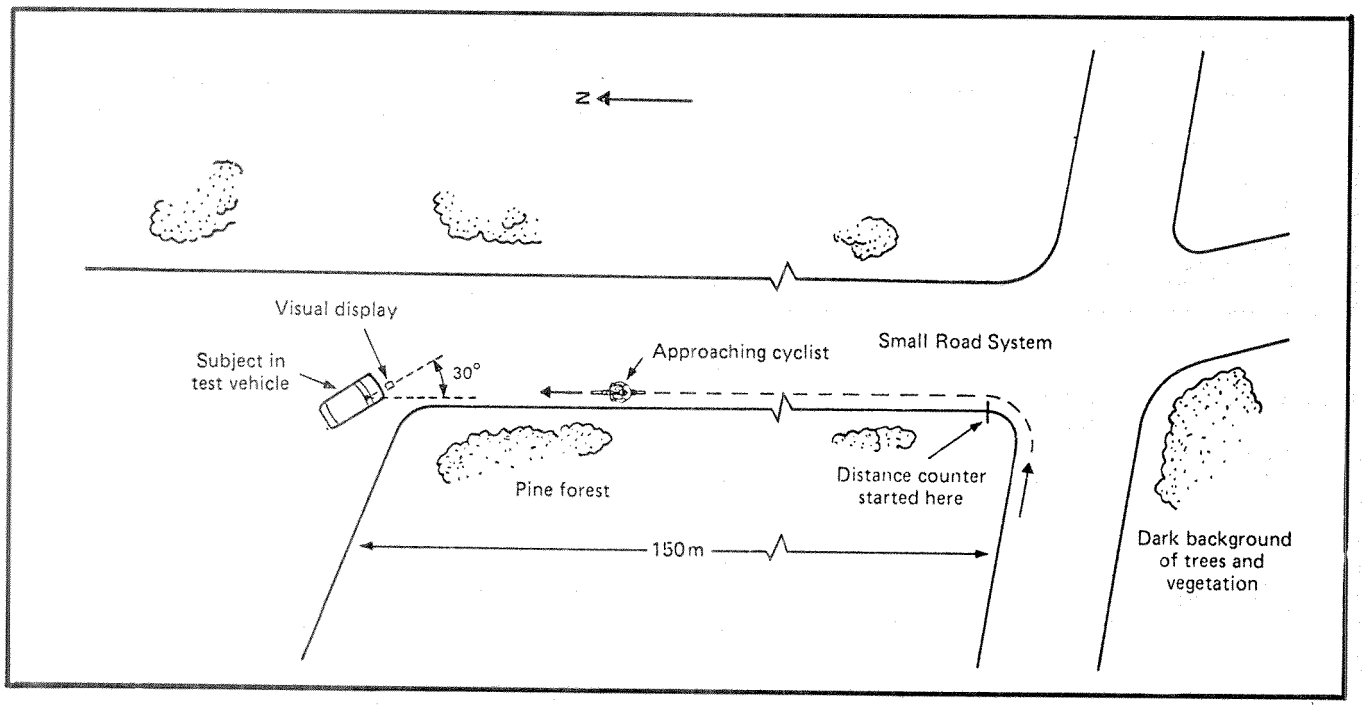

Figure 32. Test conditions for conspicuity aids

means it was shown that the jacket was most effective having a significantly longer average detection distance than the other items.

The effectiveness of conspicuity aids in the overtaking situation where the visibility of the back is likely to be important was assessed by measuring the gaps left by overtaking vehicles. It was considered that an effective aid would be one that significantly reduced the number of close passing vehicles, i.e., those passing within 0.8m of the cyclist's elbow on the off side. An ultrasonic device attached to a front carrier of a bicycle was used that, when actuated by the test cyclist, automatically recorded the closest passing distance between the bicycle and near side of the overtaking vehicle. It measured the gap to within a few centimeters and automatically recorded the distance in one of eight passing distance bands. The clothing items described above were tested in turn in daylight on four straight sections of road. The average results are given in Table 30. It can be seen the jacket had the greatest effect. The number of close passing vehicles was more than halved, compared with the control. The effect of brightness of fabric was established by making a number of jackets of similar color (greenish-yellow) but of widely different luminance factors. Results are given in Table 31. Tests were also carried out on white, yellow, and orange color jackets of similar brightnesses, and, as expected, their effects on passing vehicles were not significantly different.

In addition to providing effective conspicuity aids for the rider, there are other measures that may prove effective.

Table 30. Passing distances for clothing options of different styles

Option	Median (m)	Percentage Less Than 0.8m	Number of Readings
Jacket	1.20	8.4	547
Waistcoat	1.16	10.1	544
Hat	1.14	11.0	520
Armbands	1.13	14.1	475
Shoulder and Waist Belt	1.09	16.4	482
Black Jacket (control)	1.03	21.1	526

Table 31. Passing distances for jackets of different luminance factors

Option	Color Specification*			Median	Percentage Less Than 0.8m	Number of Readings
	x	y	Y			
Thin nylon	0.39	0.44	0.49	1.10	15.2	841
Thick nylon	0.36	0.51	0.74	1.13	12.4	833
Reinforced PVC	0.38	0.52	0.95	1.15	12.1	840
PVC	0.38	0.53	1.37	1.17	9.4	879
Black jacket	*(not measured but expected reflectance close to zero)			1.05	23.5	927

A number of factors may influence the visual observation made by drivers. The visual scene could be structured so there is less demand on a driver's limited attention span; thus, irrelevant objects that could distract or hamper the observation of the cyclist could be removed or repositioned. Glare from the sun can be annoying and dangerous, and signaling lights should have adequate luminous intensities to insure a conspicuous signal under most of these conditions.

Discussion and Conclusions—There was good agreement between the results from daytime detection and public road experiments indicating that a jacket was more effective than all other aids tested. A waistcoat-styled aid was the second most effective in both studies. When viewing from the rear, it is likely the arms of the jacket contribute only a small amount to the overall conspicuity because the backs of the arms were poorly illuminated. From the front, however, the tops of the arms were visible and relatively well illuminated, receiving direct light from the sky; therefore, they contributed significantly to the visibility of the cyclist. In this study and in a previous pilot experiment(116), a jacket was shown to be more effective than a waistcoat when viewed from the front. Drivers' increased awareness of the presence of the rider and earlier detection when approaching are possible for the larger gaps left by overtaking vehicles.

The relatively small and statistically nonsignificant effects of the armbands and belt are probably due to their small total area. For its size, the hat performed well, and this is probably due to its relatively high illumination—receiving direct light from the sky. Its domed shape resulted in high luminance or brightness levels when viewed from most directions. The jacket is preferable to other aids for the additional reasons that arm signals are more conspicuous and the sides of the rider are likely to be more visible. Road tests with jackets of various reflectances and colors indicate the importance of brightness rather than color in determining the conspicuity of clothing. However, there are likely to be a number of situations where color contrast may aid detection because luminance contrast is low; for example, where the rider is viewed against a bright desaturated background such as a concrete facade or cloudy sky. To offer maximum visibility, a conspicuous garment should be made from material having both a high luminance factor and highly saturated color. Finally, a conspicuous garment must attractively styled and comfortable to wear, as well as retailing at a reasonable price, if its use is to be encouraged.

Nighttime Conspicuity

Accident Studies—A comparison of accidents in Belgium, Denmark, Spain, Germany, and Ireland(111) showed that the percentage of casualties occurring in darkness

ranged from 18 to 33 percent for bicycles, and from 26 to 38 percent for mopeds. In The Netherlands, recent data(118) shows that 21 percent of severe injuries to cyclists involved in collisions with other vehicles and 24 percent of severe injuries to moped riders occur at dusk or at night.

It was found that accidents after dark were more serious, and the cyclists concerned were usually older and more frequently struck from behind. In Great Britain, a total of 4,549 (18 percent) pedal cyclists were reported as killed or injured on the roads during the hours of darkness in 1980(119). A study in The Netherlands(120) has shown that the risk of a fatal collision between a cyclist and a traveling motor vehicle is nearly four times greater under dark conditions. It is not known to what extent the poor conspicuity of the pedal cycle or cyclist is a factor in nighttime accidents, but, obviously, cyclists riding without adequate lights are likely to incur considerable additional accident risk.

Tests and Surveys—Cyclists in Great Britain, as in most other countries, are legally required to show a white light to the front and a red light to the rear when riding after dark. Observations were made in four towns in England to determine the extent to which cyclists comply with these lighting regulations(121). Details relating to over 2,500 bicycles were collected in a 2-week period during December 1980. Observations were made after dark, and it was shown overall that approximately 25 percent did not have complete lighting and 9 percent had no visible lights at all. Where lamps were fitted, 9 percent were off and nearly one-quarter were either dim or gave an unsteady output. Three-quarters of the lamps observed were battery-powered. It therefore appears that many cyclists at night will be inconspicuous and therefore at increased risk. Interviews with over 600 cyclists revealed some reasons for this. Many only replaced batteries when they were exhausted, and important reasons given for the poor performance of lamps were damage and poor connections.

The observations showed that dim lamps were common, and, in order to establish the importance of bicycle reflectors for safety, tests were carried out on the TRRL test track after dark to compare the detectability of two reflectors (25 and 75mm diameter) and a common type of battery lamp modified to give two levels of light output(121). These levels were low and corresponded to dim lamps where the batteries were close to being exhausted. The test track layout is given in Figure 33.

The average detection distance for the reflectors and two levels of light output against the glare source are given in Table 32, for observers closing in on the bicycle

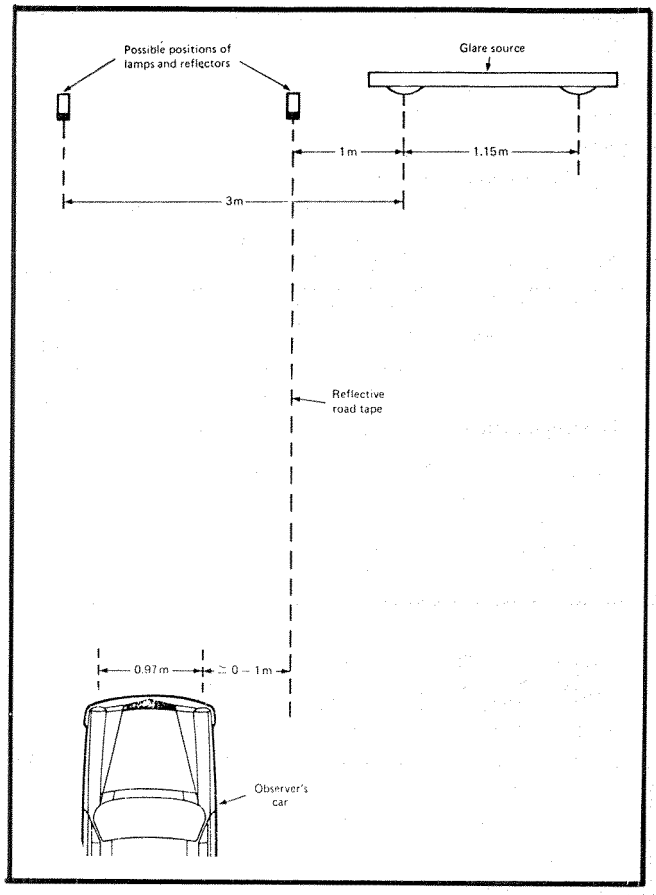

Figure 33. Layout for visibility studies

Table 32. Mean detection distances of rear lamps and reflectors

Distance of Glare Source from Bicycle	Rear Lamp Luminous Intensity (cd)		Reflectors Coefficient of Luminous Intensity (med/lx)*		No Reflectors or Lamps (Control)
(m)	0.65	0.15	1450	101	
1	358	241	247	153	41
3	635	507	399	214	64

* Coefficients of luminous intensity were measured at 0° 12' observation angle and 0° entrance angle. The observation angle is the angle between the straight lines connecting the reflector to the source of illumination and to the observer's eye. The entrance angle is the angle between the line perpendicular to the plane of the reflector face and the straight line connecting the reflector to the source of illumination.

at 35km/h. Not only is early detection of the rider by the approaching driver important but also recognition at an early stage. Early recognition of the rider can be important since for safety the driver needs to know the likely behavior of the road user he is about to overtake. In further tests, the distances at which observers were certain that a cyclist was present were used as a measure of effectiveness. Since the motion of the cyclist on the cycle was thought to provide important cues to recognition, a test cyclist rode the bicycle on rollers. The options were a commercially available flashing amber lamp designed to be attached to the cyclist's clothing, a reflective jacket, a reflective shoulder and waistbelt, a reflective spacer, and a set of pedal reflectors. Each of the options was tested in turn in conjunction with the control, i.e., rear light and mudguard reflector. The average detection and recognition distances based on results from six subjects are given in Table 33.

Table 33. Mean detection and recognition distances for conspicuity aids (glare source 3m from bicycle)

	Rear Lamp (11.1cd) and Reflector (100mcd/lx*)	Flashing Amber Beacon	Reflective Jacket (10,000mcd/lx)	Shoulder and Waist Belt (1000mcd/lx)	Spacer (500mcd/lx)	Pedal Reflectors (100mcd/lx Each)
Detection Distance	651+	588	284	185	292	182
Recognition Distance	54	59	102	68	60	124

* Coefficients of luminous intensity were measured at 0° 12′ observation angle and 0° entrance angle

\+ Maximum detection distance was limited to just over 650m corresponding to the length of the range

A survey in The Netherlands(122) has shown that 4 percent of front lamps and 4 percent of rear lamps were missing. It was also shown that 7 percent of the front lamps were defective in some way. The legally required large rear reflector was present in 93 percent of the cases.

Some indication of the effectiveness of this large rear reflector and pedal reflectors in reducing accidents can be judged from another Dutch report(123), which details the change in accident rate to cyclists following their legal requirement in November 1979. This preliminary report using only one year's after data records a drop in casualties. As accident data accumulates, it may be possible to precisely quantify their contribution to the reduction in accident risk.

The Institute of Road Safety Research SWOV(118) has carried out an analysis of accidents and concluded that a small reduction in casualties will result from the mandatory use in The Netherlands of spoke reflectors or reflective tires.

In the United States, Burg and Hulbert conducted a series of tests on bicycle spoke reflectors and reflective tires(124). Using dipped headlamps, it was found that spoke reflectors were detected at a greater distance than reflective tires when viewing the side of the bicycle. The average detection distance for the most effective spoke reflector was 354m, while for the most effective reflective tire it was 297m. However, in static viewing tests, the reflecting tires were easier to recognize. In dynamic trials where observers had to determine the direction correctly, the reflective tires were more effective at indicating direction of travel.

In West Germany, viewing trials were held to assess the contribution to conspicuity of various types of reflector(125). Spoke reflectors were judged to be superior to reflective tires.

The International Federation of Senior Police Officers (FIFSP), after a study of safety equipment for bicycles(126), concluded that a large rear reflector would be beneficial and that dynamo lighting systems should be provided that would automatically switch to battery power when the bicycle is stationary. They also attached special importance to flank protection of the bicycle rider and recommended the use of retroreflective tires(126,127).

In addition to insuring that two-wheeler lighting and reflectionization is adequate, there are other vehicle factors important for adequate visibility. The transmission of light through motor vehicle windscreens is of obvious importance since modern cars have windscreens that usually make an angle of 35° to 40° to the horizontal plane. These small angles seem to be unfavorable for the transmission of incident light coming from the traffic scene, especially where dim lamps near the threshold of perception are being viewed. A dirty, scratched, tinted, or highly raked windscreen will limit transmission of light or reduce contrast and could cause a poorly lit cyclist to be missed. Poorly aligned vehicle headlamps are a problem in that they can cause high levels of glare that can interfere with the detection of lights and can cause distraction.

Discussion and conclusions—It has been demonstrated that a reflector having a coefficient of luminous intensity of 1,450mcd/lx (75m dia reflector measured at zero entrance angle and 0° 12′ observation angle) can perform reasonably well when compared with a dim rear lamp.

In fact, under the worst conditions of glare (bicycle positioned 1m from glare source), the detection distance

of the large reflector was similar to that of the dimmest lamp. Without a reflector or rear light of any description, visibility distances are dangerously low (41 to 64m) when it is considered that, at a speed of 110km/h, a driver may need a distance of up to 200m to stop after an unexpected object becomes visible. The light output from a dim front or rear lamp when viewed from the side can be very low indeed, and side reflectors in this case can substantially improve conspicuity. The obvious disadvantage of a reflector is that its visibility depends on the illumination it receives from the driver's headlamps. If the headlamps are dim or misaligned or the two-wheeler is not directly ahead of the vehicle, then the reflectors may prove ineffective. In addition, the performance of most reflectors decreases with increasing entrance angle, although wide angle reflectors are available, and these significantly decrease the reduction in reflected light at large entrance angles.

In Great Britain and to a lesser extent in The Netherlands, it has been shown many bicycles are not equipped with adequate lights at night even though they are legally required. The widespread use of a good quality bicycle reflector might make a worthwhile contribution to safety in these and other countries where such problems exist. Should the lights flicker, dim, or go out completely, a bicycle equipped with good reflectors should be visible in a number (but by no means all) of accident situations. It is, of course, desirable that bicycle lighting performance should improve to a point where reflectors are needed only very rarely for the purpose of insuring the bicycle is visible. Bicycle reflectors are useful for aiding in detection and also for improving recognition.

After the rear light of a bicycle has been detected by an approaching driver, early recognition that a cyclist is ahead is probably important on many occasions. Pedal reflectors proved most effective at increasing recognition distance as they more than doubled the distance at which a cycle equipped with a rear lamp and mudguard reflector could be recognized. The reflective jacket was also effective; observers quickly recognized the cyclist by the side-to-side motion and outline of the cyclist. In addition, both these aids should give the driver a useful indication of the distance to the cycle. For example, the amplitude of the pedal motion can be clearly seen soon after the pedal reflectors are detected, and this is likely to be a useful cue in judging distance. Tests show that large errors in judging distance can result when only a single red light is visible, and this could be a possible cause of accidents. Reflective tires have been shown to indicate the presence and direction of travel of a two-wheeler when viewed from the side. Spoke reflectors are more effective at improving detection distance in this situation but are less efficient at improving recognition.

The need for adequate bicycle reflectors has been recognized. In The Netherlands, a high-performance rear reflector and pedal reflectors have been required on bicycles since 1979. The FIFSP has recommended the use of large rear reflectors and retroreflective tires on bicycles.

The British Standards Institution(129) has published a standard that specifies minimum requirements for bicycle reflectorization. This standard is based on the work of the International Organisation for Standardisation and specifies high-grade reflectors at the front, rear, and side of a bicycle as well as for the pedals. The British Government has been considering the possibility of insuring that all bicycles offered for sale meet these and other safety requirements.

Bicycle Spacers

Because of the inherent instability of two-wheeled vehicles, cycle and moped riders need to be given sufficient clearance by the overtaking driver to take account of possible course deviations. Experimental studies of course holding by cycle and moped riders under a range of conditions(130) show that riders need a road width in excess of lm; an additional safety margin is necessary.

A spacer is a device attached to the bicycle to discourage drivers from passing too close to the cyclist when overtaking. Commercially available spacers usually consist of a plastic rod with either a flag or disc attached at the end, the overall length being about 400mm. It is to be mounted horizontally on the rear off side of the bicycle so it projects into the road. They have been widely used in Scandinavia but have only recently gained acceptance in Great Britain.

Accident Statistics

In Great Britain, national accident data for 1980 indicate that about 30 percent of fatal pedal cycle casualties occur in situations where other road users collide with the cyclist while overtaking or strike the rear of the bicycle, both vehicles initially traveling in the same direction and going ahead. French and Danish accident studies show the dominant maneuver type involving cycles and mopeds in rural areas is that of the overtaking situation(111). It has been shown that, when lethality was calculated for bicycle-to-car accidents, the collision front of car-rear end of bicycle or moped appeared to be most severe. Attention should be given to reducing the risks in this particular accident situation.

Evaluation of Spacers

Previous studies in Great Britain, Finland, Sweden, and France(131,132,133,134) of the effects of spacers on the gaps left by overtaking drivers (used as a measure of the accident risk) have shown a range of effects from none

to an increase in average passing distance of 220mm. Differences in road conditions, driver behavior, and measurement technique could account for these differences. At TRRL, the ultrasonic range-finding technique described above was used to measure the effect of spacers of various lengths during daytime and nighttime(135). Because of the ease of measurement and subsequent analysis, it was possible to quantify for the first time the effects of spacers of various types in reducing the percentage of drivers passing very close.

For determining the effects of spacer length, a red reflective disc shape[1] 9,000mm^2 in area was employed. The shaft of the spacer was 8mm in diameter and white in color. The overall lengths of the spacers tested were 0.35, 0.40, 0.45, and 0.50m. These lengths covered the range of those commercially available and produced estimated projections beyond the rider's elbow of 25, 75, 125, and 175mm. The rider's elbow was the part closest to overtaking vehicles. For comparison purposes, the cyclist wore a black jacket of a near zero luminance factor, and this acted as the control when testing without a spacer present. Four sites were chosen for test purposes. Road width varied from 5.1 to 6.3m and speed limits from 48 to 96km/h. Broken centerline markings were present along all sections. Each spacer was tested several times at each site in a balanced order to reduce the effects of time-dependent factors.

Data collected at the four test sites were combined as there were no substantial differences between the results. Table 34 gives the averaged results for daylight and nighttime tests. Statistically significant differences at the 0.1 percent level were found under both lighting conditions.

Table 34. Passing distances for spacers of various lengths

Lighting Condition	Length of Spacer (m)	Projecting Length (from elbow) (m)	Median Gap (m)	Percent Passing Less Than 0.8m	Number of Measurements
Day	Control (no spacer)	—	1.097	14.97	855
Night	Control (no spacer)	—	1.076	16.14	477
Day	0.35	0.025	1.156	11.50	844
Night	0.35	0.025	1.198	8.85	407
Day	0.40	0.075	1.132	9.74	780
Night	0.40	0.075	1.134	11.08	415
Day	0.45	0.125	1.192	9.16	819
Night	0.45	0.125	1.194	7.28	481
Day	0.50	0.175	1.215	7.83	855
Night	0.50	0.175	1.221	6.92	492

Further tests were carried out to compare the effects of the longest spacer (0.5m) and the yellow jacket used in the detection distance studies previously described. Table 35 gives the results.

Table 35. Comparison of longest spacer with a conspicuous jacket (daylight)

Option	Median Gap (m)	Percent Passing Less Than 0.8m	Number of Measurements
Control	1.060	21.77	698
Spacer	1.157	11.37	686
Yellow Jacket	1.162	11.09	712

Discussion and Conclusion

The effects produced by spacers in increasing median overtaking distances and decreasing the percentages of vehicles passing very close are probably due to the increase in the effective width of the bicycle and rider, although some of the effect may be due to increased conspicuity. In most cases, the increase in effective width is not quite matched by a corresponding increase in median passing distance. This could be a result of the knowledge that the consequences of striking the end of the spacer when overtaking are not as severe as hitting the cyclist. The results show, that by using a spacer 0.5m in length, the percentage of overtaking vehicles passing less than 0.8m from the cyclist was approximately half that recorded when no spacer was present. This spacer had a similar effect on overtaking behavior across a wide range of road and traffic conditions. Results obtained during the day were similar to those recorded at night. As the length of the spacer decreased, effectiveness was reduced so that a spacer length of 0.35m was only about half as effective as a spacer 0.50m long. The effects on overtaking drivers of the long spacer were very similar to those of a fluorescent yellow jacket across a range of daytime road conditions. The fluorescent jacket would obviously confer extra benefits on the cyclist by increasing overall

[1] The material has a luminous factor of 0.51 and its color specification in CIE coordinates was x = 0.58, y = 0.36. Its coefficient of luminous intensity under typical viewing conditions (0° 12′ observation angle and zero entrance angle) was approximately 1,200mcd/lx.

conspicuity. However, the cost of a spacer is low and, if of sufficient length, it offers good value.

Field of View of Truck Drivers

From a Dutch study(112), it followed that most of the accidents in which a two-wheeler rider collided with the side of an HGV happened when the HGV turned to the right. From an analysis of the EEC directives on rear view mirrors, it appeared certain areas could not be seen when the vehicle was equipped only with mirrors according to these requirements (Figure 34). Therefore, additional requirements need to be recommended.

Braking

The rim brake has been fitted to bicycles for many years in some countries and is widely used on all types of bicycles. On applying the brake lever, the rubber block is forced against the metal wheel rim. The latter is normally chrome-plated steel and often gives a very low coefficient of friction when wet, which results in poor braking performance(136,137). In dry conditions, the braking force can be high, and the possibility exists of the rider going over the handlebars during emergency braking. Hub (both internal-expanding and back-pedaling) and disc brakes have a generally superior performance in wet weather because the braking surfaces are not as exposed to water. However, they are more expensive, heavier, and can make wheel removal difficult. This is perhaps the reason for many new lightweight bicycles being equipped with rim brakes.

It is difficult to obtain reliable estimates of the number of injury accidents due to inefficient brakes, but bicycle accident reports received by the Consumer Product Safety Commission of the United States (138) show many injuries to children result from the inability of the bicycle to stop quickly in emergency situations. In West Germany, Wobben(137) refers to the complaints of many cyclists concerning the inadequate braking efficiency of rim brakes in the wet. Currently, the British Government is considering setting minimum permitted wet and dry braking efficiencies for new bicycles based on the recent British standard for cycles(129). TRRL has been involved in preparing this standard and has conducted a series of tests on rim brakes.

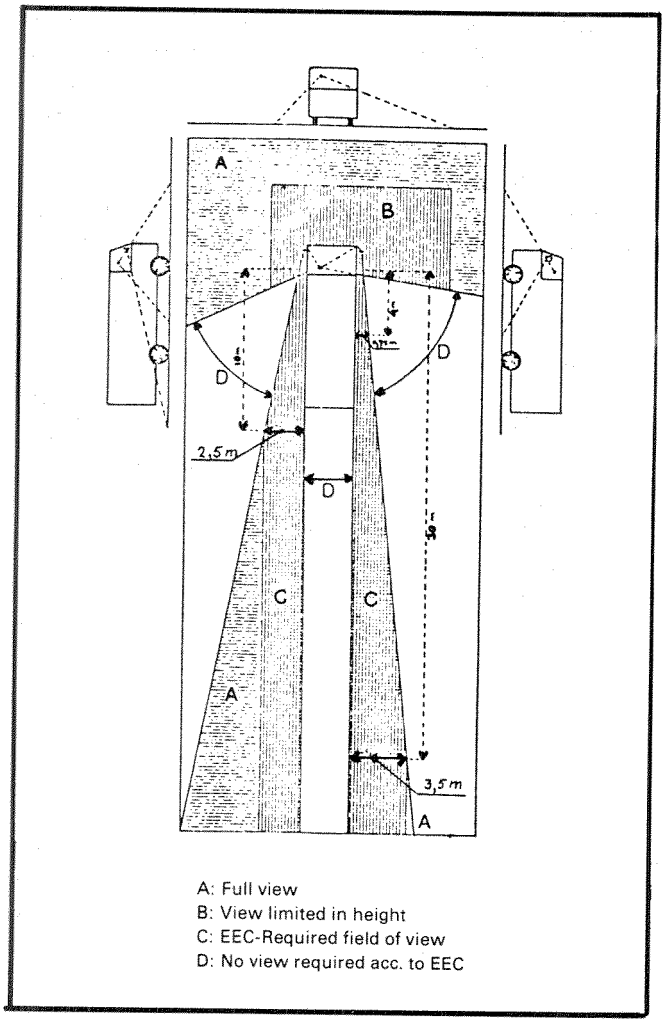

Figure 34. Field of view for HGV's right-hand traffic; right and left external mirrors according to EEC requirements(112)

Braking Studies

In one study at TRRL, the size of the problem was established by allowing children to carry out emergency braking tests under wet conditions(139). In addition, road tests were carried out to determine the performance of a common type of caliper brake, using a number of different brake blocks and wheel rims to determine whether one or more combinations would prove satisfactory in both dry and wet conditions. Recently, manufacturers have produced new types of brake blocks that are claimed to be effective in wet conditions. Nine commercially available brake block sets were tested: three synthetic blocks, five rubber blocks of various hardnesses and patterning, and one leather block. All nine sets of blocks were tested on plain chrome-plated and light alloy rings, and three sets, representing the three types of material, were further tested on dimpled and grooved chrome-plated rims. The test bicycle was a standard touring model with 686mm diameter wheels and fitted with a side pull caliper brake. To reduce variation between tests, one adult rider was used. The bicycle was equipped with a water reservoir and jets to each wheel that applied 4ml/s at each rim, and brake force was controlled by attaching brake lever stops to the ends of the handlebars. These were adjusted so that loads of 180N were effectively applied 25mm from the lever ends when the brake levers were pulled up to the stops.

(Tests have shown that loads of this magnitude are possible to achieve by male adults under emergency braking conditions. However, many children and adult females would not be expected to exert these forces.) The braking distances were measured from a speed of approximately 16km/h for each combination of block and rim. The rims were tested both dry and when continuously wetted. Table 36 gives the average deceleration achieved for each set of brake blocks under dry and wet conditions, together with the expected braking distance from a speed of exactly 16km/h. Figure 35 illustrates the relative effectiveness of the various types of block.

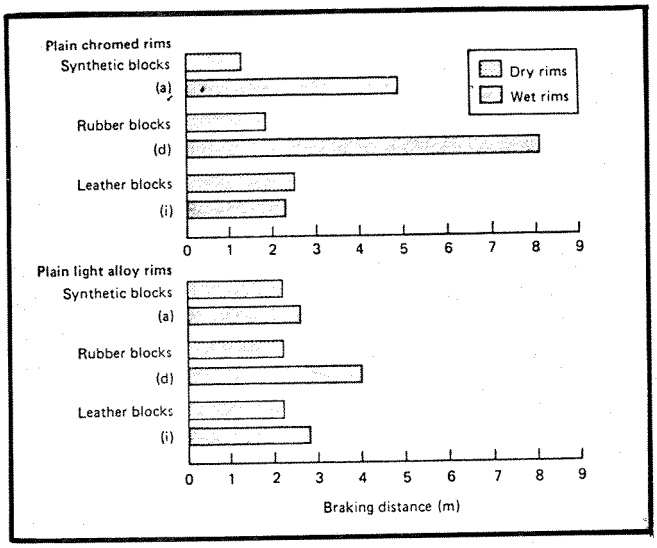

Figure 35. Expected braking distances from a speed of 16km/h

Nineteen children whose ages ranged from 6 to 11 also took part in further tests. In this case, a small bicycle was used (457mm diameter wheels) equipped with chromed rims and rubber blocks. They each made four runs under wet conditions similar to those described above. The average braking performance was 0.08g corresponding to an expected braking distance of 12.6m from a speed of exactly 16km/h. The lowest rate of 0.047g (equivalent to a braking distance of 21.4m from 16km/h) was achieved by the youngest child and the highest rate of 0.113 by the oldest.

Discussion and Conclusion

The result of the tests involving children illustrate well the very poor performance that may result in wet conditions where rubber brake blocks are used on chromed rims. This is in agreement with a previous study(140). The youngest child would have traveled over 20m in braking to a halt from the modest speed of 16km/h. This level of performance may result in an inexperienced rider failing to give way at a road junction and emerging dangerously into the major road. On hill descents, much longer stopping distances may result. Under controlled tests, braking distances were about 4-½ times those measured under dry conditions. Neither hardness nor patterning of the rubber blocks nor the use of dimpled and grooved rims significantly affected stopping distances. By contrast, leather blocks on chromed rims produced a statistically significant improvement, and adequate braking was achieved in the wet. With wet alloy rims, adequate levels of braking performance were achieved with the synthetic blocks. The leather and rubber blocks (e) and (g) (see Table 36) were slightly less effective and the other rubber blocks were less effective still.

In the dry, braking efficiencies with any of the combinations of block and rim were good; however, very high levels of braking were found with synthetic blocks on the plain chromed rims. This is potentially dangerous since the longitudinal stability of the bicycle is poor compared with other road vehicles. Calculations for the rider and bicycle employed showed that the rear wheel would be expected to lift at a deceleration of 0.56g. This is in reasonable accord with the observation that consistent rear wheel lift occurred where average decelerations were significantly greater than this value.

The reduction of accident risk in both wet and dry is likely if the correct combination of brake lock and rim is selected. Even if a collision is unavoidable, the relative velocity at impact may be reduced with better brakes. This can lead to less severe injury.

Leather blocks are now available in Great Britain, and one major manufacturer fits them to all its bicycles equipped with chromed rims. British Standard BS 6102 part 1 specifies a maximum wet braking distance of 7.5m from 16km/h, which would exclude the fitment of the worst combinations of brake block and rim. (This is a significant improvement on the ISO standard (ISO 4210) on which it is based, which specifies a braking distance twice as long (15m).) As mentioned above, the British Government is considering making the standard mandatory for all bicycles sold.

Defects and Maintenance

The two-wheeler rider will have less chance of avoiding an accident if his machine is not maintained in good condition. Defects in brakes, transmission, and tires, for example, may delay or otherwise reduce the effectiveness of accident avoidance maneuvers. Obviously, direct failure of frame or parts can be the prime cause of accidents; for example, failure of pedal crank or forks can easily lead to loss of control. Lighting that flickers, dims, or goes out completely can lead to virtual invisibility in poorly lit areas.

Table 36. Mean decelerations and expected braking distances from 16km/h

			Plain Chrome		Light Alloy		Dimpled Chrome		Grooved Chrome	
Block	Type	Condition	Deceleration (g)	Braking Distance (m)	Deceleration	Braking Distance	Deceleration	Braking Distance	Deceleration	Braking Distance
(a)	Patterned synthetic	Dry	0.76	1.3	0.46	2.2	0.58	1.7	0.58	1.7
		Wet	0.21	4.9	0.39	2.6	0.24	4.2	0.20	5.0
(b)	Plain synthetic	Dry	0.71	1.4	0.51	2.0	—	—	—	—
		Wet	0.27	3.7	0.42	2.4				
(c)	Plain synthetic	Dry	0.66	1.5	0.51	2.0	—	—	—	—
		Wet	0.28	3.6	0.43	2.3	—	—	—	—
(d)	Plain rubber	Dry	0.57	1.8	0.45	2.2	0.47	2.1	0.47	2.2
		Wet	0.12	8.1	0.25	4.0	0.13	7.5	0.12	8.5
(e)	Patterned rubber	Dry	0.54	1.9	0.47	2.2	—	—	—	—
		Wet	0.12	8.8	0.35	2.9	—	—	—	—
(f)	Patterned rubber	Dry	0.52	1.9	0.45	2.2	—	—	—	—
		Wet	0.12	8.6	0.21	4.8	—	—	—	—
(g)	Patterned rubber	Dry	0.55	1.8	0.48	2.1	—	—	—	—
		Wet	0.12	8.6	0.36	2.8	—	—	—	—
(h)	Patterned rubber	Dry	0.50	2.0	0.43	2.3	—	—	—	—
		Wet	0.11	8.9	0.26	3.9	—	—	—	—
(i)	Plain leather	Dry	0.40	2.5	0.46	2.2	0.46	2.2	0.48	2.1
		Wet	0.44	2.3	0.36	2.8	0.44	2.3	0.41	2.5

Note: Rounding errors account for apparent discrepancies between columns.

Accident Studies

TRRL carried out on-the-spot investigation of 183 accidents involving two-wheelers from 1970 to 1972(141). They considered that 14.5 percent of the bicycles and 4.7 percent of the motorcycles involved had defects that contributed to the accident. A Finnish study on 74 bicycle fatalities(142) indicated that defects were a contributory factor in 4 percent of the cases.

Maintenance Survey

To get an estimate of the size and nature of the problem, a survey was carried out by TRRL into the state of maintenance of bicycles ridden to primary and middle schools(143). It was found that, of the 439 bicycles examined, over one-third (151) were categorized as in a dangerous condition and only 36 percent were regarded by the examiners as being in good condition. A fault was categorized as dangerous if it was possible for it to be a contributory factor in an accident. The component showing the largest number of dangerous faults was the rear brake. Twelve percent were in a dangerous condition, and 9 percent of front brakes were similarly categorized.

No firm conclusion can be drawn from the existing data on the direct contribution of defects to accidents, but they do indicate the need for remedial action. This could take the form of vehicle inspection schemes and instruction on regular maintenance, especially for younger riders. The standard BS 6102 referred to above has minimum requirements for the strength of essential parts such as brake system, frame and fork assembly, wheels, pedals, and chain. It also includes requirements on sizes of protrusions and sharp edges that may come into contact with the rider during normal use. In addition, it contains a requirement that instructions be provided with each bicycle. These include, among many items, instructions on brake adjustment and recommendations for replacement of brake blocks, correct chain tension, lubrication, and recommended tightening of fasteners related to handlebar, saddle and pillar, and wheels. Also it contains recommendations for safe riding, e.g., regular checks on brakes, tires, steering, and lighting.

The design of the bicycle to aid adjustment or eliminate it would be advantageous. For example, it is often difficult to adjust brakes; yet self-adjusting brakes are already on the market(144).

Stability and Maneuverability

A certain degree of skill is required to ride any two-wheeler. To become proficient, there is a learning process, and the rider must acquire sufficient experience in a range of traffic and road conditions. To reduce accident risks,

the two-wheeler must be easy to maneuver so obstacles can be avoided quickly and must also be stable so it follows the intended course when, for example, the cyclist is signaling or is caught in a crosswind. The extent to which bicycle design affects rider performance has been examined in a number of experimental situations.

Studies of Stability and Maneuverability

In an early study at TRRL(145), an attempt was made to assess maneuverability of cycles and motor-assisted cycles by the number of faults committed on an obstacle course and on a slow-riding test. Similar tests were carried out using schoolchildren(140) on a number of bicycles, both on smooth and bumpy surfaces. These tests showed that there were large differences between the performances of riders and small differences between different cycles. A Swedish study(113) tested cyclists attempting to hold a straight course while looking behind, which was intended to simulate a common turning maneuver involving crossing the traffic stream. With three types of bicycle investigated (small-wheeled, standard touring, and rodeo type), the probability of making errors in following the course and assessing the situation behind ranged from 10 to 50 percent.

A Dutch study(130) also found differences between different machines. In one of several tests, the riders had to follow a track consisting of a sloping road section immediately followed by a sharp left turn. The riders attempted to stay within two lines 0.15m apart. The percentage of time spent outside the prescribed course was used as a measure of performance. When riding down the slope, speed increased, which made the bend more difficult to negotiate, and so both good stability and maneuverability were important for course holding. Figure 36 shows the average percentage of time outside the prescribed course when negotiating the curve with one and two hands. It can be seen that differences between the bicycles and mopeds are comparatively slight. However, the performance of the racing bicycle and standard model with high handlebars differs significantly from that of the other two bicycles. With these other models, path deviation (averaged over conditions) occurred for about 25 percent of the time. For the racing bicycle, this was nearly 50 percent; for the bicycle with high handlebars, it was 40 percent.

It appears from these studies that bicycle design has an influence on stability and maneuverability although it is not yet possible to quantify the contribution of a particular design feature to the accident risk.

Recommendations Concerning Accident Prevention Measures

When compared with motor vehicles, bicycles generally have inferior lighting and braking systems and are poorly maintained.

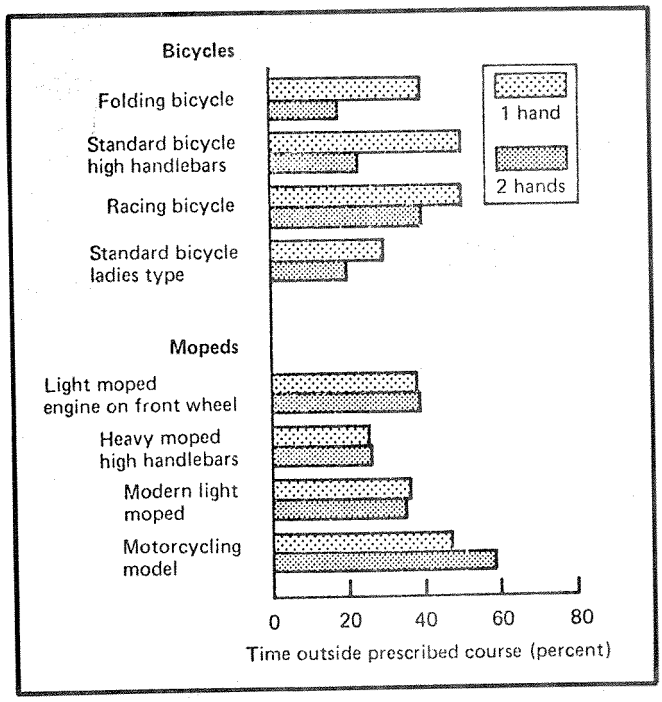

Figure 36. Time (percent) outside prescribed path in test 2, "course holding in a curve"(768 runs)

In the case of bicycle lighting, surveys and observations have demonstrated that a large problem exists. Better lighting systems are required not only to provide more reliable lighting in order that the cyclist may be easily seen at all times but also to provide an adequate beam to illuminate the road ahead. Further work in this area should be beneficial. Improvements to the nighttime visibility problem can be made by requiring that bicycles be equipped with a range of high-performance reflectors that will be readily visible in most situations and will also aid recognition. Of particular importance is an effective rear reflector and pedal reflectors. The cost of providing such reflectors is small, especially if it is carried out during manufacture. Better legal requirements for lights and reflectors are indicated.

The increasing popularity of lightweight bicycles indicates that rim brakes are now more widely fitted. It has been demonstrated that dangerously long stopping distances occur in wet conditions if rubber brake blocks are used with the chromed-steel rims. Since this is a common combination of block and rim, a legal braking requirement based on wet and dry braking standards should improve the situation. Such a requirement could apply to all new bicycles offered for sale.

Regular bicycle maintenance checks may reduce the number of poorly maintained bicycles. This could be carried out at schools or by the police. At the present time, it seems unlikely that an annual inspection similar to that required for motor vehicles would be feasible. Steps could be taken to persuade manufacturers to improve bicycle design so that maintenance is reduced to

a minimum, for example, the fitting of brakes that are automatically adjusted. Consideration should be given to a requirement that there be no sharp edges and dangerous protrusions on bicycles and mopeds, and chain guards should be fitted. In addition, there may be a case for a minimum requirement for the strength of essential parts such as brake system, frame and fork assembly, wheels, pedals, and chain. A measure that could be taken to reduce the risk of accidents to both bicycle and moped riders is the promotion of the wearing of conspicuous clothing, particularly during daytime and twilight. It would be helpful to have a standard for conspicuous clothing so that only high-visibility clothing of an adequate standard would be promoted in publicity and training courses. Consideration should also be given to encouraging the use of cycle spacers. Since they have been shown to decrease the number of vehicles passing very close, they should reduce the risks in the overtaking situation. They have the advantage of being very cheap to fit.

If a safety requirement is introduced on a large scale, it is recommended that relevant accident statistics be compared both before and after the change so the effectiveness of the measure in reducing the accident risk can be established.

References

1. Popish, L.N., and R.B. Lytel, "A study of bicycle-motor vehicle accidents," Santa Barbara Public Works Department, June 1983.
2. Koninklijke Nederlandse Toeristenbond ANWB; Stichting fiets, "De grote fietsatlas van Nederland," Kosmos B.V., Amsterdam, 1975.
3. Gibbs-Smith, C., *The Inventions of Leonardo da Vinci*, Phaidon Press Limited, London, 1978.
4. *Grote Winkler Prins Encyclopedie*, 7th edition, Elsevier Nederland B.V., 1974.
5. *Scientific American*, December 1983.
6. Rauck, M.J.B., G. Volke, and F.R. Paturi, "Mit dem Rad durch Zwei Jahrhunderte," AT Verlag, Aarau, Stuttgart, 1979.
7. Schneider, P., "Das Zweirad im Wandel der Zeit," Deutsches Zweirad Museum, Neckarsulm, Ismaning (München), Eigenverlag P. Schneider.
8. *Bundesgesetzblatt Teil II* "Gesetz zu den Übereinkommen vom 8 November 1968 über den Strassenverkehr und über Strassenverkehrszeichen, zu den Europäischen Zusatzübereinkommen vom 1., Mai 1971 zu diesen Übereinkommen sowie zum Protokoll vom 1., März 1973 über Strassenmarkierungen."
9. Horn, B.E., "Helping to identify key issues in bicycle safety through international assessment," OECD, Road Research Secretariat.
10. RAI Techniek, No. 11, October 1980, Nederlandse Vereniging de Rijwielen Automobielindustrie.
11. Roosmark, P.O., and R. Fräki, "Interview investigation of road traffic accidents," *Accident Analysis and Prevention*, Vol. 1, 1969, S.279-291.
12. Thorson, J., and J. Sande, "Hospital statistics on road traffic accidents," Proceedings 3rd Triennial Congress, 1969, Michigan, Highway Safety Research Institute, 1971.
13. Nordentoft, E., et al., "Rapportering af Trafikulykker Med Personskade," Radet for trafiksikkerhedsforsking, Rapport 13, Kopenhagen, 1972.
14. Hehlen, P., "Unfälle an Strassen-Kreuzungen und-Einmündungen," 14, Tagung des Institutes für die gesamte Unfallforschung in Zürich, April 1976 (unpublished).
15. Hobbs, C.A., et al., "Classification of injury severity by length of stay in hospital," TRRL, Report 871, 1979.
16. Maas, M.W., De Politieregistratie van Verkeersgewonden in Ziekenhuizen, SWOV, Report R-82-34, 1982.
17. Lenhart, W., "Grundauswertung des korrigierten Datenbestandes zu FP 7537," BASt, Köln, 1982 (unpublished).
18. Bunketorp, D., et al., "Traffic accident registration and analysis in Göteborg," Proceedings 7th IRCOBI Conference, Köln, 1982.
19. Pedder, J.B., et al., "A study of two-wheeled vehicle casualties treated at a city hospital," IRCOBI Conference, Salon de Provence, France, 1981.
20. Bull, J.P., and B.J. Roberts, "Road accident statistics—a comparison of police and hospital information accident analysis and prevention," 5, pp. 45-53, 1973.
21. Otte, D., and E.G. Suren, "Verletzungen und deren Langzeitfolgen bei verunfallten motorisierten Zweiradbenutzern," 1, Bochumer Workshop zur Zweiradsicherheit, February 1983.
22. Willeke, R., et al., "Ein Optimum an Sicherheit; Nutzen-Kosten-Untersuchungen für Verkehrssicherheitsmassnahmen", Schriftenreihe VDA, Heft 25, 1978.
23. Danner, M., et al., "Optimiering des passiven Unfallschutzes für motorisierte Zweiradfahrer," BASt, FP 7806 (unpublished).
24. Krupp, R., and M. Bressin, "Personenschaden infolge von Strassen verkehrsunfällen- Ein Vergleich zwischen Pkw-Insassen, motorisierten Zweiradfahrern, Fussgängern und Radfahrern," BASt, 1983 (unpublished).
25. Groepering van statistische gegevens betreffende slachtoffers van verkeersongevallen opgenomen in ziekenhuizen 1979, Ministerie van Volksgezondheid en Milieuhygiëne, 1982.

26. *ECE Statistics of Road Traffic Accidents in Europe (1981)*, United Nations, 1982.
27. Bourret, P., P. Sejourne, P. Orsoni, and C. Cavallero, "Lower limb injuries of two-wheelers," Salon de Provence Hopital, ONSER, IRCOBI, 1981.
28. Cross, K.D., and G. Fisher, "A study of bicycle/motor-vehicle accidents. Identification of problem types and countermeasures. Approaches," Vol. 1, Anacapa Sciences Inc., Santa Barbara, California, 1977.
29. McDermott, J.E., and P.A. Wood, "Pedal cycle injuries," 19th AAAM, San Diego, Emergency Department Nurses Association, Seattle, Washington, 1975.
30. EEVC Working Group 7, "Pedestrian injury accidents," Proceedings International Technical Conference on Experimental Safety Vehicles, Kyoto, 1982.
31. Grattan, E., J.A. Hobbs, and M.E. Keigan, "Anatomical sites and severities of injury in unprotected road users," IRCOBI, Amsterdam, 1976.
32. Guichon, D.M.P., and S.T. Myles, "Bicycle injuries: one year sample in Calgary Foothills Hospital," *The Journal of Trauma*, 6, Calgary, Alberta, Canada, 1975.
33. Hunter, W.W., D.G. Cole, and E.G. Leggett, "An analysis of bicycle accidents in North Carolina 1974-1976," University of North Carolina, 1978.
34. Huijbers, J.J.W., "Een beschrijving van fiets- en bromfietsongevallen ten behoeve van prioriteitsindelingen bij het letselpreventie onderzoek," SWOV (not yet published).
35. Maas, M.W., "De politieregistratie van verkeersgewonden in ziekenhuizen," SWOV, 1982.
36. Nicholl, J.P., "The use of hospital in-patient data in the analysis of the injuries sustained by road accident casualties," Transport Studies Group, University College, London, TRRL SR 628, 1980.
37. Otte, D., "A review of different kinematic forms in two-wheeler accidents. Their influence on effectiveness of protective measures," T.U. Berlin, Proceedings 24th Stapp Car Crash Conference, Troy, Michigan, 1980.
38. Pedder, J.B., S.B. Hagues, G.M. Mackay, and B.J. Roberts, "A study of two-wheeled vehicle casualties treated at a city hospital," University of Birmingham, Birmingham Hospital, IRCOBI, 1981, Salon de Provence.
39. Roland, H.E., B.J. Campbell, and W.W. Hunter, "Investigation of motor vehicle/bicycle collision parameters," Vol. 1, Final report, University of Southern California, Los Angeles, 1979.
40. Whitaker, J., "Motorcycle safety—accident survey and rider injuries," TRRL SR 239, 1976.
41. "Accidents in Great Britain 1980," Department of Transport, 1981.
42. Riley, B.S., and H.J. Bates, "Fatal accidents in Great Britain in 1976 involving heavy goods vehicles," TRRL SR 586, 1980.
43. "Strassenverkehrsunfälle 1981," Statistisches Bundesamt Wiesbaden, 1983.
44. Gauss, F., K. Langwieder, et al., "Äussere Sicherheit von Lkw und Anhängern," FAT Schriftenreihe Nr. 27.
45. OECD, "Safety of two-wheelers," OECD Research Group, Paris, France, March 1978.
46. Downing, C.S., "Pedal cycling accidents in Great Britain," Paper presented at the British Psychological Society Conference on Road Safety, Cardiff, 1981.
47. Danish Council for Road Safety Research, "Accidents with two-wheeled vehicles in traffic," Memorandum No. 89, Copenhagen, 1973.
48. Dedoyan, J., "Etude médicale et technique d'accidents impliquant des usagers de deux roues à moteur," Thèse, Lyon, 1979.
49. Kraus, J.F., R.S. Riggins, and C.E. Franti, "Some epidemiologic features of motorcycle collision injuries," *American Journal of Epidemiology*, 102, 1, pp. 74-109.
50. U.S. Department of Transportation, NHTSA, "Motorcycle accident factors study," September 1980.
51. Cross, K.D., and G. Fisher, "A study of bicycle/motor vehicle accidents; identification of problem type and countermeasure approaches," Final report, U.S. Department of Transportation, NHTSA, September 1977.
52. Roland, H.E., W.W. Hunter, J.R. Stewart, and B.J. Campbell, "Investigation of motor vehicle/bicycle collision parameters," Final report, U.S. Department of Transportation, NHTSA, February 1979.
53. Jamieson, K.G., and D. Icelly, "Crash helmets reduce head injuries," *Medical Journal of Australia*, 1973, 2, 17, pp. 806-809.
54. ONSER, "Etude des moyens de protection des usagers de 2 routes," 1976.
55. Sacreste, J., J. Masset, and A. Fayon, "Collisions expérimentales voitures/cyclemoteurs," Rapport ATP No. 1, 1979.
56. Taneda, K., "Experimental investigation of motorcycle safety," IRCOBI, pp. 270-282, 1976.
57. Chretien, B., and J.C. Cayet, "Accident de 2 roues heurtant un dispositif de retenue," ONSER, Rapport 311.79.03.
58. Dunham, T.D., "Safety helmet performance investigation," NHTSA report, November 1974.
59. Jehu, V.J., "Shock absorption test methods for protective helmets," Aspects techniques de la sécurité routière No. 58, Bruxelles, 1974.
60. Fayon, A., C. Tarriere, G. Walfish, and C. Got, "Performance of helmets and contribution to the definition of the tolerances of the human head to impact," IRCOBI, pp. 291-300, 1976.

61. Aldman, B., B. Lundell, and L. Thorngren, "Non-perpendicular impacts—an experimental study on crash helmets," IRCOBI, pp. 322-331, 1976.
62. Bastiaanse, J.C., "The natural crash helmet," IRCOBI, pp. 375-384, 1976.
63. Fleck, J.F., and F.E. Butler, "Calspan 3D crash victim simulation program," IRCOBI, pp. 283-290, 1976.
64. Janssen, E.G., and C.G. Huiskens, "Letselpreventie wielrijders," Tussen Rapport, IW-TNO, 1984.
65. Sporner, A., "Experimentelle und Mathematische Simulation von Motorradkollisionen im Vergleich zum realen Unfallgeschehen," Diss., TU München, Mai 1982.
66. Aldman, B., J. Thorson, and A. Asberg, "Bicycle accidents to children and blunt trauma to the abdomen," IAATM, 1969.
67. Juhl, M., "Bicycle spoke injuries," IRCOBI, 1976.
68. Esterer, H., A. Opitz, and E. Schima, "Intra abdominelle organverletzungen durch Sturtz auf die Fahrradlenkstange," *Unfallheilkunde 77*, 1974.
69. Melvin, J.W., P.M. Fuller, R.P. Daniel, and G.M. Pavliscak, "Human head and knee tolerance to localized impacts," SAE Paper 690477, Mid-year Meeting, Chicago, May 1969.
70. Voigt, G.E., V.R. Hodgson, and L.M. Thomas, "Breaking strength of the skull vs. impact surface curvature," Contract No. DOT HS 146.2.230, Final report, 1973.
71. Stalnaker, R.L., J.W. Melvin, G.S. Nusholtz, N.M. Alem, and J.B. Benson, "Head impact response," Proceedings 21st Stapp Car Crash Conference, SAE Paper 770921, 1977.
72. Hodgson, V.R., W.A. Lange, and R.K. Talwalker, "Injury of the facial bone," Proceedings 9th Stapp Car Crash Conference, 1965.
73. Schneider, D.C., and A.M. Nahum, "Impact studies of facial bones and skull," Proceedings 16th Stapp Car Crash Conference, SAE Paper 720965, 1972.
74. Swearingen, J.J., "Tolerance of the human face to crash impact," Federal Aviation Agency, Office of Aviation Medicine, Rept. AM 65.20, 1965.
75. Lissner, H.R., M.J. Lebow, and F.G. Evans, "Experimental studies on the relation between acceleration and intracranial pressure changes in man," *Surg. Cyn. Obst.*, Vol. III, pp. 329-338, 1960.
76. Dejeammes, M., C. Tarriere, D. Kallieris, and C. Thomas, "Exploration of biomechanical data towards a better evaluation of tolerance for children involved in automotive accidents," Proceedings 27th Stapp Car Crash Conference, 1983.
77. Yamada, H., *Strength of Biological Materials*, New York: Robert E. Krieger Pub. Co., 1973.
78. Verriest, J.P., A. Chapon, and R. Trauchessec, "Cinephotogrammetrical study of porcine thoracic response to belt applied load in frontal impact. Comparison between living and dead subjects," Proceedings 25th Stapp Car Crash Conference, 1981.
79. Walfish, G., F. Chamouard, D. Lestrelin, A. Fayon, C. Tarriere, C. Got, F. Guillon, and A. Patel, "Tolerance limits and mechanical characteristics of the human thorax in frontal and side impact and transposition of these characteristics into protection criteria," Proceedings 7th IRCOBI Conference on the Biomechanics of Trauma, September 1982.
80. Walfish, G., A. Fayon, C. Tarriere, J.C. Rosey, F. Guillon, C. Got, A. Patel, and R.L. Stalnaker, "Designing of a dummy's abdomen for detecting injuries in side impact collisions," Proceedings 5th IRCOBI Conference on the Biomechanics of Impact, September 1980.
81. Evans, F.G., *Stress and Strain in Bones*, C.C. Thomas, Publisher, pp. 92-98, 1957.
82. Cesari, D., and M. Ramet, "Pelvic tolerance and protection criteria in side impact," Proceedings 26th Stapp Car Crash Conference, 1982.
83. Young, J.W., "Applied forces of lower leg impact, 1966," reported by R.C. Snyder, Human Impact Tolerances, International Automobile Safety Conference compendium, 1970.
84. Bunketorp, O., B. Aldman, R. Jonson, B. Romanus, B. Roos, and L. Thorngren, "Experimental studies on leg injuries in car pedestrian accidents," Proceedings 6th IRCOBI Conference, 1981.
85. Ashton, S.J., J.B. Pedder, and G.M. Mackay, "Pedestrian injuries and the car exterior," SAE Transactions, SAE Paper 770092, Warrendale, Pennsylvania, 1977.
86. Aldman, B., I. Cacciola, H. Gustafsson, A. Nygren, and I. Wersäll, "The protective effect of different kinds of protective clothing worn by motorcyclists," IRCOBI, Salon de Provence, 1981.
87. "HGV side-underrun guards: a design opportunity," *Automotive Engineer*, April-May 1983.
88. Bourret, P., P. Sejourne, P. Orsoni, and C. Cavallero, "Lower limb injuries of two-wheelers," Salon de Provence Hospital, IRCOBI, Salon de Provence, 1981.
89. Gillies, N., "Helmets for use by bicycle riders," Traffic Accidents Research Unit, Department of Motor Transport, New South Wales, March 1980.
90. Hurt, H.H., J.V. Quellet, and I.J. Wagar, "Effectiveness of motorcycle safety helmets and protective clothing," AAAM, San Francisco, October 1981.
91. Rau, H., "Simulation von Zweirad Kollisionen," T.U. Berlin, from *Sicherheit bei motorisierten Zweirädern*, TÜV, Köln, 1980.
92. Riley, B.S., P.P. Chinn, and H.J. Bates, "An analysis of fatalities in heavy goods vehicle accidents," TRRL-LR 1033, 1981.

93. SWOV, "Invloed van het gebruik van helmen door bromfietsen en autogordels door inzittenden van personenauto's op de verkeersveiligheid," SWOV, 1978.
94. Taneda, K., "Experimental investigation of motorcycle safety," Japan Automobile Research Institute, Inc., IRCOBI, Amsterdam, 1976.
95. "Bicycle products, brakes, lights and helmets," Technisearch Ltd., Collingwood, Australia, June 1981.
96. AB Volvo, "Accident investigation," (Heavy commercial vehicles/unprotected road-users), Report 1, AB Volvo, Truck Division, Traffic Safety Department, December 1973.
97. Langwieder, K., "Collision characteristics and injuries to motorcyclists and moped drivers," Proceedings 21st Stapp Car Crash Conference, 1977.
98. Gauss, F., K. Langwieder, W.D. Schmidt, and M. Wrobel, "Äussere Sicherheit von LKW und Anhängern," *FAT Schriftenreihe*, Nr. 27, 1982.
99. Grattan, E., J.A. Hobbs, and M.E. Keigan, "Anatomical sites and severities of injury in unprotected road users," IRCOBI, Amsterdam, 1976.
100. Huijbers, J.J.W., "Een beschrijving van fiets- en bromfietsongevallen ten behoeve van prioriteitsindelingen bij het letselpreventie-onderzoek," SWOV (not yet published).
101. Nicholl, J.P., "The use of hospital in-patient data in the analysis of the injuries sustained by road accident casualties," Transport Studies Group, University College, London, TRRL-SR 628, 1980.
102. Otte, D., "A review of different kinematic forms in two-wheel-accidents. Their influence on effectiveness of protective measures," T.U. Berlin, Proceedings 24th Stapp Car Crash Conference, Troy, Michigan, 1980.
103. Fife, D., J. Davis, and L. Tate, "Two fatal injuries from extended rear view mirrors," *The Journal of Trauma*, Vol. 23, No. 8, 1983.
104. Appel, H., D. Otte, and E.G. Suren, "Schwerpunkte des Unfall-geschehens aus Untersuchungen am Unfallort," *Sicherheit bei Motorisierten Zweirädern*, Köln, December 1980.
105. Pedder, J.C., "A study of 93 fatal two-wheeled motor vehicle accidents," IRCOBI, Gothenburg, 1979.
106. Ramet, M., D. Cesari, and A. Dedoyan, "Two-wheeler accidents, injury mechanisms and means of prevention," IRCOBI, Salon de Provence, 1981.
107. Lewicki, L.R., and J.A. Newman, "Head protection of the bicyclist," Proceedings 19th AAAM Conference.
108. Taneda, K., "Experimental investigation of motorcycle safety," IRCOBI Conference, Amsterdam, 1976.
109. Stcherbatcheff, G., "Kinematics of a pedestrian and a two-wheeler impacted by the front of a car," IRCOBI Conference, Amsterdam, 1976.
110. Sporner, A., "Experimentelle und mathematische simulation von motorradkollisinen im vergleich zum realen unfallgeschenen," Technical dissertation at the Technischen Universität of München, September 2, 1982.
111. OECD, "Safety of two-wheelers," OECD Research Group, Paris, France, March 1978.
112. Blokpoel, A., and J.A.G. Mulder, "Het zichtveld van de bestuurders van vrachtwagens," SWOV, 1981.
113. Arnberg, P.W., E. Ohlsson, A. Westerberg, and C.A. Ostrom, "The ability of pre-school and schoolchildren to manoeuvre their bicycles," Report No. 149A, National Swedish Road and Traffic Institute, Stockholm.
114. Mackie, A.M., "Research for a road safety campaign-accident studies for advertising formulation," TRRL Report LR 432, 1972.
115. Horberg, U., and K. Rumar, "Running lights conspicuity and glare," Report 178, Department of Psychology, University of Uppsala, Sweden, 1975.
116. Watts, G.R., "The evaluation of conspicuity aids for cyclists and motorcyclists," *Human Factors in Transport Research*, Vol. I.
117. Watts, G.R., "Evaluation of conspicuity aids for pedal cycles," TRRL Report LR 1103, 1984.
118. Welleman, "Traffic safety of bicycles and mopeds," SWOV (not yet published).
119. Department of Transport, "Road accidents Great Britain 1980," HMSO, 1981.
120. Noordzij, P.C., "Cycling in the dark: an analysis of fatal bicycle accidents in The Netherlands," *Journal of Safety Research*, Vol. 8, No. 2, 1976.
121. Watts, G.R., "Pedal cycle lamps and reflectors—some visibility tests and surveys," TRRL Report LR 1108, 1984.
122. Groot, H., et al., Inventarisatie: Visuele waarneembaarheid van Tweewielers; verslag aan V & W/DVV, IWACC 1983-1, January 1983.
123. Van Minnen, J., "The effect of rear reflectors and reflecting pedals on the safety of cyclists," SWOV, Leidschendam, October 1982.
124. Burg, A., and S.F. Hulbert, "Reflectorisation of bicycle wheels," *Verkeerskunde*, Vol. 27, No. 12, pp. 590-1, 1976.
125. Masseck, K., Note on reflecting items for bicycles—private communication, 1983.
126. Kratz, G., "The effect of safety equipment for bicycles," Study by the International Federation of Senior Police Officers (FIFSP), July 1980.
127. FIFSP, "Prevention of two-wheeled vehicle accidents in the darkness," Report by the International Federation of Senior Police Officers (FIFSP), March 1977.
128. Blokpoel, A., D.A. Schreuder, and F.C.M. Wegman, "The perceptibility of the bicycle from the side in the dark," SWOV, Leidenschendam, November 1982.

129. British Standard Institution, "Cycles: specification for safety requirements for bicycles," British Standards Institution BS 6102, Parts 1 and 2, 1981.
130. Godthelp, J., and P.I.J. Wouters, "Course holding by cyclists and moped riders," *Applied Ergonomics*, 11, 4, pp. 227-235, 1980.
131. Watts, G.R., "Bicycle safety devices—effects on vehicle passing distances," TRRL Report SR 512, 1979.
132. Oranen, L., "Report on the effect of protective pennants on the behaviour of motor-vehicle drivers," Traffic Safety Research Department Pamphlet 29/1979, Traffic Safety Department, Helsinki, 1976.
133. Volkswagen Factory Wolfsburg AG, "Effect of distance bars on the distance allowed between motor vehicle and bicycle when overtaking," Biotechnological Group, Supplementary Report No. 19, 1973.
134. Centre d'Etudes Techniques de l'Equipment, "Etude d'efficacite du gabarit 2 roues ou ecarteur de danger (4 e-me-partie-mesures de distance de depassement)," CETE Bordeaux Division UTC, December 1981.
135. Watts, G.R., "Evaluation of pedal cycle spacers," TRRL Report SR 820.
136. Whitt, F.R., and D.G. Wilson, *Bicycling Science—Ergonomics and Mechanics*, MIT Press, 1962.
137. Wobben, D., "Rim brakes in the rain," Radmark + 3, pp. 88-90, 1983.
138. Marlow, D.E., "The CPSC road test of bicycle braking performance—experimental evaluation," National Bureau of Standards, Washington, D.C., 1973.
139. Watts, G.R., "Brakes on pedal cycles," Institute of Mechanical Engineers Conference on Braking of Road Vehicles, Loughborough, March 1983.
140. Lewis, G.D., "The manoeuvrability and braking performance of small-wheeled bicycles when ridden by children," TRRL Report LR 500, 1973.
141. TRRL, "Vehicle defects and their contribution to road accidents," LF 374, 1973.
142. Traffic Insurance Institute, "Light traffic (pedestrians and cyclists) accidents report in certain areas of Finland in 1971-75," Helsinki, 1976.
143. Wells, P., "The state of maintenance of bicycles ridden to primary and middle schools," TRRL Report.
144. Wouters, P.I.J., "Problems of riding on a bicycle or a moped," SWOV, Voorburg, 1980.
145. Starks, H.J.H., and R.D. Lister, "Some safety aspects of pedal and motor-assisted cycles," Road Research Technical Paper No. 38, 1957.

Section 5
Trends and Priorities in Vehicle Development in Relation to Road Safety

M.R. Dunn, Chairman, United Kingdom

Trends and Priorities in Vehicle Development in Relation to Road Safety

A. Chenevez
France

As in the first nine ESV conferences, the discussions of this Tenth Conference have largely shown that the manufacturers' research activity is not slowing down toward road safety improvements.

Such research is conducted in close cooperation with the public authorities and independent organizations. Numerous regulations have been developed from the results of that activity; they have had deep consequences on vehicle construction and have played an important role in the continuing reduction of the number of road accident victims in all countries, related to the number of kilometers driven and even in absolute figures.

Further safety progress requires new imaginative efforts. In this field, as in many others, the benefit/cost ratio is decreasing. In the 1970's, we took benefit of the most obvious and profitable measures, such as seatbelt improvements, energy absorption in front and rear ends of cars, etc. But to still improve safety through car design, we need to create much more sophisticated and expensive devices, the efficiency of which will necessarily be lower than for those invented before.

Without slowing down their efforts toward the specific safety of the vehicles, many manufacturers are wondering if the international scientific community should now concentrate on usage problems rather than just on vehicle construction.

To take just one example, I would like to mention how much the manufacturers have taken part in the seatbelt use campaigns throughout the world. Why should we provide customers with better and better restraining devices if they remain unused or can be disconnected in the case of passive restraints?

You know that in many countries more than 40 percent of the fatal accidents are caused by alcoholic drivers, so you will certainly understand why the manufacturers are in favor of more severe and more frequent controls of drunk drivers.

Similar examples could be cited in which the role of the police appears to be as important as that of the engineers. If public authorities accept that way of thinking, this will not mean the manufacturers' task would be reduced but their cooperation with public authorities will be rendered more efficient.

Prof. H.J. Kraft
Federal Republic of Germany

The round number 10 suggests the idea of a retrospect. Therefore, when treating at this Tenth ESV conference the topic of the panel discussion, "Trends and Priorities in Vehicle Development in Relation to Road Safety," the beginnings should be considered also.

The development of experimental safety vehicles originated from specifications that disproportionately emphasized occupant protection. Thus, overheavy tank-like vehicles were designed and built in which the passengers could be better protected indeed, but that

constituted a considerably higher danger for the safety of other road users. In this context, the impairment of other vehicle properties as, for instance, vehicle-handling or low-fuel consumption is mentioned only incidentally.

After construction and testing of a series of such vehicles, it was also realized by the involved governments that this was the wrong way. But before this knowledge had become generally accepted, diverse governmental delegates blamed the industry for having no interest in insuring the safety of its customers in the best possible way. However, just the opposite is the case for two reasons:

- Humanitarian reason: A sense of responsibility stimulates the automobile engineers to continuously do their very best to protect the customers against all avoidable dangers.
- Economical reason: For quite a long time, the industry has recognized that the life and health of its customers must be protected to insure also the existence of the enterprises. Vehicles can be replaced, but not lives.

Because of frank discussions between industry and government, the actual situation has improved considerably. Together we are on the right track. It is only by virtue of a well-balanced concept and special consideration of the compatibility of different vehicles that overall safety can be further improved. In this context, also, the importance of harmonization of regulations must be mentioned. Above all, legal regulations that are expected in the future (e.g., side impact) from the very beginning should specify only internationally valid requirements, and legal activities on a national basis should be avoided.

The most important tendencies toward an improvement of traffic safety can unquestionably be observed in the use of modern electronics for control systems with respect to steering, brakes, and drive. The resulting gain in safety lies in ease for the driver and an even better control of the vehicle in critical situations. We are confident we will make further gains toward our common goal, namely, the increase in safety on our roads.

Dr. E. Landsberg
Italy

The automotive industry will continue to cooperate in the promotion of improvements for road safety. In fact, cars have been greatly improved in this respect during the past 30 years. The industry has been particularly concerned to promote active or accident-avoidance features on cars. They include the many improvements to brakes, steering systems and suspensions, and lighting, quite apart from better instruments and warning signals. These advances have been achieved by the automotive industry largely without the introduction of regulations requiring them. Protective devices and features have also been introduced, and the overall safety of cars has been improved almost beyond recognition.

The latest accident-avoidance features to be proposed are the supplementary rear stoplights, which are being required in the United States, but it may be worth noting that no advantage was found for such a system when evaluated in trials in the Federal Republic of Germany.

Despite these problems, it is probably true that mechanical safety features on cars do need regulations to enforce their uniform introduction.

Sadao Takeda
Japan

I would like to present a brief summary of recent Japanese research and development in safety-related technology and also to introduce the recent development of internationalization of the Japanese road safety standards and certification system.

In general, there are four factors that influence the level of technical innovation in automobiles. First, the emergence of fundamental technologies, such as new materials and electronics, that will lead to the development of many associated technologies; second, consumer demand and the marketplace; third, social or public demands, as seen in the antipollution movement; and fourth, the desire of automakers to strengthen their competitive powers.

Regarding social or public requirements, safety-related technology has been regarded as an important aspect in this field since the 1960's. Today, safety is not only a social requirement but is necessary for the individual consumer, besides helping to differentiate one automobile product from another.

As a result, many attempts have been made to develop viable safety-related technology. Safety measures concerning vehicles are broadly divided into two categories. One is the provision of adequate protection once a

collision occurs, and another is the prevention of such collisions. Particularly in the field of accident prevention, we believe technological development has been and will be made in many areas as a result of the increasing progress being made in electronics.

The necessity of providing adequate protection for people involved in automobile accidents, including pedestrians, is a well-established fact. In Japan, studies are being carried out on seatbelts, on child-restraining chairs, and on how drivers and passengers can be afforded adequate protection from double-end collisions and side collisions. However, since this conference has focused on these issues at various sessions, I would like to concentrate on the recent technological developments in the field of accident prevention, reflecting the overall improvements made in the electronics field.

Amazing progress has been made in the electronics field in recent years. These achievements point to the possibilities of adding intelligence to machines and of applying more sophisticated control methods to driving. As a result, car electronics technology is spreading from engine control to power train, body control, and other aspects of the overall car structure. Today, many car models incorporate more than 10 chips. Safety-related technology has continually moved forward by using electronics as a major starting point.

The antiskid brake, a widely used safety feature, has been upgraded with the aid of electronics. Also, as already introduced in this ESV conference, an electronic warning system capable of sensing the driver's drowsiness and other fatigue conditions is now in practical use. Electronics technology is also applied for the brake power-maintaining system to make starting on an inclined road smoother as well as to eliminate the creep phenomena encountered in automatic transmission vehicles.

Attempts are underway to use electronics in improving running performance, such as the four-wheel steering system to achieve greater turning stability and improved response speed. Further, research on the use of supersonic waves, laser beams, and millimeter waves for detecting any obstructions located near the automobile has made important strides for future realization.

Further progress will be made in electronics, insuring a more sophisticated control system for automobiles. We anticipate development of a wide variety of systems for traffic safety, especially in the area of accident prevention.

I would like to explain three important points concerning the trouble-free development and diffusion of new technology. First is the importance of an interface between humans and machines. For example, a car provided with an antilock system is still not entirely safe if the driver is overconfident in the system's ability to prevent an accident. Drivers are all too human, and their continuing education and growing awareness in this field are important for increasing safety.

Second is the importance of developing more economical technology. This is indispensable for popularization. For example, more and more people in Japan are beginning to recognize the positive effects of antilock brakes, but their use has been limited to only 2 percent of new cars because each antilock brake system costs more than $500.

Third is the importance of exchanging information about safety technology. Although joint research and development among automakers is difficult to carry out, due to the incorporated safety measures contributing significantly to the competitiveness of each automobile product, as mentioned earlier, it is important nevertheless that information be exchanged to further the development of safety technology. Therefore, I hope the ESV conference will serve as a forum for the exchange of information concerning safety-related technology.

I would like to mention also the recent progress made in Japan concerning certification formalities as part of the overall move toward internationalization. Automobiles are so-called international merchandise, and it is of considerable importance that, as far as is possible, existing nontariff barriers be transformed into more harmonized formalities. Considerable efforts have been undertaken by Japan in this area.

As far as certification formalities are concerned, wide-ranging simplification of the Automobile Type Designation System was introduced in August 1983 with a view to increased internationalization so the system could be more accessible as far as the import of foreign automobiles is concerned. Based on the new system, the type designation was approved in 1984 for seven models and eight types of imported automobiles.

Much effort has been made to coordinate fundamental safety requirements in Europe and the United States. In October 1983, 12 items in the safety standards were amended to conform with those in Europe and the United States. Regarding 14 items of safety-related requirements, the safety standards in Europe and the United States have been treated as being at the same technological level as those in Japan. As in the past, we still feel we would like to participate wholeheartedly in ECE WP29 as one of our activities for setting up the International Uniform Safety Standard for Automobiles, which will contribute to the harmonization of standards between countries.

I had mentioned the recent developments in safety-related technology, especially the progress in electronics technology and internationalization of the safety standards and certification formalities in Japan.

I.D. Neilson
United Kingdom

Starting on a general point as a contribution to this discussion, it may be worth drawing a distinction between safety developments that are highly desirable on grounds of safety effectiveness and those that are possible. The need is to make progress, and this must clearly be done where it is readily possible. On a longer time scale, things that are highly desirable may have to wait until they can be engineered satisfactorily, but this should not delay the possible items being done first.

To balance these introductions, I have been asked to refer to trends and priorities for the improved safety of trucks, buses, and motorcycles.

For trucks, it is known that about 9 out of every 10 fatal injuries in accidents involving trucks are to road users outside the trucks—car occupants, pedestrians, and riders of two-wheelers. Only 1 in 10 are drivers and occupants of the trucks. There is a clear trend toward antilock braking systems to maintain braking stability, and these systems become even more highly desirable as the number of axles increases. There is scope for improved protection for other road users. Side guards can be designed to stop pedestrians and cyclists from being dragged under the rear wheels of trailers. There is a clear need for front underrun bumpers for trucks as a means of protecting car occupants from being killed in the many accidents where this can be avoided.

Improvements in the structural design of coaches may be anticipated, and it is to be hoped that regulations for improving structural resistance to collapse in overturning accidents will be universally adopted. Seatbelts can be fitted in coaches but, apart from some consumer resistance to using them, there are technical difficulties in designing satisfactory installations and so they may be fitted only to seats "at risk."

The largest scope for improvements in safety is in the field of motorcycle design. In particular, antilock braking should become essential equipment in the near future and in years to come even on small machines. Leg protection for riders of motorcycles is at an interesting stage of development. Progress appears to be at the point of a breakthrough in providing this much-needed item. Doubts should be resolved quickly. It seems protective wear can now be designed that gives some useful protection for the enthusiast who may choose to wear such clothing.

Ralph J. Hitchcock
United States

Several months ago, I attended a conference in the United States of various experts involved in different aspects of highway safety. Included were experts in vehicle design, human factors, driver licensing, enforcement, emergency medical services, highway design, and highway operations and maintenance. The reason I mention this conference is that a couple of suggestions were made by the emergency medical services experts on vehicle improvements that rather surprised me. The emergency medical services people are on the scene of the accident after it occurs. They said the big problem they see every day is head lacerations and head injuries caused by inside rear view mirrors and by sun visors and their mounting systems. I think it is clear to everyone at this conference that those items—the rear view mirror and sun visor—can clearly be designed so they don't cause head injury and lacerations. The fact that they do cause these kinds of injuries should tell us we need to do more in the component design areas of the car.

There were many things discussed at this conference that involved major changes and additional cost items on the car to improve safety. Such things as airbags, truck underride guards, truck side guards, antilock braking systems for motorcycles, center high-mounted stop lamps, daytime running lights, and Securi-flex windshields have been discussed and will continue to be discussed at other conferences such as this for many years. Various countries and car manufacturers will employ them as major changes in coming models to improve the safety of the vehicles. Other major potential safety improvements discussed at this conference included side impact and pedestrian impact protection. Again, these are major vehicle safety areas that will be discussed for many years. Performance criteria will be developed, and safety benefits will be weighed against costs. There is little I can add to the debate on these major safety projects. Rather, what I would like to stress are the smaller improvements that can be made, many at no additional cost, when incorporated into the basic vehicle design.

The General Motors presentation on built-in safety systems that were linked to detailed accident data and several of the papers by the British and others on smaller safety improvements in the car are notable. For example, the hood or bonnet of the car should be designed with an overlap at the fenders to provide 50 to 100mm of crush space for mitigation of pedestrian impact in injuries. As I

walked back from lunch today, I noticed that many of the European cars parked outside had hoods that overlapped while others did not. Clearly, some of them—the ones that overlapped—are probably going to be much better for pedestrian impact than the ones that do not. While it may be many years before we have a complete pedestrian impact protection requirement, new vehicle designs should have this hood overlap as a part of their basic design.

Similarly, in the United States, recessed windshield wipers were quite popular as a styling feature for several years. Again, these offer major benefits when impacted by a pedestrian. Our current stylists should try again to incorporate recessed windshield wipers into new designs.

In the interior of the car, some of the presentations at this conference have shown that steering wheel vertical displacement in a crash can be dangerous. While our national and international regulations limit the rearward displacement of the steering wheel, manufacturers certainly have the capability to limit vertical displacement as well. Similarly, padded steering wheels and steering wheel hubs are well within current technology and can prevent many serious head and facial injuries to drivers, particularly those who are wearing their safety belts. Last, soft plastic urethane bumpers have been put on many cars as a style feature. If they were designed with a foam support structure, with pedestrian protection in mind, they would do a lot to prevent pedestrian knee and leg injuries.

To summarize, I would like to encourage everyone at this conference, particularly the vehicle manufacturers, to take back to their companies or to their jobs the message that accidents result in many injuries by parts of the car that could be redesigned with little or no additional cost. I would encourage manufacturers and others at this conference to talk to the emergency medical services personnel and accident investigators in their countries to find out which little things might be done to make cars safer for people involved in accidents. If each of us does one or two small things to make cars safer, we can rest assured that many people involved in accidents will suffer fewer injuries and perhaps be alive after an accident because of our work.

Section 6
Conference Summary

C. Ashley, Motor Industry Research Association, United Kingdom

Conference Summary

Dr. C. Ashley
Motor Industry Research Association, United Kingdom

In reviewing this conference, it soon became apparent that the wealth of information cannot be summarised in any detail in 30 minutes. My comments will attempt to pick out the highlights and assess the principal trends. First, we know the conference as a whole is a considerable success. With 475 delegates and 127 papers, it has exceeded all expectations. It must now be regarded as the centre of excellence for communicating knowledge on experimental safety research in relation to vehicles.

Let us look at the value of the conference in simple monetary terms. If each paper represents $100,000 of work, then the total value of the conference is $12.7 million as a minimum. I would estimate that safety research worldwide by government and industry exceeds $100 million. That figure could be compared with the broad-band vehicle development costs of an annual $6 billion per annum, based on 40 million vehicles, $5,000 per vehicle, and 3 percent R&D costs.

Even the $6 billion on R&D is dwarfed by the $120+ billion cost of car fuel and the $12 billion cost per year if pollution measures increase fuel consumption by 10 percent. Perhaps road safety could be given a little more financial priority than less than 1 percent of the final annual cost of emission control.

Now let us return to the conference and the status reports. These are not a formality but represent a most important statement on "where we are" for each individual government agency. The United States shows a situation with a significant fall in fatalities of 11 percent 3 years ago, and this situation has been broadly maintained. There are signs of car occupant fatalities increasing, and it is to be hoped the courage of the first 13 States in bringing in mandatory seatbelt laws will be rewarded by the appropriate reduction in fatalities and injury and hence encourage the others. It would appear essential that research is carried out to show how Britain's and Germany's success in getting better than 90 percent seatbelt usage can be carried over to the United States where usage can be as low as 30 percent in mandated States. The United States gives major support of over $30 million to research and data collection. Their whole comprehensive programme in airbag development and demonstrations, crash avoidance, lighting, handling heavy vehicles, alcohol, and crashworthiness is commendable. Need I add the importance of harmonisation in this work?

The initiative of the European Experimental Vehicle Committee is well demonstrated by the work presented at the conference on the side impact dummy Eurosid, the mobile barrier, and studies on cycles and pedestrians. This work is, of course, supported by a number of countries including Germany, Italy, the United Kingdom, Holland, and Sweden.

Japan has a remarkable safety record, showing significantly lower accident rates, however measured, than other major countries. They have a slight negative trend, due to an increasing vehicle population, and it is reflected by increased motorcycle casualties. They hope to control this by increased application of existing legislation.

The accident situation in Italy, France, The Netherlands, and Germany still leaves room for improvement compared with the United States and Japan. Not that matters are static: in France, fatalities are down to the level of 20 years ago, in spite of the traffic increase. Their programme of assessment of accident Reagir, in which 10,000 injury accidents per year will be analysed, should play a major part in directing their efforts. The incentive scheme linking general subsidies of local authorities to accident reduction is novel, and we look forward to hearing of their experience in 2 years time. Like many countries, France is directing particular attention to motorcycles, heavy goods vehicles, and coaches. They are also, somewhat belatedly, introducing a road-worthiness fitness test for second-hand cars. Another logical step is the introduction of lower speed limits for wet conditions, and, again, we look forward to hearing of their experience.

An interesting proposal from Italy is for an international accident data bank. Perhaps this can be pursued in Europe as part of 1986 Road Safety Year. Italy also raised the contentious question of replacement part quality in safety-related matters and how this could be controlled—a very big question, which we expect will be looked at in many countries.

Germany outlined many interesting trends in driver education and training. We note that seatbelt usage in the rear has been made mandatory, but with no fines for the time being. This initiative will give useful evidence for other countries. Another interesting initiative will be the new Canadian legislation on running lights; this will be a valuable experience for comparison with Sweden.

Now let us turn to the conference proper, with the plenary technical session on progress with safety developments for road vehicles chaired by Mike Finkelstein. I mention the chairman because he has the important responsibility of inviting the papers and structuring his session. This particular session opened with two presentations by TRRL on modified safety vehicles. Hobbs discussed a series of modifications to an Austin Metro, making it more pedestrian-friendly through a more compliant front and bonnet or hood. Theirs was an interesting solution to the problem of reconciling standard bumper heights with reduced leg injuries. Watson's paper described the latest advances in motorcycle safety with antilock braking, leg guards, nonspill fuel tank, and an airbag. This is important because many observers are feeling that antilock braking should be available on motorcycles, perhaps starting on the big bikes of over 500cc.

The airbag panel of Breed, Maugh, Reidelbach, and Romeo discussed optimisation of airbag design for performance and cost. The experience of Ford and Daimler-Benz unit production systems will be invaluable, and the low-cost approach of Breed is exciting. I feel the use of mandatory 3-point belts, with an optional auxiliary airbag system for additional protection, is the logical route to take.

Finally, the panel of Detloff, Johanssen, Haenchen, and Sano described the wide range of automatic seatbelt designs available. The panel was convinced of the necessity to evaluate carefully automatic belt performance over a wide range of conditions. The usage rate of 98 percent in the Toyota Cressida was commendable but explicable in that people bought the car to use that feature. Perhaps increasing application of seatbelt usage laws will reduce the emphasis on automatic operation but place increased pressure on comfort, fit, and convenience.

The technical session on biomechanics and dummy development was chaired by M. Leroy. Ten papers were presented, of commendable quality. The work from the University of Pennsylvania on brain injury will be a great help in this field, as will the three papers on thorax tolerance and injury mechanism by Eppinger, Lan, and Vernir. Hoffner dealt with pelvic tolerance in side impact, and this was both a synthesis of available data and a proposed criterion based on energy. The paper by Langdon on modelling lateral impact of the thorax leads naturally to the important session on dummy development and, in particular, to the Eurosid side impact dummy, which is the result of collaboration between TRRL, ONSER, TNO, and PSA. One might expect a dummy that combines the best attributes of four groups to need careful development to produce an effective device. With the major emphasis on side impact, Eurosid is clearly designed for a need, and we will look forward with close interest to major participation in the next phase.

John Melvin described a major analytical study leading to new concepts in anthropomorphic test devices with a bold approach to a realistic dummy capable of coping with a range of impact directions. Finally, Aldman described the Chalmers/ONSER approach to an omnidirectional one-legged rationised dummy, intended to give human-like and repeatable impact response in pedestrian tests. We look forward to further reports on all three projects at the next ESV meeting.

Session three was chaired by R.M. Nicholson from the United States and was concerned with crash avoidance. It was notable for papers on three electronic devices originating from Japan: laser radar for obstacle distance measurements, a drowsiness warning device, and a tyre pressure warning system. Microwave radar devices have been demonstrated for some time but have been unable to meet size and cost targets. The lower cost 100m-range laser diode is encouraging, and I expect it to be available as an optional warning device within this decade. Quantifying fatigue or drowsiness is an almost insoluble biomedical problem, but indirect detection through steering behaviour does appear to have possibilities.

Handling was covered by aerodynamic stability computer modelling, a run fairly flat tyre bead design, practical and theoretical optimisation of four-wheel-drive vehicle handling, and further development of the Honda four-wheel steering system. The handling papers deserve close study by vehicle designers. There is still room to increase safety margins in this area, particularly under slippery conditions.

Other papers dealt with visibility, considering beam pattern and windshield condition. There were two major survey papers on statistical analysis of vehicle size involved in accidents, and on car controls for physically handicapped people.

As an incidental on accident avoidance, I asked K. Digges to reconcile the difference between the United States and German experience on high-mounted brake lights where the United States found improvement but Germany did not. He said the improvement in the United States was linked to centre-positioned high brake lights, and their experience with paired high lights mirrored that of Germany.

Although not specifically mentioned, antilock must be the most important development in crash avoidance. It is now available on a range of cars, the latest application being standard fitment to the Ford Scorpio-Granada. We look forward to lower cost mechanical systems for application to smaller cars, as promised by Lucas-Girling.

Session four on occupant protection for frontal impact was chaired by K. Digges. The key element of the presentations was growth in the use of modelling for both structures and occupants. Associated with growth was the reported accuracy and the cost-effectiveness of these techniques. Indicative of this growth is the decision of Ford Europe to invest $6 million in a Cray computer, which will give them an expanded scope in nonlinear modelling by finite elements. The exchange of information in this area between different countries was of particular value.

The principal problem addressed is that of mitigating the effect of head contact on the steering wheel for belted drivers. A test method for evaluating the severity of this impact was proposed by TRRL. Two solutions to prevent the contact were the use of airbags by Mercedes-Benz and steering wheels developed to meet the new TRRL test procedure.

The question of global, compared with subsystem, test was not addressed specifically, but it is clear that each plays its part in developing and signing off the vehicle. The actual angle and speed of a frontal impact test is still an outstanding question.

The Wilson paper, which calculates the benefits of individual treatments of parts of the vehicle, opens new perspectives in design tradeoff. His paper touches upon the friendly interior concept, which has raised so much interest.

The fifth session was organised by R. Stamm and covered accident investigation and its relevance to legislation. A significant paper by Dr. Mackay looked in detail at the effects of mandatory seatbelt use in the United Kingdom. They found a 25 percent reduction in serious injuries and deaths for car and light van occupants. They also concluded that the increase in pedestrian and pedal-cycle injuries and fatalities were statistically insignificant and did not support the hypothesis of risk compensation. They also found gross intrusion in the majority of accidents in which restrained occupants are killed and suggest that seatbelt design improvement is not a major priority. They do point out the significant reduction in fatalities and injuries that would follow fitment and use of rear seatbelts, which were also the subject of the Dutch study on seatbelts. This latter also supports the general United Kingdom experience.

Other investigation papers included the Japanese experience with a 50 percent fatality reduction from 1970 to 1980. The well-known car size effect was well detailed from the invaluable NHTSA Fatal Accident Reporting System (FARS). I have already mentioned the Italian proposals for a European data bank. Such data banks need major investment if the information is to be sufficient for valid correlations to be derived.

Finally, in the detailed trauma area, a German paper suggests a method of dealing with high scatter and uncertain limit values for crashworthiness criteria, such as HIC. This matter is important to resolve, if realistic targets are to be set for the so-called global test.

The side impact session was chaired by Ian Neilson of TRRL. This was a most significant area with nearly 20 papers, the largest section of the conference. The essential outcome of the work presented must be a harmonised side impact test procedure. Standardisation will be needed for dummy, injury criteria, barrier characteristics, and test speed, angle, and position.

Standardisation of the moving barrier is a first priority, and I feel that sufficient information and will is available to make decisions on this as soon as possible. May I suggest that the stiffness of the final model should tend to be in line with good design practice for minimising pedestrian injury and side impact aggressivity, rather than represent the current average vehicle norm, which will be a moving target. This harmonisation could be a most important consequence of the conference. It should be followed by dummy harmonisation.

There remains the discussion about whether legislative subsystem tests can be devised, instead of a full-scale test with a dummy. Conflicting ideas are still being put forward but, finally, a combination of both may be appropriate. The time for decision has arrived.

The other papers in the session significantly moved forward our modelling techniques and the study of the impact of vehicles into pedestrians.

The seventh session on safety development of goods vehicles and buses was chaired by L. Strandberg from Sweden.

A major programme on development of the tractor semitrailer unit for the future was given by M. Soret of Renault. In the VIRAGES concept vehicle, they showed development in ride, handling, stability, antilock braking, visibility, conspicuity, spray reduction, and side underrun and shielding. Spray reduction was also featured in the MVMA work (where the laser method of measurement they developed has advanced), as well as techniques for making objective comparisons.

Other papers dealt in detail with commercial vehicle-handling quantification, obstacle avoidance, front underrun, and conspicuity. A paper from my own organisation dealt with load restraint in light vans where a recommended practice has benefited both manufacturer and user.

There has been increased emphasis on PSV and coach safety, and this was reflected by papers concerned with accident analysis and the soon-to-be-legislated rollover test procedure. The discussion showed concern with the need for belts in coaches. The minimum must be belts in

the front and safety seats to absorb impact and retain the other passengers.

Much is known and agreed on how to improve safety in these vehicles, and has been clearly shown by the known concept trucks by Renault and TRRL/MIRA. Let us hope that at the next ESV conference there will be more representation by truck and coach manufacturers.

The study of severe coach accidents in France has emphasised the important hazard of fire and the need to provide easy evacuation of the vehicle. One must always remember that a significant proportion of the passengers are elderly, and experimental work must be realistically based.

Signor Rossi from Italy chaired the session on pedestrian safety and protection, a subject designated as a target area for improvement by several of the national position papers.

Thirteen papers were presented, covering a range of approaches. The problem is a complex one, with interactions between many different design aspects including frontal dimensions. This makes it difficult to specify component tests, but there are difficulties with a whole vehicle approach also in the wide range of speeds and points of impact possible.

For cars, three principal areas are important—the bumper, the bonnet leading edge, and the bonnet top. Secondary areas are the wing and windscreen. Many of the papers were concerned with optimisation, whether by experiment or analysis of these areas.

Progress on defining standards for the car-pedestrian interface must move forward with the work on side intrusion to insure engineering compatibility.

One of the techniques used by Maestripieri and others is a mobile barrier with adjustable characteristic simulating a range of vehicle front end possibilities. This enables the interaction between the frontal dimensions to be explored and quantified. The computer-based study of Harris and Grew opens up new approaches to defining these interactions.

The chairman for the final parallel session was Nakamura, and this session dealt with motorcycle safety.

Clearly five aspects are important:

1. Antilock braking
2. Leg protection for rider and passenger
3. Airbag use to control side movement in frontal impact
4. Conspicuity
5. Protective clothing and helmets

The importance of rider training has also been stressed in this status report.

All these aspects were brought out and demonstrated in the exhibition, particularly in the TRRL safety motorcycle.

The time now seems ready to move forward, and I would particularly like to encourage application of antilock braking and leg guards to motorcycles, perhaps starting with the larger machines where cost is not such a major factor.

Conclusion

I will conclude by making general comments on the conference. Some people have asked whether the scope should be enlarged to include driver behaviour and road design. Even emissions and noise have been mentioned. This will be reviewed by the committee, but I believe the tendency must be resisted so we can concentrate on the key area of safety and the vehicle.

I would like to congratulate Diane Steed on her dramatic statement that she is establishing an office of international harmonisation, reporting directly to herself. Even more encouraging is her specific reference to braking standards and side impact test methods and standards.

The final message is to ask each one of you to do your utmost within your area of professional responsibility to take advantage of the wealth of information given at this conference. When this is done, there will be a significant positive effect on vehicle safety and accidents worldwide.

Section 7
Closing Remarks

Michael M. Finkelstein, United States
John W. Furness, United Kingdom

Closing Remarks

Michael M. Finkelstein
National Highway Traffic Safety Administration

As the Tenth International Technical Conference on Experimental Safety Vehicles comes to a close, we in the auto safety community again have tangible evidence of the benefit gained from our effort to seek solutions to our common problems. As we progress beyond the development of experimental safety vehicles to the examination of the full range of vehicle safety problems facing us all, it is clear that our success to date in the ESV program must serve as a model for future cooperation.

Here in Oxford, we have had 4 days of wide-ranging discussions of vehicle safety. We have heard and discussed papers of the highest quality, papers whose importance will grow as we have time to study them and incorporate these new findings into our own future research.

We would be remiss if we did not take this opportunity on behalf of Administrator Steed and the entire U.S. delegation—I am sure I can say without fear of contradiction, on behalf of all of the conference participants—to express our gratitude for the generosity, hospitality, and remarkable efficiency of our British hosts: Her Majesty's Government and the Institution of Mechanical Engineers. Thank you all.

John W. Furness
United Kingdom

Ladies and gentlemen, it is now my task as your conference chairman to formally close this Tenth ESV Conference. In doing so, I would like to make some comments on the proceedings. First, I am sure you will agree that the conference itself and the associated social events have been both interesting and enjoyable. We have had a considerable number of reports and papers presented on a variety of topics concerning the safety design of road vehicles. Many were of high quality and have shown us some new and promising aspects of vehicle safety design to exploit. In addition, we were able to see the practical application of several of these ideas on vehicles and components exhibited here this week. The result seems to me to have fully justified the decision of the organisers to extend the scope of the conference to include motorcycles, trucks, and buses, as well as passenger cars.

On behalf of my co-chairman Michael Finkelstein and myself, I would like to thank everyone for their contribution to the success of the conference: to the U.K. Department of Transport for hosting the conference, the Planning Panel and staff of the Institution of Mechanical Engineers, and the U.S. National Highway Traffic Safety Administration for organising the event; to all who contributed papers, took part in panel discussions, chaired technical sessions, presented status reports, or made exhibits available; for the cooperation of the Society of Motor Manufacturers and Traders, the University and Colleges of Oxford, our interpreters, the catering staff, projectionists, and the secretarial and other workers behind the scenes. Even the weather was unusually kind to us, which helped the outdoor events!

I would also like to make special reference to James

Shively of NHTSA who has acted as U.S. coordinator for all ten ESV conferences and is, I understand, due to retire shortly; to Ian Neilson of the Transport and Road Research Laboratory for helping to organise the exhibition and acting as the focal point for the receipt of all the European papers, and to Dr. Cedric Ashley for his able summary of the technical highlights of the conference papers and exhibits.

In conclusion, I am most grateful to Sir Peter Lazarus, Permanent Secretary, U.K. Department of Transport, for opening the Conference, and to Miss Diane Steed, Administrator, NHTSA, U.S. Department of Transportation, for her stimulating keynote address, for presenting the NHTSA awards, and for giving us so much of her valuable time.

It only remains for me to thank you once again, to wish you all a safe journey home, and to declare the Tenth ESV Conference closed.

*U.S. GOVERNMENT PRINTING OFFICE: 1986-499-027

DOT HS 806 916
February 1986